Cairo University

CUIPA

# Cairo University International Publications Awards

Vol. 11 ( 1 )

June - 2017


# International Publications Awards
## Cairo University


# Vol. 11 Issue 1

# June 2017

## Dear colleagues,

We are pleased to introduce vol. 11(1) issue of the international publications of Cairo University. It is a further step and distinct contribution, reflecting the scientific ability of staff members, which conforms to international quality standards.

The purpose of issuing these publications is mainly to introduce this work to the academic community, demonstrate the different research abilities of CairoUniversity researchers, and encourage them to increase the quality and quantity of their research.

We would like to assure you that the administration will spare no effort to support and reinforce these goals.

We congratulate all colleagues who were granted the awards for their international publications of the year 2016 and wish them all the best for their future endeavors.

We are also pleased to inform you that this policy will continue to be in effect for the years to come.

.

**Prof. Amr adly**

**Vice - President for post-graduate studies and research**
**Cairo university**

**Prof. Gaber Nassar**

**President**
**Cairo university**

| Issue | I | II | III<br>A, B | IV<br>A, B | V | VI<br>A, B | VII | Vol. 5(1) | Vol. 5(2) | Vol. 6(1)<br>A, B, C |
|---|---|---|---|---|---|---|---|---|---|---|
| Year | Sep. 2007 | Dec. 2007 | Oct. 2008 | May 2009 | Oct. 2009 | May 2010 | Oct. 2010 | May 2011 | Oct. 2011 | May 2012 |
| Issue | Vol. 6(2) | Vol. 7(1)<br>A, B, C | Vol. 7(2) | Vol. 8(1) | Vol. 8(2) | Vol. 9(1) | Vol. 9(2) | Vol. 10(1) | Vol. 10(2) | Vol. 11(1) |
| Year | Oct. 2011 | May 2013 | Oct. 2013 | May 2014 | Oct. 2014 | May 2015 | Nov. 2015 | Jun. 2016 | Nov. 2016 | Jun. 2017 |

# *Table of Contents*


| | Page |
|---|---|
| **Preface** | i |
| **List of Publication in Journals** | |
| **1. Basic Sciences Sector** | 1 |
| 1-1 Faculty of Science | 3 |
| 1-2 Faculty of Agriculture | 124 |
| 1-3 Faculty of Veterinary Medicine | 154 |
| 1-4 National Institute of Laser Sciences | 204 |
| **2. Engineering Sciences Sector** | 211 |
| 2-1 Faculty of Engineering | 213 |
| 2-2 Faculty of Computers and Information | 268 |
| 2-3 Institute of Statistical Studies and Research | 274 |
| 2-4 Faculty of Regional and Urban Planning | 276 |
| **3. Medical Sciences Sector** | 279 |
| 3-1 Faculty of Medicine | 281 |
| 3-2 Faculty of Oral & Dental Medicine | 413 |
| 3-3 Faculty of Pharmacy | 417 |
| 3-4 National Cancer Institute | 521 |
| 3-5 Faculty of Physical Therapy | 538 |
| **4. Social Sciences Sector** | 543 |
| 4-1 Faculty of Economics and Political Science | 545 |
| 4-2 Faculty of Commerce | 551 |
| **5. Humanity Sciences Sector** | 555 |
| 5-1 Faculty of Archaeology | 557 |
| 5-2 Faculty of Arts | 564 |
| 5-3 Faculty of Kindergarten | 564 |
| 5-4 Institute of African Research and Studies | 565 |
| **List of Publication in Books and Chapters** | 573 |
| **Authors' Index** | 585 |

# ( 1 )

# Basic Sciences Sector

1-1 Faculty of Science
1-2 Faculty of Agriculture
1-3 Faculty of Veterinary medicine
1-4 National Institute of Laser Sciences

# Total No. of Publication for Basic Sciences Sector

| Faculty | 2006 | 2007 | 2008 | 2009 | 2010 | Total |
|---|---|---|---|---|---|---|
| Science | 142 | 162 | 241 | 242 | 290 | 1077 |
| Agriculture | 8 | 14 | 35 | 83 | 75 | 215 |
| Veterinary Medicine | 11 | 20 | 47 | 53 | 86 | 217 |
| National Institute of Laser Sciences | 13 | 11 | 9 | 21 | 27 | 81 |
| Total | 174 | 207 | 332 | 399 | 478 | 1590 |

| Faculty | 2011 | 2012 | 2013 | 2014 | 2015 | 2016 | Total |
|---|---|---|---|---|---|---|---|
| Science | 387 | 447 | 509 | 435 | 456 | 619 | 2853 |
| Agriculture | 136 | 148 | 128 | 52 | 96 | 81 | 641 |
| Veterinary Medicine | 136 | 95 | 118 | 71 | 161 | 137 | 718 |
| National Institute of Laser Sciences | 33 | 26 | 32 | 29 | 42 | 50 | 212 |
| Total | 692 | 716 | 787 | 587 | 755 | 887 | 4424 |

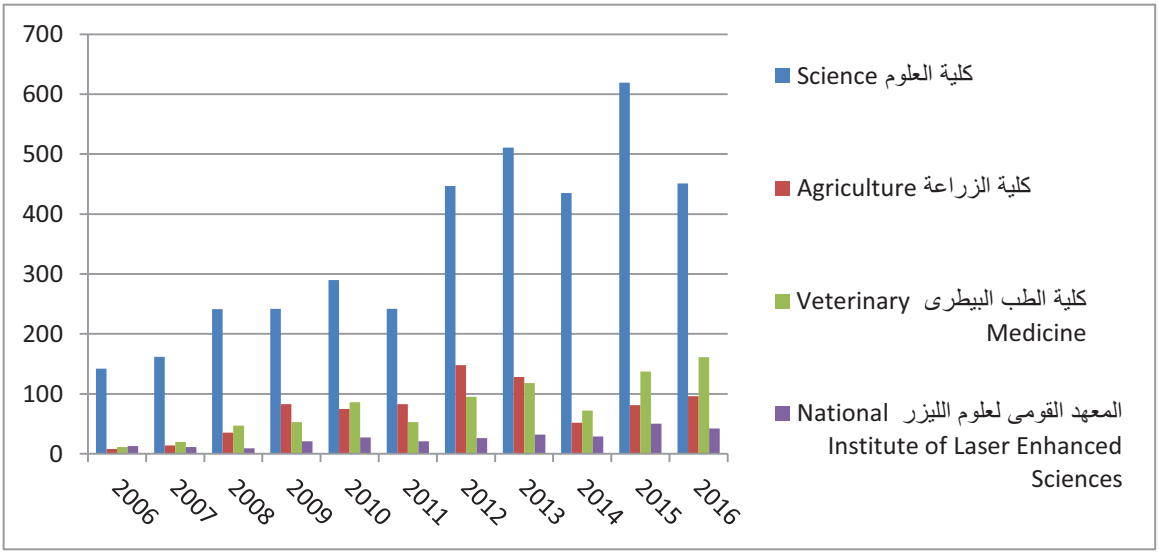

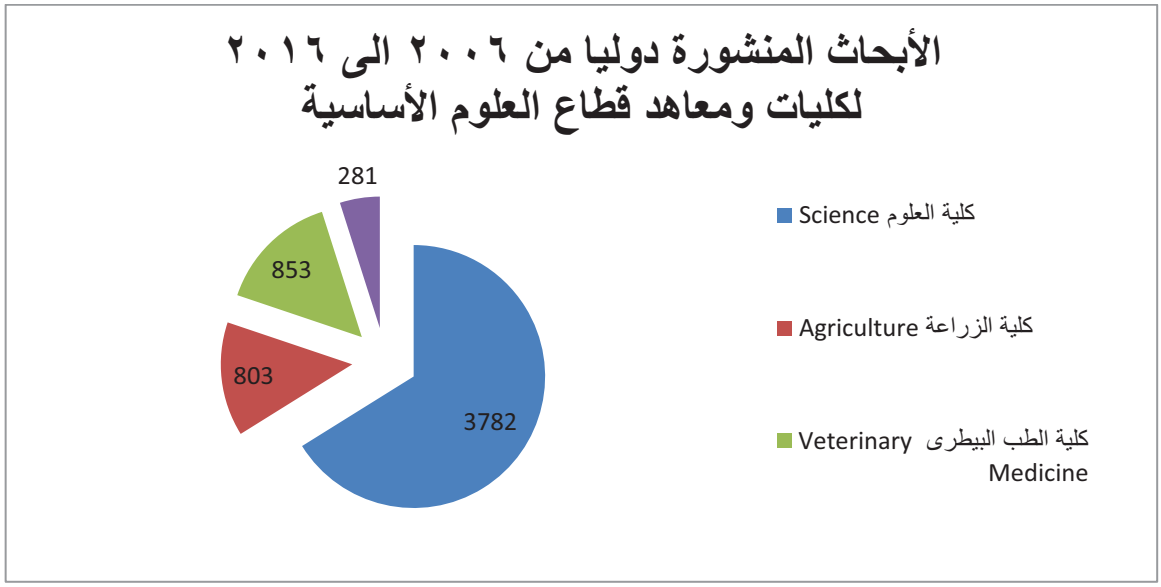
الأبحاث المنشورة دوليا من ٢٠٠٦ الى ٢٠١٦
لكليات ومعاهد قطاع العلوم الأساسية
281
853
803
3782
Science كلية العلوم
Agriculture كلية الزراعة
Veterinary Medicine كلية الطب البيطرى

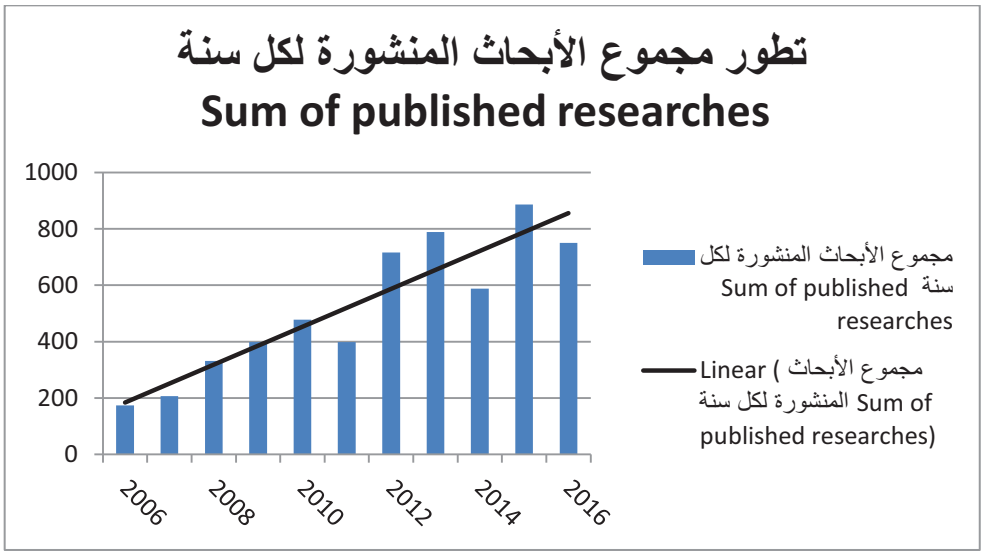
تطور مجموع الأبحاث المنشورة لكل سنة
Sum of published researches
1000
800
600
400
200
0
2006
2008
2010
2012
2014
2016
مجموع الأبحاث المنشورة لكل سنة Sum of published researches
Linear ( مجموع الأبحاث المنشورة لكل سنة Sum of published researches)

## Faculty of Science

***Dept. of Astronomy and Meteorology***

### B-1. A Database of Multi-Year (2004–2010) Quality-Assured Surface Solar Hourly Irradiation Measurements for the Egyptian Territory

Mohamed Korany, Mohamed Boraiy, Yehia Eissa, Youva Aoun, Magdy M. Abdel Wahab, Stéphane C. Alfaro, Philippe Blanc, Mossad El-Metwally, Hosni Ghedira, Katja Hungershoefer and Lucien Wald

*Earth Syst. Sci. Data, 8: 105-113, (2016), IF: 8.286*

A database containing the global and diffuse components of the surface solar hourly irradiation measured from 1 January 2004 to 31 December 2010 at eight stations of the Egyptian Meteorological Authority is presented. For three of these sites (Cairo, Aswan and El-Farafra), the direct component is also available. In addition, a series of meteorological variables including surface pressure, relative humidity, temperature, wind speed and direction is provided at the same hourly resolution at all stations. The details of the experimental sites and instruments used for the acquisition are given. Special attention is paid to the quality of the data and the procedure applied to flag suspicious or erroneous measurements is described in detail. Between 88 and 99 % of the daytime measurements are validated by this quality control. Except at Barrani where the number is lower (13 500), between 20 000 and 29 000 measurements of global and diffuse hourly irradiation are available at all sites for the 7-year period. Similarly, from 9000 to 13 000 measurements of direct hourly irradiation values are provided for the three sites where this component is measured. With its high temporal resolution this consistent irradiation and meteorological database constitutes a reliable source to estimate the potential of solar energy in Egypt. It is also adapted to the study of high-frequency atmospheric processes such as the impact of aerosols on atmospheric radiative transfer. It is planned to update regularly the current 2004–2010 database, which has been placed on the Pangaea repository (doi:10.1594/PANGAEA.848804) and contains the individual meteorological and irradiation data files of the eight stations
**Keywords:** Solar irradiation; Meteorological variables.

### B-2. Helical Kink Instability in a Confined Solar Eruption

Alshaimaa Hassanin and Bernhard Kliem

*Astrophysical Journal, 832 (2016) IF: 5.909*

A model for strongly writhing confined solar eruptions suggests an origin in the helical kink instability of a coronal flux rope which remains stable against the torus instability. This model is tested against the well observed filament eruption on 2002 May 27 in a parametric MHD simulation study which comprises all phases of the event. Good agreement with the essential observed properties is obtained. These include the confinement, terminal height, writhing, distortion, and dissolution of the filament, and the flare loops. The agreement is robust against variations in a representative range of parameter space. Careful comparisons with the observation data constrain the ratio of the external toroidal and poloidal field components to Bet/Bep1 and the initial flux rope twist to $\Phi \approx 4\pi$. Different from ejective eruptions, two distinct phases of strong magnetic reconnection can occur. First, the erupting flux is cut by reconnection with overlying flux in the helical current sheet formed by the instability. If the resulting flux bundles are linked as a consequence of the erupting rope's strong writhing, they subsequently reconnect in the vertical current sheet between them. This reforms the overlying flux and a far less twisted flux rope, offering a pathway to homologous eruptions.
**Keywords:** Instabilities; Magnetohydrodynamics (MHD); Sun: Corona; Sun; Coronal mass ejections (CMES); Sun; Flares; Sun; Magnetic Fields.

### B-3. On the Chemistry of Hydrides of N Atoms and O+ Ions

Zainab Awad, Serena Viti and David A. Williams

*The Astrophysical Journal, 826: 207-214, (2016), IF: 5.909*

Previous work by various authors has suggested that the detection by Herschel/HIFI of nitrogen hydrides along the low-density lines of sight toward G10.6-0.4 (W31C) cannot be accounted for by gas-phase chemical models. In this paper we investigate the role of surface reactions on dust grains in diffuse regions, and we find that formation of the hydrides by surface reactions on dust grains with efficiency comparable to that for H2 formation reconciles models with observations of nitrogen hydrides. However, similar surface reactions do not contribute significantly to the hydrides of O+ ions detected by Herschel/HIFI that are present along many sight lines in the Galaxy. The O+ hydrides can be accounted for by conventional gas-phase chemistry either in diffuse clouds of very low density with normal cosmic-ray fluxes or in somewhat denser diffuse clouds with high cosmic-ray fluxes. Hydride chemistry in dense dark clouds appears to be dominated by gas-phase ion–molecule reactions.
**Keywords:** Astrochemistry; Dust; Extinction; Ism; Abundances; Ism; Clouds; Ism; Molecules.

### B-4. IFU Spectroscopy of Southern Planetary Nebulae - III

A. Ali, M. A. Dopita, H. M. Basurah, M. A. Amer, R. Alsulami and A. Alruhaili

*Monthly Notices of The Royal Astronomical Society, 462: 1393-1404, (2016), IF: 4.952*

In this paper, we describe integral field spectroscopic observations of four southern Galactic planetary nebulae (PNe), M3-4, M3-6, Hen2-29 and Hen2-37 covering the spectral range 3400-7000 angstrom. We derive the ionization structure, the physical conditions, the chemical compositions and the kinematical characteristics of these PNe and find good agreement with previous studies that relied upon the long-slit technique in their co-spatial area. From their chemical compositions as well as their spatial and kinematic characteristics, we determined that Hen2-29 is of the Peimbert type I (He-and N-rich), while the other three are of type II. The strength of the nebular He II line reveals that M3-3, Hen2-29 and Hen2-37 are of mid to high excitation classes while M3-6 is a low-excitation PN. A series of emission-line maps extracted from the data cubes were constructed for each PN to describe its overall structure. These show remarkable morphological

diversity. Spatially resolved spectroscopy of M3-6 shows that the recombination lines of C II, C III, C IV and NIII are of nebular origin, rather than arising from the central star as had been previously proposed. This result increases doubts regarding the weak emission-line star (WELS) classification raised by Basurah et al. In addition, they reinforce the probability that most genuine cases of WELS arise from irradiation effects in close binary central stars.
**Keywords:** Ism; Abundances; Planetary nebulae; Individual; M3-4; Planetary nebulae; Individual; M3-6; Planetary nebulae; Individual; He2-29; Planetary nebulae; Individual; Hen2-37.

## B-5. Non-LTE Equivalent Widths for Nii with Error Estimates

A. Ahmed and T. A. A. Sigut

*Monthly Notices of the Royal Astronomical Society, 455: 1099-1114, (2016), IF: 4.952*

Non-local thermodynamic equilibrium (non-LTE) calculations are performed for NII in stellar atmospheric models appropriate to main-sequence B stars to produce new grids of equivalent widths for the strongest NII lines commonly used for abundance analysis. There is reasonable agreement between our calculations and previous results, although we find weaker non-LTE effects in the strongest optical NII transition, λ3995. We also present a detailed estimation of the uncertainties in the equivalent widths due to inaccuracies in the atomic data via Monte Carlo simulation and investigate the completeness of our model atom in terms of included energy levels. Uncertainties in the basic NII atomic data limit the accuracy of abundance determinations to ≈±0.10 dex at the peak of the NII optical spectrum near Teff ≈ 24 000 K.
**Keywords:** Line; Formation; Radiative transfer; Stars; Abundance; Stars; Atmospheres.

## B-6. Problems for the Wels Classification of Planetary Nebula Central Stars: Self-Consistent Nebular Modelling of Four Candidates

Hassan M. Basurah, Alaa Ali, Michael A. Dopita, R. Alsulami, Morsi A. Amer and A. Alruhaili

*Monthly Notices of the Royal Astronomical Society, 458: 2694-2709, (2016), IF: 4.952*

We present integral field unit (IFU) spectroscopy and self-consistent photoionization modelling for a sample of four southern Galactic planetary nebulae (PNe) with supposed weak emission-line central stars. The Wide Field Spectrograph on the ANU 2.3 m telescope has been used to provide IFU spectroscopy for NGC 3211, NGC 5979, My 60, and M 4-2 covering the spectral range of 3400-7000 angstrom. All objects are high-excitation non-Type I PNe, with strong He II emission, strong [Ne V] emission, and weak low-excitation lines. They all appear to be predominantly optically thin nebulae excited by central stars with T-eff > 10(5) K. Three PNe of the sample have central stars which have been previously classified as weak emission-line stars (WELS), and the fourth also shows the characteristic recombination lines of a WELS. However, the spatially resolved spectroscopy shows that rather than arising in the central star, the CIV and NIII recombination line emission is distributed in the nebula, and in some cases concentrated in discrete nebular knots. This may suggest that the WELS classification is spurious, and that, rather, these lines arise from (possibly chemically enriched) pockets of nebular gas. Indeed, from careful background subtraction we were able to identify three of the sample as being hydrogen rich O(H)-Type. We have constructed fully self-consistent photoionization models for each object. This allows us to independently determine the chemical abundances in the nebulae, to provide new model-dependent distance estimates, and to place the central stars on the Hertzsprung-Russell diagram. All four PNe have similar initial mass (1.5 < M/M-circle dot < 2.0) and are at a similar evolutionary stage.
**Keywords:** Plasmas; Ism; Abundances; Planetary nebulae; Individual; Ngc 3211; Planetary nebulae; Individual; NGC 5979; Planetary nebulae; Individual; My 60; Planetary nebulae; Individual; M 4-2.

## B-7. A Photometric Study of four Recently Discovered Contact Binaries: 1Swasp J064501.21 +342154.9, 1Swasp J155822.10-025604.8, 1Swasp J212808.86+151622.0, and Ucac4 436-062932

G. DjuraševiĆ, A. Essam, O. LatkoviĆ, A. Cséki, M. A. El-Sadek, M. S. Abo-Elala and Z. M. Hayman

*The Astronomical Journal, 152: 1-14, (2016), IF: 4.617*

We present new, high-quality multicolor observations of four recently discovered contact binaries, 1SWASP J064501.21+342154.9, 1SWASP J155822.10-025604.8, 1SWASP J212808.86+151622.0, and UCAC4 436-062932, and analyze their light curves to determine orbital and physical parameters using the modeling program of G. Djurašević. In the absence of spectroscopic observations, the effective temperatures of the brighter components are estimated from the color indices, and the mass ratios are determined with the q-search method. The analysis shows that all four systems are W UMa type binaries in shallow contact configurations, consisting of late-type main-sequence primaries and evolved secondaries with active surface regions (dark or bright spots) resulting from magnetic activity or ongoing transfer of thermal energy between the components. We compare the derived orbital and stellar parameters for these four variables with a large sample of previously analyzed W UMa stars and find that our results fit it well.
**Keywords:** Binaries; Eclipsing; Stars; Fundamental parameters; Stars; Individual (1Swasp J064501.21 +342154.9; 1Swasp J155822.10-025604.8; 1Swasp J212808.86+151622; Ucac4 436-062932).

## B-8. The First Photometric Analyses of the Algol Binary Systems GSC 04328-02164 and GSC 03164-01558

A. Essam, Amal S. Hamed, Shahenaz M. Youssef and Ghada F. Mohamadien

*Astronomical Journa, 151: 19-25, (2016), IF: 4.617*

The CCD observations for the eclipsing Algol type binary systems GSC 04328-02164 in wideband BVRcIc filters and GSC 03164-01558 in B and I filters have been analyzed using the PHOEBE package (v 0.31a) to determine their orbital and

physical parameters. The absolute parameters and evolutionary tracks of the two systems have been determined. The results show that the mass ratio, inclination, distance, and age for the system GSC 04328-02164 are equal to q = 0.674 ± 0.002, i = 75.997 ± 0.022, d = 375.477 ± 4.299 pc, and τ = 26.76 ± 15.65 lowast 108 years, respectively. For the other system, GSC 03164-01558, q = 0.941 ± 0.006, i = 88.0484 ± 0.030, d = 444.651 ± 9.444 pc, and τ = 53.63 ± 9.16 lowast 108 years.
**Keywords:** Binaries; Eclipsing; Stars; Evolution; Stars; Fundamental parameters; Stars; Individual (GSC 04328- 02164, GSC 03164-01558).

## B-9. Cylindrical Thin-Shell Wormholes Supported by Phantom Energy

Ali Mohamed Ali Eid

*Eur. Phys. J. Plus, 131: 298-302, (2016), IF: 1.521*

In the framework of Darmois-Israel formalism, the general equations describing the motion of cylindrical thin-shell wormholes supported by equation of state of phantom energy are derived. The linear perturbation approach is used to investigate the stability of a cylindrical thin-shell wormhole of a static solution.
**Keywords:** Astrophysics; Cosmology; General relativity.

## B-10. On the Stability of Charged Thin-Shell Wormholes

Ali Mohamed Ali Eid

*Eur. Phys. J. Plus, 131: 23-27, (2016), IF: 1.521*

In the framework of Darmois-Israel formalism, the stability of charged thin shell wormholes is discussed by linearized radial perturbations around static solutions at the wormhole throat. A wormhole is described as a limiting case of a constant density spherical shell, where the structure must be unstable to linearized radial perturbations.
**Keywords:** Astrophysics; Cosmology; General relativity.

## B-11. Daily Variation of Radon Gas and its Short-Lived Progeny Concentration Near Ground Level and Estimation of Aerosol Residence Time

M. Mohery, A. M. Abdallah, A. Ali and S. S. Baz5

*Chinese Physics B, 25: 50701-50701, (2016), IF: 1.436*

Atmospheric concentrations of radon (Rn-222) gas and its short-lived progenies Po-218, Pb-214, and Po-214 were continuously monitored every four hours at the ground level in Jeddah city, Kingdom of Saudi Arabia. The measurements were performed three times every week, starting from November 2014 to October 2015. A method of electrostatic precipitation of positively charged Po-218 and Po-214 by a positive voltage was applied for determining Rn-222 gas concentration. The short-lived Rn-222 progeny concentration was determined by using a filter holder connected with the alpha-spectrometric technique. The meteorological parameters (relative air humidity, air temperature, and wind speed) were determined during the measurements of Rn-222 and its progeny concentrations. Rn-222 gas as well as its short-lived progeny concentration display a daily and seasonal variation with high values in the night and early morning hours as compared to low values at noon and in the afternoon. The observed monthly atmospheric concentrations showed a seasonal trend with the highest values in the autumn/winter season and the lowest values in the spring/summer season. Moreover, and in parallel with alpha-spectrometric measurements, a single filter-holder was used to collect air samples. The deposited activities of Pb-214 and the long-lived Rn-222 daughter Pb-210 on the filter were measured with the gamma spectrometric technique. The measured activity concentrations of Pb-214 by both techniques were found to be relatively equal largely. The highest mean seasonally activity concentrations of Pb-210 were observed in the autumn/winter season while the lowest mean were observed in the spring/summer season. The mean residence time (MRT) of aerosol particles in the atmospheric air could be estimated from the activity ratios of Pb-210/Pb-214.
**Keywords:** Atmospheric boundary; Layer; Temporal variations; Seasonal variation; Diurnal variation; Outdoor air; Pb-210; Po-210; Thoron; Egypt; Milan.

## B-12. Bianchi Type I in F(T) Gravitational Theories

M. I. Wanas, G G L Nashed and O A Ibrahim.

*Chinese Physics B, 25: 50401-50401, (2016), IF: 1.436*

A tetrad field that is homogeneous and anisotropic which contains two unknown functions A(t) and B(t) of cosmic time is applied to the field equations of f (T), where T is the torsion scalar, T = T μ νρ S μ νρ . We calculate the equation of continuity and rewrite it as a product of two brackets, the first is a function of f (T) and the second is a function of the two unknowns A(t) and B(t). We use two different relations between the two unknown functions A(t) and B(t) in the second bracket to solve it. Both of these relations give constant scalar torsion and solutions coincide with the de Sitter one. So, another assumption related to the contents of the matter fields is postulated. This assumption enables us to drive a solution with a non-constant value of the scalar torsion and a form of f (T) which represents ΛCDM.
**Keywords:** F(T) Gravitational theory; Bianchi type I; Special solutions.

## B-13. Dynamics of Charged Shell with a Cosmological Constant

Ali Mohamed Ali Eid

*New Astronomy, 44: 17-20, (2016), IF: 1.085*

Using the Darmois–Israel formalism technique, charged thin shell in the presence of a cosmological constant is constructed. An equation governing the behavior of the radial pressure across the junction surface is deduced. The cosmological constant term and the charge term slows down the collapse of matter. The spherical N-shell model with an appropriate initial condition imitates quite well the FRW universe with $\Lambda \neq 0$.
**Keywords:** General relativity; Cosmology; Gravitation; Astrophysics.

## B-14. Helical Kink Instability in the Confined Solar Eruption on 2002 May 27

A. Hassanin, B. Kliem and N. Seehafer

*Astronomische Nachrichten, 337 (2016) IF: 0.956*

This paper presents an improved MHD modeling of the confined filament eruption in solar active region NOAA 9957 on 2002 May 27 by extending the parametric studies of the event in Torok & Kliem2005 and Hassanin & Kliem2016. Here the initial flux rope equilibrium is chosen to possess a small apex height identical to the observed initial filament height, which implies a more realistic inclusion of the photospheric line tying. The model matches the observations as closely as in the preceding studies, with the closest agreement again being obtained for an initial average flux rope twist of about 4π. Thus, the model for strongly writhing confined solar eruptions, which assumes that a kink-unstable flux rope in the stability domain of the torus instability exists at the onset of the eruption's main acceleration phase, is further substantiated.
**Keywords:** Instabilities; Magnetohydrodynamics (MHD); Sun; Corona; Sun; Coronal mass ejections (CMES); Sun; Flares.

## B-15. An AP Structure with Finslerian Flavor: Path Equations

M. I. Wanas, M. E. Kahil and Mona M. Kamal

*Gravitation and Cosmology, 22: 345-354, (2016), IF: 0.909*

The Bazanski approach to deriving paths is applied to Finsler geometry. The approach is generalized and applied to a new developed geometry called "Absolute parallelism with Finslerian Flavor" (FAP). A set of path equations is derived for the FAP. It is a horizontal (h) set. A striking feature in this set is that the coefficient of the torsion term jumps by a step of one-half from one equation to the other. It is tempting to believe that the h-set admits some quantum features. Comparisons with the corresponding sets in other geometries are given. Conditions for reducing the set of path equations obtained to well-known path equations in some geometries are summarized in a schematic diagram
**Keywords:** Bazanski approach; AP-Geometry; Finsler geometry; Quantum properties.

## B-16. Investigating Exoplanet Orbital Evolution Around Binary Star Systems with Mass Loss

Walid A. Rahoma

*Journal of Astronomy and Space Sciences, 33: 257-264 (2016)*

A planet revolving around binary star system is a familiar system. Studies of these systems are important because they provide precise knowledge of planet formation and orbit evolution. In this study, a method to determine the evolution of an exoplanet revolving around a binary star system using different rates of stellar mass loss will be introduced. Using a hierarchical triple body system, in which the outer body can be moved with the center of mass of the inner binary star as a two-body problem, the long period evolution of the exoplanet orbit is determined depending on a Hamiltonian formulation. The model is simulated by numerical integrations of the Hamiltonian equations for the system over a long time. As a conclusion, the behavior of the planet orbital elements is quite affected by the rate of the mass loss from the accompanying binary star.
**Keywords:** Exoplanet; Long period dynamics; Hierarchical system; Triple star systems.

### *Dept. of Biophysics*

## B-17. RNF8 E3 Ubiquitin Ligase Stimulates UBC13 E2 Conjugating Activity that is Essential for DNA Double Strand Break Signaling and Brca1 Tumor Suppressor Recruitment.

Hodge CD, Ismail IH, Edwards RA, Hura GL, Xiao AT, Tainer JA, Hendzel MJ and Glover JN

*Journal Biological Chemistry, 291(18): 9396-9410 (2016 ) IF:4.258*

DNA double strand break (DSB) responses depend on the sequential actions of the E3 ubiquitin ligases RNF8 and RNF168 plus E2 ubiquitin-conjugating enzyme Ubc13 to specifically generate histone Lys-63-linked ubiquitin chains in DSB signaling. Here, we defined the activated RNF8-Ubc13~ubiquitin complex by x-ray crystallography and its functional solution conformations by x-ray scattering, as tested by separation-of-function mutations imaged in cells by immunofluorescence. The collective results show that the RING E3 RNF8 targets E2 Ubc13 to DSB sites and plays a critical role in damage signaling by stimulating polyubiquitination through modulating conformations of ubiquitin covalently linked to the Ubc13 active site. Structure-guided separation-of-function mutations show that the RNF8 E2 stimulating activity is essential for DSB signaling in mammalian cells and is necessary for downstream recruitment of 53BP1 and BRCA1. Chromatin-targeted RNF168 rescues 53BP1 recruitment involved in non-homologous end joining but not BRCA1 recruitment for homologous recombination. These findings suggest an allosteric approach to targeting the ubiquitin-docking cleft at the E2-E3 interface for possible interventions in cancer and chronic inflammation, and moreover, they establish an independent RNF8 role in BRCA1 recruitment.
**Keywords:** 53Bp1; BRCA1; DNAdamage response; E3 Ubiquitin-protein ligase RNF8 (RNF8); RNF168; UBC13; Cell biology; Ubiquitylation (Ubiquitination); X-Ray Crystallography; X-Ray scattering.

## B-18. BCL10 is Recruited to Sites of DNA Damage to Facilitate DNA Double-Strand Break Repair

Ismail I H, Dronyk A, Hu X, Hendzel M J and Shaw A R

*Cell Cycle, 15(1): 84-94, (2016), IF: 3.952*

Recent studies have found BCL10 can localize to the nucleus and that this is linked to tumor aggression and poorer prognosis. These studies suggest that BCL10 localization plays a novel role in the nucleus that may contribute to cellular transformation and carcinogenesis. In this study, we show that BCL10 functions as part of the DNA damage response (DDR). We found that BCL10 facilitates the rapid recruitment of RPA, BRCA1 and RAD51 to sites of DNA damage. Furthermore, we also found that ATM phosphorylates BCL10 in response to DNA damage. Functionally, BCL10 promoted DNA double-

strand breaks repair, enhancing cell survival after DNA damage. Taken together our results suggest a novel role for BCL10 in the repair of DNA lesions.
**Keywords:**BCL10; BRCA1; HR Repair; NF-KB; RNF8/168.

## B-19. Transcranial Low-Level Infrared Laser Irradiation Ameliorates Depression Induced by Reserpine in Rats

Haitham S. Mohammed

*Lasers in Medical Science, 31: 1651-1656, (2016), IF: 2.461*

Transcranial low-level infrared laser is a modality of therapy based on the principle of photons delivered in a non-invasive manner through the skull for the treatment of some neurological conditions such as psychological disorders, traumatic brain injuries, and neurodegenerative diseases among others. In the present study, effects of low-level infrared laser irradiation with different radiation powers (80, 200, and 400 mW, continuous wave) were investigated on normal animals subjected to forced swimming test (FST). Results indicated that there are changes in FST parameters in animals irradiated with laser; the lowest dose provoked a significant increase in animal activity (swimming and climbing) and a significant decrease in animal's immobility, while the highest laser dose resulted in a complete inverse action by significantly increasing animal immobility and significantly decreasing animal activity with respect to control animals. The lowest dose (80 mW) of transcranial laser irradiation has then utilized on animals injected with a chronic dose of reserpine (0.2 mg/kg i.p. for 14 days) served as an animal model of depression. Laser irradiation has successfully ameliorated depression induced by reserpine as indicated by FST parameters and electrocorticography (ECoG) spectral analysis in irradiated animals. The findings of the present study emphasized the beneficial effects of low-level infrared laser irradiation on normal and healthy animals. Additionally, it indicated the potential antidepressant activity of the low dose of infrared laser irradiation.
**Keywords:** Depression; Ecog; FST; Low-level infrared laser; Rat.

## B-20. Role of Silver Nanoparticles in Imparting Antimicrobial Activity of Titanium Dioxide

Wafa I. Abdel-Fatah, Mohamed M. Gobara, Sherif F.M. Mustafa, Ghareib W. Ali and Osiris W. Guirguis

*Materials Letters, 179: 190-193, (2016), IF: 2.437*

In the present work, facile syntheses for titanium dioxide (TiO2), Silver (Ag), and Ag/TiO2 nanoparticles were applied through sol-gel technique. Structural and morphological characterizations were followed by UV, TEM, and SAED. The cup agar diffusion method was followed to investigate the bactericidal activities against three common bacterial strains being Escherichia coli (Gram-negative), Bacillus subtitles and Staphylococcus aureus (Gram positive). The bactericidal activities were evidenced by the inhibition zones of the bacterial growth around the resultant substrates. The results prove promising bactericidal activity of Ag and Ag/TiO2 nanophases compared to TiO2 anatase phase nanoparticles possessing no bactericidal activity. The combined presence of silver nanoparticles along with the anatase phase induced a promising bactericidal activity.
**Keywords:** Biomaterials; Nanoparticles; Sol-Gel Preparation; Antibacterial activity.

## B-21. Zika Viral Polymerase Inhibition Using Anti-Hcv Drugs Both in Market and Under Clinical Trials

Abdo A Elfiky

*Journal of Medical Virology,88 (12):2044-2051(2016)IF:1.998*

In the last few months, a new Zika virus (ZIKV) outbreak evolved in America. In accordance, World Health Organization (WHO) in February 2016 declared it as Public Health Emergency of International Concern (PHEIC). ZIKV infection was reported in more than 60 countries and the disease was spreading since 2007 but with little momentum. Many antiviral drugs are available in market or in laboratories under clinical trials, could affect ZIKV infection. In silico docking study were performed on the ZIKV polymerase to test some of Hepatitis C Virus (HCV) drugs (approved and in clinical trials). The results show potency of almost all of the studied compounds on ZIKV polymerase and hence inhibiting the propagation of the disease. In addition, the study suggested two nucleotide inhibitors (IDX-184 and MK0608) that may be tested as drugs against ZIKV infection.
**Keywords:** Molecular modeling; Zikavirus; Polymerase; Nucleotideinhibitors; IDX-184; Protein-Ligand docking.

## B-22. An Efficient Method for Measuring the Similarity of Protein Sequences

A. El-Lakkani and M. Lashin

*Sar a and osar in Environmental Research, 27(5): 363-370, (2016), IF: 1.897*

An accurate numerical descriptor for protein sequence is introduced. It is basically a set of each three successive amino acids in the sequence (triplet), starting from left to right, in addition to the distances between each two successive amino acids in the triplet such that the summation of these distances does not exceed 8. This numerical descriptor combines two features the amino acid composition and the position of each amino acid relative to the other nearby aminoacids. This numerical descriptor is used to measure the similarity between protein sequences in three sets: NADH dehydrogenase subunit 5 (ND5) proteins of different species, 24 transferrin proteins from vertebrates and 12 proteins of baculoviruses. High correlation coefficient values between our results and the results of ClustalW program are obtained. These values are higher than the values obtained in many other related works.
**Keywords:** Similarity analysis; Protein sequences; Graphical representation; Numerical descriptor; Correlation and significance analysis.

## B-23. Effect of Fast Neutrons on the Structure and Thermal Properties of PVA/HPMC Blends

Nabawia A. Abdel-Zaher, Manal T. H. Moselhey and Osiris W. Guirguis

*Journal of Thermal Analysis and Calorimetry, 126: 1289-1299, (2016), IF: 1.781*

Blends of PVA/HPMC of different mass percents are prepared using solution casting method and are subjected to fast neutron irradiation of fluence 1x107 n cm-2. Structural configuration of the blends as well as thermal properties is studied using X-ray diffraction (XRD) and thermal analyses (differential scanning calorimetry and thermal gravimetric analysis) to reveal the miscibility map and to characterize the structural properties of the blend system. The data obtained from the X-ray diffraction patterns show broadening and sharpening of peaks at different HPMC concentrations with PVA as well as by irradiation with fast neutrons. Thermal analyses show variations in the first-order thermodynamic transition temperature, the melting temperature, shape and area of thermal peaks which are attributed to the different degrees of crystallinity and the existence of polymer–polymer interactions between PVA and HPMC molecules. The data explain the possibility of miscibility existence between the amorphous components of the two homopolymers PVA and HPMC.
**Keywords:** PVA - HPMC Blends; X-Ray diffraction; Dsc; Thermogravimetric analysis; Fast neutrons irradiation.

## B-24. Drug–Polymer Interaction Between Glucosamine Sulfate and Alginate Nanoparticles: Ftir, Dsc and Dielectric Spectroscopy Studies

A S El-Houssiny, A A Ward, D M Mostafa, S L Abd-El-Messieh, K N Abdel-Nour, M M Darwish and W A Khalil

*Advances in Natural Sciences: Nanoscience and Nanotechnology, 7 (2016) IF: 1.581*

This work involves the preparation and characterization of alginate nanoparticles (Alg NPs) as a new transdermal carrier for site particular transport of glucosamine sulfate (GS). The GS–Alg NPs were examined through transmission electron microscopy (TEM), Fourier transform infrared spectroscopy (FTIR), differential scanning calorimetry (DSC) and dielectric spectroscopy. GS–Alg NPs was efficiently prepared via ionic gelation method which generates favorable conditions for the entrapment of hydrophilic drugs. The TEM studies revealed that GS–Alg NPs are discrete and have spherical shapes. FTIR studies showed a spectral change of the characteristic absorptions bands of Alg NPs after encapsulation with GS because of the amine groups of GS and the carboxylic acid groups of Alg. The DSC data showed changes in the thermal behavior of GS–Alg NPs after the addition of GS indicating signs of main chemical interaction among the drug (GS) and the polymer (Alg). The absence of the drug melting endothermic peak within the DSC thermogram of GS–Alg NPs indicating that GS is molecularly dispersed in the NPs and not crystallize. From the dielectric study, it was found modifications within the dielectric loss (ε") and conductivity (σ) values after the addition of GS. The ε" and σ values of Alg NPs decreased after the addition of GS which indicated the successful encapsulation of GS within Alg NPs. Furthermore, the dielectric study indicated an increase of the activation energy and the relaxation time for the first process in the GS–Alg NPs as compared to Alg NPs. Consequently, the existing observations indicated an initiation of electrostatic interaction among the amine group of GS and carboxyl group of Alg indicating the successful encapsulation of GS inside Alg NPs which could provide favorable circumstance for the encapsulation of GS for topical management.
**Keywords:** Alginate; Transdermal carrier; Nanoparticles; Glucosamine sulfate.

## B-25. IDX-184 is A Superior Hcv Direct-Acting Antiviral Drug: A Qsar Study

Abdo A. Elfiky and Wael M. Elshemey

*Medicinal Chemistry Research, 25: 1005-1008, (2016),IF:1.436*

Quantitative structure–activity relationship (QSAR) parameters are good indicators for the reactivity of direct-acting antiviral drugs. Since molecular structure is related to molecular function, careful selection of molecular substitutions will result in more drugs that are potent. In this work, QSAR parameters are selected in order to compare the four drugs used as nucleotide inhibitors (NIs) for non-structural 5B (NS5B) RNA-dependent RNA polymerase (RdRp) of hepatitis C virus (HCV). These drugs are: ribavirin (widely used over the last 20 years), sofosbuvir (approved on December 2013 by FDA), and finally IDX-184 and R7128 (phase IIb of clinical trial drugs). The nucleotide analogues uracil (U), guanine (G), and cytosine (C) from which these drugs are fabricated are also compared to that group of drugs. QSAR parameters suggested that the drug IDX-184 is the best among all of the studied NIs. It also shows that NIs are always more reactive than their parent nucleotide.
**Keywords:** Qsar; NS5B; Sofosbuvir; IDX-184; Nucleotide inhibitors.

## B-26. Geometrical Parameters and Scattered Radiation Effects on the Extrinsic Sensitivity and Counting Efficiency of a Rectangular Gamma Camera

Mohamed A. Ghoneim, M.H. Khedr and Wael M. Elshemey

*Applied Radiation and Isotopes, 118: 131-135, (2016), IF:1.136*

A point source is used to investigate the effect of water phantom thickness and source-to-detector distance (SDD) on the sensitivity and counting efficiency of a rectangular detector gamma camera. The increase in water thickness resulted in an increase in scatter fraction, a decrease in sensitivity, and counting efficiency. The increase in SDD resulted in a decrease in sensitivity and an increase in counting efficiency. An SDD of 0.79±0.02 m is found to provide a good compromise for acceptable sensitivity and reasonable counting efficiency
**Keywords:** Gamma camera; Scattered fraction; Extrinsic sensitivity; Counting efficiency; Calibration.

## B-27. Electroporation Parameters for Successful Transdermal Delivery of Insulin

Ebtsam A. Mohammad, Wael M. Elshemey, Anwar A. Elsayed and Amr A. Abd-Elghany

*American Journal of Therapeutics, 23 (2016) IF: 1.132*

This work investigates the effects of electroporation parameters on the transdermal delivery of insulin. Electroporation (EP) is known to induce temporal pores in the membrane, which are expected to enhance the diffusion of insulin through rabbits' skin. For such purpose, 5 different formulations of insulin and enhancers are applied to rabbit groups (5 rabbits each) with induced hyperglycemia in the presence of electroporative pulses. The blood sugar level (BSL) is followed up to 5-hour duration starting from the administration of the hyperglycemia-inducing factor. The effect of different electroporation parameters on BSL of rabbits is examined and compared with control groups. Results show that the increase in the number of pulses (from 15 up to 60 successive pulses) at an insulin concentration of 50 IU/mL, the increase in insulin concentration (from 50 to 70 IU/mL), and the decrease in applied field strength (from 200 to 100 V/cm) result in a significant decrease in BSL compared with control. Among all of the investigated formulations, the best performance is recorded for the insulin solution + EP (without enhancers) in almost all of the studied experimental conditions.

**Keywords:** Electroporation; Insulin; Hyperglycemia; Transdermal delivery.

## B-28. Molecular-Level Characterization of Normal, Benign and Malignant Breast Tissues Using Ftir Spectroscopy

Wael M. Elshemey, Alaa M. Ismail and Nihal S. Elbialy

*Journal of Medical and Biological Engineering, 36: 369-378, (2016), IF: 1.018*

The present study investigates the diagnostic capability (sensitivity, specificity, and diagnostic accuracy) of the Fourier transform-infrared (FTIR) technique as a tool for the characterization of excised breast tissues with special emphasis on the differentiation between malignant and benign tumors. For such purpose, normal, malignant, and benign excised breast tissue samples were collected. The scatter diagrams of suggested FTIR characterization parameters were plotted and the corresponding diagnostic indices were calculated, showing maximum values reaching 100 % for differentiating between normal and diseased samples. The receiver operating characteristic analysis of such indices reported that the maximum area under the curve reached a value of one, which indicates highly accurate performance. The capability of the technique to differentiate between benign and malignant samples yielded promising results. A deconvolution of the Amide I protein peak revealed a high percentage of ordered protein secondary structure elements in normal tissue compared to those for malignant and benign tumors. The results indicate that the FTIR technique is ready for application in the characterization of excised breast tissues.

**Keywords:** Breast cancer; Fourier transform; Infrared (FTIR) Spectroscopy; Receiver operating characteristic (Roc) curve; Scatter diagram; Deconvolution.

## B-29. Role of Duty Cycle on Pseudomonas Aeruginosa Growth Inhibition Mechanisms by Positive Electric Pulses

Fadel M. Ali, Reem H. Elgebaly, Mona S. Elneklawi and Amal S. Othman

*Bio-Medical Materials and Engineering, 27: 211-225 (2016) IF: 0.988*

**Background:** P. aeruginosa considered as a notoriously difficult organism to be controlled by antibiotics or disinfectants.The potential use of alternative means as an aid to avoid the wide use of antibiotics against bacteria pathogen has been recentlyarisen remarkably. **Objective:** Effect of extremely low frequency positive electric pulse with different duty cycles on Pseudomonas aeruginosa(ATCC: 27853) growth by constructed and implemented exposure device was investigated in this study. **Methods:** The exposure device was applied to give extremely low frequency in the range of 0.1 up to 20 Hz with thecapability to control the duty cycle of each pulse with variation from 10% up to 100%. Growth curves of Pseudomonas aeruginosawere investigated before and after exposure to different frequencies (0.1, 0.2, 0.3, 0.4, 0.5, 0.6, 0.7, 0.8, 0.9 Hz) throughmeasuring the optical density and cell count. Exposures to selected frequencies in the whole ranges of duty cycles were done.These studies were followed by DNA fragmentation, transmission electron microscope (TEM), antibiotic susceptibility tests,and dielectric measurements. **Results:** Findings revealed inhibition effect by 48.56% and 47.4% together with change in the DNA structural properties forsamples exposed to 0.5 Hz and 0.7 Hz respectively. Moreover the data indicated important role of duty cycle on the inhibitionmechanism. **Conclusion:** It is concluded that there are two different mechanisms of interaction between positive electric pulse andmicroorganism occurred; 0.5 Hz caused rupture in cell wall while 0.7 Hz caused denaturation of the inner consistent of the cell.

**Keywords:** Extremely low frequency; Pseudomonas aeruginosa; Duty cycle; Positive electric pulse; DNA; TEM.

## B-30. Assessment of DNA Damage in Ehlrich Carcinoma after Treatment with Doxorubicin Encapsulated in Nanoscales thermosensitive Liposomes in Combination Tith Localized Hyperthermia

Rageh M M, Shafaa M W, Elhefnawy M R and El-Nagdy M S

*General Physiology Biophysics,35(3):311-322(2016)IF:0.892*

Nanoscales thermosensitive liposomes (TSL) composed of synthetic lipids (dipalmitoylphosphatidylcholine and distearoylphosphatidylcholine), were used for doxorubicin encapsulation with 70% encapsulated efficiency. The liposomes were characterized by dynamic light scattering, transmission electron microscopy and turbidity method. Additionally, the liposomes exhibited a significant release of doxorubicin (Dox) by 60% within 5 min at 42°C. To assess the therapeutic efficacy of Dox in combination with hyperthermia, Dox free and encapsulated TSL were administered directly to Ehrlich tumor bearing mice at 1 mg/kg dose. Immediately after the drug administration, hyperthermia was applied to mention the temperature inside the tumor site at 42°C either for 5 min and

30 min. The results indicate a significant increase in the percent of apoptotic and necrotic cells in the treated group. Moreover, disrupts the integrity and the amount of intact DNA in tumor cells. In conclusion, Dox and hyperthermia may serve as a useful targeted drug delivery system for management of Ehrlich carcinoma.

**Keywords:** Thermosensitive liposomes; Hyperthermia; Doxorubicin; Cancer; Comet assay; DNA.

## B-31. Eco-Friendly Methods of Copper Nanoparticles Synthesis

Jihad Ibrahim Abd-Elkareem, Hatem Mahmoud Bassuony, Sepa Mostafa Mohammed, Heba Mohamed Fahmy and Nada Reda Abd-Elkader

*Journal of Bionanoscience, 10: 15-37 (2016)*

Metal nanoparticles were widely synthesized in the last few decades and have been shown large scales of applications. Copper nanoparticles have various applications in numerous areas such as nanofluids, biological applications, optical and nano devices due to their special properties depending on their size such as electrical conductivity, thermal and visual properties. Physical, thermal, and chemical reductions are the most preponderant synthesis methods of copper nanoparticles. These methods are complex, many steps methods with high cost and toxicity. So their contributions in biological applications will be reduced. For those reasons, using Green chemistry led to distinguish progress in nanoparticles' synthesis methods. It could resolves the problem of the high toxicity of chemical synthesized nanoparticles, offers lower cost, allows eco-friendly methods and facilitates synthesis procedures. In our work we represent an overview and comparison between different green synthesis methods of copper nanoparticles (using plants, plant leaves, microorganisms, fungi, Crustaceans and mixtures of two of them). The present review also discusses the advantages and disadvantages of these green synthesis methods in the aim of providing the researchers concerned with the copper nanoparticles synthesis and applications with a deep insight through comparing different methods of green chemistry synthesis of copper nanoparticles.

**Keywords:** Antibacterial activity; Antimicrobial effect; Copper; Cu nps; Green chemistry; Metal nanoparticles; Nontoxic nanostructures; Sem; Synthesis; Tem.

## B-32. Exposure of Chitosan to Uv/Ozone: Structural Information and Antibacterial Activity

Osiris W. Guirguis, Gehan T. El-Bassyouni, Mona A. Esawy, Nada R. Abd Elkader, Hadeer M. Mahmoud, Hend M. Mostafa and Nabawia A. Abdel-Zaher

*Journal of Applied Pharmaceutical Science, 6: 124-130 (2016)*

In the present work, variation in the group coordination of chitosan due to the exposure to UV/ozone was considered by the FTIR reflectance. Pronounced variations in the intensities of reflectance bands and shifts in their positions were detected. This could be attributed to the change in the molecular configuration of chitosan. On the other hand, the well diffusion method was used to investigate the anti-bactericidal activities against two common bacterial strains [Bacillus subtitles (B. subtilis) and Escherichia coli (E. coli)] by detecting the mean inhibition zone diameters (IZD) against the micro-organisms. The achieved data revealed that the chitosan exposed to UV/ozone confirmed a high potential of antibacterial activity.

**Keywords:** Chitosan; Structural information; FTIR; Antibacterial activity; Uv/Ozone treatment.

## B-33. Geographical Renogram Scanning for Patients of Renal Diseases

Adel M. kelany, Osiris W. Guirguis and Rania M. Abdel Halim

*Australian Journal of Basic and Applied Sciences, 10: 154-173 (2016)*

Geochemical environment is indeed a significant factor in the serious health problems.Many people have suffered from diseases that led to serious studies to find out the relationship between drinking water and chronic diseases. The chemistry of drinking water commonly has been cited as an important factor in many diseases. A strong relationship between contaminated drinking water with heavy metals from some of the governorates in Egypt and chronic diseases such as renal failure has been identified in this study. These diseases are apparently related to contaminant drinking water with heavy metals such as Fe, Pb, Cd, Mn and Ni. Renal failure is related to contaminated drinking water with lead (Pb) and cadmium (Cd). There is a relationship between chronic diseases and geologic environment. The purpose of the present study is to assess and compare drinking water quality with WHO standards and its related renal diseases in seven governorates in Egypt: Cairo, Giza, El-Sharkia, El-fayoum, Bani-Sweif, Sohag and Aswan. Water samples have been taken for each governorate from drinking water tap. Data collection based on laboratory analyses of water samples and patients with renal diseases that undergoing investigation for diagnosis in Nuclear Medicine Department using Glomerular Filtration Rate (GFR) as indicator for renal function status. Some physical and chemical parameters are examined to find out quality of drinking tap water. The data reveal that percentage of renal failure and obstructed kidneys are in progress in surveyed geographical areas. Situation was much worse for Aswan where the percentage of renal failure was about 76.41% then El- Fayoum with about 66.67%, Sohag with about 66.28%, Bani-Sweif with about 64.49%, El-Sharkia with about 64.29%, Cairo about 53.19% and Giza with about 49.65%. The patients with obstructed nephrouropathy were much worse for Giza (about 26.95%), El-Sharkia (about 26.67%) and Cairo (about 25.53%). The percentage of patients with hydronephrotic kidneys was the highest in Upper Egypt. To save local residents study suggests; regular monitoring of water quality should be practiced to provide safe drinking water and regular monitoring of renal functions to protect the kidney from different diseases.

**Keywords:** Drinking water; Nuclear medicine; Gfr and renal failure.

*Dept. of Botany*

## B-34. High Salinity Induces Different Oxidative Stress and Antioxidant Responses in Maize Seedlings Organs

Hamada Abd Elgawad Gaurav Zinta Momtaz M. Hegab Renu Pandey Han Asard and Walid Abuelsoud

*Frontiers in Plant Science, 7 (2016) IF: 4.495*

Salinity negatively affects plant growth and causes significant crop yield losses world-wide. Maize is an economically important cereal crop affected by high salinity. In this study, maize seedlings were subjected to 75 mM and 150 mM NaCl, to emulate high soil salinity. Roots, mature leaves (basal leaf-pair 1,2) and young leaves (distal leaf-pair 3,4) were harvested after 3 weeks of sowing. Roots showed the highest reduction in biomass, followed by mature and young leaves in the salt-stressed plants. Concomitant with the pattern of growth reduction, roots accumulated the highest levels of Na+ followed by mature and young leaves. High salinity induced oxidative stress in the roots and mature leaves, but to a lesser extent in younger leaves. The younger leaves showed increased electrolyte leakage (EL), malondialdehyde (MDA), and hydrogen peroxide (H2O2) concentrations only at 150 mM NaCl. Total antioxidant capacity (TAC) and polyphenol content increased with the increase in salinity levels in roots and mature leaves, but showed no changes in the young leaves. Under salinity stress, reduced ascorbate (ASC) and glutathione (GSH) content increased in roots, while total tocopherol levels increased specifically in the shoot tissues. Similarly, redox changes estimated by the ratio of redox couples (ASC/total ascorbate and GSH/total glutathione) showed significant decreases in the roots. Activities of enzymatic antioxidants, catalase (CAT, EC 1.11.1.6) and dehydroascorbate reductase (DHAR, EC 1.8.5.1), increased in all organs of salt-treated plants, while superoxide dismutase (SOD, EC 1.15.1.1), ascorbate peroxidase (APX, EC 1.11.1.11), glutathione-s-transferase (GST, EC 2.5.1.18) and glutathione reductase (GR, EC 1.6.4.2) increased specifically in the roots. Overall, these results suggest that Na+ is retained and detoxified mainly in roots, and less stress impact is observed in mature and younger leaves. This study also indicates a possible role of ROS in the systemic signaling from roots to leaves, allowing leaves to activate their defense mechanisms for better protection against salt stress.

**Keywords:** Maize; Salinity; Oxidative stress.

## B-35.Atmospheric Pressure Plasma Jet for Bacterial Decontamination and Property Improvement of Fruit and Vegetable Processing Wastewater

Abdel-Aleam H Mohamed, Samir M Al Shariff, Salama A Ouf and Mohamed Benghanem

*Journal of Physics D: Applied Physics, 49: 195-401-12, (2016), IF: 2.772*

An atmospheric pressure plasma jet was tested for decontaminating and improving the characteristics of wastewater derived from blackberry, date palm, tomato and beetroot processing industries. The jet was generated by blowing argon gas through a cylindrical alumina tube while a high voltage was applied between two electrodes surrounding the tube. Oxygen gas was mixed with argon at the rate of 0.2% and the argon mass flow was fixed at 4.5 slm. Images show that the generated plasma jet penetrated the treated wastewater samples. Plasma emission spectra show the presence of O and OH radicals as well as excited molecular nitrogen and argon. Complete decontamination of wastewater derived from date palm and tomato processing was achieved after 120 and 150 s exposure to the plasma jet, respectively. The bacterial count of wastewater from blackberry and beetroot was reduced by 0.41 and 2.24 log10 colony-forming units (CFU) per ml, respectively, after 180 s. Escherichia coli was the most susceptible bacterial species to the cold plasma while Shigella boydii had the minimum susceptibility, recording 1.30 and 3.34 log10 CFU ml−1, respectively, as compared to the 7.00 log10 initial count. The chemical oxygen demands of wastewater were improved by 57.5–93.3% after 180 s exposure to the plasma jet being tested. The endotoxins in the wastewater were reduced by up to 90.22%. The variation in plasma effectiveness is probably related to the antioxidant concentration of the different investigated wastewaters.

**Keywords:** Cold plasma Jet; Wastewater; Bacterial decontamination; Antioxidants; Endotoxins.

## B-36. Arthrocladium, an Unexpected Human Opportunist in Trichomeriaceae (Chaetothyriales

Mariana M. F. Nascimento, Laura Selbmann, Somayeh Sharifynia, Abdullah M. S. Al-Hatmi, Hermann Voglmayr, Vania A. Vicente, Shuwen Deng, Alexandra Kargl, Tarek A. A. Moussa, Hassan S. Al-Zahrani, Omar A. Almaghrabi and G. Sybren De Hoog

*Fungal Biology, 120: 207-218, (2016), IF: 2.244*

The family Trichomeriaceae (Chaetothyriales) mainly comprises epiphytic and epilithic organisms. In some species elaborate ascomata are formed, but for the great majority the species no asexual conidium formation is known other than simple fragmentation of the thallus. The present paper re-establishes the genus Arthrocladium with three non-sporulating species. One of these is described for a strain causing a fatal infection in a human patient with a rare genetic immune disorder.

**Keywords:** Black yeasts; Disseminated infection; Phylogeny; Sterile fungi.

## B-37. Fatty Acid Constituents of Peganum Harmala Plant Using Gas Chromatography–Mass Spectroscopy

Tarek A.A. Moussa and Omar A. Almaghrabi

*Saudi Journal of Biological Sciences, 23: 397-403 (2016) IF:1.781*

Fatty acid contents of the Peganum harmala plant as a result of hexane extraction were analyzed using GC–MS. The saturated fatty acid composition of the harmal plant was tetradecanoic, pentadecanoic, tridecanoic, hexadecanoic, heptadecanoic and octadecanoic acids, while the saturated fatty acid derivatives were 12-methyl tetradecanoic, 5,9,13-trimethyl tetradecanoic and 2-methyl octadecanoic acids. The most abundant fatty acid was hexadecanoic with concentration 48.13% followed by

octadecanoic with concentration 13.80%. There are four unsaturated fatty acids called (E)-9-dodecenoic, (Z)-9-hexadecenoic, (Z,Z)-9,12-octadecadienoic and (Z,Z,Z)-9,12,15-octadecatrienoic. The most abundant unsaturated fatty acid was (Z,Z,Z)-9,12,15-octadecatrienoic with concentration 14.79% followed by (Z,Z)-9,12-octadecadienoic with concentration 10.61%. Also, there are eight non-fatty acid compounds 1-octadecene, 6,10,14-trimethyl-2-pentadecanone, (E)-15-heptadecenal, oxacyclohexadecan-2 one, 1,2,2,6,8-pentamethyl-7-oxabicyclo[4.3.1] dec-8-en-10-one, hexadecane-1,2-diol, n-heneicosane and eicosan-3-ol.

**Keywords:** Peganum harmala; Unsaturated fatty acids; Saturated fatty acids; Non-fatty acids; GC–MS.

## B-38. Cinnamon Oil: A Possible Alternative for Contact Lens Disinfection.

Rasha H. Bassyounia, Zeinat Kamel, Maha Mohssen Abdelfattah and Eman Mostafa

*Contact Lens and Anterior Eye, 39(4):277-283 (2016) IF: 1.752*

**Objective:**To investigate the antibacterial activity of cinnamon oil alone and in combination with a multipurpose contact lens disinfectant solution (MPS) as well as tobramycin against multi drμg resistant conjunctival bacteria both in planktonic and sessile forms. **Methods:** Minimum inhibitory concentrations (MIC) of tobramycin and cinnamon oil against 19 bacterial strains were investigated against planktonic and sessile cells by micro-dilution methods. Synergistic effects were determined by well diffusion and micro-dilution tissue culture plate methods for planktonic and sessile cells respectively. Time kill assay was performed to study the bactericidal effect of cinnamon oil in concentrations ranging from 5% to 0.312% combined with an MPS with respect to time. **Results:** MICs of cinnamon oil against planktonic bacteria ranged from 0.04% to 1.25% versus 0.156% to 5% for sessile cells. Combination of cinnamon oil with tobramycin had a synergistic effect against most tested organisms. The MIC values of cinnamon oil in combination with tobramycin was significantly lower than cinnamon oil alone against biofilm production (P=0.004). Time kill assay revealed that combination of cinnamon oil and disinfectant successfully eradicated the tested microorganisms at all tested concentrations within 2h contact time except for 0.312% concentration (3h) versus 24h for MPS alone. **Conclusion:**Cinnamon oil has a promising antimicrobial effect. It could be a probable candidate for contact lens disinfection.

**Keywords:** Antimicrobial; Cinnamon oil; Conjunctival microbiota; Contact lens; Disinfectant.

## B-39. Antimicrobial Activity of Gold Nanoparticles (Aunps) on Deterioration of Archeological Gilded Painted Cartonnage, Late Period, Saqqara, Egypt

Hala A. M. Afifi, Neveen S. Geweely, Heba S. Galal, Shehata A. Abdelrahim and Fatma M.S. Al-Qudsid

*Geomicrobiology Journal, 33: 578-585, (2016), IF: 1.402*

A piece of polychrome and gilded cartonnage mask was excavated by the Ministry of Antiquities in Saqqara region. It belongs to the late period. The mask upon mummy presented a gilded face with heavy wig height 30–40 cm was painted with green, black eye brow and red mouth. Cartonnage is a composite material consists of organic support contains many glued layers of linen or papyri that have ground painting layers. It suffers from many deterioration aspects (microbial pigments, and flaking most likely due to inappropriate storage. Examination study was performed to analyze and investigate the ground painting and gilding layer of the cartonnage by optical light microscopy, Scanning electron microscopy (SEM) equipped with energy dispersive X-ray analysis, Fourier transform infrared spectroscopy (FTIR) and X-ray diffraction (XRD). The results confirmed that the degradation factors affecting on the painted, gilded cartonnage was attributed to the direct effects of microbial phenomena, which have led to many deterioration forms (macro- and micro cracks, flaking, coloration, scaling and defoliation microbiological spots). Three Gram-positive bacteria (Bacillus cereus, Bacillus licheniformis and Staphylococcus aureus), two Gram-negative bacteria (Escherichia coli and Pseudomonas aeruginosa) and four fungal species (Aspergillus flavus, Botrytes cinerea, Fusarium moniliforme, and Verticillium albo-atrum) were isolated from archeological gilded painted cartonnage. Antibacterial and antifungal activities of three shapes (rods, spheres and prisms) of gold nanoparticles (AuNPs) were tested against the isolated deteriorated microbial species. The rod-shaped gold nanoparticles have high potential antibacterial and antifungal activity reaching to the maximum significant inhibition (8- and 9-cm inhibition zones) against the most sensitive bacterial and fungal species (B. cereus and A. flavus, respectively) accompanied with leakage of protein and nucleic acid, sugars and electrolytes. Disturbance in the blood picture of guinea pigs infected with the most resistant species (P. aeruginosa and F. moniliforme) were showed. The rod-shaped gold nanoparticles were safe and successful in curing the tested inoculated guinea pigs.

**Keywords:** Biodegradation; Medicine; Microbe; Nanoparticles; Pathogenic.

## B-40. Review Paper: Integrated Algal Engineering for Bioenergy Generation, Effluent Remediation, and Production of High-Value Bioactive Compounds

Mohd Azmuddin Abdullah, Ashfaq Ahmad, Syed Muhammad Usman Shah, Sanaa Mahmoud Metwally Shanab, Hamdy Elsayed Ahmed Ali, Mervat Aly Mohamed Abo-State and Mohd Fariduddin Othman

*Biotechnology and Bioprocess Engineering, 21: 236-249 (2016) IF: 1.211*

Increased demand for energy worldwide has resulted in increasing interest in alternative renewable sources of biofuels. Demand for improved systems of bioenergy generation, environmental remediation, and coproduction of high value bioactive compounds has led to the potential use of algae in biomass utilization. In Malaysia, palm oil industries generate high amount of solid wastes. Palm Oil Mill Effluent (POME) is estimated to be three times of the amount of crude palm oil produced. POME is a heavily polluting wastewater due to its high chemical oxygen demand (COD), high biochemical oxygen demand (BOD), and high contents of minerals such as nitrogen and phosphorus that can cause severe pollution to the environment and water resources. A combination of wastewater

treatment and renewable bioenergy co-generation with recovery of high-value biochemicals would benefit the palm oil industry.
**Keywords:** Microalgae; Bioenergy; Biocompounds; Palm oil mill offluent; Bioremediation.

## B-41. Anti-Fungal Potential of Ozone Against some Dermatophytes

Salama A. Ouf, Tarek A. Moussa, Alshimaa M. Abd-Elmegeed and Samar R. Eltahlawy

*Brazilian Journal of Microbiology,47:697-702 (2016) IF:0.865*

Dermatophytes are classified in three genera, Epidermophyton, Microsporum and Trichophyton. They have the capacity to invade keratinized tissue to produce a cutaneous infection known as dermatophytoses. This investigation was performed to study the effect of gaseous ozone and ozonized oil on three specific properties of six different dermatophytes. These properties included sporulation, mycelia leakage of sugar and nutrients and the activity of their hydrolytic enzymes. Generally, ozonized oil was found to be more efficacious than gaseous ozone. Microsporum gypseum and Microsporum canis were the most susceptible, while Trichophyton interdigitale and T. mentagrophytes were relatively resistant. The study revealed a steady decline in spore production of M. gypseum and M. canis on application of ozonated oil. An increase in leakage of electrolytes and sugar was noticed after treatment with ozonized oil in the case of M. gypseum, M. canis, T. interdigitale, T. mentagrophytes and T. rubrum. The results also revealed loss in urease, amylase, alkaline phosphatase, lipase and keratinase enzyme producing capacity of the investigated fungi.
**Keywords:** Dermatophytes; Dermatophytosis; Ozone; Hydrolytic enzymes; Ozonized oil.

## B-42. Association Study of Single Nucleotide Polymorphism of Human Toll Like Receptor 9 and Susceptibility to Pulmonary Tuberculosis in Egyptian Population

Samia M. Omran, Zeinat K. Mohamed, Zainab Zakaria, Yasser M. Abd-Elmonem and Khaled E. El Gayar

*Afr. J. Microbiol. Res, 10 (20): 717-724 (2016)*

Toll-like receptors (TLRs) are known to play important roles in human innate immune systems. Polymorphisms in and functions of TLRs have been investigated to identify associations with specific infectious diseases including tuberculosis (TB). This study was performed for 166 samples of unrelated individual's diagnosis of pulmonary tuberculosis and 98 household healthy samples. Genomic DNA was extracted from EDTA-anticoagulated peripheral blood. The alleles of (rs352140) TLR9 gene polymorphisms were detected using polymerase chain reaction restriction fragment length polymorphism. The resulting fragments were separated in 3% agarose gel electrophoresis. The sequence results generated by the forward and reverse sequencing primers were analyzed with the software program sequencing analysis. Sequence comparisons of three genotypes AG, AA, and GG were performed using the multiple-alignment algorithm in Megalign. The direct counting was used to determine the allele and genotype frequencies of each polymorphism. Hardy-Weinberg equilibrium (HWE) tests were performed in controls by Fisher exact test. Significant deviations from the Hardy-Weinberg equilibrium in the distribution of the TLRs SNP genotypes in TB patients and controls were not detected for the SNP TLR9rs352140 for both patients and controls. These results do not indicate a major influence of these putative functional TLR SNP on the susceptibility to (or protection from) tuberculosis in Egyptian population.
**Keywords:** Association; TLR9; Tuberculosis; Egyptian population.

## B-43. Biosynthesis Characterization and Antimicrobial Activity of Silver Nanoparticles from Actinomycetes

Zeinat Kamel, Mahmoud Saleh and Noha El Namoury

*Research Journal of Pharmaceutical Biological and Chemical Sciences, (2016)*

Biosynthesis of silver nanoparticles using some Streptomyces species was reported, out of 46 strains tested, 15 strains showed ability to synthesized AgNPs. Among which the two potential Streptomyces M-13 and Streptomyces M-24 showed high potency of production of silver nanoparticles. Biosynthesized AgNPs from potent strain was characterized using UV-visible spectroscopy, FTIR analysis, Transmission Electron Microscope (TEM). TEM study indicated the formation of spherical shape distributed silver nanoparticles without aggregation varying from 10-20 nm in size. The silver nanoparticles synthesized by potential Streptomyces M-13 and Streptomyces M-24 showed good antibacterial activity against Gram-positive and Gram-negative bacteria by well diffusion method. The two potential Streptomyces species M-13 and M-24 was characterized and identified as Streptomyces graminofaciens and Streptomyces catenulae, respectively. The two Streptomyces strains reported in the present study are a newly added source for the biosynthesis of silver nanoparticles and these nanoparticles can be used potentially for biomedical application.
**Keywords:** Silver nanoparticles; Streptomyces graminofaciens; Streptomyces catenulae; Tem; Antimicrobial activity.

## B-44. Biosynthesis, Characterization, and Antimicrobial Activity of Silver Nanoparticles from Actinomycetes

Zeinat Kamel, Mahmoud Saleh and Noha El Namoury

*Research Journal of Pharmaceutical, Biological and Chemical Sciences, 7: 119-127 (2016)*

Biosynthesis of silver nanoparticles using some Streptomyces species was reported, out of 46 strains tested, 15 strains showed ability to synthesized AgNPs. Among which the two potential Streptomyces M-13 and Streptomyces M-24 showed high potency of production of silver nanoparticles. Biosynthesized AgNPs from potent strain was characterized using UV-visible spectroscopy, FTIR analysis, Transmission Electron Microscope (TEM). TEM study indicated the formation of spherical shape distributed silver nanoparticles without aggregation varying from 10-20 nm in size. The silver nanoparticles synthesized by potential Streptomyces M-13 and Streptomyces M-24 showed good antibacterial activity against Gram-positive and Gram-negative bacteria by well diffusion

method. The two potential Streptomyces species M-13 and M-24 was characterized and identified as Streptomyces graminofaciens and Streptomyces catenulae, respectively. The two Streptomyces strains reported in the present study are a newly added source for the biosynthesis of silver nanoparticles and these nanoparticles can be used potentially for biomedical application.
**Keywords:** Silver nanoparticles; Streptomyces graminofaciens; Streptomyces catenulae; Tem; Antimicrobial activity.

## B-45. Characterization of Aspergillus Flavus Ng 85 Laccase and its Dye Decolorization Efficiency

N. M. Khalil, M. I. A. Ali, S. A. Ouf and M. N. Abd El-Ghany

*Research Journal of Pharmaceutical, Biological and Chemical Sciences, 7: 817-829 (2016)*

The purified laccase of Aspergillus flavus NG85 isolated from Saint Catherine Protectorate, showed a molecular weight of 68.5 kDa. Its optimum activity obtained at enzyme concentration of 0.15 mg, substrate concentration of 10 mg/ml, temperature of 47.5 oC, pH of 5 and Km of 9.09 mg/ml. The enzyme retained 85% of its activity after 4 hours of incubation at 50 oC and 88% of its activity after 4 hours of incubation at pH 5. Copper sulfate exhibited the highest significant promotive effect on laccase activity, while sodium azide caused complete inhibition. The maximum and rapid decolorization of the purified laccase was achieved with malachite green. Among seven metallic ions tested, copper ion was the best in decolorization efficiency. Furthermore, decolorization of the real textile effluent by purified laccase predominantly occurred within the first 4 days. The putative gene for laccase was isolated, sequenced and recorded in Gene bank under accession number KM522917.2.
**Keywords:** Laccase; Optimization; Synthetic dyes; Decolorization.

## B-46. Isolation and Characterization of Two Phages Infecting Streptomyces Scabies

AlKhazindar M, Sayed ETA, Khalil MS and Zahran D

*Research Journal of Pharmaceutical, Biological and Chemical Sciences, 7: 1351-1363 (2016)*

Potato scab is an important wide spread disease caused by Streptomyces scabies. Actinophages affect the composition and diversity of bacterial population, thereby, can be used as biological control. Two specific phages against S. scabies were isolated from different potato fields in different locations in Giza, Egypt. Phages were partially characterized using electron microscopy and genome structure. The first phage is suggested to belong to family podoviridae and was named vB_StscP-G1 however, the second phage belongs to family siphoviridae and was named vB_StscS-G2. Physical properties including dilution end point, longevity invitro, thermal inactivation point and host range were studied for the two isolated phages. Both phages were thermostable and were not affected by storage up to 180 days at room temperature. Furthermore, they were infective in acidic and alkaline conditions but, were totally inhibited at high alkaline conditions. Antiviral activity was also studied using different plant extracts and chemicals. Some plant extract showed a significant inhibitory effect on the isolated phages. However, sodium chloride and copper sulphate showed significant increase in the activity of the phages. Our results provide a useful data for designing a control strategy against potato scab disease.
**Keywords:** Potato scab; Actinophages; Electron microscopy; Podoviridae; Siphoviridae; Titre; Antiviral activity.

### *Dept. of Chemistry*

## B-47. Spontaneous MirrorSymmetry Breaking in Isotropic Liquid Phases of Photoisomerizable Achiral Molecules

Mohamed Alaasar, Marko Prehm, Yu Cao, Feng Liu and Carsten Tschierske

*Angewandte Chemie International Edition, 55: 312-316, (2016), IF: 11.709*

Spontaneous mirror-symmetry breaking is of fundamental importance in science as it contributes to the development of chiral superstructures and new materials and has a major impact on the discussion around the emergence of uniform chirality in biological systems. Herein we report chirality synchronization, leading to spontaneous chiral conglomerate formation in isotropic liquids of achiral and photoisomerizable azobenzene-based rod-like molecules. The position of fluorine substituents at the aromatic core is found to have a significant effect on the stability and the temperature range of these chiral liquids. Moreover, these liquid conglomerates occur in a new phase sequence adjacent to a 3D tetragonal mesophase.
**Keywords:** Polycatenars; Azo compounds; Chirality; Mirror symmetry breaking.

## B-48. Molecularly Imprinted Polymer-Based Bulk Optode for the Determination of Itopride Hydrochloride in Physiological Fluids

F.M. Abdel-Haleem, Adel Madbouly, R.M. El Nashar and N.T. Abdel-Ghani

*Biosensors and Bioelectronics, 85: 740-742, (2016), IF: 7.476*

We report here for the first time on the use of Molecularly Imprinted Polymers as modifiers in bulk optodes, Miptode, for the determination of a pharmaceutical compound, itopride hydrochloride as an example in a concentration range of 1×10−1–1×10−4 mol L−1. In comparison to the optode containing the ion exchanger only (Miptode 3), the optode containing the ion exchanger and the MIP particles (Miptode 2) showed improved selectivity over the most lipophilic species, Na+ and K+, by more than two orders of magnitude. For instance, the optical selectivity coefficients using Miptode 2, View the MathML source, were as follow: View the MathML source−6; Na+=−4.0, which were greatly enhanced in comparison with that obtained by Miptode 3. This work opens a new avenue for using miptodes for the determination of all the pharmaceutical preparations without the need for the development of new ionophores.
**Keywords:** Molecularly imprinted polymer; Bulk optode; Itopride hydrochloride; Miptode.

## B-49. Nano-$TiO_2$ Modified Carbon Paste Sensor for Electrochemical Nicotine Detection Using Anionic Surfactant

M. Shehataa, S.M. Azab, A.M. Fekry and M.A. Ameer

*Biosensors and Bioelectronics, 79: 589-592, (2016), IF: 7.476*

A newly competitive electrochemical sensor for nicotine (NIC) detection was successfully achieved. Nano-TiO2 with a carbon paste electrode (CPE) were used for the sensor construction, where Nano-TiO2 was considered as one of the richest and highly variable class of materials. The sensor showed electrocatalytic activity in both aqueous and micellar media toward the oxidation of NIC at Britton–Robinson (B–R) buffer solution (4×10−2 M) of pH range (2.0–8.0) containing (1.0 mM) sodium dodecylsulfate (SDS) using cyclic voltammetry (CV) and electrochemical impedance spectroscopy (EIS) techniques. Scanning electron microscope (SEM) and Energy Dispersive X-Ray Analysis (EDX) techniques were also used. The linear range of detection for NIC using the new Nano-TiO2 Modified Carbon Paste sensor (NTMCP) was detected using diffrential pulse voltammetry (DPV) technique and it was found between 2×10−6 M and 5.4×10−4 M with a detection limit of 1.34×10−8 M. The obtained results clarified the simplicity, high sensitivity and selectivity of the new NTMCPE for nicotine determination in real cigarettes and urine samples.

**Keywords:** Nicotine; Nano-TiO2; Cyclic voltammetry; Scanning electron microscope.

## B-50. Deactivation of Au/Ceo2 Catalysts During Co Oxidation: Influence of Pretreatment and Reaction Conditions

A. Abd El-Moemen, Ali M. Abdel-Mageed, J. Bansmann, M. Parlinska-Wojtan, R. J. Behm and G. Kučerová

*Journal of Catalysis, 341: 160-179, (2016), IF: 7.354*

The influence of the pretreatment on the activity and deactivation behavior of a high surface area 4.5 wt.% Au/CeO2 catalyst during low temperature CO oxidation reaction (Treact = 80 °C) was studied in a multi-technique approach. Furthermore, the influence of changing from a close-to-stoichiometric (1% CO, 1% O2 rest N2), to O2-rich (1% CO, 5% O2 rest N2) and CO-rich (5% CO, 1% O2 rest N2) gas mixtures was investigated. Findings from kinetic and deactivation measurements are correlated with experimental data on the Au particle size, Au and Ce oxidation state, and on the nature of adsorbed species after the different pretreatments and during/after subsequent reaction, which were obtained by operando and in situ methods such as operando X-ray absorption spectroscopy and IR spectroscopy, as well as ex situ X-ray photoelectron spectroscopy, X-ray diffraction and transmission electron microscopy. These data revealed that the pretreatment significantly affects catalyst structure, surface composition and activity in the initial stages of the reaction. During reaction, however, the catalyst surface composition approaches a dynamic equilibrium state, which is largely reached already after 10 min time on stream and which is independent of the pretreatment. Consequently, under present reaction conditions, longer-term deactivation is not dominated by the buildup of site blocking adsorbed species such as surface carbonates, but by slow processes such as reduction/re-oxidation of the bulk support during the reaction in combination with a modest irreversible Au NP growth.

**Keywords:** Co oxidation; Catalyst pretreatment; Deactivation; Au Catalyst; Au/Ceo2; Xps; Drifts; Xas.

## B-51. Water Assisted Dispersion of Ru Nanoparticles: the Impact of Water on the Activity and Selectivity of Supported Ru Catalysts During the Selective Methanation of Co in Co2-Rich Reformate

Ali M. Abdel-Mageed, S. Eckle, D. Widmann and R. J. Behm

*Journal of Catalysis, 335: 79-94, (2016), IF: 7.354*

We have investigated the impact of realistic high water contents up to 30% on the selective methanation of CO in CO2-rich (15.5% CO2) reformates on supported Ru catalysts. Both for a Ru/γ-Al2O3 catalyst and for a highly active Ru/zeolite catalyst, the activity decreased somewhat in the presence of water, with the extent depending on the CO content and on the catalyst. Most drastic are the changes in the selectivity for CO methanation in the range of low CO contents (100 ppm) on the Ru/Al2O3 catalyst, for which it increased from 42% in the absence of water to 100% in the presence of 30% water. For the Ru/zeolite catalyst, which is 100% selective already in dry gas independent of the CO concentration, high water contents did not affect the selectivity. For the Ru/Al2O3 catalyst, time resolved operando extended X-ray absorption fine structure (EXAFS) measurements revealed that the Ru particle size increases gradually with reaction time during the first 200 min, and stays constant afterward. Under steady-state conditions the increase in selectivity observed for the Ru/Al2O3 catalyst goes along with a decrease in the Ru particle size with increasing water content, from 2.0 nm under dry conditions to 1.2 nm at 15% water in the feed (Ru/zeolite: 1.0–0.8 nm at 5% H2O under steady-state conditions). We attribute this to a water assisted disruption of Ru–Ru bonds, leading to a dispersion of the Ru nanoparticles. Consequences on the reaction and adsorption behavior, with the latter being followed by in situ diffuse reflectance infrared Fourier transform spectroscopy (DRIFTS), are discussed in terms of a mechanistic picture derived earlier, which correlates the selectivity for CO methanation with the Ru particle size, with small Ru nanoparticles exhibiting a low activity for CO2 dissociation.

**Keywords:** Selective Co methanation; CO2 dissociation; Water effect; Particle size effect; Ru catalyst; Alumina; Zeolite; Operando exafs; Ru K-Edge; Drifts.

## B-52. Mirror Symmetry Breaking in Cubic Phases and Isotropic Liquids Driven by Hydrogen Bonding

Mohamed Alaasar, Silvio Poppe, Qingshu Dong, Feng Liu and Carsten Tschierske

*Chemical Communications, 52: 13869-13872, (2016), IF: 6.567*

Achiral supramolecular hydrogen bonded complexes between rod-like 4-(4-alkoxyphenylazo)pyridines and a taper shaped 4-substituted benzoic acid form achiral (Ia3d) with combining macron]d) and chiral “Im[3 with combining macron]m-type” bicontinuous cubic (I432) phases and a chiral isotropic liquid

mesophase (Iso1). The chiral phases, resulting from spontaneous mirror symmetry breaking, represent conglomerates of macroscopic chiral domains eventually leading to uniform chirality.
**Keywords:** Polycatenars; Azo compounds; Chirality; Mirror Symmetry breaking; Self-Assembly.

## B-53. Helical Nano-Crystallite (Hnc) Phases: Chirality Synchronization of Achiral Bent-Core Mesogens in a New Type of Dark Conglomerates

Mohamed Alaasar, Marko Prehm and Carsten Tschierske

*Chemistry -A European Journal, 22:6583-6597 (2016) IF:5.771*

Spontaneous generation of macroscopic homochirality in soft matter systems by self-assembly of exclusively achiral molecules under achiral conditions is a challenging task with relevance for fundamental scientific research and technological applications. Dark conglomerate phases (DC phases), being optically isotropic mesophases composed of conglomerates of macroscopic chiral domains and formed by some non-chiral bent-core mesogens, represent such a case. Here we report two new series of non-symmetric bent-core molecules capable of forming a new type of mirror symmetry broken DC phases. In the synthesized molecules, a bent 4-bromoresorcinol core is connected to a phenyl benzoate wing and an azobenzene wing with or without additional peripheral fluorine substitution. The self-assembly was investigated by DSC, polarizing microscopy, electro-optical studies and XRD. Chiral and apparently achiral DC phases were observed besides distinct types of lamellar liquid crystalline phases with different degree of polar order, allowing the investigation of the transition from smectic to DC phases. This indicates a process in which increased packing density at first gives rise to restricted rotation and thus to growing polar order, which then leads to chirality synchronization, layer frustration and nano-scale crystallization. Topological constraints arising from the twisted packing of helical conformers in lamellar crystals is proposed to lead to amorphous solids composed of helical nano-crystallites with short coherence length (HNC phases). This is considered as a third major type of DC phases, distinct from the previously known liquid crystalline sponge phases and the helical nano-filament phases (HNF phases). Guidelines for the molecular design of new materials capable of self-assembly into these three types of DC phases are proposed.
**Keywords:** Amorphous materials;Azo compounds;Chirality;Mesophases;Self-assembly.

## B-54. Electrochemical Behavior of Surgical 316L Stainless Steel Eye Glaucoma Shunt (Ex-Press) in Artificial Aqueous Humor

Amany M. Fekry, Renad S. El-Kamel and Azza A. Ghoneim

*Journal of Materials Chemistry B, 4 (26): 4542-4548 (2016) IF: 4.872*

A novel system of electrodeposited gold nanoparticles on a carbon paste electrode was utilized as an electrochemical sensor to monitor the corrosion performance of 316L stainless steel alloy in aqueous humor containing moxifloxacin hydrochloride (MFH) drug. Electrochemical impedance spectroscopy (EIS), cyclic voltammetry (CV) and potentiodynamic polarization measurements were used to estimate the corrosion performance of 316L stainless steel alloy in aqueous humor with immersion time. The experimental data was confirmed by scanning electron microscopy (SEM), Energy dispersive X-ray analysis (EDX) and antibacterial activity. All techniques conform well to each other and confirmed that the tested alloy corrosion decreases with increasing immersion time in aqueous humor. Corrosion is more inhibited after the addition of MFH drug. In addition, as the concentration of the drug increases, the protection efficiency of the tested alloy increases. This behavior was confirmed by sensing the drug concentration with time using the modified carbon paste electrode.
**Keywords:**SEM; EDX; EIS.

## B-55. A Novel Nano-Palladium Complex Anode for Formic Acid Electro-Oxidation

Gumaa A. El-Nagar, Ahmed F. Darweesh and Ibrahim Sadiek

*Electrochimica Acta, 215: 334-338, (2016), IF: 4.803*

This study introduces a novel nano-sized palladium complex with high electrocatalytic activity and stability as a catalyst for the anodic reaction of direct Formic acid fuel cell (DFAFC). Morphologically, as prepared Pd-complex has intersected nano-rod like structure with an average particle size of 7 nm. Nano-Pd-complex modified GC electrode showed 10 times higher electrocatalytic activity and 16 times higher stability compared with the traditional Pd nanoparticles modified GC electrode with the same Pd weight. This significant improvement may be attributed to its small size and bulky structure that hinders the sintering of the active Pd atoms (i.e., obstructs the growth of Pd particle size) and impedes the adsorption of poisoning intermediate species (e.g., CO) and/or formation reversible surface hydride as evidenced by the DFT calculations. This study introduces a new promising category of Pd-based catalyst with high activity, catalyst utilization and durability for DFAFCs applications.
**Keywords:** Nano-Pd; Complex; Electrocatalysis; Fuel cells.

## B-56. Determination of Some Neurotransmitters at Cyclodextrin/Ionic Liquid Crystal/Graphene Composite Electrode

Nada F.Atta, Ekram H.El-Ads,Yousef M. A. and Ahmed Galal

*Electrochimica Acta, 199: 319-331, (2016), IF: 4.803*

A novel reduced graphene oxide (RGO) composite glassy carbon electrode modified with ionic liquid crystal (ILC), 1-Butyl-1-methylpiperidinium hexa-fluoro-phosphate and cyclodextrin (CD/ILC/RGO/ILC/GC) was fabricated via mechanical casting of each layer. The modified electrode was used for the determination of some neurotransmitters such as dopamine (DA), epinephrine (EP), norepinephrine (NEP), levodopa (L-DOPA), 3,4-dihydroxy-phenyl acetic acid (DOPAC) and serotonin (ST). This electrode anticipated the good electron mobility and large surface area of graphene, high ionic conductivity and stability of ionic liquid crystal besides the pre-concentrating effect of CD. Optimization of the sensor performance is presented and resulted in a better current signal. The linear dynamic range of the modified electrode was from $0.8\times10^{-7}$–$0.1\times10^{-4}$ mol $L^{-1}$ for determination of EP with a correlation coefficient 0.998 and LOD $0.0117\times10^{-9}$ mol $L^{-1}$.

The sensor was sensitive and successfully applied for direct determination of EP in human urine samples with good recovery results.

**Keywords:** Graphene; Ionic liquid crsytal; Cyclodextrin; Neurotransmitters; Epinephrine; Human urine.

## B-57. Highly Selective Thiourea-Based Bulk Optode for Determination of Salicylate in Spiked Urine Samples, Aspirin and Aspocid

F.M. Abdel-Haleem

*Sensors and Actuators B: Chemical, 233: 257-262 (2016) IF:4.758*

Thiourea-based bulk optodes were prepared for the determination of salicylate in biological and pharmaceutical samples; these optodes were prepared by embedding the thiourea ionophore in a plasticized poly (vinyl chloride) impregnated with the chromoionophore ETH7075 (Ob) or ETH5294 (Od). The observed optical response was explained by the salicylate extraction into the polymer via Hydrogen bond formation and simultaneous protonation of the chromoionophores yielding the absorbance change at 525 or 665 nm for Ob or Od, respectively. The developed optodes exhibited very good selectivity for salicylate over most lipophilic anions and oxoanions that can form Hydrogen bond. For instance, the optical selectivity coefficients using Ob optode, View the MathML source, were as follows: View the MathML source; Benzoate−=−2.6; View the MathML source which were greatly enhanced in comparison with that obtained by the previous work. Both Ob and Od exhibited detection limits of 3.9 × 10−5 and 1.0 × 10−4 mol L−1 with 3 and 5 min response times, respectively, at pH 4.5 using acetate buffer with very good reversibility. The developed sensors were utilized successfully for the determination of salicylate in spiked urine samples, Aspirin and Aspocid.

**Keywords:** Salicylate optodes; Thiourea ionophore; Ph Chromoionophore; Aspirin; Aspocid; Spiked urine.

## B-58. Unconventional Chd+ N Hydrogen Bonding Interactions in the Stepwise Solvation of the Naphthalene Radical Cation by Hydrogen Cyanide and Acetonitrile Molecules

Sean P. Platt, Isaac K. Attah, M. S. El-Shall, Rifaat Hilal, Shaaban A. Elroby and Saadullah G. Aziz

*Physical Chemistry and Chemical Physics, 18(4): 2580-2590, (2016), IF: 4.449*

Equilibrium thermochemical measurements using the mass-selected ion mobility (MSIM) technique havebeen utilized to investigate the binding energies and entropy changes of the stepwise association ofhydrogen cyanide (HCN) and acetonitrile (CH3CN) molecules with the naphthalene radical cation(C10H8_+) in the gas phase forming the C10H8_+(HCN)n and C10H8_+(CH3CN)n clusters with n = 1–3 and 15, respectively. The lowest energy structures of the$C_{10}H_8$_+(HCN)n and C10H8_+($CH_3CN$)n clusters forn = 1–2 have been calculated using the M062X and o97XD methods within the 6-311+G** basis set,and for n = 1–6 using the B3LYP method within the 6-311++G** basis set. In both systems, the initialinteraction occurs through unconventional CHd+...N ionic hydrogen bonds between the hydrogenatoms of the naphthalene cation and the lone pair of electrons on the N atom of the HCN or the CH3CN molecule. The binding energy of CH3CN to the naphthalene cation (11 kcal mol (1is larger than that of HCN (7 kcal mol (1due to a stronger ion–dipole interaction resulting from the large dipole moment of CH3CN (3.9 D). On the other hand, HCN can form both unconventional hydrogen bonds with the hydrogen atoms of the naphthalene cation (CHd+ NCH), and conventional linear hydrogen bonding chains involving HCN.. HCN interactions among the associated HCN molecules. HCN molecules tend to form ‘‘externally solvated’’ structures with the naphthalene cation where the naphthalene ion is hydrogen bonded to the exterior of an HCN… HCN chain. For the C10H8+ (CH3CN)n clusters‘‘‘internally solvated’’ structures are favored where the acetonitrile molecules are directly interacting withthe naphthalene cation through CHd+ N unconventional ionic hydrogen bonds. In both theC10H8+(HCN)n and C10H8)+CH3CN)n clusters, the sequential binding energy decreases stepwise toabout 6–7 kcal mol 1by three HCN or CH3CN molecules, approaching the macroscopic enthalpy ofvaporization of liquid HCN (6.0 kcal mol1).

## B-59. Chemically Modified Carbon Paste and Membrane Sensors for the Determination of Benzethonium Chloride and Some Anionic Surfactants (Sles, Sdsand Labsa): Characterization Using Sem and Afm

Yousry M. Issaa, Sabrein H. Mohamed and Mohamed Abd-El Baset

*Talanta, 155: 158-167, (2016), IF: 4.035*

Chemically modified carbon-paste (CMCP) and membrane-sensors based on incorporating benzothonium-tetraphenylborate (BT-TPB) were constructed for the analysis of benzethonium chloride, and some other surfactants such as sodium lauryl ether sulphate (SLES), sodium dodecyl sulphate (SDS), and linear alkylbenzene sulphonic acid (LABSA). All sensors showed good sensitivity and reverse wide linearity over a concentration range of 5.97×10−7 to 1.00×10−3 and 5.96×10−7 to 3.03×10−3 mol L−1 with limit of detection of 3.92×10−7and 3.40×10−7 mol L−1 for membrane and chemically modified carbon paste sensors, respectively, with respect to benzethonium chloride (BT.Cl). They could be used over a wide pH range of 2.0–10.0. The thermal coefficients of membrane and CMCP sensors are 5.40×10−4, 1.17×10−4 V/°C, respectively. The sensors indicated a wide selectivity over different inorganic cations. The effect of soaking on the surface morphology of the membrane sensor was studied using EDX-SEM and AFM techniques. The response time was <10 s The freshly prepared, exhausted membrane, and CMCP sensors were successfully applied for the potentiometric determination of the pure BT.Cl solution. They were also used for the determination of its pharmaceutical formulation Dermoplast® antibacterial spray (20% benzocaine+0.2% benzethonium chloride) with recovery values ranging from 97.54±1.70 to 101.25±1.12 and from 96.32±2.49 to 101.23±2.15%. The second goal of these sensors is the potentiometric determination of different surfactants such as SLES, SDS, and LABSA with good recovery values using

BT.Cl as a titrant in their pure forms, and in samples containing one of them (shampoo, Touri dishwashing liquid, and waste water). The statistical analysis of the obtained data was studied.
**Keywords:** Benzethonium chloride; Surfactants; Membrane sensor; Chemically modified carbon paste sensor; Ion selective sensors.

## B-60. Towards A Molecular Level Understanding of the Sulfanilamide-Soil Organic Matter-Interaction

Ashour A. Ahmed, Sören ThieleBruhn, Peter Leinweber and Oliver Kühn

*Science of The Total Environment, 559:347-35(2016)IF: 3.976*

Sorption experiments of sulfanilamide (SAA) on well-characterized samples of soil size-fractions were combined with the modeling of SAA-soil-interaction via quantum chemical calculations. Freundlich unit capacities were determined in batch experiments and it was found that they increase with the soil organic matter (SOM) content according to the order fine silt > medium silt > clay > whole soil > coarse silt > sand. The calculated binding energies for mass-spectrometrically quantified sorption sites followed the order ionic species > peptides > carbohydrates > phenols and lignin monomers > lignin dimers > heterocyclic compounds > fatty acids > sterols > aromatic compounds > lipids, alkanes, and alkenes. SAA forms H-bonds through its polar centers with the polar SOM sorption sites. In contrast dispersion and π-π-interactions predominate the interaction of the SAA aromatic ring with the non-polar moieties of SOM. Moreover, the dipole moment, partial atomic charges, and molecular volume of the SOM sorption sites are the main physical properties controlling the SAA-SOM-interaction. Further, reasonable estimates of the Freundlich unit capacities from the calculated binding energies have been established. Consequently, we suggest using this approach in forthcoming studies to disclose the interactions of a wide range of organic pollutants with SOM.
**Keywords:** Sulfanilamide (Saa); Soil organic matter (Som); Sorption isotherms; Quantum chemical calculations; Quantitative structure-Activity relationship (Qsar).

## B-61. Tailoring Optical Absorption in Silicon Nanostructures from Uv to Visible Light: A Tddft Study

Walid M.I. Hassan, M.P. Anantram, Reza Nekovei, Mahmoud M. Khader and Amit Verma

*Solar Energy, 126: 44-52, (2016), IF: 3.685*

The utilization of silicon nanostructures, from quantum dots to nanowires, for photovoltaic applications depends on understanding the effect of their physical structure on their optical absorption properties. In this work, we perform TDDFT calculations to study the length dependent optical absorption in pristine and doped silicon nanostructures. Our main findings are that: (i) The oscillator strength as a function of length is quadratic at small lengths, and then increases linearly. (ii) The exciton binding energy is seen to decrease by approximately 45% from 0.67 eV to about 0.3 eV with length increase, for a nanostructure with a cross-section diameter of approximately 12 Å. (iii) Doping and codoping with P, B, and Zr have the potential to cause the optical absorption to change from UV to the visible spectrum. The findings of this investigation demonstrate the potential to tailor silicon nanostructures for photovoltaic and optoelectronic applications.
**Keywords:** Silicon nanostructures; Exciton binding energy; Doping; Tddft.

## B-62. Pore Structure and Adsorption Properties of Carbon Xerogels Derived from Carbonization of Tannic Acid-Resorcinol-Formaldehyde Resin

Nady A. Fathya,Mahmoud S. Rizk and Reham M.S. Awad

*Journal of Analytical and Applied Pyrolysis, 119: 60-68, (2016), IF: 3.652*

The paper describes a promising route for the synthesis of carbon xerogels using tannic acid- resorcinol-formaldehyde resin (TA-RF) as novel precursors for producing carbon gels with relatively low cost as compared to conventional RF xerogel. Tannic acid as a starting material for preparing these carbon materials is cheaper than resorcinol by about a factor of eight. The effect of both carbonization temperature (773, 873 and 973 K) and reaction time (30 and 60 min) on the microstructure of produced samples was studied. Four micro-mesoporous carbons, namely CX773-30, CX873-30, CX973-30 and CX773-60, were obtained and characterized by using element compositions of carbon, hydrogen and nitrogen (C, H and N), transmission electron microscopy (TEM), fourier transform infrared spectroscopy (FTIR) and N2 adsorption-desorption at 77 K measurements. Adsorption properties of the carbon xerogels obtained toward Pb(II) ions in aqueous solution as function of carbonization temperature and time were investigated. FTIR and TEM results showed that TA-RF xerogel possesses numerous surface functional groups and different shape of interconnected particles in its network as compared to RF xerogel. Carbon xerogel prepared at 973 K and carbonization time at 30 min (CX973-30) given the maximum BET surface area (248 m2 g−1) and total pore volume (0.183 cm3 g−1). Thus the pyrolysis temperature of 973 K and time of 30 min as carbonization conditions for tannic acid-resorcinol-formaldehyde precursor (TA-RF) were the most effective for development of the pore structure of the gel. High adsorption capacity for Pb (II) ions by CX973-30 was obtained (Q = 250 mg g−1) with initial concentrations ranging from 100 to 500 mg L−1 at pH 5.5, and the adsorption isotherm for lead ions followed Langmuir model. The outcome of this study promoted that tannic acid having good potential to be used as carbon precursor and could be polymerized with resorcinol-formaldehyde for preparing carbon xerogels with highly tailored porosity and adsorption capacity.
**Keywords:** Carbon xerogels; Tannic acid; Resorcinol; Formaldehyde; Porosity; Adsorption; Pb (II) Ions.

## B-63. Design and Synthesis of New Ru-Complexes as Potential Photo-Sensitizers: Experimental and Td-Dft Insights

Walid Sharmoukh, Walid M. I. Hassan, Philippe C. Gros and Nageh K. Allam

*Rsc Advances, 6: 69647-69657, (2016), IF: 3.289*

We report density functional theory (DFT) and time-dependent density functional theory (TDDFT) calculations on a novel organic ligand and a novel class of ruthenium complexes; cis-RuL2X2 with L = 2,2′-bipyridine-6,6′-bis ethyl ester phosphonate and phosphonic acid, X = Cl, CN or NCS. The calculations show that cis-configurations are more stable than the trans-counterparts. The DFT results have been used to help design such novel complexes for potential use as sensitizers. We demonstrate the opportunity to synthesize such complexes with high purity. The synthesis of these complexes relies on the preparation of the key intermediates cis-Ru(2,2′-bipyridine-6,6′-bisdiethyl ester phosphonate)Cl2. These complexes were characterized by 1H, 13C, and 31P NMR, elemental analysis and FTIR spectroscopy. The NCS complex shows the smallest optical band gap followed by the Cl and CN complexes, respectively, with the highest performance upon use as a sensitizer in dye-sensitized solar cells.

## B-64. Electrochemical Behavior of a Novel Nano-Composite Coat on Ti Alloy in Phosphate Buffer Solution for Biomedical Applications

Amany M. Fekry

*Rsc Advances, 6: 20276-20285, (2016), IF: 3.289*

A novel nano-composite film coat of organic/inorganic composition including chitosan (CS), TiO2 nanoparticles (TO) and hydroxyapatite (HA) nanoparticles, was synthesized on a Ti–6Al–4V alloy surface. Open-circuit potential (OCP), electrochemical impedance spectroscopy (EIS) and potentiodynamic polarization measurements were used to observe the corrosion behavior of the novel synthesized nano-composite coat on titanium alloy surface in a phosphate buffer solution. The results were confirmed by scanning electron microscopy (SEM) and energy dispersive X-ray (EDX) analysis techniques. The antibacterial activity for the novel nano-coat was determined and compared with the bare Ti alloy. Electrochemical impedance spectroscopy measurements showed that the total corrosion resistance of this newly synthesized nano-coat gave the highest corrosion resistance compared to the separate CS, TO and/or HA coatings. Also, this novel nano-coat showed high antibacterial activity compared with the bare alloy. The excellent biocompatibility of this novel nano-coat may be due to its organic/inorganic composition.

**Keywords:** Corrosion; Sem; Edx.

## B-65. Kinetic Study of the Alkaline Degradation of Imidapril Hydrochloride Using a Validated Stability Indicating HPLCMethod

Shabaan A. Abdulla, Eman Y. Frag and Heba E. Ahmed

*Rsc Advances, 6: 69239-69250, (2016), IF: 3.289*

An aqueous alkaline degradation study was performed for imidapril hydrochloride (IMD) drug in the presence of its degradation products and an isocratic stability indicating method was presented using a HPLC technique. The separations were performed using an ACE Generix 5C8, 150 4.6 mm column and a mobile phase consisting of bu er solution (0.1 M potassium dihydrogen phosphate and 0.02 M tetra-N-butyl ammonium hydrogen sulphate of pH ¼ 4.5 with 1 N HCl) and acetonitrile 60 : 40 (v/v). The wavelength of the detector was adjusted at 210 nm. The method showed high sensitivity concerning accuracy, precision, linearity and speci fi city within the acceptable range from 0.1 to 100 m g mL 1 and the limit of quanti fi cation was found to be 0.0211 m g mL 1 for IMD. The proposed method was used to determine the drug in its pharmaceutical formulation and to investigate the degradation kinetics of the drug's alkaline-stressed sample. The reactions were found to follow a fi rst-order reaction. The activation energy could also be estimated. The optimized stability indicating HPLC method was validated according to ICH guidelines.

**Keywords:** HPLC; Imidapril hydrochloride.

## B-66. Mirror Symmetry Breaking in Fluorinated Bent-Core Mesogens

Mohamed Alaasar, Marko Prehm and Carsten Tschierske

*Rsc Advances, 6: 82890-82899, (2016), IF: 3.289*

Spontaneous chirality synchronization in the LC phases of achiral bent-core molecules, the so called dark conglomerate mesophases (DC phases), is a challenging task with significant importance for fundamental scientific research and potential applications. Here we report the synthesis and investigation of two new series of achiral bent-core mesogens derived from 4-bromoresorcinol and 4-chlororesorcinol with 2,3-difluorinated azobenzene-based side arms. The self-assembly of these materials was characterized by DSC, polarizing microscopy, X-ray diffraction investigations (XRD) and electro-optical studies. Depending on the type of halogen substituent at the central resorcinol core and on the terminal alkyl chain length different types of mesophases were observed, where 4-bromoresocinol derived compounds predominately show helical nanocrystallite phases, (HNC phases), representing conglomerates of chiral domains (DC[*]), whereas the related 4-chlororesorcinol based compounds form smectic C phases with a polar domain structure (SmCsPAR). Comparison with related compounds provides information about the influence of core fluorination on the mesophase behaviour and DC[*] phase formation, thus providing a step forward in uncovering the molecular design principles of LC materials capable of mirror symmetry breaking.

**Keywords:** Azobenzene;Bent-core liquid crystals;Mirror symmetry breaking.

## B-67.Novel Fuel Blends Facilitating the Electro-Oxidation of Formic Acid at a Nano-Pt/GC Electrode

Gumaa A. El-Nagar, Ahmad M. Mohammad, Mohamed S. El-Deab and Bahgat E. ElAnadouli

*Rsc Advances, 6: 29099-29105, (2016), IF: 3.289*

This paper addresses the promoting effect of the electrooxidation of formic acid (FAO) at a nano-Pt/GC electrode in the presence of selected low molecular weight alcohols (R–OH) as blending components. That is, blending FA with different molar ratios of methanol (MeOH), ethanol (EtOH), ethylene glycol (EGOH) and isopropanol (PrOH) resulted in a significant enhancement of the direct FAO to CO2 (desired pathway) with a concurrent depression of the amount of CO produced from the “non-faradaic” dissociation of FA.

Moreover, a favorable negative shift of the onset potential of the direct FAO peak at the nano-Pt/GC electrode is observed. Fuel utilization (FU ¼ amount of charge consumed during the oxidation process per mole of fuel) and the turnover number (TON ¼ number of FA molecules oxidized per platinum site per second) are significantly enhanced as well for FAO in the various FA/R–OH blends compared to pure FA. That is, the use of equimolar amounts of FA with either EtOH, MeOH, EGOH or PrOH resulted in a facile FAO at the nano-Pt/GC electrode of about 9, 7, 5 and 4 times higher FU compared to pure FA, respectively. Similar increase of TON is observed as well. The blending component is believed to adsorb at the Pt surface sites and thus disfavor the "non-faradaic" dissociation of FA to CO. Additionally; it might induce the CH-down adsorption orientation of FA, thus favoring FAO to CO2. The enhanced oxidation activity indicates that this fuel blend is a promising fuel system.

**Keywords:** Electrooxidation; Formic acid; Nanoparticles; Fuel blend.

## B-68. Synthesis, Antimicrobial, Anti-Cancer and Molecular Docking of two Novel Hitherto Unreported Thiophenes

Yahia N. Mabkhot, Nabila Abdelshafy Kheder, Assem Barakat, Muhammad I. Choudhary, Sammer Yousufe and Wolfgang Frey

*RSC Advances, 6: 63724-63729, (2016), IF: 3.289*

One pot synthesis of two novel hitherto unreported thiophenes was achieved by a facile and selective synthetic method. The crystal structures of the synthesized compounds were determined using an X-ray single crystal technique. The synthesized thiophenes were evaluated for their anti-cancer and antimicrobial activities. Molecular docking studies of the synthesized compounds were performed by (MOE). The predicted results from the molecular docking studies were in complete agreement with the experimental data for antimicrobial evaluation.

**Keywords:** Antimicrobial; Anti-cancer; Molecular docking; Thiophenes.

## B-69. Synthesis, Characterization and Antitumor Activity of Novel Tetrapodal 1,4-Dihydropyridines: P53 Induction, Cell Cycle Arrest and Low Damage Effect on Normal Cells Induced by Genotoxic Factor $H_2O_2$

Magda F. Mohamed, Ahmed F. Darweesh, Ahmed H. M. Elwahy and Ismail A. Abdelhamid

*RSC Adv, 6: 40900-40910, (2016), IF: 3.289*

Synthesis of novel tetrakis(2,6-dimethyl-4-phenyl-1,4-dihydropyridinyl)methanes 5a–d by acid-catalyzed condensation of the tetrakis-aldehydes 6a–d with eight equivalents of 3-aminobut-2-enenitrile 2 is reported. The structures of 5a–d are confirmed by different spectral tools. In vitro, cytotoxic screening assay for novel tetrapodal 1,4-dihydropyridines (5a–d) was performed on five different human cell lines (HCT116, A549, MCF7, PC3, and HEPG2). The compounds showed higher cytotoxic activity against (A549, HCT116, and MCF7) cell lines. The loss of the cytotoxic activity was observed in the case of PC3 and HEPG2 cell lines. Compound 5b showed the highest cytotoxic activity against the three lines (A549, HCT116, and MCF7). In an attempt to know the mechanism followed by the compounds to inhibit cell proliferation, compound 5b was chosen for molecular studies. Compound 5b induced apoptotic inhibition of the proliferation of human colon adenocarcinoma HCT116 cells through induction of the tumor suppressor protein p53, BAX, and through the inhibition of anti-apoptotic proteins by decreasing BCL2 gene expression using real-time PCR. Regarding cell cycle analysis, compound 5b induced G1 arrest against the three lines (MCF7, HCT116, and A549). Compound 5b has been found to reduce apoptosis of human normal melanocytes HFB4 and normal fibroblasts BHK that has been treated with genotoxic factor H2O2. Moreover, compound 5b has a potent protective effect against DNA damage, as indicated by the in vitro studying of different concentrations of 5b against two different types of healthy DNA (calf-thymus DNA and pBR322 DNA).

**Keywords:** Tetrakis(2,6-Dimethyl-4-Phenyl-1,4-Dihydropyridinyl) methanes; Cytotoxic screening.

## B-70.Synthesis, Reactions and DFT Calculations of Novel Bis(Chalcones) Linked to a Thienothiophene Core Through an Oxyphenyl Bridge

Osama M. Sayed, H. Moustafa, Ahmed E. M. Mekky, Ahmad M. Farag and Ahmed H. M. Elwahy

*RSC Adv, 6: 10949-10961, (2016), IF: 3.289*

A synthesis of novel isomeric bis(chalcones) based-thienothiophene and study of their synthetic utilities as building blocks for novel bis(dihydroisoxazoles), bis(dihydropyrazoles) and bis(dihydropyrimidines) each linked to a thienothiophene core through an oxyphenyl bridge is reported. Density functional theory (DFT) calculations at the B3LYP/6-31G level of theory have been carried out to investigate the equilibrium geometry of the novel isomeric chalcones 7 and 10. Moreover, total energy, energy of the HOMO and LUMO and Mullikan atomic charges were calculated. In addition, the dipole moment and orientation of the two p-isoelectronic chalcones 7 and 10 have been measured and their interactions with hydrazine hydrate to form dihydropyrazoles have been studied.

**Keywords:** Thienothiophene; BIS(Chalcones); BIS(Dihydroisoxazoles); BIS(Dihydropyrazoles); BIS(Dihydropyrimidines).

## B-71. Synthetic Routes to Benzosuberone-Based Fused- and Spiro-Heterocyclic Ring Systems

Thoraya A. Farghaly, Sobhi M. Gomha, Kamal M. Dawood and Mohamed R. Shaaban

*RSC Advances, 6: 17955-17979, (2016), IF: 3.289*

Natural products containing a benzosuberone nucleus are important class of medicinal and pharmaceutical compounds and have recently attracted a considerable amount of attention due to their remarkable broad-spectrum biological activity. The present review endeavors to highlight the progress in the synthesis of benzosuberones and their fused, as well as spiro, ring systems in the literature up to 2015.

**Keywords:** Benzosuberones; Benzocycloheptanone; Synthesis; Fused ring systems.

## B-72. The Effect of A-Site Doping in A Strontium Palladium Perovskite and its Applications for Non-Enzymatic Glucose Sensing

Ekram H. El-Ad, Ahmed Galalab and Nada F. Atta

*RSC Advances, 6: 16183-16196, (2016), IF: 3.289*

The catalytic activity of a strontium palladium perovskite, Sr2PdO3, toward non-enzymatic glucose sensing is strongly affected by the Sr2+ A-site partial substitution by Ca2+ ions; Sr2−xCaxPdO3 with x = 0–0.7. Scanning and transmission electron microscopies (SEM, EDAX and TEM), XRD, XPS, BET and a particle size analyzer were used to investigate the microstructure, morphology, physical–chemical and electrochemical properties of the prepared perovskites. A good-crystalline orthorhombic Sr2PdO3 phase was formed as the main phase in all the prepared samples with particle sizes in the range of nanometers as confirmed by XRD. Doping the A-site Sr2+ cations with Ca2+ ions in the Sr2PdO3 perovskite leads to the enhancement of the elecrocatalytic activity towards non-enzymatic glucose sensing showing the highest elecrocatalytic activity in the case of Sr1.7Ca0.3PdO3. This may be attributed to the higher free volume in the crystal lattice, enhanced content and mobility of surface lattice oxygen and distorted stabilized perovskite structure leading to higher catalytic activity of the prepared perovskites. In addition, synergistic interactions were achieved between Sr2+ and Ca2+ in the A-site and Pd2+ ions in the B-site resulting in improved surface activity and a stabilized structure. As a result, greater ionic and electronic conductivity and enhanced catalytic activity were achieved upon doping. Graphite/Sr1.7Ca0.3PdO3 as a free enzymatic glucose sensor exhibited good stability, a low detection limit, high sensitivity, good selectivity even in the presence of common interferents, applicability in real sample analysis and anti-interference ability.

**Keywords:** Non-enzymatic glucose sensor; Perovskite; Urine; Ca dopant; Xrd.

## B-73. The Effect of Gold Nanoparticles on the Diagnostic Polymerase Chain Reaction Technique for Equine Herpes Virus 1 (Ehv-1)

Dalia M. El-Husseini, Nashwa M.Helmy and Reham H.Tammam

*RSC Advances (The Royal Society of Chemistry, 6: 54898-54903, (2016), IF: 3.289*

Nano-biotechnology has been a noticeable research area because of its successful applications in molecular diagnostics and therapy of various genetic and microbial diseases. Although the polymerase chain reaction (PCR) technique is one of the most highlighted and promising applications in the molecular diagnosis field, it suffers from some drawbacks that affect its efficiency. For instance, as a diagnostic technique for equine herpes virus-1 (EHV-1), conventional PCR could lead to false negative results due to the low viral titer in some samples, which leads to the necessity to improve its sensitivity. In this study, we carried out experiments to determine the effects of 15 nm unmodified citrate-coated gold nanoparticles (GNPs) on the key PCR reactants in order to see if these would enhance the overall outcomes of the reaction. Our results showed that, after optimization of the GNPs, oligonucleotide primers and Taq polymerase concentrations, a specific high yield amplification with a detection limit of 102 DNA copies could be reached compared to the 105 to 104 detection limit of conventional PCR. Thus, the developed and optimized GNPs-assisted PCR technique could be used for a more efficient, highly sensitive molecular detection of EHV-1.

**Keywords:** Gold nanoparticles; Polymerase chain reaction equine herpes virus 1.

## B-74. New Dinuclear Palladium(Ii) Complexes with Formamidine and Bridged Pyrophosphate Ligands

Ahmed A. Soliman, Othman I. Alajrawy, Fawzy A. Attabi and Wolfgang Linertd

*New Journal of Chemistry, 40: 8342-8354, (2016), IF: 3.277*

A series of new dinuclear palladium( II ) complexes of the type [(PdL 1–3 ) 2 (mPPi)] xH 2 O (1–3), where L = formamidine ligands and PPi = inorganic pyrophosphate, were synthesized and characterized by elemental analyses, magnetic susceptibility, UV-Vis spectroscopy, infrared (IR) spectroscopy, and mass spectroscopy, thermal analysis, and theoretical calculations. IR spectra confirmed that the formamidine ligands act as bidentate N2 ligands. The complexes are diamagnetic and analysis of the optimized structures indicated that the geometry is a distorted square planar with O–Pd–O and N–Pd–N bond angles ranging from 90.851 to 94.221 and from 87.661 to 91.431, respectively, which are acceptable for heteroleptic complexes. The electronic energies (a.u.) of the complexes (-1246 to -1916) indicated that the complexes were stable. The energies of the HOMOs (-0.204 to -0.283) and LUMOs (-0.057 to 0.097) orbitals of the complexes were negative, which also indicated that the complexes were stable. The dipole moment of the complexes (4.14–14.08 Debye) indicated that the complexes were polarized. They were also thermally stable, as shown from their relatively higher overall activation energies (537–1002 kJ mol-1). The complexes were screened against PC-3 (prostate carcinoma cell line), HCT-116 (colon carcinoma cell line), and MCF-7 (breast carcinoma cell line). The IC50 values of the complexes were evaluated and the results showed that [(PdL1)2(mPPi)]H2O (1) had the best IC50 value.

**Keywords:** Dinuclear Pd(Ii) complexes; Formamidine; Pyrophosphate; Biological activity.

## B-75. Nickel Oxide Nanoparticles/Ionic Liquid Crystal Modified Carbon Composite Electrode for Determination of Neurotransmitters and Paracetamol

Nada F. Atta, Asmaa H. Ibrahim and Ahmed Galal

*New Journal of Chemistry, 40: 662-673, (2016), IF: 3.277*

The ionic liquid crystal 1-butyl-1-methyl-piperidinium hexafluorophosphate and nickel oxide nanoparticles were used to construct a carbon composite electrode. This novel composite was used successfully as a sensor platform for the determination of paracetamol and some neurotransmitters such as dopamine, norepinephrine, levodopa and serotonin. Several advantages are realized in this approach due to the unique properties of nanomaterials and ionic liquid crystals, and the ease of fabrication of the carbon composite electrode. The modified

sensor was evaluated and compared with nickel oxide nanoparticles/ionic liquid modified electrodes in the presence of surfactants, namely 1-n-hexyl-3-methyl imidazolium tetrafluoroborate and 1-butyl-4-methyl pyridinium tetrafluoroborate, for the electrocatalytic oxidation of paracetamol. Modification with ionic liquid crystals showed superior current signals compared to ionic liquids. The interaction of surfactants with neurotransmitters resulted in preconcentration of the drug at the ionic liquid crystal interface that allowed both ionic channeling and charge transfer mediation. Figures of merits with optimized performance are a linear dynamic range of 44.4 × 10−7–3.33 × 10−5 mol L−1 for paracetamol sensing with a correlation coefficient of 0.999 and a limit of detection of 8.61 × 10−9 mol L−1. The electrode was successfully employed for the direct determination of paracetamol in human urine samples, for paracetamol assay in pharmaceutical formulations and simultaneous determination of paracetamol and neurotransmitters. High reproducibility and selectivity in the presence of potential interfering species were ascertained for this electrode.

**Keywords:** Ionic liquid crystal; Carbon paste electrode; Nickel oxide; Paracetamol; Urine.

## B-76. Synthesis and Characterization of some New Bis-Pyrazolyl-Thiazoles Incorporating the Thiophene Moiety as Potent Anti-Tumor Agents

Sobhi M. Gomha, Mastoura M. Edrees and Farag M. A. Altalbawy

*International Journal of Molecular Science, 17(1499): 1-11, (2016), IF: 3.257*

A new series of 1,4-bis(1-(5-(aryldiazenyl)thiazol-2-yl)-5-(thiophen-2-yl)-4,5-dihydro-1H-pyrazol-3-yl)benzenes 3a-i were synthesized via reaction of 5,5'-(1,4-phenylene)bis(3-(thiophen-2-yl)-4,5-dihydro-1H-pyrazole-1-carbothioamide) (1) with hydrazonoyl halides 2a-i. In addition, reaction of 1 with ethyl chloroacetate afforded bis-thiazolone derivative 8 as the end product. Reaction of compound 8 with methyl glyoxalate gave bis-thiazolone derivative 10. The structures of the newly synthesized compounds were established on the basis of spectroscopic evidences and their alternative syntheses. All the synthesized compounds were evaluated for their anti-tumor activities against hepatocellular carcinoma (HepG2) cell lines, and the results revealed promising activities of compounds 3g, 5e, 3e, 10, 5f, 3i, and 3f with IC50 equal 1.37 ± 0.15, 1.41 ± 0.17, 1.62 ± 0.20, 1.86 ± 0.20, 1.93 ± 0.08, 2.03 ± 0.25, and 2.09 ± 0.19 μM, respectively.

**Keywords:** Bis-Heterocycles; Bis-chalcones; Hydrazonoyl halides; Anticancer agents.

## B-77. The Thermodynamic and Kinetic Properties of 2-Hydroxypyridine/2-Pyridone Tautomerization: A Theoretical and Computational Revisit

Safiyah A. Hejazi, Osman I. Osman, Abdulrahman O. Alyoubi, Saadullah G. Aziz and Rifaat H. Hilal

*InternationalJ. Molecular Sciences,17:1893-191(2016)IF:3.257*

The gas-phase thermal tautomerization reaction between 2-hydroxypyridine (2-HPY) and 2-pyridone (2-PY) was investigated by applying 6-311++G** and aug-cc-pvdz basis sets incorporated into some density functional theory (DFT) and coupled cluster with singles and doubles (CCSD) methods. The geometrical structures, dipole moments, HOMO-LUMO energy gaps, total hyperpolarizability, kinetics and thermodynamics functions were monitored against the effects of the corrections imposed on these functionals. The small experimental energy difference between the two tautomers of 3.23 kJ/mol; was a real test of the accuracy of the applied levels of theory. M062X and CCSD methods predicted the preference of 2-HPY over 2-PY by 5–9 kJ/mol; while B3LYP functional favoured 2-PY by 1–3 kJ/mol. The CAM-B3LYP and !B97XD functionals yielded mixed results depending on the basis set used. The source of preference of 2-HPY is the minimal steric hindrance and electrostatic repulsion that subdued the huge hyperconjugation in 2-PY. A 1,3-proton shift intramolecular gas-phase tautomerization yielded a high average activation of 137.152 kJ/mol; while the intermolecular mixed dimer interconversion gave an average barrier height of 30.844 kJ/mol. These findings are boosted by a natural bond orbital (NBO) technique. The low total hyperpolarizabilities of both tautomers mark out their poor nonlinear optical (NLO) behaviour. The enhancement of the total hyperpolarizability of 2-HPY over that of 2-PY is interpreted by the bond length alternation

**Keywords:** 2-Hydroxypyridine; 2-Pyridone; Tautomerization; NBO; NLO.

## B-78. Cathodic Activation of Titanium-Supported Gold Nanoparticles: an Efficient and Stable Electrocatalyst for the Hydrogen Evolution Reaction

Mohammed A. Amina, Sahar A. Fadlallah, Ghaida S. Alosaimi, Fatma Kandemirlid, Murat Saracoglue, Sabine Szuneritsf and Rabah Boukherroub

*International Journal of Hydrogen Energy, 41(15): 6326-6341, (2016), IF: 3.205*

As-polished titanium (Ti) substrates decorated with dispersed gold nanoparticles (Au NPs/Ti) of various sizes and densities were prepared here to effectively catalyze hydrogen evolution reaction (HER) in 0.5 M H2SO4. These materials were synthesized adopting a facile one-step wet chemical method without using reducing agents, stabilizers, or any chemical pre-treatment, where Ti acts as both the reducing agent and support. This was achieved via soaking the Ti substrates for 30 min in a gold precursor bath as a function of temperature (5–65 °C). Morphological characterizations of the synthesized Au NPs/Ti catalysts indicated a size decrease and density increase of loaded Au NPs with the rise of temperature. Cathodic polarization measurements revealed that the catalyst loaded with the highest density of Au NPs exhibited the best HER activity with onset potential (EHER), exchange current density (jo), and Tafel slope (βc) of −44 mV (RHE), 6.0 × 10−3 mA cm−2, and 40 mV decade−1, respectively. This activity has markedly increased upon cathodic activation (cathodic pre-polarization treatment at −2 V (SCE) for 12 h) that yielded a Ti substrate with a porous-like network structure decorated with highly dispersed Au NPs. In addition, a catalytically active TiH2 phase was formed (as evidenced from XRD and XPS) on such a porous substrate. Such cathodically pre-treated catalyst recorded HER electrochemical parameters of −18 mV (RHE),

0.117 mA cm−2, and 38 mV decade−1, thus approaching the commercial Pt/C catalyst (EHER: 0.0 mV, jo: 0.78 mA cm−2, and βc: 31 mV dec−1). The stability of the best catalyst was assessed employing cyclic polarization and chronoamperometry measurements. It exhibited a good stability with improved activity during stability testing.
**Keywords:** Titanium; Cathodic activation; Supported gold Nanoparticles; Electrocatalysis; Hydrogen generation.

## B-79. Electrocatalytic Activity of Pt-ZrO2 Supported on Different Carbon Materials for Methanol Oxidation in H2SO4 Solution

R.S. Amin, Amani E. Fetohi, R.M. Abdel Hameed and K.M. El-Khatib

*International Journal of Hydrogen Energy, 41: 1846-1858, (2016), IF: 3.205*

Different carbon supports are considered to prepare Pt-ZrO2/XC-72R carbon black, Pt-ZrO2/SWCNTs and Pt-ZrO2/MWCNTs electrocatalysts by a solide state reaction under intermittent microwave heating method using ethylene glycol and NaBH4 as mixed reducing agents. The prepared electrocatalysts are physically characterized using X-ray diffraction (XRD), energy dispersive X-ray analysis (EDX) and transmission electron microscopy (TEM). Pt particle size decreases in the order: Pt-ZrO2/C > Pt-ZrO2/MWCNTs > Pt-ZrO2/SWCNTs. Cyclic voltammetry, chronoamperometry, chronopotentiometry and electrochemical impedance spectroscopy are applied to investigate the electrochemical performance of the three electrocatalysts for methanol oxidation in H2SO4 solution. CNTs supported electrocatalysts achieve increased methanol oxidation current density and improved stability behaviour during long-time operation when compared to the one containing carbon black. Pt-ZrO2/CNTs electrocatalyst also displays lower resistance and higher electrolyte diffusion rate to infer a faster charge transfer process and better electrode accessibility for methanol oxidation. Therefore, carbon nanotubes are suggested as ideal anode electrocatalyst supporting material for the practical application of direct methanol fuel cells.
**Keywords:** Platinum; Carbon; Electro-Oxidation; Fuel cells; Metal oxide.

## B-80. Preparation and Characterization of Pt–CeO2/C and Pt–TiO2/Celectrocatalysts with Improved Electrocatalytic Activity for Methanol Oxidation.

R.M. Abdel Hameed, R.S. Amin, K.M. El-Khatib and Amani E. Fetohi

*Applied Surface Science, 367: 382-390, (2016), IF: 3.15*

tPt–TiO2/C and Pt–CeO2/C electrocatalysts were synthesized by solid state reaction of TiO2/C and CeO2/Cpowders using intermittent microwave heating, followed by chemical reduction of platinum ions usingmixed reducing agents of ethylene glycol and sodium borohydride. The crystal structure, surface morphology and chemical composition of prepared electrocatalysts were investigated using X-ray diffraction(XRD), transmission electron microscopy (TEM) and energy dispersive X-ray analysis (EDX). The phaseangle values of different Pt diffraction planes in Pt–TiO2/C and Pt–CeO2/C were shifted in the positivedirection relative to those in Pt/C. Pt particles with diameter values of 3.06 and 2.78 nm were formed inPt–TiO2/C and Pt–CeO2/C, respectively. The electrochemical performance of prepared electrocatalysts wasexamined using cyclic voltammetry, chronoamperometry and electrochemical impedance spectroscopy.Pt–CeO2/C showed an enhanced oxidation current density when compared to Pt/C. Long time oxidationtest at Pt–TiO2/C and Pt–CeO2/C revealed their improved stability. Lower charge transfer resistance valueswere estimated at Pt–metal oxide/C electrocatalysts.
**Keywords:** Methanol; Carbon; Electro-Oxidation; Metal oxide; Cyclic voltammetry; Chronoamperometry.

## B-81. Development of Polar Order in the Liquid Crystal Phases of a 4-Cyanoresorcinol-Based Bent-Core Mesogen with Fluorinated Azobenzene Wings

Mohamed Alaasar, Marko Prehm, MariaGabriela Tamba, Nerea Sebastián, Alexey Eremin and Carsten Tschierske

*Chemphyschem, 17: 278-287, (2016), IF: 3.138*

A bent-core mesogen consisting of a 4-cyanoresorcinol unit as the central core and laterally fluorinated azobenzene wings forms four different smectic LC phase structures in the sequence SmA–SmCs–SmCsPAR–M, all involving polar SmCsPS domains with growing coherence length of tilt and polar order on decreasing temperature. The SmA phase is a cluster-type de Vries phase with randomized tilt and polar direction; in the paraelectric SmCs phase the tilt becomes uniform, although polar order is still short-range. Increasing polar correlation leads to a new tilted and randomized polar smectic phase with antipolar correlation between the domains (SmCsPAR) which then transforms into a viscous polar mesophase M. As another interesting feature, spontaneous symmetry breaking by formation of a conglomerate of chiral domains is observed in the non-polar paraelectric SmCs phase.
**Keywords:** Azobenzene; Bent-core Liquid crystals; De Vries Phase; Ferroelectricity; Mirror symmetry breaking.

## B-82. Influence of Metal Oxides on Platinum Activity Towards Methanol Oxidation in H2SO4 Solution

R.M. Abdel Hameed, R.S. Amin, K.M. El-Khatib and Amani E. Fetohi

*Chemphyschem, 17: 1054-1061, (2016), IF: 3.138*

Pt–CeO2/C, Pt–TiO2/C, and Pt–ZrO2/C electrocatalysts were prepared by using a modified microwave-assisted polyol process. Physical characterization was performed by using XRD, TEM, and EDX analyses. The incorporation of different metal oxides increased the dispersion degree of Pt nanoparticles and reduced their diameter to 2.50 and 2.33 nm when TiO2 and ZrO2 were introduced to Pt/C, respectively. The electrocatalytic activity of various electrocatalysts was examined towards methanol oxidation in H2SO4 solution by using cyclic voltammetry, chronoamperometry, and electrochemical impedance spectroscopy. Among the studied composites, Pt–ZrO2/C was selected to be a candidate electrocatalyst for better electrochemical performance in direct methanol fuel cells.

**Keywords:** Acid medium; Fuel cells; Methanol; Platinum; Transition metal oxides.

## B-83. Isolation and Characterization of Chitosan from Different Local Insectsin Egypt

Narguess H. Mareia, Emtithal Abd El-Samieb, Taher Salahc, Gamal R. Saad and Ahmed H.M. Elwahy

*International Journal of Biological Macromolecules, 82 : 871-877 (2016) IF: 3.138*

Chitin was extracted from four different local sources: the shrimp (Penaeus monodon), the desert locust(Schistocerca gregaria), the honey bee (Apis mellifera) and the beetles (Calosoma rugosa). Chitosan wasthen obtained by deacetylation of chitin and physicochemically characterized using the Fourier trans-form infrared (FTIR) and X-ray diffraction. The moisture content, water binding capacity, fats bindingcapacity, ash content were determined and chitosans morphology was visualized using the scanningelectron microscope (SEM). The difference between the obtained chitosans from three insect sources and-chitosan from shrimp in terms of crystallinity, fibrous structure was discussed

**Keywords:** Chitin; Chitosan; Insects; Deacetylation; Characterization.

## B-84. Novel Antimicrobial Superporous Cross-Linked Chitosan/Pyromellitimide Benzoyl Thiourea Hydrogels

Nadia A. Mohamed, Nahed A Abd. El-Ghany and Mona M. Fahmy

*International Journal of Biological Macromolecules, 82: 589-598, (2016), IF: 3.138*

In this work, chitosan (CS) was cross-linked with different amounts of pyromellitimide benzoyl thiourea moieties. The structure of the cross-linked CS was confirmed by elemental analyses, FTIR and 1H- NMR spectroscopy. The cross-linking process proceeds via reacting of the amino groups of CS with the isothiocyanate groups of the N,N□-bis [4-(isothiocyanate carbonyl)phenyl] pyromellitimide cross-linker. The amount of the cross-linker was varied with respect to CS to produce four new pyromellitimide benzoyl thiourea cross-linked CS (PIBTU-CS) hydrogels designated as PIBTU-CS-1, PIBTU-CS-2, PIBTU-CS-3, and PIBTU-CS-4 of increasing cross-linking degree percent of 11, 22, 44 and 88%, respectively. The scanning electron microscopy observation indicates the extremely porous structure of the hydrogels. XRD results showed that the crystallinity of CS was decreased upon cross-linking. The four hydrogels exhibit a higher antibacterial activity on Bacillus subtilis and Streptococcus pneumoniae as Gram positive bacteria and against Escherichia coli as Gram negative bacteria and higher antifungal activity on Aspergillus fumigatus, Syncephalastrum racemosum and Geotricum candidum than that of the parent CS as shown from their higher inhibition zone diameters and their lower MIC values. The swell ability of the hydrogel as well as their antimicrobial activity increased with increasing cross-linking density.

**Keywords:** Chitosan hydrogels; Synthesis; Characterization; Swell ability; Antimicrobial activity.

## B-85. Nano-Alumina Powders/Ceramics Derived from Aluminum Foil Waste at Low Temperature for Various Industrial Applications

Ahmed A.M. El-Amir, Emad M.M. Ewais, Ahmed R. Abdel-Aziem, Adel Ahmed and Bahgat E.H. El-Anadouli

*Journal of Environmental Management, 183: 121-125 (2016) IF: 3.131*

In this work, nanoscale single crystalline γ- and α-alumina powders have been successfully prepared from aluminum foil waste precursor via co-precipitation method using NH4OH as a precipitant. The obtained gel after co-precipitation treatment, was calcined at different temperatures (500,700, 900, 1050, 1100, 1300 and 1500 °C) and the products were characterized by XRD, FTIR and HRTEM. The results revealed that nano-γ-Al2O3 was fully transformed to nanometer-sized α-Al2O3 (36–200 nm) after annealing at temperatures as low as 1100 °C.The thermally preheated powder at 500 °C was further pressed under 95 MPa by the uniaxial press and the obtained bodies were found to have98.82% of the theoretical density, 1.18% porosity and 708 MPa compressive strength, when sintered at temperatures as low as 1600 °C without using any sintering aid. These excellent results proved that this work will contribute to finding a commercial source for preparing sub 100 nm α-alumina through the secondary resources management and even more so to synthesizing strong α-Al2O3 bodies which are promising in terms of their structure and compression. The α-Al2O3 bodies synthesized by the present work could be used as a feedstock for fabrication of various kinds of functional and structural materials that are extensively used in high tech.

**Keywords:** Aluminium foil waste management; Nano alumina; Co-Precipitation synthesis; Alumina based ceramics; Microstructure; Compression.

## B-86. Thermogravimetric Analysis in the Evaluation of the Inhibition of Degradation of Rigid Poly(Vinyl Chloride) Using Biologically Active Phthalimido Aromatic Hydrazide Derivatives

Nadia A. M., Nahed A. Abd El-Ghany and Mona M. Fahmy

*Polymer Degradation and Stability, 128:46-54 (2016) IF: 3.12*

Four novel antimicrobial phthalimido aromatic hydrazide derivatives were synthesized from N-(4- chlorocarbonylphenyl) phthalimide with benzhydrazide, salicylhydrazide, p-aminobenzohydrazide or p-aminosalicylhydrazide. They were characterized by FTIR, 1 H NMR, mass spectra, elemental analyses and antimicrobial activities. These derivatives were investigated as thermal stabilizers for rigid PVC using thermogravimetric analysis technique, in nitrogen. The results revealed the greater stabilizing efficiency of the investigated derivatives as shown by their higher initial decomposition temperature and higher residual weight percent in relation to dibasic lead carbonate (DBLC), cadmium-barium-zinc (CdeBaeZn) stearate and n-octyltin mercaptide (n-OTM) industrial stabilizers. The stabilizing efficiency increased with the introduction of electron donating substituent groups in the aromatic ring of the phthalimido aromatic hydrazide derivatives.

**Keywords:** Phthalimido aromatic hydrazide derivatives; Antimicrobial activity; Thermal stability; PVC; Thermogravimetry.

## B-87. Catalytic Activity of Labo3 for Oer in $HClO_4$ Medium: an Approach to the Molecular Orbital Theory

Shimaa M. Ali, Nada F. Atta, Yasser M. Abd Al-Rahman and Ahmed Galal

*Journal of The Electrochemical Society, 163: 81-88 (2016) IF:3.014*

The electrocatalytic activity of transition-metal-based perovskites, LaBO3 (B = Ni, Mn, Cr, and Co), toward an oxygen evolution reaction (OER) was investigated in HClO4 medium by linear polarization and electrochemical impedance measurements. X-Rays Diffraction characterization showed that single perovskite phases were formed. Field-emission scanning electron microscopy showed that changing the type of B-site metal ion affected the morphology of the prepared perovskites. High-resolution transmission electron microscopy confirmed the formation of orthorhombic phase laCrO3 and of the rhombohedral phases of LaNiO3, LaMnO3, and LaCoO3. Results were compared with LaFeO3 and the order of the electrocatalytic activity was found to be LaNiO3 > LaFeO3 >LaMnO3. This trend agrees with the calculated activation energy values, 11.38, 20.13, and 22.01 kJ mol−1 for LaBO3 (B = Ni, Fe and Mn), respectively and is explained based on molecular orbital principles. LaCrO3 and LaCoO3 showed no catalytic activity toward OER due to the dissolution of LaCrO3 and the formation of a passive layer of Co3O4 when tested in HClO4. Ternary La1-xSrxNiO3 perovskites have higher catalytic activity for OER compared to LaNiO3, which is promoted by increasing the Sr ratio. © 2015 The Electrochemical Society

**Keywords:** Microwave synthesis Oer perovskites transition; Metal catalyst.

## B-88. Evidence of Core-Shell Formation Between Ndfeo3 Nano-Perovskite and Ionic Liquid Crystal and its Application in Electrochemical Sensing of Metoclopramide

Nada F. Attaa, Ekram H. El-Adsa and Ahmed Galala

*Journal of The Electrochemical Society 164 (2016) IF: 3.014*

A simple and sensitive electrochemical method for determination of metoclopramide was developed based on the in-situ modification of carbon paste electrode (CpE) with NdFeO3 (NF) nano-perovskite and 2-chloro-1,3-dimethyl-imidazolinium hexafluorophosphate ionic liquid crystal (ILC) in presence of sodium dodecyl sulfate (SDS); NFILCMCpE…SDS. A core-shell formation between NdFeO3 and ILC was confirmed affecting the catalytic activity of the nanocomposite. XRD, FTIR, TEM, BET, SEM and EDAX were used to elucidate the orthorhombic structure of NdFeO3 and give a complete characterization of the proposed composite sensor. Cyclic voltammetry and electrochemical impedance spectroscopy measurements revealed enhanced electrochemical activity for metoclopramide at the proposed sensor surface. The components of the composite sensor exhibit synergistic role in enhancing the sensor signal toward the drug. A linear calibration curve for metoclopramide was obtained at the proposed sensor in the concentration range of 0.4 μmol L−1 to 300 μmol L−1 with detection limit of 1.91 nmol L−1 and sensitivity of 203.56 μA/mmol L−1. NFILCMCpE…SDS was successfully applied for the sensitive determination of metoclopramide in its commercial tablets and real samples; urine and blood serum. Also, the proposed sensor exhibited anti-interference properties toward metoclopramide determination in presence of common interferents, pain relief drugs or neurotransmitters. The proposed sensor was very stable toward the electrochemical response of metoclopramide up to one month of storage.

**Keywords:** Core-Shell; Nanostructures ionic liquid crystal metoclopramide; $NdFeO_3$ sodium dodecyl sulfate.

## B-89. Hematite Nanoparticles/Ionic Liquid Crystal/Graphene–Based Nanocomposite Electrochemical Sensor for Sensitive Determination of Antipsychotic Drug

Nada F. Attaa, Yousef M. Ahmed, Mohammad H. BinSabt and Ahmed Galala

*Journal of Electrochemical Society, 163: 0-0, (2016), IF: 3.014*

Psychotic symptoms have been widely spread and several drugs have been proposed to suppress its consequences including trifluoperazine (TFP). Here we introduce an electrochemical sensor based on glassy carbon electrode modified with a composite of hematite nanoparticles (FeNPs)/ionic liquid crystal (ILC)/graphene (RGO) for simple and direct determination of TFP. The sensor proved to be highly effective and sensitive due to the synergistic effects of FeNPs, ILC and RGO. The electrocatalytic oxidation of TFP was investigated by cyclic voltammetry (CV) and differential pulse voltammetry (DPV). Surface morphology was examined by scanning electron microscopy (SEM). Various figures of merit were evaluated including effects of pH and scan rates on the voltammetric response of TFP. Under optimal operational conditions, linear response was in the concentration range of 9 × 10−10 to 1 × 10−7 mol L−1 and 2 × 10−6 to 2 × 10−4 mol L−1 for TFP with correlation coefficients 0.997 and 0.998, respectively. The lower limits of detection and quantification were 2.29 × 10−12 mol L−1 and 7.65 × 10−12 mol L−1, respectively. The sensor showed good stability, reproducibility, repeatability, anti-interference ability and selectivity. It was possible to determine TFP in real human samples and pharmaceutical formulations.

**Keywords:**Antipsychotic drug graphene hematite Nanoparticles ionic liquid crystal trifluoperazine.

## B-90. Host Guest Inclusion Complex Modified Electrode for the Sensitive Determination of a Muscle Relaxant Drug

Nada F. Attaa, Said S. Elkholy, Yousef M. A. and Ahmed Galal

*Journal of The Electrochemical Society, 163 (2016) IF: 3.014*

Electrochemical sensor based on cyclodextrin (CD)/ionic liquid crystal (ILC)/graphene (RGO) modified glassy carbon (GC)

(GC/ILC/RGO/ILC/CD) electrode was constructed for the determination of methocarbamol (MC). The enhanced electrochemical performance of the sensor is due to the synergistic effect triggered by its individual components: surface area of RGO, ionic conductivity of ILC and the concentrating effect of CD through formation of stable host-guest "CD/MC" inclusion complex which affected the electron transfer rate. In this composite the moderate viscosity of ILC that penetrates between the graphene sheets results in filling any existing voids and act as ion carriers between the graphene sheets resulting in more conductive composite and homogenous surface for further assembling of the CD in ordered form. Under optimized conditions, the LDR was 4 × 10−8–1 × 10−6 mol L−1 for MC determination (R = 0.999) and LOD 6.64 × 10−12 mol L−1. The sensor was highly sensitive and successfully applied for direct determination of MC in human urine and in pharmaceutical formulation samples with good recovery results. This procedure was also successfully applied for simultaneous determination of MC, uric acid (UA), ascorbic acid (AA) and MC, dopamine (DA) or MC, acetaminophen (APAP) in their mixtures. The GC/ILC/RGO/ILC/CD showed also high reproducibility, selectivity and anti-interference ability.

**Keywords:** Cyclodextrin graphene ionic liquid crsytal methocarbamol pharmaceutical formulations.

## B-91. UV Excitations of Halons

Ljiljana Stojanović, Abdulrahman O. Alyoubi, Saadullah G. Aziz, Rifaat H. Hilal and Mario Barbatti

*The Journal of Chemical Physics,145:184306-1(2016) IF:2.894*

In the present study, we examined the UV excitations of a newly introduced molecular set, Halons-9, composed of nine gaseous halon molecules. The performance of the density functional-based multireference configuration interaction method (DFT/MRCI) and time-dependent density functional theory with CAM-B3LYP functional (TD-CAM-B3LYP) in the computation of singlet and triplet excited states of this set was evaluated against coupled-cluster with singles and doubles (CCSD). Excited states up to the corresponding ionization limits, including both localized and delocalized excitations, have been benchmarked. TD-CAM-B3LYP significantly underestimates excitation energies of the higher mixed valence-Rydberg and Rydberg states, with computed mean absolute deviations from the equation of motion (EOM)-CCSD results 1.06 and 0.76 eV, respectively. DFT/MRCI gives a significantly better description of higher excited states, albeit still poor, compared to the TD-CAM-B3LYP. The mean absolute deviations of mixed valence-Rydberg and Rydberg states from the reference EOM-CCSD values are 0.66 and 0.47 eV, respectively. The performance of DFT/MRCI for description of strongly correlated states with valence-Rydberg mixing is still not satisfactory enough. On the other hand, oscillator strengths of most of singlet states obtained with both methods are close to the EOM-CCSD values. The largest deviations, occurring in the case of several high-lying multiconfigurational states, are of an order of magnitude.

## B-92. Novel Benzo[D]Imidazole-Based Heterocycles as Broad Spectrum Anti-Viral Agents: Design, Synthesis and Exploration of Molecular Basis of Action

Taha M.A. Eldebss, Ahmad M. Farag, Mohamed M. Abdulla and Reem K. Arafa

*Mini-Reviews in Medicinal Chemistry,16:67-83(2016) IF:2.841*

The design and synthesis of a novel series of benzo[d]imidazole-based heterocycles and their biological evaluation as antiviral agents are reported herein. 1-(1-Methyl-1H-benzo[d]imidazol-2-yl)-2-thiocyanatoethanone 2 was used as a key intermediate for the synthesis of the thiazolylhydrazine 4, the thiazolylamine 5 and the methylthiazole 7. Coupling of compounds 5 or 7 with the appropriate diazotized aromatic amines gave the diazenyl derivatives 6a-c and 8a-c,respectively. The quinazoline derivative 12 was also synthesized. On the other hand, the phenylthio 20 and the phenylsulphonyl 22 bioisosteresand their respective diazenyl derivatives 21a-c and 23a-c were prepared. The synthesized compounds were evaluated for their HIV-1, HCV, SSPE and H1N1 inhibitory activities and were found to display very promising results. Furthermore, to investigate the underlying possible mechanism of action, in vitro and in silico screening of this series of benzo[d]imidazoles was performed against the viral enzymes HIV-1 RT, HCV NS3/4A serine protease and H1N1 NA1. Overall findings of the executed investigations highlight these novel compounds as very promising potent, broad spectrum antiviral agents.

**Keywords:** Antiviral; Benzo[D]Imidazole;HCV; H1N1; HIV; Thiazolo[2,3-B]Quinazolin-5-One.

## B-93. Synthesis and some Reactions of 1-Aryl-4-Acetyl-5-Methyl-1,2,3-Triazole Derivatives with Anticonvulsant Activity

Ekhlass M. Nassar, Fathy M. Abdelrazek, Rezk R. Ayyad and Ahmed F. El-Farargy

*Mini-Reviews in Medicinal Chemistry, 2016, 16: 926-936, (2016), IF: 2.841*

The triazoles 3a-d underwent condensation reactions with 4-(piperidin-1-yl)-benzaldehyde to afford the chalcones 5a-d. Chalcone derivatives 5a-d were reacted with 2,3-diaminomaleonitrile, thiourea and hydrazine hydrate to afford the novel diazepine-dicarbonitrile derivatives 7a-d, the pyrimidine-2-thiol derivatives 9a-d and hydrazino-pyrimidines 10a-d respectively. Structures of the prepared compounds were elucidated by physical and spectral data like FT-IR, 1H NMR, 13C NMR, and mass spectroscopy. Some of the synthesized compounds were screened for their anticonvulsant activity and SAR.

**Keywords:** Anticonvulsant activity; Chalcones; Diazepines; Hydrazino-pyrimidines; Pyrimidine-thioles; 1,2,3-Triazoles; Ultrasonication.

## B-94. Synthesis, Biological Evaluation, and Molecular Docking Studies of New Pyrazol-3- one Derivatives with Aromatase Inhibition Activities

Xue-Jing Yi1, Tamer T. El-Idreesy, Taha M. A. Eldebss, Ahmad M. Farag,Mohamed M. Abdulla,Shaimaa A. Hassan and Yahia N. Mabkhot

*Chemical Biology and Drug Design,88:832-843(2016) IF:2.802*

A new series derived from 4-(2-chloroacetyl)-1,2-dihydro-1,5-dimethyl-2-phenyl-3H-pyrazol-3-one was synthesized, characterized and its pharmacological activity toward aromatase enzyme inhibition was screened and compared to the reference native ligand letrozole. The most active compound of the series was 16, showing IC50 value of 0.0023 ± 0.0002 µm compared to letrozole with IC50 of 0.0028 ± 0.0006 µm.In addition, compounds 26 and 36 exhibit good inhibition activities close to letrozole with IC50 values 0.0033 ± 0.0001 and 0.0032 ± 0.0003 µm, respectively. Moreover,molecular docking studies were conducted to support the findings.

**Keywords:** Aromatase activity inhibitors; Ic50; Letrozole; Molecular docking studies; Pyrazol-3-One.

## B-95. Geometrical Structure, Potentiometric, Molecular Docking and Thermodynamic Studies of Azo Dye Ligand and its Metal Complexes

A.A. El-Bindary, G.G.Mohamed, A.Z. El-Sonbati, M.A.Diab,W.M.I. Hassan, Sh.M. Morgan and A.K. Elkholy

*Journal of Molecular Liquids, 218: 138-149, (2016), IF: 2.74*

The ligand of 6-(4-benzenesulfonic acid azo)-3-aminophenol (HL) is prepared and characterized by elemental analyses, IR, 1 H NMR spectra, mass spectra and X-ray diffraction analysis. The proton–ligand dissociation constants of HL ligand and its metal stability constants with Mn(II), Co(II), Ni(II) and Cu(II) ions have been determined using potentiometric studies as described by Irving and Rossotti. The optimized structure and the calculated quantum chemical parameters of HL ligand were studied. The potentiometric studies were carried out in 0.1 M KCl and 20% (by volume) DMF–water mixture. The effect of different temperatures was studied and the thermodynamic functions (ΔG, ΔH and ΔS) were calculated. The dissociation process is non- spontaneous, endothermic and entropically unfavorable. The formation of the metal complexes has been found to be spontaneous, endothermic and entropically favorable. Molecular docking was used to predict the binding between azo dye ligand and the receptor of prostate cancer mutant 2q7k-hormone and the receptor of breast cancer mutant 3hb5-oxidoreductase.

**Keywords:** Potentiometry study; Stability constants; Thermodynamics parameters; Quantum chemical parameters; Molecular docking.

## B-96. Geometrical Structures, Thermal Properties and Antimicrobial Activity Studies of Azodye Complexes

A.Z. El-Sonbati , A.A. El-Bindary, G.G. Mohamed, Sh.M. Morgan,W.M.I. Hassan and A.K. Elkholy

*Journal of Molecular Liquids, 218: 16-34, (2016), IF: 2.74*

A novel series of metal complexes with 4-(2,3-dimethyl-1-phenylpyrazol-5-one azo)-3-aminophenol ligand (HL) are prepared and characterized by elemental analyses, IR, UV–Visible spectra, 1H NMR spectra, mass spectra, X-ray diffraction analysis, conductivity measurements and magnetic susceptibility measurements as well as thermal analysis. The IR spectrum revealed that the ligand (HL) coordinates as monobasic tridentate manner with ONO donor sites of nitrogen atom of azo group (-N=N), oxygen atom of the deprotonated phenolic-OH group and exocyclic carbonyl oxygen atom forming a five/six-membered chelate structures. The 1H NMR spectra data indicated that the phenolic proton is also displaced during complexation. From the magnetic and spectral studies, it was obvious that the geometrical structures of these complexes are octahedral. The molecular structures of the ligand (HL) and its metal complexes are optimized theoretically and the quantum chemical param- eters are calculated. The XRD patterns of the ligand (HL) and complex (3) are a mixture of crystalline and amorphous phases. The activation thermodynamic parameters, such as activation energy (Ea), enthalpy ($\Delta H_*$ ), entropy (ΔS), and Gibbs free energy change of the decomposition (ΔG) are calculated using Coats–Redfern and Horowitz–Metzger methods. The ligand (HL) and its metal complexes are screened for their antimicrobial activity against, four bacteria (two Gram positive, i.e. Bacillus subtilis, Streptococcus pneumoniae, and two Gram negative, i.e. Escherichia coli and Pseudomonas aeruginosa) and two fungi species (Aspergillus fumigatus and Candida albicans). The obtained data implies that all the complexes have high antimicrobial activities toward B. subtilis, S. pneumoniae, E. coli and A. fumigatus than the ligand (HL). In addition to that, complexes (1), (3) and (5) showed antifungal effect against C. albicans.

**Keywords:** Metal complexes; Molecular structures; Quantum chemical parameters; Thermodynamic parameters; Antimicrobial activities.

## B-97. Geometrical Structures, Thermal Stability and Antimicrobial Activity of Schiff Base Supramolecular and its Metal Complexes

A.Z. El-Sonbati, M.A. Diab, A.A. El-Bindary, G.G. Mohamed Sh.M. Morgan, M.I. Abou-Dobara and S.G. Nozha

*Journal of Molecular Liquids, 215: 423-442, (2016), IF: 2.74*

The 1:1 condensation of 4-amino-1-phenyl-2,3-dimethylpyrazoline-5-one and 8-hydroxy-7-formylquinoline under template condition to obtain the Schiff base ligand 4-{(8-hydroxyquinoline-7-yl)methyleneamino}-1,2- dihydro-1,5-dimethyl-2-phenylpyra-zol-3-one (HL) with NO 2 donor set. Reaction of the ligand with metal salts gives a series of novel complexes. The ligand and its metal complexes were characterized by elemental analyses, IR, 1H and 13C NMR, electronic, ESR, X-ray diffraction and mass spectral, conductivity and magnetic susceptibility measurements as well as thermal analyses. The analytical and spectroscopic tools showed that the complexes can be formulated as: [Cu(L)2] (1), [CuLX]nH2O, where X = OAc, n = 2 (2); ONO2 , n = 3 (3); NCS, n = 0 (4), [MHLX]nH2O, where M = Cu(II), X = OSO3 , n = 5 (5); M = VO(II), X = O2SO2, n = 2H2O (6) and [UO2L(ONO2)(OH2)2].2H2O (7). The X-ray diffraction (XRD) patterns of start 1, start 2, Schiff base and complex [Cu(L)2] (1) are investigated in powder forms. The molecular

and electronic structures of the ligand (HL) and its complexes have been discussed. It was found that form (A) is more stable than other forms (B and C). The HL ligand acts as a monobasic tridentate ONO donor for complexes (1–4 and 7) and neural tridentate HONO donor for complexes (5 and 6). The molar conductivity shows that the complexes are non-electrolytes nature. Electronic spectra and magnetic moments suggested varieties of geometries around the central metal atoms. The ESR spectra of complexes (2–4) show square planar of axial type symmetry (dx2–y2) with considerable ionic bond character, while complex (1) shows a spectrum of octahedral geometry. The stability of these complexes has also been investigated. The ligand is designed as a building block for larger molecule and supramolecular assemblies. Schiff base of HL and complexes were tested against four local bacterial species; namely two Gram positive bacteria (Staphylococcus aureus and Bacillus cereus) and two Gram negative bacteria (Escherichia coli and Klebsiella pneumoniae) and against four local fungal species (Aspergillus niger, Fusarium oxysporium, Penicillium italicum and Alternaria alternata). 8-Hydroxy-7-formylquinolineand 4-amino-1-phenyl-2,3- dimethylpyrazolin-5-one showed antimicrobial activities against E. coli, K. pneumoniae, P. italicum and A. alternata. The inhibitive action of this Schiff base, against the corrosion of mild steel in 2 M HCl solution has been investigated using Tafel polarization and electrochemical impedance spectroscopy (EIS).

**Keywords:** Schiff base; Supramolecular complexes; Esr; Antimicrobial activities; Eis.

## B-98. Mixed-Ligand Complex Formation of Tenoxicam Drug with Some Transition Metal Ions in Presence of Valine: Synthesis, Characterization, Molecular Docking, Potentiometric and Evaluation of the Humeral Immune Response of Calves

Gehad G. Mohamed, Ahmed A. El-Sherif, Mohamed A. Saad, Sara E.A. El-Sawy and Sh. M. Morgan

*Journal of Molecular Liquids, 223: 1311-1332 (2016)IF: 2.74*

A combined experimental and computational study of novel mixed ligand Cu(II), Ni(II), Co(II), Mn(II), Zn(II), Fe(III) and Cr(III) complexes of tenoxicam drug (H2Ten) and valine (Val) have been reported. The complexes have been characterized using elemental analyses, molar conductance, IR, UV–Vis, magnetic moment, diffused reflectance, thermal analysis and X-ray powdered diffraction. IR and UV–Vis spectra confirm that H2Ten behaves as a neutral bidentate ligand co-ordinated to the metal ions via the pyridine-N and carbonyl group of the amide moiety. Quantum chemical calculations were performed with semi-empirical method to find the optimum geometry of complexes. Also, valuable information is obtained from calculations of molecular parameters for all complexes including net dipole moment of the metal complexes, values of binding energy, which proved that the complexes are more stable than the free ligand. X-ray powder diffraction is used as a new tool to estimate the crystallinity of chelates as well as to elucidate their geometrical structures. The protonation equilibria of tenoxicam (H 2 Ten) formed in DMSO-water solution were calculated using the nonlinear least-squares program MINIQUAD-75. The concentration distribution of the various species has been evaluated. The effect of DMSO as a solvent on the protonation constants of H 2 Ten was discussed. The thermodynamic parameters ΔH o and ΔS o calculated from the temperature dependence of the equilibrium constants were investigated. The humeral immune response of calves vaccinated with inactivated IBR vaccine and ternary M-H2Ten-Val chelates was evaluated. Mo- lecular docking was used to predict the binding between tenoxicam and the receptors of prostate cancer mutant 2q7k-hormone, breast cancer mutant 3hb5-oxidoreductase, crystal structure E. coli (3T88) and crystal structure of S. aureus (3q8u).

**Keywords:** Tenoxicam; Molecular structures; Molecular docking; X-Ray; Thermodynamics parameters; Immune response.

## B-99. Potentiometric, Equilibrium Studies and Thermodynamics of Novel Thiosemicarbazones and Their Bivalent Transition Metal(Ii) Complexes

Abeer Taha Abd El-Karim and Ahmed A. El-Sherif

*J. Molecular Liquids, 219: 914-922, (2016), IF: 2.74*

Protonation constants of novel thiosemicarbazones including 2-(1-(2-phenyl-hydrazono)-propan-2-ylidene) hydrazine-carbothioamide (TPHP) and N-methyl-2-(1-(2-phenyl-hydrazono)-propan-2-ylidene)hydrazinecarbothioamide (MTPHP) ligands and their corresponding metal-ligand formation constants with Cu(II), Ni(II), Mn(II) and Co(II) ions were determined at 15 °C, 25 °C and 35 °C in 50% DMSO solution at I = 0.1 mol·dm−3 NaNO3. The stability order of complexes with reference to the metal ions has been followed this order Cu(II) N Ni(II) N Co(II) N Mn(II) in concordwith the Irving-Williams stability order. Also, chemical equilibrium studies indicated that substitution of hydrogen in thiosemicarbazone (TPHP) bymethyl group causes lowering of acidity as a result of the electron-releasing effect of the methyl group in the substituted amino group of the thiosemicarbazide moiety. The speciation of different species in solution has been evaluated as a function of pH. Additionally, the effect of temperature on protonation of thiosemicarbazone ligands and formation of their M(II)- thiosemicarbazone complexes was investigated. The thermodynamic parameters (ΔH, ΔS andΔG) were calculated anddiscussed. Itwas found that both logK1 and –ΔH1, forM(II)-thiosemicarbazone complexes are somewhat larger than log10 K2 and –ΔH2, indicating a change in the dentate character of these ligands fromtridentate (SNN-donors) in 1:1 chelates to bidentate (SN-donors) in 1:2;M:L chelates. Also, the lower values of log10 K2 and –ΔH2 than log K1 and –ΔH1 may be attributed to steric hindrance produced by the entrance of a second molecule.

**Keywords:** Thiosemicarbazone protonation; Thermodynamics Copper; Potentiometry.

## B-100. Preparation and Structure Characterization of Hematite/Magnetite Ferro-Fluid Nanocomposites for Hyperthermia Purposes

M.A. Zayed, M.A. Ahmed, N.G. Imam and Doaa H. El Sherbiny

*Journal of Molecular Liquids, 222: 895-905, (2016), IF: 2.74*

Herein, xFe2O3/(1 − x)Fe3O4 ferrofluid nanocomposites (0.0 ≤ x ≤ 1.0) prepared by sonochemical method. XRD confirms the

formation of two separate phases with average crystallite size in the range of 12–30 nm. The crystallite size varies with the hematiteweight fraction x (wt%) and shows smallest size at x=0.2. FTIR indicates that the band at 627 cm−1 could be refer to the Fe\\O stretching vibrations and the band at 535 cm−1 could be assigned to Fe\\O in Fe2O3. HRTEM and FESM show the spherical and rod-like shape of magnetite and hematite respectively with average particle size of 12 nm for Fe3O4 NPs and 11 nm for Fe2O3 NPs. XRF confirms that nominal and chemical compositions are close. VSMindicates that the prepared ferrofluid nanocomposites exhibit almost superparamagnetic behavior. The magnetic parameters varywith theweight fraction x (wt%), in addition to superior magnetic responsively with the saturation magnetization value a rising from0.74 to 67.86 emu/g. Analytical thermal analysis techniques exhibit that the ferrofluid nanocomposites show a high degree of thermal stability; also the composition 0.2 shows different behavior and superior properties. Therefore, this composition considered as the aspect ratio for hyperthermia purposes. The behavior of nano-composite (0.2Fe2O3/0.8Fe3O4) for hyperthermia was checked primary by using homemade induction coil at tested frequency of 50 Hz. It found that, 50 Hz frequency induced hyperthermia temperature of about 43 °C at very lowmagnetic (30 μT) fieldwithin 20 min. Finally, we recommend this nanocomposite due to its high magnetization, thermal stability and acceptable biocompatibility for hyperthermia purposes.

**Keywords:** Structure investigation ferrofluid; Nanocomposites Magnetite hematite hyperthermia application.

## B-101. Synthesis, Characterization, Tautomeric Structure and Solvatochromic Behavior of Novel 4-(5-Arylazo-2-Hydroxystyryl)-1-Methylpyridinium Iodide As Potential Molecular Photoprobe

Farag Altalbawy, Elham Darwish, Mohamed Medhat, Sayed El-Zaiat and Hagar Saleh

*Materials Open Access Materials Science Journal, 9: 1022-1037, (2016), IF: 2.728*

A novel series of the title compound 4-(5-arylazo-2-hydroxystyryl)-1-methylpyridinium iodide 6 has been synthesized via condensation reactions of the arylazosalicylaldehyde derivatives 4a–i with 1-methyl-picolinium iodide 5. The structures of the new arylazo compounds were characterized by 1H NMR, IR, mass spectroscopy, as well as spectral and elemental analyses. The electronic absorption spectra of arylazomerocyanine compounds 6 were measured in different buffer solutions and solvents. The pK′s and pK*′s in both the ground and excited states, respectively, were determined for the series and their correlations with the Hammett equation were examined. The results indicated that the title arylazomerocyanine dyes 6 exist in the azo form 6A in both ground and excited states. The substituent and solvent effects (solvatochromism) of the title compound arylazomerocyanine dyes were determined using the Kamlet-Taft equation and subsequently discussed.

**Keywords:** Arylazomerocyanine; Acidity constants; Azo-Hydrazonetautomerism; Solvatochromism.

## B-102. Cytotoxicity and Anti-Proliferative Properties of Heterocyclic Compounds Derived from Progesterone

Rafat M. Mohareba, Nadia Y. MegallyAbdo and Abeer A. Mohamed

*Anticancer Agent in Medicinal Chemistry, 16: 1043-1054, (2016), IF: 2.722*

The following study explored the cytotoxic effect on human cancer cells of a series of novel progesterone derivatives through the synthesis of heterocyclic compounds incorporating progesterone moiety. The reaction of progesterone (1) with cyanoacetanilide derivatives gave the condensation products 3a,b. Either of compound 3a or 3b reacted with elemental sulfur affording the thiophene derivatives 4a and 4b, respectively. In addition, progesterone (1) underwent some multi-component reactions with aromatic aldehydes and cyanomethylene reagents in triethylamine to give the pyran derivatives 10a-f. Carrying the same reactions but using ammonium acetate afforded the pyridine derivatives 11a-f. The anti-tumor evaluations of the newly synthesized products were tested against six human cancer and normal cell lines. The results showed that nine compounds (3b, 7c, 10b, 10d, 10f, 11d, 13a, 13b and 14b) revealed optimal cytotoxic effect against cancer cell lines with IC50 □ 550 nM and their cytotoxicity's were higher than that of progesterone. Moreover, the toxicity of the most active compounds was measured against shrimp larvae. In addition, the anti-proliferative evaluations of these potent compounds were measured.

**Keywords:** Progesterone; Thiophene; Pyran; Pyridine; Cytotoxicity; Anti-proliferative.

## B-103. Experimental and Quantum Mechanical Studies on the Ion–Pair of Levocetirizine and Bromocresol Green in Aqueous Solutions

Ahmed S. Abo Dena and Walid M.I. Hassan

*Spectrochimica Acta Part A: Molecular and Biomolecular Spectroscopy, 163: 108-114, (2016), IF: 2.653*

In the present work, levocetirizine dihydrochloride (LEV) was found to interact with bromocresol green (BCG) via ion–pair formation. UV–vis and FTIR spectroscopy were used to validate the data obtained from quantum mechanical calculations (QMC). The electrostatic potential maps show that the reaction is preferred through the interaction of the sulfonic acid group of BCG and the quaternary ammonium group of LEV. The optimized geometry of the product shows that there are six different intermolecular hydrogen bonds between the studied molecules resulting from the ionic attraction between the oppositely charged groups. The UV–vis spectra suggest the formation of an ion–pair. This finding is contradicting with the previous charge–transfer hypothesis.

**Keywords:** Ion–Pair; Proton–Transfer; Spectroscopy; Hydrogen bond; Triphenylmethane.

## B-104. New Formamidine Ligands and Their Mixed Ligand Palladium(Ii) Oxalate Complexes: Synthesis, Characterization, Dft Calculations and in Vitro Cytotoxicity

Ahmed A. Soliman, Othman I. Alajrawy, Fawzy A. Attabi, Mohamed R. Shaaban and W. Linert

*Spectrochimica Acta Part A, 152: 358-369, (2016), IF: 2.653*

A series of new ternary palladium(II) complexes of the type [Pd(L 1–4 )ox] xH 2 O where L = formamidine ligands and ox = oxalate, were synthesized and characterized by elemental analyses, magnetic susceptibility, UV–Vis, infrared (IR) and mass spectroscopy and thermal analysis. The spectroscopic data indicated that the formamidine ligands act as bidentate N2 donors and the oxalate as O2 ligand. The complexes (1–4) are diamagnetic and the optimization of their structures indicated that the geometry is distorted square planer with O–Pd–O and N–Pd–N bond angles ranged 82.70–83.87and 88.21–95.02; respectively which is acceptable for the heteroleptic complexes. The dipole moment of the complexes (13.97–18.77 Debye) indicating that the complexes are more polarized than the ligands (1.93–4.96 Debye). The complexes are thermally stable as shown from their relatively higher overall activation energies (441–688 kJ mol1). The ligands and the complexes are proved to have good cytotoxicity with IC50 (lM) in the range of (0.011–0.168) against MCF-7, (0.012–0.150) against HCT-116, (0.042–0.094) against PC-3 and (0.006–0.222) against HepG-2 cell lines, which open the field for further application as antitumor compounds.

**Keywords:** Ternary Pd(II) Complexes oxalate formamidine Antitumor complexes.

## 105. 2-Bromo-1-(1H-Pyrazol-4-Yl)Ethanone: Versatile Precursors for Novel Mono-, Bis- and Poly{6-(1H-Pyrazol-4-Yl)-[1,2,4]Triazolo [3,4-B][1,3,4]Thiadiazines}

Mostafa E. Salem, Ahmed F. Darweesh, Ahmad M. Farag and Ahmed H. M. Elwahy

*Tetrahedron, 72: 712-719, (2016), IF: 2.645*

A simple synthesis of novel mono-, bis- and poly{6-(1H-pyrazol-4-yl)-[1,2,4]triazolo[3,4-b][1,3,4]thiadiazines} is reported. The formation of the target compounds was achieved by the reaction of 2-bromo- 1-(5-methyl-1-phenyl-1H-pyrazol-4-yl)ethanone with the appropriate aminotriazolethiol or by the reaction of 6-pyrazolyl-7H-[1,2,4]triazolo[3,4-b][1,3,4]thiadiazine-3-thiol with the appropriate di- and poly(bromo) compounds. The structures of the newly synthesized compounds were established by spectroscopy and elemental analyses.

**Keywords:** Cyclocondensation; Alkylation; Triazolothiadiazine; Pyrazole.

## B-106. Electrooxidation of Methanol and Ethanol on Carbon Electrodeposited Ni–Mgo Nanocomposite

H. B. Hassan, Z. Abdel Hamid and Rabab M. ElSherif

*Chinese Journal of Catalysis, 37 (4): 616-627, (2016), IF:2.628*

Ni–MgO nano-composites were prepared on carbon anodes by electrodeposition from a nickel Watts bath in the presence of fine MgO reinforcement particles. Their performance as electrocatalysts for the oxidation of methanol and ethanol in alkaline medium was investigated and compared with that of carbon coated pure Ni (Ni/C). The chemical composition, phase structure, and surface morphology of the deposited nano-composites were studied by energy dispersive X-ray spectroscopy, X-ray diffractometry, and scanning electron microscopy, respectively. Different electrochemical techniques were used to estimate the catalytic activity of the prepared electrocatalyst anodes, including cyclic voltammetry (CV), chronoamperometry, and electrochemical impedance spectroscopy (EIS). The Ni/C electrocatalyst alone exhibited remarkably low catalytic activity and poor stability toward the electrooxidation process. The inclusion of MgO significantly promoted the catalytic activity of the Ni catalyst for the alcohol electrooxidation and enhanced its poisoning resistance. The EIS results confirmed those of CV and revealed a lower charge transfer resistance and enhanced roughness for the Ni–MgO/C nano-composite electrodes compared with those of Ni/C.

**Keywords:** Nickel-Modified manganese oxide; Electrooxidation; Methanol; Ethanol; Electrochemical Impedance spectroscopy; Cyclic voltammtry.

## B-107. Re-Emergence of Amantadine-Resistant Variants Among Highly Pathogenic Avian Influenza H5n1 Viruses in Egypt

Rabeh El-Shesheny, Ola Bagato, Ahmed Kandeil, Ahmed Mostafa, Sara H. Mahmoud, Hamdi M. Hassanneen, Richard J. Webby, Mohamed A. Ali and Ghazi Kayali

*Infection, Genetics and Evolution, 46:102-109, (2016), IF:2.591*

Highly pathogenic avian influenza (HPAI) H5N1 virus continues to undergo substantial evolution. Emergence of antiviral resistance among H5N1 avian influenza viruses is a major challenge in the control of pandemic influenza. Numerous studies have focused on the genetic and evolutionary dynamics of the hemagglutinin and neuraminidase genes; however, studies on the susceptibility of HPAI H5N1 viruses to amantadine and genetic diversity of the matrix (M) gene are limited. Accordingly, we studied the amantadine susceptibility of the HPAI H5N1 viruses isolated in Egypt during 2006–2015 based on genotypic and phenotypic characteristics. We analyzed data on 253 virus sequences and constructed a phylogenetic tree to calculate selective pressures on sites in the M2 gene associated with amantadine-resistance among different clades. Selection pressure was identified in the transmembrane domain of M2 gene at positions 27 and 31. Amantadine-resistant variants emerged in 2007 but were not circulating between 2012 and 2014. By 2015, amantadine-resistant HPAI H5N1 viruses re-emerged. This may be associated with the uncontrolled prescription of amantadine for prophylaxis and control of avian influenza infections in the poultry farm sector in Egypt. More epidemiological research is required to verify this observation.

**Keywords:** H5N1viruses; Amantadine-resistant; Egypt.

## B-108. Evaluation of Heterocyclic Steroids and Curcumin Derivatives as Antibreast Cancer Agents: Studying the Effect on Apoptosis in Mcf-7 Breast Cancer Cells

Gamal A. Elmegeed, Shaymaa M.M. Yahya, Mervat M. Abd-Elhalim, Mervat S. Mohamed, Rafat M. Mohareb and Ghada H. Elsayed

*Steroids, 115: 80-89, (2016), IF: 2.513*

Anticancer agents consisting of hybrid molecules are used to improve effectiveness and diminish drug resistance. The current study aimed to introduce newly synthesized hetero-steroids of promising anticancer effects. Besides, the pro-apoptotic effects of new compounds were investigated extensively. Several pyrimidino-, triazolopyrimidino-, pyridazino-, and curcumin-steroid derivatives were synthesized, elucidated and confirmed using the spectral and analytical data. The synthesized hetero-steroids, compounds 9, 10, 11, 12, 13, 14, 15, 18, 20, 21, 22 and 24, were tested for their cytotoxic effects versus human breast cancer cells (MCF-7) using neutral red supravital dye uptake assay. Compound 24 (IC50 = 18 lM) showed more inhibitory influence on MCF-7 growth. Using QRT-PCR (Quantitative real time-polymerase chain reaction), CCND1, Survivin, BCL-2, CDC2, P21 and P53, genes expression levels were investigated. The study results disclose that compounds 4, 7, 18, 24 knocked down the expression levels of CCND1, Survivin, BCL-2 and CDC2. However, P21 and P53 were up-regulated by compounds 21, 22. This study introduced promising pro-apoptotic anticancer agents acting through the modulation of key regulators of apoptosis and cell cycle genes.

**Keywords:** Apoptotic genes; Breast cancer; Cytotoxicity; Heterocycles; Steroids.

## B-109. The Knoevenagel Reaction of Cyanoacetylhydrazine with Pregnenolone Synthesis of Thiophene, Thieno[2,3-D]Pyrimidine, 1,2,4-Triazole, Pyran and Pyridine Derivatives with Anti-Inflammatory and Anti-Ulcer Activities

Nahed N.E. El-Sayed, Mahmoud A. Abdelaziz, Wagnat W. Wardakhan and Rafat M. Mohareb

*Steroids, 107: 98-111, (2016), IF: 2.513*

The reaction of pregnenolone with cyanoacetylhydrazine and ammonium acetate at 120 C gave the Knoevenagel condensation product 3. The latter reacted with different reagents to give thiophene, thieno[2,3-d]pyrimidine, 1,2,4-triazole and pyran derivatives. The anti-inflammatory and anti-ulcer evaluations of the newly synthesized products were evaluated and the results showed that compounds 4, 8c, 10, 11, 13c, 15a, 15c, 17a, 17b, 17e, 18a and 18f possessed higher activity compared to the rest of the compounds. In addition to this, the toxicity of these active compounds was studied against shrimp larvae where compounds 15a, 15c and 18a showed non-toxicity against the tested organisms.

**Keywords:** Pregnenolone; Thiophene; 1,2,4-Triazole; Pyran; Anti-Inflammatory.

## B-110. Photocatalytic Degradation of Methylene Blue with Copper(II) Oxide Synthesized by Thermal Decomposition of Flubendazole Complexes

Ahmed M. Mansour, Eslam M. El Bakry and Nour T. Abdel-Ghani

*Journal of Photochemistry and Photobiology A: Chemistry, 327: 21-24, (2016), IF: 2.477*

Novel copper(II) complexes of an anti-parasitic Flubendazole drug (FLU), [Cu(FLU)2X2]zH2O (X = Cl (1), C2H3O2 (3), and ClO4 (4), z = 1–4) and [Cu(NO3)(FLU)2(OH2)]NO32H2O (2) were synthesized and characterized using elemental analysis, TG, IR, EPR, magnetic and conductance measurements. Geometry optimization and natural bond orbital analysis were performed at DFT/B3LYP/6-31G level of theory. Electronic transitions were calculated by TD-DFT. Tenorite (CuO) nanoparticles with promising catalytic properties were prepared in air via the controlled thermal decomposition of 1–4. The polymorph and morphology of the prepared nano-tenorite particles were investigated by powder XRD and field emission scanning electron microscope. The catalytic degradation of methylene-blue (MB) dye exposed to the UV radiation in presence of CuO nanoparticles as a catalyst was studied at room temperature in water.

**Keywords:** Flubendazole TD-DFT; Methylene-Blue tenorite Nanoparticles.

## B-111. Photochemical Dissociation of Hobr. A Nonadiabatic Dynamics Study

Saadullah G. Aziza, Abdulrahman O. Alyoubi, Shaaban A. Elrobya and Rifaat H. Hilal

*Journal of Photochemistry and Photobiology A: Chemistry, 324: 8-13, (2016), IF: 2.477*

A number of single-reference post Hartree-Fock methods, namely CIS, symmetry adopted cluster configuration interaction (SA C-CI), equation of motion coupled cluster (EOM-CCSD) and time-dependent density functional theory (TDDFT), were used to investigate the excited state properties and photochemical dissociation of hypobromous acid, HOBr. Results are in good agreement with experimental data. The decay of the excited states of HOBr in the gas phase was examined by simulating the UV photoabsorption spectrum and nonadiabatic dynamics at the TDDFT M06-2X level of theory. The spectrum, composed of 10 excited states, was simulated with the nuclear ensemble approximation, sampling a Wigner distribution with 500 points. Dynamics simulations were done with the surface hopping method, started in two separate spectral windows, at 4.0 0.25 eV and 8.0 0.25 eV, to be compared to experimental UV spectral data. Three hundred trajectories were considered from each of these windows according to their excitation probabilities. The excited-state lifetime was determined. The main photochemical channel observed were HO and Br eliminations, representing 67% of all processes.

**Keywords:** Hobr excited; State dynamics; Tddft Photodissociation Non-Adiabatic dynamics.

## B-112. Synthesis and Characterization of Schiff Base Complexes Derived from Cephradine: Fluorescence, Photostability and Photobiological Applications

Nora S. Abdel-Kadera, Aida L. El-Ansary, Tarek A. El-Tayeb and Marwa M.F. Elnagdi

*Journal of Photochemistry and Photobiology A: Chemistry, 321: 223-237, (2016), IF: 2.477*

A new Schiff base derived from the condensation of 6-formyl-7-hydroxy-5-methoxy-2-methylbenzo-pyran-4-one (benzopyran – 4-one derivative) with cephradine drug (L) was prepared and characterized by elemental analyses and some spectroscopic studies. Also, Zn(II), Cu(II), Co(II) and Ni(II) complexes of that Schiff base were prepared by template reaction. Many tools of analysis such as elemental analyses, infrared, ultraviolet-visible and thermal analysis, as well as electrical conductance and magnetic susceptibility measurements were used to elucidate the structure of these complexes. The data showed that Zn(II)-L and Cu(II)-L complexes are 1:1 (M:L). The ligand was found to be monobasic bidentate. On the other hand, Ni(II)-L and Co(II)-L form binuclear complexes. All the complexes are non-electrolyte. The luminescence properties of the prepared Schiff base and its complexes were measured. The photostability of Schiff base, L, and its Zn(II)-L and Cu(II)-L complexes were also studied. The photobiological activity of cephradine, benzopyran-4-one derivative, Schiff base, L and the complexes were studied on mosquito larvae to investigate the extent of their photosensitization efficiency in controlling noxious insects using direct sunlight (larvicidal effect). In vitro cytotoxicity study of the Schiff base and its complexes against Hep G2-cell line was investigated by the MTT assay. The Schiff base, L, exhibits better activity against Hep G2 cell line than the complexes.

**Keywords:** Schiff base; Complexes; Luminescence; Photostability; Cytotoxicity.

## B-113. Computational Design, Synthesis and Application of A New Selective Molecularly Imprinted Polymer for Electrochemical Detection

Nour T. Abdel Ghani, Rasha Mohamed El Nashar, Fatehy M. Abdel-Haleem and Adel Madbouly

*Electroanalysis, 28: 153, (2016), IF: 2.471*

A computational approach was developed to find a suitable functional monomer to design a new molecularly imprinted polymer (MIP), based on which methacyrlic acid (MAA) was selected as a functional monomer to synthesize the molecular imprinted and non-imprinted polymers. All calculations were carried out using Gaussian 03 software based on the application of Hartree Fock (HF) method with 6-31G (d) basis set. The performance of the MIPs prepared with different ratios of MAA was then evaluated using equilibrium rebinding assays. The MIP with the highest binding capacity was chosen as recognition material for the fabrication of new PVC sensors and their responses were compared with each other and with previously reported modifiers in literature. The addition of the ionic surfactant (TFPB) was found to have a synergistic effect on the response mechanism of the electrodes. The results of the MIP modified sensors show that they provide an improved electrode slope, wider pH range and a highly extended life time reaching 7 months compared to 2–4 weeks in case of traditional ion-exchangers reported in literature, besides, being successfully applied for measurements in biological samples

**Keywords:** Computational studies; Itopride hydrochloride; Molecular imprinted polymer; Pharmaceutical analysis; Polyvinylchloride electrodes.

## B-114. Potentiometric Anion Selectivity and Analytical Applications of Polymer Membrane Electrodes Based on Novel Mn(Iii)- and Mn(Iv)-Salophen Complexes

Fatehy M. Abdel-Haleem, Ibrahim H. A. Badr and Mahmoud S. Rizk

*Elecroanalysis, 28: 2922-2929, (2016), IF: 2.471*

New Mn(III)-L and Mn(IV)-L complexes were prepared from the highly lipophilic salophen ligand (L): phenol 2,2′-[(4,5-dimethyl-1,2-phenylene)bis[(E)-nitrilomethylidyne]]bis[4,6-bis(1,1-dimethylethyl). The prepared complexes were fully characterized and used for the construction of thiocyanate membrane electrodes. Optimized membrane electrodes contained 33.0 mg PVC, 66.0 mg o-nitrophenyloctylether, 50 or 5 (mole %) tetrakis(trifluoromethyl)phenyl borate and 1 mg Mn(III)-L (sensor 2) or Mn-(IV)-L (sensor 12), respectively. Such electrodes exhibited linear responses toward thiocynate in a concentration range of $10^{-1}$–$10^{-5}$ M and detection limits of $8.3\times10^{-6}$, $8.9\times10^{-6}$ M for sensor 2 and 12, respectively. Optimized membrane electrodes exhbited high selectivty toward thiocayante compared to more lipophilic anions. The observed thiocyanate selectivity of the optimized membranes was confirmed by formation constant calculations for Mn(III)-L and Mn(IV)-L with $SCN^-$, $\beta$=1014.1 and 1012.5, which was measured potentiometrically using the sandwich membrane method. Furthermore, computational study using DFT calculations was performed to at DFT/B3LYP level of theory to confirm the observed selectivity data. The response times were 3 and 0.5 min for low and high concentrations. The lifetimes of the optimized electrodes were ~4–6 weeks. The analytical utility of the optimized membrane electrodes was demonstrated by the analysis of thiocyanate level in different saliva samples.

**Keywords:** Thiocyanate sensor; Pvc electrode; Salophen Complexes; Potentiometry.

## B-115. Potentiometric Sensing of Aspirin Metabolite in Human Plasma and Pharmaceutical Preparations Using Co(Iii)-Complex Based Electrodes: Experimental and Quantum Chemical Calculations

Ola R. Shehaband Ahmed M. Mansour

*Electroanalysis, 28(5): 1100-1111, (2016), IF: 2.471*

Three novel poly vinyl chloride (PVC) (A), carbon paste (CP) (B), and coated glassy carbon-MWCNT (CGC) (C) salicylate ($sal^-$) sensors based on new synthesized [Co(L2Cl)Cl3(H2O)] H2O complex (L2Cl=(1H-benzimidazol-2-ylmethyl)-N-(2-chloro-phenyl)- amine)), o-nitrophenyloctyl ether as a mediator and tridodecylmethyl ammonium chloride as a cationic additive were successfully

used for determination of sal− in human plasma and pharmaceutical formulations. The sal−-sensors exhibited enhanced sensitivity with slope of −63.5, −60.5 and −58.9 mV/decade and detection limit of 1.0×10−5, 4.0×10−7, and 1.0×10−6 mol L−1 for A–C sensors respectively. Quantum chemical calculations were carried out by HF and DFT/B3LYP methods to explore and investigate the interaction between the receptor and the different anions. The intermolecular H-bond created between the uncoordinated C[DOUBLE BOND]O of salicylate group and the secondary amino group in the complex is the key factor of the selectivity of the proposed sensor. A linear relation is established between the natural charge on the Co center and the value of the binding energy, where the decrease in positive charge is associated by an increase in the anion binding energy.

**Keywords:** Sensing; Co(III) complex; Salicylate; Mwcnt; Theoretical calculations.

## B-116. Antimicrobial Activity of some Novel Armed Thiophene Derivatives and Petra/Osiris/Molinspiration (POM) Analyses

Yahia Nasser Mabkhot, Fatima Alatibi, Nahed Nasser E. El-Sayed, Salim Al-Showiman, Nabila Abdelshafy Kheder, Abdul Wadood, Abdur Rauf, Saud Bawazeer and Taibi Ben Hadda

*Molecules, 21: 222-0, (2016), IF: 2.465*

Tetrasubstituted 2-acetylthiophene derivative 5 was synthesized and then condensed with various nitrogen nucleophiles such as 5-amino-1,2,4-triazole, 2-aminobenzimidazole, aniline or p-chloroaniline to afford the corresponding iminothiophene derivatives 6–8a,b. Condensation of thiophene 5 with malononitrile as carbon nucleophile afforded compound 9, which underwent nucleophilic addition with DMF-DMA to afford compound 10. The newly synthesized products were characterized by elemental analysis, IR, MS, 1H-13C-NMR and CHN analysis and then evaluated for their antimicrobial activity. Results of the in vitro antibacterial activity showed that thiophene derivative 7 was found to be more potent than the standard drug gentamicin against Pseudomonas aeruginosa. Some of these compounds showed potential antimicrobial activities. Molecular docking and Osiris/Molinspiration analyses show the crucial role and impact of substituents on bioactivity and indicate the unfavorable structural parameters in actual drug design: more substitution with electronic donor group doesn't guarantee more effective bioactivity. This study should greatly help in an intelligent and a controlled pharmacomodulation of antibiotics.

**Keywords:** Armed thiophenes; Antimicrobial activity; Petra; Osiris; Molinspiration (POM) Analyses.

## B-117. Hydrazonoyl Chlorides as Precursors for Synthesis of Novel Bis-Pyrrole Derivatives

Nabila Abdelshafy Kheder

*Molecules, 21: 326-0, (2016), IF: 2.465*

A convenient synthesis of some novel bis-pyrrole derivatives via hydrazonoyl halides is described. Antimicrobial evaluation of some selected examples of the synthesized products was carried out. The bis-pyrrole derivative having chloro substituents showed good activity against all of the used microbes. The molecular docking of the bis-pyrrole derivatives was performed by the Molecular Operating Environment (MOE) program.

**Keywords:** Bis-Pyrrole; Antibacterial activity; Antifungal activity; Hydrazonoyl halides; Molecular docking.

## B-118. One Pot Single Step Synthesis and Biological Evaluation of some Novel Bis(1,3,4-Thiadiazole) Derivatives as Potential Cytotoxic Agents

Sobhi M. Gomha, Nabila A. Kheder, Abdou O. Abdelhamid and Yahia N. Mabkhot

*Molecules, 21: 1-8, (2016), IF: 2.465*

A novel series of bis(1,3,4-thiadiazole) derivatives were synthesized in one step methodology with good yields by condensation reaction between bis-hydrazonoyl chloride 1 and various reagents. The structures of the prepared compounds were confirmed by spectral data (IR,NMR, and MS), and elemental analysis. The anticancer activity against human breast carcinoma (MCF-7) cancer cell lines was evaluated in MTT assay. The results revealed that the bis-thiadiazole derivatives 5c,d, 7b,c and 9c had higher antitumor activity than the standard drug Imatinib.

**Keywords:** Bis-Hydrazonoyl Chlorides; Bis(1,3,4-Thiadiazole); Anticancer activity; Methyl arylidene Dithiocarbamate; Dipolar cycloaddition reaction.

## B-119. Synthesis and Antimicrobial Activity of Some New Thiadiazoles, Thioamides, 5-Arylazothiazoles and Pyrimido[4,5-D][1,2,4]Triazolo[4,3-A]Pyrimidines

Abdou O. Abdelhamid, Ibrahim E. El Sayed, Mohamed Z. Hussein and Mangoud M. Mangoud

*Molecules, 21: 1072-0, (2016), IF: 2.465*

A novel series of 1,3,4-thiadiazoles, 5-arylazothiazoles and hexahydropyrimido-[4,5-d][1,2,4]triazolo[4,3-a]pyrimidineswere synthesized via reaction of hydrazonoyl halides with each of alkyl carbothioates, carbothioamides and 7-thioxo-5,6,7,8-tetrahydropyrimido-[4,5-d]pyrimidine-2,4(1H,3H)-diones in the presence of triethylamine. The structures of the newly synthesized compounds were established based on their spectral data, elemental analyses and alternative synthetic routes whenever possible. Also, the newly synthesized compounds were screened for their antimicrobial activity against various microorganisms.

**Keywords:** Hydrazonoyl halides; Thioamides; 1,3,4-Thiadiazoles; Thiazoles; Pyrimido[4,5-D][1,2,4]Triazolo[4,3-A]Pyrimidines; Antimicrobials.

## B-120. Synthesis and Structure-Activity Relationship of some New Thiophene-Based Heterocycles as Potential Antimicrobial Agents

Yahia Nasser Mabkhot, Fatima Alatibi, Nahed Nasser E. El-Sayed, Nabila Abdelshafy Kheder and Salim S. Al-Showiman

*Molecules, 21: 1036-0, (2016), IF: 2.465*

Several newpyrazole, pyridine, [1,2,4]triazolo[1,5-]pyrimidine, benzimidazo[1,2-a]pyrimidine and 1,2,4-

triazolo[3,4-c][1,2,4]triazine derivatives incorporating a thiophene moiety were synthesized from (E)-ethyl 5-(3-(dimethylamino)acryloyl)-4-phenyl-2-(phenylamino)thiophene-3-carboxylate (1). The structures of the newly synthesized compounds were confirmed by IR, 1H-, 13C-NMR, mass spectral data and elemental analysis. The antibacterial and antifungal activities of all the synthesized compounds were evaluated. The results indicated that compounds 9, 12, and 19 were found to be more potent than the standard drug Amphotericin B against Aspergillus fumigates. Additionally, compound 12 exhibited higher activity than the standard drug Amphotericin B against Syncephalastrum racemosum

**Keywords:** Thiophene; Enaminone; Pyrazole; Pyridine; Antimicrobial activity.

## B-121. Synthesis of New 3-Heteroarylindoles as Potential Anticancer Agents

Abdou O. Abdelhamid, Sobhi M. Gomha, Nadia A. Abdelriheem and Saher M. Kandee

*Molecules, 21: 1-15, (2016), IF: 2.465*

2-(3-(1H-Indol-3-yl)-5-(p-tolyl)-4,5-dihydro-1H-pyrazol-1-yl)-4-substituted-5-(substituted diazenyl)thiazoles and 2-(1H-indol-3-yl)-9-substituted-4,7-disubstituted pyrido[3,2-e][1,2,4]triazolo[4,3-a]pyrimidin-5(7H)-ones were synthesized via reaction of hydrazonoyl halides with each of 3-(1H-indol-2-yl)-5-(p-tolyl)-4,5-dihydro-1H-pyrazole-1-carbothioamide and 7-(1H-indol-3-yl)-2-thioxo-5-substituted-2,3-dihydropyrido[2,3-d]pyrimidin-4(1H)-ones, respectively. Also, hydrazonoyl halides were reacted with N'-(1-(1H-indol-3-yl)ethylidene)-2-cyanoacetohydrazide to afford 1,3,4-thiadiazole derivatives. Structures of the new synthesis were elucidated on the basis of elemental analysis, spectral data, and alternative synthetic routes whenever possible. Fifteen of the new compounds have been evaluated for their antitumor activity against the MCF-7 human breast carcinoma cell line. The results indicated that many of the tested compounds showed moderate to high anticancer activity when compared with doxorubicin as a reference drug.

**Keywords:** Thiazoles; Pyrazoles; Coupling reactions; Thiosemicarbazides; Molecular docking; Anti-cancer activity.

## B-122. Synthesis, Characterization and Molecular Docking of Novel Bioactive Thiazolyl-Thiazole Derivatives as Promising Cytotoxic Antitumor Drug

Sobhi M. Gomha, Taher A. Salaheldin, Huwaida M. E. Hassaneen, Hassan M. Abdel-Aziz and Mohammed A. Khedr

*Molecules, 21: 1-17, (2016), IF: 2.465*

Reactions of ethylidenethiocarbohydrazide with hydrazonoyl halides gave 1,3-thiazole or 1,3,4-thiadiazole derivatives according to the type of hydrazonoyl halides. Treatment of ethylidenethiosemicarbazide with hydrazonoyl halides and dimethylacetylene dicarboxylate (DMAD) afforded the corresponding arylazothiazoles and 1,3-thiazolidin-4-one derivatives,respectively. The structures of the synthesized products were confirmed by IR, 1H-NMR, 13C-NMR and mass spectral techniques. The cytotoxic activity of the selected products against the Hepatic carcinoma cell line (Hepg-2) was determined by MTT assay indicating a concentration dependent cellular growth inhibitory effect, especially for compounds 14c and 14e. The dose response curves indicated the IC50 (the concentration of test compounds required to kill 50% of cell population) were 0.54 M and 0.50 M, respectively. Confocal laser scanning imaging of the treated cells stained by Rhodamin 123 and Acridine orange dyes confirmed that the selected compounds inhibit the mitochondrial lactate dehydrogenase enzymes. The binding mode of the active compounds was interpreted by a molecular docking study. The obtained results revealed promising cytotoxic activity.

**Keywords:** Ethylidenethiocarbohydrazide; Ethylidenethiosemicarbazide; Hydrazonoyl halides; 1,3-Thiazole; 1,3,4-Thiadiazole; Cytotoxic activity; Molecular docking.

## B-123. Novel Schiff Base Ligand and its Metal Complexes with some Transition Elements. Synthesis, Spectroscopic, Thermal Analysis, Antimicrobial and in Vitro Anticancer Activity

Walaa H. Mahmoud, Reem G. Deghadi and Gehad G. Mohamed

*Applied Organometallic Chemistry, 30:221-230 (2016)IF:2.452*

A novel Schiff base ligand (H 2 L) was prepared through condensation of 2,6-diaminopyridine and o-benzoylbenzoic acid in a 1:2 ratio. This Schiff base ligand was characterized using elemental and spectroscopic analyses. A new series of Cr(III), Mn(II), Fe(III), Co(II), Ni(II), Cu(II), Zn(II) and Cd(II) metal complexes of H2L were prepared and characterized using elemental analysis, spectroscopy (1H NMR, mass, UV–visible, Fourier transform infrared, electron spin resonance), magnetic susceptibility, molar conductivity, X-ray powder diffraction and thermal analysis. The complexes are found to have trigonal bipyramidal geometry except Cr(III), Mn(II) and Fe(III) complexes which have octahedral geometry based on magnetic moment and solid reflectance measurements. The infrared spectral studies reveal that H2L behaves as a neutral bidentate ligand and coordinates to the metal ions via the two azomethine nitrogens. 1H NMR spectra confirm the non-involvement of the carboxylic COOH proton in complex formation. The presence of water molecules in all reported complexes is supported by thermogravimetric studies. Kinetic and thermodynamic parameters were determined using Coats–Redfern and Horowitz–Metzger equations. The synthesized ligand and its complexes were screened for antimicrobial activities against two Gram-positive bacteria (Bacillus subtilis and Staphylococcus aureus), two Gram-negative bacteria (Escherichia coli and Neisseria gonorrhoeae) and one fungus (Candida albicans). Anticancer activities of the ligand and its metal complexes against human breast cancer cell line (MCF7) were investigated.

**Keywords:** Schiff base ligand; Spectroscopic analyses; Thermal analysis; Kinetic; Antimicrobial activities; Breast cancer.

## B-124. Synthesis, Characterization and in Vitro Antimicrobial and Anti-Breast Cancer Activity Studies of Metal Complexes of Novel Pentadentate Azo Dye Ligand

Walaa H. Mahmoud, Fatma N. Sayed and Gehad G. Mohamed

*Applied Organometallic Chemistry, 30 : 959 - 973, (2016), IF:2.452*

A new azo dye with N3O2 donor set of atoms has been synthesized via coupling reaction of 2,6-diaminopyridine with p-methoxybenzaldehyde. The molecular and electronic structure of the azo dye ligand (L) was optimized theoretically and the quantum chemical parameters were calculated. Molecular docking was used to predict the binding between L and the receptors of breast cancer mutant 3hb5-oxidoreductase, crystal structure of Escherichia coli (3T88) and crystal structure of Staphylococcus aureus (3q8u). The newly synthesized L was used for complex formation with Cr(III), Mn(II), Fe(III), Co.(II), Ni(II), Cu(II), Zn(II) and Cd(II) ions. The nature of bonding and the stoichiometry of L and its mononuclear complexes were deduced from elemental analyses, spectroscopic, magnetic susceptibility, molar conductance, electron spin resonance and conductivity measurements, thermogravimetric analyses and powder X-ray diffraction. Elemental analysis data show that the complexes have composition of ML type with an octahedral geometry for all the complexes. The activation thermodynamic parameters were calculated. The prepared azo dye and its metal complexes were tested against various Gram-positive and Gram-negative bacteria and a fungus. Most complexes exhibit antibacterial and antifungal activities against these organisms. Anticancer evaluation studies against standard breast cancer cell line were performed using various concentrations. The activity index was calculated.

**Keywords:** Azo dye; Spectroscopy; Molecular structures; Quantum chemical parameters; Thermogravimetric analysis; Molecular docking; Biological activity; Anticancer activity.

## B-125. Experimental and Quantum Chemical Calculations of Novel Photoactivatable Manganese(I) Tricarbonyl Complexes

Ahmed M. Mansour andOla R. Shehab

*Journal of Organometallic Chemistry, 822(1): 91-99 (2016) IF: 2.336*

[MnBr(CO)3(TZ)] (1) and [Mn(CO)3(MZ)] (2) (TZ = Tazarotene and MZ = Metamizole) have been synthesized and characterized as new visible light photo-trigged carbon monoxide releasing molecules. The ability to deliver CO to DMSO or myoglobin solution has been studied. TZ behaves as a bidentate ligand via the pyridine N-atom and π–Ctriple bond; length of mdashC group, while MZ is a mono-negatively tridentate ligand and coordinates to Mn(I) through the pyrazolone Cdouble bond; length as m-dashO, –SO3− and tertiary amino groups. These photoCORMs cannot be stored for a long time in DMSO, but they are able to release CO fast upon the exposure to the light (412–468 nm). About one CO equivalent was delivered from CORM 1 to the myoglobin solution upon the exposure to 468 nm LED lamp for 42 min. The electronic configuration of the metal center, hybridization type and nature of bonding have been obtained by natural bond orbital analysis. TD-DFT calculations have been performed to recognize the electronic structure and to explain the related experimental findings. The CORMs have been screened for their antibacterial activity against Staphylococcus aureus and Escherichia coli in comparison to their parent drugs.

**Keywords:** Gasotransmitters; Photoactivatable; Tazarotene; Metamizole; TD-DFT.

## B-126. Gas-Phase Acidity and Dynamics of the Protonation Processes of Carbidopa and Levodopa. A Qm/Qd Study

Ghader M. Sukkera, Shaaban A. Elroby and Rifaat Hilala

*Journal of Biomolecular Structure and Dynamics, 34(10): 2268-2280, (2016), IF: 2.3*

The present work details, our efforts to investigate and compare the acid – base properties of levodopa (LD) and carbidopa (CD), a drug combination being used in the treatment of Parkinson ' s disease. Protonation and deprotonation were examined for all possible sites in the two drugs. Proton af fi nity and proton detachment enthalpies were computed at the B3LYP/6 – 311++G** level of theory. Results of the present work reveal that CD is more basic and can abstract protons in solution much more ef fi ciently than LD. Furthermore, at all deportation sites considered, CD is more acidic than LD. DFT-based ADMP, dynamic simulations have been performed to explore the dynamics of the protonation pro- cesses in LD and CD. Thus, while the dynamics of the protonation process of LD is very straightforward leading to the formation of the corresponding cation, the protonation process in CD is very complex involving a major geometry change and rearrangement. Results of the present work reveal that the active species in acid medium is not CD in its normal geometry but a carbonyl hydrazine form instead. The presence of the carbonyl group β to the hydrazine group may very well underlie its enhanced activity which allows it to bind to the active site of the DDC enzyme. The relative stabilities of various water – water – CD complexes have been computed and compared.

**Keywords:** Acid; Base properties; Proton Af Fi Nity; Carbidopa; Levodopa; Parkinson ' S diseas.

## B-127. Papain-Based Vaccination Modulates Schistosoma Mansoni Infection-Induced Cytokine Signals

N. Abdel Aziz, H. Tallima, E. A. Hafez and R. El Ridi

*Scandinavian Journal of Immunology,83:128-138(2016)IF:2.27*

We have previously shown that immunization of outbred rodents with cysteine peptidases-based vaccine elicited type 2-biased immune responses associated with consistent and reproducible protection against challenge Schistosoma mansoni. We herein start to elucidate the molecular basis of C57BL/6 mouse resistance to S. mansoni following treatment with the cysteine peptidase, papain. We evaluated the early cytokine signals delivered by epidermal, dermal, and draining lymph node cells of na€ıve, and S. mansoni -infected mice treated 1 day earlier with 0 or 50 lg papain, or immunized twice with papain only (10 lg/ mouse), papain-free recombinant S. mansoni glyceraldehyde 3-phosphate dehydrogenase and 2-Cys

peroxiredoxin peptide (10 and 15 lg/mouse, respectively = antigen Mix), or papain-adjuvanted antigen Mix. Schistosoma mansoni infection induced epidermal and lymph node cells to release type 1, type 2 and type 17 cytokines, known to counteract each other. Expectedly, humoral immune responses were negligible until patency. Papain pretreatment or papain-based vaccination diminished or shut off S. mansoni infection early induction of type 1, type 17 and type 2 cytokines except for thymic stromal lymphopoietin and programmed the immune system towards a polarized type 2 immune milieu, associated with highly significant ($P < 0.005$ – $<0.0001$) resistance to S. mansoni

**Keywords:** Schistosoma mansoni.

## B-128. Azobenzene-Containing Bent-Core Liquid Crystals: an Overview

Mohamed Alaasar

*Liquid Crystals, 43: 2208-2243, (2016), IF: 2.244*

Azo-functionalised materials are of special interest due to their photochromic nature, i.e. reversible trans–cis isomerisation upon photoirradiation. The combination of photosensitivity and liquid crystalline properties in the same molecule allows the material to be exploited for optical and optoelectronic devices. Azobenzene-based bent-core liquid crystals (BCLCs) have attracted considerable attention in recent years due to their rich mesomorphism. In this review, the main research directions and different molecular structures of bent-core molecules incorporating azobenzene unit and its subtype the so-called hockey-stick molecules are summarised. Additionally, azobenzene-based U-shaped molecules, hydrogen-bonded bent-shaped liquid crys- talline materials and some selected examples of two different types of photoswitchable meso- genic dimers are provided. The nature, number and position of the lateral substitutions able to modify the phase behaviour of such BCLCs, affording in turn interesting liquid crystalline phases are discussed. Finally, the isomerisation process of these photosensitive BCLCs in solutions or in mesophases under the effect of UV-visible irradiation is summarised.

**Keywords:** Bent-core liquid crystals; Azobenzene; Polarity; Chirality; Photosensitivity; Dimers.

## B-129. Mesophase Behaviour of 1:1 Mixtures of 4-Nalkoxyphenylazo Benzoic Acids Bearing Terminal Alkoxy Groups of Different Chain Lengths

H.A. Ahmed, M.M. Naoum and G.R. Saad

*Liquid Crystals, 43: 1259-1267, (2016), IF: 2.244*

The thermal and mesophase behaviour of all possible 1:1 mixtures (In/Im) formed from any two homologues of 4-n-alkoxyphenylazo benzoic acids bearing different alkoxy chain lengths (n and m vary between 6 and 16 carbons), were investigated by differential scanning calorimetry (DSC) and phases identified by polarised light microscopy (PLM). Phase transitions were investigated as a function of the average alkoxy chain length (n=(n + m)/2) of the mixed acids. A comparison, made between the present series and previously investigated simpler analogues, 4-n-alkoxy benzoic acids, revealed that increasing the length of the mesogenic core increased the stabilities of both the smectic C and nematic phases.

**Keywords:** 4-N-Alkoxyphenylazo benzoic acids; 4-N-Alkoxy benzoic acids; Binary mixtures; Phase transitions.

## B-130. The Effect of Orientation of the Lateral Methyl Substituent on the Mesophase Behaviour of 4-Alkoxyphenylazo Aryl Benzoates

Magdi M. Naoum, Abdelgawad A. Fahmi, Amira H. Abaza and Gamal R. Saad

*Journal Liquid Crystals, 43: 1831-1845, (2016), IF: 2.244*

Two homologous series of 4-alkoxyphenylazo 4□-(2□- (and 3□-) methyl-) 4□-substituted benzoates (IIna–f and IIIna–f, six series each) were prepared and investigated. Within each series, the length of the terminal alkoxy group varies among 6, 8, 10 and 12 carbons, while the other terminal substituent, X, is a polar group that alternatively changes between the electron-donating CH3O, CH3, and the electron-withdrawing Br, NO2 and CN groups, in addition to the un-substituted analogue, X = H, aiming to investigate the effect of the different orientations of the methyl groups substituted on the central benzene ring, on the mesophase behaviour. The mesomorphic properties were discussed in terms of steric and polarisability effects. The mesophase stability was correlated with the polarisability anisotropy of bonds to the terminal substituent X. Comparative studies were made between the prepared isomers with each other and with the previously investigated laterally neat analogues 4-(4□-alkoxyphenylazo) phenyl 4□-substituted benzoates (Ina–f).

**Keywords:** Phenylazo phenyl benzoates; Mesophase behaviour; Lateral-methyl substitution; Polarisability.

## B-131. Tazarotene Copper Complexes: Synthesis, Crystal Structure, Dft and Biological Activity Evaluation

Ahmed M. Mansour

*Polyhedron, 109: 99-106, (2016), IF: 2.108*

New mononuclear copper(II) complexes of the first topical receptor-selective retinoid drug, Tazarotene (Tz), of the type [Cu(Tz)2X2] (X = Cl (1) and Br (2a)) were synthesized, characterized (elemental analysis, TG, FT IR, UV–Vis, EPR, magnetic susceptibility, molar conductance measurements and single crystal X-ray analysis) and tested for their antimicrobial activities against Staphylococcus aureus and Escherichia coli. Tazarotene behaves as a neutral monodentate ligand via the pyridine nitrogen atom. Complex 1 crystallizes in the monoclinic P21/c space group. The environment around the metal center in 1 could be described as an intermediate between tetrahedral and square–planar geometries. Crystals of the polymeric {[Cu(Tz)(μ-Br)]}n (2b) complex were obtained by the slow evaporation of the reaction filtrate of complex 2a. The distorted tetrahedral environment around Cu(I) is formed from the pyridine N atom of Tz, the S atom of another Tz molecule as well as two bridged bromine atoms, with a Cu…Cu′ distance of 3.327 Å. Time-dependent density functional theory calculations were carried out to understand the electronic structure and to explain the related experimental findings. The electronic arrangement, type of hybridization and nature of bonding were obtained from natural bond orbital analysis.

**Keywords:** Polymeric copper complexes; Bridged halides; Tazarotene; Lanl2dz; Td-Dft.

## B-132. Organic Synthesis and Inhibition Action of Novel Hydrazide Derivative for Mild Steel Corrosion in Acid Solutions

Zeinab A. Abdallah, Mohamed S. Mohamed Ahmed and M.M. Saleh

*Materials Chemistry and Physics, 174: 91-99 (2016)IF: 2.101*

A new derivative of hydrazide family, 2-(2-hydrazinyl-1,6-dihydro-6-oxopyrimidin-4-yl) acetohydrazide (HDOP) is synthesized and used as a corrosion inhibitor for mild steel both in 1 M HCl and 0.5 M H2SO4 solutions. A facial synthesis of a novel hydrazinyl hydrazide derivative is accomplished via a one-pot synthesis. Reaction of ethyl 2-(1,2,3,6-tetrahydro-6-oxo-2-thiopyrimidin-4-yl)acetate (1) with hydrazine hydrate in an ethanol refluxing produces the target hydrazinyl hydrazide derivative in a good yield. Different techniques such as IR, NMR and mass spectroscopy are used for characterization of the obtained products. The inhibition of mild steel corrosion using HDOP in different concentrations is studied by electrochemical impedance spectroscopy and polarization measurements. The inhibition efficiency (IE) of HDOP is found to be higher in HCl than that in H2SO4 solution. This is attributed to the stronger adsorption of Cl− on the iron surface which enables better synergism between Cl− and the protonated inhibitor. The HDOP acts mainly as a cathodic inhibitor (in both acid solutions) and an inhibition efficiency of ~89% was obtained in the HCl solution. The free energy of adsorption obtained by applying Langmuir adsorption isotherm predicts physisorption of HDOP on the iron surface in the HCl solution.
**Keywords:** Organic compound; Chemical synthesis; Adsorption; Corrosion.

## B-133. 2, 7-Diarylidene-Cycloheptanone, Hydrazonoyl Chlorides and Heterocyclic Amines as Precursors for Synthesis of Bioactive New Fused Cycloheptapyrimidine Derivatives

Thoraya A. Farghaly, Magda A. Abdallah and Zeinab A Muhammad

*Current Organic Synthesis, 13: 291-299, (2016), IF: 2.05*

A series of novel cyclohepta[1,2-d][1,2,4]triazolo[4,3-a]pyrimidines was prepared by reaction of 9- arylmethylene-cycloheptapyrimidine-2-thione with hydrazonoyl halides in dioxane in the presence of triethylamine. Also, a series of fused cycloheptapyrimidines was synthesized via reaction of 2,7-diarylmethylenecycloheptanone with heterocyclic amines. The products 14a-c of the latter reaction were used as starting materials since they contain an olefinic exocyclic C=C and endocyclic C=N bonds. 1,3-Dipolar cycloaddition reaction of these products with hydrazonoyl halides in benzene in the presence of triethylamine afforded novel spiropyrazolines. All the above reactions proceeded site and regio-selectively, and the structures of the products were established based on both elemental and spectral analysis data (IR, 1H NMR, MS). In addition, the biological activity of some of the new products was evaluated and the results obtained revealed medium to high activity against some bacteria and fungi species.

**Keywords:** 2, 7-Diarylmethylene-Cycloheptanone, Hydrazonoylhalides; Site-Selectivity; Spiropyrazolines; Antimicrobial activity.

## B-134. Convergent Synthesis Strategy of Novel Fused Azines: 1H-15N Hmbc Nmr as a Tool for Assertion of the Site Selectivity of Aza-Michael Addition Reaction

Tamer S. Saleh, Ahmed E. M. Mekky and Abdullah S. Al-Bogami

*Current Organic Synthesis, 13: 278-290, (2016), IF: 2.05*

A unified convergent strategy has been developed for the facile synthesis of a series of novel fused azines bearing a phenothiazine moiety based on the aza-Michael addition reaction of an enaminone derivative to a variety of different heterocyclic amines under microwave irradiation conditions. The results of this study revealed that new methods are required to allow for the simple and efficient analysis of the fused azine products of this reaction other than single-crystal X-ray crystallography. With this in mind, 1H–15N HMBC experiments were used in the current study to allow for the unambiguous structural characterization of the fused azine products. These results provided further support in favor of the proposed structures and allowed for the resolution of several discrepancies reported in the literature regarding the structural characterization of these compounds.
**Keywords:** Microwave irradiations; Pyrazolo[1,5-A]Pyrimidines; Triazolo[1,5-A]Pyrimidine; Pyrimido[1,2-A]Benzimidazole; 1H-15N Hmbc.

## B-135. Hydrazonoyl Halides as Precursors for Synthesis of Bioactive Thiazole and Thiadiazole Derivatives: Synthesis, Molecular Docking and Pharmacological Study

Thoraya A. Farghaly, Sobhi M. Gomha, Abdelwahed R. Sayed and Mohammed A Khedr.

*Current Organic Synthesis, 13: 445-455, (2016), IF: 2.05*

New thiazole and 1,3,4-thiadiazole derivatives were synthesized from the reaction of hydrazonoyl halides and each of 3-(4-fluorophenyl)-3,4,5,6-tetrahydrobenzo[6,7]cyclohepta[1,2-c]pyrazole-2(1H)-carbothioamide and (E)-3-[mercapto(phenylamino)methylene]-thiochroman-4-one, respectively. The structures of all the newly synthesized compounds were established by elemental and spectral analyses. All of the synthesized compounds were tested for anticancer activity against colon cancer cell line HT29, human breast cancer cells MCF-7 and human hepatocellular carcinoma cell line HepG2. Many derivatives of the tested compounds showed moderate to high anticancer activity. Also, molecular docking against HER2 kinase domain revealed high free binding energy and good binding mode. The structure activity relationship (SAR) of tested compounds was studied.
**Keywords:** Carbothioamides; Hydrazonoyl halides; Benzosuberone; Thiazoles; Thiadiazoles; Antitumor agents.

## B-136. Multicomponent Synthesis of Novel Bis(2-Amino-Tetrahydro-4H-Chromene – 3-Carbonitrile) Derivatives Linked to Arene or Heteroarene Cores

Amna M. Abdella, Ahmed H. M. Elwahy and Ismail A. Abdelhamid

*Current Organic Synthesis, 13: 601-610, (2016), IF: 2.05*

An efficient and convenient route for synthesis of novel bis 4H-chromene-3- carbonitrile derivatives is reported. The synthetic pathway involves one pot, multi-component reaction of bis-aldehydes, malononitrile, and dimedone in the presence of a catalytic amount of piperidine. A stepwise approach for the synthesis of the target compounds was also investigated.
**Keywords:** Bis-Aldehydes; Bis-Arylidenemalononitriles; Multicomponent Reactions; Bis-4H-Chromene-3-Carbonitriles.

## B-137. Synthesis and Quantum Chemical Studies on the Tautomeric Structures of New Thiazole and Thiadiazine Derivatives

Sobhi M. Gomha, Fatma A. A. El-Hag, Ahmed M. El Defrawy and Thoraya A Farghaly.

*Current Organic Synthesis, 13: 907-916, (2016), IF: 2.05*

New series of thiazoles and thiadiazines incorporated with pyrazole ring were synthesized via the reaction of 2-(1-(4-cyano-1,5-diphenyl-1H-pyrazol-3-yl)ethylidene) hydrazine-carbothioamide or 4-imino-7-methyl- 2,3-diphenyl-2H-pyrazolo[3,4-d]pyridazine-5(4H)-carbothiohydrazide with different reagents. The structures of all tautomeric forms of the newly synthesized compounds were confirmed on the basis of spectral data aided with DFT and semi-empirical calculations.
**Keywords:** Thiazoles; Thiadiazines; Tautomeric structure; Dft.

## B-138. Synthesis of New Thiazole Derivatives as Antitumor Agents

Eman M. H. Abbas, Sobhi M. Gomha, Thoraya A. Farghaly and Mohamed M Abdalla.

*Current Organic Synthesis, 13: 456-465, (2016), IF: 2.05*

New series of substituted thiazole were prepared starting from thiosemicarbazone derivatives 1a,b by reacting with different reagents namely, hydrazonoyl chlorides, dimethyl acetylene dicarboxylate, phenacyl bromide, chloroacetone, and chloroacetic acid. The structures of the newly synthesized compounds were elucidated on the basis of elemental analyses and spectral data. Some representative examples of the newly synthesized compounds were screened as antitumor agents against all the 60 cell lines of the NCI-60 cell panels. The tested compounds were active only against MCF7, SF268, SF295, HT29, HT29, COLO205, COLO205, K562, HL60, A549-ATCC, H460, LOXIMVI, OVCAR3, OVCAR4, OVCAR5, OVCAR8, SKOV3, PC39, DU145 and A498 while inactive against other cell lines in the panel.
**Keywords:** Thiazole; Hydrazonoyl chlorides; Thiosemicarbazone; Antitumor activity.

## B-139. Antiosteoporotic Effect of Petroselinum Crispum, Ocimum Basilicum and Cichorium Intybus L. in Glucocorticoid-Induced Osteoporosis in Rats

Walaa G. Hozayen, Mohamed A. El-Desouky, Hanan A. Soliman, Rasha R. Ahmed and Amal K. Khaliefa

*Bmc Complementary and Alternative Medicine, 16: 165-175, (2016), IF: 1.987*

**Background**: Glucocorticoid-induced osteoporosis (GIO) is one of the serious side effects which have become the most common secondary osteoporosis. The purpose of this study is to evaluate the effect of aqueous extract of parsley, basil and chicory on glucocorticoid-induced osteoporosis in rats. **Methods** Fifty Female rats were divided into five groups and treated for 8 weeks as follow: group 1 served as control; group (2) subcutaneously injected with 0.1 mg/kg b. wt. dexamethasone dissolved in saline; group 3 received similar dose of dexamethasone together with aqueous parsley extract in a dose of 2 g/kg b. wt.; group 4 received similar dose of dexamethasone together with 400 mg/kg b. wt. aqueous basil extract and group 5 received similar dose of dexamethasone together with 100 mg/kg b. wt. aqueous chicory extract. **Results:** The dexamethasone group showed a significant decrease in serum E2, Ca, P levels and significant decrease in total BMD, BMC and a significant increase in serum PTH, ALP and ACP. Bone TBARs was significantly increased while GSH, antioxidant enzymes were significantly decreased. These changes were attenuated by parsley, basil and chicory extracts in the group 3, 4 and 5 respectively. **Conclusion:** Aqueous extracts of parsley, basil and chicory showed bone protection against glucocorticoid-induced in rats. From our results, we concluded that chicory has a potent protective effect more than parsley and basil due to containing flavonoids and inulin.
**Keywords:** Dexamethasone osteoporosis; Bone biomarkers; Histopathology and Oxidative stress.

## B-140. Certification of Caffeine Reference Material Purity by Ultraviolet/Visible Spectrophotometry and High-Performance Liquid Chromatography with Diode-Array Detection as two Independent Analytical Methods

A.B. Shehataa,M.S. Rizk and E.A. Renda

*Journal of Food and Drug Analysis,24:703-715,(2016),IF: 1.98*

Caffeine reference material certified for purity is produced worldwide, but no research work on the details of the certification process has been published in the literature. In this paper, we report the scientific details of the preparation and certification of pure caffeine reference materials. Caffeine was prepared by extraction from roasted and ground coffee by dichloromethane after heating in deionized water mixed with magnesium oxide. The extract was purified, dried, and bottled in dark glass vials. Stratified random selection was applied to select a number of vials for homogeneity and stability studies, which revealed that the prepared reference material is homogeneous and sufficiently stable. Quantification of caffeine purity % was carried out using a calibrated UV/visible spectrophotometer and a calibrated high-performance liquid chromatography with diode-array detection method. The results

obtained from both methods were combined to drive the certified value and its associated uncertainty. The certified value of the reference material purity was found to be 99.86% and its associated uncertainty was ±0.65%, which makes the candidate reference material a very useful calibrant in food and drug chemical analysis.

**Keywords:** Caffeine; Certification; Coffee; Extraction; Purity analysis.

## B-141. Synthetic Routes to Spirocyclic Pyridazines, Partially-Saturated Pyridazines and Their Condensed Derivatives

Amr M. Abdelmoniem and Ismail A. Abdelhamid

*Current Organic Chemistry, 21: 1512-1546, (2016), IF: 1.949*

Different synthetic strategies to 4,4-disubstituted pyridazines and condensed pyridazines with a special reference to the synthetic routes to their spiro analogues are comprehensively outlined in this review.

**Keywords:** Spirocyclic pyridazines; Partially-Saturated Pyridazines; Synthesis; Retro- Diels-Alder; 1,3-Dipolar Cycloaddition; Aza-michael addition; Nucleophilic reactions.

## B-142. Development of New Potentiometric Sensors for the Determination of Proguanil Hydrochloride in Serum and Urine

Fatehy M. Abdel-Haleem, Mohamed Saad and Mohamed S.Rizk

*Chinese Chemical Letters, 27: 857-863, (2016), IF: 1.947*

Potentiometric electrodes were developed for the rapid determination of proguanil hydrochloride in pure samples, pharmaceutical preparations and spiked serum and urine samples using PVC membrane, screen printed (SPE), coated wired (CWE), carbon paste (CPE) and modified carbon paste (MCPE) electrodes based on the ion-exchanger of proguanil with phosphotungestic acid (Pr-PT) as a chemical modifier. The prepared electrodes showed Nernestian slopes of 59.7, 58.1, 58.5, 58.5 and 57.0 for the PVC, SPE, CWE, CPE and MCPE for the proguanil ions in a wide concentration range of 1.0 × 10−5–1.0 × 10−2 mol L−1 at 25 °C with detection limits of 7.94 × 10−6, 1.0 × 10−5, 1.0 × 10−6, 7.07 × 10−6 and 2.5 × 10−6 mol L−1, respectively. The prepared electrodes exhibited high proguanil selectivity in relation to several inorganic ions and sugars and they could be successfully utilized for its determination in pure solutions, pharmaceutical preparations and serum and urine samples using the direct potentiometry and standard addition methods with very good recovery values.

**Keywords:** Proguanil hydrochloride; Pvc membrane Electrode; Carbon paste electrode; Screen printed electrode; Mwcnts; Coated wire electrode.

## B-143. Spectroscopic, Dft, Magnetic and Biological Activity Evaluation of Pd(Ii), Pt(Ii) and Ru(Iii) Complexes of Nitazoxanide

Ahmed M. Mansour

*Inorganica Chimica Acta, 453: 697-703, (2016), IF: 1.918*

[M(NTZ)Cl2] (M = Pd(II) (1), Pt(II) (2) and NTZ = Nitazoxanide) and [Ru(NTZ)Cl3(OH2)] (3) complexes have been synthesized and characterized by elemental analysis, thermogravimetric analysis, IR, 1H NMR, conductance and magnetic measurements. NTZ is coordinated to the metal ions as a bidentate ligand via the N-atom of the thiazole ring and amide Cdouble bond; length as m-dashO. The susceptibility of Staphylococcus aureus and Escherichia coli towards NTZ and its complexes has been evaluated. The calculated electronic structures and the related electronic transitions have been obtained at TD-DFT/B3LYP/LANL2DZ level of theory. Upon the chelation, the value of the natural charge of Ru(III) ion (+0.182e) was found to be lower than those of Pd(II) and Pt(II) ions (~+0.398e) in their complexes, which reflects the higher complexation ability of NTZ towards the high oxidation state and low-d-orbital population metal ion. Complex 3 is existing in a low-spin octahedral arrangement. The DC magnetic measurements in terms of Weiss constant revealed the presence of the intermolecular interactions among the spin carriers. The low stability of 1–3 in DMSO and the rate of the releasing of NTZ was the factor which reproduces the order of the toxicity (NTZ > 2 > 3 > 1) against the tested microbes.

**Keywords:** Nitazoxanide; Low-Spin Ru(Iii) Complexes; Magnetic; Nbo; Td-Dft; Antibacterial activity.

## B-144. Efficient, Microwave-Mediated Synthesis of Benzothiazole- and Benzimidazole-Based Heterocycles

Ahmed F. Darweesh, Ahmed E. M. Mekky, Amani A. Salman and Ahmad M. Farag

*Research on Chemical Intermediates, 42: 4341-4358 (2016) IF: 1.833*

1-(Benzothiazol-2-yl)-3-(N,N-dimethylamino)-2-* (phenylsulfonyl)prop-2-en-1-one (3) and 1-(1 methylbenzimidazol-2-yl)-3-(N,N-dimethylamino)-2-(phenylsulfonyl)prop-2-en-1-one (4) were obtained from the reaction of 1-(benzothiazothiazol-2-yl)-2-phenylsulfonyl-1-ethanone (1) and 1-(1-methyl-1H-benzimidazol-2-yl)-2-(phenylsulfonyl)-1-ethanone (2) with N,N-dimethylformamidedimethyl acetal, respectively. The enaminosulfones 3 and 4 were used as versatile building blocks for the synthesis of novel pyrazolo[1,5-a]pyrimidine and [1,2,4]-triazolo[1,5-a]pyramidine derivatives via their reactions with the appropriate aminopyrazoles and aminotriazole under both microwave and thermal reaction conditions. They have been also utilized as reactive synthons for the construction of novel pyrimido[1,2-a]benzimidazole, pyrido[1,2-a]benzimidazole, pyrimidine, isoxazole and pyrazole heterocycles pendent to benzothiazole and benzimidazole ring systems.

**Keywords:** Enaminosulfone; Benzimidazole; Benzothiazole; Pyrazolo[1,5-A]Pyrimidine; [1,2,4]-Triazolo[1,5-A]Pyramidine; Pyrimido[1,2-A]Benzimidazole; Pyrido[1,2-A]Benzimidazole.

## B-145. Facile Synthetic Approaches for New Series of Pyrazole-4-Carbonitrile Derivatives

Korany A. Ali, Eman Ali Ragab, Heba S. Abdelghafar and Ahmad M. Farag

*Research on Chemical Intermediates, 42: 3553-3566, (2016), IF: 1.833*

Aldol condensation of 3-acetyl-1-(4-fluorophenyl)-5-phenyl-1H-pyrazole-4-carbonitrile with benzaldehyde afforded 1-(4-fluorophenyl)-5-phenyl-3-((E)-3-phenylacryloyl)-1H-pyrazole-4-carbonitrile, which in turn reacted with a series of 1,2- and 1,3-binucleophiles to afford new substituted pyrazoles, pyrimidines, and condensed azolopyrimidine derivatives attached to pyrazole scaffold at position 3. Moreover, multicomponent condensation reactions (MCRs) were used as an alternative method, and 1H–13C heteronuclear single quantum coherence (HSQC) in addition to heteronuclear multiple-bond correlation (HMBC) spectra were used for full confirmation of a selected example of these compounds. The reactivity of 1-(4-fluorophenyl)-5-phenyl-3-((E)-3-phenylacryloyl)-1H-pyrazole-4-carbonitrile towards active methylene derivatives, including malononitrile and ethyl cyanoacetate, was explored and afforded 2-amino-6-(4-cyano-1-(4-fluorophenyl)-5-phenyl-1H-pyrazol-3-yl)-4-phenylpyridine-3-carbonitrile and ethyl 6-(4-cyano-1-(4-fluorophenyl)- 5-phenyl-1H-pyrazol-3-yl)-1,2-dihydro-2-oxo-4-phenylpyridine-3-carboxylate, respectively.

**Keywords:** Pyrazole-4-Carbonitrile; Binucleophiles; Chalcone; Multicomponent; Condensation reactions (Mcrs); Pyrimidine

## B-146. Spectroscopic and Thermal Characterization of Biologically and Anticancer Active Novel Schiff Base Metal Complexes

Walaa H. Mahmoud, Reem G. Deghadi and Gehad G. Mohamed

*Research on Chemical Intermediates, 42: 7869-7907, (2016), IF: 1.833*

The novel Schiff base ligand 2,20-((1Z,10Z)-(1,3-phenylenebis(azanylylidene)) –bis(phenylmethanylylidene)) dibenzoic acid (H2L) was obtained by the condensation of m-phenylenediamine with o-benzoylbenzoic acid. The molecular and electronic structure of Schiff base ligand (H2L) was optimized theoretically, and the quantum chemical parameters are calculated. Molecular docking was used to predict the binding between Schiff base ligand (H2L) and the receptors of breast cancer mutant 3hb5-oxidoreductase, crystal structure E. coli (3t88) and crystal structure of S. aureus (3q8u). The newly synthesized Cr(III), Mn(II), Fe(III), Co(II), Ni(II), Cu(II), Zn(II), and Cd(II) complexes were characterized by elemental microanalysis, molar conductance, spectroscopic techniques (IR,1H NMR, ESI-mass, ESR, UV–Vis), magnetic susceptibility, thermal (TG/DTG) and powder X-ray diffraction data to explicate their structures. The data showed that the complexes had composition of MH2L type. The IR results confirmed the bidentate binding of the ligand involving two azomethine nitrogens. 1H NMR spectral data of the ligand (H2L) and its Zn(II) and Cd(II) complexes agreed well with the proposed structures. On the basis of electronic spectra and the magnetic measurements, octahedral geometry of the complexes was proposed. Thermogravimetric data (TG and DTG) were also studied. The kinetic and thermodynamic parameters for thermal decomposition of the complexes were calculated using the Coats–Redfern and Horowitz–Metzger methods. In order to appraise the effect of antimicrobial activity of metal ions upon chelation, the newly synthesized ligand and its metal complexes were screened against a number of bacteria organisms as Bacillus subtilis, Staphylococcus aureus, Escherichia coli, and Neisseria gonorrhoeae and against one fungus, Candida albicans, to assess their inhibiting potential by using the disc diffusion method. The results showed that in some cases the antimicrobial activity of complexes was more biologically active than the Schiff base ligand. Anticancer activity of the ligand and its metal complexes were evaluated in human cancer (MCF-7 cells viability). It was found that [Cd(H2L)(H2O)2Cl2]2H2O complex showed lowest IC50 than the others, and hence was the more active. The activity index was calculated.

**Keywords:** Schiff base; M-Phenylenediamine Tg/Dtg Electronic spectra; Molecular orbital calculation; Molecular docking antimicrobial; Activity anticancer activity.

## B-147. Synthesis and Anticancer Activity of Some New Heterocyclic Compounds Based on 1-Cyanoacetyl-3,5-Dimethylpyrazole

Nadia H. Metwally,Fathy M. Abdelrazek and Salwa M. Eldaly

*Research on Chemical Intermediates, 42: 1071-1089, (2016), IF: 1.833*

The starting 3-(3,5-dimethyl-1H-pyrazol-1-yl)-3-oxopropanenitrile (1) reacts with phenyl isothiocyanate and ethyl bromoacetate to give the corresponding thiazole derivative 4. On repetition of the reaction using phenacyl bromides 5a–d (instead of ethyl bromoacetate), oxathiepine-6-carbonitriles 10a–d were obtained. Coupling of compound 1 with aryldiazonium chlorides gives the corresponding 2-(arylhydrazono)-(3,5-dimethyl-1H-pyrazol-1-yl)-3-oxopropanenitrile derivatives 12a–e, which on treatment with p-phenylenediamine, followed by reaction of hydrazine hydrate afforded pyrazole derivatives 15a–d. The reaction of 1 with 5-amino-3-(cyanomethyl)-1H –pyrazole-4-carbonitrile afforded the respective 2-cyanomethyl-pyrazolo[1,5-a]pyrimidine-3-carbonitrile derivative 18. Compound 18 reacted with phenyl isothiocyanate in the presence of potassium hydroxide at room temperature and then phenacyl bromide was added; the pyrazolopyrimidines 24 were obtained. The structures of all the newly synthesized products were confirmed based on elemental, spectral data and a plausible mechanism has been postulated to account for their formation. Also, we evaluate the anticancer activity of some representative examples of the newly synthesized compounds.

**Keywords:** 3-(35-Dimethyl-1H-Pyrazol-1-Yl)-3-Oxopropanenitrile Oxathiepine – 6-Carbonitriles Pyrazolo-[1,5-A]Pyrimidine thiazoles anticancer activity

## B-148. Complexes of Schiff Base of Benzopyran-4-One Derivative Synthesis, Characterization, Non-Isothermal Decomposition Kinetics and Cytotoxicity Studies

Nora S. Abdel-Kader, Rehab M. Amin and Aida L. El-Ansary

*Journal of Thermal Analysis and Calorimetry, 123: 1695-1706, (2016), IF: 1.781*

New metal complexes of Schiff base (L) prepared from condensation reaction of 2-aminopyridine and 6-formyl-7-hydroxy-5-methoxy-2-methylbenzopyran-4-one with metal ions; Mn(II), Co(II), Ni(II) and Cu(II) are synthesized. Different

analysis tools such as elemental analyses, FTIR, thermal analyses, conductivity, mass spectrometry, electronic spectra and magnetic susceptibility measurements are all used to elucidate the structures of the newly prepared metal complexes. The IR spectral data suggested that the ligand behaves as a monobasic bidentate ligand toward the central metal ion with ON donor atoms. The thermal decomposition kinetics of all complexes was estimated by Coats-Redfern. Ni–L and Co–L complexes were selected to study their thermal decomposition under non-isothermal conditions using Flynn–Wall–Ozawa and Starink methods at different three heating rates (5, 10 and 15 °C min−1). The values of the activation energy (E) obtained by the all methods are in good agreement. All complexes are thermally stable as reflected from the high value of their activation energies. Ni–L complex has the highest thermal stability, and Mn–L complex has the lowest one indicating that Mn–L complex has fast rate of successive decomposition. The Schiff base L, Cu–L and Mn–L compounds were screened for in vitro cytotoxicity against normal standard fibroblast cells (3T3) using MTT assay. Among these compounds, Mn–L complex enhanced growth inhibition and cell death in a concentration-dependent manner for the standard fibroblast cells (3T3). Mn–L complex was then subjected against four human cancer cell lines; human hepatocellular carcinoma (Huh-7), human Hepatoblastoma (Hep G2) and human cervical cancer cells (HeLa & HeLa-Fas) for anticancer activity. Results indicate that Mn–L complex may be useful leads for anticancer drug development in the future.

**Keywords:** Schiff base; Complexesnon-Isothermalkinetic analysiscytotoxicity.

## B-149. Novel Synthesis of 2-Imino-2H – Chromene-3-Carboximide Metal Complexes Thermal Decomposition, Spectral Studies and Antimicrobial Activity Evaluation

Madiha H. Soliman, Gehad G. Mohamed and Galal H. Elgemeie

*Journal of Thermal Analysis and Calorimetry, 123: 583-594, (2016), IF: 1.781*

New metal complexes derived from the reaction of Cr(III), Mn(II), Fe(III), Co(II), Ni(II), Cu(II) and Zn(II) chlorides with the 2-imino-2H-chromene-3-carboximide organic ligand (HL) have been synthesized. The resulting complexes have been characterized by elemental analysis (CHN), IR, magnetic susceptibility, mass spectra, 1H NMR, UV–Vis, ESR, thermal analysis (TG, DTG and DTA) and molar conductance measurements. All the complexes are 1:2 and 1:3 electrolytes according to their molar conductivities. The microanalyses and spectroscopic data showed that the metal(II)/(III) ions in these complexes achieved coordination number of six and hence have octahedral geometrical structures.This is attained by bonding to the bidentate ligand via its two amino nitrogen atoms and two imine nitrogen atoms, and two monodentate aquo groups via its oxygen atoms. The results showed that the ligand acts as neutral bidentate coordinating via amino and NH nitrogens without displacement of hydrogen. The antimicrobial activities of the chromene ligand and its complexes have been tested against a number of pathogenic bacteria and fungi to assess their inhibiting potential. Antimicrobial studies indicate that these complexes exhibit better activity than the chromene ligand.

**Keywords:** Coumarin metal complexes; Ir thermal analysis; Mass spectra antimicrobial activity.

## B-150. Synthesis and Characterization of Biodegradable Copoly(Ether-Ester-Urethane)sand Their Chitin Whisker Nanocomposites

Nadia A. Mohamed, Hend E. Salama, Magdy W. Sabaa and Gamal R. Saad

*Journal of Thermal Analysis and Calorimetry, 125: 163-173, (2016), IF: 1.781*

A series of copoly(ether-ester-urethane)s have been synthesized from poly(3-hydroxybutyrate) (PHB) diol prepolymer, as hard segments, and copoly(ε-caprolactone-ethylene glycol-ε-caprolactone) (PCL-PEG-PCL) diols with different PEG block lengths, as soft segments, with/without chitin whiskers (ChW) using hexamethylene diisocyanate, as a coupling agent, in one-step polymerization. The PHB content in the resulting copolymers was 0 and 40 %, and the content of ChW was varied from 0 to 5 %. The chemical structure of the resulting copolymers was characterized by FTIR, 1H-NMR and 13C-NMR spectra. The effect of chemical structure and ChW content on the thermal properties was studied by differential scanning calorimetry (DSC) and thermogravimetric analysis (TG). The DSC data revealed that the ΔHm of both PHB and PCL-PEG-PCL slightly increases with increasing the ChW content. The cold and melt crystallization of PHB enhanced with increasing ChW content. The TG data revealed that the thermal stability of copolymers slightly enhanced at high content of ChW. The swelling behavior of the copolymers was also investigated.

**Keywords:** Biodegradable copolymers; Nanocomposites; Synthesis; Dsc; Thermogravimetric analysis.

## B-151. Synthesis, Spectral Characterization, Thermal, Anticancer and Antimicrobial Studies of Bidentate Azo Dye Metal Complexes

Walaa H. Mahmoud, M. M. Omar and Fatma N. Sayed

*Journal of Thermal Analysis and Calorimetry, 124: 1071-1089, (2016), IF: 1.781*

As a part of systematic investigation of biologically active compound, m-phenylene diamine, new azo dye ligand was synthesized by diazotization of m-phenylene diamine and coupled with coupling compound, pmethoxy benzaldehyde. A new series of Cr(III), Mn(II), Fe(III), Co(II), Ni(II), Cu(II), Zn(II) and Cd(II) complexesderived from this azo dye ligand (L) were synthesized. The structures of the ligand and metal complexes were confirmed by elemental analysis, spectroscopic studies (IR, UV–Vis, 1H NMR, mass spectrometry, electronic spectra, magnetic susceptibility and ESR), conductivity measurements, thermogravimetric analyses (TG-DTG) and X-ray powder diffraction. The molar conductance measurements of the complexes in DMF determine electrolytic nature of the complexes. On the basis of elemental and thermal analyses, magnetic moment, electronic and ESR spectral studies, an octahedral geometry was assigned for metal complexes. XRD data reflect that azo dye ligand and its Cr(III), Mn(II), Fe(III), Co(II), Ni(II), Cu(II) and Zn(II) complexes are amorphous while Cd(II) complex is crys- talline. Also, the newly

synthesized azo dye ligand, in comparison with metal complexes, is screened for its antimicrobial and anticancer activity against breast cancer cell line (MCF7). The results showed that Mn(II), Ni(II)and Zn(II) metal complexes have higher anti-breast cancer activity than free ligand.
**Keywords:** P-Methoxybenzaldehyde; Spectroscopy kinetics studies; Antimicrobial activity anticancer activity.

## B-152. Thermal Behavior of Binary Mixtures of Isomers of Different Molecular Structures and Different Lateral Substituent Positions

Hoda Abdelrazeik Ahmed Ahmed

*Journal of Thermal Analysis and Calorimetry, 125: 823-830, (2016), IF: 1.781*

Binary systems comprising two laterally substituted azo/ester isomers, namely 2- (or 3-) methyl-(or fluoro-) substituted phenyl 40-(400-alkoxy phenylazo) benzoates (Ina–d), were thermally investigated by differential scanning calorimetry (DSC) and the phases identified by polarized light microscopy (PLM). The phase diagrams constructed were made from isomeric components that differ in the relative positions of the lateral substituent attached to the individual components. Another binary phase diagram was formed from the 3-fluoro phenyl-40-(400- alkoxyphenylazo) benzoates (Ind) and their isomers 4-(3- fluorophenylazo)-phenyl-40-alkoxybenzoates (IIn). The latter two components differ from each other in the location inversion of the ester group, as well as in the exchange of the terminal substituents. For mixtures Ina/Inb, the CH3 group distributed SmA arrangement. In the mixtures of the two structurally different isomers, Ind/IIn, the addition of one component to the other resulted in a pronounced decrease in the stability of all mesophases.
**Keywords:** 2-Substituted phenyl 40-(400-Alkoxy phenylazo) Benzoates 3-Substituted phenyl 40-(400-Alkoxy phenylazo) Benzoates phase transitions binary phase diagrams.

## B-153. Thermal, Spectral, Dft and Biological Activity Evaluation of Co(Ii), Ni(Ii) and Cu(Ii) Complexes of N,S-Chelated Benzotriazole Ligand

Ahmed M. Mansour

*Journal of Thermal Analysis and Calorimetry, 123: 571-581, (2016), IF: 1.781*

[ML2]·yC2H5OH·zH2O complexes (M=CoII (1) and NiII (2), y = 4, z = 0; M=CuII (3), y = 0, z = 3; HL = N-(2-thiazolyl)-1H-benzotriazole-1-carbothioamide) were prepared, characterized (elemental analysis, TG, FT IR, UV–Vis, EPR, magnetic and conductance measurement) and tested for their antimicrobial activity against Escherichia coli and Staphylococcus aureus. Complexes 1–3 consist of a metal center having a considerable tetrahedral distortion in the xy-plane from the square planar stereochemistry MN2S2 formed by the two deprotonated benzotriazole ligands. TD-DFT calculations were carried out at B3LYP/6-31G* level of theory to understand the electronic structure and to explain the related experimental findings. Natural bond orbital analysis was performed to provide details about the electronic arrangement, type of hybridization and the nature of bonding. Coordination of HL to CoII gave rise to inactive compound, but the development of NiII and CuII complexes did not clearly change the toxicity of the free HL.
**Keywords:** Benzotriazole; Carbothioamide; Metal complexes; Dft; Antibacterial.

## B-154. Co(II), Ni(II) and Cu(II) Complexes of Methyl-5-(Phenylthio) Benzimidazole-2-Carbamate: Molecular Structures, Spectral and DFT Calculations

Ahmed M. Mansour, Eslam M. El Bakry and Nour T. Abdel-Ghani

*Journal of Molecular Structure, 1111: 100-107, (2016), IF:1.78*

[Co(FBZ)2(H2O)]·2NO3·0.5H2O (1), [Ni(FBZ)2X2]·zH2O (X = Cl−, z = 0.5 (2) and X = CH3COO−, z = 1 (3)) and [Cu(FBZ)2(H2O) (NO3)]·NO3·1.5H2O (4) (FBZ = methyl-5-(Phenylthio) benzimidazole-2-carbamate; Fenbendazole) complexes were synthesized and characterized by elemental analysis, thermal, IR, EPR, UV–Vis, magnetic and conductance measurements. Geometry optimization, molecular electrostatic potential maps and natural bond orbital analysis were carried out at DFT/B3LYP/6-31G∗ level of theory. FBZ behaves as a neutral bidentate ligand via the pyridine-type nitrogen of the benzimidazole moiety and the carbamate group. Three-step ionization with pKa values of 3.38, 4.06 and 10.07 were reported for FBZ. The coordination of FBZ to the metal ions led to an increase in the antibacterial activity against the tested Staphylococcus aureus and Escherichia coli bacteria.
**Keywords:** Benzimidazole-2-Carbamate; Epr; Dft.

## B-155. New Binary and Ternary Platinum(Ii) Formamidine Complexes: Synthesis, Characterization, Structural Studies and in-Vitro Antitumor Activity

Ahmed A. Soliman , Othman I. Alajrawy , Fawzy A. Attaby and W. Linert

*Journal of Molecular Structure, 1115: 17-32, (2016), IF: 1.78*

A series of new binary and ternary platinum(II) complexes of the type [Pt(L1-4)Cl2].xH2O and [Pt(L1-4)ox].xH2O where L = formamidine ligands and ox ¼ oxalate, have been synthesized and characterized by elemental analyses, magnetic susceptibility, UVevis, infrared (IR), mass spectroscopy, thermal analysis and theoretical calculations. The spectroscopic data indicated that the formamidine ligands act as bidentate N2 donors. The complexes (1-8) are diamagnetic and the optimization of their structures indicated that the geometry is distorted square planar with Cl-Pt-Cl, O-Pt-O and N-Pt-N bond angles ranged 81.73-95.82 which is acceptable for the heteroleptic complexes. The electronic energies (a.u.) of the complexes (-893.53 to 1989.84) indicate that the complexes are more stable than the ligands. The energies of the HOMO (-0.218 to -0.244) and LUMO (-0.0111 to 0.134) orbitals of the complexes were negative which indicates that the complexes are stable compounds. The dipole moment of the complexes (6.23-19.89 Debye) indicates that the complexes are polarized. The complexes are thermally stable as shown from their relatively higher overall activation energies (889-2066 kJ mol-

1). The complexes are proved to have a good cytotoxicity with IC50 (mM) against MCF-7 (0.040e0.117), HCT-116 (0.085-0.119) and HepG-2 (0.058-0.131) cell lines, which open the field for further application as antitumor compounds.
**Keywords:** Pt(Ii) Complexes ternary; Complexes formamidine; Cytotoxicity Dft calculations.

## B-156. Synthesis, Spectroscopic Studies, Thermal Analyses, Biological Activity of Tridentate Coordinated Transition Metal Complexes of Bi(Pyridyl- 2-Ylmethyl)Amine]Ligand

Hanan F. Abd El-Halim and Gehad G. Mohamed

*Journal of Molecular Structure, 1104: 91-95, (2016), IF: 1.78*

A new tridentate acyclic pincer ligand, [bi(pyridin-2-methyl)amine] (bpma, HL), was synthesized and reacted to form complexes with copper(II), nickel(II), iron(II), cobalt(II) and zinc(II) ions. Both the ligand and its complexes were characterized using elemental analysis, molar conductance, infrared, 1H-NMR-spectroscopy, mass and thermal analyses. According to the spectroscopic data, all of the complexes share the same coordination environment around the metal atoms, consisting two nitrogen-pyridine entities, one nitrogen-methylamine entity, one/two water molecules and/or one/two chloride or bromide ions. Complexes also showed molar conductivity according to the presence of two halide anions outer the coordination sphere except Co(II) and Zn(II) complexes are non electrolytes. Analysis indicates that the metal ions have trigonal bipyramidal structure. Cu(II), Ni(II), Fe(II), Co(II), and Zn(II) metal complexes were screened for their antibacterial activity against Bacillus subtilis, Staphylococcus aureus (G+) and Escherichia coli, and Pseudomonas aeruginosa (G-) bacteria. They showed remarkable antimicrobial activity.
**Keywords:** Bi(Pyridyl-2-Ylmethyl)Amine] Metal complexes; Spectroscopy biological activity.

## B-157.Synthesis, Spectroscopic, Dft Calculations and Biological Activity Studies of Ruthenium Carbonyl Complexes with 2-Picolinic Acid and a Secondary Ligand

Shahera M. Shohayeb, Rania G. Mohamed, H. Moustafa and Samir M. El-Medani

*Journal of Molecular Structure, 1119: 442-450 (2016) IF: 1.78*

Thermal reaction of [Ru3(CO)12] with 2-picolinic acid (Hpic) in the absence and presence of a secondary ligand (pyridine, Py, bipyridine, Bipy, or thiourea, Tu) was investigated. Four complexes with molecular formulae: [Ru(CO)3(Hpic)], 1, [Ru2(CO)5(Hpic)(Py)], 2, [Ru2(CO)5(Hpic)(Tu)], 3 and [Ru2(CO)4(Hpic)(Bipy)], 4, were isolated. All complexes were characterized based on elemental analyses, IR, 1H NMR, magnetic studies, mass spectrometry and thermal analysis. The ligand and its complexes have been screened for antibacterial activities. Density Functional Theory (DFT) calculations at the B3LYP/6-311G (d,p)_ level of theory have been carried out to investigate the equilibrium geometry of the ligands. The optimized geometry parameters of the complexes were evaluated using B3LYP method and LANL2DZ basis set. The extent of natural charge population (core, valence and rydberg), exact electronic configuration, total Lewis and total non-Lewis are estimated and discussed in terms of natural bond orbitals (NBO) analysis.
**Keywords:** Metal Carbonyls; Nbo; Bacterial activity; Thermal analysis; Dft calculations.

## B-158. Graphene Functionalization by 1,6-Diaminohexane and Silver Nanoparticles for Water Disinfection

Abdelsattar O. E. Abdelhalim, Ahmed Galal, Mohamed Z. Hussein and Ibrahim E.-T. El Sayed

*Journal of Nanomaterials, 2016: 1-7, (2016), IF: 1.758*

Reduced graphene (G) was prepared by chemically reducing graphene oxide (GO). For the first time, the resulting G was functionalized by 1,6-diaminohexane and decorated with silver nanoparticles (AgNPs). The resulting G and modified G were characterized by X-ray diffraction (XRD), nuclear magnetic resonance (NMR), infrared (FTIR) spectroscopies, and high resolution transmission electron microscopy (HRTEM). The 1,6-diaminohexane-graphene structure was ascertained from the NMR and FTIR data. AgNPs were identified with various sizes within the graphene matrix. The resulting hybrid material was used as an effective antimicrobial contact catalyst for disinfecting water from Total Coliform and Fecal Coliform bacteria. A triple action in this respect was achieved from graphene, 1,6-diaminohexane, and AgNPs without observed release of silver that causes toxicity.
**Keywords:** Xrd; 1,6-Diaminohexane; Silver nanoparticles; Graphene; Water disinfection.

## B-159. nfluence of Metal Complex Formation on the Antimicrobial Activity of Nifuroxazide: Spectroscopic, Electrochemical, and Dft Studies

Ahmed M. Mansour

*Journal of Coordination Chemistry, 69(2): 215-226, (2016), IF: 1.756*

[M(HL)2] complexes (M = Co(II) (1), Ni(II) (2), and Cu(II) (3); H2L = 4-hydroxybenzoic [(5-nitro-2-furanyl) methylene] hydrazide acid, nifuroxazide) were synthesized, characterized (by elemental analysis, TG, IR, UV–vis., EPR, magnetic, and conductance measurements) and tested for their antimicrobial activities. H2L is a mono-negative bidentate ligand via hydrazone N and C–O− forming intermediate complexes between tetrahedral and square-planar geometries (“flattened” tetrahedron, D2d symmetry) for 1 and 2, as well as square-planar for Cu(II) complex 3. Natural bond orbital analysis revealed that the interaction of oxygen with metal ion is the main factor which determines the stability of 1–3 as the binding energy decreases with an increase in the M–O bond length. Time-dependent density functional theory calculations were carried out to understand the electronic transitions in related experimental observations. The reduction potential values of the nitro group are affected by the metal center. Ni(II) complex 2 displayed the highest activity among the tested complexes against Escherichia coli with a MIC50 value of 0.098 μmol $mL^{-1}$ compared with 0.131 (1) and 0.117 μmol $mL^{-1}$ (3).
**Keywords:** Nitrofuran; Nbo; Mep; Metal complexes; Electrochemical.

## B-160. Synthesis, X-Ray Structure, Dft and Thermodynamic Studies of Mono- and Binuclear Palladium(Ii) Complexes Involving 1,4-Bis(2-Hydroxyethyl)Piperazine, Bio-Relevant Ligands and 4,4′-Bipiperidine

Mohamed R. Shehata, Mohamed M. Shoukry, Mahmoud A. Mabrouk and Rudi Van Eldik

*Journal of Coordination Chemistry, 69(3): 522-540, (2016), IF: 1.756*

[Pd(BHEP)Cl2] (BHEp = 1,4-bis(2-hydroxyethyl)piperazine) was synthesized and characterized. The palladium center has a typical square-planar geometry with a tetrahedral distortion. The alcohol groups of the ligand do not participate in binding to Pd(II). The DFT/B3LYP method was used for geometric optimization of the ligand and the complex using the Gaussian 09 program and compared with experimental results. The stoichiometry and stability constants of the complexes formed between [Pd(BHEP)(H2O)2]2+ and some selected amino acids, peptides, and DNA constituents were investigated at 25 °C and 0.1 M ionic strength. The binuclear complex [(H2O)(BHEP)Pd(Bip)Pd(BHEP)(H2O)]4+ was detected, where Bip = 4,4′-bipiperidine. Inosine, uracil, and thymine interact with the binuclear complex via substitution of both coordinated water molecules. The potentiometric results were complimented by spectroscopic measurements. The concentration distribution diagrams of the various species formed were evaluated.

**Keywords:** 1,4-Bis(2-Hydroxyethyl)Piperazine; Palladium(Ii); Binuclear complex; Stability constants.

## B-161. Synthesis, Characterization, and Biological Activity of Cross-Linked Chitosan Biguanidine Loaded with Silver Nanoparticles

Hend E. Salama, Gamal R. Saad and Magdy W. Sabaa

*Journal of Biomaterials Science, Polymer Edition, 27:1880-1898, (2016), IF: 1.733*

Chitosan biguanidine hydrochloride (ChG) and glutaraldehyde cross-linked chitosan biguanidine (CChG) were synthesized and characterized by Fourier transform infrared spectroscopy, 1H NMR and 13C NMR, X-ray diffraction, scanning electron microscopy (SEM) and thermal analyses (TGA and DTA). The results showed that ChG and CChG had a more amorphous structure than that of chitosan, and their thermal stability were slightly lower than that of chitosan. Colloidal silver nanoparticles (AgNPs) were prepared using borohydride reduction method and then investigated as fillers in partially cross-linked chitosan biguanidine. The obtained nanoparticles were uniform and spherical with average size of 9.6 ± 0.5 nm. The prepared CChG/AgNPs composites were characterized for their morphology, thermal properties, cytotoxicity and antimicrobial activity. The SEM images showed that the AgNPs are well imbedded in the CChG matrix. The thermal stability of CChG was improved with incorporation of AgNPs. The CChG and CChG/AgNPs showed less cytotoxicity to breast cancer cells (MCF-7). Compared with chitosan and CChG, the ChG and CChG/AgNPs showed better antimicrobial activity against Streptococcus pneumoniae and Bacillus subtilis as Gram-positive bacteria, Escherichia coli as Gram-negative bacteria and Aspergillus fumigatus, Geotricum candidum and Syncephalastrum recemosum as fungi.

**Keywords:** Chitosan biguanidine; Crosslinked; Silver nanoparticles; Cytotoxicity; Antimicrobial activity.

## B-162. Mechanical, Thermal and Dielectric Properties of Poly (Lactic Acid) Chitosan Nanocomposites

Moataz A. Elsawy, Gamal R. Saad and Aisha M. Sayed

*Polymer Engineering and Science, 27: 987-994, (2016), IF:1.719*

Poly(lactic acid) (PLA) loaded with various levels of chitosan nanoparticles (CsNP) (0–5.0%) were prepared by twin-screw extrusion. The nanocomposites were investigated based on their morphology, thermal, mechanical and dielectric properties. The SEM morphology showed that CsNP was dispersed uniformly in the PLA matrix. Thermal analysis through DSC revealed that the cold crystallization temperature of PLA in the case of nanocomposites slightly decreased with increasing content of CsNP; indicating a limit nucleating effect of CsNP. TGA analysis revealed that the incorporation CsNP slightly decreased the thermal stability of the PLA matrix. The mechanical analysis indicated that the incorporation of the CsNP in the PLA matrix improved the elongation and the impact strength, but decreased the tensile strength. The dielectric properties of these materials have been investigated for the α-relaxation process as a function of the temperature and frequency. The α-relaxation process was analyzed with Vogel–Fulcher–Tamman and Havriliak–Negami models and fitting parameters and their evolution were obtained.

**Keywords:** Poly (Lactic Acid); Chitosan nanoparticles; Nanocomposites; Mechanical; Thermal and dielectric Properties.

## B-163. Biocorrosion Control of Electroless Ni-Zn-P Coating Based on Carbon Steel by the Pseudomonas Aeruginosa Biofilm

Sahar A. Fadl-allah, A.A. Montaser and Sanaa M.F. Gad El-Rab

*International Journal of Electrochemical Science, 11: 5490-5506, (2016), IF: 1.692*

Pseudomonas aeruginosa (P. aeruginosa) is considered one of the most important microorganisms that show a strong trend to growth on the metal surface and promote the biofilm formation. The present study describes the effect of P. aeruginosa (ATCC9027) on the corrosion resistance of electroless nickel-zinc-phosphorous (Ni-Zn-P) alloy coating based on carbon steel C1018. The influence of aerobic bacteria P. aeruginosa on the corrosion behavior of C1018 and Ni-Zn-P alloy in artificial sea water was studied by dielectric spectroscopy. Scanning electron microscope, SEM, and energy dispersive X-ray surface analysis techniques were used to distinguish the morphology and chemical composition of the alloy coating surface before and after 28 days of immersion in a nutrient medium. Although, the presence of P. aeruginosa in sterile media reduce the value of the corrosion resistance of C1018 to 691Ω , but it rises the corrosion resistance of Ni-Zn-P alloy up to 28KΩ. Quantitative description of the power of the morphology of alloy coating on bacterial affection and biofilm construction was investigated by the plate-counting method. The free biofilm fraction electrode

surface (1-Θ) was calculated for C1018 and Ni-Zn-P to be equal 4.016 and 0.3616, respectively. These results revealed that the antibacterial performance of the zinc alloy coating is better than the uncoated C1018 and it encourages the formation of passive biofilm protect carbon steel from biocorrosion.

**Keywords:** Carbon Steel; Pseudomonas aeruginosa; Biocorrosion; Biofilm; Ni-Zn-P Alloy; Eis; Sem; Edx.

## B-164. Determination and Speciation of Tellurium Hazardous Species in Real and Environmental Samples

Yousry M. Issa, Hussein M. Abdel-Fattah, Ola R. Shehab and Nahla B. Abdel-Moniem

*International Journal of Electrochemical Science, 11: 7475-7498, (2016), IF: 1.692*

Although tellurium is relatively rare in the environment, it is required in a number of important industrial applications such as semiconductor manufacturing, rubber industry, and solar panels. However, it has several environmental hazards and can be accumulated in the body and induce several health issues. It was reported that the toxicity of tellurium depends on its oxidation state with tellurite being the most toxic form. Determination and speciation of tellurite in real and environmental samples have been considered of primary analytical interest. Here, we have developed a simple technique for the analysis of tellurite in different chemical environments without the need for special pre-separation that is currently utilized in the standard quantitative techniques. This method depends on a carbon paste electrode modified with iron(II) phenanthrolin diclofenac (FephenD2) and iron (II) bipyridyl diclofenac (FebipyD2) as electroactive phases in carbon paste. The sensors have the following features: low detection limit (1.42×10-5 mol/L), long life time of more than 2 months, high selectivity to tellurite in the presence of a wide range of inorganic and organic ions, high thermal stability (22-56 ºC) and short response time of only 10-20 seconds. The sensors were successfully applied in the determination of tellurite in environmental and biological samples such as waste water, human serum, tellurite culture media, synthetic tellurite-cefotaxime and tellurite/tellurate mixtures. The results show high recovery rates, selective and highly reproducible response, indicating the suitability of the proposed sensors for practical applications.

**Keywords:** Tellurium; Carbon paste electrode; Environmental Samples; Speciation analysis.

## B-165. Electrochemical Deposition of Nickel Oxide Nanocatalyst on Anodically Pretreated Glassy Carbon and its Electrocatalytic Activity

A. M. Ghonim, B. E. El-Anadouli and M. M. Saleh

*International Journal of Electrochemical Science, 11: 621-639, (2016), IF: 1.692*

The effects of anodic oxidation of glassy carbon (GC) in H2SO4 and NaOH electrolytes on the electrodeposition of nickel oxide nanoparticles (NiOx) and on the electrocatalytic activity of the GC/NiOx electrode are studied. Cyclic voltammetry (CV), Tafel Plot, scanning electron microscopy (SEM) and energy dispersive X-ray spectroscopy (EDX) are used for characterization of the electrodes. The structural and electrochemical characteristic of GC/NiOx (GC is unoxidized), GCOXAC/NiOx (GC is oxidized in acid (0.1 M H2SO4)) and GCOX-AL/NiOx (GC is oxidized in alkali (0.1 M NaOH)) are different. While NiOx nanoparticles deposited on GCOX-AC reveal a bird-like shape, it shows semi-spherical shape with larger size when it is deposited on either GC or GCOX-AL. Glucose electrooxidation in alkaline medium is used as a probe reaction to study and compare the electrocatalytic activity of the GC/NiOx with GCox (GC is oxidized in acid or alkali). Enhancement of glucose oxidation on either GCOX-AC/NiOx or GCOX-AL/NiOx is evident. While glucose oxidation on either GCOX-AC/NiOx or GCOX-AL/NiOx, shows higher peak currents, it shows negative shifts in both the peak and onset potentials only on the GCOX-AL/NiOx. The enhancement and the difference in the catalytic activity on both GCOX-AC /NiOx and GCOX-AL/NiOx are discussed in the light of surface analysis of both electrodes compared to GC /NiOx.

**Keywords:** Glassy carbon; Oxidized; Nickel oxide; Nanoparticles; Glucose.

## B-166. Impurities Effect on the Charge Mobility of Yttria-Stabilized Zirconia

Menna M. Abo-Zeid, Mohamed S. El-Deab, A. Abdel Kareem, Omayma A.M. El-Kady and A. M. Daher

*International Journal of Elctrochemical Science, 11: 3137-3146, (2016), IF: 1.692*

The present study is concerned with the preparation of yttria-stabilized zirconia (YSZ) having high charge mobility. Herein, we studied the doping of zirconia with different concentrations of Y2O3. The samples were prepared by a solid state reaction at 800, 1000, and 1200°C for 2 hours. The morphology of the pellets was characterized by scanning electron microscope (SEM). Crystallinity and phase change were studied by X-ray diffraction (XRD). The electrical conductivity of the sintered pellets was measured and demonstrated that the conductivity increase as yttria content increase. We have also found that the conductivity decreased with increasing the level of the impurities in the natural ore.

**Keywords:** Yttria-Stabilized zirconia; Clusters; Composite materials; Solid state reactions; Crystal structures.

## B-167. Manufacture of Lead-Specific Screen-Printed Sensor Based on Lead Schiff Base Complex as Carrier and Multi-Walled Carbon Nanotubes for Detection of Pb(Ii) in Contaminated Water Tests

Tamer Awad Ali1, Abeer M.E. Hassan and Gehad G. Mohamed

*International Journal of Electrochemical Science, 11: 10732-10747, (2016), IF: 1.692*

A novel screen-printed electrode (SPE) based on [Pb(L)] complex (H2L = 2-((2-(2-(2-(2-hydroxy-5-methoxybenzylidene amino) phenyl)disufanyl)phenylimino) methyl) – 4-methoxyphenol) was prepared for selective determination of Pb(II)ion. The ligand and its Pb(II) complex

were prepared and characterized using elemental analysis, spectroscopic (IR and 1H NMR) and molar conductance. Different individual variables were optimized using IUPAC recommendation such as graphite powder, plasticizer, amounts of [Pb(L)] complex ionophore and multi-walled carbon nanotubes (MWCNT). Their possible interactions were investigated. In this potentiometric method, fabrication of screen-printed (SPE; electrode V) and multi-walled carbon nanotubes-screen-printed (MWCNT-SPE; electrode IX) sensors was described. [Pb(L)] complex alone or with MWCNT was used as modifier in case of electrodes V and IX, respectively. Optimum composition resulted in enhancement in the sensitivity and selectivity of the SPE toward Pb(II)ions significantly over the concentration range of 1.0 × 10-7 -1.0 × 10-1 and 4.6 × 10-8 -1.0 × 10-1 mol L-1 of Pb(II) with detection limit of 1.0 × 10 -7 and 4.6 × 10-8 mol L-1 and a Nernstian slope of 28.98±0.92 and 30.28±0.70 mV decade-1 for electrodes V and IX, respectively. No significant change in response was observed over the pH range of 3.0-8.0 and 2.5-8.5 with response time lower than 9 and 7s for electrodes V and IX, respectively. The potentiometric selectivity coefficients were calculated and the results obtained showed the good selectivity of the modified SPE electrodes (V and IX) for Pb(II) ion over other metal ions. Finally, these electrodes were precisely applied for the determination of Pb(II) ions in real spiked water samples. The results obtained using both the proposed potentiometric method and atomic absorption spectrometer (AAS) showed satisfactory agreement.

**Keywords:** Screen-Printed electrodes; Schiff base; Pb(Ii)-Schiff base Complex; Real water samples.

## B-168. Potentiometric and Equilibrium Studies on Complex-Formation Reactions of [Pd(2-Aminomethylpyridine) (H2o)2]2+ with Ligands of Biological Significance and Displacement Reactions of DNA Constituents

Abeer T. Abdelkarim

*International Journal of Electrochemical Science, 11: 4283-4299, (2016), IF: 1.692*

The stability constants of the complexes formed between various biologically relevant ligands (amino acids and DNA constituents) and [Pd(Pic)(H2O)2]2+ were investigated at 25 ºC and 0.1 M ionic strength. The concentration distribution diagrams of the various complex species as a function of pH were evaluated. DNA constituents form 1:1 and 1:2 complexes. The equilibrium constants for the substitution of representative coordinated DNA constituents by mercaptoethylamine, cysteine and glutathione were calculated. The results are expected to contribute to the chemistry of antitumour agents. The thermodynamic parameters ΔH◦ and ΔS◦ calculated from the temperature dependence of the equilibrium constants were determined for adenosine, and adenosinemonophosphate complexes with [Pd(Pic)(H2O)2]2+. The thermodynamic study of these systems is very important because it can give information about the structural environment of the complexes; moreover, it can help in outlining different noncovalent interactions such as coulombic forces and hydrogen bonds.

**Keywords:** Potentiometry; Complex-Formation; Thermodynamics;Antitumor; Speciation; Glutathione.

## B-169. Role of some Plating Parameters in the Properties of Ni-P/Al2o3 Nanocomposite Coatings on Mg Alloy

Fakiha El-Taib Heakal and Maanoum A. Maanoum

*International Journal of Electrochemical Science, 11: 7189-7215, (2016), IF: 1.692*

Electroless Ni-P/Al2O3 nanocomposite coatings on AZ91D magnesium alloy have been deposited by incorporating nanoalumina particles into Ni-P alloy matrix to stimulate the wear and corrosion resistance of the substrate. NanoAl2O3 particles were uniformly suspended in the bath for 1 h using magnetic stirring, and the Al2O3 content in the composite was determined gravimetrically. The effect of nanoparticle concentration in the plating bath on each of nanoAl2O¬3 in the deposit, its deposition rate and its micro-hardness and wear resistance was thoroughly studied. The influence of SLS surfactant as a wetting agent on the porosity of the deposit and on its content from the nanoparticles was explored. Coat micro-hardness as well as phase transition were also examined in relation to temperature of the heat treatment process. Furthermore, the impact of bath temperature on the deposition rate and on the amount of incorporated nanoparticles in the deposit was discussed. The role of other plating parameters such as stirring speed and nickel sulfate concentration of the plating bath solution in determining the amount of nanoparticles embedded in the Ni-P matrix were assessed and rationalized. Electrochemical polarization curves were measured to evaluate the corrosion performance of AZ91D alloy samples coated with different prepared nanocomposite deposits. In all cases, the obtained as-plated or heat treated Ni-P/Al2O¬3 nanocomposite coating can perfectly act as a potential physical barrier to protect AZ91D substrate from corrosion in the aggressive chloride environment.

**Keywords:** En Nanocomposite; Magnesium alloy; Xrd; Polarization curves; Corrosion protection.

## B-170.The Inhibitive Performance of Fenugreek for Corrosion of Copper and Nickel in Sulfuric Acid

Shimaa M. Ali

*International Journal of Electrochemical Science, 11: 953-966, (2016), IF: 1.692*

Fenugreek extract was examined as a corrosion inhibitor for copper and nickel in 2.0 M H2SO4 solution by gravimetric and electrochemical measurements. Scanning electron micrographs showed that the surface damage is decreased in inhibited acidic solution for both metals. The maximum inhibition efficiencies were 85.6% and 83.5% for copper and nickel, respectively, by using 20% (V/V%) of fenugreek extract in H2SO4 solution. Adsorption of fenugreek on both metals follows Langmuir adsorption isotherm. Florry-Huggins isotherm can be applied successively only in case of nickel suggesting a chemisorptions mode at later stages of adsorption process. Linear polarization and impedance measurements prove the inhibition ability of fenugreek for copper and nickel corrosion in H2SO4 solution.

**Keywords:** Natural inhibitor; Corrosion; Thermodynamics; Polarization; Impedance.

## B-171. Understanding Different Inhibition Actions of Surfactants for Mild Steel Corrosion in Acid Solution

Reham H. Tammam, Amany M. Fekry and Mahmoud M. Saleh

*International Journal of Electrochemical Science, 11: 1310-1326, (2016), IF: 1.692*

The inhibition actions of different surfactants for corrosion of mild steel were studied by electrochemical impedance spectroscopy and polarization measurements and weight loss. Cationic surfactant: cetylpyridinium bromide (CPBr), non-ionic surfactant: triton (TX-100) and anionic surfactant: dodecyl benzene sulphonate (DBS)in 1 M H2SO4.The order of the determined protection efficiency was found to be CPBr > TX-100 > DBS, due to the differences in the molecular structures of the three surfactants. The adsorption extent of CPBr was found to be higher than both TX-100 and DBS. A positive shift in the value of Epzc in presence of the CPBr was attributed to the specific adsorption of the halide ion Br- which facilitates the physical adsorption of the CP+ which is commenced by chemisorption of the pyridinium ring via its π-electrons with the surface Fe atom. Polarization curves and Weight loss measurements confirm the protection efficiency trends for the three surfactants.

**Keywords:** Mild steel; Iron; Polarization; Acid inhibition; Acid corrosion.

## B-172. Preparation, Spectroscopic, Theoretical Thermodynamic and Antimicrobial Discussions of Zr(Iv), Ce(Iii) and Th(Iv) Ibuprofen Drug Complexes

Moamen S. Refat1 , Gehad G. Mohamed, Mohamed Y. El-Sayed, Hamada M. A. Kill,Hammad Fetooh, Mohamed A. Al-Omar and Ahmed M. Naglah

*Journal of Computational and Theoretical Nanoscience, 13: 5269-5276, (2016), IF: 1.666*

The Zr(IV), Ce(III) and Th(IV) complexes of ibuprofen drug were synthesized and antimicrobial assessment. These complexes were assigned based on elemental analyses, conductivity measure- ment, and (UV-Vis, infrared and 1H-NMR) spectra as well as thermogravimetric analyses. Infrared spectroscopic tool prove that the ibuprofen acts as a monodentate chelate via the oxygen of carboxylate group after deprotonated. The elemental analyses gave the molar rations between the respective drug and (Zr(IV) and Th(IV)) and Ce(III) metal ion with 1:4 and 1:3, respectively. The thermal degradation of ibuprofen complexes were assigned and the kinetic thermodynamic values were calculated based on two an official methods. The antimicrobial tests were assessed towards some kind of bacteria and fungi.

**Keywords:** Ibuprofen; Tridentate; Tetradentate; Complexes; Thermal decomposition; Antimicrobial test.

## B-173. Photophysical Behavior and Computational Investigation of Novel 1,4-Bis(2-(2-Phenylpyrimido[1,2-A]Benzimidazol – 4-Yl)Phenoxy)Butan (Bppb) Macromolecule

Tamer S. Saleh, Mahmoud A. Hussein, Osman I. Osman, Khalid A. Alamry, Ahmed E. M. Mekky, Abdullah M. Asiri and Samy A. El-Daly.

*Journal of Fluorescence, 26: 1895-1904, (2016), IF: 1.601*

A new macromolecule pyrimido[l,2-a]benzimidazole derivative named 1,4-bis(2-(2-phenylpyrimido[1,2-a]benzimidazol-4-yl)phenoxy)butan (BPPB) has been synthesized in accepted yield using microwave assistance. The new compound BPPB has been formed by the interaction of 3,3'-((butane-1,4-diylbis(oxy))bis(2,1-phenylene))bis(1-phenylprop-2-en-1-one) (3) with 2- aminobenzimidazole (4) in the presence of potassium hydroxide as a basic catalyst in dimethylformamide (DMF) under microwave radiation for 20 min. The chemical structure of this novel compound was elucidated by elemental and spectral techniques including: FT-IR, H-1-NMR, C-13-NMR and mass spectra. The electronic absorption and emission spectra of BPPB were measured in different solvents. BPPB displayed a solvatochromic effect of the emission spectrum that is reflected by red shifts of its fluorescence emission maxima on increasing the solvent polarity, indicating a change of electronic charge distribution upon excitation. BPPB crystalline solids gave excimer-like emission at 535 nm with a bandwidth of ca. 60 nm. Ground and excited states electronic geometry optimizations using density functional theory (DFT) and time-dependent density functional theory (TD-DFT), respectively, complemented these spectral findings. The intramolecular charge transfer was investigated by natural bond orbital (NBO) technique.

**Keywords**: Photoluminescence; Effect of solvent; Photostability; DFTstudies; 1,4-Bis(2-(2-Phenylpyrimido[1,2-A]Benzimidazol-4-Yl)Phenoxy)Butan (Bppb).

## B-174. DFT Insights Into the Electronic and Optical Properties of Fluorine-Doped Monoclinic Niobium Pentoxide (B-Nb2O5:F)

Tamer S. El-Shazly, Walid M. I. Hassan, Sayed S. Abdel Rehim and Nageh K. Allam

*Applied Physics A: Materials Science and Processing, 122 (2016) IF: 1.444*

We report on the effect of fluorine doping on the electronic structure and optical properties of monoclinic niobium pentoxide (B-Nb2O5) as revealed by the first principles calculations. Density functional theory (DFT) along with generalized gradient approximation (GGA) at the revised Perdew-Burke-Ernzerhof (PBEsol) exchange–correlation functional was used in this study. The band calculations revealed that the studied materials are indirect bandgap semiconductors, with bandgap energies of 2.67 and 2.28 eV for the undoped and F-doped B-Nb2O5, respectively. Upon doping B-Nb2O5, the Fermi level shifts towards the conduction band, allowing optical absorption in the visible region with enhanced transmittance in the wavelength range 400-1000 nm. The calculated static refractive index of the undoped B-Nb2O5 is in good agreement with the reported experimental value, which is

enhanced upon F-incorporation resulting in cladding properties for the F-doped B-Nb2O5. Also, the effective mass of free charge carriers increased upon F-doping. The enhanced properties were attributed to the effect of the excessive valent electron of the incorporated F atom.

## B-175. Anticancer Activity of some [1,2,4]Triazepino[2,3-A] Quinazoline Derivatives: Monolayer and Multicellular Spheroids in Vitro Models

Hanem M. Awad, Walid Fayad, Salwa M. El-Hallouty, Thoraya A. Farghaly and Mohamad M. Abdallah

*Medicinal Chemistry Research, 25: 1952-1957 (2016)IF: 1.436*

In this study, five derivatives of triazepino[2,3-a] quinazoline-2,7(1H)-dione were synthesized and their anticancer activities were investigated both in two-dimensional-monolayer and three-dimensional-multicellular spheroids cancer models. All the five compounds showed very high anticancer activities against the 11 cancer cell types that have been investigated in the monolayer model. Comparing the results of both monolayer and multicellular spheroids models of the anticancer activity of these five compounds, we can conclude that the meta-methyl derivative induced its anticancer activity through apoptosis to give the best results in the monolayer model. However, in the multicellular spheroids model its apoptotic activity induced moderate anticancer activity (64 % cytotoxicity). On the other hand, both two nitro-derivatives either in meta-position or para-position, did not show potent pro-apoptotic activities toward the monolayer model but showed very high cytotoxic activity toward the multicellular spheroids model (100 %). These results reveal that the cell death mechanism induced by both nitro-compounds is exerted via other path than the apoptosis. Interestingly, all the tested compounds were generally safe to normal cells spheroids when tested at the same concentration.

**Keywords:** [1,2,4]Triazepino[2,3-A] Quinazolinesanticancer Activityapoptosis.

## B-176. Synthesis of Pyridine, Pyran and Thiazole Containing Thiophene Derivatives and Their Anti-Tumor Evaluations

Rafat M. Mohareb, Rehab A. Ibrahim and Wagnat W. Wardakhan

*Medicinal Chemistry Research,25: 2187-2204,(2016), IF:1.436*

The multi-component reaction of 2- acetylthiophene with aromatic aldehydes and either malononitrile or ethyl cyanoacetate gave the pyran derivatives 4a–4f and pyridine derivatives 5a–5f. On the other hand, the reaction of the 2-acetylthiophene with elemental sulfur and either malononitrile or ethyl cyanoacetate gave the thiophene derivatives 6a and 6b; respectively. Compounds 6a and 6b underwent a series of heterocyclic reactions to give thiazole and thiophene derivatives. All the products were assessed for antitumor activity towards human cancer human gastric cancer (NUGC and HR), human colon cancer (DLD1), human liver cancer (HA22T and HEPG2), human breast cancer (MCF), nasopharyngeal carcinoma (HONE1) cell lines. Compounds 4e, 4f, 5e, 5f, 7b, 8b, 10e, 10f, 11e, 11f, 14d-f, 15d-f, 16a,b and 18b exhibited optimal cytotoxic effect against cancer cell lines, with IC50's in the nM range. Moreover, 7b, 10e, 14d, 15e and 16b showed no toxicity against shrimp larvae. Anti-proliferative cell activity against cancer cell lines of the most potent compounds showed that compounds 5f and 10e achieved the highest activities among the tested compounds.

**Keywords:** Thiophene; Pyran; Pyridine; Cytotoxicity; Toxicity; Anti-Proliferative.

## B-177. Construction and Performance Characteristics of Modified Screen Printed and Modified Carbon Paste Sensors for Selective Determination of Cu(II) Ion in Different Polluted Water Samples

Tamer Awad Ali,Gehad G. Mohamed and Amal H. Said

*Chemical Engineering Communications, 203: 724-735, (2016), IF: 1.433*

Four new ion-selective electrodes (ISEs), based on N,N`-bis (salicylaldehyde)-p-phenylene diamine (SPD) as ionophore, are constructed for the determination of copper(II) ion. The modified carbon paste (MCPEs; electrodes I and II) and modified screen-printed sensors (MSPEs; electrodes III and IV) exhibit good potentiometric response for Cu(II) over a wide concentration range of 1.0x106 – 1.0x102 mol L1 for electrodes (I and II) and 4.8x107 – 1.0x102 mol L1 for electrodes (III and IV) with a detection limit of 1.0x106 mol L1 for electrodes (I and II) and 4.8x107 mol L1 for electrodes (III and IV), respectively. The slopes of the calibration graphs are 29.62±0.9 and 30.12±0.7 mV decade1 for electrode (I) (tricresylphosphate (TCP) plasticizer) and electrode (II) (o-nitrophenyloctylether o-NPOE plasticizer), respectively. Also, the MSPEs showed good potentiometric slopes of 29.91±0.5 and 30.70±0.3 mV decade1 for electrode (III) (TCP plasticizer) and electrode (IV) (o-NPOE plasticizer), respectively. The electrodes showed stable and reproducible potentials over a period of 60, 88, 120, and 145 days at the pH range from 3 to 7 for electrodes (II), (III), and (IV) and pH range from 3 to 6 for electrode (I). This method was successfully applied for potentiometric determination of Cu(II) in tap water, river, and formation water samples in addition to pharmaceutical preparation. The results obtained agree with those obtained with the atomic absorption spectrometry (AAS).

**Keywords:** Copper determination; Modified carbon paste sensors; Modified screen-Printed sensors; N,N0-Bis(Salicylaldehyde)-P- Phenylene diamine ionophore.

## B-178. A DFT Study of the Dissociation, Ionization, and Uv/Visible Spectra of Methyl Hypobromite

M. Elshakre and I. Sadiek

*Computational and Theoretical Chemistry, 1088: 32-43, (2016), IF: 1.403*

The energetics and the molecular structures of CH3OBr in the ground electronic, S0, second excited, S2, sextet excited, S6, and cationic ground, D0 + states have been investigated theoretically. The HBr elimination of CH3OBr is found to have two dissociation pathways involving two transition states with an energy difference of 5.28 kcal/mol. The B3LYP optimization of the S2 state, which is found to be 1.95 eV above the S0 state,

shows a tendency of OBr bond dissociation, resulting in CH3O and Br formation. The optimization of the S6 state, which is found to be 2.35 eV above the S0 state, shows a tendency of CO bond dissociation, forming CH3 and OBr. The ionization energy of the anticipated dissociation products was calculated and found to agree well with the values reported experimentally. For CH3OBr, which has no experimental value for the ionization energy, our ionization energy calculations predicted a value of 9.98 eV. Utilizing the excited states calculations and the ionization energy calculations, a design of a pump–probe experiment has been provided in order to explore the ultrafast dissociation dynamics of CH3OBr through S2 and S6 states. The vertical excitation energy calculations were carried out to explore the UV/Visible spectrum of CH3OBr, and the frequency calculations were performed to explore its IR spectrum. The excitation and ionization of CH3OBr result in significant molecular changes including bond lengths, bond angles, dihedral angles, atomic charges, dipole moments, and rotational constants. The excitation to the S2 results in a significant elongation of the OBr bond, which reflects its tendency for the dissociation through this bond. The excitation to the S6 state results in a remarkable elongation in the CO bond, reflecting its tendency to dissociate along this bond. The calculations of atomic charges and dipole moment indicate noticeable changes due to excitation and ionization. The electron density contour of HOMO's indicates the specific site of the HOMO from which the excitation and ionization takes place. The calculations of rotational constants A, B, and C indicated the structural changes through the three mutually perpendicular axes x, y, and z. The effect of ionization to D0 + state on CH3O, CH3, and OBr was investigated following the same thread used for the mother molecule, CH3OBr. CH3O was found to suffer dramatic changes in the molecular structure. It was found to form the CH2OH isomer upon ionization, in which the CO bond has more double bond character. Moreover, the ionization induces a significant change in the planarity of the CH3O, which changes to the fully planar CH2OH isomer.

**Keywords:** Dft methyl hypobromite; Photo-Dissociation Ionization energy Uv/Vis and Ir spectra structural changes.

## B-179. Empirical Simulation of the I-E Curves of a H2/Air Pem Fuel Cell at Asymmetric Relative Humidity

Faisal Abdellatif Al-Odail, Mahmoud M. Saleh and Takeo Ohsaka

*Bulletin of The Chemical Society of Japan, 89: 1455-1461, (2016), IF: 1.372*

The present work is dedicated to study the performance of H2/Air proton exchange membrane (PEM) fuel cells (FC) by using an empirical modeling and experimental results at symmetric and asymmetric relative humidity. The empirical modeling is presented by Kim's equation which was used in simulating the performance of the H2/Air PEM FC and in fitting the experimental data at different operating conditions. The simulation of the cell performance helps to understand the impacts of different kinetics, ohmic and mass-transfer resistances on the I-E curves and hence on the performance of the FC. By fitting the experimental data with the theoretical calculations, it is possible to extract important kinetics, ohmic and mass-transfer parameters at different temperatures and at different symmetric and asymmetric relative humidity. Although the exact physical meanings of some fitting parameters are quite clear, others are not.

**Keywords:** Empirical; Simulation; Pem fuel cell; Asymmetric; Humidity

## B-180. Preparation and Evaluation of Hyperbranched P-Chloromethyl Styrene Polymers/Montmorillonite Clay Nanocomposites as Dielectric Materials

AmalAmin, Eman H. Ahmed, Magdy W. Sabaa, Magdy M. H. Ayoub and Inas K. Battisha

*PolymerBulletin, 73: 147-162, (2016), IF: 1.371*

Hyperbranched polymers/montmorillonite clay modified with cetyl trimethyl ammonium bromide (MMT-CTAB) nanocomposites with polystyrene core were prepared by self-condensing vinyl polymerization via atom transfer radical polymerization of p-chloromethyl styrene monomer (CMS) alone or with styrene (St) and methyl methacrylate (MMA) monomers in the presence of MMT-CTAB acting as inimer with the double bond at one end and the alkyl-Cl unit at the other end. Three hyperbranched polymers/MMT-CTAB nanocomposites such as PCMS homopolymer/MMT-CTAB, PCMS-b-PSt copolymer/MMT-CTAB and PCMS-b-PSt-b-PMMA terpolymer/MMT-CTAB were prepared. The prepared hyperbranched polymers/MMT-CTAB nanocomposites were characterized via X-ray diffraction, dynamic mechanical thermal analyses and transmission electron microscopy for further applications as dielectric materials. Accordingly, several parameters were measured including dielectric permittivity (ε′), A.C. conductivity (σ) and loss tangent (tan δ) in case of frequency and temperature ranging from 0.1 Hz to 100 kHz and 20–80 °C, respectively.

**Keywords:** Hyperbranched Polymersself;Condensing Vinyl Polymerizationatom Transfer Radical Polymerizationpolymers;Clay Nanocompositesdielectric; Polymeric Materials.

## B-181. Control of Zinc Corrosion in Acidic Media: Green Fenugreek Inhibitor

Shimaa M. Ali

*Transactions of Nonferrous Metals Society of China, 26: 3034-3045, (2016), IF: 1.34*

Fenugreek seeds extract was examined as a green corrosion inhibitor for Zn in 2.0 mol/L H2SO4 and 2.0 mol/L HCl solutions by mass loss and electrochemical measurements. Scanning electron microscope (SEM) images show that the surface damage is decreased in the presence of the inhibitor. X-rays photoelectron spectroscopy (XPS) analysis was performed to identify the corrosion product, ZnO, and to prove the inhibitor adsorption mechanism. The maximum inhibition efficiency values are 90.7% after 1 h and 66.6% after 0.5 h by 200 mL/L of fenugreek extract in H2SO4 and HCl solutions, respectively. Addition of I− ion greatly improves the inhibition efficiency of fenugreek seeds extract for Zn corrosion in HCl due to the synergistic effect. Potentiodynamic polarization and EIS measurements prove the inhibition ability of fenugreek for Zn corrosion in HCl as indicated by the decreased corrosion

current density and increased charge transfer resistance values in the presence of fenugreek.
**Keywords:** Zinc; Corrosion mechanism; Inhibitor; Synergetic effect.

## B-182.Flubendazole Pd(Ii) Complexes: Structural Studies, Cytotoxicityand Quantum Chemical Calculations

Ahmed M. Mansour, Eslam M. El Bakry and Nour T. Abdel-Ghani

*Journal of Iranian Chemical Society,13:1429-1437(2016)IF:1.3*

[Pd(FLU)2X2]·yH2O·zCH3OH (FLU = flubendazole; X = Cl (1), y = 0, z = 0; X = Br (2), NO3 (3), y = 2, z = 0; X = SCN (4), y = 2, z = 3) were synthesized as potential anticancer complexes, and their structures were elucidated using elemental analysis, TG/DTA, IR, 1H NMR, UV–vis., and conductivity measurements. FLU interacts with Pd(II) ions as a neutral unidentate ligand via the pyridine-type nitrogen of the benzimidazole ring. Geometry optimization, molecular electrostatic potential maps and natural bond orbital analysis were performed by DFT/B3LYP method. FLU, in comparison to its complexes, was screened for its antibacterial and cytotoxic activity. Complexes 1–4 possess strong anticancer activity with IC50 values (4.13–3.68 μg ml−1) compared with 3.57 μg ml−1 reported for cis-platin. The cytotoxicity was shown to be affected by the nature of the anion, where the sequence is 3 > 2 > 4 > 1 in case of MCF7 cell line. Structural-activity relationships suggested that EHOMO, energy gap and dipole moment were the most significant descriptors for the correlation with the antitumor activity.
**Keywords:** Flubendazole; Dft; Biological activity; Nmr; Nbo; B3lyp.

## B-183.The Effect of Different Copper Salts on the Mechanical and Ballistic Characteristics of Double Base Rocket Propellants

Nour Abdel-Ghani, Ahmed Elbeih and Farag Helal

*Central European Journal of Energetic Materials, 13: 261-270, (2016), IF: 1.28*

This paper discusses the enhancement in the ballistic performance of double base rocket propellants (DBRPs) by the addition of different copper salts vs lead salts as burning rate modifiers through stable combustion and the formation of a plateau region in the low pressure region. Compositions based on DBRPs containing different percentages of lead stearate and different types of copper salts were prepared and studied. For comparison, a conventional DBRP was studied. The ignition temperature and heat of combustion were determined experimentally, and the mechanical properties were measured and evaluated. The performance in terms of ballistic characteristics (burning rate, operating pressure) were measured at different throat diameters (8, 8.5, 9, 9.5 mm) and at different temperatures (−20 and 50 °C). Specific impulses were calculated using the ICT thermodynamic code. The experimental data from the proportional study indicate that the compositions containing the studied burning rate modifiers are superior to the original DBRP in respect of ballistic performance and mechanical properties.
**Keywords:** Double base rocket propellant; Burning rate modifiers; Ballistic performance; Mechanical properties.

## B-184. Removal of Methylene Blue from Synthetic Aqueous Solutions with Novel Phosphoric Acid-Doped Pyrazole-G-Poly(Glycidyl Methacrylate) Particles: Kinetic and Equilibrium Studies

M.S. Mohy Eldin, K.M. Aly, Z.A. Khan, A.E.M. Mekky, T.S. Saleh and A.S. Al-Bogami

*Desalination and Water Treatment, 57: 27243-27258, (2016), IF: 1.272*

Fundamental investigations of the removal of methylene blue (MB) from aqueous solutions by synthesized orthophosphoric acid-doped pyrazole-g-poly glycidyl methacrylate (OPA-Py-g-PGMA) and poly (glycidyl methacrylate) (PGMA) particles of average size 71 and 40m, respectively, conducted under batch conditions. The kinetic and equilibrium results obtained for MB sorption with different initial MB concentrations onto synthesized OPA-Py-g-PGMA, and PGMA were analyzed. Kinetic modeling analysis with three different types of kinetic sorption models (pseudo-first-order, pseudo-second-order, simple Elovich, and intraparticle diffusion rate models) was applied to simulate the MB sorption data. The analysis of the kinetic data indicated that the sorption was a second-order process. An ion-exchange mechanism may have existed in the MB-sorption process with the synthesized OPA-Py-g-PGMA. The MB uptake by OPA-Py-g-PGMA and PGMA quantitatively evaluated with equilibrium sorption isotherms. To describe the isotherms mathematically, the experimental data of the removal equilibrium correlated with the Langmuir, Freundlich, Temkin, and Dubinin-Radushkevich (D-R) isotherm models, and the applicability of these isotherm equations to the sorption systems compared by the correlation coefficients. The maximum sorption capacities, determined from the Langmuir isotherm, were 15.15 and 8.67mg/g at 25 degrees C for OPA-Py-g-PGMA and PGMA, respectively. Moreover, diffusion mechanism of MB was described by different adsorption diffusion models. The diffusion rate equations inside particulate of Dumwald-Wagner and intraparticle models were used to calculate the diffusion rate. The actual rate-controlling step involved in the MB sorption process was determined by further analysis of the sorption data by the kinetic expression given by Boyd.
**Keywords:** Basic dye removal; Methylene blue; Acid-base Ions exchanger; Pgma; Pyrazole; Grafting; Ftir; Tga.

## B-185. Potentiometric Study of Speciation and Thermodynamics of Complex Formation Equilibria of Diorganotin(Iv) Dichloride with 1-(2-Aminoethyl)Piperazine

Ahmed A. El-Sherif, M. R. Shehata, Mohamed M. Shoukry and N. Mahmoud

*J Solution Chemistry, 45: 410-430, (2016), IF: 1.256*

The interaction of DET (diethyltin(IV)) and DVT (divinyltin(IV)) with 1-(2- aminoethyl)piperazine (AEP) was

investigated potentiometrically at different temperatures in 0.1 moldm-3 NaNO3. The hydrolysis constants of diethyltin(IV) and divinyltin(IV) cations and the stepwise formation constants of the complexes formed in solution were calculated at different temperatures and in solutions of dioxane–water solutions of different compositions. The stoichiometries and stability constants for the complexes formed are reported. The results show formation of 1:1 complexes and the corresponding hydroxide complexes. The concentration distributions of the various complex species were evaluated as a function of pH. The thermodynamic parameters DH and DS calculated from the temperature dependence of the equilibrium constants were investigated for DET and DVT complexes with AEP.

**Keywords:** Formation equilibria; Diethyltin (Iv); Divinyltin(Iv); Piperazine dioxane; Thermodynamics speciation.

## B-186. Potentiometric, Thermodynamics and Coordination Properties for Binary and Mixed Ligand Complexes of Copper(II) with Imidazole-4-Acetic Acid and Tryptophan or Phenylalanine Aromatic Amino Acids

Abeer T. Abdelkarim and Ahmed A. El-Sherif

*J. Solution Chemistry, 45: 712-731, (2016), IF: 1.256*

Binary and ternary complex formation equilibria of copper(II) with imidazole- 4-acetic acid (IMA) and some aromatic amino acids such as tryptophan and phenylalanine have been studied from 15 to 45 °C by potentiometric titration. The pH-titrations of the reaction mixtures have shown 1:1:1 (Cu:IMA:amino acid) ternary complex formation. The stability of mixed-ligand complexes was quantitatively compared with the stability of the binary complexes as Δlog10K, Δlog10β and log10X parameters. The speciation of different species in solution has been evaluated as a function of pH. The effect of temperature on protonation of the ligands and formation of mixed ligand complexes was investigated. Thermodynamic parameters were calculated and are discussed. The effect of solvent of the protonation of IMA and Cu–IMA complex formation was also investigated and discussed. Additionally, the stoichiometric protonation constants (log10β) of imidazole-4-acetic acid and its binary Cu(II)–IMA complexes were determined potentiometrically over a wide range of solvent composition.

**Keywords:** Potentiometry; Copper(Ii); Imidazole-4-Acetic Acid; Tryptophan; Thermodynamics;Species.

## B-187. Synthesis and SAR Study of the Novel Thiadiazole–Imidazole Derivatives as A New Anticancer Agents

Sobhi Mohamed Gomha, Hassan Mohamed Abdel-aziz and Khaled Dessouky Khalil

*Chemical Pharmacetical Bulletin, 64: 1356-1363, (2016), IF: 1.228*

In the present study, a novel series of 2-(2-(3-aryl-5-substituted-1,3,4-thiadiazol-2(3H)-ylidene)-hydrazinyl)-4,4-diphenyl-1H-imidazol-5(4H)-one derivatives were designed and prepared via the reaction of the most versatile, hitherto unreported 2-(5-oxo-4,4-diphenyl-4,5-dihydro-1H-imidazol-2-yl)-N-phenylhydrazinecarbothioamide with the appropriate hydrazonoyl halides. In addition, some thiazole derivatives were prepared. The structures of the newly synthesized compounds were established based on spectroscopic evidences and their alternative syntheses. Some of the newly synthesized compounds have been evaluated for their anticancer activity against a liver carcinoma cell line HEPG2-1. Moreover, their structure–activity relationship (SAR) was explored for further development in this area. The results indicated that many of the tested compounds showed moderate to high anticancer activity with respective to doxorubicin as a reference drug. Consequently, the new synthesized series of thiadiazole–imidazole derivatives are considered as powerful anticancer agents.

**Keywords:** Imidazole; 1,3,4-Thiadiazole; Hydrazonoyl halide; Cytotoxicity evaluation.

## B-188. Synthesis, Antimicrobial and Anti-Inflammatory Activity of some Newbenzoxazinone and Quinazolinone Candidates

Maher Abd El-Aziz El-Hashash, Mohammad Emad Azab, Rasha Abd El-Aziz Faty and Abd El-Galil Elsyed Amr

*Chem. Pharm. Bull., 64: 263-271, (2016), IF: 1.228*

Benzoxazinones and quinazolinones have a wide spectrum of biological activity. In this paper we focused on studying the antimicrobial and anti-inflammatory activities of some newly synthesized benzoxazinone and quinazolinone derivatives. Thus we prepared 2-[α-benzoylaminostyryl]-6,8-dibromo-3,1-benzoxazin-4(H)- one 2 which underwent a reaction with primary and secondary amines, and hydrazine hydrate to give compounds 3, 4 and 5, respectively. Treatment of 2 with hydroxylamine hydrochloride, formamide and/or NaN3/ AcOH afforded compounds 7, 8, 11 and 12, respectively. Also, compound 2 reacted with maleic anhydride, aromatic hydrocarbons and/or active methylene compounds to produce compounds 13, 15a–c and 16, respectively. Most of the newly synthesized compounds showed significant antimicrobial and anti-inflammatory activities comparable to ampicillin, mycostatine and indomethacin positive controls.

**Keywords:** Benzoxazinone; Quinazolinone; Imidazole; Tetrazole; Antimicrobial; Anti-Inflammatory.

## B-189. Thermally Stable Antimicrobial Poly(Vinyl Chloride)/ Maleimido Aromatic Hydrazide Composites

Nadia A. Mohamed, Nahed A. Abd El-Ghany, Mona M. Fahmy and Marwa H. Ahmed

*Journal of Vinyl and Additive Technology, 22: 247-258, (2016), IF: 1.219*

Antimicrobial novel substituted maleimido aromatic hydrazides were synthesized from N-[4-(chlorocarbonyl) phenyl] maleimide with salicylhydrazide, p-aminobenzohydrazide, or p-aminosalicylhydrazide. They were characterized by Fourier transform infrared (FTIR), hydrogen-1 nuclear magnetic resonance (1 H- NMR), mass spectra, elemental analyses, and antimicrobial activities. These derivatives were investigated as thermal stabilizers for rigid poly(vinyl chloride) (PVC) at 180C in air by measuring the rate of dehydrochlorination, the extent of discoloration, and the changes that occurred in the molecular

masses of the degraded PVC samples. The previously reported stabilizing efficiency data of a nonsubstituted derivative, which was synthesized from N-[4-(chlorocarbonyl) phenyl] maleimide with benzohydrazide, is also given for comparison. The results reveal the greater stabilizing efficiency of the investigated derivatives as shown by their longer thermal stability (Ts) periods and lower dehydrochlorination rates in relation to dibasic lead carbonate, cadmium-barium-zinc stearate, and n-octyltin mercaptide industrial stabilizers. The stabilizing efficiency increases with the introduction of electron donating substituent groups in the aromatic ring of the stabilizer molecules. Moreover, the investigated stabilizers impart better color stability for the degraded samples as compared with the reference stabilizers. A synergistic effect is achieved when the materials under investigation were mixed in various weight ratios with any of the reference stabilizers, reaching its maximum at equivalent weight ratio of the investigated stabilizer to the reference one.

**Keywords:** Maleimido aromatic hydrazides; Antimicrobial activity; Pvc; Dehydrochlorination rate; Discoloration degree; Molecular weight determination.

## B-190. Synthesis and Structure Elucidation of some Novel Thiophene and Benzothiophene Derivatives as Cytotoxic Agents

Rafat M. Mohareb, Amira E. M. Abdallah, Maher H. E. Helal and Somiya M. H. Shaloof

*Acta Pharmaceutica, 66: 53-68, (2016), IF: 1.212*

Att empting to produce cyclized systems with potential anti-proliferative activity, a series of novel thiophene and benzothiophene derivatives were designed and synthesized. The reactivity of the latt er derivatives towards diff erent chemical reagents was studied. Twenty-one compounds were synthesized and evaluated as anti-cancer agents. The results showed that ethyl 5-amino-3-(4-chlorostyryl)-4-cyanothiophene- 2-carboxylate (5b), ethyl 5-amino-4-((4-methoxyphenyl) carbonyl)-3-methylhiophene-2-carboxylate (8c) and 5-3-(ethoxy-3-oxopropanamido)-3-methyl – 4-(phenylcarbamoyl)thiophene-2-carboxylate (9) were the most active compounds towards three tumor cell lines – MCF-7 (breast adenocarcinoma), NCI-H460 (non-small cell lung cancer) and SF-268 (CNS cancer) and a normal fi broblast human cell line (WI-38) compared to the anti-proliferative eff ects of the reference control doxorubicin.

**Keywords:** Thiophene; Benzothiophene; Cytotoxic agents.

## B-191. Construction of Nanophase Novel Coatings-Based Titanium for the Enhancement of Protein Adsorption

Sahar A. Fadlallah, Mohammed A. Amin and Ghaida S. Alosaimi

*Acta Metallurgica Sinica (English Letters), 29(3): 243-252, (2016), IF: 1.188*

In the recent years, biological nanostructures coatings have been incorporated into orthopedic and dental implants in order to accelerate osseointegration and reducing surgical restrictions. In the present work, chemical etching, anodization and metal doping surface modification methods were integrated in one strategy to fabricate innovative titanium surfaces denominated by titanium nanoporous, anodized titanium nanoporous, silver-anodized titanium nanoporous and gold-anodized titanium nanoporous. The stability properties of nanostructures-coated surfaces were elucidated using electrochemical impedance spectroscopy (EIS) after 7 days of immersion in simulated biological fluids. Morphology and chemical compositions of new surfaces were characterized by scanning electron microscope and energy-dispersive X-ray analysis. The EIS results and data fitting to the electrical equivalent circuit model demonstrated the influence of adsorption of bovine serum albumin on new surfaces as a function of protein concentration. Adsorption process was described by the very well-known model of the Langmuir adsorption isotherm. The thermodynamic parameter ΔGADS (−50 to 59 kJ mol−1) is calculated, which supports the instantaneous adsorption of protein from biological fluids to new surfaces and refers to their good biocompatibility. Ultimately, this study explores new surface strategy to gain new implants as a means of improving clinical outcomes of patients undergoing orthopedic surgery.

**Keywords:** Titaniumnanoporoussurface;Modificationprotein Adsorptionelectrochemical; Impedance spectroscopy (Eis).

## B-192. The Relation Between Glutathione S-Transferase M1 Null-Genotype and Cardiac Problems in Beta-Thalassemia

Asem Metwally Abo-Shanab, Mohamed Ali El-Desouky, Naglaa Mohamed Kholoussi, Ghada Youssef El-Kamah, Iman Aly Helwa and Abdelgawad Ali Fahmi

*Acta Biochimica Polonica, 63: 267-271, (2016), IF: 1.187*

This work was carried out to investigate the role of Glutathione S-Transferase M1 (GSTM1) null genotype frequency in prognosis of β-thalassemia, and to detect the correlation between GSTM1 null genotype and appearance of cardiac complications in β-thalassemia. **Materials and Methods**. The studied groups in the present work were divided to three groups (group I: 20 healthy subjects, group II: 56 β-thalassemic patients and group III: 16 β-thalassemic patients with cardiac complications were taken from group II). The measurement of human high sensitive C-reactive protein (hs-CRP) was performed using nephelometry. GSTM1 genotype was detected by Polymerase Chain Reaction (PCR) and cardiac complications were determined by using Echocardiography. **Results.** A statistically significant increase in hs-CRP and interleukin-6 (IL-6) levels was found in β-thalassemic patients with cardiac complications compared to normal subjects. Results showed no relation between GSTM1 null genotype frequency neither with β-thalassemia nor with cardiac complications appearance, where the interaction between GSTM1 null genotype in β-thalassemic patients with cardiac complications and healthy subjects were insignificant compared to subjects with GSTM1 non-null genotype. **Conclusions**. GSTM1 null genotype frequency has no role in β-thalassemia or cardiac complications appearance.

**Keywords:** Gstm1; B-Thalathemia; Cardiac complications; Hs-Crp; Il-6.

## B-193. Bis(indoline-2,3-diones): Versatile precursors for Novel bis(2',6'-dimethyl – 2-oxo-1'H– spiro[indoline-3,4'-pyridine]-3',5'-dicarbonitrile) derivatives

Amr M. Abdelmoniem, Ahmed H. M. Elwahy and Ismail A. Abdelhamid

*Arkivoc, iii: 304-312, (2016), IF: 1.177*

Reaction of 3-aminocrotononitrile with a series of bis(indoline-2,3-diones) afforded the corresponding bis(2',6'-dimethyl-2-oxo-1'H-spiro[indoline-3,4'-pyridine]-3',5'-dicarbonitrile) derivatives in good to excellent yields.
**Keywords:** Bis(Indoline-2,3-Diones); Bis(Spirooxindole); 1,4-Dihydropyridine-3,5-Dicarbonitrile; Alkylation; Condensation

## B-194. New Approaches for the Synthesis, Cytotoxicity and Toxicity of Heterocyclic Compounds Derived from 2-Cyanomethylbenzo[C]Imidazole

Rafat M. Mohareb, Abeer A. Mohamed and Amira E. M. Abdallah

*Acta Chimica Slovenica, 63: 227-240, (2016), IF: 1.167*

The reaction of ethyl cyanoacetate with o-phenylenediamine gave the 2-cyanomethylbenzo[c]imidazole (1). The latter compound was used as the key starting material to synthesise biologically active heterocyclic derivatives. Thus, the reaction of 1 with cyclohexanone and either of benzaldehyde, 4-methoxybenzaldehyde or 4-chlorobenzaldehyde gave the annulated derivatives 2a–c, respectively. The antitumor evaluations of the newly synthesized products against the three cancer cell lines MCF-7 (breast adeno-carcinoma), NCI-H460 (non-small cell lung cancer) and SF-268 (CNS cancer) showed that compounds 2b, 6, 11b, 11c, 12b, 16a, 16b and 18a exhibited optimal cytotoxic effect against cancer cell lines, with IC50 values in the nM range. Bioactive compounds are often toxic to shrimp larvae. Thus, in order to monitor these chemicals in vivo lethality to shrimp larvae (Artemia salina), Brine-Shrimp Lethality Assay was used. Compounds 11b, 12b and 16b showed no toxicity against the tested organisms.
**Keywords:** Benzimidazole; Thiophene; Thiazole; Synthesis; Anti-Tumor; Toxicity.

## B-195. 1,Ω-Bis(Formylphenoxy)Alkane: Versatile Precursors for Novel Bis-Dihydropyridine Derivatives

Refaie M. Kassab , Ahmed H. M. Elwahy and Ismail Abdelshafy Abdelhamid

*Monatshefte Fur Chemie, 147: 1227-1232, (2016), IF: 1.131*

Reaction of b-aminocrotonitrile with a series of bis(aldehydes) containing ether linkages afforded the corresponding bis(2,6-dimethyl-1,4-dihydropyridine-3,5- dicarbonitrile) derivatives in good to moderate yield. Oxidative aromatization of the latter compounds into the corresponding bis(2,6-dimethylpyridine-3,5-dicarbonitrile) derivatives was achieved using ceric ammonium nitrate (CAN).
**Keywords:** Bis(Aldehyde) B; Aminocrotonitrile Bis(Dihydropyridine) cyclocondensation aromatization.

## B-196. Novel Bis(Benzothiazole-Oxime)-Based Pd(Ii)– Complex: Synthesis, Characterization, Quantum Chemical Calculations, and Catalytic Significance in Suzuki–Miyaura and Heck–Mizoroki Cross Coupling Reactions

Ahmed F. Darweesh, Ahmed M. Mansour and Ahmed H. M. Elwahy

*Monatsh Chem, 147: 1197-1205, (2016), IF: 1.131*

In the present work, a novel binuclear benzothiazole- oxime Pd(II) complex was synthesized, characterized (elemental analysis, infrared spectroscopy, thermogravimetric analysis, ultraviolet–visible spectroscopy, nuclear magnetic resonance, and conductance measurements), and explored for its catalytic activity in Suzuki–Miyaura and Heck–Mizoroki cross-coupling reactions of different aryl- and heteroaryl halides with arylboronic acids and styrene, respectively, using the microwave irradiation conditions. The electronic arrangement, type of hybridization, and nature of bonding in the Pd-complex were investigated by natural bond orbital analysis. Time-dependent density functional theory calculations were carried out to understand the electronic transitions in the related experimental observations.
**Keywords:** Coordination chemistry; Catalysis; Microwave Assisted synthesis; Density functional theory.

## B-197. Thermally Stable Antimicrobial Pvc/Maleimido Phenyl Thiourea Composites

Nadia A. Mohamed, Nahed A. Abd El-Ghany, Mona M. Fahmy and Marwa H. Ahmed

*Advances in Polymer Technology, 35:136-145,(2016), IF:1.114*

Four novel antimicrobial maleimido phenyl thiourea derivatives were synthesized from N-[4-(chlorocarbonyl) phenyl] maleimide with phenyl thiourea and its derivatives (p-methyl, o-chloro, and p-carboxy). Their structures were characterized by FTIR, 1H NMR, mass spectra, and elemental analyses. Their antimicrobial activities against three types of bacteria (Bacillus subtilis, Streptococcus pneumoniae, and Escherichia coli) and against three crop-threatening pathogenic fungi (Aspergillus fumigatus, Geotricum candidum, and Syncephalastrum racemosum) were investigated. The results revealed that these derivatives are effective in inhibiting the growth of the tested bacteria and fungi as indicated from the inhibition zone diameter and minimum inhibitory concentration. The antibacterial activities of these derivatives were more effective against Gram-positive bacteria than Gram-negative bacteria. These derivatives were investigated as thermal stabilizers for rigid poly(vinyl chloride) at 180°C in air by measuring the rate of dehydrochlorination and the extent of discoloration. The results reveal the greater stabilizing efficiency of the investigated derivatives as shown by their longer thermal stability periods (Ts) and lower dehydrochlorination rates in relation to dibasic lead carbonate, cadmium–barium–zinc stearate, and n-octyltin mercaptide industrial stabilizers. The stabilizing efficiency increases with the introduction of electron-donating substituent groups in the aromatic ring of the stabilizer molecules. Moreover, the investigated stabilizers

impart better color stability for the degraded samples as compared with the reference stabilizers.
**Keywords:** Antimicrobial activity; Dehydrochlorination rate; Discoloration degree; Maleimido phenyl thiourea derivatives; Pvc.

## B-198. Alkoxide-Directed Hydride Addition to A, Unsaturated Sultones

Kamal M. Dawood, Andrea Bramborg, Ahmed F. Darweesh, Katrin Spinde, Victor Rogachev, Anne Jäger and Peter Metz

*Heterocycles, 93: 723-736, (2016), IF: 1.107*

Seven- and eight-membered β,γ-unsaturated sultones were readily prepared by ring closing metathesis. Epoxidation of these sultones and of an analogous six-membered sultone furnished the corresponding β,γ-epoxy sultones efficiently. Treatment of these epoxides with a suitable base gave α,β-unsaturated γ-hydroxy sultones in high yields. Reduction of both the α,β-unsaturated γ-hydroxy sultones and the epoxy sultones by Red-Al is likely to proceed in a hydroxyl-directed fashion via a mixed aluminate as the reactive intermediate.
**Keywords:** Sultones; Alkoxide-Hydride addition.

## B-199. An Efficient Synthesis of 1-(4H-1,2,4-Triazol-3-Yl)-Hexahydroquinoline-3 – Carbonitrile and Their Spiro Derivatives from B-Enaminones

Ismail A. Abdelhamid, Said A. Soliman Ghozlan, Doaa M. Abdelmoniem and Amr M. Abdelmoniem

*Heterocycles, 92: 637-648, (2016), IF: 1.107*

A series of N-((1,2,4-triazol-3-yl)-enamine and N-((1,2,3-triazol-4-yl)-enamine were prepared and reacted with α,β-unsaturated nitriles yield novel N-(4H-1,2,4-triazol-3-yl)-hexahydroquinoline-3-carbonitrile and their fused and spiro derivatives. Dimroth type rearrangement of the prepared quinoline derivatives 7a,b and 15a,b was observed in acetic anhydride leading to the formation of substituted pyrimido[4,5-b]quinoline 11a,b, spiro[indoline-3,5'-pyrimido[4,5-b]quinoline] 19 and spiro[indoline-3,5'-[1,3]oxazino[4,5-b]quinoline] 22.
**Keywords:** N-((1,2,3-Triazol-4-Yl); Enamine; Hexahydroquinoline; Pyrimido[4,5-B]Quinoline; Isatin; Spiro-indoline.

## B-200. Application of Mannich and Michael Reactions in Synthesis of Pyridopyrimido[2,1 – B][1,3,5]Thiadiazinones and Pyridopyrimido[2,1-B][1,3]Thiazinones as Anticancer Agents

Sobhi M. Gomha, Magda A. Abdallah, Mahmoud A. Mourad and Mahmoud M. Elaasser

*Heterocycles, 92: 688-699, (2016), IF: 1.107*

A new series of pyrido[2',3':4,5]pyrimido[2,1-b][1,3,5]thiadiazinones were prepared by aminomethylation of pyridopyrimidinethione with a variety of primary aromatic amines and formaldehyde solution (37%) through Mannich reaction. Also, another series of pyrido[2',3:4,5]pyrimido[2,1-b][1,3]thiazinones were synthesized by Micheal addition reaction of pyridopyrimidinethione to the activated double bond of a number of arylidene malononitrile and ethyl 3-aryl-2-cyanopropenoate. The mechanism of formation of the synthesized compounds was discussed and the assigned structure was established via microanalysis and spectral data (IR, 1HNMR and Mass). In addition, the antitumor activities of the synthesized compounds were investigated in comparison with the well-known anticancer standard drugs doxorubcin and Imatinib using MTT assay. The results revealed that the tested compounds showed high variation in the inhibitory growth rates and activities against the tested tumor cell lines in a concentration dependent manner. The highest activity was measured for compound 4g against human hepatocellular carcinoma (HepG2) cells and compound 4i in case of breast carcinoma (MCF-7) cells compared with reference drug imatinib. These results revealed that these compounds exhibited promising antitumor activities
**Keywords:** Ethylidenethiosemicarbazide; Hydrazonoyl Halides; 1,3-Thiazole; 1,3,4 – Thiadiazoles.

## B-201. Dabco-Catalyzed Green Synthesis of Thiazole and 1,3-Thiazine Derivatives Linked to Benzofuran

Sobhi M. Gomha, Mohamed G. Badrey and Wael A. A. Arafa

*Heterocycles, 92: 1450-1461, (2016), IF: 1.107*

An eco-friendly and simple procedure for the reaction of 2-(1-(benzofuran-2-yl)ethylidene)hydrazinecarbothioamide with arylidenemalononitriles and hydrazonoyl halides catalyzed by using sterically hindered organic base, 1,4-diazabicyclo[2.2.2]octane (DABCO) was described. This new protocol has the advantage of good yields and short reaction times. The structure of the newly synthesized compounds was elucidated via elemental analyses and spectral data.
**Keywords:** Thiazoles; 1,3-Thiazines; Thiosemicarbazone; Hydrazonoyl halides.

## B-202. Microwave Assisted Multi-Component Synthesis of Novel Bis(1,4-Dihydropyridines) Based Arenes or Heteroarenes

Sherif M. H. Sanad, Refaie M. Kassab, Ismail A. Abdelhamid, and Ahmed H. M. Elwahy

*Heterocycle, 92: 910-924, (2016), IF: 1.107*

A synthesis of novel bis-1,4-DHPs was reported. Two possible synthetic approaches for these compounds were investigated. In the first approach the monopodal 1,4-DHPs were used as building blocks for the construction of the target molecules via a simple alkylation. In the second strategy the appropriate bis-aldehydes have been synthesized in a first step followed by reaction with four equivalents of 3-aminobut-2-enenitrile using different catalysts under microwave irradiation as well as under conventional heating to give the corresponding bis-1,4-DHPs in good to excellent yield. The oxidative aromatization of some derivatives of the latter compounds into the corresponding bis-2,6-dimethylpyridine-3,5-dicarbonitrile derivatives was achieved using ceric ammonium nitrate (CAN).
**Keywords:** Bis-1,4-Dhps; Bis-Aldehydes; Oxidative Aromatization; Oxidative aromatization.

## B-203. Synthesis and Antimicrobial Evaluations of Novel Spiro Cyclic 2-Oxindole Derivatives of N-(1H-Pyrazol-5-Yl)-Hexahydroquinoline Derivatives

Said Ahmed Soliman Ghozlan, Muhammed Ali Ramadan, Amr Mohamed Abdelmoniem and Ismail Abdelshafy Abdelhamid

*Heterocycles, 92: 1075-1084, (2016), IF: 1.107*

A novel series of interesting spiro cyclic 2-oxindole derivatives of N-(1H-pyrazol-5-yl)hexahydroquinoline derivatives were prepared via the versatile readily accessible cyclic β-enaminones incorporating pyrazole. Antimicrobial evaluations were performed on the prepared compounds. Most of these compounds exhibited high to moderate antimicrobial activity.
**Keywords:** B-Enaminone; Spiro-Oxindole; Pyrazole; Hexahydroquinoline; Antimicrobial evaluation.

## B-204. Synthesis of some Novel Thiadiazoles and Thiazoles Linked to Pyrazole Ring

Magda A. Abdallah, Sobhi M. Gomha, Mohamad R. Abdelaziz, and Nany S. Eldin Serag

*Heterocycles, 92: 649-663, (2016), IF: 1.107*

The novel compound namely ethyl 3-(1-(2-(2-cyanoacetyl)-hydrazono)ethyl)-1,5-diphenyl-1H-pyrazole-4-carboxylate 3 was used as key intermediate for synthesizing the thioanilide derivative 4 and the arylidene derivatives 6. The reaction of 4 with a number of haloketones and haloesters furnished the respective thiazole derivatives 8, 10 and 11a,b. Moreover, the reaction of 4 with N-aryl-2-oxopropane hydrazonoyl chloride 13 and ethyl (N-arylhydrazono)chloroacetate 17 in absolute ethanol in the presence of triethylamine at reflux afforded a new series of thiadiazoles 15 and 19, respectively. The mechanisms that account for formation of products 15 and 19 were discussed. Also, the structures of all the newly synthesized products were confirmed based on elemental analysis, spectral data and by alternative methods.
**Keywords:** Imidazole; 1,3,4-Thiadiazole; Hydrazonoyl halide; Cytotoxicity evaluation.

## B-205. Synthesis of some Novel Thiazole, Thiadiazole and 1,4- Phenylene – Bis-Thiazole Derivatives as Potent Antitumor Agents

Sobhi M. Gomha, Fathy M. Abdelrazek, Aly H. Abdelrahman and Peter Metz

*Heterocycles, 92: 954-967, (2016), IF: 1.107*

A novel series of 2-ethylidenehydrazono-5-arylazothiazoles 5a-h and 2-ethylidenehydrazono-5-arylazothiazolones 9a-d were prepared by cyclocondensation of hydrazonyl halides 3a-h and 7a-d with ethylidenethiosemicarbazide 2. In addition, reaction of 2 with N-phenylcarbohydrazonyl chloride (14), afforded 1,3,4-thiadiazole derivative 17 as the end product. Moreover, the thiosemicarbazide derivative 2 was reacted with various bromoacetyl compounds 19a-d and 1,1'-(1,4-phenylene)bis(2-bromoethanone) (21) furnished the respective thiazole derivatives 20a-d and 1,4-phenylene-bisthiazole derivative 22. The structures of the newly synthesized compounds were established on the basis of spectroscopic evidences and their alternative syntheses. The newly synthesized compounds were evaluated for their antitumor activities against hepatocellular carcinoma (HepG2) cell line and the results revealed promising activities of compounds 5h, 5d, 5g, 5f and 5e with IC50 equal 2.23 ± 0.28, 2.48 ± 0.34, 2.49 ± 0.24, 4.03 ± 0.11, and 5.32 ± 0.27 μM, respectively.
**Keywords:** Thiazoles; Thiadizoles; Cyclocondensation; Hydrazonyl halides.

## B-206. An efficient one-pot, three-component synthesis of 6-cyano-hexahydro-4H-thieno[3'',2'':5,6]pyrimido[1,2-a]quinoline – 2-carboxylates and their spiro derivatives from β-enaminones

Said Ahmed Soliman Ghozlan, Doaa Mohamed Abdelmoniem, Amr Mohamed Abdelmoniem and Ismail Abdelshafy Abdelhamid

*Turkish Journal of Chemistry, 40: 434-440, (2016), IF: 1.098*

A simple and efficient one-pot synthesis of novel thieno[3',2':5,6]pyrimido[1,2-a]quinoline-2-carboxylates (5a-d) and their spirooxindole derivatives (12a-d) was accomplished. Thus, the Michael addition reaction of the cyclic enaminone 3 with the corresponding α,β-unsaturated nitrile derivatives 4a-d in refluxing EtOH in the presence of piperidine afforded 5a-d in good yields. On the other hand, spirooxindole derivatives 12a-d were synthesized by the reaction of cyclic β-enaminone 3 with the corresponding 3-cyanomethylidene-2-oxoindoles 11a-d in refluxing EtOH.
**Keywords:** Cyclic enaminones; A,B-Unsaturated nitriles; Hexahydroquinolines;multicomponent reaction; Spirooxindoles.

## B-207. Ecofriendly One-Pot Synthesis and Antiviral Evaluation of Novel Pyrazolyl Pyrazolines of Medicinal Interest

Sobhi Gomha, Magda Abdallah, Mohamad Abd El-Aziz and Nany Serag

*Turkish Journal of Chemistry, 40: 484-498, (2016), IF: 1.098*

Ethyl 3-acetyl-1,5-diphenyl-1H-pyrazole-4-carboxylate reacts with a variety of arylaldehydes by grinding method in the presence of a catalytic amount of sodium hydroxide at ambient temperature to give the respective chalcones. The latter compounds react also by grinding method with nitrogen nucleophiles such as hydrazine hydrate, phenyl-hydrazine, and thiosemicarbazide to afford the corresponding pyrazol-3-yl pyrazolines. A series of 6-pyrazolylpyrimidine-2-thione derivatives were prepared by reaction of the above chalcones with thiourea by grinding method in the presence of a catalytic amount of sodium hydroxide at room temperature. In addition, 7-pyrazolylpyridopyrimidine-3-thione was prepared by reaction of chalcone with 6-aminothiouracil. All the newly synthesized compounds were characterized on the basis of elemental analysis and spectral data (IR, 1H and 13CNMR, mass). Moreover, some of the products were evaluated for their antiviral activity against the herpes virus at different concentrations. The results obtained indicated that compounds 4a, 4b, 4f, 5a, 5b, and 5c have promising activity.
**Keywords:** Chalcones; Pyrazolines; Pyrimidines; Pyridopyrimidines; Grinding; Antiviral activity.

## B-208. Synthesis and Evaluation of Some Novel Thiazoles and 1,3-Thiazines as Potent Agents Against the Rabies Virus

Magda Abdallah, Sobhi Gomha, Mohamad Abd El-aziz and Nany Serag

*Turkish Journal of Chemistry, 40: 441-453, (2016), IF: 1.098*

A series of novel thiazoles and 1,3-thiazine derivatives were synthesized in good yield via reaction of ethyl 3-(1-(2-thiocarbamoylhydrazono)ethyl)-1,5-diphenyl-1H-pyrazole-4-carboxylate with hydrazonoyl halides and arylidenemalononitriles, respectively. The structure of the newly synthesized products was elucidated via elemental analysis, spectral data, and alternative routes whenever possible. Moreover, the antiviral screening of the products was evaluated and the results revealed that some of them have strong to moderate potency against the rabies virus compared with the reference drug.
**Keywords:** Thiazoles; 1,3-Thiazines; Thiosemicarbazone; Hydrazonoyl halides; Antiviral evaluation.

## B-209. Synthetic Access to Some New Benzothiazole-Based 1,3,4-Thiadiazole and 1,3-Thiazole Derivatives

Kamal M. Dawood, Eman A. Ragab and Korany A. Ali

*Turkish Journal of Chemistry, (2016) 40: 277-282, (2016), IF: 1.098*

(Benzothiazol-2-yl)-3-phenylthiourea 2 was prepared and treated with hydrazonoyl chlorides 3a{e to yield thecorresponding 5-(benzothiazol-2-ylimino)-1,3,4-thiadiazole derivatives 6a{e, respectively. Reaction of the thiourea derivative 2 with ethyl 2-chloro-3-oxobutanoate 9 afforded the corresponding 2-(benzothiazol-2-ylimino)thiazole- 5-carboxylate derivative 11. The newly synthesized heterocyclic derivatives were conrmed from their elemental and spectral analyses.
**Keywords:** Benzothiazole; Thiazole; Thiadiazole; Thiourea; Hydrazonoyl chlorides.

## B-210. Optimizing the Preparation Conditions of Activated Carbons from Olive Cake Using Koh Activation

Nour T. Abdel Ghani, Ghadir A. ElChaghaby, Mohamed H. ElGammalq and ElShaimaa A. Rawash

*New Carbon Materials, 31 (2016) IF: 0.993*

Activated carbons were prepared from olive cake waste by KOH activation. A full factorial 23 experimental design was used to optimize their preparation conditions. The factors and levels included are activation temperature (600 and 900 益), activation time (1 and 3 h) and impregnation ratio (1 颐2 and 1 4). The surface area of the activated carbons was chosen as a measure of the optimization. The surface and pore properties of the activated carbon obtained at the optimum conditions were characterized by nitrogen adsorption, infrared spectroscopy and scanning electron microscopy. Results indicated that all factors and their interactions are significant (p<0. 05). A function was used to correlate the surface area of the activated carbons to their preparation conditions with a correlation coefficient of 99. 2% . The activated carbon prepared at the optimum conditions has a BET surface area of 672 m2 / g and an average pore size of 2. 05 nm with micro and mesopore volumes of 81. 36 and 18. 37% , respectively.
**Keywords:** Olive cake; Activated carbon; Potassium hydroxide Impregnation; Desirability function; Porosity.

## B-211. Biodegradable/Biocompatible Coated Metal Implants for Orthopedic Applications

Mohamed M. Saleh, A.H. Touny , Mohammed A. Al-Omair and M.M. Saleh

*Bio-Medical Materials and Engineering, 27: 87-99, (2016), IF: 0.988*

Biocompatible metals have been suggested as revolutionary biomaterials for bone-grafting therapies. Although metals and their alloys are widely and successfully used in producing biomedical implants due to their good mechanical properties and corrosion resistance, they have a lack in bioactivity. Therefore coating of the metal surface with calcium phosphates (CaP) is a benign way to achieve well bioactivity and get controlled corrosion properties. The biocompatibility and bioactivity calcium phosphates (CaP) in bone growth were guided them to biomedical treatment of bone defects and fractures. Many techniques have been used for fabrication of CaP coatings on metal substrates such as magnesium and titanium. The present review will focus on the synthesis of CaP and their relative forms using different techniques especially electrochemical techniques. The latter has always been known of its unique way of optimizing the process parameters that led to a control in the structure and characteristics of the produced materials.
**Keywords:** Calcium phosphate; Scaffold; Biomaterial; Biodegradable; Composite.

## B-212. Phytochemical Investigation of Boscia Angustifolia A. Rich. (Capparaceae)

Maha M. Salem , Sameh R. Hussein, Reham El-Sharawy, Eman A. Ragab , Kamal M. Dawood and Sabry I.M. El Negoumy

*Biochemical Systematics and Ecology, 65: 202-204, (2016), IF: 0.988*

Boscia angustifolia A. Rich. leaves were collected and subjected to a phytochemical investigation. Ten compounds; six flavonols, two coumarins, one methyl benzoate and one phthalate compound were isolated and identified for the first time from the studied taxa. Tamarixetin-3-O-β-sophoroside-7-O-methylether and rhamnocitrin-3-O-β-sophoroside are reported here as new natural compounds. The chemosystematic relationship between Boscia species is also discussed
**Keywords:** Boscia angustifolia; Capparaceae; Flavonoids; Chemosystematics.

## B-213. Radiation-Induced Coloration of Xylenol Blue/Film Containing Hexachloroethane for Food Irradiation Applications

Yasser S. Soliman, W. B. Beshir, A. A. Abdel-Fattah, Ramy Amer Fahim and Bahgat E. El-Anadouli

*Journal of Radioanalytical and Nuclear Chemistry, 310: 117-124, (2016), IF: 0.983*

Polyvinyl butyral films mixed with xylenol blue (XB) indicator and hexachloroethane (HCE) were prepared for possible application in food irradiation. Upon γ–irradiation the films undergo visual color change from yellow (XB, pH 8) to red (XB, pH 2.8) by H+ formation in the presence of HCE. The dosimetric characteristics of films containing different dye and HCE concentrations were investigated spectrophotometrically at λmax 555 nm. Radiation sensitivity is enhanced with HCE and, accordingly red color intensity. The prepared films can be applicable in dose range 0.25–10 kGy with uncertainty of dose reaching 4.45 % at 1σ.

**Keywords:**Xylenol blue; Hexachloroethane; Film dosimetry; Indicators.

## B-214. A Convenient Synthesis of Novel 1,3-Phenylene Bridged Bis-Heterocyclic Compounds

Hamdi M. Hassaneen, Ahmad S. Shawali and Fatma M. Saleh

*Journal of Sulfur Chemistry, 37: 241-250, (2016), IF: 0.945*

Reactions of bis-hydrazonoyl bromide 1 with each of phenyl-5-arylidene-2-thioxo-thiazol-4-one, triazinethiones and 4,6-dimethyl-2,6-dioxocyclohexane-1-thiocarboxanilide as sulfur dipolarophilic reagents led to the formation of the hitherto unreported 1,3-phenylene bis-heterocycles 4, 8 and 10, respectively. The structures of the isolated products were established on the basis of their elemental and spectral analyses. The mechanism and the site selectivity in the studied reactions are discussed.

**Keywords:** Cycloaddition; Bis-Nitrilimines; Heterocycles; Bis-Hydrazonoyl halides; Spirocycloadducts.

## B-215. Preparation, Characterization of Metallic Iron and Bimetallic Iron/Copper Nanoparticles and Their Application for the Removal of Trihalomethanes from Potable Water

Abeer M. E. Hassan, S.A. Abo El- Enein, Gehad G. Mohamed and Amr.I. Mohamed

*Jokull Journal, 66(7): 1-23, (2016), IF: 0.833*

Trihalomethanes (THMs) are formed when chlorine reacts with organic matter in water and including four compounds chloroform (CHCl3), bromodichloromethane (CHBrCl2), dibromochloromethane (CHBr2Cl) and bromoform (CHBr3). THMs are prevalent in Arab Public of Egypt Water Supplies, because more than 95% Egypt supplies are sourced from surface waters. Surface water sources contain higher levels of organic matter, compared to ground water sources, therefore surface waters have a greater THM formation potential. Also surface waters, in comparison with ground waters, vary in seasonal temperature which can also result in an increase in THMs. People can be exposed to THMs in drinking water in a number of ways; ingestion of drinking water, inhalation of indoor air largely due to volatilisation from drinking-water, inhalation and dermal exposure during showering and bathing. Acute effects of THMs in drinking water are rare. In this study, nanoscale zero-valent iron (NZVI) and Bimetallic Iron/Copper Nanoparticles were synthesized by iquid-phase reduction and used to remove THMs in actual drinking water from ElFustat plant including chloroform (CHCl3), bromodichloromethane (CHBrCl2), and dibromochloromethane (CHBr2Cl). The effects of dosage, initial pH , contact time and temperature on removal efficiency were also studied. Scanning electron microscopy showed uniformly NZVI particles with diameters less than 100 nm and also Bimetallic Iron/Copper Nanoparticles were scanned by Scanning electron microscopy. The removal efficiency was enhanced with the increasing amount of NZVI, the optimum dosage was 1.5 g/l for NZVI and 0.5 g/l for bimetallic Iron/Copper Nanoparticles. The kinetics model of the removal of THMs was in agreement with a pseudo-first-order model. Bimetallic Iron/Copper Nanoparticles accelerated removal rate of THMs over NZVI alone by its higher reactivity. The degradation products were analyzed using gas chromatography which showed that dehalogenation of THMs by NZVI and Bimetallic Iron/Copper Nanoparticles followed the order of CHBr2Cl > CHBrCl2 > CHCl3. NZVI particles and bimetallic iron/cupper are a promising sustainable material for potential application in elimination of THMs from actual drinking water.

**Keywords:** Trihalomethanes (Thms); Nanoscale; Zero-Valent Iron)Nzvi(Bimetalliciron; Copper nanoparticls.

## B-216. A New Strategy for Synthesis of Novel 1, 4-Phenylene Bridged Bis-Hetero - Cyclic Compounds

Hamdi M. Hassaneen, Ahmad S. Shawali and Lamiaa M. El Agaty

*Letters in Organic Chemistry, 13: 504-513, (2016), IF: 0.756*

Reactions of bis-hydrazonoyl chloride 1 with each of KSCN and KSeCN yielded the corresponding bis-thiadiazoline 2A and bis-selenadiazoline 2B. Bispyrazole derivatives 7a-e and 8a-b were also obtained by reactions of 1 with the appropriate active methylene compounds. Reactions of 1 with each of 1, 2-dicyanoethylene, acenaphthylene and phenyl-5-arylidene-2-thioxo-thiazol-4-one as dipolarophiles led to the formation of the corresponding cycloadducts 9, 12 and 14, respectively. Also, reaction of bis-hydrazonoyl chloride 1 with triazinethione 16a-e afforded 1,4-Bis-(1,2,4-triazolotriazin)benzene 17a-e. The structures of the compounds prepared were established on the basis of elemental and spectral analyses as well as their chemical reactions.

**Keywords:** Acenaphthalene; Acetylacetone; Bis-nitrilimine; Bis-Triazolotriazine; Bis-Pyrazole; Ethyl benzoylacetate; Malononitrile; Triazinethione.

## B-217. Modified Carbon Paste Electrode for Potentiometric Determination of Aluminium Ion in Spiked Real Water Sample

Marwa Elbadry Mohamed

*Russian Journal of Electrochemistry,52:754-761,(2016), IF:0.692*

The present paper describes the development of a new chemically modified carbon paste electrode based on azithromycin (AMC) that considered as a selective aluminium recognition agent in the CPE. This electrode was fully characterized in terms of composition, response time, usable pH range and temperature. The electrode exhibited a Nernstian response for Al+3 ion over a concentration range from 7.0 × 10–6 to 1.0 × 10–2 mol L–1 with a slope of 21.3 ± 0.18 mV decade–1 and the limit of detection was 6.0×10–6 mol L−1. It had a response time of about 6 s. The proposed sensor possesses a very good selectivity with respect to a variety of other cations. Finally this modified electrode was applied for the determination of the concentration of Al3+ ion in different water samples and the obtained results were comparable with those obtained with atomic absorption spectrometer (AAS).
**Keywords:** Aluminium determination; Potentiometry; Modified Carbon Paste Electrode; Ionophore.

## B-218. 3,4-Bis(Bromomethyl)Thieno[2,3-B]Thiophene: Versatile Precursors for Novel Bis(Triazolothiadiazines) Bis(Quinoxalines), Bis (Dihydrooxadiazoles) and Bis(Dihydrothiadiazoles)

Osama M. Sayed, Ahmed E. M. Mekky, Ahmad M. Farag and Ahmed H. M. Elwahy

*J. Heterocyclic Chem, 53: 1113-1120, (2016), IF: 0.685*

A synthesis of novel bis(triazolothiadiazines) 11–14, bis(quinoxalines) 16 and 17, bis(thiadiazoles) 24 and 25, and bis(oxadiazole) 31, which are linked to the thieno[2,3-b]thiophene core via phenoxymethyl group, was reported. Thus, reaction of the bis(α-bromoketones) 6 and 7 with the corresponding 4-amino-3-mercapto-1,2,4- triazole derivatives 8–10 in ethanol–DMF mixture in the presence of a few drops of triethylamine as a catalyst under reflux afforded the novel bis(5,6-dihydro-s-triazolo[3,4-b]thiadiazines) 11–14 in 60–72% yields. The bis (quinoxalines) 16 and 17 were also synthesized as a sole product in high yields by the reaction of 6 and 7 with o-phenylenediamine 15 in refluxing acetonitrile in the presence of piperidine as a catalyst. Cyclization of the bis(aldehyde thiosemicarbazones) 20 and 21 with acetic anhydride afforded the corresponding bis(4,5- dihydro-1,3,4-thiadiazolyl) derivatives 24 and 25 in good yield. Bis(5-phenyl-2,3-dihydro-1,3,4-oxadiazole) derivative 31 could be obtained in 67% yield by cyclization of the appropriate bis(N-phenylhydrazone) 29 in refluxing acetic anhydride for 3 h.
**Keywords:** Bis(Triazolothiadiazines); Bis(Quinoxalines); Bis(Thiadiazoles); Bis(Oxadiazole).

## B-219. Synthesis and Reactivity of Enaminones: A Facile Synthesis of Thiophene and 1,3,4-Thiadiazole Derivatives Incorporating A Thiazole Moiety

Kamal M. Dawood and Samia M. Sayed

*Journal of Heterocyclic Chemistry,53:1950-1955,(2016),IF:0.685*

Several new heterocyclic compounds such as thiophene derivatives have been synthesized by the reactions of the versatile unreported 3-mercapto-2-(4-methyl-2-(tosylamino)thiazole-5-carbonyl)-3-phenylaminopropenal () with chloroacetonitrile, ethyl 2-bromoacetate, and 1-aryl-2-bromoethanone derivatives. Reaction of potassium salt intermediate with hydrazonyl halides () to afford 1,3,4-thiadiazole derivatives incorporating a thiazole moiety has been described. All newly synthesized compounds were elucidated by considering the data of both elemental and spectral analysis.
**Keywords:** Enaminones; Thiophene; 1,3,4-Thiadiazole; Thiazole.

## B-220. A Facile Three-Component One-Pot Synthesis of some Novel Tricyclic Hetero-Ring Systems

Sobhi M. Gomha and Fathy M. Abdelrazek

*Journal of Heterocyclic Chemistry,53:1892-1896,(2016),IF: 0.685*

A novel, facile, one-pot, multicomponent reaction for the synthesis of a series of pyrano[2,3-d][1,2,4]triazolo[4,3-a]pyrimidine and pyrano[2′,3′:4,5]pyrimido[2,1-b][1,3,5]thiadiazine derivatives has been developed from reaction of 2,4-dichlorobezaldehyde, malononitrile, and the appropriate active methylene compounds in refluxing dioxane in the presence of chitosan. A plausible mechanism has been proposed for this reaction, and the structure of the newly synthesized compounds was all established on the basis of spectral data (mass, IR, and 1H-NMR) and elemental analyses.
**Keywords:** Thiazoles; Pyrazoles; Coupling reactions; Thiosemicarbazides; Anti-Cancer activity.

## B-221. An Efficient One-Pot Synthesis of Novel Spiro Cyclic 2-Oxindole Derivatives of Pyrimido[4,5-B]Quinoline, Pyrido[2,3-D:6,5-D′] Dipyrimidine and Indeno[2′,1′:5,6]Pyrido [2,3-D]Pyrimidine in Water

Amr Mohamed Abdelmoniem, Huwaida M. E. Hassaneen and Ismail Abdelshafy Abdelhamid

*Journal of Heterocyclic Chemistry,53:2084-2090,(2016),IF:0.685*

A novel and facile one-pot synthesis of spiro cyclic 2-oxindole derivatives of pyrimido[4,5-b]quinoline- 4,6-dione, pyrido[2,3-d:6,5-d′]dipyrimidine-2,4,6-trione, and indeno[2′,1′:5,6]pyrido [2,3-d]pyrimidine employing 6-aminothiouracil (or 6-aminouracil), isatin, and cyclic 1,3-diketone (e.g. 1,3-indanedione, dimedone, or barbituric acid) has been developed
**Keywords:** Spiro cyclic 2-Oxindole; Pyrimido[4,5-B]Quinoline; Pyrido[2,3-D:6,5-D′] Dipyrimidine; Indeno[2′,1′:5,6]Pyrido [2,3-D]Pyrimidine.

## B-222. Chemoselectivity in Reactions of Hydrazonoyl Halides with Ethyl 2(3H)-Permidinylideneacetate

Ahmed Sami Shawali, Thoraya A. Farghaly and Tarek M. S. Nawar

*Journal of Heterocyclic Chemistry, 5:909-914, (2016),IF:0.685*

Ethyl 2(3H)-permidinylideneacetate reacted with C-aryl-N-arylmethanehydrazonoyl and C-ethoxycarbonyl-N-arylmethanehydrazonoyl chlorides and in different ways yielding 2-(pyrazoliden-4-yl) perimidines and substituted

pyrrolo[1,2-a] perimidines , respectively. The mechanisms of the reactions studied are discussed, and the structures of the products were confirmed by spectral and elemental analyses and by alternate synthesis.
**Keywords:** 1,8-Diaminonaphthalene; Hydrazonoyl halides; Nitrilimines; Ketene aminals; Chemoselectivity.

## B-223. Green One-Pot Solvent-Free Synthesis of Pyrazolo[1,5-A]Pyrimidines, Azolo[3,4-D]Pyridiazines, and Thieno[2,3-B]Pyridines Containing Triazole Moiety

Abdou O. Abdelhamid, Tamer T. El-Idreesy, Nadia A. Abdelriheem and Huda R. M. Dawoud

*J. Heterocyclic Chemistry, 53: 710-718, (2016), IF: 0.685*

Synthesis of pyrazolo[1,5-a]pyrimidines, [1,2,4]triazolo[1,5-a]pyrimidine, 8,10-dimethyl-2-(5-methyl- 1-phenyl-4,5-dihydro-1H-1,2,3-triazol-4-yl)pyrido[2′,3′:3,4]-pyrazolo[1,5-a]pyrimidine, benzo[4,5]imidazo [1,2-a]pyrimidine via heterocyclic amines, and sodium 3-hydroxy-1-(5-methyl-1-phenyl-1H-1,2,3-triazole-4-yl) prop-2-en-1-one were carried out. Also, synthesis of isoxazoles, and pyrazoles from sodium 3-hydroxy-1- (5-methyl-1-phenyl-1H-1,2,3-triazole-4-yl)prop-2-en-1-one and hydroxymoyl chlorides and hydrazonoyl halides, respectively, were made. Analogously, (1,2,3-triazol-4-yl)thieno[2,3-b]pyridine derivatives were obtained from sodium 3-hydroxy-1-(5-methyl-1-phenyl-1H-1,2,3- triazole-4-yl)prop-2-en-1-one and cyanothioacetamide followed by its reacting with active methylene compounds. In addition to full characterization of all synthesized compounds, they were tested to evaluate their antimicrobial activities, and some compounds showed competitive activities to those of tetracycline, the typical antibacterial drug, and clotrimazole, the typical antifungal drug.
**Keywords:** Pyrazolo[1,5-A]Pyrimidines; [1,2,4]Triazolo[1,5-A]Pyrimidine; 1,2,3-Triazole.

## B-224. Hydrazononitriles as Precursors for 4-Aminotriazoles and 3-Aminoisoxazoles: One Pot Synthesis of Triazolo[1,5-A]Quinazoline Derivatives

Ismail A. Abdelhamid, Amr M. Abdelmoniem, Said A. S. Ghozlan and Holger Butenschön

*Journal of Heterocyclic Chemistry, 53: 1251-1258, (2016), IF:0.685*

The reaction of various hydrazononitriles with hydroxylamine hydrochloride yielded various products, namely, 3-aminoisoxazolone, 3-amino-1,2,4-triazole and 4-amino-1,2,3-triazole derivatives depending on the nature of substituents.
**Keywords:** Hydrazononitriles; 3-Aminoisoxazole; 3-Amino-1,2,4-Triazole; 4-Amino-1,2,3-Triazole; Triazolo[1,5-A]Quinazoline.

## B-225. Isoxazolopyrimidinethione and Isoxazolopyridopyrimidinethione Derivatives: Key Intermediates for Synthesis of Novel Fused Triazoles as Potent 5A-Reductase Inhibitors and Anti-Prostate Cancer

Sobhi M. Gomha, Mohamed G. Badry and Mohamed M. Abdallad

*Journal Heterocyclic Chemistry, 53: 558-565, (2016) IF: 0.685*

The arylideneisoxazolone derivative 1 is used for preparation of two different pyrimidinethiones 3 and 5 through interaction with thiourea and thiouracil, respectively. Compounds 3 and 5 were subjected to reaction 53with different hydrazonyl halides in basic medium to afford different triazolopyrimidines 9a–h and 13a–f, the structures were confirmed by their spectral and elemental analysis. All the newly synthesized products were screened against 5α-reductase. Some of the newly synthesized compounds showed potent 5α-reductase inhibition activities with good ED50
**Keywords:** Heterocycles; Hydrazonoyl halides; Anticancer agents.

## B-226. Regioorientation in the Addition Reaction of A-Substituted Cinnamonitrile to Enamines Utilizing Chitosan as A Green Catalyst: Unambiguous Structural Characterization Using 2D-Hmbc Nmr Spectroscopy

Said A. S. Ghozlan،Ahmed Gamal Ahmed and Ismail Abdelshafy Abdelhamid

*Journal of Heterocyclic Chemistry,53:817-823,(2016),IF: 0.685*

Hexahydroquinolines and their fused derivatives are obtained in good to excellent yields by proceeding through a simple, mild, and efficient procedure including the reaction of enamines with substituted cinnamonitriles using DABCO, piperidine, or chitosan as catalysts. The regioorientation of Michael addition was established with no doubt using the 2D-HMBC spectroscopy.
**Keywords:** Hexahydroquinolines; Cinnamonitriles; Dabco; Regioorientation; 2D-HMBC.

## B-227. Synthesis and Characterization of Bisimidazoles, Bistriazoles, Bisthiadiazoles, and Bisthiazoles from Novel Bishydrazonoyl Dichlorides

Abdelwahed R. Sayed, Sobhi M. Gomha and Thoraya A. Farghaly

*Journal of Heterocyclic Chemistry,53:255-262,(2016), IF:0.685*

We have synthesized a number of bisimidazoles, bistriazoles, and bisthiadiazoles derivatives based on new bishydrazonoylchlorides. Structures of the final products were elucidated by elemental analysis and spectral data.
**Keywords:** Bisimidazoles; Bistriazoles; Bisthiadiazoles; Bisthiazoles.

## B-228. Synthesis and Reactivity of Enaminones: A Facile Synthesis of Thiophene and 1,3,4-Thiadiazole Derivatives Incorporating a Thiazole Moiety

Kamal M. Dawood and Samia M. Sayed

*Journal of Heterocyclic Chemistry :* 53, 1950-1955 (2016). *IF:0.685*

Several new heterocyclic compounds such as thiophene derivatives have been synthesized by the reactions of the versatile unreported 3-mercapto-2-(4-methyl-2-(tosylamino)thiazole-5-carbonyl)-3-phenylaminopropenal (7) with chloroacetonitrile, ethyl 2-bromoacetate, and 1-aryl-2-bromoethanone derivatives. Reaction of potassium salt intermediate 6 with hydrazonyl halides (14a–c) to afford 1,3,4-thiadiazole derivatives incorporating a thiazolemoiety has been described. All newly synthesized compounds were elucidated by considering the data of both elemental and spectral analysis.

## B-229. Synthesis and Reactivity of Phenylthiourea Derivatives: an Efficient Synthesis of New Thiazole-Based Heterocycles

Samia M. Sayed, Mohamed A. Raslan and Kamal M. Dawood

*Journal of Heterocyclic Chemistry, 53: 508-512, (2016), IF:0.685*

Reaction of 1-(5-acetyl-4-methylthiazol–2-yl)–3-phenylthiourea with hydrazonoyl chlorides and yielded the corresponding (thiazolyl)imino–1,3,4-thiadiazole derivativesand , respectively. Reaction of with ethyl chloroacetate gave (thiazolyl)imino-1,3-thiazolidin-4-one derivative , which upon condensation with aromatic aldehyde derivatives yielded the 5-benzylidene derivatives. In addition, treatment of with 3-chloropenta-2,4-dione afforded the corresponding (thiazolyl)imino-1,3-thiazole derivative . The newly synthesized compounds were confirmed from their elemental analyses and spectral data.

**Keywords:** Phenylthiourea; 1,3-Thiazole; 1,3,4-Thiadiazole; Hydrazonoyl chloride.

## B-230. Synthesis of Pyrazolyl-Pyrazoles and Pyrazolyl-[1,2,4] – Triazolo[3,4-D][1,5]Benzothiazepines as P53 Activators Using Hydrazonoyl Chlorides

Sobhi M. Gomha, Thoraya A. Farghaly, Abdelwahed R. Sayed and Mohamed M. Abdalla

*Journal of Heterocyclic Chemistry, 53: 1503-1509, (2016), IF:0.685*

Di-pyrazoles, tripyrazoles, and pyrazolyltriazolobenzothiazepines were prepared from α,β-unsaturated ketones and hydrazonoyl chlorides. The structure of all the newly synthesized compounds was established on the bases of their spectral data and elemental analyses. The activity of all products was examined as p53 ubiquitination which showed promising activities.

**Keywords:** Pyrazoles; Triazolo[3,4-D][1,5]Benzothiazepines; Hydrazonoyl chlorides; Ic50 of P53 Ubiquitination.

## B-331. Ultrasound Assisted Synthesis of some Novel Bis-Pyridazine Derivatives

Ahmed E. M. Mekky and Abdullah S. Al-Bogami

*Journal of Heterocyclic Chemistry, 53: 595-605, (2016), IF:0.685*

Bis-enaminone 3 was coupled with aryldiazonium chlorides 4a, 4b to afford the bis-arylhydrazonopropanals 6a, 6b. Compounds 6a, 6b could be utilized for the synthesis of a variety of bis-(dimethyl 2,3-dihydropyridazine-3,4-dicarboxylate), bis-(pyridazin-3(2H)-one), bis-(2,3-dihydropyridazine-4-carbonitrile) and bis-(3-imino-2,3-dihydropyridazine) derivatives, under ultrasonic irradiation. A comparative study of aforementioned reactions was carried out under conventional method as well as under ultrasonic irradiation conditions.

**Keywords:** Biological-Activity; Irradiation; Microwave; Inhibitors; Chemistry; Sonochemistry.

## B-232. Useful Precursors for Synthesis of Some New Azolo[3,4-D]Pyridiazines, Azolo[1,5-A]Pyrimidines, Azolo[5,1-C]Triazines, Pyrazoles, and Benzo[B] [L,4]Diazepine

Abdou O. Abdelhamid, Abdelgawad A. Fahmi and Basma S. Baaiu

*J. Heterocyclic Chemistry, 53: 1917-1927, (2016), IF: 0.685*

Pyrazolo[3,4-d]pyridazines, isoxazolo[3,4-d]pyridazines, azolo[1,5-a]pyrimidines, azolo[5,1-c]triazines, pyrazoles, and benzo[b][l,4]diazepine were synthesized from the appropriate hydrazonoyl halides, hydroximoyl halides, heterocyclic amines, diazotized heterocyclic amines, arenediazonium chlorides, and o-phenylenediamines with appropriate of sodium 3-(5-bromobenzofuran-2-yl)-3-oxoprop-1-en-1-olate or 1-(5-bromobenzofuran-2-yl)-3-(dimethylamino)prop-2-en-1-one.
The newly synthesized compounds were elucidated by elemental analyses, spectral data, and alternative synthesis whenever possible.

**Keywords:** Pyrazolo[3,4-D]Pyridazines; Isoxazolo[3,4-D]Pyridazines; Azolo[1,5-A]Pyrimidines; Azolo[5,1-C]Triazines.

## B-233. Heterocyclisation of 2,5-Diacetyl-3,4-Disubstituted-Thieno[2,3-B]Thiophene Bis-Thiosemicarbazones Leading to Bis-Thiazoles and Bis-1,3,4-Thiadiazoles as Anti-Breast Cancer Agents

Sobhi M. Gomha, Mohamed G. Badrey and Mastoura M. Edrees

*Journal of Chemical Research, 40: 120-125, (2016), IF: 0.661*

In this paper, the synthesis of bis-thiazoles and bis-1,3,4-thiadiazoles linked to a thienothiophene nucleus is described. The synthesis was achieved through interaction between 2,5-diacetylthieno[2,3-b]thiophene bis-thiosemicarbazones with a variety of hydrazonyl halides in a basic medium. All the synthesised compounds were characterised by IR, 1H NMR, 13C NMR and mass spectroscopic analyses. The newly synthesised compounds represent a variety of novel

polyheteroatomic moieties containing nitrogen and sulfur. Most of the synthesised compounds were evaluated for their antitumour activity against the breast cancer MCF-7 cell line. The results revealed that four compounds are equipotent to tamoxifen (IC50 = 8.04 µg mL–1) with IC50 = 8.23, 8.26, 8.68 and 9.12 µg mL–1 respectively.

**Keywords:** Bis – Thiazoles; Thienothiophenes; Thiosemicarbazone; Hydrazonoyl halides; Anti-Breast cancer Agents.

## B-234. Hydrazonoyl Chlorides in the Synthesis of Pyrazolo[5,1-C][1,2,4]Triazole Derivatives and Their Biological Activities

Thoraya A. Farghaly, Sobhi M. Gomha, Eman K. Mousa and Mahmoud Elaasser

*Journal of Chemical Research, 40: 467-470, (2016), IF: 0.661*

A new series of 7-arylazopyrazolo[5,1-c][1,2,4]triazoles was synthesised via reaction of 3-amino-4-(arylhydrazono)-4,5-dihydropyrazol-5ones with hydrazonoyl halides using triethylamine as a basic catalyst. The structure of all the synthesised compounds was confirmed on the basis of elemental and spectral analyses. Moreover, the antimicrobial and antitumour activities of these compounds were evaluated and the results obtained indicate the weak efficacy of some of them as antibacterial agents. However, the results of antitumour activity against HepG-2 liver cancer and HCT-116 colon cancer of some derivatives showed good activity in comparison with the reference drugs.

**Keywords:** 3Aminopyrazoles; Pyrazolotriazoles; Antimicrobial activity; Antitumour activity.

## B-235. Conformation and Electronic Structure of Carbidopa. A Qm/Md Study

Ghader M. Sukker, Nuha Wazzan, Ashour Ahmed and Rifaat Hilal

*Journal of Theoretical and Computational Chemistry, 15(1): 1650002-22, (2016), IF: 0.619*

Carbidopa (CD) is a drug used in combination with L-dopa (LD) in treatment of Parkinson's disease (PD). CD is an inhibitor for enzyme decarboxylase, yet its mode of action is not entirely known although it is believed to involve enzyme shape recognition. The present work attempts to investigate the conformational preferences of CD. Tight geometry optimization at the density functional theory (DFT)/B3LYP/6-311þþG** level of theory has been carried out. The shallow nature of the potential energy surface (PES) and the presence of several local minima within a small energy range necessitate the launching of DFT-based molecular dynamics (MD) simulations. Two MD experiments were submitted for 35,000 points each. The complete trajectory in time domain of 10.5 ps is analyzed and discussed. The global minimum energy structure of CD is localized and identi¯ed by subsequent frequency calculations. The quantum theory of atom in molecules (QTAIMs) is used to extract and compare the quantum chemical topology features of the electron density distribution in CD and LD. Bonding characteristics are analyzed and discussed within the natural bond orbital (NBO) framework.

**Keywords:** Carbidopa; Parkinson's Disease; Dft calculations; Quantum dynamics; Qtaim.

## B-236. Robust and Optimal Control of Magnetic Microparticles Inside Fluidic Channels with Time-Varying Flow Rates

Islam S.M. Khalil, Hazem Abass, Mostafa Shoukry1, Anke Klingner, Rasha M. El-Nashar , Mohamed Serry and Sarthak Misra

*International Journal of Advanced Robotic Systems, 13 (2016) IF: 0.615*

Targeted therapy using magnetic microparticles and nanoparticles has the potential to mitigate the negative side-effects associated with conventional medical treatment. Major technological challenges still need to be addressed in order to translate these particles into in vivo applications. For example, magnetic particles need to be navigated controllably in vessels against flowing streams of body fluid. This paper describes the motion control of paramagnetic microparticles in the flowing streams of fluidic channels with time-varying flow rates (maximum flow is 35 ml.hr−1). This control is designed using a magnetic-based proportional-derivative (PD) control system to compensate for the time-varying flow inside the channels (with width and depth of 2 mm and 1.5 mm, respectively). First, we achieve point-to-point motion control against and along flow rates of 4 ml.hr−1, 6 ml.hr−1, 17 ml.hr−1, and 35 ml.hr−1. The average speeds of single microparticle (with average diameter of 100 µm) against flow rates of 6 ml.hr−1 and 30 ml.hr−1 are calculated to be 45 µm.s−1 and 15 µm.s−1, respectively. Second, we implement PD control with disturbance estimation and compensation. This control decreases the steady-state error by 50%, 70%, 73%, and 78% at flow rates of 4 ml.hr−1, 6 ml.hr−1, 17 ml.hr−1, and 35 ml.hr−1, respectively. Finally, we consider the problem of finding the optimal path (minimal kinetic energy) between two points using calculus of variation, against the mentioned flow rates. Not only do we find that an optimal path between two collinear points with the direction of maximum flow (middle of the fluidic channel) decreases the rise time of the microparticles, but we also decrease the input current that is supplied to the electromagnetic coils by minimizing the kinetic energy of the microparticles, compared to a PD control with disturbance compensation.

**Keywords:** TimeVarying Flow; Magnetic; Microfluidicchannel; Microparticles; Disturbance; Optimal control.

## B-237. Rp-Hplc Stability-Indicating Method for Estimation of Irbesartan and Hydrochlorothiazide in Bulk and Pharmaceutical Dosage form

Tamer Awad Ali1, Gehad G. Mohamed, Ali A. Aglan and Fakiha El-Taib Heakal

*Chinese Journal of Analytical Chemistry, 44 (2016) IF: 0.566*

A stability indicating RP-HPLC method was described and validated for the simultaneous determination of hydrochlorothiazide (HCTZ) and irbesartan (IRB) in combined pharmaceutical preparations. In this study, hydrochlorothiazide and irbesartan were degraded under different stress test conditions as recommended by the International Conference on

Harmonization (ICH). The degraded samples were used to develop a stability indicating high performance liquid chromatographic method (HPLC) for hydrochlorothiazide and irbesartan determination. The two drugs were separated from their degradation products using a reversed phase (C18) analytical column and a mobile phase consisted of 50 mM potassium di-hydrogen orthophosphate:acetonitrile (55:45, V/V) buffer (pH 2.5). The instrumental settings were optimized at flow rate of 1.3 mL min− 1, column temperature of 30 °C, detection wavelength of 210 nm and injection volume of 20 µL. The retention time of HCTZ and IRB was around 3 and 5.2 min, respectively. The method was validated for linearity, precision, accuracy, specificity, ruggedness and robustness. The results indicated that the described method was suitable for quantitative analysis of HCTZ and IRB in the presence of their degradation products formed under a variety of stress conditions. The proposed method was also applicable to the determination of stability of HCTZ and IRB drugs and was successfully used in quality control of bulk manufacturing and pharmaceutical preparations

**Keywords:** Irbesartan; Hydrochlorothiazide; High performance Liquid chromatographic; Validation methods; Stability; Degradation.

## B-238. Swelling Behavior of Cross-Linked Terephthaloyl Thiourea Carboxymethyl Chitosan Hydrogels

Nadia A. Mohamed and Nahed A. Abd El-Ghany

*Cellulose Chemistry and Technology, 50: 463-471, (2016), IF: 0.562*

Four cross-linked terephthaloylthioureacarboxymethyl chitosan (TTUCM-chitosan) hydrogels were prepared via cross-linking of carboxymethyl chitosan (CM-chitosan) with different concentrations of terephthaloyldiisothiocyanate. The swelling behaviors of the hydrogels at different pH values (4, 7 and 9) and temperatures (25, 35 and 45 ºC), as well as their electrical conductivity, have been investigated. The results reveal that the highest swellability was attained at 35ºC in acidic medium (pH 4), which indicated the dependence of the swellability of the hydrogels on pH and temperature. The results also indicated that the swellability percent of the prepared hydrogels increased with increasing of their cross-linking density, reaching their maximum values at 35ºC. On the other hand, the electrical conductivity of the hydrogels decreased with increasing cross-linking density and increased when rising the temperature up to 45ºC. It is expected that these smart hydrogels may be useful to develop drug delivery systems with improved drug loading capacity and controlled release behavior.

**Keywords:** Carboxymethyl chitosan hydrogels; Cross-Linking; Swellability; Ph-Dependent; Temperature; Dependent; Electrical conductivity.

## 239. Liquid Chromatographic Determination of Solifenacin Succinate, Flavoxate Hydrochloride and Tolterodine Tartrate in Bulk Drugs and Their Pharmaceutical Dosage Forms

Ali K. Attia, Eman Y. Z. Frag, Gehad G. Mohamed and Heba E. Ahmed

*Journal of the Chilean Chemical Society, 61(1): 2772-2776, (2016), IF: 0.429*

A simple, precise, specific and accurate reversed phase HPLC (RP-HPLC) method has been developed for the determination of solifenacin succinate (SOLS), flavoxate HCl (FLXHC) and toltoridine tartarate (TOLT) in bulk and pharmaceutical dosage forms. The proposed RP-HPLC method was carried out using Xterra RP-18 column (5 µm practical size, 25 cm x 4.6 mm i.d.). The flow rate, the injection volume and the detection wavelength were 1.0 mL/min, 20 mL and 200 nm, respectively. The mobile phase consisted of 0.05 M pentane sulfonic acid sodium salt (SOLS: pH 3.0±0.05, FLXHC and TOLT: pH 5.5±0.05) and acetonitrile (50:50 v/v). The retention times for SOLS, FLXHC and TOLT drugs were found to be 4.1±0.1 min, 4.3±0.0 min and 5.8±0.1 min, respectively. The calibration was linear over the concentration range of 0.1-100 µg/mL. The mean recoveries for SOLS, FLXHC and TOLT drugs were about 99.80%, 100.43% and 100.00%, respectively. The method was validated according to the ICH guidelines with respect to specificity, linearity, accuracy, precision and robustness.

**Keywords:** Solifenacin succinate; Flavoxate Hcl; Toltoridine Tartarate; Rp-Hplc.

## 240. Synthesis, Electronic Absorption, Fluorescence and Life Time Spectroscopic Study of Some New 3,7-Disubstituted Coumarin Derivatives as New Fluorescent Probes

F.M.A. Altalbawy, M.H. Abdelkader, E.S.S. Darwish and M.H. Elnagdi

*Asian Journal of Chemistry, 28: 2303-2310, (2016), IF: 0.325*

he synthesis of several novel 3-heterocyclic substituent-7-methoxycoumarin derivatives were carried out starting from 3-acetyl-7-hydroxy-2H-chromen-2-one (3), which reacted with DMF-DMA affords enaminone 4 which transformed into pyranone 8, pyridine derivative 12a,b, 23, 24, triaroylbenzene 22 and fuaranone 17 with treatment with hippuric acid (5), acetyl acetone (12a), ethyl acetoacetate (12b), acetic acid and ammonium acetate, 3-acetyl-7- hydroxy-2H-chromen-2-one (3), acetic acid and 1,4-naphthoquinone (15) respectively. The UV-visible, fluorescence and live time spectra for compounds were determined. Most of them displayed high fluorescence quantum yields ranging from 0.70 to 0.99 and life times in the nanosecond range, which can make these new 3-heterocyclic substituent-7-methoxycoumarin compounds very useful as new fluorescent probes. - See more at:

**Keywords:** Fluorescence; Lifetimes; Coumarin; Enaminone; Pyridine; Fuaranone.

## B-241. Development of Pvc Membranes with Clove Oil as Plasticizer for Blood Bag Applications

Ahmed M. Omer, T. M. Tamer, Abd EL Monem, Sami Abd Elmoaty, Mona Abd El Fatah and Gamal R Saad

*Journal of Applied Pharmaceutical Science, 6: 85-93 (2016)*

In the present study, Antimicrobial PVC films containing different amounts of clove oil as a plasticizer were prepared using traditional casting method. The physical and mechanical properties of the plasticized PVC membranes e.g. surface wettability were investigated. The increase of clove oil content demonstrated an increase in surface hydrophilicity and elongation to break the film. The thermogravimetric analysis revealed a decrease of polymer thermal stability by increasing clove oil concentration. The antibacterial activities against four different bacterial strains (two-gram positive: Staphylococcus aureus and Bacillus cereus & two-gram negative: Pseudomonas aeruginosa and Escherichia coli) were promoted by addition of clove oil. Although the natural source of clove oil, the bio-evaluation of plasticized membranes showed an increase in hemolysis percent (%) and thrombus weight. It can be concluded that the addition of clove to PVC need to further studies for applying in blood bags.

**Keywords:** Pvc; Membranes; Clove oil; Plasticizer; Antibacterial.

## B-242. Hypolipidemic and Anti-Fatty Liver Effects Exerted by Standardized Punica Granatum L. Peel Extract in Hepg2 Cell-Line and High-Fat Diet-Induced Mice

Omar A. Tahaa, Alaa Barakat, Heba K. Abdelhakim, Mohamed Abbas Shemis and Zainab Zakaria

*International Journal of Pharmacy and Pharmaceutical Sciences, 8: 156-161 (2016)*

**Objective:** Pomegranate, (Punica granatum L., Lythraceae) peel has concentrated amounts of lipid-lowering elements that demonstrated, in various hoary and recent studies, their effects against obesity and hyperlipidemia, which involves elevated rates of lipid and lipoprotein levels in blood and increases risks of cardiovascular diseases. We aim to study expression modulation of genes involved in lipid metabolism by the impact of standardized pomegranate peel extract (PPE) in a comprehensive research on human liver cells and experimental mice **Methods:** Using reverse-transcription real-time PCR, an in vitro study harnessing HepG2 cell line was conducted to determine the hyperlipidemia-related gene expression profiles and cytotoxic effects upon treatment with PPE. In another complementary in vivo study, male C57BL/6J mice were fed a high-fat diet (HFD) or an HFD supplemented with PPE for 14 d to define the expression of lipid metabolism related genes that control obesity. Fatty liver proportions were also estimated after treatment. **Results**: Higher mRNA expression of LDL receptor (LDL-R) and down-regulation of sterol regulatory element-binding protein (SREBF-2), (SRBEP-1c), Fatty acid synthase (FAS) and 3-hydroxy-3-methylglutaryl-CoA reductase (HMGCR) upon PPE treatment in HepG2 cell line were significantly recorded. In vivo study indicated significant weight reduction of body and liver, besides amelioration of fatty liver state detected by histological analysis. Moreover, the reverse-transcription real-time PCR assay demonstrated suppression (FAS) expression and up regulation of hormone sensitive lipase (HSL) in mice isolated liver and white adipose tissues. **Conclusion:** Our study manages to affirm the hypolipidemic and anti-fatty liver influence of Punica granatum L. peel extract, reflected by molecular evaluation above and beyond other physiological assays.

**Keywords:** Pomegranate; Peel extract; Hyperlipidemia; LDLR; SREBP; FAS; HMGCR; HS

## B-243. Pantoprazole Sodium Sesquihydrate Complexes: Synthesis, Characterization, Potentiometric Determination and DNA Interaction

W. H. Hegazy, Y. M. Issa, W. N. El-Sayed and H. I. Ahmed

*Oriental Journal of Chemistry, 32: 1085-1097 (2016)*

The synthesis and characterization of solid complexes for pantoprazole sodium sesquihydrate with Cd(II), Hg(II) and Zn(II) metals in molar ratios M:L = 1:2 was studied. The complexes are stable in the solid state and are soluble only in DMF and DMSO. The metal complexes were characterized by elemental analysis, molar conductivity measurements, magnetic susceptibility, UV spectrophotometry, IR, Mass spectra, TGA/DTG analysis. Potentiometric measurements for these metal complexes were studied.

**Keywords:** Pantoprazole; Complexes; Potentiometry; Proton Pump inhibitors; DNAinteraction.

## B-244. Protective Effects of Zingiber Officinale Against Carbon Tetrachloride Induced Liver Fibrosis

Iman H. Hasan, Mohamed A. El-Desouky, Ghada M. Abd-Elaziz and Walaa G. Hozayen

*International Journal of Pharmacy and Pharmaceutical Sciences, 8: 377-381 (2016)*

**Objective:**Liver plays a pivotal role in regulating various physiological processes in the body such as metabolism, secretion, and storage. It has a great capacity to detoxify toxic substances and synthesize useful principles. The current study was designed to investigate the possible protective effects of Zingiber officinale (ginger) extract on liver fibrosis induced by carbon tetrachloride (CCl4) in rats. **Methods:**The animals were divided into four groups with eight rats in each. To induce liver fibrosis, Wistar albino rats received CCl4 (2 ml/kg diluted in corn oil) twice weekly for eight weeks. Rats were concurrently treated with Z. officinale extract at two different doses (300 and 600 mg/kg/day). **Results:**CCl4 induced liver injury characterized by fibrotic changes, degenerated hepatocytes and focal accumulation of inflammatory cells. In addition, CCl4 administration produced a significant increase in serum aminotransferases, lipids, liver lipid peroxidation and nitric oxide. The hepatoprotective effects of Z. officinale extract were evidenced by the significant decrease in serum aminotransferases and liver lipid peroxidation. Further, concurrent treatment with either dose of Z. officinale enhanced liver glutathione and enzymatic antioxidant defenses. **Conclusion:**Z. officinale showed a marked hepatoprotective

effect against CCl4–induced liver fibrosis and injury through the abolishment of oxidative stress and potentiation of the antioxidant defense system.
**Keywords:** Antioxidant; Ginger; Fibrosis; Oxidative stress.

## B-245. Synthesis, Biological Evaluation of 1,3,4-Oxadiazole, Triazole and Uracil Derivatives from Poly (Ethylene Terephthalate) Waste

Asmaa M. Fahim, El-Sayed M.A. Yakout , Eman A. Ragab , Ahmad M. Farag and Galal A. M. Nawwar

*Egyptian Journal of Chemistry, 59: 285-303 (2016)*

Poly(ethylene terephthalate) (PET) was hydrolyzed in aqueous NaOH using solar energy. PET is used as versatile reagent for the synthesis of a variety of heterocyclic compounds. Uracil (6a, b), 1,3,4-oxadiazole (9, 12a, b), 1,3,4-triazole (10, 14), thiadiazole (11a, b and 15) derivatives were synthesized from PET. The antimicrobial and antioxidant activities of the synthesized compounds were evaluated and showed significant activities.
**Keywords:** Pet; Oxadiazole; Triazole; Thiadiazol; Uracil; Antimicrobial;, Antioxidant.

### *Dept. of Entomology*

## B-246. Molecular Characterization of A C-Type Lysozyme from the Desert Locust, Schistocerca Gregaria (Orthoptera: Acrididae)

Amr A. Mohamed, Long Zhang, Moataza A. Dorrah, Mohamed Elmogy, Hesham A. Yousef, Taha T.M. Bassal and Bernard Duvic

*Developmental and Comparative Immunology, 61: 60-69, (2016), IF: 3.62*

Lysozymes are bacteriolytic peptides that are implicated in the insect nonspecific innate immune responses. In this study, a full-length cDNA encoding a c-type lysozyme from Schistocerca gregaria (SgLys) has been cloned and characterized from the fat body of immune-challenged 5th instar. The deduced mature lysozyme is 119 amino acid residues in length, has a calculated molecular mass of 13.4 kDa and an isoelectric point (Ip) of 9.2. SgLys showed high identities with other insect lysozymes, ranging from 41.5% to 93.3% by BLASTp search in NCBI. Eukaryotic in vitro expression of the SgLys ORF (rSgLys) with an apparent molecular mass of ~16 kDa under SDS-PAGE is close to the calculated molecular weight of the full-length protein. rSgLys displayed growth inhibitory activity against Gram-negative and Gram-positive bacteria. 3D structure modeling of SgLys, based on comparison with that of silkworm lysozyme, and sequence comparison with the helix-loop-helix (α-hairpin) structure of hen egg white lysozyme (HEWL) were employed to interpret the antibacterial potencies. Phylogenetic alignments indicate that SgLys aligns well with insect c-type lysozymes that expressed principally in fat body and hemocytes and whose role has been defined as immune-related. Western blot analysis showed that SgLys expression was highest at 6–12 h post-bacterial challenge and subsequently decreased with time. Transcriptional profiles of SgLys were determined by semi-quantitative RT-PCR analysis. SgLys transcript was upregulated at the highest level in fat body, hemocytes, salivary gland, thoracic muscles, and epidermal tissue. It was expressed in all developmental stages from egg to adult. These data indicate that SgLys is a predominant acute-phase protein that is expressed and upregulated upon immune challenge.
**Keywords:** Schistocerca gregaria; C-Type Lysozyme; Cdna; Innate immunity; Antibacterial activity; Recombinant Expression; Transcriptional profiles.

## B-247. A Family of Cs Defensins and Defensin-Like Peptides from the Migratory Locust, Locusta Migratoria, and Their Expression Dynamics During Mycosis and Nosemosis

Mingyue Lv, Amr Ahmed Mohamed, Liwei Zhang, Pengfei Zhang and Long Zhang

*Plos One, (2016) IF: 3.057*

Insect defensins are effector components of the innate defense system. During infection, these peptides may play a role in the control of pathogens by providing protective antimicrobial barriers between epithelial cells and the hemocoel. The cDNAs encoding four defensins of the migratory locust, Locusta migratoria, designated LmDEF 1, 3–5, were identified for the first time by transcriptome-targeted analysis. Three of the members of this CS?? defensin family, LmDEF 1, 3, and 5, were detected in locust tissues. The pro regions of their sequences have little-shared identities with other insect defensins, though the predicted mature peptides align well with other insect defensins. Phylogenetic analysis indicates a completely novel position of both LmDEF 1 and 3, compared to defensins from hymenopterans. The expression patterns of the genes encoding LmDEFs in the fat body and salivary glands were studied in response to immune-challenge by the microsporidian pathogen Nosema locustae and the fungus Metarhizium anisopliae after feeding or topical application, respectively. Focusing on Nosema-induced immunity, qRT-PCR was employed to quantify the transcript levels of LmDEFs. A higher transcript abundance of LmDEF5 was distributed more or less uniformly throughout the fat body along time. A very low baseline transcription of both LmDEFs 1 and 3 in naïve insects was indicated, and that transcription increases with time or is latent in the fat body or salivary glands of infected nymphs. In the salivary glands, expression of LmDEF3 was 20-40-times higher than in the fat body post-microbial infection. A very low expression of LmDEF3 could be detected in the fat body, but eventually increased with time up to a maximum at day 15. Delayed induction of transcription of these peptides in the fat body and salivary glands 5–15 days post-activation and the differential expression patterns suggest that the fat body/salivary glands of this species are active in the immune response against pathogens. The ability of N. locustae to induce salivary glands as well as fat body expression of defensins raises the possibility that these AMPs might play a key role in the development and/or tolerance of parasitic infections.
**Keywords:** Defensins; Insects; Fats; Locusts; Sequence motif Analysis; Salivary glands; Nymphs; Parasitic diseases.

## B-248. Assessment of Oxidative Stress and Activities of Antioxidant Enzymes Depicts the Negative Systemic Effect of Iron-Containing Fertilizers and Plant Phenolic Compounds in the Desert Locust

David Renault, Moataza A. Dorrah, Amr A. Mohamed, Eman A. Abdelfattah and Taha T. M. Bassal

*Environmental Science and Pollution Research, 23: 21989-22000, (2016), IF: 2.76*

For herbivore insects, digesting can be somewhat challenging, as the defense mechanisms evolved by plants, including the release of phenolics like the non-protein amino acid L-3,4-dihydroxyphenylalanine (L-DOPA), can cause fitness costs. In addition, industrial and agricultural activities have elevated the amounts of iron that can be found in nature and more particularly FeSO4 that is used as fertilizer. Traces of iron can enhance the auto-oxidation of L-DOPA, in turn, generating reactive oxygen species (ROS) and consequently oxidative stress in insects. We examined the effects of the ion Fe2+ (as FeSO4) and L-DOPA on fifth instars of the desert locust Schistocerca gregaria. We measured the level of oxidative damage occurring to macromolecules (proteins and lipids) from midgut and thoracic tissues and assessed the activities of responsive antioxidant enzymes. Injected L-DOPA and redox-active metal iron generated ROS which caused oxidative damages to proteins and lipids to S. gregaria. The protein carbonyls and lipid peroxides present in tissue homogenates were elevated in treated insects. No synergism was observed when L-DOPA was co-injected with Fe2+. K m values of superoxide dismutase (SOD), glutathione reductase (GR), and glutathione peroxidase (GPx) were 4.3, 2.6, and 4.0 mM in thoracic muscles and 5.00, 2.43, and 1.66 mM in whole midgut for SOD, GR, and GPx, respectively, and 8.3 and 3.43 M for catalase (CAT) in the two tissues, respectively. These results suggest higher affinities of GPx and CAT to H2O2 in midgut than in muscles. The time-course changes in activities of antioxidant enzymes and amounts of protein carbonyls and lipid peroxides showed fluctuating patterns, suggesting complex interactions among macromolecules, L-DOPA and FeSO4, and their degradation products. Our results demonstrated the stressful effects of L-DOPA and FeSO4, proving that iron-containing fertilizers are pollutants that can strongly affect S. gregaria.

**Keywords:** Antioxidant enzymes; Insect; Lipid peroxides; Midgut; Oxidative stress; Protein carbonyls; Thoracic muscles

## B-249. Vibrio Cholerae Laboratory Infection of the Adult House Fly Musca Domestica

El-Bassiony GM, Luizzi V, Nguyen D, Stoffolano JG Jr and Purdy AE

*Medical and Veterinary Entomology, 30, (4) : 392-402, (2016), IF: 2.242*

The present study was designed to test the hypothesis that house flies may be capable of specifically harbouring ingested Vibrio cholerae in their digestive tracts. Flies were continuously fed green fluorescent protein (GFP)-labelled, non-O1/non-O139 environmental strains of V. cholerae. Bacterial burdens were quantitatively measured using plate counts and localization was directly observed using confocal microscopy. Vibrio cholerae were present in the fly alimentary canal after just 4 h, and reached a plateau of ~107 colony-forming units (CFU)/fly after 5 days in those flies most tolerant of the pathogen. However, individual flies were resistant to the pathogen: one or more flies were found to carry < 180 V. cholerae CFU at each time-point examined. In flies carrying V. cholerae, the pathogen was predominantly localized to the midgut rather than the rectal space or crop. The proportion of house flies carrying V. cholerae in the midgut was dose-dependent: the continuous ingestion of a concentrated, freshly prepared dose of V. cholerae increased the likelihood that fluorescent cells would be observed. However, V. cholerae may be a transient inhabitant of the house fly. This work represents the first demonstration that V. cholerae can inhabit the house fly midgut, and provides a platform for future studies of host, pathogen and environmental mediators of the successful colonization of this disease vector.

**Keywords:** Musca domestica; Cholera; Crop; Faecal pellets; Midgut; Peritrophic matrix.

## B-250. Mortality and Nematode Production in Spodoptera Littoralis Larvae in Relation to Dual Infection with Steinernema Riobrave, Heterorhabditis Bacteriophora, and Beauveria Bassiana, and the Host Plant

El-Sayed H. Shaurub, Naglaa F. Reyad, Horia A. Abdel-Wahab and Safia H. Ahmed

*Biological Control, 103: 86-94, (2016), IF: 2.012*

The present study aimed to evaluate the interactive applications of the promising biocontrol agents, the entomopathogenic nematodes (EPNs) Steinernema riobrave and Heterorhabditis bacteriophora and the entomopathogenic fungus (EPF) Beauveria bassiana, each at the LC25 level, to the last instars of the Egyptian cotton leafworm, Spodoptera littoralis, in either sequential or simultaneous fashion to determine whether interactions (synergistic, additive, or antagonistic) among these entomopathogens were present. Moreover, the indirect impact of two cultivated host plants (cabbage and cowpea) and three wild host plants (castor, Jew's mallow, and mallow) or their primary metabolites (total protein, carbohydrate, and lipid content) on the virulence of these entomopathogens and on nematode production also was assessed. Synergisms were observed among the different entomopathogen pairings. In case where sequential applications were made, applying the EPF first was best for infective juvenile (IJ) production; applying the EPN prior the EPF significantly reduced IJ production. Larvae raised on cabbage (the most lipid–rich diet) were most resistant for both EPN species tested. In general, not many IJs were produced from hosts that fed on mallow, but many were produced from hosts that fed on castor. In the case of EPF, B. bassiana was most effective at controlling larvae that fed on mallow, which was considered the least nutritive of the host plants. The results obtained are suggestive of an efficient control to S. littoralis. This would be achieved through the implementation of an integrated program including combining the entomopathogens studied with each other, or intercropping castor (in the case of the nematode application), or mallow (in the case of the fungus application) with cotton for enhancing the control of this insect pest in Egypt.

**Keywords:** Spodoptera littoralis Entomopathogenic nematodes Entomopathogenic fungi; Virulence host; Plant nematode production.

## B-251. Prevalence of Some Human Enteroparasites in Commonly Consumed Raw Vegetables in Tabuk, Saudi Arabia

Refaat M. Gabre and Abdelazim Shakir

*Journal of Food Protection, 79: 665-668, (2016), IF: 1.609*

The problem of parasitic contamination of food, especially fresh vegetables, is not limited to personal hygiene during food preparation but is also widely dependent on the source of the food and the handling it undergoes before it gets to the consumer. The objective of the present study was to evaluate parasitic contamination in eight common raw vegetables in Tabuk, Kingdom of Saudi Arabia. A total of 400 samples of raw vegetables obtained from wholesale and retail markets were examined for helminth eggs and larvae and for cysts of different parasites, using standard methods. The prevalence of the parasites was 20.65% in cucumber, 15.76% in cabbage, 14.67% in pea, 14.13% in cress, 13.04% in lettuce, 10.33% in carrot, 8.70% in green onion, and 2.72% in tomato. Statistical analysis showed a significant difference (P , 0.05) for Entamoeba spp. cysts, Ascaris lumbricoides eggs, Entamoeba coli cysts, and unknown isolated parasite cysts. Parasites are common in vegetables that are frequently eaten raw and, for this reason, may pose a health risk for consumers in Tabuk.
**Keywords:** Helminth eggs and larvae; Parasite cysts; Raw vegetables; Tabuk.

## B-252. Updated Checklist of Iranian Opiinae (Hymenoptera: Braconidae)

Neveen S. Gadallah, Hassan Ghahari, Francisco Javier Peris-Felipo and Maximilian Fischer

*Zootaxa, 4066: 1-40, (2016), IF: 0.994*

An updated checklist of Opiinae from Iran is provided including 101 species from 11 genera (Atormus van Achterberg, 1997, Biosteres Foerster, 1862, Eurytenes Forster, 1862, Fopius Wharton, 1987, Indiopius Fischer, 1966, Opius Wesmael, 1835, Phaedrotoma Forster, 1862, Pokomandya Fischer, 1959, Psyttalia Walker, 1860, Utetes Forster, 1862 and Xynobius Forster, 1862) belonging to two tribes (Biosterini and Opiini). Moreover, seven species Biosteres (Chilotrichia) punctiscuta (Thomson, 1895), Biosteres (Biosteres) remigii Fischer, 1971, Eurytenes (Eurytenes) abnormis (Wesmael, 1835), Opius (Hypocynodus) ponticus Fischer, 1958, Opius pygmaeator (Nees, 1811), Opius (Nosopoea) speciosus Fischer, 1959 and Phaedrotoma nitidulator (Nees, 1834) are recorded for the first time from Iran.
**Keywords:** Hymenoptera; Braconidae; Opiinae; New records; Checklist; Iran.

## B-253. Review of the Genus Defilippia Lioy (Bombyliidae, Diptera) from Egypt, with Description of A New Species, New Combinations, and A Neotype Designation for D. Pharaonis (Paramonov, 1928)

Magdi S. El-Hawagry

*Zootaxa, 4170: 149-158, (2016), IF: 0.994*

In the present study, five Defilippia species are shown to be represented in Egypt. Two species, D. efflatouni (Bezzi) and D. minos (Meigen), were already included in Defilippia; two species, D. decrepita (Wiedemann), comb. nov., and D. pharaonis (Paramonov), comb. nov., are newly combined to Defilippia; and a new species, D. elbayensis, sp. nov., is described herein. Homeotypes of Exoprosopa flava Paramonov, 1928 and Defilippia decrepita (Wiedemann, 1828), comb. nov. have been examined and it was found that the two species are not synonymous and Exoprosopa flava Paramonov, 1928, stat. rev. is rather a distinct valid species in its original genus Exoprosopa. A neotype for D. pharaonis (Paramonov, 1928) is designated.
**Keywords:** Exoprosopa; Exoprosopinae; Bee flies; Taxonomy; Defilippia elbayensis; Sp. Nov; Exoprosopa flava stat. Rev.

## B-254. An Annotated Catalogue of the Iranian Euphorinae, Gnamptodontinae, Helconinae, Hormiinae and Rhysipolinae (Hymenoptera: Braconidae)

Neveen S. Gadallah, Hassan Ghahari and Kees Van Achterberg

*Zootaxa, 2072: 1-38, (2016), IF: 0.994*

The Iranian species diversity of five braconid subfamilies, Euphorinae (54 species in 16 genera and 8 tribes), Gnamptodontinae (4 species in 1 genus and 1 tribe), Helconinae (9 species in 5 genera and 2 tribes), Hormiinae (8 species in 4 genera and 2 tribe) and Rhysipolinae (3 species in 2 genera) are summarized in this catalogue. A faunistic list is given comprising both local and global distribution of each species under study as well as host records. In the present study ten new records are added to the Iranian fauna: Centistes (Ancylocentrus) ater (Nees), Centistes cuspidatus (Haliday), Meteorus affinis (Wesmael), Meteorus rufus (DeGeer), Microctonus brevicollis (Haliday), Microctonus falciger Ruthe, Peristenus nitidus (Curtis) (Euphorinae), Aspicolpus carinator (Nees), Diospilus capito (Nees) and Diospilus productus Marshall (Helconinae s.l.). Euphorus pseudomitis Hedwig, 1957 is transferred to the subfamily Hormiinae and Hormisca pseudomitis (Hedwig, 1957) is a new combination.
**Keywords:** Braconidae; Euphorinae; Gnamptodontinae; Helconinae; Hormiinae; Rhysipolinae; New records; Iran.

## B-255. A Preliminary Account of the Fly Fauna in Jabal Shada Al-A'La Nature Reserve, Saudi Arabia, with New Records and Biogeographical Remarks (Diptera, Insecta)

Magdi S. El-Hawagry, Mahmoud S. Abdel-Dayem , Ali A. Elgharbawy and Hathal M. Al Dhafer

*Zookeys, 636: 107-139, (2016), IF: 0.938*

The first list of insects of Al-Baha Province, Kingdom of Saudi Arabia (KSA) was published in 2013 and contained a total of 582 species; an addendum to this list was published in 2015 adding 142 species and bringing the total number recorded from the province to 724 insect species representing 17 orders. The previous two studies excluded Jabal Shada al-A'la Nature Reserve (SANR), so the present study in SANR, as belonging to Al-Baha Province, are complementary to the previous two. The present study presents a preliminary list of Diptera (Insecta) in SANR, with remarks on their zoogeography, and is the first of a series of planned ecological and systematic studies on different insect orders as one of the outputs of a project proposed to study the entire insect fauna of SANR. A total number of 119 Diptera species belonging to 87 genera, 31 tribes, 42 subfamilies, and representing 30 families has been recorded from SANR in the present study. Some species have been identified only to the genus level and listed herein only because this is the first time to record their genera in KSA. Fourteen of the species are recorded for the first time for KSA, namely: Forcipomyia sahariensis Kieffer, 1923 [Ceratopogonidae]; Chaetosciara sp. [Sciaridae]; Neolophonotus sp.1; Neolophonotus sp.2; Promachus sinaiticus Efflatoun, 1934; Saropogon longicornis (Macquart, 1838); Saropogon sp. [Asilidae]; Spogostylum tripunctatum (Pallas in Wiedemann, 1818) [Bombyliidae]; Phycus sp. [Therevidae]; Hemeromyia sp.; Meoneura palaestinensis Hennig, 1937 [Carnidae]; Desmometopa inaurata Lamb, 1914 [Milichiidae]; Stomoxys niger Macquart, 1851 [Muscidae]; and Sarcophaga palestinensis (Lehrer, 1998) [Sarcophagidae]. Zoogeographic affinities of recorded fly species suggest a closer affiliation to the Afrotropical region (46%) than to the Palearctic region (23.5%) or the Oriental region (2.5%). This supports the previous studies' conclusions and emphasizes the fact that parts of the Arabian Peninsula, including Al-Baha Province, ought to be a part of the Afrotropical Region rather than of the Palaearctic Region or the Eremic Zone.

**Keywords:** Afrotropical; Al-Baha province; Al-Sarah Al-sarawat mountains; Arabian peninsula; Eremic zone; Fly species; New records; Palaearctic; Tihama.

## B-256. First Record of the Genus Pycnodictya with its Subspecies P. Galinieri Galinieri from Egypt (Orthoptera, Acrididae)

Asmaa A. Haggag

*Zookeys, 630: 105-114, (2016), IF: 0.938*

The band-winged Pycnodictya galinieri galinieri (Reiche & Fairmaire, 1849) and its genus Pycnodictya Stål, 1873 (Orthoptera: Acrididae: Oedipodinae) are recorded for the first time for the Egyptian fauna. The species was collected from Gabal Elba, in the southeastern corner of Egypt. This record expands the known distributional range of P. galinieri towards the north of Africa. Descriptions of the genus and the Egyptian subspecies are given using multiple diagnostic characters. The descriptions are supplemented by drawings and photographs of the specimen collected. It is proposed that the genus Pycnodictya belongs to the tribe Locustini.

**Keywords:** Egypt; New record; Oedipodinae; Pycnodictya galinieri introduction.

## B-257. Three New Species of the Genus Macroocula Panfilov, 1954 (Hymenoptera: Bradynobaenidae: Apterogyninae) from Saudi Arabia

Ahmed Mostafa Soliman, Neveen Samy Gadallah and Hathal Mohammed Al Dhafer

*Turkish Journal of Zoology, 40: 352-362, (2016), IF: 0.88*

Three new species of the genus Macroocula Panfilov, 1954 from Saudi Arabia are described and illustrated: M. atuberculata Soliman & Gadallah sp. nov. (Al-Quwayiyah, Al-Aflag, Al-Zulfi, and Riyadh), M. zulfiensis Soliman & Gadallah sp. nov. (Al-Zulfi and Riyadh), and M. khorimensis Soliman & Gadallah sp. nov. (Muzahimiyah and Riyadh). A key to Macroocula species with a ventral protuberance on the hind trochanter is provided.

**Keywords:** Bradynobaenidae; Apterogyninae; Macroocula; New species; Saudi arabia.

## B-258. Area Reduction and Trace Element Pollution in Nile Delta Wetland Ecosystems

Mohamed M. El-Shazly, Wael A. Omar, Yusuf A. Edmardash, Mona Sayed Ibrahim, Emad I. Elzayat, Iman I.A. El-Sebeay, Khaled M. Abdel Rahman andMustafa M. Soliman

*African Journal of Ecology, (2016) IF: 0.875*

The three main Nile Delta wetland ecosystems, Manzala, Burullus and Edku lagoons, are among the most ecologically important and productive habitats in Egypt. We studied the area degradation and the human health risks associated with trace metal accumulation in Tilapia zillii harvested from these lakes. The area of Manzala lagoon has shrunken from about 3035 km2 in 1800 to about 288 km2 in 2015, the area of Edku has shrunken from about 336 km2 in 1824 to about 18 km2 in 2014, and the area of Burullus has shrunken from about 1116 km2 in 1949 to about 546 km2 in 2014. This area degradation is attributed to drying for housing, land reclamation and fish farming. As a result, the concentration of pollutants and nutrients has subsequently increased, and large parts of the lakes have been overgrown with aquatic vegetation, which increased the rate of degradation and land transformation. Metal pollution was detected in water, sediment and edible fish harvested from the lakes. The hazard index, an indicator of human health risks associated with fish consumption, showed adverse health effects of zinc and lead metals for habitual fish consumers. The impact of the high dam on the lakes was discussed.

**Keywords:** Ecosystem degradation; Egyptian delta Lagoons; Nile river; Tilapia zillii; Trace metal pollution.

## B-259. Larvicidal, Biological and Genotoxic Effects, and Temperature-Toxicity Relationship of Some Leaf Extracts of Nerium Oleander (Apocynaceae) on Culex Pipiens (Diptera: Culicidae)

Shaurub H El-Sayed and Ghada M El-Bassiony

*J Arthropod-Borne Diseases, 10(1): 1-11, (2016), IF: 0.865*

**Background:** The present study was undertaken to study the larvicidal activity of different extracts of Nerium ole- ander

leaves, and post-treatment temperature- toxicity relationship of these extracts against Culex pipiens. Further, the most potent extract was used to evaluate its biological and genotoxic activities. **Methods:** Crude extracts of N. oleander leaves were prepared using water, chloroform, acetone and diethyl ether as solvents. Extraction was carried out using soxhlet apparatus. Bioassay test was carried out on the larvae, and the LC50 of each extract was determined. Thus, newly hatched first instar larvae were treated, and the mortality count was recorded daily till pupation (accumulated mortality). The LC50 of diethyl ether extract, as the most potent extract, was used for the further biological and genotoxic studies. **Results:** The results obtained indicated that diethyl ether extract of N. oleander leaves was the most potent extract, with LC50 of 10500 mg/l. The toxicity of the four extracts, using the LC50, at 10 °C was higher than that at 35 °C. The LC50 of diethyl ether extract significantly decreased the larval duration, pupal duration, percentage of pupation, percentage of adult emergence, longevity of females, fecundity, and oviposition activity index, whereas the growth index and the percentage of development per day of larvae and pupae were significantly increased compared to nontreated insects. Moreover, treatment with this extract induced significant dominant lethality in both male and female adults. **Conclusion:** It appears that diethyl ether extract of N. oleander leaves is potential control agent to Cx. pipiens.

**Keywords:** Culex pipiens; Genotoxicity; Larvicidal activity; Nerium oleander; Temperature-toxicity relationship.

## B-260. Water Cytotoxicity and Dioxins Bioaccumulation in an Egyptian Delta Wetland Ecosystem

MM El-Shazly, El Elzayat, WA Omar, IIA El-Sebeay, YA Edmardash, MM Soliman, KM Abdel Rahman and MS Ibrahim

*African Journal of Aquatic Science, 41: 289-296, (2016), IF:0.806*

Manzala Lake, as one of the main Egyptian wetland ecosystems, is facing risks of pollution. An in vitro cytotoxicity test using a mammalian cell line was employed to determine the toxicity of multiple pollutants in the water and Tilapia zillii fish sampled from the lake. The concentrations of seven polychlorinated dibenzo-p-dioxins and ten polychlorinated dibenzofurans were investigated in water and muscle of the fish in 2014. Cytotoxicity testing showed that the percentage inhibition of cell viability in the studied sites ranged between 56.16% and 83.22%. Dioxin analysis indicated that the average concentrations of 1,2,3,4,6,7,8,9-octachlorodibenzo-p-dioxin, 1,2,3,4,7,8-hexachlorodibenzofuran, 1,2,3,4,6,7,8-heptachlorodibenzofuran and 1,2,3,4,6,7,8,9-octachlorodibenzofuran were higher than the toxic equivalence quotients (TEQs) set by the World Health Organization (WHO) in all water and fish muscle samples; however, the average concentration of 2,3,7,8-tetrachlorodibenzofuran was higher only in fish muscle samples. The bioaccumulation factor (BAF) ranged dramatically between 2 and 58.5 for the detected dioxins. Adverse human health effects through the consumption of fish are not expected, because dioxin levels in fish muscle are deemed safe for human consumption. Implementation of a strategic multidisciplinary action plan is strongly recommended to sustain this delta wetland ecosystem.

**Keywords:** Manzala lake; Pollution; Risk assessment; Tilapia zillii; Toxicity.

## B-261. Analysis of Larval Antigens of Cephalopina Titillator in the Camel Mucus for Diagnosis of Infestation

Hesham A. Yousef, Afaf Abdel Meguid, Amira Afify and Hany M. Hassan

*Biologia, 71/4: 438-443, (2016), IF: 0.719*

Serodiagnostic test for the diagnosis of infestation of camels by the camel nasal fly, Cephalopina titillator was examined. The enzyme-linked immunosorbent assay (ELISA) technique was used to analyze and compare the production of antibodies in the camel mucus against salivary gland contents (SGc), excretory-secretory products (ESP), digestive tract contents (DTc) antigens from 2nd and 3rd larval instars of C. titillator sampled in summer and winter. ELISA characterization of larval antigens showed that the presence of C. titillator larvae in camel, Camelus dromedarius, resulted in higher antibody titer in mucus samples of infested camels collected in winter than those collected in summer in both L2 and L3. In L2, the most antigenic secretion was SGc > ESP > DTc, but in L3 ESP > SGc > DTc. The antibody titers in camel mucus are affected by the intensity of infestation with C. titillator.

**Keywords:** Cephalopina titillator; Salivary gland contents; Excretory secretory products; Digestive tract contents; Elisa; Camel mucus introduction.

## B-262. Effect of A Novel Photopesticide on Some Biological Aspects of Milkweed Bug Spilostethus Pandurus (Scopoli), with Reference to Ultrastructural Changes in the Midgut

H.A.S. Elelimy, H.H. Awad and T.A. El Tayeb

*African Entomology, 24(1): 100-111, (2016), IF: 0.521*

The Hemipteran bug Spilostethus pandurus is a serious pest infesting plant seeds. Haematoporhyrin (HPF) was successful as a novel trend for S. pandurus control in the field due to its accumulation inside their organs after incubation and exposure to sunlight in the summer season. The survival rate of nymphs decreased with increasing HPF concentration. A concentration of 1× 10 –3 M/l HPF increased the mortality of the first nymphal instar by 6.06- and 3.9-fold after 2 and 3 days as compared to the control, it produced the highest mortality that remained nearly constant throughout most of the 16 days of development. All biological parameters were affected, showing increased nymphal mortality, decreased number of deposited eggs by females and decreased percentage of egg hatchability. Light and electron microscopic studies on midgut regions (mg1–mg4) of adults resulting from treated nymphs revealed severe disorganisation and disintegration of cells and the presence of a great number of vacuoles. The basement membrane was detached. The microvilli were destroyed in the apical part and the food discharged. In addition, cell lysis appeared from mg1 to mg4 and many of cell organelles disappeared. The appearance of autophagic lysosomes was evident together with looped, vacuolated or swollen mito- chondria. It seems likely that the nuclear

membrane was ruptured or detached and clump- ing of the chromatin occurred. The muscle fibre and trachea were malformed. The obtained results might reflect the potency of HPF as a novel photoinsecticide in milkweed bug control in an integrated pest management (IPM) programme.
**Keywords:** Milkweed bug; Lygaeidae; Gut; Tem; Porphyrins; Photopesticide.

## B-263. Effects of Farnesol on the Ultrastructure of Brain and Corpora Allata, Sex Hormones and on Some Oxidative Stress Parameters in Locusta Migratoria (Orthoptera: Acridiidae)

H.H. Awad and N.A. Ghazawy

*African Entomology, 24(2): 502-512, (2016), IF: 0.521*

Farnesol, at 0.06 × 10 4 ppm concentration was tested against the fifth nymphal instar of Locusta migratoria induced antifeedant activity by 33.6 % and 45 % to males and females, respectively. Ultrastructural studies, using transmission electron microscopy, revealed marked pathological changes in the neurosecretory cells in brain and corpora allata (CA) cells of treated nymphs. The brain neurosecretion was held inside the neurosecretory cells whose axons did not liberate normally, leading to the accumulation of neurosecretory granules inside. These cells appeared ruptured and irregular. Corpora allata cells had hyper - trophied nuclei, numerous lysosomes, malformed mitochondria, Golgi bodies and some other intracellular organelles in the gland cells. Multivesicular bodies were scattered and intercellular spaces appeared within the cell matrix. The haemolymph testosterone and progesterone levels were significantly decreased in the fifth nymphal instar treated with farnesol. Moreover, haemolymph and brain superoxide dismutase (SOD) activity were significantly decreased in brains of treated males and females. On the other hand, haemolymph malondialdehyde (MAD) only declined. By contrast, the brain MDA level was significantly increased in farnesol-treated fifth nymphal instars of both sexes. The ultrastructural and biochemical changes reflect the sensitivity of L. migratoria to farnesol as a neurotoxin bioinsecticide. It appears that the changes in the biochemical macromolecules reflect the ultrastructural alterations obtained. Thus, farnesol can be used as a promising biocide against the migratory locusts as it could be mixed in bait traps in the integrated pest management programme (IPM).
**Keywords:** Brain; Corpora allata; Tem; Terpenes; Locusts; Mad; Sod; Testosterone; Proges- Terone.

## B-264. Isolation and Functional Characterisation of Antibacterial Peptide from the Mosquito, Aedes (Ochlerotatus) Caspius (Diptera: Culicidae)

G.M. El-Bassiony, W.I.M. Ahmed, M.B.E. Mahmoud and N.M.M. Elwan

*African Entomology, 24, (2): 197-207, (2016), IF: 0.521*

One antimicrobial peptide was isolated and purified to 5.50-fold from the crude lysate of immunised Aedes caspius larvae by (NH4)2SO4 fractionation, ion-exchange chromatography, and reverse-phase high performance liquid chromatography (HPLC). The peptide, named ACAm, was found to be heat stable below 80 °C and exhibited strong antimicrobial activities against Gram-positive and Gram-negative bacteria as well as against peptidoglycans and lipopolysaccharides of bacterial cell walls. The estimated molecular weight of ACAm by sodium dodecyl sulphate polyacrylamide gel (SDS-PAGE), under non-reducing conditions, was 4 kDa. Using isoelectric focusing (IEF), ACAm exhibited pI in basic pH (8.4) belonging to cationic peptides.
**Keywords:** Antimicrobial peptides; Antibacterial activity; Aedes caspius; Mosquitoes; Ion-exchange chromatography; Rp-Hplc.

## B-265. Records for the Family Ulidiidae (Diptera, Tephritoidea) in Saudi Arabia

H.M. Al Dhafer and M.S. El-Hawagry

*African Entomology, 24: 225-232, (2016), IF: 0.521*

The Diptera family Ulidiidae or picture-winged flies known from the Kingdom of Saudi Arabia are reviewed. Six species in three genera are recognised, Ceroxys confusa (Becker), C. urticae (Linnaeus), Melieria nigritarsis Becker, M. omissa (Meigen) [Otitinae], Physiphora alceae (Preyssler), and P. smaragdina (Loew) [Ulidiinae]. Only M. nigritarsis and P. alceae were previously recorded from the Kingdom. The other four species, C. confusa, C. urticae, M. omissa, and P. smaragdina represent new country records. Additionally, the above records of Ceroxys are new for the Arabian Peninsula. Physiphora smaragdina (Loew) is known for most of Africa except SouthAfrica. This is the third time this species is recorded outsideAfrica in addition to Israel and the United Arab Emirates. The Saudi Arabian genera and species are keyed and images are provided to facilitate identification.
**Keywords:** Otitidae; Picture-winged flies; Arabian peninsula; Middle east; Palaearctic region; New records; Key.

## B-266. Parageron Raydahensis, New Species and the First Record of Subfamily Usiinae (Bombyliidae: Diptera) from Saudi Arabia

Magdi Shaaban Ali El-Hawagryand Hathal Mohammed Al Dhafer

*Pakistan Journal of Zoology, 48: 1307-1310, (2016) IF: 0.478*

A new species, Parageron raydahensis sp. nov. represents the first record of the subfamily Usiinae (Bombyliidae, Diptera) from the Kingdom of Saudi Arabia (KSA) and is the first record of the genus from the Arabian Peninsula. The species was collected from Garf Raydah Protected Area, Abha, Asir Province, southwestern part of the KSA using a Malaise trap set in a site rich in Juniperus procera, Acacia etbaica, Olea spp., other typical Afrotropical trees, and introduced cactus species. This second known record of the genus Parageron supports the concept that several southwestern KSA provinces including Asir Province are part of the Afrotropical Region.
**Keywords:** Usiini; New species; Arabian peninsula; Asir; Abha; Garf raydah protected area; Afrotropical.

## B-267. Sphaerodema Urinator Duforas (Hemiptera: Belostomatidae) as A Predator of Fasciola Intermediate Host, Lymnaea Natalensis Krauss

Younes A. A., Hanaa El-Sherief, Fathia Gawish and Marwa Mahmoud

*Egyptian Journal of Biological Pest Control, 26(2): 191-196, (2016), IF: 0.152*

The water bug Sphaerodema urinator Duforas (Hemiptera: Belostomatidae), inhabits lakes, ponds, marches and rice fields, was found to predate on a wide range of other aquatic organisms like insects and snails. To evaluate the predatory potential on the Fasciola intermediate host, Lymnaea natalensis Krauss snail, laboratory studies involved searching; encounter, consumption and prey preference were achieved. Obtained results indicated that the searching time of the predator ranged between 3.4±0.5 to 7.8±0.9 min and handling time ranged between 18.8±1.01 to 25±1.0 min, depending on the snail size and the predator vulnerability. The adult water bug could kill and consume small-, medium- and largesized snails. Number of snails consumed/ day differed according to their size and density. Preference experiments showed that the adult predator prefers small size snails than medium or large ones. This study suggested that the predator , S. urinator may be potentially suitable as a bio-control agent against Fasciola intermediate host, L. natalensis.

**Keywords:** Predator; Sphaerodema urinator; Fasciola; Intermediate host; Snail.

## B-268. Comparison of Sucrose Intake and Production of Elimination Spots Among Adult Musca Domestica, Musca Autumnalis, Phormia Regina and Protophormia Terraenovae

Ghada Mohamed El-Bassiony and John George Stoffolano Jr

*Asian Pacific Journal of Tropical Biomedicine, 6, ( 8) : 640-645 (2016)*

**Objective** To compare the differences in intake and excretion between Musca domestica and other three species from families Muscidae and Calliphoridae which may help explaining the significance of house fly in the transmission of pathogens. **Methods** The four adult species were supplied with two concentrations of sucrose via modified capillary feeder assay system. The two sucrose concentrations were applied to one adult male/each experiment and the elimination spots were counted. Using 0.25 mol/L sucrose + 0.25% bromophenol blue, one active non-starved male/cup was observed carefully for 1 h to record its behavior. As a growing medium used in bacterial transmission experiments, undiluted trypticase soy broth was used to feed 3-day-old females and males of Musca domestica following two different diets upon emergence and the frequency of elimination spots was estimated. **Results** The two Musca species have half the weight of the two Phormia species. Comparing the volume of intake per hour, house fly took as much as the other species, all of which were larger. House fly produced twice, or more, the number of elimination spots/h than the other three species. Feeding the flies a sugar liquid diet resulted in producing more fecal spots than regurgitation spots. The male house flies produced less elimination spots/h when fed with trypticase soy broth than with the two sucrose solutions. **Conclusions** House flies eliminated more than the other examined fly species and most of these elimination events were defecation which implicates the fecal route for pathogen transmission by this important vector.

**Keywords:** Regurgitation; Defecation; Non-Hematophagous Diptera; Pathogen Transmission; Food Safety

## B-269. Experimental Evaluation of Odonata Nymph in the Biocontrol of Schistosomiasis Intermediate Hosts

Aly Younes, Hanaa El-Sherief, Fathia Gawish and Marwa Mahmoud

*Asian Pacific Journal of Tropical Biomedicine, 6: 995-1000 (2016)*

**Objective:** To evaluate the predatory potential of the Odonata nymph on freshwater snails that serve as intermediate hosts for Schistosoma species (Bulinus truncatus and Biomphalaria alexandrina). Methods: Observations on the searching, attacking and devouring of the two snail types with series of laboratory-based predation experiments, whose aims were to determine daily predation rate, differential predation, prey preference considering small-, mediumand large-sized snails were conducted. **Results:** Laboratory evaluation revealed that, the Odonata nymph could kill and consume the two intermediate hosts. The number of snails consumed differed according to the snail type, size and density. The times taken for searching and handling times were dependent on the snail size, type and satiation of the predator. The predation rate varied also with respect to snail type, size and density. This study also evaluated that Odonata nymphs consumed more Bulinus truncatus than Biomphalaria alexandrina per unit time, and that there may be a preference for smaller than larger snails. **Conclusions:** According to our observation, the predator, Hemianax ephippiger nymph may be a suitable biocontrol agent in connection with Schistosoma intermediate hosts.

**Keywords:** Schistosoma; Intermediate hosts; Snails; Biological control.

## B-270. In Vitro Antimicrobial Activity of Maggot Excretions/Secretions of Sarcophaga (Liopygia) Argyrostoma (Robineau-Desvoidy)

Ghada M. El-Bassionyand John G. StoffolanoJr.

*African Journal of Microbiology Research, 10(27): 1036-1043 (2016)*

The excessive usage of conventional antibiotics leads to the emergence of multidrug-resistant bacterial strains which threaten public health and stimulates searching for new sources of bio-therapeutic drugs. The aim of this study was to investigate the antimicrobial activity of maggot excretions/secretions from larvae of Sarcophaga argyrostoma, a common species of the family Sarcophagidae in Egypt. The excretions/secretions (ES) produced by third instar larvae were sterile filtered and tested against selected pathogenic strains of Gram positive (Gram+ve) bacteria, Staphylococcus aureus and Bacillus subtilis; Gram negative (Gram-ve) bacteria, Escherichia coli and Pseudomonous aeruginosa; and the

filamentous fungus Aspergillus flavus. The ES product produced by third instar maggots proved to be more effective against Gram-ve bacteria. Larval ES, at 0.125 mg/ml concentration, were significantly potent towards P. aeruginosa, E. coli and S. aureus in a descending sequence. The minimum inhibitory concentrations of S. argyrostoma ES were 0.125 mg/ml for P. aeruginosa and E. coli, using the turbidimetric assay method. Twice and four times this concentration were required to inhibit growth of S. aureus (0.25 mg/ml) and B. subtilis (0.5 mg/ml), respectively. The antibacterial properties of S. argyrostoma ES were not affected by heating or freeze-thaw cycles when tested against E. coli.

**Keywords:** Sarcophaga argyrostoma; Antimicrobial activity; Larval excretions; Larval secretions; Minimum inhibitory Concentration.

## B-271. Mineral Exploration and Basement Mapping in Areas of Deep Transported Cover Using Indicator Heavy Minerals and Paleoredox Fronts, Yilgarn Craton, Western Australia

Walid Salama, Ravi R. An and Michael Verrall

*Ore Geology Reviews, 72: 485-509, (2016), IF: 3.819*

Glacial sediments have been thoroughly integrated into mineral exploration protocols in the Northern hemisphere (e.g., Canada and Fennoscandia), but have received less attention in Australia. In Western Australia (WA), Permo-Carboniferous diamictites, buried by younger Cenozoic sediments, cover scattered areas that have potential to host gold and nickel mineralization, in the NE of the Yilgarn Craton. A systematic stratigraphic, mineralogical and geochemical study was undertaken to determine whether diamictites in the Agnew–Lawlers gold province have properties that may help target concealed mineralization. At the Agnew–Lawlers District, rocks intersected in 31 drill holes NE of the Waroonga gold mine, were interpreted in terms of lithological, textural and paleolandscape, mineralogical and geochemical variations to select the best sampling media for mineral exploration and provenance assessment. The paleotopographic variation, asymmetry of the depositional basin, polymictic composition, matrix-supported, mixed angular and rounded and poorly sorted texture of the diamictite clasts indicate mechanical dispersal from proximal and distal, heterogeneous source rocks. Ferromagnesian minerals, chromite, Cr-magnetite, magnetite and Ni–Cu–Fe sulfides are abundant in the diamictite close to mafic–ultramafic source rocks. Monazite, apatite, zircon and clasts derived from pyrite-bearing quartz veins increase in abundance in the diamictite close to the Waroonga shear zone that separates granitoid/gneiss terrain from the Scotty Creek metasediments. Ilmenite is extensively distributed in diamictites throughout the study area and its Mn content can be used to differentiate between felsic and mafic source rocks. Alteration of ilmenite to titanite, monazite to apatite and thorite, and replacement and fracture-filling of pentlandite to monazite suggest felsic, intrusive-related hydrothermal alteration of the source rocks prior to mechanical weathering. Late Paleozoic tropical weathering associated with oscillation of water table and icehouse to greenhouse climatic shift has created paleoredox fronts in the Permo-Carboniferous sequence. Below the redox fronts, diamictites are unweathered, rich in detrital sulfide and opaque oxide minerals and can be used in provenance studies and tracing mineralization. These characteristics of unweathered diamictite are the optimal sampling medium target for provenance studies and mineral exploration. These are cemented mainly by calcareous cement where they overlie mafic–ultramafic rocks and by pyrite cement where they overlie the Scotty Creek metasediments. Above the redox fronts, diamictites are variably weathered to ferruginous and bleached kaolinitic saprolites which are stable under oxidizing, circum-neutral conditions. Ferruginous diamictites are rich in recycled redox-sensitive elements derived from oxidation of ferromagnesian, sulfide and opaque oxide heavy minerals. These weathering features can be used to identify weathered diamictite for sampling for hydromorphic metal dispersion studies.

**Keywords:** Diamictites; Indicator minerals; Geochemistry; Yilgarn craton; Western australia.

## B-272. Morphologic Characteristics and Migration Rate Assessment of Barchan Dunes in the Southeastern Western Desert of Egypt

M.A. Hamdan, A.A. Refaat and M. Abdel Wahed

*Geomorphology, 257C: 57-74, (2016), IF: 2.813*

This work explores the morphologic characteristics of aeolian dune sand in the southeastern part of Western Desert of Egypt. It aims to assess the movement of barchan dunes and evaluate their environmental influence on the Toshka ProjectMorphometric investigation of barchan dunes in the Toshka area revealed that most barchans have high length/width (a/c) ratios (fat to pudgy), while one-fifth of the studied barchans have lower a/c ratios and so appear normal in their morphologic forms. Statistical analysis of the main parameters of barchan dunes in Toshka and other desert regions in the Kharga (Egypt), Kuwait, Southern Morocco, California and Southern Peru demonstrates that barchans of the Toshka area are distinctive in their appearance. They are characterized by distinct aspect with higher values of length and width and greater growth in height. The high-energy wind environment in addition to the large amount of drifting sand are principal factors responsible for the unique shape of Toshka barchans.The migration rate of barchan dunes in four chosen test locations, within the central and western Toshka area, ranges from about 3 to 10.82 m/year. The calculated average migration rate of these dunes is about 6 m/year in a SSW direction. Sand encroachment is more extensive in the central and western parts of the investigated Toshka area. Risk evaluation of sand dune movements in the southeastern part of the Western Desert points to medium to high sand encroachment risk values. These may represent serious hazards to the newly-established Toshka Project, threatening roads, as well as cultivated lands in the area.

**Keywords:** Barchan dune; Dune migration; Dune encroachment hazard; Western desert of egypt.

## B-273. Could The Conventionally Known Abu Roash "G" Reservoir (Upper Cenomanian) be A Promising Active Hydrocarbon Source in the Extreme Northwestern Part of Egypt Palynofacies, Palaeoenvironmental, and Organic Geochemical Answers

Sameh S. Tahoun and Amr S. Deaf

*Marine and Petroleum Geology, 76: 231-245, (2016) IF: 2.788*

In different areas of the Western Desert of Egypt, the Abu Roash "G" Member exhibits either a reservoir or source affinity. Thus, thirteen cutting samples covering the Abu Roash "G" Member were selected from the Nest-1A well at Matruh Basin to investigate its hydrocarbon source potential. Palynological age dating of the section that is calibrated with foraminifera and ostracodes enabled a proper identification of the "G" Member. Detailed analysis of the vertical distribution of particulate organic matter of this member shows two palynofacies types. PF-1 reflects an outer middle shelf depositional environment of prevailed reducing (suboxic-anoxic) conditions for the organic-rich shales of the lower "G" Member (samples 1–8). While, PF-2 reflects a minor regression that resulted in deposition of another organic-rich shales of the upper "G" Member (samples 9–13) in an inner middle shelf setting under the same prevailing reducing (suboxic-anoxic) conditions. Organic geochemical analysis reveals good to very good potential of the "G" Member as a hydrocarbon source rock (1.8–2.41, avg. 2.15 total organic content wt %). It also shows good to very good petroleum potential (PP: 4.8–11 , avg. 8 mg HC/g rock). Pyrolsis and palynofacies analyses show kerogen type II for the lower "G" Member (samples 1–8), which is characterized by high Hydrogen index (HI: 396 and 329 mg HC/g TOC at depths 1500 and 1560 m) and very high dominance of oil-prone material (amorphous organic matter "AOM", marine palynomorphs, and sporomorphs) and very rare occurrence of gas-prone material (brown phytoclasts). The upper "G" Member (samples 9–13) shows kerogen type II-III, which is characterized by a lower HI value of 213 mg HC/g TOC at depth 1340 m and it contains fewer amounts of gas-prone material and relatively lower AOM and marine palynomorphs in comparison to the upper "G" Member. Maturation parameters Tmax (430–433 °C), production index (PI: 0.1 mg HC/g rock), and thermal alteration index (TAI: 2+) indicate the lower "G" Member has already entered the early oil-window kitchen, and it is expected to produce oil. The upper "G" Member is expected to produce only oil with no gas shows, because it is marginally mature (Tmax 426 °C, PI 0.2, TAI 2). The source potential index (SPI: 5.3 t HC/m2) of the "G" Member shows it as currently generating moderate quantities of oil in the area of Nest-1A well. Consequently, the organic-rich shales of the "G" Member are suggested here as a promising, active oil source rock in that extreme northwestern part of the Western Desert of Egypt. However, for commercial oil recovery from the Abu Roash "G" Member, it is highly recommended to explore the depocentre of Matruh Basin at about 150 km east the Nest-1A well.

**Keywords:** Palynofacies; Palaeoenvironment; Organic geochemistry; Abu Roash "G"; Hydrocarbon potential; North Western desert; Egypt.

## B-274. Structural Regime and its Impact on the Mechanism and Migration Pathways of Hydrocarbon Seepage in the Southern Gulf of Suez Rift: an Approach for Finding New Unexplored Fault Blocks

Shawky Sakran, Muhammad Nabih, Ahmed Henaishand Abdelmohsen Ziko

*Marine and Petroleum Geology, 71: 55-75, (2016), IF: 2.788*

A Natural active oil seepage occurs at the intersection of the NW-oriented rift coastal fault and a NE-oriented cross fault which bound the southwest dipping Little Zeit tilted fault block at the southwestern side of the Gulf of Suez, Egypt. Detailed surface geological mapping followed by subsurface mapping using aeromagnetic, seismic and borehole data of Ras El Ush oilfield (the nearest oil field to the seepage) provide a reliable hydrocarbon migration pathway model of the area. The proposed model suggests that hydrocarbons migrated upward at the intersection of a NE-oriented and the NW-oriented rift coastal faults where they found their way to the surface. The Nubia Sandstone occurs south of Ras El Ush oilfield in a trap door structure and probably entrapped some of the migrating hydrocarbons while a probable oil-water-contact at −1000 m which resulted into the migration of hydrocarbon through the damage zone of the northeast fault. The original oil in place of the predicted reservoir is estimated to be more than 47.5 MMBO which encourages the design makers for more investigation of this reservoir to increase its certainty and putting it in the plan of the future investments.

**Keywords:** Gebel El Zeit; Oil seepage; Hydrocarbon migration; Fault connectivity; Gulf of suez rift.

## B-275. Fluid-Related Modifications of Cr-Spinel and Olivine from Ophiolitic Peridotites by Contact Metamorphism of Granitic Intrusions in the Ablah Area, Saudi arabia

Ahmed H. Ahmed and Adel A. Surour

*Journal of Asian Earth Sciences, 122: 58-79, (2016), IF: 2.647*

The Ablah serpentinized peridotites and overlying layered metagabbros represent an allochthonous piece of a dismembered ophiolite in the southern Hijaz terrane that belongs to the Neoproterozoic Arabian Shield in Saudi Arabia. On both sides, the ophiolite is bounded by wider domains of granitic intrusions and volcano-sedimentary successions, all together follow a N–S trend. The protolith of the Ablah serpentinized peridotites is mainly harzburgite which is partly or totally serpentinized. Carbonate veins of variable sizes invade and hydrate the serpentinized peridotites. Away from the contact with the granitic intrusions, fresh primary (igneous) olivine and Cr-spinel are preserved in the partly serpentinized peridotites. These relict primary minerals are used to infer their tectonic setting of formation as a nascent spreading center rock association of mid-ocean ridge or back-arc basin setting. Based on the re-distribution of elements related to different thermal effects, three patterns of Cr-spinel modification can be defined. The first pattern can be followed in the partly serpentinized peridotites where Cr-spinel displays simple zoning that is characterized by sharp contact between primary Al-rich cores and secondary Fe3+-rich rims. These cores and rims are

homogeneous and show progressive decrease in Mg, Al and Cr, but with remarkable increase in Fe3+ and Fe2+ toward the rims. Mineral assemblage in equilibrium with this type of Cr-spinel is primary olivine + antigorite + chlorite ± talc ± chrysotile. The second pattern of Cr-spinel modification is represented by homogeneous weakly zoned Cr-rich spinel with no distinct sharp contacts between Cr-rich cores and magnetite rims. Cr-spinel cores of this type are rich in Cr and Fe2+, and poor in Mg, Al and Fe3+. The mineral assemblage in equilibrium with this Cr-spinel type is Fe-rich olivine + antigorite + enstatite + chlorite + tremolite + anthophyllite ± talc. The third pattern is defined by pervasive heterogeneous modification in which the alteration starts from the cores outwards forming a very characteristic "atoll" textured SiO2- and Cr-rich porous spinel. This type is characterized by core-to-rim increase in Cr, Fe3+, Si, Mn, Ni and Ti, and decrease in Mg, Al and Fe2+. The mineral assemblage in equilibrium with this pattern is chlorite + carbonates + lizardite/chrysotile ± antigorite. The first modification pattern is suggested to form under nearly solid-state conditions in the distal part from the granitic intrusion. The second pattern could be formed under reducing conditions with high temperature and fluid/rock ratio near the contact zone. The peak metamorphic temperature of this stage ranges from 500 to 650 °C that indicate upper amphibolite facies conditions. During retrograde metamorphism, the hydrothermal fluids are cooler and oxidizing which lead to the precipitation of thick marble-like carbonate veins within the serpentinized peridotites. In such a case, the aqueous fluids attack the Al- and Mg-rich cores, which are less resistant and replicable than the Fe-rich rims, and form the third chemical modification pattern of porous SiO2-rich spinel. The high SiO2 content in Cr-spinel is most probably attributed to the formation of Mg- and Al-rich silicates within the sub-microscopic pores of altered Cr-spinel.

**Keywords:** Serpentinized peridotites; Contact metamorphism; Cr-Spinel; Ferritchromite; Atoll texture; Ablah; Saudi Arabia.

## B-276. Petrology of the Motaghairat Mafic–Ultramafic Complex, Eastern Desert, Egypt: A High-Mg Post-Collisional Extension-Related Layered Intrusion

Ali H. Abdel Halim, Hassan M. Helmy, Yasser M. Abd El-Rahman, Tomoyuki Shibata, Mahmoud M. El Mahallawi, Masako Yoshikawa and Shoji Arai

*Journal of Asian Earth Sciences, 116: 164-180 (2016) IF: 2.647*

The geodynamic settings of the Precambrian mafic–ultramafic complexes in the Eastern Desert of Egypt have important bearing on understanding the geotectonic evolution of the Arabian Nubian Shield. We present a detailed petrological study on a layered mafic–ultramafic intrusion that is located at the contact between the Precambrian continental crust and the Miocene Red Sea oceanic crust. The Motaghairat layered intrusion consists of basal lherzolite, orthopyroxenite, troctolite, olivine gabbro and anorthosite on the top. Variations in modal mineralogy and mineral chemistry along with the chemical composition of these units suggest their derivation from a common high-Mg tholeiitic parent melt through fractional crystallization processes. The parental magma was derived from a metasomatised mantle source. The primitive mantle-normalized patterns of the calculated melts exhibit enrichment in U relative to Th and Ba relative LREE which indicate that the enriched lithospheric mantle source was metasomatised by fluids derived from a subducted oceanic crust rather than by a sediment melt. Geological and petrological evidences suggest that the layered Motaghairat intrusion was emplaced during post-orogenic extension following subduction break-off and lithospheric delamination after the collision between the amalgamated island arc terranes and the Saharan Metacraton. The heat source required to melt the metasomatised lithospheric mantle was derived from the upwelling of hot asthenosphere after the subduction-break-off.

Keywords: Layered intrusion; High-Mg Magma; Post-Collision; Metasomatised mantle; Lithospheric delamination; Slab Break-Off

## B-277. Physical Properties and Na-Activation of Egyptian Bentonitic Clays for Appraisal of Industrial Applications

Mohamed A. Agha, Ray E. Ferrell, George F. Hart, Mohamed S. Abu El Ghar and Ali Abdel-Motelib

*Applied Clay Science, 131: 74-83, (2016), IF: 2.586*

Selected physical properties of bentonitic clays in the north Western Desert, Egypt were investigated to assess their potential use in industrial applications. Assessment tests included specific surface area (SSA), swelling index (SI), green (GCS) and dry (DCS) compressive strengths, rheological properties, and filtrate volume. The impact of Na-activation on swelling index and rheological properties was also considered. SSA, SI after Na-activation, GCS, and rheological properties were highly correlated with smectite content and a modified AgTU-CEC. Mineral impurities greatly influenced the physical properties. Quartz and feldspars reduced the rheological properties and increased the water loss. Halite and colloidal iron oxides increased swelling index and enhanced rheological properties. DCS was greatly influenced by the percentage of added water and kaolinite abundance. Na-activation improved the swelling index and rheological properties of halite-poor samples. The swelling index of Na-activated samples was a useful tool for determining the quality and grade of bentonitic clays. The suitability of the Egyptian bentonitic clays for drilling mud and bonding of foundry sands was determined by comparing the results with a standard bentonite and published industrial specifications. Egyptian bentonitic clays showed comparable compressive strengths with Wyoming Na-bentonite (SWy-1) by adding 8 and 10 wt.% clay to sand molds and can be used for most metal-type castings. Egyptian bentonitic clays with a high swelling index and low quartz and feldspar content, produced comparable rheological properties with the Wyoming Na-bentonite and met international drilling mud specifications. However, the filtrate volume measurements indicated that the samples require additional modifications to reduce water loss. Many desirable bentonitic clay properties were reduced by large quantities of kaolinite.

**Keywords:** Bentonitic clays; Egypt; Ssa; Swelling index; Na-Activation; Industrial applications.

## B-278. Geochemical Exploration for Supergene Copper Oxide Deposits, Mount Isa Inlier, Nw Queensland, Australia

Walid Salama, Michael F. Gazley and Lindsay C. Bonnett

*Journal of Geochemical Exploration, 168: 72-102, (2016), IF2.147*

Extensive, variable, and generally thick regolith is a major challenge to mineral exploration in regolith-dominated terranes. The landscape of the Mount Isa Inlier, NW Queensland, Australia, is the product of several episodes of complex weathering, erosion and sedimentation. Weathering profiles were studied from more than 100 drill holes along three traverses crossing the Lady Annie, Mount Kelly and Anthill sulfide deposits to assess the nature, lateral extent and thickness of the supergene Cu oxide mineralization. A typical regolith profile consists, from the base up, of saprock, ferruginous saprolite (Cu-oxide zone), kaolinitic saprolite and silcrete bands (leached zone), and a pedolith of mottled, lateritic duricrust and soil zones. Oxidation of sulfides (primarily pyrite) in host rocks has created an acidic pH gradient, mobilizing Fe, Mn, Cu, Mo, Zn, Co, Ni, As, Bi, In, Sb, Be, P, U and Cd. The acidic pH is buffered by calcareous lithologies of the host rocks, particularly in the vicinity of the primary sulfides at Lady Annie and Mount Kelly resulting in formation of thick, mushroom-shaped Cu oxide halo, in which Cu may reach > 15 wt.%. The Cu values decrease to < 500 ppm in the bleached kaolinitic saprolite and silcrete. Conversely, siliceous bedrock lithologies at Anthill act as a weak buffer to the acidic fluids; thus, Fe, Cu and other mobile elements are laterally dispersed from the sulfide ore body and precipitated at different lithological boundaries where they are buffered by carbonates. Therefore, thick kaolinitic saprolite and silcrete are formed over sulfide mineralization, particularly along faults. Ferruginous duricrusts marginal to fault-controlled sulfide mineralization are anomalous in Cu, Zn, Cd, Sb and Be, and thus can be used as useful medium in geochemical exploration. Gold, Ag, Pb and As are residually concentrated in pedolith and kaolinitic saprolite over the primary sulfide mineralization. Thus, these elements can be used effectively as pathfinder elements, particularly in truncated landscape, where pedolith is eroded and the exposed kaolinitic saprolite is depleted in Cu. Ferruginous soil (850–300, 300–80 and < 80 μm size fractions), lag (> 1.6 and > 7.6 mm) and termite mounds have been applied successfully as sampling media for Cu oxide exploration in Anthill. Soil and lag over sulfide mineralization are rich in Fe, As, Pb, Ag, Bi, In, V, U and Mo. The best response over sulfide mineralization is recorded in the > 7.6 mm ferruginous lag. However, broadest signature of well-defined Au, Bi and In anomalies are better detected using termite mounds than soil and lag. Successful use of soil in exploration for Cu oxide deposits in Mount Isa requires a genetic discrimination between residual and transported origin.

**Keywords:** Regolith; Soil; Mineralogy; Lady annie; Mount Kelly;Anthill.

## B-279. A New Tectono‑Sedimentary Model for Cretaceous Mixed Nonmarine–Marine Oil‑Prone Komombo Rift, South Egypt

S. S. Selim

*International Journal of Earth Sciences, 105: 1387-1415, (2016), IF: 2.133*

The Komombo Basin is a recently discovered mixed nonmarine–marine, petroliferous basin of Cretaceous age in South Egypt. It is an asymmetrical half graben, synchronous with the Neothys opening and filled with up to 4 km of continental to open marine strata ranging from Early to Late Cretaceous. Despite its great relevance, no detailed sedimentological study concerning this basin has been carried out to date. Here, we present an integrated approach to the borehole and core data, as well as unique outcrop sections to construct a new detailed sedimentological interpretation on depositional systems, controls on basin evolution, basin configuration and regional tectonic setting. Seven depositional systems were recognized: (I) a fluvial fan system, (II) a braidplain system, (III) a siliciclastic lacustrine system, (IV) a lacustrine/lagoonal system, (V) a fluvial-estuarine system, (VI) a tidally affected delta, and (VII) an open marine system. The Komombo Basin evolution can be compartmentalized into three main rifting phases: the Berriasian–Early Barremian, Late Barremian, and Aptian–Albian. The first and third rifting phases are comparable with the rifting phases reported for several basins in North and Central Africa. The second rifting phase represents a transitional event between the other two phases. The first three depositional systems consist mainly of continental siliciclastics and are dominant in the Berriasian–Early Barremian and Late Barremian rifting phases. The lacustrine/lagoon and fluvial-estuarine systems correspond to the Aptian–Albian rifting phase, while the Campanian–Maastrichtian open-shelf deposits represents the post-rift stage.
**Keywords:** Cretaceous; Nonmarine; Rift; Komombo; Egypt.

## B-280. Paleo-Redox Depositional Conditions Inferred from Trace Metal Accumulation in Two Cretaceous-Paleocene Organic-Rich Sequences from Central Egypt

Moataz El-Shafeiy, Ahmed El-Kammar, Ahmed El-Barkooky and Philip A. Meyers

*Marine and Petroleum Geology, 73: 333-349, (2016), IF: 2.13*

Cretaceous-Paleocene organic-rich sediments in Egypt occur as an east-west trending belt extending from the Quseir-Safaga district (Red Sea) to the Kharga-Dakhla (Western Desert) region. They are associated with the Duwi Formation (phosphate-bearing) and the overlying Dakhla Formation (deeper epicontinental shale/marl). This study aims to reconstruct the paleo-redox conditions during deposition of these thermally immature organic-rich sediments using carbon-sulfur-iron systematics and trace metal proxies in two cores, one each from the Quseir and Abu Tartur areas. Paleoproductivity, based on P content, seems to have been higher in the Quseir section than in the Abu Tartur section. The Quseir section also records a relatively greater occurrence of anoxic conditions during the accumulation of these sediments than the Abu Tartur section. This difference is indicated by its markedly higher total

organic carbon (TOC) content as well as higher contributions of redox-sensitive and sulfide-forming metals (Mo, U, Ni, V, and Co). A weak correlation exists between S and TOC, and a positive S intercept (>1) was observed in most of the rock units of the study sections. A high consistency between the TOC-S-Fe relations and trace metals findings was found. The uppermost Duwi and the lowermost Dakhla strata, which have the highest TOC and represent a maximum sea transgression during the Late Cretaceous, have the highest contents of redox-sensitive trace metals. The carbonate-dominated transgressive Baris and Beida members of the Dakhla Formation record relatively stronger oxygen-depleted conditions during their accumulation than others, which led to relatively higher TOC contents and redox-sensitive metal accumulations. A scenario for the environmental conditions that existed during the deposition of these organic-rich successions, based on compiled trace metals and TOC-S-Fe implications, is reconstructed here.

**Keywords:** Redox conditions; Toc-S-Fe systematics; Trace metals; Black (Oil) shale; Cretaceous-Paleocene; Egypt.

## B-281. An Exploratory Early and Middle Holocene Sedimentary Record with Palynoforms and Diatoms from Faiyum Lake, Egypt

M.A. Hamdan, M.I.A. Ibrahimb, M.A. Shiha, R.J. Flower, F.A. Hassan and S.A.M. Eltelet

*Quaternary International, 410: 3-42, (2016), IF: 2.067*

We report on the sedimentology, pollen and diatom records in a 26 m long core of Holocene sediments from the Tersa area, near the centre of the Faiyum Depression (Egypt). Two radiocarbon and one OSL dates have been obtained for the core, dates range from 9545 ± 60 Cal. BP to c. 4040 BP. These correspond respectively with the Terminal Palaeolithic (Qarunian) and Neolithic Faiyum A (Faiyumian) cultures. The core is subdivided into 3 sedimentological units: unit 1 (21–26 m) is very thinly laminated, calcareous silt deposited in a deep water lake; unit 2 (9.5–21 m) is finely laminated sand, silt and carbonates formed as a lacustrine fan delta; unit 3 (9.5 m to the core top), is formed of massive silt, sandy silt and very fine grained flood plain sands. Planktonic diatom taxa, mainly Cyclostephanos, Aulacoseira, Cyclotella and Stephanodiscus spp. were abundant in units 1 & 2-a, indicating deep, open lake conditions. Magnetic minerals increased from the base of unit 2 indicating an increasing contribution of Nile alluvium. Benthic taxa such as Fragilaria, Cocconeis, Amphora and Navicula tended to increase towards the core top, from unit 2-b; 3-a to 3-b, indicative of lake shallowing and periods of low Nile floods. Unit 3-c is barren of diatoms and is compatible with terrestrial flood plain conditions. Vegetation was mainly represented by herbaceous pollen throughout most of the core and in the topmost sediment, pollen was scarce but pteridophyte (Osmundaceae) spores increased. Arboreal vegetation had low percentages in most of the record but increased in the middle section of the core (unit 2). A depositional deltaic environment was indicated throughout most of the core (sub-units 2-a & 3-a), where high abundances of Poaceae, Cyperaceae, Chenopodiaceae, Amaranthaceae, Polypodiaceae and Osmundaceae were recorded, indicating high Nile floods and fluctuating rainfall.

**Keywords:** Diatom pollen lake; Sediments holocene faiyum egypt.

## B-282. Small Vertebrates from Khasm El-Raqaba, Late Middle Miocene, Eastern Desert, Egypt

Gregg F. Gunnell, Alisa J. Winkler, Ellen R. Miller, Jason J. Head, Ahmed N. El-Barkooky, Mohamed Abdel Gawad, William J. Sanders and Philip D. Gingerich

*Historical Biology, 28 (1-2): 159-171, (2016), IF: 2.059*

Khasm El-Raqaba (KER) (28.451°N, 31.834°E) is a large commercial limestone quarry in Egypt's Eastern Desert. The site is best known for cetacean fossils recovered from middle Eocene deposits, but remains of some geologically younger, small fossil vertebrates representing snakes, rodents and bats, have been recovered from karst fissure-fill deposits intrusive into the Eocene limestones. Comparisons with extant and extinct material reveal that the KER snakes represent two different colubrines, the rodents are referable to the ctenodactylid Africanomys, and the bats represent a new species of Hipposideros (Pseudorhinolophus). Together, faunal correlation and geological evidence are in broad agreement with a late Middle Miocene age for this KER fauna, and a palaeoenvironmental reconstruction of mixed subtropical and more arid microhabitats.

**Keywords:** Snakes; Rodents; Bats; Neogene; North Africa; Limestone.

## B- 283. Architecture and Evolution of a Tectonically-Induced Middle Eocene Clastic Wedge on the Southern Tethyan Carbonate Shelf, North Eastern Desert, Egypt

S.S. Selim, M. Darwish and A.M. Abu Khadrah

*Proceedings of the Geologists Association, 127: 377-390, (2016), IF: 1.844*

The North Eastern Desert Basin is a series of interconnected basins located within the internal zone of the Syrian arc inversion belts. Throughout the Middle Eocene the basin was subject to pulses of transpression tectonics which led to development of a Middle Eocene clastic wedge. It is well exposed in the Shabraweet area, North Eastern Desert (Egypt). Detailed sedimentological study including facies analysis, and identification paleo-drainage directions were carried out in order to evaluate the development stages and architecture of the Middle Eocene clastic wedge and response to basin inversion. This was achieved through detailed description and measurement of eight surface profiles in the Shabraweet area. Twelve facies have been identified and can be arranged into nine facies associations. The overall architecture can be differentiated into 5 discontinuity-based sequences, described from oldest to youngest. Sequence 1 shows variation from a stream-dominated delta in the north to lagoonal deposits through the delta fringes. Sequence 2 shows downstream variation from alluvial channels, to alluvial fringes, and to distal floodbasin. Sequence 3 shows downstream variation from amalgamated fluvial channels to alluvial plain deposits. Sequence 4 shows downstream variation from deltaic to lagoon margin deposits. Sequence 5 shows variation from estuarine to offshore lagoonal environments. Tectonic inversion is interpreted as the primary control of the development of Middle Eocene clastic wedge. The sequences 1–3 reflect a progressive inversion with complete emergence and establishment of an

alluvial plain, while the upper sequences 4 and 5 reflect a tectonic quiescence and gradual return to marine conditions.
**Keywords:** Middle eocene; Shabraweet; Tethyan shelf; Syrian arc; North eastern desert; Egypt.

## B-284. Geochemistry and U-Pb Zircon Dating Constraints of Some Plutonic Rocks Along Bir Tawilah Shear Zone, Central Saudi Arabia: Implication for Magma Peterogenesis and Age of Gold Mineralization

Hesham M. Harbi, Kamal A. Ali, Abdelmonem A. Eldougdoug and Nasir S. Al-Jahdli

*Chemie Der Erde -Geochemistry, 76: 309-324, (2016),IF:1.622*

The study area covered by this work is located along the Bir Tawilah fault zone which encompasses the Arabian Shield between Afif terrane and western oceanic terranes. The rocks are dominantly ophiolite assemblages, island arc metavolcanic and metasedimentary rocks, and dioritic to granitic intrusions. The diorite and granodiorite rocks are I-type granitoids, calk-alkaline, metaluminous to peraluminous, formed in a volcanic arc setting, whereas the monzogranite is classified as A-type granite, alkaline and highly fractionated calc-alkaline, generated in within-plate tectonic setting. Nb and Y relationships indicated that the diorites and granodiorites were generated by a mafic parental magma contaminated with crustal materials, and controlled by fractional crystallization, whereas the monzogranites were generated from a magma characterized by an enriched mantle (EM) source. Mineralization including gold is hosted by the carbonatized serpentinite (listvenite) and the syn-tectonic granodiorite along Bir Tawilah thrust zone. U-Pb zircon geochronology indicates that the granodiorite at Jabal Ghadarah is emplaced at ca. 630 ± 12 Ma, probably suggests that the metallic minerals associated with the granodiorite along Bir Tawilah thurst zone are the result of remobilization of pre-existing gold mineralization associated with listevenite that is related to arc accretion.
**Keywords:** U-Pb zircon dating; Arabian shield; Gold mineralization; Bir tawilah shear zone; Arabian ahield.

## B-285. Morphology and Development of Pahoehoe Flow-Lobe Tumuli and Associated Features from A Monogenetic Basaltic Volcanic Field, Bahariya Depression, Western Desert, Egypt

Ezz El Din, Abdel Hakim Khalaf and Mohamed Saleh Hammed

*Journal of African Earth Science, 113:165-180,(2016) IF:1.326*

The dimensions, landforms, and structural characteristics of pahoehoe flow-lobe tumuli from Bahariya Depression are collectively reported here for the first time. The flow-lobe tumuli documented here characterize hummocky flow surfaces. These tumuli are characterized by low, dome-like mounds, lavainflation clefts, and squeeze ups. Flow-lobe tumuli are of various shapes and sizes, which are affected by the mechanism of inflation because they formed in response to the increase of pressure within the flow when the flow's crust becomes thicker. The tumuli often appear isolated or in small groups in the middle sectors of the lava flows, whereas in the distal sectors they form large concentration, suggesting the presence of complex lava tubes inside of the flow. Tumuli exhibited by El Bahariya lava flows are between 3.0 and 50 m in length and up to 5.0 m in height with lenticular geometry in aerial view. The flow emplacement of flow-lobe tumuli is controlled by variations in local characteristics such as nature of the substrate, flow orientation, slope, interferrence with other lobes, and rate of lava supply. Their presence generally towards the terminal ends of flow fields suggests that they seldom form over the clogged portions of distributary tubes or pathways. Thus, localized inflations that formed over blockages in major lava tubes result in formation of flow-lobe tumuli. The three-tiered (crust-core-basal zone) internal structure of the flow-lobe tumuli, resembling the typical distribution of vesicles in P-type lobes, confirms emplacement by the mechanism of inflation. All the available data show that the morphology and emplacement mechanism of the studied flow-lobe tumuli may be analogous to similar features preserved within topographically confined areas of the Hawaiian and Deccan hummocky lava flows. Considering the age of the studied volcanic fields (~22 Ma) it is most probable that the structures described here may be amongst the oldest recognized examples of lava inflation.
**Keywords:** Volcanic fields; Tumuli morphotypes; Baharyia Depression dilation fractures.

## B-286. Origin of Hydrous Alkali Feldspar-Silica Intergrowth in Spherulites from Intra-Plate A2-Type Rhyolites at the Jabal Shama, Saudi Arabia

Adel A. Surour, Said A. El-Nisr and Rami A. bakhsh

*Journal of African Earth Sciences, 115:92-107, (2016),IF:1.326*

Miocene rhyolites (19.2 ± 0.9 Ma) at the Jabal Shama in western Saudi Arabia represent an example of rift-related silicic volcanism that took place during the formation of the Red Sea. They mostly consist of tuffaceous varieties with distinct flow banding, and pea-sized spherulites, obsidian and perlitized rhyolite tuffs. Although they have the geochemical signature of A2-type rhyolites, these silicic rocks are not typically alkaline but alkali-calcic to calc-alkaline. They developed in a within-plate regime and possibly derived from a recycled mafic subducted slab in depleted sub-continental mantle beneath the western Arabian plate. The Jabal Shama rhyolites are younger in age than their Miocene counterparts in Yemen and Ethiopia. The Jabal Shama spherulites consist of hydrous alkali feldspar-silica radial intergrowths with an occasional brown glass nucleus. Carbonate- and glass-free spherulites give up to 4.45 wt% L.O.I. The hydrous nature of these silicates and the absence of magnetite in the spherulites is a strong indication of oxidizing conditions. The spherulites contain hydrous feldspars with up to ~6 wt% $H_2O$, and they develop by diffusion and devitrification of glass in the rhyolite tuff at ~800 °C. Owing to higher undercooling due to supersaturation, the radial hydrous phases within spherulites might grow faster and led to coagulation. The polygonal contacts between spherulites and the ~120° dihedral angle suggest solid-state modification and recrystallization as the process of devitrification proceeds as low as ~300 °C. The sum of FeO + MgO is positively correlated with total alkalies along with magnetite oxidation in the matrix to Fe-oxyhydroxides, and to the incorporation of $OH^-$ into silicates within the spehrulites themselves. Structural $H_2O$ in glass of the Jabal Shama perlite (obsidian) is considerable (~9–12 wt%) with 3.72–5.6 wt% L.O.I. of the

whole-rock. The presence of deleterious silica impurities would lower the ore grade due to poor expansion. Zeolitization of the rhyolite tuff was limited or incomplete in comparison with that of Pliocene-Pleistocene rift-related mafic volcanics in the western Arabian plate.

**Keywords:** Jabal shama; Rhyolites; Intra-Plate; Spherulites; Hydrous feldspars.

## B-287. Newly Improved Band Ratio of Aster Data for Lithological Mapping of the Fawakhir Area, Central Eastern Desert, Egypt

Hassan Mohy , Islam Abou El-Magd and Fawzy F. Basta

*Journal of The Indian Society of Remote Sensing, 44 (5): 735-746, (2016), IF: 0.676*

This research study aims at utilizing the ASTER data for lithological mapping of the Fawakhir area, Central Eastern Desert of Egypt. Short wave infrared and thermal infrared channels were processed and interpreted for the potential mapping of the various rock types at the Fawakhir area. A newly developed ASTER band-ratio of 4/7, 4/10, 4/11 is introduced to characterize the lithological units in the area of study. Field visits and laboratory microscopic examinations of selected samples collected from the different exposed rocks in the area of study were carried out. The validation mechanism was based on both calculating statistical optimum index factor (OIF) and matching interpreted lithological boundaries to field data and previously published geologic maps.

**Keywords:** Aster; Lithological mapping; Fawakhir area; Band ratio; Egypt.

## B-288. Fracture Reopening by Micro-Earthquakes, A Mechanism for Oil Seepage in Mildly Active Rifts: A Case Study from Gemsa Oilfield, the Southern Gulf of Suez Rift, Egypt

Shawky Sakran, Muhammad Nabih, Ahmed Henaish and Abdelmohsen Ziko

*Arabian Journal of Geosciences, 9 (5), May 2016: 1-17 (2016)*

Episodic hydrocarbon seepage is present at Gemsa oilfield, southern Gulf of Suez rift, Egypt. The occurrence of the oil at this area has been known for thousands of years. The nature and origin of this seepage is the main target of the present study. Surface geological mapping substantiated by subsurface mapping using 2-D seismic lines and well log data are integrated. Moreover, the present day stress orientation and magnitudes are integrated with the mechanical properties of the reservoir rock in order to produce a coherent interpretation for the migration pathways and the main causes of the hydrocarbon seepage. The study revealed that the episodic hydrocarbon seepage at mildly active rifts such as the southern Suez rift can be resulted from the migration of entrapped hydrocarbons along the damage zone of slightly active faults with continuous micro-earthquakes. The pressure released from the micro-earthquakes causes the reopening of preexisting fractures where hydrocarbon found their easy pathway to the surface through highly fractured rocks and unconsolidated sediments. The produced migration pathway map proposes the possibility of an unexplored Hammam Faraun Member reservoir at the study area. The original oil in place of the predicted reservoir is estimated to be more than 22 MMBO which encourages the design makers for more investigation of this reservoir to increase its certainty and putting it in the plan of the future investments.

**Keywords:** Gemsa; Oil seepage; Hydrocarbon migration; Gulf of suez rift; Fault valve; Hammam faraun member; Micro-earthquakes; Seismicity.

## B-289. Preservation and Restoration of the Wadi Sura Caves in the Framework of the "Gilf Kebir National Park", Egypt

Maria Cristina Tomassetti, Giulio Lucarini, Mohamed A. Hamdan, Andrea Macchia and Giuseppina Mutri Barbara E. Barich

*International Journal of Conservation Science, 7: 913-934 (2016)*

In 2010 the Italian-Egyptian Environmental Cooperation launched a safeguarding project for the preservation of the caves with prehistoric rock art located in the Gilf Kebir plateau in southwestern Egypt. The project was part of the cooperation program developed to establish the Egyptian Gilf Kebir National Park (GKNP) protected area. Given their bad state of preservation, the Italian conservation project focused on the Caves of Swimmers and Archers, located along the Wadi Sura. Although only very few studies of this kind have been carried out in the Saharan region, our w ork in the Gilf Kebir can be considered a pilot study, the results of which should be evaluated in the long term. Results obtained to date and reported in this paper provide analytical petrographic studies of the bedrock, a complete photographic and geodet ic survey of the two sites, data from climate monitoring, along with a preliminary consolidation of some of the most at-risk areas of the two caves. Finally, laboratory experimentation led us to select the most suitable materials for the consolidation of the rock, shifting in the direction of nano-technology instead of ethyl silicate use because of the longer cross-linking process of the latter in hyper-arid environments; the use of the latter can in fact result in extremely long and expensive field seasons. These results will be valuable for the continuation and extension of the project, which is currently suspended due to safety concerns in the region.

**Keywords:** Saharan rock art; Climatic weathering; Sandstone consolidation; Petrographic analysis; P Orosimetric analysis; Laboratory experimentation on Nano -silica.

## B-290. Magmatic Underplating Beneath the Emeishan Large Igneous Province (South China) Revealed by the Comgra-Elip Experiment

Yangfan Deng, Yun Chen, Peng Wang, Khalid S. Essa, Tao Xu, Xiaofeng Liang and José Badal

*Tectonophysics, 672–673: 16-23, (2016), IF: 2.65*

Because of the abundant geological, geochemical and geophysical studies conducted on the Emeishan large igneous province (ELIP) in South China, the Permian mantle plume model associated with this region is widely accepted. Furthermore, the dome-shaped structure related with this plume has been determined with success by sedimentological data and

gravity stripping. Although the sediment thickness, upper crust, Moho depth and the lithosphere–asthenosphere boundary (LAB) are well constrained by active- and passive-source seismological results, the density anomaly in ELIP is still a poorly constrained issue that needs further attention. With the aim especially to understand the impact on surface of the magmatic processes that originated in the deep mantle, we performed the COMGRA-ELIP gravity experiment across this region. Using a stripping method, we determined the residual gravity in ELIP and surrounding areas. The residual gravity reaches a maximum value of + 150 mGal in the inner zone of ELIP and its strength decreases gradually when measuring from the inner zone to the middle and outer zones. Combining active and passive seismic results and the least-squares variance analysis method, we propose a strong density contrast of 0.2 g/cm3 (density of 3.14 g/cm3) for the 15- to 20-km-thick igneous layer accreted at the base of the crust, as evidence of crustal underplating in ELIP, to explain the present-day residual gravity anomaly.

**Keywords:** Stripping; Residual gravity; Density anomaly; Underplating; Emeishan large igneous province; South china.

## B-291. A Least-Squares Minimization Approach for Model Parameters Estimate by Using A New Magnetic Anomaly Formula

E. R. ABO-EZZ and K. S. ESSA

*Pure and Applied Geophysics,17 (4):1265-1278,(2016), IF:1.677*

A new linear least-squares approach is proposed to interpret magnetic anomalies of the buried structures by using a new magnetic anomaly formula. This approach depends on solving different sets of algebraic linear equations in order to invert the depth (z), amplitude coefficient (K), and magnetization angle (θ) of buried structures using magnetic data. The utility and validity of the new proposed approach has been demonstrated through various reliable synthetic data sets with and without noise. In addition, the method has been applied to field data sets from USA and India. The best-fitted anomaly has been delineated by estimating the root-mean squared (rms). Judging satisfaction of this approach is done by comparing the obtained results with other available geological or geophysical information.

**Keywords:** New magnetic anomaly formula; A Linear Least-Squares; Model parameters; Rms.

## B-292. Hydro/Engineering Geophysical Parameters and Design Response Spectrum for Sustainable Development in Ras Muhammed National Park, Sinai

Mohamed H. Khalil and Mohamed A. Gamal

*Pure and Applied Geophysics, 173:2101-2118,(2016),IF: 1.677*

The Egyptian government is preparing a sustainable development master plan for the Ras Muhammed National Park (RMNP), south Sinai. Noteworthy, the scarcity of the freshwater resources and close proximity to the active seismic zones of the Gulf of Aqaba implicate geophysical investigations for the fresh groundwater aquifers and construct a design response spectrum, respectively. Accordingly, 14 VESs, hydro/engineering geophysical analysis, pumping tests, downhole seismic test, a design response spectrum for buildings, and borehole data were carried out in the study area. The unconfined freshwater aquifer was effectively depicted with true resistivities, thickness, and EC ranged from 56 to 135 Ω m, 11 to 112 m, and 1.4 to 7.1 mS/m, respectively. The Northeastern part was characterized by higher aquifer potentiality, where coarser grains size, highest thickness (112 m), high true resistivity (135 Ω m), groundwater flow (0.074 m3/day), tortuosity (1.293–1.312), formation resistivity factor (4.1–4.6), and storativity (0.281–0.276). An increase in pumping rate was accompanied by an increase in well loss, increase in aquifer losses, decrease in well specific capacity, and decrease in well efficiency. Design response spectrum prognosticated the short buildings (<7 floors) in RMNP to be suffering from a high peak horizontal acceleration and shear forces for acceleration between 0.25 and 0.35 g. Therefore, appropriate detailing of shear reinforcement is indispensable to reduce the risk of structural damages at RMNP.

**Keywords:** Hydro/Engineering; design response spectrumresistivity; tortuosity; formation; resistivity factor; storativity; peak horizontal acceleration.

## B-293. Subsurface Faults Detection Based on Magnetic Anomalies Investigation: A Field Example at Taba Protectorate, South Sinai

Mohamed H. Khalil

*Journal of Applied Geophysics, 131: 123-132 (2016), IF: 1.355*

Quantitative interpretation of the magnetic data particularly in a complex dissected structure necessitates using of filtering techniques. In Taba protectorate, Sinai synthesis of different filtering algorithms was carried out to distinct and verifies the subsurface structure and estimates the depth of the causative magnetic sources. In order to separate the shallow-seated structure, filters of the vertical derivatives (VDR), Butterworth high-pass (BWHP), analytic signal (AS) amplitude, and total horizontal derivative of the tilt derivative (TDR_THDR) were conducted. While, filters of the apparent susceptibility and Butterworth low-pass (BWLP) were conducted to identify the deep-seated structure. The depths of the geological contacts and faults were calculated by the 3D Euler deconvolution. Noteworthy, TDR_THDR was independent of geomagnetic inclination, significantly less susceptible to noise, and more sensitive to the details of the shallow superimposed structures. Whereas, the BWLP proved high resolution capabilities in attenuating the shorter wavelength of the near surface anomalies and emphasizing the longer wavelength derived from deeper causative structure. 3D Euler deconvolution (SI = 0) was quite amenable to estimate the depths of superimposed subsurface structure. The pattern, location, and trend of the deduced shallow and deep faults were conformed remarkably to the addressed fault system.

**Keywords:** Magnetic; Vertical derivatives; Butterworth high-pass; Analytic signal amplitude; Total horizontal derivative of the tilt derivative; Apparent susceptibility; Butterworth low-Pass; 3D euler deconvolution.

## B-294. A Least-Squares Minimization Approach to Interpret Gravity Data Due to 2D Horizontal Thin Sheet of Finite Width

E . M. Abdelrahman, M. M. Gobashy, K. S. Essa, E. R. Abo-Ezz and T. M. El-Araby

*Arabian Journal of Geosciences, 9 (8):515-521,(2016) IF:1.224*

In the present paper, we have developed a least-squares minimization approach to estimate simultaneously the depth and the width of a buried 2D thin sheet from moving average residual gravity anomalies using the window-curves method. The method involves fitting the 2D thin sheet model convolved with the same moving average filter as applied to the observed data. As a result, our method can be applied not only to residuals but also to the Bouguer gravity data. A scheme for analysis of gravity data has been formulated to determine the model parameters of the thin sheet. The method is applied to synthetic data with and without random errors and tested on a field example from Egypt.

**Keywords:** 2D horizontal thin sheet model; Depth-Width Curves method; Least-Squares method.

## B-295. Hydraulic and Electric Anisotropy of Shallow Fresh Coastal Aquifer in Nabq, Sinai, Egypt

Mohamed H. Khalil

*Arabian Journal of Geosciences, 9:284: 2-18, (2016), IF:1.224*

The prospective of this research is to investigate the hydraulic and electric anisotropy of the fresh coastal aquifer. In this context, 44 Schlumberger DC soundings associated with the available boreholes data and numbers of measured and/or calculated hydraulic and electric parameters were carried out in Nabq area, Sinai. The inverted DC soundings revealed high potentiality of the fresh coastal aquifer toward the western part of the Quaternary and Pre-Quaternary. An increased tortuosity (T) toward the west direction was associated with coarser grains size and increase in resistivity (ρ) hydraulic conductivity (K), transmissivity (T), and a decrease in porosity (ϕ). The longitudinal hydraulic conductivity (Kl) was found to be greater than the transverse hydraulic conductivity (Kt) which implied a lower tortuosity in the horizontal direction than in the vertical direction. The decrease in the hydraulic anisotropy (λH) was associated by an increase in transmissivity. Minor variation in electric anisotropy (λe) could be observed as a result of alternating layers and intercalation of different grain sizes. Resistivity of the fresh aquifer was recognized by a liner direct relation with λH, whereas, no clear relation could be observed with λE. A polynomial relation with poor correlation coefficient could be observed between λH and λE.

**Keywords:** Hydraulic Anisotropy; Electric anisotropy; Tortuosity; Resistivity; Hydraulic conductivity Transmissivity; Porosity; Fresh coastal aquifer.

## B-296. Regional Integrated Interpretation of the Hydrocarbon Prospectivity of the Nile Delta, offshore Egypt

Said Hanafy, Shastri L. Nimmagadda, Sharaf E. Mahmoud, Walid M. Mabrouk and Khamis Farhood

*Arabian Journal of Geosciences, 9 (5): 1-18, (2016), IF: 1.224*

Interpretation of 2500 km of newly processed 2D seismic and regional potential field data has led to the identification of two new Miocene–Oligocene sedimentary basins in the northern part of offshore Egypt. The western part of the basin is deeper and has thick sedimentary cover. The upper part of the Miocene section is tested in its southern part through two wells, where the eastern subbasin is still virgin and is located at the intersection between Temsah basins and southeastern end of the Levantine basin. The main sedimentary unit of the basin is the Miocene–Oligocene sedimentary section, which was proven by the exploration and production activities in Nile Delta to be one of the hydrocarbon-generating facies. This fact is supported by 1D basin analysis using the average parameter values, which shows a hydrocarbon window, extending from lower Miocene to upper Miocene. The basin dimensions are more than 2000 km2 area and more than 4000 m of thickness, with variable petroleum system parameters' potentialities, starting from Tortonian–Serravallian to lower Oligocene section.

**Keywords:** Nile Delta; Regional interpretation.

## B-297. A Simple Method for Depth Determination from Self-Potential Anomalies Due to Two Superimposed Structures

El-Sayed M. Abdelrahman Eid R. Abo-Ezz Tarek M. El-Araby and Khalid S. Essa

*Exploration Geophysics, 47 (4): 308-314, (2016), IF: 1.197*

In this paper, we develop a method to determine the depth to two superimposed sources from a self-potential anomaly profile. The method is based on finding a relationship between the depths to the two superimposed structures from a combination of observations at symmetric points with respect to the coordinate of the sources' centre. Formulae have been derived for two classes of geometric sources: spheres and cylinders. Equations are also formulated to estimate the other model parameters, including the polarisation angle and electric dipole moment of both structures. The proposed method is tested both on synthetic data with and without random noise, as well as real self-potential data from a set of field data collected in Turkey. In all cases, the model parameters obtained are in good agreement with the actual ones.

**Keywords:** Depth-Curves method; Interpretation; Noise; Sp data; Superimposed structures

## B-298. Depth and Shape Solutions from Second Moving Average Residual Magnetic Anomalies

El-Sayed M. Abdelrahman Khalid S. Essa Tarek M. El-Araby and Eid R. Abo-Ezz

*Exploration Geophysics, 47 (1): 58-66, (2016), IF: 1.197*

We have developed a simple and fast numerical method to simultaneously determine the depth and shape of a buried structure from second moving average residual anomalies obtained from magnetic data with filters of successive window lengths. The method is similar to Euler deconvolution, but it solves for depth and shape independently. The method involves using a nonlinear relationship between the depth to the source and the shape factor, and a combination of observations at five points with respect to the coordinate of the source centre with a free parameter (window length). The method is based on computing the standard deviation of the depths determined from all second moving average residual anomalies for each value of the shape factor. The standard deviation may generally be considered a criterion for determining the correct depth and shape of the buried structure. When the correct shape factor is used, the standard deviation of the depths is less than the standard deviation using incorrect values of the shape factor. This method can be applied to residuals, as well as the observed magnetic data consisting of the combined effect of a residual component due to a purely local structure and a regional component represented by a polynomial of up to fourth-order. The method is applied to synthetic data, with and without random errors, and tested on a field example from Brazil. In all cases, the shape and depth of the buried structures are found in good agreement with the actual ones.

**Keywords:** Interpretation; Magnetic data; Noise; Standard deviation.

## B-299. Geotechnical Parameters from Seismic Measurements: Two Field Examples from Egypt and Saudi Arabia

Mohamed H. Khalil and Sherif M . Hanafy

*Journal of Environmental and Engineering Geophysics, 21: 13-28, (2016), IF: 0.619*

Geotechnical parameters were used to determine subsurface rock quality for construction purposes. We summarize the mathematical relationships used to calculate the geotechnical parameters from P- and S-wave velocities and density values. These relationships are applied to two field examples; the first is a regional seismic study in Egypt and the second is a 2-D seismic profile recorded in Saudi Arabia. Results from both field examples are used to determine the subsurface rock quality and locate zones that should be avoided during construction. We suggest combining all geotechnical parameters into one map using a normalized-weighted relation, which helps to locate the zones with high versus low rock quality for engineering purposes.

**Keywords:** Geotechnical parameters; P- and S-Wave velocities.

## B-300. A Solution to Unexploded Ordnance Detection Problem from its Magnetic Anomaly Using Kaczmarz Regularization

Maha Abdelazeem and Mohamed M. Gobashy

*Interpretation-A Journal of Subsurface Characterization, 4 (3): (2016) IF: 0.51*

Old military events pose a critical and severe problem for many countries, including the Egyptian northwestern coast. These result in extensive areas of surface/subsurface landmines that affect the economic development plans of many countries. Detection of these landmines becomes a target for many geophysical research teams. Currently, unconventional near-surface flight technologies, such as quad-hexacopters instead of regular land surveys, are used for safety reasons in the acquisition phase. We have introduced a new processing and modeling technique of magnetic data conducted over mines or near-surface geophysical targets for accurate and precise determination of location and depth. The technique is based on the application of the Kaczmarz regularization method to the ill-posed magnetic inverse problem. The advantage of this method is the optimum transformation of regularized normal equations to an equivalent augmented regularized normal system of equations. The condition number of the updated system, which determines the degree of ill posedness, is greatly lower than the original one; this improves and guarantees a good solution to the system. The method is applied to an unexploded ordnance (UXO) test site in the United Kingdom. Our results have determined that the technique is appropriate and promising in efficiently addressing a wide number of problems that are important to near-surface geophysicists, including UXO detection.

**Keywords:** Uxo; Inversion; Magnetic; Kacsmarz.

### *Dept. of Mathematics*

## B-301. Mono-Jet, -Photon and -Z Signals of a Supersymmetric (B-L) Model at the Large Hadron Collider

W. Abdallah, J. Fiaschi, S. Khalila and S. Morettic

*Journal of High Energy Physics, (2016) IF: 6.023*

Search for invisible final states produced at the Large Hadron Collider (LHC) by new physics scenarios are normally carried out resorting to a variety of probes emerging from the initial state, in the form of single-jet, -photon and -Z boson signatures. These are particularly effective for models of Supersymmetry (SUSY) in presence of R-parity conservation, owing to the presence in their spectra of a stable neutralino as a Dark Matter (DM) candidate. We assume here as theoretical framework the Supersymmetric version of the (B − L) extension of the Standard Model (BLSSM), wherein a mediator for invisible decays can be the Z′ boson present in this scenario. The peculiarity of the signal is thus that the final state objects carry a very large (transverse) missing energy, since the Z′ is naturally massive and constrained by direct searches and Electro-Weak Precision Tests (EWPTs) to be at least in the TeV scale region. Under these circumstances the efficiency in accessing the invisible final state and rejecting the Standard Model (SM) background is very high. This somehow compensates the rather meagre production rates. Another special feature of this invisible BLSSM signal is its composition, which is often dominated by sneutrino decays (alongside the more traditional neutrino and neutralino modes). Sensitivity of the CERN machine to these two features can therefore help disentangling the BLSSM from more popular SUSY models. We assess in this analysis the scope of the LHC in establishing the aforementioned invisible signals through a sophisticated signal-to-background simulation carried out in presence of parton shower, hadronisation as well as detector effects. We find that significant sensitivity exists already after 300 fb−1 during Run

2. We find that mono-jet events can be readily accessible at the LHC, so as to enable one to claim a prompt discovery, while mono-photon and -Z signals can be used as diagnostic tools of the underlying scenario.
**Keywords:** Supersymmetry phenomenology.

## B-302. A Viable Logarithmic F(R) Model for Inflation

M. Amin, S. Khalil and M. Salah

*Journal of Cosmology and Astroparticle Physics, (2016) IF:5.634*

Inflation in the framework of f(R) modified gravity is revisited. We study the conditions that f(R) should satisfy in order to lead to a viable inflationary model in the original form and in the Einstein frame. Based on these criteria we propose a new logarithmic model as a potential candidate for f(R) theories aiming to describe inflation consistent with observations from Planck satellite (2015). The model predicts scalar spectral index $0.9615 < ns < 0.9693$ in agreement with observation and tensor-to-scalar ratio r of order 10−3. Furthermore, we show that for a class of models, a natural coupling between inflation and a scalar boson is generated through the minimal coupling between gravity and matter fields and a reheating temperature less that 109 GeV is obtained.
**Keywords:** F(R) Modified gravity; Inflation.

## B-303. Numerical Study for Multi-Strain Tuberculosis (Tb) Model of Variable-Order Fractional Derivatives

Nasser H. Sweilam and Seham M. AL-Mekhlafi

*Journal of Advanced Research, 7: 271-283, (2016), IF: 3*

In this paper, we presented a novel multi-strain TB model of variable-order fractional derivatives, which incorporates three strains: drug-sensitive, emerging multi-drug resistant (MDR) and extensively drug-resistant (XDR), as an extension for multi-strain TB model of nonlinear ordinary differential equations which developed in 2014 by Arino and Soliman [1]. Numerical simulations for this variable-order fractional model are the main aim of this work, where the variable-order fractional derivative is defined in the sense of Gru¨nwald–Letnikov definition. Two numerical methods are presented for this model, the standard finite difference method (SFDM) and nonstandard finite difference method (NSFDM). Numerical comparison between SFDM and NSFDM is presented. It is concluded that, NSFDM preserves the positivity of the solutions and numerically stable in large regions than SFDM.
**Keywords:** Nonstandard finite difference; Epidemic model; Tuberculosis; M/XDR-TB; Variable-order fractional; Grunwald–Letnikov definition.

## B-304. On the "Kpkp^Kpkp^-Operator", New Extension of the Kdv6 to (M + 1)-Dimensional Equation and Traveling Waves Solutions

H. I. Abdel-Gawad

*Nonlinear Dynamics, 85: 1509-1515, (2016), IF: 3*

Very recently, the KdV6 was extended to a (2 + 1)- dimensional equation by a direct way. Here, by using the " kˆp-operator" the extension of that equation is done in a rigorous mathematical formulation. Polynomial solutions to the closed form equation are obtained via the unified method. It is found that via nonlinear interactions of traveling waves the solutions of the constructed equation may not be unique. Also, these solutions may show solitary or explosive shock waves.
**Keywords:** A Method of extension of the Kdv6 to higher; Dimensional equation; Solitary; Soliton; Elliptic; Shock Waves; Non-Uniqueness of the solutions; The unified method

## B-305. New Galerkin Operational Matrices for Solving Lane-Emden Type Equations

W.M. Abd-Elhameed, E.H. Doha, A.S. Saad and M.A. Bassuony

*Revista Mexicana De Astronomia Y Astrofisica, 52(1): 83-92, (2016), IF: 2.364*

Lane-Emden type equations model many phenomena in mathematical physics and astrophysics, such as thermal explosions. This paper is concerned with intro - ducing third and fourth kind Chebyshev-Galerkin operational matrices in order to solve such problems. The principal idea behind the suggested algorithms is based on converting the linear or nonlinear Lane-Emden problem, through the application of suitable spectral methods, into a system of linear or nonlinear equations in the expansion coefficients, which can be efficiently solved. The main advantage of the proposed algorithm in the linear case is that the resulting linear systems are specially structured, and this of course reduces the computational effort required to solve such systems. As an application, we consider the solar model polytrope with n = 3 to show that the suggested solutions in this paper are in good agreement with the numerical results.
**Keywords:** Methods: Analytical; Methods: Numerical; Stars: Solar-Type.

## B-306. Jacobi–Gauss–Lobatto Collocation Method for Solving Nonlinear Reaction–Diffusion Equations Subject to Dirichlet Boundary Conditions

A.H. Bhrawy, E.H. Doha, M.A. Abdelkawy and R.A. Van Gorder

*Applied Mathematical Modelling,40:17031716,(2016),IF:2.291*

This paper extends the application of the spectral Jacobi–Gauss–Lobatto collocation (J-GL-C) method based on Gauss–Lobatto nodes to obtain semi-analytical solutions of nonlinear timedependent reaction–diffusion equations (RDEs) subject to Dirichlet boundary conditions. This approach has the advantage of allowing us to obtain the solution in terms of the Jacobi parameters $\alpha$ and $\beta$, which therefore means that the method holds a number of collocation methods as a special case. In addition, the problem is reduced to the solution of system of ordinary differential equations (SODEs) in the time variable, which may then be solved by any standard numerical technique. We consider five applications of the general method to concrete examples. In each of the examples considered, the numerical

results show that the proposed method is of high accuracy and is efficient for solving nonlinear time-dependent RDEs.
**Keywords:** Nonlinear reaction; Diffusion equations collocation Method Jacobi; Gauss; Lobatto quadrature.

## B-307. Mssm Dark Matter in Light of Higgs and Lux Results

W. Abdallahand S. Khalil1

*Advances In High Energy Physics, (2016) IF: 1.839*

The constraints imposed on the Minimal Supersymmetric Standard Model (MSSM) parameter space by the Large Hadron Collider (LHC) Higgs mass limit and gluino mass lower bound are revisited. We also analyze the thermal relic abundance of lightest neutralino, which is the Lightest Supersymmetric Particle (LSP). We show that the combined LHC and relic abundance constraints rule out most of the MSSM parameter space except a very narrow region with very large tanbeta (~50). Within this region, we emphasize that the spin-independent scattering cross section of the LSP with a proton is less than the latest Large Underground Xenon (LUX) limit by at least two orders of magnitude. Finally, we argue that nonthermal Dark Matter (DM) scenario may relax the constraints imposed on the MSSM parameter space. Namely, the following regions are obtained: m0 = 4 TeV and m12 =600 GeV for low tanbeta (~10); m0 ~ m12 = 1 TeV or m0 = 4 TeV and m12 = 700 GeV for large tanbeta (~50).
**Keywords:** Dark matter; Suppersymmetry and Large hadron Collider.

## B-308. Deformation of an Elastic Magnetizable Square Rod Due to A Uniform Electric Current Inside the Rod and an External Transverse Magnetic Field

AR El Dhaba, AF Ghaleb andL Placidi

*Mathematics and Mechanics of Solids, 21(2): 222-241, (2016), IF: 1.836*

We find the deformation and stresses in an infinite rod of an electric conducting material with square normal crosssection, carrying uniform electric current and subjected to an external, initially uniform magnetic field. The complete solution of the uncoupled problem is obtained using a boundary integral method. The results are discussed in detail.
**Keywords:** Boundary integrals; Electric current; Long rod; Magnetic vector potential; Maxwell stress; Plane problem; Thermo-Magneto; Elasticity.

## B-309. A Novel Operational Matrix of Caputo Fractional Derivatives of Fibonacci Polynomials: Spectral Solutions of Fractional Differential Equations

Waleed M. Abd-Elhameed and Youssri H. Youssri

*Entropy, 18(10): 1-15, (2016), IF: 1.743*

Herein, two numerical algorithms for solving some linear and nonlinear fractional-order differential equations are presented and analyzed. For this purpose, a novel operational matrix of fractional-order derivatives of Fibonacci polynomials was constructed and employed along with the application of the tau and collocation spectral methods. The convergence and error analysis of the suggested Fibonacci expansion were carefully investigated. Some numerical examples with comparisons are presented to ensure the efficiency, applicability and high accuracy of the proposed algorithms. Two accurate semi-analytic polynomial solutions for linear and nonlinear fractional differential equations are the result.
**Keywords:** Fibonacci polynomials; Operational matrix; Spectral methods; Modified bessel functions; Fractional-order differential equations; Van Der Pol oscillator; Rayleigh equation.

## B-310. Numerical Approximation of L´Evy-Feller Fractional Diffusion Equation Via Chebyshev-Legendre Collocation Method

N.H. Sweilam and M.M. Abou Hasan

*The European Physical Journal Plus, 131: 251: 2-12, (2016), IF: 1.521*

This paper reports a new spectral algorithm for obtaining an approximate solution for the L´evy- Feller diffusion equation depending on Legendre polynomials and Chebyshev collocation points. The L´evy-Feller diffusion equation is obtained from the standard diffusion equation by replacing the second-order space derivative with a Riesz-Feller derivative. A new formula expressing explicitly any fractional-orderderivatives, in the sense of Riesz-Feller operator, of Legendre polynomials of any degree in terms of Jacobipolynomials is proved. Moreover, the Chebyshev-Legendre collocation method together with the implicit Euler method are used to reduce these types of differential equations to a system of algebraic equations which can be solved numerically. Numerical results with comparisons are given to confirm the reliability of the proposed method for the L´evy-Feller diffusion equation.
**Keywords:** L´Evy-Feller diffusion equation; The Riesz-feller derivative; Spectral algorithm.

## B-311. Multiple Wave Scattering by Submerged Obstacles in an Infinite Channel of Finite Depth. I. Streamlines

M.S. Abou-Dina and A.F. Ghaleb

*European Journal of Mechanics-B/Fluids, 59: 37-51, (2016), IF: 1.418*

A finite number of rigid bodies of finite extent are submerged and kept fixed in an infinite, homogeneous layer of finite depth of an inviscid fluid of constant density. The layer is bounded from above by a free surface and from below by a horizontal impermeable bottom. An incident harmonic wave of given frequency propagating in the fluid layer is partially reflected by the obstacles, while part is transmitted after multiple scattering. The problem is to determine the resulting motion of the fluid in the frame of the linearized theory. A finite Fourier transform technique is used to this end, in combination with the methods of separation of variables, fundamental solutions and boundary collocation. This yields different expressions for the solution in

different parts of the flow domain, each of which depends on a system of orthogonal functions. The obtained solution exhibits smoothness at any order in the fluid domain. It satisfies rigorously the field equation and all the boundary conditions, with the exception of the condition at the obstacle boundaries which is satisfied pointwise by boundary collocation. The method deals invariably with any finite number of obstacles, and its accuracy is clearly defined. Numerical applications with one and two circular obstacles are presented and the effects of the level of submergence are discussed. Plots are provided for the resulting system of streamlines.

**Keywords:** Wave scattering; Potential flow; Linear theory; Finite fourier transform; Fundamental solutions; Boundary collocation method.

## B-312. Spectral Solutions for Fractional Differential Equations Via A Novel Lucas Operational Matrix of Fractional Derivatives

WM Abd-Elhameed and YH Youssri

*Romanian Journal of Physics, 61(5-6):795-815(2016), IF:1.398*

In this research article, a novel operational matrix of fractional-order differentiation of Lucas polynomials in the Caputo sense is established. Based on this matrix along with the application of tau and collocation spectral methods, two efficient numerical algorithms for solving multi-term fractional differential equations are proposed and analyzed. Some new formulae for Lucas polynomials are stated and proved for investigating the new algorithms. The convergence and error analysis of the suggested Lucas expansion are investigated carefully. Some new inequalities including the modified Bessel function of the first kind and the well-known golden ratio are stated and proved. Some numerical tests are carried out for some specific and important types of problems including the Bagley-Torvik, Ricatti, Lane-Emden and oscillator equations. The results obtained are compared with some existing ones in open literature and it is noticed that the two proposed algorithms are robust, accurate and easy to apply.

**Keywords:** Lucas polynomials; Tau and collocation spectral methods; Fractional-Order; Differential equations; Error analysis.

## B-313. A New Collocation Scheme for Solving Hyperbolic Equations of Second Order in A Semi-Infinite Domain

R.M. Hafez, M.A. Abdelkawy, E.H. Doha andA.H. Bhrawy

*Romanian Reports in Physics, 68(1): 112-127, (2016), IF:1.367*

This paper reports a new fully collocation algorithm for the numerical solution of hyperbolic partial differential equations of second order in a semi-infinite domain, using Jacobi rational Gauss-Radau collocation method. The widely applicable, efficiency, and high accuracy are the key advantages of the collocation method. The series expansion in Jacobi rational functions is the main step for solving the mentioned problems. The expansion coefficients are then determined by reducing the hyperbolic equations with their boundary and initial conditions to a system of algebraic equations for these coefficients. This system may be solved analytically or numerically in a stepby-step manner by using Newton's iterative method. Numerical results are consistent with the theoretical analysis and indicate the high accuracy and effectiveness of this algorithm.

**Keywords:** Hyperbolic equations; Jacobi rational functions; Collocation method; Semi-infinite domain; Gauss-Radau quadrature.

## B-314. Singularly Perturb E D Bvp to Estimation of Diaphragm Deflection in Mems Capacitive Microphone: an Application of Adm

M.M. Khader and N.H. Sweilam

*Applied Mathematics and Computation, 281 (2016): 214-222 ) IF: 1.345*

In this paper, we implement the Adomian decomposition method (ADM) to approximate the deflection of polysilicon diaphragm with small flexural rigidity of Micro Electro Mechanical System (MEMS) capacitive microphone. We prove the existence and the uniqueness of the solution of considered problem with the help of the theory of semi-group. Special attention is given to prove the convergence of the implemented method. Numerical simulation and comparison between the approximate solutions by using the ADM with the variational iteration method are given.

**Keywords:** Adomian decomposition method; Analytical solution; Diaphragm deflection; Singular perturbation; Semi-Group theory; Capacitive microphone.

## B-315. Modified Jacobi–Bernstein Basis Transformation and its Application to Multi-Degree Reduction of Bézier Curves

A.H. Bhrawy, E.H. Dohab, M.A. Sakerc and D. Baleanud

*Journal of Computational and Applied Mathematics, 302: 369-384, (2016), IF: 1.328*

This paper reports new modified Jacobi polynomials (MJPs). We derive the basis transformation between MJPs and Bernstein polynomials and vice versa. This transformation is merging the perfect Least-square performance of the new polynomials together with the geometrical insight of Bernstein polynomials. The MJPs with indexes corresponding to the number of endpoints constraints are the natural basis functions for Least-square approximation of Bézier curves. Using MJPs leads us to deal with the constrained Jacobi polynomials and the unconstrained Jacobi polynomials as orthogonal polynomials. The MJPs are automatically satisfying the homogeneous boundary conditions. Thereby, the main advantage of using MJPs, in multi-degree reduction of Bézier curves on computer aided geometric design (CAGD), is that the constraints in CAGD are also satisfied and that decreases the steps of multi-degree reduction algorithm. Several numerical results for the multi-degree reduction of Bézier curves on CAGD are given.

**Keywords:** Basis transformation; Modified jacobi polynomials; Bernstein polynomials; Galerkin orthogonal polynomials; Multiple degree reduction of bézier curves.

## B-316. An Efficient Operational Matrix Technique for Multidimensional Variable-Order Time Fractional Diffusion Equations

M. A. Zaky, S. S. Ezz-Eldien, E. H. Doha, J. A. Tenreiro Machado and A. H. Bhrawy

*Journal of Computational and Nonlinear Dynamics, 11(6): 1-8, (2016), IF: 1.223*

This paper derives a new operational matrix of the variable-order (VO) time fractional partial derivative involved in anomalous diffusion for shifted Chebyshev polynomials. We then develop an accurate numerical algorithm to solve the 1 + 1 and 2 + 1 VO and constant-order fractional diffusion equation with Dirichlet conditions. The contraction of the present method is based on shifted Chebyshev collocation procedure in combination with the derived shifted Chebyshev operational matrix. The main advantage of the proposed method is to investigate a global approximation for spatial and temporal discretizations, and it reduces such problems to those of solving a system of algebraic equations, which greatly simplifies the solution process. In addition, we analyze the convergence of the present method graphically. Finally, comparisons between the algorithm derived in this paper and the existing algorithms are given, which show that our numerical schemes exhibit better performances than the existing ones.
**Keywords:** Operational matrix; Multidimensional variable-Order time Fractional diffusion equations.

## B-317. Bounds for Truncation and Perturbation Errors of Nonuniform Sampling Series

M. H. Annaby and R. M. Asharabi

*Bit Numerical Mathematics, 56: 807-832, (2016), IF: 1.167*

This paper introduces a comprehensive study of truncation and perturbation errors of nonuniform sampling, interpolation, representations. We derive pointwise as well as global estimates associated with the truncated nonuniform sampling formulae. The study of the perturbation error involves the estimation of the amplitude error which results from replacing the actual samples by approximate ones, as well as the jitter error arising when alternative nodes replace the original nodes, is carried out with rigorous error bounds. Numerical and geometrical verifications of the accuracy of our estimates are exhibited.
**Keywords:** Nonuniform; Sampling theoremstruncation Amplitude and Jitter errors.

## B-318. On the Optimal Control for Fractional Multi-Strain Tb Model

N. H. Sweilam1 and S. M. AL-Mekhlafi

*Optimal Control Applications and Methods, 37: 1355-1374, (2016), IF: 1.097*

In this paper, optimal control of a general nonlinear multi-strain tuberculosis (TB) model that incorporates three strains drug-sensitive, emerging multi-drug resistant and extensively drug-resistant is presented. The general multi-strain TB model is introduced as a fractional order multi-strain TB model. The fractional derivatives are described in the Caputo sense. An optimal control problem is formulated and studied theoretically using the Pontryagin maximum principle. Four controls variables are proposed to minimize the cost of interventions. Two simple-numerical methods are used to study the nonlinear fractional optimal control problem. The methods are the iterative optimal control method and the generalized Euler method. Comparative studies are implemented, and it is found that the iterative optimal control method is better than the generalized Euler method.
**Keywords:** Tuberculosis; M/XDR-TB; Pontryagin maximum principle; Caputo fractional derivatives; Fractional optimal control; Generalized euler method; Grünwald–Letnikovs Definition.

## B-319. An Elegant Operational Matrix Based on Harmonic Numbers: Effective Solutions for Linear and Nonlinear Fourth-Order Two Point Boundary Value Problems

WM Abd-Elhameed

*Nonlinear Analysis-Modelling and Control, 21(4): 448-464, (2016), IF: 1.075*

This paper analyzes the solution of fourth-order linear and nonlinear two point boundary value problems. The suggested method is quite innovative and it is completely different from all previous methods used for solving such kind of boundary value problems. The method is based on employing an elegant operational matrix of derivatives expressed in terms of the well-known harmonic numbers. Two algorithms are presented and implemented for obtaining new approximate solutions of linear and nonlinear fourth-order boundary value problems. The two algorithms rely on employing the new introduced operational matrix for reducing the differential equations with their boundary conditions to systems of linear or nonlinear algebraic equations, which can be efficiently solved by suitable solvers. For this purpose, the two spectral methods, namely, Petrov–Galerkin and collocation methods are applied. Some illustrative examples are considered aiming to ascertain the wide applicability, validity, and efficiency of the two proposed algorithms. The obtained numerical results are satisfactory and the approximate solutions are very close to the analytical solutions and they are more accurate than those obtained by some other existing techniques in literature.
**Keywords:** Shifted legendre polynomials; Harmonic numbers; Fourth-order boundary value problems; Petrov–Galerkin method; Collocation method.

## B-320. Multi-Soliton Rational Solutions for Quantum Zakharov-Kuznetsov Equation in Quantum Magnetoplasmas

M. S. Osman

*Waves in Random and Complex Media, 26: 434-443, (2016), IF: 1.061*

In this paper, the multi-soliton rational solutions are obtained for quantum Zakharov–Kuznetsov equation in quantum magnetoplasmas via the generalized unified method. Compared with the Hirota's method and the inverse scattering method, the proposed method gives more general exact multi-wave

solutions without much extra effort. The obtained results show that the generalized unified method provides a powerful mathematical tool for solving many nonlinear evolution equations arising in different branches of science. To give more physical insights into the obtained solutions, we present graphically their representative structures by setting the parameter which is proportional to the ratio of the strength of the magnetic field to the electronic Fermi temperature in the solutions of the quantum Zakharov–Kuznetsov equation as specific values.

**Keywords:** Multi-soliton rational solutions; The quantum zakharov–Kuznetsov equation; Travelling wave solutions; The generalised unified method.

## B-321. On the Extension of Solutions of the Real to Complex Kdv Equation and A Mechanism for the Construction of Rogue Waves

H. I. Abdel-Gawad, M. Tantawy and R. E. Abo Elkhair

*Waves In Random and Complex Media, 26: 397-406, (2016), IF: 1.061*

Rogue waves are more precisely defined as waves whose height is more than twice the significant wave height. This remarkable height was measured (by Draupner in 1995). Thus, the need for constructing a mechanism for the rogue waves is of great utility. This motivated us to suggest a mechanism, in this work, that rogue waves may be constructed via nonlinear interactions of solitons and periodic waves. This suggestion is consolidated here, in an example, by studying the behavior of solutions of the complex (KdV). This is done here by the extending the solutions of its real version.

**Keywords:** On the extension of Solutions of the real to Complex Kdv; Equation and A mechanism for the Construction of Rogue waves.

## B-322. Dynamic of DNA's Possible Impact on its Damage

H. I. Abdel-Gawad, M. Tantawy andM. S. Osman

*Mathematical Methods in the Applied Sciences, 39: 168-176, (2016), IF: 1.002*

In this paper, we investigate the dynamic of DNA described via DNA double-stranded model with transverse and longitudinal motions. This model admits solitary, soliton, periodic, or chirped wave solution. It is justified that the most admissible physical solution is the soliton or chirped wave solution. The stability analysis of all these solutions is performed by using the Sturm–Liouville problem and the topological invariance. We found that soliton and chirped waves are unstable so that the unbounded amplitude may occur. In the view of these models, damage of DNA membrane or bases may occur under small disturbance. Also, the suggested models will be indispensable when inhomogeneity or medium dissipation is taken into account.

**Keywords:** The dynamic of DNA; Traveling wave solutions; The unified method; Stability of solutions.

## B-323. A Space–Time Spectral Collocation Algorithm for the Variable Order Fractional Wave Equation

A. H. Bhrawy, E. H. Doha, J. F. Alzaidy and M. A. Abdelkawy

*Springerplus, 5: 1-15, (2016), IF: 0.982*

The variable order wave equation plays a major role in acoustics, electromagnetics, and fluid dynamics. In this paper, we consider the space–time variable order fractional wave equation with variable coefficients. We propose an effective numerical method for solving the aforementioned problem in a bounded domain. The shifted Jacobi polynomials are used as basis functions, and the variable-order fractional derivative is described in the Caputo sense. The proposed method is a combination of shifted Jacobi–Gauss–Lobatto collocation scheme for the spatial discretization and the shifted Jacobi–Gauss–Radau collocation scheme for temporal discretization. The aforementioned problem is then reduced to a problem consists of a system of easily solvable algebraic equations. Finally, numerical examples are presented to show the effectiveness of the proposed numerical method.

**Keywords:** Variable-Order fractional derivative; Collocation method; Jacobi polynomials; Gauss quadrature; Fractional wave equation.

## B-324. New Tchebyshev-Galerkin Operational Matrix Method for Solving Linear and Nonlinear Hyperbolic Telegraph Type Equations

W. M. Abd-Elhameed, E. H. Doha, Y. H. Youssri and M. A. Bassuony

*Numerical Methods For Partial Differential Equations, 32(6): 1553-1571, (2016), IF: 0.964*

The telegraph equation describes various phenomena in many applied sciences. We propose two new efficient spectral algorithms for handling this equation. The principal idea behind these algorithms is to convert the linear/nonlinear telegraph problems (with their initial and boundary conditions) into a system of linear/ nonlinear equations in the expansion coefficients, which can be efficiently solved. The main advantage of our algorithm in the linear case is that the resulting linear systems have special structures that reduce the computational effort required for solving them. The numerical algorithms are supported by a careful convergence analysis for the suggested Chebyshev expansion. Some illustrative examples are given to demonstrate the wide applicability and high accuracy of the proposed algorithms.

**Keywords:** Chebyshev polynomials; Galerkin and collocation methods; Hyperbolic telegraph equation; Operational matrix

## B-325. A Numerical Technique Based on the Shifted Legendre Polynomials for Solving the Time-Fractional Coupled Kdv Equations

A. H. Bhrawy, E. H. Doha, S. S. Ezz-Eldien and M. A. Abdelkawy

*Calcolo, 53(1): 1-17, (2016), IF: 0.816*

The time-fractional coupled Korteweg–de Vries (KdV) system is a generalization of the classical coupled KdV system and obtained by replacing the first order time derivatives by fractional derivatives of orders ν1 and ν2, ($0 < \nu1, \nu2 \leq 1$). In this paper, an accurate and robust numerical technique is proposed for solving the timefractional coupled KdV equations. The shifted Legendre polynomials are introduced as basis functions of the collocation spectral method together with the operational matrix of fractional derivatives (described in the Caputo sense) in order to reduce the time-fractional coupled KdV equations into a problem consisting of a system of algebraic equations that greatly simplifies the problem. In order to test the efficiency and validity of the proposed numerical technique, we apply it to solve two numerical examples.
**Keywords:** Coupled KDVequation; Operational matrix; Gauss quadrature; Collocation spectral method; Caputo derivative.

## B-326. Multi-Soliton Solutions Based on Interactions of Basic Traveling Waves with an Application to the Nonlocal Boussinesq Equation

H.I. Abdel-Gawad

*Acta Physica Polonica B, 47: 1101-1112, (2016), IF: 0.795*

It is shown that multi-waves are generated through direct or indirect nonlinear interactions of basic traveling waves. Direct and indirect nonlinear interactions are suggested via nonlinear combinations and bilinear transformations with nonlinear combinations of basic traveling wave solutions. Here, the used method is a generalization of the unified method presented by the first author in a recent work. Two- and three-soliton solutions have been obtained by the nonlocal Boussinesq equation through the simplified Hirota method very recently. Here, it is shown that they are particular cases of those found in this work. Multi-soliton waves are shown to be super-diffracted notably for higher speed of waves spreading. Further, a giant wave is formed in the region of interaction of the soliton waves.
**Keywords:** Multi-Soliton; Solutions based on interactions of basic; Traveling waves with an application to the nonlocal boussinesq equation.

## B-327. Einstein Geometrization Philosophy and Differential Identities in Pap-Geometry

M. I. Wanas, Nabil L. Youssef, W. El Hanafy and S. N. Osman

*Advances in Mathematical Physics, 235-248 (2016) IF: 0.787*

The importance of Einstein's geometrization philosophy, as an alternative to the least action principle, in constructing general relativity (GR), is illuminated. The role of differential identities in this philosophy is clarified. The use of Bianchi identity to write the field equations of GR is shown. Another similar identity in the absolute parallelism geometry is given. A more general differential identity in the parameterized absolute parallelism geometry is derived. Comparison and interrelationships between the above mentioned identities and their role in constructing field theories are discussed.
**Keywords:** Geometrization philosophy; Differential identities; Ap-Geometry; Pap-Geometry.

## B-328. On The Locus of Smooth Plane Curves with A Fixed Automorphism Group

Eslam Badr and Francesc Bars

*Mediterranean Journal of Mathematics, 13: 3605-3627, (2016), IF: 0.599*

Let $M_g$ be the moduli space of smooth, genus $g$ curves over an algebraically closed field $K$ of zero characteristic. Denote by $M_g(G)$ the subset of $M_g$ of curves $\delta$ such that $G$ (as a finite nontrivial group) is isomorphic to a subgroup of $Aut(\delta)$, and let $\widetilde{M_g(G)}$ be the subset of curves $\delta$ such that $G \cong Aut(\delta)$, where $Aut(\delta)$ is the full automorphism group of $\delta$. Now, for an integer $d\geq 4$, let $M^{Pl}_g$ be the subset of $M_g$ representing smooth, genus $g$, plane curves of degree $d$, i.e. smooth curves that admits a plane non-singular model of degree $d$, (in this case, $g= \frac{1}{2}(d − 1)(d − 2)$), and consider the sets $M^{Pl}_g(G):=M^{Pl}_g\cap M_g(G)$ and $\widetilde{M^{Pl}_g(G)}:=M^{Pl}_g\cap\widetilde{M_g(G)}$. In this paper, we study some aspects of the irreducibility of $\widetilde{M^{Pl}_g(G)}$ and its interrelation with the existence of "normal forms", i.e. non-singular plane equations (depending on a set of parameters) such that a specialization of the parameters gives a certain non-singular plane model associated to the elements of $\widetilde{M^{Pl}_g(G)}$. In particular, we introduce the concept of being equation strongly irreducible (ES-Irreducible) for which the locus $\widetilde{M^{Pl}_g(G)}$ is represented by a single "normal form". Henn (Die Automorphismengruppen dar algebraischen Functionenkorper vom Geschlecht 3. Inagural-dissertation, Heidelberg, 1976), and Komiya-Kuribayashi (On Weierstrass points and automorphisms of curves of genus three. In: Algebraic geometry (Proc. Summer Meeting, Copenhagen 1978), LNM, vol 732. Springer, New York 1979), observed that $\widetilde{M^{Pl}_3(G)}$, whenever non-empty, is ES-Irreducible. In this article, we prove that this phenomenon does not occur for any odd $d\geq5$. More precisely, let $\Z/m\Z$ be the cyclic group of order $m$, we show that $\widetilde{M^{Pl}_g(\Z/(d−1)\Z)}$ is not ES-Irreducible for any odd integer $d\geq5$, and the number of its irreducible components is at least two. Furthermore, we conclude the previous result when $d=6$ for the locus $\widetilde{M^{Pl}_{10}(\Z/3\Z)}$. Lastly, we prove the analogy of these statements when $K$ is any algebraically closed field of positive characteristic $p$ such that $p>(d−1)(d−2)+1$.
**Keywords:** Plane Non-singular curves; Automorphism groups.

## B-329. Solving Time-Fractional Order Telegraph Equation Via Sinc–Legendre Collocation Method

N. H. Sweilam, A. M. Nagy and Adel A. El-Sayed

*Mediterranean Journal of Mathematics, 13: 5119-5133, (2016), IF: 0.599*

In this paper, we introduce a numerical method for solving time-fractional order telegraph equation. The method depends basically on an expansion of approximated solution in a series of Sinc function and shifted Legendre polynomials. The fractional derivative is expressed in the Caputo definition of fractional derivatives. The expansion coefficients are then

determined by reducing the time-fractional order telegraph equation with its boundary and initial conditions to a system of algebraic equations for these coefficients. This system can be solved numerically using the Newton's iteration method. Several numerical examples are introduced to demonstrate the reliability and effectiveness of the introduced method.
**Keywords:** Spectral method; Time-fractional order telegraph equation; Sinc function; Caputo fractional derivative; Legendre polynomials.

## B-330. Linearization Formulae for Certain Jacobi Polynomials

W. M. Abd-Elhameed ,E. H. Doha and H. M. Ahmed

*Ramanujan Journal, 39: 155-168, (2016), IF: 0.563*

In this article, some new linearization formulae of products of Jacobi polynomials for certain parameters are derived. These new derived formulae are expressed in terms of hypergeometric functions of unit argument, and they generalize some existing formulae in the literature. With the aid of some standard formulae and also by employing symbolic algebraic computation, and in particular Zeilberger's algorithm, several reduction formulae for summing certain terminating hypergeometric functions of unit argument are given, and hence several linearization formulae of products of Jacobi polynomials for special parameters free of hypergeometric functions are deduced.
**Keywords:** Jacobi Polynomialslinearization Problems Generalized; Hypergeometric Functions; Algorithms by zeilberger; Petkovsek and van hoeij.

## B-331. New Ring of A Class of Bessel Integral Operators

Miloud Assal and Nasr A. Zeyada

*Integral Transforms and Special Functions, 27: 611-619, (2016), IF: 0.528*

In this paper, we introduce a new ring of ponderation functions which allowed us to describe and classify a large class of ring of Bessel integral operators. The main result is to give an explicit form of some ideals of such a ring of operators.
**Keywords:** Rings; Ideals; Bessel function; Bessel integral Operators.

## B-332. Non-Singular Plane Curves with an Element of "Large" Order in its Automorphism Group

Eslam Badr and Francesc Bars

*International Journal of Algebra and Computation, 26: 399-433, (2016), IF: 0.469*

Let $M_g$ be the moduli space of smooth, genus $g$ curves over an algebraically closed field $K$ of zero characteristic. Denote by $M_g(G)$ the subset of $M_g$ of curves $\delta$ such that $G$ (as a finite nontrivial group) is isomorphic to a subgroup of $Aut(\delta)$, and let $\widetilde{M_g(G)}$ be the subset of curves $\delta$ such that $G ≅ Aut(\delta)$, where $Aut(\delta)$ is the full automorphism group of $\delta$. Now, for an integer $d\geq 4$, let $M^{Pl}_g$ be the subset of $M_g$ representing smooth, genus $g$, plane curves of degree $d$, i.e. smooth curves that admits a plane non-singular model of degree $d$, (in this case, $g= \frac{1}{2}(d − 1)(d − 2)), and consider the sets $M^{Pl}_g(G):=M^{Pl}_g\cap M_g(G)$ and $\widetilde{M^{Pl}_g(G)}:=M^{Pl}_g\cap\widetilde{M_g(G)}$. In this paper we first determine, for an arbitrary but a fixed degree $d$, an algorithm to list the possible values $m$ for which $M^{Pl}_g(\Z/m\Z)$ is non-empty, where $\Z/m\Z$ denotes the cyclic group of order $m$. In particular, we prove that $m$ should divide one of the integers: $d−1, d, d^2−3d+3, (d−1)2, d(d−2)$ or $d(d−1)$. Secondly, consider a curve $\delta\in M^{Pl}_g$ with $g=\frac{1}{2}(d−1)(d−2)$ such that $Aut(\delta)$ has an element of "very large" order, in the sense that this element is of order $d^2−3d+3, (d−1)2, d(d−2)$ or $d(d−1)$. Then we investigate the groups $G$ for which $\delta\in\widetilde{M^{Pl}_g(G)}$ and also we determine the locus $\widetilde{M^{Pl}_g(G)}$ in these situations. Moreover, we work with the same question when $Aut(\delta)$ has an element of "large" order: $\ell d, \ell (d−1)$ or $\ell (d−2)$ with $\ell\geq 2$ an integer.
**Keywords:** Non-Singular curves; Plane models; Automorphism groups; Moduli spaces.

## B-333. Nullity Distributions Associated with Chern Connection

Nabil L. Youssef and Salah G. Elgendi

*Publicationes Mathematicae-Debrecen, 88: 235-248, (2016), IF: 0.438*

The nullity distributions of the two curvature tensors R* and P* of the Chern connection of a Finsler manifold are investigated. The completeness of the nullity foliation associated with the nullity distribution NR* is proved. Two counterexamples are given: the first shows that NR* does not coincide with the kernel distribution of R*; the second illustrates that NP* is not completely integrable. We give a simple class of a non-Berwaldian Landsberg spaces with singularities.
**Keywords**: Klein-Grifone formalism; Chern connection; Nullity distribution; Kernel distribution; Nullity foliation.

## B-334. Numerical Approach for Solving Space Fractional Order Diffusion Equations Using Shifted Chebyshev Polynomials of the Fourth Kind

Nasser Hassan Sweilam, Abdelhameed Mohamed Nagy and Adel Abd Elaziz El-Sayed

*Turkish Journal of Mathematics, 40:1283-1297,(2016),IF:0.378*

In this paper, a new approach for solving space fractional order diffusion equations is proposed. Thefractional derivative in this problem is in the Caputo sense. This approach is based on shifted Chebyshev polynomialsof the fourth kind with the collocation method. Thenite difference method is used to reduce the equations obtainedby our approach for a system of algebraic equations that can be efficiently solved. Numerical results obtained with ourapproach are presented and compared with the results obtained by other numerical methods. The numerical resultsshow the efficiency of the proposed approach.
**Keywords:** Space fractional order diffusion equation; Caputo derivative; Chebyshev collocation method; FiNite difference

method; Chebyshev polynomials of the fourth kind; Euler approximation.

## B-335. Automorphism Groups of Nonsingular Plane Curves of Degree 5

Eslam Badr and Francesc Bars

*Communications in Algebra, 44: 4327-4340, (2016), IF: 0.368*

Let $M_g$ be the moduli space of smooth, genus $g$ curves over an algebraically closed field $K$ of zero characteristic. Denote by $M_g(G)$ the subset of $M_g$ of curves $\delta$ such that $G$ (as a finite nontrivial group) is isomorphic to a subgroup of $Aut(\delta)$, and let $\widetilde{M_g(G)}$ be the subset of curves $\delta$ such that $G ≅ Aut(\delta)$, where $Aut(\delta)$ is the full automorphism group of $\delta$. Now, for an integer $d\geq 4$, let $M^{Pl}_g$ be the subset of $M_g$ representing smooth, genus $g$, plane curves of degree $d$, i.e. smooth curves that admits a plane non-singular model of degree $d$, (in this case, $g= \frac{1}{2}(d − 1)(d − 2)), and consider the sets $M^{Pl}_g(G):=M^{Pl}_g\cap M_g(G)$ and $\widetilde{M^{Pl}_g(G)}:=M^{Pl}_g\cap\widetilde{M_g(G)}$. Henn in [7 Henn, P. (1976). Die Automorphismengruppen dar algebraischen Functionenkorper vom Geschlecht 3, Inagural-dissertation, Heidelberg.] and Komiya and Kuribayashi in [10 Kuribayashi, A., Komiya, K. (1979). On Weierstrass points and automorphisms of curves of genus three. Algebraic geometry (Proc. Summer Meeting, Copenhagen 1978). LNM, Vol. 732, Springer, pp. 253–299.], listed the groups $G$ for which $\widetilde{M^{Pl}_3(G)}$ is nonempty. In this article, we determine the loci $\widetilde{M^{Pl}_6(G)}$, corresponding to nonsingular degree 5 projective plane curves, which are nonempty. Also, we present the analogy of Henn's results for quartic curves concerning nonsingular plane model equations associated to these loci (see Table 2 for more details). Similar arguments can be applied to deal with higher degrees.

**Keywords:** Automorphism groups; Plane curves.

## B-336. On Weakly-Embedded Subgroups of Finite Groups

M. Asaad and M. Ramadan

*Communications in Algebra,44(10):4564-4574,(2016) IF:0.368*

Let G be a finite group and H a subgroup of GWe say that H is an H-subgroup in G if NGH∩ Hg ≤ H for all g ∈ GH is called weakly H-subgroup in G if G has a normal subgroup K such that G = HK and H ∩ K is an H-subgroup in G. We say that H is weakly H-embedded in G if G has a normal subgroup K such that HG = HK and H ∩ K is an H-subgroup in GIn this paper, we investigate the structure of the finite group G under the assumption that some subgroups of prime power order are weakly H-embedded in GOur results improve and generalize several recent results in the literature.

**Keywords:** C-Normal subgroup; Subgroup; P-Nilpotent group; Supersolvable group; Saturated formation; Weakly ;-Subgroup.

## B-337. Simple-Direct-Projective Modules

Yasser Ibrahim, M. Tamer Koşan, Truong Cong Quynh and Mohamed Yousif

*Communications in Algebra, 44: 5163-5178, (2016), IF: 0.368*

In this paper, we introduce and study the dual notion of simple-direct-injective modules. Namely, a right R-module M is called simple-direct-projective if, whenever A and B are submodules of M with B simple and M/A ≅ B ⊆⊕M, then A ⊆⊕M. Several characterizations of simple-direct-projective modules are provided and used to describe some well-known classes of rings. For example, it is shown that a ring R is artinian and serial with J2(R) = 0 if and only if every simple-direct-projective right R-module is quasi-projective if and only if every simple-direct-projective right R -module is a D3-module. It is also shown that a ring R is uniserial with J2(R) = 0 if and only if every simple-direct-projective right R-module is a C3-module if and only if every simple-direct-injective right R -module is a D3-module.

**Keywords:** Artinian serial rings; C3-Modules; D3-Modules; Simple-Direct-injective; Simple; Direct-Projective Modules; Uniserial rings.

## B-338. New Linearization Formulae for the Products of Chebyshev Polynomials of Third and Fourth Kinds

EH Doha and WM Abd-Elhameed

*Rocky Mountain Journal of Mathematics, 46(2): 443-460, (2016), IF: 0.367*

This paper deals with the problem of finding two new closed formulae for linearization coefficients of two special nonsymmetric cases for Jacobi polynomials P(α,β)n(x)Pn(α,β)(x) corresponding to the parameters' values β=−α=±1/2β=−α=±1/2. From these two formulae, the linearization coefficients of the products of Chebyshev polynomials of the third and fourth kinds are established. Based on using algorithmic methods, such as the algorithms by Zeilberger, Petkovsek and Van-Hoeij, and two certain Whipple's transformations, six new closed formulae for summing certain terminating hyper\-geometric functions of unit argument are given.

**Keywords:** Jacobi polynomials.

## B-339. On Modules with Cyclic Socle

Ali Assem

*Journal of Algebra and its Applications/ World Scientific, 15, (09), November (2016) IF: 0.365*

The extension problem for linear codes over modules with respect to Hamming weight was already settled in [J. A. Wood, Code equivalence characterizes finite Frobenius rings, Proc. Amer. Math. Soc. 136 (2008) 699–706; Foundations of linear codes defined over finite modules: The extension theorem and MacWilliams identities, in Codes Over Rings, Series on Coding Theory and Cryptology, Vol. 6 (World Scientific, Singapore, 2009), pp. 124–190]. A similar problem arises naturally with respect to symmetrized weight compositions (SWC). In 2009, Wood proved that Frobenius bimodules have the extension

property (EP) for SWC. More generally, in [N. ElGarem, N. Megahed and J. A. Wood, The extension theorem with respect to symmetrized weight compositions, in 4th Int. Castle Meeting on Coding Theory and Applications (2014)], it is shown that having a cyclic socle is sufficient for satisfying the property, while the necessity remained an open question. Here, landing in midway, a partial converse is proved. For a (not small) class of finite module alphabets, the cyclic socle is shown necessary to satisfy the EP. The idea is bridging to the case of Hamming weight through a new weight function. Note: All rings are finite with unity, and all modules are finite too. This may be re-emphasized in some statements. The convention for left homomorphisms is that inputs are to the left. Read More: http://www.worldscientific.com/doi/abs/10.1142/S0219498816501620

**Keywords:** Macwilliams; Theorems; Linear codes; Cyclic socle; Annihilators.

## B-340. On Weakly c-Embedded Subgroups of Finite Groups

M. Asaad and M. Ramadan

*Journal of Algebra and its Applications, 15(5): 1-12, (2016), IF: 0.365*

Let G be a finite group. A subgroup H of G is said to be an HC-subgroup of G if there exists a normal subgroup T of G such that G = HT and Hg ∩NT (H) ≤ H for all g ∈ G. We say that H is weakly HC-embedded in G if there exists a normal subgroup T of G such that HG = HT and Hg ∩ NT (H) ≤ H for all g ∈ G. In this paper, we investigate the structure of the finite group G under the assumption that some subgroups of prime power order are weakly HC-embedded in G. Our results improve and generalize several recent results in the literature.

**Keywords:** C-Normal subgroup; Subgroup;Subgroup; Supersolvable group; Saturated formation.

## B-341. Rings Whose Cyclics Are C3-Modules

Yasser Ibrahim, Xuan Hau Nguyen, Mohamed F. Yousif and Yiqiang Zhou

*Journal of Algebra and Its Applications, 15: 1650152-1650152, (2016), IF: 0.365*

It is well known that if every cyclic right module over a ring is injective, then the ring is semisimple artinian. This classical theorem of Osofsky promoted a considerable interest in the rings whose cyclics satisfy a certain generalized injectivity condition, such as being quasi-injective, continuous, quasi-continuous, or CS. Here we carry out a study of the rings whose cyclic modules are C3-modules. The motivation is the observation that a ring R is semisimple artinian if and only if every 3-generated right R-module is a C3-module. Many basic properties are obtained for the rings whose cyclics are C3-modules, and some structure theorems are proved. For instance, it is proved that a semiperfect ring has all cyclics C3-modules if and only if it is a direct product of a semisimple artinian ring and finitely many local rings, and that a right self-injective regular ring has all cyclics C3-modules if and only if it is a direct product of a semisimple artinian ring, a strongly regular ring and a 2×2 matrix ring over a strongly regular ring. Applications to SI-rings, respectively, the rings whose 2-generated modules are C3-modules, and the rings whose cyclics are ADS or quasi-continuous are addressed.

**Keywords:** C3-Module; Cc3-Ring; Local ring; Semiperfect ring; Self-Injective regular ring; Strongly regular ring.

## B-342. Sampling Theorems Associated with Differential Operators with Finite Rank Perturbations

Mahmoud H. Annaby, Omar H. El-Haddad and Hassan A. Hassan

*Journal of the Korean Mathematical Society, 5: 969-990, (2016), IF: 0.356*

We derive a sampling theorem associated with first order self-adjoint eigenvalue problem with a finite rank perturbation. The class of the sampled integral transforms is of finite Fourier type where the kernel has an additional perturbation.

**Keywords:** Green'S function; Eigenfunctions expansions; Finite rank perturbations.

## B-343. A New Generalized Jacobi Galerkin Operational Matrix of Derivatives: Two Algorithms for Solving Fourth-Order Boundary Value Problems

Waleed M Abd-Elhameed and Hany M Ahmed and Youssri H Youssri

*Advances in Difference Equations, (22): 1-16 (2016), IF: 0.297*

This paper reports a novel Galerkin operational matrix of derivatives of some generalized Jacobi polynomials. This matrix is utilized for solving fourth-order linear and nonlinear boundary value problems. Two algorithms based on applying Galerkin and collocation spectral methods are developed for obtaining new approximate solutions of linear and nonlinear fourth-order two point boundary value problems. In fact, the key idea for the two proposed algorithms is to convert the differential equations with their boundary conditions to systems of linear or nonlinear algebraic equations which can be efficiently solved by suitable numerical solvers. The convergence analysis of the suggested generalized Jacobi expansion is carefully discussed. Some illustrative examples are given for the sake of indicating the high accuracy and effectiveness of the two proposed algorithms. The resulting approximate solutions are very close to the analytical solutions and they are more accurate than those obtained by other existing techniques in the literature.

**Keywords:** Generalized jacobi polynomials; Legendre polynomials; Operational matrix; Fourth-Order boundary value problems; Galerkin and collocation methods.

## B-344. Numerical Solutions of Fractional Wave Equations Using an Efficient Class of Fdm Based on the Hermite Formula

Mohamed M Khader and Mohamed H Adel

*Advances in Difference Equations, 1-10, (2016), IF: 0.297*

In this article, a numerical study is introduced for solving the fractional wave equations by using an efficient class of finite difference methods. The proposed scheme is based on the

Hermite formula. The stability and the convergence analysis of the proposed methods are given by a recently proposed procedure similar to the standard von Neumann stability analysis. A simple and accurate stability criterion valid for different discretization schemes of the fractional derivative, arbitrary weight factor, and arbitrary order of the fractional derivative, are given and checked numerically. Finally, a numerical example is presented to confirm the theoretical results.
**Keywords:** Finite difference methods; Hermite formula; Fractional wave equation; Stability and convergence analysis.

## B-345. Linearization Coefficients of Some Particular Jacobi Polynomials Via Hypergeometric Functions

Waleed M Abd-Elhameed

*Advances in Difference Equations, (91): 1-13 (2016) IF: 0.297*

The main purpose of the present paper is to establish two new linearization formulas for certain Jacobi polynomials. The new established formulas are expressed in terms of terminating hypergeometric functions of the type 4F3(1). In virtue of the well-known Pfaff-Saalschütz identity, or by using some computer algebra algorithms, and in particular, the algorithms of Zeilberger, Petkovsek and van Hoeij, the resulting 4F3(1) can be reduced for particular choices of the involved parameters. This reduction leads to obtaining several simple linearization formulas of some particular Jacobi polynomials free of any hypergeometric functions.
**Keywords:** Jacobi polynomials; Linearization coefficients; Generalized hypergeometric functions; Computer algebra algorithms.

## B-346. Comparative Study for Multi-Strain Tuberculosis (TB) Model of Fractional Order

Nasser Hassan Sweilam and Seham Mahyoub AL−Mekhlafi

*Applied Mathematics and Information Sciences, 10: 1403-1413, (2016),*

In this paper, we introduce the multi−strain TB model of fractional-order derivatives, which incorporates three strains: drug−sensitive, emerging multi−drug resistant(MDR) and extensively drug−resistant(XDR ). Numerical simulations for this extended fractional order model is the main aim of this work, where the adopted model is described by a system of non-linear ordinary differential equations and the fractional derivative is defined in the sense of the Grünwald−Letnikov definition. Two numerical methods are presented for this model, the standard finite difference method (SFDM) and the nonstandard finite difference method (NSFDM). Numerical comparisons between SFDM and NSFDM are presented. It is concluded that the proposed NSFDM preserves the positivity of the solutions, and it is numerically stable in large regions than SFDM.
**Keywords:** Nonstandard finite difference; Epidemic model; Tuberculosis; M/Xdr−TB; Fractional differential; Grünwald−letnikov definition.

## B-347. Multi-Soliton Rational Solutions for some Nonlinear Evolution Equations

Mohamed S. Osman

*Open Physics Formerly (Central European Journal of Physics), 14: 26-36, (2016),*

The Korteweg-de Vries equation (KdV) and the (2+ 1)-dimensional Nizhnik-Novikov-Veselov system (NNV) are presented. Multi-soliton rational solutions of these equations are obtained via the generalized unified method. The analysis emphasizes the power of this method and its capability of handling completely (or partially) integrable equations. Compared with Hirota's method and the inverse scattering method, the proposed method gives more general exact multi-wave solutions without much additional effort. The results show that, by virtue of symbolic computation, the generalized unified method may provide us with a straightforward and effective mathematical tool for seeking multi-soliton rational solutions for solving many nonlinear evolution equations arising in different branches of sciences.
**Keywords:** Multi-Soliton rational solution; Generalized unified method; Korteweg-De vries equation; (2+ 1)-Dimensional Nizhnik-Novikov-veselov equation.

## B-348. Solutions of the Connection Problems Between Fermat and Generalized Fibonacci Polynomials

WM Abd-Elhameed and YH Youssri

*Jp Journal of Algebra, Number Theory and Applications, 38(4): 349-362, (2016),*

This paper aims to develop innovative formulae linking Mersenne and Fermat numbers with a class of generalized Fibonacci numbers including the celebrated Fibonacci and Pell numbers. These formulae can be obtained by solving the connection problems between Fermat and generalized Fibonacci polynomials. The introduced connection formulae are obtained with the aid of the power from representations and inversion formulae of Fermat and generalized Fibonacci
**Keywords:** Fibonacci sequence; Recurrence relation; Hypergeometric functions; Connection coefficients.

## B-349. Search for Narrow Resonances Decaying to Dijets in Proton-Proton Collisions at $\sqrt{S} = 13$ Tev

Ali Yehia Ellithi Kamel (et. al.)

*Physical Review Letters, 116: 71801-0, (2016), IF: 7.645*

A search for narrow resonances in proton-proton collisions at $\sqrt{s}$=13 TeV is presented. The invariant mass distribution of the two leading jets is measured with the CMS detector using a data set corresponding to an integrated luminosity of 2.4 fb−1. The highest observed dijet mass is 6.1 TeV. The distribution is smooth and no evidence for resonant particles is observed. Upper limits at 95% confidence level are set on the production cross section for narrow resonances with masses above 1.5 TeV. When interpreted in the context of specific models, the limits exclude string resonances with masses below 7.0 TeV, scalar diquarks below 6.0 TeV, axigluons and colorons below

5.1 TeV, excited quarks below 5.0 TeV, color-octet scalars below 3.1 TeV, and W′ bosons below 2.6 TeV. These results significantly extend previously published limits.
**Keywords:** Pp collision; Dijets.

## B-350. A Search for Pair Production of New Light Bosons Decaying Into Muons

Ali Yehia Ellithi Kamel (et. al.)

*Physics Letters B, 752: 146-0, (2016), IF: 4.787*

A search for the pair production of new light bosons, each decaying into a pair of muons, is performed with the CMS experiment at the LHC, using a dataset corresponding to an integrated luminosity of 20.7 fb−1 collected in proton–proton collisions at center-of-mass energy of √s = 8 TeV. No excess is observed in the data relative to standard model background expectation and a model independent upper limit on the product of the cross section, branching fraction, and acceptance is derived. The results are compared with two benchmark models, the first one in the context of the next-to-minimal supersymmetric standard model, and the second one in scenarios containing a hidden sector, including those predicting a nonnegligible light boson lifetime
**Keywords:** Pp collision; Pair production; Light bosons.

## B-351. Combined Search for Anomalous Pseudoscalar Hvv Couplings in Vh(H → Bb) Production and H → Vv Decay

Ali Yehia Ellithi Kamel (et. al.)

*Physics Letters B, 759: 672-0, (2016), IF: 4.787*

A search for anomalous pseudoscalar couplings of the Higgs boson H to electroweak vector bosons V (= W or Z) in a sample of proton–proton collision events corresponding to an integrated luminosity of 18.9 fb−1 at a center-of-mass energy of 8 TeV is presented. Events consistent with the topology of associated VH production, where the Higgs boson decays to a pair of bottom quarks and the vector boson decays leptonically, are analyzed. The consistency of data with a potential pseudoscalar contribution to the HVV interaction, expressed by the effective pseudoscalar cross section fractions fa3 , is assessed by means of profile likelihood scans. Results are given for the VH channels alone and for a combined analysis of the VH and previously published H → VV channels. Under certain assumptions, f ZZ a3 > 0.0034 is excluded at 95% confidence level in the combination. Scenarios in which these assumptions are relaxed are also considered.
**Keywords:** Pp Collision; Higgs boson; Coupling; Electroweak Vector bosons.

## B-352. Measurement of the Ratio B(B0 S → J/Ψf0(980))/B(B0 S → J/Ψφ(1020)) in Pp Collisions at √S = 7 Tev

Ali Yehia Ellithi Kamel (et. al.)

*Physics Letters B, 756: 84-0, (2016), IF: 4.787*

A measurement of the ratio of the branching fractions of the B0 s meson to J/ψf0(980) and to J/ψφ(1020)is presented. The J/ψ, f0(980), and φ(1020) are observed through their decays to μ+μ−, π+π−, and K+K−, respectively. The f0 and the φ are identified by requiring |Mπ+π− − 974 MeV| < 50 MeV and|MK+K− − 1020 MeV| < 10 MeV. The analysis is based on a data sample of pp collisions at a centreof-mass energy of 7 TeV, collected by the CMS experiment at the LHC, corresponding to an integrated luminosity of 5.3 fb−1. The measured ratio is B(B0s→J/ψf0) B(f0→π+π−) B(B0s→J/ψφ) B(φ→K+K−) = 0.140±0.008 (stat)±0.023 (syst), where the first uncertainty is statistical and the second is systematic.
**Keywords:** Pp collision; Branching fractions; B0 S meson; J/Ψf0(980).

## B-353. Measurement of the W Boson Helicity Fractions in The Decays of Top Quark √ Pairs to Lepton + Jets Final States Produced In Pp Collisions at S = 8 Tev

Ali Yehia Ellithi Kamel (et. al.)

*Physics Letters B, 762: 512-0, (2016), IF: 4.787*

The W boson helicity fractions from top quark decays in tt events are measured using data from proton– proton collisions at a centre-of-mass energy of 8 TeV. The data were collected in 2012 with the CMS detector at the LHC, corresponding to an integrated luminosity of 19.8 fb−1. Events are reconstructed with either one muon or one electron, along with four jets in the final state, with two of the jets being identified as originating from b quarks. The measured helicity fractions from both channels are combined, yielding F0 = 0.681 ± 0.012 (stat) ± 0.023 (syst), FL = 0.323 ± 0.008 (stat) ± 0.014 (syst), and FR = −0.004 ± 0.005 (stat) ± 0.014 (syst) for the longitudinal, left-, and right-handed components of the helicity, respectively. These measurements of the W boson helicity fractions are the most accurate to date and they agree with the predictions from the standard model
**Keywords:** Pp collision; Top quarks.

## B-354. Res_Id: 1405 J Res_Wcode: 2806 Measurement of the ZZ production cross section and $Z \rightarrow \ell^{+}\ell^{-}\ell'^{+}\ell'^{-}$ branching fraction in pp collisions at $\sqrt{s} = 13$ TeV

Ali Yehia Ellithi Kamel (et. al.)

*Physics Letters B, 763: 280-303, (2016), IF: 4.787*

Four-lepton production in proton–proton collisions, pp→(Z/γ∗)(Z/γ∗)→ℓ+ℓ−ℓ′+ℓ′−, where ℓ,ℓ′=e or μ, is studied at a center-of-mass energy of 13 TeV with the CMS detector at the LHC. The data sample corresponds to an integrated luminosity of 2.6 fb−1. The ZZ production cross section, View the MathML source, is measured for events with two opposite-sign, same-flavor lepton pairs produced in the mass region 60<mℓ+ℓ−,mℓ′+ℓ′−<120 GeV. The Z boson branching fraction to four leptons is measured to be View the MathML source for the four-lepton invariant mass in the range 80<mℓ+ℓ−ℓ′+ℓ′−<100 GeV and dilepton mass mℓ+ℓ−>4 GeV for all opposite-sign, same-flavor lepton pairs. The results are in agreement with standard model predictions.

**Keywords:** CMS; Physics; Electroweak

## B-355. Measurements of TT Charge Asymmetry Using Dilepton Final States in Pp Collisions at √S = 8 TeV

Ali Yehia Ellithi Kamel (et. al.)

*Physics Letters B, 760: 365-0, (2016), IF: 4.787*

The charge asymmetry in tt events is measured using dilepton final states produced in pp collisions at the LHC at √s = 8 TeV. The data sample, collected with the CMS detector, corresponds to an integrated luminosity of 19.5 fb−1. The measurements are performed using events with two oppositely charged leptons (electrons or muons) and two or more jets, where at least one of the jets is identified as originating from a bottom quark. The charge asymmetry is measured from differences in kinematic distributions, unfolded to the parton level, of positively and negatively charged top quarks and leptons. The tt and leptonic inclusive charge asymmetries are found to be 0.011 ± 0.011 (stat) ± 0.007 (syst) and 0.003±0.006 (stat)±0.003 (syst), respectively. These results, as well as charge asymmetry measurements made as a function of the invariant mass, rapidity, and transverse momentum of the tt system, are in agreement with predictions of the standard model

**Keywords:** Pp collision; Tt Charge asymmetry; Dilepton final states.

## B-356. Search for R-Parity Violating Decays of A Top Squark in Proton–Proton Collisions at √S = 8 Tev

Ali Yehia Ellithi Kamel (et. al.)

*Physics Letters B, 760: 178-0, (2016), IF: 4.787*

The results of a search for a supersymmetric partner of the top quark (top squark), pair-produced in proton–proton collisions at √s = 8 TeV, are presented. The search, which focuses on R-parity violating, chargino-mediated decays of the top squark, is performed in final states with low missing transverse momentum, two oppositely charged electrons or muons, and at least five jets. The analysis uses a data sample corresponding to an integrated luminosity of 19.7 fb−1 collected with the CMS detector at the LHC in 2012. The data are found to be in agreement with the standard model expectation, and upper limits are placed on the top squark pair production cross section at 95% confidence level. Assuming a 100% branching fraction for the top squark decay chain, t → tχ±1 ,χ±1 → ± + jj, top squark massesless than 890 (1000) GeV for the electron (muon) channel are excluded for the first time in models with a single nonzero R-parity violating coupling λijk (i, j,k ≤ 2), where i, j,k correspond to the three generations.

**Keywords:** Pp collision; R-Parity violation; Top squark.

## B-357. Measurement of the Integrated and Differential T¯T Production Cross Sections for High-Pt Top Quarks in Pp Collisions at Ffiffi S P = 8 Tev

Ali Yehia Ellithi Kamel (et. al.)

*Physical Review D, 94: 72002-0, (2016), IF: 4.506*

The cross section for pair production of top quarks (t¯t) with high transverse momenta is measured in pp collisions, collected with the CMS detector at the LHC with ffiffi s p ¼ 8 TeV in data corresponding to an integrated luminosity of 19.7 fb−1. The measurement is performed using lepton þ jets events, where one top quark decays semileptonically, while the second top quark decays to a hadronic final state. The hadronic decay is reconstructed as a single, large-radius jet, and identified as a top quark candidate using jet substructure techniques. The integrated cross section and the differential cross sections as a function of top quark pT and rapidity are measured at particle level within a fiducial region related to the detector-level requirements and at parton level. The particle-level integrated cross section is found to be σt¯t ¼ 0.499 0.035ðstat þ systÞ 0.095ðtheoÞ 0.013ðlumiÞ pb for top quark pT > 400 GeV. The parton-level measurement is σt¯t ¼ 1.44 0.10ðstat þ systÞ 0.29ðtheoÞ 0.04ðlumiÞ pb. The integrated and differential cross section results are compared to predictions from several event generators.

**Keywords:** Pp collision; Ttbar production; Top quarks.

## B-358. Measurements of Dn2 and an1: Probing the Neutron Spin Structure

H. F. Ibrahim (et. al.)

*Physical Review D, 94: 52003-52003, (2016), IF: 4.506*

We report on the results of the E06-014 experiment performed at Jefferson Lab in Hall A, where a precision measurement of the twist-3 matrix element d2 of the neutron (dn2) was conducted. The quantity dn2 represents the average color Lorentz force a struck quark experiences in a deep inelastic electron scattering event off a neutron due to its interaction with the hadronizing remnants. This color force was determined from a linear combination of the third moments of the 3He spin structure functions, g1 and g2, after nuclear corrections had been applied to these moments. The structure functions were obtained from a measurement of the unpolarized cross section and of double-spin asymmetries in the scattering of a longitudinally polarized electron beam from a transversely and a longitudinally polarized 3He target. The measurement kinematics included two average Q2 bins of 3.2 GeV2 and 4.3 GeV2, and Bjorken-x between 0.25 and 0.90 covering the deep inelastic and resonance regions. We have found that dn2 is small and negative for Q2=3.2 GeV2, and even smaller for Q2=4.3 GeV2, consistent with the results of a lattice QCD calculation. The twist-4 matrix element fn2 was extracted by combining our measured dn2 with the world data on the first moment in x of g_n1, Gamma_n1. We found fn2 to be roughly an order of magnitude larger than dn2. Utilizing the extracted dn2 and fn2 data, we separated the Lorentz color force into its electric and magnetic components, Fy,nE and Fy,nB, and found them to be equal and opposite in magnitude, in agreement with the predictions from an instanton model but not with those from QCD sum rules. Furthermore, using the measured double-spin asymmetries, we have extracted the virtual photon-nucleon asymmetry on the neutron An1, the structure function ratio gn1/Fn1, and the quark ratios (Delta u+Delta ¯u)/(u+¯u) and (Delta d+Delta ¯d)/(d+¯d). These results were found to be consistent with deep-inelastic scattering world data and with the prediction of the constituent quark model but at odds with the perturbative quantum chromodynamics predictions at large x.

**Keywords:** Twist-3 matrix element; Deep inelastic electron scattering; 3He Target; Color force; Cross section; Quantum chromodynamics.

## B-359. Search for Dark Matter and Unparticles Produced in Association with A Z Boson in Proton-Proton Collisions at Ffiffi S P ¼ 8 Tev

Ali Yehia Ellithi Kamel

*Physical Review D, 93: 52011-0, (2016), IF: 4.506*

A search for evidence of particle dark matter (DM) and unparticle production at the LHC has been performed using events containing two charged leptons, consistent with the decay of a Z boson, and large missing transverse momentum. This study is based on data collected with the CMS detector corresponding to an integrated luminosity of 19.7 fb−1 of pp collisions at the LHC at a center-of-mass energy of 8 TeV. No significant excess of events is observed above the number expected from the standard model contributions. The results are interpreted in terms of 90% confidence level limits on the DM-nucleon scattering cross section, as a function of the DM particle mass, for both spin-dependent and spinindependent scenarios. Limits are set on the effective cutoff scale Λ, and on the annihilation rate for DM particles, assuming that their branching fraction to quarks is 100%. Additionally, the most stringent 95% confidence level limits to date on the unparticle model parameters are obtained.
**Keywords:** Pp collision; Dark matter; Z Boson.

## B-360. Search for Pair Production of First and Second Generation Leptoquarks in Proton-Proton Collisions at √ S = 8 Tev

Ali Yehia Ellithi Kamel

*Physical Review D, 93: 32005-0, (2016), IF: 4.506*

A search for pair production of first and second generation leptoquarks is performed in final states containing either two charged leptons and two jets, or one charged lepton, one neutrino and two jets, using proton-proton collision data at √s=8 TeV. The data, corresponding to an integrated luminosity of 19.7 fb−1, were recorded with the CMS detector at the LHC. First-generation scalar leptoquarks with masses less than 1010 (850) GeV are excluded for β=1.0 (0.5), where β is the branching fraction of a leptoquark decaying to a charged lepton and a quark. Similarly, second-generation scalar leptoquarks with masses less than 1080 (760) GeV are excluded for β=1.0 (0.5). Mass limits are also set for vector leptoquark production scenarios with anomalous vector couplings, and for R-parity violating supersymmetric scenarios of top squark pair production resulting in similar final-state signatures. These are the most stringent limits placed on the masses of vector leptoquarks and RPV top squarks to date.
**Keywords:** Pp collision; Scalar leptoquarks.

## B-361. Search for Pair Production of First and Second Generation Leptoquarks in Proton-Proton Collisions at Ffiffi S P ¼ 8 Tev

Ali Yehia Ellithi Kamel

*Physical Review D, 93: 32004-0, (2016), IF: 4.506*

A search for pair production of first and second generation leptoquarks is performed in final states containing either two charged leptons and two jets, or one charged lepton, one neutrino and two jets, using proton-proton collision data at ffiffi s p ¼ 8 TeV. The data, corresponding to an integrated luminosity of 19.7 fb−1, were recorded with the CMS detector at the LHC. First-generation scalar leptoquarks with masses less than 1010 (850) GeV are excluded for β ¼ 1.0 ð0.5Þ, where β is the branching fraction of a leptoquark decaying to a charged lepton and a quark. Similarly, second-generation scalar leptoquarks with masses less than 1080 (760) GeV are excluded for β ¼ 1.0 ð0.5Þ. Mass limits are also set for vector leptoquark production scenarios with anomalous vector couplings, and for R-parity violating supersymmetric scenarios of top squark pair production resulting in similar final-state signatures. These are the most stringent limits placed on the masses of vector leptoquarks and RPV top squarks to date. DOI: 10.1103/PhysRevD.93.032
**Keywords:** Pp collision; Leptoquarks.

## B-362. Search for Pair-Produced Vectorlike B Quarks in Proton-Proton Collisions at Ffiffi S P = 8 Tev

Ali Yehia Ellithi Kamel

*Physical Review D, 93: 112009-0, (2016), IF: 4.506*

A search for the production of a heavy B quark, having electric charge −1=3 and vector couplings to W, Z, and H bosons, is carried out using proton-proton collision data recorded at the CERN LHC by the CMS experiment, corresponding to an integrated luminosity of 19.7 fb−1. The B quark is assumed to be pair produced and to decay in one of three ways: to tW, bZ, or bH. The search is carried out in final states with one, two, and more than two charged leptons, as well as in fully hadronic final states. Each of the channels in the exclusive final-state topologies is designed to be sensitive to specific combinations of the B quarkantiquark pair decays. The observed event yields are found to be consistent with the standard model expectations in all the final states studied. A statistical combination of these results is performed, and upper limits are set on the cross section of the strongly produced B quark-antiquark pairs as a function of the B quark mass. Lower limits on the B quark mass between 740 and 900 GeV are set at a 95% confidence level, depending on the values of the branching fractions of the B quark to tW, bZ, and bH. Overall, these limits are the most stringent to date.
**Keywords:** Pp collision; B Quarks.

## B-363. Search for Resonant T ¯ T Production in Proton-Proton Collisions at √ S = 8 Tev

Ali Yehia Ellithi Kamel

*Physical Review D, 93: 12001-0, (2016), IF: 4.506*

A search is performed for the production of heavy resonances decaying into top-antitop quark pairs in proton-proton collisions at √s=8 TeV. Data used for the analyses were collected with the CMS detector and correspond to an integrated luminosity of 19.7fb−1. The search is performed using events with three different final states, defined by the number of leptons (electrons and muons) from the t ¯ t→ WbWb decay. The analyses are optimized for reconstruction of top quarks with high Lorentz boosts, where jet substructure techniques are used to enhance the sensitivity. Results are presented for all channels and a combination is performed. No significant excess of events

relative to the expected yield from standard model processes is observed. Upper limits on the production cross section of heavy resonances decaying to $t\bar{t}$ are calculated. A narrow leptophobic topcolor Z′ resonance with a mass below 2.4 TeV is excluded at 95% confidence level. Limits are also derived for a broad Z′ resonance with a 10% width relative to the resonance mass, and a Kaluza-Klein excitation of the gluon in the Randall-Sundrum model. These are the most stringent limits to date on heavy resonances decaying into top-antitop quark pairs.
**Keywords:** Pp collision; Ttbar production.

## B-364. Search for Supersymmetry in P P Collisions at √ S = 8 Tev in Final States with Boosted W Bosons and B Jets Using Razor Variables

Ali Yehia Ellithi Kamel

*Physical Review D, 93: 92009-0, (2016), IF: 4.506*

A search for supersymmetry in hadronic final states with highly boosted W bosons and b jets is presented, focusing on compressed scenarios. The search is performed using proton-proton collision data at a center-of-mass energy of 8 TeV, collected by the CMS experiment at the LHC, corresponding to an integrated luminosity of 19.7 fb−1. Events containing candidates for hadronic decays of boosted W bosons are identified using jet substructure techniques, and are analyzed using the razor variables MR and R2 , which characterize a possible signal as a peak on a smoothly falling background. The observed event yields in the signal regions are found to be consistent with the expected contributions from standard model processes, which are predicted using control samples in the data. The results are interpreted in terms of gluino-pair production followed by their exclusive decay into top squarks and top quarks. The analysis excludes gluino masses up to 1.1 TeV for light top squarks decaying solely to a charm quark and a neutralino, and up to 700 GeV for heavier top squarks decaying solely to a top quark and a neutralino.
**Keywords:** Pp Collision; Super symmetry; W boson; B Jets.

## B-365. Islands of Stability and Quasi-Magic Numbers for Super- and Ultra-Heavy Nuclei

M. Ismail, A. Y. Ellithi, A. Adel and Hisham Anwer

*Chinese Physics C, 40: 124102-0, (2016), IF: 3.761*

In the framework of Strutinsky's approach, we calculated the shell and the residual pairing correction energies for 5569 even-even nuclei in the range $72 \leq Z \leq 282$ and $96 \leq N \leq 540$. Quasi-magic numbers and deformed islands of stability that reside in a range defined by Green's formula and the two-neutrons drip line are introduced. We present 36 quasi-magic proton and 53 quasi-magic neutron magic numbers that contribute to the formation of 133 deformed islands of stability along the N-Z space. The quasi-magic proton and neutron magic numbers volatile as the mass number increases and other magic numbers take over. Consequently, the deformed islands of stability fail to exhibit a pattern along the search space covered.
**Keywords:** Islands of stability; Magic numbers; Superheavy nuclei.

## B-366. Electron Number Density Measurements Using Laser-Induced Breakdown Spectroscopy of Ionized Nitrogen Spectral Lines

Ashraf M. EL Sherbini, Abdelnasser M. Aboulfotouh and Christian G. Pariggerb

*Spectrochimica Acta Part B, 125: 152-158, (2016), IF: 3.289*

Spectrally broadened, singly ionized nitrogen emission lines are monitored to determine electron number densities in laser-induced plasma from aluminum, nano- and bulk-zinc monoxide, as well as hydrogen-rich plastic and wood targets. The optical emission spectra for N II at the average wavelength of 500.33 nm are recorded in standard ambient temperature and pressure environments. For time delays of 25 to 450 ns from the onset of the 1064-nm Nd:YAG radiation induced optical breakdown, the electron number densities in the range of 5.1±1×1019 to 1.22±0.04×1019cm−3 are inferred from the continuum and the nitrogen spectral line analysis. In addition, the corresponding electron temperatures of 10.1±0.6eVto1±0.2 eV are determined from the calculated absolute spectral radiance values in the near infrared region. At the early stages of plasma emission, Balmer series hydrogen lines are embedded in free electron radiation yet the broadening of the N II lines yields reliable electron number density values
**Keywords:** Nanoparticles laser ablation; Atomic spectroscopy Laser-induced; Breakdown spectroscopy.

## B-367. Nano-Material Size Dependent Laser-Plasma Thresholds

Ashraf M. EL Sherbini and Christian G. Parigger

*Spectrochimica Acta Part B, 124: 79-81, (2016), IF: 3.289*

The reduction of laser fluence for initiation of plasma was measured for zinc monoxide nanoparticles of diameters in the range of 100 to 20 nm. In a previous work by EL Sherbini and Parigger [Wavelength Dependency and Threshold Measurements for Nanoparticle-enhanced Laser-induced Breakdown Spectroscopy, Spectrochim. Acta Part B116(2016) 8-15], the hypothesis of threshold dependence on particle size leads to the interpretation of the experiments for varying excitation wavelengths with fixed, 30 nm nanomaterial. The experimental results presented in this work were obtained with 1064 nm Nd:YAG radiation and confirm and validate the suspected reduction due to quenching of the thermal conduction length to the respective sizes of the nanoparticles
**Keywords:** Nanomaterials laser ablation atomic spectroscopy; Zinc monoxide laser fluence; Laser-induced breakdown spectroscopy.

## B-368. Wavelength Dependency and Threshold Measurements for Nanoparticle-Enhanced Laser-Induced Breakdown Spectroscopy

Ashraf M. EL Sherbini and Christian G. Parigger

*Spectrochimica Acta Part B, 116: 8-15, (2016), IF: 3.289*

Nanoparticles of zinc monoxide are selected for laser-induced breakdown spectroscopy with 5 ns pulsed 1064 nm, 532 nm, and 355 nm radiation from a Nd:YAG laser device. Fluences of

2 to 20 J/cm2 are used, and plasma conditions are determined by recording emission spectra in the temporal window of 1 to 2μs after optical breakdown initiation. The bulk-versusnano-article plasmas in laboratory air show that the averaged electron density and temperature values are practically identical. Enhanced signals are recorded for nanoparticles in the amount of ×10 to ×120 for 355 nm radiation. The nanoparticles cause lower optical breakdown thresholds and show signal enhancements as evidenced from the analysis of the Zn I line at 481.0 nm. The measured Hα line at 656.3 nm usually occurs in laser-induced plasma experiments in standard ambient temperature and pressure laboratory air, and it is used in the interpretation of the bulk- and nanomaterial results. The theoretical model largely predicts and confirms the excitation wavelength-dependent experimental results

**Keywords:** Nanoparticles laser ablation; Atomic spectroscopy; Zinc monoxide laser-induced breakdown spectroscopy.

## B-369. Nuclear Spin of Odd-Odd A Emitters Based on The Behavior of A-Particle Preformation Probability

M. Ismail, A. Adel and M. M. Botros

*Physical Review C, 93: 54618-0, (2016), IF: 3.146*

The preformation probabilities of an α cluster inside radioactive parent nuclei for both odd-even and odd-odd nuclei are investigated. The calculations cover the isotopic chains from Ir to Ac in the mass regions 166≤A≤215 and 77≤Z≤89. The calculations are employed in the framework of the density-dependent cluster model. A realistic density-dependent nucleon-nucleon (NN) interaction with a finite-range exchange part is used to calculate the microscopic α-nucleus potential in the well-established double-folding model. The main effect of antisymmetrization under exchange of nucleons between the α and daughter nuclei has been included in the folding model through the finite-range exchange part of the NN interaction. The calculated potential is then implemented to find both the assault frequency and the penetration probability of the α particle by means of the Wentzel-Kramers-Brillouin approximation in combination with the Bohr-Sommerfeld quantization condition. The correlation of the α-particle preformation probability and the neutron and proton level sequences of the parent nucleus as obtained in our previous work is extended to odd-even and odd-odd nuclei to determine the nuclear spin and parities. Two spin coupling rules are used, namely, strong and weak rules to determine the nuclear spin for odd-odd isotopes. This work can be a useful reference for theoretical calculation of undetermined nuclear spin of odd-odd nuclei in the future.

**Keywords:** Preformation probabilities.

## B-370. Relative Stability and Magic Numbers of Nuclei Deduced from Behavior of Cluster Emission Half-Lives

M. Ismail, W. M. Seifand A. Abdurrahman

*Physical Review C, 94: 24316-3, (2016), IF: 3.146*

We calculated the half-life times (Tc) of the 14C, 20O, 20Ne, and 24Ne cluster emissions from heavy and superheavy nuclei. The variation of Tc with the neutron and proton numbers of daughter nuclei is studied to determine the minima in log10Tc at each neutron number for different daughter isotones. We found that each minimum for a given isotone corresponds to neutron magicity already indicated by other approaches. The proton numbers at neutron magic numbers were found to be also proton magic numbers or differ slightly from them. We arranged the different isotones at each neutron magic number according to their stability in the sense that the more stable daughter isotone corresponds to the lowest value of log10Tc. The magic neutron numbers predicted by the present study are N = 126, 148, 152, 154, 160, 162, 172, 176, 178, 180, 182, 184, and 200. The predicted magic proton numbers are Z = 82, 98, 100 102, 106, 108, 114, and 116. The values of N and Z mentioned above agree with magic numbers deduced in other studies.

**Keywords:** Cluster radioactivity.

## B-371. Laser Plasma Diagnostics and Self-Absorption Measurements of the Hβ Balmer Series Line

Ghaneshwar Gautam, Christian G. Parigger, David M. Surmickand Ashraf M. El Sherbini

*Journal of Quantitative Spectroscopy and Radiative Transfer, 170: 189-193, (2016), IF: 2.859*

In this work, the peak-separation of the Balmer series hydrogen beta line was measured to determine the electron density of laser-induced plasma from spatially and temporally resolved spectra collected in laboratory air at standard ambient temperature and pressure. The self-absorption phenomenon is investigated by using a mirror that retro-reflects the emitted radiation through the plasma. The experimental data with and without the mirror were analyzed with available hydrogen beta computer simulations. Hardly any self absorption was found as indicated by the correction factors that only marginally differ from unity. The obtained electron density values are also compared with the electron densities from nearby nitrogen lines. The hydrogen beta Hβ peak-separation method yields reliable results for an electron density of the order of 110 17 cm3 for time delays of 5μs from plasma generation, which confirms that self-absorption is insignificant for such electron densities.

**Keywords:** Laser plasma; Stark broadening hydrogen; Electron density.

## B-372. Optical Properties of Hydroxyethyl Cellulose Film Treated with Nitrogen Plasma

K.H. Mahmoud

*Spectrochimica Acta Part A: Molecular and Biomolecular Spectroscopy, 157: 153-157, (2016), IF: 2.653*

Hydroxyethyl cellulose (HEC) film has been prepared by casting technique. The prepared sample has been treatedwith nitrogen plasmaat different exposure times. The optical absorptionwas recorded at room temperature in the wavelength range of 200–800 nm. Absorbance fitting procedure curves revealed a direct allowed transition with optical band gap, Eopt, of 4.9 eV for pristine film, and this value decreases to 4.30 eV for 20min plasma treatment time. The band tail values (Ee) were found to be increased under plasma time treatment from

1.74 eV in case of the pristine film to 2.20 eV for 20min. The dispersion of refractive index and complex dielectric constants under plasma treatment was also studied. Variation of color parameters under effect of the plasma treatment is analyzed in the framework of CIE L*U*V* color space

**Keywords:** Band tail -Hec- optical properties; Plasma treatment.

## B-373. Nucleon Properties in the Quantized Linear Sigma Model at Finite Temperature and Chemical Potential

M Abu-Shady and H M Mansour

*J. Phys. G: Nucl. Part. Phys., 43: 1-22, (2016), IF: 2.448*

The linear sigma model at finite temperature and chemical potential is systematically studied using the coherent-pair approximation, in which the quantized meson fields are included. The expectation value of the chiral Hamiltonian density is minimized and the resulting equations for the nucleon are solved. The qualitative features of the quantized sigma and pion fields are strongly sensitive to the change of temperature and chemical potential and are in agreement with the mean-field approximation calculations. It is noticed that the nucleon mass increases with increasing coherence parameter x. In addition, the nucleon mass increases with increasing temperature T and the baryonic chemical potential μ, and then it decreases at higher values of the temperature and baryonic chemical potential. The obtained results show that the meansquare radius of the proton and the neutron increase with increasing temperature or baryonic chemical potential, and that the pion–nucleon coupling constant gpNN decreases with the temperature or baryonic chemical potential. We conclude that the coherent-pair approximation successfully gives a better description of the nucleon properties at finite temperature and baryonic chemical potential.

**Keywords:** Quark sigma model; Chemical potential; Nucleon properties; Finite temperature.

## B-374. On Magic Numbers for Super- and Ultraheavy Systems and Hypothetical Spherical Double-Magic Nuclei

M Ismail, A Y Ellithi, A Adel and Hisham Anwer

*Journal of Physics G: Nuclear and Particle Physics, 43: 15101-0, (2016), IF: 2.448*

Based on the calculations of the shell and the residual pairing correction energies in the framework of Strutinsky's approach, we evaluated the proton and neutron magic numbers in the range $72 \leq Z \leq 282$ and $96 \leq N \leq 540$. New magic numbers and new islands of stability lie in a range defined by Green's formula and the two-neutrons drip lines are presented. Our calculations reproduced known spherical double-magic nuclei and present evidences on new spherical double-magic nuclei in super- and ultraheavy regions.

**Keywords:** Shell correction

.

## B-375. Optimum Orientation Versus Orientation Averaging Description of Cluster Radioactivity

W M Seif, M Ismail, A I Refaie and Laila H Amer

*Journal of Physics G: Nuclear and Particle Physics, 43: 75101-75101, (2016), IF: 2.448*

While the optimum-orientation concept is frequently used in studies on cluster decays involving deformed nuclei, the orientation-averaging concept is used in most alpha decay studies. We investigate the different decay stages in both the optimum-orientation and the orientation-averaging pictures of the cluster decay process. For decays of 232,233,234U and 236,238Pu isotopes, the quantum knocking frequency and penetration probability based on the Wentzel–Kramers–Brillouin approximation are used to find the decay width. The obtained decay width and the experimental half-life are employed to estimate the clusters preformation probability. We found that the orientation-averaged decay width is one or two orders of magnitude less than its value along the non-compact optimum orientation. Correspondingly, the extracted preformation probability based on the averaged decay width increases with the same orders of magnitude compared to its value obtained considering the optimum orientation. The cluster preformation probabilities estimated by the two considered schemes are in more or less comparable agreement with the Blendowske–Walliser (BW) formula based on the preformation probability of α (${S}_{\alpha }^{{\rm{a}}{\rm{v}}{\rm{e}}})$ obtained from the orientation-averaging scheme. All the results, including the optimum-orientation ones, deviate substantially from the BW law based on ${S}_{\alpha }^{{\rm{o}}{\rm{p}}{\rm{t}}}$ that was estimated from the optimum-orientation scheme. To account for the nuclear deformations, it is more relevant to calculate the decay width by averaging over the different possible orientations of the participating deformed nuclei, rather than considering the corresponding non-compact optimum orientation.

**Keywords:** Alpha decay; Cluster decay; Preformation probability; Half-life; Deformation.

## B-376. Ternary Fission of 260No in Collinear Configuration

M. Ismail, W.M. Seif, A.S. Hashem, M.M. Botros and I.A.M. Abdul-Magead

*Annals of Physics, 372: 375-391, (2016), IF: 2.375*

We investigate the collinear ternary fission of the 260No isotope. The calculations are performed in the framework of the three cluster model for all possible accompanied light particles of even mass numbers A=4−52. The folding nuclear and Coulomb interaction potentials are used, based on the M3Y-Reid nucleon–nucleon force for the nuclear part. The deformation of the involved fragments and their relative orientations with respect to each other inside the fissioning nuclei are considered. Among all possible fragmentation channels, the suggested most probable channels are indicated as the ones showing a peak in the Q-value and a local minimum in the fragmentation potential, with respect to the mass and charge asymmetries. The indicated favored fragmentation channels from the approximate spherical calculations and those obtained after considering the deformations of the produced fragments

are discussed in detail. In addition to the preferred heavy fragments of closed shells, favored prolate ones of high deformations appear when the nuclear deformations are taken into account. Among indicated fifty six favored channels, a collinear ternary fission of the 260No isotope is indicated to be most favored through the fragmentation channels of 15058Ce+410Be+40100Zr,60152Nd+412Be+3896Sr,58150Ce +614C+3896Sr,58148Ce+616C+3896Sr,54140Xe+822O+4098 Zr,42106Mo+1848Ar+42106Mo and 41104Nb+2052Ca+41104Nb

**Keywords:** Ternary fission; Fragmentation potential; Deformed nuclei; Heavy nuclei.

## B-377. Ternary Fission of 260No in Equatorial Configuration

M. Ismail, W.M. Seif and A.S. Hashem

*The European Physical Journal A, 52:317-317, (2016),IF:2.373*

Spontaneous ternary fission is one of the observed decay modes of heavy nuclei. We systematically investigate the equatorial ternary fission of the 260No isotope. In the framework of the three-cluster model, the three-body interaction potential is calculated in terms of the folded M3Y-Reid nucleon-nucleon force and the Coulomb one. The relative orientations of the deformed heavy nuclei participating in the fragmentation process are taken into account. All possible emitted light particles with even mass numbers A=4A=4 -52 are considered. The favored fragmentation channels are estimated as the ones characterized with peaks in the Q-value and local minima in the fragmentation potential. In the absence of nuclear deformations, the closed shell effects are found to play the key role in determining the channels of minimum fragmentation potential and the involved two heavier fragments tend to be of comparable sizes. Inclusion of nuclear deformations manifest the participation of highly deformed prolate nuclei, with large mass asymmetry, as heavy fragment partners in the estimated favored fragmentation channels. The results indicate that the equatorial ternary fission of 260No is most favored with the light emitted nuclei 4,6,82He and 104Be through the fragmentation channels 15560Nd + 42He + 1010Zr, 15360Nd + 62He + 10140Zr, 15260Nd + 82He + 10040Zr, and 1520Nd + 104Be + 9838Sr,

**Keywords:** Ternary fission; Heavy ions.

## B-378. Structural and Optical Properties of P-Quaterphenyl Thin Films and Application in Organic/Inorganic Photodiodes

A.A. Attia a, M.M. Saadeldin , H.S. Soliman , A.S. Gadallah and K. Sawaby

*Optical Materials, 62: 711-716, (2016), IF: 2.183*

Para-quaterpheny1 (p-4pheny1) thin films were deposited by the thermal evaporation method on glass/quartz substrates for structural and optical investigations. The XRD of p-4phenyl thin films showed thatthe as-deposited films have a monoclinic structure. The surface morphology of p-4phenyl thin film was studied using scanning electron microscope. The absorption spectrum of p-4phenyl thin film recorded in the wavelength range 200e2500 nm. Photoluminescence measurements revealed two emission peaks at 435 and 444 nm using N2-laser (337.8 nm). The energy gap obtained from the absorption and photoluminescence data was found to be 2.87 and 2.74 eV respectively with Stokes shift value of 0.13 eV. The current-voltage characteristics of p-4phenyl/p-Si heterojunction have been recorded in the dark and under illumination of laser (337.8 nm). Responsivity, Detectivity, External quantum efficiency and Response speed of (Au/p-4pheny1/p-Si/Al) photodetector have been determined using different laser sources at -1 V bias.

**Keywords:** P-Quaterphenyl; Thin Film ;X-Ray diffraction; Optical properties; Organic/Inorganic photodiode.

## B-379. Characterization, Phase Change and Conductivity Crossover of New Luminescent Ferroelectric Mn (Ii) Organic-Inorganic Hybrid

Mohga F. Mostafa, Thana Sh. El Dean and Ahmed K. Tammam

*Materials Chemistry and Physics,180:373-382,(2016), IF:2.101*

Synthesis and characterization of new luminescent ferroelectric [(CH3)(C6H5)3P]2MnBr4 organic-inorganic hybrid (OIH) are reported. Powder x-ray diffraction showed the following phases: P2/m (280 K) Phase (IV) P21 (298 K) Phase (III) Pna21 (350 K) Phase (II) Pnma (370 K) Phase (I). Room temperature lattice parameters are a = 9.6233 (Å), b = 12.5653 (Å) c = 16.4503 (Å) and β = 105.6° (T = 298 K). UV-VIS and Ac magnetic susceptibility confirm tetrahedral symmetry of [MnBr4]2−. DSC and dielectric measurements showed four phase transitions at T4peak = 279.1 ± 1 K (ΔS = 1.03 J/mol K), T3peak = 300.1 ± 2 K (ΔS = 2.33 J/mol K), T2peakt = 353.2 ± 3 K (ΔS = 2.68 J/mol K) and T1peak = 379.1 ± 3 K (ΔS = 2.43 J/mol K). Calculated lattice potential energy values vary from 827 (kJ/mol) at 280 K to (797 kJ/mol) at 370 K. Ac conductivity measurements (220 < T(K) < 400) and (0.081 < f (kHz) < 30) are presented. It is ferroelectric with Curie temperature Tc = 309 K. Hybrid is semiconductor in the temperature range 309 ± 14 K, where conductivity follows Jonscher's universal dielectric response otherwise it is an insulator where crossover to super-linear power law prevails. Comparison to the corresponding chloride is discussed.

**Keywords:** Phase transition; Dielectric constant; Conductivity crossover.

## B-380. Res_Id: 1125 J Res_Wcode: 848 Bose–Einstein Condensation in A Two-Component Bose Gas with Harmonic Oscillator Interaction

A A Abulseoud, A H Abbas, A A Galal and Th M El-Sherbini.

*Journal of Statistical Mechanics: Theory and Experiment, 2016: 73304-0, (2016), IF: 2.091*

In this article a system containing two species of identical bosons interacting via a harmonic oscillator potential is considered. It is assumed that the number of bosons of each species is the same and that bosons belonging to the same species repel each other while those belonging to different species attract. The Hamiltonian is diagonalized and the energy spectrum of the system is written down. The behaviour of the system in the thermodynamic limit is studied within the framework of the grand canonical ensemble, and thermodynamic parameters, such as the internal energy, entropy and specific heat capacity are calculated. It is shown that the system exhibits a single species Bose–Einstein condensation

when the coupling strengths are equal and a dual species condensation when they are different.
**Keywords:** Bose einstein condensation; Quantum phase transition.

## B-381. Studying Factors Affecting the Indoor Gamma Radiation Dose Using the Mcnp5 Simulation Software

M. Orabi

*Journal of Environmental Radioactivity, 165: 54-59, (2016), IF: 2.047*

Different factors and parameters affecting the indoor gamma radiation dose are considered and investigated. The change of the dose with different positions inside the room is discussed. The relative doses are also calculated for different changes; with different room dimensions, different wall thicknesses, and different building material densities. Some other factors are also discussed. The study is carried out by executing some models designed by the MCNP version 5 simulation software. The calculations of the dose rates are performed by adopting a simple and convenient calculation model which is based on the obtained relative changes of the dose rates with the different factors.
**Keywords:** Mcnp; Modeling; Natural radiation; Radiation doses; Radioactivity concentrations; Simulation.

## B-382. Characterization and Coordination of Intercalation - Non-Intercalation Phase Transition in A New Hybrid Halide Perovskite (N-C16h33nh3)2 Zncl4

M.M. Abdelkader and W.M. Gamal

*Solid State Sciences, 61: 173-184, (2016), IF: 2.041*

The ac conductivity σ(ω,T) and the complex dielectric permittivity ε•(ω,T) as function of temperature 100 K < T < 400 K and frequency in the range 1 kHz ≤ f ≤ 100 kHz, as well as some thermal characterizations, namely the differential scanning calorimetry (DSC) and the differential thermal analysis (DTA) thermograms, were, measured and presented for polycrystalline virgin samples of the titled compound. It is one member of the long-chain of Zn hybrids of the series (n-CnH2n+1NH3)2ZnCl4 (n = 8–18) and hence it belongs to the class of thermal energy storage materials. Our data evidenced that the hybrid undergoes a first order solid-solid structural phase transition from an intercalation to a non-intercalation at ≈373 K which is associated with an increase in the interlayer spacing "d" by 19.3%. In the room temperature phase, the hybrid is intercalated and tends to crystallize in an isolated square tetrahedra of zero-dimensional (0D) but arranged in the crystal system in two-dimensional (2D) via the assisted charge hydrogen bonds Nsingle bondH…Cl. It is therefore highly packed and hence have a highly transition temperature, highly thermal energy storage compared with other hybrids of the same n but of different M. These novelties characteristics suggested that the hybrid is more suitable for solar energy research. The even-odd effect, which is only common for Zn and Co in the room temperature phase and absent for other compounds, as well as the mechanism of the phase change have been discussed. The role of the coordination of the divalent metal ion and the dimensionality of the isolated unit (MCl4)−2 (M = Zn and/or Co) are considered. Comparison of the current phase transition with that of Zn compounds (n = 8, 10, 12, and 14) has been given.
**Keywords:** Intercalation; Non-Intercalation; Organic-Inorganic hybrid perovskite; Thermal energy Storage materials - (N-C16h33nh3)2Zncl4; Ac conductivity; Dielectric permittivity; Dsc and /Or Dta thermograms.

## B-383. Synthesis and Spectroscopic Investigation of Cobalt Oxide Nanoparticles

Khaled H. Mahmoud

*Polymer Composites, 37: 1881-1885, (2016), IF: 2.004*

Hydroxyethyl cellulose and cobalt chloride are used as precursor materials for the synthesis of cobalt oxide (Co3O4) nanoparticles. A composite system from polymer and metal chloride is prepared via casting technique. The thermal decomposition of the composite is studied using thermogravimetric technique. Calcination of the composite system at 350C resulted in the formation of Co3O4 nanoparticles. X-ray diffraction analysis reveals the presence of crystalline Co3O4 with an average particle size of around 15 nm. The bonding nature and morphology of nanosized Co3O4 are examined using transmission electron microscopy and infrared spectroscopy. The Tauc's plot indicates the energy band gap for direct allowed transition as 3.2 eV and 1.4 eV.
**Keywords:** Cobalt oxide nanoparticle; Band Gap-Polymer composite film.

## B-384. Thermal and Spectroscopic Properties of the Nano-System (Zno(1−X)Sio2(X))

F. El-Kabbany , S. Taha, M. Hafez and I.S. Yahia

*Journal of Molecular Structure, 1111: 33-45, (2016), IF: 1.78*

Structural and thermal properties of the investigated nano-matrix ZnO(1−x)SiO2(x) samples were characterized by various techniques such as X-ray analysis, scanning electron microscopy (SEM), thermogravimetric analysis (TGA) and differential thermal analysis (DTA). IR spectroscopic analysis in the frequency range 400–4000 cm−1 is used here to investigate the new nano-system at room temperature. The variation of enthalpy (ΔH) with the concentration of SiO2 nanoparticles for the five systems of the ZnO(1−x)SiO2(x) matrix is determined. Seven different fundamental modes have been investigated. All of the vibrations of the investigated nano-system (ZnO(1−x)SiO2(x)) were found to be 449 cm−1, 469 cm−1, 798 cm−1, 959 cm−1, 1096 cm−1, 1630 cm−1 and 3447 cm−1 correspond to normal vibrations of stretching mode of ZnO, Si – O – Si or O – Si – O bending mode, Si – O – Si symmetric stretching, vibrational mode of Si–O – Zn, Si – O – Si asymmetric stretching, bending vibration mode of adsorbed water and stretching vibration of OH group respectively in which the variations strongly support the variation of ZnO and SiO2 nanoparticles concentration in the studied matrix. Measurements and interpretation of IR spectra as a function of ZnO and SiO2 nanoparticles concentration is reported.
**Keywords:** Thermal ir analysis Zno(1X)Sio2(X) matrix.

## B-385. Toward a Better Parameterization of Nuclear Density for A-Decay Calculation

M. Ismail, A.Y. Ellithi, A. Adel and A.R. Abdulghany

*Nuclear Physics A, 947: 64-75, (2016), IF: 1.258*

Starting from three-parameter Fermi distribution of nuclear densities, we used two formulas, for calculating the half-density radius, to study the effect of variation of radius of daughter nucleus on both α-decay half-life and α-preformation factor. We compared the results of the aforementioned two formulas with the corresponding results obtained from the nuclear densities of Hartree–Fock calculation derived from the BSk2 Skyrme force. We considered >60 isotopes of Po and Rn α-emitter elements and studied the variation of half-life and preformation factor with density parameters. We found that the variation of density parameters of daughter nuclei highly affects the calculated half-life and the extracted value of preformation factor, but the behavior of these two quantities with variation of parent neutron number is almost independent of the density parameters.
**Keywords:** Nucleon distributions.

## B-386. A Systematic Calculation of Alpha Decay Half-Lives Using A New Approach for Barrier Penetration Probability

M. Ismail, A. Y. Ellithi, A. EL-Depsy and O. A. Mohamedien

*International Journal of Modern Physics E, 25 (2016) IF: 1.229*

A systematic calculation of alpha decay half-lives of 347 nuclei is considered in the framework of the Wentzel–Kramers–Brillouin (WKB) approximation using two formulas. A recently proposed barrier penetration formula, with some modified parameters, is used first. Second, a new analytic barrier penetration formula is derived by taking into account the centrifugal potential. A good agreement with experimental data is achieved especially for spherical nuclei. The new formula reproduces experimental alpha decay half-lives with a satisfying accuracy especially for penetration energies much lower than the Coulomb barrier.
**Keywords:** Parabolic approximation; Alpha decay; Quantum tunneling; Coulomb barrier.

## B-387. Adiabatic and Coupled Channels Calculations for Near Barrier Fusion of 16O+238U Using Realistic Nucleon–Nucleon Interaction

M. Ismail, W. M. Seif and M. M. Botros

*International Journal of Modern Physics E, 25: 1650026-1650026, (2016), IF: 1.229*

We investigate the fusion cross-section and the fusion barrier distribution of 1616O+238+238U at near- and sub-barrier energies. We use an interaction potential generated by the semi-microscopic double folding model-based on density dependent (DD) form of the realistic Michigan-three-Yukawa (M3Y) Reid nucleon–nucleon (NN) interaction. We studied the role of both the static and dynamic deformations of the target nucleus on the fusion process. Rotational and vibrational degrees of freedom of 238238U-nucleus are considered. We found that the deformation and the octupole vibrations in 238238U enhance its sub-barrier fusion cross-section. The signature of the the octupole vibrational modes of 238238U appears clearly in its fusion barrier distribution profile.
**Keywords:** Fusion cross-section; Fusion barrier distribution; Double folding modes; Static and dynamic deformations; Octupole vibrations.

## B-388. Sensibility of Grey Particle Production System to Energy and Centrality in 60A and 200A Gev 1616O–Nucleus Interactions

A. Abdelsalam, M. S. El–Nagdy, B. M. BadawyW. Osman and M. Fayed

*International Journal of Modern Physics E, 25: 1650034-16500, (2016), IF: 1.229*

The grey particle production following 60 A and 200A GeV 1616O interactions with emulsion nuclei is investigated at different centralities. The evaporated target fragment multiplicity is voted as a centrality parameter. The target size effect is examined over a wide range, where the C, N and O nuclei present the light target group while the Br and Ag nuclei are the heavy group. In the framework of the nuclear limiting fragmentation hypothesis, the grey particle multiplicity characteristics depend only on the target size and centrality while the projectile size and energy are not effective. The grey particle is suggested to be a multisource production system. The emission direction in the 4ππ space depends upon the production source. Either the exponential decay or the Poisson's peaking curves are the usual characteristic shapes of the grey particle multiplicity distributions. The decay shape is suggested to be a characteristic feature of the source singularity while the peaking shape is a multisource super-position. The sensibility to the centrality varies from a source to other. The distribution shape is identified at each centrality region according to the associated source contribution. In general, the multiplicity characteristics seem to be limited w.r.t. the collision system centrality using light target nuclei. The selection of the black particle multiplicity as a centrality parameter is successful through the collision with the heavy target nuclei. In the collision with the light target nuclei it may be qualitatively better to vote another centrality parameter.
**Keywords:** Grey particle multiplicity; Dependence on target size; Dependence on centrality; Emission characteristics; Nuclear limiting fragmentation.

## B-389. Structural Properties of Heavy and Superheavy Nuclei in a Semi-Microscopic Approach

M. Ismail, A. Y. Ellithi, A. Adel and Hisham Anwer

*International Journal of Modern Physics E, 25 (2016) IF: 1.229*

The structure of some heavy and superheavy nuclei with $93 \le Z \le 126$ and $130 \le N \le 252$ is studied using a semi-microscopic model. In this approach, the macroscopic energy part of the total energy of a nucleus is obtained from the Skyrme nucleon–nucleon interaction in the semi-classical extended Thomas–Fermi approach. The microscopic shell-plus pairing correction energies are calculated in Strutinsky's approach. Within this semi-microscopic approach, the total energy surfaces are investigated in multidimensional deformation space. For each

nucleus, the model predictions for the binding energy, deformation energy, the deformation parameters and comparison with other theoretical models are presented. The proposed model shows a significant consistency with other models, and it is found to be successful in reproducing the structural properties of nuclei in heavy and superheavy region.
**Keywords:** Superheavy nuclei; Shell-Correction; Binding energy.

## B-390. Influence of Ionic Temperature on the Acoustic Dressed Soliton in Plasma with Maxwellian Positrons

E K El-Shewy, N F Abdo and M S Yousef

*Indian Journal of Physics, 90 /8: 959-963, (2016), IF: 1.166*

The dressed solitary ion waves in a collisionless unmagnetized plasma composed warm fluid of ion and Boltzmann distributed electrons and positrons are studied. For nonlinear ion acoustic waves, a reductive perturbation method is applied to deduce the KdV equation in terms of first order potential. When soliton amplitude is enlarged, the shape of the wave sidetracks from KdV equation. To improve the soliton shape, the perturbed KdV equation is obtained.The effects of ionic temperature on the electrostatic dressed soliton structures are also discussed.
**Keywords:** Ion acoustic waves; Perturbed Korteweg–De vries (Kdv) Equation; Dressed solitary solution.

## B-391. Thermal and Electrical Heating Treatments of Conductive Acrylonitrile Butadiene/Butyl Rubber Blends

Abdulkareem A Redhwan, AA El-Gamal, SA Khairy and HH Hassan

*Journal of Thermoplastic Composite Materials, 29: 92-102, (2016), IF: 0.922*

Blend of acrylonitrile butadiene/isoprene-isobutene rubber (NBR/IIR) with different compositions was prepared. Scanning electron microscopic observations confirmed the compatibilization of bromo isoprene-isobutene rubber on NBR/IIR blend. Each rubber blend was loaded with different ratios of N-326 (high-abrasion furnace (HAF)): N-774 (semi-reinforcing furnace) carbon blacks. Current–voltage curves, joule electrical heating, and temperature-dependent electrical conductivity of the prepared blends were measured. The electrical and thermal properties of the blends were enhanced upon the increase of N-326 (HAF) content.
**Keywords:** Acrylonitrile; Butyl rubber; Sem; Thermal; Electrical conductivity.

## B-392. Characterization of Organic–Inorganic Hybrid Layered Perovskite and Intercalated Compound (N- C12h25nh3)2Zncl4

M.M. Abdel-Kader, A.I. Aboud and W.M. Gamal

*Phase Transitions, 89: 448-470, (2016), IF: 0.858*

We report on some electrical properties and solid–solid phase transitions of organic–inorganic hybrid layered halide perovskite and intercalated compound (n-C12H25NH3)2ZnCl4 which is one member of the long-chain compounds of the series (n-CnH2n+1NH3)2,(n = 8–18). The complex dielectric permittivity $\epsilon^*(\omega,T)$ and the ac conductivity $\sigma(\omega,T)$ were measured as functions of temperature 100 K < T < 390 K and frequency 5 kHz < f < 100 kHz. Moreover, the differential scanning calorimetery and the differential thermal analysis thermograms were performed. The analysis of our data confirms the existence of a structural phase transition at $T \approx (362 \pm 2)$ K, where the compound changes its state from intercalation to non-intercalation with a drastic increase in the c-axis by about 16.4%. The behavior of the frequency-dependent conductivity follows the Jonscher universal power law: $\sigma(\omega, T) \alpha \omega s(\omega,T)$. The mechanism of electrical conduction in the low-temperature phase (phase II) can be described as quantum mechanical tunneling model.
**Keywords:** Organic–Inorganic Hybrid Perovskites; Intercalation Compounds; (N-C12h25nh3)2 Zncl4; Dielectric properties; Thermal parameters.

## B-393. Synthesis, Structural and Optical Properties of Tin Oxide Nanoparticles and its Cmc/Peg-Pva Nanocomposites Films

Noha H. El Fewaty, A. M. El Sayed and R. S. Hafez

*Polymer Science, Series A, 58: 1004-1016, (2016), IF: 0.76*

Polyethylene glycol–polyvinyl alcohol (PEG–PVA) blend is a multifunctional material and controlling its properties is important for various medical and industrial uses. In this paper, we report the influence of carboxymethyl cellulose (CMC) and doping with tin oxide (SnO2) nanoparticles (NPs) on the structural and optical properties of PEG–PVA. The prepared samples were investigated by X-ray diffraction (XRD), high-resolution transmission electron microscopy (HR-TEM), scanning electron microscopy (SEM), Fourier transform infrared (FTIR) and UV–Vis-NIR spectroscopies. SnO2 NPs of rutile structure, average crystallite size of ~30.2 nm and optical band gap (Eg) of 3.68 eV were prepared by a simple sol–gel process. CMC addition enhances the crystallinity of PEG–PVA that then gradually reduced by increasing SnO2 doping ratio. The optical transmittance of PEG–PVA increased from 77 to 90% after mixing with CMC and then decreased to 64% with increasing SnO2 content to 1.5%. Also, the Eg of PEG–PVA increased from 5.20 to 5.28 eV and then decreased to 4.88 eV due to CMC addition and SnO2 incorporation, respectively. The refractive index, the dispersion parameters and the optical conductivity of PEG–PVA, CMC/PEG–PVA and of its nanocomposite films are discussed. The correlation between the structural modifications and the resultant optical properties are reported.
**Keywords:** Sno2 nanoparticles; Nanocomposite; Pva-Peg Blend; Optical constants; Refractive index; Conductivity.

## B-394. Comparison Between Different Proximity Potentials and the Double-Folding Model for Spherical–Deformed Interacting Nuclei

M. Ismail and I.A.M. Abdul-Magead

*Canadian Journal of Physics, 94 (2016) IF: 0.724*

The Coulomb barrier parameters have been calculated for a spherical–deformed interacting pair of nuclei using 14 different versions of the proximity approaches and a simple analytical formula for the Coulomb part of the heavy ion potential. The results of these proximity versions have been compared with more accurate results obtained from the double-folding model (DFM). We have considered the interacting pair 48Ca + 238Pu as an example and assumed the presence of the quadrupole, octupole, and hexadecapole deformation parameters for 238Pu. The orientation angle dependence of the Coulomb barrier parameters has been computed for different sets of deformation parameters. We found that the proximity types named Prox77, BW Prox91, AW Prox95, Bass Prox77, and Bass Prox80 are the best ones of the available 14 versions of the proximity approaches for calculating the nuclear part of the interaction potential for a spherical–deformed pair of nuclei.

**Keywords:** Proximity potential; Double-Folding model; Coulomb barrier parameters; Heavy Ion potential; Deformed nuclei.

## B-395. Study and Assessment of Low Frequency Noise in Occupational Settings

Adel M. Shehap, Hany A. Shawky and Tarek M. El-Basheer

*Archives of Acoustics, 41/1: 151-160, (2016), IF: 0.661*

Low frequency noise is one of the most harmful factors occurring in human working and living envi- ronment. Low frequency noise components from 20 to 250 Hz are often the cause of employee complaints. Noise from power stations is an actual problem for large cities, including Cairo. The noise from equip- ments of station could be a serious problem for station and for environmental area. The development of power stations in Cairo leads to appearing a wide range of gas turbines which are strong source of noise. Two measurement techniques using C-weighted along side the A-weighted scale are explored. C-weighting is far more sensitive to detect low frequency sound. Spectrum analysis in the low frequency range is done in order to identify a significant tonal component. Field studies were supported by a questionnaire to determine whether sociological or other factors might influence the results by using annoyance rating mean value. Subjects included in the study were 153 (mean = 36.86, SD = 8.49) male employees at the three electrical power stations. The (C-A) level difference is an appropriate metric for indicating a potential low frequency noise problem. A-weighting characteristics seem to be able to predict quite ac- curately annoyance experienced from LFN at workplaces. The aim of the present study is to find simple and reliable method for assessing low frequency noise in occupational environment to prevent its effects on work performance for the workers. The proposed method has to be compared with European methods.

**Keywords:** Low frequency noise; A-Weighting; C-Weighting; Audible; Method of assessment.

## B-396. Application of a Folding-Model Optical Potential to Analyzing Inelastic Pion–Nucleus Scattering and the in-Medium Effect on a Pion–Nucleon Amplitude

V. K. Lukyanov, E. V. Zemlyanaya, K.V. Lukyanov and I. A. M. Abdul-Magead

*Physics of Atomic Nuclei, 79: 978-986, (2016), IF: 0.457*

The folding-model optical potential is generalized in such a way as to apply it to calculating the cross sections for inelastic scattering of $\pi^{\pm}$-mesons on 28Si, 40Ca, 58Ni, and 208Pb nuclei at the energies of 162, 180, 226, and 291 MeV leading to the excitation of the $2^+$ and $3^-$ collective states. In doing this, use is made of known nucleon-density distributions in nuclei and the pion–nucleon scattering amplitude whose parameters were obtained previously by fitting the elastic scattering cross sections for the same nuclei. Thus, the values of quadrupole ($\beta 2$) and octupole ($\beta 3$) deformations of nuclei appear here as the only adjustable parameters. The scattering cross section is calculated by solving the relativistic wave equation, whereby effects of relativization and distortion in the entrance and exit scattering channels are taken exactly into account. The cross sections calculated in this way for inelastic scattering are in good agreement with respective experimental data. The importance of the inclusion of in-medium effects in choosing parameters of the pion–nucleon amplitude is emphasized.

**Keywords:** Pion–Nucleus scattering ;In-medium effect.

## B-397. Structural and Optical Properties of Tio2 Nanoparticles/Pva for Different Composites Thin Films

A.M.Shehap and Dana S.Akil

*The Journal of Nanoelectronics and Materials,9/1:17-36 (2016)*

Polymeric films based on polyvinyl alcohol (PVA) doped with titanium dioxide nanoparticles at different weight percentage (1.25, 2.5, 5, 7.5, 10 TiO2/PVA) were prepared using the sonification and casting techniques. The structural properties of those samples were examined by XRD, FTIR, and UV-Visible .The XRD pattern revealed that the amorphous domain in PVA polymer matrix increased with raising the TiO2 content. The complexation of the dopant with the polymer was examined by FTIR studies .The absorption spectra of UV-Visible light showed irregular changes of the absorption for high doping samples in UV range (7.5, 10 TiO2 /PVA). Absorbance, transmittance and reflectance spectra were used for the determination of the optical constants. The results indicated that the optical band gap decreases with increasing TiO2 content, while the refractive index increased to high value for the composites of high dopant. Using the Wemple-DiDomenico model, we calculated the static reflection index, the oscillation energy, and the dispersion energy. The dispersion energy changes slowly as a function of TiO2 percentage .The dispersion parameters and the high frequency dielectric constant were determined. In addition the average oscillator wavelength $\lambda 0$ and oscillator strength S0 for the investigated samples were found to be strongly affected by the nanopartices dopant.

**Keywords:** Pva; Tio2; Xrd; Ftir; Uv-Visible; Wemple-didomenico.

## B-398. Origanum Majorana Attenuates Nephrotoxicity of Cisplatin Anticancer Drug Through Ameliorating Oxidative Stress

Amel M. Soliman, Shreen Desouky, Mohamed Marzouk and Amany A. Sayed

*Nutrients, 8: 1-9, (2016), IF: 3.759*

Despite the fact that cisplatin is an important anticancer drug, its clinical utilization is limited by nephrotoxicity during long term medication. Combined cisplatin chemotherapy with plant extracts can diminish toxicity and enhance the antitumor efficacy of the drug. This study evaluated the effect of Originum majorana ethanolic extract (OMEE) on cisplatin-induced nephrotoxicity. Eighteen male rats were divided into three groups as follows: a control group, a group treated with cisplatin (3 mg/kg body weight), and a group that received both cisplatin and OMEE (500 mg/kg body weight) for 14 days. Cisplatin induced a significant increase in creatinine, urea, uric acid, blood urea nitrogen, malondialdehyde, and nitric oxide levels. However, glutathione, superoxide dismutase, and catalase levels were significantly diminished. Conversely, OMEE significantly modulated the renal and oxidative markers negatively impacted by cisplatin. OMEE significantly reduced the effects of cisplatin-induced changes in renal and oxidative markers, possibly through its free radical scavenging activity. Thus, OMEE may be combined with cisplatin to alleviate nephrotoxicity in cancer chemotherapy. View Full-Text

**Keywords:** Cisplatin; Nephrotoxicity; Originum majorana; Oxidative stress.

## B-399. Inflammatory and Non-Inflammatory Breast Cancer: A Potential Role for Detection of Multiple Viral DNAs in Disease Progression

El-Shinawi M, Mohamed HT, Abdel-Fattah HH, Ibrahim SA, El-Halawany MS, Nouh MA, Schneider RJ and Mohamed MM

*Ann Surg Oncol., 23(2): 494-502, (2016), IF: 3.655*

**Background:** Inflammatory breast cancer (IBC) is the most lethal form of breast cancer. Multiple viral infections in IBC tissues were found to be associated with disease pathogenesis. OBJECTIVE: The aim of the present study was to correlate the incidence of viral DNA with breast cancer progression. **Materials and Methods:** Overall, 135 women diagnosed with breast cancer were enrolled in this study. Using polymerase chain reaction and sequencing assays, we determined the incidence of human papillomavirus types 16 and 18 (HPV-16 and -18), human cytomegalovirus (HCMV), Epstein-Barr virus, human herpes simplex virus type 1 and 2, and human herpes virus type 8 (HHV-8) in breast carcinoma tissue biopsies. We also assessed the expression of the cell proliferation marker Ki-67 by immunohistochemistry in association with the incidence of viral DNA. **Results:** HCMV and HPV-16 were the most detected viral DNAs in breast carcinoma tissues; however, the frequency of HCMV and HHV-8 DNA were significantly higher in IBC than non-IBC tissues. Moreover, the prevalence of multiple viral DNAs was higher in IBC than non-IBC tissues. The incidence of multiple viral DNAs positively correlates with tumor size and number of metastatic lymph nodes in both non-IBC and IBC patients. The expression of Ki-67 was found to be significantly higher in both non-IBC and IBC tissues in which multiple viral DNAs were detected. **Conclusions:** The incidence of multiple viral DNAs in IBC tissues was higher compared with non-IBC tissues. The present results suggest the possibility of a functional relationship between the presence of multiple viral DNAs and disease pathogenesis.

**Keywords:** Inflammatory breast cancer; Viral DNAs; Ki-67. Lymph node metastasis.

## B-400. Whipworms in Humans and Pigs: Origins and Demography

Mohamed B. F. Hawash, Martha Betson, Azmi Al-Jubury, Jennifer Ketzis, Arve LeeWillingham, Mads F. Bertelsen, Philip J. Cooper, D. Tim J. Littlewood, Xing-Quan Zhu and Peter Nejsum

*Parasites and Vectors, 48: 4-9, (2016), IF: 3.234*

**Background** Trichuris suis and T. trichiura are two different whipworm species that infect pigs and humans, respectively. T. suis is found in pigs worldwide while T. trichiura is responsible for nearly 460 million infections in people, mainly in areas of poor sanitation in tropical and subtropical areas. The evolutionary relationship and the historical factors responsible for this worldwide distribution are poorly understood. In this study, we aimed to reconstruct the demographic history of Trichuris in humans and pigs, the evolutionary origin of Trichuris in these hosts and factors responsible for parasite dispersal globally. **Methods** Parts of the mitochondrial nad1 and rrnL genes were sequenced followed by population genetic and phylogenetic analyses. Populations of Trichuris examined were recovered from humans (n = 31), pigs (n = 58) and non-human primates (n = 49) in different countries on different continents, namely Denmark, USA, Uganda, Ecuador, China and St. Kitts (Caribbean). Additional sequences available from GenBank were incorporated into the analyses. **Results** We found no differentiation between human-derived Trichuris in Uganda and the majority of the Trichuris samples from non-human primates suggesting a common African origin of the parasite, which then was transmitted to Asia and further to South America. On the other hand, there was no differentiation between pig-derived Trichuris from Europe and the New World suggesting dispersal relates to human activities by transporting pigs and their parasites through colonisation and trade. Evidence for recent pig transport from China to Ecuador and from Europe to Uganda was also observed from their parasites. In contrast, there was high genetic differentiation between the pig Trichuris in Denmark and China in concordance with the host genetics. **Conclusions** We found evidence for an African origin of T. trichiura which were then transmitted with human ancestors to Asia and further to South America. A host shift to pigs may have occurred in Asia from where T. suis seems to have been transmitted globally by a combination of natural host dispersal and anthropogenic factors.

**Keywords:** Whipworms trichuris humans; Pigs demographic History evolution.

## B-401. Use of Arius Thalassinus Fish in a Pollution Biomonitoring Study, Applying Combined Oxidative Stress, Hematology, Biochemical and Histopathological Biomarkers: A Baseline Field Study

Yousef S. Saleh and Mohamed-Assem S. Marie

*Marine Pollution Bulletin, 106: 308-322, (2016), IF: 3.099*

The present field study aimed to determine the extent of pollution in the Red Sea coast of Yemen Republic using a battery of biomarkers in sea catfish, Arius thalassinus, originating froma reference site in comparison with a polluted site.We reported the concentration of heavy metals in some vital fish organs and their effects on the morphological, hematological, biochemical and oxidative stress biomarkers accompanied by the examination of histopathological alterations. The obtained results showed clear signs of stress in fish from a polluted site. Linear correlation analysis exhibited that the biomarkers response could be linked to the detected metals bioaccumulation. In addition, principal component analysis showed a clear separation of sampling sites in two different assemblages. Semi-quantitative analysis for the observed histopathological lesions revealed that gillswere the most affected organs with signs of severe alterations. This field investigation provides a baseline data on pollution status in this region.

**Keywords:** Arius thalassinus; Red Sea; Biomarkers; Semi-Quantitative analysis; Heavy metals; Marine pollution.

## B-402. Hormonal-Receptor Positive Breast Cancer: Il-6 Augments Invasion and Lymph Node Metastasis Via Stimulating Cathepsin B Expression.

Sherif A. Ibrahim, Eslam A. El-Ghonaimy, Hebatallah Hassan; Noha Mahana, Mahmoud Abdelbaky Mahmoud, Tahani El-Mamlouk, Mohamed El-Shinawi and Mona M. Mohamed

*J Adv Res., 7(5): 661-70, (2016), IF: 3*

Hormonal-receptor positive (HRP) breast cancer patients with positive metastatic axillary lymph nodes are characterized by poor prognosis and increased mortality rate. The mechanisms by which cancer cells invade lymph nodes have not yet been fully explored. Several studies have shown that expression of IL-6 and the proteolytic enzyme cathepsin B (CTSB) was associated with breast cancer poor prognosis. In the present study, the effect of different concentrations of recombinant human IL-6 on the invasiveness capacity of HRP breast cancer cell line MCF-7 was tested using an in vitro invasion chamber assay. The impact of IL-6 on expression and activity of CTSB was also investigated. IL-6 treatment promoted the invasiveness potential of MCF-7 cells in a dose-dependent manner. Furthermore, MCF-7 cells displayed elevated CTSB expression and activity associated with loss of E-cadherin and upregulation of vimentin protein levels upon IL-6 stimulation. To validate these results in vivo, the level of expression of IL-6 and CTSB in the carcinoma tissues of HRP-breast cancer patients with positive and negative axillary metastatic lymph nodes (pLNs and nLNs) was assessed. Western blot and immunohistochemical staining data showed that expression of IL-6 and CTSB was higher in carcinoma tissues in HRP-breast cancer with pLNs than those with nLNs patients. ELISA results showed carcinoma tissues of HRP-breast cancer with pLNs exhibited significantly elevated IL-6 protein levels by approximately 2.8-fold compared with those with nLNs patients ($P < 0.05$). Interestingly, a significantly positive correlation between IL-6 and CTSB expression was detected in clinical samples of HRP-breast cancer patients with pLNs ($r = 0.78$, $P < 0.01$). Collectively, this study suggests that IL-6-induced CTSB may play a role in lymph node metastasis, and that may possess future therapeutic implications for HRP-breast cancer patients with pLNs. Further studies are necessary to fully identify IL-6/CTSB axis in different molecular subtypes of breast cancer.

**Keywords:** Cathepsin B; Epithelial-Mesenchymal transition; Hormonal-receptor; Positive breast cancer; Il-6; Invasion; Lymph node metastasis.

## B-403. Secretome of Tumor-Associated Leukocytes Augment Epithelial-Mesenchymal Transition in Positive Lymph Node Breast Cancer Patients Via Activation of Egfr/Tyr845 and Nf-Kb/P65 Signaling Pathway.

Elghonaimy EA, Ibrahim SA, Youns A, Hussein Z, Nouh MA, El-Mamlouk T, El-Shinawi M and Mostafa Mohamed M

*Tumour Biology, 37(9): 12441-12453, (2016), IF: 2.926*

Epithelial-mesenchymal transition (EMT) is an essential process in breast cancer metastasis. The aim of the present study was to determine the role of secretions of tumor-associated leukocytes (TALs) isolated from negative and positive lymph nodes (nLNs and pLNs, respectively) breast cancer patients in regulating EMT mechanism and the associated signaling pathways. We found an increased infiltration of TALs, which was associated with downregulation of E-cadherin and over-expression of vimentin in the breast carcinoma tissues of pLNs as compared to nLNs patients and normal breast tissues obtained from healthy volunteers during mammoplasty. Furthermore, TALs isolated from pLNs breast cancer patients secreted an elevated panel of cytokines by up to 2-5-fold when compared with those isolated from nLNs patients. Secretome of TALs of pLNs possessed higher TARC, IGF-1, IL-3, TNF-β, IL-5, G-CSF, IL-4, and IL-1α with more than a fivefold compared to those of nLNs. Using the human breast cancer cell lines MCF-7 and MDA-MB-231, we found that cytokines secreted by TALs isolated from nLNs and pLNs breast cancer patients promoted EMT via upregulation of TGF-β and vimentin and downregulation of E-cadherin at messenger RNA (mRNA) levels in both cell lines and at protein level in MCF-7. While TGF-β is over-expressed by MDA-MB-231 seeded in media conditioned by secretome of TALs isolated from nLNs and pLNs breast cancer patients. The downstream TGF-β signaling transcription factors, Snail, Slug, and Twist, known to be associated with EMT mechanism were over-expressed by MCF-7 and MDA-MB-231 seeded in media conditioned by secretome of TALs isolated from nLNs and pLNs breast cancer patients. Acquisition of EMT in MCF-7 cells is mechanistically attributed to the activation of EGFR(Tyr845) and NF-κB/p65(Ser276) signaling which are significantly highly expressed by MCF-7 cells seeded in media conditioned by secretome of TALs isolated from pLNs compared to nLNs patients. Overall, this study provides implications of secretome of TALs and activated

EGFR(Tyr845) and NF-κB/p65(Ser276) in EMT process that may be considered a therapeutic strategy to inhibit lymph node metastasis in breast cancer patients.
**Keywords:** Breast cancer; E-Cadherin; Egfr(Tyr845); Lymph Node metastasis; Nf-Kb/P65(Ser276); Vimentin.

## B-404. Improved Genistein Loading and Release on Electrospun Chitosan Nanofiber Blends

Sara Ibrahim, Huda M. Sayed, A.M. EL-Rafei, Azza El Amir, Mohammed Ismail and Nageh K. Allam

*Journal of Molecular Liquids, 223: 1056-1061, (2016),IF: 2.74*

Chitosan is a natural polysaccharide exhibiting excellent biocompatibility, biodegradability and nontoxicity,making Chitosan–based biomaterials ideal drug delivery systems and cell carriers for tissue engineering. The electrospinning technique, with optimized parameters, was used to fabricate chitosan/PVA as-spun mats. Field emission scanning electron microscopy (FESEM) was used to investigate the morphologies of the as-spun mats. We present a novel electrospun nanofiber-based drug delivery. In this system, genistein was loaded on nanofiber mats via three methods namely; passive loading, crosslinking after passive loading, and active loading. The way in which genistein was loaded significantly influenced its in-vitro drug release characteristics. The in-vitro release studies revealed that physical cross-linked nanofibers have a significantly delayed release demonstrating 21% progressive release after 30 min and 69% after 24 h, which is considered a superior drug delivery system compared to those reported before for genistein release.
**Keywords:** Chitosan blend; Nanofibers electrospinning genistein drug release.

## B-405. A Promising Therapeutic Potential of Cerebrolysin in 6-Ohda Rat Model of Parkinson's Disease

Neveen A. Noor , Haitham S. Mohammed , Iman M. Mourad, Yasser A. Khadrawy and Heba S. Aboul Ezz

*Life Sciences, 155: 174-179, (2016), IF: 2.685*

**Aims:** Parkinson's disease (PD) is the second most prevalent neurodegenerative disease affecting the population. The present study investigates the potential therapeutic effect of cerebrolysin (CBL), as a neurotrophic factor mimic, on the behavioral and biochemical alterations induced in 6-hydroxydopamine (6-OHDA) – lesioned rats as a model of PD. Main methods: The animals were divided into 3 experimental groups; control group, Parkinsonian model group through bilateral microinjection of 6-OHDA into substantia nigra (SN) and CBL-treated group which received a daily intraperitoneal administration of CBL (2.5 ml/kg) initiated 24 h after induction of Parkinsonism for 21 days. Key **findings:** Treatment of Parkinsonian animals with CBL succeeded in restoring the midbrain and striatum dopamine levels. In addition, it normalized the increased MDA and NO levels recorded in the Parkinsonian animals and replenished the decreased level of midbrain GSH. In addition to the recorded recovery of the biochemical parameters, there was a parallel improvement in the animal's behavioral aspects. **Significance:** The findings of the present study provide evidence for the promising therapeutic effect of CBL in the present 6-OHDA rat model of PD through counteracting oxidative stress, replenishing dopamine content and enhancing behavioral outcomes.
**Keywords:** Parkinson's disease; Cerebrolysin; 6-Hydroxydopamine; Ratsubstantia nigra.

## B-406. Mechanisms of Echinochrome Potency in Modulating Diabetic Complications in Liver.

Mohamed AS, Soliman AM and Marie MA.

*Life Sciences, 151: 41-49, (2016), IF: 2.685*

**Background:** Diabetes mellitus is one of the most public metabolic disorders. It is mainly classified into type 1 and type 2. Echinochrome is a pigment from sea urchins that has antioxidant, anti-microbial, anti-inflammatory and chelating abilities. AIMS: The present study aimed to investigate the anti-diabetic mechanisms of echinochrome pigment in streptozotocin-induced diabetic rats. **Main Methods:**Thirty six male Wistar albino rats were divided into two main groups, type 1 diabetes and type 2 diabetes groups. Each group was divided into 3 subgroups (6 rats/subgroup); control, diabetic and echinochrome groups. Diabetic model was induced by a single dose of streptozotocin (60mg/kg, i.p) for type 1 diabetes and by a high fat diet for 4weeks before the injection with streptozotocin (30mg/kg, i.p) for type 2 diabetes. Diabetic groups were treated orally with echinochrome extract (1mg/kg body weight in 10% DMSO) daily for 4weeks. KEY **Findings:** Echinochrome groups showed a reduction in the concentrations of glucose, MDA and the activities of arginase, AST, ALT, ALP and GGT. While it caused general increase in the levels of insulin, TB, DB, IB, NO and the activities of G6PD, GST, GPx, SOD and GSH. The histopathological investigation showed partial restoration of pancreatic islet cells and clear improvement in the hepatic architecture. **Significance:** The suggested mechanism of Ech action in the reduction of diabetic complications in liver involved two pathways; through the hypoglycemic activity and the antioxidant role of Ech.
**Keywords:** Diabetes; Echinochrome; Histopathology; Liver; Oxidative stress; Pancreas.

## B-407. Antihepatotoxic Efficacy of Mangifera Indica L. Polysaccharides Against Cyclophosphamide in Rats

Sohair R Fahmy, Ahmed I Amein, Fathi M. Abd Elgleel and Sara M. Elaskalany

*Chemico-Biological Interactions, 244:113-120,(2016), IF:2.618*

The present study aims to evaluate the possible protective role of polysaccharides extracted from the Egyptian mango Mangifera indica L. (MPS) and/or silymarine against cyclophosphamide (CP) toxicity in male albino rats. The MPS and/or silymarin significantly decreased the activities of serum ASAT and ALAT. However, MPS (1000 mg/kg) normalized their activities towards the normal levels recording 28.75 and 78.75 U/ml respectively. The recorded data also showed the antioxidant effect of MPS by decreasing the level of malondialdehyde (MDA) and increasing the level of reduced glutathione (GSH) as well as normalized the activities of the antioxidant enzyme GST and SOD. Histopathological examinations also confirmed the protective efficacy of MPS

against liver toxicity of CP. In conclusion, the recorded results of the present study support the protective role of MPS and/or silymarin against CP-induced hepatic damage.
**Keywords:** Mangifera indica L; Polysaccharides; Protective; Cyclophosphamide; Silymarin.

## B-408. Effect of Canagliflozin and Metformin on Cortical Neurotransmitters in a Diabetic Rat Model

Nadia M.S. Arafa, Mohamed Assem S. Marie and Sara Abdullah Mubarak AlAzimi

*Chemico-Biological Interactions, 258: 79-88, (2016), IF: 2.618*

The rapid economic development in the Arabian Gulf has resulted in lifestyle changes that have increased the prevalence of obesity and type 2 diabetes, with the greatest increases observed in Kuwait. Dyslipidemia and diabetes are risk factors for disruptions in cortical neurotransmitter homeostasis. This study investigated the effect of the antidiabetic medications canagliflozin (CAN) and metformin (MET) on the levels of cortical neurotransmitters in a diabetic rat model.
**Keywords:** Acetylcholinesterase; Canagliflozin; Cortex; Diabetic rat; Metformin; Neurotransmitters.

## B-409. Fasciola Gigantica Enolase is a Major Component of Worm Tegumental Fraction Protective Against Sheep Fasciolosis.

Mahana N, Abd-Allah HA, Salah M, Tallima H and El Ridi R.

*Acta Tropica, 158: 189-196, (2016), IF: 2.38*

Infection of cattle and sheep with the parasite Fasciola gigantica is a cause of important economic losses throughout Asia and Africa. Many of the available anthelmintics have undesirable side effects, and the parasite may acquire drug resistance as a result of mass and repeated treatments of livestock. Accordingly, the need for developing a vaccine is evident. Triton-soluble surface membrane and tegumental proteins (TSMTP) of 60, 32, and 28 kDa previously shown to elicit protective immunity in mice against challenge F. gigantica infection were found to be strongly immunogenic in sheep eliciting vigorous specific antibody responses to a titer>1:16,000 as assessed by enzyme-linked immunosorbent assay. Furthermore, the 60 kDa fraction induced production of antibodies able to bind to the surface membrane of newly excysted juvenile flukes and mediate their attrition in antibody-dependent complement- and cell-mediated cytotoxicity assays, and significant ($P<0.05$) 40% protection of sheep against F. gigantica challenge infection. Amino acid micro sequencing of the 60 kDa-derived tryptic peptides revealed the fraction predominantly consists of F. gigantica enolase. The cDNA nucleotide and translated amino acid sequences of F. gigantica enolase showed homology of 92% and 95%, respectively to Fasciola hepatica enolase, suggesting that a fasciolosis vaccine might be effective against both tropical and temperate liver flukes.
**Keywords:** Enolase; Fasciola gigantica; Fasciolosis; Vaccination.

## B-410. The Use of Biotic and Abiotic Components of Red Sea Coastal Areas as Indicators of Ecosystem Health

Wael A. Omar; Yousef S. Saleh and Mohamed-Assem S. Marie

*Ecotoxicology, 25: 253-266, (2016), IF: 2.329*

A biomonitoring study was conducted using some biotic (Pomadasys hasta and Lutjanus russellii fish) and abiotic (water and sediment) components of the Red Sea coast of Hodeida, Yemen Republic along two polluted sites (Al-Dawar beach and Urj village) in comparison to a reference site (Al-Nukhailah beach). The studied fish biomarkers included hepatosomatic index (HSI), condition factor (K), scaled mass index (SMI), catalase, glutathione-S-transferase (GST), malondialdehyde (MDA), total protein and albumin. In addition, metals (Fe, Cu, Zn, Pb and Cd) concentrations in water and sediment were measured and sediment pollution assessment was carried out using contamination factor (CF), geoaccumulation index (Igeo), pollution load index (PLI) and enrichment factor (EF). The studied metals concentration in water and sediment samples showed significant increase among the polluted sites in comparison to the reference site. Sediment pollution assessment generally confirmed that Urj village was the most contaminated site followed by Al-Dawar beach. Catalase, GST and MDA proved to be the most responsive biomarkers with increased values of GST and MDA at sites influenced by agricultural, urban and industrial activities while catalase, HSI, K, SMI, total protein and albumin showed the opposite trend. This study recommends monitoring of sediment Igeo and EF values as well as SMI, catalase, GST and MDA as sensitive indicators of different anthropogenic activities and their effects on aquatic ecosystems under complex and different gradients of metal pollution. In addition, P. hasta proved to be more sensitive towards the detected pollution condition.
**Keywords:** Marine pollution; Metals; Pomadasys hasta; Lutjanus russellii; Red Sea; Sediment quality.

## B-411. Description of two Equine Nematodes, Parascaris Equorum Goeze 1782 and Habronema Microstoma Schneider 1866 from the Domestic Horse Equus Ferus Caballus (Famisly: Equidae) in Egypt.

Kareem Morsy, Abdel Rahman Bashtar , Saleh Al Quraishy and Salma Adel

*Parasitology Research, 115(11): 4299-4306, (2016), IF: 2.027*

Parasitic gastroenteritis (PGE) caused by infection of the gut with parasitic nematodes is one of the most important diseases of livestock animals from both financial and welfare perspectives. Parascaris equorum and Habronema microstoma are of the most endemic nematodes of the world which are currently the major cause of PGE of the domestic horses in Egypt. The present investigation introduced the first morphological description of these nematodes recovered from the domestic horse, Equus ferus caballus (Equidae), in Egypt by light and scanning electron microscopy. Seven P. equorum (fifth stage) and 18 adults of H. microstoma were recovered from the gastrointestinal tracts of four young domestic horses collected during the year of 2015. Microscopic examination of the isolated fifth stage P. equorum revealed that it possessed a long body with a broad anterior end equipped by large

shamrock-like lips with deep transverse groove on medial surface set off from the rest of the body by a deep post-labial constriction giving the body a shouldered appearance. The total body length was 12–15 (14 ± 2) cm for males and 13–18 (16 ± 2) cm for females. Lips were three in number in the form of one dorsal and two sub-ventral surrounding the central stoma. The isolated adult worms of H. microstoma were whitish in color narrowed slightly at the anterior end. Single lateral ala in the cephalic region in both sexes was observed. The buccal vestibule was markedly thickened and equipped by two tridentate teeth. The adult worms had two bilobed lateral lips surrounding the mouth with four sub-median cephalic papillae and two amphids. The males were 14.5–18.0 (17.2 ± 0.3) mm long and 1.23–1.57 (1.42 ± 0.3) mm wide. The posterior end was spirally coiled and had wide caudal alae. The spicules were unequal. The females were 13.5–21.0 (16.2 ± 0.3) mm long and 1.55–1.75 (1.69 ± 0.3) mm wide. The anal pore had a thin upper rim and was located 177.0 µm from the posterior end.

**Keywords:** Nematoda – Parascaris; Equorum-Habronema microstoma-equus ferus Caballus-Light and Scanning electron microscopy.

## B-412. First Record of Anisakis Simplex Third-Stage Larvae (Nematoda, Anisakidae) in European Hake Merluccius Merluccius Lessepsianus in Egyptian Water

Yasmin Abou-Rahma, Rewaida Abdel-Gaber and Amira Kamal Ahmed

*Journal o Parasitology Research, 52: 1-8, (2016), IF: 2.027*

The prevalence of infection and the identification of anisakid larvae in European hake Merluccius merluccius lessepsianus from Hurghada City, Red Sea Governorate, Egypt, were investigated. Fish samples were collected during the period of February and November 2014. Twenty-two (36.66%) out of sixty examined fish specimens were found to be naturally infected with Anisakis type I larvae mostly found as encapsulated larvae in visceral organs. There was a positive relationship between host length/weight and prevalence of infection. Based on morphological, morphometric, and molecular analyses, these nematodes were identified as third-stage larvae of Anisakis simplex. The present study was considered as the first report of anisakid larvae from European hake in the Egyptian water.

**Keywords:** Anisakid ;Nematoda.

## B-413. Head Lice in Progress: What Could/Should Be DoneA Report on an in Vivo and in Vitro Field Study

Fathy Abdel-Ghaffar , Mohammed Abdel-Aty , Ibrahim Rizk , Saleh Al-Quraishy , Margit Semmler , Falk Gestmann and Norman-Philipp Hoff

*Parasitology Research, 115: 4245-4249, (2016), IF: 2.027*

Head lice infections are a growing problem in the light of increasing migration of large population as well as the increasing current refugee flows and concomitant poor hygienic conditions. These infections are associated with a significantly reduced quality of life and frequent medical consultations. The approved drugs for the treatment of head lice infections have some disadvantages in the treatment despite their good efficacy. In addition to irritant-toxic substances that can cause adverse reactions in patients, a partial development of resistance has occurred and a double application is necessary to achieve adequate efficacy. For this reason, we have decided to test a product without the aforementioned treatment drawbacks. We examined the effect of Licener® on the head lice treatment through individual therapy trials. We identified 65 patients with head lice infections for the treatment with Licener®. All patients were treated with Licener® and visited for a period of 2 weeks. Successfully treated patients had no relapses. Against the background of this study and based on the observations of our applications, we expect that Licener® could enhance considerably the therapeutic options for the treatment of head lice infections, as an alternative to classical products.

**Keywords:** Head lice; Children; Agent of diseases; Treatment; Neem; Shampoo.

## B-414. Henneguya Collaris Sp. Nov., (Myxosporidia), Parasite of the Greenband Parrotfish Scarus Collana Rüppell, 1835 (Actinopterygii, Scaridae) From the Red Sea, Egypt. A Light and Electron Microscopic Study.

Kareem Morsy , Margit Semmler , Ebtsam Al-Olayan and Heinz Mehlhorn

*Parasitology Research, 115(6): 2253-2261, (2016), IF: 2.027*

The phylum Myxozoa comprises more than 2180 species, almost all of which are considered to be obligate parasites of aquatic fishes. In the present study, Henneguya collaris sp. nov. is the first described histozoic myxozoan species of the genus Henneguya infecting the kidney of the greenband parrotfish Scarus collana (Actinopterygii, Scaridae). One hundred and eighty specimens of fish were collected randomly during the period from September 2014 to October 2015 from boat landing sites and the market places at Hurghada City along the Red Sea in Egypt. of these, 90 (50 %) specimens were infected. Light microscopic examination showed that the infection was detected as mature spores with two polar capsules regularly arranged at the anterior pole of each spore and extruded polar filaments free in the kidney tissue. The spore body was oval in shape, measured 7.1 ± 0.2 (6.2-8.4) µm in length and 6.3 ± 0.2 (5.8-7.0) µm in width, with a bifurcated caudal process of equal length, reaching 6.3 ± 0.2 (5.8-7.0) µm in length. Polar capsules were 3.4 ± 0.2 (3.0-4.2) µm in length and 1.9 ± 0.2 (1.6-2.4) µm in width with 6-8 (10) turns of polar filaments. Ultrastructural analysis showed that the spore development was asynchronous. Sporogenesis, capsulogensis, valvogenesis, and spore maturation of the present parasite were also described. The present species was compared morphologically with the spore characteristics of the most similar species of Henneguya spp. recorded previously from different geographical areas taking into account the stage and dimensions of the spore body, tails, and polar filament coils, including their number and the most important characteristic features that distinguish them from the present species. Considering the data obtained, the material described herein represents a new species and the name Henneguya collaris sp. nov. is proposed.

**Keywords**: Myxosporidiasis-Henneguya collaris Sp. Nov.-Scarus collana ;Fish-Ultrastructure.

## B-415. Morphological Re-Description and Molecular Characterization of Kudoa Pagrusi (Myxosporea: Multivalvulida) Infecting the Heart Muscles of the Common Sea Bream Fish Pagrus Pagrus (Perciformes: Sparidae) from the Red Sea, Egypt

Fathy Abdel-Ghaffar , Rewaida Abdel-Gaber , Sherein Maher , Saleh Al Quraishy and Heinz Mehlhorn

*Parasitology Research, 115: 3175-3184, (2016), IF: 2.027*

In the present study, 100 samples of different sizes of the common sea bream fish Pagrus pagrus were collected from the Egyptian water along the Gulf of Suez, Red Sea and examined for the prevalence of myxosporidian parasites in general and Kudoa spp. in particular. Fish samples were thoroughly externally examined. After dissection, all the internal organs were removed and examined. A total of 60 out of 100 fish specimens were found to be infected with Kudoa stages. Parasitic infection was restricted to the heart muscles of the examined fish. None of the other organs was found to be infected. Macroscopic cysts (plasmodia) heavily infested the different parts of the heart muscles. Each plasmodium measured 1.2–2.5 (1.53 ± 0.2) mm× 0.63–0.80 (0.65± 0.2) mm. Mature spores are quadratic in shape in the apical view showing four equal valves and four symmetrical polar capsules. Fresh spores were 5.0–7.1 (5.7±0.2) µm long×5.4–8.5 (6.1 ± 0.3) µm wide. On the basis of spore morphology, the present species was identified as Kudoa pagrusi. Morphometric characterization revealed that the relatively small size of this Kudoa species was the distinctive feature that separates it from all previously described species. Molecular analysis based on small subunit ribosomal DNA (SSU rDNA) sequences revealed that the highest percentage of identity was observed with K. scomberomori and followed by K. shiomitsui, K. hypoepicarclialis, K. amamiensis, and K. kenti. The kudoid spores showed morphometric variations to some extents but had essentially identical nucleotide sequences of the SSU rDNA gene sequences closest to those of K. scomberomori and K. shiomitsui recorded from elasmobranchs in the Indo- Pacific Ocean. The present findings support the identification of an ancestral marine origin of the present Kudoa species.

**Keywords:** Marine fish parasites; Pagrus pagrus; Morphology Molecular characterization.

## B-416. Morphological Re-Description and New Geographical Records for Three Digenean Parasites Infecting African Sharptooth Catfish Clarias Gariepinus (Pisces: Clariidae) in Egypt

Rewaida Abdel-Gaber , Thabet Sakarn , Gamal El-Shahawi , Hoda El-Fayoumi and Rana Mohammed

*Parasitology Research, 115: 4251-4260, (2016), IF: 2.027*

Sixty specimens of African sharptooth catfish Clarias gariepinus (Clariidae) were collected during the period of March 2014–February 2015 from boat landing sites and fishermen of the River Nile at Beni Suef Governorate, Egypt, and examined for the presence of digenean parasites. The morphology of these parasites was studied by using light microscopy to describe morphological and morphometrically measurements for different body parts. Three digenean species belonging to three different genera were collected from various organs within the examined fish species. A certain degree of site specificity was also observed, with Thaparotrema botswanensis being found only in the gall bladder of C. gariepinus, while both Pseudoholorchis clarii and Glossidium pedatum were found only in the intestine and thus seem to occupy a certain niche within their host. This study represent as the first record of T. botswanensis and G. pedatum from C. gariepinus, as well as the first report of the genera from the River Nile in Egypt. In addition, re-description of P. clarii clarifies measurements for some body parts.

**Keywords:** Freshwater fish; Clarias gariepinus; Clariidae; Digenea parasites; Morphological description

## B-417. Syphacia Obvelata (Nematode, Oxyuridae) Infecting Laboratory Mice Mus Musculus (Rodentia, Muridae): Phylogeny and Host-Parasite Relationship

Rewaida Abdel-Gaber

*Parasitology Research, 115: 975-985, (2016), IF: 2.027*

Syphacia obvelata is a pinworm nematode parasite infecting man and laboratory animals in high abundance. This parasitological study was carried out during the period of March 2014–February 2015 to investigate the helminth parasites infecting the laboratory mice Mus musculus in the Animal House at Cairo University, Egypt. The prevalence of S. obvelata in M. musculus was 75.0 %. The extent of infection with S. obvelata is analyzed according to the sex of the host mice. It was shown that the prevalence of male infection was greater than female worms. Morphological characterization revealed that the present Oxyurid species possesses a rounded cephalic end with less developed lips, esophagus divided into cylindrical corpus, and globular bulb supported internally with valvular apparatus; three mamelons are located at the ventral surface with a single chitinized spicule and a gubernaculum provided with an accessory hook in males, and ovijector apparatus opens ventrally by the vulva surrounded by protruded lips in female worms. Body of the male was 0.623–1.130(0.830±0.11)mm long and 0.092– 0.130(0.110±0.01)mm wide; the esophagus was 0.164– 0.280(0.210±0.01)mm long; the nerve ring and excretory pore are located at 0.035–0.132 (0.073±0.01) and 0.087– 0.191(0.145±0.01)mm from the anterior end, respectively, while the female measured 2.930–4.650(3.540±0.1)mm long and 0.120–0.232(0.156±0.001)mm wide; the esophagus was 0.213–0.410(0.342±0.01)mm long; the nerve ring, excretory pore, and vulval opening are located at 0.026–0.157 (0.121± 0.01), 0.134–0.243 (0.195±0.01), and 0.323–0.632(0.546± 0.11)mm from the anterior end, respectively; eggs measured 0.120–0.139(0.129±0.001)mm long and 0.030–0.052(0.045 ±0.001)mm wide. It compared morphometrically with other Syphacia species described previously and showed little differences in measurements. Molecular characterization based on small subunit ribosomal DNA (rDNA) was done to confirm the obtained morphological and morphometric results. A preliminary genetic comparison between SSU rDNA of the present parasite and other species of

Oxyuridae places it as a putative sister taxon to other S. obvelata.
**Keywords:** Laboratory Mice; Syphacia Spp; Host-Parasite Relationship; Phylogenetic relationship.

## B-418. Exploration of the Therapeutic Potential Effect of Sepia Officinalis in Animal Model of Sepsis Induced by Cecal Ligation and Puncture

Abd El-Latif AA, Sayed AA, Soliman AM and Fahmy SR

*Injury-International Journal of the Care of the Injured, 47(2016): 2709-2717, (2016), IF: 1.91*

**Objective:** The present investigation explored the therapeutic potential effect of Sepia officinalis body tissue (SOBT) and Sepia officinalis polysaccharide (SOP) extracts, in animal model of sepsis [induced by cecal ligation and puncture (CLP)]. **Materials and Methods:** Experimental animals were divided into 4 groups, Group 1: Sham control rats. Group 2: Septic rats. Group 3: Septic rats treated with methanolic extract of Sepia officinalis body tissue (SOBT) (500mg/kg body weight) for 2days. Group 4: Septic rats treated with Sepia officinalis polysaccharide (SOP) extract (200mg/kg body weight) for 2days. **Results:** The antioxidant activity of SOBT and SOP was proven by DPPH test. CLP-induced liver and kidney toxicities showed by an increase in the ALAT, ASAT, γGT, ALP, creatinine, BUN and uric acid concentrations in serum. Moreover, CLP-induced oxidative stress in liver and kidney evidenced by the increase of MDA levels, decrease in GSH concentrations and decrease in the enzymatic antioxidants (SOD, CAT, GST). In addition, CLP caused decrease in CYP1A2 content in liver. **Conclusions:** Our findings demonstrate the therapeutic efficacy of SOBT and SOP in liver and kidney disorders. Therefore this study suggests that SOBT and SOP could be a potential therapeutic agents for sepsis treatment.
**Keywords:** Histopathology; Kidney; Liver; Oxidative stress; Sepia officinalis; Sepsis.

## B-419. Studies on the Genotoxicity Behavior of Silver Nanoparticles in the Presence of Heavy Metal Cadmium Chloride in Mice

Hanan Ramadan Hamad Mohamed

*Journal of Nanomaterials, 2016: 1-12, (2016), IF: 1.758*

Incredible rapid growth in the nanoparticles applications and development increases the daily human exposure to them but humans are exposed to many other pollutants in addition to nanoparticles that forced us to evaluate the effect of heavy metal cadmium chloride (CdCl2) coinjection on silver nanoparticles induced genotoxic risk in this study. Mice were injected into the abdominal cavity with single dose of Ag nanoparticles (20, 41, and 82 mg/kg) or CdCl2 (1.5 mg/kg) either separately or together simultaneously and sacrificed 24 hours later. CdCl2 cotreatment enhanced the induced dose-dependent sperm abnormality by Ag nanoparticles different doses as shown by the statistical significant decreases in both sperm concentration and motility and increases in the frequency of abnormal sperms and also potentiated the Ag nanoparticles induced chromosomal and DNA damage indicated by the statistical significant elevations in the frequencies of micronucleated polychromatic erythrocytes (MNPCEs) and DNA damage levels. Moreover, statistical elevations in malondialdehyde level and reductions in catalase activity were observed after CdCl2 coinjection with Ag nanoparticles compared with Ag nanoparticles treated groups' values. Ag nanoparticles induced sperm abnormality, clastogenicity, and genotoxicity were potentiated by heavy metal cadmium coinjection that threatens the human life and increases silver nanoparticles genotoxic risks.
**Keywords:** Nanotoxicology; Sperm abnormality; Contaminants; Genotoxicity; Cadmium and toxic effect.

## B-420. Alterations in the Fatty Acid Profile, Antioxidant Enzymes and Protein Pattern of Biomphalaria Alexandrina Snails Exposed to the Pesticides Diazinon and Profenfos

Fayez A Bakry, Karem El-Hommossany, Mahmoud Abd El-Atti and Somaya M Ismail

*Toxicology and Industrial Health, 32 (4): 666-676, (2016), IF:1.688*

The use of pesticides is widespread in agricultural activities. These pesticides may contaminate the irrigation and drainage systems during agriculture activities and pests' control and then negatively affect the biotic and a biotic component of the polluted water courses. The present study aimed to evaluate the effect of the pesticides diazinon and profenfos on some biological activities of Biomphalaria alexandrina snails such as fatty acid profile, some antioxidant enzymes (thioredoxin reductase (TrxR), sorbitol dehydrogenase (SDH), superoxide dismutase (SOD), catalase (CAT) as well as glutathione reductase (GR) and lipid peroxidation (LP)) and protein patterns in snails' tissues exposed for 4 weeks to LC10 of diazinon and profenfos. The results showed that the two pesticides caused considerable reduction in survival rates and egg production of treated snails. Identification of fatty acid composition in snail tissues treated with diazinon and profenfos pesticides was carried out using gas–liquid chromatography (GLC). The results declared alteration in fatty acid profile, fluctuation in percentage of long chain and short chain fatty acid contributions either saturated or unsaturated ones, and a decrease in total lipid content in tissues of snails treated with these pesticides. The data demonstrate that there was a significant inhibition in the activities of tissues SOD, CAT, glutathione reductase (GR), TrxR, and SDH in tissues of treated snails, while a significant elevation was detected in LP as compared to the normal control. On the other hand, the electrophoretic pattern of total protein showed differences in number and molecular weights of protein bands due to the treatment of snails. It was concluded that the residues of diazinon and profenfos pesticides in aquatic environments have toxic effects on B. alexandrina snails.
**Keywords:** Snails; Pesticides; Antioxidants; Enzymes; Fatty Acids; Proteins;Biochemistry.

## B-421. Ameliorative Effect of Allolobophora Caliginosa Extract on Hepatotoxicity Induced by Silicon Dioxide Nanoparticles

Shimaa A Sadek, Amel M Soliman and Mohamed Marzouk

*Toxicology and Industrial Health,32:1358-1372,(2016),IF: 1.688*

This study aims to evaluate the possible ameliorative effect of earthworm (Allolobophora caliginosa) extract (EE) against silicon dioxide nanoparticles (SiNPs)-induced liver injury in male albino rats. The effectiveness of EE was compared with silymarin as a standard hepatoprotective drug. The present work demonstrates the antioxidant activity of EE by 1,1-diphenyl-2-picrylhydrazyl assay. Administration of SiNPs, for 15 consecutive days, caused changes in most of the biochemical parameters, namely, serum aminotransferase enzymes activities (alanine transaminase and aspartate transaminase), alkaline phosphatase activity, total protein, total and direct bilirubin level, malondialdehyde, glutathione reduced, catalase, superoxide dismutase, glutathione reductase, and glutathione peroxidase. In addition, administration of SiNPs induced changes in liver tissue architecture. Administration of EE, for subsequent 30 days, to SiNPs exposure demonstrated significant ameliorative effects on nearly all the studied parameters, and such effects were compatible with those of silymarin. In addition, the administration of EE repairs, to some extent, the abnormal architecture of the liver tissue induced by SiNPs.

**Keywords:** Earthworm extract; Liver injury; Oxidative stress; Silicon dioxide nanoparticles.

## B-422. Comparative Toxicity of Paraquat Herbicide and Some Plant Extracts in Lymnaea Natalensis Snails

Fayez A Bakry, Mona E Eleiwa, Samir A Taha and Somya M Ismil

*Toxicology and Industrial Health, 32 (1): 143-153, (2016), IF: 1.688*

Paraquat has been shown to be a highly toxic compound for humans and animals, and many cases of acute poisoning and death have been reported over the past few decades. The present study was undertaken to evaluate comprehensively herbicides (Paraquat) and some plant extracts to biochemical aspects of Lymnaea natalensis snails. It was found that the exposure of L. natalensis to Paraquat and plant extracts led to a significant reduction in the infectivity of Fasciola gigantica miracidia to the snail. The glucose level in hemolymph of exposed snails was elevated, while the glycogen showed a decrease in soft tissues when compared with the control group. In addition, the activity level of some enzymes representing glycolytic enzymes as hex-okinase (HK), pyruvate kinase (PK), phosphofructokinase (PFK), lactate dehydrogenase (LDH), and glucose phosphate isomerase (GPI) in snail's tissues were reduced in response to the treatment. It was concluded that the pollution of the aquatic environment by herbicide would adversely affect the metabolism of the L. natalensis snails. Snails treated with Agave attenuate, Ammi visnaga, and Canna iridiflora plant had less toxic effect compared to snails treated with Paraquat.

**Keywords:** Paraquat herbicide; Lymnaea natalensis snails; Fasciola gigantica miracidia; Agave attenuate; Ammi visnaga; Canna iridiflora plant.

## B-423. Neurochemical Impact of Bisphenol A in the Hippocampus and Cortex of Adult Male Albino Rats.

Yasser A Khadrawy, Neveen A Noor, Iman M Mourad and Heba S Aboul Ezz

*Toxicology and Industrial Health, 32: 1711-1719, (2016), IF:1.688*

Bisphenol A (BPA), an endocrine-disrupting chemical, is widely used in the manufacture of polycarbonated plastics and epoxy resins and line metal beverage cans. Growing evidence suggests that BPA acts directly on neuronal functions as it is lipophilic and could accumulate in the brain. The present study aims to investigate the effect of two doses of BPA (10 mg/kg for 6 and 10 weeks and 25 mg/kg for 6 weeks) on excitatory (glutamate and aspartate) and inhibitory (-aminobutyric acid, glycine, and taurine) amino acid neurotransmitter levels in the cortex and hippocampus. This study extends to investigate the effect of BPA on acetylcholinesterase (AchE) activity and some oxidative stress parameters in the two regions. In the cortex, a significant increase in the excitatory and a significant decrease in the inhibitory amino acids occurred after BPA (10 mg/kg for 10 weeks and 25 mg/kg for 6 weeks). This was accompanied by a significant increase in lipid peroxidation, nitric oxide, and reduced glutathione after 6 weeks of BPA (25 mg/kg). In the hippocampus, a significant increase in the excitatory and inhibitory amino acid neurotransmitters occurred after 6 weeks of BPA. Hippocampal lipid peroxidation increased significantly after BPA exposure and hippocampal reduced glutathione increased significantly after 6 weeks of BPA exposure (10 mg/kg). BPA induced a significant increase in cortical and hippocampal AchE activity. The present neurochemical changes in the cortex and hippocampus suggest that BPA induced a state of excitotoxicity and oxidative stress. This may raise concerns about the exposure of humans to BPA due to its wide applications in industry.

**Keywords:** Bisphenol A; Amino acid neurotransmitters; Oxidative stress; Cortex; Hippocampus; Rat.

## B-424. Studies on Fate and Toxicity of Nanoalumina in Male Albino Rats: Lethality, Bioaccumulation and Genotoxicity

Gamal M Morsy, Kawther S Abou El-Ala and Atef A Ali

*Toxicology and Industrial Health, 32(2): 344-359, (2016), IF:1.688*

The purpose of this study is to follow-up the distribution, lethality percentile doses (LDs) and bioaccumulation of aluminium oxide nanoparticles (Al2O3-NPs, average diameter 9.83 ± 1.61 nm) in some tissues of male albino rats, and to evaluate its genotoxicity to the brain tissues, during acute and sublethal experiments. The LDs of Al2O3-NPs, including median lethal dose (LD50), were estimated after intraperitoneal injection. The computed LD50 at 24 and 48 h were 15.10 and 12.88 g/kg body weight (b.w.), respectively. For acute experiments, the bioaccumulation of aluminium (Al) in the brain, liver, kidneys, intestine and spleen was estimated after 48 h of injection with a single acute dose (3.9, 6.4 and 8.5 g/kg b.w.), while for sublethal experiments it was after 1, 3, 7, 14 and 28 days of injection with 1.3 g/kg b.w. once in 2 days. Multi-way analysis of variance affirmed that Al uptake, in acute experiments, was significantly affected by the injected doses, organs (brain, liver, kidneys, intestine and spleen) and their interactions, while for sublethal experiments an altogether effect based on time (1, 3, 7, 14, 28 days), doses (0 and 1.3 g), organs and their interactions was reported. In addition, Al accumulated in the brain, liver, kidney, intestine and spleen of rats

administered with Al2O3-NPs were significantly higher than the corresponding controls, during acute and sublethal experiments. The uptake of Al by the spleen of rats injected with acute doses was greater than that accumulated by kidney, brain, intestine and liver, whereas the brain of rats injected with sublethal dose accumulated lesser amount of Al followed by the kidney. Bioaccumulation of Al, in all studied tissues, was positively correlated with the injected doses (in acute term) and the experimental periods (in sublethal term). In the acute and sublethal experiments, comet assay parameters such as the tail intensity (i.e. DNA percentage), tail extent moment and olive tail moment were estimated using a single cell gel electrophoresis/comet assay. The results showed significant increase in DNA percentage damage in the brain cells. The obtained results indicate that bioaccumulation of Al was associated with significantly increased levels of comet parameters that depended on the doses and the experimental periods. In conclusion, Al has a high affinity to get accumulated in tissues to a level that is able to induce genotoxicity. Therefore, bioaccumulation is time, dose and organ dependant.
**Keywords:** Nanoparticles; Accumulation; Genotoxicity; Lethality; Nanoalumina; Rats.

## B-425. Studies on Fate and Toxicity of Nanoalumina in Male Albino Rats: Oxidative Stress in the Brain, Liver and Kidney

Gamal M Morsy, Kawther S Abou El-Ala and Atef A Ali

*Toxicology and Industrial Health, 32(2): 200-214, (2016), IF:1.688*

The present work aimed to evaluate the oxidative stress of nanoalumina (aluminium oxide nanoparticles, Al2O3-NPs) with a diameter <13 nm (9.83 ± 1.61 nm) as assessed by the perturbations in the enzymatic and non-enzymatic antioxidants as well as lipid peroxidation (LPO) in the brain, liver and kidney of male albino rats, after 2 days of single acute dose (3.9 or 6.4 or 8.5 g/kg) injection and a sublethal dose of 1.3 g/kg once in 2 days for a period of 28 days. According to two-way analysis of variance, superoxide dismutase (SOD), catalase (CAT) and glutathione peroxidase (GPx) activities as well as the levels of glutathione (GSH) and LPO were significantly affected by the injected doses, organs and their interactions. On the other hand, in sublethal experiments, these parameters were affected by the experimental periods, organs and their interactions. Regression analysis confirmed that the activities of SOD, CAT, GPx and GSH levels in the brain, liver and kidney were inversely proportional with the acute doses, the experimental periods, and aluminium accumulated in these tissues, whereas the levels of LPO exhibited a positive relationship. Correlation coefficient indicated that oxidative stress mainly depends on aluminium accumulated in the studied organs, followed by injected doses and the experimental periods. In comparison with the corresponding controls, the acute and sublethal doses of Al2O3-NPs caused significant inhibition of the brain, hepatic and renal SOD, CAT, GPx activities and a severe marked reduction in the concentrations of GSH that were associated with a significant elevation in the levels of malondialdehyde (an indicator of LPO). In conclusion, our data indicated that rats injected with nanoalumina suffered from the oxidative stresses that were dose and time dependent. In addition, Al2O3-NPs released into the biospheres could be potentiating a risk to the environment and causing hazard effects on living organisms, including mammals.
**Keywords:** Nanoalumina; Acute; Oxidative stress; Rats; Sublethal.

## B-426. Studies on Fate and Toxicity of Nanoalumina in Male Albino Rats: Some Haematological, Biochemical and Histological Aspects

Gamal M Morsy, Kawther S Abou El-Ala and Atef A Ali

*Toxicology and Industrial Health, 32(4): 634-655, (2016), IF:1.688*

The work aimed to evaluate the nanoalumina toxicity on the histological architecture, some haematological and biochemical aspects in male albino rats, during acute and sublethal experiments. Rats, in acute experiments, were injected with a single-acute dose of 3.9 g or 6.4 g or 8.5 g of aluminium oxide (Al2O3) kg(-) (1), whereas those of sublethal were injected with 1.3 g of Al2O3 kg(-) (1)2 days(-) (1) One-way analysis of variance indicated that injected doses and the experimental periods were significantly affected by haemoglobin (Hb) content; haematocrit value (Hct); white blood cell (WBC) count; blood platelet (Plt) count; mean corpuscular volume (MCV); mean corpuscular Hb (MCH) and MCH concentration (MCHC). In acute experiments, Hct, WBC count, MCV and Plt were significantly higher than the corresponding controls, whereas Hb, MCH and MCHC markedly decreased. In comparison with the related controls after 1, 3 and 7 days post-injection, red blood cell count, Hb, Hct, WBC count, Plt and MCV were significantly increased, but begun to decrease after 14 or/and 28 days and were associated with a marked decrease in MCH and MCHC. In serum of rats injected with acute or sublethal dose, the concentrations of total protein (TP) and total lipid (TL) were significantly lesser than the corresponding controls, whereas the levels of urea, uric acid, creatinine and the activities of aspartate aminotransferase and alanine aminotransferase were markedly increased. The injected doses were directly proportional with all the studied biochemical parameter, except the TL and TP that exhibited a negative correlation. Histologically, the highest acute and sublethal doses of nanoalumina caused hepatic irregular disarray, necrosis to the hepatic and Kupffer cells that are associated with congested blood sinusoids. The renal tissues characterized by the appearance of inter-tubular congestion that is accompanied by the dilation of the vascular glomeruli that completely occupied Bowman's capsule and accompanied with partial disappearance of the renal tubule's brush border. The brain showed a progressive degeneration of neurons in both the experiments.
**Keywords:** Nanoalumina; Acute; Biochemical; Haematological; Histological; Rats; Sublethal.

## B-427. Infection with Plasmodium Chabaudi Diminishes Plasma Immune Complexes and Ameliorates the Histopathological Alterations in Different Organs of Female Bwf1 Lupus Mice

M.A. Abdel-Maksoud, F.A. Abdel-Ghaffar, A. El-Amir S. Al-Quraishy and G. Badr

*European Review For Medical and Pharmacological Sciences, 20: 733-744, (2016), IF: 1.575*

**Objective:** To determine the effect of Plasmodium chabaudi infection on the plasma level of circulating immune complexes (CICs), haemoglobin (Hb) content, urine profile, and histological features of female BWF1 mice, the murine model of systemic lupus erythematosus (SLE). MATERIALS AND **Methods:** A total of 30 female BWF1 lupus mice were randomly divided into three groups as follows: group (I) control group (P. chabaudi uninfected); group (II) lupus mice infected with live P. chabaudi; group (III) lupus mice infected with irradiated P. chabaudi. Urine samples were daily collected from the second week-post infection. Mice from the three groups were killed at day 14 post-infection and heparinized blood was collected for further haemoglobin contents and plasma analysis. Paraffin-embedded kidney, liver, lung, heart, brain, ovary and skin tissues were stained with Hematoxylin and Eosin (H&E) and examined under light microscope. **Results:** Our results reveal that infection of lupus mice with live P. chabaudi was associated with an increase in urinary Hb and a decrease in plasma Hb and CIC levels. Interestingly, infection of lupus mice with live P. chabaudi ameliorates the histopathological alterations mediated by lupus disease in kidney tissues. Although no parasite sequestration was observed in any of the investigated organs, P. chabaudi pigment deposition was observed in the liver of both live and irradiated P. chabaudi infected groups. **Conclusions:** This study in lupus prone BWF1 mice indicated that gamma-irradiated P. chabaudi infection has the desired lupus ameliorating effect without negative effects of malaria which assist the understanding of different responses to plasmodium sp. infection in human lupus patients.

**Keywords:** Bwf1; Haemoglobin; Immune complexes; Lupus; Malaria.

## B-428. Comparative Evaluation of Genotoxic Effects Induced by Cuo Bulk and Nano-Particles in Nile Tilapia, Oreochromis Niloticus

Amr A. Abdel-Khalek

*Water, Air and Soil Pollution, 227: 1-11, (2016), IF: 1.551*

Metal oxide nano-particles have definitely unique toxicological properties than currently investigated oxides. Therefore, this study was aimed to comparatively evaluate the genotoxicity of nano-CuO and bulk CuO particles on a model fish species Oreochromis niloticus. Fish were exposed to two selected concentrations (1/10 and 1/20 of the LC50/96 h) of both nano-CuO and bulk CuO for 30 days. Genotoxic effects associated with DNA ladder formation and chromosomal damage were investigated using DNA fragmentation and micronucleus techniques. Based on DNA fragmentation of fish hepatocytes, the two selected concentrations of bulk and nano-CuO were found to induce DNA damage. Analysis of the DNA fragments initiated by bulk CuO on agarose gel revealed DNA ladder pattern, which is commonly considered as a hallmark of apoptosis, while fish exposed to nano-CuO particles showed a molecular hallmark of necrosis which is the fragmentation of the nuclear DNA into a smear-like pattern. Also, DNA damage was further confirmed quantitatively using the image analysis software Image J. In this context, nano-CuO-treated groups exhibited a maximum DNA damage especially at the lower concentration (1/20 LC50/96 h). To ensure CuO genotoxicity, micronucleus and other nine nuclear abnormalities were studied in peripheral erythrocytes and significant ($p < 0.05$) elevation was observed in nano-CuO-exposed groups at the lower concentration followed by a decrease in extent of chromosomal damage at the higher concentration, while fish groups treated with bulk CuO showed a more or less dose-dependent effect.

**Keywords:** Cuo Nano-Particles; Genotoxicity; DNA fragmentation; Micronucleus.

## B-429. The Accumulation Potency of Bulk and Nano Zinc Metal and Their Impacts on the Hematological and Histological Perturbations of Oreochromis Niloticus

Amr Adel Abdel-Khalek, Aliaa Hamed and Mohamed Assem Marie

*Water, Air and Soil Pollution, 227: 1-13, (2016), IF: 1.551*

This study was carried out to comparatively evaluate the bioaccumulation potency of Zn bulk and nanoparticles in Oreochromis niloticus and to investigate the induced hematological and histological alterations. Fish were exposed to ½ LC50/96 h values of both bulk and nano Zn meal for 7, 14, and 28 days. Concerning metal bioaccumulation factor (BAF), the data displayed that zinc nanoparticles (Zn NPs) had more efficiency to penetrate the studied tissues such as the liver, kidneys, gills, skin, and muscle. Hematological parameters named red blood cells (RBC), hemoglobin (Hb), and hematocrit (Hct) values were altered in Zn NPs treated groups after 14th and 28th days while these hematological parameters recovered to some extent in bulk particles (BPs) treated groups at the end of the experimental period. The changes in hematological parameters were found to be time dependent. Blood indices such as mean corpuscular volume (MCV) and mean corpuscular hemoglobin (MCH) revealed the presence of normocytic normochromic anemia in the studied groups at the most exposure periods except microcytic hypochromic anemia at the 7th day of bulk particles exposed fish. Based on histological end points, several alterations in the gills, liver, and kidney tissues were observed. Severely deformations were observed at NPs treated fish groups which varied between adaptive changes to tissue damage at the end of exposure period. The deformations were recorded to be increased in NPs exposed fish compared to BPs treated fish throughout the study periods.

**Keywords:** Oreochromis niloticus; Bulk and Nano Zinc; Hematological parameters; Histopathology.

## B-430. Toxicity Evaluation of Copper Oxide Bulk and Nanoparticles in Nile Tilapia, Oreochromis Niloticus, Using Hematological, Bioaccumulation and Histological Biomarkers

Amr A. Abdel-Khalek , Shereen R. Badran and Mohamed-Assem S. Marie

*Fish Physiology and Biochemistry, 42: 1225-1236, (2016), IF:1.442*

The increased industrial applications of nanoparticles (NPs) augment the possibility of their deposition into aquatic ecosystems and threatening the aquatic life. So, this study aimed to provide a comparable toxicological effects of nano-CuO and bulk CuO on a common freshwater fish, Oreochromis niloticus. Fish were exposed to two selected doses (1/10 and 1/20 of the LC50/96 h) of both nano-/bulk CuO for 30 days.

Based on the studied hematological parameters (RBCs count, hemoglobin content and hematocrit%), the two selected concentrations of CuO in their nano- and bulk sizes were found to induce significant decrease in all studied parameters. But, nano-CuO-treated fish showed the maximum decrease in all recorded parameters among the all studied groups especially at the low concentration of 1/20 LC50/96 h. Hematological status was also confirmed using the calculated blood indices (MCV, MHC and MCHC). In case of bulk CuO-treated groups, the significant decrease in the studied hematological parameters was not followed by any change in MCV and MCH (normocytic anemia), while fish that exposed to NPs showed a significant increase in all calculated blood parameters reflecting erythrocytes swelling which is related to the intracellular osmotic disorders (macrocytic anemia). Regarding metal bioaccumulation factor, the results showed that CuO NPs had more efficiency to internalize fish tissues (liver, kidneys, gills, skin and muscle). The accumulation pattern of Cu metal was ensured by histopathological investigation of liver, kidneys and gills. The histopathological analysis revealed various alterations that varied between adaptation responses and permanent tissue damage.

**Keywords:** Oreochromis niloticuscuo (Bps and Nps)Hematological parametershistopathology.

## B-431. Skin-Derived Semiochemicals of the Lacertid Lizard Acanthodactylus Boskianus

Eraqi R. Khannoon, Kamar K.H. Mohammed and Ahmed I. Dakrory

*Amphibia-Reptilia, 37(2016): 427-436, (2016), IF: 1.396*

Skin lipids impede transcutaneous water loss in several species of squamate reptiles and act as a barrier to harmful microorganisms; they play an additional role as chemical cues involved in chemical communication eliciting behavioral responses in intra- and interspecific interactions. While studies till now give little detailed information on the nature of skin slough, the femoral gland secretions of the lacertid lizard Acanthodactylus boskianus have been analyzed and the chemical profile is known for the species. In the present study we use GC-MS analysis of skin slough to focus on the chemical composition of skin in the xeric-adapted lacertid lizard A. boskianus and compare this to its femoral secretions. In the shed skin we detected steroids, alcohols, carboxylic acids, alkanes, aldehydes, carboxylic acid esters, squalene, monoglycerides of fatty acids, glycerol monoethers of long chain alcohols, and 1,3 alkanediol, which are the same chemical groups already found in the femoral secretions of this species. However, the relative percentages of these compounds in skin slough differ from those known for femoral secretions. While the compounds characterizing skin slough are qualitatively similar to femoral secretions, they could represent an adaptation to hot and dry habitats of A. boskianus. With regard to the characteristic chemical profiles for different sexes, there is not enough evidence to support their possible role as chemosignals, and behavioral experiments should be performed to test the possible use of skin shedding in intraspecific communication.

**Keywords:** Pheromones; Shedding; Skin lipids; Lacertidae.

## B-432. The Impact of Three Herbicides on Biological and Histological Aspects of Biomphalaria Alexandrina, Intermediate Host of Schistosoma Mansoni

Fathy Abdel-Ghaffar, Amira K. Ahmed, Fayez Bakry, Ibrahim Rabei and Amina Ibrahim

*Malacologia, 59(2): 197-210, (2016), IF: 1.211*

Schistosomiasis remains a public health problem in the developing world. Biomphalaria alexandrina is the intermediate host of Schistosoma mansoni, with a widespread distribution in Egypt. In Egypt molluscicides have been important, but otherwise molluscicides have been of minor significance. They may, however, become important now that WHO talks about eradicating schistosomiasis in some countries and that WHO has finally accepted that snail control is important.The present study investigated the different effects of three commercial herbicidical compounds, Butralin (as Amex 48% EC), glyphosate isopropylammonium (Herphosate 48% SL) and Pendimethalin (Stomp 50% EC) on B. alexandrina. All three compounds were found to have a molluscicidal effect, with Pendimethalin the most toxic over the examined range of concentrations. In addition, at sublethal concentrations, these compounds reduced growth rates and reproductive output (numbers of eggs laid) in exposed B. alexandrina, and it reduced viability of those eggs. Interpretion of assay data was supported by histological changes in the digestive and hermaphrodite glands of snails exposed at a range of concentrations. Moreover, the three compounds were also shown to rapidly (with three hours exposure) induce a toxic effect in miracidiae and cercariae of Schistosoma mansoni. It can be concluded that the three herbicidical compounds have molluscicidal and antihelminth properties.

**Keywords:** Biomphalaria alexandrina; Schistosoma mansoni; Miracidiae; Cercariae; Butralin; Glyphosate Isopropylammonium; Pendimethalin; Herbicides; Molluscicidal Activity; Antihelminth activity; Schistosomiasis.

## B-433. A Study on the Possible Therapeutic Role of Panax Ginseng Extract Against A Rat Model of Parkinson'S Disease Induced by Intrastriatal Rotenone Injection

Yasser A Khadrawy, Iman M Mourad, Haitham S Mohammed, Neveen A Noor and Heba S Aboul Ezz

*International Journal of Clinical and Experimental Medicine, 9: 3831-3841, (2016), IF: 1.075*

The neuroprotective effects of Panax ginseng were extensively studied. However, the therapeutic role of Panax ginseng in rat model of Parkinson's disease (PD) has not been studied enough. In the present study, rats were divided into three groups; control, rat model of PD induced by intrastriatal injection of rotenone and rat model of PD treated daily with Panax ginseng extract (100 mg/kg for 2 weeks). Forelimb wire hanging and the traction tests scored a significant decrease in PD model rats. In ginseng extract-treated group, these behavioral parameters changed to non significant values from the control rats. In the midbrain of rat model, a state of oxidative stress was observed

as indicated from the significant increase in lipid peroxidation, nitric oxide and tumor necrosis factor-α and the decrease in reduced glutathione in comparison to control. This was accompanied by a significant decrease in dopamine and a significant increase in acetylcholinesterase activity. In the striatum, an increase in lipid peroxidation and a decrease in nitric oxide, dopamine content and acetylcholinesterase were recorded. Panax ginseng treatment improved all the midbrain and striatal changes induced by rotenone except nitric oxide. However, this improvement was partial since the measured parameters in ginseng-treated group were not significant from the rat model of PD except tumor necrosis factor-α. From the present findings, it could be concluded that Panax ginseng extract administration for 2 weeks showed a partial ameliorative effect against the rat model of PD induced by the intrastriatal injection of rotenone.

**Keywords:** Panax ginseng; Parkinson'S disease; Dopamine; Oxidative stress; Rat.

## B-434. Assessing the Awareness of Egyptian Medical Students About Responsible Conduct of Research and Research Ethics: Impact of an Educational Campaign.

Mohamed El-Shinawi, Karim Osama Mohamed, Yousef Ahmed Fouad, Yara Mohamed Fahmy, Hadeel Abdulwahed Asar, Mohamed Gomaa Khalil, Lida Anestidou Samer S. El-Kamary and Mona Mostafa Mohamed

*Accountability in Research: Policies and Quality Assurance, 23(4): 199-218, (2016), IF: 0.872*

This is a quasi-experimental pre-post assessment study utilizing an anonymous self-administered questionnaire to assess Egyptian medical students' awareness about responsible conduct of research (RCR) and research ethics. Students' were assessed before and after an RCR awareness campaign. Our results showed that most of the pre-campaign respondents were not familiar with the basic principles and terms of RCR. An increase in the awareness about RCR across all discussed topics was noted following the campaign. We concluded that an educational awareness campaign is effective in increasing medical students' awareness about RCR and should be incorporated into current medical school curricula in Egypt.

**Keywords:** Egypt; Medical students; Plagiarism; Research misconduct; Responsible conduct.

## B-435. Purification and Characterization of Two Glutathione Peroxidases from Embryo of the Camel Tick Hyalomma Dromedarii

M. A. Ibrahim, M. M. Mohamed, A. M. Ghazy, M. El-Mogy and H. M. M. Masoud

*Russian Journal of Bioorganic Chemistry, 42(3): 272-281, (2016), IF: 0.66*

Two glutathione peroxidase isoenzymes were purified from 24-day old embryos of the camel tick Hyalomma dromedarii and designated tick embryo glutathione peroxidase 1 and 2 (TEGPx1 and TEGPx2). The purification procedure involved ammonium sulfate precipitation, as well as ion exchange and gel filtration column chromatography. Glutathione peroxidase isoenzymes subunit molecular mass was determined by SDS-PAGE to be 36 ± 2 kDa and 59 ± 1.5 kDa for TEGPx1 and TEGPx2, respectively. TEGPx1 isoenzyme exhibited a dimeric structure with native molecular mass of 72 kDa while TEGPx2 was a monomeric protein. TEGPx1 and TEGPx2 displayed their pH optima at 7.6 and 8.2. Both isoenzymes cleaved preferentially H2O2 with Km values of 24 and 49 μM. Iodoacetamide competitively inhibited TEGPx1 with Ki value of 0.45 mM and 1.10; phenanthroline competitively inhibited TEGPx2 with Ki value of 0.12 mM. These results indicate the presence of two different forms of glutathione peroxidase in the developing camel tick embryos. This finding enhances our knowledge and understanding of the physiology of these ectoparasites and will encourage the development of new and untraditional control methods.

**Keywords:** Glutathione peroxidase; Purification characterization camel tick; Hyalomma dromedarii.

## B-436. New Insights Into Sepsis Therapy Using Sepia Officinalis

Amel M. Soliman, Sohair R. Fahmy, Amany A. Sayed and Asmaa A. Abd El-Latif

*Jundishapur Journal of Microbiology, 9: 1-7, (2016), IF: 0.655*

**Background**: Sepsis remains a major problem for both scientists and clinicians. Cecal ligation and puncture (CLP) is considered the gold standard for animal models of sepsis. The undesirable side effects of certain antibiotics have forced scientists to discover new, natural, and safe antimicrobial agents, such as cephalopods, which are known to display significant antimicrobial activity. Objectives: The present investigation aims to evaluate the in vitro and in vivo antibacterial and antiseptic efficacy of Sepia officinalis body tissue (SOBT) extract and S. officinalis polysaccharide (SOP) from its cuttlebone. **Materials and Methods**: Forty-eight rats were divided into 4 groups, and starting 2 hours after CLP, treatments were given for 2 days as follows: sham control rats treated orally with distilled water, septic rats treated orally distilled water, septic rats treated orally methanolic extract of SOBT (500 mg/kg b.wt) suspended in distilled water, and septic rats treated orally SOP extract (200 mg /kg b.wt) dissolved in distilled water. On the third day, half of the rats in each group were euthanized for blood collection. The other half were kept alive and used for the survival study. **Results**: The present study revealed that the SOBT and SOP extracts showed in vitro bactericidal activity against gram-positive and gram-negative bacteria. Furthermore, administration of SOBT and SOP increased the rats' survival rates by 66.7% and 83.33%, respectively, as compared to the untreated CLP-septic rats. Treatment of the CLP-septic rats with SOBT and SOP significantly alleviated alterations in procalcitonin levels and in some hematological parameters induced by CLP. **Conclusions**: SOBT and SOP had profound antiseptic efficacy.

**Keywords:** Sepsis; Antibacterial activity; Procalcitonin; Sepia officinalis body tissue extract; Sepia officinalis bone polysaccharide extract.

## B-437. Interleukin-6 Induces Secretion of Tissue Inhibitors of Etalloproteinases by Breast Carcinoma Cells

Abeer Mahmoud Badr

*Pakistan Journal of Pharmaceutical Sciences, 29: 1969-1975, (2016), IF: 0.581*

Interleukin (IL)-6 can induce matrix metalloproteinases (MMPs) expression, which may be critical factors involved in tumor metastasis. Tissue inhibitors of metalloproteinases (TIMPs) are important inhibitory enzymes of MMP. This study was designed to investigate the effect of recombinant IL-6 on the MMP/TIMP expression in MDA-MB-231 breast cancer cell line in a dose dependent manner (10, 25 and 50ng/ml) in comparison to non-treated breast cancer cells (control). The data demonstrated that low dose (10 ng/ml) of IL-6 failed to induce TIMP-1 and -2 production by breast cancer cells compared to control cells whereas moderate (25 ng/ml) and high (50ng/ml) exposure levels promoted a significant expression of TIMP-1 ($P<0.01$ and $P<0.0001$) respectively as compared to control cells. TIMP-2 was significantly released ($P<0.0001$) from breast cancer cells higher than in control cells at moderate and high exposure levels of IL-6. This up-regulation of TIMP-1 and -2 was accompanied with undetectable levels of MMP-1, -2, -3, -8, -9, - 10, and -13. Furthermore, IL-6 potentially increased the invasion potency of cancer cells significantly ($P<0.05$ and $P<0.01$) at moderate and high exposure levels respectively. These findings suggest that IL-6 could promote the invasion potency of breast cancer cells by inducing secretion of TIMP-1 and -2, causing a disturbance in TIMP/MMP balance.

**Keywords:** Interleukin-6; Matrix metalloproteinases; Tissue inhibitors of metalloproteinases; Breast carcinoma mdamb-231 Cells; Cancer invasion.

## B-438. Assessment of Metal Pollution Around Sabal Drainage in River Nile and its Impacts on Bioaccumulation Level, Metals Correlation and Human Risk Hazard Using Oreochromis Niloticus as a Bioindicator

Amr Adel Abdel-Khalek, Engy Elhaddad, Samar Mamdouh and Mohamed-Assem Saed Marie

*Turkish Journal of Fisheries and Aquatic Sicences, 16: 227-239, (2016), IF: 0.553*

This work aimed to assess the impact of Sabal drains (northern part of El-Minufiyah governorate, Egypt) on the metals load of river Nile. Four sites were selected to monitor the partitioning of metals in the aquatic components: reference site (site1); 20Km before Sabal drainage (site2); Sabal site (site3) and 20Km after Sabal drainage (site4). The maximum means of aqueous metals were observed at site3 in the following order (mg/l): Fe (0.76) >Mn (0.325) >Zn(0.07) >Pb (0.064) >Cu (0.041) >Cd (0.0035), while the trend is slightly different in sediments (mg/kg): Fe (527.9) >Mn (102.7) >Zn (17.65) >Cu (11.4) >Pb (1.26)>Cd (0.07). Tissue-specific patterns of metal accumulation in Oreochromis niloticus were observed. As indicated by the calculated metal pollution index and bioaccumulation factor, the tissues of liver, kidneys and gills were observed to be strong bioaccumulators compared to muscular tissues. Regarding the correlation study in site3, the bioaccumulated metals in most tissues showed homogenous-correlation with aqueous metals ($r>0.5$) and diverse-correlations with respect to sedimentary metals. The calculated hazard index (HI) indicated that each metal had low HI but, the cumulative impacts of all metals represented a real threat to fish consumers especially at site3. Metals elevation was highly correlated with Sabal discharges and regulations for water and fish consumption have to be applied

**Keywords:** Oreochromis niloticus; Metals toxicity; Bioaccumulation; Human risk.

## B-439. Implications Arising from the Use of Cymbopogen Proximus , Proximal on Placenta of Pregnant Albino Rats.

Amel Ramadan Omar, Eman Salah El Din and Heba Abdelrahman

*Brazilian Archives of Biology and Technology, 59 (2016) IF:0.468*

Halfa-bar (Cymbopogon proximus), is an aromatic grass widely growing in Upper Egypt. This herb is recommended for medical purposes as an effective diuretic, renal or abdominal antispasmodic agent. **Objectives of this study**: Evaluate the potential effects of Halfa-bar on the pregnant albino rats during the gestation period. **Material and methods**: The virgin female rats mated with male then the pregnant rats treated orally with Human Equivalent Dose (HED) of the proximol which equivalent 0.05 mg/ kg rat from 5th -18th Gestational Day (GD). At day 20 of pregnancy, all rats were anesthetized and killed to obtained maternal -fetal data (placenta). **Results**: The current study indicated that, there is statistically significant ($P \leq 0.05$) reduction in the treated placental weight. Also, the light microscopic examination of the placental specimens using haematoxylin and eosin (H&E) staining revealed the presence of various vacuoles in the cytoplasm and nuclei of the giant cells. There is an increase in the number of apoptotic cells and irregular dilatation of maternal sinusoids in the labyrinth zone. Else, microscopic investigation showed a depletion of the glycogen content in the basal and labyrinth layers and a positive caspase-3 in the spongitrophoblast cells. In the treated group, reduction in level of catalase activity (CAT) and significant elevation ($P \leq 0.05$) in the level of malondialdehyde (MDA) were recorded. **Conclusion**: The pathological effects in placenta may be due to the accumulation of proximal and transplacental passage.

**Keywords:** Cymbopogen proximus; Placenta; Rattus Norvegicus.

## B-440. Anatomical Studies on the Eye Muscle Nerves and Ciliary Ganglion of the Leaping Grey Mullet, Liza Saliens (Risso, 1810)

Amel Ramadan Omar, Eman Youssri Salah EL-Din, Ahmed Imam Dakrory, Ibrahim Yehia Abdelkader and Reema Emhammed Hassain

*Global Veterinaria, 17: 546-552 (2016)*

The aim of this study is to analyze the ocular muscle nerves and the ciliary ganglion of the bony fish Liza saliens. This leaping

grey mullet fish was collected from Kafr El-Sheikh and has been undergone to a serious of permanent histological preparation to be willing for examination. The ocular muscle nerves comprise the nervi oculomotorius, trochlearis and abducens. The oculomotor nerve arises from the pars peduncularis mesencephalon of the brain to leave the cranial cavity through its own foramen. It innervates four eye muscles; rectus superior, rectus inferior, rectus medialis and the obliquus inferior muscles. It carries pure somatic motor fibers and visceromotor (parasympathetic) ones. The ciliary ganglion is small and has no radix ciliaris brevis. It has only the radix ciliaris longa that originates from the ramus opthalmicus profundus. Only one ciliary nerve arises from the ciliary ganglion that terminates in the muscle of the iris. The trochlear nerve passes extracranially through its trochlear foramen and carries pure somatic motor fibers to the obliquus superior muscle. The nervus abducens arises from the medulla oblongata by a single root. It leaves the cranial cavity through its own foramen to enter the posterior eye muscle canal (myodome). It carries pure somatic motor fibers to the rectus lateralis muscle.

**Keywords:** Abducens ;Ciliary ganglion; Liza saliens ocular Muscle nerves oculomotor trochlear.

## B-441. Antiulcerogenic Efficacy of Ethanolic Extract of Vitis Vinifera Leaves on Rats

Dawlat Ahmed Sayed, Sohair R Fahmy, Amel M Soliman and Nagat S. Hussein

*International Journal of Pharmacy and Pharmaceutical Sciences, 8 (9): 163-172 (2016)*

**Objective:** The ethanolic extract of Vitis vinifera (VVE) leaves (500 mg/kg body weight), ranitidine (50 mg/kg body weight) and both of them were tested for their gastro-protective and curative effects against the incidence of peptic ulcer. **Methods:** The antiulcer effects of VVE were investigated using a combination of indomethacin and cold-stress for 2hr. To ascertain the mechanism of action of VVE, its protective and curative effects were studied on gastric volume, gastric juice acidity, ulcer index and malondialdehyde (MDA), glutathione (GSH), catalase (CAT), glutathione –S-transferase (GST), superoxide dismutase (SOD), nitric oxide (NO) activities of both stomach and duodenum of rats. Moreover histopathological effects on stomach and duodenum were determined. **Results:** The antioxidant activity of VVE was demonstrated using DPPH test. VVE was found to reduce the ulcer index, gastric volume and the level of gastric juice acidity. Also, VVE showed gastro-protective and curative activities mainly through improvement of antioxidant status and decreasing lipid peroxidation accompanied with amelioration of both stomach and duodenum architectures. **Conclusion:** The prophylactic and curative effects of VVE proved to be effective in preventing gastric and duodenal ulceration which may probably due to its antioxidant and anti-acid secretory effects.

**Keywords:** Severe gastric ulcer; Rats; Indomethacin; Cold stress and oxidative stress.

## B-442. Early Anatomical and Embryological Description of Pecten Oculi in Cattle Egret (Bubulcus Ibis)

Eman Youssri Salah El-Din and Ahmed Imam Dakrory

*Journal of Advanced Zoology, 37: 14-20 (2016)*

Early development of the pecten oculi of the cattle egret (Bubulcus ibis) was investigated. Different embryonic developmental stages of cattle were collected from eggs. Embryos were fixed in Bouin's solution, dehydrated, clearing, embedded, sectioned, and stained with Hematoxylin-Eosin and for examination using light microscopy. The early development of pecten was recorded according to Hamburger-Hamilton' s stages (HH 28, 29, 33, 34, 35 and 36). The primordial of pecten is formed by fusion of the ectodermal edges of the optic fissure inward. It grows into a tall thin plate protruding from a broad base. Vasularization appears in the broad base of the plate-like pecten, and then become numerous. Also, pigmentation becomes evidence.

**Keywords:** Eye; Pigmentation; Plated pectenp Pleated pecten.

## B-443. Echinochrome Pigment Attenuates Diabetic Nephropathy in the Models of Type 1 and Type 2 Diabetes

Soliman A.M., Mohamed A.S and Marie M.S.

*Diabetes Mellitus, 19: 464-470 (2016)*

**Background.** The main complication of diabetes mellitus is diabetic nephropathy in both types, which is a main reason for renal failure. Echinochrome substance present in sea urchin shells and spines and possesses high antioxidant activity. Aim. is to evaluate the ability of Ech to suppress the progression of diabetic complication in kidney. **Materials and methods.** Thirty-six male Wistar albino rats were divided into two main groups, type 1 diabetes mellitus and type 2 diabetes mellitus. Both groups divided into control, diabetic and echinochrome subgroups. Type 1 diabetes was induced by single dose of streptozotocin (60 mg/kg, i.p), while type 2 was induced by high fat diet for 4 weeks before the injection with streptozotocin (30 mg/kg, i.p). The treated groups were administrated by echinochrome (1mg/kg body weight in 10% DMSO) daily for 4 weeks. **Results.** Echinochrome groups showed reduction in the concentrations of glucose, malondialdehyde, urea, uric acid and creatinine. While it caused general increase in glutathione-S-transferase, superoxide dismutase, catalase, glutathione reduced, nitric oxide and creatinine clearance. The histopathological investigation showed clear improvement in the kidney architecture. **Conclusion.** Administration of echinochrome improves renal function and ameliorates renal histopathological changes possibly by improvement of glucose metabolism and inhibition of lipid peroxidation process.

**Keywords:** Diabetes mellitus; Echinochrome- Nephropathy; Oxidative stress; Kidney.

## B-444. Effects of Three Inorganic Fertilizers on the Biology and Histopathology of Infected Biomphalaria Alexandrina Snails

Rehab Mohamed Hussein, Mohamed Assem S Marie and Fatma Afifi Ali El-Deeb

*Research Journal of Pharmaceutical, Biological and Chemical Sciences, 7 (4): 2564-2574 (2016)*

The present work was carried out to calculate the half lethal concentrations (LC50) of three inorganic fertilizers (balanced, high phosphorus and high nitrogen fertilizers) on Biomphalaria alexandrina snails and to demonstrate measurable effects on infected B. alexandrina with Schistosoma mansoni miracidia that were exposed for one week to ¼ LC50 (126.4, 400 and 2375 ppm) separately of (balanced, high phosphorus and high nitrogen) fertilizers, respectively. The obtained results showed that the survival of all treated infected snail groups at the 1st shedding were significantly less than the control group. Moreover, results revealed a marked reduction in the infectivity of the infected snails especially those exposed to sublethal concentration of high nitrogen fertilizer when compared to control. In addition, the cercarial production of all treated groups was completely suppressed. These infected snails exhibited histopathological alterations, which is associated with severe damage in the digestive gland cells as well as the mother sporocysts of treated infected snails. Our study revealed the biological and histopathological effects of three inorganic fertilizers on infected Biomphalaria alexandrina snails

**Keywords:** Biomphalaria alexandrina; Infection; Inorganic Fertilizers; Histopathology.

## B-445. Establishing the First Institutional Animal Care and Use Committee in Egypt

Sohair R. Fahmy and Khadiga Gaafar

*Philosophy, Ethics, and Humanities in Medicine, 11: 1-6 (2016)*

**Background** Although animal research ethics committees (AREC) are well established in Western countries, this field is weakly developed and its concept is poorly understood in the Middle East and North Africa region. Objective Our main objective was to introduce the concept and requirements of ethical approaches in dealing with experimental animal in research and teaching in Egypt. **Methods** Due to its very recent inception, Cairo University, Faculty of Science IACUC decided to operate in accordance with Guide for the Care and Use of Laboratory Animals 8th Edition 2011 (the Guide) since Egypt has not yet compiled its own guide. **Results** Fifty protocols were reviewed in 2013–2014. Only ten protocols were reviewed in 2013, but in 2014, forty protocols were reviewed. In 2013 all protocols were approved and in 2014, number of approvals were 35, the number of deferrals were 4, and one refused protocol. Master's theses (MSc) research protocols constituted the majority of the total reviewed protocols. This is attributed to the decision of the Board of the Faculty of Science, Cairo University in September, 2013 that the approval of the IACUC is mandatory before conducting any research involving animals or theses registration. **Conclusion** The first IACUC was established in the Cairo University, Faculty of Science, since 2012. The challenges encountered by the committee were diverse, such as the absence of laws that control the use of animal models in scientific research, lack of guidelines (protocols for experimental animals in research) and, mandatory ethical approval for any experimental animal research.

**Keywords:** Animal research ethics committees; Egypt; Experimental animals; Cairo university; Faculty of science.

## B-446. Evaluation of Implications Potentials of Dietary Supplement (Yeast Tablets) on Pregnant Albino Rats and Their Offspring'S.

Amel R Omar, Eman Y Salah EL-Din and Heba A bdelrahman.

*Research Journal of Pharmaceutical, Biological and Chemical Sciences, 7 (3) (2016)*

The aim of this study to assess the effect of yeast tablets on the pregnant rats and their litters. The pregnant rats were administered orally with yeast tablets at a dose of 41.1 mg/kg rat from day 5 up to 19 of pregnancy andthe mothers were sacrificed on day 20 of pregnancy. The maternal external toxicity symptoms and external anomalies of fetuses were reported and skeletal abnormalities were investigated.Oral administration of yeast to pregnant rats resulted in the statistical differences regarding to the dams weight, fetal weight and length were significant. There are number of postimplantation resorptions and external malformationsof fetuses were recorded. Some fetal skeletal abnormalities were observed.

**Keywords:** Rattusnorvegicus; Saccharomyces cerevisiae; Skeletal abnormalities; Yeast tablets.

## B-447. Genotoxic and Mutagenic Studies of the Antiepileptic Drug Levetiracetam in Pregnant Rats and Their Fetuses

Haidan M. El-Shorbagy and Hamida Hamdi

*International Journal of Pharmacy and Pharmaceutical Sciences, 8: 82-88 (2016)*

**Objective:** Levetiracetam (LEV) is an anti-epileptic drug, initially approved as an adjunct therapy in adult patients with partial-onset seizures, and used as monotherapy treatment during pregnancy. However, very few, if none, investigations have been focused on LEV neurotoxicity or hepatotoxicity at the molecular level. This study aimed to evaluate the genotoxic and mutagenic potential of LEV, in liver and brain tissues of treated pregnant rats and their fetuses during pregnancy. **Methods:** LEV was administered to pregnant female albino rats at doses 300 and 600 mg/kg b. w, from gestation days 5-18. Comet assay, DNA fragmentation were performed for detection of DNA damage. Single-stranded conformation polymorphism (SSCP) followed by DNA sequencing were accomplished for detecting possible mutagenicity. **Results:** Administration of the two tested doses of LEV resulted in a significant increase of DNA damage as detected by alkaline Comet assay, and an appearance of both apoptotic laddered and smeared DNA in the tissues tested. Moreover, a significant incidence of mutations in exon 2 and 3 of Harvey rat sarcoma viral oncogene (HRAS) gene, were detected in fetal liver and brain tissues respectively, using single-stranded conformation polymorphism (SSCP) and were confirmed by DNA sequencing. **Conclusion:** Maternal and fetal DNA damage induced by LEV was evidenced in our study, even at the commonly used therapeutic dose (300

mg/kg), and thus these side effects should be considered when using LEV for long-term during pregnancy.
**Keywords:** Mutagenicity; Sscp; Hras Gene mutation Comet assay; Levetiracetam.

## B-448. Hazardous Effects Induced by Inhalation of Isopropanol

Rehab Mohamed Hussein and Osama Mohamed Sarhan

*Research Journal of Pharmaceutical, Biological and Chemical Sciences, 7(6): 2648-2660 (2016)*

The purpose of this study was to explore the effects induced by inhalation of isopropanol vapor for 2 and 4 weeks on the trachea, lung, liver and kidney. Thirty-two healthy Wister rats divided equally into four groups. Group 1 (G1) control rats were allowed to inhale fresh air, G2 were allowed to inhale IPA vapor at concentration of 240 ppm for two weeks, G3 and G4 were exposed to IPA as in G2 for four weeks. In addition, rats of G4 left without exposure for further two weeks as a recovery period. At the end of each experimental period, rats dissected; their tracheas, lungs, livers and kidneys extracted and processed for light microscopy. Tracheal mucosa showed focal destruction, desquamation, and the lamina propria showed oedema. Lungs showed emphysema in some air alveoli and bronchiolar hyperplasia with polyp formation. The hepatic parenchyma showed degenerated hepatocytes with some pyknotic nuclei. Degenerated kupffer cells, with dilatation and congestion in the portal veins. Renal glomeruli showed congestion, increase in their cellularity. Our results suggest that inhalation of the IPA vapor at low concentrations could have cytotoxic effects on the structure and function of these organs.
**Keywords:** Isopropanol inhalation; Rats; Trachea; Lung, Liver; Kidney.

## B-449. Immune-Molecular Identification of Giardia Intestinalis in Diarrhoeal Children: Comparison of Three Diagnostic Methods

Neveen A. Madbouly, Alya Farid, Ayman A. El-Badry and Azza M. El-Amir

*Journal of The Egyptian Society of Parasitology (Jesp), 46: 253-260 (2016)*

Giardiasis is a major health problem in both developed and developing world. A variety of methods for diagnosis of Giardia duodenalis cysts or trophozoites is available but still has certain limitations. 100 sample from diarrhoeal children who attending outpatient clinic in Abu El Rish hospital, Kasr Al Ainy, Faculty of Medicine, Cairo University, Egypt. Giardiasis was diagnosed by direct wet mount, microscopy after formal- ethyl acetate concentration, Ridascreen ELISA assay and n-PCR targeting beta giardin (bg) gene. Using ELISA as reference standard, the methods' sensitivities, specificities, positive (PPV) and negative (NPV) predictive values and positive (LR+) and negative (LR-) likelihood ratios with 95% confidence interval (95% CI) were analyzed.The diagnostic methods were evaluated to determine their impact on the posttest probability using Fagan's nomogram. All the studied methods led to a LR+ higher than 10 indicating ability to ruling in giardiasis. n-PCR recorded LR- equal 0.00 and the probability of giardiasis would be 0% if the test was negative. The methods were also ranked on basis of Multiattribute utility theory and Analytical hierarchy process with ELISA ranked better than n-PCR
**Keywords:** Giardia; Copro-DNA; Bg gene; Ridascreen ELISA; Fagan's Nomogram.

## B-450. Modulatory Effect of Wheat Germ Oil on Intestinal Oxidative Stress and DNA Damage Induced by Carbon Tetrachloride in Mice

Hanan Saleh

*Journal of Applied Pharmaceutical Science, 6(12): 67-74(2016)*

**Background/Aim:** The liver is continuously linked to the gut via the portal vein supply. Gastrointestinal complications are directly associated with liver cirrhosis. Carbon tetrachloride ($CCl_4$) caused liver toxicity is well documented in animal models, the very fewer search has been carried out on the intestinal damage in case of acute liver injury. Thus, this study aimed to investigate the intestinal alteration and subsequently the potential therapeutic role of Wheat Germ Oil (WGO) in the liver and small intestine after acute administration of $CCl_4$. **Material and Methods:** Mice were randomly divided into 4 groups; control group, WGO group: received corn oil orally for 2 days then WGO (1400mg/kg) orally for 8 days, $CCl_4$ group: received $CCl_4$ orally for 2 days then corn oil for 8 days, $CCl_4$ + WGO group: received $CCl_4$ for 2 days then WGO for 8 days. Serum lipid profile, serum lactate dehydrogenase (LDH), intestinal oxidative stress enzymes, histopathological and DNA fragmentation assays were estimated. **Results:** Acute dose (50%, 1 mL/kg body weight) of $CCl_4$-induced hyperlipidemia, hypocholesteremia, elevation in LDH, malondialdehyde (MDA), nitric oxide (NO) and intestinal DNA damage in addition to the reduction in the intestinal oxidative stress markers and an alteration in the mucosal architecture. On the contrary, WGO administration has the potency to protect not only the liver but also the small intestine in acute $CCl_4$-induced tissue damage. The valuable effect is chiefly attributed to its mechanism of reducing the lipid profile and suppressing the oxidative stress that caused DNA damage **Conclusion:** WGO administration could markedly improve the liver and the small intestine from the $CCl_4$ damage and consequently may be used as a therapeutic agent against the hepatic and intestinal toxicity.
**Keywords:** $CCl_4$; Wheat Germ Oil; Small intestine; Lipid Profile; DNAdamage.

## B-451. Prevalence of Toxoplasma Gondii in Chicken Samples From Delta of Egypt Using Elisa, Histopathology and Immunohistochemistry

Hany M. Ibrahim, Fathy Abdel-Ghaffar, Gamalat Y. Osman, Safinaz H. El-Shourbagy, Yoshifumi Nishikawa and Reham A. Khattab

*J Parasit Dis, 40 (2): 485-490 (2016)*

Estimates of the zoonotic diseases are helpful for monitoring and improving public health. Laboratorybased surveillance provides crucial information for assessing zoonotic disease trends and developments. Toxoplasmosis is considered as a zoonotic disease and has both medical and veterinary importance since it leads to abortion in humans and several animal species. In view of the worldwide importance of T. gondii, this study aimed to estimate the prevalence of T. gondii

in chickens from the Delta of Egypt. A total of 304 blood and brain samples were collected from Egyptian chickens from Gharbiya, Qalyoubiya, Minufiya, Beheira, Kafr EL-Shaykh and Dakahlia Provinces. In order to determine the serological and histopathological prevalence of T. gondii, the samples were examined by ELISA, histopathology and immunohistochemistry (IHC). The prevalence of T. gondii was 11.18, 6.91, 6.91 % by ELISA, histopathology and IHC, respectively. Statistically significant differences in the prevalence of T. gondii were observed on the basis of season, sex and habitat. These data provide valuable information regarding the epidemiology of T. gondii infections in Egyptian chickens, which can be employed in developing efficient strategies for disease management and control.

**Keywords:** Toxoplasmosis prevalence immunohistochemistry; ELISA chicken Tgsag2.

## B-452. Protective and Therapeutic Efficacy of Sodium Butyrate on Tamoxifen-Induced Non-Alcoholic Fatty Liver Disease in Male Rats.

Hanan Saleh, Basma Mohamed and Mohamed Assem S. Marie

*Research Journal of Pharmaceutical, Biological and Chemical Sciences, 7 (3): 951-965 (2016)*

This study aimed to investigate the protective and therapeutic efficacy of sodium butyrate (NaBu) to reduce lipid accumulation and liver steatosis induced by tamoxifen (TAM) in rats. Animals were divided mainly into protective and therapeutic groups. Each group were subdivided into four subgroups; (control) received saline either for 7 or 14 days, (NaBu) (300mg/kg) injected intraperitoneally for 7 days prior to or after saline administration for 14 days, (TAM) (40mg/kg) received orally for 14 days prior to or after saline administration for 7 days, (NaBu-TAM) received NaBu for 7 days then TAM for 14 days, (TAM-NaBu) received TAM orally for 14 days then NaBu for 7 days. NAFLD was assessed in TAM group by increasing the levels of total lipids, triglycerides and MDA. In addition to the reduction in AST, ALT, total protein, albumin, A/G ratio, ALP and some oxidative biomarkers. NaBu administration as a protective or therapeutic agent showed reduction in total lipids, triglycerides and MDA levels, with an increase in the tested endogenous scavengers accompanied with healthy hepatic histopathological examination. sodium butyrate exhibited protective and therapeutic effects in dissolving accumulated lipid and reducing steatosis induced by TAM in liver.

**Keywords:** Tamoxifen; Sodium butyrate; Steatosis; Liver Function; Lipid profile.

## B-453. Sodium Butyrate Attenuates Nephrotoxicity Induced by Tamoxifen in Rats

Hanan Saleh, Basma Mohamed and Mohamed Assem S. Marie

*Journal of Applied Pharmaceutical Science, 6 (6): 66-72 (2016)*

Tamoxifen (TAM) is a hormonal selective estrogen modulator used in the prevention and treatment of breast cancer. It associated with increased in the oxidative stress in cells leading to tissue injury. Sodium butyrate (NaBu) increased the glutathione redox system and diminished the oxidative stress. The purpose of this study was to elucidate the ameliorative effect of NaBu against TAM-induced kidney injury by reducing the generation of oxidative stress. Rats were divided mainly into four group as follow: control, rats received saline for 14 days orally then saline intraperitoneally (i.p.) for 7 days, NaBu, rats received saline orally for 14 days, NaBu (300mg/kg) (i.p.) for 7 days, TAM, rats received TAM (40mg/kg) orally for 14 days, then saline (i.p.) for 7 days, (TAM-NaBu) rats received TAM orally for 14 days, NaBu (i.p.) for 7 days. Kidney injury followed by TAM treatment was assessed by the elevation in the levels of creatinine, urea, uric acid and MDA and reduction in some oxidative biomarkers, in addition to the abnormal architecture of the kidney. Conversely, Administration of sodium butyrate could ameliorate all of these damaging effects in the antioxidant system in the TAM-treated group. NaBu affords significant increments in the antioxidant enzymes. In addition, it has the therapeutic capacity to protect the kidney from the oxidative stress induced by TAM through improving the kidney function and diminishing the free radicals. Supplementation of NaBu could be useful in alleviating TAM-induced kidney injury.

**Keywords:** Tamoxifen; Sodium butyrate; Kidney; Oxidative stress.

## B-454. Three Week Dietary Intervention Using Apricots Pomegranate JuiceOrand Fermented SourSobya and Impact on Biomarkers of Antioxidative Activity Oxidative Stress and Erythrocytic Glutathione Transferase.

Mostafa Gouda, Amr Moustafa, Laila Hussein and Mohamed Hamza.

*Nutrition Jouranal, 15(1), (2016) IF: 3.265*

**Background:** The beneficial effects of the polyphenol (PP) rich fruits and Lactic acid bacteria fermented foods had been reported as cost-effective strategies for health promotion. Randomized controlled trial was designed to test the hypothesis that daily intake of polyphenol rich pomegranate juice (PGJ) or/ and lactic acid bacteria fermented sobya (FS) improved selected biomarkers of relevance to heath status. **Methods:** The design of the human trial consisted of 35 healthy adults, who were distributed to 5 equal groups, The first group served as control and received no supplements, the second group received fresh apricot fruits (200 g), the third (PGJ) (250 g), the fourth a mixture of PGJ (150 g) and FS (140 g) and the fifth group received (FS) (170 g). The supplements were served daily between 5 – 6 pm for 21 days. Blood and urine samples were collected at days zero and 22 of the dietary intervention. The supplements were analyzed chemically for (PP) contents and total antioxidative activities and microbiologically for selected bacteria and yeast counts. The blood samples were assayed for plasma antioxidative activities and for erythrocytic glutathione transferase activity (E-GST). Urine samples were analyzed for the excretions of total PP, antioxidative activity and thiobarbituric acid reactive substances (TBARS). **Statistical analysis:** Two way analysis of variance (ANOVA) was conducted and included the main effects of treatment, time and treatment x time interaction. **Results:** Daily intake of (PGJ) for 3 weeks significantly increased the plasma and urinary anti-oxidative activities and reduced the urinary excretion of (TBARS). Daily intake of (FS) for 3 weeks increased only (E-GST) activity. Daily intake of a mixture of PGJ and (FS) was also effective. **Conclusions:** The daily intakes of PGJ and/ or (FS) affected positively selected biomarkers of relevance to

health status. These functional foods have potential implication for use as bio-therapeutic foods. (Continued on next page).

**Keywords:** Pomegranate Juice; Sobya; Human trial; Antioxidative activity; Oxidative stress; Erythrocytic Glutathione-S-Transferase.

## B-455. Transcriptional Profiling of Breast Cancer Cells in Response to Mevinolin: Evidence of Cell Cycle Arrest,DNA Degradation and Apoptosis.

Ali M. Mahmoud, Mourad A.M. Aboul-Soud, Junkyu Han, Yazeed A. Al-Sheikh, Ahmed M. Al-Abd and Hany A. El-Shemy.

*International Journal of Oncology, 48: 1886-1894, (2016), IF:3.018.*

The merging of high-throughput gene expression techniques, such as microarray, in the screening of natural products as anticancer agents, is considered the optimal solution for gaining a better understanding of the intervention mechanism. Red yeast rice (RYR), a Chinese dietary product, contains a mixture of hypocholesterolemia agents such as statins. Typically, statins have this effect via the inhibition of HMG-CoA reductase, the key enzyme in the biosynthesis of cholesterol. Recently, statins have been shown to exhibit various beneficial antineoplastic properties through the disruption of tumor angiogenesis and metastatic processes. Mevinolin (MVN) is a member of statins and is abundantly present in RYR. Early experimental trials suggested that the mixed apoptotic/necrotic cell death pathway is activated in response to MVN exposure. In the current study, the cytotoxic profile of MVN was evaluated against MCF-7, a breast cancer-derived cell line. The obtained results indicated that MVN-induced cytotoxicity is multi-factorial involving several regulatory pathways in the cytotoxic effects of MVN on breast cancer cell lines. In addition, MVN-induced transcript abundance profiles inferred from microarrays showed significant changes in some key cell processes. The changes were predicted to induce cell cycle arrest and reactive oxygen species generation but inhibit DNA repair and cell proliferation. This MVN-mediated multi-factorial stress triggered specific programmed cell death (apoptosis) and DNA degradation responses in breast cancer cells. Taken together, the observed MVN-induced effects underscore the potential of this ubiquitous natural compound as a selective anticancer activity, with broad safety margins and low cost compared to benchmarked traditional synthetic chemotherapeutic agents. Additionally, the data support further pre-clinical and clinical evaluations of MVN as a novel strategy to combat breast cancer and overcome drug resistance.

**Keywords:** Mevinolin; Microarray; Mcf-7; Natural products; P53.

## B-456. Physical Properties of Particulate Matter from Animal Houses—Empirical Studies to Improve Emission Modelling.

Ehab Mostafa, Christoph Nannen, Jessica Henseler, Bernd Diekmann, Richard Gates and Wolfgang Buescher.

*Environmental Science and Pollution Research, 23: 12253-12263, (2016), IF: 2.76.*

Maintaining and preserving the environment from pollutants are of utmost importance. Particulate matter (PM) is considered one of the main air pollutants. In addition to the harmful effects of PM in the environment, it has also a negative indoor impact on human and animal health. The specific forms of damage of particulate emission from livestock buildings depend on its physical properties. The physical properties of particulates from livestock facilities are largely unknown. Most studies assume the livestock particles to be spherical with a constant density which can result in biased estimations, leading to inaccurate results and errors in the calculation of particle mass concentration in livestock buildings. The physical properties of PM, including difference in density as a function of particle size and shape, can have a significant impact on the predictions of particles' behaviour. The aim of this research was to characterize the physical properties of PM from different animal houses and consequently determine PM mass concentration. The mean densities of collected PM from laying hens, dairy cows and pig barns were 1450, 1520 and 2030 kg m−3, respectively, whilst the mass factors were 2.17 × 10−3, 2.18 × 10−3 and 5.36 × 10−3 µm, respectively. The highest mass concentration was observed in pig barns generally followed by laying hen barns, and the lowest concentration was in dairy cow buildings. Results are presented in such a way that they can be used in subsequent research for simulation purposes and to form the basis for a data set of PM physical properties.

**Keywords:** Particulate matter; Particle density; Shape factor; Mass factor; Mass concentration; Livestock buildings.

## B-457. Synthesis; Spectroscopic Characterizations and Biological Activities of Vanadyl(Ii) Folate Compound as A New Anti-DNA Damage and Antioxidant Agent.

Moamen S. Refat, Samy M. El-Megharbel, Mohamed I. Kobeasy, Ghada I. Mahamoud, Mohamed A. Al-Omar and Ahmed M. Naglah.

*Journal of Molecular Liquids, 220: 468-477, (2016), IF: 2.74.*

New oxovanadium(IV) folate [(VO)2(FO)(NH4)2(SO4)2] complex was synthesized by the reaction between vanadyl(II) sulfate and folic acid vitamin B9 drug in an alkaline media. Elemental analysis shows 1:2 ligand to metal ion stoichiometry and the conductance data deduced that oxovanadium(IV) folate complex has non-electrolytic nature. IR spectrum of oxovanadium(IV) complex reveal that folic acid acts as a binuclear chelate via deprotonation of both carboxylic groups. The biological section aimed to test the toxicity of carbofuran orally for male rat and oxidative stress of the sub-lethal (2.4 mg/kg b.w, 1/25 LD50) dose on the lipid peroxidation level (LPO), reduced glutathione content (GSH), antioxidant enzymes, superoxide dismutase (SOD), catalase (CAT), glutathione peroxidase (GPx) and glutathione-S-transferase (GST) activities of testicular tissue. The protective efficiency of vanadylfolate (50 mg/kg b.w) only or combined together carbofuran was tested. The taken of carbofuran orally led to elevation in LPO level by 2.10 fold in comparable with control. The efficient of antioxidant enzymes using of vanadylfolate in combined with carbofuran or its only were decreased by (25.48%, 18.60%, 22.46% and 16.62%) but the GSH level increased by 37.18% in testicular tissue in comparison with controller sample. The DNA damaging of carbofuran and

vanadylfolate were assessed using single cell gel electrophoresis (SCGE) data.
**Keywords:** Carbofuran; Vanadyl(II) Ion; Folic acid; Testicular Tissue; Antioxidant enzymes; DNA damage.

## B-458. Enhancing Oxidative Stability of Biodiesel Samples Subjected to Cations Contamination During Storage Using Lantana Camara L. (Verbanaceae) Leaves Extracts.

Samir Abd-elmonem A. Ismail and Rehab Farouk M. Ali.

*Biochemical Engineering Journal;110:143-151,(2016), IF:2.463*

activity and free radial scavenging capacity of 80% ethanol; methanol; ethyl acetate and chloroform extracts of Lantana camara L. (Verbenaceae) leaves (LCL). Furthermore; the impact of the selected extract on the oxidative stability of biodiesel; measured as peroxide; P-anisidine and totox value; was evaluated using biodiesel samples contaminated with 1000 and 2000 ppm of Fe3+; Cu2+ and Al3+ and stored for different periods (0; 4; 8 and 12 days). The highest total phenolic contents 46.50 mg GAL/g dry weight (DW); total flavonoids (16.06 mg catechin/ g DW); DPPH radical scavenging activity (87.69%) and reducing power activity (2.90; absorbance value) were recorded for aqueous ethanol (ethanol:water; 80:20 v/v) extract. The peroxide values of biodiesel samples subjected to 1000 and 2000 ppm of Fe3+; Cu2+ and Al3+ contamination at the end of the storage period (12 day) were about (1.45;1.96); (1.27;1.61) and (1.21;1.52) times as high as in control sample without additives; respectively. Biodiesel samples subjected to 2000 ppm of Cu2+ and Fe3+ had the highest values of p-AV (17.89 and 16.37) and Totox (92.98 and 85.23) at the end of the storage period; respectively. Addition of LCL extract at level of 800 ppm caused decreases in the formation of peroxide ranged from 53.48 to 66.00%; in the formation of secondary oxidation products from 47.58 to 69.64% and in Totox values varied from 54.56 to 66.25% compared to those samples subjected to metal contamination without antioxidant.
**Keywords:** Antioxidant; Oxidative; Stability fuel metals-cations.

## B-459. Germline Recombination in A Novel Cre Transgenic Line; Prl3b1-Cre Mouse.

Al-Sayed Al-Soudy, Tsuyoshi Nakanishi, Seiya Mizuno, Yoshikazu Hasegawa, Hossam H. Shawki, Megumi C. Katoh, Walaa A. Basha, Abdelaziz E. Ibrahim, Hany A. El-Shemy, Hiroyoshi Iseki, Atsushi Yoshiki, Youhei Hiromori, Hisamitsu Nagase, Satoru Takahashi, Hisashi Oishi and Fumihiro Sugiyama.

*Genesis, 54: 389-397, (2016), IF: 2.165*

Spermatogenesis is a complex and highly regulated process by which spermatogonial stem cells differentiate into spermatozoa. To better understand the molecular mechanisms of the process, the Cre/loxP system has been widely utilized for conditional gene knockout in mice. In this study, we generated a transgenic mouse line that expresses Cre recombinase under the control of the 2.5 kbp of the Prolactin family 3, subfamily b, member 1 (Prl3b1) gene promoter (Prl3b1-cre). Prl3b1 was initially reported to code for placental lactogen 2 (PL-2) protein in placenta along with increased expression toward the end of pregnancy. PL-2 was found to be expressed in germ cells in the testis, especially in spermatocytes. To analyze the specificity and efficiency of Cre recombinase activity in Prl3b1-cre mice, the mice were mated with reporter R26GRR mice, which express GFP ubiquitously before and tdsRed exclusively after Cre recombination. The systemic examination of Prl3b1-cre,R26GRR mice revealed that tdsRed-positive cells were detected only in the testis and epididymis. Fluorescence imaging of Prl3b1-cre,R26GRR testes suggested that Cre-mediated recombination took place in the germ cells with approximately 74% efficiency determined by in vitro fertilization. In conclusion, our results suggest that the Prl3b1-cre mice line provides a unique resource to understand testicular germ-cell development. genesis 54:389–397, 2016. © 2016 Wiley Periodicals, Inc.
**Keywords:** Prl3b1; Placental lactogen; Testis; Spermatogenesis; Cre/Loxp; Mouse.

## B-460. Optimization of Growth Conditions for Purification and Production of L-Asparaginase by Spirulina Maxima.

Hanaa H., El Baky and Gamal S. El Baroty.

*Evidence-Based Complementary and Alternative Medicine,, Article ID 1785938, 7 1-0, (2016), IF: 1.931.*

L-asparaginase (L-AsnA) is widely distributed among microorganisms and has important applications in medicine and in food technology sectors. Therefore, the ability of the production, purification, and characterization of AsnA from Spirulina maxima (SM)were tested. SMcultures grown in Zarrouk mediumcontaining different N2 (in NaNO3 form) concentrations (1.25, 2.50, and 5.0 g/L) for 18 days contained a significant various quantity of dry biomass yields and AsnA enzyme levels. MS L-AsnA activity was found to be directly proportional to the N2 concentration. The cultures of SMat large scales (300 L medium, 5 g/L N ) showed a high AsnA enzyme activity (898 IU), total protein (405 mg/g), specific enzyme activity (2.21 IU/mg protein), and enzyme yield (51.28 IU/L) compared with those in low N2 cultures. The partial purification of crude MS AsnA enzyme achieved by 80% ammonium sulfate AS precipitated and CM-Sephadex C-200 gel filtration led to increases in the purification of enzyme with 5.28 and 10.91 times as great as that in SM crude enzymes. Optimum pH and temperature of purified AsnA for the hydrolyzate were 8.5 and 37 ± 0.2 C, respectively. To the best of our knowledge, this is the first report on L-asparaginase production in S. maxima.
**Keywords:**L-Asparaginase; Spirulina maxima; Enzyme activity; Enzyme purification.

## B-461. Analysis of the Dust Emissions from a Naturally Ventilated Turkey House Using Tracer Gas Method.

Ehab Mostafa, Bernd Diekmann, Wolfgang Buescher and Till Schneider.

*Environmental Monitoring and Assessment, 188: 1-15, (2016), IF: 1.633.*

Particulate matter (PM) emissions are becoming increasingly important in licensing procedures for the construction of new livestock houses or for the modernization of existing ones. Emission predictions require reliable data about emission rates. On this account, it is necessary to obtain information about the emission development and the relevant influencing factors in naturally ventilated turkey houses. The primary objective of the present research was to describe different aspects of PM emissions from a naturally ventilated turkey house. This includes the quantification of PM emissions and descriptions of the relevant influencing factors. Moreover, the tracer gas decay (TGD) method for ventilation rate estimation had to be used. To determine the emission mass flow from livestock buildings, it was necessary to measure the concentration of the target substance in the exhaust air and the airflow volume. The PM concentration measurements were carried out with a light scattering aerosol spectrometer in the exhaust air. The airflow volume was determined using the TGD method. To this purpose, tracer gas was injected into the supply air before the concentration decay was measured in the exhaust air of the building. The main influences on the PM concentration and the PM size distribution were shown to be animal activity and air volume flow. For the turkey barn, the PM emission factor averaged 0.027 g h−1 animal−1 over the entire year. If service times were to be included in the calculation, the emission factor 0.021 g h−1 animal−1, again averaged over the entire year, is well below the regulatory limit.

**Keywords:** Particulate matter emission; Rate air volume Flow Sf6; Naturally ventilated barn.

## B-462.Effects of Plant-Derived Anti-Leukemic Drugs on Individualized Leukemic Cell Population Profiles in Egyptian Patients.

Mourad A. M. Aboul-soud, Hany A. El-shemy , Khalid M. Aboul-enein , Ali M. Mahmoud, Ahmed M. Al-abd and D. A. Lightfoot.

*Oncology Letters, 11: 642-648, (2016), IF: 1.482*

Leukemias are a group of cancer types that originate from blood-forming tissues. In this disease, an abnormally large number of immature white blood cells is produced by the bone marrow. The relationship between treatments with plant-derived drugs and leukemia-associated immunophenotypes (LAIPs) of clinically isolated leukemia cells has yet to be established. The aim of the present study was to develop a preliminary clinical prognostic map for commonly expressed LAIPs in patients clinically diagnosed with leukemia, as well as to assess the potential involvement of LAIPs in the response rate to 10 natural products of plant origin. An increased expression of LAIPs, including CD4, CD14, CD33 and CD34, was considered a surrogate marker of the desired response of leukemia cells to treatment with plant-derived drugs. By contrast, the increased expression of the LAIPs, MPO and DR, was associated with poor prognostic outcomes following treatment with the plant-derived drugs. The results showed that 5 of the 10 plant-derived drugs tested induced the expression of several desirable LAIPs biomarkers. These findings clearly highlight the potential treatment efficacy of certain plant-derived drugs against leukemic cell types.

**Keywords:** Biomarkers; Immunophenotyping; Leukemia; Natural products; Surrogate markers.

## B-463. Suggested Mechanism for the Effect of Sweeteners on Radical Scavenging Activity of Phenolic Compounds in Black and Green Tea.

Emad A. Shalaby, Ghada I. Mahmoud and Sanaa M. M. Shanab

*Frontiers In Life Science, 9: 241-251, (2016), IF: 0.864*

The present work aims to evaluate the relation between the antioxidant activities and phenolic compound contents of two tea samples (green and black) mixed with or without sweeteners (sucrose or aspartame). The aqueous extracts were screened for total polyphenol and flavonoids contents. Antioxidant activities of extracts were tested using 2, 2-diphenyl-1-picrylhydrazyl (DPPH) radical method and 2, 2′-azino-bis [ethylbenzthiazoline-6-sulfonic acid] (ABTS) methods using butylated hydroxyl anisole as standard compound. In addition, we identified polyphenols compounds using high performance liquid chromatography (HPLC). The results indicated that the antioxidant activity was higher against ABTS radical more than DPPH radical. Also, there is positive correlation between the antioxidant activity and phenolic compounds content presented in water extracts of tea samples. The results also indicated that addition of table sugar to green tea significantly decreased the antioxidant activity (from 95.8% to 90.6% with 4.0% sucrose). However, the same table sugar in black tea increased the antioxidant activity (from 87.0% to 91.9% with 4.0% sucrose). The analysis using HPLC showed that caffeine was the most predominant individual compounds in green and black tea without and with 1.0% sucrose (6081.8, 8772.1, 6474 and 3755 µg/100g, respectively). However, cinnamic acid showed the lowest content in the same tea samples (0.21, 0.25, 0.19 and 0.18 µg/100g respectively). Pyrogallol, catechol, epicatechin, ellagic, protocatchuic were significantly higher in green tea than in black tea.

**Keywords:**Tea; Sweetening substances; Sucrose; Antioxidant; Phenolic compounds; Mode of Action.

## B-464. Assessment the Protective Role of Quercetin on Acrylamide-Induced Oxidative Stress in Rats.

Hossam S. El-Beltagi and Mahgoub M. Ahmed

*Journal of Food Biochemistry, 4016: 715-723, (2016), IF:0.832*

This study aimed to elucidate whether quercetin treatment could modulate acrylamide (ACR)-induced DNA damage and oxidative changes in rat brain, liver, kidneys and testes tissues. Fifty adult albino rats were divided into five groups. The first group served as normal control, second group received 50 mg/kg quercetin (QTN) and third group received 20 mg/kg ACR. Fourth and fifth groups received dose of ACR along with 25 or 50 mg/kg QTN, respectively. ACR and QTN were given by oral administrations for 30 days. The results showed that, ACR administration induced significant elevation of alanine transferase, aspartate transferase activities, urea, creatinine and Malondialdehyde levels in serum, whereas, Acetylcholine esterase and testosterone levels were reduced after ACR administration. Moreover, ACR treatment increased Glutathione-S-transferase, Myeloperoxidase, Glutathione peroxidase activity, 8-hydroxy deoxyguanosine, tumor necrosis factor-α and nitric oxide contents in all tissues. QTN significantly improved the previous parameters. It played a role in ameliorating toxic effects of ACR in rats by reducing oxidative stress.Practical Applications , Acrylamide was found

in various fried, deep fried and oven-baked foods that are regularly consumed like chips, crisps and bread, also biscuits, crackers and breakfast cereals. Acrylamide exposure led to increase of alanine transferase, aspartate transferase activities, urea, creatinine and Malondialdehyde levels in serum, whereas, Acetylcholine esterase and testosterone levels were reduced. Moreover, ACR treatment increased Glutathione-S-transferase, Myeloperoxidase, Glutathione peroxidase activity, 8-hydroxy deoxyguanosine, tumor necrosis factor-α and nitric oxide contents in all tissues. Our study revealed the protective role of quercetin on acrylamide-induced oxidative stress in rats. Quercetin regulate the generation of inflammatory markers and increasing antioxidant enzyme activity in rat liver, kidneys, brain and testes tissues.

## B-465. Synergistic Antioxidant Scavenging Activities of Grape Seed and Green Tea Extracts Against Oxidative Stress.

Hossam S. El-Beltagi, Wael El-Desouky and Rania S. Yousef.

*Notulae Botanicae Horti Agrobotanici Cluj-Napoca, 44(2): 367-374, (2016), IF: 0.451.*

Grape seed and green tea extracts are reported to produce antioxidant scavenging activities against free radical toxicity. This study aimed to investigate the hypothesis that a specific combination of these extracts presents a synergistic antioxidant scavenging activities. The extracts of grape seed, green tea and their mixtures were characterized by phytochemical studies and tested for phenolics and flavonoids. In vitro antioxidant activity for individual extract and its mixtures was determined by DPPH, hydroxyl and superoxide free radical scavenging methods. The amount of total phenolics varied among the different extracts and ranged from 43.74 to 67.68 mg of gallic acid equivalents (GAE) / g dry weight, whereas total flavonoids content ranged from 4.25 to 11.66 mg of quercetin equivalents (QU) /g dry weight. The present results suggest that both extracts reported a highly contents of total phenolic and flavonoids compounds, also the mixtures of these extracts can synergistically enhance antioxidant activity. Antioxidant potential from mixture 2 (grape seed extract 200 mg: green tea extract 100 mg) was comparable to that of standard. HPLC results showed that the most abundant components in the mixture 2 extract were epigallocatechingallate while the lowest was the procyanidine.

## B-466. Applying of Low Dose Gamma-Radiation to Enhance T. Harzianum and T. Viride Fungi for Carbofuran Pesticide Biodegradiation.

Abd El-Moneim M.R. Afify, Mohamed A. Abo-El-Seoud, Ghada M. Mohamed and Bassam W. Kassem.

*Fresenius Environmental Bulletin,25:284-291,(2016),IF: 0.372*

This investigation has been carried out to study the possibility of enhancing Trichoderma spp with low dose gamma radiation for biodegradation of carbofuran pesticide. Five fungi strains are identified as Trichoderma spp. including T. harzianum and T. viride, Aspergillus niger, Fusarium oxysporum and Penicillium cyclopium . The results showed that Trichoderma spp. reach its maximum growth using carbofuran concentration of 200 (T. harzianum, and T. viride, 167.6, 222.0 respectvely ). On the other hand Aspergillus niger reach its maimum yieled 203.2 with 20 mg/L while the growth of Fusarium oxysporum and Fusarium oxysporum were dose dependenc. This indicated that the isolates of Trichoderma spp. were potentially useful for carbofuran bioremediation after enchantment by low dose of gamma radiation . The biomass of T. spp strain were increased and reached its maximum at 250 Gy of gamma radiation with Trichoderma spp. as well as T harzianum and T. viride, respectively.

**Keywords:**Carbofuran; Trichoderma harzianum; Trichoderma Viride; Biodegradation; Gamma-Irradiation.

## B-467. Insecticidal Activities of Naphthalenemethanol, Decahydro Derivative and 1 – Phenyl,1- 0Ne, 2,4 Hexadiyne of Chloroform Extract of Artemisia Monosperma by Gc-Ms Spectroscopy.

Abd El-Moneim M.R. Afify.

*Fresenius Environmental Bulletin, 25:4747-4752 (2016) IF:0.372*

Two compounds from chloroform extract of Artemisia monosperma plant had been separated and identified as insecticidal activity. The purified fractions I and fraction II were separated and their chemical structure studied by GC-MS spectroscopic analysis . The results proved the presence of 2 – Naphthalenemethanol,decahydro - Alpha, Alpha, 4a ,8-Tetramethyl-didehydro derive.,[ 2R-( EZ Alpha, 4a alpha, 8 a , beta)} and 1-phenyl,1-0ne, 2,4 hexadiyne which having insecticidal activity against house fly. The above TLC purified fractions which had a single compound (By GC-MS analysis) gave 15 to 20 time more toxic as insecticidal than the crude chloroform extract. Then we could use these natural compounds as insecticidal activities instead of using synthetic compounds to protect human from diseases.

**Keywords:** Artemisia monosperma; Insecticidal; Bicyclohexyl-Ol Derivative; Phenyl-Diacetylene derivative.

## B-468. Comparative Study Between Formalin-Killed Vaccine and Developed Gamma Irradiation Vaccine Against Mannheimia Haemolytica in Rabbits.

Sahar Ahmed, Basem Ahmed, Ghada Mahmoud, Waleed Nemr and Emam Abdel Rahim.

*Turkish Journal of Veterinary and Animal Sciences, 40: 219-224, (2016), IF: 0.352.*

Mannheimia haemolytica is responsible for considerable economic losses to sheep, goats, and cattle and other livestock industries in Egypt. This study aimed to evaluate the effectiveness of a newly developed gamma irradiation vaccine against Mannheimia haemolytica in comparison to a formalin-killed vaccine. Three groups of rabbits were used in this study. Group 1 animals were inoculated with 4 × 109 bacterial cells per dose of the formalin-killed vaccine. Group 2 was inoculated with 2 × 109 bacterial cells per dose of gamma-irradiated vaccine. Group 3 (control group) was injected with 2 mL of sterile PBS. The vaccines were injected subcutaneously into experimental animals twice with 3-week intervals between

inoculations. Three weeks after the second vaccination dose, the animals in all groups were infected with M. haemolytica twice with 1-week intervals between inoculations. Blood samples were collected weekly after the first vaccination until one week after the second M. haemolytica infection challenge. ELISA results revealed that the gamma irradiation vaccine developed in this study provided protective effects that reached high levels at the time of challenge. Furthermore, the second dose of gamma irradiation vaccine could act as a booster dose resulting in increased antibody production.

**Keywords:** Mannheimiosis; Vaccine; Gamma radiation; Formalin-Killed; Elisa.

## B-469. Molecular Identification of Five Egyptian Lady Bird Beetles Based on 28S rDNA (Coleoptera: Coccinellidae).

Jamila Y. Atif, M. M.El-Husseini, H. A. Al-Shemi and Sayeda S. Ahmed.

*Egyptian Journal of Biological Pest Control, 26: 153-156, (2016), IF: 0.152.*

Usingmolecular tool based on 28S rDNA, this study aimed to show the relationshipamong the five coccinellid species: Coccinella undecimpunctata, C.septempunctata, Cydonia vicina isis, C. vicina nilotica, and Hippodamiavariegata, collected from Giza region throughout the years 2013 and 2014.Results revealed that the species, C. undecimpunctata, C. septempunctataand H. variegate were identical to the same specimens species in theGene Bank. Meanwhile, a monophyletic relationship appeared between the species C.v. isis and C. v. nilotica compared to the species Cheilomenessexmaculata. The sequences obtained in this study were deposited in theGene Bank. Analysis of phylogenetic tree Database was performed using UPGAMAmethod by MEGAV6 software.

**Keywords:**Coccinellidae; Cydonia; Hippodamia; Genetic Study; Phylogenic Tree; 28S Rdna Gene.

## B-470. Anti-Diabetic Effect of Chitosan in Alloxan Induced Diabetic Rats.

Abdel-Rahim E. A1, Fouad A. Ahmed, M. S. Abdel-latif and Magda W. Mostafa.

*Research Journal of Pharmaceutical, Biological and Chemical Sciences, 7: 609-6016 (2016).*

Diabetes mellitus (DM) is a complex and multi-various groups of disorders that disturb the metabolism. Chitosan as anti-diabetic agent was studied in diabetic rats. Five groups of rats (Sprague-Dawley) (8 rats for each group) were used, group 1 used as normal control fed on a standard diet whereas groups 2, 3, 4 and 5 were diabetic rats, group 2 was diabetic control. Which fed on a standard diet group 3 rats fed on semi modified Chitosan 5% in diet treatment but group 4 rats ingested 5g chitosan suspended in water by stomach tube (twice weekly) and group 5 rats were drinking drug in water. Feeding period continued for 8 weeks. At the end of the experiment fasting blood samples were obtained from animals in all groups and analyzed for several biochemical parameters. The results showed that rats in groups 3, 4 and 5 attained more body weight than group 2. Serum glucose, malondialdhyde, total lipids, total cholesterol, LDL cholesterol and triglycerides were all increased in diabetic control group. The total antioxidant capacity and HDL cholesterol were decreased. Also liver and kidney functions were elevated. Addition of either chitosan to the diet or diamicron drug in water caused a marked improvement of all three parameters and returned back to near normal values. The conclusion is chitosan supplementation can protect against health hazards exerted due to diabetic mellitus.

**Keywords:** Diabetes mellitus; Alloxan; Chitosan; Drug (Diamicron); Liver function; Kidney functions.

## B-471. Antioxidant and Antiviral Activities of Essential Oils from Callistemon Viminalis and Schinus Molle L.

Ramy M Romeilah, Sayed A Fayed and Ghada I Mahmoud

*Research Journal of Pharmaceutical, Biological and Chemical Sciences, 7: 1982-1993 (2016).*

The essential oils of Callistemon viminalis and Schinus molle leaves from plants grown in Egypt, obtained by hydrodistillation in a Clevenger type apparatus were investigated by GC/MS. The main components of C. viminalis oil were 1,8-cineole (65.92%), α-pinene (12.34%) while the results showed that the major components of S. molle oil were α-phellandrene (25.81%), elemol (11.02%). Both C. viminalis and S. molle oils exhibited strong DPPH scavenging activity, with IC50 values of 72.98 µg/mL and 172.41µg/mL respectively. The antiviral assays were performed with herpes simplex virus type 1 (HSV-1) and using RC-37 cells as a host cell. TC50 (50% cytotoxic concentration) of C. viminalis oil (676.35 µg/mL) demonstrated significantly lower toxicities towards the RC-37 cells than the S. molle oil (476.48 µg/mL). IC50 (inhibitory concentration for 50% of plaques) for HSV-1 of C. viminalis and S. molle oils were 63.73 and 48.06 µg/mL respectively, while SI (Selectivity index = TC50/IC50) of C. viminalis oil (10.61) was higher than S. molle oil (9.91). Both essential oils exhibited high anti-HSV-1 activity by direct interaction with free virus particles. To conclude, C. viminalis and S. molle oils could be a promising source of natural antioxidants and antiviral agents.

**Keywords:** Callistemon viminalis; Schinus molle; Essential Oils; Antioxidant; Antiviral.

## B-472. Bioactive Components in Black Beans for Inhibition of Cancer Cell Growth.

Kamel Eshraq B, Ali Mona M, Fayed Sayed A, and Abdel-Rahim EA.

*Research Journal of Pharmaceutical, Biological and Chemical Sciences, 7: 1068-1080 (2016).*

Legumes are the basic diet in many populations, especially in Africa. They hold high nutritional value and they promote the human health. The aim of this investigation was to study the influence of different processing methods such as soaking, cooking and germination on chemical composition, phenols, tannins , flavonoids content, antioxidant and anticancer activity of black beans .Phenolic compounds of raw and processed black beans was evaluated by HPLC. The antioxidant activity was evaluated by DPPH. Anticancer activities were evaluated on five different cell lines (colon (HCT), breast (MCF7), lung

(A5499), prostate (PC3) and Hela (HELA).The obtained results indicated that black beans showed high protein, ash and fiber content 26.54, 5.22 and 5.58% , respectively. Total phenols, tannins and flavonoids decreased with prolonged soaking time. The reduction percent increased in cooked beans. High DPPH antioxidant activity for raw black beans was observed. After 24 h of germination, phenolic compounds become higher in value. E-vanellic acid represented in highest value (56.94 mg/ 100g) followed by naringin, luteolin and kaempferol (11.31, 9.486 and 2.49 mg/100g). There were differences in total phenols, flavonoids and tannins content have been observed between raw and processed black beans samples and their antioxidant activity. Although antioxidant activity was decreased in the processed samples, ethanol extracts of different processing exhibited cytotoxicity activities on cancer cell lines, raw sample proved to be the most active in antitumoral followed by germinated sample(48h). This study demonstrated that phenolic compounds of black beans is related with soaking, cooking process and germination, and also with their anticancer activity. Strong anticancer activity toward (MCF7) cell line was observed. Anticancer activity realized a noticeable reduction of tumor inhibition after 48 h of germination.

**Keywords:**Legumes; Soaking; Germination; Cooking; Antioxidant; Cytotoxic; Cell line.

## B-473. Biochemical and Physiological Effects of Tio2 and Sio2 Nanoparticles on Cotton Plant Under Drought Stress.

Magdy A Shallan, Hazem MM Hassan, Alia AM Namich and Alshaimaa A Ibrahim.

*Research Journal of Pharmaceutical, Biological and Chemical Sciences, 7(4): 1540-1551 (2016).*

Application of nanofertilizers is one of the promising methods for increasing resources use efficiency and reducing environmental pollutions. This study was carried out to investigate the effects of nano titanium dioxide (nano-TiO2), and nano silicon dioxide (nano-SiO2) on chemical constituents and yield characteristics of cotton plant under drought stress. The cotton plants pre-treated with four concentrations of nano-TiO2 (25, 50, 100 and 200 ppm) or nano-SiO2 (400, 800, 1600 and 3200 ppm) then exposed to drought stress. In general, the drought stress reduced the pigments content, total soluble sugars content, glutathione reductase activity and yield characteristics, while increased total phenolics, total soluble proteins, total free amino acids, proline content, total reducing power, total antioxidant capacity, catalase activity, peroxidase activity and superoxide dismutase activity in comparison with control. The obtained results showed that pretreatment of cotton plants under drought stress with nano-TiO2 or nano-SiO2 caused increasing of pigments content, total soluble sugars, total phenolics, total soluble proteins, total free amino acids, proline content, total reducing power, total antioxidant capacity and antioxidant enzyme activities and enhancement of yield characteristics. The optimum concentration of nano-TiO2 and nano-SiO2 to alleviate the drought stress in cotton plant was 50 ppm and 3200 ppm, respectively. Finally, it can be concluded that foliar application of nano-TiO2 or nano-SiO2 could improve the drought tolerance of cotton plants.

**Keywords:** Drought stress; Cotton; Titanium dioxide; Silicon dioxide; Nanoparticles.

## B-474. Chemical Characterization, Antioxidant and Antihepa Totoxic Activities of Calliandra Haematocephala (Hassk.), Growing in Egypt .

Amr M. Abo-Elhamd, Ahmed M. Aboul-Enein, Samy M. Mohamed, Ahmed S. Shalaby, Usama Konsowa, Emad M. Hassan and Nadia S. Metwally.

*Journal of Chemical and Pharmaceutical Research, 8: 828-845 (2016).*

This study aims to investigate the major constituen ts of hexane fraction, of Calliandra haematocephala (Hassk.) leaves. In addition to, the hepatoprotective and antioxidant activities of the total alcohol extract against carbon tetrachloride (CCl4) -induced liver damage in vivo.C. haematocephala leaves were extracted with methanol, and hexane, fraction of methanol was separated and two major bands and were identified by GC/MS, MS,HNMR. Fatty acids were isolated, methylated and identified by GC/MS. In vivo the hepatoprotective and antioxidant activities of methanol extract against CCl4-induced liver injury was evaluated in rats based on the analysis of biochemical parameters and histopathological studies. The results illustrated that the analysis of hexane fraction led to isolation of lupeol and mixture of sterols. Four major fatty acids (palmitic,oleic, linoleic and linolenic,) were determined. Oral administration of the extract at doses 100 and 200 mg/kg bw. caused significant decrease in the levels of serum ALT, AST, GGT and bilirubin as well as albumin was significantly elevated. Moreover, the extract decreased MDA content and increased the levels of SOD, GSH and CAT compared with intoxicated rats. Also, creatinine and urea were improved as a result of the treatment of the extract. The hepatoprotective and antioxidant effect of the extract may be attributed to phenolics, flavonoids or the saponins content of the extract which may be acting as free radical scavenging effect, inhibiting lipidperoxidation and increasing antioxidant activities suggesting that the alcohol extract of C. haematocephala leaves has potential to be explored as valuable hepatoprotective and antioxidant.

**Keywords:**Calliandra haematocephala (Hassk.); Sterols; Lupeol; Fatty acid; Total phenolics; Fl Avonoids; Antioxidant; Hepatoprotective activities.

## B-475. Chemical Constituents and Antimicrobial Activity of Different Annona Species Cultivated in Egypt.

Mona A. Mohammed, Souad E. El-Gengaihi, Ahmed M. Aboul Enein, Emad M. Hassan, Osama K. Ahmed and Mohsen S. Asker.

*Journal of Chemical and Pharmaceutical Research, 8: 261-271 (2016).*

Three Annona species, A. squamosa, A. cherimola and A. Abdel Razik were investigated for their volatile oils in leaves, qualitatively and quantitatively. GC/MS recorded that A. Cherimola contains 27.59% isocaryophylline. A. squamosa contains the highest percentage of copaene, α- pinene and β pinene in the following amounts, 17.06, 9.96 and 12.99 respectively. The oil showed potent antimicrobial activity against different pathogenic organisms. The investigation

deals with the antioxidant content of the fixed and volatile oils. The fixed oil of the seeds contains higher amount of oleic and linoleic acids, where the the degree of the unsaturated fatty acids reaches over 70%.

**Keywords:** Quantitative; Qualitative analyses volatile; Fixed Oils; Antimicrobial; Antioxidant.

## B-476. Chitosan, Gymnema Sylvestre and Ascorbic Acid as Complementary Medicine Against Hypercholesterolemia in Rats.

Sayed A Fayed, Ghada I Mahmoud and Ramy M Romeilah.

*Research Journal of Pharmaceutical, Biological and Chemical Sciences, 7: 1200-1207 (2016).*

The present study was performed to evaluate the curative effects of chitosan and the combination of chitosan, Gymnema sylvestre and ascorbic acid (CGA) supplementation on oxidative stress and hypercholesterolemia induced in hypercholesterolemic rats. The plasma lipid levels, transaminases, lactate dehydrogenase activities, glucose, malondialdehyde and whole blood reduced glutathione, the activities of superoxide dismutase, glutathione peroxidase in erythrocytes and plasma glutathione reductase, glutathioneS-transferase and catalase were examined in hypercholesterolemic rats supplemented or not supplemented with chitosan or CGA. The results indicated that hypercholesterolemic rats fed basal or hypercholesterolemic diets revealed significantly higher mean plasma levels of total lipids, total cholesterol, triglycerides, low density and high density lipoprotein cholesterol, Atherogenic index, transaminases (ALT and AST), lactate dehydrogenase, malondialdehyde and glucose, in addition, significantly lower mean activities of enzymatic antioxidants and blood reduced glutathione were noted, compared to normal control. However, in hypercholesterolemic rats receiving the CGA supplement diet for two months, all these parameters were significantly better than those in hypercholesterolemic rats receiving basal or hypercholesterolemic diet. On the other hand, non significant improvement was observed by chitosan supplement diet. These results referred to possibility using CGA as curative natural supplement as hypocholesterolemic and antioxidative agents in hypercholesterolemic rats.

**Keywords:** Chitosan; Gymnema sylvestre; Ascorbic acid; Complementary medicine; Hypercholesterolemia; Oxidative stress.

## B-477. Coragen (Chlorantraniliprole) Insecticide Effects on Male Albino Rats.

Shallan Magdy A., Abdel-Mobdy Yasmin E, Hamdi Eman and Abdel Rahim Emam A.

*Research Journal of Pharmaceutical, Biological and Chemical Sciences, 7: 1536-1545 (2016).*

The study aimed to evaluate toxic effects of insecticide Coragen (Chlorantraniliprole) doses of 1/20, 1/40 and 1/60LD50 orally on albino rat males during experimental period (every 2 consecutive days for 90 days). Rats which administered coragen showed significant decrease in body weight gain and daily body weight gain. Organs weight (heart, kidney and brain) were decreased but spleen and liver showed a significant increase compared with control. Also, there were significant increase in AST and ALT activities, significant changes in the haematological indices RBC count, haemoglobin percentage, haematocrit and WBC count. Also, a slight increase in urea was recorded but creatinine almost remains stable in all intoxicated rats. Coragen 1/20LD50 rats showed mild histopathological changes in liver and kidney compared to control. The results of the present study advice to avoid exposure to any pesticide however how much it is safe to avoid hazard risk.

**Keywords:**Chlorantraniliprole; Coragen; Ast; Alt; Urea; Creatinine; Haemoglobin Rbc; Wbc.

## B-478. Determination of Antioxidant and Anti-Inflammatory Activities,as Well as in Vitro Cytotoxic Activities of Extracts of Anastatica Hierochuntica (Kaff Maryam) Against Hela Cell Lines.

Faten Abou-Elella, Eman A. Hanafy and Yahaya Gavamukulya

*Journal of Medicinal Plants Research, 10(7): 77-87 (2016).*

Anastatica hierochuntica L. is distributed throughout the Arabian Peninsula, and North Africa. It is locally called "Kaff Maryam". All parts of the plant are used in folk medicine. This study aimed to investigate possible antioxidant activity of various extracts of Kaff Mariam, anti-inflammatory activities, as well as in vitro cytotoxic activities. Five extract types were used, namely, the whole ethanolic extracts, ethyl acetate, petroleum ether, water, and butanol extracts. The explored items included determination of total phenolics using the Folin-Ciocalteu assay and total flavonoids using Muller's method, anti-oxidant activity using three assays (2, 2'-Azinobis [3-ethylbenzothiazoline-6-sulfonic acid]-diammonium salt (ABTS), reducing power, and 2, 2-diphenyl-1-picrylhydrazyl (DPPH)), membrane stabilization test for anti-inflammatory studies, as well as in vitro cytotoxic activities against HeLa cell lines using the 3-(4, 5-dimethylthiozol-2-yl)-2, 5-diphenyltetrazolium bromide (MTT) assay. The results obtained indicated high flavonoid and phenolic contents in all the five extracts types. All extracts registered high antioxidant activity using three assays, but generally, the ABTS assay recorded the highest antioxidant activity as compared to the reducing power and DPPH methods. The membrane stabilization test showed that extracts of Kaff Maryam had good anti-inflammatory activity. Extracts of Kaff Maryam also registered very good cytotoxic activities against HeLa cell lines. Kaff Maryam extracts have good antioxidant, anti-inflammatory, and cytotoxic activities and the results of this study provide the basis for further investigation of Kaff Maryam for potential identification of novel bioactive compounds with therapeutic properties.

**Keywords:**Anastatica hierochuntica; Kaff maryam; Antioxidant; Anti-Inflammatory; Hela cell lines; Cytotoxicity.

## B-479. Effect of Lead Stress on the Hydrolytic Enzyme Activities and Free Radical Formation in Radish (Raphanus Sativus L.) Plant.

Hossam S. El-Beltagi, Amal A. Mohamed, Abdel-Kader M. Abdel-Samad and Mohamed M. Rashed.

*American Journal of Biochemistry and Molecular Biology, 6: 84-94 (2016).*

**Background and Objective:** The effect of lead on several metabolic reactions in the radish plant has been investigated. The present study was conducted to evaluate the potential role of enzymes activity, their isoenzyme profile pattern and free radical formation as biomarkers of Pb pollution in the radish (Raphanus sativus L.) plant. **Materials and Methods:** Varied concentrations of Pb(NO3)2 ranging from 25-500 ppm in the growth media were used. The plant samples were collected after 40 days growth period. Lead and micronutrients concentration, the profile of electron spins resonance determination and hydrolytic enzymes activities were analyzed. **Results:** Lead concentrations in roots and leaves increased with increasing Pb concentration in the tested media, however the most accumulation were observed in leaves. Generally, the concentration of micronutrients such as Fe, Zn, Mn and Cu declined in leaves compared to the roots. Results of the profile of Electron Spin Resonance (ESR) determination showed a decrease in unstable free radical level in the roots, followed by a significant increase with increasing Pb concentrations. The Pb induced changes in some enzymes activity and its isoenzyme profiles such as acid phosphatase (AP), esterase (EST) and polyphenol oxidase (PPO) in leaves and roots of radish plant. Results of isoenzymes suggested that the staining intensities of isoform patterns were consistent with the changes of the activities assayed in solutions. **Conclusion:** These results suggested that (Raphanus sativus L.) seedlings may have a better protection against oxidative stress by increasing antioxidant enzymes activity exposed to Pb toxicity.

**Keywords:**Lead stress; Radish; Electron spins resonance; Acid phosphatase; Esterase; Polyphenol oxidase.

## B-480. Enhancement of Antioxidant Enzymes Activities, Drought Stress Tolerances and Quality of Potato Plants as Response to Algal Foliar Application.

Hanaa H. Abd El Baky, Osama A. Nofal and Gamal S. El Baroty.

*Recent Patents on Food, Nutrition and Agriculture, 8(1): 70-77 (2016).*

**Background:** Different types of environmental stress may induce several physiological, biochemical and molecular responses in several crop plants. According to a patent study, several types of low antioxidant defense compounds and the activity of various antioxidant defense enzymes are induced in plants grown under various biotic and abiotic stress actors. Methods: In this work, the responses of potatoes plant treated with algae extract to drought stress were examined by evaluating the crop yield of tuber, cellular biological compounds (total carbohydrates and proteins), mineral composition and enzyme and non-enzyme antioxidant systems and total oxidative compounds. **Results:** The yield of tuber, concentration of low antioxidant defense compounds (glutathione, ascorbate, carotenoids, total phenol, flavonoids and tocopherols) and the activity of various antioxidant defense enzymes (catalase CAT, peroxidase POD, ascorbate peroxidase APX and superoxide dismutase SOD) in tuber of treated potato plants with algae extract were significantly increased compared with that in non-treated plants. In ddition,**essential elements:** Fe, K, Ca, Mg and P were accumulated at high concentration in treated plant than that in untreated plants. The screening of antioxidant activity of the ethanolic extract of tubers potatoes treated with algae extracts using the di-(phenyl)-(2,4,6-trinitrophenyl) minoazanium radical (DPPH) assay radical-scavenging showed an appreciable reduction of the stable radical DPPH with an IC50 of 75 µg/ml. **Conclusion:** The results suggest that the algae foliar extracts application can improve non-enzymatic and enzymatic antioxidant defense systems in potatoes plant cultivated under drought stress conditions, and it may be recommended for application in arid and semiarid regions.

**Keywords:**Algal foliar application; Antioxidant compounds; Drought stress; Potato plants; Potato tuber quality.

## B-481. Evaluation of Antioxidant and Metal Chelating Activities of Protein Hydrolysates Produced from Leather Waste by Alkaline and Enzymatic Hydrolysis.

Jacob Rania H, Hassan HMM and Afify AS.

*Research Journal of Pharmaceutical, Biological and Chemical Sciences, 7: 910-919 (2016).*

The objective of this study was to evaluate antioxidant and metal chelating activities of leather protein hydrolysates (LPHs). The hydrolysates were produced from chrome-containing leather waste (CCLW) by alkaline hydrolysis (CaO or KOH) and enzymatic hydrolysis (Protease or trypsin). Degree of hydrolysis (DH), total amino acid content, amino acid composition, DPPH radical scavenging and iron and copper chelating activities of each hydrolysate were determined. Results showed that the highest DH percentage was recorded with LPH by CaO treatment (46.86%) and followed by KOH treatment (31.81%) then protease treatment (1.04%) and trypsin treatment (0.57%). The LPH obtained by CaO treatment contained the highest concentration of free amino acids (246.65 mg/g waste) and the highest Fe+2 chelating activity (85.54% at concentration 0.20 mg/ml) compared with the other treatments. The LPH obtained by enzymatic hydrolysis possessed the higher DPPH scavenging and Cu2+ chelating activities than LPH obtained by alkaline hydrolysis. It was concluded that the alkaline hydrolysis is a suitable and economically beneficial method to produce LPH. The LPH is an economic and natural source of amino acids and good antioxidant and metal chelating agents in plant and animal nutrition.

**Keywords:**Leather waste; Protein hydrolysates; Amino acids; Antioxidant; Metal chelating.

## B-482. Free Radical Scavenging Activity of Three Different Flowers-Hibiscus Rosa-Sinensis, Quisqualis Indica and Senna Surattensis.

Abd El-Moneim Mohamed Radwan Afify and Hazem Mohamed Mahmoud Hassan.

*Asian Pacific Journal of Tropical Biomedicine, 6(9): 771-777 (2016).*

**Objective:** To evaluate three flowers of Hibiscus rosa-sinensis (H. rosa-sinensis), Quisqualis indica (Q. indica) and Senna surattensis (S. surattensis) for their antioxidant activity by different methods in addition to total phenolic, flavonoid and pigment contents. **Methods:** Antioxidant activity of water, ethanol and absolute ethanol extracts of three flowers, H. rosa-

sinensis, Q. indica and S. surattensis was evaluated. The antioxidant activity was assessed by 1,1-diphenyl-2-picrylhydrazyl free radical scavenging activity, ferrous chelating activity, reducing power, nitric oxide scavenging activity, hydroxyl radical scavenging activity as well as total antioxidant capacity. Total flavonoids, total phenols and total pigments including chlorophylls and carotenoids were measured for the three flowers. **Results:** The results showed that the highest total antioxidant capacity at concentration of 500 mg/L was found in S. surattensis as 0.479 ± 0.001. Scavenging activity of H. rosasinensis, Q. indica and S. surattensis flower extracts against 1,1 diphenyl-2- picrylhydrazyl radical showed the highest activity of (90.20 ± 0.29)% with 500 mg/L. Phytochemical screening of the three flowers extracts were carried out for alkaloids, flavonoids, saponins, tannins, steroids, glycosides, terpenoids, amino acid and mucilages. H. rosa-sinensis showed the total phenolic in water extract of (235.77 ± 14.31) mg/100 g, the other two flowers Q. indica and S. surattensis had the total phenolic in ethanol extracts of (937.70 ± 25.06) and (850.30 ± 13.81) mg/100 g, respectively. On the other hand total flavonoids were identified in absolute ethanol extracts in the three flowers [(32.83 ± 1.34), (49.24 ± 4.87) and (2.79 ± 0.23) mg/100 g, respectively]. **Conclusions:** The extracts in the constituents of the three flowers could be used as additives as supplement fractions in foods.

**Keywords:**Free radical; Antioxidant; Hibiscus rosa-Sinensis; Quisqualis indica; Senna surattensis.

## B-483. Hypocholesterolemic Effects of Diets Containing Different Levels of Kishk as a Dried Fermented Milkewhole Wheat Mixture in Experimental Rats.

Rehab F.M. Ali.

*Journal of Ethnic Foods, 3: 117-123 (2016).*

**Background:** Kishk is a popular traditional functional food in Egypt. This study was performed to investigate the effects of different levels of kishk as a dried fermented milk/whole wheat mixture on growth performance, relative weight of organs, lipid profile, and some biochemical parameters in rats fed a cholesterol-rich diet. **Methods:** Forty male rats were assigned to five groups, each consisting of eight rats. The first one presents the negative control group that received the basal diet, while the second group that serves as the positive (þ) control group received a high-cholesterol diet (HCD). The last three groups received HCD supplemented with 10%, 20%, and 30% of kishk. **Results:** Rats fed diets containing various levels of kishk for 8 weeks had significantly ($p < 0.05$) lower body weights compared with the rats of both negative and positive groups. The liver/body weight ratio significantly increased in rats fed HCD compared with the control rats. Incorporation of kishk into the HCD at levels of 10%, 20%, and 30% significantly (p 0.05) decreased the change of liver/body weight ratio by 14.46%, 17.51%, and 18.78%, respectively, when compared with the HCD group. Results also indicate that rats fed HCD had a state of dyslipidemia, compared with the negative control group. Administration of HCD supplemented with various levels of kishk for 8 weeks significantly ($p < 0.05$) attenuated the increases in serum cholesterol, low-density lipoprotein cholesterol, triglyceride concentration, and atherogenic indices, and increased high-density lipoprotein cholesterol in a dose-dependent manner compared with the HCD group. Activities of liver enzymes (alanine transferase and aspartate transferase) as well as kidney function parameters (urea, uric acid, and creatinine) were elevated in the HCD group compared with the negative control group. **Conclusion:** Consumption of HCD supplemented with various levels of kishk for 8 weeks induced a significant protective effect reflected in the reductions of the serum levels of aspartate transferase and alanine transferase, as well as kidney functions (uric acid, urea, and creatinine).

**Keywords:** Biochemical; Function Food; Hypercholesterolemia; Kishk; Whole Wheat.

## B-484. Identification of Phenolic Compounds from Banana Peel (Musa Paradaisica L.) as Antioxidant and Antimicrobial Agents.

Ahmed M. Aboul-Enein, Zeinab A. Salama, Alaa A. Gaafar, Hanan F. Aly, Faten A bou-Elella1 and Habiba A. Ahmed.

*Journal of Chemical and Pharmaceutical Research, 8(4: 46-55 (2016).*

This study was carried out to investigate the chemical composition and biological activity of banana peel extracts, the efficiency of the different solvent systems: aqueous, 80 % methanol, 80% ethanol and 80% acetone was used for extraction of phenolic, flavonoid and tannin compounds. Banana peel relative antioxidants potential by four assays DPPH·, Fe2+-chelating, Reducing power and ABTS·+ inhibitor activities was evaluated. Analysis showed that the percentage of moisture, protein, crude fat and total carbohydrates were 88.10, 13.42, 7.57, 10.44 and 68.31 g/100g DW respectively. For mineral content, potassium is the major element found in banana peel was (9.39 % of DW) followed by magnesium, calcium, sodium and phosphorus were (0.71, 0.44, 0.18 and 0.09 % of DW), respectively. Also, the content of microelement including iron, manganese, zinc and copper were 96.50, 35.01, 27.95 and 3.37 ppm, respectively. Methanolic extract (80%) had the highest content of total phenolic, flavonoid and tannin were 17.89, 21.04 and 24.21 mg /g DW respectively. Most of acetone banana peel extracts (80%) was found to be highest antioxidant and antimicrobial activity at 600 ppm against gram positive and negative bacteria, fungi and yeast. The phenolic profiles of banana peel acetone extract was identified by HPLC. The main phenolic compounds was chyrsin, qurectein and catchin. These results clearly encourage the application of banana peel as a potent natural source of antioxidant and antimicrobial sources.

**Key words:** Antioxidant; Antimicrobial; banana peel; HPLC.

## B-485. Phenolic Compounds from Grape Wastes and Their Impact in Neurodegenerative Disease.

Souad El Gengaihi, Emad M. Hassan, Abeer Y. Ibrahim, Faten M. Aboul Ella and Doha H. Abou Baker

*Journal of Chemical and Pharmaceutical Research, 8 (4): 207-217 (2016).*

Twelve phenolic compounds were isolated from Thompson seedless grape and Grenache Noir (GN) wastes. These compounds were identified as quercetin 3-O-β-D-glucopyranosyl (1→2)-O-β-D-glucopyranoside, quercetin-3-O-α- L-rhamnopyranosyl (1→6)-O-β-D-glucopyranoside, quercetin-3-O-β-D-glucopyranoside, kaempferol-3-O-β-

Dglucopyranoside, kaempferol-3-O-β-D-galactopyranoside, kaempferol-7-O-β-D-glucopyranoside, quercetin, catechin, isorhamnetin, gallic acid, cinnamic acid and ferulic acid. All structures were characterized by spectroscopic analyses and comparisons with the previously reported data. Two of the isolated compounds, gallic and catechin revealed a power full antioxidant activity which due to its hydroxyl groups. The present study has been designed also to explore the possible role of grape pomace extract against aluminium chloride-induced neurotoxicity in rats. Aluminium chloride (70 mg/kg) was administered daily for six weeks that significantly increased cognitive dysfunction and oxidative damage as indicated by a rise in nitrite oxide concentration. Chronic administration of grape pomace extract (13 and 129 mg/kg) daily to rats for a period of 6 weeks significantly improved the memory performance tasks of rats, attenuated oxidative stress (superoxide dismutase and catalase), decreased acetylcholinesterase activity. Results showed that BDNF, Bcl-2 and AChE return to their normal value after administration of the extract. This study demonstrated the neuroprotective potential of grape waste extract in aluminium chloride-induced cognitive dysfunction and oxidative damage.

**Keywords:** Grape Waste; Phenolic Compounds; Antioxidant Activity; Alzheimer'S Diseas.

## B-486. Protective Effect of Zinc, Selenium, Vitamin C, E and Epicatechine on Cadmium–Induced Toxicity and Disturbances in the Kidney, Liver, Bone, Lipid Metabolism and Oxidative Stress in Rats.

Ismail SA, and Roquia I Rizk.

*Research Journal of Pharmaceutical, Biological and Chemical Sciences, 7: 647-655 (2016).*

The aim of the present study is to investigate the protective effect of zinc (6.13 mg /kg bw), selenium (0.4 mg /kg bw), vitamin C (100mg /kg bw), vitamin E (40 mg /kg bw) and epicatechine (4.5 mg /kg bw) on cadmium – exposed rats (1.23 mg /kg bw), 5 times per week for 30 days. Zn+2 significantly decreased the elevated level of urea in serum, but creatinine has still been at a higher level. Serum renal markers, β2 microglobulin (β2 MG) concentration and the activities of N-acetyl –β-D glucosaminidase (NAG) and alanine aminopeptidase (AAP) were significantly decreased by cadmium and did not return to the normal level when using the antioxidants.While epicatechine increased the NAG activity again. Bone resorption marker, Ctelopeptide of collagen-alpha-(1) chain (CTX-1) was increased by Cd and declined again by Zn+2 and all antioxidants except Se. The oxidative stress biomarkers, serum glutathione peroxidase (GPx) activity was decreased by cadmium and improved by all protective factors in the present study, while the elevated level of malonaldehyde (MDA) was ameliorated by Zn only. The protective factors, except vitamin C, decreased the elevated level of AST, in cadmium-induced toxicity. In addition, Se, vitamins C and E improved the lowered level of albumin. The used protective antioxidants improved the elevated levels of cholesterol, LDL-C and triglycerides in serum occurred by cadmium toxicity. Our results suggest that Zn+2 and some antioxidants may protect against cadmium-induced toxicity.

**Keywords:** Cadmium; Zinc; Antioxidants; Bone resorption; Nephrotoxicity; Hepatotoxicity.

## B-487.The Influence of Lithovit Fertilizer on the Chemical Constituents and Yield Characteristics of Cotton Plant Under Drought Stress.

Magdy A. Shallan, Hazem M.M. Hassan, Alia A.M. Namich and Alshaimaa A. Ibrahim.

*International Journal of Chemtech Research, 9(8): 1-11 (2016).*

Nano-fertilizers are used recently as an alternative to conventional fertilizers for slow release and efficient use by plants. This study was carried out to evaluate the effects of Lithovit (nano-CaCO3) fertilizer on chemical constituents and yield characteristics of cotton plant under drought stress. The cotton plants pre-treated with four concentrations of nano-CaCO3 (3000, 6000, 9000 and 11000 ppm) then exposed to drought stress. The obtained results showed that pretreatment of cotton plants under drought stress with nano-CaCO3 caused increase of pigments content, total soluble sugars, total phenolics, total soluble proteins, total free amino acids, proline content, total reducing power, total antioxidant capacity and antioxidant enzyme activities and enhancement of yield characteristics. The optimum concentration of nano-CaCO3 to alleviate the drought stress in cotton plant was 11000 ppm. Finally, it can be concluded that foliar application of nano-CaCO3 can reduce the adverse effects of drought on cotton plants.

**Keywords:**Drought stress; Cotton; Lithovit; Nanoparticles; Chemical constituents; Yield.

## B-488. Improved Salinity Tolerance by Phosphorus Fertilizer in Two Phaseolus Vulgaris Recombinant Inbred Lines Contrasting in Their P-Efficiency

A. Bargaz, R. M. A. Nassar, M. M. Rady, M. S. Gaballah, S. M. Thompson, M. Brestic, U. Schmidhalter and M. T. Abdelhamid

*Journal of Agronomy and Crop Science, 202: 497-507, (2016), IF: 2.565.*

Legumes' sensitivity to salt is exacerbated under growth conditions requiring nitrogen fixation by the plant. Phosphorus (P) deficiency is widespread in legumes, especially common bean (Phaseolus vulgaris L). To examine the perfor- mance of P. vulgaris under salt stress conditions, a field experiment was con- ducted using two recombinants inbred lines (RILs) 115 (P-deficiency tolerant) and 147 (P-deficiency susceptible), grown under different salinity levels (L) (1.56, 4.78, and 8.83 dS m-as LI, L2, and L3, respectively) and supplied with four P rates (0, 30, 60, and 90 kg ha-1 P as P0, P30, P60, and P90, respectively) in order to assess the impact of P on salt tolerance. Results indicate that growing both RILs at P60 or P90 under all salinity levels (especially L1) significantly increased total chlorophyll, carotenoids, total soluble sugars, total free amino acids, and proline. Increasing P supply up to P60 under all salinity levels significantly induced higher accumulation of P, K+, Ca2+ and Mg2+ leaves in both RILs. Based on quadratic response over all locations, the maximum seed yield of 1.465 t ha-1 could be obtained at could application of P 81.0 kg ha-1 in RIL115, while seed yield of 1.275 t ha-1 be obtained with P rate of 78.3 kg ha-1 in RIL147. RIL115 exhibited more salt-tolerance with positive consequence on plant biomass and grain yield stability. Improved salt tolerance

through adequate P fertilization is likely a promising strategy to improve P. vulgaris salinity tolerance and thus productivity, a response that seems to be P-rate dependent.
**Keywords:**Common bean; Phaseolus vulgaris; Phosphorus Efficiency; Salt stress.

## B-489. Dual Application of 24-Epibrassinolide and Spermine Confers Drought Stress Tolerance in Maize (Zea Mays L.) by Modulating Polyamine and Protein Metabolism.

Neveen B. Talaat and Bahaa T. Shawky

*Journal of Plant Growth Regulation, 35: 518-533, (2016), IF:2.166*

No information is available concerning the influence of dual application of 24-epibrassinolide (EBL) and spermine (Spm) on the nitrogen metabolism in plants subjected to drought conditions. As a first report, this investigation assesses the role of EBL, Spm, and their dual application on polyamine and protein pools in water-stressed plants. It explores the ameliorative effects of these foliar applications under water deficiency. Two maize hybrids (Giza 10 and Giza 129) were treated with or without EBL and/or Spm foliar applications under well-irrigated and drought-stressed conditions (75 and 50 % of field capacity). Dual application (25 mg l-1 Spm ? 0.1 mg l-1 EBL) significantly relieved the drought-induced inhibition on the activities of ribulose-1,5-bisphosphate carboxylase and nitrate reductase and the contents of relative water, nitrate, and protein, particularly in hybrid Giza 129. Changes in the content of free polyamines and in the activity of polyamine biosynthetic and catabolic enzymes were detected when water-stressed plants were treated with EBL and/or Spm. Putrescine content and arginine decarboxylase activity were significantly increased in stressed hybrid Giza 10 plants treated by the dual application. However, spermidine and Spm levels as well as ornithine decarboxylase and S-adenosylmethionine decarboxylase activities were significantly increased in stressed hybrid Giza 129 plants treated with the dual application. Diamine oxidase, polyamine oxidase, protease activity, carbonyl content, and ethylene formation were increased in response to water stress and significantly decreased when stressed plants were treated by the dual application. Total free amino acids, phenols, and flavonoids concentration were increased with the increasing water stress level, moreover, they further increased in stressed plants treated with the dual application. Overall, the combined utilization of EBL and Spm serves as complementary tools to confer plant drought tolerance by altering polyamine, ethylene, and protein levels.
**Keywords:**24-Epibrassinolide maize (Zea Mays L.) Polyamines pool protein content; Spermine water stress.

## B-490. Active Yeast Extract Counteracts the Harmful Effects of Salinity Stress on the Growth of Leucaena Plant.

Rania M.A. Nassar , Nermeen T. Shanan and Faten M. Reda

*Scientia Horticulturae, 201: 61-67, (2016), IF: 1.538*

The current investigation was carried out at the Nursery of Ornamental Horticulture Department, Faculty of Agriculture, Cairo University, Giza, Egypt during the two successive growing seasons of 2014 and 2015 in order to ameliorate the growth of leucaena plants grown under different levels of salinity in irrigation water (2000, 4000 and 8000 ppm) by foliar spray with active yeast extract (100 ml AYE/L.). The obtained results indicated that increasing salt concentration significantly decreased all investigated growth parameters (plant height, stem diameter, number of compound leaves developed/plant, fresh weight of stems/plant, fresh weight of leaves/plant and plant biomass). Likewise, concentration of chloroplast pigments and percentage of crude protein in leaves were decreased especially those plants grown under 4000 and 8000 ppm salinity. By contrast, increased salinity level more than 200 ppm induced significant increase in proline concentration in leucaena leaves. At the same time, the decrease in stem diameter which was observed due to salinity stress could be attributed mainly to the prominent decrease in all included tissues (periderm, cortex, phloem, xylem and pith). Data also revealed that leucaena plants grown under stress of different levels of salinity and sprayed with active yeast extract (AYE) had better growth behavior than those unsprayed. It was found that yeast extract treatment had the ability to induce significant recovery for the reduction occurred in vegetative growth of leucaena plants which exposed to salinity stress.
**Keywords:**Leucaena; Salinity stress; Chloroplast pigments; Stem anatomy; Yeast extract.

## B-491. Comparative Botanical Studies of Some Salvia Species (Lamiaceae) Grown in Egypt. I Morphological Characteristics.

Kassem F. El-Sahhar, Rania M. A. Nassar and Hend M. Farag.

*Research Journal of Pharmaceutical, Biological and Chemical Sciences, 7(3): 1985-2000 (2016).*

A series of botanical studies of four species of the genus Salvia L. grown in Egypt, namely, Salvia coccinea Buc'hoz ex Etl., Salvia farinacea Benth., Salvia officinalis L. and Salvia splendens Sellow ex Roem. & Schult was carried out. The present study introduce a detailed botanical information about germination of seeds and the morphology of vegetative and reproductive growth of the four investigated species of Salvia throughout the consecutive stages of their whole life span. The vegetative characters include: plant height, number of lateral branches / plant, number of leaves/ plant, total leaf area/ plant and fresh and dry weights of leaves/ plant. In addition, various parameters of the reproductive growth at flowering stage and harvest time were recorded including: number of inflorescences/ plant, number of flowers of the main inflorescence, number of flowers/ plant, number of seeds/ plant, specific weight of seeds and yield of seeds/ plant. Moreover, keen observations and descriptive morphology of the root and the shoot system were under consideration. Such knowledge would be useful to specialists in various aspects of biology of such plants.
**Keywords:**Salvia; Seed germination; Morphology; Vegetative; Reproductive growth.

## B-492. Plant Powder Teabags: A Novel and Practical Approach to Resolve Culturability and Diversity of Rhizobacteria.

Mohamed S. Sarhan, Elhussein F. Mourad, Mervat A. Hamza, Hanan H. Youssef, Ann-Christin Scherwinski, Mahmoud El-Tahan, Mohamed Fayez, Silke Ruppel and Nabil A. Hegazi.

*Physiologia Plantarum, 157: 403-413, (2016), IF: 3.52.*

We have developed teabags packed with dehydrated plant powders, without any supplements, for preparation of plant infusions necessary to develop media for culturing rhizobacteria. These bacteria are efficiently cultivated on such plant teabag culture media, with better progressive in situ recoverability compared to standard chemically synthetic culture media. Combining various plant-based culture media and incubation conditions enabled us to resolve unique denaturing gradient gel electrophoresis (DGGE) bands that were not resolved by tested standard culture media. Based on polymerase chain reaction PCR-DGGE of 16S rDNA fingerprints and sequencing, the plant teabag culture media supported higher diversity and significant increases in the richness of endo-rhizobacteria, namely Gammaproteobacteria (Enterobacteriaceae) and predominantly Alphaproteobacteria (Rhizobiaceae). This culminated in greater retrieval of the rhizobacteria taxa associated with the plant roots. We conclude that the plant teabag culture medium by itself, without any nutritional supplements, is sufficient and efficient for recovering and mirroring the complex and diverse communities of rhizobacteria. Our message to fellow microbial ecologists is: simply dehydrate your plant canopy, teabag it and soak it to prepare your culture media, with no need for any additional supplementary nutrients.

**Keywords:** Plant powder teabags; Plant-Based culture media; Dgge; 16S Rdna; Rhizobacteria.

## B-493. Plant-Based Culture Media: Efficiently Support Culturing Rhizobacteria and Correctly Mirror Their in-Situ Diversity.

Hanan H. Youssef, Mervat A. Hamza, Mohamed Fayez, Elhussein F. Mourad, Mohamed Y. Saleh, Mohamed S. Sarhan, Ragab M. Suker, Asmaa A. Eltahlawy, Rahma A. Nemr, Mahmod El-Tahan, Silke Ruppel and Nabil A. Hegazi.

*Journal of Advanced Research, 7: 305-316, (2016), IF: 3.*

Our previous publications and the data presented here provide evidences on the ability of plant-based culture media to optimize the cultivability of rhizobacteria and to support their recovery from plant-soil environments. Compared to the tested chemically-synthetic culture media (e.g. nutrient agar and N-deficient combined-carbon sources media), slurry homogenates, crude saps, juices and powders of cactus (Opuntia ficus-indica) and succulent plants (Aloe vera and Aloe arborescens) were rich enough to support growth of rhizobacteria. Representative isolates of Enterobacter spp., Klebsiella spp., Bacillus spp. and Azospirillum spp. exhibited good growth on agar plates of such plant-based culture media. Cell growth and biomass production in liquid batch cultures were comparable to those reported with the synthetic culture media. In addition, the tested plant-based culture media efficiently recovered populations of rhizobacteria associated to plant roots. Culturable populations of >106–108 cfu g−1 were recovered from the ecto- and endo-rhizospheres of tested host plants. More than 100 endophytic culture-dependent isolates were secured and subjected to morphophysiological identification. Factor and cluster analyses indicated the unique community structure, on species, genera, class and phyla levels, of the culturable population recovered with plant-based culture media, being distinct from that obtained with the chemically-synthetic culture media. Proteobacteria were the dominant (78.8%) on plant-based agar culture medium compared to only 31% on nutrient agar, while Firmicutes prevailed on nutrient agar (69%) compared to the plant-based agar culture media (18.2%). Bacteroidetes, represented by Chryseobacterium indologenes, was only reported (3%) among the culturable rhizobacteria community of the plant-based agar culture medium.

**Keywords:** Plant-Based culture media; Rhizobacteria; Cultivability; Community structure of Rhizobacteria; Cactus; Succulent plants.

## B-494. Antibacterial Activity of Papain Hydrolysed Camel Whey and its Fractions.

Mahmoud Abdel-Hamid, Hanan A. Goda, Cristian De Gobba, Håvard Jenssen and Ali Osman.

*International Dairy Journal, 61: 91-98, (2016), IF: 1.938*

Camel whey (CW) was hydrolysed with papain from Carica papaya and fractionated by size exclusion chromatography (SEC). The antibacterial activity of the CW, camel whey hydrolysate (CWH) and the obtained SEC-fractions was assessed using the disc-diffusion method. The CWH exhibited significantly higher antibacterial activity than the unhydrolysed CW. SEC-F2 (fraction 2) exhibited the highest antibacterial activity against Staphylococcus aureus, whereas Escherichia coli was the least affected. Transmission electron microscopy (TEM) micrographs showed that the SEC-F2 caused changes in the treated bacterial cells. Additionally, LC/MS analysis was used to characterise the peptides profile of CW, CWH and SEC-F2. Two major peptides (414.05 and 456.06 Da mass) were detected in CWH and SEC-F2, with higher concentration in the latter. This study has demonstrated that hydrolysis of CW with papain generates a wide range of potent antibacterial peptides against selected pathogenic bacteria.

**Keywords:**Camel whey; Papain; Antibacterial activity; Size exclusion chromatography Lc/Ms Analysis; Tem.

### *Dept. of Agricultural Zoology and Nematology*

## B-495. Morphological and Genetic Differentiation of Ereminadesertorum (Gastropoda, Pulmonata, Helicidae) in Egypt.

Reham F. Ali, Marco T. Neiber, Frank Walther and Bernhard Hausdorf

*Zoologica Scripta, 45 (1): 48-61, (2016), IF: 2.733*

To understand the processes that result in morphological and genetic diversity, we studied the differentiation of the land snails Eremina d. desertorum and Eremina desertorum irregularis in the deserts of northern Egypt. These two taxa are differentiated with regard to shell size and shape and are separated by a narrow hybrid zone west of Alexandria. The lack of differences in the genitalia and the lack of reciprocal

monophyly of the mitochondrial haplotypes of E. d. desertorum and E. desertorum irregularis support their classification as subspecies rather than distinct species. Low genetic distances indicate that the differentiation is probably less than half a million years old. The genetic data indicate a population expansion in agreement with other evidence that the Nile region in northern Egypt was more humid well into historical times than today. Shell size and shape are correlated with a climatic gradient from cooler and more humid conditions along the Mediterranean coast to arid and hot conditions in the interior. The decrease of body size with decreasing precipitation and increasing temperature might be explained by limited time for food intake in the more arid regions. The shape differences between the taxa are partly an indirect consequence of selection for body size, but are also directly affected by selection for reduction of aperture size.

**Keywords:** Eremina desertorum desertorum; Eremina desertorum irregularis; North coast; Genetic diversity.

## B-496.Effect of Silver Nanoparticles on the Mortality Pathogenicity and Reproductivity of Entomopathogenic Nematodes.

Entsar H. Taha and Noha M. Abo-Shady.

*International Journal of Zoological Research, 12(3-4): 47-50 (2016).*

Scientists are concerning about using nanomaterials, such as silver nanoparticles (AgNP) in biological control of plant parasitic nematodes. In this study, it was evaluate that the side effect of AgNP on the non target nematodes, entomopathogenic nematodes (EPNs) that found naturally in the same soil environment and contribute to the insect pests control. **Methodology**: The effect of different concentrations (1500, 500, 200, 40 and 20 ppm) of silver nanoparticles on mortality of EPNs Heterorhabditis indica, Steinernema arenarium and Steinernema abbasi for (1, 2, 3, 4 and 5 days) was studied. and the effect on pathogenic properties of EPNs on Galleria mellonella was also studied. **Results**: It was found that, mortality percentage of EPNs depended on nano-Ag. Concentrations and the exposure time. There was a slight effect on pathogenicity, while there was a significant effect on EPNs reproductivity with the two concentrations (500 and 1500 ppm). **Conclusion**: Nanosilver can be used to control plant parasitic nematodes without excessive in order to don't harm the useful nematodes, EPNs.

**Keywords:**Entomopathogenic nematodes; Heterorhabditis idica; Steinernema arenarium; Steinernema abbasi; Silver nanoparticles.

## B-497. Advanced Applications of Solar Energy in Agricultural Greenhouses.

Reda Hassanien Emam Hassanien, Ming Li and Wei Dong Lin.

*Renewable and Sustainable Energy Reviews, 54: 989-1001, (2016), IF: 6.798.*

Energy is the largest overhead cost in the production of agricultural greenhouse crops in temperate climates. Moreover, the initial cost of fossil fuels and traditional energy are dramatically increasing. The negative environmental impacts, limited sources of fossil fuels and a high consumption of energy and food have caused the increase in demand for solar energy as a green and sustainable choice. Therefore, this paper reviews the solar energy application technologies in the environmental control systems of greenhouses (cooling, heating and lighting) mainly the generated energy of photovoltaic (PV) and solar collectors, as well as the PV water pumping for irrigation. Furthermore, this paper briefly discusses the economic analyses and the challenges for this technology.

**Keywords:** PV Greenhouse; Solar Energy; Cooling systems; Heating systems; PV Pump.

## B-498. Performance and Operation Mode Analysis of A Heat Recovery and Thermal Storage Solar-Assisted Heat Pump Drying System.

Yu Qiu, Ming Li, Reda Hassanien Emam Hassaniena, Yunfeng Wang, Xi Luo and Qiongfen Yu.

*Solar Energy, 137: 225-235, (2016), IF: 3.685.*

A novel heat recovery and thermal storage solar-assisted heat pump drying system was set up. Moreover, the effect of different economic variables on payback period was investigated. The evaporator and condenser were integrated in the drying chamber and the water storage tank was set up in the system to recover the heat effectively and improve the utilization of solar energy. Based on a total required heat of 23.157 MJ for drying 10 kg of radish process, the theoretical analysis results illustrated that when the daily average radiation intensity was 0.480 kW/m2 the system run at solar drying (SD) mode, when the daily average radiation intensity ranged from 0.430 kW/m2 to 0.480 kW/m2 the system run at the solar-assisted heat pump drying (SAHPD) mode, when the daily average radiation intensity was less than 0.430 kW/m2, the system run at the heat pump drying (HPD) mode. The experimental results showed that the coefficient of performance of the drying system was ranged from 3.21 to 3.49 at the SAHPD mode. Furthermore, the SAHPD can save energy consumption by 40.53% in terms of heat recovery and thermal storage. The payback period for drying radish, pepper, and mushroom in the life span of the system was 6 years, 4 years, and 2 years, respectively. Therefore, it can be concluded that mushroom is the most suitable material to be dried in this system.

**Keywords:** Heat recovery; Thermal storage; Solar-assisted Heat pump; Solar drying.

## B-499. Experimental Investigation on the Performance of a Solar Powered Lithium Bromide–Water Absorption Cooling System.

*International Journal of Refrigeration,71:46-59(2016) IF:2.291*

The performance of solar cooling absorption system needs further research, due to its poor coefficient of performance (COP). Therefore, this study investigated the performance of a 23 kW solar powered single-effect lithium bromide–water (LiBr–H2O) absorption cooling system. Furthermore, the space heating mode was also investigated and the improvement methods were analyzed and discussed. The cooling system was driven by a parabolic trough collector of 56 m2 aperture area and used for cooling a 102 m2 meeting room. Research results revealed that the chiller's maximum instantaneous refrigeration coefficient (chiller efficiency) could be up to 0.6. Most of the

time, in sunny and clear sky days the daily solar heat fraction ranged from 0.33 to 0.41 and the collectors field efficiency ranged from 0.35 to 0.45. At the same time, chiller efficiency was varied from 0.25 to 0.7 and the daily cooling COP was varied from 0.11 to 0.27, respectively.
**Keywords:** Solar cooling; Single-Effect absorption Chiller; Lithium bromide–Water; Parabolic trough solar collector (Ptc); Cooling performance.

## B-500.Energy Conversion and Transmission Characteristics Analysis of Ice Storage Air Conditioning System Driven by Distributed Photovoltaic Energy System.

Yongfeng Xu, Ming Li and Reda Hassanien Emam Hassanien.

*International Journal of Photoenergy, 2016: 1-17, (2016), IF:1.226*

In order to reduce the investment and operation cost of distributed PV energy system, ice storage technology was introduced to substitute batteries for solar energy storage. Firstly, the ice storage air conditioning system (ISACS) driven by distributed photovoltaic energy system (DPES) was proposed and the feasibility studies have been investigated in this paper. and then, the theoretical model has been established and experimental work has been done to analyze the energy coupling and transferring characteristics in light-electricity-cold conversion process. In addition, the structure optimization analysis was investigated. Results revealed that energy losses were high in ice making process of ice slide maker with only 17.38% energy utilization efficiency and the energy efficiency and exergy efficiency of ISACS driven by DPES were 5.44% and 67.30%, respectively. So the immersed evaporator and cointegrated exchanger were adopted for higher energy utilization efficiency and better financial rewards in structure optimization. The COP and exergy efficiency of ice maker can be increased to 1.48 and 81.24%, respectively, after optimization and the energy utilization efficiency of ISACS driven by DPES could be improved 2.88 times. Moreover, ISACS has the out-of-the-box function of ordinary air conditioning system. In conclusion, ISACS driven by DPES will have good application prospects in tropical regions without power grid.
**Keywords:** ICEstorage; Distributed photovoltaic; Energy characteristics; Exergy; Optimization.

## B-501. Evaluation of Alternative Management Practices with the Annagnps Model in the Carapelle Watershed.

Ossama Mohamed Mahmoud Abdelwahab, Ronald L. Bingner, Fabio Milillo and Francesco Gentile.

*Soil Science, 181: 293-305 (2016).713.*

The Annualized Agricultural Non-point Source (AnnAGNPS) model can be used to analyze the effects of management practices on sediment loads in agricultural watersheds. The study was performed in a 506 km2 Mediterranean watershed located in Apulia, Southern Italy, planted with mostly winter wheat (83%) where runoff and sediment loads have been monitored at an in-stream gage. The AnnAGNPS model was used to predict runoff and sediment load without calibration during a 5-year period. On an annual scale, the model showed good prediction capability for runoff (R2 = 0.8, NSE [Nash and Sutcliffe coefficient of efficiency] = 0.7) and satisfactory results for sediment load (NSE = 0.5, R2 = 0.5). Based on the current conditions of the watershed as a baseline scenario, the effectiveness of alternative conservation practices applied within the watershed was also evaluated. No-tillage practices applied to the entire cropland area reduced soil erosion within fields by 44% and sediment yield from fields to streams by 20%. Reduced tillage decreased soil erosion, sediment yield, and sediment load at the gage location by 12%, 7%, and 4% respectively. Limiting the placement of alternative practices to the cropland sub-watersheds with the most erosion (Scenarios G and H) proved to be a promising and viable approach to sediment erosion reduction throughout the watershed. In this perspective, areas that produce the most sediment were identified and targeted for replacement of varying levels of cropland with forest, and consequently sediment loads were reduced from 5% to 97%. The effect of vegetated streams and riparian buffers as natural traps that can increase the in situ sediment deposition was also considered. Most, but not all of the scenarios discussed herein could realistically be implemented within the watershed, particularly if there are incentive policies. Even considering the intrinsic uncertainty of modeling results, evaluating these systems with the aid of AnnAGNPS serves as a means to provide reference information and allows watershed conservation planners to compare the impacts of different management scenarios with sustainable agriculture guidelines.
**Keywords:** Annagnps model; Soil erosion; Sediment load; Best Management practices.

## B-502. An Experimental Study of Building Thermal Environment in Building Integrated Photovoltaic (BIPV) Installation.

Wang Yunfeng, Reda Hassanien Emam Hassanien, Li Ming, Xu Guixian and Ji Xu.

*Bulgarian Chemical Communications, 48, Special Issue E1: 158-164, (2016), IF: 0.229*

A 120kWp building integrated photovoltaic (BIPV) system was installed on the south facade of the building of Solar Energy Research Institute in Yunnan Normal University in October 2014. The area of curtain wall was 1560m2 (26m×60m), which consists of 720 semi-transparent monocrystalline silicon double glazing PV panels. The windows of many rooms from the fifth to the ground floors were covered by the PV curtain wall. The PV light transmittance was about 47%. Therefore, this paper studied the monthly and seasonal variations of thermal environment for building in terms of solar data and meteorological parameters. In summer and winter, the ambient temperatures and the indoor temperatures of the covered rooms by the PV curtain wall in different floors were tested and compared to the reference rooms without PV curtain wall. Results showed that the indoor temperature was 6℃ higher than the ambient temperature in winter. Therefore, it can be concluded that the integration of semi-transparent BIPV reduces the heating demand in winter.
**Keywords:**Building-Integrated; Photovoltaic system; Building thermal environment; Experimental study.

## B-503.Performance Analysis of ICE Storage Air Conditioning System Driven by Distributed Photovoltaic Energy.

Y. F. Xu, M. Li, X. Luo, Y. F. Wang, Q. F. Yu and R. H. E. Hassanien.

*Bulgarian Chemical Communications, 48, Special Issue E1: 165-172, (2016), IF: 0.229.*

In this paper, an ice storage air conditioning system (ISACS) driven by distributed photovoltaic energy system (DPES) was proposed. Furthermore, the system structure optimization analysis was also investigated. The energy coupling and transferring characteristics in light-electricity-cold conversion process were analyzed by the theoretical calculations and experimental tests. Results revealed that the system energy utilization efficiency and exergy efficiency were 4.64% and 43.91%, respectively. The energy losses were high in photo-electric conversion process and the ice making process of ice slide machine. Therefore, the immersed evaporator and co-integrated exchanger were adopted and the ice making efficiency and solar energy utilization ratio were improved with the increasing of the system energy efficiency.
**Keywords:**Photovoltaic; ICEstorage; Energy; Exergy; Structure optimization.

## B-504.Testis-Enriched Heat Shock Protein A2 (Hspa2): Adaptive Advantages of the Birds with Internal Testes Over the Mammals with Testicular Descent.

Abinash Padhi, Mona M. Ghaly and Li Ma.

*Scientific Reports, 6: 148-153, (2016), IF: 5.228.*

The molecular chaperone heat shock protein A2 (HSPA2), a member of the 70 kDa heat shock protein (HSP70) family, plays an important role in spermatogenesis and male fertility. Although HSPA2 is evolutionarily highly conserved across the metazoan lineages, the observation of striking differences in temperature-sensitive expressions, testicular physiology,spermatogenesis, as well as its role in male fertility indicates that avian and mammalian HSPA2 may exhibit distinct evolutionary trajectory. The present study reports that while mammalian HSPA2 is constrained by intense purifying selection, avian HSPA2 has been subjected to positive selection. The majority of the positively selected amino acid residues fall on the α-helix and β-sheets of the peptide-binding domain located at the carboxyl-terminal region of the avian HSPA2. The detection of positively selected sites at the helix and β-sheets, which are less tolerant to molecular adaptation, indicates an important functional consequence and contribution to the structural and functional diversification of the avian HSPA2. Collectively, avian HSPA2 may have an adaptive advantage over the mammals in response to heat stress, and therefore, mammals with testicular descent may be at a greater risk in the event of scrotal temperature rise.
**Keywords:** Heat shock protein A2; Mammals; Avian; Evolution.

## B-505.Expression of Inflammatory and Cell Death Program Genes and Comet DNA Damage Assay Induced by Escherichia Coli in Layer Hens.

Gamal M. K. Mehaisen, Mariam G. Eshak, M. I. El Sabry and Ahmed O. Abass.

*Plos One,, (2016), IF: 3.057*

Modern methods of industrial poultry and egg production systems involve stressful practices that stimulate Escherichia coli (E. coli) activity causing endotoxic shock. This investigation was conducted to evaluate the expression of pro-inflammatory cytokines and cell death program genes and DNA damage induced by E. coli in the brain and liver tissues of laying hens. A total of two hundred and ten H&N brown layer hens with 20 week age, were used in this research. First, preliminary experiments were designed (60 hens in total) to establish the optimal exposure dose of E. coli and to determine the nearest time of notable response to be used in the remainder studies of this research. At 35-wk of age, 150 hens were randomly assigned into 2 groups with 3 replicates of 25 birds each, the first group was injected in the brachial wing vein with 107 E. coli colony/hen, while the second group was injected with saline and served as a control. The body temperature and plasma corticosterone concentration were measured 3 hr after injection. Specimens of liver and brain were obtained from each group and the gene expression of p38 mitogen-activated protein kinase, interlukin-1? (IL-1?), tumor necrosis factor alpha (TNF-?), Bax, and caspase-3 genes were measured by quantitative real-time PCR. DNA damage in the brain and liver tissues were also measured by comet assay. Hens treated with E. coli showed significant ($P<0.05$) increase of body temperature and plasma corticosterone (42.6°C and 14.5 ng/ml, respectively) compared to the control group (41.1°C and 5.5 ng/ml, respectively). Additional remarkable over-inflammation gene expression of p38, IL-1? and TNF-?.genes were also detected in the brain (2.2-fold, 2.0-fold and 3.3-fold, respectively) and the liver (2.1-fold, 1.9-fold and 3.0-fold, respectively) tissues of the infected chickens. It is also important to note that hens injected with E. coli showed an increase in DNA damage in the brain and liver cells ($P<0.05$). These results were synchronized with activating cell death program since our data showed significant high expression of Bax gene by 2.8- and 2.7-fold and caspase-3 gene by 2.5- and 2.7-fold in the brain and liver tissues of infected chickens, respectively ($P<0.05$). In conclusion, the current study indicates that E. coli injection induces inflammatory physiological response and triggers cell death program in the brain and liver. Our results provide more understanding to endotoxic shock by E. coli in chickens at cellular level. Further studies are required to confirm if such responses are destructive or protective to set the means through which a chicken mounts a successful defense against avian pathogenic E. coli.
**Keywords**: Escherichia coli; Inflammation;cell death; DNA Damage,; Laying hens.

## B-506. Identification and characterization of miRNAs in the ovaries of a highly prolific sheep breed.

Hu X, Pokharel K, Peippo J, Ghanem N, Zhaboyev I and Kantanen Jand Li MH.

*Animal Genetics, 47: 234-239, (2016), IF: 2.207.*

Until recently, there have been few studies concerning miRNAs or miRNA-mediated biological processes in sheep (Ovis aries). In the present study, we used a deep-sequencing approach to examine ovarian miRNAs and the mRNA transcriptomes in two ewes of a highly prolific breed, Finnsheep. We identified 113 known sheep miRNAs, 131 miRNAs conserved in other mammals and 60 novel miRNAs, the expression levels of which accounted for 78.22%, 21.73% and 0.05% of the total respectively. Furthermore, the 10 most abundantly expressed miRNAs in the two libraries were characterized in detail, and the putative target genes of these miRNAs were annotated using GO annotation and KEGG pathway enrichment analyses. Among the target genes, intracellular transducers (SMAD1,SMAD4, SMAD5 and SMAD9) and bone morphogenetic protein (BMP) receptors (BMPR1B and BMPR2) were involved in the transforming growth factor b (TGFb) signaling pathway in the reproductive axis, and the most significant GO terms were intracellular part (GO:0044424), binding (GO:0005488) and biological_process (GO:0008150) for cellular component, molecular function and biological process respectively. Thus, these results expanded the sheep miRNA database and provided additional information on the prolificacy trait regulated through specific miRNAs in sheep and other mammals.
**Keywords:** Deep-Sequencing; Mrna; Ewes; Prolificacy.

## B-507.Fateful Triad of Reactive Oxygen Species, Mitochondrial Dysfunction and Lipid Accumulation is Associated with Expression Outline of the Amp-Activated Protein Kinase Pathway in Bovine Blastocysts.

S. Prastowo , A. Amin, F. Rings, E. Held, D. Salilew Wondim, A. Gad, C. Neuhoff, E. Tholen, C. Looft, K. Schellander, D. Tesfaye and M. Hoelker.

*Reproduction, Fertility and Development (2016) IF: 2.135.*

Low cryotolerance is considered as the major drawback of in vitro-produced bovine embryos and is frequently associated with a triad encompassing increased cytoplasmic lipid accumulation, enhanced levels of reactive oxygen species (ROS) and mitochondrial dysfunction. The aim of the present study was to explore the role of the AMP-activated protein kinase (AMPK) pathway in the process resulting such phenotypes. Comparative analysis under different environmental conditions revealed downregulation of AMP-activated protein kinase cytalytic subunit 1alpha (AMPKA1), peroxisome proliferator-activated receptor gamma coactivator 1 alpha (PGC1A) and carnitine palmitoyltransferase 1 (CPT1) genes and upregulation of acetyl-CoA carboxylase α (ACC). In contrast, the presence of fatty acids within the culture medium resulted in a distinct molecular profile in the embryo associated with enhanced levels of ROS, mitochondrial dysfunction and elevated lipid accumulation in bovine embryos. Because AMPKA1 regulates PGC1A, CPT1 and ACC, the results of the present study reveal that AMPK in active its form is the key enzyme promoting lipolysis. Because AMPK1 activity is, in turn, controlled by the AMP : ATP ratio, it is possible to speculate that excessive uptake of exogenous free fatty acids could increase cellular ATP levels as a result of the disturbed β-oxidation of these external fatty acids and could therefore bypass that molecular feedback mechanism. Subsequently, this condition would cause enhanced generation of ROS, which negatively affect mitochondrial activity. Both enhanced generation of ROS and low mitochondrial activity are suggested to enhance the accumulation of lipids in bovine embryos.
**Keywords:** Mitochondrial activity.

## B-508.Effects of A-Tocopherol and Freezing Rates on the Quality and Heterologous in Vitro Fertilization Capacity of Stallion Sperm after Cryopreservation.

J.S. de Vasconcelos Franco, M. Faheem, A. Chaveiro and F. Moreira da Silva.

*Theriogenology, 86: 957-962, (2016), IF: 1.838.*

The effects of supplementation of α-tocopherol and different freezing rates (FRs) on the ability of stallion sperm to fertilize bovine oocytes with intact zona pellucida were investigated, in an attempt to develop a model to assess cryopreserved sperm function. Semen was obtained from four purebred Lusitano stallions (n = 4). Each ejaculate was subjected to cryopreservation with a commercial extender (Ghent, Minitub Iberia, Spain), without any supplementation (control) or supplemented with 2-mM α-tocopherol. The semen was exposed to two different FRs between 5 °C and -15 °C: slow (5 °C/min) and moderate (10 °C/min). After thawing, the viability (SYBR®-14 and propidium iodide [PI]), mitochondrial membrane potential (JC-1, 5,5',6,6'-tetrachloro-1,1',3,3'tetraethylbenzimidazolyl carbocyanine iodine) and membrane lipid peroxidation (C11-BODIPY(581/591)) of each sample were determined by flow cytometry. Moreover, the heterologous IVF rate was measured to evaluate the fertilization capacity of postthaw semen in the four different treatments. For both extenders, the viability was higher for spermatozoa cooled slowly (39.40 ± 2.17 vs. 17.59 ± 2.25-control, 31.96 ± 2.19 vs. 11.46 ± 1.34-Tocopherol, $P < 0.05$). The α-tocopherol extender improved ($P < 0.05$) postthaw lipid peroxidation (10.28 ± 0.70 vs. 15.40 ± 0.95-slow FR, 10.14 ± 0.40 vs. 13.48 ± 0.34-moderate FR), however, it did not improve viability and mitochondrial membrane potential. Regarding the IVF rate, in the moderate FR, α-tocopherol supplementation reported a higher percentage of IVF (20.50 ± 2.11, $P < 0.05$), comparing with the control (14.00 ± 1.84). Regarding the slow FR, no significance differences were observed for percentage of IVF between the two extenders and the FRs. However, it seems that the α-tocopherol supplementation improved the IVF rate. In conclusion, this research reported that bovine oocytes intact zona pellucida can be used to evaluate the quality of postthaw stallion semen and α-tocopherol supplementation in the stallion freezing extender might exert a protective effect against oxidative damage during heterologous IVF.
**Keywords:**Cryopreservation; Freezing rate; Heterologous in vitro fertilization; Spermatozoon; Stallion; A-Tocopherol.

## B-509.Quality Improvement of Transgenic Cloned Bovine Embryos Using an Aggregation Method: Effects on Cell Number, Cell Ratio, Embryo Perimeter, Mitochondrial Distribution, and Gene Expression Profile.

Bang JI, Jin JI, Ghanem N, Choi BH, Fakruzzaman M, Ha AN, Lee KL, Uhm SJ, Ko DH, Koo BC and Lee J Gand Kong IK.

*Theriogenology, 84: 509-523, (2016), IF: 1.798.*

The production of cloned embryos using conventional methods has extremely low success rates owing to low embryo quality. To improve the quality of cloned bovine embryos expressing enhanced green fluorescent protein (EGFP), we applied an aggregation culture method. The EGFP gene was transfected into bovine fetal fibroblasts using a retroviral vector system. Somatic cell nuclear transferwas performed using these cells, and the result ing embryos were cultured in aggregates or individually. Gene expression was analyzed by a microarray,and differentially expressed genes were validated by quantitative real-time polymerase chain reaction. The total number of cells per blastocyst and the ratio of inner cell mass cells to trophectoderm cells were higher inaggregated transgenic cloned blastocysts (agBL, 368.7109.6 and 1:4.8, respectively) than in in vitro–fertilized blastocysts (ivfBL, 189.8 65.8 and 1:2.6,respectively) and nonaggregated transgenic cloned blastocysts (sBL, 113.1 36.3 and 1:1.5,respectively, P<0.05and P<0.01, respectively).Moreover, the blastocystperimeterwas larger in the agBL group than in the ivfBL and sBL groups (1168.8 200.23 vs. 887.33 187.62 and 678 226.1 mm, P < 0.05). In addition,mitochondrial fluorescence intensitywas higher in the agBL group than in the ivfBL and sBL groups (P < 0.05). The number of apoptotic cells per blastocystwas lower in the ivfBL and agBL groups than in the sBL group (3.72.2 and 3.4 2.1 vs. 6.7 6.8, P < 0.05). The genes identified in the microarray belonged to 18 categories. Expression of the Krüppel-like factor 4 gene, which is associated with cell proliferation,development, and transcription,was 7.2-fold higher in the agBL group than in the ivfBL group(P<0.05) but did not differ between the sBL and ivfBL groups (P>0.05). Expression of the heat shock 70-kDaprotein1Agene,which is associated with apoptosis,was 12-fold higher in the sBL group than in the ivfBL and agBL groups (P < 0.05). Expression of a stemness-related gene(octamer-binding transcription factor 4) and trophectoderm-specific genes (homeobox protein CDX2 and keratin 18) was higher in the agBL group than in the sBL group (P < 0.05).However, expression of the stemness gene homeobox proteinNANOGdid not differ among the groups (P > 0.05). Taken together, these data suggest that the aggregation method improves the quality of cloned embryos expressing EGFP and might be helpful in animal cloning.

**Keywords:** Aggregation method; Bovine; Ivf; Microarray; Quantitative real-Time Pcr; Scnt.

## B-510. Res_Id: 1643 بدون عنوان J Res_Wcode: 773

Fakruzzaman M, Ghanem N, Bang JI, Ha AN, Lee KL, Sohn SH, Wang Z, Lee DS and Kong IK.

*Animal Reproduction Science, 159: 172-183, (2016), IF: 1.511.*

Endogenous peroxiredoxin II (PRDX II) protein plays a vital role in early embryonic development. This study assessed the beneficial effects of exogenous PRDX II on bovine embryo development at the cellular and molecular levels. To this end, in vitro maturation (IVM)medium was supplemented with various concentrations of PRDX II (0, 6.25, 12.5, 25, 50,and 100 g/mL). of these, 12.5 g/mL PRDX II was the most effective and significantly promoted embryonic development. Therefore, this concentration of PRDX II was used in subsequent experiments. The percentage of embryos that developed into Day 8 blasto-cysts and the total number of cells per blastocyst (38.2% and 150.6 ± 5.1) was higher inthe PRDX II-treated group than in the control (26.4% and 128.9 ± 3.9, respectively). More-over, the percent of TUNEL positive cells was higher (P < 0.05) in the control than in the PRDX II-treated. Furthermore, PRDX II added to the IVM media increased mitochondria content in blastocysts and decreased the intracellular ROS levels in oocytes and blastocysts compared with the control (P < 0.05). The expression of genes associated with blastocystquality (CDX2 and IFN), antioxidant activity (SOD2), and mitochondrial activity (TFAM)was higher, whereas the expression of a gene involved in the apoptotic pathway (c-FOS)was lower, in the PRDX II-treated than in the control group. In conclusion,supplementation of IVM medium with PRDX II promotes development to the blastocyst stage and improves blastocyst quality through reducing ROS, enhancing embryonic mitochondrial activity, andmodulating development-related target genes expression.

**Keywords:**Bovine; Blastocyst; Prdx Ii; Apoptosis; Mitochondria; Gene expression.

## B-511.Genetic parameters for harmony and gaits in Hispano-Arabe horses estimated by Bayesian methods and Restricted Maximum Likelihood

M.M. Gómez, L.T.Gama, J.M.León , J.Fernández, S.A.Attalla and J.V.Delgado.

*Livestockscience, 188: 159-165, (2016), IF: 1.293.*

Genetic parameters for harmony and gaits (walk, trot and canter) were estimated in the Hispano-Arabe horse breed. The data set included 12,957 records of 901 animals, collected from 2000 to 2014, and was analysed by Bayesian procedures (Gibbs Sampling) and Restricted Maximum Likelihood. The multivariate animal model with repeated records included management group, sex, combination of year and event of evaluation, season of evaluation as fixed effect, plus age at classification and proportion of Arabian genes as linear covariates and additive genetic, permanent environmental and judge as random effects. Bayesian heritability/repeatability estimates for harmony, walk, trot and canter were 0.18/0.35, 0.10/0.18, 0.13/0.27 and 0.13/0.20, respectively, with standard errors from 0.02 to 0.05. Estimates of additive genetic correlations among harmony and gaits traits ranged from 0.45 to 0.83, and were stronger between harmony and trot or canter than between walk and trot. Analyses by Restricted Maximum Likelihood yielded similar results, and correlations between breeding values estimated by both procedures ranged from 0.80 to 0.94.

**Keywords:**Horse; Conformation; Movement; REML; Bayes ian inference.

## B-512. Interaction of Donor Age, Parity and Repeated Recovery of Cumulus–Oocyte Complexes by Ovum Pick-Upon in Vitro Embryo Production and Viability after Transfer.

Jong-In Jin, Nasser Ghanem, Seong-Su Kim, Byung-Hyun Choi, A-Na Ha, Kyeong-Lim Lee, Du-Won Sun, Hyun-Tae Lim, Jung-Gyu Lee and Il-Keun Kong.

*Livestock Science, 188: 43-47, (2016), IF: 1.293.*

The objective of this study was to investigate the effect of age and number of parities on the potential of the Korean native cow (Hanwoo breed) as oocyte donor in ovum pick-up and subsequent in vitro embryo production. All animals were divided into two different groups based on age (3–6 and 7–9 years) and parity (2–3 and 4–7). Ovum pick-up (OPU) was performed to ten Korean native cows over a 4-months period at intervals of 3–4 d (twice weekly). The population of follicles (≥3 mm diameter) present in both ovaries and the grades of all cumulus-oocyte complexes (COCs) retrieved were recorded. All COCs were matured, fertilized and allowed to develop in vitro and the morphological quality of embryos was evaluated before transfer to recipients. There were 18.4±5.7 (mean ± SEM) follicles available for aspiration throughout the experiments, the population of follicles decreased from 19.1±6.3 in the first month to 16.9±4.2 in the last month ($p \leq 0.05$). However, with advancement in age and parity of animals, there was an increase in number of ovarian follicles. Furthermore, the average number of COCs retrieved was 12.5±5.6 in the first month and this number was reduced in the fourth month (10.4±5.4). The total number of recovered COCs was increased in old cows with increased number of parities. Consequently, embryo production decreased from 4.8±3.1 to 4.2±2.8 on the first and last months, while, it was increased in old cows than young ones ($p \leq 0.05$). Furthermore, animals with high number of antral follicular count produced more COCs and embryos. Therefore, we concluded that repeated OPU of Korean native cows resulted in significant decrease in the in vitro production of embryos in young compared with old cows, this has negatively impacted embryo survival after transfer.

**Keywords:** Ovum Pick-Up; Korean native cow; Follicle population; Oocyte competence; Embryo production.

## B-513. The Anti-Müllerian Hormone Profile is Linked with the in Vitro Embryo Production Capacity and Embryo Viability after Transfer but Cannot Predict Pregnancy Outcome.

N Ghanem, JI Jin, SS Kim, BH Choi, KL Lee, AN Ha, SH Song and IK Kong.

*Reproduction in Domestic Animals, 51: 301-310, (2016), IF:1.21*

The current study investigated the possibility of using the AMH concentration as a predictor of the ability of Korean Hanwoo cows to produce cumulus-oocyte complexes, embryos that survive after transfer as well as the pregnancy outcome of surrogates. Eight sessions of ovum pick-up (OPU) were performed with 19 donor cows at an interval of 3–4 days.Antral follicle count (AFC), oocyte quality and in vitro embryo development were recorded for each cow. Embryos produced from cows with different AMH profiles were transferred into recipients (n = 96). Cows in the high (≥0.25 ng/ml) and intermediate (0.1≥ to <0.25 ng/ml) AMH groups had a significantly higher AFC per OPU session (20.40 1.36 and 16.91 1.52, respectively, mean standard deviation) than cows in the low AMH group (<0.1 ng/ml, 12.19 2.14). In addition, more cumulus-oocyte complexes per donor were recovered in the high (11.46 1.22) and intermediate(7.38 0.83) AMH groups than in the low AMH group (4.77 0.44). The percentage of oocytes reached blastocyst stage was significantly higher in the intermediate (47.0%) and high (38.5%) AMH groups than in the low AMH group(32.3%). The number of embryos produced per cow was higher in the high (3.9 0.2) and intermediate (6.9 0.6)AMH groups than in the low AMH group (2.2 0.3). The percentage of embryos that gave birth to viable calves when transferred into recipients was higher for those derived from cows in the intermediate AMH group (50.7%) than for those derived from cows in the low (35.7%) and high (36.4%) AMH groups. In conclusion, a single measurement of AMH concentration predicted the in vitro embryo production potential of donor Korean native cows before OPU and is linked with embryo viability after transfer into recipients.

**Keywords:** Amh; Afc; Opu-Ivp; Embryo survival; Donor; Calving rate.

## B-514. Effects of Dietary Methionine on Performance, Egg Quality and Glutathione Redox System in Egg-Laying Ducks.

A. M. Fouad, D. Ruan, Y. C. Lin, C. T. Zheng, H. X. Zhang, W. Chen, S. Wang, W. G. Xia and Y. Li

*British Poultry Science, 57: 818-823, (2016), IF: 0.933*

1. In this study, 6 dietary DL-methionine (Met) levels (2.5, 3.0, 3.5, 4.0, 4.5 and 5.0 g/kg) were tested to estimate the dietary Met requirements of Longyan ducks from 19 to 46 weeks of age, and to investigate its effect on the glutathione redox system. 2. In total, 1080 Longyan ducks aged 19 weeks were allocated randomly to the 6 dietary treatments, where each treatment comprised 6 replicate pens with 30 ducks per pen. 3. Met had no effects on egg production, yolk weight, yolk colour or the glutathione redox system, but the egg weight, egg mass and feed conversion ratio (FCR) were improved significantly by dietary Met supplementation. As the dietary Met concentration increased, the eggshell thickness and breaking strength decreased significantly, whereas the albumen weight increased significantly. 4. According to broken-line regression analysis, the optimum Met requirements for egg weight, egg mass, FCR and albumen weight are 686, 661, 658 and 731 mg/bird/d, respectively, with a dietary crude protein level of 170 g/kg.

**Keywords:**Dl-Methionine; Glutathione redox system; Laying Duck.

## B-515.The Nutritive Value of Sugar Beet Pulp-Substituted Corn for Barki Lambs.

Adel Eid Mohamed Mahmoud and Nasr El-Sayed El-Bordeny.

*Pakistan Journal of Zoology, 48: 995-1002, (2016), IF: 0.478.*

The experiment examined the effect of partial or whole replacement of yellow corn in growing Barki lambs rations by dried sugar beet pulp (SBP) on digestibility, blood parameters and growth performance. Forty Barki lambs averaged (30 kg live body weight) and 6 months old were divided into 5 groups

of 8 lambs each for 90 days trial. All tested rations were contained concentrate feed mixture (CFM) and clover hay. Corn grains was the main source of energy in the CFM (SBP0), while 25, 50, 75 and 100% of CFM corn were substituted by SBP in SBP0, SBP50, SBP75 and SBP100, respectively. Results showed that SPB75 and SBP100 recorded higher (P<0.05) nutrients digestibilities with exception of ether extract. Rations' nutritive values as total digestible nutrients (TDN, P=0.016), digestible energy (P=0.011), metaboloizable energy (P=0.001) and digestible crude protein (DCP, P=0.001) were higher for SBP50 and SBP75 compared to the other treatments. All measured blood parameters were within normal ranges with a significant (P<0.05) effects of experimental rations on blood plasma parameters. Data of rumen parameters of showed insignificant effects of sugar beet pulp on volatile fatty acids. But there were a linear negative effect on ruminal pH and ruminal ammonia concentrations with SBP rations compared with control ration. The average daily gain indicated that SBP75 and SBP100 tended to have similar values (P=0.638) like SBP0. Feed conversion as kg DM/ kg gain was insignificantly differed (P>0.05) among the experimental rations whereas TDN and DCP per kg gain was significantly (P<0.001) higher for the animals fed SBP0. It could be concluded that SBP may be used as a partial or whole replacement of yellow corn on the rations of growing Barki lambs.

**Keywords:**Corn grains; Growing lamb; Nutrients digestibility; Sugar beet pulp.

## B-516.Evolution of a Milkshed and Role of Alternative Milk Collection Centres in Egypt.

Annabelle Daburon, Mohamed Radwan, Véronique Alary, Ahmed Ali, Sherif Abdelghany and Karim Fouad.

*Cahiers Agricultures, 25 (2016) IF: 0.384.*

In Egypt, an agro-industrial company, in association with a non-governmental organization, began setting up milk collection centres within producers' organizations in 2011. The project was very active in the Beni Suef Governorate. This article analyses the milkshed evolution over the past 50years and the project impact.Using interviews and historical data, a diachronic analysis was performed. The evolution can be divided into four phases: before 1980, dairy products were primarily sold on the local market, from 1980 to 2000, a "milkshed centred" development drove the dairy sector, from 2000 to 2011, the sector was driven by the demand in Greater Cairo, and since 2011, the arrival of the agro-industry has introduced new dynamics in local milk collection. Locally, the development of collection centres led to a rise in milk prices and improvements to milk hygienic quality. Demographic and dietary changes have stimulated demand for dairy products. Liquid milk collection has developed since the liberalization of public policies and improved infrastructure. The agro-industry is struggling to penetrate the highly competitive local milk collection sector and the model's future is uncertain.

**Keywords:** Milk collection; Regional development; Family farms; Dairy industry egypt.

## B-517. Application of Nano-Dicalcium Phosphate in Broiler Nutrition: Performance and Excreted Calcium and Phosphorus.

H.M.A. Hassan, A. Samy, A.E. El-Sherbiny, M.A. Mohamed and M.O. Abd-Elsamee.

*Asian Journal of Animal and Veterinary Advances, 8: 477-483 (2016).*

**Background:** The environmental issues related to the presence of phosphorus (P) in poultry excreta have led the researchers to manipulate the diet of poultry in order to decrease the P excretion without having any negative impact on the performance of birds. Presently, added minerals are used as nanoparticles in order to increase absorption and subsequent decreased presence in poultry excreta. Therefore, an experiment was conducted to study the effect of dietary nano-dicalcium phosphate (NDCP) compared to conventional dicalcium phosphate (CDCP) on performance and excreted calcium (Ca) and P in broiler chicken. **Materials and Methods:** Two hundred and eighty one day-old male broiler chicks were divided into seven treatment groups for a period of 26 days. Seven experimental diets were formulated having three levels of either CDCP or NDCP at 1.75, 1.31 and 0.88% and a lower level of NDCP at 0.44%. Thus, these diets contained 100, 75, 50 and 25% of the recommended non-phytate P i.e., 0.45%. The diet having 1.75% CDCP (100% recommended non-phytate P) served as a control diet. Every dietary treatment had 4 replicates of 10 chicks each. Broiler performance, Ca and P excretion were studied. **Results:** Birds fed different levels of NDCP gained significant more body weight (p<0.05) and utilized feed more efficiently than the control group (1.75% CDCP). Decreasing levels of CDCP led to decrease in body weight gain and impaired feed conversion ratio compared to the control group. Values of body weight gain and feed intake increased by about 25 and 10%, respectively, feed conversion ratio improved by about 12% for birds fed NDCP compared to those fed CDCP. Level of dietary DCP significantly (p<0.001) affected Ca and P excretion while source of DCP significantly (p<0.001) affected P excretion but had no effect on (p>0.05) Ca excretion. Feeding 0.44% NDCP in the diet decreased the excreted Ca and P by 50.74 and 46.24%, respectively, compared to the control. **Conclusion:** It could be concluded that using NDCP in broiler diets allow successfully to reduce the dietary DCP by 75%. Diet formulated containing only 25% of the required non phytate P in form of NDCP could be used instead of 100% CDCP. Also,using dicalcium phosphate in nanoparticle size allow to reduce the excreted Ca and P by about 50% which reduce the impact of poultry on environmental pollution.

**Keywords:** Broilers; Growth performance; Nano minerals; Phosphorus excretion; Pollution.

## B-518.Carcass Characteristics and Bone Measurements of Broilers Fed Nano Dicalcium Phosphate Containing Diets.

M.A. Mohamed, H.M.A. Hassan, A. Samy, M.O. Abd-Elsamee and A.E. El-Sherbiny.

*Asian Journal of Animal and Veterinary Advances, 8: 484-490 (2016).*

**Background:** A broiler experiment was carried to study the effect of using nano dicalcium phosphate (NDCP) compared with the conventional dicalcium phosphate (CDCP) on carcass characteristics and bone measurements. Materials and Methods: Seven groups of one day-old (Ross 308) male broilers were fed on seven experimental diets. Diets were formulated to contain three levels of CDCP or NDCP being, 1.75, 1.31 and 0.88% and a less level of NDCP being 0.44%. These levels supplied 100, 75, 50 or 25% of the recommended dietary available P requirement, correspondingly. Diet of 1.75% CDCP served as a control. The Ca: P ratio was kept 2:1 in all the diets. At the 26th day of age, carcass characteristics and tibia bone parameters were measurements. **Results:** No significant differences were detected on liver, heart and gizzard weights (% of live body weight) among all treatments while carcass weight represents live body weight. Using NDCP instead of CDCP showed significant ($p<0.001$) increase in the measured bone parameters. Birds fed 0.44% dietary NDCP showed comparable values of tibia weight, length, width and breaking strength as those fed 1.75% CDCP. The NDCP increased tibia ash, Ca and P% by 4.61, 3.62 and 4.28%, respectively, compared to CDCP. The results of bone mineral density reflected the values obtained for tibia ash, Ca and P%. **Conclusion:** It could be concluded that using NDCP instead of CDCP improved all the measured bone parameters. Diets formulated containing only 25% of the required available P level in form of NDCP could be used instead of using 100% of the requirements in form of CDCP. The dietary dicalcium phosphat level could be successfully decreased from 1.75-0.44% when used in form of nano particle size. Dicalcium phosphate in nanoparticle size was of about 400% as available as the conventional dicalcium phosphate.
**Keywords:**Nano minerals; Broilers chicks; Carcass Characteristics; Bone parameters.

## B-519. Effects of Dietary Copper Supplementation on Laying Performance, Egg Quality and Plasma Cholesterol Fractions in Laying Ducks.

A.M. Fouad, Y. Li, W. Chen, D. Ruan, S. Wang, W.G. Xie and Y.C. Lin.

*Pakistan Journal of Nutrition, 15: 878-882 (2016).*

This study was designed to investigate the influences of dietary copper (Cu) on laying performance, egg quality, plasma total cholesterol (TC), high-density lipoprotein cholesterol (HDLC) and low density lipoprotein-cholesterol (LDLC) concentrations in Shanma laying ducks. A total of 504 egg laying ducks aged 17 week were randomly allotted to seven groups (twelve ducks per replicate and six replicates each treatment). The control group was fed a corn-soybean meal diet, whereas the treatment groups were fed corn-soybean meal diets supplemented with 4, 8, 12, 16, 20, or 24 mg Cu-sulfate/kg. Egg production, egg weight, egg mass, feed conversion ratio, broken egg rate, abnormal egg rate, Haugh unit, yolk color, albumen height, eggshell weight, eggshell percent, eggshell breaking strength, eggshell thickness, plasma TC, HDLC and LDLC concentrations did not appear response to dietary Cu levels. Our results indicated that corn-soybean meal diet containing sufficient amount of Cu for laying performance and egg quality in laying ducks under the conditions of current experiment. Also, laying performance, plasma TC, HDLC, LDLC concentrations and egg quality were not sensitive traits to low levels of Cu.
**Keywords:**Copper; Laying ducks; Laying performance; Egg Quality; Cholesterol.

## B-520. Ffects of Dietary Manganese Supplementation on Laying Performance, Egg Quality and Antioxidant Status in Laying Ducks.

A.M. Fouad, Y. Li, W. Chen, D. Ruan, S. Wang, W. Xie, Y.C. Lin and C.T. Zheng.

*Asian Journal of Animal and Veterinary Advances, 11: 570-575 (2016).*

**Objective:** Manganese (Mn) is a crucial trace element for poultry nutrition because it has multiple physiological functions. Thus, the main goal of this study was to evaluate the effects of dietary Mn supplementation on laying performance, egg quality and antioxidant status in Shanma laying ducks. Methodology: Five hundred and four Shanma laying ducks, at 17 weeks of age, were randomly assigned to 7 treatments, with 6 replicates per treatment and 12 ducks per replicate. Birds were fed the same basal diet, which was supplemented with 0.0 (control), 15, 30, 45, 60, 75 or 90 mg Mn/kg in the form of Mn-sulfate. **Results:** Results showed that dietary Mn supplementation did not affect egg production, egg weight, feed conversion ratio, egg mass, egg quality, tibia characteristics, total antioxidant capacity, copper-zinc superoxide dismutase or lipid peroxidation (malondialdehyde), but supplementing 90 mg Mn/kg diet significantly ($p<0.05$) improved the activities of total superoxide dismutase, Mn-containing superoxide dismutase and increased Mn content in egg yolk compared with the control group. **Conclusion:** These results indicate that corn-soybean meal diet containing sufficient amount of Mn for laying performance and egg quality in Shanma laying ducks under the conditions of current experiment, but adding 90 mg Mn/kg basal diet is required to improve the activities of Mn-containing superoxide dismutase and total superoxide dismutase and elevate Mn content in their egg yolk.
**Keywords:**Manganese; Laying ducks; Laying performance; Egg quality; Manganese-Containing superoxide dismutase.

## B-521.Impact of Heat Stress on Meat, Egg Quality, Immunity and Fertility in Poultry and Nutritional Factors that Overcome these Effects: A Review.

A.M. Fouad , W. Chen , D. Ruan , S. Wang , W.G. Xia and C.T. Zheng

*International Journal of Poultry Science, 15: 81-95 (2016).*

Modern strains of poultry have been produced to meet the demands of consumers in terms of quantity and they are affected by problems associated with immunity (sensitivity to infection with different diseases), stressors (high sensitivity to different stressors) and product quality (meat and egg quality). In particular, heat stress (HS) negatively affects the productive performance, meat yield, egg yield, meat quality (visual appearance and chemical characteristics), egg quality (internal and external), reproductive performance, intestinal functions and immune response. In addition, there is increased awareness among consumers of the quality of food and the industry must

aim to satisfy the higher requirements of consumers. Thus, there is increased pressure on poultry producers to improve their production quantity and quality. As a consequence, it is important to know how HS affects the meat quality, egg quality, immune organs, intestinal functions and reproductive organs in order to protect against any negative effects. In addition, it is essential to determine the roles of nutritional factors and the possibility of using them to overcome the negative effects of HS. This review summarizes current research in these areas.
**Keywords:** Heat stress; Product quality; Nutritional factors; Poultry.

## B-522. Moringa Oleifera and Echinacea Purpurea as Supplements for Rhamani Lactating Ewe'S Diets and Their Effect on Rumen Characteristics, Nutrients Digestibility, Blood Parameters, Milk Production, Composition and its Fatty Acid Profile.

H.H. Azzaz, Eman S.A. Farahat, T.A. Morsy, Hend A. Aziz, Fatma I. Hadhoud and M.S. Abd-Alla.

*Asian Journal of Animal and Veterinary Advances, 11: 684-692 (2016).*

**Objective:** This study was designed to evaluate impact of adding M. oleifera and E. purpurea dried leaves to diets of Rhamani lactating ewes on their rumen fermentation characteristics, nutrients digestibility, blood parameters, milk yield, composition and its fatty acid profile. Materials and Methods: Fifteen Rhamani lactating ewes after 1 week of parturition were assigned randomly into three groups of 5 animals each using complete random design. The entire experimental period was 84 days. Ewes were fed dry matter according to 4% of their body weight. The first group was fed the basal diet which consisted of 30% CFM and 70% berseem (control diet). The second group was fed the control diet supplemented with Moringa oleifera (MO) dried leaves at 15 g kgG1 DM (T1), while the third group was fed the control diet supplemented with Echinacea purpurea (EP) dried leaves at 15 g kgG1 DM (T2). **Results:** The ewes fed MO supplemented diet (T1) showed significant increase in most of ruminal parameters (except ruminal pH) and nutrients digestibility coefficients followed by EP supplemented ewe's diet (T2), while MO and EP supplementation decreased ruminal protozoal count significantly. There were no significant differences among all groups in blood albumin, globulin, ALT, AST and total lipids concentrations,but the ewes fed MO supplemented diets had higher ($p<0.05$) plasma protein and glucose values than those of control. The supplemented diets with MO and EP increased ewe's milk productivity by 12.75 and 4.4%, respectively compared with the control diet. Milk component's yield were higher ($p<0.05$) for MO supplemented ewes group than the other groups (control and T2). The EP treated ewes recorded the lowest ($p<0.05$) milk somatic cells count. The supplemented diets with MO and EP increased milk total unsaturated fatty acids by 14 and 11%, respectively compared with the control diet. **Conclusion:** The supplemented diets with MO and EP enhanced the performance of Rhamani lactating ewes with no harmful effects on their health.
**Keywords:**Moringa oleifera; Echinacea purpurea; Rhamani ewes; Milk production; Milk fatty acids.

***Dept. of Dairy Sciences***

## B-523. Ethanol Production by Selected Intestinal Microorganisms and Lactic Acid Bacteria Growing Under Different Nutritional Conditions.

Fouad M. F. ElshaghabeeWilhelm BockelmannDiana Meske, Michael de Vrese, Hans-Georg Walte, Juergen Schrezenmeir and Knut J. Heller.

*Frontiers In Microbiology, 7: 1-13, (2016), IF: 4.165.*

To gain some specific insight into the roles microorganisms might play in non-alcoholic fatty liver disease (NAFLD), some intestinal and lactic acid bacteria and one yeast (Anaerostipes caccae, Bacteroides thetaiotaomicron, Bifidobacterium longum, Enterococcus fecalis, Escherichia coli, Lactobacillus acidophilus, Lactobacillus fermentum, Lactobacillus plantarum, Weissella confusa, Saccharomyces cerevisiae) were characterized by high performance liquid chromatography for production of ethanol when grown on different carbohydrates: hexoses (glucose and fructose), pentoses (arabinose and ribose), disaccharides (lactose and lactulose), and inulin. Highest amounts of ethanol were produced by S. cerevisiae, L. fermentum, and W. confusa on glucose and by S. cerevisiae and W. confusa on fructose. Due to mannitol-dehydrogenase expressed in L. fermentum, ethanol production on fructose was significantly ($P < 0.05$) reduced. Pyruvate and citrate, two potential electron acceptors for regeneration of NAD+/NADP+, drastically reduced ethanol production with acetate produced instead in L. fermentum grown on glucose and W. confusa grown on glucose and fructose, respectively. In fecal slurries prepared from feces of four overweight volunteers, ethanol was found to be produced upon addition of fructose. Addition of A. caccae, L. acidophilus, L. fermentum, as well as citrate and pyruvate, respectively, abolished ethanol production. However, addition of W. confusa resulted in significantly ($P < 0.05$) increased production of ethanol. These results indicate that microorganisms like W. confusa, a hetero-fermentative, mannitol-dehydrogenase negative lactic acid bacterium, may promote NAFLD through ethanol produced from sugar fermentation, while other intestinal bacteria and homo- and hetero-fermentative but mannitol-dehydrogenase positive lactic acid bacteria may not promote NAFLD. Also, our studies indicate that dietary factors interfering with gastrointestinal microbiota and microbial metabolism may be important in preventing or promoting NAFLD.
**Keywords:**Weissella confusa; Fructose; Arabinose; Lactulose; Inulin; Ethanol; Fecal slurries; Non-Alcoholic; Fatty liver Disease.

## B-524. Antibacterial Peptides Generated by Alcalase Hydrolysis of Goat Whey.

Ali Osman, Hanan A. Goda, Mahmoud Abdel-Hamid, Sanaa M. Badran and Jeanette Otte.

*Lwt - Food Science and Technology, 65: 480-486, (2016), IF:2.711*

Goat whey hydrolysates were produced from goat whey using Alcalase from Bacillus licheniformis. The goat whey hydrolysate (GWH) with the highest degree of hydrolysis was fractionated by size exclusion chromatography (SEC), and the antibacterial activity of the GWH and the obtained SEC-

fractions were evaluated using the disc diffusion method. The results showed that the GWH exhibited significantly higher antibacterial activity than the unhydrolysed goat whey. Among all SEC fractions obtained, only SEC-F2 and SEC-F3 showed antibacterial activity against the tested bacteria. SEC-F3 exhibited the highest antibacterial effectiveness against Escherichia coli and Bacillus cereus with MIC values of 0.09 and 0.03 mg/mL respectively, whereas, SEC-F3 and SEC-F2 had comparable MIC values against Staphylococcus aureus (~0.02 mg/mL). Transmission electron microscopy showed that the GWH caused changes in the bacterial cells affected. Additionally, LCeMS analysis was used to characterize the peptides of GWH and SEC-F3. Two major peptides were detected in GWH and SEC-F3, with higher concentration in the latter, having masses of 730 and 1183 Da, respectively. These results suggest that hydrolysis of goat whey by Alcalase is an easy tool to enhance its antibacterial activities. GWH and its effective antibacterial fractions may be used to control the undesirable bacteria in food and improve its safety.
**Keywords:** Antibacterial peptides; Goat milk; Alcalase.

## B-525. Angiotensin-Converting Enzyme Inhibition and Antioxidant Activity of Commercial Dairy Starter Cultures.

Alaa Abd El-Fattah, Sally Sakr, Samia El-Dieband Hany Elkashef.

*Food Science and Biotechnology, 25/6: 1745-1751, (2016), IF: 0.699*

In this study, skim milk fermented with 14 commercial dairy starters were evaluated for their proteolysis ability, angiotensin I-converting enzyme (ACE)-I, and antioxidant properties. The antioxidant activity was determined using DPPH radical scavenging, chelating of Fe2+ ions, and reducing power assays. The results showed that the coagulation time, pH, and titratable acidity varied among the used starters and appeared to be starter dependent. Lactobacillus helveticus Lh-B02 starter had the highest proteolytic and ACE-I activity. Lactobacillus casei-01, Yo-Fast 1, YC-281, MYE 96, and YO-MIX 205 starters had the highest DPPH radical scavenging activity. Chelating of Fe2+ ions of the L. casei-01 starter was the highest, whereas the O-114 starter was the greatest in reducing power. Regarding the yogurt starters, Yo-Fast 1 starter exhibited h igh values o f proteolytic, ACE-I, and DPPH radical scavenging activity. A positive correlation was observed between the proteolytic and ACE-I or antioxidant activities of all starters.
**Keywords:**Commercial dairy Starter; Proteolysis; ACE-I; Antioxidant.

## B-526. Reduction of Pesticide Residues in Egyptian Buffalo Milk by Some Processing Treatments.

Fawzia H.R. Abd-Rabo, Hany Elsalamony and Sally S. Sakr.

*International Journal of Dairy Science, 11: 75-80 (2016).*

This study was designed to evaluate the pesticide residues in Egypt. Buffalo milk was collected from Sharkia, Dakhlia and Giza provinces. The effect of pasteurization, sterilization, fermentation and coagulation on some organophosphorus (dimethoate and malathion) pesticides spiked in buffalo milk was studied. The obtained results showed that the sampling time and method of analysis may be behind the remarkable effect on dimethoate and malathion content of milk samples. All treatments had significant effects on the reduction of pesticides level. The pesticides degradation percentage was improved by fermentation. Pasteurization however removed malathion completely and reduced dimethoate level to a great extent.
**Keywords:**Pesticide residues; Organophosphorus; Heat treatments; Fermentation; Coagulation.

### *Dept. of Economic Entomology and Insecticides*

## B-527. Dissipation Dynamic, Residue Distribution and Processing Factor of Hexythiazox in Strawberry Fruits Under Open Field Condition.

Ayman N. Saber, Farag M. Malhat, Hany M.A. Badawy and Dalia A. Barakat.

*Food Chemistry, 196: 1108-1116, (2016), IF: 4.052.*

Two independent field trials were performed to investigate the dissipation and residue levels of hexythiazox in strawberry. The study presents a method validation for extraction and quantitative analysis of hexythiazox residues in strawberry using HPLC-DAD. The results shown that the mean recoveries ranged from 85% to 93%, furthermore the intra- and inter-day relative standard deviations were less than 10%. The results suggest that the hexythiazox dissipation curves followed the first-order kinetic and its half-life ranged from 3.43 to 3.81 days. The final residues in strawberry were below the Codex maximum residue limit (MRL) (6 mg/kg) after three days of the application. The effects of household processing and storage on the levels of hexythiazox residues were quantified, and it's useful for reducing the dietary exposure. The processing factor after each stage were generally less than 1, indicating that the whole process can reduce the residues of hexythiazox in strawberry. The results could provide guidance to safe and reasonable use of hexythiazox in agriculture.
**Keywords:** Residues dissipation; Hexythiazox strawberry Storage processing pesticides; Safety evaluation.

## B-528. Factors Affecting the Quality of Mated Honey Bee Queens Stored for Different Periods in Queen-Right Bank Colonies. Effect of Cage Level and Position on Holding Frame.

Mohammad Abd Al-Wahab Abd Al-Fattah, Hatem Ahmed Sharaf El-Din and Yasser Yehia Ibrahim.

*Journal of Apicultural Research, 55:284-291 (2016) IF: 2.084.*

The effect of storage cage level (upper or lower) and its position (peripheral or middle positions) on weight, survival rate and egg laying capacity of honey bee queens stored in queen-right colonies for various storage periods was studied. Storing mated queens in this way had a significant effect on their weight after 75 days of storage. The means of queen weight were 174.9 and 167.4 mg for the upper and lower strips, respectively showing the superiority of the upper one. A significant increase in the mean weight of queens stored in the middle position (172.5 mg) was noticed comparing to peripheral ones (169.8 mg). All the stored queens had significantly greater weight than their original weight before storage during the different periods of experiment. There were significant differences in the survival

rate of mated queens stored in different levels, as the mean survival rate of queens stored in the upper strip (69.3%) was higher than the survival rate of mated queens stored in the lower one (60.1%). The queens stored in middle position attained a significantly higher survival rate (70.7%), than those stored in peripheral ones (58.7%).The overall survival rate was negatively influenced with the increase of storing period. In respect of egg laying capacity measured as sealed worker brood area, queens stored for 45 days produced a significantly larger sealed brood area (875.5 cm2) than that produced by queens stored for 75 days (843.2 cm2).

**Keywords:**Honey bee; Queen-Right bank; Storage level; Storage position; Queen weight; Queen survival; Egg-laying.

## B-529. Resistance to Propanil in Ricefield Bulrush (Schoenoplectus mucronatus) is Conferred by a psbA Mutation, Val219 to Ile

Rafael M. Pedroso, Kassim Al-Khatib, Ibrahim Abdallah, Rocio Alarc´on-Reverte and Albert J. Fischer.

*Weed Science, 64: 562-569, (2016), IF: 1.993.*

Determining the mechanisms of herbicide resistance in weeds allows for the development and implementation of applied management practices aimed to control and to prevent further spread of herbicide-resistant populations in crop fields. This research was conducted to determine propanil resistance and cross-resistance to other photosystem II (PSII) inhibitors in ricefield bulrush biotypes and to elucidate the mechanism of propanil resistance. To this end, propanil-resistant (R) and propanil-susceptible (S) biotypes were selected from field-collected populations after propanil spraying at the field rate, and whole-plant, dose–response experiments were conducted to evaluate cross-resistance to PSII inhibitors and interactions between propanil and the insecticides malathion and carbaryl. In addition, the psbA gene from R and S biotypes was sequenced for amino acid alterations following polymerase chain reaction (PCR) amplification. Plant survival data indicated the R biotype displayed a 14-fold increase in propanil resistance relative to the susceptible (S) biotype. In addition, the propanil-R biotype also had increased resistance to the PSII-inhibitors bromoxynil, diuron, and metribuzin but was more susceptible to bentazon than were propanil-S plants. Synergism between propanil and the insecticides carbaryl and malathion was greater in the S biotype than it was in the R biotype, indicating that, unlike propanil resistance in weedy grasses, enhanced degradation of the herbicide molecule is not a mechanism of resistance for propanil in ricefield bulrush. A Val219 to Ile substitution in the propanil-R chloroplast D1 protein was identified following sequencing of the psbA gene. This research suggests a single-point mutation at the target site causes resistance to propanil, diuron, metribuzin, and bromoxynil but increasing susceptibility to bentazon in propanil-R ricefield bulrush, a novel Val219–Ile feature. To our knowledge, this is the first instance of propanil resistance in weeds because of a mechanism other than enhanced herbicide metabolism. Tank-mixing bentazon and propanil, where permitted, can control both propanil-R and propanil-S biotypes.

**Keywords:**Bentazon; Carbaryl; Herbicide resistance; Malathion; Oryza sativa L.; Propanil; Psba.

## B-530. Resistance Monitoring and Enzyme Activity in Three Field Populations of Cowpea Aphid (Aphis Craccivora) From Egypt.

Eman A. Fouad, Hala M. Abou-Yousef, Ibrahim S. Abdallah and Mohammed A. Kandil.

*Crop Protection, 81: 163-167, (2016), IF: 1.652*

The cowpea aphid (Aphis craccivora) is one of the most important sucking insect pests attacking certain legumes in Egypt particularly faba bean, cowpea and pea. In this study we monitored the resistance level of three field populations of A. craccivora to seven insecticides belonging to three different chemical classes (organophosphates, carbamates and neonicotinoids). The three populations were collected from three governorates in Egypt namely Dakahlia, Qalyobia and Beni Suef. Diagnostic concentrations (LC90 values for susceptible strain) for each insecticide were established using a leaf dipping technique. Resistance monitoring showed that the field population from Dakahlia was highly resistant to all the tested insecticides. In a similar manner, the population from Qalyobia was also resistant to all insecticides except for fenitrothion to which only moderate resistance was observed. The field population from Beni Suef exhibited a lower level of resistance to all the seven tested insecticides. Biochemical assay showed that esterase activity in these three field populations was generally higher as the enzyme activity ratio ranged from 4.3 to 7.8 fold more than that for the susceptible strain. The activity of the other measured detoxifying enzymes (glutathione -S- transferase and mixed function oxidases) was moderate in the populations from Qalyobia and Dakahlia. Nevertheless, the enzyme activity in A. craccivora collected from Beni Suef was variable and differed slightly from the activity measured in the susceptible strain. Monitoring insecticide resistance among the three aphid populations was a proactive approach to detect any shift in insecticide efficiency. The possible occurrence of resistance in the cowpea aphid to the tested insecticides may be due to the higher activity of carboxylesterases. Further studies on the resistance mechanism to these insecticides are needed to provide insights in how to manage and delay the onset of the resistance and thus prolong the performance of insecticides against A. craccivora.

**Keywords:** Aphis craccivora.

## B-531. Sublethal Effects of Spinosad and Emamectin Benzoate on Larval Development and Reproductive Activities of the Cabbage Moth, Mamestra Brassicae L. (Lepidoptera: Noctuidae)

Moataz A.M. Moustafa, Agnes Kakai, Mona Awad and Adrien Fonagy.

*Crop Protection, 90: 197-204, (2016), IF: 1.652.*

Lepidopteran insect pest management has relied heavily on synthetic chemical pesticides, but their ef- ficiency is declining as a result of emerging insecticide resistance. Recently biopesticides have become the most promising products employed in pest management strategies. We investigated the sublethal effects of two bioinsecticides, spinosad and emamectin benzoate, on larval and pupal development, and reproductive activity including calling behaviour, pheromone production, fecundity and fertility of the cabbage moth,

Mamestra brassicae. To assess sublethal effects, second instar larvae were fed with 0.005, 0.05, or 0.5 mg a.i. spinosad/g diet or 0.00005, 0.0005, or 0.005 mg a.i. emamectin benzoate/g diet. Both bioinsecticides significantly increased larval and pupal development time and negatively affected reproductive activity of M. brassicae. The calling activity of females decreased very significantly in the highest sublethal concentration of spinosad and in all treatments by emamectin benzoate. The results suggest that, both spinosad and emamectin benzoate are promising alternatives to conventional insecticides for the control of M. brassicae if successfully introduced into Integrated Pest Management (IPM) programs.

**Keywords:**Spinosad; Emamectin benzoate; Sublethal concentrations; Reproductive behaviour; Pheromone Production; Mamestra brassicae.

## B-532. Comparative Susceptibility of Corcyra Cephalonica (Lepidoptera: Pyralidae) Eggs to Carbon Dioxide and Nitrogen at Different Temperatures.

Mohamed Y. Hashem, Adel A.I. Ahmed, Sayeda S. Ahmed, Shimaa S.H. Khalil and Youssef A. Mahmoud.

*Journal of Stored Products Research, 69: 99-105, (2016), IF: 1.533.*

The aim of this study was to evaluate the susceptibility of the egg stage of the rice moth Corcyra cephalonica to modified atmospheres (MAs) enriched with CO2 or N2 at 25, 30 and 35 °C combined with various exposure times. The tested modified atmospheres containing CO2 were 20% CO2, 16% O2 and 64% N2, 40% CO2, 12% O2 and 48% N2, 60% CO2, 8% O2 and 32% N2 and 80% CO2, 4% O2 and 16% N2. The tested modified atmospheres containing N2 were 97% N2 and 3% O2and 98% N2 and 2% O2. The results showed that the hatchability responding to modified atmospheres enriched with either CO2 or N2 decreased significantly with an increase in exposure time, gas content (%) and temperature. All tested combinations provided complete (100%) egg control in less than 4 days. Based on 100% mortality, shorter exposures were obtained with 80% CO2 than with N2 at most tested temperatures. The modified atmospheres enriched with 98% N2 were more effective than 97% N2 against C. cephalonica eggs, especially at 35 °C. It is recommended to use high levels of CO2 in air (80%) and N2 (98%) in controlling 0–24-h-eggs of C. cephalonica within 24–36 h for CO2 and 18–72 h for N2.

**Keywords:**Carbon dioxide; Nitrogen; Reduced oxygen; Stored product insects; Toxicity.

## B-533. Fragments of Tenebrio Molitor Cadherin Enhance Cry3aa Toxicity for The Red Flour Beetle, Tribolium Castaneum (Herbst).

M. A. M. Moustafa, J. Vlasák and F. Sehnal.

*Journal of Applied Entomology, 140: 277-286, (2016),IF:1.517*

Bacillus thuringiensis crystalline (Cry) proteins are highly toxic to a wide range of insect pests, but some species resist their action. This is true for many economically important beetles, including stored product pests, such as Tribolium castaneum. In this article, we show that the susceptibility of T. castaneum larvae to natural as well as to a recombinant Cry3Aa-type toxin, applied in the diet, is enhanced by supplementing the diet with recombinant fragments of Tenebrio molitor cadherin, Cry toxin-binding sites occur in several cadherin repeats (CR). In our study, we used the toxin-binding region CRtb, which represents a substantial part of the repeat CR12-MPED (membrane-proximal extracellular domain). CRtb and CR12-MPED consistently increased Cry3Aa toxicity. This synergistic effect occured at diverse mass ratios between the toxin and the cadherin fragments, suggesting that optimal ratios can be found. In our 6-week-long assay with T. castaneum, we achieved mortality of up to 96.6% with toxin concentration 30 μg/g. Cadherin fragments CR11 and CR9-11 elicited small and diverse effects that require further analysis.

**Keywords:** Bacillus thuringiensis; Biocontrol; Cadherin; Cry3aa; Synergism; Toxicity modulation.

## B-534. On the Biology of Tetrastichus Galactopus (Ratzeburg) (Hymenoptera: Eulophidae) A Hyperparasitoid of Sinophorus Xanthostomus (Gravenhorst) Parasitizing Pieris Rapae L.

Askar, S. I. and M. M. El-Hussieni.

*Egyptian Journal of Biological Pest Control, 26: 523-526, (2016), IF: 0.152.*

Studies were carried out to estimate parasitism rate, emergency rate, longevity and sex ratio of the hyperparasitoid, Tetrastichus galactopus (Ratzeburg) (Hymenoptera: Eulophidae) when it attacks the primary species Sinophorus xanthostomus(Gravenhorst)(Hymenoptera:Ichneumonidae)parasitizingPierisrapaeL.(Lepidoptera:Noctuidae)under laboratoryconditions.ThehyperparasitoidadultsemergedfromP.rapaepupae.Parasitismwascompletedwhenthehost age ranged between 17 to 22 days old. T. galactopus adults' longevity averaged 8 days. Hyperparasitism rate averaged (49.40%). T. galactopus immatures lasted a mean of (16.72±0.72) days. The emerged hyperparasitoid individual adults (70.98 and 29.02%) were males and females, respectively, with a sex ratio of2.16:1.

**Keywords:**Tetrastichus galactopus; Sinophorus xanthostomus; Pieris rapae; Biology; Hyperparasitoid.

## B-535. Fruit and Vegetable Extracts as Radiation Protectants for the Beet Armyworm Nucleopolyhedrovirus.

Martin Shapiro, Said El Salamouny, B. Merle Shepard and D. Michael Jackson.

*Journal of Agricultural and Urban Entomology, 32: 91-100, (2016), IF: 0.111.*

Extracts from 37 fruits and vegetables were tested as ultraviolet (UV) protectants for the nucleopolyhedrovirus (SeMNPV) of the beet armyworm, Spodoptera exigua (Hu¨bner) (Lepidoptera: Noctuidae). Only one extract (black currant) provided almost complete protection following UVB/UVA irradiation for 30 minutes under laboratory conditions. As a group, fruit and vegetable extracts were significantly less effective than published values for herb and spice extracts. Based on analyses of antioxidant capacity and total phenolic content of selected plants, it was determined that (1) herbs and spices contained

much higher levels of antioxidants and phenolics than fruits and vegetables, (2) neither high levels of antioxidants nor high levels of phenolics alone could account for UV protection, and (3) selection of extracts with high levels of both antioxidants and total phenolics resulted in increased UV protection.
**Keywords:** Spodoptera exigua; Insecta; Ultraviolet radiation; Protectants; Semnpv.

## B-536. The Role of Detoxifying Enzymes in the Resistance of the Cowpea Aphid (Aphis Craccivora Koch) to Thiamethoxam.

Ibrahim Saleh Abdallah, Hala Mohamed Abou-Yousef, Eman Atef Fouad and Mohammed Abd El-Hady Kandil

*Journal of Plant Protection Research, 56: 67-72 (2016).*

The cowpea aphid (Aphis craccivora Koch) is considered a serious insect pest attacking several crops. We carried out biochemical studies to elucidate the role of the metabolising enzymes in conferring resistance to thiamethoxam, in two strains (resistant and susceptible) of the cowpea aphid. Bioassay experiments showed that the thiamethoxam selected strain developed a 48 fold resistance after consecutive selection with thiamethoxam for 12 generations. This resistant strain also exhibited cross-resistance to the tested carbamates, pirimicarb and carbosulfan, organophosphorus (malathion, fenitrothion, and chlorpyrifos-methyl), and the neonicotinoid (acetamiprid). Synergism studies have indicated that S,S,S-tributyl phosphorotrithioate (DEF), a known inhibitor for esterases, increased thiamethoxam toxicity 5.58 times in the resistant strain compared with the susceptible strain. Moreover, the biochemical determination revealed that carboxylestersae activity was 30 times greater in the resistant strain than in the susceptible strain. In addition, the enzyme activity of glutathione S-transferase (GST) and mixed function oxidases (mfo) increased only in the resistant strain 3.7 and 2.7 times, respectively, in relation to the susceptible (the control). Generally, our results suggest that the higher activity of the detoxifying enzymes, particularly carboxylesterase, in the resistant strain of the cowpea aphid, apparently have a significant role in endowing resistance to thiamethoxam, although additional mechanisms may contribute.
**Keywords:** Aphis craccivora; Detoxifying enzymes; Resistance; Synergism; Thiamethoxam.

## B-537. A Comparative Study of Nutmeg (Myristica Fragrans Houtt.) Oleoresins Obtained by Conventional and Green Extraction Techniques.

Nashwa F. S. Morsy.

*Journal of Food Science and Technology, 53: 3770-3777, (2016), IF: 1.241.*

This study evaluated the effect of conventional maceration and ultrasound assisted extraction techniques on the extraction yield, chemical composition and sensory characteristics of nutmeg oleoresins. Extraction was performed using material: absolute ethanol ratio 1:4, at room temperature. The volatile components of the oleoresin were identified by gas chromatography–mass spectrometry. The results of the study showed that the yield ranged from 4.55 to 9.63 %. Fifty-three compounds in the nutmeg oleoresin have been identified to account for >90 % of the total oil content. Sabinene, myristicin, elemicin, α-pinene, β-pinene, limonene, terpinen-4-ol and myristic acid were found as major compounds of all the nutmeg oleoresins obtained by different techniques. The sensory characteristics of the oleoresin were strongly influenced by the ultrasonic intensity and duration of extraction. The experimental results showed that ultrasound assisted extraction technique at 40 % of the maximal output power and 10 min produced superior quality nutmeg oleoresin with a remarkable yield.
**Keywords:**Nutmeg; Oleoresin; Ultrasonic; Maceration, B-Pinene; Myristicin.

## B-538. Antimicrobial, Biochemical, Organoleptic and Stability Properties of Cookies Fortified by Pomegranate Juice During Storage.

Lamyaa El-Seideek, Serag Farag Zaied, Magda Ibrahim Hassan and Mohamed H. Elgammal.

*Research Journal of Pharmaceutical, Biological and Chemical Sciences, 7: 288-299 (2016).*

In the present work, Pomegranate peels (PMP), Juice (PMJ) extracts were tested for antibacterial and antifungal activities (AA). GC-MS analysis was done in identifying the major phenol contents. Four concentrations of PMJ were used besides control (15%, 18%, 21% and 24%) for supplementation of cookies. Cookies samples were stored even 45 days at room temperature with studying sensory evaluation at zero time and at the end of storage besides fungal count at the end of storage. Using PMP and PMJ, either with water or alcohol showed positive response against tested bacteria and fungi. The aqueous PMJ extract was more effective in controlling the tested pathogenic microbes either bacteria or fungi than PMP extract. PMJ was more effective than PMP, whereas water was more effective than alcohol extract in controlling the microorganisms. Finally, it could be recommended that supplementation with 15% Juice of pomegranate can improve the safety and quality of cookies.
**Keywords:** Punica granatum; Antimicrobial activity; Toxigenic fungi; Pathogenic bacteria.

## B-539. Influenza Virus Targets Class I Mhc-Educated Nk Cells for Immunoevasion.

Ahmad Bakur Mahmoud, Megan M. Tu, Andrew Wight, Haggag S. Zein, Mir Munir A. Rahim, Seung-Hwan Lee, Harman S. Sekhon, Earl G. Brown and Andrew P. Makrigiannis.

*Plos Pathogens, PLoS Pathog 12(2): e1005446: 1-22, (2016), IF: 7.003.*

The immune response to influenza virus infection comprises both innate and adaptive defenses. NK cells play an early role in the destruction of tumors and virally-infected cells. NK cells express a variety of inhibitory receptors, including those of the Ly49 family, which are functional homologs of human killer-cell immunoglobulin-like receptors (KIR). Like human KIR, Ly49 receptors inhibit NK cell-mediated lysis by binding to major histocompatibility complex class I (MHC-I) molecules that are expressed on normal cells. During NK cell maturation, the interaction of NK cell inhibitory Ly49 receptors with their MHC-I ligands results in two types of NK cells: licensed

("functional"), or unlicensed ("hypofunctional"). Despite being completely dysfunctional with regard to rejecting MHC-I-deficient cells, unlicensed NK cells represent up to half of the mature NK cell pool in rodents and humans, suggesting an alternative role for these cells in host defense. Here, we demonstrate that after influenza infection, MHC-I expression on lung epithelial cells is upregulated, and mice bearing unlicensed NK cells (Ly49-deficient NKCKD and MHC-I-deficient B2m-/- mice) survive the infection better than WT mice. Importantly, transgenic expression of an inhibitory self-MHC-I-specific Ly49 receptor in NKCKD mice restores WT influenza susceptibility, confirming a direct role for Ly49. Conversely, F(ab')2-mediated blockade of self-MHC-I-specific Ly49 inhibitory receptors protects WT mice from influenza virus infection. Mechanistically, perforin-deficient NKCKD mice succumb to influenza infection rapidly, indicating that direct cytotoxicity is necessary for unlicensed NK cell-mediated protection. Our findings demonstrate that Ly49:MHC-I interactions play a critical role in influenza virus pathogenesis. We suggest a similar role may be conserved in human KIR, and their blockade may be protective in humans.

**Keywords:**Influenza virus; Nk Cell-Mediated lysis; Histocompatibility complex class I.

## B-540. Genic and Intergenic Ssr Database Generation, Snps Determination and Pathway Annotations,in Date Palm (Phoenix Dactylifera L.).

Morad M. Mokhtar, Sami S. Adawy, Salah El-Din S. El-Assal, and Ebtissam H. A. Hussein.

*Plos One, 11(7): 1-19, (2016), IF: 3.057*

The present investigation was carried out aiming to use the bioinformatics tools in order to identify and characterize, simple sequence repeats within the third Version of the date palm genome and develop a new SSR primers database. In addition single nucleotide polymorphisms (SNPs) that are located within the SSR flanking regions were recognized. Moreover, the pathways for the sequences assigned by SSR primers, the biological functions and gene interaction were determined. A total of 172,075 SSR motifs was identified on date palm genome sequence with a frequency of 450.97 SSRs per Mb. Out of these, 130,014 SSRs (75.6%) were located within the intergenic regions with a frequency of 499 SSRs per Mb. While, only 42,061 SSRs (24.4%) were located within the genic regions with a frequency of 347.5 SSRs per Mb. A total of 111,403 of SSR primer pairs were designed, that represents 291.9 SSR primers per Mb. Out of the 111,403, only 31,380 SSR primers were in the genic regions, while 80,023 primers were in the intergenic regions. A number of 250,507 SNPs were recognized in 84,172 SSR flanking regions, which represents 75.55% of the total SSR flanking regions. Out of 12,274 genes only 463 genes comprising 896 SSR primers were mapped onto 111 pathways using KEGG data base. The most abundant enzymes were identified in the pathway related to the biosynthesis of antibiotics. We tested 1031 SSR primers using both publicly available date palm genome sequences as templates in the in silico PCR reactions. Concerning in vitro validation, 31 SSR primers among those used in the in silico PCR were synthesized and tested for their ability to detect polymorphism among six Egyptian date palm cultivars. All tested primers have successfully amplified products, but only 18 primers detected polymorphic amplicons among the studied date palm cultivars.

**Keywords:** Genic; Interginic; Ssrs; Snps; Data palm database.

## B-541. Use of Posttranscription Gene Silencing in Squash To Induce Resistance Against the Egyptian Isolate of the Squash Leaf Curl Virus.

Omnia Taha, Inas Farouk, Abdelhadi Abdallah and Naglaa A. Abdallah.

*International Journal of Genomics, (2016), Article ID 6053147: 1-9, (2016), IF: 1.83.*

Squash leaf curl virus (SqLCV) is a bipartite begomovirus affecting squash plants. It is transmitted by whitefly Bemisia tabaci biotype B causing severe leaf curling, vein banding, and molting ending by stunting. In this study full-length genomic clone of SqLCV Egyptian isolated and posttranscriptional gene silencing (PTGS) has been induced to develop virus resistance. The Noubaria SqLCV has more than 95% homology with Jordon, Israel, Lebanon, Palestine, and Cairo isolates. Two genes fragment from SqLCV introduced in sense and antisense orientations using pFGC5049 vector to be expressed as hairpin RNA. The first fragment was 348 bp from replication associated protein gene (Rep). The second fragment was 879 bp representing the full sequence of the movement protein gene (BC1). Using real-time PCR, a silencing record of 97% has been recorded to Rep/TrAP construct, as a result it has prevented the appearance of viral symptoms in most tested plants up to two months after infection, while construct containing the BC1 gene scored a reduction in the accumulation of viral genome expression as appearing in real-time PCR results 4.6-fold giving a silencing of 79%, which had a positive effect on symptoms development in most tested plants.

**Keywords:** Gene silencing; Squash; Leaf curl virus.

## B-542. Overexpression of Synechocystis Glutaredoxin-2 Improves the Growth of Pseudomonas Fluorescens Under Salt Stress.

Ahmed Gaber, Mohamed El-awady, Nagwa I. Elarab and Salah A. Moustafa.

*Romanian Biotechnological Letters, 22 (6): 11983-11991, (2016), IF: 0.38.*

Plant Growth Promoting Rhizobacteria (PGPR) play an important role in agricultural systems, especially as biofertilizer. Previously, we screened one bacterial isolate as indole acetic acid (IAA) producer on the basis of IAA colorimetric assay. Based on morphological, physiological and biochemical characteristics presented in Bergey's Manual of Systematic Bacteriology and on 16SrRNA homology, this isolate identified as Pseudomonas fluorescens (accession # JQ809429). Pseudomonas Fluorescens, like other PGPR isolates, produced IAA in the presence of tryptophan, thus genes for IAA production (iaaM and iaaH) were detected in the present study. Moreover, the overexpression of Synechocystis PCC 6803 glutaredoxin-2 (ssr2061) in Pseudomonas fluorescens cells significantly enhance the growth of the recombinant cells on LB media supplemented with different concentration of NaCl. The recombinant strain was able to

produce IAA under 2% of NaCl in the medium. While, the wild type strain failed to produce IAA under same condition. Additionally, effect of the salt on the growth of recombinant and wild type cells was studied by pot culture experiments by using sterilized air dried soil supplemented with 0.5 M or 1 M NaCl. Interestingly, the cell density of the recombinant cells markedly increased even after 6 days from the irrigation with the salt water over the wild type cells. These results suggest that theglutaredoxin-2proteincould play a major role in regulating abiotic tolerance against salt stress in Pseudomonas fluorescens cell.

**Keywords:**Luria-bertani (Lb); Salt stress; Plant growth promoting rhizobacteria glutaredoxins (Grxs); Synechocystis Pcc 6803; Recombinant enzyme.

## B-543. Identification, Characterization and Genetic Improvement of Bacteriocin Producing Lactic Acid Bacteria.

Abdelhadi A. Abdelhadi, Nagwa I. Elarabi, Rasha G. Salim, Ahmed N. Sharaf and Nivien A. Abosereh.

*Biotechnology, 15,( 3-4): 76-85 (2016).*

Bacteriocin produced by lactic acid bacteria has received more scientific attention, this is due to its ability to inhibit wide range of spoilage and pathogenic microorganisms and their potential usefulness as natural substitute for chemical food preservatives. The aim of the present study isolation, identification and improvement of Lactic Acid Bacteria (LAB) that produce bacteriocin from different traditional dairy products in Egypt. **Methodology**: Isolation and identification of LAB isolates based on morphological, biochemical and molecular 16S rDNA gene. To improve LAB bacteriocin production broth and filter mating techniques were used. The RAPD were used to confirm transconjugants. **Results**: Three bacterial isolates showed a high bacteriocin activity and named (I1, I2 and I3). The three bacterial isolate were Gram positive, cocci, asporogenous, non-motile and negative to catalase and oxidase. The biochemical identification using API kit indicated that isolates I1, I2 were related to genus Enterococcus while isolate (I3) was related to genus Pediococcus (94.4 and 99.5%) respectively. On the other hand, 16S rDNA sequencing showed 99% homology with Enterococcus faecium and 97% homology of I3 with Pediococcus pentosaceus. All sequences were deposited in the GenBank nucleotide databases under accession number LC063691.1, LC063692.1 and LC063861.1. Genetic improvement of selected bacterial isolates were carried out using two different techniques of conjugation, filter and broth mating techniques. The transconjugation frequencies of the filter mating technique was higher than (4.6x10–5) the broth mating technique (2.4x10–5). The genetic variability among the transconjugants lines were tested using RAPD analysis and showed 8.25% polymorphism percentages for donor, recipient and tranconjugants lines. **Conclusion**: Results concluded that three bacteriocin producing LAB isolates Enterococcus faecium (I1-I2) and Pediococcus pentosaceus (I3) with probiotic properties could be used in wide range of different industrial application.

**Keywords:** Identification; Bacteriocin; Lactic acid bacteria.

## B-544. Improving Growth and Productivity of Olive Trees Through Raising Photosynthesis Efficiency.

ES Hegazi , NE Kasim, TA Yehia, MS Abou rayya and Thanaa Sh M.

*Research Journal of Pharmaceutical, Biological and Chemical Sciences, 7: 2697-2703 (2016).*

The application of magnesium sulphate at the rate of 100g/tree in each of January, April, June and August increased significantly vegetative growth, photosynthetic pigments, leaf mineral contents (N, P, K and Mg), carbohydrates content in leaves, flowering characteristics (density, perfect flowers %, initial and final fruit set ), fruit quality (weight, size, diameter and pulp/seed ratio. Oil content in fruit was increased (18-20 %) in comparison with (12 %) in untreated trees. Yield of treated trees with magnesium sulphate was doubled (43 kg/tree) in comparison with (20 Kg/ tree) in untreated trees. The increase of growth and productivity of Manzanillo olive trees treated with magnesium sulphate could be explained by improving photosynthesis efficiency.

**Keywords:** Olive; Magnesium sulphate; Growth; Leaf mineral; Carbohydrate; Photosynthetic pigments; Yield; Oil content.

## B-545. Possibility of Using Infrared Absorption (Ft-Ir) Spectroscopy in Studying Effect of Fertilization with Ammonium Sulphate (Nh4)2So4 on Nitrogen, Chlorophyll and Starch Contents of Manzanillo Olive Leaves.

ES Hegazi, TA Yehia, NE Kasim, GMS Elbahy and Thanaa Sh M.

*Research Journal of Pharmaceutical, Biological and Chemical Sciences, 7: 826-830 (2016).*

Fourier Transform Infrared (FT-IR) was used to study the effect of fertilization with ammonium sulphate (NH4)2SO4 on nitrogen, chlorophyll and starch contents in Manzanillo olive leaves. Ammonium sulphate was applied at rate of 1kg/tree in each of February, May, June and August respectively. Studying FT-IR spectra of leaves were recorded at the beginning of growing season in March, at full bloom in May, at final fruit set in July and before harvest in August. Careful examination of the spectra of leaves revealed that the treatment of the soil with ammonium sulphate fertilizer causes no observable changes in their spectral features of the spectra apart from slight changes in the intensities of the absorption bands. To evaluate the changes in the spectral features on quantitative bases, the absorbance of the peaks at 2921 cm-1 (C-H) methyl group, 1658 cm-1 (N-H) amides, 1155 cm-1 (C-N-C) chlorophyll (porphyrin ring) and 1049 cm-1 (C-O) starch were determined and the absorbances ratios A1658cm-1 / A2921 cm-1, A1155cm-1 / A2921cm-1 and A1049cm-1 / A2921cm-1 were calculated to track the amount of change in the contents of nitrogen, chlorophyll and starch as a result of fertilization with ammonium sulphate during the growing season. Examination of the spectra of samples show that the ratio A1658cm-1 / A2921 cm-1 (Nitrogen content) given the highest rate of change in March. The samples taken in May indicated that increasing all absorption ratios compared to the samples taken in March. The samples which taken in July showed that the rates of changes in

absorption ratios at 1658 cm-1 /2921 cm-1 (Nitrogen content) and 1155 cm-1 / 2921 cm-1(Chlorophyll) were decrease compared to the samples taken in May, while the ratio 1049 cm-1 /2921cm-1(Starch) increase with increasing the rate of nitrogen fertilization. The samples taken in August showed that the rate of increase in the absorption ratios in 1658 cm-1 /2921 cm-1 and 1155 cm-1 /2921 cm-1 have no significant changes a bit for the sample taken in July. Whereas, the rate of increasing the ratio of 1049 cm-1 /2921 cm-1 (Starch) decreased with increasing the rate of nitrogen fertilization.

**Keywords:** Olive; Manzanillo; Ammonium sulphate; Nitrogen; Chlorophyll; Starch; Ft-Ir; Infrared.

## B-546. The Impact of Magnetized Water on the Anatomical Structure, Yield and Quality of Potato (Solanum Tuberosum L.) Grown Under Newly Reclaimed Sandy Soil.

Hozayn M, Azza M Salama, Abd El-Monem AA and Alharby F Hesham.

*Research Journal of Pharmaceutical, Biological and Chemical Sciences, 7: 1059-1072 (2016).*

A great attention on the possibility of using magnetized water which has very affective effects on germination, plant growth and production. Our previous and positive results on many crops i.e., wheat, lentil, chick-pea, faba bean, flax, canola and sugar beat, led us to continue studying the application of magnetic treatments either seeds and/or water on productivity of field crops under field condition. In this study, two macro field trials using potato (var. Spunta) were conducted at Research and Production Station, National Research Centre, Alemam Malek village, Al Nubaria district, Al Behaira Governorate, Egypt in 2012/2013 and 2013/2014 winter seasons to study and evaluate the impact of magnetizing irrigation water on quantity, quality and anatomical structure of potato plant. Results indicated that, irrigation potato plants with water passed through magnetic device (Magnetron, 2 inch, production by Magnetic Technologies L.C.C. company, Russia, branch United Arab Emirates) induced positive significant effect on the most of studied parameters (anatomical structure of leaves, stem and tuber, tuber physical properties, yield components, yield and some macro and micro elements and carbohydrates fractions) compared with irrigation with normal water. The percent of increase in tuber yield per fed (fed=4200 m2) reached to 33.25%, ranged from 0.71 to 20.95 % in yield components parameters. Regarding nutritional value, the increment ranged between 2.40 to 28.57% and from 2.19 to 33.92% in macro (N, P, K, Ca & Mg) and microelements (Fe, Mn, Zn & Cu), respectively. The percent of increases reached to 7.81, 11.56 and 5.13% in the total carbohydrates, polysaccharides and starch, respectively. It could be concluded that, magnetic water treatment could be used to improve productivity of potato tuber under newly reclaimed sandy soil condition.

**Keywords:**Potato; Solanum tuberosum; Magnetized water; Anatomy; Productivity; Quality.

## B-547. Performance of A Vertical Subsurface Flow Constructed Wetland Under Different Operational Conditions.

Sara G. Abdelhakeem, Samir A. Aboulroos and Mohamed M. Kamel.

*Journal of Advanced Research, 7: 803-814, (2016), IF: 3.*

effluent treatment was studied in an eight month experiment under different operational conditions including: vegetation (the presence or absence of common reeds ‘‘Phragmites australis”), media type (gravel or vermiculite), and mode of sewage feeding (continuous or batch). Plants had a significant effect ($P<0.05$) on the removal efficiency and mass removal rate of all pollutants, except phosphorous. The average removal efficiencies of chemical oxygen demand (COD), biological oxygen demand (BOD), total suspended solids (TSS), ammonium (NH4) and total-P (TP) were 75%, 84%, 75%, 32% and 22% for the planted beds compared to 29%, 37%, 42%, 26% and 17%, respectively, for the unplanted beds. The VSSFCW was ineffective in removing nitrate (NO3). The effect of either media type or feeding mode system on the removal efficiency of COD and BOD was insignificant. Vermiculite media significantly ($P<0.05$) increased the efficiency of the wetland in removing NH4, TP and dissolved phosphorous (DP) when compared with gravel particularly in the planted beds. The batch mode was more effective in removing TSS and NH4 compared to the continuous mode. Volumetric rate constant (kV) was different for various pollutants and significantly increased due to the presence of plants. Media type had no significant effect on the values of kV for COD, BOD and TSS, while kV for NH4 and TP under vermiculite in the planted beds and kV for P in the unplanted beds were significantly higher than those under gravel.

**Keywords:** Constructed wetlands; Vegetation; Sewage Effluent; Growth media; Feeding mode; Volumetric rate constant.

## B-548. The Elnady Technique: an Innovative, New Method for Tissue Preservation

Fawzy A. Elnady

*Alternatives to Animal Experimentation, 33(3): 237-242, (2016), IF: 5.712*

At the Faculty of Veterinary Medicine, Cairo University, there is an increasing number of students but a limited avail-ability of animal cadavers for dissection, and student exposure to formalin is a known hazard. In order to address these challenges, a new method for tissue preservation was developed, the “Elnady Technique.” This method is a modified form of plastination, where the chemicals used are not patented, are inexpensive and locally available, and the process is performed at room temperature. The produced specimens are realistic, durable, have no offensive odor, and are dry, soft and flexible. They can be used to replace the use of animals killed for teaching basic anatomy, embryology, pathology, parasitology and forensic medicine. They have great potential to support training in clinical skills and surgery, including for clinical examination, endoscopy, surgical sutures, and obstetrics simulation.

**Keywords:** Veterinary anatomy; Alternatives; Plastination; Preservation

## B-550. Dromedary Milk Exosomes as Mammary Transcriptome Nano-Vehicle: Their Isolation, Vesicular and Phospholipidomic Characterizations

Aya M. Yassin , Marwa I. Abdel Hamid , Omar A. Farid , Hassan Amer and Mohamad Warda

*Journal of Advanced Research, 7 (5): 749-756, (2016), IF: 3*

Exosomes are extracellular nanovesicles that play a role in cellular trafficking and communication. Camel milk exosomes might carry the potential of recovery of several illnesses that coins the dromedary milk. This study shows for the first time their isolation and fine characterization. The differential ultracentrifugation was used for their isolation. Their recovery from dromedary milk during different lactation periods was evaluated. The vesicular characterization and stability testing of the recovered exosome were examined by transmission electron microscopy (TEM). The proteome footprinting was resolved by gel electrophoresis prior to their specific protein biomarker analysis. The immunoblotting of their specific protein biomarker TSG101 unexpectedly revealed a truncated 35 KDa protein specific for dromedary milk exosome rather than the previously reported 43 KDa mammalian one. The reversed-phase HPLC screening of their phospholipid makeup was compared with that of cattle milk exosomes at different lactation periods. Since dromedary milk exosomes reflect their mammary transcriptome outcome, further assessment of their content of αs1casein, αs2casein β-casein κ-casein mRNAs parallel with a constitutive glyceraldehyde dehydrogenase (GAPD) gene was performed using real-time PCR. The TEM scanning indicated that dromedary milk exosomes are freeze-stress unstable homogeneous with average size of 30 nm. There was no significant difference in expression level of different casein genes in mid lactation period in dromedary milk exosomes over late lactation period. The phospholipidomic survey proved that phosphatidylcholine is the major candidate of the examined phospholipids in dromedary milk exosomes. The obtained data give novel interpretation about the content of camel milk exosomes with possible insight for use as potentially-safe nano carrier.

**Keywords:** Dromedary; Milk; Exosomes; Transcriptome; Proteome; Phospholipids

## B-551. Oxidative Stress During Erythropoietin Hyporesponsiveness Anemia at end Stage Renal Disease: Molecular and Biochemical Studies.

Khalil Samar, Amer Abdelhalim Hassan, El Behairy Adel Mohamad and Warda Mohamad

*Journal of Advanced Research, 7(3): 348-358 (2016)*

Inflammation and oxidative stress are two faces of one coin in end stage renal disease patients on maintenance hemodialysis. Their interconnection induces anemia complicated with erythropoietin hyporesponsiveness. The biochemical bases behind the resistance to erythropoietin therapy with frequent hemoglobinemia, oxidative stress and iron status have not been fully understood. Here two equal groups (40 patients each) of responders and non-responders to recombinant human erythropoietin therapy (higher than 300 IU/kg/wk of epoetin) were investigated. Hematological and biochemical analyses of collected blood and serum samples were performed along with serum electrophoretic protein footprinting. The leukocytic DNA fragmentation was used to evaluate the degree of oxidative insult. The good responders showed lower erythrocyte malondialdehyde (E-MDA) level and less DNA fragmentation of circulating leukocytes than poor responders with elevated hemoglobin, albumin, A/G ratio, total iron, and ferritin levels. Contrariwise, lower erythrocyte superoxide dismutase (E-SOD) and catalase activities in EPO poor responder group were noticed. Neither other serum constituents nor electrophoretic protein pattern showed any difference between the two groups. There were higher levels of inflammatory markers, interleukin-6 and C reactive protein in EPO poor responder than good responder. The negative correlations between Hb and both IL6 and CRP levels in the present data remotely indicate a positive correlation between inflammatory markers and severity of anemia.

**Keywords:** Anemia of chronic disease; Erythropoietin Resistance; Hemodialysis; Inflammatory markers; Oxidative stress; Vitamin C

## B-552. Antioxidant Activities and Liquid Chromatography with Electrospray Ionization Tandem Mass Spectrometry Characterization and Quantification of the Polyphenolic Contents of Rumex Nervosus Vahl Leaves and Stems

Kebede Taye Desta, Won Sup Lee, Sung Joong Lee, Yun-Hi Kim, Gon-Sup Kim, Soo Jung Lee, Soo Taek Kim, A. M. Abd El-Aty, Mohamad Warda, Ho-Chul Shin, Jae Han Shim and Sung Chul Shin

*Journal of Separation Science, 38 (9): 1433-1441, (2016), IF:2.741*

In the present study, four compounds, viz. chlorogenic acid, catechin, orientin, and apigenin-O-acetylglycoside among 18 polyphenol compounds (17 flavonoids and one hydroxycinnamic acid derivative) were characterized for the first time in Rumex nervosus leaves and stems by using liquid chromatography with electrospray ionization tandem mass spectrometry. Method validation in terms of determination coefficient, limits of detection, and quantification were ≥ 0.9979, 0.68–1.61, and 2.27–5.38 mg/L, respectively. Accuracy, expressed as percent recovery for two spiking levels (10 and 50 mg/L), were in the range 78.9–110.6% with the exception of caffeic acid. The relative standard deviations were 1–17%. The total polyphenol content was higher by approximately two times in the leaf (1073 mg/kg fresh sample) than in the stem (519.86 mg/kg fresh sample). The antioxidant effects increased in a dose-dependent manner, and the scavenging activities, investigated by measuring 2,2′-azino-bis(3-ethylbenzothiazoline-6-sulfonic acid) scavenging activity, ferrous ions chelating activity, superoxide anion radical scavenging activity, and ferric reducing antioxidant power activity, were significant ($p < 0.05$) using low concentrations of the leaf extract. Overall, the present study suggests that different parts of R. nervosus have great potential for producing a range of extracts with potential applications in medicine.

**Keywords:** Antioxidant Activity; Flavonoids; Polyphenols; Rumex Nervosus; Tandem Mass Spectrometry

## B-553. Biochemical and Histological Studies on Adverse Effects of Mobile Phone Radiation on Rat'S Brain

Shaymaa Hussein, Abdel-Aleem El-Saba and Mona K. Galal

*Journal of Chemical Neuroanatomy, 78: 10-19, (2016), IF: 1.8*

With the rapid development of electronic technologies, the public concern about the potential health hazards induced by radiofrequency (RF) radiation has been grown. To investigate the effect of 1800 MHz RF radiation emitted from mobile phone on the rat's brain, the present study was performed. Forty male rats were randomly divided into two equal groups; control and exposed group. The later one exposed to 1800 MHz emitted from mobile phone with an SAR value of 0.6 W/kg for two hours/day for three months. The brain tissues were collected at the end of the experimental period and separated into hippocampus and cerebellum for subsequent biochemical, histological, immunohistochemical and electron microscopic investigations. The rats that were exposed to RF- radiation had a significant elevation in MDA content and a significant reduction in antioxidant parameters (glutathione, super oxide dismutase and glutathione peroxidase) in both regions. Degenerative changes were observed in the hippocampus pyramidal cells, dark cells and cerebellar Purkinje cells with vascular congestion. In addition a significant DNA fragmentation and over expression of cyclooxygenase-2 apoptotic gene was detected. Those results suggested that, direct chronic exposure to mobile phone caused severe biochemical and histopatholog- ical changes in the brain.

**Keywords:** Mobile phone Radiofrequency Radiation Hippocampus Cerebellum Oxidative Stress Apoptosis.

## B-552. Prediction of Desirable Genotype Patterns in Baladi Beef Cattle and Water Buffalo by Identification of New Leptin Gene Snps

M.A.Ghoneim, H.A.Ogaly, E.M.Gouda and A.M.El-Behairy

*Livestock Science, 194: 51-56, (2016), IF: 1.293*

The leptin gene is considered to be an excellent candidate gene for predicting desirable economic traits in both beef and dairy cattle. Leptin gene polymorphism has been analyzed in different livestock species and the polymorphic pattern has been demonstrated to be associated with energy balance, milk production, live body weight and reproductive performance. The present study was designed to analyze genetic polymorphisms in the coding region of leptin gene in native beef cattle and water buffalo in comparison to Holstein cattle. A total number of 180 animals (60 animals of each breed) were used for blood sampling and DNA extraction. Target sites in leptin gene (first 94 bp fragment of exon 2 and 330 bp fragment including first part of exon 3) were amplified by polymerase chain reaction (PCR) using two specific primers pairs. Genotyping for R25C single nucleotide polymorphism (SNP) in exon 2 was carried out using the Kpn21-RFLP method. Variations in the exon 3 coding sequence were investigated by PCR-SSCP analysis. Two alleles (C and T) were observed in exon 2 giving rise to three R25C variants (CC, CT and TT). The highest frequency in all populations was the homozygote genotype (CC) where it recorded 91.6%, 98.3% and 100% for Baladi cattle, Holstein cattle and buffalo, respectively. Four alleles (A, B, C and D) and six genotypes (AA, AB, BB, CC, DD and CD) were identified in all studied breeds upon exon 3 analysis. Genotype AA was found to be the most dominant in all studied breeds followed by genotype CC in Holstein and Baladi cattle but followed by AB genotype in buffalo. All observed and expected genotypes were found to be statistically significant ($P \leq 0.05$) when subjected to chi-square analysis. Two point mutations have been identified in the first part of exon 3 coding sequence (a3033>t and c3051>t) of Baladi cattle samples. Polymorphisms that were detected in this study indicated that these breeds have high genetic variability in the leptin gene. These results implicate the prospective use of leptin gene polymorphisms for association studies with different productive and reproductive performances and marker assisted selection (MAS).

**Keywords:** Leptin gene; Polymorphism; Baladi cattle; Buffalo; Genotype

## B-555. Potential Therapeutic Role of Mesenchymal Stem Cell In Delayed Wound Healing of Diabetic Rats

Abdelbary Prince, Mostafa Abdalla Gad, Ibrahim W. Hasani, Mohamad Warda and Adel Elbehairy

*Der Pharmacia Lettre, (2016)*

The aim of the present work was to investigate the effect of BM-MSCs on wound closure in STZ-induced d iabetic rats. Diabetic wound models were carried out by making a standard wound on dorsum of forty rats, which were divided into four groups with ten rats in each: Wound from diabetic and non-diabetic control rats were treated with PBS, while diabetic and non-diabetic treated rats w ere treated with BM-MSCs for 12 days. The closure rate and the ratios relative to the beta actin gene of both treated groups (diabetic and non-diabetic) were significantly increased at 7 and 12 days after wounding as compared to thei r corresponding controls ($P < 0.05$). Histologic analysis revealed complete reepithelialization in treated groups. Taken together, BM-MSCs mediated correction of the diabetic wound healing impairment is due to, partly, increased VEGF expression in the skin of STZ-induced diabetic rats.

**Keywords:**BM-MSCs; Diabetic Rats; Vegf;Wound Healing

## B-556. Use of Allicin as Feed Additive to Enhance Vaccination Capacity of Clostridium Perfringens Toxoid In Rabbits

Waleed Abu El Hammed, Hamdy Soufy, Ahmed El-Shemy, Soad M. Nasra and Mohamed I. Dessouky

*Vaccine, 34, issue 17: 2000-2007, (2016), IF: 3.413*

The present study assessed the efficacy of Clostridium perfringens (C. perfringens) toxoid and/or allicin – as feed additive – in rabbits for preventing or minimizing the severity of infection with locally isolated strain of C. perfringens type A. Serum biochemical, immunological and pathological investigations were also done. on e hundred rabbits of 6 weeks of age were divided into five equal groups (G1–G5). G1 were kept as normal control. G2 was allocated for C. perfringens type A infection. G3 was vaccinated with C. perfringens toxoid at zero time and then with a booster dose at the 3rd week of the experimental period. G4 was treated with allicin 20% added to

the ration (200 mg/kg ration) all over the experimental period. G5 was vaccinated with C. perfringens toxoid at the zero time then with a booster dose at the 3rd week of the experiment period, and treated with allicin 20% from the zero time till the end of the experiment. At the 4th week, G2, G3, G4 and G5 were challenged orally (5 ml) and subcutaneously (2 ml) with 24 h cooked meat broth containing 1 × 107 colony-forming units/ml of C. perfringens type A strain. Blood and tissue samples were collected from all groups post-vaccination then post-challenge for biochemical analysis, serum neutralization test and histopathological examinations. Results revealed that rabbits treated with both allicin and toxoid vaccine demonstrated high level of antitoxin titre post-challenge, improved liver and kidney functions, and reduced morbidity and mortality rates and the severity of histopathological changes associated with challenge of rabbits with C. perfringens type A strain. In conclusion, vaccination of rabbits with C. perfringens toxoid combined with allicin 20% gave better protection, enhanced immune response and had no adverse effects on the general health conditions against C. perfringens type A infection compared to rabbits vaccinated with C. perfringens toxoid only.

**Keywords:** Rabbits; Clostridium perfringens toxoid; Allicin; Serum biochemistry; Immunostimulant; Pathology

## B-557. Assessment of Growth Performance, Hemato-Biochemical Parameters, Immunological and Histopathological Alterations Associated with New Bacterial Multistrain Probiotic (Gro-2-Max) Supplementation on Broiler Chicken.

Abeer A. Abd El-Baky and Sherein S.A. Elgayed

*International Journal of Chemtech Research, 9 (12): 996-1016 (2016)*

Long time ago, attempts for enhancing the poultry health status, are concentrating on ways for modulating the indigenous intestinal flora by live microbial adjuncts, now called “probiotics”. In the present study 126, one-day old commercial broiler chicks were used to evaluate the effect of supplementation with new bacterial multistrain probiotic (Gro-2-Max) and were equally divided into 6 groups. Group 1 (control), were fed and drank without any treatment. Supplementation in ration was done at a rate of 500 g/ton starting from 1st day till the end of experiment (42 days) in group 2, from 15th to 42nd day in group 3, and from 1st to 10th and from 30th to 42nd day in group 4. Supplementation in drinking water was carried out at a rate of 1g/liter for 24 hours starting from 1st to 5th, 16th to 20th and from 30th to 35th day in group 5, and for 3 successive days/week till 42nd day in group 6. Evaluation included monitoring chicken performance (feed intake, body weight gain, feed conversion rate, immune index and cecal bacterial enumeration), clinicopathological alterations (hemogram and serum biochemistry), immune responses (humeral and cellular), and histopathological examinations (liver, kidney, spleen, bursa of Fabricious, thymus and ileum). Results concluded to, the positive effect of Gro-2-Max® on chicken performance especially groups 2 and 6, decreasing effect on lipogram especially total cholesterol, total triglycerides and low density lipoprotein cholesterol, nonspecific humeral and cellular immune responses, and improving effect on intestinal function through increasing the height of ileal villi.

**Keywords:** Probiotics; Chicken performance;Clinical Pathology;Immunology;Histopathology.

## B-558. Histological, Histochemical and Ultrastructural Characterizations of the Epididymal Region of the Turkey (Meleagrisgallopavo).

Shaymaa Hussein

*Research Journal of Pharmaceutical, Biological and Chemical Sciences, 7(3): 1359-1369 (2016)*

Histological, histochemical and ultrastructural studies were performed on the epididymal regions of ten adult sexually mature apparently healthy male native turkeys (Meleagrisgallopavo). The epididymis of turkey was consisted of extra testicular rete, efferent ductules, connecting ductules, and the epididymal duct. The rete testis were lined by squamous to cuboidal cells, while the proximal efferent ductules were lined by pseudo stratified columnar of ciliated, non-ciliated type I and basal cells. The distal efferent ductules were lined by pseudo stratified columnar of ciliated, non-ciliated type II and basal cells. However, the connecting ductules were wide and narrow lined by pseudo stratified columnar of ciliated, non-ciliated type III and occasional basal cells of regular lumen. Narrow connecting ductules consist mainly of ciliated cells while wide consist of non-ciliated. The epididymal duct lined by pseudo stratified non ciliated columnar and basal cells of same size and intensity. Histochemically the reactivity for PAS was detected in the supra nuclear cytoplasm and luminal borders of the efferent ductular epithelium, intraepithelial gland of the epididymal duct and the basement membrane of various ducts and ductules. While such reactivity not seen in the connecting ductules.

**Keywords:** Epididymis; Histology; Histochemical; Ultrastructure; Turkey.

## B-559. Immunohistochemical Expression of Proliferating Cell Nuclear Antigen (Pcna) in the Parotid Salivary Glands of Male Albino Rats after Long Administration of Nutmeg.

El-Sakhawy MA, Al-Sabaa A1, Abusaida H, Issa Y and Moheb M

*Research Journal of Pharmaceutical, Biological and Chemical Sciences, 7, (5) (September - October): 187-199 (2016)*

A total number of 60 adult male albino rats (average weight = 200gm) were used and were classified into two main groups: 1. The Control group (Group A): comprised 20 animals. These animals received 1ml of distilled water orally on a daily basis for the duration of the experiment (2, 4, 6 and 8 weeks). 2. The Experimental group (Group B): comprised 40 animals and was subdivided into 4 subgroups corresponding to 4 durations (2, 4, 6 and 8 weeks). Each subgroup in turn was further divided into 2 subgroups in which each rat was given 1ml of the prepared nutmeg aqueous extract orally on a daily basis in the following doses (100 and 500 mg/kg b.w.) respectively. on termination of the experiment, the parotid salivary glands were dissected out, cleaned and fixed in 10%bufferedformalin solution. Then, paraffin wax sections were obtained and stained with: Haematoxylin and Eosin (H&E) to verify histological details.

Other paraffin sections were prepared and stained immunohistochemically for the expression of PCNA.The parotid gland of the control group (Group A) was composed of parenchyma which showed normal appearance of secretory acini and ducts; and fine C.T. stroma in between lobes and lobules. As for the experimental group (Group B),the most noticeable changes were cytoplasmic vacuolations in acinar cells, dilatation of intercalated and striated ducts, congestion of blood vessels, signs of nuclear changes (pyknosis, karyolysis, karyorrhexis, hyper chromatism, etc.), lymphocytic infiltration, hyalinization of C.T. stroma. These changes gradually increased as the duration increased and as the dose administered increased. PCNA Immunohistochemical Results showed weak +ve PCNA nuclei of the acini. In the experimental groups, the nuclei of the acinar cells revealed moderate +ve PCNA expression in subgroups 1 and 2, while in subgroups 3 and 4 both the nuclei of the acinar cells and the ducts revealed intense +ve PCNA expression. The cytoplasm of the acinar cells also showed weak +ve PCNA expression in subgroups 3 and 4. Image analysis results revealed significant increase in the blue binary colour was observed in the experimental groups with the increase of duration and with the increase of the dose of nutmeg extract as well.

**Keywords:** Nutmeg; Parotid; Pcna

## B-560. Eutrophication, Ammonia Intoxication, and Infectious Diseases: Interdisciplinary Factors of Mass Mortalities in Cultured Nile Tilapia

Nermeen M. Abu-Elala, Reham M. Abd-Elsalam, Sherif Marouf, Mohamed Abdelaziz and Mohamed Moustafa

*Journal of Aquatic Animal Health, 28:187-198, (2016),IF:0.859*

The present study was designed to assess the possible causes of the mass mortalities of Nile Tilapia Oreochromis niloticus at El-Behera Governorate, Egypt, in relationship to environmental and microbiotic factors. Water samples were collected from fish farms at different locations and from Lake Edku to analyze water temperature, water pH, salinity, biological oxygen demand, dissolved oxygen, total ammonia nitrogen, and un-ionized ammonia. A number of moribund and freshly dead fish were sampled and submitted to our laboratory for microbiological, molecular, and histopathological examination. Water analysis of the fish farms revealed noticeable increases in the previously mentioned physicochemical parameters. Clinical examinations of moribund fish showed severe gill rot and massive external and internal hemorrhages. Ordinary and molecular laboratory findings confirmed the presence of Branchiomyces sp. in gill tissue and mixed bacterial fish pathogens (Streptococcus agalactiae, Vibrio alginolyticus, V. parahaemolyticus, Pseudomonas anguilliseptica, and P. aeruginosa) in visceral organs. The histopathological and transmission electron microscopic examinations revealed severe necrosis of gill filaments and blockage of branchial blood vessels and lamellar capillaries with Branchiomyces sp. hyphae and spores mixed with different shapes of bacteria. Severe inflammations were detected in liver, kidney, heart, and brain tissues. Ultimately, we can conclude that the syndrome of mass fish kills in this area is a consequence of ecological damage to the aquatic environment, which is mainly related to natural and anthropogenic factors, as well as to the presence of infectious agents.

**Keywords:** Interdisciplinary Causes of Mass Mortalities in Cultured Fish.

## B-561. Improving the Physico-Chemical and Sensory Characteristics of Camel Meat Burger Patties Using Ginger Extract and Papain

Heba H.S. Abdel-Naeem and Hussein M.H. Mohamed

*Meat Science, 118: 52-60, (2016), IF: 2.801*

The objective of the current study was to include tenderizing agents in the formulation of camel meat burger patties to improve the physico-chemical and sensory characteristics of the product. Camel meat burger patties were processed with addition of ginger extract (7%), papain (0.01%) and mixture of ginger extract (5%) and papain (0.005%) in addition to control. Addition of ginger, papain and their mixture resulted in significant (P b 0.05) increase of the collagen solubility and sensory scores (juiciness, tenderness and overall acceptability) with significant (P b 0.05) reduction of the shear force values. Ginger extract resulted in extensive fragmentation of myofibrils; however, papain extract caused noticeable destructive effect on connective tissue. Moreover, ginger and papain resulted in improvement of the lipid stability of treated burger patties during storage. Therefore, addition of ginger extract and papain powder during formulation of camel burger patties can improve their physico-chemical and sensory properties.

**Keywords:** Camel meat; Burger patties; Ginger extract; Papain; Tenderness; Collagen solubility.

## B-562. Effect of Cooking Temperature on Characteristics and Microstructure of Camel Meat Emulsion Sausages

Hussein MH Mohamed, Mohamed MT Emara and Taha M Nouman

*Journal of The Science of Food and Agriculture, 96: 2990-2997, (2016), IF: 2.076*

**Background:** The camel is an excellent source of high quality meat and camel meat might be a potential alternative for beef. This study aimed to manipulate the raw camel meat for the production of stable and acceptable emulsion sausage, as well as to study the effect of cooking at different core temperatures on the tenderness, sensory quality and microstructure of produced sausage. **Results:** Increasing the cooking temperature of sausages resulted in reduction of the shear force values from 2.67 kgf after cooking at 85 C to 1.57 kgf after cooking at 105 C. The sensory scores of sausages have been improved by increasing the cooking core temperature of meat batter. The light and scanning electron microscope micrographs revealed solubilisation of the high quantity of connective tissue of camel meat. High emulsion stability values for the camel meat batter associated with high values of water-holding capacity for raw camel meat and meat batter have been recorded. **Conclusion:** Stable and acceptable camel meat emulsion can be developed from camel meat. Increasing the cooking core temperature of meat batter improved the quality of produced sausages. Therefore, camel meat emulsion sausages might be a potential alternative for beef particularly in Asian and African countries

**Keywords:** Camel meat; Emulsion sausages; Scanning electron Microscope; Cooking temperature.

## B-563. Detection of Mechanically Recovered Poultry Meat (Mrpm) in Traditional Egyptian Luncheon (Emulsion Type Sausage)

Mai A. Mohamed, Dalia A. Zahran, Gehan M.A. Kassem, M.M.T. Emara and N.M. Mansour

*Polish Journal of Food and Nutrition Sciences, 66: 17-23, (2016), IF: 0.679*

Detection of MRPM in emulsion type products is a challenge facing meat industry. Where, most of meat products processors in Egypt illegally replace beef meat partially or totally with MRPM in meat products to reduce products cost. Commercial and experimentally produced emulsion type sausage (traditional Egyptian luncheon) formulated with 0, 10, 30, 50, 70, 90% MRPM instead of the meat mass and cooked to different core temperature (70, 80 and 90°C) were examined for technological properties, ash, bones, cartilage and calcium (Ca) content, in addition to histological sections stained with H&E and Trichrome blue. Results indicated that all market samples showed unacceptable texture and binding scores with high ash, collagen, cartilage, bone and Ca content. Histological section showed the presence of skin and cartilage. Addition of 10% MRPM to luncheon formulation could not be detected at different cooking temperatures. While the use of 30% or more MRPM to luncheon formulation, signifi cantly changed technological properties and chemical composition of the product. Thermal treatments of luncheon sausages changed their chemical composition as well as induced structural changes in bone and cartilage content.

**Keywords:** MRPM; Egyptian luncheon; Calcium; Bone and Cartilage.

## B-564. Detection of Mycobacterium Avium Subsp. Paratuberculosis In Raw Buffaloe""s Milk

Nagah M. Hafiz, Saad, M.F., Hanafy, M.H. and Eman F. Abdel - Latif

*International Journal of Chemtech Research, 9:123-128 (2016)*

Mycobacterium avium subsp.paratuberculosis(MAP) is the causative organism of paratuberculosis, a disease with extensive economic effect,superlatively on dairy cattle. on e hundred ninety-two Egyptian buffaloes' milk samples were examined for MAP.Sixteen (8.33%) samples could be detected by milk-Enzyme-Linked Immunosorbent Assay (ELISA). No samples were found positive in milk-Polymerase Chain Reaction (PCR).

**Keywords:** Buffaloe's milk; Mycobacterium avium subsp. Paratuberculosis; Enzyme - Linked Immunosorbent assay; Polymerase chain reaction.

## B-565. Influence of Selected Essential Oils on Some Pathogenic Microorganisms in White Soft Cheese

Ayah, B. Abdel - Salam and Saad, M.F

*International Journal of Chemtech Research, 9:214-220 (2016)*

This study was designed to show the effect of antimicrobial properties of some Essential Oils (EOs); cinnamon and thyme oils for four weeks on S.aureus and E.coli microorganisms in white soft cheese. The higher sensory score of cheese samples was gained at first two weeks with cinnamon oil. S.aureus and E.coli count of cinnamon and thyme oils cheese samples significantly decreased ($P<0.05$) through 3 and 4 weeks of storage. The cinnamon and thyme oils had the different degrees of antibacterial effect on the selected pathogenic microorganisms during the storage of cheese.

**Keywords:** Cinnamon oil; Thyme oil; S.Aureus; E.Coli; White Soft cheese.

## B-566. Occurrence of Escherichia Coli and Coliforms in Processed Cheese

Sallam, S. S., Salwa A. Aly and Al Banna A.

*International Journal of Chemtech Research, 9:313-319 (2016)*

One hundred and twenty samples of processed cheese representing: 60 samples of processed cheese cubes, 30 samples blocks and 30 samples spread were randomly collected from different super markets in Cairo, Giza, Alexandria and Behira Governorates, Egypt. Collected samples were subjected to Coliform count as well as biochemical and serological identification of the isolated strains. The results reveal the presence of Coliforms, in percentages of 25.8%. on the other hand, Escherichia coli (E. coli) could be detected in in percentages of 2%. on ly three isolated of E. coli could be serologically identified as E. coli O27. The degree of acceptability of the processed cheese samples vs Egyptian standards was determined the economic and public health significance of contamination of processed cheese products was discussed.

**Keywords:** Coliforms; Escherichia coli and processed cheese.

## B-567. Phylogenetic and Comparative Genomics of the Family Leptotrichiaceae and Introduction of A Novel Fingerprinting Mlva for Streptobacillus Moniliformis

Tobias Eisenberg, Ahmad Fawzy, Werner Nicklas, Torsten Semmler and Christa Ewers

*Bmc Genomics, 17: 864-0, (2016), IF: 3.867*

**Background** The Leptotrichiaceae are a family of fairly unnoticed bacteria containing both microbiota on mucous membranes as well as significant pathogens such as Streptobacillus moniliformis, the causative organism of streptobacillary rat bite fever. Comprehensive genomic studies in members of this family have so far not been carried out. We aimed to analyze 47 genomes from 20 different member species to illuminate phylogenetic aspects, as well as genomic and discriminatory properties. **Results** Our data provide a novel and reliable basis of support for previously established phylogeny from this group and give a deeper insight into characteristics of genome structure and gene functions. Full genome analyses revealed that most S. moniliformis strains under study form a heterogeneous population without any significant clustering. Analysis of infra-species variability for this highly pathogenic rat bite fever organism led to the detection of three specific variable number tandem analysis loci with high discriminatory power. **Conclusions** This highly useful and economical tool can be directly employed in clinical samples without laborious prior cultivation. Our and prospective case-specific data can now easily be compared by using a newly established MLVA database in order to gain a

better insight into the epidemiology of this presumably under-reported zoonosis.
**Keywords:** Next generation sequencing-Multi locus variable number; Tandem repeat analysis (Mvla)-Phylogeny-Typing-Fingerprinting-Streptobacillus leptotrichiaceae.

## B-568. New Polymorphisms Within the Variable Number Tandem Repeat (Vntr) 7 Locus of Mycobacterium Avium Subsp. Paratuberculosis

Ahmad Fawzy, Michael Zschöck, Christa Ewers and Tobias Eisenberg

*Molecular and Cellular Probes, 30: 132-137, (2016), IF: 1.565*

Variable number tandem repeat (VNTR) is a frequently employed typing method of Mycobacterium avium paratuberculosis (MAP) isolates. Based on whole genome sequencing in a previous study, allelic diversity at some VNTR loci seems to over- or under-estimate the actual phylogenetic variance among isolates. Interestingly, two closely related isolates on one farm showed polymorphism at the VNTR 7 locus, raising concerns about the misleading role that it might play in genotyping. We aimed to investigate the underlying basis of VNTR 7-polymorphism by analyzing sequence data for published genomes and field isolates of MAP and other M. avium complex (MAC) members. In contrast to MAP strains from cattle, strains from sheep displayed an “imperfect” repeat within VNTR 7, which was identical to respective allele types in other MAC genomes. Subspecies- and strain-specific single nucleotide polymorphisms (SNPs) and two novel (16 and 56 bp) repeats were detected. Given the combination of the three existing repeats, there are at least five different patterns for VNTR 7. The present findings highlight a higher polymorphism and probable instability of VNTR 7 locus that needs to be considered and challenged in future studies. Until then, sequencing of this locus in future studies is important to correctly assign the underlying allele types.
**Keywords:** Paratuberculosis; Mycobacterium; Imperfect snps; Vntr.

## B-569. First Report of Miru-Vntr Genotyping of Mycobacterium Avium Subsp. Paratuberculosis Isolates from Egypt

A. Fawzy, A. Fayed, H. Youssef, A. El-Sayed and M. Zschöck

*Iranian Journal of Veterinary Research, 17:130-133,(2016), IF: 0.167*

Mycobacterium avium subsp. paratuberculosis (MAP) is the causative agent of Johne's disease, an economically important disease in ruminants worldwide. It was first isolated in Egypt in 2005. Since then, the pathogen has been detected in different Egyptian provinces. In order to trace the source of infection, genotyping using simple methods of high discriminatory power such as mycobacterial interspersed repetitive unit-variable number tandem repeats (MIRU-VNTR) were carried out in different countries. Until now there is no published information about MIRU-VNTR genotyping of MAP isolates in Egypt. To address that point, 100 faecal samples were collected and cultivated from 3 different suspected dairy farms. Fourteen isolates belonging to one farm were identified as MAP and subjected to genotyping using 8 different MIRU-VNTR loci PCRs. Two different genotypes were recognized based on size polymorphism observed in one locus (VNTR-7) that was confirmed by sequencing. Our work provides a preliminary basis of constructing a MIRU-VNTR genotyping database of MAP in Egypt.
**Keywords:** Egypt; Inmv; Miru-Vntr; Paratuberculosis.

## B-570. Dispersion of the Vancomycin Resistance Genes Vana and Vanc of Enterococcus Isolated from Nile Tilapia on Retail Sale: A Public Health Hazard

Kamelia M. Osman, Mohamed N. Ali, Ismail Radwan, Fatma ElHofy, Ahmed H. Abed, Ahmed Orabi and Nehal M. Fawzy

*Frontiers In Microbiology, 7: 1-9, (2016), IF: 4.165*

Although normally regarded harmless commensals, enterococci may cause a range of different infections in humans, including urinary tract infections, sepsis, and endocarditis. The acquisition of vancomycin resistance by enterococci (VRE) has seriously affected the treatment and infection control of these organisms. VRE are frequently resistant to all antibiotics that are effective treatment for vancomycin-susceptible enterococci, which leaves clinicians treating VRE infections with limited therapeutic options. With VRE emerging as a global threat to public health, we aimed to isolate, identify enterococci species from tilapia and their resistance to van-mediated glycopeptide (vanA and vanC) as well as the presence of enterococcal surface protein (esp) using conventional and molecular methods. The cultural, biochemical (Vitek 2 system) and polymerase chain reaction results revealed eight Enterococcus isolates from the 80 fish samples (10%) to be further identified as E. faecalis (6/8, 75%) and E gallinarum (2/8, 25%). Intraperitoneal injection of healthy Nile tilapia with the eight Enterococcus isolates caused significant morbidity (70%) within 3 days and 100% mortality at 6 days postinjection with general signs of septicemia. All of the eight Enterococcus isolates were found to be resistant to tetracycline. The 6/6 E. faecalis isolates were susceptible for penicillin, nitrofurantoin, gentamicin, and streptomycin. on the other hand 5/6 were susceptible for ampicillin, vancomycin, chloramphenicol, and ciprofloxacin. The two isolates of E. gallinarum were sensitive to rifampicin and ciprofloxacin and resistant to vancomycin, chloramphenicol, and erythromycin. Molecular characterization proved that they all presented the prototypic vanC element. on the whole, one of the two vancomycin resistance gene was present in 3/8 of the enterococci isolates, while the esp virulence gene was present in 1/8 of the enterococci isolates. The results in this study emphasize the potential role that aquatic environments are correlated to proximity to anthropogenic activities in determining the antimicrobial resistance patterns of Enterococcus spp. recovered from fish in the river Nile in Giza, Elmounib, Egypt as a continuation of our larger study on the reservoirs of antibiotic resistance in the environment.
**Keywords:** Nile tilapia; Antibiotic resistance phenotype; Esp; Vana and vanc genes; E. Faecalis; E. Gallinarum.

## B-571. Prevalence of the Antibiotic Resistance Genes in Coagulase-Positive-and Negative-Staphylococcus in Chicken Meat Retailed to Consumers

Kamelia Osman, Jihan Badr, KhalidS.Al-Maary, IhabM.I.Moussa, Ashgan M.Hessain, Zeinab M.S. Amin Girah , Usama Abo-shama, Ahmed Orabi and Aalaa Saad

*Frontiers in Microbiology, 7: 1-12, (2016), IF: 4.165*

The use of antibiotics in farm management (growing crops and raising animals) has become a major area of concern. Its implications is the consequent emergence of antibiotic resistant bacteria (ARB) and accordingly their access into the human food chain with passage of antibiotic resistance genes (ARG) to the normal human intestinal microbiota and hence to other pathogenic bacteria causative human disease. Therefore, we pursued in this study to unravel the frequency and the quinolone resistance determining region, mecA and cfr genes of methicillin-susceptible Staphylococcus aureus (MSSA), methicillin-resistant S. aureus (MRSA), methicillin-resistant coagulase-negative staphylococci (MRCNS) and methicillin-susceptible coagulase-negative staphylococci (MSCNS) isolated from the retail trade of ready-to-eat raw chicken meat samples collected during one year and sold across the Great Cairo area. The 50 Staphylococcus isolated from retail raw chicken meat were analyzed for their antibiotic resistance phenotypic profile on 12 antibiotics (penicillin, oxacillin, methicillin, ampicillin-sulbactam, erythromycin, tetracycline, clindamycin, gentamicin, ciprofloxacin, chloramphenicol, sulfamethoxazole-trimethoprim and vancomycin) and their endorsement of the quinolone resistance determining region, mecA and cfr genes. The isolation results revealed 50 isolates, CPS (14) and CNS (36), representing ten species (S. aureus, S. hyicus, S. epidermedius, S. lugdunensis, S. haemolyticus, S. hominus, S. schleiferi, S. cohnii, S. intermedius and S. lentus). Twenty seven isolates were methicillin-resistant. Out of the characterized 50 staphylococcal isolates, three were MRSA but only 2/3 carried the mecA gene. The ARG that bestows resistance to quinolones, β-lactams, macrolides, lincosamides and streptogramin B (MLS(B)) in MRSA and MR-CNS were perceived. According to the available literature, the present investigation was a unique endeavor into the identification of the quinolone-resistance-determining-regions, the identification of MRSA and MR-CNS from retail chicken meat in Egypt. In addition, these isolates might indicate the promulgation of methicillin, oxacillin and vancomycin resistance in the community and imply food safety hazards.

**Keywords:** Antimicrobial resistance phenotype; Resistance in the quinolone; Resistance; Determining-Regions; BiofilmChicken meat; Meca gene.

## B-572. Determination of Virulence and Antibiotic Resistance Pattern of Biofilm Producing Listeria Species Isolated from Retail Raw Milk

Kamelia M. Osman, Ahmed Samir, Usama H. Abo-Shama, Essam H. Mohamed, Ahmed Orabi and Tara Zolnikov

*Bmc Microbiology, 16: 2-13, (2016), IF: 2.581*

**Background:** on e of the foodborne pathogens is Listeria monocytogenes, which causes serious invasive illness in elderly and immunocompromised patients, pregnant women, newborns and infants ranking second after salmonellosis because of its high case fatality rate. Listerial cow mastitis marked by abnormal milk, increased cell counts and reduced production has not been reported. Therefore, apparently healthy cows can be reservoirs of L. monocytogenes. A number of 203 udder milk samples from apparently healthy animals (buffalo, n = 100; cow, n = 103) were collected and tested for Listeria. Isolated colonies on the PALCAM agar were Listeria species confirmed according to their biochemical and the Christie–Atkins–Munch-Petersen (CAMP) reactions. The Listeria species pathogenicity of was tested by phosphatidylinositol-specific phospholipase C, DL-alanine-β-naphthylamide HCl, Dalanine-p-nitroanilide tests, chick embryo, mice inoculation tests, Vero cell cytotoxicity and biofilm formation. The virulence-associated genes, hlyA, plcB, actA and iap associated with Listeria were molecularly assayed. **Results:** The 17 isolated Listeria spp. represented a prevalence rate of 8.4 %. of these 3 (1.4 %), 2 (1 %), 5 (2.5 %), 4 (2 %) and 3 (1.5 %) were confirmed as L. monocytogenes, L. innocua, L. welshimeri, L. seelegeri, respectively. While the L. monocytogenes isolate displayed all the four virulence-associated genes, L. seelegeri carried the hlyA gene only. The L. monocytogenes had a strong in vitro affinity to form a biofilm, in particular serotype 4 which is associated with human infections. L. monocytogenes showed resistance for 9/27 antibiotics. **Conclusions:** The biofilm forming capability of the Listeria spps. makes them particularly successful in colonizing surfaces within the host thus being responsible for persistence infections and due to their antimicrobial resistant phenotype that this structure confers. In addition, strains belonging to serotypes associated with human infections and characterized by pathogenic potential (serotype 4) are capable to persist within the processing plants forming biofilm and thus being a medical hazard.

**Keywords:** Listeria species; Buffalo; Cow; Virulence genes; Biofilm formation; Antibiotic resistance.

## B-573. Different Counteracting Host Immune Responses to Clade 2.2.1.1 and 2.2.1.2 Egyptian H5n1 Highly Pathogenic Avian Influenza Viruses in Naïve and Vaccinated Chickens

Ahmed A. Samy, Mona I. El-Enbaawy, Ahmed A. El- Soad A. Nasef, Mahmoud. Naguib, E.M. Abdelwhab, Hirokazu Hikonod and Takehiko Saitod.

*Veterinary Microbiology, 183: 103-109, (2016), IF: 2.564*

In Egypt, two distinct lineages of H5N1 highly pathogenic avian influenza (HPAI) viruses, “classic 2.2.1.2” and “variant 2.2.1.1” strains, have evolved. The underlying host immune responses counteracting these viruses in chickens remain not well understood. In the present study, the cytokine responses to a classic strain (C121) and those to a variant strain (V1063) were compared in naïve and vaccinated chickens. In naïve chickens, the C121 replicated more efficiently than the V1063. Both the C121 and the V1063 increased interferon (IFN)-γ and interleukin (IL)-10 gene expression at 48 h post inoculation (hpi) in the lung and spleen but the levels of these cytokines were lower in chickens infected with the C121 than those infected with the V1063. In contrast, in chickens vaccinated with inactivated C121-based vaccine, the C121 replicated less than the V1063. Both challenge with the C121 and that with the

V1063 did not increase IFN-γ gene expression at 48 hpi; rather, the C121 increased IL-4 gene expression in the lung accompanied with lower viral titer and higher HI titers. These results suggested that the pathogenicity of HPAI viruses correlated with IFN-γ-producing helper and/or cytotoxic T cell responses in naïve chickens, whereas vaccine efficacy to HPAI viruses correlated with IL-4 producing helper T cell responses in the lung in vaccinated chickens. It implies that IL-4 in the lung, in addition to the traditional serum HI titers, could be used to screen novel vaccine strategies, such as strains, adjuvant, prime/boost protocols, against HPAI in chickens.

**Keywords:** Avian influenza (Hpai) virus subtype H5n1; The egyptian; Vaccinationi; Fnα.

## B-574. Synthesis and Molecular Modeling of Antimicrobial Active Fluoroquinolone–Pyrazine Conjugates with Amino Acid Linkers

Siva S. Panda, Oleksandr S. Detistov, Adel S. Girgis, Prabhu P. Mohapatra, Ahmed Samir and Alan R. Katritzky

*Bioorganic and Medicinal Chemistry Letters, 26: 2198-2205, (2016), IF: 2.486*

Novel fluoroquinolone–pyrazine conjugates 7a–h with amino acid linkers were synthesized in good yields utilizing benzotriazole chemistry. Antimicrobial bioassay showed that the synthesized bis-conjugates have antimicrobial properties comparable to the parent drugs. Compound 7h showed superior antibacterial activity against Staphylococcus aureus and Streptococcus pyogenes (MIC = 74.6 μM and 149.3 μM, respectively). This matched well with the estimated values obtained from 3D-pharmacophore and 2D-QSAR studies (MIC = 67 μM and 92.9 μM, respectively)

**Keywords:**Antibiotics; Conjugates; Benzotriazole; Chemistry; Computational studies.

## B-575 .Initiation and Regulation of Immune Responses to Immunization with Whole Inactivated Vaccines Prepared from Two Genetically and Antigenically Distinct Lineages of Egyptian Influenza A Virus Subtype H5n1

Samy El-Enbaawy, El-Sanousi, Nasef and Hikono Saito

*Archives of Virology, 161(10): 2797-806, (2016), IF: 2.255*

Following the introduction of highly pathogenic avian influenza (HPAI) virus subtype H5N1, the Egyptian government implemented a massive poultry vaccination campaign as the cornerstone of its policies to control the virus. The efficacy of vaccination has been evaluated primarily by measuring titers of antibodies inhibiting the hemagglutinating activity of the viral hemagglutinin (HA). However, other aspects of the host response remain poorly understood. In the present study, in addition to hemagglutination inhibition (HI) titers, cytokine profiles were examined and IFNγ concentrations were measured in vivo after immunization with a whole inactivated virus (WIV) prepared from a classical strain of clade 2.2.1.2 (C121) and an antigenic drift variant of clade 2.2.1.1 (V1063). The results revealed an earlier response and higher HI titers and IFNγ levels in sera from chickens immunized with C121, accompanied by significantly higher expression of IL8, IL10, and IL18 in the spleen and IL6 and IL10 in the bursa, compared to those immunized with V1063. Furthermore, stimulation of the HD11 cell line with C121 induced gradual upregulation of pro-inflammatory cytokines, which was observed at 24 hours post-inoculation (hpi), and became more pronounced at 48 and 72 hpi, accompanied by upregulation of IFNα. Conversely, V1063 induced very early transient higher expression of pro-inflammatory cytokines at 3 and 6 hpi accompanied by upregulation of IL10, which then decreased at 24, 48 and 72 hpi. In summary, our results provide evidence of a correlation between adaptive immune responses induced by WIVs and higher expression of IL10 and IL18 in addition to early induction of IFNα. These findings could be used to improve immune responses induced by WIVs.

**Keywords:** Avian influenza (Hpai) Virus subtype H5n1; The egyptian; Vaccinationi; Fnα.

## B-576. Comparative Studies for Serodiagnosis of Haemorrhagic Septicaemia in Cattle Sera

Jakeen K. El-Jakee, Samah Said Ali, Soumaya Ahmed El-Shafii, Ashgan M. Hessain, Abdullah A. Al-Arfaj and Moussa I. Mohamed

*Saudi Journal of Biological Sciences, 23: 48-53, (2016), IF:1.781*

Haemorrhagic septicaemia caused by Pasteurella multocida is a major epizootic disease in cattle and buffaloes in developing countries with high morbidity and mortality rate. In the present study, a total of 88 P. multocida isolates were isolated from 256 nasopharyngeal swabs and lung tissues samples (34.4%) during the period from January, 2013 to March, 2014 from different governorates located in Egypt. Dead calves showed the highest percentage of P. multocida isolation followed by the emergency slaughtered calves, diseased calves then apparently healthy ones. These isolates were confirmed as P. multocida microscopically, biochemically by traditional tests and by API 20E commercial kit then by PCR. The percentages of positive serum samples using somatic antigen and micro-agglutination test at 1/1280 diluted serum were 10%, 54.49% and 0% in apparently healthy, diseased and emergency slaughtered samples, respectively whereas, the percentages using capsular antigen and indirect haemagglutination test were 40%, 60.89% and 60% in apparently healthy, diseased and emergency slaughtered samples, respectively. The ELISA showed the highest sensitivity for diagnosing P. multocida in apparently healthy, diseased and emergencyslaughtered animals with percentages of 42%; 92.9% and 80%, respectively. The obtained results revealed that the ELISA using capsular antigen of P. multocida is a more sensitive and specific serological test for diagnosis of haemorrhagic septicaemia.

**Keywords:** Haemorrhagic septicaemia; Serodiagnosis; Hat; Ihat; ELISA.

## B-577. Coagulase-Negative Staphylococci Collected from Bovine Milk: Species and Antimicrobial Gene Diversity

kamelia. osman, khaled. abd el-razik, hanan. marie and amany arafa

*Journal of Food Safety, 36: 89-99, (2016), IF: 0.915*

The aim of this study was to examine the genetically mediated antimicrobial resistance in 94 coagulase-negative

staphylococcal (CNS) milk isolates (buffalo, n = 88, and cow, n = 6), and to determine whether antimicrobial resistance profiles differed between bacterial species. Our analysis of 94 CNS isolates from milk confirmed the well-established multiresistant character of staphylococci in the dairy setting. Resistance against oxacillin, ciprofloxacin and cefoxitin was most frequently observed. Eleven CNS species isolated from buffalo's and cow's milk samples were 100% sensitive to gentamicin, erythromycin, clindamycin and ciprofloxacin. Resistance to oxacillin was attributed to the mecA gene in 44.7% of the oxacillin-resistant isolates. The mecA gene was detected in Staphylococcus intermedius, epidermidis, hominis, hyicus, caprae, sciuri, lugdunensis and xylosus while totally absent in chromogenes, simulans and lentus. of the 11 CNS species, S. epidermidis, S. lugdunensis, S. hominis, S. xylosus and S. intermedius were the only species that exhibited multiple resistance.

**Keywords:** Meca gene; Coagulase-Negative Staphylococcal; Milk bovine.

## B-578. Production and Evaluation of Autogenous Vaccine Against Avian Colibacillosis

J. K. El Jakee, G. M. El Amry, A. M. Hessain, H. A. Hemeg S. M. Shafei and I. M. Moussa

*Journal of Animal and Plant Sciences, 26(1): 79-87, (2016), IF: 0.422*

The present investigation aimed to prepare a potent Escherichia coli vaccine to control colibacillosis in chickens. Firstly a total of 7 Escherichia coli isolates: O125: K 70, O1: K-, O146: K-, O26: K: –, O 78: K 80, O126: K58 and O128: K 67 were collected from diseased chickens. The collected strains were examined for virulent genes (stx1, stx2, eaeA and hylA) using PCR and analyzed by SDS-PAGE. Inactivated whole culture and outer membrane protein (OMP) vaccines were developed from Escherichia coli serogroups O1 and O78 and determined their potency to induce antibody response against colibacillosis in comparison to Nobilis® vaccine using Micro-agglutination test (MAT) and Enzyme Liked Immunosorbent assay (ELISA). The prepared inactivated and Escherichia coli outer membrane protein vaccines were free from bacterial and fungal contamination and both of the vaccines were found safe with no clinical symptoms when inoculated subcutaneously with double field dose into chicks. The protection rate of the inactivated vaccine was 84%, the protection rate in Nobilis® E. coli inactivated vaccine was 80% and the protection rate in OMP vaccine was 92%. Meanwhile, the mortality rate was 28% among the unvaccinated chicken. The results of this study indicate the higher protection rate of OMP and suggesting further development of OMP as a vaccine for protection of chickens against E. coli infections.

**Keywords:** Escherichia coli; Vaccine; Outer membrane Proteins (OMP); Elisa; Virulent genes.

## B-579. Detection of Virulence Genes and Antimicrobial Resistance of Bacterial Isolates of Diarrhea in Newly Borne Buffalo Calves.

Wagdy R. ElAshmawy, Sherif Maroufand Hussein M. Galal.

*Research Journal of Pharmaceutical, Biological and Chemical Sciences, 7(4): 1728-1735 (2016)*

Diarrhea in newly borne calves (Cattle or Buffalo) remains one of the important economically life threatening disease. The study was carried out on 120 buffalo calves, 80 suffered from diarrhea and 40 apparently healthy. They are aged from one day old till 2 months. The prevalence of Salmonellosis in examined calves was 15.8%. It was 21.25% in calves with diarrhea and 5% in apparently healthy ones. The prevalence of E. coli infection in examined calves was 15%. It was 18.75% in calves with diarrhea and 7.5% in apparently healthy ones. The virulence genes of Salmonella isolates including invA was detected in all isolates (100%), while bcfC gene was detected in 47% of the isolates. In contrast, avrA and ssaQ gene were identified in only 36% of the isolates. The 16 SrDNA ompA and fimH genes were identified in all E.coli isolates and Iss gene was not detected in any isolates. The antimicrobial susceptibility was carried out on isolated Salmonella and E. coli strains using 14 different antibacterials. All Salmonella isolates were resistant to lincomycin, neomycin and gentamicin but all were susceptible to ciprofloxacin and streptomycin. E. coli isolates were resistant to neomycin, sulfamethoxazole + trimethoprim and nalidixic acid but all were susceptible to ciprofloxacin, gentamicin and streptomycin.

**Keywords:** Salmonella; E.Coli, Buffalo calves; Virulence Genes; Antimicrobial resistance.

## B-580. Eucalyptus Tree: A Potential Source of Cryptococcus Neoformans in Egyptian Environment

Mahmoud Elhariri, Dalia Hamza, Rehab Elhelw and Mohamed Refai

*International Journal of Microbiology, 1-5 (2016)*

In Egypt, the River Red Gum (Eucalyptus camaldulensis) is a well-known tree and is highly appreciated by the rural and urban dwellers.The role of Eucalyptus trees in the ecology of Cryptococcus neoformans is documented worldwide.The aim of this survey was to show the prevalence of C. neoformans during the flowering season of E. camaldulensis at the Delta region in Egypt.Three hundred and eleven samples out of two hundred Eucalyptus trees, including leaves, flowers, and woody trunks, were collected from four governorates in the Delta region.Thirteen isolates of C. neoformans were recovered from Eucalyptus tree samples (4.2%). Molecular identification of C. neoformans was done by capsular gene specific primer CAP64 and serotype identification was done depending on LAC1 gene. This study represents an update on the ecology of C. neoformans associated with Eucalyptus tree in Egyptian environment.

**Keywords:** Eucalyptus tree; Cryptococcus neoformans; Lac1 Gene; Ecology; Egypt.

## B-581. Frequency of Fungal and Aflatoxin B1 Contaminants in Cattle Feed

El-Enbaawy, M. H. Soliman and Nagwa, S. Ata.

*International Journal of Pharmtech Research, 9 (10): 81-88 (2016)*

**Background** Fungal contamination of animal feed is extensively widespread as those fungi are ubiquitous in nature. Among those fungi is Aspergillus which produce aflatoxins when favored conditions of temperature and humidity are

available. There are four major types of aflatoxins B1, B2, G1 and G2. Aflatoxin B1 which considered as the most dangerous naturally occurring toxin have carcinogenic effect on both human and animals. **Method** Sixty finished cattle feed samples from Giza governorate were examined for the presence of fungi and aflatoxin B1 contaminants. Total mould count (TMC) was performed by pour platting technique while aflatoxin B1 detection was done using thin layer chromatography (TLC) technique. **Results** The total mould count / gm was calculated with mean ± standard error 5.58X104 ±2.96X104 . Our results showed that the most commonly isolated fungal genera was Aspergillus (85%). Among Aspergillus genus, A. flavus was the most frequently isolated species as it was isolated from 71.7% from total samples. TLC analysis of aflatoxin B1 revealed its presence in 18.3% from the total examined samples with range between 1.5-72.4 ppb and finally the mean ± standard error was 24.15 ± 8.16 **Conclusions in Conclusion**, Regular monitoring for the presence of aflatoxin B1 in animal feed is crucial for implementing perfect feed safety programs as aflatoxin B1 consumption can increase susceptibility to diseases, impair the reproductive performance and it can be excreted in milk in the form of aflatoxin M1 which considered of major public health concern

**Keywords:** Animal Feed; Total mould count; Aflatoxin B1; TLC.

## B-582. Phenotypic and Genotypic Characterization of Locally Isolated Salmonella Strains Used in Preparation of Salmonella Antigens in Egypt.

Hazem Mohammed Ibrahim, Dalia Ahmed Mohammed Abd El-Moaty, Hanan Ali Ahmed and Mona Ibrahim El-Enbaawy

*Journal Veterinary World, Vol 9, p1435-1440 (2016)*

**Aim:** This work was conducted to study the phenotypic and genotypic characterization of locally isolated *Salmonella* strains (*Salmonella* Pullorum, *Salmonella* Enteritidis, and *Salmonella* Typhimurium) from poultry used in the preparation of *Salmonella* antigens in Egypt. **Materials and Methods:** The phenotypic characterization of *Salmonella* strains was done using standard microbiological, biochemical, and serological techniques. Molecular identification was done using different sets of primers on different genes using different polymerase chain reaction (PCR) techniques. **Results:** The phenotypic characterization of *Salmonella* strains was confirmed. Molecular identification revealed detection of 284 bp fragment of InvA gene in all studied *Salmonella* strains. Furthermore, multiplex PCR was used for more confirmation of being *Salmonella* spp., generally at 429 bp as well as genotyping of *Salmonella* Typhimurium and *Salmonella* Enteritidis at 559 and 312 bp, respectively, in one reaction. **Conclusion:** The locally isolated field *Salmonella* strains were confirmed phenotypically and genotypically to be *Salmonella* Enteritidis, and *Salmonella* Typhimurium and could be used for the preparation of *Salmonella* antigens.

**Keywords:** Characterization; Duplex Polymerase Chain Reaction, Multiplex Polymerase Chain Reaction, *Salmonella* spp.

## B-583. Supplementation of Freezing andthawing media with brain-derivedneurotrophic factor protects humansperm from freeze-thaw-induceddamage

Atefeh Najafi, Ebrahim Asadi, Adel R. Moawad, Saideh Mikaeili, Fardin Amidi, Emmanuel Adutwum, Majid Safa and Ali Gholi Sobhani

*Fertility and Sterility, 106: 1658-16650000, (2016), IF: 4.426*

**Objective:** To investigate the effects of brain-derived neurotrophic factor (BDNF) supplementation to freezing and thawing media on frozen-thawed human sperm parameters. **Design:** Laboratory study. **Setting:** University hospital. Patient(s): Semen samples from 21 healthy fertile men. **Intervention(s):** We measured reactive oxygen species (ROS) by flow cytometry using the probes dichlorofluorescin diacetate for intracellular hydrogen peroxide (H2O2) and dihydroethidium for intracellular superoxide anion (O2 –), sperm plasma membrane integrity by flow cytometry, caspase-3 activity using ELISA, and AKT phosphorylation status using Western blot in sperm that was cryopreserved and thawed in media either supplemented with BDNF or without BDNF supplementation (control). Main Outcome Measure(s): Sperm motility, viability, ROS levels, caspase-3 activity and AKT phosphorylation**. Result(s):** The percentage of motile and viable sperm cells was significantly higher in BDNF-supplemented groups as compared with the nonsupplemented (control) group. There was a significant difference in AKT phosphorylation status between BDNF-supplemented groups and the control group. Moreover, the levels of intracellular H2O2 and caspase-3 activity were significantly lower in the sperm cells that were frozen and thawed in media supplemented with BDNF compared with in the control group. **Conclusion(s):** BDNF supplementation to sperm freezing or thawing media has protective effects against oxidative stress and apoptosis in frozen-thawed human spermatozoa and could improve sperm function, probably through the activation of AKT.

**Keywords:** Sperm cryopreservation; Ros; Apoptosis; Membrane integrity; AKT; BDNF.

## B-584. Histochemical Structure and Immunolocalisation of the Hyaluronan System in the Dromedary Oviduct

Omnia Mohey-Elsaeed, Waleed F. A. Marei, Ali A. Fouladi-Nashta and Abdel-Aleem A. El-Saba

*Reproduction, Fertility and Development, 28(7): 936-947, (2016), IF: 2.135*

We investigated the local modulation of some histochemical properties of oviducts of the dromedary (Camelus dromedarius), focusing on the immnolocalisation of hyaluronic acid (HA) synthases (HAS2 and HAS3), hyaluronidases (HYAL2 and HYAL1) and the HA receptor CD44 in the ampulla and isthmus. Abundant acidic mucopolysaccharides (glycosaminoglycans) were detected by Alcian blue staining along the luminal surface of both ciliated and non-ciliated epithelial cells (LE). Staining for HAS2 was higher in the primary epithelial folds of the ampulla compared with the isthmus, especially in secretory cells, adluminal epithelial surface and supranuclear cell domain. HAS3 staining was stronger in the LE of the isthmus than ampulla. HYAL2 was

detected in the LE in the ampulla and isthmus and was more intense in the adluminal projections of secretory cells. HYAL1 was weakly detected in the LE with no difference between the ampulla and isthmus. Strong CD44 immunostaining was present in the LE of the ampulla and isthmus. CD44 staining was higher in secretory cells than in ciliated epithelial cells and was higher in the supranuclear region than the basal region of the cytoplasm. In conclusion, we provide evidence that HA synthesis and turnover occur in the camel oviduct. Differences in HAS2 and HAS3 expression suggest regional differences in the molecular size of HA secreted in oviductal fluid that may influence oviduct–gamete interaction in the camel.
**Keywords:** Camel; CD44; Hyaluronidase.

## B-585. Localisation and Endocrine Control of Hyaluronan Synthase (Has) 2, Has3 and Cd44 Expression in Sheep Granulosa Cells

R. Chavoshinejad, W. F. A. Marei, G. M. Hartshorne and A. A. Fouladi-Nashta

*Reproduction, Fertility and Development, 28(6): 765-775, (2016), IF: 2.135*

The aim of the present study was to investigate the hormonal regulation of hyaluronan (HA) components in sheep granulosa cells. HA components are present in the reproductive tract and have a range of physical and signalling properties related to reproductive function in several species. First, abattoir-derived ovaries of sheep were used to determine the localisation of HA synthase (HAS) 1–3 and CD44 proteins in antral follicles. Staining for HAS1–3 and CD44 proteins was most intense in the granulosa layer. Accordingly, the expression of HAS2, HAS3 and CD44 mRNA was measured in cultured granulosa cells exposed to 0–50 ng mL–1 of 17β-oestradiol and different combinations of oestradiol, gonadotropins, insulin-like growth factor (IGF)-1 and insulin for 48–96 h (1 ng mL–1 FSH, 10 ng mL–1 insulin, 10 ng mL–1 IGF-1, 40 ng mL–1 E2 and 25 ng mL–1 LH.). mRNA expression was quantified by real-time polymerase chain reaction using a fold induction method. The results revealed that the hormones tested generally stimulated mRNA expression of the genes of interest in cultured granulosa cells. Specifically, oestradiol, when combined with IGF-1, insulin and FSH, stimulated HAS2 mRNA expression. Oestradiol and LH had synergistic effects in increasing HAS3 mRNA expression. In conclusion, we suggest that the hormones studied differentially regulate HAS2, HAS3 and CD44 in ovine granulosa cells in vitro. Further work is needed to address the signalling pathways involved.
**Keywords:** Follicle; Ovary; Ovine.

## B-586. Hyaluronan and Hyaluronidase, Whichi Better for Embryo Development?

Waleed F.A. Marei, Kabir A. Raheem, Mazdak Salavati, Tina Tremaine, Muhammad Khalid and Ali A. Fouladi-Nashta

*Theriogenology, 86(4): 940-948, (2016), IF: 1.838*

Our aim was to examine size-specific effects of Hyaluronan (HA) on preimplantation embryo development. We investigated the effects of Hyalovet (HA, 500–750 kDa; the size produced by HA synthase-3, which is abundant in the oviduct), or HA treated with Hyaluronidase-2 (Hyal2; also expressed in the oviduct that breaks down HA into 20 kDa fragments). In experiment 1 (in vivo), oviducts of synchronized and superovulated ewes (n = 20) were surgically exposed on Day 2 post-mating, ligated, and infused with either Hyalovet, Hyalovet + Hyal2, Hyal2, or PBS (control). Ewes were killed 5 days later for recovery of embryos and oviductal epithelial cells (OEC). Blastocyst rates were significantly higher in Hyal2 and Hyalovet + Hyal2 oviducts. Hyaluronidase-2 infusion resulted in higher blastocyst cell numbers and hatching rates. This was associated with increased HSP70 expression in OEC. In contrast, Hyalovet resulted in the lowest development to blastocyst stage and lowest hatching rates, and decreased IGF2 and IGFBP2 expression in OEC. IGF1 and IL1α expression were not affected. In experiment 2, to rule out indirect effects of oviductal factors, ovine embryos were produced and cultured with the same treatments in vitro from Day 2 to 8. Hyaluronidase-2, but not Hyalovet, enhanced blastocyst formation and reduced inner cell mass apoptosis. Hyalovet inhibited hatching. In conclusion, the presence of large-size HA (500–750 kDa) in the vicinity of developing embryos appears to disturb the oviductal environment and embryo development in vivo and in vitro. In contrast, we show evidence that breakdown of HA into smaller fragments is required to maximize embryo development and blastocyst quality.
**Keywords:** Blastocyst; Hyaluronidase-2; IGF; HSP70; Il1α.

## B-587. In Vivo and in Vitro Studies of Muc1 Regulation in Sheep Endometrium

Kabir A. Raheem, Waleed F.A. Marei, Bruce K. Campbell and Ali A. Fouladi-Nashta

*Theriogenology, 85(9): 1635-1643, (2016), IF: 1.838*

In this study, we investigated the expression of mucin 1 (MUC1) mRNA and protein in sheep endometrium at different time points during follicular and luteal phases of estrous cycle, and also determined the effect of steroid hormone treatments and interferon tau (IFNτ) on MUC1 mRNA expression in endometrial cell culture in vitro. In experiment one, 15 Welsh mountain ewes were synchronized to a common estrus and killed at precise stages of estrous cycle corresponding to (1) pre-LH peak, (2) LH peak, (3) post-LH peak, (4) early luteal, and (5) mid-luteal. Reproductive tracts were harvested and mRNA was extracted from the endometrial tissues. Parts of the uterine horns were fixed for immunohistochemistry. In experiment two, mixed populations of ovine endometrial cells (from slaughterhouse material collected at the postovulatory stage of the estrous cycle) were cultured to 70% confluence before treatment with (1) progesterone (P4, 10 ng/mL, for 48 hours), (2) estradiol (E2, 100 pg/mL, for 48 hours), or with (3) E2 priming for 12 hours (100 pg/mL) followed by P4 (10 ng/mL) for 36 hours. These were compared with: (4) IFNτ (10 ng/mL, for 48 hours), and (5) basic medium (Dulbecco Modified Eagle Medium /F12) as control. The results showed that MUC1 mRNA and protein expression in sheep endometrium were highest during the midluteal stage and very low during the post-LH period compared with the other stages ($P < 0.05$). MUC1 immunostaining in the luminal epithelium was apically restricted and was not significantly different across all stages of estrous cycle except at the post-LH peak where it was significantly low. In cell culture, MUC1 mRNA expression was significantly upregulated by both steroids either singly or in combination ($P < 0.05$), and downregulated in the presence of IFNτ. In conclusion, endometrial MUC1 expression is

cyclically regulated by both E2 and P4 in vivo and in vitro, and directly downregulated by IFNτ treatment in vitro.
**Keywords:** MUC1; Endometrium; Progesterone; Estrogen; Interferon TAU.

## B-588. Monitoring of Embryonic and Fetal Losses in Different Breeds of Goats Using Real-Time B-Mode Ultrasonography

Haney Samir, Aly Karen,Tarek Ashmawy, Mostafa Abo-Ahmed, Mohamed El-Sayed and Gen Watanabe

*Theriogenology Journal, 85(2): 207-215, (2016), IF: 1.838*

Compared to cattle and sheep, few studies had been undertaken to evaluate the incidence of embryonic and fetal losses (EFL) in goats. The objectives of the present study were to characterize the timing of EFL and to identify the factors that are associated with EFL in goats such as breed, age, parity, method of estrous synchronization, and breeding. Moreover, this study aimed to ensure whether a relationship existed between serum progesterone (P4) and EFL. Goats (n = 151) of different breeds (70 Zaraiebi, 42 Damascus, and 39 Cross goats [Baladi × Damascus]) were evaluated by ultrasonography to monitor EFL during different stages of gestation (D20-23, D26-29, D33-36, D40-45, and D47-54 after breeding). Blood samples were collected at D7, D20, and at each ultrasonographic scanning to clarify changes of serum P4 levels concurrently with EFL. Results revealed that 45 of 109 goats (41.28%) were exposed to EFL. A higher EFL % was observed between D20 to 23 and D47 to 54 (19.61%) compared with D47 to 54 to birth (11.76%). Moreover, a higher EFL % was observed in Zaraiebi goats compared with others. Age and goat parity had no significant effect on the EFL % in all goats. A high EFL % were observed in goats synchronized by P4 sponge, as well as artificially inseminated goats compared with goats with spontaneous estrus, and bred by natural mating, respectively. Serum P4 at D7 or D20 after breeding showed nonsignificant difference between normal pregnant goats and goats that experienced EFL. Unlike goats that experienced partial EFL, goats that experienced total EFL between D20 to 23 and D26 to 29 showed an abrupt P4 reduction (85.06%; $P < 0.01$) suggesting the probability of endocrine disruption of the CL. However, goats that were exposed to total EFL between D26 and 29 to D33 to 36 showed a low P4 reduction (24.90%; $P < 0.05$), which might be considered as an effect rather than a cause of EFL. In conclusion, different factors such as breed, estrous synchronization, breeding, and stage of pregnancy may be involved in EFL in goats. Therefore, improvement of the goat management in the early stage of pregnancy is important to decrease EFL % in goats. Although the P4 did not show any significant difference between normal pregnancy goats and goats that experienced EFL, CL disruption should be taken into the consideration, at least, in goats exposed to total embryonic losses.
**Keywords:** Embryonic and fetal loss; Goat; Progesterone; Ultrasonography.

## B-589. Assessment of Uterine Vascular Perfusion During the Estrous Cycle of Mares in Connection to Circulating Leptin and Nitric Oxide Concentrations

Elshymaa A. Abdelnaby, Amal M. Abo El-Maaty, Refaat S.A. Ragab and Adel A. Seida

*Journal of Equine Veterinary Science, 39: 25-32,(2016),IF:0.73*

The objective of this study was to find difference in vascular perfusion of uterine horns or uterine body throughout the estrous cycle and their relation to circulating nitric oxide and leptin concentrations. Five cyclic mares were subjected to transrectal Doppler ultrasonography and blood sampling for 18 days. Area of color and power Doppler modes was measured in pixels. Day ($P = .0001$) of the estrous cycle and ovulation ($P = .0001$) influenced uterine blood flow. Uterine body blood flow directed away from the transducer (blue, $P = .0001$) increased from day −5 until day 0 (day of ovulation), and its power ($P = .0001$) blood flow increased from day −6 until day 0; then, both decreased until days 12 and 10, respectively. Conversely to the contralateral uterine horn, ipsilateral uterine horn blood flow directed away from the transducer (blue, $P = .0001$) increased from day −5 until day −1, and its power ($P = .0001$) blood flow increased from day −6 until day 0; then, both decreased until day 10. Nitric oxide concentrations ($P = .0001$) attained two major peaks; the first on day −3 and the other persisted from day 2 until day 5. Leptin concentrations increased ($P > .001$) with a maximum value on day 0 and then decreased until a minimum value on day 9. In conclusion, during the estrous cycle, ipsilateral uterine horn and uterine body blood vessels had similar blood flow. Both leptin and nitric oxide played a role during follicle growth, ovulation, and corpus luteum development and modulated uterine blood flow before and after ovulation.
**Keywords:** Blood flow; Uterus; Estrus; Leptin; Nitric oxide; Mare

## B-590. Effect of L-Arginine Treatment on Motility, Hyperactivity, Acrosome Reaction of Ejaculated Ram Spermatozoa

K.H. El-Shahat, T.M. Ismail, M.R. Badr and K. Zaki

*Anim. Reprod., Belo Horizonte,, 13: 75-80, (2016), IF: 0.574*

The aim of this study was to evaluate the effect of in vitro treatment of ejaculated ram spermatozoa with different concentrations of L-arginine at various incubation times on motility, hyperactivity (HA) and acrosome reaction. Freshly ejaculated spermatozoa collected from three rams were pooled and subjected to the swim up technique in modified sperm Tyrode's albumin lactate pyruvate (S-TALP) medium supplemented with different concentrations of L-arginine (0.01, 0.02, 0.03,0.04 and 0.05 mM) at 30, 60,90 and 120 min of incubation. Following sperm incubation, the following parameters were examined: motility, hyperactivity (HA) and acrosome reaction (AR). The results showed that irrespective of the concentration, incubation of ram spermatozoa with L-arginine for 30min did not significantly affect the motility. However, increase the time of incubation for more than 30 min significantly decreased ($P < 0.05$) the motility of the spermatozoa as compared to the control. The lowest motility was recorded when spermatozoa were incubated with 0.05 mM

L-arginine for 120 min. Treatment of ram spermatozoa with 0.05 mM L-arginine resulted in a significant ($P < 0.05$) increase in HA% immediately after dilution compared to the control. A significant ($P < 0.05$) increase in total AR% was concomitant to the increase in the concentration of L-arginine with highest AR achieved at 0.04 mM and 90 min incubation. However, increasing the time of incubation to 120 min significantly decreased ($P < 0.05$) the percentage of spermatozoa with total AR compared to the other incubation times at 0.02, 0.04, and 0.05 mM L-arginine. In conclusion, under our experimental conditions treatment of ejaculated ram spermatozoa with 0.04 mM of L-arginine for 90 min was considered the best concentration of L-arginine to be used for in vitro induction of acrosome reaction.

**Keywords:** Acrosome reaction; Capacitation; Hyperactivation; L-Arginine; Ram sperm.

## B-591. Developmental Competence of Buffalo (Bubalus Bubalis) Oocytes: Effect of Oocytes Quality, Protein Additives, Hormonal Supplement and Type of Capacitating Agents

Waheed, El-Shahat and A.M. Hammam

*Buffalo Bulletin, 35: 427-435, (2016), IF: 0.06*

Four experiments were conducted to study the effect of media supplements on in-vitro maturation, cleavage and embryo development of buffalo oocytes. In experiment 1, oocytes were cultured in TCM-199+10% fetal calf serum (FCS) and kept at 39oC under 5% CO2 for in-vitro embryo development. In experiment 2, excellent quality oocytes were subjected to TCM-199 enriched with either 10% FCS or estrous buffalo serum (EBS; 20 to 40 pg/ml) and then fertilized using frozen semen in TALP medium containing heparin (0.02 mg/ml) and caffeine (3.89 mg/ml). In experiment 3, oocytes were cultured in-vitro maturation (IVM) medium supplemented or not with 20 IU/ml equine chorionic gonadotropins (eCG). Experiment 4 was carried out to examine the suitable capacitating agent, either heparin or caffeine or both. Excellent and good quality oocytes produced higher ($P<0.05$) maturation and morula development rates. In-vitro maturation and cleavage rates were significantly higher ($P<0.05$) in IVM medium plus EBS or eCG. Heparin and caffeine produced significantly ($P<0.05$) higher embryo developmental rates. In conclusion, excellent quality oocytes cultured with either EBS or eCG and fertilized with buffalo spermatozoa capacitated with heparin and caffeineprogressively enhanced developmental competence of buffalo oocytes

**Keywords:** Buffalo; Oocytes; Ecg; Heparin; Caffeine.

## B-592. Effect of Heparin, Caffeine and Calcium Ionophore A23187 on in Vitro Induction of the Acrosome Reaction of Fresh Ram Spermatozoa

K.H. El-Shahat, T.M. Ismail, M.R. Badr and K. Zaki

*Asian Pacific Journal of Reproduction, 5: 148-155 (2016)*

**Objective:** To determine the effect of different concentrations of heparin, caffeine or calcium ionophore and incubation time on motility, hyperactivity (HA) and acrosome reaction (AR) of ram sperm in vitro. **Methods:** Semen samples were collected by artificial vagina from three mature ram. Split fractions (0.1 mL) of the pooled semen were layered under 1 mL of S-TALP medium supplemented with either heparin (10, 25, 50, 75 and 100 mg/mL), caffeine (0.5, 0.75, 1, 2 mg/mL), or calcium ionophore A23187 (0.5, 0.75, 1, 1.55 mM/mL). Individual motility, hyperactivity percentage and acrosomal status were recorded at 0, 1, 2, 3 and 4 h post-incubation for all treatments and control. Moreover, they were examined for ability to fertilize sheep oocyte in vitro. **Results:** Heparin, caffeine and calcium ionophore A23187 at a concentration of 75 mg/ mL, 1 mg/mL, and 1.55 mM/mL respectively can be used as a protocol to provide the best results for in vitro cap citation and acrosome reaction in ram. The penetration rates of rate of oocytes inseminated with spermatozoa treated with calcium ionophore A23187,and heparin were higher as compared with caffeine. Moreover, heparin achieved higher fertilization rates but without significant difference with others. **Conclusion:** The best concentration of heparin, caffeine and ionophore A23187 are 75 mg/mL, 1 mg/mL, 1.55 mM/mL for 3, 1, 4 h incubation respectively and can be used for in vitro fertilization in sheep.

**Keywords:** Ram sperm capacitation; Hyperactivation Acrosome reaction; Hyperactivity Oocyte heparin caffeine Ca Ionophore Ivf.

## B-593.Link of A Ubiquitous Human Coronavirus to Dromedary Camels

Victor M. Cormana, Isabella Eckerle, Ziad A. Memishc, Anne M. Liljanderd, Ronald Dijkmane,f, Hulda Jonsdottire,f, Kisi J. Z. Juma Ngeiywag, Esther Kamaug, Mario Younanh, Malakita Al Masrii, Abdullah Assirii, Ilona Gluecksj, Bakri E. Musak, Benjamin Meyera, Marcel A. Müllera, Mosaad Hilalil, Set Bornsteinm, Ulrich Werneryn, Volker Thiele, Joerg Joresd, Jan Felix Drexlera and Christian Drostena.

*Pnas, 113 ( 35) 1-6 (2016)*

The four human coronaviruses (HCoVs) are globally endemic respiratory pathogens. The Middle East respiratory syndrome (MERS) coronavirus (CoV) is an emerging CoV with a known zoonotic source in dromedary camels. Little is known about the origins of endemic HCoVs. Studying these viruses' evolutionary history could provide important insight into CoV emergence. In tests of MERS-CoV–infected dromedaries, we found viruses related to an HCoV, known as HCoV-229E, in 5.6% of 1,033 animals. Human- and dromedary-derived viruses are each monophyletic, suggesting ecological isolation. on e gene of dromedary viruses exists in two versions in camels, full length and deleted, whereas only the deleted version exists in humans. The deletion increased in size over a succession starting from camelid viruses via old human viruses to contemporary human viruses. Live isolates of dromedary 229E viruses were obtained and studied to assess human infection risks. The viruses used the human entry receptor aminopeptidase N and replicated in human hepatoma cells, suggesting a principal ability to cause human infections. However, inefficient replication in several mucosa-derived cell lines and airway epithelial cultures suggested lack of adaptation to the human host. Dromedary viruses were as sensitive to the human type I interferon response as HCoV-229E. Antibodies in human sera neutralized dromedary-derived viruses, suggesting population immunity against dromedary viruses. Although no current epidemic risk seems to emanate from these viruses, evolutionary inference suggests that the endemic human virus HCoV-229E may constitute a descendant of camelid-associated viruses. HCoV-229E evolution provides a scenario for MERS-CoV emergence.

**Keywords:** Coronavirus evolution; Ecology zoonotic diseases Livestock

## B-594.Hepatitis E Virus Infection in Dromedaries, North and East Africa, United Arab Emirates, and Pakistan

Andrea Rasche, Muhammad Saqib, Anne M. Liljander, Set Bornstein, Ali Zohaib, Stefanie Renneker, Katja Steinhagen, Renate Wernery, Mario Younan, Ilona Gluecks, Mosaad Hilali, Bakri E. Musa, Joerg Jores, Ulrich Wernery, Jan Felix Drexer, Christian DrostenComments to Author and Victor Max Corman

*Emerging Infectious Diseases,22(7):1249-1252,(2016),IF:6.994*

A new hepatitis E virus (HEV-7) was recently found in dromedaries and 1 human from the United Arab Emirates. We screened 2,438 dromedary samples from Pakistan, the United Arab Emirates, and 4 African countries. HEV-7 is long established, diversified and geographically widespread. Dromedaries may constitute a neglected source of zoonotic HEV infections.
**Keywords:** Hepatitis E Virus; Dromedaries; North and East Africa; United arab emirates; Pakistan.

## B-595.Ultrastructure of Sarcocystis Bertrami Sarcocysts from A Naturally Infected Donkey (Equus Asinus) from Egypt.

Dubey, VAN Wilpe and Verma Hilali.

*Parasitology, 143: 18-23, (2016), IF: 2.41*

There is considerable confusion concerning Sarcocystis species in equids. Little is known of Sarcocystis infections in donkeys (Equus asinus). Here we describe the structure of Sarcocystis bertrami-like from the donkey by light microscopy (LM) and transmission electron microscopy (TEM). Nineteen sarcocysts from the tongue of a donkey from Egypt were studied both by LM and TEM. By LM, all sarcocysts had variably shaped and sized projections on the sarcocyst walls, giving it a thin-walled to thick-walled appearance, depending on individual sarcocyst and plane of section. By TEM, sarcocysts walls had villar protrusions (vp) of type 11. The sarcocyst wall had conical to slender vp, up to 6 µm long and 1 µm wide; the vp were folded over the sarcocyst wall. The total thickness of the sarcocyst wall with ground substance layer (gs) was 1-3 µm. The vp had microtubules (mt) that originated deeper in the gs and continued up to the tip. The apical part of the vp had electron dense granules. The mt were configured into 3 types: a tuft of electron dense mt1 extending the entire length of the vp with a tuft of medium electron dense mt2 appearing in parallel, and fine mt3 present only in the villar tips. The gs was mainly smooth with few indistinct granules. All sarcocysts were mature and contained metrocytes and bradyzoites. Bradyzoites were approximately 11-15 × 2-3 µm in size with typical organelles.
**Keywords:** Sarcocystis bertrami; Donkey (Equus asinus); Transmission electron microscopy.

## B-596.Serological Detection and Epidemiology of Neospora Caninum and Cryptosporidium Parvum Antibodies in Cattle in Southern Egypt

Fereig RM, AbouLaila MR, Mohamed SG, Mahmoud HY, Ali AO, Ali AF, Hilali M, Zaid A, Mohamed AE and Nishikawa Y.

*Acta Tropica, 162: 206-211, (2016), IF: 2.38*

Neospora caninum and Cryptosporidium parvum are intracellular protozoan parasites that are distributed worldwide and of major economical concern in cattle industry. N. caninum can cause abortion storms and high culling rates, whereas C. parvum has zoonotic implications and can cause diarrhea in calves. There are currently no data on the prevalence of neosporosis and cryptosporidiosis in humans or animals in southern Egypt. Prevalence of these two infections was determined in a sample of cattle from two different areas in southern Egypt, Sohag and Qena, using enzyme-linked immunosorbent assay. A total 301 cattle were sampled, of which 18.9% were positive for N. caninum, 35.9% were positive for C. parvum and 10.0% were positive for both. Geographical location and breeding system were considered as potential risk factors for C. parvum infection. A higher prevalence of infection was identified on small scale farms, compared with larger, intensive systems, with a prevalence of 50.2% compared with 37.8%, respectively. Animals in Sohag had a significantly higher prevalence compared with Qena, with a seroprevalence of 46.1% compared with 31.6%, respectively. In brief, marked seroprevalence recorded in this study indicates a high incidence of N. caninum and C. parvum infections in cattle, and this necessitates the application of more effective strategies for combating these types of infections on farms in Egypt.
**Keywords:** Cattle; Cryptosporidium parvum; Neospora Caninum; Elisa; Egypt

## B-597. Molecular Differentiation of Sarcocystis Buffalonis and Sarcocystis Levinei in Water Buffaloes (Bubalus Bubalis) from Sarcocystis Hirsuta and Sarcocystis Cruzi In Cattle (Bos Taurus).

Bjørn Gjerde, Mosaad Hilali and Ibrahim E. Abbas

*Parasitology Research, 115: 2459-2471, (2016), IF: 2.027*

The purpose of the present study was to obtain sarcocysts of Sarcocystis buffalonis and Sarcocystis levinei from water buffaloes and characterize the isolates by molecular methods in order to determine whether the two species were genetically different from Sarcocystis hirsuta and Sarcocystis cruzi, respectively, from cattle, which had been characterized before. About 35 macroscopically visible (3-4 × 1-2 mm) and 20 barely visible (1-3 × 0.2 mm) sarcocysts were excised from the esophagus of 18 naturally infected and freshly slaughtered adult water buffaloes at three slaughterhouses in Egypt. Genomic DNA was extracted from the sarcocysts, and all isolates were first characterized at the mitochondrial cytochrome c oxidase subunit I gene (cox1) gene through PCR amplification and direct sequencing. Selected isolates were subsequently further characterized at the 18S and 28S ribosomal (r) RNA genes and the internal transcribed spacer 1 (ITS1) region of the nuclear rDNA unit by direct sequencing or

cloning. on ly six of the isolated macroscopic sarcocysts belonged to S. buffalonis, whereas the others belonged to Sarcocystis fusiformis. Twelve of the smaller cysts belonged to S. levinei and seven to Sarcocystis sinensis. The characterization of the sarcocysts of S. sinensis and some of the sarcocysts of S. fusiformis have been reported before. Fifteen additional sarcocyst isolates of S. fusiformis were characterized at cox1 in the present study and found to be identical or closely similar to previous isolates. At cox1, the sequence identity between the six isolates of S. buffalonis was 99.8-100 % (two haplotypes), whereas the identity between the 12 isolates of S. levinei was 99.0-100 % (10 haplotypes). The identity between cox1 sequences of S. buffalonis and S. hirsuta (n = 56) was 92.9-93.6 % (on average 93.4 %), and the identity between cox1 sequences of S. levinei and S. cruzi (n = 22) was 92.9-94.0 % (on average 93.5 %). The phylogenetic analyses placed with high support the cox1 sequences of S. buffalonis and S. hirsuta into two monophyletic sister groups, and the same was true for the cox1 sequences of S. levinei and S. cruzi. Hence, the study established that S. buffalonis and S. levinei are distinct species different from S. hirsuta and S. cruzi, respectively. Nucleotide sequences of S. buffalonis could be distinguished from those of S. hirsuta also at the 28S rRNA gene (clearly different) and the ITS1 region (small and uncertain difference) but not at the 18S rRNA gene. Sequences of S. levinei could be distinguished from those of S. cruzi both at the 18S and 28S rRNA genes (ITS1 region not examined). However, the cox1 gene was superior to the 18S and 28S rRNA genes as regards the ability to unambiguously delimit the species within each species pair, since at the latter markers, the number of consistent nucleotide differences between the species was low and there was a slight overlap between the intraspecific and interspecific sequence divergence. Comparison of the newly generated 18S rRNA gene sequences of S. levinei from water buffaloes with similar sequences deposited in GenBank suggested that S. levinei and S. cruzi are not strictly intermediate host specific but might occasionally infect cattle and water buffaloes, respectively.

**Keywords:** Sarcocystis; Buffalonis; Sarcocystis levinei;Sarcocystis hirsuta;Sarcocystiscruzi;Sarcocystis fusiformis;Water buffaloe;Bublus bubalis;Cattle; Bos taurus;Egypt;Phylogeny;18S Rrna;28S Rrna;Itsi;Cox!

## B-598. Molecular Diagnosis of Eimeria Stiedae in Hepatic Tissue of Experimentally Infected Rabbits

Khaled M. Hassan, Waleed M. Arafa, Waheed M. Mousa, Khaled A.M. Shokier, Salama. Shany and Shawky M. Aboelhadid

*Experimental Parasitology, 169: 1-5, (2016), IF: 1.623*

The early detection of Eimeria stiedae in the hepatic tissue of experimentally infected rabbits was investigated using molecular assay. Forty 6-week-old male New Zealand rabbits were divided into two groups. Group A (30 animals) was infected with 2.5 104 sporulated oocysts of E. stiedae per animal on Day 0 and Group B (10 animals) was used as the uninfected controls. Three animals from Group A and one from Group B were sacrificed at 0, 3, 6, 9, 12, 15, 18, 21, 24 and 27 days post infection (PI). Gross and microscopic post-mortem findings were recorded. Polymerase chain reaction (PCR) of the E. stiedae internal transcribed spacer 1 genomic region was conducted on blood, liver tissue, and feces from the Group A experimentally infected animals. Macroscopically, the liver showed irregular yellowish white nodules pathognomonic to E. stiedae infection beginning on Day 15 PI. Hepatomegaly and ascites were obvious from Day 21e24 PI. The presence of different E. stiedae schizonts and gametocytes in the histopathological sections of the biliary epithelium were evident on Day 15 PI. The E. stiedae PCR was first positive in liver tissues on Day 12 and in fecal samples on Day 18 PI, but the blood samples were negative. In conclusion, the PCR can be used for early diagnosis and control of E. stiedae schizonts before shedding of the oocysts in feces.

**Keywords:** Eimeria stiedae; Rabbit; Experimental infection; Early Diagnosis; Pcr.

## B-599. Domestic Cats (Felis Catus) are Definitive Hosts for Sarcocystis Sinensis from Water Buffaloes (Bubalus Bubalis).

GjerdeBand Hilali M.

*Journal of Veterinary Medical Science, 78(7): 1217-1221, (2016), IF: 0.822*

The definitive hosts of Sarcocystis sinensis in water buffaloes have hitherto been unknown, but the close similarity of this species to the cat-transmitted Sarcocystis bovifelis in cattle suggested they were felids. In a previous study, two domestic cats were fed macroscopic sarcocysts of Sarcocystis fusiformis contained within or dissected from the esophageal muscles of water buffaloes, while no microscopic sarcocysts of S. sinensis were noticed. Both cats started shedding small numbers of sporocysts 8-10 days post infection (dpi) and were euthanized 15 dpi. Using a PCR-based molecular assay targeting the mitochondrial cox1 gene of S. fusiformis, both cats were shown to act as definitive hosts for this species. In the present study, DNA samples derived from oocysts/sporocysts in the intestinal mucosa of both cats were further examined by PCR for the presence of S. sinensis using 2 newly designed primers selectively targeting the cox1 gene of this species. All 6 DNA samples examined from each cat tested positive for S. sinensis. A 1,038-bp-long portion of cox1 was amplified and sequenced as 2 overlapping fragments from 5 of these DNA samples. The 5 sequences shared 99.3-100% identity with 7 previous cox1 sequences of S. sinensis obtained from sarcocysts in water buffaloes. Additionally, amplification of the ITS1 region with primers targeting various Sarcocystis spp., yielded amplicons of 2 different lengths, corresponding to those obtained from sarcocyst isolates of S. sinensis and S. fusiformis, respectively. This is the first study to show that cats act as definitive hosts for S. sinensis.

**Keywords:** Bubalus bubalis; Cat; Cox1; Sarcocystis Fusiformis; Sarcocystis sinensis.

## B-601.Parasitic Cymothoid Isopods and Their Impacts in Commercially Important Fishes from Lake Qarun, Egypt

Nisreen E. Mahmoud, M.M.Fahmy, Mai Abuowarda.M and Marwa S. Khattab

*International Journal of Chemtech Research, 9:221-229 (2016)*

Cymothoid Isopods are parasitic crustaceans cause serious impacts on the fish population and might lead to fish mortality and consequently economic loses. The present study aims to to investigate the prevalence of isopod infestation and their

histopathological alterations among three commertially important fish species in lake Qarun, Fayoum province, Egypt. A total of 150 fish samples; Dicentrarchus labrax (50) Solea vulgaris (50), and Tilapia zilli (50) ) were collected from the lake during the period from March to August 2015. Results revealed the total prevalence of 32.66% with two isopod species identified as Nerocilaor bignyi and Renocila thresherorum. Gills affected with R. thresherorum showed complete sloughing of the epithelium lining accompanied with severe congestion and edema in the secondary gill lamellae in addition to inflammatory exudates found between the gill filaments. Further studies are needed to estimate the source of isopod infestation problem and to develop a strategy for controlling such problem among Lake Qarun fishes.

**Keywords:** Cymothoidae; Isopods; Parasites; Pathology; Lake Qarun.

## B-602. Recent Progress in Applications of Nanoparticles in Fish Medicine: A Review

Mohamed Shaalan, Mona Saleh, Magdy El-Mahdy and Mansour El-Matbouli

*Nanomedicine: Nanotechnology, Biology, and Medicine, 12: 701-710, (2016), IF: 5.671*

Nanotechnology has become an extensive field of research due to the unique properties of nanoparticles, which enable novel applications. Nanoparticles have found their way into many applications in the field of medicine, including diagnostics, vaccination, drug and gene delivery. In this review, we focused on the antimicrobial effects of nanoparticles, with particular emphasis on the problem of antibiotic resistant bacteria in fisheries. The use of nanoparticle-based vaccines against many viral pathogens is a developing field in fish medicine research. Nanoparticles have gained much interest as a specific and sensitive tool for diagnosis of bacterial, fungal and viral diseases in aquaculture. Nevertheless our review also highlights the many applications of nanotechnology that are still to be explored in fish medicine.

**Keywords:** Nanoparticles; Fish diseases; Diagnosis; Antimicrobial; Fish vaccines.

## B-603. Infectious Bacterial Pathogens, Parasites and Pathological Correlations of Sewage Pollution as an Important Threat to Farmed Fishes in Egypt

Mahmoud A. Mahmoud , Mohamed Abdelsalam , Olfat A. Mahdy , Hala M.F. El Miniawy , Zakia A.M. Ahmed , Ahmed H. Osman , Hussein M.H. Mohamed , A.M. Khattab f and M.A. Zaki Ewiss

*Environmental Pollution, 219: 939-948, (2016), IF: 4.839*

This paper is a part of a multi-disciplinary research "Application of Decentralized on -Site Water Treatment System in Egypt for Use in Agriculture and Producing Safe Fish and Animal Proteins". The project aimed to investigate the environmental impact of implementing sewage water before and after treatment using the effluent of the on-site decentralized Japanese' Johkasou system, in agriculture and producing fish protein. The aim is to establish such system in Egypt to strengthen the sanitary conditions of water resources. In the present study, the impact of the sewage pollution in some fish farms at El-Fayyum, Port Said and El-Dakahlia governorates in Egypt was carried out. Water and fish (Oreochromis niloticus and Mugil cephalus) samples were collected from private fish farms of such localities. Bacteriological and chemical examination of water samples revealed the existence of coliforms and many other bacterial species of significant human health hazards. The chemical parameters of water showed a marked deviation from normal levels while examination of fish flesh specimens indicated contamination with Streptococcus Sp., Staphylococcus Sp., and Salmonella in all examined localities. Other bacterial isolates of human health importance (Morganella morganii, Pseudomonas cepacia and Enterococcos durans) were identified. The parasitological examination revealed the presence of encysted metacercariae (EMC); Diplostomatidae, Prohemistomatidae and Heterphyidae. Moreover, two protozoan parasites (Mxyoboulus tilapiae and Ichthyophthirius multifilis) were also recorded. The histopathological examination revealed mild tissue reaction in case of bacterial infection and severe pathological lesions in different organs in case of EMC infection. Lamellar hyperplasia and mononuclear cell infiltration in branchial tissue was common findings. In skeletal muscles, atrophy of muscle fibres, myolysis and myophagia were detected

**Keywords:** Water pollution; Fish; Egypt; Morganella; Pseudomonas and Enterococcus.

## B-604. Gastrin-Releasing Peptide Receptor (Grpr) Promotes Emt, Growth, and Invasion in Canine Prostate Cancer

Said M. Elshafae, Bardes B. Hassan, Wachiraphan Supsavhad, Wessel P. Dirksen, Rachael Y. Camiener, Haiming Ding, Michael F. Tweedle and Thomas J. Roso

*The Prostate, 76: 796-809, (2016), IF: 3.778*

**Background** The gastrin-releasing peptide receptor (GRPr) is upregulated in early and late-stage human prostate cancer (PCa) and other solid tumors of the mammary gland, lung, head and neck, colon, uterus, ovary, and kidney. However, little is known about its role in prostate cancer. This study examined the effects of a heterologous GRPr agonist, bombesin (BBN), on growth, motility, morphology, gene expression, and tumor phenotype of an osteoblastic canine prostate cancer cell line (Ace-1) in vitro and in vivo. **Methods** The Ace-1 cells were stably transfected with the human GRPr and tumor cells were grown in vitro and as subcutaneous and intratibial tumors in nude mice. The effect of BBN was measured on cell proliferation, cell migration, tumor growth (using bioluminescence), tumor cell morphology, bone tumor phenotype, and epithelial-mesenchymal transition (EMT) and metastasis gene expression (quantitative RT-PCR). GRPr mRNA expression was measured in primary canine prostate cancers and normal prostate glands. **Results** Bombesin (BBN) increased tumor cell proliferation and migration in vitro and tumor growth and invasion in vivo. BBN upregulated epithelial-to-mesenchymal transition (EMT) markers (TWIST, SNAIL, and SLUG mRNA) and downregulated epithelial markers (E-cadherin and β-catenin mRNA), and modified tumor cell morphology to a spindle cell phenotype. Blockade of GRPr upregulated E-cadherin and downregulated VIMENTIN and SNAIL mRNA. BBN altered the in vivo tumor phenotype in bone from an osteoblastic to osteolytic phenotype. Primary canine prostate cancers had increased GRPr mRNA expression compared to normal prostates. **Conclusion** These data demonstrated that the GRPr is important in prostate cancer

growth and progression and targeting GRPr may be a promising strategy for treatment of prostate cancer.
**Keywords:** GRPr; EMT; Metastasis; Canine; Bombesin.

## B-605. Intranasal Chromium Induces Acute Brain and Lung Injuries in Rats: Assessment of Different Potential Hazardous...

Abeer Salama, Rehab Hegazy and Azza Hassan

*Plos on e, December 20, 2016: 1-20, (2016), IF: 3.057*

Chromium (Cr) is used in many industries and it is widely distributed in the environment. Exposure to Cr dust has been reported among workers at these industries. Beside its hazardous effects on the lungs, brain injury could be induced, as the absorption of substances through the nasal membrane has been found to provide them a direct delivery to the brain. We investigated the distribution and the effects of Cr in both brain and lung following the intranasal instillation of potassium dichromate (inPDC) in rats. Simultaneously, we used the common intraperitoneal (ipPDC) rat model of acute Cr-toxicity for comparison. Thirty male Wistar rats were randomly allocated into five groups (n = 6); each received a single dose of saline, ipPDC (15 mg/kg), or inPDC in three dose levels: 0.5, 1, or 2 mg/kg. Locomotor activity was assessed before and 24 h after PDC administration, then, the lungs and brain were collected for biochemical, histopathological, and immunohistochemical investigations. Treatment of rats with ipPDC resulted in a recognition of 36% and 31% of the injected dose of Cr in the brain and lung tissues, respectively. In inPDC-treated rats, targeting the brain by Cr was increased in a dose-dependent manner to reach 46% of the instilled dose in the group treated with the highest dose. Moreover, only this high dose of inPDC resulted in a delivery of a significant concentration of Cr, which represented 42% of the instilled dose, to the lungs. The uppermost alteration in the rats locomotor activity as well as in the brain and lung histopathological features and contents of oxidative stress biomarkers, interleukin-1β (IL-1β), phosphorylated protein kinase B (PKB), and cyclooxygenase 2 (COX-2) were observed in the rats treated with inPDC (2 mg/kg). The findings revealed that these toxic manifestations were directly proportional to the delivered concentration of Cr to the tissue. In conclusion, the study showed that a comparably higher concentrations of Cr and more elevated levels of oxidative stress and inflammatory markers were observed in brain and lung tissues of rats subjected to inPDC in a dose that is just 0.13 that of ipPDC dose commonly used in Cr-induced toxicity studies. Therefore, the study suggests a high risk of brain-targeting injury among individuals environmentally or occupationally exposed to Cr dust, even in low doses, and an additional risk of lung injury with higher Cr concentrations. Moreover, the study introduces inPDC (2 mg/kg)-instillation as a new experimental animal model suitable to study the acute brain and lung toxicities induced by intranasal exposure to Cr compounds.

## B-606. Renoprotective Effect of Lactoferrin Against Chromium-Induced Acute Kidney Injury in Rats: Involvement of Il-18 and Igf-1 Inhibition

Rehab Hegazy, Abeer Salama, Dina Mansour and Azza Hassan

*Plos on e, March 18, 2016: 1-18, (2016), IF: 3.057*

Hexavalent chromium (CrVI) is a heavy metal widely used in more than 50 industries. Nephrotoxicity is a major adverse effect of chromium poisoning. The present study investigated the potential renoprotective effect of lactoferrin (Lf) against potassium dichromate (PDC)-induced acute kidney injury (AKI) in rats. Beside, because previous studies suggest that interlukin-18 (IL-18) and insulin-like growth factor-1 (IGF-1) play important roles in promoting kidney damage, the present work aimed to evaluate the involvement of these two cytokines in PDC model of AKI and in the potential renoprotective effect of lactoferrin. Adult male albino Wistar rats were pretreated with Lf (200mg/kg/day, p.o.) or (300mg/kg/day, p.o.); the doses that are usually used in the experiment studies, for 14 days followed by a single dose of PDC (15mg/kg, s.c.). PDC caused significant increase in serum urea, creatinine, and total protein levels. This was accompanied with decreased renal glutathione content, and increased renal malondialdehyde, IL-18, IL-4, nuclear factor kappa B (NFκB), IGF-1, and the phosphorylated form of forkhead box protein O1 (FoxO1) levels. Moreover, normal expression IFN-γ mRNA and enhanced expression of TNF-α mRNA was demonstrated in renal tissues. Histopathological investigations provoked deleterious changes in the renal tissues. Tubular epithelial hyperplasia and apoptosis were demonstrated immunohistochemically by positive proliferating cell nuclear antigen (PCNA), Bax, and Caspase-3 expression, respectively. Pretreatment of rats with Lf in both doses significantly corrected all previously mentioned PDC-induced changes with no significant difference between both doses. In conclusion, the findings of the present study demonstrated the involvement of oxidative stress, inflammatory reactions, tubular hyperplasia and apoptosis in PDC-induced AKI. It suggested a role of IL-18 through stimulation of IL-4-induced inflammatory pathway, and IGF-1 through triggering FoxO1-induced cell proliferation. Moreover, the study revealed that Lf protected the kidney against Cr-induced AKI in rats and significantly showed antioxidant, anti-inflammatory, and anti-proliferative properties with down-regulation of IL-18 and IGF-

## B-607. The Mitigative Effect of Raphanus Sativus Oil on Chromium-Induced Geno- and Hepatotoxicity In Male Rats

M.O. Elshazly, Ashraf M. Morgan, Merhan E. Ali, Essam Abdel-mawla and Sahar S. Abd El-Rahman

*Journal of Advanced Research, 7: 413-421, (2016), IF: 3*

To study the impact of radish oil on the possible genotoxic and hepatotoxic effects of hexavalent chromium, male rats were divided into 4 groups. Group 1 served as control, group 2 received radish oil at the recommended human therapeutic dose (0.07 mL/kg) by gavage, group 3 received sodium dichromate dihydrate (SDD) 520 mg/L in drinking water, and group 4 received both SDD and radish oil as previously mentioned in groups 2 and 3. All treatments were continued for six months. The results revealed that chromium exposure promoted oxidative stress with a consequently marked hepatic histopathological alterations, increased serum alanine aminotransferase (ALT) and alkaline phosphatase (ALP) activities, alfa fetoprotein (AFP) levels, and micronucleated erythrocytes (MNE) % in peripheral blood. Moreover, COMET assay of hepatic DNA revealed that SDD exposure significantly decreased the intact cells %, head diameter, and head DNA % compared to control, indicating DNA damage. However, radish

oil co-administration with SDD resulted in marked amendment in the altered parameters as detected by improved liver function markers (ALT and ALP) and AFP level, decreased lipid peroxidation, increased antioxidant markers, inhibited hepatic DNA damage and restored the hepatic histology by preventing the appearance of the altered hepatocytes' foci and decreasing chromium induced histopathological lesions. It could be concluded that radish oil was able to provide a convergent complete protection against the geno- and hepatotoxicity of chromium by its potent antioxidant effect.

**Keywords:** Chromium; Alfa Fetoprotein; Comet; Micronucleated Rbcs; Oxidative stress; Radish.

## B-608. Response of Triple Negative Breast Cancer to Neoadjuvant Chemotherapy: Correlation Between Ki-67 Expression and Pathological Response.

Gamal M Elnemr, Ahmed H El-Rashidy, Ahmed H Osman, Lotfi F, Osama A Abbas, Abdullah S Al-Zahrani, Sheriff M El-Seman, Amrallah A Mohammed and Abdelghani A Hassan

*Asian Pacific Journal of Cancer Prevention, 17: 807-8013, (2016), IF: 2.514*

Triple-negative breast cancers constitute about 15% of all cases, but despite their higher response to neoadjuvant chemotherapy, the tumors are very aggressive and associated with a poor prognosis as well as a higher risk of early recurrence. This study was retrospectively performed on 101 patients with stage II and III invasive breast cancer who received 6–8 cycles of neo-adjuvant chemotherapy. Out of the total, 23 were in the triple negative breast cancer subgroup. Nuclear Ki-67 expression in both the large cohort group (n=101) and triple negative breast cancer subgroup (n=23) and its relation to the pathological response were evaluated. The purpose of the study was to identify the predictive value of nuclear protein Ki-67 expression among patients with invasive breast cancers, involving the triple negative breast cancer subgroup, treated with neoadjuvant chemotherapy in correlation to the rate of pathological complete response. The proliferation marker Ki-67 expression was highest in the triple negative breast cancer subgroup. No appreciable difference in the rate of Ki-67 expression in triple negative breast cancer subgroup using either a cutoff of 14% or 35%. Triple negative breast cancer subgroup showed lower rates of pathological complete response. Achievement of pathological complete response was significantly correlated with smaller tumor size and higher Ki-67 expression. The majority of triple negative breast cancer cases achieved pathological partial response. The study concluded that Ki-67 is a useful tool to predict chemosensitivity in the setting of neoadjuvant chemotherapy for invasive breast cancer but not for the triple negative breast cancer subgroup

**Keywords:** Triple negative breast cancer; Neoadjuvant Chemotherapy; Ki-67; Pathological response.

## B-609. Feline Mammary Cancer: Novel Nude Mouse Model and Molecular Characterization of Invasion and Metastasis Genes

B. B. Hassan, S. M. Elshafae, W. Supsavhad, J. K. Simmons, W. P. Dirksen, S. M. Sokkar and T. J. Rosol

*Veterinary Pathology, 54: 32-43, (2016), IF: 2.12*

Feline mammary carcinoma (FMC) is similar to human breast cancer in the late age of onset, incidence, histopathologic features, biological behavior, and pattern of metastasis. Therefore, FMC has been proposed as a relevant model for aggressive human breast cancer. The goals of this study were to develop a nude mouse model of FMC tumor growth and metastasis and to measure the expression of genes responsible for lymphangiogenesis, angiogenesis, tumor progression, and lymph node metastasis in FMC tissues and cell lines. Two primary FMC tissues were injected subcutaneously, and 6 FMC cell lines were injected into 3 sites (subcutaneous, intratibial, and intracardiac) in nude mice. Tumors and metastases were monitored using bioluminescent imaging and characterized by gross necropsy, radiology, and histopathology. Molecular characterization of invasion and metastasis genes in FMC was conducted using quantitative real-time reverse transcription polymerase chain reaction in 6 primary FMC tissues, 2 subcutaneous FMC xenografts, and 6 FMC cell lines. The histologic appearance of the subcutaneous xenografts resembled the primary tumors. No metastasis was evident following subcutaneous injection of tumor tissues and cell lines, whereas lung, brain, liver, kidney, eye, and bone metastases were confirmed following intratibial and intracardiac injection of FMC cell lines. Finally, 15 genes were differentially expressed in the FMC tissues and cell lines. The highly expressed genes in all samples were PDGFA, PDGFB, PDGFC, FGF2, EGFR, ERBB2, ERBB3, VEGFD, VEGFR3, and MYOF. Three genes (PDGFD, ANGPT2, and VEGFC) were confirmed to be of stromal origin. This investigation demonstrated the usefulness of nude mouse models of experimental FMC and identified molecular targets of FMC progression and metastasis.

**Keywords:** Mammary cancer; Metastasis; Lung; Brain; Bone; Angiogenesis; Lymphangiogenesis; Cat; Animal model.

## B-610. Modulating Effect of Peppermint and Eucalyptus Essential Oils on Vvnd Infected Chickens

Awaad Afify, SA Zoulfekar, Faten F Mohammed Elmenawy and H M Hafez

*Pakistan Veterinary Journal, 36: 350-355, (2016), IF: 0.822*

Treatment of broiler chickens with the peppermint and eucalyptus essential oils blend improved protection and productive performance as compared with the infected positive control birds. It decreased total mortality, increased final body weight, and decreased final feed conversion ratio (FCR) ($P \leq 0.05$). The peppermint and eucalyptus essential oils blend had a positive effect on macroscopic and microscopic lesion scoring and enhanced HI and ELISA titers against Newcastle disease virus vaccine, as compared to their untreated control groups ($P \leq 0.05$). In conclusion; the peppermint and eucalyptus essential oils blend used in the present investigation significantly controlled vVND infection where it has immunomodulatory effect and positively evoked the immune response against this very hot challenging virus which is of great devastating economic impact on poultry industry.

**Keywords:** Broiler chickens; Eucalyptus; Immune response; Peppermint volatile Oils; Vvndv.

## B-611.Leaves of Cordia Boissieri A. DC. as a Potential Source of Bioactive Secondary Metabolites for Protection Against Metabolic Syndrome-Induced in Rats

Asmaa I. Owis, Amira M. Abo-youssef and Ahmed H. Osman

*Zeitschrift Für Naturforschung C A Journal of Biosciences, (2016) IF: 0.709*

Cordia boissieri A. DC. (Boraginaceae) is traditionally used as an herbal remedy for diabetes by Hispanic women in Southwestern USA. A recent investigation showed the significant protective effect of ethyl acetate extract against metabolic syndrome (MS). However, the corresponding active principles responsible for this effect and relations between their structure and biological actions remain unclear. Thus, ethyl acetate extract was subjected to column chromatography, which yielded seven compounds identified on the basis of spectroscopic data as rutin, hesperidin, kaempferol-3-O-β-d-glucopyranoside, rosmarinic acid, β-sitosterol-3-O-β-d-glucopyranoside, quercetin, and kaempferol. The isolated compounds (5 mg/kg/day) were tested in a fructose enriched-diet rat model using metformin as a standard drug. Blood samples were withdrawn for estimation of MS-associated biomarkers and liver samples were subjected to histopathological and immunohistochemical examination. The isolated compounds impaired most of the changes associated with MS as evidenced by improved insulin sensitivity, glucose tolerance, kidney function, lipid profiles and reduced oxidative stress and inflammation by different degrees. It is worth noting that quercetin and kaempferol showed the most potent effect. Structure-activity relationship study revealed that the presence of 2,3-double bond in ring C and ortho-hydroxylation in ring B increases the flavonoids activity while glycosylation or methylation decreased this activity.

**Keywords:** Cordia boissieri; Metabolic syndrome; Secondary metabolites.

## B-412. Characterization of Antiradical and Anti-Inflammatory Activities of Some Cold Pressed Oils In Carrageenan-Induced Rat Model of Acute Inflammation

Hanan Naeim Attia, Faten M. Ibrahim, Yousreya A. Maklad1, Kawkab A. Ahmed and Mohamed Fawzy Ramadan

*Der Pharma Chemica, 8: 148-158 (2016)*

Inflammation is a process involving multiple factors acting in a complex network, where a distinct cytokine cascade of pro-inflammatory and inflammatory mediators unfolds. Substantial levels of bioactive phytochemicals were found in cold-pressed oils (CPO). To evaluate the antiradical and anti-inflammatory potential of CPO including Nigella sativa oil (BCO), Coriandrum sativum oil (COO), and Syzygium aromaticum oil (CLO). Indomethacin was used as the reference standard. In vitro assays were undertaken to evaluate radical scavenging properties utilizing stable 1,1-diphenyl-2-picrylhydrazyl (DPPH˙) and galvinoxyl radicals. In vivo studies comprised carrageenan (CG)-induced rat paw edema as a model for acute inflammation. Biochemical estimations of tumor necrosis factor-α(TNFα), interleukin 6 (IL-6), and interleukin 12 (IL-12) were evaluated in paw exudates and sera of treated as well as untreated animals groups. Histopathological examination of rat paw sections was carried out. In vitro assays revealed strong radical scavenging potential of CPO against stable DPPH˙ and galvinoxyl radicals with CLO showing the highest radical quenching activity. Pro- inflammatory cytokine levels were markedly improved as compared to untreated CG group. CLO exhibited superior attenuation of pro-inflammatory release as compared to BCO, COO, and indomethacin. Rat paw sections of CPO-treated groups showed a marked improvement in histopathological alterations induced by CG injection. Attenuation of inflammatory mediators by bio active constituents of the selected CPO, together with the antioxidant potential, might represent a possible prophylactic or therapeutic target against inflammation and subsequent free radical generation.

**Keywords:** Cold pressed Oil; Coriandrum sativum; Syzygium aromaticum; Nigella sativa; Anti-Inflammatory; Indomethacin.

## B-613. Effect of a Single Dose Adminstration of Wheat Bran Extract and Its Active Components on Acute Ischemicbrain Injury

Shaaban H, Shafei A. A, Abdel Jaleel Gehad.A, Ibrahim B.M and Hassan A.H.

*International Journal of Pharmacognosy and Phytochemical Research, 8(3): 453-461 (2016)*

Three known compounds were isolated from wheat bran (Graminae)sitosterol 3-O- D-glucopyranoside (WB1), Sucrose (WB2) and 10(cis), 13(cis)-octadecadieneoic acid (WB3) for first time by successive column chromatography. The structures were determined mainly by spectroscopic method (1H, 13CNMR). This study aimed to evaluate antioxidant activity and determine the effect of ethanol extract of wheat bran and its active components on oxidative stress induced by cerebral ischemia-reperfusion injury (I/R) by occlusion of the left common carotid artery (CCA) in the rat. They restored the I/R-induced depletion of super oxide dismutase activity (SOD) and reduced glutathione (GSH) contents, with reduction of malondialdehyde (MDA) and nitric oxide (NO) contents that elevated during cerebral ischemia-reperfusion injury. In conclusion, WBI, WB3 and total ethanol Bran extract ameliorated the oxidative stress resulted from cerebral ischemia-reperfusion confirmed by histopathological examination and immunohistochemical

**Keywords:** Bran; Steroidal saponin; Unilateral carotid artery Occlusion (Cao); Histopathology; Immunohistochemistry; Cyclooxygenase-2 .

## B-614. Illicium Verum Extracts Anti-Gastro Ulcerogenic Potential on Experimentally Rat Models

Faten M. Ibrahim, Abeer Y Ibrahim, EL Gohary A. E, Mohamed S. Hussein and Kawkab A. Ahmed

*International Journal of Pharmtech Research, 9: 65-80 (2016)*

**Background:** The traditional herbal, medicinal plants, drugs are used in treating many diseases. The herbal treatment commonly used in treating most type of ulcers. Different extracts of Illicium verum were investigated for their anti-gastro ulcerogenic effect on rats. **Aims:** Evaluation of Illicium verum extracts as anti-ulcerogenic agent in rat model. Methods: plant essential oil and extracts (petroleum ether and aqueous

alcoholic), were performed and then LD50 values were determined (2500 mg/ kg b.wt. for aqueous alcoholic extract and 1250 mg/ kg for petroleum ether extract). Rats were classified into three main groups; negative control administered distilled water, positive controls administered different extracts as well as ulcerogenic sub-group and the last main group is treated animals. **Results:** in an in-vitro study, aqueous alcoholic extract exhibited the highest antioxidant properties and the lowest effect was recorded for petroleum ether extract. In an in-vivo experiment, aqueous alcoholic extract possessed potent anti-ulcerogenic effect as compared to famotin, reference drug. It enhanced the production of reduced glutathione and induced the glutathione reductase activity, superoxide dismutase activity and catalase activity determined in gastric mucosa with marked reduction in lipid peroxides productions in the two ulcerogenic models.

**Keywords:** Illicium verum; Essential oils; Antiulcer; (Alcohol and Aspirin) Ulcer;Antioxidants.

## B-615. In Vivo Study on the Hindrance Activity of Cinnamon Extract Against Aspergillus Niger in Mice

Randa Mohamed Alarousy, Sherein IsmailAbd El-Moez1, Kawkab Ahmed Ahmed and Hany Mohamed Hassan.

*International Journal of Chemtech Research, 9:962-972 (2016)*

**Aim:** The antimycotic effect and immune stimulating capacity of natural extract of Cinnamomum zeylanicum plant was evaluated against Aspergillus niger strain. **Methods and results:** the herbal extract was prepared from cinnamon park to be examined against Aspergillus niger (ATCC16404)species fungal cell suspension. Mice were injected with both fungal cell suspensions and Cinnamomum zeylanicum extract in a certain regime. Histopathological examination was applied on lung, liver and brain tissues extracted from the experimental animals and histopathological findings revealed the strong fungicidal effect of the herbal extract in the mice's tissues. Phagocytic activity, interleukins 2 & 6 (IL 2& IL6) and tumor necrosis factor(TNF) were measured in mice's blood samples as immunity stimulating efficacy parameters and also results revealed the potent immune stimulating efficacy of the extract and its safetyin vivo. **Conclusion:** According to the results of the study, Cinnamomum zeylanicum extract has a strong fungicidal activity against A. niger(ATCC16404)in addition to potent immune stimulating action confirmed experimentally. Results are supporting the efficacy of C. zeylanicum extract as prophylactic agent as well as fungicide. Significance and impact of the study: our study spotted a light on the advantages of the examined herbal extract as antimycotic substance, the promising results revealed encourages the use of C. zeylanicum extract as pharmaceutical preparation for treating and prevention of mycosis in immunocompromised patients instead of using some chemical antimycotic preparations available for commercial use to avoid the disadvantages of these chemically prepared medications.

**Keywords:** Cinnamomum Zeylanicum; Interleukin 2; Interleukin 6; Antimycotic Extract; Immunostimulant.

## B-616. Possible Therapeutic Effect of Arsenic Trioxide and L-Carnitine on Hepatocellular Carcinoma Induced in Rats

Basma Z. Emam, Amira M. Abo-Youssef, Ahmed H. Osman and Aziza M. Amer.

*International Journal of Pharmaceutical Sciences Review and Research, 41: 4-11 (2016)*

The present study aimed to evaluate the therapeutic effect of arsenic trioxide (ASO) and L-carnitine on hepatocellular carcinoma (HCC)-induced in rats using diethylnitrosamine (DENA) followed by carbon tetrachloride (CCL4). Fifty male (10-12 weeks old) Wistar albino rats were randomly assigned to five groups namely normal control, carcinogenic, cisplatin, ASO and L-carnitine groups. Assessed biomarkers included serum alkaline phosphatase (ALP), total bilirubin (tBil), alanine transaminase (ALT), aspartate transaminase (AST), albumin and total protein as hepatocyte integrity parameters, serum tumor marker alpha-fetoprotein (AFP), hepatic malondialdehyde (MDA), glutathione reduced (GSH) and superoxide dismutase (SOD) as oxidative stress biomarkers. Histopathology and immunohistochemistry of P53 were also conducted. ASO and L-carnitine significantly improved hepatic functions as indicated by significant reduction in serum ALP, tBil, ALT and AST. In addition, L- carnitine attenuated oxidative stress biomarkers. Histopathological and immunohistochemistry P53 findings strongly supported results of biochemical estimations. $AS_2O_3$ and L-carnitine have therapeutic effect on HCC- induced in rats; possibly through enhancement of tumor cells apoptosis by $AS_2O_3$ and protective effect of mitochondria by L-carnitine.

**Keywords:** Diethylnitrosamine; Carbon tetrachloride; Hepatocellular carcinoma; Cisplatin; Arsenic trioxide; L-Carnitine.

## B-617. Protective Effect of Cordia Boissieri A. Dc. (Boraginaceae) on Metabolic Syndrome

Asmaa I. Owis, Amira M. Abo-youssef, Ahmed H. Osman

*Journal of Applied Pharmaceutical Science, 6: 83-89 (2016)*

Increased fructose ingestion has been linked to obesity, hyperglycemia, dyslipidemia, and hypertension associated with metabolic syndrome. Cordia boissieri A. DC. (Boraginaceae) is a slow growing beautiful plant, used traditionally as herbal remedy by diabetic Hispanic women in the Southwestern USA. The present study aimed to elucidate the toxicity and the possible protective effect of ethyl acetate extract of C. boissieri leaves on metabolic syndrome. Three groups of rats were fed on fructose-enriched diet for 14 weeks. on e group served as fructose-enriched diet control, while the remaining groups were treated with metformin (10 mg/kg/day) and ethyl acetate extract (200 mg/kg/day) during the last 4 weeks. A fourth group was fed on normal laboratory diet. At the end of the experiment, blood samples were withdrawn for the estimation of metabolic syndrome-related markers and liver samples were subjected to histopathological and immunohistochemical examination. Induction of metabolic syndrome using fructose enriched diet was associated with increased weight gain coupled with elevated levels of blood glucose, insulin, uric acid, urea, creatinine, total cholesterol, triglycerides, malondialdehyde (MDA), nitric oxide and tumor necrosis factor in addition to, decreased level of glutathione (GSH). Four-weeks oral administration of ethyl acetate extract attenuated most of the changes associated with metabolic syndrome as marked by improved insulin sensitivity, glucose tolerance, kidney function,

lipid profiles and reduced oxidative stress and inflammation. The present study provides evidence of the potential protective effect of C. boissieri against metabolic syndrome.

**Keywords:** Cordia boissieri; Boraginaceae; Metabolic Syndrome; Ethyl aetate,

## B-618.Switching to Instant Black Coffee Modulates Sodium Selenite-Induced Cataract in Rats

E. A. El Okda, M. M. Mohamed, Shaheed and A. R. Abdel-Moemin

*Gms German Medical Science, 14: 1-11 (2016)*

The influence of daily consumption of some common beverages on the development of cataract in rats was investigated. Total phenol content was determined in the beverages and an oral standardized dose of total phenols from each beverage was given to the treated rats. Weaned male albino rats were used and divided into five groups (n=7). Rats were fed Ain 93G and administered the standardized dose of instant coffee, black tea and hibiscus beverages for 30 days. on day 14 all rats were injected with a single dose of sodium selenite (Na2SeO3) 15 µmol/kg bodyweight, except the control groups NC (negative control, did not receive Na2SeO3) and PC (positive control, was already injected on day 1 of the study). The rats were continued on Ain 93G and the standardized dose for another 16 days. Positive control rats were used. Total phenols were 210, 40, and 44 mg/g dry weight gallic acid equivalent in black coffee, black tea, and hibiscus, respectively. Decreased levels (statistically significant $P<0.05$) of malondialdehyde, total nitric oxide, Ca-ATPase, tumor necrosis factor-α, interleukin-1β, superoxide dismutase, and conversely, increased levels (statistically significant $P<0.05$) of total protein, reduced glutathione, catalase were found in the lenses of the coffee group compared to PC. There are co-phenol substances in the instant black coffee that promoted coffee to be the most effective beverage.

**Keywords:** Instant black coffee; Black tea; Hibiscus; Total Phenols; Sodium selenite; Cataract; Rats; Co-Phenols.

## B-619. The Potential Protective Impact of Spirulina platensis Against Thioacetamide-Induced Liver Fibrosis in Rats

Asmaa Khairy Mohammed Al-Mokaddem

*Asmaa K. Al-Mokaddem, Kawkab A. Ahmed, Sahar S. Abd El-Rahman and Essam Abdel-mawla*

*Journal ,: p1-p2, (2016)*

**Abstract :** The present study was carried out to investigate the possible protective role ofSpirulina platensis in modulating hepatic fibrosis induced by thioacetamide. Forty eight maleSprague-Dawley rats were randomly allocated into four groups (Gps), twelve rats each; Gp1received distilled water orally by gavage and served as control negative group, Rats of Gp2were daily administered Spirulina in distilled water at a dose of 300 mg/kg body weight, Ratsof Gp3 were intraperitoneally injected with thioacetamide (TAA) in distilled water twiceweekly at a dose of 200mg/kg body weight. While, Rats of Gp4 were co-administered Spirulinaand thioacetamide (TAA) as in Gp2 and Gp3. All treatments continued for eight weeks. Serumsamples were separated and used for estimation of hepatic function tests, body and liverweights were estimated and tissue specimens were collected for histopathological andimmunohistochemical studies. Our results revealed that Spirulina was able to improve bodyweight, liver function markers (AST, ALT, ALP and Bilirubin) and hinder the progress offibroplasia induced by TAA to great extent. Spirulina co-administration induced markeddecreased apoptotic figures among the hepatic parenchymal cells as well as decreased theimmune positivity of α-SMA, which all suggesting its role as a hepatoprotective agent

**Key words:** Spirulina platensis, Thioacetamide, Liver Fibrosis.

## B-620. A Simple Extraction Method for the Simultaneous Detection of Tetramisole and Diethylcarbamazine in Milk, Eggs, and Porcine Muscle Using Gradient Liquid Chromatography–Tandem Mass Spectrometry

Dan Zhang, Jin-A Park, Dong-Soon Kim, Seong-Kwan Kim, Soo-Jean Shin, Jae-Han Shim, Sung Chul Shin, Jin-Suk Kim, A.M. Abd El-Aty and Ho-Chul Shin

*Food Chemistry, 192: 299-305, (2016), IF: 4.052*

Analysis of residual quantities of contaminants in foods of animal origin is crucial for quality control of consumer products. This study was aimed to develop a simple and raid analytical method for detection of tetramisole and diethylcarbamazine using gradient liquid chromatography coupled with tandem mass spectrometry (LC/MS/MS). Tetramisole, diethylcarbamazine, and guaifenesin (as an internal standard) were extracted from milk, eggs, and porcine muscle using acetonitrile followed by partitioning at −20 °C for 1 h. No extract purification was deemed necessary. The analytes were separated on C18 column using ammonium formate both in water and methanol. Good linearity was achieved over the tested concentration range with R2 □ 0.974. Recovery at two fortification levels ranged between 67.47% and 97.38%. The intra- and inter-day precisions were <20%. The limit of quantification was 0.2 and 2 ng/g for tetramisole and diethylcarbamazine, respectively. An analytical survey of samples purchased from large markets showed that none of the samples contained any of the target analytes. To the best of our knowledge, this is the first report on the quantitative determination of tetramisole and diethylcarbamazine in animal food products.

**Keywords:** Anthelmintics; Tetramisole; Diethylcarbamazine; Lc/Ms/Ms; Porcine Muscle; Milk; Eggs.

## B-621.Contributing Effect of Various Washing Procedures and Additives on the Decline Pattern of Diethofencarb in Crown Daisy, A Model of Leafy Vegetables

Sung-Woo Kim, A.M. Abd El-Aty, Jeong-Heui Choi, Young-Jun Lee, Truong T.B. Lieu, Hyung Suk Chung, Md. Musfiqur

Rahman, Ok-Ja Choi, Ho-Chul Shin, Gyu-Seek Rhee, Moon-Ik Chang, Hee Jung Kim and Jae-Han Shim

*Food Chemistry, 201: 153-159, (2016), IF: 4.052*

The effects of various washing procedures, including stagnant, running, and stagnant and running tap water, and the use of washing solutions and additives, namely NaCl (1% and 2%), vinegar (2%, 5%, and 10%), detergent (0.5% and 1%), and charcoal (1% and 2%), on the reduction rate of diethofencarb were estimated in field-incurred crown daisy, a model of leafy vegetables, grown under greenhouses located in 3 different areas (Gwangju, Naju, and Muan). The original Quick, Easy, Cheap, Effective, Rugged, and Safe "QuEChERS" method was modified for extraction and liquid chromatography–tandem mass spectrometry (LC/MS/MS) was used for analysis. The recovery of diethofencarb in unwashed and washed samples was satisfactory and ranged between 84.28% and 115.32% with relative standard deviations (RSDs) of <6%. The residual levels decreased following washing with stagnant, running, and stagnant + running tap water (i.e., decline in levels increased from 65.08% to 85.02%, 69.99 to 86.79, and 74.75 to 88.96, respectively). The percentage of decline increased and ranged from 77.46% to 91.19% following washing with various solutions. Application of 1% detergent was found to be the most effective washing method for reducing the residues in crown daisy. Additionally, washing with stagnant and running tap water or even stagnant water for 5 min might reduce the residue levels substantially, making the prepared food safe for human consumption.

**Keywords:** Diethofencarb; Quechers; Washing methods; Washing solutions; Crown daisy; Lc/Ms/Ms.

## B-622. Detection of Three Herbicide, and on e Metabolite, Residues in Brown Rice and Rice Straw Using Various Versions of the Quechers Method and Liquid Chromatography-Tandem Mass Spectrometry

Young-Jun Lee, Md. Musfiqur Rahman, A.M. Abd El-Aty, Jeong-Heui Choi, Hyung Suk Chung, Sung-Woo Kim, Azza M. Abdel-Aty, Ho-Chul Shin and Jae-Han Shim

*Food Chemistry, 210: 442-450, (2016), IF: 4.052*

A single-run analytical method was developed to analyze the three herbicides azimsulfuron, bensulfuron-methyl, and mesotrione and its metabolite (4-methylsulfonyl-2-nitrobenzoic acid (MNBA)) in brown rice and rice straw using liquid chromatography-tandem mass spectrometry (LC/MS/MS). Samples extracted using various versions of Quick, Easy, Cheap, Effective, Rugged, and Safe "QuEChERS" (original unbuffered, acetate (AOAC), and citrate (EN) buffered) methods gave poor recoveries of all the tested analytes in both matrices. The extraction efficiency was improved when primary-secondary amine (PSA) sorbent was removed from the purification step, with the best recovery being achieved for EN-QuEChERS, which was subsequently used throughout the study. Overall, a determination coefficients (R2) □ 0.995 was achieved at matrix-matched calibration curves at various concentration ranges. The recovery rates at three fortification levels (limit of quantification (LOQ), 1/2 maximum residue limit (1/2MRL), and MRL) ranged from 78 to 114.5, with relative standard deviations (RSDs) < 18% for all the tested analytes in both matrices. The LOQs for all herbicides were lower than the MRL set by the Ministry of Food and Drug Safety (MFDS), Republic of Korea. Field trials with the recommended, or double the recommended dose, revealed that the herbicides can safely be applied to rice, as no residues were detected in the harvested samples at 110 days.

**Keywords:** Herbicides; Rice; Rice straw; Quechers; Lc/Ms/Ms; Residues.

## B-623. Development of A High-Performance Liquid Chromatography with Fluorescence Detection Method for Quantification of Piperazine in Animal Products by Using Precolumn Derivatization

Jin-A Park, Dan Zhang, Dong-Soon Kim, Seong-Kwan Kim, Sang-Hyun Cho, Daun Jeong, Jin-Suk Kim, Jae-Han Shim, A.M. Abd El-Aty and Ho-Chul Shin

*Food Chemistry, 196: 1331-1337, (2016), IF: 4.052*

A new high-performance liquid chromatography with fluorescence detection (HPLC-FLD) method was developed for determination of piperazine residues in food animal products. Samples were extracted with formic acid in water and purified using the PCX cartridge. Following purification, the samples were derivatized using dansyl chloride, and the analyte was separated using water/acetonitrile as a mobile phase. The calibration curves showed good linearity over a concentration range of 20–120 ng/g with coefficient of determination (R2) □ 0.996. The intra-day accuracy (presented as recovery %) and precision (presented as relative standard deviation, RSD %) were 81–97.3% and 0.83–6.87%, whereas, the inter-day values were 80.5–96.8% and 1.7–6.8%, respectively. The limit of quantification (LOQ) was 20 ng/g, which was considerably lower than the maximum residue limit (MRL). The developed method was used to monitor market samples, and piperazine was not detected in any of the samples. To our knowledge, this is the first study in which the detection of piperazine in various food and animal products by using a sensitive and reliable analytical method has been described.

**Keywords:** Piperazine; Derivatization; Sample preparation; Hplc; Livestock products; Residue analysis.

## B-624. Synthesis of New Thiazolo-Celecoxib Analogues as Dual Cyclooxygenase – 2/15-Lipoxygenase Inhibitors: Determination of Regio-Specific Different Pyrazole Cyclization by 2D Nmr

Eman K.A. Abdelall and Gehan M Kamel

*European Journal of Medicinal Chemistry, 118: 250-285, (2016), IF: 3.902*

Two new series of 1,5-diaryl pyrazoles (5a, 5b, 7a, 7b and 10) and 1,5-diaryl pyrazoline (12a and 12b) were prepared as both Cyclooxygenase-2 and 15-lipoxygenase inhibitors. Carrageenan-induced rat paw edema, ulcer index and anti-COX-1/COX-2 and 15-LOX inhibition assays were also included. Cyclization of different pyrazoles was discussed using 2D NMR such as HSQC, HMBC and NOSEY determinations. Compound 5a is more effective with ED50 = 0.98 and 3.98 μM against COX-2 and 15-lipoxygenase respectively, than the

references celecoxib (1.54 μM) and meclofenamate sodium (5.64 μM).
**Keywords:** Cyclooxygenase inhibitors; Celecoxib analogues; So2nh2 Pharmacophores; 15-Lipoxygenase inhibitors; Anti-Inflammatory; Dmfdma; Ethyl Trifloroacetate.

## B-625. Biological and Mechanistic Characterization of Novel Prodrugs of Green Tea Polyphenol Epigallocatechin Gallate Analogs in Human Leiomyoma Cell Lines

Reda Saber Ibrahim Ahmed, Gang Liu, Andrea Renzetti, Pershang Farshi, Huanjie Yang, Claire Soave, Ghassan Saed, Ashraf Ahmed El-Ghoneimy, Hossny Awad El-Banna, Robert Foldes, Tak-Hang Chan and Q. Ping Dou

*Journal of Cellular Biochemistry, 117: 2357-2369, (2016), IF:3.446*

Uterine fibroids (leiomyomas) are very common benign tumors grown on the smooth muscle layer of the uterus, present in up to 75% of reproductive-age women and causing significant morbidity in a subset of this population. Although the etiology and biology of uterine fibroids are unclear, strong evidence supports that cell proliferation, angiogenesis and fibrosis are involved in their formation and growth. Currently the only cure for uterine fibroids is hysterectomy; the available alternative therapies have limitations. Thus, there is an urgent need for developing a novel strategy for treating this condition. The green tea polyphenol epigallocatechin gallate (EGCG) inhibits the growth of uterine leiomyoma cells in vitro and in vivo, and the use of a green tea extract (containing 45% EGCG) has demonstrated clinical activity without side effects in women with symptomatic uterine fibroids. However, EGCG has a number of shortcomings, including low stability, poor bioavailability, and high metabolic transformations under physiological conditions, presenting challenges for its development as a therapeutic agent. We developed a prodrug of EGCG (Pro-EGCG or 1) which shows increased stability, bioavailability and biological activity in vivo as compared to EGCG. We also synthesized prodrugs of EGCG analogs, compounds 2a and 4a, in order to potentially reduce their susceptibility to methylation/inhibition by catechol-O-methyltransferase. Here, we determined the effect of EGCG, Pro-EGCG, and 2a and 4a on cultured human uterine leiomyoma cells, and found that 2a and 4a have potent antiproliferative, antiangiogenic, and antifibrotic activities.
**Keywords:** Uterine fibroids; Leiomyoma; Green tea; Egcg Analogs; Prodrugs; Therapy.

## B-626. Determination of Residual Levels of Naloxone, Yohimbine, Thiophanate, and Altrenogest in Porcine Muscle Using Quechers with Liquid Chromatography and Triple Quadrupole Mass Spectrometry

Dan Zhang, Jin-A Park, Seong-Kwan Kim, Sang-Hyun Cho, Soo-Min Cho, Hee Yi, Jae-Han Shim, Jin-Suk Kim, A. M. Abd El-Aty and Ho-Chul Shin

*Journal of Separation Science, 39(5): 835-841,(2016), IF:2.741*

A quick, easy, cheap, effective, rugged, and safe QuEChERS (method) was used for the simultaneous detection of four veterinary drug residues, namely naloxone, yohimbine, thiophanate, and altrenogest, in porcine muscle, using liquid chromatography with electrospray ionization triple quadrupole tandem mass spectrometry. Because of the unavailability of a suitable internal standard, matrix-matched calibrations were used for quantification, with determination coefficients ≥ 0.9542. The accuracy (expressed as recovery %) ranged from 60.53 to 83.25%, and the intra- and interday precisions (expressed as relative standard deviations) were <12%. The limits of quantification were 5, 0.5, 2, and 5 ng/g for naloxone, yohimbine, thiophanate, and altrenogest, respectively. Samples purchased from local markets in Seoul, Republic of Korea, revealed no traces of the target analytes. The developed method described herein is sensitive and reliable and can be applied to quantify the tested veterinary drugs in animal tissues.
**Keywords:** Porcine Muscle; Residue Analysis; Sample Preparation; Triple quadrupole; Tandem mass spectrometry; veterinary drugs.

## B-627. Quechers Method for the Simultaneous Quantification of Phorate and its Metabolites in Porcine and Chicken Muscle and Table Eggs Using Ultra-High Performance Liquid Chromatography with Tandem Mass Spectrometry

Md. Musfiqur Rahman Sung-Woo Kim Tae Woong Na A. M. Abd El-AtyYoung-Jun Lee Joon-Seong Park Amer Ramadan Han Sol Lee1 Hyung Suk Chung Jeong-Heui Choi1 Ho-Chul Shin Jae and Han Shim

*Journal of Separation Science, 39:2079-2086, (2016), IF:2.741*

An analytical method to detect phorate and its metabolites, including phorate sulfone, phorate sulfoxide, phoratoxon, phoratoxon sulfone, and phoratoxon sulfoxide, in porcine and chicken muscles and table eggs was developed and validated. Extraction was performed using a quick, easy, cheap, effective, rugged, and safe method and analysis was conducted using ultra-high performance liquid chromatography-tandem mass spectrometry. Matrixmatched calibrations were linear over the tested concentrations, with determination coefficient _ 0.995 for all tested analytes in the different matrices. The limits of detection and quantification were 0.001 and 0.004 mg/kg, respectively. The calculated recovery rates at three fortification levels were satisfactory, with values between 74.22 and 119.89% and relative standard deviations<10%. The method was applied successfully to commercial samples collected from locations throughout the Korean Peninsula, and none of them showed any traces of the tested analytes. Overall, the developed method is simple and versatile, and can be used for monitoring phorate and its metabolites in animal products rich in protein and fat.
**Keywords:** Chicken muscle; Metabolites; Phorate; Porcine Muscle; Table eggs.

## B-628. Simultaneous Determination of Seven Multiclass Veterinary Antibiotics in Surface Water Samples in the Republic of Korea Using Liquid Chromatography with Tandem Mass Spectrometry

Hyung Suk Chung, Jeong-Heui Choi, A. M. Abd El-Aty, Young-Jun, Han Sol, Sangdon Kim, Hee-Jung Jung, Tae-Woo Kang, Ho-Chul Shin and Jae and Han Shim

*Journal of Separation Science, 39 (24): 4688-4699, (2016), IF: 2.741*

A simultaneous determination method using solid-phase extraction and liquid chromatography with tandem mass spectrometry was developed to detect and quantify the presence of seven multiclass veterinary antibiotics (13 compounds in total) in surface water samples, which included the effluents of livestock wastewater and sewage treatment plants, as well as the reservoir drainage areas from dense animal farms. The pH of all water samples was adjusted to 2 or 6 before solid-phase extraction using Oasis HLB cartridges. The developed method was fully validated in terms of linearity, method detection limit, method quantitation limit, accuracy, and precision. The linearity of all tested drugs was good, with R2 determination coefficients ≥ 0.9931. The method detection limits and method quantitation limits were 0.1–74.3 and 0.5–236.6 ng/L, respectively. Accuracy and precision values were 71–120 and 1–17%, respectively. The determination method was successfully applied for monitoring water samples obtained from the Yeongsan River in 2015. The most frequently detected antibiotics were lincomycin (96%), sulfamethazine (90%), sulfamethoxazole (88%), and sulfathiazole (50%); the maximum concentrations of which were 398.9, 1151.3, 533.1, and 307.4 ng/L, respectively. Overall, the greatest numbers and concentrations of detected antibiotics were found in samples from the effluents of livestock wastewater, sewage treatment plants, and reservoir drainage areas. Diverse veterinary antibiotics were present, and their presence was dependent upon the commercial sales and environmental properties of the analytes, the geographical positions of the sampling points, and the origin of the water.

**Keywords:** River water; Solid-Phase extraction; Surface water; Tandem mass spectrometry; Veterinary antibiotics.

## B-629. Simultaneous Detection of Flumethasone, Dl-Methylephedrine, and 2 – Hydroxy-4,6-Dimethylpyrimidine in Porcine Muscle and Pasteurized Cow Milk Using Liquid Chromatography Coupled with Triple-Quadrupole Mass Spectrometry

Dan Zhang, Jin-A. Park, Seong-Kwan Kim, Sang-Hyun Cho, Daun Jeong, Soo-Min Cho, Hee Yi, Jae-Han Shim, Jin-Suk Kim, A.M. Abd El-Aty and Ho-Chul Shin

*Journal of Chromatography B, 1012-1013: 8-16, (2016), IF:2.687*

A simple analytical method based on liquid chromatography coupled with triple-quadrupole mass spectrometry was developed for detection of the veterinary drugs flumethasone, dl-methylephedrine, and 2-hydroxy-4,6-dimethylpyrimidine in porcine muscle and pasteurized cow milk. The target drugs were extracted from samples using 10 mM ammonium formate in acetonitrile followed by clean-up with n-hexane and primary secondary amine sorbent (PSA). The analytes were separated on an XBridge™ hydrophilic interaction liquid chromatography (HILIC) column using 10 mM ammonium formate in ultrapure water and acetonitrile. Good linearity was achieved over the tested concentrations in matrix-fortified calibrations with correlation coefficients (R2) ≥ 0.9686. Recovery at two spiking levels ranged between 73.62–112.70% with intra- and inter-day precisions of ≤20.33%. The limits of quantification ranged from 2–10 ng/g in porcine muscle and pasteurized cow milk. A survey of market samples showed that none of them contained any of the target analytes. Liquid–liquid purification using n-hexane in combination with PSA efficiently removed the interferences during porcine and milk sample extraction. The developed method is sensitive and reliable for detection of the three target drugs in a single chromatographic run. Furthermore, it exhibits high selectivity and low quantification limits for animal-derived food products destined for human consumption.

**Keywords:** Flumethasone; Dl-Methylephedrine; 2-Hydroxy-4,6-Dimethylpyrimidine; Tandem mass spectrometry; Porcine Muscle; Milk; Veterinary drugs.

## B-630. Determination of Process-Related Impurities in N-Acetylglucosamine Prepared by Chemical and Enzymatic Methods: Structural Elucidation and Quantification

Yi Soo Kim, Sung Joong Lee, Jin Young Choi, Yun-Hi Kim, Kebede Taye Desta, Zhe Piao, Su-Lim Choi, Sang-Jip Nam, Kyung-Yun Kang, A. M. Abd El-Aty, Yong Chul Shin and Sung Chul Shin

*Archives of Pharmacal Research,39(7):937-945,(2016),IF: 2.49*

β-N-acetylglucosamine (β-AG) is a monosaccharide distributed widely in living organisms with various pivotal roles. The presence of particulates and impurities can affect the safety and efficacy of a product for its intended duration of use. Thus, the current study was carried out to identify and quantify the potentially-harmful process related impurities; namely α-N,6-diacetylglucosamine (α-DAG) and α-N-acetylglucosamine (α-AG), derived from the chemical and enzymatic synthesis of β-AG. The impurities were characterized using a high resolution mass spectrometry, a nuclear magnetic resonance spectroscopy, and liquid chromatography-tandem mass spectrometry (LC/MS/MS). The developed method showed a good linearity (R2 ≥ 0.998), satisfactory precision (≤6.1 % relative standard deviation), intra- and inter-day accuracy (88.20–97.50 %), extraction recovery (89.30–110.50 %), matrix effect (89.70–105.20 %), and stability (92.70–101.60 %). The method was successfully applied to determine the level of α-DAG that was 3.04 and 0.07 % of the total β-AG, following chemical and enzymatic methods, respectively. It can be concluded that the enzymatic rather than the chemical method is more efficient for the synthesis of β-AG. Characterization of impurities heeds the signal for acquiring and evaluating data that establishes biological safety.

**Keywords:** Chitin; Nuclear magnetic resonance; Process-Related impurity; Tandem mass spectrometry; B-N-Acetylglucosamine

## B-631. Chemical and Antimicrobial Effects of Pomegranate Peel Aqueous Extract

Attia H Atta, Nermeen H. M. Hassaneen, Manal I. Abd El Fadeel, Doaa Sedky and Amany M. Mohamed

*Wulfenia, 23: 339-359, (2016), IF: 2*

This study was designed to investigate the effect of different concentration of pomegranate peel extract on chemical and microbiological quality of frozen bovine minced meat. Sixteen equal parts of minced meat were used as follows: one normal control, three POMP extract- treated parts (0.5, 1.5, and 3 % ), three inoculated parts (S. typhimurium, S. aureus or E. coli) and nine parts (3 POMP concentrations + 3 microorganisms inoculated, i.e. 3 X 3). Physical properties, chemical composition and microbiological count were performed at 0, 7, 15, 30 and 45 days of freezing at -18 ºC. The results showed that POMP aqueous extract maintained protein %, ash%, pH, thiobarbituric acid (TBA) number and total volatile nitrogen (TVN) at levels higher than non-treated non polluted samples and maintained TBA and TVN at levels lower than non-polluted or S. typhimurium or S. aureus but not E. coli - polluted samples. The results revealed that POMP has completely prevented survival of S. typhimurium and S. aureus but not E. coli during storage periods. In conclusion, POMP dried watery extract could be useful as natural preservative for bovine minced meat, since it maintained chemical and microbiological quality of minced meat.

**Keywords:** Pomegranate Peel- Additives- Natural Preservatives -S. Typhimurium -S. Aureus -E. Coli

## B-632. Comparative Biliary and Serum Kinetics of Doxycycline After Oral and Intramuscular Routes with Special Reference to its Unique Entero-Hepatic Circulation in Turkeys

K. Abo-EL-Sooud, G.A. Swielim, Y.R. Wally and Samar M. EL-Gammal

*Wulfenia, 23 (9): 206-219, (2016), IF: 2*

The present investigation was conducted to compare bile and serum concentrations of doxycycline (DOX) in turkeys after single intramuscular (IM) and oral administrations of 20 mg/kg body weight (b.w.). Furthermore, the entero-hepatic circulation and absolute bioavailability from gastrointestinal tract of DOX after oral dose were accessed. Three groups of male turkeys of five each received DOX at a dose rate of 20 mg/kg b.w. intravenously, intramuscularly and orally. Samples of serum and bile excreted were taken at predetermined intervals during 6 h. DOX concentrations of were determined by a reverse phase high-performance liquid chromatography (HPLC) with UV detection at 347 nm. After intravenous (IV) injection the elimination half-life, the total body clearance (Cltot) and the volume of distribution (Vss) were 3.90 h, 0.55 L/h/kg and 2.39 L/kg, respectively. The maximal serum concentrations (Cmax) of DOX in turkeys were 4.38 and 3.17 µg/ml, with time to peak concentration (Tmax) values of 0.74 and 1.00 h and absolute bioavailability were 71.83 % and 48.81 %, after IM and oral administrations respectively. The bile concentrations were up to 100 times higher than those in serum. The cumulative biliary excretion of the administered dose DOX was about 7% and 3% recovered from the bile within the first 6 hr after IM and oral dosing, respectively. After oral dose the entero-hepatic circulation model is based on the classical one compartment model with bile elimination half-life (T1/2k1g) of 5.36 h and the maximal bile concentrations (Cmax) was 222.39 µg/ml. Therefore DOX could be relevant for treatment of cholecyctitis and enteric infectious diseases.

**Keywords:** Doxycycline; Bile; Pharmacokinetics; Entero-Hepatic; Turkeys.

## B-633. Analysis of Mandipropamid Residual Levels Through Systematic Method Optimization Against The Matrix Complexity of Sesame Leaves Using Hplc/Uvd

Waziha Farha, Md. Musfiqur Rahman, A. M. Abd El-Aty, Sung-Woo Kim, Da-I Jung, So Jeong Im, Jeong-Heui Choi, Md. Humayun Kabir, Kang-Bong Lee, Ho-Chul Shin and Jae-Han Shim

*Biomedical Chromatography, 30 (7): 990-995,(2016), IF:1.729*

An analytical method was developed to detect mandipropamid residues in sesame leaves using high-performance liquid chromatography–ultraviolet detection. Samples were extracted with acetonitrile and were prepurified using a solid-phase extraction (SPE) cartridge with an additional dispersive-SPE (d-SPE) sorbent application. The method was validated using an external calibration curve prepared using pure solvent. The linearity was excellent with determination coefficient = 1. The limits of detection and quantification were 0.003 and 0.01 mg/kg, respectively. Recoveries at three spiking levels – 0.1, 0.5, and 1.0 mg/kg – were in the range 80.3–90.7% with relative standard deviations <2%. This method was applied to field-treated samples collected from two different areas, Gwangju and Muan, in the Republic of Korea and the half-lives were similar, 5.10 and 5.41 days, respectively. The pre-harvest residue limit was also predicted for both sites. The proposed method is sensitive and able to quantify trace amounts of mandipropamid in leafy vegetables. The combination of SPE and d-SPE effectively removed the matrix components in sesame leaves

**Keywords:** Dissipation patter; Half--Life; Mandipropamid; Method development; Residue analysis; Sesame leaves.

## B-634. Polyphenolic Profile and Antioxidant Effects of Various Parts of Artemisia Annua L.

Yi Song, Kebede Taye Desta, Gon-Sup Kim, Soo Jung, Won Sup, Yun-Hi Kim, Jong Sung Jin, A. M. Abd El-Aty, Ho-Chul Shin, Jae-Han Shim and Sung Chul Shin

*Biomedical Chromatography, 30 (4): 588-595,(2016), IF:1.729*

An annual Korean weed, Artemisia annua L., has been used as a folk medicine for the treatment of a number of diseases. Remarkably, among the 32 polyphenols characterized in various parts of plant tissue, including flowers, leafs, stems and roots, 10 compounds were detected for the first time using liquid chromatography–tandem mass spectrometry (LC/MS/MS). The quantification method was validated using structurally related external standards with determination coefficients (R2) ≥0.9995. The limits of detection and quantitation were 0.068–3.932 and 0.226–13.108 mg/L, respectively. The recoveries estimated at 50 and 100 mg/L ranged between 60.6–92.2 and 61.3–111%, respectively, with relative standard deviations <12%. The roots contained the largest concentration of identified components, while the flowers contained the least. The antioxidant capacity evaluated in terms of 1,1-diphenyl-2-

picrylhydrazyl and 2,2′-azinobis(3-ethylbenzothiazoline-6-sulfonic acid) radical cation-scavenging activities and reducing power was highest in the roots and lowest in the flowers. The findings are well correlated and suggest that the antioxidant capacities principally depend upon the polyphenol concentrations in each part of the plant.

**Keywords:** Artemisia annua L; Antioxidant activity; Liquid Chromatography-Tandem mass spectrometry; Medicinal Herb; Polyphenols.

## B-635. Residual Determination and Risk Assessment of Buprofezin in Plum (Prunus Domestica) Grown in Open-Field Conditions Following the Application of Three Different Formulations

Humayun Kabir, Abd El-Aty, Sung-Woo Kim, Han Sol, Musfiqur Rahman, Young-Jun, Hyung Suk Chung, Truong Lieu, Jeong-Heui Choi, Ho-Chul Shin, Geon-Jae Im, Su Myeong Hong and Jae-Han Shim

*Biomedical Chromatography, 30 (11): 1721-1727, (2016), IF:1.729*

This study was conducted to characterize the residual level and perform a risk assessment on buprofezin formulated as an emulsifiable concentrate, wettable powder, and suspension concentrate over various treatment schedules in plum (Prunus domestica). The samples were extracted with an AOAC quick, easy, cheap, effective, rugged, and safe, 'QuEChERS', method after major modifications. As intrinsic interferences were observed in blank plum samples following dispersive-solid phase extraction (consisting of primary secondary amine and C18 sorbents), amino cartridges were used for solid-phase extraction. Analysis was carried out using liquid chromatography with diode array detection and confirmed by liquid chromatography–tandem mass spectrometry. The method showed excellent linearity with determination coefficient (R2 = 1) and satisfactory recoveries (at two spiking levels, 0.5 and 2.5 mg/kg) between 90.98 and 94.74% with relative standard deviation (RSD) ≤8%. The limit of quantification (0.05 mg/kg) was considerably lower than the maximum residue limit (2 mg/kg) set by the Codex Alimentarius. Absolute residue levels for emulsifiable concentrates were highest, perhaps owing to the dilution rate and adjuvant. Notably, all formulation residues were lower than the maximum residue limit, and safety data proved that the fruits are safe for consumers.

**Keywords:** Buprofezin; Lc-Dad; Quechers; Emulsifiable Concentrates; Suspension concentrates; Wettable powder.

## B-636. Residue Level and Dissipation Pattern of Lepimectin in Shallots Using High-Performance Liquid Chromatography Coupled with Photodiode Array Detection

Sung-Woo Kim, Md. Musfiqur Rahman, A. M. Abd El-Aty, Lieu T. B. Truong, Jeong-Heui Choi, Joon-Seong Park, Mi-Ra Kim, Ho-Chul Shin and Jae-Han Shim

*Biomedical Chromatography, 30 (11): 1835-1842, (2016), IF:1.729*

Lepimectin, as an emulsifiable concentrate, was sprayed on shallots at the recommended dose rate (10 mL/20 L) to determine its residue levels, dissipation pattern, pre-harvest residue limits (PHRLs), and health risk. Samples were randomly collected over 10 days, extracted with acetonitrile, purified using an amino solid-phase extraction (NH2-SPE) cartridge and analyzed using a high-performance liquid chromatography–photodiode array detection method. Field-incurred samples were confirmed using ultra-performance liquid chromatography–tandem mass spectrometry. The linearity was excellent, with a determination coefficient (R2) of ≥0.9991. The recoveries at two spiking levels (0.2 and 1.0 mg/kg) ranged from 84.49 to 87.64% with relative standard deviations of ≤7.04%. The developed method was applied to field samples grown in separate greenhouses, one located in Naju and one in Muan, in the Republic of Korea. The dissipation pattern was described by first-order kinetics with half-lives of 1.9 (Naju) and 1.7 days (Muan). The PHRL curves indicated that, if the lepimectin residues are <0.18 (Naju) and <0.13 mg/kg (Muan) 5 days before harvest, the residue levels will be lower than the maximum residue limit (0.05 mg/kg) upon harvesting. The risk assessment data indicated that lepimectin is safe for use in the cultivation of shallots, with no risk of detrimental effects to the consumer.

**Keywords:** Dissipation pattern; Lepimectin; Liquid chromatography; Pre-Harvest residue limit; Shallots; Tandem mass spectrometry.

## B-637. Simultaneous Detection of Fluquinconazole and Flusilazole in Lettuce Using Gas Chromatography with a Nitrogen Phosphorus Detector: Decline Patterns at Two Different Locations

So Jeong Im, Md. Musfiqur Rahman, A. M. Abd El-Aty, Sung-Woo Kim, Humayun Kabir, Waziha Farha, Truong Lieu, Young-Jun, Da-I. Jung, Jeong-Heui Choi, Ho-Chul Shin, Geon-Jae Im, Su-Myeong Hong and Jae-Han Shim

*Biomedical Chromatography, 30 (6): 946-952, (2016), IF:1.729*

Method validations in addition to decline patterns of fluquinconazole and flusilazole in lettuce grown under greenhouse conditions at two different locations were investigated. Following the application of fluquinconazole and flusilazole at a dose rate of 20 mL/20 L water, lettuce samples were collected randomly for up to 7 days post-application, and simultaneously extracted with acetone, purified through solid-phase extraction, analyzed via gas chromatography with a nitrogen phosphorus detector, and confirmed through gas chromatography–mass spectrometry. The linearity was excellent, with determination coefficients (R2) between 0.9999 and 1.0. The method was validated in triplicate at two different spiking levels (0.2 and 1.0 mg/kg) with satisfactory recoveries between 75.7 and 97.9% and relative standard deviations of <9. The limit of quantification was 0.01 mg/kg. Both analytes declined very quickly, as can

be seen from the short half-life time of <4 days. Statistical analysis revealed significant differences between residues at different days of sampling, except at 7 days post-application (triple application). At that point, the decline patterns of fluquinconazole and flusilazole were independent of application rate, location, temperature and humidity.

**Keywords:** Gc-Npd; Decline pattern; Fluquinconazole; Flusilazole; Half-Life; Lettuce; Residue.

## B-638. The Polyphenolic Profiles and Antioxidant Effects of Agastache Rugosa Kuntze (Banga) Flower, Leaf, Stem and Root

Kebede Taye Desta, Gon-Sup Kim, Yun-Hi Kim, Won Sup Lee, Soo Jung Lee, Jong Sung Jin, A. M. Abd El-Aty, Ho-Chul Shin, Jae-Han Shim and Sung Chul Shin

*Biomedical Chromatography, 30 (2): 225-231,(2016), IF:1.729*

Agastache rugosa Kuntze (Korean mint) is used as a spice and in folk medicine in East Asia. The present study identified a total of 18 polyphenols from the flower, leaf, stem and roots of this plant using high-performance liquid chromatography–tandem mass spectrometry. Fourteen of these compounds had not previously been identified in these plant tissues. Each polyphenol was validated in comparison with external calibration curves constructed using structurally related compounds, with determination coefficients >0.9993. The limits of detection and quantification were 0.092–0.650 and 0.307–2.167 mg/L, respectively. Recoveries of 61.92–116.44% were observed at two spiking levels, with 0.91–11% precision, expressed as relative standard deviation (except anthraquinone spiked at 10 mg/L). Hydroxycinnamic acid was the most abundant compound in the root, while the flowers showed the highest total flavonoid level. Antioxidant activities, determined in terms of reducing power, Fe2+ chelating activity and the radical scavenging activities using α,α-diphenyl-β-picrylhydrazyl and 2-2□-azino-bis-3-ethylbenzothiazoline-6-sulfonic acid, increased in a concentration-dependent manner; the highest activity was identified in the stems, followed by leaves > flowers > roots. These findings indicate that A. rugosa is a good source of bioactive compounds and can be used as a functional food.

**Keywords:** Agastache rugosa kuntze; Antioxidant activity; Flavonoid; Herbal medicine; Herbal spice; Liquid Chromatography-Tandem mass spectrometry; Polyphenol.

## B-639. Various Extraction Methods for Detection of Bistrifluron Residues in Asian Pear Using High-Performance Liquid Chromatography: Application to Dissipation Patterns Under Open-Field Conditions

Lieu T. B. Truong, Sung Woo Kim, A. M. Abd El-Aty, Humayun Kabir, Musfiqur Rahman, Jeong-Heui Choi, Ho-Chul Shin, Chan-Hyeok Kwon, Kang-Bong Lee, Hae Jung Yoon and Jae Han Shim

*Biomedical Chromatography, 30 (10): 1535-1540, (2016), IF:1.729*

The present study was carried out to develop an analytical method for the detection and quantification of bistrifluron, a benzoylphenylurea compound, in pear using high-performance liquid chromatography with UV detection. Samples were extracted using conventional, AOAC and EN quick, easy, cheap, effective, rugged and safe 'QuEChERS' methods. As expected, conventional and EN-QuEChERS methods gave higher recoveries than AOAC. In addition, interference around the analyte retention time was observed in the conventional method. Thus, the EN-QuEChERS method was selected and validated by studying various parameters, including linearity, limit of detection, limit of quantification (LOQ), recovery and precision. Linearity was excellent, with a correlation coefficient of 0.9998. Recovery rates at three spiking levels (0.05, 0.2 and 1 mg/kg) ranged from 73.76 to 98.66%. Intra- and inter-day precisions, expressed as relative standard deviations, were <6%. The LOQ of 0.05 mg/kg was considerably lower than the maximum residue limit (1 mg/kg) set by the Korean Ministry of Food and Drug Safety. The developed method was successfully applied to open-field pear samples, in which the target analyte was slowly dissipated (55% decline) over 14 days with a half-life of 10.19 days. Notably, the residue levels throughout the period of sample collection (14 days) were lower than the maximum residue limit, indicating that the residue was not hazardous for consumers

**Keywords:** Quechers; Bistrifluron; Dissipation kinetics; Liquid Chromatography; Method development; Pear; Residue analysis

## B-640. A Combined Liquid Chromatography-Triple-Quadrupole Mass Spectrometry Method for the Residual Detection of Veterinary Drugs in Porcine Muscle, Milk, and Eggs

Dan Zhang, Zee-Yong Park, Jin-A Park, Seong-Kwan Kim, Daun Jeong, Sang-Hyun Cho, Jae-Han Shim, Jin-Suk Kim, A. M. Abd El-Aty and Ho-Chul Shin

*Environmental Monitoring and Assessment, 188: 348-0, (2016), IF: 1.633*

A liquid chromatography-electrospray ionization tandem mass spectrometry (LC/ESI-MS/MS) method was developed for monitoring and detection of four different drugs, namely acetanilide, pentylenetetrazole, phenacetin, and tetramethrin in porcine muscle, pasteurized milk, and table egg samples. For acetanilide and pentylenetetrazole, the samples were extracted with 0.1 % formic acid in acetonitrile, followed by defatting with n-hexane, partitioning at −20 °C for 1 h, centrifugation, and filtration, whereas the quick, easy, cheap, effective, rugged, and safe "QuEChERS" method was used for phenacetin and tetramethrin. The final extracts were combined and analyzed in a single chromatographic run using an XBridgeTM analytical column and 0.1 % formic acid and 10 mM ammonium formate in ultrapure water (A) and 0.1 % formic acid and 10 mM ammonium formate in methanol (B) as the mobile phase. Owing to the unavailability of internal standards, matrix-matched calibrations were used for analyte quantification with coefficients of determination (R2) ≥ 0.9865. The intra- and inter-day accuracies ranged from 60.75 to 90.90 % and from 63.75 to 89.30 %, respectively, while the respective analytical precisions were 1.48–17.44 % (23.3 % for porcine sample spiked with phenacetin) and 1.97–15.78 %. The limits of quantification (LOQ) were between 0.5 and 2.5 ng/g in the matrices tested. Food samples purchased from local markets in Seoul were analyzed using the developed method and none of the tested drugs was detected.

**Keywords:** Animal food products; Milk; Porcine muscle; Quechers; Table eggs; Tandem mass spectrometry; Veterinary drugs.

## B-641. An Overview on Common Aspects Influencing the Dissipation Pattern of Pesticides: A Review

Waziha Farha, A. M. Abd El-Aty, Md. Musfiqur Rahman, Ho-Chul Shin and Jae-Han Shim

*Environmental Monitoring and Assessment, 188: 693-0, (2016), IF: 1.633*

The common aspects and processes influencing dissipation kinetics of pesticides are determinants of their fate in the environment. Nowadays, with increasing population, the demand for food and fodder crops has also increased. With the development in science and technology, the methods of controlling pests may improve, but the major role played by the environment cannot be altered, i.e. the environmental factors, climatic conditions, and geology of areas under cultivation. Plants play a crucial role in the dissipation kinetics, as they may vary in species and characteristics. Differences in physico-chemical properties, such as formulation, bioavailability, and efficacy of the pesticide, may result in variable dissipation patterns even under the same environmental conditions. While modelling the dissipation kinetics for any specific pesticide applied to any specific crop, each factor must be considered. This review focusses on the variability observed across common factors, i.e. environmental aspects, plant-associated facts, and observed characteristics of chemical substances, influencing pesticide dissipation.
**Keywords:** Dissipation pattern; Environmental; Pesticide; Photodegradation; Plants; Temperature.

## B-642. Effects of Light Shading and Climatic Conditions on the Metabolic Behavior of Flonicamid in Red Bell Pepper

Da-I Jung, Waziha Farha, A. M. Abd El-Aty, Sung-Woo Kim, Md. Musfiqur Rahman, Jeong-Heui Choi, Md. Humayun Kabir, So Jeong Im, Young-Jun, Lieu. T. B. Truong, Ho-Chul Shin, Geon-Jae Im and Jae-Han Shim

*Environmental Monitoring and Assessment, 188: 144-0, (2016), IF: 1.633*

The degradation behavior of flonicamid and its metabolites (4-trifluoromethylnicotinic acid (TFNA) and N-(4-trifluoromethylnicotinoyl) glycine (TFNG)) was evaluated in red bell pepper over a period of 90 days under glass house conditions, including high temperature, low and high humidity, and in a vinyl house covered with high density polyethylene light shade covering film (35 and 75 %). Flonicamid (10 % active ingredient) was applied (via foliar application) to all fruits, including those groups grown under normal conditions (glass house) or under no shade cover (vinyl house). Samples were extracted using a Quick, Easy, Cheap, Effective, Rugged, and Safe "QuEChERS" method and analyzed using liquid chromatography-tandem mass spectrometry (LC/MS/MS). The method performance, including linearity, recovery, limits of detection (LOD), and quantitation (LOQ), was satisfactory. Throughout the experimental period, the residual levels of flonicamid and TFNG were not uniform, whereas that of TFNA remained constant. The total sum of the residues (flonicamid and its metabolites) was higher in the vinyl house with shade cover than in the glass house, under various conditions. The total residues were significantly higher when the treatment was applied under high light shade (75 %). The flonicamid half-life decreased from 47.2 days (under normal conditions) to 28.4 days (at high temperatures) in the glass house, while it increased from 47.9 days (no shade cover) to 66 days (75 % light shading) in the vinyl house. High humidity leads to decreases in the total sum of flonicamid residues in red bell pepper grown in a glass house, because it leads to an increase in the rate of water loss, which in turn accelerates the volatilization of the pesticide. For safety reasons, it is advisable to grow red bell pepper under glass house conditions because of the effects of solar radiation, which increases the rate of flonicamid degradation into its metabolites.
**Keywords:** Degradation; Flonicamid; Glass house; Half-Life; Humidity; Metabolites; Shade cover; Temperature; Vinyl house.

## B-643. Simultaneous Determination of Water-Soluble Whitening Ingredients and Adenosine in Different Cosmetic Formulations by High-Performance Liquid Chromatography Coupled with Photodiode Array Detection

Jeon JS, Kim HT, Kim MG, Oh MS, Hong SR, Yoon MH, Cho SM2, Shin, Shim JH, Ramadan and Abd El-Aty

*International Journal of Cosmetic Science, 38: 286-298, (2016), IF: 1.542*

**Objective:** The Korean Cosmetic Act regulates the use of functional cosmetics) by the law. Four functional cosmetic groups, whitening, anti-wrinkle, UV protection and combination of whitening and anti-wrinkle, were categorized according to the Korean Cosmetic Act and Functional Cosmetics Codex. In this study, highperformance liquid chromatography (HPLC) coupled with photodiode array detection (DAD) was employed for the simultaneous detection of arbutin (and its decomposition product, hydroquinone), niacinamide, ascorbyl glucoside, ethyl ascorbyl ether and adenosine in functional cosmetic products such as creams, emulsions and lotions. **Methods:** Separation by HPLC-DAD was conducted using a C18 column with a gradient elution of 5 mM KH2PO4 buffer (containing 0.1% phosphoric acid) and methanol (containing 0.1% phosphoric acid). The wavelengths for the detection of arbutin, hydroquinone, niacinamide, adenosine, ascorbyl glucoside and ethyl ascorbyl ether were 283, 289, 261, 257, 238 and 245 nm, respectively. **Results:** This method exhibited good linearity ($R2 \geq 0.999$), precision (expressed as relative standard deviation (RSD) < 2%) and mean recoveries (89.42–104.89%). The results obtained by monitoring 100 market samples showed that the detected levels of the tested materials are within the acceptable authorized concentration. **Conclusion:** The method developed herein is simple and can be used for market survey and quality control of functional cosmetics.
**Keywords:** Adenosine; Arbutin, ascorbyl glucoside; Ethyl Ascorbyl Ether; High-Performance liquid chromatography; niacinamide.

## B-644. Investigating the Potential Role of Vitamin E in Modulating the Immunosuppressive Effects of Tylvalosin and Florfenicol in Broiler Chickens

Fatma I. Abo El-Ela, S.A.S. Shany, Manal B. El-Deen, H.A. El-Banna, A.A. El-Gendy, K. Hendy and M.A. Tohamya

*Research In Veterinary Science, 118: 25-32, (2016), IF: 1.504*

Tylvalosin (TVS) is a third-generation macrolide drug used for prophylaxis and treatment of mycoplasma, however; it is supposed to possess an immunosuppressive effect. In the current study, the immunosuppressive effect of TVS and florfenicol (FFC) and the potential immunomodulatory role of Vit Ewere investigated. The experiment included one day old chick groups treatedwith either TVS, FFC, Vit E, TVS/Vit E, FFC/Vit E and control non-treated group. Chickswere vaccinatedwith inactivated H9N2 avian influenza (AI) vaccine and humoral antibody titers to viral antigen as well as innate immunity (serum lysozyme activity and nitric oxide levels) were evaluated. Total and differential leucocytic counts, serumliver enzymes level, blood leucocytic DNA damage and cellular area percentages within the lymphoid organs were also screened. Treatment with TVS and FFC significantly decreased immune response of chickens while treatment with Vit E improved the humoral immune response at 4 and 5 weeks post-vaccination. Vit E also significantly increased the cellular immune response. The combination of Vit Ewith either TVS or FFC modulated their immunosuppressive effect and resulted inmild immunostimulatory effects. TVS alone induced a genotoxic effect on chickens' blood leucocytes and the genotoxicity was inhibited by combination of TVS with Vit E. Histopathology revealed that chickens treated with either TVS or FFC exhibited toxic effect on the lymphatic tissues.

**Keywords:** Chickens; Florfenicol; Immunity; Tylvalosin; Vitamin E.

## B-645. Simultaneous Detection of Glabridin, (-)-A-Bisabolol, and Ascorbyl Tetraisopalmitate in Whitening Cosmetic Creams Using Hplc-Pad

Jong‑Sup Jeon,Han‑Taek Kim, Myeong‑Gil Kim, Moon‑Seog Oh; Se‑Ra Hong, Mi‑Hye Yoon, Ho‑Chul Shin,Jae‑Han Shim, Nehal Aly Afifi, Ahmet Hacımüftüog and A. M. Abd El‑Aty

*Chromatographia (2016), 79: 0-860, (2016), IF: 1.332*

A simultaneous analytical method was developed and validated to quantify three lipophilic compounds; namely glabridin (an isoflavonoid isolated from crude licorice), (−)-α-bisabolol (a sesquiterpene alcohol obtained from plant extracts), and ascorbyl tetraisopalmitate (a fat-soluble molecule derived from vitamin C) in functional cosmetic cream using high-performance liquid chromatography (HPLC) coupled with photodiode array detection (PAD). Cosmetic cream samples were extracted with a mixture of acetonitrile and isopropyl alcohol (45:55, v/v) and the target compounds were separated on a C18 column with a gradient mobile phase consisting of deionized water, acetonitrile, and isopropyl alcohol. The detector wavelengths were 228, 202, and 221 nm, for glabridin,(−)-α-bisabolol, and ascorbyl tetraisopalmitate, respectively. The calibration curves showed good linearity with determination coefficients (R2) ≥ 0.999. The mean recoveries were ranged between 89.8 and 103.9 % with relative standard deviations (RSDs) <5 %. The intra- and inter-day precision was <2 %. The limits of detection (LODs) were 0.03, 0.4, and 4.02 μg mL−1 for glabridin, (−)-α-bisabolol, and ascorbyl tetraisopalmitate, respectively. The method was successfully applied for monitoring 11 market samples, in which glabridin was quantified in the range of 17.5–25 mg 100 g−1, (−)-α-bisabolol in the range of 25.1– 677 mg 100 g−1, and 140.6–291.5 mg 100 g−1 for ascorbyl tetraisopalmitate. The proposed analytical method is simple, sensitive, and versatile and can be used for the quantification of lipophilic compounds in cosmetics in a single chromatographic run.

**Keywords:** High-Performance liquid chromatography; Glabridin; (−)-A-Bisabolol; Ascorbyl tetraisopalmitate; Functional cosmetic.

## B-646. Determination of Residual Levels of Metrafenone in Lettuce Grown Under Greenhouse Conditions Using Gas Chromatography with a Micro-Electron Capture Detector

Humayun Kabir, A. M. Abd El-Aty, So Jeong Im, Md. Musfiqur Rahman, Sung-Woo Kim, Waziha Farha, Jeong-Heui Choi, Da-I Jung, Young-Jun, Troung LieuHo-Chul ShinGeon-Jae ImSu-Myeong HongJae and Han Shim

*Applied Biological Chemistry, 59 (1): 43-49, (2016), IF: 0.655*

The current study was carried out to detect metrafenone residues and estimate the half-lives in lettuce grown under greenhouse conditions using gas chromatography with a micro-electron capture detector. Metrafenone was applied in two and three doses (with a 7-day interval) to two different sites in Naju (distance between sites 1 and 2 = 6.5 km) in different seasons (spring and autumn). Samples were extracted with acetone and matrix components were purified using a silica solid-phase extraction (SPE) cartridge. The calibration curve over the concentration range of 0.02–5.0 mg/L was linear with a determination coefficient (R2) = 0.9993. The limits of detection and quantification were 0.003 and 0.01 mg/L, respectively. Recoveries at two fortification levels (0.1 and 0.5 mg/kg) ranged from 78.5 to 113.3 % with a relative standard deviation <8 %. The calculated half-lives were 2.3 and 2.2 days and 4.9 and 5.0 days for the double and triple doses at sites 1 and 2, respectively. These results suggest that the method is effective and sensitive for the determination of metrafenone residues in field-incurred lettuce samples, and the difference in the reported half-lives is due to seasonal variation.

**Keywords:** Metrafenone; Lettuce; Gas chromatography-Micro Electron capture detector; Decline; Half-Life.

## B-647. Enhancement of Immune Response Against Ibd and Ib in Antibiotic Treated Mycoplasma Gallisepticum Serologically Positive Broiler Chickens

Kh.M.Elbayoumi, Zeinab M.S. Amin Girh, Eman R. Hassan, Aziza M.Amer, Ghazi .A. M. Zohair and M.M. Amer

*International Journal of Chemtech Research, 9:934-942 (2016)*

This study was carried out to study effect of antibiotics and or prebiotics on immune response of Mycoplasma gallisepticum (MG) serologically positive broiler chickens to IBD and IB live vaccine. A total number of 210, 1 day old broiler chickens were used. Chicks were divided into seven equal groups and treated

as follows: betaine, macroloids (tylosin), polymyxins (colistin), tylosin and betaine, colistin and betaine was given to group 1, 2 , 3, 4and 5; respectively. While group 6 and 7 was kept nontreated vaccinated and non vaccinated non treated (negative) control; respectively. Chickens groups 1-6 were vaccinated with vector IBD and IB commercial vaccines simulating commercial field. Evaluating antibody titers against used vaccines was done using ELISA kits on sera collected at 0 day of life and every 10 days till the end of the experiments. Results revealed that the best means ELISA titer results against IBD vaccine by the end of the experiments was 7950 in both colistin group (3) and colistin and betaine group (5), followed by group (4) received tylosin and betaine which was 7800 , followed by group (2) received tylosin which was 7750 followed by group (1) received betaine only which was 7700 , followed by 7400 in group 6 ( vaccinated non treated). The mean ELISA titers against IB live vaccine the highest was in group (5) received colistin and betain which was 1540, followed by group (3) received colistin only which was 1490, followed by group (4) received tylosin and betaine which was 1345, followed by group (1) received betaine only which was 1395, followed by group (2) which received tylosin which was 1300,while non treated vaccinated group 6 gives 1212. The recorded mean ELISA titers of MG, IBD and IB in sera of chicks at 1 day of life 5269,11000 and 5790; respectively are due to maternal derived antibodies. Maternal derived antibodies to IBD and IB was gradually decreased in non vaccinated non treated group 7 to reach 2800 and 111 at the 30th day of life. While MG antibodies was markedly increased after live vaccine application, on the other hand non observed lesions was detected in antibiotic medicated group. It could be concluded that both polymexins (colistin) and macroloids (tylosin) antibiotics used in this study has positive impacts in controlling of Mycoplasma galisepticum and on immune response of broiler chickens to IB and IBD vaccines. Prebiotic (betaine) enhanced positively immune system to produce humoral immune response. A combination between antibiotic and prebiotic can be used to minimize the possible adverse effects of excessive use of antibiotic on vital organs.

**Keywords:** Broiler;IB and IBDvaccines; ELISAtest; Colistin; Tylosin; Betaine.

## B-648. Pharmacokinetics of Tylvalosin in Healthy and Experimentally Mycoplasma Gallisepticum Infected Broiler Chickens

Ammar Haki Salman, S.A.H. Youssef, Amer Ramadan and Ahmed M. Soliman

*International Journal of Pharmtech Research, 9: 72-80 (2016)*

A study of tylvalosin pharmacokinetics was conducted in healthy and Mycoplasma gallisepticum-infected broiler chickens. Tylvalosin was administered intravenously and orally at a dose rate of (25 mg/kg b.wt.) to determine its concentrations in blood as well as its kinetic disposition. The serum concentration - time curve indicated a two compartment open model. Following intravenous injection, the mean elimination half-lives (t1/2□) of (6.666±0.285 and 3.048±0.232 h) before and after infection, respectively. The apparent volume of distribution (Vd(area)) of tylvalosin was (3.802±0.148 and 0.657±0.367 L/Kg) with body clearance CLβ (0.953±0.040 and 1.976±o.743. L/kg/h) with mean of MRT was (9.314±0.407 and 1.739±0.779 h) in healthy and M. gallisepticum -infected chickens, respectively. Following oral administration, Tylvalosin was absorbed with (t½ka) of (0.963±0.045 and 0.958±0.207 h) with peak serum concentration of (1.226±0.041 and 0.0760±0.024 µg/ml) at (tmax) of (1.723±0.04 and 1.310±0.055 h) and eliminated with (t½β) of (3.504±0.49 and 3.862±0.103 h) in healthy and infected chickens. The systemic bioavailability of Tylvalosin (F%) following oral administration was (48.39±0.001 and 72.96±0.003 %) in healthy and infected birds respectively. It is to conclude that serum and tissues Tylvalosin concentration following twice-daily dose of (25 mg/Kg b. wt./day) were suitable to maintain its therapeutic regimen for treatment of mycoplasma infection in broiler chickens, in addition mycoplasma infection significantly decrease and/or consumed serum concentration, increased elimination rate so it is recommended that dose rate is adjusted in case of mycoplasma infection.

**Keywords:** Tylvalosin; Disposition kinetics; Healthy; Broiler Chickens; Mycoplasma gallisepticum.

## B-649. Pharmacokinetics, Bio-Equivalence and Tissue Residues of two Oral Colistin Formulations in Broiler Chickens

Ahmed m. Soliman , ahmed ragab elbestawy and sherin ibrahim

*International Journal of Pharmacy and Pharmaceutical Sciences, 8 (4): 166-170 (2016)*

**Objective:** The present study was carried out to investigate and provide an overview of the pharmacokinetics, bio-equivalence and tissue residues of colistin in two oral tested products, BAC-Liquido® (Interchemi Co.) and Coline-L (Medmac Co.) in healthy broiler chickens. Methods: The comparative pharmacokinetics, bio-equivalence, blood and tissue residues of BAC-Liquido and Coline-L in broiler chickens was studied after oral administration of both products in a dose of 100.000 IU colistin base/kg. b. wt once daily for 5 consecutive days. **Results:** Colistin in both products obeyed a two compartments open model following I. V administration. The disposition kinetics of BAC-Liquido and Coline-L following oral administration of 100.000 IU colistin base/kg. b. wt revealed that the maximum blood concentration [Cmax.] were 5.10 and 4.95 µg/ml and attained at [tmax.] of 5.90 and 6.40 h, respectively. Colistin in BAC-Liquido and Coline-L was eliminated with half-lives [t1/2β] equal to 3.15 and 2.89 h, respectively. The mean systemic bioavailability of colistin in BAC-Liquido and Coline-L following oral administration in healthy chickens was 3.75 and 4.05%, respectively. The blood (µg/ml) and tissue (µg/g) residues of Coline-L and BAC-Liquido following repeated oral administrations showed that liver, kidney; lung, breast, and thigh muscles contained the limited colistin residues. Colistin in both preparations was completely disappeared from all tissues at 24 h following the last oral dose (except liver 48 h). **Conclusion:** It was concluded that Coline-L is bioequivalent to BAC-Liquido since Cmax test/Cmax reference and AUCtest/AUCreference ratios were 0.97 and 1.06, respectively. Chickens should not be slaughtered for human consumption within treatment and could be consumed after the discontinuation of the treatment (except liver, withdrawal time 48 h) of either BAC-Liquido® or Coline-L.

**Keywords:** Pharmacokinetics; Colistin; Broiler chickens; Bioavailability; Tissue residue.

## B-450. Phenotypic Identification of Pseudomonas Aeruginosa Isolated from Milk in Taif Governorate and Characterization of Resistance to Fluoroquinolones and some Medical Plant Extracts

Nashwa A. Ezzeldeen, Samar M. Mouneir, Nourah Mohammed Komaikh Al-Zahrani, Afaf Ali Amin El. Haririr, M., Mohamed A. Abdelmonem, Seida A.A and Manal F AbdelAzez

*Advances in Environmental Biology, 10(2): 56-68 (2016)*

Pseudomonas aeruginosa had been assigned as the distinct cause of otitis externa , cystitis, endocarditis, dermatitis, wound infections, conjunctivitis, equine metritis and ulcerative keratoconjunctivitis, mink haemorrhagic pneumonia, deep pyoderma,infections of the lower urinary tract, prostatitis, osteomyelitis, chronic rhinitis, pleuritic, mastitis. Results: Prevalence of Pseudomonas aeruginosa among cattle milk was investigated which covered Taif Governorate through microbiological examination of 100 various samples of milk. In positive samples, bacteriological examinations were done on 37 isolates. The result showed that the prevalence of Pseudomonas aeruginosa isolation were 60% goat milk, 41.2% sheep milk, 35.3% camel milk and 54.5% raw cow milk.Serogrouping results revealed that out of 37 isolates, [8] isolates were O1 serogroupe with percentage 21.6%, [12] isolates were O3 and O4 serogroupe with percentage of 16.2% of each, [4] isolates were serogroupe O7 in percentage of 10.8%, [3] isolates were O6 serogroupe with percentage of 8.1%, O5, O8, O10 and O11 serogroups were [2] isolates for each with percentage 5.4% and one isolate with percentage 2.7% were O2 and O9 serogroupes. The antimicrobial test revealed that most strains were sensitive to gentamicin ,pipracillin, meropenem and ciprofloxacin with percentage 100% in goat milk strains and camel milk strains. on the other hand, trimethoprim sulfamethoxazole recorded 100% resistant on cow milk strains, followed by 92.9% resistant to cefepime. The in vitro sensitivity test of Pseudomonas aeruginosa strains was done against 11 nature plant extracts. The ethanolic extracts of Coriander, Bay leaf Black pepper, Parsley and Turmeric did not show any antibacterial activity against isolated strains with different concentrations. While Hibiscus, Thyme, Black cumin, Red chili and Cinnamon gave microbicide activity against all isolated strains in concentration 100%. Using of PCR techniques proved the presence of genes of ceftazidime resistance blaVIM gene and blaPER gene. Also quinolone-resistant gene gyrA gene was proved to be existed

**Keywords:** Pseudomonas aeruginosa; Resistance gene Detection;Antimicrobial susceptibility testing.

## B-451. Phytochemical and Pharmaco-Toxicological Assessment of Hydro Ethanolic Extract of Taverniera Aegyptiaca Boiss

Salah M. El-kousy, K. Abo EL-Sooud, Khadiga F. Amer, Sayed A. El-Toumy and Ahmed R. Hassan

*International Journal of Pharmacognosy and Phytochemical Research, 8 (12): 1907-1912 (2016)*

Taverniera aegyptiaca Boiss is a wild plant is grown at the Red Sea coast, Egypt. Traditional uses of this species drive us to evaluate the phytochemical and pharmaco-toxicological aspects of the hydro ethanolic extract of the aerial parts of T. aegyptiaca. Phytochemical screening revealed the presence of various bioactive secondary metabolites as flavonoids, terpenes, glycosides, saponins and sterols compounds which might be responsible for their medicinal attributes. Alkaloids and tannins were not detected. The safety of ethanolic extract of T. aegyptiaca is evidenced by the high LD50 value of the extract (>5g/kg). In addition, there wasn't significant modification in the general behavior of the animals and deaths after 72 hours post-administration. Oral administration of 500 mg kg−1 hydro ethanolic extract of T. aegyptiaca, significantly inhibited the nociception to acetic acid-induced writhes and increases in the latency to response of tail to thermal stimulation. Furthermore, pretreatment of rats with T. aegyptiaca extract reduced the ulcer index and produced protection in ethanol induced ulceration model. The extract induced all pharmacological effects in a dose dependent manner. These findings suggested that T. aegyptiaca can be used as a promising source of new antinociceptive anti-inflammatory and anti-ulcerogenic agent.

**Keywords:** Taverniera aegyptiaca; Phytochemical; Antinociceptive; Anti-Inflammatory; Anti-Ulcerogenic.

## B-652. Potential Hepatoprotective Effect of Combining Vitamin C and L-Carnitine Against Acetaminophen Induced Hepatic Injury and Oxidative Stress in Rats.

Zeinab A. El-Gendy, Seham A. El-Batran, S.A.H.Youssef, A. Ramadan, Azza H.M. Hassan and Rania F. Ahmed.

*International Journal of Pharmtech Research, 9: 33-47 (2016)*

Acetaminophen is one of the most popular OTC analgesics and antipyretics especially among women unfortunately; its miss use can result in serious hepatic injury. In the present study hepatoprotective activity of L-carnitine plus Vitamin C against acetaminophen induced hepatic damage in Adult Female Wistar albino rats was evaluated. L-carnitine at dose levels of 25 and 50mg/kg p.o. /day plus Vitamin C 100 mg/Kg p.o. /day were administered for 21 days. on day twenty-one; hepatic injury was induced by administering a single dose of 600mg/Kg body wt. p.o. of acetaminophen. Results revealed that combining L-carnitine and vitamin C reduced serum liver enzymes; Aspartate amino Transferase (AST) and Alanine amino Transferase (ALT), decreased cholesterol level and low density lipoproteins (LDLCholesterol), increased high density lipoproteins (HDL-Cholesterol), dropped interleukin-6 (IL- 6) and tumor necrosis factor alpha (TNFα), hindered the progression of oxidative stress as foreseen by increasing glutathione (GSH) level and reducing malondialdehyde (MDA) and nitric oxide (NOx) contents. In conclusion; we can recommend the use of vitamin C in combination with l-Carnitine to protect against adverse effects that could result from over dosage of acetaminophen.

**Keywords:** L-Carnitine; Vitamin-C; Interleukein – 6; Acetaminophen; Liver Injury.

## B-653. Quercetin Protects Against Thioacetamide Induced Hepatotoxicity in Rats Through Decreased Oxidative Stress Biomarkers, the Inflammatory Cytokines; (TNF-A), (Nf-B) and DNA Fragmentation

Nehal A Afifi, A Ramadan, W El-Eraky, Abeer AA Salama, Amany A El-Fadaly and Azza Hassan

*Der Pharma Chemica, 8(9): 48-55 (2016)*

The present study aimed to investigate the hepatoprotective mechanisms of quercetin and silymarin in experimentally induced hepatic toxicity in rats. Mature Albino Wister rats were orally daily treated with quercetin (50 and 100 mg/kg), silymarin (50 mg/kg) for 21consecutive days, then were injected intraperitoneal with TAA (300 mg/Kg, i.p.) twice with 24 hours interval in the last two days of the experiment to induce hepatotoxicity. Afterwards, blood samples were withdrawn from all rats and liver tissue were isolated. Sera separated for determination of serum liver function tests. Liver homogenates were used for assessment of oxidative stress biomarkers, inflammatory cytokines, hepatocellular apoptosis and histopathological examinations. Moreover, hepatic DNA fragmentation levels were examined calorimetrically by diphenylamine (DPA) and electrophoreticaly by agarose gel electrophoresis. Results of the present study revealed that oral administration of quercetin (50 and 100 mg/kg) for 21 days significantly improved the elevated liver enzymes (AST and ALT), alkaline phosphatase and total bilirubin with significant decreased oxidative stress biomarkers measured as malondialdehyde (MDA) , nitric oxide (NO) and reduced glutathione (GSH) contents in liver homogenate. In addition, quercetin decrease the elevated inflammatory cytokine; tumor necrosis factor alpha (TNF-α), nuclear factor kappa beta (NF-κ B) and DNA fragmentation in a dose dependant manner. Finally, it can be concluded that quercetin displayed a protective effect against TAAinduced hepatic toxicity via mechanisms involving the alleviation of oxidative stress, antioxidant potential, and attenuation of inflammation and inhibition of hepatocellular apoptosis.

**Keywords:** Hepatotoxicity; Quercetin; Silymarin;Thioacetamide (TAA); Rats.

## B-654. Studies on Effect of Prebiotic on Immune Response of Broiler Chicken to Nd -Ai Combined Inactivated Vaccine

1 M.M. Amer, Kh.M.Elbayoumi, Zeinab M.S. Amin Girh, Eman R. Hassan and M.A.Bosila

*International Journal of Chemtech Research, 9: 182-190 (2016)*

Effect of prebiotic on immune response to companied inactivated ND-AI vaccine in presence of bacterial infection were studied, 160 day old Cobb broiler chicks were divided into 4 equal groups; 40 chicks in each. Group 1 negative control non vaccinated while group 2 received lysozyme while groups 3 received Betaine, finally group 4 were kept as positive vaccinated control positive group. Chickens group were vaccinated subcutaneously with the recommended dose of inactivated ND-AI combined vaccine. E.coli O78 K80 H11 strains in phosphate buffered saline )PBS) was used as a bacterial challenge strain and was used by oral infection, each chick was given 0.5ml containing 1 x 104 viable microorganism/ml. Blood samples were collected weekly for haemagllutination inhibition (HI) test , bursa and liver were collected for histopathological examination. Results of HI test against ND revealed that best mean antibody titer was 6.14±0.69 in birds received Betaine (gr 3), followed by 6.00 ±0.95 in those received lysozyme (gr 2) , followed by that of group 4 (positive vaccinated group infected with E.coli ) which showed 4.00±1.89 , then finally 4.00 ±0.58 in negative control group. Results of AI haemagllutination inhibition (HI) antibodies was the best in group 2 that received betaine which was (4.86±0.69) followed by 4.71± 0.95 in lysozyme (gr. 2) , followed by group (4) positive vaccinated group which was 4.43± 0.54 and finally 3.43±0.79 in the negative control group1. Also it was noticed that group (4) vaccinated infected with E.coli control positive showing clinical signs of E.coli infection in the form of diarrhea and subcutaneous inflammation (cellulitis ) mortality rate was 30%. Concerning histopathological findings the examined bursa, and liver stained sections of control negative group show no detectable pathological lesions until the end of the experiment, on the other hand it was found that Bursa of Fibricus of group (3) which received Betain showing moderate hyperplasic activity of the lymphoid follicle which later on become more obvious by the end of the experiment, concerning liver sections group (4) infected vaccinated non treated group showed severe hydropic degeneration other field showed severe congestion of the central vein while groups (2) and (3) were less affected as they showed mild congestion of portal vein. In conclusion building immune foundation against respiratory virus is crucial and can be fulfilled by proper vaccination programme and can be enhanced by prebiotics which could improve antibody titers of inactivated respiratory vaccine , unfortunately this need further investigations specially of studding aspects of celluler immune response with used prebiotics.

**Keywords:** Broiler vaccination; Prebiotic; E.Coli; Compined inactivated Ai and Nd; Lysozyme; Betaine.

## B-655. A Trial for Prevention of Campylobacter Jejuni Infection in Broiler Chickens Using Autogenus Bacterin

Wafaa A. Abd El-Ghany, M.H. Awaad and S.R. Nagwa

*Asian Journal of Poultry Science, 10: 78-85 (2016)*

Two strains of Campylobacter jejuni (C. jejuni) representing biotype I and II were used for preparation of bacterin. Pure, sterile and safe watery aluminium hydroxide and incomplete Freund's oil adjuvant bivalent bacterins were prepared. Both types of bacterins were evaluated in broiler chickens through subcutaneous (S/C) inoculation at one week old and boostered at three weeks of age. Results of immunoassay [mean Enzyme Linked Immuno-Sorbent Assay (ELISA) titres] and bioassay (clinical signs, mean lesion score, shedding and re-isolation rates as well as histopathological examination) proved that both types of bacterins were effective. However, oil type bacterin gave more protective effect than water type one.

**Keywords:** Campylobacter Jejuni; Bacterin; Chickens; Protection; ELISA.

## B-656. Effect of Certain Phytobiotics on the Immune Response of Newcastle Disease Vaccinated Broiler Chickens

M.M. Zaki, Wafaa A. Abd El-Ghany, Maha M. Hady and Reda M.S. Korany

*Asian Journal of Poultry Science, 10: 134-140 (2016)*

In this study, the immunopotency of dried coriander seed (Cr), turmeric (Tu) and thyme (Th) powders feed additives in broilers was investigated. **Methodology**: Three hundred, day old broiler chicks were divided into 5 groups, each of 3 replicate and kept for a period of 35 days. A basal diet was used to which Cr, Tu

and Th were added either solely at level of 0.75% or in mixture (Mx), while control fed basal diet (C). Haemagglutinating Inhibiting (HI) antibody titre against Newcastle Disease (ND) was measured in sera of all birds. By the end of the experimental period, three birds from each replicate were weighed and killed then bursa (Br), thymus (Thy) and spleen (Sp) were extracted to calculate weight indices and fixed in formol buffer for morphometric measurements. **Results**: The HI titres were higher ($p<0.05$) in Cr and Tu compared with others. The Br, Thy and Sp weight indices were higher ($p<0.05$) in all groups than C, while those of Tu, Th and Mx groups were higher ($p<0.05$) than Cr group. The morphometric measurements were higher ($p<0.05$) in all treated groups compared to C, while values of Tu were higher ($p<0.05$) than Th and Cr groups. **Conclusion**: Dried Cr and Tu feed additives had an immunomodulatory effect in broilers.

**Keywords:** Herbal feed additives; Broilers; Immunity; Newcastle disease vaccine; Hi.

## B-657. Effect of Na-Butyrate Supplementation on Electromicroscopy, Virulence Gene Expression Analysis and Gut Integrity of Experimentally Induced Salmonella Enteritidis in Broiler Chickens

M.H.H. Awaad, Wafaa A. Abd El-Ghany, S.A. Nasef, Medhat S. El-Halawany, Faten F. Mohamed and Ahmed F. Gaber

*Asian Journal of Poultry Science, 10: 126-133 (2016)*

**Objectives:** The efficacy of microencapsulated Na-butyrate (NaB) supplementation for reducing Salmonella enteritidis (S. enteritidis)infection was investigated. Methodology: on e day old broiler chicks (n = 200) were allotted into 4 equal groups. At 2nd day of age, birds of groups 3 and 4 were challenged by crop gavage with 5×108 CFU mLG1 of S. enteritidis. Groups 2 and 3 were supplemented with NaB diet while 1 and 4 were fed on a plain ration without treatment. Scanning Electron Microscopy (SEM) of re-isolated S. enteritidis of challenged NaB treated broilers revealed broken cells with morphological changes in comparison with untreated challenged group,however, Transmission Electron Microscopy (TEM) showed several lipids like bodies that barely detected in untreated group. **Results:** Results from Polymerase Chain Reaction (PCR) analyses revealed that S. enteritidis strain from untreated challenged control harbored virulence genes invA, stn and pefA with incidence rate of 100%. While, NaB supplementation resulted in detection of 100% of invA gene and only 66.6% of pefA and stn genes. Gut integrity of NaB supplemented groups showed significant (p#0.05) increase in villi height and villus height: crypt depth ratio and had positive effect in maintenance of healthy intestinal epithelial cells. **Conclusion:** NaB supplement is effective in reducing S. enteritidis in chickens.

**Keywords:** Salmonella; Butyrate; Chickens; Pcr; Electron microscopy.

## B-658. Effect of Prebiotic and/ or Antibacterial Drug on Performance of Broiler Infected with E.Coli

M.M. Amer, Kh.M.Elbayoumi, Zeinab M.S. Amin Girh, Eman R. Hassan, M.A.Bosila and Hoda M. Mekky

*International Journal of Pharmtech Research, 9: 58-69 (2016)*

This study was conducted in order to investigate the beneficial effect induced by lysozyme , betain tylosine and/or colistine on performance of broiler chickens in presence of infection with avian pathogenic E.coli (APEC) treated with tylosine and or colistine.360 one old day broiler chick divided into 9 equal groups; 40 chicks in each. Groups 2-8 experimentally infected with E.coli groups 2, 3, 4 and 6 treated with tylosine, gr 2 and 8 treated with colistine sulphate , groups 4 and 5 received lysozymes while groups 6 and 7 were given Betain. Birds of groups 1 and 9 were kept as negative and positive control; respectively. Average body weight (ABW), organ body weight (liver, intestine, Gizzard and Bursa) as well as organ body weight ratio (BWR) at 3rd, 7th and 10th dpi were calculated together with feed conversion rate (FCR) and average feed intake. Samples from liver and intestine were collected for histopathological examination. The best FCR was in group (6) that received tylosine and betain (1.44) followed by (1.46) group (7) which received betain then followed 1.49 of gr (5) received lysozyme then followed by group (2) which received tylosine and colistine and group (4) which received tylosine and lysozme those showed similar result 1.50 followed by group (3) received tylosine which was 1.51 then control negative group (1) which was 1.53 then the lowest 1.72 in E.coli infected nontreated. Organ BWR in the 10th days post challenge the highest is spleen of group 7 received betaine which was 0.15, followed similar results (0.13) of group 6 and group 5 , followed by group 4 which was 0.12 , then groups 8, control positive group group 9 and gr2 has similar results which was 0.11, finally group 1 which is 0.07. Concerning liver BWR by 10th days post challenge the highest was group 7 which was 4.09, followed by gr 6 which was 3.87, followed by group 5 which was 3.81, followed by group 4 which was 3.79, followed by group 2 which was 3.75, followed by control negative group 1 which was 3.50, followed by control positive group 9 which was 3.45, followed by group 3 which was 2.99, followed by group 8 which was 2.09. concerning intestine body weight ratio by 10th days post infection the highest was group 4 which was 7.19, followed by group 2 which was 6.66, followed by group 5 which was 6.24, then group 7 (betaine) which was 6.20, followed by group 6 which was 6.12, then group 3 received tylosine which was 6.10, followed by group 8 which was 5.96, followed by control positive group 9 which was 5.83, and finally group 1) which was 5.60. Gizzared –proventriculus BWR it was found by 10th days post infection that highest ratio was gr 4 which was 4.47 followed by group 2 which was 4.16 followed by gr 3 which was 4.07 followed by gr 5 which was 4.04, followed by group 8 which was 3.66, followed by groups 6 and group 7 which showing same results 3.65, then followed by group 1 which was 3.60 and finally group 9 which was 3.57. Bursal BWR by the 10th days post infection the highest was group 7 which was 0.21, followed by g 6 which was 0.20, followed by group 4 and group 8 which show similar results 0.18, followed by group 3 and group 5 which also show similar results 0.17, then groups 2 and group 9 are showing similar results which was 0.16, finally group 1 which was 0.15. Histopatholgical finding of liver are varied from group to another as group one shows no changes while gr 2,6,7 and 8 showed mild changes after challenge in form of mild congestion of portal vein on the other hand control positive gr 9 showed severe congestion of the portal vein and sinusoids the hepatocytes suffering from vacuolar degeneration in the cytoplasm with disorganization of the hepatic cord, groups 3,4 and 5almost showed the same lesion in the form of mild congestion of the portal vein, congestion of the central vein and

vacuolar degeneration of hepatocyte which considered a reversible condition. Concerning histopathological finding of intestine, group (1) control negative group showing no lesions and normal histopathological section as shown in fig.(6), while gr (9) control positive showing severe congestion of the blood vessels in the sub mucosa accompanied with mild edema with inflammatory cells inflation in both the mucosa and the sub mucosa, while chickens groups 2,4,5 and 8 showing mild inflammatory cell infiltration as shown in fig (8), while groups 3,6 and 7 showing inflammation with inflammatory cell infiltration in mucosa and submucosal layer as shown in fig (9).this results revealed that antibiotic colistine and lysozymes control E.coli and prevent destructive effect on intestinal mucosa. It could be concluded that antibiotics used against avian pathogenic E.coli still of value in control of infection by improving performance either single or in combination. The used prebiotic showed to play an important role in improving productivity of infected chickens. The used combinations are safe and effective. Therefore, we can advice to use of combination between antibacterial and prebiotic for prevention and control of infection in high risk facing poultry industry.

**Keywords:** Broiler performance; Prebiotic; E.Coli; Tylosine; Lysozyme; Betaine; Colistine.

## B-659. Effect of Sodium Butyrate on Salmonella Enteritidis Infection in Broiler Chickens

Wafaa A. Abd El-Ghany, M.H. Awaad, S.A. Nasef and A.F. Gaber

*Asian Journal of Poultry Science, 10: 104-110 (2016)*

This study was designed to examine the effect of using sodium butyrate encapsulated in palm fat in comparison with enrofloxacin on Salmonella Enteritidis (SE) infection in broiler chickens. Two hundred, day-old broiler chicks were allocated into 5 equal groups (n = 50). Group 1 was kept without challenge or treatment (blank control), Group 2 was fed on sodium butyrate, Group 3 was challenged and treated with enrofloxacin, Group 4 was challenged and treated with sodium butyrate and Group 5 was only challenged (positive control). Challenged groups were orally inoculated with 0.3 mL (1.5×108 SE/mL/chick) at the 2nd day of age. Enrofloxacin was given at the 3rd day of age in water (10 mg kg–1 b.wt.) for 5 successive days; however, sodium butyrate was added in doses of 1.0, 0.5 and 0.25 kg t–1 for starter, grower and finisher ration respectively from day till 5 weeks old. The results revealed no mortalities and decrease in the severity of signs and lesions in treated groups than positive control one. At the 4th week of age, sodium butyrate supplement gave significant ($p \leq 0.05$) improvement in body weight, weight gain and feed conversion than others. The re-isolation rate and enumeration of SE were lower in sodium butyrate and enrofloxacin treatments than positive control. In conclusion, sodium butyrate as an acidifier could be used as an environmentally friendly supplement when compared with enrofloxacin for treatment of SE infection in broiler chickens as it could reduce the disease picture severity, improve performance variables and decrease the intestinal colonization.

**Keywords:** Sodium butyrate; Salmonella; Chickens; Performance

## B-660. Isolation and Molecular Identification of Ibv Isolates in Different Governorates in Egypt

A. M. Ghetas, M. A. Kutkat, M. M. Amer and M. H. H. Awaad

*Journal of The Egyptian Society of Parasitology, 46: 351-356 (2016)*

Tracheal swabs and different organs are collected from 17 chicken farms showing respiratory signs and variable mortalities in different governorates. Three successive blind serial passages were performed. Four IBV isolates are detected in vaccinated chickens by RT-PCR and are identified by sequence and phylogenetic analysis of portion of S1 gene. Two IBV isolates, IBV S40 and IBV S61, are related to Mass reference strains (Egypt/F/03, M41, H120, Ma5, and M52). However, IBV S78 and IBV S82 are related to Egyptian variant 2 IBV strains Ck/Eg/BSU- 2/2011 and Ck/Eg/ BSU-3/2011.These results indicate the continuous evolution of Egyptian IBV circulating in chickens despite vaccination using H120 live attenuated vaccine.

**Keywords:** Ibv; Isolation; Identification;Vaccine; Egypt.

## B-661. Res_Id: 110J Res_Wcode: 1958

## Studies on effect of prebiotic on immune response of broiler chicken to ND -AI combined inactivated vaccine

Mohamed Mahrous Mohamed Amer

*Journal ,: p1-p2, (2016), IF: 0*

## B-662. Effect of Experimental Coronary Sinus Ligation on Myocardial Structure and Function in the Presence or Absence of Structural Heart Disease: an Insight for the Interventional Electrophysiologist

Osama Ali Diab, Mohammed Said Amer, and Rania Ahmed Salah El-Din

*Europace(The European Journal of Pacing, Arrhythmias and Cardiac Electrophysiology), 18(12): 1897-1904, (2016), IF: 4.021*

Aims To study the effect of coronary sinus (CS) occlusion on normal hearts and hearts with structural disease. Methods and results We included 32 dogs, divided into 4 groups: (1) CS ligation (CSL): subjected to CSL; (2) control group: no intervention; (3) MI-CSL group: subjected to myocardial infarction (MI) induction followed by CSL after 1 week; and (4) MI-control group: subjected to MI induction, then open thoracotomy after 1 week without CSL. Electrocardiography, echocardiography, histopathology, and immunohistochemistry were done before and after CSL. In CSL group, there were no significant electrocardiographic or echocardiographic changes after CSL, although there was interstitial oedema that decreased after 1 week with the appearance of Thebesian vessels and positive staining for vascular endothelial growth factor. In MI-CSL group, there was significant increase in left ventricular

(LV) end-systolic diameter (P ¼ 02), decrease in LV fractional shortening (P ¼ 0.0001), and LV ejection fraction (P ¼ 0.002) in comparison with MI-control group, associated with severe myocardial degeneration. Conclusion Acute CS occlusion could be compensated in normal hearts, but may be detrimental in the presence of structural heart disease.
**Keywords:** Coronary Sinus; Coronary sinus occlusion;thebesian vessels

## B-663. Regenerative Potential of Immature Permanent Non-Vital Teeth Following Different Dentin Surface Treatments

Salma H. El Ashry, Ashraf M. Abu-Seida, Amr A. Bayoumi and Ahmed A. Hashem

*Experimental and Toxicologic Pathology, 68: 181-190, (2016), IF: 1.716*

This study evaluates the regenerative potential of immature permanent non-vital teeth following different dentin surface treatments in dogs. Periapical lesions and necrotic pulps were induced in 288 roots of 144 teeth in twelve dogs. Teeth were randomly divided into 3 equal groups according to the evaluation period. Each group was subdivided into 8 subgroups according to the treatment modalities including; blood clot, blood clot and collagen, blood clot and Ethylenediaminetetraacetic acid (EDTA), blood clot, collagen and EDTA, blood clot and Mixture Tetracycline Citric Acid and Detergent (MTAD), blood clot, collagen and MTAD, positive control and negative control. Apart from control subgroups, all infected root canals were cleaned with sodium hypochlorite solution and triple antibiotics paste before different treatment protocols. After different treatments, the root length, thickness and apical diameter were evaluated by radiographic examination. Histopathological examination was carried out to evaluate the inflammation, bone/root resorption, tissue in-growth in pulp space, new hard tissue formation and apical closure. Using EDTA solution as a surface modifier showed significantly higher levels of tissue in-growth in the pulp space after 6 weeks and 3 months. Addition of collagen as a scaffold caused significantly more bone/root resorption than the other subgroups while EDTA caused significantly lower inflammatory cell counts only after 2 weeks. Final rinse with 17% EDTA solution before blood clot induction has positive impact on tissue interaction along dentinal walls without modification of the cell type. Moreover, the use of collagen as a scaffold material and MTAD as a surface modifier did not improve the quality of the regenerative process.
**Keywords:** Dentin surface treatment;
Ethylenediaminetetraaceticacid; Mixture tetracycline citric acid and detergent; Immature teeth; Necrotic pulp; Regeneration.

## B-664. Treatment of Experimental Furcation Perforations with Mineral Trioxide Aggregate, Platelet Rich Plasma or Platelet Rich Fibrin in Dogs' Teeth

Hosam E. Tawfik, Ashraf M. Abu-Seida, Ahmed A. Hashem and Mohammed M. El-Khawlani

*Experimental and Toxicologic Pathology, 68: 321-327, (2016), IF: 1.716*

This work evaluates the effect of mineral trioxide aggregate (MTA), platelet rich plasma (PRP) or platelet rich fibrin (PRF) on healing of non-contaminated and contaminated furcation perforations. A total of 192 teeth of 12 dogs was divided into three equal groups according to evaluation period. Each group was further subdivided into MTA, PRP, PRF, negative and positive control subgroups. Each experimental subgroup was further subdivided according to perforation status into non-contaminated and contaminated subdivisions. Root canal therapy was carried out and furcation perforation was made in all teeth except in negative control subgroup. The furcation perforation was repaired immediately in subdivision (1) and after 4 weeks in subdivision (2). The change in vertical bone loss was measured by radiography. Inflammatory cell count, cemental deposition, new bone formation, bone resorption and epithelial proliferation were assessed. Both PRP and PRF demonstrated statistically significant reduction in vertical bone loss and inflammatory cell count than MTA. No significant difference was found between MTA, PRP and PRF in cemental deposition, new bone formation, bone resorption and epithelial proliferation. The non-contaminated teeth demonstrated better treatment outcomes than the contaminated teeth. In conclusion, PRP and PRF are successful treatment options for repairing of furcation perforation in both non-contaminated and contaminated teeth in dogs with superior outcomes in non contaminated teeth.
**Keywords:** Cemental deposition; Dogs; Furcation perforation; MTA; PRF; PRP.

## B-665. Radiographic Evaluation of Early Periprosthetic Acetabular Bone Contrast and Prosthetic Head Acetabular Coverage after Uncemented and Cemented Total Hip Prosthesis in Dogs

Ayman A. Mostafa, Karin Lucas, Ingo Nolte and Patrick Wefstaedt

*Bmc Veterinary Research, 12: 271-279, (2016), IF: 1.643*

**Background** Coxofemoral osteoarthritis is a chronic, disabling condition affecting people and dogs, with THA providing an excellent return to function in severely affected joints. The principal role of THA is to restore an adequate range of motion to the hip joint while transferring load from the acetabulum in order to improve the survival of the implant and enhance the limb function in the short and long terms. The objectives of the study reported here were, therefore, to radiographically evaluate periprosthetic acetabular bone GV and to assess prosthetic head acetabular coverage after 4 months of uncemented and cemented THA in dogs. Means periprosthetic acetabular GV for each and combined 3 regions of interest (zones 1, 2 and 3) were calculated immediately and 4 months after THA. Prosthetic head Norberg (PHN) angle was also measured to assess the degree of prosthetic head acetabular coverage after 4 months of surgery. **Results** Zones 2 and 3 showed a significant increase in the mean bone GV after 4 months of uncemented THA. No differences in zones 1–3 after 4 months of cemented THA. Combined zones showed a significant increase in overall mean bone GV 4 months after uncemented THA; whereas, no changes were identified after 4 months of cemented THA. The PHN angles did not change after 4 months of uncemented and cemented THA and did not differ significantly between the 2 designs of hip arthroplasty. **Conclusions** Regional

periprosthetic acetabular bone GV varies with the design of THA. None of the designs showed periprosthetic acetabular bone lucency. No differences identified in the degree of prosthetic head acetabular coverage in both designs, indicating proper implant stability after 4 months of surgery. Further longer–term investigation on larger population is however still warranted.
**Keywords:** Radiographic Evaluation; Periprosthetic acetabular Contrast; Acetabular coverage; Total hip arthroplasty; Dogs.

## B-666. Effects of Denervation of The Hip Joint on Results of Clinical Observations and Instrumented Gait Analysis in Dogs with Sodium Urate Crystal–Induced Synovitis

Elham A. Hassan; Nicolaas E. Lambrechts; Hsin-Yi Weng; Paul W. Snyder and Gert J. Breur

*American Journal of Veterinary Research, 77: 1200-1210, (2016), IF: 1.124*

**Objective** To evaluate the effects of selective hip joint denervation on gait abnormalities and signs of hip joint pain in dogs. Animals 6 Healthy Adult Hound-Type Dogs. Procedures Minimally invasive denervation was performed on the right hip joint of each dog. Two weeks later, sodium urate was injected into the right hip joint to induce synovitis. Dogs were evaluated clinically and by use of instrumented gait analysis before and 2 weeks after minimally invasive denervation and 4, 8, and 24 hours after induction of synovitis. Dogs were euthanized, and necropsy and histologic examination were performed. **Results** No kinetic or kinematic gait modifications were detected 2 weeks after minimally invasive denervation. Denervation did not eliminate signs of pain and lameness associated with sodium urate–induced synovitis. Results of histologic examination confirmed that denervation was an effective method for transecting the innervation of the craniolateral and caudolateral aspects of the hip joint capsule. **Conclusions and Clinical Relevance**In this study, minimally invasive denervation did not result in gait modifications in dogs. Denervation did not abolish the signs of pain and lameness associated with generalized induced synovitis of the hip joint. Further studies are required before conclusions can be drawn regarding the clinical usefulness of hip joint denervation for dogs with hip dysplasia.
**Keywords:** Dog- Hip Joint; Denervation; Gait analysis

.

## B-667. Recent Advances in the Management of Foreign Body Syndrome in Cattle and Buffaloes: A Review

Ashraf M. Abu-Seida and Oday S. Al-Abbadi

*Pakistan Veterinary Journal, 36: 385-393, (2016), IF: 0.822*

Foreign body syndrome (FBS) is a fairly common disease of cattle and buffaloes,especially in the developing countries. This disease is caused by ingestion of indigestible metallic and non-metallic blunt or sharp foreign objects. It is associated with high economic losses and therefore an urgent science-based policy is required to control and manage this syndrome. Indiscriminate feeding habits, feed scarcity, industrialization and mechanization of agriculture are predisposing factors for FBS in bovine and bubaline. The condition is difficult to diagnose solely on the basis of clinical signs and physical examination. However, laboratory diagnosis and imaging techniques like radiography and ultrasonography can be of high diagnostic value in detecting the condition. Anemia, increased packed cell volume, neutrophilia with a left shift, increased total protein, globulin, total bilirubin, Alanine Aminotransferase, Alkaline Phosphatase, Phosphorus and decreased albumin/globulin ratio and Calcium are the common abnormal laboratory findings. Recently, ultrasonography has replaced radiography for diagnosis of FBS in bovine and bubaline due to its availability and accuracy in evaluation of features of the reticulum, detection of penetrating metallic objects, diagnosis and assessment of various sequelae of FBS including; local and diffuse traumatic reticuloperitonitis, reticular, splenic, hepatic,abdominal and thoracic abscesses, diaphragmatic hernia, traumatic pericarditis and pleuropneumonia. Although, FBS is ideally treated with rumenotomy, it can be prevented to a large extent by proper management practices, increasing the awareness among the livestock keepers, oral administration of rumen magnets at the age of one year and reapplication of a new magnet every 4 years in animals at high risk.
**Keywords:** Buffaloes; Cattle; Foreign body syndrome; Hardware disease; Traumatic reticuloperitonitis; Ultrasonography.

## B-668. Sequential Canine Neonatal Spinal Ultrasonography from Birth Till Spinal Ossification

Mohammed S Amer, Elham A Hassan, Faisal A Torad, Ashraf A Shamaa and Elsayed A Elsherpieny

*Pakistan Veterinary Journal, 36: 6-10, (2016), IF: 0.822*

The purpose of this study was to report the normal ultrasonographic appearance and spinal cord sagittal diameter of canine neonates. Longitudinal and transverse scans were done on 11 clinically normal canine neonates were performed at 3, 10, 20 and 30 days of age, using 8-10 MHz linear transducer. Measurement of the spinal cord sagittal diameter was recorded at different spinal segments. The spinal cord was recognized as an anechoic to hypoechoic tubular structure within the spinal canal, the three meningeal layers enclosing the cord were identified as hyperechoic dura and pia matters with the anechoic subarachnoid matter in between the two. The spinal cord sagittal diameter at the cervical and lumbar regions was greater than that of the thoracic region, and the cord was tapered at the mid-lumbar region forming the conus medullaris. It was difficult to visualize the spinal cord after 30 days of age. In conclusion, ultrasonographic imaging of the canine neonatal spinal cord varies with age till 30 days old.
**Keywords:** Dog; Spinal canal; Spinal cord; Ultrasound.

## B-669. Ultrasonographic Examination of Mammary Glands in Lactating Jennies (Equus Asinus)

Elham A Hassan, Ahmed I Abdelgalil, Faisal A Torad and Ashraf A Shamaa

*Pakistan Veterinary Journal, 36: 89-92, (2016), IF: 0.822*

The purpose of the present study was to describe the normal ultrasonographic characteristics of the udder and teats in lactating Jennies. Seven lactating Baladi Egyptian Jennies were examined ultrasonographically using 6-8 MHz linear probe.

Sagittal and transverse scans of the udder parenchyma and teats were performed for right and left halves through direct (transcutaneous) and indirect (modified stand-off pad) techniques. Measurements of the TCL (teat canal length), TCD (teat canal diameter), TWT (teat wall thickness) and TCD (teat cistern diameter) of both right and left teats were compared for significant difference. The udder parenchyma was identified as coarse granular hypoechoic structure with multiple anechoic cavities. The teat has 3 distinct layers; the outer hyperechoic skin, the inner hyperechoic mucosa and the hypoechoic muscle layers. No significant differences were observed between measurements of the right and the left side. In conclusion, ultrasonography is a safe, effective and non-invasive method that allowed the visualization of the mammary gland (parenchyma and teat) in donkeys. Alteration from the normal ultrasonographic appearance could be helpful for diagnosing pathological conditions of the udder and teats.

**Keywords:** Donkey; Mammary gland; Teat; Udder; Ultrasonography.

## B-670. Epidural Lidocaine, Nalbuphine and Lidocaine–Nalbuphine Combination in Donkeys

Faisal A. Torad and Elham A. Hassan

*Journal of Equine Veterinary Science, 37: 1-5, (2016), IF: 0.73*

Nalbuphine is a lipophilic semisynthetic κ-agonist/μ-antagonist opioid that has been used for epidural anesthesia in humans and dogs but not in donkeys. The purpose of the present study was to report the effect of epidural nalbuphine either alone or in combination with lidocaine compared with lidocaine alone. Six adult clinically healthy Baladi Egyptian donkeys were used. All donkeys were allocated into one of the three groups with a 2-week washout period using a Latin Square design. Group 1 injected with lidocaine hydrochloride 2% at a dose of 0.22 mg/kg. Group 2 injected with nalbuphine hydrochloride 2% at a dose of 0.4 mg/kg, and Group 3 injected with a combination of lidocaine hydrochloride 2% at a dose of 0.11 mg/kg and nalbuphine hydrochloride at a dose of 0.2 mg/kg. Epidural nalbuphine alone resulted in analgesia of significant ($P < .05$) long duration (198.3 ± 12.6 minutes) but of significant ($P < .05$) slow onset (14.3 ± 1.8 minutes). The combination of lidocaine–nalbuphine resulted in rapid onset (6.7 ± 1.2 minutes) and prolonged duration (147 ± 5.6 minutes) of analgesia. Rapid and intense analgesia was produced with lidocaine–nalbuphine combination when compared with lidocaine or nalbuphine alone. Mild ataxia was reported only in lidocaine and lidocaine–nalbuphine groups. Mild sedation was achieved after administration of nalbuphine groups either alone or in combination with lidocaine. The obtained results suggest that lidocaine–nalbuphine combination could be used efficiently for performing surgical interventions required long duration and effective analgesia.

**Keywords:** Nalbuphine; Lidocaine; Epidural; Donkey.

## B-671. The Influence of Addition of Osteogenic Supplements to Mineral Trioxide Aggregate on the Gene Expression Level of Odontoblastic Markers Following Pulp Capping in Dogs

Salma H. El Ashry, Ashraf M. Abu-Seida and Ramy A. Emara

*Veterinarski Arhiv, 86: 685-697, (2016), IF: 0.321*

This study investigates the effect of addition of dexamethasone, vitamin D3, or chitosan to mineral trioxide aggregate (MTA) on the gene expression level of dentin sialophosphoprotein (DSPP) and matrix extracellular phosphoglycoprotein (MEPE) after pulp capping in dogs. Pulp exposure was performed in sixty dogs' teeth. The teeth were classified into 3 equal groups according to the evaluation period. Group 1:7 days, group 2: 21 days and group 3: 60 days. Each group was further subdivided according to the pulp capping material used,into subgroup A: MTA + dexamethasone, subgroup B: MTA + dexamethasone + vitamin D3, subgroup C: MTA + chitosan and subgroup D: MTA. According to the group, the pulps of the capped teeth were removed for analysis of the relative mRNA expression level of DSPP and MEPE using PCR. Statistical analysis of all data was performed. In subgroup A, significant expression was observed of DSPP($P \leq 0.05$) in group 2 up to 18.8 relative fold change while in subgroup B a significant upregulated gene expression of DSPP ($P \leq 0.05$) up to 29.4 relative fold change was seen. Significant upregulated DSPP expression ($P \leq 0.05$) was recorded in groups1 and 2 up to 6.9 and 3.6 relative fold change, respectively in subgroup C. In conclusion, dexamethasone, with or without vitamin D3 and chitosan, are synergistic odontogenic inducers with MTA for differentiation of dental pulp cells in dogs. The upregulation of DSPP is a good marker for this differentiation.

**Keywords:** Chitosan; Dexamethasone; Dentin Sialophosphoprotein; Matrix extracellular Phosphoglycoprotein; Mineral trioxide aggregate; Pulp capping.

## B-672. A Systemic Review on Ultrasonographic Applications in Camels

Abu-Seida A.M.

*Journal of Camel Practice and Research, 23: 139-146, (2016), IF: 0.027*

Ultrasound is widely accepted as a safe noninvasive diagnostic imaging technique in animals and human. This review aims to shed light on the current applications and future prospect of ultrasonography in camels. To date, ultrasonography has been used efficiently to study the ovarian status in she camels such as; follicular wave, spontaneous ovulation, optimum time for mating, ovarian vasculature, superovulatory response, ovarian follicular dynamics, ovarian follicular wave synchronisation and follicular deviation. Moreover, it has been applied for collection of cumulus oocyte complexes, pregnancy diagnosis, foetometry, foetal sexing, embryo transfer programmes, assessment of somatic cell nuclear transfer and evaluation of the quality and developmental ability of dromedary embryos. Uterine involution and various reproductive disorders such as; early embryonic death, endometritis, vaginal adhesions, ovarian cysts and ovarian hydrobursitis have been diagnosed by ultrasound. In male camels, ultrasonography is a useful tool in studying the developmental changes of testes and pelvic genitalia including; bulbourethral gland, prostate, and pelvic urethra and predicting puberty and future fertility. Normal pleura, heart, fore stomach, liver, small and large intestines, kidney, eye, udder and teat, foot, carpal and tarsal joints have been successfully imaged. However, very limited affections of these structures including; infectious pleuropneumonia, peritonitis, trypanosomiasis, John's disease, intestinal obstruction and ruptured urinary bladder have been diagnosed ultrasonographically in camels. Therefore, ultrasonographic

application in camels, compared to other farm animals, is still limited. In conclusion, ultrasonography is untapped in camel practice however, it can offer veterinarians the opportunity for more precise diagnosis and treatment of numerous disorders.
**Keywords:** Camel; Dromedary; Foetometry; Ovum Pick-Up; Pregnancy diagnosis; Ultrasonography.

## B-673. A Gigantic Cutaneous Fibroadenoma in a Dog

Ashraf M. Abu-Seida and Mohamed M. Saleh

*Asian Journal of Animal Sciences, 10: 113-119 (2016)*

Mixed skin tumors are uncommon in dogs. This study reports the clinical findings, radiography, ultrasonography, histopathology and clinical outcome of a rare case of gigantic fibroadenoma in a 4-year-old American Pit Bull Terrier bitch. Four firm, painless at palpation, poorly circumscribed swellings of various sizes and shapes were observed at the left hock joint and hind canon. Mixed echo pattern of the neoplasm and central large blood vessels were observed under doppler ultrasonography. The neoplasm was surgically excised with complete remission and the dog was still disease-free after 6 months. The excised tumor weighted 2350 g. Histopathological findings included; diffuse bundles of fibrous connective tissue arranged in different direction with whorl formation, sebaceous glands adenoma with cyst formation and fibroadenoma in certain areas. Tendency of malignancy was common dented by pleomorphic cells, hyperchromacia and atypical mitotic figures. Several areas of inflammatory reaction and hemorrhages were also observed within the tumor. No evidence of metastasis was seen in both chest and abdomen. In conclusion, fibroadenoma should be listed as a mixed skin neoplasm in dogs and surgical excision is curative.
**Keywords:** Adenoma; Fibroma; Fibroadenoma; Pit Bull Dog; Sebaceous gland; Histopathology.

## B-674. Current Status and Prospect of Ultrasonographic Application in Buffaloes

Ashraf M. Abu-Seida

*Asian Journal of Animal and Veterinary Advances, 11: 144-157 (2016)*

Unlike cattle, there is a shortage of literature on ultrasonographic findings in both normal and diseased organs in buffaloes. Although ultrasonography has been used as a diagnostic imaging technique in small animal practice for several decades, ultrasound examination in buffaloes just attracted the attention of scientists in the last decade. Recently, various studies have been conducted in both normal and diseased buffaloes particularly those suffering from traumatic reticuloperitonitis, traumatic pericarditis, diaphragmatic hernia, omasal impaction, intestinal obstruction, endocarditis, thoracic, hepatic and abdominal abscesses, bronchopneumonia, lung consolidation, pleural effusion, pulmonary emphysema, pleuritis, mastitis and urolithiasis. Moreover, ultrasound is of tremendous value and provides much promise as a tool of dairy buffalo reproductive management and research. Several physiologic and pathologic conditions of the ovaries and uterus, not accurately diagnosed by rectal palpation, can easily be confirmed by ultrasound and consequently, appropriate therapies can be applied. Based on the results of the available studies, ultrasonography seems to be a valuable tool for determination of various physiologic and pathologic conditions in buffaloes. Additionally, this technique is a decision-making tool in surgery in buffaloes. Several ultrasonographic differences are recorded in buffaloes compared to cattle. Therefore, more studies should be conducted to evaluate the reliability of ultrasound in both normal and diseased uninvestigated organs in buffaloes particularly spleen, abomasum, kidneys, joints and tendons.
**Keywords:** Buffalos; Diaphragmatic hernia; Mastitis; Pericarditis; Traumatic reticuloperitonitis; Ultrasonography.

## B-675. Evaluation of Experimental Gastric Endoscopic Mucosal Resection (Emr) in Dogs

Naglaa A. Abd El-Kader and Haithem A. Farghali

*Asian Journal of Animal and Veterinary Advances, 11(9): 531-537 (2016)*

**Background:** Experimental Endoscopic Mucosal Resection(EMR) is arelatively newtherapeutic methodfor resection of certainneoplastic lesions throughoutthe gastrointestinal(GI) tract inthe veterinary practice. **Materialsand Methods:** This experimental study was applied on five mongrel dogs to evaluate the technical efficacy and possible complications of such technique as well as using canine model for educational training of EMR technique. The range of resected mucosal size was 10-25×5-20 mm with surgical time range 32-61 min. **Results**:In the first three cases (withsmaller resected mucosal sizes 15×10, 10×5 and 10×10 mm, respectively), there were no recorded complications.The fourth and fifthcases (with largerresected mucosal sizes 25×20and20×15 mm, respectively)showed postoperative vomiting. **Conclusion:** The present results were without complications such as bleeding or perforation as recorded in previous studies for human. The obtained results might be due to the application of suction followed by banding ligation.
**Keywords:** Endoscopic; Resection gastric; Banding ligation; Polyps; Neoplasms; Polypectomy; Canine Model.

## B-676. Evaluation of Low Level Laser-Activated Stromal Vascular Fraction as A Single Procedure for Treatment of Experimental Chondral Defects

Ahmed N. Abdallah, Ashraf A. Shamaa, Omar S. El-Tookhy and Eman M. Abd El-Mottaleb

*Asian Journal of Animal Sciences, 10 (1): 15-21 (2016)*

Regenerative therapies offer attractive alternatives for the treatment of chondral defects. Adipose-Derived Mesenchymal Stem Cells (AD-MSCs) found in the Stromal Vascular Fraction (SVF) allow the development of one-step surgical procedure by their abundant availability and a minimal invasive technique. Low Level Laser Irradiation (LLLI) of stem cells showed improved results on stem cell growth and proliferation. The aim of this study was to evaluate the treatment of chondral defects using single injection of laser activated SVF in a Platelet Rich Plasma (PRP) vehicle. Chondral defects were created surgically in the femoral condyle of 9 dogs, autologous adipose tissue was harvested from the abdomen and SVF was isolated, added to the PRP, laser irradiated and injected intraarticularly in the right joint. The left joint was injected normal saline as control negative. Evaluation of the treatment was done by physical

examination, radiology and histopathology. Treated joints showed marked degree of cartilage regeneration and restoration of chondral histomorphological picture on the contrary of the control joints that showed deterioration over time and defect filling with only fibrous tissue forming a fibrocartilage at the end of 6 months period. The obtained results proved that the use of low level laser activated adipose derived stem cells is a safe, feasible technique as a single step surgical procedure and a very promising option for treatment of chondral defects.

**Keywords:** Adipose; Stromal vascular fraction; Stem cells; Laser; Platelet rich plasma; Chondral defects.

## B-677. In-Vivo Assessment of Dentin Bridge Formation after Using Mta and Experimental Propolispaste as Direct Pulp Capping Material

Reham S.Saleh, Shaymaa M Nagi, Maram E Khallaf, Sameh H Abd El-Alim, Mohamed H Zaazou, Ashraf M Abu-Seida and Mokhtar N Ibrahim

*Research Journal of Pharmaceutical, Biological and Chemical Sciences, 7: 1244-1250 (2016)*

The aim of this study was to evaluate the effect of two different pulp capping materials regarding dentin bridge formation after direct pulp capping for one week and two months. A total of 32 teeth were prepared for this study using two male dogs. Class V cavities were prepared on the buccal surface then exposure was done using a small round bur. Teeth were randomly divided into two main groups according to the applied capping materials (n=16); group I: MTA and group II: experimental Propolis paste. Prepared cavities were finally restored using resin modified glass ionomer. Then these two main groups were further divided into two subgroups (n=8) according to the observation period; one week and two months. Results revealed that no dentin bridge was formed after one week with both tested materials. on the other hand at two months observation period; there was dentin bridge formation in both MTA and Propolis groups and the difference was statistically insignificant. There was no statistically significant difference between both materials at each observation period. Experimental Propolis pulp capping material was able to induce reparative dentin bridge formation after two months. Experimental Propolis paste and MTA are successful direct pulp capping materials regarding dentin bridge formation

**Keywords:** MTA; Experimental propolis; Direct pulp capping and Glass ionomer.

## B-678. Laboratory, Radiographic and Ultrasonographic Findings of Acute Traumatic Reticuloperitonitis in Buffaloes (Bubalus Bubalis)

Arafat Khalphallah, Ashraf M. Abu-Seida, Mohammed Abdelhakiem, Enas Elmeligy and Usama T. Mahmoud

*Asian Journal of Animal and Veterinary Advances, 11: 675-683, (2016), IF: 0.869*

**Background and Objective:** Traumatic reticuloperitonitis (TRP) is one of the most important diseases in buffaloes. The study objective is to describe the clinical, laboratory, radiographic and ultrasonographic findings in buffaloes suffering from acute (TRP). Methodology: This study was carried out on 20 apparently normal buffaloes (control group) and 20 buffaloes with acute TRP (diseased group). Full case history was obtained and all animals were subjected to thorough clinical examination, pain tests and electronic metal detector, complete blood pictures, blood serum biochemical analysis, radiographic and ultrasonographic examinations. Rumenotomy was performed in 13 affected buffaloes. **Results:** Diseased buffaloes showed sudden onset of anorexia, sharp drop in milk yield, fever, ruminal atony, constipation, increased respiratory and heart rates. Moreover, the animals were reluctant to lie down or move. Out of 20 diseased buffaloes, 17 had positive pain tests and 14 had positive metal detection. All diseased buffaloes shared marked leucocytosis associated with neutrophilia and shift to the left. A significant increase in the serum level of AST ($p>0.05$) was the only abnormal serum biochemical analysis. Radiographic examination revealed metallic foreign objects in the reticulum of seven buffaloes, normal sized and shaped heart with clear margins. The main ultrasonographic findings of diseased buffaloes included changes in the shape, contour and contraction of the reticulum. Buffaloes with acute TRP had a reticulum either with its even contour and its half-moon shaped structure ($n = 14$) or slight loss of its shape with slight loss of its contour ($n = 6$). The diseased buffaloes had biphasic reduced reticular contractions (1.9±0.6/5 min). The reticulum was displaced from the diaphragm with a distance of 0.7-3.4 cm in 17 buffaloes. However, reticular abscess was not imaged, peritoneal effusions were imaged in 16 buffaloes. **Conclusion:** Buffaloes with acute TRP show characteristic and complementary clinical, laboratory, radiographic and ultrasonographic findings which are helpful for diagnosis and follow up this disease.

**Keywords:** Buffaloes; Hardware disease; Reticulum; Traumatic Reticuloperitonitis; Ultrasonography.

## B-679. Physical Evaluation of A New Pulp Capping Material Developed from Portland Cement

Ahmed Negm, Ehab Hassanien, Ashraf Abu-Seida and Mohamed Nagy

*Journal of Clinical and Experimental Dentistry,8:278-283(2016)*

**Background:** This study examined the effects of addition of 10% and 25% by weight calcium hydroxide on the physicochemical properties of Portland cement associated with 20% bismuth oxide in order to develop a new pulp capping material. **Material and Methods:** The solubility, pH value, setting time, compressive strength, and push out bond strength of modified Portland were evaluated and compared to those of mineral trioxide aggregate (MTA) and Portland cement containing 20% bismuth oxide. **Results:** The statistical analysis was performed with ANOVA and Duncan's post-hoc test. The results show that the strength properties and push out bond strength of Portland cement were adversely affected by addition of calcium hydroxide especially with a ratio of 25 wt%, however, the setting time and pH were not affected. MTA showed a statistically significant lower setting time than other cements ($P\leq0.001$). Portland cement with bismuth oxide and Port Cal I showed a statistically significant higher Push out Bond strength than MTA and Port Cal II ($P=0.001$). **Conclusions:** Taking the setting time, push out bond strength and pH value into account, addition of 10 wt% calcium hydroxide to Portland cement associated with 20% bismuth oxide produces a new pulp capping material with acceptable physical and adhesive properties. Further studies are

recommended to test this cement biologically as a new pulp capping material.
**Keywords:** Calcium hydroxide; Mta; Portland cement; Setting time; Solubility; Strength.

## B-680. Role of Endothelial Progenitor Cells in Management of Myocardial Infarction Following Total Coronary Occlusion in Dogs.

Mohamed S Amer, Faisal A Torad, Ashraf A Shamaa, Omar Salah El-Tookhy, Dina Sabry Abdel Fatah, Laila Ahmed Rashed, Magdy Abdelhamid, Soheir Mahmoud Mahfouz and Doaa Mostafa Gharib

*Research Journal of Pharmaceutical, Biological and Chemical Sciences, 7(3): 1225-1237 (2016)*

Myocardial infarction caused by ischemic heart disease is a major health problem being the most prevalent cause of premature death in human. Chronic total occlusion (CTO) remains one of the most difficult challenges for coronary interventions. The currently available therapeutics only delay disease progression and mainly aim to enable patients to survive with a heart that is working at a fraction of its original capacity. Recent approaches suggest that the primary goal of cells therapy is to induce neovascularization rather than to replace myocardial tissue. In this paper, twenty dogs were subjected experimentally to CTO; only half were treated with endothelial progenitor cells (EPCs). Clinical, electrocardiographic, echocardiographic, histopathological, biochemical, and immunohistochemistry assessments were performed for 6-months at different time intervals. Results demonstrated improved systolic function. The fractional shortening (FS %) and the ejection fraction (EF) gradually decreased in both groups. In the treated group, the FS% and EF increased gradually until retaining their normal values at 6-months. ECG pattern improved with resolving of abnormal changes. Quantitative gene expression showed high significant difference between expressions on infarcted tissues versus non-infarct tissues. The intracardiac administration of EPCs is shown to be a useful cell therapy as potentially promoting both neovascularization and cardiac regeneration in ischemic heart disease. Large-scale studies should be induced to examine the potential effects of this novel approach on the risk of death and complications in patients with large acute myocardial infarctions and depressed left ventricular contractile function.
**Keywords:** Coronary, Occlusion, Endothelial Progenitor Cells, Epcs, Myocardial Infarction.

## B-681. Role of Hepatocyte Differentiated Mesenchymal Stem Cells in Treatment of Experimentally Induced Canine Liver Cirrhosis

Marwa H. Hassan, Ashraf A. Shamaa, Elham A. Hassan, Omar S. El-Tookhy, Sabry D. Abd Elfatah and Gehan G. Shehab

*Asian Journal of Animal Sciences, 10: 120-130 (2016)*

Liver cirrhosis represents the final pathway of all chronic hepatic injury. Replacement the damaged hepatocytes through cell-based therapies have been a promising therapeutic agent for tissue regeneration. This study aimed to assess the effect of treatment with Hepatocyte Differentiated Mesenchymal Stem Cells (HD-MSCs) in experimentally induced canine liver cirrhosis. Experimental induction of liver cirrhosis was done on 18 skeletally mature mongrel dogs using carbon tetrachloride (CCl4) for 16 weeks; dogs were evaluated for cirrhosis through clinical, Liver Function Tests (LFTs), ultrasonography with Portal Vein (PV) and Hepatic Vein (HV) diameter estimation and histopathological examination. Dogs were randomly allocated into one of the two study groups; Sham group: CCl4 with no HD-MSCs treatment and group II: CCl4 with HD-MSCs treatment then dogs were evaluated for the efficacy of cell treatment through clinical, LFTs, ultrasonography with PV and HV diameter estimation, postmortem examination, histopathological examination of liver tissue and relative quantitative expression of collagen I" and albumin were measured by Reverse Transcription-Polymerase Chain Reaction (RT-PCR). The HD-MSCs administration restored liver function that was confirmed by clinical, LFTs, histopathology and RT-PCR. Liver tissue ultrasonography, PV and HV diameter were improved. The study proves the ability of HD-MSCs to potentially improve cases of liver cirrhosis.
**Keywords:** Dog; Ccl4; Liver cirrhosis; Mesenchymal stem Cells;RT-PCR; Liver function Test; Hd-Mscs.

## B-682. Surgical Correction of Female Pseudohermaphroditism in Five Pit Bull Dogs

Faisal A. Torad and Elham A. Hassan

*Asian Journal of Animal Sciences, 10: 77-84 (2016)*

Congenital urogenital anomalies are well recognized but infrequent finding in dogs. Due to the complex urogenital anatomy such congenital anomalies encompasses a wide range of phenotypic variations. The most common complication associated with these anomalies includes dysuria, urinary incontinence, skin scald dermatitis and recurrent urinary tract infection. The objective of the present study was to report five Pit Bull dogs diagnosed to have female pseudohermaphroditism with special reference to their surgical management. Complete physical, radiographic and ultrasonographic examinations were done. Corrective surgery was designed individually for each case including clitorectomy, reconstruction of the vaginal floor and correction of penile direction. All surgeries resulted in uncomplicated wound healing and relieve of the associated urinary incontinence, skin scald dermatitis. Owner's satisfaction was achieved in all dogs. None of the dogs developed urinary incontinence and/or urinary tract infection following surgery. When considering surgical correction in dogs with female pseudohermaphroditism, the outcome of surgical decision is usually depend upon the course of the urethra and the position of the external urethral orifice.
**Keywords:** External genitalia; Anomaly; Hermaphrodite; Bitch.

## B-683. Transcutaneous and Transrectal Ultrasonography In Buffalo Calves with Urine Retention

Ahmed M. Abdelaal, Oday S. Al-Abbadi and Ashraf M. Abu-Seida

*Asian Journal of Animal and Veterinary Advances, 11: 79-88 (2016)*

This study describes the ultrasonographic findings of the urinary tract of buffalo calves suffered from urine retention. In this study, 25 male buffalo calves with urine retention and 8

apparently clinically healthy male buffalo calves were used. All calves were subjected to thorough clinical and ultrasonographic examinations. Based on the clinical findings, the diseased calves were classified into four groups. The first group included 8 calves with severe abdominal pain and absence of urine outflow, second group included 5 calves with mild abdominal pain and absence of urine outflow, third one included 8 calves with absence of both pain reactions and urine outflow and finally, fourth group included 4 calves with severe abdominal pain and dribbling of bloody urine. Both transcutaneous and transrectal ultrasonographic examinations were carried out by using 3.5-5.0 MHz convex and 6-8 MHz linear transducers. Ultrasonographic examination revealed distended urinary bladder in first, second and fourth groups. In third group, the urinary bladder was ruptured with anechoic to hypoechoic fluid accumulated in the abdomen. In the second group, the anechoic urine was present inside and outside the urinary bladder.Hydronephrosis of variable degrees was detected in all diseased calves. Moreover, urethral calculi could be detected in 4 calves at 3rd group. Renal calculi were seen in a calf at 4th group. Both renal and urethral calculi appeared as hyperechogenic dots with acoustic shadowing. In conclusion, ultrasonography may be considered a diagnostic and prognostic tool for urine retention in buffalo calves.

**Keywords:** Buffalo; Calves; Hydronephrosis; Ruptured urinary Bladder; Ultrasonography; Urolithiasis.

## B-684. Ultrasonographic Findings in Hardware Diseased Buffaloes (Babulus Babilus)

Ahmed M. Abdelaal, Mohamed B. Mostafa, Ashraf M. Abu-Seida, Oday S. Al-Abbadi and Salah F. Abbas

*Research Journal of Pharmaceutical, Biological and Chemical Sciences, 7: 1644-1649 (2016)*

Hardware disease is one of the most important forestomach diseases in buffaloes. This research describes the most common ultrasonographic findings in buffaloes with hardware disease. Sixty hardware diseased buffaloes were examined by ultrasound at three views; ventral abdominal view just behind xiphoid cartilage, left and right lateral views from 5th to 8th intercostal spaces (ICSs). All ultrasonographic findings of the reticulum and surrounding organs were reported. The reticular wall, distance between reticulum and abdominal wall and relaxation period in hardware diseased buffaloes were significantly increased ($P \leq 0.05$) and the reticular motility and the amplitude of contraction were significantly reduced ($P \leq 0.05$) when compared with normal values. Local peritonitis was observed in 44 buffaloes and showed echogenic strands interspersed with anechoic fluid represented the inflammatory reactions . Moreover, abscesses with different sizes were seen in 16 cases and appeared with anechoic to hypoechoic center surrounded by echogenic wall. Peritonitis and abscesses were observed between the reticulum, rumen, diaphragm and or abomasum. Liver, spleen and whole abdomen were involved in the complications of hardware disease in 11, 8 and 13 buffaloes, respectively. In conclusion, ultrasonography is a reliable technique for diagnosis and prognosis of hardware disease in buffaloes.

**Keywords:** Buffaloes; Hardware disease; Reticulum; Sharp Foreign body syndrome; Traumatic reticuloperitonitis; Ultrasonography.

## B-685. Teratogenic Effect of Cisplatin in Rats and the Protective Role of Sodium Selenate

Mohammed S. Hassan, Ashraf M. Morgan, Mohey M. Mekawy, Amr R. Zaki and Zeinab M. Ghazi

*Experimental and Toxicologic Pathology, 68: 277-287, (2016), IF: 1.716*

Eighty pregnant Sprague-Dawley rats were used in this study. They were allotted to four equal groups.Thefirst group served as a control without any treatment while the other groups were given cisplatin,sodium selenate, and cisplatin + sodium selenate, respectively. Cisplatin was injected intraperitoneally in a dose of 5 mg/kgb wt. on the 12th day of gestation while sodium selenate was administered orally in a dose of 0.5 mg/kgb wt throughout gestation. Animals were sacrificed on the 20th day of gestation for fetal examination. Cisplatin produced significant elevation in the percentages of late resorption sites and dead foetuses compared with the control group. The mean foetal and placental weights were significantly reduced. Dwarf foetuses and subcutaneous (s/c) haemorrhage were also recorded in cisplatin-treated group. Visceral abnormalities were revealed in the form of dilated nares, anophthalmia and/or microphthalmia, dilated brain ventricles, hypertrophy of the heart, hypoplasia of the lung, hepatomegaly and dilated renal pelvis. Skeletal examination showed wide open fontanel, incomplete ossification of parietal and interparietal bones, incomplete ossification of sternum, reduction in the number or even complete absence of phalanges, sacral and/or caudal vertebrae. Histopathological examination of placentas in cisplatin-treated group revealed severe pathological alterations. Administration of sodium selenate significantly alleviated the afore-mentioned adverse effects of cisplatin on the fetuses and their placentas so we conclude that sodium selenate as an antioxidant has an effective protective role in cisplatin teratogenic effects.

**Keywords:** Cisplatin; Sodium selenate; Rats; Visceral; Skeletal; Teratogenic effects.

## B-686. Protective Effect of Nano-Selenium and Ionized Selenium Against the Testicular Damage, Endocrine Disruptor and Testicular Ultrastructure of Bisphenol a in Albino Male Rats

Bhattacharjee, Basu, Ghosh, Biswas J and Bhattacharya.

*Asian Journal of Animal and Veterinary Advances, 11: 653-664 (2016)*

Cyclophosphamide (CP) is the most commonly used chemotherapeutic drug for various types of cancer. However, its use causes severe cytotoxicity to normal cells in human. It is well known that the undesirable side effects are caused due to the formation of reactive oxygen species. Selenium is an essential micronutrient for both animals and humans and has antioxidant and membrane stabilizing property, but selenium is also toxic above certain level. Nano selenium has been well proved to be less toxic than inorganic selenium as well as certain organoselenium compounds. The objective of the study is to evaluate the protective role of Nano-Se against CP-induced hepatotoxicity and genotoxicity in Swiss albino mice. CP was administered intraperitoneally (25 mg/kg b.w.) and Nano-Se was given by oral gavages (2 mg Se/kg b.w.) in concomitant and pretreatment scheme. Intraperitoneal administration of CP

induced hepatic damage as indicated by the serum marker enzymes aspartate and alanine transaminases and increased the malonaldehyde level, depleted the glutathione content and antioxidant enzyme activity (glutathione peroxidase, glutathione-s-transferase, superoxide dismutase and catalase), and induced DNA damage and chromosomal aberration. Oral administration of Nano-Se caused a significant reduction in malonaldehyde, ROS level and glutathione levels, restoration of antioxidant enzyme activity, reduction in chromosomal aberration in bone marrow, and DNA damage in lymphocytes and also in bone marrow. Moreover, the chemoprotective efficiency of Nano-Se against CP induced toxicity was confirmed by histopathological evaluation. The results support the protective effect of Nano-Se against CP-induced hepatotoxicity and genotoxicity.

**Keywords:** Nano-Se; Antioxidant Enzyme; Cyclophosphamide; Genotoxicity; Hepatotoxicity; Oxidative Stress.

## B-687. A Welfare Assessment Scoring System for Working Equids- a Method for Identifying at Risk Populations and for Monitoring Progress of Welfare Enhancement Strategies (Trialed in Egypt)

ahmed b.a.ali,mohamed. el sayed, mohamed y matoock and manal fouad, camie. heleski

*Applied Animal Behaviour Science,176:52-62,(2016), IF: 1.795*

There are an estimated 112 million horses, donkeys and mules (i.e., working equids) in developing regions of the world. Though their roles are often fundamental to the well-being of the families they work for, their welfare is often severely compromised due to the limited resources and/or limited knowledge base of owners. The main objective of this study was to develop a multifactorial welfare assessment score for accurate, comprehensive, quick and reliable assessment of these equids. A total of 5248 working equids (n = 2198 horses, 2640 donkeys, 410 mules) were assessed between February 2012–January 2014. Equids were divided into categories based on the three species involved, as well as the four work types involved (transporting goods or people by cart, ridden (e.g., in tourist locations), or working in brick kilns). Analysis of variance "ANOVA" was used to compare differences between groups with α set at 0.05. In terms of behavioral measures, the most at-risk equids appeared to be horses who pulled goods by cart with 20.7% showing a depressed attitude and 22.6% being unresponsive to an observer's approach (significantly greater than the other species and the other work types, $P < 0.05$). Mules who pulled goods by cart showed 30.8% avoiding an observer's approach, 42.7% avoiding chin contact and 14.2% showing an aggressive response to observer (significantly greater than the other species and the other work types, $P < 0.05$). In terms of physical measures, 21.6% of donkeys who pulled goods by cart had harness-induced lesions and 21.9% showed evidence of firing-type lesions (significantly greater than the other species and other work types, $P < 0.05$). Mules who pulled goods by cart had the highest prevalence of mistreatment-induced lesions at 36.7% (significantly greater than the other species and other work types, $P < 0.05$). From a positive perspective, horses used for riding or transporting people by cart (e.g., most often animals working in tourist areas) were most likely to be in a healthy physical state (over 85% for both categories; significantly greater than other species and other work types, $P < 0.05$). To conclude, this welfare assessment scoring system met our initial objective of being a useful tool in identifying which equids had the most significant welfare problems (i.e., which species, work type, age and sex). This, in turn will help in selecting appropriate interventions, and in targeting interventions toward the most vulnerable equids.

**Keywords:** Working Equids; Welfare Assessment; Equine Behavior; Equine Welfare

## B-688. Biosafety Standards for Working with Crimean- Congo Hemorrhagic Fever Virus

Manfred Weidmann, Tatjana Avsic-Zupanc, Silvia Bino, Michelle Bouloy, Felicity Burt, Sadegh Chinikar, Iva Christova, Isuf Dedushaj, Ahmed El-Sanousi, Nazif Elaldi, Roger Hewson, Frank T. Hufert, Isme Humolli, Petrus Jansen van Vuren, Zeliha Koçak Tufan, Gülay Korukluoglu, Pieter Lyssen, Ali Mirazimi, Johan Neyts, Matthias Niedrig, Aykut Ozkul, Anna Papa, Janusz Paweska, Amadou A. Sall, Connie S. Schmaljohn, Robert Swanepoel, Yavuz Uyar, Friedemann Weber and Herve Zeller

*Journal of General Virology, 97: 2799-2808, (2016), IF: 3.192*

In countries from which Crimean-Congo haemorrhagic fever (CCHF) is absent, the causative virus, CCHF virus (CCHFV), is classified as a hazard group 4 agent and handled in containment level (CL)-4. In contrast, most endemic countries out of necessity have had to perform diagnostic tests under biosafety level (BSL)-2 or -3 conditions. In particular, Turkey and several of the Balkan countries have safely processed more than 100000 samples over many years in BSL-2 laboratories. It is therefore advocated that biosafety requirements for CCHF diagnostic procedures should be revised, to allow the tests required to be performed under enhanced BSL- 2 conditions with appropriate biosafety laboratory equipment and personal protective equipment used according to standardized protocols in the countries affected. Downgrading of CCHFV research work from CL-4, BSL-4 to CL-3, BSL-3 should also be considered.

## B-689. Re-Emergence of a Novel H5n1 Avian Influenza Virus Variant Subclade 2.2.1.1 in Egypt During 2014

M. A. Rohaim, R. F. El-Naggar, M. M. Hamoud, S. A. Nasr, E. Ismael, S. E. Laban , H. A. Ahmed and M. Munir

*Transboundary and Emerging Diseases, early view: 1-7, (2016), IF: 2.714*

Large-scale surveillance is crucial for understanding the evolution and the emergence of avian influenza viruses (AIVs) in endemic areas. Circulation of highly pathogenic avian influenza (HPAI) subtype H5N1 is continuously causing significant economic losses to the Egyptian poultry industry and is a threat to public health. In this report, a HPAI H5N1 strain (A/chicken/Egypt/Fadllah-7/2014) was detected from a vaccinated flock showing clinical signs of infection. Genetic characterization of the isolate indicated a high level of nucleotide identity (95–98%) with variant and classical groups of H5N1. Moreover, multiple-nucleotide and amino acid alignments revealed several prominent and characteristic substitutions in the surface glycoprotein, which may have biological relevance to the pathobiology of the virus.

Phylogenetic analysis demonstrated that the reported isolate closely relates to H5N1 AIVs subclade 2.2.1.1 in spite of no reports of this subclade since 2011 from AI reported cases in Egyptian avian species. In conclusion, our results highlight the re-emergence of a novel H5N1 AIV variant subclade 2.2.1.1 that could escape immunity induced by vaccines. This discovery illustrates the importance of continuous monitoring of poultry in this country for controlling AIV including identifying sources of vaccine seed viruses.

**Keywords:** Surveillance; Circulation; Variant subclade 2.2.1.1; Monitoring.

## B-690. Introduction and Enzootic of A/H5n1 in Egypt: Virus Evolution, Pathogenicity and Vaccine Efficacy Ten Years on .

E.M. Abdelwhaba, M.K. Hassan, A.S. Abdel-Moneimc, M.M. Naguiba, A. Mostafae, I.T.M. Husseing, A. Arafa, A.M. Erfan, W.H. Kilany, M.G. Agourb, Z. El-Kanawatib, H.A. Husseini, A.A. Selimb, S. Kholousyb, H. El-Naggarj, E.F. El-Zoghbyb, A. Samy, M. Iqbalk, A. Eidl, E.M. Ibraheemh, S. Pleschkaf, J. Veitsa, S.A. Nasefb, M. Beera, T.C. Mettenleitera, Grunda, M.M. Alib, T.C. Hardera and H.M. Hafezm

*Infection Genetics and Evolution, 40: 80-90, (2016), IF: 2.591*

It is almost a decade since the highly pathogenic H5N1 avian influenza virus (A/H5N1) of clade 2.2.1 was introduced to Egypt in 2005, most likely, via wild birds; marking the longest endemic status of influenza viruses in poultry outside Asia. The endemic A/H5N1 in Egypt still compromises the poultry industry, poses serious hazards to public health and threatens to become potentially pandemic. The control strategies adopted for A/H5N1 in Egyptian poultry using diverse vaccines in commercialized poultry neither eliminated the virus nor did they decrease its evolutionary rate. Several virus clades have evolved, a few of them disappeared and others prevailed. Disparate evolutionary traits in both birds and humans were manifested by accumulation of clade-specific mutations across viral genomes driven by a variety of selection pressures. Viruses in vaccinated poultry populations displayed higher mutation rates at the immunogenic epitopes, promoting viral escape and reducing vaccine efficiency. on the other hand, viruses isolated from humans displayed changes in the receptor binding domain, which increased the viral affinity to bind to human-type glycan receptors. Moreover, viral pathogenicity exhibited several patterns in different hosts. This review aims to provide an overview of the viral evolution, pathogenicity and vaccine efficacy of A/H5N1 in Egypt during the last ten years.

**Keywords:** Clade 2.2.1; Egypt; Genetic evolution; H5N1; Highly pathogenic avian influenza virus; Pandemic threat.

## B-691. Epidemiology of 11 Respiratory Rna Viruses in A Cohort of Hospitalized Children in Riyadh, Saudi Arabia

Haitham M. Amer, Mohamed S. Alshaman, Mohamed A. Farrag, Moawia E. Hamad, Muslim M. Alsaadi and Fahad N. Almajhdi

*Journal of Medical Virology, 88: 1086-1091, (2016), IF: 1.998*

Respiratory tract infections are a principal cause of illness and mortality in children worldwide and mostly caused by viruses. In this study, the epidemiology of 11 respiratory RNA viruses was investigated in a cohort of hospitalized children at a tertiary referral center in Riyadh from February 2008 to March 2009 using conventional and real-time monoplex RT-PCR assays. Among 174 nasopharyngeal aspirates, respiratory syncytial virus (RSV) was detected in 39 samples (22.41%), influenza A virus in 34 (19.54%), metapneumovirus (MPV) in 19 (10.92%), coronaviruses in 14 (8.05%), and parainfluenza viruses (PIVs) in 11 (6.32%). RSV, PIVs and coronaviruses were most prevalent in infants less than 6 months old, whereas MPV and influenza A virus were more prominent in children aged 7–24 and 25–60 months, respectively. The majority of the viruses were identified during winter with two peaks observed in March 2008 and January 2009. The presented data warrants further investigation to understand the epidemiology of respiratory viruses in Saudi Arabia on spatial and temporal basis.

**Keywords:** Epidemiology; Molecular tools; Prevalence; Respiratory viruses; Riyadh.

## B-692. Molecular Epidemiology of Human Metapneumovirus in Riyadh Province,Saudi Arabia

Haitham Mohamed Amer

*Journal of Molecular Microbiology and Biotechnology, 26: 414-421, (2016), IF: 1.701*

Human metapneumovirus (HMPV) is an important cause of respiratory tract illness in children. Two HMPV subgroups, A and B, and four genotypes, A1, A2, B1 and B2, have been identified. Concurrent circulation of the different genotypes in yearly epidemics has been recorded globally, but not in Saudi Arabia. The current report was designed to study HMPV epidemiology in Saudi children and to analyze the genetic diversity and circulation patterns. Nasopharyngeal aspirates (n = 174) were collected from hospitalized children in Riyadh (2008-2009). The screening of samples using real-time RT-PCR identified 19 HMPV strains. The majority of the strains belonged to subgroup B, while all strains of subgroup A were members of genotype A2. In 2008, only subgroup B was recognized, whereas in 2009 both subgroups were identified to be cocirculating at similar rates. The full-length attachment (G) gene and a partial sequence of the fusion (F) gene of positive samples were sequenced. The G gene showed a high degree of genetic diversity and exhibited a variable number of positively selected sites in different lineages. In contrast, the F gene demonstrated an extensive genetic stability with a higher tendency toward purifying selection. This is the first report on HMPV genotype circulation in Saudi Arabia; however, the exact circulation kinetics requires further retrospective and prospective study.

**Keywords:** Attachment glycoprotein; Fusion protein; Genotypic classification; Human metapneumovirus; Phylogeny; Riyadh.

## B-693. Recombinase Polymerase Amplification Assay for Rapid Detection of Lumpy Skin Disease Virus

Mohamed A. Shalaby, Ayman El-Deeb, Mohamed El-Tholoth, Donata Hoffmann, Claus-Peter Czerny, Frank T. Hufert, Manfred Weidmann and Ahmed Abd El Wahed

*Bmc Veterinary Research, 12: 1-6, (2016), IF: 1.643*

Lumpy skin disease virus (LSDV) is a Capripoxvirus infecting cattle and Buffalos. Lumpy skin disease (LSD) leads to significant economic losses due to hide damage, reduction of milk production, mastitis, infertility and mortalities (10 %). Early detection of the virus is crucial to start appropriate outbreak control measures. Veterinarians rely on the presence of the characteristic clinical signs of LSD. Laboratory diagnostics including virus isolation, sequencing and real-time polymerase chain reaction (PCR) are performed at well-equipped laboratories. In this study, a portable, simple, and rapid recombinase polymerase amplification (RPA) assay for the detection of LSDV-genome for the use on farms was developed.

**Keywords:** Lumpy skin disease; Virus recombinase Polymerase Amplification assay point of Need; Test cattle.

## B-694. Experimental Infection of Is/885/00-Like Infectious Bronchitis Virus in Specific Pathogen Free and Commercial Broiler Chicks.

Faez Awada, Rajesh Chhabra, Anne Forrestera, Julian Chantrey, Matthew Baylisa, Stephane Lemiered, Hussein Aly Husseine and Kannan Ganapathya

*Research In Veterinary Sciences, 105: 15-22, (2016), IF: 1.504*

Pathogenesis of an IS/885/00-like (IS/885) strain of variant infectious bronchitis virus (IBV) was examined in one day old specific pathogen free (SPF) and commercial broiler chicks. Chicks were humanely euthanized at 3, 6, 9, 12, 15, 21 and 28 days post infection (dpi) for necropsy examination, and tissues were collected for histopathology and virus detection by reverse transcription polymerase chain reaction (RT-PCR). Respiratory clinical signs and gross lesions consisting of tracheal caseous exudate and plugs, and swollen kidneys (with or without) urate deposits were observed in SPF and broiler chicks. The onset of disease developed more slowly and were of lesser severity in broiler compared to SPF chicks, reflecting the inhibitory effects of the IBV maternal-antibodies in the broiler chicks or genetic/strain susceptibility, or both. Head swelling was observed in one infected broiler chick at 15 dpi and the virus was recovered by RT-PCR and isolation. In the IS/885-infected SPF chicks, cystic oviducts were found in two female chicks. IS/885 was isolated from the cystic fluid. Using ELISA, low to moderate levels of the antibodies to IBV was detected in the SPF compared to broiler infected chicks.

**Keywords:** Chicks; Cystic Oviduct; Head swelling; Ibv Is/885/00-Like; Infectious bronchitis virus.

## B-695. Surface Gene Variants of Hepatitis B Virus in Saudi Patients

Ahmed Y. Al‐Qudari, Haitham M. Amer, Ayman A. Abdo, Zahid Hussain, Waleed Al‐Hamoudi, Khalid Alswat and Fahad N. Almajhdi

*Saudi Journal of Gastroenterology, 22:133-138, (2016), IF:1.312*

**Background/Aims:**Hepatitis B virus (HBV) continues to be one of the most important viral pathogens in humans. Surface (S) protein is the major HBV antigen that mediates virus attachment and entry and determines the virus subtype. Mutations in S gene, particularly in the "a" determinant, can influence virus detection by ELISA and may generate escape mutants. Since no records have documented the S gene mutations in HBV strains circulating in Saudi Arabia, the current study was designed to study sequence variation of S gene in strains circulating in Saudi Arabia and its correlation with clinical and risk factors. **Patients and Methods:**A total of 123 HBV-infected patients were recruited for this study. Clinical and biochemical parameters, serological markers, and viral load were determined in all patients. The entire S gene sequence of samples with viral load exceeding 2000 IU/mL was retrieved and exploited in sequence and phylogenetic analysis. **Results:**A total of 48 mutations (21 unique) were recorded in viral strains in Saudi Arabia, among which 24 (11 unique) changed their respective amino acids. Two amino acid changes were recorded in "a" determinant, including F130L and S135F with no evidence of the vaccine escape mutant G145R in any of the samples. No specific relationship was recognized between the mutation/amino acid change record of HBsAg in strains in Saudi Arabia and clinical or laboratory data. Phylogenetic analysis categorized HBV viral strains in Saudi Arabia as members of subgenotypes D1 and D3. **Conclusion:** The present report is the first that describes mutation analysis of HBsAg in strains in Saudi Arabia on both nucleotide and amino acid levels. Different substitutions, particularly in major hydrophilic region, may have a potential influence on disease diagnosis, vaccination strategy, and antiviral chemotherapy.

**Keywords:** Chronic hepatitis; Hepatitis B virus; Liver cirrhosis; Phylogeny; Sequence analysis; Surface gene.

## B-696. The Matrix Gene of Influenza A H5n1 in Egypt, 2006-2016: Molecular Insights and Distribution of Amantadine-Resistant Variants.

Mahmoud M. Naguib,Naglaa Hagag, Ahmed A. El-Sanousi, Hussein Ali Hussein and Abdel-Satar Arafa

*Virus Genes, 52: 872-876, (2016), IF: 1.285*

Large-scale sequence analysis of Matrix (M) gene and its coding proteins M1 and M2 was performed for 274 highly pathogenic avian influenza viruses H5N1 circulated in Egypt from 2006 to 2016. The aim is to study the amantadine-resistant markers distribution and to estimate the evolutionary rate. 246 viruses were obtained from the Global Initiative on Sharing All Influenza Data base, and 28 additional viruses were sequenced. Maximum clade credibility (MCC) phylogenetic tree revealed that the M gene has evolved into two different lineages. Estimated Evolutionary analysis showed that the M2 protein possessed higher evolutionary rates (3.45 × 10-3) than the M1 protein (2.73 × 10-3). M gene encoding proteins revealed significant markers described to be associated with host tropism and increase in virulence: V15I, N30D, and T121A in M1 and L55F in M2 protein. Site analysis focusing attention on the temporal and host distribution of the amantadine-resistant markers was carried out and showed that vast majority of the M2 amantadine-resistant variants of clade 2.2.1.1 (n = 90) is N31 marker, in addition to G27 (n = 7), A27 (n = 5), I27 (n = 1), and S30 (n = 1). In 2010-2011, amantadine resistant frequency increased considerably resembling more than half of the resistant variants. Notably, all viruses of clade 2.2.1.1 possessed amantadine-resistant marker. However, almost all current circulating viruses in Egypt of clade 2.2.1.2 from 2014 to 2016 did not carry any amantadine-resistant markers.

**Keywords:** Amantadine resistance; Avian influenza H5n1; M1 Protein; M2 Protein; Matrix gene.

## B-697. Protective Efficacy of a Prime-Boost Protocol Using H5-DNA Plasmid as Prime and Inactivated H5n2 Vaccine as the Booster Against the Egyptian Avian Influenza Challenge Virus.

H. A. Hussein, B. M. Ahmed, S. M. Aly, A. H. El-Deeb, A. A. El-Sanousi, M. A. Rohaim, A. A. Arafa and M. R. Gadalla

*Acta Virologica, 60 (3): 307-315, (2016), IF: 1.222*

In this study, a recombinant DNA plasmid was constructed, encoding for HA1 of a selected Egyptian H5N1 virus (isolated during the 2012 outbreaks). In the immunization and challenge experiments, SPF chickens received 1 or 2 doses of H5-DNA plasmid prime, and boosted with the inactivated H5N2 vaccine. Haemagglutination inhibition (HI) titers, protection levels, and the magnitude of virus shedding were compared to that of the chickens that received either DNA plasmid or inactivated H5N2 vaccine alone. H5N1 virus A/chicken/Egypt/128s/2012 (H5N1) highly pathogenic avian influenza (HPAI) clade 2.2.1/C was used for the challenge. Chickens immunized with 1 or 2 doses of H5-DNA vaccine failed to overcome the challenge with 0% and 10% protection, respectively. Quantitative real-time reverse transcription-PCR revealed virus shedding of 2.2 x 104 PCR copies/ml 3 days post challenge (dpc) in the only surviving bird from the group that received 2 doses of plasmid. However, chickens immunized with 1 or 2 doses of H5-DNA plasmid as prime and inactivated H5N2 vaccine as booster, showed 80% protection after challenge, with a viral shedding of 1.2 x 104 PCR copies/ml (1 dose) and 1.6 x 104 PCR copies/ml (2 doses) 3 dpc. The surviving birds in both groups did not shed the virus at 5 and 7 dpc. In H5N2-vaccinated chickens, protection levels were 70% with relatively high virus shedding (1.8 x 104 PCR copies/ml) 3 dpc. HI titers were protective to the surviving chickens. This study reports the efficacy of H5-DNA plasmid to augment reduction in viral shedding and to provide better protection when applied in a prime-boost program with the inactivated AI vaccine.

**Keywords:** Avian H5n1 influenza; Inactivated H5n2 vaccine; DNAplasmid; Hemagglutinin; Prime-Boost.

## B-698. The Zoonotic Potential of Giardia Intestinalis Assemblage E in Rural Settings

Khaled A. Abdel-Moein and Hossam Saeed

*Parasitology Research, 115: 3197-3202, (2016), IF: 2.027*

Giardiasis is a globally re-emerging protozoan disease with veterinary and public health implications. The current study was carried out to investigate the zoonotic potential of livestock-specific assemblage E in rural settings. For this purpose, a total of 40 microscopically positive Giardia stool samples from children with gastrointestinal complaints with or without diarrhea were enrolled in the study as well as fecal samples from 46 diarrheic cattle (18 dairy cows and 28 calves). Animal samples were examined by sedimentation method to identify Giardia spp., and then, all Giardia positive samples from human and animals were processed for molecular detection of livestock-specific assemblage E through amplification of assemblage-specific triosephosphate isomerase (tpi) gene using nested polymerase chain reaction (PCR). The results of the study revealed high unexpected occurrence of assemblage E among human samples (62.5 %), whereas the distribution among patients with diarrhea and those without was 42.1 and 81 %, respectively. on the other hand, the prevalence of Giardia spp. among diarrheic dairy cattle was (8.7 %), while only calves yielded positive results (14.3 %) and all bovine Giardia spp. were genetically classified as Giardia intestinalis assemblage E. Moreover, DNA sequencing of randomly selected one positive human sample and another bovine one revealed 100 and 99 % identity with assemblage E tpi gene sequences available at GenBank after BLAST analysis. In conclusion, the current study highlights the wide dissemination of livestock-specific assemblage E among humans in rural areas, and thus, zoonotic transmission cycle should not be discounted during the control of giardiasis in such settings.

**Keywords:** Giardia intestinalis assemblage E; Rural settings; zoonosis.

## B-699. Evidence of Zoonotic Transmission of Helicobacter Canis Between Sheep and Human Contacts

Maha A. Sabry, Khaled A. Abdel-Moeinand Aya Seleem

*Vector-Borne and Zoonotic Diseases, 16: 650-653, (2016), IF:1.956*

Not fully understood; so, this study was conducted to investigate the possible role of ruminants in the epidemiology of these pathogens. For this purpose, fecal samples were collected from 149 animals (76 sheep, 33 goats, 21 cattle, and 19 buffaloes) and stool specimens from 10 animal caretakers in intimate contact with the examined animals. All samples were examined for the presence of Helicobacter species through detection of Helicobacter genus specific 16S rRNA using PCR. Then, all positive Helicobacter spp. amplicons were sequenced to recognize their species through BLAST analysis at GenBank. The overall prevalence of Helicobacter spp. was 14.8% while the distribution among the different animals was 26.3%, 3%, 4.8%, and 0% in sheep, goats, cattle, and buffaloes respectively. Helicobacter canis was the predominant species and detected only in sheep (21%) and goats (3%). Moreover, Helicobacter winghamensis and Helicobacter canadensis were also detected in sheep but not in other animals, whereas the only positive bovine sample was identified as Helicobacter bovis. on the other hand, 4 out of 10 humans were positive for Helicobacter spp. and all sequences were identified as H. canis. The sequences identity matrix and phylogenetic analysis of H. canis sequences from humans and sheep contacts revealed that one human sequence was identical to that of sheep and making sister group clade, which prove the zoonotic transmission of this pathogen between sheep and human contacts. However, our findings highlight sheep as a potential reservoir for H. canis, further researches are needed to address the potential role of sheep in the food-borne transmission of such emerging pathogen.

**Keywords:** Helicobacter canis; Reservoir; Sheep;Zoonosis.

## B-700. Equine Dendritic Cells Generated with Horse Serum Have Enhanced Functionality in Comparison to Dendritic Cells Generated with Fetal Bovine Serum

Anja Ziegler, Helen Everett, Eman Hamza, Mattia Garbani, Vinzenz Gerber, Eliane Marti and Falko Steinbach

*Bmc Veterinary Research, 12: 254-265, (2016), IF: 1.643*

**Background** Dendritic cells are professional antigen-presenting cells that play an essential role in the initiation and modulation of T cell responses. They have been studied widely for their potential clinical applications, but for clinical use to be successful, alternatives to xenogeneic substances like fetal bovine serum (FBS) in cell culture need to be found. Protocols for the generation of dendritic cells ex vivo from monocytes are well established for several species, including horses. Currently, the gold standard protocol for generating dendritic cells from monocytes across various species relies upon a combination of GM-CSF and IL-4 added to cell culture medium which is supplemented with FBS. The aim of this study was to substitute FBS with heterologous horse serum. For this purpose, equine monocyte-derived dendritic cells (eqMoDC) were generated in the presence of horse serum or FBS and analysed for the effect on morphology, phenotype and immunological properties. Changes in the expression of phenotypic markers (CD14, CD86, CD206) were assessed during dendritic cell maturation by flow cytometry. To obtain a more complete picture of the eqMoDC differentiation and assess possible differences between FBS- and horse serum-driven cultures, a transcriptomic microarray analysis was performed. Lastly, immature eqMoDC were primed with a primary antigen (ovalbumin) or a recall antigen (tetanus toxoid) and, after maturation, were co-cultured with freshly isolated autologous CD5+ T lymphocytes to assess their T cell stimulatory capacity. **Results** The microarray analysis demonstrated that eqMoDC generated with horse serum were indistinguishable from those generated with FBS. However, eqMoDC incubated with horse serum-supplemented medium exhibited a more characteristic dendritic cell morphology during differentiation from monocytes. A significant increase in cell viability was also observed in eqMoDC cultured with horse serum. Furthermore, eqMoDC generated in the presence of horse serum were found to be superior in their functional T lymphocyte priming capacity and to elicit significantly less non-specific proliferation. **Conclusions** EqMoDC generated with horse serum-supplemented medium showed improved morphological characteristics, higher cell viability and exhibited a more robust performance in the functional T cell assays. Therefore, horse serum was found to be superior to FBS for generating equine monocyte-derived dendritic cells.

**Keywords:** Dendritic cell; Fetal bovine serum; Horse.

## B-701. Occurrence of Clostridium Perfringens Types A, E, and C in Fresh Fish and its Public Health Significance

Maha Sabry, Khaled Abd El-Moein, Eman Hamza and Fatma Abdel Kader

*Journal of Food Protection, 79: 994-1000, (2016), IF: 1.609*

Fish remains among the most traded of food commodities, and Egypt is one of the emerging countries being recognized as an important world fish exporter. Clostridium perfringens is an important foodborne pathogen to consider in fish trade, as it has been implicated as the causative organism of two fish outbreaks. The aim of the present study was to investigate the occurrence and toxin diversity of C. perfringens associated with fresh and canned fish and to examine the public health significance of C.perfringens infection in fish. Isolation and identification of C. perfringens showed a significantly higher prevalence of the bacterium in fresh fish collected from aquaculture (54.5%) and from markets (71%) as well as in humans in contact with fish (63%) compared with water used for keeping fresh fish (27.3%) and water used in canned fish (17.8%). The isolation level was significantly higher in samples from the external surface of fresh fish (31.8% in aquaculture, 45.6% in markets) than from the intestinal contents of the same fish (9.1% in aquaculture, 6.7% in markets). Thus, markets represent a risk factor for contamination of the external surface of fish from the surrounding environment. Genotyping of the C. perfringens–positive isolates by using multiplex PCR revealed that type A enterotoxin-negative (CPE) is the predominant strain among fish (fresh and canned), humans, and water in contact with fresh fish. Interestingly, C. perfringens types A enterotoxin-positive (CPEþ) and C were found only in fresh fish, and these two strains have great health importance in humans. Strikingly, C. perfringens type E strain was detected for the first time in fish, humans, and water in contact with fresh fish. Our results demonstrate for the first time that fish act as a reservoir for C. perfringens, particularly for types A CPEþ, C, and E. The external surface of fish represents a vehicle for contamination of fish from the surrounding environment as well as a source of infection of humans, thereby representing a public health hazard.

**Keywords:** Bacterial zoonotic diseases; Canned fish; Fish; Type C clostridium perfringens; Type E clostridium perfringens

## B-702. Occurrence of Human Pathogenic Clostridium Botulinum Among Healthy Dairy Animals: an Emerging Public Health Hazard

Khaled A. Abdel-Moein and Dalia A. Hamza

*Pathogens and Global Health, 110: 25-29, (2016), IF: 1.486*

The current study was conducted to investigate the occurrence of human pathogenic Clostridium botulinum in the feces of dairy animals. Fecal samples were collected from 203 apparently healthy dairy animals (50 cattle, 50 buffaloes, 52 sheep, 51 goats). Samples were cultured to recover C. botulinum while human pathogenic C. botulinum strains were identified after screening of all C. botulinum isolates for the presence of genes that encode toxins type A, B, E, F. The overall prevalence of C. botulinum was 18.7% whereas human pathogenic C. botulinum strains (only type A) were isolated from six animals at the rates of 2, 2, 5.8, and 2% for cattle, buffaloes, sheep, and goats, respectively. High fecal carriage rates of C. botulinum among apparently healthy dairy animals especially type A alarm both veterinary and public health communities for a potential role which may be played by dairy animals in the epidemiology of such pathogen.

**Keywords:** Botulism; Clostridium botulinum; Dairy animals; Public health.

## B-703. Norway Rat (Rattus Norvegicus) as a Potential Reservoir for Echinococcus Granulosus: a Public Health Implication

Khaled A. Abdel-Moein and Dalia A. Hamza

*Acta Parasitologica, 61: 815-819, (2016), IF: 1.293*

Cystic hydatidosis is a re-emerging parasitic zoonosis with worldwide distribution. The current study was carried out to investigate the possible role of rats in the epidemiology of such disease in urban and suburban areas. For this purpose, a total of 50 feral Norway rats (Rattus norvegicus) were collected from urban and suburban settings, Cairo, Egypt. Rats were examined to be infected with cystic hydatidosis through serological examination by IHA test as well as post-mortem examination of internal organs, histopathological or molecular identification of the collected cysts. Moreover, 42 persons inhabiting suburban areas were tested for cystic hydatidosis by IHA. The overall seroprevalence rates of cystic hydatidosis in the examined rats and persons were 36% and 11.9% respectively. Cysts from 3 rats were identified as E. granulosus hydatid cysts (one via histopathological examination while the others by molecular technique and genotyped as G6 strain). The results of the current study highlight the possible role of Norway rat in the epidemiological cycle of E. granulosus especially in urban and suburban settings.

**Keywords:** Norway rat; Echinococcus granulosus; Public health.

## B-704. Listeria Monocytogenes: an Emerging Food-Borne Pathogen and its Public Health Implications

Waffa W Reda, Khaled Abdel-Moein, Ahmed Hegazi, Yasmin Mohamed and Khaled Abdel-Razik

*Journal of Infection in Developing Countries, 10: 149-154, (2016), IF: 1.139*

**Introduction:** Listeria monocytogenes is considered one of the most important food-borne pathogens transmitted to humans via contaminated food. The aim of the present study was to demonstrate the importance of L. monocytogenes as a food-borne pathogen. Methodology: A total of 340 samples were collected from different localities in El Giza Governorate, Egypt, to check the occurrence of L. monocytogenes in that area. The collected samples comprised 250 food samples, 40 swabs from food refrigerators, and 50 stool specimens from diarrheic children. L. monocytogenes was isolated from the examined samples according to the International Organization for Standardization. The isolates were tested biochemically using Listeria Microbact 12L and confirmed by polymerase chain reaction. **Results:** The isolation rates of L. monocytogenes were 8% in beef burger, 4% in minced meat, 4% in luncheon meat, while sausage samples were all negative. Eight percent of raw milk samples were positive for L. monocytogenes, whereas cheese samples and refrigerator swabs were negative. on ly Listeria grayi was isolated from human stools (2.5%). **Conclusion:** The high isolation rates of L. monocytogenes among the examined food stuffs highlight the crucial role of food as an important vehicle for this pathogen. More efforts should be made to ensure safe handling and processing of these foods to reduce the transmission of L. monocytogenes to humans.

**Keywords:** Listeria monocytogenes; Food-borne; Meat; Milk; Egypt.

## B-705. Carbapenemase-Producing Klebsiella Pneumoniae In Broiler Poultry Farming in Egypt

Eman Hamzaa, Sohad M. Dorghamb and Dalia A. Hamzaa

*Journal of Global Antimicrobial Resistance, 7: 8-10, (2016), IF: 1.087*

This study investigated the occurrence of carbapenem-resistant Klebsiella pneumoniae strains in broiler chickens, drinking water and humans working in contact with chickens and identified the carbapenem resistance determinants among isolates from different sources. Internal organs and droppings were collected from 100 broilers with signs of respiratory disease at five broiler farms in Egypt. Additionally, 20 drinking water samples and 49 faecal samples from workers and veterinarians working at these farms were included. Following culture on MacConkey agar, suspected K. pneumoniae colonies were identified by phenotypic testing. Susceptibility to carbapenems was tested in confirmed K. pneumoniae isolates by disk diffusion. Carbapenem-resistant isolates were subjected to PCR for detection of carbapenemase-encoding genes (blaKPC, blaOXA-48 and blaNDM). K. pneumoniae was isolated from 35% of broilers and 25% of water samples. of the 35 poultry isolates, 15 were carbapenem-resistant; all of them were blaNDM-positive, including 11 isolates harbouring blaKPC, blaOXA-48 and blaNDM and 4 containing either blaKPC and blaNDM (n=3) or blaOXA-48 and blaNDM (n=1). Similarly, three of five K. pneumoniae isolates from drinking water were positive for blaKPC and blaNDM (n=1) or for all three genes (n=2). Interestingly, 56% of K. pneumoniae from humans displayed carbapenem resistance; all of them were positive for the three carbapenemase genes. Carbapenemase-producing K. pneumoniae occurred at relatively high frequency among broilers, drinking water and workers at poultry farms in Egypt. Additional work is needed to confirm transmission between poultry and humans and to elucidate the direction and mechanism of transmission.

**Keywords:** Carbapenem-resistant klebsiella pneumoniae; Carbapenemase genes; Chickens; Kpc; Ndm; Oxa-48.

## B-706. Molecular Detection of Mycobacterium Tuberculosis in Cattle and Buffaloes: A Cause for Public Health Concern

Khaled A. Abdel-Moein , Osman Hamed and Heba Fouad

*Tropical Animal Health and Production, 48: 1541-1545, (2016), IF: 0.87*

Tuberculosis is a re-emerging disease causing a growing public health burden. The current study was conducted to investigate the occurrence of Mycobacterium tuberculosis among cattle and buffaloes with tuberculous lesions. Typical tuberculous lesions were collected from 34 cattle and 34 buffaloes (Bubalus bubalis) through postmortem examination of slaughtered animals in abattoirs. DNAs were extracted from samples, and M. tuberculosis was identified by PCR. Positive samples were examined for resistance against rifampicin and isoniazid using GenoType MTBDRplus. Moreover, sera from 90 slaughterhouse workers, butchers, or meat inspectors were examined for the presence of M. tuberculosis antibodies using

ELISA. Five cattle (14.7 %) and three buffaloes (8.8 %) tested positive. M. tuberculosis from one cattle was resistant to rifampicin and another was resistant to isoniazid. In addition, the seroprevalence of M. tuberculosis IgG among examined humans was 5.6 %. The occurrence of M. tuberculosis in cattle and buffaloes is a public health concern.
**Keywords:** M. Tuberculosis; Cattle; Buffaloes; Public health.

## B-707. Occurrence of Human Hepatitis E Virus in Norway Rats: A Zoonotic Potential with Great Public Health Implications

Nahed Hamed Ghoneim, Khaled Abdel-Aziz Abdel-Moein, Dalia Anwar Hamza and Naglaa Mohamed Hagag

*Asian Pacific Journal of Tropical Disease, 6: 718-721 (2016)*

**Objective** To investigate the occurrence of human hepatitis E virus genotype I among sheep and rats as well as seroprevalence of hepatitis E virus immunoglobulin G (IgG) antibodies among people live in rural settings. **Methods** Fecal samples were collected from 43 Norway rats and 30 sheep. All fecal samples were examined for the presence of human hepatitis E virus genotype I through direct detection using RT-PCR. In addition, serum samples collected from 90 apparently healthy persons live in rural settings were examined for the presence of hepatitis E virus IgG antibodies by using enzyme linked immunosorbent assay**. Results** Out of 73 examined animals, human hepatitis E virus genotype I was detected in five animals giving an overall prevalence 6.8% while only rats given positive results 11.6%. Furthermore, the overall seroprevalence of hepatitis E virus IgG antibodies among the examined individuals was 63.3% while the seroprevalence in adults (75.0%) was higher than that in children (34.6%). **Conclusions** The detection of human hepatitis E virus genotype I in the feces of Norway rats in such high prevalence highlights the possible role which may be played by such animal in the epidemiology of hepatitis E virus infections in rural settings where the virus is more prevalent among human populations.
**Keywords:** Hepatitis E Virus; Norway rat; Zoonosis; Rural settings.

## B-708. Prevalence and Phylogenetic Characterization of Listeria Monocytogenes Isolatedfrom Processed Meat Marketed in Egypt

Yasmin Mohamed, Waffa W. Reda, Khaled Abdel-Moein, Khaled A. Abd El-Razik, Ashraf M.A. Barakat, Hassan A. El Fadaly,Nawal A. Hassanain and Ahmed G. Hegazi

*Journal of Genetic Engineering and Biotechnology, 14: 119-123 (2016)*

Because of its high case fatality rate, listeriosis locates among the most frequent causes of death due to food-borne illness. In this study, a total of 150 processed meat samples were collected from Giza Governorate, Egypt. Phenotypic and genotypic identification of Listeria monocytogenes was performed using PCR incorporating listeriolysin O virulence gene hlyA followed by DNA sequence analysis. L. monocytogenes was confirmed in 4% of each of beef burger, minced meat, and luncheon samples. Phylogenetic analysis showed that all the six Egyptian isolates have high homology with Colombian isolate (EF030606), except one Egyptian isolate which showed high homology with Indian isolate (EU840690). The public health significance of these pathogens as well as recommended sanitary measures were discussed.
**Keywords:** L. Monocytogenes; Processed meat; Egypt; Phylogenetic analysis.

## B-709. Antimicrobial Blue Light Inactivation of Gram-Negative Pathogens in Biofilms: in Vitro and in Vivo Studies.

Yucheng Wang, Ximing Wu, Jia Chen, Rehab Amin, Min Lu, Brijesh Bhayana, Jie Zhao, Clinton K. Murray, Michael R. Hamblin, David C. Hooper and Tianhong Dai.

*Journal of Infectious Diseases, 214: 1380-1387(2016) IF:6.344.*

**Background:** Biofilms affect >80% bacterial infections in human and are usually difficult to eradicate because of their inherent drug resistance. **Methods**. We investigated the effectiveness of antimicrobial blue light (aBL) (wavelength, 415 nm) for inactivating Acinetobacter baumannii or Pseudomonas aeruginosa biofilms in 96-well microplates or infected mouse burn wounds. **Results**. In vitro, in 96-well microplates, exposure of 24-hour-old and 72-hour-old A. baumannii biofilms to 432 J/cm2 aBL resulted in inactivation of 3.59 log10 and 3.18 log10 colony-forming units (CFU), respectively. For P. aeruginosa biofilms, similar levels of inactivation—3.02 log10 and 3.12 log10 CFU, respectively—were achieved. In mouse burn wounds infected with 5 × 106 CFU of A. baumannii, approximately 360 J/cm2 and 540 J/cm2 aBL was required to inactivate 3 log10 CFU in biofilms when delivered 24 and 48 hours, respectively, after bacterial inoculation. High-performance liquid chromatography analysis revealed the presence of endogenous porphyrins in both A. baumannii and P. aeruginosa. TUNEL assay detected no apoptotic cells in aBL-irradiated mouse skin at up to 24 hours after aBL exposure (540 J/cm2).
**Keywords:** Acinetobacter baumannii; HPLC; Pseudomonas Aeruginosa; Tunel assay; Antimicrobial blue Light; Biofilm; Bioluminescence imaging; Burn wound; Endogenous Porphyrins; Mouse model.

## B-710. A New Biocompatible Nanocomposite as a Promising Constituent of Sunscreens.

Rehab M. Amin, Souad A. Elfeky, Thomas Verwanger and Barbara Krammer.

*Materials Science and Engineering:C, 63:46-51 (2016) IF: 3.42.*

Skin naturally uses antioxidants to protect itself from the damaging effects of sunlight. If this is not sufficient, other measures have to be taken. Like this, hydroxyapatite has the potential to be applied as an active constituent of sunscreens since calcium phosphate absorbs in the ultraviolet region (UV). The objective of the present work was to synthesize a hydroxyapatite–ascorbic acid nanocomposite (HAp/AA-NC) as a new biocompatible constituent of sunscreens and to test its efficiency with skin cell models. The synthesized HAp/AA-NC was characterized by Fourier transform infrared spectroscopy, transmission electron microscopy, absorption spectrophotometry and X-ray diffraction analysis. The protective effect of the construct was tested with respect to viability and intracellular reactive oxygen species (ROS) generation of primary human dermal fibroblasts (SKIN) and

human epidermal keratinocytes (HaCaT). Both cell lines were irradiated with UV light, λmax = 254 nm with a fluence of 25 mJ cm− 2 to mimic the effect of UV radiation of sunlight on the skin. Results showed that HAp/AA-NC had a stimulating effect on the cell viability of both, HaCaT and SKIN cells, relative to the irradiated control. Intracellular ROS significantly decreased in UV irradiated cells when treated with HAp/AA-NC. We conclude that the synthesized HAp/AA-NC have been validated in vitro as a skin protector against the harmful effect of UV-induced ROS.

**Keywords:** Nanocomposite; Hydroxyapatite; Ascorbic acid; Sunscreens; Dermal fibroblasts; Keratinocytes.

## B-711. Fair Resource Allocation Schemes for Cooperative Dynamic Free Space Optical Networks.

Abdallah S. Ghazy, Hossam A. I. Selmy and Hossam M. H. Shalaby.

*Journal of Optical Communications and Networking, 8: 822-834, (2016), IF: 2.183.*

Free space optics (FSO) presents a promising solution for the last-mile connectivity problem. However, adverse weather conditions like fog, rain, and snow, can significantly degrade the performance of FSO links. Thus, the implementation of reliable FSO networks becomes a significant issue. At the same implementation cost, dynamic (reconfigurable) FSO networks are more robust against severe weather conditions over static ones. In this paper, two resource allocation schemes are proposed for dynamic cooperative FSO networks. Each scheme is formulated as a multi objective optimization problem, where capacity,reliability-fairness, average transmitted power, and bit-error rate functions are targeted. One scheme prioritizes the reliability-fairness over capacity, while the other does the opposite. The simulation results reveal that the proposed schemes are more reliable and cost efficient than traditional relayed networks, especially under severe weather conditions.

**Keywords:** Dynamic Networks; Free Space Optics; Lexicographic; Lex-Max-Min Theory; Relayed Networks; Resource Allocation; Weighted Sum.

## B-712. Antimicrobial Blue Light Inactivation of Pseudomonas Aeruginosa by Photo-Excitation of Endogenous Porphyrins: in Vitro and in Vivo Studies.

Rehab M. Amin,Brijesh Bhayana, Michael R. Hamblin and Tianhong Dai.

*Lasers in Surgery a nd Medicine, 48: 562-368,(2016),IF: 2.135.*

Pseudomonas aeruginosa is among the most common pathogens that cause nosocomial infections and is responsible for about 10% of all hospital-acquired infections. In the present study, we investigated the potential development of tolerance of P. aeruginosa to antimicrobial blue light by carrying 10 successive cycles of sublethal blue light inactivation. The high-performance liquid chromatographic (HPLC) analysis was performed to identify endogenous porphyrins in P. aeruginosa cells. In addition, we tested the effectiveness of antimicrobial blue light in a mouse model of nonlethal skin abrasion infection by using a bioluminescent strain of P. aeruginosa. The results demonstrated that no tolerance was developed to antimicrobial blue light in P. aeruginosa after 10 cycles of sub-lethal inactivation. HPLC analysis showed that P. aeruginosa is capable of producing endogenous porphyrins in particularly, coproporphyrin III, which are assumed to be responsible for the photodynamic effects of blue light alone. P. aeruginosa infection was eradicated by antimicrobial blue light alone (48 J/cm(2) ) without any added photosensitizer molecules in the mouse model. In conclusion, endogenous photosensitization using blue light should gain considerable attention as an effective and safe alternative antimicrobial therapy for skin infections.

**Keywords:** Pseudomonas aeruginosa; Blue light; Drug Resistance; Endogenous porphyrins; Mouse.

## B-713. Performance Evaluation of Hybrid Dpsk-Mppm Techniques in Long-Haul Optical Transmission.

Abdulaziz E. El-Fiqi, Ahmed E. Morra, Salem F. Hegazy, Hossam M. H. Shalaby, Kazutoshi Kato and Salah S. A. Obayya.

*Applied Optics, 55: 5614-5622, (2016), IF: 1.598.*

In this paper, we evaluate the performance of hybrid differential phase shift keying-multipulse pulse position modulation (DPSK-MPPM) techniques in long-haul nonlinear-dispersive optical fiber transmission. An expression for the nonlinear interference variance is obtained analytically using the Gaussian noise (GN) model. We derive upper-bound expressions that take into account the fiber nonlinearity impact on the DPSK-MPPM system's performance for both bit- and symbol-error rates (BER and SER). The tightness of the BER's upper bound is verified using Monte Carlo simulation. The numerical analysis is carried out based on the proposed setup supplemented by a realistic simulation scenario for the DPSK-MPPM long-haul optical transmission system. Our results reveal that while the hybrid DPSK-MPPM technique outperforms both traditional DPSK and MPPM techniques under amplified spontaneous emission (ASE) noise (linear limit), it is less robust when fiber nonlinearity is considered. However, under the impact of low nonlinearity, the performance of a hybrid technique still surpasses the traditional ones. We also discuss the effect of some wavelength-division multiplexing (WDM) parameters on optimal system performance. The nonlinear interference penalties on the maximum reachable distances by both hybrid and traditional modulation systems are then investigated at a forward-error correction (FEC) requirement (BER=10^−3)(BER=10^−3). In particular, at an average launch power of −8 dBm−8 dBm, the hybrid DQPSK-MPPM system with a total frame length of eight time slots including two signal time slots outreaches a traditional DQPSK system by 950 km.

**Keywords:** (060.0060) Fiber Optics; Optical Communications; (060.4080) Modulation; (060.4370) Nonlinear Optics; Fibers.

## B-714. Electrical and Optical Clock and Data Recovery in Optical Access Networks: A Comparative Study.

Esraa Abd El-Khaleq, Yasmine El-Sayed, Tawfik Ismail and Hassan Mostafa.

*International Journal of Communication Systems, 29: 2555-2564, (2016), IF: 1.099.*

Clock and data recovery (CDR) is an essential part in high-speed telecommunication systems. The CDR is used to extract the clock and re-time the received data, which allows a synchronous operation to recover the transmitted signal. In optical access networks, electrical CDR or optical CDR implementations can be used. However, there are no clear guidelines or recommendations on which CDR implementation should be adopted for better performance. These missing clear recommendations are because the electrical CDR requires electronics design expertise whereas the optical CDR requires optical design expertise. Consequently, in this paper, an all-digital CDR, designed and implemented on the field-programmable gate array platform, and an optical CDR, developed by using fiber Bragg grating technology on the OptiSystem platform, are presented. Furthermore, the integration of these 2 CDR implementations with the optical access network is implemented, and their performance is evaluated for various transmission rates and communication distances. Finally, a comparative study in terms of the bit error rate between the all-digital CDR and the optical CDR is presented.

**Keywords:** Clock and data recovery; Fiber bragg grating; Field-Programmable Gate array; Optical access network.

## B-715. Numerical Analysis of Ultrafast Physical Random Number Generator Using Dual-Channel Optical Chaos.

Amr Elsonbaty, Salem F. Hegazy and Salah S. A. Obayya.

*Optical Engineering, 55: 94105-94105, (2016), IF: 0.984.*

Fast physical random number generators (PRNGs) are essential elements in the development of many modern applications. We numerically demonstrate an extraction scheme to establish an ultrafast PRNG using dual-channel optical-chaos source. Simultaneous suppression of time-delay signature in all observables of the output is verified using autocorrelation-function method. The proposed technique compares the level of the chaotic signal at time tt with M levels of its delayed version. The comparators [1-bit analog-to-digital converters (ADCs)] are triggered using a clock subject to an incremental delay. All the delays of the chaotic signal before the ADCs and the relative delays of the clock are mutually incommensurable. The outputs of the ADCs are then combined using parity-check logic to produce physically true random numbers. The randomness quality of the generated random bits is evaluated by the statistical tests of National Institute of Standards and Technology Special Publication 800-22. The results verify that all tests are passed from M=1 to M=39 at sampling rate up to 34.5 GHz, which indicates that the maximum generation rate of random bits is 2.691 Tb/s without employing any preprocessing techniques. This rate, to the best of our knowledge, is higher than any previously reported PRNG.

**Keywords:** Optical chaos; Physical random number generator; Dual-Channel chaos; Postprocessing.

## B-716. Bioluminescence-Sensing Assay for Microbial Growth Recognition.

Heba Ramadan Eed, Nora S. Abdel-Kader, Mahmoud Helmy El Tahan, Tianhong Dai and Rehab Amin

*Journal of Sensors, 2016: 1-5, (2016), IF: 0.712*

The conventional methods for microbial viability quantification require cultivation and are laborious. There is consequently a widespread need for cultivation-free methods. The adenosine triphosphate (ATP) bioluminescence-sensing assay is considered an extremely effective biosensor; hence ATP is the energy currency of all living microbes and can be used as a rapid indicator of microbial viability. We developed an ATP bioluminescence-sensing assay to detect microbial viability. A bioluminescent recombinant E. coli strain was used with luciferase extracted from transformed bacteria. Results showed that there is a direct correlation between the bioluminescence intensity of the ATP bioluminescence-sensing assay and the microbial viability. Bacterial counts from food samples were detected using the developed sensing assay and validated by the traditional plate-counting method. Compared with the plate-counting method, ATP bioluminescence-sensing assay is a more rapid and efficient approach for detecting microbial viability.

**Keywords:** Atp; Bioluminescence; Sensing assay.

## B-717. Free Space Optic and Mmwave Communications: Technologies, Challenges and Applications.

Tawfik Ismail, Erich Leitgeb and Thomas Plank.

*Ieice Transactions on Communications, E99-B: 1243-1254, (2016), IF: 0.65.*

Increasing demand in data-traffic has been addressed over the last few years. It is expected that the data-traffic will present the significant part of the total backbone traffic. Accordingly, much more transmission systems will be required to support this growth. A free space optic (FSO) communication is the greatest promising technology supporting high-speed and high-capacity transport networks. It can support multi Gbit/s for few kilometers transmission distance. The benefits of an FSO system are widespread, low cost, flexibility, immunity to electromagnetic field, fast deployment, security, etc. However, it suffers from some drawbacks, which limit the deployment of FSO links. The main drawback in FSO is the degradation in the signal quality because of atmospheric channel impairments. In addition, it is high sensitive for illumination noise coming from external sources such as sun and lighting systems. It is more benefit that FSO and mmWave are operating as a complementary solution that is known as hybrid FSO/mmWave links. Whereas the mmWave is susceptible to heavy rain conditions and oxygen absorption, while fog has no particular effect. This paper will help to better understand the FSO and mmWave technologies and applications operating under various atmospheric conditions. Furthermore, in order to improve the system performance and availability, several modulation schemes will be discussed. In addition to, the hybrid FSO/mmWave with different diversity combining techniques are presented.

**Keywords:** Free space optic; Millimeter wave; Wireless applications; Losses; Availability; Turbulence; Diversity combining; Modulations; Hybrid networks.

## B-718. A New Technique for Ultra-Fast Physical Random Number Generation Using Optical Chaos.

Amr Elsonbaty, Salem F. Hegazy and Salah S. A. Obayya.

*Proceedings of Spie - The International Society For Optical Engineering, 9892: 98921-98921 (2016).*

In this paper, we numerically demonstrate a new extraction scheme for generating ultra-fast physically random sequence of bits. For this purpose, we utilize a dual-channel optical chaos source with suppressed time delayed (TD) signature in both the intensity and the phase of its two channels. The proposed technique uses M 1-bit analog-to-digital converters (ADCs) to compare the level of the chaotic intensity signal at time t with its levels after incommensurable delay-interval Tm, where m = {1,2, … , M}. The binary output of each 1-bit ADC is then sampled by a positive-edge-triggered D flip flop. The clock sequence applied to the flip-flops is relatively delayed such that the rising edge of the clock triggering the m flip-flop precedes the rising edge of the clock of a subsequent m+1 flip-flop by a fixed period. The outputs of all flip flops are then combined by means of a parity-check logic. Numerical simulations are carried out using values of parameters at which TD signature is suppressed for chosen values of setup parameters. The 15 statistical tests in Special Publication 800-22 from NIST are applied to the generated random bits in order to examine the randomness quality of these bits for different values of M. The results show that all tests are passed from M = 1 to M = 39 at sampling rate up to 34.5 GHz which indicates that the maximum generation rate of random bits is 2.691 Tb/sec using a chaotic source of single VCSEL and without employing any pre-processing techniques.

**Keywords:** Optical Chaos; Physical Random Number Generator; Dual-Channel Chaos; Post-Processing

## B-719. Accurate Relative-Phase and Time-Delay Maps All Over the Emission Cone of Hyperentangled Photon Source.

Salem F. Hegazy, Jala El-Azab, Yehia A. Badr and Salah S. A. Obayya.

*Proceedings of Spie - The International Society for Optical Engineering, 9894: 98940-98940 (2016).*

High flux of hyperentangled photons entails collecting the two-photon emission over relatively wide extent in frequency and transverse space within which the photon pairs are simultaneously entangled in multiple degrees of freedom. In this paper, we present a numerical approach to determining the spatial-spectral relative-phase and time-delay maps of hyperentangled photons all over the spontaneous parametric down conversion (SPDC) emission cone. We consider the hyperentangled-photons produced by superimposing noncollinear SPDC emissions of two crossed and coherently pumped nonlinear crystals. We adopt a vectorial representation for all parameters of concern. This enables us to study special settings such as the self-compensation via oblique pump incidence. While rigorous quantum treatment of SPDC emission requires Gaussian state representation, in low-gain regime (like the case of the study), it is well approximated to the first order to superposition of vacuum and two-photon states. The relative phase and time-delay maps are then calculated between the two-photon wavepackets created along symmetrical locations of the crystals. Assuming monochromatic plane-wave pump field, the mutual signal-idler relations like energy conservation and transverse momentum conservation define well one of the two-photon with reference to its conjugate. The weaker conservation of longitudinal momentum (due to relatively thin crystals) allows two-photon emission directions coplanar with the pump beam while spreading around the perfect phase-matching direction. While prior works often adopt first-order approximation, it is shown that the relative-phase map is a very well approximated to a quadratic function in the polar angle of the two-photon emission while negligibly varying with the azimuthal angle.

**Keywords:** Hyperentanglement; Two – Crystal; Oblique Incidence; Phase compensation; Walkoff compensation.

## B-720. Encoding Classical Bits in the Arrival Time of Dense-Coded Photons.

Salem F. Hegazy, Ahmed E. Morra and Salah S. A. Obayya.

*Proceedings of Spie - The International Society For Optical Engineering, 9900: 99000-99000 (2016).*

We present a scheme to encode M extra classical bits to a dense-coded pair of photons. By tuning the delay of an entangled pair of photons to one of 2M time-bins and then applying one of the quantum dense coding protocols, a receiver equipped with a synchronized clock of reference is able to decode M bits (via classical time-bin encoding) + 2 bits (via quantum dense coding). This protocol, yet simple, does not dispense several special features of the used programmable delay apparatus to maintain the coherence of the two-photon state. While this type of time-domain encoding may be thought to be ideally of boundless photonic capacity (by increasing the number of available time-bins), errors due to the environmental noise and the imperfect devices and channel evolve with the number of time-bins.

**Keywords:** Time-Bin;superdense coding; Delay line; Quantum information; Channel capacity; Hybrid modulation; Quantum bit error rate.

## B-721. In Vitro and in Vivo Antimicrobial Activity of Combined Therapy of Silver Nanoparticles and Visible Blue Light Against Pseudomonas Aeruginosa.

Nour El Din S, El-Tayeb TA, Abou-Aisha K and El-Azizi M.

*International Journal of Nanomedicine.,11:1749-1758, (2016), IF: 4.32.*

Silver nanoparticles (AgNPs) have been used as potential antimicrobial agents against resistant pathogens. We investigated the possible therapeutic use of AgNPs in combination with visible blue light against a multidrug resistant clinical isolate of Pseudomonas aeruginosa in vitro and in vivo. The antibacterial activity of AgNPs against P. aeruginosa (1×10(5) colony forming unit/mL) was investigated at its minimal inhibitory concentration (MIC) and sub-MIC, alone and in combination with blue light at 460 nm and 250 mW for 2 hours. The effect of this combined therapy on the treated bacteria was then visualized using transmission electron microscope. The therapy was also assessed in the prevention of biofilm formation by P. aeruginosa on AgNP-impregnated gelatin biopolymer discs. Further, in vivo investigations were

performed to evaluate the efficacy of the combined therapy to prevent burn-wound colonization and sepsis in mice and, finally, to treat a real infected horse with antibiotic-unresponsive chronic wound. The antimicrobial activity of AgNPs and visible blue light was significantly enhanced (P<0.001) when both agents were combined compared to each agent alone when AgNPs were tested at MIC, 1/2, or 1/4 MIC. Transmission electron microscope showed significant damage to the cells that were treated with the combined therapy compared to other cells that received either the AgNPs or blue light. In addition, the combined treatment significantly (P<0.001) inhibited biofilm formation by P. aeruginosa on gelatin discs compared to each agent individually. Finally, the combined therapy effectively treated a horse suffering from a chronic wound caused by mixed infection, where signs of improvement were observed after 1 week, and the wound completely healed after 4 weeks. To our knowledge, this combinatorial therapy has not been investigated before. It was proved efficient and promising in managing infections caused by multidrug resistant bacteria and could be used as an alternative to conventional antibiotic therapy.

**Keywords:** Biofilm; Bioplastic disc; Invasive sepsis; Murine Model; Nonconventional therapy; Wound colonization.

## B-722. Gold Nanorod Synthesis Catalysed by au Clusters.

Yasser Attia Attia, Carlos Vazquez-Vazquez, María del Carmen Blanco-Varela, David Buceta and M Arturo Lopez-Quintela.

*Faraday Discussions, 191: 205-213, (2016), IF: 3.858.*

Gold nanorods have been successfully synthesized by the seed mediated method using Au clusters. This synthesis does not require silver ions to obtain large amounts of Au nanorods and has good control over their aspect ratio. Au clusters are produced with the same recipe as for Au seeds, but using shorter reaction times. This very simple scheme confirms the important catalytic influence of clusters in the anisotropic growth control.

**Keywords:** Gold nanorods; Gold clusters; Seeds mediated Method; Catalysis.

## B-723. Comparison of Nanoparticles Effects on Biogas and Methane Production from Anaerobic Digestion of Cattle Dung Slurry.

E. Abdelsalam, M. Samer, Y.A. Attia, M.A. Abdel-Hadi, H.E. Hassan and Y. Badr.

*Renewable Energy, 87, Part 1: 592-598, (2016), IF: 3.404*

Nanoparticles (NPs) of trace metals such as Co, Ni, Fe and Fe3O4 were implemented in this study to compare their effects on biogas and methane production from anaerobic digestion of livestock manure. The most effective concentrations of NPs additives were determined based on our previous studies, and were 1 mg/L Co NPs, 2 mg/L Ni NPs, 20 mg/L Fe NPs and 20 mg/L Fe3O4 NPs. These concentrations of NPs additives were further investigated and compared to each other in this study and were found to significantly ($p < 0.05$) increase the biogas yield by 1.7, 1.8, 1.5 and 1.7 times in comparison with control, respectively. The methane yield significantly ($p < 0.05$) increased by 2, 2.17, 1.67 and 2.16 times the methane volume of the control, respectively. The results of this study showed that the Ni NPs yielded the highest biogas and methane production compared to Co, Fe and Fe3O4 NPs.

**Keywords:** Nanoparticles; Biogas; Methane production; Anaerobic digestion; Trace metals; Slurry treatment.

## B-724. Laser-Induced Breakdown Spectroscopy on Metallic Samples at Very Low Temperature in Different Ambient Gas Pressures.

R.H. El-Saeid, M. Abdelhamid and M.A. Harith.

*Spectrochimica Acta B, 116: 1-7, (2016), IF: 3.289.*

Analysis of metals at very low temperature adopting laser-induced breakdown spectroscopy (LIBS) is greatly beneficial in space exploration expeditions and in some important industrial applications. In the present work, the effect of very low sample temperature on the spectral emission intensity of laser-induced plasma under both atmospheric pressure and vacuum has been studied for different bronze alloy samples. The sample was cooled down to liquid nitrogen (LN) temperature 77 K in a special vacuum chamber. Laser-induced plasma has been produced onto the sample surface using the fundamentalwavelength of Nd:YAG laser. The optical emission fromthe plasma is collected by an optical fiber and analyzed by an echelle spectrometer combinedwith an intensified CCD camera. The integrated intensities of certain spectral emission lines of Cu, Pb, Sn, and Zn have been estimated from the obtained LIBS spectra and compared with that measured at room temperature. The laserinduced plasma parameters (electron number density Ne and electron temperature Te) were investigated at room and liquid nitrogen temperatures for both atmospheric pressure and vacuum ambient conditions. The results suggest that reducing the sample temperature leads to decrease in the emission line intensities under both environments. Plasma parameters were found to decrease at atmospheric pressure but increased under vacuum conditions.

**Keywords:** Libs liquid nitrogen; Temperature vacuum plasma Parameters.

## B-725. Photo-Extracellular Synthesis of Gold Nanoparticles Using Baker's Yeast and their Anticancer Evaluation Against Ehrlich Ascites Carcinoma Cells.

Yasser A. Attia, Yassmeen E. Farag, Yasser M. A. Mohamed, Akaber T. Hussien and Tareq Youssef.

*New Journal of Chemistry, 40: 9395-9402, (2016), IF: 3.277.*

The chemical methods for the synthesis of gold nanoparticles lead to the formation of some toxic chemicals adsorbed on the surface that may have adverse effects on their medical applications. Hence, the need to develop environmentally benign nanoparticles has attracted growing interest. Gold nanoparticles with 13.0 ± 0.9 nm size have been biosynthesized using an aqueous extract of Baker's yeast (Saccharomyces cerevisiae) under visible light. The existing components in the aqueous yeast extract were identified for the first time as trimethylsilyl derivatives of butan-2,3-diol, glucose, indole-3-acetic acid and undecanoic acid. This extract acts as a capping and reducing agent for gold nanoparticles. The cytotoxicity of the biosynthesized gold nanoparticles, chemically synthesized

gold nanoparticles of ~5.0 ± 2.0 nm size and aqueous extract of Baker's yeast towards Ehrlich ascites carcinoma cancer cells has been studied using the Trypan blue exclusion method. The results show that the killed percentage of Ehrlich ascites carcinoma cells under dark incubation with an aqueous extract of Baker's yeast, chemically synthesized gold nanoparticles and the photo-biosynthesized gold nanoparticles are 9.7%, 12.5% and 24.6%, respectively. These percentages are increased to 10.63%, 60.6% and 86.5% under visible light incubation, respectively. The killing enhancement of the Ehrlich ascites carcinoma cells under visible light incubation is proposed based on the photothermal properties of the formed plasmonic gold nanoparticles that conjugated with anti-epidermal growth factor receptor antibodies beside the phagocytosis of the excess yeast extract that is present in the photo-extracellular synthesized gold nanoparticles sample. The combination between two different treatment ways can give a third one with high affinity for the treatment of cancer.

**Keywords:** Yeast extract; Gold nanoparticles; Cancer therapy; Photothermal treatment; Cytotoxicity; Chemical derivatization; Photosynthesis.

## B-726. Effect of Size, Concentration, and Type of Spherical Gold Nanoparticles on Heat Evolution Following Laser Irradiation Using Tissue-Simulating Phantoms.

Hossam Zakaria, Wessameldin S. Abdelaziz and Tareq Youssef

*Lasers In Medical Science, 31: 625-634, (2016), IF: 2.461.*

Photothermal therapy has recently gained a considerable attention particularly after the revolution of nanomaterials and nanotechnology. The aim of the present study is to assess the optimal photothermal response through investigating some effective parameters of spherical gold nanoparticles (AuNPs), e.g., type, size, and concentration, as a preclinical study for efficient photothermal treatment. Tissue-simulating phantoms based on agar and water media incorporated with two different types of AuNPs, spherical Au particles capped with citrate or spherical Au core–silica shell NPs, were built. Heat evolution for each NP type was recorded in the phantom matrix with different particle sizes at various concentrations following exposure to low laser power (irradiance 35 mW/cm2) and emitting at λ = 532 nm. Our results demonstrated that AuNPs capped with citrate recorded higher temperature elevations than those capped with silica shell. Particles with smaller sizes produced more heating effect than those having larger sizes. Also, higher temperatures were recorded at a critical concentration of NPs. Exponential decay constants based on theoretical calculations demonstrated that laser attenuation increases with the continuous increase of particle size and concentration.

**Keywords:** Tissue-Simulating; Phantoms gold nanoparticles; Photothermal treatment.

## B-727. Establishment of an in Vitro Propagation and Transformation System of Balanites Aegyptiaca.

Galal Khamis, Traud Winkelmann, Frank Schaarschmidt and Jutta Papenbrock.

*Plant Cell, Tissue and Organ Culture, (2016) 125: 457-470 .(2016) IF: 2.39.*

Balanites aegyptiaca (Balanitaceae) is a drought-tolerant but salt-sensitive tree species distributed in the tropical and arid lands in Africa and Asia. The tree contains many secondary metabolites and a high percentage of oil in the kernels that can be used for biodiesel production. This study aimed to establish an in vitro propagation system of two B. aegyptiaca provenances (El- Kharga and Wadi El-Alaqi) from nodal and cotyledon explants. The explants were placed on Murashige and Skoog medium supplemented with different concentrations of 6-benzyladenine (BA) and thidiazuron (TDZ) for shoot induction. BA was significantly more effective in shoot induction from nodal explants and treatment with BA also resulted in higher regeneration rates of about 40–60 % of adventitious shoots on cotyledon explants, whereas on TDZ-containing medium slightly higher shoot numbers per explant but a negative effect on shoot length were recorded. Rooting was achieved in 40–60 % of the shoots on medium containing between 1.2 and 4.8 lM indole-3-butyric acid. Three different Agrobacterium tumefaciens strains (EHA105, GV3101, and LBA4404) harboring the plasmid pCAMBIA2301 containing the nptII marker and gus reporter genes were used to establish a transformation system in B. aegyptiaca. Strain GV3101 resulted in the highest survival rates and highest number of explants positive in the GUS assay. This selected A. tumefaciens strain was used to introduce pBinAR containing the sequence encoding ERD10 (early responsive to dehydration 10) to produce salt-tolerant B. aegyptiaca plants. The presence of the ERD10 and the nptII gene were detected by PCR in transformed B. aegyptiaca plants.

**Keywords:** Agrobacterium tumefaciens; Balanites aegyptiaca; ERD10; Regeneration; Rooting; Salt stress.

## B-728. A Combination of Silver Nanoparticles and Visible Blue Light Enhances the Antibacterial Efficacy of Ineffective Antibiotics Against Methicillin-Resistant Staphylococcus Aureus (MRSA).

Fatma Elzahraa Akram, Tarek El-Tayeb, Khaled Abou-Aisha and Mohamed El-Azizi.

*Annals of Clinical Microbiology and Antimicrobials, 15: 48-61, (2016), IF: 2.19.*

**Background:** Silver nanoparticles (AgNPs) are potential antimicrobials agents, which can be considered as an alternative to antibiotics for the treatment of infections caused by multi-drug resistant bacteria. The antimicrobial effects of double and triple combinations of AgNPs, visible blue light, and the conventional antibiotics amoxicillin, azithromycin, clarithromycin, linezolid, and vancomycin, against ten clinical isolates of methicillin-resistant Staphylococcus aureus (MRSA) were investigated. **Methods** The antimicrobial activity of AgNPs, applied in combination with blue light, against selected isolates of MRSA was investigated at 1/2–1/128 of its minimal

inhibitory concentration (MIC) in 24-well plates. The wells were exposed to blue light source at 460 nm and 250 mW for 1 h using a photon emitting diode. Samples were taken at different time intervals, and viable bacterial counts were determined. The double combinations of AgNPs and each of the antibiotics were assessed by the checkerboard method. The killing assay was used to test possible synergistic effects when blue light was further combined to AgNPs and each antibiotic at a time against selected isolates of MRSA. **Results** The bactericidal activity of AgNPs, at sub-MIC, and blue light was significantly ($p < 0.001$) enhanced when both agents were applied in combination compared to each agent alone. Similarly, synergistic interactions were observed when AgNPs were combined with amoxicillin, azithromycin, clarithromycin or linezolid in 30–40 % of the double combinations with no observed antagonistic interaction against the tested isolates. Combination of the AgNPs with vancomycin did not result in enhanced killing against all isolates tested. The antimicrobial activity against MRSA isolates was significantly enhanced in triple combinations of AgNPs, blue light and antibiotic, compared to treatments involving one or two agents. The bactericidal activities were highest when azithromycin or clarithromycin was included in the triple therapy compared to the other antibiotics tested. **Conclusions** A new strategy can be used to combat serious infections caused by MRSA by combining AgNPs, blue light, and antibiotics. This triple therapy may include antibiotics, which have been proven to be ineffective against MRSA. The suggested approach would be useful to face the fast-growing drug-resistance with the slow development of new antimicrobial agents, and to preserve last resort antibiotics such as vancomycin.

**Keywords:** Nonconventional antimicrobials; Double and triple Combinations; Multidrug-Resistance; Checkerboard assay; Linezolid; Vancomycin; Azithromycin; Clarithromycin.

## B-729. Surface Morphology Study of Some Cueni Reference Alloys Using Laser Induced Breakdown Spectroscopy.

S.A. Sheta , G. Di Carlo , G.M. Ingo and M.A. Harith.

*Materials Chemistry and Physics, 173:516-523 (2016) IF:2.101*

In the present work a detailed study of the surface morphology of purposely-prepared CueNi reference alloys has been performed. These alloys have been prepared via tailored casting methods in order to have samples with same chemical composition and different local chemical enrichments of both metals. A micro-LIBS system for surface spatial scanning was set up based on a second harmonic Nd:YAG laser at 532 nm and using a focusing lens of focal length 7 cm to disclose the local chemical composition variation. Surface morphological scanning was performed for some of the binary CueNi reference alloys to differentiate between chemically homogeneous and heterogeneous alloys. LIBS results were compared with the information of the Scanning Electron Microscope coupled with Energy Dispersive X-ray (SEMEDS) investigation carried out to provide surface local large-area chemical analysis via EDS technique. It has been proved that LIBS is a simple, sensitive and direct technique in the determination of homogeneity or heterogeneity of the sample's surface. The LIBS results have been shown to be more sensitive and accurate in the heterogeneity determination than other used conventional analytical techniques

## B-730. Res_Id: 598J Res_Wcode: 2290

## QuantitativeanalysisofCuandCoadsorbedon fish bonesvia laser-inducedbreakdownspectroscopy

R.A.Rezk , A.H.Galmed , M.Abdelkreem , N.A.AbdelGhany , M.A.Harith

*Optics &Laser Technology, 83: 131-139, (2016), IF: 1.879*

In the present work, laser-inducedbreakdownspectroscopy(LIBS)hasbeenappliedforqualitativeand quantitativeanalysisofheavymetalsadsorbedby fish bones.Fishboneswereusedasanaturalandlow cost heavymetalsorbent(mainlyCuandCo)fromsyntheticwastewater.Theremovalefficiency ofthe adsorbent wasstudiedasafunctionofinitialmetalconcentrationandpHvalue.Optimalexperimental conditions wereevaluatedforimprovingthesensitivityofLIBStechniquethroughparametricdepen- dence studies.Furthermore,calibrationcurveswereconstructedbasedonX-ray fluorescence (XRF) analysistechnique,whereas,thelimitsofdetection(LOD)forCuand Cowerecalculated.Theresultswere validatedbycomparingLIBSdatawiththoseobtainedbyXRFspectrometry.Theresultsofthetwo techniquesarestronglycorrelatedwhichverified thefeasibilityofusingLIBStodetecttracesofheavy metals adsorbedfromwastewaterby fish bones.Thisstudyreflects thepotentialofusingLIBSin environmentalapplications.

Keywords: Libs Xrf Wastewater Heavymetals Adsorption Fish Bone

## B-731. Res_Id: 436J Res_Wcode: 15

## Fabrication and characterisation of sulfur and phosphorus (S/P) co-doped carbon nanotubes

ariq Altalhi, Amine Mezni, Ali Aldalbahi, Arwa Alrooqi, Yasser Attia, Abel Santos, Dusan Losic

*Chemical Physics Letters, 658: 92-96, (2016), IF: 1.86*

In this work, first, we aim to present a catalyst-free protocol to fabricate doped carbon nanotubes (CNTs) by S, P and S/P elements and with controlled physical and chemical properties. Then, we have explored the effect of S concentration on the morphology of CNTs. The structural and chemical composition of fabricated CNTs/NAA composites were analysed by various characterisation techniques, including transmission electron microscopy (TEM), scanning electron microscopy (SEM), EDXS and high resolution transmission electron microscopy (HRTEM).

Keywords: Carbon Nanotubes; Nanoporous Anodic Alumina; Cvd Approach And Composites Membrane; Doped Carbon Nanotubes

## B-732. Res_Id: 432J Res_Wcode: 4

## Ag/ZnO/graphene-tert-butyldimethylsilyl chloride hybrid nanocomposite as highly efficient catalyst for hydrogen production

Wessam Omara, Souad A. Elfeky

*Recent Patents On Nanotechnology,10:157-164,(2016), IF:1.576*

Background: Nanoparticles have a promising potential in electrochemical sensitivity. Polyaniline (PANI) received significant attention in the latest years owing to its high conductivity and excellent electrochemical stability. This research aims to study the effect of gold nanoparticles capped octadecyl amine (Au/ODA) on polyaniline emeraldine salt (ES) electrochemical sensitivity to formaldehyde (FA) using DPV technique. Furthermore, ES and Au-ODA/ES have been applied for the first time in sensing FA. Few relevant patents to the topic have been reviewed and cited in this article. Methods: Emeraldine salt (ES) was prepared by doping the prepared emeraldine base (EB) powder with dodecylbenzene sulfonic acid (DBSA) at a ratio of 1:2 W/W. Then ES-DBSA was dissolved in chloroform solution and added to Au/ODA nanoparticles solution to obtain Au/ES-DBSA nanocomposite. FA sensors were prepared by depositing a film from ESDBSA or Au/ES-DBSA on a working electrode and the potential was measured at FA different concentrations in Electrochemical cell kit. Results: FTIR and XRD confirmed the structure of ES-DBSA and Au/ES-DBSA. The obtained results reveal that the ESDBSA nanosensor is an efficient sensor because it can recognize the low levels of FA starting from 0.06 ppm. The recorded electrochemical oxidation current shows a linear direct relationship between the produced current and FA concentration in case of ES-DBSA nanoparticles while it illustrates a fluctuating signal with lower sensitivity in the case of the novel prepared nanocomposites (Au/ES-DBSA). This may be due to the gold capping agent (ODA), which in turn could inhibit the role of DBSA and decrease the conductivity of the nanocomposite. Conclusion: Herein we described the application of ES-DBSA and Au/ES-DBSA nanocomposite for the first time as a novel, facile, and cheap method for electrochemical sensitive detection of formaldehyde. The gold capping agent ODA hinders the ES-DBSA conductivity through interaction with the DBSA sulfo group.

Keywords: Au/Es-Dbsa, Formaldehyde, Gold Nanoparticles, Nanocomposites, Polyaniline, Potential

## B-663. Two-Dimensional Cardiothoracic Ratio for Evaluation of Cardiac Size in Cats

Elham A. Hassan and Faisal A. Torad

*Veterinary Radiology and Ultrasound, 57: 646-669, (2016), IF: 0.926*

**Introduction/Purpose:** Thoracic radiography is the most common diagnostic tool used for evaluating cats with suspected cardiac disease. Evaluation of cardiac size and silhouette is an important indicator of pathologic cardiac changes. Tracking of cardiac silhouette and calculation of cardiothoracic ratio is a novel diagnostic tool that has been used for evaluation of cardiac size in German shepherd dogs.1 The purpose of the present study was to evaluate cardiac size in cats using two-dimensional cardiothoracic ratio calculation. Methods: Clinical, radiographic, and echocardiographic data of 50 cats with normal (n = 25) as well as enlarged heart (n = 25) were used in the study. Echocardiographic examination was used as a gold standard to differentiate cats with enlarged cardiac size from those with normal cardiac size. Right lateral thoracic radiographs obtained at the point of peak inspiration were used; two-dimensional cardiothoracic area was calculated as the percentage area of the cardiac silhouette relative to the thoracic area using a computer software program. All measurements were made in triplicates by the same observer (E.A.H.) and the average was calculated. Receiver operating characteristic (ROC) curve analysis was used to determine the diagnostic accuracy of cardiothoracic ratio in evaluating cardiac size. **Results:** In right lateral thoracic radiographs obtained at the peak inspiration, the mean (±SD) cardiothoracic ratio of normal cats was 17.17% ± 1.70% while in cats with enlarged cardiac size was 26.7% ± 3.97%. The cutoff value of cardiothoracic ratio for diagnosing enlarged cardiac size was 19.97%, the area under the curve of the ROC curve analysis was 0.977 ± 0.004 with a 95% confidence of interval (0.988–1.000). **Discussion/Conclusions:** Two-dimensional cardiothoracic ratio obtained at the point of peak inspiration may provide a clinically useful objective tool for evaluating cardiac size in cats.

**Keywords:** Cardiothoracic ratio; Cat; Radiograph; Heart.

## B-658. The Relationship Between Ultrasonographic Appearance and Histopathological Findings of Lens and Posterior Segment Abnormalities in Donkeys

Faisal A. Torad and Elham A. Hassan

*Veterinary Ophthalmology, 19 (2016) IF: 1.736*

**Purpose:** Ocular ultrasonography is a rapid and non invasive diagnostic tool for assessing the equine eye when corneal, lens opacity or severe eyelid swelling precludes ophthalmoscopy of the deeper structures. The present study provides representative ultrasonographic images of the lens and posterior segment diseases in donkeys and correlates these diseases with histopathological findings. **Material/Methods:** The present study was performed on 24 eyes from 19 donkeys of different ages (2–5 years), weights (150–220 kg) and of both sexes (12 males and seven females). All cases have lens or posterior segment abnormalities and received complete ophthalmoscopic and ultrasonographic examinations using Toshiba just vision 200 with microconvex 5–8 MHz probe. The ultrasonographic appearance was correlated with the histopathologic findings collected from enucleated hopeless cases (nine eyes). **Results**: Ultrasonographic examination allowed diagnosis of the following conditions: Cataract (nine eyes), lens dislocation (six eyes), retinal detachment (five eyes) endophthalmitis (three eyes) and vitreal hemorrhage (one eye). These conditions were correlated to the histopathological findings: In the cataractous eye, the lenticular capsule showed liquefaction of its fibers. Lysis of the lenticular fibers was accompanied with release of proteinous fluid between the fibers as clefts containing necrotic

debris. The capsular epithelial cells migrated to the lens to form bladder cells. These ballooning cells appeared with pale staining cytoplasm and with or without nuclei in the plain section. In retinal detachment, progressive retinal degeneration with atrophy of retinal layer and complete absence of photoreceptors were identified. In endophthalmitis, the iris and ciliary process showed edema, congestion and leukocyte infiltration. **Discussion:** Ultrasonography provides valuable diagnostic information that could be correlated with the histopathological findings. Histopathological examination confirmed the ultrasonographic diagnosis of ocular conditions in donkeys.

**Keywords:** Ultrasonography; Eye; Lens; Posterior segment; donkey.

**24. Res_Id: 432 J Res_Wcode: 4 Ag/Zno/Graphene-Tert-Butyldimethylsilyl Chloride Hybrid Nanocomposite as Highly Efficient Catalyst For Hydrogen Production**

Yasser A. Attia

*Materials Express, 6: 211-219, (2016), IF: 1.64*

Modification of Ag/ZnO/graphene nanocomposite using tert-butyldimethylsilyl chloride (TBSCl) as a precursor of the silicon substrate to produce a highly active catalytic system under visible light for hydrogen photoproduction is created in this work. The catalytic activity of this photoresponsive nanocatalyst towards methylene blue dye degradation and hydrogen production are in detail described. The rate order of methylene blue dye photodegradation and hydrogen evolution under visible light irradiation of the samples is: Ag/ZnO/graphene-TBSCl > Ag/ZnO/graphene > Ag/ZnO > ZnO/graphene > ZnO. The hydrogen evolution rate of Ag/ZnO/graphene/TBSCl-hybrid is about 45 times, 6.6 times, 6.4 times and 2.5 times faster than that of pure ZnO nanoparticles, ZnO/graphene, Ag/ZnO and Ag/ZnO/graphene composite, respectively. By introducing Si to Ag/ZnO/graphene composites, an enhancement for photodecomposition and water splitting efficiency under visible light irradiation has been achieved. This is a new advance in the enhancement of photocatalytic activity of nanostructures and offer additional knowledge in the control of charge recombination.

Keywords: Hydrogen Photoproduction; Methylene Blue Dye; Photocatalysis; Photodegradation; Water Splitting; Zno-Based Nanocomposites

**B-734. Res_Id: 438J Res_Wcode: 20 Photobiosynthesis of Metal/Graphene Nanocomposites: New Materials for Water Desalination and Purification**

Yasser A. Attia, Yasser M.A. Mohamed and Tariq A. Altalhi

*Desalination and Water Treatment, 57: 26014-26021, (2016), IF: 1.272*

Ultra-pure water, free from metals and micro-organisms, has been easy obtained from Red seawater (Jeddah, KSA) by plasmonic-graphene hybrid nanocomposites that green synthesized using Baker's yeast (Saccharomyces cerevisiae) extract under visible light irradiation. Gas chromatography mass spectroscopy (GC/MS) analysis of aqueous yeast extract indicates the presence of significant biomolecules; butane-2,3-diol, glucose, undecanoic acid, and indole-3-acetic acid that can act under visible light as reducing and capping agent for the growth of (Ag, Au, and Ag/Au) plasmonic nanoparticles and graphene-based plasmonic nanocomposites. These nanocomposites able to absorb sunlight very strongly and converting it very efficiently into heat energy that enhancing the seawater evaporation. Bimetallic Ag/Au/reduced graphene-oxide nanocomposites show the highest gain of temperature and highest stability after three times of recycling processes. These eco-friendly nanocomposites are smart alternatives in water desalination and purification technique by taking the advantages of their excellent photothermal conversion, its energy-saving, cost-effective, and ease recyclability.

Keywords: Metal Nanoparticles, Graphene, Yeast, Photosynthesis, Water Desalination And Purification, Photothermal

**B-735. Res_Id: 448J Res_Wcode: 1489 Reaching White-Light Radiation Source of Ultrafast Laser Pulses With Tunable Peak Power Using Nonlinear Self-Phase Modulation in Neon Gas**

Walid Tawfik

*Radiation Physics And Chemistry, 125: 165-170, (2016), IF: 1.207*

A source of white-light radiation that generates few-cycle pulses with controlled peak power values has been developed. These ultrafast pulses have been observed by spectral broadening of 32 fs pulses through nonlinear self-phase modulation in a neon-filled hollow-fiber then compressed with a pair of chirped mirrors for dispersion compensation. The observed pulses reached transform-limited duration of 5.77 fs and their peak power values varied from 57 GW up to 104 GW at repetition rate of 1 kHz. Moreover, the applied method is used for a direct tuning of the peak power of the output pulses through varying the chirping of the input pulses at different neon pressures. The observed results may give an opportunity to control the ultrafast interaction dynamics on the femtosecond time scale and facilitate the regeneration of attosecond pulses.

Keywords: Ultrafast Lasers Few-Cycle Femtosecond Self-Phase Modulation

**B-736. Res_Id: 596J Res_Wcode: 2215**
**Magnetic Quadrupole (M2) X-Ray Laser Transitions from Neon-Like Arsenic As+23**

Mohammad Z. Mansour, Wessameldin S. Abdelaziz, Tharwat M. El Sherbini

*Canadian Journal of Physics, 94: 1233-1240, (2016), IF: 0.964*

Neon-like arsenic As+23 are studied theoretically where 457 energy levels are calculated. Highly energetic electrons are considered as the main pumping source for the population of the energy levels. Relativistic calculations are considered through calculations, and the possible X-ray laser transitions are determined with their gain coefficients. The soft X-ray laser transitions ($\lambda \approx 17–27$ nm) are dominated by the magnetic quadrupole M2. The results show good agreement with the observed data and, moreover, new transitions that are not given in the literature are calculated together with their gain values.
Keywords: Soft X-Ray Lasers, Neon-Like Arsenic, Magnetic Quadrupole, Fully Relativistic Energy Levels, Distorted Waves, Gain Coefficients

**B-737. Res_Id: 595J Res_Wcode: 2210**
**X-Ray Laser Lines In Nickel-Like Erbium**

Wessameldin S. Abdelaziz

*Canadian Journal of Physics, 94: 705-711, (2016), IF: 0.964*

Energy levels of 249 excited levels in nickel-like erbium are calculated using the 3s23p63d10 as a ground state and the single electron excited states from n = 3 to n = 4, 5 orbitals, calculations have been performed using FAC code (Gu. Astrophys. J. 582, 1241 (2003). doi:10.1086/344745). The populations are calculated over electron densities from 1020 to 1023 cm−3 and electron temperatures 1/2, 3/4 of the ionization potential of Ni-like Er. The gain coefficients of the transitions are calculated.
**Keywords:** Energy Levels, Excited Levels, Nickel-Like Erbium, X-Ray Laser Lines

**B-738. Res_Id: 445J Res_Wcode: 1801**
**Creation of Transform-Limited 120 Gw Optical Pulses Using Broadband Supercontinuum Generation in Optical Fiber**

walid tawfik

*Journal of Optoelectronics and Advanced Materials, 181: 201-206, (2016), IF: 0.429*

A novel procedure to produce transform-limited optical pulses with high peak power using supercontinuum generation in an optical fiber has been developed. These pulses have been created using a mode-locked Ti:Sapphire oscillator to generate 18 fs pulses at 795.3 nm with energy of 4 nJ and bandwidth of 46 nm. A high power chirped pulse amplification was used to produce femtosecond pulses of 2.6 W at 32 fs for wavelength 800 nm. To achieve extreme pulse compression in the fewcycle regime, the 32 fs pulses have been injected through a hollow-fiber filled with neon gas to generate supercontinuum pulses then temporally compressor by multilayer-chirped mirrors. This arrangement enabled the generation of a five-octavewide supercontinuum ultrafast pulses over a wide frequency range from 500 THz to 333 THz. That broad bandwidth has allowed to produce transform limited pulses of 6.01 fs time duration and 120 GW peak power that exceeds the previously observed value of 80 GW for similar pulses. The observed results may give an opportunity to generate ultrashort pulses with extreme short optical wavelength using high harmonic generation that are needed for ultrafast spectroscopy in femtochemistry.
**Keywords:** Transform-Limited, Time-Band-Width-Product, Ultrafast Pulses, Supercontinuum Generatio

**B-739. Res_Id: 444J Res_Wcode: 1802**
**Optimizing The Optical Throughput of a Neon-Filled Hollow-Core Fiber for Ultra-Broadband Sub-5 Fs Pulses**

walid tawfik

*Journal of Optoelectronics and Advanced Materials, 181: 213-219, (2016), IF: 0.383*

In this work, new optimization conditions to increasing the optical throughput of neon-filled hollow-core fiber for very broad optical bandwidth and reach extremely-short laser pulses are represented. In the used method, seed pulses from a Ti:sapphire mode locked laser of 18 fs pulses with energy 5 nJ/pulse were injected into a chirped pulse amplifier (CPA) to reach 2.6 mJ per pulse. By controlling the CPA compressor, the output pulses were tuned from 32 – 56 fs. These pulses were used to generate supercontinuum spectra through nonlinear interaction with neon gas filled hollow-fiber by self-phase modulation. The generated output pulses from the fiber were compressed using chirped mirrors to perform dispersion compensation. The observed results reveal that, the output of the fiber can be tuned from about 12 to 94 THz by varying the chirping of input pulses at different pressure of the neon gas. Under optimum conditions of broadband-width at 94 THz, the generated pulses reached the shortest possible time duration of 4.86 fs. The observed results can give an opportunity to control the progression of strong-electric-field interactions on the ultrafast time scale and can be applied to regenerate attosecond pulses in the deep ultraviolet range
Keywords: Sub-5 Fs, Ultra-Broadband, Femtosecond Laser, Self-Phase Modulation, Chirped Pulse

**B-740. Res_Id: 454J Res_Wcode: 1229**
**Quantitative Determination of Copper in a Glass Matrix Using Double Pulse Laser Induced Breakdown and Electron Paramagnetic Resonance Spectroscopic Techniques**

Ahmed A.I. Khalil and Mohamed A. Morsy

*Talanta, 154: 109-118, (2016), IF: 4.035*

A series of lithium–lead–borate glasses of a variable copper oxide loading were quantitatively analyzed in this work using two distinct spectroscopic techniques, namely double pulse laser induced breakdown spectroscopy (DP-LIBS) and electron paramagnetic resonance (EPR). DP-LIBS results measured upon a combined nanosecond lasers irradiation running at 266

nm and 1064 nm pulses of a collinear configuration directed to the surface of borate glass samples with a known composition. This arrangement was employed to predict the electron's temperature (Te) and density (Ne) of the excited plasma from the recorded spectra. The intensity of elements' responses using this scheme is higher than that of single-pulse laser induced breakdown spectroscopy (SP-LIBS) setup under the same experimental conditions. On the other hand, the EPR data shows typical Cu (II) EPR-signals in the borate glass system that is networked at a distorted tetragonal Borate-arrangement. The signal intensity of the Cu (II) peak at $g\perp=2.0596$ has been used to quantify the Cu-content accurately in the glass matrix. Both techniques produced linear calibration curves of Cu-metals in glasses with excellent linear regression coefficient (R2) values. This study establishes a good correlation between DP-LIBS analysis of glass and the results obtained using EPR spectroscopy. The proposed protocols prove the great advantage of DP-LIBS system for the detection of a trace copper on the surface of glasses.
Keywords: Borate Glass; Dp-Libs; Epr; Quantitative Analysis; Plasma Parameters

## B-741. Res_Id: 456J Res_Wcode: 1231 Laser Produced Plasma Diagnosis Of Carcinogenic Heavy Metals In Gallstones

Mohammad A. Gondal, Mohamed A. Shemis, Ahmed A. I. Khalil, Mohamed M. Nasr and Bilal Gondal

*Journal of Analytical Atomic Spectrometry, 31: 506-514, (2016), IF: 3.379*

Gall bladder cancer [GBC] is a highly fatal malignancy. Geographically, regions of high prevalence of gallstones [GSs] have shown to have higher rates of GBC, which is now a recognized risk factor for GBC. Heavy metal toxicity has also been reported to be associated with GBC. An effort therefore at recognizing and avoiding potential risk factors for GBC occurrence is therefore paramount. It is also known that over time heavy metals can accumulate in the biliary system and hence in GSs. We hereby measured the levels of heavy metals in GSs via a highly sensitive technique using a laser produced plasma by comparing the levels of heavy metals in a 29 year old man to a 65 year old man. For this direct spectral analysis of GSs, a laser produced plasma was created by focusing a 266 nm pulsed UV laser generated by fourth harmonics of a Nd:YAG laser on GS samples. For the first time to the best of our knowledge, the plasma parameters, electron temperature and electron density for the GS matrix were computed from the Boltzmann distribution of the upper energy levels and Stark broadening of selected spectral lines. The determination of plasma parameters is important to satisfy the optically thin plasma (to avoid self-absorption) and obtain local thermodynamic equilibrium (LTE) conditions, which are critical for the quantitative analysis. The heavy metal concentrations of chromium, lead, cadmium, nickel and mercury were determined in two different GS samples by recording the laser induced breakdown spectra (LIBS) and by drawing the calibration curves of the spectral lines of carcinogenic metals like chromium, lead, cadmium, nickel and mercury. The results obtained from LIBS were crosschecked using a standard inductively coupled plasma-mass spectrometer (ICP-MS) technique. The effect of delay time (time between the laser pulse and the ICCD camera gate opening) and laser energy on the intensity of the spectral lines of lead, chromium and calcium was also investigated. The system developed in this study is highly applicable for the rapid analysis of any biological or human tissue samples.
Keywords: Libs, Plasma Diagnostics, Gallstones.

## B-742. Res_Id: 603J Res_Wcode: 1626 Fluorescein Dye Derivatives and Their Nanohybrids: Synthesis, Characterization and Antimicrobial Activity

Nabel A. Negm, Maram T.H. Abou Kana, Ali A. Abd-Elaal and Ahmed H.M. Elwahy

*Journal of Photochemistry and Photobiology, B: Biology 162: 421-433, (2016), IF: 3.03*

Fluorescein (resorcinolphthalein) is a synthetic organic photoactive dye compound soluble inwater, alcohol and polar solvents. It is widely used as a fluorescent tracer inmedicinal and biological applications and tumor infected tissues tracer. In this study, fluorescein (F) was condensed by five coupling agents namely: p,p-phenylene diamine, p-hydroxy aniline, o-hydroxy aniline, p-methoxy aniline and p-methyl aniline in a molar ratio of 2(F):1 (coupling agent). The chemical structures of the synthesized fluorescein derivatives were confirmed using: microelemental analysis, FTIR spectroscopy, 1H-NMR spectroscopy, and mass spectroscopy. The synthesized compounds were loaded on chemically prepared silver nanoparticles via reduction reaction of silver nitrate. The structures and properties of the formed fluorescein derivatives silver nanohybrids were determined using: UV/Vis spectroscopy, TEM images and dynamic light scattering (DLS). The synthesized compounds and their nanohybrids were evaluated for their antimicrobial activities against different bacterial strains and fungi. The results showed that the formed fluorescein derivatives silver nanohybrids are in moderate diameter range, and the loading of the synthesized compounds protect the silver nanoparticles against coagulation. The antimicrobial activity against the studied microorganisms was comparable to the standard used. Moreover, the antimicrobial activity was increased considerably in case of using fluorescein derivatives silver nanohybrids. The antimicrobial activities were correlated to the chemical structures of the compounds, diameter of the formed nanohybrids and to the nature of the tested bacterial strains. The mechanism of the antimicrobial action of the synthesized compounds and their nanohybrids was proposed.
Keywords: Fluorescein, Tem, Dynamic Light Scattering, Nanohybrids, Antimicrobial Activity

## B-743. Res_Id: 601J Res_Wcode: 1624 Enhancement of Fluorescence, Photo-Physicalparameters and laser Performance of pyrromethene (PM597) Laser dye by Ag nanoparticles In Different media

Ibraheem A.Alhijry, A.-S.Gadallah, H.I.Abdelkader, MaramT.H.AbouKana

*Journal of Luminescence, 171: 98-105, (2016), IF: 2.693*

+++

The effectofsurfaceplasmonresonance(SPR)ofsilvernanoparticles(Ag NPs),exposuretoradiation,on the opticalandphoto-physicalpropertiesofpyrromethene(PM597)laserdyeinliquidands olidmedia wasassessed.2-hydroxyethylmethacrylatewasusedashomo-monomerandhomo-polymer,while2-hydroxyethylmethacrylate/methylmethacrylatewereusedasco-monomerandco-polymerhosts.Ag NPs waspreparedandconfirmed itssizebyhighresolutiontransmissionelectronmicroscope (HRTEM), UV/vis absorptionspectroscopyandalso,theoreticallybyusingMietheory. Themolarconcentrationof preparedNPswas C¼3.39110————————————————9 mol/L. 40%C(1.356110————————————————9 mol/L) AgNPswasfoundtohavethe optimum distancewith(1110————————————————4 mol/L PM597inliquidmediumand1110 ————————————————3 mol/L PM597insolid medium) dyemoleculesaccordingtoMetalEnhancementFluorescence(MEF )model.[40%CAgNPs: 1110————————————————3 mol/L PM597]complexsampleshad3.12cm ————————————————1 and 3.89cm————————————————1 gain valuesinhomo-andco- polymer media,whileparentPM597dyehad2.5cm ————————————————1 and 3.45cm————————————————1 gain values.Also,amplified spontaneous emission(ASE)valueofcomplexsampleswas0.455%and0.538%in caseofhomo-andco- polymer respectively.Whileitwas0.4%and0.457%incaseofparentPM597d yeinthesamesequent media. Finally,photo-stabilitiesofcomplexsampleshadhighervaluesinco-monomerandco-polymer hosts comparedwithrespecttotheirstabilitiesinhomo-monomerandhomo-polymerhosts.

**Keywords:** Silvernanoparticles; Pyrromethene (597)dyelaser; HEMA (homo-monomer,homo-polymer); HEMA/MMA (co-monomer,co-polymer); Optical andphoto-physicalproperties; Localized surface Plasmonresonance

## B-744. Timing Stability Enhancement of an Erbium Doped Mode Locked Fiber Laser Using Sesam Mirror

G. Afifi, M. Atta Khedr, Y. Badr , M. Danailov, P. Sigalotti, P. Cinquegrana, M.B. Alsous and A.R. Galaly

*Optical Fiber Technology, 29: 74-83, (2016), IF: 1.6*

We report on an examination of pulse timing stability of a home built Erbium Doped Fiber Laser (EDFL) passively mode locked via nonlinear polarization rotation by inserting semiconductor saturable absorber mirror (SESAM) in laser cavity. A very low root mean square (RMS) timing jitter (less than 27 fsec) and faster self-starting mode locking have been established. In order to get clear, low noise signal for time resolving measurements, synchronization of EDFL laser with an external high precision electronic oscillator have been established. Subsequently, it is synchronized and optically cross-correlated with a Ti:Sapphire laser source (Micra). The measured relative timing jitter was found to be less than 65 fsec. In this way, the two, well synchronized Ti:Sapphire and EDFL laser pulses prove to be a powerful tool for time resolving measurements

**Keywords:** Fiber Laser; Jitter; Timing and Mode Locking; Optical Cross Correlation.

## B-745. Acute Hematologic, Hepatologic, and Nephrologic Changes after Intraperitoneal Injections of 18 Nm Gold Nanoparticles In Hamsters

Hazem Mohamed Saleh, Omar A Soliman, Mohamed Osama Elshazly, Mohamed Osama Elshazly, Adel K Gohar and Taher A Salaheldin

*International Journal of Nanomedicine, 11: 2505-2513, (2016), IF: 4.32*

In vivo responses to gold nanoparticles (GNPs) vary not only according to the size, shape, surface charge, and capping agent of GNPs but also according to the animal model, the route of administration, and the exposure frequency and duration. We illustrate here the changes in some hematologic parameters, in the hepatic and renal functions, and in the histopathology of solid organs after multiple intraperitoneal injections of 18 nm GNPs in adult male Syrian golden hamsters. We scored the histopathological changes in the liver and kidneys to grade the deleterious effects. Multiple intraperitoneal injections of 18 nm GNPs in hamsters were nonlethal in the short term but resulted in macrocytosis and hypochromasia, leukocytosis, neutrophilia, lymphocytosis, and monocytosis. The hepatic and renal functions showed nonsignificant changes; however, histopathological examination showed hepatic and renal alterations ranging from mild to marked degeneration, with occasional necrosis of hepatocytes and tubular epithelium.
Keywords: In Vivo, Hamsters, Nanogold, Acute

## B-746. Laser acupuncture as an adjunctive therapy for spastic cerebral palsy in children

Ola A. Dabbous, Yousry M. Mostafa, Hossam A. El Noamany,Shrouk A. El Shennawy and Mohammed A. El Bagoury

*Lasers Med Sci, 31: 1061-1067, (2016), IF: 2.461*

Laser acupuncture is widely used as an alternative line of treatment in several chronic pediatric diseases. To investigate whether biostimulation by low-level laser on acupuncture points adds a clinical benefit to conventional physiotherapy in hemiplegic spastic cerebral palsy (CP) children. Forty spastic hemiplegic cerebral palsy children by age 1– 4 years were chosen from the pediatric outpatient clinic of the National Institute of Laser Enhanced Sciences (NILES), Cairo University, and Menofyia University hospitals. They were randomly divided into control and study groups; 20 children each. Both groups received physiotherapy for 3 months, while only the study group also received laser acupuncture (low-level laser 650 nm with 50 mW power was applied at each acupoint for 30 s giving an energy density of 1.8 J/cm2). Preassessment

and postassessment of muscle tone, the range of motion (ROM), and gross motor function measurements (GMFMs) were obtained, and the results were statistically analyzed. Comparison between posttreatment measures for the control vs. study groups showed significant difference in muscle tone (wrist flexors and plantar flexors) in favor of the study group, while range of motion showed no significant differences. GMFM showed no significant difference in total score while there was a significant difference in goal total score (sum of % scores for each dimension identified as goal area divided by number of goal areas) in favor of the study group. Laser acupuncture has a beneficial effect on reducing spasticity in spastic cerebral palsy and may be helpful in improving their movement.

**Keywords:** Laser; Acupuncture; Cerebral Palsy; Spasticity.

## B-747. Photodecomposition, photomutagenicity and photocytotoxicity ofretinyl palmitate under He–Ne laser photoirradiation and its effectson photodynamic therapy of cancer cells in vitro

Tarek Ibrahima, Mahmoud N.El Rouby, El-Sayed A.M. Al-Sherbinia, Amr H.El Noury and Mona E. Morsy

*Photodiagnosis and Photodynamic Therapy, 13: 316-322, (2016), IF: 2.412*

**Objective:** Our aim was to study photodecomposition, photomutagenicity and cytotoxicity of retinylpalmitate (RP), a principal storage form of vitamin A in humans and animals, under He–Ne laser pho-toirradiation. Moreover, the effect of different concentrations and timing protocol of antioxidants onphotodynamic therapy (PDT) is contradictory, so the effect of RP (as antioxidant) on the PDT cytotoxicitywas studied.Methods: Photomutagenicity was tested by Ames test. Photodecomposition was studied by UV–visspectroscopy. Cytotoxicity was measured with MTT-assay. Moreover, the effect of PDT, using hemato-porphyrin derivatives (HpD) as photosensitizer under He–Ne laser irradiation (10 J/cm2), was studiedon HeLa cells either with or without RP (1–100 1M) which incubated with the cells for short or longincubation period (1 h or 24 h) prior to PDT. **Results:** No photodecomposition of RP alone was obseved whereas there is a little photodecompositionof RP only in presence of HpD under irradiation with He–Ne laser. Moreover, no photomutagenicity wasobserved in Salmonella typhimurium strains under laser irradiation in presence or absence of HpD. RPalone (1–100 1M) significantly decrease the viability of HeLa cells. Laser irradiation of HeLa cells pre-incubated with RP alone for 24 h showed further significant decrease in viability of the cells. While RPincubations for 1 h before PDT had slight effect on the cells, 24 h incubation before PDT enhanced thecytotoxicity of PDT on HeLa cells.**Conclusions**: RP can be used 24 h before PDT to enhance its effects. RP is not mutagenic under irradiationwith He–Ne laser.

**Keywords:** Photodecompositionphotodynamic Therapy (PDT) Photomutagenicityretinyl Palmitate (RP)Vitamin

## B-748. Targeting doxorubicin encapsulated in stealth liposomes to solid tumors by non thermal diode laser

Magdy M. Ghannam, Reem El Gebaly and Maha Fadel

*Lipids In Health And Disease, 15(1):68: 1-8, (2016), IF: 2.137*

Background: The use of liposomes as drug delivery systems is the most promising technique for targeting drug especially for anticancer therapy. Methods: In this study sterically stabilized liposomes was prepared from DPPC/Cholesterol/PEG-PE encapsulated doxorubicin. The effect of lyophilization on liposomal stability and hence expiration date were studied. Moreover, the effect of diode laser on the drug released from liposomesin vitro and in vivo in mice carrying implanted solid tumor were also studied. Results: The results indicated that lyophilization of the prepared liposomes encapsulating doxorubicin led to marked stability when stored at 5 °C and it is possible to use the re-hydrated lyophilized liposomes within 12 days post reconstitution. Moreover, the use of low energy diode laser for targeting anticancer drug to the tumor cells is a promising method in cancer therapy. Conclusion: We can conclude that lyophilization of the liposomes encapsulating doxorubicin lead to marked stability for the liposomes when stored at 5°C. Moreover, the use of low energy diode laser for targeting anticancer drug to the tumor cells through the use of photosensitive sterically stabilized liposomes loaded with doxorubicin is a promising method. It proved to be applicable and successful for treatment of Ehrlich solid tumors implanted in mice and eliminated toxic side effects of doxorubicin.

**Keywords**: Liposomes, Doxorubicin, Diode Laser, Anticancer

## B-749. Evaluation of the Effectiveness of Fluorescent Visualization of Bile Ducts Using Fluorescein and Ultraviolet a at Laparoscopic Cholecystectomy

Amr Mohsen, Mahmoud S. Elbasiouny, Mostafa El-Shazli, Osama Azmy and Ahmed Amr, M

*Surgical Innovation, 23(3): 261-265, (2016), IF: 1.358*

**Background.** This work studied the diagnostic effectiveness of a new technology and device to augment visualization of bile ducts at laparoscopic cholecystectomy. It depends on excitation of fluorescein in bile by ultraviolet light to get green fluorescent light emanating from these ducts. Methods. Forty laparoscopic cholecystectomy patients received fluorescein sodium injections either in the gallbladder or intravenously, followed by exposure of the expected bile ducts area to ultraviolet light that was delivered by a specially designed device. Neutral observing surgeons were asked to judge whether or not they could see fluorescent bile ducts early in the operation before they were displayed by dissection. Accordingly, specificity, sensitivity, likelihood ratios, and predictive values of the technique were calculated. **Results**. Fluorescent bile ducts were seen at an earlier stage than their detection by dissection in 33 out of 40 operations. The technique had 100% specificity, 82.5% sensitivity, 0.18 negative likelihood ratio, 100% positive predictive value, and 85.11% negative predictive value. There were no complications related to the technique. **Conclusions**. The developing ultraviolet/fluorescein technique is helpful in early localization of bile ducts at laparoscopic cholecystectomy. When fluorescence is detected in the field, the technique can be completely relied on to denote the position of bile ducts. In a few cases fluorescence is not detected. Here further

development of the device is the need to improve its sensitivity. Otherwise, the technique is quite simple and safe.

**Keywords:** Fluorescence, Cholecystectomy, Fluorescein, Ultraviolet, Bile Ducts

## B-750. Usage of Low Level Laser Biostimulation and Platelet Rich Fibrin in Bone Healing: Experimental Study

Khaled Atef El-Hayes, Ahmed Abbas Zaky, Zeinab Amin Ibrahim, Ghada Farouk Ahmed Allam and Mohamed Farouk Allam

*Dent. Med. Probl., 53: 338-344, (2016)*

Background. Experimental studies have shown that low level laser therapy (LLLT) has a positive local biostimulative effect in the early stage of bone healing. Platelet rich fibrin (PRF) also has been shown to be effective in the treatment of intrabony periodontal defects. Objectives. The objective of our experimental study was to demonstrate the combined effects of LLLT and PRF on bone healing. Material and Methods. Our experimental study was done over 80 bony cavities in 20 adult male rabbits, aged 12 months. An incision was made for exposure of the femur bone of all rabbits. Then, by using a large, round surgical bur, a perforated hole was made in the femur. The cavities induced in these rabbits were divided into 4 groups: The control group which was neither subjected to any laser irradiation nor filled with any bone substitute (group I); The bony defects were filled with PRF (group II); The cavities were subjected to low level laser (LLL) for biostimulation (group III); The cavities were subjected to LLL for biostimulation then were filled with PRF (group IV). Histological assessments of the four groups were done using a hematoxylin and eosin stain. Statistical analysis was done using ANOVA and Bonferroni tests for comparisons between the four groups. Results. The area percentage of the newly formed bone in group IV was significantly higher than the other three groups. The area percentage of the newly formed bone in group III is significantly higher than group II. Conclusions. LLLT could induce bone formation in the bone defect at a faster rate than PRF. However, a combination of both LLLT and PRF as treatment modalities could induce bone formation in the bone defect more than that of LLLT or PRF alone (Dent. Med. Probl. 2016, 53, 3, 338–344).

**Keywords:** Low Level Laser, Biostimulation, Experimental Study, Bone Healing, Platelet Rich Fibrin.

International Publications Awards
Cairo University

# ( 2 )

# Engineering Sciences Sector

2-1 Faculty Engineering
2-2 Faculty of Computers and Information
2-3 Institute of Statistical Studies and Research
2-4 Faculty of Regional and Urban Planning

# Total No. of Publication for Engineering Sciences Sector

| Faculty | 2006 | 2007 | 2008 | 2009 | 2010 | Total |
|---|---|---|---|---|---|---|
| Engineering | 56 | 79 | 109 | 140 | 131 | 515 |
| Computers and Information | 2 | 3 | 4 | 11 | 6 | 26 |
| Regional and Urban Planning | | | | | | 0 |
| Statistical Studies and Research Institute | 8 | 6 | 11 | 7 | 4 | 36 |
| **Total** | 66 | 88 | 124 | 158 | 141 | 577 |

| Faculty | 2011 | 2012 | 2013 | 2014 | 2015 | 2016 | Total |
|---|---|---|---|---|---|---|---|
| Engineering | 198 | 228 | 240 | 167 | 196 | 227 | 1256 |
| Computers and Information | 32 | 35 | 0 | 19 | 24 | 20 | 130 |
| Regional and Urban Planning | | 1 | 0 | 0 | 0 | 6 | 7 |
| Statistical Studies and Research Institute | 17 | 43 | 43 | 5 | 13 | 10 | 131 |
| **Total** | 247 | 307 | 283 | 191 | 233 | 263 | 1524 |

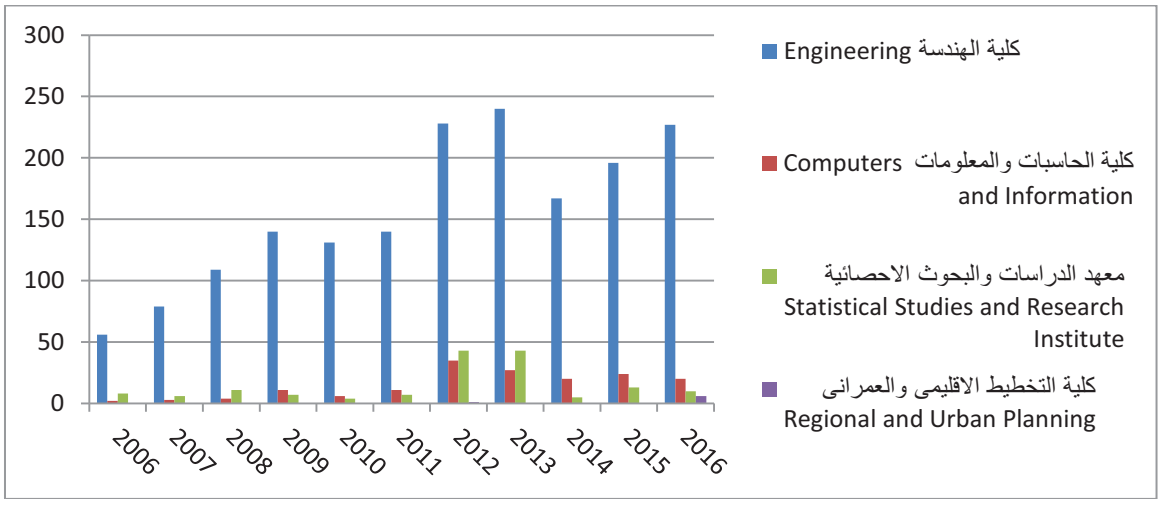

## الأبحاث المنشورة دوليا من ٢٠٠٦ الى ٢٠١٦ لكليات ومعاهد قطاع العلوم الهندسية

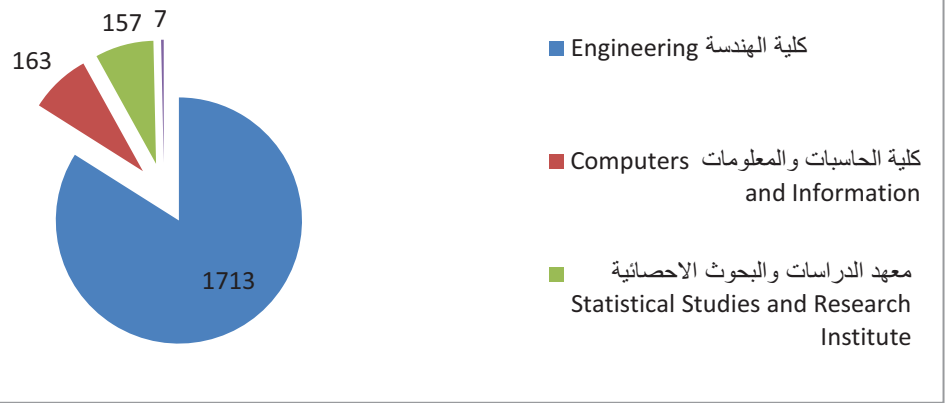


## تطور مجموع الأبحاث المنشورة لكل سنة
## Sum of published researches

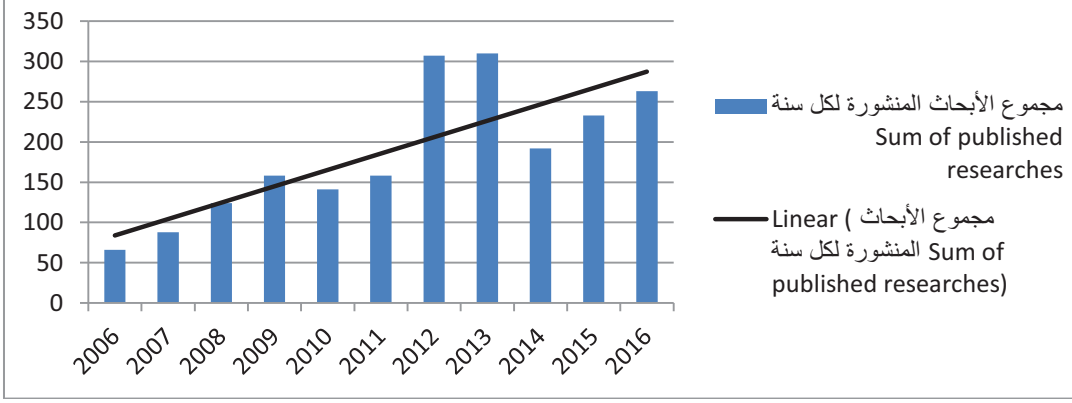

## Faculty of Engineering

### *Dept. of Architectural Engineering*

### E-1. Parametric-Based Designs for Kinetic Facades to Optimize Daylight Performance: Comparing Rotation and Translation Kinetic Motion for Hexagonal Facade Patterns

Ayman Hassaan Ahmed Mahmoud and Yomna Elghazi

*Solar Energy, 126: 111-127 (2016) IF: 3.685*

Recent literature shows that experimentation in kinetics and architectural skins is more widely introduced as a solution for environmental-related design issues. Facades and elements are transformed in kinetic living creatures changing in synchrony with the surrounding environment. Through the lens of morphology, this research explores the possibilities of kinetic composition afforded by facades in motion. It presents a method for the evaluation of kinetic facades system performance using experimental approach. The experiments investigate improving daylight performance through the design and motion of kinetic facades using various integrated software. The impact of kinetic motion of hexagonal pattern on south-facing skin to control the daylight distribution in an office space is studied using parametric simulation technique. Results demonstrate the analysis of rotational and translation kinetic motions at the early design stage compared to a traditional window (base case). Finally, possible configurations to enhance daylight performance are suggested.

**Keywords:** Kinetic facade; Daylight; Parametric Design; Building skin

### E-2. Roof Top PV Retrofitting: A Rehabilitation Assessment Towards Nearly Zero Energy Buildings in Remote Off-Grid Vernacular Settlements in Egypt

Marwa Dabaieh, Nahla N. Makhlouf and Omar M. Hosny

*Solar Energy, 123: 160-173 (2016) IF: 3.685*

Vernacular buildings in Egypt express a variety of passive low-tech approaches in design and construction to achieve human comfort and fulfil inhabitants' requirements. They have been devised to suit living in regions where local inhabitants had to invent various passive building strategies to live under severe local climatic conditions without depending on fossil fuels. This paper discusses a retrofitting approach for off-grid vernacular buildings in the Western Desert of Egypt. The study hypothesis argues that, when retrofitted and equipped with renewable energy solutions, vernacular structures can act as nearly zero energy buildings. A post occupancy evaluation was used as an assessment tool for two pilot projects that served as case studies. Results showed that combining vernacular passive strategies with affordable active renewables such as roof top solar panels results in a hybrid energy efficient retrofitting solution for deprived off-grid vernacular buildings. The intention is for the results to act as a basis for future retrofitting that would take into account the challenges and obstacles inherent in such work. This is an aim capable of contributing to a reduction of energy consumption that would also encourage retrofitting using renewable solutions for existing housing stock in Egypt.

**Keywords:** Roof Top PV; Vernacular Retrofitting; Nzeb; Energy Poverty; Post Occupancy Evaluation

### E-3. Participatory Landscape: Better Scenario for Poor Egyptian Urban Settings in Existing and New City Districts—Case of Monshaet Nasser and 6Th October City

Asmaa Abdel Aty Mohamed, Ahmed Amin and Ahmed Shalaby

*Journal of Urban Planning and Development, 142: 4015002-4015002 (2016) IF: 2.246*

Participatory landscape approaches are currently being positioned as the essential basis for sustainable landscape development. However, with the current democratic transform and the consequent decentralization of the spatial planning policy in Egypt, no practices have been conducted in this field. Accordingly, there is a vital need for coherent and integrated approaches for the practical application of participatory landscape. This paper represents one of a series of research papers targeting this aim. It focuses on poor urban settings in existing informal areas and in new cities' districts, represented by the case studies of Monashaet Nasser and the sixth district in the 6th of October city, respectively, which are used to carry out the questionnaires, followed by a statistical analysis and illustrative causal loop diagrams. The questionnaire integrates measuring local residents' willingness and participation methods together with the practitioners' recommendations for their degree of involvement as compared with the other stakeholders, with the functional, environmental, aesthetical, economic, maintainability, and sociability quality aspects of the landscape that would be achieved. The tests undertaken in this research were carried out through a statistical analysis using the statistical package for social sciences (SPSS) program, followed by an illustrative analysis for the results represented by the causal loop diagrams, which show a clear representation for the roles of each of the residents and stakeholders in the process. The results illustrate the fact that although the two case studies were from the same economic level, there were variations among most of the findings concerning the local residents' participation method. They indicated that the local residents in existing poor urban settings prefer to participate with their effort only, whereas those living in the poor new cities' districts are willing to participate with their money, time, and effort. Moreover, it was found that the landscape aspects that would be positively affected are the maintainability aspects for the existing area and the sociability aspects for the relatively new district, with traces of negative effects on the functional and aesthetical landscape qualities. This highlights the challenges for the decision makers when constructing their implementation plans, to achieve the balance among all roles of stakeholders to avoid any negative effects and overcome the distrust landscape problems that have been compositely formed upon past participatory experiences, especially in existing poor settings.

**Keywords:** Urban Development, Public Participation, Community Development, Urban Landscape.

***Dept. of Chemical Engineering***

## E-4. Identifying and Visualizing Functional Pam Diversity Across Crispr-Cas Systems

Ryan T. Leenay, Kenneth R. Maksimchuk, Rebecca A. Slotkowski, Roma N. Agrawal, Ahmed A. Gomaa, Alexandra E. Briner, Rodolphe Barrangou and Chase L. Beisel

*Molecular Cell, 62: 137-147 (2016) IF: 13.958*

CRISPR- Cas adaptive immune systems in prokaryotes boast a diversity of protein families and mechanisms of action, where most systems rely on protospacer-adjacent motifs (PAMs) for DNA target recognition. Here, we developed an in vivo, positive, and tunable screen termed PAM-SCANR (PAM screen achieved by NOT-gate repression) to elucidate functional PAMs as well as an interactive visualization scheme termed the PAM wheel to convey individual PAM sequences and their activities. PAM-SCANR and the PAM wheel identified known functional PAMs while revealing complex sequence-activity landscapes for the Bacillus halodurans I-C (Cascade), Escherichia coli I-E (Cascade), Streptococcus thermophilus II-A CRISPR1 (Cas9), and Francisella novicida V-A (Cpf1) systems. The PAM wheel was also readily applicable to existing high-throughput screens and garnered insights into SpyCas9 and SauCas9 PAM diversity. These tools offer powerful means of elucidating and visualizing functional PAMs toward accelerating our ability to understand and exploit the multitude of CRISPR-Cas systems in nature.

**Keywords:** Crispr; Cas; PAM, PAM-SCNR; Cas9; Cpf1; Cas3; CRISPR- Cas.

## E-5. Impact of Ambient Air Temperature and Heat Load Variation on the Performance of Air-Cooled Heat Exchangers in Propane Cycles in Lng Plants – Analytical Approach

M.F.M. Fahmy and H.I. Nabih

*Energy Conversion and Management,121:22-35(2016) IF:4.801*

An analytical method is presented to evaluate the air flow rate required in an air-cooled heat exchanger used in a propane pre-cooling cycle operating in an LNG (liquefied natural gas) plant. With variable ambient air inlet temperature, the air flow rate is to be increased or decreased so as to assure and maintain good performance of the operating air-cooled heat exchanger at the designed parameters and specifications. This analytical approach accounts for the variations in both heat load and ambient air inlet temperature. The ambient air inlet temperature is modeled analytically by simplified periodic relations. Thus, a complete analytical method is described so as to manage the problem of determining and accordingly regulate, either manually or automatically, the flow rate of air across the finned tubes of the air-cooled heat exchanger and thus, controls the process fluid outlet temperature required for the air-cooled heat exchangers for both cases of constant and varying heat loads and ambient air inlet temperatures. Numerical results are obtained showing the performance of the air-cooled heat exchanger of a propane cycle which cools both NG (natural gas) and MR (mixed refrigerant) streams in the LNG plant located at Damietta, Egypt. The inlet air temperature variation in the summer time has a considerable effect on the required air mass flow rate, while its influence becomes relatively less pronounced in winter.

**Keywords:** Air-Cooled Heat Exchangers Lng Propane Cycle

## E-6. Enhancement of the Efficiency of the Open Cycle Phillips Optimized Cascade Lng Process

M.F.M. Fahmy , H.I. Nabih and M. El-Nigeily

*Energy Conversion and Management, 112: 308-318 (2016) IF: 4.801*

This study aims to improve the performance of the Open Cycle Phillips Optimized Cascade Process for the production of liquefied natural gas (LNG) through the replacement of Joule–Thomson (JT) valves by expanders. The expander has a higher thermodynamic efficiency than the JT valve. Moreover, the produced shaft power from the expander is integrated into the process. The study is conducted using the Aspen HYSYS-V7 simulation software for simulation of the Open Cycle Phillips Optimized Cascade Process having the JT valves. Simulation of several proposed cases in which expanders are used instead of JT valves at different locations in the process as at the propane cycle, ethylene cycle, methane cycle and the upstream of the heavies removal column is conducted. The optimum cases clearly indicate that expanders not only produce power, but also offer significant improvements in the process performance as shown by the total plant power consumption, LNG production, thermal efficiency, plant specific power and CO2 emissions reduction. Results also reveal that replacing JT valves by expanders in the methane cycle has a dominating influence on all performance criteria and hence, can be considered as the main key contributor affecting the Phillips Optimized Cascade Process leading to a notable enhancement in its efficiency. This replacement of JT valves by liquid expanders at different locations of the methane cycle encounters power savings in the range of 4.92–5.72%, plant thermal efficiency of 92.64–92.97% and an increase in LNG production of 5.77–7.04%. Moreover, applying liquid expanders at the determined optimum cases for the different cycles, improves process performance and shows a plant power saving of 5.80%, plant thermal efficiency of 92.81% and an increase in LNG production of 7.0%.

**Keywords:** Natural Gas Liquefaction Process Lng Jt Valves

## E-7. Conceptual Insights to Debottleneck the Network Pinch in Heat- Integrated Crude Oil Distillation Systems without Topology Modification

Mamdouh A. Gadalla, Omar Y. Abdelaziz and Fatma H. Ashour

*Energy Conversion and Management, 126: 329-341 (2016) IF: 4.801*

Heat exchanger network pinch sets the limitations of heat recovery for existing network topologies. Improving the heat recovery within a pinched-network is independent of the areas of individual exchangers present in the network, rather the topology of the network must be altered. Such a change in the topology can be very capital intensive and in many cases seems not easy to implement. This research aims to overcome the Network Pinch through proposing process operation changes, avoiding network topology alterations; hence, debottlenecks the heat-integrated systems towards further energy savings beyond

the maximum heat recovery limitations. A new graphical representation is recently proposed to simulate existing preheat trains/networks with all energy equipment. The recent graphical representation is employed in this work to identify the pinching matches that limit heat recovery. Therefore, such graphs are key tools to identify potential process changes by which the Network Pinch is overcome. New graphs are constructed involving hot stream temperatures against cold stream temperatures. Existing exchangers are described by straight lines, with slopes related to flows of process streams and heat capacities. Exchanger matches touching the line where hot outlet stream temperature equals cold inlet stream temperature are pinching matches; this condition corresponds to absolute maximum heat recovery ($\Delta T = 0$). Potential process changes within a distillation unit are identified to relax the Network Pinch and further heat recovery is maximised. The slope of such an exchanger match is decreased or the location of the pinching match is altered keeping the same slope. These changes are translated into process changes within the crude oil distillation unit. Accordingly, the process changes are determined based on which match is pinched besides its location within the network. An illustrative example shows that process changes overcome the Network Pinch and energy recovery is increased by 14% beyond the maximum level achieved for the existing process conditions. Capital investments imposed are minor compared with substantial energy cost savings.

**Keywords:** Network Pinch; Energy Efficiency; Retrofit; Heat Exchanger Network; Crude Distillation Unit; Process Integration

## E-8. Pressure Influence on Pyrolysis Product Properties of Raw and Torrefied Miscanthus: Role of Particle Structure

A. Wafiq, D. Reichel and M. Hanafy

*Fuel, 179: 156-167 (2016) IF: 3.611*

Compared to coal, few studies were performed on biomass pyrolysis at elevated pressures, high heating rates, and moderate temperatures, the conditions usually prevailing in commercial fluidized bed gasifiers. In this work, Miscanthus is selected as one of the most promising biomass energy crops which is characterized by high annual yield and energy ratio. The effect of pressure on the product yields, gas composition, and char structure for pyrolysis of pulverized raw and torrefied Miscanthus was investigated in a drop tube reactor. Torrefaction was carried out at 250 C for 30 min, while pyrolysis of raw and torrefied Miscanthus was performed at 800 C in a pressure range of 1–30 bar. The gases were analyzed using a micro-GC, while the chars were characterized using proximate and ultimate analysis, porosity and BET surface area measurements, and Scanning Electron Microscopy (SEM). It was found that the pyrolysis pressure significantly affects the yields and properties of products, and that torrefaction significantly changes properties and pyrolysis behavior of Miscanthus. The torrefied Miscanthus was found to have higher char yields and char porosities at all the investigated pressures, while the raw Miscanthus was found to have higher gas yields, and higher liquid yields at high pressures. The char yield of both raw and torrefied Miscanthus increases till 10 bar and did not show any further changes at higher pyrolysis pressures. The yield of CO2 increased with pyrolysis pressure for both raw and torrefied Miscanthus, while the yield of the high molecular weight gases like C2H4 and C2H6 decrease with increasing pyrolysis pressure and totally disappear at 30 bar. Hydrogen represented the major difference in the gas yield trend for raw and torrefied Miscanthus. A non-monotonous trend with pressure was observed for the liquid product yield of raw Miscanthus, while a decreasing trend with asymptote-like nature took place for torrefied Miscanthus. The different pyrolysis behavior of raw and torrefied Miscanthus evidenced in the liquid product yield trend, char porosity and SEM images might be attributed to the force balance on the particles' structure which led to extensive fragmentation occurrence in the 10–15 bar range for raw Miscanthus chars, and its absence in the whole pressure range for torrefied Miscanthus chars, a hypothesis that is to be confirmed in future research work. The results obtained in this study are important inputs for modeling industrial fluidized bed gasifiers working on Miscanthus.

**Keywords:** Miscanthus, Pyrolysis, Pressure, Torrefaction, Fragmentation, Char

## E-9. The Rmodynamic Analysis for the Sorptive Removal of Cesium and Strontium Ions Onto Synthesized Magnetic Nano Zeolite

O.A. Abdel Moamen, H.A. Ibrahim, N. Abdelmonem and I.M. Ismail

*Microporous and Mesoporous Materials, 223: 187-195 (2016) IF: 3.349*

The present study aims at examining the feasibility of using synthesized magnetic nano zeolite for the sorptive removal of cesium and strontium ions existing in the liquid radwaste stream. Csþ/Naþ and Sr2þ/ Naþ binary ion exchange experiments were performed in the batch mode at different three temperatures (298,303 and 313 K), optimized proton concentration (pH), equilibrium time and constant total normality. The thermodynamic analysis of both binary systems was performed using four types of model equations: Langmuir; Freundlich; Radlish-Peterson and thermodynamic equilibrium models. The extended DebyeeHuckel relation and the Wilson equation were used to estimate the solution and the solid phase activity coefficients, respectively. The results obtained during this study demonstrated the correlation of the four examined models with the experimental equilibrium data, which proved to be satisfactory. On the other hand, the thermodynamic non-idealities was found to give the best results. Thermodynamic parameters such as enthalpy change, Gibbs free energy change and entropy change were also calculated. The obtained affirmative results demonstrated that the synthesized magnetic nano zeolite can be used as an efficient sorbent for the removal of Csþ and Sr2þ ions from the contaminated solutions.

**Keywords:** Radioactive Waste Stream; Cs+ and Sr2+ Ions; Magnetic Nano-Sized Zeolite; Kiellend Plot.

## E-10. Preparation of Al2o3/Alf3-Supported Ruthenium Catalysts for the Hydrogenolysis of Biodiesel-Derived Crude Glycerol

Tamer S. Ahmed, Omar Y. Abdelaziz and George W. Roberts

*Industrial and Engineering Chemistry Research, 55 (19): 5536-5544 (2016) IF: 2.567*

Hydrogenolysis of biodiesel-derived glycerol to value-added chemicals has emerged as an innovative approach to biowaste valorization for a more sustainable society. In the present work, Ru catalysts on Al2O3/AlF3 supports with different AlF3 content were prepared by the aqueous incipient wetness method and tested in the reaction of glycerol hydrogenolysis for the first time. The prepared catalysts were characterized by neutron activation analysis, N2 physisorption, and H2 chemisorption techniques. The catalytic hydrogenation of crude glycerol was performed at a temperature of 473 K and a hydrogen pressure of 4.0 MPa, using a 5 wt□% glycerol aqueous solution for 4 h with comprehensive characterization of liquid- and gas-phase products. Texture, structure, and activity of the prepared catalysts were significantly affected by the fluoridation. To understand the mechanism of possible reactions for glycerol hydrogenolysis better, the effects of pH and individual hydrogenolysis of most of the products of the glycerol reaction were investigated

**Keywords:** Glycerol Hydrogenolysis; Ruthenium; Catalysts; Biodiesel; Gamma Alumina; Fluorinated Alumina

## E- 11. Investigation and Performance Improvement of the Propane Precooling Cycle in the Propane Precooled Mixed Refrigerant Cycle Liquefaction Process

M. F. M. Fahmy, H. I. Nabih and M. R. Abd El-Aziz

*Industrial and Engineering Chemistry Research, 55: 2769-2783 (2016) IF: 2.567*

This study aims to improve the performance of the propane precooling cycle used for precooling of both natural gas and mixed refrigerant in the Propane Precooled Mixed Refrigerant Cycle (PPMRC) in an LNG plant. The unit is simulated by Aspen HYSYS version 7.3 for optimization of the propane precooling cycle to provide the minimum energy consumption of the propane compressors and the two aircoolers. The effect of subcooling temperature in the propane air-cooler, the number of compression stages in the propane cycle, and the quality of the natural gas feed are investigated. Results reveal the extent of reduction in power consumption on decreasing the subcooling temperature of liquid propane. The optimal subcooling temperature of liquid propane and number of compression stages in the propane cycle is determined. The positive impact attained in the performance of the propane cycle is higher for lean feed gas than for rich feed gas. The decrease of liquid propane subcooling temperature has a dominating influence on all performance criteria and, hence, can be considered as the key contributor affecting the propane precooling cycle in the PPMRC liquefaction process.

**Keywords:** Natural Gas ; Liquefaction ; Ppmrc Cycle.

## E-12. Investigation of Silicates as a Catalyst in Biodiesel Production: A Review

Hassan I. El Shimi, Nahed K. Attia, Guzine I. El Diwani and Shakinaz T. El Sheltawy

*International Journal of Energy Research, 40: 1743-1756 (2016) IF: 2.529*

Hiking of crude oil prices and diesel fuel shortage is incentive for the researchers to develop bioenergy sources. Biodiesel has environmental beneficial attributes, and its production processes are worthy of continued studies. Many biodiesel production processes are available but, most of them are not on a commercial scale. Biodiesel production using solid catalysts involved fewer unit operations compared with homogeneous catalyzed processes. Many heterogeneous catalysts have been extensively investigated in the recent years and well established. Researchers' focus is how to obtain active and more stable silicates catalyst that can be recycled for several times in the process. Silicates catalyst activity and stability are critically discussed in this work to assess their industrial application, as excessive purification steps could be avoided. This review provides a brief overview on semi-novel heterogeneous catalyst types 'silicates' used in the transesterification of vegetable oils for biodiesel production. Process conditions and leaching out of catalyst active sites are also highlighted. Product quality analysis is presented, in addition to concluded remarks regarding silicates as a selected catalyst. A preliminary economic assessment of biodiesel production catalyzed by the suggested catalyst 'silicates' compared with potassium hydroxide (KOH) and lime (CaO) is performed.

**Keywords:** Biodiesel; Heterogeneous; Catalyst Activity and Stability; Transesterification; Leaching-Out; Silicates; Preliminary Economic Assessment; Quality Analysis

## E-13. Three-Dimensional CFD Simulation of Industrial Claus Reactors

Abdel-Samea Abdel-Fattah, Seif-Eddeen K. Fateen,Tarek M. Moustafa and Mai M.K. Fouad

*Chemical Engineering Research and Design, 112: 78-87 (2016) IF: 2.525*

The Claus process is used extensively in the industry to recover elementary sulfur from hydrogen sulfide present in gases from refineries and natural gases. It involves thermal oxidation of hydrogen sulfide and its reaction with sulfur dioxide to form sulfur and water vapor. In this study, we used a computational fluid dynamics (CFD) tool to build a three-dimensional finite-element model that describes the detailed flow fields and chemical reactions for two different industrial cases. The first case consisted of three Claus industrial reactors in series (R1A, R1B and R1C) and the second case consists of two Claus industrial reactors in series (R2A and R2B), each having one inlet and one outlet with different operating temperatures and feed concentrations. The flow behavior and the outlet compositions of the partially packed Claus reactors at temperature range of 458–570 K, with varying SO2and H2S feed concentrations are presented and discussed. We present two sets of empirical kinetic rate equations, both of which give good agreement with the available industrial data.

**Keywords:** Claus Reactor, Comsol, Cfd Simulation, Reaction Kinetics

## E-14. Grafting of Acrylamide Onto Polysaccharides Blend Using Photo-Initiators

El-sayed, Marwa M Sorour, H Abd, Nabil Moneem, El Shalaan, Hayam Marsafy and Sahar El

*Journal of Polymers and The Environment, 24 (2016) IF: 1.969*

The present paper comprises of hydrogel synthe- sis processes using a blend of three natural polysaccharides (PsB) ''starch, chitosan and alginate'' grafted acrylamide (PsB-g-Am) using ultraviolet (UV) irradiation. The grafting process has been undergo using three different photo-ini- tiators [Dimethoxy-2-phenylacetophenone (DMPA), ben- zoin methyl ether (BME) and benzophenone (BP)]. Furthermore, different PsB/Am weight ratios have been used. The prepared hydrogel has been characterized using XRD and SEM. Grafting percentage (%G), grafting effi- ciency (%GE), grafting yield (%GY) also have been com- pared. Among the three used photo-initiators, DMPA gave the maximumattained values of%G (130 %), %GE (72 %) and %GY (89 %) followed by BME and BP, respectively. Swelling water ratio (SWR) for the grafted hydrogels in distilled water (DW) has been studied. Grafted hydrogel using DMPA photo-initiator gave the maximum SWR of 30 g/g.Am/PsBweight ratio and the used photo-initiator had a direct effect on SWR of the produced hydrogel.

**Keywords:** Polysaccharide; Hydrogel; Photo-Initiator; Ultraviolet.

## E-15. Critical Point Calculations of Multi-Component Reservoir Fluids Using Nature-Inspired Metaheuristic Algorithms

Moataz N. Shehataa, Seif-Eddeen K. Fateen and Adrian Bonilla-Petriciolet

*Fluid Phase Equilibria, 409: 280-290 (2016) IF: 1.846*

This study introduces the application of nature-inspired metaheuristic algorithms for performing critical point calculations in multicomponent reservoir fluids. These algorithms are Monkey – Krill Herd Hybrid (MAKHA), Intelligent Firefly Algorithm (IFA), Covariance Matrix Adaptation Evolution Strategy (CMAES), Artificial Bee Colony (ABC), Cuckoo Search (CS), Bare Bones Particle Swarm Optimization (BBPSO) and Flower Pollination Algorithm (FPA). Capabilities and limitations of these optimizers have been analyzed using black oil, volatile oil, and condensate reservoir fluids with fifty components. Results showed that BBPSO, IFA and FPA outperformed other nature-inspired methods for critical point calculations in tested fluids. In particular, BBPSO offered the best efficiency-reliability tradeoff for the accurate prediction of critical points in multicomponent mixtures.

**Keywords:** Critical Point Calculations; Reservoir Fluids; Stochastic Global Optimization; Nature-Inspired Method.

## E-16. Performance Analysis of Stopping Criteria of Population-Based Metaheuristics for Global Optimization in Phase Equilibrium Calculations and Modeling

Jorge Adán Fernández-Vargas, Adrián Bonilla-Petriciolet, Gade Pandu Rangaiah and Seif-Eddeen K. Fateen

*Fluid Phase Equilibria, 427: 104-125 (2016) IF: 1.846*

This paper investigates the numerical behavior of several stochastic optimization methods in phase equilibrium modeling and calculations using different stopping (also known as termination and convergence) criteria. Several optimization methods, namely, Ant Colony Optimization, Particle Swarm Optimization, Differential Evolution and Harmony Search, and some of their variants, were used to compare the capabilities and limitations of different stopping criteria in phase stability problems, phase equilibrium calculations, reactive phase equilibrium calculations and parameter estimation for local composition models. The termination conditions included improvement-, movement- and distribution-type stopping rules that track the values of objective function and/or decision variables. Drawbacks and implications of tested stopping criteria were analyzed, and results showed that the selection of the stopping condition is a key factor for reliable thermodynamic calculations via global optimization using these metaheuristics. In particular, improvement-type criteria based on the tracking of the objective function values are recommended for identifying the convergence of stochastic methods in solving new phase equilibrium problems, where the global optimum is unknown.

**Keywords:** Global Optimization; Phase Stability; Gibbs Free Energy Minimization; Parameter Estimation; Stochastic Optimization Methods; Metaheuristics; Stopping Criterion

## E-17. Gravitational Search, Monkey, and Krill Herd Swarm Algorithms for Phase Stability, Phase Equilibrium, and Chemical Equilibrium Problems

Ahmed M. E. Khalil, Seif-Eddeen K. Fateen and Adrian Bonilla-Petriciolet

*Chemical Engineering Communications, 203: 389-406 (2016) IF: 1.433*

Phase equilibrium calculations (PECs) and phase stability (PS) analysis of reactive and nonreactive systems problems are important for the simulation and design of chemical engineering processes. These problems, which are challenging, multi-variable, and non-convex, require optimization techniques that are both efficient and effective in finding the solution. Stochastic global optimization algorithms, especially swarm algorithms, are promising tools for such problems. In this study, monkey algorithm (MA), gravitational search algorithm (GSA), and Krill Herd algorithm (KHA) were used to solve PS, phase equilibrium, and chemical equilibrium problems. We have also studied the effect of adding a local optimizer at the end of the stochastic optimizer run. The results were compared to determine the strengths and weaknesses of each algorithm. When a local optimizer was used, MA was found to be a reliable algorithm in solving the problems. GSA had relatively the least numerical effort for all problems among the three algorithms but with low reliability. KHA was more reliable than other two algorithms without the use of a local optimizer. The performance of GSA, MA, and KHA was compared with firefly algorithm and cuckoo search (CS). In summary, this study found that CS algorithm was more reliable than the newly tested algorithms. Nevertheless, MA and GSA algorithms, when combined with a local optimizer, solve the thermodynamic problems as reliably and efficiently as CS.

**Keywords:** Gravitational Search Algorithm; Krill Herd Algorithm; Monkey Algorithm; Phase and Chemical Equilibrium Calculations; Phase Stability Analysis; Stochastic Swarm Algorithms.

## E-18. Unconstrained Gibbs Minimization for Solving Multireaction Chemical Equilibria Using a Stochastic Global Optimizer

Seif-Eddeen K. Fateen

*Computer Applications In Engineering Education, 24: 899-904 (2016) IF: 0.935*

This paper presents a simple method for solving multireaction chemical equilibrium problems via Gibbs Minimization through the use of a stochastic global optimizer. The method is explained at the level of upper-undergraduate chemistry or chemical engineering students. Its matlab code is also presented and explained. Four examples with varying difficulties illustrate the versatility and robustness of the method, which is simple, general, and scalable and can be easily extended to simultaneous chemical and phase equilibrium problems.

**Keywords:** Upper-Division Undergraduate; Graduate Education/Research; Chemical Engineering; Physical Chemistry; Computer-Based Learning; Equilibrium; Reactions; Thermodynamics

## E-19. A Scope on Microalgae as Potential Source of Biofuel

El-mekkawi, Samar A El-ardy, Ola A Abdelmonem, Nabil M Elahwany and Ahmed H

*Arpn Journal of Engineering and Applied Sciences, 11: 11421-11432 (2016)*

Biofuel is expected to have a role in creating a renewable, practical and environmentally intact source of energy. Biomass is converted into biofuels either via: chemical, thermo chemical, or biochemical processes. The choice of conversion process and feedstock depends on the desired product and the form of energy. The potentiality of microalgae as a biofuel source is high comparing to other sorts of biomass. However there are several basics needed for the development of this trend. Firstly, the suitable microalgae strain. Secondly, the type of cultivation system that is agreeable to the environmental consideration and ideal for energy conservation. Finally, the physical and chemical factors affect the cultivation of microalgae. Greenhouse gas emissions and energy utilization potential are pertinent to biofuel production. Life cycle assessment of biofuel production from microalgae proposes them to be preferable to fossil fuel. However; the algal technologies need more improvements to be attractive economically.

**Keywords:** Biodiesel, Biofuel, Cultivation Systems, Fatty Acids, Microalgae, Photo Bioreactor, Triacylglycerides

## E-20. Optimum Photobioreactor Design Via Optimizing Cultivation Conditions of September – October

El-mekkawi, Samar A El-ardy, Ola A Abelmonem, Nabil M Elahwany and Ahmed H

*Research Journal of Pharmaceutical, Biological and Chemical Sciences, 7: 303-311 (2016)*

Biodiesel production is considered one of the global issues. In recent years, cyanobacterial biodiesel have attracted much attention and investments. The cultivation technique using photobioreactor is mandatory for optimizing the biomass production and oil content also for producing specific products with high purity. In this research, the variance in light sources affects algal growth is recorded through fluorescent, white LED, red LED and blue LED illumination. The result oil of this diversity is analyzed using gas chromatography GC-Mass, while the protein and carbohydrates of the biomass are analyzed in order to enrich the added value. The results revealed that illumination using white LED optimizes the biomass, oil, protein and carbohydrates contents. The carbon chains have the most suitable configuration for biodiesel specifications. Finally, photo- bioreactor unit is designed in capacity of 6.4 L, composite of 8 bubble column each of volume 1L with cavity 20%. This unit produces 31.36 g dry algae per month. It can be repeated several times according to the amount of desired product.

**Keywords:** Photobioreactor; Microcystis Aeruginosa; Led; Biodiesel; Gc-Mass; Biomass.

## E-21. Preliminary Economic Estimation for Microcystis Aeruginosa Cultivated in Two Closed Cultivation Systems

El-mekkawi, Samar A El-ibiari, N N El-ardy, Ola A Abdelmonem and Nabil M Ahmed H

*Research Journal of Pharmaceutical , Biological and Chemical Sciences, 7: 2113-2117 (2016)*

In recent years, cyanobacterial cultivation has paid much attention and investments. Since cyanobacteria can be used for biodiesel production. It also has abundant bio-refinery products. The cultivation technique using photobioreactor is mandatory to ensure production of specific products with high purity. In this research, the cultivation process requirements to cultivate Microcystis aeruginosa and an economic estimation of the designed system of cultivation are discussed in details. Comparing the economic benefit of cultivation in flat plate photobioreactor with that of cultivation in bubble column photobioreactor; the results revealed that in spite of the validity of bubble column system on bench scale this system is not applicable on scaling up cultivation. Scaling up Flat Plate photobioreactor recorded positive return on investment (ROI).

**Keywords:** Economic Estimation; Microcystis Aeruginosa; Photobioreactor; Bubble Column; Flat Plat; Bio- Refinery Corresponding

## E-22. Phycoremediation of Olive Wastewater for Sustainable Production

Moustafa, S and El Shimi, H.

*International Journal of Chemtech Research, 9:567-579 (2016)*

The dual role of cyanobacteria in wastewater phycoremediation for sustainable biomass production combined with biorefinery approach is a feasible option. Phycoremediation is the process of employing algae for removing excess nutrient load from wastewater and subsequently diminish the pollution load. Industrial processes for olive production generate a considerable amount of oil wastewater, designated "olive mill wastewater" (OMW) known as alpechin, it caused serious environmental problems particularly in the Mediterranean areas

where it is generated in huge quantities in short periods of time. The objective of this research was to study the ability of three cyanobacteria strains (Nostoc muscorum, Anabaena oryzae and Spirulina platensis) to grow, either individually or in a mixture, on relatively high olive mill wastewater (OMW) concentrations of 50, 75 and 100%. The highest phenolic compounds biodegradability and maximum biomass production have been taken as main criteria in the selection of the best treatment in this study. Best results of all growth parameters and phenolic compounds degradation were obtained by mixed culture and 50% OMW and these parameters make the potential of bio-formulating such these wastes into sources for olive trees bio-organic fertilizer is the most preferable methods for the agrosustainable system. The cultivated algal species are suggested to be a promising feedstock for biodiesel, food and animal feed production according to the biochemical composition.

**Keywords:** Cyanobacteria, Phycoremediation, Sustainable, Biorefinery, Omw, Biodiesel

## E-23. Feasibility Study of Biodiesel Production From Microalgae Grown on Domestic Wastewater: A Case Study of Egypt

El Shimi, H and Moustafa S.

*International Journal of Chemtech Research, 9:904-913 (2016)*

First test diesel engines using blends with algal biodiesel are already carried out but still optimized. The purpose of microalgae growing is mainly for food and feed markets, but algal biofuel has much attention in recent years worldwide. Technical data about feasibility of cultivation system, lipids extraction and conversion into biodiesel are still limited. Potentials of microalgae have incentive the Egyptian scientists to conduct a preliminary economic assessment for 0.25 Million tons biodiesel production from microalgae grown in wastewater, which had a range of expected accuracy ±20%. Process units required have been sized. Total capital investment (TCI), total manufacturing cost (TMC), net profit, rate on return (ROR) and payback period were all calculated to be USD138134136, USD576517352, USD121584271, 88% and one year, respectively based on feedstock cost of USD400/ton and biodiesel selling price of USD2000/ton. As well, sensitivity and break-even analyses were evaluated on variations in feedstock cost, product prices and microalgae lipids content using ROR and payback time. Results recommended that for profitable algal biodiesel business, the biomass cost cannot be higher than USD530/ton, algal biodiesel price and biomass lipids content must be above USD1578/ton and 30% on dry basis, respectively.

**Keywords:** Algal Biodiesel, Transesterification, Preliminary Economic Assessment, Sensitivity and Break-Even Analyses, Rate of Return

## E-24. Phycoremediation of Olive Oil Wastes Using Cyanobacteria for Sustainable Biofertilizer and Biodiesel Production

Hassan I. El Shimi and Soha S. Mostafa

*Arpn Journal of Engineering and Applied Sciences, 11: 10259-10272 (2016)*

The dual role of cyanobacteria in wastewater phycoremediation for sustainable biomass production combined with biorefinery approach is a feasible option. Phycoremediation is the process of employing algae for removing excess nutrient load from wastewater and subsequently diminish the pollution load. Industrial processes for olive production generate a considerable amount of oil wastewater, designated "olive mill wastewater" (OMW) known as alpechin, it caused serious environmental problems particularly in the Mediterranean areas where it is generated in huge quantities in short periods of time. The objective of this research was to study the ability of three cyanobacteria strains (Nostoc muscorum, Anabaena oryzae and Spirulina platensis) to grow, either individually or in a mixture, on relatively high olive mill wastewater (OMW) concentrations of 50, 75 and 100%. The highest phenolic compounds biodegradability and maximum biomass production have been taken as main criteria in the selection of the best treatment in this study. Best results of all growth parameters and phenolic compounds degradation were obtained by mixed culture and 50% OMW and these parameters make the potential of bio-formulating such these wastes into sources for olive trees bio-organic fertilizer is the most preferable methods for the agro-sustainable system. The cultivated algal species are suggested to be a promising feedstock for biodiesel, food and animal feed production according to the biochemical composition.

**Keywords:** Cyanobacteria, Phycoremediation, Sustainable, Biorefinery, Omw, Biodiesel

## E-25. Evaluation of Biodiesel Production from Spent Cooking Oils: A Techno-Economic Case Study of Egypt

Hassan I. El Shimi, Ahmed S. Fawzy, Nahed K. Attia, Guzine I. El Diwani and Shakinaz T. El Sheltawy

*Arpn Journal of Engineering and Applied Sciences, 11: 10280-10290 (2016)*

Biodiesel is one of the feasible alternatives to minimize the diesel shortage in Egypt and worldwide. It produced by transesterification of oils and fats in presence of homogenous or heterogeneous catalysts. Feedstock is the controlling factor of biodiesel industry. However, virgin vegetal oils are expensive to obtain biodiesel, so utilization of spent cooking oils (SCO) is considered a cheap alternative for biodiesel production. In this research, techno-economic appraisal was performed on the Egyptian biodiesel business using SCO as feedstock, and homogeneous (KOH) and heterogeneous (Phosphate rock, Na2SiO3 and CaO) catalysts. The economic analyses were then compared; to determine the most effective technique for biodiesel production. Also, sensitivity and break-even analyses were evaluated for all catalysts on the variations in SCO and biodiesel prices using simple rate of return (SRR). PR is recommended to be the ideal catalyst for biodiesel industry according to the current situation in Egypt.

**Keywords:** Biodiesel, Transesterification, Techno-Economic Appraisal, Sensitivity and Break-Even Analyses, Simple Rate of Return.

## E-26. Modelling of Coal - Biomass Blends Gasification and Power Plant Revamp Alternatives in Egypt ' S Natural Gas Sector

Dalia A. Ali, Mamdouh A. Gadalla, Omar Y. Abdelaziz and Fatma H. Ashour

*Chemical Engineering Transactions, 52: 49-54 (2016)*

Recently, there has been a growing research interest in the co-gasification of biomass with coal to produce syngas and electricity in a sustainable manner. Co-gasification technology do not only decrease potentially the exploitation of a significant amount of conventional coal resources, and thus lower greenhouse gases (GHG) emissions, but also boost the overall gasification process efficiency. In the present work, a rigorous simulation model of an entrained flow gasifier is developed using the Aspen Plus® software environment. The proposed simulation model is tested for an American coal and the model validation is performed in good agreement with practical data. The feedstocks used in the proposed gasifier model are dry Egyptian coal and a blend of an Egyptian coal and rice straw that is gathered locally. The proposed gasifier model mainly consists of three reactors. The first one is a yield reactor where the coal pyrolysis occurs, the second reactor is a stoichiometric reactor where the gasification reactions arise, and the third reactor is a Gibbs reactor where the water-gas and steam-methane reforming reactions take place. The influence of using a feed mixture of 90 % coal and 10 % rice straw on the gasifier efficiency is investigated. The developed model provides a robust basis for revamping of an existing Egyptian natural gas-based power plant to replace its standard fuel with a coal-rice straw blend, in case of low natural gas supply. The model is further employed to assess different revamping scenarios and alternatives within the natural gas power plant. For a dry blend of (90 % Egyptian coal and 10 % rice straw), the cold gas efficiency is estimated as 85.7 %, while for dry Egyptian it is calculated as 79.61 %. The revamped Egyptian natural gas power plant decreases the total annualized cost (TAC) by 52.7 % with respect to a new constructed integrated gasification combined cycle (IGCC) plant. Besides, the payback period decreases to 1.24 y rather than 12 y in case of the construction of a new IGCC power plant.

**Keywords:** Gasification, Co-Gasification, Power Plant Revamp

## E-27. Supply Chain Design Network Model for Biofuel and Petrochemicals from Biowaste

Ismaail A. Emara, Mamdouh Gadallab and Fatma Ashour

*Chemical Engineering Transactions, 52: 1069-1074 (2016)*

Supply Chain (SC) is the effective coordination and integration of all activities performed by several business lines and their infrastructures; such as raw material suppliers, manufacturers, distributors and retailers till delivering the products to the customer. The supply chain facilities location is an important issue which is needed to be solved as it is one of the important pillars in the supply chain design model. Therefore, it is critical for supply chain managing teams and designers to adopt the latest scientific and most effective methods to locate a facility by carrying different scenarios and trade-offs assessment, the used tools are only a decision supporting tools. This paper concentrates on the development status of a decision-support tool for solving supply chain design including location problem of various facilities, using the MILP mixed integer linear problem solving programming model by constructing a generic analytical algorithm to solve this problem. EXECL SOLVER TOOL, MATLAB SOFTWARE with a GUI (graphical user input interface) programmed by the C# (C SHARP) programming software are used. In the MILP programming model iterative algorithm methods are used, where every iteration would generate a whole different new set of solutions to match some constrains, conditions and service levels added by the programmer. The first solution only matches some previous added criteria, resulting in a new set of solutions in the iteration, until finally an optimal solution rises under dynamic environment. In this paper, a typical three layers medium term planning mixed integer linear Programme MILP model for supply chain design is presented and applied for chemicals and biofuel production from rice straw biomass. These three stages are commonly: raw materials collecting areas, distribution center and manufacturing plant locations. With the aid of ASPEN HYSYS simulation software and CAPCOST TOOL, Economic feasibility studies are done for designing supply chain design model. Different scenarios are examined which is a good way to price out potential solutions.

**Keywords:** Biofuel, Biowaste, Supply Chain

## E-28. Revamping of Heat Exchanger Network of an Egyptian Refinery Plant Using New Temperature Driving Force (Tdf) Graphical Technique

Dina A. Kamel, Mamdouh A. Gadalla and Fatma H. Ashour

*Chemical Engineering Transactions, 52: 337-342 (2016)*

This paper introduces a new graphical approach for revamping of existing heat exchanger networks (HENs) based on pinch analysis rules. The HEN is represented on a simple graph, where the cold stream temperatures are plotted on the X-axis against the driving forces for each exchanger plotted on the Y-axis. This graphical technique can describe the energy analysis problems in term of temperature driving force inside the heat exchanger, which is an important factor in the revamping process as the differences in these driving forces are involved in calculating the area of heat exchangers, and consequently affecting the revamping cost. Also, each exchanger is represented in this graph as a straight line with a slope related to the heat capacity flows and length as function of the heat duty. An algorithm for revamping is also proposed. The temperature driving force new representation is applied on an existing HEN in an Egyptian refinery (EORU) to boost its energy efficiency. The graphical revamping in application on the HEN shows savings of approximately 10 % in the energy demand with minor structural modifications.

**Keywords:** Revamping, Heat Exchanger Network, Temperature Driving Force (Tdf)

### *Dept. of Computer Engineering*

## E-29. A Bias and Variance Analysis for Multistep-Ahead Time Series Forecasting

Souhaib Ben Taieb and Amir F. Atiya

*IEEE Transactions on Neural Networks and Learning Systems, 27: 1-15 (2016) IF: 4.854*

Multistep-ahead forecasts can either be produced recursively by iterating a one-step-ahead time series model or directly by estimating a separate model for each forecast horizon. In addition, there are other strategies; some of them combine aspects of both aforementioned concepts. In this paper, we present a comprehensive investigation into the bias and variance behavior of multistep-ahead forecasting strategies. We provide a detailed review of the different multistep-ahead strategies. Subsequently, we perform a theoretical study that derives the bias and variance for a number of forecasting strategies. Finally, we conduct a Monte Carlo experimental study that compares and evaluates the bias and variance performance of the different strategies. From the theoretical and the simulation studies, we analyze the effect of different factors, such as the forecast horizon and the time series length, on the bias and variance components, and on the different multistep-ahead strategies. Several lessons are learned, and recommendations are given concerning the advantages, disadvantages, and best conditions of use of each strategy.

**Keywords:** Forecasting, Predictive Models, Time Series Analysis, Computational Modeling, Joints, Artificial Neural Networks, Analytical Models

## E-30. Analytical Solutions to the Dynamic Pricing Problem for Time-Normalized Revenue

Michael Nawar Ibrahim and Amir F Atiya

*European Journal of Operational Research, 254: 632-643 (2016) IF: 2.679*

In this work we consider dynamic pricing for the case of continuous replenishment. An essential ingredient in such a formulation is the use of time normalized revenue or profit function, in other words revenue or profit per unit time. This provides the incentive to sell many items in the shortest time (and of course at a high price). Moreover, for most firms what matters most is how much revenue or profit is achieved in a certain time frame, for example per year. This changes the problem qualitatively and methodologically. We develop a new dynamic pricing model for this formulation. We derive an analytical solution to the pricing problem in the form of a simple-to-solve ordinary differential equation (ODE) equation. The trajectory of this ODE gives the optimal pricing curve. Unlike many of the models existing in the literature that rely on computationally demanding dynamic programming type solutions, our model is relatively simple to solve. Also, we apply the derived equation to two commonly used price-demand functions (the exponential and the power functions), and derive closed-form pricing curves for these functions.

**Keywords:** Pricing; Dynamic Pricing; Time-Normalized Revenue; Nonhomogeneous Poisson Process; Calculus of Variations

## E-31. Hsbs: A Human's Heat Signature and Background Subtraction Hybrid Approach for Crowd Counting and Analysis

Nermin Kamal Abdel-Wahab Negied, Elsayed B. Hemayed and Magda Fayek

*International Journal of Pattern Recognition and Artificial Intelligence, 30(8): 1655025-1655025 (2016) IF: 0.9*

This work presents a new approach for crowd counting and classification based upon human thermal and motion features. The technique is efficient for automatic crowd density estimation and type of motion determination. Crowd density is measured without any need for camera calibration or assumption of prior knowledge about the input videos. It does not need any human intervention so it can be used successfully in a fully automated crowd control systems. Two new features are introduced for crowd counting purpose: the first represents thermal characteristics of humans and is expressed by the ratio between their temperature and their ambient environment temperature. The second describes humans motion characteristics and is measured by the ratio between humans motion velocity and the ambient environment rigidity. Each ratio should exceed a certain predetermined threshold for human beings. These features have been investigated and proved to give accurate crowd counting performance in real time. Moreover, the two features are combined and used together for crowd classification into one of the three main types, which are: fully mobile, fully static, or mix of both types. Last but not least, the proposed system offers several advantages such as being a privacy preserving crowd counting system, reliable for homogeneous and inhomogeneous crowds, does not depend on a certain direction in motion detection, has no restriction on crowd size. The experimental results demonstrate the effectiveness of the approach.

**Keywords:** Emissivity; Apparent Temperature; Heat Signature; Motion Detection; Privacy Preserving

## E-32. Enhanced Bag of Words Using Multilevel K-Means for Human Activity Recognition

Motasem Elshourbagy, Elsayed Hemayed and Magda Fayek

*Egyptian Informatics Journal, 17(2): 227-237 (2016)*

This paper aims to enhance the bag of features in order to improve the accuracy of human activity recognition. In this paper, human activity recognition process consists of four stages: local space time features detection, feature description, bag of features representation, and SVMs classification. The k-means step in the bag of features is enhanced by applying three levels of clustering: clustering per video, clustering per action class, and clustering for the final code book. The experimental results show that the proposed method of enhancement reduces the time and memory requirements, and enables the use of all training data in the k-means clustering algorithm. The evaluation of accuracy of action classification on two popular datasets (KTH and Weizmann) has been performed. In addition, the proposed method improves the human activity recognition accuracy by 5.57% on the KTH dataset using the same detector, descriptor, and classifier.

**Keywords:** Multilevel K-Means; Human Activity Recognition; Bag Words.

***Dept. of Electric Power and Machines***

## E-33. Gallium - Nitride - Based Submodule Integrated Converters for High - Efficiency Distributed Maximum Power Point Tracking Pv Applications

Omair Khan, Weidong Xiao and Hatem H. Zeineldin

*IEEE Transactions on Industrial Electronics, 63: 966-975 (2016) IF: 6.383*

Distributed maximum power point tracking (MPPT) photovoltaic (PV) systems have drawn increased attention since the inhomogeneous irradiance on PV modules can significantly deteriorate the effectiveness of solar energy harvest. To address the issue, this paper focuses on developing a highly efficient submodule integrated converter (subMIC), which is connected across each submodule of a PV panel. Gallium nitride (GaN) field-effect transistors are utilized in the synchronous buck converter topology to achieve high conversion efficiency and reduced size. A converter prototype, which is digitally controlled using a microcontroller for MPPT, is developed and tested, considering various irradiation conditions. The peak efficiency of the proposed GaN-based subMIC is measured to be higher than 99% at 400-kHz switching frequency, whereas the accuracy of MPPT is above 99% considering low-power conditions.

**Keywords:** Dc / Dc Power Conversion, Energy Harvesting, Photovoltaic (Pv) Power Systems.

## E-34. A Novel Ten-Switch Topology for Unified Power Quality Conditioner

Abdul Mannan Rauf, Amit Vilas Sant, Vinod Khadkikar and H. H. Zeineldin

*IEEE Transactions on Power Electronics,31:6937-6946 (2016) IF: 4.953*

This paper proposes a new topological configuration for a unified power quality conditioner (UPQC). Generally, the power structure of the three-phase three-wire UPQC consists of two back-to-back connected six-switch inverters. For this configuration, out of 12 switches, six of the series inverter switches will be underutilized most of the time. To improve the semiconductor utilization and consequently to reduce the total switch count, this paper proposes a new reduced switch topology for the UPQC. The proposed topology is realized using only ten switches and retains all the performance merits of the 12-switch UPQC while minimizing its underutilization without increasing the switch VA rating. The paper provides a detailed analytical study and evaluation by comparing the proposed topology with the twelve- and nine-switch-based UPQC system configurations. The feasibility of the proposed topology is validated through experimental investigation.

**Keywords:** Power Quality, Ten-Switch Converter, Unified Power Quality Conditioner (Upqc), Voltage Sag, Zero Sequence.

## E-35. Solar Parabolic Dish Stirling Engine System Design, Simulation and Thermal Analysis

A.Z. Hafez, Ahmed Soliman, K.A. El-Metwally and I.M. Ismail

*Energy Conversion and Management, 126: 60-75 (2016) IF: 4.801*

Modeling and simulation for different parabolic dish Stirling engine designs have been carried out using Matlab®. The effect of solar dish design features and factors such as material of the reflector concentrators, the shape of the reflector concentrators and the receiver, solar radiation at the concentrator, diameter of the parabolic dish concentrator, sizing the aperture area of concentrator, focal Length of the parabolic dish, the focal point diameter, sizing the aperture area of receiver, geometric concentration ratio, and rim angle have been studied. The study provides a theoretical guidance for designing and operating solar parabolic dish Stirling engines system. At Zewail city of Science and Technology, Egypt, for a 10 kW Stirling engine; The maximum solar dish Stirling engine output power estimation is 9707 W at 12:00 PM where the maximum beam solar radiation applied in solar dish concentrator is 990 W/m2 at 12:00 PM. The performance of engine can be improved by increasing the precision of the engine parts and the heat source efficiency. The engine performance could be further increased if a better receiver working fluid is used. We can conclude that where the best time for heating the fluid and fasting the processing, the time required to heat the receiver to reach the minimum temperature for operating the Solar-powered Stirling engine for different heat transfer fluids; this will lead to more economic solar dish systems. Power output of the solar dish system is one of the most important targets in the design that show effectiveness of the system, and this has achieved when we take into account many factors in the design of the solar dish system. One of these factors is the reflector material of the concentrator and using the results from the Matlab simulation program; where the Polymeric Film, Non Metal reflectors, with a net conversion power of more than 97.07%, still holds the conversion record than the Anod Aluminum reflectors, which has a net conversion power 85.97% with respect to the polished stainless reflectors with a net conversion power 49.52% from the 10 kW Stirling engine. Where the power output differ as 9707, 4952, 8597 W, respectively from the 10 kW Stirling engine. It is shown that there are changes in Stirling power output for different materials, which guide us to select the optimum material, based on the targeted power output and cost. Our target to reach the optimum power that we need it in the design 10 kW power output design as an example from the solar dish Stirling engine.

**Keywords:** Solar Dish; Design; Thermal Analysis; Stirling; Simulation; Matlab; Gui

## E-36. Enhanced Flicker Mitigation in Dfig-Based Distributed Generation of Wind Power

Moataz Ammar and Mohammed E. Ammar

*IEEE Transactions on Industrial Informatics, 12: 2041-2049 (2016) IF: 4.708*

Upon the connection of wind generators to distribution grids, significant flicker emission can appear, due to the low X/R ratios and low short-circuit levels at the points of connection.

This paper proposes a reactive-power-based control scheme that aims for accurate cancellation of voltage flicker resulting from the grid connection of DFIG-based wind power. The control scheme operation is based on constructing the two-bus equivalent network of the detailed power system, via local measurements of voltage and active and reactive power flows at the DFIG terminals. The reactive power flow at the DFIG terminals is adjusted accordingly to cancel voltage flicker, based on the constructed equivalent network equations. The proposed control scheme avoids the use of power flow approximations at the connection point, and hence is free of the inaccuracies implicated in the conventional reactive-power-based flicker mitigation approaches (based on power factor control and voltage control). The proposed control scheme is shown, by comparative results, to provide superior performance to those conventional flicker mitigation approaches, as well as flicker mitigation capability independent of the connection point parameters.

**Keywords:** Dfig, Distributed Generation (Dg), Flicker, Power Quality, Reactive Power Control, Wind Power

## E-37. A Novel Approach to Solve Power Flow for Islanded Microgrids Using Modified Newton Raphson with Droop Control of Dg

Faisal Mumtaz, M. H. Syed , Mohamed Al Hosani and H. H. Zeineldin

*IEEE Transactions on Sustainable Energy, 7: 493-503 (2016) IF: 3.727*

The study of power flow analysis for microgrids has gained importance where several methods have been proposed to solve these problems. However, these schemes are complicated and not easy to implement due to the absence of a slack bus as well as the dependence of the power on frequency as a result of the droop characteristics. This paper proposes simple and effective modifications to the conventional method (Newton Raphson) to compute the power flow for microgrids. The presented method provides a simple, easy to implement, and accurate approach to solve the power flow equations for microgrids. The proposed method is applied to two test systems: a 6-bus system and a 38-bus system. The results are compared against simulation results from PSCAD/EMTDC which validate the effectiveness of the developed method. The proposed technique can be easily integrated in current commercially available power system software and can be applied for power system studies.

**Keywords:** Distributed Generation (Dg), Islanded Microgrid, Power Flow.

## E-38. Wind-Turbine Collective-Pitch Control Via a Fuzzy Predictive Algorithm

Ahmed Lasheen and Abdel Latif Elshafei

*Renewable Energy, 87: 298-306 (2016) IF: 3.404*

This paper proposes a new fuzzy predictive algorithm for collective pitch control of large wind turbines. Collective pitch controllers operate in region three to harvest the rated power and maintain the rated speed. The wind turbine model is represented by a Takagi–Sugeno (T–S) fuzzy model. The number of T–S fuzzy rules is reduced based on a gap – metric criterion. A model predictive controller is designed based on the fuzzy model taking into consideration the pitch actuator constraints. The proposed controller is coupled with conventional PI controllers for individual pitch control so as to minimize the moments on the turbine blades. A Kalman observer is designed to estimate the immeasurable states. The performance of the proposed fuzzy-predictive controller is compared to a gain schedule PI controller and a mixed H2/H∞ controller. Simulation results, based on a typical 5-MW offshore wind turbine, demonstrate the superiority of the proposed fuzzy-predictive controller.

**Keywords:** Wind Turbines; Collective Pitch Control; Predictive Control; T–S Fuzzy Models

## E-39. A Dynamic Economic Emission Dispatch Considering Wind Power Uncertainty Incorporating Energy Storage System and Demand Side Management

M.H. Alham, M. Elshahed, Doaa Khalil Ibrahim and Essam El Din Abo El Zahab

*Renewable Energy, 96: 800-811 (2016) IF: 3.404*

Reducing carbon emissions is an important goal for the whole world; a high penetration of wind energy can help in reducing emissions. However, great increase in wind energy usage raises some issues concerning its variability and stochastic nature. These issues increase the importance of studying methods of wind energy representation, and in the same time studying the effect of using some flexible resources in decreasing those issues. This paper proposes a dynamic economic emission dispatch (DEED) model incorporating high wind penetration considering its intermittency and uncertainty. Energy storage system (ESS) and demand side management (DSM) are implemented in order to study their effect on the cost, emission, and wind energy utilization. The GAMS software has been utilized to solve this DEED problem. The achieved results show the importance of using ESS and DSM in decreasing both cost and emission, and increasing the wind energy utilization.

**Keywords:** Energy Storage; Demand Side Management; Dynamic Economic Emission Dispatch; Wind Energy.

## E-40. Maximization of Generated Power from Wind Energy Conversion System Using a New Evolutionary Algorithm

T.A. Boghdady, M.M. Sayed and E.E. Abu Elzahab

*Renewable Energy, 99: 631-646 (2016) IF: 3.404*

In this paper, a grid-connected Doubly Fed Induction Generator controlled by a Sliding Mode Controller (SMC) is used to maximize the Wind Energy Conversion System (WECS) output power. A SMC is implemented using a PID controller that is tuned using a new algorithm based on hybrid Differential Evolution with a Linearized Biogeography-Based Optimization (LBBO-DE). Biogeography-Based Optimization (BBO) is an evolutionary optimization algorithm based on a mathematical model of organism distribution. BBO permits a recombination of the solutions features by migration. A new migration model based on the sigmoid function is proposed. An analysis of the LBBO-DE is conducted using six different models, including the sigmoid model. Their performance were tested with 23

benchmark functions. The comparison reveals that the sigmoid model has the best performance. Therefore, the LBBO-DE with a sigmoid model is used to optimize the controller parameters to maximize the WECS output power. The LBBO-DE with the sigmoid model is compared with the Tyreus-Luyben tuning method, Genetic Algorithm (GA) and Linearized BBO (LBBO). The results showed that the LBBO-DE has the best performance. The proposed algorithm is verified using an experimental setup for the maximization of the generated power from the WECS and reducing power loss.
**Keywords:** Biogeography-Based Optimization; Differential Evolution; Sliding Mode Control; Wind Energy Conversion System.

## E-41. Stability Evaluation of Interconnected Multi-Inverter Microgrids Through Critical Clusters

Iraklis P. Nikolakakos, Hatem H. Zeineldin, Mohamed Shawky El-Moursi and Nikos D. Hatziargyriou

*IEEE Transactions on Power Systems, 31: 3060-3072 (2016) IF: 3.342*

This paper proposes the notion of "critical cluster" in inverter based droop controlled microgrids, thus representing the neighborhood of the distributed generation units that determines the small signal stability margin of the entire system. The clustering starts from the lowest impedance electrical connection between distributed generators, termed as "critical line". At first, the systematic study of few similar microgrids by means of the eigenvalue analysis of their small signal models reveals the correlation between the location of their dominant low frequency modes and the individual connections between neighboring inverters. Second, the sensitivity analysis of active power droop gain with respect to network parameters confirms the previous findings and shows the dominating effect of the critical line's impedance. Simulations and small signal analysis studies assess the impact of the choice of various interconnection points when two individual droop controlled islanded microgrids are connected to form a single microgrid. At the same time, simplified models on the basis of critical clusters allow the effective approximation of the stability margin corresponding to the original systems. The results reveal that different interconnection points lead to strong variations in the performance of the coupled microgrid both in terms of transient response and small signal stability.
**Keywords:** Distributed Generation (DG), Droop Control, Islanded Microgrid, Parallel Inverters, Small-Signal Stability.

## E-42. Planning the Coordination of Directional Overcurrent Relays for Distribution Systems Considering Dg

Łukasz Huchel and Hatem H. Zeineldin

*IEEE Transactions on Smart Grid, 7:1642-1649 (2016) IF:3.19*

Introduction of distributed generation (DG) to the power system may lead to nonselective protection actions. For every future DG installation, the relay settings need to be modified to guarantee protection coordination that can lead to numerous changes in relay settings. This paper presents a novel approach to plan relay protection coordination considering future DG installations. Thus, this paper aims at proposing a method capable of optimally identifying one set of relay settings valid for all possible future DG planning scenarios. The proposed algorithm is formulated as a linear programming problem and the simplex algorithm is utilized to solve it. The proposed approach is tested on the distribution part of the modified meshed IEEE 14-bus system and the IEEE 13-bus radial test system. Comparative studies have been conducted to highlight the advantages of the proposed approach under various planning scenarios considering application of fault current limiters.
**Keywords:** Coordination Time Interval (CTI), Fault Current Limiters (FCLS), Linearization, Protection Coordination.

## E-43. An Analytical Approach to Design the Pm in Pmarel Motors Robust Toward the Demagnetization

Nicola Bianchi and Hanafy Mahmoud

*IEEE Transactions on Energy Conversion, 31: 800-809 (2016) IF: 2.596*

In the permanent magnet (PM)-assisted reluctance motors, low-energy PM, such as Ferrite PM, is used to get a cheap rotor. As far as the design choices are concerned, the PM width has to be selected so as to achieve the desired air-gap flux density at no-load condition and the PM thickness has to be selected to avoid the demagnetization of the PM under full-load conditions. This paper presents a practical analytical approach to compute PM width and thickness according to a given air-gap flux density and stress on the PM itself. Two approaches based on a complete model and a simplified model are considered and compared. As an example, a 36-slot 4-pole machine is designed. Finite element analysis confirms the results achieved by means of both analytical analyses.
**Keywords:** Finite Element Analysis, Pmarel Motors, Demagnetization, Permanent Magnet-Assisted Reluctance Motors, Ferrite PM, Air-Gap Flux Density

## E-44. Bat Inspired Algorithm Based Optimal Design of Model Predictive Load Frequency Control

M. Elsisi, M. Soliman, M.A.S. Aboelela and W. Mansour

*Electrical Power and Energy Systems, 83: 426-433 (2016) IF: 2.587*

Bat inspired algorithm (BIA) has recently been explored to develop a novel algorithm for distributed optimization and control. In this paper, BIA-based design of model predictive controllers (MPCs) is proposed for load frequency control (LFC) to enhance the damping of oscillations in power systems. The proposed model predictive load frequency controllers are termed as MPLFCs. Two-area hydro-thermal system, equipped with MPLFCs, is considered to accomplish this study. The suggested power system model considers generation rate constraint (GRC) and governor dead band (GDB). Time delays imposed to the power system by governor-turbine, thermodynamic process, and communication channels are accounted for as well. BIA is utilized to search for optimal controller parameters by minimizing a candidate time-domain based objective function. The performance of the proposed controller has been compared to those of the conventional PI

controller based on integral square error (ISE) technique and the PI controller optimized by genetic algorithms (GA), in order to demonstrate the superior efficiency of the BIA-based MPLFCs. Simulation results emphasis on the better performance of the proposed MPLFCs compared to conventional and GA-based PI controllers over a wide range of operating conditions and system parameters uncertainties.

**Keywords:** Bat Inspired Algorithm (BIA); Load Frequency Control (LFC); Model Predictive Control (MPC); Time Delays; Nonlinearities.

## E-45. An Inverse Approach for Interturn Fault Detection in Asynchronous Machines Using Magnetic Pendulous Oscillation Technique

Hanafy Mahmoud, Ahmed Abou-Elyazied Abdallh, Nicola Bianchi, S. M. El-Hakim, Adel Shaltout and Luc Dupré

*IEEE Transactions on Industry Applications, 52: 226-233 (2016) IF: 1.901*

In this paper, a coupled experimental-mathematical inverse problem based methodology for the detection of interturn faults in an asynchronous induction machine is presented. The fault detection is accomplished by interpreting well-defined measurements into the machine mathematical model. First, the studied machine is modeled by means of a dynamic state-space model in the abc reference frame. This model simulates the machine behavior under healthy and faulty cases in both transient and steady-state conditions. The signature of the interturn fault is captured using the magnetic pendulous oscillation technique. The proposed inverse problem is validated numerically and experimentally. The results show the robustness of the proposed scheme against the measurement noise.

**Keywords:** Steady-State Conditions, Interturn Fault Detection, Asynchronous Induction Machine, Magnetic Pendulous Oscillation Technique, Experimental-Mathematical Inverse Problem Based Methodology, Machine Mathematical Model, State-Space Mode, Transient Conditions.

## E-46. Enhancement Low-Voltage Ride Through Capability of Permanent Magnet Synchronous Generator-Based Wind Turbines Using Interval Type-2 Fuzzy Contro

Haitham Mahmoud Yassin, Hanafy Hassan Hanafy and Mohab M. Hallouda

*Iet Renewable Power Generation, 10: 339-348 (2016) IF: 1.56*

Increased penetration level of the wind power generation has brought new issues and challenges of power quality. One of these issues is low-voltage ride through (LVRT). This study proposes an LVRT scheme for the permanent magnet synchronous generator (PMSG) variable speed wind turbine at grid faults. The machine side converter controller is used to control the dc-link voltage using interval type-2 fuzzy logic control taking into account the non-linear relationship between the generator speed and the dc-link voltage. Under grid faults, there is a power mismatch between the generated active power and the active power delivered to the grid. This excess power is stored in the generator inertia to keep the dc-link voltage constant. To validate the proposed control strategy, simulation results for 1.5 MW PMSG-based wind energy conversion system are carried out by MATLAB-Simulink under symmetrical and asymmetrical faults.

**Keywords:** Low-Voltage Ride Through (LVRT), Permanent Magnet Synchronous Generator (PMSG), Interval Type-2 Fuzzy Logic Control

## E-47. Automatic Tuning of Robust Constrained Cross-Direction Controllers

Mohammed E. Ammar and Guy A. Dumont

*International Journal of Adaptive Control and Signal Processing, 30: 1550-1567 (2016) IF: 1.368*

The paper machine cross-directional (CD) process is a large-scale spatially distributed system. It is known to be severely ill-conditioned as the gain rolls down to zero for some of the process directions. Model uncertainties in the process are inevitable resulting in a challenging robust control design problem. CD actuators are subject to min–max constraints while slice lip actuators are subject to additional bending moment limits. Because of the large number of input constraints, the industrial practice is to tune the CD controller assuming inactive constraints. The robustness of CD feedback loops to model uncertainties under constrained internal model control satisfies an integral quadratic inequality. This work develops an automatic tuning algorithm that guarantees robust stability and performance of the constrained CD feedback loop. Spatial response models are identified in a prediction error frame delivering bounds on the CD process pseudo-singular values. The CD controller is synthesized online through a linear matrix inequalities feasibility problem taking into consideration the modal space uncertainty rising from the uncertainties in the estimated parameters and the expected variations in the dynamic response. The developed tuning technique is suitable for paper machines producing different grades of paper as the CD process spatial and dynamic responses change for each grade. The performance of the tuned constrained internal model control controller is validated through comparing it to an industrial CD controller that has been implemented in paper mills as part of a commercial product.

**Keywords:** Cross-Direction Control; CD Model Identification; Internal Model Control; Linear Matrix Inequalities

## E-48. Fast Synthesis of Permanent Magnet Assisted Synchronous Reluctance Motors

Nicola Bianchi and Hanafy Mahmoud

*Iet Electric Power Applications, 10: 312-318 (2016) IF: 1.211*

This paper describes a procedure for a practical synthesis of both a synchronous reluctance motor and a permanent magnet assisted synchronous reluctance motor. The procedure is completely analytical, yielding a rapid drawing of the motor geometry, taking into account both magnetic and mechanical considerations. From the application requirements, the external volume of the motor is computed. The further practical needs, such as maximum outer space, maximum available length, existing stator lamination, and so on are considered. Then, the design of the rotor geometry is carried out. The PM size is

determined considering the demagnetisation limit according to the maximum current loading.
**Keywords:** Demagnetisation Limit, Fast Permanent Magnet Assisted Synchronous Reluctance Motor Synthesis, Motor Geometry, Magnetic Considerations, Mechanical Considerations, Maximum Outer Space, Maximum Available Length, Existing Stator Lamination, Rotor Geometry Design

## E-49. Design and Implementation of a Variable-Structure Adaptive Fuzzy-Logic Yaw Controller for Large Wind Turbines

Farag, Wael El-Hosary, Hanan El - Metwally and Khaled Kamel Ahmed

*Journal of Intelligent and Fuzzy Systems, 30: 2773-2785 (2016) IF: 1.16*

The current trend of wind energy generation industry is to use large and ultra-large wind turbines that can reach more than 10 MW in ratings; especially in off-shore wind farms. Therefore, more emphasis is being given by researchers to increase the harvested energy by each individual wind turbine. Previously, more focus has been given to pitch control techniques of turbine blades for improving the harvested energy and lowering the turbine maintenance cost. However, still not enough work is done to investigate the effectiveness of nacelle yaw control in improving the harvested energy specifically for large wind turbines. In this paper, we introduce a new yaw controller based on adaptive fuzzy systems. The control objective of the proposed controller is to effectively track of the wind direction by yaw motion of the turbine nacelle. For that reason, it is a fuzzy-logic-based controller that has the capability to adaptively tune its rule base online. The change in the fuzzy rule base is done using a variable structure direct adaptive control algorithm to achieve the pre-defined control objectives. This algorithm has two advantages. First, it has a good performance in the training phase as it makes use of the initial rule base defined for the fuzzy logic yaw controller. Second, it has a robust estimator since it depends on a variable structure technique. The adaptive nature of the proposed controller significantly reduces the rule base size and improves its performance. The previous statement is verified through three levels of testing. The first level is Model-In-the-Loop (MIL) MATLAB/SIMULINK extensive simulations, with the performance results get compared to that of a carefully tuned Proportional-Integral-Differential (PID) controller. The second level of testing is through Software-In-the-Loop (SIL) testing using the same use cases. The last level is the Processor-In-the-Loop (PIL) experimental tests using a Texas Instruments TMS320F28335 digital signal processing board.
**Keywords:** Wind Turbine, Fuzzy Logic Control (Flc), Yaw Control, Adaptive Control, Model-In-The-Loop, Software-In-The-Loop, Processor-In-The-Loop

## E-50. Electrothermal Analysis of Low- and Mediumvoltage Cable Joints

Osama E. Gouda and Adel Zein El Dein

*Electric Power Components and Systems,1:1-10(2016) IF:0.747*

In this article, an analytical method to calculate the steady-state temperature distribution along the joint of a three-phase distribution cable is presented. The results of this method are compared with those obtained by an experimental study and by the finite element method. It is found that the results of the analytical method are in good agreement with those obtained by an experimental study and by the finite- element method. The effects of connector dimensions as well as the effect of the ambient temperature and cable load current on the maximum temperature of the joint are discussed in detail. From the present analysis, it is found that the increasing of the connector length is more effective than the connector thickness in the reduction of the maximum temperature of conductor inside the joint.
**Keywords:** Analytical Method, Cable Joint, Finite-Element Method, Temperature

## E-51. Vector Hysteresis Modeling in Arbitrarily Shaped Objects Using an Energy Minimization Approach

Amr A. Adly and Salwa K. Abd-El-Hafiz

*ACES Journal, 31(7): 765-770 (2016) IF: 0.389*

It is known that proper and efficient modeling of vector hysteresis is crucial to the precise design and performance estimation of electric power devices and magnetic recording processes. Recently, discrete Hopfield neural networks have been successfully utilized in the construction of vector hysteresis models. This paper presents a novel energy-minimization Hopfield neural network approach to implement Stoner-Wohlfarthlike vector hysteresis operators in triangular sub-regions. Advantages of the approach stem from the nonrectangular nature of such operators, which could mimic major hysteresis loops as well as their implementation in the most commonly used triangular discretization subdomains. Details of the approach are given in the paper.
**Keywords:** Discrete Hopfield Neural Network, Energy Minimization, Shape Anisotropy, Vector Hysteresis.

## E-52. Discrete Wavelet Transform and Support Vector Machine-Based Parallel Transmission Line Faults Classification

Saber, Ahmed Emam and Ahmed Amer Rabah

*Ieej Transactions on Electrical and Electronic Engineering, 11: 43-48 (2016) IF: 0.261*

This paper presents a scheme for classification of faults on double circuit parallel transmission lines using combination of discrete wavelet transform and support vector machine (SVM). Only one cycle post fault of the phase currents was employed to predict the fault type. Two features for each phase current were extracted using discrete wavelet transform. Thus, a total of 12 features were extracted for the six phase currents. The training data were collected, and SVM was employed to establish the fault classification unit. After that, the fault classification unit was tested for different fault states. The power system simulation was conducted using the MATLAB/Simulink program. The proposed technique took into account the mutual coupling between the parallel transmission lines and the randomness of the faults on transmission line considering time of occurrence, fault location, fault type, fault resistance, and loading conditions. The results show that the proposed

technique can classify all the faults on the parallel transmission lines correctly.
**Keywords:** Support Vector Machine; Transmission Line; Wavelet Transform

## E-53. Application of Multi - Objective Pid Controller for Load Frequency Control in Two - Area Nonlinear Electric Power Systems

Magdy Aboelela

*International Journal of Power and Energy Conversion, 7: 139-156 (2016)*

Design of optimal controllers is indeed a multi-objective optimisation problem. Non-dominated sorting in genetic algorithms-II (NSGA-II) is a popular algorithm for solving multi-objective optimisation problems. This paper investigates the application of NSGA-II technique for the tuning of a proportional-integral-derivative (PID) controller for a class of identical two area-thermal power stations including the generation rate constraint (GRC) and boiler nonlinear dynamics as well as the governor dead band (GDB). The design objective is to improve the damping of frequency fluctuation in two-area power system when subjected to a disturbance in their loads. The proposed technique is applied to generate Pareto set of global optimal solutions to the given multi-objective optimisation problem. Further, the two PID controllers in each area are assumed to have identical structures (same parameters). Simulation results using the tuned multi-objectives-based GA PID controller are presented. The effectiveness of the proposed scheme is confirmed using MATLAB-Simulink software.
**Keywords:** Load Frequency Control; Lfc; Electric Power System; Pid Controllers; Multi-Objective Genetic Algorithm; Nonlinear Systems.

## E-54. An Analysis of Migration Models for Linearized Biogeography - Based Optimization Applied for Pid Tuning Problem

Tarek A. Boghdady , Mahmoud M. Sayed and Essam E. Abouelzahab

*Journal of Electrical Engineering, 1/2016: 257-268 (2016)*

Linearized Biogeography-Based Optimization (LBBO) is a new version of Biogeography-Based Optimization (BBO). BBO is an evolutionary optimization algorithm based on the mathematical model of organism distribution of Biological systems. BBO permits a recombination for the features of candidate solutions (habitats) by means of emigration and immigration. This paper presents a new migration model based on the sigmoid function (S curve) to be one of the nonlinear migration models. This paper also presents an analysis of three linear and three nonlinear different migration models, including the sigmoid model, in LBBO and tests their performance with the non-noisy 23 benchmark functions that have been accepted for 2005 Congress on Evolutionary Computation (CEC). Another test with seven transfer functions is carried out and the performance study explores that sigmoid migration model has the best performance between the different models that will be discussed. The proposed LBBO algorithm with the sigmoid migration function (LBBO-S) had been tested with 23 benchmarks and then compared with the 20 algorithms that have been accepted for 2005 CEC. The proposed algorithm achieved advanced rank between them and it gave better results and lower variance, which proved to have competitive performance with stateof- the-art evolutionary algorithms. An application of the proposed sigmoid model is applied here to tune Proportional Integral Derivative (PID) controller, which is widely used in industrial control systems. Enhancement the performance and ensuring the system stability of an industrial process by tuning PID controller parameters is an important issue. By using Matlab/Simulink and the objective function is chosen to be the squared error integral criteria, LBBO algorithm with the sigmoid migration model is applied to the seven transfer functions, and a comparison with Particle Swarm Optimization (PSO), BBO, and Modified Biogeography-Based Optimization (MBBO) is carried out. The results of the simulation proved that the proposed algorithm (LBBO-S) is an effective tuning method and has better performance compared with other algorithms
**Keywords:** Biogeography-Based Optimization (BBO), Evolutionary Algorithm (EA), and Proportional Integral Derivative Control.

## E-55. Evaluating the Energy System in Yemen

Maged M. Al-Barashi, Doaa K. Ibrahim and Essam El-Din Abo El-Zahab

*Journal of Electric Engineering, Jee, 16 (Edition 1): 338-342 (2016)*

This paper presents a deep analysis for the energy system in Yemen, which consists of thermal power plants taking into account the strengths and weaknesses of its power system. The investigation results show that Yemen power system suffers lacking of energy efficiency (EE), weak institutional capacity, high losses in the generation, transmission and distribution grids, and currently the disability to invest in renewable energy (RE). Yemen should focus on foundational activities to build institutional capacity and mobilize resources to initiate suitable energy efficiency policies and measures.Yemen should also focus on exploring the opportunities of designing innovative energy systems based on decentralized small-scale power generation. Microgrids could enable power supply to remote areas at lower costs than required by traditional infrastructure.
**Keywords:** Energy Efficiency, Renewable Energy, Yemen Power System, Al-Mukha Wind Farm.

## E-56. Assessment of Sudden Voltage Changes and Flickering for a Grid-Connected Photovoltaic Plant

Mostafa Ahmed Elshahed

*International Journal of Renewable Energy Research, 6: 1328-1335 (2016)*

In this paper, sudden voltage changes studies are carried out for a 20 MW grid-connected photovoltaic plant to assess the impact of energization of the step-up transformers, which may cause a voltage dip that could be a nuisance to the point of common coupling (PCC) of the transmission system. In addition, the flicking performance of the plant is checked. At the design stage, these studies are necessary to verify compliance of the photovoltaic plant and to design its connection with regulatory grid codes and international standards. The photovoltaic plant is

compliant with the FICHTNER standard for long-term flicker severity and with the short-term flicker severity requirements of Engineering Standard P28. Based on the study results, the main breaker which is connected to the PCC should be ordered with 150 Ohm Pre-Insertion Resistor to make the Photovoltaic plant comply with grid code requirements of sudden voltage changes.
**Keywords:** Grid Codes; Grid-Connected Photovoltaic Plants; Energization; Flickering

## E-57. Implementation of Model Predictive Control for Three-Phase Inverter with Output Lc Filter on Ezdsp F28335 Kit Using Hil Simulation

Ihab S. Mohamed, Sherif A. Zaid, M.F. Abu-Elyazeed and Hany M. Elsayed

*International Journal of Modelling Identification and Control, 25(4): 301-312 (2016)*

The control of UPS inverters has a special importance in applications where a high quality output voltage is needed. Several control schemes have been proposed for the control of three-phase inverter. This paper presents a simple and powerful control scheme using model predictive control (MPC). It uses a discrete-time model of the system to predict the behaviour of the output voltage for all possible switching states generated by the inverter. Then, a cost function is used for selecting the optimal switching state that will be applied at the next sampling instant. The simulation results under linear and nonlinear loads are presented, using MATLAB/Simulink tools, verifying the feasibility and good performance of the proposed control scheme. Finally, experimental results are presented, using HIL simulation, to verify the feasibility and good performance of the proposed MPC under realistic conditions.
**Keywords:** Dsp; Hil Simulation; Power Conversion; Model Predictive Control; Mpc; Uninterruptible Power Systems.

## E-58. New Current Trajectory for Field Weakening Control of Pmsm in Wide Speed Range

Mohamed H. Abouelella, Sherif A. Zaid, Osama A. Mahgoub and Abdelatif M. El-Shafei

*International Review of Electrical Engineering, 11(1): 45-54 (2016)*

Permanent Magnet Synchronous Motors (PMSMs) have received great attention recently. Many industrial applications require PMSM to operate in the constant power range above the rated motor speed, called the field-weakening region. In this paper, a new current trajectory is proposed to enhance the dynamic performance of the PMSM in the field-weakening region. This is accomplished by selecting a predefined value of the direct axis current from a Lookup Table (LUT) according to the desired speed then a transition between this value and the optimum required current takes place in order to improve the dynamic performance of the overall drive system. The system is simulated using Matlab/Simulink and tested experimentally to confirm the effectiveness of the proposed trajectory.
**Keywords:** Pmsm; Field Weakening; Mtpa; Dsp

## E-59. Fuzzy Pid Controller for Fast Direct Torque Control of Induction Motor Drives

Mohamed E. El-Shimy and S.A. Zaid

*Journal of Electrical Systems, 12(4): 687-700 (2016)*

Direct torque control (DTC) has been employed to give fast torque response, which is very important in traction and electric vehicle applications, in high dynamic performance Induction Motor (IM) drives. Fast torque response can be achieved by optimizing the selection of the inverter voltage vectors in the conventional DTC. This paper introduces a method for selecting voltage vectors; in DTC controlled IM drives, to achieve fast torque response at constant switching frequency. Also, the application of the Fuzzy PID (FPID) control technique improves the system speed and torque responses. Simulation results show that both torque and speed responses are faster with the proposed controller than the conventional DTC.
**Keywords:** Direct Torque Control (Dtc); Fuzzy Pid Controller (Fpid); Induction Motor (Im); Conventional Pid Controller.

### *Dept. of Electronics and Communication Engineering*

## E-60. Single-Readout High-Density Memristor Crossbar

M. A. Zidan, H. Omran, R. Naous, A. Sultan, H. A. H. Fahmy, W. D. Lu and K. N. Salama

*Scientific Reports, 60 (2016) IF: 5.228*

High-density memristor-crossbar architecture is a very promising technology for future computing systems. The simplicity of the gateless-crossbar structure is both its principal advantage and the source of undesired sneak-paths of current. This parasitic current could consume an enormous amount of energy and ruin the readout process. We introduce new adaptive-threshold readout techniques that utilize the locality and hierarchy properties of the computer-memory system to address the sneak-paths problem. The proposed methods require a single memory access per pixel for an array readout. Besides, the memristive crossbar consumes an order of magnitude less power than state-of-the-art readout techniques.
**Keywords:** Memristors, Crossbar Memories, Sneak-Paths, Single Reading

## E-61. Fronthaul Cell Outage Compensation for 5G Networks

Mohamed Selim, Ahmed E. Kamal, Khaled Elsayed, Heba M. Abdel-Atty and Mohammed Alnuem

*IEEE Communications Magazine, 54: 169-175 (2016) IF: 5.125*

5G networks are expected to bring the gigabits per second throughput level per user to reality by 2020. This is done using a combination of new and well known technologies such as C-RAN, self-organizing networks, ultra dense networks, massive MIMO, and millimeter waves. In new RAN architectures, C-RAN has been viewed as a promising 5G architecture that centralizes baseband processing units and virtualizes them into a resource pool. The baseband units are connected to the remote radio heads via high speed fronthaul links. Failure of any 5G cell site fronthaul means the loss of hundreds of gigabits, or even terabits. In this article, we present a novel cell outage

compensation approach using new SHRs added to each cell site in the 5G network. These SHRs operate only in case of fronthaul/ backhaul failure of any cell site in the network. A new software defined controller is introduced to handle the self-healing procedures. The article also introduces a high-level simulation study that is carried out to assess the proposed approach. The simulation results confirm the advantages of the proposed approach in terms of the degree of recovery from failures.

**Keywords:** Computer Architecture, Microprocessors, 5G Mobile Communication, Macrocell Networks, Wireless Communication, Baseband, Interference

## E-62. Stability Analysis of Slotted Aloha with Opportunistic Rf Energy Harvesting

Abdelrahman M. Ibrahim, Ozgur Ercetin and Tamer ElBatt

*IEEE Journal on Selected Areas in Communications, 34, No. 5: 1477-1490 (2016) IF: 3.672*

Energy harvesting (EH) is a promising technology for realizing energy-efficient wireless networks. In this paper, we utilize the ambient RF energy, particularly interference from neighboring transmissions, to replenish the batteries of the EH enabled nodes. However, RF energy harvesting imposes new challenges into the analysis of wireless networks. Our objective in this paper is to investigate the performance of a slotted Aloha random access wireless network consisting of two types of nodes, namely Type I, which has unlimited energy supply and Type II, which is solely powered by an RF energy harvesting circuit. The transmissions of a Type I node are recycled by a Type II node to replenish its battery. We characterize an inner bound on the stable throughput region under half-duplex and full-duplex energy harvesting paradigms as well as for the finite capacity battery case. Additionally, we analyze the case where RF energy harvesting serves as a backup for an unlimited energy source. We present numerical results that validate our analytical results, and demonstrate their utility for the analysis of the exact system.

**Keywords:** Wireless Networks, Slotted Aloha, Opportunistic Energy Harvesting, Interacting Queues

## E-63. Rmp: Reduced-Set Matching Pursuit Approach for Efficient Compressed Sensing Signal Reconstruction

Michael M. Abdel-Sayed, Ahmed Khattab and Mohamed F. Abu-Elyazeed

*Journal of Advanced Research, 7(6): 851-861 (2016) IF: 3*

Compressed sensing enables the acquisition of sparse signals at a rate that is much lower than the Nyquist rate. Compressed sensing initially adopted ℓ1 minimization for signal reconstruction which is computationally expensive. Several greedy recovery algorithms have been recently proposed for signal reconstruction at a lower computational complexity compared to the optimal ℓ1 minimization, while maintaining a good reconstruction accuracy. In this paper, the Reduced-set Matching Pursuit (RMP) greedy recovery algorithm is proposed for compressed sensing. Unlike existing approaches which either select too many or too few values per iteration, RMP aims at selecting the most sufficient number of correlation values per iteration, which improves both the reconstruction time and error. Furthermore, RMP prunes the estimated signal, and hence, excludes the incorrectly selected values. The RMP algorithm achieves a higher reconstruction accuracy at a significantly low computational complexity compared to existing greedy recovery algorithms. It is even superior to ℓ1 minimization in terms of the normalized time-error product, a new metric introduced to measure the trade-off between the reconstruction time and error. RMP superior performance is illustrated with both noiseless and noisy samples.

**Keywords:** Compressed Sensing, Matching Pursuit, Sparse Signal Reconstruction, Restricted Isometry Property

## E-64. Accurate Dynamic Power Estimation for Cmos Combinational Logic Circuits with Real Gate Delay Model

Omnia S. Fadl, Mohamed F. Abu-Elyazeed, Mohamed B. Abdelhalim, Hassanein H. Amer and Ahmed H. Madian

*Journal of Advanced Research, 7: 89-94 (2016) IF: 3*

Dynamic power estimation is essential in designing VLSI circuits where many parameters are involved but the only circuit parameter that is related to the circuit operation is the nodes' toggle rate. This paper discusses a deterministic and fast method to estimate the dynamic power consumption for CMOS combinational logic circuits using gate-level descriptions based on the Logic Pictures concept to obtain the circuit nodes' toggle rate. The delay model for the logic gates is the real-delay model. To validate the results, the method is applied to several circuits and compared against exhaustive, as well as Monte Carlo, simulations. The proposed technique was shown to save up to 96% processing time compared to exhaustive simulation.

**Keywords: Keywords:** Cmos Combinational Logic Circuits Logic Pictures Real-Delay Model Switching Activity Dynamic Power Estimation Toggle Rate

## E-65. Distributed Beamforming and Autonomous Participation Decision Making in Cooperative Cr Systems in Presence of Asynchronous Interference

Mai H. Hassan, Jahangir Hossain and Vijay K. Bhargava

*IEEE Transactions on Wireless Communications, 15: 5016-5029 (2016) IF: 2.925*

We propose a distributed beamforming for cooperative cognitive radio (CR) networks, that reduces the required feedback overhead in terms of sharing the channel state information (CSI) between the cooperating CR relays. Assuming the reciprocity of the channels of each cooperating CR node toward the CR receiver, as well as toward the primary receiver, the proposed beamforming technique only requires sharing the location information of the CR relays among the cooperating CR relays, rather than the global CSI. Reducing the required feedback overhead provides enhanced scalability of the cooperative CR network with lower deployment cost. In this paper, we also propose two autonomous decision making strategies that can help each CR user to independently decide whether to participate in the cooperative transmission or not. This participation decision is tackled from a game theoretic approach, by quantifying the reward and cost functions of each CR relay. The first proposed strategy, named regret testing-

based strategy, is proved to asymptotically achieve an approximate Nash equilibrium state of the system. However, it has higher complexity and slower convergence time. So we also propose a suboptimal decision making strategy, named learning-based strategy, that has lower complexity and faster convergence time.

**Keywords:** Nash Equilibrium, Asynchronous Interference, Autonomous Participation Decision, Cognitive Radio, Distributed Beamforming.

## E-66. Energy - Aware Cooperative Wireless Networks with Multiple Cognitive Users

Mahmoud Ashour, Muhammad Majid Butt, Amr Mohamed, Tamer ElBatt and Marwan Krunz

*IEEE Transactions on Communications, 64(8) : 3233-3245 (2016) IF: 2.298*

In this paper, we study and analyze cooperative cognitive radio networks with arbitrary number of secondary users (SUs). Each SU is considered a prospective relay for the primary user (PU) besides having its own data transmission demand. We consider a multi-packet transmission framework that allows multiple SUs to transmit simultaneously because of dirty-paper coding. We propose power allocation and scheduling policies that optimize the throughput for both PU and SU with minimum energy expenditure. The performance of the system is evaluated in terms of throughput and delay under different opportunistic relay selection policies. Toward this objective, we present a mathematical framework for deriving stability conditions for all queues in the system. Consequently, the throughput of both primary and secondary links is quantified. Furthermore, a moment generating function approach is employed to derive a closed-form expression for the average delay encountered by the PU packets. Results reveal that we achieve better performance in terms of throughput and delay at lower energy cost as compared with equal power allocation schemes proposed earlier in the literature. Extensive simulations are conducted to validate our theoretical findings.

**Keywords:** Cognitive Relaying, Opportunistic Communication, Throughput, Delay, Relay Selection

## E-67. Maximum Secondary Stable Throughput of A Cooperative Secondary Transmitter–Receiver Pair: Protocol Design and Stability Analysis

Ahmed Elshafie, Tamer Khattab, Amr Elkeyi and Mohammed Nafie

*IEEE Transactions on Vehicular Technology, 65: 4937-4951 (2016) IF: 2.243*

In this paper, we investigate the impact of cooperation between a secondary transmitter-receiver pair and a primary transmitter on the maximum stable throughput of the primary-secondary network. Each transmitter, either primary or secondary, has a buffer for storing its own traffic. In addition to its own buffer, the secondary transmitter has a buffer for storing a fraction of the undelivered primary packets due to channel impairments. Moreover, the secondary destination has a relaying queue (buffer) for storing a fraction of the undelivered primary packets. In our proposed cooperative system, the secondary transmitter and the secondary destination increase the spectrum availability for the secondary packets by relaying the unsuccessfully transmitted packets of the primary transmitter. We consider two multiple-access strategies to be used by the secondary transmitter and the secondary destination to utilize the silence sessions of the primary transmitter. Numerical results demonstrate the gains of our proposed cooperative system over the noncooperation case and the systems when the secondary transmitter is the only cooperating node in the network.

**Keywords:** Receivers, Radio Transmitters, Stability Analysis, Decoding, Buffer Storage, Cognitive Radio.

## E-68. Effective Capacity of Delay - Constrained Cognitive Radio Links Exploiting Primary Feedback

Ahmed H. Anwar, Karim G. Seddik, Tamer ElBatt and Ahmed H. Zahran

*IEEE Transactions on Vehicular Technology, 65, (9): 7334-7348 (2016) IF: 2.243*

In this paper, we study the effective capacity (EC) of cognitive radio (CR) networks operating under statistical quality of service (QoS) constraints in an attempt to support real-time applications at the secondary users (SUs). In particular, we analyze the performance gains, in terms of EC and average transmitted power, attributed to leveraging the primary user (PU) feedback overheard at the SU, at no additional complexity or hardware cost. We characterize the EC performance improvement for the SU, in the presence of a feedback-based sensing scheme, under the signal-to-interference-plus-noise ratio (SINR) interference and collision models. Toward this objective, we develop a Markov chain model for feedback-based sensing to compare the performance of a two-link network, a single secondary link, and a primary network abstracted to a single primary link, with and without primary-feedback exploitation. We prove that exploiting the primary feedback at the secondary transmitter improves the EC of the SU under the SINR interference model. On the other hand, interestingly, exploiting the PU feedback messages does not enhance the EC of the SU under the collision model. Nevertheless, exploiting the PU feedback reduces the SU average transmitted power under the two aforementioned models. Finally, we present numerical results, for plausible scenarios, that support our analytical findings.

**Keywords:** Arq Feedback, Cognitive Radio, Collision Channel, Effective Capacity, Interference Channel, Packet Delay

## E-69. Random Aerial Beamforming for Underlay Cognitive Radio with Exposed Secondary Users

Ahmed M. Alaa, Mahmoud H. Ismail and Hazim Tawfik

*IEEE Transactions on Vehicular Technology, 65: 5364-5383 (2016) IF: 2.243*

In this paper, we introduce the exposed secondary-user (SU) problem in underlay cognitive radio systems, where both the secondary-to-primary and primary-to-secondary channels have a line-of-sight (LoS) component. Based on a Rician model for the LoS channels, we show, both analytically and numerically, that LoS interference hinders the achievable SU capacity when interference constraints are imposed at the primary user (PU)

receiver. This is caused by the poor dynamic range of interference channel fluctuations when a dominant LoS component exists. To improve the capacity of such a system, we propose the use of an electronically steerable parasitic array radiator (ESPAR) antenna at the secondary terminals. An ESPAR antenna involves a single radio frequency (RF) chain and has a reconfigurable radiation pattern that is controlled by assigning arbitrary weights to M orthonormal basis radiation patterns via altering a set of reactive loads. By viewing the orthonormal patterns as multiple virtual dumb antennas, we randomly vary their weights over time, creating artificial channel fluctuations that can perfectly eliminate the undesired impact of LoS interference. This scheme is termed as random aerial beamforming (RAB) and is well suited for compact and low-cost mobile terminals as it uses a single RF chain. Moreover, we investigate the exposed-SU problem in a multiuser setting, showing that LoS interference hinders multiuser interference diversity and affects the growth rate of the SU capacity as a function of the number of users. Using RAB, we show that LoS interference can, in fact, be exploited to improve multiuser diversity by boosting the effective number of users.

**Keywords:** Underlay Cognitive Radio, Aerial Degrees of Freedom (Dofs), Cognitive Radio, Dumb Antennas, Line-Of-Sight (Los) Channels, Multiuser Diversity (Md)

## E-70. Closed - form Exact and Asymptotic Expressions for the Symbol Error Rate and Capacity of the H-Function Fading Channel

Husam R. Alhennawi , Moataz M. H. El Ayadi , Mahmoud H. Ismail and Hebat-Allah M. Mourad

*IEEE Transactions on Vehicular Technology, 65: 1957-1974 (2016) IF: 2.243*

In this paper, we derive closed-form exact and asymptotic expressions for the symbol error rate (SER) and channel capacity when communicating over Fox's H-function fading channel. The SER expressions are obtained for numerous practically employed modulation schemes in case of single-branch and three multiple-branch diversity receivers: maximal ratio combining (MRC), equal gain combining (EGC), and selection combining (SC). The derived exact expressions are given in terms of the univariate and multivariate Fox's H-functions for which we provide a portable and efficient Python code. Since Fox's H-function fading channel represents the most generalized fading model ever presented in the literature, the derived expressions subsume most of those previously presented for all the known simple and composite fading models. Moreover, easy-to-compute asymptotic expansions are provided to easily study the behavior of the SER and channel capacity at high values of the average signal-to-noise ratio (SNR). The asymptotic expansions are also useful in comparing different modulation schemes and receiver diversity combiners. Numerical and simulation results are also provided to support the mathematical analysis and prove the validity of the obtained expressions.

**Keywords:** Channel Capacity, Symbol Error Rate, Fox'S H-Distribution, Asymptotic Analysis, Diversity Systems

## E-71. Novel 10-Bit 2.8-Mw Tdc Design Using Sar with Continuous Disassembly Algorithm

Karim O. Ragab, Hassan Mostafa and Ahmed Eladawy

*IEEE Transactions on Circuits and Systems Ii (Tcas Ii), 63: 909-913 (2016) IF: 1.136*

This brief introduces a successive approximation time-to-digital converter based on a novel algorithm denoted as successive approximation register with continuous disassembly (SAR-CD). The main advantage of the proposed SAR-CD algorithm is that it moves the conditioning between the evaluated bits to the digital domain, after all the bits are evaluated. Simulation results show promising enhancements in power consumption compared with the state-of-the-art designs. A full 10-bit architecture is introduced using 65-nm CMOS technology as a case study with simulation power consumption of 2.8 mW at a sampling rate of 29.4 Msample/s from 1-V power supply with an effective number of bits value of 8.63 bits and a maximum differential nonlinearity of 1 least significant bit.

**Keywords:** Cmos, Data Converters, Successive Approximation Analog-To-Digital Converter (Adc), Time-To-Digital Converters (Tdcs), Time Interval Measurement

## E-72. A Low-Distortion High-Efficiency Class-D Audio Amplifier Based on Sliding Mode Control

Ahmed I. Hussein, Ahmed Nader Mohieldin, Faisal Hussien and Ahmed Eladawy

*IEEE Transactions on Circuits and Systems Ii, 63: 713-717 (2016) IF: 1.136*

This brief presents a low-power low-distortion high-efficiency class-D audio amplifier. The proposed architecture uses an integral sliding mode controller with a novel on-chip continuous current sensor. A full-bridge output stage is used to increase the output power, and an adaptive nonoverlapping-clock generation technique is presented to eliminate the short circuit current. Moreover, the switching frequency is chosen to achieve the highest possible linearity without efficiency degradation. The proposed architecture contains the minimum number of loop amplifiers to reduce quiescent current consumption. The proposed class-D audio amplifier has been implemented using 65-nm CMOS technology and operated from a single 2.7-V voltage supply (using thick oxide transistors) while occupying an active area of 0.31 mm2. Post-layout simulations show that the proposed architecture achieves a total harmonic distortion of 0.002% for a 2.2 Vpp 1-kHz input signal. It achieves a peak efficiency of 96% and a maximum output power of 400 mW at an 8-Ω differential load.

**Keywords:** Sliding Mode Control (Smc), Class-D Audio Amplifier, Current Sensor, High-Efficiency, Low-Distortion, Low-Power

## E-73. Process Variation Aware Design of Multi - Valued Spintronic Memristor - Based Memory Arrays

Hassan Mostafa and Yehea Ismail

*IEEE Transactions on Semiconductor Manufacturing (Tsm), 29: 145-152 (2016) IF: 1.045*

The missing fourth passive element, predicted by L. Chua and denoted by memristor, has recently been in the research focus since its titanium dioxide thin film realization is reported by HP. Following that, the spintronic memristor, which is based on the magnetic tunneling junction, is presented as an alternative to the thin film memristor. The nano-scale geometry size of the memristor makes it hard to control its dimensions due to the process variation resulting from the fabrication process. This process variation results in yield degradation in the spintronic memristor-based memory arrays. This yield degradation is more significant when the spintronic memristor is utilized as a multi-valued memory elements. In this paper, the impact of the process variation on the spintronic memristor-based memory yield is discussed for the 1-bit, 2-bit, and n-bit memory element. Moreover, two approaches are introduced to enhance the memory yield.

**Keywords:** Process Variation, Statistical Yield, Memristor, Non-Volatile Memory.

## E-74. Using Network Coding to Achieve the Capacity of Deterministic Relay Networks with Relay Messages

Ahmed Zewail, Yahay Mohasseb, Mohammed Nafie and Hesham Elgamal

*Wireless Communications and Mobile Computing, 16: 2390-2405 (2016) IF: 0.922*

In this paper, we derive the capacity of the deterministic relay networks with relay messages. We consider a network that consists of five nodes, four of which can only communicate via the fifth one. However, the fifth node is not merely a relay as it may exchange private messages with the other network nodes. First, we develop an upper bound on the capacity region based on the notion of a single-sided genie. In the course of the achievability proof, we also derive the deterministic capacity of a four-user relay network (without private messages at the relay). The capacity achieving schemes use a combination of two network coding techniques: the simple ordering scheme and detour scheme. In the simple ordering scheme, we order the transmitted bits at each user such that the bi-directional messages will be received at the same channel level at the relay, while the basic idea behind the detour scheme is that some parts of the message follow an indirect paths to their respective destinations. This paper, therefore, serves to show that user cooperation and network coding can enhance throughput, even when the users are not directly connected to each other. Finally, we make a conjecture about the capacity region of the general K-node relay network with relay messages.

**Keywords:** Network Coding, Relay Networks, Deterministic Capacity

## E-75. Distributed Opportunistic Scheduling for Mimo Underlay Cognitive Radio Networks

Manal El Tanab, Walaa Hamouda and Yasmine Fahmy

*Wireless Communications and Mobile Computing, 16: 2212-2224 (2016) IF: 0.922*

Cognitive radio networks have emerged to improve the utilization of the scarce spectrum. In this paper, we propose a distributed resource allocation algorithm that allocates resources opportunistically to the secondary users in a multiple-input multiple-output environment. In order to reduce the complexity and cost, antenna selection schemes are employed to allow the secondary communication using a single radio frequency chain. The proposed algorithm is proved theoretically and using simulations, to give a performance very close to that of a centralized one with lower delay and overhead. Furthermore, we introduce two techniques for the proposed algorithm based on the allowable data rates referred to as limited and maximum rates. We derive closed-form expression for the consumed power and tight upper bounds for the average throughput achieved by each technique. A comparison between the proposed techniques is also provided. Both simulations and analytical results show that the proposed algorithm achieves high throughput with low complexity. Moreover, the results show that the tightness of the bounds improves with the diversity order. Finally, the proposed techniques are compared with two suggested random schemes to investigate their effectiveness.

**Keywords:** Distributed Opportunistic Scheduling, Mimo, Underlay Cognitive Radio Networks

## E-76. Offset Calibration Technique for Capacitive Transimpedance Amplifier Used in Uncooled Infrared Detection

A.S.H. Ahmed, M.M. Aboudina and S.E.D. Habib

*Microelectronics Journal, 53: 56-64 (2016) IF: 0.876*

This paper presents a novel readout circuit of uncooled, bolometer-based, focal plane arrays (FPAs).The offset and flicker noise are the design challenges of microbolometer readout circuits (ROCs). The ROC is not only required to apply careful noise cancellation techniques, but also to be insensitive to process and supply voltage variations. The proposed circuit involves a new offset cancellation technique which overcomes process variations, noise, random, and systematic offset.

**Keywords:** Focal Plane Array, Microbolometers, Read-Out Circuits, Offset Cancellation Technique, Uncooled Infrared Detectors

## E-77. Memristor Based Bpsk and Qpsk Demodulators with Nonlinear Dopant Drift Model

N.E. Elashkar, M.Aboudina, H.A.H.Fahmy, G.H.Ibrahim and A.H.Khalil

*Microelectronics Journal, 56: 17-24 (2016) IF: 0.876*

In this paper, the dependence of the instantaneous memristance value and its I–V characteristics on a periodic signal phase are studied. Hence, expression for the instantaneous memristance as a function of the periodic input phase is derived. This derivation is based on the memristor linear dop ant drift model and is provided for sinusoidal input waveforms. To prove the tendency, simulations using linear and nonlinear dopant drift memristor models are performed in the Cadence simulation environment. Based on those, asset of digital communication demodulators are proposed and investigated exploiting the change of the average memristance with the initial phase of applied signal. The experimental-based 'nonlinear' dopant drift model is used in designing the proposed demodulators for Binary Phase Shift Keying(BPSK) and Quadrature Phase Shift

Keying (QPSK) modulation schemes. Since all proposed de-modulators are asynchronous, the proposed circuits do not need any carrier recovery circuits. Moreover, transient simulations have been executed showing the proper matching to the expected performance.
**Keywords:** Bpsk, Memristor Based Demodulator, Nonlinear Dopant Drift Model, Qpsk

## E-78. On the Use of a Programmable Front-End for Multi-Band / Multi-Standard Applications

Hoda Abdelsalam, Hassan Mostafa and Yehea Ismail

*Microelectronics Journal, 49: 1-9 (2016) IF: 0.876*

Modern wireless devices require a compact wireless receiver that can access all the available services with fewer bulky off-chip passive components. This advocates the need for multi-band multi-standard receivers. This paper proposes a reconfigurable such receiver front-end controlled by its driving clocks. The receiver adopts charge sampling and impedance translation techniques. Its driving clocks are adjusted based on the targeted frequency. The receiver is tested over the existing standards specifications: GSM 2G (850 MHz, 900 MHz, 1.8 GHz and 1.9 GHz), UMTS 3G (850 MHz, 1.8 GHz, 1.9 GHz and 2.1 GHz), Bluetooth (2.4 GHz) and LTE (700 MHz→5 GHz) and Wi-Fi (2.4 GHz and 5 GHz). The proposed front-end architecture achieves NF of 8 dB, out-of-band IIP3 of 0 dBm and in-band IIP3 of −5 dBm across the tested frequencies in 65 nm CMOS technology. The design occupies 0.45 mm2.
**Keywords:** Receiver; Rf; Multiband; Lte

## E-79. Statistical Yield Improvement Under Process Variations of Multi-Valued Memristor-Based Memories

Hassan Mostafa and Yehea Ismail

*Microelectronics Journal, 51: 46-57 (2016) IF: 0.876*

Memristor, the missing fourth element predicted by L. Chua, has recently been in the research focus since HP Lab reported the first TiO2 thin film memristor realization. The nano-scale geometry size of the memristor makes it difficult to control its dimensions due to the process variation incurred in the fabrication process. This process variation results in yield degradation in the memristor-based memories. This yield degradation is more severe when the memristor device is used as a multi-valued memory element. In this paper, the impact of the process variation on the memristor-based memory yield is investigated for the 1-bit, 2-bit, and n-bit memristor memory element. In addition, two approaches are proposed to improve the memory yield. Therefore, the main objective of this work is to introduce a statistical yield simulation flow to calculate the memory statistical yield under process variations and investigate the effect of different design knobs on this statistical yield regardless of the memristor models and the process variation models used. Simulation results reveal that for 1-bit memristor-based memories, the nominal write voltage should be increased by 30% and the nominal threshold value (i.e., the midway memristance value between the memristor ON resistance and the memristor OFF resistance) should be increased by 65% to achieve the maximum yield. Finally, the paper lists the minimum memristor size that should be used to achieve a 99.9% memory yield for n-bit memories. These results show how the process variation imposes limitations on the minimum memristor device size when multi-valued memories are to be designed.
**Keywords:** Memristor-Based Memory; Process Variation; Statistical Yield Improvement; Multi-Valued Memory

## E-80. Capacity of Fox's H-Function Fading Channel with Adaptive Transmission

Y. Abo Rahama, Mahmoud H. Ismail and M.S. Hassan

*Electronics Letters, 52: 976-978 (2016) IF: 0.854*

Novel closed-form exact expressions for the capacity of the recently-introduced Fox's H-function fading channel are derived. The expressions are obtained assuming different types of adaptive transmission strategies, namely, channel inversion with fixed rate, truncated channel inversion with fixed rate, optimum rate adaptation with fixed power and optimum power and rate adaptation. The obtained expressions are versatile and can be used to evaluate the capacity for virtually any fading channel one might be interested in as a special case.
**Keywords:** H-Function Fading Channel, Optimum Rate Adaptation, Truncated Channel Inversion, Adaptive Transmission Strategies, Novel Closed-Form Exact Expressions

## E-81. Defeating the Eavesdropper: On the Achievable Secrecy Capacity Using Reconfigurable Antennas

Ahmed Alaa and Yasmine Fahmy

*Wireless Personal Communications,91:729-738(2016)IF: 0.701*

In this paper, we consider the transmission of confidential messages over slow fading wireless channels in the presence of an eavesdropper. We propose a transmission scheme that employs a single reconfigurable antenna at each of the legitimate partners, whereas the eavesdropper uses a single conventional antenna. A reconfigurable antenna can switch its propagation characteristics over time and thus it perceives different fading channels. It is shown that without channel side information (CSI) at the legitimate partners, the main channel can be transformed into an ergodic regime offering a secrecy capacity gain for strict outage constraints. If the legitimate partners have partial or full CSI, a sort of selection diversity can be applied boosting the maximum secret communication rate. In this case, fading acts as a friend not a foe.
**Keywords:** Channel State Information (Csi), Outage Probabilit, Outage Secrecy Capacity, Reconfigurable Antennas, Secrecy Capacity

## E-82. Carrier Aggregation-Based Dynamic Spectrum Access Framework for Lte-A Primary Operators

Khaled Qorany AbdelFadeel, Ahmed Khattab, Khaled Elsayed and Fadel Digham

*Iet Communications, 10(13): 1596-1604 (2016) IF: 0.624*

In this study, the authors tackle the dynamic spectrum access (DSA) problem for primary operators (POs) for long-term

evolution-advanced (LTE-A) systems. They propose an auction-based DSA framework that exploits the capabilities of carrier aggregation to efficiently utilise the under-utilised spectrum which varies with time and space. Their proposed dynamic access framework defines the LTE-A resource allocation problem as a bounded knapsack auction (BKA). They solve such a BKA by converting it to a 0–1 knapsack problem that is solved using dynamic programming. Unlike prior work, they are the first to introduce an accurate model for estimating the bandwidth required to satisfy the traffic demands of an LTE-A operator's subscribers for a projected demand model. Using extensive simulations of such a realistic network model, the results of their framework show more than 20% reduction in the required spectrum and up to 80% reduction in the average under-utilised spectrum compared with traditional static spectrum access widely adopted by spectrum regulation authorities. The reduction in the average under-utilised spectrum becomes 93.3% with 250% higher revenue compared with existing dynamic allocation strategies that are directly formulated as 0–1 knapsack auctions.

**Keywords:** Resource Allocation, Long Term Evolution, Radio Spectrum Management, Dynamic Programming

## E-83. Unified Approach for Probability of Detection Evaluation Over Generalised Fading Channels

Moataz M.H. El Ayadi, Mahmoud H. Ismail and Husam R. Alhennawi

*Iet Communications, 10: 1532-1541 (2016) IF: 0.624*

In this study, the authors revisit energy detection-based spectrum sensing cognitive radio systems operating over generalised fading channels. In particular, they derive closed-form exact expressions as well as low- and high-signal-to-noise ratio asymptotic expansions for the misdetection probability over the Fox's H-function fading channel. The closed-form expression is given in terms of the bivariate Fox's H-function and subsumes most of the expressions previously presented in the literature. Also, the obtained asymptotic expressions are very easy to compute and can be used to get various performance insights. We verified, theoretically and numerically, the validity of the exact expression for important special cases previously reported in the literature, namely the Nakagami-m and the extended generalised-K fading distributions. Numerical results also demonstrate the high accuracy of the asymptotic expansions.

**Keywords:** Signal Detection, Cognitive Radio, Probability, Radio Spectrum Management

***Dept. of Engineering Mathematics and Physics***

## E-84. Power and Energy Analysis of Fractional-Order Electrical Energy Storage Devices

M.E. Fouda, A.S. Elwakil, A.G. Radwan and A. Allagui

*Energy, 111: 785-792 (2016) IF: 4.292*

Characterizing and modeling electrical energy storage devices is essential for their proper integration in larger systems. However, basic circuit elements, i.e. resistors, inductors, and capacitors, are not well-suited to explain their complex frequency-dependent behaviors. Instead, fractional-order models, which are based on non-integer-order differential equations in the time-domain and include for instance the constant phase element (CPE), are mathematically more fit to this end. Here, the electrical power and energy of fractional-order capacitance and inductance are derived in both steady-state and transient conditions, and verified using a number of commercial supercapacitors and fractional-order coils. A generalized expression for the energy stored in a supercapacitor/fractional-order inductor is derived and found to depend on the capacitance/inductance and the dispersion coefficient of the device, as well as on the properties of the applied voltage waveform.

**Keywords:** Power; Energy; Capacitor; Supercapacitor; Fractional-Order Inductor

## E-85. Symmetric Encryption Algorithms Using Chaotic and Non-Chaotic Generators: A Review

A. G. Radwan, Sherif H. AbdElHaleem and Salwa K. Abd-El-Hafiz

*Journal of Advanced Research, 7: 193-208 (2016) IF: 3*

This paper summarizes the symmetric image encryption results of 27 different algorithms, which include substitution-only, permutation-only or both phases. The cores of these algorithms are based on several discrete chaotic maps (Arnold's cat map and a combination of three generalized maps), one continuous chaotic system (Lorenz) and two non-chaotic generators (fractals and chess-based algorithms). Each algorithm has been analyzed by the correlation coefficients between pixels (horizontal, vertical and diagonal), differential attack measures, Mean Square Error (MSE), entropy, sensitivity analyses and the 15 standard tests of the National Institute of Standards and Technology (NIST) SP-800-22 statistical suite. The analyzed algorithms include a set of new image encryption algorithms based on non-chaotic generators, either using substitution only (using fractals) and permutation only (chess-based) or both. Moreover, two different permutation scenarios are presented where the permutation-phase has or does not have a relationship with the input image through an ON/OFF switch. Different encryption-key lengths and complexities are provided from short to long key to persist brute-force attacks. In addition, sensitivities of those different techniques to a one bit change in the input parameters of the substitution key as well as the permutation key are assessed. Finally, a comparative discussion of this work versus many recent research with respect to the used generators, type of encryption, and analyses is presented to highlight the strengths and added contribution of this paper.

**Keywords:** Permutation Matrix; Symmetric Encryption; Chess; Chaotic Map; Fractals

## E-86. Novel Permutation Measures for Image Encryption Algorithms

Salwa K. Abd-El-Hafiz, Sherif H. AbdElHaleem and Ahmed G. Radwan

*Optics and Lasers in Engineering, 85: 72-83 (2016) IF: 2.319*

This paper proposes two measures for the evaluation of permutation techniques used in image encryption. First, a general mathematical framework for describing the permutation phase used in image encryption is presented. Using this

framework, six different permutation techniques, based on chaotic and non-chaotic generators, are described. The two new measures are, then, introduced to evaluate the effectiveness of permutation techniques. These measures are (1) Percentage of Adjacent Pixels Count (PAPC) and (2) Distance Between Adjacent Pixels (DBAP). The proposed measures are used to evaluate and compare the six permutation techniques in different scenarios. The permutation techniques are applied on several standard images and the resulting scrambled images are analyzed. Moreover, the new measures are used to compare the permutation algorithms on different matrix sizes irrespective of the actual parameters used in each algorithm. The analysis results show that the proposed measures are good indicators of the effectiveness of the permutation technique.
**Keywords:** Chaos; Chess Horse Movement; Image Encryption; Pixel Permutations

## E-87. Effect of Self Assembled Quantum Dots on Carrier Mobility, with Application to Modeling the Dark Current in Quantum Dot Infrared Photodetectors

Sarah Youssef, Yasser M. El-Batawy and Ahmed A. Abouelsaood

*Journal of Applied Physics (Aip), 120: (2016) IF: 2.101*

A theoretical method for calculating the electron mobility in quantum dot infrared photodetectors is developed. The mobility calculation is based on a time-dependent, finite-difference solution of the Boltzmann transport equation in a bulk semiconductor material with randomly positioned conical quantum dots. The quantum dots act as scatterers of current carriers (conduction-band electrons in our case), resulting in limiting their mobility. In fact, carrier scattering by quantum dots is typically the dominant factor in determining the mobility in the active region of the quantum dot device. The calculated values of the mobility are used in a recently developed generalized drift-diffusion model for the dark current of the device [Ameen et al., J. Appl. Phys. 115, 063703 (2014)] in order to fix the overall current scale. The results of the model are verified by comparing the predicted dark current characteristics to those experimentally measured and reported for actual InAs/GaAs quantum dot infrared photodetectors. Finally, the effect of the several relevant device parameters, including the operating temperature and the quantum dot average density, is studied.
**Keywords:** Quantum Dots, Dark Current, Photodetectors, Electron Mobility, Carrier Scattering.

## E-88. Time-Dependent Congestion Pricing System for Large Networks: Integrating Departure Time Choice, Dynamic Traffic Assignment and Regional Travel Surveys in the Greater Toronto Area

Aya Aboudina, Hossam Abdelgawad, Baher Abdulhai and Khandker Nurul Habib

*Transportation Research Part A: Policy and Practice, 94: 411-430 (2016) IF: 1.994*

Congestion pricing is one of the widely contemplated methods to manage traffic congestion. The purpose of congestion pricing is to manage traffic demand generation and supply allocation by charging fees (i.e., tolling) for the use of certain roads in order to distribute traffic demand more evenly over time and space. This study presents a framework for large-scale variable congestion pricing policy determination and evaluation. The proposed framework integrates departure time choice and route choice models within a regional dynamic traffic assignment (DTA) simulation environment. The framework addresses the impact of tolling on: (1) road traffic congestion (supply side), and (2) travelers' choice dimensions including departure time and route choices (demand side). The framework is applied to a simulation-based case study of tolling a major freeway in Toronto while capturing the regional effects across the Greater Toronto Area (GTA). The models are developed and calibrated using regional household travel survey data that reflect the heterogeneity of travelers' attributes. The DTA model is calibrated using actual traffic counts from the Ontario Ministry of Transportation and the City of Toronto. The case study examined two tolling scenarios: flat and variable tolling. The results indicate that: (1) more benefits are attained from variable pricing, that mirrors temporal congestion patterns, due to departure time rescheduling as opposed to predominantly re-routing only in the case of flat tolling, (2) widespread spatial and temporal re-distributions of traffic demand are observed across the regional network in response to tolling a significant, yet relatively short, expressway serving Downtown Toronto, and (3) flat tolling causes major and counterproductive rerouting patterns during peak hours, which was observed to block access to the tolled facility itself.
**Keywords:** Congestion-Pricing; Dynamic Traffic Assignment Simulation; Departure Time Choice; Large-Scale Network; Schedule-Delay Cost

## E-89. What are the Correct Results for the Special Values of the Operands of the Power Operation?

Wafaa S. Sayed and Hossam A. H. Fahmy

*Acm Transactions on Mathematical Software (Toms), Volume 42 Issue 2: 14-14 (2016) IF: 1.879*

Language standards such as C99 and C11, as well as the IEEE Standard for Floating-Point Arithmetic 754 (IEEE Std 754-2008) specify the expected behavior of binary and decimal floating-point arithmetic in computer-programming environments and the handling of special values and exception conditions. Many researchers focus on verifying the compliance of implementations for binary and decimal floating-point operations with these standards. In this article, we are concerned with the special values of the operands of the power function Z = X^Y. We study how the standards define the correct results for this operation, propose a mathematically justified definition for the correct results of the power function on the occurrence of these special values as its operands, test how different software implementations for the power function deal with these special values, and classify the behavior of different programming languages from the viewpoint of how much they conform to the standards and our proposed mathematical definition. We present inconsistencies between the implementations and the standards, and discuss incompatibilities between different versions of the same software.
**Keywords:** Floating-Point Arithmetic, Nan, Indeterminate, Limits, L'Hˆopital'S Rule, Inconsistency, Incompatibility

## E-90. Dipole–Octupole Polarisability of Uranium Hexafluoride and the oretical Prediction of Anisotropic Light-Scattering Spectrum Using New Intermolecular Potential

M.S.A. El-Kader and Y.N. Kalugina

*Molecular Physics, 114: 44-52 (2016) IF: 1.837*

The higher order dipole–octupole polarisability of uranium hexafluoride has been determined from anisotropic collision-induced light scattering (CILS) of gaseous UF6. A new isotropic intermolecular potential was proposed. The CILS spectra were analysed using present and literature intermolecular potentials. Our estimates for the dipole–octupole polarisability is |E| = 507.3 a.u., which is in a good agreement with our new ab initio value and literature theoretical estimates. Our best theoretical values of (hyper)polarisabilities calculated at the CCSD(T) level of theory are as follows: $\alpha$ = 54.63 a.u., E=−555.3 a.u., C = 595.1 a.u., and $\gamma$ = 2103 a.u.

**Keywords:** Collision-Induced Light Scattering; Intermolecular Potential; Multipolar Polarisabilities; Uf6

## E-91. Enhanced Model of Conductive Filament-Based Memristor Via Including Trapezoidal Electron Tunneling Barrier Effect

Amr Mahmoud Hassan, Hossam A. H. Fahmy, Nadia Hussein and Rafat Ahmed

*IEEE Transactions on Nanotechnology, 15: 484-491 (2016) IF: 1.702*

Memristors exhibit very promising features such as nonvolatility and small area. Several types of memristors have been developed in the last decade using different materials along with physical models explaining their behaviors. In this paper, we modify a previously published model to account for a trapezoidal electron tunneling barrier rather than a zero field or constant potential barrier. The model is verified against experimental data showing better agreement. We then perform a study to find out the effect of different memristors parameters on its I-V characteristics and how to shape the characteristics to fit the applications. Finally, we provide a SPICE model which takes into account the tunneling capacitance and clarify that any fabricated memristor has, inherently, a memcapacitor in parallel. The dominant element may be the memristor or the memcapacitor depending on the frequency of operation.

**Keywords:** Memristors, Mathematical Model, Tunneling, Integrated Circuit Modeling, Electrodes, Data Models, Platinum

## E-92. Mhd Flow Due to a Linearly Stretching Sheet with Induced Magnetic Field

Tarek M. A. El-3Mistikawy

*Acta Mechanica, 227: 3049-3053 (2016) IF: 1.694*

The full MHD equations, governing the flow due to a linearly stretching sheet in the presence of a transverse magnetic field, can be cast in a self similar form involving two parameters—the magnetic Prandtl number Pm and the magnetic interaction number $\beta$. The leading-order problem, as Pm $\sim$ 0, is of hierarchical type allowing the solution first for the velocity field and then for the induced magnetic field. Solutions of the full problem tend readily to the hierarchical solutions as Pm gets smaller, thus justifying the use of the hierarchical approach even at not so small Pm.

**Keywords:** Mhd Flow; Linearly Stretching Sheet; Induced Magnetic Field; Self Similarity

## E-93. Artificial Neural Network Modeling of Plasmonic Transmission Lines

R. Andrawis, M. Swillam, M. El-Gamal and E. Solliman

*Applied Optics, 55: 2780-2790 (2016) IF: 1.66*

In this paper, new models based on Artificial Neural Network (ANN) are developed to predict the propagation characteristics of plasmonic nanostrip and coupled nanostrips transmission lines. The trained ANNs are capable of providing the required propagation characteristics with good accuracy and almost instantaneously. The nonlinear mapping performed by the trained ANNs is written as closed-form expressions, which facilitate the direct use of the results obtained in this research. The propagation characteristics of the investigated transmission lines include the effective refractive index and the characteristic impedance. The time needed to simulate 1000 different versions of the transmission line structure is about 48 hours using full-wave solver compared to 3 seconds using the developed ANN model.

**Keywords:** Neural Networks, Transmission Lines

## E-94. A Novel Surrogate-Based Approach for Optimal Design of Electromagnetic-Based Circuits

Abdel-Karim S.O. Hassan, Ahmed S.A. Mohamed, Azza A. Rabie and Ahmed S. Etman

*Engineering Optimization, 48: 185-198 (2016) IF: 1.38*

A new geometric design centring approach for optimal design of central processing unit-intensive electromagnetic (EM)-based circuits is introduced. The approach uses norms related to the probability distribution of the circuit parameters to find distances from a point to the feasible region boundaries by solving nonlinear optimization problems. Based on these normed distances, the design centring problem is formulated as a max–min optimization problem. A convergent iterative boundary search technique is exploited to find the normed distances. To alleviate the computation cost associated with the EMbased circuits design cycle, space-mapping (SM) surrogates are used to create a sequence of iteratively updated feasible region approximations. In each SM feasible region approximation, the centring process using normed distances is implemented, leading to a better centre point. The process is repeated until a final design centre is attained. Practical examples are given to show the effectiveness of the new design centring method for EM-based circuits.

**Keywords:** Em-Based Circuit Design; Design Centring; Normed Distances; Optimal Design; Space-Mapping Surrogates; Yield Optimization.

## E-95. Oscillation of Third Ordern on linear damped delay differential equations

Martin Bohner, Said R. Grace, Ilgin Sager and ErcanTunç

*Applied mathematics and computation, 278: 21-32 (2016) IF: 1.345*

This paper is concerned with the oscillation of certain third-order nonlinear delay differential equations with damping. We give new characterizations of oscillation of the third-order equation in terms of oscillation of a related, well-studied, second-order linear differential equation without damping. We also establish new oscillation results for the third-order equation by using the integral averaging technique due to Philos. Numerous examples are given throughout.

**Keywords:** Oscillation; Delay; Third order; Functional differential equation

## E-96. Statistical Design Centering Optimization of 1D Photonic Crystal Filters

Abdel-Karim S. O. Hassan, Ahmed S. A. Mohamed, Mahmoud M. T. Maghrabi and Nadia H. Rafat

*Progress In Electromagnetics Research M, 49: 153-165 (2016) IF: 1.315*

A statistical design centering approach is introduced, to achieve the optimal design center point of one-dimensional photonic crystal-based filters which are parts of several optoelectronic systems. Up to our knowledge, it is the first time that a design centering approach is applied to such a design problem. The proposed approach seeks nominal designable parameter values that maximize the probability of satisfying the design specifications (yield function). Thus, the achieved optimal design center point is much more robust to unavoidable designable parameter variations, occurring during fabrication process, for example. The yield maximization problem is formulated as an unconstrained optimization problem solved by derivative-free based-algorithm (NEWUOA) coupled with a variance reduction yield estimator to reduce large number of required system simulations. The flexibility and efficiency of the proposed design centering approach are demonstrated by two practical examples: band pass optical filter and spectral control filter. A comparison with Minimax optimization technique is also given.

**Keywords:** Simulated-Driven Optimization, Optimal System Design, Design Centering, Photonic Filters Design, Photonic Crystals

## E-97. New Insights from an Empirical Multi-Property Interatomic Potential and Predicted Collision-Induced Light Scattering Spectra for Hg-Rare Gas Van Der Waals Complexes

Mohamed S. A. El-Kader and George Maroulis

*(Zeitschrift Für Physikalische Chemie) Z.Phys.Chem., 230: 15-34 (2016) IF: 1.183*

An empirical interatomic potentials for the interaction of Hg with inert gases are developed by simultaneously fitting the modified Tang–Toennies (MTT) potential function to spectroscopic data, thermo-physical and transport properties over a wide temperature range. The two-body anisotropic collision induced light scattering spectra of mercury vapor with mixtures of rare gas has never been measured. The lineshape calculations through quantum mechanical methods have been used to predict a reasonable experimental spectra of the induced light scattering at t = 500 K using these models of potentials and a suitable models for the anisotropy. The results of calculations show that these models of the interactions and the induction mechanisms are the most accurate models reported to date for these mixtures.

**Keywords:** Collision-Induced Light Scattering Spectra, Interatomic Potential, Thermo-Physical and Transport Properties, Hg-Rare Gas.

## E-98. Theoretical Calculation of the Roto translational Collision - Induced Absorption (Cia) Spectra in O2 – O2 Pairs

Mohamed S. A. El-Kader

*(Zeitschrift Für Physikalische Chemie) Z.Phys.Chem., 230: 1099-1109 (2016) IF: 1.183*

Quantum mechanical lineshapes of collision-induced absorption (CIA) at room temperature are computed for gaseous molecular oxygen using theoretical values for induced dipole moments and new isotropic interatomic potential as input. Comparison with measured spectra of the rototranslational collision induced absorption shows good agreement over the full range of frequencies. Empirical models of the dipole moment which reproduce the experimental spectra and the first two spectral moments more closely than the fundamental theory are also given. The quality of the present potential has been checked by comparing between calculated and experimental thermo-physical and transport properties over a wide temperature range, which are found to be in good agreement.

**Keywords:** Far-Infrared Absorption, Induced Dipole Moment, Potential, Oxygen.

## E-99. Fundamentals of Fractional-Order Lti Circuits and Systems: Number of Poles, Stability, Time and Frequency Responses

Mourad S. Semary, Ahmed G. Radwan and Hany N. Hassan

*International Journal of Circuit Theory and Applications, 44: 2114-2133 (2016) IF: 1.179*

This paper investigates some basic concepts of fractional-order linear time invariant systems related to their physical and non-physical transfer functions, poles, stability, time domain, frequency domain, and their relationships for different fractional-order differential equations. The analytical formula that calculates the number of poles in physical and non-physical s-plane for different orders is achieved and verified using many practical examples. The stability contour versus the number of poles in the physical s-plane for different fractional-order systems is discussed in addition to the effect of the non-physical poles on the steady state responses. Moreover,time domain responses based on Mittag-Leffler functions for both physical and non-physical transfer functions are discussed for different cases, which confirm the stability analysis. Many fractional-order linear time invariant systems based on fractional-order differential equations have been discussed numerically in both

time and frequency domains to validate the previous fundamentals.
**Keywords:** Fractional-Order Systems; Stability Analysis; Control; Poles; Physical-Plane; filters; Timeinvariant; Linear System

## E-100. Fractional-Order Mutual Inductance: Analysis and Design

Ahmed Soltan, Ahmed G. Radwan and Ahmed M. Soliman

*International Journal of Circuit Theory and Applications, 44: 85-97 (2016) IF: 1.179*

This paper introduces for the first time the generalized concept of the mutual inductance in the fractional-order domain where the symmetrical and unsymmetrical behaviors of the fractional-order mutual inductance are studied. To use the fractional mutual inductance in circuit design and simulation , an equivalent circuit is presented with its different conditions of operation. Also, simulations for the impedance matrix parameters of the fractional mutual inductance equivalent circuit using Advanced Design System and MATLAB are illustrated. The Advanced Design System and MATLAB simulations of the double-tunedfilter based on the fractional mutual inductance are discussed. A great matching between the numerical analysis and the circuit simulation appears, which confirms the reliability of the concept of the fractional mutual inductance. Also, the analysis of the impedance matching using the fractional-order mutual inductance is introduced.
**Keywords:** Mutual Inductance; Fractional Elements; Double-Tuned filter; Equivalent Circuit

## E-101. Fractional Order Oscillator Design Based on Two-Port Network

Lobna A. Said, Ahmed G. Radwan, Ahmed H. Madian and Ahmed M. Soliman

*Circuits Systems and Signal Processing, 35: 3086-3112 (2016) IF: 1.178*

In this paper, a general analysis of the generation for all possible fractional order oscillators based on two-port network is presented. Three different two-port network classifications are used with three external single impedances, where two are fractional order capacitors and a resistor. Three possible impedance combinations for each classification are investigated, which give nine possible oscillators. The characteristic equation, oscillation frequency and condition for each presented topology are derived in terms of the transmission matrix elements and the fractional order parameters α and β. Mapping between some cases is also illustrated based on similarity in the characteristic equation. The use of fractional order elements α and β adds extra degrees of freedom, which increases the design flexibility and frequency band, and provides extra constraints on the phase difference. Study of four different active elements, such as voltage-controlled current source, gyrator, op-amp-based network, and second-generation current-conveyor-based network, serve as a two-port network is presented. The general analytical formulas of the oscillation frequency and condition as well as the phase difference between the two oscillatory outputs are derived and summarized in tables for each designed oscillator network. A comparison between fractional order oscillators with their integer order counterparts is also illustrated where some designs cannot work in the integer case. Numerical Spice simulations and experimental results are given to validate the presented analysis.
**Keywords:** Fractional-Order; Two-Port Network; Oscillator; Gyrator; Ccii

## E-102.Guest Editorial: Fractional-Order Circuits and Systems: Theory, Design and Applications

Costas Psychalinos, Ahmed S. Elwakil, Ahmed G. Radwan and Karabi Biswas

*Circuits Systems, and Signal Processing, 35: 1807-1813 (2016) IF: 1.178*

Nowadays, there is a significant research interest in the area of fractional-order circuits. This originates from the fact that they find applications in biochemistry, medicine, electrical engineering, and many other fields. For example, the modeling of viscoelasticity as well as of biological cells and tissues has been performed through the utilization of fractional-order calculus. This special issue is focused on the theory, design, and applications of fractional-order circuits and systems, with the purpose of offering to the circuits and systems community the opportunity to explore recent advances in fractional-order circuits and systems theory and design as well as of their applications. A total of 20 papers have been accepted in this special issue and are arranged to cover the following subjects: circuit theory of fractional-order circuits, fractional-order filter and oscillator design and applications, digital circuits and systems approximating fractional-order systems as well as fractional-order circuit applications in renewable energy.
**Keywords:** Fractional-Order; Theory; Design; Applications

## E-103. On the Optimization of Fractional Order Low-Pass Filters

Lobna A. Said, Samar M. Ismail, Ahmed G. Radwan, Ahmed H. Madian, Mohamed F. Abu El-Yazeed and Ahmed M. Soliman

*Circuits Systems and Signal Processing, 35: 2047-2039 (2016) IF: 1.178*

This paper presents three different optimization cases for normalized fractional order low-pass filters (LPFs) with numerical, circuit and experimental results. A multi-objective optimization technique is used for controlling some filter specifications, which are the transition bandwidth, the stop band frequency gain and the maximum allowable peak in the filter pass band. The extra degree of freedom provided by the fractional order parameter allows the full manipulation of the filter specifications to obtain the desired response required by any application. The proposed mathematical model is further applied to a case study of a practical second- generation current conveyor (CCII)-based fractional low-pass filter. Circuit simulations are performed for two different fractional order filters, with orders 1.6 and 3.6, with cutoff frequencies 200 and 500 Hz, respectively. Experimental results are also presented for LPF of 4.46 kHz cutoff frequency using a fabricated fractional capacitor of order 0.8, proving the validity of the proposed design approach.

**Keywords:** Fractional Order Element; Low-Pass Filter; Optimization; Ccii

## E-104. Hyperbolic Model for the Classical Navier-Stokes Equations

Samir Abohadima and Amr Guaily

*The Canadian Journal of Chemical Engineering, 94: 1396-1401 (2016) IF: 1.1*

A new formulation of the classical Navier-Stokes equations is presented, which overcomes the equations' main disadvantage: being a mixed parabolic-hyperbolic system. The new model is achieved by adopting the compressible codeformational time derivative in the stress-strain constitutive relation, resulting in a consistency with the principle of material frame indifference. The main advantage of the new formulation is that the resulting system of equations is purely hyperbolic. The proposed formulation is used to model the benchmark problem of the shock/boundary layer/expansion fan interaction with an apparent degree of success.
**Keywords:** Navier-Stokes, Stress Relaxation, Codeformational Time Derivative, Viscous, Shock Reflection

## E-105. Modified Kinetic-Hydraulic Uasb Reactor Model for Treatment of Wastewater Containing Biodegradable Organic Substrates

Mostafa M. El-Seddik, Mona M. Galal, A. G. Radwan and Hisham S. Abdel-Halim

*Water Science and Technology, 73.7: 1560-1571 (2016) IF: 1.064*

This paper addresses a modified kinetic-hydraulic model for up-flow anaerobic sludge blanket (UASB) reactor aimed to treat wastewater of biodegradable organic substrates as acetic acid based on Van der Meer model incorporated with biological granules inclusion. This dynamic model illustrates the biomass kinetic reaction rate for both direct and indirect growth of microorganisms coupled with the amount of biogas produced by methanogenic bacteria in bed and blanket zones of reactor. Moreover, the pH value required for substrate degradation at the peak specific growth rate of bacteria is discussed for Andrews' kinetics. The sensitivity analyses of biomass concentration with respect to fraction of volume of reactor occupied by granules and up-flow velocity are also demonstrated. Furthermore, the modified mass balance equations of reactor are applied during steady state using Newton Raphson technique to obtain a suitable degree of freedom for the modified model matching with the measured results of UASB Sanhour wastewater treatment plant in Fayoum, Egypt.
**Keywords:** Acetic Acid Degradation; Bacterial Growth; Biogas Modeling; Modified Uasb.

## E-106. Oscillation Criteria for Nth-Order Nonlinear Delay Differential Equations with Amiddle Term

S. R. Gracea and A. Zaferb

*Mathematical Methods in The Applied Sciences, 39: 1150-1158 (2016) IF: 1.002*

In this article, we establish some new criteria for the oscillation of nth-order nonlinear delay differential equations of the form

$$\left(r_2(t)\left(r_1(t)\left(y^{(n-2)}(t)\right)^{\alpha}\right)'\right)' + p(t)\left(y^{(n-2)}(t)\right)^{\alpha} + q(t)f(y(g(t))) = 0, \quad n \text{ even},$$

provided that the second-order equation

$$(r_2(t)z')' + \frac{p(t)}{r_1(t)}z = 0$$

is either nonoscillatory or oscillatory. Examples are given to illustrate the results.
**Keywords:** Oscillation; Nth-Order; Delay Differential Equation; Comparison

## E-107. Ion Slip Effect on Unsteady Couette Flow of A Dusty Fluid in the Presence of Uniform Suction and Injection with Heat Transfer

Hazem Ali Attia , W. Abbas and Mostafa A. M. Abdeen

*Journal of The Brazilian Society of Mechanical Science and Engineering, 38: 2381-2391 (2016) IF: 0.963*

The combined effects of Hall current, ion slip, viscous dissipation, and Joule heating on unsteady magnetohydrodynamic Couette flow with heat transfer of a dusty viscous incompressible electrically conducting fluid are studied under a constant pressure gradient. The fluid is subjected to an external uniform magnetic field and a uniform suction and injection perpendicular to the plates (y-direction). Numerical solutions for the constitutive equations are obtained using the method of finite differences. The effects of the magnetic field, Hall parameter, and ion slip parameter on the velocity and temperature distributions for both the fluid and particle phases are investigated in details and shown graphically. It is found that, the Hall current and ion slip parameters have a great effect on the fluid and dust velocities and temperature.
**Keywords:** Dusty Viscous Incompressible Fluid · Unsteady Magnetohydrodynamic Couette Flow · Hall Currents · Ion Slip Currents · Joule Dissipation

## E-108. A Simulation Study for the Use of Transistor Contacts for Sub-Terahertz Radiation Detection

Nihal Ibrahim , Nadia H. Rafat and Salah El-Din Elnahwy

*Iet Microwaves, Antennas and Propagation, 10: 784-790 (2016) IF: 0.88*

Despite the increasing evidence that on-chip metallisation layer plays the role of an antenna in field effect transistor terahertz detectors, sufficient study and analysis of this role remain lacking. Three-dimensional (3D) simulation is used to study the efficiency of sub-terahertz electromagnetic radiation coupling to

on-chip metallisation layer components. The results suggest that on-chip metallisation, especially the contacts of the field effect transistor, can be used as an effective antenna with reasonable efficiency. The two basic structures tested are the laterally stacked as well as vertically stacked contacts. The effect of varying a number of design parameters of the suggested test structures (e.g. substrate/inter-metal-dielectric thickness, and contacts dimensions) is studied using 3D simulation, and the overall detection efficiency is extracted in each case. These results are used to extract broad guidelines for the efficient use of the on-chip metallisation layer as an effective detecting antenna in sub-terahertz radiation detectors.

**Keywords:** Metallisation; Terahertz Wave Detectors; Electronic Engineering Computing; Submillimetre Wave Detectors; Electrical Contacts; Radiation Detection; Submillimetre Wave Antennas; Submillimetre Wave Transistors; Field Effect Transistors

## E-109. An Optimal Linear System Approximation of Nonlinear Fractional-Order Memristor–Capacitor Charging Circuit

Mourad S. Semary, Hany L. Abdel Malek, Hany N. Hassan and Ahmed G. Radwan

*Microelectronics J., 51: 58-66 (2016) IF: 0.876*

The analysis of nonlinear fractional-order circuits is a challenging problem. This is due to the lack of nonlinear circuit theorems and designs particularly in the presence of memristive elements. The response of a series connection of a simple resistor with fractional order capacitor and its analytical formulation in both charging and discharging phases is considered. The numerical simulation of fractional order HP memristor in series with a fractional order capacitor is also discussed. It is a demonstration of a simple nonlinear fractional-order memristive circuit in both charging and discharging cases. Furthermore, this paper introduces an approach to approximate nonlinear fractional-order memrisitve circuits by linear circuits using a minimax optimization technique. Hence, the new circuit can be analyzed using the conventional linear circuit theorems. The charging and discharging of a series fractional-order memristor with a fractional-order capacitor are discussed numerically. The effect of fractional-order parameters and memristor polarity are also investigated. Using a suitable optimization technique, an accurate approximation by a circuit that include a resistor and a fractional-capacitor is obtained for both charging and discharging cases. A great matching was observed between the frequency responses of the fractional-order nonlinear low pass filter based on fractional-order memristor and fractional-order capacitor and that of the optimized linear fractional order case. Similar matching is observed for the nonlinear and optimized cases when a periodic triangular waveform is applied using Fourier series expansion.

**Keywords:** Memristor; Fractional Element; Nonlinear Fractional-Order System; Memristor–Capacitor Charging Circuit; Low-Pass Filter; Optimal Solution.

## E-110. Two-Port Two Impedances Fractional Order Oscillators

Lobna A Said, Ahmed G Radwan, Ahmed H Madian and Ahmed M Soliman

*Microelectronics Journal, 55: 40-52 (2016) IF: 0.876*

This paper presents a study for general fractional order oscillator based on two port network where two topologies of oscillator structure with two impedances are discussed. The two impedances are chosen to be fractional elements which give four combinations for each topology. The general oscillation frequency, condition and the phase difference between the two oscillatory outputs are deduced in terms of the transmission matrix parameter of a general two port network. As a case study: two different networks are presented which are op-amp based circuit and non-ideal gyrator circuit. The oscillation parameters for each case have been derived, and discussed numerically using Matlab. Spice simulations are presented for some cases to validate the proposed idea. Experimental results for the op-amp network are introduced to validate the reliability of the presented oscillator. The extra degree of freedom provided by the fractional order parameter enables the oscillation frequency band to cover from small Hz to hundreds MHz which is suitable range for most of measuring applications.

**Keywords:** Fractional-Order Circuits; Two-Port Network; Oscillators

## E-111. Mhd Flow Due to the Nonlinear Stretching of A Porous Sheet

Tarek M. A. El-Mistikawy

*Advances In Mathematical Physics, (2016) IF: 0.787*

The MHD flow due to the nonlinear stretching of a porous sheet is investigated. A closed form solution is obtained when the stretching rate is inversely proportional to the distance from the origin. Otherwise a uniformly valid asymptotic expansion, for large magnetic interaction number $\beta \sim \infty$, is developed. It coincides with a homotopy perturbation expansion for the problem. The asymptotic/homotopy perturbation expansion gives results in excellent agreement with accurate numerical results, for large as well as small values of $\beta$. For large $\beta$, the expansion, being asymptotic, needs a small number of terms, regardless of the mass transfer rate or the degree of nonlinearity. For small $\beta$, the expansion is a homotopy perturbation one. It needs considerably increasing number of terms with higher injection rates and/or with stretching rates approaching the inverse proportionality. It may even fail.

**Keywords:** Mhd; Nonlinear Stretching; Porous Sheet; Asymptotic Expansion; Homotopy Perturbation

## E-112. Oscillation Criteria for Third-Order Functional Differential Equations with Damping

Martin Bohner, Said R. Grace and Irena Jadlovska

*Electronic Journal of Di Erential Equations, 2016: 1-15 (2016) IF: 0.769*

This paper is a continuation of the recent study by Bohner et al [9] on oscillation properties of nonlinear third order functional

differential equation under the assumption that the second order differential equation is nonoscillatory. We consider both the delayed and advanced case of the studied equation. The presented results correct and extend earlier ones. Several illustrative examples are included.
**Keywords:** Oscillation; delay; advance; third order; damping; functional differential equation.

## E-113. Oscillatory Behavior of a Third-Order Neutral Dynamic Equation with Distributed Delays

Said R. Grace, John R. Graef and Ercan Tunç

*Electronic Journal of Qualitative Theory of Differential Equations, 14: 1-14 (2016) IF: 0.732*

The authors present some new oscillation criteria for the third-order neutral dynamic equation with distributed delays

$$\left[r(t)\left(\left[x(t)+\int_a^b p(t,\eta)x\left[\tau(t,\eta)\right]\Delta\eta\right]^{\Delta\Delta}\right)^{\alpha}\right]^{\Delta}+\int_c^d q(t,\xi)f\left(x\left[\phi(t,\xi)\right]\right)\Delta\xi=0$$

on a time scale T, where a is the quotient of odd positive integers. Using a Riccati type transformation and a comparison technique, they establish some new sufficient conditions to ensure that a solution x of this equation either oscillates or satisfies.
**Keywords:** Oscillation, Time Scales, Third-Order Neutral Dynamic Equation, Asymptotic Behavior, Distributed Delays.

## E-114. Asymptotic Behavior of Solutions of Forced Fractional Differential Equations

Said R. Grace, John R. Graef and Ercan Tunç

*Electronic Journal of Qualitative Theory of Differential Equations, 71: 1-10 (2016) IF: 0.732*

The authors study the boundedness of nonoscillatory solutions of forced fractional differential equations of the form

$${}^{C}D_c^{\alpha}y(t)=e(t)+f(t,x(t)),\qquad c>1,\quad \alpha\in(0,1),$$

where $y(t)=(a(t)x'(t))'$, $c_0=\frac{y(c)}{\Gamma(1)}=y(c)$, and $c_0$ is a real constant. The technique used in obtaining their results will apply to related fractional differential equations with Caputo derivatives of any order. Examples illustrate the results obtained in this paper.
**Keywords:** Integro-Differential Equations, Fractional Differential Equations, Asymptotic Behavior, Nonoscillatory Solutions

## E-115. Characterizing Software Development Method Using Metrics

Doaa M. Shawky and Salwa K. Abd-El-Hafiz

*Journal of Software: Evolution and Process, 28: 82-96 (2016) IF: 0.729*

This work investigates whether the development methodology affects some metrics that are related to the quality of the generated code. Trying to characterize the development methodology using software metrics could be beneficial to developers who use agile approaches extensively. Therefore, this study sheds light on the metrics that might be highly affected by following agile approaches. The values of these metrics need to be tracked, because they might result in a quality-related issue, such as error-proneness, for example. The proposed approach employs different feature selection and classification methods, which include artificial neural networks. We used 11 object-oriented systems of various sizes and functionalities. Five of the used systems were developed using agile approaches, while the rest were developed using non-agile methodologies. The classes and methods of the used systems were represented by a set of metrics that shows some complexity, cohesion, and coupling features of the systems. The generated metrics are used as features to classify between the two different types of the development methodologies using a feed-forward artificial neural network. The obtained high classification accuracy shows the strong relationship between the used metrics and the type of the followed development process.
**Keywords:** Agile Development; Classification; Feature Selection; Software Metrics; Ann.

## E-116. Analytical Solutions for Timoshenko Beam-Columns on Elastic Foundations

Taha. M.H and Abdeen M.A.M.

*Arabian Journal for Science and Engineering, 41: 4053-4064 (2016) IF: 0.728*

In the present work, static and dynamic stability parameters of a Timoshenko beam-column resting on a two parameters foundation are investigated. Analytical solutions using recursive differentiation method (RDM) are obtained considering both the angular inertia and shear stress induced from the axial load. Obtained solutions are verified and then used to capture the significance of different beam-foundation parameters on the stability parameters. Different approaches used to deal with the shear stress induced from the axial load are investigated. Solutions based on Euler-Bernoulli beam and Timoshenko beam theories are compared. It is indicated that the solutions of the two theories converge as the slender ratio of the beam increases. In case of beams resting on soils, it is indicted that the soil influence on stability parameters may be neglected for beams with slenderness ratio less than 20. It is highlighted that the proposed solutions are simple, straightforward and accurate compared with the available solutions in literature.
**Keywords:** Recursive Differentiation Method; Stability Parameter; Timoshenko Beam; Two Parameter Foundations.

## E-117. Optimization of Multilayer Cylindrical Cloaks Using Genetic Algorithms and Newuoa

Ahmed A. Sakr and Alaa K. Abdelmageed

*The European Physical Journal Applied Physics, 74: 30301-30301 (2016) IF: 0.669*

The problem of minimizing the scattering from a multilayer cylindrical cloak is studied. Both TM and TE polarizations are considered. A two-stage optimization procedure using genetic algorithms and NEWUOA (new unconstrained optimization algorithm) is adopted for realizing the cloak using homogeneous isotropic layers. The layers are arranged such that they follow a repeated pattern of alternating DPS and DNG

materials. The results show that a good level of invisibility can be realized using a reasonable number of layers. Maintaining the cloak performance over a finite range of frequencies without sacrificing the level of invisibility is achieved.
**Keywords:** Electromagnetic Scattering; Cloaking; Optimization

## E-118. Asymptotic Behavior of Certain Integrodifferential Equations

Said Grace and Elvan Akin

*Discrete Dynamics in Nature and Society, 1-6 (2016) IF: 0.646*

This paper deals with asymptotic behavior of nonoscillatory solutions of certain forced integrodifferential equations of the form: $(a(t)x'(t))' = e(t) + \int_c^t (t-s)^{\alpha-1}k(t,s)f(s,x(s))ds,\ c > 1,\ 0 < \alpha < 1.$

From the obtained results, we derive a technique which can be applied to some related integrodifferential as well as integral equations.
**Keywords:** Asymptotic Behavior, Integro-Differentil Equations

## E-119. Comparison Criteria for Nonlinear Functional Dynamic Equations of Higher Order

Taher S. Hassan and Said R. Grace

*Discrete Dynamics in Nature and Society, 1-9 (2016) IF: 0.646*

We will consider the higher order functional dynamic equations with mixed nonlinearities of the form $x^{[n]}(t) + \sum_{j=0}^{N} p_j(t)\phi_{\gamma_j}(x(\varphi_j(t))) = 0$, on an above-unbounded time scale $\mathbb{T}$, where $n \geq 2$, $x^{[i]}(t) := r_i(t)\phi_{\alpha_i}[(x^{[i-1]})^{\Delta}(t)]$, $i = 1, \ldots, n-1$, with $x^{[0]} = x$, $\phi_\beta(u) := |u|^\beta \operatorname{sgn} u$, and $\alpha[i,j] := \alpha_i \cdots \alpha_j$. The function $\varphi_i : \mathbb{T} \to \mathbb{T}$ is a rd-continuous function such that $\lim_{t\to\infty}\varphi_i(t) = \infty$ for $j = 0, 1, \ldots, N$. The results extend and improve some known results in the literature on higher order nonlinear dynamic equations.
**Keywords:** Oscillation; Nth-Order; Delay Differential Equation; Comparison

## E-120. Fractional-Order Two-Port Networks

M. E. Fouda, A. S. Elwakil, A. G. Radwan and B. J. Maundy

*Mathematical Problems in Engineering, 2016: 1-5 (2016) IF: 0.644*

We introduce the concept of fractional-order two-port networks with particular focus on impedance and admittance parameters. We show how to transform a 2x2 impedance matrix with fractional-order impedance elements into an equivalent matrix with all elements represented by integer-order impedances; yet the matrix rose to a fractional-order power. Some examples are given.
**Keywords:** Fractional - Calculus; Impedance; Two - Port Networks

## E-121. Asymptotic Behavior of Even-Order Damped Differential Equations with P-Laplacian Like Operators and Deviating Arguments

Qingmin Liu, Martin Bohner, Said R Grace and Tongxing Li

*Journal of Inequalities and Applications, 2016: 1-18 (2016) IF: 0.63*

We study the asymptotic properties of the solutions of a class of even-order damped differential equations with p-Laplacian like operators, delayed and advanced arguments. We present new theorems that improve and complement related contributions reported in the literature. Several examples are provided to illustrate the practicability, maneuverability, and efficiency of the results obtained. An open problem is proposed.
**Keywords:** Asymptotic Behavior; Functional Differential Equation; Even-Order; Damping Term; P-Laplacian Equation

## E-122. Oscillation Criteria for Certain Fourth-Order Nonlinear Delay Differential Equations

Said R. Grace, Shurong Sun and Elvan Akın

*Mediterr. J. Math., 13: 2383-2396 (2016) IF: 0.599*

In this article, we establish some new criteria for the oscillation of fourth-order nonlinear delay differential equations of the form

$$(r_2(t)(r_1(t)(y''(t))^{\alpha})')' + p(t)(y''(t))^{\alpha} + q(t)f(y(g(t))) = 0$$

provided that the second-order equation

$$(r_2(t)z'(t))' + \frac{p(t)}{r_1(t)}z(t) = 0$$

is nonoscillatory or oscillatory.

**Keywords:** Oscillation, Fourth Order, Functional Differential Equation

## E-123. On the Oscillatory and Asymptotic Behavior of Solutions of Certain Integral Equations

Said R. Grace

*Mediterr. J. Math., 13: 2721-2732 (2016) IF: 0.599*

We present the conditions under which every positive solution x(t) of the integral equation

$$x(t) = a(t) + \int_c^t (t-s)^{\alpha-1}[e(s) + k(t,s)f(s,x(s))]\,\mathrm{d}s, \quad c > 1, \alpha > 0$$

Satisfies

$$x(t) = O(a(t)) \quad \text{as} \quad t \to \infty, \quad \text{i.e.,} \limsup_{t\to\infty}\frac{x(t)}{a(t)} < \infty,$$

From the obtained results, we derive a technique which can be applied to some related integral equations that are equivalent to certain fractional differential equations of Caputo derivative of any order. We also establish new oscillation criteria for such fractional differential equations.

**Keywords:** Asymptotic Behavior, Oscillation, Nonoscillatation, Caputo Derivative, Fractional Differential Equations

## E-124. Non-Darcy Unsteady Mhd Hartmann Flow in a Porous Medium with Heat Transfer

Hazem Ali Attia, Mostafa A. M. Abdeen and Karem M. Ewis

*Mechanics and Industry, 17: 112-112 (2016) IF: 0.559*

The time varying magneto-hydrodynamic (MHD) Hartmann non-Darcy flow with heat transfer through a porous medium of an electrically conducting, viscous, incompressible fluid between two infinite parallel insulating porous plates is studied. A non-Darcy model that obeys the Forchheimer extension is assumed for the characteristics of the porous medium. A uniform suction and injection as well as an externally applied uniform magnetic field are applied in the direction normal to the plates where a uniform and constant pressure gradient is imposed in the axial direction. The two plates are kept at different but constant temperatures while the Joule and viscous dissipations are considered in the energy equation. The effect of the magnetic field, the Hall current, the porosity of the medium, and the uniform suction and injection on both the velocity and temperature distributions are studied and interesting results are presented for various values of the existing parameters.
**Keywords:** Porous Medium; Non-Darcy Model; Forchheimer Model ; Hartmann Flow; Magnetohydrodynamic; Hall Current; Numerical Solution

## E-125. On a Sum with a Three-Parameter Mittag-Leffler Function

D.S. de Oliveira, E. Capelas de Oliveira and Sarah Deif

*Integral Transforms and Special Functions, 27: 639-652 (2016) IF: 0.528*

The bounding of the two-parameter Mittag-Leffler function is discussed. As a particular consequence, we present two proofs for a sum involving a three-parameter Mittag-Leffler function. This sum can be seen as a generalization of a relation involving a product of two exponential functions. Particular cases are recovered.
**Keywords:** Mittag-Leffler Functions, Laplace Transform, Volterra Integral Equation, Error Bounds, Sum of Series

## E-126. Fractional-Order Multi-Phase Oscillators Design and Analysis Suitable for Higher-Order Psk Applications

Mohammed E. Fouda, Ahmed Soltan, Ahmed G. Radwan and Ahmed M. Soliman

*Analog Integrated Circuits and Signal Processing, 87: 301-312 (2016) IF: 0.417*

Recently, multi-phase oscillator design witnesses a lot of progress in communication especially phase shift keying based systems. Yet, there is a lack in design multi-phase oscillator with different fractional phase shifts. Thus, in this paper, a new technique to design and analyze a multi-phase oscillator is proposed. The proposed procedure is built based on the fractional-order elements or constant phase elements in order to generate equal or different phase shifts. The general characteristics equation for any oscillator is studied to derive expressions for the oscillation conditions and oscillation frequency. Also, stability analysis is introduced to guarantee the oscillation. Then, different examples of oscillators for equal and different phase shifts are introduced with their simulations.
**Keywords:** Oscillator; Multi-Phase; Fractional; Psk; Stability; Oscillator Analysis.

## E-127. Unsteady Flow of a Dusty Bingham Fluid Through a Porous Medium in a Circular Pipe

H. A. Attia, W. Abbas, A. L. Aboul-Hassan, M. A. M. Abdeen and M. A. Ibrahim

*Journal of Applied Mechanics and Technical Physics, 57: 596-602 (2016) IF: 0.274*

A time-varying flow through a porous medium of a dusty viscous incompressible Bingham fluid in a circular pipe is studied. A constant pressure gradient is applied in the axial direction, whereas the particle phase is assumed to behave as a viscous fluid. The effect of the medium porosity, the non-Newtonian fluid characteristics, and the particle phase viscosity on the transient behavior of the velocity, volumetric flow rates, and skin friction coefficients of both the fluid and particle phases is investigated. A numerical solution is obtained for the governing nonlinear momentum equations by using the method of finite differences.
**Keywords:** Unsteady Flow, Circular Pipe, Porous Medium, Non-Newtonian Fluid, Bingham Fluid.

## E-128. Non-Darcyeffect on Non-Newtonian Bingham Fluid with Heat Transfer Between two Parallel Plates

W. Abbas, Hazem Ali Attia and Mostafa A. M. Abdeen

*Bulgarian Chemical Communications, 48: 497-505 (2016) IF: 0.229*

The non-Darcy model for the Bingham fluid has a wide range of applications in energy systems and magnetic material processing. This work investigated the effect of unsteady non-Darcy flow on the velocity and temperature distributions for non-Newtonian Bingham fluid between two infinite parallel porous plates with heat transfer considering the Hall Effect. A constant pressure gradient is applied in the main axial direction and an external uniform magnetic field and uniform suction and injection are applied in the direction perpendicular to the plates. The dimensionless governing coupled momentum and energy equations taking the Joule and viscous dissipations into consideration are derived and solved numerically using the finite difference approach. The effect of porosity of the medium, Hartmann, and Hall current parameters on the velocity and temperature distributions with a Reynolds number fixed at 10 (For R_e≥10, non-Darcy model is sufficient) is investigated. It is found that the porosity and inertial effects have a marked effect on decreasing the velocity distribution in an inverse proportionality manner. Furthermore, increasing the non-Darcian parameter decreases the temperature values for each value of the porosity.
**Keywords:** Non-Newtonian Fluid, Bingham Model, Non-Darcyflow, Heat Transfer, Hall Current

## E-129. Oscillation Criteria for Fourth Order Nonlinear Positive Delay Differential Equations with A Middle Term

Said Grace and Elvan Akin

*Dynamic Systems and Applications, 25:431-438 (2016) IF: 0.213*

In this article, we establish some new criteria for the oscillation of fourth order nonlinear delay differential equations of the form $x(4)(t) + p(t)x(2)(t) + q(t)f(x(g(t))) = 0$ provided that the second order equation $z(2)(t) + p(t)z(t) = 0$ is nonoscillatiory or oscillatory. This equation with $g(t) = t$ is considered in [8] and some oscillation criteria for this equation via certain energy functions are established. Here, we continue the study on the oscillatory behavior of this equation via some inequalities

**Keywords:** Oscillation, Differential Equations, Higher Order, Delay.

## E-130. Approximate Analytical Technique to Design Reflectarray Antenna

Hesham M. Yamani, Ahmed M. Attiya and Alaa K. Abdelmageed

*Advanced Electromagnetics, 5: 41-45 (2016)*

This paper presents an analysis and design for a reflectarray antenna composed of an array of rectangular patches printed on a grounded dielectric slab. A simple analytical technique based on equivalent surface impedance is used to determine the reflection of the elements in reflectarray antenna. This equivalent surface impedance is obtained analytically in a closed form. The effect of the angle of incidence on each element in the reflectarray is included in calculations. To author's knowledge, this property has not been included in previous analysis techniques of reflectarray antenna.

**Keywords:** Reflectarray- Grounded Slab

### *Dept. of Irrigation & Hydraulics Engineering*

## E-131. Event - Based Stormwater Management Pond Runoff Temperature Model

F. Sabouria, B Gharabaghi, Ahmed A Sattar and J Thompsona

*Journal of Hydrology, 540: 306-316 (2016) IF: 3.043*

Stormwater management wet ponds are generally very shallow and hence can significantly increase (about 5.4 °C on average in this study) runoff temperatures in summer months, which adversely affects receiving urban stream ecosystems. This study uses gene expression programming (GEP) and artificial neural networks (ANN) modeling techniques to advance our knowledge of the key factors governing thermal enrichment effects of stormwater ponds. The models developed in this study build upon and compliment the ANN model developed by Sabouri et al. (2013) that predicts the catchment event mean runoff temperature entering the pond as a function of event climatic and catchment characteristic parameters. The key factors that control pond outlet runoff temperature, include: (1) Upland Catchment Parameters (catchment drainage area and event mean runoff temperature inflow to the pond); (2) Climatic Parameters (rainfall depth, event mean air temperature, and pond initial water temperature); and (3) Pond Design Parameters (pond length-to-width ratio, pond surface area, pond average depth, and pond outlet depth). We used monitoring data for three summers from 2009 to 2011 in four stormwater management ponds, located in the cities of Guelph and Kitchener, Ontario, Canada to develop the models. The prediction uncertainties of the developed ANN and GEP models for the case study sites are around 0.4% and 1.7% of the median value. Sensitivity analysis of the trained models indicates that the thermal enrichment of the pond outlet runoff is inversely proportional to pond length-to-width ratio, pond outlet depth, and directly proportional to event runoff volume, event mean pond inflow runoff temperature, and pond initial water temperature.

**Keywords:** Event; Stormwater; Runoff;

## E-132. Event-Based Total Suspended Sediment Particle Size Distribution Model

Jennifer Thompsona, Ahmed A Sattar, B Gharabaghi and Ed Mac Bean

*Journal of Hydrology, 536: 236-246 (2016) IF: 3.043*

One of the most challenging modelling tasks in hydrology is prediction of the total suspended sediment particle size distribution (TSS–PSD) in stormwater runoff generated from exposed soil surfaces at active construction sites and surface mining operations. The main objective of this study is to employ gene expression programming (GEP) and artificial neural networks (ANN) to develop a new model with the ability to more accurately predict the TSS–PSD by taking advantage of both event-specific and site-specific factors in the model. To compile the data for this study, laboratory scale experiments using rainfall simulators were conducted on fourteen different soils to obtain TSS–PSD. This data is supplemented with field data from three construction sites in Ontario over a period of two years to capture the effect of transport and deposition within the site. The combined data sets provide a wide range of key overlooked site-specific and storm event-specific factors. Both parent soil and TSS–PSD in runoff are quantified by fitting each to a lognormal distribution. Compared to existing regression models, the developed model more accurately predicted the TSS–PSD using a more comprehensive list of key model input parameters. Employment of the new model will increase the efficiency of deployment of required best management practices, designed based on TSS–PSD, to minimize potential adverse effects of construction site runoff on aquatic life in the receiving watercourses.

**Keywords:** Suspended Sediment; Erosion.

## E-133. Prediction of Timing of Watermain Failure Using Gene Expression Models

Sattar, A.M.A., Gharabaghi and B. McBean

*Water Resources Management, 30: 1635-1651 (2016) IF: 2.437*

An innovative predictive equation characterizing watermain failure timing developed from datasets of historical failures in Greater Toronto Area (GTA), Ontario, Canada is described. Gene expression programming (GEP) is used to develop empirical relations between the time to failure and control variables including protection methods for three types of pipes, Cast Iron, Ductile Iron, and Asbestos Cement. The developed

GEP model has a correlation coefficient of 0.68, and with the advantage for predicting not only the time to first break, but also subsequent breaks. The prediction uncertainties of the developed GEP were 38 % of the median value for time to next failure. A parametric analysis is performed for further verification of the developed GEP model showing the relation is simple, yet effectively forecasts watermain timing to first failure and subsequent failures. Simulated failure scenarios indicate a return to high failure rates if cement mortar lining and cathodic protection are not extended to all candidate pipes in the distribution system.

**Keywords:** Infrastructurewatermainpipe Failurepredictiondata Mininggene Expression Programmingasset Rehabilitation

## E-134. Harold Edwin Hurst: the Nile and Egypt, Past and Future

John Sutcliffe, Stephen Hurst, Ayman G. Awadallah, Emma Brown and Khaled Hamed

*Hydrological Sciences Journal, 61: 1557-1570 (2016) IF: 2.182*

H.E. Hurst spent some 60 years studying the Nile for the Egyptian government, and laid the foundation for a monumental set of hydrological records and investigations. His studies of the size of over-year reservoirs needed to maintain a given yield from Nile flows showed that this was greater than that based on random series. This finding, known as the Hurst phenomenon, was confirmed by other natural series and led to important advances in practical and theoretical statistics. His work led to the design of the Aswan High Dam and to continued research in Egypt.

**Keywords:** Nile, Hurst Phenomenon, Aswan High Dam.

## E-135. The Distribution of Spearman'S Rho Trend Statistic for Persistent Hydrologic Data

K. H. Hamed

*Hydrological Sciences Journal, 61: 214-223 (2016) IF: 2.182*

Spearman's rho, a distribution-free statistic, has been suggested in the literature for testing the significance of trend in time series data. Although the use of the test based on Spearman's rho (also known as the Daniels test) is less widespread than that based on Kendall's tau (the Mann-Kendall test), the two tests have been shown in the literature to be equivalent for time series with independent observations. The distribution of the Mann-Kendall trend statistic for persistent data has been previously addressed in the literature. In this paper, the distribution of Spearman's rho as a trend test statistic for persistent data is studied. Following the same procedures used for Kendall's tau in earlier work, an exact expression for the variance of Spearman's rho for persistent data with multivariate Gaussian dependence is derived, and a method for calculating the exact full distribution of rho for small sample sizes is also outlined. Approximations for moderate and large sample sizes are also discussed. A case study of testing the significance of trends in a group of world river flow station data using both Kendall's tau and Spearman's rho is presented. Both the theoretical results and those of the case study confirm the equivalence of trend testing based on Spearman's rho and Kendall's tau for persistent hydrologic data.

**Keywords:** Spearman'S Rho, Kendall'S Tau, Persistence, Trend Test, Autocorrelation

## E-136. Prediction of Organic Micropollutant Removal in Soil Aquifer Treatment System Using Gep

Ahmed M. A. Sattar

*Journal of Hydrologic Engineering, 21: 1-15 (2016) IF: 1.53*

With constrained Nile water and the cruel drop in per capita freshwater share in Egypt, soil aquifer treatment (SAT) appears an attractive, low-cost, unconventional water resource that is environmentally friendly and relatively easy to operate. Nevertheless, organic micropollutants (OMPs) in treated wastewater pose environmental and health risks if not properly attenuated through vadose zone infiltration. Thus, determination of OMP removal in a SAT system is important for sustainable groundwater management. In this study, a new, simple equation for the prediction of organic micropollutant removal in SAT systems was developed using gene expression programming (GEP). A wide range of 15 OMPs and aquifer conditions were examined along with various real operational aspects of SAT systems, including hydraulic loading rate and dry/wet ratio. The effect of spatial heterogeneity on saturated hydraulic conductivity was considered. Developed GEP models had an average coefficient of determination R 2 R2 of 0.92. Monte Carlo simulation (MCS) with 50,000 realizations was used to propagate uncertainty in SAT parameters in order to generate stochastic inputs for the GEP model. It was found that the removal of OMPs in SAT systems is mostly affected by biodegradation rate and soil-saturated hydraulic conductivity, in addition to dry/wet ratio. Finally,the developed GEP models were applied to enhance the criteria for selecting potential sites for SAT systems in Egypt considering OMP. It was shown that a SAT system would perform well at three sites, with a OMP removal efficiency reaching 100%, whereas it would have a removal of only 50% in the other two sites. Uncertainties in predictions were quantified with an average value of 35%. The developed GEP models can serve as basis for preliminary SAT site selection and design, and can substitute for complex commercial modeling software, especially for practitioners and decision makers in feasibility studies. However, for SAT implementation in a selected location, results can be confirmed only through field column tests

**Keywords:** Health Hazards, Soil Treatment, Aquifers, Environmental Issues, Model Analysis, Water Treatment, Developing Countries, Water Resources, Egypt, Europe, Monte Carlo, Africa, Monac

## E-137. A Probabilistic Projection of the Transient Flow Equations with Random System Parameters and Internal Boundary Conditions

Ahmed M. A. Sattar

*Journal of Hydraulic Research, 54: 342-359 (2016) IF: 1.471*

This paper presents a novel probabilistic approach based on the polynomial chaos expansion that can model the uncertainty propagation from the beginning of a waterhammer simulation and not as an afterthought. Uncertainties are considered in pipe diameter, friction coefficient, and wave speed, as well as

internal boundary conditions of leaks and blockages. The polynomial chaos expansion solver results are in an excellent agreement with those calculated by using a model employing the traditional method of characteristics. The probabilistic polynomial chaos approach has the advantage of being robust and more efficient than other non-intrusive methods such as Monte Carlo simulation, which requires thousands of iterations for sharp solutions. The polynomial chaos approach is further extended to solve for randomness in frequency domain using the transfer matrix method with results of comparable accuracy. With further developments, this probabilistic approach can be integrated within existing network modelling software for practical hydraulic engineering problems.
**Keywords:** Blockages, Leaks, Pipelines, Polynomial Chaos Expansion, Probabilistic Analysis, Random Variable, Transient Flow, Water-Hammer Equations

## E-138. Closure to "Gene Expression Models for The Prediction of Longitudinal Dispersion Coefficients in Transitional and Turbulent Pipe Flow by Ahmed M. A. Sattar

Ahmed M. A. Sattar

*Journal of Pipeline Systems Engineering and Practice 7: 1-2 (2016) IF: 0.89*

In the study developed by Sattar (2014b), the writer applied the gene expression programming (GEP) on a data set of 220 pipe dispersion coefficient measurements spanning the transitional and turbulent pipe flow. He developed four simple GEP models for the prediction of longitudinal dispersion coefficient. Sattar (2014b) presented validation criteria and performed uncertainty analysis for GEP model predictions. The GEP models showed their superiority over existing analytical models. Moreover, Sattar (2014b) showed that among the presented GEP models, some produce better results than others when scored against various proposed criteria.
**Keywords:** Dispersion, Gep

## E-139. Assessing Groundwater Storage Changes in The Nubian Aquifer Using Grace Data

Ahmed M. Yosri, Mohamed A. Abd-Elmegeed and Ahmed E. Hassan

*Arabian Journal of Geosciences, 9: 567-575 (2016)*

Gravity Recovery and Climate Experiment (GRACE) level two (L2) data is used in estimating the groundwater storage changes (GWSC) in the Nubian Sandstone Aquifer System (NSAS). This set of data consists of spherical harmonics coefficients with specific degree and order. The GRACE data is decorrelated using a sixth degree polynomial in order to reduce the effect of the noise error resulting from the correlation between the spherical harmonics coefficients with the same degree parity. The GRACE estimates of GWSC are smoothed using Gaussian filter with half width of 1000 km. This half width is chosen in order to maximize the correlation between the GRACE estimates of GWSC and previous modeling results of the NSAS. The loss in groundwater storage occurring in each of the four countries sharing the NSAS is calculated to assess the sustainability of using the NSAS as a water resource in each country. The overarching finding in this study is that NSAS is losing its groundwater storage at a very high rate. Also, it is found that Egypt is the fastest in losing its groundwater storage from the NSAS. This loss of groundwater storage in Egypt may not necessarily be resulting from in-country extractions because of the transboundary nature of this aquifer. The GRACE-based estimates are found to be close to available data and previous modeling results of the NSAS.
**Keywords:** Groundwater Storage . Grace . Nubian Aquifer . Arid Regions

### *Dept. of Mechanical Design and Production*

## E-140. Visible Light Photocatalytic Reduction of Cr(Vi) By Surface Modified Cnt / Titanium Dioxide Composites Nanofibers

Alaa Mohamed, T.A. Osman, M.S. Toprak, M. Muhammed, Eda Yilmaz and A. Uheida

*Journal of Molecular Catalysis A: Chemical, 424: 45-53 (2016) IF: 3.958*

In this work we report a highly efficient photocatalytic reduction of Cr(VI) based on PAN-CNT/TiO2-NH2 composite nanofibers fabricated by using electrospinning technique followed by chemical crosslinking of surface modified TiO2 NPs functionalized with amino group. The structure and morphology of the fabricated composite nanofibers were characterized by FTIR, SEM, TEM, TGA, and XPS. The results indicate that the composite nanofibers possess excellent photoreduction performance for Cr(VI) under visible light (125 W) after 30 min, which is much faster than previous reports. The effects of various experimental parameters such as catalyst dose, irradiation time, initial concentration of Cr(VI), and pH on the photoreduction efficiency of Cr(VI) were investigated. The highest photoreduction efficiency of Cr (VI) was obtained at low acidity and low amount of TiO2/CNT photocatalyst. The kinetic experimental data was attained and fitted well with a pseudo-first-order model. The UV–vis spectrophotometer and XPS analyses proved that chromate Cr(VI) was reduced to Cr(III). In addition, it can be concluded that the addition of the phenol enhances the photocatalytic reduction of Cr(VI). Furthermore, the photoreduction mechanism has also been discussed. Finally, the fabricated composite nanofibers were found to be stable after at least five regeneration cycles.
**Keywords:** Photocatalytic Reduction; Chromium (Vi); Composite Nanofibers; Visible Light

## E-141. Composite Nanofibers for Highly Efficient Photocatalytic Degradation of Organic Dyes from Contaminated Water

Alaa Mohamed, Ramy El-Sayed, T.A. Osman, M.S. Toprak and M. Muhammed A. Uheida

*Environmental Research, 145: 18-25 (2016) IF: 3.088*

In this study highly efficient photocatalyst based on composite nanofibers containing polyacrylonitrile (PAN), carbon nanotubes (CNT), and surface functionalized TiO2 nanoparticles was developed. The composite nanofibers were fabricated using electrospinning technique followed by chemical crosslinking. The surface modification and

morphology changes of the fabricated composite nanofibers were examined through SEM, TEM, and FTIR analysis. The photocatalytic performance of the composite nanofibers for the degradation of model molecules, methylene blue and indigo carmine, under UV irradiation in aqueous solutions was investigated. The results demonstrated that high photodegradation efficiency was obtained in a short time and at low power intensity compared to other reported studies. The effective factors on the degradation of the dyes, such as the amount of catalyst, solution pH and irradiation time were investigated. The experimental kinetic data were fitted using pseudo-first order model. The effect of the composite nanofibers as individual components on the degradation efficiency of MB and IC was evaluated in order to understand the overall photodegradation mechanism. The results obtained showed that all the components possess significant effect on the photodegradation activity of the composite nanofibers. The stability studies demonstrated that the photodegradation efficiency can remain constant at the level of 99% after five consecutive cycles.

**Keywords:** Photocatalytic; Composite Nanofibers; Organic Contaminants; Electrospinning; Carbon Nanotubes (Cnts)

## E-142. Adaptive Learning of Human Motor Behaviors: an Evolving Inverse Optimal Control Approach

Haitham El-Hussieny, A.A. Abouelsoud, Samy F. M. Assala and Said M. Megahed.

*Engineering Applications of Artificial Intelligence, 50: 115-124 (2016) IF: 2.368*

Understanding human behaviors has received considerable attention in neuroscience literature. Existing research addressed the main question: given measurements of a certain human movement, what is the underlying optimality criteria that human has optimized to fulfill this movement? Inverse Optimal Control (IOC) is a well-established approach to understand the biological movements in terms of the optimal control theory. IOC learns the criterion that best describes the demonstrated human behavior. Thus far, gradient-based techniques have been used to obtain the unknown behavior cost. However, these techniques are limited by locating only local optimum parameters. In this paper, behavior learning is modeled as an Inverse Linear Quadratic Regulator (ILQR) problem, where linear behavior dynamics and a quadratic cost are assumed. An efficient meta-heuristic technique, Particle Swarm Optimization (PSO), is used to retrieve the unknown cost in the proposed ILQR problem. Moreover, an evolving-ILQR algorithm is proposed to refine the learned cost once new unseen demonstrations exist to overcome the over-fitting problem. The reach-to-grasp behavior is studied to quantify the proposed approaches. Results are encouraging and show consistency with that in neuroscience literature. Meanwhile, the evolving-ILQR algorithm has quantified in successive scenarios, where the so far retrieved behavior cost has incrementally refined once new unseen demonstrations are available.

**Keywords:** Inverse Optimal Control; Linear Quadratic Regulator; Behavior Modeling; Particle Swarm Optimization; Incremental Learning

## E-143. Assessment of Corrosion Damage Acceptance Criteria in Api579-Asme/1 Code

M. S. Attia and M. M. Megahed

*Int J Mechanics of Materials and Design, 12: 141-151 (2016) IF: 1.926*

This study presents a comparative evaluation of the various acceptance criteria in API579- ASME/1 fitness-for-service (FFS) code for equipment suffering from metal loss, using a case of severe corrosion in a pipe subjected to internal pressure and supplemental loads. All three assessment levels were conducted to evaluate the remaining life of the pipe under various acceptance criteria assuming constant corrosion rate. In particular, Level-3 assessment was performed using three-dimensional parametric limit finite element analysis to evaluate the remaining life. The model accounts for the observed metal loss, with the aim of evaluating the plastic collapse pressure of the corroded pipe. The remaining life was estimated using both global and local failure criteria and the conservatism of various methods and criteria is assessed. Results showed a potential trade-off of continued operation at the original design pressure for shorter period against a pressure de-rating procedure for extended operat

**Keywords:** Fitness-For-Service Corrosion Remaining Life Assessment Limit Analysis Finite Element Analysis Li

## E-144. The Influence of Temperature and Humidity on the Sensitivity of Torque Transducers

K.M. khaled, D.Roske, A.E. Abuelezz and M.G. El-Sherbiny

*Measurement, 94: 186-200 (2016) IF: 1.742*

This paper presents a study of the effect of temperature and relative humidity on the sensitivity and the characteristics of torque transducers such as residual zero torque, reversibility and creep. Temperature and humidity coefficients of the sensitivity take positive as well as negative values. Linear dependence is found between the influence of temperature/relative humidity and the applied load. For some torque transducers, under temperature change the sensitivity has a transient overshoot reaching up to 3 times the steady amplitude. Also there is a small effect of temperature/relative humidity on the transducer's parameters such as residual zero torque, reversibility and creep. Equations are presented to predict the effect of temperature/relative humidity changes on the sensitivity of torque transducers.

**Keywords:** Torque Transducers Sensitivity Relative Humidity

## E-145. Optimum Solar Humidification – Dehumidification Desalination for Microgrids and Remote Area Communities

Khalid M. Abd El-Aziz, Karim Hamza, Mohamed El-Morsi, Ashraf O. Nassef, Sayed M. Metwalli and Kazuhiro Saitou

*Journal of Solar Energy Engineering, 138 (2016) IF: 1.571*

This paper presents the optimization of a solar-powered humidification–dehumidification (HDH) desalination system for remote areas where it is assumed that only minimal external electric power (for operating control systems and auxiliaries) is available. This work builds on a previous system by

disconnecting the condenser from the saline water cycle and by introducing a solar air heater (SAH) to further augment the humidification performance. In addition, improved thermal simulation models for the condenser and the humidifier are used to obtain more accurate productivity estimations. The heuristic gradient projection (HGP) optimization procedure is also refactored to reduce the number of function evaluations, to reach the minimum unit cost of produced fresh water, compared to genetic algorithms (GAs). A case study which assumes a desalination plant on the Red Sea near the city of Hurghada, Egypt, is presented. The optimum systems are shown to significantly reduce the unit cost of fresh water production below the reported minimum ($1.3/m3 compared to $3/m3), while keeping specific energy consumption within the reported range, 120–550 kWh/m3, for solar HDH systems.
**Keywords:** Dehumidification , Humidifiers , Optimization , Solar Energy , Condensers (Steam Plant) , Water , Flow (Dynamics) , Significant Wave Heights , Temperature , Microgrids

## E-146. The Plastic Instability of Clamped-Clamped Conical Thin-Walled Pipe Reducers

Ibrahim Awad, Ch.A.R. Saleh and A.R. Ragab

*International Journal of Pressure Vessels and Piping, 146: 87-94 (2016) IF: 1.432*

The analytical study for plastic deformation of clampede clamped conical reducer pipe under internal pressure does not deduce a closed form expression for the pressure at plastic instability. The presented study employs finite element analysis (FEA) to estimate the internal pressure at instability for conical reducers made of different materials and having different dimensional configurations. Forty dimensional configurations, classified as medium type, and five types of materials have been included in the analysis using ABAQUS package. A correlation expression is derived by nonlinear regression to predict the instability pressure. The proposed expression is verified for other dimensional configurations out of the above used forty models and for other materials. Experiments have been conducted by pressurizing conical clamped-clamped reducers until bursting in order to verify the finite element models. Comparison of instability pressures, strains and deflections at specific points along the conical surface shows satisfactory agreement between analysis and experiments.
**Keywords:** Plastic Instability Limit Load Conical Shells

## E-147. 3D Finite Element Modeling of in-Service Sleeve Repair Welding of Gas Pipelines

Ahmed R. Alian, Mostafa Shazly and Mohamad M. Megahed

*International Journal of Pressure Vessels and Piping, 146: 216-229 (2016) IF: 1.432*

The present work investigates the influence of welding sequence and scheme on residual stresses induced during in-service sleeve repair welding of gas pipelines. For this purpose, a 3D thermo-mechanical FE analysis is conducted on an 8″-Schedule-20, API 5L-X65 steel pipe. Two welding sequences for the sleeve-pipe circumferential fillet welds are compared in the present study: sequential welding in which one side of the sleeve is welded first and then the other side is welded by the same welder, and simultaneous welding in which both sides of the sleeve are welded concurrently by two welders. Within the simultaneous welding sequence, four different welding schemes, designed to investigate the influence of the number of welders and welding directions on residual stresses, are investigated. The results show that the sequential welding sequence induces less residual stresses and distortions. Within the simultaneous welding sequence, the back-step welding scheme is found to induce the least average residual stresses as compared to other welding schemes.
**Keywords:** Sleeve Repair; Pipe Line; Finite Elements; Residual Stresses; Welding

## E-148. Maximizing Wind Energy Capture for Speed-Constrained Wind Turbines During Partial Load Operation

Zeyu Yan, Victor Yu, Mohamed L. Shaltout, Matthew Chu Cheong and Dongmei Chen

*Journal of Dynamic Systems, Measurement, and Control, 138: 0-0 (2016) IF: 0.975*

With the development of wind turbine technology, more wind turbines operate in the partial load region, where one of the main objectives is to maximize captured wind energy. This paper presents the development of an optimal control framework to maximize wind energy capture for wind turbines with limited rotor speed ranges. Numerical optimal control (NOC) techniques were applied to search for the achievable maximum power coefficient, thus maximum wind energy capture. Augmentations of these optimal techniques significantly reduced the computational cost. Simulation results show that, in comparison with the traditional torque feedback and conventional optimal control algorithms, the proposed augmented optimal control algorithm increases the harvested energy while minimizing the computational expense for speed-constrained wind turbines during partial load operation.
**Keywords:** Torque , Wind Velocity , Stress , Algorithms , Optimal Control , Optimization , Rotors , Turbines , Wind Energy , Wind Turbines

## E-149. Tribological Properties of Dispersed Carbon Nanotubes in Lubricant

Waleed Khalil, Alaa Mohamed, Mohamed Bayoumi and T.A. Osman

*Fullerenes, Nanotubes and Carbon Nanostructures, 24: 479 - 485 (2016) IF: 0.812*

This study examined the tribological properties of two lubricating oils, mobil gear 627 and paraffinic mineral oils, with multi-walled carbon nanotubes (MWCNTs) nanoparticles used as additives with various concentrations (0.1, 0.5, 1, and 2 wt.%). The friction and wear experiments were performed using a four ball tribotester. The samples were tested for their anti-wear, load carrying capacity, and friction coefficients according to ASTM D-2783, ASTM D-2596, and ASTM D-5183 standards. The experimental results show that the addition of MWCNTs to base oils exhibit good friction reduction and anti-wear properties. The wear test results show a decreased wear by 68% and 39% in the case of MWCNTs-based mineral oil as compared with base mobil gear 627 and paraffinic mineral oils,

respectively. Furthermore, the friction reduction results show a decrease of friction about 57% and 49% in the case of MWCNTs-based mineral oil as compared with base mobil gear 627 and paraffinic mineral oils, respectively. The weld load of the base oil containing 1% MWCNTs was found to be 400 kgf and 125 kgf as compared with base mobil gear 627 and paraffinic mineral oils, respectively, which got welded at 200 kgf and 100 kgf. The morphologies and typical element distribution of the worn surfaces were characterized by scanning electron microscope (SEM) and energy-dispersive X-ray (EDX). The SEM micrographs and EDX chemical analysis confirm the formation of a tribolayer composed of the elements from the nanoparticles.

**Keywords:** Nanolubricant, Carbon Nanotubes, Tribological Properties, Lubricant Additive, Anti-Wear, Friction Coefficients

## E-150. Rheology and Thermal Conductivity of Calcium Grease Containing Multi-Walled Carbon Nanotube

Kamel, B.M. Mohamed, A. El Sherbiny and M. Abed, K.A.

*Fullerenes, Nanotubes and Carbon Nanostructures, 24: 260-265 (2016) IF: 0.812*

Recently, nanofluids attract considerable interest for enhanced rheological behavior and thermal performance. The aim of this research is to study the influence of additives Multi-Walled Carbon Nanotubes (MWCNTs) on the rheological behavior and its structure, thermal conductivity, and the influence of shear thinning rate on oil separation at different temperatures for calcium grease. Various concentrations of MWCNTs (0.5, 1, 2, 3, and 4%) have been added to the grease to obtain the best percentages that improve the properties of nanofluid. The microstructure of MWCNTs and nanofluid were examined by X-ray diffraction (XRD), Transmission Electron Microscope (TEM), and Scanning Electron Microscope (SEM). These experimental investigations were evaluated with a Brookfield programmable Rheometer DV-III ULTRA. The results indicated that the optimum concentration of MWCNTs was 3%, and the dropping point increasing about 11%. The rheological behaviors of the nanofluids show that the grease with various concentrations of MWCNTs demonstrates non Newtonian behaviors and the results indicated that the shear stress, apparent viscosity and thermal conductivity increase with the increase of volume concentration of MWCNTs to 65%, 52%, and% 56, respectively.

**Keywords:** Grease; Multi-Walled Carbon Nanotubes; Rheological Behavior; Thermal Conductivity

## E-151. Tribological Behaviour of Calcium Grease Containing Carbon Nanotubes Additives

Kamel, bahaa M mohamed, Alaa sherbiny and M El Abed, K A

*Industrial Lubrication and Tribology, 68: 723-728 (2016) IF: 0.406*

**Purpose :** The purpose of this paper is to fabricate composite nanogrease for tribological applications. Multi-walled carbon nanotubes (MWCNTs) with a size 10 nm average diameter and 5 m in length were used as additives to calcium grease. **Design/methodology/approach :** The tribological four-ball machine was used to evaluate calcium grease with carbon nanotubes (CNTs) as an additive. The interaction between CNT and calcium grease (nanogrease) were studied by transmission electron microscopy and X-ray diffraction. **Findings –** MWCNTs composite nanogrease was manufactured for tribological applications. The effectiveness of the fabricated grease in improving the tribological performance at different concentrations and under different loads was tested. The results are summarized as follows. CNT nanoparticle additive dispersed in calcium grease significantly improve its anti-wear performance, reducing friction, increasing load-carrying capacity and extreme pressure (EP) property. The friction is reduced by about 50 per cent, the wear scar diameter (WSD) decreased to 32 per cent and the EP properties increases about 38 per cent, with only 3 wt.%. The modified grease with CNTs additives of 3 wt.% showed the most favorable results. Energy dispersive x-ray (EDX) analysis shows that C was present on the worn scar surface, with atomic concentration of about 22 per cent. The presence of C suggests that a lubricating film is likely formed because of the presence of CNTs and very likely prevented the steel-to-steel direct contact. Originality/value – The results indicated that a 3 wt.% of MWCNT nanogrease is an excellent antiwear, with EP and low friction coefficient. It was also found that the friction coefficient was reduced to about 50 per cent, the WSD decreased by about 32 per cent and the EP properties increased about 38 per cent. The mating surfaces were investigated with scanning electron microscopy and EDX. The results show that a boundary film mainly composed of CNTs, Cr and Fe was formed on the rubbed surfaces.

**Keywords:** Additives; Carbon Nanotubes; Friction Welding; Gears; Greases Paper Type Research Paper; Lubricant Additives; Lubrication; Nanotribology; Wear Testing

## E-152. The Effect of Process Parameters on the Mechanical Properties of A356 Al – Alloy / Zro2 Nanocomposite

A. Shash, A. E. Amer, I. S. El-Mahallawi and M. A. El-Saeed

*Journal of Nano Research, 38: 1-8 (2016) IF: 0.366*

In this study the effect of zirconia (ZrO2) nanoparticles (40 nm) in reinforcing A356 aluminum alloys as a base metal matrix were investigated. Zirconia nanopowders were stirred in the A356 matrix with different fraction ratios ranging from (0, 1, 2, 3, 5%) by weight at variable stirring speeds ranging from (270, 800, 1500, 2150 r.p.m) at a mushy zone (600°C) and liquid state (700°C) using a constant stirring time for one minute. The microstructure revealed the change of grains from dendritic to spherical shape with increasing stirring speed. The Scanning Electron Microscopy of the fractured surface revealed the presence of nanoparticles at the interdendritic spacing of the fracture surface and was confirmed with EDX analysis of these particles.The results of the study showed that the mechanical properties (strength, elongation and hardness) using ZrO2 as reinforcements were increased at the following parameters: 1500 r.p.m stirring speed in semi-solid state (600oC) and adding 3 wt.% of ZrO2.

**Keywords:** Nano-Metal Matrix Composites; Zro2 Nano-Powders; Mushy Zone; Mechanical Properties

## E-153. Mechanical Properties and Wear Resistance of Semisolid Cast Al2o3 Nano Reinforced Hypo and Hyper-Eutectic Al–Si Composites

I. S. El-Mahallawi and A. Y. Shash

*Advanced Structured Materials, 33: 13-30 (2016)*

The present investigation studies the prospects of using nanoparticles as reinforcement ceramic powders to gain improved performance of hypo and hyper eutectic Al cast alloys. A series of castings were prepared using A356 and A390 as the matrix alloy and alumina nano-powder in 40 nm size as the reinforcement. The nanoparticles were added to the molten slurries with stirring with different fraction ratios ranging from (0, 1, 2 and 4 wt%) in the mushy zone using a constant stirring time for one minute. To evaluate the results, the alloys were further characterized by various tribological and mechanical characterization methods. The results showed higher strength values with improved ductility compared to the monolithic alloys under the same casting conditions. The results also showed improvement in the wear resistance of the nano-reinforced alloys. The scanning electron microscopy of the fracture surface and the wear surface revealed the presence of nanoparticles in the interdendritic spacing and this confirmed with EDX analysis of these particles. The data obtained from the experimental work in this study together with previous published work by the authors were statistically analyzed using analysis of variance (ANOVA) to define the significant factors on both ultimate tensile strength and ductility and their level of confidence, using the orthogonal array L8. Response surface methodology (RSM) was used to build a model relating the type of matrix and nanoparticles addition to the ultimate tensile strength (UTS). The results have shown that the percent of the nanoparticles additions have a significant effect on the tensile properties of the alloys.

**Keywords:** Nano-Metal Matrix Composites; Al2o3 Nano-Powders; Wear Resistance; Mushy Zone; Mechanical Stirring

## E-154. Options for Nanoreinforced Cast Al–Si Alloys with Tio2 Nanoparticles

A. Y. Shash, I. S. El-Mahallawi and A. E. Amer

*Advanced Structured Materials, 33: 1-12 (2016)*

This study presents a new concept of refining and enhancing the properties of cast aluminium alloys by adding nanoparticles. In this work the effect of adding titanium dioxide (TiO2) nano-particles (40 nm) to the aluminum cast alloy A356 as a base metal matrix was investigated. Titanium dioxide nano-powders were stirred into the A356 matrix with different fraction ratios ranging from (0, 1, 2, 3, 4, 5 %) by weight at variable stirring speeds ranging from (270, 800, 1500, 2150 rpm) in both the semisolid (600 °C) and liquid state (700 °C) using a constant stirring time of one minute. The cast microstructure exhibited change of grains from dendritic to spherical shape when increasing stirring speed. The fracture surface showed the presence of nanoparticles at the interdendritic spacing of the fracture surface and was confirmed with EDXS analysis of these particles. The results of the study showed that the mechanical properties (strength, elongation and hardness) for the nanoreinforced castings using TiO2 were enhanced for the castings made in the semi-solid state (600 °C) with 3 % weight% of TiO2 at 1500 rpm stirring speed.

**Keywords:** Nanoreinforced Castings; Semisolid Casting; Hypoeutectic Aluminium Alloys

### *Dept. of Mechanical Power Engineering*

## E-155. Effects of Oxidizer Flexibility and Bluff-Body Blockage Ratio on Flammability Limits of Diffusion Flames

Islam A. Ramadan, Abdelmaged H. Ibrahim, Tharwat W. Abou-Arab, Sherif S. Rashwan, Medhat A. Nemitallah and Mohamed A. Habib

*Applied Energy, 178: 19-28 (2016) IF: 5.746*

Concerns about global warming have encouraged the interest in hydrocarbon combustion techniques that allow easy capture of carbon dioxide. One technique for achieving this objective is through the use of pure oxygen instead of air for combustion or what is called oxy-combustion carbon capture technology. The main goal of the manuscript is to study flammability limits, visual flame appearance and exhaust emissions of diffusion flame stabilized over a bluff body over ranges of operating and design conditions. The operating conditions include flow Reynolds number, equivalence ratio and oxidizer composition. The design parameter considers the change of blockage ratio (BR) of the bluff body namely, BR = 0.36, 0.5, 0.67 and 0.82. Based on this, three sets of experiments were performed utilizing compressed natural gas (CNG) as a fuel to be burned with three different oxidizers including air, oxygen-enriched-air and oxy-fuel mixtures (O2 plus CO2 with a controlled oxygen fractions, OF). The three sets of experiments were performed to identify ranges for stable flame operation considering different oxidizers under different operating conditions. Stability limits, visual flame appearance and extinction limits of these flames are quantified and analyzed. Furthermore, three different regions were observed; precisely, jet flames, central-jet dominated flames and recirculation zone flames, depending on the ratio between oxidizer and fuel momentum. The flame color changed from yellow for air combustion, to bright white for oxygen-enriched-air combustion and finally to blue with yellow tips for oxy-combustion. The flame length was the highest for air combustion, then lower for oxy-combustion and the lowest for oxygen-enriched-air combustion. This was attributed to the effect of oxygen-enrichment which results in increase in the flame speed making flame length shorter. For the sake of comparison, the flammability limits of the three sets were reported and the results revealed that oxygen-enriched-air-flames have higher stability than air-flames and oxy-flames, respectively.

**Keywords:** Air Combustion; Oxygen-Enriched Combustion; Oxy-Combustion; Flammability Limits; Diffusion Flames; Bluff-Body.

## E-156. Experimental Investigation of Partially Premixed Methane–Air and Methane–Oxygen Flames Stabilized Over a Perforated-Plate Burner

Sherif S. Rashwan, Abdelmaged H. Ibrahim, Tharwat W. Abou-Arab, Medhat A. Nemitallah and Mohamed A. Habib

*Applied Energy, 169: 126-137 (2016) IF: 5.746*

In this work, two sets of experiments were performed including air and oxy-combustion premixed flames stabilized over a perforated-plate burner. A set of experiments was performed considering air–fuel combustion in order to identify a range of equivalence ratio for stable flame operation at fixed oxidizer Reynolds number and over a range of premixing ratio (namely 7, 25, 45, 67 and 128). Also, effects of premixing ratio (L/D) on lower and upper flammability limits over a range of oxidizer Reynolds number were investigated. Another set of experiments was performed considering oxy-fuel combustion in order to identify a range of equivalence ratio for stable flame operation at fixed oxidizer Reynolds number. The study documents the visual flame length, appearance and color and identifies the extinction mechanism outside the flammability limits for both air and oxy-combustion flames over wide ranges of operating equivalence and premixing ratios. For air combustion flames, the results showed wide ranges of flammability limits at lower premixing ratios and tight ranges of flammability limits at higher premixing ratios. This can be attributed to the increase in the degree of flame diffusivity while reducing the premixing ratio and, as a result, more stable flame is obtained. Reductions in the emissions of NO and CO were observed while increasing the premixing ratio for the air combustion case. For the oxy-combustion flames, the results showed stable flame operation at oxygen fraction of 36%; however, the flammability limits were approximately 20% lower as compared to those of air combustion flames. Flash back was observed when operating oxygen fraction exceeded 40% and flame stability was affected badly with the decrease of oxygen fraction. The visual flame length was longer in cases of oxy-combustion flames as compared to those of air combustion.

**Keywords:** Air–Fuel Combustion; Oxy-Fuel Combustion; Flammability Limits; Perforated-Plate Burner; Partially Premixed Flames

## E-157. Heat Transfer and Friction Characteristics of Shell and Tube Heat Exchanger with Multi Inserted Swirl Vanes

Mhmoud Galal Yehia, Ahmed A.A.Attia, Osama Ezzat Abdelatif and Essam E.Khalil

*Applied Thermal Engineering, 102: 1481-1491 (2016) IF: 3.04*

The effect of friction characteristics of the heat exchanger model when using different number of swirl vanes at different locations along the pipe length to enhance the heat transfer rate will be discussed through a simulation for shell and tube heat exchanger using ANSYS FLUENT CFD techniques. The number of swirl vanes inserted into each tube is three swirl vanes and six swirl vanes distributed along the pipe length with variable diameter (10 mm, 15 mm, 19 mm) and different blade angle (15, 30, 45) for each case. The results show that the numerical results reasonably agree well with the available literature. The case of six swirl vanes with 19 mm diameter and 45 blade angle gives the maximum heat transfer enhancement, friction factor, and thermal enhancement factor compared with plain tube case. A correlation for Nusselt number and friction factor is developed.

**Keywords:** Numerical Simulation; Shell and Tube Heat Exchanger; Turbulence Model; Swirl Vane

## E-158. Review on Premixed Combustion Technology: Stability, Emission Control, Applications and Numerical Case Study

Sherif S. Rashwan, Medhat A. Nemitallah and Mohamed A. Habib

*Energy and Fuels, 30(12): 9981-10014 (2016) IF: 2.835*

Recently, premixed combustion dominated the field of combustion research worldwide. The current work is a review that addresses the stability, approaches, and emission control of premixed flames in different applications. The study addresses the recent developments made to overcome the combustor operability issues, including flame stability and emission control. The influences of oxidizer and fuel flexibility using oxy-fuel combustion and hydrogen enrichment on combustion efficiency and flame stability are investigated. Furthermore, the influences of operating and combustor design conditions on flame characteristics are discussed. Recent developments in swirl-stabilized combustor are analyzed and summarized. The effect of premixing on emissions is investigated, considering a variety of design and operating conditions in different applications. As per this survey, the application of fully premixed combustion in the industrial area is even so defined; all the same, promising designs are under development. The challenges regarding the application of the premixed combustion technology in the industrial field are discussed. The role of numerical CFD techniques to predict the reacting flow field and heat release in premixed combustion mode is addressed. A numerical case study is presented to address the premixed combustion characteristics in a swirl stabilizer gas turbine combustor.

**Keywords:** Premixed Combustion; Review.

## E-159. The Flow Field Structure of Highly Stabilized Partially Premixed Flames in a Concentric Flow Conical Nozzle Burner with Coflow

A.M. Elbaz, M.F. Zayed, M. Samy, W.L. Roberts and M.S. Mansour

*Experimental Thermal and Fluid Science, 73: 2-9 (2016) IF:2.128*

The stability limits, the stabilization mechanism, and the flow field structure of highly stabilized partially premixed methane flames in a concentric flow conical nozzle burner with air co-flow have been investigated and presented in this work. The stability map of partial premixed flames illustrates that the flames are stable between two extinction limits. A low extinction limit when partial premixed flames approach non-premixed flame conditions, and a high extinction limit, with the partial premixed flames approach fully premixed flame conditions. These two limits showed that the most stable flame conditions are achieved at a certain degree of partial premixed. The stability is improved by adding air co-flow. As the air co-flow velocity increases the most stable flames are those that approach fully premixed. The turbulent flow field of three flames at 0, 5, 10 m/s co-flow velocity are investigated using Stereo Particle Image Velocimetry (SPIV) in order to explore the improvement of the flame stability due to the use of air co-flow. The three flames are all at a jet equivalence ratio (Phij) of

2, fixed level of partial premixing and jet Reynolds number (Rej) of 10,000. The use of co-flow results in the formation of two vortices at the cone exit. These vortices act like stabilization anchors for the flames to the nozzle tip. With these vortices in the flow field, the reaction zone shifts toward the reduced turbulence intensity at the nozzle rim of the cone. Interesting information about the structure of the flow field with and without co-flow are identified and reported in this work.
**Keywords:** Partially Premixed, Flames, Combustion, Stability, Flow Field

## E-160. Classification of the Mixing Field of Partially Premixed Flames Using Regime Diagram

Mohy S Mansour

*Combustion Science and Technology, 188: 667-683 (2016) IF: 1.193*

Partially premixed combustion is one of the common combustion modes for many practical combustion systems where the mixture is classified as nonhomogeneous. The available experimental data show that the nature of mixing affects significantly the flame stability and structure of partially premixed flames at the same level of turbulence and local stoichiometry. Quantitative description of the mixing field is not yet available in order to discuss and analyze the effect of mixing on the flame structure and stability. The broad range of fluctuations in mixture fraction space within this mode requires proper classification into sub-ranges with common characteristics. This classification should be applicable for both laminar and turbulent flames. Accordingly a new diagram classifying the mixing field of partially premixed combustion into eight regimes within and partially within the flammability limits is proposed. The local mean and range of mixture fraction fluctuations are used to construct this diagram. One of those regimes covers the triple flames where the fluctuations lie within the flammability limits. The link between the stability and the proposed regimes is investigated using quantitative experimental data of turbulent flames. The data show promising correlation between stability and location of the flames within the diagram. The proposed regime diagram can be used as a platform for the classification of the mixing field of partially premixed flames.
**Keywords:** Mixing Field, Regime Diagram, Partially Premixed, Flames

## E-161. Review of Flow-Excited Resonance of Acoustic Trapped Modes in Ducted Shallow Cavities

Kareem Aly and Samir Ziada

*Journal of Pressure Vessel Technology, 138(4): 40803-40803 (2016) IF: 0.499*

Flow-excited resonances of acoustic trapped modes in ducted shallow cavities are reviewed in this paper. The main components of the feedback mechanism which sustains the acoustic resonance are discussed with particular emphasis on the complexity of the trapped mode shapes and the strong three-dimensionality of the cavity flow oscillations during the resonance. Due to these complexities of the flow and sound fields, it is still difficult to theoretically or numerically model the interaction mechanism which sustains the acoustic resonance. Strouhal number and resonance amplitude charts are therefore included to help designers avoid the occurrence of resonance in new installations, and effective countermeasures are provided which can be implemented to suppress trapped mode resonances in operating plants.
**Keywords:** Resonance , Flow (Dynamics) , Acoustics , Shear (Mechanics) , Cavities , Oscillations , Excitation.

## E-162. Numerical Modeling and Performance Investigation for Compact Heat Exchangers in Different Fin Arrangement and Fluid Flow Conditions

Waleed A. Abdelmaksoud and Mahmoud A. Kassem

*Computational Thermal Sciences: An International Journal, 8: 469-482 (2016)*

This paper presents a computational fluid dynamics (CFD) parametric study to investigate the effect of various parameters such as the fin arrangement (or spacing) and the inlet flow conditions (velocity and temperature) on the performance of compact finned-tube heat exchangers, which can be found in many HVAC industrial applications. In the present study, the heat exchanger's performance is expressed in terms of heat transfer and pressure drop. Both heat transfer and pressure drop are presented here in dimensionless forms; the Nusselt number and the pressure coefficient. An additional factor, the ratio of the Colburn factor to friction factor, combining the effects of the heat transfer and the pressure drop, is also presented to complete the performance assessment. Several CFD cases were studied using a commercial software package for the investigation of flow and thermal behavior in the heat exchanger under various modeling conditions. To ensure accurate numerical results, grid independence analysis and model validation against previously published experimental data were performed. Using the results generated from the CFD cases, two useful mathematical correlations were developed and presented in the dimensionless form. These correlations can be used to predict the performance of typical heat exchangers.
**Keywords:** Heat Exchangers, CFD, Heat Transfer, Pressure Drop

### *Dept. of Mining, Petroleum and Metallurgy*

## E-163. Influence of Friction Stir Processing on the Microstructure and Mechanical Properties of a Compocast AA2024-Al2O3 Nanocomposite

W. Hoziefa, S. Toschi,M.M.Z. Ahmed, Al. Morri, A.A.Mahdy, M.M. El-Sayed Seleman, I. El-Mahallawi and L. Ceschini A. Atlam

*Materials and Design, 106: 273-284 (2016) IF: 4*

The effect of friction stir processing (FSP) on the microstructure and mechanical properties of a semi-solid cast AA2024-1wt%Al2O3 nanocomposite was investigated. For comparison, plates of unreinforced AA2024 alloy were also cast and processed at the same FSP conditions (400 rpm, 20 mm/min). The microstructure of all the produced materials was investigated using optical microscopy (OM), scanning electron microscopy (SEM) and electron backscattered diffraction

(EBSD). Microhardness and tensile tests were carried out on the unreinforced AA2024 alloy and AA2024-Al2O3 nanocomposite before and after FSP. The addition of 1 wt% of Al2O3 nanoparticles significantly reduced the grain size of both the cast and FSPed microstructures, leading to a grain size reduction from 28 µm to 18 µm in the cast condition, and from 3.7 µm to 2.3 µm after FSP. The application of FSP to AA2024-Al2O3 nanocomposite enhanced the tensile strength and yield strength by 71% and 30%, respectively, in comparison to the as cast matrix, as a result of the uniform distribution of Al2O3 reinforcement and grain refinement of Al matrix. The combined application of compocasting and FSP resulted to be a promising method to treat casting defects and to produce nanocomposites characterised by good reinforcement dispersion and high strength and ductility.

**Keywords:** Compocasting, Friction Stir Processing, Microstructure, Mechanical Properties.

## E-164. Testing Microwave Dewatering As a Solution for Reducing Clay Disposal Pond Areas

H.El-Shall and A.A.El-Midany

*Drying Technology : An International Journal, 34: 1957-1963 (2016) IF: 1.854*

Phosphate processing plants produce an excessive amount of phosphatic clay. This clay represents a serious environmental problem due to their disposal in huge ponds. Finding a feasible method to reduce the clay disposal area is needed. Although the flocculation process, in the presence of fibrous material, seems to be a good dewatering process for phosphatic clay wastes, the maximum solid % of flocculated clay does not exceed 18% (starting from 3-4%). Recently, the microwave proved a better performance in several research areas as compared to the conventional drying. In this study, clay dewatering by microwave was investigated. Several factors affecting the dewatering process were studied such as heating time, microwave power efficiency and fiber %. Using the microwave, the solid content significantly increases in a reasonably short time. The time and power are the most significant among the studied factors. In addition, sand-clay mix was tested to improve the solid % to be used as a filling material. The results showed that the presence of sand enhances the clay drying due to the transparency of sand to the microwave irradiation as well as increasing the clay bed porosity, which facilitates migration of liquid water and/or water vapor toward the surface of dried material.

**Keywords:** Clay Waste; Dewatering; Microwave; Flocculation; Solid %.

## E-165. Enhancing Phosphate Grade Using Oleic Acid–Sodium Dodecyl Sulfate Mixtures

A. A. El-Midany and Y. Arafat

*Chemical Engineering Communications, 203: 660-665 (2016) IF: 1.433*

Upgrading of calcareous phosphate ores by reverse flotation in acidic media depends mainly on the chemical reagents used especially the collectors. Anionic collectors are commonly used in phosphate flotation circuits, however, in the most cases each collector was tested separately. Although, using the mixture of the anionic collectors in salt-type minerals flotation is very limited, it has several advantages over using each collector alone. Therefore, in the present paper, the mixture of oleic acid and sodium dodecyl sulphate (SDS) was tested and compared to the usage of each collector individually. A number of experiments was conducted to find out the optimal reverse flotation conditions for each collector in terms of collector dose, pH and oleic to SDS mixing ratio as main variables using factorial design. The design results showed that the oleic-SDS mixture, particularly at 1:1 mixing ratio, improves the phosphate grade with slight decrease in recovery in comparison to using each collector separately. The highest concentrate grade (> 33 % P2O5), with a recovery of 85%, was obtained at pH 6, (1:1) oleic:SDS mixing ratio and collector dose 3.5 kg/t. In addition, using (1:1) mixing ratio drastically lowers the collector dose from 3.5 to 2 kg/t or even lower depending on the pH to achieve the concentrate grade required by phosphate industry (30% P2O5).

**Keywords:** Calcareous Phosphate; Reverse Flotation; Oleic Acid; Sodium Dodecyl Sulphate.

## E-166. Production of Grain-Refined Ac7a Al−Mg Alloy Via Solidification in Ultrasonic Field

W. Khalifa and Y. Tsunekawa

*Trans. Nonferrous Met. Soc. China, 26: 930-937 (2016)IF: 1.34*

The objective of the current study was to investigate the use of ultrasonic melt treatment technology in the production of grain-refined billets of the AC7A alloy, which was intended for subsequent use as a feedstock in forming operations. The experiments included the application of ultrasonic vibrations to the molten alloys via direct and indirect techniques. Several process parameters such as pouring temperatures (several temperatures between 740 and 660 °C), and treatment time (from 12 min down to 2 min) were investigated. The experiment included continuous ultrasonic treatment from the liquid to the semisolid states. The results showed that both treatment techniques were viable for producing billets with the desirable microstructural characteristics. The optimum treatment conditions were the short treatment time (2 to 3 min), from about 660 °C down to 615 °C for the indirect treatment technique, and from 660 °C to 635 °C for the direct treatment technique. The resulting microstructures, at three positions along the height of the ingot, were characterized by fine, non-dendritic α(Al) grains in the order of a hundred microns, as compared to few thousands of microns for the conventional cast ingots. The intermetallic particles were also refined in size and modified in morphology by the ultrasonic treatment. The operating mechanisms by which the ultrasonic vibrations altered the ingot microstructures were discussed and analyzed.

**Keywords:** Al−4.5Mg Alloy; Ultrasonic Melt Treatment; Grain Refining; Intermetallics

## E-167. Microstructure, Hardness and Impact Toughness of Heat-Treated Nanodispersed Surface and Friction Stir-Processed Aluminum Alloy Aa7075

M. Refat, A. Elashery, S. Toschi, M.M.Z. Ahmed, A. Morri, I. El-Mahallawi and L. Ceschini

*Journal of Materials Engineering and Performance, 25: 5087-5101 (2016) IF: 1.1*

Friction stir processing (FSP) is a recent surface engineering processing technique that is gaining wide recognition for manufacturing nanodispersed surface composites, which are of high specific strength,hardness and resistance to wear and corrosion. Herein, four-pass FSP was applied on aluminum alloy 7075 (AA7075-O) with and without the addition of alumina nanoparticles (Al2O3) of average size 40 nm. All FSP parameters were constant at 40 mm/min transverse speed, 500 rpm and tilt angle of 3. FSP rotation direction was reversed every other pass. The friction stir-processed materials were sectioned and solution treated at 515 C for 1.5 h, followed by age hardening at 120 C for 12, 24, 36, 48 and 60 h. The effect of heat treatment regimes on microstructure, hardness and toughness was examined, as well as the fracture mode. The new friction stir-processed surfaces without and with nanodispersion showed enhancement in the hardness of the surface of the AA7075-O material (65 HV) to almost a double (100 and 140 HV) after four-pass FSP (before heat treatment) without and with incorporating nanoalumina particles, respectively. After 48-h aging at 120 C, a significant enhancement in impact toughness was achieved for both the friction stir-processed without and with nanodispersion (181 and 134 J, respectively), compared to the reference material AA7075 in T6 condition (104 J).

**Keywords:** AA7075, Friction Stir Processing, Hardness, Heat Treatment, Microstructure, Surface Nanocomposites, Toughness

## E-168. Interrelation of Steel Composition, Hardening Route, and Tempering Response of Medium Carbon Low-Alloy Steels

Abdel-Hamid A. Hussein, Mahmoud T. Abdu, El-Sayed M. El-Banna, Saied E. Soliman and Mahmoud M. Tash

*Journal of Materials Engineering and Performance, 25: 1463-1473 (2016) IF: 1.094*

Four medium carbon and low-alloy steels were hardened through oil and forced air cooling. Tempering was then performed in the temperature range 250-600 °C. The martensite content increased with an increased hardenability and/or the rate of cooling. Tempering at T > Ms caused a gradual decline in both hardness and strength and an improvement in the Charpy V-notch impact toughness. The low-alloy steels underwent tempered martensite embrittlement (as a result of the formation of carbides at the martensite interlaths and prior austenite grain boundaries) and enhancement of phosphorus segregation (particularly in the presence of Ni). Higher hardenability steels were found to be better hardened via the more recent forced air quenching rather than the conventional oil quenching. In this work, a modest, novel attempt is presented to empirically correlate the impact toughness with the hardness measurements to enable future prediction of impact toughness from hardness measurements.

**Keywords:** Heat Treatment, Microscopy, Modeling and Simulation, Optical Metallography, Steel

## E-169. Optimizing Thewelding Parameters of Reinforcing Steel Bars

Tamer Moustafa , Waleed Khalifa , M. Raafat El-Koussy and Nahed Abd El-Reheem

*Arab J Sci Eng, 41: 1699-1711 (2016) IF: 0.73*

Welding is highly recommended for splicing concrete reinforcing bars in all concrete structures. SMAW lap-welded and butt-welded joints made from Tempcore and hot-rolled reinforcing steel bars were studied. The results give an insight into the effect of metallurgical structure and the chemical composition on the effective lap weld length of reinforcing steel bars. It was found that the hot-rolled bars gave shorter acceptable lap length than the Tempcore bars. This was because of the higher amount of pearlite/bainite phases in weld area. In the other hand, the HAZ hardening resulted in the most pronounced changes in ductility of hot-rolled joints. Preheating the hot-rolled bars up to 200 °C was insufficient to prevent the formation of HAZ hard phases.

**Keywords:** Rebarwelding microstructure tensilehaz Structurelap Weld Lengthbutt

## E-170. Optimization of Dye Removal by Activated Carbon Prepared from Sawdust

Yasser Sh. Mahrous and Ayman A. El-Midany

*Mp Materials Testing, 58: 155-160 (2016) IF: 0.27*

Industrial dyes disposal represents one of the major environmental problems. Although the different techniques were used for its removal, the adsorption technique proved to be the most effective. In the current paper, removal of the disperse dye using activated carbon was investigated. The controlling factors of the removal process were studied by experimental design. Initially, the factors; namely: dye concentration, pH, etching time, agitation speed, carbon concentration and organic to aqueous solution ratio were screened using Placket Burman design. Then the significant factors, coming from screening design, were investigated using full factorial design to find the optimum removal conditions. The results indicated that dye concentration, carbon concentration and organic to aqueous solution ratio are the most significant factors among the screened ones. The complete dye removal can be achieved for low dye concentration, while for high dye concentration, the dye removal depends on the activated carbon concentration where the removal percent ranges from 51.7 up to 97 %.

**Keywords:** Disperse Dye, Activated Carbon, Dye Removal, Adsorption Process

## E-171. Ultrasonic Rheo-Diecasting of A383 Aluminum Alloy

Waleed Khalifa, Yoshiki Tsunekawa and Shimaa El-Hadad

*Solid State Phenomena, 256: 282-287 (2016)*

In this study, un-refined A383 aluminum alloy was cast at different temperatures using ultrasonic melt treatment. The liquid alloy was treated by ultrasonic vibrations in the crucible and/or in the shot sleeve of a pressure diecasting machine. The treatment temperature extended to the semisolid temperature range. The UST melt could be injected into the die cavity while being in the semisolid state which is known as rheodiecasting. The results showed that ultrasonic treatment resulted in finer microstructure, globular Fe-intermetallic particles and partially modified eutectic Si. For samples solidified in shot sleeve: Fe-intermetallics become compacted with UST at all positions of ingot. Si particles are compacted in less acicular form near to horn and acicular at other positions. For the rheo-diecasting experiments, with UST treatment in the crucible and die casting, at 600-588 C and 588-578C, Fe-intermetallics were observed in compact form, and Si particles were highly modified.

**Keywords:** Ultrasonic, Rheodiecasting, Aluminum, A383, Microstructure

## E-172. Thixocasting of a l- 7%Si Alloy Billets Prepared by Ultrasonic Treatment

Waleed Khalifa and Yoshiki Tsunekawa

*Solid State Phenomena, 256: 276-281 (2016)*

The feasibility of using the ultrasonic melt treatment to prepare billets for thixocasting process of hypoeutectic Al-7%Si alloys was studied in this paper. The work covered the billet preparation, soaking treatments and thixocasting process, with focus on the microstructural features in each case. The results showed that the use of ultrasonic treatment in billet preparation resulted in highly uniform, fine and non-dendritic microstructures. Billets with globule sizes as small as 58 µm, and roundness of more than 0.7 were obtained by ultrasonic melt treatment. Different soaking conditions before thixocasting were done and the optimum from which was the soaking for 5 min at 580oC, which resulted in thixocast parts with excellent combination of fine globules of 80 µm and roundness of 0.7 - 0.81. The eutectic Si, as well, was greatly refined by the ultrasonic thixocasting process. Furthermore, high-Fe ultrasonic treated billets, which were thixocasted successfully, exhibited Fe-intermetallic particles in highly desirable fine compacted form. These results reveal the feasibility and competence of UST as a potential route for feedstock production.

**Keywords:** Thixocasting, Ultrasonic, Globular, Soaking, Al-7%Si, Fe, Intermetallic.

### *Dept. of Public Works*

## E-173. Modeling of Phenol and Cyanide Removal in a Full-Scale Coke-Oven Wastewater Treatment Plant

Abdelsalam elawwad, Ahmed naguib and Hisham Abdel-Halim

*Desalination and Water Treatment, 57(52): 25181-25193 (2016) IF: 1.272*

The BioWin general activated sludge (AS) model (EnviroSim Associates, Ltd, Canada) was extended to predict the kinetics of phenol and cyanide removal from coke-oven wastewater mixed with sewage. To apply the modeling for this type of wastewater, a different model structure and an accurate estimation of the stoichiometric and kinetic parameters are required. In this study, additional processes for the phenol and cyanide were added to the BioWin AS model. Due to the inhibitory effect phenol and cyanide have on biological processes, the Haldane equation was used rather than the Monod equation that is typically used in wastewater modeling. A sensitivity analysis was performed to select the most sensitive parameter in the extended model. The model was calibrated under steady-state conditions and validated under dynamic-flow conditions. Adjustments were made only to the most sensitive parameters of the extended model processes related to phenol and cyanide. The new calibrated parameters were compared to the existing parameters from the literature, which were based on batch lab-scale experiments with synthetic wastewater. The extended model was capable of describing COD, ammonium, phenol, and cyanide removal in a full-scale coke-oven wastewater treatment plant under dynamic conditions.

**Keywords:** Coke-Oven Wastewater, Phenol, Cyanide, Nitrification, Biowin As Model

## E-174. Comparison and Database Development of four Recent Asm3 Model Extensions

Nagwan G. Mostafa, Mona M. Galal, Ahmed G. Radwan and Ehab M. Rashed

*Journal of Environmental Engineering, 142: 1-9 (2016) IF: 1.125*

In the last decade, many Activated Sludge Model No. 3 (ASM3) extensions were proposed to adopt new concepts such as simultaneous storage and growth of heterotrophic organisms and two-step nitrification-denitrification processes. From these ASM3 model extensions, four are included in this study: ASM3 with two-step nitrification-denitrification, ASM3 for simultaneous autotrophic and heterotrophic storage-growth, ASM3 extension for two-step nitrification-denitrification, and ASM3 for simultaneous storage-growth and nitrification-denitrification. The four models are analyzed and compared to the original ASM3 model with respect to the modeling concepts adopted, the process kinetic rates modified, and the kinetic parameters and stoichiometric coefficients introduced. A new schematic representation of the modeling concepts concerning the organisms' activities is introduced. A database of all parameters and coefficients of the four considered model extensions is developed using a unified notation system to reduce effort and confusion of the future researchers using their values as initial calibration or guidance values. Finally, the four models and the original ASM3 model are implemented using the parameters' values from the developed database, then the simulation results are compared with actual field measurements.

**Keywords:** ASM3 Model Extensions; Practical Database; Modeling Concepts; Process Kinetics; Kinetic Parameters; Stoichiometric Parameters.

## E-175. Performance of Single-Chamber Microbial Fuel Cells Using Different Carbohydrate-Rich Wastewaters and Different Inocula

Safwat Ahmed, Ehab Rozaik and Hisham Abdel-Halim

*Polish Journal of Environmental Studies, 25 (2): 503-510 (2016) IF: 0.79*

A microbial fuel cell (MFC) can use wastewater as a substrate; hence, it is essential to understand its performance when seeded with different inocula and during the treatment of carbohydrate-rich wastewaters to simultaneously optimize electricity production and wastewater treatment. This study investigates the performance of single-chamber membraneless MFCs used to treat three different carbohydrate-rich synthetic wastewaters (glucose, sucrose, and soluble starch) while seeding with two different inocula (a microbial solution containing different species of microorganisms, and anaerobic sludge). The results showed that the highest voltages, power densities, and COD removal effi ciencies were obtained using microbial fuel cells fed with glucose-based synthetic wastewater, and were 351 mV, 218 mW/m2, and 98.8%, respectively, for the microbial solution, and 508 mV, 456.8 mW/m2, and 94.3%, respectively, for the anaerobic sludge. The lowest results of voltages, power densities, and COD removal effi ciencies were obtained using microbial fuel cells fed with the soluble starch-based synthetic wastewater, and were 281 mV, 139.8 mW/m2, and 86.4%, respectively, for the microbial solution, and 396 mV, 277.6 mW/m2, and 79.4%, respectively, for the anaerobic sludge. In all experiments, the voltages and power densities obtained for the anaerobic sludge were higher than those obtained for the microbial solution, and the COD removal effi ciencies obtained for the anaerobic sludge were less than those obtained for the microbial solution. This study determined that voltage generation, power densities, and COD removal effi ciencies were inversely proportional to the complexity of the carbohydrate used in single-chamber microbial fuel cells.

**Keywords:** Microbial Fuel Cell, Anaerobic Sludge, Glucose, Sucrose, Soluble Starch.

***Dept. of Structural Engineering***

## E-176. Estimating Water Treatment Plants Costs Using Factor Analysis and Artificial Neural Networks

Mohamed Marzouk and Mostafa Elkadi

*Journal of Cleaner Production, 112:4540-4549(2016) IF: 4.959*

The cost of construction project is a fundamental input for decision making process set by owner during procurement stage. The paper identifies the cost drivers that are used in parametric cost estimation model for water treatment plants. Cost estimation at planning stage of projects is important for the success of the next stages in the projects. It is also very useful at the design stage of a project when information is incomplete and detailed designs are limited in such an early stage. Literature has been reviewed and interviews were conducted with experts and officials in water treatment plants to explore all variables that influence the construction cost of water treatment plants. A questionnaire survey was then conducted to assess the impact of the identified factors on construction costs of water treatment plants. Datasets that consist of 160 water treatment plant projects in Egypt were collected. Construction cost drivers have been nominated through two different procedures. The first technique is descriptive statistics ranking of variables by evaluating Mean Score and Relative Importance Index based on respondents' feedback in conducting questionnaire. The second technique utilizes exploratory factor analysis on the collected dataset. These cost drivers are used to construct two predictive models for estimating the construction cost of water treatment plants models using artificial neural networks. Analysis of results was performed to validate the models and demonstrate their effectiveness. The proposed methodology aids public authorities to perform comparative analysis and evaluate the different alternatives of water treatment plant projects.

**Keywords:** Parametric Cost Estimation; Water Treatment Plant; Cost Driver; Descriptive Statistics Ranking; Principal Component Analysis; Artificial Neural Networks.

## E-177. Framework for Sustainable Low-Income Housing Projects Using Building Information Modeling

Mohamed Marzouk, Shimaa Azab and Mahmoud Metawie

*Journal of Environmental Informatics,28:25-38(2016)IF: 3.857*

Governments in developing countries serve low income people by constructing low income housing projects. Most of total life cycle cost (LCC) of these projects is incurred during the operational phase, making these projects lose their economic aspect of sustainability. Decreasing the cost of low income housing projects and taking into consideration the available resources are two crucial facets that should be taken into consideration. Therefore, this paper focuses on two aspects of the sustainability of building through its life cycle, which are environmental and economic aspects using environmentally friendly materials in construction. To accomplish this aim, a framework is developed that integrates Building Information Modeling (BIM) with computer simulation, optimization and system dynamics in Low Income Housing (LIH) projects. The developed framework helps in determining LIH project duration and selecting the optimum alternative with to material systems. The sustainability aspects of building are achieved by considering a LCC of these buildings and the number of points that can be awarded under the Leadership in Energy and Environmental Design (LEED) rating system. It aids government and/or contractors in adopting BIM technology to minimize life cycle cost while achieving maximum LEED materials credits points for LIH projects. Social Housing project in Badr City-Egypt is considered as a case study to demonstrate the use of the developed prototype and to illustrate its essential features. The results have shown that selection of sustainable building materials for the construction has a crucial role in the formation of a sustainable building as they affect the performance of building. Therefore, the Egyptian government should consider building materials with sustainable properties and a low LCC in the design phase to mitigate the negative impacts of LIH projects.

**Keywords:** Building Information Modeling, Computer Simulation, Optimization, System Dynamics, Low Income Housing

## E-178. Comparison of Actions and Resistances in Different Building Design Codes

Mourad M. Bakhoum, Sherif A. Mourad and Maha M. Hassan

*Journal of Advanced Research, 7: 757-767 (2016) IF: 3*

Structural design codes of different countries provide engineers with data and procedures for design of the various structural components. Building design codes from USA, Europe, and

Egypt are considered. Comparisons of the provisions for actions (loads), and for the resistance (strength) of sections in flexural and compressive axial loading are carried out. Several parameters are considered including variable actions for occupancy and different material strengths. The comparison is made considering both concrete and steel structures. Issues and consequences of mixing actions from one code and resistance from another code are also discussed.
**Keywords:** Concrete Elements; Design Codes; Loads; Strength; Steel Elements

## E-179. Investigating Sustainability Parameters of Administrative Buildings in Saudi Arabia

Khalid Al-Gahtani, Ibrahim Alsulaihi, Mostafa El-Hawary and Mohamed Marzouk

*Technological Forecasting and Social Change, 105: 41-48 (2016) IF: 2.678*

Cultural differences have always been considered a crucial factor in the implementation of ready-made models. Following international interest, Arabian communities have promoted the need to adopt sustainability strategies in construction, with the vital goal of minimizing environmental impacts and overcoming resource limitations. This paper presents a generic framework for selecting the key sustainability parameters for office and administrative buildings in Saudi Arabia because these types of buildings consume huge amounts of resources and generate a massive amount of waste and carbon dioxide emissions. The framework building blocks start with benchmarking regional and international rating systems. Next, a swift review of regional literature and emerging concepts is performed. The results are then tabulated to establish a pool of criteria. For this effort, a total of 112 criteria have been identified and grouped into five main groups. The next step involves industry engagement, which is best investigated through a questionnaire. The final step is the survey results analysis using two techniques: severity index (SI) and exploratory factor analysis. The resulting factors are considered to be key parameters when constructing a new rating system that considers cultural differences.
**Keywords:** Rating Systems; Green Buildings; Sustainability; Environment; Statistical Analysis; Severity Index; Exploratory Factor Analysis; Principal Component Analysis

## E-180. Evaluating the New Can/Csa-S806-12 Torsion Provisions for Concrete Beams with Frp Reinforcements

M. M. Hassan and A. Deifalla

*Materials and Structures, 49: 2715-2729 (2016) IF: 2.453*

Recently, the Canadian Standards Association proposed the first and only torsion design provisions for the case of beams with fiber reinforced polymer (FRP) reinforcements within the Canadian standard “Design and construction of building structures with fiber-reinforced polymers” (CAN/CSA-S806-12). The evaluation of the shear provisions of this code has shown more accurate and consistent shear predictions compared with other codes. The purpose of this study is to evaluate the torsion provisions of the CAN/CSA-S806-12. Such evaluation is performed considering the available experimental database from four different studies examining over 20 concrete beams with FRP or mixed (i.e. FRP and steel) reinforcements, tested under torsion. The cracking and ultimate torque as well as the failure mode predicted using the CAN/CSA-S806-12 were compared with the experimentally observed ones. The CAN/CSA-S806-12 was found to be overly conservative. Thus, modifications were proposed to the current CAN/CSA-S806-12, which were found to provide slightly better results.
**Keywords:** Concrete; Beam; Designglass Frp; (Gfrp); Carbon Frp (Cfrp); Frp; Torsion

## E-181. Decision Support for Tower Crane Selection with Building Information Models and Genetic Algorithms

Mohamed Marzouk and Ahmed Abubakr

*Automation in Construction, 61: 1-15 (2016) IF: 2.442*

Tower cranes are major construction equipment that is highly demanded in construction projects. The planning process for tower cranes utilization starts in early stages of the construction projects. Poor selection could incur extra costs on the construction projects or cause delays in project duration. The planning procedures for tower cranes include selection, allocation and operation. This paper presents a framework for the selection of tower cranes types and locations at construction sites. The framework considers three main models: 1) decision making model to select the tower crane type, 2) optimization model for the selection of the ideal number and location of tower cranes, and 3) 4D simulation model to simulate tower crane operations. Several clash detection scenarios are presented to assure the safety operation of the tower crane group. A case study is shown herein to demonstrate the capabilities of the developed framework.
**Keywords:** Decision Making; Tower Cranes; Building Information Modeling; Analytical Hierarchy Process; Genetic Algorithms

## E-182. Target-Free Approach for Vision-Based Structural System Identification Using Consumer-Grade Cameras

Hyungchul Yoon, Hazem Elanwar, Hajin Choi, Mani Golparvar-Fard and Billie F. Spencer Jr.

*Structural Control Health Monitoring, 23: 1405-1416 (2016) IF: 2.082*

Recent reports on America's infrastructure have emphasized the importance of structural health monitoring of civil infrastructures. System identification is a key component of many structural health monitoring strategies. Current system identification methods estimate models of a structure by measuring displacements, accelerations, and strains with wired or wireless sensors. However, these methods typically involve installation of a limited number of sensors at discrete locations and require additional data acquisition devices. To overcome these limitations, computer vision-based techniques have been introduced recently that employ high-speed and high-resolution cameras. Such cameras can be quite costly and require tedious installation of targets. This paper investigates the potential of using consumer-grade cameras for structural system identification without the need to install targets. The underlying

methods for target-free displacement measurements are introduced, including region of interest selection, feature detection, point tracking, and outlier removal. A set of experiments are conducted to assess the efficacy of the proposed approach by comparing the accuracy of the identified model with one obtained using a conventional wired system. Careful comparison of the results demonstrates the significant potential of the proposed approach.
**Keywords:** Structural Health Monitoring; System Identification; Computer Vision; Feature Tracking; Consumer-Grade Cameras

## E-183. Experimental Study on the Rotation Capacity of Cold-Formed Steel Beams

Mohammed H. Serror, Emad M. Hassan and Sherif A. Mourad

*Journal of Constructional Steel Research, 121: 216-228 (2016) IF: 2.033*

The rotation capacity of cold-formed steel (CFS) beams has been evaluated through experimental investigation. Studies on different structural levels have been performed. At the element level, different profile slenderness ratios have been considered, and different section shapes have been investigated by increasing the number of flange bends: C-section and curved-section,which represents an infinite number of flange bends. At the connection level, aweb boltedmoment resistant type of connection using through plate has been adopted. Inweb bolted connectionswithout out-of-plane stiffeners, prematureweb buckling results in early loss of strength. Hence, outof- plane stiffeners have been examined to delayweb and flange buckling and to produce relatively high moment strength and ductility. The experimental results have been compared with numerical results obtained by the authors in another paperwork. The results revealed that increasing the number of flange bends will not in all cases enhance the behavior. Meanwhile, the use of out-of-plane stiffeners can increase the seismic energy dissipation, the moment strength and the ductility, when compared with the case without stiffeners.
**Keywords:** Experimental Study; Cold-Formed Steel Beam; Rotation Capacity; Slenderness Ratio; Section Shape; Out-Of-Plane Stiffeners

## E-184. Automated Community-Based Housing Response: Offering Temporary Housing Solutions Tailored to Displaced Populations Needs

Omar El-Anwar and Lei Chen

*Journal of Computing in Civil Engineering, 30(6): 4016019-4016019 (2016) IF: 1.855*

Following disasters, emergency management agencies are under immense pressure to make quick decisions regarding the provision of temporary housing, including their locations and types. Such decisions can significantly impact the socioeconomic recovery of displaced families and available budgets for other postdisaster activities. To address these challenges, a new holistic temporary housing planning framework is proposed to offer customized housing plans tailored to the specific social, economic, and psychological needs of displaced families while controlling expenditures. This paper presents the theoretical formulation and implementation details of the community-based housing response pool, which is a comprehensive framework that aims at (1) quantifying the specific needs and preferences of each displaced family, (2) evaluating the ability of housing alternatives to meet those needs, (3) computing temporary housing life cycle costs, and (4) optimizing housing decisions accordingly. The paper also presents an application example to demonstrate and evaluate the optimization model capabilities.
**Keywords:** Temporary Housing, Decision-Support-System, Automation

## E-185. Behavior of Concrete-Filled Double Skin Steel Tube Beam-Columns

Maha M. Hassan, Ahmed A. Mahmoud and Mohammed H. Serror

*Steel and Composite Structures, 22: 1141-1162 (2016) IF: 1.796*

Concrete-filled double skin steel tube (CFDST) beam-columns are widely used in industrial plants, subways, high-rise buildings and arch bridges. The CFDST columns have the same advantages as traditional CFT members. Moreover, they have lighter weight, higher bending stiffness, better cyclic performance, and have higher fire resistance capacities than their CFT counterparts. The scope of this study is to develop finite element models that can predict accepted capacities of double skin concrete-filled tube columns under the combined effect of axial and bending actions. The analysis results were studied to determine the distribution of stresses among the different components and the effect of the concrete core on the outer and inner steel tube. The developed models are first verified against the available experimental data. Accordingly, an extensive parametric study was performed considering different key factors including load eccentricity, slenderness ratio, concrete compressive strength, and steel tube yield strength. The results of the performed parametric study are intended to supplement the experimental research and examine the accuracy of the available design formulas.
**Keywords:** Beam-Columns; Concrete-Filled Tube; Double-Skin; Parametric Study

## E-186. Numerical Study on Buckling of Steel Web Plates with Openings

Mohammed H. Serror, Ahmed N. Hamed and Sherif A. Mourad

*Steel and Composite Structures, an International Journal, 22: 1417-1443 (2016) IF: 1.796*

Cellular and castellated steel beams are used to obtain higher stiffness and bending capacity using the same weight of steel. In addition, the beam openings may be used as a pass for different mechanical fixtures such as ducts and pipes. The aim of this study is to investigate the effect of different parameters on both elastic and inelastic critical buckling stresses of steel web plates with openings. These parameters are plate aspect ratio; opening shape (circular or rectangular); end distance to the first opening; opening spacing; opening size; plate slenderness ratio; steel grade; and initial web imperfection. The web/flange interaction has been simplified by web edge restraints representing simply supported boundary conditions. A numerical parametric study has been performed through linear and nonlinear finite element

(FE) models, where the FE results have been verified against both experimental and numerical results in the literature. The web plates are subject to in-plane linearly varying compression with different loading patterns, ranging from uniform compression to pure bending. A buckling stress modification factor (β-factor) has been introduced as a ratio of buckling stress of web plate with openings to buckling stress of the corresponding solid web plate. The variation of β-factor against the aforementioned parameters has been reported. Furthermore, the critical plate slenderness ratio separating elastic buckling and yielding has been identified and discussed for two steel grades of DIN-17100, namely: ST-37/2 and ST-52/3. The FE results revealed that the minimum β-factor is 0.9 for web plates under uniform compression and 0.7 for those under both compression and tension.

**Keywords:** Numerical Study; Web Plate With Openings; Elastic and Inelastic Buckling; Buckling Stress Modification Factor

## E-187. Finite Element Analysis of Circular Concrete Filled Tube Connections

Hazem M. Ramadan, Maha M. Hassan, Mohamed A. Mooty and Sherif A. Mourad

*Journal of Constructional Steel Research, 120: 33-44 (2016) IF: 1.702*

A parametric study based on finite element technique is performed to investigate the performance of different connection configurations between circular concrete filled steel tube (CCFT) columns and gusset plates subjected to axial compression loadings. The study focuses on the effect of the pipe and gusset plate dimensions on the connection behavior. The modeling assumptions and techniques used to perform the analysis are detailed. The models are verified using experimental test data performed earlier by the authors. A notable effectwas observed on the behavior of the connections due to its detailing changes with respect to failure mode, yield and ultimate capacity, stress distribution and initial and final stiffness.

**Keywords:** Finite Element; Concrete Filled Tube; Connections

## E-188. Influence of Floor Diaphragm – Wall Coupling on the System -Level Seismic Performance of an Asymmetrical Reinforced Concrete Block Building

Ahmed Ashour and Wael El-Dakhakhni.

*Journal of Structural Engineering, 142 (2016) IF: 1.7*

Understanding the inelastic seismic response of reinforced masonry shear walls (RMSW) is the first step to develop predictive models of the system-level (i.e., complete building) response under different levels of seismic demand. Such predictive models will not only have to be capable of accurately accounting for the different system-level-specific aspects but will also have to be easy enough to be adopted by design engineers. In this respect, the influence of the floor diaphragms on a building's seismic response is typically recognized only through the role of the former in distributing the shear forces on the building's seismic force resisting system (SFRS) as a result of the diaphragms' in-plane stiffness. Subsequently, the current paper focuses on analyzing experimental data of a series of RMSW tested as individual components and within two asymmetrical building systems. The analyses showed that the out-of-plane stiffness of the floor diaphragms played an important role in flexurally coupling the RMSW aligned along the loading direction with those walls aligned orthogonally. This system-level aspect affected not only the different wall strength and displacement demands but also the failure mechanism sequence and the building's twist response. For the building system under consideration, the diaphragm-wall coupling resulted in doubling the building's initial stiffness, and also significantly increasing the building's strength. The results of the study show that neglecting diaphragm out-of-plane coupling influence on the RMSW at the system-level may result in unconservative designs and possibly undesirable component-level failure modes as a result of violating capacity design principles. To develop an analytical model that can account for the aforementioned influences, simplified load-displacement relationships were developed to predict RMSW component- and system-level responses under lateral seismic loads. In the current study, three approaches were proposed to account for the diaphragm coupling influences on the RMSW response. The developed analytical model presents a useful system-level response prediction tool for displacement- and performance-based seismic design of RMSW buildings.

**Keywords:** Asymmetrical Building; Backbone Model; Coupled-Walls; Diaphragm Coupling; Masonry Building; Displacementbased Design; System-Level Response; Shear Walls; Concrete and Masonry Structures.

## E-189. Experimental Evaluation of the System - Level Seismic Performance and Robustness of an Asymmetrical Reinforced Concrete Block Building

Ahmed Ashour, Wael El-Dakhakhni and Marwan Shedid

*Journal of Structural Engineering, 142 (2016) IF: 1.7*

In recent years, research interests in studying the response of different seismic force-resisting systems have been shifting from component-level to system-level studies. Building on the existing knowledge of component-level performance of reinforced masonry shear walls (RMSW), the current study evaluates some similarities and discrepancies between RMSW system-level and component-level responses under seismic loading. The study also focuses on evaluating the system-level seismic robustness of a RMSW building by quantifying key relevant robustness indicators proposed in the literature. To meet the study objectives, an experimental asymmetrical two-story reduced-scale RMSW building was tested to failure under simulated seismic loading. Subsequently, the study first presents a brief summary of the experimental program followed by a discussion of the damage sequence and the load-displacement hysteretic behavior of the RMSW building. In general, the experimental results demonstrated the impact of both the floor slab-induced twist and wall flexural coupling through the floor slabs on the building response, with the latter significantly influencing the building response compared to the former. In addition, the robustness indexes quantified for five key robustness indicators (drift ratio, strength, stiffness, strain energy, and residual drift ratio) can provide a means by which the system-level performance of RMSW buildings can be assessed from different perspectives under a wide range of seismic demands.

**Keywords:** Concrete and Masonry Structures; Masonry Buildings; Robustness; Seismic Loads; Shear Walls; Slab Coupling; System-Level Performance.

## E-190. Improved Hybrid Boundary Solution for Shell Elements

Taha H.A. Naga and Youssef F. Rashed

*Engineering Analysis with Boundary Elements, 71: 70-78 (2016) IF: 1.251*

In this paper, a new finite element for shell structures is developed using an improved hybrid boundary solution. First the variational boundary integral equation for shear-deformable plate bending problems is developed based on quadratic boundary elements. Hence such a formulation is coupled to a similar formulation for 2D plane stress problems to produce the developed shell elements. Numerical examples are presented to demonstrate the accuracy and validity of the proposed formulation. 
**Keywords:** Finite Element Method; Boundary Element Method; Variational Formulation; Stiffness Matrix; Shear-Deformable Plates; Shell Structures.

## E-191. Bim Standards for Automated Bem Structural Analysis and Design of Rc Plates

Mostafa E. Mobasher, Youssef F. Rashed and Wael Elhaddad

*Journal of Computing In Civil Engineering, Asce, 30: 4015054-4015054 (2016) IF: 1.219*

This paper introduces a new system that utilizes the advantages of boundary element analysis in structural engineering applications. A standardized building information model (BIM) for automated structural analysis and design of reinforced concrete plates based on the boundary element method (BEM) is proposed. Based on the model view definition approach, BIM standards are presented for the preprocessing and postprocessing of BEM analysis. Furthermore, standards are proposed for automated structural design of structural slab and beam elements based on the BEM analysis results. For each of the BIM components, standards are provided for the object structure, data flow, and graphical user interface (GUI). The extensibility of the software and applicability for a wide range of research and practical applications are considered in all the proposed standards. The system created can act as the basis for structural analysis and design of building floor and foundation problems. Object-oriented programming is used to implement the standards in a prototype. The prototype was verified by application to the solution of practical structural engineering problems. The performance of the proposed system is evaluated in terms of the modeling and the processing time required to analyze typical structural engineering applications using the prototype.
**Keywords:** Building Information Modeling; Boundary Element Method; Building Slabs and Foundations; Software Tools In Structural Engineering; Automation; Computer-Aided Design.

## E-192. Application of in-Test Model Updating to Earthquake Structural Assessment

Hazem H. Elanwar and Amr S. Elnashai

*Journal of Earthquake Engineering, 20: 62-79 (2016) IF: 0.922*

Analytical methods are frequently utilized for structural assessment due to their simplicity and cost-effectiveness. However, modeling of material inelasticity and geometric nonlinearity under reversed inelastic deformations is still very challenging and its accuracy is difficult to quantify. On the other hand, realistic experimental assessment is costly, time-consuming, and impractical for large or spatially extended structures. Hybrid simulation has been developed as an approach that combines the realism of experimental techniques with the economy of analytical tools. In hybrid simulation, the structural is divided into several modules such that the critical components are tested in the laboratory, while the rest of the structure is simulated numerically. The equations of motion solved in the computer enable the integration of the analytical and experimental components at each time increment. The objective of this article is to apply a newly developed identification and model updating scheme to acquire the material constitutive relationship from the physically tested specimen during the analysis to two complex hybrid simulation case studies. The identification scheme is developed and verified in a companion article, while the two experiments presented in this article are selected such that they address different structural engineering applications. First, a beam-column steel connection with heat treated beam section is analyzed. Afterwards, the response of a multi-bay concrete bridge is investigated. The results of these two examples demonstrate the effectiveness of model updating to improve the numerical model response as compared to the conventional hybrid simulation approaches.
**Keywords:** Model Updating, Pseudo-Dynamic Tests, Hybrid Simulations, Constitutive Relationships, Optimization Algorithms

## E-193. Framework for Online Model Updating in Earthquake Hybrid Simulations

Hazem H. Elanwar and Amr S. Elnashai

*Journal of Earthquake Engineering, 20: 62-79 (2016) IF: 0.922*

Hybrid simulation has been effectively utilized to assess structural response subjected to intense dynamic loads. The process comprises dividing the structure into experimental and numerical modules. The experimental modules represent the critical components responses, which cannot be idealized reliably through analytical approaches. The responses of the different modules are combined through a stepwise integration scheme. In conventional hybrid simulations, the number of experimental components is restricted by the capacity of the test facility; usually 1–3 components, and the numerical simulation does not benefit from the information acquired from the tested component during the analysis. In this article, a framework is proposed to identify the material constitutive relationship from the tested component(s) and to update the corresponding numerical parts that share close characteristics with the physical tests. Optimization tools and neural networks are presented as alternatives for the identification procedure; the framework is

however extendable and scalable. The communication protocol between the different structural components is also discussed within the proposed framework. Several analytical examples are presented to prove the feasibility of the presented framework, while experiments are used to verify the process in a companion article.
**Keywords:** Model Updating, Hybrid Simulation, Constitutive Model, Optimization Tools, Neural Networks, Nonlinear Analysis

## E-194. Establishing Multi - Levels Performance Condition Indices for Public Schools Maintenance Program Using Ahp and Fuzzy Logic

Mohamed Marzouk and Ehab Awad

*Studies in Informatics and Control, 25: 343-352 (2016)IF:0.723*

This research targets the creation of indices to enforce standard assessment for group of educational buildings and to set common understanding of facilities' condition among different stakeholders. This model contains four levels of performance assessment that deal with program, facility, package, and element. AHP-fuzzy model is built using linguistic expression to represent condition of asset. The proposed model generates standard indices for three levels (element, package, and facility) which are aggregated to provide realistic condition assessment for a group of facilities (program). For evaluation of this model, a case study is presented with data from 21 schools in Giza governorate-Egypt to provide these indices. Example for assessment of two elements is worked out to illustrate the feasibility of this model. Outputs could be used by management as part of the decision support system.
**Keywords:** Ahp, Fuzzy Logic, Facility Assessment, Educational Facilities, Condition Index

## E-195. Modeling Housing Supply and Demand Using System Dynamics

Mohamed Marzouk and Ismail Hosny

*Housing, Care and Support, 19: 64-80 (2016)*

Purpose The housing sector in Egypt represents a considerable share of the gross domestic product (GDP) and accordingly the economy. Further, it is considered vital for any population around the world, because it provides the shelter needed by people. Egyptian housing market is facing many problems which need to be solved. The paper aims to discuss these issues. Design/methodology/approach This research reviews and analyzes the Egyptian public and private housing market's key variables. As such, it highlights the importance of informed decision making through detailed analysis and study of the market, especially when planning for the future by any housing market stakeholder. The research proposes the use of system dynamics (SD) modeling to analyze the market by creating a stock and flow model using STELLA modeling and simulation software. Findings The results reveal that the expected newly established families will be nearly 800,000 families in year 2015/2016. Out of these numbers, 600,000 families require economic housing units, while the expected supply is nearly 300,000 units. Originality/value A study is made for the economic housing market, which is a very big housing market and population segment that has been suffering from negligence for years.
**Keywords:** Egypt, Forecasting, System Dynamics, Sensitivity Analysis, Economic Housing, Informed Decision Making

***Dept. of Systems and Biomedical Engineering***

## E-196. Free - Breathing Slice-Interleaved Myocardial T2 Mapping with Slice-Selective T2 Magnetization Preparation

Tamer A. Basha, Steven Bellm, Sebastien Roujol, Shingo Kato and Reza Nezafat

*Magnetic Resonance in Medicine, 76: 555-565 (2016) IF: 3.782*

**Purpose:** To develop and evaluate a free-breathing slice-interleaved T2 mapping sequence by proposing a new slice-selective T2 magnetization preparation (T2 prep) sequence that allows interleaved data acquisition for different slices in subsequent heartbeats. **Methods:** We developed a slice-selective T2 prep for myocardial T2 mapping by adding slice-selective gradients to a conventional single-slice T2 prep sequence. In this sequence, five slices are acquired during five consecutive heartbeats, each using a slice-selective T2 prep. The scheme was repeated four times using different T2 prep echo times. We compared the performance of the proposed slice-interleaved T2 mapping sequence and the conventional single-slice T2 mapping sequence in term of accuracy, precision, and reproducibility using phantom experiments and in vivo imaging in 10 healthy subjects. We also evaluated the feasibility of the proposed sequence in 28 patients with cardiovascular disease, and the quality of the maps was scored subjectively. Furthermore, we investigated the impact of through-plane motion by comparing T2 measurements acquired during end-systole versus mid-diastole. **Results:** T2 measurements using a slice-interleaved T2 mapping sequence were correlated with a spin echo ($r(2) = 0.88$) and single-slice T2 mapping sequence ($r(2) = 0.98$). The mean myocardial T2 values were correlated between slice-interleaved (48 ms) and single-slice (51 ms) T2 mapping sequences. Subjective scores of T2 map quality were good to excellent in 81% of the maps in patients. There was no difference in T2 measurements between end-systole versus mid-diastole. **Conclusions:** The proposed free-breathing slice-interleaved T2 mapping sequence allows T2 measurements of five left ventricular slices in 20 heartbeats with similar reproducibility and precision as the single-slice T2 mapping sequence but with a four-fold reduction in acquisition time.
**Keywords:** Myocardial T2 Mapping; Precision; Quantitative Myocardial Tissue Characterization; Reproducibility; Slice-Interleaved T2 Mapping; Slice-Selective T2prep

## E-197. Identification of Rheumatoid Arthritis Biomarkers Based on Single Nucleotide Polymorphisms and Haplotype Blocks: A Systematic Review and Meta - Analysis

Mohamed N. Saad, Mai S. Mabrouk, Ayman M. Eldeibb and Olfat G. Shaker

*Journal of Advanced Research – Cairo University, 7(1): 1-16 (2016) IF: 3*

Genetics of autoimmune diseases represent a growing domain with surpassing biomarker results with rapid progress. The exact cause of Rheumatoid Arthritis (RA) is unknown, but it is thought to have both a genetic and an environmental bases. Genetic biomarkers are capable of changing the supervision of RA by allowing not only the detection of susceptible individuals, but also early diagnosis, evaluation of disease severity, selection of therapy, and monitoring of response to therapy. This review is concerned with not only the genetic biomarkers of RA but also the methods of identifying them. Many of the identified genetic biomarkers of RA were identified in populations of European and Asian ancestries. The study of additional human populations may yield novel results. Most of the researchers in the field of identifying RA biomarkers use single nucleotide polymorphism (SNP) approaches to express the significance of their results. Although, haplotype block methods are expected to play a complementary role in the future of that field.

**Keywords:** Haplotype Block; Linkage Disequilibrium; Major Histocompatibility Complex; Rheumatoid Arthritis; Single Nucleotide Polymorphism

## E-198. Comparison of Spoiled Gradient Echo and Steady-State Free-Precession Imaging for Native Myocardial T1 Mapping Using the Slice - Interleaved T1 Mapping (Stone) Sequence

Jihye Jang, Steven Bellm, Sébastien Roujol, Tamer A. Basha, Maryam Nezafat, Shingo Kato, Sebastian Weingärtner and Reza Nezafat

*Nmr in Biomedicine, 29: 1486-1496 (2016) IF: 2.983*

Cardiac T1 mapping allows non-invasive imaging of interstitial diffuse fibrosis. Myocardial T1 is commonly calculated by voxel-wise fitting of the images acquired using balanced steady-state free precession (SSFP) after an inversion pulse. However, SSFP imaging is sensitive to B1 and B0 imperfection, which may result in additional artifacts. A gradient echo (GRE) imaging sequence has been used for myocardial T1 mapping; however, its use has been limited to higher magnetic field to compensate for the lower signal-to-noise ratio (SNR) of GRE versus SSFP imaging. A slice-interleaved T1 mapping (STONE) sequence with SSFP readout (STONE-SSFP) has been recently proposed for native myocardial T1 mapping, which allows longer recovery of magnetization (>8 R-R) after each inversion pulse. In this study, we hypothesize that a longer recovery allows higher SNR and enables native myocardial T1 mapping using STONE with GRE imaging readout (STONE-GRE) at 1.5T. Numerical simulations and phantom and in vivo imaging were performed to compare the performance of STONE-GRE and STONE-SSFP for native myocardial T1 mapping at 1.5T. In numerical simulations, STONE-SSFP shows sensitivity to both T2 and off resonance. Despite the insensitivity of GRE imaging to T2 , STONE-GRE remains sensitive to T2 due to the dependence of the inversion pulse performance on T2 . In the phantom study, STONE-GRE had inferior accuracy and precision and similar repeatability as compared with STONE-SSFP. In in vivo studies, STONE-GRE and STONE-SSFP had similar myocardial native T1 times, precisions, repeatabilities and subjective T1 map qualities. Despite the lower SNR of the GRE imaging readout compared with SSFP, STONE-GRE provides similar native myocardial T1 measurements, precision, repeatability, and subjective image quality when compared with STONE-SSFP at 1.5T.

**Keywords:** Balanced Steady-State Free Precession; Cardiovascular Mr (Cmr) Methods; Myocardial T1 Mapping; Relaxometry; Slice-Interleaved T1 Mapping; Spoiled Gradient Echo

## E-199. Breast Cancer Classification Using Deep Belief Networks

Ahmed M. Abdel-Zaher and Ayman M. Eldeib

*Journal of Expert Systems with Applications, 46: 139-144 (2016) IF: 2.981*

Over the last decade, the ever increasing world-wide demand for early detection of breast cancer at many screening sites and hospitals has resulted in the need of new research avenues. According to the World Health Organization (WHO), an early detection of cancer greatly increases the chances of taking the right decision on a successful treatment plan. The Computer-Aided Diagnosis (CAD) systems are applied widely in the detection and differential diagnosis of many different kinds of abnormalities. Therefore, improving the accuracy of a CAD system has become one of the major research areas. In this paper, a CAD scheme for detection of breast cancer has been developed using deep belief network unsupervised path followed by back propagation supervised path. The construction is back-propagation neural network with Liebenberg Marquardt learning function while weights are initialized from the deep belief network path (DBN-NN). Our technique was tested on the Wisconsin Breast Cancer Dataset (WBCD). The classifier complex gives an accuracy of 99.68% indicating promising results over previously-published studies. The proposed system provides an effective classification model for breast cancer. In addition, we examined the architecture at several train-test partitions.

**Keywords:** Breast Cancer Diagnosis; Cad; Classification; Deep Learning Based Classifier; Pattern Recognition

## E-200. Evaluating Validity of Various Acupuncture Device Types: A Random Sequence Clinical Trial

Jungtae Leem, Jimin Park, Gajin Han, Seulgi Eun, Meena M. Makary, Kyungmo Park, Junhee Lee and Sanghoon Lee

*Bmc Complementary and Alternative Medicine, 16-43 (2016) IF: 1.987*

**Background** Although various placebo acupuncture devices have been developed and used in acupuncture research, there is controversy concerning whether these devices really serve as appropriate placebos for control groups. **Methods/Design** The proposed study is a single-center prospective random sequence participant- and assessor-blinded trial with two parallel arms. A total of 76 participants will be randomly assigned to Group 1 or Group 2 in a 1:1 ratio. Group 1 will consist of Sham Streitberger's needle, Real Streitberger's needle, and Phantom acupuncture session. Group 2 will consist of Park Sham device with real needle, Park Sham device with sham needle, and no treatment session. Participants will have a total of three acupuncture sessions in a day. The primary endpoint is blinding test questionnaire 1. Secondary endpoints are the Bang's blinding index, the Massachusetts General Hospital

Acupuncture Sensation Scale index, and physiological data including heart rate, heart rate variability, and skin conductance response. **Discussion** This trial will evaluate the relevance of using placebo acupuncture devices as controls using a validation test procedure.
**Keywords:** Placebo Acupuncture, Blinding Validation, Park Sham Device, Streitberger'S Needle, Phantom Acupuncture

## E-201. Accurate Harmonic Phase Tracking of Tagged Mri Using Locally-Uniform Myocardium Displacement Constraint

Safaa M. ElDeeb and Ahmed S. Fahmy

*Medical Engineering and Physics, 38: 1305-1313 (2016) IF: 1.619*

Harmonic phase (HARP) tracking is one of the most commonly used techniques for estimating the myocardium regional function from tagged cardiac Magnetic Resonance Imaging sequences. Nevertheless, tag fading and phase distortion can severely limit the tracking accuracy of the technique. In this work, we propose to modify the HARP tracking algorithm to impose a constraint of locally uniform displacement field while tracking the different myocardium points. A numerical contracting phantom and a dataset of 11 patients are used to study the performance of the proposed technique at the different cardiac phases, slices, and regions. The results show that the proposed method improves the tracking accuracy and the reliability of the conventional HARP technique.
**Keywords:** Cardiac Function; Phase-Based Tracking; Harp; Myocardium Tagging; Mri

## E-202. Image Encryption Via Discrete Fractional Fourier-Type Transforms Generated by Random Matrices

M. H. Annaby, M.A. Rushdi and E.A. Nehary

*Signal Processing: Image Communication, 49: 25-46 (2016) IF: 1.602*

One of the major application areas of the fractional Fourier transform (FrFT) and the discrete fractional Fourier transforms (DFrFT) is in signal and information security, particularly in signal and image encryption. Recently, many researchers proposed techniques that implemented not only the fractional transforms, but also various randomized versions of the DFrFT, which add more security features to signal's encryption. In this paper, we propose new DFrF-type transforms whose eigensystems are generated using a novel random-matrix scheme. We give theoretical justifications for the importance of our transforms and show their statistical significance in comparison to recently proposed transforms in the context of image encryption. Experimental results show also that the encryption keys based on the proposed transforms have high sensitivities against decryption attacks.
**Keywords:** Discrete Fractional Fourier Transform; Spectral Decomposition; Image Encryption; Random Matrices; Entropy and Permutation Tests

## E-203. Improved Estimation of the Cardiac Global Function Using Combined Long and Short Axis Mri Images of the Heart

Hossam El-Rewaidy and Ahmed S. Fahmy

*Biomedical Engineering Online, 15 (2016) IF: 1.382*

**Background** Estimating the left ventricular (LV) volumes at the different cardiac phases is necessary for evaluating the cardiac global function. In cardiac magnetic resonance imaging, accurate estimation of the LV volumes requires the processing a relatively large number of parallel short-axis cross-sectional images of the LV (typically from 9 to 12). Nevertheless, it is inevitable sometimes to estimate the volume from a small number of cross-sectional images, which can lead to a significant reduction of the volume estimation accuracy. This usually encountered when a number of cross-sectional images are excluded from analysis due to patient motion artifacts. In some other cases, the number of image acquisitions is reduced to accommodate patients who cannot withstand long scan times or multiple breath-holds. Therefore, it is required to improve the accuracy of estimating the LV volume from a reduced number of acquisitions. **Methods** In this work, we propose a method for accurately estimating the LV volume from a small number of images. The method combines short-axis (SAX) and long axis (LAX) cross sectional views of the heart to accurately estimate the LV volumes. In this method, the LV is divided into a set of consecutive chunks and a simple geometric model is then used to calculate the volume of each chunk. Validation and performance evaluation of the proposed method is achieved using real MRI datasets (25 patients) in addition to CT-based phantoms of human hearts. **Results** The results show a better performance of the proposed method relative to the other available techniques. It is shown that, at the same number of cross-sectional images, the volume calculation error is significantly lower than that of current methods. In addition, the experiments show that the results of the proposed model are reproducible despite variable orientations of the imaged cross-sections. **Conclusion** A new method for calculating the LV volume from a set of SAX and LAX MR images has been developed. The proposed method is based on fusing the SAX and LAX segmented contours to accurately estimate the LV volume from a small number of images. The method was tested using simulated and real MRI datasets and the results showed improved accuracy of estimating the LV volume from small number of images.
**Keywords:** Cardiac Function Volume Estimation Geometric Models Mri

## E-204. Robust Computer-Aided Detection of Pulmonary Nodules from Chest Computed Tomography

Zaid Abduh, Manal Abdel Wahed and Yasser M. Kadah

*Journal of Medical Imaging and Health Informatics, 6: 693-699 (2016) IF: 0.877*

Detection of pulmonary nodules in chest computed tomography scans play an important role in the early diagnosis of lung cancer. A simple yet effective computer-aided detection system is developed to distinguish pulmonary nodules in chest CT scans. The proposed system includes feature extraction,

normalization, selection and classification steps. One hundred forty-nine gray level statistical features are extracted from selected regions of interest. A min–max normalization method is used followed by sequential forward feature selection technique with logistic regression model used as criterion function that selected an optimal set of five features for classification. The classification step was done using nearest neighbor and support vector machine (SVM) classifiers with separate training and testing sets. Several measures to evaluate the system performance were used including the area under ROC curve (AUC), sensitivity, specificity, precision, accuracy, F1 score and Cohen-k factor. Excellent performance with high sensitivity and specificity is reported using data from two reference datasets as compared to previous work.

**Keywords:** Computed Tomography; Computer Aided Diagnosis; Pulmonary Nodules

## E-205. Segmentation of the Right Ventricle in Mri Images Using a Dual Active Shape Model

Hossam El-Rewaidy, El-Sayed Ibrahim and Ahmed S Fahmy

*Iet Image Processing, 10: 717-723 (2016) IF: 0.86*

Active shape models (ASM) showed to have potential for segmenting the right ventricle (RV) in cardiac magnetic resonance images (MRIs). Nevertheless, the large variability and complexity of the RV shape do not allow for concisely capturing all possible shape variations among patients and anatomical cross-sections. Noticeably, the latter increases the number of iterations required to converge to a proper solution and reduces the segmentation accuracy. In this study, the authors propose a new ASM framework that can model the RV shape in short-axis cardiac MRI images. In this framework, the RV contour is split into two simpler segments, septal (SP) and free wall, whose shape variations are independently modelled using two separate (dual) ASM models. The contour splitting is done at the location of the RV insertion points into the SP wall. Further, instead of using the conventional Procrustes method, the RV contours are aligned using the Bookstein coordinate transformation, which uses the RV insertion points as landmarks to linearly align the RV contours. The results from a dataset of 14 patients show that the proposed framework outperforms the conventional ASM framework and can model complex RV shape variation with more accuracy and in less iteration steps.

**Keywords:** Biomedical Mri; Image Segmentation; Medical Image Processing

## E-206. A Novel Computerized System to Simulate Orthodontic Treatment Plan

Kadry Ali Ezzat , Ahmed H. Kandil and Sahar Ali Fawzi

*International Journal of Applied Engineering Research, 11: 5673-5681 (2016)*

Detection and treatment of malocclusions and other dental deformities are a considerable field of work in the plan of orthodontic treatment. Severe malformations of the mid face such as maxillary or mandibular deformity can be treated by the distraction and reformation of skull bones. During an operation, the appropriate bony part of the mid-face is separated from the rest of the skull (osteotomy), slowly moved into the ideal position by way of a distraction device. In the current clinical practice, planning for orthodontic treatment and orthognathic surgery was based on Computed Tomography (CT)data sets. CT images are inefficient for helping the orthodontists and surgeons in treatment and surgical planning. A tool is needed to help the physicians and surgeons in the treatment planning in order to anticipate the results and give the accurate decision, in this paper there are preliminary descriptive studies on DICOM images of the skull to help the orthodontists by providing the following algorithms: Segmentation of the lower jaw (mandible), Segmentation of the upper jaw (maxilla) from CT data, Segmentation of upper teeth, each tooth and computation of mandible volume.

**Keywords:** Ct-Scans, Threshold, K-Mean, Region Growing, Dicom.

## E-207. Determination of Displacements in the Biomechanical Orthodontic System by Using Finite Element Method

Kadry Ali Ezzat, Ahmed H. Kandil, Sahar Ali Fawzi and Ahmed M. El-Bialy

*International Journal of Applied Engineering Research, 11: 6794-6799 (2016)*

Orthodontic tooth movement is a physiologic reaction to remotely connected forces; intention forces are principally mechanical. The ideal use of orthodontic force empowers most extreme movement of teeth with the negligible irreversible harm of the alveolar bone, and teeth. Since Archwires are the primary power framework in orthodontics, it is imperative in clinical practice that they convey suitable, predictable and repeatable forces amid treatment. These specific wires even guarantee shape memory properties and the likelihood of super elastic behaviour, which fundamentally affects clinical practices. Since, Titanium, Nickel and Cobalt Archwires are still the materials of decision in numerous phases of treatment. They provide an alluring blend of stiffness, flexibility and formability. In any case, clinical specialists have remarked on the variability of Archwire behaviour for quite a long time. Conflicting Archwire properties can add to eccentric treatment term and results.This paper analyzes the mechanical and physical attributes of Titanium, Nickel and Cobalt wires to evaluate their variability in engineering terms. From the outcomes for those sorts of wires, the testing technique gives the data required by originators wishing to enhance the Archwires properties and provide important data to clinicians for their practice.

**Keywords:** Orthodontics, Mechanical Properties, Tensile Properties, Orthodontic Wires, Titanium, Stainless Steel.

## Faculty of Computers and Information

***Dept. of Computer Science (CS)***

### E-208. Comparative Optimizer Rank and Score: A Modern Approach for Performance Analysis of Optimization Techniques.

Ahmed S. Tawfik, Amr A. Badr and Ibrahim F. Abdel-Rahman

*Expert Systems with Applications, 45: 118-130(2016) IF: 2.981*

The performance analysis of optimization techniques is very important to understand the strengths and weaknesses of each technique. It is not very common to find an optimization technique that performs equally on all optimization problems, and the numbers offered by the most common performance measures, the achieved function value (fitness) and the number of function evaluations, are not representative by their own. For instance, reporting that an optimization technique O on a benchmark function B achieved a fitness F after a number of evaluations E is not semantically meaningful. Some of the logical questions that would arise for such report are: (a) how other techniques performed on the same benchmark, and (b) what are the characteristics of this benchmark (for example, modality and separability). The comparative optimizer rank and score (CORS) proposes an easy to apply and interpret method for the investigation of the problem solving abilities of optimization techniques. CORS offers eight new performance measures that are built on the basic performance measures (that is, achieved fitness, number of function evaluations, and time consumed). The CORS performance measures represent the performance of an optimization technique in comparison to other techniques that were tested under the same benchmarks, making the results more meaningful. Besides, these performance measures are all normalized in a range from 1 to 100, which helps the results to keep well-interpretable by their own. Furthermore, all the CORS performance measures are aggregatable, in which the results are easily accumulated and represented by the common characteristics defining optimization problems (such as dimensionality, modality, and separability), instead of a per benchmark function basis (such as F1, F2, and F3). In order to demonstrate and validate the CORS method, it was applied to the performance data of eight novel optimization techniques of the recent contributions to metaheuristics, namely, the bat algorithm (BA), cuckoo search (CS), differential search (DS), firefly algorithm (FA), gravitational search algorithm (GSA), one rank cuckoo search (ORCS), separable natural evolution strategy (SNES), and exponential natural evolution strategy (xNES). These performance data were generated by 96 tests of 16 benchmark functions and 6 dimensionalities. Along with the basic and CORS performance data, the aggregated CORS results were found to offer a very helpful knowledge regarding the performance of the examined techniques.

**Keywords:** Metaheuristics; Nature-Inspired Algorithms; Optimization; Performance Analysis; Swarm Intelligence.

### E-209. A Modified Flower Pollination Algorithm for Global Optimization.

Emad Nabil.

*Expert Systems with Applications, 57: 192-203 (2016) IF: 2.981*

Expert and intelligent systems try to simulate intelligent human experts in solving complex real-world problems. The domain of problems varies from engineering and industry to medicine and education. In most situations, the system is required to take decisions based on multiple inputs, but the search space is usually very huge so that it will be very hard to use the traditional algorithms to take a decision; at this point, the metaheuristic algorithms can be used as an alternative tool to find near-optimal solutions. Thus, inventing new metaheuristic techniques and enhancing the current algorithms is necessary. In this paper, we introduced an enhanced variant of the Flower Pollination Algorithm (FPA). We hybridized the standard FPA with the Clonal Selection Algorithm (CSA) and tested the new algorithm by applying it to 23 optimization benchmark problems. The proposed algorithm is compared with five famous optimization algorithms, namely, Simulated Annealing, Genetic Algorithm, Flower Pollination Algorithm, Bat Algorithm, and Firefly Algorithm. The results show that the proposed algorithm is able to find more accurate solutions than the standard FPA and the other four techniques. The superiority of the proposed algorithm nominates it for being a part of intelligent and expert systems.

**Keywords:** Nature-Inspired Algorithms; Clonal Selection Algorithm; Flower Pollination Algorithm; Global Optimization.

### E-210. Computational Determination of the Effects of Virulent Escherichia Coli and Salmonella Bacteriophages on Human Gut.

Marwa Mostafa Mostafa, Mohammad Nassef and Amr Badr.

*Computer Methods and Programs in Biomedicine, 135:27-35 .(2016) IF: 1.862.*

Background and objective: Salmonella and Escherichia coli are different types of bacteria that cause food poisoning in humans. In the elderly, infants and people with chronic conditions, it is very dangerous if Salmonella or E. coli gets into the bloodstream and then they must be treated by phage therapy. Treating Salmonella and E. coli by phage therapy affects the gut flora. This research paper presents a system for detecting the effects of virulent E. coli and Salmonella bacteriophages on human gut. Methods: A method based on Domain–Domain Interactions (DDIs) model is implemented in the proposed system to determine the interactions between the proteins of human gut bacteria and the proteins of bacteriophages that infect virulent E. coli and Salmonella. The system helps gastroenterologists to realize the effect of injecting bacteriophages that infect virulent E. coli and Salmonella on the human gut. **Results**: By testing the system over Enterobacteria phage 933W, Enterobacteria phage VT2-Sa and Enterobacteria phage P22, it resulted in four interactions between the proteins of the bacteriophages that infect E. coli O157:H7, E. coli O104:H4 and Salmonella typhimurium and the proteins of human gut bacterium strains. Conclusion: Several effects were detected such as: antibacterial activity against a number of bacterial species in human gut, regulation of cellular differentiation and organogenesis during gut, lung, and heart development, ammonia assimilation in bacteria, yeasts, and plants, energizing defense system and its function in the detoxification of lipopolysaccharide, and in the prevention of bacterial translocation in human gut.

**Keywords:** Salmonella; Escherichia Coli (E. Coli); Bacteriophage; Domain–Domain Interactions (DDI); Human Gut; Protein–Protein Interaction (PPI).

## E-211. A Binary Clonal Flower Pollination Algorithm for Feature Selection.

Safinaz AbdEl-Fattah Sayed, Emad Nabil and Amr Badr.

*Pattern Recognition Letters, 77: 21-27 (2016) IF: 1.586*

Feature selection problem has been detected essentially in the last years. It is a step that is considered the prerequisite of the classification step. For the feature selection problem, the goal is to find out the most important subset of features that represent the original features in a certain domain. The selected features are used in optimization of a certain fitness function, so the feature selection problem can be seen as an optimization problem. This paper presents a new hybrid algorithm that combines Clonal Selection Algorithm (CSA) with Flower Pollination Algorithm (FPA) to compose Binary Clonal Flower Pollination Algorithm (BCFA) to solve the feature selection problem. The accuracy of the Optimum-Path Forest (OPF) classifier is used as an objective function. The experiments were implemented on three public datasets and demonstrated that the proposed hybrid algorithm achieved remarkable results in comparison with other well-known algorithms such as Binary Cuckoo Search Algorithm (BCSA), Binary Bat Algorithm (BBA), Binary Differential Evolution Algorithm (BDEA) and Binary Flower Pollination Algorithm (BFPA).
**Keywords:** Feature Selection; Clonal Selection Algorithm; Flower Pollination Algorithm; Optimum Path Forest.

### *Dept. of Information System (IS)*

## E-212. Search for the standard model Higgs boson produced through vector boson fusion and decaying to b(b)over-bar.

Khachatryan, V. Sirunyan, A. M. Tumasyan, A. Adam, W. Asilar, E. Bergauer, T. Brandstetter, J. Brondolin, E. Dragicevic, M. Ero J. Flechl, M. Friedl, M Fruhwirth, R. Ghete, V. M. and Hartl, C. et al.

*Phys. Rev. D 92, 10(4): 123-125 (2016) IF: 5.*

A first search is reported for a standard model Higgs boson (H) that is produced through vector boson fusion and decays to a bottom-quark pair. Two data samples, corresponding to integrated luminosities of 19.8 fb−1 and 18.3 fb−1 of proton-proton collisions at √s=8 TeV were selected for this channel at the CERN LHC. The observed significance in these data samples for a H→b¯b signal at a mass of 125 GeV is 2.2 standard deviations, while the expected significance is 0.8 standard deviations. The fitted signal strength μ=σ/σSM=2.8+1.6−1.4. The combination of this result with other CMS searches for the Higgs boson decaying to a b-quark pair yields a signal strength of 1.0±0.4, corresponding to a signal significance of 2.6 standard deviations for a Higgs boson mass of 125 GeV.
**Keywords:** Significance of 2.6 Standard Deviations For A Higgs Boson Mass of 125 Gev.

## E-213. Pair-Wise Association Measures for Categorical and Mixed Data.

Ayman Taha and Ali S. Hadi.

*Information Sciences- Elsevier Publisher, 346–347: 73-89 (2016) IF: 3.364.*

We introduce two measures for the strength of the association between two categorical variables. The measures, denoted by η1 and η2, take values in the interval [0, 1]. A value of zero means there is no association between the two categorical variables, while a value of 1 means there is a perfect association (e.g., when we associate a variable with itself, we obtain η=1). The measures are symmetric with respect to the order of variables, invariant with respect to permutations of the categories of the variables, and scalable for large number of observations. In addition, extensions of the proposed measures are presented for measuring the strength of association between pair of mixed variables, one quantitative and the other is categorical. The performance of the proposed measures compared to other association measures is investigated using simulated as well as real data.
**Keywords:** Categorical Data; Variables Correlation; Attributes Association; Data Analytics.

## E-214. Analyzing and Repairing Overlapping Work Items in Process Logs.

Ahmed Awad, Nesma M. Zakia and Chiara Di Frances comarino.

*Information and Software Technology, 80: 110-123 (2016) IF: 1.569*

**Context**: In real life logs, it often happens that some human resources appear to have more than one task active concurrently, thus resulting in human multitasking. However, tasks that require some intellectual effort cannot be executed in parallel in real life. This misalignment between what actually happens and what is registered in the logs, however, is not reflected in the output of the different log-based performance measuring approaches, thus compromising the quality of the computed metrics. **Objective**: We introduce a novel approach to rewrite events in process execution logs for multitasking human resources. The approach is based on two typical human work patterns, the queuing and stacking patterns. The rewrite aims at serializing multi tasks for the same resource based on the work pattern detected. Thus, possibly better performance measures can be obtained. **Method**: We defined a quantitative approach to detect multitasking human performers and resolve them by serialization. The approach is prototyped and evaluated on a set of real-life software development process logs. **Results**: Our results show that the proposed approach contributes to find better results when log-based performance analysis techniques are applied to the repaired logs in comparison to the original logs. **Conclusions**: The work shows that based on the human work patterns, stacking or queuing, logs can be enhanced, so as to be possibly closer to what happened in the reality and to allow for more accurate performance measures.
**Keywords:** Process Logs; Humans Work Patterns; Performance Measurement; Business Processes; Log Analysis.

*Dept. of Information Technology (IT)*

## E-215. A Predictive Model for Toxicity Effects Assessment of Biotransformed Hepatic Drugs Using Iterative Sampling Method.

Alaa Tharwat, Yasmine S. Moemen and Aboul Ella Hassanien

*Scientific Reports (Nature), 38660 (2016) IF: 5.578*

Measuring toxicity is one of the main steps in drug development. Hence, there is a high demand for computational models to predict the toxicity effects of the potential drugs. In this study, we used a dataset, which consists of four toxicity effects:mutagenic, tumorigenic, irritant and reproductive effects. The proposed model consists of three phases. In the first phase, rough set-based methods are used to select the most discriminative features for reducing the classification time and improving the classification performance. Due to the imbalanced class distribution, in the second phase, different sampling methods such as Random Under-Sampling, Random Over-Sampling and Synthetic Minority Oversampling Technique are used to solve the problem of imbalanced datasets. ITerative Sampling (ITS) method is proposed to avoid the limitations of those methods. ITS method has two steps. The first step (sampling step) iteratively modifies the prior distribution of the minority and majority classes. In the second step, a data cleaning method is used to remove the overlapping that is produced from the first step. In the third phase, Bagging classifier is used to classify an unknown drug into toxic or non-toxic. The experimental results proved that the proposed model performed well in classifying the unknown samples according to all toxic effects in the imbalanced datasets.

**Keywords:** Machine Learnning; A Predictive Model; Toxicity Effects Assessment; Biotransformed Hepatic Drugs; Iterative Sampling Method.

## E-216. Brain Mri Tumor Segmentation with 3D Intracranial Structure Deformation Features.

Shang-Ling Jui, Shichen Zhang, Weilun Xiong, Fangxiaoqi Yu, Mingjian Fu, Dongmei Wang, Aboul Ella Hassanien and Kai Xiao.

*IEEE Intelligent Systems, 31(2): 66-76 (2016) IF: 3.5.*

Extraction of relevant features is of significant importance for brain tumor segmentation systems. To improve brain tumor segmentation accuracy, the authors present an improved feature extraction component that takes advantage of the correlation between intracranial structure deformation and the compression resulting from brain tumor growth. Using 3D nonrigid registration and deformation modeling techniques, the component measures lateral ventricular (LaV) deformation in volumetric magnetic resonance images. By verifying the location of the extracted LaV deformation feature data and applying the features on brain tumor segmentation with widely used classification algorithms, the authors evaluate the proposed component qualitatively and quantitatively with promising results on 11 datasets comprising real and simulated patient images.

**Keywords:** 3D Intracranial Structure; Brain Mri Tumor Segmentation; Deformation Features.

## E-217. Feature Selection Via Chaotic Antlion Optimization.

Zawbaa HM, Emary E and Grosan C.

*Plos One, 11: 1-21 (2016) IF: 3.057*

Selecting a subset of relevant properties from a large set of features that describe a dataset is a challenging machine learning task. In biology, for instance, the advances in the available technologies enable the generation of a very large number of biomarkers that describe the data. Choosing the more informative markers along with performing a high-accuracy classification over the data can be a daunting task, particularly if the data are high dimensional. An often adopted approach is to formulate the feature selection problem as a biobjective optimization problem, with the aim of maximizing the performance of the data analysis model (the quality of the data training fitting) while minimizing the number of features used.

**Keywords:** Optimization- Random Walk-Natural Selection.

## E-218. Impact of Chaos Functions on Modern Swarm Optimizers.

E. Emary and Hossam M. Zawbaa.

*Plos One, 11: 1-26 (2016) IF: 3.057.*

Exploration and exploitation are two essential components for any optimization algorithm. Much exploration leads to oscillation and premature convergence while too much exploitation slows down the optimization algorithm and the optimizer may be stuck in local minima. Therefore, balancing the rates of exploration and exploitation at the optimization lifetime is a challenge. This study evaluates the impact of using chaos-based control of exploration/ exploitation rates against using the systematic native control. Three modern algorithms were used in the study namely grey wolf optimizer (GWO), antlion optimizer (ALO) and moth-flame optimizer (MFO) in the domain of machine learning for feature selection. Results on a set of standard machine learning data using a set of assessment indicators prove advance in optimization algorithm performance when using variational repeated periods of declined exploration rates over using systematically decreased exploration rates.

**Keywords:** Chaotic Optimizers, Feature Selection.

## E-219. Computational Identification of Tissue-Specific Splicing Regulatory Elements in Human Genes From Rna-Seq Data.

Eman Badr , Mahmoud ElHefnawi and Lenwood S. Heath.

*Plos One, 11: 1-18 (2016) IF: 3.057.*

Alternative splicing is a vital process for regulating gene expression and promoting proteomic diversity. It plays a key role in tissue-specific expressed genes. This specificity is mainly regulated by splicing factors that bind to specific sequences called splicing regulatory elements (SREs). Here, we report a genome-wide analysis to study alternative splicing on multiple tissues, including brain, heart, liver, and muscle. We propose a pipeline to identify differential exons across tissues and hence tissue-specific SREs. In our pipeline, we utilize the DEXSeq package along with our previously reported

algorithms. Utilizing the publicly available RNA-Seq data set from the Human BodyMap project, we identified 28,100 differentially used exons across the four tissues. We identified tissue-specific exonic splicing enhancers that overlap with various previously published experimental and computational databases. A complicated exonic enhancer regulatory network was revealed, where multiple exonic enhancers were found across multiple tissues while some were found only in specific tissues. Putative combinatorial exonic enhancers and silencers were discovered as well, which may be responsible for exon inclusion or exclusion across tissues. Some of the exonic enhancers are found to be co-occurring with multiple exonic silencers and vice versa, which demonstrates a complicated relationship between tissue-specific exonic enhancers and silencers.

**Keywords:** Alternative Splicing; Splicing Regulatory Elements; Enhancers; Silencers; Tissue Specificity.

## E-220. Pqsar: the Membrane Quantitative Structure-Activity Relationships in Cheminformatics.

Ammar Adl, Moustafa Zein and Aboul Ella Hassanien.

*Expert Systems With Applications, 54: 219-227(2016) IF:2.981.*

The applications of quantitative structure activity relationships (QSAR) are used to establish a correlation between structure and biological response. Similarity searching is one of QSAR major phases. Innovating new strategies for similarity searching is an urgent task in cheminformatics research for three reasons: (i) the increasing size of chemical search space of compound databases; (ii) the importance of similarity measurements to (2D) and (3D) QSAR models; and (iii) similarity searching is a time consuming process in drug discovery. In this study, we introduce theoretical similarity searching strategy based on membrane computing. It solves time consumption problem. We adopt a ranking sorting algorithm with P System to rank probabilities of similarity according to a predefined similarity threshold. That bio-inspired model, simulating biological living cell, presents a high performance parallel processing system, we called it PQSAR. It relies on a set of rules to apply ranking algorithm on probabilities of similarity. The simulated experiments show how the effectiveness of PQSAR method enhanced the performance of similarity searching significantly; and introduced a standard ranking algorithm for similarity searching.

**Keywords:** Quantitative Structure Activity Relationships (Qsar); Similarity Measurements; Similarity Searching Strategy; P System; Chemical Search Space; Drug Discovery.

## E-221. Binary Grey Wolf Optimization Approaches for Feature Selection.

E. Emary, Hossam M. Zawbaa and Aboul Ella Hassanien.

*Neurocomputing, 172(8): 371-381 (2016) IF: 2.392.*

In this work, a novel binary version of the grey wolf optimization (GWO) is proposed and used to select optimal feature subset for classification purposes. Grey wolf optimizer (GWO) is one of the latest bio-inspired optimization techniques, which simulate the hunting process of grey wolves in nature. The binary version introduced here is performed using two different approaches. In the first approach, individual steps toward the first three best solutions are binarized and then stochastic crossover is performed among the three basic moves to find the updated binary grey wolf position. In the second approach, sigmoidal function is used to squash the continuous updated position, then stochastically threshold these values to find the updated binary grey wolf position. The two approach for binary grey wolf optimization (bGWO) are hired in the feature selection domain for finding feature subset maximizing the classification accuracy while minimizing the number of selected features. The proposed binary versions were compared to two of the common optimizers used in this domain namely particle swarm optimizer and genetic algorithms. A set of assessment indicators are used to evaluate and compared the different methods over 18 different datasets from the UCI repository. Results prove the capability of the proposed binary version of grey wolf optimization (bGWO) to search the feature space for optimal feature combinations regardless of the initialization and the used stochastic operators.

**Keywords:** Grey Wolf Optimization; Binary Grey Wolf Optimization; Feature Selection; Bio-Inspired Optimization; Evolutionary Computation.

## E-222. Binary Ant Lion Approaches for Feature Selection.

E. Emary, Hossam M. Zawbaa and Aboul Ella Hassanien.

*Neurocomputing, 213(12): 54-65 (2016) IF: 2.39.*

In this paper, binary variants of the ant lion optimizer (ALO) are proposed and used to select the optimal feature subset for classification purposes in wrapper-mode. ALO is one of the recently bio-inspired optimization techniques that imitates the hunting process of ant lions. Moreover, ALO balances exploration and exploitation using a single operator that can adaptively searches the domain of solutions for the optimal solution. Binary variants introduced here are performed using two different approaches. The first approach takes only the inspiration of ALO operators and makes the corresponding binary operators. In the second approach, the native ALO is applied while its continuous steps are threshold using suitable threshold function after squashing them. The proposed approaches for binary ant lion optimizer (BALO) are utilized in the feature selection domain for finding feature subset that maximizing the classification performance while minimizing the number of selected features. The proposed binary algorithms were compared to three common optimization algorithms hired in this domain namely particle swarm optimizer (PSO), genetic algorithms (GAs), binary bat algorithm (BBA), as well as the native ALO. A set of assessment indicators is used to evaluate and compare the different methods over 21 data sets from the UCI repository. Results prove the capability of the proposed binary algorithms to search the feature space for optimal feature combinations regardless of the initialization and the used stochastic operators.

**Keywords:** Binary Ant Lion Optimizer; Ant Lion Optimizer; Feature Selection; Bio-Inspired Optimization.

## E-223. On the use of Terminal and Inline Conversion in Planar Optical Interconnection Networks.

Haitham S. Hamza.

*IEEE/OSA Journal of Optical Communications and Networking, 8: 844-853 (2016) IF: 2.183.*

Optical wavelength converters (WCs) are used in the design of most optical interconnection networks to improve blocking performance. Typical network architectures make use of WCs at the terminal of the network (i.e., at the input and/or output ports). Recently, inline conversion has been introduced where WCs are deployed and shared between the stages of the network. Sharing conversion among stages can lead to architectures with reduced complexity and hence lower cost. However, sharing inline conversion requires crossovers of interstage links to enter and exit the shared inline converters. As a result, inline conversion can be difficult to implement in planar switching networks with no crossover between interstage links. In this paper, we study, for the first time to the best of our knowledge, the use of combined terminal and inline WCs in planar optical interconnection networks. In particular, we show that terminal conversion has limited scalability even when fixed-range WCs are used. Accordingly, we propose a new design approach that improves scalability while preserving the noncrossover property of planar interconnection networks. It is shown that all conversion processes in the new design are independent of the number of wavelengths in the network, and hence high scalability is achieved.
**Keywords:** Optical Switches; Optical Wavelength Conversion; Complexity Theory; Optical Interconnections; Ports (Computers); Optical Fiber Networks.

## E-224. Optimized Hierarchical Routing Technique for Wireless Sensors Networks.

Shaimaa Ahmed El-said, Asmaa Osamaa and Aboul Ella Hassanien.

*Soft Computing, 20(11): 4549-4564 (2016) IF: 1.6.*

Wireless sensor networks are battery-powered ad hoc networks in which sensor nodes that are scattered over a region connect to each other and form multi-hop networks. Since these networks consist of sensors that are battery operated, care has to be taken so that these sensors use energy efficiently. This paper proposes an optimized hierarchical routing technique which aims to reduce the energy consumption and prolong network lifetime. In this technique, the selection of optimal cluster head (CHs) locations is based on artificial fish swarm algorithm that applies various behaviors such as preying, swarming, and following to the formulated clusters and then uses a fitness function to compare the outputs of these behaviors to select the best CHs locations. To prove the efficiency of the proposed technique, its performance is analyzed and compared to two other well-known energy efficient routing techniques: low-energy adaptive clustering hierarchy (LEACH) technique and particle swarm optimized (PSO) routing technique. Simulation results show the stability and efficiency of the proposed technique. Simulation results show that the proposed method outperforms both LEACH and PSO in terms of energy consumption, number of alive nodes, first node die, network lifetime, and total data packets received by the base station. This may be due to considering residual energies of nodes and their distance from base station , and alternating the CH role among cluster's members. Alternating the CH role balances energy consumption and saves more energy in nodes.
**Keywords:** Wireless Sensors Networks (Wsn) Energy Efficient Routing Techniques; Artificial Fish Swarm Algorithm (Afsa); Hierarchical Routing Technique.

## E-225. A Large Vocabulary System for Arabic Online Handwriting Recognition.

Ibrahim Abdelaziz, Sherif Abdou and Hassanin Al-Barhamtoshy.

*Pattern Analysis and Applications,19:1129-1141(2016) IF: 1.1.*

The success of using Hidden Markov Models (HMMs) for speech recognition application has motivated the adoption of these models for handwriting recognition especially the online handwriting that has large similarity with the speech signal as a sequential process. Some languages such as Arabic, Farsi and Urdo include large number of delayed strokes that are written above or below most letters and usually written delayed in time. These delayed strokes represent a modeling challenge for the conventional left-right HMM that is commonly used for Automatic Speech Recognition (ASR) systems. In this paper, we introduce a new approach for handling delayed strokes in Arabic online handwriting recognition using HMMs. We also show that several modeling approaches such as context based tri-grapheme models, speaker adaptive training and discriminative training that are currently used in most state-of-the-art ASR systems can provide similar performance improvement for Hand Writing Recognition (HWR) systems. Finally, we show that using a multi-pass decoder that use the computationally less expensive models in the early passes can provide an Arabic large vocabulary HWR system with practical decoding time. We evaluated the performance of our proposed Arabic HWR system using two databases of small and large lexicons. For the small lexicon data set, our system achieved competing results compared to the best reported state-of-the-art Arabic HWR systems. For the large lexicon, our system achieved promising results (accuracy and time) for a vocabulary size of 64k words with the possibility of adapting the models for specific writers to get even better results.
**Keywords:** Online Handwriting Recognition Arabic Large Vocabulary Adaptive Training Hidden Markov Models Advanced Modeling.

## E-226. A Deep Neural Networks (Dnn) Based Models for a Computer Aided Pronunciation Learning System.

Mohamed S Elaraby, Mustafa Abdallah, Sherif Abdou and Mohsen Rashwan.

*Lecture Notes in Computer Science (Lncs), 9811: 51-58 (2016)*

Gaussian Mixture Models (GMM) has been the most common used models in pronunciation verification systems. The recently introduced Deep Neural Networks (DNN) has proved to provide significantly better discriminative models of the acoustic space. In this paper, we introduce our efforts to upgrade the models of a Computer Aided Language Learner (CAPL) system that is used to teach the Arabic pronunciation for Quran recitation

rules. Four major enhancements were introduced, firstly we used SAT to reduce the inter-speakers variability, secondly, we integrated a hybrid DNN-HMM models to enhance the acoustic model and decrease the phone error rate. Third, we integrated Minimum Phone Error (MPE) with the hybrid DNN. Finally, in the testing phase, we used a grammar-based decoding graph to limit the search space to the frequent errors types. A comparison between the performance of the conventional GMM-HMM and the hybrid DNN-HMM was performed with results showing significant performance improvements.
**Keywords:** Pronunciation Learning Deep Neural Networks Speaker Adaptive Training.

***Dept. of Operation Research and Decision Support***

### E-227. A Multiobjective Distance Separation Methodology to Determine Sector-Level Minimum Separation for Safe Air Traffic Scenarios.

Ayman Ghoneim and Hussein A. Abbass.

*European Journal of Operational Research, 253: 226-240 (2016) IF: 2.679.*

A precursor question to increase the capacity of an airspace is to determine the minimum distance separation required to make this airspace safe. A methodology to answer this question is proposed in this paper. The methodology takes sector volume, number of crossings and crossing angles of routes, and the number of aircraft as input, and generate air traffic scenarios which satisfy the input values. A stochastic multi-objective optimization algorithm is then used to optimize separation values. The algorithm outputs the set of non-dominated solutions representing the trade-off between separation values and the best attainable target level of safety. The results show that the proposed methodology is successful in determining the minimum distance separation values required to make an air traffic scenario safe from a collision risk perspective, and in illustrating how minimum separation values are affected by different sector/traffic characteristics.
**Keywords:** Air Traffic Management; Evolutionary Optimization; Air Traffic Scenario Design; Airspace Safety; Air Traffic Collision Risk.

## Institute of Statistical Studies and Research

***Dept. of Applied Statistics and Econometrics***

### E-228. The Power Lomax Distribution with an Application to Bladder Cancer Data

El-Houssainy A. Rady, W. A. Hassanein and T. A. Elhaddad

*Springerplus, 5:1838 (2016) IF: 0.982*

A three-parameters continuous distribution, namely, Power Lomax distribution (POLO) is proposed and studied for remission times of bladder cancer data. POLO distribution accommodate both inverted bathtub and decreasing hazard rate. Several statistical and reliability properties are derived. Point estimation via method of moments and maximum likelihood and the interval estimation are also studied. The simulation schemes are calculated to examine the bias and mean square error of the maximum likelihood parameter estimators. Finally, a real data application about the remission time of bladder cancer is used to illustrate the usefulness of the proposed distribution in modelling real data application. The characteristics of the fitting data using the proposed distribution are compared with known extensions of Lomax distribution. The comparison showed that the POLO distribution outfit most well-known extensions of Lomax distribution.
**Keywords:** Power lomax distribution; Maximum likelihood; Bladder cancer; Hazard function; Goodness of fit.

### E-229. A New Non Parametric Estimator for PDF Based on Inverse Gamma Distribution

A. M. Mousa, M. Kh. Hassan and A.Fathi

*Communications in Statistics - Theory and Methods, 45: 7002-7010 (2016) IF: 0.3*

The non parametric approach is considered to estimate probability density function (Pdf) which is supported on $(0, \infty)$. This approach is the inverse gamma kernel. We show that it has same properties as gamma, reciprocal inverse Gaussian, and inverse Gaussian kernels such that it is free of the boundary bias, non negative, and it achieves the optimal rate of convergence for the mean integrated squared error. Also some properties of the estimator were established such as bias and variance. Comparison of the bandwidth selection methods for inverse gamma kernel estimation of Pdf is done.
**Keywords:** Boundary bias; Inverse gamma kernel; Density estimation; Bandwidth.

***Dept. of Computer Sciences and Information***

### E-230. Channel-Aware Routing and Priority-Aware Multi-Channel Scheduling for Wsns-Based Smart Grid Applications

Melike Yigit, V. Cagri Gungor, Etimad Fadel, Laila Nassef, Nadine Akkari and Ian F. Akyildiz

*Jounal of Network and Computer Applications, 71: 50-58 (2016) IF: 2.229*

Wireless Sensor Networks (WSNs) are one of the most promising solutions for smart grid applications due to advantages, such as their low-cost, different functionalities, and successful adoption to smart grid environments. However, providing quality of service (QoS) requirements of smart grid applications with WSNs is difficult because of the power constraints of sensor nodes and harsh smart grid channel conditions, such as RF interference, noise, multi-path fading and node contentions. To address these communication challenges, in this paper link-quality-aware routing algorithm (LQ-CMST) as well as the priority and channel-aware multi-channel (PCA-MC) scheduling algorithm have been proposed for smart grid applications. Furthermore, the effect of different modulation and encoding schemes on the performance of the proposed algorithms has been evaluated under harsh smart grid channel conditions. Comparative performance evaluations through extensive simulations show that the proposed algorithms significantly reduce communication delay and the choice of encoding and modulation schemes is critical to meet the requirements of envisioned smart grid applications.
**Keywords:** Smart grid; Data prioritization; Multi-channel Scheduling; Routing.

## E-231. Large-Scale Nonlinear Mixed-Binary Goal Programmingmodel to Assess Candidate Locations for Solar Energystations: an Improved Real-Binary Differential Evolutionalgorithm with a Case Study

Said Ali Hassan ElQuliti and Ali Wagdy Mohamed

*Journal of Computational and Theoretical Nanoscience, 13(12): 7864-7878 (2016) IF: 1.666*

This paper proposes a large-scale nonlinear integer goal programming model (LSNLIGPM) for solving the general problem of admission capacity planning at the national and/or institutional level and for a given long-term planning horizon. The model aims to satisfy the required key objectives of the Ministry of Education (MEO) and/or 5-year national plan related to the higher education enrollment problem. The model is described in a general form that can be adopted for any country taking into considerations its special requirements. The national plans for higher education together with relevant data for Saudi Arabia are used as a case study. Many relative objectives of national admission capacity planning have been taken into consideration. In this paper, an improved Differential Evolution (DE) algorithm for solving constrained optimization, named IDECO, is developed to solve the proposed non-linear integer GP problem. The proposed algorithm introduces a new search mutation to improve both the local search tendency and the global exploration capability, and to accelerate the convergence of DE technique. Besides, adaptive crossover rate and randomized scale factors will be introduced as uniformly random numbers to enhance the population diversity.
**Keywords:** Large-scale; Nonlinear; Mixed-binary model; Goal programming; Locations for solarenergy stations.

## E-232. Multistage Procedure for Optimal Distribution of Preparatory-Year Students to Faculties and Departments: a Mixed Integer Nonlinear Goal Programming Model with Enhanced Differential Evolution Algorithm

Said Ali El-Qulity, Ali Wagdy Mohamed, Abdullah O. Bafail, and Reda M. S. Abdelaal

*Journal of Computational and Theoretical Nanoscience, 13: 7847-7863 (2016) IF: 1.666*

Higher education sector in the Kingdom of Saudi Arabia has observed great leaps during the last National development plan (2011–2015) and the new one (2016–2020). The higher education authority always tries to solve the question of conflicting aspects concerning the distribution of preparatory-year students among faculties and departments while respecting available capacity, resources, GPA, and student desires and capabilities. Goal Programming (GP) is considered as one of the most powerful techniques for many applications comprising conflicting objectives. This paper proposes a Mixed Integer Nonlinear Goal Programming Model (MINLIGPM) for solving the problem of admission planning both at the faculty and departmental levels. The model aims to satisfy the required key objectives stated by higher authority related to the distribution of preparatory year students among various faculties and departments in a University. The model is described in a general form that can be adopted for any university taking into considerations its special requirements. The requirements, resources and constraints together with relevant data for the Faculty of Engineering and Department of Industrial Engineering at King Abdulaziz University, Saudi Arabia will be used as a case study. The simple linear GP model can be solved using many computerized software such as: Microsoft Excel Solver add-ins, Linear Program Solver (Tora), QM for Windows. However, such software fails to solve a model such that proposed in this paper. Therefore, an enhanced Differential Evolution (DE) algorithm for solving constrained optimization, named EDECO, will be developed to solve the proposed non-linear integer GP problem. The proposed algorithm introduces a new search mutation to improve both the local search tendency and the global exploration capability, and to accelerate the convergence of DE technique. Besides, adaptive crossover rate and randomized scale factors will be introduced as uniformly random numbers to enhance the population diversity.
**Keywords:** Higher education; Admission capacity planning; Large-scale nonlinear goal programming; Differential evolution algorithm.

## E-233. A Time-Stamp Based Approach for Decrypting the Encrypted Xml Documents Partially

A.A. Abd EL-Aziz

*Jökull Journal, 66 (2), (2016) IF: 1.342*

When a SOAPWeb Service is receiving an encrypted XML document, it decrypts the key and uses it to decrypt all the parts of the document containing encrypted data. Finally, the data are parsed with an XML parser and the whole document is forwarded to the next module. In this case, the XML Security processing module typically does not know which parts of the decrypted data are later processed by the business logic due to the absence of time-stamp during the decryption process. Thus, it could also happen that the encrypted data are decrypted, parsed, and not processed further for security analysis. In this research, we use a temporal model for XML representation using a combination of valid time and transaction time through tuple time-stamping. In addition to the time-stamp, we use one attribute of the key components of the encrypted elements to distinguish among them. The time-stamp and the selected attribute will guide the receiver to decrypt the required parts of the encrypted XML documents instead of decrypting all the parts. Moreover, they can be used to retrieve the parts that must be decrypted to contribute to the query results over the encrypted XML documents. The proposed technique not only reduces decryption time, but also it increases the security of the data.
**Keywords:** XML Security, Time-Stamp, XML Encryption, XML Decryption

## E-234. A Generalized National Planning Approach for Admission Capacity in Higher Education: a Nonlinear Integer Goal Programming Model with a Novel Differential Evolution Algorithm

Said Ali El-Qulity and Ali Wagdy Mohamed

*Computational Intelligence and Neuroscience, 21: 1-14 (2016) IF: 0.43*

This paper proposes a nonlinear integer goal programming model (NIGPM) for solving the general problem of admission capacity planning in a country as a whole. The work aims to satisfy most of the required key objectives of a country related to the enrollment problem for higher education. The system general outlines are developed along with the solution methodology for application to the time horizon in a given plan.The up-to-date data for Saudi Arabia is used as a case study and a novel evolutionary algorithm based on modified differential evolution (DE) algorithm is used to solve the complexity of the NIGPM generated for different goal priorities. The experimental results presented in this paper show their effectiveness in solving the admission capacity for higher education in terms of final solution quality and robustness.

### E-235. A New Modified Binary Differential Evolution Algorithmand its Applications

Ling Wang, Xiping Fu, Yunfei Mao, Muhammad Ilyas Menhas and Minrui Fei

*Applied Mathematics and Information Sciences an International Journal, 10(5): 1965-1969 (2016)*

This paper proposes a novel discrete version of Differential Evolution (NBDE) algorithm to solve combinatorial optimization problems with binary variables. A new binary mutation rule is introduced derived from the table of the basic DE mutation strategy and the value of scaling factor F is 1. The eight different combinations of the three randomly selected individuals using binary encoding are deduced. The developed mutation operator enables NBDE to explore and exploit the search space efficiently and effectively which are verified in applications to discrete optimization problems. Numerical experiments and comparisons on One-Max problem and Knapsack problem with two different sizes demonstrate that NBDE outperforms other existing algorithms in terms of final solution quality, search process efficiency and robustness.

**Keywords**: Differential evolution; Discrete optimization; Binary mutation rule.

***Dept. of Mathematical Statistics***

### E-236. Weibull Quasi Lindley Distribution and its Statistical Properties with Applications to Lifetime Data

Amal S. Hassan, I. Elbatal and Saeed E. Hemeda

*International Journal of Applied Mathematics and Statistics, 55: 63-80 (2016)*

In this article, a new four-parameter lifetime model named the Weibull quasi Lindley distribution based on the Weibull G-family is introduced. It is more flexible than several recently introduced lifetime distributions. Various structural properties of the new distribution are derived including moments, moment generating function, quantile function, reliability, hazard rate function and mean residual life. Expressions for the R´enyi, q-entropies and density function of order statistics are also obtained. The model parameters are estimated by the method of maximum likelihood and the observed information matrix is determined. Two real data sets are presented to illustrate the advantage of the new distribution. In fact, the new model provides a better fit to this data than some of the most important distributions.

**Keywords**: Hazard rate; Reliability; Entropies; Moments; Maximum likelihood estimation.

### E-237. The New Kumaraswamy Kumaraswamy Weibull Distribution with Application

Mahmoud R. Mahmoud, El-Sayed A. El-Sherpieny and Mohamed A. Ahmed

*Pakistan Journal of Statistics and Operation Research, 12: 165-184 (2016)*

The Weibull distribution has been used over the past decades for modeling data in many fields so finding generalization of the Weibull distribution becomes very useful to fit more cases or get better fits than before. In this paper, the Kumaraswamy Kumaraswamy Weibull (Kw Kw W) distribution is presented for the first time and we show that it generalizes many important distributions. The probability density function (pdf), the cumulative distribution function (cdf), moments, quantiles, the median, the mode, the mean deviation, the entropy, order statistics, L-moments, extreme value and parameters estimation based on maximum likelihood are obtained for the Kw Kw W distribution. An illustration study and a real data set are used to illustrate the potentiality and application of the new Kw Kw W distribution

**Keywords:** The Weibull distribution; The Kumaraswamy family; Moments; Order statistics; L-Moments; Entropy; Extreme values; Maximum likelihood estimation.

## Faculty of Regional and Urban Planning

***Dept. of Essential and Engineering Sciences***

### E-238. A Comprehensive Statistical Study on Daytime Surface Urban Heat Island During Summer in Urban Areas, Case Study: Cairo and its New Towns

Hamid Taheri Shahraiyni, Sahar Sodoudi, Abbas El-Zafarany, Tarek Abou El Seoud, Hesham Ashraf and Kristin Krone

*Remote Sensing, 8(8): 643-643 (2016) IF: 3.036*

Surface urban heat island (SUHI) is defined as the elevated land surface temperature (LST) in urban area in comparison with non-urban areas, and it can influence the energy consumption, comfort and health of urban residents. In this study, the existence of daytime SUHI, in Cairo and its new towns during the summer, is investigated using three different approaches; (1) utilization of pre-urbanization observations as LST references; (2) utilization of rural observations as LST references (urban–rural difference); and (3) utilization of the SIUHI (Surface Intra Urban Heat Island) approach. A time series of Landsat TM & ETM+ data (46 images) from 1984 to 2015 was employed in this study for daytime LST calculation during summer. Different statistical hypothesis tests were utilized for the evaluation of LST and SUHI in the case studies. The results demonstrated that there is no significant LST difference between the urban areas studied, and their corresponding built-up areas. In addition, daytime LST in new towns during the summer is 2 K warmer than in Cairo. Utilization of a pre-

urbanization observations approach, alongside an evaluation of the long-term trend, demonstrated that there is no daytime SUHI during the summer in the study areas, and construction activities in the study areas do not result in cooling or warming effects. Utilization of the rural observations approach showed that LST is lower in Cairo than its surrounding areas. This demonstrates why the selection of suitable rural references in SUHI studies is an important and complicated task, and how this approach may lead to misinterpretation in desert city areas with significant landscape and surface difference with their most surrounding areas (e.g., Cairo). Results showed that, although SIUHI technique can be representative for the changes of variance of LST in urban areas, it is not able to identify the changes of mean LST in urban areas.

**Keywords:** Land Surface Temperature; Landsat; Urban Areas; Surface Urban Heat/Cool Island; Statistical Hypothesis Tests; Cairo

***Dept. of Regional Development***

## E-239. Driving Factors of Urban Sprawl In Giza Governorate of Greater Cairo Metropolitan Region Using Ahp Method

Taher Osman, Prasanna Divigalpitiya and Takafumi Arima

*Land Use Policy, 58: 21-31 (2016) IF: 2.768*

Based on questionnaire surveys and the AHP method, this paper determines the driving forces of urban sprawl and analyzes their relative influence on sprawl in the middle, north, and south sectors of Giza Governorate, which is located in the western part of the Greater Cairo Metropolitan Region. Sprawl patterns in the study area were influenced by seven driving forces: geographical characteristics, availability of life facilities, economic incentives, land demand and supply, population increases, administrative functions, and development plans. These forces have varying degrees of influence in each sector. Amongst these forces, economic incentives in the middle sector, population increases in the north sector, and administrative functions in the south sector were the forces most influential in urban sprawl.

**Keywords:** Informal Urbanization; Development Policy; Urban Modeling; Analytical Hierarchy Process; Questionnaire Survey

## E-240. Measuring Urban Sprawl Patterns in Greater Cairo Metropolitan Region

Taher Osman, Takafumi Arima and Prasanna Divigalpitiya

*Journal of The Indian Society of Remote Sensing, 44: 287-295 (2016) IF: 0.676*

On the subject of informal sprawl in recent Egypt, this research takes Greater Cairo Region (GCR) as a case and puts forward that informal urban sprawl can be estimated from spatial disposition, informal sprawl efficacy and outer influences; and then evolves a geo-spatial indicators system for quantifying sprawl. So as to estimating these indicators, various data sources are selected, including land use maps, digitized map of the highways and town centers, and population statistical data, etc. GIS spatial analysis methods are used to spatialize these indicators into 120 m × 120 m cells. In addition, an incorporated sprawl index (ISI) is estimated by weight sum of these indicators. The results demonstrated that geo-spatial indicators system can captivate most of the exemplary attributes and interior differentia of urban sprawl. Building land in Cairo has kept quick growing with considerable amount of low efficacy and dysfunctional spatial disposition. The subsequent sprawl attributes are determined by each indicator's exemplary spatial disposition of urban sprawling, conspicuous fragmentation and unevenness of landscape due to ineffective implementation of land use planning, improper pattern of exemplary discontinuous development, strip development and leapfrog development, low efficacy of sprawl, low development density, low population density output in newly developed areas; and unfavorable influences on agriculture and environment and population life.

**Keywords:** Informal Urbanization, Geo-Spatial Indices, Quantifying Urban Sprawl, Greater Cairo Region, Egypt

## E-241. Driving Factors of Urban Sprawl in Giza Governorate of the Greater Cairo Metropolitan Region Using A Logistic Regression Model

Taher Osman , Prasanna Divigalpitiy and Takafumi Arima

*International Journal of Urban Sciences, 20: 206-225 (2016)*

Since the 1950s, The Greater Cairo Metropolitan Region (GCMR) has witnessed an unprecedented rate of urban sprawl that has been mainly concentrated in arable lands against urban planning regulations, and has presented a critical challenge to the urban environment and serious corrosion for arable lands. Thus, the need to identify the driving factor of sprawl is crucial to understand the future of the GCMR urban environment and to overcome the serious challenges of rapid urbanization. We focused on the Giza governorate as a critical area in the GCMR and divided it into three sub-sectors to collect data and analyse. A primary list of driving factors was identified by literature review. Later this list was narrowed down to seven factors after interviews with local urban experts and consideration of the availability of data. Next, a logistic regression analysis was used to evaluate those factors with data derived from existing maps and remotely sensed data for the period of 2004–2013. An operating characteristic (ROC) evaluation of the logistic regression analysis gave high accuracy rates for the entire study area. The findings of the research revealed decreasing significance of the CBD and Nile River as drivers of sprawl. The most significant factors according to the analysis were neighbourhood factors, local urban centres, and accessibility factors of distances to urban uses and major roads. The research suggests more future urban expansion by the existing urban cores and along major roads, leading to more informal urban settlements. It also points to the possibility of persistent deterioration in the urban built environment and agricultural lands. Thus, these findings should be applied to actual urban planning policies, and development regulations should be strengthened to protect the urban environment from further deterioration.

**Keywords:** Urban Sprawl; Driving Factors; Logistic Regression; GCMR

## E-242. Using the Sleuth Urban Growth Model to Simulate the Impacts of Future Policy Scenarios On Land Use in the Giza Governorate, Greater Cairo Metropolitan Region

Taher Osman , Prasanna Divigalpitiy and Takafumi Arima

*International Journal of Urban Sciences, 20: 407-426 (2016)*

The goal of this paper was to find an appropriate urban policy to preserve arable land that is being consumed by highly accelerated urban growth in the Giza Governorate of the Greater Cairo Metropolitan region for the last 50 years. We simulated three different urban policies and relevant growth scenarios for Giza from 2015 to 2035 by using the SLEUTH model to investigate their effects on arable lands. The first scenario used historical growth trends to simulate the persistent growth trends under existing conditions. The second was a compact growth scenario with robust restrictions on development in areas outside of designated growth centres. The third scenario considered officially planned growth that integrated stricter growth plans and stronger protections on lands with natural resources at a level that could be realistically accomplished with strong political commitments. The input data required by the model, including slope, land use, exclusion, and urban growth, transportation, and hill shade were derived from three Landsat satellite images from 1984, 2000, and 2013, according to supervised classifications. The simulation results found that the compact growth policy scenario had the least negative impact on arable lands, while the historical growth scenario had the worst impact.

**Keywords:** Informal Urbanization; Development Policies; Spatial Modelling; Transportation Networks; Developing Countries

## E-243. Applying A Hybrid Model of Markov Chain And Logistic Regression to Identify Future Urban Sprawl in Abouelreesh, Aswan: A Case Study

Omar Hamdy, Shichen Zhao, Taher Osman, Mohamed A Salheen and Youhansen Y Eid

*Geosciences, 6: 1-17 (2016)*

Urban sprawl has become a very complex process, because it has many factors affecting its directions and values. The study of relative research shows that the driving forces that lead and redirect future urban sprawl require the application of a statistical method. In our study, logistic regressions were used to analyze and class the driving forces for urban sprawl. Identifying the driving forces, which is the most important step in predicting the future of urban sprawl in 2037, was performed using the cellular automata models. This study takes the Aswan area as a case study in the period from 2001 to 2013 by analyzing the official detailed plan and Google Earth historical imagery. Almost all data was prepared for logistic regression analysis using ArcGIS software and IDRISI® Selva. In our study, a hybrid model of the Markov chain and logistic regression models was applied to identify future urban sprawl in 2037. The findings of this paper simulate the increase in urban area over 24 years from 1.85 to 2.59 km2. These findings highlight the growing risks of urban sprawl and the difficulties opposing the sustainable urban development plans officially proposed for this area.

**Keywords:** Urban Planning; Logistic Regression; Markov; Urban Sprawl; Aswan

# ( 3 )

# Medical Sciences Sector

3-1 Faculty Mediccine
3-2 Faculty of Oral & Dental Medicine
3-3 Faculty of Pharmacy
3-4 National Cancer Institute
3-5 Faculty of Physical Therapy

# Total No. of Publication for Medical Sciences Sector

| Faculty | 2006 | 2007 | 2008 | 2009 | 2010 | Total |
|---|---|---|---|---|---|---|
| Medicine | 49 | 64 | 124 | 154 | 226 | 617 |
| Pharmacy | 27 | 40 | 77 | 104 | 126 | 374 |
| National Cancer Institute | 9 | 16 | 16 | 27 | 37 | 105 |
| Oral and Dental Medicine | | | 1 | 15 | 19 | 35 |
| Physical Therapy | | | 0 | 0 | 1 | 1 |
| Nursing | | | 1 | 4 | 2 | 7 |
| **Total** | 85 | 120 | 219 | 304 | 411 | 1139 |

| Faculty | 2011 | 2012 | 2013 | 2014 | 2015 | 2016 | Total |
|---|---|---|---|---|---|---|---|
| Medicine | 350 | 338 | 388 | 324 | 406 | 403 | 2209 |
| Pharmacy | 224 | 261 | 297 | 240 | 15 | 14 | 1051 |
| National Cancer Institute | 52 | 46 | 57 | 37 | 293 | 346 | 831 |
| Oral and Dental Medicine | 23 | 21 | 20 | 17 | 53 | 46 | 180 |
| Physical Therapy | 3 | 30 | 10 | 18 | 34 | 46 | 141 |
| Nursing | 6 | 5 | 20 | 30 | 52 | 5 | 118 |
| **Total** | 658 | 701 | 792 | 666 | 853 | 860 | 4530 |

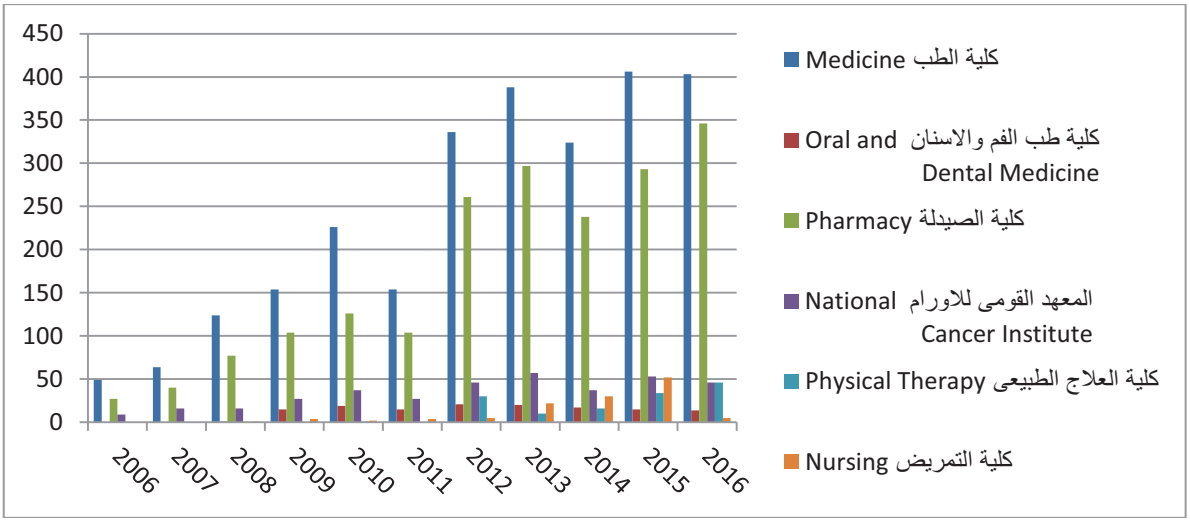

## الأبحاث المنشورة دوليا من ٢٠٠٦ الى ٢٠١٦
## لكليات ومعاهد قطاع العلوم الطبية

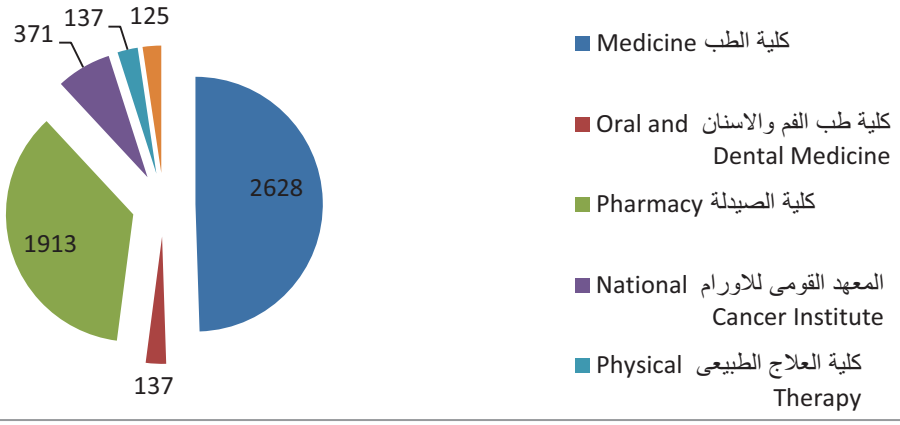


## تطور مجموع الأبحاث المنشورة لكل سنة
## Sum of published researches

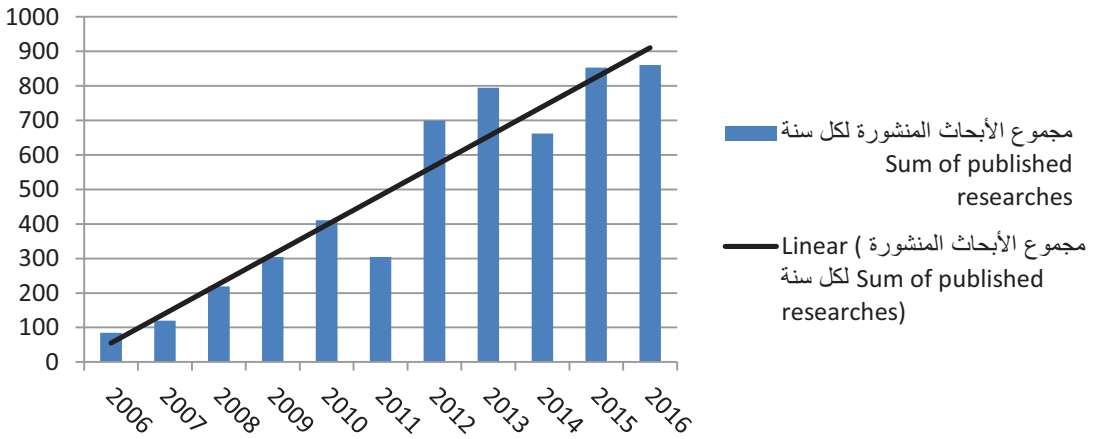

# Total No. of Publication for Social Sciences Sector

| Faculty | 2006 | 2007 | 2008 | 2009 | 2010 | Total |
|---|---|---|---|---|---|---|
| Economics and Political Science | 13 | 14 | 13 | 8 | 10 | 58 |
| Commerce | 4 | 2 | 1 | 4 | 6 | 17 |
| Mass Communication | | | 1 | 0 | 3 | 4 |
| Law | | | | | | |
| **Total** | 17 | 16 | 15 | 12 | 19 | 79 |

| Faculty | 2011 | 2012 | 2013 | 2014 | 2015 | 2016 | Total |
|---|---|---|---|---|---|---|---|
| Economics and Political Science | 6 | 10 | 42 | 29 | 36 | 31 | 154 |
| Commerce | 17 | 24 | 15 | 11 | 17 | 9 | 93 |
| Mass Communication | 1 | 0 | 0 | 0 | 0 | 3 | 4 |
| Law | 1 | 1 | 0 | 5 | 1 | 0 | 8 |
| **Total** | 25 | 35 | 57 | 45 | 54 | 43 | 259 |

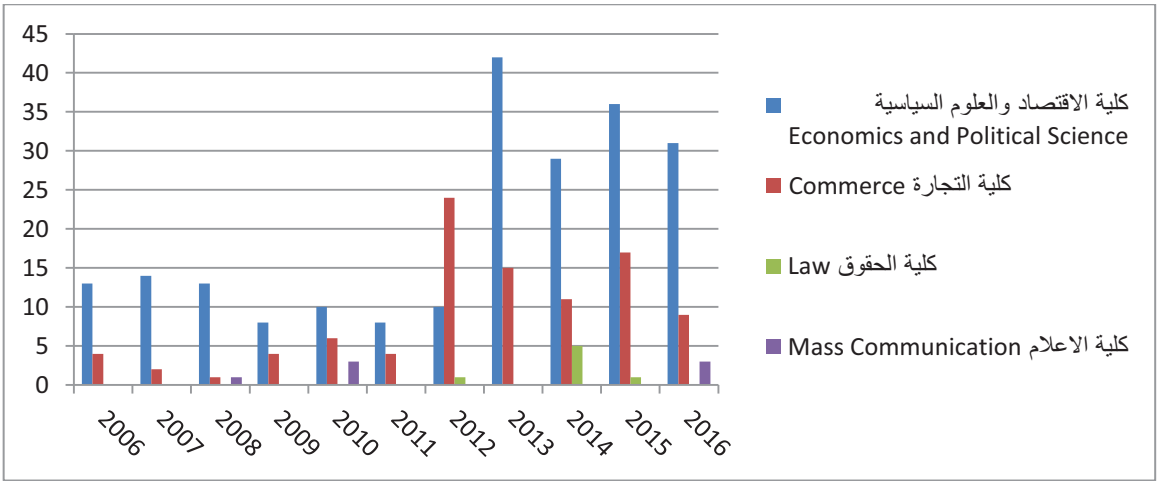

## الأبحاث المنشورة دوليا من ٢٠٠٦ الى ٢٠١٦
## لكليات ومعاهد قطاع العلوم الاجتماعية

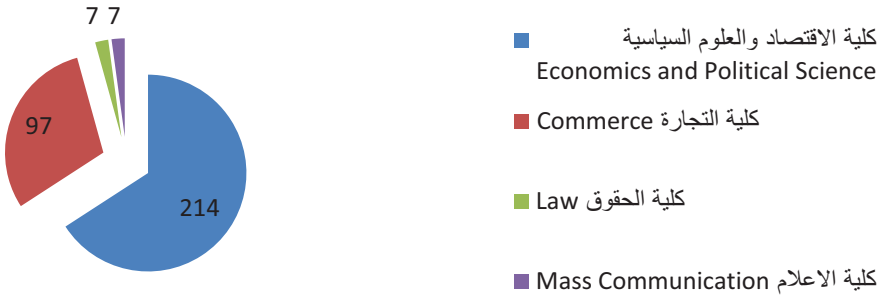


## تطور مجموع الأبحاث المنشورة لكل سنة
## Sum of published researches

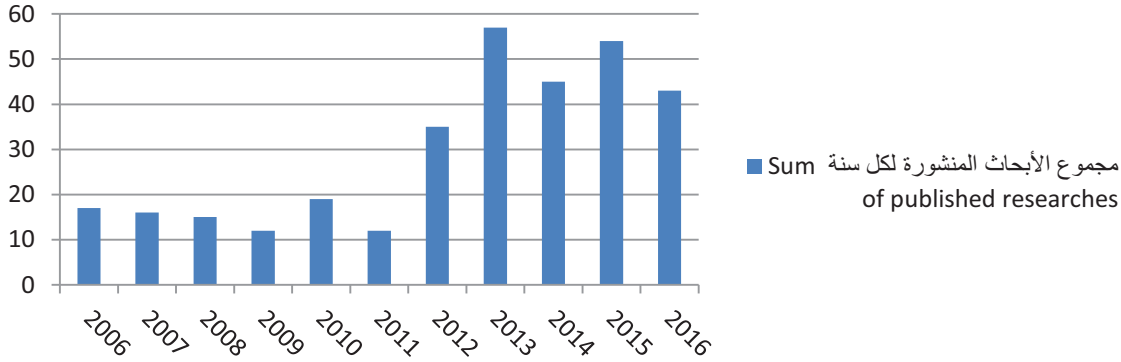

## Faculty of Medicine

***Dept. of Anatomy***

### M-1. Tensile Properties of the Deep Transverse Metatarsal Ligament in Hallux Valgus: A Consort-Compliant Article.

Sahar Abdalbary, Ehab A A El-Shaarawy and Bahaa E.A. Khalid's

*Medicine, Feb;95(8) (2016) IF: 2.133*

The deep transverse metatarsal ligament (DTML) connects the neighboring 2 metatarsal heads and is one of the stabilizers connecting the lateral sesamoid and second metatarsal head. In this study, we aimed to determine the tensile properties of the DTML in normal specimens and to compare these results with hallux valgus specimens. We hypothesized that the tensile properties of the DTML would be different between the 2 groups of specimens. The DTML in the first interspace was dissected from 12 fresh frozen human cadaveric specimens. Six cadavers had bilateral hallux valgus and the other 6 cadavers had normal feet. The initial length (L0) and cross-sectional area (A0) of the DTML were measured using a digital caliper, and tensile tests with load failure were performed using a material testing machine. There were significant between-groups differences in the initial length (L0) P = 0.009 and cross-sectional area (A0) of the DTML P = 0.007. There were also significant between-groups differences for maximum force (N) P = 0.004, maximum distance (mm) P = 0.005, maximum stress (N/mm2) P = 0.003, and maximum strain (%) P = 0.006. The DTML is an anatomical structure for which the tensile properties differ in hallux valgus

**Keywords:**Deep Transverse metatarsal ligament; Hallux valgu; Tensile prpoperties.

### M-2. Changes in Rat Testis Morphologyand Androgen Receptor Expression Around the Age of Puberty.

Nabila A. Abd EL-Meseeh, Ehab A.A. El-Shaarawy, Ahmed F. Al-Domairy and Reem A. Abou Sehly

*Annals of Anatomy, 205: 37-44 (2016) IF: 1.308*

**Background:** Androgens are the keystone in fertility and intact sexual functions in males. It exerts its actions via androgen receptors extensively present in testicular cells, only its presence in germ cells is controversial. The alteration of androgen receptors in different testicular cells is usually accompanied by different sexual disorders. On the other hand, many sexual disorders are treated with androgens. Puberty, being the juncture of hormonal blossom, is an important stage to evaluate the evolution of testicular cells including androgen receptors. The aim of the work was to investigate the morphological and androgen receptor changes in different testicular cells during puberty in the rat testis using histological and immunohistochemical techniques. **Material and Methods:** This study was carried out on 45 male albino rats (Sprague-Dawley). The rats were divided into three age groups; group I (prepubertal) 21 days old, group II (peripubertal) 35 days and group III (postpubertal) 90 days old. The rat testes were examined histologically and immuneohistochemically. Cells and androgen receptors were counted using Leica Qwin 500 image analyzer computer system. Data were analyzed using univariate ANOVA and Bonferroni post hoc test. **Results:**Histological examination of the different ages showed developmental changes of different testicular cells. Immunohistochemical examination revealed the presence of AR in spermatogenic cells in pubertal and postpubertal groups and partially in prepubertal group. AR was clearly expressed in both Sertoli and Leydig cells in the three groups. The maximum expression in Sertoli cells was at 90 days while that of Leydig cells was at the age of 35 days. **Conclusion:** Androgen receptors should not be excluded as an effective factor on germ cells through its direct action on AR, clearly expressed in spermatogenic cells and its surge at the age of puberty. Studies and treatments should respect the AR expected levels according to age in other testicular cells as well. Sertoli cells show a linear increase of AR expression throughout life, while Leydig cells show a peak at the age of puberty.

**Keywords:** Androgen receptors; Immunohistochemistry; Puberty; Testis

### M-3. NT-ProBNP in Children with Left to Right Shunt and Dilated Cardiomyopathy

Hala Mahmoud Koura, Neamat M Abdalla, Mona Hamed Ibrahim, Maha M A Abo Hashishand and Sherif Mohamed Zaki

*Iranian Journal of Pediatrics, 26(3):e4485 (2016) IF: 0.521*

**Background:** B-type natriuretic peptide (BNP) levels are elevated in children with congenital heart disease involving a left-to-right shunt (LRS) and are also raised in dilated cardiomyopathy (DCM). As far as we know, there are few reports in the literature comparing the change of the NT-proBNP in LRS and DCM especially in the pediatric age group. **Objectives:** The aim of the study was to compare the changes of the NT-proBNP in pediatric patients with LRS and DCM. Correlation between the levels of NT-proBNP and the echocardiographic parameters in both groups was determined. Patients and Methods: A total of 30 children (13 males and 17 females) participated in the study. There were 11/30 (36.7%) DCM and 19/30 (63.3%) LRS. The control group consisted of 44 healthy infants and children. Manifestations of heart failure (decompensation) were recorded. The NT-pro BNP levels were measured. The following Echo parameters were assessed: systolic function (ejection fraction and fraction shortening), pulmonary to systemic flow (Qp/Qs) in LRS, pulmonary flow and pulmonary artery pressure (SPAP) and LV diastolic function (E-wave, A-wave, E/A ratio and deceleration time). **Results:** Clinically 17/30 (56.7%) (11 of the LRS and 5 of the DCM) were decompensated. Significant shunt was present in 15/19 (78.9%) in LRS. Systolic dysfunction was presented in 5/30 (16.7%) cases (4 patients were DCM and one case was LRS). Two types of diastolic dysfunction, impaired relaxation in 5/22 (22.7%) patients and restrictive-like filling pattern in 5/16 (31.2 %) were observed. The NT-Pro BNP level was significantly elevated 11 and 16 times in the LRS and DCM groups respectively. Negative significant correlations were observed between the levels of NT-ProBNP and the following echo variables; EDD, LAD, E wave and E/A ratio in the LRS patients. Positive significant correlations were observed between the levels of NT-ProBNP and the following echo variables; PAP and QP/QS in the LRS. Both the PAP and QP/QS were higher in the elevated NT-Pro BNP group compared to the normal level group. The NT-Pro BNP level was elevated in all 17/30 (56.7%)

decompensated patients (11 were LRS, 6 were DCM) (P = 0.002). However, the level was elevated in only 7/13 (23.3%) of the compensated patients (3 were LRS, 4 were DCM) (P = 0.002). The NT-Pro BNP level was also elevated in 18/19 cases with pulmonary hypertension (P = 0.01). Finally, we conclude that the NT-ProBNP level is elevated in both LRS and DCM in pediatric age. This elevation is more remarkable with heart failure and increased PAP in both diseased groups. The level was also elevated and correlated to Qp/Qs in the LRS patients. **Conclusions:** So, we recommend the use of NT-ProBNP as a routine marker for following up patients with heart failure and pulmonary hypertension in LRS and DCM

**Keywords:** Nt-Probnp; Left To right shunt; Dilated cardiomyopathy.

## M-4. Morphological and Morphometric Study of the Cartilaginous Framework of the Dorsum and Tip of the Nose Among Egyptian Populations: A Cadaveric Study.

Ehab A A El-Shaarawy

*Folia Morphologica, 75 (3): 316-325 (2016) IF: 0.469*

**Background:** Success or failure of rhinoplasty depends mainly on the awareness of the surgeon with the construction of the nasal cartilaginous framework and the knowledge of the morphology and different dimensions of these cartilages. The current study aimed at evaluation of the morphology of the nasal cartilages and to address their different measurements as well as observation of anatomical variations of these cartilages and elucidation of their implications in rhinoplasty. **Materials and Methods:** Thirty adult human cadaveric noses, males and females aged 20-70 years were used in the current study. The specimens were dissected; cartilages were exposed and examined morphologically for shape, parts and attachments. Different nasal cartilage measurements were done. **Results:**The examination of nasal cartilage revealed that the mean length of upper lateral cartilage was variable. The mean width and thickness were 12.8 ± 1.29 mm and 1.34 ± 0.14 mm, respectively. The mean length, width and thickness of alar cartilage were assessed. Angle of divergence was observed to be 23-44°. Statistically, there were no significant differences between genders. **Conclusions:** Data obtained from this study confirmed the anatomical varia-tions of the nasal cartilages among the Egyptians and confirmed the differences with several ethnic groups. This has important surgical implications giving the attention required during different techniques in rhinoplasty in order to maintain dorsal aesthetic lines of the nose and proper respiratory function.

**Keywords:** Domal angle; Lower lateral nasal cartilage; Nasal cartilages; Measurements; Upper lateral nasal cartilage.

## M-5. Helicobacter Pylori Infection in Children with Sickle Cell Disease: IgG Versus Combined IgA and IgG Serology.

Hala M Koura, Mona El-Ghamrawy, Sonia Adolf, Mona Hamed and Sherif M Zaki.

*Research Journal of Pharmaceutical, Biological and Chemical Sciences, 7(2): 1307-1316 (2016)*

Serological tests are cheap and non-invasive, so they are used in the diagnosis of Helicobacter pylori infection and more preferred than other invasive methods. Although the diagnostic utility of IgG antibodies to H. pylori is well established, the usefulness of IgA tests is less well documented. Determine the prevalence of H. pylori infection and find the frequency of IgA-positive IgG-negative cases in children with SCD, thus assessing the clinical utility of IgA testing in those patients. Forty children with SCD having a mean age of 10.3years ±5.07 years were recruited from the pediatric hematology clinic of the new children's hospital Cairo University. They underwent clinical evaluation including duration of illness, recurrent abdominal pain (RAP) and peptic like features. They were also subjected to H. pylori serological tests using IgA and IgG antibodies. Thirty normal subjects matched for age and sex served as control group and for whom IgG and IgA serology was done. The prevalence of H. pylori in SCD children was 52.5% using IgG antibody test and 65% using combined serology(IgG + IgA), the same for controls, from 26.7% prevalence to 40%.A high frequency of IgA-positive IgG-negative cases was detected in both patients and controls (12.5% and 13.33% respectively).The age of the patients and their duration of illness were strongly associated to H. pylori seropositivity while RAP and peptic like features were not. Great care should be taken not to underestimate the prevalence of H. pylori infection in children with SCD from the results of IgG serology and it's mandatory to do IgA antibodies in any patient with suspected H. pylori infection and having negative IgG antibodies.

**Keywords:** Sickle cell disease; Helicobacter pylori; Iga-Igg.

## M-6. Non-Traditional Laboratory Markers and Disease Activity in Patients with Systemic Lupus Erythematosus

H.M. Koura, Manal Elshamaa and A. GalalS.M. Zak

*Research Journal of Pharmaceutical, Biological and Chemical Sciences, 7(2): 72-78 (2016)*

While the history and physical examination are most important in assessing systemic lupus erythematosus (SLE) disease activity; laboratory tests are helpful in organ systems that cannot be assessed clinically and can be used to correlate with the disease activity. The aim of the study was to assess the usefulness of some non-traditional lab markers versus the traditional lab markers in the SLE disease activity. A total of 28 SLE patients participated in the current study. Assessing SLE disease activity has been created using the SLE Disease Activity Index (SLEDAI). Two types of lab markers were measured; the first was the traditional lab markers (urea, creatinine, ALT, AST, ESR (1st hour), CRP, C3, C4, Albuminuria, ANA, Anti DNA) and the second was some non-traditional lab markers (granzyme B, fas ligand and neopterin). Six cases (21.4%) were Lupus without nephritis, while 22 cases (78.6%) were diagnosed as Lupus Nephritis. Nine cases (32.1%) were non-active disease, while 19 cases (67.9%) were in disease activity. The ESR levels were elevated in all the active disease cases (67.9%) and in only 3 cases (10.7%) of the non-active disease cases (P=0.000). The mean level of the granzyme B was 341.10±38.04 pg/ml in active disease patients. Its level increased 70 % during the disease activity as compared to that of the control group (P= 0.000). Concerning the mean level of the Fas Ligand, it was 505.05±201.63pg/ml in the active disease patients, while it was

220.44±205.46pg/ml in the non-active disease patients. Its level increased more than two and half folds in the active patients (P=0.000) as compared to that of the control group. Finally, the mean level of the neopterin was 26.31±7.52 nmol/L in the active disease patients. Its level increased more than eight folds in the active disease as compared to that of the control group (P=0.000). The levels of the non-traditional lab markers (granzyme B, fas ligand and neopterin) are sensitive and wellcorrelated to the disease activity in SLE patients.
**Keywords:** Non-traditional lab markers; Sle Activity

***Dept. of Andrology and Sexology***

## M-7. Shaeer"s Corporal Rotation III: Shortening-Free Correction of Congenital Penile Curvature-the Noncorporotomy Technique

Osama Shaeer and Kamal Shaeer

*European Urology, 69(1): 129-134 (2016) IF: 14.976*

**Background:** Shortening-free correction of congenital ventral penile curvature by rotation of the corpora cavernosa was first introduced in 2006 (Shaeer's corporal rotation I). The basic principle was shifting the concavity of both corpora cavernosa from the ventral aspect of the penis to the lateral aspects, in opposition. Rotation was achieved by approximating short parallel incisions on the dorsum of both corpora cavernosa. In 2008, we reported modification of the technique (Shaeer's corporal rotation II), in which the incisions spanned the whole length of the corpora cavernosa**. Objective:**The current modification, Shaeer's corporal rotation III (the noncorporotomy technique) simplifies corporal rotation further and addresses shortcomings. **Design, Setting, and Participants:**This is a retrospective study of 127 cases of congenital ventral penile curvature 25-90° operated at Kamal Shaeer Hospital, Cairo, Egypt, from 2009 to 2015. SURGICAL PROCEDURE: The neurovascular bundle was mobilized, and the corpora were rotated by approximating premarked respective points on either side of the deep dorsal vein using polyester sutures without incising the tunica albuginea. **Outcome Measurements and Statistical Analysis:** Intraoperative postrotation angle and erect length and girth. **Results and Limitations:** On-table measurements showed a mean prerotation erection angle of 66.5° ± 17.9° (range: 25-90°; median 65°). Following rotation, the angle was 0.47° ± 1.8° ($p<0.001$) and length was 0.06 ± 0.25 cm longer ($p=0.007$), whereas girth was 0.77 ± 0.9 cm narrower ($p<0.001$). Complications included 11 cases (8.7%) of ventral wound gaping and 3 (2.4%) with mild recurrence not requiring correction. The International Index of Erectile Function was 24.99 ± 0.9, with an increase of 13.35 ± 3.4 over the preoperative state ($p<0.001$). **Conclusions:** Shaeer's corporal rotation III enables correction of any degree of ventral congenital penile curvature, with neither shortening nor erectile dysfunction. **Patient Summary:**Shaeer's corporal rotation is a surgical technique for correction of severe degrees of innate downward curvature of the penis, without shortening.
**Keywords:** Congenital penile curvature; Corporal rotation; Curved penis; Penile deviation; Rotation of The corpora Cavernosa; Shaeer's technique

## M-8. TNF-α -308 Polymorphisms and Male Infertility Risk: A Meta-Analysis and Systematic Review

Taymour Mostafa and Mai Taymour

*Journal of Advanced Research, 7: 185-192 (2016) IF: 3*

This study aimed to conduct a systematic review and meta-analysis of prospective studies discussing TNF-α -308 polymorphism and male infertility. This study was conformed to Preferred Reported Items for Systematic Reviews and Meta-Analyses guidelines. PubMed, Embase and Scopus databases were searched to identify relevant studies by two independent reviewers. Hazard ratios were pooled using fixed-effect or random-effects models when appropriate. Q-test was performed to evaluate study heterogeneity and publication bias appraised using funnel plots. The search yielded five studies (three of Caucasians ethnicity and 2 of Asian ethnicity) comprising 2939 men (2262 infertile men and 677 fertile controls). Most of the studied cases were carried out on TNF-α promoter region at positions -308 G/A (four studies) where -308 C/T was dealt with in one study. Overall, significant associations between TNF-α -308 gene polymorphisms and idiopathic male infertility risk were observed (fixed effect: OR = 0.472, 95% CI: 0.378-0.589; P = 0.001; random effect: OR = 0.407, 95% CI: 0.211-0.785; P = 0.007) with robust findings according to sensitivity analyses. Funnel plot inspections did not give evidences of publication bias. A stratified analysis performed for ethnic groups revealed significant association in both Caucasian and Asian populations. It is concluded that there are evidences of associations between TNF-α -308 gene polymorphisms and male infertility risk.
**Keywords:** Male Infertility; Meta-Analysis; Polymorphism; Semen; Sperms; Tnf-A

## M- 9. Total Phallic Reconstruction Using the Radial Artery Based Forearm Free Flap after Traumatic Penile Amputation

Marco Falcone, Giulio Garaffa, Amr Raheem, Nim A. Christopher and David J. Ralph

*Journal of Sexual Medicine, 13: 1119-1124 (2016) IF: 2.884*

**Introduction** Although genital injuries in civilian centers are rare, the scenario is completely different in the battlefield. If the penile distal stump is not adequate for primary reimplantation or it cannot be found, then delayed penile reconstruction needs to be considered. **Aim** To report a single-center experience with total phallic reconstruction using radial artery based forearm free flap (RAFFF) after penile traumatic loss. **Methods** We retrospectively reviewed the clinical records of 10 patients who underwent total phallic reconstruction with the use of the RAFFF from September 2001 through August 2015 after traumatic amputation of the penis. Main Outcome Measures Patients' baseline features, surgical outcomes, complications, and satisfaction are reported. **Results** The average age at the time of penile reconstruction was 36 years (range = 27–52 years). The causes of penile loss were self-amputation owing to an acute schizophrenic episode (n = 2), road traffic accident (n = 3), blast injury (n = 3), donkey bite (n = 1), and Fournier gangrene (n = 1). The average time from the trauma to reconstruction with the RAFFF was 7 years (range = 2–15 years). The urethral stump was adequate for primary

anastomosis, with phallic neourethra construction in six patients. The remaining patients had complete avulsion of the penis and were voiding though a perineal urethrostomy. In consequence, they required a two-stage urethroplasty. An acute arterial thrombosis of the microsurgical anastomosis occurred in two patients and was managed successfully with immediate exploration. A neourethra stricture and fistula occurred in one patient, which needed revision. All patients who underwent complete urethral reconstruction could void and ejaculate from the tip of the phallus. After a median follow-up of 51 months (range = 1–114 months), all patients were satisfied with the size, cosmetic appearance, and sensation of the phallus. Six patients underwent inflatable penile prosthesis implantation and could engage in penetrative sex. However, revision surgery was needed in three patients (infection, n = 2; mechanical failure, n = 1). **Conclusion** Despite the high incidence of postoperative complications and the possible need for multiple operations, in expert hands and in large-volume centers, penile reconstruction with the RAFFF after traumatic loss of the penis yields excellent results and allows patients to regain sexual and urinary functions.

**Keywords:** Phalloplasty; Radial Artery Forearm Free Flap; Penile Trauma; Penile Amputation.

## M-10. Does Being Overweight Affect Seminal Variables in Fertile Men?

Emad A. Taha, Sohair K. Sayed, Hisham D. Gaber, Hatem K. Abdel Hafez, Nagwa Ghandour, Asmaa Zahran and Taymour Mostafa

*Reprod Biomed Online, 33: 703-708 (2016) IF: 2.796*

The effect of being overweight on seminal variables was assesed in 165 fertile men. Participants were divided into three groups: fertile men with normal body mass index (BMI) (18.5-24.9 kg/m2), fertile overweight men (BMI 25-29.9 kg/m2) and fertile obese men (BMI >30 kg/m2). Medical history was taken, a clinical examination conducted. Semen analysis was undertaken and BMI measured. Seminal reactive oxygen species (ROS) was estimated by chemiluminescent assay, sperm vitality by the hypo-osmotic swelling test and sperm DNA fragmentation by propidium iodide staining with flowcytometry. Fertile obese men had significantly lower sperm concentration, progressive sperm motility and sperm normal morphology, with significantly higher seminal ROS and sperm DNA fragmentation compared with fertile normal-weight men and overweight men (all $P < 0.05$). BMI was negatively correlated with sperm concentration ($r = -0.091$; $P = 0.014$), progressive sperm motility ($r = -0.697$; $P = 0.001$), normal sperm morphology ($r = -0.510$; $P = 0.001$), sperm vitality ($r = -0.586$; $P = 0.001$), but positively correlated with sperm DNA fragmentation percentage ($r = 0.799$; $P = 0.001$) and seminal ROS ($r = 0.673$; $P = 0.001$). Increased BMI was found to affect semen parameters negatively even in fertile men.

**Keywords:** BMI; Male Infertility; Obesity; Oxidative Stress; Semen; Sperm DNA Fragmentation.

## M-11. Seminal miRNA Relationship with Apoptotic Markers and Oxidative Stress in Infertile Men with Varicocele

Taymour Mostafa, Laila A. Rashed, Nashaat I. Nabil, Ihab Osman, Rashad Mostafa and Mohamed Farag

*Biomed Research International, 2016: 1-9 (2016) IF: 2.134*

**Aim.** This study aimed to assess seminal miRNA relationship with seminal apoptotic markers and oxidative stress (OS) in infertile men associated with varicocele (Vx). Methods. In all, 220 subjects were divided into the following groups: fertile normozoospermic men, fertile normozoospermic men with Vx, infertile oligoasthenoteratozoospermic (OAT) men without Vx, and infertile OAT men with Vx. They were subjected to history taking, clinical examination, and semen analysis. In their semen, the following were estimated: miRNA-122, miRNA-181a, and miRNA-34c5 using quantitative real-time PCR, apoptotic markers (BAX, BCL2) protein expression, and OS markers [malondialdehyde (MDA) and glutathione peroxidase (GPx)]. **Results.** The mean levels of seminal miRNA-122, miRNA-181a, and miRNA-34c5 were significantly reduced in infertile OAT men with Vx compared with other groups coupled with Vx grade and Vx bilaterality. Seminal miRNA-122, miRNA-181a, and miRNA-34c5 were positively correlated with sperm concentration, total sperm motility, sperm normal morphology, seminal GPx, and seminal BCL2 and negatively correlated with seminal MDA and seminal BAX. Conclusions. Seminal miRNA-122, miRNA-181a, and miRNA-34c5 are decreased in infertile OAT men with Vx associated with increased Vx grade and Vx bilaterality. In addition, they are positively correlated with sperm parameters and negatively correlated with OS, apoptotic markers.

**Keywords:** miRNA; Male Infertility; Semen; Oxidative Stress; Varicocele

## M-12. Seminal Corynebacterium Strains in Infertile Men with and Without Leucocytospermia.

M. Mashaly, D. T. Masallat, A. A. Elkholy, I. A. Abdel-Hamid and T. Mostafa

*Andrologia, 48: 335-339 (2016) IF: 1.441*

This study aimed to identify seminal Corynebacterium strains in infertile men with and without leucocytospermia. Semen samples from 60 infertile men were allocated into two equal groups: semen samples with leucocytospermia and semen samples without leucocytospermia. Semen culture for Corynebacterium species was carried out on Columbia agar medium confirmed by Gram-stained film and biochemical tests followed by analytical profile index biotyping and antibiotic susceptibility. Bacterial isolates were detected in 20/60 semen cultures (33.3%) as Corynebacteria, Staphylococci, Alpha haemolytic streptococci and E. coli. In all, 12/60 (20%) had Corynebacterium positive semen culture, whereas C. seminal was the major isolated species followed by C. amycolatum, C. jekium and C. urealyticum. There was nonsignificant difference between patients with/without Corynebacterium positive culture regarding sperm concentration and normal sperm morphology; however, in positive cultures sperm motility was significantly lower compared with negative cultures. Antimicrobial sensitivity among Corynebacteria strains was highest for vancomycin,

rifampicin then imipenem, ampicillin + sulbactam, ciprofloxacin. It is concluded that positive semen cultures for different Corynebacteria species were demonstrated in infertile men, whereas Corynebacterium seminale was the most common isolated species. Vancomycin, rifampicin then imipenem and ampicillin + sulbactam are recommended as sensitive antibiotics.
**Keywords:** Antibiotics; Corynebacteria; Leucocytospermia; Male Infertility; Semen.

## M-13. Seminal Cyclooxygenase Relationship with Oxidative Stress in Infertile Oligoast henoteratozoos permic Men with Varicocele.

T. Mostafa, L. Rashed and M. Taymour

*Andrologia, 48: 137-142 (2016) IF: 1.441*

This study aimed to assess the relation of seminal cyclooxygenase COX-1, COX-2 with oxidative stress in infertile oligoasthenoteratozoospermic (OAT) men with varicocele (Vx). In all, 128 men were allocated into fertile men, fertile men with Vx, infertile OAT men without Vx and infertile OAT men with Vx. They were subjected to history taking, clinical examination and semen analysis. Also, seminal COX-1, COX-2, malondialdehyde (MDA) and glutathione peroxidase (GPx) were estimated. Mean levels of seminal COX-1, COX-2 were over-expressed, the mean level of seminal MDA was significantly increased, and the mean level of seminal GPx was significantly decreased in infertile OAT men with Vx compared with other groups. Seminal COX-1 and COX-2 were over-expressed in cases with Vx grade III compared with Vx grades I, II cases and in cases with bilateral Vx compared with unilateral Vx. There was significant negative correlation between seminal COX-1 and COX-2 with sperm concentration, sperm motility, sperm normal morphology, seminal GPx and significant positive correlation with seminal MDA. It is concluded that seminal COX-1 and COX-2 are over-expressed in infertile OAT men with Vx compared with fertile men with/without and infertile OAT men without Vx being associated with oxidative stress, Vx grade and Vx laterality.
**Keywords:** COX; Male Infertility; Oxidative Stress; Semen; Varicocele

## M-14. Precocious Puberty: A Question to be Answered

Mostafa Taymour

*Human Andrology, 6: 31-37 (2016)*

Precocious puberty (PP) is allied with accelerated growth, advanced bone age, development of secondary sex characteristics, and early closure of epiphysis. This article aimed to review PP in both sexes. A search for a review of published articles was carried out using PubMed, medical subject heading databases, and Scopus engine. Keywords used to accomplish these concerned associations were puberty, PP, adolescence, adrenarche, menarche, pubarche, and thelarche. Etiologically, PP is divided into gonadotropin-releasing hormone (GnRH)-dependent and GnRHindependent causes. GnRH-dependent PP [central precocious puberty (CPP)] is based on hypothalamic–pituitary–gonadal axis activation associated with progressive pubertal development, accelerated growth rate, and advanced skeletal age. CPP is one of the common forms of PP resembling the normal route of puberty at an age less than 8 and 9 years for girls and boys, respectively. Peripheral precocious puberty is related to sex steroid exposure independent of hypothalamic–pituitary–gonadal axis activation. Therapy is indicated in children with CPP with accelerated bone age, height progress, or psychosocial stress to halt puberty succession to a socially satisfactory age, allowing the child to achieve optimal height potential. GnRH analog is the treatment of preference, with best height result if initiated before 6 years of age.
**Keywords:** Adolescence; Adrenarche; Menarche; Precocious Puberty; Pubarche; Puberty; Thelarche.

## M-15. The Drug Treatment of Delayed Ejaculation

Moustafa El-Saied, Ibrahim A Abdel-Hamid and Tahia B. Mostafa

*Translational Andrology and Urology, 5: 576-591 (2016)*

Delayed ejaculation (DE) is an uncommon and a challenging disorder to treat. It is often quite concerning to patients and it can affect psychosocial well-being. Here we reviewed how DE is treated pharmacologically .We also highlighted specific settings where drugs could be introduced to medical practice. Electronic databases were searched from 1966 to February 2016, including PubMed MEDLINE, EMBASE, EBCSO Academic Search Complete, Cochrane Systematic Reviews Database, and Google Scholar using key words; delayed ejaculation, retarded ejaculation, inhibited ejaculation, drugs, treatment, or pharmacology. To achieve the maximum sensitivity of the search strategy and to identify all studies, we combined "delayed ejaculation" as Medical Subject Headings (MeSH) terms or keywords with each of "testosterone" or "cabergoline" or "bupropion" or "amantadine" or "cyproheptadine" or "midodrine" or "imipramine" or "ephedrine" or "pseudoephedrine" or "yohimbine" or "buspirone" or "oxytocin" or "bethanechol" as MeSH terms or keywords. There are a number of drugs to treat patients with DE including: testosterone, cabergoline, bupropion, amantadine, cyproheptadine, midodrine, imipramine, ephedrine, pseudoephedrine, yohimbine, buspirone, oxytocin, and bethanechol. Although there are many pharmacological treatment options, the evidence is still limited to small trials, case series or case reports. Review of literature showed that evidence level 1 (Double blind randomized clinical trial) studies were performed with testosterone, oxytocin, buspirone or bethanechol treatment. It is concluded that successful drug treatment of DE is still in its infancy. The clinicians need to be aware of the pathogenesis of DE and the pharmacological basis underlying the use of different drugs to extend better care for these patients. Various drugs are available to address such problem, however their evidence of efficacy is still limited and their choice needs to be individualized to each specific case.
**Keywords:** Ejaculation; Delayed Ejaculation (De); Drugs; Inhibited Ejaculation; Treatment

## M-16. The Impact of Chronic Testicular Inflammatory Infiltration on Spermatogenesis in Azoospermic Men, Evidence-Based Pilot Study

Ahmed M Hassanin and Essam Ayad

*Middle East Fertility Society Journal, 21: 31-35 (2016)*

**Introduction:** The testes are immune privileged organs but they are subjected to acute and chronic inflammations that can impair spermatogenesis. Spermatogonial stem cells are less sensitive to injury, capable of self-renewal, and act as a reservoir that can restart impaired spermatogenesis. **Objective:** To study the association of chronic testicular inflammatory infiltration with an area of complete spermatogenesis in testicular biopsies of men with non-obstructive azoospermia (NOA). Design: Retrospective study. **Patients and methods:** Review of 109 archived Bouin fixed, paraffin embedded and hematoxylin and eosin stained open testicular biopsies of azoospermic men. **Main outcome measure:** The absence/presence (focal/widespread) of chronic interstitial inflammatory infiltration and absence/presence of late spermatids. **Results:** Obstructive picture was found in 25 (22.9%) whereas non-obstructive patterns were found in 84 (77.1%) of the reviewed biopsies. Focal interstitial lymphocytic infiltration (ILI) was found in 9 (36%) obstructive biopsies whereas in non-obstructive patterns 32 (38.1%) had focal and 27 (32.1%) had wide spread ILI. In NOA late spermatids were present in 32 (38.1%) biopsies. Finding late spermatids was significantly highest when the infiltrate was focal and significantly lowest when the infiltrate was wide spread. **Conclusion:** In NOA, the possibility of finding an area of complete focal spermatogenesis in the open testicular biopsy is significantly highest when there is a focal type of ILI, but the possibility is significantly lowest when the infiltrate is widespread. This may guide the clinical testicular sperm extraction (TESE) procedure.

**Keywords:** Spermatogenesis; Lymphocytic Inflammatory Infiltration; Testis; Azoospermia.

## M-17. Useful Implications of Low-Dose Long-Term Use of PDE-5 Inhibitors.

Taymour Mostafa

*Sexual Medicine Reviews, 4: 270-284 (2016)*

**Introduction:** Phosphodiesterase type 5 (PDE-5) hydrolyzes cyclic guanylate monophosphate (cGMP) specifically to 5' GMP, promoting successful corporeal vascular relaxation and penile erection during sexual stimulation. Oral PDE-5 inhibitors such as sildenafil, vardenafil, tadalafil, and avanafil have provided noninvasive, effective, well-tolerated treatment for erectile dysfunction (ED) patients and, at the same time, stimulated both academic and clinical interests. Lately, some oral PDE-5 inhibitors were released as low-dose preparations with the concept of potential daily administration and long-term use. **AIM:** To highlight the possible potential implications of low-dose long-term use of PDE-5 inhibitors. **Method:** A systematic review was carried out until December 2015 based on a search of all concerned articles in MEDLINE, medical subjects heading (MeSH) databases, Scopus, The Cochrane Library, EMBASE, and CINAHL databases without language restriction. Key words used to assess the outcome and estimates for concerned associations were: PDE-5 inhibitors; erectile dysfunction; low-dose; long-term; sildenafil; tadalafil; vardenafil; avanafil. **Main Outcome Measures:**Demonstrating different implications for low-dose long-term use of PDE-5 inhibitors. **Results:**Low-dose and/or long-term use of PDE-5 inhibitors was shown to put forth beneficial sound effects in different medical implications with potentials that could be extended for different utilities. These implications included sexual, urogenital, cardiovascular, pulmonary, cutaneous, gastrointestinal, and reproductive, as well as neurological disorders. However, it is evident that most potential appliances were carried out experimentally on preclinical studies with off-label indications. **Conclusion:** Making use of and exploring low-dose and/or long-term use of several PDE-5 inhibitors for their possible implications seem to be valuable in different medical disorders. Increased knowledge of the drug characteristics, comparative treatment regimens, optimal prescribing patterns, and well-designed clinical trials are needed before these agents can be recommended for use.

**Keywords:** Avanafil; Chronic Use; Erectile Dysfunction; Low-Dose; PDE-5 Inhibitors; Sildenafil; Tadalafil; Vardenafil

### *Dept. of Anesthesiology*

## M-18. The Effects of Perineural Dexmedetomidine on the Pharmacodynamic Profile of Femoral Nerve Block: A Dose-Finding Randomised, Controlled, Double-Blind Study

M. Abdulatif, M. Fawzy, H. Nassar, A. Hasanin and M. Ollaek and H. Mohamed

*Anaesthesia, 71: 1177-85 (2016) IF: 3.794*

This randomised, controlled, double-blind study investigated the effects of different doses of perineural dexmedetomidine on the pharmacodynamic profile of femoral nerve block in patients undergoing arthroscopic knee surgery. Ultrasound-guided femoral nerve block was performed before general anaesthesia using 25 ml of bupivacaine 0.5% combined with normal saline in the control group, and 25 μg, 50 μg or 75 μg of dexmedetomidine in three treatment groups (n = 15 for each group). All patients received a standard general anaesthetic and multimodal postoperative analgesic regimen. The use of the 50 μg and 75 μg dose levels of dexmedetomidine was associated with reduction of the onset time, extension of the duration of block, prolonged time to the first postoperative request for rescue analgesia, and reduced postoperative morphine requirements. The times to first request for postoperative analgesia were mean (SD) 10.8 (1.6) h in the control group and 11.0 (7.1), 21.8 (3.0) and 28.6 (10.0) in the 25 μg, 50 μg and 75 μg treatment groups, respectively. These times were significantly longer in the 50 μg and 75 μg treatment groups compared with the 25 μg ($p < 0.0001$) and control group ($p < 0.0001$). The total 24-h postoperative morphine consumption was 7.6 (5.1) mg in the control group, and 6.5 (3.5), 3.9 (3.4), 1.8 (2.6) in the 25 μg, 50 μg and 75 μg treatment groups, respectively. Postoperative morphine consumption was significantly higher in the control group compared with the 50 μg ($p = 0.045$) and the 75 μg ($p = 0.001$) treatment groups. The best analgesic profile was achieved at the 75 μg dose, but this was associated with increased risk of hypotension.

**Keywords:** Adrenergic Alpha-2 Receptor Agonists; Anaesthetics; Bupivacaine; Dexmedetomidine; Femoral; Local; Peripheral Nerves

## M-19. Diagnostic Values of CD64, C-Reactive Protein and Procalcitonin in Ventilator-Associated Pneumonia in Adult Trauma Patients: A Pilot Study

Habib SF, Ahmed S, Skelly R, Bhatt K, Patel B, Lowe D, Tuson J and Rogers SN.

*Clinical Chemistry and Laboratory Medicine Journal, 54: 889-895 (2016) IF: 3.017*

**Background:** Ventilator-associated pneumonia (VAP) is one of the most common nosocomial infections; however, its diagnosis remains difficult to establish in the critical care setting. We investigated the potential role of neutrophil CD64 (nCD64) expression as an early marker for the diagnosis of VAP. **Methods:** Forty-nine consecutive patients with clinically suspected VAP were prospectively included in a single center study. The levels of nCD64, C-reactive protein (CRP), and serum procalcitonin (PCT) were analyzed for diagnostic evaluation at the time of intubation(baseline), at day 0 (time of diagnosis), and at day 3. The receiver operating characteristic curves were analyzed to identify the ideal cutoff values. **Results:** VAP was confirmed in 36 of 49 cases. In patients with and without VAP, the median levels (interquartile range, IQR) of nCD64 did not differ either at baseline [2.4 (IQR, 1.8–3.1) and 2.6 (IQR, 2.3–3.2), respectively; p = 0.3] or at day 0 [2 (IQR, 2.5–3.0) and 2.6 (IQR, 2.4–2.9), respectively; p = 0.8]. CRP showed the largest area under the curve (AUC) at day 3. The optimum cutoff value for CRP according to the maximum Youden index was 133 mg/dL. This cutoff value had 69% sensitivity and 76% specificity for predicting VAP; the AUC was 0.73 (95% CI, 0.59–0.85). The nCD64 and PCT values could not discriminate between the VAP and non-VAP groups either at day 0 or day 3. **Conclusions:** The results of this pilot study suggest that neutrophil CD64 measurement has a poor role in facilitating the diagnosis of VAP and thus may not be practically recommended to guide the administration of antibiotics when VAP is suspected.

**Keywords:** Biomarkers; Cd64; Crp; Procalcitonin; Ventilator-Associated Pneumonia.

## M-20. Modulation of Splanchnic Circulation: Role in Perioperative Management of Liver Transplant Patients.

Ahmed Mukhtar and Hany Dabbous

*World Journal of Gastroenterology, 22:1582-1592 (2016) IF:2.787*

Splanchnic circulation is the primary mechanism that regulates volumes of circulating blood and systemic blood pressure in patients with cirrhosis accompanied by portal hypertension. Recently, interest has been expressed in modulating splanchnic circulation in patients with liver cirrhosis, because this capability might produce beneficial effects in cirrhotic patients undergoing a liver transplant. Pharmacologic modulation of splanchnic circulation by use of vasoconstrictors might minimize venous congestion, replenish central blood flow, and thus optimize management of blood volume during a liver transplant operation. Moreover, splanchnic modulation minimizes any high portal blood flow that may occur following liver resection and the subsequent liver transplant. This effect is significant, because high portal flow impairs liver regeneration, and thus adversely affects the postoperative recovery of a transplant patient. An increase in portal blood flow can be minimized by either surgical methods (e.g., splenic artery ligation, splenectomy or portocaval shunting) or administration of splanchnic vasoconstrictor drugs such as Vasopressin or terlipressin. Finally, modulation of splanchnic circulation can help maintain perioperative renal function. Splanchnic vasoconstrictors such as terlipressin may help protect against acute kidney injury in patients undergoing liver transplantation by reducing portal pressure and the severity of a hyperdynamic state. These effects are especially important in patients who receive a too small for size graft. Terlipressin selectively stimulates V1 receptors, and thus causes arteriolar vasoconstriction in the splanchnic region, with a consequent shift of blood from splanchnic to systemic circulation. As a result, terlipressin enhances renal perfusion by increasing both effective blood volume and mean arterial pressure.

**Keywords:** Liver Transplant; Perioperative Renal Function; Portal Blood Flow; Splanchnic Circulation; Vasopressin Agonists

## M-21. Incidence and Outcome of Cardiac Injury in Patients with Severe Head Trauma

Ahmed Hasanin, Email author, Amr Kama, Shereen Amin, Dina Zakaria, Riham El Sayed, Kareem Mahmoud and Ahmed Mukhtar

*Scandinavian Journal Trauma Resuscitation and Emergency Medicine, 24: 58-63 (2016) IF: 2.31*

**Background:** Although cardiac injury has been reported in patients with various neurological conditions, few data report cardiac injury in patients with traumatic brain injury (TBI). The aim of this work is to report the incidence of cardiac injury in patients with TBI and its impact on patient outcome. **Methods:** A prospective observational study was conducted on a cohort of 50 patients with severe TBI. Only patients with isolated severe TBI defined as Glascow coma scale (GCS) < 8 were included in the study. Acute physiology and chronic health evaluation (APACHE) II score, GCS, hemodynamic data, serum Troponin I, electrocardiogram (ECG), and echocardiographic examination, and patients' outcome were recorded. A neurogenic cardiac injury score (NCIS) was calculated for all patients (rising troponin = 1, abnormal echocardiography = 1, hypotension = 1). Univariate and multivariate analyses for risk factors for mortality were done for all risk factors. **Results** AND **Discussion:** Fifty patients were included; age was 31 ± 12, APACHE II was 21 ± 5, and male patients were 45 (90 %). Troponin I was elevated in 27 (54 %) patients, abnormal echocardiography and hypotension were documented in 14 (28 %) and 16 (32 %) patients, respectively. The in-hospital mortality was 36 %. Risk factors for mortality by univariate analysis were age, GCS, APACHE II score, serum troponin level, NCIS, and hypotension. However, in multivariate analysis, the only two independent risk factors for mortality were APACHE II score (OR = 1.25, 95 % confidence interval: 1.02-1.54, P = 0.03) and NCIS score (OR = 8.38, 95 % confidence interval: 1.44-48.74, P = 0.018). **Conclusions:**Cardiac injury is common in patients with TBI and is associated with increased mortality. The association of high NCIS and poor outcome in these patients warrants a further larger study.

**Keywords:** Severe Head Injury; Cardiac Injury; Echocardiography; Tsroponin.

## M-22. National Surveillance of Health Care–Associated Infections in Egypt: Developing a Sustainable Program in a Resource-Limited Country

Talaa El-Shokry, El-Kholy Ismail Kotb and Hafez Attia.

*American Journal of Infection Control, 44: 1296-1301 (2016) IF: 1.995*

**Background:** Health care–associated infections (HAIs) are a major global public health concern. The lack of surveillance systems in developing countries leads to an underestimation of the global burden of HAI. We describe the process of developing a national HAI surveillance program and the magnitude of HAI rates in Egypt. **Methods:** The detailed process of implementation of a national HAI surveillance program is described. A 3-phase surveillance approach was implemented in intensive care units (ICUs). This article focuses on results from the phase 2 surveillance. Standard surveillance definitions were used, clinical samples were processed by the hospital laboratories, and results were confirmed by a reference laboratory. **Results:** Ninety-one ICUs in 28 hospitals contributed to 474,544 patient days and 2,688 HAIs. of these, 30% were bloodstream infections, 29% were surgical site infections, 26% were pneumonia, and 15% were urinary tract infections. Ventilator-associated pneumonia had the highest incidence of device associated infections (4.3/1,000 ventilator days). The most common pathogens reported were Klebsiella spp (28.7%) and Acinetobacter spp (13.7%). of the Acinetobacter spp, 92.8% (157/169) were multidrug resistant, whereas 42.5% (151/355) of the Klebsiella spp and 54% (47/87) of Escherichia coli were extendedspectrum β-lactamase producers. **Conclusions:** Implementation of a sustainable surveillance system in a resource-limited country was possible following a stepwise approach with continuous evaluation. Enhancing infection prevention and control programs should be an infection control priority in Egypt.

**Keywords:** Health Care–Associated Infections, Surveillance System; Resource-Limited Country

## M-23. Caudal Extradural Catheterization in Pediatric Renal Transplant and its Effect on Perioperative Hemodynamics and Pain Scoring: A Prospective Randomized Study

Sherif M. Soaida, Mohammed S. ElSheemy , Ahmed M. Shouman, Ahmed I. Shoukry, Hany A. Morsi, Doaa M. Salah,· Fatina I. Fadel and Hafez M. Bazaraa

*Journal of Anesthesia, 30: 47-54 (2016) IF: 1.343*

**Purpose** 'Hockey stick incision' used in renal transplant is large enough to cause severe postoperative morbidity especially in pediatric recipients. Although epidural analgesia is known to be effective in pain control, the resulting sympathectomy might affect hemodynamics interfering with the transplant process. In our study, we evaluated the feasibility and safety of inserting an epidural catheter to the thoracic level via the caudal route, and the effect of using epidural local anesthetics at low concentrations on hemodynamics. **Methods** After approval from the ethical committee at Kasr Al Ainy University Hospital and consent from parents/legal guardians, sixty patients aged 3–12 years who were scheduled for renal transplant were randomly divided into two equal groups. Group I (epidural group) received continuous caudal epidural bupivacaine 0.125 % with fentanyl together with intravenous (IV) fentanyl and paracetamol. Group II (control group) received only IV fentanyl and paracetamol. Intraoperative data included heart rate (HR), mean arterial blood pressure (MAP) and central venous pressure (CVP). Postoperative variables included HR, MAP, CVP, pain score and complications. **Results** Threading failure via the caudal route occurred in 6.67 % of cases. Intraoperative differences in hemodynamics and CVP were not clinically significant between groups. Postoperative HR, MAP, and CVP were generally higher in the control group. Pain control was more satisfactory and postoperative complications were less in the epidural group. **Conclusion** Caudal epidural anesthesia in pediatric renal transplant is a valuable addition to general anesthesia as it provides stable perioperative hemodynamics, excellent postoperative analgesia and is associated with fewer complications than narcotic-dependent analgesia. Clinical trial registration number: NCT02037802

**Keywords:** Anesthesia Transplant Pediatrics Caudal Epidural Renal.

## M-24. The Intraoperative Therapeutic Equivalence of Balanced Vs Saline-Based 6% Hydroxyethyl Starch 130/0.4 and their Influence on Perioperative Acid-Base Status and Renal Functions

Ahmed Helmy, Ahmed Mukhtar, Abeer Ahmed, Nazmy Edward Sief and Amr Hussein

*Journal of Clinical Anesthesia, 32: 267-273 (2016) IF: 1.284*

Study objective This study was designed to evaluate the therapeutic equivalence of balanced 6% hydroxyethyl starch (HES) 130/0.4 (Tetraspan) vs saline-based 6% HES 130/0.4 (Voluven) regarding the volume effect and the effect on acid-base status and renal functions in patients undergoing major urologic procedures. Design Randomized comparative trial. Setting Operating room and ward. Patients Forty patients, American Society of Anesthesiologists statuses 1 and 2. Intervention Patients were randomly allocated to receive either Voluven (n = 20) or Tetraspan (n = 20). Measurements Hemodynamic variables. Laboratory variables in the form of arterial blood gases, serum chloride and sodium levels, hemoglobin level, international normalized ratio, and kidney and liver functions were measured after induction of anesthesia (T1), at the end of surgery (T2), and on the first postoperative day (T3). Main results Both groups were comparable regarding the total amount of study drugs and crystalloid consumption. No significant difference in hemoglobin levels between both groups, but there were significant differences between T1 and T2 hemoglobin within both groups and T3 hemoglobin in the Tetraspan group. Both groups were comparable regarding the renal functions, but there was a significant difference between T1 and T2 creatinine within both groups. No significant differences between both groups in liver functions and coagulation profile, but there were significant differences between values at T1, T2 and T3 within each group. Relative to baseline, both pH and bicarbonate decrease significantly in both groups. In the Voluven group, bicarbonate decreased significantly at the end of surgery relative to the Tetraspan group. Serum electrolytes did not vary between both groups. Conclusion Both balanced 6% HES 130/0.4 (Tetraspan) and saline-based 6% HES 130/0.4 (Voluven) were equally effective for hemodynamic stabilization of patients undergoing major

urologic procedures without any significant impact on acid-base status or renal functions.
**Keywords:** Hydroxyethyl Starch; Intraoperative Fluid; Colloids; Crystalloids; Safety; Volume Effect.

***Dept. of Cardiology***

## M-25. Pacemaker Malfunction Attributed to Multidetector Cardiac Computed Tomography

Abdalla Amin Selim Elagha

*Journal ,: p1-p2 (2016) IF: 17.201999664*

Recent. A 32-year-old man, with known VATER syndrome, presented with a history of previous cardiac surgery (tetralogy of Fallot repair 20 years ago), which was complicated by a complete heart block, and therefore a permanent pacemaker was implanted. His pacemaker was replaced twice in the following years; the latest was a dual-chamber with rate-modulation pacemaker (DDDR) that was placed transvenously (Medtronic, ADDR06 Adapta DR, implanted in 2009). He had severe pulmonary regurgitation and was primarily experiencing increasing dyspnea. He was referred to computed tomography (CT) coronary angiography to rule out coronary artery disease and for anatomic definition postrepair and quantification of ventricular volumes and function. MRI was not considered appropriate because of the presence of epicardial leads. The patient was pacemaker dependent. Initially, the pacemaker was functioning well in DDD mode, with regular synchronized pacing. After appropriate preparation, the CT examination was conducted with the use of a 256-slice multidetector CT scanner. Helical scanning with low pitch (0.2) and retrospective gating was used because functional information was to be obtained. Scout images show the pacemaker and its connected leads within normal position, and the abandoned epicardial leads placed from an infradiaphragmatic location, as well. The pacer was within the scan field (Figure 1). The patient did not experience any symptoms during the examination. Surprisingly, during the scan, pacemaker malfunction was detected in the form of oversensing, which inhibited ventricular pacing, and dropped pacemaker beats were noted, as shown in ECG strips (Figure 2). Multidetector CT images show normal anatomy of coronary arteries (Figure 3) and normal leads position (online-only Data Supplement Movie I). There was a period of transient ventricular asystole as the CT gantry (contains high-voltage x-ray tube) was rotating around the pacer, disturbing its electric circuit, whereas the native atrial contraction proceeded unchanged (online-only Data Supplement Movies II and III). This inhibitory effect was transient, lasting only while the width of the x-ray beam directly irradiated the pacemaker, a time that was <2 s in duration. It was terminated spontaneously, as the gantry moved away from the location of the pacemaker generator (online-only Data Supplement Movie IV). Interrogation of the device after the scan demonstrated a sensed arrhythmia with a cycle length of 271 ms (the gantry rotation speed of the scanner) that inhibited ventricular pacing. Although it has been traditionally believed to be a safe and harmless procedure in pacemaker patients, computed tomography scanning uses high doses of ionizing radiation and can trigger pacemaker malfunction, when the radiation is directed on the device.
**Keywords:**

## M-26. Scar Quantification by Cardiovascular Magnetic Resonance as an Independent Predictor of Long-Term Survival in Patients with Ischemic Heart Failure Treated by Coronary Artery Bypass Graft Surgery.

Krishna Kancharla, Gaby Weissman, Abdalla A. Elagha, Kalyan Kancherla, Swetha Samineni, Peter C. Hill, Steven Boyce and Anthon R. Fuisz

*Journal of Cardiovascular Magnetic Resonance,18 (2016) IF:5.752*

**Background:**Scar burden by late gadolinium enhancement (LGE) cardiovascular magnetic resonance (CMR) is associated with functional recovery after coronary artery bypass surgery (CABG). There is limited data on long-term mortality after CABG based on left ventricular (LV) scar burden. **Methods:**Patients who underwent LGE CMR between January 2003 and February 2010 within 1 month prior to CABG were included. A standard 16 segment model was used for scar quantification. A score of 1 for no scar, 2 for≤50 % and 3 for>50 % transmurality was assigned for each segment. LV scar score (LVSS) defined as the sum of segment scores divided by 16. All-cause mortality was ascertained by social security death index.
**Keywords:** SCAR; CMR.

## M-27. Segmental Peri-Coronary Epicardial Adipose Tissue Volume and Coronary Plaque Characteristics

Mohamed Hassan, Karim Said, Hussien Rizk, Fatma ElMogy, Mohamed Donya and Mohamed Houseniand Magdi Yacoub

*European Heart Journal-Cardiovascular Imaging, 17: 1169-1177 (2016) IF: 4.293*

**Aims:** Epicardial adipose tissue (EAT) has been proposed to modulate underlying coronary plaque features. The study aimed to determine the relation between segmental EAT (sEAT) volume, assessed by cardiac magnetic resonance (CMR), and underlying coronary plaque characteristics, as estimated by multidetector computed tomography (CT) (MDCT). **Methods and Results:** The study included 32 male patients with stable angina pectoris and 11 age-matched healthy controls. For each CAD patient, sEAT volume around 8 coronary segments (3 in left anterior descending artery, 3 in right coronary artery, and 2 in left circumflex artery) was quantified by CMR. by MDCT, plaques in each coronary segment were characterized in terms of plaque volume, type, CT attenuation, and severity of luminal stenosis. Serum levels of adipokines were measured. Total EAT volume was significantly higher in CAD patients than in control group. Serum resistin showed significant correlation with EAT volume (r=0.69, P < 0.001). Analysis of 256 coronary segments showed larger sEAT volume with increasing luminal stenosis of the corresponding segment (mild: 8.2 cm3; moderate: 11 cm3; severe: 11.8 cm3, P <0.001). sEAT volume was larger in segments with mixed than those with calcified or non-calcified plaques (12.1 vs. 10.2 vs. 9.5 cm3, respectively, P = 0.015). sEAT volume was larger in segments with low CT attenuation non- calcified plaques compared with non-calcified plaques with CT attenuation .30 HU (10.5 vs. 8.2 mm3, P < 0.001). **Conclusion:** Peri-coronary epicardial adipose tissue volume is significantly associated with the extent and severity of coronary

atherosclerosis and may be a determinant of plaque vulnerability.
**Keywords:** Epicardial Adipose Tissue; Coronary Plaque Characteristics; Atherosclerosis; Resistin.

## M-28. Detection of Left Atrium Myopathy Using Two- Dimensional Speckle Tracking Echocardiography in Patients with End-Stage Renal Disease on Dialysis Therapy

Noha Hassanin and Alkhateeb Alkemary

*Echocardiography, 33: 233-241 (2016) IF: 1.432*

phy (2DSTE) has recently been proposed to evaluate left ventricular (LV) filling pressure in dialysis patients. Aim: The purpose of this study was to study the LA function in dialysis patients using two-dimensional speckle tracking echocardiography correlated to prevalence of atrial fibrillation, echocardiographically pulmonary capillary wedge pressure, and right ventricle systolic pressure. Methods: Hundred adult patients aged 49.3 13.9 years on regular hemodialysis and 40 healthy individuals were enrolled in the study. Left ventricular dimensions, ejection fraction, and mass index were studied. Left atrium volume index (LAVI) was calculated by dividing left atrium volumes by body surface area. Left ventricle filling pressure was evaluated according to E/E'. Left atrium global systolic strain (LASS) was studied using 2DSTE. Left atrium stiffness was calculated noninvasively based on the ratio of E/E' to LASS. Right ventricle systolic pressure was estimated with the Bernoulli equation formula. Results: Left atrium diameter, left ventricle indexed mass, mitral (E/E'), and LA stiffness were increased in dialysis group 4.4 0.2 cm, 126.5 24.6 g/m2, 16.9 4.4, and 0.5 0.1, respectively, $P < 0.001$ for all. Left atrium systolic strain was significantly decreased in dialysis patients (26.6 1.9 vs. 33.7 2.1%, $P < 0.001$). Left atrium stiffness was significantly higher in dialysis patients with atrial fibrillation (AF) compared to those without AF. Conclusion: Assessment of LA deformation parameters predicts LV diastolic dysfunction and right ventricle systolic pressure in dialysis patients. Left atrium function in dialysis patients was impaired before the occurrence of left atrium dilatation.
**Keywords:** Hemodialysis; Atrial Fibrillation, Left Atrium Systolic Strain.

## M-29. Early Detection of Subclinical Uremic Cardiomyopathy Using Two-Dimensional Speckle Tracking Echocardiography.

Noha Hassanin and Alkhateeb Alkemary

*Echocardiography, 33: 527-536 (2016) IF: 1.432*

evaluate left ventricular (LV) systolic and diastolic dysfunction in patients with various stages of chronic kidney disease (CKD) using conventional, tissue Doppler and two-dimensional speckle tracking echocardiography (2DSTE). **Methods:** Forty controls and 90 CKD patients, aged 49.3 14 years old, were enrolled in the study. Patients were divided into 3 groups depending on their glomerular filtration rate. Group 1 (≥60 mL/min per 1.73 m2), group 2 (≤60 mL/min per 1.73 m2), and group 3 (≤60 mL/min per 1.73 m2 and on regular dialysis for at least 12 months). Pulsed-Doppler and tissue Doppler studies were used to estimate LV filling pressure E/E0. Using 2DSTE, circumferential, radial, and longitudinal functions of the LV have been measured. **Results:** LV longitudinal systolic strain, early, and late diastolic strain rates were significantly reduced in CKD patients 16.9 3.8%, 1.6 0.5%, and 1.3 0.4% in CKD vs. 22.5 0.6%, 2.3 0.2%, and 1.9 0.1% in controls, $P < 0.001$ for all), and no difference was observed in terms of the circumferential LV functions 22.4 1.7 vs. 22.5 1.4, $P = 0.567$). Severity of the kidney dysfunction appears to parallel with the rise of E/E0 significantly ($P < 0.001$). **Conclusion:** In CKD, although the longitudinal and radial systolic functions were reduced, LV ejection fraction may remain within normal limits due to the preservation of the circumferential functions. Early detection of uremic cardiomyopathy might provide useful information for the risk stratification and decide the proper dialysis therapy in these patients.
**Keywords:** End-Stage Renal Disease; Left Ventricle; Speckle Tracking Echocardiography; Systolic Function.

## M-30. Giant Left Atrial Appendage Aneurysm Compressing the Left Anterior Descending Coronary Artery

Kerolos Wagdy, Amir Samaan, Soha Romeih, Walid Simry, Ahmed Afifi and Mohamed Hassan

*Echocardiography, 33: 1790-1792 (2016) IF: 1.432*

Le atrial appendage aneurysm (LAAA) is a rare congenital structural heart disease. It is often diagnosed by echocardiography; however, other imaging modalities can add to its diagnosis and its potential effects on the surrounding structures. A 16-year-old boy presented with dyspnea and palpitation. Transthoracic echocardiography showed a large LAAA communicating with the LA through a narrow neck with impaired left ventricular (LV) systolic function. Multi-detector cardiac tomography showed that the LAAA is compressing the left anterior descending artery. The LAAA was surgically resected followed by improvement of the LV systolic function.
**Keywords:** Aneurysm; Computed Tomography; Coronary Artery; Left Atrial Appendage Function; Transthoracic Echocardiography.

## M-31. Evaluation of Pulmonary Artery Pressure and Resistance by Pulsed Doppler Echocardiography in Patients with End-Stage Renal Disease on Dialysis Therapy

Noha Hassaninand Alkemary

*Journal of The Saudi Heart Association, 28: 101-112 (2016)*

**Background:** Pulmonary hypertension (PH) is one of the most important comorbidities in patients undergoing hemodialysis (HD). The goal of the present work is to determine the possible etiologic factors for its occurrence. Methods: The prevalence of PH was estimated by Doppler echocardiography in a cohort of 100 patients aged 49.3 13.9 years on regular HD. Mean pulmonary artery pressure was estimated from pulmonary acceleration time by Mahan's regression equation. Pulmonary vascular resistance and pulmonary capillary wedge pressure were calculated. We focused on the effect of HD on left and right ventricle diastolic and systolic function. Right ventricle

systolic function was assessed by tricuspid annular systolic excursion and pulsed Doppler myocardial performance index. Since impaired endothelial function was postulated as an underlying cause of PH, we studied the effects of HD on brachial artery endothelial function. **Results:** The current study found that pulmonary hypertension was prevalent in 70% of patients on dialysis. Left atrium diameter, left ventricle mass indexed to body surface area, and mitral E/E0 were increased in the dialysis group (4.4 0.2 cm, 126.5 24.6 g/m2, and 16.9 4.4, respectively, p < 0.001 for all). Pulmonary artery systolic pressure was positively correlated to duration of dialysis and negatively correlated to glomerular filtration rate (p < 0.001 and r = 0.991). Pulmonary vascular resistance was significantly increased in dialysis patients (1.9 0.2 Wood units vs. 1.2 Wood units in controls, p < 0.001). Endothelial dysfunction, defined as brachial artery flow mediated dilatation <6%, was found in 46% of dialysis group. **Conclusion:** Increased pulmonary artery systolic pressure in the HD population could be attributed to left atrium dilatation and left ventricle diastolic dysfunction. Pulmonary vascular resistance was significantly increased in dialysis group. This might be explained by impaired endothelial nitric oxide synthesis that not only caused systemic vasoconstriction but also affected the pulmonary vasculature.

**Keywords:** Hemodialysis; End Stage Renal Disease; Pulmonary Artery Pressure; Pulmonary Vascular Resistance; Pulsed Doppler Echocardiography

***Dept. of Chemical Pathology***

## M-32. Signal Transducer and Activator of Transcription 5 is Implicated in Disease Activity in Adult and Juvenile Onset Systemic Lupus Erythematosus

Safa Meshaa, Rasha El Refai, Ahmed El Saie and Rabab El Hawary

*Clinical Rheumatology, 35: 1515-1520 (2016) IF: 2.042*

The Janus kinase/signal transducers and activators of transcription (JAK/STAT) pathway is one of a handful of pleiotropic cascades used to transduce a multitude of signals for development and homeostasis in humans. It is the principal signaling mechanism for a wide array of cytokines and growth factors. Dysregulated cytokine action on immune cells plays an important role in the initiation and progress of systemic lupus erythematosus (SLE). In this study, we tried to assess the role of STAT5 in systemic lupus erythematosus and correlate its phosphorylation level with the disease activity. The activation of the STAT5 was assessed by measuring the level of expression of phosphorylated STAT5 (pSTAT5) using flow cytometry on the peripheral blood T and B cells in 58 SLE patients (40 adult and 18 juvenile onset) and on 23 healthy age- and sex-matched controls for both groups. Serum prolactin level was also assessed in the patients and control by ELISA. The study revealed that the level of pSTAT5 was higher in adult SLE patients than in healthy control (p= 0.001) and in juvenile-onset SLE patients versus age-matched control (p = 0.031). A positive correlation existed between the pSTAT5 levels and Systemic Lupus Activity Measure (SLAM) score and also with multiple clinical manifestations indicating a potential role of STAT5 signaling in pathogenesis SLE. The pSTAT5 signaling is implicated in the disease activity of SLE and may be a useful target of therapy by correcting the dysregulation of cytokines involved in the disease pathogenesis.

**Keywords:** Phosphorylated Stat5; Prolactin; Signaling Pathway; Systemic Lupus Erythematosus

***Dept. of Clinical and Chemical Pathology***

## M-33. Cystinosin Deficiency Causes Podocyte Damage and Loss Associated with Increased Cell Motility

Ekaterina A. Ivanova, Fanny O. Arcolino, Mohamed A. ElmonemMaria P. Rastaldi, Laura Giardino, Elisabeth M. Cornelissen and Lambertus P. van den Heuvel

Elena N. Levtchenk*Kidney International, 89: 1037-1048 (2016) IF: 7.683*

The involvement of the glomerulus in the pathogenesis of cystinosis, caused by loss-of-function mutations in cystinosin (CTNS, 17p13), is a matter of controversy. Although patients with cystinosis demonstrate glomerular lesions and high-molecular-weight proteinuria starting from an early age, a mouse model of cystinosis develops only signs of proximal tubular dysfunction. Here we studied podocyte damage in patients with cystinosis by analyzing urinary podocyte excretion and by in vitro studies of podocytes deficient in cystinosin. Urine from patients with cystinosis presented a significantly higher amount of podocytes compared with controls. In culture, cystinotic podocytes accumulated cystine compatible with cystinosin deficiency. The expression of podocyte specific genes CD2AP, podocalyxin, and synaptopodin and of the WT1 protein was evident in all cell lines. Conditionally immortalized podocyte lines of 2 patients with different CTNS mutations had altered cytoskeleton, impaired cell adhesion sites, and increased individual cell motility. Moreover, these cells showed enhanced phosphorylation of both Akt1 and Akt2 (isoforms of protein kinase B). Inhibition of Akt by a specific inhibitor (Akti inhibitor 1/2) resulted in normalization of the hypermotile phenotype. Thus, our study extends the list of genetic disorders causing podocyte damage and provides the evidence of altered cell signaling cascades resulting in impaired cell adhesion and enhanced cell motility in cystinosis.

**Keywords:** Cell Adhesion; Cell Motility; Glomerular Damage; Nephropathic Cystinosis; Podocyturia

## M-34. Development of Molecularly Targeted Agents and Immunotherapies in Small Cell Lung Cancer

Adam Sharp, Jaishree Bhosle, Fatma Abdelraouf, Sanjay Popat, Mary O'Brien and Timothy A. Yap

*European Journal of Cancer, 60: 26-39 (2016) IF: 6.163*

Small cell lung cancer (SCLC) is a smoking-induced malignancy with multiple toxin associated mutations, which accounts for 15% of all lung cancers. It remains a clinical challenge with a rapid doubling time, early dissemination and poor prognosis. Despite multiple clinical trials in SCLC, platinum-based chemotherapy remains the mainstay of treatment in the first line advanced disease setting; good initial responses are nevertheless inevitably followed by disease relapse and survival ultimately remains poor. There are currently no molecularly targeted agents licenced for use in SCLC. Advances in sequencing the cancer genome and other high-throughput profiling technologies have

identified aberrant pathways and mechanisms implicated in SCLC development and progression. Novel anti-tumour therapeutics that impact these putative targets are now being developed and investigated in SCLC. In this review, we discuss novel anti-tumour agents assessed in SCLC with reference to the complex molecular mechanisms implicated in SCLC development and progression. We focus on novel DNA damage response inhibitors, immune checkpoint modulators and antibody-drug conjugates that have shown promise in SCLC, and which may potentially transform treatment strategies in this disease. Finally, we envision the future management of SCLC and propose a biomarker-driven translational treatment paradigm for SCLC that incorporates next generation sequencing studies with patient tumours, circulating plasma DNA and functional imaging. Such modern strategies have the potential to transform the management and improve patient outcomes in SCLC.

**Keywords:** Small Cell Lung Cancer; Targeted Therapies; Precision Medicine; Molecular Analysis; Angiogenesis; Cell Signalling; Apoptosis; Immunotherapies; Dna Repair; Antibody-Drug Conjugate.

## M-35. Sunitinib (SU11248) in Patients with Chemo Naive Extensive Small Cell Lung Cancer or who Have A 'Chemosensitive' Relapse: A Single-Arm Phase II Study (EORTC-08061)

Fatma Abdelraouf, Egbert Smit, Baktiar Hasan, Jessica Menis, Sanjay Popat, Jan P. van Meerbeeck, Veerle F. Surmont, Paul Baasand Mary O'Brien

*European Journal of Cancer, 54: 35-39 (2016) IF: 6.163*

**Background:**Targeted therapies have to date not been successful in the treatment of small cell lung cancer (SCLC). This study aimed to assess the therapeutic activity of sunitinib (an oral, multi-targeted tyrosine kinase inhibitor) using positron emission tomography (PET)–computed tomography (CT) imaging as an early indicator of response. **Methods** This was a single-arm phase II study of sunitinib in patients with SCLC who are either chemo naive (extensive disease) or have a 'sensitive' relapse. A loading dose of 150 mg sunitinib was given orally followed by 37.5 mg/d. The primary end-point was disease control rate (DCR) at 8 weeks after the start of treatment and secondary end-points included toxicity of treatment and overall response. PET–CT was carried out at 4 weeks into the treatment. The study was closed early because of low accrual with only 9 of required 48 patients (19%) accrued. **Results** Nine patients were registered, seven females and two males with a median age of 65 years and a median duration of sunitinib treatment of 7.4 weeks. DCR at 8 weeks was achieved in two patients, both of whom went on to long periods of disease control, one patient achieved a partial response which lasted 10 months and a second patient had stable disease (minor shrinkage) which lasted 20 months. One of these patients proved to have an atypical carcinoid tumour at rebiopsy after 10 months. DCR and PET–CT imaging both predicted these responses. Grade III–IV toxicities were encountered during treatment, most commonly neutropenia (n = 3), thrombocytopenia (n = 3) and hypermagnesaemia (n = 2). One toxic death occurred due to bronchial haemorrhage. **Conclusion** This study emphasises the need for alternate study design and end-points for new drug assessment in SCLC.

**Keywords:** Sclc; Sunitinib; Tyrosine Kinase Inhibitor; Targeted Therapy; Phase Ii Study; Second-Line Treatment.

## M-36. Altered mTOR Signalling in Nephropathic Cystinosis

Ivanova EA, van den Heuvel LP, Elmonem MA, De Smedt H, Missiaen Pastore A Mekahli and Bultynckand Levtchenko

*Journal of Inherited Metabolic Disease, 39: 457-464 (2016) IF:3.541*

Lysosomes play a central role in regulating autophagy via activation of mammalian target of rapamycin complex 1 (mTORC1). We examined mTORC1 signalling in the lysosomal storage disease nephropathic cystinosis (MIM 219800), in which accumulation of autophagy markers has been previously demonstrated. Cystinosis is caused by mutations in the lysosomal cystine transporter cystinosin and initially affects kidney proximal tubules causing renal Fanconi syndrome, followed by a gradual development of end-stage renal disease and extrarenal complications. Using proximal tubular kidney cells obtained from healthy donors and from cystinotic patients, we demonstrate that cystinosin deficiency is associated with a perturbed mTORC1 signalling, delayed reactivation of mTORC1 after starvation and abnormal lysosomal retention of mTOR during starvation. These effects could not be reversed by treatment with cystine-depleting drug cysteamine. Altered mTORC1 signalling can contribute to the development of proximal tubular dysfunction in cystinosis and points to new possibilities in therapeutic intervention through modulation of mTORC-dependent signalling cascades.

**Keywords:** Mtor Signalling; Cystinosis; Autophagy; Proximal Tubular Dysfunction

## M-37. Role of Flow Cytometry in the Diagnosis of Chronic Granulomatous Disease: the Egyptian Experience

Rabab El Hawary Email, Safa Meshaal, Caroline Nermeen Galal, Mahitab Abdelkawy, Radwa Alkady, Dalia Abd Elaziz, Tomas Freiberger, Barbora Ravcukova, Jiri Litzman, Jacinta Bustamante, Jeannette Boutros and Taghrid Gaafarand Aisha Elmarsafy

*Journal of Clinical Immunology, 36: 610-618 (2016) IF: 3.094*

**Introduction:**Chronic granulomatous disease (CGD) is an inherited mutational defect in any of the NADPH oxidase complex, CYBB (gp91-phox), NCF1 (p47-phox), CYBA (p22-phox), NCF2 (p67-phox), or NCF4 (p40-phox) leading to inability of phagocytes to perform effective respiratory burst and thus diminished killing of bacteria and fungi. The identification of defective proteins aids in establishing a diagnosis prior to genetic analysis, which is rather labor-intensive, expensive, and time-consuming. **Aim** The present study aims at assessing the NADPH proteins by performing the intracellular staining with specific monoclonal antibodies and their assessment on flow cytometry. The use of flow cytometry is less laborious and faster to perform than western blot. It also confirms the diagnosis of CGD and detects the affected components allowing proper management of patients. **Materials and Methods** Twenty-eight patients from 25 different kindred, clinically suspected as CGD were recruited in Egypt. Dihydrorhodamine test was performed

to confirm the diagnosis of the patients. Intracellular staining of NADPH components using specific monoclonal antibodies was performed followed by flow cytometric analysis. **Results** The present study revealed that the most common defective protein in our cohort is p22-phox, found in 13 patients (46.4 % of cases) followed by p47-phox in 8 patients (28.6 %), gp91-phox in 5 patients (17.9 %), and finally p67- phox in 2 patients (7.1 %). **Conclusion** In countries with limited resources and yet large number of CGD patients, the analysis of the defective proteins by flow cytometry is an optimum solution for confirming the diagnosis and is a step for targeted sequencing in families seeking prenatal diagnosis.

**Keywords:** Chronic Granulomatous Disease; Flow Cytometry; Ncf1; Ncf2; Cyba; Cybb

## M-38. Ca2+ Signalling in Human Proximal Tubular Epithelial Cells Deficient for Cystinosin

Ekaterina A. Ivanova, Mohamed A. Elmonem, Inge Bongaerts, Tomas Luyten, Ludwig Missiaen, Lambertus P. van den Heuvel, Elena N. Levtchenko and Geert Bultynck

*Cell Calcium, 60: 282-287 (2016) IF: 2.909*

Nephropathic cystinosis is an autosomal recessive lysosomal storage disorder caused by loss-of-function mutations in the CTNS gene coding for the lysosomal cystine transporter, cystinosin. Recent studies have demonstrated that, apart from cystine accumulation in the lysosomes, cystinosin-deficient cells, especially renal proximal tubular epithelial cells are characterized by abnormal vesicle trafficking and endocytosis, possible lysosomal dysfunction and perturbed intracellular signalling cascades. It is therefore possible that Ca2+ signalling is disturbed in cystinosis, as it has been demonstrated for other disorders associated with lysosomal dysfunction, such as Gaucher, Niemann-Pick type C and Alzheimer's diseases. In this study we investigated ATP-induced, IP3-induced and lysosomal Ca2+ release in human proximal tubular epithelial cells derived from control and cystinotic patients. No major dysregulation of intracellular Ca2+ dynamics was found, although ATP-induced Ca2+ release appeared slightly sensitized in cystinotic cells compared to control cells. Hence, these subtle changes in Ca2+ signals elicited by agonists may contribute to the pathogenesis of the disease.

**Keywords:** Lysosomal Storage Disorders; Nephropathic Cystinosis; Calcium Homeostasis

## M-39. Circulating Maternal Total Cell-Free Dna, Cell-Free Fetal Dna and Soluble Endoglin Levels in Preeclampsia: Predictors of Adverse Fetal Outcome? A Cohort Study

Radwa Marawan Abdel Halim, Dalia Ibrahim Ramadan, Reham Zeyada, Ahmed Soliman Nasr and Iman Atef Mandour

*Molecular Diagnosis and Therapy, 20:135-149 (2016) IF: 2.602*

**Background:** The diagnosis of preeclampsia (PE) is based on the measurement of maternal blood pressure and proteinuria; however, these parameters are not used in the prediction of adverse fetal outcomes that may occur due to fetal stress. The plasma concentrations of total cell-free DNA (cf-DNA), cell-free fetal DNA (cff-DNA) and soluble endoglin (sEng) are higher in women with established PE th0an in normotensive controls, and the increase is particularly marked in those with severe PE. We aimed to evaluate the levels of cf-DNA, cff-DNA and sEng in pregnant Egyptian women with PE in order to assess the severity of the disease and to detect their potential utility in the future prediction of time of delivery and adverse fetal outcome. **Subjects and Methods:** The study included 107 pregnant females with established PE during their third trimester (51 with mild PE and 56 with severe PE), together with 93 normotensive pregnant women. Absolute quantitation of the hemoglobin subunit beta (HBB) and testis-specific protein, Y-linked 1 (TSPY1) genes for the measurement of cf-DNA and cff-DNA in maternal blood, respectively, was carried out using real-time polymerase chain reaction (PCR) together with the measurement of serum sEng using ELISA. **Results:** An almost twofold increase in cf-DNA and cff-DNA was detected in the severe PE group over the mild group, and both were significantly different from the control group. Significantly higher levels of cf-DNA, cff-DNA and sEng, with variable magnitudes, were detected in the preterm labor and unfavorable fetal outcome groups compared with the term and favorable outcome groups, respectively. The three markers were almost equivalent with regard to the area under the curve for predicting adverse fetal outcome in the severe PE group. The same was also true for cf-DNA and cff-DNA within the mild PE group. **Conclusions:** Incorporation of cf-DNA, cff-DNA and sEng into the prenatal care service should be considered as a serious addition for the screening and detection of adverse pregnancy outcomes in view of their significant elevations in cases of preeclamptic women whose babies ultimately suffered a poor outcome.

**Keywords:** Preeclampsia; Cell Free Dna; Cell Free Fetal Dna; Soluble Endoglin

## M-40. Impact of Prothrombotic Risk Factors in a Cohort of Egyptian Hemophilia a Patients

Mona Salah El-Din Hamdy, Aml Soliman Nasr, Manal Mohamed Makhlouf, Zainab Ali El-Saadany, Magy Samir and Dalia Saber Morgan

*Molecular Diagnosis and Therapy, 20:151-159 (2016) IF: 2.602*

**Introduction:**Hemophilias are a group of related bleeding disorders that show an X-linked pattern of inheritance. The clinical phenotype of severe hemophilia may vary markedly among patients as a result of many factors, including genetic prothrombotic risk factors. **Objectives:**Our objective was to study the incidence of the most common prothrombotic risk factors for additive effects among Egyptian patients with hemophilia A and their impact on clinical phenotype; annual bleeding frequency and severity of hemophilic arthropathy, as well as the effect of a single variation in these patients. **Methods:** This study was carried out in 100 patients with hemophilia A. Genotyping for factor V Leiden (FVL) G1691A, prothrombin G20210A, MTHFR C677T, and A1298C mutations was conducted using a real time-polymerase chain reaction (RT-PCR) assay. **Results:** Our study revealed mutations in hemophilia patients as follows: prothrombin G20210A (3 %), FVL (14 %), MTHFR C677T (42 %), and A1298C (59 %). Despite a lack of statistical significance when each gene was analysed separately, heterozygosity of prothrombin G20210A or FVL was always associated with either a mild or moderate, but never a severe, clinical presentation. The lowest bleeding frequency (less than once per month) was identified among patients with two heterozygous variants irrespective of the

involved genes. In addition, the incidence of hemarthrosis was significantly higher among patients with a wild genotype of the prothrombin gene and FVL, and the average number of affected joints was significantly higher among patients with wild-type prothrombin and FVL genes than among heterozygous patients. **Conclusion:** These prothrombotic mutations have a cumulative effect in amelioration of the severity of bleeding in hemophiliacs. The most prominent effect is that of prothrombin G20210A and FVL, while MTHFR C677A and A1298C gene mutations are less conclusive.

**Keywords:** Rt-Pcr; Hemophilia A; Fvl; P G20210a; Mthfr C677a; Mthfr A1298c

## M-41. Boronic Acid Disk Diffusion for the Phenotypic Detection of Polymerase Chain Reaction-Confirmed, Carbapenem-Resistant, Gram-Negative Bacilli Isolates

Elsherif Ismail Elawady, Jastaniah Al-Masaudi Harakeh and Karrouf G

*Bmc Microbiology, 16: 135-0 (2016) IF: 2.581*

**Background** The Middle East is regarded as a secondary reservoir for OXA-48 and New Delhi metallo-β-lactamase (NDM) carbapenemases. One of the main challenges in clinical microbiology diagnostics is the detection of carbapenemases. For this reason simple screening methods have been sought to detect carbapenemase producers to determine appropriate therapeutic measures and implement infection control interventions. The present study aimed to evaluate the efficacy of the modified Hodge test (MHT) and a boronic acid-based combined disk test using carbapenems as substrates for the phenotypic determination of OXA-48 and NDM type carbapenemases in 45 epidemiologically unrelated carbapenem-resistant clinical isolates of Klebsiella pneumoniae (13 isolates), Acinetobacter baumanii (20 isolates), and Pseudomonas aeruginosa (12 isolates). **Results** Boronic acid disk test using meropenem as substrate and 600 µg of 3- aminophenylboronic acid (APB) was the most sensitive method (83.33 %) for detection of OXA-48, while the most specific method was MHT (100 %). As regards NDM carbapenemase, boronic acid disk tests using imipenem and 600 µg of APB per disk, and meropenem with 300 or 600 µg of APB were the most sensitive methods (87.50 %), while the most specific method was the MHT (100 %). **Conclusions** The results of the present study indicate that phenotypic screening with the MHT and the boronic acid disk test may be used to detect OXA-48 and NDM carbapenemases in Gram-negative bacilli clinical isolates, and that these tests can be easily applied in tertiary care settings with minimal infrastructure

**Keywords:** Boronic Acid; Carbapenem; Disk Diffusion Enterobacteriaceae ;Phenotypic Screening.

## M-42. Significant Association Between Fasl Gene -844T/C Polymorphism and Risk to Hepatocellular Carcinoma in Egyptian Patients

Rania H. Khalifaa, Dina M. Rasheed Bahgat, Hatem Abdel Hamid Darwish and Rasha Mohamad Hosny Shahin

*Immunology Letters, 172: 84-88 (2016) IF: 2.483*

Fas/Fas ligand (FasL) system is the most critical apoptotic signaling entity in the extrinsic apoptotic pathway; hence mutations affecting this pathway may prevent the immune system from the removal of newly-formed tumor cells, and thus lead to tumor formation. The present study investigated the association between the FasL -844T/C polymorphism and the risk of hepatocellular carcinoma (HCC) in a cohort of Egyptian patients and explored the relationship of various clinical and pathological parameters with this single nucleotide polymorphism (SNP). Blood samples were withdrawn from hundred HCC patients and 100 age-, sex- and ethnically matched controls. The FasL -844T/C (rs763110) gene polymorphism was typed from genomic DNA using polymerase chain reaction restriction fragment length polymorphism (PCR-RFLP) assay. Genotype distributions and allelic frequencies between patients and control subjects showed that the TT homozygous patients were two times more likely to develop HCC (p=0.011). Also, the T allele was found to be a significant risk factor for the disease (OR 1.970, 95% CI 1.250-3.105, p=0.003). No association was detected between different parameters of the disease and the SNP. For the first time, our results suggest that the -844T/C polymorphism in the FasL gene confers risk to HCC. The alarming increase in the incidence of HCC in Egypt encourages further studies to document our results in a larger sample, and recommends more genetic studies hoping to define a genomic risk prediction specific to this cancer in our population.

**Keywords:** Fas/Fas Ligand; Polymorphism; Hepatocellular Carcinoma; Pcr-Rflp; Egypt

## M-43. Association of Chitotriosidase Enzyme Activity and Genotype with the Risk of Nephropathy in Type 2 Diabetes

Mohamed A. Elmonem, Hanan S. Amin, Riham A. El-Essawy, Dina A. Mehaney, Malak Nabil, Laila N. Kamel and Ibtisam M. Farid

*Clinical Biochemistry, 49: 444-448 (2016) IF: 2.382*

**Objective.:** The immune-inflammatory system has been implicated in the pathogenesis of diabetic nephrop- athy; however, many of the mechanisms involved remain unclear. Chitotriosidase enzyme is an active human chitinase and a major protein product of activated macrophages. Although playing an important role in innate and acquired immunity, chitotriosidase involvement in the development of diabetic nephropathy is unknown. **Design and methods:** Chitotriosidase enzyme activity and the presence of the functional 24-bp duplication mutation of the chitotriosidase gene (CHIT1) were assessed in 262 Egyptian type 2 diabetic patients with and without nephropathy and 90 non-diabetic controls. In diabetic patients, multiple linear regression models were adapted to assess the association of chitotriosidase activity with two important measures of renal disease progression: urinary albumin/creatinine ratio and eGFR, while the association of the CHIT1 genotype with the in- cidence of nephropathy was evaluated by multiple logistic regression. **Results:** In diabetic patients, chitotriosidase enzyme activity showed a statistically significant elevation as compared to controls and correlated positively with the progression of nephropathy. A significant association of chitotriosidase activity with both urinary albumin/creatinine ratio and eGFR was detected after adjusting for age, gender, duration of diabetes, body mass index, hypertension status, total cholesterol,

triglycerides and HbA1c levels, P b 0.001. We also identified a protective association between the CHIT1 mutated genotype and di- abetic nephropathy after adjusting for the same confounders (odds ratio: 0.517, 95% CI: 0.289–0.924, P = 0.026). **Conclusions:** This study demonstrates for the first time that the immunomodulatory effects of chitotriosidase enzyme could be implicated in the development of nephropathy in type 2 diabetes.
**Keywords:** Type 2 Diabetes; Diabetic Nephropathy; Chitotriosidase; Chit1 Genotype; 24-Bp Duplication.

## M-44. Jaundice, Phototherapy and Dna Damage in Full-Term Neonates

N Ramy, E A Ghany, W Alsharany, A Nada, R K Darwish, W A Rabie and H Aly

*Journal of Perinatology, 36: 132-6 (2016) IF: 2.087*

**Objective:** Phototherapy is the standard therapeutic approach for neonatal hyperbilirubinemia. Oxidative effects of phototherapy may have potential harms, including DNA damage. Unconjugated bilirubin (UCB) might also possess antigenotoxic potential. Intensive phototherapy is more efficacious than conventional phototherapy in treating hyperbilirubinemia. This study aimed to assess the impact of hyperbilirubinemia and the two different types of phototherapy on DNA damage in peripheral blood mononuclear cells of neonates. **Study Design:** The study was conducted on term neonates with non-hemolytic hyperbilirubinemia and control healthy neonates. Genotoxicity was assessed using single-cell gel electrophoresis (Comet assay) in peripheral mononuclear cells. Blood samples were obtained at enrollment in all infants and after intensive or conventional phototherapy in jaundiced infants. **Result:** DNA damage did not significantly differ between jaundiced and non-jaundiced neonates (11.4±8.7 and 10.9±8.3 arbitrary units (AU), respectively, P=0.58). It increased significantly after exposure to phototherapy compared with prephototherapy values (45.6±14.7 vs 11.4±8.7 AU, respectively, P<0.001). The duration of phototherapy correlated positively with markers of DNA damage (r=0.86, P<0.001); however, the intensity of used light did not significantly impact genotoxicity. **Conclusion:** Hyperbilirubinemia does not influence DNA damage, whereas both conventional and intensive phototherapy are associated with DNA damage in term infants with hyperbilirubinemia
**Keywords:** Dna; Commet Assay; Phototherapy

## M-45. Impact of CYP3A5 and MDR-1 Gene Polymorphisms on the Dose and Level of Tacrolimus Among Livingdonor Liver Transplanted Patients: Single Center Experience

Mona Fathy, Manal Kamal, Abeer Mohy and Ahmad Nabil

*Biomarkers, 21: 335-341 (2016) IF: 2.016*

**Aim of work:** To assess the impact of Cytochrome P450 3A5 (CYP3A5) and multidrug resistance- 1 gene (MDR-1) single nucleotide polymorphisms on the dose and blood level of tacrolimus among liver transplanted patients. Patients and methods: We enrolled a prospective study of 41 liver transplanted patients. Doseadjusted trough blood concentration (C/D ratio) was calculated. Polymerase chain reactionrestriction fragment length polymorphism followed by sequencing was done for genotyping of CYP3A5*3 (6986A4G). **Results:** At 1 week, 1 and 3 months C/D ratio were significantly lower in CYP3A5 expressers *1/*1 patients compared to non-expressers *3/*3. **Conclusion:** CYP3A5 (6986A4G) genotype, rather than MDR-1 (2677G4A/T) variant, has an impact on tacrolimus pharmacokinetics.
**Keywords:** Cytochrome P450; Liver Transplantation; Multidrug Resistance-1; Tacrolimus.

## M-46. Molecular Characterization of Exons 6, 8 and 9 of Abcb4 Gene in Children with Progressive Familial Intrahepatic Cholestasis Type 3

Mona Fathy, Manal Kamal, Marwa Al-Sharkawy, Hanaa Al-Karaksy and Nora Hassan

*Biomarkers, 21: 573-577 (2016) IF: 2.016*

**Aim of work:** To estimate the frequency of mutations involving exons 6, 8 and 9 of Adenosine triphosphate- binding cassette, subfamily B, member 4 (ABCB4) gene among children with progressive intrahepatic cholestasis with high c-GT activity (PFIC3). **Subjects and methods:** Cross sectional study was conducted on 30 children with PFIC3. Genotyping was performed by sequencing analysis of exons 6, 8 and exon 9 of ABCB4 gene. **Results:** Heterozygous synonymous polymorphic variant was detected in exon 6 (rs 1202283) and in exon 8 (rs 2109505). No mutations in studied exons were detected. **Conclusion:** Exons 6, 8 and 9 mutations of ABCB4 gene are not common among Egyptian children with PFIC3.
**Keywords:** Abcb4 Transporter; Children; Genotyping; Progressive Familial Intrahepatic Cholestasis 3.

## M-47. The Clinical Relevance and Prognostic Significance of Microsomal Epoxide Hydrolase Gene Polymorphisms and their Susceptibility to Acquired Aplastic Anemia: An Egyptian Study

Manal Mohamed Makhlouf and Rania Ismail Magdy

*Biomarkers, 21: 416-423 (2016) IF: 2.016*

**Background:** Microsomal epoxide hydrolase enzyme (mEPHX) is involved in xenobiotics detoxification. Two variants of mEPHX, Tyr113His and His139Arg, have been described. Both may lead to acquired aplastic anemia (AA). OBJECTIVES: Assessing mEPHX genetic polymorphisms and detecting their impact on susceptibility and prognosis in Egyptian AA patients. **Participants and Methods:**mEPHX 113 and 139 genotypes were determined by polymerase chain reaction-restriction fragment length polymorphism (PCR-RFLP) in 100 patients with AA and 100 control subjects. **Results:** Both mEPHX Tyr113His and His139Arg gene polymorphisms were associated with increased risk of developing AA, and have a significant impact of bad prognosis (p value < 0.01). **Conclusions:** These mEPHX gene polymorphisms can be considered as risk factors and predictive molecular markers for prognosis in AA patients.
**Keywords:** Acquired Aplastic Anemia; Pcr-Rflp; Genetic Polymorphisms; Mephx His139arg; Mephx Tyr113his.

## M-48. Down-Regulation of Expression of Retinoid Acid-Related Orphan Receptor C (Rorc) in Systemic Lupus Erythematosus.

Safaa M. El-Karaksy, Hala A. Raafat, Marianne Nabil Y. Abadir and Mariam Onsy F. Hanna

*Journal of Receptors and Signal Transduction, 36(2): 207-212 (2016) IF: 1.782*

**Context:** Retinoic acid-related orphan receptor C (RORC), the key factor orchestrating the transcription of genes encoding interleukin 17, plays a critical role in the regulation of inflammatory responses. **Objective:** The objective of this study was to analyze the expression of RORC in the peripheral blood of patients with systemic lupus erythematosus (SLE) for a better understanding of the pathogenesis of SLE especially in relation to disease activity and clinical and biochemical findings. **Methods:**The study included 24 patients with SLE and a control group of 18 healthy gender- and age-matched individuals. Evaluation of the level of expression of RORC mRNA was performed by real-time polymerase chain reaction. RESULTS: The results showed that patients with SLE had lower RORC gene expression levels compared with healthy subjects that were not correlated with disease activity. The down-regulation of RORC was significantly lower in patients with lupus nephritis in remission than active lupus nephritis and nonrenal patients. **Conclusions:** The findings suggest that RORC plays a significant role in the dysregulated immune response associated with SLE. Deciphering the intricate regulatory network and the target genes of RORC will help unravel new specific treatments for SLE.

**Keywords:** Autoimmunity; Expression; Interleukin 17; Retinoic Acid-Related Orphan Receptor C; Systemic Lupus Erythematosus

## M-49. Inborn Errors of Metabolism Detectable by Tandem Mass Spectrometry in Egypt: the First Newborn Screening Pilot Study

Fayza A Hassan, Fatma El-Mougy, Sahar A Sharaf, Iman Mandour, Marian F Morgan, Laila A Selim, Sawsan A Hassan, Fadia Salem, Azza Oraby, Marian Y Girgis, Iman G Mahmoud, Amira El-Badawy, Ibrahim El-Nekhely, Nadia Moharam, Dina A Mehaney and Mohamed A Elmonem

*Journal of Medical Screening, 23(3) (2016) IF: 1.75*

**Objectives:**To estimate the burden of metabolic disorders detectable by tandem mass spectrometry in Egypt, through a pilot expanded newborn screening programme at Cairo University Children's Hospital in 2008, and examining the results of 3,900 clinically at-risk children, investigated at Cairo University Children's Hospital for the same disorders over the past 7 years using the same technology. **Methods:** Dried blood spots of 25,276 healthy newborns from three governorates in Upper, Middle, and Lower Egypt were screened, to give a representative sample of the Egyptian newborn population. Based on the pilot study outcomes and the results of clinically suspected children, we estimated the total birth prevalence of tandem mass spectrometry detectable metabolic disorders, and the relative frequency of several individual disorders. **Results:** Among the healthy newborns, 13 metabolic disorder cases (five phenylketonuria [1:5,000], two methylmalonic acidemia, and isovaleric acidemia [1:12,500], one each of maple syrup urine disease, propionic acidemia, β-ketothiolase deficiency, and primary carnitine deficiency [1:25,000]) were confirmed, giving a total birth prevalence of 1:1944 live births. Among the clinically suspected children, 235 cases were diagnosed, representing a much wider disease spectrum. **Conclusions:**Egypt has one of the highest reported birth prevalence rates for metabolic disorders detectable by tandem mass spectrometry. Early diagnosis and management are crucial for the survival and well-being of affected children. A nationwide NBS programme by tandem mass spectrometry is recommended.

**Keywords:** Inborn Errors of Metabolism; Tandem Mass Spectrometry; Newborn Screening.

## M-50. Significance of CD99 Expression in T-Lineage Acute Lymphoblastic Leukemia

Enein A, Rahman HA, Sharkawy NE, Elhamid SA, Abbas SM, Abdelfaatah and Khalil Fathalla.

*Cancer Biomarkers, 17: 117-123 (2016) IF: 1.736*

**Background:**CD99 was first isolated as an antigen on the T acute lymphoblastic leukemia cells. It has been shown to participate in T cell adhesion and is widely expressed on a variety of hematopoietic and non-hematopoietic cell types. AIM of WORK: Detection of the expression pattern of CD99 on leukemic and normal T cells and assessing the possibility of its use as a tool for the diagnosis and monitoring of T-ALL cases. **Methodology:** We used flow cytometry technique to determine the expression level of CD99 in 62 newly diagnosed TALL patients. Patients were followed up for the presence of minimal residual disease on day 15 and day 42 post-therapy. 20 age and sex matched healthy controls were enrolled in our study. **Results:** CD99 was expressed in all T-ALL patients, with a higher median expression level when compared to controls (58.5% versus 1.38%, $p < 0.001$). On day 42 post-therapy, 100% of follow up patients who had initial CD99 expression 50% had no minimal residual disease, while only 45.5% of those who had initial CD99 expression > 50% had no minimal residual disease ($P = 0.03$). There was no significant influence of CD99 expression on the 1-year overall survival probability ($P = 0.82$). **Conclusion:** CD99 could be used to complement current strategy relying on TdT for diagnosis and monitoring of minimal residual disease during the post-therapy follow up of T-ALL patients. Further studies are needed to confirm these findings.

**Keywords:** Cd99; T Acute Lymphoblastic Leukemia; Disease Free Survival.

## M-51. Survivin and Cyclin E2 Genes Expression in A Cohort of Egyptian Acute Leukemia Patients: Clinical Importance and Future Prospects

Makhlouf M.M

*Cancer Biomarkers, 16: 181-189 (2016) IF: 1.736*

**Background:** Abnormalities in the control of apoptosis play an important role in leukemogenesis. Survivin is a member of inhibitor of apoptosis proteins family, it prevents apoptosis by blocking caspase activity and play a role in cell proliferation. While, cyclin E2 is one of the cyclins proteins family that controls progression of cell cycle by activation of cyclin dependant-kinase. **Objective:** Was to assess survivin and cyclin

E2 genes expression in acute leukemia (AL) patients, and to define their role in the susceptibility of AL, and their correlation with the clinical presentation, laboratory findings, as well as treatment outcome. **Patients and Methods:**This study included 60 de novo AL patients and 40 control subjects to study the expression of survivin and cyclin E2 genes using RT-PCR. RESULTS: Survivin and cyclin E2 genes expression was significantly higher in leukemic patients compared with control subjects (P< 0.001), both genes separately were associated with increased risk of leukemia development and treatment failure (P< 0.01). Moreover, when combining the 2 genes expression, a significant elevation of the risk of leukemia and treatment failure was found (P < 0.01). **Conclusions:**Survivin and cyclin E2 genes expression may have clinical relevance and can be considered as molecular risk factors for AL. Also they may be useful as predictive markers for treatment outcome in leukemic patients.

**Keywords:** RT-PCR; Survivin; Acute Leukemia; Cyclin E2.

## M-52. Prevalence of Polyoma Bk Virus Infection Among Living-Donor Renal Transplant Recipients

M. El Ansary, S. Abd Elhamid, G. Saadi, W. Ismail, N. Ibrahim, N. Bahaa El-Din and S. Alhsyek

*Transplant Infectious Disease, 18: 529-537 (2016) IF: 1.459*

**Background:** Polyomavirus nephropathy (PVN) mainly caused by BK polyomavirus (BKPyV) remains the most common productive viral infection of the kidney in immunosuppressed patients. The diagnosis of PVN is based on the detection of BK viruria and BK viremia in conjunction with histological findings in the graft biopsy. **Methods:** Our study was aimed to estimate the prevalence of productive BKPyV infection among renal transplant patients within the first year post-transplant and identify those at risk of developing PVN. Our cross-sectional study was conducted on 134 kidney transplant patients. Evidence of BKPyV replication was assessed by viral quantification of blood and urine samples of studied patients using a quantitative real-time polymerase chain reaction (Q-PCR)PCR), detection of decoy cells in urine cytology smears, histological examination of graft biopsies from Q-PCR BKPyV-positive patients, and immunohistochemical staining by simian virus 40 (SV40) antibody. **Results:** Significant BKPyV infection was prevalent in 8% (n = 11) of our patients, with a peak of BKPyV infection about 8 months post transplant. BKPyV viral load by Q-PCR assay in these patients varied from 1350 to 20,000,000 (1.35 × 10(3) to 2 × 10(7) ) copies/mL for urine samples and 935 to 18,920 (9.35 × 10(2) to 1.89 × 10(4) ) copies/mL for blood samples. All the 11 patients were positive for decoy cells but only 3 developed PVN based on histology and positive SV40 staining. BKPyV infection was more prevalent in older patients. All patients responded to reduction in their immunosuppressive regimens, apart from 2 patients who required replacement of calcineurin inhibitors-based regimen with mammalian target of ramapycin inhibitors with an overall good response. **Conclusion:** Protocol screening programs based on detection of viral replication by viruria, viremia, and decoy cells in urine are necessary to shed light on patients with high virus replication and hence increased risk of developing PVN, and to allow early diagnosis and intervention

**Keywords:** Polyomavirus; Bk Nephropathy; Quantitative Pcr; Immunohistochemistry; Renal Transplantation.

## M-53. Molecular Screening of Cftr Gene in Egyptian Patients with Congenital Bilateral Absence of the Vas Deferens: A Preliminary Study

Mona Fathy, Tarek Ramzy, Last Dina A. Mehaney and Mohamed A Elmonem

*Andrologia, 48: 1307-1312 (2016) IF: 1.441*

In the current study, we enrolled 14 Egyptian infertile males with isolated congenital bilateral absence of the vas deferens (CBAVD). Screening for the most commonly reported 36 CFTR mutations, and the intron 8 (T)n splice variant was performed by multiplex PCR followed by reversed hybridisation. Samples with the 5T variant were picked for DNA sequencing of intron 8/exon 9 region to identify the number of adjacent TG repeats. The p.Phe508del and the p.Ser1251Asn mutations were detected in heterozygous state in three patients (10.7% of alleles) and in one patient (3.6% of alleles), respectively, while the 5T variant was detected in five patients (28.6% of alleles). Among those five patients, four had TG12 repeats and one had TG13 repeats confirming the pathogenic penetrance of all 5T alleles in Egyptian CBAVD patients. The allelic frequencies of the mutations p.Phe508del, p.Ser1251Asn and the 5T variant in 60 Egyptian cystic fibrosis patients were 24.2%, 3.3% and 2.5% respectively. The mutation p.Ser1251Asn was detected for the first time in isolated CBAVD patient in our study. Due to the high prevalence of p.Phe508del mutation and 5T variant in Egyptian CBAVD patients, we recommend their screening initially, ideally followed by full CFTR gene sequencing in unidentified patients.

**Keywords:** Azoospermia; Cbavd; Cftr Gene; Egyptian Males; Infertility.

## M-54. Indoleamine 2,3-Dioxygenase and Regulatory T Cells in Acute Myeloid Leukemia

Mansour I, Zayed RA, Said F and Latif LA

*Hematology, 21: 447-453 (2016) IF: 1.385*

**Background and objectives:** The microenvironment of acute myeloid leukemia (AML) is suppressive for immune cells. Regulatory T cells (Tregs) have been recognized to play a role in helping leukemic cells to evade immunesurveillance. The mesenchymal stem cells (MSCs) are essential contributors in immunomodulation of the microenvironment as they can promote differentiation of Tregs via the indoleamine 2,3-dioxygenase (IDO) pathway. The aim of the present work was to evaluate the expression of IDO in bone marrow derived MSCs and to study its correlation to percentage of Tregs. Methods: Thirty-seven adult bone marrow samples were cultured in appropriate culture medium to isolate MSCs. Successful harvest of MSCs was determined by plastic adherence, morphology, and positive expression of CD271 and CD105; negative expression of CD34 and CD45 using flowcytometry. MSCs were examined for IDO expression by immunocytochemistry using anti-IDO monoclonal antibody. CD4+ CD25+ cells (Tregs) were measured in bone marrow samples by flowcytometry. **Results:** MSCs were successfully isolated from 20 of the 37 bone marrow samples cultured. MSCs showed higher expression of IDO and Tregs percentage was higher in AML patients compared to control subjects (P = 0.002 and P < 0.001, respectively). A positive correlation was found between IDO expression and Tregs percentage (P value = 0.012, r = 0.5). **Conclusion:** In this

study, we revealed an association between high IDO expression in MSCs and elevated levels of Tregs which could have an important role in the pathogenesis of AML, providing immunosuppressive microenvironment.
**Keywords:** Mesenchymal Stem Cells; T Regulatory Cells; Acute Myeloid Leukemia; Indoleamine 2, 3-Dioxygenase

## M-55. The Association of Cytokine Genes Polymorphisms and Susceptibility to Aplastic Anemia in Egyptian Patients

Rania A. Zayed, Samah M. Abdel-Hamid and Hend El-Lithy

*Hematology, 21: 106-112 (2016) IF: 1.385*

**Background and objective:** Aplastic anemia (AA) remains a rare disease, with very interesting pathophysiology that is being investigated for years now. The present study aimed to determine the association between cytokine gene polymorphisms (TGF-β1 −509 C/T, TNF-α −308 G/A, IFN-γ +874 A/ T) and susceptibility to AA in Egyptian patients. Methods: The study included 80 participants subjected to determination of gene polymorphisms on genomic DNA using polymerase chain reaction-restriction fragment length polymorphism assay. **Results:** It was found that IFN-γ +874 A/T gene polymorphism is associated with three-fold increased risk of development of AA (odds ratio (OR) 3.116, P = 0.019), while TNF-α −308 G/A gene polymorphism is associated with decreased risk (OR 0.318, P = 0.026). TGF-β1 −509 C/T gene polymorphism showed comparable risk between patients and controls (P = 0.263). **Conclusion:** IFN-γ +874 A/T gene polymorphism is associated with the etiology of AA in Egyptian patients.
**Keywords:** Aplastic Anemia; Cytokine Gene Polymorphism; TGF-B1 −509 C/T; TNF-A −308 G/A; Ifn-Γ +874 A/T.

## M-56. Contribution of Protein Z Gene Single-Nucleotide Polymorphism to Systemic Lupus Erythematosus in Egyptian Patients

Yousry SM, Shahin RM and El Refai RM.

*Blood Coagulation and Fibrinolysis, 27:691-795(2016) IF:1.242*

Protein Z has been reported to exert an important role in inhibiting coagulation. Polymorphisms in the protein Z gene (PROZ) may affect protein Z levels and thus play a role in thrombosis. This study aimed to investigate the prevalence and clinical significance of protein Z gene G79A polymorphism in Egyptian patients with systemic lupus erythematosus (SLE). We studied the distribution of the protein Z gene (rs17882561) (G79A) single-nucleotide polymorphism by PCR-restriction fragment length polymorphism in 100 Egyptian patients with SLE and 100 age, sex, and ethnically matched controls. There was no statistically significant difference in the distribution of the genotypes between SLE patients and the control group in our study (P=0.103). But a statistically significant difference in the frequency of the alleles between SLE patients and controls was observed (P=0.024). Also a significant association was detected between protein Z genotypes (and also A allele) and thrombosis, which is one of the manifestations of SLE (P=0.004 and P=0.001, respectively). Moreover, we observed a significant association between the protein Z AA and GA genotypes (and also A allele) and the presence of anticardiolipin antibodies (P=0.016 and P=0.004, respectively). The minor A allele of the G79A polymorphism in the protein Z gene might contribute to the genetic susceptibility of SLE in Egyptian patients. Also, an influence for this polymorphism on some of the disease manifestations has been elucidated, so protein Z G79A AG/AA may be a risk factor for thrombosis.
**Keywords:** Pcr-Rflp; Protein Z Gene G79a Polymorphism; Systemic Lupus Erythematosus; Thrombosis.

## M-57. Endothelial Cell Protein C Receptor Gene 6936A/G and 4678G/C Polymorphisms as Risk Factors for Deep Venous Thrombosis.

Zoheir Eldanasouri N, Abdel-Aal, Hosny and Abdel-Ghany.

*Blood Coagulation and Fibrinolysis, 27(3): 259-265 (2016) IF:1.242*

Endothelial cell protein C receptor (EPCR) enhances the generation of activated protein C by the thrombin-thrombomodulin complex. A soluble form of EPCR (sEPCR) is present in plasma. Two polymorphisms in the EPCR gene (6936A/G and 4678G/C) have been reported to influence the risk of venous thromboembolism. We aimed to investigate the relation between EPCR gene polymorphisms (6936A/G and 4678C/G) and deep venous thrombosis (DVT) and their relations to sEPCR level. This study involved 90 patients with DVT and 90 age and sex-matched healthy controls. Plasma levels of sEPCR were measured in 45 cases of the primary DVT by ELISA. PCR-restriction fragment length polymorphism (RFLP) was used for detection of EPCR polymorphisms (6936A/G and 4678G/C). Regarding 6936A/G, our results demonstrated that mutant genotypes (AG, GG) were associated with an increased risk for DVT [P<0.001, odds ratio (OR) 4.125, 95% confidence interval (95% CI) 2.198-7.740] as well as its mutant allele G (P<0.001, OR 2.549, 95% CI 1.601-4.061). The mutant genotypes were associated with increased levels of sEPCR. Although in 4678G/C, our results demonstrated that the mutant genotype (CC) was considered as a protective factor against DVT (P=0.014, OR 0.289, 95% CI 0.108-0.776) as well as its mutant allele C (P=0.02, OR 0.600, 95% CI 0.388-0.927), but it had no effect on sEPCR level. Our data suggest that 6936A/G polymorphism is a risk factor for DVT and is associated with elevated plasma levels of sEPCR, while 4678G/C polymorphism plays a role in protection against DVT.
**Keywords:** Deep Venous Thrombosis; Endothelial Cell Protein C Receptor; Polymorphisms

## M-58. Prevalence and Risk Factors of Mrsa, Esbl and Mdr Bacterial Colonization Upon Admission to an Egyptian Medical ICU

Fouda R, Soliman MS, ElAnany MG, Abadeer M and Soliman G

*Journal of Infection in Developing Countries, 10, (4): 329-336 (2016) IF: 1.139*

**Introduction:** Bacterial colonization of the skin and mucous membranes of intensive care unit (ICU) patients with virulent organisms such as methicillin-resistant Staphylococcus aureus (MRSA), extended-spectrum beta-lactamase (ESBL) producers, and multidrug-resistant Gram- negative bacteria (MDR-GNB) frequently results in life-threatening infections. Universal screening of ICU patients upon admission has been suggested. The aim of the current study was to evaluate the prevalence and

pattern of MRSA, ESBL, and MDR-GNB colonization in patients upon admission to an Egyptian medical ICU, along with the related demographic and clinical risk factors. **Methodology:** Throat, axillary, and groin swabs were obtained from all study participants in addition to rectal swabs from consenting patients. These swabs were screened for MRSA, ESBL, and MDR-GNB. Results: of the patients included in the study, 33%, 13%, and 63% were colonized with ESBL, MDR-GNB, and MRSA organisms, respectively. Those suffering from a more severe disease with a simplified acute physiology score II (SAPS II) > 29 demonstrated higher levels of MDR- GNB colonization upon admission, while MDR-GNB or ESBL colonization upon admission was associated with higher ICU mortality. **Conclusions:** Colonization of ICU patients with superbugs upon admission has an impact on outcome and mortality. In this Egyptian example, colonization rates were higher than in other literature reports, demonstrating the need for routine screening and decolonization, if applicable.
**Keywords:** Icu; Colonization; Mdr-Gnb; Mrsa; Esbl.

## M-59. Genetic Mutations Affecting the First Line Eradication Therapy of Helicobacter Pylori-Infected Egyptian Patients

Iman Ramzy, Hassan Elgarem, Iman Hamza, Doaa Ghaith, Tamer Elbaz, Waleed Elhosary, Gehan Mostafa and Mohammad A. Mohey Eldin Elzahry

*Revista Do Instituto De Medicina Tropical De São Paulo, 58: (2016) IF: 1.114*

**Introduction:** Several genetic mutations affect the first-line triple therapy for Helicobacter pylori. We aimed to study the most common genetic mutations affecting the metronidazole and clarithromycin therapy for H. pylori-infected Egyptian patients. **Patients and Methods:** In our study, we included 100 successive dyspeptic patients scheduled for diagnosis through upper gastroscopy at Cairo's University Hospital, Egypt. Gastric biopsies were tested for the presence of H. pylori by detection of the 16S rRNA gene. Positive biopsies were further studied for the presence of the rdxA gene deletion by Polymerase Chain Reaction (PCR), while clarithromycin resistance was investigated by the presence of nucleotide substitutions within H. pylori 23S rRNA V domain using MboII and BsaI to carry out a Restricted Fragment Length Polymorphism (RFLP) assay. **Results:** Among 70 H. pylori positive biopsies, the rdxA gene deletion was detected in 44/70 (62.9%) samples, while predominance of the A2142G mutations within the H. pylori 23S rRNA V domain was evidenced in 39/70 (55.7%) of the positive H. pylori cases. No statistically significant difference was found between the presence of gene mutations and different factors such as patients 'age, gender, geographic distribution, symptoms and endoscopic findings. **Conclusion:** Infection with mutated H. pylori strains is considerably high, a finding that imposes care in the use of the triple therapy to treat H. pylori in Egypt, since the guidelines recommend to abandon the standard triple therapy when the primary clarithromycin resistance rate is over 20%.
**Keywords:** 16S rRNA; Metronidazole Resistance; Rdxa Gene; Clarithromycin Resistance

## M-60. Emerging New Delhi Metallo-B-Lactamase-1-Type-Producing Gram-Negative Bacteria Isolated from Cairo University Pediatric Hospital, Cairo, Egypt

Mona Wassef, Mona Abdelhaleim, Doaa Ghaith and Doaa Ghaith

*Journal of Global Antimicrobial Resistance, 7:84-87 (2016) IF:1.087*

New Delhi metallo-b-lactamase (NDM) compromises the efficacy of almost all b-lactam antibiotics, including carbapenems. This study aimed to screen for the blaNDM-1-type gene and NDM-1-type carbapenemase production among Gram-negative bacteria in Cairo University Pediatric Hospital (Cairo, Egypt). Among 382 Gram-negative clinical isolates collected over the period October 2013 to May 2014, 100 clinical isolates showing reduced carbapenem (imipenem and meropenem) susceptibility were included in this study. Initial phenotypic screening for NDM enzyme production was performed by Etest for metallo-b-lactamases (EMBL). Genotypic detection of the blaNDM-1-type gene was done by TaqMan real-time PCR. Metallo-b-lactamase production was detected in 23% of the isolates by EMBL, whereas 24% of the isolates were found to be positive for the blaNDM-1-type gene by real-time PCR. The EMBL sensitivity was 79.2%, specificity was 94.7%, positive predictive value was 82.6%, negative predictive value was 93.5% and overall accuracy was 91.0%. Seventeen (70.8%) of blaNDM-1-type-positive cases were hospital-acquired in origin, whilst 7 cases (29.2%) were community-acquired. Eleven isolates (45.8%) harbouring blaNDM-1-type were found in critical care units. In conclusion, the high prevalence of blaNDM-1- type carbapenemase gene among Gram-negative bacteria, with its great potential for spread in intensive care units, warrants the attention of a nationwide surveillance programme to contain its spread.
**Keywords:** Ndm-1-Type; Carbapenemase; Mic; Etest, Mbl; Imipenem

## M-61. Production of Endothelial Progenitor Cells Obtained from Human Wharton""s Jelly Using Different Culture Conditions

SA Zayed, TM Gaafar, RM Samy, D Sabry, AS Nasr and FA Abdel Maksoud

*Biotechnic & Histochemistry, 91: 532-539 (2016) IF: 1.078*

Endothelial progenitor cells (EPC) participate in revascularization and angiogenesis. EPC can be cultured in vitro from mononuclear cells of peripheral blood, umbilical cord blood or bone marrow; they also can be transdifferentiated from mesenchymal stem cells (MSC). We isolated EPCs from Wharton ' s jelly (WJ) using two methods. The fi rst method was by obtaining MSC from WJ and characterizing them by fl ow cytometry and their adipogenic and osteogenic differentiation, then applying endothelial growth differentiating media. The second method was by direct culture of cells derived from WJ into endothelial differentiating media. EPCs were characterized by morphology, Dil-LDL uptake/UEA-1 immunostaining and testing the expression of endothelial markers by fl ow cytometry and RT-PCR. We found that MSC derived from WJ

differentiated into endothelial-like cells using simple culture conditions with endothelium induction agents in the medium.
**Keywords:** Culture; Endothelium; Human Tissue; Markers; Mesenchymal Stem Cells; Progenitor Cells; Wharton's Jelly

## M-62. Prevalence of Mutations Within Major Hydrophilic Region of Hepatitis B Virus and their Correlation with Genotypes Among Chronically Infected Patients in Egypt.

Abu Zeid W M, Ramadan D I and Shemis M A

*Arab Journal of Gastroenterology, 17(1):34-40 (2016) IF:0.644*

**Background and Study Aims:** Mutations within the major hydrophilic region (MHR) of the hepatitis B surface antigen (HBsAg) have been reported in relation to viral persistence by evasion from vaccine and immunotherapy, severity of liver disease and lack of detection by commercial kits. The aim of this study was to elucidate the circulation of hepatitis B virus (HBV) genotypes, subgenotypes and serotypes in Egypt, with recognition of the pattern and prevalence of MHR mutations possibly occurring during the course of the disease. **Patients and Methods:** Eighty-eight samples from patients with chronic HBV infection were included in the study. The surface protein-encoding gene (S gene) in the HBV genome was subjected to amplification and partial sequencing. **Results:** Based on phylogenetic analysis, only genotype D was found circulating among patients. The majority of isolates belonged to subgenotype D3 (86.3%), followed by D7 (8%), then D5 (3.4%) and lastly D1 (2.3%). Two subtypes were identified: ayw2 (97%) and ayw3 (2%). The 'w' sub-determinant was not defined in one isolate (1%). A significant proportion of patients (13/88, 14.8%) exhibited mutations in the MHR, 10 of whom harboured mutations in the 'a' determinant region and three outside. The first loop comprised four patients with three mutations (P127S, P127T and Y134F). The second loop contained six patients, all with one mutation, S143L, which was most frequently encountered in this study (6.8%). **Conclusions:** We conclude that genotype D, subgenotype D3 and HBsAg subtype ayw2 are the most common types circulating in Egypt, which account for 100%, 86.3% and 97% of the population, respectively, with a moderate degree of MHR mutations.
**Keywords:** Hbv Genotypes; Hbsag Subtypes; Mhr Variants; Major Hydrophilic Region.

## M-63. Study of the Clinical Relevance of Helicobacter Pylori Virulence Genes to Gastric Diseases Among Egyptian Patients

Mona El-Khlousy, Eiman A. Rahman, Sally Mostafa,Amira Bassam,Heba A. Elgawad, Mohamed S. Elnasr, Mohammad Mohey and Doaa Ghaith

*Arab Journal of Gastroenterology, 17: 90-94 (2016) IF: 0.644*

**Background and study aims:** Helicobacter pylori infection is common in Egypt. It has been associated with gastritis, ulcers and it is a risk factor for gastric cancer. We aimed to study the correlation between the presence of H. pylori virulence factors and the histopathological and endoscopic findings in gastric biopsies. **Patients and methods:** Gastric biopsies from thirty seven patients scheduled for diagnostic endoscopy in Cairo University hospital were included in the study. All gastric biopsies were subjected to histopathological examination and PCR assay for detection of 16S rRNA gene to diagnose H. pylori infection, detection of H. pylori virulence factors by PCR for cagA and vacA genotypes and serological analysis of H. pylori (cagA, vacA, P25, and P19) IgG antibodies by immunoblot assay were done. **Results:** H. pylori infection was detected in 23 (62.2%) cases by histopathology while 28/37 (75.7%) were positive for H. pylori 16S rRNA gene by PCR. By PCR seventeen samples out of 37 (45.9%) were positive for cagA gene and five (13.5%) for cag empty site gene. **Conclusion:** The most common vacA genotype identified was vacA s2m2 genotype in 10 (27.02%). No statistical correlation was found between IgG antibodies against different antigens of H. pylori virulence factors (cagA, vacA, p25, and p19) and the degree of gastritis except for IgG antibodies against the UreA antigen.
**Keywords:** Helicobacter Pylori, Gastritis, Caga, Vaca, Immunoblot

## M-64. Expression of Toll-Like Receptors 3 and 9 in Egyptian Systemic Lupus Erythematosus Patients

Aml Nasr- Samar Fawzy and Engy El Khateeb-Prof. Gheita

*Zeitschrift Für Rheumatologie, 75: 502-507 (2016) IF: 0.569*

**Background** Systemic lupus erythematosus (SLE) is a common complex disease characterized by chronic generalized inflammation which may involve several tissues and organs. **Objective** The aim of this work was to study the expression of Toll-like receptors (TLR) 3 and 9 in SLE patients, and to investigate their relationship to clinical features, disease activity,and damage. **Patients and methods** The current study included 24 Egyptian female SLE patients and 15 matched controls. Disease activity was assessed using the SLE Disease Activity Index (SLEDAI) and damage using the Systemic Lupus International Collaborating Clinics (SLICC) index. Expression of TLR3 and TLR9 in B- (CD19-positive) and T-lymphocytes (CD3-positive) was studied using flow cytometry. Results Patient age ranged between 17 and 42 years (mean $26.17 \pm 5.78$ years). There was a significant difference between patients and controls regarding TLR3/CD3, TLR3/CD19, TLR9/CD3, and TLR9/CD19 expression ($p < 0.0001$). There were significant correlations of TLR3/CD3, TLR3/CD19, and TLR9/CD19 with serum creatinine ($r = 0.52$, $p = 0.009$; $r = 0.504$, $p = 0.012$; and $r = 0.58$, $p = 0.003$; respectively) and negative correlations with ALT levels ($r = -0.42$, $p = 0.04$; $r = -0.49$, $p = 0.016$; and $r = -0.472$, $p = 0.02$; respectively). **Conclusion** The results of the study suggest that TLR3 and TLR9 play a role in the pathogenesis of SLE, and have an impact on organ involvement in this disease. More studies concerning the biology and function of TLRs are required in larger patient cohorts, and may lead to development of a new class of drugs.
**Keywords:** Flow Cytometry; Creatinine; Alanine Transaminase; T-Lymphocytes; B-Lymphocytes.

## M-65. Association of DNA Methyltransferase 3B Promotor Polymorphism with Childhood Chronic Immune Thrombocytopenia

Gouda HM, Kamel NM and Meshaal SS

*Labmedecine, 47(4): 312-317 (2016) IF: 0.561*

**Background:** DNA methylation is an epigenetic process that refers to chromatin-based mechanisms in the regulation of gene expression without DNA alternation. It is mediated by DNA methyltransferases (DNMTs). The DNA methyltransferase 3B (DNMT3B) gene contains a C-to-T single nucleotide polymorphism (SNP; rs2424913) in the Promotor region, 149 base pairs from the transcription start site, which is reported to significantly increase the Promotor activity. **Objective:** To investigate the prevalance of rs2424913 single nucleotide polymorphism located in the DNMT3B gene Promotor. **Methods:** In the present study, we investigated the prevalence of rs2424913 single nucleotide polymorphism located in DNMT3B gene Promotor by restriction fragment length polymorphism (PCR-RFLP) in Egyptian pediatric chronic immune thrombocytopenia (ITP) patients and controls. Results: The homozygous genotype (TT) was significantly higher in our patient and conferred almost 3-fold increased risk of chronic ITP when compared to controls. **Conclusion:** The present study shows that DNMT3B rs2424913 promotor polymorphism represents a genetic risk factor that may play an important role in understanding the pathogenesis of chronic ITP.
**Keywords:** Chronic ITP; DNA Methylation; Methyltransferases; Rs2424913

## M-66. Mitochondrial Neurogastrointestinal Encephalopathy: Clinical, Biochemical and Molecular Study in Three Egyptian Patients

Selim, Van Coster, R. Mehaney, Hassan, F. Vanlander, A. Smet, J. De Latter, Vandemeule broecke, Abdou Mohamed Nakhla, Mostafa Habets, Bakker and Bary Abdel

*Genetic Counseling, 27(2): 193-205 (2016) IF: 0.384*

**Background:** Mitochondrial Neurogastrointestinal Encephalopathy syndrome is a rare autosomal recessive disorder. The disease is caused by mutations in the thymidine phosphorylase gene. This article reports the clinical, biochemical and molecular findings in three Egyptian patients with Mitochondrial Neurogastrointestinal Encephalopathy syndrome from two different pedigrees. **Subjects and methods:**The three patients were subjected to thorough neurologic examination, Brain Magnetic Resonance Imaging. Histochemical and biochemical assay of the mitochondrial respiratory chain complexes in muscle homogenate was performed (1/3). Thymidine Phosphorylase enzyme activity was performed in 2/3 patients and Thymidine Phosphorylase gene sequencing was done (2/3) to confirm the diagnosis. **Results:** All patients presented with symptoms of severe gastrointestinal dysmotility with progressive cachexia, neuropathy, sensory neural hearing loss, asymptomatic leukoencephalopathy. Histochemical analysis of the muscle biopsy revealed deficient Cytochrome C oxidase and mitochondrial respiratory chain enzyme assay revealed isolated complex I deficiency (1/3). Thymidine Phosphorylase enzyme activity revealed complete absence of enzyme activity in 2/3 patients. Direct sequencing of Thymidine Phosphorylase gene revealed c.3371A>C homozygous mutation. Molecular screening of both families revealed heterozygous mutation in both parents and 4 siblings. **Conclusions:** Mitochondrial Neurogastrointestinal Encephalopathy syndrome is a rare mitochondrial disorder with an important diagnostic delay. In case of pathogenic mutations in Thymidine Phosphorylase gene in the family, carrier testing and prenatal diagnosis of at risk members is recommended for early detection. The possibility of new therapeutic options makes it necessary to diagnose the disease in an early state.
**Keywords:** Mitochondrial Disease; Gastrointestinal; Encephalomyopathy; Thymidine Phosphorylase.

## M-67. Association of Macrophage Migration Inhibitory Factor Promoter Polymorphism –173G/C with Susceptibility to Childhood Asthma

Tarek Z. El-Adly, Sally Kamal, Hala Selim and Shahira Botros

*Central European Journal of Immunology, 41: 268-272 (2016) IF: 0.309*

**Introduction** Macrophage migration inhibitory factor (MIF) is a proinflammatory cytokine that plays an important role in the pathogenesis of asthma. Polymorphisms associated with inflammatory diseases exist in the promoter region of MIF, which alter its expression. We aimed to study the association of MIF promoter polymorphism –173G/C with childhood asthma. Material and methods In this case-control study, we recruited 60 pediatric patients with bronchial asthma and 90 age- and sex-matched healthy controls. MIF-173G/C was genotyped using polymerase chain reaction-restriction fragment length polymorphism (PCR-RFLP). **Results** Genotype distribution between cases and healthy controls was statistically evaluated. Our results revealed that the frequency of the MIF-173C allele was significantly higher in children with asthma than in the control group ($p = 0.002$, odds ratio [OR] = 3.61, 95% confidence interval [CI] = 1.63-7.97). The frequency of the MIF-173CC genotype was higher in the asthmatic children than in the controls ($p = 0.028$, OR = 6.24, 95% CI = 1.24-31.29). Comparing carriage of the MIF-173C allele in pediatric patients with asthma with that observed in healthy controls (GC + CC vs. GG) revealed a positive association with the disease ($p = 0.019$, OR = 3.12, 95% CI = 1.22-7.99). **Conclusions** These results suggest that MIF-173G/C polymorphism confers an increased risk of susceptibility to the development of childhood asthma in an Egyptian population.
**Keywords:** Children; Polymorphism; Asthma; Promoter; Macrophage Migration Inhibitory Factor.

## M-68. Study of KCNJ11 Gene Mutations in Association with Monogenic Diabetes of Infancy and Response to Sulfonylurea Treatment in a Cohort Study in Egypt

Hanan Madani

*ACTA Endocrinologica-Bucharest,xII(2):157-160(2016) IF:0.235*

**Introduction.** KCNJ11 gene activating mutations play a major role in the development of neonatal diabetes mellitus (NDM). KCNJ 11 gene encodes the Kir 6.2 subunit of ATP- sensitive potassium channel which is a critical regulator of pancreatic beta-cell insulin secretion. **Aim.** To study KCNJ11 gene mutations in infants with NDM and the effect of sulfonylurea treatment on the glycemic control in patients with KCNJ11 gene mutation. Subjects and methods. Thirty infants with NDM were screened for KCNJ11 gene mutations by DNA sequencing, insulin therapy was replaced by sulfonylurea treatment in patients with mutations. **Results.** R201C heterozygous mutation was found in one patient who was successfully shifted from

insulin therapy to sulfonylurea treatment, while E23k, I337V, and S385C polymorphisms were detected in 14 patients. **Conclusion.** Screening for KCNJ 11 gene mutations could lead to identification of patients with mutations who can be successfully shifted from insulin therapy to sulfonylurea treatment improving their quality of life.
**Keywords:** Kcnj11 Gene Mutations; Neonataldiabetes Mellitus; Sulfonylurea Therapy Versus Insulintherapy.

## M-69. Genotypic Analysis of Giardia Duodenalis in Children at Egypt

Marwa Ahmed Ghieth, Ayman A. El-BadryEnas Y. Abu Sarea Samah S. Abdel Gawad and Marwa M. Elsharkawy

*Comparative Clinical Pathology, 25: 1241-1246 (2016)*

Giardia duodenalis is among the most common and frequent intestinal protozoan infecting Egyptian children. The present study aims to identify the genotypic features of G. duodenalis among children fecal samples complaining of diarrhea at Beni-Suef Governorate, Egypt, and to study the association between Giardia assemblages and clinical presentation of the disease among this category. One hundred thirty diarrheic stool samples were subjected to direct stool examination, and positive samples for Giardia were subjected to copro-DNA extraction and amplification targeting the triose phosphate isomerase (tpi) gene using nested polymerase chain reaction (nPCR) technique. Then amplified DNA products were purified and sequenced. Out of 36 microscopically positive samples for Giardia, 28 samples were successfully purified and sequenced; subassemblages AII, BIII, and BIV were detected (10.7, 14,3, and 17,8 %, respectively), and it was difficult to subgroup 16 samples that belong to assemblage B (57 %). Children below the age of 6 are significantly 16 times at risk of infection with assemblage B than assemblage A (p value = .001). Flatulence and presence of fat particles on microscopic examination were significantly associated with infection (p value = 0.001, 0.027, respectively). However, assemblage B was associated with variations of symptomology than A. The present study focuses on giardiasis among Beni-Suef community. Infection is due to both assemblages: assemblage B is more prevalent (89.3 %) than A (10.7 %) and assemblage AI was not recorded. More studies are needed to identify source of infection
**Keywords:** Giardiasis; Giardia Duodenalis; TPI; Assemblage; Genotyping; Egypt.

## M-70. Immunomodulatory Effects of Chitotriosidase Enzyme

Mohamed A Elmonem, Lambertus P. van den H and Elena Levtchenko

*Enzyme Research, 1-9 (2016)*

Chitotriosidase enzyme (EC: 3.2.1.14) is the major active chitinase in the human body. It is produced mainly by activated macrophages, in which its expression is regulated by multiple intrinsic and extrinsic signals. Chitotriosidase was confirmed as essential element in the innate immunity against chitin containing organisms such as fungi and protozoa; however, its immunomodulatory effects extend far beyond innate immunity. In the current review, we will try to explore the expanding spectrum of immunological roles played by chitotriosidase enzyme in human health and disease and will discuss its up-to-date clinical value.
**Keywords:** Chitotriosidase; Human Immunity; Macrophages.

## M-71. Interleukin 10 (− 1082 G/A) and (− 819 C/T) Gene Polymorphisms in Egyptian Women with Polycystic Ovary Syndrome (Pcos)

Talaat RM, Mohamed YA, Mohamad EH and Elsharkawy Mand Guirgis AA1.

*Meta Gene, 9: 254-258 (2016)*

Cytokines play critical roles in the pathogenesis of Polycystic Ovarian Syndrome (PCOS). This work was designed to study the implication of IL10 gene polymorphisms (−1082 G/A and −819 C/T) on the susceptibility of Egyptian women to have PCOS. Rotterdam consensus criteria were used to diagnose PCOS patients. Genotyping was performed by single-stranded polymorphism-polymerase chain reaction (SSP-PCR) in 61 PCOS patients and 80 healthy controls, and IL-10 serum levels were measured using Enzyme linked immunosorbent assay (ELISA). The frequency of IL10 −1082 G/G (46%) genotype was significantly increased (p b 0.001) while the frequency of −1082 A/A (16%) genotype was significantly decreased (p b 0.05) in PCOS patients compared to controls (14% and 35% for G/G and A/A genotypes; respectively). G allele (65%) is significantly increased (p b 0.01( in PCOS patients while A allele (61%) is significantly increased (p b 0.001( in control subjects. The distribution of IL10 -819 T/ T genotype was significantly increased (p b 0.05) in PCOS group. G/G genotype (odd ratio (OR = 5.322) with con- fidence interval (CI = 2.364–11.982) and the G allele (OR = 2.828 with CI = 1.73–4.61) of −1082 G/A and T/T genotype of −819 C/T (OR = 4.18 with CI = 1.26–13.86) could be considered as risk factors for PCOS. IL-10 levels were significantly lower among PCOS patients (313.42 ± 30.10) compared to normal controls (4914.36 ± 303.72). Depending on our preliminary work, IL10 −1082 G/G might be considered as a host genetic factor for PCOS susceptibility in Egyptian women. Studies concerning other cytokine gene polymorphisms are required to get a better understanding of the pathogenesis of PCOS disease.
**Keywords:** Pcos Cytokines Il-10 Polymorphism Snp

## M-72. Prevalence of Hepatitis C Among Egyptian Children with Sickle Cell Disease and the Role of Il28b Gene Polymorphisms in Spontaneous Viral Clearance

Somaia Mohammed Mousa, Mona Kamal El-Ghamrawy, Heba Gouda, Mervat Khorshied, Dina Abd El-Salam Ahmed and Hala Shiba

*Mediterranean Journal of Hematology and Infectious Diseases, 8: 1-6 (2016)*

**Background and Objectives:** Hepatitis C virus (HCV) is a major health problem in Egypt with its prevalence estimated to be 14.7% among the general population in 2008. Patients receiving frequent blood transfusions like those with sickle cell disease (SCD) are more exposed to the risk of acquiring HCV. IL28B gene polymorphisms have been associated with spontaneous HCV clearance. This study aims to determine the

prevalence of HCV infection among children with SCD and to investigate the relation between IL28B gene polymorphisms and spontaneous HCV clearance. **Methods:** Seventy SCD patients were screened for HCV antibody. HCV-positive patients were tested for the level of HCV RNA using quantitative real-time PCR. IL28B polymorphisms (rs 12979860 SNP and rs 12980275 SNP) were detected using TaqMan QRT-PCR and sequence-specific primers PCR respectively. **Results:** Sixteen patients (23%) were HCV antibody positive, 9 of them (56.3%) had undetectable HCV RNA in serum, and 7 (43.7%) had persistent viremia. Genotypes CC/CT/TT of rs12979860 were found in 30 (42.9%), 29 (41.4%) and 11 (15.7%) patients and rs12980275 AA/AG/GG were found in 8 (11.4%), 59 (84.3%) and 3 (4.3%) patients. There was no significant difference in the frequency of IL28B (rs 12979860 and rs12980275) genotypes among HCV patients who cleared the virus and those with persistent viremia (p=0.308 and 0.724 respectively) **Conclusion:** Egyptian SCD patients have a high prevalence of HCV. Multi-transfused patients still exposed to the risk of transmission of HCV. IL28B gene polymorphisms are not associated with spontaneous clearance of HCV in this cohort of Egyptian children with SCD.
**Keywords:** Hcv; Sickle Cell Disease; Il28b Gene Polymorphism; Spontaneous Clearance.

## M-73. RECK Gene Promoter Rs10814325 Polymorphism in Egyptian Patients with Hepatocellular Carcinoma on Top of Chronic Hepatitis C Viral Infection.

Amal Bahgat Fakhry, Asmaa Ismail Ahmed, Mahmoud Abdo AbdelAlim and Dalia Ibrahim Ramadan

*Asian Pacific Journal of Cancer Prevention, 17: 2383-2388 (2016)*

**Background:**The reversion-inducing-cysteine-rich protein with Kazal motifs (RECK) gene is a novel transformation suppressor gene that was linked to several malignancies. **Objective:** To analyze any association between RECK gene rs10814325 single-nucleotide polymorphism (SNP) and HCC susceptibility along with it is association wiht various clinico-pathological and laboratory data. **Materials and Methods:**RECK gene rs10814325 SNP was estimated, using real-time PCR technique, in 30 HCC patients on top of chronic HCV infection, 30 HCV related cirrhotic patients and 30 healthy controls. **Results:** No special pattern of association could be detected on comparing the RECK gene rs10814325 genotypes(P=0.5), or alleles(P=0.49) among the studied groups. HCC patients with TT genotype had younger age (mean of 54.1±6.0 years vs 60.6±10.2 years for TC/CC genotypes, P=0.035). Abdominal distension was significantly greater in TT genotype patients (75% vs 30% of TC/CC genotypes, P=0.045). TT genotype was present in 75% of patients with lymph node metastasis. Serum GGT levels were higher in TT genotype patients [80 of (48.5-134.8) vs 40 IU/l (33-87.5) for TC/CCgenotypes], and lower limb edema was observed in 60% of TT vs 20% of TC/CCgenotypes, however, both just failed to reach significance (P=0.05 and P=0.06, respectively). **Conclusions:**RECK gene rs10814325 T>C could not be considered a risk factor for HCC development on top of HCV, but may be related to the disease progression and metastasis.

**Keywords:** Hepatocellular Carcinoma ; Hcv Related-Cirrhosis ; Reck Gene ; Gene Polymorphism ; Real Time Pcr.

## M-74. Role of CD134 and Fas and Fas Ligand Genes Polymorphism as Biomarkers for Disease Activity in Lupus Nephritis: A Preliminary Egyptian Study

Hala I El Gendy, Mona N Abdel Gawad, Aml S Nasr and Elham A Ghoneim

*Indian Journal of Rheumatology, 11: 129-135 (2016)*

**Objective:** To illustrate the role of CD134 and FAS and FAS ligand genes polymorphism as biomarkers for disease activity in Egyptian patients with Lupus Nephritis. **Materials and Methods:** Twenty-five patients with biopsy-proven LN, 25 patients with SLE with no evidence of nephritis, and fifty patients matched apparently healthy volunteers. Levels of CD134 were measured using flow cytometry. FAS and FASL gene polymorphisms were detected using polymerase chain reaction-restriction fragment length polymorphism. Furthermore, carotid artery intima-media thickness (IMT) measurements were done. **Results:** LN group had highest level of CD134 compared to other two groups, and also higher among SLE compared to controls with highly significant differences in between. Frequency of AA genotype of FASA-670G polymorphism was significantly higher in LN and SLE patients than in controls. The frequency of A allele was statistically higher in LN and in SLE group than in controls. Furthermore, the frequency of CC genotype of C-844T polymorphism of FASL gene was significantly higher in LN and SLE patients than in healthy controls. The frequency of C allele was statistically higher in LN and in SLE group than in controls. **Conclusion:** Co-stimulatory molecules on CD4+ T-cells together with FAS, and FASL polymorphisms are associated with disease activity in this preliminary study.
**Keywords:** Cd134; Fas; Fas Ligand Genes Polymorphism; Lupus Nephritis.

### *Dept. of Clinical Oncology and Nuclear Medicine*

## M-75. Targeting mTOR Pathway in Gynecological Malignancies: Biological Rationale and Systematic Review of Published Data

Loay Kassemand Omar Abdel-Rahman.

*Critical Reviews in Oncology Hematology, 108: 1-12 (2016) IF: 5.039*

**Background:** mTOR inhibitors are widely used in different malignancies with several trials testing their efficacy and safety in gynecological malignancies. We aimed to review the current evidence that support the expansion of using such drugs in the treatment of advanced gynecological cancers. **Methods:**A comprehensive systematic review of literature has been conducted to include prospective trials that used everolimus, temsirolimus or ridaforolimus in the management of gynecological cancers and have available efficacy and toxicity results. **Results:** A total of 23 studies including 980 patients were considered eligible for our review. Our review included 16 phase II and 7 phase I studies with the majority of patients having uterine cancers. Regarding Endometrial cancer, the CBR ranged from 21% to 60% and median PFS from 2.8 months to 7.3 months. In Ovarian cancers, CBR ranged from 24% to 50% and median PFS from 3.2 months to 5.9 months. In the single phase II study in cervical cancer the CBR was 61% and median

PFS was 3.5 months. The toxicity profile was consistent with what was observed previously in other malignancies with fatigue, mucositis, and hematological toxicities being the most common adverse events observed. **Conclusion:** mTOR inhibitors seem to be a promising option in the second line management of advanced gynecological cancers with best safety and efficacy outcomes when given as a single agent or in combination with hormonal treatment. More research is needed for better patient selection.

**Keywords:** Cervical Cancer; Endometrial Cancer; Everolimus; Ovarian Cancer; Temsirolimus.

## M-76. Analysis of PI3K/mTOR Pathway Biomarkers and Their Prognostic Value in Women with Hormone Receptor–Positive, Her2-Negative Early Breast Cancer

Azim HA, Kassem L, Treilleux I, Wang Q, El Enein MA, Anis SE and Bachelot T.

*Translational Oncology, 9: 114-123 (2016) IF: 3.077*

**Background:** The PI3K/AKT/mTOR pathway alterations have been shown to play significant roles in the development, progression, and metastatic spread of breast cancer. Furthermore, they have been implicated in the process of drug resistance, especially endocrinal therapies. In this study, we aimed to define the correlation between the PI3K mutations and the expression of the phosphorylated forms of different downstream molecules in women with estrogen receptor (ER)–positive, human epidermal growth factor receptor 2–negative (luminal) early breast cancer treated at Cairo university hospitals. **Methods:** Next-generation sequencing was used to detect mutations in the PIK3CA hotspots (in exons 9 and 20). Immunohistochemistry was performed on tissue microarray blocks prepared from samples of 35 Egyptian luminal breast cancer patients in the pathology department of Centre Léon Bérard (CLB). The intensity and the percentage of stained tumor cells were integrated to define high versus low biomarker expression. The cytoplasmic and nuclear stainings were graded separately. Patients were followed for a median of 4.7 years (2.1 to 6.9 years). Correlation was done between PI3K mutations and the immunohistochemistry expression of pAKT, LKB1, p4EBP1, and pS6 ribosomal protein (pS6RP) with the clinicopathologic features and disease free survival (DFS) of the patients. **Results:** Median age at diagnosis was 51.3 years (range, 25 to 82 years). Tumors were larger than 20 mm in 79.2% of the cases, whereas 57.9% had axillary lymph node deposits. Only 12.3% of the patients had SBR grade I tumors, 50.8% had grade II, and 36.8% had grade III. ERs were negative in 6 patients (17%) after pathology review. Thirty-two cases were assessable for LKB1 and pAKT, 33 for p4EBP1 and pS6RP, and 24 for PI3K mutations. Nuclear LKB1, cytoplasmic LKB1, nuclear pAKT, cytoplasmic pAKT, nuclear p4EBP1, and cytoplasmic pS6RP expression was high in 65.6%, 62.5%, 62.5%, 68.8%, 42.4%, and 57.6%, respectively. PIK3CA mutations were found in 7 patients (29.2%). PI3K mutations were correlated with nuclear localization of pAKT (i.e., decreased cytoplasmic pAKT, P = .04; and increased nuclear pAKT, P = .10). There was a tendency toward an inverse correlation between PI3K mutations and the expression of pS6RP (P = .10) and p4EBP1 (P = .19). Nuclear LKB1 expression was a marker of good prognosis. It was associated with smaller tumors (P = .05), more ER (P = .08) and progesteron receptor (PgR) positivity (P = .002). In the Kaplan Meier (KM) model, patients with high nuclear LKB1 had longer DFS (hazard ratio = 0.36; 95% confidence interval, 0.15-1.10; P = .08). Nuclear pAKT high expression also carried a tendency toward longer DFS (hazard ratio = 0.51; 95% confidence interval, 0.11-1.16; P = .13). The expression of p4EBP1, pS6RP, and the PI3K mutational status did not show any prognostic significance in our cohort. **Conclusion:** Among the studied biomarkers, only nuclear expression of LKB1 and pAKT tended to predict better survival in breast cancer patients. PI3K mutation was correlated with the expression of nuclear pAKT but not pS6RP or p4EBP1.

**Keywords:** Breast Cancer; Pi3k; Mtor.

## M-77. High Dose Chemotherapy and Autologous Stem Cell Transplantation for Relapsed or Refractory Nodular Lymphocyte Predominant Hodgkin Lymphoma

Akhtar Elhassan Edesa, Rauf Zahir and Maghfoor I.

*Annals of Hematology, 95: 49-54 (2016) IF: 3.022*

Nodular lymphocyte predominant Hodgkin lymphoma (NLPHL) is a distinct subtype of Hodgkin lymphoma. We report our results of relapsed/refractory NLPHL patients who received high-dose chemotherapy and autogenic stem cell transplantation (HDC auto-SCT). Seventeen NLPHL patients received HDC auto-SCT (1996–2014): male 14 andfemale 3, with median age at diagnosis of 22 years, at HDC auto-SCT 28 years (15–58 years). At the time of relapse/progression, 13 (76 %) had NLPHL and 4 (24 %) had transformed diffuse large B cell lymphoma. The reason for HDC auto-SCT was refractory NLPHL in 12 patients and relapsed in 5 patients. Salvage chemotherapy was etoposide, methylprednisolone, cisplatinum, and Ara-C (ESHAP); eight patients also received rituximab with ESHAP. HDC was carmustine, etoposide, cytarabine, and melphalan (BEAM).Post-auto-SCT, complete remission was achieved in 14(82 %), partial remission in 1 (6 %), and progressive diseasein 2 (12 %) patients. The median follow-up is 63 months fromauto-SCT (6–124 months). of the nine patients who receivedonly ESHAP, four had post-auto-SCT events versus no eventin all eight patients who received rituximab+ESHAP.Kaplan–Meier estimates of 5-year event-free survival for thewhole group is 76 %: rituximab+salvage (100 %) versus salvagealone (56 %), P=0.041. Overall survival is 94 %: 100versus 89 %, respectively, P=not significant (NS). Even in refractory NLPHL patients, long-term disease-free survival is possible after HDC auto-SCT. Post-auto-SCT relapse or progression can still be managed withchemo/chemo+immunotherapy/ radiation. These encouraging results of rituximab in salvage setting should be explored further in a clinical trialsetting for this patient population

**Keywords:** Autologous Stem Cell Transplantation . Nodular Lymphocyte Predominant Hodgkin Lymphoma . Hodgkin Lymphoma; Refractory Hodgkin Lymphoma; Rituximab-Containing Salvage; Eshap Chemotherapy.

## M-78. Technetium-99M Thyroid Scan; Does it Have a Diagnostic Aid in Sub-Clinical Auto-Immune Thyroid Disease in Systemic Lupus Erythematosus Patients?

A Amin, A Alkemary and M Abdo

*Lupus, 25: 155-161 (2016) IF: 2.783*

**Purpose:** Technetium-99m (Tc-99m) thyroid scintigraphy is a well known diagnostic tool that shows the entire gland in a single image. We aimed to evaluate its additive diagnostic value in subclinical autoimmune thyroid disease (S-AITD) in systemic lupus erythematosus (SLE) patients. **Methods:** We investigated 100 systemic lupus erythematosus (SLE) patients without overt thyroid involvement (eight men and 92 women; mean age 40±6.5 years) and 50 age and sex matched controls. All were subjected to thyroid evaluation using anti-thyroglobulin (anti-TG) and anti-thyroid peroxidase (anti-TPO) antibodies; hormones (FT3; FT4 and TSH) and Tc-99m thyroid scintigraphy. RESULTS: 14/100 (14%) and none (0%) were positive for S-AITD in SLE and control groups, respectively (P = 0.0001). They were classified by thyroid scintigraphy and hormonal profile into 2/14 Hashimoto; 10/14 atrophic thyroiditis and 2/14 Graves' disease. Anti-TPO was elevated in 12 SLE cases, while anti-TG was elevated in only 2/14 (P = 0.0001). Thyroid scintigraphy showed statistically significant associations with FT4, TSH and anti-TPO. **Conclusion:** Tc-99m thyroid scintigraphy may have an additional diagnostic role in S-AITD among SLE patients, with an impact on patient management. This potential needs to be further evaluated in a larger series on a multicenter basis.

**Keywords:** Systemic Lupus Erythematosus; Tc-99M; Thyroid Scan; Auto-Immune Thyroiditis.

## M-79. High Symptom Burden Among Patients with Newly Diagnosed Incurable Cancer in a Developing Country.

Samy Alsirafy, Hesham H. Abd El-Aal, Radwa Fawzy and Dina E. Farag

*Journal of Pain and Symptom Management, 51 (2016) IF: 2.649*

Palliative care (PC) is ideally integrated into the care of patients with incurable cancer as early as a diagnosis is made.1 This is supported by the evidence that earlier PC is associated with significantly better patient-reported outcomes.2 Many cancer patients, especially in developing countries with limited resources, present in an advanced incurable stage and the only realistic treatment option for them is PC.1 Although PC is needed most in developing countries, little evidence to illustrate the need for PC and its early integration comes from these countries.

**Keywords:** Advanced Cancer; Palliative Care; Symptom Burden;Developing Countries.

## M-80. Implication of Different Clinical and Pathological Variables in Patients with Differentiated Thyroid Cancer on Successful Ablation for 3700 Mbq (131)I: A Single Egyptian Institutional Experience Over 14 Years

Maha Abd Elkareem Husseini

*Annals of Nuclear Medicine, 30: 468-476 (2016) IF: 1.467*

**Objective:** Is to investigate possible factors predicting success of ablation for 3700 MBq radioactive iodine 131 in patients with differentiated thyroid cancer (DTC) following near total thyroidectomy. **Methods:** This retrospective study enrolled 272 patients between 2000 and 2014. The success or failure of ablation was assessed 6 months after given the dose and our criteria for complete successful remnant ablation defined as: Negative (131)I whole body scan with no residual functioning thyroid tissue or distant functioning metastases and stimulated thyroglobulin (Tg) level less than 2 ng/ml. Different clinical and pathological factors, such as age, gender, tumor histology, grade and variants, size of primary malignant lesion, stage, and risk assessment according to the American (ATA) and European Thyroid Association (ETA) guidelines, associated pathology, tumor mutifocality, lymph node (LN) metastases and their number, invasiveness of the tumor (capsular invasion of the nodule, extra-thyroidal extension, and vascular invasion), baseline stimulated Tg level, and pre-ablative diagnostic scan were assessed. **Results:**There were 185 successful ablations (68 %). The baseline-stimulated Tg measured before the ablation was the only independent predictor of ablation success in multivariate analysis (P < 0.0001) with odds ratio (OR) of 2.64 (95 % CI: 1.54-4.54) and the optimal cutoff for this was 3.8 ng/mL. On the univariate analysis, LN metastases was predictor of ablation failure (P value = 0.03). **Conclusion:** Baseline-stimulated Tg level is clinically important and had a significant predictive value for successful ablation; therefore, higher pre-ablation Tg should potentially be incorporated in the decision making for (131)I dosage or other treatment. In accordance with other studies, this is also applicable to cervical lymph nodal involvement and thyroid capsule invasion.

**Keywords:** Differentiated Cancer Thyroid; Radioactive Iodine 131; Successful Ablation; Thyroglobulin Level

## M-81. An Interatrial Tunnel: A Rare Form of Atrial Septal Defects

Hani M. Mahmoud, Mohamed Hosny, Peter Philip, Kerolos Wagdy, Ahmed Kharabish, Wesam EL Mozy and Magdi Yacoub

*Echocardiography-A Journal of Cardiovascular Ultrasound and Allied Techniques, 33 (2016) IF: 1.432*

Atrial septal defects (ASDs) account for approximately 6%–10% of congenital heart defects. The well-known types of atrial septal communications are the ostium secundum, ostium primum, sinus venosus types, and coronary sinus defects. A 50-year- old female was referred for TEE for better assessment of MR severity and mechanism. 2D/3D-TEE showed a rare combination of different abnormalities; bi-leaflet mitral valve prolapse, cleft P2, cor triatriatum sinister, and a tunnel-shaped IAS communication. To the best of our knowledge, this is a very rare case with a rare

form of atrial septal defect that was not described before. We named this defect an interatrial tunnel.
**Keywords:** Atrial Septal Defect; Cleft In Left Atrioventricular Valve; Congenital Heart Defects; Cor Triatriatum.

## M-82. Emergency Department Visits at the End of Life of Patients with Terminal Cancer: Pattern, Causes, and Avoidability.

Samy A. Alsirafy, Ahmad A. Raheem and Abdullah S. Al-Zahrani

*American Journal of Hospice and Palliative Medicine, 33: 658-662 (2016) IF: 1.296*

Frequent emergency department visits (EDVs) by patients with terminal cancer indicates aggressive care. The pattern and causes of EDVs in 154 patients with terminal cancer were investigated. The EDVs th at started during working hours and ended by home discharge were considered avoidable. During the last 3 months of life, 77% of patients had at least 1 EDV. In total, 309 EDVs were analyzed. The EDVs occurred out of hour in 67%, extended for an average of 3.6 hours, and ended by hospitalization in 52%. The most common chief complaints were pain (46%), dyspnea (13%), and vomiting (12%). The EDVs were considered avoidable in 19% of the visits. The majority of patients with terminal cancer visit the ED before death, mainly because of uncontrolled symptoms. A significant proportion of EDVs at the end of life is potentially avoidable.
**Keywords:** Avoidable; Emergency Department; End of Life; Pain; Palliative Care; Symptoms; Terminal Cancer

## M-83. Cardiovascular Magnetic Resonance is Successfully Feasible in Many Patients Aged 3 to 8 Years Without General Anesthesia or Sedation

Ahmed Kharabish, Naira Mkrtchyan, Christian Meierhofer, Stefan Martinoff, Peter Ewert Stern and Sohrab Fratz

*Journal of Clinical Anesthesia, 34: 11-14 (2016) IF: 1.284*

**Objectives:** Patients younger than 8 years are usually examined by cardiovascular magnetic resonance (CMR) under general anesthesia (GA) or sedation without intubation. Therefore, we sought to study the feasibility of CMR in patients aged 3 to 8 years without GA or sedation. Patients: Data sets of 71 consecutive patients aged 3 to 8 years were studied retrospectively. **Design:** The total cohort was divided into 2 groups: a no-GA or sedation without intubation group (no-GA or sedation) and a GA or sedation without intubation group (GA or sedation). Measurements: The patients' age, scan durations for each group, successfully answered clinical question, and number of sequences per study were compared between both groups. **Main results:** Scan duration in the no-GA or sedation group (n = 44) was 35 ± 20 minutes, and that in the GA or sedation group (n = 27) was 60 ± 31 minutes (P < .001). The percentage of successful reports was 95% (42/44) in the no-GA or sedation group and 89% (24 of 27) in the GA or sedation group (P = 0.29). **Conclusion:** CMR in patients aged 3 to 8 years is usually successfully feasible without GA or sedation.
**Keywords:** CMR; CHD; Sedation.

## M-84. Intraindividual Validation of Ventricular Volume Measurement by Aortic and Pulmonary Arterial Flow Measurements in Routine Clinical Cardiovascular Magnetic Resonance of Congenital Heart Disease

Ahmed Kharabish, Fransis Ghandour, Naira Mkrtchyan, Christian Meierhofer, Stefan Martinoff, Peter Ewert, Heiko Stern and Sohrab Fratz

*Progress in Pediatric Cardiology, 43: 151-154 (2016)*

**Introduction:** To validate right and left ventricular stroke volume (RVSV & LVSV) measurements by forward flow stroke volume from aortic (AoSV) and pulmonary arterial (MPASV) measurements during routine cardiovascular magnetic resonance (CMR) in congenital heart disease (CHD). **Methods:** Retrospectively studied CMR of 147 consecutive patients (median age 22 years, range (0.5 – 64 years) with CHD. Patients with ventricular septal defects, mitral valve regurgitation or severe tricuspid-valve-regurgitation were excluded. 126 LVSV were compared to the AoSV. 99 RVSV were compared to the MPASV. Ventricular SV was determined using a routine standard stack of cine axial slices. Arterial forward flow SV was determined using a routine standard phase-velocity quantitative flow sequence. **Results:** AoSV correlated with LVSV by ($r^2$=0.9, $p<0.0001$) and showed upper and lower limits of agreement in Bland Altman analysis of 11ml and -12 ml, mean difference -1ml. Similarly RVSV correlated with the accompanying MPASV ($r^2$=0.8,$p<0.0001$) and showed upper and lower limits of agreement in Bland Altman analysis of 18ml and -26ml, and mean difference - 4ml. **Conclusion:** Measured ventricular SV correlates closely with SV, assessed by CMR flow measurement in the originating great artery in CMR of CHD.
**Keywords:** Congenital Heart Disease ;Cardiovascular Magnetic Resonance ;Stroke Volumes;Phase Contrast

## M-85. The Coronary Arterial Anatomy of the 17-Segment Model Using 3-Tesla Cardiac Magnetic Resonance Imaging

Mohamed Talaat, Ahmed Kharabish, Mohamed D. Homos and Mohamed

*The Egyptian Journal of Radiology and Nuclear Medicine, 47: (2016)*

**Aim:** To analyze the correspondence of the 17 left ventricular myocardial segments with each coronary artery by using late gadolinium contrast enhanced cardiovascular magnetic resonance (CMR) imaging. **Material and methods:** A total number of 58 patients with known or suspected ischemic heart disease were enrolled in this study. Those patients were scheduled for CMR and conventional coronary angiography. The correspondence between the coronary artery distribution and the supplied myocardium was assessed according to the 17-segment model. **Results:** The segments 1, 2, 3, 7, 8, 13, 14 and 17 were totally specific for LAD, segments 6 and 12 were totally specific for LCX, and segment 10 was specific for RCA. There was overlap between LAD and RCA for segments 9 and 15. There was overlap between LCX and RCA for segments 4, 5 and 11. The segment 16 was shared by the all territories (LAD, LCX and RCA) with slight LCX predominance. **Conclusions:** Our

study concluded that the LAD territory on CMR bases is larger than the American Heart Association (AHA) proposed 17-segment model.
**Keywords:** Cmri; LGE; IHD

## M-86. The Use of the Chuangs Prognostic Scale to Predict the Survival of Metastatic Colorectal Cancer Patients Receiving Palliative Systemic Anticancer Therapy

Samy A Alsirafy, Omar Zaki, AmrY Sakr and Abha A Mohammed

*Indian Journal of Palliative Care, 22: 312-316 (2016)*

**Background:**With the increasing number of agents active against cancer, advanced cancer patients including metastatic colorectal cancer (mCRC) patients may continue receiving palliative systemic anticancer therapy (PSAT) near the end-of-life. Validated palliative prognostic models, such as the Chuang's prognostic scale (CPS), may be helpful in identifying mCRC patients with limited survival who are unlikely to benefit from PSAT. AIM: To test the ability of the CPS to predict the survival of mCRC under treatment with PSAT. **Methods:**CPS was prospectively assessed in 36 mCRC patients who were receiving PSAT. The scale is based on eight items: ascites, edema, cognitive impairment, liver and lung metastases, performance status, tiredness, and weight loss. The total CPS score ranges from 0 to 8.5 with the higher score indicating worse prognosis. **Results:** Patients were divided into two groups using a CPS cutoff score of 5, Group 1 with a CPS score ≤5 and Group 2 with a CPS score >5. Using this cutoff value, 3-month mortality was predicted with a positive predictive value of 71%, a negative predictive value of 77%, a sensitivity of 67%, a specificity of 81% and an overall accuracy of 75%. Group 1 patients had a longer median survival of 149 days (95% confidence interval [CI]: 82-216) in comparison to Group 2 patients who had a median survival of 61 days (95% CI: 35-87). The difference in survival was statistically significant (P = 0.01). **Conclusion:** CPS may be useful in identifying mCRC patients with limited survival who are unlikely to benefit from PSAT.
**Keywords:** Chuang's Prognostic Scale; End-Of-Life Care; Metastatic Colorectal Cancer; Palliative Systemic Anticancer Therapy; Prognosis.

## M-87. Ultrasound: Can it Replace MRI in the Evaluation of the Rotator Cuff Tears?

Samira Saraya and Rehab El Bakry

*The Egyptian Journal of Radiology and Nuclear Medicine, Volume 47: 193-201 (2016)*

**Objective** To assess ultrasound accuracy in rotator cuff tears detection with delineation of the extent of the injury (partial/full thickness tear) compared to MRI. **Methods** Forty patients were referred with clinical suspicion of rotator cuff tear. Human ethics committee approval was obtained. Ultrasound and MRI were done for all patients by 2 different radiologists being blind to the results of the other examination to minimize the bias. Surgery or arthroscopy was considered when conservative treatment failure for 6 months, or when rotator cuff repair was indicated. Results Ultrasound detected different tendon pathologies (tendinitis, partial and full thickness tears), in addition to the causal factors. Compared to MRI, ultrasound sensitivity for tendinitis detection was 85% with 86% NPV and 90% accuracy, while for partial thickness tears, its sensitivity, specificity, PPV, NPV and accuracy were 88%, 89%, 94%, 80% and 83% respectively. But in full thickness tears its sensitivity and specificity were 100% each. **Conclusion** Ultrasound and MRI are comparable in both sensitivity and specificity. Since US is less expensive and more available, it could be considered as the screening method when rotator cuff integrity is the main question, if well-trained radiologists and high resolution equipments are available.
**Keywords:** Ultrasound; Mri; Rotator Cuff Tears; Shoulder Impingement.

## M-88. Voluntary Reporting to Assess Symptom Burden Among Yemeni Cancer Patients: Common Symptoms are Frequently Missed.

Samy A Alsirafy, Khalil A Al-Alimi, Salem M Thabet, Afif Al-Nabhi and Nahla A Aklan

*Journal of Community and Supportive Oncology, 14: 117-121 (2016)*

**Background:** Adequate symptom assessment is necessary to relieve the high symptom burden experienced by cancer patients. However, health care professionals may depend only on patient's voluntary reporting (VR) to assess symptoms and therefore some symptoms may be missed. **Objective:** To assess the symptom burden experienced by Yemeni cancer patients by using VR and systematic assessment (SA). **Methods:** 50 cancer patients were asked an open question to voluntarily report their symptoms. This was followed by an SA of a list of 20 common physical symptoms that was drawn up based on the literature. **Results:** From 375 symptom entries related to the 20 symptoms, VR accounted for 66 entries (18%) and SA for 309 (82%). The mean number of VR symptoms/patient was 1.3, and the mean number of VR plus SA symptoms was 7.5 ($P$< .001). In all, 74% of VR symptoms and 57% of SA symptoms were moderate or severe. For each symptom, the percentage of patients who experienced it and did not report it voluntarily (missed) was 100% for bleeding, constipation, early satiety, hoarseness, taste changes, and weight loss. These were followed by anorexia (97%), skin symptoms (92%), dry mouth (91%), edema (89%), dyspnea (88%), sore mouth (88%), fatigue/weakness (85%), diarrhea (80%), dysphagia (80%), nausea (76%), cough (75%), urinary symptoms (75%), vomiting (62%), and pain (18%). Pain was the most common voluntarily reported symptom (56% of patients), the most commonly distressing (42%), and the least under-reported (18%). **Limitations:** Relatively small sample size; the SA included only 20 symptoms. **Conclusions:** SA of symptoms yields a more accurate estimation of symptom burden than does VR. As with many developing countries where the majority of cancer patients present at an incurable disease stage, Yemeni cancer patients suffer a high symptom burden, especially pain.
**Keywords:** Yemen; Cancer; Pain; Palliative Care; Symptoms; Systematic Assessment; Voluntary Reporting.

*Dept. of Clinical Pathology*

## M-89. Contribution of Toll-Like Receptor 9 Gene Single-Nucleotide Polymorphism to Systemic Lupus Erythematosus in Egyptian Patients.

Rasha Mohamad Hosny Shahin, Engy El Khateeb, Rania Hassan Khalifa and Rasha Mahmoud El Refai

*Immunological Investigations, 45: 235-242 (2016) IF: 1.78*

**Background:** Systemic lupus erythematosus (SLE) is an autoimmune disease, with multiple genetic and environmental factors involved in its etiology. The toll-like receptor 9 (TLR9) gene has been reported to have important roles in the development and progression of SLE. In this case-control study, the effect of TLR9 polymorphism on susceptibility to SLE was investigated in Egyptian patients**. Methods:**We studied the distribution of the TLR9 rs352139 (G + 1174A) single nucleotide polymorphism (SNP) by allele-specific polymerase chain reaction (PCR) in 104 Egyptian patients with SLE and 108 age-, sex-, and ethnically matched controls. **Results:** There was no statistically significant difference in the distribution of the AA genotype and alleles between SLE patients and the control group in our study; however, the GA heterozygous patients were three times more likely to develop SLE ($P < 0.001$). A significant association was detected between TLR9 genotypes and some of the disease manifestations as myositis ($p = 0.032$), psychosis ($p = 0.014$), photosensitivity ($p = 0.002$), and pleurisy ($p = <0.001$). Moreover, we observed a significant association between the TLR9 AA and GA genotypes and the presence of antinuclear antibodies (ANA) ($p = 0.038$). **Conclusion:** The G + 1174A SNP in the toll receptor 9 gene may contribute to the genetic susceptibility of SLE in Egyptian patients. Also, an influence for this polymorphism on disease manifestations has been elucidated.

**Keywords:** Polymorphis; TLR9; Systemic Lupus Erythematosus

## M-90. Evaluation of a Novel Commercial Quaternary Ammonium Compound for Eradication of Mycobacteria, Hcv and Hbv in Egypt

Yasmine Samy Elkholy, Asmaa Sayed Hegab, Dalia Kadry Ismail and Reem Mostafa Hassan

*Journal of Microbiology, 54: 39-43 (2016) IF: 1.621*

Endoscopes are a common source of outbreaks of healthcare-associated infections. It is therefore important to identify high-level disinfectants capable of eliminating or killing all vegetative bacteria, mycobacteria, and viruses. Aldehydebased disinfectants are most commonly used in clinical practice but resistance has recently been detected and side effects associated with these disinfectants are well documented. In this study, we evaluated Virusolve+® EDS, a novel quaternary ammonium compound formulation supplied by Amity international, against Mycobacterium bovis (ATCC-27289), hepatitis C virus (HCV)-positive serum and hepatitis B surface antigen-positive serum. We also compared its efficacy against Cidex® (glutaraldehyde 2%), an aldehyde-based disinfectant. M. bovis showed no growth after 10 weeks with either Virusolve+® or Cidex®. Virusolve+® achieved a 104- fold reduction in the initial 106 HCV load under clean conditions (without red blood cells) for 20 min, whereas Cidex® achieved this reduction under clean and dirty conditions (without and with red blood cells, respectively) after both 10 and 20 min. Both Virusolve+® and Cidex® were able to eradicate hepatitis B virus (HBV) infectivity under clean conditions after 10 and 20 min, whereas under dirty conditions they were only able to eradicate virus infectivity after 20 min. Virusolve+® EDS when compared with Cidex® showed equal mycobactericidal activity completely eradicating M. bovis. However, both showed comparable virucidal activity against HBV, which was more effective under clean conditions, emphasizing the importance of the cleaning step in endoscope reprocessing. Cidex® was more effective at eradicating HCV under dirty conditions after a short contact time.

**Keywords:** Virusolve+ Eds; Cidex; High-Level Disinfectants.

## M-91. The Role of 16S Rrna Gene Sequencing in Confirmation of Suspected Neonatal Sepsis

El Gawhary, El-Anany, Hassan and Ali El Gameel

*Journal of Tropical Pediatrics, 62: 75-80 (2016) IF: 1.059*

Different molecular assays for the detection of bacterial DNA in the peripheral blood represented a diagnostic tool for neonatal sepsis. We targeted to evaluate the role of 16S rRNA gene sequencing to screen for bacteremia to confirm suspected neonatal sepsis (NS) and compare with risk factors and septic screen testing. Sixty-two neonates with suspected NS were enrolled. White blood cells count, I/T ratio, C-reactive protein, blood culture and 16S rRNA sequencing were performed. Blood culture was positive in 26% of cases, and PCR was positive in 26% of cases. Evaluation of PCR for the diagnosis of NS showed sensitivity 62.5%, specificity 86.9%, PPV 62.5%, NPV 86.9% and accuracy of 79.7%. 16S rRNA PCR increased the sensitivity of detecting bacterial DNA in newborns with signs of sepsis from 26 to 35.4%, and its use can be limited to cases with the most significant risk factors and positive septic screen.

**Keywords:** Neonatal Sepsis; 16S Rrna Sequencing; Septic Screen.

*Dept. of Dermatology*

## M-92. Interventions for Acne Scars

Rania Abdel Hay, Khalid Shalaby, Hesham Zaher, Vanessa Hafez, Ching Chi Chi, Sandra Dimitri, Ashraf F Nabhan and Alison M Layton

*Cochrane Database of Systematic Reviews, 4 (2016) IF: 6.103*

**Background** Acne scarring is a frequent complication of acne and resulting scars may negatively impact on an affected person's psychosocial and physical well-being. Although a wide range of interventions have been proposed, there is a lack of high-quality evidence on treatments for acne scars to better inform patients and their healthcare providers about the most effective and safe methods of managing this condition. This review aimed to examine treatments for atrophic and hypertrophic acne scars, but we have concentrated on facial atrophic scarring. **Objectives** To assess the effects of interventions for treating acne scars. Search methods We searched the following databases up to November 2015: the Cochrane Skin Group Specialised Register, the Cochrane Central Register of Controlled Trials (CENTRAL) in the Cochrane Library (2015, Issue 10),MEDLINE (from 1946), EMBASE (from 1974), and LILACS (from 1982). We also searched five trials registers, and checked the reference lists of

included studies and relevant reviews for further references to randomised controlled trials. Selection criteria We include randomised controlled trials (RCTs) which allocated participants (whether split-face or parallel arms) to any active intervention (or a combination) for treating acne scars. We excluded studies dealing only or mostly with keloid scars. Data collection and analysis Three review authors independently extracted data from each of the studies included in this review and evaluated the risks of bias. We resolved disagreements by discussion and arbitration supported by a method expert as required. Our primary outcomes were participant reported scar improvement and any adverse effects serious enough to cause participants to withdraw from the study. Main results We included 24 trials with 789 adult participants aged 18 years or older. Twenty trials enrolled men and women, three trials enrolled only women and one trial enrolled only men. We judged eight studies to be at low risk of bias for both sequence generation and allocation concealment. With regard to blinding we judged 17 studies to be at high risk of performance bias, because the participants and dermatologists were not blinded to the treatments administered or received; however, we judged all 24 trials to be at a low risk of detection bias for outcome assessment. We evaluated 14 comparisons of seven interventions and four combinations of interventions. Nine studies provided no usable data on our outcomes and did not contribute further to this review's results. For our outcome 'Participant-reported scar improvement' in one study fractional laser was more effective in producing scar improvement than non-fractional non-ablative laser at week 24 (risk ratio (RR) 4.00, 95% confidence interval (CI) 1.25 to 12.84; n = 64; very low quality evidence); fractional laser showed comparable scar improvement to fractional radiofrequency in one study at week eight (RR 0.78, 95% CI 0.36 to 1.68; n = 40; very low-quality evidence) and was comparable to combined chemical peeling with skin needling in a different study at week 48 (RR 1.00, 95% CI 0.60 to 1.67; n = 26; very low-quality evidence). In a further study chemical peeling showed comparable scar improvement to combined chemical peeling with skin needling at week 32 (RR 1.24, 95% CI 0.87 to 1.75; n= 20; very low-quality evidence). Chemical peeling in one study showed comparable scar improvement to skin needling at week four (RR 1.13, 95%CI 0.69 to 1.83; n = 27; very low-quality evidence). In another study, injectable fillers provided better scar improvement compared to placebo at week 24 (RR 1.84, 95% CI 1.31 to 2.59; n = 147 moderate-quality evidence). For our outcome 'Serious adverse effects' in one study chemical peeling was not tolerable in 7/43 (16%) participants (RR 5.45, 95% CI 0.33 to 90.14; n = 58; very low-quality evidence). For our secondary outcome 'Participant-reported short-term adverse events', all participants reported pain in the following studies: in one study comparing fractional laser to non-fractional non-ablative laser (RR 1.00, 95% CI 0.94 to 1.06; n = 64; very low-quality evidence); in another study comparing fractional laser to combined peeling plus needling (RR 1.00, 95% CI 0.86 to 1.16; n = 25; very low-quality evidence); in a study comparing chemical peeling plus needling to chemical peeling (RR 1.00, 95% CI 0.83 to 1.20; n = 20; very low-quality evidence); in a study comparing chemical peeling to skin needling (RR 1.00, 95% CI 0.87 to 1.15; n = 27;very low-quality evidence); and also in a study comparing injectable filler and placebo (RR 1.03, 95% CI 0.10 to 11.10; n = 147; low quality evidence). For our outcome 'Investigator-assessed short-term adverse events', fractional laser (6/32) was associated with a reduced risk of hyperpigmentation than non-fractional non-ablative laser (10/32) in one study (RR 0.60, 95% CI 0.25 to 1.45; n = 64; very low-quality evidence); chemical peeling was associated with increased risk of hyperpigmentation (6/12) compared to skin needling (0/15) in one study (RR 16.00, 95% CI 0.99 to 258.36; n = 27; low-quality evidence). There was no difference in the reported adverse events with injectable filler (17/97) compared to placebo (13/50) (RR 0.67, 95% CI 0.36 to 1.27; n = 147; low-quality evidence). Authors' conclusions There is a lack of high-quality evidence about the effects of different interventions for treating acne scars because of poor methodology, underpowered studies, lack of standardised improvement assessments, and different baseline variables. There is moderate-quality evidence that injectable filler might be effective for treating atrophic acne scars; however, no studies have assessed long-term effects, the longest follow-up being 48 weeks in one study only. Other studies included active comparators, but in the absence of studies that establish efficacy compared to placebo or sham interventions, it is possible that finding no evidence of difference between two active treatments could mean that neither approach works. The results of this review do not provide support for the first-line use of any intervention in the treatment of acne scars. Although our aim was to identify important gaps for further primary research, it might be that placebo and or sham trials are needed to establish whether any of the active treatments produce meaningful patient benefits over the long term.

**Keywords:** Acne Scars; Systematic Review.

## M-93. Propranolol Versus Captopril in the Treatment of Infantile Hemangioma (Ih): A Randomized Controlled Trial.

Hesham Zaher, Hoda Rasheed, Mohamed M. El-Komy, Rehab A. Hegazy, Heba I. Gawdat, Dalia M. Abdel Halim, Rania M. Abdel Hay, Ranya A. Hegazy and Abeer M. Mohy

*Journal of The American Academy of Dermatology, 74: 499-505 (2016) IF: 5.621*

**Background:** Renin-angiotensin system components have been demonstrated in the biology of infantile hemangioma (IH). Captopril, an angiotensin-converting enzyme inhibitor, is proposed as a therapeutic alternative to oral propranolol. **Objectives:** We sought to compare the benefit of propranolol and captopril in the treatment of IH, and to assess angiotensin-converting enzyme gene polymorphism in patients with IH and in control subjects. **Methods:** Thirty patients with IH and 35 healthy control subjects were enrolled in this study. Patients were randomly assigned to treatment with either propranolol or captopril. Assessment was done clinically and by measurement of serum vascular endothelial growth factor and angiotensin II in patients and control subjects. Angiotensin-converting enzyme gene polymorphism was also studied. **Results:** Clinical improvement was significantly better and faster in the patients treated with propranolol. Both groups showed reduced vascular endothelial growth factor and angiotensin II levels posttreatment, with a significantly higher percentage reduction in the propranolol-treated group. Cardiac side effects were reported only in the captopril-treated group. Baseline vascular endothelial growth factor level was significantly higher, and baseline angiotensin II level was significantly lower, in patients than control subjects. **Limitations:** We studied a relatively small number of patients and control subjects. Conclusion: Propranolol shows greater benefit than captopril in the treatment of IH.

**Keywords:** Angiotensin Ii; Captopril; Efficacy; Infantile Hemangioma; Propranolol; Side Effects; Vascular Endothelial Growth Factor.

## M-94. Association of Interleukin (IL)18 and Il10 Gene Polymorphisms with Oral Lichen Planus Risk; A Case-Control Study

Rania Abdel Hay, Laila Rashed, Rehab Hegaz and Nesrin Samir

*Journal of Dermatological Science, 83:244-247(2016) IF: 3.739*

Expression of both pro- and anti-inflammatory cytokines has been reported in oral lichen planus (OLP). Interleukin-18 (IL18) an interferon gamma (INFg) inducing agent is involved in OLP as it is a potent pro-inflammatory cytokine besides its inhibitory effect on the synthesis of IL10. IL-10 is an anti-inflammatory cytokine having a direct ability to down-regulate IL18 and INFg, which makes it an important immunoregulator as well as a mediator of inflammatory process. Genetic factors producing disproportions in pro- and antiinflammatory cytokine production have been anticipated to increase the susceptibility for OLP.
**Keywords:** Cytokine; Interleukin; Lichen Planus.

## M-95. Serum Vitamin D and Vitamin D Receptor Gene Polymorphism in Mycosis Fungoides Patients: A Case Control Study.

Hoda Rasheed, Rehab A. Hegazy, Heba I. Gawdat, Dina A. Mehaney, Marwa M. Kamel, Marwa M. Fawzy, Mohammed M. Nooh and Hebatallah A. Darwish

*Plos One, (2016) IF: 3.057*

**Background:** Vitamin D has been considered a key player in various malignancies including cutaneous cancers. To date, mycosis fungoides (MF) has been the least studied in relation to vitamin D. Furthermore, the vitamin D receptor (VDR) single nucleotide polymorphisms (SNPs) have not been tackled before in the context of MF, despite their incrimination in numerous diseases. **Aim Of Study:**To assess the role of vitamin D in MF by measuring its serum level, and studying VDR SNPs (TaqI, BsmI, FokI) in different stages of MF. **Patients and Methods:**48 patients with various stages of MF, and 45 healthy controls were included. Complete history, full clinical examination and a five mm punch skin biopsy were performed to all recruited patients. Venous blood samples were withdrawn from both patients and controls to determine the serum vitamin D level and VDR gene polymorphisms. **Results:**Serum vitamin D level was significantly lower in patients (5.3-33.7 nmol/L)] compared to controls (8.3-90.1 nmol/L)] (P<0.001). A significant difference was observed between patients and controls regarding the FokI polymorphism only, being higher in patients (P = 0.039). Also Vitamin D serum levels differed significantly in patients with FokI genotypes (P = 0.014). No significant correlations were detected between any of the studied parameters and the demographic and clinical data of the included subjects. **Conclusion:** Depressed vitamin D and FokI polymorphism are potentially involved in the context of MF. VDR gene polymorphisms warrant further larger scale investigations to detect the exact genes involved in the pathogenesis of such an enigmatic disease.

**Keywords:** Vitamin D; Vdr Gene Polymorphism; Cutaneous Cancers; Mycosis Fungoides.

## M-96. Evaluation of Exposure of Pemphigus Vulgaris Patients to Mycobacterium Tuberculosis and Aspergillus Fumigatus

R. A. Ali, R. H. Elsherif, M. A. Salehand M. H. Ismail1

*European Journal of Clinical Microbiology and Infectious Diseases, 35: 1749-1752 (2016) IF: 2.857*

The purpose of this study was to screen pemphigus vulgaris (PV) (autoimmune bullous skin disease) for the presence of immunoglobulin G against Mycobacterium tuberculosis and Aspergillus fumigatus. The sera of 60 PV patients and 28 controls were screened for the presence of immunoglobulin G against M. tuberculosis and A. fumigatus by enzyme-linked immune-sorbent assay. Forty patients were females and 20 were males. The range of IgG against M. tuberculosis was from 0.9 to 152.6 (median = 2.95) in the patients and was from 0 to 2.2 (median = 1.6) in the controls. Seven (11.7 %) patients and none of the controls exceeded the cut-off value. Four patients were on systemic steroids and azathioprine and three did not receive treatment before. The results showed that PV patients had significantly more IgG against M. tuberculosis than the controls; the p value was 0.006. The range of IgG against A. fumigatus was from 1.3 to 76.3 (median = 4.9) in the patients and was from 1 to 105.3 (median = 5.25) in the controls. Six (10 %) patients and eight (28.6 %) controls exceeded the cut-off value. The six patients were on systemic steroids and azathioprine. No significant difference was detected between PV patients and controls regarding exposure to A. fumigatus; the p value was 0.308. PV patients showed significantly more exposure to the M. tuberculosis than the controls. This suggests that M. tuberculosis may contribute to the pathogenesis of PV.
**Keywords:** Aspergillus; Exposure; Mycobacterium Tuberculosis; Pemphigus.

## M-97. Fractional Carbon Dioxide Laser Versus Low-Dose Uva-1 Phototherapy for Treatment of Localized Scleroderma: A Clinical and Immunohistochemical Randomized Controlled Study

S. M. Shalaby, M. Bosseila, M. M. Fawzy, D. M. Abdel Halim and S. S. Sayed and R. S. H. M. Allam

*Lasers in Medical Science, 31: 1707-1715 (2016) IF: 2.461*

Morphea is a rare fibrosing skin disorder that occurs as a result of abnormal homogenized collagen synthesis. Fractional ablative laser resurfacing has been used effectively in scar treatment via abnormal collagen degradation and induction of healthy collagen synthesis. Therefore, fractional ablative laser can provide an effective modality in treatment of morphea. The study aimed at evaluating the efficacy of fractional carbon dioxide laser as a new modality for the treatment of localized scleroderma and to compare its results with the well-established method of UVA-1 phototherapy. Seventeen patients with plaque and linear morphea were included in this parallel intra-individual comparative randomized controlled clinical trial. Each with two comparable morphea lesions that were randomly assigned to

either 30 sessions of low-dose (30 J/cm2) UVA-1 phototherapy (340–400 nm) or 3 sessions of fractional CO2 laser (10,600 nm-power 25 W). The response to therapy was then evaluated clinically and histopathologically via validated scoring systems. Immunohistochemical analysis of TGF-ß1 and MMP1 was done. Patient satisfaction was also assessed. Wilcoxon signed rank test for paired (matched) samples and Spearman rank correlation equation were used as indicated. Comparing the two groups, there was an obvious improvement with fractional CO2 laser that was superior to that of low-dose UVA-1 phototherapy. Statistically, there was a significant difference in the clinical scores ($p = 0.001$), collagen homogenization scores ($p = 0.012$), and patient satisfaction scores ($p = 0.001$). In conclusion, fractional carbon dioxide laser is a promising treatment modality for cases of localized morphea, with proved efficacy of this treatment on clinical and histopathological levels

**Keywords:** Fractional Carbon Dioxide Laser; Localized Scleroderma; Mmp1; Randomized Controlled Trial; Tgf-B1; Treatment; Uva-1 Phototherapy.

## M-98. Treatment of Hypertrophic Scars and Keloids by Fractional Carbon Dioxide Laser: A Clinical, Histological, and Immunohistochemical Study

Azzam OA, Bassiouny DA, El-Hawary MS, El Maadawi ZM, Sobhi RM and El-Mesidy MS.

*Lasers in Medical Science, 31: 9-18 (2016) IF: 2.461*

Treatment of keloids (K) and hypertrophic scars (HTS) is challenging. A few case reports reported good results in HTS treated by fractional CO2 laser. The aim of the present study was the assessment of the clinical response as well as histological changes in K and HTS treated by fractional CO2 laser and the role of matrix metalloproteinase 9 (MMP9) in the response. A randomized half of the scar was treated by fractional CO2 laser in 30 patients (18 K, 12 HTS) for a total of four sessions 6 weeks apart. Vancouver scar score (VSS) was done before and 1, 3, and 6 months after the last laser session by a blinded observer. Biopsies taken from normal skin, untreated scar, and treated scar tissue 1 and 3 months after the laser sessions were stained by HX & E for histological changes and Masson trichrome for collagen fiber arrangement. Immunohistochemical staining for MMP9 was done in before and 1 month after samples. Quantitative morphometric analysis was done for collagen and MMP9 by image analyzer. Nineteen patients completed the 6-month follow-up period (12 K, 7 HTS). VSS score was significantly lower in the treated compared to untreated areas after 3 and 6 months in both K and HTS but was mainly due to improved pliability of the scar. Histologically, dense inflammatory infiltrate and increased vascularity was apparent 1 month after laser sessions and disappeared at 3 months. Thinner better organized collagen bundle could be seen in 3 months after samples. MMP9 was significantly increased in after treatment samples but without significant correlation with VSS. Fractional CO2 resurfacing is safe but affects mainly pliability of K and HTS with collagen remodeling apparent 3 months after therapy. MMP9 may play a role in mechanism of action of CO2 laser in K and HTS.

**Keywords:** Fractional Co2 Laser; Hypertrophic Scars; Keloids; Mmp9; Masson'S Trichrome

## M-99. Phototherapy: the Vitiligo Management Pillar

Samia Esmat, Wedad Mostafa-Rehab A. Hegazy, Suzan Shalaby, Vaneeta Sheth, Randa Youssef and Medhat El-Mofty

*Clinics in Dermatology, 34: 594-602 (2016) IF: 2.367*

Phototherapy has been the mainstay of vitiligo therapy for several decades. A variety of wavelengths and modalities are available, but narrowband ultraviolet B remains the safest and most commonly used treatment. Acting on multiple steps in vitiligo pathogenesis, narrowband ultraviolet B is one of the few therapies that can effectively induce stabilization and stimulate repigmentation. Achievement of optimal results involves using a combination of appropriate treatment protocols, careful patient selection, and patient education to set expectations. Individual patient characteristics, including disease activity, vitiligo phenotype, lesion location, and skin phototype, should all be considered, along with combination therapies.

**Keywords:** Phototherapy; Vitligo.

## M-100. B Cell Activating Factor and T-Helper 17 Cells: Possible Synergistic Culprits in the Pathogenesis of Alopecia Areata.

Mostafa A. Elela, Heba I. Gawdat, Rehab A. Hegazy, Marwa M. Fawzy, Rania M. Abdel Hay and Dina Saadiand Olfat Shaker

*Arch Dermatol Res, 308: 115-121 (2016) IF: 2.146*

The role of T-helper 17 cells (Th17) and regulatory T-cells (Tregs) in the pathogenesis of alopecia areata (AA) has not been clearly elucidated. B cell activating factor (BAFF) being a regulator of T cell activation could be involved in this pathologic process as well. The current study evaluated the expression of IL-17, IL-22, Foxp3 and BAFF in tissue and sera of AA patients. Forty AA patients and 40 age and sex matched healthy controls were included. Tissue and serum levels of IL-17, IL-22, BAFF as well as serum level of Foxp3 were measured by enzyme-linked immunosorbent assay (ELISA). Immunohistochemical staining was used for assessment of tissue level of Foxp3. Tissue and serum levels of IL-17, tissue levels of IL-22 and BAFF were significantly higher in patients. Serum levels of IL-22, Foxp3 and BAFF were non-significantly higher in patients. Foxp3 immunostaining showed negativity in tissue of patients and controls. A significant positive correlation was found between both tissue levels of IL-17 and BAFF ($r = 0.474$, $P = 0.035$) and tissue level of IL-22 and disease duration ($r = 0.766$, $P < 0.001$) in AA patients. Th17 cells and BAFF are synergistically involved in the pathogenesis of AA. BAFF represents a promising therapeutic target for such a challenging disease. Defective Tregs number and/or function in AA warrants further studies.

**Keywords:** Alopecia Areata; B Cell Activating Factor; Pathogenesis; Regulatory T Cells; T Helper 17 Cells.

## M-101. Expression of Sirtuins 1, 6, Tumor Necrosis Factor, and Interferon-? in Psoriatic Patients.

H Rasheed, MHM El-Komy, RA Hegazy, HI Gawdat, AM AlOrbani and OG Shaker

*Int J Immunopathol Pharmacol., 29: 764-768 (2016) IF: 1.47*

Sirtuins (SIRT) have been regarded as culprits in the pathogenesis of various diseases. Their exact role has not been explained. This study aimed to assess the expression of SIRT1, SIRT6, tumor necrosis factor (TNF)-α, and interferon (IFN)-γ in psoriatic patients. Thirty psoriatic patients and 22 controls were enrolled. Clinical examination and Psoriasis Area and Severity Index (PASI) were obtained. Two skin biopsies (lesional, peri-lesional) and one from controls were obtained. Tissue levels of SIRT1, SIRT6, TNF-α, and IFN-γ were measured using ELISA. SIRT1 was significantly lower in lesional skin with gradual increase in perilesional followed by control skin (P <0.001). SIRT6, TNF-α, and IFN-γ were significantly higher in lesional than perilesional and control skin (P <0.001). Significant positive correlations were found between SIRT1 and TNF-α, IFN-γ and between SIRT6 and TNF-α in peri-lesional skin. SIRT1 and SIRT6 are potentially involved in the pathogenesis of psoriasis. Modulating their action could offer a novel therapy for such disease.

**Keywords:** Ifn-Γ; Pathogenesis; Psoriasis; Sirtuins 1and6; TnfA

## M-102. Dermoscopic and Immunohistochemical Changes in Acquired Melanocytic Nevi Following Narrow-Band Ultraviolet B Therapy

Zaher H. Bassiouny D, Abdel Hay R, Samir N. Ragab and N. Sayed S.

*Dermatology, 232: 273-278 (2016) IF: 1.449*

**Background:**Acquired melanocytic nevi (AMN) have been reported to undergo morphological and dermoscopic changes following exposure to narrow-band ultraviolet B (NB-UVB) radiation. **Objective:** To study the morphological, dermoscopic and immunohistochemical changes in AMN following NB-UVB radiation. **Methods:** Suberythemogenic NB-UVB sessions were delivered to 40 patients with AMN. For each patient, a minimum of 2 nevi were selected. One nevus was surgically removed from each patient prior to sessions as control; for the other nevus, dermoscopic images were captured before and after NB-UVB sessions. The images were evaluated for changes. At the end, another nevus was surgically removed for immunohistochemical assessment of Ki-67 and melan-A. **Results:**Our study showed a statistically significant increase in the size of AMN following NB-UVB radiation. Benign dermoscopic changes were observed. Statistically significant positive correlations were found between some dermoscopic findings and the total cumulative dose of NB-UVB. Immunohistochemical analysis did not show any significant change in the exposed AMN. **Conclusion:** AMN irradiated with repeated suberythemogenic doses of NB-UVB showed benign morphological and dermoscopic changes, and this was confirmed by our immunohistochemical study.

**Keywords:** Dermatoscopy; Immunohistochemistry; Melanogenesis; Nevus.

## M-103. Expression of Angiopoietin-1, Angiopoietin-2, and their Receptor Tie2 in Verruca Vulgaris (Common Skin Warts)

Eman A. El-Nabarawy, Ghada M. El-Hanafy, Laila A. Rashed and Fatma S. Yasin

*International Journal of Dermatology, 55: 0-0 (2016) IF: 1.415*

**Background** Angiogenesis and vasodilatation are reported associated with the development of verruca vulgaris, yet vascular endothelial growth factor overexpression was not detected in the lesions of common warts. Angiopoietins, as angiogenesis factors, have not been studied before in warts. **Objectives** To assess tissue expression of angiopoietin 1 (Ang1), angiopoietin 2 (Ang2), and their receptor Tie2 in the lesions of common warts to try to identify their role as pro-angiogenic factors in the development of these lesions. **Patients and methods** Fifty patients with common skin warts and 50 age- and sex-matched controls were included in this study. Four millimeter punch skin biopsies were taken from warts and from normal skin of controls for the detection of gene expression of Ang1, Ang2, and Tie2 using real-time polymerase chain reaction. Results The mean levels of Ang1, Ang2, and Tie2 were significantly higher in the lesions of common warts compared to the normal skin of controls (P < 0.001 for all). **Conclusions** Upregulation of Ang1, Ang2, and Tie2 seems to play a possible role in the angiogenesis associated with common skin warts.

**Keywords:** Angiogenesis in Warts.

## M-104. Pathologic Features of Anogenital Precancerous High-Grade Squamous Intraepithelial Lesion (Squamous Cell Carcinoma in Situ)

Ruzeng Xue, Amira Elbendary, Manuel Valdebran, Soham Chaudhari and Dirk Elston

*Journal of Cutaneous Pathology, 43(9): 735-73 (2016) IF: 1.409*

**Background** Precancerous high-grade squamous intraepithelial lesion (HSIL), the current consensus terminology for anogenital squamous cell carcinoma in situ (SCCIS), often presents with distinctive histopathologic findings that may be a function of anatomic site or associated human papillomavirus infection. **Methods** Fifty-six specimens of anogenital HSIL were compared with an equal number of specimens of SCCIS from non-anogenital sites in regard to the presence of parakeratosis, flag sign in the stratum corneum, compact stratum corneum, hypergranulosis, koilocytes, small blue cells, clonal populations of keratinocytes, pagetoid scatter of atypical keratinocytes, clear cell change, glassy red cytoplasm, pigmentation, nuclear/cytoplasmic(N/C) ratio >2/1, nuclear hyperchromasia, pleomorphic nuclei, mitotic figures, abnormal mitotic figures, dyskeratotic keratinocytes, involvement of skin appendages, acantholysis and amyloid deposition. **Results** Hypergranulosis, koilocytes, small blue cells, pigmentation, nuclear hyperchromasia, dyskeratotic keratinocytes and amyloid deposition were more frequently noted in anogenital HSIL. Parakeratosis, clear cell change, pleomorphic nuclei, skin appendages involvement and acantholysis were strongly associated with non-anogenital location. There was no significant difference in the incidence of the remaining features. **Conclusion** The strongest predicators of an anogenital location included hypergranulosis, koilocytes, small blue cells and nuclear hyperchromasia. Pigmentation and amyloid deposition were also strongly associated with an anogenital location.

**Keywords:** Anogenital, Bowen'S Disease, High-Grade Squamous

## M-105. Hidradenoma Papilliferum with Oncocytic Metaplasia: A Histopathological and Immunohistochemical Study.

Elbendary A1, Cochran E, Xie Q, Kabigting F, Pereira L and Elston Heilman E.

*The American Journal of Dermatopathology, 38 (6): 444-447 (2016) IF: 1.396*

Hidradenoma papilliferum is a benign cutaneous adnexal neoplasm, commonly occurring in the vulva and perianal region of adult women. It has characteristic histopathological features composed of anastomosing and branching tubules, lined by columnar cells, and a basal layer of myoepithelial cells. A 39-year-old woman was evaluated for 2 asymptomatic labial masses. The histopathological examination revealed a Bartholin's cyst and a hidradenoma papilliferum. The latter contains a distinct area of oncocytic/ oxyphilic metaplasia. Immunohistochemical stains revealed positive staining for gross cystic disease fluid protein (GCDFP)-15 and androgen receptor. GATA-3, a protein expressed in sweat glands, highlights a similar positive staining pattern with weaker staining in areas of oncocytic metaplasia. P63 highlighted the myoepithelial differentiation. In situ hybridization for Human Papilloma Virus 6, 11, 16, and 18 was negative. P53 was negative and Ki- 67 was low, confirming its benign nature. Oncocytes are enlarged epithelial cells with voluminous eosinophilic granular cytoplasm resulting from staining of nonribosomal cytoplasmic components. Few reports documented it in hidradenoma papilliferum. Our case demonstrated a florid distinct appearance of this metaplasia. The immunoprofiles of this oncocytic metaplasia such as p53 negativity and positivity for androgen receptor and GCDFP-15 demonstrates similarity to apocrine metaplasia in the breast. The authors' case demonstrates the benign nature of oncocytic metaplasia and supports the common origin of oncocytic cells and columnar cells in hidradenoma papilliferum.

**Keywords:** Oncocytic Metaplasia; Oxyphilic Change; Hidradenoma Papilliferum; Gcdfp-15; Gata-3; Hpv; P63; P53.

## M-106. Linear Sclerodermoid Lupus Erythematosus Profundus in a Child.

Elbendary A, Griffin J, Li S, Tlougan B and Junkins-Hopkins JM.

*The American Journal of Dermatopathology, 38: 904-909 (2016) IF: 1.396*

Lupus erythematosus panniculitis, also known as lupus profundus, is a variant in the clinicopathological spectrum of lupus erythematosus (LE) affecting about 2%–3% of LE patients. A linear configuration of LE panniculitis has been reported rarely with rare reports describing the coexistence of different forms of cutaneous LE and localized morphea. In this study, the authors present a 9-year-old girl with linear arrangement of subcutaneous nodules on her left forearm. Microscopic findings from 2 biopsies included lymphocytes at the dermoepidermal junction with mild interface dermatitis, a dense lymphocytic infiltrate that was concentrated around adnexae and subcutaneous fat in concert with thickened collagen bundles and mild widening of fibrous septae surrounding fat lobules. Although the clinical differential diagnosis included panniculitis or a sporotrichoid infection, 1 biopsy showed a dense lymphocytic infiltrate histologically bordered on that of cutaneous lymphoid hyperplasia or a late stage of Lyme disease, and a second also demonstrated more prominent sclerodermoid collagen bundles rendering the diagnosis of linear sclerodermoid LE profundus.

**Keywords:** Linear; Lupus; Erythematosus; Profundus; Scleroderma.

## M-108. Polarized Microscopy in Lesions with Altered Dermal Collagen

Elbendary, Amira Valdebran, Manuel Parikh, Kruti Elston and Dirk M.

*The American Journal of Dermatopathology, 38 (8): 593-597 (2016) IF: 1.396*

Alterations in dermal collagen are noted in dermatofibroma, dermatofibrosarcoma protuberans, morphea, lichen sclerosus et atrophicus, hypertrophic scars, and keloids. The authors sought to determine whether variations in birefringence of collagen by polarized microscopy could be of help in diagnosing such conditions. Representative hematoxylin and eosin sections of 400 cases, including dermatofibroma, dermatofibrosarcoma protuberans, hypertrophic scars, keloid, morphea, and lichen sclerosus, were examined under polarized microscopy. Distinct patterns of birefringence of collagen for each disease were noted under polarized microscopy. This study highlights the use of polarized microscopy as adjunctive tool in differentiating different diseases with collagen alteration.

**Keywords:** Polarized Microscopy; Birefringence; Dermatofibroma;Dermatofibrosarcoma Protuberans; Morphea; Lichen Sclerosus; Hypertrophic Scar; Keloid.

## 107. Nevus Sebaceous of Jadassohn with Eight Secondary Tumors of Follicular, Sebaceous and Sweat Gland Differentiation

Yeqiang Liu, Manuel Valdebran, Jia Chen, Amira Elbendary, Fei Wu and Minyuan Xu

*The American Journal of Dermatopathology, 38 (11): 861-866 (2016) IF: 1.396*

**abstract** rupture of the follicles and inflammation. The other possible mechanism is the traumatic injury of the follicles induced by plucking the hairs projecting from nevi, the procedure frequently done for cosmetic reasons on facial skin. This traumatically induced inflammation creates appropriate milieu for metaplastic bone formation, what finely explains the affinity of osteonevi for the presentation in head and neck region. The authors have statistically confirmed this postulation showing that perifollicular foreign body reaction is significantly more likely encountered in head and neck nevi than in control group of nevi.5 The superficial skin inflammation related to the shaving procedure with the occasional involvement of deep dermal structures may explain the high proportion of osteonevi on facial skin of the males in this study. Sasaki et al4 reported signs of inflammation in half of their reviewed cases of osteonevi, with hair shafts in the bone areas observed in several cases. Having compared the osteonevi with the control group of nevi, we found higher percentage of coexistent perilesional chronic inflammatory reaction in the group of osteonevi, but the difference was insignificant (6.1% vs. 2.7%). In the largest

reported series of osteonevi, Moulin et al1 found coexistent histopathological signs of inflammation in only 6.5% cases of osteonevi. These findings are not unexpected because it is likely that inflammation had occurred previously and subsided in all osteonevi.

**Keywords:** No Key Words

## M-109. Treatment of Dystrophic Epidermolysis Bullosa with Bone Marrow Non-Hematopoeitic Stem Cells: A Randomized Controlled Trial

El-Darouti, Fawzy Amin, Abdel HayHegazy and Gabr El Maadawi

*Dermatologic Therapy, 29: 96-100 (2016) IF: 1.268*

Patients with dystrophic epidermolysis bullosa (DEB) have mutations in type VII collagen gene. Type VII collagen is synthesized by keratinocytes and fibroblasts. Based on the ability of bone marrow non-hematopoeitic stem cells (NHBMSC) to develop into fibroblasts, we decided to investigate the use of NHBMSC in the treatment of recessive DEB (RDEB). This study included fourteen patients with RDEB; the first seven of them were given cyclosporine after the infusion of NHBMSC. As cyclosporine has been used for the treatment of RDEB we decided not to use cyclosporine for the second group of seven patients. Skin biopsies from the lesions were studied by electron microscopy before and after treatment. The number of new blisters decreased significantly after treatment in both groups ($p = 0.003$ and 0.004 respectively) and the rate of healing of new blisters became significantly faster after treatment in both groups ($p < 0.001$) with no significant difference between the two groups. Electron microscopic examination revealed increased number of anchoring fibrils after treatment in both groups. No major side effects were reported during the 1-year follow-up period. Our findings highlight the efficacy as well as the safety of NHBMSC in the treatment of RDEB.

**Keywords:** Bullous Disease; Cyclosporine; Epidermolysis Bullosa; Stem Cells

## M-110. Assessment of Tissue Level of Histone Deactylase-2 (HDAC-2) in Patients with Mycosis Fungoides

Amira El Tawdy, Iman Amin, Rania Abdel Hay, Laila Rashed and Zeiad Gad

*Journal of Cutaneous Medicine and Surgery, 20: 40-43 (2016) IF: 1.191*

**Background:**Histone deactylases (HDAC) have a role in the pathogenesis of mycosis fungoides (MF) through their actions on different apoptosis pathways. OBJECTIVE: To assess the possible role played by HDAC-2 in MF by estimating the tissue expression of HDAC2 mRNA in different stages of MF. **Methods:** This study included 28 MF patients and 30 controls. The HDAC-2 levels were detected by real-time polymerase chain reaction (PCR). Correlations of HDAC-2 levels with clinical presentation and different stages of MF were analyzed. **Results:** Mean HDAC-2 level was significantly higher in patients ($P < .001$) than in controls. HDAC-2 highest mean value was significantly detected in patients with stage IIb, and the lowest mean value was detected in patients with stage Ia ($P < .001$). **Conclusion:** Up-regulation of tissue HDAC-2 in MF patients might develop a new approach in the understanding of the pathogenesis of MF. Histone deactylases are important targets for molecular cancer therapeutics.

**Keywords:** Apoptosis, Cancer Therapeutics, Cell Cycle, Hdac-2, Mycosis Fungoides

## M-111. Assessment of Tissue Levels of Dickkopf-1 in Androgenetic Alopecia and Alopecia Areata

Fawzi Mahmoud and Shaker Saleh MA.

*Journal of Cosmetic Dermatology, 15(1): 10-15(2016) IF: 1.126*

**Background:** Androgenetic alopecia (AGA) is the commonest form of hair loss in men. Alopecia areata (AA) is an organ-specific autoimmune disease. Studies revealed that Dickkopf 1 (DKK-1), a powerful suppressor of the Wnt/β-catenin signaling pathway, induced anagen-to-catagen transition in mice. Moreover, in vitro studies suggested that DKK-1 played a role in dihydrotestosterone (DHT)-induced balding. AIM: To evaluate the tissue levels of DKK-1 in patients with AGA and AA, to assess its possible role as a pathogenetic mechanism in both disorders. **Methods:** This study included 24 patients with AGA, 31 patients with AA, and 33 healthy controls. Scalp biopsies were taken from all participants for the detection of tissue DKK-1 levels**. Results:** Tissue DKK-1 levels were significantly higher in patients with AGA than in controls ($P = 0.000$) as well as in patients with AA than in controls ($P = 0.001$). In addition, they were significantly higher in patients with AGA than in patients with AA ($P = 0.000$). DKK-1 was higher in male than in female patients with AGA. DKK-1 was negatively correlated with disease duration in AGA. **Conclusion:** In conclusion, this study suggests an important role for DKK-1 in the pathogenesis of AGA and AA through documenting higher tissue DKK-1 levels in patients with both hair disorders compared to controls and suggests that DKK-1 may be a promising therapeutic target for these hair diseases.

**Keywords:** Alopecia Areata; Androgenetic Alopecia; Dickkopf

## M-112. Assessment of Vitamin D Receptors in Alopecia Areata and Androgenetic Alopecia

Fawzi MM, Mahmoud SB, Ahmed SF and Shaker OG.

*Journal of Cosmetic Dermatology, 15(4): 318-323 (2016) IF: 1.126*

**Background** Alopecia areata (AA) is a frequent autoimmune disease, the pathogenesis of which is still unknown. Androgenetic alopecia (AGA) is a noncicatricial type of patterned hair loss. Expression of vitamin D receptors (VDRs) on keratinocytes is essential for maintenance of normal hair cycle, especially anagen initiation. **Objective** To assess VDRs in the skin and blood of AA and AGA patients, in order to evaluate their possible role in these hair diseases. **Methods** This study recruited 20 patients with AA, 20 patients with AGA, and 20 healthy controls. Blood samples and lesional scalp biopsies were taken from all participants for detection of VDR levels. **Results** Serum and tissue VDR levels were lower in AA as well as AGA patients when compared to controls ($P = 0.000$). Serum and tissue VDR were positively correlated in each group. Tissue VDR was significantly lower in female patients

with AA than males (P = 0.046) although serum and tissue VDR levels were significantly higher in female AGA patients than males (P = 0.004). **Conclusion** This study suggests an important role for VDR in the pathogenesis of AA and AGA through documenting lower serum and tissue VDR levels in AA and AGA patients in comparison with controls.
**Keywords:** Vitamin D Receptors; Alopecia Areata; Androgenetic Alopecia.

## M-113. Salty and Spicy Food; are they Involved in the Pathogenesis of Acne Vulgaris? A Case Controlled Study

M. A. El Darouti Md, O. A. Zeid Md, D. M. Abdel Halim, R. A. Hegazy, D. Kadry, D. I. Shehab, H. S. Abdelhaliem and M. A. Saleh

*Journal of Cosmetic Dermatology, 15: 145-149 (2016) IF: 1.126*

**Background:** Many studies have suggested a strong relation between diet and acne. Many patients with acne believe that spicy and salty foods exacerbate acne. **Aim:**To assess the relationship between the dietary intake of salty and spicy food and the onset, severity, duration of acne. **Methods:** Two hundred patients with acne vulgaris and 200 age- and gender-matched controls were subjected to a detailed questionnaire taking, clinical examination and dietary assessment through using "24 h recall" method. Sodium content of the 24-h food intake was computed by a computer program connecting participants' dietary information to the food composition table of National Nutrition Institute data base. **Results:** Patients with acne consumed significantly higher daily amounts of sodium chloride (NaCl) (median 3367.54 mg) compared to the controls (median 2271.8 mg) (P < 0.001). A negative correlation between the amount of NaCl in the diet of patients with acne and the age of onset of acne lesions was detected (r = -0.216, P = 0.031). However, neither salty nor spicy food correlated with duration or severity of the disease. **Conclusion:** Consumption of salty foods was significantly higher among patients with acne compared to acne free subjects, making the consumption of salty food a possible participating factor in the development of acne.
**Keywords:** Acne; Diet; Sodium Chloride; Spicy Food.

## M-114. Vitiligo – the Story from Within: A Transmission Electron Microscopic Study Before and after Narrow-Band Ultraviolet B

Marwa M. Fawzy, PhD, Zeinab M. El Maadawi, Rehab A. Hegazy and Nesrin S. Abd El Fatah

*Ultrastructural Pathology, 40: 265-275 (2016) IF: 0.828*

Melanocyte loss is the main feature of vitiligo, but evidence refers to pathological multiplayers. Transmission electron microscopy was utilized to further explore vitiligo before and after narrow-band ultraviolet B (NB-UVB) therapy. Skin biopsies were retrieved from lesional and perilesional skin and compared to normal control skin. Sections were examined for melanocytes and keratinocytes and the number of melanosomes and thickness of basal lamina were measured. In lesional skin, keratinocytes revealed two types of degeneration with a significant increase in the mean thickness of basal lamina and decrease in the number of melanosomes. After treatment, lesional and perilesional skin showed variable ultrastructural features.
**Keywords:** Narrow-Band Ultraviolet B; Transmission Electron Microscopy; Vitilig

## 115. Is There A Link Between Human Herpesvirus Infection and Toll-Like Receptors in the Pathogenesis of Pityriasis Rosea? A Case-Control Study.

Mostafa Abou El-Ela, Eman Shaarawy, Mohamed El-Komy, Marwa Fawzy, Rania Abdel Hay, Rehab Hegazy, Amin Sharobim, Nadine Moustafa, Laila Rashed and Khalda Sayed Amr

*Acta Dermatovenerologica Croatica,24:282-287(2016)IF :0.469*

Human herpesvirus (HHV) 6 and 7 are involved in the pathogenesis of pityriasis rosea (PR). Our aim was to evaluate the role of the innate immune response in PR through the detection of Toll-like receptors (TLR) 2, 3, 4, 7, 8, and 9 expression in the skin of affected patients and to detect the possibility of being induced by HHV-6 and/or HHV-7 viral coexistence in these patients. Twenty-four patients with PR and 24 healthy controls were included in this case-control study. Biopsy was obtained from the PR lesion and from the healthy skin of controls for detection of HHV-6 and 7 as well as TLRs 2, 3, 4, 7, 8, and 9 gene expression using real-time polymerase chain reaction (PCR). Significantly elevated expression of all studied TLRs and significantly higher viral load of HHV-6 and 7 in PR cases were detected. A significant higher expression of TLR2 and 4 in HHV-7 positive cases and a significant positive correlation between TLR9 and HHV-7 viral load were documented. HHV6 and 7 may also be involved in the pathogenesis of PR via TLR pathways.
**Keywords:** Innate Immunity; Pattern Recognition Receptors; Rt-Pcr; Viral Coexistence; Viral Reactivation.

## M-116. In-Vitro Differentiation of Adipose-Derived Stem Cells Into Melanocytic Lineage: A Possible New Alternative Treatment for Vitiligo

El Maadawi, Zeinab M. Fawzy, Marwa M. Metwally and Hala G

*The Egyptian Journal of Histology, 39: 260-268 (2016)*

**Introduction** Adipose tissue has been shown to contain adipose-derived stem cells (ADSCs), which constitute a very convenient source of stem cells because it can be obtained easily in large quantities. Vitiligo is a pigmentation disorder caused by loss of skin melanocytes and can be treated by grafting autologous melanocytes. However, it is difficult to obtain sufficient skin for autologous cell transplantation. If ADSCs can differentiate into melanocytes, adipose tissue could be used as an alternative source of melanocytes in vitiligo treatment. Aim The aim of this study was to evaluate the potential differentiation of ADSCs into melanocyte precursor cells. Materials and methods Human subcutaneous adipose tissue was obtained. Isolation and culture of ADSCs was done. After 1 week, differentiation of ADSCs into melanocytic lineage was initiated using basic medium M254 supplemented with Human Melanocyte Growth Supplement, which was replaced every other day for 3 weeks. C-kit immunocytochemistry and Melan-A/MART-1

immunofluorescence were performed to assess the differentiation of ADSCs into melanocytic lineage. Functional characterization of melanocytic differentiation was validated by detecting tyrosinase activity assay after 1, 2, and 3 weeks of differentiation. Data obtained from quantitative morphometric study and tyrosinase activity assay were statistically analyzed. Results After 1 week of culture in the differentiation medium, ADSCs began to exhibit melanocytic morphology with multiple cytoplasmic processes, which became more apparent by the end of the third week. Melanocytic differentiation was confirmed by positive C-kit and Melan-A/MART-1 immunophenotyping as well as by positive tyrosinase activity, which increased significantly by the end of week 3 after differentiation. Conclusion ADSCs could be differentiated into morphological and functional melanocytic lineages, which might be useful as an alternative treatment for vitiligo.
**Keywords:** Adipose-Derived Stem Cells; Cell Culture; Melanocytes

***Dept. of Diagnostic Radiology***

## 116. Doppler Ultrasonography in Living Donor Liver Transplantation Recipients: Intra- and Post-Operative Vascular Complications

Abdelaziz O and Attia H.

*Word Journal of Gastroenterology, 22(27): 6145-6172 (2016) IF: 2.787*

Living-donor liver transplantation has provided a solution to the severe lack of cadaver grafts for the replacement of liver afflicted with end-stage cirrhosis, fulminant disease, or inborn errors of metabolism. Vascular complications remain the most serious complications and a common cause for graft failure after hepatic transplantation. Doppler ultrasound remains the primary radiological imaging modality for the diagnosis of such complications. This article presents a brief review of intra- and post-operative living donor liver transplantation anatomy and a synopsis of the role of ultrasonography and color Doppler in evaluating the graft vascular haemodynamics both during surgery and post-operatively in accurately defining the early vascular complications. Intra-operative ultrasonography of the liver graft provides the surgeon with useful real-time diagnostic and staging information that may result in an alteration in the planned surgical approach and corrections of surgical complications during the procedure of vascular anastomoses. The relevant intra-operative anatomy and the spectrum of normal and abnormal findings are described. Ultrasonography and color Doppler also provides the clinicians and surgeons early post-operative potential developmental complications that may occur during hospital stay. Early detection and thus early problem solving can make the difference between graft survival and failure.
**Keywords:** Us; Intraoperative; Post operative Living donor liver transplantation; Complications.

## M-117. International Consortium on Mammographic Density: Methodology and Population Diversity Captured Across 22 Countries

Valerie A. McCormack, Anya Burton, Isabel dos-Santos-Silva, John H. Hipwell, Caroline Dickens, Dorria Salem, Dorria Salem, Rasha Kamal, Mikael Hartman and Charmaine Pei Ling Lee

*Cancer Epidemiology, 40: 141-151 (2016) IF: 2.644*

Mammographic density (MD) is a quantitative trait, measurable in all women, and is among the strongest markers of breast cancer risk. The population-based epidemiology of MD has revealed genetic, lifestyle and societal/environmental determinants, but studies have largely been conducted in women with similar westernized lifestyles living in countries with high breast cancer incidence rates. To benefit from the heterogeneity in risk factors and their combinations worldwide, we created an International Consortium on Mammographic Density (ICMD) to pool individual-level epidemiological and MD data from general population studies worldwide. ICMD aims to characterize determinants of MD more precisely, and to evaluate whether they are consistent across populations worldwide. We included 11755 women, from 27 studies in 22 countries, on whom individual-level risk factor data were pooled and original mammographic images were re-read for ICMD to obtain standardized comparable MD data. In the present article, we present (i) the rationale for this consortium; (ii) characteristics of the studies and women included; and (iii) study methodology to obtain comparable MD data from original re-read films. We also highlight the risk factor heterogeneity captured by such an effort and, thus, the unique insight the pooled study promises to offer through wider exposure ranges, different confounding structures and enhanced power for sub-group analyses.
**Keywords:** International Consortium; Breast Density; Breast Cancer

## M-118. Value of Diffusion-Weighted Magnetic Resonance Imaging in the Characterization of Small Solid Renal Lesions

Sally Emad-Eldin and Iman M Hamdy Ibrahim

*Kasr Al-Ainy Medical Journal, 22(2): 49-55 (2016) IF: 2*

**Aim of the study** Our aim was to assess the value of diffusion-weighted imaging (DWI) and apparent diffusion coefficient (ADC) measurement for the characterization of small solid renal lesions. **Patients and methods** We prospectively evaluated 30 patients (18 men and 12 women). Their age ranging from 18 to 65 years (mean age of 49.6±12.9). They were examined by conventional MRI and DWI with b factors of 0, 600 and 1000 s/mm2. Mean ADC values of the normal renal parenchyma, benign, malignant small solid renal lesions were calculated **Results** The mean ADC value of normal renal parenchyma was significantly higher that of benign and malignant lesions. No statistical significance noted between the mean ADC values of benign and malignant renal lesions (P value=0.5). Among malignant lesions, the mean ADC value was highest in the RCC lesions (1.4±0.22) and lowest in the lymphoma lesions (0.679±0.08) showing statistical significance (P value=0.0001). The mean ADC values of RCC and TCC showed no statistical significance, whereas there was statistical significance was noted between RCC and pyelonephritis (P value=0.0004) , RCC and

Angiomyolipomas (P value=0.0001), lesions. **Conclusion** DWI is a fast sequence that can be easily added to a routine MR imaging protocol. DWI is notably valuable in lesion detection and evaluation when gadolinium contrast medium cannot be administered. However, due to the overlap of ADC values between benign and malignant lesions, it cannot be used as a single diagnostic tool and should be concurrently interpreted in conjunction with conventional MRI for optimal characterization of renal lesions

**Keywords:** Benign; Diffusion-Weighted Imaging; Malignant; Renal Lesions; Small; Solid

## M-119. Can we Apply the Mri Bi-Rads Lexicon Morphology Descriptors on Contrast-Enhanced Spectral Mammography?

Kamal Helal Mansour Haggag and Nada Farahat Alieldin.

*British Journal of Radiology, 89: 20160157-20160157 (2016) IF: 1.84*

**Objective:** To assess the feasibility of using the MRI breast imaging reporting and data system (BI-RADS) lexicon morphology descriptors to characterize enhancing breast lesions identified on contrast-enhanced spectral mammography (CESM). **Methods:** The study is a retrospective analysis of the morphology descriptors of 261 enhancing breast lesions identified on CESM in 239 patients. We presented the morphological categorization of the included lesions into focus, mass and non-mass. Further classifications included (1) the multiplicity for "focus" category, (2) the shape, margin and internal enhancement for "mass" category and (3) the distribution and internal enhancement for "non-mass" category. Each morphology descriptor was evaluated individually (irrespective of all other descriptors) by calculating its sensitivity, specificity, positive-predictive value (PPV) and negative-predictive value (NPV) and likelihood ratios (LRs). **Results:** The study included 68/261 (26.1%) benign lesions and 193/261 (73.9%) malignant lesions. Intensely enhancing foci, whether single (7/12, 58.3%) or multiple (2/12, 16.7%), were malignant. Descriptors of "irregular"-shape (PPV: 92.4%) and "non-circumscribed" margin (odds ratio: 55.2, LR positive: 4.77; p-value: 0.001) were more compatible with malignancy. Internal mass enhancement patterns showed a very low specificity (58.0%) and NPV (40.0%). Non-mass enhancement (NME) was detected in 81/261 lesions. Asymmetrical NME in 81% (n552/81) lesions was malignant lesions and internal enhancement patterns indicative of malignancy were the heterogeneous and clumped ones. **Conclusion:** We can apply the MRI morphology descriptors to characterize lesions on CESM, but with few expectations. In many situations, irregular-shaped, non-circumscribed masses and NME with focal, ductal or segmental distribution and heterogeneous or clumped enhancement are the most suggestive descriptors of malignant pathologies. Advances in knowledge: (1) The MRI BI-RADS lexicon morphology descriptors can be applied in the characterization of enhancing lesions on CESM with a few exceptions. (2) Multiple bilateral intensely enhancing foci should not be included under the normal background parenchymal enhancement unless they are proved to be benign by biopsy. (3) Mass lesion features that indicated malignancy were irregular-shaped, spiculated and irregular margins and heterogeneous internal enhancement patterns. The rim enhancement pattern should not be considered as a descriptor of malignant lesions unless CESM is coupled with an ultrasound examination

**Keywords:** Can We Apply The Mri Bi-Rads Lexicon Morphology Descriptors on Contrast-Enhanced Spectral Mammography?

## 120. The Diagnostic Utility of Combined Diffusion-Weighted Imaging and Conventional Magnetic Resonance Imaging for Detection and Localization of Non Palpable Undescended Testes

Emad-Eldin Abo-Elnagaa and Hanna Abdel-Satar.

*Journal of Medical Imaging and Radiation Oncology, 60(3): 344-351 (2016) IF: 1.182*

**Introduction** We aimed to evaluate the diagnostic performance of combined diffusion weighted imaging (DWI) and conventional magnetic resonance imaging (MRI), including fat-suppression T2WI for identification and localization of non palpable undescended testes (UDTs). Methods This prospective study included 40 consecutive patients, with 47 non-palpable undescended testes (unilateral in 33 cases and bilateral in seven cases). Their age ranged from 5 months to 18 years, mean = 7.5 ± 5.9 years. MRI examinations included T1WI, T2WI, fat-suppression T2WI and DWI at b value of 50, 400 and 800 s/mm2. All patients underwent laparoscopic exploration. Results According to the laparoscopy findings, the final diagnoses of the location of UDTs were: intra-canalicular (n = 18, 38%), low intra-abdominal (n = 6, 13%), high intra-abdominal (n = 5, 11%). Absent or vanishing testes were detected in 18 cases (38%). The diagnostic accuracy, sensitivity, specificity of combined DWI and conventional MRI were 95.7%, 93.5% and 100% respectively. Conclusion Combined DWI and MRI showed a greater performance compared to conventional MRI alone for identification of non-palpable UDTs. Based on our findings, we can obviate the need for diagnostic laparoscopy in patients who had preoperative detection of inguinal testes or nubbins. However, laparoscopy is still needed to confirm an absent rather than undetected non-viable abdominal testes.

**Keywords:** Dw; Mri; Undesended Testes.

## M-121. Usefulness of Diffusion-Weighted Magnetic Resonance Imaging for the Characterization of Benign and Malignant Renal Lesions

Sally Emad-Eldin, Shady Rakha, Sameh A.Z. Hanna and Hesham Badawy

*The Egyptian Journal of Radiology and Nuclear Medicine, 47(1): 325-333 (2016)*

**Purpose** Our aim was to evaluate the diagnostic potential of diffusion-weighted magnetic resonance imaging (DW-MRI) and quantitative assessment of apparent diffusion coefficient (ADC) value for the characterization of renal lesions and differentiation into benign and malignant. **Patients and methods** A total of 87 consecutive patients with 107 renal lesions were enrolled in this prospective study. MRI examinations including DWI with b factors of 0, 600 and 800 s/mm2 were performed at 1.5 T MRI unit. The mean ADC values of normal renal parenchyma, solid and cystic lesions were calculated. **Results** There was statistical significance difference between ADC value of normal renal

parenchyma with that of benign (n = 60, 56%) and malignant (n = 47, 44%) renal lesions (P value < 0.0001). ADC values differed significantly between solid (n = 74, 69.2%) and cystic lesions (n = 33, 30.8%) (P value < 0.0001). There was significant difference between ADC values of all benign (n = 60, 56%) and malignant renal lesions (n = 47, 44%) (P value < 0.0001) but not between benign solid (n = 27, 36.5%) and malignant solid renal lesions (n = 47, 63.5%) (P value = 0.784). **Conclusion** There is overlap between the ADC values of benign and malignant lesions. The use of ADC value alone may lead to inaccurate assessment of renal lesions. Thus, DW-MRI should be interpreted in conjunction with conventional MRI sequences to allow for better characterization of renal lesions.
**Keywords:** Dwi; Renal; Benign; Malignant.

## M-122. Detection and Diagnosis of Breast Lesions: Performance Evaluation of Digital Breast Tomosynthesis and Magnetic Resonance Mammography

Rasha Kamal, Sahar Mansour, Dalia ElMesidy and Kareem Moussaand Ahmed Hussien

*The Egyptian Journal of Radiology and Nuclear Medicine, 47: 1159-1172 (2016)*

**Objective:** To assess the impact of digital breast tomosynthesis (DBT) and magnetic resonance mammography (MRM) in enhancing the performance of digital mammography (DM) in the detection and evaluation of different breast lesions. **Patients and methods:** In this retrospective study, 98 patients with 103 breast lesions were assessed by DM, DBT and MRM. Mammography images were acquired using the ‘‘combo mode", where both DM and DBT scanned in the same compression. MRM was performed by 1T open system. Each lesion was assigned a blinded category in an individual performance for each modality. The resultant BI-RADS categories were correlated with reports of the pathology specimens or outcome of 18-month follow-up. **Results:** Both DBT and MRM showed equivalent sensitivity of 92%. The specificity for DBT and MRM was 80.7% and 89.7% respectively. The efficacy of DM was raised from 61% to 83.5% with DBT and 90.2%withMRM. The results of the three modalities and the final diagnosis revealed a significant correlation (p=0.035).The association between the results of DBT and those of MRM showed statistically significant difference between DBT and MRM for diagnosing breast lesions (p=0.001). **Conclusion:** Both MRM and DBT provide better performance than classic DM. Adding either of these modalities to the classic examination enhances diagnosis and precise disease distribution.
**Keywords:** Breast Cancer; Digital Mammography; Digital Breast Tomosynthesis; Magnetic Resonance Mammography

## M-123. Mri and Three Dimensional Ultrasonography in the Assessment of Pulmonary Hypoplasia in Fetuses with Urinary Tract Anomalies

Mariam Raafat, Mona El-Kalioubie and Sahar Mahmoud Mansour

*The Egyptian Journal of Radiology and Nuclear Medicine, 47: 1753-1764 (2016)*

**Purpose:** To analyze the correlation and agreement between three dimensional (3D) US and MRI in the assessment of pulmonary volumes of fetuses with different types of urinary tract malformations (UTM) and high-risk of pulmonary hypoplasia (PH). **Patients and methods:** Thirty-nine fetuses with various UTM, at risk for PH were involved in this cross-sectional study. 3D volume US data sets of the fetal lungs were acquired. The right, left and total lung volumes were calculated separately using the virtual organ computer-aided analysis (VOCAL) method with a 30_ rotation. MRI of fetal lung was obtained with assessment of signal intensity and lung volumetry. Comparison between mean lung volumes was performed using unpaired t test. Agreement between the 3D-US and MRI methods was done using Cohen kappa test. **Results:** Good agreement was detected between the two methods (Kappa = 0.629, p = 0.001). The measured lung volumes by 3D-US were smaller than those measured by MRI (p > 0.05, non-significant). MRI showed greater specificity, PPV and diagnostic accuracy (100% each) than 3D-US (50%, 88.9% and 90% respectively). **Conclusion:** There is a good concordance between 3D-US and MRI in the evaluation of PH in fetuses with UTM. MRI could be reserved for borderline cases of pulmonary hypoplasia and the difficult diagnostic situations.
**Keywords:** Fetal Mri; Pulmonary Hypoplasia; Three-Dimensional Ultrasound; Urinary Tract Anomalies

## M-124. Subtraction Mri Versus Diffusion Weighted Imaging: Which is More Accurate in Assessment of Hepatocellular Carcinoma after Trans Arterial Chemoembolization (Tace)?

Noha Abd ElShafy ElSaid, Randa Osama Kaddah, Marwa Shaker Abdel Fattah and Nada Mohsen Salama

*The Egyptian Journal of Radiology and Nuclear Medicine, 47: 1251-1264 (2016)*

This study aims to compare the role of both subtraction MRI and Diffusion weighted images in assessment of HCC after trans-arterial chemo embolization (TACE). Patients and methods: 32 patients having 54 HCC lesions underwent TACE. Ages ranged between 59 and 73 years (mean age 59.6); there were 26 males and 6 females. All examinations were performed using Philips 1.5 T MRI (Achieva). Pre contrast: T1, T2W and In phase and out phase gradient echo sequence, dynamic: eTHRIVE technique performed. Subtraction of an unenhanced T1-weighted was from the identical post enhancement sequences in early angiographic and late arterial phases. Diffusion imaging: it was performed using single-shot spin-echo echo-planar imaging with b = 0, 300, 600 mm/s2. DWI was used to create ADC maps. Two readers blinded to each other assessed subtraction of dynamic study and DWI technique to evaluate post treatment response. Results: Reader 1 subtraction dynamic MRI sensitivity = 97%, specificity = 100% PPV = 100% and NPV = 95% compared to 70.59%, 75%, 82.76% and 60% respectively in DWI. Reader 2 subtraction dynamic MRI sensitivity = 97%, specificity = 100% PPV = 100% and NPV = 95% compared to 76.5%, 90%, 92.8% and 69% respectively in DWI. Conclusion: DW-MRI had lower accuracy measures compared to subtraction MRI with increased false negative. DWI may act as a supplementary sequence to compensate for the dynamic MRI in patients who couldn't hold their breath adequately.
**Keywords:** Subtraction Mri; Dwi; Post Tace Hcc

## M-125. Role of Diffusion Weighted Imaging in Characterization of Pancreatic Pathology

Eman Salah Mohammed Abdallah, Mohamed Ibrahim Mahmoud Ali, Maryse Yousef Awadallah, Hamed Samir and Hamed El Ghawabi

*Egyptian Journal of Radiology and Nuclear Medicine, 47(3): 723-727 (2016)*

**Purpose** The purpose of the study was to show the value of combination of conventional MRI with DWI to raise the sensitivity and specificity considering the differentiation between pancreatic benign and malignant lesions. **Patients and methods** Study included 30 patients performed in the radiology department, Cairo University, as well as in a private center: 21 males and 9 females. Age of patients ranged between 27 and 76 years. The study was performed between August 2012 and April 2014. Patients were subjected to proper history taking, conventional MRI and DWI. **Result** In our study using combined qualitative analysis of diffusion weighted imaging and quantitative analysis of ADC values we found that results of diffusion weighted MRI are approaching that of contrast enhanced MRI not only in detecting pancreatic tumors but also in detection of tumor necrosis and liver metastasis which are essential information to reflect disease prognosis and treatment strategies. **Conclusion** Conventional MRI in combination with functional diffusion weighted imaging gave us helpful information regarding the characterization of pancreatic benign and malignant lesions. Diffusion weighted imaging may detect small masses better than conventional MRI although it has poor spatial resolution.

**Keywords:** Pancreas; Adc; Pancreatic Neoplasms;Diffusion

## M-126. Mr Spectroscopy Evaluation of White Matter Signal Abnormalities of Different Non-Neoplastic Brain Lesions

Randa O. Kaddah and Mohsen E. Khalil

*The Egyptian Journal of Radiology and Nuclear Medicine, 47(1): 233-242 (2016)*

**Objectives:** Our aim was to evaluate the efficacy of MR Spectroscopy in characterization of white matter signal abnormalities diagnosed by MRI detect changes in different metabolites and peaks of inflammation. **Patients and methods**: 93 patients (49 females and 44 males) age ranging from 2 to 63 years with average (37± 2.34 years) presented with white matter hyperintense lesions on T2 and T2 FLAIR and/or contrast enhanced T1WI diagnosed on MRI are included our study. **Results:** In Infectious group: Average Cho/NAA ratio: 0.79 ±0.19, Cho/Cr ratio: 0.95 ± 0.17, NAA/Cr 1.89 ±0.69, in inflammatory group Cho/NAA ratio: 0.65 ±0.15, Cho/Cr ratio: 0.98 ± 0.29, Average NAA/Cr ratio 1.69 ± 0.19. In ischemic group: Average Cho/NAA ratio: 0.83 ± 0.09, Cho/Cr ratio: 0.81± 0.23, Average NAA/Cr 1.54 ± 0.39, in metabolic group: Average Cho/NAA ratio: 0.57 ± 0.13, Cho/Cr ratio: 0.76 ±0.26; NAA/Cr ratio was 1.73 ± 0.44, in mitochondrial group, Average Cho/NAA ratio: 0.62 ± 0.19, Cho/Cr ratio: 0.54 ± 0.14, NAA/Cr ratio was 1.49 ±0.59, in inherited dysmyelinating; Cho/NAA ratio: 0.51 ±0.17, Cho/Cr ratio: 0.63 ± 0.13; Average NAA/Cr ratio was 1.87± 0.65. Glutamate and myoinositol peak raised in inflammatory, infectious, metabolic, inherited, and ischemic group mainly in the acute and subacute stage. Amino acids and succinate peak specifically are raised in brain abscesses. **Conclusion:** MRS is a noninvasive additional MRI technique to define the nature of non-neoplastic brain lesions. Together with image analysis, it may be the key to etiologic diagnosis or, at least, definition of the group where the lesion is classified, by detecting changes in different metabolites and peaks of inflammation.

**Keywords:** Mr Spectroscopy; White Matter; Non-Neoplastic

## M-127. Adult Thoracic and Abdominal Aortic Coarctation, Combined Value of Mscta and Conventional Angiography in Endovascular Management

Randa O. Kaddah, Magdy A. Haggag and Usama Lotfy

*The Egyptian Journal of Radiology and Nuclear Medicine, 47(2): 509-520 (2016)*

**Objective:** To detect the value of MSCTA in diagnosis and preplanning in endovascular management of adult thoracic and abdominal coarctation. The additional value of conventional angiography before or during the procedures is explained. The follow-up by either techniques is evaluated for early detection of re-coarctation and re-intervention. **Patients and methods:** This retrospective study included 22 patients, 9 females and 13 males, age ranging from 17 to 49 years. The main clinical presentation was hypertension (n= 15). All patients were evaluated by MSCTA and conventional angiography with pressure gradient studies for preoperative evaluation and planning of treatment. Follow-up MSCTA was done at 6 months interval for 3 years. **Results:** MSCTA detected suprarenal MAS (n= 3), infrarenal and juxtarenal MAS (n= 10), preand post-coarctation dilatation of the thoracic aorta and subclavian (n= 4), thoracic collateral pathways (n= 5). Mean narrowest diameter is 2.3 mm (1.2–4.5 mm). In conventional angiography peak systolic gradient decreased from 33 to 2 mmHg. Successful endovascular repair was done in n= 15, PTA was done alone in 6 and PTA and stenting were done in n=9. Endovascular reintervention was done in n= 3. **Conclusion:** Aortic COA could be found in any segment of the aorta. Proper identification of the anatomical details and pressure gradient studies are important factors affecting the plan of management.

**Keywords:** Coarctation; Adult; Multislice Ct; Angiography.

## M-128. Multidetector Ct Evaluation of Alternative Diagnosis of Clinically Suspected Acute Appendicitis, Appendicular and Nonappendicular Lesions

Randa O. Kaddah and Amr M. Ayad

*The Egyptian Journal of Radiology and Nuclear Medicine, 47(3): 669-677 (2016)*

**Objective:** To assess the accuracy of MDCT in diagnosis and preoperative evaluation of alternatives of acute appendicitis causing RLQP and associated complications. **Patients and methods:** 350 consecutive patients (250 males and 100 females) with ARLQP underwent MDCT examinations with contrast. Each scan was evaluated independently for the presence of inflammatory process (appendicitis), associated complications and for the detection of other findings rather than acute

appendicitis causing RLQP. The radiological findings were compared with histopathological results for operated cases. **Results:** 146 typical cases out of 350 patients received CT diagnosis of acute appendicitis, 62 with complications such as appendicular abscess (n= 32), appendicolith (n=7), mucocele (n=15), retrocecal appendix (n= 5), and retroileal appendix (n= 3); 63 patients received nonappendicular GIT causes, and 79 patients received alternative diagnosis of extra-GIT causes; patients who were operated upon based on either clinical diagnosis or US findings or both, with negative CT findings and pregnant women were excluded from the study. **Conclusion:** MDCT can be used effectively in the preoperative evaluation of appendicitis, provides high accuracy for detecting complications, detects other findings causing RLQP, and better guides physicians for proper management of these patients.
**Keywords:** Multidetector Ct; Appendicitis; Right Lower Quadrant Pain (Rlqp)

## M-129. Triangular Fibrocartilage and Ligamentous Injury of the Wrist Joint: Does Mr Arthrography Improve Diagnosis Over Standard Mri?

Randa Osama Kaddah, Noha Abd ElShafy Elsaid and Marwa Shaker Abdel Fatah

*The Egyptian Journal of Radiology and Nuclear Medicine, 47 (4): 1501-1509 (2016)*

To detect the added value of magnetic resonance arthrography (MRA) over MRI in different triangular fibrocartilage complex (TFCC) and intrinsic wrist ligament lesions. **Patients and methods:** MRI and MRA were achieved in 57 patients presented with wrist pain. Another symptompless Ten control individuals with negative MRI and MRA findings were included. Images were assessed for the presence of TFCC, scapholunate ligament (SCL) and lunotriquetral ligament (LTL) lesions. Imaging findings were compared with arthroscopic findings in all cases. **Results:** Out of fifty-seven patients, 38 males (66.6%) and 19 females (33.3%) (age range 19– 61 years (mean = 34.3 years) were included in the study, The sensitivity, specificity and accuracy of MRI and MRA for TFCC peripheral tears were 79.16%, 100%, 85.29% and 91.66%, 100%, and 94.11% respectively, the sensitivity, specificity and accuracy of MRI and MRA for TFCC central tears were 60%, 100%, 80% and 90%, 100%, and 95% respectively. Sensitivity, specificity and accuracy of MRI and MRA for SCL partial tears were 63.15%, 100%, 75.86% and 94.73%, 100% and 96.55%, respectively. For LTL partial tears, the values were 20%, 100%, 73.33% and 80%, 100%, and 93.33% respectively. **Conclusion:** MR arthrography is highly accurate for the evaluation of TFCC and ligamentous injury of the wrist joint.
**Keywords:** Wrist Pain Mr Arthrography Tfcc Ligaments

## M-130. Role of High Resolution Computed Tomography (Hrct) of the Chest in the Diagnosis of Lymphangioleiomyomatosis (Lam) – A Serial Study of 15 Patients

Youssriah Y. Sabri, Iman M. Hamdy Ibrahim, Heba Mostafa Ahmed and Hebatallah H. Assal.

*The Egyptian Journal of Radiology and Nuclear Medicine, 47: 765-769 (2016)*

**Aim of work:** To highlight the characteristic high resolution computed tomography (HRCT) findings in 15 patients diagnosed with lymphangioleiomyomatosis (LAM), narrowing the wide range of ILD and allowing accurate diagnosis preventing unnecessary interventional procedures. **Patients and methods:** 15 female patients ranged in age from 17 to 55 years (mean age = 40.33 years). ILD was suspected based on clinical examination and chest radiographs. They were referred to do HRCT chest for further assessment. A 64 MSCT scanner was used. **Results:** All patients showed bilateral multiple cysts showing upper lobar predominance in 13.3% of cases and lower lobar one in 6.7%. The size of the cysts ranged from few mms to 3 cm with variable wall thickness. Pneumothorax was reported in three patients and pulmonary hypertension in 15 cases. **Conclusion:** HRCT is a valued diagnostic tool for diagnosis of LAM showing characteristic features for the disease.
**Keywords:** Hrct; Lam; Cystic Lung; Ild.

## M-131. Preoperative Embolization of Nasopharyngeal Angiofibromas:The Role of Direct Percutaneous Injection of Cyanoacrylate Glue in Conjunction with Particulate Endovascular Approach

Mohamed Abdel Hakim, Osman Kasem, Ahmed Sayed Awad, Hussam Al Dein Mahmoud Al Bosraty and Ayman Ismail Kamel

*The Egyptian Journal of Radiology and Nuclear Medicine, 47: 1431-1441 (2016)*

**Purpose** The aim of this study was to assess the clinical application, extent of tumour devascularization and surgical outcome after embolization of nasopharyngeal angiofibromas prior to surgery by using percutaneous cyanoacrylate glue and endovascular particulate material. We discuss our primary experience, and describe technical considerations and potential complications of the procedure. Subjects and methods This study reports 29 patients with juvenile nasopharyngeal angiofibromas; that were embolized prior to surgical resection with percutaneous glue and endovascular particulate material; with surgery performed 24–72 h later. Preoperative and postoperative imaging studies were reviewed. Documented intraoperative blood loss was obtained and analysed. Results Almost complete radiographic devascularization was encountered in 26 of 29 tumours. An average of 3.2 spinal needles was placed in the tumours. An average of 4.2 mL of cyanoacrylate glue was injected into each tumour. The estimated mean of the blood transfused during the operations was 150 mL. The embolization procedure proved to be safe and effective with no major or serious complications. Conclusion The embolization of nasopharyngeal angiofibromas before surgery using percutaneous cyanoacrylate glue with endovascular particulate material proved to efficiently devascularize these tumours with lower blood loss during surgery and no major procedural complications.
**Keywords:** Nasopharyngeal Angiofibromas; Direct Percutaneous Embolization; Cyanoacrylate Glue

## M-132. In Utero Mri Diagnosis of Fetal Malformations in Oligohydramnios Pregnancies

Ahmed Hesham Said, Eman El-Kattan, Ahmed K. Abdel-Hakeem and Sahar Saleem

*The Egyptian Journal of Radiology and Nuclear Medicine, 47: 1733-1742 (2016)*

**Objective** To evaluate the role of MRI in assessing Ultrasonographically (US)-suspected fetal malformations associated with oligohydramnios. **Methods** We performed MRI in 43 oligohydramnios pregnancies referred with US- suspected fetal malformations at a mean of 22.5 weeks' gestation. MRI findings were correlated with US data and outcome measures. **Results** MRI correctly diagnosed one normal foetus suspected to have posterior cephalocele. In the remaining 42 foetuses who had malformations involving their urinary systems (n=36), brain (n=23), bones (n=4), hearts (n=3), and hepatobiliary (n=3). MRI confirmed diagnosis in 25 foetuses (58.1%), and added US-occult findings in 14 (32.5%) that were mainly related to the brain urinary and hepatobiliary system. in 2 foetuses (4.7%), MRI added findings but missed data correctly detected by US in another 2 fetuses. MRI missed metal skeletal and cardiac function abnormalities correctly detected by US. MRI accurately detected multiple body system abnormalities that aided prenatal correct diagnosis of syndromes including Meckel Gruber (n=15) and Joubert syndrome and related cerebellar disorders (n=1). **Conclusion:** MRI is valuable in evaluating suspected fetal malformations especially those related to brain and urinary system when ultrasound is inconclusive going to oligohydramnios. Fetal MRI can add findings that may modify prenatal diagnosis.

**Keywords:** Oligohydramnios; Fetal Mri; Fetal Malformations

## M-133. Do We Need 18F-Fdg Pet/Ct Scan in Staging and Management of Testicular Tumors?

Tamer W. Kassem

*The Egyptian Journal of Radiology and Nuclear Medicine, 47: 445-452 (2016)*

**Objective** The aim of this study was to assess the role of positron emission tomography/computed tomography (PET/CT) scan in preoperative staging of testicular tumors and therefore determining the line of appropriate management. **Patients and methods** During two year duration we prospectively evaluated 34 patients with testicular tumors diagnosed by histopathology after biopsy or orchidectomy. All patients underwent PET/CT examinations following a preset protocol that included low dose non contrast study, whole body scanning post 18F-FDG injection and post IV contrast CT scan. The images obtained were reconstructed using dedicated software and workstations. Results of PET/CT examinations were compared with histopathology and serum markers. **Results** Out of 34 cases all masses were malignant (germ cell tumors). 20 masses (58.8%) were diagnosed by histopathology as seminoma subtype while 14 masses (41.2%) were diagnosed as non seminomatous germ cell tumors (NSGCT) subtype. There were 16 true positives, 14 true negatives, 2 false positive, and 2 false negative cases. Sensitivity, specificity, positive predictive value and negative predictive values were 88.9%, 87.5%, 88.9% and 87.5% respectively. **Conclusion** Positron emission tomography/computed tomography (PET/CT) has a major role in preoperative staging of testicular tumors and defines the need of post operative adjuvant therapy.

**Keywords:** 18F-Fdg Pet/Ct; Staging; Management; Testicular Tumors

## M-134. Up and Down Staging of Tcc Using 18F-Fdg Pet/Ct Scan

Tamer W. Kassem

*The Egyptian Journal of Radiology and Nuclear Medicine, 47: 1095-1102 (2016)*

**Objective** The purpose of this study was to investigate the ability of PET/CT to restage urinary bladder transitional cell carcinoma (TCC) whether up or down after initial staging by histopathology and other imaging modalities. **Patients and methods** During three year duration 27 patients with urinary bladder TCC were prospectively evaluated. They were previously diagnosed by histopathology after biopsy and had prior imaging for initial staging. All patients underwent PET/CT examinations following a preset protocol. The images obtained were reconstructed using dedicated software and workstations. Results of PET/CT examinations were confirmed by histopathology. **Results** Prior imaging and PET/CT findings were matched in 17 patients (63%) with no changes regarding their initial TNM stages and differed in 10 patients (37%). Six patients (22.2%) showed new sites of distant metastasis and unchanged initial stages. Two patients (7.4%) were up staged and 2 patients (7.4%) were down staged for whom the plan of clinical management was justified. **Conclusion** 18F-FDG PET/CT can up and down stage TCC and can detect new sites of nodal or distant metastasis leading to optimal therapy planning.

**Keywords:** Staging; Tcc; 18F-Fdg Pet/Ct

## M-135. Upper Limb Dvt after Hemodialysis Avf Creation: Role of Ct Venography

Tamer W. Kassem

*The Egyptian Journal of Radiology and Nuclear Medicine, 47: 897-902 (2016)*

**Objective** The aim of this study was to assess the role of CT venography (CTV) in diagnosis of upper limb deep venous thrombosis (DVT) after arterio-venous fistula (AVF) creation for patients with chronic renal failure (CRF) under regular hemodialysis. Patients and methods During two years duration 22 patients with upper limb hemodialysis arterio-venous fistulas suspected to have deep venous thrombosis were prospectively evaluated. All patients underwent CTV examinations following a preset protocol. The images obtained were reconstructed using dedicated software and workstations. **Results** of CTV examinations were compared with those of Color Doppler (CD) examinations. **Results** Out of 22 examined cases, 20 cases (90.9%) had autogenous AVF and 2 cases (9.1%) had synthetic grafts. Diagnosis of proximal upper limb segment DVT including brachial, axillary and subclavian veins recorded 12 TP (54.5%), 8 TN (36.4%), 2 FP (9.1%) and no FN cases. Sensitivity, specificity, positive predictive value (PPV) and negative predictive value (NPV) were 100%, 80%, 85.7% and 100% respectively. Diagnosis of central venous segment DVT including innominate veins and SVC recorded 14 TP (63.6%), 8 TN (36.4%) and neither FP nor FN cases. Sensitivity, specificity,

PPV and NPV were 100%, 100%, 100% and 100% respectively. **Conclusion** CTV has a major role in diagnosis of deep venous thrombosis particularly the central innominate veins/SVC segment after upper limb AVF creation for patients with CRF under hemodialysis.
**Keywords:** Upper Limb; Thrombosis; Hemodialysis Avf; Ct Venography.

## M-136. Diffusion-Weighted Mri in Adrenal Lesions: A Warranted Adjunct?

Mona El-Kalioubie, Sally Emad-Eldin and Omar Abdelaziz

*The Egyptian Journal of Radiology and Nuclear Medicine, 47: 599-606 (2016)*

**Purpose** We assessed the value of adding Diffusion-weighted (DW) sequences to conventional MR in the diagnostic adrenal algorithm, particularly in patients with indeterminate adrenal mass. We compared the predictive capabilities of apparent diffusion coefficient values (ADC), lesion size and signal drop on chemical shift MRI (CS MRI) for differentiating benign and malignant lesions. **Materials and methods** Fifty-five patients with 59 adrenal lesions were evaluated. Lesion size, signal loss on CSMRI and ADCs were assessed. Sensitivity, specificity and accuracy were calculated for each parameter. We compared the predictive capability of ADC, CS signal drop, and lesion size for malignancy with receiver operating characteristic (ROC) curves. **Results** Considering all lesion subtypes, ADC values showed overlap. Benign and malignant masses had statistically different mean ADCs, with greater mean ADC values in benign lesions ($1.78 \pm 0.5$ versus $0.97 \times 10{-}3$ mm2/s $\pm$ 0.3). ADC had the lowest accuracy (71.2%) but highest specificity (100%). Lack of signal drop had the greatest sensitivity (100%); lesion size was the most accurate (88.1%). On ROC curves, ADC had the lowest prediction for malignancy. **Conclusion** Lesion size and signal drop were stronger predictors of adrenal malignancy than ADC. ADC shows poor significance in individual cases due to overlapping values.
**Keywords:** Mri; Diffusion-Weighted Imaging; Adrenal Benign Lesions; Adrenal Malignant Lesions; Apparent Diffusion Coefficient.

### *Dept. of Ear Nose & Throat*

## M-137. Thyroid and Parathyroid Dysfunction after Total Laryngectomy in Patients with Laryngeal Carcinoma

Hesham Negm, Mohamed Mosleh, Hesham Fathy and Ahmed Awad

*European Archives of Oto-Rhino-Laryngology, 273(10): 3237-3241 (2016) IF: 1.627*

The objective of this study is to investigate thyroid and parathyroid functions in patients with laryngeal carcinoma after total laryngectomy with hemithyroidectomy with or without irradiation, and to determine if irradiation when following surgery has an additive effect contributing to either or both glands hypo function. This study included 17 patients with laryngeal squamous cell carcinoma who were subjected to surgery. Nine of them were further justified for postoperative radiotherapy as well. All patients were subjected to Clinical assessment, including adequate history taking and physical examination, to detect the presence of hypothyroidism or hypoparathyroidism. Laboratory assessment of thyroid function included TSH and T4 assay, and parathyroid function included corrected serum calcium and parathormone levels. Eight (48 %) patients were treated with surgery alone, and 9 (52 %) patients received postoperative radiotherapy. In this study, 13 out of the 17 patients (78 %) were found to be hypothyroid and 4 (22 %) were euthyroid, while 7 (42 %) were found to have hypoparathyroidism. The study showed; among the 8 patients who were treated by surgery only, 5 (62.5 %) of them developed hypothyroidism and 3 (37.5 %) were euthyroid and 3 (37.5 %) developed hypoparathyroidism and 5 (62.5 %) were normal. Among the 9 patients who were treated by surgery and radiotherapy, 8 (88.9 %) developed hypothyroidism and 1 (11.1 %) was euthyroid and 4 (44.4 %) developed hypoparathyroidism and 5 (55.6 %) were normal. The study confirms the development of hypothyroidism with or without hypoparathyroidism after total laryngectomy with a higher incidence in those treated by combined surgery and radiotherapy and in supraglottic tumors.
**Keywords:** Hypothyroidism Hypoparathyroidism Tsh T4 Calcium Total Laryngectomy Laryngeal Carcinoma

## M-138. Identification and Prevalence of Allergic, Nonallergic, and Local Allergic Rhinitis Patients in Western Area, Saudi Arabia

Hatem Badran, Ahmed Hussein, Mohamad Salah and Wassim T Lotfi

*Annals of Otology, Rhinology and Laryngology, 125: 634-643 (2016) IF: 1.171*

**Objectives:** To evaluate the diagnostic yield of skin prick test (SPT) and serum total immunoglobulin E (IgE) antibodies level in patients with allergic rhinitis (AR) and the role of nasal provocation test (NPT) for the determination of local allergic rhinitis (LAR) in patients with nonallergic rhinitis (NAR). **Methodology:** This multi-center study included 1230 patients with clinical manifestations for ≥2 years. Patients were classified according to the Allergic Rhinitis and Its Impact on Asthma (ARIA) and scored according to the quantitative Score for Allergic Rhinitis (SFAR). The SPT and total IgE antibody levels were done for all patients. Patients gave negative SPT underwent NPT, and its result was interpreted using Lebel Symptom Score Scale. **Results:** The SPT was positive in 77.8% of patients, mostly for grass pollen and dust mites. All patients were sensitive to multiple allergens. Median serum IgE antibody level for total study population was 162 IU/ml. Forty-two patients (3.4%) with negative SPT showed a weak response to NPT, while 231 patients (18.7%) with negative SPT had a high response to NPT and were considered to have LAR. **Conclusion:** The SPT could discriminate between AR and NAR patients. The NPT could identify LAR in 84.6% of patients with rhinitis among those considered as NAR.
**Keywords:** Allergic Rhinitis, Local Allergic Rhinitis, Nonallergic Rhinitis, Skin Pricking Test, Nasal Provocation Test

## M-139. Palatal Eversion for the Treatment of Combined Nasopharyngeal Stenosis and Tonsillar Pillars Adhesion

Gamal Abdel-Fattah

*International Journal of Pediatric Otorhinolaryngology, 90: 227-230 (2016) IF: 1.125*

**Objective** Rarely the tonsillar pillars and the soft palate became adherent to the posterior nasopharyngeal wall by strong fibrous tissue due to excessive dissection and cauterization during surgery leading to nasopharyngeal stenosis. Therefore, many treatment modalities are being tried to cure this problem. The aim of this study is to explore our results of modifying the basic technique to accommodate those patients with combined nasopharyngeal stenosis and tonsillar pillars adhesions in one stage. **Study Design:** Case series. **Methods** This study was conducted on 10 patients with combined nasopharyngeal stenosis and tonsillar pillars adhesions after adenotonsillectomy. They were subjected to treatment by palatal eversion through dividing the soft palate in the midline to separate each pillar from the pharyngeal wall in continuation with each half of soft palate and removal of the fibrous tissue causing stenosis. This was followed by eversion and fixation of the two palatal divisions on either side to allow complete epithelialization of the stenotic area. Postoperative follow-up was done for one year by the flexible nasopharyngoscopy, perceptual speech analysis, and polysomnography. **Results** The flexible nasopharyngosopic examination of the 10 patients at the end of post-operative period revealed a freely mobile soft palate with no nasopharyngeal stenosis or palatal fistula. Velopharyngeal function and speech assessment by perceptual speech analysis was normal in all 10 cases. No obstructive episodes were recorded in polysomnograms. **Conclusions** Palatal eversion is a promising technique in the treatment of post-adenotonsillectomy of combined nasopharyngeal stenosis and tonsillar pillars adhesion. It is recommended to be used on a wider scale of patients and other indications as nasopharyngeal stenosis following uvulopalatoplasty and post nasopharyngeal radiotherapy. The level of evidence: 4 (case series).

**Keywords:** Nasopharyngeal Stenosis; Palatal Eversion; Adenotonsillectomy Complications.

## M-140. Mucocele of the Hard Palate in Children

Mosaad Abdel-Aziz,Badawy Khalifa, Ahmed NassarAhmed Nassar, Ahmed Kamel and Nader Naguib

*International Journal of Pediatric Otorhinolaryngology, 85: 46-49 (2016) IF: 1.125*

**Objective** Mucus retention cyst of the hard palate may result from obstruction of the ducts of the minor salivary glands, and it was defined as a mucocele. Although, the disease is not common in the hard palate, it was previously reported by many authors in the soft palate. The aim of our study was to present pediatric patients who were diagnosed to have mucocele of the hard palate, and to evaluate the outcome of the surgical excision of this lesion. **Methods** This is a case series study included 8 pediatric patients who presented with cystic lesions on the hard palate which were removed surgically, and were diagnosed as mucoceles. Preoperative data, surgical procedures, and postoperative outcome were presented. Follow up of patients was performed for at least one year. **Results** The swelling was detected as a single isolated lesion, on the side of the hard palate, covered with healthy mucosa, not tender, oval or round in shape, and measuring 0.4 to 1.7 cm in its greatest dimension. Computed tomography showed a well defined cavity which was not invading the bone, and not disrupting the muscles of the palate. Histopathological examination confirmed that the lesion was a cavity that is lined with an epithelial layer with pseudoepitheliomatous hyperplasia. No patients developed intraoperative or postoperative complications, and no recurrence was detected in any patient. **Conclusions** Oral mucoceles can develop on the hard palate of the children, the lesions are mucus retention cysts. Complete surgical removal of the lesions with their cystic wall is a good treatment options, it carries no risk of recurrence.

**Keywords:** Oral Mucocele; Mucus Retention Cyst; Hard Palate; Palatal Cysts.

## M-141. Trans-Oral Endoscopic Partial Adenoidectomy Does Not Worsen the Speech after Cleft Palate Repair

Mosaad Abdel-Aziz, Badawy Khalifa, Ahmed Shawky, Mohammed Rashed, Nader Naguibb and Asmaa Abdel-Hameed

*Brazilian Journal of Otorhinolaryngology, 82(4): 422-426 (2016) IF: 0.73*

**Introduction:** Adenoid hypertrophy may play a role in velopharyngeal closure especially in patients with palatal abnormality; adenoidectomy may lead to velopharyngeal insufficiency and hyper nasal speech. Patients with cleft palate even after repair should not undergo adenoidectomy unless absolutely needed, and in such situations, conservative or partial adenoidectomy is performed to avoid the occurrence of velopharyngeal insufficiency. Trans-oral endoscopic adenoidectomy enables the surgeon to inspect the velopharyngeal valve during the procedure. Objective: The aim of this study was to assess the effect of transoral endoscopic partial adenoidectomy on the speech of children with repaired cleft palate. **Methods:** Twenty children with repaired cleft palate underwent transoral endoscopic partial adenoidectomy to relieve their airway obstruction. The procedure was completely visualized with the use of a 70◦ 4 mm nasal endoscope; the upper part of the adenoid was removed using adenoid curette and St. Claire Thompson forceps, while the lower part was retained to maintain the velopharyngeal competence. Preoperative and postoperative evaluation of speech was performed, subjectively by auditory perceptual assessment, and objectively by nasometric assessment. Results: Speech was not adversely affected after surgery. The difference between preoperative and postoperative auditory perceptual assessment and nasalance scores for nasal and oral sentences was insignificant (p = 0.231, 0.442, 0.118 respectively).

**Keywords:** Endoscopicadenoidectomy;Cleft Palate;Adenoid Hypertrophy;Velopharyngealinsufficiency

## M-142. Lateralization of the Pharyngeal Flap for Treatment of Lateral Velopharyngeal Gap

Mosaad Abdel-Aziz, Mohammed Rashed, Nader Naguib and Ahmed Shawky

*Journal of Craniofacial Surgery, 27(1): 101-104 (2016) IF: 0.7*

Pharyngeal flap is usually used for treatment of velopharyngeal insufficiency (VPI); it is bridged between the posterior pharyngeal wall and the soft palate traversing the central part of the velopharyngeal port. The aim of this study was to assess the efficacy of lateralization of the pharyngeal flap for treatment of VPI in patients with lateral velopharyngeal gap. Fifteen patients with VPI due to lateral velopharyngeal gap were subjected to closure of the gap by pharyngeal flap that was lateralized to fill the gap. Preoperative and postoperative assessment of velopharyngeal functions including flexible nasopharyngoscopy, auditory perceptual assessment (APA), and nasometric assessment were performed. Postoperatively, flexible nasopharyngoscopy showed complete velopharyngeal closure in all the patients, with significant improvement of speech parameters as measured by APA. Also, nasalance score showed significant improvement for oral and nasal sentences that was measured by nasometry. Lateralization of the pharyngeal flap for treatment of VPI in patients with lateral velopharyngeal gap is an effective method; it improves the velopharyngeal closure and the speech of the patients.

**Keywords:** Hypernasality; Lateral Velopharyngeal Gap; Pharyngeal Flap; Velopharyngeal Insufficiency

## M-143. Cochlear Microphonics Recording During Abr Threshold Testing in Children

Abeir Osman Dabbous

*Hearing, Balance and Communication, 14: 163-182 (2016)*

**Objective:** It is agreed that the cochlear microphonic (CM) arises mainly from the normal outer hair cells (OHCs) in cochlea. The aim of this research is to study the CM characteristics in different hearing profiles and reflect the usefulness of recording CM simultaneously during Auditory Brainstem Response (ABR) threshold testing in children. **Methods:** This is a retrospective study that included 33 cases comprised of children with autism spectral disorders (ASD), children with cochlear sensorineural hearing loss (SNHL), children with auditory neuropathy spectrum disorder (ANSD) and 41 normal hearing healthy children as controls. The children's ages ranged from 0.5 to 96 months. Both the CM and ABR waves were simultaneously recorded using alternating split polarity ABR. **Results:** CM amplitudes and thresholds in normal hearing children with ASD did not significantly differ from normal hearing healthy children. CM were preserved in children with ANSD despite the absence of distortion product OAE responses, but in a significantly lower amplitude than those with DPOAE. There was no statistically significant correlation between the children's ages and CM amplitude at any intensity level and in any of the different child groups, except in the controls where there was a statistically significant negative correlation between the children's ages and CM amplitude at 70dBnHL, while there was a statistically significant positive correlation between the children's ages and CM threshold. There were no differences in the CM amplitude between the two ears at any intensity level in all of the different groups of children. **Conclusion:** Children with ASD showed comparable outer hair cell function to normal hearing healthy children, reflecting absence of any peripheral hyperacusis due to loudness recruitment. CM should always be searched for when testing young children when there is absence of ABR response with absence or presence of otoacoustic emissions, to avoid any false negative results for ANSD. CM can be preserved in children with SNHL with loudness recruitment. This finding could be confused with ANSD, so CM should be traced down to its threshold for an appropriate diagnosis.

**Keywords:** Auditory Brainstem Response; Autism Spectral Disorders; Auditory Neuropathy Spectral Disorder; Cochlear Microphonics; Sensorineural Hearing Loss.

### *Dept. of Emergency Medicine*

## M-144. Left Ventricular Scar Impact on Left Ventricular Synchronization Parameters and Outcomes of Cardiac Resynchronization Therapy

Walid Ahmed, Wael Samy, Osama Tayeh and Noha Behairy

*International Journal of Cardiology,222:665-670(2016)IF:4.638*

**Background** Left ventricular scar, including global scar and lateral wall, plays an important role in predicting response to cardiac resynchronization therapy (CRT). **Materials and methods** Thirty patients underwent CRT implantation. Assessment of left ventricular (LV) dyssynchrony was done through Gated SPECT LV phase analysis. Pre-implantation cardiac magnetic resonance (CMR) with late gadolinium enhancement technique to examine LV scar burden. Echocardiographic examination of LV end-systolic volume (LVES) prior to CRT and 6 months later. **Results** Thirty patients received CRT (mean age 58.7±9.0, 24 males). Reverse LV remodeling (decline ≥15% from baseline VES) was documented in 19 patients. Temporal changes in LV dyssynchrony parameters were correlated to LV reverse remodeling. Applying ROC for predicting CRT non-response showed a cutoff 36.5% of global LV scar burden had a sensitivity of 81.8% and specificity of 68.4%. A cutoff for lateral wall scar burden 40.5% of whole lateral wall had a sensitivity of 72.7% and specificity of 68.4%. **Conclusion** Reverse LV remodeling is associated with temporal improvements in LV dyssynchrony parameters. LV scar had an unfavorable impact on CRT response. Both global and lateral wall scar burden could predict CRT nonresponse status.

**Keywords:** Cardiac Resynchronization Therapy; Phase Analysis Gated Spect; Left Ventricular Dyssynchrony; Cardiac Magnetic Resonance; Left Ventricular Scar; Lateral Wall Pacing

### *Dept. of Endemic*

## M-145. Diagnostic Accuracy of the Γ-Glutamyl Transpeptidase to Platelet Ratio to Predict Liver Fibrosis in Egyptian Patients with Hcv Genotype 4

Yusuke Shimakawa, Philippe Bonnard, Mohamed El Kassas, Mohamed Abdel-Hamid,Gamal Esmat and Arnaud Fontanet

*Gut, 65: 1577-1578 (2016) IF: 14.921*

Given the high disease burden with viral hepatitis, and the advent of highly effective direct-acting antivirals against HCV infection, the WHO is now developing a global strategy to eliminate viral hepatitis by 2030.1 Increasing the uptake of HCV diagnosis and treatment will become a key intervention in achieving this goal. Although antiviral drugs should be considered for all persons with chronic HCV infection, those with significant liver fibrosis, and especially cirrhosis, should be prioritised for treatment, as they are at increased risk of hepatic complications. Current WHO guidelines for HCV recommend

aspartate aminotransferase (AST)-to-platelet ratio index (APRI) or Fib-4 for the fibrosis assessment in low/middle-income countries (LMIC), because of their low cost and wide availability.2 Recently, Lemoine et al 3 developed a novel simple index called γ-glutamyl transpeptidase (GGT) to platelet
**Keywords:** Hcv; Predictive

## M-146. Excess Mortality Rate Associated with Hepatitis C Virus Infection: A Community-Based Cohort Study in Rural Egypt.

Aya Mostafa, Yusuke Shimakawa, Ahmed Medhat, Nabiel N. Mikhail, Cédric B. Chesnais, Naglaa Arafa, Iman Bakr, Mostafa El Hoseiny, Mai El-Daly, Gamal Esmat, Mohamed Abdel-Hamid, Mostafa K. Mohamed and Arnaud Fontanet

*Journal of Hepatology, 64 (2016) IF: 10.59*

>80% of people chronically infected with hepatitis C virus (HCV) live in resource-limited countries, yet the excess mortality associated with HCV infection in these settings is poorly documented. **Methods:** Individuals were recruited from three villages in rural Egypt in 1997-2003 and their vital status was determined in 2008-2009. Mortality rates across the cohorts were compared according to HCV status: chronic HCV infection (anti-HCV antibody positive and HCV RNA positive), cleared HCV infection (anti-HCV antibody positive and HCV RNA negative) and never infected (anti-HCV antibody negative). Data related to cause of death was collected from a death registry in one village. **Results:** Among 18,111 survey participants enrolled in 1997-2003, 9.1% had chronic HCV infection, 5.5% had cleared HCV infection, and 85.4% had never been infected. After a mean time to follow-up of 8.6years, vital status was obtained for 16,282 (89.9%) participants. When compared to those who had never been infected with HCV in the same age groups, mortality rate ratios (MRR) of males with chronic HCV infection aged <35, 35-44, and 45-54years were 2.35 (95% CI 1.00-5.49), 2.87 (1.46-5.63), and 2.22 (1.29-3.81), respectively. No difference in mortality rate was seen in older males or in females. The all-cause mortality rate attributable to chronic HCV infection was 5.7% (95% CI: 1.0-10.1%), while liver-related mortality was 45.5% (11.3-66.4%). **Conclusions:** Use of a highly potent new antiviral agent to treat all villagers with positive HCV RNA may reduce all-cause mortality rate by up to 5% and hepatic mortality by up to 40% in rural Egypt.
**Keywords:** Africa; Cohort Studies; Egypt; Hepatitis C; Mortality

## M-147. Associations of Human Leucocyte Antigen Class Ii-Dqb1 Alleles with Hepatitis C Virus Infection in Egyptian Population: A Multicentre Family-Based Study

M. El-Bendary, M. Neamatallah, G. Esmat, E. Kamel, H. Elalfy, H. Elalfy, T. Besheer, D. Eldeib, A.-H. Eladl, M. El-Setouhy, A.-H. El-Gilany and A. El-Waseef

*Journal of Viral Hepatitis, 23: 961-970 (2016) IF: 4.179*

Hepatitis C infection is a global pandemic. HLA-DQB1 alleles are believed to have an effective role in immune response against HCV including susceptibility to or protection from this infection. The aim of this study was to investigate the contribution of HLA-DQB1 alleles in the outcome of HCV genotype-4 infection through a family-based association study. Egyptian families with HCV (324) were recruited for this study (324 index positive for RNA-HCV, 225 positive relatives representing chronic hepatitis C cases and 582 family members negative for HCV-RNA [control], 63 of whom spontaneously cleared the virus. All subjects were genotyped for HLA-DQB1 alleles by sequence-specific primers (SSP-PCR) and sequence-based typing (SBT) methods. The frequency of DQB1*02:01:01 carriage was significantly higher in infected patients when compared to controls and those who spontaneously cleared virus (OR=5.47, P<.0001 and OR= 6.5234, P<.0001, respectively), and the carriage of the DQB1*03:01:01:01 allele was significantly higher in those who cleared and controls when compared to the infected patients (OR=0.2889, P<.0001 and OR=0.3016, P<.0001, respectively). On the other hand, the frequency of DQB1*06:01:01 and QB1*05:01:01:01 alleles was not associated with infection (comparison of infected and cleared patients showed OR of 2.1598 [P<.01]), but it becomes nonsignificant after adjustments with the Bonferroni formula (PC >0.05) and OR= 1.3523, P>.05, respectively. This study shows that clearance of HCV is associated with DQB1*03:01:01:01 allele and chronicity of HCV infection associated with the risk allele: DQB1*02:01:01.
**Keywords:** HCV; HLA; DNA Sequencing; Dqb1; Allele; Gene Polymorphism; High Resolution; Intrafamilial; Persistence; Viral Clearance

## M-148. Therapeutic Outcome of 6198 Interferon-Naïve Egyptian Patients with Chronic Hepatitis C: A Real-Life Experience and Lessons to be Learned in Daas' Era

Zayed, Gamal Eldeen, Elmakhzangy, Seif, El-Akel, Awad, Esmat G and Mabrouk.

*Journal of Viral Hepatitis, 23(7): 506-511 (2016) IF: 4.179*

Antiviral therapy for HCV infection has been validated in randomized controlled clinical trials, but its value in the real world is less well studied. There is relatively little data on real-world responses to interferon-based therapies for patients with genotype 4 infection. We aimed to examine experience with large-scale access to antiviral therapy in chronic HCV in a real-life clinical setting in Egypt. Detailed pretreatment data of 6198 IFN-naïve chronic HCV patients who had received PEG-IFN/RBV therapy at Cairo-Fatemic Hospital, Egypt, between 2009 and 2012 were obtained from the HCV database. At week 12, 95.7% of patients had undetectable HCV RNA, and by week 24 and 48, breakthrough was 6% and 4%, respectively. However, 43.7% of patients discontinued treatment prematurely, and intent to treat end of treatment response was 44.6% (79.3% per protocol). Sustai-ned response data were available from only 1281 patients and was 84.9%. Haematological abnormalities were comparable in patients who did or did not comply with therapy. This is the first real-world, large-scale experience of antiviral therapy in chronic HCV in Egypt. Suboptimal response in HCV predominantly genotype 4 was mainly driven by noncompliance as well as gaps in the healthcare system leading to treatment discontinuation. These results need to be considered in the era of all oral antiviral regimes.
**Keywords:** Egypt; Hcv; Real Experience; Treatment

## 149. An Endoscopic Strategy Combining Mega Stents and Over-the-Scope Clips for the Management of Post-Bariatric Surgery Leaks and Fistulas (with Video).

Hany M. Shehab, Sherif M. Hakky and Khaled A. Gawdat

*Obesity Surgery, 26 (2016) IF: 3.346*

**Background and Aims** Endoscopic stenting has proved effective in the management of post-surgical leaks but is strongly hampered by the high rate of stent migration. In this study, we evaluate our experience with a new approach involving the use of novel ultra-large expandable stents tailored for bariatric surgery leaks (Mega stents), combined with the use of the innovative over-the-scope clips (OTSC). **Methods** Retrospective analysis of patients with post-bariatric surgery leaks managed at our institution by an approach combining Mega stents and over-the-scope clips. **Results** Twenty-two patients were treated for post-bariatric surgery leaks; 13 (59 %) had a sleeve gastrectomy while nine (41 %) had a RYGB. A total of 30 stents were inserted. Successful endoscopic insertionand removal were achieved in all patients. OTSC clips were applied in 12 patients (55 %); five simultaneously with stents and seven after stent removal. Primary closure (after one endoscopic procedure) was achieved in 13 patients (59 %) and in a total of 18 patients after multiple endoscopic procedures (82 %). An average of 1.4 stents and 2.8 endoscopic procedures were required per patient. Stent migration occurred in four patients (18 %), and all were retrievable endoscopically. Other complications included retrosternal pain and vomiting in 20 patients (91 %) including one necessitating early removal, bleeding in two patients (9 %), and perforation and esophageal stricture in one patient each (5 %). Two mortalities were encountered, and one of them was stent-related (bleeding). **Conclusion** Mega stents are effective in the management of post-bariatric surgery leaks. The combined use of Mega stents and OTSC clips is associated with a low incidence of migration and a low number of stents and procedures required per patient.

**Keywords:** Sleeve Gastrectomy; Gastric Bypass; Fistula; Leak; Stent; Esophageal Stent; Oesophageal Stent; Clips; Over-The-Scope Clips; Surgical Obesity Complications; Gastric Leak

## M-150.Circulating Serum Mirnas as Diagnostic Markers for Colorectal Cancer.

Abdel-Rahamn Zekri, Amira S Youssef, Mai Lotfy and Abeer A Bahnassy

*Plos One, 11: 1-14 (2016) IF: 3.057*

**Aim** The study was designed to assess the possibility of using circulating miRNAs (serum miRNAs) as diagnostic biomarkers in colorectal cancer (CRC) and to identify their possibility as candidates for targeted therapy. **Methods** The study involved two sample sets: 1- a training set which included 90 patients with colorectal related disease (30 with CRC, 18 with inflammatory bowel disease (IBD), 18 with colonic polyps (CP) and 24 with different colonic symptoms but without any colonoscopic abnormality who were enrolled as control group) and 2- a validation set which included 100 CRC patients. Serum miRNAs were extracted from all subjects to assess the expression profiles for the following miRNAs (miR-17, miR-18a, miR-19a, miR-19b, miR-20a, miR-21, miR-146a, miR-223, miR-24, miR-454, miR-183, miR-135a, miR- 135b and miR-92a) using the custom miScript miRNA PCR-based sybergreen array. The area under the receiver operating characteristic curve (AUC) was used to evaluate the diagnostic performance of the studied miRNAs for colorectal cancer diagnosis. **Results** Data analysis of miRNA from the training set showed that; compared to control group, only miR-19b was significantly up-regulated in patients with IBD group (fold change = 5.24, p = 0.016), whereas in patients with colonic polyps, miR-18a was significantly up-regulated (fold change = 3.49, p-value = 0.018). On the other hand, miR-17, miR-19a, miR-20a and miR-223 were significantly up-regulated (fold change = 2.35, 3.07, 2.38 and 10.35; respectively and p-value = 0.02, 0.015, 0.017 and 0.016; respectively in CRC patients. However,the validation set showed that only miR-223 was significantly up-regulated in CRC patients (fold change = 4.06, p-value = 0.04). **Conclusion** Aberrant miRNA expressions are highly involved in the cascade of colorectal carcinogenesis. We have found that (miR-17, miR-19a, miR-20a and miR-223) could be used as diagnostic biomarkers for CRC. On the other hand, miR-19b and miR-18a could be used as diagnostic biomarkers for CP and IBD respectively.

**Keywords:** Circulating Mirnas, Colorectal Cancer, Inflammatory Bowel Disease, Colonic Polyps Diagnostic Biomarkers

## M-151. Transcriptional Dysregulation of Upstream Signaling of Ifn Pathway in Chronic Hcv Type 4 Induced Liver Fibrosis

Marwa K. Ibrahim ,Ghada Maher Salum, Noha G. Bader El Din, Reham M. Dawood Ahmed Barakat, Ahmed Khairy and Mostafa K. El Awady

*Plos One, (2016) IF: 3.057*

IFN orchestrates the expression of various genes to halt hepatitis C virus (HCV) replication with the possibility of either reduced or increased liver fibrosis; due to controlled viral replication or overproduction of inflammatory mediators, repectively. In this study, we examined the transcriptional profiling of type I IFN related genes in HCV-chronically infected patients with varying degrees of liver fibrosis. PCR array was used to examine the expression of 84 type I IFN related genes in peripheral blood mononuclear cells (PBMCs) RNA from 12 treatment-naïve chronic HCV patients (5 F0-F1 and 7 F2-F4) and 5 healthy subjects. We further validated our results by quantitative real time PCR (qRT-PCR) in 103 treatment-naïve chronic HCV patients (43 F0-F1 and 60 F2-F4) and 15 controls. PCR array data revealed dysregulation in TLR7 pathway. The expression of TLR7 was decreased by 4 folds and MyD88 was increased by 3 folds in PBMCs of F2-F4 patients when compared to the healthy volunteers (p = 0.03 and 0.002, respectively). In addition, IRF7 and TLR7 showed dramatic downregulation (6 and 8 folds, respectively) in F2-F4 patients when compared to F0-F1 ones. qRT-PCR confirmed the altered expression patterns of TLR7 and MyD88 in F2-F4 patients when compared to either controls or F0-F1 patients. However, by qRT-PCR, IRF7 and NF-?B1 (TLR7 pathway transcription factors) exhibited similar mRNA abundance among F2-F4 and F0-F1 patients. These results suggest that TLR7 and MyD88 are possible candidates as biomarkers for the progression of HCV-induced liver fibrosis and/ or targets for therapeutic intervention.

**Keywords:** Hcv; Genotype 4; Fibrosis; Ifn

## M-152. Safety of Direct Antiviral Agents in the Management of Hepatitis C

Mohamed El Kassas, Tamer Elbaz, Enas Hafez and Gamal Esmat

*Expert Opinion on Drug Safety, 15: 1643-1652 (2016) IF: 2.896*

**Introduction:** Hepatitis C virus is a hepatotropic virus that generally leads to chronic hepatitis and various harmful sequelae. The lone standard of treatment has been pegylated interferon and ribavirin, which produces a modest response and many side effects. However, a new era of management was declared with the introduction of various directly acting antiviral agents. **Areas covered:** Recent direct antiviral agents (DAAs) primarily target the non-structural proteins of the virus and affect its replication. These agents successfully achieve a sustained virologic response. However, some serious side effects were reported, which may or may not be drug-related effects. Important drug-drug interactions were also reported. The treating physician should be reasonably familiar with these effects. We review the safety profile of these agents in the management of HCV**. Expert opinion:** Cautious concomitant drug intake is necessary for the new HCV therapies. Future HCV management will depend on interferon-free and likely ribavirin-free regimens. The co-administration of direct antiviral agents of different classes increases the probability of side effects and drug-drug interactions.

**Keywords:** Direct Antiviral Agents; Drug Interactions Hepatitis C (Hcv); Safety; Side Effects.

## M-153. Tumor Necrosis Factor-? -G308a Polymorphism is Associated with Liver Pathological Changes in Hepatitis C Virus Patients

Noha G Bader El Din, Sally Farouk, Reem El-Shenawy, Marwa K Ibrahim, Reham M Dawood, Mostafa M Elhady, Ahmed M Salem, Naglaa Zayed, Ahmed Khairy and Mostafa K El awady

*World J Gastroenterology, (2016) IF: 2.787*

**AIM:** To investigate the association of tumor necrosis factor alpha (TNF?) -G308A polymorphism with different liver pathological changes in treatment-naïve Egyptian patients infected with hepatitis C virus (HCV) genotype 4. **Methods:**This study included 180 subjects, composed of 120 treatment-naïve chronic HCV patients with different fibrosis grades (F0-F4) and 60 healthy controls. The TNF? -G308A region was amplified by PCR and the different genotypes were detected by restriction fragment length polymorphism analysis. The TNF? protein was detected by enzyme-linked immunosorbent assay. The influence of different TNF? -G308A genotypes on TNF? expression and liver disease progression were statistically analyzed. The OR and 95%CI were calculated to assess the relative risk confidence. **Results:** Current data showed that the TNF? -G308A SNP frequency was significantly different between controls and HCV infected patients (P = 0.001). Both the AA genotype and A allele were significantly higher in late fibrosis patients (F2-F4, n = 60) than in early fibrosis patients (F0-F1, n = 60) (P = 0.05, 0.04 respectively). Moreover, the GA or AA genotypes increased the TNF? serum level greater than the GG genotype (P = 0.002). The results showed a clear association between severe liver pathological conditions (inflammation, steatosis and fibrosis) and (GA + AA) genotypes (P = 0.035, 0.03, 0.04 respectively). The stepwise logistic regression analysis showed that the TNF? genotypes (GA + AA) were significantly associated with liver inflammation (OR = 3.776, 95%CI: 1.399-10.194, P = 0.009), severe steatosis (OR = 4.49, 95%CI: 1.441-14.0, P = 0.010) and fibrosis progression (OR = 2.84, 95%CI: 1.080-7.472, P = 0.034). Also, the A allele was an independent risk factor for liver inflammation (P = 0.003), steatosis (P = 0.003) and fibrosis (P = 0.014). **Conclusion:** TNF? SNP at nucleotide -308 represents an important genetic marker that can be used for the prognosis of different liver pathological changes in HCV infected patients.

**Keywords:** Cytokine Expression; Hepatitis C Virus Immune Response; Liver Disease Progression; Single Nucleotide Polymorphisms; Tumor Necrosis Factor Alpha

## M-154. Simple Predictive Model for Identifying Patients with Chronic Hepatitis C and Hepatitis C Virus Genotype 4 Infection with a High Probability of Sustained Virologic Response with Peginterferon Alfa-2A/Ribavirin: Pooled Analysis of Data from Two Large, International Cohort Studies.

Tarik Asselah, Gamal Esmat, Faisal M S and Imam Waked

*Advances in Therapy, 10: 1797-1813 (2016) IF: 2.503*

**Introduction:** Wherever access to direct-acting antiviral agents is restricted, dual peginterferon/ribavirin (PegIFN/RBV) therapy remains an option for treatment of hepatitis C virus (HCV) genotype 4 (GT4) infection, which predominates in the Middle East and Sub-Saharan Africa. Our goal was to develop a baseline scoring system to identify GT4-infected patients with a low or high probability of achieving a sustained virologic response (SVR) with PegIFN alfa-2a/RBV using data from two large cohort studies. **Methods:** Associations between baseline characteristics and SVR were explored by generalized additive models and multiple logistic regression analysis to develop a predictive model, which was then checked by bootstrapping. The score comprised four factors with points assigned thus: age ≤40, 3 points; >40 but ≤55, 2 points; alanine aminotransferase ≤1 or >3× the upper limit of normal, 1 point; no cirrhosis, 1 point; HCV RNA <50,000 IU/mL, 2 points; 50,000 to <400,000 IU/mL, 1 point. The values for a given patient are summed to produce a score from 0 to 7 where higher scores indicate higher chances of SVR. **Results:**Among the 459 patients, 28 (6%), 50 (11%), 92 (20%), 121 (26%), 103 (22%), and 65 (14%) patients had scores of 0-1, 2, 3, 4, 5, and 6-7, respectively, with respective SVR rates of 11%, 28%, 50%, 57%, 63%, and 83%. Relapse rates decreased with increasing prediction score (80%, 39%, 15%, 19%, 5%, and 7%, respectively). SVR rates were consistently higher in Caucasian than Black patients and in patients with a rapid virologic response HCV RNA <50 IU/mL at week 4); however, the trend toward higher SVR rates with increasing score remained apparent in each subgroup. **Conclusion:** In conclusion, a simple scoring system can be used to identify GT4-infected patients with a high probability of achieving an SVR with PegIFN alfa-2a/RBV.

**Keywords:** Access To Treatment; Genotype 4; Hcv; Hepatology; Infectious Diseases; Peginterferon Alfa; Predictors; Ribavirin; Sustained Virologic Response.

## M-155. Elbasvir and Grazoprevir for Chronic Hepatitis C Genotypes 1 and 4.

Al-Salama ZT and Deeks ED

*Expert Review of Clinical Pharmacology, 9: 1413-1421 (2016) IF: 2.488*

**Introduction:** During the last few years, treatment of hepatitis C virus (HCV) revolutionized with the appearance of direct antiviral agents especially for patients with HCV genotypes 1 and 4 infections. Elbasvir (NS5A inhibitor) and grazoprevir (NS3/4A protease inhibitor) are newly developed drugs that are presented in fixed dose combination tablets. **AreasCovered:** This review covers the mechanism of action, pharmacokinetic and pharmacodynamics properties, clinical uses, safety and efficacy of elbasvir/grazoprevir in managing a wide variety of easy and difficult to treat populations (such as presence of cirrhosis, treatment experienced, co-infection with HIV and patients with inherited blood disorders). Expert commentary: Elbasvir/grazoprevir combination showed great efficacy with high rates of sustained virological response rates in genotypes 1 and 4 HCV infection. In addition, it retained a good safety profile and is generally well tolerated

**Keywords:** Hcv; Elbasvir and Grazoprevir; Genotype 1; Genotype 4

## M-156. Contradicting Roles of Mir-182 in Both Nk Cells and Their Host Target Hepatocytes in Hcv

Shereen A. El Sobky, Nada M. El-Ekiaby, Radwa Y.Mekky. Noha M. Elemam, Mohammad A. Mohey Eldin, Mohammed El-sayed and Gamal Esmat.

*Immunology Letters, 169: 52-60 (2016) IF: 2.483*

**Background and Aim:**Natural killer cells are part of the innate immunity involved in viral eradication and were shown to be greatly affected by HCV infection. Epigenetic regulation of NK cell function by microRNAs was not efficiently studied before and was never studied in HCV infection; therefore the aim of this study was to assess for the first time the role of microRNAs in regulating the function of NK cells of HCV-infected patients and hence viral replication in the target HCV-infected Huh7 cells. **Methodology:** NK cells were isolated from PBMCs of HCV-infected patients as well as controls, and HCV-infected liver biopsies as well as Huh7 cells infected with the virus were used. For the infection of Huh7 cells, first viral vector was in-vitro transcribed into viral RNA that was then used to infect naïve Huh7 cells. Supernatant from the infected cells was then collected and used for further infection. For manipulation of NK cells or Huh7 cells, miR-182 mimics and inhibitors were transfected via lipofection method. RNA was extracted from each cell population, reverse transcribed. Gene expression as well as viral load was quantified using qPCR. **Results:**Screening of NKG2A and NKG2D between patients and controls showed no difference in expression of NKG2A, while NKG2D was found to be downregulated. In view of that, bioinformatics analysis was performed and showed that miR-182 has potential binding sites on both the inhibitory receptor NKG2A and the activating receptor NKG2D, and on its ligand ULBP2, as well as on the viral genome itself. In NK cells of HCV-infected patients, miR-182 was found to be over-expressed compared to controls; its ectopic expression was found to decrease NKG2D mRNA level, while miR-182 inhibitors were able to decrease NKG2A mRNA compared to untransfected cells. In addition, co-culturing genotype 4 or 2 HCV-infected Huh7 cells with miR-182 mimicked NK cells of HCV-infected patients showed decreased viral replication, suggesting an enhanced NK cell function. On the other hand, miR-182 and ULBP2 were both found to be downregulated in HCV liver tissues and HCV-infected Huh7 cells compared to their controls. miR-182 mimics were found to decrease ULBP2 mRNA and increase viral replication in genotypes 4 and 2 HCV-infected target (Huh7) cells compared to controls, while miR-182 inhibitor decreased viral replication in the cell models. **Conclusion:** miR-182 was never investigated before, neither in HCV infection nor in NK cells, and we found it to have dysregulated expression in both liver tissues and NK cells of HCV-infected patients compared to control. In addition to that, miR-182 was found to have a contradicting effect in both effector cell and its HCV-infected target cell regarding HCV replication.

**Keywords:** HCV; NKG2A; NKG2D; Natural Killer Cells; ULBP2; miR-182

## M-157. Thyroid Dysfunction in Chronic Hepatitis C Patients Treated with the Combined Pegylated Interferon-Ribavirin Therapy

Iman Hamza, Yara Eid, Mohammad El-Sayed, Raghda Marzaban and Shaimaa Abdul-Kareem

*Journal of Interferon and Cytokine Research, 36: 527-533 (2016) IF: 2.135*

Hepatitis C virus (HCV) is an Egyptian serious national health problem. The combination of pegylated interferon (PEG-IFN) with ribavirin (RIB) was considered the established therapy for chronic hepatitis C (CHC), and it was associated with several adverse effects, including thyroid dysfunction (TD). The aim of this work was to study TD in CHC patients receiving PEG-IFN+ RIB therapy. This retrospective study included 100 adult patients attending the outpatient clinics at AL-Kahera Al-Fatemya hospital and were eligible candidates for PEG-IFN+ RIB therapy. Thyroid hormonal profile (thyroid-stimulating hormone, free triiodothyronine, and free thyroxine) was done before initiation of treatment (week 0) and at weeks 12, 24, 48, and 72. The incidence of TD was more evident by the end of treatment (week 48); it was found to be 35%, mostly in the form of hypothyroidism, while the least incidence was detected by week 12 (2%), all in the form of hyperthyroidism. Generally, hypothyroidism was higher than hyperthyroidism in multiple folds. Thyroid profile was not significantly related to viral load

**Keywords:** Thyroid Dysfunction - HCV - Pegylated Interferon-Ribavirin Therapy.

## M-158. Predictors of Virological Response in 3,235 Chronic Hcv Egyptian Patients Treated with Peginterferon Alpha-2A Compared with Peginterferon Alpha-2B Using Statistical Methods and Data Mining Techniques

Maissa El Raziky, Waleed Fouad Fathalah, Zeinab Zakaria, Hadeel Gamal Eldeen, Amr Abul-Fotouh, Ahmed Salama, Abubakr Awad, Gamal Esmat and Mahasen Mabrouk

*Journal of Interferon and Cytokine Research, 36: 338-346 (2016) IF: 2.135*

Despite the appearance of new oral antiviral drugs, pegylated interferon (PEG-IFN)/RBV may remain the standard of care therapy for some time, and several viral and host factors are reported to be correlated with therapeutic effects. This study aimed to reveal the independent variables associated with failure of sustained virological response (SVR) to PEG-IFN alpha-2a versus PEG-IFN alpha-2b in treatment of naive chronic hepatitis C virus (HCV) Egyptian patients using both statistical methods and data mining techniques. This retrospective cohort study included 3,235 chronic hepatitis C patients enrolled in a large Egyptian medical center: 1,728 patients had been treated with PEG-IFN alpha-2a plus ribavirin (RBV) and 1,507 patients with PEG-IFN alpha-2b plus RBV between 2007 and 2011. Both multivariate analysis and Reduced Error Pruning Tree (REPTree)-based model were used to reveal the independent variables associated with treatment response. In both treatment types, alpha-fetoprotein (AFP) >10 ng/mL and HCV viremia >600 × 10(3) IU/mL were the independent baseline variables associated with failure of SVR, while male gender, decreased hemoglobin, and thyroid-stimulating hormone were the independent variables associated with good response ($P < 0.05$). Using REPTree-based model showed that low AFP was the factor of initial split (best predictor) of response for either PEG-IFN alpha-2a or PEG-IFN alpha-2b (cutoff value 8.53, 4.89 ng/mL, AUROC = 0.68 and 0.61, $P = 0.05$). Serum AFP >10 ng/mL and viral load >600 × 10(3) IU/mL are variables associated with failure of response in both treatment types. REPTree-based model could be used to assess predictors of response.

**Keywords:** Predictors; PEG-IFN Alpha-2B; PEG-IFN Alpha-2A; Data Mining.

## M-159. Three Gene Signature for Predicting the Development of Hepatocellular Carcinoma in Chronically Infected Hepatitis C Virus Patients.

Marwa K Ibrahim, Hosny Salama, Mohamad Abd El Rahman, Reham M Dawood, Noha G Bader El Din, Heba F Salem, Mohamed E A Abdelrahim, Dalia Omran, Moataza H Omran, Khaled Helmi El-Wakeel, Tawfeek H Abdelhafez, Ahmed Khedr and Mostafa K El Awady

*Journal of Interferon and Cytokine Research, 36: 698-705 (2016) IF: 2.135*

Hepatitis C virus (HCV) is the leading cause of liver fibrosis and hepatocellular carcinoma (HCC). At present, there is no predictive biomarker for the patients at high risk of developing HCC. In this study, we examined the association between single-nucleotide polymorphisms (SNPs) in 3 innate immunity genes [2'-5'oligoadenylate synthetase 1 (OAS1) rs10774671, interleukin 28B (IL28B) rs12979860, and low molecular mass polypeptide 7 (LMP-7) at codon 49] besides cytomegalovirus (CMV) coinfection and susceptibility to HCC in genotype 4 (GT4) chronically infected Egyptian patients. SNPs were determined using restriction fragment length polymorphism analysis in DNA from HCC patients ($n = 34$) and compared with either controls ($n = 70$) or patients with early grades of liver fibrosis ($n = 49$). Our results demonstrated that patients bearing the genetic combination consisting of LMP-7 CA/AA [OR 4.75, 95% confidence interval (CI) 1.443-15.631, $P = 0.007$] and IL28B rs12979860 CT/TT (OR 6.00, 95% CI 1.603-22.455, $P = 0.004$) and positive for CMV viremia (OR 3.11, 95% CI 1.151-8.412, $P = 0.02$) were more likely to have HCC. However, OAS1 rs10774671 does not seem to contribute to the development of HCC. Binary regression analysis indicated that HCC risk significantly increases with the presence of each unfavorable genotype (LMP-7 CA/AA, IL28B rs12979860 CT/TT), when accompanied by the existence of CMV coinfection (probability of HCC risk is 0.8 for combined factors versus 0.14, 0.07, and 0.07 for individual factor IL28B, LMP-7, and CMV; respectively). These data suggest that the 2 SNPs and the coinfection in concert have potential in predicting the risk of HCC development in patients infected with HCV GT4.

**Keywords:** Hcc; Hcv; Il28b; Lmp7; Oas1; Liver Fibrosis.

## M-160. Enhancing NK Cell Cytotoxicity by Mir-182 in Hepatocellular Carcinoma.

Mohamed M. Abdelrahman, Injie O. Fawzy, Aya A. Bassiouni Asmaa I. Gomaa, Gamal Esmat, Imam Waked and Ahmed I. Abdelaziz

*667-673 (2016) IF: 2.127*

**Background and Aim:** NK-cells are the principle defense line against different malignancies. Their activation status is determined by the balance between activating and inhibitory receptors such as NKG2D and NKG2A, respectively. MicroRNAs are crucial post-transcriptional regulators of gene expression, playing key roles in modulating NK-cell development and function. The aim of this study is to investigate the role of miRNAs in regulating the activation and cytotoxic function of NK-cells in HCC. **Methods:** In silico analysis was performed to predict a potential miRNA that might target NKG2D and NKG2A mRNAs. NK-cells were isolated from HCC patients and healthy controls, after which miRNA and mRNA were quantified. Manipulating miRNA expression was performed followed by investigating downstream targets and the cytotoxic activity of NK-cells against Huh-7 cell lines. **Results:** NK-cells of HCC patients showed miR-182 overexpression compared to controls. NKG2D and NKG2A were upregulated and downregulated, respectively, in HCC NK-cells. Upon forcing miR-182 expression in the HCC NK-cells, upregulation of both receptors was observed. Finally, miR-182 was reported to induce NK-cell cytotoxicity represented in Perforin-1 upregulation and increase in cytolytic killing of co-cultured Huh-7 cells. **Conclusion:** Our findings suggest that miR-182 may augment NK-cell cytotoxicity against liver cancer via modulating NKG2D and NKG2A expressions.

**Keywords:** HCC; miR-182; Micrornas; NKG2A; NKG2D; Natural Killer Cells

## M-161. Abrogating the Interplay Between Igf2bp1, 2and 3 and Igf1r by Let-7I Arrests Hepatocellular Carcinoma Growth.

Fawzy IO, Hamza MT, Hosny KA, Esmat G and Abdelaziz AI.

*Growth Factors, 34: 42-50 (2016) IF: 2.043*

IGF2BP 1, 2 and 3 control the fate of many transcripts. Immunoprecipitation studies demonstrated the IGF2BPs to bind to IGF1R mRNA, and our laboratory has recently shown them to post-transcriptionally regulate IGF1R. This study sought to identify a microRNA regulating the IGF2BPs and consequently IGF1R. All three IGF2BPs were among the top-ranked predicted targets of let-7i. Let-7i was downregulated in HCC tissues, and transfection of HuH-7 with let-7i inhibited malignant cell behaviors and decreased IGF2BPs transcripts. Direct binding of let-7i to IGF2BP2 and IGF2BP3 3'UTRs was confirmed, and the effect of let-7i caused a decrease in the IGF2BPs' target gene, the IGF1R. IGF1R mRNA was inversely correlated with let-7i in HCC tissues and was reduced upon let-7i transfection into HuH-7. Reporter assays validated IGF1R as a target of let-7i. Therefore, let-7i may control HCC tumorigenesis by regulating IGF1R directly and indirectly by interrupting the interplay between IGF1R and the IGF2BPs.

**Keywords:** Insulin-Like Growth Factor 1 Receptor; Hepatocellular Carcinoma; Insulin-Like Growth Factor-2-Mrna-Binding Protein; Let-7I; Microrna; Post-Transcriptional Regulation

## M-162. Seroprevalence of Hcv Among Cairo University Students in Egypt

Gamal Esmat, Maissa El Raziky, Mohammed M. Nabeel, Rabab Maher and Zeinab Zakaria

*Journal of Medical Virology, 88: 1384-1387 (2016) IF: 1.998*

**Background and study aim:** Egypt has the highest prevalence of hepatitis C virus (HCV) worldwide. This study aimed to determine the seroprevalence of hepatitis C virus among Cairo University students. **Results:** Overall prevalence rate of antibody to HCV (anti-HCV) was 4.6%.It showed that the prevalence was relatively higher among females(86/1660,5,2%)while males (51/1340,3,8%)with no significant difference .PCR for HCV RNA was detected in 31.4%of the anti-HCV positive subjects.which showed statistical significant difference between males (29/51)and females (14/86)at P=0.001. **Conclusions:** despite the prevalence rate reported in the present study was similar to anti HCV prevalence among persons in the same age group,confirmed the presence of HCV infection among the students of Cairo University.

**Keywords:** Hepatitis C Virus (HCV)- Anti-HCV- Prevalence-Polymerase Chain Reaction (PCR)

## M-163. Influence of Delta Virus Infection on the Virologic Status in Egyptian Patients with Chronic Hepatitisb Virus Genotype D

Rabab Fouad, Mahmoud Abdo, Hadeel Gamal Eldeen, Dina Sabry, Mira Atef, Rasha Ahmed and Naglaa Zayed

*Journal of Medical Virology, 88: 837-842 (2016) IF: 1.998*

Hepatitis delta virus (HDV) usually have an unfavorable clinical outcome in chronic hepatitis B virus (HBV) patients. In Egypt, data about epidemiology, the spectrum of disease, and impact of HDV on HBV infection are rare. To assess the prevalence, clinical and virological characteristics of HDV infection among Egyptian patients with chronic HBV. Adult patients with Hepatitis B surface antigen (HBsAg)-positive were evaluated for the presence of HDV using anti HDV-IgG and HDV RNA by RT-PCR. Routine laboratory investigations, genotypes and subtypes for both HBV and HDV, abdominal sonography, and transient elastography (TE) were done. Liver biopsy was performed only in whenever indicated. One hundred and twenty-one treatment-naïve chronic HBV patients were included. Wild HBV genotype-D2 was found in 98.2% and 81.9% were HBeAg negative. Prevalence of HDV was 8.3% by anti-HDV IgG and 9.9% by RT-PCR. Wild HDV genotype-IIb was reported in 83.3%. HDV infection was more common in males, 90.9% of delta patients were HBeAg negative. Compared to the mono-infected HBV, concomitant HBV/HDV infection was not associated with more derangment in ALT nor advanced stage of fibrosis. 66.7% of HDV patients had significantly lower HBV-DNA level compared to the non-delta patients ($P < 0.001$). HDV is not uncommon in Egypt. HBV genotype-D was associated with HDV genotype-IIb. Delta infection was associated with negative HBeAg status, reduction of HBV replication, but neither influenced the clinical course nor increased significant liver damage risk.

**Keywords:** Egypt; HBV; HDV; Genotype

## M-164. Accurate Prediction of Advanced Liver Fibrosis Using the Decision Tree Learning Algorithm in Chronic Hepatitis C Egyptian Patients

Somaya Hashem, Gamal Esmat, Wafaa Elakel, Shahira Habashy, Safaa Abdel Raouf, Samar Darweesh, Mohamad Soliman, Mohamed Elhefnawi, Mohamed El-Adawy and Mahmoud ElHefnawi

*Gastroenterology Research and Practice, 1-7 (2016) IF: 1.742*

**Background/Aim**. Respectively with the prevalence of chronic hepatitis C in the world, using noninvasive methods as an alternative method in staging chronic liver diseases for avoiding the drawbacks of biopsy is significantly increasing. The aim of this study is to combine the serum biomarkers and clinical information to develop a classification model that can predict advanced liver fibrosis. **Methods.** 39,567 patients with chronic hepatitis C were included and randomly divided into two separate sets. Liver fibrosis was assessed via METAVIR score; patients were categorized as mild to moderate (F0–F2) or advanced (F3-F4) fibrosis stages. Two models were developed using alternating decision tree algorithm. Model 1 uses six parameters, while model 2 uses four, which are similar to FIB-4 features except alpha-fetoprotein instead of alanine aminotransferase. Sensitivity and receiver operating characteristic curve were performed to evaluate the performance of the proposed models. **Results.** The best model achieved 86.2% negative predictive value and 0.78 ROC with 84.8% accuracy which is better than FIB-4. **Conclusions.** The risk of advanced liver fibrosis, due to chronic hepatitis C, could be predicted with high accuracy using decision tree learning algorithm that could be used to reduce the need to assess the liver biopsy.

**Keywords:** Liver Fibrosis; Serum Biomarkers; Decision Tree Learning Algorithm; Chronic Hepatitis C.

## M-165. MicroRNA-486-5P Enhances Hepatocellular Carcinoma Tumor Suppression Through Repression of IGF-1Rand its Downstream mTOR, STAT3andC-Myc

Rana Ahmed Youness, Hend Mohamed El-Tayebi, Reem Amr Assal, Karim Hosny, Gamal Esmat and Ahmed Ihab Abdelaziz

*Oncology Letters, 12: 2567-2573 (2016) IF: 1.482*

The insulin-like growth factor (IGF)-axis has been paradigmatically involved in hepatocellular carcinoma (HCC) tumor initiation, progression and drug resistance. Consequently, members of the IGF-axis and most importantly, IGF-1 receptor (IGF-1R) have been considered as intriguing targets for HCC therapy. Few miRNAs have been recently reported to be associated with IGF-1R regulation. The present study aimed to investigate the role of microRNA (miRNA/miR)-486-5p in the regulation of IGF-1R and its downstream signaling cascades. miR-486-5p was markedly downregulated in hepatitis C virus-induced HCC tissues and Huh-7 cells. Forcing the expression of miR-486-5p in Huh-7 cells resulted in the repression of IGF-1R, mammalian target of rapamycin (mTOR), signal transducer and activator of transcription 3 (STAT3) and c-Myc mRNA levels. Ectopic expression of miR-486-5p in Huh-7 cells markedly repressed cellular viability, proliferation, migration and clonogenicity in a similar pattern to IGF-1R small interfering RNAs, and were evaluated using 3-(4,5-dimethylthiazol-2-yl)-2,5-diphenyltetrazolium bromide, BrdU incorporation, wound healing and colony forming assays, respectively. Overall, the study findings demonstrated that miR-486-5p acts as a tumor suppressor in HCC through the repression of essential members of the IGF-axis, including IGF-1R and its downstream mediators mTOR, STAT3 and c-Myc.

**Keywords:** HCC; IGF-1R; Stat3; C-Myc; Mtor; Microrna-486-5P.

## M-166. Mutations Affecting Domain V of the 23S Rrna Gene in Helicobacter Pylori from Cairo, Egypt

Ghaith D, Elzahry M, Mostafa G, Mostafa S, Elsherif R and Ramzy I.

*Journal of Chemotherapy, 28 (2016) IF: 1.333*

**Background:** Clarithromycin is a main component of the recommended first-line triple therapy for Helicobacter pylori in Egypt. We aimed in our study to investigate the prevalence of clarithromycin-resistant H. pylori strains due to the point mutations at domain V of the H. pylori 23S rRNA among the Egyptian population using the polymerase chain reaction/restricted fragment length polymorphism (PCR/RFLP) assay. **Methods:** Gastric biopsies obtained from 100 dyspeptic patients who consecutively attended at Cairo University Hospital during the period from January to November 2013 were subjected to PCR/RFLP in order to detect the point mutations at domain V of the H. pylori 23S rRNA associated with clarithromycin resistance. The PCR amplicon of the 23S H. pylori rRNA is restricted with MboII for detection of A2142G mutation and with BsaI for A2143G mutation. **Results:** The prevalence of H. pylori infection among 100 patients was 70%; clarithromycin resistance was detected in 39/70 (57.7%) of positive H. pylori isolates. Occurrence of 23S rRNA A2142G mutations resulted in two DNA fragments (418 and 350 bp) by PCR-RFLP; on the other hand, no A2143G mutations were detected. **Conclusions:**The high prevalence of clarithromycin resistance (57.7%) caused by A2142G mutations at domain V of the H. pylori 23S rRNA may mandate changing of the standard clarithromycin-containing triple therapy. The PCR/RFLP assay was a rapid and accurate method for molecular detection of H. pylori infection in addition to determination of different nucleotide mutations causing clarithromycin resistance.

**Keywords:** 23S Rrna; Clarithromycin Resistance; Helicobacter Pylori; Rflp-Pcr

## M-167. Low Molecular Mass Polypeptide 7 Single Nucleotide Polymorphism is Associated with the Progression of Liver Fibrosis in Patients Infected with Hepatitis C Virus Genotype 4

Mostafa K. El Awady, Moataza H. Omran, Marwa K. Ibrahim, Amr M. Moustafa, Reham M. Dawood, Noha G. Bader El Din, Aisha Elsharkawy, Mohamad S. Abdel Aziz, Reem El Shenawy, Yasmine S. El Abd and Ashraf O. Abdel Aziz

*Clinical Laboratory, 62: 381-387 (2016) IF: 0.936*

**Background:** The hepatitis C virus (HCV) is a leading cause of liver disease and the consequent complications of cirrhosis. However, there is no precise biomarker to predict the patients at high risk of developing progressive disease. We showed previously the implication of low molecular mass polypeptide-7 (LMP-7) single nucleotide variations in the response to combined pegylated IFN and ribavirin therapy in patients infected with HCV genotype 4. In this study, we examined the possible relationship between LMP-7 genotypes and both the degree of liver fibrosis and the transition from end stage of fibrosis to hepatocellular carcinoma (HCC). **Methods:** LMP-7 single nucleotide variation at codon 49 (substitution from A to C) was determined using restriction fragment length polymorphism analysis in leucocyte DNA from healthy subjects (n = 36) and HCV-chronically infected patients of genotype 4 either with different grades of liver fibrosis (n = 77) or with hepatocellular carcinoma (n = 25). Chronic HCV-infected patients having liver fibrosis were categorized into two groups based on the degree of fibrosis, early fibrosis (F0 - F2, n = 37) and late fibrosis (F3 - F4, n = 40). **Results:** Our results demonstrated that patients with the LMP-7 CA/AA genotypes were more likely to have advanced fibrosis scores than those bearing the CC genotype, although LMP-7 polymorphism does not seem to contribute to the progression from the late stage of fibrosis to hepatocellular carcinoma. **Conclusions:** These results suggest that LMP-7 polymorphism is a candidate prognostic marker in mathematical models designed for predicting the progression of HCV-related liver disease. Nevertheless, the mechanism whereby LMP-7 leads to the progression of liver fibrosis remains to be determined.

**Keywords:** Lmp-7, Snp Analysis, Liver Fibrosis, Hcv, Hcc, Cirrhosis, Chronic Viral Infection.

## M-168. Fibroscan, APRI, FIB4,and GUCI: Role in Prediction of Fibrosisand Response to Therapy in Egyptian Patients with HCV Infection

Ayman Yosry, Rabab Fouad, Shereen A. Alem, Aisha Elsharkawy, Mohammad El-Sayed, Noha Asem, Ehsan Hassan, Ahmed Ismail and Gamal Esmat

*Arab Journal of Gastroenterology, 17(2):78-83 (2016) IF: 0.644*

**Background and study aims** Multiple noninvasive methods have been used successfully in the prediction of fibrosis. However, their role in the prediction of response to hepatitis C virus (HCV) antiviral therapy is debatable. The aim of this study was to validate and compare the diagnostic performance of FibroScan, APRI (aspartate aminotransferase (AST)-to-platelet ratio index), FIB4, and GUCI (Göteborg University Cirrhosis Index) for the prediction of hepatic fibrosis and treatment outcome in HCV-infected patients receiving pegylated interferon and ribavirin (PEG-IFN/ribavirin). **Patients and methods** This study included 182 Egyptian patients with chronic HCV infection. They were classified into two groups based on the stages of fibrosis: mild to significant fibrosis (F1–F2) and advanced fibrosis (F3–F4). The APRI, FIB4, and GUCI scores were calculated before the antiviral treatment. The FibroScan was performed for all patients before treatment. **Results** Stiffness and FIB4 have greater sensitivity and specificity in detecting advanced fibrosis of 80%, 77% and 88%, 84%, respectively. Based on multivariate regression analysis, FIB4, body mass index (BMI), and alpha-fetoprotein (AFP) level were found to be statistically significant predictors of advanced fibrosis (p-value: 0.000, 0.011, and 0.001, respectively) with odds ratio (OR: 3.184, 1.170, and 1.241, respectively). With respect to virological response, the stiffness, APRI, FIB4, and GUCI were significantly lower in sustained virological responders. However, these are not good predictors of response to PEG-IFN/ribavirin therapy. AFP was the only statistically significant predictor of response ($p = 0.002$) with OR of 1.141 in multivariate regression analysis. **Conclusion** FibroScan and noninvasive scores such as APRI, FIB4, and GUCI can be used as good predictors of liver fibrosis in chronic hepatitis C. However, they are not good predictors of response to PEG-IFN/ribavirin therapy.

**Keywords:** Chronic Hepatitis C Virus; Fibroscan; Aspartate Aminotransferase-To-Platelet Ratio Index; FIB4; Göteborg University Cirrhosis Index

## M-169. Aggressive Treatment of Performance Status 1and 2 Hcc Patients Significantly Improves Survival - an Egyptian Retrospective Cohort Study of 524 Cases.

Aziz Ao, Omran D, Nabeel Mm, Elbaz Tm, Abdelmaksoud Ah, Attar Ie and Shousha Hi

*Asian Pacific Journal of Cancer Prevention, 17: 2539-2543 (2016)*

**Background:** In the Barcelona Clinic Liver Cancer (BCLC) system, only sorafenib is suggested for HCC patients having performance status (PS) 1 or 2 even if they have treatable lesions. In the current study, we aimed to explore the outcome of using aggressive treatment for HCC patients with PS 1 and 2. **Materials and Methods**: Five hundred and twenty four patients with HCC were enrolled in this study and divided into 2 groups: 404 PS 1 and 120 PS 2. of the included 524 patients, 136 recceived non-aggressive supportive treatment and sorafenib, while 388 patients were offered aggressive treatment in the form of surgical resection, transplantation, percutaneous ablation, trans-arterial chemoembolization and/or chemoperfusion. All the patients were followed up for a period of 2 years to determine their survival. **Results:** Most HCC patients were CHILD A and B grades (89.4% versus 85.0%, for PS1 and PS2, respectively). Patients with PS1 were significantly younger. Out of the enrolled 524 patients, 388 were offered aggressive treatment, 253 (65.2%) having their lesions fully ablated, 94 (24.2%) undergoing partial ablation and 41 patients with no ablation (10.6%). The median survival of the patients with PS 1 who were offered aggressive treatment was 20 months versus 9 months only for those who were offered supportive treatment and sorafenib (<0.001). Regarding HCC patients with PS 2, the median survivals were similarly 19.7 months versus 8.7 months only (<0.001). Conclusions: Aggressive treatment of HCC patients with PS 1 and 2 significantly improves their survival. Revising the BCLC guidelines regarding such patients is recommended.

**Keywords:** Hcc; Performance Status; Aggressive Treatment; Outcome; Prognosis.

## M-170. Real-Time Elastography as a Noninvasive Assessment of Liver Fibrosis in Chronic Hepatitis C Egyptian Patients: A Prospective Study

Lamiaa Mobarak, Mohammed M. Nabeel, Ehsan Hassan, Dalia Omran and Zeinab Zakaria

*Annals of Gastroenterology, 29: 358-362 (2016)*

**Background** Hepatitis C virus is a worldwide problem. Noninvasive methods for liver fibrosis assessment as ultrasound-based approaches have emerged to replace liver biopsy. The aim of this study was to evaluate the diagnostic accuracy of real-time elastography (RTE) in the assessment of liver fibrosis in patients with chronic hepatitis C (CHC), compared with transient elastography and liver biopsy. **Methods** RTE, FibroScan and liver biopsy were performed in 50 CHC patients. In addition, aspartate aminotransferase to platelet ratio index (APRI) and routine laboratory values were included in the analysis. **Results** RTE was able to diagnose significant hepatic fibrosis ($F \geq 2$) according to METAVIR scoring system at cut-off value of 2.49 with sensitivity 100%, specificity 66%, and area under the receiver-operating characteristics (AUROC) 0.8. FibroScan was able to predict significant fibrosis at cut-off value 7.5 KPa with sensitivity 88%, specificity 100%, and AUROC 0.94.APRI was able to predict significant hepatic fibrosis ($F \geq 2$) with sensitivity 54%, specificity 80%, and AUROC 0.69. There was a significant positive correlation between the FibroScan score and RTE score ($r=0.6$, $P=0.001$). **Conclusions** Although FibroScan is superior in determining significant hepatic fibrosis, our data suggest that RTE may be a useful and promising noninvasive method for liver fibrosis assessment in CHC patients especially in cases with technical limitations for FibroScan.

**Keywords:** Hepatitis C Virus, Liver Fibrosis, Real-Time Elastography, Transient Elastography, Liver Biopsy, Aspartate Aminotransferase To Platelet Ratio Index

## M-171. RegulatoryandActivated Effector T Cells in Chronic Hepatitis C Virus: Relation to Autoimmunity

Hanan Fouad, Maissa El Said El Raziky, Eman Medhat Hassan, Ghada Mahmoud Abdel Aziz, Samar K Darweesh and Ahmed Reda Sayed

*World Journal of Hepatology, 8 (2016)*

**AIM** To investigate how Tregs are regulated in chronic hepatitis C virus (HCV) patients via assessment of Tregs markers (granzyme 2, CD69 and FoxP3), Teffs markers [TNFRSF4 (OX40), INFG] and CD4 , CD25 genes. **Methods** A prospective study was conducted on 120 subjects divided into 4 groups: Group Ⅰ (n = 30) treatment naïve chronic HCV patients; Group Ⅱ (n = 30) chronic HCV treated with Peg/Riba; Group Ⅲ (n = 30) chronic HCV associated with non-organ specific autoantibody and Group Ⅵ (n = 30) healthy persons as a control group. Tregs and Teffs markers were assessed in peripheral blood mononuclear cells by quantitative real time reverse transcriptase-polymerase chain reaction. **Results** Chronic HCV patients exhibited significant higher levels of both Teffs and Tregs in comparison to healthy control group. Tregs markers were significantly decreased in Peg/Riba treated HCV patients in comparison to treatment naïve HCV group. In HCV patients with antinuclearantibody (ANA) + ve, Tregs markers were significantly decreased in comparison to all other studied groups. Teffs markers were significantly elevated in all HCV groups in comparison to control and in HCV group with ANA + ve in comparison to treatment naïve HCV group. **Conclusion** Elevated Tregs cells in chronic HCV patients dampen both CD4+ and CD8+ autologous T cell immune response. Interferon-α and ribavirin therapy suppress proliferation of Tregs. More significant suppression of Tregs was observed in HCV patients with autoantibodies favoring pathological autoimmune response.

**Keywords:** Autoimmunity; T Regulatory Cells; Hepatitis C Virus; T Activator Cells; Interferon

## M-172. Interplay Between Microrna-17-5P, Insulin-Like Growth Factor-Ii Through Binding Protein-3 in Hepatocellular Carcinoma

Danira Ashraf Habashy, Hend Mohamed El Tayebi, Injie Omar Fawzy, Karim Adel Hosny, Gamal Esmat and Ahmed Ihab Abdelaziz

*World Journal of Hepatology, 8: 976-984 (2016)*

**AIM:** To investigate the effect of microRNA on insulin-like growth factor binding protein-3 (IGFBP-3) and hence on insulin-like growth factor-II (IGF-II) bioavailability in hepatocellular carcinoma (HCC). **Methods:** Bioinformatic analysis was performed using microrna.org, DIANA lab and Segal lab softwares. Total RNA was extracted from 23 HCC and 10 healthy liver tissues using mirVana miRNA Isolation Kit. microRNA-17-5p (miR-17-5p) expression was mimicked and antagonized in HuH-7 cell lines using HiPerFect Transfection Reagent, then total RNA was extracted using Biozol reagent then reverse transcribed into cDNA followed by quantification of miR-17-5p and IGFBP-3 expression using TaqMan real-time quantitative PCR. Luciferase reporter assay was performed to validate the binding of miR-17-5p to the 3'UTR of IGFBP-3. Free IGF-II protein was measured in transfected HuH-7 cells using IGF-II ELISA kit. **Results:** Bioinformatic analysis revealed IGFBP-3 as a potential target for miR-17-5p. Screening of miR-17-5p and IGFBP-3 revealed a moderate negative correlation in HCC patients, where miR-17-5p was extensively underexpressed in HCC tissues (P = 0.0012), while IGFBP-3 showed significant upregulation in the same set of patients (P = 0.0041) compared to healthy donors. Forcing miR-17-5p expression in HuH-7 cell lines showed a significant downregulation of IGFBP-3 mRNA expression (P = 0.0267) and a significant increase in free IGF-II protein (P = 0.0339) compared to mock untransfected cells using unpaired t-test. Luciferase assay validated IGFBP-3 as a direct target of miR-17-5p; luciferase activity was inhibited by 27.5% in cells co-transfected with miR-17-5p mimics and the construct harboring the wild-type binding region 2 of IGFBP-3 compared to cells transfected with this construct alone (P = 0.0474). **Conclusion:** These data suggest that regulating IGF-II bioavailability and hence HCC progression can be achieved through targeting IGFBP-3 via manipulating the expression of miRNAs.

**Keywords:** Hepatocellular Carcinoma; Insulin-Like Growth Factor Binding Protein-3; Insulin-Like Growth Factor Signaling Pathway; Insulin-Like Growth Factor-II; Microrna

## M-173. Serum Mirna Panel in Egyptian Patients with Chronic Hepatitis C Related Hepatocellular Carcinoma

Ahmed Khairy, Iman Hamza, Olfat Shaker and Ayman Yosry

*Asian Pacific Journal of Cancer Prevention, 17: 2699-2703 (2016)*

**Background:**Primary hepatocellular carcinoma (HCC) is one of the most common malignancies worldwide. MicroRNAs (miRNAs) have great HCC diagnostic potential and circulating miRNAs have been reported as promising biomarkers for various pathologic conditions. AIM: To explore the potential benefit of serum miR-126, miR-129, miR-155, miR-203 and miR-223 as non-invasive diagnostic markers of hepatitis C virus (HCV)-related HCC. **Materials and Methods:**The expression of miRNA was evaluated using real-time quantitative RT-PCR in 78 serum samples (30 treatment-naive chronic HCV, 25 post-HCV compensated cirrhosis and 23 treatment- naive HCC cases). **Results:**Comparing miRNA fold changes in the HCC group vs the non HCC groups, there was significant fold decrease in miR-126 (P= 0.034), miR-129 (P= 0.006), miR-155 (P= 0.011), miR-203 (<0.001) and miR-223 (P= 0.013). The highest AUC to differentiate HCC patients from non-HCC was 0.76 for miR-203. **Conclusions:**Among studied miRNAs, serum miR-203 has the highest potential as a non-invasive biomarker of HCC.

**Keywords:** Hcc Diagnosis; Chronic Hcv Infection; Serum Mirnas; Egypt.

## M-174. Noninvasive Assessment of Liver Fibrosis in Egyptian Children with Chronic Liver Diseases.

Tawhida Abdel Ghaffar, Azza Youssef, Khalid Zalata, Aisha ElSharkawy, Mohamed Mowafy, Abdel Aziz Abdel Wanis and Gamal Esmat

*Current Pediatric Research, 20: 57-63 (2016)*

**Aim:** to evaluate Liver stiffness measurement LSM and aspartate transaminase to platelet ratio APRI score as non invasive means of fibrosis assessment in children with chronic liver disease. **Methods:** Liver biopsy was done for 42 children (20 boys and 22girls with mean age of 11.5 ± 3.9 years) suffering from various chronic liver diseases. The stage of fibrosis was assessed according to METAVIR system. APRI score was calculated for 42 of the children and LSM by transient elastography was performed to each of the children as well as to 18 healthy age and sex matched controls. The correlation between METAVIR fibrosis stage and each of the APRI score and LSM was studied. Cutoff points for differentiation of no or mild fibrosis from significant fibrosis in the group as a whole was calculated for APRI and LSM using ROC curves. **Results:** fifteen children had no or mild fibrosis (=F2 METAVIR) (G 2). The mean APRI score of the patients was 0.71 +/- 0.48. It was significantly higher in G2 vs G1 patients (0.71 vs 0.3) and showed significant correlation with METAVIR staging (r= +0.53, P<0.001). At a cut off of 0.58 it had 63%, 73%, 70.4%, 66.7% sensitivity, specificity, PPV and NPV respectively for significant fibrosis. LSM was significantly higher in patients vs controls (38.8 vs 11.1 kPas and P<0.000) and in G2 vs G1 (15.4 vs 6.9 KPas and P<0.000). It showed significant positive correlation with both METAVIR staging and APRI score (r=0.58, 0.69 respectivelyand P<0.001). A cut off of 8.1KPas had a 78%, 73%, 77.8% and 73.3% sensitivity, specificity, PPV and NPV respectively for significant fibrosis. **Conclusion:** In children, APRI score and LSM perform reasonably well in fibrosis assessment. Diseases with different etiologies have different cutoff values for significant fibrosis.

**Keywords:** Liver Stiffness Measurement, Fibroscan, Apri Score, Liver Fibrosis, Children

***Dept. of Forensic and Toxicology***

## M-175. Padova Charter on Personal InjuryandDamage Under Civil-Tort Law : Medico-Legal Guidelines on Methods of AscertainmentandCriteria of Evaluation.

Santo Davide Ferrara, Eric Baccino, Rafael Boscolo-Berto, Giovanni Comandè, Ranieri Domenici, Claudio Hernandez-Cueto, Mete Korkut Gulmen, George Mendelson, Massimo Montisci, Gian Aristide Norelli, Vilma Pinchi, Mohammed Ranavaya, Dina A. Shokry, Vera Sterzik, Yvo Vermylen, Duarte Nuno Vieira, Guido Viel and Riccardo Zoja .

*International Journal of Legal Medicine, 130(1): 1-12 (2016) IF: 2.862*

Compensation for personal damage, defined as any pecuniary or non-pecuniary loss causally related to a personal injury under civil-tort law, is strictly based on the local jurisdiction and therefore varies significantly across the world. This manuscript presents the first "International Guidelines on Medico-Legal Methods of Ascertainment and Criteria of Evaluation of Personal Injury and Damage under Civil-Tort Law". This consensus document, which includes a step-by-step illustrated explanation of flow charts articulated in eight sequential steps and a comprehensive description of the ascertainment methodology and the criteria of evaluation, has been developed by an International Working Group composed of juridical and medico-legal experts and adopted as Guidelines by the International Academy of Legal Medicine (IALM).

**Keywords:** Civil Law; Ialm; Law of Delict; Methods of Ascertainment; Non-Pecuniary Loss; Pecuniary Loss; Personal Damage; Personal Injury; Tort Law.

## M- 176. The Role of PON1andCYP2D6 Genes in Susceptibility to Organophosphorus Chronic Intoxication in Egyptian Patients

Amr Mohamed Tawfik Khattab, Abeer Ahmed Zayed, Asmaa Ismail Ahmed, Aly Gamaleldin Abdelaal and Alaa AbdelHamid Mekdad

*Neurotoxicology, 53: 102-107 (2016) IF: 2.738*

**Background** Paraoxonase-1 (PON1) activity toward organophosphorus(OP) compounds shows inter-individual variations, rendering the identification of individuals' PON1 allozymes valuable in treating patients suffering from organophosphorus intoxication. One of the most important cytochrome P450 monooxygenases (CYPs) is CYP2D6. The CYP2D6 G1934A polymorphism leads to good, poor or no enzyme activity. Genetic testing helps identification of high risk individuals as well as management of chronic intoxicated patients. Objective to investigate a possible association between genetic polymorphisms of PON1 Q192R, and CYP2D6 G1934A as well as PON1 and pseudo-cholinesterase (PChE) enzyme activity levels and chronic organophosphate exposed patients, and hence, susceptibility for organophosphorus chronic poisoning. **Design and methods** Thirty chronic organophosphate exposed farm workers were compared to 29 healthy controls as regards PON1 Q192R and CYP2D6 G1934A polymorphisms using PCR-RFLP technique. Also serum PON1 and PChE activities were determined spectrophotometrically. **Results** Serum PChE was significantly reduced in chronic intoxicated patients compared to the control group (p = 0.02), while PON1 activity was increased, but just failed to reach significance (p = 0.06). PON1 192 RR genotype and R allele were significantly increased in chronic OP intoxicated patients (p = 0.005 & p = 0.002 respectively). CYP2D6 1934 A allele was significantly increased in chronic OP patients (p = 0.045). combining the two SNPs showed a significant statistical difference between the two groups with PON1QQ and CYP2D6 GG genotypes being more represented in the healthy controls (p = 0.001). Fatigue and motor weakness were the most prevalent neurological symptoms seen in chronic cases (56.7%), followed by headache and lacrimation (30% each), depression (23%), tingling and sensory symptoms (20%), sleep disorders and limb pain (13%). The mean duration of environmental exposure to organophosphates was 7.7 ± 5.2 years and no association was found between chronic symptoms of intoxication and duration of exposure, provided that all workers were exposed for at least 3 years. **Conclusion** PON1 192RR genotype and CYP2D6 1934 A allele were found to be related to the susceptibility to organophosphate chronic toxicity in Egyptians. Larger scale gene-environmental interaction studies are recommended to confirm results and Genotyping is recommended during selection of agricultural pesticide workers to exclude high risk group.

**Keywords:** PON-1; CYP2D6; Organophosphates; Chronic Intoxication

## M-177. Synthesis of High-Quality Graphene Oxide from Spent Mobile Phone Batteries

Sayed M. Badawy

*Environmental Progress and Sustainable Energy, 35: 1485-1491 (2016) IF: 1.631*

Synthesis of high-quality graphene oxide from waste graphite recovered from spent mobile phone batteries was investigated. Graphite powders were easily removed from the anodic copper foil of lithium ion batteries opposed to being sent to landfills. Graphene oxide (GO) was prepared by leaching and oxidation of the graphite with a mixture of potassium permanganate and concentrated sulfuric acid. The structure of GO has been studied using Infrared spectroscopy (FT-IR), X-ray diffraction (XRD), scanning electron microscopy (SEM) and Transmission electron microscopy (TEM). FT-IR spectra of GO indicate the existence of –OH, ketone and -O- groups. Crystalline monolayer and multilayer nano-sized structures of exfoliated graphene oxide sample exhibiting atomically smooth edges were observed by SEM and TEM

**Keywords:** Graphene Oxide, Graphite, Spent Mobile Batteries

## M-178. Age Estimation in Living Egyptians Using Signal Joint T-Cell Receptor Excision Circle Rearrangement

Samah F. Ibrahim, Iman F. Gaballah and Laila A. Rashed.

*Journal of Forensic Sciences, 4: 1-5 (2016) IF: 1.322*

Age estimation is one of the challenges in forensic sciences. There are many techniques to estimate the age. Molecular biology approach is one of these techniques. Signal joint T-cell receptor excision circles gene (sjTRECs), is one of this approach. We aimed to use sjTRECs as a suitable marker for age estimation among Egyptian population. TaqMan qPCR approach was used to quantify sjTREC levels in blood samples obtained from 153 healthy Egyptian individuals ranging from a few weeks to 70 years. Our results showed a significant negative correlation between sjTREC levels and age with $p \leq 0.05$. Moreover, the individual's age can be determined through this formula Age = 30.671+ (5.998Y) (Y is dCtTBP sjTREC) with standard error 7.35 years. Within the forensic context, sjTREC' levels can be used to estimate the Egyptian individual's age accurately.

**Keywords:** Forensic Science, Dna Typing, Signal Joint T-Cell Receptor Excision Circles, Egyptian, Age Estimation, Polymerase Chain

## M-179. Application of Acacia Modestaand Dalbergia Sissoo Gums as Green Matrix for Silver Nanoparticle Binding

Hira Munir, Muhammad Shahid, Fozia Anjum, Muhammad Nadeem Akhtar, Sayed M. Badawy and Ahmed El-Ghorab

*Green Processing and Synthesis, 5: 101-105 (2016) IF: 1.291*

A low-cost, efficient, and ecofriendly method for the synthesis of silver nanoparticles (AgNPs) using gums as reducing agent was performed. The obtained nanoparticles were characterized by UV-visible spectroscopy. The antibacterial activity of the prepared nanoparticles was tested against Gram-negative and Gram-positive bacteria. The in vitro toxicity was evaluated by performing hemolytic analysis. The mutagenic activity was evaluated using Ames test. The prepared nanoparticles possessed high antibacterial potential and also inhibited the biofilm formation. Under the conditions of this study, it is concluded that the prepared AgNPs were nontoxic and nonmutagenic and possessed pharmaceutical applications.

**Keywords:** Acacia Modesta; Dalbergia Sissoo; Green Matrix; Gums; Silver Nanoparticles.

## M-180. Laboratory Freezing Desalination of Seawater.

Sayed M. Badawy

*Desalination and Water Treatment, 57: 11040-11047 (2016) IF: 1.272*

Freeze desalination of samples of seawater from Umluj beach, Red Sea, in Saudi Arabia, was investigated by laboratory experiments using nondirect freezing. The influence of kinetic parameters including degree of crystallization, freezing–melting cycles, and gradual melting on the total dissolved solids (TDS) and salt rejection was examined. The melted ice water produced by partial crystallization of single-stage freezing has two times less salt concentration than the feed seawater (TDS, 40,916 mg/l). Continuous cycling of the freezing–melting process reduced the dissolved salts to 1.5% with TDS 610 mg/l, in the level of drinking water. The TDS of the melted ice decreased with gradual melting time and reached 693 mg/l after 6 h. The results indicated that the laboratory freezing desalination could decrease sea ice salinity from 4.1 to 0.06% without using chemical additives.

**Keywords:** Seawater; Freezing; Desalination; Salt Rejection; Tds

## M-181. Adsorption of Direct Green 26 Onto Fix 3500 Treated Sawdust: Equilibrium, Kineticand Isotherms

A. Hashem, F. Ahmad and Sayed M. Badawy

*Desalination and Water Treatment, 57: 13334-13346 (2016) IF: 1.272*

Cationized sawdust (CSD) was prepared by the reaction of sawdust (SD) with cationizing agent. Three levels of CSD having different nitrogen content were prepared. The CSD samples were characterized by estimation of nitrogen content. The feasibility of CSD to remove C.I. Direct Green (DG 26) dye from aqueous solutions was examined. The impacts of several operating parameters such as adsorbent dose, adsorption time, and adsorbate concentration on the adsorption capacity were investigated. The CSD was effectively used in adsorption of DG 26 dye from aqueous solutions. In order to determine the best fit isotherm, the experimental equilibrium data were analyzed using eight adsorption isotherm models including Langmuir, Freundlich, Temkin, and Dubinin–Radushkevich (two parameter models), Redlich–Peterson, Toth, Sips and Khan (three parameter models) using non-linear regression technique. Tempkin and Sips isotherms were found to best represent the data for DG 26 dye than other isotherms. The kinetics of adsorption of DG 26 dye have been discussed using six kinetic

models, i.e., the pseudo-first-order model, the pseudo-second-order model, Batacharia–Venkobachar, the Elovich equation, the intraparticle diffusion model, and Bangham equation. The removal of DG 26 dye onto CSD particles could be well described by the pseudo–second-order model. CSD dye was found to be inexpensive and effective adsorbent for removal of DG 26 dye from aqueous solutions.

**Keywords:** Sawdust; Direct Green 26; Adsorption Isotherm; Cationized Sawdust; Wastewater Treatment

***Dept. of Internal Medicine***

## M-182. International Diagnostic Guidelines for Patients with HCV-Related Extrahepatic Manifestations: A Multidisciplinary Expert Statement

Clodoveo Ferri, Manuel Ramos-Casals, Anna Linda Zignego, Luca Arcaini, Dario Roccatello, Alessandro Antonelli, David Saadoun, Anne Claire Desbois, Marco Sebastiani, Milvia Casato, Peter Lamprecht, Alessandra Mangia, Athanasios G Tzioufas, Zobair M Younossi and Patrice Cacoub

*Autoimmunity Reviews, 15(12): 1145-1160 (2016) IF: 8.49*

Hepatitis C virus (HCV) infection is responsible for both hepatic and extra-hepatic disorders (HCV-EHDs); these latter are correlated on one hand clearly with HCV lymphotropism causing immune-system dysregulation as well as with viral oncogenic potential, and on the other hand probably with chronic inflammatory status causing cardio-metabolic complications as well as neurocognitive disturbances. The spectrum of HCV-EHDs ranges from mild or moderate manifestations, such as arthralgia, sicca syndrome, peripheral neuropathy, to severe, life-threatening complications, mainly vasculitis and neoplastic conditions. Given the clinical heterogeneity of HCV-EHDs, HCV-infected individuals are inevitably referred to different specialists according to the presenting/prevalent symptom(s); therefore, the availability of comprehensive diagnostic guidelines is necessary for a patient's whole assessment that is decisive for early diagnosis and correct therapeutic approach of various hepatic and HCV-EHDs, regardless of the specific competencies of different physicians or referral centers. In this respect, a multidisciplinary network of experts, the International Study Group of Extrahepatic Manifestations Related to Hepatitis C Virus Infection (ISG-EHCV), was organized with the intention to formulate diagnostic guidelines for the work-up of possible HCV-EHDs. There was a broad consensus among ISG-EHCV members on the proposed guidelines, which essentially are based on two main levels of patient's assessment. At the referral stage, it is proposed that all patients with HCV infection should be invariably examined by means of first-line diagnostic procedures including virological and hepatic parameter evaluation, as well as the detection of clinical findings that may suggest one or more HCV-EHDs. This preliminary assessment should reveal specific HCV-EHDs, which will be deeper analyzed by means of second-line, targeted investigations. The proposed multidisciplinary expert statement represents the first attempt to draw comprehensive diagnostic guidelines for HCV-infected individuals encompassing the entire spectrum of HCV-related disorders, namely typical hepatic manifestations along with less common, often unpredictable HCV-EHDs. The HCV-EHDs may compromise to a substantial degree the overall disease outcome in a significant number of HCV-infected individuals that renders their timely identification and treatment an imperative. In conclusion, the application of standardized but thorough diagnostic guidelines of HCV-EHDs is advisable at the referral stage as well as during the follow-up period of HCV infected patients. It is envisioned that the proposed strategy will result in improvement of clinical outcomes in such patients.

**Keywords:** Hepatitis C Virus; Hcv; Extrahepatic Disorders; Diagnostic Guidelines; Autoimmunity; Hepatitis; Mixed Cryoglobulinemia; Vasculitis; Lymphoma; Neuropathy; Sicca Syndrome; Sjögren's Syndrome; Arthritis; Diabetes; Thyroid; Porphyria.

## M-183. The Schistosome Glutathione S-Transferase P28gst, A Unique Helminth Protein, Prevents Intestinal Inflammation in Experimental Colitis Through a Th2-Type Response with Mucosal Eosinophils.

V Driss, M El Nady, M Delbeke, C Rousseaux, C Dubuquoy, A Sarazin, S Gatault, A Dendooven, G Riveau, JF Colombel, P Desreumaux and L Dubuquoy M Capron

*Mucosal Immunology, 9: 322-335 (2016) IF: 6.103*

Intestinal helminth parasites are potent inducers of T helper type 2 (Th2) response and have a regulatory role, notably on intestinal inflammation. As infection with schistosomes is unlikely to provide a reliable treatment of inflammatory bowel diseases, we have investigated the beneficial effect of a schistosome enzymatic protein, the 28-kDa glutathione S-transferase (P28GST), on the modulation of disease activity and immune responses in experimental colitis. Our results showed that immunization with recombinant P28GST is at least as efficient as established schistosome infection to reduce colitis lesions and expression of pro-inflammatory cytokines. Considering underlying mechanisms, the decrease of inflammatory parameters was associated with the polarization of the immune system toward a Th2 profile, with local and systemic increases of interleukin (IL)-13 and IL-5. Dense eosinophil infiltration was observed in the colons of P28GST-immunized rats and mice. Depletion of eosinophils by treatment with an anti-Siglec-F monoclonal antibody and use of IL-5-deficient mice led to the loss of therapeutic effect, suggesting the crucial role for eosinophils in colitis prevention by P28GST. These findings reveal that immunization with P28GST, a unique recombinant schistosome enzyme, ameliorates intestinal inflammation through eosinophil-dependent modulation of harmful type 1 responses, representing a new immuno-regulatory strategy against inflammatory bowel diseases.

**Keywords:** Inflammatory bowel diseases ; Helminthic Proteins ; Inflammatory cytokines ; Eosinophils.

## M-184. Comparing Different Calcification Scores to Detect Outcomes in Chronic Kidney Disease Patients with Vascular Calcification

Mohamed M. NasrAllah, Amr Nassef, Tarik H. Elshaboni, Fadia Morise, Noha A. Osman and Usama A. Sharaf El Din

*International Journal of Cardiology,220:884-889(2016)IF:4.638*

**Background** There is no consensus on the most appropriate technique to diagnose vascular calcification in chronic kidney disease. This is primarily because of the absence of direct comparisons of predictive values of the various calcification scores, especially outside the coronary vascular beds, to detect clinical outcomes. **Methods** We included 93 haemodialysis patients and performed 6 vascular calcification scores: two scores utilised simple X-rays of abdominal aorta and peripheral vessels. CT scans of the thoracic, upper abdominal and lower abdominal aorta were performed to calculate the aortic calcification index and CT of the pelvis for calcification of iliac vessels. Patients were followed for 63 months (mean 46.8 months) for first major cardiovascular events and mortality. **Results** Nineteen cardiovascular events and 28 deaths occurred. Calcification was detected more sensitively in central and peripheral beds using CT scans compared to X-rays ($p<0.001$). CT scans detected calcification more frequently in distal than proximal vascular beds ($p<0.001$). Calcification of the pelvic vessels and lower abdominal aorta were most predictive of events including pre-existing cardiovascular disease O.R. 6.5 (95% C.I. 2–22; $p=0.001$) and O.R. 3 (95% C.I. 1.1–9; $p=0.035$); new major cardiovascular events H.R. 4.2 (95% C.I. 1.5–11; $p=0.006$) and H.R. 2 (95% C.I. 0.8–5.3; $p=0.1$) as well as mortality H.R. 2.8 (95% C.I. 1.3–6; $p=0.01$) and H.R. 2.2 (95% C.I. 1.04–5; $p=0.04$) respectively. **Conclusions** CT based techniques are more sensitive than plain X-rays at detecting peripheral and aortic vascular calcifications. Distal CT scans of the aorta and pelvic vessels have the highest predictive value for cardiovascular events and mortality.
**Keywords:** Aortic Calcification, Vascular Calcification, Kidney Disease

## M-185. Correlation Between JAK2 Allele Burden and Pulmonary Arterial Hypertension and Hematological Parameters in Philadelphia Negative JAK2 Positive Myeloproliferative Neoplasms. an Egyptian Experience

Mattar MM, Morad MA, El Husseiny NM, Ali NH and El Demerdash DM

*Ann Hematol, 95(10): 1611-1616 (2016) IF: 3.022*

Myeloproliferative neoplasms are characterized by a common stem cell-derived clonal proliferation, but are phenotypically diverse. JAK2 is mutated (V617F) in more than 90 % of patients with polycythemia vera (PV) and approximately 60 % of patients with essential thrombocythemia (ET) or primary myelofibrosis (PMF). Pulmonary arterial hypertension (PAH) is a major complication of several hematological disorders. Chronic myeloproliferative disorders associated with PAH have been included in group five for which the etiology is unclear and/or multifactorial. Theaimo fthisstudyisto screen Egyptian Philadelphia negative JAK2 positive myeloproliferative neoplasm patients for the presence of PAH and its correlation with JAK2 allele burden. We also made a review for correlation of JAK2 allele with hematological parameters comparing our results to others. We enrolled 60 patients with Philadelphia negative myeloproliferative neoplasms. All patients enrolled in the study were subjected to laboratory and imaging workup in the form of CBC, liver, kidney profile, bone marrow examination, abdominal ultrasonography, and transthoracic echocardiography. Our results revealed that 7 patients out of 60 (11.67 %) had pulmonary arterial hypertension, 3 patients with PMF, 2 patients with PRV, and 2 patients with ET, and its correlation with JAK2 allele burden was not statistically significant. Correlation analysis between JAK2 V617F allele burden and other parameters revealed: statistical significant correlation with age, HB, HCT, PLT, UA, LDH, and splenic diameter but insignificant correlation with WBCs and PAH. Pulmonary arterial hypertension prevalence in our study was 11.67 % and no significant correlation with JAK 2 allele burden. Our study is the largest one up to our knowledge that studies the association between its prevalence and JAK2 burden.
**Keywords:** JAK2 Mutation; Myeloproliferative Neoplasm; Pulmonary Hypertension.

## M-186. Antiviral Treatment Prioritization in HCV-Infected Patients with Extrahepatic Manifestations – an Egyptian Perspective

Hussein El-Fishawy, Gamal Saadia, May Hassaballa, Mohamed Hussein, Wahid Doss, Gaafar Ragab and Rashad Barsoum

*Journal of Advanced Research, 7 (3): 391-402 (2016) IF: 3*

Egypt, the single country with highest incidence of HCV infection in the world, has embarked on a government-sponsored mass treatment program using several combinations of DAAs. Recognizing the importance of extrahepatic manifestations, independently of the hepatic, a subcommittee was assigned to develop national guidelines for respective prioritizing indications and protocols. It evaluated the benefit of treating patients with different extrahepatic manifestations, and reviewed relevant clinical trials and guidelines concerning DAA combinations available in Egypt. The latter included Sofosbuvir plus either peg-interferon, Simeprevir, Ledipasvir or daclatasvir, and the Viekera family comprising paritaprevir/ritonavir + ombitasvir with (GT-1) or without (GT-4) Dasabuvir. Any of these protocols may be used with or without Ribavirin according to indication. A blueprint was subjected to peer debate in dedicated workshops in two national meetings and subsequently to an online professional review, eventually leading to a final report that was adopted by the health authorities. Seven compelling and 10 optional indications were identified for treating patients with predominantly extrahepatic manifestations. The former include kidney disease at different stages, cryoglobulinemic vasculitis and non-Hodgkin lymphoma. Selected treatment protocols, were encoded and their use was prioritized on the basis of evidence of efficacy and safety. We concluded that any of the studied protocols may be used, preferably with ribavirin, for 12-week treatment in all patients with extrahepatic manifestations without cirrhosis and with eGFR above 30 ml/min/1.73 sqm. Ribavirin should be included in protocols for treating patients with compensated cirrhosis. Daclatasvir-based protocols are recommended for decompensated cirrhosis, while the Viekera family is recommended in patients with eGFR < 30 ml/min/1.73 sqm, including those on dialysis. In kidney-transplanted patents, caution is due to avoidance of the pharmacokinetic interaction with the Cytochrome-P450 enzyme system, in-between immunosuppressive agents and most DAAs, particularly the Viekera family.
**Keywords:** DAAs; Cryoglobulinemia; Chronic Kidney Disease; Dialysis; Transplantation.

## M-187. Urinary A1 -Microglobulin and Albumin Excretion in Children and Adolescents with Type 1 Diabetes

Aasem Saif and Neveen Soliman

*Journal of Diabetes, 9: 61-64 (2016) IF: 2.5*

**Background:** We investigated the correlation of urinary alpha 1-microglobulin, as a marker of tubular dysfunction, with albumin excretion in children and adolescents with type 1 diabetes. **Methods:** Ninety two Egyptian patients with type 1 diabetes were included in the study (Mean age was 14.14±5.13 years); all of them had type 1 diabetes for more than 5 years (Mean duration of diabetes was 8.28±2.62 years) and normal renal function. Forty healthy subjects were also included as a control group. All patients had their urinary albumin excretion assessed. Urinary alpha 1-microglobulin of both patients and control groups was measured in the morning urine specimen. **Results:** Analysis of the results showed that patients had significantly higher levels of urinary alpha 1-microglobulin compared with the control group ($p < 0.01$). Among the patients, there was a strong positive correlation between urinary alpha 1-microglobulin and urinary albumin excretion ($p < 0.01$). Positive correlations were also found between urinary alpha 1-microglobulin and diabetes duration ($p < 0.01$), glycated hemoglobin ($p < 0.05$), fasting ($p < 0.05$) and postprandial blood glucose ($p < 0.05$). **Conclusion:** Our study that urinary alpha 1-microglobulin strongly correlates with urinary albumin excretion in children and adolescents with type 1 diabetes. It also demonstrates the importance of tubular dysfunction, as an early and integral component of the diabetic nephropathy syndrome, in those patients. The results of our study emphasize the value of tight glycemic control in slowing the progress of tubular dysfunction, especially in patients with longer diabetes duration.

**Keywords:** Adolescents; Albumin Excretion; Children; Type 1 Diabetes; A1-Microglobulin

## M-188. CD28and PTPN22 are Associated with Susceptibility to Rheumatoid Arthritis in Egyptians

Mohsen M. Hegab, Aml Fawzy Abdelwahab, Ali M. El-Sayed Yousef, Mohamed Nabil Salem, Walaa El-Baz, Sherry Abdelrhman, Fatemah Elshabacy, Abdelazim Alhefny, Wagida Abouraya, Saleh Mohamed Ibrahim and Gaafar Ragab

*Human Immunology, 77: 522-526 (2016) IF: 2.127*

**Objective** Limited data are available on the genetics of rheumatoid arthritis (RA) in Egyptians. Therefore, we investigated whether the confirmed genetic risk factors for RA in Europeans and/or Asians contribute to RA susceptibility in Egyptians. Subjects and methods A set of seven single-nucleotide polymorphisms (SNPs) in the vicinity of CD28, TNFAIP3, PTPN22, PADI4 and HLA-DRA were tested in a large multi-centric RA cohort in Egypt, consisting of 394 cases and 398 matched controls. Patients were stratified based on the positivity of either anti-citrullinated protein antibodies (ACPAs) or rheumatoid factor (RF). **Results** Significant association was evident for three SNPs in this cohort: the CD28 (rs1980422) variant showed a strong association in the whole cohort ($P = 0.000119$) and in seropositive subsets of the disease (PACPA+ = 0.004; PRF+ = 0.0005). Upon stratification, the PTPN22 (rs2476601) and TNFAIP3(rs5029939) variants showed association only with ACPA positive (PACPA+ = 0.00573) and negative (PACPA− = 0.00999) phenotypes, respectively. **Conclusion** Our results suggest that CD28(rs1980422) and PTPN22(rs2476601) contribute to RA-susceptibility in Egyptians. Failure to replicate the association of PADI4(rs2240340)/(PADI4_94) in Egyptian RA patients provides further support for the notion that genetic architecture of RA is different in multiple populations of European, Asian, African, and Middle Eastern ancestries. Further investigation using large-scale studies is thus needed to maximize the power of genetic association.

**Keywords:** Rheumatoid Arthritis; Egyptians; Snps; Acpas; Rf

## M-189. Gastrointestinal Manifestations in Systemic Lupus Erythematosus

M Fawzy, A Edrees, H Okasha, A El Ashmaui and G Ragab

*Lupus, 25(13): 1456-1462 (2016) IF: 2.118*

Systemic lupus erythematosus (SLE) is an autoimmune disorder characterized by multisystem involvement, including the gastrointestinal (GI) tract. There is a significant variation in the clinical presentation and severity of GI disorders. When GI symptoms present as the initial manifestation of SLE, there is likely to be a delay in the diagnosis. The cause of these GI manifestations in SLE may be the disease, or the side effects of medications, or infections. In this study we investigated the GI manifestations in a group of SLE patients. Our study was conducted on 40 SLE patients and 30 healthy controls to assess the prevalence of GI symptoms in SLE patients. The prevalence of gastrointestinal manifestations in our study was 42.5%. GI manifestations in our SLE patients were: acute abdominal pain (due to pleurisy and peritonitis), 6%; diffuse abdominal pain, 23.5%; epigastric pain, 29%; epigastric pain with vomiting, 23.5%; epigastric pain with chronic constipation, 6%; chronic constipation, 6%; and diffuse abdominal pain with bleeding per rectum, 6%. In our study, we found a higher incidence of Giardia infestation in SLE patients than in healthy controls, and 10% of these patients were asymptomatic. There was more Giardia infestation in patients with GI symptoms as compared with patients with no GI symptoms, with a P value of 0.009. In our study SLE patients with GI symptoms had a peak systolic velocity (cm/s) with a mean of $108.4 \pm 32.1$ standard deviation (SD) in the celiac Doppler study. Patients without GI symptoms had a peak systolic velocity with a mean of $111.9 \pm 37.7$ SD, meaning that our patients mostly had no evidence of celiac trunk stenosis, but there was significant difference between SLE patients without GI symptoms and controls, as the mean was higher in SLE patients than in the controls. Also, the celiac end diastolic velocity was higher in both groups of SLE patients with GI symptoms and those without GI symptoms, compared to controls.

**Keywords:** Systemic Lupus Erythematosus; Gastrointestinal Manifestations; Giardiasis.

## M-190. Prognostic Value of the Biomarker Copeptin in Critically Ill Patients with Sepsis

Elham M Sobhy, Mervat M Naguib, Mohamed G Hammad and Laila A Rashed

*Kasr Al Ainy Medical Journal, 22 (3): 123-128 (2016) IF: 2*

**Objective** The aim of this study was to evaluate copeptin as a predictor of short-term ICU mortality in patients with sepsis and its relation with disease severity. Design This study was an observational case–control one. Methods The study included 60 patients admitted to the ICU with sepsis: 20 patients with sepsis, 20 patients with severe sepsis, and 20 patients with septic shock. Baseline characteristics, serum copeptin, and APACHE II score were determined at the time of admission. They were prospectively followed up for 7 days to determine improvement, development of multiple organ failure, or death. Copeptin level in patients with sepsis was compared with its level in the control group comprising 10 patients with congestive heart failure, 10 patients with post-acute myocardial infarction, and 10 healthy individuals. **Results** The mean copeptin level was 48.4 (15.1) pmol/l in patients with sepsis, 69.2 (15.4) pmol/l in severe sepsis, and 120.9 (31.2) pmol/l in septic shock. It was significantly higher than its level in post-acute myocardial infarction [21.1 (8.0) pmol/l], congestive heart failure [20.6 (9.8) pmol/l], and healthy controls [8 (4.3) pmol/l] (P<0.001). Spearman correlation analysis showed a positive correlation between copeptin and total leukocytic count (r=0.466; P<0.001), urea (r=0.496; P<0.001), creatinine (r=0.552; P<0.001), alanine aminotransferase (r=0.451; P<0.001), and APACHII (r=0.661; P<0.001). Improved patients significantly had lower copeptin [43.5 (8.7) pmol/l] than those who died [103.8 (36.2) pmol/l] (P<0.001). Area under the curve of copeptin for predicting mortality was 0.880 (P<0.001). A cutoff value of 58.1 pmol/l had 96.6% sensitivity and 61.3% specificity. **Conclusion** Serum copeptin is a sensitive predictor of mortality in critically ill patients with sepsis. Moreover, it could be a promising biomarker for disease severity and development of multiple organ failure in this group of patients

**Keywords:** Apache Ii Score; Copeptin; Multiple Organ Failure; Mortality, Sepsis.

## M-191. Is Low Cystatin C in Acute Stroke a Blessing or a Curse? A Pilot Study on Egyptian Patients

Elham M Sobhy, Yasser M Abdelhamid, Enas Hamdy and Mona M Adam

*Kasr Al Ainy Medical Journal, 22: 7-11 (2016) IF: 2*

**Introduction** Cerebrovascular stroke is a costly disease. Elevated cystatin C levels were independently associated with both ischemic and hemorrhagic stroke. In contrast, cystatin C has been found to play protective roles in the nervous system. Aim The aim of the present study was to find out the relationship between serum cystatin C level and the outcome of acute cerebrovascular stroke in middle aged and elderly Egyptian patients. Patients and methods This study was conducted on 49 patients with recent stroke and normal kidney functions and 30 healthy matched controls. All patients were followed up for 1 week. Cystatin C was determined for both patients and controls. **Results** Cystatin C level tended to be lower in patients than in controls, both below and above the age of 60. Females tended to have higher levels of cystatin C. There was a gradual decrease in the cystatin C level according to the outcome, being least in the deteriorated group. However, the differences were insignificant. **Conclusion** The results suggest that low cystatin C level - in a patient with normal kidney function - may predict worse prognosis. Accordingly, creatinine estimation is mandatory in assessing the kidney function in these patients and cystatin cannot replace it, as it may represent another risk factor.

**Keywords: Keywords:** Cerebrovascular, Cystatin, Stroke.

## M-192. Thyroid Dysfunction Among Type 2 Diabetic Female Egyptian Subjects

Ibrahim N Elebrashy. Amr El Meligi, Laila Rashed, Randa F Salam, Elham Youssef and Shaimaa A Fathy

*Therapeutic and Clinical Risk Management, 12: 1757-1762 (2016) IF: 1.903*

**Purpose:** High prevalence of thyroid disorders is more common in type 1 diabetes compared to type 2 diabetes, due to associated autoimmunity. Hypothyroidism is the most common disorder. The objective was to assess the prevalence of thyroid dysfunction among type 2 diabetic Egyptian females and to find the correlation between metabolic syndrome components and autoimmune thyroid dysfunction. Materials and methods: The study included 62 type 2 diabetic Egyptian females and 27 sex- and age-matched controls. All patients in the study were subjected to anthropometric measures, including HbA1c, lipid profile, serum uric acid, thyroid-stimulating hormone (TSH), free triiodothyronine, free thyroxine, anti-thyroid peroxidase (TPO), antithyroglobulin (anti-Tg), and thyroid ultrasound. **Results:** Hypothyroidism was found in 45.2% of patients (5.49±3.37 μIU/mL) versus 11.1% of controls (1.79±1.21 μIU/mL) (P,0.001). Anti-TPO was found in 75.8% (347.15±244.87 IU/mL) of patients versus 7.4% (32.89±33.26 IU/mL) of controls (P,0.001). Anti-Tg was found in 61.3% (508.03±369.16 IU/mL) of patients versus 0 (51.26±35.53 IU/mL) controls (P,0.001). A significant positive correlation was found between TSH and antithyroid antibodies (anti-Tg, anti-TPO; P=0.002 and P=0.043, respectively) and between TSH and thyroid-gland volume (P=0.002) in diabetic patients. No correlation was found between any components of metabolic syndrome and thyroid antibodies in diabetic patients. **Conclusion:** Autoimmune thyroid disease is more common in Egyptian women with type 2 diabetes than nondiabetic women, and thus points to a role of autoimmunity in the pathogenesis of type 2 diabetes.

**Keywords:** Autoimmune Thyroid Dysfunction, Tsh, Anti-Tpo, Anti-Tg, T2 Diabetes, Metabolic Syndrome

## M-193. Endothelial Nitric Oxide Synthase Gene Polymorphismsand the Risk of Vasculopathy in Sickle Cell Disease

Sherif M. Yousry, Hend N. Ellithy and Gehan H. Shahin

*Hematologt, 21: 359-367 (2016) IF: 1.385*

**Background:** Sickle cell disease (SCD) is one of the major health problems in many parts of the world. SCD is characterized by multisystem complications with marked variability in its severity between patients, probably linked to nitric oxide (NO). Endothelial nitric oxide synthase (eNOS) enzyme which is responsible for NO synthesis may be implicated in SCD pathophysiology. Aim of the study: To explore the possible association between the eNOS gene polymorphisms and severity of SCD. Furthermore, we examined the genomic diversity of these polymorphisms in SCD patients. **Methods:** We genotyped 100 SCD patients and 80 controls were

genotyped for eNOS 4a/b and eNOS 786T>C polymorphisms, using allele-specific polymerase chain reaction (PCR) and PCR-restriction fragment length polymorphism assay, respectively. Polymorphisms were analyzed in relation to severity of SCD manifestations. **Results:** The homozygous mutant eNOS-786T>T genotype was significantly associated with high risk of acute chest syndrome (ACS). The wild-type eNOS-4a/4b genotype was protective against vaso-occlusive crisis (VOC) and pulmonary hypertension (PHTN). The mutant homozygous haplotype (C –4a) was significantly associated with the risk of ACS, VOC, and PHTN. **Conclusion:** eNOS intron 4 and eNOS T>C gene polymorphisms may be used as a genetic marker of prognostic value in SCD, as they are associated with unfavorable clinical outcomes.

**Keywords:** Sickle Cell Disease, Nitric Oxide Synthase, Gene Polymorphisms, Vasculopathy

## M-194. Leprosy Masquerading as Systemic Rheumatic Diseases

Hala El-Gendy, Rasmia M. El-Gohary, Kyrillus S. Shohdy and Gaafar Ragab

*Jcr-Journal of Clinical Rheumatology, 22: 264-271 (2016) IF: 1.245*

Rheumatologic manifestations not only are encountered in leprosy but also can be the first and even the sole presenting manifestation. The hallmark of leprosy is skin and peripheral nerve affection; however, it can affect a wide range of other organs, with the joints being the commonest. We have searched PubMed with the key words leprosy, arthritis, vasculitis, rheumatic diseases, and autoantibodies in a proper combination. Relevant studies were retrieved from scanning of their abstracts. The relevant references provided in these articles were also selected and reviewed. We summarize the clinical and laboratory manifestations that make leprosy masquerade as a systemic rheumatic disease. Moreover, we report 4 Egyptian patients who presented with rheumatologic manifestations, namely, arthritis and vasculitis that turned out to be leprosy related.

**Keywords:** Leprosy, Rheumatologic Manifestations, Arthritis, Vasculitis, Autoantibodies.

## M-195. Burden of End-Stage Kidney Disease: North Africa

Rashad S Barsoum

*Clinical Nephrology, 86 (S1): 14-17 (2016) IF: 1.065*

Geographical, ecological, and genetic factors result in many similarities among the six main countries of the African Sahara, including the epidemiology of kidney disease. With an average incidence of 182 and prevalence of 522 patients with end-stage kidney disease (ESKD) per million population, North Africa (NA) spends $650 million on dialysis and transplantation despite an estimated annual loss of 600,000 life years. The health burden of ESKD is not limited to its directly-related morbidity and mortality but affects even more significantly other body systems, particularly the cardiovascular system. In addition, dialysis units are reservoirs for infectious agents, such as hepatitis-C (HCV) and -B (HBV) viruses, and methicillin-resistant staphylococci (MRSA), which threaten the health of the community. Shortage of financial resources eventually creates inequity of health care at large since only the rich are able to find their way around the limited public services. ESKD is no exception; inequity being even further augmented by the trade of organs, particularly in Egypt. This is attributed to high demand in the absence of a deceased donor program and in the presence of a pool of young, healthy, unemployed potential donors who have no access to any social security plans. Many attempts to face the challenge of accommodating ESKD management in NA are underway, including relevant legislations, promoting deceased donor transplants, chronic kidney disease (CKD) prevention and early detection programs, and generating nontraditionally directed financial resources.

**Keywords:** Life Years Lost, Economics of CKD, Health Burden, Kidney Transplantation, Dialysis

## M-196. Validation of Urinary Pd-1andFoxp3 Mrna in Cohort of Egyptian Renal Allograft Recipients

Mohamed momtaz Abd Elaziz, Seham Bakry Abd ElAal M. Abd ElAal, Laila Rashed and Dina Hesham

*Annals of Transplantation, 21: 17-21 (2016) IF: 1.032*

**Background:** We investigated the diagnostic and prognostic value of urinary programmed death 1 (PD-1) and FOXP3 (Forkhead transcription factors) mRNA in acute renal allograft rejection. **Material/Methods:** Urine samples from 31 acute renal allograft rejection subjects and 23 stable recipients were collected. Messenger RNA of PD-1 and FOXP3 were analyzed with real-time RT-PCR. The associations with acute rejection, disease severity, and outcome were investigated. **Results:** Both PD-1 and FOXP3 mRNA were higher in acute rejection than subjects with stable grafts. In acute rejection, PD-1 and FOXP3 mRNA were significantly correlated with serum creatinine and Banff histological grade. Both PD-1 and FOXP3 mRNA performed well in diagnosing acute rejection (AUC 0.81 and 0.91, respectively). However, a combination of both FOXP3 mRNA at cutoff level 1.5 and PD-1 mRNA at cutoff level 2.6 had 94% sensitivity, 97% specificity, and AUC 0.98 in diagnosing acute rejection. Only FOXP3 mRNA was correlated with rejection reversibility and predicted graft salvage (98% sensitivity, 87% specificity, and AUC 0.93) at cutoff level 1.7. **Conclusions:** PD-1 and FOXP3 mRNA were high in acute rejection, and performed well in diagnosing rejection episodes, and were correlated with rejection severity. The combination of FOXP3 and PD-1 mRNA had better sensitivity and specificity in diagnosing acute rejection than each separately. Only FOXP3 anticipated rejection outcome.

**Keywords:** Forkhead Transcription Factors; Graft Rejection; Programmed Cell Death 1 Receptor

## M-197. Microparticles (Cd146)and Arterial Stiffness Versus Carotid Intima Media Thickness as an Early Predictors of Vascular Affection in Systemic Lupus Patients

Sahar Nassef, Hala El Guindey, Mary Fawzy, Amal Nasser, Rasha Reffai and Doa Shemiy

*Arch Rheumatol, 31(1): 31-40 (2016) IF: 0.22*

**Objectives:** This study aims to evaluate cluster of differentiation 146 (CD146) and pulse wave velocity (PWV) as non-invasive

methods for prediction of early vascular affection in systemic lupus erythematosus (SLE) patients without symptoms of vascular disease, to detect the outcome and reproducibility of these methods, and to correlate CD146 and PWV with lipid profile, intima media thickness (IMT), and ankle brachial index. Patients and methods: Thirty female SLE patients (mean age 26.6±6.6 years; range 15 to 35 years) fulfilling the American College of Rheumatology 1997 revised criteria for SLE classification, and 15 age and sex matched healthy controls were included. All participants were performed full clinical assessments including measurement of Systemic Lupus Erythematosus Disease Activity Index, lipid profile, CD146, carotid IMT, PWV, and rise time as an indication of how fast the waveform rises. **Results:** Cluster of differentiation 146 levels were elevated in patients with SLE compared to controls ($p<0.001$). There was a statistically significant difference between patients and controls in the femoral, lower thigh, and ankle rise time. There was a statistically significant correlation between IMT and ages of patients, Systemic Lupus Erythematosus Disease Activity Index, and brachial-below knee PWV, while there was no correlation between IMT and disease duration, lipid profile, brachial-femoral PWV, and brachial-ankle PWV. There was statistically significant correlations between brachial-femoral PWV and serum cholesterol level, and between brachial-ankle PWV and low density lipoprotein cholesterol. **Conclusion:** Our results showed that SLE vascular affection is more pronounced in small arteries. Also, elevated CD146 and brachial-femoral PWV are useful early markers of vascular affection in SLE as well as rise time may be a marker for arterial stiffness.

**Keywords:** Arterial Stiffness; Cluster of Differentiation 146; Pulse Wave Velocity; Systemic Lupus Erythematosus.

## M-198. Polyglandular Dysfunction in Patients with Type 1 Diabetes: Recurrent Hypoglycemia is an Alarming Symptom

Aasem Saif

*Clinical Diabetes, 34: 113-114 (2016)*

A 35-year-old man known to have type 1 diabetes for 8 years presented to the emergency department with disturbed conscious level. He gave a history of recurrent similar attacks during the previous 8 months. All of these attacks were proved to be due to hypoglycemia. Some of the episodes were mild and treated by oral glucose only, whereas others were severe, requiring hospital admission and treatment with an intravenous glucose infusion. The patient had been taking human mixed insulin for the past 2 years. His insulin doses were reviewed by his primary care providers and decreased after each episode of hypoglycemia. His total daily insulin dose had been decreased from 70 to 10 units during the previous 8 months. The patient gave a history of darkening of the skin of his face and extremities associated with significant weight loss throughout the previous year. He had no family history of type 1 diabetes or thyroid or adrenal diseases. On admission to the emergency department, the patient had disturbed conscious level with no signs of lateralization. His blood pressure was 70/40 mmHg, pulse was 72 bpm and regular, weight was 60 kg, and BMI was 20.7 kg/m². Hyperpigmentation of the face, oral mucosa, and exposed areas of upper and lower limbs was evident, especially when compared to old photographs of the patient. No other significant clinical findings were noticed. His random blood glucose was 32 mg/dL. The patient was admitted to the intensive care unit. After receiving dextrose 25% intravenously, his conscious level improved significantly and was back to normal within 2 hours. Serum cortisol and free thyroxin (FT4) were very low. Thyroid-stimulating hormone (TSH) and adrenocorticotropic hormone (ACTH) were very high—150 mIU/mL (normal 0.35–5.5 mIU/mL) and 972 pg/mL (normal 10–46 pg/mL), respectively. Renal function was normal. Thyroid peroxidase (TPO) antibodies were highly positive. The patient was diagnosed to have polyglandular autoimmune syndrome type II (PAS II). He was started on hormonal replacement therapy (hydrocortisone before levothyroxine to avoid precipitating an adrenal crisis), with dose adjustments made during the following weeks. His general condition, blood pressure, and blood glucose showed significant improvement within 3 weeks. His insulin doses were gradually increased to achieve optimum blood glucose control

**Keywords:** Polyglandular Dysfunction, Type 1 Diabetes, Hypoglycemia.

## M-199. Vkorc1 Gene (Vitamin K Epoxide Reductase) Polymorphisms are Associated with Cardiovascular Disease in Chronic Kidney Disease Patients on Hemodialysis

Noha A Osman, Nevine El-Abd and Mohamed Nasrallah

*Saudi Journal of Kidney Diseases and Transplantation, 27: 908-915 (2016)*

Vitamin K is necessary for the carboxylation of clotting factors and matrix Gla protein (MGP). Vitamin K epoxide reductase (VKOR) is the enzyme responsible for recirculation of Vitamin K increasing its tissue availability. Polymorphisms of VKOR may alter the function of MGP, thereby influencing vascular calcification. We conducted this study to investigate the relationship of VKORC1 gene single nucleotide polymorphisms (SNP's) to vascular calcification and clinically overt cardiovascular disease in chronic kidney disease (CKD) patients on hemodialysis (HD). The study included 54 CKD patients on HD. We excluded those with diabetes or on anticoagulant therapy. Vascular calcifications were measured using computerized tomography scans and roentgenograms. Prevalent clinically overt cardiovascular disease was reported based on the evidence of documented preexisting major cardiovascular events. Genotype detection for the gene VKORC1 C1173T and G-1639A polymorphisms was carried out by polymerase chain reaction. We found a significant association between C1173T polymorphisms and vascular calcification (odds ratio [OR] = 43, P = 0.001). The mutant T allele was also linked with higher odds of vascular calcification (OR = 8.880, 95% confidence interval [CI] = 3.1–25.4, P = 0.001) and clinically overt cardiovascular disease (OR = 4.7, 95% CI = 1.5–14.7, P = 0.005). VKORC1 G-1639A polymorphisms were not associated with vascular calcification and had lower prevalence of clinically overt cardiovascular disease (OR = 0.07, 95% CI = 0.01–0.4, P = 0.001). In patients with CKD on HD, we found that VKORC1 gene polymorphisms did have an association with prevalent cardiovascular calcification and clinically overt cardiovascular disease, C1173T polymorphisms with higher risk for disease, and G-1639A with lower risk.

**Keywords:** Vitamin K, Cardiovascular Outcome, Chronic Kidney Disease

## M-200. Cinacalcet Versus Parathyroidectomy in the Treatment of Secondary Hyperparathyroidism Post Renal Transplantation

Amin R. Soliman, Hoda A. Maamoun, Mahmoud A. Soliman, Hatem Darwish and Esam Elbanna

*Romanian Journal of Internal Medicine, 54(3): 184-189 (2016)*

**Background:** Persistent hyperparathyroidism (HPT) with hypercalcemia is prevalent after transplant and is considered a risk factor for progressive bone loss and fractures and vascular calcification, as well as the development of tubulointerstitial calcifications of renal allografts and graft dysfunction. The subtotal parathyroidectomy is the standard treatment, although currently it has been replaced by the calcimimetic cinacalcet. **Aim.** The hypothesis of this study is that subtotal parathyroidectomy is superior to cinacalcet for treatment of persistent secondary parathyroidectomy post renal transplant, with minimal morbidity and significantly it reduces the cost of treatment after transplantation. **Methods.** We report our long-term clinical experience with either cinacalcet or parathyroidectomy in 59 kidney transplant recipients with hyperparathyroidism. Group one included medical treatment with cinacalcet and had 45 patients while parathyroidectomy patients (group 2) were 16 patients with two of them excluded because of surgical failure. **Results.** No difference was found between groups for any parameter. A greater short-term change of calcium and phosphorus homeostasis obtained by surgery than by cinacalcet, and in long term change, no significant difference between the two groups. **Conclusions:** The main findings of this study are that correction of severe hyperparathyroidism was similar in both surgical and cinacalcet groups with the absence of a difference of long-term serum iPTH 1-84 levels between the two groups

**Keywords:** Hyperparathyroidism, Cinacalcet Hydrochloride, Parathyroidectomy, Kidney Transplantation.

### *Dept. of Medical Biochemistry and Molecular Biology*

## M-201. Fibrogene: A Gene-Based Model for Staging Liver Fibrosisq

Mohammed Eslam, Ahmed M. Hashem, Manuel Romero-Gomez, Thomas Berg, Gregory J. Dore6, Alessandra Mangia, Henry Lik Yuen Chan, William L. Irving, David Sheridan, Maria Lorena Abate, Leon A. Adams, Martin Weltman, Elisabetta Bugianesi, Ulrich Spengler, Olfat Shaker, Janett Fischer, Lindsay Mollison, Wendy Cheng, Jacob Nattermann, Stephen Riordan, Luca Miele, Kebitsaone Simon Kelaeng and Javier

*Journal of Hepatology, 64 (2): 390-398 (2016) IF: 10.59*

**Background & Aims:** The extent of liver fibrosis predicts longterm outcomes, and hence impacts management and therapy. We developed a non-invasive algorithm to stage fibrosis using non-parametric, machine learning methods designed for predictive modeling, and incorporated an invariant genetic marker of liver fibrosis risk. **Methods:**Of 4277 patients with chronic liver disease, 1992 with chronic hepatitis C (derivation cohort) were analyzed to develop the model, and subsequently validated in an independent cohort of 1242 patients. The model was assessed in cohorts with chronic hepatitis B (CHB) (n = 555) and non-alcoholic fatty liver diseas (NAFLD) (n = 488). Model performance was compared to FIB-4 and APRI, and also to the NAFLD fibrosis score (NFS) and Forns' index, in those with NAFLD. **Results:** Significant fibrosis (PF2) was similar in the derivation (48.4%) and validation (47.4%) cohorts. The FibroGENE-DT yielded the area under the receiver operating characteristic curve (AUROCs) of 0.87, 0.85 and 0.804 for the prediction of fast fibrosis progression, cirrhosis and significant fibrosis risk, respectively, with comparable results in the validation cohort. The modelperformed well in NAFLD and CHB with AUROCs of 0.791, and 0.726, respectively. The negative predictive value to exclude cirrhosis was >0.96 in all three liver diseases. The AUROC of the FibroGENE-DT performed better than FIB-4, APRI, and NFS and Forns' index in most comparisons. **Conclusion:** A non-invasive decision tree model can predict liver fibrosis risk and aid decision making.

**Keywords:** Chronic Hepatitis C; Chronic Hepatitis B; Non-Alcoholic Steatohepatitis; Nash; Ifnl; Fibrosis; Data Mining Analysis.

## M-202. The Role of Protamine 2 Gene Expressionand Caspase 9 Activity in Male Infertility

Adel A. Zalata, Naglaa Mokhtar, Amany Atwa, Mohamed Khaled and Olfat G. Shaker

*The Journal of Urology, 195: 796-800 (2016) IF: 4.7*

**Purpose:** Approximately 15% of couples are affected by infertility with the man responsible in almost half of the cases. PRMs (protamines) confer a higher order of DNA packaging in sperm than that in somatic cells. Because of the critical roles of PRMs in spermatid differentiation, aberrations in PRM expression or changes in protein structure could be causes of certain types of idiopathic human male infertility. The aim of this study was to give insight into the role of PRM2 gene expression and caspase 9 activity in the pathogenesis of male infertility. **Materials and Methods:** The current study included 70 men with idiopathic infertility and 64 fertile men who attended the andrology outpatient clinic at Mansoura University Hospital. Semen sample analyses were done according to WHO recommendations. The acrosome reaction of spermatozoa recovered from each sample was assessed. Samples were separated using discontinuous gradient separation. From each semen sample mature sperm were separated from immature sperm. The resulting samples were divided into 2 parts, including one to determine caspase 9 activity and the other for RNA extraction and reverse transcriptase-polymerase chain reaction of PRM2 gene expression. The polymerase chain reaction product was electrophoresed on 2% agarose gel. **Results:** PRM2 gene expression was significantly decreased in immature sperm extracted from the fertile and infertile groups. Caspase 9 activity was significantly increased in immature sperm extracted from both groups. **Conclusions:** Low levels of PRM2 may be associated with morphological abnormalities, initiation of the apoptotic pathway and decreasing sperm motility. PRM2 may be an important marker to better understand the key regulatory pathway of spermatogenesis and it may act as a crucial part of fertilization

**Keywords:** Testis; Spermatozoa; Infertility, Male; Protamines; Caspase 9

## M-203. Therapeutic Efficacy of Amniotic Membrane Stem Cellsand Adipose Tissue Stem Cells in Rats with Chemically Induced Ovarian Failure

Hanan Fouad, Dina Sabry, Khaled Elsetohy and Naglaa Fathy

*Journal of Advanced Research, 7: 233-241 (2016) IF: 3*

The present study was conducted to compare between the therapeutic efficacies of human amniotic membrane-derived stem cells (hAM-MSCs) vs. adipose tissue derived stem cells (ADMSCs) in cyclophosphamide (CTX)-induced ovarian failure in rats. Forty-eight adult female rats were included in the study; 10 rats were used as control group. Thirty-eight rats were injected with CTX to induce ovarian failure and divided into four groups: ovarian failure (IOF) (IOF group), IOF+phosphate buffer saline (PBS group), IOF+hAM-MSCs group and IOF+AD-MSCs group. Serum levels of FSH and estradiol (E2) were assessed. Histopathological examination of the ovarian tissues was performed and quantitative gene expressions of Oct-4, Stra8 and integrin beta-1 genes were conducted by quantitative real time PCR. **Results** showed that IOF and IOF+PBS rat groups exhibited decreased ovarian follicles, increased interstitial fibrosis with significant decrease of serum E2, significant increase serum FSH level and significant down-regulation of Stra8 and integrin beta-1. In hAM-MSCs and AD-MSCs rat groups, there were increased follicles and corpora with evident the presence of oocytes, significant increase in serum E2, significant decrease in serum FSH levels (in hAMMSCs treated group only) and significant up-regulation of the three studied genes with higher levels in hAM-MSCs treated rats group when compared to AD-MSCs treated rats group. In **Conclusion** administration of either hAM-derived MSCs or AD-MSCs exerts a significant therapeutic efficacy in chemotherapy induced ovarian insult in rats. hAM-MSCs exert higher therapeutic efficacy as compared to AD-MSCs.

**Keywords:** Ovarian Failure ;Ovarian Insufficiency; Chemotherapy; Ham-Mscs; Ad-Mscs.

## M-204. Effect of Silibininand Vitamin E on the Ask1-P38 Mapk Pathway in D-Galactosamine/Lipopolysaccharide Induced Hepatotoxicity.

Hashem RM, Hassanin KM, Rashed LA, Mahmoud MO and Hassan MG.

*Experimental Biology and Medicine,11:1250-1257(2016) IF:2.542*

Apoptosis signal-regulating kinase 1 (ASK1), a redox-sensor mitogen-activated protein kinase kinase kinase (MAPKKK) that activates p38 MAPK pathways in oxidative stress-induced hepatotoxicity in D-galactosamine/lipopolysaccharide (D-GalN/LPS) model, is a key central pathway in which specific targeting of ASK1 deactivation is of a great therapeutic potential. We tested the effect of silibinin and vitamin E in curative and prophylactic manner of treatment on the negative modulators of ASK1, thioredoxin1 (Trx1), thioredoxin reductase1 (TrxR1), and the protein phosphatase (PP5), whereas they have previously proven to have hepatoprotective effect. Either curative or prophylactic silibinin and vitamin E groups significantly decreased ASK1 and p38 MAPK levels through increasing the gene expression of Trx1, TrxR1, and PP5 to reduce the oxidative stress as demonstrated by decreasing the levels of NADPH oxidase 4 (NOX4), TBARS and conjugated diene with a concomitant increase in the levels of GSH, CAT, and SOD. These results were confirmed by histopathology examination which illustrated progressive degenerative changes of hepatocytes such as hydropic degeneration, vacuolation, pyknosis, karyolysis, and loss of architecture of some cells in D-GalN/LPS treatment, and these features were alleviated with silibinin and vitamin E administration. In conclusion, silibinin and vitamin E decreased ASK1-p38 MAPK pathway through deactivating the upstream signalling ASK1 molecule via increasing the levels of Trx1 and TrxR1 as well as the PP5 to alleviate in D-GalN/LPS induced hepatotoxicity

**Keywords:** Ask1; Pp5; Trx1; Trxr1; Hepatotoxicity; P38 Mapk

## M-205. Bone Marrow-Derived Mesenchymal Stem Cells Effectively Regenerate Fibrotic Liver in Bile Duct Ligation Rat Model

Mohamed HE, Elswefy SE, Rashed LA, Younis NN and Shaheen MA and Ghanim AM

*Exp Biol Med, 6: 581-591 (2016) IF: 2.542*

Mesenchymal stem cells (MSCs) have attracted lots of attention for the treatment of acute liver failure and end-stage liver diseases. This study aimed at investigating the fundamental mechanism by which bone marrow-derived MSCs (BM-MSCs) induce liver regeneration of fibrotic liver in rats. Rats underwent bile duct ligation (BDL) surgery and four weeks later they were treated with either BM-MSCs (3 × 10(6) cells /rat, once, tail vein injection) or silymarin (100 mg/kg, daily, orally) for four weeks. Liver function tests and hepatic oxidative stress were determined. Hepatic injury and fibrosis were assessed by H and E, Sirus red staining and immunohistochemical expression of α-smooth muscle actin (α-SMA). Hepatocyte growth factor (HGF) and the gene expression of cytokeratin-19 (CK-19) and matrix metalloproteinase-2 (MMP-2) in liver tissue were determined. BDL induced cholestatic liver injury characterized by elevated ALT and AST activities, bilirubin and decreased albumin. The architecture damage was staged as Metavir score: F3, A3. Fibrosis increased around proliferating bile duct as indicated by sirus red staining and α-SMA immunostaining. Fibrogenesis was favored over fibrolysis and confirmed by decreased HGF with increased expression of CK-19, but decreased MMP-2 expression. BM-MSCs treatment restored deteriorated liver functions and restored the histological changes, resolved fibrosis by improving liver regenerative capabilities ($P < 0.001$), increases in HGF and MMP-2 mRNA and downregulating CK-19 mRNA. Sliymarin, however, induced similar but less prominent effects compared to BM-MSCs. In conclusion, liver regenerative capabilities can be stimulated by BM-MSCs via augmentation of HGF that subsequently up-regulate MMP-2 mRNA while downregulating CK-19 mRNA.

**Keywords:** Bone Marrow-Derived Mesenchymal Stem Cells; Bile Duct Ligation; Cytokeratin-19; Hepatic Regeneration; Hepatocyte Growth Factor; Matrix Mettaloproteinase-2.

## M-206. ULBP3: A Marker for Alopecia Areata Incognita.

Moftah NH, El-Barbary RA, Rashed L and Said M

*Arch Dermatol Res, 6: 415-421 (2016) IF: 2.146*

Alopecia areata incognita (AAI) is a type of diffuse hair fall with no confirmatory diagnostic test. The UL16 binding protein-3 (ULBP3) is ligands for natural-killer group 2, member D (NKG2D) receptor. It is a key regulator of both innate and adaptive immune responses. In the normal hair follicle, ULBP3 is turned off. However, different studies reported its high level in alopecia areata (AA). Therefore, this study was done to evaluate ULBP3 in AAI in comparison with telogen effluvium (TE), female pattern hair loss (FPHL), and normal hair. Biopsy specimens from 36 females suffering from AAI, 15 with FPHL, nine with TE, and ten healthy female controls were subjected to the immunogenetic detection of ULBP3 levels by real-time polymerase chain reaction (PCR). A high statistically significant increase in ULBP3 level in AAI patient group compared with FPHL, TE, and normal hair was detected. ULBP3 levels were positively correlated with the age and duration of the disease. Accordingly, ULBP3 may act as a confirmatory test for AAI. ULBP3 may be implicated in the disease pathogenesis, progression, and chronicity, and AAI may be a subtype of AA
**Keywords:** Alopecia Areata; Alopecia Areata Incognita; Androgenetic Alopecia; Dermoscopy; Telogen Effluvium; Ulbp3.

## M-207. Hepatitis C Viral Kinetic Changes in a Retrospective Cohort Study of Chronic Hepatitis C Virus Egyptian Patients on Pegylated Interferonand Ribavirin Therapy

Gamal Eldeen Esmat, Wafa Al Akel, Rasha Ahmed Abdel Aziz, Ahmed Al Sayed Taha, Dina Sabry, Laila A. Rashed, Aya Mostafa, Amany Y. El Kazaz and Sahar H. Ahmed

*Journal of Interferon and Cytokine Research, 36: 149-158 (2016) IF: 2.135*

The aim of this study was to determine the relative importance of the kinetics of antiviral response compared to baseline host and virological factors for predicting treatment outcome. A retrospective analysis of 285 chronic hepatitis C virus (HCV) patients, encompassing genotypes 4 treated with peginterferon alpha-2a and ribavirin, was performed. Baseline characteristics were compared across HCV genotypes and pretreatment factors associated with rapid virological response (RVR) were identified. The relative significance of RVR compared to other baseline factors for predicting sustained virological response was analyzed by multiple logistic regression analysis. Ninety-seven percent of the patients harbored HCV genotype 4a patients. The positive predictive value (PPV) of RVR for end-of-treatment response (ETR) was 88% and of early virological response (EVR) was 85%, which means that achievement of both RVR and EVR is a good positive predictive factor of response. The negative predictive value (NPV) of RVR for ETR was low and equals 26.77%, which means that approximately two-thirds of patients were able to achieve ETR despite not experiencing RVR, which means RVR is a bad negative predictive factor of response. The NPV of EVR for ETR was high and equals 90%, which means that only 10% of patients were able to achieve an ETR despite not experiencing EVR, which explains that EVR is a very good negative predictive factor of response. In univariate logistic regression analysis, which included the following: female gender, alanine aminotransferase, aspartate transaminase, α-fetoprotein, baseline HCV-RNA levels, grade of activity, stage of fibrosis, and positive HCV-RNA, by polymerase chain reaction at week 4, none of the previous factors was a significant independent factor of failure of response to treatment. The current study demonstrated that a viremia at week 4 has a good PPV, but it has a very low NPV. The NPV of EVR was more robust for ETR (90%). EVR is regarded as a robust indicator of treatment outcome, and a 12-week stopping rule for patients is strongly evident.
**Keywords:** Hcv; Interferon; Ribavirin.

## M-208. Molecular Assessment of Vitamin D Receptor Polymorphism as A Valid Predictor to the Response of Interferon/Ribavirin-Based Therapy in Egyptian Patients with Chronic Hepatitis C.

Abdelsalam A, Rashed L, Salman T, Hammad L and Sabry D.

*Journal of Digestive Diseases, 8: 547-553 (2016) IF: 1.887*

**Objective:**The aim of this study was to find an association between serum concentration of vitamin D and vitamin D receptor (VDR) polymorphisms to achieve a sustained virological response (SVR). **Methods:** We conducted a case-control study in which 250 participants were recruited and divided into three groups (100 chronic hepatitis C [CHC] patients who achieved SVR, 100 CHC patients who did not achieve SVR and 50 apparently healthy individuals as controls). Blood samples were collected to measure serum vitamin D concentration, and four VDR polymorphisms (FokI, ApaI, TaqI, and BsmI) were detected using polymerase chain reaction-restriction fragment length polymorphism. **Results:** Non-responders were found to have significantly low vitamin D concentration compared with responders and control groups. Concerning VDR polymorphisms, both FokI and TaqI polymorphisms were associated with successful treatment. **Conclusion:** Vitamin D concentration, FokI, and TaqI may be considered as the predictors for the response of CHC patients to a combination therapy of pegylated interferon and ribavirin. © 2016 Chinese Medical Association Shanghai Branch, Chinese Society of Gastroenterology, Renji Hospital Affiliated to Shanghai Jiaotong University School of Medicine and John Wiley & Sons Australia, Ltd.
**Keywords:** Hepatitis C Virus; Interferons; Ribavirin; Single Nucleotide Polymorphism; Vitamin D Receptor

## M-209. Sirt-1Expression is Associated with Expression of Nanog in Patients with Colorectal Adenocarcinoma

Amany Osamaa, Dina Sabryb, Sahar M. Hassany, Soha Saoud Abdelmoneim and Abeer Sabry

*Cancer Biomarkers, 17: 155-163 (2016) IF: 1.736*

**AIMS:** The study aimed to investigate the quantitative expression of NANOG, p38 α, NCF2, ELF and TGF-β genes in patients with colorectal adenocarcinoma, adenoma and normal colonic tissue and their correlation with SIRT-1 protein level expression. **Method:** This study enrolled one hundred sixty seven patients; group A: 87 patients with colonoscopic findings

of no adenoma or adenocarcinoma and group B: 80 patients with colorectal mass. Consecutive colonoscopic examinations were conducted, and tissue samples were taken from the colonic lesions/masses. Total RNA was isolated and mRNA expression level of NANOG, mitogen activated p38α, Neutrophil Cytosol Factor 2 (NCF2), Embryonic Liver Fodrin (ELF) and Transforming Growth Factor Beta (TGF-β) genes were quantified by qRT-PCR. Sirt-1 protein expression level was assessed by quantitative western blot. **Results:** There were significantly high level of mRNA transcripts expression of the genes studied in patients with adenocarcinoma and adenoma compared with normal tissue (P value < 0.01), NANOG, NCF2, ELF and TGF-β at a cut of > 0.314, > 0.392, 0.349 and 0.333 respectively showed sensitivity (96.5%, 98.8%, 95.3%, 98.8%) and specificity of (95.3%, 92.6%, 89.5%, 93.8%) respectively in diagnosing colonic adenocarcinoma. Sirt-1 protein level was significantly highly expressed in colorectal adenocarcinoma compared to normal and adenoma colonic tissue and positively correlated with NANOG. **Conclusion:** Over expression of NANOG, p38α, NCF2, ELF and TGF-β genes in both cases of adenocarcinoma and adenoma could have a diagnostic value. SIRT-1 and NANOG are high correlated biological markers for diagnosis and prognosis follow up in patients with adenocarcinoma.

**Keywords:** ELF; NANOG; NCF2; SIRT-I; Tgf-B; Colon Adenocarcinoma; P38α.

## M-210. Comparative Evaluation of Plga Nanoparticle Delivery System for 5-Fluorouraciland Curcumin on Squamous Cell Carcinoma.

Shaimaa M. Masloub, Mohamed H. Elmalahy, Dina Sabry, Wael S. Mohamed and Sahar H. Ahmed

*Archives of Oral Biology, 64: 1-10 (2016) IF: 1.733*

**Purpose:** The purpose of this study is to assess the effect of 5-fluorouracil nanoparticles and curcumin naoparticles on cell proliferation and the expression of the apoptotic marker (caspase 3) in squamous cell carcinoma cell line. **Material and Methods:** PLGA 5-fluorouracil nanopartciles and PLGA curcumin nanoparticles were prepared and applied for 24 and 48h on human laryngeal squamous carcinoma cell line (Hep-2) as regard IC 50 concentration. MTT assay was used for evaluation of cytotoxicity of prepared nanoparticles. Quantitaive reverse transcriptase polymerase chain reaction (QRT-PCR) was used for the assessment of caspase-3 expression in the treated cell line. **Results:** The drug release rate profiles was dependent upon polymer to drug ratio, noting that the higher PLGA polymer ratio to 5-fluprouracil or curcumin drug showed faster release rates. On the other hand, the least PLGA polymer ratio to 5-fluprouracil or curcumin drug showed the slowest release rates. MTT assay revelaed that 5-fluorouracil nanoparticels or curcumin nanoparticels showed a clear cytotoxic effect on Hep-2 cell line compared to non treated cancer cells. The RT-PCR assessment of caspase-3 expression revealed that there was a significant increase in caspase-3 expression in Hep-2 cell line treated with 5-fluorouracil nanoparticles or curcumin compared to non treated cancer cells. **Conclusion:** Curcumin nanoparticles could be more active in inducing apoptosis in short term assays (24h) than long term assays (48h) due to differential cellular uptake. While 5-fluorouracil nanoparticles induced higher significant apoptosis in long term (48h) compared to curcumin group.

**Keywords:** Apoptosis; Caspase-3; Hep-2; Nanotechnology.

## M-211. Impact of Foki (Rs10735810)and BsmI (Rs1544410) on Treatment of Chronic HCV Patients with Genotype 4

Olfat Shaker, Yasser Nassar, Shymaa Ayoub, Maissa Elrazki and Amr Zahra

*Journal of Clinical Laboratory Analysis, 30 (6): 1021-1027 (2016) IF: 1.549*

**Background and Aim:** Chronic infection with hepatitis C virus (HCV) is a huge problem both globally and at the level of the individual patient. Our aim is to detect the influence of vitamin D receptor gene polymorphisms (BsmI and Fok1) and vitamin D level in HCV patients under treatment with interferon. **Subject and Methods:** Blood samples were taken from 103 HCV patients all of them are genotype 4. They were divided into responders (n = 63) and nonresponders (n = 40) according to their response to interferon treatment. Also 120 subjects with matched age and sex were enrolled as controls. All subjects were subjected to history taking, general examination, liver function tests, hepatitis markers, HCV quantitation by real-time polymerase chain reaction (PCR), DNA extraction from whole blood, PCR-restriction fragment length polymorphism (RFLP) for genotyping, and quantitation of vitamin D level by ELISA. **Results:** There were significant differences between responders and nonresponders in the mean values of vitamin D (P = 0.001) as well as the prevalence of single nucleotide polymorphism (SNP) BsmI (Bb) (P = 0.02). Meanwhile, no significant differences in Fok1 genotype between responders and nonresponders to interferon therapy of HCV patients in all genotypes [FF, Ff, ff) (P = 0.34, 0.091, and 0.43), respectively. **Conclusion:** BsmI and vitamin D level in chronic liver disease patients are predictors of response to combination therapy of HCV.

**Keywords:** Hepatitis C; Vitamin D; Polymorphism

## M-212. Braf, Kras and Helicobacter Pylori Epigenetic Changes-Associated Chronic Gastritis in Egyptian Patients with and Without Gastric Cancer

Dina Sabry, Rasha Ahmed, Sayed Abdalla, Wael Fathy, Ahmed Eldemery and Azza Elamir

*World Journal Microbiology and Biotechnology, 32: 92-99 (2016) IF: 1.532*

We aimed to study MLH1 and MGMT methylation status in Helicobacter pylori-associated chronic gastritis in Egyptian patients with and without gastric cancer. 39 patients were included in our study. They were divided into 2 groups; patients without (group I) and with gastric adenocarcinoma (group II). Patients were subjected to clinical examination, abdominal ultrasound and upper endoscopy for gastric biopsy. Biopsies were subjected to urease test, histological examination, and DNA purification. H. pylori, Braf, Kras,MLH1 andMGMTmethylation were assessed by quantitative PCR. DNA sequencing was performed to assess Braf and Kras genes mutation. qPCR of H. pylori was significantly higher in patients with adenocarcinoma (group II) than those without adenocarcinoma (group I); with a p\0.001 as well as in patients with age above 50 years with a p value = 0.008. By applying

logistic regression analysis it was reported that the H. pylori qPCR is a significant predictor to the adenocarcinoma with OR = 1.025 (95 % CI: 1. 002–1.048), with sensitivity of 90 % and specificity of 100 %. Adenocarcinoma patients had a significantly higher mean age and levels of H. Pylori, Braf, K-ras, methylated MGMT and methylated MLH1 than those of gastritis patients. DNA sequence analysis of Braf (codon 12) and Kras (codon 600) had genes mutation in gastric adenocarcinoma versus chronic gastritis. **Conclusion:** H. pylori may cause epigenetic changes predisposing the patients to cancer stomach. Estimation of H. pylori by qPCR can be a good predictor to adenocarcinoma. Braf and Kras genes mutation were reveled in gastritis and adenocarcinoma patients.
**Keywords:** H.Pylori; Braf; Kras Epigenetics.

## M-213. Molecular Mechanisms Underlying FibrosisandElastin Destruction Inchildhood Interstitial Lung Diseases

Enas A. Hamed, Mostafa M. El-Saied, Khaled Saad, Hazem Abu-Zeid Yousef, Amany O. Mohamed and Dina Sabry

*Pathophysiology, 23: 275-283 (2016)*

**Objective:**This study aimed to evaluate fibrosis and elastin destruction in childhood interstitial lung disease (chILD) patients. **Methods:** Sixty patients and twenty healthy children were recruited. On admission, evaluation of chILD severity was made using Fan chILD score. Participants provided urine and blood samples. Plasma levels of transforming growth factor (TGF)-β1, connective tissue growth factor (CCN2), soluble factor related apoptosis (sFas) and long non-coding RNAs and urinary levels of desmosine/urinary creatinine (UDes/UCr) were measured. **Results:** In patients, clinical findings were crackles (100.00%), tachypnea (65.00%), cardiomegaly (45.00%), digital clubbing (43.30%), cough (33.00%), cyanosis (26.70%), hepatomegaly (28.30%) and wheezes (23.30%). Categorizing of the patients with Fan chILD clinical score revealed that most patients 33.30% scored (3, symptomatic with abnormal saturation/cyanosis during exercise) then 28.30% scored (5, symptomatic with clinical and echocardiographic features of pulmonary hypertension), 18.30% scored (2, symptomatic with normal room air saturations), 15.00% scored (1, asymptomatic) and 5.00% scored (4, symptomatic with abnormal room air saturation/cyanosis at rest). TGF-β1, CCN2, sFas, lncrRNA-2700086A05Rik relative gene expression and UDes/UCr levels were higher in patients than controls (P=0.002, P=0.001, P=0.001, P=0.001, P=0.001, respectively). In patients, significant positive correlations were found between TGF-β1 and CCN2, sFas, UDes/UCr; between CCN2 and both sFas and UDes/UCr; between UDes/UCr and sFas. Morbidity and mortality rates were 46.70% and 10.00%, respectively. **Conclusion:**Markers of fibrosis (TGF-β1, sFas, CCN2) and elastin destruction (UDes/UCr) were increased in chILD especially in patients with long disease duration. So blockage of their pathways signals may offer novel therapeutic targets.
**Keywords:** Connective Tissue Growth Factor (CCN2); Interstitial Lung Disease of Children; Long Non-Coding Rnas; Transforming Growth Factor (TGF)B-(1); Urinary Desmosine (UDes).

## M-214. Comparison of the Therapeutic Effectiveness of Human Cd34+and Rat Bone Marrow Mesenchymal Stem Cells on Improvement of Experimental Liver Fibrosis in Wistar Rats

Hayam G Sayyed, Amany Osama, Naglaa K Idriss, Dina Sabry, Azza S Abdelrhim and Rania Bakry

*International Journal of Physiology, Pathophysiology and Pharmacology, 8: 128-139 (2016)*

Human umbilical cord blood (UCB) cells and bone marrow mesenchymal stem cells (BM-MSCs) have numerous advantages as grafts for cell transplantation. We hypothesized differing impacts of human UCB cells and rat BM-MSCs on reversal of hepatic injury and revival of liver function in carbon tetrachloride (CCl4)-induced liver fibrosis. **Methods:** Forty rats were divided into 4 groups; control group, CCl4 group, CCl4/CD34+ group and CCl4/BM-MSCs group. Blood samples were driven from rats at 4, 8 and 12 weeks to measure serum concentration of albumin and alanine aminotransferase (ALT). Quantitative expression of collagen Iα, TGF-β, α-SMA, albumin, MMP-2, MMP-9 and TNF-α were assessed by polymerase chain reaction. Histopathological examination of the liver tissue was performed. GFP labeled cells were detected in groups injected with stem cells. **Results:** Regarding liver function, CD34+ were more efficient than BM-MSCs in elevating albumin ($P<0.05$) and reducing ALT ($P<0.05$) concentrations. Concerning gene expression, CD34+ were more effective than BM-MSCs in reducing gene expressions of collagen Iα ($P<0.01$), TGF-β1 ($P<0.01$) and α-SMA ($P<0.01$). Both CD34+ and BM-MSCs have the same efficacy in reducing TNF-α ($P<0.001$ and $P<0.01$, respectively). Furthermore, CD34+ were more valuable than BM-MSCs in increasing gene expression of albumin ($P<0.05$) and MMP-9 ($P<0.01$). **Conclusion:** Taken together; human UCB CD34+ stem cells were more efficient in improvement of experimental liver injury than BM-MSCs. This study highlighted an important role of human UCB CD34+ stem cells in liver fibrosis therapy.
**Keywords:** Ccl4 Liver Fibrosis; Bone Marrow Stem Cell; Stem Cell Therapy; Umbilical Cord Blood Cd34.

## M-215. Heat Shock Protein-70 Expression in Vitiligoand its Relation to the Disease Activity

Doss RW, El-Rifaie AA, Abdel-Wahab AM, Gohary YM and Rashed LA.

*Indian Journal of Dermatology, 4: 408-412 (2016)*

**Background:** Vitiligo is a progressive depigmenting disorder characterized by the loss of functional melanocytes from the epidermis. The etiopathogenesis of vitiligo is still unclear. Heat shock proteins (HSPs) are prime candidates to connect stress to the skin. HSPs were found to be implicated in autoimmune diseases such as rheumatoid arthritis and other skin disorders as psoriasis. **Aim and Objectives:**The aim of this study was to map the level of HSP-70 in vitiligo lesions to declare its role in the pathogenesis and activity of vitiligo. **Materials and Methods:** The study included thirty patients with vitiligo and 30 age- and sex-matched healthy controls. Vitiligo patients were divided as regards to the disease activity into highly active, moderately active, and inactive vitiligo groups. Skin biopsies were taken from the lesional and nonlesional skin of patients and from the

normal skin of the controls. HSP-70 messenger RNA (mRNA) expression was estimated using quantitative real-time polymerase chain reaction. **Results:** Our analysis revealed a significantly higher expression of HSP-70 mRNA in lesional skin biopsies from vitiligo patients compared to nonlesional skin biopsies from vitiligo patients ($P < 0.001$) and compared to skin biopsies from healthy controls ($P < 0.001$). The level of HSP-70 was not found to be correlated with age, sex, or disease duration. The expression of HSP-70 was correlated with the disease activity and patients with active vitiligo showed higher mean HSP-70 level compared to those with inactive disease. **Conclusions:** HSP-70 plays a role in the pathogenesis of vitiligo and may enhance the immune response in active disease.
**Keywords:** Heat Shock Protein-70; Messenger Rna; Real-Time Polymerase Chain Reaction; Vitiligo.

## M-216. Comparative Evaluation for Potential Differentiation of Endothelial Progenitor CellsandMesenchymal Stem Cells Into Endothelial-Like Cells

Dina Sabry, Olfat Noh and Mai Samir

*International Journal of Stem Cells, 9: 44-52 (2016)*

Understanding the mechanisms of vascular remodeling could lead to more effective treatments for ischemic conditions. We aimed to compare between the abilities of both human Wharton jelly derived mesenchymal stem cells (hMSCs) and human cord blood endothelial progenitor cells (hEPCs) and $CD34^+$ to induce angiogenesis in vitro. hMSCs, hEPCs, and $CD34^+$ were isolated from human umbilical cord blood using microbead (MiniMacs). The cells characterization was assessed by flow cytometry following culture and real-time PCR for vascular endothelial growth factor receptor 2 (VEGFR2) and von Willebrand factor (vWF) to prove stem cells differentiation. The study revealed successful isolation of hEPCs, $CD34^+$, and hMSCs. The hMSCs were identified by gaining $CD29^+$ and $CD44^+$ using FACS analysis. The hEPCs were identified by having $CD133^+$, $CD34^+$, and KDR. The potential ability of hEPCs and $CD34^+$ to differentiate into endothelial-like cells was more than hMSCs. This finding was assessed morphologically in culture and by higher significant VEGFR2 and vWF genes expression ($p<0.05$) in differentiated hEPCs and $CD34^+$ compared to differentiated hMSCs. hEPCs and $CD34^+$ differentiation into endothelial-like cells were much better than that of hMSCs
**Keywords:** $Cd34^+$; Endothelial Cell Differentiation; Human Endothelial Progenitor Cells; Human Mesenchymal Stem Cells

### *Dept. of Medical BioChemsitry*

## M-217. Combined Effect of Bone Marrow Derived Mesenchymal Stem Cellsand Nitric Oxide Inducer on Injured Gastric Mucosa in A Rat Model

Laila Rashed, Doaa Mostafa Gharib, Rania Elsayed Hussein, Ola Tork and Azza Abusree

*Tissue and Cell, 48: 644-652 (2016) IF: 1.258*

**Aim** To study the effect of intravenous injection of bone marrow mesenchymal stem cells (BMMSCs), alone and combined with NO inducer in gastric ulcer healing in a rat model. **Methods** Rats were divided into controls, gastric ulcer, gastric ulcer receiving mesenchymal stem cells (MSCs), gastric ulcer receiving NO inducer (l-Arginine), gastric ulcer receiving MSCs plus NO inducer (l-Arginine) groups. MSCs were given in a dose of (106cells) by intravenous injection. l-Arginine was given 300 mg/kg body weight intraperitoneally. 24 h and 7 days after BMMSCs and NO inducer injection, VEGF, PGE, TNF-α were assessed by ELISA. Gene expression of HGF, caspase-3, eNOS and BAX/Bcl-2 in gastric tissues were studied by real time PCR. Histopathology staining of gastric tissues was performed. **Results** Injection of MSCs or NO inducer or both to the gastric ulcer group significantly decreased caspase-3 and BAX genes expression (apoptotic factors) and increased Bcl-2 gene expression (anti-apoptotic factor) compared to that of the gastric ulcer group after both 24 h and 7 days with more significant results in the gastric group received both MSCs and NO inducer. HGF gene expression was significantly increased in the groups injected with MSCs or NO inducer or both compared with the corresponding gastric ulcer group ($p < 0.05$, $p < 0.05$ & $p < 0.001$ respectively). There was a significant decrease in the mean PGE2 and TNF-α levels in the gastric ulcer group receiving MSCs, the gastric ulcer group receiving NO and the gastric ulcer group receiving both MSCs and NO compared to the gastric ulcer group after both 24 h and 7 days. Histopathological examination of gastric tissue of groups that received stem cells or NO alone, showed mucosal regenerative changes with increased thickness together with reduced inflammatory cellular infiltrate in the submucosa and decreased congestion. There was complete restoration in gastric mucosa in the group that received both stem cells and NO. **Conclusion** Administration of MSCs, NO, or MSCs plus NO may exert a therapeutic effect on the mucosal lesion in gastric ulcer through their anti-inflammatory, angiogenic and antiapoptotic actions.
**Keywords:** Mesenchymal Stem Cells; No; Refractory Peptic Ulcer; Stem Cells Therapy; E-Nos

### *Dept. of Neurology*

## M-218. Global, Regional,and National Comparative Risk Assessment of 79 Behavioural, Environmentaland Occupational, and Metabolic Risks or Clusters of Risks, 1990–2015: A Systematic Analysis for the Global Burden of Disease Study 2015

Foad Abd-Allah, et al.

*The Lancet, 388(10053): 1659-1724 (2016) IF: 44.002*

**Background:** The Global Burden of Diseases, Injuries, and Risk Factors Study 2015 provides an up-to-date synthesis of the evidence for risk factor exposure and the attributable burden of disease. By providing national and subnational assessments spanning the past 25 years, this study can inform debates on the importance of addressing risks in context. **Methods:** We used the comparative risk assessment framework developed for previous iterations of the Global Burden of Disease Study to estimate attributable deaths, disability-adjusted life-years (DALYs), and trends in exposure by age group, sex, year, and geography for 79 behavioural, environmental and occupational, and metabolic risks or clusters of risks from 1990 to 2015. This study included 388 risk-outcome pairs that met World Cancer Research Fund-defined criteria for convincing or probable evidence. We extracted relative risk and exposure estimates from randomised controlled trials, cohorts, pooled cohorts, household

surveys, census data, satellite data, and other sources. We used statistical models to pool data, adjust for bias, and incorporate covariates. We developed a metric that allows comparisons of exposure across risk factors-the summary exposure value. Using the counterfactual scenario of theoretical minimum risk level, we estimated the portion of deaths and DALYs that could be attributed to a given risk. We decomposed trends in attributable burden into contributions from population growth, population age structure, risk exposure, and risk-deleted cause-specific DALY rates. We characterised risk exposure in relation to a Socio-demographic Index (SDI). **Findings:** Between 1990 and 2015, global exposure to unsafe sanitation, household air pollution, childhood underweight, childhood stunting, and smoking each decreased by more than 25%. Global exposure for several occupational risks, high body-mass index (BMI), and drug use increased by more than 25% over the same period. All risks jointly evaluated in 2015 accounted for 57·8% (95% CI 56·6-58·8) of global deaths and 41·2% (39·8-42·8) of DALYs. In 2015, the ten largest contributors to global DALYs among Level 3 risks were high systolic blood pressure (211·8 million [192·7 million to 231·1 million] global DALYs), smoking (148·6 million [134·2 million to 163·1 million]), high fasting plasma glucose (143·1 million [125·1 million to 163·5 million]), high BMI (120·1 million [83·8 million to 158·4 million]), childhood undernutrition (113·3 million [103·9 million to 123·4 million]), ambient particulate matter (103·1 million [90·8 million to 115·1 million]), high total cholesterol (88·7 million [74·6 million to 105·7 million]), household air pollution (85·6 million [66·7 million to 106·1 million]), alcohol use (85·0 million [77·2 million to 93·0 million]), and diets high in sodium (83·0 million [49·3 million to 127·5 million]). From 1990 to 2015, attributable DALYs declined for micronutrient deficiencies, childhood undernutrition, unsafe sanitation and water, and household air pollution; reductions in risk-deleted DALY rates rather than reductions in exposure drove these declines. Rising exposure contributed to notable increases in attributable DALYs from high BMI, high fasting plasma glucose, occupational carcinogens, and drug use. Environmental risks and childhood undernutrition declined steadily with SDI; low physical activity, high BMI, and high fasting plasma glucose increased with SDI. In 119 countries, metabolic risks, such as high BMI and fasting plasma glucose, contributed the most attributable DALYs in 2015. Regionally, smoking still ranked among the leading five risk factors for attributable DALYs in 109 countries; childhood underweight and unsafe sex remained primary drivers of early death and disability in much of sub-Saharan Africa. **Interpretation:** Declines in some key environmental risks have contributed to declines in critical infectious diseases. Some risks appear to be invariant to SDI. Increasing risks, including high BMI, high fasting plasma glucose, drug use, and some occupational exposures, contribute to rising burden from some conditions, but also provide opportunities for intervention. Some highly preventable risks, such as smoking, remain major causes of attributable DALYs, even as exposure is declining. Public policy makers need to pay attention to the risks that are increasingly major contributors to global burden.

**Keywords:** Comparative Risk Assessment, Behavioural, Environmental, Occupational, Metabolic Risks

## M-219. Global, Regional, and National Disability-Adjusted Life-Years (DALYS) For 315 Diseases and Injuries and Healthy Life Expectancy (HALE), 1990-2015: A Systematic Analysis for the Global Burden of Disease Study 2015.

Foad Abd-Allah, et al.

*The Lancet, 388(10053): 1603-1658 (2016) IF: 44.002*

**Background:** Healthy life expectancy (HALE) and disability-adjusted life-years (DALYs) provide summary measures of health across geographies and time that can inform assessments of epidemiological patterns and health system performance, help to prioritise investments in research and development, and monitor progress toward the Sustainable Development Goals (SDGs). We aimed to provide updated HALE and DALYs for geographies worldwide and evaluate how disease burden changes with development. **Methods:** We used results from the Global Burden of Diseases, Injuries, and Risk Factors Study 2015 (GBD 2015) for all-cause mortality, cause-specific mortality, and non-fatal disease burden to derive HALE and DALYs by sex for 195 countries and territories from 1990 to 2015. We calculated DALYs by summing years of life lost (YLLs) and years of life lived with disability (YLDs) for each geography, age group, sex, and year. We estimated HALE using the Sullivan method, which draws from age-specific death rates and YLDs per capita. We then assessed how observed levels of DALYs and HALE differed from expected trends calculated with the Socio-demographic Index (SDI), a composite indicator constructed from measures of income per capita, average years of schooling, and total fertility rate. FINDINGS: Total global DALYs remained largely unchanged from 1990 to 2015, with decreases in communicable, neonatal, maternal, and nutritional (Group 1) disease DALYs offset by increased DALYs due to non-communicable diseases (NCDs). Much of this epidemiological transition was caused by changes in population growth and ageing, but it was accelerated by widespread improvements in SDI that also correlated strongly with the increasing importance of NCDs. Both total DALYs and age-standardised DALY rates due to most Group 1 causes significantly decreased by 2015, and although total burden climbed for the majority of NCDs, age-standardised DALY rates due to NCDs declined. Nonetheless, age-standardised DALY rates due to several high-burden NCDs (including osteoarthritis, drug use disorders, depression, diabetes, congenital birth defects, and skin, oral, and sense organ diseases) either increased or remained unchanged, leading to increases in their relative ranking in many geographies. From 2005 to 2015, HALE at birth increased by an average of 2·9 years (95% uncertainty interval 2·9-3·0) for men and 3·5 years (3·4-3·7) for women, while HALE at age 65 years improved by 0·85 years (0·78-0·92) and 1·2 years (1·1-1·3), respectively. Rising SDI was associated with consistently higher HALE and a somewhat smaller proportion of life spent with functional health loss; however, rising SDI was related to increases in total disability. Many countries and territories in central America and eastern sub-Saharan Africa had increasingly lower rates of disease burden than expected given their SDI. At the same time, a subset of geographies recorded a growing gap between observed and expected levels of DALYs, a trend driven mainly by rising burden due to war, interpersonal violence, and various NCDs. **Interpretation:** Health is improving globally, but this means more populations are spending more time with functional health

loss, an absolute expansion of morbidity. The proportion of life spent in ill health decreases somewhat with increasing SDI, a relative compression of morbidity, which supports continued efforts to elevate personal income, improve education, and limit fertility. Our analysis of DALYs and HALE and their relationship to SDI represents a robust framework on which to benchmark geography-specific health performance and SDG progress. Country-specific drivers of disease burden, particularly for causes with higher-than-expected DALYs, should inform financial and research investments, prevention efforts, health policies, and health system improvement initiatives for all countries along the development continuum.
**Keywords:** National, Disability-Adjusted Life-Years (DALYS)

## M-220. Global, Regional, and National Incidence, Prevalence, and Years Lived with Disability For 310 Diseases and Injuries, 1990-2015: A Systematic Analysis for the Global Burden of Disease Study 2015.

Foad Abd-Allah, et al.

*The Lancet, 388(10053): 1545-1602 (2016) IF: 44.002*

**Background:** Non-fatal outcomes of disease and injury increasingly detract from the ability of the world's population to live in full health, a trend largely attributable to an epidemiological transition in many countries from causes affecting children, to non-communicable diseases (NCDs) more common in adults. For the Global Burden of Diseases, Injuries, and Risk Factors Study 2015 (GBD 2015), we estimated the incidence, prevalence, and years lived with disability for diseases and injuries at the global, regional, and national scale over the period of 1990 to 2015. **Methods:** We estimated incidence and prevalence by age, sex, cause, year, and geography with a wide range of updated and standardised analytical procedures. Improvements from GBD 2013 included the addition of new data sources, updates to literature reviews for 85 causes, and the identification and inclusion of additional studies published up to November, 2015, to expand the database used for estimation of non-fatal outcomes to 60 900 unique data sources. Prevalence and incidence by cause and sequelae were determined with DisMod-MR 2.1, an improved version of the DisMod-MR Bayesian meta-regression tool first developed for GBD 2010 and GBD 2013. For some causes, we used alternative modelling strategies where the complexity of the disease was not suited to DisMod-MR 2.1 or where incidence and prevalence needed to be determined from other data. For GBD 2015 we created a summary indicator that combines measures of income per capita, educational attainment, and fertility (the Socio-demographic Index [SDI]) and used it to compare observed patterns of health loss to the expected pattern for countries or locations with similar SDI scores. FINDINGS: We generated 9·3 billion estimates from the various combinations of prevalence, incidence, and YLDs for causes, sequelae, and impairments by age, sex, geography, and year. In 2015, two causes had acute incidences in excess of 1 billion: upper respiratory infections (17·2 billion, 95% uncertainty interval [UI] 15·4-19·2 billion) and diarrhoeal diseases (2·39 billion, 2·30-2·50 billion). Eight causes of chronic disease and injury each affected more than 10% of the world's population in 2015: permanent caries, tension-type headache, iron-deficiency anaemia, age-related and other hearing loss, migraine, genital herpes, refraction and accommodation disorders, and ascariasis. The impairment that affected the greatest number of people in 2015 was anaemia, with 2·36 billion (2·35-2·37 billion) individuals affected. The second and third leading impairments by number of individuals affected were hearing loss and vision loss, respectively. Between 2005 and 2015, there was little change in the leading causes of years lived with disability (YLDs) on a global basis. NCDs accounted for 18 of the leading 20 causes of age-standardised YLDs on a global scale. Where rates were decreasing, the rate of decrease for YLDs was slower than that of years of life lost (YLLs) for nearly every cause included in our analysis. For low SDI geographies, Group 1 causes typically accounted for 20-30% of total disability, largely attributable to nutritional deficiencies, malaria, neglected tropical diseases, HIV/AIDS, and tuberculosis. Lower back and neck pain was the leading global cause of disability in 2015 in most countries. The leading cause was sense organ disorders in 22 countries in Asia and Africa and one in central Latin America; diabetes in four countries in Oceania; HIV/AIDS in three southern sub-Saharan African countries; collective violence and legal intervention in two north African and Middle Eastern countries; iron-deficiency anaemia in Somalia and Venezuela; depression in Uganda; onchoceriasis in Liberia; and other neglected tropical diseases in the Democratic Republic of the Congo. **Interpretation:**Ageing of the world's population is increasing the number of people living with sequelae of diseases and injuries. Shifts in the epidemiological profile driven by socioeconomic change also contribute to the continued increase in years lived with disability (YLDs) as well as the rate of increase in YLDs. Despite limitations imposed by gaps in data availability and the variable quality of the data available, the standardised and comprehensive approach of the GBD study provides opportunities to examine broad trends, compare those trends between countries or subnational geographies, benchmark against locations at similar stages of development, and gauge the strength or weakness of the estimates available.
**Keywords:** National Incidence, Prevalence, Disability.

## M-221. Global, Regional, and National Levels of Maternal Mortality, 1990-2015: A Systematic Analysis for the Global Burden of Disease Study 2015.

Foad Abd-Allah, et al.

*The Lancet, 388(10053): 1775-1812 (2016) IF: 44.002*

**Background:** In transitioning from the Millennium Development Goal to the Sustainable Development Goal era, it is imperative to comprehensively assess progress toward reducing maternal mortality to identify areas of success, remaining challenges, and frame policy discussions. We aimed to quantify maternal mortality throughout the world by underlying cause and age from 1990 to 2015. **Methods:** We estimated maternal mortality at the global, regional, and national levels from 1990 to 2015 for ages 10-54 years by systematically compiling and processing all available data sources from 186 of 195 countries and territories, 11 of which were analysed at the subnational level. We quantified eight underlying causes of maternal death and four timing categories, improving estimation methods since GBD 2013 for adult all-cause mortality, HIV-related maternal mortality, and late maternal death. Secondary analyses then allowed systematic examination of drivers of

trends, including the relation between maternal mortality and coverage of specific reproductive health-care services as well as assessment of observed versus expected maternal mortality as a function of Socio-demographic Index (SDI), a summary indicator derived from measures of income per capita, educational attainment, and fertility. **Findings:** Only ten countries achieved MDG 5, but 122 of 195 countries have already met SDG 3.1. Geographical disparities widened between 1990 and 2015 and, in 2015, 24 countries still had a maternal mortality ratio greater than 400. The proportion of all maternal deaths occurring in the bottom two SDI quintiles, where haemorrhage is the dominant cause of maternal death, increased from roughly 68% in 1990 to more than 80% in 2015. The middle SDI quintile improved the most from 1990 to 2015, but also has the most complicated causal profile. Maternal mortality in the highest SDI quintile is mostly due to other direct maternal disorders, indirect maternal disorders, and abortion, ectopic pregnancy, and/or miscarriage. Historical patterns suggest achievement of SDG 3.1 will require 91% coverage of one antenatal care visit, 78% of four antenatal care visits, 81% of in-facility delivery, and 87% of skilled birth attendance. **Interpretation:** Several challenges to improving reproductive health lie ahead in the SDG era. Countries should establish or renew systems for collection and timely dissemination of health data; expand coverage and improve quality of family planning services, including access to contraception and safe abortion to address high adolescent fertility; invest in improving health system capacity, including coverage of routine reproductive health care and of more advanced obstetric care-including EmOC; adapt health systems and data collection systems to monitor and reverse the increase in indirect, other direct, and late maternal deaths, especially in high SDI locations; and examine their own performance with respect to their SDI level, using that information to formulate strategies to improve performance and ensure optimum reproductive health of their population.

**Keywords:** National Levels, Maternal Mortality.

## M-222. Global, Regional,and National Life Expectancy, All-Cause Mortality, and Cause-Specific Mortality for 249 Causes of Death, 1980-2015: A Systematic Analysis for the Global Burden of Disease Study 2015.

Foad Abd-Allah, et al.

*The Lancet, 388(10053): 1459-1544 (2016) IF: 44.002*

**Background:** Improving survival and extending the longevity of life for all populations requires timely, robust evidence on local mortality levels and trends. The Global Burden of Disease 2015 Study (GBD 2015) provides a comprehensive assessment of all-cause and cause-specific mortality for 249 causes in 195 countries and territories from 1980 to 2015. These results informed an in-depth investigation of observed and expected mortality patterns based on sociodemographic measures. **Methods:** We estimated all-cause mortality by age, sex, geography, and year using an improved analytical approach originally developed for GBD 2013 and GBD 2010. Improvements included refinements to the estimation of child and adult mortality and corresponding uncertainty, parameter selection for under-5 mortality synthesis by spatiotemporal Gaussian process regression, and sibling history data processing. We also expanded the database of vital registration, survey, and census data to 14 294 geography-year datapoints. For GBD 2015, eight causes, including Ebola virus disease, were added to the previous GBD cause list for mortality. We used six modelling approaches to assess cause-specific mortality, with the Cause of Death Ensemble Model (CODEm) generating estimates for most causes. We used a series of novel analyses to systematically quantify the drivers of trends in mortality across geographies. First, we assessed observed and expected levels and trends of cause-specific mortality as they relate to the Socio-demographic Index (SDI), a summary indicator derived from measures of income per capita, educational attainment, and fertility. Second, we examined factors affecting total mortality patterns through a series of counterfactual scenarios, testing the magnitude by which population growth, population age structures, and epidemiological changes contributed to shifts in mortality. Finally, we attributed changes in life expectancy to changes in cause of death. We documented each step of the GBD 2015 estimation processes, as well as data sources, in accordance with Guidelines for Accurate and Transparent Health Estimates Reporting (GATHER). **Findings:** Globally, life expectancy from birth increased from 61·7 years (95% uncertainty interval 61·4-61·9) in 1980 to 71·8 years (71·5-72·2) in 2015. Several countries in sub-Saharan Africa had very large gains in life expectancy from 2005 to 2015, rebounding from an era of exceedingly high loss of life due to HIV/AIDS. At the same time, many geographies saw life expectancy stagnate or decline, particularly for men and in countries with rising mortality from war or interpersonal violence. From 2005 to 2015, male life expectancy in Syria dropped by 11·3 years (3·7-17·4), to 62·6 years (56·5-70·2). Total deaths increased by 4·1% (2·6-5·6) from 2005 to 2015, rising to 55·8 million (54·9 million to 56·6 million) in 2015, but age-standardised death rates fell by 17·0% (15·8-18·1) during this time, underscoring changes in population growth and shifts in global age structures. The result was similar for non-communicable diseases (NCDs), with total deaths from these causes increasing by 14·1% (12·6-16·0) to 39·8 million (39·2 million to 40·5 million) in 2015, whereas age-standardised rates decreased by 13·1% (11·9-14·3). Globally, this mortality pattern emerged for several NCDs, including several types of cancer, ischaemic heart disease, cirrhosis, and Alzheimer's disease and other dementias. By contrast, both total deaths and age-standardised death rates due to communicable, maternal, neonatal, and nutritional conditions significantly declined from 2005 to 2015, gains largely attributable to decreases in mortality rates due to HIV/AIDS (42·1%, 39·1-44·6), malaria (43·1%, 34·7-51·8), neonatal preterm birth complications (29·8%, 24·8-34·9), and maternal disorders (29·1%, 19·3-37·1). Progress was slower for several causes, such as lower respiratory infections and nutritional deficiencies, whereas deaths increased for others, including dengue and drug use disorders. Age-standardised death rates due to injuries significantly declined from 2005 to 2015, yet interpersonal violence and war claimed increasingly more lives in some regions, particularly in the Middle East. In 2015, rotaviral enteritis (rotavirus) was the leading cause of under-5 deaths due to diarrhoea (146 000 deaths, 118 000-183 000) and pneumococcal pneumonia was the leading cause of under-5 deaths due to lower respiratory infections (393 000 deaths, 228 000-532 000), although pathogen-specific mortality varied by region. Globally, the effects of population growth, ageing, and changes in age-standardised death rates substantially differed by cause. Our analyses on the expected associations between cause-specific mortality and SDI show the regular shifts

in cause of death composition and population age structure with rising SDI. Country patterns of premature mortality (measured as years of life lost [YLLs]) and how they differ from the level expected on the basis of SDI alone revealed distinct but highly heterogeneous patterns by region and country or territory. Ischaemic heart disease, stroke, and diabetes were among the leading causes of YLLs in most regions, but in many cases, intraregional results sharply diverged for ratios of observed and expected YLLs based on SDI. Communicable, maternal, neonatal, and nutritional diseases caused the most YLLs throughout sub-Saharan Africa, with observed YLLs far exceeding expected YLLs for countries in which malaria or HIV/AIDS remained the leading causes of early death. **Interpretation:**At the global scale, age-specific mortality has steadily improved over the past 35 years; this pattern of general progress continued in the past decade. Progress has been faster in most countries than expected on the basis of development measured by the SDI. Against this background of progress, some countries have seen falls in life expectancy, and age-standardised death rates for some causes are increasing. Despite progress in reducing age-standardised death rates, population growth and ageing mean that the number of deaths from most non-communicable causes are increasing in most countries, putting increased demands on health systems.

**Keywords:** Global, Regional, National Life Expectancy, Mortality.

## M-223. Global, Regional, National,andSelected Subnational Levels of Stillbirths, Neonatal, Infant,andUnder-5 Mortality, 1980-2015: A Systematic Analysis for the Global Burden of Disease Study 2015.

Foad Abd-Allah, et al.

*The Lancet, 388(10053): 1725-1774 (2016) IF: 44.002*

**Background:** Established in 2000, Millennium Development Goal 4 (MDG4) catalysed extraordinary political, financial, and social commitments to reduce under-5 mortality by two-thirds between 1990 and 2015. At the country level, the pace of progress in improving child survival has varied markedly, highlighting a crucial need to further examine potential drivers of accelerated or slowed decreases in child mortality. The Global Burden of Disease 2015 Study (GBD 2015) provides an analytical framework to comprehensively assess these trends for under-5 mortality, age-specific and cause-specific mortality among children under 5 years, and stillbirths by geography over time. **Methods:** Drawing from analytical approaches developed and refined in previous iterations of the GBD study, we generated updated estimates of child mortality by age group (neonatal, post-neonatal, ages 1-4 years, and under 5) for 195 countries and territories and selected subnational geographies, from 1980-2015. We also estimated numbers and rates of stillbirths for these geographies and years. Gaussian process regression with data source adjustments for sampling and non-sampling bias was applied to synthesise input data for under-5 mortality for each geography. Age-specific mortality estimates were generated through a two-stage age-sex splitting process, and stillbirth estimates were produced with a mixed-effects model, which accounted for variable stillbirth definitions and data source-specific biases. For GBD 2015, we did a series of novel analyses to systematically quantify the drivers of trends in child mortality across geographies. First, we assessed observed and expected levels and annualised rates of decrease for under-5 mortality and stillbirths as they related to the Soci-demographic Index (SDI). Second, we examined the ratio of recorded and expected levels of child mortality, on the basis of SDI, across geographies, as well as differences in recorded and expected annualised rates of change for under-5 mortality. Third, we analysed levels and cause compositions of under-5 mortality, across time and geographies, as they related to rising SDI. Finally, we decomposed the changes in under-5 mortality to changes in SDI at the global level, as well as changes in leading causes of under-5 deaths for countries and territories. We documented each step of the GBD 2015 child mortality estimation process, as well as data sources, in accordance with the Guidelines for Accurate and Transparent Health Estimates Reporting (GATHER). FINDINGS: Globally, 5·8 million (95% uncertainty interval [UI] 5·7-6·0) children younger than 5 years died in 2015, representing a 52·0% (95% UI 50·7-53·3) decrease in the number of under-5 deaths since 1990. Neonatal deaths and stillbirths fell at a slower pace since 1990, decreasing by 42·4% (41·3-43·6) to 2·6 million (2·6-2·7) neonatal deaths and 47·0% (35·1-57·0) to 2·1 million (1·8-2·5) stillbirths in 2015. Between 1990 and 2015, global under-5 mortality decreased at an annualised rate of decrease of 3·0% (2·6-3·3), falling short of the 4·4% annualised rate of decrease required to achieve MDG4. During this time, 58 countries met or exceeded the pace of progress required to meet MDG4. Between 2000, the year MDG4 was formally enacted, and 2015, 28 additional countries that did not achieve the 4·4% rate of decrease from 1990 met the MDG4 pace of decrease. However, absolute levels of under-5 mortality remained high in many countries, with 11 countries still recording rates exceeding 100 per 1000 livebirths in 2015. Marked decreases in under-5 deaths due to a number of communicable diseases, including lower respiratory infections, diarrhoeal diseases, measles, and malaria, accounted for much of the progress in lowering overall under-5 mortality in low-income countries. Compared with gains achieved for infectious diseases and nutritional deficiencies, the persisting toll of neonatal conditions and congenital anomalies on child survival became evident, especially in low-income and low-middle-income countries. We found sizeable heterogeneities in comparing observed and expected rates of under-5 mortality, as well as differences in observed and expected rates of change for under-5 mortality. At the global level, we recorded a divergence in observed and expected levels of under-5 mortality starting in 2000, with the observed trend falling much faster than what was expected based on SDI through 2015. Between 2000 and 2015, the world recorded 10·3 million fewer under-5 deaths than expected on the basis of improving SDI alone. **Interpretation:** Gains in child survival have been large, widespread, and in many places in the world, faster than what was anticipated based on improving levels of development. Yet some countries, particularly in sub-Saharan Africa, still had high rates of under-5 mortality in 2015. Unless these countries are able to accelerate reductions in child deaths at an extraordinary pace, their achievement of proposed SDG targets is unlikely. Improving the evidence base on drivers that might hasten the pace of progress for child survival, ranging from cost-effective intervention packages to innovative financing mechanisms, is vital to charting the pathways for ultimately ending preventable child deaths by 2030.

**Keywords:** Selected Subnational, Levels of Stillbirth

## M-224. Measuring the Health-Related Sustainable Development Goals in 188 Countries: A Baseline Analysis from the Global Burden of Disease Study 2015.

Foad Abd-Allah, et al.

*The Lancet, 388(10053): 1813-1850 (2016) IF: 44.002*

**Background:** In September, 2015, the UN General Assembly established the Sustainable Development Goals (SDGs). The SDGs specify 17 universal goals, 169 targets, and 230 indicators leading up to 2030. We provide an analysis of 33 health-related SDG indicators based on the Global Burden of Diseases, Injuries, and Risk Factors Study 2015 (GBD 2015). **Methods:** We applied statistical methods to systematically compiled data to estimate the performance of 33 health-related SDG indicators for 188 countries from 1990 to 2015. We rescaled each indicator on a scale from 0 (worst observed value between 1990 and 2015) to 100 (best observed). Indices representing all 33 health-related SDG indicators (health-related SDG index), health-related SDG indicators included in the Millennium Development Goals (MDG index), and health-related indicators not included in the MDGs (non-MDG index) were computed as the geometric mean of the rescaled indicators by SDG target. We used spline regressions to examine the relations between the Socio-demographic Index (SDI, a summary measure based on average income per person, educational attainment, and total fertility rate) and each of the health-related SDG indicators and indices. FINDINGS: In 2015, the median health-related SDG index was 59·3 (95% uncertainty interval 56·8-61·8) and varied widely by country, ranging from 85·5 (84·2-86·5) in Iceland to 20·4 (15·4-24·9) in Central African Republic. SDI was a good predictor of the health-related SDG index (r2=0·88) and the MDG index (r2=0·92), whereas the non-MDG index had a weaker relation with SDI (r2=0·79). Between 2000 and 2015, the health-related SDG index improved by a median of 7·9 (IQR 5·0-10·4), and gains on the MDG index (a median change of 10·0 [6·7-13·1]) exceeded that of the non-MDG index (a median change of 5·5 [2·1-8·9]). Since 2000, pronounced progress occurred for indicators such as met need with modern contraception, under-5 mortality, and neonatal mortality, as well as the indicator for universal health coverage tracer interventions. Moderate improvements were found for indicators such as HIV and tuberculosis incidence, minimal changes for hepatitis B incidence took place, and childhood overweight considerably worsened. **Interpretation:**GBD provides an independent, comparable avenue for monitoring progress towards the health-related SDGs. Our analysis not only highlights the importance of income, education, and fertility as drivers of health improvement but also emphasises that investments in these areas alone will not be sufficient. Although considerable progress on the health-related MDG indicators has been made, these gains will need to be sustained and, in many cases, accelerated to achieve the ambitious SDG targets. The minimal improvement in or worsening of health-related indicators beyond the MDGs highlight the need for additional resources to effectively address the expanded scope of the health-related SDGs.

**Keywords:** Health-Related, Sustainable Development,Baseline Analysis

## M-225. Global Burden of Stroke and Risk Factors in 188 Countries, During 1990-2013: A Systematic Analysis for the Global Burden of Disease Study 2013

Foad Abd-Allah, et al.

*The Lancet Neurology, 15(9): 913-924 (2016) IF: 23.648*

**Background:** The contribution of modifiable risk factors to the increasing global and regional burden of stroke is unclear, but knowledge about this contribution is crucial for informing stroke prevention strategies. We used data from the Global Burden of Disease Study 2013 (GBD 2013) to estimate the population-attributable fraction (PAF) of stroke-related disability-adjusted life-years (DALYs) associated with potentially modifiable environmental, occupational, behavioural, physiological, and metabolic risk factors in different age and sex groups worldwide and in high-income countries and low-income and middle-income countries, from 1990 to 2013. **Methods:** We used data on stroke-related DALYs, risk factors, and PAF from the GBD 2013 Study to estimate the burden of stroke by age and sex (with corresponding 95% uncertainty intervals [UI]) in 188 countries, as measured with stroke-related DALYs in 1990 and 2013. We evaluated attributable DALYs for 17 risk factors (air pollution and environmental, dietary, physical activity, tobacco smoke, and physiological) and six clusters of risk factors by use of three inputs: risk factor exposure, relative risks, and the theoretical minimum risk exposure level. For most risk factors, we synthesised data for exposure with a Bayesian meta-regression method (DisMod-MR) or spatial-temporal Gaussian process regression. We based relative risks on meta-regressions of published cohort and intervention studies. Attributable burden for clusters of risks and all risks combined took into account evidence on the mediation of some risks, such as high body-mass index (BMI), through other risks, such as high systolic blood pressure (SBP) and high total cholesterol. FINDINGS: Globally, 90·5% (95% UI 88·5-92·2) of the stroke burden (as measured in DALYs) was attributable to the modifiable risk factors analysed, including 74·2% (95% UI 70·7-76·7) due to behavioural factors (smoking, poor diet, and low physical activity). Clusters of metabolic factors (high SBP, high BMI, high fasting plasma glucose, high total cholesterol, and low glomerular filtration rate; 72·4%, 95% UI 70·2-73·5) and environmental factors (air pollution and lead exposure; 33·4%, 95% UI 32·4-34·3) were the second and third largest contributors to DALYs. Globally, 29·2% (95% UI 28·2-29·6) of the burden of stroke was attributed to air pollution. Although globally there were no significant differences between sexes in the proportion of stroke burden due to behavioural, environmental, and metabolic risk clusters, in the low-income and middle-income countries, the PAF of behavioural risk clusters in males was greater than in females. The PAF of all risk factors increased from 1990 to 2013 (except for second-hand smoking and household air pollution from solid fuels) and varied significantly between countries. **Interpretation:**Our results suggest that more than 90% of the stroke burden is attributable to modifiable risk factors, and achieving control of behavioural and metabolic risk factors could avert more than three-quarters of the global stroke burden. Air pollution has emerged as a significant contributor to global stroke burden, especially in low-income and middle-income countries, and therefore reducing exposure to air pollution should be one of the main priorities to reduce stroke burden in these countries.

**Keywords:** Stroke,Global Burden of Disease,

## M-226. Health in Times of Uncertainty in the Eastern Mediterranean Region, 1990-2013: A Systematic Analysis for the Global Burden of Disease Study 2013.

Foad Abd-Allah, et al.

*The Lancet Global Health, 4(10): 0-713 (2016) IF: 14.722*

**Background:** The eastern Mediterranean region is comprised of 22 countries: Afghanistan, Bahrain, Djibouti, Egypt, Iran, Iraq, Jordan, Kuwait, Lebanon, Libya, Morocco, Oman, Pakistan, Palestine, Qatar, Saudi Arabia, Somalia, Sudan, Syria, Tunisia, the United Arab Emirates, and Yemen. Since our Global Burden of Disease Study 2010 (GBD 2010), the region has faced unrest as a result of revolutions, wars, and the so-called Arab uprisings. The objective of this study was to present the burden of diseases, injuries, and risk factors in the eastern Mediterranean region as of 2013. **Methods:** GBD 2013 includes an annual assessment covering 188 countries from 1990 to 2013. The study covers 306 diseases and injuries, 1233 sequelae, and 79 risk factors. Our GBD 2013 analyses included the addition of new data through updated systematic reviews and through the contribution of unpublished data sources from collaborators, an updated version of modelling software, and several improvements in our methods. In this systematic analysis, we use data from GBD 2013 to analyse the burden of disease and injuries in the eastern Mediterranean region specifically. **Findings:** The leading cause of death in the region in 2013 was ischaemic heart disease (90·3 deaths per 100 000 people), which increased by 17·2% since 1990. However, diarrhoeal diseases were the leading cause of death in Somalia (186·7 deaths per 100 000 people) in 2013, which decreased by 26·9% since 1990. The leading cause of disability-adjusted life-years (DALYs) was ischaemic heart disease for males and lower respiratory infection for females. High blood pressure was the leading risk factor for DALYs in 2013, with an increase of 83·3% since 1990. Risk factors for DALYs varied by country. In low-income countries, childhood wasting was the leading cause of DALYs in Afghanistan, Somalia, and Yemen, whereas unsafe sex was the leading cause in Djibouti. Non-communicable risk factors were the leading cause of DALYs in high-income and middle-income countries in the region. DALY risk factors varied by age, with child and maternal malnutrition affecting the younger age groups (aged 28 days to 4 years), whereas high bodyweight and systolic blood pressure affected older people (aged 60-80 years). The proportion of DALYs attributed to high body-mass index increased from 3·7% to 7·5% between 1990 and 2013. Burden of mental health problems and drug use increased. Most increases in DALYs, especially from non-communicable diseases, were due to population growth. The crises in Egypt, Yemen, Libya, and Syria have resulted in a reduction in life expectancy; life expectancy in Syria would have been 5 years higher than that recorded for females and 6 years higher for males had the crisis not occurred. **Interpretation:** Our study shows that the eastern Mediterranean region is going through a crucial health phase. The Arab uprisings and the wars that followed, coupled with ageing and population growth, will have a major impact on the region's health and resources. The region has historically seen improvements in life expectancy and other health indicators, even under stress. However, the current situation will cause deteriorating health conditions for many countries and for many years and will have an impact on the region and the rest of the world. Based on our findings, we call for increased investment in health in the region in addition to reducing the conflicts.

**Keywords:** Health; Eastern Mediterranean Region; Global Burden of Disease.

## M-227. GlobalandNational Burden of Diseases and Injuries Among Children and Adolescents Between 1990 and 2013: Findings from the Global Burden of Disease 2013 Study.

Foad Abd-Allah, et al.

*Jama Pediatrics, 170: 267-287 (2016) IF: 9.528*

**Importance:** The literature focuses on mortality among children younger than 5 years. Comparable information on nonfatal health outcomes among these children and the fatal and nonfatal burden of diseases and injuries among older children and adolescents is scarce. **Objective:** To determine levels and trends in the fatal and nonfatal burden of diseases and injuries among younger children (aged <5 years), older children (aged 5-9 years), and adolescents (aged 10-19 years) between 1990 and 2013 in 188 countries from the Global Burden of Disease (GBD) 2013 study. **Evidence Review:**Data from vital registration, verbal autopsy studies, maternal and child death surveillance, and other sources covering 14,244 site-years (ie, years of cause of death data by geography) from 1980 through 2013 were used to estimate cause-specific mortality. Data from 35,620 epidemiological sources were used to estimate the prevalence of the diseases and sequelae in the GBD 2013 study. Cause-specific mortality for most causes was estimated using the Cause of Death Ensemble Model strategy. For some infectious diseases (eg, HIV infection/AIDS, measles, hepatitis B) where the disease process is complex or the cause of death data were insufficient or unavailable, we used natural history models. For most nonfatal health outcomes, DisMod-MR 2.0, a Bayesian metaregression tool, was used to meta-analyze the epidemiological data to generate prevalence estimates. **Findings:**of the 7.7 (95% uncertainty interval [UI], 7.4-8.1) million deaths among children and adolescents globally in 2013, 6.28 million occurred among younger children, 0.48 million among older children, and 0.97 million among adolescents. In 2013, the leading causes of death were lower respiratory tract infections among younger children (905.059 deaths; 95% UI, 810,304-998,125), diarrheal diseases among older children (38,325 deaths; 95% UI, 30,365-47,678), and road injuries among adolescents (115,186 deaths; 95% UI, 105,185-124,870). Iron deficiency anemia was the leading cause of years lived with disability among children and adolescents, affecting 619 (95% UI, 618-621) million in 2013. Large between-country variations exist in mortality from leading causes among children and adolescents. Countries with rapid declines in all-cause mortality between 1990 and 2013 also experienced large declines in most leading causes of death, whereas countries with the slowest declines had stagnant or increasing trends in the leading causes of death. In 2013, Nigeria had a 12% global share of deaths from lower respiratory tract infections and a 38% global share of deaths from malaria. India had 33% of the world's deaths from neonatal encephalopathy. Half of the world's diarrheal deaths among children and adolescents occurred in just 5 countries: India, Democratic Republic of the Congo, Pakistan, Nigeria, and Ethiopia. **Conclusions and Relevance:**Understanding the levels and trends of the leading causes of death and disability among

children and adolescents is critical to guide investment and inform policies. Monitoring these trends over time is also key to understanding where interventions are having an impact. Proven interventions exist to prevent or treat the leading causes of unnecessary death and disability among children and adolescents. The findings presented here show that these are underused and give guidance to policy makers in countries where more attention is needed.
**Keywords:** National Burden, Children, Diseases, Injuries

## M-228. Estimates of Global, Regional, and National Incidence, Prevalence, and Mortality of Hiv, 1980-2015: the Global Burden of Disease Study 2015.

Foad Abd-Allah, et al.

*Lancet HIV, 3(8): 0-387 (2016) IF: 8.364*

**Background:** Timely assessment of the burden of HIV/AIDS is essential for policy setting and programme evaluation. In this report from the Global Burden of Disease Study 2015 (GBD 2015), we provide national estimates of levels and trends of HIV/AIDS incidence, prevalence, coverage of antiretroviral therapy (ART), and mortality for 195 countries and territories from 1980 to 2015. **Methods:** For countries without high-quality vital registration data, we estimated prevalence and incidence with data from antenatal care clinics and population-based seroprevalence surveys, and with assumptions by age and sex on initial CD4 distribution at infection, CD4 progression rates (probability of progression from higher to lower CD4 cell-count category), on and off antiretroviral therapy (ART) mortality, and mortality from all other causes. Our estimation strategy links the GBD 2015 assessment of all-cause mortality and estimation of incidence and prevalence so that for each draw from the uncertainty distribution all assumptions used in each step are internally consistent. We estimated incidence, prevalence, and death with GBD versions of the Estimation and Projection Package (EPP) and Spectrum software originally developed by the Joint United Nations Programme on HIV/AIDS (UNAIDS). We used an open-source version of EPP and recoded Spectrum for speed, and used updated assumptions from systematic reviews of the literature and GBD demographic data. For countries with high-quality vital registration data, we developed the cohort incidence bias adjustment model to estimate HIV incidence and prevalence largely from the number of deaths caused by HIV recorded in cause-of-death statistics. We corrected these statistics for garbage coding and HIV misclassification. FINDINGS: Global HIV incidence reached its peak in 1997, at 3·3 million new infections (95% uncertainty interval [UI] 3·1-3·4 million). Annual incidence has stayed relatively constant at about 2·6 million per year (range 2·5-2·8 million) since 2005, after a period of fast decline between 1997 and 2005. The number of people living with HIV/AIDS has been steadily increasing and reached 38·8 million (95% UI 37·6-40·4 million) in 2015. At the same time, HIV/AIDS mortality has been declining at a steady pace, from a peak of 1·8 million deaths (95% UI 1·7-1·9 million) in 2005, to 1·2 million deaths (1·1-1·3 million) in 2015. We recorded substantial heterogeneity in the levels and trends of HIV/AIDS across countries. Although many countries have experienced decreases in HIV/AIDS mortality and in annual new infections, other countries have had slowdowns or increases in rates of change in annual new infections. **Interpretation:** Scale-up of ART and prevention of mother-to-child transmission has been one of the great successes of global health in the past two decades. However, in the past decade, progress in reducing new infections has been slow, development assistance for health devoted to HIV has stagnated, and resources for health in low-income countries have grown slowly. Achievement of the new ambitious goals for HIV enshrined in Sustainable Development Goal 3 and the 90-90-90 UNAIDS targets will be challenging, and will need continued efforts from governments and international agencies in the next 15 years to end AIDS by 2030.
**Keywords:** HIV, Incidence, Prevalence, Mortality

## M-229. Repetitive Transcranial Magnetic Stimulation Versus Botulinum Toxin Injection in Chronic Migraine Prophylaxis: A Pilot Randomized Trial

Hatem S Shehata, Eman H Esmail, Ahmad Abdelalim, Shaimaa El-Jaafary, Alaa Elmazny, Asmaa Sabbah and Nevin M Shalaby

*Journal of Pain Research, 9: 771-777 (2016) IF: 2.363*

**Background:** Chronic migraine is a prevalent disabling disease, with major health-related burden and poor quality of life. Long-term use of preventive medications carries risk of side effects. OBJECTIVES: The aim of this study was to compare repetitive transcranial magnetic stimulation (rTMS) to botulinum toxin-A (BTX-A) injection as preventive therapies for chronic migraine. **Methods:** A pilot, randomized study was conducted on a small-scale sample of 29 Egyptian patients with chronic migraine, recruited from Kasr Al-Aini teaching hospital outpatient clinic and diagnosed according to ICHD-III (beta version). Patients were randomly assigned into two groups; 15 patients received BTX-A injection following the Phase III Research Evaluating Migraine Prophylaxis Therapy injection paradigm and 14 patients were subjected to 12 rTMS sessions delivered at high frequency (10 Hz) over the left motor cortex (MC, M1). All the patients were requested to have their 1-month headache calendar, and they were subjected to a baseline 25-item (beta version) Henry Ford Hospital Headache Disability Inventory (HDI), Headache Impact Test (HIT-6), and visual analogue scale assessment of headache intensity. The primary efficacy measures were headache frequency and severity; secondary measures were 25-item HDI, HIT-6, and number of acute medications. Follow-up visits were scheduled at weeks 4, 6, 8, 10, and 12 after baseline visit. **Results:** A reduction in all outcome measures was achieved in both the groups. However, this improvement was more sustained in the BTX-A group, and both the therapies were well tolerated. **Conclusion:**BTX-A injection and rTMS have favorable efficacy and safety profiles in chronic migraineurs. rTMS is of comparable efficacy to BTX-A injection in chronic migraine therapy, but with less sustained effect
**Keywords:** Botulinum Toxin-A; Chronic Migraine; Prophylaxis; Rtms.

## M-230. Ultrasound Evaluation of Internal Jugular Valve Incompetence (IJVI) in Egyptian Patients with Idiopathic Intracranial Hypertension (IIH)

Ibtessam M. Fahmy, Noha T. Abokrysha, Sandra M. Ahmed and Haidy M. El-Shebawy

*Journal of the Neurological Sciences,360:18-22(2016) IF: 2.126*

**Background**: Idiopathic intracranial hypertension (IIH) is a clinical syndrome with no identified causative factor. Internal jugular valve incompetence (IJVI) has been linked to many neurological disorders such as idiopathic intracranial hypertension (IIH), transient global amnesia and cough-induced headache. Intact valves prevent efficiently retrograde flow into the internal jugular vein. Aim: The aimof this study is to evaluate the competence of the jugular vein valves and its relationship to age, BMI, opening CSF pressure and MRV findings in IIH patients. Subjects andmethods: Twenty-five Egyptian female patients diagnosedwith IIH according to the modified Dandy criteria, and 24 female controls,matched for age and BMI,were included and examined using color-coded duplex for IJVI during the Valsalva maneuver. The patients underwent lumbar puncture to measure the opening pressure, MRV, ophthalmic examination and laboratory work-up. **Results:** There was no statistically significant difference in the proportion of IJVI among the patients and controls (P=0.7). Therewas a statistically significant increase in the opening pressure and proportion ofMRV abnormalities in the patients with IJVI compared to the patients without IJVI (P=0.03 and 0.007, respectively), but there were no statistically significant difference with regard to age, BMI, grade of papilledema and perimetry findings. **Conclusion:** This study showed that there is no relationship between IJVI and IIH; thus, IJVIwould be a rather normal finding. Further studies are recommended to confirm or rule out a possible relationship.

**Keywords:** Color Coded Duplex; Idiopathic Intracranial Hypertension; Internal Jugular Valve Incompetence.

## M-231. Interleukins 17and 10 in a Sample of Egyptian Relapsing Remitting Multiple Sclerosis Patients

TZ Tawfik, et al.

*Journal of The Neurological Sciences,369:36-38(2016) IF:2.126*

**Background**: Cytokines are major contributors in the immune disruption in multiple sclerosis (MS).**Objective:** Evaluating the proinflammatory (IL-17A) and anti-inflammatory (IL-10) cytokines in relapsing-remitting (RR) MS patients at time of relapse and during remission.**Subjects and Method:** A case-control study including 30 RRMS patients and 15 controls. Patients were recruited from the Kasr Al-Ainy MS research unit (KAMSU), Cairo University, Egypt. Levels of IL-17A and IL-10 were assessed in patients' sera, during relapse and 30days after IV methylprednisolone, and in control subjects using enzyme linked immunosorbent assays (ELISA).**Results:** IL-17 was higher in patients during relapse and remission phases when compared with controls (P=0.001), whereas, IL-10 was higher in patients during remission but normal during relapse (P=0.01; 0.86 respectively). IL-17 increased during relapses (P=0.001) while IL-10 increased during remissions (P=0.028). No significant correlations were found between both interleukins and age at onset; disease duration, number of relapses; or EDSS.**Conclusion:** RRMS patients can have a regulatory imbalance between both pro-and antiinflammatory cytokines, which could be a target for treatment strategies rather than focusing on a single cytokine.

**Keywords:** Relapsing; Remitting multiple sclerosis.

## M-232. Motor Cortex rTMS Improves Dexterity in Relapsing-Remittingand Secondary Progressive Multiple Sclerosis

Eman Elzamarany, Lamia Afifi, Neveen M. El-Fayoumy, Husam Salah and Mona Nada

*ACTA Neurologica Belgica, 116: 145-150 (2016) IF: 1.495*

The motor cortex (MC) receives an excitatory input from the cerebellum which is reduced in patients with cerebellar lesions. High-frequency repetitive transcranial magnetic stimulation (rTMS) induces cortical facilitation which can counteract the reduced cerebellar drive to the MC. Our study included 24 relapsing-remitting multiple sclerosis (RRMS) and secondary progressive multiple sclerosis (SPMS) patients with dysmetria. The patients were divided into two groups: Group A received two sessions of real MC rTMS and Group B received one session of real rTMS and one session of sham rTMS. Ten healthy volunteers formed group C. Evaluation was carried out using the nine-hole pegboard task and the cerebellar functional system score (FSS) of the expanded disability status scale (EDSS). Group A patients showed a significant improvement in the time required to finish the pegboard task (P = 0.002) and in their cerebellar FSS (P = 0.000) directly after the second session and 1 month later. The RRMS patients showed more improvement than the SPMS patients. Group B patients did not show any improvement in the pegboard task or the cerebellar FSS. These results indicate that MC rTMS can be a promising option in treating both RRMS or SPMS patients with cerebellar impairment and that its effect can be long-lasting.

**Keywords:** Repetitive Transcranial Magnetic Stimulation Dysmetria Multiple Sclerosis Motor Cortex Cerebellum Rtms

### *Dept. of NeuroSurgery*

## M-233. Neuroendoscopic Stent Placement for Cerebrospinal Fluid Pathway Obstructions in Adults

Sascha Marx, Steffen K. Fleck, Ehab El Refaee, Jotham Manwaring, Christina Vorbau, Michael J. Fritsch, Michael R. Gaab, Henry W. S. Schroeder and Joerg Baldauf

*Journal of Neurosurgery, 125: 576-584 (2016) IF: 3.443*

**Objective** Since its revival in the early 1990s, neuroendoscopy has become an integral component of modern neurosurgery. Endoscopic stent placement for treatment of CSF pathway obstruction is a rarely used and underestimated procedure. The authors present the first series of neuroendoscopic intracranial stenting for CSF pathway obstruction in adults with associated results and complications spanning a long-term follow-up of 20 years. **Methods** The authors retrospectively reviewed a prospectively maintained clinical database for endoscopic stent placement performed in adults between 1993 and 2013. **Results** of 526 endoscopic intraventricular procedures, stents were placed for treatment of CSF disorders in 25 cases (4.8%). The

technique was used in the management of arachnoid cysts (ACs; n = 8), tumor-related CSF disorders (n = 13), and hydrocephalus due to stenosis of the foramen of Monro (n = 2) or aqueduct (n = 2). The mean follow-up was 87.1 months. No deaths or infections occurred that were related to endoscopic placement of intracranial stents. Late stent dislocation or migration was observed in 3 patients (12%). **Conclusions** Endoscopic intracranial stent placement in adults is rarely required but is a safe and helpful technique in select cases. It is indicated when reliable and long-lasting restoration of CSF pathway obstructions cannot be achieved with standard endoscopic techniques. In the treatment of tumor-related hydrocephalus, it is a good option to avoid reclosure of the restored CSF pathway by tumor growth. Currently, routine stent placement after endoscopic fenestration of ACs is not recommended. Stent placement for treatment of CSF disorders due to tumor is a good option for avoiding CSF shunting. To avoid stent migration and dislocation, and to allow for easy removal if needed, the device should be fixed to a bur hole reservoir.
**Keywords:** Ac = Arachnoid Cyst; Csf Disorders; Etv = Endoscopic Third Ventriculostomy; Hydrocephalus; Intracranial Stenting; Neuroendoscopy

## M-234. The Value of Lateral Spread Response Monitoring in Predicting the Clinical Outcome after Microvascular Decompression in Hemifacial Spasm: A Prospective Study on 100 Patients.

Ahmed El Damaty, Christian Rosenstengel, Marc Matthes, Joerg Baldauf and Henry W. S. Schroeder

*Neurosurgical Review, 39: 455-466 (2016) IF: 2.166*

Microvascular decompression represents an effective treatment for hemifacial spasm. The use of lateral spread response (LSR) monitoring remains a useful intraoperative tool to ensure adequate decompression of the facial nerve. The aim of this study was to assess the value of LSRs intraoperative monitoring as a prognostic indicator for the outcome of microvascular decompression in hemifacial spasm. Our study included 100 patients prospectively. The patients were classified into four groups whether LSRs were totally, partially, not relieved, or not detected from the start. According to clinical outcome, the patients were classified into four groups depending on the clinical course after surgery and the residual symptoms if any. Then, correlations were made between LSR events and treatment outcome to detect its reliability as a prognostic indicator. LSRs were relieved totally in 56 % of the patients, partially relieved in 14 %, not relieved in 10 %, and were not detected in 20 % of the patients from the start. HFS was relieved directly after operation in 62 % with clinical improvement of 90-100 %. Thirty-one percent described 50-90 % improvement over the next 3 months after surgery. Almost all of these 31 % (28 out of 31 patients) reported further clinical improvement of 90-100 % within 1 year after surgery. Three percent suffered from a relapse after a HFS-free period, and 4 % reported minimal or no improvement describing 0-50 % of the preoperative state. The percentage of the satisfied patients with the clinical outcome who reported after 1 year a clinical improvement of 90-100 % was 90 %. Statistical analysis did not find a significant correlation between the relief of LSRs and clinical outcome. LSRs may only represent an intraoperative tool to guide for an adequate decompression but failed to represent a reliable prognostic indicator for treatment outcome.
**Keywords:** Endoscope-Assisted; Hemifacial Spasm; Intraoperative Monitoring; Lsr; Lateral Spread; Microvascular Decompression.

## M-235. Role of Surgery for Small Petrous Apex Meningiomas Causing Refractory Trigeminal Neuropathy in the Minimally Invasive Era.

Ahmed Hegazy, Ahmed Alfiki, M. Fathy Adel, M. FM Alsawy, M. Fouad AlDash, Mostafa Zein, Sameh M. Amin, Hieder AlShami and Arundhati Biswas

*Neurology India, 64: 973-979 (2016) IF: 1.41*

**Background:** Radiosurgery seems to be a very appealing option for patients having a small petrous apex meningioma and presenting with trigeminal neuralgia, presumably because of the lower risk and cost involved. The aim of this study was to analyze the results of our surgical series of petrous apex meningioma presenting with trigeminal neuralgia, and to determine the efficacy of neurosurgical treatment with regard to pain control. The procedure-related complication and morbidity rates were also evaluated. **Materials and Methods**: This is a retrospective study of 17 patients with a small (<3 cm) petrous apex meningioma. The included patients were refractory to medical treatment for trigeminal neuralgia and were deemed as surgical candidates. Postoperatively, the patients were assessed for pain relief according to the Barrow Neurological Institute (BNI) scale. A P value of less than 0.05 was considered significant. Magnetic resonance imaging was also performed after 6 weeks to assess the radicality of resection. **Results:** In a median follow-up of approximately 2 years, the study showed that 14 of the 17 (82.4%) patients had complete pain relief, with very low morbidity and no mortality, and 100% tumor control. According to the Barrow Neurological Institute (BNI) scale for the assessment of postoperative pain relief, 52.9, 23.5, 5.9, 11.8, and 5.9% of patients had grades I, II, IIIa, IIIb, and IV in terms of their pain relief, respectively. **Conclusions:** In our population of patients, surgery proved to be successful in providing symptomatic relief, with low morbidity and no mortality, and was comparable with other studies involving the minimally invasive modalities. However, these results warrant further follow-up, with recruitment of more patients, to demonstrate whether or not, surgery should be the primary choice of treatment in this subgroup of patients.
**Keywords:** Petrous Apex Lesions; Stereotactic Radiosurgery; Trigeminal Neuralgia

## M-236. Composite Vascular Pedicled Middle Turbinate Flap for Reconstruction of Sellar Defects

Sameh M Amin, Tamer O Fawzy and Ahmed A Hegazy

*Annals of Otology, Rhinology and Laryngology, 125: 770-774 (2016) IF: 1.171*

**Objectives:** Herein, we describe our experience in simple harvest of the vascular pedicled middle turbinate flap (MTF) sufficient for sellar defect reconstruction. **Methods:** An anatomical feasibility study is done in 10 sides of 5 preserved injected cadaveric heads. The middle turbinate is separated from the skull base and the basal lamella with or without retrograde

dissection of its tail as a composite flap based on the middle turbinate and posterolateral nasal arteries. The technique was applied in 25 cases of cerebrospinal fluid (CSF) leak after endoscopic transsphenoidal surgery. **Results:** The mean area of MTF with and without medial mucosal dissection was 9.53 cm2 and 7.6 cm2, respectively. The mean length between anterior end of MT and basal lamella and the latter and the sella was 3.67 cm and 2.33 cm, respectively. The mean area of sella was 2.2 cm2. The MTF covered the sella, planum, and tuberculum sella corridors in 10 head sides. Partial dissection of MT medial mucosa was needed in 3 head sides to cover sella, planum, and tuberculum sella. Follow-up for 26 to 37 month revealed control of CSF leak in 24 cases. Conclusion: Composite MTF is a simple rapid reproducible option for sellar defects reconstruction.

**Keywords:** Endoscopic Sinus Surgery, Endoscopic Skull Base Surgery, Minimally Invasive Csf Leak Closure, Minimally Invasive Skull Base Surgery, Nasal and Sinus Surgery, Surgery, Surgical Outcomes

## M-237. Percutaneous Transpedicular Fixation: Technical Tips and Pitfalls of Sextantand Pathfinder Systems

Mohamed M. Mohi Eldin and Ahmed Salah Aldin Hassan

*Asian Spine Journal, 2016 Feb;10(1): 111-122 (2016)*

**Study Design:** The efficacy of the operative techniques, possible benefits as well as pitfalls and limitations of the techniques are discussed. Potential drawbacks are also detected. Purpose: This study aims to report indications, techniques, and our experience with the use of the Sextant and PathFinder percutaneous transpedicular screw fixation systems. Overview of Literature: Percutaneous pedicle screw insertion is a novel technique. Successful percutaneous placement of pedicle screws requires surgical skill and experience because of lack of anatomic surface landmarks. Fluoroscopy-guided percutaneous placement of pedicle screws is effective. Many systems are now available. **Methods:** We conducted a prospective operative and postoperative analysis of 40 patients with absolute indication for thoracic or lumbar instability between January 2009 and June 2013. All procedures were performed with the Sextant (group A) and PathFinder (group B) systems under fluoroscopic guidance. Operative techniques are discussed and the results compared. **Results:** Percutaneous transpedicular screw fixation minimizes the morbidity associated with open techniques without compromising the quality of fixation. A total of 190 screws were inserted. There was no additional morbidity. Postoperative computed tomography images and plain X-rays were analyzed. Reduction of visual analog scale scores of back pain was evident. **Conclusions:** Fluoroscopy-guided percutaneous pedicular screws are feasible and can be safely done. Current systems allow multisegmental fixation with significantly less difficulties. The described techniques have acceptable intra- and postoperative complication rates, and overall sufficient pain control with early mobilization of patients.

**Keywords:** Percutaneous; Transpedicular; Screw Fixation; Minimally Invasive.

## M-238. Surgical Resection of Low-Grade Gliomas in Eloquent Areas with the Guidance of the Preoperative Functional Magnetic Resonance Imagingand Craniometric Points

Ahmed Abdullah, Hisham El Shitany, Waleed Abbass, Amr Safwat, Amr K Elsamman and Ehab El Refaee

*Journal of Neurosciences in Rural Pracric, 7: 571-576 (2016)*

**Objectives:** Surgical resection of low-grade gliomas (LGGs) in eloquent areas is one of the challenges in neurosurgery, using assistant tools to facilitate effective excision with minimal postoperative neurological deficits has been previously discussed (awake craniotomy and intraoperative cortical stimulation); however, these tools could have their own limitations thus implementation of a simple and effective technique that can guide to safe excision is needed in many situations. **Materials and Methods:** The authors conducted a retrospective analysis of a prospectively collected data of 76 consecutive surgical cases of LGGs of these 21 cases were situated in eloquent areas. Preoperative functional magnetic resonance imaging (fMRI), pre- and post-operative MRI with volumetric analysis of the tumor size was conducted, and intraoperative determination of the craniometric points related to the tumor (navigation guided in 10 cases) were studied to evaluate the effectiveness of the aforementioned tools in safe excision of the aforementioned tumors. **Results:** Total-near total excision in 14 (66.67%) subtotal in 6 (28.57%), and biopsy in 1 case (4.57%). In long-term follow–up, only one case experienced persistent dysphasia. **Conclusion:** In spite of its simplicity, the identification of the safe anatomical landmarks guided by the preoperative fMRI is a useful technique that serves in safe excision of LGGs in eloquent areas. Such technique can replace intraoperative evoked potentials or the awake craniotomy in most of the cases. However, navigation-guided excision might be crucial in deeply seated and large tumors to allow safe and radical excision.

**Keywords:** Craniometric Points, Eloquent Areas, Functional Magnetic Resonance Imaging, Glioma, Low-Grade Glioma, Surgery

### *Dept. of Obstetrics and Gynecology*

## M-239. Recombinant Versus Urinary Human Chorionic Gonadotrophin for Final Oocyte Maturation Triggering in IVF and ICSI Cycles.

Youssef MA, Abou-Setta AM and Lam WS.

*Cochrane Database Syst Rev, 4:CD003719 (2016) IF: 6.103*

**Background:**For the last few decades urinary human chorionic gonadotrophin (uhCG) has been used to trigger final oocyte maturation in cycles of in vitro fertilization (IVF) and intracytoplasmic sperm injection (ICSI). Recombinant technology has allowed the production of two drugs, recombinant human chorionic gonadotrophin (rhCG) and recombinant luteinising hormone (rLH), that can be used for the same purpose, to mimic the endogenous luteinising hormone (LH) surge. This allows commercial manufacturers to adjust production according to market requirements and to remove all urinary contaminants, facilitating the safe subcutaneous administration of a compound with less batch-to-batch variation. However, prior to a change in practice, it is necessary to

compare the effectiveness of the recombinant drugs to the currently used urinary human chorionic gonadotrophin (uhCG). **Objectives:**To assess the effects of subcutaneous rhCG and high dose rLH versus uhCG for inducing final oocyte maturation in subfertile women undergoing IVF and ICSI cycles. **Search Methods:** We searched the Cochrane Menstrual Disorders and Subfertility Group Trials Register (April 2015), the Cochrane Central Register of Controlled Trials (CENTRAL) (2015, Issue 3), MEDLINE (1946 to April 2015), EMBASE (1980 to April 2015) and PsycINFO (1806 to April 2015) as well as trial registers at ClinicalTrials.gov on 13 May 2015 and the World Health Organization International Clinical Trials Registry Platform (WHO ICTRP) search portal on 14 May 2015. **Selection Criteria:**Two review authors independently scanned titles and abstracts and selected those that appeared relevant for collection of the full paper. We included randomised controlled trials comparing rhCG and rLH with urinary hCG for final oocyte maturation triggering in IVF and ICSI cycles for treatment of infertility in normogonadotropic women. **Data Collection and Analysis:** Two authors independently performed assessment for inclusion or exclusion, quality assessment and data extraction. We discussed any discrepancies in the presence of a third author to reach a consensus. The primary review outcomes were ongoing pregnancy/live birth and incidence of ovarian hyperstimulation syndrome (OHSS). Clinical pregnancy, miscarriage rate, number of oocytes retrieved and adverse events were secondary outcomes. We combined data to calculate pooled odds ratios (ORs) and 95% confidence intervals (CIs) and assessed statistical heterogeneity using the I(2) statistic. We evaluated the overall quality of the evidence for the main comparisons using GRADE methods. **Main Results:**We included 18 RCTs involving 2952 participants; 15 compared rhCG with uhCG, and 3 compared rhLH with uhCG. The evidence for different comparisons ranged from very low to high quality: limitations were poor reporting of study methods and imprecision. Pharmaceutical companies funded 9 of the 18 studies, and 5 studies did not clearly report funding source. Ongoing pregnancy/live birthThere was no conclusive evidence of a difference between rhCG and uhCG (OR 1.15, 95% CI 0.89 to 1.49; 7 RCTs, N = 1136, I(2) = 0%, moderate quality evidence) or between rhLH and uhCG (OR 0.95, 95% CI 0.51 to 1.78, 2 RCTs, N = 289, I(2) = 0%, very low quality evidence) for ongoing pregnancy/live birth rates. OHSS There was no evidence of a difference between rhCG and uhCG in the incidence of OHSS: moderate to severe OHSS (OR 1.76, 95% CI 0.37 to 8.45; 3 RCTs, N = 417, I(2) = 0%, low quality evidence), moderate OHSS (OR 0.78, 95% CI 0.27 to 2.27; 1 RCT, N = 243, I(2) = 0%, low quality evidence), mild to moderate OHSS (OR 1.00, 95% CI 0.42 to 2.38; 2 RCTs, N = 320, I(2) = 0%, low quality evidence) or undefined OHSS (OR 1.18, 95% CI 0.50 to 2.78; 3 RCTs, N = 495, I(2) = 0%, low quality evidence). Likewise, there was no evidence of a difference between rhLH and uhCG in OHSS rates for moderate OHSS (OR 0.82, 95% CI 0.39 to 1.69, 2 RCTs, N = 280, I(2) = 5%, very low quality evidence). Other adverse events There was no evidence of a difference in miscarriage rates between rhCG and uhCG (OR 0.72, 95% CI 0.41 to 1.25; 8 RCTs, N = 1196, I(2) = 0%, low quality evidence) or between rhLH and uhCG (OR 0.95, 95% CI 0.38 to 2.40; 2 RCTs, N = 289, I(2) = 0%, very low quality evidence). For other adverse effects (most commonly injection-site reactions) rhCG was associated with a lower number of adverse events than uhCG (OR 0.52, 95% CI 0.35 to 0.76; 5 RCTS, N = 561; I(2) = 67%, moderate quality evidence). However, when we used a random-effects model due to substantial statistical heterogeneity, there was no evidence of a difference between the groups (OR 0.56, 95% CI 0.27 to 1.13). Only one study comparing rLH and uhCG reported other adverse events, and it was impossible to draw conclusions. **Authors' Conclusions:** We conclude that there is no evidence of a difference between rhCG or rhLH and uhCG for live birth or ongoing pregnancy rates or rates of OHSS.

**Keywords:** HCG; OHSS

## M-240. Volume Expanders for the Prevention of Ovarian Hyperstimulation Syndrome.

Youssef M A and Mourad S

*Cochrane Database Syst Rev, 2016 Aug 31;(8):CD001302 (2016) IF: 6.103*

**Background:**Ovarian hyperstimulation syndrome (OHSS) is a serious and potentially fatal complication of ovarian stimulation which affects 1% to 14% of all in vitro fertilisation (IVF) or intracytoplasmic sperm injection (ICSI) cycles. A number of clinical studies with conflicting results have reported on the use of plasma expanders such as albumin, hydroxyethyl starch (HES), mannitol, polygeline and dextran as a possible intervention for the prevention of OHSS. Women with very high estradiol levels, high numbers of follicles or oocytes retrieved, and women with polycystic ovary syndrome (PCOS), are at particularly high risk of developing OHSS. Plasma expanders are not commonly used nowadays in ovarian hyperstimulation. This is mainly because clinical evidence on their effectiveness remains sparse, because of the low incidence of moderate and severe ovarian hyperstimulation syndrome (OHSS) and the simultaneous introduction of mild stimulation approaches, gonadotropin-releasing hormone (GnRH) antagonist protocols and the freeze-all strategy for the prevention of OHSS. **Objectives:**To review the effectiveness and safety of administration of volume expanders for the prevention of moderate and severe ovarian hyperstimulation syndrome (OHSS) in high-risk women undergoing IVF or ICSI treatment cycles. **Search Methods:**We searched databases including the Cochrane Gynaecology and Fertility Group Specialised Register of controlled trials, the Cochrane Central Register of Controlled Trials (CENTRAL), MEDLINE, Embase and trial registers to September 2015; no date restrictions were used as new comparators were included in this search. The references of relevant publications were also searched. We attempted to contact authors to provide or clarify data that were unclear from trial or abstract reports. **Selection Criteria:**We included randomised controlled trials (RCTs) comparing volume expanders versus placebo or no treatment for the prevention of OHSS in high-risk women undergoing ovarian hyperstimulation as part of any assisted reproductive technique. **Data Collection and Analysis:** Two review authors independently selected the studies, assessed risk of bias and extracted relevant data. The primary review outcome was moderate or severe OHSS. Other outcomes were live birth, pregnancy and adverse events. We combined data to calculate pooled Peto odds ratios (ORs) and 95% confidence intervals (CIs) for each intervention. Statistical heterogeneity was assessed using the I(2) statistic. We assessed the overall quality of the evidence for each comparison, using GRADE methods. **Main Results:**We included nine RCTs (1867 women) comparing human albumin (seven RCTs) or HES (two RCTs) or mannitol (one RCT) versus placebo or no treatment for

prevention of OHSS. The evidence was very low to moderate quality for all comparisons. The main limitations were imprecision, poor reporting of study methods, and failure to blind outcome assessment.There was evidence of a beneficial effect of intravenous albumin on OHSS, though heterogeneity was substantial (Peto OR 0.67 95% CI 0.47 to 0.95, seven studies, 1452 high risk women; $I^2$ = 69%, very low quality evidence) . This suggests that if the rate of moderate or severe OHSS with no treatment is 12%, it will be about 9% (6% to12%) with the use of intravenous albumin. However, there was evidence of a detrimental effect on pregnancy rates (Peto OR 0.72 95% CI 0.55 to 0.94, $I^2$ = 42%, seven studies 1069 high risk women, moderate quality evidence). This suggests that if the chance of pregnancy is 40% without treatment, it will be about 32% (27% to 38%) with the use of albumin.There was evidence of a beneficial effect of HES on OHSS (Peto OR 0.27 95% CI 0.12 to 0.59, $I^2$ = 0%, two studies, 272 women, very low quality evidence). This suggests that if the rate of moderate or severe OHSS with no treatment is 16%, it will be about 5% (2% to 10%) with the use of HES. There was no evidence of an effect on pregnancy rates (Peto OR 1.20 95% CI 0.49 to 2.93, one study, 168 women, very low quality evidence).There was evidence of a beneficial effect of mannitol on OHSS (Peto OR 0.38, 95% CI 0.22 to 0.64, one study, 226 women with PCOS, low quality evidence). This means that if the risk of moderate or severe OHSS with no treatment is 52%, it will be about 29% (19% to 41%) with mannitol. There was no evidence of an effect on pregnancy rates (Peto OR 0.85 95% CI 0.47 to 1.55; one study, 226 women, low quality evidence).Live birth rates were not reported in any of the studies. Adverse events appeared to be uncommon, but were too poorly reported to reach any firm conclusions. **AUTHORS' Conclusions:**Evidence suggests that the plasma expanders assessed in this review (human albumin, HES and mannitol) reduce rates of moderate and severe OHSS in women at high risk. Adverse events appear to be uncommon, but were too poorly reported to reach any firm conclusions, and there were no data on live birth. However, there was evidence that human albumin reduces pregnancy rates. While there was no evidence that HES, or mannitol had any influence on pregnancy rates, the evidence of effectiveness was based on very few trials which need to be confirmed in additional, larger randomised controlled trials (RCTs) before they should be considered for routine use in clinical practice.

**Keywords:** Volume Expander; OHSS.

## M-241. Tramadol Versus Celecoxib for Reducing Pain Associated with Outpatient Hysteroscopy: A Randomized Double-Blind Placebo-Controlled Trial

A.Hassan, A.Wahba and H.Haggag

*Human Reproduction, 31 (2016) IF: 4.621*

**Study Question:**Which is better, Tramadol or Celecoxib, in reducing pain associated with outpatient hysteroscopy? **Summary Answer:**Both Tramadol and Celecoxib are effective in reducing pain associated with outpatient hysteroscopy but Celecoxib may be better tolerated. **What Is Known Already:** Pain is the most common cause of failure of outpatient hysteroscopy. A systematic review and meta-analysis showed that local anaesthetics were effective in reducing pain associated with hysteroscopy but there was insufficient evidence to support the use of oral analgesics, opioids and non-steroidal anti-inflammatory drugs, to reduce hysteroscopy-associated pain and further studies were recommended. **Study Design, Size, Duration**: This was a randomized double-blind placebo-controlled trial with balanced randomization (allocation ratio 1:1:1) conducted in a university hospital from May 2014 to November 2014. **Participants/Materials, Setting, Methods:** Two hundred and ten women who had diagnostic outpatient hysteroscopy were randomly divided into three equal groups: Group 1 received oral Tramadol 100 mg, group 2 received Celecoxib 200 mg and group 3 received an oral placebo. All the drugs were given 1 h before the procedure. A patient's perception of pain was assessed during the procedure, immediately afterwards and 30 min after the procedure with the use of a visual analogue scale (VAS). **Main Results and the Role of Chance:** There was a significant difference in the pain scores among the groups during the procedure, immediately afterwards and 30 min after the procedure (P< 0.001, 0.001, <0.001 respectively). Tramadol had significantly lower pain scores when compared with the placebo during the procedure (mean difference = 1.54, 95% confidence interval (CI) (0.86, 2.22), P < 0.001), immediately after the procedure (mean difference = 1.09; 95% CI (0.5, 1.68), P < 0.001) and 30 min later (mean difference = 0.95, 95% CI (0.48, 1.41), P < 0.001). Celecoxib administration also led to significantly lower pain scores than the placebo during the procedure (mean difference = 1.28, 95% CI (0.62, 1.94), P < 0.001), immediately after the procedure (mean difference = 0.72; 95% CI (0.13, 1.32), P = 0.016) and 30 min later (mean difference = 0.77, 95% CI (0.3, 1.24), P = 0.001). There were no significant differences in pain scores between Tramadol and Celecoxib at any time. Time until no pain differed significantly among the groups (P = 0.01); it was shorter with both Tramadol and Celecoxib groups when compared with placebo (P = 0.002 and 0.046, respectively). The procedure failed to be completed in one patient in the placebo group but no failure to complete the procedure occurred in Tramadol and Celecoxib groups. Four women in the Tramadol group reported nausea but no side effects were reported with Celecoxib group and no complications were reported in any group of patients. LIMITATIONS, REASONS FOR CAUTION: All results were based on the subjective perception of pain, which varies among individuals and is related to the individuals' previous pain experience and level of anxiety. **Wider Implications of the Findings:**Tramadol and Celecoxib are effective in reducing pain in outpatient hysteroscopy. Celecoxib may be better tolerated as no side effects were reported in the study, however further research on a larger sample size is required before drawing firm conclusions about lack of side effects. **Study Funding/Competing Interests:** This research did not receive any specific grant from any funding agency in the public, commercial or not-for-profit sector. All authors declare no conflict of interest.

**Keywords:** Celecoxib; Tramadol; Cyclo-Oxygenase-2 Inhibitors; Outpatient Hysteroscopy; Pain

## M-242. Optimal Timing of Misoprostol Administration in Nulliparous Women Undergoing Office Hysteroscopy: A Randomized Double-Blind Placebo-Controlled Study.

Usama M. Fouda, Sherine H. Gad Allah and Hesham S Elshaer

*Fertility and Sterility., 106(1): 196-201 (2016) IF: 4.426*

**Objective:** To determine the optimal timing of vaginal misoprostol administration in nulliparous women undergoing office hysteroscopy. **Design:** Randomized double-blind placebo-controlled study. **Setting:**University teaching hospital. **Patient(S):**One hundred twenty nulliparous patients were randomly allocated in a 1:1 ratio to the long-interval misoprostol group or the short-interval misoprostol group. **Intervention(S):**In the long-interval misoprostol group, two misoprostol tablets (400 µg) and two placebo tablets were administered vaginally at 12 and 3 hours, respectively, before office hysteroscopy. In the short-interval misoprostol group, two placebo tablets and two misoprostol tablets (400 µg) were administered vaginally 12 and 3 hours, respectively, before office hysteroscopy. **Main Outcome Measure(S):** The severity of pain was assessed by the patients with the use of a 100-mm visual analog scale (VAS). The operators assessed the ease of the passage of the hysteroscope through the cervical canal with the use of a 100-mm VAS as well. **Result(S):** Pain scores during the procedure were significantly lower in the long-interval misoprostol group (37.98 ± 13.13 vs. 51.98 ± 20.68). In contrast, the pain scores 30 minutes after the procedure were similar between the two groups (11.92 ± 7.22 vs. 13.3 ± 6.73). Moreover, the passage of the hysteroscope through the cervical canal was easier in the long-interval misoprostol group (48.9 ± 17.79 vs. 58.28 ± 21.85). **Conclusion(S):**Vaginal misoprostol administration 12 hours before office hysteroscopy was more effective than vaginal misoprostol administration 3 hours before office hysteroscopy in relieving pain experienced by nulliparous patients undergoing office hysteroscopy.

**Keywords:** Pain,Office Hysteroscopy, Misoprostol

## M-243. Does the Addition of Growth Hormone to the in Vitro Fertilization/Intracytoplasmic Sperm Injection Antagonist Protocol Improve Outcomes in Poor Responders? A Randomized, Controlled Trial.

Yasmin Ahmed Bassiouny, Dina Mohamed Refaat Dakhly, Yomna Ali Bayoumi and Nawara Mohamed Hashish

*Fertility and Sterility, 105: 697-702 (2016) IF: 4.426*

**Objective:** To evaluate the effectiveness of the addition of growth hormone (GH) to the antagonist protocol in IVF/intracytoplasmic sperm injection cycles in poor responders. **Design:** Parallel randomized, controlled, open-label trial. SETTING: University hospital. PATIENT(S): A total of 141 patients (GH, n = 68; gonadotropins only, n = 73) were enrolled. Twenty-five patients had their cycles cancelled. Analysis was performed per cycle start as well as per ET. **Intervention(S):** Patients received the antagonist protocol with or without GH supplementation. **Main Outcome Measure(S):** Mean number of cumulus complexes, metaphase II oocytes retrieved and fertilized, chemical and clinical pregnancy rates, early miscarriage rate, ongoing pregnancy and live birth rates. **Result(S):** The addition of GH significantly lowered duration of hMG treatment, duration of GnRH antagonist treatment, and dose of gonadotropin. It significantly increased mean E2 levels on the day of hCG administration, number of collected oocytes (7.58 ± 1.40 vs. 4.90 ± 1.78 [mean ± SD]), number of metaphase II oocytes (4.53 ± 1.29 vs. 2.53 ± 1.18), number of fertilized oocytes (4.04 ± 0.96 vs. 2.42 ± 1.03), and number of transferred embryos (2.89 ± 0.45 vs. 2.03 ± 0.81). There was no significant difference in the clinical pregnancy rate per cycle (22.1% vs. 15.1%) or live birth rate per cycle (14.7% vs. 10.9%). **Conclusion(S):** Growth hormone as an adjuvant treatment in IVF/intracytoplasmic sperm injection cycles for poor responders should be cautiously used with the antagonist protocol, because there is still no identified impact on pregnancy outcomes. However, evaluation of the clinical pregnancy and live birth rates in our data was limited by low statistical power. clinical trial registration number: Clinicaltrials.gov identifier: nct02195947.

**Keywords:** Antagonist Protocol; IVF/ICSI; Poor Ovarian Response; Poor Responders

## M-244. Diclofenac Plus Lidocaine Gel for Pain Relief During Intrauterine Device Insertion. A Randomized, Double-Blinded, Placebo-Controlled Study.

Usama M. Foud, Noha M. Salah Eldin, Khaled A. Elsetohy, Hoda A. Tolba, Mona M. Shaban and Sherin M. Sobh

*Contraception, 93(6): 513-518 (2016) IF: 2.788*

**Objective:** To determine the effectiveness of diclofenac potassium combined with 2% lidocaine gel in reducing the pain of intrauterine device (IUD) insertion. Study design: We randomized 90 parous women requesting copper T380A IUD insertion in a 1:1 ratio to active or placebo treatment. Active treatment included administration of two 50-mg diclofenac potassium tablets 1 h before IUD insertion, application of 3 mL of 2% lidocaine gel on the anterior cervical lip 3 min before IUD insertion and placement of a cotton swab soaked in 2% lidocaine gel in the cervical canal 3 min before IUD insertion. Women in the placebo group received placebo tablets and gel. Participants assessed pain intensity using a 10-cm visual analog scale (VAS). We considered a 2-cm difference in VAS pain score between both groups during IUD insertion to be a clinically significant difference. **Results:** Subjects receiving active treatment, as compared to placebo, experienced less pain during tenaculum placement (1.66±0.85 vs. 2.33±1.19, p=.003) and IUD insertion (3.14±0.92 vs. 3.94±1.3, p=.001). Women who delivered only by cesarean section had higher pain scores with IUD insertion compared with women with previous vaginal deliveries (4.41±1.24 vs. 3.29±1.05, p=.001). **Conclusion:** Diclofenac potassium combined with 2% lidocaine gel slightly reduced pain scores during tenaculum application and copper IUD insertion in parous women; however, the reduction in pain scores lacked clinical significance. Implications: Although we found a statistically significant lowering of pain scores with pretreatment with diclofenac potassium and lidocaine gel in parous women having copper IUD placement, the reduction is not clinically relevant. These findings may be more relevant for nulliparous women who experience more pain than parous women with IUD insertion and support studies of diclofenac potassium and lidocaine gel in this population.

**Keywords:** Diclofenac Potassium; Lidocaine Gel; IUD; Pain; Visual Analog Scale.

## M-245. GnRH Antagonist Rescue Protocol Combined with Cabergoline Versus Cabergoline Alone in the Prevention of Ovarian Hyperstimulation Syndrome: A Randomized Controlled Trial.

Usama M. Fouda, Ahmed M. Sayed, Hesham S. Elshaer, Bahaa Eldin M. Hammad, Mona M. Shaban, Khaled A. Elsetohy and Mohamed A. Youssef

*Journal of Ovarian Research, 9:29 (2016) IF: 2.502*

**Background:** The aim of this study was to compare the efficacy of antagonist rescue protocol (replacing GnRH agonist with GnRH antagonist and reducing the dose of gonadotropins) combined with cabergoline versus cabergoline alone in the prevention of ovarian hyperstimulation syndrome (OHSS) in patients pretreated with GnRH agonist long protocol who were at high risk for OHSS. **Methods:** Two hundred and thirty six patients were randomized in a 1:1 ratio to the cabergoline group or the antagonist rescue combined with cabergoline group. Both groups received oral cabergoline (0.5 mg/day) for eight days beginning on the day of HCG administration. In the antagonist rescue combined with cabergoline group, when the leading follicle reached 16 mm, GnRH agonist (triptorelin) was replaced with GnRH antagonist (cetrorelix acetate) and the dose of HP-uFSH was reduced to 75 IU/day. HCG (5,000 IU/I.M) was administered when the serum estradiol level dropped below 3500 pg/ml. The study was open label and the outcome assessors (laboratory staff and the doctor who performed oocyte retrieval) were blind to treatment allocation. **Results:** The incidence of moderate/severe OHSS was significantly lower in the antagonist rescue combined with cabergoline group [5.08 % Vs 13.56 %, P value =0.025, OR = 0.342, 95 % CI, 0.129–0.906]. Four cycles were cancelled in the cabergoline group. There were no significant differences between the groups with respect to the number of retrieved oocytes, metaphase II oocytes, high quality embryos and fertilization rate. Moreover, the implantation and pregnancy rates were comparable between both groups. **Conclusion:** GnRH antagonist rescue protocol combined with cabergoline is more effective than cabergoline alone in the prevention of OHSS.

**Keywords:** Cabergoline, Ivf-Et, Ovarian Hyperstimulation Syndrome, Gnrh Antagonist.

## M-246. Endometrial Scratch Injury Induces Higher Pregnancy Rate for Women with Unexplained Infertility Undergoing Iui with Ovarian Stimulation: A Randomized Controlled Trial

Ahmed M. Maged, Hesham Al-Inany, Khaled M. Salama, Ibrahim I. Souidan, Hesham M. Abo Ragab and Noura Elnassery

*Reproductive Sciences, 23: 239-243 (2016) IF: 2.429*

**Objective:** To explore the impact of endometrial scratch injury (ESI) on intrauterine insemination (IUI) success. **Methods:** One hundred and fifty four infertile women received 100 mg of oral clomiphene citrate for 5 days starting on day 3 of the menstrual cycle. Patients were randomized to 2 equal groups: Group C received IUI without ESI and group S had ESI. Successful pregnancy was confirmed by ultrasound. **Results:** 13, 21, and 10 women got pregnant after the first, second, and third IUI trials, respectively, with 28.6% cumulative pregnancy rate (PR). The cumulative PR was significantly higher in group S (39%) compared to group C (18.2%). The PR in group S was significantly higher compared to that in group C at the second and third trials. The PR was significantly higher in group S at the second trial compared to that reported in the same group at the first trial but nonsignificantly higher compared to that reported during the third trial, while in group C, the difference was nonsignificant. Eight pregnant women had first trimester abortion with 18.2% total abortion rate with nonsignificant difference between studied groups. **Conclusion:** The ESI significantly improves the outcome of IUI in women with unexplained infertility especially when conducted 1 month prior to IUI

**Keywords:** IUI; Endometrial Injury; Ovarian Stimulation; Unexplained Infertility.

## M-247. Accuracy of Hysteroscopic Endomyometrial Biopsy in Diagnosis of Adenomyosis

Dina M. R. Dakhly, Ghada A. F. Abdel Moety, Waleed Saber, Sherine H. Gad Allah, Ahmed T. Hashem and Lubna O. E. Abdel Salam

*The Journal of Minimally Invasive Gynecology, 23: 364-371 (2016) IF: 2.39*

**Objectives:** To investigate the diagnostic accuracy of endomyometrial biopsy obtained via office hysteroscopy for the diagnosis of adenomyosis. Study Design: Cross-sectional study. Setting: Cairo University Teaching Hospital, Cairo, Egypt. **Patients:** A total of 404 premenopausal women with symptoms clinically suggestive of having adenomyosis. Interventions: All patients were subjected to 2-dimensional transvaginal sonography (TVS) in-office hysteroscopy examination with endomyometrial biopsy. Patients who subsequently underwent hysterectomy were included in the final analysis. Main **Measurements and Results:** Accuracy of diagnostic modalities was represented using the terms sensitivity, specificity, positive predictive value, negative predictive value, and overall accuracy. A total of 292 patients were eligible for final analysis. of these, 162 (55.47%) were diagnosed with adenomyosis based on hysterectomy specimens. TVS had a high sensitivity (83.95%) and a moderate specificity (60%). In contrast, endomyometrial biopsy was more specific (78.46%) than sensitive (54.32%). Hysteroscopic appearance of the endometrial cavity had low sensitivity (40.74%) and specificity (44.62%). Adding endomyometrial biopsy to TVS improved specificity (89.23%). **Conclusion:** Endomyometrial biopsy obtained via office hysteroscopy can diagnose adenomyosis with a high specificity and is recommended after TVS. Journal of Minimally Invasive Gynecology (2016) 23, 364–371 2016 AAGL. All rights reserved.

**Keywords:** Adenomyosis; Endomyometrial Biopsy; Office Hysteroscopy; Sensitivity; Specificity.

## M-248. Barbed Versus Conventional Suture: A Randomized Trial for Suturing the Endometrioma Bed after Laparoscopic Excision of Ovarian Endometrioma.

Usama M. Fouda, Khaled A. Elsetohy and Hesham S. Elshaer

*Journal of Minimally Invasive Gynecology., 23(6): 962-968 (2016) IF: 2.39*

**Objectives:** To determine whether the unidirectional knotless barbed suture can be used to control bleeding from the endometrioma bed after laparoscopic excision of ovarian endometrioma, and to detect whether the use of the unidirectional barbed suture is associated with shorter suturing time of the endometrioma bed compared with the continuous conventional smooth suture with intracorporeal knot tying. Design: Randomized clinical trial (Canadian Task Force classification I). Setting: Tertiary hospital. Patients: Forty patients with unilateral ovarian endometrioma (mean diameter, 3–10 cm) were randomized in a 1:1 ratio to the barbed suture group or the conventional suture group. Interventions: The endometrioma bed was sutured either with unidirectional barbed suture (V-Loc 180; Covidien, Mansfield, MA) or conventional suture (Vicryl; Ethicon, Somerville, NJ). Two layers of continuous sutures were used to control bleeding from the endometrioma bed and to reapproximate the ovarian edges. **Measurements and Main Results:** The degree of suturing difficulty was evaluated by the surgeons using a visual analog scale (VAS) ranging from 1 (least difficult suturing) to 10 (most difficult suturing). Operating time and suturing time were significantly shorter in the barbed suture group (43.3 6 10.54 vs 52.8 6 9.69 minutes; p 5 .005 and 8.85 6 2.52 vs 15.7 6 4.12 minutes; p, .001, respectively). Suturing with barbed suture was less difficult than suturing with conventional suture (3.68 6 1.37 vs 4.77 6 1.56; p 5 .025). Intraoperative blood loss was similar in the 2 groups. No perioperative complications were reported in either group. A nonsignificant decrease in serum anti-mullerian hormone (AMH) levels was observed after the operation in the barbed suture group and the conventional suture group (3.04 6 1.5 vs 2.52 6 1.31 ng/mL; p 5 .252 and 2.76 6 1.48 vs 2.13 6 1.14 ng/mL; p 5 .139, respectively). The rate of decline in serum AMH levels after the operation was 18.32% in the barbed suture group and 22.84% in the conventional suture group. Conclusion: The unidirectional knotless barbed suture (V-Loc) facilitates suturing of the endometrioma bed after laparoscopic excision of ovarian endometrioma. Compared with conventional smooth suture (Vicryl), the unidirectional barbed suture reduces the time needed to suture the endometrioma bed and the total operating time.

**Keywords:** Barbed Suture; Conventional Suture; Endometrioma; Endometriosis; Laparoscopy; Ovarian Reserve; Suturing Time

## M-249. Role of Oral Tramadol 50 Mg in Reducing Pain Associated with Outpatient Hysteroscopy: A Randomised Double-Blind Placebo-Controlled Trial.

Abdelgany Hassan and Hisham Haggag

*Austrailian and New Zealand Journal of Obstetrics and Gynecology, 56 (2016) IF: 1.738*

**Background:** Several drugs have been used to reduce hysteroscopy-associated pain. Although the Royal College of Obstetricians and Gynaecologists has recommended against the use of opiates in outpatient hysteroscopy, we wished to investigate if opioids can be used if the appropriate opioid was given in the appropriate dose. Aim To study the effectiveness of tramadol 50 mg in reducing pain associated with outpatient hysteroscopy. **Materials and Methods:** A prospective randomised double-blind placebo-controlled trial conducted in the outpatient hysteroscopy clinic at Cairo University Hospital. Main outcome measures were the severity of pain during the procedure, immediately after the procedure and 30 minutes later assessed by a visual analogue scale (VAS). VAS of 0 indicates no pain and VAS of 10 indicates the worst possible pain. **Results** A total of 140 women who had diagnostic outpatient hysteroscopy were randomised to receive oral tramadol 50 mg or placebo one h before performing outpatient hysteroscopy. There was no difference between the groups in the age, parity, duration of the procedures or indications of hysteroscopy. The median pain score was significantly lower in the tramadol group during the procedure (5 vs 6; P = 0.013), immediately after the procedure (3 vs 4; P < 0.036), and 30 minute later (1 vs 2; P = 0.034). Two women in the tramadol group reported nausea, but this was mild and did not warrant cancelling the procedure. **Conclusions** Oral administration of tramadol 50 mg before hysteroscopy reduces the pain evoked by the procedure and the drug was well tolerated by women

**Keywords:** Hysteroscopy; Pain; Tramadol.

## M-251. The Impact of Altering Filling Pressures in Diagnostic Outpatient Hysteroscopy on the Procedure Completion Ratesand Associated Pain: A Randomised Double-Blind Controlled Trial

Haggag HM and Hassan AM

*Austrailian and New Zealand Journal of Obstetrics and Gynecology, 56 (2016) IF: 1.738*

**Background:** Several studies have compared different distension media and analgesics to optimise the efficiency of outpatient hysteroscopy. However, studies comparing different uterine filling pressures are scarce. Aim The objective of this study was to evaluate and compare different uterine filling pressures during diagnostic outpatient hysteroscopy in an attempt to find the optimal pressure allowing adequate visualisation while minimising pain and increasing patient satisfaction. **Materials and Methods**: This was a double-blind randomised controlled trial. A total of 240 women who had diagnostic outpatient hysteroscopy were randomly divided into three equal groups: the uterine filling pressure was 30 mm Hg in group 1, 50 mm Hg in group 2 and 80 mm Hg in group 3. The primary outcome was adequate visualisation, and secondary outcomes were the proportion of completed procedures, pain perceived during the procedure, immediately after the procedure and 30 min later. **Results:** Adequate visualisation was lower in group 1 (88.7% vs 97.5% and 98.7%; P = 0.009), but was not different between groups 2 and 3 (P > 0.999). The proportion of completed procedures was not different among the groups. There was a progressive increase in pain scores from the lower to the higher pressure groups during the procedure, immediately after the procedure and 30 min after completing the procedure. **Conclusion:** Uterine filling pressure of 50 mm Hg was associated with better visualisation than 30 mm Hg and lower

pain scores than that of 80 mmHg with no difference in the proportion of completed procedures.
**Keywords:** Filling pressure; Hysteroscopy; Pain.

## M-252. Prevalence of Human Papilloma Virus (HPV) and its Genotypes in Cervical Specimens of Egyptian Women by Linear Array HPV Genotyping Test.

Youssef MA, Abdelsalam L, Harfoush RA, Talaat IM, Elkattan E, Mohey A, Abdella RM, Farhan MS, Foad HA, Elsayed AM, Elkinaai NA, Ghaith D, Rashed ME, Ghafar MA, Khamis Y and Hosni AN.

*Infect Agent Cancer, 32 (2016) IF: 1.718*

**Background:** The association of human papillomavirus (HPV) with cervical cancer is well established. AIM: To investigate HPV genotype distribution and co-infection occurrence in cervical specimens from a group of Egyptian women. **Methods:** A group of 152 women with and without cervical lesions were studied. All women had cervical cytology and HPV testing. They were classified according to cytology into those with normal cytology, with squamous intraepithelial lesions (SIL) and invasive squamous cell carcinoma (SCC). Cervical samples were analyzed to identify the presence of HPV by PCR, and all positive HPV-DNA samples underwent viral genotype analysis by means of LINEAR ARRAY HPV Genotyping assay. **Results:**A total of 26 HPV types with a prevalence of 40.8 % were detected. This prevalence was distributed as follows: 17.7 % among cytologically normal females, 56.5, 3.2, and 22.6 % among those with LSIL, HSIL and invasive SCC respectively. Low-risk HPV types were detected in 81.8 % of the cytologically-normal women, in 5.7 % of those in LSIL women, and in 14.3 % of infections with invasive SCC, while no low-risk types were detected in HSIL. High-risk HPV types were detected in 18.2 % of infections in the cytologically normal women, 14.3 % of infections in LSIL, and in 21.4 % of invasive lesions. The probable and possible carcinogenic HPV were not detected as single infections. Mixed infection was present in 80 % of women with LSIL, in 100 % of those with HSIL, and in 64.3 % of those with invasive SCC. This difference was statistically significant. HPV 16, 18 and 31 were the most prevalent HR HPV types, constituting 41.9, 29.03 and 12.9 % respectively, and HPV 6, 62 and CP6108 were the most prevalent LR HPV types constituting 11.3, 9.7 and 9.7 % respectively. Conclusion: These data expand the knowledge concerning HPV prevalence and type distribution in Egypt which may help to create a national HPV prevention program. HPV testing using the LINEAR ARRAY HPV Genotyping assay is a useful tool when combined with cytology in the diagnosis of mixed and non-conventional HPV viral types.
**Keywords:** Hpv; Cancer Cervix

## M-253. Carbetocin Versus Oxytocin in the Management of Atonic Post Partum Haemorrhage (PPH) after Vaginal Delivery: A Randomised Controlled Trial.

Ahmed Mohamed Maged, AbdelGany M. A. Hassan and Nesreen A. A. Shehata

*Archives of Gynecology and Obstetrics, 293: 993-999 (2016) IF: 1.68*

**Objective:** The objective of this study is to compare the effectiveness and safety of carbetocin vs. oxytocin in the management of atonic post partum haemorrhage (PPH) after vaginal delivery. **Methods:** A prospective randomised study was conducted in which 100 pregnant women were randomised into 2 equal groups: group 1 received Carbetocin 100 µgm (Pabal(®) Ferring, UK) and group 2 received oxytocin 5 IU (Syntocinon(®), Novartis, Switzerland). **Results:** The amount of blood loss and the need for other uterotonics were significantly lower in the carbetocin group (811 ± 389.17 vs. 1010 ± 525.66 and 10/50 vs. 21/50). There was no significant difference between the carbetocin and oxytocin groups regarding occurrence of major PPH (6 vs. 11), the need for blood transfusion (6 vs. 9), the difference between blood haemoglobin levels before delivery and 24 h after delivery (0.6 ± 0.28 vs. 0.56 ± 0.25), respectively. There was no significant difference between the 2 study groups regarding both systolic and diastolic blood pressure measured immediately after the drug administration and at 30 and 60 min later. Regarding the drugs side effects, there was no significant difference between the 2 groups in the occurrence of nausea, vomiting, tachycardia, flushing, dizziness, headache, shivering, metallic taste, dyspnea, palpitations and itching. **Conclusions:**Carbetocin is a better alternative to oxytocin in management of atonic PPH with non-significant hemodynamic changes or side effects
**Keywords:** Atonic Postpartum Haemorrhage; Carbetocin; Oxytocin; Vaginal Deliver.

## M-254. A Novel Protocol for Postpartum Magnesium Sulphate in Severe Pre-Eclampsia: A Randomized Controlled Pilot Trial

Waleed El-Khayat, Adel Atef, Sahar Abdelatty and Ali El-semary

*The Journal of Maternal-Fetal and Neonatal Medicine, 29: 154-158 (2016) IF: 1.674*

**Objective:** Magnesium sulphate is the preferred anticonvulsant used to prevent the development of fits in severe pre-eclampsia; we aim to compare between three different protocols of postpartum magnesium sulphate in the effectiveness of preventing the development of fits in severe pre-eclampsia. **Methods:** Double-blind randomized controlled pilot trial, done in Cairo university hospital, Cairo, Egypt during 2013-2014, on 240 women with severe pre-eclampsia. Magnesium sulphate intravenous infusion was given in the postpartum period to all the patients, women were randomly allocated to group I (Single loading dose only), group II (12 h abbreviated protocol) or group III (24 h standard protocol) (n = 80 in each group). **Results:** There were no significant difference between the three groups as regards the incidence of eclampsia, elevated liver enzymes and low platelets syndrome, maternal ICU admission and; however

The incidence of flushing was significantly higher in group III than group II and I (24 [30%] versus 12 [15%] versus 4 [5%]; $p < 0.001$) respectively. **Conclusion:** The pilot study demonstrates that the single-loading dose of postpartum magnesium sulphate is a promising alternative to the standard and the abbreviated protocol in preventing eclampsia; however, a large clinical trial is necessary to prove this.
**Keywords:** Abbreviated Regimen; Eclampsia; Magnesium Sulphate; Pre-Eclampsia.

## M-255. A Randomized Controlled Trial of Clomifene Citrate, Metformin, and Pioglitazone Versus Letrozole, Metformin, and Pioglitazone for Clomifene - Citrate- Resistant Polycystic Ovary Syndrome

Waleed El-khayat, Ghada Abdel Moety, Maged Al Mohammady and Dalia Hamed

*International Journal of Gynecology and Obstetrics, 132: 206-209 (2016) IF: 1.674*

**Objective:** To examine the efficacy of clomifene citrate, metformin, and pioglitazone versus letrozole, metformin, and pioglitazone among women with polycystic ovary syndrome (PCOS) resistant to clomifene citrate. **Methods:** A prospective double-blind randomized controlled trial of women younger than 40 years who had primary/secondary infertility associated with PCOS and had not ovulated in response to clomifene citrate regimens previously was conducted at a center in Cairo, Egypt, between August 1, 2013, and December 31, 2014. Computer-generated random number tables and opaque envelopes were used to assign participants to group A or group B. Participants allocated to group A received 100mg clomifene citrate daily for 5 days from the third day of the menstrual cycle, whereas those in group B received 5mg letrozole daily in the same regimen. All patients received 850 mg metformin and 15 mg pioglitazone for 10 days from the first day of the menstrual cycle. The primary outcome was cumulative ovulation rate. Analyses were by intention to treat. **Results:** Fifty women were assigned to each group. Ovulation occurred in 108 (92.3%) of 117 cycles in group A and 93 (86.9%) of 107 cycles in Group B (P=0.184). **Conclusion:** Combined treatment with letrozole, metformin, and pioglitazone was efficacious among women with PCOS resistant to clomifene citrate. ClinicalTrials.gov: NCT01909141.
**Keywords:** Clomifene Citrate; Clomifene Citrate Resistance; Letrozole; Metformin; Pioglitazone; Polycystic Ovary Syndrome

## M-256. Carbetocin Versus Oxytocin for Prevention of Postpartum Hemorrhage after Vaginal Delivery in High Risk Women.

Ahmed Mohamed Maged, Abdel Gany MA Hassan and Nesreen AA Shehata

*Journal of Maternal-Fetal and Neonatal Medicine, 29: 532-536 (2016) IF: 1.674*

**Objective:** To compare effectiveness and tolerability of carbetocin versus oxytocin in prevention of postpartum hemorrhage (PPH) after vaginal delivery. **Methods:** A prospective double-blinded randomized study conducted on 200 pregnant women randomized into two groups: Group 1 (100 women) received single 100 μg IM dose of carbetocin and Group 2 received of 5 IU oxytocin IM. Both groups received their drug after fetal and before placental delivery. **Results:** There was a statistically significant difference between the two study groups regarding amount of bleeding ($337.73 \pm 118.77$ versus $378 \pm 143.2$), occurrence of PPH (4 versus 16%), need for other uterotonics (23 versus 37%) and hemoglobin difference between before and after delivery ($0.55 \pm 0.35$ versus $0.96 \pm 0.62$) (all being lower in carbetocin group) and measured hemoglobin 24 h after delivery (being higher in carbetocin group); however, there was no significant difference between the two study groups regarding occurrence of major PPH and the need for blood transfusion. Women in carbetocin group showed a statistically significant lower systolic and diastolic blood pressure immediately after delivery and at 30 and 60 min than women in oxytocin group. There was no significant difference between the two study groups regarding occurrence of nausea, vomiting, flushing, dizziness, headache, shivering, metallic taste, dyspnea, palpitation and itching. Women in carbetocin group experienced tachycardia more than women in oxytocin group. **Conclusions:**Carbitocin is a better alternative to traditional oxytocin in prevention of PPH after vaginal delivery with minimal hemodynamic changes and similar side effects.
**Keywords:** Carbetocin; Oxytocin; Postpartum Hemorrhage; Vaginal Delivery

## M-257. Comparing Vaginal Misoprostol Versus Foley Catheter Plus Vaginal Isosorbide Mononitrate for Labor Induction.

Waleed El-Khayat, Heba Alelaiw, Abdallah El-kateb and Ali Elsemary

*The Journal of Maternal-Fetal and Neonatal Medicine, 29: 487-492 (2016) IF: 1.674*

**Objective (S):** To compare the effectiveness and safety of intra-cervical Foley catheter combined with intra-vaginal isosorbide mononitrate (IMN) versus intra-vaginal misoprostol for cervical ripening and labor induction in pregnant women with unripe cervices. **Methods:** Open-labeled randomized controlled trial in Cairo university hospital, Cairo, Egypt during 2012-2014. Three hundred and ninety-five pregnant women at term or post-term with an indication for labor induction and unripe cervix were included in the study. The subjects were randomly divided into two groups. Vaginal misoprostol was used in group 1 ($n = 197$) and intra-cervical Foley catheter plus vaginal IMN in group 2 ($n = 198$). Our main outcome measure was cesarean section rate. **Results:** Among the 395 included patients there were significantly lower duration of induction of labor ($p < 0.001$) in group 1with lower cesarean section rates [22.8% in group 1versus 33.3% in group 2; RR 0.7 (0.6-0.9), ($p = 0.020$)]. Whereas the uterine hyperstimulation ($p < 0.001$) was significantly higher in group 1. There were no significant differences between both groups as regard patients' demographic characteristics. **Conclusions(S):** Vaginal misoprostol is more effective but less safe than Foley catheter combined with vaginal IMN for induction of labor in term and post-term pregnancy. **Trial Registration:** ClinicalTrials.gov NCT01506388.
**Keywords:** Cervical Ripening, Foley Catheter, Isosorbide Mononitrate, Labor Induction, Misoprostol.

## M-258. Could First-Trimester Assessment of Placental Functions Predict Preeclampsia and Intrauterine Growth Restriction? A Prospective Cohort Study.

Abdel Moety GA, Almohamady M, Sherif NA, Raslana AN, Mohamed TF, El Moneam HM, Mohy AM and Youssef MA

*J Matern Fetal Neonatal Med., 29 (2016) IF: 1.674*

**Bjective:** To examine the role of first-trimester uterine artery Doppler, serum β-hCG and pregnancy-associated placental protein-A (PAPP-A) in prediction of preeclampsia and IUGR. **Methods:** A total of 100 pregnant women in the 11-14 weeks' gestation were examined using uterine artery Doppler, serum β-hCG and PAPP-A. All women were followed-up for development of preeclampsia or IUGR. **Results:** A total of 94 women completed the study of which 7 (7.4%) developed complications. Uterine artery PI and RI were significantly higher whereas serum β-hCG and PAPP-A levels were significantly reduced in patients who developed complications when compared with those who did not. Uterine artery PI had the highest sensitivity (100%) but a low specificity (56% and 45%) in prediction of preeclampsia and IUGR, respectively. Adding PAPP-A to uterine artery PI elevated the specificity into 94.44% and 95.51%, respectively. Combined PI and β-hCG elevated the specificity into 88.89% and 89.89%, respectively. Conclusion: Our study suggests that first-trimester uterine artery impedance, as measured by Doppler ultrasound as well as low serum biomarkers (β-hCG and PAPP-A) can be used for prediction of preeclampsia and IUGR. The most sensitive is uterine artery PI. Adding β-hCG to PI improves specificity in prediction of both preeclampsia and IUGR. Uterine artery PI plus PAPP-A is the best combination for prediction of both preeclampsia and IUGR.
**Keywords:** IUGR; PAPP-A; Preeclampsia; Serum B-Hcg; Uterine Artery Doppler.

## M-259. Intralipid Supplementation in Women with Recurrent Spontaneous Abortionand Elevated Levels of Natural Killer Cells

Dina M.R. Dakhly, Yomna A. Bayoumi, Mohamed Sharkawy, Sherine H. Gad Allah, Mohamed A. Hassan, Hisham M. Gouda, Ahmed T. Hashem, Dina L. Hatem, Mona F. Ahmed and Waleed El-Khayat

*International Journal of Gynecology and Obstetrics, 135: 324-327 (2016) IF: 1.674*

**Objective:** To investigate the efficacy of intralipid supplementation in women with recurrent spontaneous abortion (RSA) and elevated natural killer cell activity undergoing in vitro fertilization/intracytoplasmic sperm injection. **Methods:** Between February 10, 2013, and April 30, 2015, a double-blind randomized controlled study was conducted at a center in Egypt. Women with unexplained secondary infertility, RSA, and elevated levels of natural killer cells (>12%) were enrolled and randomly assigned to receive intralipid (2mL diluted at 20% in 250mL saline) or saline (250mL) infusion on the day of oocyte retrieval using random numbers and sealed envelopes. Patients and attending physicians were masked to group assignment. The infusions were repeated within 1week of a positive pregnancy test and then every 2weeks until the end of the first trimester. The primary outcome was chemical pregnancy 14days after embryo transfer. Analyses were by intention-to-treat. **Results:** Overall, 296 women were enrolled. Chemical pregnancy was recorded for 84 (58.3%) of 144 women in the intralipid group and 76 (50.0%) of 152 in the control group (P=0.129). **Conclusion:** Intralipid supplementation did not increase frequency of chemical pregnancy. However, findings related to ongoing pregnancy and live birth should be investigated further. ClinicalTrials.gov:NCT01788540
**Keywords:** In Vitro Fertilization; Intracytoplasmic Sperm Injection; Intralipid; Natural Killer Cells; Recurrent Spontaneous Abortion.

## M-260. Is There A Difference in the Maternaland Neonatal Outcomes Between Patients Discharged after 24 H Versus 72 H Following Cesarean Section? A Prospective Randomized Observational Study on 2998 Patients.

Yomna Ali Bayoumi, Yasmin Ahmed Bassiouny, Ayman Ahmed Hassan, Hisham Mohamed Gouda, Sherif Sameh Zaki and Abdelrahman Ahmed Abdelrazek

*The Journal of Maternal-Fetal and Neonatal Medicine, 29: 1339-1343 (2016) IF: 1.674*

**Objective:** To compare the incidence of postpartum maternal and neonatal complications and hospital readmission in patients discharged 24 versus 72 h after cesarean section. **Methods:** Using randomization, 1495 patients were discharged after 24 h and 1503 patients were discharged after 72 h. All patients fulfilled the discharge criteria. Patients were assessed 6 weeks after delivery, any maternal or neonatal problems or hospital readmissions during this time interval were reported. **Results:** There was no difference in maternal hospital readmission between the two groups, but there was a significantly higher neonatal readmission rate in the 24-h group mainly due to neonatal jaundice. As for the complications reported after 6 weeks, the only two significant outcomes were initiating breast feeding, being significantly higher in the 72-h group [OR and 95% CI 0.77 (0.66-0.89)] and the mood swings being significantly lower in the 72-h group [OR and 95% CI 2.28 (1.94-2.68)]. Conclusion: Our recommendation is still in favor of late discharge, after cesarean delivery. Bearing in mind, that an early 24-h discharge, after cesarean delivery is feasible, but with special care of the neonate, with early visit to the pediatrician and early establishment of effective lactation.
**Keywords:** Cesarean Section Discharge; Hospital Readmission; Maternal Outcome; Neonatal Outcome; Postpartum Complications

## M-261. Periconceptional Risk Factors of Spina Bifida Among Egyptian Population: A Case-Control Study.

Ahmed Maged, Moutaz Elsherbini, Wafaa Ramadan, Rasha Elkomy, Omneya Helal, Dina Hatem, Mona Fouad and Hassan Gaafar

*Journal of Maternal-Fetal & Neonatal Medicine, 29: 2264-2267 (2016) IF: 1.674*

**Objective:** To study the preconceptual & early conceptional risk factors predisposing to the development of spina bifida (SB)

among Egyptian population. **Study Design:** The study involved 197 pregnant women undergoing fetal anatomy scan; 97 women proved to have fetal SB and 100 women with normal fetuses as a control group. The control group was recruited randomly in the same period from patients undergoing anatomical scan. Risk factors that might lead to SB were investigated including maternal age, gravidity, parity, residence, history of diabetes mellitus or drug intake, smoking, infections, exposure to X-ray, history of congenital anomalies in other offspring, parental consanguinity, positive family history, and folate supplementations. **Results:**SB affected the lumbo-sacral region in the majority of cases (89.7%). It was associated with hydrocephalus in 66 cases (68%), polyhydramnios in 12 cases (12.4%). The SB group showed significantly higher parity ($p = 0.005$), more frequent history of drug intake ($p < 0.001$), higher frequency of infection with CMV ($p = 0.004$), and HSV ($p = 0.013$) and less proportion of folate supplementation ($p < 0.001$). **Conclusion:**The rate of SB in the tested group was five per 1000. Risk factors were lack of folate supplementation and history of antiepileptic drugs intake.

**Keywords:** 3D Ultrasound; Consanguinity; Hydrocephalus; Spina Bifida

## M-262. Role of Antioxidants in Gestational Diabetes Mellitusand Relation to Fetal Outcome: A Randomized Controlled Trial

Ahmed M. Maged, Haitham Torky, Mona A. Fouad, Sherine H. GadAllah, Nevien M. Waked, Ahmed S. Gayed and Ashraf K. Salem

*Journal of Maternal-Fetal and Neonatal Medicine, 29: 4049-4054 (2016) IF: 1.674*

**Objective:** To examine the effect of antioxidant administration on the oxidative parameters in both blood and placental tissue and its relation to fetal outcome in women with GDM. **Patients and Methods:**Two-hundred pregnant women with gestational diabetes mellitus (GDM) were randomized into 2 groups, Group1 received 1 gram L-ascorbic acid per day and Group2 received placebo. **Results:**The use of antioxidants significantly lower the needed insulin dose for blood sugar control ($25.6 \pm 20.3$ versus $40.5 \pm 23.7$, respectively). In placental tissue homogenates, glutathione (GSH) was $49.6 \pm 5.9$ versus $62.34 \pm 4.99$, malondialdahyde (MDA) was $165.7 \pm 9.2$ versus $264.15 \pm 12$, superoxide dismutase (SOD) was $0.3 \pm 0.3$ versus $0.054 \pm 0.16$ while catalase (CAT) was $14.06 \pm 2.4$ versus $15.52 \pm 3.97$ and glutathione peroxidase (GPx) was $14 \pm 4.1$ versus $26.3 \pm 4.26$ in antioxidant group compared to the control group ($p < 0.001$). In maternal blood, GSH was $1.5 \pm 0.3$ versus $0.74 \pm 0.088$, CAT was $380.7 \pm 11$ versus $325.44 \pm 21.8$, GPx was $52.3 \pm 8.7$ versus $75.82 \pm 6.84$ and SOD was $188 \pm 15.3$ versus $98.56 \pm 11.05$ in antioxidant group compared to control group ($p < 0.001$). In neonatal blood, the level of MDA and SOD showed a statistically significant difference between antioxidants and control groups ($4 \pm 0.7$ versus 6.6 7 $\pm 0.66$ and1 8 $8 \pm 15.3$ versus $98.5 \pm 11.05$, respectively) ($p < 0.001$). The neonatal blood sugar after 1 and 2 hours of delivery was more stable in antioxidant group ($56.7 \pm 10.9$ versus $39.7 \pm 11.1$ and $58.5 \pm 10.8$ versus $41.7 \pm 13.1$, respectively) ($p < 0.05$). The neonates NICU admission was lower in antioxidant group (5 versus 11) ($p < 0.05$). **Conclusion:**The use of antioxidants markedly reverses the oxidative stresses in women with GDM with marked improvement on neonatal outcome

**Keywords:** Antioxidants; Fetal Outcome; Gestational Diabetes; Oxidative Stress

## M-263. Does Dehydroepiandrosterone Improve Pregnancy Rate in Women Undergoing Ivf / Icsi with Expected Poor Ovarian Response According to the Bologna Criteria? A Randomized Controlled Trial.

Mohamed Kotb, AbdelGany Hassan and Ahmed AwadAllah

*European Journal of Obstetrics, Gynecology and Reproductive Biology, 200: 11-15 (2016) IF: 1.662*

**Objective:** To provide the best available evidence on the role of dehydroepiandrosterone (DHEA) treatment in improving the outcome of in vitro fertilization (IVF)/intracytoplasmic sperm injection (ICSI) in women with poor ovarian response (POR). **Study Design:** A randomized controlled trial conducted in Cairo University hospitals and Dar Al-Teb subfertility and assisted conception centre, Giza, Egypt. 140 women undergoing IVF/ICSI with POR according to the Bologna criteria were randomly divided into 2 equal groups. The study group received DHEA 25mg three times daily for 12 weeks before the IVF/ICSI cycles and the control group did not receive DHEA. Controlled ovarian stimulation (COH) was started on the second day of menstruation using human menopausal gonadotropins, cetrotide 0.25mg was started when the leading follicle reached 14mm. The main outcome measures were the clinical pregnancy rate, ongoing pregnancy rate, retrieved oocytes, fertilization rate, gonadotropins doses and COH days. **Results:** The DHEA group had significantly higher clinical pregnancy rate (32.8% vs 15.7%, p=0.029), ongoing pregnancy rate (28.5% vs 12.8%), retrieved oocytes (6.9±3 vs 5.8±3.1, p=0.03), fertilization rate (62.3±27.4 vs 52.2±29.8, p=0.039), significantly less gonadotropins doses (3383±717.5IU vs 3653.5±856IU, p=0.045) and COH days (11.6±1.8 vs 12.6±1.06, p=0.001). **Conclusion:** DHEA increases the number of oocytes, fertilization rate, fertilized oocytes, and clinical pregnancy rate and ongoing pregnancy rate in women with POR according to the Bologna criteria. DHEA was well tolerated by the patients and was associated with less COH days and gonadotropins doses.

**Keywords:** Dhea; Bologna Criteria; IVF; ICSI

## M-264. Effect of Hydrosalpinx on Uterineand Ovarian Hemodynamics in Women with Tubal Factor Infertility

Akmal El-Mazny, Wafaa Ramadan, Ahmed Kamel and Sherine Gad-Allah

*European Journal of Obstetrics and Gynecology and Reproductive Biology, 199: 55-59 (2016) IF: 1.662*

**Objective:** To evaluate the effect of hydrosalpinx on uterine and ovarian blood flows in women with tubal factor infertility. **Study Design:** In a cross-sectional study at a university teaching hospital, 60 women with hydrosalpinx-related tubal infertility (hydrosalpinx group) were compared with 60 women with male or unexplained infertility (non-hydrosalpinx group). In the mid-luteal (peri-implantation) phase of the cycle,

endometrial thickness, uterine and ovarian artery pulsatility index (PI) and resistance index (RI), and endometrial and ovarian volume and 3D power Doppler vascularization index (VI), flow index (FI), and vascularization flow index (VFI) were measured in both groups. **Results:** The endometrial VI (p=0.002), FI (p=0.041), and VFI (p=0.018), and ovarian VI (p=0.011), and VFI (p=0.015) were significantly lower in the hydrosalpinx group than in the non-hydrosalpinx group. However, the endometrial thickness, uterine artery PI and RI, ovarian artery PI and RI, endometrial volume, and ovarian volume and FI were not significantly different between the two groups. **Conclusion:** Hydrosalpinx is associated with impaired endometrial and ovarian blood flows which may adversely affect endometrial receptivity and oocyte quality.

**Keywords:** 3D Power Doppler; Hydrosalpinx; Tubal Infertility; Uterine and Ovarian Blood Flow

## M-265. Misoprostol Versus Uterine Straightening by Bladder Distension for Pain Relief in Postmenopausal Patients Undergoing Diagnostic Office Hysteroscopy: A Randomised Controlled Non-Inferiority Trial

Usama M. Fouda, Hesham S. Elshaer, Khaled A. Elsetohy and Mohamed A. Youssef

*European Journal of Obstetrics & Gynecology and Reproductive Biology, 203: 326-330 (2016) IF: 1.662*

**Objective:** To compare the effectiveness of misoprostol with uterine straightening by bladder distension in minimising the pain experienced by postmenopausal patients during diagnostic office hysteroscopy. Study design: Seventy-six postmenopausal patients were randomly allocated in a 1:1 ratio to the misoprostol group or to the bladder distension group. Patients in the misoprostol group were instructed to insert two misoprostol tablets (400 mg) in the vagina 12 h before office hysteroscopy. Patients in the bladder distension group were instructed to drink one litre of water and to avoid urination during a period of 2 h before office hysteroscopy. The severity of pain experienced by the patients during and at 30 min after the procedure was measured using a 100-mm visual analogue scale (VAS). The ease of passing the hysteroscope through the cervical canal was assessed by the hysteroscopists using a 100-mm VAS. **Results:** The passage of the hysteroscope through the cervical canal was easier in the misoprostol group [60.37 15.78 vs. 50.05 19.88, p = 0.015]. The mean VAS pain score during the procedure was significantly lower in the misoprostol group [39.47 13.96 vs. 50.18 15.44, p = 0.002]. The mean VAS pain score 30 min post-procedure was comparable between both groups [11.82 3.71 vs. 12.61 4.06, p = 0.379]. **Conclusion:** Vaginal misoprostol is more effective than uterine straightening by bladder distension in relieving the pain experienced by postmenopausal patients during office hysteroscopy.

**Keywords:** Bladder Distension, Misoprostol, Office Hysteroscopy, Pain, Uterine Straightening.

## M-266. The Role of Prophylactic Use of Low Dose Aspirinand Calheparin in Patients with Unexplained Recurrent Abortion

Ahmed M. Maged, Aly Abdelhafiz, Walaa AI Mostafa, Noura El-Nassery, Mona Fouad, Emad Salah and Amal Kotb

*Gynecological Endocrinology, 32: 970-972 (2016) IF: 1.413*

**Objective:** To study the effect of prophylactic use of low dose aspirin and heparin on patients with recurrent unexplained pregnancy loss. **Methods:** Prospective case control study conducted on 180 pregnant women randomized into two equal groups. Group 1 received low-dose aspirin 75 mg and heparin 5000 IU subcutaneous every 12 h. Group 2 received no treatment. **Results:** There was a statistically significant difference between the two study groups regarding number of patients who completed their first trimester (66 versus 39) (p values 0.018). The outcome regarding completion of first trimester was not related to age, BMI or number of previous abortions in both the study groups. Complications of the use of aspirin calheparin occurred in 60% of the patients. The most common complication was bruising at injection site occurring in 60% of the patients followed by bleeding gums (14.4%), gastrointestinal troubles (12.2%), epistaxis (10%) and transient thrombocytopenia in only 2.22% of the patients (Table 4). **Conclusion:**The use of prophylactic dose of calheparin and aspirin is associated with increased chance of passing 1st trimester safely regardless the age, body mass index or number of abortion in women with unexplained recurrent spontaneous abortion

**Keywords:** Aspirin; Calheparin; Unexplained Recurrent Abortion.

## M-267. Which is the Best Ivf / Icsi Protocol to Be Used in Poor Responders Receiving Growth Hormone As an Adjuvant Treatment? A Prospective Randomized Trial

Dina M. R. Dakhly, Yomna A. Bayoumi and Sherine H. Gad Allah

*Gynecological Endocrinology, 32: 116-119 (2016) IF: 1.413*

This open label randomized study aims to define the best protocol to be used with growth hormone in poor responders, with comparison performed to delineate which protocol offers the best cycle outcomes. Two-hundred eighty-seven poor responders were included. The patients were randomly allocated into four groups receiving growth hormone (GH) as an adjuvant therapy added to either long or short agonist protocol, miniflare or antagonist protocols. The short/GH gave significantly lower mean number of oocytes when compared with the long/GH, antagonist/GH and miniflare/GH (4 ± 1.69 versus 5.06 ± 1.83, 4.95 + / = 1.90 and4.98 ± 2.51, respectively p = 0.005). Considering the number of fertilized oocytes, the long/GH showed significantly higher levels than short/GH and antagonist/GH (3.73 ± 1.47 versus 3.02 ± 1.52 and 2.89 ± 1.14, respectively). The main drawback is that it required significantly higher HMG dose and longer duration of stimulation. The long/GH was superior when compared with the three protocols regarding the number of oocytes retrieved and fertilized. But, when considering the clinical pregnancy rates, there was a difference in favor of the long/GH but not reaching a statistically significant value (ClinicalTrials.gov Identifier: NCT01897324)

**Keywords:** Antagonist Protocol; Ivf/Icsi; Growth Hormone; Long Agonist Protocol; Miniflare Protocol; Poor Responders; Short Agonist Protocol

## M-268. Three-Dimensional Ultrasonographyand Power Doppler for Discrimination Between Benign and Malignant Endometrium in Premenopausal Women with Abnormal Uterine Bleeding

Mohamed El-Sharkawy, Akmal El-Mazny, Wafaa Ramadan, Dina Hatem, Aly Abdel-Hafiz, Mohamed Hammam and Adel Nada

*BMC Women's Health, 16 (2016) IF: 1.353*

**Background:** Ultrasonography has been extensively used in women suspected of having a gynecological malignancy. The aim of this study is to evaluate the efficacy of 3D ultrasonography and power Doppler for discrimination between benign and malignant endometrium in premenopausal women with abnormal uterine bleeding. **Methods:** This cross-sectional study included 78 premenopausal women with abnormal uterine bleeding scheduled for hysteroscopy and endometrial curettage. The endometrial thickness (ET), uterine artery pulsatility index (PI) and resistance index (RI), and endometrial volume (EV) and 3D power Doppler vascularization index (VI), flow index (FI), and vascularization flow index (VFI) were measured and compared with hysteroscopic and histopathologic findings. **Results:** The ET (P <0.001), EV (P <0.001), and endometrial VI (P <0.001) and VFI (P = 0.043) were significantly increased in patients with atypical endometrial hyperplasia and endometrial carcinoma (n = 10) than those with benign endometrium (n = 68); whereas, the uterine artery PI and RI and endometrial FI were not significantly different between the two groups. The best marker for discrimination between benign and malignant endometrium was the VI with an area under the ROC curve of 0.88 at a cutoff value of 0.81%. **Conclusion:** 3D ultrasonography and power Doppler, especially endometrial VI, may be useful for discrimination between benign and malignant endometrium in premenopausal women with abnormal uterine bleeding.

**Keywords:** 3D Ultrasonography; Doppler; Endometrial Carcinoma; Hysteroscopy; Premenopausal Bleeding.

## M-269. The Effect of Loading Dose of Magnesium Sulfate on Uterine, Umbilical, and Fetal Middle Cerebral Arteries Doppler in Women with Severe Preeclampsia: A Case Control Study

Ahmed M. Maged, Ahmed M. T. Hashem, Sherine H. Gad Allah, Mohamed El Mahy, Walaa A. I. Mostafa and Amal Kotbb

*Hypertension in Pregnancy, 35: 91-99 (2016) IF: 1.211*

SYNOPSIS IV MgSO4 administration in women with severe preeclampsia resulted in a decrease in umbilical artery, uterine artery, and fetal middle cerebral artery Doppler indices. **Objective:** To evaluate Doppler parameters of the umbilical artery (UmA), uterine artery (UA), and fetal middle cerebral artery (MCA) before and after MgSO4 administration in women with severe preeclampsia. **Methods:** A case control study included 100 pregnant women with severe preeclampsia. Umbilical artery, uterine artery, and fetal middle cerebral artery Doppler were measured before and 20 minutes after intravenous administration of 6 g of magnesium sulfate. **Results:** There was a significant difference between maternal systolic blood pressure (173.20 ± 22.72 vs. 156.60 ± 19.18), diastolic blood pressure (109.60 ± 9.14 vs. 101.90 ± 10.05), and heart rate (80.52 ± 11.52 vs. 88.48 ± 12.08) before and after administration of MgSO4 in the studied patients (p value < 0.001). There was a significant difference between umbilical artery, middle cerebral artery, and uterine artery Doppler parameters before and after administration of MgSO4 in the studied patients (p value < 0.001). There was no significant difference between umbilical artery/middle cerebral artery with regard to RI and PI. However, there was significant difference with regard to the S/D ratio (p value < 0.001). The decrease in the values of Doppler parameters before and after administration of MgSO4 was more in the middle cerebral artery than in the umbilical artery. **Conclusion:**Intravenous administration of magnesium sulfate in pregnant women with severe preeclampsia resulted in a decrease in umbilical artery, uterine artery, and fetal middle cerebral artery Doppler indices with reduced resistance to blood flow in these vessels.

**Keywords:** Doppler Ultrasound; Hypertension; Magnesium Sulfate; Middle Cerebral Artery; Preeclampsia; Umbilical Artery; Uterine Artery.

## M-270. Effect of Ovarian Endometrioma on Uterineand Ovarian Blood Flow in Infertile Women

Akmal El-Mazny, Ahmed Kamel, Wafaa Ramadan, Sherine Gad-Allah, Suzy Abdelaziz and Ahmed M Hussein

*International Journal of Women'S Health, 8: 677-682 (2016)*

**Background:** Angiogenesis has been found to be among the most important factors in the pathogenesis of endometriosis. The formation of new blood vessels is critical for the survival of newly implanted endometriotic foci. The use of 3-D power Doppler allows for the demonstration of the dynamic vascular changes that occur during the process of in vitro fertilization (IVF). We aimed to evaluate the effect of ovarian endometrioma on uterine and ovarian blood flow in infertile women. **Materials and Methods**: In a case-control study at a university teaching hospital, 138 women with unilateral ovarian endometrioma scheduled for IVF were compared to 138 women with male-factor or unexplained infertility. In the mid-luteal (peri-implantation) phase of the cycle, endometrial thickness, uterine and ovarian artery pulsatility index and resistance index, endometrial and ovarian volume, 3-D power Doppler vascularization index (VI), flow index (FI), and vascularization FI (VFI) values were measured in both groups. **Results:** There were no significant differences (P>0.05) in endometrial thickness, uterine ovarian artery pulsatility index and resistance index, endometrial and ovarian volume, or VI, FI, and VFI between the two groups. Furthermore, the endometrial and ovarian Doppler indices were not influenced by endometrioma size. No significant differences were observed in the ovarian Doppler indices between endometrioma-containing ovaries and contralateral ovaries. **Conclusion:** Ovarian endometrioma is not associated with impaired endometrial and ovarian blood flows in infertile women scheduled for IVF, and it is not likely to affect endometrial receptivity or ovarian function through a vascular mechanism.

**Keywords:** 3-D Power Doppler; IVF; Endometrioma; Uterine and Ovarian Blood Flow.

## M-271. Maternal Urinary Cell Free Fetal Dna in Relation to Gestational Age

Mona Mohamed Shaban, Noha Mohamed Salah Eldin, Hisham Omar Kandil, Zeinab Aly Hassan, Walaa A. Rabie, Wael Elgarf and Mohamed Talaat Elrayes

*Middle East Fertility Society Journal, 21: 241-245 (2016)*

**Objectives:** To evaluate the presence of cell-free fetal DNA in the maternal urine in relation to gestational age as a potential source for non-invasive prenatal diagnosis. Material and methods: One hundred and sixty normal pregnant women were included in the study; 80 women pregnant with male fetuses and 80 women pregnant with female fetuses. Maternal urine of all patients was examined at 12, 16 and 20 wks' gestation for the SRY gene (sex-determining region Y) as a cffDNA (cell free fetal DNA) marker and Ribonuclease P RNA component H1 (RPPH1) as a total cfDNA (cell free DNA) marker using a quantitative real-time PCR assay. **Results:** SRY gene was detected in maternal urine of those pregnant with male fetuses starting from 16 weeks in 25% (20/80) of cases only and in 80% of cases (64/80) at 20 weeks, but it was not detected at 12 weeks. All women female fetuses were negative for SRY gene. **Conclusions:** Cell free fetal DNA in maternal urine was not detected in early gestational age using SRY gene alone despite the use of extraction kit specific for extraction of Free-circulating nucleic acids and highly sensitive reported PCR technique. Further studies should be done to evaluate whether cell free fetal DNA in maternal urine can be detected after reaching a certain threshold in blood.

**Keywords:** Cell Free Fetal Dna, Maternal Urine, Gestational Age, Prenatal Diagnosis.

### *Dept. of Ophthalmology*

## M-272. Retinal Nerve Fiber Layerand Ganglion Cell Complex Thicknesses are Reduced in Children with Type 1 Diabetes with no Evidence of Vascular Retinopathy

Dina El-Fayoumi, Nashwa M. Badr Eldine, Amanne F. Esmael, Dalia Ghalwash and Hend M. Soliman

*Investigative Ophthalmology and Visual Science, 57: 5355-5360 (2016) IF: 3.427*

**Purpose:** To determine whether type 1 diabetes (T1DM) in children with a mean age of 12.21 ± 3.04 years affects the retinal nerve fiber layer (RNFL) and ganglion cell complex (GCC) when compared to age- and sex-matched healthy children. **Methods:** Forty-six children with T1DM with no diabetic retinopathy (DR) and 50 normal age- and sex-matched controls underwent full clinical ophthalmic and spectral-domain optical coherence tomography (SD-OCT) examination. Using RTVue Fourier-Domain OCT (version 6.11.0.12) average, superior, and inferior RNFL and GCC thicknesses (in µm) were measured. Mean values of patients and the control group were compared. **Results:** In children with T1DM with no DR, the mean average RNFL thickness was 110.9 µm ± 10.46, and the mean GCC thickness was 95.59 µm ± 5.13; both were significantly thinner than the control group (115.62 µm and 99.30 µm, respectively). The retinal nerve fiber layer and GCC thickness showed no correlation to either age of onset, duration of the disease, or glycosylated hemoglobin (HbA1c). A positive correlation was found between the daily insulin dose and the average RNFL thickness (r = 0.378, P = 0.01). The average GCC in children with dyslipidemia was thinner than those with normal lipid profile (91.29 ± 6.46 µm, 97.11 ± 3.59 µm, respectively) with a P value of 0.011. **Conclusions:** Thinning of the RNFL and GCC in children with T1DM with no DR compared to healthy controls suggests that neurodegenerative changes occur in the absence of vascular changes. It also shows that neurodegeneration is not related to either disease duration, onset, or control

**Keywords:** Type 1 Diabetes Mellitus, Children, Optical Coherence Tomography, Retinal Nerve Fiber Layer, Ganglion Cell Complex, Neuro-Degeneration, Vasculopathy.

## M-273. Intravitreal Infliximab in Refractory Uveitis in Behcets Disease: A Safety and Efficacy Clinical Study.

Mostafa M.E. Hamza, Tamer A. Macky, Mohamed Karim Sidky, Gaafar Ragab andMahmoud M. Soliman

*Retina-The Journal of Retinal and Vitreous Diseases, 36(12): 2399-2408 (2016) IF: 3.039*

**Purpose:** To assess the safety and efficacy of intravitreal infliximab (1 mg/0.05 mL) in patients with refractory posterior uveitis in Behcet's disease. **Methods:** Twenty patients were included in this study. Best corrected visual acuity (BCVA), vitreous haze (graded 0–4), vasculitis, retinitis, and papillopathy (presence or absence) were assessed at baseline, Day 1 and Week 2, 4, 6, 8, 12, and 18. Optical coherence tomography (OCT) central foveal thickness, fluorescein angiography, and flash electroretinogram were done at baseline and 4, 12, and 18 weeks. **Results:** Mean baseline logMAR BCVA was 0.94 (20/160), had improved significantly by Week 2 to 0.6 (20/80) (P, 0.0001), and reached 0.36 (20/40) by Weeks 18 with three injections (P, 0.0001). Mean central foveal thickness OCT decreased significantly from baseline 361 mm to 180 mm at the end of follow-up (P , 0.0001). Profound decrease in mean vitreous haze gradings from two to 0.2 by the end follow-up (P , 0.05). There was a significant reduction in the number of patients with vasculitis (15 at baseline to 1 weeks at 18 weeks), retinitis (nine at baseline to none at 4 weeks), and papillitis (two at baseline to none at 4 weeks) (P , 0.05). No significant electrophysiological changes or ocular adverse inflammatory reactions were observed during the study period. **Conclusion:** Intravitreal infliximab appeared to be safe and effective in treating uveitis in Behcet's disease and should be considered as an alternative to systemic therapies.

**Keywords:** Intravitreal, Infliximab, Uveitis, Behcets Disease.

## M-274. Primary Trabeculotomy Compared to Combined Trabeculectomy–Trabeculotomy in Congenital Glaucoma: 3-Year Study

Dalia H. Khalil and Mohamad Amr Salah Eddin Abdelhakim

*Acta Ophthalmologica, 94: 550-554 (2016) IF: 3.032*

Purpose To compare the outcome of primary trabeculotomy with that of combined trabeculectomy–trabeculotomy (CTT) with mitomycin C (MMC) in children with congenital glaucoma. Methods This is a prospective comparative study, carried out on a cohort of 28 eyes (28 infants) with congenital glaucoma.

Infants with proved congenital glaucoma [based on intra-ocular pressure (IOP), cup/disc (C/D ratio), corneal diameter and axial length measurements] were randomly allocated to either group A (trabeculotomy) or group B (CTT with MMC). Postoperatively, all patients were followed regularly for 3 years; for IOP and C/D evaluation. Criteria for successful outcome included resolution of corneal oedema, reversal of disc cupping, and IOP 18 mmHg or less. **Results** Success rate in each group was 85.7% (p = 1.00). All preoperative parameters, including horizontal corneal diameter, axial length, IOP and C/D ratio, were not statistically significantly different between the two groups. Also, postoperative C/D ratio, IOP, IOP difference and percentage difference (compared to preoperative values), at different follow-up visits, were not statistically significantly different between both surgical techniques. Comparing preoperative to postoperative IOP and C/D ratio in each group was statistically significant. **Conclusion** Both primary trabeculotomy and CTT with MMC had similar outcomes, which could mean that trabeculotomy could be resorted to first.

**Keywords:** Combined Trabeculotomy–Trabeculectomy – Congenital Glaucoma – Success Rate – Trabeculotomy.

## M-275. Trabeculectomy with Ologen in Secondary Glaucomas Following Failed Trabeculectomy with Mmc: Comparative Study

Heba Magdy El-Saied and Mohamad Amr Salah Eddin Abdelhakim

*Eye, 30: 1126-1134 (2016) IF: 2.213*

**Purpose** We aimed to assess the IOP-lowering effect of trabeculectomy with ologen in refractory secondary glaucoma following failed trabeculectomy with mitomycin C (MMC), and to compare its surgical outcome between open angle (SOAG) and angle closure (SACG) cases. **Methods** This is a prospective interventional comparative study conducted on 40 eyes (40 patients) with medically uncontrolled secondary glaucoma. Patients were divided into group A: 18 eyes (18 patients) with SOAG, and group B: 22 eyes (22 patients) with SACG. All patients underwent trabeculectomy with insertion of ologen implant. Intraocular pressure (IOP) measurement, SITA standard perimetry (Central 24-2), spectral domain optical coherence tomography (OCT) for retinal nerve fiber layer (RNFL) thickness, and anterior segment OCT for bleb morphology, were all done pre- and postoperatively. Primary outcome measures were comparing preoperative to postoperative measurements and also comparing these measurements between SOAG and SACG. All patients were examined up to 1 year. **Results** When preoperative IOP was compared with postoperative IOP, in each group, there was a statistically significant difference (P<0.001). IOP percentage difference was statistically insignificantly different between both groups except at 1 month. According to Moorfields bleb grading system; postoperative bleb was better than the bleb of the previously failed trabeculectomy (P<0.001), and there was a significant difference between group A and B regarding bleb area. Total success rate was 100%; in group A, complete success was 100%, while in group B it was 72.7% (P=0.016). **Conclusion** Our results suggest that Ologen may be a useful alternative to MMC in repeat trabeculectomy.

**Keywords:** Trabeculectomy; Soag; Sacg; Ologen.

## M-276. Excision of Tenon Capsule in Pediatric Trabeculectomy: A Controlled Study

Ahmed Awadein and Yasmine M. El Sayed

*Journal of Glaucoma, 25: 39-44 (2016) IF: 2.102*

**Purpose:** To compare the results of trabeculectomy alone and combined with partial tenonectomy in pediatric glaucoma patients. **Methods:** This was a prospective, controlled, cohort study that included 64 eyes of 46 children younger than 12 years with uncontrolled glaucoma, who underwent trabeculectomy with mitomycin C in an institutional setting. Patients were randomized to undergo a trabeculectomy either with (group A) or without (group B) tenonectomy. Children were followed up prospectively for 24 months. Kaplan-Meier survival analysis and mean survival times with 95% confidence intervals (CIs) were calculated. Postoperative results were compared at 3, 6, 12, and 24 months of follow-up. The main outcome measures were: intraocular pressure (IOP), surgical success, postoperative interventions, and complications in both groups. **Results:** Mean postoperative IOP was lower in group A at all postoperative visits (19.2 mm Hg in group A vs. 22.1 mm Hg in group B at 24 mo, P=0.05). There was a tendency toward greater use of glaucoma medications in group B (P<0.001). Cumulative probability of survival at 24 months was 70% (95% CI, 48%-86%) for group A, and 45% (95% CI, 28%-63%) for group B (P=0.09). Mean survival time was significantly longer (P=0.04) in group A (16.6 mo) than in group B (11.6 mo). Encapsulation occurred more frequently (P=0.03) in group B (25%) than in group A (3%). **Conclusions:**Excision of the Tenon capsule could help achieve better IOP control in pediatric glaucoma surgery.

**Keywords:** Glaucoma; Tenon; Trabeculectomy; Children.

## M-277. Goldmann Versus Disposable Applanation Tonometer Tips in Glaucoma Patients and Normal Subjects.

Eldaly MA

*Current Eye Research, 41: 521-525 (2016) IF: 2.025*

**Purpose:** To assess agreement of intraocular pressure (IOP) measured with Goldmann applanation and disposable Luneau SA applanation prisms in glaucoma patients compared with normal subjects. **Methods:** In a prospective comparative study, one eye per primary open-angle glaucoma (POAG) patient was measured for IOP using Goldmann and disposable Luneau SA (Tonojet) applanation tonometry prisms. Glaucoma patients found with IOP < 21mmHg were compared to an age-matched group of normal subjects. The main outcomes measured were IOP and the difference in IOP between either prism. Bland-Altman plots were used to study the agreement between measurements. Regression analysis was applied to either group. **Results:** One hundred and four POAG patients (eyes) were enrolled into this study. Seventy-one of them were found with IOPs < 21?mmHg, and were compared to 71 normal subjects (eyes). The mean difference between either prism was almost similar, 2.0?±?2.0 and 2.1?±?1.7?mmHg in the glaucoma and normal eye groups, respectively. Bias of two SD from the mean ranged from -1.8 to 5.8?mmHg in glaucoma group and -1.2 to 5.4?mmHg with normal subjects (p?<?0.0001 in either group). The inaccuracy was non-systematic with glaucoma patients

while was systematic with normal subjects. **Conclusions:** The disagreement between disposables and standard Goldmann tips followed different patterns in glaucoma patients when compared with normal subjects. The use of the Goldmann tip is advised with glaucoma patients

**Keywords:** Disposable, Goldmann, Glaucoma, Intraocular Pressure, Normal Subjects.

## M-278. The Effect of Laser Panretinal Photocoagulation on Diabetic Macular Edema Using the Pascal Photocoagulator Versus the Conventional Argon Laser Photocoagulator.

Mohamed M. Mahgoub and Tamer A. Macky

*Ophthamologica, 235: 137-140 (2016) IF: 1.515*

**Purpose:** The aim of this study was to compare the effect of panretinal photocoagulation for proliferative diabetic retinopathy (PDR) on diabetic macular edema (DME) using a Pascal ® Photocoagulator (PP) or a conventional argon laser photocoagulator (CALP). **Methods:** Eighty eyes with PDR and center-involving DME were randomized to PP or CALP. Both groups had baseline assessment of best-corrected visual acuity (BCVA) and were examined with optical coherence tomography and fluorescein angiography. **Results:** The mean number of laser shots for the PP and CALP groups was 1,726.10 and 752.00 at session 1 and 1,589.00 and 830.00 ($p < 0.001$) at session 2, respectively. The mean central foveal thickness (CFT) at baseline was 306 ± 100 and 314 ± 98 for the PP and CALP groups, respectively. At 8 weeks, the mean CFT was 332 ± 116 and 347 ± 111 for the PP and CALP groups, respectively ($p > 0.05$). The mean BCVA was similar during the study period with no significant difference between the groups ($p > 0.05$). **Conclusion:** PP and CALP had similar effects on DME in PDR eyes and were equally safe with no significant increase in CFT.

**Keywords:** Pascalphotocoagulator ; Conventional Argon Laser •Proliferative Diabetic Retinopathy ; Diabetic Maculopathy ; Panretinal Photocoagulation.

## M-281. Epidemiological Features of Pediatric Ocular Trauma in Egypt

Ebrahim Abdullah Yehia Al Wadeai, Amr Abdellatif Osman, Tamer A. Macky and Mahmoud M. Soliman

*Journal of Ophthalmology, 2016: 1-6 (2016) IF: 1.463*

**Purpose.** To review the epidemiology of serious pediatric ocular trauma presenting to Kasr El Aini Hospital, Cairo University. **Methods.** Children with serious ocular trauma during a six-month period were examined and their data was analyzed. **Results.** Eighty eyes of 75 patients were included in this study, with 64% males ($P< 0.001$) and average age of 5 years (5 months–15 years). There were 67 (83.75%) open globe injuries, 11 (13.75%) closed globe injuries, and 2 (2.5%) chemical injuries. of the open globe injuries, 24 (30%) were ruptured globes and 43 (53.75%) were lacerations (31 penetrating injuries (38.75%), 6 IOFBs (7.5%), and 6 perforating injuries (7.5%)). of the closed globe injuries, 3 had hyphema (3.75%), 5 had traumatic cataracts (6.25%), and 3 had vitreous hemorrhage with retinal detachment (3.75%). Forty-two patients (56%) presented within 24 hours, 28 patients (37.33%) presented between 24 hours and 1 week, and 5 patients (6.6%) presented after one week from the time of trauma. Seven eyes developed posttraumatic endophthalmitis (10% of open globe injuries). On leaving the hospital, 55 (68.75%) eyes had poor vision, 13 (16.25%) had moderate vision, and 12 (15%) had good vision. **Conclusion.** Children at a higher risk of trauma are males, >5 years, unsupervised, and involved in street activities. Immediate comprehensive primary management and secondary rehabilitation are mandatory in these cases

**Keywords:** Ocular Trauma, Pediatric, Epidemiology, Egypt

## M-279. The Effectiveness of Intraocular Methotrexate in the Treatment of Posterior Uveitis in Behçet'S Disease Patients Compared to Retrobulbar Steroids Injection

Hossam El Din Mohamed Khalil, Heba A. El Gendy, Hala Ahmed Raafat Youssef, Hazem Effat Haroun, Tamer Atef Gheita and Hossam Mahmoud Bakir

*Journal of Ophthalmology, 2016(2016): 1-5 (2016) IF: 1.463*

**AimofWork.** To evaluate the efficacy of intravitreal methotrexate (MTX) compared to retrobulbar triamcinolone acetonide (TAA),in controlling posterior segment involvement and inducing remissions among Behc¸et's disease (BD) patients. Study **Design.**This is a cross-sectional nonrandomized comparative study. Patients andMethods. 31 adult BDmale patients with amean disease duration of 5.45 years who presented with bilateral posterior segment involvement were included. Each patient received intravitreal injection of 400 $\mu$g/0.1mL (MTX) for the right eye (Group A) and 1mL of retrobulbar 40mg/mL TAA for the left eye (Group B). **Results:** 90% of eyes showed complete improvement of anterior chamber reaction, whereas an improvement in vitreous activity in 77% with no significant differences between both groups ($p \leq 0.1$). BCVA improved in 77.4% eyes (Group A) compared to 87.1% (Group B)($p \leq 0.4$).Relapseswere noted in 11 eyes (35.5%), in groupA,with themean duration of remission being 19.1 weeks ± 2.13 compared to 7.35 ± 2.8 in 20 eyes (64.5%) in group B ($p \leq 0.1$). **Conclusion.** No statistical differences were found between both treatment modalities; however, based on clinical observations, intravitrealMTX may ensure better control of inflammatory reaction and may encourage longer remission as compared to retrobulbar TAA in BD patients.

**Keywords:** Bechet's Disaese, Methotrexate, Intravitreal Injection, Retrobulbar Steroids.

## M-280. Endoscopic-Assisted Scleral Fixated Iol in the Management of Secondary Aphakia in Children

Heba A. El Gendy, Hossam Eldin Khalil, Hazem Effat Haroun, and Mohamed Wagieh El Deeb

*Journal of Ophthalmology, 2016(2016): 1-6 (2016) IF: 1.463*

**Purpose.** To evaluate the short-term postoperative outcomes in endoscopic-assisted sclera fixation intraocular lens (IOL) for the management of secondary aphakia in children. **Methods.**This is a prospective study, whereas 40 aphakic eyes with absence of a good capsular support were implanted by endoscopy-assisted sclera fixation technique. **Results.** No major intraoperative complications were recorded. All cases were followed up for 6 months. Only transient ocular hypertension occurred in 10 (25%)

eyes. Lens decentration and/or tilting were clinically detected in 2 eyes (5%). Ultrasonic biomicroscopic (UBM) examination revealed lens tilting in 2 (5%) of the operated eyes, despite the proper haptics positioning in the ciliary sulcus. Postoperative vitreous hemorrhage was reported in 5 eyes (12.5%) in the early postoperative period and retinal detachment in one eye.A postoperative refractive astigmatism ranging from 0.75D to 3.75D (mean 1.7D ± 0.79) was recorded, as compared to mean preoperative values of 2.00D,with no statistically significant differences being recorded ($p \geq 0.05$). An improvement of BCVA, 1-2 lines on Snellen chart at the end of the follow-up period, was detected in 23 eyes (57.5%) with a mean of 0.6 ± 0.08 SD, as compared to a preoperative mean values of 0.5 ± 0.07 SD ($p \geq 0.05$). **Conclusion.** Using an endoscope for transscleral suturing of intraocular lenses in aphakic pediatric eyes might be considered as being an effective technique that can reduce surgical complications, especially postoperative lens decentration.

**Keywords:** Aphakia, Scleral Fixation, Endoscopy, Secondary Implantation.

## M-281. A Controlled Study on the Correlation Between Tear Film Volumeand Tear Film Stability in Diabetic Patients

Iman M. Eissa, Noha M Khalil and Heba A El-Gendy

*Journal of Ophthalmology, 2016(2016): 1-5 (2016) IF: 1.463*

**Purpose.** To assess the tear filmquantity and correlate itwith the quality and stability of the tear filmin diabetics and compare them to age matched controls. Introduction. Diabetes affects tear film parameters in multiple ways. Poor metabolic control and neuropathy are postulated factors. To further understand how diabetes affects tear film parameters this study was conducted. **Subjects and Methods.** Tear meniscus height was measured by anterior segment OCT, along with tear thinning time, a subtype of noninvasive tear break-up time, and blinking rate per minute which were all recorded for 22 diabetic patients. Correlations between these tear film parameters were studied and then compared to 16 agematched controls. **Results.** A statistically significant difference was found in blinking rate between the diabetic and the control group ($P = 0.002$), with higher blinking rate among diabetics. All tear film parameters were negatively correlated with duration of diabetes. A positive correlation was found between tear film volume and stability. **Conclusion.** Diabetes affects the tear film in various ways. Diabetics should be examined for dry eye signs even in absence of symptoms which may be masked by associated neuropathy. Duration of diabetes has an impact on tear film status.

**Keywords:** Dry Eye; Diabetes; Tear Break Up Time; Oct.

## M-283. Association of Vascular Endothelial Growth Factor -634G/Cand Receptor for Advanced Glycation End Products G82S Gene Polymorphisms with Diabetic Retinopathy

Asmaa Kamal, Khaled Abu Eleinen and Ibrahem Siam

*International Journal of Ophthalmology, 9(8): 1106-1111(2016) IF: 0.939*

**AIM** To investigate the association of receptor for advanced glycation end products (RAGE) G82S and vascular endothelial growth factor (VEGF) -634 G/C gene polymorphisms with diabetic retinopathy (DR). **Methods** Our cross-sectional study included 61 diabetic patients, 12 of them had proliferative diabetic retinopathy (PDR), 15 had non proliferative diabetic retinopathy (NPDR), 34 had no diabetic retinopathy (NDR) and 61 healthy controls. Participants were tested for RAGE G82S and VEGF -634 G/C polymorphisms by polymerase chain reaction-restriction fragment length polymorphism. **Results** We found a significant association between VEGF -634 G/C polymorphism and PDR as PDR patients had increased incidence of VEGF -634 CC genotype compared to NDR patients [odds ratio for CC vs (GC+GG)=6.5, 95% CI=1.5-27.8, P=0.021]. Also VEGF -634 CC genotype and C allele were significantly higher in the PDR than in NPDR patients, which is a novel finding in our study (P=0.024, 0.009 respectively). The mean triglycerides level was significantly higher in diabetic patients with CC genotype (P=0.01) as compared to patients with other genotypes. All cases and control subjects were of the same heterozygous RAGE 82G/S genotype**.** **Conclusion** Patients carrying VEGF -634 C polymorphism have a higher risk of PDR development, so VEGF -634 G/C polymorphism could be used as a predictive marker for PDR in diabetic patients. We could not find a significant association between RAGE G82S polymorphism and DR.

**Keywords:** diabetic retinopathy, vascular endothelial growth factor, receptor for advanced glycation end products, gene polymorphism

## M-284. Changes in the Axis of Astigmatismand in Fundus Torsion Following Inferior Oblique Muscle Weakening

Ahmed Awadein, Dina El-Fayoumi and Rasha H. Zedan

*Journal of Aapos, 20: 289-294 (2016) IF: 0.931*

**Purpose:**To study the changes in fundus torsion and in the axis of astigmatism following inferior oblique (IO) myectomy in patients with inferior oblique overaction (IOOA). **Methods:**The degree of fundus torsion and corneal astigmatism were prospectively evaluated before and 3 months after IO myectomy in patients with IOOA grade +2 or more in one or both eyes and an astigmatic error of ≥1 D. Fundus torsion was evaluated by measuring the disk foveal angle (DFA) using fundus photography. The axis of astigmatism was identified from the anterior sagittal map using Pentacam corneal imaging. **Results:**A total of 54 eyes of 27 patients were included. Patients were divided into two groups: those with esotropia and those with exotropia. All patients had a preoperative DFA >8°, which decreased postoperatively in both groups (P < 0.01). Postoperatively, there was incyclorotation of the axis of astigmatism by >5° in 80% of the esotropic group and 75% of the exotropic groups (P < 0.01). **Conclusions:** Incyclorotation of the axis of astigmatism occurs after IO myectomy. Measurement of the change in the axis of astigmatism can be used to assess the torsional changes after IO myectomy in patients with IOOA.

**Keywords:** Inferior Oblique - Astigmatism - Pentacam - Fundus Torsion

## M-285. Comparison Between Medial Rectus Pulley Fixationand Augmented Recession in Children with Convergence Excessand Variable-Angle Infantile Esotropia

Heba M. Fouad, Mohamad A. Abdelhakim, Ahmed Awadein and Hala Elhilali

*Journal of Aapos, 20: 405-409 (2016) IF: 0.931*

**Purpose:** To compare the outcomes of medial rectus (MR) muscle pulley fixation and augmented recession in children with convergence excess esotropia and variable-angle infantile esotropia. **Methods:** This was a prospective randomized interventional study in which children with convergence excess esotropia or variable-angle infantile esotropia were randomly allocated to either augmented MR muscle recession (augmented group) or MR muscle pulley posterior fixation (pulley group). In convergence excess, the MR recession was based on the average of distance and near angles of deviation with distance correction in the augmented group, and on the distance angle of deviation in the pulley group. In variable-angle infantile esotropia, the MR recession was based on the average of the largest and smallest angles in the augmented group and on the smallest angle in the pulley group. Pre- and postoperative ductions, versions, pattern strabismus, smallest and largest angles of deviation, and angle disparity were analyzed. **Results:** Surgery was performed on 60 patients: 30 underwent bilateral augmented MR recession, and 30 underwent bilateral MR recession with pulley fixation. The success rate was statistically significantly higher ($P = 0.037$) in the pulley group (70%) than in the augmented group (40%). The postoperative smallest and largest angles and the angle disparity were statistically significantly lower in the pulley group than the augmented group ($P < 0.01$). **Conclusions:**Medial rectus muscle pulley fixation is a useful surgical step for addressing marked variability of the angle in variable angle esotropia and convergence excess esotropia.

**Keywords:** Pulley Fixation; Augmented Recession; Convergence Excess and Variable-Angle Infantile Esotropia.

## M-286. Brinzolamide/Timolol Versus Dorzolamide/Timolol Fixed Combinations: A Hospital – Based, Prospective, Randomized Study

Mary S Galose, Heba M Elsaied, Tamer A Macky and Pakinam H Fouad

*Indian Journal of Ophthalmology,64(2):127-131(2016)IF: 0.825*

**Purpose:** To compare the efficacy and tolerability of brinzolamide/timolol (BT) and dorzolamide/ timolol (DT) fixed combinations on intraocular pressure (IOP) reduction. **Methods:** Patients with primary open angle glaucoma or normal tension glaucoma were randomized to receive either BT or DT. IOPs were measured at baseline, 2 weeks, and 1, 2, and 3 months. The primary outcome measures were the mean change in IOP from baseline at each visit. Secondary outcome measures included the tolerability of each fixed combination. **Results:** Seventy-three patients (73 eyes) were included; 37 eyes in BT group and 36 eyes in DT group. Baseline mean IOP were $24.14 \pm 4.5$ and $29.53 \pm 6$ mmHg for BT and DT, respectively ($P < 0.001$). Both BT and DT provided statistically significant mean IOP reductions from baseline values within each group at all study visits ($P < 0.001$). DT provided greater mean IOP reductions from baseline than BT at each visit which was statistically significant at 2 weeks ($P = 0.037$). Mean percentage of IOP reduction was 24.35% and 46.33% at 2 weeks ($P < 0.001$), and 24.65% and 47% at 3 months ($P < 0.001$) for BT and DT, respectively. Patients' tolerability appeared to be better for DT than for BT with complete ocular comfort without any ocular adverse effects in 31 patients (81.1%) in DT group and 11 patients (29.7%) in BT group ($P < 0.001$). **Conclusion:** Both drops provide effective IOP reduction which was greater, and patients were more likely to achieve lower target pressures with DT than with BT.

**Keywords:** Brinzolamide/Timolol, Dorzolamide/Timolol, Fixed Combinations.

## M-288. Vascular Endothelial Growth Factor Gene Polymorphism is Not Associated with Diabetic Retinopathy in Egyptian Patients

Rana Ahmed Abdel Fattah, Rasha Mounir Eltanamly, Mostafa Hamed Nabih and Manal Mohammed Kamal

*Middle East African Journal of Ophthalmology, 23: 75-78 (2016)*

**Purpose:** Vascular endothelial growth factor (VEGF) was implicated as a major contributor to the development of diabetic retinopathy (DR). This study investigated whether single nucleotide polymorphisms of A allele of rs699947 or G allele of rs10434 in the VEGF gene were associated with DR in Egyptian patients with type 2 diabetes mellitus (DM). **Methods:** This is a case–controlled study which was performed at Cairo University Hospital in 2012 on Egyptian patients with type 2 DM with and without DR. Healthy adults without diabetes comprised the comparison group. Patients underwent an ophthalmological examination and fundus photography. Genotyping was performed for the A allele of rs699947 and the G allele of rs10434 polymorphisms using real-time polymerase chain reaction. **Results:** A total of 128 patients were enrolled in this study and divided into three groups: Group A included 46 patients with type 2 DM and DR; Group B included 41 patients with type 2 DM without DR; and Group C included 41 healthy controls. There was no significant association between rs699947 or rs10434 and any of the three groups ($P = 0.5$, $P = 0.7$, respectively). Allelic frequency in the three groups was not statistically significant for rs699947 or rs10434 ($P = 0.6$, $P = 0.6$, respectively). **Conclusion:** Rs699947 or rs10434 polymorphism was not associated with the presence of DR in Egyptian patients. Further studies are required before genetic testing for polymorphism can be used clinically to correlate with DR.

**Keywords:** Diabetic Retinopathy; Gene; Polymorphism.

## M-287. A New Ultrasound Biomicroscopic Sign Seen after Deep Sclerectomy (Dolphin Head Sign)

Abdelrahman AM, Cheweikh HM, El-Fayoumi DM and Allam RS

*Journal of Current Glaucoma Practice, May-Aug;10(2): 56-59 (2016)*

**Purpose:**To describe a new ultrasound biomicroscopic (UBM) sign seen in patients who underwent deep sclerectomy (DS) as a surgical procedure for the management of uncontrolled primary open-angle glaucoma (POAG). The presence of this sign in

ultrasound biomicroscopy is suggested to be an indicator of successful surgery. We would like to name this sign as the "dolphin head sign." **Design:** Prospective interventional study. **Materials and Methods:** Twenty-eight eyes of 17 patients with POAG underwent DS with intraoperative mitomycin C (MMC) 0.3% applied for 2 minutes under the superficial scleral flap. Patients were followed up for a minimum of 6 months. Ultrasound biomicroscopy was done at the third postoperative month to evaluate the surgical area in both successful and failed cases. **Results:** The study included 28 eyes of 17 patients. The mean age of the study group was 42.90 ± 14.37 years (20-64 years). The study included 10 females and 7 males. The mean preoperative intraocular pressure (IOP) was 24.57 ± 6.37 mm Hg (20-38 mm Hg). The mean best corrected visual acuity (BCVA) was 0.57 ± 0.3 (0.05-1.00). Complete success has been achieved in 21 eyes (75%) during the follow-up period, with a mean IOP of 12.00 ± 3.86 mm Hg (6-20 mm Hg). The dolphin head sign was demonstrated only in successful cases, whereas the unsuccessful cases failed to show the typical sign. **Conclusion:** The presence of a "dolphin head" configuration in UBM images could be taken as an indicator of successful DS. How to cite this article: Abdelrahman AM, El Cheweikh HM, El-Fayoumi DMS, Allam RSHM. A New Ultrasound Biomicroscopic Sign seen after Deep Sclerectomy (Dolphin Head Sign).

**Keywords: Keywords:** Deep Sclerectomy; Dolphin Head Sign; Glaucoma; Glaucoma Surgery; Ultrasound Biomicroscopy

***Dept. of Orthopaedic***

## M-289. Clinical Outcome of Conventional Versus Biological Fixation of Subtrochanteric Fractures by Proximal Femoral Locked Plate

Ihab I El-Desouky, Molham M Mohamed and Ahmed E Kandil

*Injury, 47(6): 1309-1317 (2016) IF: 1.91*

**introduction** Surgical fixation is the standard management of the subtrochanteric fractures. Proximal femoral locked plating (PF-LCP) provides a strong construct for fixation with a high success rate. However, some studies reported implant failure due to loss of the postero-medial bone support and recommended an anatomical reduction. Other studies reported excellent to good results with indirect (biological) fixation without anatomical reduction. In this study, we reviewed the short-term clinical results of PF-LCP fixation for subtrochanteric fractures using both conventional and biological fixation. **Materials and Methods** Forty six patients (34 males and 12 females) with comminuted subtrochanteric fractures were included aged between 18 and 74 (mean 44.3 years). They were treated in a single-blind random manner by either conventional (open, direct) or biological (indirect) reduction method and internal fixation with PF-LCP. Intra-operative variables including; duration of surgery, blood loss, fluoroscopy time and any complications were recorded. Post-operative differences including; duration of healing, implant failure, complications and the final clinical outcome by Harris Hip Score (HHS) were documented. **Results** 44 cases continued to the final follow-up (23 of the open fixation group and 21 of the biological fixation group). Patients of open group demonstrated greater blood loss (756 ± 151 vs. 260 ± 39 ml; P < 0.0001), longer operative times (129 ± 16.9 vs. 91 ± 8 min; P < 0.0001) and incisions (s) length (20.4 ± 3 vs. 13.4 ± 1 cm; P < 0.0001). More patients needed blood transfusion in open group (11 patients vs. six in closed group; P < 0.0001). Patients of biological group demonstrated longer fluoroscopy time (80.9 ± 7.3 vs. 47.2 ± 5.8 sec.; P < 0.0001). For each group, one case of implant failure was recorded. Low patient compliance was a detrimental factor for the implant failure in both cases. No much difference was demonstrated for the healing rate (open group; 18.3 ± 3.7 vs. biological group16.5 ± 4 weeks; P < 0.058) and for the functional outcome (open group; excellent/good: 54%/37%, biological group; excellent/good: 57%/33%; P = 0.766). **Conclusion** PF-LCP provided a strong construct for fixation of the comminuted subtrochanteric fractures either by open or biological techniques. Low patient compliance is an influential factor for implant failure in both types.

**Keywords:** Subtrochanteric Fractures; Proximal Femoral Plate; PF-LCP; Patient Compliance.

## M-290. Percutaneous Iliosacral Screw Fixation in Vertically Unstable Pelvic Injuries, A Refined Conventional Method.

Ihab I. El-Desouky, Molham M. Mohamed and Ahmed E. kandil

*Acta Orthopædica Belgica, 82: 52-59 (2016) IF: 0.837*

Percutaneous ilio-sacral screw fixation is a well-established method for fixation of unstable posterior pelvic lesions. Due to unavailability of the navigation system in our institute and the limits of using CT-guided method, we tried to refine the conventional method. Between March 2011 and Nov. 2012, twenty patients with closed vertical pelvic injuries were admitted. They were 17 males and three females with an average age of 34 years (range from 27 to 55). Percutaneous ilio-sacral screw fixation was done in the supine position using a Schanz screw marking of a fixed entry point in the outer iliac table. Closed reduction was done in all cases with excellent reduction in 14 cases, good in two and fair in four cases. The mean duration of screw insertion was 17 minutes (ranged from 10 to 25). One case of injury of the superior gluteal vessels was present and one case with misplacement through the ventral part of contra-lateral sacral ala. No neurological complications were detected. Ilio-sacral screw fixation by this refined technique allows safe stabilization of vertical pelvic lesions with an acceptable complication rate.

**Keywords:** Ilio-Sacral; Vertical Shear; Pelvic Fracture.

***Dept. of Parasitology***

## M-291. Molecular Seasonality of Giardia Lamblia in A Cohort of Egyptian Children: A Circannual Pattern

Mousa A.M. Ismail , Dina M.H. El-Akkad , Enas M.A. Rizk1 , Hala M. El-Askary and Ayman A. El-Badry

*Parasitology Research, 115(11): 4221-4227 (2016) IF: 2.027*

Giardia lamblia (G. lamblia) is the mostworldwide prevailing intestinal parasite, notorious for its broad range of seasonal and age-related prevalence. The potentially lethal nature of giardiasis makes it essential that the seasonality,the groups at risk, and other potential risk factors are identified.The present molecular epidemiological study was designed to determine the genetic diversity of G. lamblia infection,taking into account seasonal peaks, age distribution, and associated symptoms in a cohort of

Egyptian diarrheic patients. Stool samples were collected from 1187 diarrheic patients attending outpatient clinics of Cairo University hospitals,of all age groups over a 12-month period. The patients were examined microscopically for fecal G. lamblia cysts,and/or trophozoites, and for copro-DNA detection using nested polymerase chain reaction (nPCR) assays targeting beta giardin gene. PCR-positive samples were characterized molecularly by nPCR restriction fragment length polymorphism(RFLP) to determine Giardia assemblages. The findings revealed circannual prevalence of Giardia, with a seasonal pattern peaking in mid-summer and late winter, with the summer peak preceded by a peak in temperature. Infection was prevailing in 224 (18.9 %) cases, mainly assemblage B (81.2 %)followed by assemblage A (18.8 %). There were statistically significant associations between the detection of Giardia and flatulence, persistent diarrhea, vomiting, and abdominal pain,while gender and intermittent diarrhea showed no association.The pre-school age group was the most vulnerable. This is the first study of molecular characterization of Giardia to determine its circannual prevalence in Egypt, a finding which carries promising potential for the diagnosis, treatment, and elimination of the disease.

**Keywords:** Giardia Lamblia ; Molecular Seasonality ; Diarrheic Egyptian ;Circannual Pattern.

## M-292. Immunomodulatory Impression of AntiandPro-Inflammatory Cytokines in Relation to Humoral Immunity in Human Scabies

Amany Ahmed Abd El-Aal, Marwa Adel Hassan, Heba Ismail Gawdat, Meran Ahmed Ali and Manal Barakat

*International Journal of Immunopathology and Pharmacology, 29(2): 188-194 (2016) IF: 1.47*

The chief manifestations of scabies are mediated through hypersensitivity-like reactions and immune responses which are so far not well understood and remain poorly characterized. The aim of this study is to investigate the role of inflammatory cytokines in relation to humoral immunity in patients with scabies. Serum levels of total IgE, specific IgG, IL-10, IL-6, INF-γ, and TNF-α were investigated in a cross-sectional study including 37 patients with manifestations suggestive of scabies and serologically positive for anti-Sarcoptes IgG, in addition to 20 healthy controls. The median value of total IgE was 209 (range, 17–1219 IU/mL), reflecting its wide range within cases. IL-10 showed significant higher levels (287 ± 139) in cases than in controls (17.4 ± 11.32). A positive correlation was reported between total IgE and severity of manifestations ($r = 0.429$, $P < 0.005$). A significant positive correlation was observed between total IgE and both IgG and IL-6. On the contrary, a negative correlation was recorded between IL-6 and TNF-α which makes us suggested anti-inflammatory rather than pro-inflammatory effect of IL-6. Moreover, a negative correlation was noticed between the anti-inflammatory cytokine IL-10 and severity of manifestations, specific IgG, total IgE, and INF-γ. Therefore, the current study theorized a regulatory role of IL-10 in inflammatory responses of scabietic patients suggesting further future analysis of its therapeutic potential.

**Keywords:** Immune Response, Inflammatory Cytokines, Interferon, Interleukin, Scabies

## M-293. Electron Microscopic Alterations in Pediculus Humanus Capitis Exposed to Some Pediculicidal Plant Extracts

Dina M. H. El Akkad, Naglaa Saad M. El-Gebaly, Hebat-Allah Salah A. Yousof and Mousa A. M. Ismail

*The Korean Journal of Parasitology, 54(4): 527-532 (2016) IF:1.027*

Head lice, Pediculus humanus capitis, infestation is an important public health problem in Egypt. Inadequate application of topical pediculicides and the increasing resistance to the commonly used pediculicides made the urgent need for the development of new agents able to induce irreversible changes in the exposed lice leading to their mortality. The aim of the present work is to evaluate pediculicidal efficacy of some natural products such as olive oil, tea tree oil, lemon juice, and ivermectin separately in comparison with tetramethrin-piperonyl butoxide (licid), as a standard pediculicide commonly used in Egypt. The effects of these products were evaluated by direct observation using dissecting and scanning electron microscopes (SEM). Results showed that after 1 hr exposure time in vitro, absolute (100%) mortalities were recorded after exposure to 1% ivermectin and fresh concentrate lemon juice. The mortalities were decreased to 96.7% after exposure to tea tree oil. Very low percentage of mortality (23.3%) was recorded after 1 hr of exposure to extra virgin olive oil. On the other hand, the reference pediculicide (licid) revealed only mortality rate of 93.3%. On the contrary, no mortalities were recorded in the control group exposed to distilled water. By SEM examination, control lice preserved outer smooth architecture, eyes, antenna, respiratory spiracles, sensory hairs, and legs with hook-like claws. In contrast, dead lice which had been exposed to pediculicidal products showed damage of outer smooth architecture, sensory hairs, respiratory spiracles and/or clinching claws according to pediculicidal products used.

**Keywords:** Pediculus Humanus Capitis, Pediculicide, Plant Extract, In Vitro, Scanning Electron Microscope.

## M-294. Post-Immunization Immunohistochemical Expression of Caspase 3and P53 Apoptotic Markers in Experimental Hydatidosis

Amany Ahmed Abd El-Aal, Naglaa Saad Mahmoud El-Gebaly, Abeer Said Al-Antably, Marwa Adel Hassan and Marwa Ahmed El-Dardiry

*Revista Brasileira De Parasitologia Veterinária, 25: 333-340 (2016) IF: 0.99*

Th aim of this study was to investigate post-immunization apoptotic changes in experimental hydatidosis, using Caspase 3 and p53 immunohistochemical markers. Two groups of rabbits were immunized with a crude antigen (group 1) or a partially purifid antigen (group 2) and were compared to an infected non-immunized control group. More effctive immune responses were obtained in group 2 than group 1, signifid by fewer and smaller cystic lesions and more severe destructive changes. Normal growth of cysts was attained in the control group, with no expression of apoptotic markers. Signifiantly higher expression of Caspase 3 and p53 were observed in group 1 compared to group 2, as indicated by OD and area percentage, respectively (Group 1 Caspase 3: 0.89±0.21, 93.5%±6.2; Group 1 p53: 0.46±0.18, 53.26%±11.6; Group 2 Caspase 3: 0.52±0.15,

49.23%±11.7; Group 2 p53: 0.19±0.4, 18.17%±7.3). Vaccine-induced immune responses and cellular damage may underlie the expression of apoptotic markers that appeared to result in a degenerative and atrophic course of action upon immunization. Th results of the current study emphasize the importance of immunization for the stimulation of protective immune responses and in preventing mechanisms of evasion to ensure normal cell growth. A cost/benefi control program that implements proper vaccine preparations should be further assessed for complete elimination of severe infections in endemic areas

**Keywords:** Experimental Hydatidosis, Caspase 3, P53, Apoptosis

## M-295. Comparative Study on Immunoblot Versus Pcr in Diagnosis of Schistosomiasis Mansoni in Experimental Infected Mice

Mousa A.M. Ismail, Wahed Mohammed Ali Mousa, Enas Yahia Abu-Sarea, Maha M. A. Basyouni and Samah Sayed Mohammed

*Journal of The Egyptian Society of Parasitology, 46(1): 101-108 (2016)*

This study compared PCR and Western blot techniques in diagnosis of schistosomiasis mansoni. Forty Swiss albino mice were used, thirty two mice were infected with cercariae of S. mansoni and eight mice were kept uninfected which were used as a control. Blood was obtained from four infected mice weekly beginning from the 1st week to the 8th week post infection. The study found that PCR was positive from the first week post infection, while Western blot technique was positive from the second week post infection. Thus, PCR diagnosed schistosomiasis mansoni earlier than Western blot technique, but both were able to diagnose.

**Keywords:** Egypt; Schistosoma Mansoni; Pcr; Western Blot Technique.

## M-296. Copro - Molecular Characterization of Cryptosporidium SPPandGenotypes Among Egyptian Children

Noha M. Abdelrazek, Abeer S. A. Al-Antably, Mona M. Fathy, and Ayman A. El-Badry

*Journal of The Egyptian Society of Parasitology, 46: 375-386 (2016)*

Stool samples from 182 diarrhoeic (symptomatic) children and 100 apparently healthy (asymptomatic) children, matched for age, from Aboul-Reesh Cairo University Pediatrics Hospital were examined by ELISA and by nPCR (targeting COWP gene) for the detection of Cryptosporidium. The demographic and environmental data of the diarrhoeic group was recorded. The PCR amplified product of positive cases was then subjected to RFLP by digesting it with the restriction enzyme RsaI. The obtained fragments were resolved by electrophoresis and the bands were visualized and characterized versus a standard. ELISA results demonstrated a prevalence rate of 13.2% (24/182) among diarrhoeic group, and 8% (8/100) among nondiarrheic group, with overall detection rate of 11.3% (32/282). Higher rates of detection were obtained by nested PCR assay among diarrhoeic group 25.8% (47/182) and 16% (16/100) among non-diarrhoeic group with overall detection rate of 22.3% (63/282). Considering nPCR as the reference method, ELISA had a sensitivity of 47.6% and a specificity of 99.1%. RsaI digestion of nPCR product of COWP gene revealed the presence of 2 genotypes: genotype 1 with 4 bands (34, 106, 125 and 285) and genotype 2 in which 3 bands (34, 106 and 401). Among the 63 cases with cryptosporidiosis, 53 (88.3%) had genotype 1, and 7 (11.7%) had genotype 2. The higher prevalence of genotype 1 suggests a relatively greater risk of human source of infection than zoonosis

**Keywords:** Cryptosporidium; Elisa; Nested PCR.

## M-297. Egyptian Eosinophilicand Infectious Meningoencephalitis and Their Impact on Psychological Aspects

Mamdouh M. M. El-Bahnasawy, Mohammad Reda El Feky, Ayman T. A. Morsy, Mousa A. M. Ismail and Tosson A. Morsy

*Journal of The Egyptian Society of Parasitology, 46(1): 67-80 (2016)*

Meningoencephalitis is an acute inflammation of the brain and spinal cord & their covering protective membranes. Meningitis can be life-threatening because of the inflammation's proximity to the brain and spinal cord; therefore, the condition is classified as a medical emergency. The commonest symptoms of meningitis are headache and neck stiffness associated with fever, confusion or altered consciousness, vomiting, and an inability to tolerate light (photophobia) or loud noises (phonophobia). Children often exhibit only nonspecific symptoms, such as irritability and drowsiness. If a rash is present, it may indicate a particular cause of meningitis; for instance, meningitis caused by meningococcal bacteria may be accompanied by a characteristic rash. A broad variety of allergic, infectious, neoplastic, and idiopathic diseases are associated with increased blood and/or tissue eosinophilia and range in severity from self-limited conditions to life-threatening disorders. Although accepted upper limits of normal blood eosinophil numbers vary somewhat, a value above 600 eosinophils /microL of blood is abnormal in the vast majority of cases. Generally speaking, there are several possible causes of eosinophils in the CSF; undoubtedly parasitic infection is one of the main causes.

**Keywords:** Egypt; Meningoencephalitis; Central Nervous System; Parasitosis; Psychology.

## M-298. Modified Culture Methodology for Specific Detection of Blastocystis Hominis in Stool Samples

Marwa A. Hassan, Enas M. Rizk and Rita M. Wassef

*Journal of The Egyptian Society of Parasitology, 46: 541-548 (2016)*

Blastocystis hominis provides major challenges for laboratory diagnosis due to its polymorphic nature in wet mounts which can result in confusion with other protozoa, yeast or even fat globules. Studies revealed that simple smears were less sensitive than in vitro cultivation using different media for the detection of B. hominis in stool specimens. Cultures of B. hominis are usually enriched by different types of sera to enhance growth and multiplication of the parasite. The aim of this study is to assess the use of two sera types other than horse serum that is

commonly used in culture media for the growth, multiplication and detection of B. hominis in examined stool samples and comparing the results with those obtained using horse serum. Fifty stool samples were collected from patients suffering from different colonic manifestations attending Cairo University Hospitals. The samples were freshly cultured in three different culture media using horse serum (in Jones' medium), donkey serum (as a modification in Jones' medium) and human plasma (in modified Pavlova's medium) in adequate preparations. Cultures were then left for incubation and examined by direct microscopy to detect Blastocystis hominis. The results showed of 50 stool samples studied, 18 samples (36%) were positive results for B. hominis. The number of positive results obtained by horse serum, donkey serum and human plasma were 13,18and 11 respectively. Paired comparisons were made between each 2 cultures with each culture set as a reference once to detect the most appropriate one for diagnosis. When horse was set as the reference method, donkey serum showed a sensitivity of 100% and specificity of 86.5% with a 90% agreement between the 2 methods. While human plasma showed a sensitivity of 46.2% and specificity of 86.5% with an agreement of 76%. In addition, the vacuolar form was the commonest pattern observed in this study throughout all the three cultures.

**Keywords:** Blastocystis Hominis, Culture, Horse Serum, Donkey Serum, Human Plasma.

## M-299. Nematodes Ultrastructure: Complex Systems and Processes

Maha M.A.Basyoni and Enas M.A.Rizk

*Journal of Parasitic Diseases, 40 (4): 1130-1140 (2016)*

Nematode worms are among the most ubiquitous organisms on earth. They include free-living forms as well as parasites of plants, insects, humans and other animals. Recently, there has been an explosion of interest in nematode biology, including the area of nematode ultrastructure. Nematodes are round with a body cavity. They have one way guts with a mouth at one end and an anus at the other. They have a pseudocoelom that is lined on one side with mesoderm and on the other side with endoderm. It appears that the cuticle is a very complex and evolutionarily plastic feature with important functions involving protection, body movement and maintaining shape. They only have longitudinal muscles so; they seem to thrash back and forth. While nematodes have digestive, reproductive, nervous and excretory systems, they do not have discrete circulatory or respiratory systems. Nematodes use chemosensory and mechanosensory neurons embedded in the cuticle to orient and respond to a wide range of environmental stimuli. Adults are made up of roughly 1000 somatic cells and hundreds of those cells are typically associated with the reproductive systems. Nematodes ultrastructure seeks to provide studies which enable their use as models for diverse biological processes including; human diseases, immunity, host-parasitic interactions and the expression of phylogenomics. The latter has, however, not been brought into a single inclusive entity. Consequently, in the current review we tried to provide a comprehensive approach to the current knowledge available for nematodes ultrastructures.

**Keywords:** Nematodesultrastructureelectron Microscope.

## M-300. Protozoa Causing Food Poisoning

Mahfouz Ahmad Al-Agroudi, Ayman T. A. Morsy, Mousa A. M. Ismail and Tosson A. Morsy

*Journal of The Egyptian Society of Parasitology, 46(3): 497-508 (2016)*

Food poisoning also called foodborne illness, or illness caused by eating contaminated food is a term used to cover an unpleasant range of illnesses. Food poisoning symptoms vary with the source of contamination. Most types of food poisoning cause one or more of the following signs and symptoms: nausea, vomiting, watery diarrhea, abdominal pain and cramps and fever Signs and symptoms may start within hours after eating the contaminated food, or they may begin days or even weeks later. Sickness caused by food poisoning generally lasts from a few hours to several days.

**Keywords:** Food Poisoning, Protozoa

## M-301. Socio-Demographic Risk Factors of Schistosomiasis Mansoni in Patients with Gastrointestinal Symptoms: A Seroprevalance Study in Egypt

Abeer S.A. Al-Antably, Shawky A. Fouad, Maha M.A. Basyoni, and Marwa A.Hassan

*Journal of The Egyption Society of Parasitology, 46: 377-384 (2016)*

Limited data is available on the epidemiologic status of schistosomiasis mansoni in Egypt. The present work aimed to explore the seroepidemiological status of Schistosoma mansoni infection in Egypt by screening inhabitants of different Egyptian governorates and its correlation with morbid symptoms and risk factors. Health questionnaires and indirect haemagglutination test (IHAT) were performed upon a cross-sectional study of 1788 individuals from 22 governorates. Socio-demographic variables included sex, age, residence and canal water contact. A multivariate regression model was used to assess associations between S.mansoni infection and socio-demographic variables. S.mansoni significant titre ≥ 1:160 was detected in 43% of samples. S. mansoni showed the highest prevalence in Al-Fayoum (15.2%), Kafr El-Sheikh (11.2%) then Assiut (10.9%) while the least positive results were from Matrouh (0.2%). This may be the first indication to emerging foci in Cairo, Luxor, Aswan, Suez, Port Said and the Red Sea Governorates. Anti-S.mansoni antibodies were least detected at 11 -20ys while they were the highest at 41 -50ys, the highest titres (1/1280) were achieved by the age group 31 -40ys.Male gender was a risk factor as 48.2% of males were IHAT +ve. Contacting canal water tends to be advantageous for schistosomiasis mansoni as 72.6% had a history of canal contact and 96.7% of them achieved the highest titre. The alteration in the actual prevalence of schistosomiasis mansoni in Egypt with emergence of new foci including Cairo, Luxor, Aswan, Mersa-Matrouh and the north-eastern province alongside Suez Canal that may be explained by the associated socioepidemiologic risk factors

**Keywords:** Egypt, Schistosoma Mansoni, Seroepidemiology, Ihat

## M-302. The Antigenic Relationship Between Schistosoma Mansoniand its Intermediate Snail Host

Shaimaa M. Abdel Aal, Jomana A. Ahmed, Mousa A. M. Ismail and Sahar Z. Abdel Maogood

*Journal of The Egyptian Society of Parasitology, 46(3): 663-670 (2016)*

Schistosomiasis is a public health problem in many developing countries including Egypt, Determination of the antigenic relationship between S. mansoni and its intermediate snail host (IMH) Biomphalaria alexandrina can open a new field for diagnosis and control of the disease. In the present study infected and non-infected B. alexandrina foot and visceral hump tissue as well as S. mansion crude Ag (SWAg) were fractionated using SDS-PAGE. It's specific and cross reacted protein fractions were determine using EITB versus experimentally prepared mice hyper immune sera (HIS) versus each antigen. After treatment of fractionated S.mansoni crude worm antigens (SWAg) versus HIS produced after vaccination of mice by the same Ag, 8 kda protein fractions ranged from 35-140 kda were reacted specifically. Treatment of fractionated B.alexandrina infected and non-infected foot and visceral hump Ag versus previous HIS revealed presence of common polypeptides bands between SWAg and non-infected snail antigens. The fraction at 135 kda, 68 kda, were detected in all cases, while that at 40-42 kda and that at 35 kda was diagnosed in SWAg and that of infected snails only. The fraction at 68 kda was reacted specifically between SWAg and all tested fractionated snail antigens either that of foot or visceral hump when they treated separately by HIS of mice vaccinated by each snail Ag separately. The fraction at 135 kda was common between SWAg and snail (infected and non-infected) visceral hump antigen. The fraction at the level of 110 kda was diagnosed in SWAg, in non-infected foot antigen and visceral hump Ag. The fraction at the level of 46-48 kda are common between SWAg and snail foot and visceral hump Ag after treated by HIS of mice vaccinated by foot Ag, Presence of common antigenic fractions between snail tissues and Schistosoma species can prefer an easily source of antigen valuable for diagnosis or vaccination as well as can be considered as new tool for determination to the snail IMH of new discovered trematode parasites.

**Keywords:** S.Mansoni; B.Alexandrina; Eitb; Common Fractions.

## M-303. Therapeutic Effect of Mefloquine on Schistosoma Mansoni in Experimental Infection in Mice

Omaima Mohammed Abou-Shady, Soheir Sayed Mohammed, Samar Sayed Attia, Hebat-Allah Salah Yusuf and Dina Omar Helmy

*Journal of Parasitic Disease, 40(2): 259-267 (2016)*

Schistosomiasis is one of the most prevalent parasitic infections worldwide. Praziquantel is the drug of choice for treatment of schistosomiasis for its high efficacy. The present work was carried out on 160 mice to evaluate the therapeutic effect of mefloquine on experimental schistosomiasis mansoni. Mice were classified into 3 groups; group I (20 infected non-treated mice), group II included 60 infected mice which were further divided into group IIm (20 mice treated with 400 mg/kg mefloquine), group IIp (20 mice treated with 1,000 mg/kg/2 days praziquantel) and group IIpm (20 mice treated with 200 mg/kg mefloquine and 500 mg/kg praziquantel), group III included 80 non-infected mice subdivided into group IIIn (20 non-treated mice), group IIIm (20 mice treated with 400 mg/kg mefloquine), group IIIp (20 mice treated with 1,000 mg/kg/2 days praziquantel), group IIIpm (20 mice treated with 200 mg mefloquine and 500 mg praziquantel). Mefloquine significantly reduced worm burden, tissue egg load, number of liver granulomas and increased the percent of dead ova within granulomas. Combination of mefloquine and praziquantel gave better curative effects than praziquantel or mefloquine given alone.

**Keywords:** Scistosoma Mansoni, Mefloquine , Praziquantel.

### *Dept. of Pathology*

## M-304. Does the Human Papilloma Virus Affect the Prognosis of Laryngeal Squamous Cell Carcinoma? an Immunohistochemical Study

Maha E. Salama

*Kasr Al Ainy Medical Journal, 22(3): 147-152 (2016) IF: 2*

Context The worldwide increase in the prevalence of laryngeal cancer is a major health problem. Human papilloma virus (HPV) infection is a major cause for laryngeal carcinoma, especially in nonsmokers. Aim This study investigated the effect of HPV on laryngeal carcinoma prognosis and whether HPV-associated carcinoma cases carry a better or worse outcome. This was approached by studying the relationship between HPV infection (indicated by p16 immunoreactivity) and various prognostic markers of laryngeal carcinoma such as patients' age, tumor grade, lymph node metastasis, thyroid cartilage infiltration, and immunohistochemical markers of tumor proliferation such as cyclin D1 and p53. Materials and methods This was a preliminary study that included paraffin blocks of 40 cases of laryngeal squamous cell carcinoma, obtained either as laryngoscopic biopsies or laryngectomy samples with or without selective neck dissection. All cases were immunostained using antibodies against p16, cyclin D1, and p53. Statistical analysis The clinical, histopathological, and immunohistochemical data are summarized as percentages and means±SD. The $\chi 2$-test was used to assess differences between qualitative variables, whereas the t-test and analysis of variance were used for quantitative variables. A P-value less than 0.05 was considered to be significant. **Results** A statistically significant correlation was observed between p16 expression and tumor grade, lymph node metastasis, thyroid cartilage infiltration, and immunoexpressions of cyclin D1 and p53. No other prognostic markers correlated with p16 expression. **Conclusion** HPV-induced squamous cell carcinoma may carry a worse prognosis in the larynx.

**Keywords:** Carcinoma, Immunohistochemistry, Laryngeal, P16.

## M-305. Chronic Mastitis in Egyptand Morocco: Differentiating Between Idiopathic Granulomatous Mastitis andIgG4-Related Disease.

Steven G. Allen, Amr S. Soliman, Kathleen Toy, Omar S. Omar, Tamer Youssef, Mehdi Karkouri, Essam Ayad, Azza Abdel-Aziz, Ahmed Hablas, Ali Tahri, Hanna N. Oltean, Celina G. Kleer and Sofia D. Merajver

*Breast Journal, 2016 Sep;22(5): 501-509 (2016) IF: 1.92*

Idiopathic granulomatous mastitis (IGM) is a benign, frequently severe chronic inflammatory lesion of the breast. Its etiology remains unknown and reported cases vary in their presentation and histologic findings with an optimal treatment algorithm yet to be described owing mainly to the disease's heterogeneity. IgG4-related disease (IgG4-RD) is a newly recognized systemic fibroinflammatory condition characterized by a dense lymphoplasmacytic infiltrate with many IgG4-positive plasma cells, storiform fibrosis, and obliterative phlebitis. Immunosuppressive therapy is considered to be an effective first-line therapy for IgG4-RD. We sought to clarify and classify chronic mastitis according to the histologic findings of IgG4-RD mastitis with respect to IGM and to develop a robust diagnostic framework to help select patients for optimal treatment strategies. Using the largest collection to date (43 cases from Egypt and Morocco), we show that despite sharing many features, IGM and IgG4-RD mastitis are separate diseases. To diagnostically separate the diseases, we created a classification schema-termed the Michigan Classification-based upon our large series of cases, the consensus statement on IgG4-RD, and the histologic description of IGM in the literature. Using our classification, we discerned 17 cases of IgG4-RD and 8 cases of IGM among the 43 chronic mastitis cases, with 18 indeterminate cases. Thus, our Michigan Classification can form the basis of rational stratification of chronic mastitis patients between these two clinically and histopathologically heterogeneous diseases.
**Keywords:** Chronic Mastitis, Egypt, Morocco, Idiopathic Granulomatous Mastitis, IgG4

## M-306. Chronic Renal Allograft Dysfunction in Egyptian Population: HistopathologicalandImmuno histochemi cal Study

Wael M. Hamza, Hanan H. Ali, Samia M. Gabal and Sawsan A. Fadda

*Saudi Journal of Kidney Diseases and Transplantation, 27: 921-928 (2016)*

The chronic dysfunction stands as the most common cause of renal allograft loss. During the nineties of the past century, this condition was referred to as chronic allograft nephropathy (CAN). Since 2005, CAN has been assigned by the eighth Banff schema to four main categories via histopathological and immunohistochemical findings including chronic antibodymediated rejection (CAMR), chronic T-cell-mediated rejection (CTMR), chronic cyclosporine toxicity (CNITOX), and "interstitial fibrosis (IF)/tubular atrophy; not otherwise specified (NOS)" to eliminate the term CAN. We conducted a retrospective study of renal allograft cases with biopsy-proven chronic damage diagnosed at our nephropathology units, between January 2007 and September 2013, to assign them to the defined categories. Differences between groups were tested using one-way analysis of variance. The frequencies of the diagnostic categories were as follow: CNITOX (43.1%), CAMR (27.5%), CTMR (17.6%), and NOS (11.8%). The serum creatinine level, time posttransplant, and global sclerosis frequency were insignificant among the categories. Nine categorized cases showed transplant glomerulopathy; five of them were seen in association with CAMR. There was a positive relationship between the number of interstitial CD8 + T cells and the degree of IF in CTMR cases. Two cases showed combined features of CAMR and CTMR. Protocol renal allograft biopsy starting 3 months after transplantation with proper monitoring and adjustment of the calcineurin inhibitors level may reduce the potential risk of chronic damage in renal allograft.
**Keywords:** Renal Transplantation, Chronic Allograft Nephropathy, Banff Schema

## M-307. MDM2 Expression in SerousandMucinous Epithelial Tumors of the Ovary

Shereen E Abdelaal, Fahima M Habib, Amina A Gamal el Din, Samia M Gabal, Nabila S Hassan and Nihad A Ibrahim

*Asian Pacific Journal of Cancer Prevention, 17: 3295-3300 (2016)*

**Background:**Different types of cancer exhibit abnormalities in cell cycle regulators. The murine double minute2(MDM2) cell cycle regulator is a protooncogene that negatively regulates the P53 tumour suppressor gene. Surface epithelial tumours constitute approximately two thirds of ovarian neoplasms. Each histologic type can be classified as benign, borderline and malignant. This study aimed to examine immunohistochemical expression of the MDM2 protein in ovarian serous and mucinous epithelial tumours (benign, borderline and malignant). **Materials and Methods:**This study included forty five ovarian tumours, subdivided into fifteen cystadenomas (5 serous and 10 mucinous), fifteen borderline tumours (11 serous and 4 mucinous) and fifteen cystadenocarcinomas (9 serous and 6 mucinous). Paraffin sections were stained with haematoxylin and eosin for histopathologic study, and with mouse monoclonal antiMDM2 antibody for immunohistochemistry. **Results:** MDM2 positivity was detected in 28.9% of the studied ovarian tumours. All benign tumours were negative and positivity was significantly higher in malignant than borderline tumours (P value of chisquare test =0.000). Significantly, all MDM2 positive mucinous tumours were malignant with no positive mucinous borderline tumours. Malignant tumours showed positive MDM2 expression in 83.3% of mucinous type and in 55.6% of serous type. Borderline serous tumours showed negative MDM2 in 72.7% of cases (P value of Z test =0.04). **Conclusions:**Alterations in the expression of the cell cycle regulator (MDM2) occur early in the process of tumourigenesis in serous and mucinous ovarian tumours. We suggest that MDM2 may be used in those tumours as a marker for risk stratification and identification of cases with cancer development and progression. We recommend further studies on MDM2 immunohistochemistry, in conjunction with adjuvant methods as DNA ploidy and FISH gene amplification, focusing on the mucinous tumours and differentiating between the three tumour categories, benign, borderline and malignant.
**Keywords:** MDM2; Ovarian Cancer; Eithelial Tumors of Ovary; Immunohistochemistry.

***Dept. of Pediatrics***

## M-308. A Randomized Trial of Factor Viii and Neutralizing Antibodies in Hemophilia A.

*F. Peyvandi, P.M. Mannucci, I. Garagiola, A. El?Beshlawy, M. Elalfy, V. Ramanan, P. Eshghi, S. Hanagavadi, R. Varadarajan, M. Karimi, M.V. Manglani, C. Ross, G. Young, T. Seth, S. Apte, D.M. Nayak, E. Santagostino, M.E. Mancuso, A.C. Sandoval Gonzalez, J.N. Mahlangu, S. Bonanad Boix, M. Cerqueira, N.P. Ewing, C. Male, T. Owaidah, V. Soto Arellano, N.L. Kobrinsky, et al.*

*The New England Journal of Medicine; 374: 2054-2064 (2016) IF: 59.558*

**Background :** The development of neutralizing anti–factor VIII alloantibodies (inhibitors) in patients with severe hemophilia A may depend on the concentrate used for replacement therapy. **Methods** We conducted a randomized trial to assess the incidence of factor VIII inhibitors among patients treated with plasma-derived factor VIII containing von Willebrand factor or recombinant factor VIII. Patients who met the eligibility criteria (male sex; age <6 years; severe hemophilia A; and no previous treatment with any factor VIII concentrate or only minimal treatment with blood components) were included from 42 sites. **Results** of 303 patients screened; 264 underwent randomization and 251 were analyzed. Inhibitors developed in 76 patients; 50 of whom had high-titer inhibitors (≥5 Bethesda units). Inhibitors developed in 29 of the 125 patients treated with plasma-derived factor VIII (20 patients had high-titer inhibitors) and in 47 of the 126 patients treated with recombinant factor VIII (30 patients had high-titer inhibitors). The cumulative incidence of all inhibitors was 26.8% (95% confidence interval [CI]; 18.4 to 35.2) with plasma-derived factor VIII and 44.5% (95% CI; 34.7 to 54.3) with recombinant factor VIII; the cumulative incidence of high-titer inhibitors was 18.6% (95% CI; 11.2 to 26.0) and 28.4% (95% CI; 19.6 to 37.2); respectively. In Cox regression models for the primary end point of all inhibitors; recombinant factor VIII was associated with an 87% higher incidence than plasma-derived factor VIII (hazard ratio; 1.87; 95% CI; 1.17 to 2.96). This association did not change in multivariable analysis. For high-titer inhibitors; the hazard ratio was 1.69 (95% CI; 0.96 to 2.98). When the analysis was restricted to recombinant factor VIII products other than second-generation full-length recombinant factor VIII; effect estimates remained similar for all inhibitors (hazard ratio; 1.98; 95% CI; 0.99 to 3.97) and high-titer inhibitors (hazard ratio; 2.59; 95% CI; 1.11 to 6.00). **Conclusions** Patients treated with plasma-derived factor VIII containing von Willebrand factor had a lower incidence of inhibitors than those treated with recombinant factor VIII. (Funded by the Angelo Bianchi Bonomi Foundation and others; ClinicalTrials .gov number; NCT01064284; EudraCT number; 2009-011186-88.).

**Keywords:** Factor vIII; Neutralizing antibodies; Hemophilia A.

## M-309. Clinical Outcomes in 3343 Children and Adults with Rheumatic Heart Disease from 14 Low and Middle Income Countries: 2-Year Follow-Up of the Global Rheumatic Heart Disease Registry (the REMEDY Study).

Liesl Zühlke, Ganesan Karthikeyan, Mark E. Engel, Sumathy Rangarajan, Pam Mackie, Blanche Cupido, Katya Mauff, Shofiqul Islam, Rezeen Daniels, Veronica Francis, Stephen Ogendo, Bernard Gitura, Charles Mondo, Emmy Okello, Peter Lwabi, Mohammed M. Al-Kebsi, Christopher Hugo-Hamman, Sahar S. Sheta, Abraham Haileamlak, Wandimu Daniel, Dejuma Yadeta Goshu, Senbeta G. Abdissa, Araya G. Desta, Bekele A. Shasho, Dufera M. Begna, Ahmed ElSayed, Ahmed S. Ibrahim, John Musuku, Fidelia Bode-Thomas, Christopher C. Yilgwan, et al.

*Circulation; 134 (19): 1456-1466 (2016) IF: 17.202*

**Background :** There are few contemporary data on the mortality and morbidity associated with rheumatic heart disease (RHD) or information on their predictors. We report the two year follow-up of individuals with RHD from 14 low and middle income countries in Africa and Asia. **Methods** Between January 2010 and November 2012; we enrolled 3343 patients from 25 centers in 14 countries and followed them for two years to assess mortality; congestive heart failure (CHF); stroke or transient ischemic attack (TIA); recurrent acute rheumatic fever (ARF); and infective endocarditis (IE). **Results** Vital status at 24 months was known for 2960 (88.5%) patients. Two thirds were female. Although patients were young (median age 28 years; interquartile range 18 to 40); the two year case fatality rate was high (500 deaths; 16.9%). Mortality rate was 116.3/1000 patient-years in the first year and 65.4/1000 patient-years in the second year. Median age at death was 28.7 years. Independent predictors of death were severe valve disease (hazard ratio (HR) 2.36; 95% confidence interval (CI) 1.80-3.11); CHF (HR 2.16; 95% CI 1.70-2.72); New York Heart Association functional class III/IV (HR 1.67; 95% CI 1.32-2.10); atrial fibrillation (AF) (HR 1.40; 95% CI 1.10-1.78) and older age (HR 1.02; 95% CI 1.01-1.02 per year increase) at enrolment. Post-primary education (HR 0.67; 95% CI 0.54-0.85) and female sex (HR 0.65; 95%CI 0.52-0.80) were associated with lower risk of death. 204 (6.9%) had new CHF (incidence; 38.42/1000 patient-years); 46 (1.6%) had a stroke or TIA (8.45/1000 patient-years); 19 (0.6%) had ARF (3.49/1000 patient-years); and 20 (0.7%) had IE (3.65/1000 patient-years). Previous stroke and older age were independent predictors of stroke/TIA or systemic embolism. Patients from low and lower-middle income countries had significantly higher age- and sex-adjusted mortality compared to patients from upper-middle income countries. Valve surgery was significantly more common in upper-middle income than in lower-middle- or low-income countries. **Conclusions** Patients with clinical RHD have high mortality and morbidity despite being young; those from low and lower-middle income countries had a poorer prognosis associated with advanced disease and low education. Programs focused on early detection and treatment of clinical RHD are required to improve outcomes.

**Keywords:** Countries; Developing; Heart; Morbidity; Mortality; Outcome Assessment; Patient; Rheumatic Heart Disease; Valves.

## M-310. FAT1 Mutations Cause A Glomerulotubular Nephropathy.

Heon Yung Gee, Carolin E. Sadowski, Pardeep K. Aggarwal, Jonathan D. Porath, Toma A. Yakulov, Markus Schueler, Svjetlana Lovric, Shazia Ashraf, Daniela A. Braun, Jan Halbritter, Humphrey Fang, Rannar Airik, Virginia Vega-Warner, Kyeong Jee Cho, Timothy A. Chan, Luc G.T. Morris, Charles ffrench-Constant, Nicholas Allen, Helen McNeill, Rainer Bu¨scher, Henriette Kyrieleis, Michael Wallot, Ariana Gaspert, Thomas Kistler, David V. Milford, Moin A. Saleem, Wee Teik Keng, Stephen I. Alexander, Rudolph P. Valentini, Christoph Licht, Jun C. Teh, Radovan Bogdanovic, Ania Koziell, Agnieszka Bierzynska, Neveen A. Soliman, Edgar A. Otto, Richard P. Lifton, et al.

*Nature Communications; 7: 1-11 (2016) IF: 11.329*

Steroid-resistant nephrotic syndrome (SRNS) causes 15% of chronic kidney disease (CKD). Here we show that recessive mutations in FAT1 cause a distinct renal disease entity in four families with a combination of SRNS; tubular ectasia; haematuria and facultative neurological involvement. Loss of FAT1 results in decreased cell adhesion and migration in fibroblasts and podocytes and the decreased migration is partially reversed by a RAC1/CDC42 activator. Podocyte-specific deletion of Fat1 in mice induces abnormal glomerular filtration barrier development; leading to podocyte foot process effacement. Knockdown of Fat1 in renal tubular cells reduces migration; decreases active RAC1 and CDC42; and induces defects in lumen formation. Knockdown of fat1 in zebrafish causes pronephric cysts; which is partially rescued by RAC1/CDC42 activators; confirming a role of the two small GTPases in the pathogenesis. These findings provide new insights into the pathogenesis of SRNS and tubulopathy; linking FAT1 and RAC1/CDC42 to podocyte and tubular cell function.
**Keywords:** SRNS; CKD; FAT1; Pathogenesis; Tubulopathy; Podocyte.

## M-311. Mutations in SLC 39 A14 Disrupt Manganese Homeostasis and Cause Childhood - Onset Parkinsonism - Dystonia.

Karin Tusch, Esther Meyer, Leonardo E. Valdivia, Ningning Zhao, Chris Dadswell, Alaa Abdul-Sada, Christina Y. Hung, Michael A. Simpson, W. K. Chong, Thomas S. Jacques, Randy L. Woltjer, Simon Eaton, Allison Gregory, Lynn Sanford, Eleanna Kara, Henry Houlden, Stephan M. Cuno, Holger Prokisch, Lorella Valletta, Valeria Tiranti, Rasha Younis, Eamonn R. Maher, John Spencer, Ania Straatman-Iwanowska, Paul Gissen, Laila A. M. Selim, Guillem Pintos-Morell, Wifredo Coroleu-Lletget, Shekeeb S. Mohammad, et al.

*Nature Communications; 7: 1-16 (2016) IF: 11.329*

Although manganese is an essential trace metal; little is known about its transport and homeostatic regulation. Here we have identified a cohort of patients with a novel autosomal recessive manganese transporter defect caused by mutations in SLC39A14. Excessive accumulation of manganese in these patients results in rapidly progressive childhood-onset parkinsonism–dystonia with distinctive brain magnetic resonance imaging appearances and neurodegenerative features on post-mortem examination. We show that mutations in SLC39A14 impair manganese transport in vitro and lead to manganese dyshomeostasis and altered locomotor activity in zebrafish with CRISPR-induced slc39a14 null mutations. Chelation with disodium calcium edetate lowers blood manganese levels in patients and can lead to striking clinical improvement. Our results demonstrate that SLC39A14 functions as a pivotal manganese transporter in vertebrates.
**Keywords:** Hypermanganesemia; Childhood; Dystonia.

## M-312. Rapid Progression and Mortality of Lysosomal Acid Lipase Deficiency Presenting in Infants.

Simon A. Jones, Vassili Valayannopoulos, Eugene Schneider, Stephen Eckert, Maryam Banikazemi, Martin Bialer, Stephen Cederbaum, Alicia Chan, Anil Dhawan, Maja Di Rocco, Jennifer Domm, Gregory M. Enns, David Finegold, J. Jay Gargus, Ornella Guardamagna, , Christian Hendriksz, Iman G. Mahmoud, Julian Raiman, Laila A. Selim, Chester B. Whitley, Osama Zaki and Anthony G. Quinn,

*Genetics In Medicine; 18: 452-458 (2016) IF: 7.71*

**Purpose:** The purpose of this study was to enhance understanding of lysosomal acid lipase deficiency (LALD) in infancy. **Methods:** Investigators reviewed medical records of infants with LALD and summarized data for the overall population and for patients with and without early growth failure (GF). Kaplan–Meier survival analyses were conducted for the overall population and for treated and untreated patients.**Results:** Records for 35 patients; 26 with early GF; were analyzed. Prominent symptom manifestations included vomiting; diarrhea; and steatorrhea. Median age at death was 3.7 months; estimated probability of survival past age 12 months was 0.114 (95% confidence interval (CI): 0.009-0.220). Among patients with early GF; median age at death was 3.5 months; estimated probability of survival past age 12 months was 0.038 (95% CI: 0.000-0.112).
Treated patients (hematopoietic stem cell transplant (HSCT); n = 9; HSCT and liver transplant; n = 1) in the overall population and the early GF subset survived longer than untreated patients; but survival was still poor (median ageat death; 8.6 months). **Conclusions:**These data confirm and expand earlier insights on the progression and course of LALD presenting in infancy. Despite variations in the nature; onset; and severity of clinical manifestations; and treatment attempts; clinical outcome was poor.

**Keywords:** cholesteryl ester storage disease; infants; lysosomal acid lipase deficiency; natural history.

## M-313. Controversies and research agenda in nephropathic cystinosis: conclusions from a "Kidney Disease: Improving Global Outcomes" (KDIGO) Controversies Conference

Craig B. Langman, Bruce A. Barshop, Georges Desche^nes, Francesco Emma, Paul Goodyer, Graham Lipkin, Julian P. Midgley, Chris Ottolenghi, Aude Servais, Neveen A. Soliman, Jess G. Thoene and Elena N. Levtchenk

Neveen A Soliman Elshakhs

*Journal ,: p1-p2 (2016) IF: 7.6830000877*

**Background:** Nephropathic cystinosis is an autosomal recessive metabolic, lifelong disease characterized by lysosomal cystine accumulation throughout the body that commonly presents in infancy with a renal Fanconi syndrome and, if untreated, leads to end-stage kidney disease (ESKD) in the later childhood years. The molecular basis is due to mutations in CTNS, the gene encoding for the lysosomal cystine-proton cotransporter, cystinosin. During adolescence and adulthood, extrarenal manifestations of cystinosis develop and require multidisciplinary care. Despite substantial improvement in prognosis due to cystine-depleting therapy with cysteamine, no cure of the disease is currently available. Kidney Disease: Improving Global Outcomes (KDIGO) convened a Controversies Conference on cystinosis to review the state-of-the-art knowledge and to address areas of controversies in pathophysiology, diagnostics, monitoring, and treatment in different age groups. More importantly, promising areas of investigation that may lead to optimal outcomes for patients afflicted with this lifelong, systemic disease were discussed with a research agenda proposed for the future.
**Keywords:** Biomarker; cell Signaling; Chronic kidney disease; Cystinosin; End-stage kidney disease; Rare kidney diseases.

## M-314. Whole Exome Sequencing Identifies Causative Mutations in the Majority of Consanguineous or Familial Cases with Childhood-Onset Increased Renal Echogenicity.

Daniela A. Braun, Markus Schueler, Jan Halbritter, Heon Yung Gee, Jonathan D. Porath, Jennifer A. Lawson, Rannar Airik, Shirlee Shril, Susan J. Allen, Deborah Stein, Adila Al Kindy, Bodo B. Beck,4 Nurcan Cengiz, Khemchand N. Moorani, Fatih Ozaltin, Seema Hashmi, 0 John A. Sayer, Detlef Bockenhauer, Neveen A. Soliman, Edgar A. Otto, Richard P. Lifton and Friedhelm Hildebrandt

*Kidney International; 89: 468-475 (2016) IF: 7.683*

Chronically increased echogenicity on renal ultrasound is a sensitive early finding of chronic kidney disease that can be detected before manifestation of other symptoms. Increased echogenicity; however; is not specific for a certain etiology of chronic kidney disease. Here; we performed whole exome sequencing in 79 consanguineous or familial cases of suspected nephronophthisis in order to determine the underlying molecular disease cause. In 50 cases; there was a causative mutation in a known monogenic disease gene. In 32 of these cases whole exome sequencing confirmed the diagnosis of a nephronophthisis-related ciliopathy. In 8 cases it revealed the diagnosis of a renal tubulopathy. The remaining 10 cases were identified as Alport syndrome (4); autosomal-recessive polycystic kidney disease (2); congenital anomalies of the kidney and urinary tract (3); and APECED syndrome (1). In 5 families; in whom mutations in known monogenic genes were excluded; we applied homozygosity mapping for variant filtering; and identified 5 novel candidate genes (RBM48; FAM186B; PIAS1; INCENP; and RCOR1) for renal ciliopathies. Thus; whole exome sequencing allows the detection of the causative mutation in 2/3 of affected individuals; thereby presenting the etiologic diagnosis and allows identification of novel candidate genes.
**Keywords:** Chronic Kidney Disease; Pediatric Nephrology; Genetic Kidney Disease; Whole Exome Sequencing; Mutation Analysis; Monogenic Diseases; Increased Renal Echogenicity; Nephronophthisis.

## M-315. Large-Scale Targeted Sequencing Comparison Highlights Extreme Genetic Heterogeneity in Nephronophthisis-Related Ciliopathies.

Markus Schueler, Jan Halbritter, Ian G Phelps, Daniela A Braun, Edgar A Otto, Jonathan D Porath, Heon Yung Gee, Jay Shendure, Brian J O'Roak, Jennifer A Lawson, Marwa M Nabhan, Neveen A Soliman, Dan Doherty and Friedhelm Hildebrandt

*Journal of Medical Genetics; 53: 208-214 (2016) IF: 5.65.*

**Background :** The term nephronophthisis-related ciliopathies (NPHP-RC) describes a group of rare autosomal-recessive cystic kidney diseases; characterised by broad genetic and clinical heterogeneity. NPHP-RC is frequently associated with extrarenal manifestations and accounts for the majority of genetically caused chronic kidney disease (CKD) during childhood and adolescence. Generation of a molecular diagnosis has been impaired by this broad genetic heterogeneity. However; recently developed high-throughput exon sequencing techniques represent powerful and efficient tools to screen large cohorts for dozens of causative genes. **Methods:** Therefore; we performed massively multiplexed targeted sequencing using the modified molecular inversion probe strategy (MIPs) in an international cohort of 384 patients diagnosed with NPHP-RC. **Results:** As a result; we established the molecular diagnoses in 81/384 unrelated individuals (21.1%). We detected 127 likely disease-causing mutations in 18 of 34 evaluated NPHP-RC genes; 22 of which were novel. We further compared a subgroup of current findings to the results of a previous study in which we used an array-based microfluidic PCR technology in the same cohort. While 78 likely disease-causing mutations were previously detected by the array-based microfluidic PCR; the MIPs approach identified 94 likely pathogenic mutations. Compared with the previous approach; MIPs redetected 66 out of 78 variants and 28 previously unidentified variants; for a total of 94 variants. **Conclusions**: In summary; we demonstrate that the modified MIPs technology is a useful approach to screen large cohorts for a multitude of established NPHP genes in order to identify the underlying molecular cause. Combined application of two independent library preparation and sequencing techniques; however; may still be indicated for Mendelian diseases with extensive genetic heterogeneity in order to further increase diagnostic sensitivity.
**Keywords:** Nephronophthisis; Ciliopathy; Multiplex Targeted Sequencing; Genetics; Modified Molecular Inversion Probe Strategy.

## M-316. Targeted Sequencing of 96 Renal Developmental MicroRNAs in 1213 Individuals from 980 Families with Congenital Anomalies of the Kidney and Urinary Tract.

Stefan Kohl, Jing Chen, Asaf Vivante, Daw-Yang Hwang, Shirlee Shril, Gabriel C. Dworschak, Amelie Van Der Ven, Simone Sanna-Cherchi, Stuart B. Bauer, Richard S. Lee, Neveen A. Soliman, Elijah O. Kehinde, Heiko M. Reutter, Velibor Tasic and Friedhelm Hildebrandt

*Nephrology Dialysis Transplantation; 31: 1280-1283 (2016) IF: 4.085*

**Background :** Congenital anomalies of the kidney and urinary tract (CAKUT) are the most common cause of chronic kidney diseases in children and young adults; accounting for ~50% of cases. These anomalies represent maldevelopment of the genitourinary system and can be genetically explained in only 10–16% of cases by mutations or by copy number variations in protein coding sequences. Knock-out mouse models; lacking components of the microRNA (miRNA) processing machinery (i.e. Dicer; Drosha; Dgcr8); exhibit kidney malformations resembling human CAKUT. **Methods** Given the Dicer-null mouse phenotype; which implicates a central role for miRNAs gene regulation during kidney development; we hypothesized that miRNAs expressed during kidney development may cause CAKUT in humans if mutated. To evaluate this possibility we carried out Next-Generation sequencing of 96 stem-loop regions of 73 renal developmental miRNA genes in 1248 individuals with non-syndromic CAKUT from 980 families. **Results** We sequenced 96 stem-loop regions encoded by 73 miRNA genes that are expressed during kidney development in humans; mice and rats. Overall; we identified in 31/1213 individuals from 26 families with 17 different single nucleotide variants. Two variants did not segregate with the disease and hence were not causative. Thirteen variants were likely benign variants because they occurred in control populations and/or they affected nucleotides of weak evolutionary conservation. Two out of 1213 unrelated individuals had potentially pathogenic variants with unknown biologic relevance affecting miRNAs MIR19B1 and MIR99A. **Conclusions** Our results indicate that mutations affecting mature microRNAs in individuals with CAKUT are rare and thus most likely not a common cause of CAKUT in humans.

**Keywords:** Cakut; Microrna; Mirna; Stem-Loop Topic: Phenotype Congenital Abnormality Mutation Genes Nucleotides Urinary Tract Genitourinary System Kidney Mice Micro Rna Massively-Parallel Genome Sequencing Kidney Development.

## M-317. Cystinosis: A Review.

Mohamed A. Elmonem, Koenraad R. Veys, Neveen A. Soliman, Maria van Dyck, Lambertus P. van den Heuvel and Elena Levtchenko

*Orphanet Journal of Rare Diseases; 11: 1-17 (2016) IF: 3.29*

Cystinosis is the most common hereditary cause of renal Fanconi syndrome in children. It is an autosomal recessive lysosomal storage disorder caused by mutations in the CTNS gene encoding for the carrier protein cystinosin; transporting cystine out of the lysosomal compartment. Defective cystinosin function leads to intra-lysosomal cystine accumulation in all body cells and organs. The kidneys are initially affected during the first year of life through proximal tubular damage followed by progressive glomerular damage and end stage renal failure during mid-childhood if not treated. Other affected organs include eyes; thyroid; pancreas; gonads; muscles and CNS. Leucocyte cystine assay is the cornerstone for both diagnosis and therapeutic monitoring of the disease. Several lines of treatment are available for cystinosis including the cystine depleting agent cysteamine; renal replacement therapy; hormonal therapy and others; however; no curative treatment is yet available. In the current review we will discuss the most important clinical features of the disease; advantages and disadvantages of the current diagnostic and therapeutic options and the main topics of future research in cystinosis.

**Keywords:** Nephropathic Cystinosis; Diagnosis; Cysteamine; Fanconi Syndrome; Esrd.

## M-318. Patterns of Primary Immunodeficiency Disorders Among a Highly Consanguineous Population: Cairo University Pediatric Hospitals 5-Year Experience.

Galal N, Meshaal S, Elhawary R, ElAziz DA, Alkady R, Lotfy S, Eldash A, Boutros J and Elmarsafy A

*Journal of Clinical Immunology; 36(7): 649-65 (2016) IF:3.094*

**Introduction :** Primary immunodeficiency disorders (PIDs) are heterogeneous disorders that mainly present with severe; persistent; unusual; or recurrent infections in childhood. Reports from different parts of the world indicate a difference between Western and Eastern populations. AIM: The aim of this study was to report on the different patterns of PIDs and identify subgroup characteristics in a highly consanguineous population in Egypt. **Methods:** We performed a retrospective chart review for children below 18 years diagnosed with PID at Cairo University Pediatric Hospital from 2010 to 2014. **Results**: Four hundred seventy-six children were diagnosed with PID disorders. Major categories included combined immunodeficiency disorders; which constituted a large proportion (30 %) of cases; along with predominantly antibody disorders (18 %) followed by syndromic combined disorders (16.8 %); phagocytic disorders (13.2 %); immune dysregulation disorders (10.5 %); and autoinflammatory disorders (9 %). **Conclusion:** PIDs have different patterns within inbred populations with high consanguinity.

**Keywords:** Primary Immunodeficiency Disorders; Children; Consanguineous Populations; Patterns.

## M-319. Patterns of Nutrition and Dietary Supplements use in Young Egyptian Athletes: A Community-Based Cross-Sectional Survey.

Safaa Tawfik, Nehal El Koofy and Eman Mohamed Ibraheim Moawad

*Plos One; 11: 1-12 (2016) IF: 3.057*

The aim of this study was to investigate the pattern of basic and sport nutrition as well as perspectives of young Egyptian athletes. Structured interview survey measuring knowledge; attitudes; beliefs and behaviors about basic and sport nutrition was administered to adolescent athletes recruited from 4 sport clubs and 2 fitness centers in Greater Cairo governorate. A total

of 358 participants aged 13–18 years completed questionnaires. Basic nutrition knowledge was reasonable in almost all domains except fast food. Fixed breakfast (78.5%); home meals (lunch; 70.7%); and healthy snacks (55.8%) were the most positive features of the basic dietary pattern. More than 70% perceived themselves as knowledgeable about sport nutrition. The prevalence rate of sport supplement intake was (48.9%; n = 175); predominantly sport drinks (66.9%) and creatine (54.3%). Coaches were the primary source of sport nutrition information. Forty-four percent of participants (n = 77/175) reported supplement consumption during competition seasons only. Better physical appearance and enhancement of athletic performance were the major motivations for supplement intake. These findings indicate the necessity of a comprehensive nutrition education program targeting not only athletes and parents; but also coaching staff; health trainers and all sport team officials.

**Keywords:** Young Athletes; Supplements; Nutrition Knowledge; Nutrition Practices; Attitudes.

## M-320. The use of Multiplex PCR for the Diagnosis of Viral Severe Acute Respiratory Infection in Children: A High Rate of Co-Detection During the Winter Season.

Amani A. El Kholy, Nadia A. Mostafa, Aliaa A. Ali, May M.S. Soliman, Seham A. El-Sherbini, Reem I. Ismail, Nousa El Basha, Rania I. Magdy, Nihal El-Rifai and Dina H. Hamed

*European Journal of Clinical Microbiology and Infectious Diseases; 35 (10): 1607-1613 (2016) IF: 2.857*

Respiratory tract infection is a major cause of hospitalization in children. Although most such infections are viral in origin; it is difficult to differentiate bacterial and viral infections; as the clinical symptoms are similar. Multiplex polymerase chain reaction (PCR) methods allow testing for multiple pathogens simultaneously and are; therefore; gaining interest. This prospective case-control study was conducted from October 2013 to February 2014. Nasopharyngeal (NP) and oropharyngeal (throat) swabs were obtained from children admitted with severe acute respiratory infection (SARI) at a tertiary hospital. A control group of 40 asymptomatic children was included. Testing for 16 viruses was done by real-time multiplex PCR. Multiplex PCR detected a viral pathogen in 159/177 (89.9 %) patients admitted with SARI. There was a high rate of co-infection (46.9 %). Dual detections were observed in 64 (36.2 %); triple detections in 17 (9.6 %); and quadruple detections in 2 (1.1 %) of 177 samples. Seventy-eight patients required intensive care unit (ICU) admission; of whom 28 (35.8 %) had co-infection with multiple viruses. AdV; HBoV; HRV; HEV; and HCoV-OC43 were also detected among asymptomatic children. This study confirms the high rate of detection of viral nucleic acids by multiplex PCR among hospitalized children admitted with SARI; as well as the high rate of co-detection of multiple viruses. AdV; HBoV; HRV; HEV; and HCoV-OC43 were also detected in asymptomatic children; resulting in challenges in clinical interpretation. Studies are required to provide quantitative conclusions that will facilitate clinical interpretation and application of the results in the clinical setting.

**Keywords:** Severe Acute Respiratory Infection (Sari); Children; Multiplex Pcr; Viruses.

## M-321. Limitations of Serum Ferritin to Predict Liver Iron Concentration Responses to Deferasirox Therapy in Patients with Transfusion-Dependent Thalassaemia.

John B. Porter, Mohsen Elalfy, Ali Taher, Yesim Aydinok, Szu-Hee Lee and Pranee Sutcharitchan

*European Journal of Haematology; 98:280-288 (2016) IF:2.544*

**Background**: In transfusion-dependent anaemias; while absolute serum ferritin levels broadly correlate with liver iron concentration (LIC); relationships between trends in these variables are unclear. These relationships are important because serum ferritin changes are often used to adjust or switch chelation regimens when liver magnetic resonance imaging (MRI) is unavailable. **Objectives andMethods:** This post hoc analysis of the EPIC study compared serum ferritin and LIC in 317 patients with transfusiondependent thalassaemia before and after 1 yr of deferasirox. **Results:** Serum ferritin responses (decreases) occurred in 73% of patients; 80% of whom also have decreased LIC. However; 52% of patients without a serum ferritin response did decrease LIC and by >1 mg Fe/g dw (median 3.9) in 77% of cases. Absolute serum ferritin and LIC values correlated significantly only when serum ferritin was <4000 ng/mL ($r = 0.59$; $P < 0.0001$) and not at higher levels (≥4000 ng/mL; $r = 0.19$). Serum ferritin response was accompanied by decreased LIC in 89% and 70% of cases when serum ferritin was <4000 or ≥4000 ng/mL; respectively. **Conclusions:** As serum ferritin nonresponse was associated with LIC decrease in over half of patients; use of liver MRI may be particularly useful for differentiating true from apparent non-responders to deferasirox based on serum ferritin trends alone.

**Keywords:** Serum Ferritin; Liver Iron Concentration; Deferasirox; Thalassaemia; Chelation.

## M-322. Association of TLR Polymorphisms with Bronchopulmonary Dysplasia.

Amr Hosny Malash, Aliaa Adel Ali, Rania Mohamed Samy and Radwa ahmed Shamma

*Gene; 592: 23-28 (2016) IF: 2.319*

**Background** : Bronchopulmonary dysplasia (BPD) remains a leading cause of morbidity and mortality during infancy. Evidence suggests that the Toll-like receptor (TLR) signaling pathway plays an integral role in lung inflammation and injury. This study aimed to detect single nucleotide polymorphisms (SNPs) in TLR pathway genes [TLR5 and Toll-interleukin 1 receptor domain-containing adaptor protein (TIRAP)] among preterm neonates and to determine their association with the development and severity of bronchopulmonary dysplasia.

**Keywords:** Bronchopulmonary Dysplasia; Neonatal Mortality; Oxygen Therapy; Preterm Neonates; Sepsis; Toll-Like Receptors.

## M-323. Safety and Efficacy Osafety and Efficacy of Combined Treatmentwith Pegylated Interferon Alpha-2B and Ribavirinfor Hcv Genotype 4 in Children.

El-Karaksy HM, Mogahed EA, El-Raziky MS, Doaa Saleh, Besheer M and Mubarak S

*Journal of Interferon and Cytokine Research; 36(1): 1-8 (2016) IF: 2.135*

Combined treatment with pegylated interferon (PEG-IFN)-α2b and ribavirin (RBV) is the only currently approved treatment for hepatitis C virus (HCV) infection in children. The aim of this study was to assess the safety and efficacy of combined treatment with PEG-IFN-α2b and RBV in Egyptian children and adolescents with genotype 4 (GT4) HCV infection. The study included 66 patients (3-17 years of age); of both sexes; infected with HCV GT4; treated with PEG-IFN-α2b (60 µg/m(2)); subcutaneously once weekly plus RBV (15 mg/kg/day) in 2 divided oral doses. Efficacy was assessed by achievement of sustained virological response (SVR). Safety was assessed by questionnaires directed to the patients at specific intervals; growth assessment and laboratory tests. SVR was achieved in 28 patients (42.4%). Nonresponders had significantly commoner history of treated malignancies (P = 0.03); baseline lower absolute neutrophil count (ANC; P = 0.009); higher gamma glutamyl transpeptidase (GGT; P = 0.003); and higher viral load (P = 0.03). Fever was the most frequently reported side effect occurring in 98.5% of the patients followed by musculoskeletal symptoms. Neutropenia was observed in 36 patients (54.6%) and necessitated treatment discontinuation in 1 patient. Decline in both weight and height percentiles was observed in 70% of children who received the combined therapy for a total of 48 weeks. In conclusion; the currently available treatment for HCV GT4 in pediatric patients has modest SVR with numerous adverse events necessitating meticulous monitoring to optimize care of the patients. Side effects could be managed with dose modifications and specific treatment when necessary.

**Keywords:** Pegylated Interferon Alpha; Hcv ;Genotype 4; Children.

## M-324. A Case Report of Biotin-Thiamine-Responsive Basal Ganglia Disease in a Saudi Child: is Extended Genetic Family Study Recommended?

Mohammad F. Aljabri, Naglaa M. Kamal, Moinuddin Arif, Asrar M. AlQaedi and Enas Y.M. Santali

*Medicine; 95 (2016) IF: 2.133*

Biotin-thiamine-responsive basal ganglia disease (BTRBGD) is a neurometabolic autosomal recessive (AR) disorder characterized by subacute encephalopathy with confusion; convulsions; dysarthria; and dystonia. The disease is completely reversible if treated early with biotin and thiamine; and can be fatal if left untreated.We herein present our experience with in an extended family study of an index case of BTRBGD aiming to support its AR mode of inheritance; diagnose asymptomatic and missed symptomatic cases; and provide family screening with proper genetic counseling. **Methods:** An index case of BTRBGD and his family underwent thorough clinical and radiological assessment along with genetic molecular testing. **Results**: Two-and-half years old Saudi male child whose parents are consanguineous fulfilled the clinical and magnetic resonance imaging (MRI) criteria of BTRBGD. He was proved by molecular genetic testing to have homozygous mutation of c.1264A>G (p.Thr422Ala) in the SLC19A3 gene of BTRBGD. Extended clinical; radiological; and genetic family study revealed 2 affected members: a neglected symptomatic cousin with subtle neurological affection and an asymptomatic brother carrying the disease mutation in homozygous status. Heterozygous pattern was detected in his parents; his grandma and grandpa; his aunt and her husband; 2 siblings; and 1 cousin while 1 sibling and 2 cousins were negative to this mutation.Treatment of the patient and his diseased cousin with biotin and thiamine was initiated with gradual improvement of symptoms within few days. Treatment of his asymptomatic brother was also initiated. Conclusion: BTRBGD requires high index of suspicion in any child presenting with unexplained subacute encephalopathy; abnormal movement; and characteristic MRI findings. Extended family study is crucial to diagnose asymptomatic diseased cases and those with subtle neurological symptoms.

**Keywords:** Biotin ; Thiamine; Responsive Basal Ganglia Disease; Saudi; Children; Genetic.

## M-325. Environmental and Occupational Lead Exposure Among Children in Cairo; Egypt a Community-Based Cross-Sectional Study.

Eman Mohamed Ibraheim Moawad, Nashwa Mostafa Badawy and Marie Manawill

*Medicine; 95: 1-8 (2016) IF: 2.133*

The aim of this study was to assess childhood lead exposure in a representative sample of Cairo; and to investigate the possible risk factors and sources of exposure. This cross-sectional study was conducted from November 2014 through April 2015. The target population was children aged 6 to 18 years; recruited into 4 groups; garbage city; moderate-living standard area; urban and suburban schools; and workshops in the city of Cairo. Blood lead levels (BLLs) and hemoglobin (Hb) concentrations were measured. Also; potential local environmental sources were assessed for hazardous lead contamination. Analysis on 400 participants has been carried out. A total of 113 children had BLLs in the range 10 to 20mg/dL. Smoking fathers; housing conditions; playing outdoors; and exposure to lead in residential areas were significantly correlated with high BLLs. The mean values of hemoglobin were inversely correlated with BLLs. Children involved in pottery workshops had the highest BLLs and the lowest Hb values with a mean of (43.3mg/dL and 8.6 g/dL; respectively). The mean value of environmental lead in workshop areas exceeded the recommended levels. Also; those values measured in dust and paint samples of garbage city were significantly high. Moreover; the mean lead levels in the soil samples were significantly higher in urban schools (P ¼ 0.03) than the suburban ones. Childhood lead poisoning accounts for a substantial burden in Egypt; which could be preventable. Development of national prevention programs including universal screening program should be designed to reduce incidence of lead toxicity among children.

**Keywords:** Children; Lead Toxicity; Urban; Suburban; Workshop; Anemia; Cairo.

## M-326. Perceptions; Practices; and Traditional Beliefs Related to Neonatal Jaundice Among Egyptian Mothers a Cross-Sectional Descriptive Study.

Eman Mohamed Ibraheim Moawad, Enas Abdallah Ali Abdallah and Yahia Zakaria Abdelalim Ali

*Medicine; 95: 1-7 (2016) IF: 2.133*

Neonatal jaundice (NNJ) is one of the most common neonatal disorders worldwide. It is still a main cause of avoidable brain damage; physical and mental impairment; and probable death in newborns. We aimed to assess perceptions; practices; and traditional beliefs among Egyptian mothers toward NNJ that may contribute to delayed presentation and inappropriate management of hyperbilirubinemia. This descriptive; cross-sectional study was conducted from January to May 2015. We interviewed 400 Egyptian mothers who gave birth in <1 month before the study using a structured questionnaire. Participants were recruited from outpatients of Cairo University Teaching Hospital. This study revealed unexpected moderate knowledge and attitude scores of Egyptian mothers in most domains with a mean of 6.6 and 20.6; respectively; although the majority of them were illiterate or had low educational attainment. In terms of knowledge; 52.3% of participants had adequate knowledge about NNJ in the aspects of awareness; risk factors; management; and complications. Almost all participants exhibited moderate (89.8%) and high levels (10%) of positive attitudes toward NNJ. Maternal sociodemographic factors influenced knowledge level; attitudes; and behaviors related to NNJ in Egypt. Working mothers and those residing in urban areas were significantly more knowledgeable (P=0.023 and 0.021; respectively); and attained higher attitude scores (P<0.001 and P<0.001; respectively) than housewives and rural ones. Moreover; significantly higher attitude scores (P< 0.001) were attained by those who had completed their university [22.3 (SD=3.1)] or postgraduate education [22.2 (SD=3.6)]. The majority of Egyptian mothers have a satisfactory level of knowledge and attitudes related to NNJ. However; cultural beliefs and traditional infant care practices still have an impact on mothers regardless of their educational level.

**Keywords:** Attitude; Egypt; Knowledge; Mothers; Neonatal Jaundice.

## M-327. Prevalence and Clinical Significance of Nonorgan Specific Antibodies in Patients with Autoimmune Thyroiditis as Predictor Markers for Rheumatic Diseases.

Basant M. Elnady, Naglaa M. Kamal, Raneyah H.M. Shaker, Amal F. Soliman, Waleed A. Hasan, Hamed A. Alghamdi, Mohammed M. Algethami and Mohamed Bilal Jajah

*Medicine; 95 (2016) IF: 2.133*

Autoimmune diseases are considered the 3rd leading cause of morbidity and mortality in the industrialized countries. Autoimmune thyroid diseases (ATDs) are associated with high prevalence of nonorgan-specific autoantibodies; such as antinuclear antibodies (ANA); antidouble-stranded deoxyribonucleic acid (anti-dsDNA); antiextractable-nuclear antigens (anti-ENAs); rheumatoid factor (RF); and anticyclic-citrullinated peptides (anti-CCP) whose clinical significance is unknown.We aimed to assess the prevalence of various nonorgan-specific autoantibodies in patients with ATD; and to investigate the possible association between these autoantibodies and occurrence of rheumatic diseases and; if these autoantibodies could be considered as predictor markers for autoimmune rheumatic diseases in the future.This study had 2 phases: phase 1; in which 61 ATD patients free from rheumatic manifestations were assessed for the presence of these nonorgan-specific autoantibodies against healthy 61 control group; followed by 2nd phase longitudinal clinical follow-up in which cases are monitored systematically to establish occurrence and progression of any rheumatic disease in association to these autoantibodies with its influences and prognosis.Regarding ATD patients; ANA; anti-dsDNA; Anti-ENA; and RF were present in a percentage of (50.8%); (18%); (21.3%); and (34.4%); respectively; with statistically significance difference (P<0.5) rather than controls. Nearly one third of the studied group (32.8%) developed the rheumatic diseases; over 2 years follow-up. It was obvious that those with positive anti-dsDNA had higher risk (2.45 times) to develop rheumatic diseases than those without. There was a statistically significant positive linear relationship between occurrence of disease in months and (age; anti-dsDNA; anti-CCP; RF; and duration of thyroiditis). Anti-dsDNA and RF are the most significant predictors (P<0.0001).ATD is more associated with rheumatic diseases than previously thought. Anti-dsDNA; RF; and anti-CCP antibodies may be used as predictive screening markers of systemic lupus erythematosus and RA; with early referral to rheumatologists for close follow-up and early diagnoses for appropriate disease management of the disease; as early disease control will allow better quality of life.

**Keywords:** Nonorgan Specific Antibodies; Autoimmune Thyroiditis; Rheumatic Diseases.

## M-328. Lipid Peroxides in the Serum of Asphyxiated Neonates.

N Ramy, W Al Sharany, MA Mohamed, H Madani, E Saleh and H Aly

*Journal of Perinatology; 36: 849-852 (2016) IF: 2.087*

**Objective:** Lipid peroxides (LPOs) are released when free radicals react with unsaturated fatty acids in cell membranes during hypoxic ischemic insult in neonates. We aimed to assess LPO concentrations in the serum of asphyxiated and non-asphyxiated neonates and examine their correlation with the severity of asphyxia. **Study Design:** This prospective cross-sectional study was conducted on a group of asphyxiated neonates and controls. Serum LPO concentrations was measured by enzyme-linked immunosorbent assay at 4-6 h of life in all subjects. Encephalopathy was classified according to Sarnat's stages into mild; moderate and severe at 12-24 h of life. LPO was compared between groups and was correlated with severity of encephalopathy and mortality. **Results**: A total of 90 infants were enrolled; of them 45 had asphyxia. Serum LPO (nmol ml(-1)) was significantly greater in the asphyxia group (6.9±3.01 vs 1.78±1.09; P<0.001). It correlated positively with severity of encephalopathy (P<0.001) and negatively with Apgar score at 5 min (r=-0.532; P<0.001) and with initial blood gases pH (r=-0.664; P<0.001). LPO measured greater concentrations in infants who died compared with asphyxiated survivors (11.64±1.31 vs 6.18±2.48; P=0.0004). Conclusion: LPO was

increased and correlated with severity of asphyxia as well as with mortality. Further studies are warranted to examine whether it is only a marker for outcome or a contributor in the pathogenesis of hypoxic-ischemic brain injury.
**Keywords:** Lipid Peroxides,Asphyxiated Neonates,Hypoxic Ischemic Insult,Free Radicals.

## M-329. Molybdenum Cofactor and Isolated Sulphiteoxidase Deficiencies: Clinical and Molecularspectrum Among Egyptian Patients.

Maha S. Zaki, Laila Selim, Hala T. EL-Bassyouni, Mahmoud Y. Isaa, Iman Mahmoud,Samira Ismail, Mariane Girgis, Abdelrahim A. Sadek, Joseph G. Gleeson d and Mohamed S. Abdel Hamid

*European Journal of Paediatric Neurology; 20(5): 1-9 (2016) IF: 1.923*

**Aim :** Molybdenum cofactor deficiency (MoCD) and Sulfite oxidase deficiency (SOD) are rare autosomal recessive conditions of sulfur-containing amino acid metabolism with overlapping clinical features and emerging therapies. The clinical phenotype is indistinguishable and they can only be differentiated biochemically. MOCS1; MOCS2; MOCS3; and GPRN genes contribute to the synthesis of molybdenum cofactor; and SUOX gene encodes sulfite oxidase. The aim of this study was to elucidate the clinical; radiological; biochemical and molecular findings in patients with SOD and MoCD. Methods Detailed clinical and radiological assessment of 9 cases referred for neonatal encephalopathy with hypotonia; microcephaly; and epilepsy led to a consideration of disorders of sulfur-containing amino acid metabolism. The diagnosis of six with MoCD and three with SOD was confirmed by biochemical tests; targeted sequencing; and whole exome sequencing where suspicion of disease was lower. **Results** Novel SUOX mutations were detected in 3 SOD cases and a novel MOCS2 mutation in 1 MoCD case. Most patients presented in the first 3 months of life with intractable tonic–clonic seizures; axial hypotonia; limb hypertonia; exaggerated startle response; feeding difficulties; and progressive cystic encephalomalacia on brain imaging. A single patient with MoCD had hypertrophic cardiomyopathy; hitherto unreported with these diseases. Interpretation Our results emphasize that intractable neonatal seizures; spasticity; and feeding difficulties can be important early signs for these disorders. Progressive microcephaly; intellectual disability and specific brain imaging findings in the first year were additional diagnostic aids. These clinical cues can be used to minimize delays in diagnosis; especially since promising treatments are emerging for MoCD type A.
**Keywords:** Molybdenum Cofactor Deficiency; Sulfite Oxidase Deficiency; Microcephaly; Epilepsy; Mocs1 Genemocs2 Gene; Suox Gene.

## M-330. Detection of Mediterranean Fever Gene Mutations in Egyptian Children with Inflammatory Bowel Disease.

Samia Salah, Mortada El-Shabrawi, Hala Mohamed Lotfy, Hala Fathy Shiba, Maha Abou-Zekri and Yomna Farag

*International Journal of Rheumatic Diseases; 19(8): 806-813 (2016) IF: 1.914*

**Aim :** The aim of the current study is to investigate the prevalence of familial Mediterranean fever gene (MEFV) mutations in a cohort of Egyptian children with inflammatory bowel disease (IBD); and to characterize familial Mediterranean fever (FMF)-IBD patients; helping better understanding of IBD pathogenesis. **Methods** The study enrolled 17 patients with ulcerative colitis (UC); 15 with Crohn's disease(CD); 10 with indeterminate colitis (IC) and 33 healthy children as controls. All cases and controls were tested for 12 FMF gene mutations by reverse hybridization after multiplex polymerase chain reaction amplification and DNA sampling. **Results** Eighty-eight percent of the IBD patients carried the mutations; with Sequence variant V627A being the commonest versus 42.4% of controls. No associations were found between MEFV gene mutations; and phenotypic characteristics of IBD patients. **Conclusion** IBD patients; in populations with a high Background carrier rate of MEFV variants; should be screened for MEFV gene mutations; especially those diagnosed as indeterminate colitis. Testing larger numbers of healthy Egyptian children for MEFV gene mutation is important to further determine the allele frequency in Egypt.
**Keywords:** Disease; Etiology and Pathogenesis - Human; Immunogenetics; Paediatric Rheumatology; Pediatric Rheumatology; Basic Sciences.

## M-331. A Randomized Clinical Trial Comparing 3 Different Replacement Regimens of Vitamin D in Clinically Asymptomatic Pediatrics and Adolescents with Vitamin D Insufficiency.

Iman M. Talaat, Naglaa M. Kamal, Hamed A. Alghamdi, Abdulla A. Alharthi and Mohamed A. Alshahrani

*Italian Journal of Pediatrics; 42: 106-113 (2016) IF: 1.614*

**Background :** Pediatric and Adolescent populations both have special needs for vitamin D especially for growing bone. Inadequate vitamin D is defined as 25 (OH) D(25hydroxy vitamin D) < 30 ng/ml. **Methods:** We conducted a randomized; controlled clinical trial from July 2014 over 1 year; aiming to assess the changes in 25 (OH) D and biochemical outcome on calcium and PTH(parathyroid hormone) using 3 different regimens of vitamin D replacement. Initial and 4 month 25 (OH) D; calcium; PTH and 12 month 25 (OH) D levels were assayed. Participants divided into 3 groups: 1) given 400 IU daily; 2) given 45000 IU weekly for 2 months then 400 IU daily; 3) given 2000 IU daily for 3 months then 1000 IU daily. **Results**: The results showed significant difference between the 3 groups as regards 25 (OH) D at 4 and 12 months ($P < 0.001$). Regimens used in group 2 and 3 caused increase in 25 (OH) D after 4 month (median increase is 225% and 200% respectively). 25 (OH) D dropped in group 1 and 2 (median decrease is 42 and 53% respectively) but continued to increase in group 3 (median change is 6%). In group 2 serum calcium median change was 1.2% with few cases of hypercalcuria. 94.9; 76.1 and 7.7 are the percent of vitamin D deficient participants in groups 1; 2 and 3 respectively after 12 months follow up. Conclusion: We advise as a replacement for vitamin D insufficiency; low loading dose with high maintaince dose rather than the opposite to achieve steady increase in serum 25 (OH) D with no hypercalcemic side effects.
**Keywords:** 25 (Oh) D; Replacment Regimens; Vitamin D Deficiency; Vitamin D Insufficiency.

## M-332. Giardia Assemblages a and B in Diarrheic Patients: A Comparative Study in Egyptian Children and Adults.

Noussa R. El Basha, Mayssa M. Zaki, Omayma M. Hassanin, Mohamed K. Rehan and Dalia Omran

*The Journal of Parasitology; 102: 69-74 (2016) IF: 1.394*

Giardia duodenalis is considered the most common intestinal parasite in humans worldwide. Children are especially affected; with more severe consequences than adults. The present study was designed to determine the distribution of assemblages A and B Giardia infection in children and adults; with the use of light microscopy and polymerase chain reaction-restriction fragment length polymorphism (PCR-RFLP) as diagnostic procedures; and to investigate its associations with clinical and epidemiological data collected from children and adult groups. This cross-sectional study was conducted from October 2012 to October 2013 by collecting fecal samples from 200 children and 200 adults complaining of diarrhea. Samples were subjected to parasitological examination by direct wet smear and formol-ether methods. Genotyping of G. doudenalis samples was conducted by PCR-RFLP analysis. Giardia duodenalis infection caused by assemblages A and B was identified in 60 samples; 34 from children and 26 from adults. Assemblage B was detected in 38 patients (63.34%); and assemblage A was detected in 22 patients (36.66%). Assemblage A was significantly more frequent in children with age range 2-8 yr; and assemblage B was higher in children with age range 6-16 yr old. Diarrhea frequency/day and recurrences per month affected patients infected with assemblage A (P value < 0.001) more frequently. Children infected with assemblage A presented significantly more severe diarrhea and dehydration than those infected with assemblage B (P value < 0.001). Although both Giardia assemblages A and B were identified in children and adults; assemblage A infected younger children more frequently and was more closely related to severe clinical manifestations than assemblage B.

**Keywords:** Giardia Duodenalis; Assemblage A; Assemblage B; Genotyping; Diarrhea.

## M-333. Urinary Transforming Growth Factor B-1 as a Marker of Renal Dysfunction in Sickle Cell Disease.

Emad E. Ghobria, Hanan A. Abdel-Aziz, Ahmed M. Kaddah and Nesma A. Mubarak

*Pediatrics and Neonatology; 57: 174-180 (2016) IF: 1.319*

**Background** : Sickle cell disease (SCD) is a genetic disorder that results in deformity of red blood cells. Renal dysfunction affects 5–18% of patients with SCD. To date; few studies have described urinary levels of transforming growth factor β-1 (TGF-β1); which is a marker of fibrosis; as a biomarker in identifying patients at risk of developing renal disease in SCD. The aim of this study is to determine prevalence of sickle cell nephropathy in Egyptian SCD patients. We aimed also to evaluate the association of urinary TGF-β1 with other conventional biomarkers of renal damage in SCD patients to identify a novel renal biomarker for early diagnosis of sickle nephropathy. Methods We examined 40 SCD patients; 21 with sickle cell anemia; 16 sickle thalassemia; and three with sickle trait. We compared them to 20 control children with matched age and sex. The study was held in the time period between May 2013 and December 2013 in the Hematology Clinic; New Cairo University Children Hospital; Cairo; Egypt. **Results** Urinary excretion of TGF-β1 was 7.07 ± 1.91 ng/mL in SCD patients versus 2.23 ± 0.76 ng/mL in control children (p < 0.001). SCD patients had elevated estimated glomerular filtration rate (177.44 ± 35.6 mL/min/1.73 m2); denoting a state of glomerular hyperfiltration. 47.5% of SCD patients had microalbuminuria. Urinary TGF-β1 correlated positively with microalbuminuria and estimated glomerular filtration rate (p = 0.001 and p = 0.018; respectively). **Conclusion** We concluded that urinary TGF-β1 may serve as a marker of early renal injury in SCD

**Keywords:** Biomarkers; Sickle Cell Nephropathy; Transforming Growth Factor B-1.

## M-334. Fas/Fas Ligand Pathways Gene Polymorphisms in Pediatric Renal Allograft Rejection.

Fatina I. Fadel, Manal F. Elshamaa, Ahmed Salah, Marwa Nabhan, Maha Rasheed, Solaf Kamel, Dina Kandil and Eman H. Thabet

*Transplant Immunology; 37: 28-34 (2016) IF: 1.317*

**Background** : An essential milestone in pediatric transplantation is to find noninvasive biomarkers to monitor acute rejection (AR). In this retrospective (Case-control) study; we examined the role of Fas -670A/G and Fas Ligand (FasL) -843C/T gene polymorphisms in allograft nephropathy in pediatric renal transplant recipients. **Methods:** In 47 pediatric kidney transplant recipients and 20 healthy controls; Fas -670A/G and FasL -843C/T gene polymorphisms as well as serum soluble Fas Ligand level (sFasL) were measured. **Results**: Serum sFasL levels were significantly higher in transplant recipients children than that in controls (548.25±298.64pg/ml vs 143.17±44.55pg/ml; p=0.0001). There was no significant difference between patients with AR and those without AR in regards to serum sFasL levels (567.70±279.87pg/ml vs 507.85±342.80pg/ml; p=0.56). Fas -670A/G genotypes or alleles were not significantly different between controls and transplant recipients and among transplant recipients with and without AR. (P>0.05 for all). FasL -843C/T genotypes were not different between transplant recipients and controls and among transplant recipients with and without AR (P>0.05 for all). However; Frequency of C allele in transplant patients was significantly higher than that in the control group (44.68% vs 25%; P=0.03). FasL -843C/T alleles were significantly different between patients with and without AR (P=0.03). The percentages of C allele were higher in children with AR (58.82% vs 36.67%). We found that serum FasL and serum creatinine were variables that were independently associated with AR. Conclusion: This study suggests that FasL gene polymorphisms in peripheral blood might be accurate in detecting cellular AR.

**Keywords:** Cellular Rejection; Fas Ligand; Genetic Polymorphism; Pediatric Transplantation.

## M-335. Polymorphisms of Immunoglobulin G Fcreceptors in Pediatric Guillain–Barré Syndrome.

Lobna A. Mansour, Marian Y. Girgis, Mohamed Abdulhay, Ehab I. Abou ElEinein, Rabab ElHawary, Mariam Onsy and F. Hanna

*Neuropediatrics; 47: 151-156 (2016) IF: 1.291*

Guillain–Barré syndrome (GBS) is an autoimmune peripheral neuropathy characterized by demyelination and axonal damage. Biallelic functional polymorphisms in the immunoglobulin G Fc receptors (FcγR)–FcγRIIA: H131/R131; FcγRIIIA: V158/ F158; and FcγRIIIB: NA1/NA2 affect the affinity of the IgG–FcγR interaction; therefore; diseases such as GBS in which this interaction plays a critical rolemight be influenced by the polymorphisms. Methods We evaluated the role of FcγR polymorphisms in susceptibility to GBS in Egyptian pediatric patients and the association of the variant alleles with neurophysiological types; severity; and outcome of the disease. A total of 50 patients with GBS and 50 controls were examined for FcγR polymorphisms by allele-specific polymerase chain reaction. **Results** FcγRIIA H131 allele (p ¼ < 0.0001; odds ratio [OR] ¼ 4.78; 95% confidence interval [CI]; 2.62–8.70) and FcγRIIA H/H131 genotype (p ¼ < 0.0001; OR ¼ 10.56; 95% CI; 3.59–31.06) were significantly increased in GBS patients while FcγRIIIA and FcγRIIIB allelic distributions were similar among patients and controls. The FcγR genotypes showed no association with neurophysiological types of GBS; severity or outcome of the disease. **Conclusions** These findings reflect that FcγRIIA H131 allele may represent a risk marker for susceptibility to GBS.

**Keywords:** Allele; Specificpolymerase Chainreaction; Fc Receptors; Guillain; Barré; Immunoglobulin G; Infection; Polymorphism.

## M-336. Coagulation; Thrombophilia and Patency of Arteriovenous Fistula in Children Undergoing Haemodialysis Compared With Healthy Volunteers: A Prospective Analysis.

Fatina I. Fadela, Manal F. Elshamaa, Safaa M. Abdel-Rahman, Eman H. Thabet, Solaf Kamel, Dina Kandil, Mona H. Ibrahim and Mostafa El-Ahmady

*Blood Coagulation and Fibrinolysis;27:190-198(2016) IF:1.242*

This study aimed to assess whether markers of coagulation; fibrinolysis or thrombophilia are increased in children on haemodialysis compared with controls and whether measurement of any of these factors could help to identify patients at an increased risk of arteriovenous fistula (AVF) occlusion. Blood samples were taken from 55 children immediately before a session of haemodialysis and from 20 healthy volunteers. Thrombin-antithrombin (TAT); D-dimer; plasmin-antiplasmin (PAP) and anticardiolipin immunoglobulin G (ACA-Ig G) were measured by ELISA. Factor V Leiden mutation (G1691A) was determined by gene polymorphism [restriction fragment length polymorphism (RFLP)]. Determination of the patency of the AVF was prospectively followed up for a minimum of 4 years or until the AVF was nonfunctioning. Fifty-five patients were studied with a median follow-up of 659 days (range 30-1670 days). A significant increase was found in the levels of D-dimer; PAP and ACA-Ig G in haemodialysis patients with thrombosed and nonthrombosed native AVFs vs CONTROLS: There was a significant difference between both chronic haemodialysis patients with thrombosed and nonthrombosed native AVF with regard to ACA-IgG levels. At 1 year follow-up; primary patency was 61.4% (27 patients). In multivariate analysis; D-dimer was inversely associated with secondary patency.Thrombophilia may predispose children with end stage renal disease to access failure. The promising finding is that in children on haemodialysis; D-dimer levels were increased and inversely correlated with secondary patency. Further evaluation is required into the possible role of D-dimer as a biomarker of AVF occlusion.

**Keywords:** Children; Coagulation; Fibrinolysis; Haemodialysis; Native Arteriovenous Fistula Thrombosis.

## M-337. Respiratory Syncytial Virus and Human Metapneumovirus in Severe Lower Respiratory Tract Infections in Children Under Two.

Heba T Othman, Walaa A Abu Elhamed, Dina M Hassan2 May S Soliman and Radwa W Abdel Baset

*The Journal of Infection in Developing Countries; 10(3): 283-289 (2016) IF: 1.139*

**Introduction**: Viruses are the most important causative agents of acute lower respiratory tract infections (ALRTIs); ranked as the second leading cause of death and the primary cause of hospitalization in children. Respiratory syncytial virus (RSV) and human metapneumovirus (hMPV) are among the commonest viral causes of severe ALRTI. In this study; we aimed to study the burden of both RSV and hMPV in causing severe ALRTI in children younger than two years of age admitted to the pediatric intensive care unit (PICU). METHODOLOGY: Nasopharyngeal swabs were collected from children admitted to the PICU with a diagnosis of community-acquired ALRTI who were two years of age or younger. Real-time polymerase chain reaction (RT-PCR) was used to test for RSV and hMPV. **Results**: A total of 127 swabs were screened for RSV and hMPV; of which 49.6% were negative for RSV and hMPV; 46.4% were positive for RSV; and 3.9% were positive for hMPV. With respect to RSV; the mean age of cases (4.01 ± 5.05) and the monthly distribution (mainly January) were the most important risk factors. There were no statistically significant differences between the RSV group and control group regarding duration of hospital stay; mechanical ventilation need or duration; and underlying chronic conditions. **Conclusions**: RSV is important viral cause of severe ALRTIs in children younger than two years of age during this study period; hMPV played a minor role.

**Keywords:** Ower Respiratory Tract Infections; Respiratory Syncytial Virus; Human Metapneumovirus; Pediatric Icu

## M-338. Anti-Oxidant Profiles and Markers of Oxidative Stress in Preterm Neonates.

Eman Abdel Ghany Abdel Ghany, Walaa Alsharany Abu Elhamed, Aliaa Adel Ali,Eman Rafaat Younass and Jihan Seid Hussein

*Paediatrics and International Child Health; 36: 134-140 (2016) IF: 1.103*

**Background**: Preterm birth is associated with an increased oxidant burden which places these infants at a higher risk of injury. Aims: This prospective study aimed to assess levels of antioxidants and a marker of oxidative stress in preterm neonates. **Objectives:** (i) To compare levels of anti-oxidants [vitamin A**;** vitamin E**;** catalase**;** total anti-oxidant status (TAS)] as well as malondialdehyde level (MDA) (a marker of lipid peroxidation) between preterm and full-term neonates; (ii) to determine changes in the values of measured vitamins at birth and at discharge among preterm neonates; and (iii) to compare levels of anti-oxidants with MDA levels in relation to complications of prematurity and outcome. **Methods:** The study was undertaken in 100 preterm neonates and 100 full-term neonates as a control group. MDA was estimated by a thiobarbituric acid-reactive technique; TAS was determined using a Randox assay kit; catalase activity was measured spectrophotometrically and vitamin A and E levels were estimated by high performance liquid chromatography. **Results:** The plasma levels of vitamin A**;** vitamin E**;** TAS and catalase were significantly lower in the preterm than in the full-term group (Pv0.01)**;** and the plasma level of MDA was significantly higher in preterm than full-term neonates (Pv0.01). Vitamin A and E levels in preterm neonates were significantly higher at discharge than at birth (Pv0.01). Vitamin A**;** vitamin E and catalase levels at birth were significantly lower in patients who developed necrotizing enterocolitis or bronchopulmonary dysplasia than in those who did not. **Conclusion:** Preterm neonates are exposed to increased oxidant stress at birth and are susceptible to anti-oxidant deficiencies. A higher dose of enteral vitamin A supplementation in preterm neonates might reduce morbidity and improve outcome. Further studies are warranted to evaluate the appropriate dose of oral vitamin E supplementation for preterm neonates.
**Keywords:** Preterm Neonates**;** Oxidative Stress**;** Antioxidants**;** Vitamin A**;** Vitamin E**;** Total Antioxidant Status**;** Malondialdehyde**;** Nicu.

## M-339. Association Between the Specific Ugt1a1 Promoter Sequence Variant (C-3279T>G) and Unconjugated Neonatal Hyperbilirubinemia.

Rania Hosny Tomerak, Nahed Fahmy Helal, Olfat Gameel Shaker and Mohamed Abdelhamid Yousef

*Journal of Tropical Paediatrics**;** 62: 457-463 (2016) IF: 1.059*

We investigated the association between c-3279T>G and unconjugated neonatal hyperbilirubinemia. In all**;** 141 neonates were recruited; 63 had hyperbilirubinemia necessitating treatment**;** and 78 with bilirubin < 7 mg/dl served as the control group. The frequency of occurrence of c-3279T > G allele was significantly higher in the hyperbilirubinemic (49.2%) than in the control group (25.6%). The homozygous (p = 0.001**;** OR = 17.7 and CI = 3.9–79.3) rather than the heterozygous state (p = 0.3**;** OR = 0.7 and CI = 0.3–1.6) was associated with hyperbilirubinemia. Among the hyperbilirubinemic group**;** comparison between the three genotypes**;** homozygous mutation**;** heterozygous mutation and the normal allele**;** revealed that the former was associated with significantly higher mean peak total serum bilirubin [mean ± standard deviation (SD): 33.7 ± 8.2**;** 26.9 ± 2.8 and 21 ± 2.7**;** respectively**;** p-value = 0.0001]**;** higher bilirubin/albumin ratio (p = 0.000) and a longer duration of hospital stay (p = 0.001). Homozygous c-3279T > G mutation represents an important risk factor for the development of neonatal hyperbilirubinemia.
**Keywords:** Neonatal Hyperbilirubinemia**;** Ugt1a1 Gene**;** C-3279T>G Mutation**;** Neonatal Jaundice**;** Genetics of Neonatal Hyperbilirubinemia.

## M-340. Mutation Spectrum of Egyptian Children with Cystic Fibrosis.

Walaa Aboulkasem Shahin, Dina Ahmed Mehaney and Mona Mostafa ElFalaki

*Springerplus**;** 5: 686-0 (2016) IF: 0.982*

**Objective**: To know the common CFTR mutations in the Egyptian patients with cystic fibrosis as it was previously thought to be uncommon disease in Egypt. **Methods:** This is a cross sectional study of 60 patients diagnosed as cystic fibrosis by sweat chloride testing. They were enrolled from the Allergy and Pulmonology Unit Children's Hospital Cairo University. They were screened for the presence of the frequent 36 mutations in Caucasians by reverse hybridization line probe technique**;** using INNO-LiPACFTR19 and CFTR17 + Tn kits. **Results**: Most of patients presented with classic manifestations of CF such as variable pulmonary disease and pancreatic insufficiency**;** and hepatomegaly with or without ascites. The mutations detected were F508 del (58 %)**;** 2183AA/G (10 %)**;** N1303K (6 %)**;** I148T (4 %)**;** W1282X (4 %)**;** G155D (2 %)**;** CFTRdel2-3 (21 KB) (2 %)**;** 3199del6 (2 %)**;** R347P (2 %). Unique to the Egyptian population are these mutations R1162X and A544E (6**;** 4 %) respectively they were found in our cohort study and were not reported elsewhere in the Arab population till now. There was no association between the initial clinical presentation of CF and the genotypes detected. **Conclusion**: The F508 del is still the most commonly encountered mutation (58 %)**;** however other rare mutations were identified where each ranged from (2 to 10 %).
**Keywords:** CFTR Mutations; Cystic Fibrosis; Egypt; F508del

## M-341. Value of Ultrasound in Detecting Urinary Tract Anomalies after First Febrile Urinary Tract Infection in Children.

Emad E. Ghobrial, Doaa M. Abdelaziz, Maha F. Sheba and Yasser S. Abdel-Azeem

*Clinical Pediatrics**;** 55: 415-420 (2016) IF: 0.954*

**Background** : Urinary tract infection (UTI) is an infection that affects part of the urinary tract. Ultrasound is a noninvasive test that can demonstrate the size and shape of kidneys**;** presence of dilatation of the ureters**;** and the existence of anatomic abnormalities. The aim of the study is to estimate the value of ultrasound in detecting urinary tract anomalies after first attack of UTI. Methods. This study was conducted at the Nephrology Clinic**;** New Children's Hospital**;** Faculty of Medicine**;** Cairo University**;** from August 2012 to March 2013**;** and included 30 children who presented with first attack of acute febrile UTI. All patients were subjected to urine analysis**;** urine culture and sensitivity**;** serum creatinine**;** complete blood count**;** and imaging in the form of renal ultrasound**;** voiding cysto-urethrography**;** and renal scan. Results. All the patients had fever with a mean of 38.96°C ± 0.44°C and the mean duration of illness was 6.23 ± 5.64 days. Nineteen patients (63.3%) had an

ultrasound abnormality. The commonest abnormalities were kidney stones (15.8%). Only 2 patients who had abnormal ultrasound had also vesicoureteric reflux on cystourethrography. Sensitivity of ultrasound was 66.7%; specificity was 37.5%; positive predictive value was 21.1%; negative predictive value was 81.8%; and total accuracy was 43.33%. Conclusion. We concluded that ultrasound alone was not of much value in diagnosing and putting a plan of first attack of febrile UTI. It is recommended that combined investigations are the best way to confirm diagnosis of urinary tract anomalies.
**Keywords:** Urinary Tract Infection; Ultrasound; Urinary Tract Anomalies.

## M-342. Relationship Between Visceral Obesity and Plasma Fibrinogen in Obese Children.

Mona Hafez, Sahar ElMasry, Noha Musa, Marwa Fathy, Mona Hassan, Nayera Hassan, Mohamed El Husseiny and Mahmoud Tareef

*Journal of Pediatric Endocrinology and Metabolism; 29: 289-296 (2016) IF: 0.912*

**Background**: The prevalence of obesity in children and adolescents has increased significantly worldwide with an alarming rise of its co-morbidities. The excess of visceral adipose tissue is associated with hypertension; prothrombotic and pro-inflammatory states. Our aim was to find a possible association between visceral obesity and plasma fibrinogen; as one of the cardiovascular risk factors; in obese children. **Methods:** Forty-three obese children and 40 non-obese controls were studied regarding their history; complete physical examination; anthropometric assessment; body composition analysis; ultrasonographic measurement of visceral adipose tissue and subcutaneous fat as well as laboratory measurement of plasma fibrinogen. **Results:** Our study revealed significant higher levels of fibrinogen in obese children than controls (14.5+5.1 and 2.9+0.52 mg/mL; respectively) with p-value <0.01. Moreover; the obese group had statistically significant difference in visceral fat (5.96+0.77 cm) and subcutaneous fat (2.66+0.70 cm) than controls (2.45+0.65 and 0.70+0.18 mg/mL; respectively) with p-value <0.01. In addition; fibrinogen had significant positive correlation with body mass index (r=0.327); waist/hip ratio (r=0.394); fat percentage (r=0.301); visceral adipose tissue (r=0.323) and subcutaneous fat (r=0.301). **Conclusions:** There was highly significant increase in the fibrinogen level; visceral and subcutaneous abdominal fat in the obese group with insignificant sex differences. Fibrinogen had a significant positive correlation with the different adiposity markers; blood pressure; visceral and subcutaneous fat. Visceral adipose tissue is a stronger predictor for cardiovascular risk compared to subcutaneous fat.
**Keywords:** Body Mass Index; Fibrinogen; Obesity; Subcutaneous Fat; Visceral Fat.

## M-343. Blind Percutaneous Liver Biopsy in Infants and Children:Comparison of Safety and Efficacy of Percussion Technique and Ultrasound Assisted Technique

Engy A. Mogahed, Yasmeen A. Mansy, Yasmeen Al Hawi, Rokaya El-Sayed, Mona El-Raziky and Hanaa El-Karaksy

*Arab Journal of Gastroenterology;17(4):168-175(2016)IF:0.644*

**Background and study aims :** Liver biopsy remains the most reliable method to diagnose various hepatic disorders in children. We aimed to assess the technical success and complication rate of ultrasound (US) assisted percutaneous liver biopsy versus transthoracic percussion guided technique in paediatrics. Patients and methods This randomized controlled study included all cases performing liver biopsy at Paediatric Hepatology Unit; Cairo University Paediatric Hospital over 12 months. **Results** Patients were 102 cases; 62 were males; with age range 18 days to 12 years. Fifty seven procedures were done using the percussion guided technique and 45 cases were US assisted. The total number of complicated biopsies was 14 (13.7%); with more serious complications occurring in the percussion group. Complications were more frequent with younger age; lower platelet count; number of passes and occurrence of hypotension. **Conclusion** US assisted percutaneous liver biopsy; although more costly; but may be safer to perform particularly in younger age.
**Keywords:** Children; Liver Biopsy; Percussion Technique; Ultrasound Assisted.

## M-344. Haemophagocytic Lymphohistiocytosis Presenting as Neonatal Liver Failure: A Case Series

Hala Abdullatif, Nabil Mohsen, Rokaya El-Sayed, Fatma El-Mougy and Hanaa El-Karaksy

*Arab Journal of Gastroenterology; 17: 105-109(2016) IF: 0.644*

**Background and study aim:** Haemophagocytic lympho-histiocytosis (HLH) is a life-threatening clinical syndrome with liver involvement varying from mild dysfunction to severe fulminant failure. The aim of this study was to present a case series of four HLH patients presenting with acute liver failure (ALF) in the neonatal period. **Patients andMethods:** All four patients were neonates at the onset of symptoms. They presented to Cairo University Pediatric Hospital with ALF; they underwent prompt investigations including determination of ferritin; fibrinogen; and triglyceride levels as part of our ALF workup. Further investigations were tailored according to the associated clinical features and the results of preliminary investigations. **Results:** HLH was diagnosed according to HLH-2004 criteria. Three patients fulfilled at least five out of eight criteria. Fever; splenomegaly; elevated ferritin levels; and low fibrinogen levels were present in all patients. The fourth patient had a serum ferritin level >10,000 ng/ml; favouring the diagnosis of HLH; despite fulfilling only four out of eight criteria. For three patients; positive consanguinity and previous sibling death were reported; suggesting a genetic aetiology of HLH. **Conclusion:** ALF can be the presenting feature of HLH; thus; a high index of suspicion is necessary. Fever is a hallmark; especially in neonates. Diagnosis is important for this potentially treatable condition.

**Keywords:** Acute Liver Failure;Ferritin;Haemophagocytic Lymphohistiocytosis; HLH; Neonates.

## M-345. Evaluation of Epicardial Fat and Carotid Intima-Media Thickness in Obese Children

Hatem Hamed Elshorbagy, ElSaeed R. Fouda, Naglaa M. Kamal, Mohammed M. Bassiouny and Waleed M. Fathi

*Iranian Journal of Pediatrics; 26: 0-0 (2016) IF: 0.521*

**Background**: Epicardial fat has a role in cardiovascular diseases. **Objectives**: To assess epicardial fat and its relation with carotid intima-media thickness (IMT) in obese adolescents with metabolic syndrome (MetS). **Patients and Methods:**The study included 60 obese adolescents and 25 control subjects. According to the presence or absence of MetS; obese subjects were divided into two subgroups. We measured weight; height; calculated Body Mass Index; waist circumference; hip circumference; systolic blood pressure; diastolic blood pressure and biochemical parameters (fasting glucose; total cholesterol; triglycerides; high density lipoprotein cholesterol; and low density lipoprotein cholesterol; High sensitivity C-reactive protein; fasting insulin; a homeostasis model assessment index of insulin resistance. plus an echocardiographic examination with measurement of epicardial adipose tissue thickness (EATT). **Results**: Left ventricular mass index measurements were significantly higher in MetS group than both non-MS and control groups. The MetS and non-MetS obese patients had significantly higher carotid IMT in comparison to the control group. Carotid IMT measurements were significantly higher in MetS group had than both non-MetS and control groups. Also; EATT was significantly increased in patients with MetS compared to control group. Among MetS obese group; EATT was positively correlated with body mass index-standard deviation score; waist circumference; fasting glucose; fasting insulin; insulin resistance; triglyceride levels; left ventricular thickness; left ventricular mass index and myocardial performance index. EATT was found to be the only predictor of carotid IMT. **Conclusions**: EATT is closely related to carotid IMT and early cardiac dysfunction in obese adolescents with MetS.

**Keywords:** Echocardiography; Epicardial Adipose Tissue Thickness; Metabolic Syndrome.

## M-346. Language Profile in Congenital Hypothyroid Children Receiving Replacement Therapy

Hend Soliman, Aisha Fawzy Abdel Hady, Asmaa Abdel Hamid and Heba Mahmoud

*Folia Phoniatrica Et Logopaedica; 68: 67-72 (2016) IF: 0.391*

**Objective:** The aim of this work was to evaluate receptive and expressive language skills in children with congenital hypothyroidism receiving early hormonal replacement treatment before the age of 3 months and to identify any subtle areas of weaknesses in their language development to check the necessity for future language intervention. **Patients andMethods:** The study was conducted on 30 hypothyroid children receiving hormonal replacement. They were subdivided into group I (5–8 years 11 months; 12 cases) and group II (9–12 years 11 months; 18 cases). All patients were subjected to a protocol of assessment applied in the Diabetes; Endocrine and Metabolism Pediatric Unit (DEMPU) and evaluation of language skills by the REAL scale. **Results:** The younger group reached average Arabic language scores; while the older group showed moderate language delay. Conclusion: Early replacement therapy supports language development in young children. However; longitudinal and follow-up studies are required to identify difficulties presenting at older ages that may affect children in the academic settings.

**Keywords:** Congenital; Hypothyroidism; Hormonal Replacement; Language development.

## M-347. Clinical; Molecular; and Therapeutic Aspects of Ndm in Ten Cases with Diabetes in 1St 6 Months of Life

Noha MusS, Mona Hafez, Mona Hassan, Fatma El-Mougy, Sahar Sharaf, Michael Polak, Helene Cave and Sherif Mofeed

*International Journal of Diabetes In Developing Countries; 36: 81-88 (2016) IF: 0.366*

Neonatal diabetes mellitus (NDM) is defined as hyperglycemia occurring within the first 6 months of life; it may be permanent or transient. Diagnosis of NDM is vital for prognosis; genetic counseling; and treatment. The aim of this study was to study clinical; biochemical; molecular; and therapeutic aspects of diabetes presenting in the first 6 months of life. Ten cases with NDM were studied regarding perinatal and family history; clinical features and biochemical tests on admission and follow-up; HLA typing and molecular studies; and mode of therapy. Molecular studies for the common mutations associated with NDM (KCNJ11; INS; ABCC8 and methylation defects) were done using PCR amplification and gene sequencing. Ten cases developed diabetes in the first 6 months of life (three in the first 8 weeks; seven between 8 and 24 weeks). All presented with ketoacidosis; one had developmental delay with convulsions. Molecular studies revealed methylation defect in two cases; KCNJ11 in three cases; INS mutations in two cases; and no detectable defect in three cases. Insulin was stopped on follow-up in three cases (TND); successfully substituted with sulfonylurea (SU) in three cases; and continued in four cases (PND). Molecular genetic testing is essential in cases with NDM for guiding mode of therapy as SU receptor defects can be successfully treated with oral SU instead of insulin injections. SU was more effective in achieving diabetes control in cases with KCNJ11 mutations.

**Keywords:** Neonatal Diabetes; Molecular Diagnosis; Sulfonylurea; Insulin.

## M-348. Arginine Dimethylation Products in Pediatric Patients with Chronic Kidney Disease

Akram E. El-Sadek, Eman G. Behery, Ahmed A. Azab, Naglaa M. Kamal, Mostafa A. Salama, Waleed E. Abdulghany and Enas A.A. Abdallah

*Annals of Medicine and Surgery; 9: 22-27 (2016)*

**Background** : arginine and its metabolites have been linked to pediatric chronic kidney disease (CKD). We aimed to estimate serum levels of argninine (Arg); asymmetric dimethylarginine (ADMA) and symmetric dimethylarginine (SDMA) in pediatric CKD patients and its relation to altered kidney function.

**Patients and Methods:** 132 pediatric patients with CKD and 120 healthy age and sex matched controls were compared regarding; serum Arg; ADMA and SDMA levels. **Results**: In comparison to their values in control subjects; serum Arg levels were significantly lower; serum ADMA levels were non-significantly higher; but serum SDMA levels were significantly higher in CKD patients (p values: < 0.000; = 0.054; <0.000; respectively). Calculated Arg/ADMA and Arg/SDMA ratios were significantly higher in patients compared to controls (p values: 0.001; and <0.000; respectively). However ADMA/SDMA ratio was significantly lower in patients compared to controls (p = 0.001. Serum Arg levels showed positive significant correlation; while serum ADMA and SDMA levels showed negative significant correlation with eGFR. Moreover; Arg/ADMA ratio showed negative significant correlation; while ADMA/SDMA ratio showed positive significant correlation with eGFR of patients. Regression analysis defined high serum SDMA level as persistently significant predictor for low eGFR. **Conclusion:** Disturbed serum levels of arginine and its dimethyl derivatives may underlie development and/or progression of CKD. Elevated serum SDMA level is strongly correlated with impaired kidney functions and could be considered as a predictor for kidney functions deterioration and CKD progression.

**Keywords:** Chronic Kidney Disease; Kidney Functions; Serum Arginine; Serum Dimethyl Arginine Derivatives.

## M-349. Early Detection of Myocardial Dysfunction in Poorly Treated Pediatric Thalassemia Children and Adolescents: Two Saudi Centers Experience.

Mohamed H. Ibrahim, Ahmed A. Azab, Naglaa M. Kamal, Mostafa A. Salama, Soha A. Ebrahim, Ashraf M. Shahin, Akram E. El-Sadek, Waleid E. Abdulghany, Laila M. Sheriefand Enas A.A. Abdallah

*Annals of Medicine and Surgery; 9: 6-11 (2016)*

**Background & Objective:** Cardiac complications are among the most serious complications in Beta Thalassemia Major Patients. Our aim was to evaluate the value of tissue Doppler imaging (TDI) for early detection of myocardial dysfunction in pediatric and adolescent patients with B-TM before development of overt heart failure or cardiomyopathy. **Patients And Methods:**100 thalassemic patients below 18 years old and 100 healthy; age & sex matched controls were enrolled in our case-control study. Cases were selected from those attending outpatient clinics and inpatient wards; King Abdulaziz University hospital and Alhada Armed Forces Hospital; Saudi Arabia; between January 2014 and January 2015. They were subjected to echo-Doppler examination for both septal and lateral walls of the basal mitral and tricuspid annuli assessing the systolic myocardial velocity (S wave); early diastolic myocardial velocity (Ea wave) and late diastolic myocardial velocity (Aa wave). **Results**: Patients with thalassemia have RV and LV dysfunction on the basis of abnormal TDI derived myocardial velocities. There was a statistically significant differences between patients and controls regarding (Aa) and (S) of the septal wall of the basal mitral annulus and (Ea) of the lateral wall of the mitral annulus. Also patients with thalassemia have significantly higher (S) of the basal tricuspid annulus. These abnormalities were not detected by conventional echo-Doppler. **Conclusion:** Clinically asymptomatic thalassemic children and adolescents who had normal global functions by conventional echo-Doppler were found to have abnormal left ventricular and right ventricular dysfunctions detected by TDI. TDI is superior to Echo-Doppler in detection of early myocardial damage in asymptomatic thalassaemic patients.

**Keywords:** Echo-Doppler; Myocardial Dysfunction; Pediatric; Thalassaemia; Tissue Doppler Imaging.

## M-350. Evaluation of Cardiac Functions of Cirrhotic Children using Serum Brain Natriuretic Peptide and Tissue Doppler Imaging.

Aya M Fattouh, Mortada H El-Shabrawi, Enas H Mahmoud and Wafaa O Ahmed

*Annals of Pediatric Cardiology; 9(1): 22-28 (2016)*

**Background** : Cirrhotic cardiomyopathy (CCM) is described as the presence of cardiac dysfunction in cirrhotic patients. In children with chronic liver disease; CCM has been very rarely investigated. The Aim of the Study: Is to evaluate the cardiac function of cirrhotic children to identify those with CCM. **Patients and Methods:** Fifty-two cirrhotic patients and 53 age and sex matched controls were assessed using serum brain-type natriuretic peptide (BNP); conventional echocardiography; and tissue Doppler imaging. **Results:** Patients' mean ages were 7.66 ± 4.16 years (vs. 6.88 ± 3.04 years for the controls). The study included 27 males and 25 females (28 and 25 respectively for the controls). Patients had larger left atrium and right ventricle (RV) (P value 0.05) and increased LV posterior wall thickness than controls (P value 0.04). They had higher late atrial diastolic filling velocity (A) of tricuspid valve (TV) inflow (0.59 ± 0.17 vs. 0.5 ± 0.1 m/s P < 0.001) and lower ratios between the early diastolic filling velocity (E) and A wave velocity (E/A) of both mitral valve and TV inflow (1.7 ± 0.35 vs. 1.87 ± 0.34 and 1.3 ± 0.3 vs. 1.5 ± 0.3 P < 0.005 and 0.0008; respectively). Patients had significantly longer isovolumic relaxation time of LV (45.5 ± 11.1 vs. 40.5 ± 7.7 ms P0.008); higher late diastolic peak myocardial velocity (A□) (11.8 ± 3.6 vs. 9.5 ± 2.7 ms P 0.0003) and systolic velocity (S□) of the RV (14.5 ± 2.7 vs. 13.2 ± 2.9; P 0.01) and significantly higher myocardial performance index of both LV and RV (P 0.001 and 0.01). BNP levels were significantly higher in cases than controls (5.25 ng/l vs. 3.75 ng/l; P < 0.04) and was correlated with the E wave velocity of the TV (r 0.004) and the E/E□ ratio of the RV (r 0.001). None of the clinical or laboratory data were correlated with the BNP level. **Conclusion:** Cirrhotic children have cardiac dysfunction mainly in the form of diastolic dysfunction. There is a need that CCM be more accurately described in children.

**Keywords:** Brain-Type Natriuretic Peptide; Cirrhotic Cardiomyopathy; Liver Cirrhosis; Tissue Doppler Imaging.

## M-351. First Report of Co-Morbidity of Pantothenate Kinase - Associated Neurodegeneration and Three Types of Chronic Hemolytic Anemias.

Iman M. Talaat, Naglaa M. Kamal, Ebtessam H.K. El Melegy, Hamed A. Alghamdi, Mohammed F. Aljabri, Enas A.A. Abdallah, Mohammed Sarar and Mohamed A. Alshahranib

*Annals of Medicine and Surgery; 5: 11-13 (2016)*

**Background**: Pantothenate kinase-associated neurodegeneration (PKAN)**;** sickle cell anemia**;** and thalassemia are autosomal recessive disorders that can cause iron deposition in tissues during childhood. PKAN is characterized by accumulation of iron in the basal ganglia causing progressive extrapyramidal manifestations. Thalassemia and sickle cell disease can cause iron overload and deposition in tissues**;** including central nervous system. **Presentation of Case**: we herein report the first report of comorbidity of PKAN**;** β-thalassemia-major**;** sickle cell and glucose-6-phosphate dehydrogenase deficiency (G6PD) anemias in a 9 years old Saudi female patient who presented with gait disturbance**;** speech difficulty**;** and progressive movement disorders of the neck**;** upper and lower limbs. **Conclusion:** Although extremely rare**;** β-thalassemia-major**;** sickle cell and G6PD anemias can be associated with PKAN. It is unknown whether this association is random or due to an unknown factor that may have caused several mutations.
**Keywords:** Eye of The Tiger Sign; Hemosiderosis; Pantothenate Kinase-Associated Neurodegeneration; Sickle Cell Disease; B-Thalaasemia.

## M-352. Heart-Type Fatty Acid-Binding Protein as A Predictor of Cardiac Ischemia in Intractable Seizures in Children.

Hatem H El Shorbagy, Mostafa A Elsayed, Naglaa M Kamal, Ahmed A Azab, Mohamed M Bassiouny and Ibrahim A Ghoneim

*Journal of Pediatric Neurosciences**;** 11: 175-181 (2016)*

**Background:** Children with intractable epilepsy have chronic dysfunction of the autonomic nervous system causing myocardial ischemia. Heart-type fatty acid-binding protein (H-FABP) is a sensitive biomarker for myocardial ischemia. AIMS: We aimed to evaluate serum levels of H-FABP during seizures compared to their interictal levels and healthy controls and changes in heart rate (HR) and HR variability (HRV) in epileptic children with intractable seizures. **Materials and Methods:** We included 30 epileptic seizures in 25 children with intractable epilepsy and 30 matched controls. They were subjected to video-electroencephalography monitoring simultaneously with Holter electrocardiogram and measurement of H-FABP. **Results**: Mean serum levels of H-FABP were increased significantly in patients either in the ictal or interictal periods compared to that in the controls ($P < 0.001$ and $P< 0.01$**;** respectively). There is no significant difference in serum levels of the H-FABP in the ictal and interictal periods. The basal time domain measures of HRV were significantly lower in the patient group compared to the control group. **Conclusion:** H-FABP might suggest a degree of myocardial ischemia in intractable epilepsy. HRV is impaired in patients with refractory seizures.
**Keywords:** Heart; Type Fatty Acid; Binding Protein; Myocardial Ischemia; Refractory Seizures.

## M-353. Stunted Growth. Proceedings of the 23rd Aschauer Soiree, Held at Aschauhof, Germany, November 7th 2015.

Mortada Hassan Fakhri El-Shabrawi

*Journal ,: p1-p2 (2016)*

Recent. Twenty-four scientists met at Aschauhof, Altenhof, Germany, to discuss the associations between child growth and development, and nutrition, health, environment and psychology. Meta-analyses of body height, height variability and household inequality, in historic and modern growth studies published since 1794, highlighting the enormously flexible patterns of child and adolescent height and weight increments throughout history which do not only depend on genetics, prenatal development, nutrition, health, and economic circumstances, but reflect social interactions. A Quality of Life in Short Stature Youth Questionnaire was presented to cross-culturally assess health-related quality of life in children. Changes of child body proportions in recent history, the relation between height and longevity in historic Dutch samples and also measures of body height in skeletal remains belonged to the topics of this meeting. Bayesian approaches and Monte Carlo simulations offer new statistical tools for the study of human growth.

**Key words**: Adolescent growth, Peer group, Growth hormone, Community effect, Body height 481.

## M-354. The Effect of Nutritional Status on Outcome of Hospitalization in Paediatric Liver Disease Patients.

Yasmeen Mansi,Shereen Abdel Ghaffar, Shaymaa Sayed and Hanaa El-Karaksy

*Journal of Clinical and Diagnostic Research**;** 10(12): 1-5 (2016).*

**Introduction:** Liver is an important organ for metabolism. It has a major role in integrating the various biochemical pathways of metabolism. Thus**;** children with chronic liver disease are at high risk for developing undernutrition**;** with important prognostic implications. Aim: To evaluate the nutritional status of hospitalized paediatric liver disease patients and its effect on outcome. **Materials and Methods:** We prospectively analysed the nutritional status of 59 consecutive patients during their first 24 hours of admission**;** at the Hepatology Unit**;** using the following indices: weight/age**;** height/age**;** weight/height**;** Body Mass Index (BMI)**;** arm circumference and triceps skinfold**;** subcapular skinfold**;** and mid upper arm circumference. **Results:** According to the measurements: 35.6% were underweight**;** 49% were stunted**;** 10% were wasted by weight for length/height percentile and 5% were wasted by body mass index**;** 49% had percentage of ideal body weight below normal**;** 27% had head circumference below 3rd percentile**;** 59.4% had triceps skinfold thickness below 5th percentile**;** 66% had subscapular skinfold thickness below 5th percentile; 56% had arm circumference below 5th percentile. There was no correlation between these growth parameters and mortality. However**;** we found a positive correlation between decreased triceps skinfold thickness and prolonged hospital stay. Malnourished patients**;** according to triceps skinfold thickness**;** were significantly younger and they were the ones who suffered from cholestatic disorders of infancy. Conclusion: Only triceps skinfold thickness was found to be a useful predictor for a prolonged hospital stay. Serial measurements may be more effective.
**Keywords:** Hospitalized Children with Liver Disease**;** Nutritional Assessment**;** Skin Fold Thickness.

## M-355. Value of Electroencephalographic Monitoring in Newborns with Hypoxic-Ischemic Encephalopathy Treated with Hypothermia.

Hatem Hamed Elshorbagy, Ahmed A. Azab, Naglaa M. Kamal, Naglaa Fathy Barseem, Mohamed M. Bassiouny, Mostafa A. Elsayed and Tohamy H. Elkhouly

*Journal of Pediatric Neurosciences; 11: 309-315 (2016)*

**Background** : The values of electroencephalography (EEG) in neonatal hypoxic-ischemic encephalopathy (HIE) during therapeutic hypothermia (TH) are still uncertain. AIMS: The aim of this study is to detect EEG Background:; the prevalence of seizures during cooling; and to determine different EEG patterns that can predict brain injury in magnetic resonance imaging (MRI). **Patients and Methods**: Thirty-nine newborns with HIE were subjected to TH. Continuous monitoring by video-EEG was carried out throughout cooling and during rewarming. MRI was done for all newborns after rewarming. The predictive value of EEG Background : for MRI brain injury was evaluated at 6-h intervals during cooling and rewarming. **Results**: At all-time intervals; normal EEG was associated with no or mild MRI brain injury. At the beginning of cooling; normal Background : was more predictive of a favorable MRI outcome than at later time points. After 24 h of monitoring; diffuse burst suppression and depressed patterns had the greatest prognostic value. In most patients; a discontinuous pattern was not associated with poor prognosis. Thirty-one percent developed electrical seizures; and 8% developed status epilepticus. Seizures were subclinical in 42%. There is a significant association between duration of seizure patterns detected on the EEG and severity of brain injury on MRI. **Conclusions**: Continuous EEG monitoring in newborns with HIE under cooling has a prognostic value about early MRI brain injury and identifies electrographic seizures; approximately 50% of which are subclinical. Treatment of clinical and subclinical seizure results in a reduction of the total duration of seizure pattern supports the hypothesis that subclinical seizures should be treated.

**Keywords:** Electroencephalographic Monitoring; Hypoxic-Ischemic Encephalopathy; Therapeutic Hypothermia

### *Dept. of Pharmacology*

## M-356. Role of Selective Blocking of Bradykinin Receptor Subtypes in Attenuating Allergic Airway Inflammation in Guinea Pigs.

Mohamed M. El-Kady, Zarif I. Girgis, Eman A. Abd El-Rasheed, Olfat Shaker, Magdy I. Attallah and Ahmed A. Soliman

*European Journal of Pharmacology;788:152-159(2016)IF:2.73*

The present study was designed to evaluate the potential role of bradykinin antagonists (R-715; bradykinin B1 receptor antagonist and icatibant; bradykinin B2 receptor antagonist) in treatment of allergic airway inflammation in comparison to dexamethasone and montelukast. R-715 as dexamethasone significantly decreased peribronchial leukocyte infiltration; bronchoalveolar lavage fluid (BALF) albumin and interleukin 1β as well as serum OVA-specific IgE level. Also; R-715 like montelukast significantly decreased BALF cell count (total and eosinophils). Icatibant showed negative results. The current findings suggest that selective bradykinin B1 receptor antagonists may have the therapeutic potential for the treatment of allergic airway inflammation.

**Keywords:** Bradykinin; R-715; Icatibant; Airway Hyperresponsiveness; Bronchoalveolar Lavage; Asthma

## M-357. Effects of Telmisartan and Pioglitazone on High Fructose Induced Metabolic Syndrome in Rats.

Mary Girgis Shahataa, Gomaa Mostafa-Hedeab, Esam Fouaad Ali, Emad ahmed Mahdi and Fatma Abd Elhaleem Mahmoud

*Canadian Journal of Physiology and Pharmacology; 94(8): 907-917 (2016) IF: 1.704*

Metabolic syndrome (MS) is a cluster of hypertension; insulin resistance; dyslipidaemia; and hyperuricemia. This study was designed to assess the effect of telmisartan and pioglitazone on high fructose induced MS. Thirty-five male albino rats were classified into 5 groups: A; normal diet; B; high-fructose diet (HFD) subdivided into B1 (HFD only); B2 (telmisartan; 5 mg/kg); B3 (pioglitazone; 10 mg/kg); and B4 (telmisartan + pioglitazone). Administration of the drugs was started after the rats had been on HFD for 4 weeks and continued for 4 weeks. Body mass (BM); blood pressure (BP); uric acid (UA); total cholesterol; triglycerides (TG); high-density lipoprotein (HDL-c); low-density lipoprotein (LDL-c); blood urea nitrogen (BUN); creatinine; and nitric oxide (NO) were measured and the levels of fasting glucose and fasting insulin were estimated. Compared with group B1; telmisartan treatment significantly decreased BP; BM; serum glucose; insulin; UA; urea; cholesterol; TGA; and LDL and significantly increased HDL; whereas pioglitazone treatment significantly decreased BP; serum glucose; insulin; UA; urea; creatinine; cholesterol; TGA; and LDL and significantly increased HDL. Co-administration of pioglitazone + telmisartan significantly decreased insulin; urea; and creatinine compared with telmisartan alone. Combined telmisartan + pioglitazone allowed better control of BP; hyperglycaemia; insulin resistance; and the amelioration of BM increase that may be associated with pioglitazone treatment.

**Keywords:** Metabolic Syndrome; Telmisartan; Pioglitazone; Body Mass; Blood Pressure; Dyslipidaemia; Uric Acid; Insulin Resistance.

### *Dept. of Physiology*

## M-358. Effect of Gamma-Carboxylase Inhibition on Serum Osteocalcin May be Partially Protective Against Developing Diabetic Cardiomyopathy in Type 2 Diabetic Rats.

Gamal SM, Sadek NB, Rashed LA, Shawky HM and Gamal El-Din MM.

*Diabetes and Vascular Disease Research;13:405-417(2016) IF:3.035*

**Aims:** To investigate the possible protective effect of elevated undercarboxylated osteocalcin on diabetic cardiomyopathy mechanisms and risk factors. **Methods:** In all; 32 male rats were divided into four groups: control; diabetic; diabetic warfarin and normal warfarin-treated groups. Isolated heart functions were assessed; fasting serum insulin; glucose and glycosylated haemoglobin; homeostasis model assessment insulin resistance

and lipid profile were investigated. Serum undercarboxylated osteocalcin and adiponectin were also measured. In cardiac tissue; malondialdehyde content; acyl-CoA dehydrogenase gene expression; Bax/Bcl2 ratio; sarcoendoplasmic reticulum calcium ATPase and osteocalcin receptor (G protein-coupled receptor family C group 6 member A) genes expression were investigated. **Results**: Prophylactic elevation of undercarboxylated osteocalcin was accompanied by improved insulin sensitivity and lipid profile; increased serum adiponectin; upregulated myocardial osteocalcin receptor with preserved left ventricular function; decreased cardiac malondialdehyde content; acyl-CoA dehydrogenase and Bax/Bcl2 ratio. **Conclusion:** Undercarboxylated osteocalcin was suggested to have protective effects against diabetic cardiomyopathy; possibly through direct action on upregulated G protein-coupled receptor family C group 6 member A and indirectly via adiponectin. These effects may be mediated through antagonizing oxidative stress and apoptosis.

**Keywords:** Diabetes Mellitus; Adiponectin; Diabetic Cardiomyopathy; Undercarboxylated Osteocalcin; Warfarin.

## M-359. Analysis of Microcirculation Measurements by Novice Users Trained by a Standardized Interactive Tutorial: an Inter-Observer Variability Study.

Vladimir Cerny, Islam Abdo, Ronald B. George, Liivi Maddison, Nivin Sharawi and Christian Lehmann

*Clinical Hemorheology and Microcirculation; 62: 123-8 (2016) IF: 1.815*

Excessive time for analysis may impede microcirculatory studies with large amounts of video data. Engaging more personnel in the analyses seems to be a rational approach in that scenario and could shorten the time-interval between capturing images and obtaining results. Our hypothesis was that novice users would be able to determine standard microcirculatory parameters using a semi-automated software with an acceptable degree of variability after participating in a standardized interactive training session. 14 volunteers were included in the study. All volunteers analyzed separately the same sample video after the training. The kappa statistic was calculated for the primary outcome parameter microvascular flow index (MFI) within small and large vessels and indicated a fair level of agreement in the results of the novice users. A standardized interactive tutorial can be useful to teach microcirculatory analysis in previously untrained subjects.

**Keywords:** Microcirculation; Analysis; Education; Tutorial.

## M-360. Effect of Undifferentiated Versus Hepatogenic Partially Differentiated Mesenchymal Stem Cells on Hepatic and Cognitive Functions in Liver Cirrhosis.

Dalia Azmy Elberry, Shaimaa Nasr Amin, Reham Shehab El Nemr Esmail, Laila Ahmed Rashed and Maha Mohamed Gamal

*Excli Journal; 15: 652-670 (2016) IF: 1.292*

Liver cirrhosis is the outcome of chronic liver injury. The current study aimed to investigate the therapeutic effect of undifferentiated mesenchymal stem cells versus in vitro partially differentiated mesenchymal stem cells on liver cirrhosis and hepatic encephalopathy. 50 adult male albino rats constituted the animal model and were divided into the following groups: control; thioacetamide; undifferentiated mesenchymal stem cells and hepatocyte growth factor-differentiated mesenchymal stem cells groups. Cognitive assessment was achieved by open field test and Y-maze task. We measured serum alanine aminotransferase; albumin and transforming growth factor-beta1; gene expression of α-smooth muscle actin; matrix metalloprotein-2; its tissue inhibitor and apoptotic markers: Bax and Bcl2; brain glial fibrillary acidic protein; synaptophysin; and dopaminergic receptors.

**Keywords:** Liver; Hepatic Encephalopathy; Stem Cells; Hippocampus; Basal Ganglia.

## M-361. Interaction Between Renin Angiotensin System and Apelin/APJ System in Hypertensive Rats.

Rehab A. Mohamed, Maha M. Sabry, Heba M. Shawky, Amal F. Tawadrous and Doaa M. Gharib

*Der Pharma Chemica; 8(4): 32-49 (2016)*

White adipose tissue (WAT) is now recognized as the largest endocrine organ of the body. WAT secretes a number of bioactive peptides and proteins; collectively termed “adipokines”. Adipokines have different biological effects; including blood pressure control. Dysregulated production and release of specific adipokines; namely renin angiotensin system (RAS) peptides &apelin; from WAT in the setting of obesity may contribute to hypertension. Based on previous concepts; the present study aimed to clarify role of RAS and Apelin/APJ system in obesity-induced hypertension through modulation of Angiotensin type 1 receptor (AT1R); Angiotensin 1-7/Mas receptor and Apelin/ APJ receptor expression and to elucidate the possible interaction between the two systems. 48rats were used in this study divided into 6 groups; group 1(control group) given standard rat chow; group 2(control + captopril group):given standard rat chow + captopril 40mg/kg; group 3(Control + L-NAME group): given standard rat chow + L-NAME 20mg/kg; group 4(control hypertensive group):fed high fat high sucrose diet (HF-HS) for 10 weeks; Group 5: (hypertensive + captopril group): Fed HF-HS diet & received captopril (40mg/kg) for 10weeks; Group 6: (hypertensive + LNAME group): Fed HF-HS diet & received L-NAME (20mg/kg) for 10 weeks. At the end of experiment; body weight; fat weight and systolic blood pressure were measured. Visceral adipose tissue (epididymal fat) was collected for gene expression of AT1R; Ang1-7 R and apelin/APJ. Results of this study demonstrated activation of the adipose (RAS) and Apelin/APJ system in rats with diet-induced hypertension; consistent with a strong link between visceral obesity and hypertension. Obesity induced hypertension was associated with marked upregulation in AT1R; apelin /APJ R expression and down regulation of Ang-(1-7)/Mas R in adipose tissue. Captopril treatment showed significant decrease in body weight; fat weight and systolic blood pressure associated with significant increase in adipose tissue gene expression of Apelin/APJ receptor and Ang 1-7/Mas receptor. Whereas L-NAME significantly increased blood pressure and decreased body weight; fat weight with significant increased AT1R expression. Obesity induced hypertension was associated with increased AT1R & apelin receptor expression

and decreased Ang-(1-7) R expression which provides evidence that apelin/APJ upregulation by HFHS diet could not antagonize hypertensive effect of AngII/AT1R. This may be explained by apelin resistance or high expression of Ang II. ACE inhibition decreased blood pressure significantly in obese hypertensive rats through increased Ang-(1-7) R & apelin/APJ receptor expression. L-NAME raised blood pressure significantly in obese rats through increased AT1R expression and possible inhibition of nitric oxide (NO)- mediated vasodilator action of Ang-(1-7) &apelin. These results suggest an interaction between Apelin and RAS peptides to regulate ABP in obese subjects.
**Keywords:** Ras; Apelin; Obesity Induced Hypertension

***Dept. of Public Health***

## M-362. PM2.5 As A Marker of Exposure to Tobacco Smoke and Other Sources of Particulate Matter in Cairo; Egypt.

Loffredo CA, Tang Y, Momen M, Makambi K, Radwan GN and Aboul-Foutoh A

*International Journal of Tuberculosis and Lung Disease; 20: 417-422 (2016) IF: 2.148*

**Setting:**Cairo and Giza governorates of Egypt. **Background** Particulate matter under 2.5 μm in diameter (PM2.5) arises from diverse sources; including tobacco smoke from cigarettes and waterpipes; and is recognized as a cause of acute and chronic morbidity and mortality. **Objective**: To measure PM2.5 in workplaces with different intensities of smoking and varying levels of smoking restrictions. **Design:** We conducted an air sampling study to measure PM2.5 levels in a convenience sample of indoor and outdoor venues in 2005-2006. **Results**: Using a calibrated SidePak instrument; 3295 individual measurements were collected at 96 venues. Compared to indoor venues where tobacco smoking was banned (PM2.5 levels 72-81 μg/m(3)); places offering waterpipes to patrons of cafes (478 μg/m(3)) and Ramadan tents (612 μg/m(3)) had much higher concentrations; as did venues such as public buildings with poor enforcement of smoking restrictions (range 171-704 μg/m(3)). Both the number of waterpipe smokers and the number of cigarette smokers observed at each venue contributed significantly to the overall burden of PM2.5. **Conclusion:**Such data will support smoke-free policies and programs aimed specifically at reducing environmental tobacco exposure and improving air quality in general; and will provide a baseline for monitoring the impact of tobacco control policies.
**Keywords:** Tobacco- PM2.5 - Waterpipe-Egypt.

## M-363. Prognostic Markers Among Egyptian Children with Sepsis in the Intensive Care Units; Cairo University Hospitals.

Ibrahiem SK, Galal YS, Youssef MR, Sedrak AS, El Khateeb EM and Abdel-Hameed ND

*Allergologia Et Immunopathologia; 44: 46-53 (2016) IF: 1.689*

**Background :** Early identification of septic patients at risk of mortality is important in their prognosis. **Objective:** Identification of septic patients at risk of mortality in Pediatric Intensive Care Units (PICUs) at Cairo University Hospitals; through measuring the levels of certain immunological parameters. **Methods:** A hospital-based prospective cohort study was conducted in two PICUs at Cairo University Hospitals; all patients with diagnosis of severe sepsis or septic shock on admission were included. A total of 57 patients were prospectively followed at the selected PICUs and their demographic and clinical data were recorded. Microbiological and immunological workup (at days 1 and 7) was conducted for all patients to detect the causative organism of sepsis and to measure the levels of immunoglobulins (IgG; IgM and IgA); complement factors (C3 and C4); mature lymphocyte subpopulations (CD3+) and natural killer (NK) cells (CD3-CD16+CD56+); respectively. **Results:** Mortality rate was 24.6%; the most frequent causes of death were multi-organ dysfunction and refractory shock. PELOD and PRISM III scores were significantly higher among non-survivors. At day 1; non-survivors had significantly higher levels of IgG; C4 and NK cells than survivors. However; from day 1 to day 7; survivors had a progressive increase in most of the immunological parameters (IgG; IgM; C4and CD3+ T lymphocytes). Survival curve analysis revealed the significant predictive ability of NK cells to detect early mortality. **Conclusion:** Monitoring the levels of cellular and humoral immunological parameters together with assessing PELOD and PRISM III scores can significantly affect prognosis and survival of septic children.
**Keywords:** Immunological Parameters; Outcome; Pediatric Intensive Care Units; Sepsis; Survival

## M-364. Parental Perceptions of Congenital Cardiovascular Malformations in Their Children.

Sameera Ezzat, Osamah Saeedi, Doaa A. Saleh, Hala Hamzeh, Mohamed A. Hamid, Nancy Crowell, Camille Boostrom, Christopher A. Loffredo and Irene A. Jillson

*Cardiology In The Young; 26: 1158-1167 (2016) IF: 0.825*

We assessed parental attitudes towards congenital cardiovascular malformations in their children in a cross-sectional study in Egypt. Parents face many problems related to concerns about their child's prognosis; but these associations with parental stress have never been evaluated in Egypt or examined in relation to religiosity in a predominantly Muslim society. Accordingly; we conducted interviews in Cairo with mothers of 99 sequential infants born with conotruncal heart malformations (cases) and 65 mothers of age-matched controls. The survey assessed healthcare access and usage; knowledge of congenital cardiovascular malformations; religiosity; the Locus of Control Scale; and the Parenting Stress Index. Results showed that 45% of the mothers of cases had correct knowledge about their child's diagnosis; 85% were satisfied with the clinical care; and 79% reported that the cost of care was burdensome. Compared with parents of cases; parents of controls were more likely to report stress overall and all its subscales. Regarding belief about locus of control over health; God as a determining factor was given the highest endorsement. Mothers in the congenital cardiovascular malformations group reported a higher level of parental locus of control than did those in the control group. The correlations between stress and locus of control were stronger in the control than in the case group. Religiosity was related neither to stress nor to locus of control. Future studies can explore the roles that personal; familial; and societal factors play in exacerbating or reducing stress levels among parents of sick children; particularly in developing countries where economic pressures are acute.

**Keywords:** Chd; Cardiovascular Malformations; Parental Stress; Religio.

## M-365. Cancer Screening Knowledge and Attitudes of Under- and Post-Graduate Students at Kasr Al Ainy School of Medicine; Cairo University; Egypt.

Amal Samir Sedrak, Yasmine Samir Galal and Tarek Tawfik Amin

*Asian Pacific Journal of Cancer Prevention;17:3807-3814 (2016)*

**Background** : Increasing knowledge and awareness of cancer screening significantly influence health promotion behavior which could markedly reduce incidence rates. In many countries; health care providers are the principal source of information concerning cancer screening. This study was carried out to assess the level of knowledge concerning cancer screening among medical students; house officers and residents and to explore their attitude towards cancer screening practices. **Materials and Methods:** This cross-sectional study was conducted in Kasr Al Ainy Medical School at Cairo University in Egypt; with 300 undergraduate medical students and 150 postgraduates (interns and residents) enrolled. A pre-tested self-administered questionnaire was used to collect data from the study participants regarding personal and education-related information; knowledge about cancer screening and its sources; and attitude towards cancer screening. **Results:** More than 64% of participants had knowledge scores of ≤ 10 points (out of 24). The total knowledge score (out of 6 points) for breast cancer screening increased from 1.9±1.0 to 2.3±1.2 and 2.4±1.1 for 4th; 5th and 6th year respectively; interns showed the highest score of 2.6 ±1.1; P= 0.001. Year of enrollment at medical school was a significant positive predictor of acquiring knowledge about cancer screening (post graduate vs. undergraduate students) (OR= 1.30; C.I =1.01-1.63); lack of or none receiving of orientation/training about cancer screening was the sole negative significant predictor for proper knowledge about cancer screening (OR=0.50; C.I=0.31-0.82). Over 92% of students agreed that they had insufficient knowledge about cancer screening; 88.2% appraised the need to have enough knowledge in order to direct/advice patients; relatives and friends; and 93.7% required that the faculty should emphasize the importance of cancer screening in the delivered curricula at medical school. **Conclusions:** A relatively low to moderate level of knowledge about cancer screening was detected among the selected medical students regardless of their year of enrollment at medical school or their graduation status; which may implicate a negative impact on early cancer detection especially in a low resource country like Egypt

**Keywords:** Cancer Screening - Health Promotion Behaviors - Knowledge - Attitude - Medical Students.

## M-366. Colon Cancer Among Older Saudis: Awareness of Risk Factors and Early Signs; and Perceived Barriers to Screening.

Yasmine Samir Galal, Tarek Tawfik Amin and Rehab Ahmed AbdelHai

*Asian Pacific Journal of Cancer Prevention;17:1837-1846 (2016)*

**Background**: Colon cancer screening (CRCS) uptake is markedly affected by public awareness of the disease. This study was conducted to assess levels of knowledge of CRC; to explore the pattern of CRCS uptake and identify possible barriers to screening among Saudis older than 50 years of age and primary care providers (PCPs) in Al Hassa region; Saudi Arabia. **Materials and Methods:** This cross-sectional study was conducted in randomly selected primary health care (PHC) centers; 884 Saudis and 39 PCPs being enrolled for data collection. Structured interviews were conducted to obtain information regarding socio-demographic characteristics; personal information relevant to CRC; awareness about early signs/symptoms and risk factors; and barriers to CRCS. Also; a self- administered data collection form was used to assess barriers to CRCS from the physicians' perspectives. **Results:** More than 66% of participants were lacking knowledge about CRC. Participants with higher educational levels; having ever heard about CRC; and having relatives with CRC had a significantly higher awareness of the disease. The rate of reported CRCS was low (8.6%). After conducting a logistic regression analysis; it was observed that female gender (OR=0.28; 95% CI=0.14-0.57; P=0.001); being unmarried (OR=0.11; 95% CI=0.10-0.23; P=0.001); lower levels of education (OR=0.36; 95% CI=0.16-0.82; P=0.015); and having no relatives with CRC (OR=0.30; 95% CI=0.17-0.56; P=0.001) were significantly associated with a lower CRCS uptake. There was a significant difference between most of the perceived barriers to CRCS and gender. Exploratory factor analysis showed that personal fear (especially fear of the screening results and shyness) was the major factor that hindered CRCS with high loading Eigen value of 2.951; explaining 34.8% of the barriers of the included sample toward utilization of CRCS; followed by lack of awareness of both person and providers (high Eigen value of 2.132; and explaining 23.7% of the barriers). The most frequently cited barriers to CRCS from the physicians' perspectives were lack of public awareness; lack of symptoms and signs; and fear of painful procedures. **Conclusions:** Poor levels of knowledge about CRC were found among older Saudis attending PHC centers in Al Hassa; Saudi Arabia. It is crucial to implement an organized national screening program in Saudi Arabia to increase public awareness.

**Keywords:** Colorectal Cancer; Risk Factors; Screening Programs; Barriers; Public Awareness.

### *Dept. of Pulmonary Medicine and Tuberculosis*

## M-367. Multidetector Ct Scan of the Chest Versus Transthoracic Ultrasound in Diagnosis of Pleural Diseases.

Yamamah H, Sobhy K, Kamel K, Ahmed S and Hareedy A

*International Journal of Pharmaceutical and Clinical Research; 8: 1470-1476 (2016)*

Pleural diseases (as pleural effusions; pleural masses; pleural plaques; diffuse pleural thickening and pleural tumors) affect over 3000 subjects per million populations each year. Diseases of the pleura can be broadly classified into benign and malignant. The incidence of malignant pleural mesothelioma is increasing worldwide. Imaging of the pleura can be challenging and it plays an important role in the diagnosis and subsequent management of patients with pleural diseases. This study aimed to compare the efficiency and reliability of Multidetector Computed tomography (MDCT) and Transthoracic Ultrasound

(TUS) in diagnosis of pleural disease. **Patients and Methods:** This study included 71 patients with pleural disease. All patients were subjected to complete history taking; full clinical examination; MDCT chest and TUS examination. The patients included in the study were classified according to the pathology of the lesions into Group A (51 patients with malignant lesions) and Group B (included 20 patients with non- malignant lesions); The malignant patients included in the study were classified according to the pathology of the lesions into Group A1 (24 patients with primary malignant lesions) and Group A2 (27 patients cases with secondary malignant lesions). **Conclusion:** MDCT scan of the pleura is less sensitive than TUS in detection of pleural nodules; masses; pleural thickening; adhesion and also in detecting lung masses. However TUS examination of the pleura – in the presence of adequate window –could suspect nature of lung mass by Dupplex study; Yet TUS examination of the pleura is a localized examination and can't be applied to whole chest without prior guidance by radiology either CXR or MDCT.

**Keywords:** Pleural Diseases; Multidetector CT Scan; Transthoracic Ultrasound; Pleural Nodules; Pleural Masses.

### *Dept. of Radiation*

## M-368. Role of Diffusion Weighted Imaging and Dynamic Contrast Enhanced Mr Mammography to Detect Recurrence in Breast Cancer Patients after Surgery.

Safaa Ibrahim Saif El-nasr a, Rasha Wessam Abdel Rahman, Sherif Fathy Abdelrahman, Maha Hussein Helal and Soha Talaat Hamed

*The Egyptian Journal of Radiology and Nuclear Medicine; 47: 1151-1157 (2016)*

**Objective:** To assess role of Diffusion weighted imaging (DWI) in addition to dynamic contrast-enhanced magnetic resonance mammography (DCE-MRM) in detection of breast cancer recurrence after surgery. **Patients and methods**: Sixty female patients who underwent breast surgery were included in this prospective study. Patients were examined by sonomammography followed by DCE-MRI to exclude recurrence. DWI was performed using b values of 0; 50; and 850 s/mm2. Patients with suspected recurrence were subjected to histopathological confirmation. **Results:** Twenty seven patients had pathologically proven recurrence and thirty three patients showed spectrum of post operative changes. DCE-MRI was superior to DWI with 2 false positive (FP) cases and no false negative (FN) cases; while DWI showed 3 (FN) cases and 4 (FP) cases. DCE-MRI & DWI showed sensitivity (100%; 88.9%); specificity (93.9%; 87.9%); positive predictive value (PPV) (93.1%; 88.9%); negative predictive value (NPV) (100%; 90.6%) & accuracy (96.7%; 88.3%) respectively. **Conclusion:** Our study showed better diagnostic performance for DCE-MRI compared to DWI in post operative breast assessment. However; DWI can provide an alternative diagnostic tool to contrast administration ''if interpreted in association with conventional MR sequences" thus can be used when contrast media is contraindicated.

**Keywords:** DWI; DCE-MRI; Breast Cancer Recurrence.

## M-369. Utility of Cardiac Mri in the Assessment of Myocardial Viability: Evaluating its Role Using 3-T Machine in Correlation with Spect.

Sherif Fathy Abdelrahman, Mohamed Talaat Ali, Mohamed Ali Salem and Sherif Sabri

*The Egyptian Journal of Radiology and Nuclear Medicine; (2016) 47: 73-81 (2016).*

**Background** : Assessment of viable myocardium has important prognostic value in patients with coronary artery disease (CAD). The aim of this study was to compare 3 T cardiac magnetic resonance (CMR) with single-photon emission computed tomography (SPECT). **Methods:** Thirty-three patients with coronary artery disease were involved in this study. All patients were examined using coronary angiography to determine the degree of the coronary artery disease. Then; they underwent 3 T CMR examination; after administration of intravenous gadolinium and the segmental extent of myocardial enhancement was determined; followed by SPECT evaluation. Comparison of myocardial viability was performed in 99 coronary territories. **Results:** Agreement between two modalities was obtained in 88 segments (88.9%); resulting in a kappa value of 0.725. In 99 segments; we had eleven discordant results. Eleven SPECT viable segments were non-viable according to CMR. **Conclusion:** SPECT was comparable to 3 T CMR for myocardial viability assessment; C-MRI detected more non-viable segments with high definition to the thickness of the myocardial scar tissue than the SPECT.

**Keywords:** 3 T Magnetic Resonance Imaging; Single Photon Emission Computed Tomography; Coronary Artery Disease; Myocardial Viability.

### *Dept. of Rheumatology*

## M-370. Prevalence of Comorbidities and Evaluation of Theirscreening in Spondyloarthritis: Results of Theinternational Cross-Sectional Asas-Comospa Study

Anna Molt, Adrien Etcheto, Désirée van der Heijde, Robert Landewé, Filip van den Bosch, Wilson Bautista Molano, Ruben Burgos-VargasPeter P Cheung Eduardo Collantes-Estevez, Atul Deodhar, Bassel El-Zorkany Shandor Erdes, Jieruo Gu, Najia Hajjaj-Hassouni, Uta KiltzTae-Hwan Kim, Mitsumasa Kishimoto, Shue-Fen Luo, Pedro M Machado Walter P and et al.

*Annals of The Rheumatic Diseases; 75(6): 1016-1023 (2016) IF: 12.384*

**Background**: Increased risk of some comorbidities has been reported in spondyloarthritis (SpA). Recommendations for detection/management of some of these comorbidities have been proposed; and it is known that a gap exists between these and their implementation in practice. **Objective** To evaluate (1) the prevalence of comorbidities and risk factors in different countries worldwide; (2) the gap between available recommendations and daily practice for management of these comorbidities and (3) the prevalence of previously unknown risk factors detected as a result of the present initiative. Methods Cross-sectional international study with 22 participating countries (from four continents); including 3984 patients with SpA according to the rheumatologist. Statistical analysis The prevalence of comorbidities (cardiovascular; infection; cancer;

osteoporosis and gastrointestinal) and risk factors; percentage of patients optimally monitored for comorbidities according to available recommendations and percentage of patients for whom a risk factor was detected due to this study. **Results** The most frequent comorbidities were osteoporosis (13%) and gastroduodenal ulcer (11%). The most frequent risk factors were hypertension (34%)**;** smoking (29%) and hypercholesterolaemia (27%). Substantial intercountry variability was observed for screening of comorbidities (eg**;** for LDL cholesterol measurement: from 8% (Taiwan) to 98% (Germany)). Systematic evaluation (eg**;** blood pressure (BP)**;** cholesterol) during this study unveiled previously unknown risk factors (eg**;** elevated BP (14%))**;** emphasising the suboptimal monitoring of comorbidities. **Conclusions** A high prevalence of comorbidities in SpA has been shown. Rigorous application of systematic evaluation of comorbidities may permit earlier detection**;** which may ultimately res METHODS Study design Observational**;** cross-sectional**;** multicentric and international study**;** with 22 participating countries from four continents (Africa**;** America**;** Asia and Europe).ult in an improved outcome of patients with SpA.

**Keywords:** Ard (Ann Rheum Dis)

## M-371. Clinical Significance of Angiopoietin-1 in Behcet's Disease Patients with Vascular Involvement.

Iman H. Bassyouni, Mohammed Sharaf, Iman E. Wali and Hossam M. Mansour

*Heart and Vessels**;** 31: 918-924 (2016) IF: 2.293*

**Objective** Behcet's Disease (BD) is a chronic multisystem inflammatory disorder of unclear etiology. Vascular inflammation**;** endothelial dysfunction and angiogenesis may be in part responsible for the pathogenesis of BD. The aim of the present study was to assess Angiopoietin-1 (Ang-1) concentrations as a recent angiogenic mediator in plasma of BD patients and to analyze its association with disease clinical**;** laboratory parameters as well as disease activity. Methods The present study included 47 BD patients and 30 age and gender matched healthy controls. Demographic**;** clinical**;** disease Activity and severity were prospectively assessed. Plasma Ang-1 levels were measured using enzyme-linked immunosorbent assay (ELISA). **Results** The plasma level of Ang-1 in BD patients was significantly lower than healthy controls (p=0.005). Plasma Ang-1 level in patients with vascular affection was significantly lower than those without vascular affection (p=0.045). Levels of Ang-1 showed a significant positive correlation with steroid dose. Patients who received cyclophosphamide or steroids showed a significant increase in plasma Ang-1 level. This was further confirmed by the results of the multivariate analysis. There was no significant association between plasma Ang-1 levels and other clinical manifestations nor disease activity or severity. **Conclusion** Plasma Ang-1 levels were diminished in our BD patients especially in patients with vascular involvement. Larger studies with further investigations of the precise role of Ang-1 in the pathogenesis of BD are needed and might lead to novel therapies for the clinical management of BD.

**Keywords:** Angiogenesis; Angiopoietin; Behcet'S Disease; Vasculitis

## M-372. Therapeutic Antioxidant and Anti-Inflammatory Effects of Laser Acupuncture on Patients with Rheumatoid Arthritis.

Atef M. M. Attia, Fatma A. A. Ibrahim, Noha A. Abd El-Latif, , Samir W. Aziz, Azhar M. Elwan, Abdel Aziz A. Abdel Aziz, Aliaa Elgendy and Fatema T. Elgengehy

*Lasers in Surgery and Medicine**;** 48: 490-497 (2016) IF: 2.135*

**Background and Objective:** The laser acupuncture has many potential therapeutic effects. Currently**;** they are not evaluated for their therapeutic effects on rheumatoid arthritis (RA) patients. The aim of this study was to investigate the effects of laser acupuncture on the oxidative and antioxidative markers**;** as well as the inflammatory markers and disease activity of RA patients. **Design/Materials and Methods:** The study was conducted on 30 RA patients and 20 healthy subjects. The patients were subjected to laser acupuncture (904 nm**;** 100 mW power output**;** 1 minute irradiation time**;** beam area of 1 cm(2); total energy per point 6 J**;** energy density 6 J/ cm(2); irradiance 0.1 W/cm(2); frequency 10000 Hz**;** duty-cycle 100%) for 3 days/week for duration of 4 weeks. The acupuncture points of exposure were LI4**;** TE5**;** LI 11**;** DU 14**;** LIV3**;** SP6**;** GB34**;** and S36. The levels of oxidative and antioxidant markers were determined by spectrophotometric methods whereas the inflammatory markers were determined by ELISA methods. Lastly**;** using DAS28 scores the disease activity was assessed. **Results**: After laser acupuncture**;** the study group revealed significantly increased plasma superoxide dismutase (SOD)**;** glutathione reductase (GR)**;** catalase activities**;** blood glutathione (GSH)**;** and plasma ATP concentrations**;** compared to those before treatment ($P < 0.0005$). Moreover**;** the results revealed significantly reduced plasma malondialdehyde (MDA)**;** serum nitrate and nitrite**;** serum C-reactive protein (CRP)**;** plasma interleukin-6 (IL-6) levels and significantly reduced glutathione peroxidase (GPx) activity and erythrocyte sedimentation rate (ESR) in laser exposed patients**;** compared to those before treatment ($P < 0.0005$). The RA patients subjected to laser acupuncture showed highly significant reduction in disease activity ($P < 0.0005$) based on DAS28 score. **Conclusion:** Our study results confirmed the effectiveness of laser acupuncture in alleviating oxidative stress and inflammation**;** improving antioxidant and energy metabolic status**;** while also suppressing the disease activity in RA patients. Laser acupuncture is a promising treatment modality to reduce the pain and suffering of RA patients because of its efficiency in inhibiting most of the main factors involved in the pathogenesis of this disease.

**Keywords:** Atp; Antioxidants; Disease Activity; Inflammation; Laser Acupuncture; Oxidative Stress; Rheumatoid Arthritis.

## M-373. Genetic Polymorphisms of Interleukin 6 and Interleukin 10 in Egyptian Patients with Systemic Lupus Erythematosus.

RM Talaat, SA Alrefaey, IH Bassyouni, ME Ashour and AA Raouf

*Lupus**;** 25 (3): 255-264 (2016) IF: 2.118*

Systemic lupus erythematosus (SLE) is a complex autoimmune disease. Cytokine gene polymorphisms play an important role in SLE. Thus**;** this study aimed to investigate the associations between interleukin 6 (IL-6) and interleukin 10 (IL-10) promoter

single-nucleotide polymorphisms (SNPs) and their susceptibility to SLE and the implications for plasma levels. We genotyped IL-6-174G/C (rs1800795) using mutagenically separated polymerase chain reaction (MS-PCR) and IL-10-1082G/A (rs1800896) and -819C/T (rs1800871) using sequence specific primer polymerase chain reaction (SSP-PCR) in 100 Egyptian patients and 119 controls. The plasma levels of IL-6 and IL-10 were measured by enzyme-linked immunosorbent assay (ELISA). There was significant increase in the frequency of IL-6 (-174) GG genotype ($P < 0.05$) and G allele ($P < 0.01$) compared to controls. A significant increase in the distribution of IL-10 (-1082G/A) GG ($P < 0.05$) and AA ($P < 0.05$) genotypes and a significant reduction in the frequency of GA genotype ($P < 0.05$) was found in SLE patients. The mean serum concentration of IL-6 ($P < 0.001$) and IL-10 ($P < 0.001$) was significantly elevated in SLE patients compared to healthy controls. There was no significant association of the most common clinical findings and IL-6 and IL-10 gene polymorphisms in SLE patients. In conclusion; our preliminary study indicated that both GG genotype and G allele of IL-6 (-174G/C) could be considered as risk factors for SLE. In addition; the polymorphisms at IL-10 (-1082 G/G and AA) may play a role in SLE susceptibility in Egyptian patients. Larger prospective studies are needed to confirm our findings.

**Keywords:** SLE; IL-10; IL-6; Cytokines Polymorphism.

## M-374. Possible Risk Factors Associated with Greater Damage in Systemic Lupus Erythematosus Patients: An Egyptian Multicenter Study

M Hammad, M Eissa and S Fathi

*Lupus; 25: 1019-1027 (2016) IF: 2.118*

**Objectives** Systemic lupus erythematosus (SLE) is a prototypic multisystem autoimmune disorder. The total damage in a patient with SLE may result from SLE itself or from any other pathologic process. The aim of this study was to assess risk factors of greater damage in a sample of Egyptian SLE patients. Methods This Egyptian multicenter retrospective study included 100 SLE patients: 64 patients from Cairo University Hospitals and 36 patients from Zagazig University Hospitals. The Systemic Lupus International Collaborative Clinics (SLICC)/American College of Rheumatology (ACR) Damage Index (ACR-DI) was used to document the damage in each patient. **Results** The total SLICC/ACR-DI score ranged from 0 to 8. A higher DI score was found in hypertensive patients; compared to normotensive patients; and among those with positive anti-phospholipid antibodies; compared to those with negative anti-phospholipid antibodies. This difference was statistically significant ($p < 0.01$). Also; a higher DI score was found in cyclophosphamide users; compared to non-users; and in those with proteinuria and seizures; compared to those without; and the difference was statistically significant ($p < 0.05$). There was a significant positive correlation between the DI and patient age ($p < 0.05$). **Conclusions** Damage in SLE cannot be prevented completely; as SLE disease is considered an aggressive disease treated by aggressive medications; but rheumatologists should try to minimize damage as much as possible to maintain the patients' health; functioning and general wellbeing.

**Keywords:** Age; Blood Pressure; Damage Index; Egypt; Lupus; Proteinuria; Risk Factors; Seizures; Systemic Lupus Erythematosus

## M-375. Comparison of Comorbidities of the Egyptian Rheumatoid Arthritis Patients to the Global Cohort of the Comora Study: A Post-Hoc Analysis.

assel El-Zorkany, Abir Mokbel, Sherif M. Gamal, Maha Mousa, Mohamed Youssef and Ihsane Hmamouchi

*Clin Rheumatol; 35: 1153-1159 (2016) IF: 2.042*

The aims of this study are to present the results of Egyptian RA patients included in COMORA cohort and compare it to general COMORA cohort; concerning prevalence of comorbidities; and level of application of recommendations related to detection/prevention of comorbidities. Threehundred eight Egyptian RA patients included in the crosssectional; observational; multi-center; international study BCOMORA^; were compared to the total number of 3612 RA patients. The CRF of COMORAwas used in all patients. CRF collects demographic and disease characteristics; comorbidities; risk factors; and compliance with recommendations regarding management of comorbidities. Data were analyzed according to COMORA protocol. Egyptian RA patients were significantly younger; had more active disease; and were more functionally disabled. They showed more frequent use of NSAIDs; methotrexate and steroids and significantly lower use of bDMARDs when compared to non-Egyptians. Egyptian patients had the highest ever HCV prevalence; while depression; hypertension; smoking and dyslipidemia were less prevalent in Egyptians. Prevalence of malignancy risk factors was highly deficient among Egyptians; primarily due to lack of screening. Further; following recommendations for monitoring comorbidities is significantly deficient among Egyptian patients. Egyptian patients had more active disease and more functional impairment than the rest of the COMORA cohort; with lower use of bDMARDs; that is possibly related to the economic situation. Also; there is a clear gap in screening and monitoring comorbidities. Awareness among Egyptian healthcare providers (and possibly similar third-world countries) to detect and manage RA-related comorbidities is required.

**Keywords:** Comora ; Comorbidities ; Egypt ; Ra .

## M-376. Enhancing the Care of Women with Rheumatic Diseases During Pregnancy: Challenges and Unmet Needs in the Middle East.

S. Al-Emadi . Abutiban,B. El Zorkany, N. Ziad, A. Al-Herz, M. Al-Maini, B. Khan , A. Ghanem, H. Al Rayes, J. Al Saleh, H. Al-Osaimi and M. Stensen

*Clin Rheumatol; 35(1): 25-31 (2016) IF: 2.042*

Pregnancy in women with rheumatic disorders is known to be associated with risks for both the mother and fetus; however; these risks can be minimized with proper planning and careful management of the disease. In the Middle East; there are specific cultural challenges that may have a negative impact on the care that women with rheumatic disorders receive. There is a need for cross-collaboration between specialist physicians;

improved awareness of rheumatic disorders among the general public and more open discussion with patients about the potential complications of pregnancy. Women in the region are often unwilling to discuss their disease with their partner and are even less likely to seek advice regarding family planning from their physician. The objective of this review is to highlight the specific challenges of pregnancy management and to discuss why establishing specialist pregnancy clinics for women with rheumatic disorders could be an effective solution. Such clinics can provide high quality care before; during and after pregnancy as shown in several European and US centers. Additionally; such clinics could be useful for the collection of pregnancy outcomes data from the Middle East; which may currently be lacking in the region; in order to highlight where further improvements can be made. With specialist care and analysis of pregnancy outcomes; the standard of care for women with rheumatic disorders in this area could be significantly improved.
**Keywords:** Autoimmune Rheumatic Diseases; Counselling; Interdisciplinary Management; Pregnancy; Systemic Lupus; Women'S Health

## M-377. Association of Vdr Apai and Taqi Gene Polymorphisms with the Risk of Scleroderma and Behçet'S Disease.

Asmaa Kamal, Sherif M. Gamal, Fatema T. Elgengehy, Alkhateeb K. Alkemary and Ibrahem Siam

*Immunological Investigations; 45: 531-542 (2016) IF: 1.78*

Vitamin D deficiency and vitamin D receptor (VDR) gene polymorphisms have been reported in autoimmune diseases. However; their role in Behçet's disease (BD) and scleroderma remains inconclusive. Our aim was to evaluate vitamin D receptor (ApaI; TaqI) gene polymorphisms in relation to Behçet's disease and scleroderma in Egyptians. The study was conducted on 54 patients with BD; 30 scleroderma patients; and 60 healthy control subjects. VDR (ApaI; TaqI) gene polymorphisms were investigated using polymerase chain reaction-restriction fragment length polymorphism technique. The "a" allele of ApaI (A/a) polymorphism was significantly associated with increased BD risk (OR = 2.09; 95% CI = 1.18–3.71; p = 0.011); while the TaqI "tt" genotype was significantly lower in BD patients as compared to control subjects (OR = 0.35; 95% CI = 0.13–0.9; p = 0.026). Carriage of "aT" VDR haplotype was significantly associated with higher BD risk (OR = 2.28; 95% = 1.14–4.56; p = 0.022). In conclusion; our findings suggest that VDR gene polymorphisms have a significant association with BD in Egyptian patients.
**Keywords:** Behçet'S Disease; Gene Polymorphism; Scleroderma; VDR

## M-378. Serum and Synovial Cartilage Oligomeric Matrix Protein Levels in Early and Established Rheumatoid Arthritis.

Tamer A. Gheita, Safaa Sayed, Heba A. Gheita and Sanaa A. Kenawy

*Zeitschrift Für Rheumatologie; 75: 917-923 (2016) IF: 0.569*

**Objective**: To assess cartilage oligomeric matrix protein (COMP) levels in serum and synovial fluid in patients with early and established rheumatoid arthritis (RA); and to correlate the levels with clinical; laboratory and radiological characteristics. **Patients and Methods:** The study included 24 female RA patients. Full medical history was taken; thorough clinical examination and laboratory investigations performed; and body mass index (BMI) recorded. Radiological damage was assessed according to the modified Larsen score. Disease activity score 28 (DAS28) was calculated. The control group comprised 30 age- and gender-matched healthy subjects. Serum and synovial COMP levels were determined by enzyme-linked immunosorbent assay (ELISA). **Results**: Mean patient age was 44.04 ± 10.5 years. of the 24 patients; 12 had early RA and 12 had established disease with joint destruction; 5 of each group had knee effusion. Serum COMP was significantly higher in patients (19.54 ± 5.47 μg/ml) compared to controls (5.93 ± 1.95 μg/ml; $p < 0.001$) and was also significantly higher in patients with established disease (23.9 ± 3.1 μg/ml) compared to those in early stages (15.1 ± 3.2 μg/ml; $p < 0.001$). Synovial COMP was also significantly increased in established compared to early-stage RA (31.2 ± 9.8 μg/ml vs. 51.6 ± 10.4 μg/ml; $p = 0.013$). Serum and synovial COMP significantly correlated with age; disease duration; BMI; DAS28 and modified Larsen score. On performing regression analysis in RA patients; only BMI could predict the serum level of COMP ($p = 0.02$). **Conclusion:** COMP is a promising biomarker for disease activity in RA; making it a potential therapeutic target. The obvious correlation with the BMI throws light on the importance of weight control not only in osteoarthritis (OA); but also in RA.
**Keywords:** Biomarker; Body Mass Index; Enzyme-Linked Immunosorbent Assay; Inflammation; Osteoarthritis

### *Dept. of Surgery*

## M-379. Establishing the Feasibility of Face Transplantation in Granulomatosis with Polyangiitis.

A. M. Hashem, G. S. Hoffman,B. Gastman, S. Bernard, R. Djohan, M. Hendrickson, G. Schwarz, G. Doumit, B. B. Gharb, A. Rampazzo, J. E. Zins, M. Siemionow and F. Papay

*American Journal of Transplantation; 16(7): 2213-2223 (2016) IF: 5.669*

Granulomatosis with polyangiitis (GPA; formerly Wegener's granulomatosis) is a rare vasculitis that commonly starts in the craniofacial region. We report a case that was masked by prior facial trauma and associated with pyoderma gangrenosum (PG). Disease progression and aggressive debridements led to severe facial tissue loss. The decision to perform a face transplant was controversial because of the risk of disease relapse on the facial allograft. We reviewed renal transplant outcomes in GPA for possible relevance. A PubMed search retrieved 29 studies. Patient and graft survival; relapse; morbidity; mortality; rejection and immunosuppression were assessed. Ten-year patient survival and graft survival were 84.4% and 72.6%; respectively. GPA relapse occurred in 31.5%; and upper airway/ocular relapse occurred in 17.8% (resolved in 76.9%). Mortality was 12.3%. Acute and chronic rejection rates were 14.9% and 6.8%; respectively. Traditional posttransplant immunosuppression was effective. Our review suggests that GPA renal transplant outcomes are comparable to general renal transplant cohorts. Furthermore; transplanted GPA patients exhibit lower disease relapse secondary to lifelong immunosuppression. This supported our decision to perform a

face transplant in this patient; which has been successful up to the present time (1-year posttransplantation). Untreated GPA and PG are potential causes of worse surgical outcomes in the craniofacial region.

**Keywords:** Facial Transplantation; Granulomatosis with Polyangiitis; Wegener's Granulomatosis; Craniofacial Reconstruction

## M-380. Malignant Pyoderma Associated with Granulomatosis with Polyangiitis (Wegener Granulomatosis) as A Unique Indication for Facial Vascularized Composite Allotransplantation: Part I.

Gastman, Brian , Hashem, Ahmed M. , Djohan, Risal , Bernard, Steven , Hendrickson, Mark , Schwarz, Graham , Gharb, Bahar B, Rampazzo, Antonio, Fernandez, Anthony, Zins, James, Hoffman, Gary S , Doumit, Gaby , Siemionow, Maria and Papay Francis

*Plastic and Reconstructive Surgery; 137(6): 1007-1015 (2016) IF: 3.087*

**Background**: Granulomatosis with polyangiitis (Wegener granulomatosis) is a rare disease that commonly starts in the craniofacial region and can lead to considerable facial disfigurement. Granulomas and vasculitis; however; can involve many other tissues (especially pulmonary and renal). Dermatologic and subcutaneous components can lead to malignant pyoderma. **Methods:** The authors describe a unique pathologic condition; where significant Le Fort type trauma was associated with subsequent development of granulomatosis with polyangiitis and malignant pyoderma. Successive operations to excise necrotic tissue and reconstruct the defects were followed by worsening inflammation and tissue erosions. Trauma and surgery in proximity to the eye and sinuses masked the initial clinical presentation and led to delay in diagnosis and disease progression. The resultant facial disfigurement and tissue loss were substantial. **Results**: Despite multiple confounding factors; accurate diagnosis was eventually established. This was based on persistence of sinus inflammations in the absence of infective agents; proven sterility of lung lesions; and antineutrophil cytoplasmic antibody positivity with proteinase 3 specificity. Skin lesion biopsy specimens were identified as pyoderma gangrenosum and later as malignant pyoderma. Institution of immunosuppressive therapy allowed successful control of the disease and wound healing. The resulting craniofacial destruction; however; necessitated facial vascularized composite allotransplantation. **Conclusion:** Recognition of this rare pathologic association is essential; to prevent delays in diagnosis and treatment that can lead to major craniofacial tissue loss.

**Keywords:** Malignant Pyoderma; Face Transplantation; Granulomatosis With Polyangiitis; Wegener's Granulomatosis; Craniofacial Reconstruction

## M-381. Active Range of Motion Outcomes after Reconstruction of Burned Wrist and Hand Deformities.

Ahmed M. Afifi, Tarek A. Mahboub, Amr Ibrahim Fouad, Kodi Azari, Haitham H. Khalil and James E. McCarthy

*Burns; 42: 783-789 (2016) IF: 1.904*

This works aim is to evaluate the efficacy of skin grafts and flaps in reconstruction of post-burn hand and wrist deformities. A prospective study of 57 burn contractures of the wrist and dorsum of the hand was performed. Flaps were used only if there was a non-vascularized structure after contracture release; otherwise a skin graft was used. Active range of motion (ROM) was used to assess hand function. The extension deformity cohort uniformly underwent skin graft following contracture release with a mean improvement of 71 degrees ($p<0.0001$). The flexion deformity cohort was treated with either skin grafts (8 patients) or flaps (9 patients) with a mean improvement of 44 degrees ($p<0.0001$). Skin grafts suffice for dorsal hand contractures to restore functional wrist ROM. For flexion contractures; flaps were more likely for contractures >6 months. Early release of burn contracture is advisable to avoid deep structure contracture.

**Keywords:** Flap; Hand Burn; Hand Reconstruction; Reconstruction

## M-382. Timing and Outcome Concerns Regarding Feminizing Genitoplasty from the Perspective of Egyptian Families of Girls with Virilized External Genitalia.

Mahmoud M. Marei, Ahmed E. Fares, Noha Musa, Ayman H. Abdelsattar, Amal Sharaf, Mona M. Hassan, Montasser Elkotby, Gamal Eltagy, Mona Hafez and Mohamed M. Elbarbary

*Hormone Research in Paediatrics; 85: 49-57 (2016) IF: 1.661*

**Background**: Congenital adrenal hyperplasia in females leads to virilization of external genitalia and persistent urogenital sinus. There are controversies regarding the timing and outcomes of surgery. Deferring surgeries beyond childhood is difficult to implement in conservative societies; and may result in stigmatization and distress to individuals with disorders of sexual differentiation and their families. **Methods:** Thirty girls with virilization due to congenital adrenal hyperplasia were admitted for single-stage feminizing genitoplasty; between 2011 and 2014. We prospectively studied the concerns and input of the families represented by the mothers. After comprehensive counselling; the mothers completed a questionnaire to clarify their priorities and concerns related to surgery. **Results:** Surgeries were performed at a mean age of 22 months. Most cases ranged between Prader's degrees III and IV. Egyptian families believe that early surgical reconstruction is in the best interest of their girls. They are marginally more concerned about functional outcomes and future child bearing than external appearance and cosmetic outcomes. **Conclusions:** Social difficulties noticeably add challenges to the management plan within conservative societies. Early genital reconstructive surgery; when reasonably indicated; needs to remain a viable option. Comprehensive psychosocial support within a multidisciplinary approach is needed to defer feminizing genitoplasty in selected cases to adolescence.

**Keywords:** Feminizing Genitoplasty; Genital Reconstructive Surgery; Congenital Adrenal Hyperplasia; Disorders of Sexual Development; Ambiguous Genitalia; Egypt.

## M-383. Aortic Bypass Surgery Using Synthetic Conduits in a Child with Mycotic Aneurysmal Disease.

A Sayed, M Mashaal, SA Soliman and H Elwan

*Annals of Royal College of Surgeons of England; 98: 59-61 (2016) IF: 1.332*

A six-year-old child developed multiple aortic aneurysms as a consequence of fungal infection following thoracic aortic surgery for coarctation. Several repairs of both the thoracic and abdominal aorta were carried out using synthetic material combined with long-term postoperative antifungal treatment. We describe the surgical interventions performed and follow-up. The choice of conduit continues to be the main concern; however; when other alternatives are not available; synthetic material combined with indefinite antifungal treatment can produce satisfactory medium-term results.

**Keywords:** Paediatric; Aorta; Aneurysm; Infection; Surgery.

## M-384. Anatomical Measurements of the Urogenital Sinus in Virilized Female Children Due to Congenital Adrenal Hyperplasia.

M.M. Marei, A.E. Fares, A.H. Abdelsattar, K.S. Abdullateef, H. Seif, M.M. Hassan, M. Elkotby, G. Eltagy and M.M. Elbarbary

*Journal of Pediatric Urology (2016) IF: 1.17*

**Background** : Virilized females due to congenital adrenal hyperplasia represent the most common form of female disorders of sexual development. The anomaly therein is an external virilization to resemble male genitalia and a persistent urogenital sinus. **Objectives**: To study the anatomical details of the virilized female cases operated upon between 2011 and 2015. This anatomical description is presented to support the current surgical strategy of partial urogenital mobilization to correct this anomaly. **Methods:** Thirty cases (presenting to a single tertiary center) were prospectively studied by genitography; cysto-urethroscopy; and operated upon via a single-stage feminizing genitoplasty. A single surgical team operated upon all cases. External virilization was assessed by the Prader classification. The internal anatomy was studied by measuring the length of the urethra proximal to the confluence; and the vertical depth of the vaginal-urethral confluence from the perineum. The correlation coefficients between the external virilization and the internal anatomical measurements were derived. **Results**: The median age at surgery was 19 months (range 6-42 months). External virilization did not obviously correlate with the length of the proximal (prejunctional) urethra ($r = -0.03$; $P = 0.5$); or strongly with the depth of the vaginal-urethral confluence ($r = 0.2$; $P = 0.2$). The mean length of the proximal urethra was 22 mm (range 10-32 mm); and the mean vertical depth of the vaginal-urethral confluence from the perineum was 16 mm (range 8-31 mm). **Discussion:** Due to limitations of the radiological and endoscopic evaluation; the accurate anatomical assessment of this condition may be challenging. In order to assess or compare the anatomy of these cases; there are two important points to address: (1) the length of the urethra proximal to the urogenital sinus; as this will impact the urinary outcome; and (2) the depth (level) of vaginal entry into the urogenital sinus; as this will affect the mobilization required to exteriorize the vagina. **Conclusion:** The degree of external virilization does not totally correlate with the internal anatomy. The depth of the vaginal-urethral confluence from the perineum is an indicator of the required mobilization for the current perineal approach. In 90% of cases in this age group (1-3 years old); this depth is ?20 mm. This supports the current understanding that partial urogenital mobilization could be suitable for most cases.

**Keywords:** Congenital Adrenal Hyperplasia; Urogenital Sinus; Feminizing Genitoplasty; Urogenital Mobilization; Disorders of Sexual Development.

## M-385. Reconstructive Surgery and Patients with Spinal Cord Injury: Perioperative Considerations for the Plastic Surgeon.

Jacqueline S. Israel, Anna R. Carlson, Laura A. Bonneau, Steve J. Kempton, Timothy W. King, Michael L. Bentz and Ahmed M. Afifi

*Journal of Plastic Surgery and Hand Surgery; 50: 44-49 (2016) IF: 0.791*

**Background** : Patients with spinal cord injury (SCI) requiring reconstructive surgery; particularly for pressure ulcers; are ubiquitous in Plastic and Reconstructive Surgery practices. Much of the current literature focuses on operative techniques; antibiotic indications; sitting protocols; and dressing and bedding choices. **Methods:** This paper reviews normal neuroanatomy; outlines changes in neurophysiology observed in spinal cord injury; and addresses concepts related to perioperative care that are highly relevant but often under-emphasised. **Results**: Vascular disturbances such as autonomic dysreflexia and orthostatic hypotension are dangerous phenomena occurring in this patient population that; if not properly recognised and treated; may result in complications such as haematoma; flap loss; inadequate tissue perfusion; and death. The management of spasticity; deep venous thrombosis; and perioperative pain are also relevant and discussed in this paper. **Conclusion:** A basic understanding of these concepts is essential for the Plastic Surgeon involved in the care of patients with SCI and pressure ulcers; particularly before and after debridement or reconstruction.

**Keywords: :** Autonomic Dysreflexia; Neuropathic Pain; Pressure Ulcer; Reconstructive; Spinal Cord Injury.

## M-386. Is Peripheral Arterial Disease Associated with Carotid Artery Disease in Egyptians? A Pilot Study.

Ahmed Sayed, Sandra M. Ahmed, Ahmed M. Abdelalim, Martin Nagah and Hussein Khairy

*The Egyptian Journal of Neurology; Psychiatry and Neurosurgery; 53: 12-18 (2016)*

**Background**: Atherosclerosis involves various vascular segments. The association of carotid artery disease (CAD) to peripheral arterial disease (PAD) is not well investigated in Egyptian patients. Objective In this pilot study; our aim was to examine the relationship between PAD and CAD in an Egyptian population. Patients and methods We examined 37 consecutive patients with PAD for the presence of CAD. Vascular and neurologic examination and duplex assessment of extracranial

and intracranial carotid system and ankle–brachial index measurement were carried out to determine whether CAD is symptomatic or not. **Results** CAD was found in 20 (54.1%) patients. Eight (21.6%) patients had signifi cant extracranial internal carotid stenosis and 13(37%) had intracranial stenosis and were more signifi cantly above the age of 60 years. All patients with intracranial stenosis were men. PAD with RC6 was signifi cantly associated with cerebrovascular events (P = 0.001) and signifi cant extracranial stenosis (P = 0.013) and intracranial internal carotid stenosis (P = 0.001). **Conclusion** Intracranial and extracranial carotid stenoses are commonly present in patients with critical PAD. Duplex ultrasound screening for CAD presence and severity may be of great benefi t; especially in the elderly and patients with critical limb ischemia. These fi ndings need to be further confi rmed in a study on larger population of Egyptians.

**Keywords:** Carotid Stenosis Intracranial Stenosis; Peripheral Arterial Disease

***Dept. of Urology Dept***

## M-387. Reoperations Following Robot-Assisted Radical Cystectomy: A Decade of Experience.

Ahmed A. Hussein, Zishan Hashmi, Seyedeh Dibaj, Tareq Altartir, Thomas Fiorica, Joseph Wing, Mohammad Durrani, John Binkowski, Lesley Boateng, Gregory Wilding and Khurshid A. Guru

*The Journal of Urology; 195: 1368-1376 (2016) IF: 4.7*

**Purpose:** There is a paucity of data regarding the operative management of complications after robot-assisted radical cystectomy. We reviewed operative management of robot-assisted radical cystectomy specific complications during our 10-year experience with this procedure and assessed the feasibility; safety and outcomes of robot-assisted reoperations. **Materials and Methods**: We retrospectively reviewed the records of all patients who underwent surgical interventions for robot-assisted radical cystectomy specific complications between 2005 and 2015. Univariable and multivariable logistic regression models were fit to evaluate predictors of surgical intervention after robot-assisted radical cystectomy. Kaplan-Meier curves were used to describe time to surgical interventions. **Results:** A total of 92 patients (23%) underwent surgical intervention after robotassisted radical cystectomy. Mean followup was 27 months. Average time to any surgical intervention after cystectomy was 14 months. The reoperation rate was 5%; 2% and 16% at 30; 31 to 90 and greater than 90 days; respectively. Using the Kaplan-Meier method surgical interventions occurred at a rate of 30% at 2 years and 46% at 5 years. Interventions for ureteroileal complications were the most common (48 cases) followed by interventions for bowel obstruction; fistulas and abdominal wall related complications (11 cases). Clavien 3 or greater complications and neoadjuvant chemotherapy were associated with surgical intervention. **Conclusions:** Even in experienced hands the long-term complications of robotassisted radical cystectomy are notable. of our patients 23% required surgical interventions after the procedure. Our initial experience with robot-assisted management of robot-assisted radical cystectomy complications appears safe and feasible; although the decision to proceed is determined primarily by surgeon experience.

**Keywords:** Urinary Bladder Neoplasms; Cystectomy; Robotic Surgical Procedures; Complications; Reoperation.

## M-390. Technical Mentorship During Robot-Assisted Surgery: A Cognitive Analysis.

Ahmed A. Hussein, Somayeh B. Shafiei, Mohamed Sharif, Ehsan Esfahani, Basel Ahmad, Justen D. Kozlowski, Zishan Hashmi and Khurshid A. Guru

*BJU International; 118: 429-436 (2016) IF: 4.387*

**Objective** To investigate cognitive and mental workload assessments; which may play a critical role in defining successful mentorship. **Materials and Methods** The 'Mind Maps' project aimed at evaluating cognitive function with regard to surgeon's expertise and trainee's skills. The study included electroencephalogram (EEG) recordings of a mentor observing trainee surgeons in 20 procedures involving extended lymph node dissection (eLND) or urethrovesical anastomosis (UVA); with simultaneous assessment of trainees using the National Aeronautics and Space Administration Task Load index (NASA-TLX) questionnaire. We also compared the brain activity of the mentor during this study with his own brain activity while actually performing the same surgical steps from previous procedures populated in the 'Mind Maps' project. **Results** During eLND and UVA; when the mentor thought the trainee's mental demand and effort were low based on his NASA-TLX questionnaire (not satisfied with his performance); his EEG-based mental workload increased (reflecting more concern and attention). The mentor was mentally engaged and concerned while he was engrossed in observing the surgery. This was further supported by the finding that there was no significant difference in the mental demands and workload between observing and operating for the expert surgeon. **Conclusions** This study objectively evaluated the cognitive engagement of a surgical mentor teaching technical skills during surgery. The study provides a deeper understanding of how surgical teaching actually works and opens new horizons for assessment and teaching of surgery. Further research is needed to study the feasibility of this novel concept in assessment and guidance of surgical performance.

**Keywords:** Cognition; Assessment; Training; Surgery; Robot-Assisted; Eeg.

## M-388. Ambulatory Movements; Team Dynamics and Interactions During Robot-Assisted Surgery.

Nabeeha Ahmad, Ahmed A. Hussein, Lora Cavuoto, Mohamed Sharif, Jenna C. Allers, Nobuyuki Hinata, Basel Ahmad, Justen D. Kozlowski, Zishan Hashmi, Ann Bisantz and Khurshid A. Guru

*BJU International; 118: 132-139 (2016) IF: 4.387*

**Objective** To analyse ambulatory movements and team dynamics during robot-assisted surgery (RAS); and to investigate whether congestion of the physical space associated with robotic technology led to workflow challenges or predisposed to errors and adverse events. Methods With institutional review board approval; we retrospectively reviewed 10 recorded robot-assisted radical prostatectomies in a single operating room (OR). The OR was divided into eight zones; and all movements were tracked and described in terms of start and end zones; duration; personnel and purpose. Movements were further classified into avoidable (can be eliminated/improved) and unavoidable (necessary for completion of the procedure). **Results** The mean operating time was 166 min; of which

ambulation constituted 27 min (16%). A total of 2 896 ambulatory movements were identified (mean: 290 ambulatory movements/procedure). Most of the movements were procedure-related (31%); and were performed by the circulating nurse. We identified 11 main pathways in the OR; the heaviest traffic was between the circulating nurse zone; transit zone and supply-1 zone. A total of 50% of ambulatory movements were found to be avoidable. **Conclusion** More than half of the movements during RAS can be eliminated with an improved OR setting. More studies are needed to design an evidence-based OR layout that enhances access; workflow and patient safety.

**Keywords:** Disruption; Error; Layout; Operating Time; Robot; Robotic Surgery; Surgical Flow.

## M-389. Outcomes of Living Donor Renal Transplantation in Children with Lower Urinary Tract Dysfunction: A Comparative Retrospective Study.

Ismail R. Saad, Enmar Habib, Mohammed S. ElSheemy, Mahmoud Abdel-Hakim, Mostafa Sheba, Aziz Mosleh, Doaa M. Salah, Hafez Bazaraa, Fatina I. Fadel, Hany A. Morsi and Hesham Badawy

*Bju International; 118(2): 320-326 (2016) IF: 4.387*

**Objectives** To compare outcomes of renal transplantation (RTx) in children with end-stage renal disease (ESRD) resulting from lower urinary tract dysfunction (LUTD) vs other causes. **Patients and Methods** A database of children (<18 years old) who underwent RTx between May 2008 and April 2012 was reviewed. Patients were divided into those with LUTD (group A; n = 29) and those with other causes of ESRD (group B; n = 74). RTx was performed after achieving low intravesical pressure (<30 cmH2O) with adequate bladder capacity and drainage. The groups were compared using Student's t-test; Mann– Whitney; chi-squared or exact tests. Graft survival rates (GSRs) were evaluated using Kaplan–Meier curves and the log-rank test. **Results** The mean SD (range) age of the study cohort was 5.05 12.4 (2.2–18) years. Causes of LUTD were posterior urethral valve (PUV; 41.4%); vesico-ureteric reflux (VUR; 37.9%), neurogenic bladder (10.3%); prune belly syndrome (3.4%), obstructive megaureter (3.4%) and urethral stricture disease(3.4%). There was no significant difference in age; dialysis duration or donor type. In group A; 25 of the 29 patients (86.2%) underwent ≥1 surgery to optimize the urinary tract for allograft. Pretransplant nephrectomy was performed in 15 of the 29 patients (51.7%); PUV ablation in nine patients (31%) and ileocystoplasty in four patients (13.7%). The mean SD follow-up was 4.52 1.55 and 4.07 1.27 years in groups A and B; respectively. There was no significant difference in creatinine and eGFR between the groups at different points of follow-up. The GSRs at the end of the study were 93.1 and 91.1% in groups A and B; respectively (P = 1.00). According to Kaplan–Meier survival curves; there was no significant difference in the GSR between the groups using the log-rank test (P = 0.503). No graft was lost as a result of urological complications. In group B; one child died from septicaemia. The rate of urinary tract infections was 24 and 12% in groups A and B; respectively; but was not significant. No significant difference was found between the groups with regard to the incidence of post-transplantation hydronephrosis. of the 22 patients who had hydronephrosis after transplantation; three were complicated by UTI. Injection of bulking agents was required in two patients for treatment of grade 3 VUR. In the third patient; augmentation cystoplasty was needed. **Conclusion** Acceptable graft function; survival and UTI rates can be achieved in children with ESRD attributable to LUTD. Thorough assessment and optimization of LUT; together with close follow-up; are key for successful RTx.

**Keywords:** Renal Transplantation; Live Donor; Lower Urinary Tract Dysfunctions; Children.

## M-391. A Prospective Evaluation of High-Resolution Ct Parameters in Predicting Extracorporeal Shockwave Lithotripsy Success for Upper Urinary Tract Calculi.

Mahmoud Abdelhamid, Ashraf A. Mosharafa, Hamdy Ibrahim, Hany M. Selim, Mohamed Hamed, Mohamed N. Elghoneimy, Hosny K. Salem, Mohamed S. Abdelazim and Hesham Badawy

*Journal of Endourology; 30: 1227-1232 (2016) IF: 2.107*

**Objective:** To evaluate the ability of noncontrast CT parameters (stone size; stone attenuation; and skin-to-stone distance [SSD]) to predict the outcome of extracorporeal shockwave lithotripsy (SWL) in a prospective cohort of patients with renal and upper ureteric stones. **Patients and Methods:** Patients with stones 5 to 20 mm were prospectively enrolled from 2011 to 2014. Patients had NCCT with recording of stone size; stone mean attenuation; and SSD; as well as various stone and patient parameters. The numbers of needed sessions as well as the final outcome were determined; with SWL failure defined as residual fragments >3 mm. Predictors of SWL failure were assessed by multiple regression analysis. **Results:** Two hundred twenty patients (mean ± standard deviation [SD] age 41.5 ± 12.4 years) underwent SWL. Mean ± SD stone size was 11.3 ± 4.1 mm; while mean ± SD stone attenuation was 795.1 ± 340.4 HU. Mean ± SD SSD was 9.4 ± 2.1 cm. The average number of sessions was 1.64. SWL was effective in 186 (84.5%) patients (group A); while 34 (15.5%) patients had significant residual fragments (>3 mm). On univariate analysis; predictors of SWL failure included stone attenuation >1000 HU; older age; higher body mass index; higher attenuation value; larger stone size; and longer SSD. Increased SSD and higher stone attenuation retained their significance as independent predictors of SWL failure ($p < 0.05$) on multiple regression analysis both after first session and as final SWL outcome. A positive correlation was found between number of SWL sessions and mean stone attenuation ($r = 0.6$; $p < 0.001$) and SSD ($r = 4$; $p < 0.001$). **Conclusions:** Stone mean attenuation and SSD on noncontrast CT are significant independent predictors of SWL outcome in patients with renal and ureteric stones. These parameters should be included in clinical decision algorithms for patients with urolithiasis. For patients with stones having mean attenuation of >1000 HU and/or large SSDs; alternatives to SWL should be considered.

**Keywords:** Computed Tomography; Stone Attenuation; Urinary Calculi.

## M-392. The Loud Surgeon Behind the Console: Understanding Team Activities During Robot-Assisted Surgery.

Judith Tiferes, Ahmed A. Hussein, Ann Bisantz, Justen D. Kozlowski, Mohamed A. Sharif, Nathalie M. Winder, Nabeeha Ahmad, Jenna Allers, Lora Cavuoto and Khurshid A. Guru

*Journal of Surgical Education; 73: 504-512 (2016) IF: 1.95*

**Objectives**: To design a data collection methodology to capture team activities during robot-assisted surgery (RAS) (team communications; surgical flow; and procedural interruptions); and use relevant disciplines of Industrial Engineering and Human Factors Engineering to uncover key issues impeding surgical flow and guide evidence-based strategic changes to enhance surgical performance and improve outcomes. **Design:** Field study; to determine the feasibility of the proposed methodology. **Setting:** Recording the operating room (OR) environment during robot-assisted surgeries (RAS). The data collection system included recordings from the console and 3 aerial cameras; in addition to 8 lapel microphones (1 for each OR team member). Questionnaires on team familiarity and cognitive load were collected. **Participants:** In all; 37 patients and 89 OR staff members have consented to participate in the study. **Results**: Overall; 37 RAS procedures were recorded (130 console hours). A pilot procedure was evaluated in detail. We were able to characterize team communications in terms of flow; mode; topic; and form. Surgical flow was evaluated in terms of duration; location; personnel involved; purpose; and if movements were avoidable or not. Procedural interruptions were characterized according to their duration; cause; mode of communication; and personnel involved. **Conclusion**: This methodology allowed for the capture of a wide variety of team activities during RAS that would serve as a solid platform to improve nontechnical aspects of RAS.

**Keywords:** Communication; Team Interactions, Robot-Assisted Surgery, Non Technical Skills; Flow; Interruptions.

## M-393. Lower Calyceal and Renal Pelvic Stones in Preschool Children: A Comparative Study of Mini-Percutaneous Nephrolithotomy Versus Extracorporeal Shockwave Lithotripsy.

Mohammed S ElSheemy, Kareem Daw, Enmar Habib, Waseem Aboulela, Hesham Fathy, Ahmed M Shouma N, Mohamed El Ghoneimy, Ahmed I Shoukry, Hany A Morsi and Hesham Badawy

*International Journal of Urology;23;(7):564-570(2016)IF:1.878*

**Objectives:** To compare outcomes of the mini-percutaneous nephrolithotripsy technique and extracorporeal shockwave lithotripsy for lower calyceal and renal pelvicstones in preschool children. **Methods:** From January 2010 to December 2014; single renal pelvic or lower calycealcalculi 10–25 mm in size in children (age ≤6 years) treated by either extracorporeal shockwave lithotripsy (64 patients) or the mini-percutaneous nephrolithotripsy technique (54 patients) were included. Extracorporeal shockwave lithotripsy was carried out byusing a Dornier electromagnetic lithotripter. The mini-percutaneous nephrolithotripsytechnique was through 14-Fr renal access using a 9.5-Fr semirigid ureteroscope withholmium:yttrium aluminium garnet lithotripsy. The two study groups were comparedusing Mann–Whitney; v2-test or Fisher's exact test.**Results:** Stone parameters were similar in the mini-percutaneous nephrolithotripsy technique and extracorporeal shockwave lithotripsy groups in all patients; and in thepelvic (39 Miniperc; 52 extracorporeal shockwave lithotripsy) and lower calyceal (15Miniperc; 12 extracorporeal shockwave lithotripsy) subgroups. Stone-free rates in themini-percutaneous nephrolithotripsy technique and extracorporeal shockwave lithotripsygroups were 88.9% versus 43.8% ($P < 0.001$) and 94.4% versus 81.2% ($P = 0.032$) afterfirst and last sessions; respectively. In the renal pelvis; they were 87.2% versus 50%($P < 0.001$) and 94.9% versus 84.6% ($P = 0.179$); whereas in the lower calyx; they were93.3% versus 16.7% ($P < 0.001$) and 93.3% versus 66.7% ($P = 0.139$) after first and lastsessions; respectively. Retreatment rates in the mini-percutaneous nephrolithotripsytechnique versus extracorporeal shockwave lithotripsy were 7.4% versus 50% ($P < 0.001$),7.7% versus 46.2% ($P < 0.001$); and 6.7% versus 66.7% ($P = 0.003$) in all patients; renalpelvic and lower calyceal stones; respectively. No significant difference was found incomplications ($P = 0.521$). Auxiliary procedures were required in 9.4% and 1.9% ofchildren in the extracorporeal shockwave lithotripsy and mini-percutaneous nephrolithotripsy technique groups; respectively. **Conclusions:** The mini-percutaneous nephrolithotripsy technique has significant lyhigher stone-free rates than extracorporeal shockwave lithotripsy for renal pelvic andlower calyceal stones (10–25 mm); with a lower retreatment rate and without asignificant increase in complications.

**Keywords:** Lower Calyx; Miniperc; Preschool Children; Renal Calculi; Shockwave Lithotripsy

## M-394. Effect of Endourological Procedures on Erectile Function: A Prospective Cohort Study.

Ashraf Mosharafa, Mahmoud Abd El Hamid, Mohamed Tawfik and Omar Abd El Rzzak

*International Urology and Nephrology; 48 (2016) IF: 1.292*

**Introduction** Many patients offered endourological procedures are concerned about potential sexual dysfunction following endoscopy; and there are scarce published data to support an evidence-based response. We aim to assess possible effects of endourological procedures on sexual activity and erectile function. Patients and methods Sexually active men undergoing cystoscopy and/or upper tract endourological procedures were enrolled and evaluated using the IIEF-5 score and the IPSS; filled the day before and 10 days and 45–60 days after the procedure. Patients' characteristics (age; chronic medical condition; smoking; and medications) were recorded. The primary outcome was the change in the IIEF-5 score. **Results** One hundred patients aged 24–60 years (mean 37.4) underwent endourological procedures (42 PCNLs; 30 ureteroscopies; 22 retrograde ureteropyelographies ± stenting; and 6 cystolitholapaxies) between January and August 2014. Preoperative IPSS ranged from 0 to 32 (mean [SD] 11.93 [8.64]); while IIEF-5 ranged from 14 to 25 (mean [SD] 21.63 [2.96]); with eight patients in the mild to moderate (12–16) ED range; 31 mild ED (17–21); and 59 no ED (22–25). Following the procedure; the IPSS improved (mean IPSS down from 11.9 to 6.1 at 10 days and 6.2 at 45 days; $P < 0.001$); while the IIEF remained unchanged [21.6 preoperative to 21.0 at 10 days ($P = 0.43$) and 21.7 at 45 days ($P = 0.81$)]. Patients with indwelling ureteric stents (28 patients) had significant LUTS

postoperatively with a mean [SD] IPSS of 9.8 [7.2] at 10 days and 11.6 [7.8] at 45 days. The IIEF-5 score was not affected with a mean [SD] of 21.5 [3.3] at 10 days and 21.8 [3.1] at 45 days; compared to 22.0 [3.0] preoperatively (P = 0.44). **Conclusion** Endoscopic procedures did not negatively impact erectile function and sexual activity.
**Keywords:** Erectile Function; Endourology; Iief; Stents.

## M-395. Technical Refinements to Improve Outcomes Following Distal Hypospadias Repair.

John M. Lacy, Lauren N. Hendrix, Raevti Bole, MA, Enmar Habib, Cole W. Wootton and Ali M. Ziada

*Canadian Journal of Urology; 23(1): 8184-8187 (2016) IF: 1.006*

Hypospadias complications; most notably meatal stenosis; are commonly reported to occur after tubularized incised plate (TIP) hypospadias repair. We focus on a point of technique in TIP repair and its effect on outcome of this possible complication; as well as other commonly reported complications. Meatal stenosis after TIP can be avoided if the urethra and overlying glans are dissected and sutured separately with no attempt at cross suturing whether the urethra ends below; behind; or above the glans sutures. This hypothesis was evaluated by a prospective data collection before and after implementation to evaluate the effect of a technical refinement on rates of meatal stenosis in TIP hypospadias repair.All cases of coronal to midpenile hypospadias repair during two periods were included in our study. Group 1 included 140 consecutive patients over a 30 month period. Group 2 included 122 consecutive patients over a 36 month period during which the above mentioned technical changes were implemented by all participating pediatric urologists. Rates of complications between the two groups were compared with special emphasis on meatal stenosis.Median follow up for both groups was > 1 year. Overall complication rate in Group 1 was 31.5% compared to 9.8% in Group 2. Meatal stenosis was significantly reduced from 13 patients (9.3%) in Group 1 to 2 patients (1.6%) in Group 2; p = 0.008.The technical refinements described resulted in reduction of complication rates and a decrease in incidence of meatal stenosis.
**Keywords:** Meatal Stenosis; Hypospadias; Pediatric Urology; Reconstruction; Urethra.

## M-397. Conservative Management of Colonic Injury During Percutaneous Nephrolithotomy.

M. Elghoneimy, M. Abdel-Rassoul, H. Elfayoumy and A. Mosharafa

*African Journal of Urology; 22: 101-105 (2016)*

**Objectives** Colonic injury is a rare but serious complication of percutaneous renal surgery. Its clinical course may be elusive and an awareness of the various presentations is of great importance. We describe how early diagnosis and a diligent conservative approach have resulted in a favorable outcome in our series. Patients and methods From 2005 to 2015; 2150 percutaneous nephrolithotomy (PNL) procedures were performed in our center. Patients' records were searched for the occurrence of colonic injury. Records were reviewed and we report on the preoperative data; the clinical presentation and the management approach in these cases. **Results** Three patients (0.14%) were identified with colonic injury following PNL; the three injuries were in male patients with a median age of 36.6 (range 28–45 years). Two injuries were on the left side and one on the right. Two of our patients had a low BMI. The renal puncture was in the lower posterior calyx in two and in the middle calyx in one. The diagnosis was established postoperatively in all and confirmed using antegrade or retrograde pyelography. All patients were managed conservatively with a favorable outcome. **Conclusion** An approach combining a high degree of suspicion for early diagnosis and a diligent conservative management results in a favorable outcome in patients with colonic injury during PNL.
**Keywords:** Percutaneous Nephrolithotomy; Complication; Colonic Injury; Urolithiasis; Kidney Calculi.

## M-396. Fertility Preservation Options for Prepubertal Boys Facing Gonadotoxic Therapies.

Ahmed Hussein, Pamel Yango, Youseff Ezz, James Smith and Nam D Tran

*Minerva Ginecologica; 68: 668-674 (2016).*

Infertility is a common disease affecting 10-15% of reproductive couples with significant psychological and financial impacts to both patients and society. Approximately 80 million people worldwide are infertile; with an increasing incidence of male infertility. Semen cryopreservation in adults is a proven method of fertility preservation for male patients undergoing gonadal toxic therapies. Unlike adults who can cryopreserve sperm at any time prior to gonadal toxic treatments; there are no effective fertility preservation options for children undergoing cancer treatment; a time when semen cryopreservation is not feasible. Thus; most of the childhood cancer survivor will develop irreversible azoospermia due to the gonadal toxicity of the treatment on spermatogononial stem cells. This review will summarize the possible options and challenges of fertility preservation in this vulnerable population.
**Keywords:** Fertility Preservation; Gonadotoxic Therapy; Sperm; Spermatogonial Stem Cell.

## Faculty of Oral Dental Medicine

### *Dept. of Dental Material*

### M-398. Color-Matching and Blending-Effect of Universal Shade Bulk-Fill-Resin-Composite in Resin-Composite-Models and Natural Teeth

Rasha M. Abdelraouf and Nour A. Habib

*Biomed Research International, 1-8(2016) IF: 2.134*

**Objectives**: To assess visually color-matching and blending-effect (BE) of a universal shade bulk-fill-resin-composite placed in resin-composite-models with different shades and cavity sizes and in natural teeth (extracted and patients' teeth). **Materials and Methods.** Resin-composite-discs (10 mm × 1 mm) were prepared of universal shade composite and resin-composite of shades: A1, A2, A3, A3.5, and A4. Spectrophotometric-color-measurement was performed to calculate color-difference (Δ□) between the universal shade and shaded-resin-composites discs and determine their translucency-parameter (TP). Visual assessment was performed by seven normal-color-vision-observers to determine the color-matching between the universal shade and each shade, under Illuminant D65. Color-matching visual scoring (VS) values were expressed numerically (1–5): 1: mismatch/totally unacceptable, 2: Poor-Match/hardly acceptable, 3: Good-Match/acceptable, 4: Close-Match/small-difference, and 5: Exact-Match/no-color-difference. Occlusal cavities of different sizes were prepared in teeth-like resin-composite-models with shades A1, A2, A3, A3.5, and A4. The cavities were filled by the universal shade composite. The same scale was used to score color-matching between the fillings and composite-models. BE was calculated as difference in mean-visual-scores in models and that of discs. Extracted teeth with two different class I-cavity sizes as well as ten patients' lower posterior molars with occlusal caries were prepared, filled by universal shade composite, and assessed similarly. **Results.** In models, the universal shade composite showed close matching in the different cavity sizes and surrounding shades ($4 \leq VS < 5$)) (BE = 0.6–2.9 in small cavities and 0.5–2.8 in large cavities). In extracted teeth, there was good-to-close color-matching (VS = 3.7–4.4 in small cavities, BE = 2.5–3.2) (VS = 3–3.5, BE = 1.8–2.3 in large cavities). In patients' molars, the universal shade composite showed good-matching (VS = 3–3.3, BE = −0.9–2.1). **Conclusions:** Color-matching of universal shade resin-composite was satisfactory rather than perfect in patients' teeth.
**Keywords:** Color matching; Blending effect; Universal shade; Bulk fill; Resin composite.

### *Dept. of Oral and Maxillofacial Surgery*

### M-399. Long-Term Effectiveness of the Pedicled Buccal Fat Pad in the Closure of a Large Oroantral Fistula

Emad T. Daif

*Journal of Oral and Maxillofacial Surgery, 74: 1718-1722 (2016) IF: 1.631*

**Purpose**: This study evaluated the long-term effectiveness of the pedicled buccal fat pad (BFP) in the closure of a large oroantral fistula (OAF). **Materials and Methods:** Twenty-five consecutive patients with OAFs larger than 5 mm were treated with a pedicled BFP. They were followed clinically and radiographically for 10 years after surgery to monitor the durability and effectiveness of the pedicled BFP in the closure of the OAF. **Results:** The procedure was successful in all patients. The healing process was satisfactory, with no breakdown or liquefaction necrosis postoperatively. No complications were observed during the follow-up period. **Conclusions:** The results of this study support the view that the use of the pedicled BFP is a durable, straightforward, convenient, and reliable method for the treatment of a large OAF.
**Keywords**: Pedicled buccal fat pad; Oro-antral fistula.

### M-400. Correlation of Age, Sex, and Location with Recurrence of Oral Giant Pyogenic Granuloma After Surgical Excision

Emad Tawfik Daif

*Journal of Craniofacial Surgery, 27: 0-0 (2016) IF: 0.7*

**Objectives**: This study was carried out to correlate age and sex of the patient as well as location of the oral giant pyogenic granuloma (PG) with the recurrence rate after surgical excision. **Methods:** Seventy-two patients having oral giant PGs were treated by a conservative surgical excision. Information on sex, age, lesion site, and recurrence was collected. Data were reviewed and analyzed to correlate the recurrence rate with sex and age of the patient as well as the location of the lesion. **Results:** Recurrence of the oral giant PG was occurred in 22.2% of patients. The highest rates of recurrence were observed in the third (33.3%) and fourth (19%) decades of life. The recurrence rate was more common in females (24%) than males (18.2%) and it was predominant in mandibular lesions (25%) than maxillary one (8.3%). **Conclusions:** On the basis of their results the authors concluded that recurrence of oral giant PG has an obvious correlation with age and sex of the patient as well as location of the lesion.
**Keywords:** Inflammatory hyperplasia; Oral pyogenic granuloma; Recurrence rate.

### *Dept. of Oral Medicine and Periodontology*

### M-401. Serum and Salivary Levels of Chemerin and Mmp-9 in Oral Squamous Cell Carcinoma and Oral Premalignant Lesions.

Noha A. Ghallab and Olfat G. Shaker

*Clinical Oral Investigations, May: 1-11 (2016) IF: 2.207*

**Objectives**: The objective of this study was to investigate serum and salivary levels of chemerin and MMP-9 as early diagnostic biomarkers for patients with oral premalignant lesions (OPMLs) and oral squamous cell carcinoma (OSCC). **Methods:**This study included 45 individuals; 15 healthy control, 15 patients with OPMLs, and 15 patients with early stage OSCC. Chemerin and MMP-9 were determined in serum and saliva samples utilizing enzyme-linked immunosorbent assays. **Results:**Serum and salivary levels of chemerin and MMP-9 in patients with OSCC were significantly higher than OPMLs and control group. Patients with OPMLs showed also elevated profiles for serum and salivary chemerin and MMP-9 compared to control group. Receiver operator characteristic curve analysis revealed that all tested biomarkers have 100 % sensitivity and 100 % specificity with area under the curve (AUC) of 1.00 in detecting early stage OSCC and OPMLs. In distinguishing OSCC from OPMLs,

salivary MMP-9, serum chemerin, and salivary chemerin showed AUC of 0.99, 0.92, and 0.88, respectively, showing higher sensitivity and specificity compared with serum MMP-9 (AUC; 0.6) which failed to differentiate between the two conditions. **Conclusion:**Chemerin and MMP-9 might be considered as salivary diagnostic biomarkers for OPMLs and early detection of OSCC and also for detecting early cancerization of OPMLs. **Clinical Relevance:** This research implied that salivary chemerin was a novel diagnostic factor for patients with OPML and early stage OSCC patients, and chemerin could be a new therapeutic target for regulating cancer angiogenesis and blocking malignization of OPMLs.
**Keywords:** Angiogenesis; Chemerin; MMP-9; Oral squamous Cell carcinoma; Premalignant; Saliva.

## M-402.Malondialdehyde, Superoxide Dismutase and Melatonin Levels in Gingival Crevicular Fluid of Aggressive and Chronic Periodontitis Patients

NA Ghallab, E Hamdy and OG Shaker

*Australian Dental Journal, 61, (1): 53-61 (2016) IF: 1.272*

**Background** The aim of this study was to investigate malondialdehyde (MDA), superoxide dismutase (SOD) and melatonin levels in the gingival crevicular fluid (GCF) of patients with chronic periodontitis (CP) and generalized aggressive periodontitis (GAgP) as biomarkers for oxidative stress. **Methods** The study comprised 65 subjects: 15 healthy individuals, 25 CP patients and 25 GAgP patients. Plaque index, gingival index, pocket depth, clinical attachment level measurements and GCF samples were obtained from all subjects. MDA, SOD and melatonin levels were determined utilizing enzyme-linked immunosorbent assay. **Results** GCF-MDA levels were significantly higher in the GAgP group compared to the CP and control groups ($p < 0.001$) and significantly higher in the CP group than the C group ($p < 0.001$). SOD and melatonin GCF levels were significantly higher in the control than the GAgP and CP groups ($p < 0.05$), and significantly lower in the GAgP than the CP group ($p < 0.05$). The CP group demonstrated a significant negative correlation between GCF-MDA and melatonin concentrations. A positive correlation was observed between SOD and CAL in the CP group and PD in the GAgP group. **Conclusions** MDA, melatonin and SOD could be considered as biomarkers for oxidative stress in periodontal diseases and might be useful diagnostic aids in distinguishing CP and GAgP patients.
**Keywords:** Aggressive periodontitis; ELISA; Malondialdehyde; Melatonin; Superoxide dismutase.

## M-403. Molecular Underpinnings of Corneal Angiogenesis: Advances Over the Past Decade

Nizar Saleh Abdelfattah, Mohamed Amgad, Amira A. Zayed, Heba Hussein and Nawal Abd El-Baky

*International Journal of Ophthalmology, 9(5): 768-779 (2016) IF: 0.939*

The cornea is maintained in an avascular state by maintaining an environment whereby anti-angiogenic factors take the upper hand over factors promoting angiogenesis. Many of the common pathologies affecting the cornea involve the disruption of such equilibrium and the shift towards new vessel formation, leading to corneal opacity and eventually-vision loss. Therefore it is of paramount importance that the molecular underpinnings of corneal neovascularization (CNV) be clearly understood, in order to develop better targeted treatments. This article is a review of the literature on the recent discoveries regarding pro-angiogenic factors of the cornea (such as vascular endothelial growth factors, fibroblast growth factor and matrix metalloproteinases) and anti-angiogenic factors of the cornea (such as endostatins and neostatins). Further, we review the molecular underpinnings of lymphangiogenesis, a process now known to be almost separate from (yet related to) hemangiogenesis.
**Keywords:** Cornea; Neovascularization; Angiogenesis; Lymphangiogenesis; Vascular endothelial growth factor .

### *Dept. of Pedodontics*

## M-404. Comparative Evaluation of Passive, Active, and Passive-Active Distraction Techniques on Pain Perception During Local Anesthesia Administration in Children.

Soad A. Abdelmoniem and Sara A. Mahmoud

*Journal of Advanced Research, 7: 551-556 (2016) IF: 3*

Local anesthesia forms the backbone of pain control techniques and is necessary for a painless dental procedure. Nevertheless, administering a local anesthetic injection is among the most anxiety-provoking procedures to children. This study was performed to compare the efficacy of different distraction techniques (passive, active, and passive-active) on children's pain perception during local anesthesia administration. A total of 90 children aged four to nine years, requiring inferior alveolar nerve block for primary molar extraction, were included in this study and randomly divided into three groups according to the distraction technique employed during local anesthesia administration. Passive distraction **group:** the children were instructed to listen to a song on headphones; Active distraction **group:** the children were instructed to move their legs up and down alternatively; and Passive-active distraction group: this was a combination between both techniques. Pain perception during local anesthesia administration was evaluated by the Sounds, Eyes, and Motor (SEM) scale and Wong Baker FACES® Pain Rating Scale. There was an insignificant difference between the three groups for SEM scale and Wong Baker FACES Pain Rating Scale at $P = 0.743$ and $P = 0.112$ respectively. The examined distraction techniques showed comparable results in reducing pain perception during local anesthesia administration.
**Keywords:** Active; Children; Distraction; Local anesthesia; Pain perception; Passive; Passive-Active.

### *Dept. of Prosthetic Dentistry*

## M-405. A Systematic Review on Immediate Loading of Implants Used to Support Overdentures Opposed by Conventional Prostheses: Factors that Might Influence Clinical Outcomes.

Kostas Zygogiannis, Daniel Wismeijer, Irene H.A. Aartman and Reham B. Osman

*The International Journal of Oral and Maxillofacial Implants, 31: 63-72 (2016) IF: 1.859*

**Purpose:** Different treatment protocols in terms of number, diameter, and suprastructure design have been proposed for immediately loaded implants that are used to support mandibular overdentures opposed by maxillary conventional dentures. The aim of this study was to investigate the influence of these protocols on survival rates as well as clinical and prosthodontic outcomes. **Materials and Methods:** Several electronic databases were searched for all relevant articles published from 1966 to June 2014. Only randomized controlled trials and prospective studies with a minimum follow-up of 12 months were selected. The primary outcomes of interest were the success and survival rates of the implants. Prosthodontic complications were also evaluated. **Results:** Fourteen studies fulfilled the inclusion criteria. of the studies identified, nine were randomized controlled trials and five were prospective studies. The mean follow-up period was 3 years or less for the vast majority of the studies. The reported survival and success rates were comparable to that of conventional loading for most of the included studies. No specific immediate loading protocol seemed to perform better in terms of clinical and prosthodontic outcomes. **Conclusion:** Immediate loading protocols of mandibular overdentures seem to be a viable alternative to conventional loading. It was not possible to recommend a specific treatment protocol related to the number, diameter of the implants, and attachment system used. Long-term, well-designed studies comparing different immediate loading modalities could help to establish a protocol that delivers the most clinically predictable, efficient, and cost-effective outcome for edentulous patients in need of implant overdentures.
**Keywords:** Dental implants; Implant supported/retained overdentures; Immediate loading; Mandible; Systematic review.

## M-406. A Technique for Retrieving Cement-Retained Implant Prostheses

Iman Abd-Elwahab Radi and Adnan Alfahd

*Journal of Prosthetic Dentistry, 116: 848-850 (2016) IF: 1.515*

Lack of retrievability is one of the most important disadvantages of cement-retained implant restorations. A straightforward and cost-effective technique for accessing the abutment screw channel and unscrewing the abutment and cement-retained prosthesis as 1 unit is described. The technique does not jeopardize the integrity of the restoration, screw, abutment, or implant. A guiding acrylic resin index is fabricated for locating and guiding the access to the screw channel of the abutment, provided that the patient's cast with the implant analog is available. The procedure could be extrapolated to computer-aided designed and computer-aided manufactured (CAD-CAM) implant prostheses, whereby a CAD-CAM index could be fabricated on the digital model.
**Keywords:** Cement retained implant prosthesis; Acrylic guide; Retrievability.

## M-407. Effect of Two Different Soft Liners and Thicknesses Mediating Stress Transfer for Immediately Loaded 2-Implant Supported Mandibular Overdentures: A Finite Element Analysis Study

Iman Abd-Elwahab Radi and Nesrin Elmahrouky

*Journal of Prosthetic Dentistry, 116: 356-361 (2016) IF: 1.515*

**Statement of problem**. The use of soft liners as female receptacles for ball attachments retaining immediately loaded implant overdenture has been recommended to enhance osseointegration and provide a shock absorbing effect. However, which liner and which thickness is still unclear. **Purpose.** The purpose of this finite element analysis (FEA) study was to evaluate the effect of a 2- and 4-mm thickness of thermoplastic resin (TRL) and silicone-based liners (SBL) on the displacement and stresses transmitted to immediately loaded implants retaining a mandibular overdenture. Material and methods. Four 3-dimensional (3D) FEA models of a mandibular implant overdenture retained by 2 ball attachments (2 models for each lining material with 2- or 4-mm liner thicknesses) were developed. Implants were placed in the canine regions and surrounded by a 1-mm cylinder of immature bone simulating immediate loading. A vertical and an oblique load of 150 N were applied in the right premolar molar regions. Stresses and displacement were set as output variables. **Results.** Replacing the TRL by the SBL was associated with a decrease in stresses by 73% and in displacement by at least 46%. Increasing the thickness of any liner decreases stresses by 45% during vertical loading and by 25% during oblique loading and decreases displacement by 61.5% during vertical loading and by an average of 32.5% during oblique loading. None of the liners exceeded the experimental risk limits for micromotion at the bone-implant interface (50 mm). **Conclusion.** In immediately loaded mandibular implant overdentures, both SBL and TRL decrease the micromotion of implants and the stresses at the bone-implant interface. However, SBL is more effective. The thickness of both liners seems to play a major role in decreasing the stresses and displacement of periimplant tissues.
**Keywords:** Soft liner; Finite element analysis; Implant retained overdentures; Immediate loading.

## M-408. Effects of Build Direction on the Mechanical Properties of 3D-Printed Complete Coverage Interim Dental Restorations

Nawal Alharbi, Reham Osman and Daniel Wismeijer

*The Journal of Prosthetic Dentistry,115:760-767(2016) IF:1.515*

Statement of problem The application of 3-dimensional printing technology is emerging in dentistry and is being increasingly used to fabricate dental restorations. To date, scientific evidence is lacking regarding the effect of different factors on the mechanical properties of the printed restorations with the additive manufacturing technique. Purpose The purpose of this in vitro study was to evaluate the effect of build direction (layer orientation) on the mechanical properties of a novel 3-dimensionally (3D)-printed dental restorative material. Material and methods Based on the printing direction, 2 groups were tested. In the first group (n=20), the specimens were vertically printed with the layers oriented perpendicular to the load direction. In the second group (n=20), the specimens were horizontally printed with the layers oriented parallel to the load direction. All specimens were fabricated using the DW028D 3D-printer. The specimens were loaded with a universal testing machine at a crosshead speed of 1 mm/min with a 10-kN load cell. The test was performed at room temperature (22°C) under dry testing conditions. The compressive strength was calculated for both groups, and the results were compared using the unpaired t test (α=.05). **Results** The mean ±SD compressive strength for the vertically printed specimens was 297 MPa (±34)

compared with 257 MPa (±41) for the horizontally printed specimens (P=.002). **Conclusions** Within the limitations of this study, the layer orientation was found to influence the compressive strength of the material. Vertically printed specimens with the layers oriented perpendicular to load direction have improved mechanical properties more than horizontally printed specimens with the layers oriented parallel to load direction.

**Keywords:** Additive manufacturing;CAD/CAM; 3D-Printing; Build orientation; Printing direction; Layer orientation; Digital; Provisional dental restoration.

## M-409. Factors Influencing the Dimensional Accuracy of 3D-Printed Full-Coverage Dental Restorations Using Stereolithography Technology

Nawal Alharbi, Reham Osman and Daniel Wismeijer

*The International Journal of Prosthodontics, 29: 503-510 (2016) IF: 1.487*

**Purpose:** The aim of the present study was to evaluate the effect of the build angle and the support configuration (thick versus thin support) on the dimensional accuracy of 3D-printed full-coverage dental restorations. **Materials and Methods:** A full-coverage dental crown was digitally designed and 3D-printed using stereolithography-additive manufacturing (SLA-AM) technology. Nine different angles were used during the build **process:** 90, 120, 135, 150, 180, 210, 225, 240, and 270 degrees. In each angle, the crown was printed using a thin and a thick support type, resulting in 18 specimens. The specimens were digitally scanned using a highresolution optical surface scanner (IScan D104i; Imetric 3D). The dimensional accuracy was evaluated by digital subtraction technique. The 3D digital files of the scanned printed crowns (test model), exported in standard tessellation language (STL) format, were superimposed with the STL file of the designed crown (reference model) using Geomagic Studio 2014 (3D Systems). **Results:** The root mean square estimate value and color map results suggest that the build angle and support structure configuration have an influence on the dimensional accuracy of 3D-printed crown restorations. Among the tested angles, the 120-degree build angle showed a minimal deviation of 0.029 mm for thin support and 0.031 mm for thick support, indicating an accurate fit between the test and reference models. Furthermore, the deviation pattern observed in the color map was homogenously distributed and located further away from the critical marginal area. **Conclusions:** Within the limitations of this study, the selection of build angle should offer the crown the highest dimensional accuracy and self-supported geometry. This allows for the smallest necessary support surface area and decreases the time needed for finishing and polishing. These properties were mostly observed with a build angle of 120 degrees combined with a thin support type

**Keywords:** Additive manufacturing; Stereolithography (SLA); Building orientation; Support type; 3D-Printing dental Restorations.

## M-410. No Clear Evidence of the Effect of Cantilevered Implant Supported Fixed Restorations on the Marginal Bone or the Prosthetic Complications

Iman Abd-Elwahab Radi

*The Journal of Evidence-Based Dental Practice, 16: 53-55 (2016) IF: 1.474*

**Study Selection and Data Extraction** An electronic literature search was conducted by two independent reviewers in the PubMed database for articles written in English from June 2003 to January 2013. The key words used in this search were “dental implant,” “cantilever,” “mesial cantilever,” “distal cantilever,” and “partial fixed prosthesis.” A manual search of implant-related journals, including Clinical Implant Dentistry and Related Research, International Journal of Oral and Maxillofacial Implants, Clinical Oral Implants Research, Implant Dentistry, Journal of Oral Implantology, International Journal of Oral and Maxillofacial Surgery, Journal of Oral and Maxillofacial Surgery, International Journal of Prosthodontics, and Journal of Prosthetic Dentistry, from 2010 to 2013 was also performed. The inclusion criteria were prospective human clinical trials in which implant-supported fixed partial prostheses with cantilevers were studied. Furthermore, the articles included had to display the MBL around the implants supporting these prostheses for at least 12 months after loading, the extension of the cantilever, the type of implant placed supporting the occlusal forces, and the antagonist dentition (natural dentition, removable prosthesis, fixed prosthesis, or implant-supported prosthesis). Case reports, systematic reviews, animal studies, and those studies in which information was not clear enough or confusing were excluded from this meta-analysis. Moreover, studies including patients who underwent any type of bone augmentation at the implant area were also excluded. Screening by title and abstract and then by full text was carried out. **MainResults and Data Analysis** Only four prospective cohort studies fulfilled the inclusion criteria. For the pooled MBL in cantilevered restorations, random effects meta-analyses of the selectedby methodological differences among studies. For the MBL around implant-supported restorations with and without cantilevers, only two studies were included in the metaanalysis. The weighted mean difference of MBL between the two groups was 0.10 mm (favoring the noncantilever group), with a 95% confidence interval (CI) of 20.18 to 0.39 mm (p 5 0.47), showing no significant difference between two groups. The chi-square test of heterogeneity among the studies was not statistically significant (p 0.97). The most commonly reported complication was fracture of porcelain facings (39.2%). **Conclusion** The dearth of scientific evidence in this matter does not permit clear conclusions to be drawn. However, within the limitations, marginal bone loss does not seem to be influenced by the presence of cantilever extensions. Moreover, minor technical complications were found when a cantilever was present when compared to the control groups.

**Keywords:** Fixed implant prosthesis; Cantilever; Marginal bone loss; Systematic review.

## M-411. No Clear Evidence Regarding the Effect of Osteoporosis on Dental Implant Failure

Ahmed Yaseen Alqutaibi and Iman Abd-Elwahab Radi

*Journal of Evidence-Based Dental Practice, 16: 124-126 (2016)*
*IF: 1.474*

**Selection Criteria**: Electronic searching, with English language restriction, was performed in MEDLINE (via PubMed) and EMBASE databases through May 2014. A manual search was conducted in the electronic databases of four dental implant journals. The Cochrane Central Register of Controlled Trials and ClinicalTrials.gov were also examined Titles and abstracts of the identified articles were read independently by six examiners. Disagreements were resolved by consulting a seventh reviewer. Rejected studies were recorded with the reason for exclusion. The inclusion criteria included case reports, case series, randomized clinical trials (RCTs), and clinical trial studies reporting outcomes from subjects with osteoporosis presenting for oral rehabilitation with dental implants. Studies without follow-up, animal studies, and reviews were excluded from this study. Data were extracted by the authors. Risk of bias was not assessed. Implant failure and histological implant bone contact were the outcomes measured. Neither qualitative nor quantitative syntheses were performed. **Key Study Factor** To examine the effect of osteoporosis and or osteopenia on the implant failure and implant bone contact area. **Main Outcome Measure** Two outcome measures were considered in this systematic review: (1) dental implant failure; and (2) bone-to-implant contact, which was assessed histologically among implants that had been removed due to failure. **Main Results:** Twelve studies were included in the review (6 retrospective studies, 4 case reports, one prospective study and one cross-sectional study). Eight studies reported implant failure (five retrospective studies; one prospective study; one cross-sectional study and one case report). A total of 133 subjects (367 implants) with osteoporosis, 73 subjects (205 implants) diagnosed with osteopenia and 708 healthy subjects (2981 implants) were evaluated. of the total dental implants installed, 40 (10.9%) dental implants were lost in osteoporotic, 17 (8.29%) in osteopenic and 341 (11.43%) in healthy subjects.

**Keywords:** Osteoporosis; Dental implants failure.

## Faculty of Pharmacy

***Dept. of Analytical Chemistry***

### M-412. Screen-Printed Disposable Electrodes: Pharmaceutical Applications and Recent Developments

Heba M. Mohamed

*Trac-Trends in Analytical Chemistry, 82: 1-11 (2016) IF:7.487*

Miniaturization is crucial for the development of the current analytical tools. Several types of disposable electrochemical sensors based on the technology of screen printing have been designed for economic and practical feasibility. In the past few decades, several advances have been made in the setup and assembly of printing materials for screen-printed electrodes (SPEs). Due to their excellent material properties, simplicity, disposability, and short response times, SPEs have been efficiently used for rapid in situ analysis. This review aims to describe the elementary fabrication principles, the different designs of SPEs, and the different analytical methods based on SPEs. We particularly focus on the electrochemical application of SPEs in pharmaceutical analysis, including the determination of drugs, metabolites, and degradation products in different matrices.

**Keywords:** Disposable electrodes; Screen-printed electrodes; Electrochemical applications; Pharmaceutical analysis; Pharmaceutical residues.

### M-413. Just – Dip-it (Potentiometric Ion-Selective Electrode): An Innovative Way of Greening Analytical Chemistry

Mohamed K. Abd El-Rahman, Hala E. Zaazaa, Norhan Badr ElDin and Azza A. Moustafa

*ACS Sustainable Chemistry and Engineering, 4 (6): 3122-3132 (2016) IF: 5.267*

“Green analytical chemistry” (GAC) is a vitalarea towards the concept of sustainability. As a consequence of the widespread application of HPLC in drug-related analytical investigations and the resulting contamination of the environment with organic solvents questions have been raised about the toxicity/greenness of HPLC in the ecosystem. Traditional analytical separation technologies yield approximately 50 mL of waste per analytical data point. To this end, the pharmaceutical community continues to search for greener opportunities to markedly reduce the amount of organic waste produced and move from conventional offline separation based methodologies to greenerin-line alternatives. In this contribution, we’re adopting a“Just-Dip-It”approach with the ultimate goal of advancing and exploiting the potentiometric sensors to their most effective use in different disciplines of drug development. The unique abilities of these ion-selective electrodes (ISEs) for in-line measurements is the key driver for adoption of GAC principles to improve environmental friendliness of the analytical methods. For a meaningful comparison, this work compares the organic waste resulting from ISEs versus HPLC for degradation kinetics monitoring of active pharmaceutical ingredients (APIs) with respect to the 12 principles of GAC. Ipratropium bromide (IP) was chosen as a hydrolyzable anticholinergic drug, and its degradation kinetics were monitored by the two techniques. Thefirst in-line strategy is attained by dipping a highly integrated IP membrane sensor for continuous monitoring of the hydrolysis kinetics of IP by tracing the emf decline over the time scale. The second off-line strategy utilizes a separation-based chromatographic HPLC method via discontinuous tracking the decrease of IP peak area spectroscopically at 220 nm over time. The advantages and shortcomings of each strategy considering GAC principles are highlighted. The merits of these benign real-time analyzers (ISEs) that can deliver equivalent analytical results as HPLC while significantly reducing solvent consumption/waste generation are described. Finally, an applicable strategy for expansion of the Just-Dip-It approach to different disciplines of drug-related analytical investigations is addressed.

**Keywords:** Calix[6]Arene; GAC; HPLC; Hydrolysis kinetics; In-Line monitoring; Ion-Selective electrode; Ipratropium Bromide; Off-Line monitoring.

### M-414. In-Line Potentiometric Monitoring of Dissolution Behavior of Verapamil Hydrochloride Versus Traditional Pharmacopeial Method: A Comparative Study

Eman S. Elzanfaly, Said A. Hassan, Maissa Y. Salem and Badr A. El-Zeany

*Sensors and Actuators B:Chemical,228:587-594(2016)IF: 4.758*

The possibility of obtaining analytical signals without sample pre-treatment or derivatization is the most environmentally friendly method of analysis. In this work a comparison between potentiometric methods and traditional spectrophotometric and HPLC methods for monitoring of dissolution of drugs was established. As an example, an electro-analytical procedure was developed and validated for studying the dissolution of sustained release capsules containing verapamil hydrochloride (VER) by in-line potentiometric measurement system without sample pre-treatment. A sensor was fabricated for determination of VER in its dissolution medium using a poly(vinyl chloride) (PVC) based membrane and tetraphenylborate (TPB) as a cation exchanger. Nitrophenyl octyl ether (NPOE) was used as a plasticizer. The ion pair was obtained in situ by soaking the PVC membranes in 1 × 10−3 mol/L VER solution. The sensor was validated according to the IUPAC recommendations. The proposed sensor showed fast, stable near Nernstian responses across a relatively wide VER concentration range (4 × 10−5 to 1 × 10 −2 mol/L). The dissolution method was developed according to FDA regulations using USP apparatus I, 75 rpm rotation speed, at 37.0 ± 0.5 °C and 1000 ml of water, pH 3.0 (adjusted with 2.0 N HCl) as the dissolution medium. Dissolution profiles were generated over 24 h and compared to those obtained by the official spectrophotometric method. The transpose of a Nikolskii–Eisenman type function performed the conversion of potential to percentage of dissolution. The proposed sensor can be used as bench-top real-time analyzer for in-process tracking of the concentration of VER in monitoring its dissolution and in its pharmaceutical dosage forms. The proposed method was validated and it is considered to be a green eco-friendly technique that neither require sample pre-treatment nor consume any solvents.

**Keywords:** Dissolution monitoring; Green chemistry; In-Line Potentiometry; In-process Monitoring; Real-Time analyzer; Verapamil.

## M-415. Development and Validation of a Modified QuEChERS Protocol Coupled to LC–MS/MS for Simultaneous Determination of Multi-Class Antibiotic Residues in Honey

Amr H. Shendy, Medhat A. Al-Ghobashy, Sohair A. Gad Alla and Hayam M. Lotfy

*Food Chemistry, 190: 982-989 (2016) IF: 4.052*

LC–MS/MS assay was developed and validated according to EU guidelines for determination of nitrofuran metabolites and nitroimidazole residues in honey. Crude samples were acid-treated to liberate matrix-bound residues and a modified QuEChERS protocol was employed. Nitrofurantoin, furazolidone, furaltadone and nitrofurazone were determined via analysis of their metabolites AHD, AOZ, AMOZ and SEM, respectively while nitroimidazole residues; ronidazole (RNZ) and dimetridazole (DMZ) were determined directly. For all analytes, neat standard calibration curves, after correction for matrix effect were successfully employed. Decision limit (CCα) and detection capability (CCβ) were below the MRPL for nitrofurans (1.00 μg kg−1) and the recommended concentration for nitroimidazole (3.00 μg kg−1), respectively. The CCα, CCβ, percentage recovery and CV% ranges were 0.12–0.74 μg kg−1, 0.21–1.27 μg kg−1, 90.96–104.80% and 2.65–12.58%, respectively. This work is part of the national initiative for establishing a national monitoring program for drug residues in Egyptian honey.

**Keywords:**LC–MS/MS; Honey; Veterinary Drug Residues; Nitrofuran; Nitroimidazoles; Ronidazole; Dimetridazole; AHD; AOZ; AMOZ; SEM

## M-416.Simultaneous Determination of 200 Pesticide Residues in Honey Using Gas Chromatography–Tandem Mass Spectrometry in Conjunction with Streamlined Quantification Approach

Amr H. Shendy, Medhat A. Al-Ghobashy, Moustapha N. Mohammed, Sohair A. Gad Alla and Hayam M. Lotfy

*Journal of Chromatography A, 1427: 142-160 (2016) IF: 3.926*

A sensitive, accurate and reliable multi-class GC–MS/MS assay protocol for quantification and confirmation of 200 common agricultural pesticides in honey was developed and validated according to EU guidelines. A modified extraction procedure, based on QuEChERS method (quick, easy, cheap, effective, rugged and safe) was employed. Mass spectrophotometric conditions were individually optimized for each analyte to achieve maximum sensitivity and selectivity in MRM mode. The use of at least two reactions for each compound allowed simultaneous identification and quantification in a single run. The pesticides under investigation were separated in less than 31 min using the ultra-inert capillary column (DB-35MS). For all analytes, neat standard calibration curves in conjunction with correction for matrix effect were successfully employed. The detection limits of the assay ranged from 1.00 to 3.00 ng mL−1 for the studied pesticides. The developed assay was linear over concentration range of 10.00–500.00 ng mL−1, with correlation coefficient of more than 0.996. At the LOQ, 81% of the studied pesticides were efficiently recovered in the range of 70.00–120.00%, with CV% less than 15.00% while 99.3% compounds had mean percentage recovery of 60.00–140.00%, with CV% less than 21.00% (N = 18, over three different days). The proposed assay was successfully applied for the analysis of the studied pesticide residues in one PT sample and 64 commercial honey samples collected over 1 year from different districts around Egypt. Results revealed that only one honey sample out of the 64 analyzed samples was contaminated with tau-Fluvalinate (10.00 μg kg−1). This wide scope assay protocol is applicable for monitoring pesticide residues in honey by national regulatory authorities and accredited labs; that should help ensure safety of such widely used product.

**Keywords:**GC–MS/MS; Honey; Pesticide Residues; Quechers; Multi-Class-Multi-Residue; Egyptian honey.

## M-418. Detection and Characterization of Ponatinib Reactive Metabolites by Liquid Chromatography Tandem Mass Spectrometry and Elucidation of Bioactivation Pathways

Adnan A. Kadi, Hany W. Darwish, Mohamed W. Attwa and Sawsan M. Amer

*Rsc Advances, 6: 72575-72585 (2016) IF: 3.289*

Ponatinib (PNT), as a multi-targeted tyrosine kinase inhibitor, is active against T315I and other BCR-ABL mutants. PNT is registered in the U.S. and EU under the trade name of Iclusig®. The current study reports the identification and characterization of in vitro metabolites of PNT, which were produced by its incubation with rat liver microsomes (RLMs). PNT and its metabolites were extracted from the incubation mixture by the protein precipitation procedure and the supernatants were injected into high performance liquid chromatography tandem mass spectrometry (LC-MS/MS) equipment. Reversed phase liquid chromatography resolved seven in vitro PNT metabolites. Each metabolite displayed one or more metabolic reaction pathways including N-demethylation, N-oxide formation, oxidation, reduction and hydroxylation. Structures of the PNT metabolites showed high liability to form reactive metabolites. Since bioactivation is often speculated to be responsible for observed idiosyncratic toxicities including hepatotoxicity, incubation of PNT with RLMs was carried out in the presence of 1.0 mM GSH or 1.0 mM KCN to check its reactive metabolites. No GSH adduct was found while four cyano adduct metabolites were determined and their structures were proposed based on the mass scan and product ion data for each metabolite.

**Keywords:**BCR-ABL LC-MS/MS Ponatinib.

## M-420.Chromatographic Analysis of Multicomponent Mixture of Vitamins B1, B6, B12, Benfotiamine and Diclofenac; Part Ii: Lc-Tandem Ms/Ms Method for Simultaneous Quantification of Five Components Mixture in Pharmaceutical Formulations and Human Plasma

Ahmed Salah Fayed and Maha Abdel-Monem Hegazy

*Rsc Advances, 6: 39409-39423 (2016) IF: 3.289*

A novel high performance liquid chromatography coupled with tandem mass spectrometry (LC-MS/MS) method was established for the simultaneous determination of multivitamins, namely thiamine hydrochloride (B1), pyridoxine (B6), cyanocobalamin (B12) and benfotiamine (BEN) and their co-

formulated drug, diclofenac sodium (DIC) using torsemide as internal standard (IS). Chromatographic separation was accomplished on Shimadzu LC-20 AT Series HPLC, equipped with Sunfire C18 column (Waters) (50 4.6 mm, 5 mm) using methanol : 0.02 M ammonium acetate (80 : 20, v/v) pH 6.0 for B1, B12, BEN and DIC, while using methanol : acetonitrile : 0.01 M ammonium formate (80 : 10 : 10, v/v/v) pH 6.25 for B6 on separate runs at a flow rate of 1.0 mL min1. Sample preparation involves extraction with methanol using 30 ng mL1 of IS. Electrospray ionization (ESI) source was operated in the positive ion mode. The multiple reaction monitoring (MRM) mode on a triple quadrupole mass spectrometer was used to quantify the drugs utilizing the transitions of 265.07/122.10, 170.01/152.20, 678.64/147.01, 467.18/122.10, 296.02/214.20, 348.99/263.90 (m/z) for B1, B6, B12, BEN, DIC and IS, respectively. The proposed method was effectively applied for the analysis of laboratory prepared mixtures, in spiked human plasma as well as in their combined pharmaceutical formulations. A detailed analytical and bioanalytical validation was conducted in compliance with the FDA and ICH guidelines proving the method to be selective, linear, precise and accurate over the concentration ranges of 0.01–20.00, 0.02–50.00, 15.00–500.00, 5.00–500.00 and 10.00–500.00 ng mL1 for the five compounds, in order. The simplicity and sensitivity of this method allows its use in the quality control of the cited drugs.

**Keywords:** B1; B6; B12; Vitamins; Benfotiamine and Diclofenac.

## M-419.Rapid and Selective Determination of Pitavastatin Calcium in Presence of its Degradation Products and Co-Formulated Drug by First-Derivative Micelle-Enhanced and Synchronous Fluorimetric Methods

Ahmed S. Fayed, Maha A. Hegazy, Enas E. Abbas and Nahla N. Salama

*Rsc Advances, 6 (2016) IF: 3.289*

New spectrofluorimetric methods are presented for the rapid and selective determination of pitavastatin calcium (PIT) in the presence of its hydrolytic degradation products and the co-formulated drug ezetimibe (EZE). In the first method (method A), PIT was determined in the presence of its hydrolytic degradation products by measuring the first derivative (1D) of its enhanced native fluorescence using sodium dodecyl sulfate (SDS) as an anionic micelle enhancer at a pH of 4.1, which was adjusted using Britton–Robinson buffer in aqueous media. PIT was subjected to stress conditions of 5 M hydrochloric acid and 5 M sodium hydroxide. The 1D peak amplitude was measured at a lem of 415 nm using a lex of 252 nm. The effect of different surfactants on the fluorescence of PIT was studied; the quantum yield of PIT was in the following order: SDS (0.30) > cetrimide (0.23) > Tween (0.02). A second method (method B) was developed for the simultaneous determination of PIT and the co-formulated drug EZE in the presence of degradation products of PIT. This method utilized synchronous fluorescence spectroscopy (SFS) in an acetonitrile medium. The wavelengths that were used were lex ¼ 260 nm and lem ¼ 330 and 272 nm for PIT and EZE, respectively, using Dl ¼ 40 nm. Validation of the proposed methods was performed according to the ICH guidelines. The methods were employed for the determination of PIT (methods A and B) and EZE (method B) in bulk powder, pharmaceutical preparations of co-formulated drug substances and laboratory-prepared mixtures containing hydrolytic degradation products of PIT. Statistical analysis proved that the investigated assays were excellent. It was concluded that method A was inexpensive and environmentally friendly.

**Keywords:** Fluorescence; Pitavastatin; First derivative; Micelles

## M-420.Removal of Cationic and Anionic Dyes from Aqueous Solution with Magnetite/Pectin and Magnetite/Silica/Pectin Hybrid Nanocomposites: Kinetic, Isotherm and Mechanism Analysis

Olivia A. Attallah, Medhat A. Al-Ghobashy, Marianne Nebsen and Maissa Y. Salem

*Rsc Advances, 6: 11461-11480 (2016) IF: 3.289*

Novel adsorbents, magnetite nanoparticles modified with pectin shell and silica/pectin double shell, were fabricated and tested for single dye and dye mixture adsorption from water samples. Cationic dyes methylene blue (MB) and crystal violet (CV) and anionic dyes methyl orange (MO) and Eriochrome black T (EBT) were employed to assess dye removal efficiency. The influence of pH, amount of adsorbent, initial dye concentration and contact time was investigated. Results indicated that the optimum pH for removing cationic dyes was 8.0 and 2.0 for anionic dyes. The kinetic studies showed rapid sorption dynamics following a second-order kinetic model. Dye adsorption equilibrium data were fitted well to the Sips isotherm for cationic and anionic dyes. The maximum monolayer capacity, (qmax) for MB, CV, EBT and MO was calculated from Sips as 197.18, 180.29, 65.35 and 26.75 mg g−1 respectively for magnetite/silica/pectin NPs and 168.72, 140.49, 72.35 and 27.22 mg g−1 respectively for magnetite/pectin nanoparticles. For dye mixture adsorption, a new HPLC assay was proposed for quantitation of dyes in treated samples. The results came in accordance with that of single dye adsorption where the magnetite/pectin NPs showed preferred adsorption to anionic dyes while the magnetite/silica/pectin NPs had more affinity to cationic dyes. Thus, our proposed NPs can be used as cheap and efficient adsorbents for removal of cationic and anionic dyes from aqueous solutions.

## M-421. Development and Validation of Sensitive and Rapid UPLC-MS/MS Method for Quantitative Determination of Daclatasvir in Human Plasma: Application to A Bioequivalence Study

Mamdouh R. Rezk, Ehab R. Bendas, Emad B. Basalious and Iman A. Karim

*Journal of Pharmaceutical and Biomedical Analysis, 128: 61-66 (2016) IF: 3.169*

A rapid and sensitive UPLC–MS/MS method was developed and validated for determination of daclatasvir (DAC) in human plasma using sofosbuvir (SOF) as an internal standard (IS). The Xevo TQD LC–MS/MS was operated under the multiple-reaction monitoring mode using electrospray ionization. Precipitation with acetonitrile was used in sample preparation. The prepared samples were chromatographed on Acquity UPLC HSS C18 (50 × 2.1 mm, 1.8 m) column by pumping 10 mM ammonium formate (pH 3.5) and acetonitrile in an isocratic

mode at a flow rate of 0.30 ml/min. Method validation was performed as per the FDA guidelines and the standard curves were found to be linear in the range of 5–4000 ng/ml for DAC. The intra-day and inter-day precision and accuracy results were within the acceptable limits. A very short run time of 1.2 min made it possible to analyze more than 500 human plasma samples per day. The wider range of quantification of DAC allowed the applicability of the developed method for its determination in a bio equivalence study in human volunteers.
**Keywords:** Daclatasvir; UPLC–MS/MS; Plasma; Validation; Pharmacokinetics; Bioequivalence.

## M-422. Validated LC-MS/MS Method for the Quantification of Ponatinib in Plasma: Application to Metabolic Stability

Adnan A. Kadi, Hany W. Darwish, Mohamed W. Attwa and Sawsan M. Amer

*Plos One, 11 (2016) IF: 3.057*

In the current work, a rapid, specific, sensitive and validated liquid chromatography tandem mass-spectrometric method was developed for the quantification of ponatinib (PNT) in human plasma and rat liver microsomes (RLMs) with its application to metabolic stability. Chromatographic separation of PNT and vandetanib (IS) were accomplished on Agilent eclipse plus C18 analytical column (50 mm × 2.1 mm, 1.8 µm particle size) maintained at 21±2°C. Flow rate was 0.25 mLmin-1 with run time of 4 min. Mobile phase consisted of solvent A (10 mM ammonium formate, pH adjusted to 4.1 with formic acid) and solvent B (acetonitrile). Ions were generated by electrospray (ESI) and multiple reaction monitoring (MRM) was used as basis for quantification. The results revealed a linear calibration curve in the range of 5–400 ngmL-1 (r2 ≥ 0.9998) with lower limit of quantification (LOQ) and lower limit of detection (LOD) of 4.66 and 1.53 ngmL-1 in plasma, 4.19 and 1.38 ngmL-1 in RLMs. The intra- and inter-day precision and accuracy in plasma ranged from1.06 to 2.54% and -1.48 to -0.17, respectively. Whereas in RLMs ranged from 0.97 to 2.31% and -1.65 to -0.3%. The developed procedure was applied for quantification of PNT in human plasma and RLMs for study metabolic stability of PNT. PNT disappeared rapidly in the 1st 10 minutes of RLM incubation and the disappearance plateaued out for the rest of the incubation. In vitro half-life (t1/2) was 6.26 min and intrinsic clearance (CLin) was 15.182± 0.477.
**Keywords:** Ponatinib RLMS LC-MS/MS.

## M-424. Green Approach Using Monolithic Column for Simultaneous Determination of Coformulated Drugs

Ali M. Yehia and Heba M. Mohamed

*Journal of Separation Science, 39: 2114-2122 (2016) IF: 2.741*

Green chemistry and sustainability is now entirely encompassed across the majority of pharmaceutical companies and research labs. Researchers' attention is careworn toward implementing the green analytical chemistry principles for more eco-friendly analytical methodologies. Solvents play a dominant role in determining the greenness of the analytical procedure. Using safer solvents, the greenness profile of the methodology could be increased remarkably. In this context, a green chromatographic method has been developed and validated for the simultaneous determination of phenylephrine, paracetamol, and guaifenesin in their ternary pharmaceutical mixture. The chromatographic separation was carried out using monolithic column and green solvents as mobile phase. The use of monolithic column allows efficient separation protocols at higher flow rates, which results in short time of analysis. Two-factor three-level experimental design was used to optimize the chromatographic conditions. The greenness profile of the proposed methodology was assessed using eco-scale as a green metrics and was found to be an excellent green method with regard to the usage and production of hazardous chemicals and solvents, energy consumption, and amount of produced waste. The proposed method improved the environmental impact without compromising the analytical performance criteria and could be used as a safer alternate for the routine analysis of the studied drugs.
**Keywords:** Eco-Scale / Experimental Design; Green Analysis; Monolithic Column; Pharmaceutical Combination.

## M-423. Development and Validation of a Generic High-Performance Liquid Chromatography for the Simultaneous Separation and Determination of Six Cough Ingredients: Robustness Study on Core–Shell Particles

Ali Mohamed Yehia and Hebatallah Mohamed Essam

*Journal of Separation Science, 39: 3357-3367 (2016) IF: 2.741*

A generally applicable high-performance liquid chromatographic method for the qualitative and quantitative determination of pharmaceutical preparations containing phenylephrine hydrochloride, paracetamol, ephedrine hydrochloride, guaifenesin, doxylamine succinate, and dextromethorphan hydrobromide is developed. Optimization of chromatographic conditions was performed for the gradient elution using different buffer pH values, flow rates and two C18 stationary phases. The method was developed using a Kinetex® C18 column as a core–shell stationary phase with a gradient profile using buffer pH 5.0 and acetonitrile at 2.0 mL/min flow rate. Detection was carried out at 220 nm and linear calibrations were obtained for all components within the studied ranges. The method was fully validated in agreement with ICH guidelines. The proposed method is specific, accurate and precise (RSD% < 3%). Limits of detection are lower than 2.0 µg/mL. Qualitative and quantitative responses were evaluated using experimental design to assist the method robustness. The method was proved to be highly robust against 10% change in buffer pH and flow rate (RSD% < 10%), however, the flow rate may significantly influence the quantitative responses of phenylephrine, paracetamol, and doxylamine (RSD% > 10%). Satisfactory results were obtained for commercial combinations analyses. Statistical comparison between the proposed chromatographic and official methods revealed no significant difference.
**Keywords:** Core-Shell Particles / Cough medicine; Experimental design; Gradient chromatography; Robustness Study.

## M-427. Phospholipidomic Identification of Potential Serum Biomarkers in Dengue Fever, Hepatitis B and Hepatitis C Using Liquid Chromatography-Electrospray Ionization-Tandem Mass Spectrometry

Alaa Khedr, Maha A. Hegazy, Ahmed K. Kammoun and Mostafa A. Shehata

*Journal of Chromatography B, 1009-1010:44-54(2016)IF: 2.687*

The serum phospholipid (PL) profiles of healthy volunteers (HE) and patients with recently diagnosed dengue fever (DF), hepatitis B (HBV), and hepatitis C (HCV) were investigated using liquid chromatography-ion trap-mass spectrometry (LC-IT-MS) and liquid chromatography-triple quad-mass spectrometry (LC-TQ-MS). Major PLs, including lyso-phosphatidylcholins (LPCs), phosphatidylcholins (PCs), phosphatidylinositols (PIs), phosphatidylethanolamines (PEs) and phosphatidylserines (PSs), were characterized in human serum using LC-IT-MS. Thirty-five PLs were quantified using seven non-endogenous odd-carbon PL standards. An MS search protocol for the identification of PLs is described. The analytical method was optimized to achieve maximum recovery and detection. PLs were detected with minimal ionization suppression. The PLs species were characterized on the basis of (i) MS2 peaks due to polar head, (ii) precursor ion or neutral loss scans, (iii) identification of fatty acid, (iv) identification of sn-1 and sn-2 fatty acid. The quantitation data were subjected to principal component analysis (PCA), and a significant difference was observed between the PL profiles of the investigated diseases and those of HE subjects. The significance of the changes in each lipid among the four groups was statistically assessed using one-way analysis of variance (ANOVA) followed by Bonferroni post hoc multiple comparison. The serum profiles of 28 PLs were determined to be significantly different and enabled the discrimination between HE individuals and the studied patients. Potentially dysregulated PLs were considered as differentiating biomarkers to diagnose DF, HBV, and HCV.

**Keywords:** Phospholipids; Lc-Esi-Ms/Ms; Differentiating Biomarkers; Dengue Fever; Hepatitis B; Hepatitis C.

## M-428. Quantification of Sofosbuvir and Ledipasvir in Human Plasma by Uplc-Ms/Ms Method: Application to Fasting and Fed Bioequivalence Studies

Mamdouh R. Rezk, Ehab R. Bendas, Emad B. Basalious and Iman A. Karim

*Journal of Chromatography B Analytical Technologies in The Biomedical and Life Sciences, 1028: 63-70 (2016) IF: 2.687*

A rapid and sensitive LC–MS/MS method was developed, optimized and validated for quantification of sofosbuvir (SF) and ledipasvir (LD) in human plasma using eplerenone as an internal standard (IS).Analytes and IS were extracted from plasma by simple liquid–liquid extraction technique using methyl tertiary butyl ether. The prepared samples were chromatographed on Acquity UPLC BEH C18 column.Separation was done using a mobile phase formed of 0.1% formic acid and acetonitrile (50:50, v/v) in an isocratic mode at a flow rate of 0.4 ml/min. The Xevo TQD LC–MS/MS was operated under the multiple-reaction monitoring mode using electrospray ionization. A full validation of the method was performedaccording to the FDA guidelines. Linearity was found to be in the range of 0.25–3500 ng/ml for SF and5–2000 ng/ml for LD. The intra-day and inter-day precision and accuracy results were within the accept-able limits. A short run time of 2 min allows analysis of more than 400 plasma samples per day. Thedeveloped method was successfully applied to both fasting and fed bioequivalence studies in healthyhuman volunteers.

**Keywords:** Sofosbuvir; Ledipasvir; Uplc–Ms/Ms; Plasma; Validation; Bioequivalence.

## M-426. Immunoaffinity Extraction Using Conformation-Dependent Antibodies Coupled to SE-HPLCfor the Development of Stability and Potency-Indicating Assay for Quadrivalent Human Papillomavirus Vaccine

Moushira M. Mostafa, Medhat A. Al-Ghobashy, Faten A. Fathalla and Maissa Y. Salem

*Journal of Chromatography B Analytical Technologies in the Biomedical and Life Sciences, 1032: 211-217 (2016) IF: 2.687*

Quadrivalent human papillomavirus (HPV) vaccine is formulated of four types of non-infectious recombinant virus like particles (VLPs) that are structurally and immunologically similar to the corresponding infectious HPV virus types 6, 11, 16 and 18. With almost identical physical, chemical and structural properties of the four types of VLPs, ELISA remains the only approved in vitro potency testing assay. In this study, an alternative industry-friendly, stability- and potency-indicating assay protocol was developed and validated for the determination of HPV vaccine. Vacuum-driven immunoaffinity extraction (IAE) was employed using type-specific, conformation-dependent antibodies against each type of HPV VLPs. ELISA assay was employed to evaluate the ability of IAE columns to specifically separate each of the four types of VLPs from their quadrivalent mixture. Mean percentage recoveries of 76.76 ± 2.69, 69.12 ± 5.79, 84.86 ± 5.25 and 71.14 ± 4.50% were obtained for VLPs types 6, 11, 16 and 18, respectively with no significant interference in each case. Antigen content was then determined using SE-HPLC over a concentration range of 5.00–20.00 μg/mL ($r > 0.998$) for VLPs type 6, 11, 16 and 18, respectively. The SE-HPLC assay was found accurate and precise (RSD < 10.00%) with LOD ranging from 1.23–3.85 μg/mL. The assay protocol was found superior to conventional ELISA assay with respect to simplicity, total analysis time and cost. Good correlation between the results of analysis obtained using IAE—SE-HPLC and ELISA demonstrated the suitability of the suggested assay protocol for stability and potency assessment with a good potential for implementation for batch release. This approach should be applicable for quality assessment of other vaccine preparations based on VLPs.

**Keywords:** Immunoaffinity extraction; Size exclusion Chromatography; Human papillomavirus vaccine; Virus Like Particles; Potency-Indicating assay.

## M-430. Development and Validation of LC–MS/MS Assay for the Simultaneous Determination of Methotrexate, 6-Mercaptopurine and its Active Metabolite 6-Thioguanine in Plasma of Children with Acute Lymphoblastic Leukemia: Correlation with Genetic Polymorphism

Medhat A. Al-Ghobashy, Said A. Hassan, Doaa H. Abdelaziz, Noha M. Elhosseiny, Nirmeen A. Sabry, Ahmed S. Attia and Manal H. El-Sayed

*Journal of Chromatography B Analytical Technologies in the Biomedical and Life Sciences, 1038: 88-94 (2016) IF: 2.687*

Individualized therapy is a recent approach aiming to specify dosage regimen for each patient according to its genetic state. Cancer chemotherapy requires continuous monitoring of the plasma concentration levels of active forms of cytotoxic drugs and subsequent dose adjustment. In order to attain optimum therapeutic efficacy, correlation to pharmacogenetics data is crucial. In this study, a specific, accurate and sensitive liquid chromatography tandem mass spectrometry (LC–MS/MS) has been developed for determination of methotrexate (MTX), 6-mercaptopurine (MP) and its metabolite 6-thioguanine nucleotide (TG) in human plasma. Based on the basic character of the studied compounds, solid phase extraction using a strong cation exchanger was found the optimum approach to achieve good extraction recovery. Chromatographic separation was carried out using RP-HPLC and isocratic elution by acetonitrile: 0.1% aqueous formic acid (85:15 v/v) with a flow rate of 0.8 mL/min at 40 °C. The detection was performed by tandem mass spectrometry in MRM mode via electrospray ionization source in positive ionization mode. Analysis was carried out within 1.0 min over a concentration range of 6.25–200.00 ng/mL for the studied analytes. Validation was carried out according to FDA guidelines for bioanalytical method validation and satisfactory results were obtained. The applicability of the assay for the monitoring of the MTX, MP and TG and subsequent application to personalized therapy was demonstrated in a clinical study on children with acute lymphoblastic leukemia (ALL). Results confirmed the need for implementation of reliable analysis tools for therapeutic dose adjustment.

**Keywords:** 6-Mercaptopurine; Acute lymphoblastic leukemia; Individualized therapy; LC–MS/MS; Leukemia; Methotrexate.

## M-429. Advanced Stability Indicating Chemometric Methods for Quantitation of Amlodipine and Atorvastatin in their Quinary Mixture with Acidic Degradation Products

Hany W. Darwish, Said A. Hassan , Maissa Y. Salem and Badr A. El-Zeany

*Spectrochimica Acta Part A: Molecular and Biomolecular Spectroscopy, 154: 58-66 (2016) IF: 2.653*

Two advanced, accurate and precise chemometric methods are developed for the simultaneous determination of amlodipine besylate (AML) and atorvastatin calcium (ATV) in the presence of their acidic degradation products in tablet dosage forms. The first method was Partial Least Squares (PLS-1) and the second was Artificial Neural Networks (ANN). PLS was compared to ANN models with and without variable selection procedure (genetic algorithm (GA)). For proper analysis, a 5-factor 5-level experimental design was established resulting in 25 mixtures containing different ratios of the interfering species. Fifteen mixtures were used as calibration set and the other ten mixtures were used as validation set to validate the prediction ability of the suggested models. The proposed methods were successfully applied to the analysis of pharmaceutical tablets containing AML and ATV. The methods indicated the ability of the mentioned models to solve the highly overlapped spectra of the quinary mixture, yet using inexpensive and easy to handle instruments like the UV-VIS spectrophotometer.

**Keywords:** Amlodipine; Artificial neural networks; Atorvastatin; Genetic algorithm; Partial least squares; Stability indicating.

## M-432. Mean Centering of Double Divisor Ratio Spectra, A Novel Spectrophotometric Method for Analysis of Ternary Mixtures

Said A. Hassan, Eman S. Elzanfaly, Maissa Y. Salem and Badr A. El-Zeany

*Spectrochimica Acta Part A: Molecular and Biomolecular Spectroscopy, 153: 132-142 (2016) IF: 2.653*

A novel spectrophotometric method was developed for determination of ternary mixtures without previous separation, showing significant advantages over conventional methods. The new method is based on mean centering of double divisor ratio spectra. The mathematical explanation of the procedure is illustrated. The method was evaluated by determination of model ternary mixture and by the determination of Amlodipine (AML), Aliskiren (ALI) and Hydrochlorothiazide (HCT) in laboratory prepared mixtures and in a commercial pharmaceutical preparation. For proper presentation of the advantages and applicability of the new method, a comparative study was established between the new mean centering of double divisor ratio spectra (MCDD) and two similar methods used for analysis of ternary mixtures, namely mean centering (MC) and double divisor of ratio spectra-derivative spectrophotometry (DDRS-DS). The method was also compared with a reported one for analysis of the pharmaceutical preparation. The method was validated according to the ICH guidelines and accuracy, precision, repeatability and robustness were found to be within the acceptable limits.

**Keywords:** Mean Centering; Double divisor ratio spectra; Derivative spectrophotometry; Amlodipine; Aliskiren; hydrochlorothiazide.

## M-434. Evaluation of Multivariate Calibration Models with Different Pre-Processing and Processing Algorithms for a Novel Resolution and Quantitation of Spectrally Overlapped Quaternary Mixture in Syrup

Azza A. Moustafa, Maha A. Hegazy, Dalia Mohamed and Omnia Ali

*Spectrochimica Acta Part A: Molecular and Biomolecular Spectroscopy, 154: 76-83 (2016) IF: 2.653*

A novel approach for the resolution and quantitation of severely overlapped quaternary mixture of carbinoxamine maleate (CAR), pholcodine (PHL), ephedrine hydrochloride (EPH) and

sunset yellow (SUN) in syrup was demonstrated utilizing different spectrophotometric assisted multivariate calibration methods. The applied methods have used different processing and pre-processing algorithms. The proposed methods were partial least squares (PLS), concentration residuals augmented classical least squares (CRACLS), and a novel method; continuous wavelet transforms coupled with partial least squares (CWT-PLS). These methods were applied to a training set in the concentration ranges of 40–100 µg/mL, 40–160 µg/mL, 100–500 µg/mL and 8–24 µg/mL for the four components, respectively. The utilized methods have not required any preliminary separation step or chemical pretreatment. The validity of the methods was evaluated by an external validation set. The selectivity of the developed methods was demonstrated by analyzing the drugs in their combined pharmaceutical formulation without any interference from additives. The obtained results were statistically compared with the official and reported methods where no significant difference was observed regarding both accuracy and precision.

**Keywords:** Carbinoxamine pholcodine ephedrine cyrinol syrup Multivariate Calibration Methods Continuous Wavelet Transforms Coupled With Partial Least Squares (CWT-PLS).

## M-438. Novel Pure Component Contribution, Mean Centering of Ratio Spectra and Factor Based Algorithms for Simultaneous Resolution and Quantification of Overlapped Spectral Signals: an Application to Recently Co-Formulated Tablets of Chlorzoxazone, Aceclofenac and Paracetamol

Safaa S. Toubar, Maha A. Hegazy, Mona S. Elshahed and Marwa I. Helmy

*Spectrochimica Acta Part A: Molecular and Biomolecular Spectroscopy, 163: 89-95 (2016) IF: 2.653*

In this work, resolution and quantitation of spectral signals are achieved by several univariate and multivariate techniques. The novel pure component contribution algorithm(PCCA) along with mean centering of ratio spectra (MCR) and the factor based partial least squares (PLS) algorithms were developed for simultaneous determination of chlorzoxazone (CXZ), aceclofenac (ACF) and paracetamol (PAR) in their pure form and recently coformulated tablets. The PCCAmethod allows the determination of each drug at its λmax.While, the mean centered values at 230, 302 and 253 nm, were used for quantification of CXZ, ACF and PAR, respectively, byMCR method. Partial least-squares (PLS) algorithm was applied as a multivariate calibration method. The threemethods were successfully applied for determination of CXZ, ACF and PAR in pure form and tablets. Good linear relationships were obtained in the ranges of 2–50, 2–40 and 2–30 µg mL−1 for CXZ, ACF and PAR, in order, by both PCCA andMCR, while the PLS modelwas built for the three compounds each in the range of 2–10 µgmL−1. The results obtained from the proposed methods were statistically compared with a reported one. PCCA and MCR methods were validated according to ICH guidelines, while PLS method was validated by both cross validation and an independent data set. They are found suitable for the determination of the studied drugs in bulk powder and tablets.

**Keywords:** Chlorzoxazone; Aceclofenac paracetamol; PCCAMCR PLS.

## M-435. Evaluation of the Efficiency of Continuous Wavelet Transform as Processing and Preprocessing Algorithm for Resolution of Overlapped Signals in Univariate and Multivariate Regression Analyses; an Application to Ternary and Quaternary Mixtures

Maha A. Hegazy, Hayam M. Lotfy, Shereen Mowaka and Ekram Hany Mohamed

*Spectrochimica Acta Part A: Molecular and Biomolecular Spectroscopy, 164: 15-23 (2016) IF: 2.653*

Wavelets have been adapted for a vast number of signal-processing applications due to the amount of information that can be extracted froma signal. In thiswork, a comparative study on the efficiency of continuouswavelet transform (CWT) as a signal processing tool in univariate regression and a pre-processing tool in multivariate analysis using partial least square (CWT-PLS) was conducted. These were applied to complex spectral signals of ternary and quaternary mixtures.CWT-PLS method succeeded in the simultaneous determination of a quaternary mixture of drotaverine (DRO), caffeine (CAF), paracetamol (PAR) and p-aminophenol (PAP, the major impurity of paracetamol). While, the univariate CWT failed to simultaneously determine the quaternary mixture components and was able to determine only PAR and PAP, the ternary mixtures of DRO, CAF, and PAR and CAF, PAR, and PAP. During the calculations of CWT, different wavelet families were tested. The univariate CWT method was validated according to the ICH guidelines. While for the development of the CWT-PLS model a calibration set was prepared by means of an orthogonal experimental design and their absorption spectra were recorded and processed by CWT. The CWT-PLS model was constructed by regression between the wavelet coefficients and concentration matrices and validation was performed by both cross validation and external validation sets. Both methods were successfully applied for determination of the studied drugs in pharmaceutical formulations.

**Keywords:** Continuous Wavelet Transform Quaternary Mixtures Drotaverine Caffeine Paracetamol Para-Amino Phenol.

## M-445. Validated Spectrophotometric Methods for Simultaneous Determination of Omeprazole, Tinidazole and Doxycycline in their Ternary Mixture

Hayam M. Lotfy, Maha A. Hegazy, Shereen Mowaka and Ekram Hany Mohamed

*Spectrochimica Acta Part A: Molecular and Biomolecular Spectroscopy, 153: 321-332 (2016) IF: 2.653*

A comparative study of smart spectrophotometric techniques for the simultaneous determination ofOmeprazole (OMP), Tinidazole (TIN) and Doxycycline (DOX) without prior separation steps is developed. These techniques consist of several consecutive steps utilizing zero/or ratio/or derivative spectra. The proposed techniques adopt nine simple different methods, namely direct spectrophotometry, dual wavelength, first derivative-zero crossing, amplitude factor, spectrumsubtraction, ratio subtraction, derivative ratio-zero crossing, constant center, and successive derivative ratio

method. The calibration graphs are linear over the concentration range of 1–20 µg/mL, 5–40 µg/mL and 2–30 µg/mL forOMP, TIN and DOX, respectively. These methods are tested by analyzing synthetic mixtures of the above drugs and successfully applied to commercial pharmaceutical preparation. The methods that are validated according to the ICH guidelines, accuracy, precision, and repeatability, were found to bewithin the acceptable limits.

**Keywords:** Ternary mixture spectrophotometry; Constant Center Amplitude Factor Successive Derivative Ratio.

## M-436. Full Spectrum and Selected Spectrum Based Multivariate Calibration Methods for Simultaneous Determination of Betamethasone Dipropionate, Clotrimazole and Benzyl Alcohol: Development, Validation and Application on Commercial Dosage form

Hany W. Darwish, Eman S. Elzanfaly, Ahmed S. Saad and Abdelaziz El-Bayoumi Abdelaleem

*Spectrochimica Acta Part A: Molecular and Biomolecular Spectroscopy, 169,: 50-57 (2016) IF: 2.653*

Five different chemometric methods were developed for the simultaneous determination of betamethasone dipropionate (BMD), clotrimazole (CT) and benzyl alcohol (BA) in their combined dosage form (Lotriderm® cream). The applied methods included three full spectrum based chemometric techniques; namely principal component regression (PCR), Partial Least Squares (PLS) and Artificial Neural Networks (ANN), while the other two methods were PLS and ANN preceded by genetic algorithm procedure (GA-PLS and GA-ANN) as a wavelength selection procedure. A multilevel multifactor experimental design was adopted for proper construction of the models. A validation set composed of 12 mixtures containing different ratios of the three analytes was used to evaluate the predictive power of the suggested models. All the proposed methods except ANN, were successfully applied for the analysis of their pharmaceutical formulation (Lotriderm® cream). Results demonstrated the efficiency of the four methods as quantitative tool for analysis of the three analytes without prior separation procedures and without any interference from the co-formulated excipient. Additionally, the work highlighted the effect of GA on increasing the predictive power of PLS and ANN models.

**Keywords:** Betamethasone dipropionate; Clotrimazole; Benzyl Alcohol; PCR; PLS; ANN; GA.

## M-442. Simultaneous Determination of Mebeverine Hydrochloride and Chlordiazepoxide in their Binary Mixture Using Novel Univariate Spectrophotometric Methods Via Different Manipulation Pathways.

Hayam M. Lotfy, Yasmin M. Fayez, Adel M.Michael and Christine K. Nessim

*Spectrochimica Acta Part A: Molecular and Biomolecular Spectroscopy, 155: 11-20 (2016) IF: 2.653*

Smart, sensitive, simple and accurate spectrophotometric methods were developed and validated for the quantitative determination of a binary mixture of mebeverine hydrochloride (MVH) and chlordiazepoxide (CDZ) without prior separation steps via different manipulating pathways. These pathways were applied either on zero order absorption spectra namely, absorbance subtraction (AS) or based on the recovered zero order absorption spectra via a decoding technique namely, derivative transformation (DT) or via ratio spectra namely, ratio subtraction (RS) coupledwith extended ratio subtraction (EXRS), spectrumsubtraction (SS), constant multiplication (CM) and constant value (CV) methods. The manipulation steps applied on the ratio spectra are namely, ratio difference (RD) and amplitude modulation (AM) methods or applying a derivative to these ratio spectra namely, derivative ratio (DD1) or second derivative (D2). Finally, the pathway based on the ratio spectra of derivative spectra is namely, derivative subtraction (DS). The specificity of the developedmethodswas investigated by analyzing the laboratory mixtures and was successfully applied for their combined dosage form. The proposed methods were validated according to ICH guidelines. These methods exhibited linearity in the range of 2–28 µg/mL for mebeverine hydrochloride and 1–12 µg/mL for chlordiazepoxide. The obtained resultswere statistically compared with those of the official methods using Student t-test, F-test, and one way ANOVA, showing no significant difference with respect to accuracy and precision.

**Keywords:** Absorbance subtraction; Amplitude modulation; Chlordiazepoxide and mebeverine hydrochloride; Decoding technique; Derivative subtraction; Derivative transformation.

## M-441. Simultaneous Determination of Fluticasone Propionate and Azelastine Hydrochloride in the Presence of Pharmaceutical Dosage form Additives

Hanan A. Merey, Sally S. El-Mosallamy, Nagiba Y. Hassan and Badr A. El-Zeany

*Spectrochimica Acta Part A: Molecular and Biomolecular Spectroscopy, 160: 50-57 (2016) IF: 2.653*

Fluticasone propionate (FLU) and Azelastine hydrochloride (AZE) are co-formulated with phenylethyl alcohol (PEA) and Benzalkonium chloride (BENZ) (as preservatives) in pharmaceutical dosage form for treatment of seasonal allergies. Different spectrophotometric methods were used for the simultaneous determination of cited drugs in the dosage form. Direct spectrophotometric method was used for determining of AZE, while Derivative of double divisor of ratio spectra (DD-RS), Ratio subtraction coupled with ratio difference method (RS-RD) and Mean centering of the ratio spectra (MCR) are used for the determination of FLU. The linearity of the proposed methods was investigated in the range of 5.00-40.00 and 5.00-80.00µg/mL for FLU and AZE, respectively. The specificity of the developed methods was investigated by analyzing laboratory prepared mixtures containing different ratios of cited drugs in addition to PEA and their pharmaceutical dosage form. The validity of the proposed methods was assessed using the standard addition technique. The obtained results were statistically compared with those obtained by official or the reported method for FLU or AZE, respectively showing no significant difference with respect to accuracy and precision at p=0.05.

**Keywords:** Azelastine hydrochloride fluticasone; Propionate direct spectrophotometry derivative of Double divisor of ratio Spectra mean centering.

## M-440. Chemometrics Resolution and Quantification Power Evaluation: Application on Pharmaceutical Quaternary Mixture of Paracetamol, Guaifenesin, Phenylephrine and P-Aminophenol

Ali M. Yehia and Heba M. Mohamed

*Spectrochimica Acta Part A: Molecular and Biomolecular Spectroscopy, 152: 491-500 (2016) IF: 2.653*

Three advanced chemmometric-assisted spectrophotometric methods namely; Concentration Residuals Augmented Classical Least Squares (CRACLS), Multivariate Curve Resolution-Alternating Least Squares (MCR-ALS) and Principal Component Analysis-Artificial Neural Networks (PCA-ANN) were developed, validated and benchmarked to PLS calibration; to resolve the severely overlapped spectra and simultaneously determine; Paracetamol (PAR), Guaifenesin (GUA) and Phenylephrine (PHE) in their ternary mixture and in presence of p-aminophenol (AP) the main degradation product and synthesis impurity of Paracetamol. The analytical performance of the proposed methods was described by percentage recoveries, root mean square error of calibration and standard error of prediction. The four multivariate calibration methods could be directly used without any preliminary separation step and successfully applied for pharmaceutical formulation analysis, showing no excipients' interference.

**Keywords:** Paracetamol; Guaifenesin; Phenylephrine; Chemometric methods; Artificial neural networks.

## M-441. Ratio Manipulating Spectrophotometry Versus Chemometry as Stability Indicating Methods for Cefquinome Sulfate Determination

Ali M. Yehia, Reham M. Arafa, Samah S. Abbas and Sawsan M. Amer

*Spectrochimica Acta Part A: Molecular and Biomolecular Spectroscopy, 153: 231-240 (2016) IF: 2.653*

Spectral resolution of cefquinome sulfate (CFQ) in the presence of its degradation products was studied. Three selective, accurate and rapid spectrophotometric methods were performed for the determination of CFQ in the presence of either its hydrolytic, oxidative or photo-degradation products. The proposed ratio difference, derivative ratio and mean centering are ratio manipulating spectrophotometric methods that were satisfactorily applied for selective determination of CFQ within linear range of 5.0–40.0 μg mL− 1. Concentration Residuals Augmented Classical Least Squares was applied and evaluated for the determination of the cited drug in the presence of its all degradation products. Traditional Partial Least Squares regression was also applied and benchmarked against the proposed advanced multivariate calibration. Experimentally designed 25 synthetic mixtures of three factors at five levels were used to calibrate and validate the multivariate models. Advanced chemometrics succeeded in quantitative and qualitative analyses of CFQ along with its hydrolytic, oxidative and photo-degradation products. The proposed methods were applied successfully for different pharmaceutical formulations analyses. These developed methods were simple and cost-effective compared with the manufacturer's RP-HPLC method.

**Keywords:** Cefquinome Sulfate; Stability Study; Ratio Difference; Derivative Ratio; Mean Centering; Concentration Residuals Augmented Classical Least Squares; Partial Least Squares

## M-443. Stability-Indicating Spectrophotometric Methods for Determination of the Anticoagulant Drug Apixaban in the Presence of its Hydrolytic Degradation Product

Mahmoud A. Tantawy, Nariman A. El-Ragehy, Nagiba Y. Hassan and Mohamed Abdelkawy

*Spectrochimica Acta Part A: Molecular and Biomolecular Spectroscopy, 159: 13-20 (2016) IF: 2.653*

Apixaban (a novel anticoagulant agent) was subjected to a stress stability study including acid, alkali, oxidative, photolytic, and thermal degradation. The drug was found to be only liable to acidic and alkaline hydrolysis. The degradation product was then isolated and identified by IR and GC–mass spectrometry. Four spectrophotometric methods, namely; first derivative (D1), derivative ratio (DR), ratio difference (RD) and mean centering of ratio spectra (MCR), have been suggested for the determination of apixaban in presence of its hydrolytic degradation product. The proposed methods do not require any preliminary separation step. The accuracy, precision and linearity ranges of the proposed methods were determined, and the methods were validated as per ICH guidelines and the specificity was assessed by analyzing synthetic mixtures containing different percentages of the degradation product with the drug. The developed methods were successfully applied for the determination of apixaban in bulk powder and its tablet dosage form.

**Keywords:** Anticoagulant; Apixaban; Degradation; Spectrophotometry; Stability-Indicating

## M-443. Novel Ratio Difference at Coabsorptive Point Spectrophotometric Method for Determination of Components with Wide Variation in their Absorptivities

Ahmed S. Saad , Nisreen F. Abo-Talib and Mohamed R. El-Ghobashy

*Spectrochimica Acta Part A: Molecular and Biomolecular Spectroscopy, 152: 480-484 (2016) IF: 2.653*

Different methods have been introduced to enhance selectivity of UV-spectrophotometry thus enabling accurate determination of co-formulated components, however mixtures whose components exhibit wide variation in absorptivities has been an obstacle against application of UV-spectrophotometry. The developed ratio difference at coabsorptive point method (RDC) represents a simple effective solution for the mentioned problem, where the additive property of light absorbance enabled the consideration of the two components as multiples of the lower absorptivity component at certain wavelength (coabsorptive point), at which their total concentration multiples could be determined, whereas the other component was selectively determined by applying the ratio difference method in a single step. Mixture of perindopril arginine (PA) and amlodipine besylate (AM) figures that problem, where the low absorptivity

of PA relative to AM hinders selective spectrophotometric determination of PA. The developed method successfully determined both components in the overlapped region of their spectra with accuracy 99.39 ± 1.60 and 100.51 ± 1.21, for PA and AM, respectively. The method was validated as per the USP guidelines and showed no significant difference upon statistical comparison with reported chromatographic method.

**Keywords:** Spectrophotometry, Perindopril Arginine, Amlodipine, Ratio Difference Method and Coabsorptive Point

## M-444.Successive Ratio Subtraction Coupled with Constant Multiplication Spectrophotometric Method for Determination of Hydroquinone in Complex Mixture with its Degradation Products, Tretinoin and Methyl Paraben

Mohamed R. Elghobashy, Lories I. Bebawy, Rafeek F. Shokry and Samah S. Abbas

*Spectrochimica Acta Part A: Molecular and Biomolecular Spectroscopy, 157: 116-123 (2016) IF: 2.653*

A sensitive and selective stability-indicating successive ratio subtraction coupled with constant multiplication (SRS-CM) spectrophotometric methodwas studied and developed for the spectrumresolution of five component mixture without prior separation. The components were hydroquinone in combination with tretinoin, the polymer formed fromhydroquinone alkali degradation, 1,4 benzoquinone and the preservative methyl paraben. The proposed method was used for their determination in their pure form and in pharmaceutical formulation. The zero order absorption spectra of hydroquinone, tretinoin, 1,4 benzoquinone and methyl paraben were determined at 293, 357.5, 245 and 255.2 nm, respectively. The calibration curves were linear over the concentration ranges of 4.00–46.00, 1.00–7.00, 0.60–5.20, and 1.00–7.00 μg mL−1 for hydroquinone, tretinoin, 1,4 benzoquinone and methyl paraben, respectively. The pharmaceutical formulation was subjected to mild alkali condition and measured by this method resulting in the polymerization of hydroquinone and the formation of toxic 1,4 benzoquinone. The proposed method was validated according to ICH guidelines. The results obtained were statistically analyzed and compared with those obtained by applying the reported method.

**Keywords:** Stability Study, Hydroquinone, Tretinoin, Benzoquinone, Spectrophotometric Successive Ratio Subtraction Method Coupled With Constant Multiplication

## M-445. Application and Validation of Superior Spectrophotometric Methods for Simultaneous Determination of Ternary Mixture Used for Hypertension Management

Heba M. Mohamed and Nesrine T. Lamie

*Spectrochimica Acta Part A: Molecular and Biomolecular Spectroscopy, 155: 103-110 (2016) IF: 2.653*

Telmisartan (TL), Hydrochlorothiazide (HZ) and Amlodipine besylate (AM) are co-formulated together for hypertension management. Three smart, specific and precise spectrophotometric methods were applied and validated for simultaneous determination of the three cited drugs. Method A is the ratio isoabsorptive point and ratio difference in subtracted spectra (RIDSS) which is based on dividing the ternary mixture of the studied drugs by the spectrum of AM to get the division spectrum, from which concentration of AM can be obtained by measuring the amplitude values in the plateau region at 360 nm. Then the amplitude value of the plateau region was subtracted from the division spectrum and HZ concentration was obtained by measuring the difference in amplitude values at 278.5 and 306 nm (corresponding to zero difference of TL) while the total concentration of HZ and TL in the mixture was measured at their isoabsorptive point in the division spectrum at 278.5 nm (Aiso). TL concentration is then obtained by subtraction. Method B; double divisor ratio spectra derivative spectrophotometry (RS-DS) and method C; mean centering of ratio spectra (MCR) spectrophotometric methods. The proposed methods did not require any initial separation steps prior the analysis of the three drugs. A comparative study was done between the three methods regarding their; simplicity, sensitivity and limitations. Specificity was investigated by analyzing the synthetic mixtures containing different ratios of the three studied drugs and their tablets dosage form. Statistical comparison of the obtained results with those found by the official methods was done, differences were non-significant in regard to accuracy and precision. The three methods were validated in accordance with ICH guidelines and can be used for quality control laboratories for TL, HZ and AM.

**Keywords:** Ratio Isoabsorptive; Ratio Difference; Double Divisor; Mean Centering; Spectrophotometry

## M-446.Enhancing Prediction Power of Chemometric Models Through Manipulation of the Fed Spectrophotometric Data: A Comparative Study

Ahmed S. Saad, Abdallah M. Hamdy, Fathy M. Salama and Mohamed Abdelkawy

*Spectrochimica Acta Part A: Molecular and Biomolecular Spectroscopy, 167: 12-18 (2016) IF: 2.653*

Effect of data manipulation in preprocessing step proceeding construction of chemometric models was assessed. The same set of UV spectral data was used for construction of PLS and PCR models directly and after mathematically manipulation as per well known first and second derivatives of the absorption spectra, ratio spectra and first and second derivatives of the ratio spectra spectrophotometric methods, meanwhile the optimal working wavelength ranges were carefully selected for each model and the models were constructed. Unexpectedly, number of latent variables used for models' construction varied among the different methods. The prediction power of the different models was compared using a validation set of 8 mixtures prepared as per the multilevel multifactor design and results were statistically compared using two-way ANOVA test. Root mean squares error of prediction (RMSEP) was used for further comparison of the predictability among different constructed models. Although no significant difference was found between results obtained using Partial Least Squares (PLS) and Principal Component Regression (PCR) models, however, discrepancies among results was found to be attributed to the variation in the discrimination power of adopted spectrophotometric methods on spectral data.

**Keywords:** Chemometrics; Caffeine; Propyphenazone; Paracetamol; Ratio Spectra; Derivatives.

## M-447. Comparative Study Between Recent Methods Manipulating Ratio Spectra and Classical Methods Based on Two-Wavelength Selection for the Determination of Binary Mixture of Antazoline Hydrochloride and Tetryzoline Hydrochloride

Lamia M. Abdel-Halim, Mohamed K. Abd-El Rahman, Nesrin K. Ramadan, Hoda F.A. EL Sanabary and Maissa Y. Salem

*Spectrochimica Acta Part A: Molecular and Biomolecular Spectroscopy, 159: 98-105 (2016) IF: 2.653*

A comparative study was developed between two classical spectrophotometric methods (dual wavelength method and Vierordt's method) and two recent methods manipulating ratio spectra (ratio difference method and first derivative of ratio spectra method) for simultaneous determination of Antazoline hydrochloride (AN) and Tetryzoline hydrochloride (TZ) in their combined pharmaceutical formulation and in the presence of benzalkonium chloride as a preservative without preliminary separation. The dual wavelength method depends on choosing two wavelengths for each drug in a way so that the difference in absorbance at those two wavelengths is zero for the other drug. While Vierordt's method, is based upon measuring the absorbance and the absorptivity values of the two drugs at their λmax (248.0 and 219.0 nm for AN and TZ, respectively), followed by substitution in the corresponding Vierordt's equation. Recent methods manipulating ratio spectra depend on either measuring the difference in amplitudes of ratio spectra between 255.5 and 269.5 nm for AN and 220.0 and 273.0 nm for TZ in case of ratio difference method or computing first derivative of the ratio spectra for each drug then measuring the peak amplitude at 250.0 nm for AN and at 224.0 nm for TZ in case of first derivative of ratio spectrophotometry. The specificity of the developed methods was investigated by analyzing different laboratory prepared mixtures of the two drugs. All methods were applied successfully for the determination of the selected drugs in their combined dosage form proving that the classical spectrophotometric methods can still be used successfully in analysis of binary mixture using minimal data manipulation rather than recent methods which require relatively more steps. Furthermore, validation of the proposed methods was performed according to ICH guidelines; accuracy, precision and repeatability are found to be within the acceptable limits. Statistical studies showed that the methods can be competitively applied in quality control laboratories.

**Keywords:** Antazoline; Tetryzoline; Dual Wavelength; Vierordt's Method; Ratio Difference; Derivative Ratio

## M-448. Utility of Gold Nanoparticles/Silica Modified Electrode for Rapid Selective Determination of Mebeverine in Micellar Medium: Comparative Discussion and Application in Human Serum

Nahla N. Salama,Hala E. Zaazaa, Shereen M. Azab, Shimaa A. Atty, Naglaa M. El-Kosy and Maissa Y. Salem

*Ionics, 22(6) (2016) IF: 2.119*

A novel electrochemical sensor for the selective determination of mebeverine hydrochloride (MEB) in drug substance, products, and human plasma was introduced. The prepared nanoparticle sensor was based on a carbon paste electrode chemically modified with silica and gold nanoparticles. The surface morphology of the modified electrode was characterized by scanning electron microscope. Several parameters such as pH, scan rate, and accumulation time were optimized in order to determine the best conditions for analysis. A good linear response was obtained in the range of 4.0 × 10−8−1 × 10−5 mol L−1 with detection limit of 1.5 × 10−9 mol L−1. The obtained results are in good agreement with those obtained by official method. The method was applied for determination of mebeverine hydrochloride in different pharmaceutical dosage forms containing MEB alone or in mixtures with sulpiride or chlordiazepoxide as well as in human plasma. The developed method was simple, rapid, economic, and challenging to green chemistry.

**Keywords:** Sensorcarbon Paste Electrodegold Nanoparticles; Silicamicellar Mediamebeverine Hydrochlorideco formulated Drugs.

## M-447. Strategy Approach for Direct Enantioseparation of Hyoscyamine Sulfate and Zopiclone on a Chiral Ál-Acid Glycoprotein Column and Determination of their Eutomers: Thermodynamic Study of Complexation

Hala E. Zaazaa, Nahla N. Salama, Lobna M. Abd El Halim, Maissa Y. Salem and Laila E. Abd El Fattah

*Chirality, 28(1): 0-0 (2016) IF: 2.025*

Rapid and simple isocratic high-performance liquid chromatographic methods with UV detection were developed and validated for the direct resolution of racemic mixtures of hyoscyamine sulfate and zopiclone. The method involved the use of αl -acid glycoprotein (AGP) as chiral stationary phase. The stereochemical separation factor (ά) and the stereochemical resolution factor (Rs ) obtained were 1.29 and 1.60 for hyoscyamine sulfate and 1.47 and 2.45 for zopiclone, respectively. The method was used for determination of chiral switching (eutomer) isomers: S-hyoscyamine sulfate and eszopiclone. Several mobile phase parameters were investigated for controlling enantioselective retention and resolution on the chiral AGP column. The influence of mobile phase, concentration and type of uncharged organic modifier, ionic strength, and column temperature on enantioselectivity were studied. Calibration curves were linear in the ranges of 1-10 µg mL(-1) and 0.5-5 µg mL(-1) for S-hyoscyamine sulfate and eszopiclone, respectively. The method is specific and sensitive, with lower limits of detection and quantifications of 0.156, 0.515 and 0.106, 0.349 for S-hyoscyamine sulfate and eszopiclone, respectively. The method was used to identify quantitatively the enantiomers profile of the racemic mixtures of the studied drugs in their pharmaceutical preparations. Thermodynamic studies were performed to calculate the enthalpic ΔH and entropic ΔS terms. The results showed that enantiomer separation of the studied drugs were an enthalpic process.

**Keywords:** Enantioseparation; Al-Acid Glycoprotein; Hyoscyamine Sulfate; Zopiclone, Chiral Switching; Thermodynamic Studies

## M-448. A Highly Efficient and Sensitive Lc- Ms/Ms Method for the Determination of Afatinib in Human Plasma: Application to A Metabolic Stability Study

Adnan A. Kadi, Ali S. Abdelhameed Hany W. Darwish, Mohamed W. Attwa and Nasser S. Al-Shakliah

*Biomedical Chromatography, 30: 1248-1255 (2016) IF: 1.729*

Afatinib (AFT) is a new tyrosine kinase inhibitor approved for the treatment of nonsmall cell lung cancer. In the present study, a simple, specific, rapid and sensitive liquid chromatography tandem mass-spectrometric method for the quantification of AFT in human plasma, was developed and validated. Chromatographic separation of the analytes was accomplished on a reversed-phase Luna®-PFP 100Å column (50 × 2.0mm; 3.0 µm) maintained at ambient temperature. Isocratic elutionwas carried out using acetonitrile–water (40:60, v/v) containing 10mM ammoniumformate buffer (pH4.5) adjusted with formic acid at a flow rate of 0.4mLmin1. The analytes were monitored by electrospray ionization in positive ion multiple reaction monitoring mode. The method yields a linear calibration plot (r2 = 0.9997) from a quantification range of 0.5–500 ngmL1 with the lower limit of quantification and lower limit of detection of 1.29 and 0.42ngmL1, respectively. The intra- and inter-day precision and accuracy were estimated and found to be in the ranges of 1.53–4.11% for precision and 2.80–0.38% for accuracy. Finally, quantification of afatinib in a metabolic stability study in rat liver microsomes was achieved through the proposed method

**Keywords:** Afatinib; LC-MS/MS; Human Plasma; Metabolic Stability Study

## M-450. Stability-Indicating Chromatographic Methods for Determination of Flecainide Acetate in the Presence of its Degradation Products; Isolation and Identification of Two of its Impurities

Nariman A. El-Ragehy, Nagiba Y. Hassan, Mahmoud A. Tantawy and Mohamed Abdelkawy

*Biomedical Chromatography, 30: 1541-1548 (2016) IF: 1.729*

In this work, two stability-indicating chromatographic methods have been developed and validated for determination of flecainide acetate (an antiarrhythmic drug) in the presence of its degradation products (flecainide impurities; B and D). Flecainide acetate was subjected to a stress stability study including acid, alkali, oxidative, photolytic and thermal degradation. The suggested chromatographic methods included the use of thin layer chromatography (TLC-densitometry) and high-performance liquid chromatography (HPLC). The TLC method employed aluminum TLC plates precoated with silica gel G.F254 as the stationary phase and methanol–ethyl acetate–33% ammonia (3:7:0.3, by volume) as the mobile phase. The chromatograms were scanned at 290 nm and visualized in daylight by the aid of iodine vapor. The developed HPLC method used a RP-C18 column with isocratic elution. Separation was achieved using a mobile phase composed of phosphate buffer pH 3.3–acetonitrile–triethylamine (53:47:0.03, by volume) at a flow rate of 1.0 mL/min and UV detection at 292 nm. Factors affecting the efficiency of HPLC method have been studied carefully to reach the optimum conditions for separation. The developed methods were validated according to the International Conference on Harmonization guidelines and were applied for bulk powder and dosage form.

**Keywords:** Flecainide Acetate; Flecainide Impurity B; Flecainide Impurity D; HPLC; TLC-Densitometry

## M-449. Novel and Sensitive UPLC–MS/MS Method for Quantification of Sofosbuvir in Human Plasma: Application to a Bioequivalence Study

Mamdouh R. Rezk, Emad B. Basalious and Mohammed E. Amin

*Biomedical Chromatography, 30: 1354-1362 (2016) IF: 1.729*

A novel and sensitive LC–MS/MS method was developed and validated for determination of sofosbuvir (SF) using eplerenone as an internal standard. The Xevo TQD LC–MS/MS was operated under the multiple-reaction monitoring mode using electrospray ionization. Extraction with tert-butyl methyl ether was used in sample preparation. The prepared samples were chromatographed on Acquity UPLC BEH C18 (50 × 2.1mm, 1.7 µm) column by pumping 0.1% formic acid and acetonitrile in an isocratic mode at a flow rate of 0.35mL/min. Method validation was performed as per the US Food and Drug Administration guidelines and the standard curves were found to be linear in the range of 0.25–3500ng/mL for SF. The intra- and inter-day precision and accuracy resultswerewithin the acceptable limits. A very short run time of 1minmade it possible to analyzemore than 500 human plasma samples per day. A very low quantification limit of SF allowed the applicability of the developed method for determination of SF in a bioequivalence study in human volunteers.

**Keywords:** Sofosbuvir; UPLC-MS/MS; Plasma; Validation; Bioequivalence

## M-451.Optimization and Validation of ELISA Immunoassay for the Evaluation of In-Vitro Relative Potency of a Four-Component Human Papillomavirus Vaccine Products

Moushira M. Mostafa, Medhat A. Al-Ghobashy, Faten A. Fathalla and Maissa Y. Salem

*Biologicals, 44(6): 596-599 (2016) IF: 1.69*

A sandwich-type ELISA was optimized and validated to determine the in-vitro relative potency of the four-component prophylactic Human papillomavirus (HPV) vaccine. The vaccine contains the non-infectious virus like particles (VLP) corresponding to HPV Types 6, 11, 16 and 18. A modification of the desorption step required to release the VLPs from the aluminum adjuvant was carried out. Samples were incubated with citrate buffer for two hours at 37 °C instead of overnight incubation at room temperature. Assay validation was then carried out according to ICH guidelines. The assay was linear over a concentration range of 0.30–2000.00 ng/mL for the four HPV types. The assay was accurate and precise with a LOD of 0.092, 0.081, 0.086 and 0.068 ng/mL for type 6, 11, 16 and 18 respectively. Results were also statistically compared to those obtained using the reported ELISA assay and no significant difference was noted. In contrary to the reported ELISA protocol, this optimized immunoassay was superior with respect to analysis time, without affecting the accuracy and precision

(RSD < 5%). This assay has proven to be useful for evaluating the efficacy of the quadrivalent HPV vaccine and is applicable for quality control and batch release purposes.
**Keywords:** Human Papillomavirus Vaccine; Virus-Like Particles (VLP); ELISA; In-Vitro Relative Potency; Validation; Desorption.

## M-452.Correlation of in Vivo and in Vitro Assay Results for Assessment of Free Radical Scavenging Activity of Green Tea Nutraceuticals

Abd-ElSalam HA, Al-Ghobashy MA, Al-Shorbagy M, Nassar N, Zaazaa HE and Ibrahim MA

*Journal of Food Science, 81(7): 0-0 (2016) IF: 1.649*

Green tea (GT)-derived catechins; epigallocatechin gallate (EGCG) in particular are commonly used nutraceuticals for their free-radical scavenging activity (FRSA). The influence of photodegradation on the protective power of GT nutracenticals against oxidative stress was thoroughly explored. Photodegradation of GT extracts was carried out and monitored using orthogonal stability-indicating testing protocol; in vitro and in vivo assays. Total polyphenol content (TPC) and FRSA were determined spectrophotometrically while EGCG was selectively monitored using SPE-HPLC. In vivo assessment of photodegraded samples was investigated via measuring a number of biomarkers for hepatic oxidative stress and apoptosis (caspase-3, inducible nitric oxide synthase, nitric oxide, mitogen-activated protein kinase, glutathione, thiobarbituric acid reactive substances, nuclear factor kappa beta, and nuclear factor erythroid 2-related factor) as well as liver damage (alanine transaminase and aspartate transaminase) in serum of rats previously subjected to oxidative stress. Results showed complete degradation of EGCG in photodegraded green tea samples with no correlation with either TPC or FRSA. On the other hand, in vivo assay results revealed not only loss of activity but formation of harmful pro-oxidants. Photostability was found crucial for the protective effect of GT extract against lead acetate insult. Results confirmed that careful design of quality control protocols requires correlation of chemical assays to bioassays to verify efficacy, stability, and most importantly safety of nutraceuticals.
**Keywords:** Folin-Ciocalteu; Spe-Hplc; Free Radical Scavenging Activity; Green Tea Nutraceuticals; Photostability

## M-453. Comparative Study of Novel Ratio Spectra and Isoabsorptive Point Based Spectrophotometric Methods: Application on a Binary Mixture of Ascorbic Acid and Rutin

Hany W. Darwish, Ahmed H. Bakheit and Ibrahim A. Naguib

*Journal of Analytical Methods In Chemistry, (2016) IF: 1.369*

This paper presents novel methods for spectrophotometric determination of ascorbic acid (AA) in presence of rutin (RU) (coformulated drug) in their combined pharmaceutical formulation. The seven methods are ratio difference (RD), isoabsorptive_RD (Iso_RD), amplitude summation (A_Sum), isoabsorptive point, first derivative of the ratio spectra (1DD), mean centering (MCN), and ratio subtraction (RS). On the other hand, RU was determined directly by measuring the absorbance at 358 nm in addition to the two novel Iso_RD and A_Sum methods. The work introduced in this paper aims to compare these different methods, showing the advantages for each and making a comparison of analysis results. The calibration curve is linear over the concentration range of 4–50 μg/mL for AA and RU. The results show the high performance of proposed methods for the analysis of the binary mixture. The optimum assay conditions were established and the proposed methods were successfully applied for the assay of the two drugs in laboratory prepared mixtures and combined pharmaceutical tablets with excellent recoveries. No interference was observed from common pharmaceutical additives.
**Keywords:** Ascorbic Acid Rutin.

## M-455. Determination of Febuxostat in Human Plasma Using RP-LC–UV Method

Kareem M. Younes, Ehab F. El-Kady and Eman S. Elzanfaly

*Journal of Chromatographic Science, 54 (6): 1022-1027 (2016) IF: 1.32*

A simple and sensitive bioanalytical high-performance liquid chromatographic method with ultraviolet detection was developed and validated for the quantification of febuxostat (FEB) in human plasma. Ketoprofen was used as an internal standard. The analytes were extracted from human plasma samples by precipitation with acetonitrile. The reconstituted samples were chromatographed on C18 Bondapack 10 μm, 250 × 4.6 mm, Waters Column (Ireland) by using a mixture of acetonitrile and 0.5% aqueous phosphoric acid (pH 3) (52 : 48, v/v) as the mobile phase. The chromatographic separation was isocratically performed at room temperature at a flow rate of 1.0 mL/min with UV detection at 315 nm. The method exhibited a linear dynamic range over 0.05–5.00 μg/mL FEB in human plasma. The lower limit of quantification was 0.05 μg/mL. The results of the intra- and interday precision and accuracy studies were within the acceptable limits. The validated method was successfully applied for the determination of FEB in human plasma samples for application in bioequivalence studies.
**Keywords:** Febuxostat, Human Plasma, LC-MS,MS

## M-456. Development and Validation of HPLC and HPTLC Methods for Determination of Cefoperazone and its Related Impurities

Abdelaleem EA, Naguib IA, Zaazaa HE and Hussein EA

*Journal of Chromatographic Science, 54(2): 179-186 (2016) IF: 1.32*

Validated sensitive and highly selective methods were developed for the quantitative determination of cefoperazone sodium (CEF) in the presence of its reported impurities; 7-aminocephalosporanic acid (7-ACA) and 5-mercapto-1-methyl-tetrazole (5-MER). Method A is high-performance liquid chromatography (HPLC), where the mixture of CEF and the reported impurities; 7-ACA and 5-MER were separated on a C8 column (5 μm ps, 250 mm × 4.6 i.d.) using methanol:0.05 M KH2PO4 buffer (22.5:77.5 v/v, pH 7.5) as a mobile phase. The three components were detected at 254 nm with a concentration range of 10-90 μg mL(-1) and the mean percentage recovery 99.67% (SD 1.465). Method B is high-performance thin layer chromatography (HPTLC), where the mixture of CEF and the

reported impurities were separated on silica gel HPTLC F254 plates using (acetone:methanol:ethyl acetate:2% sodium lauryl sulfate:glacial acetic acid) (3:2:3:0.8:0.2, by volume) as a developing system and scanning at 254 nm over a concentration range of 1-10 µg per band with the mean percentage recovery 99.95% (SD 1.335). The proposed methods were statistically compared with a reported HPLC method with no significant difference regarding accuracy and precision; indicating the ability of the proposed methods to be reliable and suitable for routine analysis of drug product. The proposed HPTLC method proved to be more sensitive, while the HPLC gave more reproducible results besides saving time.
**Keywords:** Cefoperazone Sodium, Impurities, HPLC and HPTLC

## M-457. Micellar Electrokinetic Chromatography (MEKC) with Multiresponse Chemometric Optimization for the Determination of Hydrochlorothiazide and Coformulated Antihypertensives in the Presence of Hydrochlorothiazide Major Impurity

Yasmin M. Fayez and Maha A. Hegazy

*Journal of Chromatographic Science, 54: 1050-1060 (2016) IF:1.32*

In this work, micellar electrokinetic chromatographic method was developed and optimized for the determination of hydrochlorothiazide (HCT) in the presence of irbesartan (IRB), bisoprolol (BISO) and HCT main impurity. Four factors affecting the separation—sodium dodecyl sulphate (SDS) concentration, buffer concentration, temperature and voltage—were studied. Optimization studies were performed with the aid of a central composite design with six central points. The optimal separation conditions were obtained by applying Derringer's desirability function, and the conditions were borate buffer 17 mM (pH = 9), SDS 5.2 mM, temperature 25°C and voltage 12 kV. HCT, IRB and BISO were successfully determined in their pure form and pharmaceutical formulations with separation in <8 min. Calibration curves (R > 0.999) were prepared and complete method validation was performed according to ICH guidelines. The results obtained were statistically compared with that of the official methods.
**Keywords:** Hydrochlorthiazide; Irbesartan; Chlorthiazide; SDS

## M-458. Simultaneous Determination of Aspirin, Dipyridamole and Two of their Related Impurities in Capsules by Validated Tlc-Densitometric and HPLC Methods

Nariman A. El-Ragehy, Nagiba Y. Hassan, Mahmoud A. Tantawy and Mohamed Abdelkawy

*Journal of Chromatographic Science, 54: 1120-1128 (2016) IF: 1.32*

Aspirin (ASP) and dipyridamole (DIP) are widely used as a combination in pharmaceutical formulations for treatment of strokes. Many of these formulations are containing tartaric acid as an excipient (in DIP pellets formulation for sustained release), which increases the probability of formation of dipyridamole tartaric acid ester impurity (DIP-I). On the other hand, salicylic acid (SAL) is considered to be one of the synthesis impurities and a degradation product of ASP. In this work, two chromatographic methods, namely, TLC-densitometry and HPLC, have been established and validated for simultaneous determination of ASP, DIP, SAL and DIP-I. Good separation was achieved by using silica gel as stationary phase and toluene–methanol–ethyl acetate (2:3:5, by volume) as mobile phase in the case of TLC-densitometry and Zorbax ODS column with mobile phase consisting of phosphate buffer (pH 3.3)–acetonitrile–triethylamine (40:60:0.03, by volume) for HPLC. Influence of different organic solvents in mobile phase composition has been studied to optimize the separation efficiency in TLC densitometry. Moreover, factors affecting the efficiency of HPLC, like pH of the buffer used, organic solvent ratio in the mobile phase and flow rate, have been carefully studied using one variable at a time approach. Finally, the proposed methods were validated as per ICH guidelines.
**Keywords:** Aspirin; Dipyridamole; HPLC; TLC

## M-459.Simultaneous Determination of Cinnarizine and Dimenhydrinate in Binary Mixture Using Chromatographic Methods

Nesrine T. Lamie and Hany H. Monir

*Journal of Chromatographic Science, 54: 36-42 (2016) IF: 1.32*

Two accurate and sensitive chromatographic methods have been developed and validated for simultaneous determination of cinnarizine (CIN) and dimenhydrinate (DIM). The first method utilizes simultaneous quantitative TLC spectrodensitometric evaluation of them, using ethyl acetate: methylene chloride (8: 2 by volume) as a mobile phase. Chromatograms are scanned at 254 nm. This method analyses cinnarizine in a concentration range of 0.5 – 6 µg/band with mean percentage recovery of 99.78±1.001 and dimenhydrinate in a concentration range of 1 – 6 µg/band with mean percentage recovery of 99.87±1.319. The second method is an HPLC method using methanol: acetonitrile: water (85: 10: 5; by volume + 0.5% TEA) as a mobile phase. The linearity was found to be in the range of 10-60 µg mL-1 and 5-60 µg mL-1 for CIN and DIM; respectively. The methods were successfully applied to the simultaneous determination of CIN and DIM in bulk powder, laboratory-prepared mixtures and pharmaceutical dosage forms. The validity of results was assessed by applying standard addition technique. The results obtained are found to agree statistically with those obtained by a reported method, showing no significant difference with respect to accuracy and precision.
**Keywords:** Cinnarizine; Dimenhydrinate; Densitometry; HPLC; TLC

## M-460. Stability-Indicating Method and LC–MS-MS Characterization of Forced Degradation Products of Sofosbuvir

M. Nebsen and Eman S. Elzanfaly

*Journal of Chromatographic Science, 54 (9): 1631-1640 (2016) IF: 1.32*

Sofosbuvir is a novel direct acting antiviral agent against hepatitis C virus. In the present work, a rapid, specific and reproducible isocratic reversed phase high performance liquid chromatography (RP-HPLC) method has been developed and

validated for the determination of sofosbuvir in the presence of its stressed degradation products. Sobosbuvir was subjected to hydrolysis (acidic, alkaline and neutral), oxidation, photolysis and thermal stress, as per international conference on harmonization (ICH) conditions. The drug showed degradation under oxidative, photolysis, acid and base hydrolysis stress conditions. However, it was stable under thermal and neutral hydrolysis stress conditions. Chromatographic separation of the drug from its degradation products was performed on Inertsil ODS-3 C18 (250 mm × 4.6 mm i.d., 5 µm) column using a green mobile phase of methanol:water 70:30 (v/v). The degradation products were characterized by LC–MS-MS and the fragmentation pathways were proposed. The developed method was validated as per ICH guidelines. No previous method was reported regarding the degradation behavior of sofosbuvir.

**Keywords:** Sofosbuvir, Stability-Indicating, LC–MS-MS

## M-461. Validated UPLC and TLC-Densitometry Stability Indicating Methods for the Determination of Rafoxanide in the Presence of its Degradation Products

Ahmed S. Saad, Abdallah M. Hamdy, Fathy M. Salama and Mohamed Abdelkawy

*Journal of Chromatographic Science, 54(9): 1661-1669 (2016) IF: 1.32*

Two sensitive and accurate stability-indicating chromatographic methods were developed and validated for the determination of rafoxanide (RFX). Degradation products were identified by mass spectrometry and IR spectroscopy. The first is ultra-performance liquid chromatography method where separation was performed using acetonitrile:0.005 M potassium dihydrogen orthophosphate (pH 3.5) in a ratio of 80:20 by volume as a mobile phase using a Hypersil GOLD™ C8 column 1.9 mm (50 × 2.1 mm), UV detection was adjusted at 220 nm and the flow rate was 0.6 mL min−1. The other is a thin-layer chromatography-densitometry method where separation was achieved using a mobile phase composed of chloroform:ethyl acetate:toluene:ammonia (5:4:3:0.1 by volume) on silica gel 60 F254 plates, and densitometric detection was done at 280 nm. Validation was achieved as per the ICH guidelines. The proposed methods proved to be accurate, robust, specific and suitable for application as stability-indicating methods for routine analysis of RFX in quality control laboratories.

**Keywords:**UPLC; TLC-Densitometry; Chromatography; Stability Indicating

## M-462.Chromatographic Determination of Aminoacridine Hydrochloride, Lidocaine Hydrochloride and Lidocaine Toxic Impurity in Oral Gel

Lories I. Bebawy, Mohamed R. Elghobashy, Samah S. Abbas and Rafeek F. Shokry

*Journal of Chromatographic Science, 54 (4): 492-499 (2016) IF: 1.32*

Two sensitive and selective analytical methods were developed for simultaneous determination of aminoacridine hydrochloride and lidocaine hydrochloride in bulk powder and pharmaceutical formulation. Method A was based on HPLC separation of the cited drugs with determination of the toxic lidocaine-related impurity 2,6-dimethylaniline. The separation was achieved using reversed phase column C18, 250 × 4.6 mm, 5 µm particle size and mobile phase consisting of 0.05 M disodium hydrogen phosphate dehydrate (pH 6.0 ± 0.2 adjusted with phosphoric acid) and acetonitrile (55 : 45, v/v). Quantitation was achieved with UV detection at 240 nm. Linear calibration curve was in the range of 1.00–10.00, 13.20–132.00 and 1.32–13.20 µg mL−1 for aminoacridine hydrochloride, lidocaine hydrochloride and 2,6-dimethylaniline, respectively. Method B was based on TLC separation of the cited drugs followed by densitometric measurement at 365 nm on the fluorescent mode for aminoacridine hydrochloride and 220 nm on the absorption mode for lidocaine hydrochloride. The separation was carried out using ethyl acetate–methanol–acetic acid (65 : 30 : 5 by volume) as a developing system. The calibration curve was in the range of 25.00–250.00 ng spot−1 and 0.99–9.90 µg spot−1 for aminoacridine hydrochloride and lidocaine hydrochloride, respectively. The results obtainedwere statistically analyzed and compared with those obtained by applying the manufacturer's method.

**Keywords:** Aminoacridine Hydrochloride, Lidocaine Hydrochloride , HPLC, Toxic Lidocaine-Related Impurity, TLC

## M-462. Development and Validation of HPLC and CE Methods for Simultaneous Determination of Amlodipine and Atorvastatin in the Presence of their Acidic Degradation Products in Tablets

Said A. Hassan, Eman S. Elzanfaly, Badr A. El-Zeany and Maissa Y. Salem

*Acta Pharmaceutica, 66: 479-490 (2016) IF: 1.212*

Two methods were developed for separation and quantitation of amlodipine (AML) and atorvastatin (ATV) in the presence of their acidic degradation products. The first method was a simple isocratic RP-HPLC method while the second was capillary electrophoresis (CE). Degradation products were obtained by acidic hydrolysis of the two drugs and their structures were elucidated for the first time by IR and MS spectra. Degradation products did not interfere with the determination of either drug and the assays were therefore stability-indicating. The linearity of the proposed methods was established over the ranges 1-50 µg mL-1 for AML and ATV in the HPLC method and in the range of 3-50 and 4-50 µg mL-1 for AML and ATV, respectively, in the CE method. The proposed methods were validated according to ICH guidelines. The methods were successfully applied to estimation of AML and ATV in combined tablets.

**Keywords:** Atorvastatin; Amlodipine; Capillary Zone Electrophoresis; HPLC; Stability; Acidic Degradation

## M-463.Simultaneous Quantitative Analysis of Olmesartan, Amlodipine and Hydrochlorothiazide in their Combined Dosage form Utilizing Classical and Alternating Least Squares Based Chemometric Methods

Hany W. Darwish, Ahmed H. Bakheit and Ali S. Abdelhameed

*Acta Pharmaceutica, 66: 83-95 (2016) IF: 1.212*

Simultaneous spectrophotometric analysis of a multi-component dosage form of olmesartan, amlodipine and hydrochlorothiazide used for the treatment of hypertension has been carried out using various chemometric methods. Multivariate calibration methods include classical least squares (CLS) executed by net analyte processing (NAP-CLS), orthogonal signal correction (OSC-CLS) and direct orthogonal signal correction (DOSC-CLS) in addition to multivariate curve resolution-alternating least squares (MCR-ALS). Results demonstrated the efficiency of the proposed methods as quantitative tools of analysis as well as their qualitative capability. The three analytes were determined precisely using the aforementioned methods in an external data set and in a dosage form after optimization of experimental conditions. Finally, the efficiency of the models was validated via comparison with the partial least squares (PLS) method in terms of accuracy and precision.

**Keywords:** Multivariate Calibration Methods; Olmesartan Medoxomil; Amlodipine Besylate; Hydrochlorothiazide; Spectrophotometry; Pharmaceutical Tablets

## M-464. On-Column Decaffeination and HPLC Analysis of Epigallocatechin Gallate in Green Tea Nutraceuticals

Heba-Alla H. Abd-ElSalam, Medhat A. Al-Ghobashy, Hala E. Zaazaa and Mohamed A. Ibrahim

*Separation Science and Technology, 51(4) (2016) IF: 1.083*

Green tea (GT) derived epigallocatechin gallate (EGCG) is a commonly used nutraceutical for its antioxidant activity. Caffeine is the second major component and interferes with extraction of EGCG. On-column decaffeination was optimized to enable selective enrichment of EGCG, though less retained than caffeine. EGCG recovery and loss in caffeine were determined using RP-HPLC. Results indicated a significant improvement in caffeine removal and EGCG recovery. The SPE-HPLC protocol represents a model for an efficient and economic approach for improving dynamic capacity, selectivity, and sensitivity towards less retained analytes. This is particularly important for analysis of inherently complex samples of nutraceutical products.

**Keywords:** Catechins, Epigallocatechin Gallate, On-Column Decaffeination, Solid Phase Extraction

## M-465. Determination of Cefoperazone Sodium in Presence of Related Impurities by Improved Classical Least Squares Chemometric Methods: A Comparative Study

Ibrahim A. Naguib and HanyW. Darwish

*Journal of Chemistry, (2016) IF: 0.996*

A comparative study is established among 4 chemometric models depending on classical least squares (CLS) approach, namely, spectral residual augmented CLS (SRACLS), net analyte processing CLS (NAP-CLS), orthogonal signal correction CLS (OSC-CLS), and direct orthogonal signal correction CLS (DOSC-CLS). The comparison is expressed through analysis of a case study dataset of UV spectral data of Cefoperazone Sodium (CEF) and its two related impurities: in pure powder form and in pharmaceutical dosage form. Four-level three-factor experimental design was established for optimum analysis. The adopted experimental design gave rise to a training set consisting of 16 mixtures (containing different ratios of interfering species). To test the prediction power of the suggested models, an independent test set consisting of 9 mixtures was used. The presented results show the ability of the proposed models to quantify CEF in presence of two related impurities with high accuracy and selectivity (, , , and for SRACLS, NAP-CLS, OSC-CLS, and DOSC-CLS, resp.). Dosage form analysis results were compared statistically to a published HPLC methodology showing insignificant difference in terms of precision and accuracy, indicating the suggested models reliability and their suitability for quality control analysis of drug product. Compared to other models, OSC-CLS and DOSC-CLS models gave more accurate results with lower prediction error for test set samples.

**Keywords:** SRACLS; OSC-CLS

## M-466. Highly Sensitive Micellar Enhanced Spectrofluorimetric Method for Determination of Mirtazapine in Tablets and Human Urine: Application to in Vitro Drug Release and Content Uniformity Test

Hany W. Darwish, Ahmed H. Bakheit and Raed M. Alharbi

*Journal of Chemistry, (2016) IF: 0.996*

A highly sensitive and simple micelle enhanced spectrofluorimetric method was developed for assaying mirtazapine (MRZ) in REMERON® tablets and spiked human urine directly without the need of derivatizing agent. The basis of the current procedure is the examination of the relative fluorescence intensity (RFI) of MRZ in sodium lauryl sulphate (SLS) micellar medium. The RFI of MRZ in water was enhanced markedly on addition of SLS. The RFI was measured at 403 nm after excitation at 320 nm. The fluorescence-concentration relationship was linear over the range 1–500 ng/mL, with lower detection limit of 0.399 ng/mL. The proposed method was successfully applied to the determination of MRZ in dosage form and spiked human urine. Recovery percentages of MRZ utilizing the current method were , , and % for pure powder, pharmaceutical dosage form, and spiked human urine, respectively. The application of the proposed method was extended to test content uniformity and the in vitro drug release of REMERON tablets, according to USP guidelines.

**Keywords:** Mirtazapine Fluorescence Urine

## M-469.Chromatographic Analysis of a Multicomponent Mixture of B1, B6, B12, Benfotiamine, and Diclofenac; Part I: HPLCand UPLC Methods for the Simultaneous Quantification of these Five Components in Tablets and Capsules

Fayed AS, Hegazy MA and Wahab NS

*Journal of Aoac International, 99: 1513-1521 (2016) IF: 0.918*

New, simple, highly sensitive, precise, and accurate gradient reversed-phase chromatographic methods were developed using HPLC and ultra-HPLC (UPLC) systems for the determination of five components, namely thiamine, pyridoxine, cyanocobalamin, benfotiamine, and diclofenac in tablets and capsules. The

methods were compared for their efficiency in the separation and determination of these five compounds using two different C18 columns (250 × 4.6 mm, 5 µm; and 100 × 4.6 mm, 2.6 µm) for HPLC and UPLC, respectively. Chromatographic separation was performed with a mobile phase containing acetonitrile and 0.025 M phosphate buffer (pH 3.5), with a gradient program and a flow rate of 1.5 and 1.0 mL/min for both methods, respectively. The methods were validated according to International Conference on Harmonization guidelines. Linearity was achieved in the range of 5.00 to 150.00 µg/mL for each of the five compounds. Ruggedness and intermediate precision were confirmed by different analysts on different columns on different days. Moreover, the components were subjected to an accelerated stability study under acidic, alkaline, and oxidative stress conditions and no interfering peaks were observed. The five compounds were efficiently separated in <20 min by HPLC, whereas for UPLC, separation was achieved in <8 min, which dramatically decreased the consumption of organic solvents.

**Keywords:** B1; B6; B12; Vitamins; Benfotiamine and Diclofenac

## M-476.Validated Stability-Indicating RP-HPLC Method for Simultaneous Determination of Clorsulon and Ivermectin Employing Plackett-Burman Experimental Design for Robustness Testing

Saad AS, Ismail NS, Soliman M. and Zaazaa HE

*Journal of Aoac International, 99(2): 0-0 (2016) IF: 0.918*

A sensitive and highly selective stability-indicating gradient HPLC method was developed and validated for simultaneous determination of clorsulon (CLO) and ivermectin (IVM) in the presence of their degradation products. The drugs were subjected to different stress conditions, including acid and alkaline hydrolysis, oxidative, thermal, and photolytic forced degradation. The robustness of the proposed method was assessed using the Plackett-Burman experimental design, the factors affecting system performance were defined, and nonsignificant intervals for the significant factors were determined. The separation was carried out on a ZORBAX SB phenyl analytical column (250 × 4.6 mm id, 5 µm particle size), with gradient elution utilizing 10 mM sodium dihydrogen phosphate and acetonitrile as mobile phase. UV detection was performed for CLO and IVM at 254 nm over a concentration range of 4-140 and 5-50 µg/mL, respectively, with mean percentage recoveries of 99.90 ± 1.30 and 98.59 ± 1.16%, respectively. The proposed method was successfully applied to a pharmaceutical dosage form containing the investigated drugs. The results were statistically compared with the official HPLC methods, and no significant differences were found.

**Keywords:** Stability-Indicating, HPLC,Clorsulon (CLO) and Ivermectin.

## M-472.Partial Least-Squares and Linear Support Vector Regression Chemometric Methods for Simultaneous Determination of Amoxicillin Trihydrate and Dicloxacillin Sodium in the Presence of their Common Impurity

Naguib IA, Abdelaleem EA, Zaazaa HE and Hussein EA.

*Journal of Aoac International, 99(4): 0-0 (2016) IF: 0.918*

Two multivariate chemometric models, namely, partial least-squares regression (PLSR) and linear support vector regression (SVR), are presented for the analysis of amoxicillin trihydrate and dicloxacillin sodium in the presence of their common impurity (6-aminopenicillanic acid) in raw materials and in pharmaceutical dosage form via handling UV spectral data and making a modest comparison between the two models, highlighting the advantages and limitations of each. For optimum analysis, a three-factor, four-level experimental design was established, resulting in a training set of 16 mixtures containing different ratios of interfering species. To validate the prediction ability of the suggested models, an independent test set consisting of eight mixtures was used. The presented results show the ability of the two proposed models to determine the two drugs simultaneously in the presence of small levels of the common impurity with high accuracy and selectivity. The analysis results of the dosage form were statistically compared to a reported HPLC method, with no significant difference regarding accuracy and precision, indicating the ability of the suggested multivariate calibration models to be reliable and suitable for routine analysis of the drug product. Compared to the PLSR model, the SVR model gives more accurate results with a lower prediction error, as well as high generalization ability; however, the PLSR model is easy to handle and fast to optimize.

**Keywords:** Multivariate Chemometric Models ,Impurities; Amoxicillin Trihydrate and Dicloxacillin Sodium.

## M-475.Stability Study and Kinetic Monitoring of Cefquinome Sulfate Using Cyclodextrin-Based Ion-Selective Electrode: Application to Biological Samples

Ali M. Yehia, Reham M. Arafa, Samah S. Abbas and Sawsan M. Amer

*Journal of AOAC International, 99: 73-81 (2016) IF: 0.918*

Two novel cefquinome sulfate (CFQ)-selective electrodes were performed with dibutyl sebacate as a plasticizer using a polymeric matrix of polyvinyl chloride. Sensor 1 was prepared using sodium tetraphenylborate as a cation exchanger without incorporation of ionophore, whereas 2-hydroxy propyl β-cyclodextrin was used as ionophore in sensor 2. A stable, reliable, and linear response was obtained in concentration ranges 3.2 × 10(-5) to 1 × 10(-2) mol/L and 1 × 10(-5) to 1 × 10(-2) mol/L for sensors 1 and 2, respectively. Both sensors could be sufficiently applied for quantitative determination of CFQ in the presence of degradation products either in bulk powder or in pharmaceutical formulations. Sensor 2 provided better selectivity and sensitivity, wider linearity range, and higher performance. Therefore it was used successfully for accurate determination of CFQ in biological fluids such as spiked plasma and milk samples. Furthermore, an online kinetic

study was applied to the CFQ alkaline degradation process to estimate the reaction rate and half-life with feasible real-time monitoring. The developed sensors were found to be fast, accurate, sensitive, and precise compared with the manufacturer's reversed-phase chromatographic method.
**Keywords:** Cefquinome Sulfate; Potentiometry; Stability Study; Kinetic Study.

## M-470.Comparative Study of PVC-Free All-Solid-State, PVC Membrane, and Carbon Paste Ion-Selective Electrodes for the Determination of Dapoxetine Hydrochloride in Pharmaceutical Formulation

Azza Aziz and Nesrin Khamees

*Journal of Aoac International, 99: 1499-1504 (2016) IF: 0.918*

The potentiometric response characteristics and analytical applications of a poly(vinyl chloride) (PVC)-free all-solid-state ion-selective electrode for dapoxetine hydrochloride (DAP) are examined. The Nernstian response of the electrode was evaluated by comparison with PVC-based liquid membrane and carbon paste electrodes. The PVC-free electrode is prepared by direct incorporation of dapoxetine-tetraphenyl borate (DAP–TPB) as a sensing element into a commercial nail varnish containing cellulose acetate propionate. The composite was applied onto a 3 mm diameter graphite disk electrode. The electrode exhibited a Nernstian slope of 56.0 mV/decade in the concentration range of 1 × 10−4 to 1 × 10−2 mol/L with an LOD of 2 × 10−5 mol/L. The electrode is independent of pH in the range of 2 to 6 and showed good selectivity for DAP with respect to a large number of inorganic cations and amino acids. Comparable Nernstian slope, sensitivity, pH range, and selectivity pattern were obtained with a PVC membrane and a carbon paste incorporating DAP–TPB as a sensing element and dioctylphthalate as a solvent mediator. The electrodes were used for the determination of DAP in pure solution and in tablets without extraction with high accuracy and precision (RSD ≤ 2%). The nail varnish solid-state electrode is simple, economical, and rapid
**Keywords:**PVC Membrane, Carbon Paste, Ion Selective Electrode, Dapoxetine Hydrochloride

## M-474. For Stability-Indicating Analysis of Agomelatine and its Degradation Products: A Comparative Study

Ibrahim A. Naguib, Maha M. Abdelrahman, Mohamed R. El Ghobashy and Nesma A. Ali

*Journal of AOAC International, 99: 386-395 (2016) IF: 0.918*

Two accurate, sensitive, and selective stability indicating methods are developed and validated for simultaneous quantitative determination of agomelatine (AGM) and its forced degradation products (Deg I and Deg II), whether in pure forms or in pharmaceutical formulations. Partial least squares regression (PLSR) and spectral residual augmented classical least-squares (SRACLS) are two chemometric models that are being subjected to a comparative study through handling UV spectral data in range (215–350 nm). For proper analysis, a three-factor, four-level experimental design was established, resulting in a training set consisting of 16 mixtures containing different ratios of interfering species. An independent test set consisting of eight mixtures was used to validate the prediction ability of the suggested models. The results presented indicate the ability of mentioned multivariate calibration models to analyze AGM, Deg I, and Deg II with high selectivity and accuracy. The analysis results of the pharmaceutical formulations were statistically compared to the reference HPLC method, with no significant differences observed regarding accuracy and precision. The SRACLS model gives comparable results to the PLSR model; however, it keeps the qualitative spectral information of the classical least squares algorithm for analyzed components.
**Keywords:** Partial Least Squares Regression, Spectral Residual Augmented Classical Least-Squares, Agomelatine

## M-475.Chemometrics Tools in Detection and Quantitation of the Main Impurities Present in Aspirin/Dipyridamole Extended-Release Capsules

Nariman A. El-Ragehy, Ali M. Yehia, Nagiba Y. Hassan, Mahmoud A. Tantawy and Mohamed Abdelkawy

*Journal of Aoac International, 99: 948-956 (2016) IF: 0.918*

Aspirin (ASP) and dipyridamole (DIP) in combination is widely used in the prevention of secondary events after stroke and transient ischemic attack. Salicylic acid is a well-known impurity of ASP, and the DIP extended-release formulation may contain ester impurities originating from the reaction with tartaric acid. UV spectral data analysis of the active ingredients in the presence of their main impurities is presented using multivariate approaches. Four chemometric-assisted spectrophotometric methods, namely, partial least-squares, concentration residuals augmented classical least-squares (CRACLS), multivariate curve resolution (MCR) alternating least-squares (ALS), and artificial neural networks, were developed and validated. The quantitative analyses of all the proposed calibrations were compared by percentage recoveries, root mean square error of prediction, and standard error of prediction. In addition, r2 values between the pure and estimated spectral profiles were used to evaluate the qualitative analysis of CRACLS and MCR-ALS. The lowest error was obtained by the CRACLS model, whereas the best correlation was achieved using MCR-ALS. The four multivariate calibration methods could successfully be applied for the extended-release formulation analysis. The application results were also validated by analysis of the stored dosage-form solution, which showed a susceptibility of DIP esterification in the extended-release formulation. Statistical comparison between the proposed and official methods showed no significant difference.
**Keywords:** Aspirin; Dipyridamole; Chemometry

## M-476. Analytical Eco-Scale for Assessing the Greenness of A Developed Rp-Hplc Method Used for Simultaneous Analysis of Combined Antihypertensive Medications

Heba M. Mohamed and Nesrine T. Lamie

*Journal of Aoac International, 99: 1260-1265 (2016) IF: 0.918*

In the past few decades the analytical community has been focused on eliminating or reducing the usage of hazardous chemicals and solvents, in different analytical methodologies, that have been ascertained to be extremely dangerous to human health and environment. In this context, environmentally friendly, green, or clean practices have been implemented in different research areas. This study presents a greener alternative of conventional RP-HPLC methods for the simultaneous determination and quantitative analysis of a pharmaceutical ternary mixture composed of telmisartan, hydrochlorothiazide, and amlodipine besylate, using an ecofriendly mobile phase and short run time with the least amount of waste production. This solvent-replacement approach was feasible without compromising method performance criteria, such as separation efficiency, peak symmetry, and chromatographic retention. The greenness profile of the proposed method was assessed and compared with reported conventional methods using the analytical Eco-Scale as an assessment tool. The proposed method was found to be greener in terms of usage of hazardous chemicals and solvents, energy consumption, and production of waste. The proposed method can be safely used for the routine analysis of the studied pharmaceutical ternary mixture with a minimal detrimental impact on human health and the environment.

**Keywords:** Green Analysis; Hazardous Solvents; Telmisartan; Hydrochlorothiazide; Amlodipine; Analytical Eco-Scale.

## M-477. Stability Indicating Determination of Human Growth Hormone by Novel SE-LC Method

Mamdouh R. Rezk, Mostafa A. Shehata, Marwa F. Mohamed and Faten Abdel Aziz Fathalla

*Journal of Aoac International, 99: 1266-1272 (2016) IF: 0.918*

A selective, rapid size-exclusion chromatographic method was developed and validated for the separation of the human growth hormone (hGH) somatropin from its high-molecular-weight aggregates. Separation was achieved using a nontoxic mobile phase compared with the official method of the European Pharmacopoeia that uses 2-propanol in a mobile phase. The developed method used a YMC-Pack Diol (YMC Karasuma, Kyoto, Japan; 300 × 8.0 mm, 5 μm) analytical column. The mobile phase was formed with a pH 7 phosphate buffer that was pumped at a flow rate of 1 mL/min with UV detection at 214 nm. The overall run time was 20 min and the average retention times were found to be 10.21 min for the monomer peak, 9.52 min for the dimer peak, and 9.14 min for the higher aggregate. This method was validated in terms of selectivity, linearity, and intra- and inter day variations according to the International Conference on Harmonization guidelines. The developed method was applied as a rapid tool for evaluating the stability of stressed samples of hGH subjected to different temperature, agitation, and repeated freeze–thaw cycles. The developed method was successfully applied for the assessment of the quality and quantity of hGH during downstream processing, formulation, and storage.

**Keywords:** Human Growth Hormone; Size-Exclusion Chromatography; Stability.

## M-478.Robust Assessment of Molecular Size Distribution of Meningococcal Ac Vaccine

Asmaa R. Hussein, Mamdouh R. Rezk, Faten Abdel Aziz Fathalla and Mostafa A. Shehata

*Journal of Aoac International, 99: 1589-1595 (2016) IF: 0.918*

The molecular size of meningococcal polysaccharides is an important physicochemical parameter that is related to immunogenicity and efficacy. A simple method for size-exclusion chromatography was developed, optimized, and applied for safe and rapid fractionation of meningococcal polysaccharide AC vaccine. Pooling of the fractions collected from size-exclusion chromatography was investigated and evaluated, rather than analyzing each fraction separately, for determining the percentages of meningococcal polysaccharide A and C that were eluted before the distribution coefficient of 0.5. Pooling is preferred rather than analyzing each fraction individually, as it is easily handled, faster, simpler, less expensive, more accurate, safe, and applicable. The developed method was validated and successfully applied for the determination of meningococcal polysaccharide vaccine serotype A and C in quality-control and commercial samples.

**Keywords:** Meningococcal; Vaccine; Molecular Size Distribution.

## M-478. Stability Indicating Spectrofluorimetric Analysis of Metopimazine by Signal Enhanced - Partial Least Squares Chemometric Models: A Comparative Study

Hany W. Darwish, Ibrahim A. Darwish and Ahmed H. Bakheit

*Current Pharmaceutical Analysis, 12: 234-243 (2016) IF: 0.885*

**Introduction:** Predictability of partial least squares regression (PLSR) method is improved by four multivariate signal processing modelling approaches; including genetic algorithm PLS (GAPLS), net analyte processing PLS (NAP-PLS), orthogonal signal correction PLS (OSC-PLS) and direct orthogonal signal correction PLS (DOSC-PLS). The objective of the introduced work is to establish a comparison among proposed chemometric models; indicating the constituent algorithm of each and setting a comparison of analysis results. **Method:** The proposed models are compared through stability indicating analysis of mixtures of metopimazine (MTP) and its reported degradation products via handling spectrofluorimetric data, at excitation wavelength of 268 nm and working emission range of 420-520 nm. The degradation products include the oxidative degradation product (OMTP) and the alkaline hydrolysis degradation product (AMTP). A 3-factor 5-level experimental design was set; ending up with a training set of 25 mixtures containing different ratios of the interfering components. A test set composed of 12 mixtures was implemented to validate the predictive ability of the proposed models. Leave one out- cross validation procedure (LOO-CV) was used to predict optimum number of PLS components. **Result:** The 4 introduced models were successfully applied to assay MTP in raw material and the best results were given by GA-PLSR (test set 99.00% ± 2.980). **Conclusion:** The 4 models were applied to analysis of pharmaceutical tablets, then statistically compared to a reported spectrofluorimetric method; showing no significant difference regarding accuracy and

precision; indicating the ability of the suggested models to be trusted for routine quality control analysis of pharmaceutical product.
**Keywords:** DOSC-PLS; GA-PLS; NAP-PLS; OSC-PLS; Metopimazine; Spectrofluorimetry.

## M-480. Determination of Aliskiren Hemifumarate and Amlodipine Besylate in their Combined Dosage form by Different Spectrophotometric Methods

Mohamed Refaat Elghobashy, Nancy Wahid Nashat, Samah Sayed Abbas and Azza Aziz Moustafa

*Current Pharmaceutical Analysis, 12: 391-398 (2016) IF: 0.885*

**Background:** Aliskiren hemifumarate and amlodipine besylate are two anti-hypertensive drugs. They are used together in pharmaceutical dosage froms to lower blood pressure and relieve anginal pain. **Method:** Five simple, sensitive and rapid spectrophotometric methods were presented for the determination of aliskiren hemifumarate and amlodipine besylate in their combined dosage form. These methods were based on direct measurement of amlodipine besylate at 360 nm; due to lack of interference of aliskiren hemifumarate, over a concentration range of 5-35 µg mL-1 with mean recovery percentage 100.41±0.65. Aliskiren hemifumarate was determined without prior separation by; first derivative values at 290 nm (A), ratio difference method using values at 249 nm and 286.4 nm with 35 µg mL-1 of amlodipine besylate as a divisor (B), derivative ratio values at 290.6 nm utilizing 35 µg mL-1 of amlodipine besylate as a divisor (C), ratio subtraction method using values at 280.4 nm (D), measuring absorbance at isosbestic point 270.1 nm (E). **Results:** These methods were found linear for aliskiren hemifumarate over a concentration range of 30- 150 µg mL-1. The suggested methods were validated according to ICH guidelines using laboratoryprepared mixtures. Statistical analysis of the results showed no significant difference between the proposed and the reported methods with respect to accuracy and precision. **Conclusion:** The suggested methods were found to be simple, accurate and selective regarding the two cited drugs. This allows for their incorporation in the quality control analysis where time and economy are of great value.
**Keywords:** Aliskiren Hemifumarate; Amlodipine Besylate; Derivative Spectrophotometry; Ratio Difference; Isosbestic Point, Ratio Subtraction.

## M-481. Development and Validation of Stability-Indicating Methods for Determination of Torsemide

H. E. Zaazaa, S. S. Abbas, H. M. Essam and M. G. El-Bardicy

*Bulletin of The Chemical Society of Ethiopia, 30(1): 13-25 (2016) IF: 0.623*

Four sensitive and precise methods for determination of torsemide in presence of its degradation product and in pharmaceutical formulation were developed and validated. Method A is the second derivative spectrophotometry at 262.4 nm with mean percentage recoveries 100.06±0.75. Method B is first derivative of the ratio spectra spectrophotometry, at 232.4, 244.6 nm and at the total peak amplitude from the maximum at 232.4 nm to the minimum at 244.6 nm (1DD232.4+244.6nm). Method C is a TLC-densitometric one, for torsemide separation using acetone : chloroform : ethyl acetate (4:4:2 v/v) as a developing system. Method D is HPLC one, it provides complete separation of torsemide from its degradation product on C8 column with UV detection at 287 nm and recovery 99.98±0.76. The proposed methods have been successfully applied to the analysis of torsemide in pharmaceutical formulations without interference from other additives and the results were statistically compared with the official method.
**Keywords:** Hplc, Stability-Indicating, Spectrophotometry, Tlc-Densitometry, Torsemide.

## M-482. A Validated Direct Thin-Layer Chromatographic Separation and Enantioselective Determination of Racemic Centrally Acting Drugs Using Ion-Pair and Ligand-Exchange Chiral Selectors: A Thermodynamic Study of Complexation

Nahla N. Salama, Hala E. Zaazaa, Lobna M. Abd El Halim, Maissa Y. Salem, and Laila E. Abd El Fattah

*Jpc-Journal of Planar Chromatography-Modern Tlc, 29(3): 176-183 (2016) IF: 0.611*

A rapid, inexpensive, and stereoselective densitometric—thin-layer chromatographic (TLC) method using l-(+)-tartaric acid and l-histidine—Cu complex as chiral mobile phase additive for the enantioseparation of atracurium besylate and atropine sulfate, respectively, and quantitative determination of their chiral switching (eutomer) isomers, cisatracurium besylate and hyoscyamine sulfate, were used in this study. The effect on resolution of different chiral selector concentrations, temperatures, and pH values was investigated. The spots were detected with ultraviolet (UV) lamp followed by densitometric measurements at 280 nm and 215 nm for cisatracurium besylate and hyoscyamine sulfate, respectively. The mobile phases enabling successful resolution were acetonitrile—methanol—dichloromethane—glacial acetic acid—H2O containing 70 mg l-(+)-tartaric acid (7:1:0.5:0.7:1, by volume), pH 5 for atracurium besylate, and methanol—H2O containing 40 mmol l-histidine and 20 mmol copper(II) acetate (8.8:1.2, by volume), pH 6.5 for atropine sulfate. Thermodynamic parameters, enthalpy ΔH and entropy ΔS were investigated to study the effect of temperature on the enantioseparation using the Van't Hoff plot.
**Keywords:** Chiral Separation; Cisatracurium Besylate; Hyoscyamine Sulfate; Chiral Selector; Thermodynamic Functions.

## M-481. Determination of Dantrolene Sodium in the Presence of its Process-Related Impurity by High-Performance Thin-Layer Chromatography Spectrodensitometry

Nada S. Abdelwahab, Mohammed T. Elsaady, Aml G. Korany and Maha A. Hgazy

*Journal of Planar Chromatography, 29:462-468(2016)IF: 0.611*

Dantrolene sodium (DAN) is widely used as a muscle relaxant drug for the treatment of malignant hyperthermia. 5-(4-Nitrophenyl)- 2-furaldehyde is reported to be DAN-related compound C (DC), and it is the synthetic precursor of DAN that may be presented as process-related impurity in a

pharmaceutical formulation. Also, it is considered to be the acidic and photolytic degradation product of DAN. The synthesis of DC has been performed from p-nitroaniline with good yield and high purity; structure elucidation has been confirmed by infrared (IR), mass spectrometry (MS), and nuclear magnetic resonance (NMR) analyses. In the present study, high-performance thin-layer chromatography (HPTLC) technique was developed and validated for the separation and quantification of DAN along with DC. Separation was carried out on HPTLC silica gel 60 F254 plates using a developing system consisting of chloroform–ethylacetate–acetic acid (10:0.5:0.01, by volume) with ultraviolet (UV) scanning at 380 nm. The method was highly sensitive and could be used for the determination of DAN and DC in the range of 0.1–1.5 μg band−1 and 0.1–2.0 μg band−1, respectively. The method has been validated in compliance with the International Conference on Harmonization (ICH) guidelines and was successfully applied to a pharmaceutical formulation. The method was compared favorably with the reported British Pharmacopoeia high-performance liquid chromatography (BP HPLC) method.

**Keywords:** Dantrolene Dantrolene Impurity High-Performance Thin-Layer Chromatography Validation Synthesis

## M-484. Rapid Validated Liquid Chromatographic Method Coupled with Tandem Mass Spectrometry for Quantification of Nintedanib in Human Plasma

Hany W. Darwish, Mohamed W. Attwa and Adnan A. Kadi

*Tropical Journal of Pharmaceutical Research, 15: 2467-2473 (2016) IF: 0.543*

**Purpose:** To develop and validate a fast, sensitive, and simple liquid chromatographic method coupled with tandem mass spectrometry for the determination of the potent tyrosine kinase inhibitor, ninetedanib (NTB) in plasma, utilizing cyclobenzaprine (CBP) as internal standard (IS). **Methods:** Separation of the two components (NTB and CBP) was performed on a pentafluorophenyl (PFP) reversed phase column (50 × 2 mm, 3μm) at ambient temperature using isocratic elution with acetonitrile-water (60:40, v/v) containing 0.01 M ammonium formate buffer (pH 4.2) at a flow rate of 0.4 mL/min. NTB and CBP were monitored by a triple quadrupole tandem mass spectrometer with electrospray ionization source in the positive ion mode. The current method was validated following the European Medicines Agency (EMA) guidelines **Results:** The proposed method allowed rapid and specific quantification of NTB in the calibration range of 2 - 150 ng/mL and determination coefficient of ≥ 0.999. Intra- and inter-day accuracy and precision were < 4 % in all cases. **Conclusion:** The developed procedure is rapid, specific, reliable, and validated for quantification of NTB in human plasma, and thus can be applied efficiently for the analysis of clinical samples containing NTB.

**Keywords:** Nintedanib Assay; Cyclobenzaprine; Lc-Ms/Ms; Validation.

## M-483.A Novel Method to Determine New Potent Angiotensin Inhibitor, Azilsartan, in Human Plasma Via Micelle-Enhanced Spectrofluorimetry Using Cremophor RH 40

Hany W. Darwish, Ahmed H. Bakheit, Ali S. Abdelhameed and Bakheit Mustafa

*Tropical Journal of Pharmaceutical Research, 15: 1003-1012 (2016) IF: 0.543*

**Purpose:** To develop a micelle-enhanced spectrofluorimetric method for the assay of azilsartan (AZL) in bulk form and spiked human plasma without the need for derivatization procedure. Method: The proposed method was based on studying the fluorescence behavior of AZL in Cremophor RH 40 (Cr RH 40) micellar system. The fluorescence intensity was measured at 371 nm after excitation at 264 nm. The proposed procedure was validated according to International Council on Harmonization (ICH) guidelines. **Results:** In aqueous solution, the fluorescence intensity of AZL was greatly enhanced by more than 3- fold in the presence of Cr RH 40. The fluorescence – concentration plot was linear over the range of 10 – 500 ng.mL-1, with a limit of detection of 3.287 ngmL-1. The proposed method was successfully applied to the determination of AZL in pure powder form and spiked human plasma. The mean recovery of AZL in spiked human plasma using the proposed method was 90.54 ± 1.17 %. Conclusion: The suggested method is highly sensitive and simple, and can easily be applied for the quantification of AZL in pure powder form as well as in biological fluids such as plasma

**Keywords:** Azilsartan, Spectrofluorimetry, Spiked Human Plasma, Micellar System.

## M-482. A New Spectrofluorimetric Assay Method for Vandetanib in Tablets, Plasma and Urine

Hany W. Darwish and Ahmed H. Bakheit

*Tropical Journal of Pharmaceutical Research, 15: 1319-1326 (2016) IF: 0.543*

**Purpose:** To develop a simple and sensitive spectrofluorimetric method for the determination of vandetanib (VDB) in tablets (containing 100 mg of the drug) and biological fluids (spiked human plasma and urine). **Methods:** The proposed method is based on examining the intrinsic fluorescence intensity of VDB in acetonitrile at 480 nm after excitation at 330 nm. Factors affecting fluorescence intensity of the cited drug (VDB), including the influence of pH, diluting solvent and time, were studied and optimized by one factor at a time approach. A calibration curve was constructed by plotting VDB fluorescence intensity at 480 nm versus VDB concentrations in ng mL-1. The method was validated according to the recommendations of International Conference on Harmonisation (ICH) for validation of the analytical procedures **Results:** The linearity range of the method was 20 – 600 ng mL-1, with limits of quantification (LOQ) and of detection (LOD) of 30.45 and 10.05 ng mL-1, respectively. The adopted method was applied successfully to the quantitation of VDB in pure powder form (100.90 ± 0.91 %), laboratory prepared tablets (97.86 ± 1.42 %), spiked human plasma (97.97 ± 2.36 %) and urine (97.59 ± 0.87 %). Comparison of the proposed method with that of liquid chromatography-tandem mass spectrometry showed that there

was no significant difference ($p < 0.05$) between the two methods in terms of accuracy and precision. **Conclusion**: The proposed method is simple and highly sensitive and, consequently, can be applied to assay VDB in biological samples as well as in dosage form.
**Keywords:** Vandetanib; Spectrofluorimetry; Assay; Validation; Human Plasma; Human Urine; Dosage Forms.

## M-484. Enhanced Spectrofluorimetric Determination of the Multitargeted Tyrosine Kinase Inhibitor, Crizotinib, in Human Plasma Via Micelle-Mediated Approach

Hany W. Darwish, Ahmed H. Bakheit and Ibrahim A. Darwish

*Tropical Journal of Pharmaceutical Research, 15: 1319-1326 (2016) IF: 0.543*

**Purpose:** To quantify the multi-targeted tyrosine kinase inhibitor, crizotinib, in human plasma and bulk powder by highly sensitive micellar enhanced spectrofluorimetric procedure. **Method:** The developed procedure was based on measuring the fluorescence intensity of crizotinib (CRZ) in sodium dodecyl sulphate (SDS) micellar system at 404 nm after excitation at 271 nm. Validation of the developed procedure was carried out following ICH (International Council for Harmonization) guidelines. **Results:** Maximum fluorescence intensity (FI) was attained by addition of 0.2 mL SDS and 0.2 mL HCl (1N) to CRZ aliquots and then dilution with distilled water. There was a linear relationship between the FI of CRZ and its concentration over the range, 5 – 400 ng/mL, with limit of detection and of quantification of 1.857 and 5.628 ng/mL respectively. The developed procedure was successfully applied to assay CRZ in pure powder form and spiked human plasma with mean recovery of 100.68 ± 0.37 and 99.98 ± 0.20 %, respectively. **Conclusion:** The developed procedure is simple and sensitive, and can be applied to routine analysis of CRZ in pure powder form as well as in clinical laboratories for the determination of CRZ in plasma.
**Keywords:** Crizotinib; Spectrofluorimetry; Micelle; Human Plasma; Sodium Dodecyl Sulphate.

## M-486. Spectrophotometric Method for the Determination of two Coformulated Drugs with Highly Different Concentrations. Application on Vildagliptin and Metformin Hydrochloride

H. E. Zaazaa, E. S. Elzanfaly, A. T. Soudi and M. Y. Salem

*Journal of Applied Spectroscopy, 83(1),(2016) IF: 0.51*

A new smart simple validated spectrophotometric method was developed for the determination of two drugs one of which is in a very low concentration compared to the other. The method is based on spiking and dilution then simple mathematical manipulation of the absorbance spectra. This method was applied for the determination of a binary mixture of vildagliptin and metformin hydrochloride in the ratio 50:850 in laboratory prepared mixtures containing both drugs in this ratio and in pharmaceutical dosage form with good recoveries. The developed method was validated according to ICH guidelines and can be used for routine quality control testing.
**Keywords:** Vildagliptinmetformin Hclfirst Derivativespiking and Dilutionspectrophotometric Method

## M-487.Quantification of Total Mercury in Compact Fluorescent Lamps in Saudi Arabia Using Inductively Coupled Plasma Mass Spectrometry (ICP-MS)

Darwish Hany W Al-Osaimi, Ali Ahmed and Kamal O. Bakheit Ahmed

*Main Group Chemistry, 15: 117-124 (2016) IF: 0.355*

Human health is at risk due to exposure to mercury vapors that arise from breakage of compact fluorescent lamps (CFLs). Mercury content of CFLs, according to the United States Environmental Protection Agency (US EPA), varies from 2 to 5 mg with average value of 4 mg. If the amount of mercury exceeds this limit, it may be dangerous to the human health and these CFLs will fall into the hazardous waste category. Most of the currently available CFLs in the Saudia Arabia (S.A.) market are manufactured in China and by well-known, worldwide brands. To ensure the commitment of these companies to the US EPA regulations, total mercury content was determined using Inductively Coupled Plasma Mass Spectrometry (ICP-MS). Nineteen different types of CFLs were purchased from local stores and analyzed by ICP-MS. The surprising results was that most of the Chinese CFLs had values of mercury up to three times than the maximum limit recommended by US EPA. This study was devoted to highlight the risk factor that CFLs may have for public health.
**Keywords:** Metallic Mercury; Mercury Analysis; Compact Fluorescent Lamps (CFLS); Inductively Coupled Plasma Massspectrometry (ICP-MS)

## M-491.Synchronous Fluorescence Spectroscopy Coupled with Continuous Wavelet Transforms and Savitzky-Golay Derivatization Technique for the Simultaneous Determination of Tadalafil and Dapoxetine HCl

Maha Hegazy, Amira Kessiba, Mohamed Abdelkawy and Ahmed Elgendy

*International Journal of Pharmacy and Pharmaceutical Sciences, 8: 32-38 (2016)*

**Objective:** A novel combination of Tadalafil (TAD) and Dapoxetine HCl (DAP) has been recently introduced into the market for the treatment of premature ejaculation. The aim of this work is the development and validation of simple, sensitive and accurate analytical methods for the determination of TAD and DAP in their binary mixture without prior separation. **Methods:** Synchronous fluorescence spectroscopic (SFS) methods coupled with continuous wavelet transforms (CWT) and Savitzky-Golay (SAVGOL) derivatization technique have been developed. **Results:** Under optimum conditions, TAD and DAP were determined in the concentration ranges of 0.01–3 µg/ml and 0.01–1.2 µg/ml, respectively. **Conclusion:** The developed methods have the requisite accuracy, selectivity, sensitivity and precision and were satisfactorily applied for the simultaneous determination of TAD and DAP in bulk powder and pharmaceutical preparations. The results obtained for the

analysis of both drugs in their pure forms by the proposed methods were statistically compared to those obtained by applying a reported high performance liquid chromatographic method (HPLC) method. The statistical comparison showed that there is no significant difference between the proposed methods and the reported one with respect to accuracy and precision.
**Keywords:** Synchronous Fluorescence Spectroscopy; Tadalafil, Dapoxetine HCL; Continuous Wavelet Transforms; Savitzky-Golay Technique.

## M-490. Development and Validation of Stability Indicating TLC Densitometric and Spectrophotometric Methods for Determination of Clobetasol Propionate

Yasmine Farouk Bassuoni , Eman Saad Elzanfaly, Hebatallah Mohamed Essam and Hala El-Sayed Zaazaa

*Bulletin of Faculty of Pharmacy, Cairo University, 54(2): 165-174 (2016)*

Two simple analytical techniques that manipulate the inherent spectroscopic properties of the drug differently were developed for Clobetasol propionate (CP) determination in the presence of its alkaline hydrolytic degradation products. The first method depends on TLC-densitometric determination of the UV–visualized bands after TLC separation of CP in the presence of its alkaline degradation products in its bulk and pharmaceutical formulation. Separation was performed on preactivated silica gel 60 F254 TLC plates using ethyl acetate:hexane:ammonia (5:5:0.2, by volume) as a developing system followed by scanning at 240 nm. Linear correlation was obtained in the range of 0.10–0.50 μg/band. The second method was ratio difference spectrophotometry. It was applied by measuring the difference in peak amplitude of the ratio spectra at 243.40 and 256.40 nm. The selectivity of both methods was checked by analyzing laboratory prepared mixtures containing different concentrations of CP and its alkaline degradation products. The methods were validated in compliance with ICH guidelines. The methods determined CP in its bulk powder with average percentage recoveries of 99.60% ± 1.09 and 99.44% ± 1.60 for densitometry and ratio difference, respectively. Both methods were successfully applied for quantification of CP in its commercial cream.
**Keywords:** Clobetasol Propionate; Stability Indicating Method; Tlc-Densitometry; Spectrophotometry; Alkaline Degradation Products

## M-491. HPLC and TLC Chromatographic Methods for Simultaneous Determination of Binary Mixture of Isoconazole Nitrate and Diflucortolone Valerate

Mohamed R. El-Ghobashy, Yasmin M. Fayez, Zeinab M. Goda and Mostafa A. Shehata

*Bulletin of Faculty of Pharmacy, Cairo University, 54: 33-37 (2016)*

HPLC and TLC-densitometric methods were used to determine a binary mixture of isoconazole (ISO) and diflucortolone (DIF). For HPLC method a rapid separation could be achieved on a C18 column using mobile phase of 80% acetonitrile–20% methanol. The components were monitored at 230 nm over a concentration range of 10–90 lg mL 1 for ISO and 2–18 lg mL 1 for DIF with mean percentage recoveries 99.95 ± 0.866 and 99.98 ± 0.744, respectively. The second method is TLC-densitometric, where ISO and DIF are separated on silica gel plates using ethyl acetate: chloroform: toluene (60:10:10 by volume) as a developing system and scanning of the separated bands at 215 nm over a concentration range of 0.1–4 lg spot 1 for ISO and scanning of the separated bands at 237 nm over a concentration range of 0.1–1.4 lg spot 1 for DIF with mean percentage recoveries 100.19± 0.956 and 100.1 ±0.689 for ISO and DIF, respectively. The suggested methods were used to determine both drugs binary mixture in pure form and dosage form. The validity of the proposed methods was further assessed by applying standard addition technique. The obtained results were statistically compared with official HPLC method, showing no significant difference with respect to accuracy and precision.
**Keywords:** Isoconazole; Diflucortolone; HPLC; TLC-Densitometry.

## M-492. Novel Membrane Sensors for the Determination of Quetiapine Fumarate in Plasma and in Presence of its Related Compounds

Marianne Nebsen,, Christine M. El-Maraghy, Hesham Salem, and Sawsan M. Amer

*Analytical & Bioanalytical Electrochemistry, 8: 51-63 (2016)*

Two sensitive and selective polyvinyl chloride (PVC) matrix membrane sensors were developed and investigated for determination of the cationic drug Quetiapine Fumarate (QTF) in pure form, in plasma and in presence of its two related compounds namely Quetiapine N-oxide and Des-ethanol Quetiapine. The two sensors (I and II) were developed using sodium tetraphenyl borate as a cation exchanger with dioctyl phthalate (DOP) as a plasticizer. Selective molecular recognition component, β-cyclodextrin (β-CD), was used as ionophore to improve the selectivity of sensor II. The proposed sensors had a linear dynamic range of 1×10-6-1×10-2 mol L-1 for sensor I and 1×10-7-1×10-2 mol L-1 for sensor II with Nernstian slopes of 27.50±0.45 and 39.85±0.3 mV/decade for sensors I and II, respectively over the pH ranges of 2.5-7. The method was validated according to ICH guidelines. Statistical comparison between the results from the proposed method and the results from the reference HPLC method showed no significant difference regarding the accuracy and precision.
**Keywords:** Quetiapine Fumarate; Ion Selective Electrode; Membrane Sensors; Cationic Exchanger; Related Compounds; Plasma.

## M-493. Recent Development in Ultraviolet Spectrophotometry Through the Last Decade (2006–2016): A Review

Hayam M. Lotfyand Sarah S. Saleh

*International Journal of Pharmacy and Pharmaceutical Sciences, Vol 8, Issue 10,: 40-56 (2016)*

Several techniques have been proposed for treatment of spectrophotometric data, with the objective of extracting the largest amount of analytical information from spectra composed of unresolved bands. The instrumental development and analytical applications of UV regions absorption

spectrophotometry produced in the last 10 y (since 2006) are reviewed. The methods were classified according to the spectra data used, including zero order absorption, derivative and ratio amplitudes. The proposed methods were applied to solve different complex pharmaceutical mixtures and the obtained results were accepted when compared to other reported methods.
**Keywords:** Spectral Manipulation, Ratio Spectra, Amplitude, Differential, Successive, Absorptivity

## M-494. Simple Spectrophotometric Methods for the Simultaneous Determination of Antipyrine and Benzocaine

Hanan A. Merey

*Bulletin of Faculty of Pharmacy, Cairo University, 54(2): 181-189 (2016)*

Antipyrine and benzocaine are formulated together for the treatment of ear inflammation and to relieve pain. Four spectrophotometric methods were developed for the simultaneous determination of antipyrine (AN) and benzocaine (BE) in their combined dosage form. Method A depends on applying dual wavelength method where antipyrine was determined by measuring the absorbance at 254.1 and 309.1 nm (corresponding to zero difference of benzocaine), while the absorbance difference at 230.1 and 263.5 nm (corresponding to zero difference of antipyrine) was selected for benzocaine determination in the laboratory prepared spectrum. Method B depends on measuring the peak amplitude of first derivative at 305 nm for calculating benzocaine concentration then the total concentration of both drugs was determined using isoabsorptive point at 257.4 nm (antipyrine concentration was then calculated by subtraction). Method C is based on measuring the peak difference of the ratio spectra at Δp (239.1–285 nm) and Δp (301.4–250 nm) for the determination of antipyrine and benzocaine, respectively. Method D depends on measuring peak to peak amplitude of the first derivative of ratio spectra at (234.5 + 244.2 nm) and peak amplitude at 295.5 nm for the determination of antipyrine and benzocaine, respectively. The proposed methods were validated and applied for the analysis of antipyrine and benzocaine in their laboratory prepared mixtures and pharmaceutical formulation. Statistical comparison between the results of the proposed methods and those of the reported methods showed no significant difference.
**Keywords:** Antipyrine; Phenazone; Bezocaine; Dual Wave Length; Isoabsorptive Point; Different Spectrophotometric Method

## M-495. Stability Indicating Spectrophotometric Methods for Determination of Nicardipine in the Presence of its Alkaline Induced Degradation Products

Hayam Mahmoud Lotfy, Maha Abd El-Monem Hegazy, Mai M. Abd El-Aziz and Laila Elsayed Abdel Fattah

*International Journal of Pharmacy and Pharmaceutical Sciences, 8: 62-66 (2016)*

**Objective:** Derivative, ratio spectra derivative and ratio difference spectrophotometric methods were developed and validated for simultaneous determination of Nicardipine (NIC) in the presence of its alkaline induced degradation products. **Methods:** In these methods the overlapped spectra of NIC and its alkaline induced degradation products were well resolved by measuring the amplitudes of first derivative (DP1P) spectra and the second derivative (DP2P) at 382.3 and 239 nm, respectively. NIC was determined by ratio spectra derivative by measuring the amplitude at 244 nm. The ratio difference spectrophotometric method was developed in which the difference between amplitudes at 237.5 nm and 260 nm of the ratio spectra were recorded. The linearity range for the applied methods was 2-18 µg/ml. **Results:** All the developed methods were validated according to ICH Guidelines, NIC was determined with acceptable accuracy and precision. **Conclusion:** These methods were suitable as stability indicating methods for the determination of NIC in the presence of its alkaline induced degradation products either in bulk powder or in a pharmaceutical formulation. Statistical analysis of the results with those obtained by applying a reported method has been carried out revealing high accuracy and good precision.
**Keywords:** Nicardipine, Spectrophotometry, Pharmaceutical Preparations, Stability Indicating, Derivative, Ratio Derivative and Ratio Difference

## M-496. Stability Indicating Spectrophotometric Methods for the Determination of Oxetacaine in the Presence of its Hydrolytic and Oxidative Degradation Products

Eman S Elzanfaly, Enas A Amer, Sara A Galal and Hala E Zaazaa

*Der Pharma Chemica, 8(22): 32-37 (2016)*

In this study, the overlapped spectra of Oxetacaine (OXT), its hydrolytic and oxidative degradation products were well resolved using two simple spectrophotometric methods. The first method depends on measuring the peak amplitudes of first derivative of the ratio spectra (1DD) at 224.3 for selective determination of Oxetacaine in the presence of its degradation products. While in the second method, it was determined by measuring the difference between amplitudes at 216.1 nm and 227.9 nm of the recorded ratio spectra. All the developed methods were validated according to ICH Guidelines, OXT was determined with acceptable accuracy and precision.
**Keywords:** Oxetacaine, Degradation Products, Derivative Ratio, Spectrophotometry

## M-498. Validated Chromatographic Methods for the Simultaneous Determination of Mometasone Furoate and Formoterol Fumarate Dihydrate in a Combined Dosage form

Hanan A. Merey, Sally S. El-Mosallamy, Nagiba Y. Hassan and Badr A. El-Zeany

*Bulletin of Faculty of Pharmacy, Cairo University, 54: 99-106 (2016)*

Two chromatographic methods were developed and validated for the simultaneous determination of Mometasone furoate (MO) and Formoterol fumarate dihydrate (FOR). Combination of MO and FOR is used for the treatment of asthma in patients suffering from reversible obstructive airway disease. The first

chromatographic method was based on using aluminum TLC plates pre-coated with silica gel GF254 as the stationary phase and chloroform:ethyl acetate:methanol:toluene:formic acid (5:2:2:2:0.1, by volume) as the mobile phase followed by densitometric measurement of the separated bands at 233 nm. The second method is a high performance liquid chromatographic method for the separation and determination of MO and FOR using reversed phase C18 column with isocratic elution. The mobile phase composed of methanol: 0.5% ammonium acetate pH adjusted with acetic acid (80:20, v/v) at a flow rate of 1.0 mL/min. Quantitation was achieved with UV detection at 220 nm. The specificity of the developed methods was investigated by analyzing the pharmaceutical dosage form. The validity of the proposed methods was assessed using the standard addition technique. The obtained results were statistically compared with those obtained by the reported methods, showing no significant difference with respect to accuracy and precision at p = 0.05.

**Keywords:** Mometasone Furoate; Formoterol Fumarate Dihydrate; TLC-Densitometry; High Performance Liquid Chromatography; Isocratic Elution.

## M-497. Comparative Study on four Spectrophotometric Methods Manipulating Ratio Spectra for the Simultaneous Determination of Binary Mixture of Diflucortolone Valerate and Isoconazole Nitrate

Yasmine M. Fayez, Mohamed R. Elghobashy, Zeinab M. Goda and Mostafa A. Shehata

*Bulletin of Faculty of Pharmacy, Cairo University, 54: 39-47 (2016)*

Four simple, accurate, reproducible and non-sophisticated spectrophotometric methods manipulating ratio spectra were developed and validated for the simultaneous determination of diflucortolone valerate (DIF) and isoconazole nitrate (ISO) without preliminary separation in pure powder form and in their cream formulation. Method A, is constant center spectrophotometric method (CC), method B is a ratio difference spectrophotometric one (RD), method C is the first derivative of the ratio spectra (1DD), while method D is the mean centering of ratio spectra (MC). Linearity correlations ranges were 5–60 µg mL−1 for DIF and 65–850 µg mL−1 for ISO. The mean percentage recoveries of DIF were 101.60 ± 1.056 for method A, 101.33 ± 0.702 for method B, 101.31 ± 1.476 for method C and 102.69 ± 1.009 for method D, respectively. For ISO were 100.59 ± 0.525 for method A, 99.68 ± 0.721 for method B, 99.67 ± 0.742 for method C and 101.37 ± 0.958 for method D, respectively. Assessment of the specificity was achieved by analyzing synthetic mixtures containing the cited drugs. The four methods were applied for the determination of the cited drugs in cream formulation and the statistical comparison of the obtained results was made with each other and with those of official methods. The comparison in pure powder form showed that there is no significant difference between the proposed methods and the official methods regarding both accuracy and precision.

**Keywords:** Isoconazole Nitrate; Diflucortolone Valerate; Constant Center; Ratio Difference; Ratio Derivative; Mean Centering.

## M-498. Comparative Study of four Ion Selective Membrane Electrodes for Potentiometric Determination of Ivabradine Hydrochloride in Pharmaceutical Formulations and Plasma

Nadia M. Mostafa, Yasmin M. Fayez, Joliana F. Farid and Abd El-Aziz B. Abd El-Alim

*Analytical & Bioanalytical Electrochemistry, 8: 207-218 (2016)*

Four different polyvinyl chloride (PVC) membrane sensors were investigated for the determination of ivabradine HCl in pure drug substance, pharmaceutical formulations and plasma. These sensors were fabricated using sodium tetraphenyl borate (TPB) [sensor 1a,1b,1c] or ammonium reineckate (RNC) [sensor 2a,2b] or sodium phosphotungestate (PTA) [sensor 3a,3b] or tetrakis(4-chlorophenyl)borate (TpClPB) [sensor 4a,4b] as ion exchanger. The proposed sensors showed fast and stable nernstian response range from 55.1- 59.8 mV/decade across a concentration range 10-5 -10-2 M in pH range 4.5-7.5. These electrodes exhibit good selectivity for ivabradine HCl with respect to a large number of inorganic, organic cations, sugars and amino acids. The results were statistically compared with a reported method. The comparison showed no significant difference between the proposed methods and the reported method regarding both accuracy and precision.

**Keywords:** Ivabradine, Sodium Tetraphenyl Borate, Ammonium Reineckate, Sodium Phosphotungestate, Tetrakis(4-Chlorophenyl)Borate

### *Dept. of BioChemsitry*

## M-499. Bone Marrow-Derived Endothelial Progenitor Cells Protect Against Scopolamine-Induced Alzheimer-Like Pathological Aberrations

Marwa M. Safar, Hany H. Arab, Sherine M. Rizk and Shohda A. El-Maraghy

*Mol Neurobiol, 53: 1403-1418 (2016) IF: 5.397*

Vascular endothelial dysfunction plays a key role in the pathogenesis of Alzheimer's disease (AD). Patients with ADhave displayed decreased circulating endothelial progenitor cells (EPCs) which repair and maintain the endothelial function. Transplantation of EPCs has emerged as a promising approach for the management of cerebrovascular diseases including ischemic stroke, however, its impact on AD has been poorly described. Thus, the current study aimed at investigating the effects of bone marrow-derived (BM) EPCs transplantation in repeated scopolamine-induced cognitive impairment, an experimental model that replicates biomarkers of AD. Intravenously transplanted BM-EPCs migrated into the brain of rats and improved the learning and memory deficits. Meanwhile, they mitigated the deposition of amyloid plaques and associated histopathological alterations. At the molecular levels, BM-EPCs blunted the increase of hippocampal amyloid beta protein (Aβ), amyloid precursor protein (APP) and reinstated the Aβ-degrading neprilysin together with downregulation of p-tau and its upstream glycogen synthase kinase-3β (GSK-3β). They also corrected the perturbations of neurotransmitter levels including restoration of acetylcholine and associated esterase along with dopamine, GABA, and the neuroexitatory glutamate. Furthermore, BM-EPCs induced behavioral recovery via boosting of vascular endothelial growth factor (VEGF), nerve

growth factor (NGF), brainderived neurotrophic factor (BDNF) and its upstream cAMP response element binding (CREB), suppression of the proinflammatory tumor necrosis factor-α (TNF-α) and interleukin- 1β (IL-1β), and upregulation of interleukin-10 (IL-10). BMEPCs also augmented Nrf2 and seladin-1. Generally, these actions were analogous to those exerted by adipose tissuederived mesenchymal stem cells (AT-MSCs) and the reference anti-Alzheimer donepezil. For the first time, these findings highlight the beneficial actions of BM-EPCs against the memory deficits and AD-like pathological dysfunction

**Keywords:** Endothelial Progenitor Cells; Alzheimer ; Amyloid B-Protein; Neurotrophic Factors; Neurotransmitters; Neuroinflammation.

## M-500.A Novel Small Molecule Ameliorates Ocular Neovascularisation and Synergises with Anti-Vegf Therapy

Rania S. Sulaiman, Stephanie Merrigan, Judith Quigley, Xiaoping Qi, Bit Lee, Michael E. Boulton, Breandán Kennedy, Seung-Yong Seo and Timothy W. Corson

*Scientific Reports, 6: 25509, (2016) IF: 5.228*

Ocular neovascularisation underlies blinding eye diseases such as retinopathy of prematurity, proliferative diabetic retinopathy, and wet age-related macular degeneration. These diseases cause irreversible vision loss, and provide a significant health and economic burden. Biologics targeting vascular endothelial growth factor (VEGF) are the major approach for treatment. However, up to 30% of patients are non-responsive to these drugs and they are associated with ocular and systemic side effects. Therefore, there is a need for small molecule ocular angiogenesis inhibitors to complement existing therapies. We examined the safety and therapeutic potential of SH-11037, a synthetic derivative of the antiangiogenic homoisoflavonoid cremastranone, in models of ocular neovascularisation. SH-11037 dose-dependently suppressed angiogenesis in the choroidal sprouting assay ex vivo and inhibited ocular developmental angiogenesis in zebrafish larvae. Additionally, intravitreal SH-11037 (1 μM) significantly reduced choroidal neovascularisation (CNV) lesion volume in the laser-induced CNV mouse model, comparable to an anti-VEGF antibody. Moreover, SH-11037 synergised with anti-VEGF treatments in vitro and in vivo. Up to 100 μM SH-11037 was not associated with signs of ocular toxicity and did not interfere with retinal function or pre-existing retinal vasculature. SH-11037 is thus a safe and effective treatment for murine ocular neovascularisation, worthy of further mechanistic and pharmacokinetic evaluation.

**Keywords:** Small Molecules; Angiogenesis; Ocular Diseases.

## M-501. Identification of Novel Transplantable Gpcr Recycling Motif for Drug Discovery

Mohammed M. Nooh, Salvatore Mancarella and Suleiman W. Bahouth

*Biochemical Pharmacology, 120: 22-32 (2016) IF: 5.091*

β1-Adrenergic receptor (β1-AR) agonists and antagonists are widely used in the treatment of major cardiovascular diseases such as heart failure and hypertension. The β1-AR like other G protein-coupled receptors (GPCRs) are endocytosed in response to intense agonist activation. Recycling of the agonist-internalized β1-AR is dependent on its carboxy-terminal type-1 PSD-95/DLG/ZO1 (PDZ) and on phospho-serine312 in the third intracellular loop of the β1-AR. Progressive elongation of the β1-AR at its C-tail inactivated the PDZ-biding domain and inhibited the recycling of the β1-AR. However, fusing a twenty amino acid peptide derived from the multiple cloning region of the mammalian expression vector pCDNA3 to the C-tail of the β1-AR (β1-AR[+20]) produced a chimeric β1-AR that recycled rapidly and efficiently. The β1-AR[+20] recycled in a type-1 PDZ and phospho-Ser312-independent manner, indicating that this peptide provided a general GPCR recycling signal. Fusing the enhanced yellow fluorescent protein (EYFP) down-stream of β1-AR[+20] generated a β1-AR-EYFP chimera that was expressed on the membrane and recycled efficiently after agonist-induced internalization. This construct trafficked in a PDZ-SNX27/retromer-independent manner. We also fused EYFP to the N-terminus of the β1-AR to created EYFP-WT β1-AR. This construct recycled in PDZ and SNX27/retromer dependent manner. These β1-AR-EYFP constructs would be useful for high throughput screening (HTS) programs to identify new entities that would interfere with the recycling of agonist internalized GPCR that traffic in PDZ-dependent vs. PDZ-independent roadmaps.

**Keywords:** Gpcr; B-Adrenergic Receptors; Trafficking; Pdz; Snx27; Confocal Microscopy.

## M-502. Modulation of Tamoxifen Cytotoxicity by Caffeic Acid Phenethyl Ester in MCF-7 Breast Cancer Cells

Tarek K. Motawi, Samy A. Abdelazim, Hebatallah A. Darwish, Eman M. Elbaz and Samia A. Shouman

*Oxidative Medicine and Cellular Longevity, 2016: 1-13 (2016) IF: 4.492*

Although Tamoxifen (TAM) is one of the most widely used drugs in managing breast cancer, many women still relapse after long-term therapy. Caffeic acid phenethyl ester (CAPE) is a polyphenolic compound present in many medicinal plants and in propolis. The present study examined the effect of CAPE on TAM cytotoxicity in MCF-7 cells. MCF-7 cells were treated with different concentrations of TAM and/or CAPE for 48 h. This novel combination exerted synergistic cytotoxic effects against MCF-7 cells via induction of apoptotic machinery with activation of caspases and DNA fragmentation, along with downregulation of Bcl-2 and Beclin 1 expression levels. However, the mammalian microtubule-associated protein light chain LC 3-II level was unchanged. Vascular endothelial growth factor level was also decreased, whereas levels of glutathione and nitric oxide were increased. In conclusion, CAPE augmented TAM cytotoxicity via multiple mechanisms, providing a novel therapeutic approach for breast cancer treatment that can overcome resistance and lower toxicity. This effect provides a rationale for further investigation of this combination.

**Keywords:** Tamoxifen; Caffeic Acid Phenethyl Ester; Mcf-7 Breast Cancer Cells.

## M-503. Angiotensin-Converting Enzyme Insertion/Deletion Polymorphism Association with Obesity and some Related Disorders in Egyptian Females: A Case-Control Observational Study

Tarek K. Motawi, Olfat G. Shaker, Nancy N. Shahin and Nancy M. Ahmed

*Nutrition and Metabolism, 13: 1-11 (2016) IF: 3.28*

**Background** According to the WHO report in 2015, obesity is the fifth leading cause of death worldwide, and the prevalence of Egyptian female obesity is 37.5 %. Since obesity is highly influenced by genetics, and adipose tissue renin-angiotensin system is over-activated in obesity, the effect of angiotensin-converting enzyme (ACE) insertion/deletion (I/D) polymorphism on obesity and related disorders was studied in several populations, because of its effect on ACE activity. Our objective was to study the association of ACE I/D polymorphism with obesity and certain related disorders, namely hypertension, insulin resistance and metabolic syndrome, in Egyptian females. **Methods** Eighty female volunteers were recruited, blood pressure and body measurements were recorded and a fasting blood sample was obtained for the quantitation of glucose, lipid profile, insulin, leptin and identification of ACE I/D polymorphs. Subjects were grouped based on hypertension and obesity states. Comparisons of continuous parameters were made with independent sample t-test between two groups. The frequencies of ACE genotypes and alleles, and the association between gene polymorphism and metabolic parameters were assessed using chi-square or Fisher's exact test. **Results** Genotype frequencies were in Hardy-Weinberg equilibrium for all groups. Genotype distribution did not differ significantly between controls and cases of all the studied disorders. Although DD carriers had apparently higher parameters of blood pressure, lipid profile and insulin resistance, only diastolic blood pressure was almost significant ($p = 0.057$). I-carriers were significantly less susceptible to hypertension than DD carriers having normal waist/hip ratio ($p = 0.007$, OR = 17.29, CI = 1.81–164.96) and normal conicity index ($p = 0.024$, OR = 7.00, CI = 1.36–35.93). In DD genotype carriers, a significant association was found between insulin resistance and high body mass index ($p = 0.004$, OR = 8.89, CI = 1.94–40.71), waist circumference ($p = 0.003$, OR = 9.63, CI = 2.14–43.36) and waist/height ratio ($p = 0.034$, OR = 6.86, CI = 1.25–37.61), although the variations in percentages between DD and I-carriers were not high enough to conclude an effect of ACE I/D on such an association. **Conclusions** In this sample of Egyptian females, ACE I/D polymorphism was not significantly associated with obesity nor with any of its related disorders studied. The I allele seemed protective against hypertension in subjects with normal, not high, waist/hip ratio and conicity index compared to DD genotype carriers.

**Keywords:** Ace I/D Polymorphism; Obesity; Hypertension; Insulin Resistance; Metabolic Syndrome; Egypt.

## M-504. Curcumin, Silybin Phytosome(®) and A-R-Lipoic Acid Mitigate Chronic Hepatitis in Rat by Inhibiting Oxidative Stress and Inflammatory Cytokines Production.

Shimaa O. Ali, Hebatallah A. Darwish and Nabila A. Ismail

*Basic and Clinical Pharmacology and Toxicology, 118: 369-380 (2016) IF: 3.097*

Chronic hepatitis is recognized as a worldwide health problem that gradually progresses towards cirrhosis and hepatocellular carcinoma. Despite the large number of experiments using animal models for allergic hepatitis, it is still difficult to produce a picture of chronic hepatitis. Therefore, this study was conducted to introduce an animal model approximating to the mechanism of chronicity in human hepatitis. The study also aimed to examine the hepatoprotective effects of curcumin, silybin phytosome(®) and α-R-lipoic acid against thioacetamide (TAA)-induced chronic hepatitis in rat model. TAA was administered intraperitoneally at a dose of 200 mg/kg three times weekly for 4 weeks. At the end of this period, a group of rats was killed to assess the development of chronic hepatitis in comparison with their respective control group. TAA administration was then discontinued, and the remaining animals were subsequently allocated into four groups. Group 1 was left untreated, whereas groups 2-4 were allowed to receive daily oral doses of curcumin, silybin phytosome(®) or α-R-lipoic acid, respectively, for 7 weeks. Increases in hepatic levels of malondialdehyde associated with TAA administration were inhibited in groups receiving supplements. Furthermore, glutathione depletion, collagen deposition, macrophage activation and nuclear factor κappa-B expression as well as tumour necrosis factor-α and interleukin-6 levels were significantly decreased in response to supplements administration. Serological analysis of liver function and liver histopathological examination reinforced the results. The above evidence collectively indicates that the antioxidant and anti-inflammatory activities of curcumin, silybin phytosome(®) and α-R-lipoic acid may confer therapeutic efficacy against chronic hepatitis.

**Keywords:** Hepatitis; Thiacetamide; Curcumin; Silibin Phytosome; Lipoic Acid.

## M-505. Association Between Sirt1 Gene Polymorphisms and Breast Cancer in Egyptians

Sherine M. Rizk , Nancy N. Shahin and Olfat G. Shaker

*Plos One, 11: 1-19 (2016) IF: 3.057*

**Background** Breast cancer is reported to cause the highest mortality among female cancer patients. Previous studies have explored the association of silent mating-type information regulator 2 homolog 1 (SIRT1) gene expression with prognosis in breast cancer. However, no studies exist, so far, on the role of SIRT1 gene polymorphism in breast cancer risk or prognosis. The present study aimed to assess the association between SIRT1 gene polymorphisms and breast cancer in Egyptians. **Methods** The study comprised 980 Egyptian females divided into a breast cancer group (541 patients) and a healthy control group (439 subjects). SIRT1 gene single nucleotide polymorphisms (SNPs) rs3758391, rs3740051 and rs12778366 were genotyped using real-time polymerase chain reaction (RT-

PCR). Allelic and genotypic frequencies were determined in both groups and association with breast cancer and clinicopathological characteristics was assessed. **Results** Breast cancer patients exhibited elevated serum SIRT1 levels which varied among different tumor grades. SIRT1 rs3758391 and rs12778366 TT genotypes were more frequent, exhibited higher SIRT1 levels than CC and CT genotypes and were associated with histologic grade and lymph node status. SIRT1 rs12778366 TT genotype also correlated with negative estrogen receptor (ER) and progesterone receptor (PR) statuses. The T allele frequency for both SNPs was higher in breast cancer patients than in normal subjects. Combined GG and AG genotypes of rs3740051 were more frequent, showed higher serum SIRT1 levels than the AA genotype, and were associated with ER and PR expression. Furthermore, inheritance of the G allele was associated with breast cancer. **Conclusions** Our findings reveal that rs3758391 and rs12778366 polymorphisms of SIRT1 gene are associated with breast cancer risk and prognosis in the Egyptian population.

**Keywords:** Sirt1 Gene Polymorphism; Breast Cancer; Egyptians

## M-506. Impact of Genetic Polymorphism of Methylenetetrahydrofolate Reductase C677t on Development of Hyperhomocysteinemia and Related Oxidative Changes in Egyptian Beta-Thalassemia Major Patients

Mai A. Abd-Elmawl, Sherine M. Rizk, Ilham Youssry and Amira A. Shaheen

*Plos One, 11 (2016) IF: 3.057*

**Background** beta-thalasemia major (beta-TM) patients often suffer from various vascular complications together with increased oxidative stress. Hyperhomocysteinemia (Hhcy) has been defined as a risk factor for these complications. Genetic polymorphism of methylenetetrahydrofolate reductase (MTHFR) C677T has been shown to cause Hhcy particularly in individuals with low B-vitamins. However, the status of homocysteine (hcy) in beta-TM has not yet been adequately defined. Aim To evaluate the genetic polymorphism of MTHFR C677T among beta-TM patients and its prospective contribution to Hhcy and related oxidative changes. Subjects and Methods Genotyping for MTHFR C677T was done by PCR-RFLP technique. Plasma hcy, vitamin B12, folate, malondialdehyde (MDA), total antioxidant capacity (TAC), oxidized low density lipoprotein (oxLDL), total nitric oxide (NOx) and lipid profile were determined in 66 beta-TM patients and 66 control subjects of matched age and sex. **Results** The prevalence of MTHFR 677TT genotype was significant among beta-TM patients (12%) compared to (3%) controls (OR = 4.9, 95%CI:1.2–24.2,P = 0.03). A strong association between Hhcy and MTHFR TT genotype was observed (OR = 7.7, 95%CI:2.8–20.9) where all beta-TM patients with TT genotype were hyperhomocystienemic (≥ 15 μmol/l) and having sub-optimal folate level than those with CT or CC genotypes. Hyperhomocystienemic patients have suffered from increased oxidative stress characterized by significant increase in plasma MDA and oxLDL, and a significant reduction of plasma TAC and total NOx. Lipid profile of those patients was severely affected indicated by reduction in HDL and HDL/LDL and elevation in atherogenic index as compared with CC genotype. Other measured parameters were not significantly different among beta-TM patients with different MTHFR genotypes. **Conclusion** This study suggests that Egyptian beta-TM patients with MTHFR 677TT genotype could be at increasing risk of developing Hhcy particularly with folate deficiency. This state of Hhcy may account potentially for most oxidative changes and atherogenic vascular complications frequently reported in beta-TM patients.

**Keywords:** Mthfr; Thalassemia Major; Hyperhomocystienemia.

## M-508. Comparative Study of the Effects of Pegylated Interferon-Alpha 2A Versus 5-Fluorouracil on Cancer Stem Cells in a Rat Model of Hepatocellular Carcinoma

Tarek Kamal Motawi, Noha Ahmed El-Boghdady, Abeer Mostafa El-Sayed and Hebatullah Samy Helmy

*Tumor Biology, 37: 1617-1625 (2016) IF: 2.926*

Cancer stem cells (CSCs) in hepatocellular carcinoma (HCC) possess tumor-initiating, metastatic, and drug resistance properties. This study was conducted to evaluate the effects of PEGylated interferon-alpha 2a (PEG-IFN-alpha 2a) and 5-fluorouracil (5-FU) on the expression of CSC markers and on specific pathways that contribute to the propagation of CSCs in HCC. HCC was initiated in rats using a single intraperitoneal dose of diethylnitrosamine (DENA) (200 mg/kg) and promoted by weekly subcutaneous injections of carbon tetrachloride (CCl4) for 6 weeks. After the appearance of dysplastic nodules, the animals received PEG-IFN-alpha 2a or 5-FU for 8 weeks. CSC markers (OV6, CD90) and molecules related to transforming growth factor beta(TGF-beta) and other signaling pathways were assessed in hepatic tissues. The PEG-IFN-alpha 2a treatment effectively suppressed the hepatic expression of OV6 and CD90, ameliorated the diminished hepatic expression of TGF-beta receptor II (TGF-beta RII) and beta 2-spectrin (beta 2SP), and significantly reduced the elevated hepatic expression of TGF-beta 1, interleukin6 (IL6), signal transducer and activator of transcription3 (STAT3), and vascular endothelial growth factor (VEGF). In contrast, the 5-FU treatment failed to reduce the overexpression of CSC markers and barely affected the disrupted TGF-beta signaling. Furthermore, it had no effect on angiogenesis or nitrosative stress. PEG-IFN-alpha 2a, but not 5-FU, could reduce the propagation of CSCs during the progression of HCC by upregulating the disrupted TGF-beta signaling, suppressing the IL6/STAT3 pathway and reducing angiogenesis.

**Keywords:** Hepatocellular Carcinoma; Pegylated Interferon-Alpha 2A; 5-Fluorouracil; Cancer Stem Cells.

## M-509. Elevated Serum MicroRNA-122/222 Levels are Potential Diagnostic Biomarkers in Egyptian Patients with Chronic Hepatitis C but not Hepatic Cancer

Tarek M. K. Motawi, Nermin A. H. Sadik, Olfat G. Shaker and Maggy H. Ghaleb

*Tumor Biology, 37: 9865-9874 (2016) IF: 2.926*

MicroRNAs (miRNAs) are a class of endogenous small non-coding RNAs that regulate gene expression at the post-transcriptional level. Because of their size, specificity, and

relative stability in plasma, miRNAs can be used as diagnostic and prognostic biomarkers to monitor liver injury, such as that caused by hepatitis C virus (HCV) and liver cancer. In this study, we investigated miRNA expression patterns from the serum of Egyptian patients with HCV and liver cancer compared with matched healthy controls. Using microarray-based expression profiling followed by real-time quantitative polymerase chain reaction validation, we compared the levels of circulating miRNA-122 and miRNA-222 in serum from patients with hepatitis C virus (n = 40) and liver cancer (n = 60) to matched healthy controls (n = 30). MiRNA SNORD68 was the housekeeping endogenous control. We found that the serum levels of miR-122 and miR-222 were significantly elevated in HCV patients, but not in liver cancer patients, compared with controls. Receiver operating characteristic analysis revealed that miR-122 and miR-222 have a high diagnostic potential in discriminating patients with HCV from controls. Serum miR-222 was significantly higher in HCV patients compared to liver cancer patients. Our results indicate that serum miR-122 and miR-222 are elevated in Egyptian patients with chronic HCV, and these miRNAs have a strong potential to serve as novel biomarkers for liver injury but not specifically for liver cancer.
**Keywords:** Mirna-122, Mirna-222, Hepatitis C, Liver Cancer.

## M-510. Evaluation and Screening of Mrna S100a Genes as Serological Biomarkers in Different Stages of Bladder Cancer in Egypt

Manal F. Ismail, Noha A. El Boghdady, Marwa I. Shabayek, Heba A. Awida and Hamdy Abozeed

*Tumor Biology, 37: 4621-4631 (2016) IF: 2.926*

Calcium-binding proteins S100A are multifunctional proteins that show altered expression in various diseases and cancers. This study aimed at validating an easier and less time-consuming technique to evaluate the value of combined use of messenger RNA (mRNA) S100A genes in comparison and combination with voided urine cytology in detection of bladder cancer patients. Blood and urine specimens were collected from patients (n = 120) with histologically confirmed bladder carcinoma who are classified according to bladder cancer stage into four groups and from healthy volunteers (n = 30). Histopathology examination, bilharzias antibody detection, urine cytology, and mRNA expression of S100A genes were estimated for all subjects by real time polymerase chain reaction (RT-PCR). Results indicate that each of the investigated S100A genes can be used as diagnostic marker for bladder cancer. Both S100A4 and S100A6 can be used to differentiate between different stages of bladder cancer. S100A7 can be used for the diagnosis of squamous cell carcinoma. Both S100A8 and S100A9 can be used for detection of invasive bladder carcinoma while S100A11 can be used for early detection of superficial bladder carcinoma. The overall sensitivity and specificity for the studied S100A genes ranged from 73 to 90 and 84 to 92, respectively. The combined use of urine cytology with the investigated S100A genes increased sensitivity from 56 % up to a range of 87–96 %. In conclusion, serum S100A genes can be useful as potential serological biomarkers for bladder cancer, and combined use of urine cytology with S100A genes can improve the sensitivity for detection of bladder cancer.
**Keywords:** Bladder Cancer. S100. Cytology; Sensitivity; Specificity.

## M-507. Are SMAD7 Rs4939827 and CHI3L1 Rs4950928 Polymorphisms Associated with Colorectal Cancer in Egyptian Patients?

Amal Ahmed Abd El-Fattah, Nermin Abdel Hamid Sadik, Olfat Gamil Shaker and Amal Mohamed Kamal

*Tumour Biology, 37(7): 9387-9397 (2016) IF: 2.926*

A wide variety of genes have been associated with colorectal cancer (CRC) development and progression. The SMAD7 gene encodes an intracellular protein, which inhibits the transforming growth factor beta (TGF-β) signaling pathway, thereby having a key role in the control of neoplastic processes in various organs. The CHI3L1 gene encodes glycoprotein YKL-40, which plays a role in cell proliferation, anti-apoptosis, and angiogenesis. The present study aimed to evaluate the association of single nucleotide polymorphisms (SNPs) SMAD7 rs4939827 and CHI3L1 rs4950928, as well as circulating TGFβ-1 and YKL-40 levels with CRC in an Egyptian population of 77 CRC patients and 36 healthy controls. Polymorphisms in the SMAD7 rs4939827 and the CHI3L1 rs4950928 genes were determined using the real-time polymerase chain reaction (RT-PCR). Both the SMAD7 rs4939827 TT genotype and the CHI3L1 rs4950928 C allele were associated with the rectal but not the colon cancer. In addition, the C allele of both SMAD7 rs4939827 and CHI3L1 rs4950928 was associated with increased serum levels of TGF-β1 and YKL-40, respectively. In conclusion, our data suggest that SMAD7 rs4939827 and CHI3L1 rs4950928 SNPs have no significant association with CRC. A significant association of SNP in SMAD7 rs4939827 and CHI3L1 rs4950928 was revealed between the rectal cancer and colon cancer patients.
**Keywords:** Chi3l1; Colorectal Cancer; Smad7; Single Nucleotide Polymorphism; Tgf-B1; Ykl-40

## M-511. Resveratrol and Curcumin Ameliorate Di-(2-Ethylhexyl) Phthalate Induced Testicular Injury in Rats

Amal Ahmed Abd El-Fattah, Atef Tadros Fahim, Nermin Abdel Hamid Sadik and Bassam Mohamed Ali

*General and Comparative Endocrinology, 1(225): 45-54 (2016) IF: 2.667*

The present study aimed to evaluate the protective role of resveratrol and curcumin on oxidative testicular damage induced by di-(2-ethylhexyl) phthalate (DEHP). Male Wistar rats were divided into six groups; three groups received oral daily doses of DEHP (2g/kgBW) for 45days to induce testicular injury. Two of these groups received either resveratrol (80mg/kgBW) or curcumin (200mg/kgBW) orally for 30days before and 45days after DEHP administration. A vehicle-treated control group was also included. Another two groups of rats received either resveratrol or curcumin alone. Oxidative damage was observed by decreased levels of total antioxidant capacity (TAC) and glutathione (GSH) and increased malondialdehyde (MDA) level in the testes of DEHP-administered rats. Serum testosterone level as well as testicular marker enzymes activities; acid and alkaline phosphatases (ACP and ALP) and lactate dehydrogenase (LDH) showed severe declines. DEHP administration caused significant increases in the testicular gene expression levels of Nrf2, HO-1, HSP60, HSP70 and HSP90 as well as a significant decrease in c-Kit protein when compared

with the control group. Histopathological observations provided evidence for the biochemical and molecular analysis. These DEHP-induced pathological alterations were attenuated by pretreatment with resveratrol and curcumin. We conclude that DEHP-induced injuries in biochemical, molecular and histological structure of testis were recovered by pretreatment with resveratrol and curcumin. The chemoprotective effects of these compounds may be due to their intrinsic antioxidant properties along with boosting Nrf2, HSP 60, HSP 70 and HSP 90 gene expression levels and as such may be useful potential tools in combating DEHP-induced testicular dysfunction.

**Keywords:** Curcumin; Dehp; Ho-1; Hsps; Nrf2; Rat; Resveratrol; Testes

## M-512. MicroRNA-21, MicroRNA-181A and Microrna-196A As Potential Biomarkers in Adult Egyptian Patients with Systemic Lupus Erythematosus

Tarek K. Motawi, Dahlia A. Mohsen, Shohda A. El-Maraghy and Mona A. Kortam

*Chemico-Biological Interactions, 260: 110-116 (2016) IF: 2.618*

Dysregulation of miRNAs has been described in systemic lupus erythematosis (SLE), however the clinical relevance of using miRNAs as biomarkers for SLE or predictors of disease progression is poorly investigated. This study investigated the expression signature of plasma miR-21, miR-181a and miR-196a among seventy SLE patients with different systemic lupus erythematosis disease activity index (SLEDAI) scores and thirty healthy controls using quantitative real-time PCR. Plasma IL-10 level was also measured in patients and control groups. The expression levels of all selected miRNAs were significantly increased in SLE patients as compared to healthy controls. MiR-196a was superior to differentiate patients from controls, whereas miR-21 was superior to discriminate mild from severe patients. Multivariate logistic analysis revealed miR-196a as independent predictor SLE diagnosis, it also suggest the strength of miR-21 and miR-196a as predictive biomarkers for development of SLE from mild severe form. Plasma IL-10 level was higher in SLE patients than in controls but it was not correlated with disease activity however; it showed a significant correlation with miR-21 expression. These miRNAs represent potential biomarkers in SLE. MiR-21 could serve as predictor of disease progression, while MiR-196a emerges as a novel valuable biomarker to predict both SLE risk and progression, this would be a critical tool for personalizing therapy and to avoid irreversible organ damage associated with SLE.

**Keywords:** Sle; Sledai; Mir-21; Mir-181A; Mir-196A

## M-513. Design, Synthesis and Biological Evaluation of Photoaffinity Probes of Antiangiogenic Homoisoflavonoids

Bit Lee, Wei Sun, Hyungjun Lee, Halesha Basavarajappa, Rania S Sulaiman, Kamakshi Sishtla, Xiang Fei, Timothy W Corson and Seung-Yong Seo

*Bioorganic and Medicinal Chemistry Letters, 26: 4277-4281 (2016) IF: 2.486*

A naturally occurring homoisoflavonoid, cremastranone (1) inhibited angiogenesis in vitro and in vivo. We developed an analogue SH-11037 (2) which is more potent than cremastranone in human retinal microvascular endothelial cells (HRECs) and blocks neovascularization in animal models. Despite their efficacy, the mechanism of these compounds is not yet fully known. In the course of building on a strong foundation of SAR and creating a novel chemical tool for target identification of homoisoflavonoid-binding proteins, various types of photoaffinity probes were designed and synthesized in which benzophenone and biotin were attached to homoisoflavanonoids using PEG linkers on either the C-3′ or C-7 position. Notably, the photoaffinity probes linking on the phenol group of the C-3′ position retain excellent activity of inhibiting retinal endothelial cell proliferation with up to 72 nM of GI50.

**Keywords:** Chemistry, Affinity Reagents

## M-515. Could Caffeic Acid Phenethyl Ester Expand the Antitumor Effect of Tamoxifen in Breast Carcinoma?

Tarek K. Motawi, Samy A. Abdelazim, Hebatallah A. Darwish, Eman M. Elbaz and Samia A. Shouman

*Nutrition and Cancer, 68: 435-445 (2016) IF: 2.241*

Despite tamoxifen (TAM) is beneficial in treating a significant proportion of patients with breast cancer, many women still relapse after long-term therapy. Caffeic acid phenethyl ester (CAPE) is a component of honeybee propolis, with a plethora of important biological actions including anticancer activity. This study aimed to explore the cytotoxicity, the type of drugs interaction as well as the apoptotic and autophagic pathways of the combined treatment of TAM and CAPE in MCF-7 cells. Their antitumor activity and effect on survival of mice bearing Ehrlich tumor were also analyzed. The results showed synergistic cytotoxic effects, manifested by significant activation of apoptotic machinery, along with downregulation of protein levels of Bcl-2 and beclin-1, upon using the combination regimen. However, the ratio between microtubule-associated protein light chain 3-II and -I was not altered. Moreover, a decrease in vascular endothelial growth factor level was detected. Similarly, TAM + CAPE increased the life span of tumor-bearing animals and caused a marked regression in their tumor size and weight compared with those treated with either TAM or CAPE alone. In conclusion, CAPE relatively improved the anticancer activity of TAM in both in vitro and in vivo models via its apoptotic and angiostatic potentials.

**Keywords:** Caffeic Acid Phenethyl Ester, Tamoxifen, Breast Carcinoma

## M-516. Ozone Therapy in Ethidium Bromide-Induced Demyelination in Rats: Possible Protective Effect

Neveen A. Salem, Naglaa Assaf, Manal F. Ismail, Yasser A. Khadrawy and Mohga Samy

*Cellular and Molecular Neurobiology, 36: 943-954 (2016) IF: 2.328*

Multiple sclerosis, an autoimmune inflammatory disease of the central nervous system, is characterized by excessive

demyelination. The study aimed to investigate the possible protective effect of ozone (O3) therapy in ethidium bromide (EB)-induced demyelination in rats either alone or in combination with corticosteroids in order to decrease the dose of steroid therapy. Rats were divided into Group (1) normal control rats received saline, Group (2) Sham-operated rats received saline, Group (3) Sham-operated rats received vehicle (oxygen), Group (4) EB-treated rats received EB, Group (5) EB-treated rats received O3, Group (6) EB-treated rats received methylprednisolone (MP), and Group (7) EB-treated rats received half the dose of MP concomitant with O3. EB-treated rats showed a significant increase in the number of footfalls in the grid walk test, decreased brain GSH, and paraoxonase-1 enzyme activity, whereas brain MDA, TNF-α, IL-1β, INF-γ, Cox-2 immunoreactivity, and p53 protein levels were increased. A significant decline in brain serotonin, dopamine, norepinephrine, and MBP immunoreactivity was also reported. Significant improvement of the above-mentioned parameters was demonstrated with the administration of either MP or O3, whereas best amelioration was achieved by combining half the dose of MP with ozone.

**Keywords:** Ethidium Bromideozonemethylprednisolonemultiple Sclerosisoxidative Stresscox-2P53rat

## M-517. Study of Micrornas-21/221 As Potential Breast Cancer Biomarkers in Egyptian Women

Tarek Mohamed Kamal Motawi, Nermin Abdel Hamid Sadik , Olfat Gamil Shaker, Maha Rafik El Masry and Fady Mohareb

*Gene, 590: 210-219 (2016) IF: 2.319*

microRNAs (miRNAs) play an important role in cancer prognosis. They are small molecules, approximately 17–25 nucleotides in length, and their high stability in human serum supports their use as novel diagnostic biomarkers of cancer and other pathological conditions. In this study, we analyzed the expression patterns of miR-21 and miR-221 in the serum from a total of 100 Egyptian female subjects with breast cancer, fibroadenoma, and healthy control subjects. Using microarray-based expression profiling followed by real-time polymerase chain reaction validation, we compared the levels of the two circulating miRNAs in the serum of patients with breast cancer (n = 50), fibroadenoma (n = 25), and healthy controls (n = 25). The miRNA SNORD68 was chosen as the housekeeping endogenous control. We found that the serum levels of miR-21 and miR-221 were significantly overexpressed in breast cancer patients compared to normal controls and fibroadenoma patients. Receiver Operating Characteristic (ROC) curve analysis revealed that miR-21 has greater potential in discriminating between breast cancer patients and the control group, while miR-221 has greater potential in discriminating between breast cancer and fibroadenoma patients. Classification models using k-Nearest Neighbor (kNN), Naïve Bayes (NB), and Random Forests (RF) were developed using expression levels of both miR-21 and miR-221. Best classification performance was achieved by NB Classification models, reaching 91% of correct classification. Furthermore, relative miR-221 expression was associated with histological tumor grades. Therefore, it may be concluded that both miR-21 and miR-221 can be used to differentiate between breast cancer patients and healthy controls, but that the diagnostic accuracy of serum miR-21 is superior to miR-221 for breast cancer prediction. miR-221 has more diagnostic power in discriminating between breast cancer and fibroadenoma patients. The overexpression of miR-221 has been associated with the breast cancer grade. We also demonstrated that the combined expression of miR-21 and miR-221can be successfully applied as breast cancer biomarkers.

**Keywords:** Mirna; Mir-21; Mir-221; Breast Cancer; Fibroadenoma.

## M-518. Co-Occurrence of Primary Microcephaly Caused by A Novel Homozygous Aspm Mutation Along with X-Linked Ichthyosis in the Same Patient

Abdel-Hamid, M.F. Ismail, H.A. Darwish, L.K. Effat, M.S. Zaki and G.M.H. Abdel-Salam

*Genetic Counseling, 27(1): 25-33 (2016) IF: 0.384*

Autosomal recessive primary microcephaly is a heterogeneous genetic disorder caused by genes that affect neurogenesis. This form of microcephaly has not been associated with other congenital anomalies. ASPM mutations have been identified as the major cause implicated in autosomal recessive primary microcephaly. X-linked recessive ichthyosis, is an inborn error of steroid sulfatase metabolism characterized by dark and adhesive scaly skin. Here, we examined an Egyptian boy presenting with microcephaly and simplified gyral pattern. Additionally, he had ichthyosis that goes with the X-linked type. Mutation analyses of the ASPM gene for autosomal recessive primary microcephaly and STS gene of X-linked recessive ichthyosis were conducted revealing a co-occurrence of a novel homozygous splice site mutation of ASPM gene (c.2936+1G>A) and a partial deletion of STS spanning from exon 7-10. We propose that the phenotype of our patient results from the combined effects of mutations in both ASPM and STS that account for the neurological signs and skin manifestations, respectively. The association of isolated X-linked recessive ichthyosis and autosomal recessive primary microcephaly has never been reported in the literature. Careful clinical and genetic assessment of patients with atypical clinical phenotypes is crucial for detecting such rare double mutations and thus proper genetic counseling.

**Keywords:** Autosomal Recessive – Primary Microcephaly – X-Linked Recessive Ichthyosis – Aspm Gene – Sts Gene – Two Genetic Disorders.

## M-519. Molecular and Phenotypic Spectrum of Aspm-Related Primary Microcephaly: Identification of Eight Novel Mutations

Mohamed S. Abdel-Hamid, Manal F. Ismail, Hebatallh A. Darwish, Laila K. Effat, Maha S. Zaki and Ghada M. H. Abdel-Salam

*American Journal of Medical Genetics Part A, 170A: 2133-2140 (2016) IF: 2.082*

Autosomal recessive primary microcephaly (MCPH) is an abnormal proliferation of neurons during brain development that leads to a small brain size but architecturally normal in most instances. Mutations in the ASPM gene have been identified to be the most prevalent. Thirty-seven patients from 30 unrelated families with a clinical diagnosis of MCPH were enrolled in this study. Screening of ASPM gene mutations was performed by targeted linkage analysis followed by direct sequencing. Thirteen protein truncating mutations of the ASPM were

identified in 15 families (50%), eight of which were novel mutations. The mutations detected were eight nonsense, four frameshift, and one splice site. Two of these mutations (p.R1327* and p.R3181*) were recurrent and shared similar haplotypes suggesting founder effect. Patients with ASPM mutations had mild to severe intellectual disability and variable degrees of simplified gyral pattern and small frontal lobe. In addition, hypoplasia of corpus callosum (18 patients), mildly small cerebellar vermis (10 patients), and relatively small pons (13 patients) were found in 85.7%, 47.6%, and 61.9%, respectively. Furthermore, one patient had porencephaly and another had a small midline cyst. Epilepsy was documented in two patients (9.5%). Non-neurologic abnormalities consisted of growth retardation (four patients), and co-incidental association of oculo-cutaneous albinism (one patient). Our study expands the mutation spectrum of ASPM. Moreover, the simplified gyral pattern and small frontal lobe together with hypoplastic corpus callosum, small cerebellum and pons enable ASPM mutated patients to be distinguished.

**Keywords:** Autosomal Recessive; Primary Microcephaly; Aspm Gene; Novel Mutations; Founder Effect; Egyptian

## M-520. Circulating MicroRNAs, Mir-92A, Mir-100 and Mir-143, as Non-Invasive Biomarkers for Bladder Cancer Diagnosis

Tarek Kamal Motawi, Sherine Maher Rizk, Taghreed Mahmoud Ibrahim and Ihab Abdel-Rahman Ibrahim

*Cell Biochemistry and Function, 34: 142-148 (2016) IF: 2.016*

The application of microRNAs (miRNAs) as potential biomarkers and therapy targets has been widely investigated in many kinds of cancers. Recent advantages of serum miRNAs open a new realm of possibilities for non-invasive diagnosis and prognosis of bladder cancer (BC). The aim of our study was to identify plasma miR-92a, miR-100 and miR-143 expression signatures in patients with BC to introduce new markers for establishing BC diagnosis and prognosis. Blood samples were collected from 70 BC patients and 62 controls. An expression of three target miRNAs (miR-92a, miR-100 and miR-143) was measured using quantitative real-time PCR method. Results were correlated with clinicopathological data and analysed. Plasma levels of miR-92a, miR-100 and miR-143 were significantly lower in BC patients than in control group. Receiver operator characteristic analysis revealed that the sensitivity and specificity values of miR-92a were 97·1% and 76·7%, respectively, with a cut-off value of 0·573. The sensitivity and specificity values of miR-100 were 90% and 66·7%, respectively, with a cut-off value of 0·644. The sensitivity and specificity values of miR-143 were 78·6% and 93·3%, respectively, with a cut-off value of 0·164. This study explores the existence of specific plasma miRNAs as early diagnostic biomarkers for BC in Egyptian patients; and these findings suggest that plasma miR-92a, miR-100 and miR-143 could be promising novel circulating biomarkers in clinical detection of BC.

**Keywords:** Bladder Cancer; Microrna; Molecular Marker; Diagnosis; Prognostic Factor; Rt-Pcr

## M-519. Combination of Melatonin and Certain Drugs for Treatment of Diabetic Nephropathy in Streptozotocin-Induced Diabetes in Rats

Tarek K. Motawi, Samia A. Ahmed, Manal A. Hamed, Shohda A. El-Maraghy and Wessam M. Aziz

*Diabetology International, 7: 413-424 (2016)*

Diabetic nephropathy is a major complication of diabetes and a leading cause of end-stage renal failure in many developed countries. The study aimed to evaluate the efficiency of certain drugs and melatonin in the treatment of nephropathy secondary to diabetes. Diabetes was induced in rats by a single intraperitoneal injection of streptozotocin (50 mg/kg body weight). Three days after induction of diabetes (460–500 mg/dl), rats were treated daily for 60 days with Rowatinex, melatonin, Rowatinex + melatonin, Amosar (Losartan Potassium) (LSP) and LSP + melatonin. The evaluations were made by measuring blood urea nitrogen (BUN), serum uric acid, serum creatinine, urine creatinine, creatinine clearance, nitric oxide, malondialdehyde, superoxide dismutase, glutathione, total antioxidant capacity, kidney injury molecule-1, heat shock protein-70, caspase-3, transforming growth factor β1, and DNA degradation by comet assay and total protein contents. The histopathological picture of the kidneys and pancreases was confirmed in our results. Diabetic rats showed drastic changes in all the measured parameters. Treatment with melatonin and the selected drugs revealed amelioration levels with variable degrees. In conclusion, the combination of LSP and melatonin had the most potent effect on treating the deleterious action of diabetes on rat kidney.

**Keywords:** Diabetic Nephropathy, Melatonin, Rowatinex, Rowatinex, Lsp

### *Dept. of Clinical Pharmacy*

## M-520. AllosterismBased Simultaneous, Dual Anticoagulant and Antiplatelet Action: Allosteric Inhibitor Targeting the Glycoprotein IbαBinding and HeparinBinding Site of Thrombin

A. Y. Mehta, B. M. Mohammed, E. J. Martin, D. F. Brophy, D. Gailani and U. R. Desai

*Journal of Thrombosis and Haemostasis, 14(4): 828-838 (2016) IF: 5.565*

**Background:** Allosteric inhibition is a promising approach for developing a new group of anticoagulants with potentially reduced bleeding consequences. Recently, we designed sulfated β-O4 lignin (SbO4L) as an allosteric inhibitor that targets exosite 2 of thrombin to reduce fibrinogen cleavage through allostery and compete with glycoprotein Ibα to reduce platelet activation. **Objective:** To assess: (i) the antithrombotic potential of a novel approach of simultaneous exosite 2-dependent allosteric inhibition of thrombin and competitive inhibition of platelet activation; and (ii) the promise of SbO4L as the first-in-class antithrombotic agent. **Methods:** A combination of whole blood thromboelastography, hemostasis analysis, mouse arterial thrombosis models and mouse tail bleeding studies were used to assess antithrombotic potential. **Results AndConclusions:** SbO4L extended the clot initiation time, and reduced maximal clot strength, platelet contractile force, and the clot elastic modulus, suggesting dual anticoagulant and antiplatelet effects.

These effects were comparable to those observed with enoxaparin. A dose of 1 mg of SbO4L per mouse prevented occlusion in 100% of arteries, and lower doses resulted in a proportionally reduced response. Likewise, the time to occlusion increased by ~ 70% with a 0.5-mg dose in the mouse Rose Bengal thrombosis model. Finally, tail bleeding studies demonstrated that SbO4L does not increase bleeding propensity. In comparison, a 0.3-mg dose of enoxaparin increased the bleeding time and blood volume loss. Overall, this study highlights the promise of the allosteric inhibition approach, and presents SbO4L as a novel anticoagulant with potentially reduced bleeding side effects.
**Keywords:** Allosterism, Thrombin, Glycoprotein, Coagulation

## M-521. Coated Platelet Assay: A Feasible Approach to A Complicated Science

B. M. Mohammed, D. Contaifer Jr., K. K. Lastrapes, E. J. Martin, M. A. Mazepa, M. Hoffman, D. M. Monroe and D. F. Brophy

*Haemophilia, 22(1) (2016) IF: 2.673*

Coated platelets (CP) are a subpopulation of platelets with enhanced prothrombinase complex activity that develop following simultaneous dual activation with agonists (collagen and thrombin). Previous methods used to quantify CP have been described in the literature, however, they involved non-clinical standard blood collection procedures, multistep platelet preparation techniques including several labelling and washing steps, and/or the use of agonists of animal origin. In addition, these reports often lack completeness and/or clarity thus limiting reproducibility of the assay. Herein, we report a simple, reproducible assay that can bring CP screening closer to clinical laboratory practice and help standardize the methodology. We used clinic-standard blood collection procedures, minimum platelet manipulation techniques including a single-step platelet labelling procedure. Moreover, unlike previous methods that used bovine thrombin to boost CP signal detection, we used human thrombin, which is more physiologically relevant, to obtain a detectable CP signal.
**Keywords:** Coated Platelets, Hemophilia, Bleeding

## M-522. Coated Platelets and Severe Haemophilia a Bleeding Phenotype: Is There a Connection ?

K. K. Lastrapes, B. M. Mohammed, M. A. Mazep, E. J. Martin, J. C. Barrett, G. V. Massey, J. G. Kuhn, M. E. Nolte, M. Hoffman, D. M. Monroe and D. F. Brophy

*Haemophilia, 22(1): 148-151 (2016) IF: 2.673*

**Introduction:**Coated platelets are a subpopulation of platelets that possess highly prothrombotic properties. Previous observational data suggest that bleeding phenotype in severe haemophilia A is associated with coated platelet levels. Haemophilia A patients with higher coated platelet levels may have a mild bleeding phenotype; those with lower levels may have a more severe bleeding phenotype. AIM: The aim of the study was to test the hypothesis that coated platelet levels are correlated with clinical bleeding phenotype. **Methods:** This cross-sectional, observational study enrolled 20 severe haemophilia A patients, including 15 with severe and five with a mild bleeding phenotype, and a control group of 12 healthy volunteers. The haemophilia bleeding phenotype was determined by the patient's medical history and haemophilia treatment centre records. Blood was obtained from each patient by venipuncture and platelets were analysed by flow cytometry. **Results:** Patients categorized as having a severe bleeding phenotype experienced a median eight bleeds per year compared to one bleed annually in the mild bleeding phenotype group. Both groups had similar total platelet counts and fibrinogen levels. There was no difference in coated platelet percentage between severe and mild bleeding phenotype (17 and 16% respectively), however, both groups had significantly lower % coated platelets compared to controls (44%, $P < 0.0001$). **Conclusion:** Coated platelet levels were not associated with bleeding phenotype in this study; however, these data may suggest coated platelet levels are lower in haemophilia patients relative to healthy volunteers.
**Keywords:** Coated Platelets; Hemophilia; Bleeding.

## M-523. Association Between Combined Presence of Hepatitis C Virus and Polymorphisms in Different Genes with Toxicities of Methotrexate and 6-Mercaptopurine in Children with Acute Lymphoblastic Leukemia.

Doaa H. Abdelaziz, Noha M. Elhosseiny, Sahar A. Khaleel, Nirmeen A. Sabry, Ahmed S. Attia and Manal H. El-Sayed

*Pediatric Blood & Cancer, 63: 1539-1545 (2016) IF: 2.634*

**Background.** The aim of the present study is to determine the correlation of hepatitis C virus (HCV) infection and polymorphisms in different genes with toxicity of either methotrexate (MTX) or 6-mercaptopurine (6-MP) administered to children with acute lymphoblastic leukemia (ALL). Procedure. One hundred children with low-risk ALL, who were treated according to the St. Jude Total therapy XV, were recruited. The recruited children were receiving MTX and 6-MP during maintenance phase. Patients were excluded from the study if they had other types of leukemia. Genotyping analyses for the thiopurine methyltransferase (TPMT), methylenetetrahydrofolate reductase (MTHFR), and glutathione S-transferase (GST) genes were performed using a combination of polymerase chain reaction (PCR) and PCR-RFLP (where RFLP is restriction fragment length polymorphism) protocols. Relevant clinical data on adverse drug reactions were collected objectively (blinded to genotypes) from the patient medical records. **Results.** There was a significant correlation between the combined presence of HCV and TPMT*3B G460A gene polymorphisms and grades 2–4 hepatotoxicity as aspartate aminotransferase (AST) elevation ($P < 0.04$). The same observation was seen when comparing either the presence of HCV alone or the presence of the gene polymorphism alone. A significant association between the combined presence of HCV and MTHFR C677T polymorphism and grades 2–4 hepatotoxicity as alanine aminotransferase (ALT), AST, and alkaline phosphatase (ALP) elevation was observed (P values <0.001, 0.02, and 0.001, respectively). The presence of HCV infection had a significant negative effect on hepatic transaminases. **Conclusions.** The present data support a role for combining analysis of genetic variation in drugmetabolizing enzymes and the presence of HCV in the assessment of specific drugs toxicities in multiagent chemotherapeutic treatment regimens.

**Keywords:** Acute Lymphoblastic Leukemia; Chemotherapy; Children; Genetic Polymorphism; Hcv; Toxicities.

## M-524. Vitamin C Promotes Wound Healing Through Novel Pleiotropic Mechanisms.

Bassem M. Mohammed, Bernard J. Fisher, Donatas Kraskauskas, Susan Ward, Jennifer S. Wayne, Donald F. Brophy, Alpha A. Fowler, Dorne R. Yager and Ramesh Natarajan

*International Wound Journal, 13(4): 572-584 (2016) IF: 2.594*

Vitamin C (VitC) or ascorbic acid (AscA), a cofactor for collagen synthesis and a primary antioxidant, is rapidly consumed post-wounding. Parenteral VitC administration suppresses pro-inflammatory responses while promoting anti-inflammatory and pro-resolution effects in human/murine sepsis. We hypothesised that VitC could promote wound healing by altering the inflammatory, proliferative and remodelling phases of wound healing. Mice unable to synthesise VitC (Gulo−/−) were used in this study. VitC was provided in the water (sufficient), withheld from another group (deficient) and supplemented by daily intra-peritoneal infusion (200 mg/kg, deficient + AscA) in a third group. Full thickness excisional wounds (6 mm) were created and tissue collected on days 7 and 14 for histology, quantitative polymerase chain reaction (qPCR) and Western blotting. Human neonatal dermal fibroblasts (HnDFs) were used to assess effects of In conclusion, VitC favorably on proliferation. Histological analysis showed improved wound matrix deposition and organisation in sufficient and deficient +AscA mice. Wounds from VitC sufficient and deficient + AscA mice had reduced expression of pro-inflammatory mediators and higher expression of wound healing mediators. Supplementation of HnDF with AscA induced the expression of self-renewal genes and promoted fibroblast proliferation. VitC favourably impacts the spatiotemporal expression of transcripts associated with early resolution of inflammation and tissue remodelling.

**Keywords:** Wound Healing, Vitamin C, Tensile Strength

## M-525. Conducting Economic Evaluations Alongside Randomised Trials: Current Methodological Issues and Novel Approaches

Hughes D, Charles J, Dawoud D, Edwards RT, Holmes E, Jones C, Parham P, Plumpton C, Ridyard C, Lloyd-Williams H, Wood E and Yeo ST

*Pharmacoeconomics, 34: 447-461 (2016) IF: 2.566*

Trial-based economic evaluations are an important aspect of health technology assessment. The availability of patient-level data coupled with unbiased estimates of clinical outcomes means that randomised controlled trials are effective vehicles for the generation of economic data. However there are methodological challenges to trial-based evaluations, including the collection of reliable data on resource use and cost, choice of health outcome measure, calculating minimally important differences, dealing with missing data, extrapolating outcomes and costs over time and the analysis of multinational trials. This review focuses on the state of the art of selective elements regarding the design, conduct, analysis and reporting of trial-based economic evaluations. The limitations of existing approaches are detailed and novel methods introduced. The review is internationally relevant but with a focus towards practice in the UK.

**Keywords:** Pharmacoeconomics, Randomised Controlled Trials, Economic Evaluation.

## M-526. A Systematic Review of Patients' Perspectives on the Subcutaneous Route of Medication Administration

Colin H. Ridyard, Dalia M. M. Dawoud, Lorna V. Tuersley and Dyfrig A. Hughes

*Patient - Patient-Centered Outcomes Research, 9: 281-292 (2016) IF: 2.227*

**Background** Subcutaneous injections allow for self-administration, but consideration of patients' perspectives on treatment choice is important to ensure adherence. Previous systematic reviews have been limited in their scope for assessing preferences in relation to other routes of administration. Objective Our objective was to examine patients' perspectives on subcutaneously administered self-injectable medications when compared with other routes or methods of administration for the same medicines. **Methods** Nine electronic databases were searched for publications since 2000 using terms pertaining to methods of administration, choice behavior, and adverse effects. Eligibility for inclusion was determined through reference to specific criteria by two independent reviewers. **Results** were described narratively. Results of the 1726 papers screened, 85 met the inclusion criteria. Studies were focused mainly on methods of insulin administration for diabetes but also included treatments for pediatric growth disorders, multiple sclerosis, HIV, and migraine. Pen devices and autoinjectors were favored over administration with needle and syringe, particularly with respect to ergonomics, convenience, and portability. Inhalation appeared to be more acceptable than subcutaneous injection (in the case of insulin), but how subcutaneous infusion, intramuscular injection, and needle-free injection devices compare with subcutaneous injections in terms of patient preference is less certain. **Conclusions** The review identified a number of studies showing the importance of the methods and routes of drug delivery on patient choice. However, studies were prone to bias, and further robust evidence based on methodologically sound approaches is required to demonstrate how patient choice might translate to improved adherence.

**Keywords:** Subcutaneous, Patient Preferences, Injection, Systematic Review, Route of Administration

## M-527. Efficacy of Different Perioperative Statin Regimens on Protection Against Post-Coronary Artery Bypass Grafting Major Adverse Cardiac and Cerebral Events

Aya G. Elmarsafawi, Maggie M. Abbassi, Sameh Elkaffas, Hassan M. Elsawy and Nirmeen A. Sabry

*Journal of Cardiothoracic and Vascular Anesthesia, 30 (6): 1461-1470 (2016) IF: 1.519*

**Objectives:**Comparing different perioperative statin regimens for the prevention of post-coronary artery bypass grafting adverse events. **Design:** A randomized, prospective study. **Setting:** Cardiothoracic surgical units in a government hospital.

**Participants:** The study comprised 94 patients scheduled for elective, isolated on- or off- pump coronary artery bypass grafting. **Interventions:** Patients were assigned randomly to 1 of the following 3 treatment groups: group I (80 mg of atorvastatin/day for 2 days preoperatively), group II (40 mg of atorvastatin/day for 5-9 days preoperatively), or group III (80 mg of atorvastatin/day for 5-9 days preoperatively). The same preoperative doses were restarted postoperatively and continued for 1 month. **Measurements and MainResults:** Cardiac troponin I, creatine kinase, and C-reactive protein (CRP) levels were assayed preoperatively; at 8, 24, and 48 hours postoperatively; and at discharge. CRP levels at 24 hours ($p = 0.045$) and 48 hours ($p = 0.009$) were significantly lower in group III compared with the other 2 groups. However, troponin I levels at 8 hours ($p = 0.011$) and 48 hours ($p = 0.025$) after surgery were significantly lower in group II compared with group III. The incidence of postoperative major adverse cardiac and cerebrovascular events was assessed, and there was no significant difference among the 3 groups. **Conclusion:** The 3 regimens did not result in any significant difference in outcomes, but only simple trends. The higher-dose regimen resulted in a significant reduction in the CRP level. Thus, more studies are needed to confirm the benefit of higher-dose statins for the protection from post-coronary artery bypass grafting adverse events.

**Keywords:** Coronary Artery Bypass Grafting, Major Adverse Cardiac and Cerebral Events, Statins

## M-528. Obesity Does Not Affect Propofol Pharmacokinetics During Hypothermic Cardiopulmonary Bypass.

Iman A. El-Baraky, Maggie M. Abbassi, Tarek A. Marei and Nirmeen A. Sabry

*Journal of Cardiothoracic and Vascular Anesthesia, 30: 876-883 (2016) IF: 1.519*

**Objective:** Because of the lack of data regarding the impact of obesity on propofol pharmacokinetics in patients undergoing cardiac surgery using hypothermic cardiopulmonary bypass (CPB), the authors sought to explore propofol pharmacokinetics and develop a predictive pharmacokinetic model that characterizes and predicts propofol pharmacokinetics in this population. Design: A prospective, observational study. Setting: A teaching hospital. Participants: The study comprised 17 obese and 17 control (nonobese) patients undergoing hypothermic CPB. Intervention: None. **Measurements and Main Results:** Patients mainly underwent valve surgery. On initiation of hypothermic CPB (281C- 321C), patients received a propofol (1%) bolus (1 mg/kg) immediately followed by a 2 mg/kg/h infusion. Blood samples were withdrawn at the following times: before dosing; 1, 3, 5, and 7 minutes after the propofol bolus dose; every 20 minutes during infusion; just before discontinuation of the infusion; and at 1, 3, 5, 7, 10, 20, 30, and 60 minutes after discontinuation of the infusion. The plasma propofol concentration was determined using high-performance liquid chromatography, and then data were imported into Monolix (Lixoft, Antony, France) for population pharmacokinetic modeling and pharmacokinetic parameters estimation. A 2-compartment pharmacokinetic model with age as a covariate on the peripheral volume of distribution (V2) best described the pooled data. The pooled data was internally evaluated successfully to describe and predict propofol pharmacokinetics in the addressed population. Propofol clearance, intercompartmental clearance, and central volume of distribution were 805 mL/min, 1140 mL/min and 18.8 L, respectively. V2 was calculated as 9.86 exp.(1.88 [age/40]) L. **Conclusion:** Propofol pharmacokinetic parameters were similar in obese and nonobese patients undergoing hypothermic CPB. Age was the major determinant of propofol V2 in the obese population.

**Keywords:** Propofol; Pharmacokinetics; Obesity; Cardiopulmonary Bypass.

## M-529.Adverse Drug Reactions Reporting: A Questionnaire-Based Study on Egyptian Pharmacists' Attitudes Following an Awareness Workshop

Nehal A Alraie, Amr A Saad, Nirmeen A Sabry and Samar F Farid

*Journal of Evaluation In Clinical Practice, 22: 349-355 (2016) IF: 1.053*

Rationale, aims and objectives Hospital pharmacists can promote medication safety through spontaneous reporting of adverse drug reactions (ADRs). However, different educational interventions and different factors (socio-demographic and professional) have been implicated to influence the reporting process. The aims of this study were to assess the impact of pharmacovigilance awareness workshop on knowledge of hospital pharmacists;and to identify the main factors and barriers that influence ADRs reporting. **Methods** Two validated self-administered questionnaires were distributed to pharmacists attending an awareness workshop (pre and post); and a telephone survey was completed three months after the workshop. ADR reports (yellow cards) received from participating pharmacists were monitored for six months, and analysed for quality (validity and serious- ness) and reporter demographic and professional factors. **Results** Two hundred and eighty-one pharmacists (95.25%) and 270 pharmacists (91.52%) completed pre- and post-workshop questionnaires respectively. A comparison of their knowledge of ADRs to report before and after the workshop showed significant difference (Wilcoxon test $P < 0.05$). Two hundred and four pharmacists (72.6%) completed the follow-up questionnaire, with lack of time, administrative barriers and inability to complete patient details being the most frequent reasons for not reporting. A total of 163 yellow cards were received from 49 pharmacists (17.44%) over 6 months, of which 126 reports (77.3%) were serious ADRs. Demographics of reporting pharmacists showed significance for completion of post-graduate studies, ministry of health hospitals and pharmacist post in hospital. **Conclusion** Despite pharmacists' adequate knowledge after the workshop, they failed to maintain consistent reporting. Addressing the barriers to reporting and the personal factors influencing the process may be needed.

**Keywords:** Adverse Drug Reactions, Egypt, Hospital Pharmacists, Spontaneous Reporting.

## M-530.The Impact of A 600-Mg Loading Dose of Clopidogrel in Diabetic and Non-Diabetic Patients Undergoing Elective PCI.

Mina W. Mohareb , Mohamed Abd Elghany, Nirmeen A. Sabry and Samar F. Farid

*Minerva Cardioangiologica, 64: 375-382 (2016) IF: 0.752*

**Background:** High platelet reactivity (HPR) and suboptimal response to dual antiplatelet therapy (DAPT) may explain high recurrent rates of ischemic events in type 1 and 2 diabetes mellitus (DM) patients undergoing percutaneous coronary intervention (PCI). The aim of this study was to determine the effect of diabetes mellitus on clopidogrel activity in cardiac patients undergoing PCI. **Methods:** This is an observational study. Patients were categorized according to DM status into diabetic group (N.=30) and non-diabetic group (N.=33). All patients received clopidogrel in a loading dose of 600 mg before PCI. Platelet function was assessed using light transmittance aggregometry (LTA) technique at baseline (before clopidogrel administration), 24 hour after clopidogrel loading dose administration and 7-10 days after PCI. All patients were followed up for at least one year after PCI for recurrence of acute cardiac events. **Results:** There was no statistically significant difference between the two groups with respect to 10 µm adenosine diphosphate (ADP)-induced platelet aggregation measured at baseline (P=0.64), 24 hours after PCI (P=0.874), and 7-10 days after PCI (0.643). Diabetics were not significantly different from non-diabetics in terms of post-PCI acute stent thrombosis (P=0.945), sub-acute stent thrombosis (P=0.945), unstable angina (P=0.29) and cardiac death (P=0.64). There was a statistically significant difference between patients with and without post-PCI acute events regarding ADP aggregation measured 24 hours and 7-10 days after PCI. **Conclusions:** The use of a high loading dose of clopidogrel (600 mg) in patients undergoing elective PCI can overcome the significant increase in post-PCI platelet aggregation and rate of acute cardiac events induced by diabetes mellitus as co-morbidity in those patients.
**Keywords:** Clopidogril -Diabetes Mellitus -Percutaneous Coronary Intervention -Adenosine Diphosphate

## M-531.Drug-Related Problems in Cardiac Children

Nirmeen Sabry, Samar Farid and Dalia Dawoud

*Minerva Pediatrica, 68: 89-95 (2016) IF: 0.532*

**Background:** A drug-related problem (DRP) may be defned as “an event or circumstance involving drug therapy that actually or potentially interferes with the desired health outcome”. Our aim was to determine the frequency and char- acteristics of drPs in pediatric patients admitted to a tertiary cardiac care center in the egyptian capital, cairo. **Methods:** A prospective observational cohort study involving review of case notes for children aged 0-18 years, admitted to the medical ward and intensive care unit (icU), was conducted at a tertiary cardiac care center in egypt. data collection took place over a three-month period. daily reviews of patients’ records, medication charts and laboratory data were undertaken by the clinical pharmacists to identify drPs. **Results:** A total of 60 patients were included in the study (mean age 4.8 years; 53.33% males). Over a three-month period, a total of 313 drPs were recorded corresponding to an average of 5.22 problems per patient. the most commonly recorded problems related to drug-drug interaction (45.69%), prescribing unnecessary medication (31.95%), under-dosing (21.09%), inappropriate medication (0.96%) and adverse drug reaction (0.32%). Prophylactic antibiotics represented the only unnecessarily prescribed medications. of the pharmacist suggested interventions, 65% were accepted by the responsible physician. **Conclusions:** drPs occurred frequently during the study period. drug-drug interactions, drug choice and drug dosing problems represented the majority of the identifed DRPs, necessitating targeted prescriber education interventions in these areas. there is a clear need for clinical pharmacists’ involvement on the ward level to identify and rectify these frequently occurring and very costly problems
**Keywords:** Child Abuse; Drug-Related Side Effects and Adverse Reactions; Pharmacy Service, Hospital; Egypt; Observational Study; Pediatrics.

## M-532. A Pharmacokinetic Study of Digoxin Holiday Dosing Practice in Egypt: A Prospective-Randomized Trial

S.A. Alshabasy, M.M. Abbassi, M.S. Mohamed and S.F. Farid

*Bulletin of Faculty of Pharmacy, Cairo University, 54: 157-164 (2016)*

**Background** Because of the narrow therapeutic index of digoxin, most cardiologists in Egypt give digoxin holiday for atrial fibrillation and heart failure, it is not clear if the interrupted digoxin regimens are effective since serum digoxin concentrations might fall below the therapeutic range. **Objective** To evaluate and compare the digoxin serum concentration and patient’s quality of life in the continuous versus interrupted digoxin dosing regimens. **Methods** Patients were randomized to receive one of four regimens: regimen 1: 0.25 mg daily except Friday (N = 17); regimen 2: 0.25 mg daily except Thursday and Friday (N = 17); regimen 3: 0.125 mg daily (N = 17); and regimen 4: a tailored dose was calculated based on renal function and given daily (N = 23). After reaching steady state in the two holiday regimens, two plasma samples were collected (preholiday and post holiday trough concentrations); in the other two groups one trough plasma sample was collected. Quality of life questionnaire for atrial fibrillation (QLAF), was administered to all patients at baseline and then after at least one month of digoxin therapy. **Results** There was a statistically significant difference between the preholiday trough concentration and the trough steady state concentration across the four regimens (p = 0.002). There was no significant difference in the QLAF questionnaire domains, total scores at baseline, or after the follow up between the four regimens. **Conclusion** Once daily tablet (0.25 mg) was suitable in maintaining digoxin serum concentration in the recommended therapeutic range, fluctuation in digoxin serum concentration did not affect quality of life for atrial fibrillation patients.
**Keywords:** Digoxin; Interrupted Regimens; Atrial Fibrillation; Digoxin Holiday; Quality of Life

## M-533. Knowledge, Attitude, and Prevalence of Use of Hormone Replacement Therapy Among Women in United Arab Emirates

Osama Mohamed Ibrahim and Rand N Hussein

*Asian Journal of Pharmaceutical and Clinical Research,9(2016)*

**Objectives:** The purpose of this study is to investigate the knowledge and attitude of women living in the United Arab Emirates (UAE) about hormone replacement therapy (HRT) and their associated health benefits and risks. **Methods:** A cross-sectional study was performed among 220 women aged 20-70 years old in the UAE mainly in Abu Dhabi and Sharjah. The survey included 21 items; socio-demographic profiles, medical and menstrual histories, and questions related to their knowledge, attitude toward HRT use,benefits, and risks. **Results:** Among females participated in the study, (48%) were using a variety of HRT for managing menopausal symptoms. Health care professionals were chosen the most as their main source of information in both Abu Dhabi and Sharjah (68%, 39%, p<0.0001). 26% of women living in Abu Dhabi and 19% in Sharjah thought that HRT was a good solution for women with menopausal symptoms. The percentages of women who had a negative attitude toward HRT were almost equal in both cities (Abu Dhabi 10.78%, Sharjah 14.41%). However, the overall knowledge of the participants aboutHRT risks and benefits was average. Conclusion: The study indicated that there was a positive attitude toward HRT use and good knowledge of its possible benefits and risks among the participants which could be because physicians were their major source of information.

**Keywords:** Hormone Replacement Therapy, Menopause, Prevalence Knowledge and Attitude, United Arab Emirates, Sharjah, Abu Dhabi.

## M-534.Perceptions of Egyptian Physicians About Drug Shortage During Political Disturbances: Survey in Greater Cairo

Ammar A. Abdelrahman, Amr A. Saad, Nirmeen A. Sabry and Samar F. Farid

*Bulletin of Faculty of Pharmacy, Cairo University, 54: 191-196 (2016)*

**Background:** Drug shortage is a problem that entangles health systems. In Egypt, many complaints arose due to drug shortage in the period following the 25th January revolution. Physicians play a vital role in dealing with this crisis. **Objectives:** Our aim was to investigate physicians' perspective of the drug shortage problem and its impact on the healthcare system. **Methods:** A questionnaire was adopted and distributed by hand to physicians in customers' waiting areas in Medical Syndicates Union. The questionnaire covered general participant information, drug shortage effects, physicians' responses to the problem, the magnitude of the problem and its development three years around the revolution. **Results:** of the 319 distributed questionnaires, 192 responses were valid with a response rate of 60%. Most of participants expressed the dire impact of drug shortage on patients' health. Death as a result of drug shortage was reported by 67 physicians !35% of participants. A significant difference between internal medicine specialists and surgical medicine specialists in perception of drug related deaths was found (p-value = 0.004). A significant negative correlation between number of years of experience and agreement to analogues therapeutic equivalency was found (Spearman's correlation coefficient = !0.207, P-value = 0.006). About two thirds of participants viewed drug shortages as a cause of inter-professional conflicts. Generally, participants denoted that drug shortage problem is worsening with time since the revolution. **Conclusion:** Prospective studies are required to quantitatively estimate drug shortage related mortality. Enhanced drug shortage communication by drug authorities and targeted education may relieve inter-professional conflicts resulting from drug shortages

**Keywords:** Healthcare Services Research; Healthcare Personnel; Drug Shortage; Survey; Developing Country.

### *Dept. of Microbiology and Immunology*

## M-535.Comparative Genome-Scale Modelling of Staphylococcus Aureus Strains Identifies Strain-Specific Metabolic Capabilities Linked to Pathogenicity

Emanuele Bosi, Jonathan M. Monk, Ramy K. Aziz, Marco Fondi, Victor Nizet and Bernhard O. Palsson

*Proceedings of The National Academy of Sciences Usa, 113 (2016) IF: 9.423*

Staphylococcus aureus is a preeminent bacterial pathogen capable of colonizing diverse ecological niches within its human host. We describe here the pangenome of S. aureus based on analysis of genome sequences from 64 strains of S. aureus spanning a range of ecological niches, host types, and antibiotic resistance profiles. Based on this set, S. aureus is expected to have an open pangenome composed of 7,411 genes and a core genome composed of 1,441 genes. Metabolism was highly conserved in this core genome; however, differences were identified in amino acid and nucleotide biosynthesis pathways between the strains. Genome-scale models (GEMs) of metabolism were constructed for the 64 strains of S. aureus. These GEMs enabled a systems approach to characterizing the core metabolic and panmetabolic capabilities of the S. aureus species. All models were predicted to be auxotrophic for the vitamins niacin (vitamin B3) and thiamin (vitamin B1), whereas strain-specific auxotrophies were predicted for riboflavin (vitamin B2), guanosine, leucine, methionine, and cysteine, among others. GEMs were used to systematically analyze growth capabilities in more than 300 different growth-supporting environments. The results identified metabolic capabilities linked to pathogenic traits and virulence acquisitions. Such traits can be used to differentiate strains responsible for mild vs. severe infections and preference for hosts (e.g., animals vs. humans). Genome-scale analysis of multiple strains of a species can thus be used to identify metabolic determinants of virulence and increase our understanding of why certain strains of this deadly pathogen have spread rapidly throughout the world.

**Keywords:** Systems Biology, Mathematical Modeling, Pathogenicity, Core Genome, Pangenome.

## M-537.Adaptation to Potassium-Limitation is Essential for Acinetobacter Baumannii Pneumonia Pathogenesis

Reham Samir, Salma H. Hussein, Noha M. Elhosseiny, Marwa S. Khattab, Alaa E. Shawky and Ahmed S. Attia

*Journal of Infectious Diseases, 214: 2006-2013 (2016) IF:6.344*

**Background** Acinetobacter baumannii is challenging the healthcare community as the cause of a wide range of untreatable infections. New targets need to be explored for the development of therapeutics. Methods The potassium-dependent

protein (Kdp) system was investigated via bioinformatics and genetic tools. An isogenic mutant was constructed in kdpE and complemented in trans. Gene expression and the ability to grow under potassium-limited conditions were investigated. Finally, the role of KdpE in virulence was examined in the murine pneumonia model. **Results** The A. baumannii Kdp system has a distinct arrangement and is well conserved among A. baumannii strains. The genes encoding the 5 members of the system are transcriptionally linked. kdpE is upregulated >70-fold under potassium-limited conditions. The ΔkdpE mutant showed a significant growth defect under potassium-limited conditions and in the colonization of mice lungs. These defects could be restored upon introducing kdpE on a multiple-copy plasmid. Proteomic analyses indicated that KdpE could be regulating several proteins with potential involvement in pathogenesis. **Conclusions** For the first time, A. baumannii KdpE is shown to be crucial to pneumonia onset, and targeting this system can be a viable approach to treating these fatal infections.

**Keywords:** A. Baumannii, Kdpe, Virulence, Pneumonia, Pathogenesis, Potassium, Drug Targets.

## M-538.Immunoinformatics Identifies A Lactoferrin Binding Protein a Peptide as a Promising Vaccine with a Global Protective Prospective Against Moraxella Catarrhalis

Gehad M. Yassin, Magdy A. Amin and Ahmed S. Attia

*Journal of Infectious Diseases, 213: 1938-1945 (2016) IF: 6.344*

**Background.** Moraxella catarrhalis is an established pathogen that is causing substantial infections to both children and adults. However, so far there is no effective vaccine to halt the spread of these infections. **Methods.** Immunoinformatics tools were used to predict M. catarrhalis epitopes that could offer immunoprotection among major proportions of human populations worldwide. Mice were immunized with the best 3 peptides and then challenged with M. catarrhalis in the pulmonary clearance model. Finally, antibodies against these epitopes were detected in humans. **Results.** Immunoinformatics analyses identified 44 epitopes that are predicted to be good major histocompatibility complex class II binders and at the same time show high population coverage worldwide. After intraperitoneal immunization of mice with the best 3 peptides, peptide A, derived from lactoferrin-binding protein A, showed superior activity in immunogenicity and in clearing M. catarrhalis from mouse lungs. Higher clearance was obtained by combining intraperitoneal and intranasal immunization. In the serum samples from children with otitis media infected with M. catarrhalis , antibody levels against peptide A were significantly lower than in samples from children without otitis media. **Conclusions.** Peptide A is the first promising peptide-based vaccine against M. catarrhalis . Immunoinformatics predicts that it should have a global protection around the world.

**Keywords:** Immunoinformatics, Vaccine, Moraxella Catarrhalis, LBPA, Otitis Media.

## M-540.HCV RNA Activates Apcs Via Tlr7/Tlr8 While Virus Selectively Stimulates Macrophages without Inducing Antiviral Responses

Yuwei Zhang, Mohamed El-Far, Franck P. Dupuy, Mohamed S. Abdel-Hakeem, Zhong He, Francesco Andrea Procopio, Yu Shi, Elias K. Haddad, Petronela Ancuta, Rafick-Pierre Sekaly and Elias A. Said

*Scientific Reports, 6: 1-13 (2016) IF: 5.228*

The innate and adaptive immune systems fail to control HCV infection in the majority of infected individuals. HCV is an ssRNA virus, which suggests a role for Toll-like receptors (TLRs) 7 and 8 in initiating the anti-viral response. Here we demonstrate that HCV genomic RNA harbours specific sequences that initiate an anti-HCV immune response through TLR7 and TLR8 in various antigen presenting cells. Conversely, HCV particles are detected by macrophages, but not by monocytes and DCs, through a TLR7/8 dependent mechanism; this leads to chloroquine sensitive production of proinflammatory cytokines including IL-1β, while the antiviral type I Interferon response is not triggered in these cells. Antibodies to DC-SIGN, a c-type lectin selectively expressed by macrophages but not pDCs or mDCs, block the production of cytokines. Novel anti-HCV vaccination strategies should target the induction of TLR7/8 stimulation in APCs in order to establish potent immune responses against HCV.

**Keywords:** Hepatitis C Virus (HCV), Antigen Presenting Cells(APCS), Toll-Like Receptors (TLRS), Innate Immunity.

## M-541.Molecular Typing and Virulence Analysis of Multidrug Resistant Klebsiella Pneumoniae Clinical Isolates Recovered from Egyptian Hospitals

Reham Wasfi, Walid F. Elkhatib and Hossam M. Ashour

*Scientific Reports, 6:38929 (2016) IF: 5.228*

Klebsiella pneumonia infection rates have increased dramatically. Molecular typing and virulence analysis are powerful tools that can shed light on Klebsiella pneumonia infections. Whereas 77.7% (28/36) of clinical isolates indicated multidrug resistant (MDR) patterns, 50% (18/36) indicated carpabenem resistance. Gene prevalence for the AcrAB efflux pump (82.14%) was more than that of the mdtK efflux pump (32.14%) in the MDR isolates. FimH-1 and mrkD genes were prevalent in wound and blood isolates. FimH-1 gene was prevalent in sputum while mrkD gene was prevalent in urine. Serum resistance associated with outer membrane protein coding gene (traT) was found in all blood isolates. IucC, entB, and Irp-1 were detected in 32.14%, 78.5% and 10.7% of MDR isolates, respectively. We used two Polymerase Chain Reaction (PCR) analyses: Enterobacterial Repetitive Intergenic Consensus (ERIC) and Random Amplified Polymorphic DNA (RAPD). ERIC-PCR revealed 21 and RAPD-PCR revealed 18 distinct patterns of isolates with similarity ≥80%. ERIC genotyping significantly correlated with resistance patterns and virulence determinants. RAPD genotyping significantly correlated with resistance patterns but not with virulence determinants. Both RAPD and ERIC genotyping methods had no correlation with the capsule types. These findings can help up better predict MDR Klebsiella pneumoniae outbreaks associated with specific genotyping patterns.

**Keywords:** Virulence, Outbreaks, Infections, Resistance, Efflux Pump, Genotyping.

## M-542. Viruses-to-Mobile Genetic Elements Skew in the Deep Atlantis II Brine Pool Sediments.

Mustafa Adel, Ali H. A. Elbehery, Sherry K. Aziz, Ramy K. Aziz, Hans-Peter Grossart and Rania Siam

*Scientific Reports, 6: 1-9 (2016) IF: 5.228*

The central rift of the Red Sea has 25 brine pools with different physical and geochemical characteristics. Atlantis II (ATIID), Discovery Deeps (DD) and Chain Deep (CD) are characterized by high salinity, temperature and metal content. Several studies reported microbial communities in these brine pools, but few studies addressed the brine pool sediments. Therefore, sediment cores were collected from ATIID, DD, CD brine pools and an adjacent brine-influenced site. Sixteen different lithologic sediment sections were subjected to shotgun DNA pyrosequencing to generate 1.47 billion base pairs (1.47 × 10(9) bp). We generated sediment-specific reads and attempted to annotate all reads. We report the phylogenetic and biochemical uniqueness of the deepest ATIID sulfur-rich brine pool sediments. In contrary to all other sediment sections, bacteria dominate the deepest ATIID sulfur-rich brine pool sediments. This decrease in virus-to-bacteria ratio in selected sections and depth coincided with an overrepresentation of mobile genetic elements. Skewing in the composition of viruses-to-mobile genetic elements may uniquely contribute to the distinct microbial consortium in sediments in proximity to hydrothermally active vents of the Red Sea and possibly in their surroundings, through differential horizontal gene transfer.
**Keywords:** Brine Pool, Sediments, Atlantis and Discovery Deeps, Red Sea, Metagenomics, Microbial Communities, Functional Genes.

## M-543. Cancer Derived Peptide of Vacuolar Atpase 'A2' Isoform Promotes Neutrophil Migration by Autocrine Secretion of Il-8

Safaa A. Ibrahim, Arpita Kulshrestha, Gajendra K. Katara, Magdy A. Amin and Kenneth D. Beaman

*Scientific Reports, 6 (2016) IF: 5.228*

Neutrophils play significant regulatory roles within the tumor microenvironment by directly promoting tumor progression that leads to poor clinical outcomes. Identifying the tumor associated molecules that regulate neutrophil infiltration into tumors may provide new and specific therapeutic targets for cancer treatment. The a2-isoform of vacuolar ATPase (a2V) is uniquely and highly expressed on cancer cell plasma membrane. Cancer cells secrete a peptide from a2V (a2NTD) that promotes the pro-tumorigenic properties of neutrophils. This provides a2V the propensity to control neutrophil migration. Here, we report that the treatment of human neutrophils with recombinant a2NTD leads to neutrophil adherence and polarization. Moreover, a2NTD treatment activates surface adhesion receptors, as well as FAK and Src kinases that are essential regulators of the migration process in neutrophils. Functional analysis reveals that a2NTD can act as a chemo-attractant and promotes neutrophil migration. In addition, a2Neu$^{\Phi}$ secrete high levels of IL-8 via NF-κB pathway activation. Confirmatory assays demonstrate that the promoted migration of a2Neu$^{\Phi}$ was dependent on the autocrine secretion of IL-8 from a2Neu$^{\Phi}$. These findings demonstrate for the first time the direct regulatory role of cancer associated a2-isoform V-ATPase on neutrophil migration, suggesting a2V as a potential target for cancer therapy.

## M-544. The Secretome of Acinetobacter Baumannii ATCC 17978 Type II Secretion System Reveals a Novel Plasmid Encoded Phospholipase that Could be Implicated in Lung Colonization

Noha M. Elhosseiny, Ossama M. El-Tayeb, Aymen S. Yassin, Stephen Lory and Ahmed S. Attia

*International Journal of Medical Microbiology, 306: 633-641 (2016) IF: 3.898*

Acinetobacter baumannii infections are compounded with a striking lack of treatment options. In many Gram-negative bacteria, secreted proteins play an important early role in avoiding host defences. Typically, these proteins are targeted to the external environment or into host cells using dedicated transport systems. Despite the fact that medically relevant species of Acinetobacter possess a type II secretion system (T2SS), only recently, its significance as an important pathway for delivering virulence factors has gained attention. Using in silico analysis to characterize the genetic determinants of the T2SS, which are found clustered in other organisms, in Acinetobacter species, they appear to have a unique genetic organization and are distributed throughout the genome. When compared to other T2SS orthologs, individual components of the T2SS apparatus showed the highest similarity to those of Pseudomonas aeruginosa. A mutant of Acinetobacter baumannii strain ATCC 17978 lacking the secretin component of the T2SS (ΔgspD), together with a trans-complemented mutant, were tested in a series of in vitro and in vivo assays to determine the role of T2SS in pathogenicity. The ΔgspD mutant displayed decreased lipolytic activity, associated with attenuated colonization ability in a murine pneumonia model. These phenotypes are linked to LipAN, a novel plasmid-encoded phospholipase, identified through mass spectroscopy as a T2SS substrate. Recombinant LipAN showed specific phospholipase activity in vitro. Proteomics on the T2-dependent secretome of ATCC 17978 strain revealed its potential dedication to the secretion of a number of lipolytic enzymes, among others which could contribute to its virulence. This study highlights the role of T2SS as an active contributor to the virulence of A. baumannii potentially through secretion of a newly identified phospholipase.
**Keywords:** A. Baumannii; T2ss; Virulence; Phospholipase.

## M-546. Inactivation of Rabies Virus by Hydrogen Peroxide

Asmaa A. Abd-Elghaffar, Amal E. Ali , Abeer A. Boseila and Magdy A. Amin

*Vaccine, 34: 798-802 (2016) IF: 3.413*

Development of safe and protective vaccines against infectious pathogens remains a challenge. Inactivation of rabies virus is a critical step in the production of vaccines and other research reagents. Beta-propiolactone (PL); the currently used

inactivating agent for rabies virus is expensive and proved to be carcinogenic in animals. This study aimed to investigate the ability of hydrogen peroxide (H2O2) to irreversibly inactivate rabies virus without affecting its antigenicity and immunogenicity in pursuit of finding safe, effective and inexpensive alternative inactivating agents. H2O2 3% rapidly inactivated a Vero cell adapted fixed rabies virus strain designated as FRV/K within 2 h of exposure without affecting its antigenicity or immunogenicity. No residual infectious virus was detected and the H2O2-inactivated vaccine proved to be safe and effective when compared with the same virus harvest inactivated with the classical inactivating agent PL. Mice immunized with H2O2-inactivated rabies virus produced sufficient level of antibodies and were protected when challenged with lethal CVS virus. These findings reinforce the idea that H2O2 can replace PL as inactivating agent for rabies virus to reduce time and cost of inactivation process.
**Keywords:** Rabies; Hydrogen Peroxide; Inactivation; Immunity.

## M-546. Assessment of Vitamin D Status in A Group of Egyptian Children with Non Alcoholic Fatty Liver Disease (Multicenter Study).

Amal Mohamed Ahmed, Maha Abdel Ghany, Gehan Lotfy Abdel Hakeem, Aya Kamal, Rania Khattab, Asmaa Abdalla, Laila El Morsi Abou El Fotoh, Abdel Azeem El Mazary, Madiha Abdalla Sayed and Ashraf Mohamed Abdel Fadil

*Nutrition and Metabolism, 13:53: 1-6 (2016) IF: 3.28*

**Background:** Nonalcoholic fatty liver disease (NAFLD) is one of the health problems with great burden on the liver that may end with liver cirrhosis and hepatocellular carcinoma. The aim of this work was to assess serum vitamin D level in nonalcoholic fatty liver disease children. **Methods:** This cross sectional case control study involved 47 patients with nonalcoholic fatty liver disease selected while recruiting the pediatric hepatology clinics. Their ages ranged from 5–15 years and were compared with 23 healthy age and sex matched children. All involved patients were subjected to careful history taking, clinical examination and for patients and control, anthropometric measures for body mass index (BMI) calculation (plotted on WHO percentile growth charts), aspartate aminotransferase (AST), alanine aminotransferase (ALT), alkaline phosphatase (ALP), gamma glutamyl transferase (GGT), bilirubin (total and direct), serum albumin, creatinine, triglycerides, cholesterol, high density lipoprotein (HDL),low density lipoprotein (LDL), fasting blood glucose and fasting insulin (for calculation of insulin resistance), C reactive protein and serum vitamin D all were assayed. NAFLD was detected by ultrasonography and graded as absent, mild, moderate and severe. **Results:** Ninety-three percent of NAFLD patients were obese. Significant differences were found between patients and control regarding AST, ALT, ALP, GGT, total and direct bilirubin, serum albumin, creatinine, triglycerides, cholesterol, HDL, fasting blood glucose, fasting insulin, the homeostatic model assessment for insulin resistance (HOMA-IR) and serum vitamin D levels. Significant negative correlation was found between serum vitamin D level and grades of steatosis. **Conclusions:** Serum vitamin D level decreases in children with NAFLD. This low serum vitamin D level is associated with higher stages of steatosis but not with BMI.
**Keywords:** Nonalcoholic Fatty Liver Disease, Vitamin D, Children

## M-547. Optimization of Rhamnolipid Production by Biodegrading Bacterial Isolates Using Plackett–Burman Design

Mariam Hassan, Tamer Essam, Aymen S. Yasmin and Aisha Salama

*International Journal of Biological Macromolecules, 82: 573-579 (2016) IF: 3.138*

Biosurfactants are biological surfactants produced by microorganisms. Pseudomonas species are well known for the production of the rhamnolipid biosurfactant. In this work, the production of rhamnolipid biosurfactant by Pseudomonas spp. was investigated and further optimized. Two Plackett–Burman designs to study the effect of carbon source, nitrogen source, C/N ratio, iron concentration, magnesium concentration, phenol toxicity, pH, temperature, agitation and sampling time were tested. The first design revealed an optimization that increased biosurfactant productivity by almost two to fivefolds for the tested isolates. However, using the second design showed no remarkable increase in biosurfactant productivity. An additional validation run was adopted using the predicted optimal medium with predicted optimal conditions. The validation run showed remarkable increase in the productivity of the tested isolates. The use of microorganisms with biodegradation ability coupled with optimization of the parameters affecting productivity provides an efficient strategy for biosurfactant production.
**Keywords:** Multifactorial; Plackett–Burman; Rhamnolipid.

## M-548. The Effect of A1-Antitrypsin Deficiency Combined with Increased Bacterial Loads on Chronic Obstructive Pulmonary Disease Pharmacotherapy: A Prospective, Parallel, Controlled Pilot Study

Marwa G. Hennawy, Noha M. Elhosseiny, Hussein Sultan, Wael Abdelfattah, Yousry Akl, Nirmeen A. Sabry and Ahmed S. Attia

*Journal of Advanced Research, 7: 1019-1028 (2016) IF: 3*

Chronic obstructive pulmonary disease (COPD) is caused by α1-antitrypsin deficiency (AATD) genetic susceptibility and exacerbated by infection. The current pilot study aimed at studying the combined effect of AATD and bacterial loads on the efficacy of COPD conventional pharmacotherapy. Fifty-nine subjects (29 controls and 30 COPD patients) were tested for genetic AATD and respiratory function. The bacterial loads were determined to the patients' group who were then given a long acting beta-agonist and corticosteroid inhaler for 6 months. Nineteen percent of the studied group were Pi∗ MZ (heterozygote deficiency variant), Pi∗ S (5%) (milder deficiency variant), PiZZ (10%) (the most common deficiency variant), and PiMmalton (2%) (very rare deficiency variant). The patients' sputum contained from 0 to 8 × 108 CFU/mL pathogenic bacteria. The forced vital capacity (FVC6) values of the AAT non-deficient group significantly improved after 3 and 6 months. Patients lacking AATD and pathogenic bacteria showed significant improvement in forced expiratory volume (FEV1), FEV1/FVC6, FVC6, and 6 min walk distance (6MWD) after 6 months. However, patients with AATD and pathogenic bacteria showed only significant improvement in FEV1 and FEV1/FVC6. The findings of this pilot study highlight for the

first time the role of the combined AATD and pathogenic bacterial loads on the efficacy of COPD treatment.
**Keywords:** Aat Deficiency; Chronic Obstructive Pulmonary Disease; Bacteria; Genotyping; Pharmacotherapy.

## M-549. Antibiotic Resistome: Improving Detection and Quantification Accuracy for Comparative Metagenomics

Ali H. A. Elbehery, Ramy K. Aziz and Rania Siam

*Omics: A Journal of Integrative Biology, 20 : 229-238 (2016) IF:2.896*

The unprecedented rise of life-threatening antibiotic resistance (AR), combined with the unparalleled advances in DNA sequencing of genomes and metagenomes, has pushed the need for in silico detection of the resistance potential of clinical and environmental metagenomic samples through the quantification of AR genes (i.e., genes conferring antibiotic resistance). Therefore, determining an optimal methodology to quantitatively and accurately assess AR genes in a given environment is pivotal. Here, we optimized and improved existing AR detection methodologies from metagenomic datasets to properly consider AR-generating mutations in antibiotic target genes. Through comparative metagenomic analysis of previously published AR gene abundance in three publicly available metagenomes, we illustrate how mutation-generated resistance genes are either falsely assigned or neglected, which alters the detection and quantitation of the antibiotic resistome. In addition, we inspected factors influencing the outcome of AR gene quantification using metagenome simulation experiments, and identified that genome size, AR gene length, total number of metagenomics reads and selected sequencing platforms had pronounced effects on the level of detected AR. In conclusion, our proposed improvements in the current methodologies for accurate AR detection and resistome assessment show reliable results when tested on real and simulated metagenomic datasets.
**Keywords:** Antibiotic Resistance, Metagenomics, Pipeline, Mutational Antibiotic Resistance Genes, Normalization

## M-550.Gut Microbiome Alterations in Patients with Stage 4 Hepatitis C

AbdelRahman Mahmoud Aly, AbdelReheem Adel, Ahmed Osama El-Gendy, Tamer M. Essam and Ramy K. Aziz

*Gut Pathogens, 8: 1-12 (2016) IF: 2.816*

**Background:** Hepatitis C virus (HCV) causes debilitating liver diseases, which may progress to cirrhosis and cancer, and claims 500,000 annual lives worldwide. While HCV epidemiology, pathophysiology, and therapy are being deeply studied, rare attention is given to reciprocal interactions between HCV infection , HCV-induced chronic liver diseases, and the human gut microbiome. As Egypt has the world's highest prevalence of HCV infections, we launched this study to monitor differences in the gut microbial community composition of Egyptian HCV patients that may affect, or result from, the patients' liver state. **Results:** To this end, we analyzed stool samples from six stage 4-HCV patients and eight healthy individuals by high-throughput 16S rRNA gene sequencing using Illumina MiSeq. Overall, the alpha-diversity of the healthy persons' gut microbiomes was higher than those of the HCV patients. Whereas members of phylum Bacteroidetes were more abundant in HCV patients, healthy individuals had higher abundance of Firmicutes, Proteobacteria, and Actinobacteria. Genus-level analysis showed differential abundance of Prevotella and Faecalibacterium (higher in HCV patients) vs. Ruminococcus and Clostridium (healthy group), indicating that the higher abundance of Bacteroidetes in HCV patients is most likely due to Prevotella overabundance. The probiotic genus, Bifidobacterium, was only observed in the microbiotas of healthy individuals. **Conclusions:** To the best of our knowledge, this study provides a first overview of major phyla and genera differentiating stage 4-HCV patients from healthy individuals and suggests possible microbiome remodeling in chronic hepatitis C, possibly shaped by bacterial translocation as well as the liver's impaired role in digestion and protein synthesis. Future studies will investigate the microbiome composition and functional capabilities in more patients while tracing some potential biomarker taxa (e.g., Prevotella, Faecalibacterium vs. Bifidobacterium).
**Keywords:** Microbiome, Infectious Diseases, Virology, Liver Disease, Gastro-Intestinal Tract, High-Throughput Sequencing, Next-Generation Sequencing.

## M-551.Self-Nanoemulsifying Drug Delivery System (SNEDDS) with Enhanced Solubilization of Nystatin for Treatment of Oral Candidiasis: Design, Optimization, in Vitro and in Vivo Evaluation

Ahmed Alaa Kassem, Amira Mohamed Mohsen, Reham Samir Ahmed and Tamer Mohamed Essam

*Journal of Molecular Liquids, 218: 219-232 (2016) IF: 2.74*

The aim of the present study is to develop and optimize self-nanoemulsifying drug delivery systems (SNEDDSs) to improve the per-oral bioavailability of poorly soluble polyene antifungal drug, nystatin (NYS), and to evaluate its in vitro and in vivo performance. Solubility of NYS was estimated in various vehicles to select proper components combinations. Oleic acid (oil), Tween 20 (Tw20) and Tween 40 (Tw40) (surfactants) as well as dimethyl sulfoxide (DMSO) and propylene glycol (PG) (co-surfactants) were employed to construct pseudo-ternary phase diagrams. Thermodynamic stability, dispersibility and robustness to dilution tests were performed to optimize formulations from phase diagram. Five optimized formulations composed of oleic acid, Tw20 and DMSO or PG at Smix ratios (1:1, 2:1 or 3:1) were selected. They were spherical in shape of mean droplet size < 100 nm with negatively charged zeta potential < − 15 mV. The in vitro release profile of NYS-SNEDDSs was found significant in comparison to the plain NYS suspension. In vitro and in vivo evaluations against Candida albicans depicted promoted antifungal efficacy of selected NYS-SNEDDS formulations compared to marketed and plain NYS suspensions. The results indicate that NYS loaded SNEDDS, with enhanced solubilization and nanosizing, has potential to improve the absorption of drug and increase its oral antifungal efficacy.
**Keywords:** Nystatin; Self-Nanoemulsifying Drug Delivery System (Snedds); Poorly Water Soluble Drug; Pseudo-Ternary Phase Diagram; Immunosuppressed Mouse-Model; Oral Candidiasis.

## M-552. Bacterial Enzymes Involved in Lignin Degradation

Gonzalo de Gonzalo, Dana I. Colpa, Mohamed H.M. Habib and Marco W. Fraaije

*Journal of Biotechnology, 236: 110-119 (2016) IF: 2.667*

Lignin forms a large part of plant biomass. It is a highly heterogeneous polymer of 4-hydroxyphenylpropanoid units and is embedded within polysaccharide polymers forming lignocellulose. Lignin provides strength and rigidity to plants and is rather resilient towards degradation. To improve the (bio)processing of lignocellulosic feedstocks, more effective degradation methods of lignin are in demand. Nature has found ways to fully degrade lignin through the production of dedicated ligninolytic enzyme systems. While such enzymes have been well thoroughly studied for ligninolytic fungi, only in recent years biochemical studies on bacterial enzymes capable of lignin modification have intensified. This has revealed several types of enzymes available to bacteria that enable them to act on lignin. Two major classes of bacterial lignin-modifying enzymes are DyP-type peroxidases and laccases. Yet, recently also several other bacterial enzymes have been discovered that seem to play a role in lignin modifications. In the present review, we provide an overview of recent advances in the identification and use of bacterial enzymes acting on lignin or lignin-derived products.
**Keywords:** Lignin Degradation; Dyp; Peroxidases; Laccases; Dioxygenases

## M-553. Surveillance, Epidemiological, and Virological Detection of Highly Pathogenic H5N1 Avian Influenza Viruses in Duck and Poultry from Bangladesh.

Ansari WK, Parvej MS, El Zowalaty ME, Jackson S, Bustin SA, Ibrahim AK, El Zowalaty AE, Rahman MT, Zhang H, Khan MF, Ahamed MM, Rahman MF, Rahman M, Nazir KH, Ahmed S, Hossen ML, Kafi MA, Yamage M, Debnath NC, Ahmed G, Ashour HM, Masudur Rahman M, Noreddin A and Rahman MB

*Veterinary Microbiology, 193: 49-59 (2016) IF: 2.564*

Avian influenza viruses (AIVs) continue to pose a global threat. Waterfowl are the main reservoir and are responsible for the spillover of AIVs to other hosts. This study was conducted as part of routine surveillance activities in Bangladesh and it reports on the serological and molecular detection of H5N1 AIV subtype. A total of 2169 cloacal and 2191 oropharyngeal swabs as well as 1725 sera samples were collected from live birds including duck and chicken in different locations in Bangladesh between the years of 2013 and 2014. Samples were tested using virus isolation, serological tests and molecular methods of RT-PCR. Influenza A viruses were detected using reverse transcription PCR targeting the virus matrix (M) gene in 41/4360 (0.94%) samples including both cloacal and oropharyngeal swab samples, 31 of which were subtyped as H5N1 using subtype-specific primers. Twenty-one live H5N1 virus isolates were recovered from those 31 samples. Screening of 1,868 blood samples collected from the same birds using H5-specific ELISA identified 545/1603 (34%) positive samples. Disconcertingly, an analysis of 221 serum samples collected from vaccinated layer chicken in four districts revealed that only 18 samples (8.1%) were seropositive for anti H5 antibodies, compared to unvaccinated birds (n = 105), where 8 samples (7.6%) were seropositive. Our result indicates that the vaccination program as currently implemented should be reviewed and updated. In addition, surveillance programs are crucial for monitoring the efficacy of the current poultry vaccinations programs, and to monitor the circulating AIV strains and emergence of AIV subtypes in Bangladesh.
**Keywords:** Avian Influenza; H5n1; Surveillance; Bangladesh; Duck; Wild Birds; Poultry; Live Bird Markets; Virus Isolation; Reverse Transcription Polymerase Chain Reaction; Influenza A Virus

## M-554. Development and Evaluation of a Novel Vaccine Against Prevalent Invasive Multi-Drug Resistant Strains of Streptococcus Pneumoniae

Rehab H. Bahy, Hayam M. Hamouda, Amal S. Shahat, Aymen S. Yassin and Magdy A. Amin

*Peerj, 4 (2016) IF: 2.183*

Streptococcus pneumoniae is a pathogen that causes serious invasive infections, such as septicemia, meningitis and pneumonia in addition to mild upper respiratory tract infections. Protection from pneumococcal diseases is thought to be mediated mainly by serotype-specific antibodies to capsular antigens. Pneumococcal conjugate vaccine consists of sugars (polysaccharides) from the capsule of the bacterium S. pneumoniae that are conjugated to a carrier protein. Three pneumococcal conjugated vaccines, each directed against a group of serotypes, are registered in Egypt; however, local vaccine production is required to cover the most prevalent serotypes. In this work, capsular polysaccharide from the most current and prevalent serotypes in Egypt were extracted, purified and conjugated to bovine serum albumin (BSA). The polysaccharide protein conjugate was purified through ultrafiltration technique and molecular size distribution was compared to an available vaccine. The immunogenicity of the prepared vaccine was examined via two methods: First, by measuring the levels of the elicited antibodies in the sera of the vaccinated mice; second, by challenging the vaccinated groups of mice with approximately 107 CFU of each specific serotype and determining the degree of protection the developled vaccine offers. Our results show that the developed conjugated capsular polysaccharide vaccine is highly immunogenic and protective in mice. This finding illustrates the importance of tracking the most recent and predominant peneumococcal serotypes to generate effective vaccines, instead of using expensive imported vaccines with large number of serotypes which might not be even present in the community.
**Keywords:** Capsular Polysaccharide; S. Pneumoniae; Serotyping; Vaccine.

## M-555. T4 Lysozyme Fused with Cellulose-Binding Module for Antimicrobial Cellulosic Wound Dressing Materials

A. Abouhmad, G. Mamo, T. Dishisha, M.A. Amin and R. Hatti-Kaul

*Journal of Applied Microbiology, 121 (2016) IF: 2.156*

**Aims** Bacterial infection is a major challenge in wound care. Antimicrobial wound dressings are of great value for treating

wound infections. Endolysins are evolving as a new class of antimicrobials with multiple applications. This study describes the production and evaluation of T4 lysozyme (T4Lyz), product of gene e of the T4 bacteriophage, fused with Cellulose Binding Module (CBM) for facile immobilization to cellulosic wound dressing. **Methods and Results** Genes encoding T4Lyz-CBM and T4Lyz were cloned and expressed in Escherichia coli and the enzymes were purified by cation exchange chromatography. While the CBM tag did not alter the optimum pH and stability features of T4Lyz, the lytic activity of the fusion protein was lowered. The bactericidal activity of T4Lyz-CBM, determined by viable count plating assay after 1 h incubation with Micrococcus lysodeikticus was 97·5% with 10 μg ml−1, and 99·96% and 95% for E. coli and Pseudomonas mendocina, respectively, with 200 μg ml−1 enzyme. T4Lyz-CBM was immobilized to wound dressing gauze with a capacity of 5·5 μg mg−1 matrix, whereas the unmodified T4Lyz did not exhibit any binding. The immobilized protein retained its bactericidal activity against Gram-positive and Gram-negative bacteria. Both free and immobilized T4Lyz-CBM, after heat denaturation, retained their bactericidal activities against Gram-negative bacteria only. The immobilized enzyme exhibited higher stability than the free enzyme when stored in dry form or in the presence of polyol stabilizers. **Conclusion** Tagging T4Lyz with CBM provides a facile, irreversible binding to cellulosic wound dressing while retaining its activity. This approach may be suitable even for other antimicrobial enzymes and -peptides. Significance and Impact of the Study The spread of antibiotic resistance requires innovative strategies for discovery and development of effective antimicrobial alternatives. This report presents a novel strategy for producing antimicrobial wound dressing materials.

**Keywords:** Antimicrobial Activity, Cellulose Binding Module, Fusion Protein, Immobilization, Storage Stability, T4 Lysozyme, Wound Dressing.

## M-556. Chitosan and Sodium Alginate Combinations are Alternative, Efficient and Safe Natural Adjuvant Systems for Hepatitis B Vaccine in Mouse Model

Nourhan H. AbdelAllah, Nourtan F. Abdeltawab, Abeer A. Boseila and Magdy A. Amin

*Evidence-Based Complementary and Alternative Medicine, 2016: 1-8 (2016) IF: 1.931*

Hepatitis B viral (HBV) infections represent major public health problem and are an occupational hazard for healthcare workers. Current alum-adjuvanted HBV vaccine is the most effective measure to prevent HBV infection. However, the vaccine has some limitations including poor response in some vaccinee and being a frost-sensitive suspension. The goal of our study was to use an alternative natural adjuvant system strongly immunogenic allowing for a reduction in dose and cost. We tested HBV surface antigen (HBsAg) adjuvanted with chitosan (Ch) and sodium alginate (S), both natural adjuvants, either alone or combined with alum in mouse model. Mice groups were immunized subcutaneously with HBsAg adjuvanted with Ch or S, or triple adjuvant formula with alum (Al), Ch, and S, or double formulations with AlCh or AlS. These were compared to control groups immunized with current vaccine formula or unadjuvanted HBsAg. We evaluated the rate of seroconversion, serum HBsAg antibody, IL-4, and IFN-γ levels. The results showed that the solution formula with Ch or S exhibited comparable immunogenic responses to Al-adjuvanted suspension. The AlChS gave significantly higher immunogenic response compared to controls. Collectively, our results indicated that Ch and S are effective HBV adjuvants offering natural alternatives, potentially reducing dose.

**Keywords:** Hepatitis B Vaccine, Adjuvant, Alum, Chitosan, Sodium Alginate

## M-557. Biodegradation of Ketoprofen Using a Microalgal–Bacterial Consortium

Maha M. Ismail, Tamer M. Essam, Yasser M. Ragab and Fathia E. Mourad

*Biotechnology Letters, 38: 1493-1502 (2016) IF: 1.639*

**Objective** To test the toxicity of ketoprofen (a commonly-used NSAIDs) using two microalgal strains and Artemia sp. following the isolation of bacterial and microalgal strains and testing their ability to biodegrade and tolerate ketoprofen. **Results** Chlorella sp. was the most resistant to ketoprofen. A defined bacterial consortium (K2) degraded 5 mM ketoprofen as a sole carbon source both in the dark or continuous illumination. Ketoprofen did not undergo photodegradation. In the dark, biodegradation was faster with a lag phase of 10 h, 41% COD removal and 82 % reduction in toxicity. The consortium degraded up to 16 mM ketoprofen. The consortium was composed of four bacterial isolates that were identified. MS/MS analysis suggested a ketoprofen biodegradation pathway that has not been previously reported. Combining Chlorella sp. and the K2 consortium, ketoprofen was degraded within 7 days under a diurnal cycle of 12 h light/12 h dark. **Conclusion** The feasibility of using a microalgal–bacterial system to treat pharmaceutical wastewater is promising for the reduction of the process cost and providing a safer technology for pharmaceutical wastewater treatment.

**Keywords:** Artemia, Biodegradation, Chlorella, Ketoprofen, Nsaids, Spirulina, Wastewater

## M-558. Evaluation of Patients with Dry Eye Disease for Conjunctival Chlamydia Trachomatis and Ureaplasma Urealyticum.

Maha Mohssen Abdelfattah, Rania Abdelmonem Khattab, Magda H. Mahran and Ebrahim S. Elborgy

*International Journal of Ophthalmology, 9(10): 1457-1465 (2016) IF: 0.939*

**Aim:**To determine the possibility of the development of dry eye disease (DED) as a result of persistent infection with Chlamydia trachomatis and Ureaplasma urealyticum in the conjunctiva of patients. **Methods:** This study was conducted on 58 patients of age range 20-50y, diagnosed with DED. The diagnosis was confirmed by Schirmer I test and tear breakup time. The non-dry eye control group included 27 subjects of the same age. Ocular specimens were collected as conjunctival scrapings and swabs divided into three groups: the first used for bacterial culture, the second and third taken to detect Chlamydia trachomatis and Ureaplasma urealyticum by direct fluorescent antibody (DFA) assay and polymerase chain reaction (PCR) method. **Results:**Chlamydia trachomatis was detected in 65.5% and 76% of DED patients by DFA and PCR methods respectively.

Ureaplasma urealyticum was found in 44.8% of DED infected patients using the PCR method. Both organisms were identified in only 37.9% of DED patients found to be infected. Control subjects had a 22% detection rate of Chlamydia trachomatis by DFA assay versus a 7% detection rate by PCR; while Ureaplasma urealyticum was detected in 3.7% of the controls by PCR method. The conjunctival culture revealed that gram positive microorganisms represented 75% of isolates with coagulase negative Staphylococci the most common (50%) followed by Staphylococcus aureus (20%), whereas gram negative microorganisms occurred in 25% of cases, isolating Moraxella spp. as the most frequent organism. **Conclusion:** Our results tend to point out that Chlamydia trachomatis and Ureaplasma urealyticum were detected in a moderate percentage of patients with DED, and could be a fair possibility for its development. PCR is more reliable in detecting Chlamydia trachomatis than DFA technique. The presence of isolated conjunctival bacterial microflora can be of some potential value.

**Keywords:** Dry Eye Disease; Conjunctiva; Chlamydia Trachomatis; Ureaplasma Urealyticum; Direct Fluorescent Antibody; Polymerase Chain Reaction

## M-559. Study of the Prevalence and Association of Ocular Chlamydial Conjunctivitis in Women with Genital Infection by Chlamydia Trachomatis, Mycoplasma Genitalium and Candida Albicans Attending Outpatient Clinic.

Rania Abdelmonem Khattab and Maha Mohssen Abdelfattah.

*International Journal of Ophthalmology, 9(8): 1176 - 1186 (2016) IF: 0.939*

**Aim:**To determine the association between chlamydial conjunctivitis and genital infection by Chlamydia trachomatis, Mycoplasma genitalium and Candida albicans, in addition to the possible relationship between cultured bacterial pathogens and oculogenital chlamydial infection. **Methods:**This study was performed on 100 (50 symptomatic and 50 asymptomatic) women attending the Gynecological and Obstetric outpatient clinic of Alzahra hospital, Alazhar University. Simultaneously a conjunctival swab was taken from these patients. Polymerase chain reaction (PCR) was done on DNA extracted from both vaginal and conjunctival swab samples. Culture for both vaginal and conjunctival swabs was also done. Candida albicans was the predominant organism isolated by culture in 20% and 40% of conjunctival and vaginal swabs respectively. By the PCR method, ocular Chlamydia trachomatis was present in 60% of symptomatic women, while genital Chlamydia trachomatis infection was present in 30% of symptomatic women. **Results:** The results of this method also indicated that 25/50 (50%) vaginal swabs were positive with PCR for Candida albicans versus 15/50 (30%) were PCR positive in conjunctival swab. Mycoplasma genitalium was present in only 10% of vaginal swabs. Concomitant oculogenital PCR positive results for Chlamydia trachomatis and Candida albicans were 30% and 28% respectively. **Conclusion:** We can conclude that ocular Chlamydia trachomatis was associated with genital Chlamydia trachomatis in a high percentage of women followed by Candida albicans. Cultured bacterial organisms do not play a role in enhancement of Chlamydia trachomatis infection.

**Keywords:** Chlamydia Trachomatis; Mycoplasma Genitalium; Candida Albicans; Vaginal Swabs; Polymerase Chain Reaction.

## M-560. Emergence of Neoteric Serotypes Among Multidrug Resistant Strains of Streptococcus Pneumoniae Prevalent in Egypt

Rehab H. Bahy, Hayam M. Hamouda, Amal S. Shahat, Aymen S. Yassin and Magdy A. Amin

*Jundishapur Journal of Microbiology, 9(4) (2016) IF: 0.655*

**Background:**Streptococcus pneumoniae is still one of the major causes of morbidity and mortality worldwide. The prevalent serotype distribution had shown variation along different studies conducted at different time intervals. In order to efficiently assess the epidemiology of the diseases for effective preventive and treatment strategies, serotype prevalence need to be periodically reassessed. **Objectives:**Conducting a reassessment of the prevalent S. pneumoniae serotypes in Egypt as an essential step in the search for a regional vaccine. In addition, monitoring the antibiotic susceptibility patterns of pneumococcal strains currently causing infections as an evaluation of therapeutic strategies applied. **Materials** and **Methods:** A total of 100 specimens of different sources were collected in Cairo, Egypt, from 2011 to 2013, representing almost all different types of diseases caused by S. pneumoniae such as meningitis, pneumonia, otitis media and sinusitis. Conventional and molecular identification methods were performed, the antimicrobial susceptibility patterns were assessed and serotyping was done using PCR assays to identify the most prevalent types. In addition, detection of certain virulence genes for the most prevalent serotypes was carried out. **Results:** Our results revealed that in Egypt, currently, the most prevalent serotypes were serogroup 6 and serotype 19F as they represented 58% of all isolates. High rates of resistance were found to different antibiotic classes. The lytA and psaA genes were found to be more sensitive for S. pneumoniae identification than ply. **Conclusions:** Our study illustrates the importance of constantly monitoring the prevalent serotypes in any region in order to aid in the development of more effective vaccines.

**Keywords:** Antibiotic Resistance, Serotyping, Virulence, Bacterial Vaccines, Streptococcus Pneumoniae

## M-561. Anti-HSV Type-1 Activity of Olive Leaves Extract Crude form Acting as a Microemulsion Dosage form

Rania Abdelmonem Khattab, Alaa El-Din Shawky Hosny, Mostafa Ali Abdelkawy, Rania Hassan Fahmy and Nariman Alaa ElMenoufy

*African Journal of Microbiology Research, 10(22): 820-828 (2016)*

Olea europeae (L.) has been reported to have antibacterial, antifungal and antiviral activities. The aim of the present study is to evaluate antiviral activity of olive leaves extract (OLE) against herpes simplex viruses (HSV) type-1 virus. Screening of antiviral activity was assessed by measuring inhibition of viralinduced cytopathic effect of in vero cells of different OLE fractions that have been successively extracted using solvents of increasing polarities, against HSV type-1 virus. Negligible antiviral activity has been shown of different fractions, except for ethyl acetate and n-butanol fractions, showing strong and moderate anti-HSV type -1 activity, respectively. High performance liquid chromatography (HPLC) chromatographic

analysis of both fractions revealed high oleuropein content in ethyl acetate fraction in addition to other phenolic and flavonoid contents, whereas n-butanol fraction showed only high content of other phenolic and flavonoid compounds. Cytotoxicity of ethyl acetate fraction was assessed in vero cell line, the mean cytotoxic concentration CC50, was reported to be 610 µg/ml. On the other hand, the 50% inhibitory concentration (IC50), against HSV-1, was of value as low as 40 µg/ml (SI = 15.2). This concentration could be more reduced to 33 µg/ml (SI = 16.9); that is, 17% reduction in dose, by formulating a microemulsion dosage form, with particle size of 13 to 19 nm, being assessed by Malvern Zetasizer Ver. 6.2 and electron microscopy. Acyclovir, a recommended anti-HSV agent, was used as a positive control. Oleuropein pure standard and the main phenolic component of OLE, was also assessed for its anti-HSV type-1 virus. As conclusion, microemulsion formulation enhanced antiviral activity of crude OLE.

**Keywords:** Olive Leaves Extract, Ole, Acyclovir, Anti-Hsv Activity, Microemulsion, Oleuropein.

## M-563. Single Step Biotransformation of Corn Oil Phytosterols to Boldenone by a Newly Isolated Pseudomonas Aeruginosa

Mohamed Eisaa, Heba El-Refaib and Magdy Aminc

*Biotechnology Reports, 11: 36-43 (2016)*

A new potent Pseudomonas aeruginosa isolate capable for biotransformation of corn oil phytosterol (PS) to 4-androstene-3, 17-dione (AD), testosterone (T) and boldenone (BOL) was identified by phenotypic analysis and 16S rRNA gene sequencing. Sequential statistical strategy was used to optimize the biotransformation process mainly concerning BOL using Factorial design and response surface methodology (RSM). The production of BOL in single step microbial biotransformation from corn oil phytosterols by P. aeruginosa was not previously reported. Results showed that the pH concentration of the medium, (NH4)2SO4 and KH2PO4 were the most significant factors affecting BOL production. By analyzing the statistical model of three-dimensional surface plot, BOL production increased from 36.8% to 42.4% after the first step of optimization, and the overall biotransformation increased to 51.9%. After applying the second step of the sequential statistical strategy BOL production increased to 53.6%, and the overall biotransformation increased to 91.9% using the following optimized medium composition (g/l distilled water) (NH4)2SO4, 2; KH2PO4, 4; Na2HPO4. 1; MgSO4·7H2O, 0.3; NaCl, 0.1; CaCl2·2H2O, 0.1; FeSO4·7H2O, 0.001; ammonium acetate 0.001; Tween 80, 0.05%; corn oil 0.5%; 8-hydroxyquinoline 0.016; pH 8; 200 rpm agitation speed and incubation time 36 h at 30 °C. Validation experiments proved the adequacy and accuracy of model, and the results showed the predicted value agreed well with the experimental values.

**Keywords:** Androstenedione; Boldenone; Corn Oil Phytosterols; Factorial Design; Pseudomonads Aeruginosa.

## M-562. Development of Safe Effective and Immunogenic Vaccine Candidate for Diarrheagenic Escherichia Coli Main Pathotypes in a Mouse Model

Asmaa Gohar, Nourtan F. Abdeltawab, Ali Fahmy and Magdy A. Amin

*BMC Research Notes, 9: 1-18 (2016)*

**Background** Enteric and diarrheal diseases are important causes of childhood death in the developing world. These diseases are responsible for more than 750 thousand deaths in children under 5 years old worldwide, ranking second cause of death, after lower respiratory diseases, in this age group. Among the major causative agents of diarrhea is Escherichia coli. There are several vaccine trials for diarrheagenic E. coli. However, diarrheagenic E. coli has seven pathotypes and vaccines are directed for one or two of the five main pathotypes-causing diarrhea. Currently, there are no combined vaccines available in the market for all five diarrheagenic E. coli pathotypes. Therefore, we aimed to develop a low-cost vaccine candidate combining the five main diarrheagenic E. coli to offer wide-spectrum protection. We formulated a formalin-killed whole-cell mixture of enteroaggregative, enteropathogenic, enteroinvasive, enterohemorrhagic, and enterotoxigenic E. coli pathotypes as a combined vaccine candidate. **Results** We immunized Balb/C mice subcutaneously with 109 CFU of combined vaccine candidate and found a significant increase in survival rate post challenge compared to unimmunized controls (100 % survival). Next we aimed to determine the immunological response of mice to the combined vaccine candidate compared to each pathotype immunization. To do so, we immunized mice groups with combined vaccine candidate and monitored biomarkers levels over 6 weeks as well as measured responses post challenge with relevant living E. coli. We found significant increase in specific systemic antibodies (IgG), interferon gamma (IFNγ) and interleukin 6 (IL-6) levels elicited by combined vaccine candidate especially in the first 2 weeks after mice immunization compared to controls ($p < 0.05$). We also evaluated alum and cholera toxin B subunit (CTB) as potential adjuvant systems for our candidate vaccine. We found that CTB-adjuvanted combined vaccine candidate showed significantly higher IgG and IFNγ levels than alum. **Conclusions** Overall, our combined vaccine candidate offered protection against the five main diarrheagenic E. coli pathotypes in a single vaccine using mouse model. To the best of our knowledge, this is the first combined vaccine against the five main diarrheagenic E. coli pathotypes that is cost-effective with promise for further testing in humans.

**Keywords:** Escherichia Coli Enteroaggregative; Enteropathogenic; Enteroinvasive; Enterohemorrhagic Enterotoxigenic; Diarrhea Immunization; Whole-Cell Vaccine Formalin-Killed Interleukin 6 Interferon; Gamma Adjuvant System Alum Cholera Toxin Subunit B.

### *Dept. of Pharmaceutical Chemistry*

## M-564.Novel Liquid Chromatographic Methods for the Determination of Vareniclinetartrate

Ramzia I. El-Bagary, Nisreen F. Abo-Talib and Marwa A. El-Wahab Mohamed

*Talanta, 146 (2016): 83-92 (2016) IF: 4.035*

Two simple, sensitive, rapid, and stability-indicating liquid chromatographic (LC) methods have been developed for the determination of varenicline tartrate. They comprised the determination of varenicline (VRC) in the presence of its oxidative degradates and related impurity (N-formyl varenicline) (NFV). The first method was a LC with diode array detection (DAD) at 235 nm using Ristek-Ultras C18 column (100 mm 2.1 mm, 5 mm). Isocratic elution of VRC was employed using a mobile phase consisting of buffer mixture (1.2% potassium dihydrogen phosphate and 0.08% octane sulphonic acid): acetonitrile (86:14, v/v), pH (5.0). In the second method; a fluorimetric detection technique was developed, based on precolumn derivatization of VRC using 7-chloro-4-nitrobenzo-2-oxa-1, 3-diazole (NBD-Cl). The fluorescence detector (FLD) was operated at 474 nm for excitation and 539 nm for emission. Isocratic elution was applied with a mobile phase consisting of methanol-distilled water (70:30, v/v). Separation was achieved using Symmetrys Waters C18 column (150 mm 4.6 mm, 5 mm). Linearity, accuracy and precision were found to be acceptable over the concentration ranges of 0.5–20.0 mg mL1 and 0.2– 20.0 mg mL1 with the first and the second method, respectively. The optimized methods were validated and proved to be specific, simple, and accurate for the quality control of the drug in its pharmaceutical preparation.

**Keywords:** Varenicline Tartrate-Diode Array Detector-Fluorescence Detector-NBD-Cl.

## M-569. Design and Synthesis of some Novel 4-Chloro-N-(4-(1-(2-(2-Cyanoacetyl)Hydrazono) Ethyl) Phenyl) Benzenesulfonamide Derivatives as Anticancer and Radiosensitizing Agents

Mostafa M. Ghorab, Fatma A. Ragab, Helmy I. Heiba and Aiten M. Soliman

*European Journal of Medicinal Chemistry, 117: 8-18 (2016) IF: 3.902*

A Novel series of sulfonamide derivatives 4e21 have been synthesized starting from the strategic starting material (E)-4-Chloro-N-(4-(1-(2-(2-cyanoacetyl)hydrazono)ethyl)phenyl) benzenesulfonamide 4. Two series of hydrazone 5e9, and pyridone 10e21 derivatives bearing a sulfonamide moiety were obtained. All the newly synthesized compounds were evaluated for their in vitro cytotoxic activity against human liver cancer cell line (HepG2). Compounds 4e6, 8, 9, 10e14 and 16e18 showed higher activity compared to doxorubicin as a positive control. The radiosensitizing ability of the most promising compounds 4, 10 and 12 was studied which showed an increase in the cell killing effect of g-radiation after combination with these derivatives. The molecular design was performed to predict the binding mode of the most promising compounds 4, 10 and 12 with the active site of hCA IX, that showed appropriate fitting with the relevant amino acids in the binding pocket on the basis of standard bond lengths, angles, S score and E conformation data.

**Keywords:** Sulfonamide Anticancer Radio Sensitizers.

## M-567. Synthesis and Cytotoxic Activities of some Pyrazoline Derivatives Bearing Phenyl Pyridazine Core as New Apoptosis Inducers

Riham F. George, Marwa A. Fouad and Iman E.O. Gomaa

*European Journal of Medicinal Chemistry, 112: 48-59 (2016) IF: 3.902*

The cyclization of chalcones 3a-3u with 3-hydrazinyl-6-phenylpyridazine 7 under basic condition led to the formation of new pyrazoline derivatives 8a-8u. All final compounds were characterized by spectral and elemental analyses. They were screened for their antiproliferative activities against A549 (lung), HepG-2 (liver), CaCo-2 (intestinal) and MCF-7 (breast) cancer cell lines. Some of the synthesized compounds exhibited promising antiproliferative activities especially compound 8k with IC50 values of 8.33, 1.67 and 10 μM against HepG-2, MCF-7 and CaCo-2 cancer cell lines, respectively. Moreover, their antiproliferative activity was due to apoptosis rather than necrosis induction except compound 8h which exhibited equal apoptotic and necrotic properties. Compound 8k showed 5 fold increase in caspase-3 activity indicating that the apoptosis proceeds via caspase-3 activation.

**Keywords:** Pyrazolylpyridazines; Chalcones; MTT Assay; Apoptosis; Caspase-3.

## M-568.Bis-Isatin Hydrazones with Novel Linkers: Synthesis and Biological Evaluation as Cytotoxic Agents

Hany S Ibrahim, Sahar M Abou-Seri, Nasser SM Ismail, Mahmoud M Elaasser, Mohamed H. Aly and Hatem A. Abdel-Aziz

*European Journal of Medicinal Chemistry, 108: 415-422 (2016) IF: 3.902*

Many bis-isatins and isatins with hydrazide extension were reported to have a potential anti-proliferative effects against different cancer cell lines and cancer targets. In this study, four series of bis-isatins with hydrazide linkers were synthesized. These compounds were investigated for their antitumor activity by assessing their cytotoxic potency against HepG2, MCF-7 and HCT-116 cancer cell lines. Compound 21c possessed significant cytotoxic activity against MCF-7 (IC50 = 1.84 μM) and HCT-116 (IC50 = 3.31 μM) that surpasses the activity of doxorubicin against both cell lines (MCF-7; IC50 = 2.57 μM and HCT-116; IC50 = 3.70 μM). Cell cycle analysis and annexin V-FITC staining of MCF-7 cells treated with 21c suggested that the cytotoxic effect of the compound could be attributed to its pro-apoptotic activity.

**Keywords:** Bis-Isatin Hydrazones; Cell Cycle; Cytotoxic; Pro-Apoptotic

## M-566.3-Hydrazinoindolin-2-One Derivatives: Chemical Classification and Investigation of their Targets as Anticancer Agents

Hany S. Ibrahim, Sahar M. Abou-Seri and Hatem A. Abdel-Aziz

*European Journal of Medicinal Chemistry, 122: 366-381 (2016) IF: 3.902*

Isatin is a well acknowledged pharmacophore in many clinically approved drugs used for treatment of cancer. 3-Hydrazinoindolin-2-one, as a derivative of isatin, represents a pharmacophore of an important class of biologically active pharmaceutical agents by virtue of their diverse biological activities. In this review, anticancer activity will be on focus for compounds derived from 3-hydrazinoindolin-2-one. They are classified according to their chemical structure into nine different classes. In each class, different compounds were browsed, showing their anticancer activity and their potential targets. Moreover, crystallographic data or docking studies were highlighted for some compounds, when available, to provide a deep understanding of their mechanisms of action.
**Keywords:** Isatin; 3-Hydrazinoindolin-2-One; Anticancer.

## M-565. Piperazinylphthalazines as Potential Vegfr-2 Inhibitors and Anticancer Agents: Synthesis and in Vitro Biological Evaluation

Sahar M Abou-Seri, Wagdy M Eldehna, Mamdouh M Ali and Dalal A Abou El Ella

*European Journal of Medicinal Chemistry, 107: 165-179 (2016) IF: 3.902*

In our endeavor towards the development of effective VEGFR-2 inhibitors, three novel series of phthalazine derivatives based on 1-piperazinyl-4-arylphthalazine scaffold were synthesized. All the newly prepared phthalazines 16a-k, 18a-e and 21a-g were evaluated in vitro for their inhibitory activity against VEGFR-2. In particular, compounds 16k and 21d potently inhibited VEGFR-2 at sub-micromolar IC50 values 0.35 ± 0.03 and 0.40 ± 0.04 μM, respectively. Moreover, seventeen selected compounds 16c-e, 16g, 16h, 16j, 16k, 18c-e and 21a-g were evaluated for their in vitro anticancer activity according to US-NCI protocol, where compounds 16k and 21d proved to be the most potent anticancer agents. While, compound 16k exhibited potent broad spectrum anticancer activity with full panel GI50 (MG-MID) value of 3.62 μM, compound 21d showed high selectivity toward leukemia and prostate cancer subpanels [subpanel GI50 (MG-MID) 3.51 and 5.15 μM, respectively]. Molecular docking of compounds16k and 21d into VEGFR-2 active site was performed to explore their potential binding mode.
**Keywords:** Synthesis; 1-Piperazinylphthalazines; Vegfr-2 Inhibitors; Anticancer Activity.

## M-567. Amido/Ureidosubstituted Benzenesulfonamides-Isatin Conjugates as Low Nanomolar/Subnanomolar Inhibitors of the Tumor-Associated Carbonic Anhydrase Isoform XII

Wagdy M. Eldehna, Mohamed Fares, Mariangela Ceruso, Hazem A. Ghabbour, Sahar M. Abou-Seri, Hatem A. Abdel-Aziz, Dalal A. Abou El Ella and Claudiu T. Supuran

*European Journal of Medicinal Chemistry, 110: 259-266 (2016) IF: 3.902*

By using a molecular hybridization approach, two series of amido/ureidosubstituted benzenesulfonamides incorporating substituted-isatin moieties were synthesized. The prepared derivatives were in vitro evaluated for their inhibitory activity against human carbonic anhydrase (hCA, EC 4.2.1.1) I, II (cytosolic) and IX, XII (transmembrane, tumor-associated) isoforms. All these isoforms were inhibited in variable degrees by the sulfonamides reported here. hCA I was inhibited with KIs in the range of 7.9–894 nM, hCA II in the range of 7.5–1645 nM (with one compound having a KI > 10 μM); hCA IX in the range of 5.0–240 nM, whereas hCA XII in the range of 0.47–2.83 nM. As all these isoforms are involved in various pathologies, in which their inhibition can be exploited therapeutically, the derivatives reported here may represent interesting extensions to the field of CA inhibitors of the sulfonamide type.
**Keywords:** Carbonic Anhydrase; Tumor-Associated Isoforms; Amido/Ureido Sulfonamides; Isatin.

## M-571. Increasing the Binding Affinity of VEGFR-2 Inhibitors by Extending their Hydrophobic Interaction with the Active Site: Design, Synthesis and Biological Evaluation of 1-Substituted-4-(4-Methoxybenzyl)Phthalazine Derivatives

Wagdy M. Eldehna, Sahar M. Abou-Seri, Ahmed M. El Kerdawy, Rezk R. Ayyad, Abdallah M. Hamdy, Hazem A. Ghabbour, Mamdouh M. Ali and Dalal A. Abou El Ella

*European Journal of Medicinal Chemistry, 113: 50-62 (2016) IF: 3.902*

A series of anilinophthalazine derivatives 4a–j was initially synthesized and tested for its VEGFR-2 inhibitory activity where it showed promising activity (IC50 = 0.636–5.76 μM). Molecular docking studies guidance was used to improve the binding affinity for series 4a–j towards VEGFR-2 active site. This improvement was achieved by increasing the hydrophobic interaction with the hydrophobic back pocket of the VEGFR-2 active site lined with the hydrophobic side chains of Ile888, Leu889, Ile892, Val898, Val899, Leu1019 and Ile1044. Increasing the hydrophobic interaction was accomplished by extending the anilinophthalazine scaffold with a substituted phenyl moiety through an uriedo linker which should give this extension the flexibility required to accommodate itself deeply into the hydrophobic back pocket. As planned, the designed uriedo-anilinophthalazines 7a–i showed superior binding affinity than their anilinophthalazine parents (IC50 = 0.083–0.473 μM). In particular, compounds 7g–i showed IC50 of 0.086, 0.083 and 0.086 μM, respectively, which are better than that of the reference drug sorafenib (IC50 = 0.09 μM).
**Keywords:** Phthalazine; VEGFR-2; Hydrophobic Interaction.

## M-572. Novel Pyrazolo[3,4-D]Pyrimidines as Dual Src-Abl Inhibitors Active Against Mutant form of Abl and the Leukemia K-562 Cell Line

Samir M. El-Moghazy, Riham F. George, Essam Eldin A. Osman, Ahmed A. Elbatrawy, Miroslava Kissova, Ambra Colombo, Emmanuele Crespan and Giovanni Maga

*European Journal of Medicinal Chemistry, 123: 1-13 (2016) IF: 3.902*

Some novel 6-substituted pyrazolo[3,4-d]pyrimidines 4, 5, 6a-d, 7a-c, 8 and pyrazolo[4,3-e][1,2,4]triazolo[4,3-a]pyrimidines 9a-c, 10a-c, 11, 12a,b, 13a-c and 14 were synthesized and characterized by spectral and elemental analyses. They were screened for their biological activity in vitro against Abl and Src

kinases. Compounds 7a and 7b revealed the highest activity against both wild and mutant Abl kinases as well as the Src kinase and the leukemia K-562 cell line. They can be considered as new hits for further structural optimization to obtain better activity.
**Keywords:** Pyrazolo[3,4-D]Pyrimidines; Src Inhibition; Abl Inhibition; K-562 Cell Line; Molecular Modeling.

## M-574. Synthesis, Vasorelaxant Activity and 2D-QSAR Study of some Novel Pyridazine Derivatives

Riham F. George and Dalia O. Saleh

*European Journal of Medicinal Chemistry, 108: 663-673 (2016) IF: 3.902*

Novel 3,6-disubstituted pyridazines were synthesized by facile method and screened for their vasorelaxant properties utilizing isolated thoracic rat aortic rings. Compounds 8a and 11a exerted potent vasorelaxant activity (IC50 = 198 and 177 μM, respectively) relative to doxazosin mesylate (used reference standard, IC50 = 226 μM), that, they may represent promising hits for treatment of cardiovascular disorders. The observed activity was validated by a statistically significant QSAR model (N=32, n=6, R2=0.811782, R2cvOO = 0.7153, R2cvMO = 0.7209, F=17.9708, s2=9.65226x10-8) that was obtained employing CODESSA-Pro software.
**Keywords:** Pyridazines; Vasodilator; QSAR.

## M-570. Identification of New Potent Phthalazine Derivatives with VEGFR-2 and EGFR Kinase Inhibitory Activity

Kamilia M. Amin, Flora F. Barsoum, Fadi M. Awadallah and Nehal E. Mohamed

*European Journal of Medicinal Chemistry, 123: 191-201 (2016) IF: 3.902*

Efforts to develop new antitumor agents are now directed towards multitarget therapies that are believed to have high potency and low tendency to resistance compared to conventional drugs. Herein, we highlighted the synthesis and antitumor activity of five series of phthalazine-based compounds featuring a variety of bioactive chemical fragments at position 1 of the phthalazine nucleus. The antitumor activity of the target compounds was performed against fourteen cancer cell lines where all compounds were active in the nanomolar level. In addition, the mechanism of action of the target compounds was investigated through an enzymatic inhibitory assay against VEGFR-2 and EGFR kinases, revealing potent and preferential activity toward VEGFR-2. Binding mode of the most active compounds was studied using docking experiment.
**Keywords:** Phthalazine; Cytotoxicity VEGFR-2 EGFR; Docking.

## M-575. Forced Degradation of Mometasone Furoate and Development of two Rp-Hplc Methods for its Determination with Formoterol Fumarate or Salicylic Acid

Ramzia I. El-Bagary, Marwa A. Fouad, Manal A. El-Shal and Enas H. Tolba

*Arabian Journal of Chemistry, 9: 493-505 (2016) IF: 3.613*

Two simple, selective and precise stability-indicating reversed-phase liquid chromatographic methods were developed and validated for the determination of mometasone furoate in two binary mixtures, with formoterol fumarate (Mixture 1) and salicylic acid (Mixture 2). Also, a forced degradation study of mometasone furoate was carried out including acid and alkali hydrolysis, oxidation, thermal and photo-degradation. For mixture 1, the method was based on isocratic elution using a mobile phase consisting of (Acetonitrile: 3 mM Sodium lauryl sulfate) (60:40, v/v) at a flow rate of 1 ml min−1. Quantitation was achieved applying dual wavelength detection where mometasone furoate and its degradation products were detected at 247 nm and formoterol fumarate and its degradation product were detected at 214 nm at 30 °C. For mixture 2 and for the forced degradation study, separation was based on isocratic elution of mometasone furoate, its degradation products and salicylic acid on a reversed phase C8 column using a mobile phase consisting of acetonitrile:water:methanol:glacial acetic acid (60:30:10:0.1, v/v) at a flow rate of 2 mL min−1. Quantitation was achieved with UV detection at 240 nm. In addition, products from alkaline forced degradation of mometasone furoate were verified by LC–MS. Linearity, accuracy and precision were found to be acceptable over the concentration range of 10–800 μg mL−1 and 5–60 μg mL−1 for mometasone furoate and formoterol fumarate, respectively and over the concentration range of 5–320 μg mL−1 and 20–1280 μg mL−1 for mometasone furoate and salicylic acid, respectively. The two proposed methods could be successfully applied for the routine analysis of the studied drugs in their pharmaceutical preparations without any preliminary separation step.
**Keywords:** Mometasone Furoate; Formoterol Fumarate; Salicylic Acid; Stability-Indicating Assay; Forced Degradation.

## M-578.Synthesis and Molecular Modeling Studies of Indole-Based Antitumor Agents

Riham F. George, Siva S. Panda, El-Sayed M. Shalaby, Aladdin M. Srour, I. S. Ahmed Farag and Adel S. Girgis

*Rsc Advances, 6: 45434-45451 (2016) IF: 3.289*

Indole-based compounds 30–63 were synthesized by the multi-component 1,3-dipolar cycloaddition reaction of 1-alkyl-3,5-bis(arylidene)-4-piperidones 11–25 with azomethine ylides (generated by the condensation of isatins 26–28 with sarcosine 29). The single crystal X-ray studies of 46 and 48 supported the regio- and stereoselectivity of the reaction. Most of the synthesized spiro-indoles exhibited potent antitumor properties against the HeLa (cervical cancer) cell line through in vitro sulforhodamine- B bioassay, higher than that of cisplatin. Only compound 54 showed bio-potency against the HepG2 (hepatocellular cancer) cell line, comparable to that of doxorubicin hydrochloride (standard reference). 3D-Pharmacophore and 2D-QSAR studies were used to validate the

observed biological data and determine the most important parameters controlling activity. The estimated bio-properties from the computational studies showed high approximations to the experimental data.
**Keywords:** Indole, Piperidone, Antitumor, Pharmacophore, QSAR.

## M-577. Rational Design, Synthesis and 2D-Qsar Studies of Antiproliferative Tropane-Based Compounds

Nasser S. M. Ismail, Riham F. George, Rabah A. T. Serya, Fady N. Baselious, May El-Manawaty, ElSayed M. Shalaby and Adel S. Girgis

*Rsc Advances, 6: 101911-101923 (2016) IF: 3.289*

3,4-Diaryl-11-methyl-7-[(aryl)methylidene]-4,5,11-triazatricyclo[6.2.1.0*2,6*]undec-5-enes 14a–s were synthesized through reaction of 2,4-bis[(aryl)methylidene]-8-methyl-8-azabicyclo[3.2.1]octan-3-ones 12a–f with aryl hydrazines in the presence of catalytic amount of thiamine hydrochloride. Meanwhile, the 4-acetyl analogs 16a,b were obtained through reaction of 12b,e and hydrazine hydrate in acetic acid. Good support for the structure was received from single crystal X-ray studies of 14a. Some of the synthesized tropane containing-compounds showed promising antitumor properties during the in vitro MTT bio-assay against HepG2 (hepatocellular) and MCF7 (breast) human tumor carcinoma cell lines, with potency higher than that of doxorubicin (DNA intercalating agent, standard reference). Statistically significant 2D-QSAR model describes the antitumor properties against MCF7.
**Keywords:** Tropane, 4,5,11-Triazatricyclo[6.2.1.0*2,6*]Undec-5-ENE, DFT, Antitumor, QSAR.

## M-576. Discovery of Novel Quinazolinones and their Acyclic Analogues as Multi-Kinase Inhibitors: Design, Synthesis, Sar Analysis and Biological Evaluation

Nehad A. El Sayed, Amal A. Eissa, Ghada F. El Masry, Mohamed M. Abdullah and Reem K. Arafa

*Royal Society of Chemistry, 6: 111767-111786 (2016) IF: 3.289*

This work deals with the design and synthesis of some novel 6-iodo-2-(pyridin-3/4-yl)-3-substituted quinazolin-4-one derivatives 8a–l, 10a–h, 13–18 in addition to certain acyclic analogues thereof viz. 9a– n and 12a–h. The molecular design strategy was based on structural analogy between the new compounds and reported quinazolines and their acyclic analogues. This design scheme led to the synthesis of 8 new intermediates and 58 new final quinazolinones. The target compounds were evaluated for their antitumor activity against a panel of nine cancer cell lines viz. breast cancer (MCF-7, MDAMB-231, MDAMB-435 and HS-578T), colon cancer (HT-29 and HCC-2998) and leukemia (CCRFCEM, K-562 and HL-60). The quinazolinones 10a–h displayed exceptional antitumor activity and compounds 12a–h showed superior potency against MCF-7. These compounds were further subjected to in vivo study. Kinase inhibitory assay was also carried out to investigate the mechanism of action of the target compounds and they displayed the highest activity against ABL, ALK and c-RAF kinases. The 3- substituted quinazolinones 10a–h showed the highest kinase activity inhibitory potency against ABL, ALK and c-RAF with the most active compound in this study being the fluoro-3-pyridyl derivative 10a. These results are in compliance with the observed antitumor activity. Finally, a molecular modeling study was performed to interpret the potential molecular interactions of these chemotypes with the most responsive biomolecular target ABL.
**Keywords:** Acyclic Analogues-Quinazolines-Kinase Inhibitory Assay-Molecular Modeling.

## M-579. Synthesis of (Benzimidazol-2-Yl) Aniline Derivatives as Glycogen Phosphorylase Inhibitors

Shadia A. Galal, Muhammad Khattab, Fotini Andreadaki, Evangelia D. Chrysina, Jean-Pierre Praly, Fatma A. F. Ragab and Hoda I. El Diwani

*Bioorganic and Medicinal Chemistry, 24: 5423-5430(2016) IF:2.923*

A series of (benzimidazol-2-yl)-aniline (1) derivatives has been synthesized and evaluated as glycogen phosphorylase (GP) inhibitors. Kinetics studies revealed that compounds displaying a lateral heterocyclic residue with several heteroatoms (series 3 and 5) exhibited modest inhibitory properties with IC50 values in the 400–600 μM range. Arylsulfonyl derivatives 7 (Ar: phenyl) and 9 (Ar: o-nitrophenyl) of 1 exhibited the highest activity (series 2) among the studied compounds (IC50 324 μM and 357 μM, respectively) with stronger effect than the p-tolyl analogue 8.
**Keywords:** Benzimidazole Heterocycles Glycogen Phosphorylase Enzyme Inhibition.

## M-580. Simultaneous Determination of Timolol Maleate in Combination with some Other Anti-Glaucoma Drugs in Rabbit Aqueous Humor by High Performance Liquid Chromatography–Tandem Mass Spectroscopy

Sonia T. Hassib, Ehab F. Elkady and Rawda M. Sayed

*Journal of Chromatography B-Analytical Technologies in The Biomedical and Life Sciences, 1022: 109-117 (2016) IF: 2.687*

In this work, a sensitive, selective, accurate and precise LC–MS/MS method has been developed for the simultaneous determination of an anti-glaucoma ß-blocker, timolol maleate (TIM) with other co-administered anti-glaucoma drugs of different classes, namely; dorzolamide hydrochloride (DOR), brinzolamide (BRZ) and brimonidine tartrate (BRM) in rabbit aqueous humor (AH) using eslicarbazepine as an internal standard (IS). Liquid-liquid extraction was used for the purification and pre-concentration of analytes from rabbit AH matrix. The chromatographic separation was achieved using a mobile phase consisting of 10 mM ammonium formate pH = 7: methanol: acetonitrile (5: 50: 45, v/v/v) in isocratic mode of elution at a flow rate of 0.8 mL/min on an INERTSIL® C18 ODS-3 column (150 mm × 4.6 mm, 3.5 μm). The method was operated using electrospray ionization source in the positive ionization mode prior to detection by multiple reaction monitoring (MRM) at the following transitions: m/z 317.2 → 261.0 for TIM, m/z 325.1 → 199.0 for DOR, m/z 384.2 → 281.0

for BRZ, m/z 292.1 → 212.0 for BRM and m/z 255.0 → 237.0 for IS. The separation was done in only 3 min and the lower limit of quantitation (LLOQ) was (50 ng/ml) for all cited drugs. A detailed validation of the bio-analytical method was performed as mentioned in US-FDA and EMA guidelines and the standard calibration curves were found to be linear in the range (50–5000 ng/ml) for all drugs with good mean regression coefficient for all drugs.

**Keywords:** Timolol Maleate; Anti-Glaucoma Drugs; Rabbit Aqueous Humor; Liquid Chromatography; Tandem Mass Spectroscopy

## M-581. Resolution of Overlapped Spectra for the Determination of Ternary Mixture Using Different and Modified Spectrophotometric Methods

Bahia Abbas Moussa, Asmaa Ahmed El-Zaher, Marianne Alphonse Mahrouse and Maha Said Ahmed

*Spectrochimica Acta Part A: Molecular and Biomolecular Spectroscopy, 165: 127-137 (2016) IF: 2.653*

Four new spectrophotometric methods were developed, applied to resolve the overlapped spectra of a ternary mixture of [aliskiren hemifumarate (ALS)–amlodipine besylate (AM)–hydrochlorothiazide (HCT)] and to determine the three drugs in pure form and in combined dosage form. Method A depends on simultaneous determination of ALS, AM and HCT using principal component regression and partial least squares chemometric methods. In Method B, a modified isosbestic spectrophotometric method was applied for the determination of the total concentration of ALS and HCT by measuring the absorbance at 274.5 nm (isosbestic point, Aiso). On the other hand, the concentration of HCT in ternary mixture with ALS and AM could be calculated without interference using first derivative spectrophotometric method by measuring the amplitude at 279 nm (zero crossing of ALS and zero value of AM). Thus, the content of ALS was calculated by subtraction. Method C, double divisor first derivative ratio spectrophotometry (double divisor 1DD method), was based on that for the determination of one drug, the ratio spectra were obtained by dividing the absorption spectra of its different concentrations by the sum of the absorption spectra of the other two drugs as a double divisor. The first derivative of the obtained ratio spectra were then recorded using the appropriate smoothing factor. The amplitudes at 291 nm, 380 nm and 274.5 nm were selected for the determination of ALS, AM and HCT in their ternary mixture, respectively. Method D was based on mean centering of ratio spectra. The mean centered values at 287, 295.5 and 269 nm were recorded and used for the determination of ALS, AM and HCT, respectively. The developed methods were validated according to ICH guidelines and proved to be accurate, precise and selective. Satisfactory results were obtained by applying the proposed methods to the analysis of pharmaceutical dosage form.

**Keywords:** Aliskiren Hemifumarate; Amlodipine Besylate; Double Divisor; Hydrochlorothiazide; Isosbestic; Mean Centering.

## M-582. Synthesis of Novel Thiadiazole Derivatives as Selective COX-2 Inhibitors

Fatma A. Ragab, Helmi I. Heiba, Marwa G. El-Gazzar, Sahar M. Abou-Seri, Walaa A. El-Sabbagh and Reham M. El-Hazek

*Medchemcomm, 7: 2309-2327 (2016) IF: 2.319*

A novel series of thiadiazole derivatives were designed and synthesized for evaluation as selective COX-2 inhibitors in vitro and were investigated in vivo as anti-inflammatory and analgesic agents against carrageenan-induced rat paw oedema model in irradiated rats, since it is well-known that ionizing radiation plays an important role in exaggerating the inflammatory responses in experimental animals. Ulcerogenic activity and acute toxicity were evaluated for the most potent compounds. In order to understand the binding mode of the synthesized compounds into the active site of the COX-2 enzyme, a docking study was performed. Most of the tested compounds showed high inhibitory ability against COX- 2. Among them, thiadiazole derivatives bearing sulfonamide moieties, 7b, c and 13c, e, were the most potent COX-2 inhibitors, with extremely high selectivity indices (SI) compared to celecoxib; they showed high safety margins on gastric mucosa with no ulceration effects, and they were found to be non-toxic in experimental rats. The docking study showed a similar orientation of these compounds to that of celecoxib within the active site of the COX-2 enzyme, and a similar ability to immerge deeply into the additional pocket and bind with Arg513 and His90, the key amino acids responsible for selectivity.

**Keywords:** Synthesis of Novel Thiadiazole Derivatives.

## M-583. Stability-Indicating Rp-Hplc Methods for the Determination of Fluorometholone in its Mixtures with Sodium Cromoglycate and Tetrahydrozoline Hydrochloride

Ramzia I. El-Bagary, Marwa A. Fouad, Manal A. El-Shaland Enas H. Tolba

*Journal of Chromatographic Science, 54:923-933(2016) IF:1.32*

Two stability-indicating reversed-phase liquid chromatographic methods were developed and validated for the determination of fluorometholone (FLU) in its mixtures with sodium cromoglycate (SCG) and tetrahydrozoline hydrochloride (THZ). The first HPLC method (Method 1) was based on isocratic elution of FLU and SCG along with their alkaline degradation products on a reversed phase C18 column (250 × 4.6 mm id)ACE Generix 5, using a mobile phase consisting of methanolwater (70 : 30, v/v), pH adjusted to 2.5 using orthophosphoric acid at a flow rate of 1.2 mL min−1. Quantitation was achieved with UV detection at 240 nm. The second HPLC method (Method 2) was based on isocratic elution of FLU, its alkaline degradation product and THZ on a reversed phase C8 column (250 × 4.6 mm)—ACE Generix 5, using a mobile phase consisting of acetonitrile–50 mM potassium dihydrogen orthophosphate (40 : 60, v/v) at a flow rate of 2 mL min−1. Quantitation was achieved by applying dual-wavelength detection, where FLU and its alkaline degradation product were detected at 240 nm and THZ was detected at 215 nm at ambient temperatures. Linearity, accuracy and precision were found to be acceptable over the concentration range of 5–50 and 10–500 µg mL−1 for FLU and SCG (Method 1) and over the concentration

range of 5–80 and 5–60 μg mL−1 for FLU and THZ (Method 2), respectively. Besides, the FLU alkaline degradation product was verified using IR, NMR and LC–MS spectroscopy. The two proposed methods could be successfully applied for the routine analysis of the studied drugs either in their pure bulk powders or in their pharmaceutical preparations without any preliminary separation step.

**Keywords:** Fluorometholone; HPLC; Pharmaceutical Preparations; Sodium Cromoglycate; Stability-Indicating Assay; Tetrahydrozoline Hydrochloride.

## M-584. UPLC–MS-MS Method for the Determination of Vilazodone in Human Plasma: Application to A Pharmacokinetic Study

Ramzia El-Bagary, Hanaa Hashem, Marwa Fouad and Sally Tarek

*Journal of Chromatographic Science, 54: 1365-1372 (2016) IF: 1.32*

A sensitive, rapid and simple liquid chromatographic–electrospray ionization tandem mass spectrometric (LC–ESI–MS-MS) method was developed for the quantitative determination of vilazodone in human plasma and for the study of the pharmacokinetic behavior of vilazodone in healthy Egyptian volunteers. With escitalopram as internal standard (IS), liquid–liquid extraction was used for the purification and preconcentration of analytes from human plasma matrix using diethyl ether. The separation was performed on an Acquity UPLC BEH shield RP C18 column (1.7 μm, 2.1 × 150 mm). Isocratic elution was applied using methanol–0.2% formic acid (90:10, v/v). Detection was performed on a triple-quadrupole tandem mass spectrometer with multiple reaction monitoring mode via an electrospray ionization source at m/z 442.21 → 155.23 for vilazodone and m/z 325.14 → 109.2 for escitalopram. Linear calibration curves were obtained over the range of 1–200 ng/mL with the lower limit of quantification at 1 ng/mL. The intra- and inter-day precision showed relative standard deviation ≤3.3%. The total run time was 1.5 min. This method was successfully applied for clinical pharmacokinetic investigation, and a preliminary metabolic study was also carried out.

**Keywords:** Vilazodone; Uplc-Ms/Ms; Method Validation; Human Plasma; Pharmacokinetics.

## M-585. Novel Quinolines Carrying Pyridine, Thienopyridine, Isoquinoline, Thiazolidine, Thiazole and Thiophene Moieties as Potential Anticancer Agents

Mostafa M. Ghorab, Mansour S. Alsaid, Mohammed S. Al-Dosari, Fatma A. Ragab, Abdullah A. Al-Mishari and Abdulaziz N. Almoqbil

*Acta Pharmaceutica, 66: 155-171 (2016) IF: 1.212*

As a part of ongoing studies in developing new anticancer agents, a class of structurally novel 1,2-dihydropyridine 4, thienopyridine 5, isoquinolines 6-20, acrylamide 21, thiazolidine 22, thiazoles 23-29 and thiophenes 33-35 bearing a biologically active quinoline nucleus were synthesized. The structure of newly synthesized compounds was confirmed on the basis of elemental analyses and spectral data. All the newly synthesized compounds were evaluated for their cytotoxic activity against the breast cancer cell line MCF7. 2,3-Dihydrothiazole-5-carboxamides 27, 25, 4,5,6,7-tetrahydrobenzo[b]thiophene-3-carboxamide (34), 1,2-dihydroisoquinoline-7-carbonitrile (7), 5,6,7,8-tetrahydro-4H-cyclohepta[b]thiophene-3-carboxamide (35), 1,2-dihydroisoquinoline-7-carbonitrile (6), 2-cyano-3-(dimethylamino)-N-quinolin-3-yl)acrylamide (21), 1,2-dihydroisoquinoline-7-carbonitriles (11) and (8) exhibited higher activity (IC50 values of 27-45 μmol L–1), compared to doxorubicin (IC50 47.9 μmol L–1). (Quinolin-3-yl)-1,2-dihydroisoquinoline-7-carbonitrile (12), 2-thioxo-2,3-dihydrothiazole-5-carboxamide (28) and (quinolin-3-yl)-1,2-dihydroisoquinoline-7-carbonitrile (15) show comparable activity to doxorubicin, while (quinolin-3-yl)-1,2-dihydroisoquinoline-7-carbonitrile (9), 2, 3-dihydrothiazole-5-carboxamide (24), thieno [3,4-c] pyridine-4(5H)-one (5), cyclopenta[b]thiophene-3-carboxamide (33) and (quinolin-3-yl)-6-styryl-1,2-dihydroisoquinoline-7-carbonitrile (10) exhibited moderate activity, lower than doxorubicin.

**Keywords:** Quinolines, Pyridine, Thienopyridine, Isoquinoline, Acrylamide, Thiazole, Thiophene, Anticancer Activity

## M-587. Simultaneous Determination of Metformin, Glipizide, Repaglinide, and Glimepiride or Metformin and Pioglitazone by A Validated Lc Method: Application in the Presence of Metformin Impurity (1-Cyanoguanidine).

Asmaa A. El-Zaher and Ehab F. Elkady, Hanan m. Elwy and Mahmoud A. Saleh

*Journal of AOAC International, 99, ( 4) 2016: 957-963 (2016) IF: 0.918*

A rapid, simple, and precise RPLC method was developed for the simultaneous determination of the widely used oral antidiabetic, metformin hydrochloride (MTF), with some commonly coadministered oral antidiabetics from different pharmacological classes-glipizide (GPZ), pioglitazone hydrochloride (PGZ), glimepiride (GLM), and repaglinide (RPG)-in bulk, laboratory-prepared mixtures and pharmaceutical formulations in the presence of metformin-reported impurity [1-cyanoguanidine (CNG)]. Chromatographic separation was achieved using isocratic elution mode with a mobile phase of acetonitrile: 0.02 M potassium dihydrogen phosphate (pH 3.17; 50-50, v/v) flowing through a CN Phenomenex column (Phenosphere Next, 250 × 4.6 mm, 5 μm) at a rate of 1.5 mL/min at ambient temperature. UV detection was carried out at 220 nm. The method was validated according to International Conference on Harmonization guidelines. Linearity, accuracy, and precision were satisfactory for concentration ranges: 0.175-350 μg/mL for MTF, 0.0525-105 μg/mL for GPZ, 0.125-250 μg/mL for PGZ, and 0.05-100 μg/mL for GLM and RPG. Correlation coefficients were >0.99 for all analytes. LOQs were 0.009 μg/mL for MTF, 0.009 μg/mL for GPZ, 0.04 μg/mL for GLM, 0.124 μg/mL for PGZ, and 0.044 μg/mL for RPG. The developed method is specific, accurate, and suitable for the QC and routine analysis of the cited drugs in their pharmaceutical products.

**Keywords:** Oral Antidiabetic, Liquid Chromatography, 1-Cyanoguanidine, Pharmaceutical Products

## M-586.A Rapid and Optimized Lc-Ms/Ms Method for the Simultaneous Extraction and Determination of Sofosbuvir and Ledipasvir in Human Plasma

Ehab F. Elkady and Ahmed A. Aboelwafa

*Journal of Aoac International, 99 (5): 1252-1259 (2016) IF:0.918*

A new validated bioanalytical method based on LC tandem MS has been developed for the simultaneous extraction and determination of sofosbuvir and ledipasvir in human plasma using antiviral daclatasvir as an internal standard (IS). Liquid-liquid extraction of samples was used for the purification and preconcentration of the analytes from a human plasma matrix. Good and consistent recoveries were obtained, with average extraction recoveries of 91.61 and 88.93% for sofosbuvir and ledipasvir, respectively. The chromatographic separation of the three analytes was achieved within only 2.8 min by an isocratic mobile phase consisting of 10 mM ammonium acetate, which was then adjusted to pH 4.0 by acetic acid-acetonitrile-0.1% methanolic formic acid (12 + 25 + 63, v/v/v) flowing through a C18 Zorbax eclipse plus column (5 µm, 100 × 4.6 mm; Agilent). Multiple reaction monitoring transitions were measured in positive ion mode for sofosbuvir, ledipasvir, and daclatasvir (IS). A detailed validation of the method was performed and the standard curves were found to be linear in the range of 0.5 to 2500 and 5 to 2100 ng/mL for sofosbuvir and ledipasvir, respectively, applying weighted (1/X(2)) linear regression. The developed method was applied to the analysis of the two drugs after a single oral administration of Harvoni 400/90 mg film-coated tablets containing 400 mg sofosbuvir and 90 mg ledipasvir to four healthy volunteers.

**Keywords:** Sofosbuvir, Ledipasvir, Bioanalytical, Liquid Chromatography-Tandem Mass.

## M-588. Stereoselective Synthesis, Structural and Spectroscopic Study of 4,5,11-Triazatricyclo[6.2.1.0*2,6*]Undec-5-Ene

Ahmed F. Mabied, Adel S. Girgis, El-Sayed M. Shalaby, Riham F. George, Bahaa El-Dien M. El-Gendy and Fady N. Baselious

*Journal of Heterocyclic Chemistry, 53:1074-1080(2016) IF:0.685*

3-(2,4-Dichlorophenyl)-7-[(2,4-dichlorophenyl)methylidene]-11-methyl-4-phenyl-4,5,11-triazatricyclo[6.2.1.0*2,6*]undec-5-ene (3) was synthesized in a stereoselective manner. Single crystal X-ray study of 3 revealed that the structure belongs to the triclinic system with space group P1. The structure is further stabilized by an intermolecular C[BOND]H…π interaction. Molecular mechanics force field (MM+), followed by either semi-empirical AM1 or PM3, was used to calculate the optimized geometrical parameters of 3. The determined theoretical geometry parameters were found to be in good agreement with the parameters obtained by a single-crystal study. Vibrational frequencies and gauge-independent atomic orbital, 1H-NMR and 13C-NMR chemical shifts were computed at B3LYP/6-31G(d) level of theory. Moreover, the molecular electrostatic potential of 3 has been calculated exhibiting that the most electrophilic site of 3 is the N-3 atom; however, the nucleophilic site is distributed on the H atoms of dichlorophenyl groups. The frontier molecular orbitals of 3 have been determined by the same technique.

**Keywords:** Tropenones; 4,5,11-Triazatricyclo[6.2.1.0*2,6*] Undec-5-Enes; X-Ray Crystal Structure.

## M-589.Simultaneous Determination of Metformin, Vildagliptin, and 3-Amino-1-Adamantanol in Human Plasma: Application to Pharmacokinetic Studies

Ramzia I. El Bagary, Hassan M.E. Azzazy, Ehab F. El Kady and Faten Farouk.

*Journal of Liquid Chromatography & Related Technologies, 39, (4) (2016) IF: 0.669*

Metformin (MET) and vildagliptin (VLD) are coformulated in tablets for the management of diabetes mellitus. The aim of this study is the development of a new fast ultraperformance liquid chromatography method with tandem mass detection (UPLC–MS/MS) for their simultaneous determination with 3-amino-1-adamantanol (starting compound for vildagliptin synthesis; VLI) in human plasma. Separation of MET, VLD, and VLI was performed on a 5 cm UPLC-C18 column using a mobile phase of 0.5% acetic acid in methanol and 0.02 M aqueous ammonium acetate (10:90, v/v). The injection volume was 10 µL and electrospray positive ionization was applied. Extraction from human plasma was carried out by acid precipitation of plasma proteins using pregabalin as an internal standard. The assay was validated according to ICH guidelines. The developed method is valid, fast, and simple and was successfully applied in pharmacokinetic studies in human volunteers.

**Keywords:** 3-Amino-1-Adamantanol, Metformin, Pharmacokinetics, Vildagliptin.

## M-590. Synthesis and Biological Evaluation of Novel Coumarin Derivatives as Potential Antimicrobials Agents

Kamilia M. Amin, Sahar M. Abou-Seri, Rana M. Abdelnaby, Heba S. Rateb, Mahmoud A. F. Khalil and Mohamed M. Hussein

*International Journal of Pharmacy and Pharmaceutical Sciences, 8: 109-116 (2016)*

**Objective:** Synthesize new series of 7-hydroxy-4-methylcoumarin and 7-alkoxy-4-methylcoumarin derivatives featuring thiosemicarbazone or thiazolidin-4-one moieties and to evaluate their antimicrobial activity against two strains of Gram-positive bacteria (Staphylococcus aureus and Bacillus subtilis), two Gram-negative bacteria (Escherichia Coli and Pseudomonas aeruginosa), and Candida albicans. **Methods:** Preparation of the new coumarin derivatives was done by adopting Pechmann condensation and attaching different isothiocyanates to give coumarin-thiosemicarbazone hybrids. Thiosemicarbazones were cyclized into thiazolidine-4-ones using chloroacetic acid or diethyl bromo malonate. **Results:** Compounds VIb, Xb, XIVb, and XVc gave the highest inhibition zones (>20 mm) against Staphylococcus aureus. Their MIC (minimum inhibitory concentration) values ranging from 0.19-0.36 µg/ml were better than the reference drug tobramycin with MIC= 2µg/ml. Conclusion: The newly synthesized compounds with the 7-

hydroxyl group showed better antimicrobial activity than those with the 7-alkoxy groups.
**Keywords:** Coumarin, Thiosemicarbazones, Thiazolidin-4-Ones, Antimicrobial Activity

## M-591.Synthesis, Antibreast Cancer Activity and Docking Study of some Novel 4-(Benzo [D] Thiazol-2-Yl) Phenyl Moiety as CDK2 Inhibitors

Kamelia M. Amin. Eman A. Abd El-Meguid. Samy A. El-Assaly and Wageeh S. El-Hamouly

*International Journal of Pharmacy and Technology, 8: 10853-10871 (2016)*

Some novel sulfonamides, Schiff's bases and pyrrole derivatives attached to 4-benzo[d]thiazol-2-yl were prepared. Some of the newly synthesized compounds have been evaluated for their potential cytotoxicity against breast cancer cell line (MCF-7) in comparison with doxorubicin; the urea derivative 6a exhibited the highest activity. Molecular docking into CDK2 has been done for lead optimization of the compounds in study as potential CDK2 inhibitors;compound 8b showed the lowest binding score.
**Keywords:** 4-Benzo[D]Thiazol-2-Yl; Sulfonamides; Schiff's Bases; Pyrrole;MCF-7; CDK2

***Dept. of Pharmaceutical Organic Chemistry***

## M-592.Synthesis of New Thieno[2,3-B]Pyridine Derivatives As Pim-1 Inhibitors

Bassem H. Naguib and Hala B. El-Nassan

*Journal of Enzyme Inhibition and Medicinal Chemistry, 31: 1718-1725 (2016) IF: 3.428*

Three series of 5-bromo-thieno[2,3-b]pyridines bearing amide or benzoyl groups at position 2 were prepared as pim-1 inhibitors. All the prepared compounds were tested for their pim-1 enzyme inhibitory activity. Two compounds (3c and 5b) showed moderate pim-1 inhibitory activity with IC50 of 35.7 and 12.71 mM, respectively. Three other compounds (3d, 3g and 6d) showed poor pim-1 inhibition. The most active compounds were tested for their cytotoxic activity on five cell lines [MCF7, HEPG2, HCT116, A549 and PC3]. Compound 3g was the most potent cytotoxic agent on almost all the cell lines tested.
**Keywords:** Cytotoxic Activity, Pim-1, Thieno[2,3-B]Pyridine.

## M-593. Synthesis, Antitumor Screening and Cell Cycle Analysis of Novel Benzothieno[3,2-B]Pyran Derivatives

Ashraf F. Zaher, Suzan M. Abuel-Maaty, Hala B. El-Nassan, Samir A.S. Amer and Tamer M. Abdelghany

*Journal of Enzyme Inhibition and Medicinal Chemistry, 31(S4): 145-153 (2016) IF: 3.428*

Three series of benzothiophene derivatives were designed and synthesized as cytotoxic agents. The compounds were subjected to in vitro antitumor screening at the National Cancer Institute (NCI), Bethesda, MD. The results of the single dose screening indicated that only the benzothieno[3,2-b]pyran series 3a–f exhibited potent and broad spectrum cytotoxic activity and was subjected to five dose cytotoxic screening. The most active compound in this study was 2-amino-6-bromo-4-(4-nitrophenyl)-4H-[1]benzothieno[3,2-b]pyran-3-carbonitrile (3e) with MG-MID GI50, TGI, and LC50 values of 0.11, 7.94 and 42.66 mM, respectively. Compound 3e exhibited broad spectrum anticancer activity against a panel of 59 cell lines. To elucidate the underlying mechanism of compound 3e cytotoxic activity, we examined its effect on cell cycle progression and its ability to induce apoptosis using human colon adenocarcinoma cell line (HCT-116). The effect of compound 3e on the cell cycle progression indicated that exposure of HCT-116 cells to compound 3e for 24 and 48 h, induced a significant disruption in the cell cycle profile including time dependent decrease in cell population at G1 phase with concomitant increase in pre-G and G2/M cell population. Moreover, compound 3e induced time dependent increase in the percentage of early and late apoptotic and necrotic cell population. In conclusion, we were able to successfully design a new series of benzothieno[3,2-b]pyran derivatives with potent cytotoxic activity and their mechanism of cytotoxicity was examined.
**Keywords:** Antitumor Activity, Apoptosis, Benzothieno[3,2-B]Pyran, Cell Cycle Analysis.

## M-594.Synthesis of Novel Substituted Thiourea and Benzimidazole Derivatives Containing A Pyrazolone Ring as Anti-Inflammatory Agents

Ashraf A. Moneer, Khaled O. Mohammed and Hala B. El-Nassan

*Chemical Biology and Drug Design, 87:784-793(2016) IF:2.802*

Two series of new 1-(alkyl/aryl)-3-{2-[(5-oxo-4,5-dihydro- 1H-pyrazol-3-yl)amino]phenyl}thioureas 2a–h and 5-[2-(substituted amino)-1H-benzimidazol-1-yl]-4H-pyrazol- 3-ols 3a–i were designed and synthesized as antiinflammatory agents. The cyclooxygenase inhibitory activity of the newly synthesized compounds was investigated. All the compounds showed non-selective inhibition of COX-1 and COX-2 enzymes which was consistent with their docking results. Compounds 2c, 2f, 2g, 3b, and 3g that showed the highest COX-2 inhibitory activity were selected for further in vivo testing as anti-inflammatory agents using diclofenac as a reference drug. Two of the test compounds (2c and 3b) showed potent anti-inflammatory activity comparable to that of diclofenac with lower ulcerogenic effect relative to indomethacin. SAR study of the two series as cyclooxygenase inhibitors and anti-inflammatory agents was also provided.
**Keywords:** Anti-Inflammatory Activity, Benzimidazole, Cox Inhibitors, Pyrazolone, Thiourea

## M-595.Synthesis of Novel S-Acyl and S-Alkylpyrimidinone Derivatives as Potential Cytotoxic Agents

Makaram M. Said, Azza T. Taher, Hala B. El-Nassan and Eman A. El-Khouly

*Research on Chemical Intermediates, 42: 6643-6662 (2016) IF: 1.833*

Two series of 4-phenyl-5-cyanopyrimidin-6-one derivatives bearing various S-alkyl or S-acyl moieties at position 2 were prepared as cytotoxic agents. All compounds were tested for possible anti-cancer activity on two cell lines (MCF-7 and HCT-116). The MCF-7 cell line was found to be more sensitive than the HCT-116 cell line to the action of the compounds. Compound 8g was the most potent on the MCF-7 cell line with IC50 18.3 nM/mL, whereas its IC50 on the normal cell line (MRC-5) was 64.38 nM/mL, indicating its safety and selectivity towards the MCF-7 cell line. On the other hand, compound 8d was the most potent compound on the HCT-116 cell line with IC50 23.8 nM/mL. Compound 8g was screened against five kinases. The compound showed selective inhibitory activity against pim1 kinase with IC50 11.62 µM.

**Keywords:** Pyrimidine/ Antitumor Activity/ Mcf-7/ Hct-116/ Pim1

## M-598.Synthesis, Anticancer Activity, Effect on Cell Cycle Profile, and Apoptosis-Inducing Ability of Novel Hexahydrocyclooctathieno[2,3-D]Pyrimidine Derivatives

Asmaa Elsayed Kassab, Ehab Mohamed Gedawy, Afaf Ali El-Malah,Tamer Mohamed Abdelghany and Mohamed Sadek Abdel-Bakky

*Chemical and Pharmaceutical Bulletin, 64, (5): 490-496 (2016) IF: 1.228*

A novel series of hexahydrocyclooctathieno[2,3-d]pyrimidines was synthesized. Investigation of the anticancer activity of these derivatives revealed that compounds 2a and b showed broad-spectrum anticancer activity in nanomolar to micromolar concentrations. In particular, compound 2b showed a concentration required for 50% inhibition of cell growth (GI50) value of less than 1 µM against 20 cancer cell lines. Compounds 2a and b induced G2/M- and S-phase cell cycle arrest in human colon adenocarcinoma (HCT116) and human breast adenocarcinoma (MCF7) cell lines with a concomitant increase in the pre-G cell population in a time-dependent manner. Furthermore, compound 2b increased the nuclear expression of the proapoptotic protein cleaved caspase-3, indicating that apoptosis has an important role, at least in part, in the cancer cell death induced by the new compounds.

**Keywords:** Thieno[2,3-D]Pyrimidine; Synthesis; Anticancer Activity; Cell Cycle Arrest; Apoptosis; Caspase-3.

## M-597. Design, Synthesis and Biological Evaluation of some 5-Arylthieno[2,3-D]- Pyrimidines as Potential Anti-Cancer Agents

Afaf Kamal El-Ansary, Aliaa Mohammed Kamal and Mokhtar Abd-Hafiz Al-Ghorafi

*Chemical Pharmaceutical and Bulletin, 64: 1172-1180 (2016) IF: 1.228*

Structure-based design, synthesis and biological evaluation of new small molecules anti-cancer agents were described. On continuation of applying scaffold hopping theory, a series of 5-arylthieno[2,3-d]pyrimidines based on the structural features of lapatinib was designed, synthesized and characterized using IR, 1H-NMR, 13C-NMR, mass and microanalyses. Biological evaluation of the cytotoxic activity against MCF-7 cell line and the inhibition of the enzymatic activity of epidermal growth factor tyrosine kinase were carried out in vitro for the target compounds. Substituting the 4-anilino-5-arylthieno[2,3-d]pyrimidines with different pharmacophoric groups at ortho, meta and/or para positions led to discovery of two potent lead compounds 3b and f with excellent cytotoxic activity and enzymatic inhibition activity.

**Keywords:** Anti-Tumor Agent; Nucleophilic Substitution; Scaffold Hopping Theory; Sulfonamide; Thieno[2,3-D]Pyrimidine

## M-599.Design, Synthesis, Antitumor and Antimicrobial Activity of some Novel 6,7-Dimethoxyquinazoline Derivatives

Asmaa E. Kassab, Ehab M. Gedawy, Zienab Mahmoudand Rania A. Khattab

*Heterocycles, 92 (2), 272-290 (2016) IF: 1.107*

Novel 4-substituted-6,7-dimethoxyquinazolines 3, 4a and 4b were synthesized via reacting the corresponding 4-chloro derivative 2 with 2-(4-aminopiperazin-1-yl)ethanol, ethylpiperazine or benzylpiperidine. Quinazolines 6a-c and 8a-d were obtained through reacting 4-hydrazinylquinazoline 5 with different aromatic aldehydes or aromatic isothiocyanates. An attempt to synthesize 6,7-dimethoxyquinazolin-4-yl hydrazinecarboxamides via reacting the hydrazinyl derivative 5 with certain aromatic isocyanates was unsuccessful and the unexpected triazoloquinazoline 7 was obtained regardless to the isocyanate used .The anticancer activity of 4 compounds, namely 3, 4a, 4b and 7 was evaluated by National Cancer Institute (USA) at single dose (10-5 M) utilizing 59 different human tumor cell lines. Moreover, the antimicrobial activity of all the newly synthesized quinazolines was screened against Gram positive bacteria (Staphylococcus aureus and Bacillus subtilis), Gram negative bacteria (Escherichia coli and Klebsiella) and a fungal strain (Candida albicans).

**Keywords:** Synthesis; Antitumor Activity; Antimicrobial Activity; 6,7-Dimethoxyquinazoline.

## M-600. Synthesis, Characterisation and Biological Screening of some 2-Substituted Benzimidazole Derivatives as Potential Anticancer Agents

Mohammed Abed-Elrahman Shaaban, Aliaa Mohammed Kamal and Heba El-Sayed Teba

*Journal of Chemical Research, 40: 228-234 (2016) IF: 0.661*

Twenty two new polycyclic compounds containing a 2-substituted benzimidazole core were synthesised, characterised and evaluated in vitro against the three most widespread cancers. Seven compounds showed outstanding antitumor activity towards breast, lung or central nervous system cancer cell lines.

**Keywords:** Heterocyclic Synthesis, 2-Substituted Benzimidazole Derivatives, Nucleophilic Reactions, Anticancer Agents

## M-601. Design, Synthesis and in Vitro Anticancer Activity of Novel S-Alkyl Thieno[2,3-D] Pyrimidinone Derivatives

Samir Botros, Omneya M. Khalil, Mona M. Kamel and Yara El-Dash

*Der Pharma Chemica, 8: 380-393 (2016)*

In continuation to our research program concerned with structural modification of thieno[2,3-d] pyrimidines with the purpose of enhancing their anticancer activity, a series of S-alkyl thieno[2,3-d] pyrimidinone was designed and synthesized to investigate the effect of varying the linker and aliphatic or aromatic amine on the anticancer activity. The structure of the synthesized compounds has been elucidated on the basis of elemental analyses and spectroscopic methods (IR, 1H-NMR, 13C-NMR and MS). The in vitro cytotoxic activity of the newly synthesized compounds was evaluated against two human cell lines: prostate cancer (PC-3) and colon cancer (HCT-116). Compounds 4a, 4b, 11b and 11c exhibited potent anticancer activity against PC-3 cell line while 11b and 11c displayed promising anticancer activity against HCT-116. Compound 4a exhibited 5.78 fold more potent activity against PC-3 while compound 11b displayed 3.62 fold higher activity against HCT-116 compared to Imatinib.

**Keywords:** Synthesis, Thieno[2,3-D]Pyrimidines, Anticancer Activity, Prostate Cancer, Colon Cancer.

## M-603. Synthesis and Pharmacological Screening of New Thienopyridines for the Treatment of Alzheimer'S Disease

Afaf El-Malah, Zeinab Mahmoudand Mai A. AbdEl Fattah

*Der Pharma Chemica, 8: 1-12 (2016)*

Alzheimer is a multitargeting brain-hitting disease. The need to prepare and screen new agents is endless. Novel thienopyridine-tacrine analogues 4a,b – 8a,b and 9 have been designed, synthesized and biologically screened against cholinesterase inhibition activity. Two compounds 7a and 7b were found active. Compound 7b exceeded tacrine as a cholinesterase inhibitor. The docking studies explained this activity as compound 7b exhibited similar binding affinity to the acetylcholinesterase enzyme as with tacrine in addition to an extra hydrogen bonding

**Keywords:** Acetylcholine; Thienopyridines; Anti-Alzheimer'S Agents.

***Dept. of Pharmaceutical Technology and Industerial Pharmacy***

## M-605.Intraperitoneal Chemotherapy of Ovarian Cancer by Hydrogel Depot of Paclitaxel Nanocrystals

Bo Sun, Maie S. Taha, Benjamin Ramsey, Sandra Torregrosa-Allen, Bennett D. Elzeyand Yoon Yeo

*Journal of Controlled Release, 235: 91-98 (2016) IF: 7.441*

Intraperitoneal (IP) chemotherapy is a promising post-surgical therapy of ovarian cancer, but the full potential is yet to be realized. To facilitate IP chemotherapy of ovarian cancer, we developed an in-situ crosslinkable hydrogel depot containing paclitaxel (PTX) nanocrystals (PNC). PNC suppressed SKOV3 cell proliferation more efficiently than microparticulate PTX precipitates (PPT), and the gel containing PNC (PNC-gel) showed a lower maximum tolerated dose than PPT-containing gel (PPT-gel) in mice, indicating greater dissolution and cellular uptake of PNC than PPT. A single IP administration of PNC-gel extended the survival of tumor-bearing mice significantly better than Taxol, but PPT-gel did not. These results support the advantage of PNC over PPT and demonstrate the promise of a gel depot as an IP drug delivery system.

**Keywords:** Nanocrystals; Intraperitoneal Chemotherapy; Hydrogel Depot; Drug Delivery; Ovarian Cancer.

## M-606.Newly Established Myeloma-Derived Stromal Cell Line Msp-1 Supports Multiple Myeloma Proliferation, Migration, and Adhesion and Induces Drug Resistance More Than Normal-Derived Stroma

Pilar de la Puente, Nancy Quan, Ryan Soo Hoo, Barbara Muz, Rebecca C. Gilson, Micah Luderer, Justin King, Samuel Achilefu, Noha Nabil Salama, Ravi Vij and Abdel Kareem Azab

*Haematologica, 101 (2016) IF: 6.671*

**Introductory Paragraph:** The effects of a normal bone marrow (BM) microenvironment compared to a malignant microenvironment on multiple myeloma (MM) are significantly different, where BM stromal cells (BMSCs) play a key role. We established, characterized and compared a myeloma-derived stromal cell line (Myeloma Stromal Puente-1, MSP-1) with two normal stromal cell lines (HS-5 and HS-27A). MSP-1 was found to affect MM proliferation, adhesion, migration and drug resistance in a more profound manner than HS-5 and HS-27A. These results demonstrated the importance of malignant versus normal BM microenvironment on several key MM processes, providing a new myeloma-derived stromal cell line to study the effect of tumor microenvironment on MM.

**Keywords:** Malignant Microenvironment; Multiple Myeloma; New Cell Line; Stroma.

## M-607.The Alpha7 Nicotinic Agonist Abt-126 in the Treatment of Cognitive Impairment Associated with Schizophrenia in Nonsmokers: Results from a Randomized Controlled Phase 2B Study

George Haig, Deli Wang, Ahmed A Othman and Jun Zhao

*Neuropsychopharmacology, 41: 2893-2902 (2016) IF: 6.399*

A double-blind, placebo-controlled, parallel-group, 24-week, multicenter trial was conducted to evaluate the efficacy and safety of 3 doses of ABT-126, an α7 nicotinic receptor agonist, for the treatment of cognitive impairment in nonsmoking subjects with schizophrenia. Clinically stable subjects were randomized in 2 stages: placebo, ABT-126 25 mg, 50 mg or 75 mg once daily (stage 1) and placebo or ABT-126 50 mg (stage 2). The primary analysis was the change from baseline to week 12 on the MATRICS Consensus Cognitive Battery (MCCB) neurocognitive composite score for ABT-126 50 mg vs placebo using a mixed-model for repeated-measures. A key secondary measure was the University of California

Performance-based Assessment-Extended Range (UPSA-2ER). A total of 432 subjects were randomized and 80% (344/431) completed the study. No statistically significant differences were observed in either the change from baseline for the MCCB neurocognitive composite score (+2.66 [±0.54] for ABT-126 50 mg vs +2.46 [±0.56] for placebo at week 12; P>0.05) or the UPSA-2ER. A trend for improvement was seen at week 24 on the 16-item Negative Symptom Assessment Scale total score for ABT-126 50 mg (change from baseline −4.27±[0.58] vs −3.00±[0.60] for placebo; P=0.059). Other secondary analyses were generally consistent with the primary end point results. Adverse event rates were similar for ABT-126 and placebo. ABT-126 did not demonstrate a consistent effect on cognition in nonsmoking subjects with schizophrenia; however, a trend toward an effect was observed on negative symptoms.

**Keywords:** Abt-126, Non-Smokers, Phase 2B, Nicotinic Receptors, Cognitive Impairment, Schizophrenia.

## M-608. Second-Generation Phenylthiazole Antibiotics with Enhanced Pharmacokinetic Properties

Mohammed A. Seleem, Ahmed S. Mancy, Mohamed N. Seleem,Ahmed M. Disouky, Sammar A. Bayoumi, Haroon Mohammad, Ahmed Elshafeey, Abdelrahman S. Mayhoub, Tamer M. Abdelghany and Ahmed El-Morsy

*Journal of Medicinal Chemistry,59: 4900-4912 (2016 )IF: 5.589*

A series of second-generation analogues for 2-(1-(2-(4-butylphenyl)-4-methylthiazol-5-yl)ethylidene)amino- guanidine (1) have been synthesized and tested against methicillin-resistant Staphylococcus aureus (MRSA). The compounds were designed with the objective of improving pharmacokinetic properties. This main aim has been accomplished by replacing the rapidly hydrolyzable Schiff-base moiety of first-generation members with a cyclic, unhydrolyzable pyrimidine ring. The hydrazide-containing analogue 17 was identified as the most potent analogue constructed thus far. The corresponding amine 8 was 8 times less active. Finally, incorporating the nitrogenous side chain within an aromatic system completely abolished the antibacterial character. Replacement of the n-butyl group with cyclic bioisosteres revealed cyclohexenyl analogue 29, which showed significant improvement in in vitro anti-MRSA potency. Increasing or decreasing the ring size deteriorated the antibacterial activity. Compound 17 demonstrated a superior in vitro and in vivo pharmacokinetic profile, providing compelling evidence that this particular analogue is a good drug candidate worthy of further analysis.

**Keywords:** Phenylthiazole Antibiotics; Second-Generation, Enhanced Pharmacokinetic

## M-610. Inhalable Nanocomposite Microparticles: Preparation, Characterization and Factors Affecting Formulation

Ibrahim Elsayed and Mohamed Hassan Hany AbouGhaly

*Expert Opinion On Drug Delivery, 13: 207-222 (2016)IF: 5.434*

Introduction: Nanocomposite microparticles are intelligent carriers utilised for pulmonary drug delivery. These carriers are composed of drug-encapsulated nanoparticles dispersed in microstructures of polysaccharides. Upon administration, the inhaled microparticles can penetrate and be deposited deeply in the lung due to their adjusted aerodynamic particle size. Subsequently, the nanoparticles are released into the lung and are retained there for a prolonged time due to their resistance to immunological opsonisation, engulfment and digestion. Area covered: Nanocomposite microparticles may be prepared by spray drying, spray freeze drying, spray drying fluidised bed granulation or dry coating techniques. The selection of the included excipients, preparation technique and optimisation of the operational parameter play a significant role in the determination of the aerodynamic particle size, redispersibility of the nanoparticles, morphology, yield, moisture content, flowability and in vitro drug release. Moreover, the in vivo behaviour of this novel carrier may be optimised and traced by studying the lung deposition of the inhaled particles and the biological activity of the encapsulated drug. Expert opinion: Nanocomposite microparticles have been found to be superior to both nanoparticles and microparticles and may represent a promising carrier for pulmonary drug delivery.

**Keywords:** Aerodynamic Particle Size, Lung Deposition, Nanocomposite Microparticles, Spray Drying.

## M-609. Combined Mixture-Process Variable Approach: A Suitable Statistical Tool for Nanovesicular Systems Optimization

Basant A. Habib and Mohamed H. H. AbouGhaly

*Expert Opinion on Drug Delivery,13(6):777-788(2016) IF:5.434*

**Objectives:** This study aims to illustrate the applicability of combined mixture-process variable (MPV) design and modeling for optimization of nanovesicular systems. **Methods:** The D-optimal experimental plan studied the influence of three mixture components (MCs) and two process variables (PVs) on lercanidipine transfersomes. The MCs were phosphatidylcholine (A), sodium glycocholate (B) and lercanidipine hydrochloride (C), while the PVs were glycerol amount in the hydration mixture (D) and sonication time (E). The studied responses were Y1: particle size, Y2: zeta potential and Y3: entrapment efficiency percent (EE%). Polynomial equations were used to study the influence of MCs and PVs on each response. Response surface methodology and multiple response optimization were applied to optimize the formulation with the goals of minimizing Y1 and maximizing Y2 and Y3. **Results:** The obtained polynomial models had prediction R2 values of 0.645, 0.947 and 0.795 for Y1, Y2 and Y3, respectively. Contour, Piepel's response trace, perturbation, and interaction plots were drawn for responses representation. The optimized formulation, A: 265 mg, B: 10 mg, C: 40 mg, D: zero g and E: 120 s, had desirability of 0.9526. The actual response values for the optimized formulation were within the two-sided 95% prediction intervals and were close to the predicted values with maximum percent deviation of 6.2%. **Conclusions:** This indicates the validity of combined MPV design and modeling for optimization of transfersomal formulations as an example of nanovesicular systems.

**Keywords:** Combined Mixture-Process Variable Approach; Response Surface Methodology; Piepel'S Response Trace Plots; Perturbation Plot; Numerical Optimization; Lercanidipine Nanovesicles.

## M-611. ABT-126 Monotherapy in Mild-To-Moderate Alzheimer'S Dementia: Randomized Double-Blind, Placebo and Active Controlled Adaptive Trial and Open-Label Extension

Laura M. Gault, Robert A. Lenz, Craig W. Ritchie, Andreas Meier, Ahmed A. Othman, Qi Tang, Scott Berry, Yili Pritchett, and Weining Z. Robieson

*Alzheimer's Research and Therapy, 8:44: 1-13 (2016) IF: 5.197*

**Background** Results from a phase 2a study indicated that treatment with the novel α7 nicotinic acetylcholine receptor agonist ABT-126 25 mg once daily (QD) was associated with a trend for improvement in cognition in subjects with mild-to-moderate Alzheimer's dementia (AD). A phase 2b program was designed to evaluate a broader dose range of ABT-126 as monotherapy in subjects with mild-to-moderate AD. The program consisted of a double-blind, placebo and active controlled study of ABT-126 (dose range 25–75 mg) and an open-label extension study (75 mg). Methods The randomized double-blind study enrolled 438 subjects (Mini-Mental Status Examination score of 10–24, inclusive) not currently taking acetylcholinesterase inhibitors or memantine. Subjects received 24 weeks of ABT-126 25 mg QD (n = 77), ABT-126 50 mg QD (n = 108), ABT-126 75 mg QD (n = 73), donepezil 10 mg QD (n = 76), or placebo (n = 104). The primary endpoint was the change from baseline to week 24 in the 11-item Alzheimer's Disease Assessment Scale—Cognitive subscale (ADAS-Cog) total score. Subjects completing the double-blind study could enroll in the 28-week open-label extension study. Adverse events (AEs) and other safety parameters were monitored in both studies. **Results** A total of 367 patients (83.8 %) completed the double-blind study and 349 (79.7 %) entered the open-label study. Compared with placebo, donepezil significantly improved ADAS-Cog 11-item total scores from baseline to week 24 (−2.29 ± 0.95; one-sided P = 0.008). No ABT-126 dose demonstrated a statistically significant improvement vs placebo at week 24 in the ADAS-Cog total score: ABT-126 25 mg, −0.47 ± 0.94 (P = 0.309); ABT-126 50 mg, −0.87 ± 0.85 (P = 0.153); and ABT-126 75 mg, −1.08 ± 0.94 (P = 0.127). Rates of serious AEs and discontinuations due to AEs were similar across treatment groups. The most frequently reported AEs in both studies were constipation, fall, and headache. No clinically meaningful changes were observed in other parameters. **Conclusions** In the double-blind trial, donepezil significantly improved ADAS-Cog scores but no statistically significant improvement was seen with any ABT-126 dose. ABT-126 had an acceptable safety profile in subjects with mild-to-moderate AD in both studies.

**Keywords:** Abt-126; Randomized Controlled Trial; Alzheimer'S Disease; Assessment of Cognitive Disorders; Dementia; Alzheimer'S Dementia; Drug Therapy; Nicotinic Agonists; Adaptive Design.

## M-610.Effervescent Tablet Formulation for Enhanced Patient Compliance and the Therapeutic Effect of Risperidone

Kareem Abu Bakr Mohammed, Howida Kamal Ibrahim and Mahmoud Mohammed Ghorab

*Drug Delivery, 23: 297-306 (2016) IF: 4.843*

Risperidone is a poorly water soluble atypical antipsychotic drug. This work investigated the potential of developing risperidone effervescent tablets to facilitate drug administration and mask drug taste. The solid dispersion technique was selected to improve drug solubility due to its ease of scaling up, reproducibility and affordable cost. Thirty formulas were prepared adopting a 5(1).2(1).3(1) full factorial design. Trehalose, Inulin, pregelatinized starch, carboxymethylcellulose sodium and Eudragit E100 were used as hydrophilic carriers at different ratios. Rotovap, lyophilization and the kneading-oven were applied as solvent evaporation techniques. Differential scanning calorimetry, X-ray powder diffraction, Fourier transform infrared spectroscopy and scanning electron microscopy showed that the drug was present as amorphous material entrapped within the carrier matrix. Eight tablet blends were prepared using different effervescent mixture ratios with or without binder and lubricant/glidant mixture. All of the blends had acceptable flowability, acceptable effervescence times and immediate drug release that could not be achieved by any of the control formulas. The formula of choice contained 40% effervescent mixture, 5% starch, 1% boric acid, 1% aspartame and sufficient lactose. The relative bioavailability (RB) of risperidone from this formula was 161.41% with a significantly higher extent of absorption compared to the market conventional tablets. This formula may be promising in improving patient compliance and drug efficiency.

**Keywords:** Bioavailability; Dissolution; Factorial Design; Psychiatric Patients; Solid Dispersion.

## M-611.Tretinoin-Loaded Liposomal Formulations: from Lab to Comparative Clinical Study in Acne Patients

Salwa Abdel Rahman, Nevine Shawky Abdelmalak, Alia Badawi, Tahany Elbayoumy and Nermeen Sabryand Amany El Ramly

*Drug Delivery, 23(4): 1184-1193 (2016) IF: 4.843*

Topical tretinoin is the most commonly used retinoid for acne. However, its irritative potential on the applied area and the barrier properties of the stratum corneum limit its use. The objective of the present study was to formulate tretinoin liposomal gel to obtain a formula with lower skin irritation potential and greater clinical effect. A statistical 2(4) factorial design was adopted. Sixteen formulae prepared and were properly evaluated. A candidate formula (F13G) prepared with 0.025% tretinoin, phospholipid- cholesterol-dicetylphosphate (9:1:0.01) and incorporated in 1% carbopol gel was selected for skin irritation test. Clinical study was conducted on acne patients and compared to marketed product. All liposomes formulations were spherical in shape. The addition of cholesterol in the film hydration method significantly decreased the vesicle size, and increased the percentage of incorporation efficiency at ($p < 0.05$). The presence of dicetylphosphate significantly increased drug release but did not affect the percentage of incorporation efficiency and vesicle size. The results of the clinical study in acne patients revealed that F13G showed significantly higher efficacy when compared to marketed product ($p < 0.05$).

**Keywords:** Acne; Clinical Study; Liposomal Gel; Skin Irritation; Tretinoin

## M-612.Novel Non-Ionic Surfactant Proniosomes for Transdermal Delivery of Lacidipine: Optimization Using 23 Factorial Design and in Vivo Evaluation in Rabbits

Sara M. Soliman, Nevine S. Abdelmalak, Omaima N. El-Gazayerly and Nabaweya Abdelaziz

*Drug Delivery, 23 (5): 1608-1622 (2016) IF: 4.843*

**Context:**Proniosomes offer a versatile vesicle drug delivery concept with potential for delivery of drugs via transdermal route.**Objectives**:To develop proniosomal gel using cremophor RH 40 as non-ionic surfactant containing the antihypertensive drug lacidipine for transdermal delivery so as to avoid its extensive first pass metabolism and to improve its permeation through the skin.Materials and methods:Proniosomes containing 1% lacidipine were prepared by the coacervation phase separation method, characterized, and optimized using a 2(3) full factorial design to define the optimum conditions to produce proniosomes with high entrapment efficiency, minimal vesicle size, and high-percentage release efficiency. The amount of cholesterol (X1), the amount of soya lecithin (X2), and the amount of cremophor RH 40 (X3) were selected as three independent variables.**Results and Discussion:** The system F4 was found to fulfill the maximum requisite of an optimum system because it had minimum vesicle size, maximum EE, maximum release efficiency, and maximum desirability. The optimized system (F4) was then converted to proniosomal gel using carbopol 940 (1% w/w). In vitro permeation through excised rabbit skin study revealed higher flux (6.48 ± 0.45) for lacidipine from the optimized proniosomal gel when compared with the corresponding emulgel (3.04 ± 0.13) mg/cm(2)/h. The optimized formulation was evaluated for its bioavailability compared with commercial product. Statistical analysis revealed significant increase in AUC (0 - α) 464.17 ± 113.15 ng h/ml compared with 209.02 ± 47.35 ng h/ml for commercial tablet. Skin irritancy and histopathological investigation of rat skin revealed its safety.**Conclusion:**Cremophor RH 40 proniosomal gel could be considered as very promising nanocarriers for transdermal delivery of lacidipine.

**Keywords:** 23 Full Factorial Design; Bioavailability Study; Lacidipine; Proniosomal Gel; Transdermal Delivery

## M-613.Intranasal Brain-Targeted Clonazepam Polymeric Micelles for Immediate Control of Status Epilepticus: in Vitro Optimization, Ex Vivo Determination of Cytotoxicity, in Vivo Biodistribution and Pharmacodynamics Studies

Samia A. Nour, Nevine S. Abdelmalak, Marianne J. Naguib, Hassan M. Rashed and Ahmed B. Ibrahim

*Drug Delivery, 23(9): 3681-3695 (2016) IF: 4.843*

Clonazepam (CZ) is an anti-epileptic drug used mainly in status epilepticus (SE). The drug belongs to Class II according to BCS classification with very limited solubility and high permeability and it suffers from extensive first-pass metabolism. The aim of the present study was to develop CZ-loaded polymeric micelles (PM) for direct brain delivery allowing immediate control of SE. PM were prepared via thin film hydration (TFH) technique adopting a central composite face-centered design (CCFD). The seventeen developed formulae were evaluated in terms of entrapment efficiency (EE), particle size (PS), polydispersity index (PDI), zeta potential (ZP), and in vitro release. For evaluating the in vivo behavior of the optimized formula, both biodistrbution using 99mTc-radiolabeled CZ and pharmacodynamics studies were done in addition to ex vivo cytotoxicty. At a drug:Pluronic® P123:Pluronic® L121 ratio of 1:20:20 (PM7), a high EE, ZP, Q8h, and a low PDI was achieved. The biodistribution studies revealed that the optimized formula had significantly higher drug targeting efficiency (DTE = 242.3%), drug targeting index (DTI = 144.25), and nose-to-brain direct transport percentage (DTP = 99.30%) and a significant prolongation of protection from seizures in comparison to the intranasally administered solution with minor histopathological changes. The declared results reveal the ability of the developed PM to be a strong potential candidate for the emergency treatment of SE

**Keywords:** Brain, Micelles, Clonazepam, Central Composite, Intranasal

## M-614.Duodenum-Triggered Delivery of Pravastatin Sodium: Ii. Design, Appraisal and Pharmacokinetic Assessments of Enteric Surface-Decorated Nanocubosomal Dispersions

Saadia Ahmed Tayel, Mohamed Ahmed El-Nabarawi and Mina Ibrahim Tadrosand Wessam Hamdy Abd-Elsalam

*Drug Delivery, 23: 3266-3278 (2016) IF: 4.843*

**Context:** Pravastatin sodium (PVS) is a freely water-soluble HMG-CoA inhibitor that suffers from instability at gastric pH, extensive first pass metabolism, short elimination half-life (1–3 h) and low oral bioavailability (18%). **Objective:** To overpower these drawbacks and to maximize drug absorption at its main site of absorption at the duodenum, enteric surface-coated PVS-loaded nanocubosomal dispersions were presented**. Materials and methods:** Glyceryl monooleate (GMO)-based dispersions were developed by the fragmentation or the liquid precursor methods using Pluronic F127 or Cremophor EL as surfactants. As a challenging entericcoating approach, the promising dispersions were surface-coated via lyophilization with Eudragit L100-55; a duodenum-targeting polymer. The drug content, particle size, zeta potential, morphology and release studies of PVS-loaded dispersions were evaluated before and after surface-coating. Compared to an aqueous PVS solution, the pharmacokinetics of the best achieved system (E-F8) was evaluated (UPLC-MS/MS) in rats. **Results:** The enteric surfacecoated nanocubosomal dispersions were more or less spherical in shape and showed high drug-loading, negative zeta potential values and fine-tuned biphasic drug-release patterns characterized by retarded (2 h) and sustained (10 h) phases in pH 1.2 and pH 6.8, respectively. E-F8 system showed significantly (p50.05) higher oral bioavailability, delayed Tmax and prolonged MRT01 following oral administration in rats. **Conclusions:** The duodenum-triggering potential and the controlled-release characteristics of the best achieved system for smart PVS delivery were revealed.

**Keywords:** Enteric Surface-Coating, Fragmentation Method, Liquid Precursor Method, Nanocubosomes, Pravastatin Sodium

## M-615.Ketoprofen Mesoporous Silica Nanoparticles Sba-15 Hard Gelatin Capsules: Preparation and in Vitro/in Vivo Characterization

Ahmed A. Abd-Elrahman, Mohamed A. El Nabarawi, Doaa H. Hassan and Amal A. Taha

*Drug Delivery, 23(9): 3387-3398 (2016) IF: 4.843*

SBA-15 is used to enhance the bioavailability of poorly soluble ketoprofen (KP) through stabilization of its amorphous state. Additionally, the current work provides a complete in vitro and in vivo study on preformulated KP-SBA-15 sample and formulated KP-SBA-15 in hard gelatin capsule. Loading of KP was done by a novel method called immersion-rotavapor method. KP was quantified by extraction and thermal gravimetric analysis (TGA). Characterization of the loaded SBA-15 sample was done by high resolution transmission electron microscopy (HRTEM), small angle X-ray diffraction (SAXRD), nitrogen adsorption/ desorption isotherms, differential scanning calorimetry (DSC), Fourier transform infrared (FT-IR) spectroscopy and dissolution profiles. The loaded sample was formulated in hard gelatin capsule. The anti-inflammatory and analgesic studies were carried out on 24 adult male albino rats. TGA and extraction results showed 54.4 wt% of drug incorporated. Characterization of KP-SBA-15 sample confirmed the successful encapsulation of KP into the carrier pores in a molecular amorphous state. Additionally, loading of KP did not affect the mesoporous internal structure. During the first 5 min, the dissolution study showed very high release rates; nearly 50% of KP was released. These results were reflected on the in vivo study resulting in 82% inhibition in edema after 1 h and maximum analgesia after 30 min from the administration of the formulated sample. SBA-15 mesoporous silica nanoparticle proved to be a very promising drug delivery carrier that can be used as a facile way to enhance the bioavailability of poorly soluble drugs.

**Keywords:** In Vitro In Vivo Study, Immersion-Rotavapor Loading Method, Loading Method Mesoporous Silica Nanoparticle, Sba-15

## M-616.Particle Engineering/Different Film Approaches for Earlier Absorption of Meloxicam

Motaz Farid, Doaa Ahmed El-Setouhy, Mohamed Ahmed El-Nabarawi and Tahany El-Bayomi

*Drug Delivery, 23: 2309-2317 (2016) IF: 4.843*

Meloxicam (Mel) is a non-steroidal potent anti-inflammatory drug with effective analgesic effect for various situations; e.g. postoperative pain. The early systemic exposure to Mel and hence the rapid onset of pharmacological action is limited by its poor water solubility; a situation which may be more pronounced during acute pain episode because of reduced gastric motility that affects disintegration and dissolution of solid dosage forms. To overcome delayed absorption of Mel, improvement in the dissolution behavior of Mel is essential. Firstly, Mel spherical crystalline agglomerates (SCA) were prepared. Secondly, selected Mel SCA were integrated into intraoral fast disintegrating (OF) and edible (EF) films, they possess larger surface area that leads to rapid disintegration and release of the drug into the oral cavity within seconds and hence a rapid onset of action could be achieved. Stability study of formulations resulting in faster and higher extent of dissolution and suitable mechanical properties (G3 and G12) revealed their physical and chemical stability after three months of storage under different conditions. Both G3 and G12 successfully offered rapid absorption rate and accordingly an earlier systemic exposure to Mel compared to Mobic tablets as revealed by significantly earlier T max and higher AUC0–0.5h and AUC0–4h. T max following G3 fast disintegrating film administration was comparable to that reported following Mel parenteral administration but avoiding patient inconvenience. Both films may be suitable alternative to conventional oral and intramuscular Mel especially when earlier onset of action is required (in acute conditions).Meloxicam (Mel) is a non-steroidal potent anti-inflammatory drug with effective analgesic effect for various situations; e.g. postoperative pain. The early systemic exposure to Mel and hence the rapid onset of pharmacological action is limited by its poor water solubility; a situation which may be more pronounced during acute pain episode because of reduced gastric motility that affects disintegration and dissolution of solid dosage forms. To overcome delayed absorption of Mel, improvement in the dissolution behavior of Mel is essential. Firstly, Mel spherical crystalline agglomerates (SCA) were prepared. Secondly, selected Mel SCA were integrated into intraoral fast disintegrating (OF) and edible (EF) films, they possess larger surface area that leads to rapid disintegration and release of the drug into the oral cavity within seconds and hence a rapid onset of action could be achieved. Stability study of formulations resulting in faster and higher extent of dissolution and suitable mechanical properties (G3 and G12) revealed their physical and chemical stability after three months of storage under different conditions. Both G3 and G12 successfully offered rapid absorption rate and accordingly an earlier systemic exposure to Mel compared to Mobic tablets as revealed by significantly earlier T max and higher AUC0–0.5h and AUC0–4h. T max following G3 fast disintegrating film administration was comparable to that reported following Mel parenteral administration but avoiding patient inconvenience. Both films may be suitable alternative to conventional oral and intramuscular Mel especially when earlier onset of action is required (in acute conditions).

**Keywords:** Bioavailability, Edible Films, Fast Disintegrating Films, Meloxicam, Spherical Agglomeration

## M-617. Enhanced Corneal Permeation and Antimycotic Activity of Itraconazole Against Candida Albicans Via a Novel Nanosystem Vesicle

Aliaa N. ElMeshad and Amira M. Mohsen

*Drug Delivery, 23: 2115-2123 (2016) IF: 4.843*

The objective of this study was to investigate the potential of spanlastics as an ophthalmic delivery system to improve the corneal permeability and antimycotic activity of itraconazole (ITZ). Spanlastics containing edge activators, including Tween 20 or 80, were produced by modified ethanol injection method and exhibited a particle size of approximately 287 nm and an entrapment efficiency of more than 88%. Less than 13% ITZ was released from spanlastics over 6 h compared to 35% from conventional niosomes. Spanlastics exerted a 1.34-fold increase in the amount of ITZ permeated through excised bovine cornea after 24 h compared to conventional niosomes. Antimycotic

study revealed a significant ($p < 0.05$) increase in the zone of inhibition of Candida albicans culture demonstrated by spanlastics compared to ITZ powder at the same concentration level (10 mg). In vivo Draize test showed no signs of acute ocular toxicity upon application of the selected spanlastic formulation to the rabbit eye. Results revealed that spanlastics loaded with itraconazole could be a potential nanosystem in ocular drug delivery systems.

**Keywords:** Candida Albicans, Elasticity, Itraconazole, Niosomes, Spanlastics.

## M-613. A Pharmaceutical Study on Chlorzoxazone Orodispersible Tablets: Formulation, in-Vitro and in-Vivo Evaluation

Hela Abdo Moqbel, Aliaa Nabil El-Meshad and Mohamed Ahmed El-Nabarawi

*Drug Delivery, 23 (8): 2998-3007 (2016) IF: 4.843*

**Context:** Muscle spasm needs prompt relief of symptoms. Chlorzoxazone is a centrally muscle relaxant. **Objectives:** The aim of this study was to prepare chlorzoxazone orodispersible tablets (ODTs) allowing the drug to directly enter the systemic circulation and bypassing the first-pass metabolism for both enhancing its bioavailability and exerting a rapid relief of muscular spasm. Materials and methods: ODTs were prepared by direct compression method using Pharmaburst500, Starlac, Pearlitol flash, Prosolvodt and F-meltas co-processed excipients. Three ratios of the drug to the other excipients were used (0.5:1, 1:1 and 2:1). **Results and Discussion:** All ODTs were within the pharmacopeial limits for weight and content. ODTs containing Pharmaburst500 showed the shortest wetting time (45.33 s), disintegration time (DT) (43.33 s) and dissolution (Q15min 100.63%). By increasing the ratio of CLZ: Pharmaburst500 from 0.5:1 to 1:1 and 2:1, the DT increased from 26.43 to 28.0 and 43.33 s, respectively. By using Prosolvodt, ODTs failed to disintegrate in an acceptable time4180 s. DT of ODTs using different co-processed excipients can be arranged as follows: Pharmaburst5005F-melt5Pearlitol flash5Starlac5Prosolvodt. Pharmacokinetic study of the optimum formula F1 (50mg CLZ) in rabbits using HPLC-UV detector revealed a shorter Tmax (0.333 h) compared with Myofencapsules (250mg CLZ) (1.083 h) which is considered a promising treatment, especially for the rapid relief of muscle spasm. **Conclusion:** It could be concluded that orodispersible tablets are a promising carrier for CLZ designed for management of muscle spasm due to the enhanced dissolution and rapid absorption of the drug through the oral mucosa.

**Keywords:** Bioavailability, Co-Processed Excipients, Disintegration Time, Fast Dissolving Tablets, Muscle Relaxant.

## M-616. Design of Freeze-Dried Soluplus/Polyvinyl Alcohol-Based Film for the Oral Delivery of an Insoluble Drug for the Pediatric Use

Rehab Shamma and Nermeen Elkasabgy

*Drug Delivery, 23: 489-499 (2016) IF: 4.843*

Spironolactone (SL) is a poorly water-soluble drug. Being poorly soluble affects its dissolution rate which in turn affects its oral bioavailability. This work aimed to prepare freeze-dried SL-Soluplus/polyvinyl alcohol (PVA) oral thin film in an attempt to enhance the drug solubility on one hand and at the same time prepare a solid dosage form convenient for the pediatric use. SL-Soluplus/PVA films were prepared using polyethylene glycol 400 (PEG 400) as a plasticizer applying the solvent-casting technique. The prepared films were evaluated for their thickness, tensile strength, and in vitro dissolution studies. Box–Behnken design (17 runs) was applied to optimize the effects of the formulation variables on the film properties. The optimized film formulation was freeze-dried after casting so as to enhance the drug dissolution. Moreover, the optimized freeze-dried film was re-characterized in vitro and evaluated in vivo in human volunteers to investigate its palatability and satisfaction. The results showed that the optimized formulation composed of 10% polymer concentration containing Soluplus:PVA (0.33:0.66) and plasticized with 30% PEG 400 possessed the highest desirability value (0.836). Freeze-drying of the optimized formulation succeeded to improve SL in vitro dissolution due to the preparation of a more porous film compared to the non-freeze-dried one. In vivo evaluation of the optimized freeze-dried film showed high satisfaction among the participating volunteers concerning the ease of administration and sensation thereafter, where all the film specimens dissolved without the need for water and no film residues remained in the mouth following film dissolution. In conclusion, freeze-dried Soluplus/PVA-based oral thin film proved to be a successful carrier for the oral delivery of insoluble drugs like SL for pediatrics.

**Keywords:** Oral Film, Pediatrics, Polyvinyl Alcohol, Soluplus, Spironolactone

## M-615. Comparative Pharmaceutical Study on Colon Targeted Micro-Particles of Celecoxib: in-Vitro- in-Vivo Evaluation

Lamyaa Bazan, Ehab R. Bendas, Omaima N. El Gazayerly and Sabry Sayed Badawy

*Drug Delivery, 23: 3339-3349 (2016) IF: 4.843*

In order to target celecoxib which is a COX2 inhibitor, with potentials in the prevention and treatment of colitis and colon cancer, it was formulated as microparticles using the solvent/evaporation method and various pH-dependent Eudragit polymers. The in-vitro evaluation of the prepared microparticles showed spherical and smooth morphology. The encapsulation efficiency and yield were high, indicating that the method used is simple and efficient at this scale. The in-vitro release study showed no release in the acidic medium for 2 h followed by the release of the drug in pH 6.8 in case of Eudragit L100-55 and L100 and pH 7.4 in case of Eudragit S100. The pharmacokinetic parameters were calculated and method validation was performed to insure that it is suitable and reliable. Pharmacokinetic parameters were investigated by determining the Cmax, Tmax, AUC0–t, Kel, and t1/2 of the drug as a suspension and as microparticles. There was a significant difference ($p < 0.05$) in Tmax between the drug as a suspension and as microparticles. The effect of celecoxib on the degree of inflammation was examined on acetic acid induced colitis rat model and the drug was given as a suspension and as microparticles. The evaluation was done using macroscopical, microscopical and biochemical examination. There was a significant difference between the acetic acid control group and the treatment groups regarding all examination criteria in the order microparticles formulated using Eudragit S100 followed

by Eudragit L100-55 while microparticles using Eudragit L100 and drug suspension showed almost the same results.
**Keywords:** Acetic Acid Induced Colitis, Celecoxib, Colon Targeting, Microparticles, Pharmacokinetic Parameters

## M-621.Transdermal Delivery of Vancomycin Hydrochloride Using Combination of Nano-Ethosomes and Iontophoresis: in Vitro and in Vivo Study

Magdy I. Mohammed, Amna M. A. Makky, Mahmoud H. M. Teaima, Menna M. Abdellatif, Mohamed A. Hamzawy and Mahmoud A. F. Khalil

*Drug Delivery, 23(5): 1558-1564 (2016) IF: 4.843*

This study aimed to evaluate transdermal delivery of vancomycin hydrochloride using the combination of ethosomes as an encapsulating vesicle and iontophoresis. Ethosomes were prepared and evaluated in terms of electrochemical stability. Cathodal iontophoresis of negatively charged ethosomes and anodal iontophoresis of free drug solution and positively charged vesicles were conducted. The effect of current mode, density, concentration of drug and ionic strength was studied. In vivo study was performed by inducing mediastinitis in Sprague-Dawley rats using methicillin-resistant Staphylococcus aureus as infected pathogen, the mean bacterial count was compared between groups of rats, one of the treated groups received drug intramuscularly while the other group received vancomycin using iontophoretic delivery of optimized ethosomal formula. Ethosomes showed efficient electrochemical stability, cathodal iontophoresis of negatively charged vesicle (F2) showed maximum transdermal flux (550 μg/cm2/h) compared to free drug solution and other ethosomal formulae, transdermal flux was reduced by altering current mode from continuous to ON/OFF mode, reducing current density and by using normal saline as drug solvent; on the other hand, flux was potentiated by increasing drug concentration from 25 to 75 mg/ml. In vivo study revealed that there was a significant difference in terms of bacterial count between untreated and treated groups, while there was no statistically significant difference between the I.M. vancomycin treatment and treatment conducted by iontophoretic delivery of vancomycin encapsulated in ethosomal formula. Combination between ethosomes and iontophoresis had succeeded in delivering vancomycin transdermally.
**Keywords:** Ethosomes, Iontophoresis, Mediastinitis, Transdermal, Vancomycin Hydrochloride

## M-614. Baclofen Novel Gastroretentive Extended Release Gellan Gum Superporous Hydrogel Hybrid System: in-Vitro and in-Vivo Evaluation

Ibrahim A. El-said, Ahmed A. Aboelwafa, Rawia M. Khalil and Omaima N. ElGazayerly

*Drug Delivery, 23: 101-112 (2016) IF: 4.843*

Baclofen is a centrally acting skeletal muscle relaxant with a short elimination half-life, which results in frequent daily dosing and subsequent poor patient compliance. The narrow absorption window of baclofen in the upper gastrointestinal tract limits its formulation as extended release dosage forms. In this study, baclofen extended release superporous hydrogel (SPH) systems, including conventional SPH, SPH composite and SPH hybrid (SPHH), were prepared aiming to increase the residence of baclofen at its absorption window. The applicability of different polymers, namely, gellan gum, guar gum, polyvinyl alcohol and gelatin, was investigated in preparation of SPHH systems. The prepared SPH systems were evaluated regarding weight and volume swelling ratio, porosity, mechanical properties, incorporation efficiency, degree of erosion and drug release. In vivo assessment was performed in dogs to evaluate gastric residence time by X-ray studies. In addition, the oral bioavailability of baclofen relative to commercially available Lioresal® immediate release tablets was also investigated. The novel baclofen gellan SPHH cross linked with calcium chloride was characterized by optimum mechanical properties, acceptable swelling properties as well as extended drug release. It also exhibited a prolonged plasma profile when compared to twice daily administered Lioresal.
**Keywords:** Baclofen, Dogs, Gastroretentive, Gellan Gum, Pharmacokinetics, Superporous.

## M-623. Utilization of Ionotropic Gelation Technique for Bioavailability Enhancement of Cinnarizine: in Vitro Optimization and in Vivo Performance in Human

Samar M. Abouelatta, Ahmed A. Aboelwafa, Rawia M. Khalil and Omaima N. El- Gazayerly

*Drug Delivery, 23: 2736-2746 (2016) IF: 4.843*

Gastro retentive drug delivery system techniques were adopted to deliver drugs having narrow absorption window from a particular site in the GIT. Therefore, gastro retentive dosage forms were retained in the stomach, thus improving absorption and bioavailability would be improved consequently. In this study, cinnarizine (CNZ) was employed as the model drug. CNZ is a poorly soluble basic drug, suffering from low and erratic bioavailability. This is attributed to its pH-dependant solubility (highly soluble at pH < 4). CNZ is characterized by short half-life (3–6 h). Accordingly, floating CNZ emulsion gel calcium pectinate beads were developed. A mixture design was employed to study the effect of the percent of LM pectin (A), the percent of GMO (B) and the percent of Labrafac Lipophile (C) simultaneously on the percent of drug released and loaded. The optimized floating CNZ emulsion gel calcium pectinate beads and Stugeron® (the marketed reference product) were compared through a pharmacokinetic study carried on healthy human volunteers. Fortunately, simple floating CNZ emulsion gel calcium pectinate beads were prepared with zero-order release profile for 12 h. A promising in-vivo CNZ controlled release dosage form with higher bioavailability, when compared to once daily administration of Stugeron® tablets was achieved.
**Keywords:** Gastro Retentive Dosage Form, Gmo, Labrafac Lipophil, Lm Pectin, Mixture Design

## M-624. Bile Salts-Containing Vesicles: Promising Pharmaceutical Carriers for Oral Delivery of Poorly Water-Soluble Drugs and Peptide/Protein-Based Therapeutics or Vaccines

Mona Hassan Aburahma

*Drug Delivery, 23:6: 1847-1867 (2016) IF: 4.843*

Most of the new drugs, biological therapeutics (proteins/peptides) and vaccines have poor performance after oral administration due to poor solubility or degradation in the gastrointestinal tract (GIT). Though, vesicular carriers exemplified by liposomes or niosomes can protect the entrapped agent to a certain extent from degradation. Nevertheless, the harsh GIT environment exemplified by low pH, presence of bile salts and enzymes limits their capabilities by destabilizing them. In response to that, more resistant bile salts-containing vesicles (BS-vesicles) were developed by inclusion of bile salts into lipid bilayers constructs. The effectiveness of orally administrated BS-vesicles in improving the performance of vesicles has been demonstrated in researches. Yet, these attempts did not gain considerable attention. This is the first review that provides a comprehensive overview of utilizing BS-vesicles as a promising pharmaceutical carrier with a special focus on their successful applications in oral delivery of therapeutic macromolecules and vaccines. Insights on the possible mechanisms by which BS vesicles improve the oral bioavailability of the encapsulated drug or immunological response of entrapped vaccine are explained. In addition, methods adopted to prepare and characterize BS vesicles are described. Finally, the gap in the scientific researches tackling BS-vesicles that needs to be addressed is highlighted.

**Keywords:** Bile Salts, Bile Salts-Containing Liposomes, Bilosomes, Immune Response, Lipophilic Drugs, Proteins and Peptides, Vesicular Carriers.

## M-621. Insights on Novel Particulate Self-Assembled Drug Delivery Beads Based on Partial Inclusion Complexes Between Triglycerides and Cyclodextrins

Mona Hassan Aburahma

*Drug Delivery, 23:7: 2205-2219 (2016) IF: 4.843*

Most of the newly designed drug molecules are lipophilic in nature and often encounter erratic absorption and low bioavailability after oral administration. Finding ways to enhance the absorption and bioavailability of these lipophilic drugs is one of the major challenges that face pharmaceutical industry nowadays. In view of that, the purpose of this review is to shed some light on a novel particulate self-assembling system named ‘‘beads’’ than can act as a safe carrier for delivering lipophilic drugs. The beads are prepared simply by mixing oils with cyclodextrin (CD) aqueous solution in mild conditions. A unique interaction between oil components and CD molecules occurs to form in situ surface-active complexes which are prerequisites for beads formation. This review mainly focuses on the fundamentals of beads preparation through reviewing present, yet scarce, literature. The key methods used for beads characterization are discussed in details. Also, the potential mechanisms by which beads increase the bioavailability of lipophilic drugs are illustrated. Finally, the related research areas that needs to be addressed in future for optimizing this promising delivery system are briefly outlined.

**Keywords:** Beads, Cyclodextrin, Lipid-Based Formulation, Mineral Oils, Partial Inclusion Complex, Soybean Oil, Triglycerides

## M-626. Trans-Nasal Zolmitriptan Novasomes: in-Vitro Preparation, Optimization and in-Vivo Evaluation of Brain Targeting Efficiency.

Radwa M. A. Abd-Elal, Rehab N. Shamma, Hassan M. Rashed and Ehab R. Bendas

*Drug Delivery, 23: 3374-3386 (2016) IF: 4.843*

Migraine attack is a troublesome physiological condition associated with throbbing, intense headache, in one half of the head. Zolmitriptan is a potent second-generation triptan, prescribed for patients with migraine attacks, with or without an aura, and cluster headaches. The absolute bioavailability of zolmitriptan is about 40% for oral administration; due to hepatic first metabolism. Nasal administration would circumvent the pre-systemic metabolism thus increasing the bioavailability of zolmitriptan. In addition, due to the presence of microvilli and high vasculature, the absorption is expected to be faster compared to oral route. However, the bioavailability of nasal administered drugs is particularly restricted by poor membrane penetration. Thus, the aim of this work is to explore the potential of novel nanovesicular fatty acid enriched structures (novasomes) for effective and enhanced nasal delivery of zolmitriptan and investigate their nose to brain targeting potential. Novasomes were prepared using nonionic surfactant, cholesterol in addition to a free fatty acid. A 23 full factorial design was adopted to study the influence of the type of surfactant, type of free fatty acid and ratio between the free fatty acid and the surfactant on novasomes properties. The particle size, entrapment efficiency, polydispersity index, zeta potential and % zolmitriptan released after 2 h were selected as dependent variables. Novasomes were further optimized using Design Expert® software (version 7; Stat-Ease Inc., Minneapolis, MN), and an optimized formulation composed of Span® 80:Cholesterol:stearic acid (in the ratio 1:1:1) was selected. This formulation showed zolmitriptan entrapment of 92.94%, particle size of 149.9 nm, zeta potential of -55.57 mV, and released 48.43% zolmitriptan after 2 h. The optimized formulation was further examined using transmission electron microscope, which revealed non-aggregating multi-lamellar nanovesicles with narrow size distribution. DSC, XRD examination of the optimized formulation confirmed that the drug have been homogeneously dispersed throughout the novasomes in an amorphous state. In-vivo bio-distribution studies of 99mTc radio-labeled intranasal zolmitriptan loaded novasomes were done on mice, the pharmacokinetic parameters were compared with those following administration of intravenous 99mTc-zolmitriptan solution. Results revealed the great enhancement in zolmitriptan targeting to the brain, with drug targeting potential of about 99% following intranasal administration of novasomes compared with the intravenous drug solution. Zolmitriptan loaded novasomes administered via the nasal route may therefore constitute an advance in the management of acute migraine attacks.

**Keywords:** Brain Targeting; Factorial Design; Intranasal Route; Novasomes; Pharmacokinetics; Radio-Labeling; Zolmitriptan

## M-627. Localized Rosuvastatin Via Implantable Bioerodible Sponge and its Potential Role in Augmenting Bone Healing and Regeneration

Howida Kamal Ibrahim and Rania Hassan Fahmy

*Drug Delivery, 23: 3181-3192 (2016) IF: 4.843*

**Objective:** Statins proved potential bone healing properties. Rosuvastatin is a synthetic,hydrophilic, potent and highly efficacious statin. In the current work, an attempt was investigated to develop, evaluate various bioerodible composite sponges enclosing rosuvastatin and explore their potential in augmenting bone healing and regeneration. **Method:** Twelve lyophilized sponge formulae were prepared adapting a 41.31 full factorial design. Xanthan gum, polycarbophil, Carbopoland sodium alginate were investigated as anionic polymers, each at three chitosan:anionic polymer ratios (1:3, 1:1, 3:1). The formula of choice was implanted in fractured rat femora. **Results:** Visual and microscopic examination showed flexible homogenous porous structures with considerable bending ability. Polyelectrolyte complex formation was proved by DSC and FT-IR for all chitosan/anionic combinations except with xanthan gum where chitosan probably bound to the drug rather than xanthan gum. Statistical analysis proved that anionic polymer type and chitosan: polymer ratio, as well as, their interactions, exhibited significant effects on the release parameters at p0.05. The optimum chitosan/anionic polymer complexation ratios were 3:1 for polycarbophil and 1:1 for Carbopol and alginate. The release at these ratios followed Fiction diffusion while other ratios had anomalous diffusion. Imwitor900K and HPMC K100M were added as release retarardants for further release optimization. The formula of choice was implanted in fractured rat femora. Histopathological examination revealed advanced stages of healing in treated femora compared to control ones. **Conclusion:** Biodegradable sponges for local rosuvastatin delivery proved significantly enhanced wound healing and regeneration properties to fractured bones.

**Keywords:** Bioerodible, Biodegradable Sponge, Bone Healing, Polyelectrolyte Complex, Rosuvastatin.

## M-628. Fluorouracil Shell-Enriched Solid Lipid Nanoparticles (SLN) for Effective Skin Carcinoma Treatment

Rasha A. Khallaf, Heba F. Salem and Ahmed Abdelbary

*Drug Delivery, 23: 3452-3460 (2016) IF: 4.843*

**Context:** The effective treatment of skin carcinoma is warranted for targeting the chemotherapeutic agents into tumor cells and avoiding unwanted systemic absorption. **Objective:** This work was dedicated to the purpose of engineering highly penetrating shell-enriched nanoparticles that were loaded with a hydrophilic chemotherapeutic agent, 5-fluorouracil (5-FU). **Methods:** Varying ratios of lecithin and poloxamer188 were used to produce shell-enriched nanoparticles by enabling the formation of reversed micelles within this region of the SLN. The localization of 5-FU within the shell region of the SLN, was confirmed using 5-FU nanogold particles as a tracer. SLN were introduced within sodium carboxy methylcellulose hydrogel, and then applied onto the skin of mice-bearing Ehrlich's ascites carcinoma. The mice were treated with the gel twice daily for 6 weeks. **Results:** The transmission electron microscope (TEM) revealed the formation of uniform nanoparticles, which captured reversed micelles within their shell region. The SLNs' had particle size that ranged from 137 ± 5.5 nm to 800 ± 53.6, zeta potential of −19.70 ± 0.40 mV and entrapment efficiency of 47.92 ± 2.34%. The diffusion of the drug-loaded SLN (269.37 ± 10.92 μg/cm2) was doubled when compared with the free drug (122 ± 3.09 μg/cm2) when both diffused through a hydrophobic membrane. SLN-treated mice exhibited reduced inflammatory reactions, with reduced degrees of keratosis, in addition to reduced symptoms of angiogenesis compared to 5-FU-treated mice. Conclusion: SLN possesses the capacity to be manipulated to entrap and release hydrophilic antitumor drugs with ease.

**Keywords:** 5-Fluorouracil, Erlich'S Tumor, Gold Nanoparticles, Reversed Micelles, Sln.

## M-620. In Vitro/in Vivo Evaluation of an Optimized Fast Dissolving Oral Film Containing Olanzapine Coamorphous Dispersion with Selected Carboxylic Acids

Eman Magdy Maher, Ahmed Mahmoud Abdelhaleem Ali, Heba Farouk Salem and Ahmed Abdelbary Abdelrahman

*Drug Delivery, 23: 3088-3100 (2016) IF: 4.843*

Improvement of water solubility, dissolution rate, oral bioavailability, and reduction of first pass metabolism of OL (OL), were the aims of this research. Co-amorphization of OL carboxylic acid dispersions at various molar ratios was carried out using rapid solvent evaporation. Characterization of the dispersions was performed using differential scanning calorimetry (DSC), Fourier transform infrared spectrometry (FTIR), X-ray diffractometry (XRD), and scanning electron microscopy (SEM). Dispersions with highest equilibrium solubility were formulated as fast dissolving oral films. Modeling and optimization of film formation were undertaken using artificial neural networks (ANNs). The results indicated co-amorphization of OL-ascorbic acid through H-bonding. The co-amorphous dispersions at 1:2 molar ratio showed more than 600-fold increase in solubility of OL. The model optimized fast dissolving film prepared from the dispersion was physically and chemically stable, demonstrated short disintegration time (8.5 s), fast dissolution (97% in 10 min) and optimum tensile strength (4.9 N/cm2). The results of in vivo data indicated high bioavailability (144 ng h/mL) and maximum plasma concentration (14.2 ng/mL) compared with the marketed references. Therefore, the optimized co-amorphous OL-ascorbic acid fast dissolving film could be a valuable solution for enhancing the physicochemical and pharmacokinetic properties of OL.

**Keywords:** Amorphous, Bioavailability, Fast Dissolving Film, Neural Networks, Olanzapine, Pharmacokinetics, Solid Dispersion.

## M-630. Nanotransfersomes of Carvedilol for Intranasal Delivery: Formulation, Characterization and in Vivo Evaluation

Heba M. Aboud, Adel Ahmed Ali, Shahira F. El-Menshawe and Ahmed Abd Elbary

*Drug Delivery, 23: 2471-2481 (2016) IF: 4.843*

**Context:** Development of carvedilol-loaded transfersomes for intranasal administration to overcome poor nasal permeability and hepatic first pass effect so as to enhance its bioavailability. **Objective:** The purpose of this study was to develop carvedilol-loaded transfersomes containing different edge activators (EAs) then evaluating the in vivo behavior of the optimized formula in rabbits. **Methods:** The vesicles were prepared by incorporating different EAs including Span 20, Span 60, Tween 20, Tween 80, and sodium deoxycholate (SDC) in the lipid bilayer and each EA was used in three different ratios with respect to phosphatidylcholine (PC) including 95:5%, 85:15%, and 75:25% w/w (PC:EA). Evaluation of transfersomes was carried out in terms of shape, size, entrapment efficiency (EE), in vitro release, ex vivo permeation, confocal laser scanning microscopy (CLSM), and stability studies. The pharmacokinetic study of the optimized formula was conducted in rabbits. **Results:** The mean diameter of the vesicles was in the range of 295–443 nm. Transfersomes prepared with 95:5% (w/w) (PC:EA) ratio showed highest EE% where Span 60 gave the highest values. Whereas those prepared using 85:15% w/w ratio showed highest percentages of drug release where SDC was superior to other EAs. The developed transfersomes exhibited significantly higher amounts of carvedilol permeated through nasal mucosa. CLSM of formula T14 containing SDC with 85:15% (w/w) (PC:EA) ratio revealed high permeation across the nasal mucosa. **Conclusion:** The nanotransfersomal vesicles were significantly more efficient in nasal delivery of carvedilol with absolute bioavailability of 63.4%.
**Keywords:** Carvedilol, Edge Activators, Intranasal, Nanotransfersomes, Pharmacokinetic Study.

## M-631.Pharmacokinetics, Safety and Tolerability of Abt-494, A Novel Selective Jak 1 Inhibitor, in Healthy Volunteers and Subjects with Rheumatoid Arthritis

Mohamed-Eslam F. Mohamed, Heidi S. Camp, Ping Jiang, Robert J. Padley, Armen Asatryan and Ahmed A. Othman

*Clinical Pharmacokinetics, 55: 1547-1558 (2016) IF: 4.829*

**Background** ABT-494 is a potent and selective Janus kinase (JAK) 1 inhibitor being developed for the treatment of several autoimmune disorders, with potential for an improved safety profile compared with non-selective JAK inhibitors. This work characterized the pharmacokinetics, safety, and tolerability of ABT-494 following single and multiple dosing of the immediate-release formulation. **Methods** ABT-494 single (1–48 mg or placebo; n = 56) and multiple (3–24 mg or placebo twice daily for 14 days; n = 44) doses in healthy subjects, as well as multiple doses (3–24 mg or placebo twice daily for 27 days; n = 14) in subjects with rheumatoid arthritis (RA) on a background of methotrexate were evaluated. Pharmacokinetic samples were collected and safety and tolerability were assessed. **Results** ABT-494 followed bi-exponential disposition, with a terminal elimination half-life of 6–16 h and a functional half-life, calculated from maximum observed plasma concentration (Cmax) to trough plasma concentration (Ctrough) ratio at steady state, of 3–4 h. ABT-494 exposure was approximately dose proportional over the 3–36 mg dose range, with no significant accumulation with repeated dosing. In subjects with RA, no pharmacokinetic interaction between ABT-494 and methotrexate was observed. The fraction of ABT-494 dose eliminated in urine as unchanged ABT-494 was 14–25 %. All treatment-emergent adverse events (TEAEs) were mild or moderate in severity, with headache being the most frequently observed TEAE (15.6 % for ABT-494 vs. 16.7 % for placebo) after multiple twice-daily administration to healthy subjects. No clinically significant changes in laboratory parameters, vital signs, or electrocardiogram findings in healthy or RA subjects were observed. **Conclusions** The favorable pharmacokinetics, safety, and tolerability results from these studies supported further evaluations of ABT-494 in phase IIb dose-ranging trials in RA and Crohn's disease.
**Keywords:** ABT-494, Pharmacokinetics, Rheumatoid Arithritis, Autoimmune Disorders.

## M-632.Blockade of the High-Affinity Interleukin-2 Receptors with Daclizumab High-Yield Process: Pharmacokinetic/Pharmacodynamic Analysis of Single- and Multiple-Dose Phase I Trials

Mukul Minocha, Jonathan Q. Tran, James P. Sheridan and Ahmed A. Othman

*Clinical Pharmacokinetics, 55: 121-130 (2016) IF: 4.829*

**Background and Objective** Daclizumab high-yield process (DAC HYP) is a humanized monoclonal antibody that selectively blocks the α-subunit (CD25) of the high-affinity interleukin-2 receptors, and has shown robust efficacy as a treatment for multiple sclerosis (MS). This work quantitatively characterized the relationship between DAC HYP serum concentrations and saturation of CD25 expressed on antigen-rich target T cells in blood. **Methods** Serial pharmacokinetic and 968 CD25 measurements from three double-blind, randomized, placebo-controlled, phase I studies of DAC HYP (50–300 mg subcutaneous and 200–400 mg intravenous doses or placebo) in healthy volunteers (n = 95) were analyzed using nonlinear mixed-effects modeling. CD25 occupancy was determined using flow cytometry and a fluorescently-labeled DAC HYP-competing antibody. **Results** CD25 occupancy was described using a direct inhibitory sigmoidal maximum effect (Emax) model (where DAC HYP fully inhibited CD25 labeling with competing antibody). Two IC50 (serum concentration corresponding to 50 % of maximal inhibition) parameters were used to describe rapid CD25 saturation at initiation of dosing and apparently slower desaturation during DAC HYP washout. Parameter estimates (95 % bootstrap confidence intervals) were: baseline CD25 labeling, 47 % (45–48); DAC HYP IC50(saturation), 0.023 µg/mL (0.005–0.073); IC50(desaturation) 0.86 µg/mL (0.74–0.98); Hill coefficient 5.6 (4.3–6.8). **Conclusions** Based on the developed model, the 150 mg monthly subcutaneous regimen of DAC HYP in subjects with MS is predicted to saturate CD25 on target effector T cells within a few hours of dosing and maintain CD25 saturation during the entire dosing interval. Free CD25 levels return to baseline within 4–6 months of the last DAC HYP dose.
**Keywords:** Daclizumab Hyp, Cd25, Receptor Occupancy, Multiple Sclerosis.

## M-633. Population Pharmacokinetics of Daclizumab High-Yield Process in Healthy Volunteers and Subjects with Multiple Sclerosis: Analysis of Phase I–Iii Clinical Trials

Lei Diao, Yaming Hang, Ahmed A. Othman, Ivan Nestorov and Jonathan Q. Tran

*Clinical Pharmacokinetics, 55: 943-955 (2016) IF: 4.829*

**Background and Objectives** Daclizumab high-yield process (HYP) is a humanized IgG1 monoclonal antibody that binds to the α-subunit (CD25) of the interleukin-2 receptor. The present work characterized the population pharmacokinetics of daclizumab HYP in healthy volunteers (HVs) and subjects with relapsing–remitting multiple sclerosis (RRMS) and evaluated the effects of covariates on daclizumab HYP exposure. **Methods** Measurable serum concentrations (n = 17,139) from 1670 subjects in seven clinical studies (three phase I, one immunogenicity, one phase II with extension, and one phase III) were included in this pharmacokinetic analysis using non-linear mixed–effects modeling. The three phase I studies evaluated single or multiple doses that ranged from 50 to 400 mg with either intravenous or subcutaneous (SC) administration in HVs (n = 71). The phase II with extension studies evaluated doses of 150 or 300 mg SC every 4 weeks (n = 567), and the immunogenicity (n = 113) and the phase III (n = 919) studies evaluated 150 mg SC every 4 weeks, all in RRMS patients. **Results** A two-compartment model with first-order absorption and elimination adequately described daclizumab HYP pharmacokinetics. Clearance (CL) was 0.212 L/day and the central volume of distribution was 3.92 L, scaled by [body weight (kg)/68] with exponents of 0.87 and 1.12, respectively. The peripheral volume of distribution was 2.42 L. Absorption lag time, mean absorption time, and absolute bioavailability (100–300 mg SC) were 1.61 h, 7.2 days, and 88 %, respectively. The daclizumab HYP terminal half-life was 21 days. Baseline CD25, age, and sex did not influence daclizumab HYP pharmacokinetics. Body weight explained 37 and 27 % of the inter-individual variability for CL and central volume of distribution, respectively. Neutralizing antibody (NAb)-positive status (included as a time-varying covariate) increased daclizumab HYP CL by 19 %. **Conclusions** Consistent with previous findings in HVs, this analysis including extensive data from RRMS patients demonstrates that daclizumab HYP is characterized by slow CL, linear pharmacokinetics at doses above 100 mg, and high SC bioavailability. The pharmacokinetics of daclizumab HYP were not influenced by age (range 18–66 years), the sex of adult subjects, or the baseline CD4+CD25+ T cells (target level). The impact of covariates (body weight, NAb) on daclizumab HYP pharmacokinetics is unlikely to be clinically relevant.

**Keywords:** Daclizumab Hyp; Population Pharmacokinetics; Nonmem; Multiple Sclerosis.

## M-634. MEK Inhibitor, TAK-733 Reduces Proliferation, Affects Cell Cycle and Apoptosis, and Synergizes with Other Targeted Therapies in Multiple Myeloma.

P de la Puente, B Muz, A Jin, F Azab, M Luderer, N N Salama and A K Azab

*Blood Cancer Journal, 6(2): 0-0 (2016) IF: 4.411*

**Introductory Paragraph:** The RAS/RAF/MEK (mitogen-activated protein kinase)/ERK (extracellular-signal-regulated kinase) pathway is one of the main signaling systems that manage proliferation, differentiation and cell survival, as well as cell cycle and apoptosis. In this pathway, a cascade of phosphorylation events affects three key kinases: RAF, MEK (MAPK kinase) and ERK (MAP kinase). While MEK is not frequently mutated in human cancer, aberrant expression of MEK is observed in many different cancers. Multiple myeloma (MM) is the second most common hematological malignancy with a 45% five-year survival rate of patients based on the 2004–2010 myeloma cancer statistics from SEER (Surveillance, Epidemiology, and End Results Program). The RAS/RAF/MEK/ERK pathway is often deregulated in MM cells and the prevalence of RAS mutations in myeloma is reported to be about 20–40%. MEK is a serine/threonine kinase responsible for the phosphorylation of ERK1/2. ERK1/2 are unique targets of MEK, making MEK an interesting target for anticancer therapeutics. An advantage of targeting MEK is that RAF/MEK/ERK pathway is a conjunction point where several upstream signaling pathways can be blocked with the inhibition of a single kinase, MEK. MEK1/2 inhibition against MM cells has been probed to affect progression, cell cycle and apoptosis, as well as synergizes with other anti-MM agents.

**Keywords:** Multiple Myeloma, Mek Inhibitor, Tak-733.

## M-635. Nano Spray Drying Technique as a Novel Approach to Formulate Stable Econazole Nitrate Nanosuspension Formulations for Ocular Use.

Amr Maged, Azza A. Mahmoud and Mahmoud M. Ghorab

*Molecular Pharmaceutics, 13(9): 2951-2965 (2016) IF: 4.342*

The effect of using methyl-β-cyclodextrin and hydroxypropyl-β-cyclodextrin as carriers for econazole nitrate nanoparticles prepared by nano spray dryer was explored in this work. Stabilizers, namely, poly(ethylene oxide), polyvinylpyrrolidone k30, poloxamer 407, Tween 80, and Cremophor EL, were used. The nano spray dried formulations revealed almost spherical particles with an average particle size values ranging from 121 to 1565 nm and zeta potential values ranging from -0.8 to -2.5 mV. The yield values for the obtained formulations reached 80%. The presence of the drug in the amorphous state within the nanosuspension matrix system significantly improved drug release compared to that for pure drug. Combination of hydroxypropyl-β-cyclodextrin with Tween 80 achieved an important role for preserving the econazole nanosuspension from aggregation during storage for one year at room temperature as well as improving drug release from the nanosuspension. This selected formulation was suspended in chitosan HCl to increase drug release and bioavailability. The in vivo evaluation on albino rabbit's eyes demonstrated distinctly superior bioavailability of the selected formulation suspended in chitosan

compared to its counterpart formulation suspended in buffer and crude drug suspension due to its mucoadhesive properties and nanosize. The nano spray dryer could serve as a one step technique toward formulating stable and effective nanosuspensions.
**Keywords:** Eye Drops; Nano Spray Dryer; Nanoparticles.

## M-636. Effect of Different Polymers on Avanafil-B-Cyclodextrin Inclusion Complex: in Vitro and in Vivo Evaluation.

Kareem AbuBakr Soliman, Howida Kamal Ibrahim and Mahmoud Mohammed Ghorab

*International Journal of Pharmaceutics, 512: 168-177 (2016) IF: 3.994*

In this study, we examined the effect of different polymers on the chemical, physical and pharmacokinetic properties of avanafil-β-cyclodextrin (β-CD) inclusion complex. Equimolar mixtures of drug and β-CD were used to prepare 25 ternary drug-β-CD-polymer inclusion complexes using five different polymers, polyethylene glycol (PEG 4000), polyvinyl pyrrolidone (PVP K-30), chitosan, hydroxypropylmethyl cellulose, and hydroxyethyl cellulose, each in five different concentrations, 1, 3, 5, 7, and 10% (w/w). The addition of 10% (w/w) PEG 4000 resulted in a significant decrease of drug solubility, where the infrared spectra and differential scanning thermograms revealed an interaction between PEG 4000 and avanafil which hindered drug inclusion. In contrast, addition of 7% (w/w) PVP K-30 facilitated drug inclusion as concluded from differential scanning thermograms, X-ray diffraction patterns and scanning electron micrographs. This resulted in a subsequent improvement in drug solubility and in vitro dissolution. This formula was chemically and physically stable for 6 months under accelerated storage conditions. The formula had a relative bioavailability of 125.56% in rabbits as compared to conventional commercially available avanafil tablets (Spedra(®)).
**Keywords:** Bioavailability; Crystallinity; Polyethylene Glycol; Polyvinyl Pyrrolidone; Stability

## M-637. Fabrication of Novel Ultradeformable Bilosomes for Enhanced Ocular Delivery of Terconazole: in Vitro Characterization, Ex Vivo Permeation and in Vivo Safety Assessment

Aly A. Abdelbary, Wessam H. Abd-Elsalam and Abdulaziz M. Al-mahallawi

*International Journal of Pharmaceutics, 513: 688-696 (2016) IF: 3.994*

The objective of this work was to encapsulate terconazole (TCZ), a water insoluble antifungal drug, into novel ultradeformable bilosomes (UBs) for achieving enhanced ocular delivery. In addition to the constituents of the conventional bilosomes; namely, Span 60, cholesterol, and the bile salts, UBs contain an edge activator which imparts extra elasticity to the vesicles and consequently hypothesized to result in improved corneal permeation. In this study, TCZ loaded UBs were prepared utilizing ethanol injection method according to 23 full factorial design. The investigation of the influence of different formulation variables on UBs properties and selection of the optimum formulation was done using Design-Expert® software. The selected UBs formulation (UB1; containing 10 mg bile salt and 5 mg Cremophor EL as an edge activator) showed nanosized spherical vesicles (273.15 ± 2.90 nm) and high entrapment efficiency percent (95.47 ± 2.57%). Results also revealed that the optimum UBs formulation exhibited superior ex vivo drug flux through rabbit cornea when compared with conventional bilosomes, niosomes, and drug suspension. Furthermore, in vivo ocular tolerance and histopathological studies conducted using male albino rabbits proved the safety of the fabricated UBs after topical ocular application. Overall, the obtained results confirmed that UBs could be promising for ocular drug delivery.
**Keywords:** Ultradeformable Bilosomes, Corneal Permeation, Histopathology, Antifungal, Edge Activator

## M-638. Novel Instantly-Soluble Transmucosal Matrix (ISTM) Using Dual Mechanism Solubilizer for Sublingual and Nasal Delivery of Dapoxetine Hydrochloride: In-Vitro/In-Vivo Evaluation

Shahinaze A. Fouad, Rehab N. Shamma, Emad B. Basalious, Mohamed A. El-Nabarawi and Saadia A. Tayel

*International Journal of Pharmaceutics, 505: 212-222 (2016) IF: 3.994*

Dapoxetine (D) suffers from poor oral bioavailability (42%) due to extensive first pass metabolism. The usefulness of transmucosal (sublingual and intranasal) drug delivery to improve bioavailability of D, a weak basic drug, has been hampered by its poor solubility in the neutral pH of the body fluids. In this study, instantly-soluble transmucosal matrices (ISTMs) of D, containing dual mechanism solubilizer (Pluronic F-127/citric acid mixture), were prepared by lyophilization technique to enhance matrix disintegration, dissolution and transmucosal permeation. The matrices were evaluated for in-vitro disintegration, wetting time, in-vitro dissolution, ex vivo transmucosal permeation, scanning electron microscopy and in-vivo studies. Dissolution studies confirmed the higher ability of ISTMs to enhance the early time point dissolution and maintain complete drug dissolution in pH 6.8 compared to conventional lyophilized matrices. The optimized ISTM gave approximately 77.54 and 88.40 folds increase of D dissolution after 1 and 3 min relative to the drug powder in pH 6.8. ISTMs containing the highest F127 concentration (2%) and the lowest gelatin and mannitol concentrations (1%) exhibited the shortest in-vitro disintegration times ( < 10 s), the fastest dissolution in the neutral pH of body fluids (~ 99% in 3 min) and the highest enhancement of transmucosal permeation. The relative bioavailabilities of D after sublingual and intranasal administration of ISTMs to rabbits were about 124.58% and 611.15%, respectively, in comparison to the oral market tablet. The significant increase of drug dissolution in nasal fluids, rapid permeation rate together with the improved bioavailability propose that ISTMs could be promising for intranasal delivery of drugs suffering from oral hepatic metabolism and have limited solubility in nasal fluids.
**Keywords:** Weak Basic Drug; Dapoxetine; Premature Ejaculation; Instantly-Soluble Transmucosal Matrices; Intranasal; Dual Mechanism Solubilizer

## M-639. Efficacy and Safety of ABT-126 in Subjects with Mild-to-Moderate Alzheimer'S Disease on Stable Doses of Acetylcholinesterase Inhibitors: A Randomized, Double-Blind, Placebo-Controlled Study

Hana Florian, Andreas Meier, Serge Gauthier, Stanley Lipschitz, Yunzhi Lina, Qi Tang, Ahmed A. Othman, Weining Z. Robieson and Laura M. Gault

*Journal of Alzheimer's Disease, 51: 1237-1247 (2016) IF: 3.92*

**Background:** ABT-126 is a potent, selective α7 nicotinic acetylcholine receptor agonist with putative procognitive effects as a monotherapy in treating Alzheimer's disease (AD). **Objective:** This randomized, double-blind, placebo-controlled multicenter study (NCT01549834) investigated the efficacy and safety of ABT-126 in subjects with mild-to-moderate AD who were taking stable doses of acetylcholinesterase inhibitors (AChEIs). **Methods:** Subjects received 25 mg ABT-126 (n = 143), 75 mg ABT-126 (n = 145), or placebo (n = 146) once daily for 24 weeks. Subjects who completed the 24-week double-blind study were eligible to enroll in a 28-week open-label extension study (NCT01690195) and received 75 mg ABT-126 daily. The primary efficacy endpoint was the change from baseline to week 24 in the 11-item total score of the Alzheimer's Disease Assessment Scale– Cognitive Subscale (ADAS-Cog). **Results:** Neither dose of ABT-126 demonstrated significant improvement compared with placebo in the primary efficacy endpoint. However, 25 mg ABT-126 demonstrated significant improvement compared with placebo in ADAS-Cog scores at week 4 (least squares mean difference, –1.21; standard error, 0.51; $p < 0.010$, one-sided); 75 mg ABT-126 did not demonstrate significant improvements in ADAS-Cog scores compared with placebo at any time point. A treatment effect was not observed for any secondary efficacy measures of cognition, function, or global improvement. ABT-126 was generally well tolerated; the most common adverse events were agitation, constipation, diarrhea, fall, and headache. **Conclusions:** Overall, the efficacy profile of ABT-126 did not warrant further development as add-on therapy to AChEIs to treat mild-to-moderate AD.

**Keywords:**ABT-126, Nicotinic Receptors, Alzheimer'S Disease, Cognition

## M-640. Therapeutic Protein–Drug Interaction Assessment for Daclizumab High-Yield Process in Patients with Multiple Sclerosis Using a Cocktail Approach

Jonathan Q. Tran, Ahmed A. Othman, Paul Wolstencroft and Jacob Elkins

*British Journal of Clinical Pharmacology, 82: 160-167 (2016) IF: 3.83*

**Aims** To characterize the potential effect of daclizumab high-yield process (DAC HYP), a monoclonal antibody that blocks the high-affinity interleukin-2 receptors for treatment of multiple sclerosis, on activity of cytochrome P450 (CYP) enzymes. **Methods** Twenty patients with multiple sclerosis received an oral cocktail of probe substrates of CYP1A2 (caffeine 200 mg), CYP2C9 (warfarin 10 mg/vitamin K 10 mg), CYP2C19 (omeprazole 40 mg), CYP2D6 (dextromethorphan 30 mg) and CYP3A (midazolam 5 mg) on two sequential occasions: 7 days before and 7 days after subcutaneous administration of DAC HYP 150 mg every 4 weeks for three doses. Serial pharmacokinetic blood samples up to 96 h post dose and 12-h urine samples were collected on both occasions. Area under the curve (AUC) for caffeine, S-warfarin, omeprazole and midazolam, and urine dextromethorphan to dextrorphan ratio were calculated. Statistical analyses were conducted on log-transformed parameters using a linear mixed-effects model. **Results** The 90% confidence intervals (CIs) for the geometric mean ratio (probe substrate with DAC HYP/probe substrate alone) for caffeine AUC from 0–12 h (0.93–1.15), S-warfarin AUC from 0 to infinity (AUC[0–inf]) (0.95–1.06), omeprazole AUC(0–inf) (0.88–1.13) and midazolam AUC(0–inf) (0.89–1.15) were within the no-effect boundary of 0.80–1.25. The geometric mean ratio for urine dextromethorphan to dextrorphan ratio was 1.01, with the 90% CI (0.76–1.34) extending slightly outside the no-effect boundary, likely due to high variability with urine collections and CYP2D6 activity. **Conclusions** DAC HYP treatment in patients with multiple sclerosis had no effect on CYP 1A2, 2C9, 2C19, 2D6 and 3A activity.

**Keywords:** Cyp, Daclizumab High-Yield Process, Drug Cocktail, Therapeutic Protein–Drug Interaction

## M-641. Population PK–PD Analyses of CD25 Occupancy, CD56bright NK Cell Expansion, and Regulatory T Cell Reduction by Daclizumab Hyp in Subjects with Multiple Sclerosis

Lei Diao, Yaming Hang, Ahmed A. Othman, Devangi Mehta, Lakshmi Amaravadi, Ivan Nestorov and Jonathan Q. Tran

*British Journal of Clinical Pharmacology, 82: 1333-1342 (2016) IF: 3.83*

**Aim** Daclizumab high yield process (HYP) is a humanized IgG1 monoclonal antibody that binds to the α-subunit of the interleukin-2 receptor and is being developed for treatment of multiple sclerosis (MS). This manuscript characterized the pharmacokinetic–pharmacodynamic (PK–PD) relationships of daclizumab HYP in subjects with MS. Methods Approximately 1400 subjects and 7000 PD measurements for each of three biomarkers [CD25 occupancy, CD56bright natural killer (NK) cell count, regulatory T cell (Treg) count] from four clinical trials were analyzed using non-linear mixed effects modelling. Evaluated regimens included 150 or 300 mg subcutaneous (s.c.) every 4 weeks. **Results** CD25 occupancy was characterized using a sigmoidal maximum response (Emax) model. Upon daclizumab HYP treatment, CD25 saturation was rapid with complete saturation occurring after approximately 7 h and maintained when daclizumab HYP serum concentration was ≥5 mg l-1. After the last 150 mg s.c. dose, unoccupied CD25 returned to baseline levels in approximately 24 weeks, with daclizumab HYP serum concentration approximately ≤1 mgl-11L. CD56bright NK cell expansion was characterized using an indirect response model. Following daclizumab HYP 150 mg s.c. every 4 weeks, expansion plateaus approximately at week 36, at which the average maximum expansion ratio is 5.2. After the last dose, CD56bright NK cells gradually declined to baseline levels within 24 weeks. Treg reduction was characterized by a sigmoidal Emax model. Average maximum reduction of 60% occurred approximately 4 days post 150 mg s.c. dose. After the last dose, Tregs were projected to return to

baseline levels in approximately 20 weeks. **Conclusions** Robust PK–PD models of CD25 occupancy, CD56bright NK cell expansion and Treg reduction by daclizumab HYP were developed to characterize its key pharmacodynamic effects in the target patient population.
**Keywords:**CD56bright NK Cells, Daclizumab Hyp, Multiple Sclerosis, PK–PD, CD25 Occupancy, Regulatory T Cells

## M-642. Formulation of Avanafil in a Solid Self-Nanoemulsifying Drug Delivery System for Enhanced Oral Delivery

Kareem AbuBakr Soliman, Howida Kamal Ibrahim and Mahmoud Mohammed Ghorab

*European Journal of Pharmaceutical Sciences, 93: 447-455 (2016) IF: 3.773*

Avanafil was incorporated into solid self-nanoemulsifying systems with the aim of improving its oral bioavailability. Labrafil, Labrafac, and Miglyol 812 N were investigated as oils, Tween 80 and Cremophor EL as surfactants, and Transcutol HP as a co-surfactant. Nine formulations produced clear solutions of 13.89-38.09nm globules after aqueous dilution. Adsorption of preconcentrate onto Aeroperl 300 Pharma at a 2:1 ratio had no effect on nanoemulsion particle size. Differential scanning calorimetry, X-ray diffraction, and scanning electron microscopy indicated that avanafil was molecularly dispersed within the solid nanosystems. A formulation containing 10% Labrafil, 60% Tween 80, and 30% Transcutol HP had the highest drug loading (44.48mg/g) and an acceptable in vitro dissolution profile (96.42% within 30min). This formulation was chemically and physically stable for 6months under accelerated storage conditions and it produced a 3.2-fold increase in bioavailability in rabbits, as compared to conventional commercially available avanafil tablets (Spedra(®)).
**Keywords:** Aeroperl; Amorphous; Bioavailability; Dissolution; Nanoemulsion; Stability

## M-643. Intranasal Haloperidol-Loaded Miniemulsions for Brain Targeting: Evaluation of Locomotor Suppression and in-Vivo Biodistribution

El-Setouhy DA, Ibrahim AB, Amin MM, Khowessah OM and Elzanfaly ES.

*European Journal of Pharmaceutical Sciences, 92: 244-254 (2016) IF: 3.773*

Haloperidol is a commonly prescribed antipsychotic drug currently administered as oral and injectable preparations. This study aimed to prepare haloperidol intranasal miniemulsion helpful for psychiatric emergencies and exhibiting lower systemic exposure and side effects associated with non-target site delivery. Haloperidol miniemulsions were successfully prepared by spontaneous emulsification adopting 23 factorial design. The effect of three independent variables at two levels each namely; oil type (Capmul®-Capryol™90), lipophilic emulsifier type (Span 20–Span 80) and HLB value (12–14) on globule size, PDI and percent locomotor activity inhibition in mice was evaluated. The optimized formula (F4, Capmul®, Tween 80/Span 20, HLB 14) showed globule size of 209.5 ± 0.98 nm, PDI of 0.402 ± 0.03 and locomotor inhibition of 83.89 ± 9.15% with desirability of 0.907. Biodistribution study following intranasal and intravenous administration of the radiolabeled 99mTc mucoadhesive F4 revealed that intranasal administration achieved 1.72-fold higher and 6 times faster peak brain levels compared with intravenous administration. Drug targeting efficiency percent and brain/blood exposure ratios remained above 100% and 1 respectively after intranasal instillation compared to a maximum brain/blood exposure ratio of 0.8 post intravenous route. Results suggested the CNS delivery of major fraction of haloperidol via direct transnasal to brain pathway that can be a promising alternative to oral and parenteral routes in chronic and acute situations. Haloperidol concentration of 275.6 ng/g brain 8 h post intranasal instillation, higher than therapeutic concentration range of haloperidol (0.8 to 5.15 ng/ml), suggests possible sustained delivery of the drug through nasal route
**Keywords:** Haloperidol; Psychiatric Emergencies; Intranasal Delivery;Miniemulsions

## M-644. Laminated Sponges as Challenging Solid Hydrophilic Matrices for the Buccal Delivery of Carvedilol Microemulsion Systems: Development and Proof of Concept Via Mucoadhesion and Pharmacokinetic Assessments in Healthy Human Volunteers

Ahmed Abd-Elbary, Amna M.A. Makky, Mina Ibrahim Tadros and Ahmed Adel Alaa-Eldin

*European Journal of Pharmaceutical Sciences, 82: 31-44 (2016) IF: 3.773*

Carvedilol (CVD) suffers from low absolute bioavailability (25%) due to its limited aqueous solubility and hepatic first-pass metabolism. Hydroxypropyl methylcellulose (HPMC) laminated buccal sponges loaded with CVD microemulsions (CVD-ME) were exploited to surmount such limitations. Six pseudoternary-phase diagrams were constructed using Capmul® MCM C8/Capmul® PG8, Tween® 80, propylene glycol and water. Six CVD-ME systems (0.625% w/v) were incorporated into HPMC core sponges backed with Ethocel® layers. The sponges were preliminary evaluated via FT-IR, DSC and XRD. The surface pH, morphology and in vitro drug release studies were evaluated. In vivo mucoadhesion and absorption studies of the best achieved laminated sponges (F4) were assessed in healthy volunteers. CVD-ME systems displayed nano-spherical clear droplets. The sponges showed interconnecting porous matrices through which CVD was dispersed in amorphous state. No intermolecular interaction was detected between CVD and HPMC. The surface pH values were almost neutral. The sponges loaded with CVD-ME systems showed more sustained-release profiles than those loaded with CVD-powder. Compared to Dilatrend® tablets, the significantly ($P < 0.05$) higher bioavailability (1.5 folds), delayed Tmax and prolonged MRT(0–∞) unraveled the dual-potential of F4 sponges for water-insoluble drugs, like CVD, in improving drug oral bioavailability and in controlling drug release kinetics via buccal mucosa.
**Keywords:** Carvedilol; Buccal Delivery; Solidification of Microemulsions; Laminated Sponges.

## M-645. Transbuccal Delivery of Betahistine Dihydrochloride from Mucoadhesive Tablets with a Unidirectional Drug Flow: in Vitro, Ex Vivo and in Vivo Evaluation

Mohamed A El-Nabarawi, Adel A Ali, Heba M Aboud and Amira H Hassanand Amany H Godah

*Drug Design, Development and Therapy, 10: 4031-4045 (2016) IF: 2.881*

**Objective:** Betahistine dihydrochloride (BH.2HCl), an anti-vertigo histamine analog used in the treatment of Ménière's disease, undergoes extensive first-pass metabolism and suffers from short biological half-life. The aim of the present work was to develop and estimate controlled release mucoadhesive buccal tablets of BH.2HCl with a unidirectional drug flow to overcome this encumbrance. **Methods:** A direct compression method was adopted for preparation of the tablets using mucoadhesive polymers like guar gum, hydroxypropyl methyl cellulose K4M, sodium carboxymethyl cellulose and their combinations. The tablets were coated from all surfaces except one surface with a solution of 5% (w/v) cellulose acetate and 1% (w/v) dibutyl phthalate. Different permeation enhancers like 2% sodium deoxycholate, 2% sodium cholate hydrate (SCH) and 5% menthol were tested. Swelling index, ex vivo residence time, mucoadhesion strength, in vivo testing of mucoadhesion time, in vitro dissolution and ex vivo permeation were carried out. Furthermore, compatibility and accelerated stability studies were performed for the drug excipients. Finally, drug bioavailability of the BH.2HCl-optimized buccal mucoadhesive formulation was compared with that of the orally administered Betaserc® 24 mg tablet in six healthy male volunteers. **Results:** Formulation F10, which contained a combination of 35% guar gum and 5% sodium carboxymethyl cellulose, exhibited long adhesion time, high adhesion strength and diminished irritation to volunteers and showed zero-order release kinetics. SCH produced a significant enhancement in permeation of BH.2HCl across buccal mucosa. BH.2HCl-optimized buccal mucoadhesive formulation showed percentage relative bioavailability of 177%. **Conclusion:** The developed mucoadhesive tablets represent a promising alternative for the buccal delivery of BH.2HCl.
**Keywords:** Betahistine Dihydrochloride, Transbuccal Delivery, Unidirectional Drug Flow, Permeation Enhancer, Relative Bioavailability

## M-646. HPLC–DAD–MS/MS Profiling of Standardized Rosemary Extract and Enhancement of its Anti-Wrinkle Activity by Encapsulation in Elastic Nanovesicles

Shahira M. Ezzat, Maha M. Salama, Aliaa N. ElMeshad, Mahmoud H. Teaima and Laila A. Rashad

*Archives of Pharmacal Research, 39(7): 912-925 (2016)IF: 2.49*

The anti-wrinkle activity of defatted rosemary extract (DER) was assessed, and its effect was optimized by encapsulation in transferosomes (TFs). DER was standardized to a rosmarinic acid content of 4.58 ± 0.023 mg% using reversed-phase high performance liquid chromatography (Rp-HPLC), and its components were identified by HPLC-diode array detection-tandem mass spectrometry. In vitro free radical scavenging assays showed DER had high free radical scavenging activity against 2,2-diphenyl-2-picryl hydrazyl, 2,2′-azino-bis(3-ethylbenzothiazoline-6-sulfonic acid), and superoxide radicals. DER also inhibited bleaching of β-carotene with high Fe(III) and Fe(II) chelating ability. In vivo anti-wrinkle activities of topically applied DER (20, 50, and 100 mg) and a TF formulation (TF4, 20 mg of DER) were evaluated in UVB-irradiated mice using a wrinkle scoring method, metalloproteinase (MMP) expression, and histopathology. Among the nanovesicles, TF4 was the most deformable, and had an acceptable size and encapsulation efficiency and enhanced permeation of DER through rat skin compared with unencapsulated DER. DER (50 and 100 mg) and TF4 significantly inhibited MMP-2 and MMP-9 expression and improved wrinkle scores. DER and TF4 moderately decreased epidermal thickness without pigmentation. DER is a potent natural antioxidant for combating skin aging. Moreover, encapsulation of DER in TFs will enhance its skin permeation and anti-wrinkle activity.
**Keywords:**HPLC–DAD-MS/MS-Transferosome-Antioxidant-Anti-Wrinkle-Skin Permeability

## M-647. Nanoparticles as Tool for Enhanced Ophthalmic Delivery of Vancomycin: A Multidistrict-Based Microbiological Study, Solid Lipid Nanoparticles Formulation and Evaluation

Carol Yousry, Rania Hassan Fahmy, Tamer Essam, Hanan M. El-laithy and Seham A. Elkheshen

*Drug Development and Industrial Pharmacy, 42: 1752-1762 (2016) IF: 2.429*

**Context:** A microbiological multidistrict-based survey from different Egyptian governorates was conducted to determine the most prevalent causative agents of ocular infections in the Egyptian population. Antibiotic sensitivity testing was then performed to identify the most potent antimicrobial agent. Vancomycin (VCM) proved the highest activity against gram-positive Staphylococcus bacteria, which are the most commonly isolated causative agents of ocular infection. However, topically applied VCM suffers from poor ocular bioavailability because of its high molecular weight and hydrophilicity. **Objective:** The aim of the present study was to develop VCM-loaded solid lipid nanoparticles (SLNs) using water-in-oil-in-water (W/O/W) double emulsion, solvent evaporation technique to enhance ocular penetration and prolong ophthalmic residence of VCM. Method: Two consecutive full factorial designs (24 followed by 32) were adopted to study the effect of different formulation and process parameters on SLN formulation. The lipid type and structure, polyvinyl alcohol (PVA) molecular weight and concentration, sonication time, as well as lipid:drug ratio were studied as independent variables. The formulated SLN formulae were evaluated for encapsulation efficiency (EE%), particle size (PS), and zeta potential as dependent variables. **Results:** The statistically-optimized SLN formula (1:1 ratio of glyceryltripalmitate:VCM with 1% low molecular weight PVA and 1 min sonication time) had average PS of 277.25 nm, zeta potential of −20.45, and 19.99% drug encapsulation. Scanning and transmission electron micrographs showed well-defined, spherical, homogenously distributed particles. **Conclusion:** The present study suggests that VCM incorporation into SLNs is successfully achievable; however, further studies with different

nanoencapsulation materials and techniques would be valuable for improving VCM encapsulation.
**Keywords:** Egypt, Multi-District Microbiological Survey, Ocular Infection, Solid Lipid Nanoparticles, Vancomycin

## M-648.Development of a Taste-Masked Oral Suspension of Clindamycin Hcl Using Ion Exchange Resin Amberlite IRP 69 for Use in Pediatrics

Alaadin Alayoubi, Baher Daihom, Hitesh Adhikari, Sanjay Mishra, Richard Helms and Hassan Almoazen

*Drug Development and Industrial Pharmacy, 42, (10): 1579-1589 (2016) IF: 2.429*

**Purpose:** The purpose of this study is to develop an oral suspension of clindamycin resin complex for the potential use in pediatrics. **Methods:** Several types of Ion exchange resins were screened for their binding efficiency with clindamycin. In order to develop a suspension formulation, several thickening agents, surfactants, sweeting, and flavoring agents were evaluated for their influence on the release of clindamycin from resinate. Rheological studies were also conducted to select the optimum amounts of the suspending agents. The release profiles of clindamycin in SGF and SIF were also evaluated from freshly prepared suspension and from suspension formulation after storage for 1 month at 25 °C and 40 °C. Clindamycin bitterness threshold was determined based on volunteers' evaluation, and taste evaluation was conducted in 12 adult volunteers who evaluated the taste of the optimized suspension against clindamycin solution. **Results:** Among all resins tested, Amberlite IRP 69 showed the highest binding efficiency to clindamycin. Several excipients were selected into the suspension formulation based on no or minimum influence on the release of clindamycin from the resinate complex. Moreover, xanthan gum was selected as the optimal suspending agent for the suspension. Clindamycin release profiles in SGF or SIF showed 90% release within 30 min from freshly prepared sample. Clindamycin exhibited good stability profiles at 25 °C and 40 °C over 1 month storage. The mean bitterness threshold of clindamycin was 12.5 µg/ml, and taste evaluation study in adults showed sustainable taste improvement for suspension over clindamycin solution. **Conclusion:** Clindamycin/resin complexation has shown to be an efficient method to mask the taste of clindamycin and was developed into a suspension formulation that can be used in pediatrics.
**Keywords:** Amberlite IRP 69, Clindamycin, Ion Exchange Resin, Pediatric Formulations, Taste Masking

## M-649. Development and Physicochemical Characterization of Clindamycin Resinate for Taste Masking in Pediatrics

Baher Daihom, Alaadin Alayoubi, Dejian Ma, Lijia Wang, Sanjay Mishra, Richard Helms and Hassan Almoazen

*Drug Development and Industrial Pharmacy, 42 (10): 1600-1608 (2016) IF: 2.429*

**Purpose:** To evaluate the physicochemical characteristics of clindamycin HCl in a complex form (resinate) with ion exchange resin (IER) (Amberlite IRP69). **Methods:** Drug–resin complex was prepared by simple aqueous binding method. Drug binding study was carried out at different drug and resin concentrations. Several physicochemical characterization studies were conducted to evaluate the resinate complex. These studies included flow properties, in vitro drug release in SGF and SIF, DSC, TGA, mass spectroscopy and XPRD evaluations. In addition, stability study of resinate complex was conducted at 25 and 40 °C for up to 1 month. **Results:** Clindamycin and Amberlite IRP69 have formed a complex (resinate) and have shown good flow properties, good thermal properties and chemical stability (short term over 4 weeks) at 25 and 40 °C. Clindamycin release profiles from resinate in SGF and SIF have shown immediate release characteristics and release in simulated saliva has shown dependence on water volume. **Conclusion:** The clindamycin stable complex with IER (Amberlite IRP69) has the potential for further development as a compatible pediatric liquid formulation (suspension) or a fast disintegrating tablet.
**Keywords:** Clindamycin Hcl, Ion Exchange Resin, IRP69, Pediatric Formulations, Taste Masking

## M-650.Development, Optimization, and Evaluation of Carvedilol-Loaded Solid Lipid Nanoparticles for Intranasal Drug Delivery

Heba M. Aboud, Mohammed H. El komy, Adel A. Ali, Shahira F. El-Menshawe and Ahmed Abd Elbary

*AAPS Pharmscitech, 17: 1353-1365 (2016) IF: 1.954*

Carvedilol, a beta-adrenergic blocker, suffers from poor systemic availability (25%) due to firstpass metabolism. The aim of this work was to improve carvedilol bioavailability through developing carvedilol-loaded solid lipid nanoparticles (SLNs) for nasal administration. SLNs were prepared by emulsion/solvent evaporation method. A 23 factorial design was employed with lipid type (Compritol or Precirol), surfactant (1 or 2% w/v poloxamer 188), and co-surfactant (0.25 or 0.5% w/v lecithin) concentrations as independent variables, while entrapment efficiency (EE%), particle size, and amount of carvedilol permeated/unit area in 24 h (Q24) were the dependent variables. Regression analysis was performed to identify the optimum formulation conditions. The in vivo behavior was evaluated in rabbits comparing the bioavailability of carvedilol after intravenous, nasal, and oral administration. The results revealed high drug EE% ranging from 68 to 87.62%. Carvedilol-loaded SLNs showed a spherical shape with an enriched core drug loading pattern having a particle size in the range of 66 to 352 nm. The developed SLNs exhibited significant high amounts of carvedilol permeated through the nasal mucosa as confirmed by confocal laser scanning microscopy. The in vivo pharmacokinetic study revealed that the absolute bioavailability of the optimized intranasal SLNs (50.63%) was significantly higher than oral carvedilol formulation (24.11%). Hence, we conclude that our developed SLNs represent a promising carrier for the nasal delivery of carvedilol.
**Keywords:** Bioavailability; Carvedilol; Factorial Design; Intranasal; Solid Lipid Nanoparticles.

## M-651. Design, Optimization, and Evaluation of A Novel Metronidazole-Loaded Gastro-Retentive Ph-Sensitive Hydrogel

Galal M. El-Mahrouk, Mona H. Aboul-Einien and Amal I. Makhlouf

*AAPS Pharmscitech, 17: 1285-1297 (2016) IF: 1.954*

Floating pH-sensitive chitosan hydrogels containing metronidazole were developed for the eradication of Helicobacter pylori from the stomach. Hydrogels were prepared by crosslinking medium or high molecular weight chitosan in lyophilized solutions containing metronidazole using either citrate or tripolyphosphate (TPP) salts at 1% or 2% concentration. A 2^3 factorial design was developed to study the influence of formulation parameters on the physical characteristics of the prepared hydrogels. The interaction between hydrogel components was investigated. The morphology of the prepared hydrogels was inspected and their percentage swelling, release pattern, and moisture content were evaluated. The results revealed the absence of interaction between hydrogel components and their highly porous structure. Percentage swelling of the hydrogels was much higher, and drug release was faster in gastric pH compared with intestinal pH. The formula prepared using 2% high molecular weight chitosan and 2% TPP significantly swelled (700%) within the first 4 h and released the loaded drug over a period of 24 h. Its moisture content was not affected by storage at high relative humidity. Therefore, this formula was selected to be tested in dogs for its gastric retention (using X-ray radiography) and efficacy in the eradication of H. pylori (using histopathological and microbiological examination). The results revealed that the prepared hydrogel formula was retained in dog stomach for at least 48 h, and it was more effective against H. pylori than the commercially available oral metronidazole tablets (Flagyl®).

**Keywords:** Chitosan, Floating Drug Delivery System, Gastric Retention, Metronidazole, Ph-Sensitive Swelling

## M-652. Formulation of Venlafaxine for Once Daily Administration Using Polymeric Material Hybrids

Howida Kamal Ibrahim and Salwa Salah

*Journal of Microencapsulation, 33: 299-306 (2016) IF: 1.631*

**Objective:** Controlled release venlafaxine for once daily administration. **Methods:** Drug resin complexation followed by polymer encapsulation. A 41.21 factorial design was used to study the effect of polymer type and core: coat ratio on the release profile and kinetics. Polymer combinations were tried for optimisation adapting the desirability function. The optimised formula was tested in rabbits against commercial extended release capsules. **Results:** Poly-epsilon-caprolactone, poly(D, L-lactide-co-glycolide) ester and poly(D, L-lactide) ester polymers were more efficient in lowering the release rate and the initial burst release than EudragitVRRS100.Encapsulation at 1:1 ratio ensured complete coats and drug release sustainment. Formula prepared using 50:50 PLA/Eudragit at 1:1 ratio sustained the drug release up to 24 h with low burst release. This formula had higher venlafaxine absorption in rabbits compared to the commercial capsules. **Conclusions:** The optimised formula is superior to the available once-daily trials regarding enhanced bioavailability, dosage form versatility and ease of scaling up.

**Keywords:** Once Daily Dosing; Microcapsules; Drug Resinate; Venlafaxine Hcl; Mathematical Modelling

## M-653. Rapidly Disintegrating Vagina Retentive Cream Suppositories of Progesterone: Development, Patient Satisfaction and in Vitro/in Vivo Studies

Ehab Rasmy Bendas and Emad B. Basalious

*Pharmaceutical Development and Technology, 21: 288-295 (2016) IF: 1.566*

Our objective was to develop novel vagina retentive cream suppositories (VRCS) of progesterone having rapid disintegration and good vaginal retention. VRCS of progesterone were prepared using oil in water (o/w) emulsion of mineral oil or theobroma oil in hard fat and compared with conventional vaginal suppositories (CVS) prepared by hard fat. VRCS formulations were tested for content uniformity, disintegration, melting range, in vitro release and stability studies. The most stable formulation (VRCS I) was subjected to scaling-up manufacturing and patients' satisfaction test. The rapid disintegration, good retentive properties are applicable through the inclusion of emulsified theobroma oil rather than hydrophilic surfactant into the hard fat bases. The release profile of progesterone from VRCS I showed a biphasic pattern due to the formation of progesterone reservoir in the emulsified theobroma oil. All volunteers involved in patients' satisfaction test showed high satisfactory response to the tested formulation (VRCS). The in vivo pharmacokinetic study suggests that VRCS of progesterone provided higher rate and extent of absorption compared to hard fat based suppositories. Our results proposed that emulsified theobroma oil could be promising to solve the problems of poor patients' satisfaction and variability of drug absorption associated with hard fat suppositories.

**Keywords:** Dropping Out, Emulsified Oil, Hard Fat, Polyoxylglycerides, Rapidly Disintegrated Suppositories, Vagina Retentive

## M-654. Sumatriptan Succinate Sublingual Fast Dissolving Thin Films: Formulation and in Vitro/in Vivo Evaluation

Saadya A. Tayel, Mohamed A. El Nabarawi, Maha M. Amin and Mohamed H. Abou Ghaly

*Pharmaceutical Development and Technology, 21(3): 328-337 (2016) IF: 1.566*

Sumatriptan succinate (SS) is a 5-HT1 receptor agonist used in the treatment of migraine having poor bioavailability (15%) due to its extensive first-pass effect. The aim of this work was to prepare SS sublingual fast dissolving thin films (SFDTFs) allowing the drug to directly enter the systemic circulation and bypassing the first-pass metabolism. Plain thin films were prepared using solvent casting technique adopting 23x3 factorial design to study the effect of polymer and plasticizer type and concentration on mechanical properties and in vitro disintegration time of the plain prepared films using Design-Expert. Medicated films were prepared after addition of 35mg SS to each of the two selected plain formulae (F6 and F7) having desirability values above 0.9 showing the values of: 0.038, 0.039 kgf/mm2 and 156.24, 164.16% and 0.0248, 0.0240 kgf/mm2 as

tensile strength, percent elongation and elastic modulus, respectively. PVP K30 was efficient as crystallization inhibitor in retarding SS crystallization. Pharmacokinetic study of the optimum formula F7 (PVP K30:SS (1:1 w/w)) in healthy human volunteers using LC/MS/MS revealed a shorter tmax (0.25 h) compared to Imitrex tablet 25mg (2 h) which is considered promising especially for the rapid relief of acute migraine attacks.

**Keywords:** Crystallization Inhibition, Lc/Ms/Ms, Modified In Vitro Disintegration Test, Sublingual Film, Sumatriptan Succinate

## M-655. Effect of Formulation Variables on Design, In-Vitro Evaluation of Valsartan Snedds and Estimation of its Antioxidant Effect in Adrenaline Induced Acute Myocardial Infarction in Rats

Maha M. Amin, Omaima N. El Gazayerly, Nabaweya A. Abd El-Gawad, Shady M. Abd El-Halim and Sally A. El-Awdan

*Pharmaceutical Development and Technology, 21: 909-920 (2016) IF: 1.566*

Valsartan is a specific angiotensin II antagonist used for the treatment of hypertension. It suffers from low aqueous solubility and high variability in its absorption after oral administration. The aim of this study was to improve the dissolution and thereby the bioavailability of Valsartan through the development of self nano-emulsifying drug delivery systems. Four ternary phase diagrams were constructed to identify the self-emulsification region of Capmul® MCM, Labrafil® M1944, Capryol™ 90 and Labrafac® PG together with Cremophore® RH 40 and Transcutol™ HP as oil, surfactant and co-surfactant, respectively. The effect of oil type, oil and surfactant concentration on droplet size and in vitro Valsartan dissolution were studied. The protective effect of the optimum formula F5 in adrenaline-induced oxidative stress in rats during myocardial infarction was determined. Formula F5 exhibited globule size of (13.95 nm) with 76.07% ± 1.10 of Valsartan dissolved after five minutes compared to Disartan 80 mg capsules (13.43%). Results revealed a significant reduction ($p < 0.05$) in serum aspartate transaminase, creatine kinase myocardial band and malondialdehyde levels, while a significant increase ($p < 0.05$) in serum glutathione in F5. Therefore, self nano-emulsifying drug delivery systems could be considered as a promising approach to improve the dissolution and thereby the bioavailability of Valsartan.

**Keywords:** Angiotensin Ii Antagonist, Bcs Class Ii, Oxidative Stress, Ternary Phase Diagram

## M-656.Ufasomes Nano-Vesicles-Based Lyophilized Platforms for Intranasal Delivery of Cinnarizine: Preparation, Optimization, Ex-Vivo Histopathological Safety Assessment and Mucosal Confocal Imaging

Alaa Hamed Salama and Mona Hassan Aburahma

*Pharmaceutical Development and Technology, 21:6: 706-715 (2016) IF: 1.566*

To circumvent the low and erratic absorption of orally administrated cinnarizine (CN), intranasal lyophilized gels containing unsaturated fatty acid liposomes (ufasomes) and encapsulating CN were prepared from oleic acid using a simple assembling strategy. The effects of varying drug concentration and cholesterol percentage on ufasomes size, polydispersity index and entrapment efficiency were investigated using 3141 full factorial design. The optimized ufasomes that contained 14% cholesterol relative to oleic acid displayed spherical morphology with average size of 788nm and entrapment efficiency of 80.49%. To overcome the colloidal instability of CN-loaded ufasomes dispersions and their short residence time in the nasal cavity, the ufasomes were incorporated into mucoadhesive hydrogels that were lyophilized into unit dosage forms for accurate dosing. Scanning electron micrographs of the lyophilized gel revealed that the included ufasomes were intact, non-aggregating and maintained their spherical morphology. Rheological characterization of reconstituted ufasomal lyophilized gel ensured ease of application. Furthermore, the gel induced minor histopathological alterations in sheeps' nasal mucosa. Ex-vivo confocal laser imaging confirmed the ability of ufasomes to penetrate deep through nasal mucosa layers. The results highlighted in the current work confirm the feasibility of using CN-loaded ufasomal gels for intranasal drug delivery.

**Keywords:** Cinnarizine, Confocal Laser Scanning Microscopy, Intranasal Drug Delivery, Oleic Acid, Ufasomal Lyophilized Gel, Ufasomes, Unsaturated Fatty Acid Vesicles

## M-657. Formulation and Evaluation of Nanocrystals of A Lipid Lowering Agent

Dina Louis

*Iranian Journal of Pharmaceutical Research, 15(1): 71-82 (2016) IF: 1.352*

Atorvastatin calcium, the lipid lowering agent, is taken as a model drug characterized by poor water solubility and bioavailability. In this study an attempt was made for preparation of nanocrystals using high pressure homogenization. A number of stabilizers were included as well as polymers at different concentrations, and the formulations were homogenized for ten cycles at a pressure of 1000 bars. The obtained nano crystals were evaluated by determining their size, zeta potential, saturated solubility and dissolution rate. Results revealed that Formulation 3, containing (10: 1) drug to sodium lauryl sulphate ratio, possessed the highest saturated solubility and dissolution rate, and hence was analyzed by X-ray diffraction analysis, differential scanning calorimetry, Fourrier transform infrared spectroscopy and scanning electron microscopy. An in-vivo study was carried out on the successful formulation in comparison to drug powder using rats as experimental animals. A significant increase in the area under the concentration-time curve Cpmax and MRT for nanocrystals was observed in comparison to the untreated atorvastatin calcium.

**Keywords:** Atorvastatin; Bioavailability; Hhomogenization; Nanocrystals; Stabilizer.

## M-658. Labeling of Clomiphene and Biodistribution Studies for Possible Use as A Mode Li Nbreast Cancer Maging

I.T.Ibrahim, M.T.El-Kolaly, M.H.Aboumanei and A.Abdelbary

*Applied Radiation and Isotopes, 115: 37-44 (2016) IF: 1.136*

Clomiphene has growth-inhibitory effects of breast cancer cells, clomiphene was successfully labeled with 125I via direct electrophilic substitution reaction with labeling yield 97%. It was obtained at optimum substrate amount of 0.5 mg, Chloramine-T was used as an oxidizing agent at optimum amount of 25 µg. Labeling reactions was done at pH 5 at ambient temperature. This study showed good in vitro and in vivo stability of the 125I-clomiphene. The radiolabeled compound showed high ascetic fluid uptake of 18.12±0.27% at 30 min post-injection. Solid tumor uptake of 125I-clomiphene was 12.48±0.32% at 30 min post-injection. This data revealed the localization of tracer in tumor tissue with high percent sufficient to use 125I-clomiphene as a promising tool for the diagnosis of breast cancer.

**Keywords:** Antiestrogen; 125I-Clomiphene; Labeling; Biodistribution; Solid Tumor

## M-659. Chitosan-Based Thermosensitive Hydrogel for Controlled Drug Delivery to the Temporomandibular Joint

Talaat Wael M, Haider Mohamed Kawas, Sausan Al, Kandil, Nadia G, Harding and David R. K

*Journal of Craniofacial Surgery, 27: 735-740 (2016) IF: 0.7*

Intra-articular injections of hyaluronic acid (HA) and corticosteroids have been extensively used in treating temporomandibular disorders. However, rapid clearance from the site of injection is a major concern that is commonly managed by frequent dosing, which is not without complications. This study aimed to determine the suitability of thermosensitive chitosan-based hydrogels for intra-articular controlled release of drugs in the rabbit temporomandibular joint (TMJ). A series of hydrogels were prepared using different chitosan (Ch) to β-glycerophosphate (β-GP) ratios. The gelation time, swelling ratio, the shape, and surface morphology of the prepared gels were investigated to select the formulation with optimum characteristics. The left TMJ in 13 adult male New Zealand white rabbits was injected with 0.2 mL of Chitosan/β-glycerophosphate/HA while the right TMJ was injected with 0.2 mL of control solution of HA. Hyaluronic acid concentrations in experimental and control groups were measured using Hyaluronan Quantikine Enzyme-Linked Immunosorbent Assay Kit. In vitro characterization showed that both the Ch:β-GP ratio and incorporation of HA had a significant effect on gelation time, degree of swelling, and surface morphology of the hydrogels. No morphological changes were observed in the joints in both groups. The mean concentration of HA in the experimental joints after 7 days (1339.79 ± 244.98 µg/g) was significantly higher than that in the control (474.52 ± 79.36 µg/g). In conclusion, the chitosan-based thermosensitive hydrogel can be considered as a promising controlled drug release system to the TMJ in a rabbit model that would potentially overcome many of the current limitations of intra-articular formulations.

**Keywords:** Chitosan Glycerophosphate, Controlled Release, Hyaluronic Acid, Temporomandibular Disorders, Temporomandibular Joint

## M-660. Novel Mixed Hydrotropic Solubilization of Zaleplon: Formulation of Oral Tablets and in-Vivo Neuropharmacological Characterization by Monitoring Plasma Gaba Level

Ghada A. Abdelbary, Maha M. Amin and Mostafa Abdelmoteleb

*Journal of Drug Delivery Science and Technology, 33: 98-113 (2016) IF: 0.62*

Zaleplon (ZP) is a poorly water-soluble non-benzodiazepine hypnotic drug indicated for the short-term treatment of insomnia having a bioavailability of about 30%. The aim of the present study is to enhance the solubility and consequently the bioavailability of ZP using hydrotropic agents (HA). The solubility of ZP increased about 350- and 2000-fold, respectively, when 1 M of sodium benzoate and resorcinol were used as hydrotropic agents. The optimized mixed hydrotropic tablet formula (F5) composed of Resorcinol:Sodium benzoate microparticles prepared by solvent evaporation technique in a ratio of 4:1 w/w exhibits a significantly higher ($p < 0.05$) in-vitro dissolution (Q5 min) of 31.7 ± 0.11% after five minutes (Q5min) compared to 10.0 ± 0.10% for Sleep aid (5 mg) respectively. The optimized formula (F5) showed significantly higher ($p < 0.05$) GABA concentration of 122.5 ± 5.5 mg/mL in plasma compared to 118 ± 1.00 and 27.8 ± 1.5 mg/mL for Sleep aid (5 mg) and control taking only saline respectively suggesting a higher neuropharmacological effect of ZP following hydrotropic solubilization.

**Keywords:** Zaleplon; Hydrotropic Solubilization; Mixed Hydrotropy; Insomnia; Plasma Gaba Level

## M-661. Novel Chewable Colon Targeted Tablets of Bumadizone Calcium for Treatment of Ulcerative Colitis: Formulation and Optimization

Samia A. Nour, Nevine Shawky Abdelmalak and Marianne J. Naguib

*Journal of Drug Delivery Science and Technology, 35: 172-183 (2016) IF: 0.62*

The aim of the present study was the formulation of a novel chewable tablet containing the non-steroidal anti-inflammatory bumadizone calcium (BZ) to deliver the drug to the colon for the local treatment of ulcerative colitis. Colon targeted granules were prepared following 32 full factorial design. The effect of two independent variables, namely, polymer type (Eudragit ® S100, Eudragit ® L100, and a mixture of both in the ratio of 4:1) and drug to polymer ratio (1:1, 1:3& 1:5) on the % of BZ released for 12 h was studied. In order to produce chewability, candidate formulae were then mixed with different amount of maize starch and mannitol, and compressed into tablets. F11 tablets(composed of drug: Eudragit® S100 in the ratio of 1:3, 250 mg mannitol and 50 mg maize starch with a desirability of 0.925) achieved the required release profile i.e: lowest release before target area (pH 1.2 & 6.8) reaching only 11.00% at the end of the fourth hour, and 100.27% after 12 h (pH7.4).

Histopathological studies results declared clearly the ability of the chewable colon targeted tablets F11 to locally treat acetic acid induced colitis. Furthermore, the measurements of myeloperoxidase enzyme activities in colon specimens showed that F11 achieved a significantly lower levels in comparison to both untreated group and group that received the marketed tablets ($p<0.05$).
**Keywords:** Colon Targeting; Chewable Tablets; Bumadizone; Optimization; Histopathology; Myeloperoxidase

## M-662. Studies on Cleaning Validation for a Cream and Ointment Manufacturing Line

Aliaa A Badawi, Khaled Hegazy and Dina Louis

*Tropical Journal of Pharmaceutical Research, 15 (11): 2329-2335 (2016) IF: 0.543*

**Purpose:** To validate a new and simple method for cleaning a manufacturing line for creams and ointments. **Methods:** The worst case product of the line chosen was a cream containing three practically insoluble ingredients: betamethasone, tolnaftate and cliquinol. The cleaning method utilized hot water and a commercial detergent, followed by rinsing. Validation methods included the visual inspection of the machine surface, swab sampling, microbial bioburden determination and testing the final rinse for conductivity, pH and total organic carbon (TOC) limits. Acceptance limit calculations depended on the figure tip unit (FTU). **Results:** No visual residue or chemical residue was detected above 674.37 ppm, which is the maximum allowable carry-over level of the drug. Similarly, microbial bioburden was < 25 CFU/swab - the acceptable limit. Conclusion: The method adopted to get rid of insoluble drug residue and microorganism from the cream and ointment production facility was successful. The method is simple and reproducible as indicated by the results of the three cleaning cycles.
**Keywords:** Validation, Worst Case Product, Swab Sampling, Finger-Tip Unit, Acceptance Limits, Cream and Ointment Manufacturing Line

## M-663. Pharmacokinetics of Daclizumab High-Yield Process with Repeated Administration of the Clinical Subcutaneous Regimen in Patients with Relapsing-Remitting Multiple Sclerosis

Jonathan Q Tran, Ahmed A Othman, Alvydas Mikulskis, Paul Wolstencroft and Jacob Elkins

*Clinical Pharmacology: Advances and Applications,8:9-13(2016)*

**Background:** Daclizumab high-yield process (DAC HYP), a humanized immunoglobulin G1 monoclonal antibody specific for the a subunit (CD25) of the high-affinity interleukin-2 receptor, has demonstrated efficacy for treatment of relapsing forms of multiple sclerosis in Phase II and III clinical trials. **Objective:** To characterize the pharmacokinetics (PK) of DAC HYP following repeated administration of the 150 mg subcutaneous (SC) dose every 4 weeks (q4wk), the proposed clinical regimen in patients with relapsing-remitting multiple sclerosis (RRMS). **Methods:** Twenty-six patients with RRMS received DAC HYP 150 mg SC q4wk for a total of six doses. Serial PK blood samples were collected over the first and last dosing intervals and trough PK samples were collected between these doses. Blood samples for immunogenicity assessment were collected throughout the study. Serum DAC HYP levels and anti-DAC HYP antibodies were characterized using validated immunoassays. PK parameters were estimated using noncompartmental analysis. **Results:** DAC HYP showed slow SC absorption with a median time to reach maximum observed concentration (Cmax) value of ~1 week. Steady state was reached by the fourth injection. At steady state, DAC HYP mean serum Cmax, minimum observed concentration (Cmin), and area under the concentration–time curve within a dosing interval (AUCtau) values were 29.1 µg/mL, 14.9 µg/mL, and 638 µg · day/mL, respectively, with intersubject variability of 35%–40%. The AUC accumulation ratio was ~2.5 at steady state. DAC HYP had a long elimination half-life of ~22 days and low apparent clearance (0.274 L/day). Nine patients tested positive for anti-DAC HYP antibodies, with no impact on DAC HYP clearance in this limited data set. Conclusion: The PK of DAC HYP in patients with RRMS are consistent with those previously reported in healthy volunteers. The half-life of ~3 weeks and the low fluctuations in peak and trough concentrations of serum DAC HYP support the once-monthly SC dosing regimen.
**Keywords:** Pharmacokinetics, Daclizumab High-Yield Process, Multiple Sclerosis

## M-667. Formulation, Evaluation and Clinical Assessment of Gemifloxacin in Situ Gel for the Treatment of Chronic Periodontitis

Wedian Younis Abdelgawad, Magdy Ibrahim Mohamed, Mary Kamal Gad and Enji Ahmed

*International Journal of Pharmaceutical Sciences Review and Research, 38: 78-85 (2016)*

A smart drug delivery system for localized controlled release of the broad spectrum antimicrobial agent, Gemifloxacin Mesylate (GM) following insertion into the periodontal pocket was developed using the thermosensetive polymer, poloxamer 407 and the ion activated polymer, gellan gum. Many drugs do not reach the site of action in the therapeutic concentrations intended. So, in the present study, works have been done for administering the drug directly to the target site so that the efficacy of treatment can be improved. This site specific delivery of drug can thus overcome the problems faced during systemic administration of antimicrobials for the treatment of chronic periodontitis, where the drug get diluted many times before it reaches the site of action. This also reduces frequency of administration and dose size, thereby, improves patient compliance and minimizes systemic side effects. GM in situ gels were prepared by different concentrations of polymers and evaluated for physical appearance, drug content uniformity, syringeability, rheological properties, pH, gelation time, gelation temperature, in vitro gelling capacity and in vitro drug release. Drug excipients compatibility study was done by FTIR. Results showed no evidence of interaction between the drug and excipients. The selected formulation was clinically tested and the results revealed that, GM in situ gel (Containing 18 % w/w poloxamer 407 and 0.8% w/w gellan gum) showed reasonable in vitro results and good clinical improvement.
**Keywords:** : Periodontitis, Gemifloxacin Mesylate, Poloxamer 407, Gellan Gum, In Situ.

==++==

***Dept. of Pharmacognosy***

## M-670. Isoeugenol is A Selective Potentiator of Camptothecin Cytotoxicity in Vertebrate Cells Lacking TDP1

Elsayed W, El-Shafie L, Hassan MK, Farag MA and El-Khamisy SF

*Scientific Reports, 6 (2016) IF: 5.228*

Camptothecin, a topoisomerase inhibitor exhibits anti tumor activity against a wide range of tumors. Redundancy of TOP mediated repair mechanisms is a major challenge facing the efficiency of TOP targeting therapies. This study aims to uncover new TOP targeting approaches utilising a selection of natural compounds in the presence or absence of tyrosyl DNA phosphodiesterase a key TOP mediated protein-linked DNA break repair enzyme. We identify isoeugenol a phenolic ether found in plant essential oils, as a potentiator of CPT cytotoxicity in Tdp deficient but not proficient cells. Consistent with our cellular data, isoeugenol did not inhibit Tdp1 enzymatic activity in vitro nor it sensitized cells to the PARP inhibitor olaparib.
**Keywords:** Isoeugenol, Topoisomerase.

## M-666. A Comparative Metabolomics Approach Reveals Early Biomarkers for Metabolic Response to Acute Myocardial Infarction

Ali S E Farag, MA, Holvoet, P Hanafi RS and Gad. MZ

*Scientific Reports, 6: 36359-0 (2016) IF: 5.228*

Discovery of novel biomarkers is critical for early diagnosis of acute coronary syndrome (ACS). Serum metabolite profiling of ST-elevation myocardial infarction (STEMI), unstable angina (UA) and healthy controls was performed using gas chromatography mass spectrometry (GC/MS), solid-phase microextraction coupled to gas chromatography mass spectrometry (SPME-GC/MS) and nuclear magnetic resonance (H-1-NMR). Multivariate data analysis revealed a metabolic signature that could robustly discriminate STEMI patients from both healthy controls and UA patients. This panel of biomarkers consisted of 19 metabolites identified in the serum of STEMI patients. One of the most intriguing biomarkers among these metabolites is hydrogen sulfide (H2S), an endogenous gasotransmitter with profound effect on the heart. Serum H2S absolute levels were further investigated using a quantitative double-antibody sandwich enzyme-linked immunosorbent assay (ELISA). This highly sensitive immunoassay confirmed the elevation of serum H2S in STEMI patients. H2S level discriminated between UA and STEMI groups, providing an initial insight into serum-free H2S bioavailability during ACS. In conclusion, the current study provides a detailed map illustrating the most predominant altered metabolic pathways and the biochemical linkages among the biomarker metabolites identified in STEMI patients. Metabolomics analysis may yield novel predictive biomarkers that will potentially allow for an earlier medical intervention
**Keywords:** Metabolomics; Markers; Myocardial Infarction; Hydrogen Sulphide

## M-671.Hepatoprotective Effect and Chemical Assessment of a Selected Egyptian Chickpea Cultivar.

Reham H. Mekky, Mostafa R. Fayed, Mohamed R. El-Gindi, Azza R. Abdel-Monem, María del Mar Contreras, Antonio Segura-Carretero and Essam Abdel-Sattar

*Frontiers In Pharmacology, 7: 344-344 (2016) IF: 4.418*

Chickpea (Cicer arietinum) is a legume of the family Fabaceae, subfamily Faboideae. In Egypt, chickpea seeds are usually consumed at raw green and tender stage, or in the form of mature dry seeds. In our previous study, 'Giza 1' seeds exhibited stronger antioxidant activity and higher total phenol content than those from other Egyptian cultivars. In order to assess the biological potential of 'Giza 1' seeds in vivo, the extraction procedure was reproduced here. The extract was standardized using liquid chromatography coupled to diode array detector and tandem mass spectrometry (MS/MS) to evaluate their hepatoprotective effect on carbon tetrachloride (CCl4)-induced hepatotoxicity in rats and acute toxicity. Administration of the extract to rats in doses up to 2 g/Kg) did not cause any mortalities or observable signs of toxicity. Further, the plant extract showed a strong hepatoprotective activity based on assessing serum alanine aminotransferase, aspartate aminotransferase, and alkaline phosphatase and levels of albumen, globulin, total protein, total cholesterol, high density lipoprotein, triglycerides, and low density lipoprotein. The antioxidative activity was evaluated by assessing hepatic catalase and superoxide dismutase activity as well as reduced glutathione, and malondialdehyde levels. Additionally, anti-inflammatory activity was observed as the extract significantly lowered the hepatic tumor necrosis factor α content. Histopathological examination of liver tissues indicated that the extract-treated animals showed almost normal hepatic architecture with fewer pathological changes. In conclusion, the current results suggest that the chickpea extract possesses an excellent safety profile with very low acute toxicity. Also, it exhibits a significant hepatoprotective effect against CCl4-induced liver injury in rats. This can be attributed, at least partly, to the antioxidant and anti-inflammatory activity of the isoflavones and phenolic acids content of the extract.
**Keywords:** Chickpea, Cicer Arietinum, Hepatoprotection, Antioxidation, Cytotoxicity, Ld50

## M-672. Soft Corals Biodiversity in the Egyptian Red Sea Soft Corals Biodiversity in the Egyptian Red Sea: A Comparative Ms and Nmr Metabolomics Approach of Wild and Aquarium Grown Species?

Farag MA, Porzel A, Al Hammady MA, Hegazy ME, Meyer A, Mohamed TA, Westphal H and Wessjohann LA

*Journal of Proteome Research, 15: 1274-1287 (2016) IF: 4.173*

Marine life has developed unique metabolic and physiologic capabilities and advanced symbiotic relationships to survive in the varied and complex marine ecosystems. Herein metabolite composition of the soft coral genus Sarcophyton was profiled with respect to its species and different habitats along the coastal Egyptian Red Sea NMR and ultra performance liquid chromatography mass spectrometry large scale metabolomics analyses. The current study extends the application of

comparative secondary metabolite profiling from plants to corals revealing for metabolite compositional differences among its species via a comparative MS and NMR approach.
**Keywords:** Nmr, Lcms, Corals

## M-673.The Cardenolide Glycoside Acovenoside A Affords Protective Activity in Doxorubicin-Induced Cardiotoxicity in Mice

Shahira M. Ezzat, Menna El Gaafary, Abeer M. El Sayed, Omar M. Sabry, Zeinab Y. Ali, Susanne Hafner, Michael Schmiech, Lu Jin, Tatiana Syrovets and Thomas Simmet

*The Journal of Pharmacology and Experimental Therapeutics, 358: 262-270 (2016) IF: 3.76*

The current study aimed to investigate the protective effect of the cardenolide glycoside acovenoside A (AcoA) against doxorubicin-induced cardiotoxicity in mice. AcoA was isolated from the pericarps of Acokanthera oppositifolia to chemical homogeneity and characterized by means of one- and two-dimensional nuclear magnetic resonance spectroscopy. AcoA exhibited relatively low toxicity in mice (LD50 = 223.3 mg/kg bw). Repeated administration of doxorubicin induced cardiotoxicity manifested by reduced activity of myocardial membrane-bound ion pumps and elevated serum biomarkers of myocardial dysfunction, oxidative stress, and inflammation. Pretreatment of doxorubicin-exposed mice with AcoA (11.16 or 22.33 mg/kg bw, i.p.) for 2 weeks after 2 weeks of combined administration of AcoA and doxorubicin protected the animals dose dependently against doxorubicin-induced cardiotoxicity as indicated by normalization of the levels of different myocardial markers of oxidative stress (malondialdehyde, nitric oxide, total antioxidant capacity, and cardiac glutathione), serum myocardial diagnostic marker enzymes (serum cardiac troponin T, creatine kinase isoenzyme MB, aspartate aminotransferase, and lactate dehydrogenase), and inflammatory markers (c-reactive protein, tumor necrosis factor-α, and interleukin-6), as well as myocardial Na(+)/K(+)-ATPase activity. These effects were attributed to the negative impact of AcoA on transcription factors nuclear factor κB and interferon regulatory factor 3/7. Thus acovenoside A might act as a cardioprotective agent to prevent doxorubicin-induced cardiotoxicity.
**Keywords:** Acovenoside A, Doxorubicin-Induced Cardiotoxicity, Na/K Atpase

## M-674. Protocol: A Fast, Comprehensive and Reproducible One-Step Extraction Method for the Rapid Preparation of Polar and Semi-Polar Metabolites, Lipids, Proteins, Starch and Cell Wall Polymers from A Single Sample

Mohamed A. Salem, Jessica Jüppner, Krzysztof Bajdzienko and Patrick Giavalisco

*Plant Methods, 12:45: 1-15 (2016) IF: 3.449*

**Background:** The elucidation of complex biological systems requires integration of multiple molecular parameters. Accordingly, high throughput methods like transcriptomics, proteomics, metabolomics and lipidomics have emerged to provide the tools for successful system-wide investigations. Unfortunately, optimized analysis of different compounds requires specific extraction procedures in combination with specific analytical instrumentation. However, the most efficient extraction protocols often only cover a restricted number of compounds due to the different physico-chemical properties of these biological compounds. Consequently, comprehensive analysis of several molecular components like polar primary metabolites next to lipids or proteins require multiple aliquots to enable the specific extraction procedures required to cover these diverse compound classes. This multi-parallel sample handling of different sample aliquots is therefore not only more sample intensive, it also requires more time and effort to obtain the required extracts. **Results:** To circumvent large sample amounts, distributed into several aliquots for the comprehensive extraction of most relevant biological compounds, we developed a simple, robust and reproducible two-phase liquid-liquid extraction protocol. This one-step extraction protocol allows for the analysis of polar-, semi-polar and hydrophobic metabolites, next to insoluble or precipitated compounds, including proteins, starch and plant cell wall components, from a single sample. The method is scalable regarding the used sample amounts but also the employed volumes and can be performed in microcentrifuge tubes, enabling high throughput analysis. The obtained fractions are fully compatible with common analytical methods, including spectroscopic, chromatographic and mass spectrometry-based techniques. To document the utility of the described protocol, we used 25 mg of Arabidopsis thaliana rosette leaves for the generation of multi-omics data sets, covering lipidomics, metabolomics and proteomics. The obtained data allowed us to measure and annotate more than 200 lipid compounds, 100 primary metabolites, 50 secondary metabolites and 2000 proteins. **Conclusions:** The described extraction protocol provides a simple and straightforward method for the efficient extraction of lipids, metabolites and proteins from minute amounts of a single sample, enabling the targeted but also untargeted high-throughput analyses of diverse biological tissues and samples.
**Keywords:** Primary Metabolites, Secondary Metabolites, Lipids, Mtbe, Starch, Cell Wall, Proteins, Metabolomics, Lipidomics, Proteomics, Systems Biology

## M-676. Mirabolides A and B, New Cytotoxic Glycerides from the Red Sea Sponge Theonella Mirabilis

Dina R. Abou-Hussein and Diaa T. A. Youssef

*Marine Drugs, 14(8), 155: 1-11 (2016) IF: 3.345*

As a part of our continuing work to find out bioactive lead molecules from marine invertebrates, the CHCl3 fraction of the organic extract of the Red Sea sponge Theonella mirabilis showed cytotoxic activity in our primary screen. Bioassay-guided purification of the active fractions of the sponge's extract resulted in the isolation of two new glycerides, mirabolides A and B (1 and 2), together with the reported 4-methylene sterols, conicasterol (3) and swinhosterol B (4). The structures of the compounds were assigned by interpretation of their 1D (1H, 13C), 2D (COSY, HSQC, HMBC, ROESY) NMR spectral data and high-resolution mass determinations. Compounds 1–4 displayed marked cytotoxic activity against human breast adenocarcinoma cell line (MCF-7) with IC50 values of 16.4, 5.18, 6.23 and 3.0 g/mL, respectively, compared to 5.4 g/mL observed by doxorubicin as reference drug.

**Keywords:** Red Sea Sponge Theonella Mirabilis; Glycerides; Mirabolides A and B; 4-Methylene Sterols; Breast Cancer Cell Line; Cytotoxic Activity

## M-672. Antiproliferative Scalarane-Based Metabolites from the Red Sea Sponge Hyrtios Erectus

Sameh S. Elhady, Ahmed M. Al-Abd, Ali M. El-Halawany, Abdulrahman M. Alahdal, Hashim A. Hassanean and Safwat A. Ahmed

*Marine Drugs, 14: 130-0 (2016) IF: 3.345*

Two new sesterterpenes analogs, namely, 12-acetoxy,16-epi-hyrtiolide (1) and 12β-acetoxy,16β-methoxy,20α-hydroxy-17-scalaren-19,20-olide (2), containing a scalarane-based framework along with seven previously reported scalarane-type sesterterpenes (3–9) have been isolated from the sponge Hyrtios erectus (order Dictyoceratida) collected from the Red Sea, Egypt. The structures of the isolated compounds were elucidated on the basis of their spectroscopic data and comparison with reported NMR data. Compounds 1–9 exhibited considerable antiproliferative activity against breast adenocarcinoma (MCF-7), colorectal carcinoma (HCT-116) and hepatocellular carcinoma cells (HepG2). Compounds 3, 5 and 9 were selected for subsequent investigations regarding their mechanism of cell death induction (differential apoptosis/necrosis assessment) and their influence on cell cycle distribution.
**Keywords:** Red Sea Sponge; Hyrtios Erectus; Scalarane Framework; Cell Based Assay; Antiproliferative Activity

## M-677. Anti-Acetylcholinesterase Potential and Metabolome Classification of 4 Ocimum Species as Determined Via UPLC/qTOF/MS and Chemometric Tools

Farag MA, Ezzat SM, Salama MM and Tadros MG

*Journal of Pharmaceutical and Biomedical Analysis, 125: 292-302 (2016) IF: 3.169*

Ocimum is a plant of considerable commercial importance in traditional medicine worldwide as well as for the flavor and food industry. The goal of this study was to examine Ocimum extracts anti-acetylcholinesterase activity and to correlate the activity with their secondary metabolites profiles via a metabolome based ultraperformance liquid chromatography-mass spectrometry approach coupled to chemometrics. The metabolomic differences in phenolics from leaves derived from 4 Ocimum species: Ocimum basilicum, Ocimum africanum, Ocimum americanum and Ocimum minimum were assessed. Under optimized conditions, 81 metabolites were identified including 21 hydroxy cinnamic acids, 4 benzoic acid conjugates, 14C/O flavonoid conjugates, 2 alcohols, 5 acyl sugars, 4 triterpenes and 12 fatty acids. Several salviolanic acid derivatives including salviolanic acid A, B, C & I found in Salvia, were found in Ocimum herein for the first time. Unsupervised principal component analysis PCA and supervised orthogonal projection to latent structures-discriminant analysis OPLSDA were further used for comparing and classification of samples. A clear separation among the four investigated Ocimum species was revealed, with O. africanum samples found most enriched in hydroxy cinnamates conjugates and flavonoids. To the best of our knowledge, this is the first report for compositional differences among Ocimum leaves via a metabolomic approach revealing that among examined species O. africanum leaves present a better source of Ocimum bioactive metabolites. The anticholinesrase activity of examined species was further assessed with a potent IC50 values for O. americanum, O. africanum, O. basilicum ranging from 2.5 to 6.6 mgml, whereas O. minimum was least active with IC50 of 31.4 mgml. Furthermore, major HC , caftaric, chlorogenic and rosmarinic acids identified in extracts via UPLC-MS analysis exhibited IC50 values of 24, 0.5 and 7.9 mgml respectively, suggesting that HCs are likely to mediate for the anticholinesterase effect in Ocimum extracts.
**Keywords:** Ocimum; LCMS; Metabolomics

## M-679. Metabolite Profiling in Trigonella Seeds Via UPLC-MS and GC-MS Analyzed Using Multivariate Data Analyses

Farag MA, Rasheed DM, Kropf M and Heiss AG

*Analytical and Bioanalytical Chemistry, 408: 8065-8078 (2016) IF: 3.125*

Trigonella foenum-graecum is a plant of considerable value for its nutritive composition as well as medicinal effects. This study aims to examine Trigonella seeds using a metabolome-based ultra-performance liquid chromatography-mass spectrometry (UPLC-MS) in parallel to gas chromatography-mass spectrometry (GC-MS) coupled with multivariate data analyses. The metabolomic differences of seeds derived from three Trigonella species, i.e., T. caerulea, T. corniculata, and T. foenum-graecum, were assessed. Under specified conditions, we were able to identify 93 metabolites including 5 peptides, 2 phenolic acids, 22 C/O-flavonoid conjugates, 26 saponins, and 9 fatty acids using UPLC-MS. Several novel dipeptides, saponins, and flavonoids were found in Trigonella herein for the first time. Samples were classified via unsupervised principal component analysis (PCA) followed by supervised orthogonal projection to latent structures-discriminant analysis (OPLS-DA). A distinct separation among the investigated Trigonella species was revealed, with T. foenum-graecum samples found most enriched in apigenin-C-glycosides, viz. vicenins 1/3 and 2, compared to the other two species. In contrast to UPLC-MS, GC-MS was less efficient to classify specimens, with differences among specimens mostly attributed to fatty acyl esters. GC-MS analysis of Trigonella seed extracts led to the identification of 91 metabolites belonging mostly to fatty acyl esters, free fatty acids followed by organic acids, sugars, and amino acids. This study presents the first report on primary and secondary metabolite compositional differences among Trigonella seeds via a metabolomics approach and reveals that, among the species examined, the official T. foenum-graecum presents a better source of Trigonella secondary bioactive metabolites.
**Keywords:** Trigonella; Secondary Bioactive Metabolites; Lcms; Gcms

## M-678. Comparative Metabolite Profiling and Fingerprinting of Genus Passiflora Leaves Using A Multiplex Approach of UPLCMS and NMR Analyzed by Chemometric Tools

Farag MA, Otify A, Porzel A, Michel CG, Elsayed A and Wessjohann LA

*Analytical and Bioanalytical Chemistry, 408: 3125-3143 (2016) IF: 3.125*

Passiflora incarnata as well as some other Passiflora species are reported to possess anxiolytic and sedative activity and to treat various CNS disorders. The medicinal use of only a few Passiflora species has been scientifically verified. There are over 400 species in the Passiflora genus worldwide, most of which have been little characterized in terms of phytochemical or pharmacological properties. Herein large scale multi targeted metabolic profiling and fingerprinting techniques were utilized to help gain a broader insight into Passiflora species leaves chemical composition. Nuclear magnetic resonance spectroscopy and mass spectrometry spectra of extracted components derived from 17 Passiflora accessions and from different geographical origins were analyzed using multivariate data analyses

**Keywords:** Passiflora, Anxiolytic, PCA

## M-680. Metabolomics Driven Analysis of Erythrina Lysistemon Cell Suspension Culture in Response to Methyl Jasmonate Elicitation

Farag MA, Mekky H and El-Masry S

*Journal of Advanced Research, 7: 681-689 (2016) IF: 3*

An MS based metabolomic approach was used to profile the secondary metabolite of the ornamental plant Erythrina lysistemon via ultra-performance liquid chromatography coupled to photodiode array detection and high resolution qTOF mass spectrometry . Cultures maintained the capacity to produce E. lysistemon flavonoid subclasses with pterocarpans amounting for the most abundant ones suggesting that it could provide a resource of such flavonoid subclass. In contrast, alkaloids, major constituents of Erythrina genus, were detected at trace levels in suspension cultures. Methyl jasmonate (MeJA), phytohormone, was further supplied to culture with the aim of increasing secondary metabolites production and with metabolite profiles subjected to multivariate data analysis to evaluate its effect. Results revealed that triterpene oleanolic acid and fatty acid hydroxyoctadecadienoic acid were elicited in response to methyl jasmonate, whereas pterocarpans isoneorautenol showed a decline in response to elicitation suggesting for the induction of terpenoid biosynthetic pathway and concurrent with a down regulation of pterocarpans.

**Keywords:** Erythrina, Methyl Jasmonate, Pterocarpans, Cell Culture

## M-681. Estrogenic Activity Including Bone Enhancement and Effect on Lipid Profile of Luteolin-7-O-Glucoside Isolated from Trifolium Alexandrinum L. in Ovariectomized Rats

N. M. Ammar, S. S. El-Hawary, D. A. Mohamed, A. M. El-Halawany, A. A. El-Anssary, L. T. Abou El-Kassem, R. A. Hussein, G. A. Abdel Jaleel and A. H. El-Dosoky

*Phytotherapy Research, 30: 768-773 (2016) IF: 2.694*

Luteolin-7-O-glycoside (LG), an abundant component in many edible plants, was found to be one of the major constituents of the aqueous methanol extract of Trifolium alexandrinum L. family Fabaceae, a fodder plant widely cultivated in Egypt. The estrogenic activity of LG concerning the effect on uterotrophy, lipid profile, weight gain and bone enhancement activity was determined in ovariectomized rat model at a dose of 5 mg/kg. Luteolin-7-O-glycoside showed significant estrogenic effect through the preservation of normal uterine weight and plasma estradiol level. It also significantly inhibited the bone turnover markers plasma bone-specific alkaline phosphatase, plasma osteocalsin, type I procollagen N-terminal, and C-telopeptide of type II collagen levels. It induced a significant improvement in plasma lipid profile. The effect of LG was comparable with estradiol with lower effect on uterine weight. Liver and kidney functions revealed a wide safety of LG at this dose level. The present study revealed that LG may be a promising hormone replacement therapy after being examined thoroughly on human

**Keywords:** Trifolium Alexandrinum; Luteolin-7-O-Glucoside; Estrogenic Activity; Bone Enhancement Activity.

## M-682. Metabolite Profiling in Saudi Date Palm Fruit Cultivars and their Antioxidant Potential Via UPLC-qTOF-MS and Multivariate Data Analyses

Farag MA, Handoussa H, Fekry MI and Wessjohann LA

*Food and Function, 7: 1077-1086 (2016) IF: 2.686*

Date palm fruit Phoenix dactylifera is not only one of the most economically significant plants in the Middle East, but also valued for its nutritional impact, and for which development of analytical methods is ongoing to help distinguish its many cultivars. This study attempts to characterize the primary and secondary metabolite profiles of date cultivars from Saudi Arabia. A total of metabolites extracted from the fruit peel were evaluated in a UPLCMS based metabolomics analysis including flavonoids, phenolic acids and fatty acids. The predominant flavones were glycosides of luteolin and chrysoeriol, as well as quercetin conjugates, whereas caffeoyl shikimic acid was the main hydroxycinnamic acid conjugate. GCMS was further utilized to identify the primary metabolites in fruits with glucose and fructose among most cultivars. PCA and OPLS analyses revealed that flavone versus flavonol distribution in fruit were the main contributors for cultivar segregation

**Keywords:** Date Fruit, Phenolics, UPLCMS

## M-683. Naturally Occurring Thiophenes: Isolation, Purification, Structural Elucidation, and Evaluation of Bioactivities

Sabrin R. M. IbrahimHossam M. AbdallahAli M. El-Halawany and Gamal A. Mohamed

*Phytochemistry Reviews, 15: 197-220 (2016) IF: 2.686*

Thiophenes are a class of heterocyclic aromatic compounds based on a five-membered ring made up of one sulfur and four carbon atoms. The thiophene nucleus is well established as an interesting moiety, with numerous applications in a variety of different research areas. Naturally occurring thiophenes are characteristic secondary metabolites derived from plants belonging to the family Asteraceae, such as Tagetes,Echinops,Artemisia, Balsamorhiza,Blumea, Pluchea, Porophyllum and Eclipta. Furthermore, naturally occurring thiophenes are generally composed of one to five thiophene rings that are coupled together through their α-carbons, and carry alkyl chains on their free ortho-positions. Thiophene-containing compounds possess a wide range of biological properties, such as antimicrobial, antiviral, HIV-1 protease inhibitor, antileishmanial, nematicidal, insecticidal, phototoxic and anticancer activities. This review focuses on naturally occurring thiophene derivatives; their sources, physical and spectral data, and biological activities.

**Keywords:** Thiophenes, Biosynthesis, Nmr Data, Anti Microbial, Cytotoxic

## M-684.The Wild Egyptian Artichoke as a Promising Functional Food for the Treatment of Hepatitis C Virus As Revealed UPLCMSand Clinical Trials

Elsebai MF, Abass K, Hakkola J, Atawia AR and Farag MA.

*Food and Function, 7: 3006-3016 (2016) IF: 2.686*

Infection by hepatitis C virus and its subsequent complications are a major cause of mortality worldwide. The water extract of the wild Egyptian artichoke Cynara cardunculus leaves is a freely available herbal product that is used for treatment of HCV infection complications such as jaundice and ascites. The purpose of this study was to evaluate whether WEA exhibits activity against HCV, identify bioactive chemicals in its extract and to tentatively examine the potential inhibitory interactions of WEA with human drug-metabolizing enzymes. The current pilot clinical trial revealed that the water extract of a WEA plant decreased the HCV viral load below the detection level in 12 out of 15 patients. Furthermore, the liver enzymes ALT and AST, as well as the level of bilirubin were normalized. The total WEA extract inhibited CYP2B6 and CYP2C19 with high affinity

**Keywords:** Artichoke, UPLCMS, Terpenes, Hepatitis.

## M-685. Russelioside B, A Pregnane Glycoside Ameliorates Hyperglycemia in Streptozotocin Induced Diabetic Rats by Regulating Key Enzymes of Glucose Metabolism

Essam Abdel-Sattar, Shohda A. EL-Maraghy, Riham Salah El-Dine and Sherine M. Rizk

*Chemico-Biological Interactions, 252: 47-53 (2016) IF: 2.618*

An alternative strategy to treat diabetes mellitus is the use of various natural agents possessing hypoglycemic effect. Caralluma quadrangula has been used in Saudi traditional medicine in cases of thirst and hunger and for the treatment of diabetes. The present study was designed to evaluate the improving effect of russelioside B, a pregnane glycoside isolated from Caralluma quadrangula on glucose metabolism in the liver of streptozotocin-induced diabetic rats. Diabetes mellitus was induced in rats by a single intraperitoneal injection of streptozotocin (50 mg/kg body weight). Experimental rats were administered russelioside B at a dose of 50 mg/kg body weight once a day for 30 days. The results showed that RB improved the fasting serum glucose level, glycated hemoglobin percent, serum insulin level and lipid profile. A significant improvement was observed upon the administration of russelioside B on the activities of the key enzymes of carbohydrate metabolism (glucokinase, glucose-6-phosphatase, glucose-6-phosphate dehydrogenase, and glycogen phosphorylase) in the liver of diabetic rats. Further, russelioside B administration to diabetic rats reverted gene expression of glucokinase, glucose-6-phosphatase, glycogen synthase and glycogen synthase kinase-3β to near normal levels. In conclusion, russelioside B possess antidiabetic and antihyperlipidemic effect in streptozotocin induced diabetic rats. Hence, administration of russelioside B may represent a potentially useful strategy for the management of diabetes.

**Keywords:** Antihyperglycemic; Caralluma Quadrangula; Carbohydrate Metabolizing Enzymes; Diabetes; Russelioside B

## M-686. A New Bioactive Metabolite Isolated from the Red Sea Marine Sponge Hyrtios Erectus

Sameh S. Elhady, Ali M. El-Halawany, Abdulrahman M. Alahdal, Hashim A. Hassanean and Safwat A. Ahmed

*Molecules, 21: 82-0 (2016) IF: 2.465*

Chemical investigation of the lipophilic fraction of Hyrtios erectus, a Red Sea sponge, yielded a new pentacyclic nitrogen-containing scalarane; 24-methoxypetrosaspongia C (1), together with the previously reported scalaranes sesterstatin 3 (2), 12-deacetyl-12-epi-scalaradial (3) and 12-deacetyl-12,18-di-epi-scalaradial (4). The compounds were identified using HRESIMS, 1D and 2D NMR experiments. The isolated compounds showed growth inhibitory activity against hepatocellular carcinoma (HepG2), colorectal carcinoma (HCT-116) and breast adenocarcinoma cells (MCF-7).

**Keywords:** Red Sea Sponge; Hyrtios Erectus; 24-Methoxypetrosaspongia C; Scalarane Sesterterpenes; Cancer Cell Lines; Growth Inhibitory Activity

## M-687. Gingerol Synergizes the Cytotoxic Effects of Doxorubicin Against Liver Cancer Cells and Protects from its Vascular Toxicity

Fahad A. Al-Abbasi, Eman A. Alghamdi, Mohammed A. Baghdadi, Abdulmohsin J. Alamoudi, Ali M. El-Halawany, Hany M. El-Bassossy, Ali H. Aseeri and Ahmed M. Al-Abd

*Molecules, 21: 886-0 (2016) IF: 2.465*

Hydroxyphenylalkanes and diarylheptanoids possess potential therapeutic value in different pathophysiological conditions, such as malignancy. In the current study, naturally isolated

hydroxyphenylalkane and diarylheptanoid compounds were investigated for potential chemo-modulatory effects in addition to potential vascular protective roles with doxorubicin. Diarylheptanoids showed stronger antioxidant effects, in comparison to hydroxyphenylalkanes, as demonstrated by DPPH assay and amelioration of CCl4-induced disturbed intracellular GSH/GSSG balance. Shogaol and 4′-methoxygingerol showed considerable cytotoxic effects against HCT116, HeLa, HepG2 and MCF7 cells, with IC50 values ranging from 3.1 to 19.4 μM. Gingerol significantly enhanced the cytotoxic profile of doxorubicin against HepG2 and Huh7, cells decreasing its IC50s by 10- and 4-fold, respectively. Cell cycle distribution was studied using DNA cytometry. Doxorubicin alone induced cell accumulation at S-phase and G2/M-phase, while in combination with gingerol it significantly induced cell cycle arrest at the G2/M-phase. Additionally, the vascular protective effect of gingerol against doxorubicin (10 μM) was examined on isolated aortic rings. Co-incubation with 6-gingerol (30 μM) completely blocked the exaggerated vasoconstriction and impaired vascular relaxation induced by doxorubicin. In conclusion, despite its relatively weak antioxidant properties, gingerol protected from DOX-induced vascular damage, apparently not through a ROS scavenging mechanism. Besides, gingerol synergized the cytotoxic effects of DOX against liver cancer cells without influencing the cellular pharmacokinetics.

**Keywords:** Hydroxyphenylalkanes; Diarylheptanoids; Gingerol; Doxorubicin; Liver Cancer; Vascular Protection

## M-688. Phenolics from Garcinia Mangostana Inhibit Advanced Glycation Endproducts Formation: Effect on Amadori Products, Cross-Linked Structures and Protein Thiols

Hossam M. Abdallah, Hany El-Bassossy, Gamal A. Mohamed, Ali M. El-Halawany, Khalid Z. Alshali and Zainy M. Banjar

*Molecules, 21: 251-0 (2016) IF: 2.465*

Accumulation of Advanced Glycation Endproducts (AGEs) in body tissues plays a major role in the development of diabetic complications. Here, the inhibitory effect of bioactive metabolites isolated from fruit hulls of Garcinia mangostana on AGE formation was investigated through bio-guided approach using aminoguanidine (AG) as a positive control. Including G. mangostana total methanol extract (GMT) in the reaction mixture of bovine serum albumin (BSA) and glucose or ribose inhibited the fluorescent and non-fluorescent AGEs formation in a dose dependent manner. The bioassay guided fractionation of GMT revealed isolation of four bioactive constituents from the bioactive fraction; which were identified as: garcimangosone D (1), aromadendrin-8-C-glucopyranoside (2), epicatechin (3), and 2,3′,4,5′,6-pentahydroxybenzophenone (4). All the tested compounds significantly inhibited fluorescent and non-fluorescent AGEs formation in a dose dependent manner whereas compound 3 (epicatechin) was found to be the most potent. In search for the level of action, addition of GMT, and compounds 2–4 inhibited fructosamine (Amadori product) and protein aggregation formation in both glucose and ribose. To explore the mechanism of action, it was found that addition of GMT and only compound (3) to reaction mixture increased protein thiol in both glucose and ribose while compounds 1, 2 and 4 only increased thiol in case of ribose. In conclusion, phenolic compounds 1–4 inhibited AGEs formation at the levels of Amadori product and protein aggregation formation through saving protein thiol.

**Keywords:** Advanced Glycation Endproducts; Mangosteen; Amadori Product; Epicatechin; Benzophenone; Garcimangosone D; Aromadendrin

## M-689. Synthesis and Cytotoxic Activity of Biphenylurea Derivatives Containing Indolin-2-One Moieties

Wagdy M. Eldehna, Mohamed Fares, Hany S. Ibrahim, Muhammad A. Alsherbiny, Mohamed H. Aly, Hazem A. Ghabbour and Hatem A. Abdel-Aziz

*Molecules, 21: 762-0 (2016) IF: 2.465*

In our endeavor towards the development of potent anticancer agents, two different sets of biphenylurea-indolinone conjugates, 5a–s and 8a,b were synthesized. The in vitro cytotoxicity of the synthesized compounds was examined in two human cancer cell lines, namely MCF-7 breast cancer and PC-3 prostate cancer cells using the sulforhodamine B (SRB) colorimetric assay. In particular, the MCF-7 cancer cell line was more susceptible to the synthesized compounds. Compound 5o (IC50 = 1.04 ± 0.10 μM) emerged as the most active member in this study against MCF-7, with 7-fold increased activity compared to the reference drug, doxorubicin (IC50 = 7.30 ± 0.84 μM). Compounds 5l, 5q and 8b also exhibited superior cytotoxic activity against MCF-7 with IC50 values of 1.93 ± 0.17, 3.87 ± 0.31 and 4.66 ± 0.42 μM, respectively. All of the tested compounds were filtered according to the Lipinski and Veber rules and all of them passed the filters. Additionally, several ADME descriptors for the synthesized compounds 5a–s and 8a,b were predicted via a theoretical kinetic study performed using the Discovery Studio 2.5 software.

**Keywords:** Biphenylurea; Cytotoxic Activity; Indolinone; Adme

## M-690. Synthesis, Biological Evaluation and Molecular Docking of Certain Sulfones As Potential Nonazole Antifungal Agents

Mohamed Fares, Mohamed A. Said, Muhammad A. Alsherbiny, Radwa A. Eladwy, Hadia Almahli, Marwa M. Abdel-Aziz, Hazem A. Ghabbour, Wagdy M. Eldehna and Hatem A. Abdel-Aziz

*Molecules, 21: 114-0 (2016) IF: 2.465*

We reported herein the synthesis, antifungal activity, docking and in silico ADME prediction studies of four novel series of sulfones 6a–f, 8a–c, 10a–f and 12a–c. All the newly synthesized sulfones were tested against four strains of Candida (including fluconazole-resistant Candida), two strains of Aspergillus, two dermatophytic fungi (Trichophytons mentagrophyte and Microsporum canis) and Syncephalastrum sp. with fluconazole as a reference drug. In general, compounds 8a and 10b showed selective and potent anticandidal activity (MIC: 0.19–0.81 μM) relative to fluconazole (MIC = 1.00 μM). Furthermore, 10e and 12a elicited a remarkable and selective antifungal activity against Aspergillus sp. and the dermatophytic fungi (MIC: 0.16–0.79 μM) relative to fluconazole (MIC: 2–2.6 μM). Moreover, the docking results of the sulfones 6a, 8a, 10a and 10b at the active site of CYT P450 14α-sterol demethylase showed a

comparable binding interaction (interaction Energy = −34.87 to −42.43 kcal/mol) with that of fluconazole (IE = −40.37 kcal/mol).
**Keywords:** Synthesis; Sulfone; Antifungal; Anticandidal; Docking

## M-691.Gingerol Protects Against Experimental Liver Fibrosis in Rats Via Suppression of Pro-Inflammatory and Profibrogenic Mediators

Mardi M. Algandaby Ali M. El-halawany Hossam M. Abdallah Abdulrahman M. Alahdal Ayman A. Nagy Osama M Ashour and Ashraf B. Abdel-Naim

*Naunyn-Schmiedeberg"s Archives of Pharmacology, 39: 419-428 (2016) IF: 2.376*

6-Gingerol (Gin) is known to possess hepatoprotective effects. Liver fibrosis is a major health concern that results in significant morbidity and mortality. There is no FDA-approved medication for liver fibrosis. The present work aimed at exploring the beneficial effects of Gin against liver fibrosis in rats. Experimental fibrosis was induced by challenging animals with CCl4 for 6 weeks. Gin significantly ameliorated the increase in serum alanine aminotransferase (ALT) and aspartate aminotransferase (AST) activities, albumin, total cholesterol (TC) and triglyceride (TG) concentrations, and liver index. These effects were confirmed by light and electron microscopic examinations. The antifibrotic effects were confirmed by examining Masson trichrome-stained liver sections which indicated reduced collagen deposition in Gin-treated animals. Further, Gin administration hampered alpha-smooth muscle actin (α-SMA) expression and significantly reduced hepatic content of transforming growth factor-beta (TGF-β). Also, Gin elicited profound antioxidant actions as indicated by preventing reduced glutathione (GSH) depletion and lipid peroxide accumulation. The observed antifibrotic activities involved decreased production of nuclear factor κB (NF-κB), tumor necrosis factor alpha (TNF-α), expression of toll-like receptor 4 (TLR4), intercellular adhesion molecule (ICAM), and vascular cell adhesion molecule (VCAM). Involvement of Gin anti-inflammatory activity was verified by the decreased expression of inducible nitric oxide synthase (iNOS) and cyclooxygenase-2 (COX-2) in livers of animals treated with Gin. Thus, it can be concluded that Gin protects against CCl4-induced liver fibrosis in rats. This can be ascribed, at least partly, to its antioxidant, anti-inflammatory effects as well as the inhibition of NF-κB/TLR-4 expression.
**Keywords:** Gingerolhepatic Fibrosisnuclear Factor Kbtoll-Like Receptor 4

## M-692. Anti-Arthritic Activity of 11-O-(4'-O-Methyl Galloyl)-Bergenin and Crassula Capitella Extract in Rats

Seham S. El-Hawary, Rabab Mohammed, Sameh Abouzid, Zeinab Y. Ali and Ahlam Elwekeel

*Journal of Pharmacy and Pharmacology, 68: 834-844 (2016) IF: 2.363*

**Objectives** Isolation and identification of phytochemicals of Crassula capitella (Thunberg), evaluation of the anti-arthritic potential of the extract and the major isolated compound; 11-O-(40-O-methyl galloyl)-bergenin and underlying their mechanism on rat model of rheumatoid arthritis (RA). **Methods** Different fractions were subjected to column chromatography giving fourteen compound identified by mass and NMR spectroscopic techniques. RA was induced by intraplantar injection of complete Freund's adjuvant into the right hind paw of rats. Influence of tested samples in comparable to methotrexate on paw oedema, body weight gain, serum diagnostic markers, cartilage and bone degeneration enzymes, pro-inflammatory mediators and oxidative stress biomarkers in arthritic rats. Key findings Fourteen phenolic compounds were isolated and identified for the first time from C. capitella. The major compound identified as 11-O-(40-Omethyl galloyl)-bergenin. Treatment of arthritic rats with extract or 11-O-(40-Omethyl galloyl)-bergenin with the tested doses can reduce the progression and severity of RA. **Conclusion** Crassula capitella is a new natural and abundant source for 11-O- (40-O-methyl galloyl)-bergenin for resolving chronic inflammatory diseases as RA through antioxidant, anti-inflammatory and membrane stabilizing mechanism.
**Keywords:** 11-O-(40-O-Methyl Galloyl)-Bergenin;

## M-693.Carteritins A and B, Cyclic Heptapeptides from the Marine Sponge Stylissa Carteri

Ahmed H. Afifi, Ahmed H. El-Desoky, Hikaru Katoa, Remy E.P. Mangindaanc, Nicole J. de Voogdd, Nagwa M. Ammarb, Mohammed S. Hifnawy and Sachiko Tsukamoto

*Tetrahedron Letters, 75(11): 1285-1288 (2016) IF: 2.347*

Two new cyclic heptapeptides, carteritins A and B (1 and 2), were isolated from the marine sponge Stylissa carteri along with three known cyclic heptapeptides, phakellistatin 13 (3) and hymenamides C and D (4 and 5). Their structures were elucidated based on data obtained using 2D NMR, HRESIMS, and ESIMS/MS, in addition to Marfey's analysis. Carteritin A (1) showed cytotoxicities against HeLa, HCT116, and RAW264 cells with IC50 values of 0.70–1.5 μM.
**Keywords:** Cyclic Heptapeptide; Marine Sponge; Stylissa Carteri; Cytotoxic

## M-694. Solamargine Production by A Fungal Endophyte of Solanum Nigrum

S.S. El-Hawary, R. Mohammed, S.F. Abou Zid, W. Bakeer and R. Ebeland A.M. Sayed

*Journal of Applied Microbiology, 120: 900-911 (2016) IF: 2.156*

**Aims:** The aim was to isolate, identify and characterize endophytes from Solanum nigrum L. as a new source of the cytotoxic steroidal alkaloid solamargine. **Methods and Results:** Three endophytic fungi; SNFSt, SNFL and SNFF were isolated from S. nigrum and identified by molecular methods. Preliminary TLC screening showed a common metabolite between the plant and one of these fungi, SNFSt which was identified as Aspergillus flavus based on the phylogenetic analysis of its ITS sequence. Subsequent LC-HRESIMS analysis unambiguously established the identity of the compound based on its molecular formula and its characteristic MS2 fragmentation pattern as solamargine. To ascertain its identity, fungal solamargine was isolated using preparative TLC and its structure was fully characterized using NMR spectroscopic

techniques and high-resolution mass spectrometric analysis. Solamargine production could be followed and quantified for a total of 11 generations of this fungus with a titer of ~250–300 lg l 1. This study represents one of the first examples where host plant-derived compounds have been demonstrated to be steadily produced by an endophytic fungi in sizeable quantities. **Conclusions:** The production of solamargine (found in the host plant) by a cultivable fungal endophyte at a significant yield is a new observation. Further experiments such as media optimization, OSMAC (One Strain Many Compounds) or epigenetic modifiers could be applied to enhance the fungal solamargine production. Significance and Impact of the Study: The endophytic fungus SNFSt isolated from S. nigrum may be utilized for quantitative production of the potent cytotoxic metabolite solamargine.

**Keywords:** Aspergillus Flavus, Endophytes, Solamargine,Steroidal Alkaloids.

## M-695.Sesquiterpene Lactones from Cynara Cornigera: Acetyl Cholinesterase Inhibition and in Silico Ligand Docking.

Mohamed-Elamir F. Hegazy, Abeer Y. Ibrahim, Tarik A. Mohamed, Abdelaaty A. Shahat, Ali M. El Halawany, Nahla S. Abdel-Azim, Mansour S. Alsaid and Paul W. Paré

*Planta Medica, 82: 138-146 (2016) IF: 1.99*

Wild artichoke (Cynara cornigera), a thistle-like perennial belonging to the Asteraceae family, is native to the Mediterranean region, northwestern Africa, and the Canary Islands. While the pleasant, albeit bitter, taste of the leaves and flowers is attributed to the sesquiterpene lactones cynaropicrin and cynarin, a comprehensive phytochemical investigation still needs to be reported. In this study seven sesquiterpene lactones were isolated from an aqueous methanol plant extract, including a new halogenated metabolite (1), the naturally isolated compound sibthorpine (2), and five metabolites isolated for the first time from C. cornigera. Structures were established by spectroscopic methods, including HREIMS, 1H, 13C, DEPT, 1H-1H COSY, HMQC, and HMBC‐NMR experiments as well as by X-ray analysis. The isolated bioactive nutrients were analyzed for their antioxidant and metal chelating activity. Compound 1 exhibited a potent metal chelating activity as well as a high antioxidant capacity. Moreover, select compounds were effective as acetyl cholinesterase inhibitors presenting the possibility for such compounds to be examined for anti-neurodegenerative activity. A computational pharmacophore elucidation and docking study was performed to estimate the pharmacophoric features and binding conformation of isolated compounds in the acetyl cholinesterase active site

**Keywords:** Cynara Cornigera L " Asteraceae L " Sesquiterpene Lactones L " Acetyl Cholinesterase Inhibition L " In Silico Ligand Docking

## M-696. Use of Random Amplified Polymorphic Dna (Rapd) Technique to Study the Genetic Diversity of Eight Aloe Species

Shahira M.Ezzat, Abeer M.ElSayed and Maha M.Salama

*Planta Medica, 82(15): 1381-1386 (2016) IF: 1.99*

The genus Aloe comprises over 400 species of flowering succulent plants. Aloe leaves are used in the treatment of asthma, gastrointestinal ulcers, cardiovascular disease, tumors, burns, and diabetes. They are rich in anthraquinones, such as aloin, aloe-emodin, chrysophanol, aloinoside A, and aloinoside B. The various species of Aloe show chemical and morphological similarity and diversity, which depend on the genotype and environmental conditions. In a continuity to our interest in the genus Aloe, this study targets the authentication of eight different Aloe species, Aloe vera (A1), Aloe arborescens (A2), Aloe eru (A3), Aloe grandidentata (A4), Aloe perfoliata (A5), Aloe brevifolia (A6), Aloe saponaria (A7), and Aloe ferox (A8), grown in Egypt by using the technique of random amplified polymorphic DNA. Twelve decamer primers were screened in amplification with genomic DNA extracted from all species, of which five primers yielded species-specific reproducible bands. Out of 156 loci detected, the polymorphic, monomorphic, and unique loci were 107, 26, and 23, respectively. Based on a dendrogram and similarity matrix, the eight Aloe species were differentiated from each other and showed more divergence. Aloe species prevailed similarity coefficients of 54-70 % by which they could be classified into three major groups. Thus, this technique may contribute to the identification of these Aloe species that have great morphological similarity in the Egyptian local markets.

**Keywords:** Aloe Species,Xanthorrhoeaceae,Authentication,Dna Markers,Clustering.

## M-697. Phenolics from Garcinia Mangostana Alleviate Exaggerated Vasoconstriction in Metabolic Syndrome Through Direct Vasodilatation and Nitric Oxide Generation

Hossam M. Abdallah, Hany M. El-Bassossy, Gamal A. Mohamed, Ali M. El-halawany, Khalid Z. Alshali and Zainy M. Banjar

*Bmc Complementary and Alternative Medicine, 16: 359-0 (2016) IF: 1.987*

**Background** Exaggerated vasoconstriction plays a very important role in the hypertension, a major component of metabolic syndrome (MetS). In the current work, the potential protective effect of methanol extract of fruit hulls of Garcinia mangostana L. on the exaggerated vasoconstriction in MetS has been investigated. In addition, the bioactive fraction and compounds as well as the possible mechanism of action have been illustrated. **Methods** The effect of methanol extract of G. mangostana (GMT) fruit hulls on the vascular reactivity of aorta isolated from animals with MetS was investigated through bioassay-guided fractionation procedures. GMT was partitioned with chloroform (I) and the remaining mother liquor was fractionated on a Diaion HP-20 with H2O, 50 and 100 % methanol to give fractions II, III, and IV, respectively. The effect of total extract (GMT), bioactive fraction and the bioactive compounds on the vasoconstriction were examined in aortae isolated from animals with MetS by incubation for 30 min before exposing aortae to cumulative concentrations of phenylephrine (PE). The direct relaxant effect was also examined by adding cumulative concentrations of the bioactive fraction and its bioactive compounds to PE precontracted vessels. In addition, aortic nitric oxide (NO) and reactive oxygen species (ROS) production was investigated. **Results** Bioassay-

guided fractionation of GMT revealed isolation of garcimangosone D (1), aromadendrin-8-C-β-D-glucopyranoside (2), 2,4,3′-trihydroxy benzophenone-6-O-β-D-glucopyranoside (3), maclurin-6-O-β-D-glucopyranoside (rhodanthenone) (4), epicatechin (5), and 2,3′,4,5′,6-pentahydroxy benzophenone (6). Only compounds 2, 4, and 5 significantly alleviated the exaggerated vasoconstriction of MetS aortae and in the same time showed significant vasodilation of PE pre-contracted aortae. To further illustrate the mechanism of action, the observed vasodilation was completely blocked by the nitric oxide (NO) synthase inhibitor, Nω-nitro-L-arginine methyl ester hydrochloride and inhibited by guanylate cyclase inhibitor, methylene blue. However, vasodilation was not affected by the potassium channel blocker, tetraethylammonium or the cyclooxygenase inhibitor, indomethacin. In addition, compounds 2, 4, and 5 stimulated NO generation from isolated aortae to levels comparable with acetylcholine. Furthermore, 4 and 5 inhibited reactive oxygen species generation in MetS aortae. **Conclusion** The phenolic compounds 2, 4, and 5 ameliorated the exaggerated vasoconstriction in MetS aortae through vasodilatation-NO generation mechanism.

**Keywords:** Metabolic Syndrome Garcinia Mangostana Relaxation Benzophenone Flavonoids

## M-700. Isolation of Major Phenolics from Launaea Spinosa and their Protective Effect on HepG2 Cells Damaged with t-BHP.

Hossam Abdallah, Mohamed Farag, Samir Osman, Da hye Kim, Kyungsu Kang, Cheol-Ho Pan and Essam Abdel-Sattar

*Pharmceutical Biology, 54: 536-541 (2016) IF: 1.546*

**Context:** Some Launaea species (Asteraceae) are used traditionally to treat liver oxidative stress. **Objective:** The present study investigates the protective effects of isolated compounds from Launaea spinosa Sch. Bip. (Asteraceae) against oxidative stress on t-BHP-induced HepG2 cells. **Materials and Methods:** Major phenolic content from flowering aerial parts of L. spinosa was isolated and identified. The protective effects of isolated compounds (10 and 20 μM) against oxidative stress induced by tert-butyl hydroperoxide (t-BHP) in HepG2 cells were investigated through the measurement of aspartate aminotransferase (AST), alanine transaminase (ALT), and superoxide dismutase (SOD) levels. **Results:** A new phenolic compound identified as 2,3-diferulyl R,R-(+) methyl tartrate (6), in addition to five known metabolites, esculetin (1), esculetin-7-O-d-glucoside (cichoriin) (2), fertaric acid (3), acacetin-7-O-d-glucoside (4), and acacetin-7-O-d-glucuronic acid (5), were isolated. Oxidant-induced damage by 200 μM t-BHP in HepG2 cells was inhibited by compounds 1, 4, and 5 (10 and 20 μM), or quercetin (10 μM; positive control). The protective effects of compounds 1, 4, and 5 were associated with decreasing in AST, ALT, and SOD levels. Compound 4 (20 μM) decreased the AST level from 128.5 ± 13.9 to 7.9 ±1.8 U/mL. Meanwhile, compound 1 (20 μM) decreased ALT activity from 20.3 ± 7.0 to 7.6 ± 2.4 U/mL, while compound 5 decreased SOD levels from 41.6 ± 9.0 to 28.3 ± 3.4 mU/mg. **Conclusion:** The major phenolic compounds isolated from L. spinosa displayed a significant cytoprotective effect against oxidative stress, leading to maintenance of the normal redox status of the cell.

**Keywords:** Cytoprotection; Diferulyl Methyl Tartrate Ester; Oxidative Stress

## M-701.Metabolic Profile and Hepatoprotective Activity of the Anthocyanin-Rich Extract of Hibiscus Sabdariffa Calyces.

Shahira M. Ezzat, Maha M. Salama, Sayed H. Seif el-Din, Samira Saleh, Naglaa M. El-Lakkany, Olfat A. Hammam, Maha B. Salem and Sanaa S. Botros

*Pharmaceutical Biology, 54: 3172-3181 (2016) IF: 1.546*

**Context:** Hibiscus sabdariffa L. (Malvaceae) is a common traditional tea that has many biological activities. **Objectives:** To evaluate the hepatoprotective effect and study the metabolic profile of the anthocyanin-rich extract of H. sabdariffa calyces (HSARE). **Materials and Methods:** The hepatoprotective activity of HSARE was assessed (100 mg/kg/d for 4 weeks) by examining the hepatic, inflammatory, oxidative stress markers and performing a histopathological examination in rats with thioacetamide (TAA)-induced hepatotoxicity. HSARE was analyzed using ultra-performance liquid chromatography-quadrupole-time-of-flight-photodiode array-mass spectrometry (UPLC-qTOF-PDA-MS). **Results:** The UPLC-qTOF-PDA-MS analysis of HSARE enabled the identification of 25 compounds represented by delphinidin and its derivatives, cyanidin, kaempferol, quercetin, myricetin aglycones and glycosides, together with hibiscus lactone, hibiscus acid and caffeoylquinic acids. Compared to the TAA-intoxicated group, HSARE significantly reduced the serum levels of alanine aminotransferase, aspartate aminotransferase and hepatic malondialdehyde by 37.96, 42.74 and 45.31%, respectively. It also decreased hepatic inflammatory markers, including tumour necrosis factor alpha, interleukin-6 and interferon gamma (INF-γ), by 85.39, 14.96 and 70.87%, respectively. Moreover, it decreased the immunopositivity of nuclear factor kappa-B and CYP2E1 in liver tissue, with an increase in the effector apoptotic marker (caspase-3 positive cells), restoration of the altered hepatic architecture and increases in the activities of superoxide dismutase (SOD) and glutathione by 150.08 and 89.23%, respectively. **Discussion andConclusion:** HSARE revealed pronounced antioxidant and anti-inflammatory potential where SOD and INF-γ were significantly improved. HSARE possesses the added value of being more water-soluble and of natural origin with fewer side effects expected compared to silymarin.

**Keywords:** Ultra-Performance Liquid Chromatography-Quadrupole- Time-Of-Flight-Pdamass Spectrometry; Delphinidin; Hibiscuslactone; Caspase-3; Nuclear Factor Kappa-B; Cyp2e1

## M-698. Antibacterial Antioxidant and Topical Anti Inflammatory Activities of Bergia Ammannioides a Wound Healing Plant

Shahira M. Ezzat, Mouchira A. Choucry and Zeinab A. Kandil

*Pharmaceutical Biology, 54: 215-224 (2016) IF: 1.546*

**Context:** Despite the traditional use of Bergia ammannioides Henye ex Roth. (Elatinaceae) for the treatment of wounds in India, there is a scarcity of scientific data supporting this use. **Objective:**The objective of this study is to assess wound-healing potentiality of the plant, to study pharmacological activities that may contribute in eliminating wound complications, and to

investigate the biologically active fractions. Material and methods: The ethanolic extract (EtOH) of the aerial parts was fractionated to obtain n-hexane (HxFr), chloroform (ClFr), ethyl acetate (EtFr), and n-butanol (BuOH) fractions. EtOH and its fractions were formulated in strength of 5 and 10% w/w ointment and tested for wound-healing activity using the excision model. The topical anti-inflammatory, in vitro antioxidant, and antibacterial activities were evaluated. HxFr and EtFr were chemically investigated to isolate their constituents. **Results:** Application of EtOH, HxFr, and EtFr (10% w/w ointments) leads to 71.77, 85.62, and 81.29% healing of the wounds with an increase in the collagen content. HxFr had the strongest anti-inflammatory (64.5% potency relative to Voltaren®) and antibacterial activity (MIC = 104 µg/ml against Staphylococcus aureus), while EtFr showed the strongest antioxidant activity against DPPH, ABTS•+, and super oxide radical with an IC50 value of 10.25 ± 0.01, 66.09 ± 0.76, and 167.33 ± 0.91 µg/ml, respectively. β-Sitosterol, lupeol, cyclolaudenol, and cycloartenol were isolated from HxFr. Quercetin, ellagic acid, kaempferol-3-O-α-l-rhamnoside, and quercetin-3-O-α-l-rhamnoside were isolated from EtFr. Discussion and conclusion: Our study presents scientific evidence for the efficacy of B. ammannioides in enhancing wound healing, and the first isolation of cyclolaudenol and cycloartenol from Bergia.

**Keywords:** Cycloartenol, Cyclolaudenol, Wound Complications

## M-699. In Vivo Anti-Inflammatory Activity of Caffeoylquinic Acid Derivatives from Solidago Virgaurea in Rats.

Amira Abdel Motaal, Shahira M. Ezzat, Mariane G. Tadros and Hesham I. El-Askary

*Pharmaceutical Biology, 54: 2864-2870 (2016) IF: 1.546*

**Context:**Solidago virgaurea L. (Asteraceae) is traditionally used as an anti-inflammatory for the treatment of various symptoms including cystitis. However, little is known concerning the constituents responsible for this activity and the mechanism of their action. **Objective:** To assess the anti-inflammatory activity of the phenolic-rich fraction of S. virgaurea aerial parts in rats, isolate and assess the activity of the major compounds present. **Materials and Methods:**An HPLC method was developed for the analysis of the phenolic-rich fraction (EtFr). The in vivo anti-inflammatory activity of the EtFr and four isolated compounds (at 25 and 50 mg/kg) were assessed in adult male rats using the carrageenan-induced rat paw oedema model. The levels of the pro-inflammatory cytokines (TNF-α and IL-1β) were measured using ELISA. **Results:** 3,5-O-Dicaffeoylquinic acid (1), 3,4-O-dicaffeoylquinic acid (2), 3,4,5-O-tricaffeoylquinic acid (3) and 4,5-O-dicaffeoylquinic acid (4) were isolated from EtFr. Compound 3 (50 mg/kg) showed a highly significant activity in inhibiting the oedema volume after 3 h (88% of the activity of indomethacin at 10 mg/kg). The EtFr and the isolated compounds largely inhibited the excessive production of the inflammatory mediators TNF-α and IL-1β. DISCUSSION AND **Conclusion:** This is the first report of 3,4,5-tri-O-caffeoylquinic acid (3) in Solidago species. The tricaffeoylquinic acid (3) showed a significantly higher activity than the other three dicaffeoylquinic acids (1, 2, 4) and indomethacin in reduction of TNF-α and IL-1β concentrations (8.44 ± 0.62 and 5.83 ± 0.57 pg/mL compared to 12.60 ± 1.30 and 52.91 ± 5.20 pg/mL induced by indomethacin, respectively).

**Keywords:** Asteraceae; Il-1B; Tnf-A; Goldenrod; Tricaffeoylquinic Acid

## M-702. Phenolic Content and Anti-Hyperglycemic Activity of Pecan Cultivars from Egypt

ypt Seham S. El Hawary, Soumaya Saad, Ali Mahmoud El Halawany, Zeinab Y. Ali and Mahitab El Bishbishy

*Pharmaceutical Biology, 54: 788-798 (2016) IF: 1.546*

**Context:** Pecans are commonly used nuts with important health benefits such as anti-hyperglycemic and anti-hyperlipidemic effects. **Objective:** A comparative investigation of the antihyperglycemic and total phenolic content of the leaves and shells of four pecan cultivars growing in Egypt was carried out. The selected cultivars (cv.) were Carya illinoinensis Wangneh. K. Koch. cv. Wichita, cv. WesternSchely, cv. Cherokee, and cv. Sioux family Juglandaceae. Materials and methods: Total phenolic and flavonoid contents of the leaves and shells of pecan cultivars were carried out using Folin–Ciocalteu's and aluminum chloride assays, respectively. Moreover, HPLC profiling of phenolic and flavonoid contents was carried out using RP-HPLC-UV. In addition, in vivo anti-hyperglycemic activity of the ethanolic extracts (125 mg/kg bw, p.o.) of C. illinoinensis cultivars was carried out using streptozotocin (STZ)-induced diabetes in Sprague–Dawley rats for 4 weeks. **Results and discussion:** Phenolic contents were higher in shells than leaves in all studied cultivars, while flavonoids were higher in leaves. Leaves and shells of cv. Sioux showed the highest phenolics (251.7 µg gallic acid equivalent (GAE)/g), and flavonoid contents (103.27 µg rutin equivalent (RE)/g and 210.67 µg quercetin equivalent (QE)/g), respectively. The HPLC profiling of C. illinoinensis cultivars resulted in the identification of eight flavonoids (five of these compounds are identified for the first time from pecan), and 15 phenolic acids (six are identified for the first time from pecan). Leaves of cv. Sioux revealed the most potent decrease in blood glucose and glycated hemoglobin (HbA1c%) (194.9 mg/dl and 6.52%, respectively), among other tested cultivars. Moreover, leaves of cv. Sioux significantly elevated serum total antioxidant capacity (TAC) and reduced glutathione (GSH) (0.33 mMol/l and 30.68 mg/dl, respectively), and significantly suppressed the markers of both lipid peroxidation (malondialdehyde, MDA) and protein oxidation (protein carbonyl, PC) (14.25 µmol/ml and 3.18 nmol/mg protein, respectively). **Conclusion:** Different pecan cultivars showed significant variation in its phenolic and flavonoid contents and consequently their antioxidant and anti-hyperglycemic effects.

**Keywords:** Antidiabetes, Carya Illinoinensis, Glycated Hemoglobin, Hplc, Phenolics, Protein Carbonyl

## M-703.Kinetics and Molecular Docking of Vasicine from Adhatoda Vasica: an Acetylcholinesterase Inhibitor for Alzheimers Disease

S.K. Ali, A.R. Hameda, M.M. Soltan, A.M. El-Halawany, U.M. Hegazyand A.A. Hussein

*South African Journal of Botany, 104: 118-124 (2016) IF:1.244*

The alcoholic extract of Adhatoda vasica showed strong and reversible inhibition of the enzyme acetyl cholinesterase (AChE) with an IC50 = 294 µg/mL. Phytochemical study of the total alcoholic extract of A. vasica yielded four known compounds

vasicine, vasicinone, vasicole and anisotine. Vasicine reversibly and competitively inhibited AChE with ki value 11.24 µM. On the other hand, rest of isolated alkaloids showed no/or weak inhibitory effect on AChE. Vasicine showed binding similarity to both galantamine and tacrine in the catalytic site. The obtained results support the multi-pharmacological properties of vasicine, which can be considered as a promising inhibitor for acetyl cholinesterase where it can be used directly or indirectly for the development of efficient anti-Alzheimer drug.

**Keywords:** Adhatoda Vasica; Vasicine; Acetyl Cholinesterase; Alzheimer Disease

## M-704.Kinetic and Thermodynamics Studies for Castor Oil Extraction Using Subcritical Water Technology.

Wael Abdelmoez, Eman Ashour, Shahenaz M. Naguib, Amr Hilal, Dalia A. Al Mahdy, Engy A. Mahrous and Essam Abdel-Sattar

*Journal of Oleo Science, 65: 477-485 (2016) IF: 1.108*

In this work both kinetic and thermodynamics of castor oil extraction from its seeds using subcritical water technique were studied. It was found that the extraction process followed two consecutive steps. In these steps, the oil was firstly extracted from inside the powder by diffusion mechanism. Then the extracted oil, due to extending the extraction time under high temperature and pressure, was subjected to a decomposition reaction following first order mechanism. The experimental data correlated well with the irreversible consecutive unimolecular-type first order mechanism. The values of both oil extraction rate constants and decomposition rate constants were calculated through non-linear fitting using DataFit software. The extraction rate constants were found to be 0.0019, 0.024, 0.098, 0.1 and 0.117 min(-1), while the decomposition rate constants were 0.057, 0.059, 0.014, 0.019 and 0.17 min(-1) at extraction temperatures of 240, 250, 260, 270 and 280°C, respectively. The thermodynamic properties of the oil extraction process were investigated using Arrhenius equation. The values of the activation energy, Ea, and the frequency factor, A, were 73 kJ mol(-1) and 946, 002 min(-1), respectively. The physicochemical properties of the extracted castor oil including the specific gravity, viscosity, acid value, pH value and calorific value were found to be 0.947, 7.487, 1.094 mg KOH/g, 6.1, and 41.5 MJ/Kg, respectively. Gas chromatography analysis showed that ricinoleic acid (83.6%) appears as the predominant fatty acid in the extracted oil followed by oleic acid (5.5%) and linoleic acid (2.3%).

**Keywords:** In This Work Both Kinetic and Thermodynamics of Castor Oil Extraction From Its Seeds Using Subcritical Water Technique Were Studied.

## M-705. A New Acylated Flavonol from the Aerial Parts of Asteriscus Maritimus (L.) Less (Asteraceae)

Marwa I. Ezzat, Shahira M. Ezzat, Kadriya S. El Deeb and Ahlam M. El Fishawy

*Natural Product Research, 30(15): 1753-1761 (2016) IF: 1.057*

Phytochemical investigation of the flowering aerial parts of Asteriscus maritimus (L.) Less (Asteraceae) led to the isolation of a new compound: patuletin 7-O-β-D-[(2‴S) 6″(3‴-hydroxy-2‴-methyl-propanoyl)] glucopyranoside, together with five known metabolites; β-sitosterol 2, chlorogenic acid 3, P-hydroxy -methylbenzoate 4, luteolin 5 and protocatechuic acid 6. The structures of the isolated compounds were determined by comprehensive analyses of its 1D and 2D NMR, HRMS and compared with previously known analogues. The ethanolic extract of the flowering aerial parts of A. maritimus was found to be safe (LD50 = 4.6 mg/kg) and possess significant antioxidant and anti-inflammatory activities and this was in accordance with its high phenolic content (107.36 ± 0.051 mg GAE/g extract).

**Keywords:** Asteriscus Maritimus, Acylated Flavonol, Antioxidant, Anti-Inflammatory

## M-706. A New Antibacterial Lupane Ester from the Seeds of Acokanthera Oppositifolia Lam.

Abeer M. El Sayed, Shahira M. Ezzat and Omar M. Sabry

*Natural Product Research, 30: 2813-2818 (2016) IF: 1.057*

As a part of ongoing investigation of Acokanthera oppositifolia (Lam.) Codd., four compounds were isolated from its seeds, a new compound; lup-20(29)-en-3β-O-(3'-β-hydroxy) palmitate (1), three known compounds; a triterpene; lupeol (2), a cardiac glycoside; acovenoside A (3) and a sterol; β-sitosterol (4). Their structures were investigated using 1D & 2D- 1H and 13CNMR spectroscopy. Antimicrobial potential of the compounds was evaluated against 10 microorganisms responsible for endocarditis. The minimum inhibitory concentration (MIC) of the compounds was determined using broth microdilution method. The new compound (1) evidenced significant antibacterial activity especially aganist Pseudomonas aeruginosa with (MIC 7.81 µg/ml). Lupeol (2) exhibited remarkable antimicrobial activity against Methicillin-resistant Staphylococcus aureus, Aspergillus fumigates and Candida albicans (MIC 3.9, 0.24 and 3.9 µg/ml, respectively). On the other hand, acovenoside A (3) inhibited the growth of Escherichia coli (MIC 0.98 µg/ml). We herein present the potential of A. oppositifolia as a cardioprotective agent against the microorganisms responsible for endocarditis.

**Keywords:** Cardenolide, Lupeol Ester, Acokanthera, Antimicrobial, Endocarditis

## M-707. A Cytotoxic C-Glycosylated Derivative of Apigenin from the Leaves of Ocimum Basilicum Var. Thyrsiflorum

Mohamed I.S. Abdelhady and Amira Abdel Motaal

*Revista Brasileira De Farmacognosia-Brazilian Journal of Pharmacognosy, 26: 763-766 (2016) IF: 0.956*

The standardized 80% ethanolic extract of the leaves of Ocimum basilicum var. thyrsiflorum (L.) Benth., Lamiaceae, growing in KSA, exhibited a significant antioxidant activity compared to the ethyl acetate and butanol extracts, which was correlated to its higher phenolic and flavonoid contents. Chromatographic separation of the 80% ethanol extract resulted in the isolation of ten known compounds; cinnamic acid, gallic acid, methylgallate, ellagic acid, methyl ellagic acid, apigenin, luteolin, vitexin, isovitexin, and 3″-O-acetylvitexin. Compound 3″-O-acetylvitexin, a C-glycosylated derivative of apigenin, was isolated for the first time from genus Ocimum. The 80%

ethanolic extract and 3″-O-acetylvitexin showed significant cytotoxic activities against the HCT116 human colon cancer cell line [IC50 values 22.3 ± 1.1 and 16.8 ± 2.0 µg/ml (35.4 µM), respectively].

**Keywords:** Ocimum Basilicum; HCT116; Cytotoxic; Antioxidant; C-Glycosylation; Apigenin Derivative

## M-708. Cytotoxic Activity of Phenolic Constituents from Echinochloa Crus-Galli Against four Human Cancer Cell Lines

Sayed Gad El Molla, Amira Abdel Motaal, Hala El Hefnawy and Ahlam El Fishawy

*Revista Brasileira De Farmacognosia-Brazilian Journal of Pharmacognosy, 26 (1): 62-67 (2016) IF: 0.956*

Echinochloa crus-galli (L.) P. Beauv., Poaceae, grains are used as a feed for birds and millet for humans.The sulforhodamine B assay was used to assess its cytotoxicity against four human cancer cell lines. Theethanolic extract (70%) proved to be most active against HCT-116 and HELA cell lines (IC50= 11.2 ± 0.11and 12.0 ± 0.11 g/ml, respectively). On the other hand, the chloroform and ethyl acetate fractionsexhibited their highest activities against HCT-116 cell lines. The chloroform and ethyl acetate frac-tions were subjected to several chromatographic separations to render pure phenolic compounds(1–8). Compounds 1–8 were identified as: 5,7-dihydroxy-3,45-trimethoxy flavone, 5,7,4trihydroxy-35dimethoxy flavone (tricin), quercetin, flavone, apigenin-8-C-sophoroside, 2-methoxy-4-hydroxycinnamic acid, p-coumaric acid and quercetin-3-O-glucoside. All the isolated phenolic compounds exhib-ited various significant activities against the four human carcinoma where the methoxylated flavones(1 and 2) were the most active, in a way comparable to the anticancer drug Doxorubicin®. Thus, thesemethoxylated flavonoids may be considered as lead compounds for the treatment of cancer, which sup-ports previous claims of E. crus-galli traditional use. This is the first report of the occurrence of thesephenolic compounds in E. crus-galli.IntroductionCancer is a leading cause of death in economically developedcountries and the second leading cause of death in developedcountries. Lung, stomach, liver, colon and breast cancer cause themost cancer deaths each year. Breast cancer in females, and lungand prostate cancer in males are the most frequently diagnosedcancers and the leading causes of cancer death for each sex. About30% of cancer deaths are due to the five leading behavioral anddietary risks; high body mass index, low fruit and vegetable intake,lack of physical activity, tobacco use, and alcohol use (Jemal et al.,2011).Plant derived compounds have played a major role in thedevelopment of several useful cytotoxic agents viz. vinblastine, vin-cristine, and paclitaxel (Taxol®). Other promising new agents arein clinical development stage, including flavopiridol and combre-tastatin, which clarifies the urge for screening native flora in searchfor new bioactive phytochemical compounds (Reddy et al., 2003;Cragg and Newman, 2005). Corresponding author.E-mail: amira.abdelmotaal@hu.edu.eg (A. Abdel Motaal).Echinochloa crus-galli (L.) P. Beauv., Poaceae, is a problematicsummer weed found in rice fields and known as Barnyard grass.The grains are known as fodder for livestock and as millet forpeople in many Asian countries (Boulos and El Hadidi, 1984). Itis known traditionally to reduce body weight, blood sugar, treathypertension and help to detoxify liver and kidney. It is also usedfor carbuncles, hemorrhage, sores, spleen trouble, wounds and can-cer (’t Mannetje and Jones, 1992). It was previously reported thatthe 70% hydroalcoholic extract of the grains of E. crus-galli showedsignificant antidiabetic activity in normal and alloxan induced dia-betic rats (Devi et al., 2012), and that the methanol and aqueousextracts exhibited significant antioxidant activities (Ho et al., 2012;Mehta and Vadia, 2014). Several phenolic compounds; flavones,flavone glycosides, caffeoyl quinic acid derivatives were isolatedfrom other Echinochloa species such as E. utilis, E. frumentacea andE. colona (Watanabe, 1999; Kim et al., 2008; Lazaro, 2009; Gomaaand Abd Elgawad, 2012; Hegab et al., 2013).This study was carried out in order to prove the ethnophar-macological use of E. crus-galli grains as a remedy for cancer(’t Mannetje and Jones, 1992), and to specify the compoundsresponsible for its cytotoxic activity against four human cancer celllines; MCF-7 (breast carcinoma), HCT-116 (colon carcinoma), HELA(cervical carcinoma) and HEPG-2 (liver carcinoma). The use of such http://dx.

**Keywords:** Barnyard Grass,HCT-116, HELA, HEPG-2,Methoxylated Flavonoids

## M-709. In Vivo Diabetic Wound Healing Effect and HPLC-DAD-ESI-MS/MS Profiling of the Methanol Extracts of Eight Aloe Species

Abeer M.ElSayed, Shahira M.Ezzat, Moataz M.El-Naggar and Seham S.El Hawary

*Revista Brasileira De Farmacognosia-Brazilian Journal of Pharmacognosy, 26: 352-362 (2016) IF: 0.956*

Genus Aloe, Xanthorrhoeaceae, is well distributed all over Egypt, and many species have been used as medicinal plants; mainly reported to prevent cardiovascular diseases, cancer and diabetes. This study attempts to analyze the secondary metabolites in the methanol extract of the leaves of eight Aloe species; A. vera (L.) Burm. f., A. arborescens Mill., A. eru A. Berger, A. grandidentata Salm-Dyck, A. perfoliata L., A. brevifolia Mill., A. saponaria Haw. and A. ferox Mill. growing in Egypt. For this aim HPLC–DAD–MS/MS in negative ion mode was used. Although belonging to the same genus, the composition of each species presented different particularities. Seventy one compounds were identified in the investigated Aloe species, of which cis-p-coumaric acid derivaties, 3,4-O-(E) caffeoylferuloylquinic acid and caffeoyl quinic acid hexoside were the most common phenolic acids identified. Aloeresin E and isoaloeresin D, 2'-O-feruloylaloesin were the common anthraquinones identified. Lucenin II, vicenin II, and orientin were the common identified flavonoids in the investigated Aloe species. 6'-Malonylnataloin, aloe-emodin-8-O-glucoside, flavone-6,8-di-C-glucosides could be considered as chemotaxonomic markers for the investigated Aloe species. The eight Aloe species had significant anti-inflammatory activity, in addition to the significant acceleration of diabetic wound healing in rats following topical application of the methanol extracts of their leaves. This is the first simultaneous characterization and qualitative determination of multiple phenolic compounds in Aloe species from locally grown cultivars in Egypt using HPLC–DAD–MS/MS, which can be applied to standardize the quality of different Aloe species and the future design of nutraceuticals and cosmetic preparations.

**Keywords:** Aloe; HPLC–DAD–MS/MS; Chemotaxonomic; Anti-Inflammatory; Wound Healing.

## M-710. Phytochemistry, Biological Activities and Economical Uses of the Genus Sterculia and the Related Genera: A Reveiw

Moshera Mohamed El-Sherei, Alia Yassin Ragheb, Mona El Said Kassem, Mona Mohamed Marzouk, Salwa Ali Mosharrafa and Nabiel Abdel Megied Saleh

*Asian Pacific Journal of Tropical Disease, 6: 492-501 (2016) IF: 0.841*

The genus Sterculia is represented by 200 species which are widespread mainly in tropical and subtropical regions. Some of the Sterculia species are classified under different genera based on special morphological features. These are Pterygota Schott & Endl., Firmiana Marsili, Brachychiton Schott & Endl., Hildegardia Schott & Endl., Pterocymbium R.Br. and Scaphium Schott & Endl. The genus Sterculia and the related genera contain mainly flavonoids, whereas terpenoids, phenolic acids, phenylpropanoids, alkaloids, and other types of compounds including sugars, fatty acids, lignans and lignins are of less distribution. The biological activities such as antioxidant, anti-inflammatory, antimicrobial and cytotoxic activities have been reported for several species of the genus. On the other hand, there is confusion on the systematic position and classification of the genus Sterculia. However, the wide range of the reported flavonoids in the present review is quite significant and can act as a guide for further studies from the chemosystematic point of view. Also the value of the genus Sterculia and its related genera in the traditional medicine and their effective biological activities led to the possibilities of finding new sources of drugs for prospect applications.

**Keywords:** Sterculia Pterygota Firmiana Brachychiton Pterocymbium Scaphium Sterculiaceae Biological Activities.

## M-711. Antihepatotoxic Effect and Metabolite Profiling of Panicumturgidum Extract Via UPLC-qTOF-MS

Mohamed A Farag, Ahlam M El Fishawy, Sayed A El-Toumy, Khadiga F Amer, Ahmed M Mansour and Hala E Taha

*Pharmacognosy Magazine, 12 (2016) IF: 0.831*

**Background** Panicum turgidum, desert grass, has not reported any detailed phytochemical or biological study as yet Objective To establish P. turgidum secondary metabolite profile and to assess its antihepatotoxic effect **Materials and Methods** Ultra-performance liquid chromatography coupled to quadrupole high-resolution time of flight mass spectrometry was used for large-scale secondary metabolites profiling in P. turgidum extract, alongside assessing median lethal dose and hepatoprotective effect against carbon tetrachloride intoxication **Results** metabolites were identified with flavonoids as the major class present as glycosides of luteolin, apigenin, isorhamnetin and naringenin, most of which are first time to be reported in Panicum sp. Antihepatotoxic effect of P. turgidum crude extract was revealed via improving several biochemical marker levels and mitigation against oxidative stress in the serum and liver tissues, compared with CCl4 intoxicated group and further confirmed by histopathological examination. **Conclusion** This study reveals that P. turgidum, enriched in Cflavonoids, presents a novel source of safe antihepatotoxic agents and further demonstrates the efficacy of UPLC-MS metabolomics in the field of natural products drug discovery.

**Keywords:** Panicum; Hepatotoxic, Flavonoids, UPLC

## M-712. New Abietane Diterpenes from Euphorbia Pseudocactus Berger (Euphorbiaceae) and their Antimicrobial Activity

Azza Ramy Abdel‐Monem and Enas Hussein Abdelrahman

*Pharmacognosy Magazine, 12 (2016) IF: 0.831*

**Background:** Euphorbia is the largest genus in Euphorbiaceae. Terpenoids were isolated from most species of this genus. **Objective:** Since no previous study was reported about Euphorbia pseudocactus Berger, we started here a phytochemical investigation on this species to isolate and identify its terpenoid constituents and to estimate the antimicrobial activity of the isolated compounds. **Materials and Methods:** The n‐hexane fraction of the ethanolic extract of E. pseudocactus Berger was chromatographed on silica gel columns, the structures of the isolated compounds (1–5) were identified based on their MS, 1 D, and 2 D NMR spectral data. The antimicrobial activity of the n‐hexane fraction and the isolated compounds (1–4) was investigated using diffusion plate method against Gram‐positive (Staphylococcus aureus [12600] and Bacillus subtilis [6051]) and Gram‐negative (Pseudomonas aeruginosa [10145] and Escherichia coli [11775]) bacteria, yeast (Candida albicans [7102]), and fungi (Aspergillus flavus). **Results:** Two triterpenes (glut‐5‐en‐3 β‐ol [1] and olean‐12,15 ‐diene‐3 β‐ol [2]) and three abietane diterpene (3‐hydoxy‐19‐cyclopropenoyloxy‐abietane [3], ent‐abieta‐9,12,14‐triene‐12,16‐olide [4], and 12,19‐dihydroxy‐abieta‐5‐ene [5]) were isolated. Compound 1 exhibited no antibacterial activity against the tested bacteria, compound 2 and n‐hexane fraction exhibited weak activity, whereas compounds 3 and 4 showed moderate activity. All samples showed no activity against the tested yeast and fungi. **Discussion and Conclusion:** Five compounds were isolated for the 1st time from E. pseudocactus Berger, three of them (3–5) are new natural compounds. As the major isolated compound (1) exhibited no antimicrobial activity, the observed activity of the n‐hexane fraction is mainly due to its diterpenoid constituents.

**Keywords:** Abietane, Antimicrobial, Diterpene, Euphorbia Pseudocactus, Triterpene

## M-713. Anti-Acetylcholinesterase Activity of Essential Oils and their Major Constituents from four Ocimum Species.

Farag MA, Ezzat SM, Salama MM, Tadros MG and Serya RA.

*Zeitschrift Fur Naturforschung Section C-A Journal of Biosciences, 71: 393-402 (2016) IF: 0.709*

Ocimum is a genus of considerable importance in traditional medicine worldwide. The goal of this study was to examine the anti-acetylcholinesterase activity of Ocimum essential oils and to correlate the activity with their chemical profiles using a metabolome based GC-MS approach coupled to chemometrics. Further, molecular docking was adopted to rationalize the

activity of some essential oil isolates. Essential oil prepared from the four species O. basilicum, O. africanum, O. americanum, and O. minimum exhibited significant anti-acetylcholinesterase activity with (IC50 0.22, 0.175, 0.57 and 0.152 mg/mL, respectively) comparable to that of physostigmine (IC50 0.27 mg/mL). The phenylpropanoids (i.e. estragole) constituted the most dominant chemical group in O. basilicum (sweet basil) and O. minimum, whereas camphor (a ketone) was the most abundant in O. africanum and O. americanum. Supervised and unsupervised multivariate data analyses clearly separated O. africanum and O. americanum from other accessions, with estragole, camphor and, to less extent, β-linalool contributing to species segregation. Estragole was found the most active AchE inhibitor (IC50 0.337 µM) followed by cineole (IC50 2.27 µM), camphor (IC50 21.43 µM) and eugenol (IC50 40.32 µM). Molecular docking revealed that these compounds bind to key amino acids in the catalytic domain of AchE, similar to standard drugs.

**Keywords:** Anti-Acetylcholinesterase; Chemometrics; Ocimum; Volatiles.

## M-714. Phytochemical Investigation of the Bioactive Extracts of the Leaves of Ficus Cyathistipula Warb.

Fatma El-Sakhawy, Hanaa Kassem, Dina Abou-Hussein, Sabah El-Gayed, Mayy Mostafa and Rania Ahmed

*Zeitschrift Fur Naturforschung Section C-A Journal of Biosciences, 71: 141-154 (2016) IF: 0.709*

Ethanolic and aqueous leaf extracts of Ficus cyathistipula significantly reduced bloodglucose level, improved triglycerides and cholesterol levels of dyslipidemia in diabeticrats. They similarly reduced the inflammation of pawedema and stomachulcers in rats. Fractions obtained by successive partition of ethanolic extract were assessed for their cytotoxicity, antioxidant and antimicrobial activities; Petroleum ether fraction was the most cytotoxic (IC50 = 4.43 +/0.2, 17.3 +/2.22 and 15.5 +/3.67 mu g/ml on MCF7, HepG2 and HeLa cell lines, respectively). Ethyl acetate fraction was the strongest antioxidant in DPPH assay (IC50 = 100 mu g/ml). All samples exhibited low to strong antimicrobial activity. Chemical investigation of leaf extracts led to the isolation of alphaamyrin palmitate (1), lupeol acetate (2), taraxerol (3), alphasitosterol (4), protocatechuic acid (5) and 3Ocaffeoyl quinic acid (6) that were identified via spectral and chromatographic analyses. Metabolite profiling was performed via UPLCPDAMS and revealed the presence of flavonoid glycosides, phenolic acids, isoflavones, coumarins and fatty acids. Quantitative determination revealed 593 +/0.5 mg BSE, 348.1 +/0.09 mg GAE, 238.7 +/0.5 mg rutin and 9 +/0.5 g tannins per 100 g d. wt. of leaves. GLC analysis of lipid fraction revealed identification of phytosterols (15.6%), saturated (51.71%) and unsaturated (41.9%) fatty acids. Galactose, glucose, arabinose and glucoronic acid (36.98%, 28.86%, 22.56% and 1.06%, respectively) were identified by HPLC analysis of mucilagehydrolysate.

**Keywords:** Alpha-Amyrin Palmitate; Antidiabetic; Ficus Cyathistipula; Leaf Metabolites

## M-715. Plicosepalin A, A New Antioxidant Catechin–Gallic Acid Derivative of Inositol from the Mistletoe Plicosepalus Curviflorus

Jihan M. Badr, Sabrin R.M. Ibrahim and Dina R. Abou-Hussein

*Zeitschrift Fur Naturforschung Section C-A Journal of Biosciences, 71(11-12)c: 375-380 (2016) IF: 0.709*

Phytochemical investigation of the semi-parasitic plant, Plicosepalus curviflorus (Loranthaceae)growing in Saudi Arabia resulted in the isolation of a new catechin–gallic acid derivative of inositol, plicosepalin A (1) [(+) catechin-4′-O-(1″-O-galloyl-5″-O-methyl)-myoinositol], along with seven known compounds: methyl gallate (2), catechin (3), quercetin (4), gallic acid (5),lupeol (6), β-sitosterol (7), and ursolic acid (8). Their structures were elucidated on the basis of spectroscopic analyses, including HRESIMS, ESIMS, 1H and 13C NMR,HSQC, and HMBC, as well as comparison with reported data. The antioxidant and antimicrobial activities of 1 were evaluated using 2,2-diphenyl-1-picrylhydrazyl(DPPH) and the disc diffusion assay, respectively. Compound 1 exhibited potent free radical scavenging activity with an IC50 value of 9.0 ± 0.27 µM. Moreover, significant activities against Staphylococcus aureus and Bacillus subtilis were recorded.

**Keywords:** Antimicrobial; Antioxidant; Catechin Derivative; Plicosepalin A; Plicosepalus Curviflorus.

## M-716.Effect of Viscum Schimperi on Advanced Glycation Endproducts Formation

Hossam Mohamed Abdallah, Doha Omar ALGhamdi, Maab Siddiq Al-Salem, Maryam Alattas, Hany Mohamed El-Bassossy, Abdulrahman Mohammed Alahdal, Ibrahim Ateya Shehata and Essam Abdel-Sattar

*Pakistan Journal Pharmaceutical Science, 29: 2307-2316 (2016) IF: 0.581*

complication due to a reaction between sugar and amino acid of proteins to form advanced glycation endproducts (AGEs) in different tissues. Medicinal plants are considered as a great source of bioactive compounds that affect many ailments. In this regard; AGEs formation could be inhibited by many bioactive compounds isolated from medicinal plants. Viscum schimperi Engl. is a plant belongs to Loranthaceae and known for its antidiabetic activity. In this study; total methanol extract of V. schimperi (VT) was prepared, suspended in water and subjected to fractionation with chloroform followed by n-butanol to give (VC) and (VB) fractions respectively. The aqueous mother liquor was evaporated to form (VA) fraction. The inhibitory effect of all prepared fraction on the formation of advanced glycation endproducts (AGEs) was studied. The results revealed that V. schimperi extract and its different fractions inhibited protein glycation and oxidation of BSA induced by ribose together with decrease of protein aggregation. In conclusion; V. schimperi will be useful in management of diabetic complications based on its inhibition of advanced glycation endproduct formation.

**Keywords:** Viscum Schimperi, Advanced Glycation Endproducts, Diabetic Complications, Anti-Diabetic, Saudi

## M-717. Bioactive Metabolites from the Egyptian Red Sea Fungi with Potential Anti-HCV Protease Effect

Usama W. Hawas, Eman F. Ahmed, Ali Halwany, Ahmed Atif, Waill Ahmed and Lamia T. Abou El-Kassem

*Chemistry of Natural Compounds, 52: 104-110 (2016) IF: 0.473*

HCV protease (HCV PR) inhibition is considered to be one of the important targets for designing drugs to treat HCV [1]. Endophytic fungi have proved to be promising sources of new and biologically active natural products that are of interest for specific medicinal applications [2–4]. One hundred anticancer compounds have been separated from endophytic fungi between 1990 and 2010 [5]. Besides its anticancer activity, fungal endophytes serve as a source of antiviral substances. The current study was conducted to isolate endophytic fungi with anti-HCV protease and antimicrobial and anticancer activities from living symptomless tissues of Red Sea marine animals. Marine invertebrates such as sponges, algae, and soft corals are well known to house numerous microorganisms within their tissues, including fungi which may be detected directly by microscopy or indirectly by metagenomic surveys [6]. The fermentation broths of 51 endophytic fungi isolated from the fresh tissues of 30 collected marine organisms (Table 1) were screened for antimicrobial, anticancer, and anti-HCV protease

**Keywords:** HCV, Marine Endophytes

## M-718.Antimicrobial and Antiradical Potential of four Agro-Waste Citrus Peels Cultivars

Samia M. Abd-Elwahab, Nebal D. El-Tanbouly, Mohamed Y. Moussa, Azza R. Abdel-Monem and Nesrin M. Fayek

*Journal of Essential Oil Bearing Plants, 19: 1932-1942 (2016) IF: 0.313*

The peels essential oil profiles of four new cultivars of Citrus species have been studied by GC- MS. The hydro-distilled oils yield was 0.1 - 1.0 % (w/w) with the highest yield in lime peel. Out of the forty-one characterized components, limonene was the major monoterpene hydrocarbons detected in all tested samples (89.3 ± 0.0, 88.5 ± 0.2, 78.1 ± 0.3 and 53.0 ± 0.0 % in grapefruit, orange, mandarin and lime oils, respectively). Both β-pinene (16.0 ± 0.5 %) and p-cymene (13.9 ± 0.2% ) were major in lime oil, while mandarin oil was rich with γ-terpinene (9.0 ± 0.5 %). Concentration of volatile oils constituents was calculated based on the average of 3 determination ± standard deviation (S.D.). Three citrus oils; orange (100 µl/ml), lime and grapefruit (250 µl/ml), demonstrate relatively equivalent antiradical potential (inhibit 70 % of DPPH) as vitamin E (5.2 µl/ml), having IC50 of 110 ± 10.0, 142 ± 2.5 and 155 ± 5.0 µl/ml, respectively. Lime peel essential oil showed the highest antimicrobial activity recording MIC90 of 14, 11, 12 and 9 µl/ml against Staphylococcus aureus, E. coli, Candida albicans and Aspergillus flavus, respectively, while other tested oils demonstrated moderate antimicrobial activity against the eight pathogenic microorganisms.

**Keywords:** Citrus Peels, Essential Oil Composition; Gc-Ms, Radical Scavenging Activity, Antimicrobial, Waste Products.

## M-719. Biological and Chemical Investigation of the Soft Coral Lobophytum Pauciflorum Collected from the Egyptian Red Sea

Hassan M H A, Mohammed R, Hetta M H, Abdelaziz T A, El-Gendy A O and Sleim M A5

*International Journal of Pharmacognosy and Phytochemical Research, 8(6): 906-911 (2016)*

Soft corals of the genus Lobophytum, a marine invertebrate, have shown diverse biological activities as antiinflammatory, cytotoxic, and antibacterial. Our research is concerning with biological screening and discovering bioactive substances from the Red Sea soft coral Lobophytum pauciflorum. In vitro cyclooxygenase inhibitory activity using COX-1 and COX-2 kits and antimicrobial screening were carried out for n-hexane, dichloromethane, ethyl acetate and methanol fractions. The isolated compounds were elucidated using different spectroscopic methods including nuclear magnetic resonance and mass spectrometry. Also n-hexane fraction was subjected to GC/MS analysis. Bioassay guided fractionation resulted in isolation and characterization of two bio-active metabolites nephthenol (2) and gorgost-5-ene-3β-ol (3) with significant in vitro antiinflammatory activity against COX-1 and COX-2 compared to Indomethacin and Celecoxib. Four other compounds were also isolated: Heptadecan-1-ol (1), palmitic acid (4), stearic acid (5) and batilol (6). The isolated compounds showed antimicrobial activity ranging from 25 µg/ml to 50 µg/ml against the tested microorganisms. The fatty acid constituents of the n-hexane fraction were identified by GC/MS analysis; results revealed the presence of hexadecanoic acid, methyl ester as major saturated fatty acid and 7,10-hexadecadienoic acid, methyl ester as major unsaturated fatty acid.

**Keywords:** Lobophytum Pauciflorum, Gorgost-5-Ene-3B-Ol, Nephthenol, COX-1, COX-2 and GC/MS.

## M-720. Biological Investigations of a New Natural Recipe Expected to Promote Healing of Superficial Burns

Nabil Mohamed aboul-Fotouh selim

*Journal ,: p1-p2 (2016)*

Burns expose the deeper tissues of the skin or body to invasive microbes. Topical preparations for treating burn wounds, to be useful, should ideally have antibiotic power and promote healing by different mechanisms like their anti-inflammatory and antioxidant effects. Silver compounds have been the mainstay of topical burn treatment for decades. However, most chemical substances retard wound healing. Several natural agents such as honey and moist exposed burn ointment (β-sitosterol; MEBO are believed to protect wounds from infection and promote healing of burns without causing any of the adverse effects of purified chemicals. In this study, we investigated the antimicrobial, anti-inflammatory and antioxidant characteristics of a new natural recipe expected to promote healing of superficial burns and also determined the safety of its topical pharmaceutical use. Moreover, we compared the healing properties of the recipe with the commercial drugs; silver sulphadiazine (SSD; Dermazin a long-standing conventional burn dressing, and also with (β-sitosterol; MEBO a herbal preparation of Chinese origin widely

used in Asia and the Middle East. Biological investigations and trials had been made and conducted on experimental animals that were obtained from the animal house colony of National Research Centre, Dokki, Cairo, Egypt. All animals were kept on a standard laboratory diet and under the same hygienic and healthy conditions. They were acclimatized for two weeks in the laboratory in equal light and darkness periodicity, with liberal access to food and water. Animals were housed in separate hygienically maintained cages. For induction of superficial burns, one hundred and twenty adult male Murine albino rats weighing 130-150 g. were divided into four groups; each group consisted of 30 animals. They were housed in separate cages and received partial-thickness burn wounds on their dorsal skin in accordance to the Modified Murine model of partial thickness scald burn injury (A Standardized Model of Partial Thickness Scald Burns in Rats). Animals within each group were numbered then treated three times a day (t.i.d) with our new natural recipe, two times a day with (SSD; Dermazin ®), three times a day with (β-sitosterol; MEBO ®) in addition to three times a day treatment with a placebo plain gel (negative control). The burn wounds were visually inspected daily until day 14. It was found that animals in the first three groups were well preserved. No clinical infections occurred. Wound healing was at an advanced stage by the day 14 in all animals except the placebo group. Clinical examination showed that the three agents gave comparable protection and healing possibilities for the experimental animals. It is concluded that our new natural recipe is a suitable and efficacious alternative to conventional silver-based topical therapies and MEBO for treating partial-thickness burn wounds.

**Keywords:** Natural treatment of burns; Superficial burns; Calendula officinalis; Cleome droserifolia; Natural recipes.

## M-721. Chemical Composition and Evaluation of Possible Alpha Glucosidase Inhibitory Activity of Eight Aloe Species

Abeer M.El-Sayed, Shahira M.Ezzat, Mohamed Nabil Khalil and Seham S. El-Hawary

*Journal of Medicinal Plant Research, 10(13): 167-178 (2016)*

Many of the health benefits associated with Aloe species have been attributed to the polysaccharides contained in the gel of the leaves. The aim of this study was to investigate the chemical composition as well as the biological evaluation of polysaccharides isolated from the leaves of eight different Aloe species, A. vera (A1), A. arborescens (A2), A. eru (A3), A. grandidentata (A4), A. perfoliata (A5), A. brevifolia (A6), A. saponaria (A7) and A. ferox (A8) grown in El Orman Botanical Garden, Giza, Egypt. Polysaccharides from the plants were isolated using hot extraction method and then hydrolyzed. The polysaccharide hydrolysates were identified using high performance liquid chromatographic technique. Maximum yield of total polysaccharides identified were obtained from A7 (12.04%), A1 (8.51%), A8 (8.03%), A2 (5.32%) and A6 (2.18%) respectively. The isolated polysaccharides were tested for antihyperglycemic activity in alloxan-induced diabetic rats and alpha glucosidase inhibitory activity. Chromatographic investigation of the polysaccharides recorded the presence of 18 saccharides, glucuronic acid, stachyose, galacturonic acid, sucrose, glucose, xylose, galactose, rhamnose, mannose, arabinose, fructose polyol, mannitol and sorbitol in the eight Aloe species, but their quantitative composition differed among the species. Glucuronic acid, stachyose and galacturonic acid were the major detected saccharides. The results of the biological activities revealed significant antihyperglycemic activities with variable degrees. After four weeks of daily administration, polysaccharides isolated from A. vera (A1) and A. arborescens (A2) were the most active with 40 and 44% reduction in blood glucose level, respectively. All the tested polysaccharides showed significant alpha glucosidase inhibitory activity with IC50 (µg/ml) 11.70, 14.60 and 15.80 for A7, A6 and A1 respectively. In conclusion, the tested polysaccharides contribute to the antidiabetic action of these Aloe species.

**Keywords:** Aloe, Alpha Glucosidase Inhibitors, Antidiabetic, Polysaccharide.

## M-722. Chemical Investigation of Bauhinia Vahlii Wight and Arnott Leaves Grown in Egypt

Ahmed H. Elbanna, Engy A. Mahrous, Amal E. Khaleel and Taha S. El-Alfy

*International Journal of Pharmacy and Pharmaceutical Sciences, 8: 269-272 (2016)*

**Objective:** Plants of genus Bauhinia are famous for their rich flavonoid content. Several phytochemical and biological investigations affirmed the role of flavonoids in the different biological impacts exerted by Bauhinia plants. The present study aims to investigate the major phytoconstituents of the leaves of B. vahlii Wight and Arnott. **Methods:** Powdered leaves were extracted with n-hexane (HE) and the defatted marc was extracted with 70% ethanol. The defatted ethanolic extract (DEE) was further partitioned with solvents of increasing polarities. The HE and polar fractions of DEE were purified using different chromatographic techniques and isolated compounds were identified through their melting points, 1D and 2D NMR, UV and MS spectral data. **Results:** A total of nine compounds were isolated and identified. Taraxerol (1), a pentacyclic triterpene, and β-sitosterol (2) were isolated from HE. Investigation of polar fractions of DEE yielded six flavonoids and a phenolic acid, namely luteolin (3), quercetin (4), gallic acid (5), avicularin (6), quercitrin (7), hyperoside (8) and quercetin-3-O-β-sophoroside (9). Conclusion: Flavonols of the quercetin nucleus were the major detected constituents in B. vahlii leaves. Taraxerol, avicularin and quercetin-3-O-β-sophoroside are isolated for the first time from the genus Bauhinia. Results of this study encourage future pharmacological investigation of B. vahlii due to the presence of biologically active flavonoids and phytosterols.

**Keywords:** Bauhinia Vahlii Wight, Arnott., Polar Extractives, Flavonols, Quercetin, Taraxerol

## M-723.Comparative Botanical Study and Dna Finger Printing of Certain Eugenia Species Growing in Egypt

Seham S El-Hawary, Kamilia F Taha, Shahira M Ezzat and Amira Y Eissa

*International Journal of Pharmaceutical and Clinical Research, 8(8): 1135-1149 (2016)*

**Objective:** to discriminate between six Eugenia species growing in Egypt based on their micro-morphological and genetic characterization. **Methods:** For establishment of different botanical and genetic criteria, this study presents a comparative

investigation of the botanical features of the leaves and stems through microscopically investigation of the prepared entire, transverse sections and isolated elements of these organs. Furthermore, the DNA of the six Eugenia species was extracted from leaf samples and Inter Simple Sequence Repeat (ISSR) analysis using six primers of arbitrary sequences. **Results:** Comparative botanical characters of the different organs were identified. On the other hand, the total number of amplified product was 68 fragments, which were generated by the six primers; the primer HB-09 recorded 55.5% as the highest percentage of polymorphism. As well as, the primer HB-44 recorded 54.5% polymorphism. The primer HB-15 recorded the lowest percentage of polymorphism (10%) and the highest degree of similarity (90%). Conclusion: For the present study, microscopical characters, as well as, DNA fingerprinting can be considered as the identifying parameters to authenticate and differentiate between the six Eugenia species under study.
**Keywords:** Eugenia Species, Myrtaceae, Botanical Profiling, Dna Fingerprinting, ISSR.

## M-724.Evaluation of the Phenolic and Flavonoid Contents, Antimicrobial and Cytotoxic Activities of Some Plants Growing in Al Jabal Al-Akhdar in Libya

Seham S El Hawary, Abd El Rahman El Shabrawy and Shahira M Ezzat

*International Journal of Pharmacognosy and Phytochemical Research, 8(7): 1083-1087 (2016)*

The methanolic extract of the aerial part of two Libyan medicinal plants Arbutus pavarii. Pampan (Ericaceae) and Sarcopoterium spinosium. L. (Rosaceae) growing in El-Jabal Al Akhdar area were studied for their phenolic and flavonoid content, antimicrobial and cytotoxic activitie. Total polyphenol contents ranged from 61.7±2.7to 163.6±0.85 µg gallic acid equivalent / g (A. pavarii Pampan and S. spinosium. L.) and total flavonoid contents ranged from 126.9±2.98 to 206.1±1.09 µg rutin equivalent (A. pavarii Pampan and S. spinosium L.). Qualitative and quantitative analysis of major phenolic and flavonoids in the extracts were conducted by high-performance liquid chromatography (HPLC). Finally, antimicrobial activities of the two plants were measured using the disc diffusion method. While, cytotoxic properties were tested against the HEPG2 and T47D cell lines. Arbutus pavarii extract proved to be the most cytotoxic extract in this study with IC50 19.7±2.8 and 19±0.65 (µg/ml) on HEPG2 and T47D respectively.
**Keywords:** Phenolics, Flavonoids, Antimicrobial, Cytotoxic.

## M-725. GC/MS Analysis and Potential Cytotoxic Activity of Haplophyllum Tuberculatum Essential Oils Against Lung and Liver Cancer Cells

Sabry, M., Mohamed, O., El Sayed, A. M.and Alshalmani S. K.

*Pharmacognosy Journal, 8(1): 66-69 (2016)*

**Background:** Haplophyllum tuberculatum is a plant belongs to family rutacee. It is rich in volatile oils, fixed oils, alkaloids, and furanocoumarins. It is well known for the huge number of folkloric uses in middle east. **Objective:** The aim of this study is to establish the chemical composition of the essential oils of Libyan H. tuberculatum and to investigate their cytotoxic potentialities. **Materials and Methods:** The essential oils of the aerial parts and flowers of H. tuberculatum growing in Libya were prepared by hydrodistillation. GC/MS analyses were performed on a Shimaduz capillary gas chromatograph (GC 17A ver.3) instrument directly coupled to mass spectrometer-MS QP5050A. Oil A and F of H. tuberculatum at different concentrations (0-50 µg/ml) in DMSO were tested for cytotoxicity against human tumor cell lines. **Results:** Oil yield was found 0.4 and 1.5 (v/w %) on dry weight basis respectively. GC/MS analysis resulted in identification of total 35 compounds. 15 compounds were common to both oils. oil A of H. tuberculatum exhibited antitumor activities against. liver carcinoma cell line (HEPG2) and lung carcinoma cell line (H1299) 4.7 µg/ml and 4.1 µg/ml. Conclusion: Essential oil of the aerial parts of H. tuberculatum is potentially active against lung (H-1299), and liver (HEPG2) carcinoma cell lines. The observed cytotoxic, activities can be attributed to the dominance of α and γ-terpinene in this oil.
**Keywords:** Cytotoxicity, Essential Oils, Haplophyllum Tuberculatum, Liver Cancer, Lung Cancer

## M-726.Leaves of Schinus Polygamus (Cav.)Cabrera (Anacardiaceae) are Apotential Source of Hepatoprotective and Antioxidant Phytochemicals

Abeer M.El-Sayed

*Journal of Medicinal Plant Research, 10(17): 223-231 (2016)*

Phytochemical investigation of the crude ethanol extract of the leaves of Schinus polygamus (Cav.) Cabrera (Anacardiaceae) results in isolation of eight compounds identified as triterpenoids, 3-O-acetyllupeol (I), βeta-sitosterol (II), lupeol (III). In addition to the polyphenols, gallic acid (IV), methyl gallate (V), quercetin-3-α-O-rhamnoside (VI), kaempferol (VII) and quercetin (VIII). In Egypt, degenerative diseases in general and toxic hepatitis in particular remain a serious public health problem. The hepatoprotective, curative and anti-oxidant properties of the major phytochemicals, compounds III and IV isolated from leaves of S. polygamus were investigated. Liver damage was induced by CCl4 (1 mlkg-1); a well-known toxicant and exposure to this chemical is known to induce oxidative stress and causes tissue damage by the formation of free radicals. Silymarin (25 mgkg-1) and vitamin E (7.5 mgkg-1) were used as standard drugs to compare hepatoprotective and antioxidant effects of the phytochemicals, respectively. Oral administration of 50 to 100 mgkg-1 body weight of compounds III and IV were significantly protected from CCl4 induced elevation in aspartate aminotransferase (AST), alanine aminotransferase (ALT) and alkaline phosphatase (ALP) in adult male albino rats. The antioxidant effect in the liver was estimated by measuring the activity of antioxidant enzyme reduced glutathione. Detection of gallic acid and lupeol in S. polygamus as a member of family Anacardiaceae support the claim that both compounds could be considered as chemotaxonomic markers for plants belong to family Anacardiaceae. Results of the present study strongly reveal that both compounds III and IV have potent antioxidant and hepatoprotective effects against CCl4-induced hepatic intoxication.
**Keywords:** Schinus Polygamus (Cav.) Cabrera, Anacardiaceae, Triterpenes, Phenolics, Hepatoprotective, Antioxidant Effect.

## M-727. Morphological and Anatomical Features of Bauhinia Vahlii Wight and Arnott. Grown in Egypt

Ahmed Hassan Elbanna , Engy Abdel-hamid Mahrous, Amal El-Sayed Khaleel and Taha Shahat El-alfy

*Journal of Applied Pharmaceutical Science, 6: 84-93 (2016)*

Leaves and stems of plants of genus Bauhinia, family Fabaceae subfamily Caesalpinoideae, have been used as folk remedies for treatment of numerous health problems mainly diabetes. The genus is famous for the characteristic camel's foot shape of its leaves and bearing flowers ranging from white, yellow to purple. The shape and size of both flower and leaf are essential for species characterization. This study targets the morphological and histological profiling of Bauhinia vahlii Wight & Arnott. due to its recently evidenced biological importance. Morphologically, B. vahlii can be distinguished by being a huge evergreen climber with numerous pairs of coiled revolute tendrils. Its branches bear numerous large bilobed hairy leaves and white flowers that turns buff by time. The flowers show three long fertile stamens and two short staminodes. The commonly used parts, leaves and stems, were subjected to a deeper investigation. Microscopically, they are characterized by long non-glandular hairs with three small basal cells and an elongated distal one and that are rare in Caesalpinoideae. B. vahlli was recently segregated into a separate genus; Phanera based on the presence of tendrils, nature of its flower's androceum and phylogenetic data.

**Keywords:** Bauhinia Vahlii, Phanera Vahlii, Leaf, Stem, Macromorphology, Micromorphology, Hair.

## M-728. Phytochemical Composition, in Vitro Antioxidant and Cytotoxic Activities of Seeds of Convolvulus Arvensis Linn.

Taghreed A. Ibrahim, Atef A. El-Hela, Nevein M. Abd Elhady and Nabil M. Abo-Elfetoh

*International Journal of Pharma and Bio Sciences, 7(2): 107-116 (2016)*

In vitro antioxidant and cytotoxic activities of methanol extract of the seeds of Convolvulus arvensis Linn. and its successive fractions; chloroform, ethyl acetate and n-butanol were evaluated. Total phenolics and flavonoid contents of methanol extract and ethyl acetate fraction were estimated. The highest antioxidant activity was achieved in ethyl acetate fraction (120.3±0.55 mg GAE) followed by methanol extract (84.8±0.62 mg GAE). The ethyl acetate fraction showed the strongest DPPH and nitric oxide free radical scavenging activities (IC50 28.16±0.45 and 51.92±1.45 for DPPH and nitric acid, respectively). Ethyl acetate fraction showed the highest cytotoxic effect against Hela cell line (IC50 17.33±0.58). From ethyl acetate fraction seven compounds were isolated and identified; gallic acid (1), ferulic acid (2), chlorogenic acid (3), quercetin (4), apigenin-7-O-glucoside (5), quercetin-7-O-rhamnoside (6) and quercetin-3-O-rutinoside (7) using different spectroscopic techniques. Therefore, methanolic extract and the ethyl acetate fraction of the seeds of Convolvulus arvensis are recommended to be used as natural antioxidant and cytotoxic agents.

**Keywords:** Antioxidant, Convolvulus Arvensis, Cytotoxic, Seeds, Phenolic Acids, Flavonoid

## M-729. Phytochemical Investigation of Phoenix Canariensis Hort. Ex Chabaud Leaves and Pollen Grains

Mohamed S. Hifnawy, Amr M. K. Mahrous and Rehab M. S. Ashour

*Journal of Applied Pharmaceutical Science, 6: 103-109 (2016)*

Phoenix canariensis is a commonly grown, yet understudied, palm plant. The phytochemical screening of leaves and pollens revealed the presence of flavonoids, saponins, tannins, sterols and/or triterpenes. Quantitative estimation of constituents, revealed that the total polyphenolics were higher in the leaves (69.9) than in pollens (29.98) expressed in mg gallic acid equivalent/g d.wt, the total flavonoids calculated as rutin equivalent were (23.86 mg/g) in leaves and (17.20 mg/g) in pollens, the total tannins content were 55.18 and 3.31 mg tannic acid equivalent/g fresh wt, while the total steroids content were 2.6 and 12.4 mg β-sitosterol equivalent/g d.wt, in leaves and pollens, respectively. Eighteen phenolic compounds and ten flavonoids were identified by HPLC. GLC analysis of lipids, revealed the identification of phytosterols (4.93 and 28.90%), saturated (35.35 and 40.56%) and unsaturated (62.42 and 59.01%) fatty acids in leaves and pollens, respectively. Proximate analysis revealed a total moisture content of (6.4 and 7.7 %), crude fiber (32.22 and 39.50%), total ash (12.1 and 8.1%) and acid insoluble ash (4.7 and 7.6 %) for leaves and pollens, respectively. Moreover, spathe headspace volatile analysis combined with GC-MS revealed the presence of fifty-two compounds constituting 72.84% of the total oil composition where α- copaene predominates (18.72%).

**Keywords:** Phoenix Canariensis, Lipids, Headspace Volatiles, Flavonoids, Phenolics, Steroids.

***Dept. of Pharmacology and Toxicology***

## M-730. Role of Rho Kinase Inhibition in the Protective Effect of Fasudil and Simvastatin Against 3-Nitropropionic Acid-Induced Striatal Neurodegeneration and Mitochondrial Dysfunction in Rats

Ahmed LA, Darwish HA, Abdelsalam RM and Amin HA.

*Molecular Neurobiology, 53(6): 3927-3938 (2016) IF: 5.397*

3-Nitropropionic acid (3-NP)-induced neurotoxicity is an experimental model which mimics the pathology and motor abnormalities seen in Huntington's disease (HD) in human. The present investigation was directed to estimate the role of rho kinase (ROCK) inhibition in the possible protective effect of fasudil and simvastatin in 3-NP-induced striatal neurodegeneration in rats. Animals were injected s.c. with 3-NP (20 mg/kg/day) for 1 week with or without administration of fasudil (10 mg/kg/day, p.o.) or simvastatin (20 mg/kg/day, p.o.). At the end of experiment, motor and behavioral abnormalities were evaluated. Animals were then sacrificed for measurement of mitochondrial membrane potential as well as succinate dehydrogenase (SDH) and caspase-3 activities in striatum. Moreover, tumor necrosis factor-alpha (TNF-α) level and protein expressions of proliferator-activated receptor gamma coactivator

1-alpha (PGC-1α), ROCK, phosphorylated-Akt (p-Akt), endothelial and inducible nitric oxide synthase (eNOS and iNOS), Bax, and Bcl-2 were estimated. Finally, histological changes as demonstrated by striatum injury score, glial activation, and percentage of altered mitochondria were assessed. Both fasudil and simvastatin effectively inhibited 3-NP-induced behavioral, biochemical, and histological changes through inhibition of ROCK activity. However, fasudil provided more amelioration in histological changes, mitochondrial membrane potential and SDH activity in addition to p-Akt and PGC-1α protein expressions. The present study highlights a significant role of ROCK/p-Akt/eNOS pathway in the protective effects of fasudil and simvastatin on neurotoxicity and mitochondrial dysfunction induced by 3-NP in rats. Thus, specific inhibition of ROCK may be considered a promising new approach in the management of HD.

**Keywords:** Fasudil; Mitochondria; Nitropropionic Acid; Simvastatin; Striatum

## M-731.Ursodeoxycholic Acid Ameliorates Apoptotic Cascade in the Rotenone Model of Parkinson'S Disease: Modulation of Mitochondrial Perturbations

Noha F. Abdelkader, Marwa M. Safar and Hesham A. Salem

*Molecular Neurobiology, 53: 810-817 (2016) IF: 5.397*

The recent emergence of ursodeoxycholic acid (UDCA) as a contender in modifying neurotoxicity in human dopaminergic cells as well as its recognized anti-apoptotic and anti-inflammatory potentials in various hepatic pathologies raised impetus in investigating its anti-parkinsonian effect in rat rotenone model. UDCA prominently improved motor performance in the open field test and halted the decline in the striatal dopamine content. Meanwhile, it improved mitochondrial function as verified by elevation of ATP associated with preservation of mitochondrial integrity as portrayed in the electron microscope examination. In addition, through its anti-inflammatory potential, UDCA reduced the rotenone-induced nuclear factor-κB expression and tumor necrosis factor alpha level. Furthermore, UDCA amended alterations in Bax and Bcl-2 and reduced the activities of caspase-8, caspase-9, and caspase-3, indicating that it suppressed rotenone-induced apoptosis via modulating both intrinsic and extrinsic pathways. In conclusion, UDCA can be introduced as a novel approach for the management of Parkinson's disease via anti-apoptotic and anti-inflammatory mechanisms. These effects are probably linked to dopamine synthesis and mitochondrial regulation.

**Keywords:** Ursodeoxycholic Acid, Rotenone, Caspases, Dopamine, Nuclear Factor-Kb, Atp

## M-732. Wharton'S Jelly-Derived Mesenchymal Stem Cells Combined with Praziquantel as a Potential Therapy for Schistosoma Mansoni-Induced Liver Fibrosis

Olfat A. Hammam, Nagwa Elkhafif, Yasmeen M. Attia and Mohamed T. Mansour

*Scientific Reports, 6: 1-13 (2016) IF: 5.228*

Liver fibrosis is one of the most serious consequences of S. mansoni infection. The aim of the present study was to investigate the potential anti-fibrotic effect of human Wharton's jelly-derived mesenchymal stem cells (WJMSCs) combined with praziquantel (PZQ) in S. mansoni-infected mice. S. mansoni-infected mice received early (8th week post infection) and late (16th week post infection) treatment with WJMSCs, alone and combined with oral PZQ. At the 10th month post infection, livers were collected for subsequent flow cytometric, histopathological, morphometric, immunohistochemical, gene expression, and gelatin zymographic studies. After transplantation, WJMSCs differentiated into functioning liver-like cells as evidenced by their ability to express human hepatocyte-specific markers. Regression of S. mansoni-induced liver fibrosis was also observed in transplanted groups, as evidenced by histopathological, morphometric, and gelatin zymographic results besides decreased expression of three essential contributors to liver fibrosis in this particular model; alpha smooth muscle actin, collagen-I, and interleukin-13. PZQ additionally enhanced the beneficial effects observed in WJMSCs-treated groups. Our results suggest that combining WJMSCs to PZQ caused better enhancement in S. mansoni-induced liver fibrosis, compared to using each alone.

**Keywords:** Wharton'S Jelly; Mesenchymal Stem Cells; Praziquantel; Schistosoma Mansoni; Liver Fibrosis.

## M-733. 17β-Estradiol Augments Antidepressant Efficacy of Escitalopram in Ovariectomized Rats: Neuroprotective and Serotonin Reuptake Transporter Modulatory Effects.

Weam W. Ibrahim, Marwa M. Safar, Mahmoud M. Khattab and Azza M. Agha

*Psychoneuroendocrinology, 74: 240-250 (2016) IF: 4.704*

The prevalence or recurrence of depression is seriously increased in women during the transition to and after menopause. The chronic hypo-estrogenic state of menopause may reduce the response to antidepressants; however the influence of estrogen therapy on their efficacy is still controversial. This study aimed at investigating the effects of combining escitalopram with 17β-estradiol on depression and cognitive impairment induced by ovariectomy, an experimental model of human menopause. Young adult female Wistar rats were subjected to either sham operation or ovariectomy. Ovariectomized animals were treated chronically with escitalopram (10mg/kg/day, i.p) alone or with four doses of 17β-estradiol (40μg/kg, s.c) given prior to the behavioral tests. Co-administration of 17β-estradiol improved escitalopram-induced antidepressant effect in forced swimming test verified as more prominent decrease in the immobility time without opposing its memory enhancing effect in Morris water maze. 17β-estradiol augmented the modulatory effects of escitalopram on the hippocampal levels of brain-derived neurotrophic factor and serotonin reuptake transporter as well as tumor necrosis factor-alpha without altering its effects on the gene expressions of serotonin receptor 1A, estrogen receptors alpha and beta, or acetylcholinestearase content. This combined therapy afforded synergistic protective effects on the brain histopathological architecture, particularly, the hippocampus. The antidepressant effect of 17β-estradiol was abolished by pretreatment with estrogen receptor antagonist, tamoxifen (10mg/kg, p.o). In conclusion, 17β-estradiol-induced antidepressant effect was

confined to intracellular estrogen receptors activation. Moreover, 17β-estradiol enhanced escitalopram's efficiency in ameliorating menopausal-like depression, via exerting synergistic neuroprotective and serotonin reuptake transporter modulatory effects, without impeding escitalopram-mediated cognitive improvement.

**Keywords:** Estrogen Receptor Antagonist; Estrogen Receptors; Forced Swimming Test; Selective Serotonin Reuptake Inhibitor; Serotonin Receptor; Serotonin Transporter

## M-734. Exercise Modulates Oxidative Stress and Inflammation in Aging and Cardiovascular Diseases

Nada Sallam and Ismail Laher

*Oxidative Medicine and Cellular Longevity,1-32 (2016 IF: 4.492*

Despite the wealth of epidemiological and experimental studies indicating the protective role of regular physical activity/exercise training against the sequels of aging and cardiovascular diseases, the molecular transducers of exercise/physical activity benefits are not fully identified but should be further investigated in more integrative and innovative approaches, as they bear the potential for transformative discoveries of novel therapeutic targets. As aging and cardiovascular diseases are associated with a chronic state of oxidative stress and inflammation mediated via complex and interconnected pathways, we will focus in this review on the antioxidant and anti-inflammatory actions of exercise, mainly exerted on adipose tissue, skeletal muscles, immune system, and cardiovascular system by modulating anti-inflammatory/proinflammatory cytokines profile, redox-sensitive transcription factors such as nuclear factor kappa B, activator protein-1, and peroxisome proliferator-activated receptor gamma coactivator 1-alpha, antioxidant and prooxidant enzymes, and repair proteins such as heat shock proteins, proteasome complex, oxoguanine DNA glycosylase, uracil DNA glycosylase, and telomerase. It is important to note that the effects of exercise vary depending on the type, intensity, frequency, and duration of exercise as well as on the individual's characteristics; therefore, the development of personalized exercise programs is essential.

**Keywords:** Ageing, Cardiovascular Diseases, Exercise, Oxidative Stress, Inflammation, Mitochondrial Dysfunction

## M-735.Dapoxetine Attenuates Testosterone-Induced Prostatic Hyperplasia in Rats by the Regulation of Inflammatory and Apoptotic Proteins

Rabab H. Sayed, Muhammed A. Saad and Ayman E. El-Sahar

*Toxicology and Applied Pharmacology, 311: 52-60(2016) IF:3.847*

Serotonin level plays a role in suppressing the pathological findings of benign prostatic hyperplasia (BPH). Thus a new selective serotonin reuptake inhibitor, dapoxetine was used to test its ability to ameliorate the pathological changes in the rat prostate. A dose response curve was constructed between the dose of dapoxetine and prostate weight as well as relative prostate weight, then a 5mg/kg dose was used as a representative dose for dapoxetine administration. Rats were divided into four groups; the control group that received the vehicle; the BPH-induced group received daily s.c injection of 3mg/kg testosterone propionate dissolved in olive oil for four weeks; BPH-induced group treated with finasteride 5mg/kg/day p.o and BPH-induced group treated with dapoxetine 5mg/kg/day p.o. Injection of testosterone increased prostate weight and relative prostate weight which were both returned back to the normal value after treatment with dapoxetine as well as finasteride. Testosterone also upregulated androgen receptor (AR) and proliferating cell nuclear antigen gene expression. Furthermore, testosterone injection elevated cyclooxygenase-II (COX II), inducible nitric oxide synthase (iNOS), B-cell lymphoma-2 (Bcl2) expression and tumor necrosis factor alpha content and reduced caspase-3 activity, Bcl-2-associated X protein (Bax) expression and Bax/Bcl2 ratio. Dapoxetine and finasteride administration reverted most of the changes made by testosterone injection. In conclusion, the current study provides an evidence for the protective effects of dapoxetine against testosterone-induced BPH in rats. This can be attributed, at least in part, to decreasing AR expression, and the anti-proliferative, anti-inflammatory and pro-apoptotic activities of dapoxetine in BPH

**Keywords:** Apoptosis; Benign Prostatic Hyperplasia; Dapoxetine; Inflammation; Proliferating Cell Nuclear Antigen

## M-737.Combination of Metformin and 5-Aminosalicylic Acid Cooperates to Decrease Proliferation and Induce Apoptosis in Colorectal Cancer Cell Lines

Mona M. Saber, May A. Galal, Afaf A. Ain-Shoka and Samia A. Shouman

*Bmc Cancer, 16:126: 1-12 (2016) IF: 3.265*

**Background:** The link between inflammation and cancer has been confirmed by the use of anti-inflammatory therapies in cancer prevention and treatment. 5-aminosalicylic acid (5-ASA) was shown to decrease the growth and survival of colorectal cancer (CRC) cells. Studies also revealed that metformin induced apoptosis in several cancer cell lines. **Methods:** We investigated the combinatory effect of 5-ASA and metformin on HCT-116 and Caco-2 CRC cell lines. Apoptotic markers were determined using western blotting. Expression of pro-inflammatory cytokines was determined by RT-PCR. Inflammatory transcription factors and metastatic markers were measured by ELISA. **Results:** Metformin enhanced CRC cell death induced by 5-ASA through significant increase in oxidative stress and activation of apoptotic machinery. Moreover, metformin enhanced the anti-inflammatory effect of 5-ASA by decreasing the gene expression of IL-1β, IL-6, COX-2 and TNF-α and its receptors; TNF-R1 and TNF-R2. Significant inhibition of activation of NF-κB and STAT3 transcription factors, and their downstream targets was also observed. Metformin also enhanced the inhibitory effect of 5-ASA on MMP-2 and MMP-9 enzyme activity, indicating a decrease in metastasis. **Conclusion:** The current data demonstrate that metformin potentiates the antitumor effect of 5-ASA on CRC cells suggesting their potential use as an adjuvant treatment in CRC.

**Keywords:** 5-ASA, Inflammation, CRC, NF-KB, STAT3, Metformin.

## M-738.Imipramine and Amitriptyline Ameliorate the Rotenone Model of Parkinsons Disease in Rats.

Esraa A. Kandil, Noha F. Abdelkader, Bahia M. El-Sayeh and Samira Saleh

*Neuroscience, 332: 26-37 (2016) IF: 3.231*

Amitriptyline (AMI), a commonly prescribed tricyclic antidepressant (TCA) to parkinsonian patients, specifically showed a significant delay in dopaminergic therapy initiation and improvement in motor disability in parkinsonian patients. Moreover, it was recently shown that AMI has neuroprotective properties; however, the mechanisms underlying this effect in Parkinson's disease (PD) are not fully understood. The current study aimed to investigate the possible neuroprotective mechanisms afforded by AMI in the rotenone model of PD and to assess whether another TCA member, imipramine (IMI), shows a corresponding effect. Rats were allocated into seven groups. Four groups were given either saline, dimethyl sulfoxide, AMI or IMI. Three rotenone groups were either untreated or treated with AMI or IMI. Rats receiving rotenone exhibited motor impairment in open field and rotarod tests. Additionally, immunohistochemical examination revealed dopaminergic neuronal damage in substantia nigra. Besides, striatal monoamines and brain derived neurotrophic factor levels were declined. Furthermore, oxidative stress, microglial activation and inflammation were evident in the striata. Pretreatment of rotenone groups with AMI or IMI prevented rotenone-induced neuronal degeneration and increased striatal dopamine level with motor recovery. These effects were accompanied by restoring striatal monoamines and brain-derived neurotrophic factor levels, as well as reducing oxidative damage, microglial activation and expression of proinflammatory cytokines and inducible nitric oxide synthase. The present results suggest that modulation of noradrenaline and serotonin levels, up-regulation of neurotrophin, inhibition of glial activation, anti-oxidant and anti-inflammatory activities could serve as important mechanisms underlying the neuroprotective effects of the used drugs in the rotenone model of PD.

**Keywords:** Parkinson'S Disease; Amitriptyline; Imipramine; Neuroprotection; Rotenone

## M-739. Role of Adenosine A2A Receptor in Cerebral Ischemia Reperfusion Injury: Signaling to Phosphorylated Extracellular Signal-Regulated Protein Kinase (pERK1/2).

R. A. Mohamed, A. M. Agha, A. A. Abdel-Rahman and N. N. Nassa

*Neuroscience, 314: 145-159 (2016) IF: 3.231*

Following brain ischemia reperfusion (IR), the dramatic increase in adenosine activates A2AR to induce further neuronal damage. Noteworthy, A2A antagonists have proven efficacious in halting IR injury, however, the detailed downstream signaling remains elusive. To this end, the present study aimed to investigate the possible involvement of phospho-extracellular signal-regulated kinase (pERK1/2) pathway in mediating protection afforded by the central A2A blockade. Male Wistar rats (250-270 g) subjected to bilateral carotid occlusion for 45 min followed by a 24-h reperfusion period showed increased infarct size corroborating histopathological damage, memory impairment and motor incoordination as well as increased locomotor activity. Those events were mitigated by the unilateral intrahippocampal administration of the selective A2A antagonist SCH58261 via a decrease in pERK1/2 downstream from diacyl glycerol (DAG) signaling. Consequent to pERK1/2 inhibition, reduced hippocampal microglial activation, glial tumor necrosis factor-alpha (TNF-α) and brain-derived neurotropic factor (BDNF) expression, glutamate (Glu), inducible nitric oxide synthase (iNOS) and thiobarbituric acid reactive substances (TBARS) were evident in animals receiving SCH58261. Additionally, the anti-inflammatory cytokine interleukin-10 (IL-10) increased following nuclear factor (erythroid-derived 2)-like 2 (Nrf-2). Taken all together, these events suppressed apoptotic pathways via a reduction in cytochrome c (Cyt. c) as well as caspase-3 supporting a crucial role for pERK1/2 inhibition in consequent reduction of inflammatory and excitotoxic cascades as well as correction of the redox imbalance.

**Keywords:** A(2A); Apoptosis; Ischemia Reperfusion; Microglia; Oxidative Stress; pERK1/2

## M-740. Photothermal Therapy Mediated by Gum Arabic-Conjugated Gold Nanoparticles Suppresses Liver Preneoplastic Lesions in Mice

Gamal-Eldeen AM, Moustafa D, El-Daly SM, El-Hussieny EA, Saleh S, Khoobchandani M, Bacon KL, Gupta S, Katti K, Shukla R and Katti KV.

*Journal of Photochemistry and Photobiology B: Biology, 163: 47-56 (2016) IF: 3.035*

This study validates the utility of Gum Arabic-conjugated gold nanoparticles (GA-AuNPs) and laser to induce photothermal inhibition of hepatocarcinogenesis, via employing a diethylnitrosamine (DEN)-mediated hepatocellular carcinoma model. This work included both of in vitro and in vivo studies; to investigate the GA-AuNPs cytotoxicity and phototoxicity in hepatic cell line; to delineate the GA-AuNPs therapeutic efficiency in DEN-induced preneoplastic lesions (PNLs) in the liver of Balb-C mice. The therapeutic effects of GA-AuNPs on the mediators of apoptosis, inflammation, and tumor initiation, as well as the histopathological changes in preneoplastic liver have been investigated. Our results infer that GA-AuNPs in combination with laser irradiation led to a significant reduction in the cell viability and in histone deacetylase activity in hepatocarcinoma HepG2 cells. In chemically-induced PNLs mice model our results have demonstrated that GA-AuNPs, with or without laser irradiation, induced cancer cell apoptosis through the activation of death receptors DR5 and caspase-3 and inhibited both of the PNLs incidence and the initiation marker (placental glutathione S-transferase; GST-P). The laser-stimulated GA-AuNPs significantly reduced the tumor necrosis factor-α levels. In summary, GA-AuNPs with laser treatment inhibited liver PNLs via the induction of the extrinsic apoptosis pathway and the inhibition of inflammation

**Keywords:** Apoptosis; Gst-P; Gold Nanoparticles; Gum Arabic; Photothermal; Preneoplastic Lesions.

## M-741. Resveratrol and Fenofibrate Ameliorate Fructose-Induced Nonalcoholic Steatohepatitis by Modulation of Genes Expression

Enas A Abd El-Haleim, Ashraf K Bahgat and Samira Saleh

*World Journal of Gastroenterology, 22: 2931-2984 (2016) IF:2.787*

**AIM:** To evaluate the effect of resveratrol, alone and in combination with fenofibrate, on fructose-induced metabolic genes abnormalities in rats. **Methods:** Giving a fructose-enriched diet (FED) to rats for 12 wk was used as a model for inducing hepatic dyslipidemia and insulin resistance. Adult male albino rats (150-200 g) were divided into a control group and a FED group which was subdivided into 4 groups, a control FED, fenofibrate (FENO) (100 mg/kg), resveratrol (RES) (70 mg/kg) and combined treatment (FENO + RES) (half the doses). All treatments were given orally from the 9th week till the end of experimental period. Body weight, oral glucose tolerance test (OGTT), liver index, glucose, insulin, insulin resistance (HOMA), serum and liver triglycerides (TGs), oxidative stress (liver MDA, GSH and SOD), serum AST, ALT, AST/ALT ratio and tumor necrosis factor-α (TNF-α) were measured. Additionally, hepatic gene expression of suppressor of cytokine signaling-3 (SOCS-3), sterol regulatory element binding protein-1c (SREBP-1c), fatty acid synthase (FAS), malonyl CoA decarboxylase (MCD), transforming growth factor-β1 (TGF-β1) and adipose tissue genes expression of leptin and adiponectin were investigated. Liver sections were taken for histopathological examination and steatosis area were determined. **Results:** Rats fed FED showed damaged liver, impairment of glucose tolerance, insulin resistance, oxidative stress and dyslipidemia. As for gene expression, there was a change in favor of dyslipidemia and nonalcoholic steatohepatitis (NASH) development. All treatment regimens showed some benefit in reversing the described deviations. Fructose caused deterioration in hepatic gene expression of SOCS-3, SREBP-1c, FAS, MDA and TGF-β1 and in adipose tissue gene expression of leptin and adiponectin. Fructose showed also an increase in body weight, insulin resistance (OGTT, HOMA), serum and liver TGs, hepatic MDA, serum AST, AST/ALT ratio and TNF-α compared to control. All treatments improved SOCS-3, FAS, MCD, TGF-β1 and leptin genes expression while only RES and FENO + RES groups showed an improvement in SREBP-1c expression. Adiponectin gene expression was improved only by RES. A decrease in body weight, HOMA, liver TGs, AST/ALT ratio and TNF-α were observed in all treatment groups. Liver index was increased in FENO and FENO + RES groups. Serum TGs was improved only by FENO treatment. Liver MDA was improved by RES and FENO + RES treatments. FENO + RES group showed an increase in liver GSH content. **Conclusion:** When resveratrol was given with half the dose of fenofibrate it improved NASH-related fructose-induced disturbances in gene expression similar to a full dose of fenofibrate.

**Keywords:** Fructose, Nonalcoholic Steatohepatitis, Suppressor of Cytokine Signaling-3, Sterol Regulatory Element Binding Protein-1C, Fatty Acid Synthase, Malonyl Coa Decarboxylase, Leptin, Adiponectin, Transforming Growth Factor-B, Tumor Necrosis Factor-A

## M-742.Effects of Combined PPAR-Gamma and Ppar-Alpha Agonist Therapy on Fructose Induced NASHin Rats: Modulation of Gene Expression

Enas A.AbdEl-Haleim, AshrafK.Bahgat and SamiraSaleh

*European Journal of Pharmacology, 773: 59-70 (2016) IF: 2.73*

Peroxisome proliferator-activated receptors (PPARs) gamma and alpha have been shown to play key roles in maintaining glucose and lipid homeostasis by acting as insulin sensitizers and lipid-lowering agents respectively, which would make them potential candidates for the treatment of non-alcoholic steatohepatitis (NASH) characterized by insulin resistance, hyperglycemia, and hypertriglyceridemia. The effects of pioglitazone, a PPAR-γ agonist, and fenofibrate, a PPAR-α agonist, as monotherapy and in combination on the expressions of key genes linked to the development of NASH were studied in rats with fructose-induced NASH. Fructose-enriched diet was given to rats for 12 weeks. Fenofibrate (100mg/kg), pioglitazone (4 mg/kg) and combined treatment with both in half doses were given. Body weight, liver index, insulin resistance indices, triglycerides, oxidative stress markers, AST/ALT ratio and TNF-α were measured. Additionally, hepatic genes expressions of SOCS-3, sterol regulatory element binding protein-1c, fatty acid synthase, malonyl CoA decarboxylase, TGF-β1, and adipose tissue genes expressions of leptin and adiponectin were investigated. The combination of both drugs, in half doses, improved NASH-related disturbances similar to, or even better than, a full dose of fenofibrate alone possibly due to attenuating effects of pioglitazone on expression of genes responsible for insulin resistance, fatty acid synthesis and fibrosis in addition to correcting the balance between leptin and adiponectin. Histopathology confirmed the ability of this combination to decrease steatosis area and to normalize hepatic tissue structure. In Conclusion, dual activation of PPAR-γ and PPAR-α has remarkable effect in ameliorating NASH by modulation of some hepatic and adipose tissue genes expressions.

**Keywords:** Adiponectin; Leptin; Nash; Ppar; Socs-3; Srebp-1C

## M-743. The Potential of Genetically Guided Treatment in Behçet'S Disease

Tamer A Gheita, Heba A Gheita and Sanaa A Kenawy

*Pharmacogenomics, 17: 1165-1174 (2016) IF: 2.71*

Continuous identification of specific targets and candidate genes together with novel approaches offers new promises for the future of gene therapy design in Behçet's disease (BD). Personalized medicine based on pharmacogenomics is being developed at the clinical stage to improve treatment response. Screening the whole gene and regulatory regions is important when searching for novel variants associated with such complex diseases. Different host genetic factors play significant roles in susceptibility to BD. Thus, identifying these genes responsible for susceptibility and resistance to BD may offer a notable contribution toward understanding its pathogenesis, and may lead to the development of novel prophylactic and treatment strategies. Evidencedbased treatment strategy is recommended for the management in BD patients. This review sheds light on the immunopathogenesis and pharmacogenetics of BD with special attention to the treatment targeting gene polymorphisms. In conclusion, the potential of genetically guided treatment in BD takes us back to the future for an accurate management

strategy of this serious rheumatic disease. The ongoing discovery of pivotal genes related to the susceptibility, manifestations, disease activity and treatment options provide substantial hope to the reduced frequency of BD, effective control and improvement in the prognosis. Targeted gene therapy could be a leading option in the treatment armamentarium of BD.

**Keywords:** Behçet'S Disease; Gene Therapy; Immunopathogenesis; Pharmacogenomics.

## M-744. Carvedilol Alleviates Testicular and Spermatological Damage Induced by Cisplatin in Rats Via Modulation of Oxidative Stress and Inflammation

Ahmed H. Eid, Noha F. Abdelkader, Ola M. Abd El-Raouf, Hala M. Fawzy and Ezz-El-Din S. El-Denshary

*Archives of Pharmacal Research, 39: 1693-1702(2016) IF: 2.49*

The clinical application of the anticancer drug cisplatin is limited by its deleterious side effects, including male reproductive toxicity. In this context, the potential protective effect of carvedilol on testicular and spermatological damage induced by cisplatin in male Sprague–Dawley rats was investigated. Carvedilol was orally administered at a dose of 10 mg/kg for 2 weeks, and cisplatin was given as a single intraperitoneal injection of 10 mg/kg on the 12th day to induce toxicity. Cisplatin significantly reduced reproductive organ weight, sperm count and sperm motility, and increased sperm abnormalities and histopathological damage of testicular tissue. In addition, it resulted in a significant decline in serum testosterone as well as levels of testicular enzymatic and non-enzymatic antioxidants (superoxide dismutase, catalase, glutathione peroxides, and reduced glutathione). Moreover, cisplatin remarkably augmented malondialdehyde, nitric oxide, tumor necrosis factor-α, and nuclear factor-kappa B contents in testicular tissue. Conversely, carvedilol administration markedly mitigated cisplatin-induced testicular and spermatological injury as demonstrated by suppression of oxidative/nitrosative and inflammatory burden, amendment of antioxidant defenses, enhancement of steroidogenesis and spermatogenesis, and mitigation of testicular histopathological damage. The current study reveals a promising protective action of carvedilol against cisplatin-induced reproductive toxicity by virtue of its anti-inflammatory and antioxidant properties.

**Keywords:** Cisplatin;Testicular Damage; Carvedilol; Oxidative Stress; Inflammation

## M-745. Anti-Diabetic and Renoprotective Effects of Aliskiren in Streptozotocin-Induced Diabetic Nephropathy in Female Rats

Amal M. Mahfoz, Hekma A. Abd El-Latif, Lamiaa A. Ahmed, Nahed M. Hassanein and Afaf A. Shoka

*Naunyn-Schmiedebergs Arch Pharmacol, 389: 1315-1324 (2016) IF: 2.376*

Since chronic kidney disease due to diabetic nephropathy (DN) is becoming an ever larger health burden worldwide, more effective therapies are desperately needed. In the present study, the anti-diabetic and renoprotective effects of aliskiren have been evaluated in streptozotocin (STZ)- induced DN in rats. DN was induced by a single intraperitoneal injection of STZ (65 mg/kg). Three weeks after STZ, rats were divided into four groups; normal, diabetic, diabetic treated with gliclazide (10 mg/kg/day) for 1 month, and diabetic treated with aliskiren (50 mg/kg/day) for 1 month. At the end of the experiment, mean arterial blood pressure and heart rate were recorded. Rats were then euthanized and serum was separated for determination of glucose, insulin, kidney function tests, superoxide dismutase activity (SOD), adiponectin, and tumor necrosis factor-alpha (TNF-α). One kidney was used for estimation of malondialdehyde (MDA), reduced glutathione (GSH), and nitric oxide (NO) contents. Other kidney was used for histopathological study and immunohistochemical measurement of caspase-3 and transforming growth factor beta (TGF-β). In addition, islets of Langerhans were isolated from normal rats by collagenase digestion technique for in vitro study. Aliskiren normalized STZ-induced hyperglycemia, increased insulin level both in vivo and in vitro, normalized kidney function tests and blood pressure, and alleviated STZ-induced kidney histopathological changes. This could be related to the ability of aliskiren toward preserving hemodynamic changes and alleviating oxidative stress and inflammatory and apoptotic markers induced by STZ in rats. However, aliskiren was more effective than gliclazide in relieving STZ-induced DN. These findings support the beneficial effect of aliskiren treatment in DN which could be attributed to its anti-diabetic, renoprotective, antioxidant, antiinflammatory, and anti-apoptotic effects. Moreover, clinical studies are required to establish the effectiveness of aliskiren treatment in patients suffering from hypertension and diabetes.

**Keywords:** Renin-Angiotensin System; Diabetic Nephropathy; Oxidative Stress; Gliclazide; Aliskiren

## M-746. Tempol and perindopril protect against lipopolysaccharide-induced cognition impairment and amyloidogenesis by modulating brain-derived neurotropic factor, neuroinflammation and oxido-nitrosative stress.

Mahmoud Mohammed Khattab

*Journal ,: p1-p2 (2016) IF: 2.3759999275*

Recent. We aim to evaluate the protective role of the central angiotensin-converting enzyme (ACE) inhibitor perindopril, compared with the standard reactive oxygen species (ROS) scavenger tempol, against lipopolysaccharide (LPS)-induced cognition impairment and amyloidogenesis in a simulation to Alzheimer's disease (AD). Mice were allocated into a control group, an LPS control group (0.8 mg/kg, i.p., once), a tempol (100 mg/kg/day, p.o., 7 days) treatment group, and two perindopril (0.5 and 1 mg/kg/day, p.o., 7 days) treatment groups. A behavioral study was conducted to evaluate spatial and nonspatial memory in mice, followed by a biochemical study involving assessment of brain levels of Aβ and BDNF as Alzheimer and neuroplasticity markers; tumor necrosis factor-alpha (TNF-α), nitric oxide end-products (NOx), neuronal nitric oxide synthase (nNOS), and inducible nitric oxide synthase (iNOS) as inflammatory markers; and superoxide dismutase (SOD), malondialdehyde (MDA), glutathione reduced (GSH), and nitrotyrosine (NT) as oxido-nitrosative stress markers. Finally, histopathological examination of cerebral cortex, hippocampus, and cerebellum sections was performed using

both routine and special staining. Tempol and perindopril improved spatial and nonspatial memory in mice without affecting locomotor activity; decreased brain Aβ deposition and BDNF depletion; decreased brain TNF-α, NOx, nNOS, iNOS, MDA, and NT levels; and increased brain SOD and GSH contents, parallel to confirmatory histopathological findings. Tempol and perindopril may be promising agents against AD progression via suppression of Aβ deposition and BDNF decline, suppression of TNF-α production, support of brain antioxidant status, and amelioration of oxido-nitrosative stress and NT production.

**Keywords:** Amyloidogenesis; Brain-derived neurotropic factor; Neuroinflammation Oxido-nitrosative stress; Perindopril; Tempol.

## M-747.Co-administration of 3-Acetyl-11-Keto-Beta-Boswellic Acid Potentiates the Protective Effect of Celecoxib in Lipopolysaccharide-Induced Cognitive Impairment in Mice: Possible Implication of Anti-Inflammatory and Antiglutamatergic Pathways

Aya Shoukry Sayed and Nesrine Salah El-Dine El Sayed

*Journal of Molecular Neuroscience,59(1):58-67(2016) IF:2.352*

Neuro-inflammation is known to initiate the underlying pathogenesis of several neurodegenerative disorders which may progress to cognitive, behavioral, and functional impairment. Boswellia serrata is a well-known powerful antiinflammatory agent used to treat several inflammatory diseases. The aim of the current study is to investigate the effect of the combination therapy of 3-acetyl-11-keto-β-boswellic acid (AKBA), a 5-lipoxygenase (5-LOX) inhibitor and celecoxib, and a selective cyclooxygenase-2 (COX-2) inhibitor as dual enzyme inhibitors compared tomonotherapies with celecoxib and AKBA. Cognitive dysfunction is induced by intraperational injection of lipopolysaccharide (LPS) in mice. Radial maze, Y maze, and novel object recognition (NOR) were performed to evaluate the possible behavioral changes. Moreover, estimation of glutamate and tumor necrosis factor alpha (TNF-α), as well as an immunohistochemical investigation of amyloid beta peptide (Aβ) was performed to evaluate the molecular changes that followed the LPS or drug treatment. The results showed that the combination therapy of AKBA and celecoxib reversed the behavioral and molecular changes caused by LPS cognitive dysfunction model that predispose cognitive dysfunction in mice. This study showed the effectiveness of the dual therapy with AKBA and celecoxib as anti-inflammatory, antiglutamatergic, and anti-amyloidogenic agents in the management of cognitive dysfunction.

**Keywords:** Cognitive Dysfunctionlipopolysaccharide3-Acetyl-11-Keto-B-Boswellic Acidamyloid Beta Peptideglutamatetumor Necrosis Factor-Alpha

## M-748.Vitamin D Status in Rheumatoid Arthritis Patients: Relation to Clinical Manifestations, Disease Activity, Quality of Life and Fibromyalgia Syndrome

Tamer A. Gheita, Safaa Sayed, Heba A. Gheita and Sanaa A. Kenawy

*International Journal of Rheumatic Diseases, 19: 294-299 (2016) IF: 1.914*

**Aim:** To assess vitamin D levels in rheumatoid arthritis (RA) patients and to find their relation to clinical parameters, fibromyalgia syndrome (FMS), quality of life (QoL) and disease activity. **Methods:** The study included 63 RA patients and 62 controls. Clinical examination and laboratory investigations were performed. For patients, the Disease Activity Score (DAS-28), QoL index, Health Assessment Questionnaire II (HAQ II) and Modified Larsen score were calculated. 25-OH-vitamin D was measured in patients and controls. **Results:** The patients' mean age was 41.59 9.69 years and disease duration 5.89 3.67 years. The level of vitamin D in RA patients was significantly lower (23.11 12.71 ng/mL) than that in the controls (32.59 13.06 ng/mL) ($P = 0.005$) being deficient in 50.8%, insufficient in 23.8% and normal in 25.4%. The RA patients with FMS ($n = 33$) had significantly lower levels of vitamin D (19.08 10.59 ng/mL) than those without (27.55 13.51 ng/mL) ($P = 0.008$). The difference was significant on comparing those receiving hydroxychloroquine (17.39 7.84 ng/mL) to those not (31.85 13.85 ng/mL) ($P < 0.001$). Vitamin D significantly correlated with QoL index ($r = 0.58$, $P < 0.001$) and negatively with HAQ II ($r = 0.36$, $P = 0.004$) and BMI ($r = 0.39$, $P = 0.001$). **Conclusion:** Special attention is required regarding vitamin D levels in RA patients with FMS and decreased QoL. Vitamin D should be corrected and supplementation considered among the RA management armamentarium.

**Keywords:** Disease Activity (Das-28), Fibromyalgia Syndrome, Haq Ii, QoL, Rheumatoid Arthritis, Vitamin D.

## M-749. Is Coenzyme Q10 Effective in Protection Against Ulcerative Colitis? an Experimental Study in Rats

Mohamed Gamal Ewees, Basim Anwar Shehata Messiha, Ali Ahmed Abo-Saif and Hekma Abd El-Tawab Abd El-Latif

*Biol. Pharm. Bull, 39, ( 7): 1159-1166 (2016) IF: 1.574*

Coenzyme Q10 (Co-Q10) is a vitamin-like supplement which appears to be safe, with minimal side effects and low drug interaction potential. Co-Q10 is used in the treatment of a variety of disorders related primarily to suboptimal cellular energy metabolism and oxidative injury. Studies supporting the efficacy of Co-Q10 appear most promising for a variety of diseases, including ulcerative colitis (UC). The present investigation aims to elucidate the possible protective effects of Co-Q10 against UC, as induced by the administration of iodoacetamide to adult male albino rats. In our study, Co-Q10 showed potent anti-oxidant and anti-inflammatory activities through a significant increase in catalase activity and glutathione content. In addition, it significantly decreased myeloperoxidase activity, malondialdehyde content and nitrate/nitrite production. These results suggest that Co-Q10 protects against UC in rats via anti-

oxidant and anti-inflammatory potentials, and therefore seems promising for use in further clinical trials.
**Keywords:** Coenzyme Q10; Ulcerative Colitis; Iodoacetamide; Oxidative Stress; Rat; Sulfasalazine

## M-750. Protective Effect of Ursodeoxycholic Acid, Resveratrol, and N-Acetylcysteine on Nonalcoholic Fatty Liver Disease in Rats

Mahmoud Hussein Hassan Ali, Basim Anwar Shehata Messiha and Hekma Abdel-Tawab Abdel-Latif

*Pharm Biol, 54(7): 1198-1208 (2016) IF: 1.546*

**Context:** Nonalcoholic fatty liver disease (NAFLD) is the most common chronic liver disease. Resveratrol (RSV) and N-acetylcysteine (NAC) are safe representatives of natural and synthetic antioxidants, respectively. **Objective:** The objective of this study was to evaluate protective effects of RSV and NAC, compared with ursodeoxycholic acid (UDCA), on experimental NAFLD. Materials and methods: NAFLD was induced by feeding rats a methionine choline-deficient diet (MCDD) for four cycles, each of 4 d of MCDD feeding and 3 d of fasting. Animals were divided into normal control, steatosis control, and five treatment groups, receiving UDCA (25 mg/kg/d), RSV (10 mg/kg/d), NAC (20 mg/kg/d), UDCA + RSV, and UDCA + NAC orally for 28 d. Liver integrity markers (liver index and serum transaminases), serum tumor necrosis factor-a (TNF-a), glucose, albumin, renal functions (urea, creatinine), lipid profile (total cholesterol; TC, triglycerides, high density lipoproteins, low density lipoproteins; LDL-C, very low density lipoproteins, leptin), and oxidative stress markers (hepatic malondialdehyde; MDA, glutathione; GSH, glutathione-S-transferase; GST) were measured using automatic analyzer, colorimetric kits, and ELISA kits, supported by a liver histopathological study. **Results:** RSV and NAC administration significantly improved liver index (RSV only), alanine transaminase (52, 52%), TNF-a (70, 70%), glucose (69, 80%), albumin (122, 114%), MDA (55, 63%), GSH (160, 152%), GST (84, 84%), TC (86, 86%), LDL-C (83, 81%), and leptin (59, 70%) levels compared with steatosis control values. A combination of RSV or NAC with UDCA seems to ameliorate their effects. Discussion and conclusion: RSV and NAC are effective on NAFLD through antioxidant, antiinflammatory, and lipid-lowering potentials, where as RSV seems better than UDCA or NAC.
**Keywords:** Dyslipidemia, Inflammation, Methionine– Choline-Deficient Diet, Oxidative Stress, Steatohepatitis, Steatosis

## M-751. Pyrrolidinedithiocarbamate Attenuates Bleomycin-Induced Pulmonary Fibrosis in Rats: Modulation of Oxidative Stress, Fibrosis, and Inflammatory Parameters

Zaafan MA, Zaki HF, El-Brairy AI and Kenawy SA

*Experimental Lung Research, 42: 408-416 (2016) IF: 1.374*

**Objective:** The current study aimed to investigate the modulatory effects of pyrrolidinedithiocarbamate (PDTC; 100 mg/kg) on bleomycin-induced pulmonary fibrosis (5 mg/kg; intratracheal) in rats. **Materials and Methods:** Rats were randomly assigned to three groups: normal control, bleomycin control, and PDTC-treated groups. Lung injury was evaluated through histological examination, immunohistochemical detection of inducible nitric oxide synthase (iNOS) in lung tissue and evaluating the total and differential leucocytes count in bronchoalveolar lavage fluid. Lung tissue was used for biochemical assessment of lung content of hydroxyproline, transforming growth factor beta-1 (TGF-β1), tumor necrosis factor-alpha (TNF-α) as well as analysis of lipid peroxides, reduced glutathione (GSH), and total nitrite contents. **Results:** PDTC attenuated bleomycin-induced pulmonary fibrosis as evidenced by histological observations, decreased iNOS expression and prevention of bleomycin-induced altered total and differential leukocytes count. Additionally, PDTC caused a significant decrease in lung contents of hydroxyproline, TGF-β1, TNF-α, lipid peroxides, and total nitrite coupled with increase in lung GSH content as compared to bleomycin control group. **Conclusion:** PDTC attenuated bleomycin-induced pulmonary fibrosis in rats via its anti-inflammatory, antioxidant, and antifibrotic activities.
**Keywords:** Bleomycin; Nitric Oxide; Pulmonary Fibrosis; Pyrrolidinedithiocarbamate; Tumor Necrosis Factor-Alpha

## M-752. Lipoic Acid and Coenzyme Q10 Protect Against Lead-Induced Toxicity in Rats with Metabolic Syndrome

Hany A. Omar, Waleed H. Almalki, Hanan Shamard, Abeer Y. Mahdy and Hekma A. Abd El-Latif

*International Journal of Pharmacology, 12 (3)146-153(2016) IF: 0.536*

Obesity may lead to Metabolic Syndrome (MS). The MS is often characterized by oxidative stresswhich contributes to cellular damage and dysfunction. Lead toxicity is a major health problem especially in obese individuals. Therefore the aim of the current study was to investigate the biochemical and cardiovascular effects caused by lead exposure in rats with metabolic syndrome and suggesting possible protective measures. The MS was induced by feeding rats with high fat diet and fructose in drinking water for 90 days. Matched normal group was used as a control. Rats with metabolic syndrome were allowed to drink water containing lead acetate for 30 days either alone, with alpha-Lipoic Acid (LA) or coenzyme Q10 (CoQ10). At the end of experiment, body weight, systolic blood pressure and heart rate were assessed. Creatinine and uric acid were also determined. Lipid profile, oxidative stress biomarkers, nitric oxide, TNFα, calcium, insulin and glucose were determined. The exposure to lead worsens kidney function, oxidative stress and metabolic effects caused by metabolic syndrome. The use of LA or CoQ10 could ameliorate these harmful effects of lead. In conclusion, lead worsens the MS cases due to its ability to induce oxidative stress in rat tissues. The LA and CoQ10 beneficial effects could be attributed to their antioxidant capacity.
**Keywords:** Lipoic Acid, Coenzyme Q10, Lead, Kidney Function, Oxidative Stress, Metabolic Syndrome.

### M-753. Protective Effects of Alpha-Lipoic Acid and Coenzyme Q10 on Lipopolysaccharide-Induced Liver Injury in Rats

Amr M. Emam, Gehan S. Georgy, Olfat G. Shaker, Hala M. Fawzy and Hala F. Zaki

*Der Pharmacia Lettre, 8(9): 176-182 (2016)*

Lipopolysaccharide (LPS) is a major cell wall component of gram-negative bacteria known to stimulate the synthesis and secretion of several toxic metabolites, such as reactive oxygen species and cytokines. In this study, the protective effect of alpha-lipoic acid (ALA) and coenzyme Q10 (CoQ10) were evaluated in LPS-induced hepatic injury in rats. To this end, male adult Sprague Dawley rats were divided into five groups; normal control, LPS control where rats were injected with an initial dose of LPS (4 mg/kg; i.p.) on the 1stday of the experiment followed by a challenging dose (2 mg/kg; i.p.) on the 8th day, ALA (50 mg/kg), CoQ10 (10 mg/kg) and ALA plus CoQ10. Treatments continued for 15 days and the last three groups also received LPS. At the end of the study, liver function tests, as well as interleukin-6 (IL-6) were estimated in serum. Liver lipid peroxides (MDA), reduced glutathione (GSH), superoxide dismutase (SOD) and total antioxidant capacity (TAC) were also assessed, in addition to histological examination of liver sections from all groups. The obtained data revealed that LPS markedly elevated activities of serum aminotransferases, alkaline phosphatase and gamma-glutamyl transferase, as well as, total bilirubin and interleukin-6 levels. LPS-treated rats showed an increase in MDA liver content versus decrease in GSH content, SOD activity and TAC. Oral administration of ALA, CoQ10 and their combination ameliorated LPSinduced increases in liver function enzymes and IL-6, coupled by hampering of oxidative biomarkers. This was supported by histopathological evaluation results. In conclusion, administration of ALA, CoQ10 and their combination improved pathological abnormalities in liver tissues and reversed the deleterious effects induced by LPS.

**Keywords:** Alpha-Lipoic Acid, Co-Enzyme Q10, Hepatotoxicity, Lipopolysaccharide, Oxidative Stress.

### M-754. The Impact of Omega-3 and Saccharomyces Cerevisiae on Amikacin-Induced Nephrotoxicity in Rats

Aya Shaheen, Abeer A. A. Salama, Hala Fahmy Zaki, Somaia Ahmed Nada and Ezz El-Din Saeed El-Denshary

*Der Pharma Chemica, 8(1): 223-234 (2016)*

Aminoglycosides as Amikacin (AMK) are widely used antibiotics however they are reported to cause considerable nephrotoxicity mediated via increased oxidative stress. The present study aimed to assess the impact of omega-3 and Saccharomyces cerevisiae (Sc) on AMK-induced nephrotoxicity in rats. Sixty Sprague Dawley rats of both sexes were assigned to ten equal groups.Group1received saline (normal control), groups 2-4 received Sc (109 CFU ml-1; p.o.), omega-3 (200 or 400 mg/kg; p.o.), respectively, group 5 received AMK (35mg/kg/day; i.p.), groups 6- 8received AMK with Sc, omega-3 (200or 400 mg/kg), respectively and groups 9-10 received AMK and Sc combined withomega-3 (200or 400 mg/kg), respectively for 4 weeks. At the end of experiments, blood samples were collected and kidneys were isolated and used for biochemical and histological studies. AMK-induced nephrotoxicity was shown by elevations in serum urea, creatinine and blood urea nitrogen parallel to decrease in serum total protein. AMK induced oxidative stress manifested by increases in kidney malondialdehyde and nitric oxide contents parallel to decreases in reduced glutathione content and superoxide dismutase activity. Besides, AMK increased kidney hydroxyproline and tumor necrosis factor-alpha contents as well as caspase-3 immunostaining. Sc, omega-3 and their combinations attenuated AMK-induced changes in kidney function tests, oxidative stress, inflammatory, apoptotic and fibrotic biomarkers. The tested agents even improved markers of kidney damage in normal animals. Histological examinations of kidney tissues confirmed the biochemical findings. Sc and omega -3 could be of therapeutic value against nephrotoxicity induced by AMK

**Keywords:** Amikacin, Saccharomyces Cerevisiae, Omega-3, Nephrotoxicity, Oxidative Stress, Tumor Necrosis Factoralpha

## The National Cancer Institute

***Dept. of Clinical Pathology***

### M-755. Evaluation of Annexin A2 and as Potential Biomarkers for Hepatocellular Carcinoma

Nevine El-Abd, Amal Fawzy, Tamer Elbaz and Sherif Hamdy

*Tumor Biology, 37(1): 211-216 (2016) IF: 2.926*

Hepatocellular carcinoma (HCC) ranks as the fifth most common malignancy worldwide. Early detection of HCC is difficult due to the lack of reliable markers. We aimed to assess the diagnostic role of annexin A2 (ANXA2) and follistatin as serum markers for HCC patients. This study included 50 patients with confirmed diagnosis of HCC, 30 patients with chronic liver disease, and 20 normal persons. Subjects performed thorough assessment and laboratory investigations. Serum levels of alpha fetoprotein (AFP), annexin A2, and follistatin were measured using ELISA technique. Annexin A2 significantly increased in the sera of HCC patients (median, 69.6 ng/ml) compared to chronic liver disease patients (median, 16.8 ng/ml) and control group (median, 9.5 ng/ml) ($p < 0.001$). Follistatin was higher in sera of HCC patients (median, 24.4 ng/ml) compared to the control group (median, 4.2 ng/ml) ($p = 0.002$) while no such significant difference was achieved between HCC and chronic liver disease patients. At a cutoff level 29.3 ng/ml, area under the receiver-operating characteristic curve for ANXA2 was 0.910 (95 % confidence interval (CI) 0.84-0.97). For follistatin, it was 0.631 (95 % confidence interval 0.52-0.74) at cutoff level 15.7 ng/ml. Combining both annexin A2 and AFP increased the diagnostic efficiency (98 % specificity, LR + 41 and 97.6 % PPV). Follistatin combined with AFP provided 92 % specificity while lower sensitivity (50 %) was observed. Serum ANXA2 is a promising biomarker for HCC, certainly when measured with AFP. Follistatin could not differentiate between HCC and chronic liver disease, but its combination with AFP improved the specificity for HCC diagnosis.

**Keyword:** AFP; Annexin A2; Follistatin; Hepatocellular carcinoma.

## M-756. Plasma DNA Integrity Index as A Potential Molecular Diagnostic Marker for Breast Cancer

Azza M. Kamel, Salwa Teama, Amal Fawzy and Mervat El-Deftar

*Tumor Biology, 37: 7565-7572 (2016) IF: 2.926*

Plasma DNA integrity index is increased in various malignancies including breast cancer, the most common cancer in women worldwide; early detection is crucial for successful treatment. Current screening methods fail to detect many cases of breast cancer at an early stage. In this study, we evaluated the level of plasma DNA integrity index in 260 females (95 with breast cancer, 95 with benign breast lesions, and 70 healthy controls) to verify its potential value in discriminating malignant from benign breast lesions. The criteria of the American Joint Committee on Cancer were used for staging of breast cancer patients. DNA integrity index was measured by real-time PCR. DNA integrity index was significantly higher in breast cancer than in benign breast patients and healthy subjects (P = <0.001). DNA integrity index is correlated with TNM stage. Given 100 % specificity, the highest sensitivity achieved in detecting cancer group was 85.3 % at 0.55 DNA integrity index cutoff. In conclusion, the plasma DNA integrity index may be a promising molecular diagnostic marker of malignancy in breast lesions.

**Keyword:** Breast cancer; Dna integrity Index; Real time PCR.

## M-757. Evaluation of Therapeutic Effect of Low Dose Naltrexone in Experimentally-Induced Crohn's Disease in Rats

Dina Ibrahim Tawfik, Afaf Sayed Osman, Hedayat Mahmoud Tolba, Aida Khattab, Lubna O. Abdel-Salam and Mahmoud M. Kamel

*Neuropeptides, 59: 39-45 (2016) IF: 2.726*

**Background and Aim:** Crohn's disease is a relapsing inflammatory condition afflicting the digestive tract. Drugs used for treatment of Crohn's disease may be associated with serious side effects. Endogenous opioid peptides modulate inflammatory cytokine production. Opioid antagonists have been shown to play a role in healing and repair of tissues. This work was designed to detect the possible beneficial effects of opioid antagonist naltrexone in indomethacin-induced Crohn's disease in rats. **Experimental Approach:** Enteritis was induced in male albino rats by two subcutaneous injection of indomethacin in a dose of 7.5mg/kg 24h apart started on day one. Salfasalazine, naltrexone and their combination were administered orally from day one of induction of enteritis to day 10. Disease activity index, serum levels of C-reactive protein and tumor necrosis factor-α, macroscopic and microscopic pathological scores and in vitro motility studies were evaluated. **Results:** Induction of enteritis resulted in significant increase of disease activity index, significant elevation of serum levels of C-reactive protein and tumor necrosis factor-α, significant deterioration of pathological scores and significant increase in the mean contractility response of the isolated ileal segments compared with normal untreated rats. Treatment with sulfasalazine, low dose of natrexone or their combination resulted in significant improvement of all measured parameters compared with enteritis group. **Conclusion:** The current finding could provide new interesting opportunity for developing new therapeutic approaches for treatment of Crohn's disease. Use of naltrexone, especially in small dose, has little side effects making it of interest for treatment of Crohn's disease. Also, it provides the possibility of reduced doses of other drugs if it is used as combined therapy.

**Keyword:** Crohn's Disease; Dai; Indomethacin; Naltrexone; Sulfasalazine.

## M-758. KIAA0101 mRNA Expression in the Peripheral Blood of Hepatocellular Carcinoma Patients: Association with some Clinicopathological Features

Iman A. Abdelgawad, Noha H. Radwan and Hala R. Hassanein

*Clinical Biochemistry, 49: 787-791 (2016) IF: 2.382*

**Objectives:** The development of hepatocellular carcinoma (HCC) is multi-factorial, multi-step and involving many genes. Recent studies have revealed the involvement of KIAA0101 in HCC development and progression. KIAA0101 is involved in the regulation of DNA repair, cell cycle progression, and cell proliferation.This study aims to elucidate the clinicopathological significance of KIAA0101 mRNA expression in the whole blood of HCC patients. Design and methods This study was conducted on 77 patients with proven HCC who presented to the outpatient clinic at the National Cancer Institute — Cairo University over a period of 8 consecutive months. Thirty patients with cirrhosis and forty apparently healthy volunteers were included as control groups. Detection of KIAA0101 mRNA was done on whole blood collected on EDTA for all patients and control subjects using real-time PCR. **Results** KIAA0101 mRNA was over-expressed in the HCC group compared to the control groups. Overexpression of KIAA0101 mRNA was significantly associated with distant metastasis, advanced stage, high serum alkaline phosphatase and low serum albumin levels. Both sensitivity and specificity of KIAA0101 mRNA were higher than those of AFP and CEA. **Conclusion** Being associated with some of the prognostic factors of HCC which reflect tumor progression; as advanced stage, distant metastasis, hypoalbuminemia and elevated serum alkaline phosphatase, together with its relatively high diagnostic performance; KIAA0101 mRNA might be nominated to play a probable role in the diagnosis and prognosis prediction of HCC. Further studies on a wider scale are recommended to confirm these results.

**Keyword:** HCC; KIAA0101; Real-Time PCR.

## M-759. Immunophenotypic Characterization of Cytogenetic Subgroups in Egyptian Pediatric Patients with B-Cell Acute Lymphoblastic Leukemia

Shady Adnan Awad, Mahmoud M. Kamel, Mahmoud A. Ayoub,Ahmed M. Kamel, Essam H. Elnoshokaty and Niveen El-Hifnawi

*Clinical Lymphoma, Myeloma and Leukemia, 16: 19-24 (2016) IF: 2.316*

**Background:** Identification of prognostic factors in acute lymphoblastic leukemia (ALL) patients is important for stratifying patients into risk groups and tailoring treatment

accordingly. Molecular and cytogenetic abnormalities are the most important prognostic factors. Minimal residual disease (MRD) is also an important predictor of relapse in ALL. However, the correlation of both prognostic variables has not been thoroughly studied. **Methods:** We investigated the correlation between defined cytogenetic abnormalities and selected new MRD markers (CD79b, CD123, and CD200) in 56 newly diagnosed Egyptian pediatric B-cell ALL patients. **Results:** CD123 found to be expressed in 45% of patients, CD200 in 80.3%, and CD79b in 67.9%. MRD analysis during treatment showed stable expression patterns of CD200. There was significant association of CD123 expression with the hyperdiploid ALL group (P = .017). Another association (P = .029) was found between CD79b negativity and the t(12;21) group. CD200 was widely expressed in all groups. **Conclusion:** There is a significant correlation between some markers, and certain ALL recurrent cytogenetic subgroups (CD123 and hyperdiploidy, CD79b negativity, and ETV-RUNX1 group) have good prognostic value. CD200 can be used as MRD markers in ALL patients and can also can serve as therapy targets.

**Keyword:** ALL; CD123; CD200; CD79B; Hyperdiploidy;MRD.

## M-760.Screening of Human Bocavirus in Surgically Excised Cancer Specimens

Ahmed S. Abdel-Moneim ,Hosam A. El-Fol,Mahmoud M. Kamel, Ahmed S. A. Soliman, Emad A. Mahdi, Ahmed S. El-Gammal and Taha Z. M. Mahran

*Archives of Virology, 161: 2095-2102 (2016) IF: 2.255*

Human bocavirus (HBoV) is a prevalent virus worldwide and is mainly associated with respiratory disorders. Recently, it was detected in several disease conditions, including cancers. Colorectal cancer (CRC) is the third main cause of cancers worldwide. Risk factors that initiate cell transformation include nutritional, hereditary and infectious causes. The aim of the current study was to screen for the presence of HBoV in solid tumors of colorectal cancer and to determine the genotypes of the detected strains. Surgically excised and paraffin-embedded colorectal cancer tissue specimens from 101 male and female patients with and without metastasis were collected over the last four years. Pathological analysis and tumor stages were determined. The presence of HBoV was screened by polymerase chain reaction, and the genotype of the detected HBoV was determined by direct gene sequencing. Most of the examined specimens were adenocarcinoma with mucinous activity in many of them. Twenty-four out of 101 (23.8 %) CRC tissue specimens were found to contain HBoV-1. Low sequence diversity was recorded in the detected strains. The virus was detected in both male and female patients with an age range of 30-75 years. It is proposed that HBoV-1 could play a potential role in the induction of CRC.

**Keyword:** Colorectal cancer; Human bocavirus; Direct gene sequencing.

## M-761.A Novel Primer Set for Improved Direct Gene Sequencing of Human Bocavirus Genotype-1 from Clinical Samples

Ahmed S. Abdel-Moneim, Mahmoud M. Kamel, Dina H. Hamedd, Safaa S. Hassan,May S. Solimane, Saleh A. Al-Quraishy and Amani A. El Kholye

*Journal of Virological Methods, 228: 108-113 (2016) IF: 1.508*

Human bocavirus genotype (HBoV-1) is a parvovirus associated with respiratory tract infections in children with different degrees of severity. The current study intended to improve the direct gene sequencing of the HBoV-1 using a newly developed primer set. Screening the presence of human bocavirus infection among in-patients children suffering from lower respiratory tract infections was another aim of the current study. Nasopharyngeal swab samples from in-patients children suffering from lower respiratory tract infections were examined. The real-time polymerase chain reaction was used for the initial screening as a highly sensitive method to detect the HBoV. Genotyping of real-time positive samples was attempted by direct sequencing of PCR amplicons using NP, VP1/2 and the newly developed VP/NC primers. HBoV-1 was present in 56.8% of the examined children. The newly developed primer set successfully amplified all real-time PCR positive samples, however, the other primer pairs did not reliably detect real-time PCR positive samples. The gene sequences of the detected HBoV-1 showed conserved sequences to each other with a low rate of discrepancies. The high rate of infection and the similarity between the detected strains strongly suggest nosocomial infections.

**Keyword:** Egypt; Genotyping; Human bocavirus; Nosocomial Infection; Respiratory tract infection in children.

## M-762.FLT3 Internal Tandem Duplication Mutation, Cmpl and CD34 Expressions Predict Low Survival in Acute Myeloid Leukemia Patients.

Eman K. Ebrahim, Magda M. Assem, Ahmed I. Amin, Mahmoud M. Kamel, Yomna M. El Meligui and AymanM. Metwally

*Annals of Clinical and Laboratory Science, 46: 592-600 (2016) IF: 0.846*

**Objectives:** To detect FMS-like tyrosine kinase-3 internal tandem duplicate (FLT3 ITD) mutation, Myeloproliferative leukemia virus oncogene (cMPL) and Ephrin A 4 receptor (EphA4) expressions in Acute myeloid leukemia (AML) and their correlation to patient's clinicopathological characteristics and survival. **Methods:** RNA was extracted from blood samples of 58 AML patients (39 adults and 19 children) and 20 age and sex matched controls. FLT3 ITD mutation, cMPL and EphA4 expression was studied using RT-PCR and correlated to the clinical and survival data of the patients. **Results:** FLT3 ITD mutation, cMPL and EphA4 expression was positive in 35.9%, 76.9% and 56.4% of adult AML patients respectively and in 15.8%, 47.4% and 36.8% of pediatric AML patients respectively. 76.9% of adult and 89.5% of pediatric patients expressed CD33. 64.1 % of adults and 42.1% of children expressed CD34. CD34 expression was significantly associated with both FLT3 ITD mutation and cMPL expression. CD34, FLT3 and cMPL negative cases have significantly higher overall survival than positive cases. **Conclusion:** CD34 expression is

significantly associated with both FLT3 ITD mutation and cMPL expression which could be used as a marker for low survival. Normal FLT3 and negative expression of CD34 and cMPL may predict a longer overall survival. Further studies are needed to investigate the mechanism that may correlate CD34 to both markers.
**Keyword:** Acute myeloid leukemia; CD34; EPHA4; FLT3 ITD; CMPL; survival.

## M-763.Circulating DNAin Egyptian Women with Breast Cancer.

Iman Hassan Ibrahim, Mahmoud M Kamel and Mohamed Ghareeb

*Asian Pacific Journal of Cancer Prevention, 17: 2989-2993 (2016)*

The commonest cancer in Egyptian females occurs in the breast cfDNA is a non-invasive marker for tumor detetion and prognostic assessment in many types of cancer including breast cancer. This study aimed to assess the role of cfDNA and its fragmentation pattern in breast cancer prognosis and treatment response. Forty female patients with malignant breast tumors and a comparable group of healthy blood donors were enrolled prospectively. cfDNA levels and fragmentation patterns were investigated after cfDNA extraction, gel electrophoresis and gel analysis. The percentage of breast cancer patients positive for cfDNA (92.5%) was significantly higher than that of controls (55%). Also, mean concentration of cfDNA was significantly higher than in the control group ($P<0.05$). Most Her-2 positive patients had long cfDNA fragments, this being significant as compared to Her-2 negative patients ($P<0.05$). Metastasis was also positively linked to significantly higher cfDNA ($P<0.05$) and the mean cfDNA integrity index was significantly higher in non-responders compared to treatment responders ($P<0.05$). In conclusion, both qualitative and quantitative aspects of cfDNA and its different fragments in breast cancer patients could be related to prognosis, metastasis and treatment response. Long cfDNA fragments could be particularly useful for prediction purposes.
**Keyword:** Breast cancer; Circulating DNA; DNAfragments; Treatment response.

## M-764.Clinical Impact of Overexpression of FOXP3 and WT1on Disease Outcome in Egyptian Acute Myeloid Leukemia Patients

Magda M Assem, Ahmed Osman, Eman Z Kandeel, Reham A A Elshimy, Hanan R Nassar and Radwa E Ali

*Asian Pacific Journal of Cancer Prevention, 17: 4699-4711 (2016)*

**Background:** In the last decade, it has become clear that change of gene expression may alter the hematopoietic cell quiescent state and consequently play a major role in leukemogenesis. WT1 is known to be a player in acute myeloid leukemia (AML) and FOXP3 has a crucial role in regulating the immune response. **Objectives:** To evaluate the impact of overexpression of WT1and FOXP3 genes on clinical course in adult and pediatric AML patients in Egypt. **Patients and methods:** Bone marrow and peripheral blood samples were obtained from 97 de novo non M3 AML patients (63 adult and 34 pediatric). Real-time quantitative PCR was used to detect overexpression WT1 and FOXP3 genes. Patient follow up ranged from 0.2 to 39.0 months with a median of 5 months. **Results:** In the pediatric group; WT1 was significantly expressed with a high total leukocyte count median 50X109/L ($p=0.018$). In the adult group, WT1 had an adverse impact on complete remission induction, disease-free survival and overall survival ($p=0.02$, $p=0.035$, $p=0.019$ respectively). FOXP3 overexpression was associated with FAB subtypes AML M0 +M1 vs. M2, M4+M5 ($p =0.039$) and the presence of hepatomegaly ($p=0.005$). **Conclusions:** WT1 and FOXP3 overexpression has an adverse impact on clinical presentation, treatment response and survival of pediatric and adult Egyptian AML patients.
**Keyword:** AML; WT1; FOXP3.

## M-765. Increased Endoglin and Transforming Growth Factor B1 Mrna Expression and Risk of Hepatocellular Carcinoma in Cirrhotic Egyptian Patients.

Teama S, Fawzy A, Teama S, Helal A, Drwish AD, Elbaz T and Desouky E.

*Asian Pacific Journal of Cancer Prevention, 17: 2429-2434 (2016)*

Transforming growth factor-B1 (TGF-β1 )and its coreceptor endoglin (ENG) have been shown to contribute to hepatocellular tumor development and malignant progression. Our aim was to evaluate the serum expression levels of ENG/ TGF-β1 mRNAs and risk of hepatocellular carcinoma in cirrhotic Egyptian patients. Our study included 77 subjects. Real time polymerase chain reaction was used to evaluate the expression level of ENG and TGF-β1mRNAs. The relative expression ratio of ENG mRNA was 0.82 (0.1 -3.2), 0.66 (0.15-5.3), 0.38(0.007-2.8) and 0.12 (0.00-0.22) and the relative expression ratio of TGF-β1mRNA was 1.4 (0.19 -6.2), 1.2 (0.22-4.3), 1.0 (0.15-4.4) and 0.6 (0.00-2.2) for cirrhotic HCC cirrhotic, HCC only and healthy control groups respectively. Increased ENG and TGF-β1 mRNA gene expression was correlated with TNM clinical stage. The expression ratio in TNM stage III-IV 1.1 (0.07-3.2), 1.55 (0.15-6.2) was statistically significantly higher than that in stage I-II 0.47 (0.007-2.8), 1.0 (0.31-4.4) (<0.05). Our data suggested that increased ENG and TGF-β1 gene expression may participate in hepatocarcinogenesis and increased risk of HCC in individuals with cirrhosis. Early screening for evidence of cirrhosis and consideration of ENG and TGF-β1 as targets for therapy and treatment strategies are warranted.
**Keyword:** Endoglin; Tgfß1; Mrna; Quantitative PCR; Hepatocellular carcinoma.

## M-766. Quantitative Analysis of Plasma Cell-Free DNA and its DNA Integrity in Patients with Metastatic Prostate Cancer Using ALU Sequence.

Amal Fawzy, Karima M. Sweify, Hany M. El-Fayoumy and Nagwa Nofal

*Journal of The Egyptian National Cancer Institute, 28(4): 235-242 (2016)*

**Background:** Prostate cancer (PC) is the most common cancer affecting men, it accounts for 29% of all male cancer and 11% of all male cancer related death. DNA is normally released from an apoptotic source which generates small fragments of cell-free

DNA, whereas cancer patients have cell-free circulating DNA that originated from necrosis, autophagy, or mitotic catastrophe, which produce large fragments. **Aim Of Work:** Differentiate the cell free DNA levels (cfDNA) and its integrity in prostate cancer patients and control group composed of benign prostate hyperplasia (BPH) and healthy persons. **Methodology:** cf-DNA levels were quantified by real-time PCR amplification in prostate cancer patients (n= 50), (BPH) benign prostate hyperplasia (n= 25) and healthy controls (n= 30) using two sets of ALU gene (product size of 115bp and 247-bp) and its integrity was calculated as a ratio of qPCR results of 247bp ALU over 115bp ALU. **Results:** Highly significant levels of cf-DNA and its integrity in PC patients compared to BPH. Twenty-eight (56%) patients with prostate cancer had bone metastasis. ALU115 qpcr is superior to the other markers in discriminating metastatic patients with a sensitivity of 96.4% and a specificity of 86.4% and (AUC=0.981) **Conclusion:** ALU115 qpcr could be used as a valuable biomarker helping in identifying high risk patients, indicating early spread of tumor cells as a potential seed for future metastases.

**Keyword:** Alu sequence; Cancer prostate; Dna integrity; Plasma Cell-Free DNA.

## M-767. Significance of Proliferation Markers and Prognostic Factors in Egyptian Patients with Multiple Myeloma

Iman A. Abdelgawad, Noha H. Radwan, Roxan E. Shafik and Hala A. Shokralla

*Asian Pacific Journal of Cancer Prevention, 17: 2389-2394 (2016)*

**Background:** Multiple myeloma (MM) is influenced by genetic and micro-environmental changes. Malignant plasma cells produce an abnormal monoclonal immunoglobulin, as well as cytokines, such as IL-10 and IL-6 which stimulate cells of the bone marrow microenvironment (BMM) and cause dysfunction and failure of many organs. B cell activating factor (BAFF), IL6, IL10 are known to influence the growth and survival of the malignant clone. **Aim:** The objectives of the present study were to investigate the circulating levels of BAFF , IL-10 and IL-6 , correlate them with well-known parameters of disease activity in patients with MM, and to detect their impact on the patients' survival. **Materials and Methods:** This study was conducted on 89 newly diagnosed MM patients and seventy apparently healthy volunteers as a normal control group. BAFF, IL6, IL10 were measured by ELISA for both groups. Survival analysis was performed for all patients. **Results:** Studied markers were higher in the MM patients compared to the normal control subjects. Patients' survival was improved by high serum BAFF levels. **Conclusions:** High levels of BAFF were found to improve patients' survival. BAFF and IL-6 can be considered probable diagnostic markers for MM.

**Keyword:** Multiple Myeloma; BAFF; IL6; IL10.

## M-768. The Role of Genetic Polymorphisms in Nrf2 and P73 in Egyptian Women with Breast Cancer

Nevin M Al Azhary, Mahmoud M Kamel, Yahia M Ismail, Amal A Mahmoud and Enas M Radwan

*Asian Pacific Journal of Cancer Prevention, 17: 4945-4949 (2016)*

Breast cancer is the commonest cancer in Egyptian females. Nrf2 is involved in oxidative stress while P73 functions in response to DNA damage. This study aimed to assess the role of Nrf2 promoter and P73 G4C14 to A4T14 SNPs in breast cancer in Egypt. Patients: Eighty-five female patients with breast tumours (41 malignant, 44 benign) were included. Nrf2 (rs6721961) and p73 (G4A) SNPs were determined by PCR-CTPP assay. **Results:** Genotype frequencies of the Nrf2 promoter SNP were 34.2% and 37.9% for AA in benign and malignant groups respectively, and 43.9% and 40.5% for CC and, 21.9 % and 21.6% for CA. Genotype frequencies for the P73 G4A SNP were 52.9% and 44.7% for GA in benign and malignant groups respectively, and 47.1% and 55.3% for GG. Discussion: Nrf2 genotypes in pre - and post-menopausal patients, showed significantly different distributions in the 2 patient groups, the AA genotype being significantly more common in pre-menopausal patients. The P73 G4A SNP showed no relation to age of disease onset. Conclusion: The Nrf2 (rs6721961) AA genotype might be related to early breast cancer onset. In contrast the P73 G4A polymorphism showed no relation to either disease risk or age at presentation.

**Keyword:** Breast cancer; Polymorphisms; Nrf2; P73; Genotype.

## M-769. Tissue CA125 and HE4 Gene Expression Levels Offer Superior Accuracy in Discriminating Benign from Malignant Pelvic Masses.

Amal Fawzy, Mohamed R Mohamed, Mohamed AM Ali, Mohamed H AbdEl-Magied and Amany M Helal

*Asian Pacific Cancer Prevention, 17(1): 323-333 (2016)*

**Background:** Ovarian cancer remains a major worldwide health care issue due to the lack of satisfactory diagnostic methods for early detection of the disease. Prior studies on the role of serum cancer antigen 125 (CA125) and human epididymis protein 4 (HE4) in detecting ovarian cancer presented conflicting results. New tools to improve the accuracy of identifying malignancy are urgently needed. We here aimed to evaluate the diagnostic utility of tissue CA125 and HE4 gene expression in comparison to serum CA125 and HE4 in discriminating benign from malignant pelvic masses. **Materials and Methods:** One-hundred Egyptian women were enrolled in this study, including 60 epithelial ovarian cancer (EOC) patients and 20 benign ovarian tumor patients, as well as 20 apparently healthy women. Preoperative serum levels of CA125 and HE4 were measured by immunoassays. Tissue expression levels of genes encoding CA125 and HE4 were determined by quantitative real time polymerase chain reaction (qRT-PCR). The diagnostic performance of CA125 and HE4, measured either as mRNA or protein levels, was evaluated by receiver operating characteristic (ROC) curves. **Results:** The serum CA125+HE4 combination and serum HE4, with area under the curve (AUC) values of 0.935 and 0.932, respectively, performed significantly better than serum CA125 (AUC=0.592; P<0.001). Tissue CA125 and HE4 (AUC=1) performed significantly better than serum CA125

(P<0.001), serum HE4 (P=0.016) and the serum CA125+HE4 combination (P=0.018). **Conclusions:** Measurement of tissue CA125 and HE4 gene expression not only improves discriminatory performance, but also broadens the range of differential diagnostic possibilities in distinguishing EOC from benign ovarian tumors

**Keyword:** Pelvic mass; Differential diagnosis; Cancer antigen 125; Human epididymis protein 4.

## M-770. Vitamin D Receptor Gene Polymorphism in Egyptian Pediatric Acute Lymphoblastic Leukemia Correlation with Bmd

Maha Tantawy, Mahmoud Amer, Tarek Raafat and Nayera Hamdy

*Meta Gene, 9: 42-46 (2016)*

**Introduction** We studied the frequencies of the 3′ and 5′-end vitamin D receptor (VDR) gene polymorphisms and their correlation with bone mineral density (BMD) in Egyptian pediatric acute lymphoblastic leukemia (ALL) patients receiving calcium and vitamin D supplements. The purpose of this study is to find out the relation between VDR polymorphism and the response to vitamin D intake in pediatric ALL cases who receive corticosteroid therapy which predispose to osteoporosis. This study might shed the light on some genetic variants that are effect the response of individuals to vitamin D therapy. **Methods** Forty newly diagnosed pediatrics ALL cases were studied. Three SNPs at the 3′-end of the VDR gene (BsmI rs1544410, ApaI rs739837and TaqI rs731236) and two SNPs at the 5′-end (Cdx-2 rs11568820 and GATA rs4516035) were analyzed by Allelic discrimination assay. of those twenty-six cases with initial BMD data available were further analyzed with regards to the effect of various VDR genotypes/haplotypes on BMD. **Results** The genotype frequencies at 3′-end of VDR gene were, TaqI TT 23%, Tt 54% and tt 23%, BsmI bb 19.2%, Bb 65.4% and BB 15.4% and ApaI AA 12%, Aa 27% and aa 61%. The frequencies at the 5′-end were Cdx-2 GG 34.5%, GA 54% and AA 11.5% and GATA AA 8%, AG 50% and GG 42%. Eight and four possible haplotypes were observed at the 3′ and 5′-ends of the VDR gene respectively. The Tt genotype was significantly correlated with high BMD as compared to other TaqI genotypes (P = 0.0420). There was a trend towards higher BMD with the genotype Bb as compared to other BsmI genotypes. No statistical significance was found between the other VDR genotypes or haplotypes studied and BMD. **Conclusions** This is the first report on VDR gene polymorphisms in Egyptian pediatric ALL patients. The Tt genotype was associated with increased BMD. Our study showed marked genetic heterogeneity in VDR gene in Egyptian pediatric ALL patients.

**Keyword:** Acute lymphoblastic leukemia; Osteoporosis; Vitamin D Receptor; Polymorphism; Bone mineral density.

***Dept. of Diagnostic Radiation Oncology***

## M-771. Posterior Reversible Encephalopathy Syndrome in Cancer Patients: A Single Institution Retrospective Study

Carlos Kamiya-Matsuoka, Asif M. Paker, Linda Chi, Ayda Youssef, Sudhakar Tummala and Monica E. Loghin

*Journal of Neuro-Oncology, 128: 75-84 (2016) IF: 2.754*

Posterior reversible encephalopathy syndrome (PRES) is a clinico-radiologic entity. Its management and outcome in the oncology population is limited because it is still difficult to identify despite an increasingly recognized occurrence. This is the largest retrospective study of PRES in cancer patients reported from a single institution. We explore the clinical manifestations and radiologic features to comprehensively assess PRES in order to prevent permanent neurologic deficits and mortality. We retrospectively identified 69 patients with cancer who developed PRES at MDACC between 01/2006 to 06/2012. Clinical and radiographic data were abstracted from their records and reviewed for our analysis. Mean age at PRES onset was 52 ± 17.8 years. Fifty-two (75 %; $p < 0.001$) patients were women. Most common diagnoses were leukemia (30%) and lymphoma (12%). Forty-eight (70%) patients were treated with chemotherapy, 21 (30 %) bone marrow transplant and 14 (20 %) tacrolimus. Most common clinical presentation was seizures (67%). PRES was associated with hypertension in 62 (90 %) patients. On brain MRI, 33 (44 %) patients had some evidence of hemorrhage, 22 (73 %) of these were thrombocytopenic. Thirty-five (51%) patients fully recovered and 19 (28%) had permanent neurological deficits. Morbidity and mortality were associated with continuation with offending agent, thrombocytopenia, variations in mean arterial pressure ≥20 mmHg, electrographic seizures at onset, atypical MRI pattern and delay in diagnostic imaging (7.4 ± 4.8 days vs. 1.9 ± 1.8 days; $p = 0.031$) as half of them did not receive a prompt intervention. Special attention should be given to patients who present with high-risk factors in order to prevent development of PRES or decrease patient morbidity and mortality. Management of PRES should be guided by the radiographic findings. Overall, early recognition, discontinuation of the offending agents, correction of thrombocytopenia and blood pressure control are still the main strategies to manage PRES.

**Keyword:** Bone marrow transplant; Cancer; Chemotherapy; Neurotoxicity; Posterior reversible encephalopathy syndrome; tacrolimus.

***Department of Medical Oncology***

## M-772. Eight Cycles of ABVD Versus four Cycles of BEACOPPescalated Plus four Cycles of BEACOPPbaseline in Stage III to IV, International Prognostic Score ? 3, High-Risk Hodgkin Lymphoma: First Results of the Phase III EORTC 20012 Intergroup Trial.

Carde P, Karrasch M, Fortpied C, Brice P, Khaled H, Casasnovas O, Caillot D, Gaillard I, Bologna S, Ferme C, Lugtenburg PJ, Morschhauser F, Aurer I, Coiffier B, Meyer R, Seftel M, Wolf M, Glimelius B, Sureda A and Mounier N.

*J Clin Oncol. Jun 10;34(17):2028-36(2016) IF: 20.982*

**Purpose:**To compare patients with high-risk stage III to IV Hodgkin lymphoma (HL) in the phase III European Organisation for Research and Treatment of Cancer 20012 Intergroup trial (Comparison of Two Combination Chemotherapy Regimens in Treating Patients With Stage III or Stage IV Hodgkin's Lymphoma) who were randomly assigned to either doxorubicin, bleomycin, vinblastine, and dacarbazine (ABVD) or to bleomycin, etoposide, doxorubicin, cyclophosphamide, vincristine, procarbazine, and prednisone (BEACOPP).**Patients and Methods:**Patients with clinical stage III or IV HL, International Prognostic Score of 3 or higher, and age 60 years or younger received ABVD for eight cycles (ABVD8) or escalated-dose BEACOPP (BEACOPPescalated) for four cycles followed by baseline BEACOPP (BEACOPPbaseline) for four cycles (BEACOPP4+4) without radiotherapy. Primary end points were event-free survival (EFS), treatment discontinuation, no complete response (CR) or unconfirmed complete response (CRu) after eight cycles, progression, relapse, or death. Secondary end points were CR rate, overall survival (OS), quality of life, secondary malignancies, and disease-free survival in CR/CRu patients.**Results:**Between 2002 and 2010, 549 patients were randomly assigned to ABVD8 (n = 275) or BEACOPP4+4 (n = 274). Other characteristics included median age, 35 years; male, 75%; stage IV, 74%; "B" symptoms, 81%; and International Prognostic Score ? 4, 59%. WHO performance status was 0 (34%), 1 (48%), or 2 (17%). Median follow-up was 3.6 years. CR/CRu was 82.5% in both arms. At 4 years, EFS was 63.7% for ABVD8 versus 69.3% for BEACOPP4+4 (hazard ratio [HR], 0.86; 95% CI, 0.64 to 1.15; P = .312); disease-free survival was 85.8% versus 91.0% (HR, 0.59; 95% CI, 0.33 to 1.06; P = .076), and OS was 86.7% versus 90.3% (HR, 0.71; 95% CI, 0.42 to 1.21; P = .208). Death as a result of toxicity occurred in six and five patients, early discontinuation (before cycle 5) in 12 and 26 patients, treatment crossovers in five and 10 patients, and secondary malignancies in eight and 10 patients in the ABVD8 and BEACOPP4+4 arms, respectively.**Conclusion:**ABVD8 and BEACOPP4+4 resulted in similar EFS and OS in patients with high-risk advanced-stage HL. Because BEACOPP4+4 did not demonstrate a favorable effectiveness or toxicity ratio compared with ABVD8, treatment burden, immediate and late toxicities, and associated costs must be considered before selecting one of these regimens on which to build future treatment strategies.

## M-773. Efficacy and toxicity of plasmonic photothermal therapy (PPTT) using gold nanorods (GNRs) against mammary tumors in dogs and cats.

Abdoon AS, Al-Ashkar EA, Kandil OM, Shaban AM, Khaled HM, El Sayed MA, El Shaer MM, Shaalan AH, Eisa WH, Eldin AA, Hussein HA, El Ashkar MR, Ali MR and Shabaka AA.

*Nanomedicine. Nov;12(8):2291-2297. (2016) IF: 5.671*

Plasmonic photothermal therapy (PPTT) was introduced as a promising treatment of cancer. This work was conducted to evaluate the cytotoxic effect of intratumoral (IT) injection of 75?g gold nanorods (GNRs)/kg of body weight followed by direct exposure to 2 w/cm2 near infra-red laser light for 10min on ablation of mammary tumor in 10 dogs and 6 cats. Complete blood count (CBC), liver and kidney function were checked before the start of treatment and one month after injection of GNRs. Results showed that 62.5% (10/16), 25% (4/16) and 12.5% (2/16) of treated animals showed complete remission, partial remission and no response, respectively. Tumor was relapsed in 4 cases of initially responding animals (25%). Overall survival rate was extended to 315.5±20.5days. GNRs have no toxic effect on blood profile, liver or kidney functions. In conclusion, GNRs can be safely used for treatment of mammary tumors in dogs and cats.

**Keyword:** Cytotoxicity; Dogs and cats; Gold nanorods; Mammary tumors; Near infra-red light; Toxicity.

## M-774. A review on thyroid cancer during pregnancy: Multitasking is required.

Khaled H, Al Lahloubi N and Rashad N

*J Adv Res. Jul;7(4):565-70 (2016) IF: 3*

Thyroid cancer is the second most common cancer diagnosed during pregnancy after breast cancer. The goal of management is to control malignancy and prevent maternal and fetal complications as a result of maternal hypothyroidism. The role of female sex hormones as an etiologic factor was investigated, with no clear association. Pregnancy can cause an increase in size of a previously existed thyroid nodule through the structural similarity between TSH and BHCG, and the normally expressed estrogen receptors on thyroid gland cells. Effect of pregnancy on development and prognosis of differentiated thyroid malignancies (papillary and follicular) has also been studied. The prognosis of thyroid cancer is not worse in patients diagnosed during pregnancy or those who got pregnant after curative treatment. Termination of pregnancy is not indicated at all, surgery can be delayed till after delivery except in rapidly growing aggressive tumors. While radioactive iodine ablation is absolutely contra-indicated, the new systemic therapies are not well studied during pregnancy. However, almost all these new agents are classified as FDA category C or D and are better to be avoided. The effect of pregnancy on other types of thyroid cancer (medullary and anaplastic thyroid tumors) is not well studied because of very low incidence with pregnancy. The endocrinological management of thyroid cancer during pregnancy is of utmost importance. The hypothyroidism after total thyroidectomy can cause fetal hypothyroidism. Therefore, the management of thyroid cancer related to pregnancy needs a multidisciplinary team.

**Keyword:** Pregnancy; Pregnancy related disorders; Radioactive iodine; Thyroid cancer; Tyrosine kinase inhibitors

## M-775. Aromatase inhibitors induced autoimmune disorders in patients with breast cancer: A review.

Zarkavelis G, Kollas A, Kampletsas E, Vasiliou V, Kaltsonoudis E, Drosos A, Khaled H and Pavlidis N.

*J Adv Res. 2016 Sep;7(5):719-726.(2016) IF: 3*

Subacute cutaneous lupus erythematosus (SCLE) is characterized by particular cutaneous manifestations such as non-scaring plaques mainly in sunlight exposed parts of the body along with specific serum autoantibodies (i.e. antinuclear antibodies (ANA), Ro/SSa, La/SSb). It is considered either idiopathic or drug induced. The role of chemotherapeutic agents in causing SCLE has been investigated with the taxanes being the most common anticancer agents. However, recent data emerging point toward antiestrogen therapies as a causative

factor not only for SCLE but also for a variety of autoimmune disorders. This is a report of a case of a 42 year old woman who developed clinical manifestations of SCLE after letrozole treatment in whom remission of the cutaneous manifestations was noticed upon discontinuation of the drug. In addition, an extensive review of the English literature has been performed regarding the association of antiestrogen therapy with autoimmune disorders. In conclusion, Oncologists should be aware of the potential development of autoimmune reactions in breast cancer patients treated with aromatase inhibitors.
**Keyword:** Aromatase inhibitors; Arthralgias; Breast cancer; Rheumatoid arthritis; Subacute cutaneous lupus erythematosus; Systemic lupus erythematosus.

## M-776. Review on renal cell carcinoma and pregnancy: A challenging situation.

Khaled H, Lahloubi NA and Rashad N.

*J Adv Res. Jul;7(4):575-80. (2016) IF: 3*

Renal cell carcinoma is rarely diagnosed during pregnancy. Its management is a real challenge due to the sparse literature and lack of standard guidelines. In this situation, the diagnosis is often delayed as the clinical presentation might resemble other pregnancy-related disorders but it should be one of the diagnostic possibilities in women with recurrent or refractory urinary tract symptoms, renal pain, or mass that could be palpated. Diagnostic approach may include ultrasound examination and sometimes magnetic resonance imaging. If localized, surgery would be the preferred line of treatment. Other treatment modalities, end results of treatment, and review of literature of this rare association will be presented.
**Keyword:** Oncology; Pregnancy; Pregnancy related disorders; Renal cancer.

### *Dept. of Radiation Oncology*

## M-777. Vaginal Dose De-Escalation in Image Guided Adaptive Brachytherapy for Locally Advanced Cervical Cancer.

Sandy Mohamed, Jacob Christian Lindegaard, Astrid A.C. de Leeuw, Ina Jürgenliemk-Schulz, Kathrin Kirchheiner, Christian Kirisits, Richard Pötter and Kari Tanderup

*Radiotherapy and Oncology, 120(3): 480-485 (2016) IF: 4.817*

**Purpose:** Vaginal stenosis is a major problem following radiotherapy in cervical cancer. We investigated a new dose planning strategy for vaginal dose de-escalation (VDD). **Materials and Methods:** Fifty consecutive locally advanced cervical cancer patients without lower or middle vaginal involvement at diagnosis from 3 institutions were analysed. External beam radiotherapy was combined with MRI-guided brachytherapy. VDD was obtained by decreasing dwell times in ovoid/ring and increasing dwell times in tandem/needles. The aim was to maintain the target dose (D90 of HR-CTV□85Gy EQD2) while reducing the dose to the surface of the vagina to <140% of the physical fractional brachytherapy dose corresponding to a total EQD2 of 85Gy. **Results:** The mean vaginal loading (ovoid/ring) was reduced from 51% to 33% of the total loading with VDD, which significantly reduced the dose to the vaginal dose points ($p<0.001$) without compromising the target dose. The dose to the ICRU recto-vaginal point was reduced by a mean of 4±4Gy EQD2 ($p<0.001$), while doses to bladder and rectum (D2cm3) were reduced by 2±2Gy and 3±2Gy, respectively ($p<0.001$). **Conclusions:** VDD significantly reduces dose to the upper vagina which is expected to result in reduction of vaginal stenosis.
**Keyword:** Brachytherapy; Cervical cancer; Dose De escalation; MRIguided; Radiation dose; Vaginal dose.

## M-778.Single-Session Gamma Knife Radiosurgery for Optic Pathway/Hypothalamic Gliomas

Amr M. N. El-Shehaby, Wael A. Reda, , Khaled M. Abdel Kari, Reem M. Emad Eldin and Ahmed M. Nabee

*Journal of Neurosurgery, 125: 50-57 (2016) IF: 3.443*

**Objective:** Because of their critical and central location, it is deemed necessary to fractionate when considering irradiating optic pathway/hypothalamic gliomas. Stereotactic fractionated radiotherapy is considered safer when dealing with gliomas in this location. In this study, the safety and efficacy of single-session stereotactic radiosurgery for optic pathway/hypothalamic gliomas were reviewed. **Methods** Between December 2004 and June 2014, 22 patients with optic pathway/hypothalamic gliomas were treated by single-session Gamma Knife radiosurgery. Twenty patients were available for follow-up for a minimum of 1 year after treatment. The patients were 5 to 43 years (median 16 years) of age. The tumor volume was 0.15 to 18.2 cm3 (median 3.1 cm3). The prescription dose ranged from 8 to 14 Gy (median 11.5 Gy). **Results** The mean follow-up period was 43 months. Five tumors involved the optic nerve only, and 15 tumors involved the chiasm/hypothalamus. Two patients died during the follow-up period. The tumors shrank in 12 cases, remained stable in 6 cases, and progressed in 2 cases, thereby making the tumor control rate 90%. Vision remained stable in 12 cases, improved in 6 cases, and worsened in 2 cases in which there was tumor progression. Progression-free survival was 83% at 3 years. **Conclusions** The initial results indicate that single-session Gamma Knife radiosurgery is a safe and effective treatment option for optic pathway/hypothalamic gliomas.
**Keyword:** Gamma knife; Optic; Hypothalamic; Glioma; Fractionation; Single session; Stereotactic radiosurgery.

## M-779. Evaluation of the Algorithm'S Accuracy in the Computation of the Dose Distribution in the Brain Tumors

A. S. Ahmed, M. E. Abdelwanis, E. M. Attalla,Y. Saddeek and E. Shaaban

*Biosciences Biotechnology Research Asia, 13: 221-229 (2016)*

To compare dosimetric calculation using Clarkson, Convolution, Superposition and Fast Superposition algorithms in Three-Dimensional Conformal Radiotherapy (3DCRT), and to study the suitability of algorithms with respect to brain tumors and technique. Fifteen brain tumor cases for treatment plans were created using 6 MV Photon beam quality using the CMS XiO (Computerized Medical System, St. Louis, MO) treatment planning system. Patients divided into two sections according to volume of target more or less than 150cc represented by PTV. Six different points were selected to measure the dose. Mean

Dose, and Mean Relative Difference have been used Maximum percentage of variation recorded between algorithms was 43.7%, recorded with a surface dose point in case of PTV less than 150 cc. The fast superposition algorithm showed excellent results in cases of PTV less than 150cc by considering the mean relative differences with a prescribed dose with four algorithms and minimum relative difference with a prescribed dose in different PTV and treatment techniques. The superposition algorithm showed better results in all techniques. The Clarkson algorithm showed monotonically variation in the dose calculation points and histogram parameters. The other three algorithms are approximately similar in results. Present study has explained the dosimetric results of different algorithms.

**Keyword:** Algorithm; Brain tumors; Homogeneity index; Treatment planning system.

## M-780. Prediction of Dose Calculation of Breast and Chest Tumors Using Different Algorithms

A.S. Ahmed, E.M. Attalla, M.E. Abdelwanis,Y. Saddeek and E. Shaaban

*Biosciences Biotechnology ResearchAsia,13(4):2379-2385 (2016)*

This work significantly observes the suitable of algorithms by comparing the dose calculation of breast and chest tumors using Clarkson, Convolution, Superposition and Fast Superposition algorithms in three-dimensional Conformal Radiotherapy (3DCRT). Thirteen post-operative breast cases and fifteen cancer chest patients were taken in this work. Treatment plans were created using 6 and 15 MV Photon beam quality with the CMS XiO treatment planning system (Computerized Medical System, St. Louis, MO). Statistical analysis was done by relating the mean relative difference, conformity index, and homogeneity index for target structures. The percentage of difference noted between algorithms were 9.4%, recorded with a low density point in case of breast. Superposition and fast superposition algorithm were presented very good results in both cases in view of the mean relative variances using a prescribed dose with four algorithms and the lowest relative variable using a given dose in different treatment techniques PTV. Superposition algorithm exposed good calculations in all techniques. Clarkson algorithm showed monotonically variation in the dose calculation points and histogram parameters. The other three algorithms are shown approximately similar results. We found from the dosimetric results a considerable difference among four algorithms. Conferring to this study, the algorithms varied. Significant upkeep must be occupied when calculating treatment plans, as the selection of the dose computation algorithm may affected on treatment planning as well as clinical effects.

**Keyword:** Algorithm; Chest tumors; Cancer breast; Homogeneity index; Treatment planning system.

### *Dept. of Surgical Oncology*

## M-781.Appropriate Timing of Surgery after Neoadjuvant Chemoradiation Therapy for Locally Advanced Rectal Cancer

Waheed Yousry Garrer, Hisham Abd El Kader El Hossieny, Zeiad Samir Gad,Alfred Elias Namour and Sameh Mohammed Ahmed Abo Amer

*Asian Pacific Journal of Cancer Prevention, 17: 4381-4389 (2016)*

**Background:** Surgery is the corner stone for the management of rectal cancer. The purpose of this study was to demonstrate the optimal time of surgical resection after the completion of neoadjuvant chemo-radiotherapy (CRT) in treatment of locally advanced rectal cancer. **Materials and Methods:** This study compared 2 groups of patients with locally advanced rectal cancer, treated with neoadjuvant CRT followed by surgical resection either 6-8 weeks or 9-14 weeks after the completion of chemo-radiotherapy. The impact of delaying surgery was tested in comparison to early surgical resection after completion of chemo-radiotherapy. **Results:** The total significant response rate that could result in functional preservation was estimated to be 3.85% in group I and 15.4% in group II. Some 9.62% of our patients had residual malignant cells at one cm surgical margin. All those patients with positive margins at one cm were in group I (19.23%). There was less operative time in group II, but the difference between both groups was statistically insignificant (P0.845). The difference between both groups regarding operative blood loss and intra operative blood transfusion was significantly less in group II (P0.044). There was no statistically significant difference between both groups regarding the intra operative complications (P0.609). The current study showed significantly less post-operative hospital stay period, and less post-operative wound infection in group II (P0.012 and 0.017). The current study showed more tumor regression and necrosis in group II with a highly significant main effect of time F61.7 (P<0.001). Pathological TN stage indicated better pathological tumor response in group II (P0.04). The current study showed recurrence free survival for all cases at 18 months of 84.2%. In group I, survival rate at the same duration was 73.8%, however none of group II cases had local recurrence (censored) (P0.031). Disease free survival (DFS) during the same duration (18 months) was 69.4 % for patients in group I and 82.3% for group II (P0.429). **Conclusions:** Surgical resection delay up to 9-14 weeks after chemo-radiation was associated with better outcome and better recurrence free survival.

**Keyword:** Rectal cancer; Timing of surgery; Neoadjuvnat Chemo-radiation therapy.

### *Dept. of Tumor Biology*

## M-782.Loss of CHD1 Causes DNA Repair Defects and Enhances Prostate Cancer Therapeutic Responsiveness

Vijayalakshmi Kari, Wael Yassin Mansour, Sanjay Kumar Raul, Simon J Baumgart, Andreas Mund, Marian Grade, Hüseyin Sirma, Ronald Simon, Hans Will, Matthias Dobbelstein,Ekkehard Dikomey and Steven A Johnsen

*Embo Reports, 17: 1609-1623 (2016) IF: 7.739*

The CHD1 gene, encoding the chromo- domain helicase DNAbinding protein1, is one of the most frequently deleted genes in prostate cancer. Here, we examined the role of CHD1 in DNA doublestrand break (DSB) repair in prostate cancer cells. We show that CHD1 is required for the recruitment of CtIP to chromatin and subsequent end resection during DNA DSB repair. Our data support a role for CHD1 in opening the chromatin around the DSB to facilitate the recruitment of homologous recombination (HR) proteins. Consequently, depletion of CHD1 specifically affects HRmediated DNA repair but not nonhomologous end joining. Together, we provide evidence for a previously unknown role of CHD1 in DNA DSB repair via HR and show that CHD1 depletion sensitizes cells to PARP inhibitors, which has potential therapeutic relevance. Our findings suggest that CHD1 deletion, like BRCA1/2 mutation in ovarian cancer, may serve as a marker for prostate cancer patient stratification and the utilization of targeted therapies such as PARP inhibitors, which specifically target tumors with HR defects.

**Keyword:** CHD; Chromatin; DNA repair; Parp inhibitor; Prostate cancer

## M-783. Functional Crosstalk Between Dna Damage Response Proteins 53BP1and BRCA1 Regulates Double Strand Break Repair Choice

Ali Bakr, Sabrina Köcher, Jennifer Volquardsen, Rudolph Reimer, Kerstin Borgmann,Ekkehard Dikomey, Kai Rothkamm and Wael Y. Mansour

*Radiotherapy and Oncology, 119: 276-281 (2016) IF: 4.817*

**Purpose** The aim of this study was to elucidate the impact of DNA damage response (DDR) proteins 53BP1 and BRCA1 on the double-strand break (DSB)-repair choice. This is important not only in order to understand the underlying mechanisms of DSB-repair pathway regulation but also to determine the therapeutic implications for BRCA1-associated tumors. **Materials and methods** Human tumor cell lines A549 and HeLa were used. Non-homologous end-joining (NHEJ) and homologous recombination (HR) were assessed using NHEJ and HR reporter constructs. Colocalization of HR-proteins RPA and RAD51 with 53BP1 was evaluated by confocal microscopy and 3D-analysis. **Results** We demonstrate a specific crosstalk between 53BP1 and BRCA1. While 53BP1 does not colocalize with RPA or RAD51 and prohibits the recruitment of BRCA1 to DSBs to stimulate NHEJ, BRCA1 promotes the 53BP1 displacement specifically in S/G2-phase to allow end-resection, initiating HR. HR-efficiency was restored in BRCA1-depleted cells upon additional 53BP1-knockdown. Further, we found that 53BP1-mediated end protection precedes BRCA1-dependent end-resection. **Conclusion** These results demonstrate that the interplay between 53BP1/NHEJ and BRCA1/HR is of great relevance for tumor treatment, as the 53BP1 status would be highly important for the treatment response of BRCA1-associated tumors.

**Keyword:** 53BP1; BRCA1; DSB-Repair Choice.

## M-784. The Combination of A-Tocopheryl Succinate and Sodium Selenite on Breast Cancer: A Merit or A Demerit?

Doaa M. Badr, Hafez F. Hafez, Azza M. Aghaand Samia A. Shouman

*Oxidative Medicine and Cellular Longevity, (2016): 1-14 IF: 4.492*

α-Tocopheryl succinate (α-TOS), a mitochondria-targeting agent, induces apoptosis in malignant cells in vitro and in vivo. Selenite is a nutritional supplement that has been shown to stimulate apoptosis in cancer cells. This study was designed to investigate the cytotoxic effect of combined treatment of α-TOS and sodium selenite (SSe) in vitro and in vivo and to explore their effect on apoptosis and autophagy in breast cancer. The type of interaction between α-TOS and SSe was evaluated and levels of oxidative stress and apoptotic and autophagic markers were determined. SSe alone showed varying degrees of cytotoxicity on all the tested cell lines. Its combination with α-TOS was antagonistic in vitro in MCF7 and in vivo in mice bearing Ehrlich tumor compared to α-TOS-treated one. Combination of TOS with 2 μM of SSe increased the level of glutathione without changes in antiapoptotic markers Bcl-2 and Mcl-1 at 16 and 48 hrs. SSe decreased caspase 3 activity and protein level of caspases 7 and 9, while it increased autophagic markers beclin-1 and LC3B protein levels of MCF7 cells treated with α-TOS. In conclusion, SSe antagonizes α-TOS-induced apoptosis via inhibition of oxidative stress and promoting prosurvival machinery of autophagy.

**Keyword:** A-Tocopheryl succinate; Sodium selenite cytotoxicity oxidative; Stress autophagy.

## M-785. The Protective Properties of the Strawberry (Fragari Aananassa) Against Carbon Tetrachloride-Induced Hepatotoxicity in Rats Mediated by Anti-Apoptotic and Upregulation of Antioxidant Genes Expression Effects

SherifS.Hamed, NoufA.AL-Yhya, ManalF.El-Khadragy, Ebtesam M.Al-Olayan , ReemA.Alajmi, ZeinabK.Hassan, SalwaHassan andAhmed E.AbdelMoneim

*Frontiers in Physiology, Aug 5;7:325 (2016) IF: 4.031*

The strawberry (Fragaria ananassa) has been extensively used to treat a wide range of ailments in many cultures. The present study was aimed at evaluating the hepatoprotective effect of strawberry juice on experimentally induced liver injury in rats. To this end, rats were introperitoneally injected with carbon tetrachloride (CCl4) with or without strawberry juice supplementation for 12 weeks and the hepatoprotective effect of strawberry was assessed by measuring serum liver enzyme markers, hepatic tissue redox status and apoptotic markers with various techniques including biochemistry, ELISA, quantitative PCR assays and histochemistry. The hepatoprotective effect of the strawberry was evident by preventing CCl4-induced increase in liver enzymes levels. Determination of oxidative balance showed that strawberry treatment significantly blunted CCl4-induced increase in oxidative stress markers and decrease in enzymatic and non-enzymatic molecules in hepatic tissue. Furthermore, strawberry supplementation enhanced the anti-apoptotic protein, Bcl-2, and restrained the pro-apoptotic

proteins Bax and caspase-3 with a marked reduction in collagen areas in hepatic tissue. These findings demonstrated that strawberry (F. ananassa) juice possessed antioxidant, anti-apoptotic and anti-fibrotic properties, probably mediated by the presence of polyphenols and flavonoids compounds.
**Keyword:** Strawberry; Carbon tetrachloride; Oxidative stress; Gene expression; Fibrosis; Liver.

## M-786. Combinatorial Synthesis, in Silico, Molecular and Biochemical Studies of Tetrazole-Derived Organic Selenides with Increased Selectivity Against Hepatocellular Carcinoma

Saad Shaaban , Amr Negm, Abeer M. Ashmawy, Dalia M. Ahmed and Ludger A. Wessjohann

*European Journal of Medicinal Chemistry, 122: 55-71 (2016) IF: 3.902*

Novel tetrazole-based diselenides and selenoquinones were synthesized via azido-Ugi and sequential nucleophilic substitution (SN) strategy. Molecular docking study into mammalian TrxR1 was used to predict the anticancer potential of the newly synthesized compounds. The cytotoxic activity of the compounds was evaluated using hepatocellular carcinoma (HepG2) and breast adenocarcinoma (MCF-7) cancer cells and compared with their cytotoxicity in normal fibroblast (WI-38) cells. The corresponding redox properties of the synthesized compounds were assessed employing 2,2-diphenyl-1-picrylhydrazyl (DPPH), glutathione peroxidase (GPx)-like activity and bleomycin dependent DNA damage. In general, diselenides showed preferential cytotoxicity to HepG2 compared to MCF-7 cells. These compounds exhibited also good GPx catalytic activity compared to ebselen (up to 5 fold). Selenoquinones 18, 21, 22 and 23 were selected to monitor the expression levels of caspase-8, Bcl-2 and Ki-67 molecular biomarkers. Interestingly, these compounds downregulated the Bcl-2 and Ki-67 expression levels and activated the expression of caspase-8 in HepG2 cells compared to untreated cells. These results indicate that some of the newly synthesized compounds possess anti-HepG2 activity
**Keyword:** Organoselenium; Diselenides; Quinone; Tetrazole; Azido-Ugi Reaction; Redox modulators; Caspase-8; Apoptosis; Ki-67; Bcl-2.

## M-787. Circulating Serum miRNAs as Diagnostic Markers for Colorectal Cancer.

Abdel-Rahman N. Zekri, Amira Salah El-Din Youssef, Mai M. Lotfy, Reham Gabr, OlaS. Ahmed, Auhood Nassar, Nehal Hussein, Dalia Omran, Eman Medhat, Salam Eid,Marwa Mahmoud Hussein, Maha Yahia Ismail, Faris Q. Alenzi and Abeer A. Bahnassy

*Plos One, (2016) IF: 3.057*

**Aim:**The study was designed to assess the possibility of using circulating miRNAs (serum miRNAs) as diagnostic biomarkers in colorectal cancer (CRC) and to identify their methods: ossibility as candidates for targeted therapy.**Methods:**The study involved two sample sets: 1- a training set which included 90 patients with colorectalrelated disease (30 with CRC, 18 with inflammatory bowel disease (IBD), 18 withcolonic polyps (CP) and 24 with different colonic symptoms but without any colonoscopicabnormality who were enrolled as control group) and 2- a validation set which included 100CRC patients. Serum miRNAs were extracted from all subjects to assess the expressionprofiles for the following miRNAs (miR-17, miR-18a, miR-19a, miR-19b, miR-20a, miR-21,miR-146a, miR-223, miR-24, miR-454, miR-183, miR-135a, miR- 135b and miR-92a)using the custom miScript miRNA PCR-based sybergreen array. The area under thereceiver operating characteristic curve (AUC) was used to evaluate the diagnostic performanceof the studied miRNAs for colorectal cancer diagnosis.**Results**Data analysis of miRNA from the training set showed that; compared to control group, onlymiR-19b was significantly up-regulated in patients with IBD group (fold change = 5.24, p =0.016), whereas in patients with colonic polyps, miR-18a was significantly up-regulated(fold change = 3.49, p-value = 0.018). On the other hand, miR-17, miR-19a, miR-20a andmiR-223 were significantly up-regulated (fold change = 2.35, 3.07, 2.38 and 10.35; respectivelyand p-value = 0.02, 0.015, 0.017 and 0.016; respectively in CRC patients. Howeverthe validation set showed that only miR-223 was significantly up-regulated in CRC patients(fold change = 4.06, p-value = 0.04).**Conclusion**Aberrant miRNA expressions are highly involved in the cascade of colorectal carcinogenesis.We have found that (miR-17, miR-19a, miR-20a and miR-223) could be used as diagnosticbiomarkers for CRC. On the other hand, miR-19b and miR-18a could be used asdiagnostic biomarkers for CP and IBD respectively.

## M-788. Depletion of Histone Demethylase Jarid1a Resulting in Histone Hyperacetylation and Radiation Sensitivity Does Not Affect DNA Double-Strand Break Repair.

Corina Penterling, Guido A. Drexler, Claudia Böhland, Ramona Stamp,Christina Wilke, Herbert Braselmann, Randolph B. Caldwell, Judith Reindl,Stefanie Girst, Christoph Greubel, Christian Siebenwirth, Wael Y. Mansour,Kerstin Borgmann, Günther Dollinger, Kristian Unger and Anna A. Friedl

*Plosone, june 2: 1-24 (2016) IF: 3.057*

Histone demethylases have recently gained interest as potential targets in cancer treatment and several histone demethylases have been implicated in the DNA damage response. We investigated the effects of siRNA-mediated depletion of histone demethylase Jarid1A (KDM5A, RBP2), which demethylates transcription activating tri- and dimethylated lysine 4 at histone H3 (H3K4me3/me2), on growth characteristics and cellular response to radiation in several cancer cell lines. In unirradiated cells Jarid1A depletion lead to histone hyperacetylation while not affecting cell growth. In irradiated cells, depletion of Jarid1A significantly increased cellular radiosensitivity. Unexpectedly, the hyperacetylation phenotype did not lead to disturbed accumulation of DNA damage response and repair factors 53BP1, BRCA1, or Rad51 at damage sites, nor did it influence resolution of radiation-induced foci or rejoining of reporter constructs. We conclude that the radiation sensitivity observed following depletion of Jarid1A is not caused by a deficiency in repair of DNA double-strand breaks.
**Keyword:** Histone demethylase jarid1a; Dsb repair; Radiation sensitivity.

## M-789.Serum MicroRNA Panels as Potential Biomarkers for Early Detection of Hepatocellular Carcinoma on Top of HCV Infection.

Zekri AN, Youssef AS, El-Desouky ED, Ahmed OS, Lotfy MM, Nassar AA and Bahnassey AA

*Tumour Biol, 37(9): 12273-12286 (2016) IF: 2.926*

The identification of new high-sensitivity and high-specificity markers for hepatocellular carcinoma (HCC) is essential. We aimed at identifying serum microRNAs (miRNAs) as potential biomarkers for early detection of HCC on top hepatitis C virus (HCV) infection. We investigated serum expression of 13 miRNAs in 384 patients with HCV-related chronic liver disease (192 with HCC, 96 with liver cirrhosis (LC), and 96 with chronic hepatitis C (CHC)) in addition to 96 healthy participants enrolled as a control group. The miRNA expression was performed using real-time quantitative PCR-based SYBR Green custom miRNA arrays. The area under the receiver operating characteristic curve (AUC) was used to evaluate the diagnostic performance of miRNA panels for early detection of HCC. Using miRNA panel of miR-122, miR-885-5p, and miR-29b with alpha fetoprotein (AFP) provided high diagnostic accuracy (AUC = 1) for early detection of HCC in normal population while using miRNA panel of miR-122, miR-885-5p, miR-221, and miR-22 with AFP provided high diagnostic accuracy (AUC = 0.982) for early detection of HCC in LC patients. However, using miRNA panel of miR-22 and miR-199a-3p with AFP provided high diagnostic accuracy (AUC = 0.988) for early detection of HCC in CHC patients. We identified serum miRNA panels that could have a considerable clinical use in early detection of HCC in both normal population and high-risk patients.

**Keyword:** Early detection; HCC; HCV; Panel; Serum; Mirnas.

## M-790. Early Detection of Hepatocellular Carcinoma Co-Occurring with Hepatitis C Virus Infection: A Mathematical Model.

Abdel-Rahman Nabawy Zekri, Amira Salah El-Din Youssef, Yasser Mabrouk Bakr, Reham Mohamed Gabr,Ola Sayed Ahmed, Mostafa Hamed Elberry, Ahmed Mahmoud Mayla, Mohamed Abouelhoda and Abeer A Bahnassy

*World J Gastroenterol., 22(16): 4168-4182 (2016) IF: 2.787*

**Aim:**To develop a mathematical model for the early detection of hepatocellular carcinoma (HCC) with a panel of serum proteins in combination with α-fetoprotein (AFP).**Methods:** Serum levels of interleukin (IL)-8,soluble intercellular adhesion molecule-1 (sICAM-1),soluble tumor necrosis factor receptor Ⅱ (sTNF-R Ⅱ ), proteasome, and β-catenin were measured in479 subjects categorized into four groups: (1) HCCconcurrent with hepatitis C virus (HCV) infectionCase Control StudyORIGINAL ARTICLE(n = 192); (2) HCV related liver cirrhosis (LC) (n =96); (3) Chronic hepatitis C (CHC) (n = 96); and (4)Healthy controls (n = 95). The R package and differentmodules for binary and multi-class classifiers based ongeneralized linear models were used to model the data.Predictive power was used to evaluate the performanceof the model. Receiver operating characteristic curveanalysis over pairs of groups was used to identify thebest cutoffs differentiating the different groups.**Results:** We revealed mathematical models,based on a binary classifier, made up of a uniquepanel of serum proteins that improved the individualperformance of AFP in discriminating HCC patientsfrom patients with chronic liver disease either with orwithout cirrhosis. We discriminated the HCC group fromthe cirrhotic liver group using a mathematical model(-11.3 + 7.38 × Prot + 0.00108 × sICAM + 0.2574 ×β-catenin + 0.01597 × AFP) with a cutoff of 0.6552,which achieved 98.8% specificity and 89.1% sensitivity.For the discrimination of the HCC group from the CHCgroup, we used a mathematical model [-10.40 + 1.416× proteasome + 0.002024 × IL + 0.004096 × sICAM-1+ (4.251 × 10-4) × sTNF + 0.02567 × β-catenin +0.02442 × AFP] with a cutoff 0.744 and achieved96.8% specificity and 89.7% sensitivity. Additionally,we derived an algorithm, based on a binary classifier,for resolving the multi-class classification problem byusing three successive mathematical model predictionsof liver disease status.**Conclusion:** Our proposed mathematical modelmay be a useful method for the early detection ofdifferent statuses of liver disease co-occurring with HCVinfection.

**Keyword:** Mathematical model; Hepatocellular carcinoma; α-fetoprotein; Soluble intercellular adhesion molecule-1; β-catenin; Interleukin-8; Soluble tumor necrosis factor receptor; Proteasome.

## M-791. Promoter SNPs rs116896264 and rs73933062 form A Distinct Haplotype and are Associated with Galectin-4 Overexpression in Colorectal Cancer

Reham Helwa, Mohamed Ramadan, Abdel-Hady A. Abdel-Wahab,Stian Knappskog and Andrea S. Bauer

*Mutagenesis, 31: 401-408 (2016) IF: 2.297*

Galectin-4 is a member of the galectin family which consists of 15 galactoside-binding proteins. Previously, galectin-4 has been shown to have a role in cancer progression and metastasis and it is found upregulated in many solid tumours, including colorectal cancer (CRC). Recently, the role in the metastatic process was suggested to be via promoting cancer cells to adhere to blood vascular endothelium. In the present study, the regulatory region of LGALS4 (galectin-4) in seven colon cell lines was investigated with respect to genetic variation that could be linked to expression levels and therefore a tumourigenic effect. Interestingly, qRT-PCR and sequencing results revealed that galectin-4 upregulation is associated with SNPs rs116896264 and rs73933062. By use of luciferase reporter- and pull-down assays, we confirmed the association between the gene upregulation and the two SNPs. Also, using pull-down assay followed by mass spectrometry, we found that the presence rs116896264 and rs73933062 is changing transcription factors binding sites. In order to assess the frequencies of the two SNPs among colon cancer patients and healthy individuals, we genotyped 75 colon cancer patients, 12 patients with adenomatous polyposis and 17 patients with ulcerative colitis and we performed data mining in the 1000 genomes databank. We found the two SNPs co-occuring in 21% of 75 CRC patients, 0 out of 12 patients of adenomatous polyposis, and 6 out of 17 patients (35%) with ulcerative colitis. Both in the patient samples and in the 1000 genomes project, the two SNPs were found to co-occur whenever present (D′ = 1).

**Keyword:** Polymerase chain reaction; Colorectalcancer; Cell lines; Haplotype;luciferase.

## M-792. Bibliometric Analysis of Egyptian Publications on Hepatitis C Virus from Pubmed Using Data Mining of an in-House Developed Database (HCVDBegy)

Hanaa M. H. Alam El-Din, Ahmed Sharaf Eldin and Amro M. S. A. Hanora

*Scientometrics, 108 (2): 895-915 (2016) IF: 2.084*

Bibliometric analysis of Egyptian literature on HCV provides the intelligence needed for decision makers and gives an insight into research productivity in this area. We propose our database (HCVDBegy) on MS-SQL server by querying PubMed for "HCV and Egypt" with time limit till 31st March 2013. Fifty eight out of the 716 records were excluded and the rest 658 were divided into 22 domains. Analysis used data mining add-ins for Microsoft Excel, including association and regression algorithms. A fluctuation in numbers of papers was noticed from 2004 to 2009 with a steady increase onward. Eighty six percent of publications were the contribution of three or more authors. Top publishing bodies were Cairo and Ain Shams Universities, Faculty of Medicine, National Research Center and National Cancer Institute. Three Egyptian journals came on top, whereas other publishing journals were mainly from the USA. Few controlled clinical trials and meta-analyses were published. HCV epidemiology, review articles and sequence analysis domains were the most cited. Forecasting model showed a breakthrough in numbers of publications on 2013 and 2014 than those forecasted. Dependency network based on association rule model of MeSH topics was also extensively analyzed. Number of publications showed a promising increase which points to the better national awareness of HCV problem. Studying MeSH terms clustering showed some hot topics. We recommend that the PubMed should alarm authors of the challenges of author affiliations. HCVDBegy availability opens the door for more drill down analysis for decision makers

**Keyword:** Bibliometricsdata miningdata; Baseassociation ruleregression; Analysisclusteringhcv and Egyptpubmed.

## M-793. The Liver MicroRNA Expression Profiles Associated with Chronic Hepatitis C Virus (HCV) Genotype-4 Infection: A Preliminary Study

Nadia Mohamed El-Guendy, Reham Helwa, Medhat Salah El-Halawany, Shimaa Abdel Rahman Ali,Marwa Tantawy Aly, Nelly Hasan Alieldin, Shawky Abdel Hamid Fouad, Hany Saeid and Abdel-Hady Ali Abdel-Wahab

*Hepat Mon., (2016) IF: 1.932*

**Background:** MicroRNAs (miRNAs) have been repeatedly shown to play important roles in liver pathologies, including hepatitis, liver cirrhosis, and liver cancer. Egypt has the highest hepatitis C virus (HCV) infection rate worldwide, predominantly involving genotype-4. **Objectives:** In this study, we attempted to characterize the miRNA profile of the poorly studied genotype 4 of HCV in chronically infected Egyptian patients to obtain a better understanding of the disease and its complications and help in the design of better management protocols. Patients and Methods:We analyzed the expression levels of a selected panel of 94 miRNAs in fresh liver biopsies collected from 50 Egyptian patients diagnosed with chronic HCV infection using quantitative real-time polymerase chain reaction (PCR) assay. Nonparametric tests were used to analyze the expression level of each miRNA and association with the clinicopathological features of enrolled patients in this study. **Results:** Our results revealed differential expression levels of the analyzed miRNAs compared to the normal controls. Twenty-seven miRNAs (including miR-105, miR-147, miR-149-3p, and miR-196b) showed up-regulation, while 17 miRNAs (including miR-21, miR-122, miR-199a-3p, and miR-223) showed down-regulation. An inverse correlation was observed between levels of miR-95, miR-130a, and miR-142-5p with the blood albumin level. Increased expression levels of seven miRNAs (miR-29c, miR-30c, miR-126, miR-145, miR- 199a, miR-199a-3p, and miR-222) were observed with severe chronic hepatic inflammation. Several deregulated miRNAs found in this study have been previously linked to chronic liver inflammation and the risk of hepatocellular carcinoma (HCC) development. **Conclusions:** The identified expression profiles of some examined miRNAs might offer important points to consider for the treatment of naive patients and the management of chronically infected HCV patients in Egypt and around the world.

**Keyword:** Hepatitis C; Micrornas; Genotype-4; Real-Time Polymerase chain reaction; Liver cirrhosis.

## M-794.Synthesis, Characterization and Cytotoxic Evaluation of Chitosan Nanoparticles: in Vitro Liver Cancer Model

Samah A Loutfy, Hanaa M Alam El-Din, Mostafa H Elberry, Nanis G Allam, M T M Hasanin and Ahmed M

*Advances in Natural Sciences: Nanoscience and nanotechnology 7: 1-9 (2016) IF: 1.581*

To evaluate the cytotoxic effect of chitosan nanoparticles (CS-NPs) on an in vitro human liver cancer cell model (HepG2) and their possible application as a drug delivery system, we synthesized water-soluble CS-NPs, investigated their properties and extensively evaluated their cytotoxic activity on the cellular and molecular levels. A human liver cancer cell line was used as a model of human liver cancer. The CS-NPs were characterized using transmission electron microscopy, Fourier transform infrared spectroscopy, and zeta analysis. The cytotoxic effects of the CS-NPs on HepG2 cells were monitored by sulforhodamine B colorimetric assays for cytotoxicity screening and flow cytometric analysis. Molecular investigations including DNA fragmentation and the expression of some apoptotic genes on the transcriptional RNA level were conducted. Treatment of HepG2 with different concentrations of 150 nm diameter CS-NPs did not show alteration of cell morphology after 24 h of cell exposure. Also, when cells were treated with 100 μg ml−1 of CS-NPs, 12% of them were killed and IC50 reached 239 μg ml−1 after 48 h of cell exposure. Flow cytometry evaluation of the CS-NPs revealed mild accumulation in the G2/M phase followed by cellular DNA fragmentation after 48 h of cell exposure. Extensive evaluation of the cytotoxic effect of the CS-NPs showed messenger RNA (mRNA) apoptotic gene expression (p53, Bak, Caspase3) after 24 h of cell exposure with no expression of the mRNA of the caspase 3 gene after 48 h of cell exposure, suggesting the involvement of an intrinsic apoptotic caspase-independent pathway by increasing the exposure time of 100 μg ml−1 of the CS-NPs. The engineered CS-NPs were controlled to a 150 nm size and charges of 40 mV and a concentration of 100 μg ml−1 revealed a genotoxic effect on HepG2 after 48 h of cell exposure through intrinsic apoptotic

caspase-independent mechanisms. Further quantitative analysis on the molecular and protein levels is still required to confirm the impact of chitosan size and time on genotoxic effect before reaching a final conclusion and starting its biomedical application.
**Keyword:** Chitosan nanoparticles; HepG2; Flow cytometry; Apoptotic gene expression.

## M-795. Differential Expression of Viral Agents in Lymphoma Tissues of Patients with ABC Diffuse Large B-Cell Lymphoma from High and Low Endemic Infectious Disease Regions.

Therese Högfeldt, Crystal Jaing, Kevin Mc Loughlin, James Thissen, Shea Gardner, Abeer A. Bahnassy, Baback Gharizadeh, Joachim Lundahl, Anders Österborg, Anna Porwit, AbdelRahman N. Zekri, Hussein M. Khaled, Håkan Mellstedt and Ali Moshfegh

*Oncol Lett., 12(4): 2782-2788 (2016) IF: 1.482*

Diffuse large B-cell lymphoma (DLBCL), the most common type of non-Hodgkin's lymphoma (NHL) in adults, accounts for approximately 30-40% of newly diagnosed lymphomas worldwide. Environmental factors, such as viruses and bacteria, may contribute to cancer development through chronic inflammation and the integration of oncogenes, and have previously been indicated in cervical cancer, hepatocellular carcinoma, gastric cancer and lymphoproliferative disorders. In the present study, the presence of microbial agents was analyzed in the lymphoma tissue of patients with activated B-cell like (ABC) DLBCL. The present study compared two groups of patients from geographically varied regions that possess a difference in the prevalence of viral and other microbial agents. The patient populations were from Sweden (a low endemic infectious disease region) and Egypt (a high endemic infectious disease region). A differential expression of several viruses in lymphoma tissues was noted when comparing Swedish and Egyptian patients. JC polyomavirus (JCV) was detected in Swedish and Egyptian patients and, uniquely, the complete hepatitis B virus (HBV) genome was detected only in Egyptian lymphoma patients. None of these viruses were detected in control lymph tissues from Sweden or Egypt. In total, 38% of the Egyptian patients were found to have HBV surface antigens (HBsAgs) in their serum; however, HBsAgs were not found in any of the Swedish patients. The percentage of serum HBsAgs in Egyptian patients with ABC DLBCL was significantly increased compared with the general Egyptian population ($P<0.05$). The present study may support a notion that viral agents, including JCV and HBV, may be involved in the tumorigenesis of DLBCL in regions of high infectious disease.
**Keyword:** Gene array; Hepatitis B virus; Lymphoma and hodgkin disease; Molecular genetics; Virus.

## M-796. Arabinoxylan Rice Bran (Biobran) Suppresses the Viremia Level in Patients with Chronic HCV Infection: A Randomized Trial.

Hosny Salama, Eman Medhat, Magda Shaheen,Abdel-Rahman N Zekri, Tarneem Darwishand Mamdooh Ghoneum

*Int J. Immunopathol Pharmacol, 29(4): 647-653 (2016) IF: 1.47*

Current treatments for Hepatitis C virus (HCV) have severe side effects and are very expensive. There is a need to explore effective natural therapies against HCV that are less toxic and more cost-effective. In the current study, 37 chronic HCV patients were randomized into two groups and treated with either pegylated interferon (PEG IFN) plus ribavirin (n = 21) or Biobran, an arabinoxylan from rice bran (1 g/day) (n = 16). We examined viremia, liver enzymes, interferon-γ (IFN-γ) levels in serum, and toxicity before and three months after treatment. Both groups showed a significant and similar reduction in viral load after three months of treatment relative to the baseline viral load ($P <0.05$). In addition, treatment with Biobran resulted in a significant increase in the level of IFN-γ ($P <0.001$). Patients in the PEG IFN plus ribavirin group showed fever, anemia, thrombocytopenia, and easy fatigue. Patients in the Biobran group showed no side effects and reported good health. We conclude that Biobran is a potential novel therapeutic regimen that has a similar effect to PEG IFN plus ribavirin and is safe and cost-effective in the treatment of chronic HCV. Our finding of Biobran's efficacy against HCV infection warrants further investigation in multiple clinical trials (Clinical Trials Registration: NCT02690103).
**Keyword:** Biobran; Hepatitis C Virus (HCV); Arabinoxylan; Pegylated interferon (PEG IFN); Viremia.

## M-797. E1/E2 of Hepatitis C Virus Genotype4 and Apoptosis.

Abdel-Rahman N Zekri, Esraa Sobhy, Nehal Hussein, Ola S Ahmed, AmiraHussein, Sahar Shoman, Amira H Soliman and Hanaa M Alam El-Din

*Asian Pac J Cancer Prev, 17(7): 3131-3138 (2016)*

Several studies have addressed the possible role of hepatitis C virus genotype4 (HCV GT4) in apoptosis. However, this still not fully understood. In the current study a reconstructed clone of E1/E2 polyprotein region of the HCV GT4 was transfected into the Huh7 cell line and a human apoptotic PCR array of 84 genes was used to investigate its possible significance for apoptosis. Out of the 84 genes, only 35 showed significant differential expression, 12 genes being upregulated and 23 downregulated. The highestup regulated genes were APAF1 (apoptotic peptidaseactivating factor 1), BID (BH3 interacting domain death agonist) and BCL 10 (Bcell CLL/ lymphoma protein 10) with fold regulation of 33.2, 30.1 and 18.9, respectively. The most downregulated were FAS (TNF receptor super family), TNFRSF10B (tumor necrosis factor receptor superfamily member 10b) and FADD (FASassociated death domain) with fold regulation of 30.2, 27.7 and 14.9, respectively. These results suggest that the E1/E2 proteins may be involved in HCVinduced pathogenesis by modulating apoptosis through the induction of the intrinsic apoptosis pathway and disruption of the BCL2 gene family.

## M-798. Leptin Influences Estrogen Metabolism and Increases DNA Adduct Formation in Breast Cancer Cells

Samia Shouman, Mohamed Wagih and Marwa Kamel

*Cancer Biology and Medicine, 13, (4): 505-513 (2016)*

**Objective:** The elevated incidence of obesity has been paralleled with higher risks of breast cancer. High adiposity increases leptin secretion from adipose tissue, which in turn increases cancer cell proliferation. The interplay between leptin and estrogen is one of the mechanisms through which leptin influences breast carcinogenesis. An unbalanced estrogen metabolism increases the formations of catechol estrogen quinones, DNA adducts, and cancer mutations. This study aims to investigate the effect of leptin on some estrogen metabolic enzymes and DNA adduction in breast cancer cells. **Methods:** High performance liquid chromatography (HPLC) was performed to analyze the DNA adducts 4-OHE1[E2]-1-N3 adenine and 4-OHE1[E2]-1-N7 guanine. Reporter gene assay, real time reverse transcription polymerase chain reaction (real time RT-PCR), and Western blot were used to assess the expression of estrogen metabolizing genes and enzymes: Cytochrome P-450 1B1 (CYP1B1), Nicotinamide adenine dinucleotide phosphate-quinone oxidoreductase1 (NQO1), and Catechol-O-methyl transferase (COMT). **Results:** Leptin significantly increased the DNA adducts 4-OHE1[E2]-1-N3 adenine and 4-OHE1[E2]-1-N7 guanine. Furthermore, leptin significantly upregulated CYP1B1 promoter activity and protein expression. The luciferase promoter activities of NQO1 and mRNA levels were significantly reduced. Moreover, leptin greatly reduced the reporter activities of the COMT-P1 and COMT-P2 promoters and diminished the protein expression of COMT. **Conclusions:** Leptin increases DNA adduct levels in breast cancer cells partly by affecting key genes and enzymes involved in estrogen metabolism. Thus, increased focus should be directed toward leptin and its effects on the estrogen metabolic pathway as an effective approach against breast cancer.

**Keyword:** Breast Cancer; Leptin; Estrogen metabolism; DNA Adducts.

***Dept. of Tumor Pathology***

## M-799. Differential Expression of E-Cadherin and Catenins in Ovarian Sex Cord Stromal Tumours

Stavroula Stavrinou, Ashleigh Clark, Julie Irving, Cheng-Han Lee, Esther Oliva,Robert Young, Ruethairat Sriraksa, Nesreen Magdy, Susan Van Noorden,W Glenn McCluggage and Mona El-Bahrawy

*Histopathology, 69(2): 298-306 (2016) IF: 3.425*

**AIMS:** Sex cord stromal tumours (SCSTs) of the ovary encompass several histological tumour subtypes that are defined by characteristic histological features. Some can show morphological overlap with other subtypes of SCSTs, as well as with non-SCSTs. The E-cadherin/catenin complex constitutes the adherens junction, which is well developed in epithelial tissue, but the constituent molecules are also expressed in several non-epithelial tumours. The aim of this study was to determine whether the expression patterns of E-cadherin and catenins in ovarian SCSTs can be of diagnostic utility. **Methods and Results:** We studied the expression of E-cadherin, α-, β- and γ-catenin in 55 tumours using immunohistochemistry. We found that all tumour subtypes showed nuclear expression of E-cadherin, while only microcystic stromal tumours (MCSTs) displayed a distinct profile, with nuclear localization of all three catenins in almost all cases. **Conclusions:** We conclude that the E-cadherin expression profile in SCSTs can assist in distinguishing between SCSTs and non-SCSTs in which there is no nuclear expression of E-cadherin. The nuclear localization of catenins may be of potential use in distinguishing MCST from other subtypes of SCST.

**Keyword:** E-Cadherin; Catenin; Ovary; Sex cord; Stromal; Tumour.

## M-800.Rare Skin Adnexal and Melanocytic Tumors Arising in Ovarian Mature Cystic Teratomas: A Report of 3 Cases and Review of the Literature

Alexandra A. Moulla, Nesreen Magdy, M.B.Bc.H, Nicholas Francis, F.R.C.Path.,Janis Taube, Brigitte M. Ronnett and Mona El-Bahrawy

*International Journal of Gynecological Pathology, 35 (5): 448-455 (2016) IF: 1.473*

Mature teratoma of the ovary is the most common primary ovarian tumor accounting for 15% (10%–20%) of all ovarian neoplasms. Skin and skin adnexal structures are the most common elements identified in mature teratomas. Benign and malignant skin tumors can arise in ovarian teratomas, the most common being epithelial tumors. Melanocytic and adnexal tumors developing in a teratoma are rare and can be easily overlooked. We report 3 cases and review melanocytic and skin adnexal tumors encountered in ovarian teratomas.

**Keyword:** Teratoma; Ovary; Adnexal tumours.

## M-801. Expression of Cyclooxygenase 2 and Vascular Endothelial Growth Factor in Gastric Carcinoma: Relationship with Clinicopathological Parameters

Nesreen H. Hafez and Neveen S. Tahoun

*Journal of The Egyptian National Cancer Institute, 28: 149-156 (2016)*

**Background:** Gastric cancer is one of the most common cancers and the second most common cause of cancer-related death worldwide. Identification of specific prognostic indicators might allow a better prognostic stratification and more effective therapy. **Aim:** To assess the expression and relationship between COX-2 and VEGF protein in gastric adenocarcinoma and whether these markers are useful in predicting clinicopathological prognostic parameters. **Materials and methods:** The study included 83 formalin-fixed paraffin embedded tissue samples of excised gastric adenocarcinoma and 20 non tumorous tissue controls. The slides were subjected to COX-2 and VEGF immunohistochemical staining using a streptavidin–biotinperoxidase according to the manufacturer's protocol. The results were assessed independently by two pathologists. The relationships among COX-2 and VEGF expression and clinicopathological parameters were statistically analyzed. **Results:** COX-2 and VEGF expressions were obviously higher in carcinoma tissues compared to normal mucosae ($p< 0.001$). The expression rate of COX-2 was 54.2% and of VEGF was 68.7%. COX-2 positive tumors were significantly correlated with Lauren classification, tumor depth and Helicobacter pylori infection ($p< 0.001$, $p= 0.008$, $p =0.035$). VEGF was significantly associated with lymph node metastasis and tumor depth ($p<0.001$). There was a positive association between VEGF and COX-2 expression in gastric

adenocarcinoma (Kappa value =0.55). **Conclusion:** In gastric adenocarcinoma, COX-2 expression might serve as a powerful indicator for intestinal type carcinoma, locally advanced disease and H. pylori infection, while VEGF was related to loco-regional progression. COX-2 might be involved in the development of angiogenesis in gastric carcinoma through VEGF upregulation.
**Keyword:** Gastric adenocarcinoma; COX-2; VEGF; IHC

## M-802. Expression of Vascular Endothelial Growth Factor Protein in Both Serum Samples and Excised Tumor Tissues of Breast Carcinoma Patients

Halla Mohamed Ragab, HebatAllah Mohamed Shaaban, Nabila Abd El Maksoud, Samah Mohamed Radwan, Wafaa Abd Elaziz and Nesreen Hassan Hafez

*International Journal of Cancer Research, 12 (3-4): 152-161 (2016)*

**Background and Objective:** This study examined the correlation between immunohistochemistry (IHC) expression of the Vascular Endothelial Growth Factor (VEGF) in primary breast carcinoma tissue and its concentration in blood samples of the same patients preoperatively and to the other established clinicopathological parameters namely, tumor size, grade, lymph node status, Estrogen Receptor (ER), Progesterone Receptor (PR) status and human epidermal growth factor receptor 2 (Her2-neu) score. The current study also stressed on whether the ELISA detection is more sensitive and effective in diagnosis of breast cancer. **Materials and Methods:** Serum concentration of VEGF was measured using Enzyme Linked Immune Sorbent Assay (ELISA) in 92 primary breast cancer patients and compared with 25 benign breast disease patients. Also, tissue expression of VEGF was measured by immunohistochemistry. **Results:** Serum VEGF levels were significantly elevated in patients with malignant breast cancer ($p = 0.000$). The median serum level in the malignant group was 579 pg mL–1 and in the control group 200 pg mL–1. On the other hand no correlation was found between concentrations of serum VEGF and clinicopathological parameters. A significant association was showed between VEGF expression and lymph node metastasis, tumor size more than 2 cm and Her2-neu status ($p<0.0001$). No significant association was found between VEGF and patient age, histology, grade, ER and PR status ($p>0.05$). All positive cases for VEGF with strong positivity (score ++) were grade 2 and 3. **Conclusion:** The VEGF is overexpressed in breast carcinomas compared to the benign breast disease. Tissue expression of VEGF can be used as a prognostic marker due to the significant association with the large tumor size, lymph node metastasis and positive Her2-neu status. Tissue expression of VEGF can be used as a prognostic marker due to the significant association with the large tumor size, lymph node metastasis and positive Her2-neu status.
**Keyword:** Angiogenesis; VEGF; Immunohistochemistry; Enzyme linked immune sorbent assay; Breast carcinoma; Tumor grade; Prognosis; Her2-Neu.

## M-803. Nuclear and Cytoplasmic Expression of Survivin in Breast Carcinoma: Correlation with Clinicopathological Parameters

HebatAllah Mohamed Shaaban, Nesreen Hassan Hafez, Halla Mohamed Ragab andAreeg Ibrahim El Abadi

*International Journal of Cancer Research, 12 (3-4): 128-139 (2016)*

**Background:** Survivin, a member of the inhibitor of apoptotic protein family is involved in cell proliferation and apoptotic suppression. Survivin is highly expressed in many cancers and correlated with more aggressive disease. **Objective:** Assessment of survivin expression in breast carcinoma and its association with clinicopathological factors. **Materials and Methods:** One hundred and eight breast carcinoma and 22 control benign specimens were used for survivin immunohistochemical assessment. Survivin expression was evaluated according to staining intensity and percentage of positive cells. A numerical score was calculated by multiplying them. Cases with scores of ≥1 were considered positive. **Results:** Survivin expression was obviously higher in malignant cases compared to the control cases ($p<0.001$). Among the clinicopathological parameters analyzed, significant correlations were established with the patient's age ($p<0.001$), the size of the tumors ($p = 0.005$) and HER2 status ($p = 0.05$). Cytoplamic staining was detected in all positive cases, either alone (62.0%) or associated with nuclear staining (38.0%). Cytoplasmic staining only was significantly correlated with good prognostic parameters; small sized tumor, grade II, ER-positive and HER2-negative tumors ($p<0.05$). All triple negative cases (100%), 90% of luminal B and 72.2% of HER2 subtype showed survivin positivity, while only 48.7% of luminal A was positive. The association between survivin expression and molecular classification was insignificant ($p = 0.069$). **Conclusion:** Survivin has a potential role in diagnosis of malignancy. Survivin expression is associated with younger age, large tumor size, HER2-positive tumor and triple negative molecular subtype. Cytoplasmic staining was correlated with good prognostic parameters.
**Keyword:** Survivin; Immunohistochemistry; Breast carcinoma; Tumor grade; Molecular types; Prognosis; Cell Proliferation; Anti apoptotic gene.

## M-804. The Role of Napsin-A and Desmocollin-3 in Classifying Poorly Differentiating Non-Small Cell Lung Carcinoma

Noha El-Sayed Ezzat and Neveen Tahoun

*Journal of Egyptian National Cancer Institute, 28: 13-22 (2016)*

There is increased need for classification of non-small cell lung cancer (NSCLC) into its major subtypes, adenocarcinoma (AC) and squamous cell carcinoma (SCC). Such a classification is enabled in poorly differentiated tumours based on routine morphology due to overlapping morphologic features. In such cases, the use of immunohistochemistry (IHC) can differentiate between the two subtypes. Purpose: To test the ability of the two markers; Napsin-A and Desmocollin-3, in differentiating poorly differentiated (AC) from poorly differentiated SCC in small biopsies. Patients and methods: This is a retrospective study including 60 patients who presented with pulmonary nodules. Cases with biopsy specimens diagnosed as poorly differentiated non-small cell lung cancer, and had corresponding resection

specimens were included. Cell blocks were stained with anti Napsin-A, and anti Desmocollin-3. Cytoplasmic immunoreactivity for both markers was considered specific. Sensitivity, specificity, positive and negative predictive values, total accuracy and combined accuracy of both markers were calculated. **Results:** Napsin A showed a sensitivity of 89.3%, a specificity of 96.9%, PPV of 96.2%, NPV of 91.2%, and a total accuracy of 93.3% for AC, while Desmocollin-3 achieved 90.6% sensitivity, 96.4% specificity, 96.7% PPV, 90% NPV, and 93.3% total accuracy. Both markers achieved a total accuracy of 90%. Conclusion: Napsin-A, and Desmocollin-3 were sensitive and specific markers for the diagnosis of AC and SCC, respectively. Both markers allowed classification of 54/60 cases into either AC or SCC.

**Keyword:** Napsin-A; Desmocollin-3; Lung; Poorly differentiating carcinoma.

## M-805. The Role of S100p and Imp3 in the Cytologic Diagnosis of Pancreatic Adenocarcinoma

Noha E. Ezzat, Neveen S. Tahoun and Yahia M. Ismail

*Journal of Egyptian National Cancer Institute, 28: 229-234 (2016)*

**Purpose:** The aim of this study was to assess the role of the two markers, S100P and IMP3, in differentiating between pancreatic ductal adenocarcinoma (PDA) and non-neoplastic pancreatic tissue in (fine needle aspiration cytology) FNAC. **Patients and methods:** This is a retrospective study that included 72 cases presented with pancreatic mass, where endoscopic guided FNAC was taken from pancreatic lesions. The final histopathologic diagnosis was considered the gold standard. Cell blocks were stained with anti S100P, and IMP3. Nuclear immunoreactivity with or without cytoplasmic staining for the first marker, and cytoplasmic staining for the second marker was considered specific. Sensitivity, specificity, positive predictive value (PPV), negative predictive value (NPV), and total accuracy of the two markers, as well as the combined accuracy of both markers were calculated. **Results:** S100P achieved 96.4% sensitivity, 93.3% specificity, 98.2% PPV, 87.5% NPV and 95.8% total accuracy, while IMP3 achieved 91.2% sensitivity, 86.7% specificity, 96.2% PPV, 72.2% NPV and 90.3% total accuracy for PDA. Both markers showed a total combined accuracy of 89%. S100P showed strong and diffuse staining pattern in most of cases, while the staining pattern for IMP3 was moderate and focal in most of cases. **Conclusion:** Both markers were sensitive and specific for diagnosis of PDA. The staining pattern for S100P was easier to evaluate than IMP3.

**Keyword:** S100; IMP3; Cell Block; Pancreatic Adenocarcinoma

## Faculty of Physical Therapy

***Dept. of Physical Therapy for Neuromuscular Disorder***

### M-798. Bilateral Arm Training Improve Reaching Kinematics in Hemiparetic Patients

Youssef M. El balawy, Hoda M. Zakaria, Moataz M. Talaat and OlfatI.Ali

*International Journal of Pharmtech Research, 9(12): 866-872 (2016)*

**Background and Purpose:**Motor recovery after stroke is depending on the balance between neural network activity of both affected and non affected motor cortices. Bilateral arm training induce the rebalanced of inter hemispheric activation and inhibition. The aim of the study was to determine the improvement in reaching kinematics after bilateral arm training in hemiparetic patients. **Patients and Methods:** Twenty male patients with ischemic stroke included in this study and their age ranged between 40-55 years. Patients were divided randomly into two equal groups. The first group received bilateral arm training plus a selected physical therapy program. The second group received the selected physical therapy program only. Assessing kinematics of reaching movement of the affected upper limb was done before and after treatment using three-dimensional analysis. **Results:** Within the first group (before and after treatment) the results revealed that a statistically significant decrease in compensatory trunk displacement and decrease time of reach to grasp after treatment (P=<0.0002and P= 0.0001 respectively). Within the second group (before and after treatment) the results revealed that a statistically significant increase in compensatory trunk displacement(P=0.004) while there was no significance difference in time of reach to grasp after treatment (P=0.40). Between both groups, there was significant difference of trunk displacement and time of reach to grasp post treatment(P=0.0001 and p=0.0004 respectively) favouring first group. **Conclusion:** Bilateral arm training improves movement control and kinematics of reaching movement in affected upper limb in hemiparesis.

**Keywords:** Stroke, Neural Network, Bilateral Arm Training, Time of Reach, Trunk Displacement and Reaching Kinematics.

### M-799. Using Biomechanical Principles in Collar Selection for Patients Complaining Cervical Disc Prolapse

Usama M Rashad , Hoda M Zakaria and Walaa M Ragab

*International Journal of Pharmtech Research, 9: 1058-1068 (2016)*

**Objective :** Using cervical collar in management of cervical disc prolapsed has a controversial and different outcomes. So, proper selection of collar is very important for obtaining best results. **Design:** One hundred subjects suffered from cervical disc prolapse; complaining neck pain and brachialgia; were participated in this study. They were classified into five equal groups; group one had no collar, group two applied soft collar, group three applied hard collar (one piece), group four applied Philadelphia collar and group five applied two pieces variable length collar (Adjusted according to length of patient's neck to be put in a slight flexion). Visual analogue scale was applied for all patients to measure the degree of brachialgia. Electronic Goniometer or Cervical range of motion (CROM) was used also to determine painless range of motion (ROM) of neck extension. Assessment was performed before and after treatment (Twelve sessions; three times per week). **Results:** Results revealed a significant improvement in patients applied both Philadelphia and variable length collar in both VAS and ROM with more evidence for variable length collar. **Conclusion:** Variable length collar is the best choice for patients complaining cervical disc prolapsed with brachialgia.

**Keywords:** Soft Collar; One and Two Pieces Hard Collar ; Philadelphia Collar ;Cervical Disc

### M - 800. Efficacy of Biofeedback Training on Bladder Dysfunction and Quality of Life in Paraplegic Patients

Moataz M. El Semary, Hoda Zakria, Youssef Balawy and Mohamed S. Abdel-Azim

*International Journal of Pharmtech Research, 9(12): 799-805 (2016)*

**Objectives:** To evaluate efficacy of biofeedback training on treatment of bladder dysfunction and quality of life in paraplegic patients. Methods: Thirty male paraplegic patients within 6 to 18 months after injury, ages ranged from 20 to 35 years, participated in this study for a treatment period of six weeks; they were divided into two equal groups. Patients in group I were treated with pelvic floor exercises two times weekly, while patients in group II were treated with biofeedback training plus pelvic floor exercises two times weekly. All subjects were assessed for; 1) voiding cystometry, 2) EMG of pelvic-floor muscles, 3) QUALIVEEN questionnaire (short version). **Results:**There was significant improvement in group II and nonsignificant improvement in group I in values of an EMG biofeedback assessment of pelvicfloor muscles. There was highly significant improvement in group II in the bladder volume at the first desire to void and at maximum cystometric capacity, the detrusor pressure at maximum flow rate, the maximum flow rate, detrusor stability and significant improvement in bladder compliance while there was no significant difference in group I in the bladder volume at the first desire to void and at maximum cystometric capacity, the bladder compliance and detrusor stability & significant improvement the detrusor pressure at maximum flow rate & highly significant improvement in the the maximum flow rate. There was highly significant improvement in group II and non-significant improvement in group I in the Qualiveen questionnaire. **Conclusion:** Biofeedback training should be considered as valuable adjacent to conventional treatment in the control of bladder dysfunction & optimizing quality of life in paraplegic patients.

**Keywords:** Biofeedback- Bladder-Erectile-Paraplegia

*Dept. of Physical Therapy for Basic Science*

## M-801. Addition of A Sagittal Cervical Posture Corrective Orthotic Device to A Multimodal Rehabilitation Program Improves Short- and Long-Term Outcomes in Patients with Discogenic Cervical Radiculopathy

Ibrahim M. Moustafa, Aliaa A. Diab, Shimaa Taha and Deed E. Harrison

*Archives of Physical Medicine and Rehabilitation, 97: 2034-2044 (2016) IF: 3.045*

**Objective** To investigate the immediate and 1-year effects of a multimodal program, with cervical lordosis and anterior head translation (AHT) rehabilitation, on the intensity of pain, disability, and peripheral and central nervous system function in patients with discogenic cervical radiculopathy (CR). Design A randomized controlled trial with 1-year and 10-week follow-up. Setting University research laboratory. Participants Patients (N=60; 27 men) with chronic discogenic CR, a defined hypolordotic cervical spine, and AHT posture were randomly assigned to a control group (n=30; mean age, 43.9±6.2y) or an intervention group (n=30; mean age, 41.5±3.7y). Interventions Both groups received the multimodal program; in addition, the intervention group received the Denneroll cervical traction device. **Main Outcome Measures** AHT distance, cervical lordosis, arm pain intensity, neck pain intensity, and disability (Neck Disability Index [NDI]), dermatomal somatosensory evoked potentials (DSSEPs), and central somatosensory conduction time (N13–N20). Measures were assessed at 3 time intervals: baseline, 10 weeks, and 1-year follow-up. Results After 10 weeks of treatment, between-group analysis showed equal improvement in arm pain intensity (P=.40), neck pain intensity (P=.60), and latency of DSSEPs (P=.60) in both intervention and control groups. However, also at 10 weeks, there were significant differences between groups, favoring the intervention group for cervical lordosis (P<.0005), AHT distance (P<.0005), amplitude of DSSEPs (P<.0005), N13 to N20 conduction time (P<.0005), and NDI (P<.0005). Although at 1-year follow-up, between-group analysis identified a regression back to baseline values for the control group. Thus, all variables were significantly different, favoring the intervention group at 1-year follow-up: cervical lordosis (P<.0005), AHT distance (P<.0005), latency and amplitude of DSSEPs (P<.0005), N13 to N20 conduction time (P<.0005), intensity of neck and arm pain, and NDI (P<.0005). **Conclusions** The addition of the Denneroll cervical orthotic device to a multimodal program positively affected discogenic CR outcomes at long-term follow-up. We speculate that improved cervical lordosis and reduced AHT contributed to our findings.

**Keywords:** Lordosis, Radiculopathy, Randomized Controlled Trial, Rehabilitation, Traction

## M-802. Cryolipolysis Versus Laser Lipolysis on Adolescent Abdominal Adiposity

Mohamed Serag Eldein Mahgoub Mostafa and Mohamed Ali Elshafey

*Lasers in Surgery and Medicine, 48: 365-370 (2016) IF: 2.135*

**Background** Noninvasive body contouring is one of the fastest growing segments of the cosmetic aesthetic industry. There is increased public demand for procedures with fewer side effects and shorter recovery times. Cryolipolysis and Laser lipolysis have been used as treatments for localized body contouring. **Objective** To compare the effect of Cryolipolysis versus Laser lipolysis on adolescent's abdominal adiposity. Design Randomized, controlled trial. Subjects Forty-five obese adolescents of both sexes ranged in age from 13 to 16 years participated in this study were to be categorized into three groups of equal number (each group 15 subjects) randomly selected from population. **Methods** Participants were randomly assigned to three groups. Group A was received (Cryolipolysis and diet), Group B was received (Laser lipolysis and diet), Group C was received (only diet) all groups were observed for 8 weeks. Weight and height scale for (change in weight), tape measurement for (waist-hip ratio), skinfold caliper, and MRI. **Results** There was no significant difference between three groups post-treatment in BMI and body weight P-value were (0.2, 0.42, 0.67), respectively. There was a significant improvement for Cryolipolysis group in waist-hip ratio, Suprailiac skin fold, and subcutaneous adipose tissue than other groups P-value (0.001). **Conclusions** Cryolipolysis has a favorable effect than Laser lipolysis in the reduction of waist-hip ratio, skin folds at Suprailiac level and subcutaneous adipose tissue (SAT), there is no significant difference between them in the reduction of BMI and body weight. All groups did not have an effect on VAT.

**Keywords:** Abdominal Adiposity; Cryolipolysis; Laser Lipolysis; Subcutaneous Adipose Tissue.

## M-803. Axillary Ultrasound and Laser Combined with Postisometric Facilitation in Treatment of Shoulder Adhesive Capsulitis: A Randomized Clinical Trial

Haytham M. Elhafez and Salam M. Elhafez

*Journal of Manipulative and Physiological Therapeutics, 39 (5): 330-338 (2016) IF: 1.587*

**Objectives** The purpose of this study was to compare axillary ultrasound, laser, and postisometric facilitation technique with standard care in the management of shoulder adhesive capsulitis. **Methods** This is a randomized clinical trial study. Fifty-nine participants with shoulder adhesive capsulitis were selected and randomly assigned for eligibility. Forty-five participants were assigned into 3 equal groups of 15, and 14 participants were excluded from the study. The participants were blinded to their group allocation. Standard care group (A) received traditional physical therapy treatment in the form of pulsed ultrasound, scanning laser, supervised exercise program, and home exercise program; group B received the same physical therapy program as group A, except that the ultrasound and scanning laser were applied to the axillary region of the painful shoulder; and group C received the same modified physical therapy program as group B plus postisometric facilitation technique to the painful shoulder. All dependent variables were measured by the second author, who was blinded to the participant's intervention group. The first author administered treatment to all 3 groups. All participants received 12 sessions (3 times/wk for 4 weeks). Pain level and shoulder range of motion (ROM; flexion, abduction, and external rotation) were recorded 3 times (pretreatment, immediately posttreatment, and 4 weeks of treatment). **Results** Mixed-design multivariate analysis of variance indicated significant pain reduction with significant ROM increase in all

groups posttreatment and after 4 weeks. Post hoc analysis for within groups revealed that shoulder ROM and pain levels improved significantly posttreatment compared with pretreatment ROM in all groups, with the greatest improvement in group C. Between-group analysis revealed that pain-free shoulder flexion, abduction, external rotation, and pain level improved significantly in group C compared with groups A and B immediately after treatment and after 4 weeks of follow-up (P < .05). Improvements reported in group B is more than in group A, and C is more than in groups A and B. **Conclusions** Combining axillary ultrasound and laser with postisometric facilitation had a greater effect in reducing pain and improving shoulder ROM in patients with shoulder adhesive capsulitis compared with axillary ultrasound and laser with traditional exercise.

**Keywords:** Bursitis; Adhesive Capsulitis; Frozen shoulder.

## M-804. Ultrasound Cavitation Versus Cryolipolysis fornon-invasive body contouring

Mohamed Taher Mahmoud ELdesoky, Enas ELsayed Mohamed Abutaleb andGihan Samir Mohamed Mousa

*Australasian Journal of Dermatology, 57: 288-293 (2016) IF: 1.305*

**Background/Objectives:** The demand for nonsurgical and non-invasive devices is continuous and increasing. Such devices have gradually gained ground in the reduction of localised fat and the improvement of body contouring. The study aimed to compare the effects of ultrasound cavitation and cryolipolysis on localised abdominal fat. **Methods:** In total, 60 participants with a body mass index (BMI) over 30 kg/m2, whose age ranged between 25 and 45 years, were included. The participants were randomly assigned to three groups of 20 each, using ultrasound cavitation and diet, cryolipolysis and diet, and diet only (the control group), respectively. Measures were bodyweight, BMI, waist circumference and suprailiac skinfold were measured at the beginning of the study and 2 months later. **Results:** The three groups showed significant improvements in all measured variables after 2 months. There was no statistically significant difference in bodyweight or in BMI among the groups after treatment. However, the groups using ultrasound cavitation and cryolipolysis showed better post-treatment improvement than the diet-only group in waist circumference and suprailiac skinfold. There was no statistically significant difference post-treatment between the cavitation and cryolipolysis groups in waist circumference or suprailiac skinfold. **Conclusion:** Both ultrasound cavitation and cryolipolysis are safe and effective for the reduction of abdominal fat thickness and for abdominal contouring.

**Keywords:** Body Contouring, Cryolipolysis, Fat Reduction, Ultrasound Cavitation.

## M-805. Efficacy of Lumbar Mobilization on Postpartum Low Back Pain in Egyptian Females: A Randomized Control Trial

Dalia M. Kamel, Neveen A. Abdel Raoof and Sayed A. Tantawy

*Journal of Back and Musculoskelet Rehabilitation, 29: 55-63 (2016) IF: 0.956*

**Background**: Low back pain (LBP) is a common complaint in the postnatal period. Physiotherapy has many techniques to apply for such cases. **Objective:** To investigate the effect of central postero-anterior (PA) lumbar mobilization on muscle activity in postpartum LBP. **Methods:** Forty-five females with chronic LBP at least three months postnatal. Participants divided randomly and equally into three groups. Group A (Study group) received PA lumbar mobilization plus traditional treatment which consisted of Ultrasonic and Infra-red. Group B (Placebo group) received placebo mobilization plus traditional treatment. Group C (Control group) received traditional treatment only. All patients received 3 sessions/week for 4 weeks. Pain intensity, functional disabilities and Surface EMG for recording para spinal muscle activity were measured before and after intervention. Statistical analysis was done by ANOVA and paired t-test. **Results:** Central PA mobilization showed a significant reduction (P < 0.05) in the average surface EMG activity of the erector spinae musculature compared with the other groups as well as improvement in functional ability and reduction in pain intensity. **Conclusion:** A central PA mobilization significantly reduced pain intensity and surface EMG activity of erector spinae musculature as well as improvement in functional ability in mechanical low back pain in postnatal females.

**Keywords:** Mechanical Low Back Pain, Mobilization, Postpartum, Electromyography

## M-806. Sex Differences of Knee Joint Repositioning Accuracy in Healthy Adolescents

Rania N. Karkousha

*Bulletin of Faculty of Physical Therapy, 21: 56-60 (2016)*

**Introduction** Sex differences in the knee joint have long been known and impaired proprioceptive accuracy is an important risk factor that could be associated with knee joint injury. This study was conducted to compare the accuracy of knee repositioning between healthy male and female adolescents. Participants and methods A total of 64 healthy adolescents (32 males, 32 females) aging from 15 to 18 years participated in this study. Active angle repositioning test was used to assess the proprioceptive accuracy of the right knee joint at 45° knee flexion by using a Biodex system 3 pro-isokinetic dynamometer. **Results** The statistical analysis revealed that the repositioning accuracy of the knee joint was significantly lower in female participants than in males, as the mean values of repositioning errors were 3.54±1.20 for males and 4.76±1.29 for females (P< 0.05). **Conclusion** Sex-based difference in the accuracy of knee joint proprioception may imply that knee proprioceptive sensitivity might potentially contribute to the high incidence of knee injury in females compared with males, particularly during adolescence.

**Keywords:** Biodex Isokinetic System, Healthy Participants, Knee Joint, Proprioception, Sex

## M-807. Effect of Whole-Body Vibration on Motor Neuron Excitability in Healthy Young Men

Salah Eldin B. Elsayed, Neveen A. Abdel Raoof and Omnia M. Elsayed

*Bulletin of Faculty of Physical Therapy, 21: 48-55 (2016)*

**Background** Whole-body vibration (WBV) has been increasingly used for performance enhancement as well as for treatment of some conditions. There is much focus on the study of muscular performance accompanied by WBVs; however, little is known about its effect on motor units – whether it has excitatory or inhibitory effects. The purpose of this study was to investigate the effect of a single bout of WBV on motor neuron excitability in healthy individuals immediately and 30 min after application. **Participants and methods**Sixty healthy men participated in this study; their ages ranged between 18 and 25 years. They were randomly divided into two equal groups – the study group and the control group – each containing 30 men who were selected by drawing ballots from sealed envelopes. The experimental group received WBV with a frequency of 50–60 Hz and amplitude of 0–10 mm for 1 min, with a 1 min rest period between each vibration set, which was repeated five times. The control group stood on the WBV device for the same duration while it was off. Hoffman reflex amplitude and H/M ratio were measured from the soleus muscle (posterior tibial nerve) before and 0 and 30 min after application in both groups using surface electromyography. **Results** There was significant decrease in Hoffman reflex amplitude at 0 and 30 min in the study group compared with the control group (P = 0.002 and 0.01, respectively). Moreover, there was significant decrease in H/M ratio at 0 and 30 min in the study group compared with the control group (P = 0.0001 and 0.03, respectively). **Conclusion** WBV decreases motor neuron excitability and thus may have therapeutic implications for people with central nervous system disorders, in whom spasticity is a major manifestation.
**Keywords:** H-Reflex, Motor Neurons, Whole-Body Vibration

## M-808. Progressive Pressure Release Versus Dry Needling on Cervical Latent Trigger Points

Mary K. Nassif Takla, Omnia A. Atwa and Neveen A. El-Latif

*Bulletin of Faculty of Physical Therapy, InPress (2016)*

**Background** Latent myofascial trigger points (L-MTrPs) may account for the development of muscle cramps, restricted joint range of motion, muscle weakness, and accelerated fatigability. Progressive pressure release (PPR) and dynamic deep dry needling(DDDN) are two recognized techniques used in the management of myofascial trigger points. Aim The aim of this study was to compare the effect of both PPR and DDDN on pain and range of motion in upper trapezius L-MTrPs. Setting and design Single-blinded randomized trial design was used, in which 60 pain-free participants with more than two L-MTrPs in the upper trapezius were allocated randomly to two equal groups. Primary measurement outcome included pressure pain threshold (PPT) using an electronic digital algometer. Secondary outcome included active cervical lateral flexion and rotation using a baseline bubble inclinometer. Data were collected before the first treatment and at the end of the 8-week trial. Participants and materials There were fibve dropouts. The PPR group included 28 participants who received passive stretch and PPR, and the DDDN group included 27 participants who received passive stretch and DDDN. Both groups received 3 sessions/week for eight consecutive weeks. Results The PPR group showed a significant increase in PPT values (P<0.01), cervical lateral flexion (P<0.006), and rotation (P<0.027) compared with the DDDN group. **Conclusion** Within the scope of our study, we have concluded that both techniques have been effective in increasing PPT, cervical lateral flexion, and rotation. However, the PPR technique has been considered to be superior to DDDN in the management of cervical L-MTrPs.
**Keywords:** Dry Needling, Myofascial Trigger Points, Pressure Pain Threshold, Progressive Pressure Release

## M-809. A Comparison Between Different Modes of Real-Time Sonoelastography in Visualizing Myofascial Trigger Points in Low Back Muscles

Mary Kamal Nassif Takla, Naglaa Mohamed Abdel Razek, Omaima Kattabei and Marzouk Abdel Fattah El-Lythy

*Journal Journal of Manual and Manipulative Therapy, 24: 253-256 (2016)*

**Objective:** Currently, there is a lack of objective means to quantify myofascial trigger points (MTrPs) and their core features. Our research compares (1) MTrPs and surrounding myofascial tissue using twodimensional grayscale ultrasound (2DGSUS) and vibration sonoelastography (VSE); (2) the accuracy of both modes in visualizing MTrPs; (3) 'active' and 'latent' MTrPs, using VSE; and (4) the accuracy of both modes in visualizing deep and superficially located MTrPs. Methods: Fifty participants with more than two MTrPs in their quadratus lumborum, longissimus thoracis, piriformis, and gluteus medius muscles were assigned to an active MTrP (low back pain) group or a latent (currently pain free) MTrP group. MTrP identification was based on their essential criteria. An electronic algometer measured repeatedly the tenderness of MTrPs with reference to pressure pain threshold values. A handheld vibrator was applied over MTrPs, while VSE and 2DGSUS readings were taken using an EUB- 7500 ultrasound scanner. **Results:** There was a significant difference between MTrP strain and that of the immediately surrounding myofascial tissue, as measured using VSE (P50.001). VSE visualized all superficial and deep MTrPs with an accuracy of 100% (for both groups); the blinded results obtained using 2DGSUS achieved 33% and 35% accuracy, respectively. There was no significant difference found between the tissue strain ratios of active and latent MTrPs (P50.929). **Discussion:** Sonoelastography can visualize superficial and deep MTrPs, and differentiate them from surrounding myofascial structure through tissue stiffness and echogenicity. VSE was more accurate than 2DGSUS in visualizing and imaging MTrPs.
**Keywords:** Low Back Pain, Myofascial Trigger Points, Two-Dimensional Grayscale Ultrasound, Vibration Sonoelastography.

## M-810. Effect of Sex and Neck Positions on Hand Grip Strength in Healthy Normal Adults:Cross Sectional Observational Study

Doaa I. Amin, Moath Z. Hawari, Hamada E.S. Hassan and Haytham M. Elhafez

*Bulletin of Faculty of Physical Therapy, 21: 42-47 (2016)*

**Purpose** The purpose of this study was to assess the effect of sex and neck positions on hand grip strength in healthy normal adults. Materials and methods One hundred healthy adults of both sexes participated in this study. They were recruited from the students of the faculty of physical Therapy. Their ages ranged between 17 and 25 years. They were assigned to two equal groups according to their sex. Hand grip strength was measured in several neck positions. Grip strength was measured by using the Jamar handheld dynamometer, and the neck range

of motion was measured by using the cervical range of motion. **Results** Among females, there was a significant difference between the hand grip strength in neutral position and in other neck positions (P=0.036). Among males, there was a significant difference between the hand grip strength in the neutral position and in other neck positions. Within neck positions, there was a significant difference (P<0.001). In addition, there was a significant difference in the hand grip strength in various neck positions between the female and male groups (P<0.001). **Conclusion** Hand grip strength was affected by changing the neck positions in both sexes and the maximum grip strength measurement was in the neutral position of the neck.
**Keywords:** Hand Strength, Head Movement, Muscle Strength Dynamometer

## M-811. Inter-Rater and Intra-Rater Reliability of Kinovea Software for Measurement of Shoulder Range of Motion

Reham M. Abd Elrahim, Eman A. Embaby, Mohamed F. Ali and Ragia M. Kamel

*Bulletin of Faculty of Physical Therapy, 21: 80-87 (2016)*

**Background** Goniometry is a tool used frequently for measuring and documenting range of motion (ROM) during a physical therapy examination. With modern innovations in technology, new methods other than the universal goniometer have been applied. Kinovea software is a recent video-based method that uses a virtual goniometer to obtain values for the ROM of joints. However, the software's reliability in measuring shoulder joint ROM has not been studied. **Purpose** This study was conducted to investigate the inter-rater and intrarater reliability of Kinovea software for measuring shoulder joint ROM in healthy individuals. **Materials and methods** Shoulder joint ROM was measured in 52 healthy individuals (mean±SD age was 26.7±4.2 years) using Kinovea photographic measurements by three trained raters. Intrarater reliability was examined by a single rater within the same day. Shoulder flexion, abduction, and external and internal rotation ROM were measured with the patient in supine position. Results The inter-rater reliability ranged from an intraclass correlation coefficient value of 0.95 to 0.98, whereas the intrarater reliability ranged from an intraclass correlation coefficient value of 0.98 to 0.99. **Conclusion** This study showed highly reliable shoulder joint ROM measurements in healthy adults using the Kinovea software.
**Keywords:** Goniometry, Movement, Photography, Reliability, Upper Limb

## M-812. Shock Wave Versus Phonophoresis for Mechanical Neck Dysfunction

Mohamed Serag Eldein Mahgoub Mohamed and Tarek Abd Elrahman Ali Ammar

*Journal of Pain Management, 9 (2016)*

Mechanical neck dysfunction (MND) affects approximately two thirds of people in the middle age due to bad postural habits. purpose: to compare the efficacy of extracorporeal shock waves (ESWT) versus phonophoresis on pain intensity, cervical range of motion and disability in patients with MND. **Design:** randomized controlled trial. Methods: 45 patients with MND participated in this study. They were assigned randomly into three groups: Control group (A) received traditional exercises, group B received phonophoresis and the traditional exercises and group C received ESWT once a week for four sessions and the traditional exercises. Subjects received three sessions a week for four weeks. The authors measured pain intensity, cervical range of motion and neck disability by the visual analogue scale, Myrin OB goniometer and neck disability index, respectively at baseline and after four weeks of treatment. **Results:** There were significant improvements in all groups after intervention in favor of group C. **Conclusion:** It was concluded that the group that received ESWT had the greatest improvement in pain intensity, cervical range of motion and neck disability in patients with MND
**Keywords:** Neck Dysfunction, Phonophoresis, Shock Waves

## M-813. Effect of Sequential Pneumatic Compression Therapy on Venous Blood Velocity, Refilling Time, Pain and Quality of Life in Women with Varicose Veins: A Randomized Control Study

Abeer Yamany and Bassant Hamdy

*Journal of Physical Therapy Science, 28: 1981-1987 (2016)*

[**Purpose**] The aim of this study was to investigate the effects of sequential pneumatic compression therapy on venous blood flow, refilling time, pain level, and quality of life in women with varicose veins. [**Subjects and Methods**] Twenty-eight females with varicose veins were selected and randomly allocated to a control group, and experimental group. Maximum and mean venous blood velocities, the refilling time, pain by visual analog scale and quality of life by Aberdeen Varicose Veins Questionnaire were measured in all patients before and after six weeks of treatment. Both groups received lower extremity exercises; in addition, patients in the experimental group received sequential pneumatic compression therapy for 30 minutes daily, five days a week for six weeks. [**Results**] All measured parameters improved significantly in both groups, comparison of post treatment measurements between groups showed that the maximum and mean blood flow velocity, the pain level, and quality of life were significantly higher in the experimental group compared with the control group. On the other hand there was no significant difference between groups for refilling time. [**Conclusion**] Sequential pneumatic compression therapy with the applied parameters was an effective modality for increasing venous blood flow, reducing pain, and improving quality of women life with varicose veins.
**Keywords:** Varicose Veins, Pneumatic Compression Therapy, Quality of Life

## M-814. Reflexology Versus Traditional Physical Therapy Program in Pre-Eclampsic Pregnant Women with Ankle Oedema

Khadyga S. Abdulaziz and Amira H. Draz

*International Journal of Pharmtech Research, 9: 8-15 (2016)*

**Purpose:** This study was conducted to examine the effect of foot reflexology on preeclampsic women with ankle edema. Methods: Sixty mild preeclampsic women were selected from the outpatient clinic of Gynecology and Obstetrics Kasr El Ani Hospital. Their ages were ranged from 25-35 years old; their

gestational age was more than 20weeks and less than 25 weeks' and their BMI didn't exceed 35 kg/m². They were assigned into two groups, traditional exercises groupand reflexology group. Both groups were having the same antihypertensive drug (Methyldopa) and group (reflexology) under a program of foot reflexology for 3 times per week for 6 weeks. Blood pressure (systolic & diastolic) and ankle edema were evaluated for both groups. Results of this study revealed that, there was a statistically significant decrease in systolic blood pressure, diastolic blood pressure and edema volume in both groups after 6 weeks of management. Also, there was a statistically significant difference between both groups after treatment in systolic blood pressure, diastolic blood pressure and edema volume more decrease in reflexology group. **Conclusion:** Foot reflexology is an effective treatment intervention in the management of preeclampsic pregnant woman with ankle edema.

**Keywords:** Reflexology; Preeclampsia; Hypertension; Ankle Edema.

## M-815. The Effect of Knee Osteoarthritis on Lumbar Proprioception

Fatma M. Alfeky, Amira H. Draz and Wadida H. Elsayed

*International Journal of Pharmtech Research, 9: 80-91 (2016)*

**Background:** Knee osteoarthritis (OA) is a common chronic disease affecting weight bearing joints. It alters kinetics and kinematics of all lower limb joints and lumbar spine. **Purpose:** The purpose of this study was to study the effect of chronic knee osteoarthritis on lumbar proprioception. Methods: Sixty subjects participated in the study. Their age were ranged between 40 and 60 years. The subjects were assigned into two equal groups; Study group (A): It was consisted of 30 chronic unilateral grade II knee osteoarthritic patients. Control group (B): It was consisted of 30 healthy subjects matched for age, sex, weight and height to the OA participants. Lumbar proprioception was measured by Biodex system III. **Results:** There was a significant decrease in lumbar proprioception in the study group compared to control group where the level of significance was (P<0.001). he mean of the absolute angular error in the study group was 8.73± 5.31 while the mean of the absolute angular error in the study group was 1.33± 1.24. **Conclusion:** There was a deficit of lumbar proprioception in chronic knee osteoarthritis.

**Keywords:** Lumbar Proprioception, Knee Osteoarthritis, Isokinetic.

### *Dept. of Physical Therapy for BioMechanics*

## M-816. Effect of Unilateral and Bilateral Use of Laterally Wedged Insoles with Arch Supports on Impact Loading in Medial Knee Osteoarthritis

Amira Abdallah Abd El Megeid Abdallah

*Prosthetics and Orthotics International, 40(2): 231-239 (2016) IF: 0.93*

**Background:** Increased impact loading is implicated in knee osteoarthritis development and progression. **Objectives:** This study examined the impact ground reaction force (GRF) peak, its loading rate, its relative timing to stance phase timing, and walking speed during unilateral and bilateral use of laterally wedged insoles with arch supports. Study design: Within-subject design. Methods: Thirty-three female patients with medial knee osteoarthritis were examined with (unilateral 6° and 11°, and bilateral 0°, 6°, and 11°) and without insole use. **Results:** Repeated measures MANOVA revealed that the impact force increased significantly in bilateral 11° versus unilateral 6° and without-insole conditions. The loading rate decreased significantly in unilateral 11° versus bilateral 6° insoles. The relative timing increased significantly in each of bilateral 6°, bilateral 11°, and unilateral 11° versus bilateral 0° insoles and in each of bilateral 11° and unilateral 11° versus without-insole condition. There were significant positive correlations between the walking speed and each of the force and loading rate. The Chi-square test revealed insignificant association between the insole condition and the presence of impact forces. **Conclusion:**Unilateral 11° insoles are capable of reducing impact loading possibly through increasing foot pronation. Walking slowly is another possible strategy to reduce loading.

**Keywords:** Impact Loading, Wedged Insoles, Osteoarthritis

## M-817. Efficacy of Deep Neck Flexor Exercise for Neck Pain: A Randomized Controlled Study

Amr Almaz Abdel-aziem and Amira Hussin Draz

*Turkish Journal of Physical Medicine and Rehabilitation, 62: 107-115 (2016) IF: 0.094*

**Objectives:** This study aims to investigate the efficacy of deep neck f lexor exercises in the management of neck pain. **Patients and methods:** Sixty patients with non-specific neck pain of at least six-week duration were randomized into one of three groups: group 1 - physical therapy agents including transcutaneous electrical nerve stimulation, continuous ultrasound and infra-red irradiation; group 2 - physical therapy agents + isometric, stretching, and scapulothoracic exercises; and group 3 - physical therapy agents + deep neck flexor exercise. The patients were evaluated with a visual analog scale (VAS), Neck Disability Index (NDI), and the range of motion in the three planes at baseline and after one month of treatment, and at three-month follow-up period. **Results:** Compared to baseline, all groups showed a significant decrease in VAS scores at one month. However, this improvement was achieved only in group 3 at three months indicating a significant difference among the groups (p<0.05). During the study, the improvement in disability was significant in group 3, as assessed by the NDI and range of motion (p<0.05). **Conclusion:** This study demonstrates the superiority of the deep neck f lexor exercise, which offers several advantages in pain, disability, and range of motion outcomes, compared to isometric, stretching, and scapulothoracic exercises in combination with physical therapy agents for the management of neck pain.

**Keywords:** Neck Muscle; Neck Pain; Strengthening Exercise; Stretching Exercise

## M-818. Exercise Training and Postural Correction Improve Upper Extremity Symptoms Among Touchscreen Smartphone Users

Abeer Ahmed Abdelhameed and Amr Almaz Abdel-aziem

*Hong Kong Physiotherapy Journal, 35: 37-44 (2016)*

**Background** Repetitive movements and poor posture are associated with over-use of smartphones when texting or playing games and significantly contribute to the symptoms of pain and discomfort in the upper extremities. **Objective** This study investigated the effect of exercise training and postural correction on disabilities of the arm, shoulder, and hand (DASH), hand grip and key pinch strength among smartphone users. **Methods** One hundred university students were randomly divided into two groups; the experimental group participated in a 12-week programme of exercise training and postural corrections. The control group were instructed to follow their usual routine for smartphone utilization. Measurements of DASH scores, hand grip strength, and key pinch grip strength were conducted before and after 12 weeks for both groups. **Results** There were no significant differences between the start values of both groups for DASH scores, hand grip strength, and key pinch strength ($p > 0.05$). However, there was a significant improvement in all outcomes measured in the experimental group ($p < 0.05$), with significant changes in the outcomes of the control group. **Conclusion** Postural correction combined with a selected exercise training programme improved the hand grip, key pinch grip strength, and upper extremity disability and symptoms associated with smartphone use among university students.
**Keywords:** Exercise Training; Hand Grip; Smartphone; Upper Extremity Symptoms

## M-819. Effect of Wiihabilitation on Strength Ratio of Ankle Muscles in Adults

Aya A. Khalil, , Ghada A. Mohamed, Soheir M. Abd El Rahman, Salam M. Elhafez and Nagui S. Nassif,

*Journal of Physical Therapy Science, 28(10): 2862-2866 (2016)*

[**Purpose**] This study was conducted to investigate the effect of Wiihabilitation on the ankle dorsiflexion/plantar flexion strength ratio in adults. [**Subjects and Methods**] Thirty-two healthy male volunteers were randomly assigned to two equal groups (experimental and control). Participants in the experimental group received a Wiihabilitation training program for six weeks. Data were collected using a Biodex system 3 Isokinetic dynamometer. Peak torques of the dorsiflexors and plantar flexors were measured at an angular velocity of 60°/sec which in turn were used to derive the ankle dorsiflexion/plantar flexion strength ratio. [**Results**] The mean values of the ankle dorsiflexion/plantar flexion strength ratio decreased significantly between before and after the training in the experimental group, meanwhile there was no significant difference between before and after the training period in the control group . [**Conclusion**] Wiihabilitation has an impact on the ankle dorsiflexion/plantar flexion strength ratio, so it can be considered an effective training tool in terms of the ankle strength ratio. Thus, it could be recommended for both prevention and rehabilitation of ankle instability patients.
**Keywords:** Wiihabilitation, Strength Ratio, Ankle Instability.

## 820. Isokinetic Parameters of Shoulder Joint in Tennis Elbowversus Golfr''s Elbow

Bassam Ahmed Nabil Abd Elmaboud, Hamada Ahmed Hamada, and Mariem Abd-Elmoneim

*International Journal of Pharmtech Research, 9, (9),: 97-103 (2016)*

**Purposes:** The aim of our study is to analyze the difference between normal subjects and patients with elbow problems (tennis elbow or golfer's elbow) in shoulder isokinetic parameters. **Material and Methods:** Thirty male athletes participated in our study and divided into equally three groups. The first group (A) suffered from tennis elbow, the second group (B) suffered from golfer elbow, and the third group (C) is normal subjects. Each of them consisted of ten participants. Their age ranged from 20 - 35 years. Open kinetic chain shoulder flexion and extension peak torque were measured at angular velocity (60º/sec) with concentric/eccentric mode by Biodex System 3 Multi-Joint system testing and rehabilitation (Biodex Medical system, Shirley, NY, USA). **Results:** The statistical analysis revealed that there was no significant differences in the mean values of the "eccentric peak torque of shoulder flexors" among three groups with ($P>0.05$). While, there was a significant difference in the mean values of the eccentric peak torque of shoulder extensors among three groups with ($P<0.05$). Multiple pairwise comparison tests revealed that there were no significant differences of eccentric peak torque of shoulder extensors between (Group A Vs. group B) and (Group A Vs. group C) with ($p=>0.05$) and there was a significant difference of eccentric peak torque of shoulder extensors between (Group B Vs. group C). **Conclusions:** It can be concluded that there is no difference in the shoulder flexors' peak torque between athletic patients suffered from tennis elbow, golfer's elbow and normal subjects, but there is a difference in shoulder extensors' peak torque between athletic patients suffered from golfer's elbow, and normal subjects. This was significant reduction in favor to group (B).
**Keywords:** Tennis Elbow, Golfer'S Elbow, Isokinetic Parameters, Shoulder Joint.

## M-821. Effect of Backpack Shoulder Straps Length on Cervical Posture and Upper Trapezius Pressure Pain Threshold

Osama Ragaa Abdelraouf, Hamada Ahmed Hamada, Ali Selim, Wael Shendy andHoda Zakaria

*The Journal of Physical Therapy Science,28;(9):2437-2440(2016)*

[**Purpose**] This study was performed to investigate the effect of the length of backpack shoulder straps on upper trapezius muscle pain threshold and craniovertebral angle. [**Subjects and Methods**] There were 25 participants, with ages from 15 to 23 years old. Upper trapezius pain threshold and craniovertebral angle were measured for all subjects without the backpack then re-measured after walking on a treadmill for 15 min under 2 conditions: 1) wearing a backpack with short straps; and 2) wearing a backpack with long straps. [**Results**] there was a significant reduction in upper trapezius pain threshold and craniovertebral angle while carrying a backpack with long shoulder straps, compared to use of a backpack with short shoulder straps or no backpack. [**Conclusion**] A backpack with

short straps is less harmful than a backpack with long straps. This result should be considered in ergonomic design of backpacks to reduce the incidence of various physiological and biomechanical disorders.
**Keywords:** Backpack, Shoulder Straps, Cervical Posture

## M-822. The Weight-Bearing Exercise for Better Balance Program Improves Strength and Balance in Osteopenia: A Randomized Controlled Trial

Azza M. Abd El Mohsen, Hossam Eddien F. Abd El Ghaffar, Nagui S. Nassif and Ghada M. Elhafez

*Journal of Physical Therapy Science, 28: 2576-2580 (2016)*

[**Purpose**] This study investigated the effect of the Weight-bearing Exercise for Better Balance program on the strength of hip flexors, extensors, abductors, adductors, and knee flexors and extensors and balance in osteopenia. [**Subjects and Methods**] Twenty-four postmenopausal females with osteopenia volunteered to participate in this study and were randomly assigned into two equal groups of 12: the experimental and control groups. The Weight-bearing Exercise for Better Balance program was applied to the experimental group, while the control group did not receive any treatment. Isokinetic peak torque per body weight values of the hip flexors, extensors, abductors, adductors, and knee flexors and extensors were measured by Biodex System 3 isokinetic dynamometer for both groups before and after six weeks of the program. Balance was assessed in both groups using the Berg Balance Scale. [**Results**] There was a statistically significant increase in post-intervention mean values of all measured variables compared with pre-intervention values in the experimental group. Also, there was a statistically significant increase in post-intervention mean values of all measured variables except for those of the hip extensors in the experimental group compared with the control group. [**Conclusion**] The weight-bearing exercise for better balance program has significant effects on lower extremity muscle strength and body balance in postmenopausal females with osteopenia.
**Keywords:** Weight-Bearing, Strength, Osteopenia

## M-823. Efficacy of Virtual Reality-Based Balance Training Versus the Biodex Balance System Training on the Body Balance of Adults

Ibrahim MS, Mattar AG and Elhafez SM

*Journal of Physical Therapy Science, 28: 20-26 (2016)*

[**Purpose**] This study investigated efficacy of virtual reality (VR)-based balance training on enhancing balance and postural reactions of adults as a low-cost new modality compared to the established Biodex Balance System (BBS). [Subjects] Thirty normal adults of both genders were divided randomly into two equal-sized experimental groups of 15: BBS balance training and VR balance training. [**Methods**] The training programmes were conducted in 12 sessions, three 15-min sessions per week. The Nintendo® Wii Fit Plus (NWFP) and its balance board were used to train of the VR group. Each participant answered a questionnaire concerning usability, enjoyment, balance improvement, and fatigue at the end of the training programs. [Results] The study found a significant increase the measure of mean overall balance (OLB) in both groups. No significant difference was found between the groups, but a significant decrease in the mean balance-test time was found for both groups, with no significant difference between the two training methods. The VR program was rated highly enjoyable by 81.8% of the group. [**Conclusion**] The Wii Fit Plus system with the balance board as a new VR balance-training technique, can be considered an effective and enjoyable tool for the training of adults' body balance.
**Keywords:** Virtual Reality, Biodex Balance Training, Adults

## M-823. Effect of Specific Training Programmes on Hip Musculature Peak Torque in Osteoporotic Patients

Mohamed Mostafa M. Essa and Salam Mohamed El-hafez

*International Journal of Pharmtech Research,9: 103-109(2016)*

**Objectives:** The aim of this study was to investigate the effect of core and treadmill training programmes on hip musculature strength in osteoporotic postmenopausal women. **Methods:** Twenty osteoporotic postmenopausal women ageing between 50 to 60 years with BMI between 20.2 to 24.9 kg/m2 participated in this study. They were assigned randomly into equal groups. Participants of the group (A) received core training programme, while the group (B) received treadmill training programme lasting three months period. Hip flexors and extensors strength were assessed by Biodex system 3-pro dynamometer multi-joint testing and rehabilitation system, which measure the peak torques. The participants were tested twice; before and after the training programmes. **Results:** The statistical analysis revealed that there was a significant increase of the peak torque of hip extensors in the post-treatment condition compared with the pre-treatment one in both groups ($p<0.05$). Moreover, there was a significant increase of the hip flexors peak torque in the post-treatment condition compared with the pretreatment one in group (B) only ($p <0.05$). However, there were no significant differences in the hip extensors peak torque between both groups ($p>0.05$). **Conclusions:** It can be concluded that the treadmill training programme is an effective treatment policy to strengthen the hip flexors and extensors in postmenopausal women.
**Keywords:** Core Training, Treadmill Training, Hip Muscles, Peak Torque, Osteoporosis.

### *Dept. of Physical Therapy for Cardio Vascular, Respiratory Disorders and Geriatrics*

## M-824. Adipokines Response to Continuous Versus Interval Aerobic Training in Ischaemic Heart Disease Patients

Haytham Hamed Mahmoud, Nesreen Ghareeb Mohamed, Amany Rafaat Mohamed and Esam Balegh Ewas

*International Journal of Pharmtech Research, 9: 53-59 (2016)*

**Background:**Coronary artery disease (CAD) is the single most common cause of death in the developed world, responsible for about 1 in every 5 deaths and it is expected that the rate of CAD will accelerate in the next decade. The aim: of the current study was to find out adipokines response to continuous versus interval aerobic training in ischemic heart disease Patients. **Methods:** Forty men patients with an ischemic heart disease with age ranged from 50- 60 years old participated in this study. Patients

were assigned into two groups equal in number: Group A included 20 patients received high intensity interval aerobic training on treadmill 3 times per week for 12 week. Group B included 20 patients received moderate intensity continuous aerobic training on treadmill 3 times per week for 12 week. **Results:** The mean values of adiponectin, leptin and six minute walk distance were significantly improved from 8.46 ± 0.3 mg/ml, 38.83 ± 0.08 ng/ml and 433.72 ± 2.84 m to 10.85 ± 0.25 mg/ml, 35.26 ± 0.21 ng/ml and 505.52 ± 1.39 m respectively, in group A and from 8.44 ± 0.32 mg/ml, 38.95 ± 0.38 ng/ml and 434.02 ± 2.92 m to 9.65 ± 0.33 mg/ml, 37.13 ± 0.22 ng/ml and 479.05 ± 1.44 m respectively, in group B. Also, there was a significant difference between the groups after treatment on all measured variables. **Conclusion:** It is suggested that Interval are more effective than continuous aerobic training for the improvement fo adipokines, functional capacity in patients with ischemic heart disease.
**Keywords:** Adipokines, High Intensity Interval Aerobic Training, Moderate Intensity Continuous Aerobic Training, Ischemic Heart Disease

## M-825. Laser Versus Reflexology on Kidney Functions in Patients with Hypertension Enrolled Under Dash Diet

Sally Mohamed, Zahra Serry, NesreenElnahas and Sally Hakim

*International Journal of Pharmtech Research,9: 102-107 (2016)*

Kidney functions increased in hypertensive patients. Objectives of this study were to determine the difference between effect of reflexology and laser on kidney functions and blood pressure.
**Keywords:** Laser; Reflexology; Kidney Functions; Hypertension; Dash.

## M-826. Efficacy of Cardiac Rehabilitation After Percutaneous Coronary Intervention

Ali Mohammed Hassan and Neseren Ghareeb El Nahas

*International Journal of Pharmtech Research, 9: 134-141(2016)*

Cardiovascular disease (CVD) is the major health problem in developed countries. Cardiac rehabilitation (CR) programs have become an integral part of the standard of care in modern cardiology. Their scope has shifted from the emphasis on exercise therapy to comprehensive secondary prevention strategies managing risk factors, nutritional, psychological, behavioral and social factors that can affect patient outcomes. The aim of this study was to determine the efficacy of CR after percutaneous coronary intervention (PCI).
**Keywords:** Percutaneous Coronary Intervention, Cardiac Rehabilitation, Functional Capacity, Cardiovascular Risk Factors, Quality of Life.

## M-827. Infleunce of Combined Low Frequency Ultrasound and Lymphatic Drainage Techniques on Body Fat Mass and Triglycerides in Atherosclerotic Patients

Manar M. Badawy and Nesreen G. Elnahas

*International Journal of Pharmtech Research, 9: 37-45 (2016)*

The aim of this study is to find out the effect of low frequency ultrasound and lymphatic drainage on body fat mass composition and blood triglycerides and testing the strength of the relationship, between the response of fat mass and the changes in the Total Body Triglycerides, Methods: Forty women patients with age ranged from 40 to 50 years were selected from
**Keywords:** Low Frequency Ultrasound/ Lymphatic Drainage/ Triglycerides/ Fat Mass/ Coronary Atherosclerosis.

## M-828. Impact of Cold Laser on Lipid Profile in Abdominal Obese Women

Mohamed Taha Said and Nesreen G. Elnhas

*International Journal of Pharmtech Research, 9: 115-120 (2016)*

Regional body fat distribution has an important influence on metabolic and cardiovascular risk factors. High cholesterol serum levels associated with the risk of coronary heart disease. LLLT may suppress cholesterologenesis and thereby reduce cholesterol and triglyceride serum levels by altering gene expression and inducing cellular modifications. The purpose of this study was to find out the effect of low level laser therapy on lipid profile in women with abdominal obesity.
**Keywords:** Low Level Laser; Cholesterol; Lipoproteins; Triglycerides;Abdominal Obesity.

## M-829. Serum Serotonin Response to Aerobic Exercise Verus Phoenix

Zainab S.A Abdelhamid, Zahra M.Serry, Nesreen M.G.Elnahas and Nagwa M.Ammar

*International Journal of Pharmtech Research, 9: 108-114 (2016)*

Aerobic training and Phoenix (dates) for elderly subjects with mild depression can alter the level of serum serotonin either by increasing its synthesis or increasing its uptake by the serotonergic receptors. This alteration of the serum serotonin level improves the subject's depression symptoms on the geriatric depression scale with a return to the normal scores. The effects of 24 weeks aerobic exercise and date consumption on the serum serotonin level and on subjects' score on the geriatric depression scale were studied.
**Keywords:** Serum Serotonin; Aerobic Exercise; Phoenix.

## M-830. Efficacy of Noninvasive Respiratory Techniques in the Treatment of Children with Bronchial asthma: A Randomized Controlled Trial

Ragab K. Elnaggara and Mohammed A. Shendy

*Bulletin of Faculty of Physical Therapy, Cairo University, 2016, 21: 1-10 (2016)*

**Background and purpose** Although the effects of the respiratory techniques are appreciated, it is yet in need to be defined for the treatment of children with bronchial asthma. Thus, this study aimed to compare the effects of the active cycle of breathing technique (ACBT), Buteyko breathing technique (BBT), and thoracic lymphatic pump technique (TLPT) on the total serum immunoglobulin (Ig) E, ventilatory function, and

asthma perception in children with bronchial asthma. **Materials and methods** In a randomized controlled trial, 54 children with bronchial asthma randomly allocated to three equal groups. The groups were then randomly assigned to the following interventions: the ACBT group, the BBT group, or the TLPT group. Total serum IgE, ventilatory function, and perception of asthma were evaluated before treatment and after 3 consecutive months of treatment. **Results** No significant differences were found between groups at entry (P>0.05). There were nonsignificant differences as regards all outcome measures within the ACBT group (P>0.05) and significant differences within the BBT group and the TLPT group (P<0.05). Significant difference in total serum IgE in favor of the BBT group was recorded when compared with ACBT group (P=0.046) and the TLPT group (P=0.036). Moreover, significant differences in ventilatory function measures favoring the BBT group in comparison with the ACBT group and the BBT group(P<0.05) were recorded. Finally, asthma control was significantly higher in the BBTgroup than ACBT group (P=0.017) but not BBT group (P=0.081)ConclusionThe BBT and TLPT are more advantageous compared with the ACBT in the treatment of children with bronchial asthma, and Buteyko breathing is potentiallymore valuable.

**Keywords:** Asthma Perception, Bronchial Asthma, Respiratory Techniques, Total Serum Ige, Ventilatory Function

***Dept. of Physical Therapy for Growth and Developmental Disorder***

## M-831. Effect of Electromyographic Biofeedback Training on Pain, Quadriceps Muscle Strength, and Functional Ability in Juvenile Rheumatoid Arthritis

Mohamed Ahmed Mahmoud Eid, Sobhy M. Aly and Shamekh M. El-Shamy

*American Journal of Physical Medicine and Rehabilitation, 95: 921-930 (2016) IF: 2.064*

**Objective:**To investigate the effects of electromyographic (EMG) biofeedback training on pain, quadriceps strength, and functional ability in juvenile rheumatoid arthritis (JRA). **Design:**This is a randomized controlled study; 36 children (11 boys and 25 girls) with polyarticular JRA, with ages ranging from 8 to 13 years, were selected and assigned randomly, using computer-generated random numbers, into 2 groups. The control group (n = 18) received the conventional physical therapy program, whereas the study group (n = 18) received the same program as the control group in addition to EMG biofeedback-guided isometric exercises for 3 days a week for 12 weeks. Pain, peak torque of quadriceps strength, and functional ability were evaluated before, after 6 weeks, and at the end of 12 weeks of the treatment program. **Results:** By 6 weeks, significant differences were observed in the study group (P < 0.05) in all measured variables except pain levels, whereas nonsignificant differences were observed in all measured variables in the control group. By 12 weeks, each group demonstrated significant improvements in pain, quadriceps strength, and functional ability (P < 0.05), with significantly greater improvements seen in the study group compared to the control group (P < 0.05). Both groups showed significant improvement at 12 weeks compared to that at 6 weeks. **Conclusions:** Electromyographic biofeedback may be a useful intervention modality to reduce pain, improve quadriceps strength, and functional performance in JRA.

**Keywords:** Emg Biofeedback, Pain, Muscle Strength, Functional Ability, Juvenile Rheumatoid Arthritis

## M-832. Effects of Combined Resistive Underwater Exercises and Interferential Current Therapy in Patients with Juvenile Idiopathic Arthritis: A Randomized Controlled Trial

Ragab K. Elnaggar and Mohammed A. Elshafey

*American Journal of Physical Medicine and Rehabilitation, 95(2): 96-102 (2016) IF: 2.064*

**Objective:**The objective of this study was to verify the effects of combined resistive underwater exercises and interferential current on the peak torque of the quadriceps and hamstrings and pain levels in patients with juvenile idiopathic arthritis. **Design:**This is a randomized controlled study; 30 children with polyarticular juvenile idiopathic arthritis were randomly distributed into two groups: the control group (n = 15) received the traditional physical therapy program and the study group (n = 15) received resistive underwater exercises and interferential current therapy. Peak torque of the quadriceps and hamstrings and pain levels were evaluated before treatment, 1 mo later, and after 3 mos using the HUMAC NORM, CSMI Testing and Rehabilitation Isokinetic System and visual analog scale, respectively. **Results:** In the control group, all measures showed significant differences (P < 0.05) after 1 mo except peak torque of left quadriceps and pain levels, and significant differences were found after 3 mos (P < 0.05) in all. In the study group, all measures showed significant differences after 1 and 3 mos (P < 0.05) and there were significant differences between groups after 1 and 3 mos in favor of the study group (P < 0.05). **Conclusion:** The combination of resistive underwater exercises and interferential current therapy is a potentially valuable treatment for patients with juvenile idiopathic arthritis.

**Keywords:** Juvenile Idiopathic Arthritis, Resistive Underwater Exercises, Interferential Current Therapy, Peak Torque, Pain

## M-833. Effect of Plyometric Training on Shoulder Strength and Active Movements in Children Witherb''s Palsy

Maya Galal Abd Al-Wahab, Elham El-Sayed Salem, Eman Ibrahim El-Hadidy and Hassan Magdy El-Barbary

*International Journal of Pharmtech Research, 9, (4): 25-33 (2016)*

**Background:** Children with Erb's palsy often have residual weakness of the affected shoulder musculature and limitation in arm movements resulting in difficulties of their functional activities. **Aim:** This study aimed to determine the effect of plyometric training on shoulder strength and active movements in children with Erb's palsy. **Methods:** A total of 40 children with Erb's palsy (3-6 years) were randomly assigned into two groups; a control group received a selected physical therapy program and a study group received the same program as the control group in addition to plyometric training. All children were assessed pre and post 6 successive weeks of training using hand-held dynamometer for shoulder flexors and external rotators strength and active movement scale for active shoulder flexion and external rotation movements. **Results:** Significant

improvement was found in all measured variables of the control and study groups when comparing their pre and post treatment mean values except for the active shoulder external rotation movement of the control group. Comparing the post treatment mean values of all measured variables showed no significant difference between both groups, while the percent of improvement was greater in the study than the control group in all the measured variables. **Conclusion:** Plyometric training is an effective training for improving strength and active movements in children with Erb's palsy.
**Keywords:** Plyometric Training, Erb's Palsy, Shoulder Strength, Active Movement Scale.

***Dept. of Physical Therapy for Gynecology and Obstetrics***

## M-834. The Relationship Between Trunk and Pelvis Kinematics During Pregnancy Trimesters

Abeer M. Eldeeb, Hamada A. Hamada, Amr A. Abdel-Aziem and Amel M. Youssef

*Acta of Bioengineering and Biomechanics, 18: 79-85 (2016) IF: 0.767*

**Purpose:** Pregnancy is characterized by many musculoskeletal changes that affect daily living activities and walking. The purpose of this study was to examine the effect of pregnancy on pelvic and trunk kinematics, and their relationship during the three pregnancy trimesters. **Methods:** Three-dimensional pelvis and trunk motions were measured using Qualisys Gait Analysis System in the first, second and third trimesters of pregnancy. The maximum anterior pelvic tilt and maximum trunk flexion during stance phase, pelvic tilt, obliquity and rotation, as well as trunk flexion-extension, lateral bending and rotation were measured. **Results:** Repeated-measures analysis of variance showed a significant increase in the maximum anterior pelvic tilt during stance phase (p=0.005), and a significant decrease in the pelvic obliquity (p=0.011), maximum trunk flexion during stance phase (p=0.0006), trunk lateral bending (p=0.005) and trunk rotation (p=0.004). A significant negative correlation was found between maximum anterior pelvic tilt and maximum trunk flexion in the first (r=-0.72, p=0.008), second (r=-0.61, p=0.03), and third (r=-0.61,p=0.03) trimesters of pregnancy. Also, there was a significant positive correlation found between pelvic obliquity and trunk lateral bending in the first (r=0.76, p=0.04), second (r=0.59, p=0.04), and third (r=0.59, p=0.04) trimesters of pregnancy. **Conclusions:** The pregnant women walk with an increased maximum anterior pelvic tilt, a decreased maximum trunk flexion, a decreased pelvic obliquity, as well as a decreased trunk lateral bending and rotation. Pregnancy does not affect the relationship between pelvis and trunk motions.
**Keywords:** Pregnancy, Pelvis, Motion Analysis, Trunk

## M-835. Effect of Moderate Exercise on Breast Milk Leukocytes in Exclusively Breast-Feeding Mothers

Doaa Osman, Amel Yousef, Salwa El-Badry and Amal El-Taweel

*International Journal of Pharmtech Research, 9: 1-8 (2016)*

Although it is well documented that moderate exercise enhances cell-mediated immunity, effect of moderate exercise on breast milk leukocytes has not been studied yet. So, the aim of this study was to investigate the effect of moderate exercise on breast milk leukocytes in exclusively breast-feeding mothers. Forty-seven exclusively breast-feeding mothers at 1st to 5th month postpartum were randomized into two groups. Group A received breast-feeding and nutritional counseling and engaged in moderate aerobic exercise for 4 weeks with a total of 12 sessions. Group B received only the same breast-feeding and nutritional counseling for 4 weeks. Both groups were evaluated pre and post-intervention. The outcome measures were maternal anthropometric parameters and breast milk total and differential leukocytes counts. Post-intervention, there was a non-significant difference in the maternal anthropometric parameters ($P > 0.05$) while there was a highly significant increase in breast milk total and differential leukocytes counts ($P = 0.001$) in favor of group A. There was a significant inverse relationship between maternal anthropometric parameters and lymphocytes count in group A. This study explored that moderate aerobic exercise during exclusive breast-feeding was associated with increased breast milk total and differential leukocytes counts.
**Keywords:** Moderate Exercise, Exclusive Breast-Feeding, Breast Milk, Immune, Leukocytes

## M-836. Impact of Different Wave Lengths of Low Level Laser Therapy on Bone Repair: Histological Study in Rats

Ahmed El Prince Mohamed, Yousry Mahmoud Mostafa, Nashwa Taher Abdel Aziz and Engy Mohamed El Nahas

*International Journal of Pharmtech Research, 9: 18-29 (2016)*

This study was conducted to determine the effect of different wave lengths of low level laser therapy (LLLT) on bone repair in rats. Seventy two female rats were assigned randomly into three groups, group (A) consisted of twenty four rats whose bone fracture didn't receive laser therapy, group (B) consisted of twenty four rats whose bone fracture received He-Ne laser (632.8 nm) and group (C) consisted of twenty four rats whose bone fracture received Ga-As laser (905 nm). Each group was subdivided into three subgroups according to their sacrificing day on 15th, 30th and 45th post- operative days. Assessment of bone fracture healing was done through radiological analysis and histopathological analysis. The results of this study revealed that group (C) showed more complete bone regeneration on 15th and 30th post-operative days when compared with groups (A&B) according to the radiological findings. On 15th and 30th postoperative days, there was no statistically significant difference between groups (A&B) ($p > 0.05$) in newly formed blood vessels, fibroblasts, osteiod and bone formation scores. While, there was a significant difference between groups (A&C) and (B&C) in favor of group (C) (p value $< 0.05$). So, it could be concluded that infrared laser showed a biostimulating effect on bone repair by stimulating the modulation of the initial inflammatory response and anticipating the resolution to normal condition at the earlier periods. However, there were no differences between groups on 45th post-operative day.
**Keywords:** Low Level Laser Therapy- Bone Repair.

## M-837. The Effect of Kinesio Taping with Exercise Compared with Exercise Alone on Pain, Range of Motion, and Disability of the Shoulder in Postmastectomy Females: A Randomized Control Trial

Sayed A TantawyandDalia M Kamel

*Journal of Physical Therapy Science, 28: 3300-3305 (2016)*

[**Purpose**] The aim of the study was to investigate the effect of kinesio tape on pain, range of motion, and disability of the shoulder. [**Subjects and Methods**] Seventy-four female patients who underwent modified radical mastectomy participated in this study. They were randomly divided into two groups, an experimental group that received kinesio tape for the shoulder joint in addition to a conventional physiotherapy program and a control group that received the physiotherapy program only. Outcome measures included the Visual Analogue Scale, shoulder range of motion, and Shoulder Pain and Disability Index. [**Results**] The experimental group showed significant differences in all outcome measures both within and between groups. The control group only showed a significant within group difference in shoulder flexion. [**Conclusion**] Clinicians should be able to recognize the benefits achieved through the use of adjunct treatment options such as kinesio tape in comparison with benefits that can be obtained through the use of individual modalities in physical therapy. Kinesio tape can be suggested and recommended for postmastectomy patients, especially for shoulder pain, range of motion, and disability.

**Keywords:** Mastectomy, Shoulder Pain, Kinesio Tape

## M-838. Effect of Laser Puncture Combined with a Diet-Exerciseintervention on Obese Polycystic Ovarian Females

Asmaa M. El-Bandrawy and Hassan O. Ghareeb

*International Journal of Pharmtech Research, 9: 60-65 (2016)*

**Background:** Polycystic ovary syndrome (PCOS) is a common endocrine disorder, affecting 8–12% of women. Lifestyle modification is the first-line approach in managing PCOS. Acupuncture has been shown to have also beneficial effects on PCOS. Purpose: To evaluate the effect of laser acupuncture combined with a diet-exercise intervention on obese polycystic ovarian females. Methods: Sixty obese females diagnosed with PCOS. They were divided into study (N=30) and control (N=30) groups. The control group received the dietexercise intervention and the study group received the same intervention and sessions of laser acupuncture, 2 times /week for three months. The tools used to assess the outcome were anthropometric measurement, fasting blood insulin, endocrine hormones and follicular size. **Results:** The results of the study show that participants in the study group revealed a significantly greater decrease in (BMI, waist / hip ratio, fasting insulin level, LH, LH/FSH) and significant more increase in FSH and follicular size as compared to the control group , while AMH was significantly decreased after treatment only in the study group. Conclusion: Laser acupuncture combined with the diet-exercise intervention decreases BMI, waist hip circumferences, improves both metabolic and endocrine features as well as increasing the follicular size in obese polycystic ovarian women.

**Keywords:** Diet, Exercise, Laser Acupuncture, Obesity, Polycystic Ovarian Syndrome.

### *Dept. of Physical Therapy for Musculoskeletal Disorder*

## M-839. Iliopsoas Flexibility in Subjects with Bilateral Flexible Flatfoot

Samah Saad Zahran and Nadia Abdul Azim Fiyaz

*International Journal of Pharmtech Research, 9(12): 1-6 (2016)*

**Purpose:** to investigate iliopsoas flexibility in subjects with bilateral flexible flatfoot. **Methods:** comparison was held between a flexible flatfoot group (15 subjects) and normal foot alignment group (15 subjects). Navicular drop test was used to evaluate the medial longitudinal arch of both groups. The modified Thomas test was used to assess iliopsoas flexibility for both groups. The differences between both groups were assessed by using an unpaired t test. **Results:** there was a significant decrease in iliopsoas flexibility on both sides in the bilateral FFF group compared to the normal group. Conclusion: Reduction in iliopsoas flexibility was observed in subjects with bilateral flexible flatfoot when compared to normal controls. Considering that iliopsoas has a direct attachment to the spine, the pelvis and the femur, our results may support that foot misalignment can be a contributing factor to the dysfunction of the lumbopelvic-hip complex.

**Keywords:** Flatfoot, Iliopsoas, Hip, Low Back Pain, Flexibility

### *Dept. of Physical Therapy of Surgery*

## M-840. Effect of Kinesio Taping on Pain and Functional Disability in Chronic Nonspecific Low Back Pain

Amal T. Al-Shareef, Mohammed T.A. Omar and Amal H.M. Ibrahim

*Spine, 41: 821-828 (2016) IF: 2.439*

**Study Design.**A randomized controlled trial with 2-week Kinesio taping intervention.Objective. The aim of the study was to investigate the effectiveness of Kinesio taping application on pain, functional disability, and trunk flexion range of motion (ROM) in patientswith chronic nonspecific low back pain (chronic NSLBP). Summary of Background Data. Kinesio taping is a therapeutic tool used for treatment of chronic NSLBP. However, there is little scientific evidence that describes its clinical efficacy. **Methods.** Forty-four patients with chronic NSLBP were randomized into experimental group (n¼21) and placebo group (n¼23). The experimental group was treated with Erector Spinae Taping, whereas the placebo group was treated with placebo taping. The primary endpoint was pain intensity on visual analog scale. Secondary endpoints were functional disability on Arabic version of Oswestry disability index (ODI) and trunk flexion ROM on Modified Schober's test. All measurements were recorded at baseline (W0), after 2-week intervention (W2), and at 4-week (W4) follow-up. **Results.** Both group were comparable at baseline (P>0.05). The experimental group had a greater decrease in pain than the placebo group after W2 of intervention (mean between group difference 2.05 cm, 95% confidence interval [CI]=1.38–2.71 points). This was maintained to W4 follow-up (2.25 cm, 95% CI=1.67–2.82 points). At W2, the experimental group had significantly greater improvement in disability, by 3.90 points(95% CI=1.68–8.54

points). This effect was significant at W4 follow-up (5.6, 95% CI=2.65–8.54 points). Similarly trunk flexion ROM was significantly better at W2 0.71 cm, 95% CI0.85 to 0.56) and W4 follow-up 0.73 cm, 95% CI=0.88 to 0.58). **Conclusion.** Kinesio taping reduces pain and disability and improves trunk flexion ROM after 2 weeks of application. However, thesis effects were very small to be considered clinically relevant and meaningful when compared with placebo taping.
**Keywords:** Elastic Tape, Functional Disability, Kinesio Taping, Nonspecific Low Back Pain, Trunk Flexion Range of Motion

## M-841. Response of Bladder Reservoir Function to Low Level Laser Acupuncture in Primary Monosymptomatic Nocturnal Enuresis

Hussein Gamal Hussein Mogahed, Wafaa Hussein Borhan, Sherif Ahmed Gabr Sowar and Ashraf Hassan Mohamed

*International Journal of Pharmtech Research, 9, (2): 30-39 (2016)*

**Objective:** To investigate the response of bladder reservoir function to low level laser acupuncture in primary monosymptomatic nocturnal enuresis. **Materials and Methods :** Fifty patients with ages ranging from 5 – 19 years were randomly assigned into two groups of equal numbers suffering from primary monosymptomatic nocturnal enuresis. Patients in group (A) received helium neon laser operating at a wavelength of 632,8 nm and 10 mW power on acupuncture points and behavioral therapy. While Patients in group (B) received sham laser (placebo) and behavioral therapy. Both groups were treated for one month (3 sessions/week) and were evaluated initially and every 2 weeks. Informed consent was signed by all patients. **Results:** There was a non-significant difference in the pre-treatment mean values of Vavg , Vmax , Vn between both groups (A and B) where the the p-value was (0.109), (0.192), (0.761) respectively. While there was a significant difference after 1 week of treatment where p-value was (0.04), (0.037), (0.013) respectively and finally there was a significant difference after 3 weeks of treatment where p-value was (0.005), (0.016), (0.003) respectively. The results of this study supports the expectation that low level laser acupuncture has an effect on bladder reservoir function and decreasing bedwetting in primary monosymptomatic nocturnal enuresis. **Conclusion:** low level laser acupuncture has an effect on bladder reservoir function in primary monosymptomatic nocturnal enuresis.
**Keywords:** (Low Level Laser, Acupuncture, Primary Monosymptomatic Nocturnal Enuresis).

## M-842. Effect of Extracorporeal Shock Wave Therapy on Post Burn Scars

Mahmoud S Zaghloul, Mohammed M Khalaf, Wael N Thabet and Haidy N Asham

*International Journal of Pharmtech Research, 9,no.3: 78-85 (2016)*

**Introduction:** Hypertrophic scarring is a difficult problem for burn patients, and scar management is an essential aspect of outpatient burn therapy. Post burn pathologic scars involve functional and aesthetic limitations that have a dramatic influence on the patient's quality of life. The purpose was to investigate the effect of extracorporeal shock wave therapy (ESWT) on post burn scars. **Experimental**: forty patients with post burn scars were assigned randomly into two equal groups; their ages ranged from 20 to 45 years. The study group received ESWT and traditional physical therapy program (deep friction massage and stretching exercises). Control group received traditional physical therapy program (deep friction massage and stretching exercises). All groups received two sessions per week for six successful weeks. The data were collected before and after the same period of treatment for both groups. Assessment: Evaluation procedures were carried out to measure scar thickness using ultrasonography and Vancouver Scar Scale (VSS) was completed before and after treatment. **Results:** Post treatment results showed that there was a significant improvement difference in scar thickness in both groups in favor of the study group. Percentage of improvement of scar thickness in the study group was 42.55%, while it was 12.15% in the control group. There was also a significant improvement difference between results obtained using VSS in both groups in favor of the study group. **Conclusion:** Extracorporeal shock wave therapy is effective in management of post burn scars.
**Keywords:** Extracorporeal Shock Wave Therapy, Post Burn Scars, Ultrasonography, Vancouver Scar Scale.

Wolman disease At a glance Figures First | 1-1 of 2 | Last View all figures left Figure 1 Figure 2 right **Introduction** Abstract• **Introduction**• Materials and Methods• Results• Discussion• Disclosure• References• Acknowledgments• Author information• Supplementary information Lysosomal acid lipase deficiency (LALD; OMIM 278000; ref. 1) is an autosomal-recessive disorder caused by mutations of the LIPA gene located on chromosome 10q23.2-q23.3.2 Lysosomal acid lipase (LAL) is essential for the breakdown of cholesteryl esters and triglycerides in the lysosomes; and deficiency of LAL results in accumulation of these lipids in the tissues of affected individuals.1,3 The disease presents across an age continuum; from infants to adults; with common features including hepatomegaly; elevated serum transaminase concentrations; and progressive liver fibrosis and cirrhosis.4,5,6,7 In infants; growth failure (GF) and rapidly progressive hepatic disease are prominent features of LALD (historically known as Wolman disease) and key contributors to mortality; with death typically occurring within the first 6 months of life.2,8,9,10 Clinical familiarity with LALD is low; and many aspects of its clinical presentation; progression; and medical management are poorly understood. In addition; systematic analysis of the presentation of LALD in infants is lacking; current descriptions are largely based on case reports and small case series; many from more than 30 years ago.5,6,7,11,12 Medical records of infants with confirmed LALD were systematically reviewed to develop a more detailed understanding of the clinical manifestations and course of LALD presenting in infancy; including characterization of patient survival; to provide data to serve as a historical reference for efficacy studies of this population.
**Keywords:** Cholesteryl Ester Storage Disease; Infants; Lysosomal Acid Lipase Deficiency; Natural History; Wolman Disease.

++--++

**********

***0-2617-45***


International Publications Awards

Cairo University


# ( 4 )

# Medical Sciences Sector

**4-1 Faculty of Economics and Political Science**
**4-2 Faculty of Commerce**

## Faculty of Economics and Political Science

***Dept. of Economics***

### S-1. Structural Breaks and Monetary Dynamics: A Time Series Analysis

Alaa El-Shazly

*Economic Modelling, 53: 133-143 (2016) IF: 0.997*

This article investigates the stability of money demand and implications for the conduct of monetary policy in Egypt. The econometric procedures include testing for structural breaks at unknown dates and conditioning on the most recent break for estimation and forecasting. Test results provide evidence for regime shifts and lend support to the use of short-term interest rate as the main policy instrument. Sources of structural change are detected by a state-space model. Also, using a structural vector autoregressive (VAR) model for short-run dynamics, it is found that narrow money is a more appropriate monetary aggregate for policy analysis.

**Keywords:** Money demand; Structural breaks; State-space model; Structural VAR analysis.

### S-2. Do Sps Measures Matter for Margins of Trade? Evidence from Firm-Level Data

Hoda El-Enbaby, Rana Hendy and Chahir Zaki

*Applied Economics, 48: 1949-1964 (2016) IF: 0.586*

According to the World Trade Organization (WTO) standards, countries are allowed to adapt regulations under the Sanitary and phyto-sanitary (SPS) and technical barriers to trade (TBT) agreements in order to protect human, animal and plant health, as well as environment and human safety. Yet, these measures can become an impediment in international trade, especially for developing countries. Therefore, using an Egyptian firm-level data set and a new database on specific trade concerns raised in the TBT and SPS committees at the WTO, we analyse the effects of product standards on two related aspects: first, the probability to export (firm-product extensive margin), and second, the value exported (firm-product intensive margin). We merge this data set with a new database on specific trade concerns raised in the TBT and SPS committees at the WTO. Our main findings show that SPS measures imposed on Egyptian exporters have a negative impact on the probability of exporting a new product to a new destination. By contrast, the intensive margin of exports is not significantly affected by such measures.

**Keywords:** Non-tariff measures; SPS measures; WTO.

### S-3. How Did Wars Dampen Trade in the Mena Region?

Fida Karamand Chahir Zaki

*Applied Economics, 48: 5909-5930 (2016) IF: 0.586*

The article investigates the impact of wars on trade in the Middle East and North African region. Using an augmented gravity model that controls for the endogeneity problem in our estimation, we introduce a war variable and distinguish between different types of conflicts. The results show that wars have a significantly negative impact on exports, imports and trade. Civil conflicts hinder exports, imports and trade significantly. The disaggregated version of the gravity model shows that non-state conflicts have a detrimental effect on bilateral trade flows in manufacturing, and that none of the conflicts do affect trade in services. We also find that, on average, a conflict is equivalent to a tariff of 5% of the value of trade.

**Keywords:** Trade; Gravity model; Wars; Conflicts; Mena.

### S-4. Budgetary Institutions and Fiscal Performance in Egypt: Is There a Link?

Israa A. El Husseiny

*Public Budgeting and Finance, 36: 85-105 (2016)*

Budgetary institutions have been playing a crucial rule in explaining the varying fiscal performance among different countries. Both theoretical and empirical literature support the idea that budgetary institutions matter for the distribution of power among the key relevant players involved in the budgeting processes, and that they are expected to affect the ultimate outcomes of the fiscal policy. In light of this context, this paper assesses the quality of Egypt's budgetary institutions alongside each of the main phases of the budget cycle, and it analyzes how such institutions may affect the country's overall fiscal performance. The analysis shows that Egypt's fiscal performance can be improved if budgetary institutions, especially those related to transparency and sustainability issues, are strengthened.

**Keywords:** Fiscal targets; Budget integration; Fiscal transparency; Budget institutions; Egypt's state budget; Fiscal reforms.

### S-5. Environmental Challenges, Externalities and Sustainable Policies in Transport Sector in Egypt

Dalia M. Ibrahiem

*Journal of Applied Economic Sciences, XI4 (42):647-660 (2016)*

The study analyzes the environmental effects, externalities and energy consumption in transport sector in Egypt. It focuses on external costs from transport sector and its economic impact on society expressed in monetary terms, and these external costs are mainly congestion, road accidents and air pollution caused by carbon dioxide emissions. The Human Capital approach is applied to estimate economic costs of road accidents in 2014 in terms of injuries, fatalities, damages in vehicles, suffer and loss and these economic costs are estimated to be 3.75 billion dollars. Moreover, the economic costs of air pollution mainly due to carbon dioxide emissions are estimated to be 2.8 billion dollars in 2014, and these estimated economic costs of both road accidents and air pollution are about 5% of GDP. In addition, environmental and safety transport policies are discussed. Also, internalization of externalities and policies adopted in transport sector in Egypt are illustrated and finally possible sustainable transport policies are recommended

**Keywords:** Externalities; Environmental effects; Sustainable; Internalization.

## S-6. Environmental Kuznets Curve: an Empirical Analysis for Carbon Dioxide Emissions in Egypt

Dalia M. Ibrahiem

*International Journal of Green Economics, 10 (2):136-150 (2016)*

The aim of the study is to address the relationship between environmental degradation and economic growth in Egypt. In this regard, the study examines the relationship between carbon dioxide emissions ($CO_2$), economic growth (real GDP per capita), energy consumption, trade openness and population density employing Johansen cointegration analysis over time series data of 1980-2010. Specifically, the study investigates the existence of Environmental Kuznets Curve (EKC) hypothesis, the relationship between $CO_2$ emissions and real GDP per capita. The results of the study confirm the existence of long-run relationship between the variables. In addition, the study does not support the existence of EKC either in the short or the long run. Also, it is concluded that energy consumption is correlated positively with $CO_2$ emissions, while trade openness and population are correlated negatively with it. Granger causality test indicates bilateral causality between economic growth and $CO_2$ emissions and unilateral causality running from economic growth to energy consumption and from trade openness to economic growth. Important policy implications will be recommended based on these results.

**Keywords:** Environmental kuznetscurve; EKC; Carbon dioxide; CO2; Carbon emissions; Economic growth; Trade openness; Energy consumption; Population density; Cointegration; Egypt; Environmental degradation.

## S-7. On Bringing Down Egypt's Budget Deficit to Gdp Ratio: Are Expenditure Cuts Required?

Israa A. El Husseiny

*International Journal of Economics and Business Research, 12:91-102 (2016)*

It is a common argument for a developing country like Egypt that the adoption of a contractionary fiscal policy that aims at reducing the level of government expenditure and its various components is necessary to lower the budget deficit as a percentage of GDP. However, such an argument can be flawed due to the fact that changes in the government expenditure might lead to unexpected changes in both the budget deficit and GDP. Accordingly, the net effect on the budget deficit-to-GDP ratio should depend on the elasticity of both the budget deficit and GDP with respect to changes in the government expenditure. This study aims to test empirically whether cutting the government expenditure in Egypt should actually be expected to lower the budget deficit-to-GDP ratio; it employs a mathematical framework that is based on differential calculus and the concept of elasticity using a time series dataset for the Egyptian economy for the period from fiscal year 1981/1982 to fiscal year 2013/2014. The findings indicate that lowering the government expenditure so as to decrease the budget deficit-to-GDP ratio might not achieve the expected aims and thus may not be the proper policy option.

**Keywords:** Fiscal (budget) deficit; Egypt'sstate budget; Government expenditure; Fiscal policy; Egypt.

## S-8. The Nexus of Regional Poverty and Education in Egypt: A Micro Analysis

Heba Nassar and Marwa Biltagy

*International Journal of Economics and Financial 6: 1446-1453 (2016)*

The poverty pattern has changed from an urban/rural pattern to a geographical/regional pattern. These changes may be explained by several aspects. The employment aspect is one of the main determinants for socioeconomic status. The inability of household members to participate in income-generating activities is considered an important explanation of poverty trends and the relationship between poverty and employment can be explained by the loss of earnings or the decline in real incomes. This can be related to several aspects, pattern of jobs and its regularity, human resource development indicators and investment indicators. The objective of this paper is to understand the changes in poverty levels in Egypt in total and by region by studying their relationship to regional composition and trends of employment and educational characteristics. The study starts a theoretical review about poverty and employment, which will constitute the basis for the micro level analysis in order to propose a framework for a pro-poor employment strategy.

**Keywords:** Regional poverty; Education; Egypt; Investment in schooling.

### *Dept. of Political Science*

## S-9. Media, Cultural Consumption and Support for Democracy in Post-Revolutionary Egypt'

Mazen Hassan, Elisabeth Kendall and Stephen Whitefield

*Political Studies, 64: 534-551 (2016) IF: 1.156*

While much of the commentary about the Arab Spring, and the Egyptian revolution in particular, points to the importance of new social media and engagement with literary genres in generating support for democracy, the comparative literature remains ambivalent on this question. The aim of this article is to put the connection between cultural consumption of various sorts and democratic support to a rigorous test using data from a survey conducted by the authors in 2012 after the first parliamentary elections in Egypt after the revolution. The research design involves a hard test, in which we estimate the significance of cultural consumption after controlling for a broad range of 'usual suspects' affecting democratic attitudes. The results show positive effects for new social media on support for democracy, but little or no effect for literary genres.

**Keywords:** Arab spring; Democracy; Public opinion; Cultural consumption; Egypt.

## S-10. The Grand Ethiopian Renaissance Dam: A Benefit-Sharing Project in the Eastern Nile?

Rawia Tawfik

Pages 574-592 /Rece*Water International, 41 (4): 574-592 (2016) IF: 1.04*

Negotiations over the GERD have not transformed thedebate in the Eastern Nile from sharing water to sharing benefits.

Nationalistic discourse used by the three governments,the political sensitivity of the Nile issue, cautious Egyptian approach towards Eastern Nile cooperation beyond the project, divisions within policy circles in Egypt on dealing with the project and with the NBI as a framework of cooperation, the failure of Egypt to adapt its water policies to expected changes in the post-GERD era, and the new power asymmetries in the Eastern Nile have affected and will continue to affect, positions in ongoing negotiations, making it more diffcult to reach a benefit-sharing deal.

**Keywords:** GERD; Benefit-sharing; Transbound aryrivers; Eastern nile.

## S-11. Reconsidering Counter-Hegemonic Dam Projects: the Case of the Grand Ethiopian Renaissance Dam

Rawia Tawfik

*Water Policy, 18: 1033-1052 (2016) IF: 0.952*

The paper questions the argument of the hydro-hegemony framework that counter-hegemonic mechanisms used by non-hegemons in transboundary rivers lead to a more equitable order of water and benefit-sharing, using the case of the Grand Ethiopian Renaissance Dam (GERD). It agrees with hydro-hegemony scholars that the GERD is a 'game changer' that challenges Egypt's hegemonic position, and an important step in the transition towards a new order in the Nile basin. However, it scrutinises how Ethiopia and Egypt manage this transition through their policies to implement or contest the dam, and the conditions under which the GERD could lead to a more equitable order in the basin, and create incentives for cooperation beyond the project. It argues that Ethiopia's planning and implementation of the project, and Egypt's inconsistent response to it, have increased uncertainties about the benefits of the project to downstream countries, and even to Ethiopia, and fuelled the historical mistrust between the two countries. It suggests steps to build trust and translate the recent Declaration of Principles between the three Eastern Nile riparians into a benefit-sharing deal.

**Keywords:** Benefit-sharing; Counter-hegemony; Dams; Eastern Nile; GERD; Transbound aryrivers.

## S-12. EU Action in the Mediterranean: Structural Impediments Post-2011

Sally Khalifa Isaac

*Middle East Policy Journal, 23: 92-102 (2016) IF: 0.477*

The experience of Euro-Mediterranean relations in general, in the post-2011 period in particular, suggests that some structural factors influence the capacity and efficiency of the EU in the southern Mediterranean area. This paper attempts to focus on three structural factors that have represented over the past two decades illusive European assumptions about the Mediterranean. These are, first, the early assumptions on "region building," which stressed a workable European project to construct the Euro-Mediterranean area as a "region." Such an assumption omits the multiple de facto structural features that separate the two shores of the Mediterranean into distinctive regions. Second, there is the assumption that the southern Mediterranean area constitutes primarily the EU's "Southern Neighborhood," implicitly omitting (or marginalizing) the roles of regional and international powers. These powers include the United States, some Arab Gulf monarchies, Russia and China, whose policies and actions, especially post-2011, were highly visible and influential in the wider MENA region. Third, there is an implicit assumption that "Europe" or "the EU" enjoys a high level of unity in both policy formulation and implementation. This assumption seems to ignore the obvious structural impediment of European incoherence.

**Keywords:** European neighborhood policy; Arab uprisings; Euro mediterran eanrelations; Structural factors.

## S-13. Egypt and the Transformations of the Pan-African Movement: the Challenge of Adaptation

Rawia Tawfik

*African Studies, 75 (3): 297-315 (2016) IF: 0.273*

The Pan-African movement and the contribution of the Egyptian state and society to this movement have witnessed a significant change over the last five decades. The article traces the transformations in the meaning of Pan-Africanism from liberation from discrimination and colonialism to liberation from authoritarianism and a struggle for democracy and human rights. It argues that the position of the Egyptian state has changed from a progressive force that supported the Pan-African ideals of anti-imperialism and the struggle for independence to a conservative force that defends traditional concepts of sovereignty and expresses little enthusiasm for the African Union's new governance instruments. It explores the short lived potential that the January 25 revolution presented for restoring the role of the Egyptian state and revitalising the role of its civil society at the heart of the Pan-African struggle for political and economic rights. The memoirs of Egyptian leaders and officials and the reports and statements of AU organs as well as the Egyptian ministry of foreign affairs are analysed in this article to uncover the Egyptian government's position and the comparative stance of the continental organisation. Primary and secondary sources are examined to provide an assessment of the role of non-state actors in Egypt in the Pan-African movement.

**Keywords:** Egypt; Pan-africanism;Organisation of africanunity;africanunion; Unconstitutional changes of government; January 25 revolution.

## S-14. Changing Hydro-Political Relations in the Nile Basin: A Protracted Transition

Rawia Tawfik

*International Spectator, 51(3): 67-81 (2016)*

A new hydro-political order is emerging in the Nile Basin. Upstream riparian states have improved their bargaining power vis-à-vis downstream countries by adopting a common position in the negotiations over a new framework agreement to govern the utilisation of the Nile waters. Some upstream riparians have unilaterally constructed hydraulic projects that threaten Egypt's hegemonic position in the basin, the most notable of which is the Grand Ethiopian Renaissance Dam (GERD). Whether these developments will lead to a more equitable utilisation of water resources and a more cooperative order will depend on the policies of the riparian states, especially in the Eastern Nile. Respect of the Declaration of Principles on the GERD signed

between Egypt, Ethiopia and Sudan could help build trust between the three countries after years of tensions around the project. Beyond that, a basin-wide plan for the utilisation of water resources would not only maximise the benefits from the river and address the common challenges facing the basin, but also reduce the political costs of tensions on future projects.
**Keywords:** Nile basin; Historical agreements; Hydropolitics; GERD; Water resources.

## S-15. Fiscal Transparency Puzzle and Electoral Institutions: Applying a 3Ds Approach for Tracking the Action Cycle in Egypt

Lobna Abdel Latif, Mazen Hassan, Noha Youssef and Mohamed Zaky

*The Journal of Legislative Studies, 22: 424-444 (2016).*

This article aims at contributing to the discussion on the fiscal transparency puzzle. The authors challenge the idea that fiscal disclosure can directly increase fiscal accountability. Using an original data set at the level of individual members of parliament (MPs) in the Egyptian parliament, constructed from content analysis of budgetary discussions during the period 2000–10, it is shown that political incentives determined by a majoritarian electoral system curbed the willingness to check government fiscal behaviour, even among opposition MPs. This is because MPs still favoured pork-barrel behaviour to boost their re-election chances. Moreover, fiscal data disclosed could not be communicated to voters and the opposition showed a relatively higher avoidance against fiscal disclosure. The authors conclude that the electoral system is a dominant factor in shaping the final effect of transparency given its influence on the structure of political incentives.
**Keywords:** Fiscal transparency; Fiscal accountability; Electoral systems; Egypt; Legislatures.

### *Dept. of Public Administration*

## S-16. The Effect of Political Decentralization on School Leadership in German Vocational Schools

Michael Gessler and Iman K Ashmawy

*Educational Management Administration and Leadership, 44(2): 184-204 (2016) IF: 0.692*

In this explorative qualitative study the effect of political decentralization on vocational school leadership is investigated. Through conducting structural interviews with 15 school principals in the states of Bremen and Lower Saxony in Germany, the study was able to conclude that political decentralization entails the creation of elected bodies through which various stakeholders are involved in the decision-making process, and that schools are able to discretionally plan their own goals and objectives. As a result, it can be seen that school leadership adopts a participatory leadership model.
**Keywords:** Education; Political decentralization; School; Participatory; Leadership.

### *Dept. of Statictics*

## S-17. An Evaluation of the Crosier'sCusum Control Chart with Estimated Parameters

Maureen Hany and Mahmoud A. Mahmoud

*Quality and Reliability Engineering International, 32(5): 1825-1835 (2016) IF: 1.457*

We evaluate the performance of the Crosier's cumulative sum (C-CUSUM) control chart when the probability distribution parameters of the underlying quality characteristic are estimated from Phase I data. Because the average run length (ARL) under estimated parameters is a random variable, we study the estimation effect on the chart performance in terms of the expected value of the average run length (AARL) and the standard deviation of the average run length (SDARL). Previous evaluations of this control chart were conducted while assuming known process parameters. Using the Markov chain and simulation approaches, we evaluate the in-control performance of the chart and provide some quantiles for its in-control ARL distribution under estimated parameters. We also compare the performance of the C-CUSUM chart to that of the ordinary CUSUM (O-CUSUM) chart when the process parameters are unknown. Our results show that large number of Phase I samples are required to achieve a quite reasonable performance. Additionally, the performance of the C-CUSUM chart is found to be superior to that of the O-CUSUM chart. Finally, we recommend the use of a recently proposed bootstrap procedure in designing the C-CUSUM chart to guarantee, at a certain probability, that the in-control ARL will be of at least the desired value using the available amount of Phase I data.
**Keywords:** Average run length (ARL); Sdarl; Bootstrap; Cumulative sum (CUSUM); Statistical process control.

## S-18. Different Estimation Methods for Constant Stress Accelerated Life Test Underthe Family of the Exponentiated Distributions

Alaa Abdel-hamid and Essam K. Al-Hussaini

*Quality and Reliability Engineering International Journal, 32: 1095-1108 (2016) IF: 1.457*

The Accelerated Life Testing (ALT) has been used for a long time in several fields to obtain information on the reliability of product components and materials under operating conditions in a much shorter time. One of the main purposes of applying ALT is to estimate the failure time functions and reliability performance under normal conditions. This paper concentrates on the estimation procedures under ALT and how to select the best estimation method that gives accurate estimates for the reliability function. For this purpose, different estimation methods are used, such as maximum likelihood, least squares (LS), weighted LS, and probability weighted moment. Moreover, the reliability function under usual conditions is predicted. The estimation procedures are applied under the family of the exponentiated distributions in general, and for the exponentiated inverted Weibull (EIW) as a special case. Numerical analysis including simulated data and a real life data set is conducted to compare the performances between these four methods. It is found that the ML method gives the best results among other estimation methods. Finally, a comparison between the EIW and the Inverted Weibull (IW) distributions based on a

real life data set is made using a likelihood ratio test. It is observed that the EIW distribution can provide better fitting than the IW in case of ALT.

**Keywords:** Accelerated life testing; Maximum likelihood Method; Least squares method; Weighted least squares method; Probability weighted moments method; Exponentiated distributions.

## S-19. The Performance of the Multivariate Adaptive Exponentially Weighted Moving Average Control Chart with Estimated Parameters

Aya A. Aly, Mahmoud A. Mahmoud and Ramadan Hamed

*Quality and Reliability Engineering International, 32: 957-967 (2016) IF: 1.457*

The multivariate adaptive exponentially weighted moving average control chart (MAEWMA) can detect shifts of different sizes while diminishing the inertia problem to a large extent. Although it has several advantages compared to various multivariate charts, previous literature has not considered its performance when the parameters are estimated. In this study, the performance of the MAEWMA chart with estimated parameters is studied while considering the practitioner-to practitioner variation. This kind of variation occurs due to using different Phase I samples by different practitioners in estimating the unknown parameters. The simulation results in this paper show that estimating the parameters results in extensively excessive false alarms and as a result a large number of Phase I samples is needed to achieve the desired incontrol performance. Using small number of Phase I samples in estimating the parameters may result in an in-control ARL distribution that almost completely lies below the desired value. To handle this problem, we strongly recommend the use of a bootstrap-based algorithm to adjust the control limit of the MAEWMA chart. This algorithm enables practitioners to achieve, with a certain probability, an in-control ARL that is greater than or equal to the desired value while using the available number of Phase I samples.

**Keywords:** Arl; Bootstrap; Estimation; Inertia; Maewma; Statistical process control.

## S-20. On Point Estimation of the Abnormality of aMahalanobis Index

Fadlalla G. Elfadaly, Paul H. Garthwaite and John R. Crawford

*Computational Statistics and Data Analysis, 99: 115-130 (2016) IF: 1.179*

Mahalanobis distance may be used as a measure of the disparity between an individual's profile of scores and the average profile of a population of controls. The degree to which the individual's profile is unusual can then be equated to the proportion of the population who would have a larger Mahalanobis distance than the individual. Several estimators of this proportion are examined. These include plug-in maximum likelihood estimators, medians, the posterior mean from a Bayesian probability matching prior, an estimator derived from a Taylor expansion, and two forms of polynomial approximation, one based on Bernstein polynomial and one on a quadrature method. Simulations show that some estimators, including the commonly-used plug-in maximum likelihood estimators, can have substantial bias for small or moderate sample sizes. The polynomial approximations yield estimators that have low bias, with the quadrature method marginally to be preferred over Bernstein polynomials. However, the polynomial estimators sometimes yield infeasible estimates that are outside the 0–1 range. While none of the estimators are perfectly unbiased, the median estimators match their definition; in simulations their estimates of the proportion have a median error close to zero. The standard median estimator can give unrealistically small estimates (including 0) and an adjustment is proposed that ensures estimates are always credible. This latter estimator has much to recommend it when unbiasedness is not of paramount importance, while the quadrature method is recommended when bias is the dominant issue.

**Keywords:** Bernstein polynomials; Mahalanobisdistance; Median estimator; Plug-In maximum likelihood; Quadrature approximation; Unbiasedestimation.

## S-21. CUSUM Charts with Controlled Conditional Performance Under Estimated Parameters

Nesma A. Saleh, Inez M. Zwetsloot, Mahmoud A. Mahmoud and William H. Woodall

*Engineering, 28: 402-415 (2016) IF: 0.883*

We study the effect of the Phase I estimation error on the cumulative sum (CUSUM) chart. Impractically large amounts of Phase I data are needed to sufficiently reduce the variation in the in-control average run lengths (ARL) between practitioners. To reduce the effect of estimation error on the chart's performance we design the CUSUM chart such that the in-control ARL exceeds a desired value with a specified probability. This is achieved by adjusting the control limits using a bootstrap-based design technique. Such approach does affect the out-of-control performance of the chart; however, we find that this effect is relatively small.

**Keywords:** Average of arl (AARL); Bootstrap; Effect of estimation error; Standard deviation of average run length (SDARL); Statistical process control (SPC); Statistical process monitoring (SPM).

## S-22. Statistical Inference for a Step-Stress Partially-Accelerated Life Test Model with an Adaptive Type-I Progressively Hybrid Censored Data Fromweibull Distribution

Ali A. Ismail

*Statistical Papers, 57: 271-301 (2016) IF: 0.781*

In this paper, a new censoring scheme, namely, adaptive Type-I progressively hybrid censoring scheme under a step-stress partially accelerated test model is introduced. It has some advantages over the progressively hybrid censoring schemes already discussed in the literature. Based on this censoring scheme, themaximum likelihood estimations of Weibull distribution parameters and the acceleration factor are considered. The biases and mean squared errors of themaximum likelihood estimators of the model parameters are computed to evaluate their performances in the presence of censoring scheme developed in this paper through aMonte Carlo simulation study. The results obtained under the adaptive Type-I progressively hybrid censoring scheme are compared with those produced

under the non-adaptive Type-I progressively hybrid censoring scheme using three different progressive censoring schemes. Moreover, the confidence intervals lengths and their associated coverage probabilities are obtained for both adaptive and non-adaptive Type-I progressively hybrid censoring scheme. In addition, Optimum test plans are also developed to improve/guarantee the quality of the statistical inference.
**Keywords:** Quality and reliability; Step-stress partially accelerated life test;Weibulldistribution; Adaptive type-I progressively hybrid censoring scheme; Coverage probability; Optimum test plans.

## S-23. Optimum Failure-Censored Step-Stress Life Test Plans for the Lomax Distribution

Ali A. Ismail

*Strength of Materials, 48: 437-443 (2016) IF: 0.462*

This article studies partially accelerated life testing (PALT) under step-stress supposing that the time to failure has Lomax distribution with failure-censoring. Maximum likelihood estimators of PALT model parameters with the associated mean square error are obtained. Also, confidence intervals estimations of the parameters with the associated coverage probabilities are calculated. In addition, optimal test designs are considered. To validate the theoretical results simulation studies are performed.
**Keywords:** Stress; Lomax distribution; Partial acceleration; Interval estimation; Coverage probabilities; Optimal design; Type-II censoring; Newton–raphsonequations; Non-linearity; Monte carlosimulation.

## S-24. On Designing Time-Censored Step-Stress Life Test for Lomax Distribution

Ali A. Ismail

*Journal of Testing and Evaluation, 44: 230-236 (2016) IF: 0.423*

This article presents optimum time step-stress partially accelerated life tests (SSPALTs) where a pre-specified censoring time is considered. The time to failure is assumed to have Lomax distribution. Maximum likelihood estimates (MLEs) of SSPALT model parameters are obtained. Moreover, a confidence intervals estimation for the parameters with associated coverage probabilities is obtained. In addition, optimum test plans for SSPALT are also developed. Such test plans minimize the generalized asymptotic variance (GAV) of the MLEs of the model parameters. To demonstrate the theoretical results, Monte Carlo simulations are introduced and a real life example is provided.
**Keywords:** Reliability; Lomax distribution; Step-stress partially accelerated life tests; Maximum likelihood estimation; Confidence intervals; Coverage probabilities; Optimum test plans; Type-I censoring; Monte carlosimulation.

## S-25. Reliability Analysis Under Constant-Stress Partially Accelerated Life Tests Using Hybrid Censored Data from Weibull Distribution

Ali A. Ismail

*Hacettepe Journal of Mathematics and Statistics, 45: 181-193 (2016) IF: 0.277*

This article discusses the estimation of Weibull distribution parameters based on hybrid censored data under constant-stress partially accelerated test model. Two estimation methods; maximum likelihood (ML) and percentile bootstrap (PB) are used to make statistical inference on the Weibull distribution parameters and the acceleration factor. The mean square errors of the estimators are calculated to evaluate their performances through a Monte Carlo simulation study. Moreover, the confidence intervals lengths (CILs) and their associated coverage probabilities (CPs) are obtained. Finally, to demonstrate the proposed methodology, an arithmetic example is given.
**Keywords:** Statistics; Reliability; Percentile bootstrap; Confidence interval; Coverage rate; Hybrid censoring; Mean square error.

## S-26. Mathematical Programming Model for Selecting Generalized Ridge Regression Parameter

Aya Farag, Ragaa Kassem and Ramadan Hamed Mohamed

*Advances and Applications in Statistics, 48: 391-409 (2016)*

Ridge regression technique is used to estimate the regression coefficients instead of least squares method when there is multicollinearity in the data. Generalized ridge regression is more realistic than ordinary ridge regression as it assumes separate ridge parameters for each explanatory variable according to its nature. This study proposes nonlinear mathematical programming model in order to estimate the generalized ridge parameter such that to minimize both generalized cross validation and mean square error functions. The results of the proposed mathematical programming model are checked through a simulation study. In addition, the suggested model is compared to other models. The proposed model has good performance in terms of measures, mean square error and generalized cross validation.
**Keywords:** Generalized ridge regression; Mean square error; Generalized cross validation function; Mathematical programming model.

## S-27. The Use of Conditional Probability Integral Transformation Method for Testing Accelerated Failure Time Models

A. A. Abdel-Ghaly, Hanan Mohamed Aly Hasan and Elham Abdel-Rahman

*Pakistan Journal of Statistics and Operation Research, XII: 369-387 (2016)*

This paper suggests the use of the conditional probability integral transformation (CPIT) method as a goodness of fit (GOF) technique in the field of accelerated life testing (ALT), specifically for validating the underlying distributional

assumption in accelerated failure time (AFT) models. The CPIT method is based on transforming the data into independent and identically distributed (i.i.d) Uniform (0, 1) random variables and then applying a certain GOF technique to test the uniformity of the transformed random variables. In this paper, the CPIT method is used to validate each of the exponential and lognormal distributions' assumptions in an AFT model under constant stress and complete sampling. The performance of this method is investigated via a simulation study. Moreover, a real life example is presented to illustrate the application of it. Concluding comments about the good performance of the CPIT method are made.
**Keywords:** Accelerated life testing; Accelerated failure time model; Constant stress; Goodness of fit techniques; Conditional probability integral transformation method.

## Faculty of Commerce

### *Dept. of Accounting*

### S-28. Are Regulatory Capital Adequacy Ratios Good Indicators of Bank Failure Evidence from us Banks

Heba Abou-El-Sood

*International Review of Financial Analysis, 48: 292-302 (2016) IF: 0.896*

Motivated by massive bank failures during the financial crisis, this paper examines whether capital adequacy ratios required by regulators are associated with bank failure. It investigates whether the association is affected by the bank's proximity to the minimum required capital ratios. If results show a significant association between regulatory capital and failure of banks falling below the minimum capital ratios, then the ratios are set at an adequate level. Examining a sample of 560 US bank holding companies for the period 2003–2009, results reveal that the association between the core (Tier 1) capital ratio and bank failure becomes significant only if the bank holding company has a Tier 1 capital ratio of less than 6%. This is the level below which US bank regulators do not regard banks as being well capitalized. During the financial crisis period of 2007–2009, there is a significant association only when the criterion is set at or above 8%. Market-based probability of default is more significantly associated with failure relative to Tier 1 capital ratio. The findings of this paper are relevant to regulatory policy discussions and Basel III deliberations on capital adequacy at times of financial turmoil.
**Keywords:** Failure; Regulatory capital adequacy; Bank holding Companies; Distress; Financial crisis.

### S-29. Accounting Discretion and the Market Disciplining of Bank Risk-Taking Behavior: an Assessment of the Effectiveness of Egyptian Banking Reforms from an Accounting Perspective

Mohamed A. Elbannan

*Accounting and Finance Research, 5: 1-29 (2016)*

The purpose of this study is to empirically delineate significant economic consequences associated with observable differences in discretion permitted to banks under the existing Egyptian Banking Act. More specifically, the study investigates whether accounting discretion is associated with earnings quality and risk-taking in the Egyptian banking sector. In light of this increased accounting discretion caused by the banking reforms, study questions the extent to which the Egyptian banking reforms facilitate market disciplining of banks. Based on a sample of 46 banks providing 634 bank-quarters over the period 2000-2015, the results indicate that, during non-crisis (crisis) years, bank managers smooth out earnings leading to higher quality earnings but also to higher (lower) earnings volatility and (lower) bank risk, consistent with managerial efficiency and not managerial opportunism explanation of accounting discretion. It is concluded that the economic reforms created conditions whereby bank earnings attributes are improved but where prudential market monitoring and oversight over bank risk-taking behavior may suffer.
**Keywords:** Accounting discretion; Banks; Risk-taking.

### S-30. IFRS Adoption, Legal Systems and the Voluntary Disclosure of Human Capital: Cross-Country Evidence from the Banking Industry

Mohamed A. Elbannan

*Accounting and Finance Research, 5: 30-48 (2016)*

This study examines the value relevance of voluntary human capital disclosures by banks and the effect of the adoption of International Financial Reporting Standards (IFRS) on the value relevance of these disclosures. Human capital disclosures allow capital market participants to evaluate the intellectual capital of the disclosing banks, which in theory may enable market participants to assess the competitiveness of the bank's human resource strategy and the productivity of the workforce vis-à-vis benchmark performance. While IFRS does not mandate particular form of voluntary human capital disclosures (VHCD), VHCD is expected to possess information content that is useful to market participants in their equity pricing decisions. The study is conducted using a cross-country sample of 10,199 bank-years that reported labor costs. Market participants, however, are found to relate VHCD negatively to prices and returns in common and civil law countries alike. Results also suggest that IFRS adoption reduces the value relevance of VHCD due to the abundance of alternative information provided under the more comprehensive IFRS framework that helps in the prediction of future cash flows. Finally, market participants find VHCD value relevant after IFRS adoption in common law countries potentially because it reduces uncertainty about an important determinant of the bank's future performance. On the other hand, market participants in civil law countries view VHCD as value relevant but coming at added time and financial investment. As an application of the results to an emerging economy, the implications for the Egyptian accounting profession, banking sector and capital markets are discussed.
**Keywords:** IFRS; Disclosure; Banks.

### S-31. The Use of Sustainability Incentives in Executive Remuneration Contracts: Firm Characteristics and Impact on the Shareholders' Returns

Heba Abdel Motaal and Magdy Abdel-Kader

*Journal of Applied Accounting Research, 17: 311-330 (2016)*

**Purpose** The purpose of this paper is to examine which firm characteristics affect the usage of sustainability incentives in executive remuneration contracts, and whether these sustainability incentives have an impact on shareholders' return. **Design/methodology/approach** The analysis is based on a sample of 212 firms from the FTSE 350 firms over the period of 2009-2011. Findings The results indicate that there is a significant relationship between the adoption of sustainability incentives in executive remuneration and firm size, compensation committee independence, the corporate social responsibility (CSR) sustainability committee, CSR sustainability index, and resource efficiency policy variables. Further, there is evidence to support a positive impact on the shareholders' return. **Research limitations/implications.** Theresults of this study should be interpreted within two limitations. First, the limited numbers of the sample years due to the limited number of firms used sustainability incentives. Second, the use of a dummy variable in the measurement of the adoption of sustainability incentives in the analysis.**Practical implications**The paper includes implications for the development of sustainability incentives within the performance measurement system and compensation contracts that could be a solution for the agency problem. **Originality/value** This study provides empirical evidence on an increased use of sustainability incentives in UK firms, and identifies firm's characteristics that explain such increase in the sustainability incentives, finally its positive impact on the shareholders' return.
**Keywords:** Firm characteristics; Executive remuneration contracts; Shareholder returns; Sustainability incentive.

### *Dept. of Business Administration*

### S-32. Deception in Advertising Revisited: Antecedents and Differences in Perception Across Consumer Groups

DoaaFathy, Tamer H. Elsharnouby and Ehab Abou Aish

*International Journal of Business and Emerging Markets, 8: 403-425 (2016) IF: 0.29*

This research aims to examine antecedents of consumers' perception of deception in advertising. It also empirically examines deception in advertising among different gender and age groups. The researchers adopt a mixed-method approach, in which both qualitative and quantitative research methods are employed. Interview data from a sample of ten university students as well as questionnaire data from a sample of 369 consumers from the Egyptian telecommunication sector were collected and analysed. The findings suggest that consumers' perception of deception in advertising is related to three predictors: perceived information reliability and usefulness, product experience, and consumer skepticism. The findings further reveal that female and young consumers are less likely to detect deception in advertising than male and older consumers. It also provides three sets of recommendations to consumers, advertisers and policy makers.
**Keywords:** Advertising deception; Perceived deception; Marketing ethics; Telecoms; Telecommunications industry; Egypt; Consumer perceptions; Gender; Age groups; Information reliability; Perceived reliability; Perceived usefulness; Product experience; Consumer scepticism.

### S-33. Examining the Impact of the Attractiveness of Alternatives on Customers' Perceptions of Price Tolerance: Moderation and Mediation Analyses

Mohamed Sobhy Temerak

*Journal of Financial Services Marketing, 21: 284-297 (2016)*

The current literature provides mixed support for the positive influence of competitors on customers' perceptions of price tolerance (Herrmann et al, Psychology & Marketing, 200421(7), 533–551). This paper examines a number of mediators and moderators of this relationship, such as positive switching barriers, negative switching barriers and customer satisfaction. A total of 162 valid responses was collected from the financial brokerage context by means of a random sample. The data were analysed using the Partial-least square (PLS) approach to structural equation modelling. The findings show that customers' satisfaction with the service provider partially mediates the positive effect of alternatives on price tolerance. Negative, not positive, switching barriers were found to weaken the effect on price tolerance of the attractiveness of alternatives.
**Keywords:** Switching barriers; Price tolerance; Customer satisfaction; Attractiveness of alternatives.

### S-34. Implications of the Use of Social Media for Pre-Purchase Information Searches for Automobiles

Abeer A. Mahrous

*International Journal of Technology Marketing, 11: 254-275 (2016)*

Previous research in the information search of pre-purchase literature has indicated that the impact on information search behaviour of using social media as a source of information source should be investigated. This paper attempts to address this gap by examining the implications of social media information searching for pre-purchase search for information on automobiles. A sample of 384 current and prospective buyers was drawn from the Egyptian automobile market. Data were analysed using structural equation modelling. The results suggest that social media-based information searching has an impact on information quality, consideration sets and selection criteria. Accordingly, consumers are tending to use the social media as their initial and major source of information before they make a purchase. Moreover, the incidence of using offline information searches at this point is tending to decline. Some managerial insights into these results are provided.
**Keywords:** Social media; Pre-purchase search; Automobiles; Information sources; Emerging markets; Pre-purchase iInformation; Vehicle purchasing; Automobile industry; Automotive purchases; Information retrieval; Egypt; Structural equation modelling; SEM.

### *Dept. of Mathoimatics and Insurance*

### S-35. The Impact of Intellectual Capital on Corporate Performance: Evidence from the Egyptian Insurance Market

Mohamed Sherif and Mahmoud Elsayed

*International Journal of Innovation Management, 20: 0-0 (2016)*

This paper examines, using various econometric techniques, the impact of intellectual capital (IC) on the performance of Egyptian insurance companies listed between 2006 and 2011. We measure IC using the value added intellectual coefficient (VAIC) approach and its components developed by Pulic (2000), and both a direct and a moderating relationship between VAIC and corporate performance are investigated. Our results show a direct relationship between (IC-VAIC) and the performance of Egyptian insurance companies, particularly with capital employed efficiency (CEE), and to a lesser extent with human capital efficiency. In addition, a positive relationship between IC (capital employed and structural capital) and performance in the prior and current years is found. Evidence also suggests the possibility of a moderating relationship between IC and physical and financial capital, which in turn impacts on corporate performance. Our study also reveals the importance of taking into account any unobservable heterogeneity and endogeneity issues when analysing corporate performance.
**Keywords:** Intellectual capital; Financialperformance; Insurance companies; Egypt.

## S-36. Determinants of Capital Adequacy at the Egyptian Investors Compensation FUND

Ahmed Saad and Mahmoud Elsayed

*Corporate Ownership and Control Journal, 13: 31-36 (2016)*

The purpose of this study is to investigate the protection system of investors in the Egyptian stock markets, using a number of econometric techniques and hand-collected data of Egyptian Investor Protection Fund over the period from 2006 to 2014. We measure the capital adequacy through two variables, which may be a benchmark in it selves or can be compared to similar regimes at developed stock markets, these variables are: the fund reserves as a percentage of market capitalisations and fund reserves available to compensate owners of the market capitalisations, which in turn depend upon the number of customers accounts subject to compensations, number of the market portfolio owners, the value of the investor securities account at every compensation fund member, number of stock traders, number of listed shares and number of transactions. Overall, there is significant positive coefficient/relationship between market capitalisation, retained earnings and reserve. However, there is significant negative coefficient/relationship between Number of listed companies and fund reserves capital.
**Keywords:** Investor protection fund; Capital adequacy; Stock markets; Insurance companies; Egypt.

## S-36. The Impact of Intellectual Capital on Corporate Performance: Evidence from the Egyptian Insurance Market

Mohamed Sherif and Mahmoud Elsayed

*Contribution to Journal Article, (2016)*

This paper examines, using various econometric techniques, the impact of intellectual capital (IC) on the performance of Egyptian insurance companies listed between 2006 and 2011. We measure IC using the value added intellectual coefficient (VAIC) approach and its components developed by Pulic (2000), and both a direct and a moderating relationship between VAIC and corporate performance are investigated. Our results show a direct relationship between (IC-VAIC) and the performance of Egyptian insurance companies, particularly with capital employed efficiency (CEE), and to a lesser extent with human capital efficiency. In addition, a positive relationship between IC (capital employed and structural capital) and performance in the prior and current years is found. Evidence also suggests the possibility of a moderating relationship between IC and physical and financial capital, which in turn impacts on corporate performance. Our study also reveals the importance of taking into account any unobservable heterogeneity and endogeneity issues when analysing corporate performance.

**Keywords:** Intellectual capital; Financial performance; insurance; Companies; Egypt.

# ( 5 )

# Humanity Sciences Sector

5-1 Faculty of Archaeology
5-2 Faculty of Arts
5-3 Faculty of Kindergarten
5-4 Faculty of African Research and Studies

# Total No. of Publication for Humanity Sciences Sector

| Faculty | 2006 | 2007 | 2008 | 2009 | 2010 | Total |
|---|---|---|---|---|---|---|
| Arts | 7 | 7 | 17 | 15 | 15 | 61 |
| Archaeology | 1 | 2 | 5 | 16 | 19 | 43 |
| Educational Studies and Research | 0 | 0 | 0 | | 2 | 2 |
| Dar Al-Oloum | 1 | 0 | 0 | | | 1 |
| African Research and Studies Institute | | 1 | 2 | | | 3 |
| Kindergarten | | | | | | |
| **Total** | 9 | 10 | 24 | 31 | 36 | 110 |

| Faculty | 2011 | 2012 | 2013 | 2014 | 2015 | 2016 | Total |
|---|---|---|---|---|---|---|---|
| Arts | 22 | 20 | 24 | 23 | 44 | 5 | 138 |
| Archaeology | 26 | 32 | 0 | 16 | 25 | 28 | 127 |
| Educational Studies and Research | 2 | 4 | 0 | 5 | 1 | 0 | 12 |
| Dar Al-Oloum | 0 | 1 | 0 | 0 | 0 | 0 | 1 |
| African Research and Studies Institute | 3 | 8 | 11 | 8 | 3 | 20 | 53 |
| Kindergarten | | | 1 | 1 | 3 | 5 | 10 |
| **Total** | 53 | 65 | 36 | 53 | 76 | 58 | 341 |

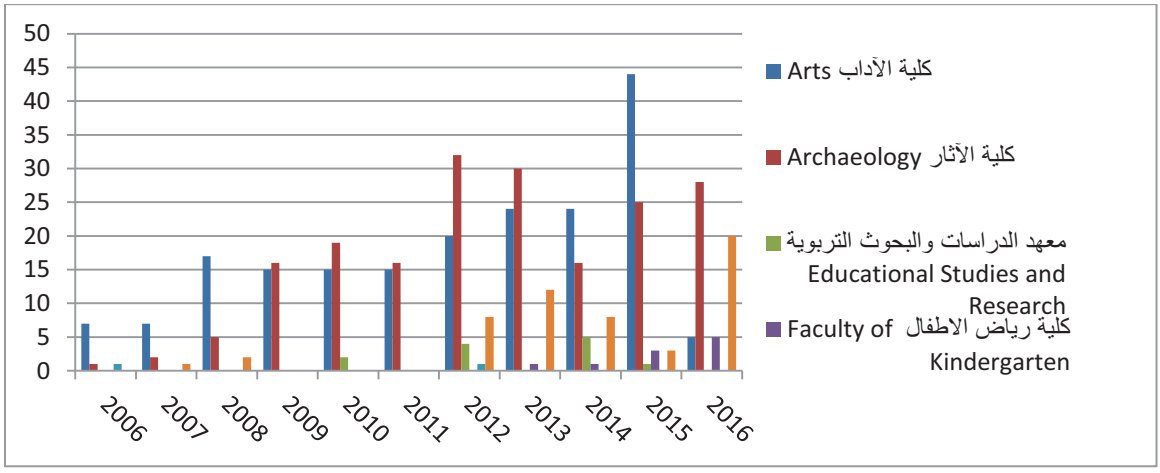

## الأبحاث المنشورة دوليا من ٢٠٠٦ الى ٢٠١٦ لكليات ومعاهد قطاع العلوم الانسانية

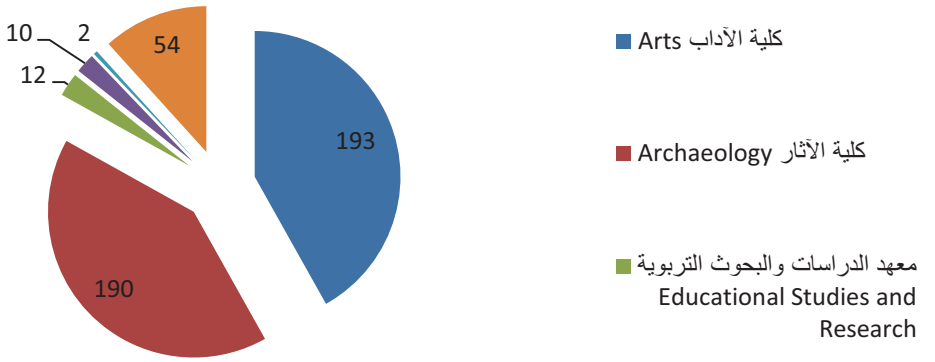


## تطور مجموع الأبحاث المنشورة لكل سنة
## Sum of published researches

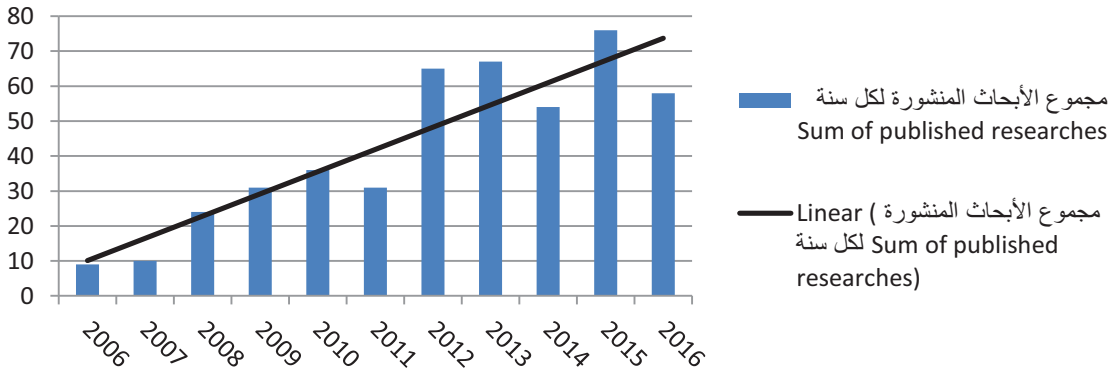

## Faculty of Arts

***Dept. of French Language and its Literature***

### T-1. Histoire et Symbolique Architecturale: Lecture du Compagnon du Tour de France de George Sand

Rania Gado

*Australian Journal of French Studies, 53: 205-219 (2016)*

This article examines the symbolic treatment of architecture in Le Compagnon du Tour de France, a historical novel by George Sand published in 1840. The novelist creates an architectural space which allows us to read the political history of her age and the social conflicts within it. Thus, the castle of the Villepreux family appears not as a solid block but as a torn edifice where different time-frames intertwine. It evokes the past through its nature as a ruin, it suggests the present through the restoration of the chapel, and it announces the future through its building sites. Inhabited by socially different characters, the manor becomes a place which reflects the complex relations between social classes.
**Keywords:** Historical novel; Architecture; Ruin; Restoration.

## Faculty of Archaeology

***Dept. of Conservation***

### T-2. Calcium Carbonate Precipitation Induced by Ureolytic Bacteria Bacillus Licheniformis

Fatma M. Helmi, Hemdan R. Elmitwalli, Sherif M. Elnagdy and Abeer F. El-Hagrassy.

*Ecological Engineering, 90: 367-371 (2016) IF: 2.74*

In this study, we report a novel approach for preparing precipitated calcium carbonate for the first time by Bacillus licheniformis using different types of media containing urea as a source of urease enzyme and for the first time using particles of pure calcium. The bacteria used in this study produced urease which catalyzes the hydrolysis of urea (CO(NH2)2) into ammonium (NH4) and carbonate (CO32−) leading to the precipitation of calcium carbonate. Calcium carbonate precipitation was experimentally studied by spontaneous precipitation at various pH (8–12), temperatures (30, 35, 40, 45, 50 °C), and at different concentrations of urease enzyme (1, 5, 10 mg mL−1). The XRD results showed a mixture of calcite and vaterite. The morphology of calcium carbonate particles prepared was studied under SEM after using it as a bioconsolidation of degraded fresco wall paintings.
**Keywords:** Biomeniralization; Calcium carbonate; Ureolytic bacteria; Bacillus licheniformis; Calcium particles; Bioconsolidation.

### T-3. Antifungal Activities of Two Essential Oils Used in the Treatment of Three Commercial Woods Deteriorated by Five Common Mold Fungi

Mohamed Z.M. Salem, Yassin E. Zidan, Maisa M.A. Mansour, Nesrin M.N. El Hadidi and Wael A.A. Abo Elgat.

*International Biodeterioration and Biodegradation, 106: 88-96 (2016) IF: 2.429*

In the past ten years natural extracts have been used as important potential applications to prevent mold growth on in-service wood. The growth of fungal hyphae of five common mold fungi (Alternaria alternata, Fusarium subglutinans, Chaetomium globosum, Aspergillus niger, and Trichoderma viride) on wood surface of Pinus sylvestris, Pinus rigida and Fagus sylvatica treated with the essential oil (EO) of P. rigida (wood) and Eucalyptus camaldulensis (leaves) was visually estimated. EOs were applied by vapor method and the mold growth inhibition was measured. The chemical constituents of the EOs was analyzed by GC/MS, which referred to the presence of α-terpineol (34.49%), borneol (17.57%), and fenchyl alcohol (14.20%) as the major components in P. rigida wood oil, and eucalyptol (60.32%), α-pinene (13.65%), and γ-terpinene (8.77%) in E. camaldulensis leaves. Complete inhibition against the growth of A. alternata, F. subglutinans, C. globosum, and A. niger except of T. viride by applying P. rigida wood EO at 5000 ppm and complete growth with all the studied fungi except of C. globosum at 156.25 ppm was found. Good inhibitions against C. globosum at 5000 ppm and 156.25 ppm and no inhibition against A. niger and T. viride and little inhibition against F. subglutinans at high concentration was found by the application of EO from E. camaldulensis leaves. These findings support the potential use of the EOs for wood protection against mold infestation for surface-treatment or fumigation of wood products.
**Keywords**: Commercial woods; Wood mold fungi; Biodeterioration; Antifungal activity; Essential oils.

### T-4. Evaluation of Usage Three Natural Extracts Applied to Three Commercial Wood Species Against Five Common Molds

Mohamed Z.M. Salem, Yassin E. Zidan, Nesrin M.N. El Hadidi, Maisa M.A. Mansour and Wael A.A. Abo Elgat.

*International Biodeterioration and Biodegradation, 110: 206-226 (2016) IF: 2.429*

Natural extracts have become of high interest in the past ten years for their inhibiting the growth of molds over wood and wood products surfaces in service or during the storage of building materials. In the present study, the antifungal effects of three natural extracts applied to three woods against five common molds were assessed. The growth of fungal hyphae of Alternaria alternata, Fusarium subglutinans, Chaetomium globosum, Aspergillus niger, and Trichoderma viride on the surfaces of Pinus sylvestris, Pinus rigida and Fagus sylvatica woods treated with extracts of Pinus rigida (heartwood), Eucalyptus camaldulensis (leaves) and Costus speciosus (rhizomes) was visually estimated. GC/MS and FTIR analyses were used to identify the chemical constituents and the functional groups of extracts. aterpineol (24.91%), borneol (10.95%), terpin hydrate (9.60%), D-fenchyl alcohol (5.99%), and limonene glycol (5.05%), which are the main constituents of P. rigida heartwood methanol extract. The main chemical compounds of methanol extract from Eucalyptus camaldulensis leaves were spathulenol (18.89%), cryptone (5.79%), 4,6,6-trimethyl-2-(3-methylbuta-1,3-dienyl)-3-oxatricyclo [5.1.0.0(2,4)] octane (5.79%), (3,3-dimethylcyclohexylidene)-(E)-acetaldehyde (5.57%), and ascaridole (4.32%). The main constituents identified in the distilled water extract from Costus speciosus rhizomes were meso-erythritol (12.21%), methyl-2-methyl-1,3-oxothiolan-2-yl-ketone (11.61%), (all-Z)-5,8,11,14,17-eicosapentaenoic acid-methyl ester (9.74%), diosgenin (5.07%), 2-ethyl-3-hydroxy-4H-

pyran-4-one (4.43%), 30 ,40 ,7- trimethylquercetin (3.17%), and digitoxin (2.77%). Wood specimens treated at the level of 2% concentration of P. rigida heartwood extract observed good inhibition to the mold growth under laboratory conditions. These findings support the potential use of natural extracts for natural wood protection against mold infestation for surface treatment of wood. The results indicate that wood extracts may be useful for reducing the incidence of mold on wood products, but none of the materials evaluated completely inhibited the test fungi. These extracts may provide a useful value-added application for byproducts of lumber production from these species

**Keywords**: Biodeterioration; Natural extracts; Commercial woods; Molds; Antifungal activity.

## T-5. Surface and Stratigraphic Elemental Analysis of an Ancient Egyptian Cartonnage Using Laser-Induced Breakdown Spectroscopy (Libs)

O. Aied Nassef, Harby E. Ahmed and M. A. Harith

*Analytical Methods, 8: 7096-7106 (2016) IF: 1.915*

An archeological Egyptian cartonnage dating back to the Greco-Roman period around the third century BC was elementally analyzed via the sample-friendly technique, Laser-Induced Breakdown Spectroscopy (LIBS). The unique characteristics of LIBS as being a simple and fast technique, has been exploited to obtain surface elemental distribution and depth profiles for the investigated sample. An Nd:YAG laser operating at the fundamental wavelength of 1064 nm has been used as the excitation source along with an echelle spectrometer coupled to an ICCD detector for spectral dispersion and detection. Under the experimental conditions, four distinct regions were studied as ten elements were analyzed for spatial distribution along the surface and also for their depth profiles. Rapid and comprehensive visualization of the investigated regions are provided. The most relevant elements i.e. carbon, calcium, silicon, oxygen and iron suggest that the cartonnage was manufactured via the traditional method, mainly dependent on natural pigments such as metal oxides and calcium carbonate (calcite) which is consistent with the previous results of other conventional techniques used in the field of Archaeology. Supporting studies obtained by both scanning electron microscopy with energy dispersive X-ray micro-analysis (SEM-EDX) and X-ray diffraction (XRD) have been presented for comparison purposes.

**Keywords:** LIBS; Cartonnage; Elements; Pigments; Historic; SEM-EDX.

## T-6. Implementation of Spectroscopic Techniques for Characterization of Icons of Deir El Sankoria, El Minia, Egypt

Gomaa Abdel-Maksoud, Yousry M. Issa and Mina Magdy

*Measurement, 91: 210-220 (2016) IF: 1.742*

Four icons from church of Saint Theodore El Shatby, Deir El Sankoria, El Minia, Egypt, have studied by micro-destructive spectroscopic methods: Attenuated Total Reflection–Fourier Transform Infrared Spectroscopy (ATR–FTIR), Raman Spectroscopy (RS), Field Emission Scanning Electron Microscopy– Energy Dispersive X-ray Spectroscopy (FESEM–EDX), X-ray Photoelectron Spectroscopy (XPS) and Inductively Coupled Plasma–Optical Emission Spectroscopy (ICP–OES). This study gave information about the materials used in the icons painting, state of the icons, and evaluation of the effect of environmental conditions. ATR–FTIR and Raman methods showed the characteristic bands of lithopone and lead white as a ground material, gum Tragacanth as a binder, and chrome oxide green, mars yellow, mars red as a pigment. EDX microanalysis exhibited the elements of mars yellow and mars red pigments, and ICP–OES method showed the concentration of chromium element that is characteristic for chrome oxide green pigment. The results were authenticated by XPS method to ensure the materials used in the painting. SEM images showed the cracking of the paint surface. Degradation of the chemical structure of gum Tragacanth binder was attributed to metal oxides of the pigments in presence of sunlight and artificial light which led to promotion of the oxidation process and then deterioration of the painting through peeling of the painting surface and cracking of the paint film.

**Keywords:** Icon; Spectroscopic techniques; Deterioration; Characterization.

## T-7. A Preliminary Study on Using Linseed Oil Emulsion in Dressing Archaeological Leather

Rushdya Rabee Ali Hassan

*Journal of Cultural Heritage, 21: 786-795 (2016) IF: 1.533*

The main goal of this study was to study and evaluate the effect of linseed oil and glycerine emulsion a surface treatment on appearance and chemical composition of archaeological leather samples, which were taken from a historical leather book binding back to 1858, 1653 & 1472 A.D, have been treated with linseed emulsion then a visual assessment, pH measurements, thermal analysis methods (TGA), infrared spectroscopy (FTIR) study and mechanical properties determination were undertaken, to see if any significant structural or chemical differences could be detected between “untreated” and “treated” leather. No dramatic changes in functional groups on the leather surface, as monitored by infrared spectroscopy, occurred in the samples before and after treatment; pH values, however, show that emulation may give good results in decreasing the acidity of the treated leather. The emulsion enhanced thermal & mechanical properties of treated samples.

**Keywords:** Archaeological leather; Linseed oil; Thermal analysis (Tg); Ph value; Dressing.

## T-8. A New Method for the Preparation of Gelatin Nanolayer: A Possible Approach to the in Situ Consolidation of Damaged Gelatin Photographic Emulsions

Maha Ahmed Ali and Mona Fouad Ali

*Applied Physics A: Materials Science and Processing, 122:552: 1-6 (2016) IF: 1.444*

A major objective of all conservation treatments is to increase the physical and chemical stability of the objects being treated. Given that photographic gelatin emulsions are highly susceptible to different forms of damage such as flaking, cracking, and powdering, consolidation treatments often form an important part of the stabilization process. The application of nanomaterials is a new approach in photograph conservation, which will hopefully

enable the control of the properties of traditional consolidants, thus improving their performance. In this study, gelatin nanoparticles and nanolayers were prepared and characterized by scanning electron microscopy, transmission electron microscopy, and dynamic light scattering for testing on damaged gelatin emulsion. The nanolayers were prepared by a two-step desolvation method, in order to obtain gelatin nanoparticles, followed by a third step involving rapid solvent evaporation. The prepared particles were found to have a spherical shape with sizes varying from 33 to 216 nm and a mean size of 42 nm depending on the conditions of synthesis. This research showed that both pH and temperature are very effective on particle size. Further studies are being planned to evaluate the benefits and potential problems of in situ consolidation of damaged gelatin emulsion using gelatin nanolayer technique.

**Keywords**: Silver gelatin prints; Damage; Consolidation; Nanolayer; Sem; Tem; DLS.

## T-9. The Use of Chitosan in Protecting Wooden Artifacts from Damage by Mold Fungi

Rehab El-Gamal, Efstratios Nikolaivits, Georgios I. Zervakis, Gomaa Abdel-Maksoud and Evangelos Topakas

*Electronic Journal of Biotechnology, 24: 70-78 (2016) IF: 1.403*

**Background:** Many buildings in Egypt e.g. museums, mosques and churches, do not possess controlled environments for minimizing the risks of damage of wooden artifacts due to the growth of fungi. Fungal damage usually appears as change in wood color, appearance of stains, and sometimes deformation of wooden surfaces. In this study we focused on the effect that some fungi exert on the properties of wooden artifacts and evaluated the effectiveness of different concentrations of chitosan on their protection against damage by mold fungi. **Results:** Samples were collected from different monuments and environments, and fungi growing on them were isolated and identified. The isolated Penicillium chrysogenum, Aspergillus flavus and Aspergillus niger strains were used for the infestation of new pitch pine samples. The results revealed that the lightness of samples infected with any of the tested fungi decreased with increasing incubation times. XRD analysis showed that the crystallinity of incubated samples treated individually with the different concentrations of chitosan was lower than the crystallinity of infected samples. The crystallinity index measured by the first and the second method decreased after the first and second months but increased after the third and fourth months. This may due to the reducing of amorphous part by enzymes or acids produced by fungi in wooden samples. **Conclusions:** The growth of fungi on the treated wood samples decreased with increasing the concentration of chitosan. Hence, it was demonstrated that chitosan prevented fungal growth, and its use could be recommended for the protection of archeological wooden artifacts.

**Keywords**: Archeological wood; Crystallinity index; Damage of wooden artifacts; Chitosan protection; Filamentous fungifungal damage; Prevention of fungal growth; Uv spectrophotometry; Wood deterioration; Xrd.

## T-10. Alternative Lime Based Grouts Used in Re-Pointing of Deteriorated Ancient Mortars and their Structural Effects on Composite Unreinforced Masonry Walls of Mekaad Radwan, Ottoman Cairo, Egypt (Case Study)

Mona F. Ali, Abubakr Moussa and Mahmoud Abdelhafez.

*Procedia - Social and Behavioral Sciences, 225: 410-420 (2016)*

Mortars and plasters of Mekaad Radwan are badly affected by decay hazards, therefore; they were studied by means of XRD and polarized microscope to detect their chemical composition, physical and petrographic properties, in addition to identify their characteristics. The analyses revealed gypsum mixed with lime as dominant component with some aggregates of sand particles, sodium chloride was detected in all the studied samples. Standardized alternative mortars were prepared, exposed to artificial aging and tested in order to select the most suitable type to replace the old mortars and plasters at Mekaad Radwan.

**Keywords**: Mekaad radwan; Building materials; Xrd; Polarized microscope; Alternative mortars; Lime based grouts; Re-pointing

## T-11. An Investigation of the Biological Fungicidal Activity of Some Essential Oils Used as Preservatives for a 19th Century Egyptian Coptic Cellulosic Manuscript

Wafika Nashyua, Eman Osman and Maisa Mansour

*International Journal of Conservation Science, 7(1):41-56 (2016)*

The main goal of this work was to investigate the biological fungicidal activity of some commercial essential oils of tea tree, lavender and thyme, which were to be applied as alternative preservatives for ancient manuscripts. To achieve our goal, model samples of cellulosic paper were made to mimic the original manuscript, which was a Coptic manuscript known as Pascha (the sacred week), dated 1812. Twenty-three microorganism strains were isolated representing twelve fungal taxa and one bacterial taxa which were identified in all collected and analyzed in samples, which included Trichoderma viride, Penicillium roqueforti, Eurotium chevalieri, Aspergillus flavus and Bacillus subtilis. A scanning electron microscope (SEM) was used to investigate the growth of the associated microorganisms and their effect on the sample paper structure. Different concentrations of the aforementioned essential oils were applied on the mimic samples, which were then subjected to accelerated ageing corresponding to 25 or 50 years of a natural one. To characterize the applied oils on the samples, we made records by using FTIR-ATR, color measurements according to CIELAB system, and analyzed the mechanical properties of the tested samples. The results revealed that the samples treated with either tea tree oil or lavender oil, had δE values that decreased as the oil concentration increased. However, when samples were treated with thyme oil the reverse was obtained. For the treated samples exposed to 25 years of light ageing, we noticed that the higher obtained tensile strength and % elongation of treated samples followed the ranking order: thyme > lavender > tea tree oils. For the treated samples that were exposed to 50 years of natural light ageing, we observed that almost all tensile strength and elongation values of the treated samples were higher than that of the untreated ones. Moreover, we noticed that the inhibition of growth of the microorganisms was obtained at a low concentration of tea tree

oil (0.25% v/v). This treatment was esthetically acceptable for archaeological objects, because it was colorless, transparent and safe. Based on the results we obtained, the optimized essential oil, which is the oil with an appropriate concentration, was selected to be added to the cellulosic pulp used for the leaf casting. Moreover, the same optimized essential oil was applied on the paper samples to be used as separators between the ancient manuscript pages. After dismantling, cleaning, leaf casting and rebinding of the damaged parts, the manuscript is then preserved.
**Keywords**: Essential oil; Fungicidal; Coptic manuscript; Leaf casting; binding; Conservation.

## T-12. Analysis of Archaeological Bones from Different Sites in Egypt by a Multipletechniques (Xrd, Edx, Ftir)

Gomaa Abdel-Maksoud and Alaa El-Sayed

*Mediterranean Archaeology and Archaeometry, 16 (2) :149-158 (2016)*

Archaeological bones were collected from different sites and conditions in Egypt to be analyzed by multitechniques to determine the reaction of bones in different burial environments (dry and moist conditions). Different analytical techniques have been used to accurately recognize archaeological bones such as X-ray diffraction, energy dispersive X-ray (EDX) and Fourier transform infrared spectroscopy (FTIR). The results revealed that XRD confirms that all bone samples taken from archaeological sites have high crystallinity. EDX analysis showed different types of elements. It also proved the increasing of calcium and phosphor elements in archaeological samples compared to the control sample. FTIR indicated deterioration of amides groups compared to the control sample.
**Keywords**: Archaeological bone; Deterioration; Analysis; Xrd; EDX; FTIR.

## T-13. Analytical Study and Conservation of Gilded Mummiform Cartonnage from the Grecoroman Period in Cairo Museum

Mona F. Ali, Ahmed M. El Sheikh and Alaa E. Ali

*Mediterranean Archaeology and Archaeometry, 16(2): 127-137 (2016)*

The state of preservation of the Cartonnage collection stored in the basement of the Egyptian museum in Cairo, is very poor; it is suffering biodeterioration as a result of inappropriate storage. The analytical techniques utilized in this study : optical microscopy (OM), Scanning Electron Microscopy (SEM) equipped with an energy dispersive X-ray detector (EDS), X-ray diffraction (XRD), and Fourier transform infrared spectroscopes (FTIR). These analytical techniques aim to specify the layer structure of the cartonnage (preparation layer, painted layer and gilded layer),they also identify the adhesives used to paste the layers of textile and in binding pigments and gilding. The treatment plan started with consolidating the fragile parts, removing the cotton bandages which we used to maintain the shape of the mask. Japanese tissue adhered with Klucel G is used to support the mask. Lenin ruptures were fixed and consolidated using Chitosan 5%.
**Keywords**: Cartonnage; Pigments; Storage; Gilded; Linen; Consolidation; Ruptures; Refilling.

## T-14. Characterization of Archaeological Wood Stained with Bat Excretions Using Various Analytical Techniques

Mourad Fawzy

*International Journal of Conservation Science, 7(3): 647-658 (2016)*

This study was conducted to diagnose and evaluate the deterioration of archaeological wood caused by bat excretions. The samples were collected from the ceiling of Mohamed Ali palace (1812), which is located in Suez, and Baron Empain palace (1911), which is located in Cairo, Egypt. The wooden samples were covered with a preparation layer (gesso) on one side. Parts from both sides of the wooden samples that suffered from the accumulation of bat excretions were examined. The effects of bat excretions on the anatomical structure and chemical composition of the wooden samples were examined and evaluated using various analytical methods, such as scanning electron microscopy (SEM), Fourier transform infrared spectroscopy (FTIR), and X-ray diffraction (XRD). In addition, a microbiological study was undertaken to identify microbial activity on the wood surface. The results showed that the wood suffered changes in its anatomical structure in addition to scratches on the wood surface that were caused by the bats' claws. Changes in the molecular bonds of both lignin and cellulose were noted in the wood. In addition, the polymerization degree of cellulose was reduced
**Keywords**: Archaeological wood; Bat excretion; Sem; Ftir; Xrd; Microbial activity.

## T-15. Evaluating Laser Cleaning of Corroded Archaeological Silver Coins

Omar Abdel-Kareem, Awad Al-Zahrani, Amal Khedr and Mohamed Abdel Harith

*Mediterranean Archaeology and Archaeometry,16:135-143 (2016)*

The present work aims at evaluating the use of laser in cleaning and analysis of archaeological corroded silver coins. The selected corroded silver coins used in this study have been excavated from burial soil in Najran excavation site where there were more than 2500 rare coins dating back to pre-Islamic eras.. Laser cleaning tests were performed on 2 different types of corroded coins using a Q-switched Nd: YAG laser at 1064 nm. LIBS diagnostics was used to monitor the laser ablation process during the removal of different kinds of corrosion products with the aim of stopping the process once the cleaned surface is reached. XRD analysis was done to characterize the corrosion crust on the coin surface. For evaluating the usefulness of using laser in this study for analytical and cleaning of the selected corroded coins, the same coins were investigated, before and after laser cleaning, with (SEM - EDX). The results showed that for analysis of the corrosion products on the crust on the surface of coin, the best LIBS spectra have been obtained after the first laser shot. The number of laser shots needed for surface cleaning depends essentially on the corrosion layer thickness. Only 5 laser shots were needed for the removal of thin corrosion layers while for thick layers 15 laser shots were used. Laser is successful, effective and safer cleaning technique for removing corrosion products of the studied archaeological coins.

**Keywords**: Laser cleaning; Nd: YAG laser; Corroded archaeological silver coins; Corrosion products; Xrd; Sem-edx; Libs.

## T-16. Evaluating the Use of Laser in Analysis and Cleaning of the Islamic Marine Archaeological Coins Excavated from the Red Sea

Omar Abdel-Kareem, A.Al-Zarani, Amal Khedr and M. Abdel Harith

*International Journal of Conservation Science, 7, (2): 511-522 (2016)*

This study aims to evaluate the use of laser in cleaning and LIBS analysis of the Islamic Marine Archaeological coins excavated from under the Red Sea water. Laser tests using a Q-switched Nd:YAG laser at 1064 nm were performed on 2 different types of corroded coins. For evaluating the usefulness of the suggested setup protocol of laser used in this study, the coins taken into study were investigated, before and after the laser cleaning, with Scanning Electron Microscope with attached energy-dispersive x-ray analyzer (SEM-EDX). The results show that the number of shots of LIBS is a very important task while acquiring LIBS spectra. The first shot is very useful for investigating the corrosion layer. The fourth and the fifth shot are useful for investigating the core of the coins with a medium layer of corrosion. The second shot is the best for the coins covered with very thin layers of tarnish. This study confirms that the fifth shot (20 pulses) is the best condition to clean the coin with a medium layer of corrosion, while the second shot (2 pulses) is the best condition to clean the coin with a very thin layer of corrosion.
**Keywords**: Marine archaeological coins; Laser cleaning; Nd:YAG laser; LIBS; SEM-EDX.

## T-17. Examination and Analyses of a Wooden Face a the Museum Storage at the Faculty of Archaeology, Cairo University

Yassin Zidan, Nesrin N.M. El Hadidi and Mohamed

*Mediterranean Archaeology and Archaeometry,16(2):1-11 (2016)*

The aim of this paper is to examine and analyze a wooden face that was covered with a transparent layer of wax after finishing the mask. The use of wax and encaustic painting was used in Ancient Egypt during the Greco – Roman period, but it was an extremely rare technique in the Egyptian dynasties. The wooden face that was chosen for this study was carefully examined using light microscopy to identify the wood, which proved to be native sycomore fig (Ficus sycomorus). Digital microscope and Scanning Electron Microscope (SEM) were used to assess decay of the outer exposed surface that had been covered in the past with a preparation layer composed of calcium carbonate. SEM micrographs showed clear decay of the cell walls due to the penetration of both the preparation layer and fungal hyphae. Microbiological investigation indicated the presence a bacterial and fungal infestation. The wood was infected infected by Aspergillus niger and Ulocladium sp fungi and Pediococcus dextrinicus bacteria. Further assessment was done by X- Ray Diffraction (XRD) to calculate the decrease of cellulose crystallinity according to Segal and Fourier Transform spectroscopy (FTIR) to detect the changes of the main wood components (cellulose, hemicellulose, lignin).

**Keywords**: Wood decay; XRD; FTIR; SEM; Microbiology; Cellulose crystallinity.

## T-18. Geognostic Investigation on Damage and Deterioration Evolution of Soil and Architectural Materials of Mekaad Radwan, Ottoman Cairo, Egypt (Case Study)

Mona F. Ali, Mahmoud Alnabaawy, Abubakr Moussa and Mahmoud Abdel Hafez

*Procedia - Social and Behavioral Sciences, 225: 421-432 (2016)*

This study determines which factors play roles of deterioration in Mekaad Radwan. The study also makes it possible to know the real response of the masonry structure to the deformation imposed at the base of the foundation condition. The used methodology included the identification of the seismicity situation and the possible damage effects of the Cairo (1992) earthquake through discussion of situation before and after earthquake as well as the controlling factors, in addition to the analysis and determination of the types, geometry of the types, deformation and other deterioration patterns, using the direct observation and primitive monitoring evaluation.
**Keywords**: Mekaad radwan; Geognostic investigation; Deterioration evolution; Seismicity situation; Architectural materials.

## T-19. Investigation the Microbial Deterioration of Sandstone from the Osirion's Sarcophagus Chamber as Affected by Rising Ground Water Level

Abdou A.O.D. El-Derby Maisa M.A. Mansour and Mohamed Z.M. Salem

*Mediterranean Archaeology and Archaeometry,16 : 273-281 (2016)*

In the present study, the microbial deterioration of sandstone from the Osirion's Sarcophagus Chamber as affected by rising ground water level was investigated by means of SEM micrograph of fungal hyphae, X-ray diffraction (XRD), and Energy-dispersive X-ray spectroscopy (EDX). The following Fungi; Cladosporium cladosporioides, Aspergillus terreus, Curvularia lunata, and Acremonium falciforme were identified on the deteriorated stone surfaces and these findings were tested by SEM investigations. The hyphae penetration of the identified microfungi caused mechanical exfoliation of building stone material as well as changing in color.
**Keywords**: Biodegradation; Osirion's sarcophagus; Fungi; sandstone.

## T-20. Microscopic Investigation for Condition Assessment of Archaeological Bones from Different Sites in Egypt

Gomaa Abdel-Maksoud and Alaa El-Sayed

*International Journal of Conservation Science, 7(2): 381-394 (2016)*

Bones are found in different archaeological sites in Egypt. The bones samples examined in this study were collected from eight archaeological sites and two museum store houses. The samples

were collected from different environments (dry and moist). Collected samples suffer from adverse deterioration, which was mainly due to burial environments. Many aspects of deterioration are found on the surface of the bones such as darkness, stains which may be derived from different sources, pitting etc. This study focuses on the changes that occur on the surface of bones in burial environments and in museum storehouses. Digital, optical, polarized and scanning electron microscopes were used to evaluate studied samples. (The results revealed that most environmental conditions in most locations let to many aspects of deterioration) such as pitting, erosion, change of color and etc. Humid environmental are more aggressive on the studied bone samples than dry conditions.

**Keywords**: Bones; Archaeological sites; Deterioration; Microscopy.

## T-21. Nanocomposites for the Protection of Granitic Obelisks at Tanis, Egypt

Fatma M. Helmi and Yasser K. Hefni

*Mediterranean Archaeology and Archaeometry, 16:87-96 (2016)*

Granite has widely been used in the fields of architecture and sculpture in Egypt, especially in the carving of obelisks, which were one of the most important features of ancient Egyptian civilization. Many granitic obelisks of Ramses II, were found in the ancient city Tanis (San el-Hagar), Nile Delta, Egypt, that has been considered one of the most important ancient Egyptian cities. Unfortunately, the granitic obelisks at Tanis have been subjected to many deterioration factors, which resulted in numerous deterioration aspects, such as granular disintegration, scaling or spalling, cracking, efflorescence, soiling, microbiological colonization. From this standpoint, the materials which are used in the protection of those granitic obelisks must have the property of hydrophobicity in order to protect them from the harmful effects of water. In the last decade, polymer-nanoparticle composites have attracted great interest in the field of culture heritage conservation due to their unique multifunctional properties, resulting from the high surface area and chemical activity of the nanoparticles dispersed in the polymers. In this paper, three types of nanocomposites (PF 4, Fluotanium, Fluozinc) were used for the protection of granitic samples collected from Tanis. The petrographical, mineralogical, and chemical study of the granitic samples were determined by means of polarizing microscope, X-ray diffraction, and X-ray fluorescence, respectively. The properties of the treated samples were estimated by visual examination, colormetric measurements, static water contact angle, total immersion water absorption, abrasion resistance, scanning electron microscope, and self-cleaning test. The durability of the nanocomposites used in this study was evaluated by repeating the measurement of static water contact angle for the treated granitic samples after exposure to ultraviolet irradiation.

**Keywords**: Nanocomposites; Granite; Protection; Obelisks; Hydrophobicity; Water contact angle; Superhydrophobic; Self-cleaning; Tanis.

## T-22. Non-Linear Static Analysis and Seismic Performance of Modern Architectural Heritage in Egypt

Sayed Hemeda

*Mediterranean Archaeology and Archaeometry, 16.3:1-16 (2016)*

The objective of this paper is the investigation of the behavior of historic masonry structures subjected to static and seismic forces and the formulation of numerical models for use in structural analysis. The case study presented herein regards the seismic analysis of El-Sakakini palace (1892 AC) in Cairo, Egypt (damaged by the earthquakes occurred in 1992 and 1995). Firstly, we collected all data regarding the site, the geometry of manufact, the characteristics of materials of construction, the structure and the soil medium, etc. The paper presents the next part which includes the investigation of the static and seismic performance of these structures according to statistical data from recent earthquakes and finally the development of an analytical model of describing their performance. An analytical, plasticity-based Model is presented for the inelastic analysis of traditional masonry structures. The proposed Model is applied to the analysis of the El-Sakakini palace in Cairo. A non-linear model is developed, aiming to capturing the key in elastic mechanisms. The analytical model is implemented in the finite element code Autodesk Robot™ Structural Analysis Professional and validated against experimental results. The results obtained suggest that for such structures non-linear static analysis provides a reasonable prediction of damage at the base of the palace, but is not however suitable for predicting the overall damage along the palace‘s entire height. The conclusive aim of the project is then to develop guidelines for the evaluation of the static and seismic vulnerability of historic masonry palaces. Ultimately, the analysis presents the optimal structural interventions to remedy the existing damage, also to prevent the formation of the same mechanisms under the action of future earthquake.

## T-23. The Adobe Barrel Vaulted Structures in Ancient Egypt: A Study of Two Case Studies for Conservation Purposes

The Abdou A.O.D. El-Derby and Ahmed Elyamani

*Mediterranean Archaeology and Archaeometry,16:295-315(2016)*

This research aims at throwing the light on one of the few survived examples of Ancient Egyptian vaulted structures; those are the storerooms of the temples of the Ramesseum and Sety I built in the 13th century BC. In the first case, only some of the adobe vaults and walls are still standing; whereas in the second case all the vaults collapsed and only the walls exist. Due to lack of maintenance and also scientific research on this topic, the survival remains may be lost forever. The research started with tracking the chronological development, the architecture and the construction of the adobe barrel vault in Ancient Egypt. The two case studies of the research were visually inspected and the existing damage symptoms and causes were reported and investigated. A structural analysis were carried out to understand the structural behavior and the causes of damage. Finally, a number of interventions were proposed that may help the existing ruins to survive.

**Keywords:** Adobe; Vault; Storerooms; Ramesseum temple; Sety I temple; Damage; Conservation.

## T-24. Using Nanocomposites in the Consolidation and Protection of Sandstone

Fatma Mohamed Helmi and Yasser Kamal Hefni

*International Journal of Conservation Science, 7: 19-40 (2016)*

In the last few years, nanoparticles have widely been used in the field of restoration and conservation of artworks. The minimizing of particles size into nanoscale, results in better properties from the large grain size materials of the same chemical composition. In this paper, pure and nanoparticles modified silicon-based polymers, were used to consolidate and protect sandstone samples. Silicon dioxide ($SiO_2$), and zinc oxide (ZnO) nanoparticles, were added to different types of the silicon-based polymers (Wacker OH 100, Dow Corning MTMOS, Mega Protec 1, Mega Protec 2) in order to improve their physiochemical and mechanical properties, which produced a significant improvement in the ability of the polymers to consolidate and protect the stone. The properties of the treated sandstone samples were evaluated comparatively by visual appraisal, colorimetric measurements, measuring of static contact angle of water droplets on the surface of the samples, total immersion water absorption, compressive strength, and scanning electron microscope. Results demonstrated that the addition of nanoparticles to silicon-based polymers enhanced their capability to consolidate and protect the sandstone samples.

**Keywords:** Nanoparticles; Silicon dioxide; Zinc oxide; Hydrophobic; Superhydrophobic; Nanocomposites.

### *Dept. of Egyptian Archaeology*

.

## T-25. Pottery: Prelimenary Report in M. Bommas, "Qubbet El-Hawa, 2016"

Emarr Khalifa

*The Journal of Egyptian Archaeology, 102: 38-40 (2016)*

Report of two short field seasons of the joint University of Birmingham / Egypt Exploration Society mission at Qubbet el-Hawa in February and September 2016. In the area of the northern necropolis, below the upper terrace of rock cut tombs, three excavation areas were identified that have not been investigated before. Among the monuments unearthed are a protection wall close to the edge of the cliff, a causeway leading to this wall, and the long-sought causeway of Sarenput I. Amongst the finds presented here, two Middle Kingdom reliefs and pottery are discussed in further detail

**Keywords**: Qubbet; E-hawa pottery.

## T-26. The Visitors Graffiti in Two Tombs of Beni Hassan (Ameny and Khnumhotep II)

Khaled Hassan

*Journal of The American Research Center in Egypt, 52-1: 33-52 (2016)*

The tombs of Beni Hassan contain distinctive scenes of daily life, thus they have been attractive for both ancient and modern visitors. The hieratic graffiti that were left by the ancient visitors reflects the significance of these tombs. Thus, this article examines the New Kingdom visitors' graffiti in two tombs of Beni Hassan (Ameny and Khnumhotep II). It also sheds more light on the location of these graffiti on the walls and their connections with the original decoration of the tombs.

**Keywords**: Visitors; Geaffiti; Beni hassan; 18$^{Th}$ Dynasty.

## T-27. Three Shabtis of the Vizier Paser (UC39724-39726)

Ahmed Ouda

*Journal of The American Research Center in Egypt, 52: 303-318 (2016)*

This paper publishes three shabti figures of the vizier Paser held in the Petrie Museum of the Egyptian Archaeology (UC39724-39726), together with another nineteen shabtis which are dispersed in four Museums (Egyptian Museum Berlin, Louvre Museum, Metropolitan Museum of Art, Penn Museum). It presents a set of criteria by which to distinguish the shabtis of Paser from those of other individuals who have the same name. It also investigates the archaeological context of these three shabtis missing from Petrie's publication in 1935 and using these parallels, attempts to identify their provenance. The function of the shabtis of the vizier Paser is also examined.

**Keywords**: Vizier; Paser; Shabtis; Berlin; Louvre.

## T-28. Two Administrative Hieratic Ostraca from Deir El-Bahri (Late 20$^{Th}$ and Early 21$^{St}$ Dynasties)

Khaled Hassan

*Studien Zur Altägyptischen Kultur, 45: 125-136 (2016)*

The documents that were found at Deir el-Medina provided us with detailed information on the lives of the small group of people who were responsible for creating the royal tombs in the Valley of the Kings throughout Ramesside times. However, at the end of the 20$^{th}$ dynasty such documents were quite rare, particularly when the workmen moved to be resettled at the temple of Ramses III at Medinet-Habu and abandoned their village due to frequent disturbances. At the same time, it seems that they took the Temple of Hatshepsut at Deir el-Bahri as a new base of work. Many unpublished hieratic ostraca have been found in the same area and dated back to the same timeframe, in addition to the graffiti of the workmen that are scattered around the area of Deir el-Bahri and are also considered to be evidence for their activities. The current paper deals with two hieratic ostraca of the late 20th and early 21st dynasties. Ostracon 450 is a list of 22 names. Ostracon 524 is a necropolis journal that is an account of about 87 workmen from various places such as Abydos. They were most probably there to do specific tasks, other than erecting new royal tombs, an activity that had actually ceased.

**Keywords**: Ostraca; Deir el-bahri; Deir el-medina; Late hieratic.

## T-29. Un Roi Sheshonq À Hermopolis

Hassan Nasr el-Dine

*Journal of The American Research Center in Egypt, 52: 115-123 (2016)*

The subject of this paper is a piece of faience, restored at the Ashmounein magazine in Middle Egypt. This piece contains hieroglyphic inscriptions that mention the name and titles of a king Sheshonq. This is the only document that preserves the names and titles of that Libyan king at Touna el-Gebel.
**Keywords**: Touna el-gebel; Ashmounein magazine; King sheshonq; Faience; Hieroglyphic inscriptions; Libyan king.

## Faculty of Kindergarten

***Dept. of Essential Sciences***

### T-30. Numerical and Experimental Investigation on Co-Combustion Characteristics of Hydrothermally Treated Municipal Solid Waste with Coal in a Fluidized Bed

Liang Lu, T.M. Ismail, Yuqi Jin, M. Abd El-Salam and Kunio Yoshikaw

*Fuel Processing Technology, 154: 52-65 (2016) IF: 3.847*

This research describes numerical and experimental studies on the co-combustion characteristics of hydrothermally treated municipal solid waste (HT MSW) with coal by utilizing a bubbling fluidized bed (BFB) reactor. The developed model is supported by some experimental test on co-combustion of coal with HT MSW to simulate the combustion process in a BFB and to evaluate the possibility of co-combustion application in a BFB reactor with different MSW blending ratios. HT MSW mixing ratios of 10, 20, 30, and 50% are chosen and examined at 700, 800, and 900 °C to determine at which temperature coal could be substituted with the HT MSW regarding emissions, such as CO, SO2 and HCl. Emissions of NO, N2O, NH3 and HCN from the mixtures are measured, simulated, and contrasted with the results of only combustion of coal. Hydrodynamics and heat and mass transfer, along with reactions during combustion, e.g., coal/waste devolatilization, volatile combustion and char combustion, are taken into account. The results obtained in this part of the study ensure the possibility of accepting the mixing ratio of the hydrothermally treated MSW, co-combusted with coal up to 30% (wt.%) without major modification of the coal-fired BFB reactor. The simulation results are compared with experimental data, which show that the gas species versus time at different heights from the fluidized bed is reasonably simulated. This indicates that the numerical model presented is valid and provides a promising way to simulate the combustion of solid waste in a BFB, which is the predominant technology for co-combustion of waste. The advantage of the theoretical study lies in its ability to reveal features of the detailed structure of the combustion process inside a solid bed.
**Keywords:** Combustion modeling; HT MSW; Bubbling fluidized BED; COAL; CFD.

### T-31. Effect of Ash Content on the Combustion Process of Simulated Msw in the Fixed Bed

Rui Sun, Tamer M. Ismail, Xiaohan Ren and M. Abd El-Salam

*Waste Management, 48: 236-249 (2016) IF: 3.829*

This paper experimentally and numerically investigates the effects of ash content on the combustion process of simulated Municipal Solid Waste (MSW). A fixed-bed experimental reactor was utilized to reveal the combustion characteristics. Temperature distributions, ignition front velocity, and the characteristics of gas species' release were measured and simulated during the combustion process. In the present work, the two-dimensional unsteady mathematical heterogeneous model was developed to simulate the combustion process in the bed, including the process rate model as well as NOx production model. The simulation results in the bed are accordant with the experimental results. The results show that as ash content increases, the lower burning rate of fuel results in char particles leaving the grate without being fully burned, causing a loss of combustible material in the MSW in a fixed bed and therefore reducing the combustion efficiency and increasing the burning time of the MSW.
**Keywords:** Municipal solid waste; Ash content; Fixed-Bed combustion; Mathematical modeling.

### T-32. Influence of Simulated Msw Sizes on the Combustion Process in a Fixed BED: CFD and Experimental Approaches

Rui Sun, Tamer M. Ismail, Xiaohan Ren and M. Abd El-Salam

*Waste Management, 49: 272-286 (2016) IF: 3.829*

This work presents the effect of the simulated sizes of Municipal Solid Waste (MSW) on the combustion process in a fixed bed experimentally and numerically. The effect of temperature, gas emissions, flame front velocity and process rate are discussed for three different sizes of MSW: 10, 30, and 50 mm. The study found that for the operating conditions of the current model, when the diameter of particles is decreased, the bulk density of the material is increased, resulting in a decrease of convective heat transfer as well as combustion speed. As the diameter size of the material particles increase, the height of the post-combustion zone is increased, while the temperature in a high temperature area is decreased, due to the decrease in the material's bulk density and the excessive increase in porosity. Results also show that the average emission concentration of CO and CO2 decreases gradually with an increase in the particle diameter size.
**Keywords:** Municipal solid waste; Fixed-Bed; Combustion; Mathematical modeling; Simulated MSW Sizes.

### T-33. Eulerian – Eulerian Cfd Model on Fluidized Bed Gasifier Using Coffee Husks as Fuel

Tamer M. Ismail, M. Abd El-Salam, Eliseu Monteiro and Abel Rouboa

*Applied Thermal Engineering, 106: 1391-1402 (2016) IF: 3.043*

A two-dimensional CFD computational model has been developed to describe the gasification process of coffee husks within a fluidized bed reactor. The Eulerian - Eulerian method is used for both gas and solid phases to provide an explanation for mass exchange, energy, and momentum. The results were obtained after comparing both the numerical model and the experimental data for validation. The current model also predicts the effects of equivalence ratio and moisture content on gasification temperature, and provides sensitive analysis of the model of the produced syngas composition in addition to the higher heating value and cold gas efficiency. The simulated syngas composition was found to be in good agreement with the experiment. The high moisture content of coffee husk has

negative effects on cold gas efficiency and HHV, an effect that decreases as the equivalence ratio increases.
**Keywords:** Pilot scale gasification plant; CFD; Fluidized Bed gasifier; Equivalence ratio; Moisture content.

## Institute of African Research and Studies

### T-34. Serological, Molecular and Ultrastructural Studies on Tobacco Rattle Virus-Infected Potato Plants in Egypt

H.F. El-Kammar, O.M. El-Banna, A.H. Hamed, M.S. Abbas and A.K. El-Attar

*Journal of Plant Pathology, 98: 15-24 (2016) IF: 1.034*

The aims of the present study were to survey, isolate and identify Tobacco rattle virus (TRV) affecting potato plants under the Egyptian conditions. TRV was isolated from naturally infected potato during two successive seasons (2012-2013 and 2013-2014) in five Egyptian governorates. Symptomatic plants were tested by indirect enzyme linked immune sorbent assay (ELISA). The identity of the virus as TRV was confirmed by host range, modes of transmission, serological diagnosis and morphology of virus particles. RT-PCR was used for the molecular detection of TRV using specific primers. Cytopathological effects of TRV on potato plants were studied. The percentages of tuber transmission ranged from 35 to 55% and transmission by the nematode (Paratrichodorus spp.) reached 17.83%. The obtained results indicated that dot-blotting immune binding assay (DBIA) and tissue-blotting immune binding assay (TBIA) tests were useful to confirm the identification of the virus. Examination of dip preparation by electron microscopy (EM) revealed rod-shaped particles with average length 48-114 nm and 180-197 nm, and 22 nm width. EM analysis showed changes in nucleus, phloem tissue, mitochondria, cell wall, and chloroplast. According to the available data, this is the first isolation of TRV from potato plants in Egypt.
**Keywords:** TRV; Transmission; Serology; Electron microscopy; PCR

### T-35. Geochemical Characteristics of Organic Matter from Rudeis and Kareem Source Rocks, Ras Budran Oilfield, Central Gulf of Suez, Egypt

Mohamed M. El Nady, Fatma M. Harb and Naglaa S. Mohamed

*Energy Sources, Part A: Recovery, Utilization and Environmental Effects, 38-22: 3273-3282 (2016) IF: 0.358*

The organic matters of Rudeis and Kareem formation from Ras Budran oilfield in the central Gulf of Suez, Egypt, were investigated throughout the study of biomarkers and infrared spectrometric analyses. The results showed that Pr/Ph, Pr/n-C17, and Ph/n-C18 ratios indicated marine source organic matters deposited under reduced condition with a less effect of biodegradation and mature stage of occurrence. The gammacerane index indicated a low-salinity environment of deposition for the initial organic matters existed in the analyzed samples. Steranes distributions show high percentage of C28 steranes and C29 steranes compared with C27 steranes, and low-concentration C27 diasteranes show generally low ratios indicating anoxic carbonate source rocks. The diasteranes/steranes showed generally low ratios indicating most marine carbonate sources. The tricyclic terpane reflects mature organic matters and originated from marine organic sources.
**Keywords:** Egypt; Gulf of Suez; Organic matters; Ras budran Oilfield; Steranes; Tricyclic terpanes.

### T-36. Source Rocks Evaluation and Timing of Petroleum Generation of Selected Wells in Meleiha Area, North Western Desert, Egypt

Mohamed M. El Nady and Naglaa S. Mohamed

*Energy Sources, Part A: Recovery, Utilization and Environmental Effects, 38-9: 1246-1254 (2016) IF: 0.358*

Fifteen rock samples were subjected to comprehensive organic geochemical studies aiming to evaluate potential source rocks as well as to predict the time of petroleum generation and expulsion of Kharita, Alam El Bueib, and Khataba Fms. in some wells in Meleiha area. The study revealed the Kharita Fm. is immature and has fair potential to produce gas. The organic matter is derived from terrestrial origin. Alam El Bueib Fm. is mature with fair to good capability of producing mixed oil and gas. The organic matter is originated mainly from mixed organic sources. Khatatba Fm. is mature and has good potentiality for generating oil. The organic matter is derived mainly from marine origin. The geothermal profile revealed that Kharita Fm. reached only the early stage of hydrocarbon generation and did not enter the oil widow till the present time. Alam El Bueib Fm. entered the oil window during Late Eocene time. Khatatba Fm. entered the oil window during Late Cretaceous. Consequently, Khatatba Fm. in Meleiha area can be considered as effective source rocks for generating both oil and gas.
**Keywords:** Egypt; Gc; Gc/Ms; Geothermal models; Meleiha Area; Nwd; Rock-Eval/Toc Pryolysis.

### T-37. Source - Rock Potential of Miocene-Paleozeoic Sediments in Gh - 376 Oilfield, South Gulf of Suez, Egypt

Mohamed M. El Nady, Naglaa S Mohamed and Ahmed N Shahin

*Energy Sources, Part A: Recovery, Utilization and Environmental Effects , 38-1: 100-109 (2016) IF: 0.358*

Twenty-two ditch samples were collected from GH-376-1 well, representing the Miocene and Paleozeoic rocks of GH-376 oilfield in the South Gulf of Suez. These were subjected to TOC, S2, Tmax, HI, and OI, and gas chromatography analyses. The results showed that Kareem Formation source rocks are immature and have fair to good potential of type III/II of kerogen for generating mixed gas and oil, but mainly gas. The organic matters are derived mainly from marine contribution from algae and bacteria deposited under reducing environments. Rudies Formation is immature and has poor to fair potential of type II/III kerogen for generating gas. The organic matter is derived mainly from marine and terrestrial sources deposited under oxidizing-reducing environments. Sudr Formation has poor to fair potential of type III kerogen to generate gas. The organic matter has been derived mainly from terrestrial sources deposited under oxidizing conditions. Matulla Formation is immature and has good to very good potential for generating mixed oil and gas. The organic matter has originated mainly from mixed organic sources deposited under oxidizing condition. Nubia Formation has poor generating potential of type II/III kerogen for generating gas. The

organic matter was derived from mixed sources deposited under an oxidizing environment.
**Keywords:** Egypt; Gh-376-1 well; Gulf of suez; Hydrocarbon potenial; Maturation; Organic richness.

## T-38. Utilizing the Rock-Eval Pyrolysis and Biomarkers Parameters to Characterize the Organic Matters of Selected Wells in the Central Gulf of Suez, Egypt

Naglaa S. Mohamed and Mohamed M. El Nady

*Energy Sources, Part A: Recovery, Utilization and Environmental Effects, 38-21: 3158-3166 (2016) IF: 0.358*

Organic matters from the KK 85-1and HH 83-1wells in the Central Gulf of Suez were analyzed by two well-proven organic geochemical methods: Rock-Eval pyrolysis and gas chromatography–mass spectrometry (GC–MS) analyses. These techniques were used to obtain independent parameters of organic matter composition, thermal maturity, and environment of deposition. The study reveals a close concordance between Rock-Eval pyrolysis data and biomarkers parameters such as steranes and triterpanes. Rock-Eval pyrolysis in conjunction with GC–MS analyses shows that the organic matters contain two types of kerogen (Type-II/III and Type III), which lie dominantly prior to the peak stage of the conventional oil window (end of diagensis–beginning of catagensis). The case study shows that these methods are suitable for a proper assessment of the petroleum potential of source rocks and the rapid geochemical characterization of sedimentary organic matter.
**Keywords:** Egypt; Gulf of suez; Organic matters; Rock-eval Pyrolysis; Steranes; Triterpanes.

## T-39. Enzyme Activity and Biochemical Changes Associated with Induction of Systematic Resistance of Faba Bean Against Damping off Disease

Neamat A. Khalifa, M. Abou-Zeid, A. Mahmoud Noher and H. M. Sobhy

*Egyptian Journal of Biological Pest Control, 26 (2): 395-404 (2016) IF: 0.152*

Damping-off and root-rot diseasesin faba bean caused by Rhizoctoniasolani Kuhn and Fusarium solani Mart are considered the most destructive diseases. These pathogenic fungi were found tobe associated with root-rot and wilt symptoms of faba bean plants collectedfrom various locations at different governorates in Egypt. The efficacy of thechemical inducer, i.e. salicylic acid (SA) and the biocontrol agents, i.e.Trichodermahamatum and Bacillus subtilis individually used and/or incombination against the incidence of faba bean damping-off disease caused by F.solani El-Menia (FS4) and R. solani El-Nubaria (R20), wasevaluated by soaking faba bean seeds and soil drenching, compared to untreatedcontrol treatment under greenhouse conditions. All the tested treatmentssignificantly reduced the percentages of damping-off diseases. The combinationamong salicylic acid, T.hamatum-2and B.subtilis-1was the most effective treatment for decreasing the percentages of damping-offfollowed by the other combination treatments, while applying each of T.hamatum-2andB.subtilis-1 individually recorded the lowest effect forreducing percentages of damping off under greenhouse conditions compared tocontrol. Also, the effects of biotic (T.hamatum-2 and B.subtilis-1) and abiotic inducers (salicylic acid), individually or in combination on the activity of lytic enzymes (protease and β-1,3-glucanase), oxidative reductive enzymes (polyphenoloxidase, catalase andperoxidase) as well as the changes in phenol compounds were determined in theleaves and the roots of faba bean plants.
**Keywords:** Fababean; Damping-off and Root-rot diseases; Induced resistance; Enzyme activitiesand phenolic compounds.

## T-40. Induction of Systemic Resistance in Faba Bean Plants Against Fusarium Ixysporum the Causal of Wilt Disease

*Neamat A. K., Abbas M. S, Sobhy H. M., Abou-Zeid, N. M and Mahmoud N. A.*

*Egyptian Journal of Biological Pest Control, 26(3): 431-438 (2016) IF: 0.152*

Faba bean wilt caused by Fusarium oxysporum Schlecht is considered the most destructive plant disease inEgypt. Salicylic acid (SA) as chemical inducer and the biocontrol agents of Trichodermahamatum and Bacillus subtilis individually and/or in combinationagainst the incidence of faba bean wilt, caused by F. oxysporumBeni-Seuf (Fo19) was evaluated as faba bean seed soaking and soildrenching, compared to untreated control treatment under greenhouse conditions.All the treatments of biotic (T. hamatum-2andB. subtilis-1) and abiotic inducer (salicylic acid)significantly reduced the incidence of wilt disease. Salicylic acid incombination with T. hamatum-2and B. subtilis-1was the most effective treatment. The lowest effect as percentage reduction of early and late wilt under greenhouse conditions compared to control wasrecorded at individual application of each of T. hamatum-2and B. subtilis-1.Also, changes in the activity of lytic enzymes (protease and β-1, 3-glucanase),oxidative reductive enzymes (polyphenoloxidase, catalase and peroxidase) andcertain phenol compounds caused by individual or combination of biotic andabiotic inducers were determined in the leaves and the roots of faba beanplants.
**Keywords:** Faba bean; Fusariumwilt; Induced resistance; Enzyme activities; Phenolic compounds.

## T-41. Assessment of Threats to Vegetation Cover in Wadi El Rayan Protected Area, Western Desert, Egypt

Abdelwahab A. Afefe, El-Bialy E. Hatab, Mohamed S. Abbas and El-Sayed I. Gaber

*International Journal of Conservation Science, 7 (3): 691-708 (2016)*

Wadi El Rayan is located in the African Sahara ecoregion of the Palearctic eco-zone, the world's largest hot desert. The total area of Wadi El Rayan is 1759km². The objective of the present study is to enrich the knowledge on the vegetation cover along the shores of Wadi El Rayan lakes and to identify the different threats, underlying causes and recommended solutions for the conservation of natural vegetation cover in Wadi El Rayan Protected Area (WRPA). Based on field surveys, we found that current pressures of human activities on natural vegetation include overgrazing, irresponsible tourism, land encroachment,

water pollution, water over-use, fire, an d habitat change and destruction. The reduction of water levels due to decreased water incoming is considered the main threat facing ecosystems and biodiversity in the lakes area. We found that the perimeter of the lower lake has decreased from 48.6km² in 2007 to 34.09km² in 2013 (a loss of 29.8 % of the total lake area), due to lake decreased water level. The most underlying causes of vegetation loss in the study area were found to be the lack of awareness, weak law enforcement, lack of suitable strategies, weak financial support and lack of stakeholders' cooperation. Survey results show that vegetation cover in the area of the connecting channel and northeastern of the lower lake represents the highest impacted area by human pressures compared to other locations. Moreover, the role of WRPA is important in achieving good cooperation between governmental authorities, local community, and owners of different economic activities and in finding new ways to improve potential future cooperation with other stakeholders. We also provide some suggested activities for conserving vegetation cover in WRPA

**Keywords:** Vegetation; Protected area; Wadi el rayan; Threats; Conservation.

## T-42. Chemical, Rheological, and Physical Properties of Germinated Wheat and Naked Barley

Abd El-Moneim Afify, Mohamed S. Abbas, Bothyna M. Abd El-Lattefi and Ashgan M. Ali

*International Journal of Chemtech Research,9(9):521-531 (2016)*

The effect of germination on chemical composition, dough raising capacity, gluten changes and folic acid of wheat" variety Gammeza 7" and naked barley "variety Giza 131" were investigated. Crude protein ranged from 9.08 to 11.70% in germinated barley and wheat. Barley was the highest in ether extract and ash. Wheat was the highest in crude fiber. Flour extract (82%) was the highest in carbohydrate. Wheat was the highest in Na, K, Fe, and Ca. Dough raising capacity was highest in 75% germinated wheat flour. Wet, dry gluten in flour extracted (82%) have the highest percentages. While 75% ubstituted germinated wheat for flour 72% extraction was the highest in wet and dry gluten. Fresh germinated wheat and barley were higher in folic content than other treatments. Germination seems to be a natural and sustainable way to improving nutritional quality and functional food compound in wheat and barley.

**Keywords:** Folic acid; Gluten; Naked barley; Nutritive value and Wheat.

## T-43. Effect of Diethyl Sulphate and Sodium Azide on Tolerance of Ex-Vitro Banana to Salt Stress

Dalia A. Kishk, Adel A. Abul-Soad, Mohamed S. Abbas, Hattem M. El-Shabrawi, El -Sayed I. Gaber and Tarek M. Noor El-Deen

*International Journal of Chemtech Research, 9(12):81-99 (2016)*

Banana is a cash crop sensitive to the salinity and problem increases by water shortage especially in arid and semi-arid regions and this can severely limit plant growth and productivity. The aim of current study was to develop mutants of banana Grande Nain cv. tolerant to salinity stress. In vitro shoots of banana Grande Nain cv. were treated with different concentrations of diethyl sulphate (DES) and sodium azide (NaN3) duringthe multiplication stage (in the third subculture) and then with NaCl in the rooting stage. After then, the transplanted banana was more stressed by adding the sea water to the irrigation water every time for 6 months. Three factors were investigated in this study, mutagen type, concentrations plus duration and salinity levels. The recorded vegetative growth parameters after six months in acclimatization stage showed that DES had less negative impact on the vegetative growth parameters than NaN3. In addition, the low concentration of DES and NaN3 gave healthy ex vitro plants of 22.88 and21.60 cm as plant height/plant, 5.78 and 7.00 as number of leaves/plant, 24.62 and 21.80cm2 as leaf area, 5.22 and 6.89 as number of roots/plant, and 7.31 and 2.98 cm as psudostem circumference respectively at all duration periods. However, using the high concentration of DES (400µm) and NaN3 (8µm) produced the most viable plants at 10 min Concerning the effect of salinity levels in the greenhouse, all measured growth parameters decreased by increasing salinity levels. There was a great variance regarding the double interactions between the three studied factors, but the triple interaction among the three factors indicated that DES at 100 and 200 µM for 10, 20 or 30 min as well as at 400 µM for 10 or 20 min with all studied salinity levels produced the best results when compared with the other treatments. Also, a fingerprinting based on ISSR was used to detect any genetic variation occurred in the stressed plants. Using different mutagens under different salinity levels, on the other hand, led to induce a great effects in terms of ions accumulation (K+ and Na+) and proline contents. According to PCR ISSR and SDS-PAGE test results; there were genetic variations in the stressed plants as a result to use DES mutagen. This study could be a base to use diluted sea water in irrigating banana plants produced from in vitro culture and treated with DES mutagens

**Keywords:** Banana CV. Grande Nain, Diethyl Sulphate, Des, Sodium Azide, Nan3, Mutagens, Salinity, Vegetative Growth, Issr

## T-44. Effect of Different Nitrogen Levels and Vermicompost on Cabbage (Brassica Oleraceae Var. Capitata L.) Growing in Rice Straw Under Greenhouse Conditions

Tarek M Younis, A A Farag, Y M Ahmed, Mohamed S Abbas and El-Sayed I Gaber

*Research Journal of Pharmaceutical, Biological and Chemical Sciences, 7 (2): 2163-2197 (2016)*

The current study was carried out during two seasons in 2012/2013 and 2013/2014 at the experimental site of Central Laboratory for Agricultural Climate, Agricultural Research Center, Egypt. The experiment aims to evaluate the ability of using rice straw as growing media, different levels of nitrogen and vermicompost on vegetative growth and quality of cabbage (Brassica oleraceae var. capitata L.) cv. OS Cross. The experimental design was a split-split plot design with three replications. The first factor was four growing media comber to control soil (old rice straw, 50% old + 50% new rice straw, new rice straw and bale rice straw), the second factor was three different nitrogen levels (10, 12 and 14 g N/plant) and the third factor was three vermicopmost addition time (30 and 60 days after transplanting and without addition). The obtained results showed that the highest significant values of vegetative growth and head cabbage quality dry weight obtained in plants grown in soil followed by old straw without significant differences between them while, the lowest value was recorded in bale straw. Increasing nitrogen levels and vermicompost addition times led to

increase all vegetative growth, head quality, dry weight and NPK content in head cabbage. The highest plant parameters recorded in plants grown in soil received 14 g N/plant and vermicompost at two times (400 cm3).Whereas, the lowest values obtained in plants grown in bale straw received 10 g N/plant without vermicopmpot addition in both growing seasons.It can concluded that using the old straw to cultivate cabbage due to the same vegetative growth and head cabbage quality that obtained in plants grown in soil without significant differences and the Increasing of nitrogen levels and vermicompost addition times led to increase all vegetative growth, head quality, dry weight and NPK content in head cabbage.

**Keywords:** Cabbage; Rice straw; Nitrogen and vermicompost.

## T-45. Effect of Nano and Molecular Phosphorus Fertilizers on Growth and Chemical Composition of Baobab (Adansonia Digitata L.)

Amira Sh. Soliman, M. Hassan, Faten Abou-Elella, A.H. Hanafy Ahmed and Souad A. El-Feky

*Journal of Plant Sciences, 11: 52-60 (2016)*

**Objective:** This study was carried out to investigate the effectiveness of foliar application of different sources of P on growth performance of Adansonia digitata in Egypt. **Materials and Methods:** Different sources of P [monoammonium phosphate (MAP), diammonium phosphate (DAP) or hydroxyapatite nanoparticles (nHA)] and unfertilized seedlings (control) were used as a foliar application to study growth parameters and chemical composition of Adansonia digitata grown in a sandy soil during two successive seasons (2014 and 2015). **Results:** Baobab plants sprayed with nHA showed a significant increase in plant growth characters (plant height, stem diameter, number of leaves per plant, leaf area, root length, total fresh and dry weights) when compared to control plants. Moreover, significant increase in total chlorophyll, carotenoids concentration, total carbohydrates percentage, vitamin C, macro-elements (N, P and K%), crude protein and total phenols content. The anticancer activity of Adansonia digitata leaves against Ehrlich Ascites Carcinoma Cells (EACC) and the antioxidant activity of leaves over control plants were recorded in the same treatment. Meanwhile, it had significant reducing power methods. **Conclusion:** It is recommended to spray with nHA for increasing plant growth, nutrition status, DPPH and anticancer activity besides, their safety for either environment or human health.

**Keywords:** Adansonia digitata; Nanofertilizers; Foliar application; FTIR; DPPH; Anticancer activity.

## T-46. Effect of Using Guar Korma Meal as a New Source of Protein on Productive Performance of Buffalos

Walaa M. Abdel-Wahab, Salah K. Sayed, Reda A.M. Sabek, Mohamed S. Abbas and Hassan M. Sobhy

*Asian Journal of Animal Sciences, 10 (6): 300-306 (2016)*

Guar korma meal (Cyamopsis tetragonoloba) is one of some nutritional sources of feed proteins which contain high protein, approximately 50% or more. This study aimed to evaluate the effect of using Guar Korma Meal (GKM) as a new source of protein in rations on productive performance for Egyptian buffalos. Materials and Methods: The first trial was carried out to determine the in vitro disappearance gas production of dry and organic matter (IVDMD and IVOMD) of the different experimental Concentrate Feed Mixtures (CFM) containing different levels of GKM instead of Sunflower Meal (SM). The second trial, depending on the results of first experiment 20 buffalos averaging 450 kg Live Body Weight (LBW) were chosen into four similar groups in the same lactation season. Animal groups were receive four experimental rations containing CFM which included GKM at the rate of 0, 6, 8 and 10% in rations R1, R2, R3 and R4 replacement with SM. Results: The results obtained from the first experiment revealed that the IVDMD and IVOMD in gas production increased with increasing the replacement level of GKM in concentrate feed mixture. The second experiment indicated that the digestibility of Dry Matter (DM), Organic Matter (OM), Crude Protein (CP) and nutritive value expressed as Total Digestible Nutrients (TDN) increased ($p<0.05$) with increasing the replacement level of GKM in the rations. Average actual milk and Fat Corrected Milk (FCM) yield were increasing with increasing level of GKM. Blood parameters were within normal range and improve lipid profile. Average feed cost per kilogram milk yield decreased with increasing GKM levels. Conclusion: Conclusively, it could be recommended that substitution SM by GKM in Egyptian buffalo's rations seems to be the best for the digestibility, improve lipid profile and productive performance.

**Keywords:** Guar korma meal; Egyptian buffalos; Digestibility; Milk production.

## T-47. Effects of Feeding Diets Containing of Some Aromatic and Medicinal Plants Remnants on Meat Quality, Fatty and Amino Acids Fractions of New Zealand White Rabbits

Hemat S. Mohamed, Adel E.M. Mahmoud, Mohamed S. Abbas and Hassan M. Sobhy

*Asian Journal of Animal Sciences, 10(4-5): 255-261 (2016)*

One hundred and eight weaned NZW rabbits used to investigate the effect of using remnants of mint, fennel, basil and anise with or without probiotic to replace 50% from alfalfa hay in rabbit's diets. This part of study had shown the effects of experimental diets on rabbit meat composition and its fatty and amino acids. Materials and Methods: The four remnants were obtained after oil extraction and were incorporated in rabbit diets, rabbits randomly assigned in to 9 experimental groups, the experimental period lasted for 8 weeks. Chemical composition, fatty and amino acids were analyzed. Results: Chemical composition of meat fed different experimental diets were in the normal structure in rabbit meat with slight differences among them. Data of fatty acids fractions observed that Poly Unsaturated Fatty Acids (PUFA) were the highest proportion of total fatty acid (41.90%) after that the percent of Saturated Fatty Acids (SFA) (40.39%) then the percent of Mono Unsaturated Fatty Acids (MUFA) (17.71%). The highest value of the total non-essential amino acids was found in anise and anise with probiotic treatment (67.65 and 67.49 g/100 g) treatment, whereas, the lowest value was found in control, fennel and fennel with probiotics (62.73, 62.13 and 62.13 g/100 g, respectively) treatment. Conclusion: Summing up, using of that medicinal plants remnant to replace 50% from alfalfa hay in rabbit diets did not have any adverse effects on chemical composition of rabbit meat and its fractions of fatty and amino acids.

**Keywords:** Rabbit; Mint; Fennel; Basil; Anise; Fatty acids; Amino acids.

## T-48. Genetic Selection for Salt Tolerance in some Egyptian Wheat Genotypes (Triticum Aestivum L.) Via Tissue Culture

Ahmed MS El-Sayed, Hoda MH El-Naggar, Mohamed S Abbas and El-Sayed I Gaber

*Plant Tissue Culture and Biotechnology, 26 (1): 25-36 (2016)*

Five wheat genotypes and their hybrids under four salinity (sea water) levels were considered for tissue culture and randomly amplified polymorphic DNA (RAPD). The genotypes and the hybrids differed in their ability to callus induction, callus fresh weight and regeneration. Among the genotypes, Sakha 93 (P1) followed by Line WB19 (P5) was the most tolerant genotypes for salinity and gave the highest growth rate (46.6%) and (46.3%), respectively while Giza 168 (P3) was the most sensitive one to salinity with lowest growth rate (26.6%). All hybrids scored higher averages in callus growth rate than their parents. P1 × P5 followed by P1 × P2 and P1 × P4 produced the highest growth rate 75.6, 59.1 and 52.6% over hybrids while P3 × P4 had the lowest rate 28.5%, respectively. The hybrid P1 × P5 gave the highest percentage of plant regeneration over all genotypes and their hybrids followed P2 × P5, P1 × P2 and P4 × P5. The highest number of RAPD specific markers scored for hybrid P1 × P5 was (6 markers), while Line WB19 (P5), P1 × P2 and P2 × P5 were (4 markers). These markers can be verified as the RAPD markers associated with salt tolerance.

**Keywords:** Triticum aestivum; Callus induction; Plant regeneration.

## T-49. In Vitro Selection and Characterization of Salt Tolerant Cell Lines in Cassava Plant (Manihot Esculenta Crantz)

Alaa M. El-Minisy, Mohamed S. Abbas,Usama I. Aly and Hattem M. El-Shabrawi

*International Journal of Chemtech Research, 9 (5): 215-227 (2016)*

To identify and characterized a tolerant cassava cell lines for salt stress. Cassava suspension culture grow on MS media containing 50, 100, 150, 200 and 250 mM NaCl were established from cassava callus cultures and some traits, including viability percentage, average and concentration of total viability cells and biochemical indicators including sodium, potassium, calcium and chloride (Na+ , K+, Ca2+, Cl-), proline content, peroxidase, glutathione reductase and glutathione peroxidase enzymes were all dramatically induced in response to salt treatment. The results indicated that the high concentration of NaCl 200 and 250 mM decrease the viable cell number one fold comparing to lower concentrations of NaCl and control sample. Surprisingly at 50, 100 mM and 150 mM NaCl we found that the number of viable cells was higher than the control sample. However, the cell viability in 12 days under NaCl stress shows high tolerance against salt stress and the cell numbers also higher comparing to other NaCl concentrations. Ionic status suggested that 200 mM NaCl accumulated less Na+, Cl- and Ca2+ and maintained better K+ in comparison to other NaCl stress cell samples. The ion homeostasis data of cassava cell culture under NaCl stress showed that the Na+ and K+ accumulation increased very much under lower concentrations of NaCl and gradually decrease in higher concentration. There is a positive relationship between salt tolerance and proline content in in cassava cultures up to 200 mM NaCl stress and the highest proline content compared to other treatments. Gel activity assay of superoxide dismutase (SOD), peroxidase (GPX) and Total peroxidase (POX) activity increased in tolerant cell lines as compared to control. Analysis of the above enzymes suggests that selected cassava cell lines possessed more efficient scavenging system of reactive oxygen species under 200 mL NaCl. we can concluded that in cassava suspension culture we can realize that viability of cell under 200 mM NaCl stress after 15 day will be the perfect time to isolate and identify the intercellular and extracellular protein or/and peptides which could be produced abundantly.

**Keywords:** Cassava; Salt stress; Cell viability; Ion concentrations; Detoxification enzyme; Proline.

## T-50. Quality and Yield Traits of Three Sugar Cane Promising Varieties as Affected by Different Levels of Nitrogen and Potassium Fertilizations in Egypt

Ibraheem A Abd Elateef, Mohamed S Abbas, El-Sayed I Gaber, Laila MA Saif and brahim H El-Geddawy

*Research Journal of Pharmaceutical, Biological and Chemical Sciences, 7 (2): 1253-1263 (2016)*

To evaluate the performance of three sugar cane varieties as affected by nitrogen and potassium fertilizations, field experiment was carried out at Malawy Agricultural Research Station in the two successive seasons of 2012/2013 and 2013/2014. Each field trail included twenty seven treatments, three sugarcane varieties (G.T.54-9 the commercial variety as a control, G.2001-79and G. 99 -103), three nitrogen levels (220, 280 and 340 kg N/fed.) and three potassium levels (24, 48 and 72 K2O kg/fed.). Results indicated that the increasing of nitrogen rate from 220 to 280 up to 340 attained a significant increment in cane yield. Also, the increasing of potassium level slightly increased cane yield /fed, in the 1st season only. Sugar cane variety G.99-103 over passed significantly the other two varieties and the promising variety G.99-103 attained additional increase over the commercial one by 5.11 and 4.88 ton/fed in the 1st and 2nd seasons respectively. The sugar yield increased significantly by increasing of nitrogen rates and the highest sugar yield was recorded with 340 kg N /fed. There is a positive and significant increase in sugar recovery percentage in the 1st season, where increasing of potassium was accompanied by significant decrease in the values of sugar recovery percentage.

**Keywords:** Sugar cane; Nitrogen; Potassium; Yield; Juice Quality

## T-51. Soil–Vegetation Relationships in Wadi El-Rayan Protected Area, Western Desert, Egypt

Mohamed S. Abbas, Abdelwahab A. Afefe, El-Bialy E. Hatab and El-Sayed I. Gaber

*Jordan Journal of Biological Sciences, 9 (2): 97-107 (2016)*

The present study provides an analysis of the soil and vegetation composition at 10 sites in Wadi El Rayan Protected Area and concentrates on the environmental factors that affect plant species

distribution. A total of 17 vascular plant species belonging to 13 botanical families was recorded. Poaceae, Chenopodiaceae, and Zygophyllaceae were the largest families identified. Chorological analysis revealed that 47% of the studied species are Pluri-regional, 41% are Bi-regional and 12% are Mono- regional. The recorded species extend their distribution all over the Saharo-Arabian (33%) followed by Irano-Turanian (24%), Mediterranean (22%) Palaeotropical (8%), Sudano-Zambezian (5%), Neotropical (5%), and Euro-Siberian (3%). The life -form spectrum revealed that the phanerophytes (35%) and geophytes helophytes (23%) are the most frequent, followed by chamaephytes (18%), therophytes (12%), hemicryptophytes (6%), and helophytes (6%). The dominant species were Phragmites australis, Tamarix nilotica and Zygophyllum album; while the co-dominant species were Juncus rigidus, Nitraria retusa, Alhagi graecorum, Typha domingensis, Zygophyllum coccineum and Eucalyptus camaldulensis. Variation in species diversity among different locations were evident, the Northeast of the Lower Lake (9 species), followed by the Southwest of the Lower Lake and the Northeast of the Upper Lake (6 species each) showed highest species richness, while the Southeast of the Lower Lake showed the lowest recorded species richness (one species). Detrended Correspondence Analysis (DCA) and Canonical Correspondence Analysis (CCA) Ordination techniques were used to examine the relationship between the vegetation and soil parameters; pH, electric conductivity, CaCO3, organic matter and relative concentrations of cations. CCA analysis showed positive correlations of species and sites along the most important ecological gradients. Both ordination techniques clearly indicated the importance of these ecological factors on the distribution of the vegetation pattern in the area

**Keywords:** Vegetation; Plant distribution; Wadi El Rayan; Soil; Desert; Egypt; Protected area.

+++

CAIRO UNIVERSITY

# Publicatin in Book & Chapters

## Basic Sciences Sector

## Faculty of Science

***Dept. of Chemistry***

### C-1. Polymers as Drug Delivery Systems 323

Magdy Sabaa Wadid

*Biodegradable and Biobased Polymers for Environmental and Biomedical Applications, Wiley- Scrivener Publishing*, (2016)

One major challenge in the field of pharmacokinetics is to sustain the therapeutic level of a drug in body tissue as long as possible during the entire length of treatment. This is achieved using the technology of controlled drug delivery (CDD), with themain aim to increase the effectiveness of drug therapy. Moreover, controlled release systems aim to improve the effectiveness of drug therapy, as the attached drugs can be targeted to specific organs, tissues or cells. Thus the applications of CDD systemsinclude both sustained delivery and targeted delivery as a one-time. In the present chapter, the different types of modified drug delivery systems (DDS) together with the concept of drug delivery matrix whether it is a hydrophobic or hydrophilic matrix are discussed in details. Polymeric materials as carriers for DDS including polysaccharides, modified polysaccharides and celluloses nanocrystals (or so called cellulose whiskers ) are also reported. In addition, examples for pH-sensitive DDS in both acidic and alkaline pH's, thermo-sensitive and light-sensitive DDS are also reported. Applications of these classes of DDS as potential carriers for controlled release drugs and for antitumor drugs are also discussed.

**Keywords:** Drug delivery systems; Controlled drug delivery; Ph-Sensitive Drug delivery systems; Thermo-sensitive drug delivery systems; Light-sensitive drug delivery system.

### C-2. Chitosan and Starch-Based Hydrogels Via Graft Copolymerization

Magdy Sabaa Wadid

*Polymeric Hydrogels as Smart Biomaterials, Springer International Publishing Switzerland*, (2016)

Graft copolymerization is an attractive method for surface functionalization of natural polymers and can be initiated by chemical methods, radiation technique, and other systems. Graft copolymerization of vinyl monomers onto polysaccharides is an efficient route for the preparation of superabsorbent. Depending upon the type of monomers and the conditions employed the properties of graft copolymers vary to a large extent. Chitosan is a non-toxic, biocompatible polysaccharide and starch is a natural hydrophilic biopolymer. Both these are most abundant natural organic materials which are extensively investigated in the development of biodegradable and environment friendly materials. Their hydrogels are of utmost importance for wide use in many fields including structural transplants, target drug delivery, tissue engineering, biosensors, adsorbents etc. In this chapter, the various techniques used for the synthesis of chitosan/starch graft copolymers, their properties and possible applications are discussed in detail.

**Keywords:** Chitosan; Starch; Graft copolymers; Hydrogel; Ion Exchangers; Biomedical applications.

### C-3. Advanced Titanium Surfaces and its Alloys for Orthopedic and Dental Applications Based on Digital Sem Imaging Analysis

Sahar Ahmed Ali Fadlallah

*Advanced Surface Engineering Materials, Wiley- Scrivener Publishing*, (2016)

The biological benefit of titanium and its alloys surfaces are highly depend on the surface morphology and chemical structures. Over the last ten years, the research was directed to improve the titanium surfaces to be highly ordered nanostructures surface) tubes, pores, channels, sponges) for a wide range of biomedical purposes. The objective of this chapter is to summarize, discuss and evaluate the titanium (Ti) surfaces developed under anodization conditions for improvement its osseointegration after implantation surgery process. Smooth implant surfaces are not beneficial for osseointegration due to poor interaction with tissues. Anodic oxidation electrochemical process in aqueous solution was used to fabricate novel anodic conversion layer with poroustitanium oxide surfaces.The porous-surface implants contributed to the osseointegration because they provide a larger contact area with surface roughness at implant-bone interface can help into the formation of physico-chemical bondage with the surrounding hard tissues and enhance the longevity of implant. The surface features can be characterized by means of scanning electron microscopy (SEM) and energy dispersive X-ray analysis. Furthermore, in vitro administration strategies for surfaces interfacial integrity and compositional variation along the implant–bone interface were examined. The electrochemical impedance measurement (EIS) results confirmed the initial stability for the Ti modified implant surface and hence could be used as indicator for fasterhealing. Accurate measurement of the nanostructures morphology enables the consistent characterization of their properties. Consequently, intensive image analysis of the SEM images can be considered an extensive stage for efficient nanostructures characterization. This morphological image analysis is consists of: contours identification, image segmentation, shapes classification, and thickness measurements. In this chapter, we discuss the role of image processing analysis to test, evaluate and confirm the morphology of implanted surfaces. As the SEM is a standard device for comparing between the morphology of implant surfaces and selects the best surface conditions using necked eye. Therefore, automated and enhanced SEM images using Imaging processing analysis techniques to support the optimal preparation condition of implanted surfaces will consider as a future aspect in the field of biomaterials.

**Keywords:** Titanium and titanium alloys implants; Nanostructures; Electrochemical impedance spectroscopy eis; Corrosion resistance; Physiological solutions; Digital sem images analysis; Image processing; Images segmentation; Image classification; Contour detection.

## Faculty of Agriculture

### *Dept. of Agricultural Botany*

#### C-4. Polyamines and Brassinosteroids in Drought Stress Responses and Tolerance in Plants

Neveen Bahaa El-Din Talaat Shawky

*Water Stress and Crop Plants: A Sustainable Approach Volume 2, Wiley and Sons*, (2016)

This chapter highlights the recent advances concerning the role of polyamines and brassinosteroids in stress tolerance of plants with a special accent on drought. Alterations of the endogenous polyamine and brassinosteroid levels and their function in alleviation of drought stress are discussed. Possibilities for application of exogenous polyamines and brassinosteroids to lessen the stress injuries and to increase drought tolerance are also summarized. Genetic and molecular approaches for improving planttolerance to drought via modification of polyamine levels and involvement of brassinosteroids in signal transduction pathways under stress are presented. Interaction of polyamines and brassinosteroids with phytohormones and osmolytes under drought stressis reviewed. We describe also the recent investigations in Bulgaria and Egypt concerning the modulation of plant reactions to drought stress by application of polyamines and brassinosteroids.

**Keywords:** Polyamines; Brassinosteroids; Drought stress.

### *Dept. of Agronomy*

#### B-5. Abatement Techniques for Reducing Emissions from Livestock Buildings

Mohamed Samer

*Book Published By Springer*, (2016)

This book identifies future scientific research priorities for developing emissions inventories, emissions abatement techniques and mitigation strategies in order to improve and sustain livestock production that is in line with climate change adaptation. Livestock production is a major source of atmospheric pollutants and greenhouse gases, such as methane, nitrogen oxides, carbon dioxide and ammonia, all of which directly contribute to global warming and climate change. Air pollutant emissions from agricultural practices have a negative environmental impact and are of relevant political importance, as highlighted in both the Kyoto and Gothenburg Protocols. This book provides solutions on how to abate these emissions by using effective abatement techniques such as additives, manure storage covers, aerobic and anaerobic treatments, and dietary manipulation. Each chapter in the book provides valuable, up-to-date information on abatement techniques, thus allowing the reader to better understand the issues involved. Recent advances and new perspectives in the field are also discussed.

**Keywords:** Emissions abatement techniques; Gaseous emissions; Greenhouse gases; Ammonia; Livestock buildings.

#### B-6. Dynamics and Resilience of Informal Areas: International Perspectives

Attia S., Shabka S., Shafik Z. and Ibrahim A.A.A.M.

*Book Published By Springer, (2014)*

This book presents discussions and debates that address Dynamics; Management; and Strategies in different contexts of informal settlements. The discussion is based on the serious work presented in fourteen different research papers that investigate related issues around the globe. The discussions are distributed on three thematic chapters; each chapter focuses on specific facets in the scope of informal urbanism. The first theme is titled “The Dynamics of Informal Settlements”; the second is “Production, Management and Operation of Urban Space”; and the last theme is titled “Innovative Policies and Strategies in informal urbanism”. In the book young authors present their views and experiences in a variety of contexts, and debate their research about informal settlements. This book presents 15 different papers distributed on three main chapters; each chapter focuses on a specific theme in the scope of informal settlements. The themes are titled as follows; the first theme is titled “The Dynamics of Informal Settlements”; the second theme is “Production, Management and Operation of Urban Space” and the last theme is titled “Innovative Policies and Strategies”. In the book young authors debate and present their research, and views about informal settlements.

**Keywords:** Informal settlements; Resilience; Urban spaces; Strategies.

#### C-7. A Proposed Statistical Model for Real Estate Appraisal in Historical Mixed Use

Asmaa Ibrahim Affiliation

*Dynamics and Resilience of Informal Areas: International Perspectives, Springer, (2014)*

This chapter (This chapter was published in the International Journal of Sustainable Development and Planning.) introduces a new statistical methodologi-cal approach for the real estate appraisal based on the consideration of the changing purchasing power of money, by deducing an equation based mainly on all the affecting urban context variables other than the market, cost and income approach that are currently used for that purpose. This is achieved through testing the pro-posed statistical model using these urban variables on one of the most important districts in downtown Cairo, Maspiro (next to Tahrir Square incorporating 1,130 land lots), together with comparing its predicted values with a sample evaluated by professional real estate appraisers to ensure its validity. Maspiro district confronts the Nile River, and faces the Egyptian Union of Radio and Television Building, Ministry of Foreign Affairs, Embassy of Brazil, Embassy of Italy and others. Accordingly, the chapter finally illustrates that all theoretical approaches dealing with the real estate appraisal are subject to some defects ignoring the changing cir-cumstances of each district and the urban planning

variables that constitute its real value. They mainly depend on factors that are subject to change from time to time in accordance with the surrounding political, social, and economic circumstances. Over or under estimations may lead to economic loss and mislead the proposed developmental plans for the regions. The urban variables, on the other side, once measured for each real estate are not subject to these changes. Therefore, the research tests the validity of finding strong correlation between these variables and their real value, in the form of an equation by using statistical methods.

**Keywords:** Real estate appraisal; Informal historic districts; Mixed use; Statistical method.

## Engineering Sector

## Faculty of Engineering

### *Dept. of Architectural Engineering*

### *Dept. of Chemical Engineering*

### C-8. Co2 Transport and Storage Technologies

لا يوجد

*Carbon Dioxide Capture: Processes, Technology and Environmental Implications, Nova Science Publications, (2014)*

This chapter focuses on the transport and storage of CO2. It discusses the different transportation options and presents some guidelines for the pipeline transportation of CO2. The storage of CO2 is discussed with some details; Different types of trapping, physical trapping, residual trapping, solubility trapping, and ionic and mineral trapping, are introduced and discussed. Geological storage, in particular, is gaining increased interest due to efficiency and economical reasons. Different types of geological storage mechanisms such as storage of $CO_2$ in depleted hydrocarbon reservoirs or the use of $CO_2$ in enhanced oil and gas recovery are presented. The risks and evironmental aspects of $CO_2$ storage are also presented at the end of this chapter.

**Keywords**: Carbon dioxide; Transport; Storage; Injection technologies.

### *Dept. of Electric Power and Machines*

### B-9. Environmental Impacts on Underground Power Distribution

Osama El-Sayed

*Book Published by Idea Group Publishers (Igi), (2014)*

The successful transmission of electrical power beneath the surface of the earth depends on a number of factors including ambient temperature, sheath bonding, cable laying depth, and especially the formation of dry zones around underground cables. Environmental Impacts on Underground Power Distribution studies the factors which affect the maximum current rating of subterranean power cables as well as various methods to maximize electrical current transmission. Focusing on the latest tools, methodologies, and research in the field, this publication is designed for use by electrical engineers, academicians, researchers, and upper-level students.

**Keywords:** Underground power cables; Dry zone formation; Cable losses; Cable grounding; Fault location.

### C-10. Swarm Intelligence Pid Controller Tuning for Avr System

Naglaa K Bahgaat and M A Moustafa Hassan

*Advances in Chaos Theory and Intelligent Control, Springer, (2014)*

The voltage regulator is designed to automatically maintain a constant voltage level in the power system. It may be used to regulate one or more AC or DC voltages in power systems. Voltage regulator may be designed as a simple “feedforward” or may include “negative feedback” control loops. Depending on the design, it may use an electromechanical mechanism, or electronic components. The role of an AVR is to keep constant the output voltage of the generator in a specified range. The PID controller can used to provide the control requirements.The chapter discusses the methods to get the best possible tuning controller parameters for an automatic voltage regulator (AVR) system of a synchronous generator. It was necessary to use PID controller to increase the stability margin and to improve performance of the system. Some modern techniques were defined. These techniques as Particle Swarm Optimization (PSO), also it illustrates the use of a Adaptive Weight Particle Swarm Optimization (AWPSO), Adaptive Acceleration Coefficients based PSO, (AACPSO), Adaptive Acceleration Coefficients based PSO (AACPSO). Furthermore, it introduces a new modification for AACPSO technique, Modified Adaptive Acceleration Coefficients based PSO (MAAPSO) is the new technique which will be discussed inside the chapter, A comparison between the results of all methods used will be given in this chapter. Simulation for comparison between the proposed methods will be displayed. The obtained results are promising.

**Keywords**: Automatic voltage regulator pid controller; Particle swarm optimization; Adaptive weight; Particle swarm optimization; Adaptive acceleration coefficients based; Particle swarm optimization; Modified adaptive acceleration coefficients based pso.

### C-11. Load Frequency Control Based on Evolutionary Techniques in Electrical Power Systems

Naglaa K. Bahgaat M. I. El-Sayed, M. A. Moustafa Hassan and F. Bendary

*Advances in Chaos Theory and Intelligent Control Volume, Springer, (2014)*

Load Frequency Control (LFC) used to regulate the power output of the electric generator within an area as the response of changes in system frequency and tie-line loading. Thus the LFC helps in maintaining the scheduled system frequency and tie-line power interchange with the other areas within the prescribed limits. Most LFCs are primarily composed of an integral controller. The integrator gain is set to a level that compromises between fast transient recovery and low overshoot in the dynamic response of the overall system. The disadvantage of this type of controllers that there are slow and does not allow the controller designer to take into account possible changes in operating conditions and non- linearities in the generator unit. Moreover, it lacks robustness. So there are many modern techniques used to tune the controller. This chapter discusses the application of evolutionary techniques in Load Frequency Control (LFC) in power systems. It gives introduction to evolutionary techniques. Then it presents the problem formulation for load frequency control with Evolutionary Particle Swarm Optimization (MAACPSO). It gives the application of Particle Swarm Optimization (PSO) in load frequency control, also it illustrates the use of a Adaptive Weight Particle Swarm Optimization (AWPSO), Adaptive Accelerated Coefficients based PSO, (AACPSO) Adaptive Accelerated Coefficients based PSO (AACPSO). Furthermore, it introduces a new modification for AACPSO technique (MAACPSO). The new technique will be explained inside the chapter, it is abbreviated to Modified Adaptive Accelerated Coefficients based PSO (MAACPSO). A well done comparison will be given in this chapter for these above mentioned techniques. A reasonable discussion on the obtained results will be displayed. The obtained results are promising.

**Keywords**: Modified Adaptive Accelerated Coefficients Based Pso; Adaptive Accelerated Coefficients Based Particle Swarm Optimization; Adaptive Weight Particle Swarm Optimization; Load Frequency Control; Particle Swarm Optimization Technique.

***Dept. of Electronics and Communication Engineering***

## C-12. Self-Healing in 5G Hetnets

لا يوجد

*Opportunities in 5G Networks: A Research and Development Perspective, Crc Press, (2014)*

The main requirements of the fifth generation (5G) are emerging through the efforts of diverse groups such as 4G America in the United States, the IMT-2020 (5G) promotion group in China, and the 5G Private Public Partnership (5G PPP) in Europe. The 5G requirements will greatly increase the network complexity, which will demand auto-integration and self-management capabilities that are well beyond today's self-organizing network (SON) features. Additionally, ultrareliable communications impose very stringent latency and reliability requirements on the architecture. The main challenges for 5G networks are the continued evolution of mobile broadband and the addition of new services and requirements, for example, anything-to-anything communication, very low latency (< 1 ms), as well as reduced signaling overhead and energy consumption (greener network). Future mobile networks will not only have significantly increased traffic volumes and data transmission rates, but also many more use cases. These include not only traffic between humans and between humans and the cloud, but also between humans, sensors, and actuators in their environment, as well as between sensors and actuators themselves. Small access nodes, with low transmitting power and no planning requirements, are conceived to be densely deployed, resulting in an ultradense network (UDN). UDNs are also called heterogeneous networks (HetNets), that is, multilayered networks with high-power macrocells and very dense small cells (SCs) with low power. This approach improves spectral efficiency per area by reducing the distance between transmitters and receivers, and improves macrocell service by offloading wireless traffic. UDNs are a step further toward low-cost, plug-and-play, self-configuring, and self-optimizing networks. 5G will need to deal with many more base stations (BSs), deployed dynamically and in a heterogeneous manner, combining different radio technologies that need to be flexibly integrated. Moreover, a massive deployment of small access nodes introduces several challenges, such as additional backhaul and mobility management requirements, which 5G needs to address (CROWD project: http://www.ictcrowd.eu/). The Mobile and Wireless Communications Enablers for the Twenty-Twenty Information Society (METIS) provides a consolidated 5G vision. According to this vision, the most prominent requirements of 5G are: (1) total capacity increased 1000-fold; (2) 10–100 times more connected devices; (3) end user data rates expected to increase by 10–100 times; (4) latency reduced by five times; and (5) requirements (1)–(4) at today's cost or less. The road toward 5G is gradual. But perhaps, a key 5G qualification that dominates all these requirements is network flexibility and reliability. These qualifications can be achieved by integrating SONs in upcoming 5G networks. The purpose of this chapter is to cover the topic of self-healing in 5G networks. Self-healing is an important functionality of SONs, and it means that networks migrate from manual operation to automated operation (minimizing human interaction). SON defines three areas: self-configuration (plug-and-play network elements [NEs]), self-optimization (automatically optimizing NEs and parameters), and self-healing (automatically detecting and mitigating failures in NEs).

**Keywords:** 5G Networks; Self-healing; Network design; Self-organizing networks.

***Dept. of Irrigation and Hydraulics Engineering***

Sayed

## C-13. Bed Morphological Changes of the Nile River Ds Major Barrages

Ahmed M. Abdel Sattar

*The Handbook of Environmental Chemistry, Springer, (2014)*

Despite being the longest alluvial river in the world with longest path of sediment, the River Nile has received the least attention regarding the bed morphological changes especially downstream large man-made hydraulic structures such as barrages. Flow sediment interaction is expected to cause a wide range of bed geomorphologic changes in the River Nile affecting river navigation and major hydraulic structures on course. This chapter aims at providing an example of the extent of bed

morphological changes downstream of the new Naga-Hammadi barrage as a result of controlled flow releases using 2D numerical modeling. A stochastic procedure is further presented that deals with the uncertainty emerging from scarcity of available measured data for sediment in the River Nile.

**Keywords:** 2D Model; Bed load; Naga-hammadi barrage; River nile; Suspended load.

***Dept. of Mechanical Design and Production***

## C-14. Influence of Al2o3 Nano-Dispersions on Mechanical and Wear Resistance Properties of Semisolid Cast A356 al Alloy

Ahmed Y. Shash, Amer E. Amer and Moataz El-Saeed

*Mechanical and Materials Engineering of Modern Structure and Component Design, Springer, (2014)*

The present investigation studies the prospects of using nanoparticles as reinforcement ceramic powders to gain improved performance of A356 Al cast alloy. Alumina nano-powder of 40 nm size was stirred into the A356 matrix with different fraction ratios ranging from (0, 1, 2 and 4 wt%) in a mushy zone (600 °C) using a constant stirring time for one minute. To evaluate the results, the alloys were further characterized by various tribological and mechanical characterization methods. The results showed higher strength values with improved ductility when compared to the monolithic alloy under the same casting conditions. Also, the wear resistance has been positively enhanced as the amount of the Al2O3 nano-particles addition increases from 1 to 4 wt% leading to a decrease in the weight loss ranging from 5.5 to 4.0 mg, respectively. The Scanning Electron Microscopy of the fracture surface and the wear surface revealed the presence of nanoparticles at the interdendritic space of the fracture surface and was confirmed with an EDX analysis of these particles.

**Keywords:** Nano-metal matrix composites; Al2o3 nano-powders; Wear resistance; Mushy zone; Mechanical stirring.

***Dept. of Mechanical Power Engineering***

## C-15. Solar Thermal Collectors with Low and High Concentration

Matteo Bortolato, Ahmed Aboulmagd, Andrea Padovan Davide Del Col

*Renewable Energy in The Service of Mankind, Vol Ii, Springer, (2014)*

This chapter describes the performance analysis of different concentrating technologies through experimental and numerical modeling activities. Two solar thermal systems with different designs and, accordingly, different concentration ratios have been studied. The first solar device is a stationary compound parabolic concentrator (CPC) collector: it is provided with truncated or full CPC reflectors and evacuated tubes. Each evacuated tube is composed of an outer glass envelope and a glass absorber with selective coating in thermal contact, via absorber fin, with a U-shaped channel for the liquid flow. The second system is a parabolic trough concentrator (PTC) with two-axis solar tracking: the primary optics consists of a segment of parabolic cylinder which concentrates the direct normal irradiance (DNI) on a linear receiver. In this system, two types of flat receivers have been tested. One receiver has been designed for thermal energy extraction, and it consists of a canalized roll-bond plate provided with a semi-selective coating. The other receiver has been designed for cogeneration of electricity and heat (CPVT), and it is equipped with triple-junction photovoltaic cells, which are actively cooled by an aluminum roll-bond heat exchanger. The performance of the described collectors has been experimentally characterized at the Solar Energy Conversion Laboratory of the University of Padova (45.4°N, 11.9°E), Italy. The collectors have also been mathematically modeled, and the numerical data have been validated against the experimental measurements.

**Keywords:** Cpc; Parabolic trough; Concentrating collectors.

***Dept. of Mining, Petroleum and Metallurgy***

## B-16. Electrodeposition of Composite Materials

لا يوجد

*Book Published by Intec, (2014)*

This chapter presents an overview of research efforts focused on both fabrication and properties of nanocomposites prepared by electrodeposition. The nanoparticles can improve the base material in terms of wear resistance, damping properties, and mechanical strength as well as electrical properties. Different kinds of matrix, such as metals, polymers, and ceramic matrix, have been employed for the production of composites reinforced by nano-ceramic particles such as carbides, nitrides, and oxides as well as carbon nanotubes. Theoretical aspects and mechanisms related to the electrodeposition process of nanocomposite films, from aqueous solutions, are discussed.

**Keywords:** Nano-structured coatings; Electrocodeposition; theoretical models; characterization techniques; application.

## C-17. Fabrication of Nanoporous Alumina

Ahmed R. Abdel-Karim and S. M. El-Raghy

*Nanofabrication Using Nanomaterials, one, (2014)*

Aluminium and other nonferrous metals, such as magnesium and titanium are ideally suited to anodizing. Nanoporous alumina AAO films produced during electrochemical anodizing of aluminium has been studied for many years, and has continued to attract interest from various researchers because of its unique chemical and physical properties. These unique properties have made it possible for a wider application such as electronic devices, magnetic storage disks, sensors in hydrogen detection, adsorption of volatile organic compounds, bio devices and in drug delivery, etc. The pore formation during the anodizing process varies with the electrolyte type, concentration,

temperature and applied anodizing potential. Depending on the combination of these parameters, different pore sizes and inter-pore distances can be achieved. The nanostructure is well defined and has a highly ordered nano architecture that enables these structures to be used as templates. There are several advantages of AAO membranes, including high porosity and uniform pore size from 5 up to 300 nm, high hydraulic conductivity (water permeability),uniform distribution of pores less than (1% variation),excellent pore structure and high resistance to chemical and temperature degradation. One of the greatest advantages of template based synthesis for the growth of nanotubes and nanotube arrays is the independent control of the length, diameter, and the wall thickness of the nanotubes. While the length and diameter of resulted nanotubes are dependent on the templates used for the synthesis, the wall thickness of nanotubes can be readily controlled by the growth duration. Another great advantage of template-based synthesis is the possibility of multilayered hollow nanotube or solid nanoscable structures formation.

**Keywords**: Anodizing; Porous layer; Valve metals; Nanowires.

## C-18. Heat Treatment: Post-Weld

لا يوجد

*Encyclopedia of Iron, Steel, and Their Alloys, Taylor and Francis, (2014)*

This entrye present article aims at providing some key concepts on post-weld heat treatment (PWHT), as well as presenting some case studies. Two examples will be given to illustrate the significance of PWHT and importance of controlling its parameters as well as showing the role of PWHT on inducing metallurgical changes on the weld joints. The role of PWHT on the precipitation behavior and formation of reversed austenite in a precipitation hardening type of stainless steel (X4CrNiMo 16-5-1) will be examined and correlated to the microstructure and hardness of the heat-affected zone (HAZ), showing its effect on obtaining homogeneity in hardness between HAZ and BM. A comparison between two filler metals (on the mechanical properties and the microstructures) after post-weld tempering treatment at 475°C and 600°C for 4 hr will be also shown. Also, typical industrial applications for PWHT will be shown in this work.

**Keywords:** Post-weld heat treatment; Stainless steels; Pwht equipment.

## C-19. Welding-Associated Failures in Power Boilers

لا يوجد

*Handbook of Materials Failure Analysis with Case Studies from The Chemicals, Concrete and Power Industries, Elsevier Science, (2014)*

The function of a boiler is to produce superheated steam by transferring the heat produced by the combustion of oil or natural gas to water and steam flowing through the tubes that form the boiler. The super-heaters consist of banks of tubes suspended in the combustion gas flow path in the upper parts of the boiler. The steam flows from the super-heaters through the main steam header to the main turbine, where it drives the turbine-generator. The service conditions involved in boilers, which are mainly governed by alternating high temperatures and induced thermal stresses;residual stresses in welds; as well as the harsh corrosive environments, promotes failure causes such as thermal fatigue; stress-corrosion cracking (SCC); corrosion; and premature creep failures due to stress raisers at welding defects. The common welding problems encountered in SSs are ensitization, SCC, hot cracking, HAZ cracking, weld metal solidification cracking, and fissuring. These problems are discussed briefly in the following sections.

**Keywords:** Welding-associated failures; Power boilers; Stainless steels.

## C-20. Effect of Soaking Treatment on the Microstructure and Wear Behavior of the Ultrasonic Melt-Treated B390 Hypereutectic Al-Si Alloy

Mona Fad, Waleed Khalifa and Shimaa El-hadad

*Light Metals 2016, John Wiley and Sons, (2014)*

The hypereutectic Al-Si alloys constitute an important family of alloys because of their excellent wear resistance and low thermal expansion. The current work aimed at studying the effect of soaking treatment on the microstructure and wear behavior of the ultrasonic melt-treated B-390 hypereutectic Al-Si alloy. The results showed that the ultrasonic treatment resulted in uniform distribution and refinement of the primary silicon particles. The soaking treatment resulted in coarsening of the primary silicon particles, with larger particles obtained at longer soaking times. It was also observed that particle coalescence is the primary ripening mechanism for the primary Si, especially in the ultrasonic-treated samples. The wear weight loss changed with the soaking time, with the ultrasonic-treated samples exhibiting more consistent trend with little variations of weight loss at different soaking times. The optimum particle size and distribution is obtained after 5 min. soaking of the conventionally cast samples, and 10 min. for the ultrasonic-treated samples. The worn surface of these conditions is characterized by fine and shallow wear scratches with little particle detachments. Soaking at high temperature leads to reducing the volume fraction of the primary silicon, which consequently, caused high weight losses during wear test.

**Keywords:** Soaking; hypereutectic; Al-Si; Wear; Microstructure; Ultrasonic.

## C-21. Electrochemical Fabrication of Nanostructures

R. Abdel-Karim

*Handbook of Nanoelectrochemistry, Springer, (2014)*

Electrodeposition is a unique technique in which a variety of materials can be produced including metals, ceramics, and polymers. In the current chapter, the advantages of electrochemical deposition techniques in fabricating various

nanomaterials with superior properties compared with conventional materials will be highlighted. The properties of various nanostructured coatings produced by electrodeposition are discussed. Some models describing nucleation and growth mechanism are presented. Finally, the importance of some nanocrystalline electrodeposits in many industrial applications as well as their potential role in the planned future technologies is emphasized. The potential of highly ordered nanomaterials for future technological applications includes the field of various nanophotonic, catalytic, microfluidic, and sensing devices, as well as functional electrodes and magnetic recording media. Another application is template assisted electrodepositiion employing a variety of nanoporous membranes and films such as nanoporous alumina membranes used for the synthesis of high-density, ordered arrays of nanodots, nanotubes, and nanowires.

**Keywords:** Electrocrystallization; Nucleation and growth; Metals; Alloys; Nanocomposites; Nanorods; Nanowires; Nanoporous membranes.

## C-22. Effect of High Intensity Ultrasonic Treatment on the Microstrcture Corrosion and Mechanical Behavior of Ac7a Aluminum Alloy

A. M. El-Aziz, M. A. El-Hady and W. Khlifa

*Light Metals , John Wiley, (2014)*

Ultrasonic treatment is one of the most efficient and cost effective processes that are developing in today's technology. It improves mechanical properties, corrosion resistance and homogeneity of the microstructure. In this study, the effect of casting conditions and ultrasonic treatment on the microstructure, hardness and corrosion behaviour of the Al-4.5%Mg alloy was investigated. Alloy ingots were melted in resistance furnace at 750C, and then cast into metallic molds. Pouring temperatures were 750C (superheated) and 639C (liquidus temperature). One sample was poured at 655C and left to solidify in ultrasonic field down to 615C within 2-3 minutes. The microstructure showed a completely coarse dendritic morphology for casting at 750C, and less dendritic morphology with finer grain size when cast at 639C. The finest and most globular aluminum grains and intermetallic particles were obtained by ultrasonic treatment during solidification. Higher hardness values and corrosion resistance were recorded for ultrasonic treated sample in comparison to cast one.

**Keywords**: Ultrasonic treatment; Aluminum alloy; Microstructure; Corrosion Mechanical.

## Medical Sciences Sector

## Faculty of Medicine

### *Dept. of Diagnostic Radiology*

### C-24. Scanning of the Pharaohs: Ct Imagingof the New Kingdom Royal Mummies

Sahar Nasr Abdu Saleem

*Book Published by Cambridge University Press*, (2016)

The royal mummies in the Cairo Museum are an important source of information about the lives of the ancient Egyptians. The remains of these pharaohs and queens can inform us about their age at death and medical conditions from which they may have suffered ،as well as the mummification process and objects placed within the wrappings. Using the latest technology, including Multi-Detector Computed Tomography and DNA analysis, co-authors Zahi Hawass and Sahar Saleem present the results of the examination of royal mummies of the Eighteenth to Twentieth Dynasties. New imaging techniques not only reveal a wealth of information about each mummy, but render amazingly lifelike and detailed images of the remains. In addition, utilizing 3D images, the anatomy of eachface has been discerned for a more accurate interpretation of a mummy's facial features. This latest research has uncovered some surprising results about the genealogy of, and familial relationships between, these ancient individuals, as well as some unexpected medical finds. Historical information is provided to place the royal mummies in context, and the book with its many illustrations will appeal to Egyptologists, paleopathologists, and non-specialists alike, as the authors seek to uncover the secrets of these most fascinating members of the New Kingdom royal families.

**Keywords:** CT, Mummy, Egypt, Royal.

### C-25. How to read and to Report a Fetal Mri Examination

Sahar Nasr Abdu Saleem

*Mr* of *Fetal and Maternal Diseases in Pregnancy, Springer*, (2016)

Fetal MRI is an interactive scanning of the moving fetus owed to the use of ultrafast MRI sequences. T2 single- shot fast spin echo (SSFSE) is the standard sequence; balanced steady-state free precession (SSFP) demonstrates well the fetal anatomy and cardiovascular system, and T1-weighted gradient echo sequence is primarily used to show hemorrhage, calcification, fat, and meconium. Advanced MRI techniques, such as diffusion-weighted imaging (DWI), diffusion tensor imaging (DTI), and mag- netic resonance spectroscopy (MRS), have been increasingly used lately]. The use of fetal MRI is not designed to replace ultrasound as the obstetric diagnostic tool of choice, but rather to act as an adjunct in certain indications. The aim of fetal MRI is to help to reachan accurate and complete prenatal diagnosis.

**Keywords:** Fetal; MRI; Pregnancy.

### *Dept. of Ear Nose and Throat*

### C-26. Surgical Anatomy in Transoral Robotic Procedure: Basic Fundamentals

Hesham Mohamed Ahmed Negm

*Transoral Robotic Surgery for Obstructive Sleep Apnea, Springer*, (2016)

Transoral robotic procedures gained wide acceptance in the treatment of different lesions involving several sub-sites of the head and neck, with the oropharynx the most commonly addressed one. The most evident consequence has been the need "to see" the anatomical structures from a new perspective, with a less important role played by the traditional, well-known, surgical landmarks. This "inside-out" vision must be well understood by those surgeons dealing with transoral robotic-assisted procedures

**Keywords:** Robotic; Sleep apnea.

### *Dept. of Histology*

### C-27. A Tale of Two Cells: Telocyte and Stem Cell Unique Relationship

Zeinab Mohamed El Moghazy El Maadawi

*Telocytes Connecting Cells, Springer*, (2016)

Telocytes have been identified as a distinctive type of interstitial cells and have been recognized in most tissues and organs. Telocytes are characterized by having extraordinary long cytoplasmic processes, telopodes, that extend to form three-dimensional networks and commonly constitute specialized forms of cell-to cell junctions with other neighboring cells. Telocytes have been localized in the stem cell niche of different organs such as the heart, lung, skeletal muscle, and skin. Electron microscopy and electron tomography revealed a specialized link between telocytes and stem cells that postulates a potential role for telocytes during tissue regeneration and repair. In this review, the distribution of telocytes in different stem cell niches will be explored, highlighting the intimate relationship between the two types of cells and their possible functional relationship.

**Keywords:** Telocyte; Stem cell; Relationship.

***Dept. of Pediatrics***

### C-28. Aspna

Mohamed Hesham Mohamed Abdrabou Safouh

*Pediatric Nephrology, Springer*, (2016)

Asia is the largest continent in the world with an estimated population approaching 4.165 billion in 2010, of which 34 % or approximately 1.433 billion are aged 19 years and under [1]. Moreover, the world's most populous countries, China and India, are anintegral part of this large continent. Unfortunately, health care delivery across the Asian continent is very uneven. Childhood mortality and morbidity are important indicators of the quality of health care delivery. Most childhood deaths occur in less developed countries and poorer sectors of the community in more developed countries, reflecting enormous disparities among different geographical areas and population groups. Despite improvement in child health in many of the emerging economies in Asia, the United Nations Children's Fund (UNICEF) estimates that childhood mortality rate is still more than twice the rate in Latin America and the Caribbean, though much lower than sub-Saharan Africa. In fact in South Asia, 1 in 16 children die before the age of 5 years. Thus the Millennium Development Goal is to reduce by two-thirds the under-five mortality rate of children between the years 1990 and 2015 [2]. To achieve this, health policy reform is needed to ensure that competent staff is available in ruralhealth facilities and that services and transportation are made affordable for these rural communities. Therefore the major challenges in pediatric nephrology practice in many of the emerging economies in Asia still include the management of children withacute kidney injury due to diarrheal diseases with severe dehydration, sepsis, and toxins. On the other hand, the prevention and treatment of children with chronic kidney disease is also emerging as the new challenge for this millennium especially in themore urban communities.

**Keywords:** Pediatric nephrology; Asia; Developing countries.

***Dept. of Urology Dept***

### C-29. Is Surgery Still Necessary for Prostate Cancer?

Ahmed Aly Hussein Aly

*Prostate Cancer, Second Edition: Science and Clinical Practice, Academic Press London / Oxford (an Imprint of Elsevier Science)*, (2016)

Management options of localized prostate cancer principally include active surveillance and active treatment options including radical prostatectomy (RP) and radiation therapies (RT). Treatment should be tailored to each patient, taking in consideration the patient's overall health, life expectancy, and disease risk; clinicians' skills and experience; and the patients' preferences and priorities. Comparative effectiveness research on these different treatments is crucial with regard to oncological efficacy, short- and long-term side effects, effects on health-related quality of life (HRQOL), and cost. Multiple well-conducted, retrospective studies suggest better cancer-specific and overall survival for RP compared to RT, especially for higher-risk disease. HRQOL outcomes are not clearly better for one modality over the other, and costs generally favor surgery over radiation. RP should be considered, particularly in the context of multimodal treatment strategies, for men with high-risk disease. Treatmentsneed to be targeted to the patients most likely to benefit, and the way forward likely will involve more use of active surveillance for low-risk disease and multimodal treatment for high-risk disease.

**Keywords:** Prostate; Surgery; Aggressive; Localized.

## Faculty of Pharmacy

***Dept. of Clinical Pharmacy***

### C-30. Economic Evaluation and Its Types

Dalia Mohamed Mohamed Dawoud

*Economic Evaluation* of *Pharmacy Services ,Chapter 4. Elsevier Science*, (2016)

In this chapter, we provide a basic introduction to the different forms of economic evaluation, including cost-minimization analysis, cost-effectiveness analysis, cost–benefit analysis, and cost–utility analysis. In particular, we discuss the measurementof costs and outcomes in these types of economic evaluation and explain how the perspective of an evaluation affects these forms of analysis. We discuss the measurement of costs and patient outcomes and introduce the main measurement tools used by healtheconomists. The chapter also introduces the concepts of incremental analysis, the cost-effectiveness plane, and cost-effectiveness acceptability curves. Finally, we discuss how the results of economic evaluations can be used in decision-making.

**Keywords:** Pharmaco economics; Pharmacy Services, Economic Evaluation; Cost effectiveness analysis.

***Dept. of Pharmaceutical Organic Chemistry***

### C-31. Green Pharmacy Education

Salwa El-Sayed Mohamed El-Meligie

*Book Published by Lambert Academic Publishing*, (2016)

The biggest challenge of green chemistry in pharmacy education is to use its rules in practice. We believe that green chemistry in pharmacy education could provide in depth insight, as well as, actionable and practical tools to brainstorm, discover new ideas, search for new skills and present a platform to show the capabilities and discoveries to the pharmacy students worldwide. Our book represents a role model all around the academic institutions, healthcare institutes, other pharmaceutical institutes as well as academic scholars and researchers to establish our ideas and find new and more effective ways of action to evaluate the results and impact. Currently, our interest is focused on

adopting green chemistry principles as a recent trend in pharmaceutical teaching and learning methods as well as research plan to afford pharmaceutical products. This book discusses green chemistry in life with its basic principles and green chemistry applications; green chemistry in education; green chemistry prospective and challenges in pharmacy education and finally our vision. As one of the professors of pharmacy education, I know that the success of this book depends ultimately on all tools that deals with the important aspects of green chemistry in pharmacy education and how apply them.

**Keywords:** Green chemistry, Sustainable development, Green pharmacy education, Prospective and challenges.

### *Dept. of Pharmacology and Toxicology*

### C-32. Protective Effect of Exercise on Age-Related Oxidant and in flammatory Events

Nada Abdelmoneim Abdelhalium Sallam

*Inflammation, Aging, and Oxidative Stress, Springer*, (2016)

Aging is associated with a chronic state of oxidative stress and inflammation that is mediated by complex and interconnected pathways. Regular exercise counteracts the deleterious effects of aging through its antioxidant and anti-inflammatory actions. Theinflammatory actions of exercise are mainly exerted on adipose tissue (by reducing its mass and inflammatory environment), on the immune system (by shifting immune cells towards the less inflammatory phenotype, modulating the cytokines profiles towards more anti-inflammatory and reduced proinflammatory cytokines, and stimulating glucocorticoids), and on skeletal muscle (by stimulating mitochondrial biogenesis, improving muscle mass and strength, reducing pro-inflammatory cytokines and increasing the anabolic myokine IL-15 and protective heat shock proteins). It is likely that regular exercise exerts the most substantial anti-inflammatory effects in patients having high baseline inflammatory biomarkers, particularly when associated with visceral fat loss. Exercise exerts antioxidant effects by suppressing inflammatory pathways and therefore inhibiting prominent sources of reactive oxygen species and reactive nitrogen species generation. Importantly, exercise also activates redox-sensitive transcription factors, mainly nuclear factor kappa B, activator protein-1 and peroxisome proliferator-activated receptor gamma coactivator 1-alpha, leading to the enhancement of the antioxidant defense mechanisms by modulating the expression and activities of superoxidedismutase, catalase, glutathione peroxidase, and thioredoxinre ductase 1. Exercise also upregulates repair proteins such as heat shock proteins, proteasome complex, oxoguanine DNA glycosylase, uracil DNA glycosylase and telomerase. It is important to note that the effects of exercise depends on the type, intensity, frequency and duration, and also on the individual's age, health status and endurance capacity.

**Keywords:** Aging, Exercise, Oxidative Stress, Mitochondrial Dysfunction and inflammation

## Faculty of Nursing

### *Dept. of Community Health Nursing*

### C-33. Disaster Preparedness, Planning and Management in the Community: The Role of Community Health Nurse

Ebtesam Moawad Elsayed

*Book Published by Creat*, (2016)

As disasters are increasing in number and severity each year, community health nurses need to be adequately prepared now than ever before. The goal of disaster management is to prevent or minimize death, injury, suffering and destruction. It is an interdisciplinary, collaborative team effort and community health nurse are integral in planning and responding to disaster. So community health nurse must be disaster aware, maintain emergency skills & equipment assist in the education of the public in personaldisaster preparedness, and get involved in disaster plan.This review discusses nature, types, characteristics, stages, and effects of disaster as well as role of community health nurse in disaster planning and management.

**Keywords:** Disaster preparedness, Planning, management, Community health nurse.

### C-34. Issues and Challenges of Community Health Nursing in Egypt

Ebtesam Moawad Elsayed

*Book Published by Create Space Independent Publishing Platform*, (2016).

Components of community health nursing practice include health promotion of individuals, families as well as groups, prevention of health problems, treatment of disorders, rehabilitation and research. Community health nursing practice in Egypt faces manychallenges. For examples, the dual disease burden of both communicable and non-Communicable diseases. Issues and challenges such as chronic diseases, disabled population, needs of special groups such as working population, elderly and children, communityviolence, mental health problems, environmental health problem and community empowerment will also be discussed within this text. Community health nurses roles including clinician, educator, advocate, manager, collaborator, leader, and researcher role will also be covered in this text.

**Keywords:** Issues; Challenges; Community health nursing; Egypt.

## C-35. Managing Information Systems and Informatics in Community Health Nursing Practice

Ebtesam Moawad Elsayed

*Book Published by Create Space Independent Publishing Platform*, (2016).

The future of nursing informatics and electronic health in Egypt is bright and promising. Innovation in nursing science combined with advances in information and communication technologies should provide community health nurses with tools that increasingcontact with the communities they serve could be also through community health nursing web-sites resources.In Egypt, much work remains to be done to make nursing informatics a reality. Through hardware, software and personnel; a multi-facet learning program that utilizes distance learning, interactive cable TV, and the internet to connect learning environments to homes, place of work, and the community at large, and by establishing-updating community nursing resources web sites. This text cover areas suchas concepts, benefits and challenges of nursing informatics in Egypt as well as application informatics into community health nursing practice

**Keywords:** Managing information systems; Informatics; Community health nursing.

***Dept. of Medical-Surgical Nursing***

## C-36. Bronchial Hygiene Therapy: Modalities and Techniques

Sameh Elsayed Mohamed Elhabashy

*Book Published by Princeton University Press*, (2016)

Pulmonary complications are major causes of morbidity and mortality for patients with compromised airway clearance. Bronchial hygiene therapy referred to any technique utilized to maintain lung sterility by loosening/removing retained secretions for enhancing ventilation and gas exchange. This book focuses on airway clearance techniques and different modalities have been used to assist those who are unable to clear pulmonary secretions effectively, after given a basic background about respiratory system anatomy and physiology. The following information will be useful for respiratory therapist, critical care nurses, and paramedics. I hope that you find this book enjoyable and clinically relevant that because of the simple presentation of ideas and supported figures.

**Keywords:** Bronchial hygiene therapy; Modalities; Techniques; Gas exchange.

***Dept. of Nursing Administration***

## C-37. Nursing as a Profession and Patient Leading, Guidance and Support

Sherin Gaber Mohamed Elassal

*Book Published by Yale University Press*, (2016)

Nurses work to promote health, prevent disease and help patients cope with illness. They are advocates and health educators for patients, families and communities. When providing direct patient care, they observe, assess and record patient symptoms, reactions and progress. Nurses collaborate with physicians in the performance of treatments and examinations, the administration of medications and the provision of direct patient care in convalescence and rehabilitation. This is why nursing considered as a profession. Patient guidance has been an essential component of Registered Nurses' professional role. In today's healthcare delivery system, patient guidance and leading is becoming increasingly important. The public demands more information and control over their health care. Moreover, illness and limited knowledge about medicine, nursing and the healthcare system mean that patients are often vulnerable and powerless. Furthermore, the development of medicine and advanced technology has resulted in aggressive and swift use of technologies, which is becoming the norm in the contemporary hospital environment.

**Keywords:** Nursing profession; Advocacy; Patient leading; Guidance; Support.

# Faculty of Economics and Political Science

***Dept. of Economics***

## C-38. The Institutional Curse of Natural Resources in the Arab World

Chahir Zaki

*Understanding and Avoiding the Oil Curse in Resource-Rich Arab Economies, Cambridge University Press*, (2016)

This paper argues that the resource curse in the Arab world is primarily an "institutional curse", even though it has several macroeconomic manifestations. An empirical investigation, using an augmented growth model, confirms the conditional resource curse hypothesis. The results suggest that on their own; political institutions do not always have an effect on growth but, when interacted with natural resources, they reduce the negative effect of natural resources on growth but do not offset it. The analysis also shows that the curse has operated in different ways within the Arab world. In the GCC, large rents per capita have been utilized to increase government legitimacy and foster regime stability. Indeed, the curse is expressed subtly through a clear segmentation of the labor markets which acts as an efficient mechanism of rent distribution in the form of well-remunerated public sector jobs and other generous social welfare

schemes to national citizens. In contrast, in the populous group comprises of poorer rentier states that have experienced conflict, violence and social unrest. Moreover, the limited resources seem to have led to more dire economic consequences: Resource busts tend to drive them to engage in excessive borrowing while booms seem to have almost eliminated their manufacturing sectors. Moreover, in a context of low rent per capita, excessive consumption resulted in massive deficiencies in infrastructure investments and an underdeveloped financial sector.

**Keywords:** Institutional curse; Natural resources; Arab world.

## C-39. Egypt as a Leading Nation: Regional Imperatives and Domestic Constraints

Riham Bahi

*Diplomatic Strategies* of *Nations in the Global South: The Search for Leadership , Palgrave*, (2016)

Egypt has been pursuing an active foreign policy to deal with regional issues as part of a strategy for creating regime legitimacy. Egypt's motivation in pursuing such a policy is closely related to its dire need for international aid in order to cope with its economic problems. The government is well aware of the incompatibility between economic dependence and the ability to pursue an independent foreign policy; therefore, it has been active in diversifying its dependence and balancing its internationalrelationships. However, Egypt's success in playing a leading regional role will depend on several factors, including its ability to attain a sustainable level of development, to deal successfully with political and security challenges, and to consolidateits democratization and good governance in a way that can be emulated and promoted elsewhere. It will also depend on the recovery of its reputation as a pragmatic moderator able to exert influence on regional issues.

**Keywords:** Egypt; Foreign policy; Regional leadership.

***Dept. of Political Science***

## C-40. Islamism as a Post-Hegemonic Discourse

Riham Bahi

*The State* of *Social Progress* of *Islamic Societies: Social, Economic, Political, and Ideological Challenges, Springer*, (2016)

A combination of critical ideas and transnationalism has been transforming the Muslim public sphere toward a pluralistic, negotiated, exchange of the sacred meaning. In this emergent public sphere, Muslim women are becoming the catalysts for transformation in Muslim thought and practice related to gender issues. Muslim women intellectuals are well positioned to challenge authoritarian, oppressive, regimes and to create a peaceful global ethos putting an end to the "clash of civilizations" and the threatsof fundamentalism and international terrorism. The contribution of Muslim women working from within to transform Muslim societies should affect the way the West thinks about Islam and Muslims ending the clash/jihadist paradigm and creating a peaceful global ethos with a genuine universality. To provide insights into the significance of the evolving, transnational, Muslim dialogue on gender equality in which the underlying concern is to empower Muslim women to claim the public sphere as their medium of struggle for justice and inclusion. This chapter advocates the need to broaden our political imagination to incorporate religious perspectives as well as alternative, discursive), forms and spaces of politics that were previously overlooked because they didnot fit a predetermined Westphalian notion of the "political".

**Keywords:** Islamism; International relations; Post-hegemonic; Public sphere.

## C-41. Copts'' Role in Modern Egypt

Mai Mogib Abdel MoneimMosad

*Egypt Beyond Tahrir Square, Indiana University Press*, (2016)

One of the distinguishing sub-themes of the Egyptian uprising on January 25th, 2011, has been the proliferation of Coptic political participation in the country. Christian movements and political participation had largely, though not entirely, been guidedby the church during the Mubarak era. During the January 25th revolution, Christian Egyptians joined their Muslim counterparts as "one hand"to challenge state authorities in pursuit of "freedom, bread, social justice and human dignity." After successfully deposing the former President, many of these Christian Egyptians continued on with their revolutionary ambitions. For years Copts presented their demands to the state primarily through the person of their Pope Shenouda III. When pressed to demonstrate for their demands, either by events or by clergy, they did so mostly within the confines of church walls. The 2011 revolution changed this tradition, and the unity expressed in over throwing Mubarak gave Copts a new sense of participation in the rebuilding Egypt. Some Christian participation remained along the lines of revolutionary values, enveloped in the youth movements that populated Tahrir Square. Others began sensing a threat to their full participation from the emergence and rise of Islamic tendencies, and rallied behind a liberal and civil cause. Still others took the opportunities afforded to them by the "Revolution"to organize and demonstrate for particular Coptic issues. Regardless of these differences, there were new givens introduced that influenced the position of Copts in contemporary Egypt: the rise of Political Islamic tendencies, the frequent sectarian clashes and incidences, the Church's retreating role in political affairs, the new Pope and Egypt's newly-elected President Morsi and, finally, the Copts'participation in the June 30th demonstrations and its outcomes on both the political and social levels and their place under the newly elected president. This chapter seeks to analyze the triangular relationship between Regime, Church and Copts. This triangular relationship helps in understanding the position of Copts before and after the so-called "Revolution,"and, second, in discovering the key factors that influenced these three actors after 25th January. Among the factors to consider are how this triangular relationship was framed and its impact on the on the Coptic community; moreover, how, the regime regarded all Copts as a single homogeneous bloc represented by the Pope. This chapter discusses the pre-revolutionary history of the Regime Church Copts relationship, traces its development after the fall of Mubarak, and continues on to the present in order to

examine the current factors and events that influence such an interrelated and complicated rapport.

**Keywords:** Copts; Egypt; Revolution.

## Faculty of Mass Communications

### *Dept. of Press*

#### C-42. Social Media in Egyptian Newspapers: New Opportunity or Credibility Threat ?

Hanaa Farouk Saleh

*Book Published by Lambert*, (2016)

The popularity of social media has revolutionized the way journalists work and the profession as a whole, these tools help to build two-way communications which made public voice louder than ever.The book examines the role playing by social media in the Egyptian newspapers, using a survey of journalists in a different position in those newspapers to know when the beginning of using was? Are these tools really integrated into newsroom routines? What forms of these tools are most used by journalists? How they profit from social media to develop their stories? studies concentrated more in exploring users' characteristics and their motivations, and rare are studies which explore journalists usage of these tools and to what degree and for what reasons? Moststudies adopt content analysis tool to explore journalist's usage of social media, so my exploratory research aims to discover to what extent may journalists use social media and their perceptions of these tools credibility, which represents a great dilemma in their journalistic work, so can they rely on it? The research is especially useful for professionals in Communications fields, news organizations, media practitioners or anyone else who may be considering utilizing online communities for professional purposes.

**Keywords:** Journalists and social media; Social media credibility; News organizations credibility; Social media use during reporting process; Social media role in egyptian context; Social media role in media; Social media use in egyptian newsroom; Egyptian journalists and their perceptions of social media; Journalistic environment; Social media adoption in profession; Media context in Egypt; New media in Egypt; Egyptian revolution; Egypt.

#### C-43. The Neo-Liberal Islamic Preachers it is not Enough to Believe but you Must Act on your Faith

لايوجد

*My Library My History Books on Google Play Political Islam and Global Media: The Boundaries* of *Religious Identity, Routledge*, (2016)

Not only believe in, but also to be active: The role of new preachers in Enforcing Islamic teachings Dr. Nermeen N. Alazrak Dr. Alamira Samah F. Saleh Assistant professor Assistant professor Cairo University Cairo University Abstract: How can you be a good Muslim and also enjoy life? How can you acquire God's satisfaction and at the same time don't deprive yourself from happiness. This is the basis of new patterns of enforcing Islamic teachings implemented by new preachers. Over the last decade a new waveof moderate Muslim preachers have emerged in Egypt with a clear goal; to persuade Muslims, specially Arabs, to not only believe in God, but also to be active in order to improve their societies, the new youthful Muslim televangelists such as Mustafa Hosny, Amr Khalid and Amr Mahran are preaching a combination of piety and modern life and it was so clear that there was a great, may be unexpected, positive response to their distinguished efforts. The chapter which we aim to accomplish should be two-fold : The new preachers' strategies and techniques to affect people and to persuade them to follow Islamic teachings by exploiting face to face communication, satellite channels and perfect using of new media. This section will discuss their creative intellectual approaches to let their audience more involved in their societal activities by using presentations of case studies as a model- Islamic songs- modern appearance) to develop their interests, life style, and their actions. How do Egyptian youth evaluate the new preachers efforts for supporting Islam and Islamic communities? and to what.

**Keywords:** Arabic nedia; Islamic speech; New preachers.

### *Dept. of Radio and Television*

#### C-44. Uploading Ideology: Reading Egyptian Social Capital Using a Facebook Lens

Alamira Samah Farag Abdalfattah

*Debates for The Digital Age (Vol.2): The Good, The Bad and The Ugly* of *Our on Line World, Praeger*, (2016)

Books about Internet culture usually focus on the people, places, sites, and memes that constitute the "cutting-edge" at the time the book is written. That approach, alas, renders such volumes quickly obsolete. This provocative work, on the other hand, focuses on overarching themes that will remain relevant for the long term. The insights it shares will highlight the tremendous impact of the Internet on modern civilization and individual lives well after specific players and sites have fallen out of favor. Content is presented in two volumes. The first emphasizes the positive impact of Internet culture for example, 24-hour access to information, music, books, merchandise, employment opportunities, and even romance. The second discusses the Internet's darker consequences, such as a demand for instant news that often pushes journalists to prioritize being first over being right, online scams, and invasions of privacy that can affect anyone who banks, shops, pays bills, or posts online. Readers of the set will clearly understand how the Internet has revolutionized communications and redefined human interaction, coming away with a unique appreciation of the realities of today's digital world for better and for worse.

**Keywords:** Facebook; Egyptian social capital; Polarization; 30$^{Th}$ of june.

-

***0-1936-1***

الاثار المصرية

**. . Prehistoric Contacts between Central Asia and India**

ابوالحسن محمودبكرىموسى

#N/A

BK or ch

*(2016),IF: ML*

This article .
**Keywords:** Rest.

-

***0-2640-30***

***Physical Therapy for Basic Science***

**. . Effect of induced fatigue on dynamic postural balance**

ايناسالسيدمحمدابوطالب

#N/A

*(2016),IF: ML*

This article .
**Keywords:** Rest.

-

***0-2617-45***

بيولوجيا الاورام

**. . Impaired 53BP1/RIF1 DSB mediated end-protection stimulates CtIP-dependent end resection and switches the repair to PARP1-dependent end joining in G1**

وائلياسينمنصورخلفالله

#N/A

*(2016),IF: ML*

This article .
**Keywords:** Rest.

-

***0-2621-46***

بيولوجيا الاورام

**. . PARP1 inhibition radiosensitizes HNSCC cells deficient in homologous recombination by disabling the DNA replication fork elongation response**

وائل ياسين منصورخلف الله

#N/A

*(2016),IF: ML*

This article .
**Keywords:** Rest.

**-**

***0-2620-47***
بيولوجيا الاورام

**. . Dual targeting of PI3K and MEK enhances the radiation response of K-RAS mutated non-small cell lung cancer**

وائلياسينمنصورخلفالله

#N/A

*(2016),IF: ML*

This article .
**Keywords:** Rest.

+++

***0-0-318***
طب الاطفال

**. . Serial serum alkaline phosphatase as an early biomarker for osteopenia of prematurity**

ايناسعبداللهعلىعبدالله

#N/A

*(2016),IF: ML*

This article .
**Keywords:** Rest.

++++

***0-0-10***
الباثولوجيا الإكلينيكية

**. . Diagnostic and Prognostic Relevance of Bone Marrow Microenvironment Components in Non Hodgkin's Lymphoma Cases Before and After Therapy**

امير هحنفىحسنسليمان

#N/A

*(2016),IF: ML*

This article .
**Keywords:** Rest.

## Engeniering Sciences Sector

## Faculty of Engineering

***Architectural Engineering***

**6-** 1431**B1458**

*Dynamics and Resilience of Informal Areas: International Perspectives*

(2016)
**Abstract**

**Keywords:**

***Architectural Engineering***

**7-** 1424**C1428**
**A Proposed Statistical Model for Real Estate Appraisal in Historical Mixed Use**

Asmaa Abdel Aty Mohamed Ibrahim

*Dynamics and Resilience of Informal Areas: International Perspectives*

(2016)
**Abstract**

**Keywords:**

***Chemical Engineering***

**8-** 1245**C1415**
**CO2 Transport and Storage Technologies**

Seif-Eddeen Fateen

*Carbon Dioxide Capture: Processes, Technology and Environmental Implications*

(2016)
**Abstract**

**Keywords:**

***Electric Power and Machines***

**9-** 564**B1846**

Ossama Elsayed Yousf Gouda

*Environmental Impacts on Underground Power Distribution*

(2016)

**Abstract**

**Keywords:**

***Electric Power and Machines***

**10-** 3228**C1413**

**Swarm Intelligence PID Controller Tuning for AVR System**

Mohamed Ahmed Moustafa Hassan

*Advances in Chaos Theory and Intelligent Control*

(2016)

**Abstract**

**Keywords:**

***Electric Power and Machines***

**11-** 3229**C1414**

**Load Frequency Control Based on Evolutionary Techniques in Electrical Power Systems**

Mohamed Ahmed Moustafa Hassan

*Advances in Chaos Theory and Intelligent Control Volume*

(2016)

**Abstract**

**Keywords:**

***Electric Power and Machines***

**12-** 564**C1845**

Ossama Elsayed Yousf Gouda

*Environmental Impacts on Underground Power Distribution*

(2016)

**Abstract**

**Keywords:**

***Electronics and Communication Engineering***

**13-** 2030**C1431**

**Self-Healing in 5G HetNets**

Khaled Mohamed Fouad Elsayed

*Opportunities in 5G Networks: A Research and Development Perspective*

(2016)

**Abstract**

**Keywords:**

***Irrigation & Hydraulics Engineering***

**14-** 1250**C1423**

**Bed Morphological Changes of the Nile River DS Major Barrages**

Ahmed Mohamed ABdel Sattar

*The Handbook of Environmental Chemistry*

(2016)

**Abstract**

**Keywords:**

***Mechanical Design and Production***

**15-** 2959**C1411**

**Influence of Al2O3 Nano-dispersions on Mechanical and Wear Resistance Properties of Semisolid Cast A356 Al Alloy**

Ahmed Yehia Shash

*Mechanical and Materials Engineering of Modern Structure and Component Design*

(2016)

**Abstract**

**Keywords:**

***Mechanical Power Engineering***

**16-** 807**C1420**
**Solar Thermal Collectors with Low and High Concentration**

*Renewable Energy in the Service of Mankind, Vol II*

(2016)

**Abstract**

**Keywords:**

***Mining, Petroleum and Metallurgy***

**17-** 2833**B1983**

Randa Abdel-Karim

*Electrodeposition of Composite Materials*

(2016)

**Abstract**

**Keywords:**

***Mining, Petroleum and Metallurgy***

**18-** 2829**C1984**
**Fabrication of Nanoporous Alumina**

Randa Abdel-Karim

*Nanofabrication using Nanomaterials*

(2016)

**Abstract**

**Keywords:**

***Mining, Petroleum and Metallurgy***

**19-** 660**C1416**
**Heat Treatment: Post-Weld**

Iman Salah Eldin El-Mahallawi

*Encyclopedia of Iron, Steel, and Their Alloys*

(2016)

**Abstract**

**Keywords:**

***Mining, Petroleum and Metallurgy***

**20-** 658**C1417**
**Welding-associated failures in power boilers**

Iman Salah Eldin El-Mahallawi

*Handbook of Materials Failure Analysis with Case Studies from the Chemicals, Concrete and Power Industries*

(2016)

**Abstract**

**Keywords:**

***Mining, Petroleum and Metallurgy***

**21-** 2260**C1410**
**Effect of Soaking Treatment on the Microstructure and Wear Behavior of the Ultrasonic Melt-Treated B390 Hypereutectic Al-Si Alloy**

Waleed Khalifa

*Light Metals 2016*

(2016)

**Abstract**

**Keywords:**

***Mining, Petroleum and Metallurgy***

**22-** 2831**C1412**
**Electrochemical Fabrication of Nanostructures**

Randa Abdel-Karim

*Handbook of Nanoelectrochemistry*

(2016)

**Abstract**

**Keywords:**

***Mining, Petroleum and Metallurgy***

**23-** 2259**C1842**
**Effect of High Intensity Ultrasonic Treatment on the Microstrcture Corrosion and Mechanical Behavior of AC7A Aluminum Alloy**

Waleed Khalifa

*Light Metals*

(2016)

**Abstract**

**-**

# Authors' Index

**Aamer, Ahmed:** M-433, M-436, M-439, M-461
**Abbas, Mohamed:** T-34, T-39, T-40, T-41, T-42, T-43, T-44, T-46, T-47, T-48, T-49, T-50, T-51
**Abbas, Samah:** M-440, M-444, M-454, M-475, M-477, M-479
**Abbassi, Maggie:** M-527, M-528, M-532
**Abd Alfatah, Mohamed:** B-528
**Abd El -Fattah, Alaa:** B-525
**Abd El-Aziz, Abd El-Aziz:** E-233
**Abd El-Ghany, Wafaa:** B-655, B-656, B-657, B-659
**Abd- Elhameed, Waleed:** B-305, B-309, B-312, B-319, B-324, B-330, B-338, B-343, B-344, B-348
**Abd El-Rahman, Yasser:** B-276
**Abd Rabo, Fawzia:** B-526
**Abd-Alla , Mamdouh:** B-522
**Abdallah, Aynam:** M-260
**Abd-Allah, Foad:** M-219, M-220, M-221, M-222, M-223, M-224, M-225, M-226, M-227, M-228, M-229
**Abdallah, Hossam:** M-683, M-688, M-691, M-697, M-700, M-716
**Abdallah, Magda:** B-133, B-200, B-204, B-207, B-208
**Abdallah, Mahmoud:** M-443, M-450, M-458, M-468
**Abdeen, Mostafa:** E-108, E-124, E-127, E-128
**Abdel Baky, Abeer Abdel Baky:** B-557
**Abdel Fattah, Amal:** M-507, M-511
**Abdel Harith, Mohamed:** B-724, B-729, B-730, T-15, T-16, T-5
**Abdel Kader, Mohamed:** B-382, B-392
**Abdel?Riheem, Nadia:** B-121, B-223
**Abdel-Aal, Asmaa:** M-57
**Abdel-Aty, Abdel-Aty:** B-552, B-620, B-621, B-622, B-623, B-626, B-627, B-628, B-629, B-630, B-633, B-634, B-635, B-636, B-637, B-638, B-639, B-640, B-641, B-642, B-643, B-645, B-646, B-654
**Abdel-Aziem, Amr Almaz:** M-825, M-830, M-843
**Abdel-Azim, Hamdy:** M-76
**Abdelaziz, Ashraf:** M-168, M-170
**Abdelaziz, Dalia:** M-318, M-37
**Abdel-Aziz, Khaled:** T-26, T-28
**Abdelaziz, Mohamed:** M-197
**Abdel-Aziz, Mosaad:** M-140, M-142, M-143
**Abdelaziz, Omar:** M-117, M-124
**Abdelaziz, Wessameldin:** B-726, B-737
**Abdelbaky, Ahmed:** M-139
**Abdelbary, Aly:** M-638
**Abdelbary, Ghada:** M-665
**Abd-El-Fattah, Mai:** M-603, M-737
**Abdel-Gaber, Rewaida:** B-412, B-415, B-416, B-417
**Abdel-Ghaffar, Fathy:** B-413, B-427, B-432, B-451
**Abdelghaffar, Shereen:** M-354, M-68
**Abd-Elghani, Abd:** B-385
**Abdel-Ghani, Nour:** B-110, B-113, B-154, B-182, B-183, B-210, B-48
**Abdelghany, Mona:** T-10, T-13, T-18, T-8
**Abdel-Hadi, Abdel-Hadi:** B-541, B-543
**Abd-El-Hafiz, Salwa:** E-87
**Abdel-Hakeem, Mohamed:** M-540
**Abdelhamid, Abdou:** B-118, B-119, B-121, B-219, B-223, B-232
**Abdelhamid, Ismail:** B-136, B-141, B-193, B-195, B-199, B-202, B-203, B-206, B-221, B-224, B-226, B-69
**Abdel-Hamid, Mahmoud:** B-524
**Abdelkader, Noha:** M-731, M-744
**Abdel-Kader, Nora:** B-112, B-148
**Abdelkareem, Omar:** T-15, T-16
**Abdel-Karim, Abeer:** B-168, B-186, B-99
**Abdelkawy, Mohamed:** M-433, M-452, M-461, M-497
**Abdelkawy, Mostafa:** M-561
**Abdel-Khalek, Amr:** B-428, B-429, B-430, B-438
**Abd-Ellatif, Mohamed:** M-18
**Abd-Ellatif, Noha:** M-804, M-805
**Abdelmageed, Alaa:** E-118, E-130
**Abdel-Mageed, Ali:** B-50, B-51
**Abdelmaksoud, Ahmed:** M-170
**Abdel-Maksoud, Gomaa:** T-12, T-20, T-6, T-9
**Abdel-Moein, Khaled:** B-698, B-699, B-701, B-702, B-703, B-704, B-706, B-707, B-708
**Abdelmoety, Ghada:** M-248, M-255, M-258
**Abdelmonem, Nabil:** E-14, E-19, E-23, E-26, E-9
**Abdelrahman, Ahmed:** M-287
**Abdelrahman, El-Sayed:** B-294, B-297, B-298
**Abdelrahman, Yasser:** M-536, M-543

**Abdelraouf, Osama:** M-826
**Abdel-Rassoul, Mohammed:** M-397
**Abdel-Razek, Abdel:** M-260
**Abdelrazek, Fathy:** B-147, B-205, B-220, B-93
**Abdelrazik, Noha:** M-296
**Abdelsalam, Mohamed:** B-603
**Abdelsalam, Rania:** M-730, M-732
**Abd-Elsalam, Reham:** B-560
**Abdel-Sattar, Ahmed:** E-131, E-132, E-133, E-136, E-137, E-138
**Abdel-Sattar, Essam:** M-671, M-685, M-700, M-704, M-716
**Abdelwahab, Abdel:** M-791
**Abdel-Wahab, Yasser:** B-337, B-341
**Abdo, Ahmed:** B-158, B-56, B-72, B-75, B-87, B-88, B-89, B-90
**Abdulazim, Mohammed:** M-391
**Abdulgawad, Nesreen:** M-799, M-800
**Abdulmagead, Ibrahim:** B-376, B-394, B-396
**Abdulrazzak, Omar:** M-394
**Aboeleela, Magdy:** , E-44, E-55
**Aboelwafa, Ahmed:** M-586, M-614, M-631
**Abo-Ezz, Eid:** B-291, B-294, B-297, B-298
**Abo-Kaila, Khaled:** B-372, B-383
**Abolnasr, Ahmad:** E-8
**Aboud, Aboud:** B-392
**Abou-Dina, Moustafa:** B-311
**Abouelsaood, Ahmed:** E-142
**Aboulela, Waseem:** M-393
**Aboul-Enein, Ahmed:** B-474, B-475, B-484
**Aboulfotouh, Abdel-Nasser:** B-366
**Abou-Seri, Sahar:** M-565, M-566, M-567, M-568, M-571, M-582, M-590
**Abu El-Ela, Faten:** B-478, B-484, B-485
**Abu-Elala, Nermeen:** B-560
**Abuelhamed, Walaa:** M-328, M-337, M-338, M-44
**Abu-Elyazeed, Mohamed:** E-64
**Abul-Fotouh, Amr:** M-158
**Aburahma, Mona:** M-621, M-659
**Abu-Seida, Ashraf:** B-663, B-664, B-667, B-671, B-672, B-673, B-674, B-677, B-678, B-679, B-683, B-684
**Abuzeid, Ola:** M-113
**Adel, Mohamed:** B-345
**Adly, Amr:** E-51
**Afifi, Lamia:** M-233
**Afify, Abd El Moneim:** B-466, B-467, B-482
**Agha, Aza:** M-733, M-739, M-784
**Ahmad, Neveen:** B-252, B-254, B-257
**Ahmed, Aasem:** M-188, M-200
**Ahmed, Ahmed:** B-67
**Ahmed, Ahmed:** B-110, B-115, B-125, B-131, B-143, B-153, B-154, B-159, B-182, B-196
**Ahmed, Amira:** B-412, B-432
**Ahmed, Ashour:** B-60
**Ahmed, Eman:** M-596, M-602
**Ahmed, Esayed:** B-69
**Ahmed, Hanan:** M-333
**Ahmed, Haney:** B-588
**Ahmed, Harby:** T-5
**Ahmed, Hoda:** B-129, B-152
**Ahmed, Ibrahim:** B-529, B-530, B-536
**Ahmed, Kawkab:** B-612, B-614, B-615, B-619
**Ahmed, Maha:** T-8
**Ahmed, Maha:** M-581
**Ahmed, Mahmoud:** S-35, S-36
**Ahmed, Mohamed:** B-132
**Ahmed, Mohamed:** B-560
**Ahmed, Nadia:** B-150, B-189, B-197, B-238, B-84, B-86
**Ahmed, Nadia:** E-92
**Ahmed, Olfat:** B-600, B-603
**Ahmed, Osama:** B-474, B-475
**Ahmed, Rhaam:** B-495
**Ahmed, Safwat:** E-175
**Ahmed, Sally:** M-119, M-121, M-124, M-137
**Ahmed, Samar:** M-64
**Ahmed, Sayeda:** B-469, B-532
**Ahmed, Tamer:** E-11
**Ahmed, Wael:** B-258, B-260
**Ahmed, Youssri:** B-309, B-312, B-324, B-343, B-348
**Ahmed, Zakia:** B-603
**Alaasar, Mohamed:** B-128, B-47, B-52, B-53, B-66, B-81
**Alalkamy, Essam:** M-357
**Alanani, Naglaa:** M-324, M-327, M-331, M-345, M-348, M-349, M-351, M-352, M-355
**Al-Antably, Abeer:** M-294, M-296, M-301
**Algarem, Hasan:** M-59
**Al-Ghobashy, Medhat:** M-415, M-416, M-420, M-425, M-426, M-451, M-452, M-464
**Al-Hameed, Salah:** B-648, B-652
**Alharery, Mahmoud:** B-580
**Ali, Adel:** B-275, B-286

**Ali, Aliaa:** M-320, M-322, M-338
**Ali, Amany:** B-398, B-418, B-436
**Ali, Maha:** B-748
**Ali, Maisa:** T-11, T-19, T-3, T-4
**Ali, Mohamed:** B-45
**Ali, Rehab:** B-458, B-483
**Ali, Shimaa:** B-170, B-181, B-87
**Ali, Yomna:** M-259, M-267
**Alieldin, Nelly:** M-120
**Al-Inany, Hesham:** M-247
**Alkhazindar, Maha:** B-46
**Allah, Elham:** B-666, B-668, B-669, B-670, B-681, B-682
**Alllam, Riham:** M-287, M-97
**Al-Mahallawi, Abdulaziz:** M-638
**Al-Mokaddem, Asmaa:** B-619
**Alsaadi, Mohamed:** M-187, M-52
**Alsherbiny, Muhammad:** M-689, M-690
**Al-Shorbagy, Muhammad:** M-452
**Alsirafy, Samy:** M-79, M-82, M-86, M-88
**Altalbawy, Farag:** B-101, B-240, B-76
**Aly, Ahmed:** M-154, M-175
**Aly, Mahmoud:** B-603
**Aly, Salwa:** B-566
**Aly, Samir:** M-572
**Ameer, Magda:** B-49
**Amer, Aziza:** B-616, B-647
**Amer, Haitham:** B-691, B-692, B-695
**Amer, Mohammed:** B-662, B-668, B-680
**Amin, Ahmed:** B-407
**Amin, Amr:** M-78
**Amin, Iman:** M-109, M-110
**Amin, Kamilia:** M-570, M-590, M-591
**Amin, Magdy:** M-554, M-555, M-556, M-560, M-562, M-563
**Amin, Maha:** M-645, M-655, M-658
**Amin, Mona:** B-399, B-402, B-403, B-434, B-435
**Amin, Shaimaa:** M-360
**Amir, Azza:** B-404, B-449
**Anany, Mervat:** M-58, M-91
**Anis, Shady:** M-76
**Ansary, Mervat:** M-378, M-52
**Arab, Hany:** M-499
**Arafa, Reem:** B-92
**Asaad, Mohamed:** B-336, B-340
**Ashmawey, Abeer:** M-786
**Ashour, Ahmed:** E-188, E-189
**Ashour, Fatma:** E-22, E-27, E-28, E-5
**Ashour, Hani:** B-527
**Ashour, Hossam:** M-541, M-553
**Ashour, Rehab:** M-729
**Assem, Magda:** M-762, M-764
**Atiya, Amir:** E-29, E-30
**Atta, Attia:** B-631
**Atta, Nada:** B-56, B-72, B-75, B-87, B-88, B-89, B-90
**Attaby, Prof.:** B-104, B-155, B-74
**Attalla, Ehab:** M-779, M-780
**Attalla, Sherief:** B-511, B-516
**Attia, Ahmed:** M-425, M-523, M-537, M-538, M-544, M-548
**Awaad, Mohamed:** B-610, B-657, B-659, B-660
**Awad, Ahmed:** E-214
**Awad, Hanan:** B-262, B-263
**Awad, Mona:** B-531
**Awad, Naglaa:** B-675
**Awad, Zainab:** B-3
**Awadallah, Fadi:** M-570
**Awadein, Ahmed:** M-276, M-284, M-285
**Azim, Fadwa:** M-54
**Aziz, Mohamed:** M-168
**Aziz, Ramy:** M-535, M-542, M-549, M-550
**Aziz, Rasha:** M-163, M-208
**Azzam, Omar:** M-98
**Badawey, Amr:** M-436
**Badawi, Alia:** M-630
**Badr, Abeer:** B-437
**Badr, Amr:** E-209, E-210, E-211
**Badr, Eslam:** B-328, B-332, B-335
**Badran, Snaa:** B-524
**Bahaa, Nevien:** M-50, M-52
**Bahaa, Sara:** M-111, M-112
**Bakr, Eman:** B-618
**Baky, Heba:** B-31
**Barakat, Dalia:** B-527
**Barsoum, Rashad:** M-187, M-196, M-198
**Basalious, ?Emad:** M-421, M-428, M-449, M-640, M-657
**Bashtar, Abdel:** B-411
**Bashtar, Abdel-Rahman:** B-388
**Bassal, Taha:** B-246, B-248
**Bassiouny, Dalia:** M-102, M-98
**Bassiouny, Yasmin:** M-243, M-260
**Bassyouni, Iman:** M-371, M-373
**Basta, Fawzy:** B-287
**Bastawros, Nabil:** B-327, B-333
**Basyoni, Maha:** M-295, M-299, M-301
**Baz, Tamer:** M-153, M-156, M-170, M-59
**Bazaraa, Hafez:** M-389
**Bebawi, Hany:** M-459
**Bendas, Ehab:** M-657
**Beshlawy, Amal:** M-308, M-321

**Biltagy, Marwa:** S-8
**Boghdady, Noha:** M-508, M-510
**Bossiela, Manal:** M-97
**Botros, Manal:** B-369, B-376, B-387
**Botros, Shahira:** M-67
**Dabbous, Abeir:** M-144
**Daif, Emad Tawfik:** M-399, M-400
**Dakrory, Ahmed:** B-431, B-440, B-442
**Damaty, Ahmed:** M-235
**Darouti, Mohammad:** M-109, M-113
**Darweesh, Ahmed:** B-105, B-144, B-196, B-198, B-55, B-69
**Darweesh, Samar:** M-165, M-174
**Darwish, Elham:** B-101, B-240
**Darwish, Hany:** M-418, M-422, M-429, M-436, M-448, M-453, M-463, M-465, M-466, M-478, M-482, M-483, M-484, M-485, M-487
**Darwish, Hebatallah:** M-502, M-504, M-515, M-516, M-518, M-730, M-95
**Dawood, Dalia:** M-525, M-526, M-531
**Dawood, Kamal:** B-198, B-209, B-212, B-228, B-229, B-71
**Deeb, Kadriya:** M-705
**Demerdash, Doaa:** M-186
**Dessouky, Mohamed:** B-556
**Diab, Aliaa:** M-809
**Doha, Eid:** B-305, B-306, B-313, B-315, B-316, B-323, B-324, B-325, B-330, B-338
**Dorrah, Moataza:** B-246, B-248
**Doss, Essam:** M-16, M-305
**Doss, Waheed:** M-187
**Draz, Amira:** M-820, M-823, M-825
**Eddin, Mohamad:** M-274, M-275, M-285
**Edesa, Wael:** M-77
**Edmardash, Yusuf:** B-258, B-260
**Eid, Mohamed:** M-840
**Eissa, Amal:** M-576
**Eissa, Mervat:** M-374
**Ekladious, Sherif:** M-347
**El Barkooky, Ahmed:** B-282
**El Hadidi, Nesrin:** T-17, T-3, T-4
**El Hussieny, Noha:** M-186
**El Refaee, Ehab:** M-234, M-239
**El Sayed, Nesrine:** M-747
**El Sherbini, Ashraf:** B-366, B-367, B-368, B-371
**El Sherbiny, Tharwat:** B-380
**Elagha, Abdalla:** M-25, M-26
**Elakel, Wafaa:** M-149, M-165, M-208
**El-Alfy, Taha:** M-722, M-727
**Elalla, Mostafa:** M-100, M-115
**El-Anadouli, Bahgat:** B-165, B-213, B-67, B-85
**Elansary, Afaf:** M-597
**El-Ansary, Aida:** B-112, B-148
**El-Anwar, Omar:** E-184
**Elaraby, Zeinab:** M-158, M-164, M-173
**El-Askary, Hesham:** M-699
**El-Assal, Salah El-Din:** B-540
**Elattar, Inas:** M-170
**Elawwad, Abdelsalam:** E-173
**El-Ayadi, Moataz:** E-68, E-84
**El-Badry, Ayman:** B-449, M-291, M-296, M-69
**El-Bagary, Ramzia:** M-564, M-575
**Elbannan, Mohamed:** S-29, S-30
**Elbaroty, Gamal:** B-460, B-480
**Elbasha, Noussa:** M-332
**Elbasiouny, Mahmoud:** B-749
**El-Batawy, Yasser:** E-88
**Elbatt, Tamer:** E-63, E-67, E-69
**El-Beltagi, Hossam:** B-464, B-465, B-479
**Elbialy, Nihal:** B-28
**Elbnna, Hossny:** B-625, B-644
**Eldaly, Mohamed:** M-277
**Eldanasouri, Nabiel:** M-57
**El-Deab, Prof.:** B-166, B-67
**Eldebss, Taha:** B-92, B-94
**Eldeeb, Abeer:** M-843
**Eldeib, Ayman:** E-197, E-199
**El-Denshary, Ezz:** M-744, M-754
**El-Dieb, Samia:** B-525
**Eldin, Hanaa:** M-792, M-794
**El-Din, Hebat:** M-423, M-479
**Eldin, Lamiaa:** M-730
**El-Dosouky, Mohamed:** B-139, B-192, B-244
**El-Eyoun, Ihab:** M-335
**Elfadaly, Fadlalla:** S-20
**El-Fattah, Hussein:** B-164
**El-Fayoumi, Dina:** M-272, M-287
**Elfayoumy, Hany:** M-397, M-766
**Elfeky, Souad:** B-733
**Elfishawy, Ahlam:** M-705, M-708, M-711
**Elfowy, Fayza:** M-49, M-53, M-66
**El-Gamal, Mohamed:** E-94
**El-Gammal, Samar:** B-632
**El-Gawad, Hossam:** E-89
**El-Gebaly, Reem:** B-29
**El-Ghany, Nahedabd:** B-189, B-197, B-238, B-84, B-86
**El-Ghobashy, Mohamed:** M-439, M-444, M-454, M-471, M-477, M-489, M-491
**El-Glil, Ahmed:** B-669
**Elhafez, Salam:** M-811, M-827, M-828,

M-829
**El-Halawany, Ali:** M-675, M-681, M-683, M-686, M-687, M-688, M-691, M-695, M-697, M-702, M-703, M-717
**El-Hanafi, Ghada:** M-103
**El-Hawagry, Magdi:** B-253, B-255, B-265, B-266
**Elhawary, Rabab:** M-318, M-32, M-335, M-37
**El-Hawary, Seham:** M-681, M-692, M-694, M-702, M-709, M-721, M-723, M-724
**Elhelw, Rehab:** B-573, B-575, B-581, B-582
**Elhelw, Rehab:** B-580
**Elhifnawy, Niveen:** M-759
**Elhilali, Hala:** M-285
**El-Idreesy, Tamer:** B-223, B-94
**Elkabbany, Farouk:** B-384
**Elkady, Ehab:** M-455, M-580, M-586, M-587, M-589
**El-Kammar, Ahmed:** B-280
**El-Karaksy, Hanaa:** M-323, M-343, M-344, M-354, M-46
**Elkasabgy, Nermeen:** M-616
**El-Kashif, Amr:** M-82
**El-Kattan, Eman:** M-126, M-252
**El-Khatib, Aiman:** M-732, M-736
**El-Khayat, Waleed:** M-254, M-255, M-257, M-259
**Elkholy, Nesrin:** M-114
**Elkholy, Said:** B-90
**Elkomy, Rasha:** M-261
**El-Lakkani, Ali:** B-22
**El-Latif, Hekmat:** M-745, M-749, M-750, M-752
**Ellithi, Ali:** B-349, B-350, B-351, B-352, B-353, B-354, B-355, B-356, B-357, B-359, B-360, B-361, B-362, B-363, B-364, B-365, B-374, B-385, B-386, B-389
**Ellithy, Hend:** M-194, M-55
**Elmaadawi, Zeinab:** M-114, M-116, M-98
**El-Mahallawi, Iman:** E-163, E-167
**Elmahdy, Magdy:** B-602
**Elmahrouk, Galal:** M-652
**Elmakhzangy, Hesham:** M-149
**Elmalah, Afaf:** M-598, M-603
**El-Maraghy, Shohda:** M-499, M-519, M-685
**El-Marsafy, Aisha:** M-318, M-37
**El-Mazny, Akmal:** M-264, M-268, M-270
**Elmegeid, Marwa:** B-384
**Elmelegie, Slawa:** M-596, M-602
**Elmeshad, Aliaa:** M-613, M-619, M-648
**El-Midany, Ayman:** E-164, E-165, E-170
**Elminiawy, Hala:** B-603
**El-Mistikawy, Tarek:** E-112, E-93
**Elmogy, Mohamed:** B-246
**El-Nagar, Gumaa:** B-55, B-67
**Elnagdy, Sherif:** T-2
**El-Nassan, Hala:** M-592, M-593, M-594, M-595
**El-Nebrawy, Eman:** M-103
**Elnoshokaty, Esam:** M-759
**Elragehy, Nariman:** M-443, M-450, M-458, M-468
**Elrahman, Ahmed:** M-612, M-620, M-625, M-646, M-653, M-661
**El-Rahman, Mahassen:** M-149, M-158
**El-Rahman, Mohamed:** M-413, M-432
**El-Rahman, Sahar:** B-607, B-619
**El-Rahman, Sherif:** M-368, M-369
**El-Raziky, Maissa:** M-158, M-164, M-174, M-212
**El-Refay, Basant:** M-815
**El-Rehem, Fouad:** B-470
**El-Rifai, Nihal:** M-320
**Elsaadany, Zinab:** M-271, M-40
**El-Sabaa, Abdel-Aleem:** B-553, B-559
**El-Sahar, Ayman:** M-735
**El-Said, Alyaa:** B-449
**El-Saied, Heba:** M-275, M-286
**Elsakhawy, Mohamed:** B-559
**El-Sanousi, Ahmed:** B-573, B-575, B-688, B-696, B-697
**El-Sayed, Abeer:** M-508
**Elsayed, Abir:** M-375
**Elsayed, Anwar:** B-27
**El-Sayed, Ekram:** B-56, B-72, B-88
**Elsayed, Gamal:** M-141
**Elsayed, Hadeel:** M-149, M-158, M-163
**Elsayed, Khaled:** E-62
**Elsayed, Nehad:** M-576
**El-Sayeda, Aly:** M-678
**Elsetohy, Khaled:** M-245, M-246, M-249, M-265
**Elsetouhy, Doaa:** M-627, M-645
**El-Shaarawy, Ehab:** M-1, M-2, M-4
**El-Shabrawi, Mortada:** M-330, M-350, M-353
**El-Shabrawy, Abdel:** M-724
**Elshafeey, Ahmed:** M-608
**El-Shafeiy, Moataz:** B-280
**Elshaghabee, Foad:** B-523
**Elshahat, Khaled:** B-590, B-591, B-592
**Elshahed, Mostafa:** E-38, E-56
**El-Shakankiry, Nayera:** M-770

**Elshakhs, Neveen:** M-188, M-310, M-313, M-314, M-315, M-316, M-317
**Elshamy, Noha:** M-425, M-523, M-537, M-544, M-548
**El-Shamy, Shamekh:** M-840
**Elsharkawy, Aisha:** M-168, M-169, M-172
**Elsharkawy, Marwa:** M-69, M-71
**El-Sharkawy, Mohamed:** M-259, M-268
**El-Shazly, Alaa:** S-1
**El-Shazly, Mohamed:** B-258, B-260
**El-Sheikh, Mohamed:** T-30, T-31, T-32, T-33
**Elshemey, Wael:** B-25, B-26, B-27, B-28
**El-Shemy, Hany:** B-455, B-459, B-462, B-469
**El-Sherbini, Seham:** M-320
**El-Sherbiny, Mahmoud:** E-144, E-149, E-151
**El-Sherei, Moshera:** M-710
**El-Sherif, Ahmed:** B-185, B-186, B-98, B-99
**Elsherif, Rasha:** M-167, M-96
**Elsherpieny, Elsayed:** B-668, E-236
**Elshimy, Mohammed:** M-389, M-393
**El-Shkra, Mohamed:** B-178
**El-Soud, Walid:** B-34
**Eltanamly, Rasha:** M-288
**Eltayeb, Osama:** M-544
**Eltoukhy, Omar:** B-676, B-680, B-681
**Elwahy, Ahmed:** B-105, B-136, B-193, B-195, B-196, B-202, B-218, B-69, B-70, B-83
**El-Zahab, Essam Abo:** E-38, E-39, E-57
**El-Zaher, Asmaa:** M-581, M-587
**Elzanfaly, Eman:** M-414, M-436, M-437, M-455, M-460, M-462, M-490, M-496, M-645
**El-Zeany, Badr:** M-414, M-429, M-437, M-441, M-462
**Elzorkani, Bassel:** M-370, M-375, M-376
**Emara, Aya:** S-19
**Emira, Ahmed:** E-73
**Esmail, Eman:** M-230
**Esmat, Gamal:** M-146, M-147, M-148, M-149, M-153, M-155, M-156, M-157, M-158, M-161, M-162, M-164, M-165, M-166, M-169, M-171, M-208
**Esmat, Samia:** M-99
**Essa, Khalid:** B-290, B-291, B-294, B-297, B-298
**Ezz, Heba:** B-405, B-423, B-433
**Ezzat, Shahira:** M-648, M-673, M-677, M-698, M-699, M-701, M-705, M-706, M-709, M-713, M-721, M-723, M-724
**Ezzeldeen, Nashwa:** B-650
**Fadda, Sawsan M H:** M-306
**Faheem, Mena:** B-564, B-565
**Fahmay, Mohamed:** B-160, B-185
**Fahmi, Abdel Gawad:** B-130, B-192, B-219, B-232
**Fahmy, Ahmed:** E-201, E-203, E-205
**Fahmy, Hossam:** E-61
**Fahmy, Magdy:** B-601
**Fahmy, Mona:** B-189, B-197, B-84, B-86
**Fahmy, Rania:** M-561, M-624, M-651
**Fahmy, Yasmine:** E-75, E-82
**Farag, Ahmad:** B-105, B-144, B-145, B-218, B-245, B-70, B-92, B-94
**Farag, Aya:** S-26
**Farag, Magdi:** B-129, B-130
**Farag, Mohamed:** M-669, M-670, M-672, M-677, M-678, M-679, M-680, M-682, M-684, M-700, M-711, M-713
**Farag, Randa:** B-106
**Farag, Randa:** B-79, B-80, B-82
**Farag, Sherif:** , E-53, E-58, E-59, E-60
**Farghali, Haithem:** B-675
**Farghaly, Thoraya:** B-133, B-135, B-137, B-138, B-175, B-222, B-227, B-230, B-234, B-71
**Farhan, Marwa:** M-252
**Farid, Ibtisam:** M-43
**Farid, Samar:** M-529, M-530, M-531, M-532, M-534
**Fateen, Seif:** E-15, E-16, E-17, E-18
**Fathalah, Waleed:** M-158
**Fathy, Hesham:** M-393
**Fathy, Hesham:** M-138
**Fathy, Mona:** M-296, M-45, M-46, M-53
**Fawzi, Marwa:** M-111, M-112
**Fawzi, Marwa:** M-100, M-109, M-114, M-115, M-116, M-97
**Fayed, Adel:** B-569
**Fayed, Dr.:** M-417, M-419, M-469
**Fayed, Sayed:** B-471, B-472, B-476
**Fayek, Nesrin:** M-718
**Fayez, Mohamed:** B-492, B-493
**Fayez, Yasmin:** M-442, M-457, M-488, M-489, M-491
**Fekry, Mostafa:** M-682
**Fishawy, Hussein:** M-187
**Foad, Marwa:** M-573, M-575, M-583, M-584

**Foad, Pakinam:** M-286
**Fouad, Hanan:** M-174
**Fouad, Shawky:** M-301
**Fouda, Ragai:** M-58
**Fouda, Usama:** M-244, M-245, M-246, M-249, M-265
**Frag, Eman:** B-239, B-65
**Gaafar, Hassan:** M-261
**Gaafar, Taghrid:** M-37, M-61
**Gaber, Ahmed:** B-542
**Gad, Ahmed:** B-507
**Gad, Zeiad:** M-110, M-781
**Gado, Rania:** T-1
**Gahleb, Ahmed:** B-308, B-311
**Galal, Hussein:** B-579
**Galal, Mona:** B-553
**Galal, Nermeen:** M-318, M-37
**Gamala, Wafia:** B-382, B-392
**Gawad, Hamdy:** B-304, B-321, B-322, B-326
**Gawad, Iman:** M-758, M-767
**Gawad, Mohamed:** B-282
**Gawdat, Heba:** M-100, M-101, M-93, M-95
**Gazayerly, Omaima:** M-614, M-615, M-626, M-631, M-655
**Gazzawi, Nervina:** B-263
**Gedawy, Ehab:** M-598, M-599
**Genidy, Gehad:** B-123, B-124, B-146, B-149, B-156, B-167, B-172, B-177, B-215, B-237, B-239, B-95, B-96, B-97, B-98
**George, Riham:** M-572, M-573, M-574, M-577, M-578, M-588
**Geweely, Neveen:** B-39
**Ghaith, Doaa:** M-167, M-19, M-252, M-59, M-60, M-63
**Ghallab, Noha:** M-401, M-402
**Ghamrawy, Mona:** M-212, M-5, M-72
**Ghany, Eman:** M-338, M-44
**Gheita, Tamer:** M-282, M-378, M-743, M-748
**Ghobrial, Emad:** M-333, M-341
**Ghoneim, Nahed:** B-707
**Ghorab, Dalia:** M-639, M-656, M-663
**Ghorab, Mahmoud Mohamed:** M-618, M-636, M-637, M-644
**Ghozlan, Said:** B-199, B-203, B-206, B-224, B-226
**Girgis, Marian:** M-329, M-335, M-49
**Gobashy, Mohamed:** B-294, B-300
**Gomaa, Ahmed:** E-4
**Gomaa, Sobhy:** B-118, B-121, B-122, B-135, B-137, B-138, B-187, B-200, B-201, B-204, B-205, B-207, B-208, B-220, B-225, B-227, B-230, B-233, B-234, B-71, B-76
**Goniem, Azza:** B-54
**Gouda, Eman:** B-554
**Gouda, Heba:** M-65, M-72
**Gouda, Iman:** M-120
**Gouda, Ossama:** E-50
**Grace, Said R.:** E-107, E-113, E-114, E-115, E-119, E-120, E-122, E-123, E-129, E-96
**Guaily, Amr:** E-105
**Habib, Basant:** M-609
**Habib, Enmar:** M-389, M-393, M-395
**Habib, Serag:** E-78
**Hafez, Ebtisam Hafez:** B-127
**Hafez, Mona:** M-342, M-347, M-382
**Hafez, Rania:** B-393
**Hafez, Vanessa:** M-92
**Hafeza, Nesreen:** M-801, M-802, M-803
**Hafiz, Nagah:** B-564
**Halim, Dalia:** M-93, M-97
**Halim, Mona:** M-60
**Hamad, Hanan:** B-419
**Hamad, Mohamed:** B-285
**Hamdan, Mohamed:** B-272, B-281, B-289
**Hamdy, Ebtehal:** M-402
**Hamdy, Mona:** M-40
**Hamed, Dina:** M-163, M-204, M-208, M-209, M-210, M-211, M-213, M-214, M-215, M-217, M-61
**Hamed, Khaled:** E-134, E-135
**Hamed, Safaa:** T-14
**Hamza, Eman:** B-700, B-701, B-705
**Hamza, Haitham:** E-223
**Hamza, Hala:** M-364
**Hamza, Iman:** M-160, M-175, M-59
**Hanafy, Riham:** M-19
**Hanfy, Eman:** B-478
**Hanna, Mariam:** M-335, M-48
**Harb, Emad:** E-208, E-211
**Harb, Gamal:** B-424, B-425, B-426
**Hareedy, Amal:** M-367
**Hashem, Ahmed:** M-248, M-259, M-269
**Hashem, Mohamed:** B-532
**Hashish, Nawara:** M-243
**Hassan, Ahmed:** B-379
**Hassan, Amal:** E-237
**Hassan, Azza:** B-605, B-606, B-613, B-652, B-653
**Hassan, Dr.:** B-103, B-174, B-61, B-63,

B-95, B-96
**Hassan, Eman:** M-151, M-174, M-796
**Hassan, Fatina:** M-23, M-334
**Hassan, Hassan:** T-29
**Hassan, Hazem:** B-473, B-481, B-482, B-487
**Hassan, Hebatallah:** B-402
**Hassan, Hossam:** B-391
**Hassan, Maha:** E-178, E-180, E-185, E-187
**Hassan, Mazen:** S-15, S-9
**Hassan, Mohamed:** E-117
**Hassan, Mohamed:** M-27, M-30
**Hassan, Nagiba:** M-441, M-443, M-450, M-458, M-468
**Hassan, Naglaa:** T-35, T-36, T-37, T-38
**Hassan, Reem:** M-90, M-91
**Hassan, Rushdya:** T-7
**Hassan, Said:** M-414, M-425, M-429, M-437, M-462
**Hassan, Samira:** M-740, M-741, M-742
**Hassan, Seham:** M-197
**Hassan, Zeinab:** M-785
**Hassaneen, Hamdi:** B-107, B-214, B-216
**Hassaneen, Huwaida:** B-122, B-221
**Hassanien, Aboul:** E-215, E-216, E-220, E-221, E-222, E-224
**Hassanien, Reda:** B-497, B-498, B-499, B-500, B-502, B-503
**Hassib, Sonia:** M-580
**Hay, Rania:** M-100, M-102, M-109, M-110, M-115, M-92, M-93, M-94
**Heakal, Fakiha:** B-169, B-237
**Hefnawi, Hala:** M-708
**Hegazi, El-Saeed:** B-544, B-545
**Hegazi, Nabil:** B-492, B-493
**Hegazy, Maha:** M-417, M-419, M-427, M-434, M-435, M-438, M-445, M-457, M-469, M-481, M-495, M-497
**Hegazy, Rania:** M-93
**Hegazy, Rehab:** M-100, M-109, M-113, M-114, M-115, M-93, M-95, M-99
**Hegazy, Salem:** B-713, B-715, B-718, B-719, B-720
**Helal, Maha:** M-120, M-368
**Helal, Nahed:** M-339
**Helmi, Fatma:** T-2, T-21, T-24
**Hemayed, Elsayed Essa:** E-31, E-32
**Hemeda, Sayed:** T-22
**Hilal, Rifaat:** B-111, B-126, B-235, B-58, B-77, B-91
**Hilali, Mosaad:** B-593, B-594, B-595, B-596, B-597, B-599
**Hosny, Alaa:** M-537, M-561
**Hosny, Karim:** M-162, M-166, M-57
**Hussein, Ahmed:** M-387, M-388, M-390, M-392, M-396
**Hussein, Ebtissam:** B-540
**Hussein, Hanaa:** B-106
**Hussein, Heba:** M-403
**Hussein, Mohammed:** M-590
**Hussein, Rehab:** B-444, B-448
**Husseiny, Israa:** S-4, S-7
**Husseni, Maha:** M-80
**Hussin, Hussin:** B-689, B-690, B-694, B-696, B-697
**Iamail, Hamida:** B-447
**Ibrahem, Mohamed:** M-138
**Ibrahim, Hassan:** B-358
**Ibrahim, Hayam:** M-415, M-416, M-435, M-445, M-493, M-495
**Ibrahim, Heba:** M-285
**Ibrahim, Ihab:** M-517
**Ibrahim, Khaled:** B-632, B-651
**Ibrahim, Marwa:** B-550
**Ibrahim, Mohamed:** M-33, M-36, M-38, M-53, M-70
**Ibrahim, Nevine:** M-622, M-626, M-630, M-664
**Ibrahim, Nihal:** E-109
**Ibrahim, Norhan:** M-413
**Ibrahim, Safaa:** M-539
**Ibrahim, Samah:** M-794
**Ibrahim, Sherif:** B-399, B-402, B-403
**Ibrashy, Ibrahim:** M-193
**Isaac, Sally:** S-12
**Iskander, Marianne:** M-420, M-492
**Ismail, Ali:** S-22, S-23, S-24, S-25
**Ismail, Dina:** M-113
**Ismail, Ismail:** B-17, B-18
**Ismail, Mahmoud:** E-68, E-71, E-81, E-84
**Ismail, Mahmoud:** B-365, B-369, B-374, B-376, B-377, B-385, B-386, B-387, B-389, B-394
**Ismail, Manal:** M-510, M-516, M-518
**Ismail, Mohamed:** B-588
**Ismail, Nabila:** M-504
**Ismail, Reem:** M-320
**Ismail, Somaya:** B-420, B-422
**Ismail, Tawfik:** B-714, B-717
**Ismial, Samir:** B-458, B-486
**Issa, Yousry:** B-164, B-243, B-59, T-6
**Jakee, Jakeen:** B-576, B-578
**Kamal, Aliaa:** M-597, M-600
**Kamal, Asmaa:** M-283, M-377

**Kamala, Rasha:** M-118, M-120, M-123
**Kamel, Azza:** M-756
**Kamel, Gehan:** B-624
**Kamel, Manal:** M-288, M-45, M-46
**Kamel, Marwa W.:** M-798
**Kamel, Mona:** M-601
**Kamel, Nermin:** M-328, M-44, M-65
**Kamel, Osama:** M-533
**Kana, Maram:** B-742, B-743
**Kandil, Hisham:** M-271
**Kassab, Asmaa:** M-598, M-599
**Kassem, Hanaa:** M-714
**Kassem, Loay:** M-75, M-76
**Kenawy, Sanaa:** M-732, M-743, M-748, M-751
**Khairy, Hussein:** M-386
**Khalaf, Ezz:** B-285
**Khalafb, Abd:** B-686
**Khaled, Hussein:** M-772, M-773, M-774, M-775, M-776, M-795
**Khaleel, Amal:** M-722, M-727
**Khalial, Gamal:** B-129, B-130, B-150, B-161, B-162, B-241, B-83
**Khalifa, Badawy:** M-140, M-142
**Khalifa, Eman:** T-25
**Khalifa, Waleed:** E-166, E-169, E-171, E-172
**Khalifa, Yasser:** B-722, B-725, B-731, B-732, B-734
**Khalil, Ahmed:** E-77
**Khalil, Ahmed:** B-740, B-741
**Khalil, Ali:** B-277
**Khalil, Essam:** E-157
**Khalil, Mohamed:** B-292, B-293, B-295, B-299
**Khalil, Mohammed:** M-721
**Khalil, Nadia:** M-596
**Khalil, Neveen:** B-45
**Khalil, Wafaa:** B-24
**Khatab, Rania:** M-546, M-558, M-559, M-561, M-599
**Khateeb, Engy:** M-89
**Khattab, Ahmed:** E-65, E-83
**Khattab, Amr:** M-177
**Khattab, Mahmoud:** M-733, M-736, M-746
**Kheder, Nabila:** B-116, B-117, B-118, B-120, B-68
**Khedr, Amal:** T-15, T-16
**Khedr, Mohamed:** B-744
**Kholy, Amani:** M-320, M-761
**Khorshied, Mervat:** M-19, M-72
**Kobeasy, Mohamed:** B-457
**Komy, Mohamed:** M-115, M-93
**Koofy, Nehal:** M-319
**Louis, Dina:** M-660, M-666
**Maamoun, Hoda:** M-199
**Mabrouk, Walid:** B-296
**Macky, Tamer:** M-273, M-278, M-281, M-286
**Magdi, Rania:** M-320, M-47
**Magdy, Ayman:** B-665
**Maged, Ahmed:** M-247, M-253, M-256, M-261, M-262, M-266, M-269
**Mahana, Noha:** B-402, B-409
**Mahdy, Dali:** M-704
**Mahgoub, Osama:** E-60
**Mahmood, Hala:** B-39
**Mahmoud, Adel:** B-515
**Mahmoud, Ayman:** E-1
**Mahmoud, Ayman:** B-693, B-697
**Mahmoud, Enas:** M-191, M-350
**Mahmoud, Ghada:** B-457, B-463, B-468, B-471, B-476
**Mahmoud, Hanafy:** E-43, E-45, E-48
**Mahmoud, Maha:** B-699, B-701
**Mahmoud, Nisreen:** B-601
**Mahmoud, Samia:** M-330
**Mahmoud, Sherif:** M-755
**Mahmoud, Walaa:** B-123, B-124, B-146, B-151
**Mahmoud, Zeinab:** M-599, M-603
**Mahrous, Abeer:** S-34
**Mahrous, Engy:** M-704, M-722, M-727
**Mahrus, Mona:** M-245, M-246, M-271
**Makary, Meena:** E-200
**Makhlouf, Amal:** M-652
**Makhlouf, Manal:** M-40, M-47, M-51
**Mandour, Iman:** M-39, M-49
**Mansour, Hesham:** B-373
**Mansour, Lobna:** M-335
**Mansour, Mohie:** E-159, E-160
**Mansour, Sahar:** M-120, M-123, M-128
**Mansour, Wael:** M-782, M-783, M-788
**Marei, Waleed:** B-584, B-585, B-586, B-587
**Marie, Mohamed-Assem.:** B-401, B-406, B-408, B-410, B-429, B-430, B-438, B-443, B-444, B-453
**Marouf, Hala:** M-330
**Marouf, Sherief:** B-560, B-579
**Marzaban, Raghda:** M-160
**Marzouk, Mohamed:** E-176, E-177, E-179, E-181, E-194, E-195
**Mattar, Mervat:** M-186
**Megahed, Mohammad:** E-143, E-146
**Megahed, Said:** E-142
**Meguid, Afaf:** B-261

**Mehaney, Dina:** M-43, M-49, M-53, M-66
**Mekawy, Mohey:** B-685
**Mekky, Ahmed:** B-134, B-144, B-173, B-184, B-218, B-231, B-70
**Merey, Hanan:** M-441, M-494, M-498
**Meshaal, Safa:** M-318, M-32, M-37, M-65
**Metwalli, Sayed:** E-145
**Metwally, Hala:** M-109, M-116
**Metwally, Hayman:** B-7
**Metwally, Nadia:** B-147
**Moawad, Adel:** B-583
**Mofty, Medhat:** M-99
**Mohamed, Abdo:** B-21, B-25
**Mohamed, Abeer:** M-151, M-795
**Mohamed, Ahmed:** B-365, B-369, B-374, B-385, B-389
**Mohamed, Ahmed:** E-95, E-97
**Mohamed, Ahmed:** B-572, B-574
**Mohamed, Ahmed:** B-570, B-571, B-572
**Mohamed, Amany:** B-171, B-49, B-54, B-64
**Mohamed, Amr:** B-246, B-248
**Mohamed, Dawlat:** B-441
**Mohamed, Dr.:** B-217
**Mohamed, Heba:** M-412, M-424, M-430, M-431, M-467
**Mohamed, Howida:** M-618, M-624, M-637, M-644, M-654
**Mohamed, Hussein:** B-561, B-562
**Mohamed, Ibrahim:** M-610
**Mohamed, Khaled:** M-594
**Mohamed, Magdi:** M-628, M-667
**Mohamed, Mahmoud:** E-39, E-54
**Mohamed, Marwa:** B-508
**Mohamed, Mervat S.:** B-108
**Mohamed, Mohamed:** B-378
**Mohamed, Noha:** M-606, M-635
**Mohamed, Sabrein:** B-59
**Mohamed, Sandy:** M-777
**Mohamed, Shaymaa:** B-553, B-558
**Mohamed, Zeinat:** B-38, B-42, B-44
**Mohammed, Ashraf:** M-851
**Mohammed, Bassem:** M-520, M-521, M-522, M-524
**Mohammed, Faten:** B-610
**Mohammed, Haitham:** B-19, B-405, B-433
**Mohareb, Rafat:** B-102, B-108, B-109, B-176, B-190, B-194
**Mohey, Abeer:** M-252, M-45, M-93
**Mohey, Muhammed:** M-157, M-167
**Mohi Eldin, Mohamed:** M-238
**Mohieldin, Ahmed:** E-73
**Mohsen, Rokaya:** M-343, M-344
**Mokhtar, Omnia:** M-120
**Moneer, Ashraf:** M-594
**Monem, Azza:** M-671, M-712
**Morad, Mohamed:** M-186
**Morsy, Hany:** M-23, M-389, M-393
**Morsy, Nashwa:** B-537
**Mosharafa, Ashraf:** M-391, M-394, M-397
**Mostafa, Azza:** M-413, M-434, M-470, M-477
**Mostafa, Hassan:** E-72, E-74, E-79, E-80
**Mostafa, Mohamed:** B-684
**Mostafa, Mohga:** B-379
**Mostafa, Nadia:** M-320
**Mostafa, Taymour:** M-10, M-11, M-12, M-13, M-14, M-15, M-17, M-8
**Mostafa, Walaa:** M-266
**Mostafa, Wedad:** M-99
**Motaal, Amira:** M-699, M-707, M-708
**Motawi, Tarek:** M-502, M-503, M-508, M-509, M-512, M-514, M-515, M-517, M-519
**Mougi, Fatma:** M-27, M-344, M-347, M-49
**Mourad, Iman:** B-405, B-423, B-433
**Mousa, Mahmoud:** M-757, M-759, M-760, M-761, M-762, M-763, M-768
**Mousa, Somaia:** M-72
**Moussa, Abubakr:** T-10, T-18
**Moussa, Bahia:** M-581
**Moussa, Tarek:** B-36, B-37, B-41
**Mukhtar, Ahmed:** M-19, M-20, M-21, M-24
**Mustafa, Prof.:** B-157, B-70
**Nabarawi, Mohammed:** M-613, M-617, M-623, M-627, M-640, M-647, M-658
**Nabhan, Marwa:** M-315, M-334
**Nabih, Hoda:** E-10, E-6, E-7
**Nafie, Mohammed:** E-70, E-76
**Naguib, Bassem:** M-592
**Nashar, Rasha:** B-113, B-236, B-48
**Nasr, Aml:** M-198, M-40, M-64, M-74
**Nasr, Shimaa:** B-689
**Nassar, Hanan:** M-764
**Nassar, Noha:** M-452, M-739
**Nassar, Rania:** B-488, B-490, B-491
**Nassar, Yasser:** M-212
**Nassef, Olodia:** T-5
**Nasser, Ghanem:** B-506, B-509, B-510, B-512, B-513
**Nassif, Nagui:** M-828, M-832
**Negm, Hesham:** M-138
**Nooh, Mohammed:** M-501
**Noor, Neveen:** B-405, B-423, B-433

**Nour, Samia:** M-622, M-664
**Ogaly, Hanan:** B-554
**Okasha, Hussein:** M-190
**Omar, Mohamed:** B-151
**Omar, Mohammed:** M-849
**Omar, Rabab:** M-163, M-169
**Omar, Waleed:** B-301, B-307
**Omran, Dalia:** M-151, M-159, M-170, M-173, M-332
**Osman, Kamelia:** B-570, B-571, B-572, B-577
**Osman, Mohamed:** B-320, B-322, B-347
**Othman, Ahmed:** M-604, M-607, M-611, M-632, M-633, M-634, M-641, M-642, M-643, M-668
**Ouda, ?Ahmed:** T-27
**Ouf, Salama:** B-35, B-41, B-45
**Raafat, Hala:** M-282, M-48
**Rabie, Walaa:** M-271, M-44
**Radwan, Ahmed:** E-100, E-101, E-102, E-103, E-104, E-106, E-110, E-111, E-121, E-126, E-85, E-86
**Radwan, Ghada:** M-362
**Radwan, Noha:** M-758
**Ragab, Eman:** B-209, B-212, B-245
**Ragab, Fatma:** M-569, M-579, M-582, M-585
**Ragab, Gaafar:** M-183, M-187, M-189, M-190, M-195, M-273
**Ragab, Refaat:** B-589
**Ragab, Yasser:** M-557
**Rageh, Monira:** B-30
**Ragheb, Marianne:** M-581
**Rahman, Enas:** M-712
**Rahman, Khaled:** B-258, B-260
**Rahoma, Walid:** B-16
**Ramadan, Dalia:** M-39, M-62, M-73
**Ramadan, Mohamad:** M-791
**Ramadan, Nesrin:** M-432, M-470
**Ramadan, Sohair:** B-407, B-418, B-436, B-441, B-445
**Rashed, Laila:** M-103, M-11, M-110, M-115, M-13, M-179, M-192, M-193, M-197, M-205, M-206, M-207, M-208, M-209, M-216, M-358, M-360, M-648
**Rashed, Youssef:** E-190, E-191
**Rasheed, Hoda:** M-93, M-95
**Raslan, Ayman:** M-258
**Raziky, Mona:** M-323, M-343
**Reda, Wafaa:** B-704, B-708
**Refaat, Ahmed:** B-272
**Refai, Mohamed:** B-580
**Rehiem, Ayman:** M-169, M-175
**Rehim, Emam:** B-468, B-470, B-472, B-477
**Rezk, Mahmoud:** B-114, B-140, B-142, B-62
**Rezkallah, Nesrine:** M-430, M-459, M-467
**Ridi, Rashika:** B-127, B-409
**Rizk, Hussien:** M-27
**Rizkb, Sherine:** M-499, M-505, M-506, M-517, M-685
**Romeilah, Ramy:** B-471, B-476
**Saad, Adel:** B-589
**Sabry, Mohamed:** B-505
**Sabry, Nirmeen:** M-425, M-523, M-527, M-528, M-529, M-530, M-531, M-534, M-548, M-630
**Sabry, Omar:** M-673, M-725
**Sadik, Nermin:** M-507, M-509, M-511, M-514
**Sadik, Nermin:** M-358
**Safar, Marwa:** M-499, M-731, M-733
**Said, Abeer:** M-24
**Said, Amal:** M-755, M-756, M-765, M-766, M-769
**Said, Kareem:** B-411, B-414
**Said, Karim:** M-27
**Salah, Doaa:** M-23, M-389
**Salaheldin, Eman:** B-439, B-440, B-442, B-446
**Salama, Ahmad:** M-158
**Salama, Hosny:** M-159, M-796
**Salama, Maha:** M-648, M-677, M-696, M-701, M-713
**Salama, Walid:** B-271, B-278
**Salamouny, Said:** B-535
**Saleem, Sahar:** M-126
**Saleh, Doaa:** M-364
**Saleh, Hanan:** B-450, B-452, B-453
**Saleh, Hazem:** B-745
**Saleh, Mahmoud:** B-132, B-165, B-171, B-179, B-211
**Saleh, Marwah:** M-111, M-113, M-96
**Saleh, Nesma:** S-21
**Saleh, Osiris:** B-20, B-23, B-32, B-33
**Saleh, Samah:** M-50, M-52, M-55
**Salem, Doria:** M-118
**Salem, Fadia:** M-49
**Salem, Hesham:** M-731
**Salem, Hosni:** M-391
**Salem, Maissa:** M-414, M-420, M-426, M-429, M-432, M-437,

| | |
|---|---|
| | M-446, M-447, M-451, M-462, M-480 |
| **Salem, Mohamad:** | M-369 |
| **Salem, Suzan:** | M-593, M-602 |
| **Samy, Rania:** | M-322, M-61 |
| **Sayed, ?Abeer:** | M-673, M-696, M-706, M-709, M-721, M-725, M-726 |
| **Sayed, Ahmed:** | M-383, M-386 |
| **Sayed, Ahmed:** | M-39, M-61 |
| **Sayed, Rabab:** | M-735 |
| **Sayed, Riham:** | M-685 |
| **Sayed, Safaa:** | M-748 |
| **Sayed, Safinaz:** | M-102, M-97 |
| **Sayed, Yasmine:** | M-276 |
| **Seif, Walaa:** | B-370, B-375, B-376, B-377, B-387 |
| **Selim, Laila:** | M-311, M-312, M-329, M-49, M-66 |
| **Selim, Mohamed:** | M-719 |
| **Serror, Mohammed:** | E-183, E-186 |
| **Shaaban, Hebat:** | M-802, M-803 |
| **Shaaban, Mohamed:** | B-104, B-71 |
| **Shady, Omayma:** | M-303 |
| **Shaeer, Kamal:** | M-7 |
| **Shaeer, Osama:** | M-7 |
| **Shaheen, Amira:** | M-506 |
| **Shahin, Mohamed:** | B-336, B-340 |
| **Shahin, Nancy:** | M-503, M-505 |
| **Shahin, Rasha:** | M-42, M-56, M-89 |
| **Shahin, Walaa:** | M-340 |
| **Shaker, Olfat:** | M-100, M-111, M-112, M-175, M-202, M-203, M-339, M-356, M-401, M-402, M-503, M-505, M-507, M-509, M-514, M-753 |
| **Shalaby, Emad:** | B-463 |
| **Shalby, Mohamed:** | B-693 |
| **Shallan, Magdy:** | B-473, B-477, B-487 |
| **Shamaa, Ashraf1:** | B-668, B-669, B-676, B-680, B-681 |
| **Shamma, Rehab:** | M-616, M-629, M-640 |
| **Shanab, Sanaa:** | B-40 |
| **Sharaf, Sahar:** | M-254, M-347, M-49 |
| **Sharawi, Nivin:** | M-359 |
| **Shash, Ahmed:** | E-152, E-153, E-154 |
| **Shaurub, El-Sayed:** | B-250, B-259 |
| **Shawali, Ahmad:** | B-214, B-216, B-222 |
| **Shawky, Doaa:** | E-116 |
| **Shawky, Heba:** | M-358 |
| **Shawky, Sara:** | E-125 |
| **Shehab, Hany:** | M-150 |
| **Shehab, Ola:** | B-115, B-125, B-164 |
| **Shehata, Mohamed:** | B-160, B-185 |
| **Shehata, Mostafa:** | M-427, M-474, M-489, M-491 |
| **Sherein S.A. Elgayed:** | B-557 |
| **Sherif, Nadine:** | M-258 |
| **Sherif, Sherif:** | M-375, M-377 |
| **Sheta, Sahar:** | M-309 |
| **Shiba, Hala:** | M-330, M-72 |
| **Shokry, Dina:** | M-176 |
| **Shoukry, Ahmed:** | M-23, M-393 |
| **Shouman, Ahmed:** | M-23, M-393 |
| **Shouman, Samia A.:** | M-502, M-515, M-798 |
| **Shousha, Hend:** | M-170 |
| **Shresher, Mohamed:** | M-82 |
| **Sidky, Mohamed:** | M-273 |
| **Slim, Tarek:** | E-140, E-141, E-150 |
| **Soaida, Sherif:** | M-23 |
| **Soliman, Ahmed:** | B-104, B-155, B-74 |
| **Soliman, Ahmed:** | B-648, B-649 |
| **Soliman, Amel:** | B-398, B-406, B-418, B-421, B-436, B-441, B-443 |
| **Soliman, Amin:** | M-199 |
| **Soliman, Amira:** | T-45 |
| **Soliman, Mohamed:** | M-157, M-160, M-165, M-169 |
| **Sulaiman, Rania:** | M-500, M-513 |
| **Sweilam, Nasser:** | B-303, B-310, B-314, B-318, B-329, B-334, B-346 |
| **Tadros, Chahir:** | S-2, S-3 |
| **Tadros, Mina:** | M-617, M-646 |
| **Taha, Dalia:** | B-580, B-702, B-703, B-705, B-707 |
| **Taher, Azza:** | M-595 |
| **Tahoun, Neveen:** | M-801, M-804, M-805 |
| **Tahoun, Sameh:** | B-273 |
| **Talaat, Neveen:** | B-489 |
| **Tammam, Reham:** | B-171, B-73 |
| **Tawfik, Mohamed:** | E-71 |
| **Tayeb, Tarek:** | B-112, B-262, B-721, B-728 |
| **Tayel, Saadia:** | M-617, M-640, M-658 |
| **Teaima, Mahmoud:** | M-628, M-648 |
| **Tomerak, Rania:** | M-339 |
| **Torad, Faisal:** | B-668, B-669, B-670, B-680, B-682 |
| **Wadid, Magdy:** | B-150, B-161, B-180 |
| **Wahab, Mohamed:** | B-1 |
| **Wahab, Mohamed:** | B-398, B-421 |
| **Wahba, Amr:** | M-242 |
| **Wahed, Manal:** | E-204 |
| **Wanas, Mamdouh:** | B-12, B-15, B-327 |
| **Warda, Mohamad:** | B-550, B-551, B-552 |
| **Wassef, Mona:** | M-60 |
| **Yamany, Samar:** | B-650 |

**Yassin, Aymen:** M-544, M-547, M-554, M-560
**Yehia, Ali:** M-423, M-424, M-431, M-440, M-468, M-475
**Yehia, Taher:** B-544, B-545
**Younis, Mohamed:** E-91, E-98, E-99
**Yousef, Hesham:** B-246, B-261
**Yousef, Mamdouh:** M-421, M-428, M-449, M-473, M-474
**Yousef, Mohamed:** B-390
**Yousef, Randa:** M-99
**Yousef, Shahinaz:** B-8
**Yousif, Ahmed:** B-514, B-519, B-520, B-521
**Yousif, Tamer:** M-547, M-550, M-551, M-557, M-651
**Youssef, Mohamed:** M-240, M-241, M-246, M-252, M-258, M-265
**Yusuf, Mohammed:** M-164, M-170, M-173
**Zaazaa, Hala:** M-413, M-446, M-447, M-452, M-456, M-464, M-472, M-476, M-479, M-480, M-486, M-490, M-496
**Zaher, Ashraf:** M-593
**Zaher, Hesham:** M-102, M-92, M-93
**Zaher, Mostafa:** B-258, B-260
**Zaki, Hala:** M-751, M-753, M-754
**Zaki, Sherif:** M-3, M-5, M-6
**Zayed, Abeer:** M-177
**Zayed, Mohamed:** B-100
**Zayed, Naglaa:** M-149, M-154, M-163
**Zayed, Rania:** M-54, M-55
**Zayed, Shahira:** M-61
**Zein, Haggag:** B-539
**Zeineldin, Hatem:** E-33, E-34, E-37, E-41, E-42

General Scientific Research Department
Phone: +(202)35704943 - 35676918 - 35675597
Fax: +(202)37745324
Web site: http://gsrd.cu.edu.eg.
www.cu.edu.eg
E-mail: resinfo@cu.edu.eg